PROCEEDINGS OF THE 15TH

INTERNATIONAL MARINE DESIGN CONFERENCE

EDITOR: Austin A. Kana

AMSTERDAM, NL

TU Delft OPEN

TU Delft

IMDC 2024
INTERNATIONAL MARINE DESIGN CONFERENCE

Colophon

Proceedings of the 15th International Marine Design Conference (IMDC-2024)

Editor:
Austin A. Kana[1]
[1] Department of Maritime and Transport Technology, Delft University of Technology
a.a.kana@tudelft.nl orcid: 0000-0002-9600-8669

Keywords:
Marine design; Design methodology; Novel marine design concepts; Maritime energy transition; Maritime unmanned and autonomous transition; Maritime digital transition; Maritime regulations; Maritime design education

Published by:
TU Delft OPEN Publishing | Delft University of Technology, The Netherlands

DOI: https://doi.org/10.59490/mg.113
ISBN: 978-94-6366-896-5

Peer Review Statement:
The editor of the proceedings warrants that 1) they adhere to TU Delft OPEN Policy on publishing integrity and good scientific publishing practices; 2) all papers have been subject to blind review by at least 2 reviewers, of which one from the International Committee, and the other from either the National Organizing Committee or the list of additional reviewers, administered by the editor; 3)

Reviews were conducted by expert referees who were requested to provide unbiased comments aimed at improving the work.

Preface

The ***15th International Marine Design Conference (IMDC-2024)*** was organized by the Department of Maritime and Transport Technology, Delft University of Technology, and was hosted by the Netherlands Defence Materiel Organisation at the Marine Etablissement Amsterdam (MEA). The aim of the IMDC is to promote all aspects of marine design as an engineering discipline. The focus of IMDC-2024 is on the key design challenges and opportunities in the maritime field with special emphasis on the following themes.

- **Ship design methodology** issues such as: design spiral, systems engineering, set-based design, design optimisation, concurrent design, modular design, configuration based design, or "fuzzy" design aspects.

- **Novel marine design concepts**, such as: hull form design, transport ships, service vessels, naval vessels, yachts and cruise ships, or specialized and complex vessels.

- **Offshore design methodology**, such as applications to: offshore wind turbines, semi-submersibles, floating fish farms, or floating cities.

- Influence of **energy transition** on maritime design, including both zero emission and high power and energy systems.

- Influence of **unmanned and autonomous transition** on maritime design.

- Influence of **digital transition** on maritime design, such as: digital shadows and twins, model-based systems engineering, AI, ML and big data.

- Influence of **regulations** on maritime design.

- Maritime **design education**

Professor Stein Ove Erikstad

Chair, International Committee
Department of Marine Technology
Norwegian University of Science and Technology
Norway

Associate Professor Austin A. Kana

Chair, National Organizing Committee
Department of Maritime and Transport Technology
Delft University of Technology
The Netherlands

Acknowledgements

IMDC-2024 would like to acknowledge the following individuals and organizations for their support.

INTERNATIONAL COMMITTEE

- **Chair: Professor Stein Ove Erikstad**, Norwegian University of Science and Technology, Norway
- **Prof. David Andrews**, University College London, UK
- **Prof. Richard Birmingham**, Newcastle University, UK
- **Adj. Prof. Per Olaf Brett**, Norwegian University of Science and Technology, Norway
- **Julie Chalfant, PhD**, Massachusetts Institute of Technology, USA
- **Kelly Cooper**, US Navy Office of Naval Research, USA
- **Prof. Hans Hopman**, Delft University of Technology, the Netherlands
- **Prof. Stefan Krüger**, Hamburg University of Technology, Germany
- **Associate Prof. Taiga Mitsuyuki**, Yokohama National University, Japan
- **Prof. Apostolos Papanikolaou**, National Technical University of Athens, Greece
- **Patrik Rautaheimo, PhD**, Elomatic, Finland
- **Prof. Myung-il Roh**, Seoul National University, Korea
- **Associate Prof. David Singer**, University of Michigan, USA
- **Prof. Dracos Vassalos**, University of Strathclyde, UK

NATIONAL ORGANIZING COMMITTEE

- **Chair: Associate Prof. Austin A. Kana**, Delft University of Technology
- **Venue chair: Bart van Oers, PhD,** Dutch Command Materiel and IT (COMMIT)
- **Nikoleta Dimitra Charisi**, Delft University of Technology
- **Koen Droste,** Damen Naval
- **Etienne Duchateau, PhD,** Dutch Command Materiel and IT (COMMIT)
- **Sietske de Geus**, Delft University of Technology
- **Agnieta Habben Jansen, PhD**, Dutch Command Materiel and IT (COMMIT)
- **Prof. Hans Hopman**, Delft University of Technology
- **Carmen Kooij, PhD**, NHL Stenden Hogeschool
- **Ben Noble**, Delft University of Technology
- **Zacharias-Panagiotis Oikonomou**, Delft University of Technology
- **Joan le Poole, PhD**, Delft University of Technology, Dutch Command Materiel and IT (COMMIT)
- **Associate Prof. Jeroen Pruyn**, Delft University of Technology
- **Evelien Scheffers**, Delft University of Technology
- **Apostolos Souflis-Rigas**, Delft University of Technology
- **Jesper Zwaginga**, Delft University of Technology
- **Secretarial and management support staff,** Department of Maritime and Transport Technology, Delft University of Technology
- **Conference organizing staff,** Marine Etablissement Amsterdam (MEA)

ADDITIONAL SCIENTIFIC REVIEWERS

- **Richmond Anku,** Delft University of Technology
- **Assistant Prof. Lindert van Biert**, Delft University of Technology
- **Anna Boon**, Delft University of Technology
- **Miguel Calvache**, Delft University of Technology
- **Associate Prof. Andrea Coraddu**, Delft University of Technology
- **Sanne van Essen**, Delft University of Technology
- **Assistant Prof. Daniele Fiscaletti**, Delft University of Technology
- **Jaap Gelling**, Delft University of Technology
- **Robert Hekkenberg**, Netherlands Ministry of Infrastructure and Water Management
- **Joseph van Houten**, University of Michigan
- **Herbert Koelman, PhD**, NHL Stenden Hogeschool
- **Benjamin Lagemann**, Norwegian University of Science and Technology, Norway
- **Anna-Louise Nijdam**, Delft University of Technology
- **Erin van Rheenen**, Delft University of Technology
- **Assistant Prof. Harleigh Seyffert**, Delft University of Technology
- **Assistant Prof. Cornel Thill**, Delft University of Technology
- **Assistant Prof. Peter de Vos**, Delft University of Technology
- **Niels de Vries**, Delft University of Technology
- **Associate Prof. Peter Wellens**, Delft University of Technology

FUNDING SPONSORS

Platinum Sponsor

Gold Sponsors

Silver Sponsors

Table of Contents

Part 1:
KEYNOTES

Part 2:
DESIGN METHODOLOGY

Part 3:
NOVEL CONCEPTS

Part 4:
OFFSHORE DESIGN METHODOLOGY

Part 5:
ENERGY TRANSITION

Part 8:
INFLUENCE OF REGULATIONS

Part 9:
DESIGN EDUCATION

Part 1:
KEYNOTES

Ship Design in the Era of Digital Transition - A State-of-the-Art Report

Apostolos Papanikolaou[1,*], Evangelos Boulougouris[2], Stein-Ove Erikstad[3], Stefan Harries[4] and Austin A. Kana[5]

ABSTRACT

The evolution of ship design from a manual toward a computer-aided, digital approach has been drastic after the 1970s, with the explosive development of computer hardware and software systems. In today's era of smart digitalization in the frame of Industry 4.0, recently introduced digital/software tools and systems increase the efficiency and quality of the life-cycle ship design process, but also the operational complexity and the demand for proper training of users of software platforms. Parametric optimisation and simulation-driven design, product lifecycle management, digital twins and artificial intelligence are nowadays frequently used by the maritime industry during the commissioning/quality control activities and in the various phases of ship design, ship operation and ship production. This paper presents an overview of notable developments in the above areas and the way ahead to respond to present and future challenges of the maritime industry.

KEY WORDS

State-of-the-Art report; Ship Design Methodologies and Tools; Holistic Ship Design; Multi-objective & Parametric Optimisation; Simulation-Driven Ship Design; Product Lifecycle Management; Digital Twins; Artificial Intelligence.

PREAMBLE

The design methodology (DM) state-of-the-art reports (DM-SoA) are inherent constituents of the International Marine Design Conference (IMDC) and its long history. A synopsis of the DM-SoA timeline from the start of the IM(S)DC until 2018 was given by Andrews et al (2018) at the 13th IMDC, held in Helsinki. This timeline shows a large variety of interpretations of what the SoA report at the IMDC should or rather could comprise, ranging from reviews of the ship design history, different variants of "Design-for-X" (Papanikolaou et al, 2009, Andrews et al., 2012), as well as challenges related to the design of particular ship types.

Recognizing the importance of the DM-SoA as a binding thread between the tri-annual IMDC conferences, and the so far lack of a clear consensus on style, form and structure, the last SoA report (Erikstad & Lagemann, 2022) has more clearly formulated the goals and purpose of the DM-SoA reports, namely to "*analyze and summarize, on behalf of the marine systems design community, the current state and key developments within our field, based on a review of current research and technology achievements, as well as feedback from academia and industry*". *Regarding form, style and structure, a set of characteristics was proposed. It should be focused on marine systems design, with a clear emphasis on design methodology within the larger*

[1] National Technical University of Athens (Naval Architecture and Marine Engineering, Ship Design Laboratory, Athens, Greece); ORCID: 0000-0001-7464-9476

[2] Strathclyde University (Naval Architecture, Ocean and Marine Engineering, Glasgow, United Kingdom); ORCID: 0000-0001-5730-007X

[3] Norwegian University of Science and Technology (Trondheim, Norway); ORCID: 0000-0001-7323-6901

[4] FRIENDSHIP SYSTEMS AG (Strategy and R&D, Potsdam, Germany); ORCID: 0009-0000-8022-989X

[5]Delft University of Technology (Department of Maritime and Transport Technology, Delft, the Netherlands); ORCID: 0000-0002-9600-8669

* Corresponding Author: papa@deslab.ntua.gr

Submitted: 1 March 2024, Revised: 15 April 2024, Accepted: 1 May 2024, Published: 7 May 2024

Conference paper, DOI: https://doi.org/10.59490/imdc.2024.784 e-ISSN: 3050-4864

framework of engineering design/systems design. It should be contemporary, giving priority to what have been key topic areas and achievements since the last conference, as well as ongoing research developments towards the next venue. It should be opinionated, to the extent that the authors of the report need to make an educated prioritization of what are the most important developments, as well as provide a basis for discussions and comments at the conference. Finally, it should also balance the focus between academia and industry and look into how research and technology developments are adopted in industry and actual design practice.

In this year's DM-SoA paper, we have aimed at following up on these principles. The focus will be on recent and emerging developments as well as on state-of-the-art, mature and *smart* ship design methodologies in the frame of *smart digitalization of the maritime industry (Industry 4.0)*. Parametric optimisation and simulation-driven ship design, ship product lifecycle management, digital twins and artificial intelligence are nowadays frequently used by the maritime industry during the commissioning/quality control of marine products and in the various phases of life-cycle ship design, ship operation, ship production and decommissioning/scrapping. This paper presents an overview of notable developments in the above areas and the way ahead to respond to the present and future challenges of the maritime industry.

INTRODUCTION

The evolution of ship design from a manual toward a computer-aided, digital approach has been drastic after the 70s, with the explosive development of computer hardware and software systems. In today's era of smart digitalization in the frame of Industry 4.0, recently introduced digital/software tools and systems increase the efficiency and quality of the life-cycle ship design process, but also the operational complexity and the demand for proper training of users of software platforms. It is evident that the international maritime industry and its representatives (shipping and shipbuilding industry, class societies, design companies, research institutes and academia) have widely adopted the smart digitalization concept in ship design, shipbuilding, and ship operation, long before Industry 4.0 was formally introduced, mainly in production processes. This is due to the very strong competition in the worldwide shipping and shipbuilding market. However, the degree of adoption the smart digitalization concept of Industry 4.0 strongly varies, depending on the size and competitiveness of the specific maritime industry and its representatives.

Typical forerunners in the introduction of smart technologies and associated digital services to the maritime industry are all major classification societies (e.g., Det Norske Veritas/DNV, 2023, Class NK, 2023, American Bureau of Shipping/ABS, 2023, Lloyds Register/LR, 2023, Bureau Veritas, 2023). The same applies to all major software vendors (e.g., NAPA, 2023, Dassault, 2023, Siemens, 2023) offering software tools for all phases (or part of) of the ship's life cycle (ship design, construction, operation). In between the end users/customers (shipyards and shipping companies) are in general the design offices/consultants, fitting the offered software tools to the needs of the end users or running specific software tools on their behalf. Of course, large shipyards and shipping companies may have their own specialists/software engineers to work directly with advanced software tools and adjust them to the needs of their companies. Finally, research institutes and academia may be in the forefront of initial developments of software tools, the marketing of which is however left to software vendors and partly class societies.

When looking at the level of digitalization, the maritime industry and particularly shipbuilding is often considered as one of the least digitally advanced industries. It is, however, important to understand the differences between digitization, digitalization and digital transformation:

- *Digitization*: is the conversion of information into a computer-readable format. A prime example of digitization in shipbuilding is moving from a drawing board to a CAD procedure or more generally, transforming a document or piece of information that was originally not in digital form into a computerized representation. With respect to ship lines, their digital form does not only serve as a digital drawing board that speeds up drafting and reduces the required time to create and modify technical drawings. This digital representation is the nucleus of all software tools dealing with ship design, production, and operation and the first step in creating a digital twin (DT). This stage of development is nowadays common in both the shipping and shipbuilding industry.
- *Digitalization*: is the use of digital technologies to optimize ship design, ship operation and business processes. It particularly refers to changes in the design work and in the way stakeholders of a maritime product engage and interact. It goes well beyond the implementation of technology for certain tasks and optimizes the global-scale performance of organizations, yielding a significant competitive advantage for them. This stage of development is nowadays quite advanced in all major shipping companies and class societies and to a lesser degree in some major shipbuilders.
- *Digital Transformation*: in the sense of Industry 4.0, it is the holistic, overall societal effect and wide-spread digitalization of the industry. It refers to the transformation of business models, socio-economic structures, legal and policy measures, organizational patterns, and so forth. The present stage of development of the maritime industry has

only a few "shining" examples of digital transformation, e.g., major class societies and shipping companies, software vendors.

There are only very few published studies on the digital transformation of the maritime industry, with emphasis on virtual prototyping and cyber security. According to Diaz (Diaz et al, 2023), "*the evolution of maritime and shipbuilding supply chains toward digital ecosystems increases operational complexity and needs reliable communication and coordination. As labor and suppliers shift to digital platforms, interconnection, information transparency, and decentralized choices become ubiquitous. In this sense, Industry 4.0 enables "smart digitalization" in these environments. Many applications exist in two distinct but interrelated areas related to shipbuilding design and shipyard operational performance. New digital tools, such as virtual prototypes and augmented reality, begin to be used in the design phases, during the commissioning/quality control activities, and for training workers and crews".* Ichimura et al (2022) rather focus on Artificial Intelligence (AI), Big Data Analytics (BDA), Cloud Computing and the Internet of Things (IoT), which are already used by the maritime industry, particularly in a variety of applications of the shipping industry. The maritime transport industry is already transitioning into a new operations paradigm, often termed as *"shipping in the era of digitalization".* Shipping companies promote digitalization as the future of the maritime industry and their efforts to set up strategies are already in progress. Examining those visions and strategies in relation to digitalization would be beneficial to better understand the way towards which the maritime industry is heading.

Turning to *smart* ship design methodologies and independently of a variety of professional software tools addressing main parts and specific aspects of ship design, the recently completed Horizon 2020 European Research project – HOLISHIP – Holistic Optimisation of Ship Design and Operation for Life Cycle (2016-2020) (Papanikolaou et al, 2022), in which 40 major representatives of the European Maritime industry participated (http://www.holiship.eu/), introduced an innovative, holistic approach to ship design and the development of integrated design software platforms and tools, which were used by the European maritime industry in a series of practical applications (demonstration studies). In the era of the 4th industrial revolution, the project set out to substantially advance ship design by the introduction of a fully computerized, multi-disciplinary optimisation approach to ship design and life-cycle operation. The approach enables the exploration of the huge design space in relatively short time, the distributed/multi-site working and the virtual reality testing, thus it is a strong asset for the development of innovative maritime concepts in response to the needs of the 21st century. The HOLISHIP approach is based on an open architecture scheme and the buildup of flexible s/w platforms (like CAESES®) with simple communication protocols and a long list of integrated external s/w tools. This includes, also, communication with professional naval architectural s/w platforms (like NAPA®) and interchange of data through macros. A comparison of the conventional ship design approach with a contemporary, fully computerized design procedure, as implemented in the HOLISHIP project, is shown in Figure 1, reproduced from (Papanikolaou, 2022).

Criterion	Conventional	HOLISHIP
Concept design	Empirical approach; supported by available computer-added calculation and graphics processing procedures, manual generation of 1…3 variants of baseline design and intuitive selection of the most promising variant	Automated parametric generation of hundreds of variants (*digital siblings*; cloning) and comparison to baseline design, including their documentation; *global optimisation* of main ship dimensions and main characteristics; rational (mathematical) identification of most promising variants on the basis of set criteria
Preliminary/ Contract design	Sequential processing of design steps (design spiral); individual optimisation of design properties (hydrodynamics, structures, machinery, economics) of just a few design variants	Parallel processing of design steps and design synthesis; multi-objective and multi-disciplinary optimisation of several/hundreds of design variants; local hull form optimisation
Accuracy of calculation methods	Low at concept design level (mostly empirical modelling); high at contract design level	High at any design level depending on the capability of the employed s/w tools; use of surrogate models for intensive calculation tasks
Design lead time and person months effort	*Assuming the availability of a baseline design*: Concept design: some person days, depending on the experience of the design team Contract design: several person months, depending on the experience of the design team *If no baseline is available*: Concept design: many person days of collecting information, identifying and analyzing similar ships already built from public data	*Assuming the availability of suitable parametric models*, e.g. from a previous design campaign: Concept and contract design: lead times are significantly reduced by a factor > 5 (est.); smaller design team with less need for experience of all team members *If no parametric models are at hand*:

		Several days to weeks for building up robust and meaningful parametric models, depends on modeler's experience
Costs	The effect of design variants on cost is done at early design stage intuitively by designer's experience or at best by checking the costs of only a few design variants	Early assessment of the effect of hundreds of design variants on cost leads to significant cost reductions in the production cost (CAPEX) and operational cost (OPEX) or maximization of the Net Present Value (NPV)
Quality of design (concept and contract)	Highly depend on the designer's and yards' experience	Superior quality thanks to systematic optimisation and selection of the best out of hundreds of variants; consolidated standard design documentation; Quality assurance via consistency in the assessment of variants
Safety of ship & the marine environment	Rules-based design with undefined safety level	Risk-based design with quantifiable risk consequences and safety level
Energy efficiency	Studies on energy efficiency are commonly done at contract design stage and mostly refer to the hull-propeller interaction; individual studies on overall energy consumption are nowadays common for high energy consumers (passenger ships, high-powered, special type of ships)	Improved energy efficiency in view of the integration of s/w tools for the simulation of energy consumption, including the machinery-propeller-hull interaction at early design stage
Life-cycle Performance and Assessment	Mostly restricted to the economics of an investment (shipowner's side); environmental impact is only considered by enforced regulations (considering the set IMO targets as constraints)	Life-cycle assessment and optimisation of economics and environmental impact at early design stage
Innovations in ship design	Limited, due to the lack of baseline designs to build upon	Enabled in view of the simulation-based (first principles) ship design approach; main design problem issue: definition of parametric model (transfer of innovation idea to a mathematical model)
Software platforms	Professional naval architectural software platforms with limited or no collaboration with external software tools; strict communication protocols	Flexible s/w platforms with simple communication protocols; long list of integrated external s/w tools, including communication with professional naval architectural platforms (CAESES); interchange of data with NAPA® through macros
Design workflow procedures	In general, manual planning of design workflow, which depends on designer's experience; limited coded design workflow procedures	Enables coding of design workflow procedures by macros; HOLISHIP demonstrated more than ten (9+3) coded design procedures for several ship types and marine assets
Distributed working/cloud communication	Not known in ship design	Enabled through cloud communication (IoT) and demonstrated through the RCE/CAESES HOLISHIP platforms
Virtual prototyping	Not known/limited in ship design	Demonstrated by simulation of the maneuverability of a ship with alternative rudders on MARIN's bridge simulator and feedback by the captain (man-machine interaction)
Acceptance by industry	Trivial, as conventional	At present the acceptance is limited to the HOLISHIP partners and knowledgeable academia; growing acceptance; education of future naval architects is essential; HOLISHIP book and dissemination through partnership

Figure 1: Conventional vs. an Advanced, Holistic Approach to Ship Design (Papanikolaou, 2022)

The present paper aims at an overview of notable, recent developments in methodologies of *smart ship design and operation* and a description of the way ahead to respond to present and future challenges of the maritime industry. It has a particular focus on the impact of the digital transformation on ship design methodologies, as of the remit of IMDC, but extending on ship production and ship operation with applications nowadays common to the maritime industry. After a brief introduction, Apostolos Papanikolaou presents an advanced parametric ship design optimisation, as implemented in project HOLISHIP, its historical development, and applications. Stefan Harries deals next with simulation-driven ship design (SDSD), what is closely related to ship design optimisation and the HOLISHIP project. Stein Ove Erikstad elaborates on the impact of digitalization on ship production and life cycle management. Austin Kana presents an overview of recent developments in the field of digital twins (DT) in the design and retrofit of ships and last, but not least, Evangelos Boulougouris presents methods and tools of Artificial Intelligence (AI) with applications in ship design and operation.

PARAMETRIC SHIP DESIGN OPTIMISATION

Ship Design Optimisation

Inherent to design is design optimisation, namely the identification of the best out of all feasible solutions for a set design problem. The progress in ship design optimisation in the last five decades has been revolutionary and in line with developments in hardware and software, moving from a single-objective optimisation for the minimum required freight rate (RFR) of a tanker (Nowacki et al, 1970), to multi-objective ship design optimisation of various types of ships for a variety of criteria and constraints (Figures 2 and 3).

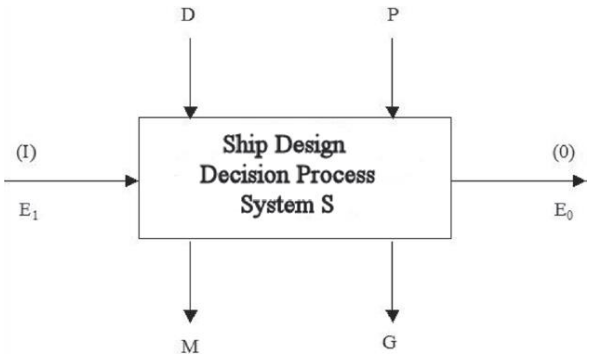

Figure 2: Single Objective Ship Design Optimisation for RFR (M: merit function, D: design variables, P: parameters, G: constraints) (Nowacki et al., 1970)

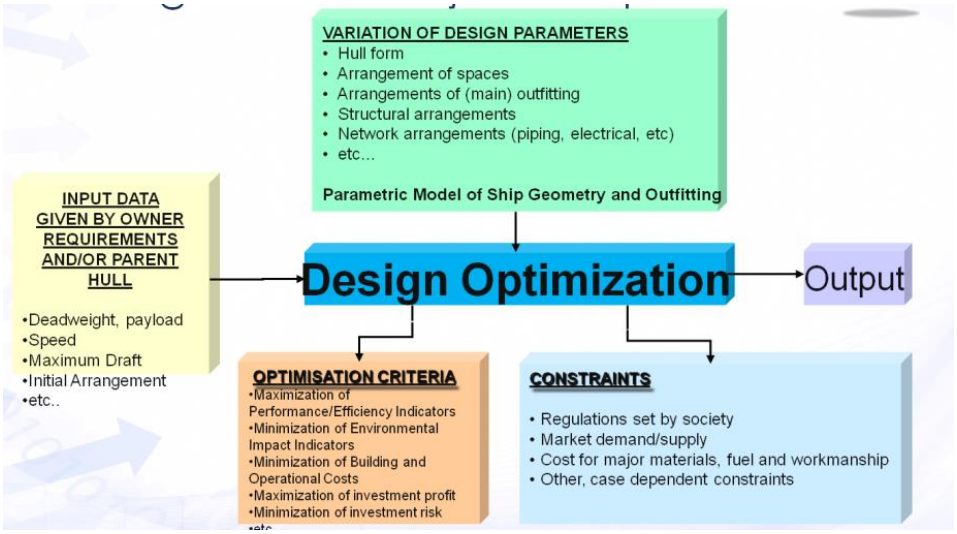

Figure 3: Multi-objective Ship Design Optimisation for multiple criteria (Papanikolaou, 2010)

The holistic approach to ship design and multi-objective ship design optimisation was introduced by A. Papanikolaou in a Special Issue of Journal CAD, which was dedicated to the 75th birthday of Professor Horst Nowacki (Papanikolaou, 2010). The outlined approach was later implemented in the EU funded project HOLISHIP (2016-2020).

Parametric Modelling - Digital Siblings

An important feature of the multi-objective optimisation procedure presented in Figure 3 is the *Parametric Ship Modelling*, namely the systematic variation of design parameters for the generation of digital "siblings". This generally refers to the variation of ship's geometry (e.g., of the wetted hull form, Figure 4), of main internal spaces (e.g., for a RoPax, Figure 5), of main structural elements (e.g., for a RoPax design, Figure 6), of ship's machinery/propulsion and main outfitting arrangements, as necessary for the processing of selected design parameters that are optimised in the frame of a defined optimisation procedure.

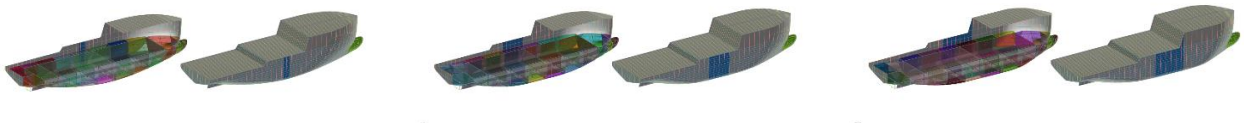

Figure 4: Three hull forms with lengthened and shortened *parallel mid-body* (shown in blue) but *identical displacement* and *longitudinal centers of buoyancy* by CAESES® (Courtesy Claus Abt, Friendship Systems, 2023)

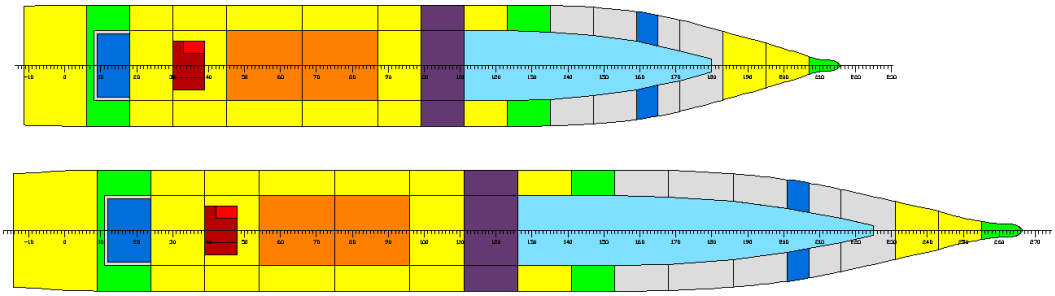

Figure 5: Internal subdivision for two RoPax hulls of different length, but identical arrangement of spaces concept, for damage stability calculation and assessment by NAPA® (Zaraphonitis et al., 2012, project HOLISHIP)
Top layout for LBP=170m, bottom layout for LBP=210m.

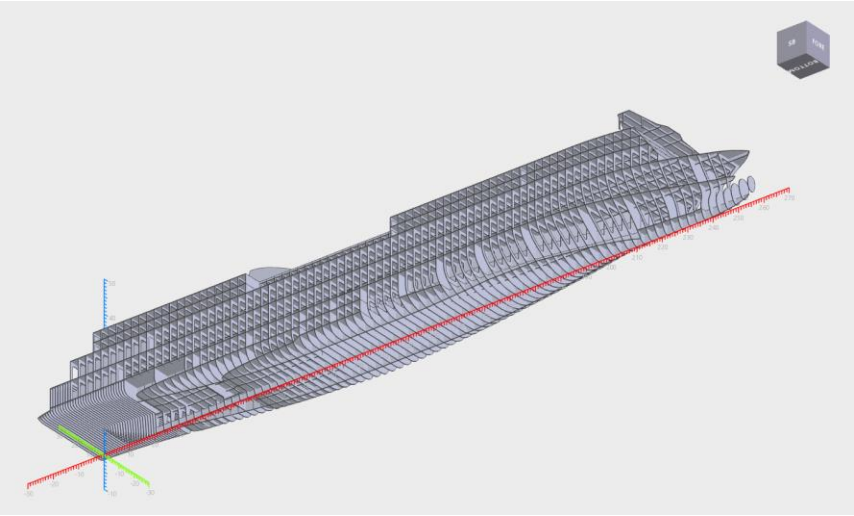

Figure 6: Parametric structural design of RoPax by NAPA Steel® (Basic model, Tuzcu et al., 2021, project HOLISHIP)

Historically and conceptually, the *parametric* optimisation of ship design was introduced by Murphy et al. (1965), when varying ship's main dimensions by systematic permutation within a certain range and identifying manually (graphically at that time) the best variant corresponding to the ship *of lowest cost*. A few years later, Nowacki et al. (1970) applied also parametric modelling by the variation of ship's main dimensions and form parameters to the optimisation of a tanker design to find the variant with the minimum required freight rate (RFR), while solving the ensuing optimisation problem by a Tangent Search Algorithm (TSA). It took about 10 years for the parametric modelling to be formally introduced into the hydrodynamic optimisation of ships by *variation of ship's hull form*, next to ship's main dimensions, in the frame of a *continuous function optimisation*. This was first applied to slender ship hull forms (mathematical hull forms, e.g., SWATH-like forms) by Kusaka et al. (1980), Salvesen et al. (1985), Papanikolaou & Nowacki et al. (1989), Papanikolaou & Androulakakis (1991) and it was later extended to a wider range of slender, high-speed vessels (Papanikolaou et al. 1996, Zaraphonitis et al., 2003). Applications to a wider class of conventional ship hull forms were first shown by Harries (1998).

The parametric modelling refers in general not only to the variation of a ship's wetted surface geometry, when dealing with hydrodynamic optimisation, but also to the internal subdivision and space arrangements of ships, when dealing with ship's damage stability of RoPax ships (Boulougouris-Papanikolaou-Zaraphonitis, 2004), while also including the parametrization of main structural elements (Tuzcu et al., 2021), or when dealing with the probability of oil-outflow of damaged tankers (Figure 7), etc. Thus, it covers both continuous, integer and discrete optimisation problems and associated techniques. It depends on the completeness of the ensuing parametric model with respect to the specific design parameters that are to be optimised in the frame of a defined optimisation problem and its processing in the frame of a simulation-driven design procedure.

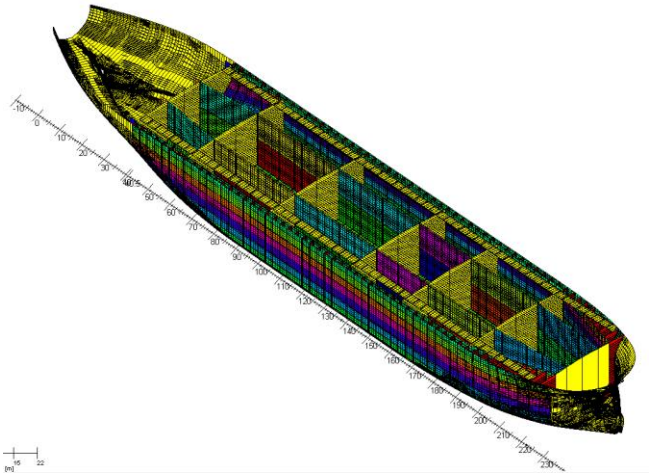

Figure 7: Parametric structural design of AFRAMAX tanker by use of POSEIDON® s/w for minimization of structural weight and of oil outflow (Papanikolaou et al, 2010, project BEST)

Parametric modelling is inherently related to *Digital Siblings*. Digital "siblings" may be seen related to digital "*twins*". However, they are of different origins and are differently used. The concept of *Digital Twin*, namely of a virtual, digital equivalent to a physical product, was introduced in 2003 by Grieves (2015). It is a virtual replica (model) of a real-world asset and it is based, besides on a digitised description of a real-world asset (here a ship), on a continuously enriched database of performance data transmitted to the virtual model from the real-world asset. This allows the virtual object to exist simultaneously with the physical one and it can be readily used in the virtual prototyping and testing of new products, e.g., in the optimisation of ship's operation after refitting a bulbous bow or of a new propulsive device; thus, it is a powerful tool of the contemporary manufacturing industry (Sharma et al., 2022, Mauro & Kana, 2022).

Digital Siblings, on the other side, are not based on the feeding with a continuous transmission of performance data of the physical asset, but are generated by the use of the design data of a *basic* digital model that is modified by systematic variation of its design parameters, *resembling the biological process of mutation, crossover and selection*. The extent of the design parameters is associated to the complexity and completeness of the ensuing parametric model that is set up by the use of a CAD software system (e.g., CAESES®, NAPA®, etc.). They should have enough modelling accuracy to allow the exploration of the huge design space in the frame of a *global* optimisation procedure, aiming at determining the object's main characteristics (Papanikolaou, 2024).

Following an advanced, conceptual/preliminary ship design approach, a ship's optimal main dimensions and main characteristics may be determined by the conduct of a properly set-up multi-stage optimisation procedure (Figure 8), as also outlined in Figure 3.

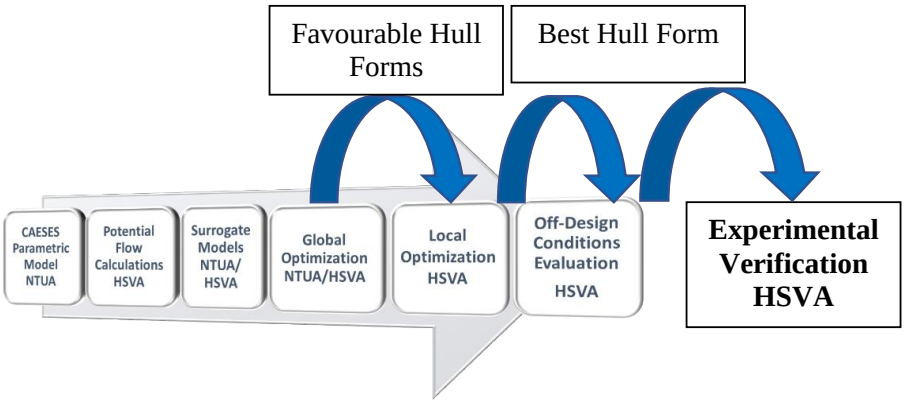

Figure 8: Multi-stage optimisation procedure applied to the hydrodynamic optimisation of a fast catamaran (project TrAM, Papanikolaou et al., 2020)

Following the *global optimisation*, in which the optimal main dimensions (length, beam, draft, and separation distance of the catamaran's demi-hulls) were identified, a *local* optimisation procedure generally follows. This can be the ship's bow (fitting or optimisation of a bulbous bow) or ship's stern or both. In the case of the optimisation of a fast catamaran, it was the transom stern region, while considering various transom stern geometries and the interaction between the ship's hull, propeller, propeller shaft, shaft-brackets and rudder (Figure 9).

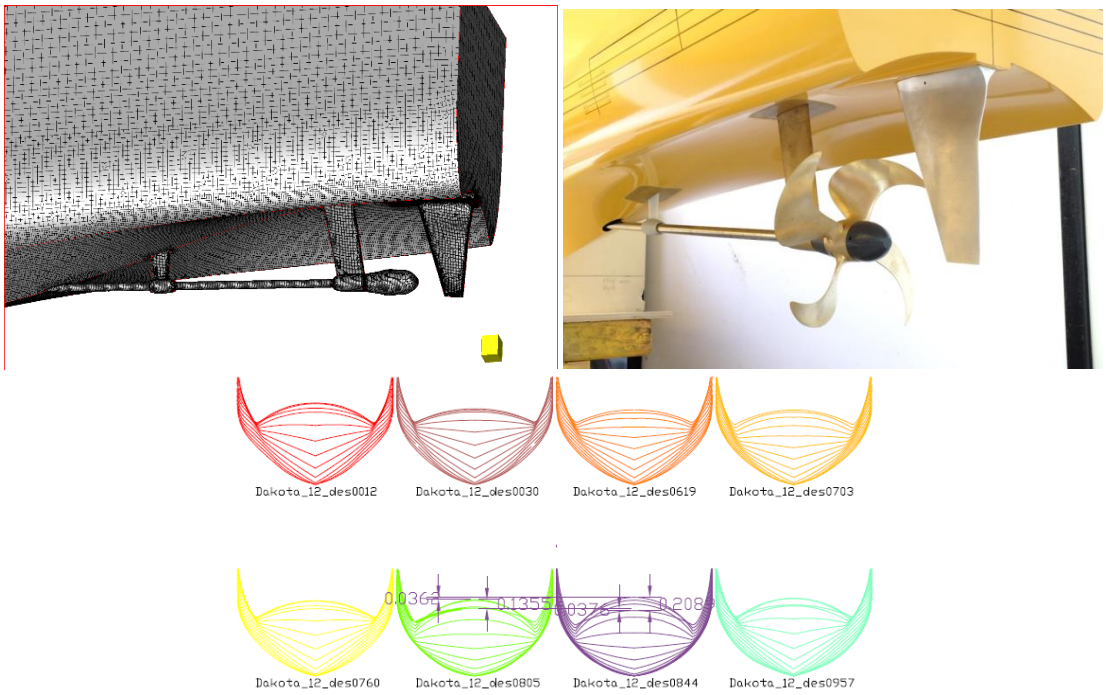

Figure 9: Local optimisation of the stern tunnel area of the Stavanger Demonstrator (catamaran *Medstraum*) by use of FreSCo+ (5.7M) - Project TrAM (Xing-Kaeding & Papanikolaou, 2021)

Because large sets of design variants need to be generated and independently assessed by partly computer-intensive procedures (e.g., CFD calculations) to determine their performance, Designs-of-Experiments (DoE), such as a SOBOL or a Latin hypercube sampling technique, are being utilized to generate variants for pre-selected free variables; the superset of all free variables representing the design space for the design task is used to generate *surrogates* of the directly calculated models. For

surrogate modelling, different techniques are available such as kriging, artificial neural network analysis and polynomial regression (Harries & Abt, 2019).

Application / Demonstration Study

A variety of application case studies, which were developed in the frame of the HOLISHIP and earlier projects, are presented in details in the co-authored book Papanikolaou (ed.) (2021). A typical representative of these studies is briefly elaborated in the following. It refers to the multi-objective optimization of the design of a RoPax ship, assumed to operate between the ports of Patras (Greece) and Ancona (Italy), with a route length of 520 nm. The vessel's capacity has been specified by the end user, Tritec Marine. The service speed should be 24 knots at design draught, even keel and in deep water, with a 15% sea margin and with the main engines operating in the region of 85% MCR. The ship will be operated for 30 years, and at the end of this period, it is assumed to be sold at a value of 15% of its CAPEX.

For this optimization study of the RoPax vessel, the parametric models developed in HOLISHIP have been applied. The parametric model for the elaboration of the hullform was created in CAESES®, while the parametric models for the internal layout (the watertight subdivision and the internal arrangement of the upper decks) and for the structural arrangement were developed in NAPA® (Figures 6 and 7).

The adopted optimisation process is outlined in Figure 10.

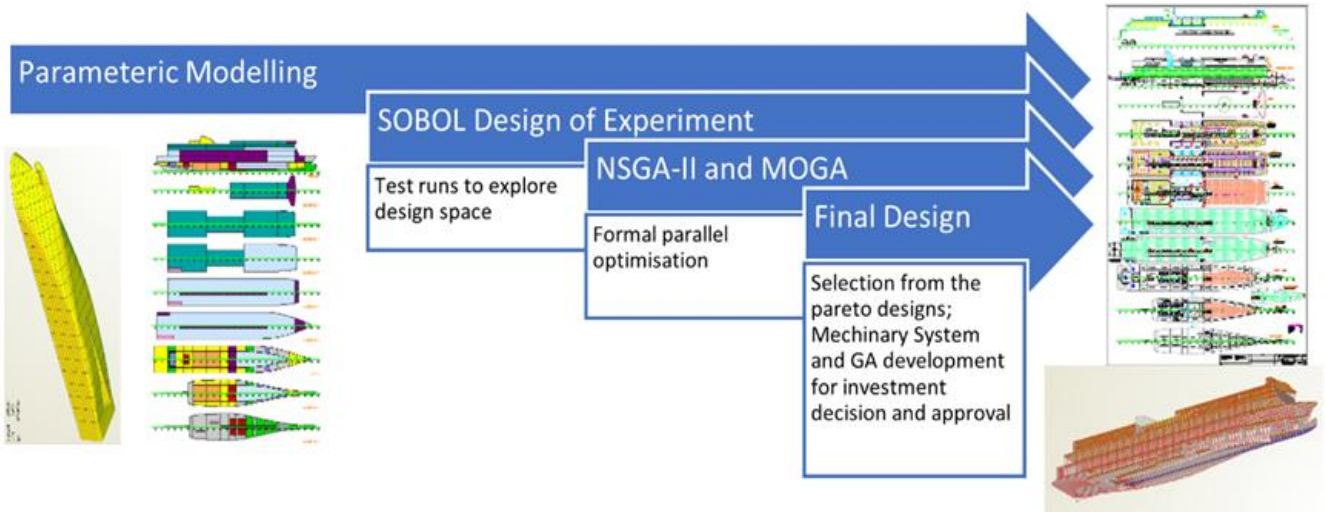

Figure 10: RoPax Optimisation Process (project TrAM)

The minimization of the payback period was selected as the objective of the optimisation, as it is a comprehensive Key-Performance Indicator (KPI), which takes into account the CAPEX as well as the yearly earnings and expenses. The implemented, most important constraints were related to intact and damage stability regulations and the EEDI requirements. With respect to the probabilistic damage stability, the Attained Subdivision Index should be greater than the Required Index by a margin of 0.01. In addition, each Partial Attained Index should be larger than 90% of the Required Index by the same margin. The attained EEDI should be less than the required Phase 2 EEDI by at least 0.2 g/tm. This is a modest requirement from the operator's point of view, presently not addressing yet Phase 3 requirements until the preferred green fuel option has been clarified.

As a first step, before the formal optimization, a Design-of-Experiment was carried out to identify significant correlations (or lack thereof) between the variables of interest within the design space, in addition to verifying the robustness of the parametric models. To this end, the well-known SOBOL algorithm was used for a total of 450 designs. Main design variables were varied within the limits, specified in Table 1.

Table 1: Design variables of RoPax Case Study (project HOLISHIP)

Design variable	Lower limit	Upper limit
Length PP	170 m	210 m
Beam	26.0 m	28.5 m
Depth to deck 3	9.0 m	9.4 m
Block coefficient	0.58	0.62

Next, a formal, global optimization for the ship's main dimensions was carried out. Two runs were conducted in parallel, one with the Non-Dominated Sorting Genetic Algorithm (NSGA-II, Deb et al., 2002) and another using the Dakota toolkit (https://dakota.sandia.gov/), which is embedded within CAESES® and uses the Multi-Objective Genetic Algorithm (MOGA) algorithm. A total of 3,000 designs were generated and assessed on top of the 450 generated during the DoE.

Typical results of the conducted multi-objective optimisation while considering 3,000 design siblings are shown in Figure 11 and the best ones with respect to specific predefined objectives and criteria were identified. The payback period of investment is about 13 years for a ship with a length of about 190m.

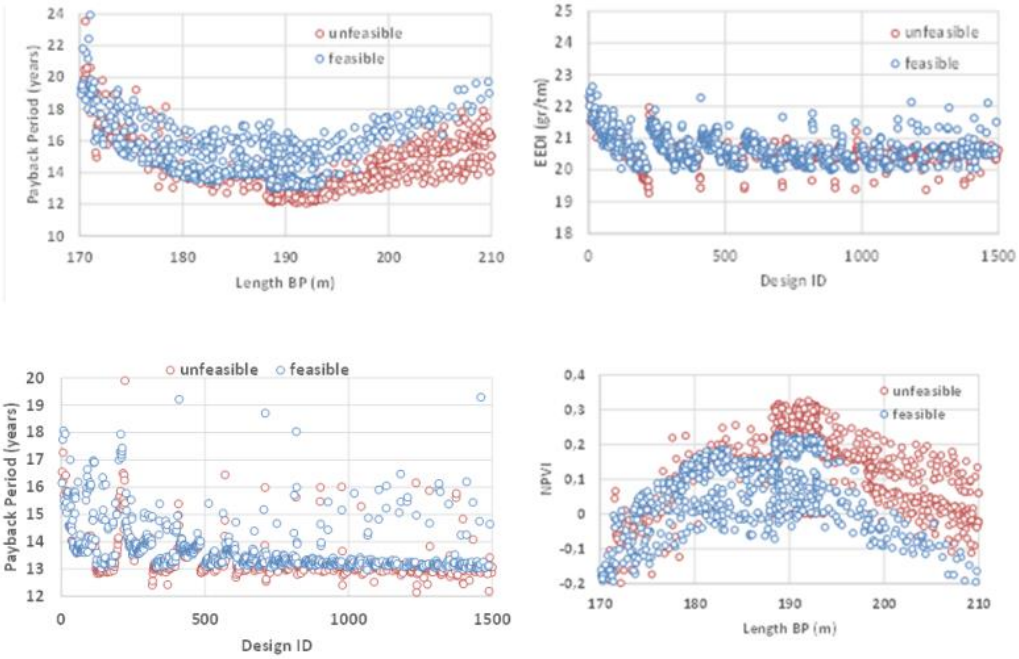

Figure 11: Sample of results of RoPax Optimisation (Project HOLISHIP)
Economic (payback period and NPVI) and Environmental Impact Indicators (EEDI)

The Net Present Value Index (NPV/investment) is about 22%. The Energy Efficiency Design Index (EEDI) converges to about 20 gr/ton-miles. Optimisation studies with respect to more objective functions and other ship types can be found in the co-authored book of Papanikolaou (ed.) (2021), further illustrating the potential of holistic and formal design optimisation.

SIMULATION-DRIVEN SHIP DESIGN (SDD)

Introduction to SDD

Over the last two decades, simulation-driven ship design has gained considerable momentum and is now used at different levels as well as at various phases, from globally scanning promising candidates early on to fine-tuning specific components just before a design freeze. While the previous section gave an introduction and an overview along with an elaboration of holistic simulation-driven ship design, taking into account different disciplines, this section will give further details, focusing on hydrodynamics as a decisive element. Let us start with a definition and a clarification:

According to Funke and Jonsson (2019) "*simulation-driven design (SDD) is an approach where simulations are performed throughout the entire design process with the intention to explore options and guide the user, as opposed to just verify or falsify a design in the later stages of the process.*" This means that simulations are utilized to actively bring about design variants, shifting the usage of simulations from late cycles towards the front, see Figure 12, while enriching the set of proposals that design teams would typically come up with by traditionally combining their specific knowledge, experience and creativity (see also Figure 1).

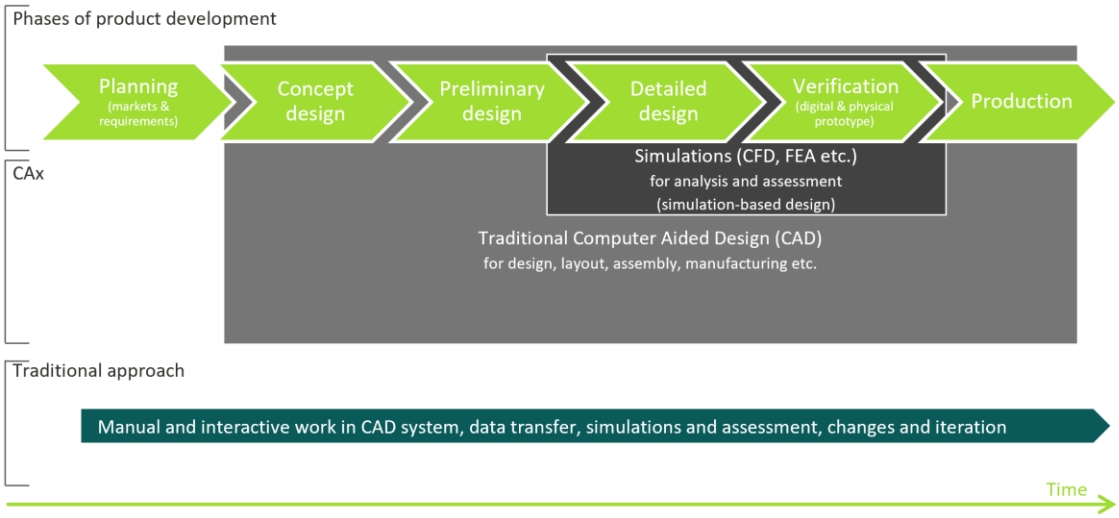

(A) Traditional design approach, using simulation-based design

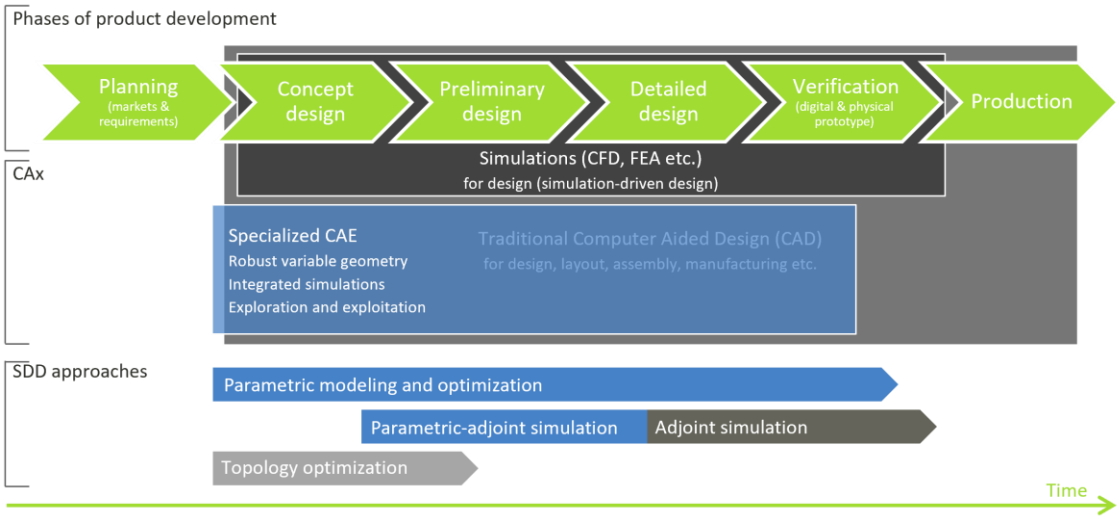

(B) Simulation-driven design, complementing the traditional approach

Figure 12: Phases of product development and utilization of simulations

While manual design work rarely surpasses the creation and analysis of more than a handful of options, SDD typically results in many variants, often several dozens and sometimes hundreds or even thousands, see section above. Clearly, this differs from simulation-based design (SBD) in which just one or several rather mature designs undergo some selected simulations to ensure sufficient performance or to identify problems to be mitigated manually within another design iteration. Figure 12 (A) and (B) illustrate differences between the traditional approach and the various SDD approaches available so far. It should be noted that SDD does not replace traditional design as such but rather complements it. (In this sense Figure 12 (B) can be seen as an overlay to Figure 12 (A).)

Traditional design is typically built on using one or combining several CAx systems. Geometry is created interactively by means of Computer Aided Design (CAD), introducing parameters while doing so. Components and systems are added and assemblies are established step by step, making changes increasingly tedious and expensive to realize. The CAD systems employed mostly originate from a time in which computer resources and simulation tools were not yet advanced enough to incorporate sophisticated simulations – e.g., Finite Element Analysis (FEA), Computational Fluid Dynamics (CFD) and, in ship design, damage stability analyses – tightly and at an early stage.

Many of today's CAD systems were production-oriented when started, see Harries et al. (2015), and most follow a history-based modelling approach in which the interactive modelling steps taken by the user are "recorded." The systems are very powerful and many of them now cover several if not all phases of product development. However, they frequently fail to

regenerate shapes readily when several input parameters are changed at a time and the history-based model is replayed for an update. Failures can be fixed interactively by the CAD user but any need of manual interference hinders the creation of large sets of variants as is representative of SDD.

The previous section of this paper describes how preliminary design can benefit from SDD by building synthesis models, and partially replacing expensive simulations with surrogates. In preliminary design, the focus is to identify the main dimensions and to find the best topology for the expected operational profile. The purpose is to make the right decision globally. Once the concept and the preliminary design are established SDD comes into play again with the aim of improving the product even further. Within this section, this local application of SDD shall be explained in more detail. Special attention is given to hydrodynamics as a key for energy-efficient operations. On most commercial ships resistance and propulsion account for more than two thirds of energy consumption, see for instance Harries et al. (2023).

As done in preliminary design and at a global level, the overwhelming majority of SDD applications at local level are built on parameters. Parameters are meaningful descriptors of a product that can be addressed and, interpreted as free variables, modified during the development process, see Harries et al. (2015) and Harries (2020). As shown in Figure 12 (B) there are parameter-free approaches like topology optimization and adjoint simulations, too.[1] However, they are not easily applied in multi-objective or even multi-disciplinary optimization campaigns while parametric modelling readily allows mixing objectives and disciplines by creating supersets of free variables from the various parametric models.

Since simulation results form an essential part of the SDD process there is one decisive prerequisite: The simulation(s) employed need to be good enough to ensure the correct ranking of variants. While high absolute accuracy is desirable it is often sufficient that the simulations yield correct relative accuracy. If that was not the case SDD would very likely mislead the design team. Therefore, before engaging SDD it is critical to ensure that an improvement found in a simulation would also materialize in real life.

In ship hydrodynamics, this has been regularly done by comparing simulation results with measurements from model tests. However, an additional challenge is that results at model scale, particularly for energy-saving devices attached to the aftbody, are not easily transferable to full-scale. Moreover, not many full-scale measurements are available but for a recent industry initiative, see Ponkratov (2023) and https://jores.net, to provide suitable benchmarks. For direct comparisons between two ships that are identical except for only one design element there is even less data to be found. Çelik et al. (2022) reported sea trials in which a conventional rudder was compared to a Gate rudder system that had been optimized using SDD, see Gürkan et al. (2023).

Let us assume for the sake of discussing SDD further that the chosen simulations are good enough. This has been the situation in several industries for quite some time, e.g., for selected applications in naval architecture like optimization of calm-water resistance and propulsion, in turbo-machinery for increasing efficiency and operating range as well as in automotive and engine design for better aerodynamics and cleaner combustion, respectively.[2]

[1] In topology optimization – sometimes also referred to as generative design – a volume is provided that is sequentially filled with material, for example, to find a light-weight structure for clearly known load cases. While this is applied for the design of components it has not become popular (yet) for the large structures that ships and even boats are made of. In fluiddynamics topology optimization is used to identify meaningful flow paths within enclosed spaces for which inlets and outlets are prescribed. The available space is iteratively filled up, constricting the fluid domain, until an objective is minimized, e.g., pressure drop. Again, this is rather done for internal flows at component level.

In adjoint simulations some of the boundaries of a geometry to be optimized are considered to be free to change, primarily in normal direction to the original shape. From the adjoints so-called shape sensitivities are derived that suggest which parts of the boundary have to be pulled out and which have to pushed in so as to improve a chosen objective. This is mostly undertaken at the stage of fine-tuning an already good design as adjoint simulations inherently identifies a local optimum close to the original shape. See Harries and Abt (2019) for more details and references.

[2] Success stories have been reported by users of high-fidelity CFD codes such as ANSYS CFX, Cadence® FidelityTM CFD (formerly known as FINE/Marine), SHIPFLOW, Siemens Simcenter STAR-CMM+ and certain OpenFOAM set-ups as well as Process Integration and Design Optimization (PIDO) systems such as CAESES®, modeFRONTIER, Optimus®, and optiSLang to mention a few.

Standard Ingredients of SDD

The standard ingredients of SDD are versatile parametric models, accurate simulations, formal strategies of exploration and exploitation and, since a few years, surrogates:

- A parametric model is any model that captures the information of interest about a system within a finite set of descriptors, i.e., the parameters. This may be a product's geometric representation as needed for engineering.[3] It may also be just an empirical relationship between certain inputs and required outputs.
- Simulations are predictions of aspects of system behaviour via an approximate (mathematical) model, omitting less important characteristics. Potential flow analysis of seakeeping behaviour may serve as an example in which viscosity is neglected yet the numerical results are of sufficient practical value. RANS simulations capture viscous flows by averaging the influence of turbulence, giving a close enough account of the flow field for many design purposes.
- Exploration is the automated scanning of a design space within the bounds chosen for the free variables, i.e., a sub-set of parameters that can be controlled by the design team. The purpose is to understand correlations between inputs and outputs, to identify promising regions (for further exploitation) and to provide data for building surrogates and/or to feed machine learning. The algorithms are those of Design-of-Experiments (DoE), for instance, the quasi-random Sobol sequence, allowing repetition and extension, and Latin Hypercube sampling. An illustration from a Sobol sequence is shown in Figure 13. The idea of a DoE is to spend as few resources as possible while getting a good overview. In recent years adaptive sampling algorithms have been introduced that place additional variants where the expected error and/or lack of information is still (the) high(est).
- Surrogates are the replacement of simulations by means of approximating models, also known as meta-models and response surfaces. Polynomial regression, Kriging and Artificial Neural Networks are popular surrogates. Upon computing a surrogate, for instance, by training on data produced during exploration, the execution of a rather expensive simulation can be sidestepped. Surrogates take just split-seconds to execute but do not necessarily yield the result that the actual simulation would give, introducing additional errors. Occasionally, a supplementary simulation is run once a promising design candidate was found, checking and, if need be, improving the surrogate afterwards.
- Exploitation is the automated improvement within the chosen design space with respect to one or several objectives, observing inequality (and sometimes equality) constraints. Exploitations can be run on the basis of simulations, surrogates or a mixture of both. Depending on which algorithm is utilized, deterministic and stochastic strategies are distinguished. Popular are local optimization based on pattern search, like the Nelder-Mead Simplex due to its simplicity, and global searches via genetic algorithms, like the NSGA-II. Global strategies cover the design space widely and advance towards non-dominated variants, yielding a Pareto frontier.[4]
- Exploration, surrogates and exploitation are combined in advanced and encapsulated strategies. Here, an initial set of variants is produced and analysed via simulations from which then a first surrogate can be derived. Additional variants are produced by further populating the design space while reducing the deviation between the surrogate(s) and the underlying simulation(s).

Ingredients and benefits of SDD are also summarized by Massobrio (2023) and are elaborated in Harries (2020).

Importantly, when commencing with an SDD campaign the people involved need to get together and agree on the following: Which key performance indicator(s) should be improved (objectives) and which should be observed and complied with (constraints), what parameters are really under the control of the design team and shall be deliberately modified (free variables) and what can actually be simulated within the given time, the available resources and with acceptable accuracy. While this seems trivial at first glance it more often than not turns out to be complex and is, frequently, no subject of spontaneous agreement.

Furthermore, SDD should not be understood solely as another term for optimization. A Design-of-Experiment, for instance, helps to understand cause-and-effect, getting an appreciation of the potential for improvement and yields insight into which of the free variables are important and which could possibly be fixed subsequently to reduce the design task's dimensionality. A surrogate built from a DoE allows capturing, providing and storing expert knowledge for a certain type of simulation by summarizing results in terms of a simple mapping between inputs and outputs, e.g., saved in csv-files. A complex simulation is taken care of by the specialist with software whose license may be expensive and whose usage may require a lot of experience. This unloads the burden from the design team and may even help improve the quality of the outcome, see Harries and Abt

[3] This may well differ from a parametric model suitable for production.

[4] A Pareto frontier is formed by the set of non-dominated variants, i.e., variants which cannot be further improved with regard to one objective without deteriorating the performance of one or several other objectives at the same time.

(2019). It also paves the ground to combine various design solutions that could not be simulated concurrently, see for instance RETROFIT55 (2024) and Marzi et al (2024), albeit at the cost of neglecting mutual influences of higher order.

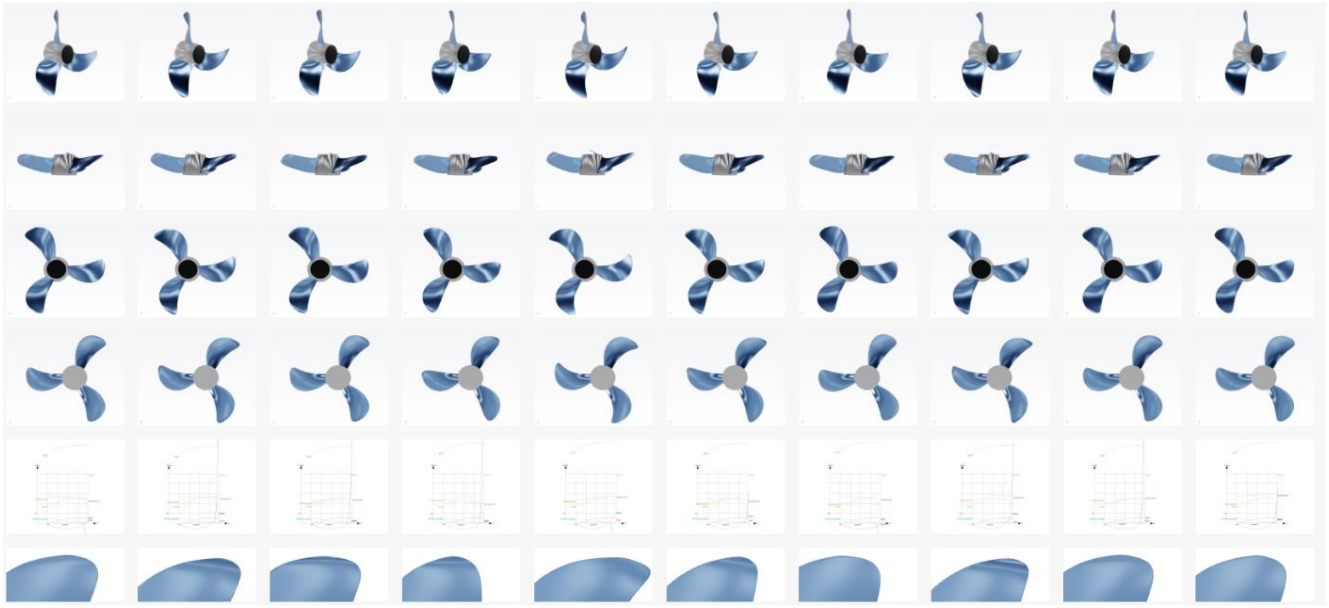

Figure 13: Excerpt from a DoE for the SDD of a propeller
(Differences can be best seen at the tip in the bottom row where various tip rakes occur)

Moreover, in situations in which many components need to play together in a concerted way like in retrofitting a ship in operation – such as changing a bulbous bow, placing a wind-assistance device on deck and modifying the propeller – the behaviour of each system can be captured without the need to already know the influence of all other systems beforehand. Thus, the interdependence can be left to finding the most favourable balance at a later stage when employing the surrogates. This is not only faster but also allows replacing quickly certain components with alternatives and/or adjusting the design task to changing requirements. Additionally, it helps reduce the complexity of the design task.

Illustrating Example of SDD

For the sake of a better appreciation let us take a closer look at a selected example: The hull form of a fast pilot boat was to be optimized for its design speed of 27.5kn at 9.5 tons of displacement. Details of the project are presented in Ahmed et al. (2023) and a thorough elaboration is given in Harries et al. (2024). Here, just the general SDD process shall be explained, see Table 2. Additional SDD examples can be found in Harries (2020), covering naval architecture, turbo-machinery and related fields of application.

Table 2: Typical SDD process

Step	General	Illustrating example
1	Discuss and define the objective(s), constraints, free variables and their bounds; decide which less important characteristics are to be omitted	The shipyard wants to build a fast monohull with conventional propulsion – diesel engine, shaft, bracket, propeller and rudder – with high energy-efficiency at 27.5kn, estimating weight to be 9.5 tons. The pilot boat is to operate in protected waters by professionals, allowing to focus on calm-water performance.
2	Build parametric model(s); balance freedom to change the design (i.e., degrees-of-freedom) with resources available (time and budget)	The hull features two propellers and tunnels for their accommodation. A parametric model, ready for simulation, is created (here in CAESES®) with eight parameters for the bare hull and ten parameters of the tunnel as free variables, see Figure 14 (A) and (B).
3	Set-up simulation(s); check the accuracy of simulation (unless already proven) and possibly reduce simulation effort per variant	Calm-water RANS simulations are set-up (here in Simcenter STAR-CCM+), see Figure 14 (C) to (F). A systematic comparison to model tests shows very good agreement for free trim and sinkage. Grid variation studies are performed to identify a compromise between accuracy and effort per variant. Appendages are found to be negligible for the optimization runs since they do not disturb the correct ranking of variants.
4	Undertake exploration; identify promising designs (and favourable regions in the design space)	Many dozens of variants are automatically generated and analysed without manual interference (hereby coupling STAR-CCM+ to CAESES® as a PIDO environment).
5	Study correlations; possibly adjust bounds and/or eliminate less important free variables	As depicted in Figure 15 thrust (see first row) as objective along with other key performance indices depends on all free variables. Some free variables have a very strong influence, e.g., lowerTransom which controls the bare hull's stern geometry (see second-to-last column in Figure 15).
6	Discuss potential for improvements; possibly redefine, swap and/or drop objectives and constraints	First improvements are found during the DoE, see Figure 16, giving an appreciation of optimization potential.
7	Build surrogate(s) and train machine-learning models	Kriging is used for a surrogate of thrust as a function of all free variables. For further machine learning (ML) see Ahmed et al. (2023). As illustrated in Figure 17 a ML model allows estimating the flow field, too.
8	Undertake exploitation directly on simulation(s) and/or on surrogate(s)	Starting from a particularly good design, i.e., variant number 15 as shown in Figure 16, two local searches, one using simulations and another using the surrogate are performed.
9	Pick promising designs; possibly repeat some of the previous steps	Various other exploitations are run (not shown here). Details can be found in Harries et al. (2024).
10	Determine performance of promising designs; refine simulation(s), study other design aspects not taken into account during the SDD campaign; possibly repeat some of the previous steps	Additional simulations with higher grid resolution, also with appendages, are run to confirm the improvements found during the optimization, see Figure 14 (C) to (F). For thrust as an objective, using an actuator model for the propeller, a reduction of about 10% could be found for the so-called 3rd optimized design when compared to the new baseline.

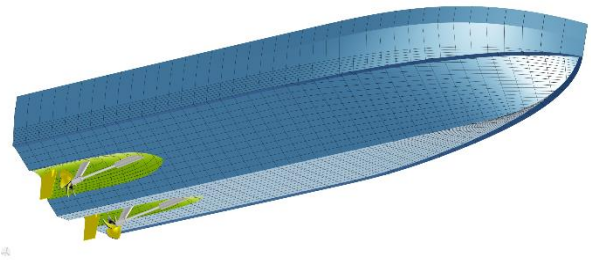

(A) New baseline

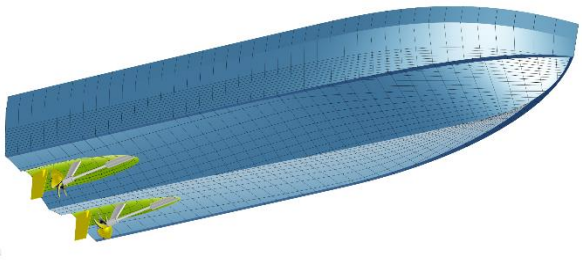

(B) 3rd optimized design

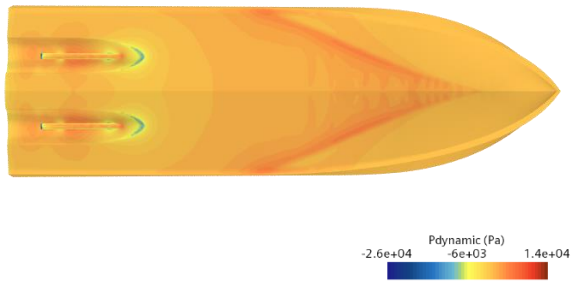

(C) Pressure distribution for new baseline

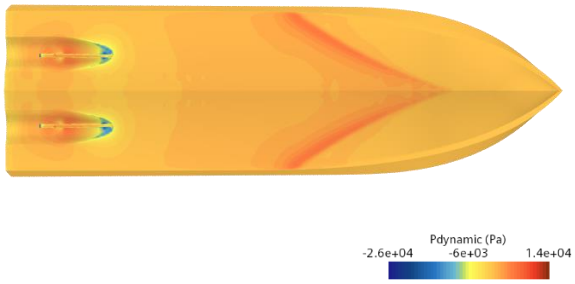

(D) Pressure distribution of 3rd optimized design

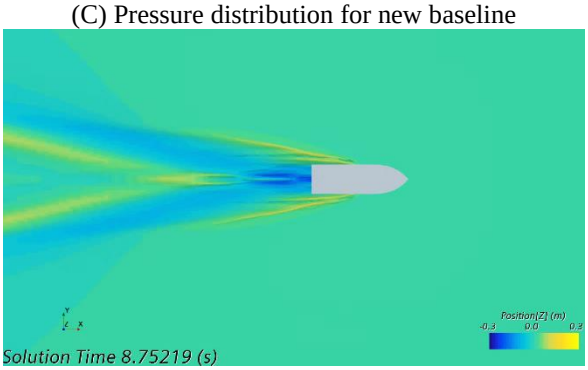

(E) Wave field of new baseline

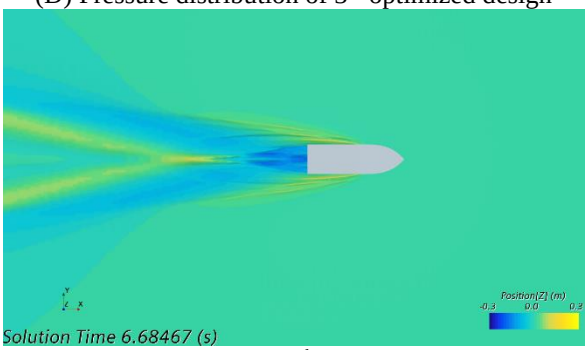

(F) Wave field of 3rd optimized design

Figure 14: Parametric model built from assembly of bare hull, tunnel and propulsion train and associated flow fields

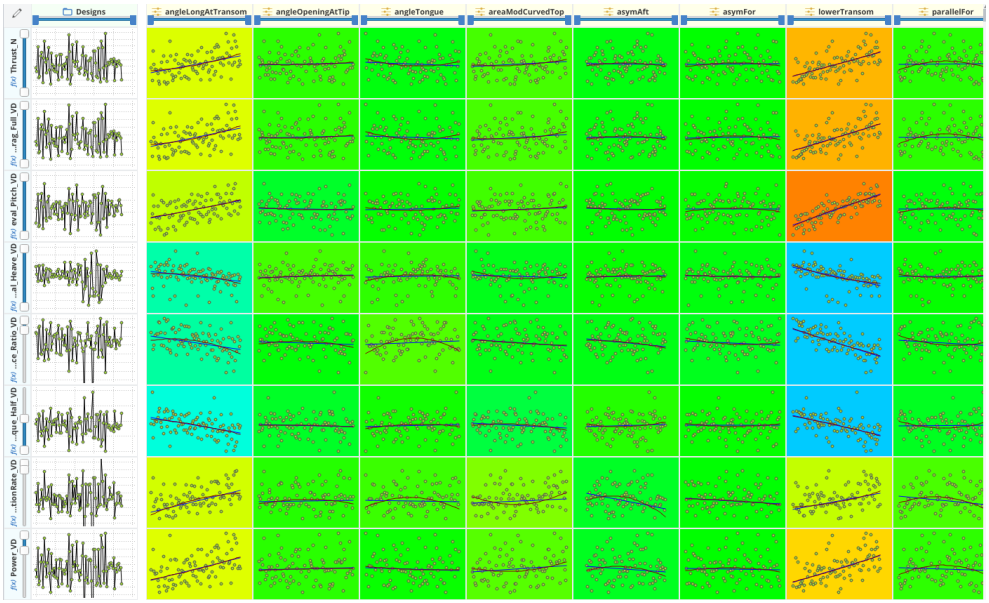

Figure 15: Excerpt of results from DoE (thrust, drag, pitch, heave etc. as functions of several free variables)

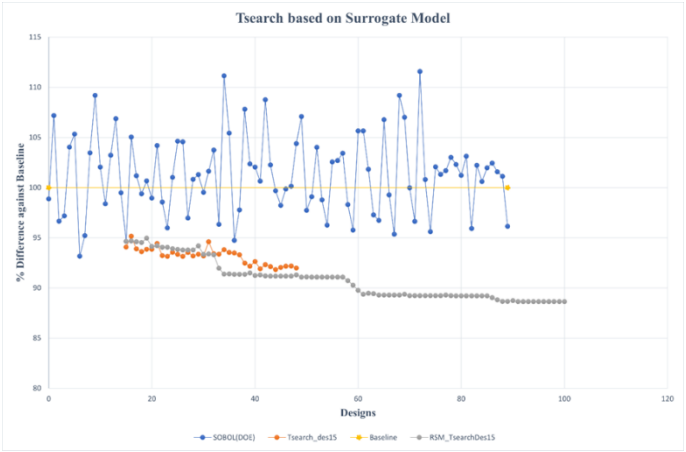

Figure 16: History of DoE and deterministic local searches run on simulation (orange) and on surrogate (grey)

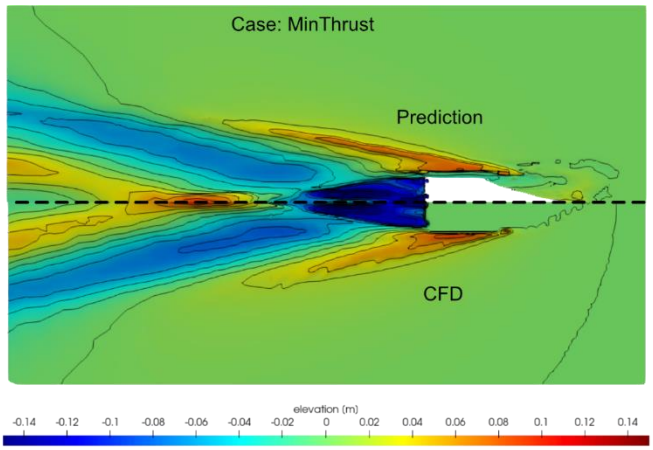

Figure 17: Wave fields for the prediction from a machine learning model (upper part) and corresponding CFD simulation (lower part) for a fast monohull giving minimum thrust

SHIP PRODUCTION AND LIFECYCLE MANAGEMENT

Lifecycle aspects of marine systems design methodology

In the previous IMDC state-of-the-art report (2022), specific lifecycle aspects were discussed under the headings of "design for sustainability" and "design for uncertainty and flexibility". The former of these now permeates every aspect of the ship and fleet development process as the industry aims towards net zero by 2050. The latter is simply a consequence of the road ahead being neither constant nor known. Since 2022 the importance of lifecycle aspects has continued and even strengthened, as well as increased in scope and complexity by the introduction of market-based mechanisms in the EU.

In this section, we will define the concept of "Design for Lifecycle" (DfLC) from the point of specific design methodology developments in various phases of the ship design process.

A pertinent question to begin with is, what is "design for lifecycle"? The 30-year-old definition by Ishii (1995) is still valid: "*Life-cycle engineering seeks to incorporate various product life-cycle values into the early stages of design. These values include functional performance, manufacturability, serviceability, and environmental impact*".

Often, this concept is tied to "Product Lifecycle Management", or PLM for short. PLM, and its sibling Product Data Management (PDM) is basically about managing all data about a product from cradle to grave. PLM is an important pre-requisite for digital twins and is a key part of what is often termed "Industry 4.0" or "Shipbuilding 4.0". However, PLM as such is not particularly about *design*, but rather how to manage the *outcome* from the design process throughout the lifecycle.

Thus, DfLC is here understood as "all activities within the overall design process that explicitly takes into account the lifecycle aspects of the ship". But do we not always design for the lifecycle? As stated in (Papanikolaou, 2019): "*One of the most important design objectives is to minimize total cost over the life cycle of the product, taking into account maintenance, refitting, renewal, manning, recycling, environmental footprint, etc*.". We typically assume a certain longevity of the vessel, say, 25 years, and this indeed drives many design parameters. Still, in the design process we need to make simplified assumptions about the operational life of the vessel. For instance, it is common to assume a fixed deployment or contract, even when there is a positive probability that the vessel will change missions. We may define a static external operating context, such as prices, fuels, technologies, regulations, etc., while in reality these are highly uncertain and vary substantially. More basically, we implicitly act as if we know and understand the future, by capturing this in a model or a set of parameters. However, while we are *always* designing for the future, the future is intrinsically uncertain, and this should be explicitly captured in a DfLC process.

Thus, a more fitting interpretation of DfLC would be "design aspects related to explicitly taking into account an extended set of design parameters that are dynamic, multi-faceted and uncertain". To cater for this, there are four distinct aspects of the design process we need to address:

1. The capturing of needs and requirements that have an impact on lifecycle value creation and compliance.
2. The appropriate modelling of the anticipated future technical, commercial, and regulatory context in which the ship or fleet is going to operate, considering that this future is both uncertain and changing.
3. The development of design solutions that are capable of delivering value and meeting stakeholder expectations throughout this changing and uncertain lifecycle.
4. Prepare for the continued management of all aspects of the ship´s future operation, bridging the gap between the ship "as-designed" and "as-operated".

Needs and requirements in a lifecycle perspective

The ship design process starts with understanding the needs and requirements of key stakeholders, (Brett and Ulstein, 2015). We have seen a gradual development towards an increased emphasis on lifecycle aspects of this step in the design process.

First, needs and requirements have become more dynamic and long term. This is a shift from a more static set of needs and requirements towards a situation with partly known and partly anticipated requirement changes along the vessel´s lifecycle, with a "license-to-operate" level of criticality. Largely, this is a consequence of the planned stepwise reduction in greenhouse gas emissions from shipping and the net zero ambitions by 2050.

With global warming at the top of the political agenda, and the IMO goal of near zero emission shipping by 2050, design-for-sustainability becomes the most important lifecycle element of the design process. For ships to be designed and delivered during the next couple of years the powering technology and fuels required for meeting the 2050 targets is simply not commercially available in the market. This implies that needs and requirements will change throughout the lifetime of the vessel (Erikstad, 2022).

The revised IMO strategy that was adopted in July 2023 calls for international shipping to achieve net zero by 2050, which is a significantly more ambitious goal than the 50% reduction that was the previous target. Along this way, there is a goal of 20% reduction by 2030, and 70% reduction by 2040. Thus, from a design perspective, we are in a somewhat new situation with explicit and changing requirements with a 25 year perspective, i.e., still within the lifespan of ships designed and built within the next few years.

In the shorter term, IMO has also adopted non-static requirements such as EEDI, EEXI, and, most recently, CII. These are all measurable index requirements that are tightened stepwise. The Energy Efficiency Design Index (EEDI) defines minimum energy efficiency level requirements for new ships, motivating for energy-efficient equipment and engines. A similar measure is the Energy Efficiency Existing Ship Index (EEXI) covering the energy efficiency of existing vessels. The more recent Carbon Intensity Indicator (CII) rates ships on a scale from A to E based on their CO_2 emissions during operations. Even if a new vessel has an adequate rating at delivery time, the gradual tightening of the CII indicator is likely to require that the vessel is retrofitted at regular times during its lifecycle. To ensure this a Ship Energy Efficiency Management Plan (SEEMP) is required for the monitoring of the ship's energy efficiency over time in order to comply with CII targets.

This focus on carbon efficiency in the short term, and zero emission for the longer perspective can also be traced to the shipowner´s fleet renewal processes. Some examples from the stated strategies of major shipowners illustrate this, e.g., "*Our ambition is to continue as a frontrunner, providing carbon-efficient freight 'right here, right now', and to enable zero-emission shipping in the medium-to long term"* (Klaveness, 2024), and "*Net zero across the business in 2040*" (Maersk, 2024).

Capturing the lifecycle operating scenario of the vessel

A prerequisite for finding preferable design solutions from a lifecycle perspective is that we are able to model the future external operating context at a level of detail sufficient for deriving relevant performance indicators for the system of interest, whether this being monetary, environmental or technical. Key players in the maritime industry have put substantial efforts into this, using a wide array of methods and strategies. One example is DNV´s annual "Energy Transition Outlook" which presents forecasts to 2050 covering renewable energy technology cost and implementation schedules, prognosis on regulatory framework and policies, fuel availability and prices, to name a few (DNV, 2023). Interestingly, DNV´s approach in this report is to present a "single best estimate" forecast of the future energy situation, based on what they call a "comprehensive system-dynamics model". Thus, this is a deterministic rather than a stochastic model, using expected value input parameters towards one particular output, corresponding to what is called a "maximum likelihood model" in risk analysis. The benefit of this is simplicity and improved transparency. One drawback is that even if this is the most likely forecast, it is still rather unlikely given the model´s complexity and the stochastic input parameters. Further, if used as part of a systems design process, the value of incorporating flexibility towards alternative, uncertain futures becomes zero for a single scenario model (de Neufville & Scholtes, 2011).

The alternative to this modelling approach is to explicitly model multiple futures as scenarios, and then evaluate a prospective design towards a (probability-weighted) distribution of the outcomes from each. There have been multiple examples of this in the maritime design literature (see Gaspar, 2012). One interesting recent example is based on the exploration of market uncertainty towards the design of offshore wind foundation installation vessels. To reduce the levelized cost of energy (LCOE), the offshore wind energy market has seen an increase in market demand, turbine size and distance from shore. According to Zwaginga (2021), "*this makes it difficult for ship designers to design a construction vessel that has the right size and capabilities for use over multiple decades.*" Designing for the first contract is likely to make a vessel increasingly less competitive over time, though how far and how fast this will go is highly uncertain. As a consequence, a large number of scenarios were generated with variations of characteristics such as range, sizes, contract types and market parameters, to be used for evaluating alternative concept designs, see Figure 18.

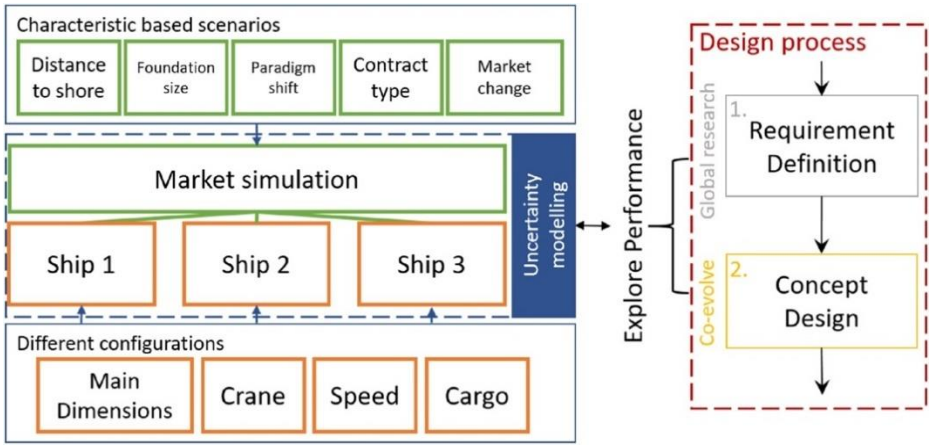

Figure 18: Scenario development for HLCV (Zwaginga et al, 2021)

Again related to lifecycle sustainability considerations, it is perhaps the uncertainty related to the availability and cost of fuel alternatives along the lifetime of the vessel that has become the most serious challenge in the conceptual design phase (Lagouvardou et al, 2023). According to DNV (2023), in order to meet the IMO GHG goals of 2030 shipping will require 30%-40% of the estimated annual global supply of carbon-neutral fuels, in competition with other sectors. Adding to complexity is the inclusion of shipping into the European Emission Trading System (ETS). In ETS, the price for carbon emissions is not set directly, but by the market in a cap-and-trade system. The FuelEU directive is likely to take this some steps further, possibly allowing across- and between-fleet emission caps, thus opening up for strategic collaboration and alliances to be considered as part of the fleet renewal and retrofit process. As a consequence, making informed decisions today that are dependent on, say, the cost and availability of a certain fuel in 2030 or 2040, becomes difficult.

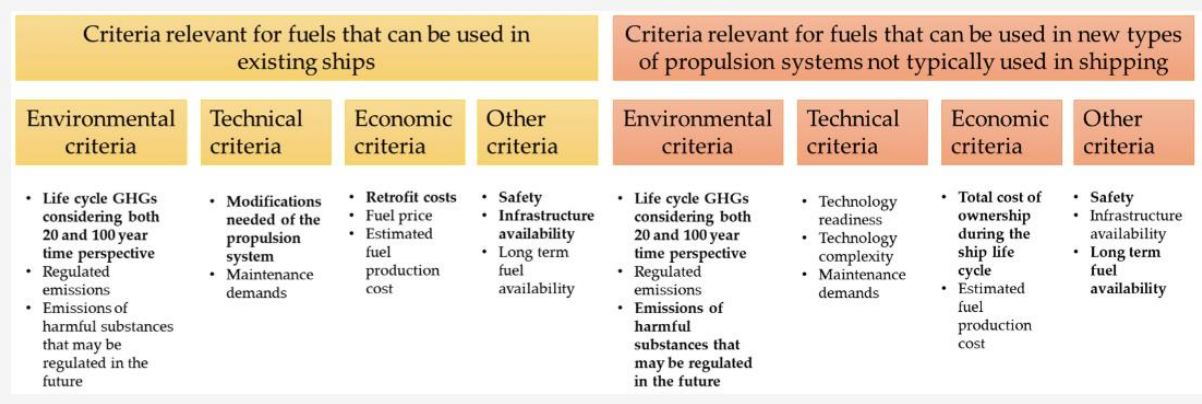

Figure 19: Criteria relevant for forecasting fuel cost and availability (Lagouvardou et al, 2023)

Developing design solutions for lifecycle value delivery

In the two previous sections, we have pointed to the changing needs and requirements along the lifecycle timeline of the vessel, as well as the uncertainty and variability of the external operating context. This leads to the question: How can we, as ship designers, find system solutions that are capable of providing sustained value along this timeline?

First, lifecycle-oriented system performance indicators, such as changeability, flexibility, adaptability and robustness, should be integrated into the design process. However, it is often difficult to make the connection between these high-level concepts and the main design decision variables. One interesting contribution is the efforts by Maggiancalda (2019) towards developing a Life Cycle Performance Assessment (LCPA) tool for the assessment of both the economic and environmental performance of a vessel over its life cycle. More specifically, an effort to quantify the changeability performance of a vessel is developed by Rehn et al. (2018), by making it possible to compare alternative design solutions towards their ability to deliver the required performance over a range of possible future operating scenarios. The changeability concept is closely tied to flexibility and retrofitability, which are both lifecycle-oriented performance concepts that takes into account the value for the shipowner of being able to have cost-efficient options that can be exercised after the outcome of a particular uncertain operating aspect has been revealed, (Lagemann 2023), as illustrated in Figure 20. The basis for the quantification of this value is based on real options models.

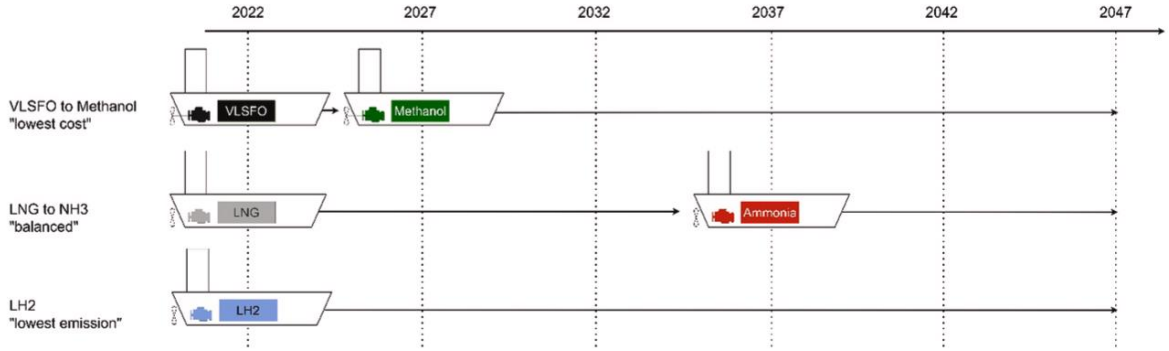

Figure 20: Pareto-optimal lifecycle machinery-fuel configuration with carbon pricing uncertainty (Lagemann et al., 2023)

Lifecycle stewardship consideration at the design stage

Lifecycle aspects of ship design also include those measures taken at the design stage for the continued management of the ship beyond delivery. For ship designers and shipbuilders this also represents a business opportunity. Traditionally, their responsibility for the delivered vessel was capped by the guarantee period. So was also the income stream. Recent developments in digitalization and the Internet of Things (IoT), having fostered a wide array of different digital twin solutions, have provided a platform for ship designers, equipment manufacturers and shipbuilders to maintain a tighter relationship with the customer throughout the lifecycle. Basically, the idea is to provide value-adding services based on both an intimate knowledge of the

ship itself combined with real-time data streams from onboard sensors. One example of such services might be the tracking vessel "inventory" all the way to scrapping, proactively offering docking services for repairs, upgrades and retrofits. Another example is online shore-based operations centers which can offer both deep expertise and economy-of-scale by the concurrent management of multiple vessels. Both these examples would benefit from action taken already at the design stage, in which both the digital twin of the vessel is born, and the control and sensor architecture of the vessel is determined. In addition, these operation stage, value-adding services should themselves be designed, preferably according to the same design methodology as the ship itself, (Erikstad 2019).

To summarize, this section has focused on the lifecycle perspectives on ship design. With our common goal of zero emission shipping by 2050, this "cradle to grave" holistic approach, where we explicitly face the uncertainty inherent in the 25-30 years lifetime of the vessel has become even more important.

DIGITAL TWINS IN THE DESIGN AND RETROFIT OF SHIPS

This section provides a review of digital twins (DTs) in the *design* and *retrofit* of ships. It also covers lessons learned from other industries, a proposal for digital twin modelling, and concludes with areas for future research and application of DTs.

Background on Digital Twins for Ship Design and Retrofit

The concept of the digital twin has existed since the beginning of space explorations when NASA implemented similar concepts to a digital twin in the 1960's (Ibrion et al, 2019). However, DTs really became a widespread concept after Grieves (2014) developed a framework of the DT where the information of the physical entity and the virtual entity are synchronized. The DT is envisioned to assist in all phases of the lifecycle but up until now research has primarily focused on the *manufacturing* and *operation* phase and has been specifically lacking in the *design* and *retire* phase. When analysing a ship's life-cycle, Mauro and Kana (2023) suggest incorporating retrofitting into the decommissioning phase of a ship. Therefore this section aims to explore this research gap and determine the state-of-the-art and current limitations related to DT-enabled ship *design* and *retrofit*.

Before proceeding, an overview of DTs is presented. Grieves (2014) provides a clear definition of a DT that is composed of three main parts:

1. a physical product in the real environment composed of information about itself
2. a virtual product in a virtual environment representing the physical product
3. a data connection between these two product actively flowing in both ways as so-called mirroring or twinning

The function of this bi-directional data connection is to process the information from the physical product, update the virtual product, assess the current state, predict the future state, and provide further instructions for the physical product, all in an automated way.

Based on this definition, unfortunately, the term "digital twin" has traditionally been used inconsistently throughout literature, with many virtual and computer models often falsely labelled as a DT. Kritzinger et al. (2018) have provided three distinct types of models to support the nomenclature (see Figure 21), which this state-of-the-art report argues should also be adopted throughout ship design DT-related literature:

- A *digital model* (DM) is a virtual representation of the physical product, but with no formal automated exchange of data between the physical and virtual entity. Data exchange could occur but only performed manually. The DM is mostly used for simulation and planning-based operations which does not require automatic data integration.
- A *digital shadow* (DS) is an extended version of a DM including only an automated data flow from the physical product towards the virtual product by which it is actively updated.
- A *digital twin* (DT) is composed of a physical and virtual product including an automated bi-directional data flow between both entities.

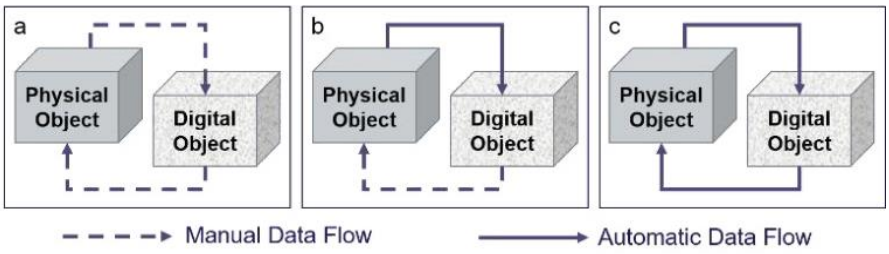

Figure 21: Integration levels between virtual and physical environment for (a) digital models, (b) digital shadows, and (c) digital twins (Kritzinger et al., 2018; Mauro and Kana, 2023)

The bi-directional communication is a crucial element because this enables a mirroring between the virtual and physical entity (Grieves, 2014). This creates opportunities to improve each stage of the ship life cycle through direct monitoring, decision making, and advanced predictive algorithms. Importantly the direct response of the DT creates an opportunity to actively improve ship operation and learn from the responses of the physical entity for future design and manufacturing.

Figure 22 provides a high-level overview of the tasks necessary between the virtual and physical entities to enable a DT:

- *Task 1*: The acquisition of data from the physical to the virtual entity obtained from employed sensors on the physical entity.
- *Task 2*: Perform a virtual test or optimization process in order to improve the performance or decrease the risk of malfunctions or failures of the physical entity.
- *Task 3*: Enacting corrective measures on the physical entity by transmitting data to the actuators of the physical entity using a specified protocol.

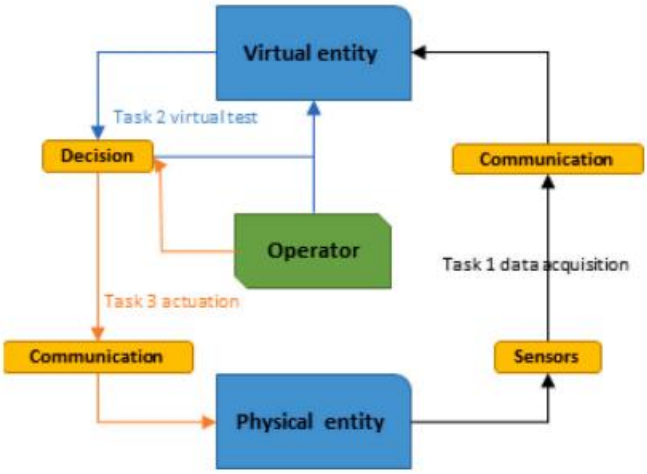

Figure 22: Schematic representation of a DT with the interconnection between virtual and physical entities (Mauro and Kana, 2023)

Sensors could measure characteristics onboard such as the engine room temperature, strain, pressure, electricity consumption or exhaust gas composition which will provide data that can be used to improve the efficiency of the operation of the ship to decrease GHG emissions. Also, environmental sensors can be deployed to measure for example the wind and sea state, outside temperature, sea salinity and GPS to directly respond to environmental changes for optimal operation in changing environments. In order to respond to such environmental and onboard changes task two is crucial to establish a corrective measurement. Lastly, this corrective measurement needs to be translated to the physical entity to alter the operation for improved performance. Such as reducing the speed during increasingly heavy sea state, winds or reducing noise pollution when entering certain (marine) protected areas.

From a ship design perspective, DT based design is not a term commonly used in literature. Especially not in the maritime industry where the concept of DT alone is underrepresented compared to other complex engineering industries (Mauro and Kana, 2023). Even in other industries such as aerospace, civil, and automotive the method for DT-based design is very premature and as a result, is inconsistent and does not have a standardized framework (Psarommatis and May, 2022). There are multiple reasons why it is so challenging to create a detailed DT framework focused on design for new builds. The main challenges provided by previous literature studies suggest three main reasons why:

1. Most importantly the definition of DT has been used inconsistently intertwining the concept of DT with other versions of digital entities.
2. The concept of DT-enabled design with the synchronised DT from Grieves (2014) is relatively new and in a very early stage of development globally.
3. The developments have mainly focused on the operation and maintenance stage and not on design (or retrofit).

This paper proposes an additional reason:

4. When designing a new vessel, the physical entity does not, by definition, exist yet. Thus, properly adhering to the DT definition requiring bi-directional communication between the physical and virtual entity is not possible. Thus, this paper discussed DT-based design to suggest a design process that eventually enables true DT capabilities once the vessel is built.

Mauro and Kana (2023) conclude that there is a large delay in the *design* and *retrofit* phase for DTs, and thus it is necessary to evaluate the state-of-the-art and limitations of DTs in these phases in more detail.

DT-based New Build Design

Currently, most research publications containing conceptual DT applications focus on parts of a ship instead of the total ship itself. A systematic review of the literature finds only two available publications which address a DT theoretical framework considering new-build methods, and of which only one is associated with the design of the whole ship (Xiao et al., 2022).
The authors propose a DT framework proposing the use of a vertical-horizontal design method of a new-build regarding the total ship throughout its life-cycle phases. This framework is still under development. Even though it provides promising conclusions, it is still a theoretical framework with in-depth research still being conducted as mentioned by the authors. Nevertheless, no articles are available regarding concrete applications of DTs linked to new-build design methods, only for theoretical and conceptual cases.

The remaining articles concern mostly subsystems of a vessel and relate to conceptional applications or only provide a general description of such an application (Arrichiello & Gualeni, 2020; Nikolopoulos & Boulougouris, 2020; Pérez Fernández, 2021; Stachowski & Kjeilen, 2017). Erikstad (2017) has also identified this trend of subsystem DT application but indicated the potential of getting closer to achieving a DT of a complete ship when such subsystem DTs are merged.

Additionally, very few papers include essential information such as specific methods, input data, output data or reliability of the design. Following the classification by Tao et al (2019) and used by Mauro and Kana (2023) the current literature on DT-based ship design is in a so-called formation stage, meaning, “very few papers are published as the technological foundations are not mature enough to support effective applications”. As a result, it will likely be challenging to iterate and develop these methods further within the maritime community outside of the specific research groups where they were developed, hampering overall progress.

Finally, a distinction can be made between (1) the design of a physical entity while consequently designing a DT specifically tailored to the physical entity and (2) developing a virtual space in which DTs can be developed for different types of ships. A choice needs to be made to establish a development direction. This distinction has been pointed out by Wang et al (2022); however, they do not mention an argument to which development direction is favourable. This state-of-the-art report argues, nevertheless, for the second direction, as it provides the potential for generality and reusability of the virtual space, enabling greater usability potential.

DT-based Retrofit Design

Even though it is not performed for every ship and therefore not considered as a general life-cycle phase, retrofitting is common to perform when aiming to reduce emissions or to improve the onboard systems (RINA, 2020). There are limited available publications linked directly to DT application for ship retrofitting, which can be explained by the fact that the retire or retrofit phase (including multiple retrofits) is the last stage of a ship’s life-cycle and subsequently will also be the last stage to be fully investigated with regard to DTs. In order to fill this gap it is proposed to examine research done on DTs in the operational phase which will provide sufficient information on design decisions linked to retrofitting. With ship data acquired during the operational phase of the vessel and processed by a DT, design decisions for a retrofit can be derived throughout the DT.

Two publications have been identified which present a conceptual framework to integrate DTs with an existing ship (Zhang et al., 2022) and virtual system (Mouzakitis et al., 2023). Zhang et al (2022) propose the construction of a DT for an already existing research vessel, ‘Gunnerus’. Although the project is still ongoing, the article provides a DT architecture including the data-driven design building block method using the Open Simulation Platform, an open-source simulation platform. Even though a unique vessel is being considered, the authors aim is to provide a standardized DT concept for the maritime industry.

Additionally, Mouzakitis et al. (2023) address the importance of using high-performance computing together with big data analytics to develop, and therefore contribute to high-level digital products for the maritime industry. The DT architecture includes a proposed data integration into the existing unified system within the 'VesselAI' project. Additionally, the Digital Twin for Green Shipping (DT4GS, 2024) project aims to develop DTs for existing commercial vessels, with applications in container ships, bulk carriers, tankers, and RO-PAX ferries. This project is still ongoing.

With maritime DT applications still being relatively new, it is logical to assume publications regarding retrofitting will become available in the future. This paper argues for additional research on DTs in the operational phase to support information regarding a possible retrofit, given the fact retrofitting is being performed to extend the life-time (e.g., operational phase) of a ship.

For both new-build and retrofit designs a clear research gap is identified regarding the application of DTs. When examining the current state-of-the-art of DTs for ship design and retrofit, the literature showed that scientific research into maritime DT applications is still in the early stages of development but is rapidly growing. Regarding new-builds, publications only cover conceptual DTs or consider a subsystem of the ship, not the total ship. Furthermore, limited available publications were found regarding DTs for retrofit design. A research gap is identified for DT application of new-build design considering the total ship and retrofitting in general.

Lessons Learned from Other Industries

In other industries, there are DT-based design challenges that have been researched but have not been addressed yet in the ship design industry. A large amount of literature referencing DT-based design is not specifically aimed at a certain industry. As a result, the proposed design methods are not very detailed. However, some important frameworks have been developed which could influence ship design as well. For example one of the ship design challenges stated by Fonseca and Gaspar (2020) is the complexity of determining the business value of the DT. Newrzella et al (2022) propose a method to define a selection of use cases and data sources to start a pilot phase, derived from the market needs and the most impactful data sources. Since the shipping industry is relatively sensitive to market needs and business value, an approach to determine what DT use cases to develop from the early design stage is fundamental.

Additionally, in the literature review by Psarommatis and May (2022) it is concluded that the manufacturing industry, which is furthest ahead of other industries, also encounters the same problem as the ship design industry specifically related to the research gap exploring DT-based design methods. The majority of DT-based design papers either develop technologies for only one-time occurrences or are not stated. The definition of the communication within the DT has been categorized as unstated or manual, with manual being the most common, which is in contradiction to the formal definition of DTs proposed by Grieves (2014). The large majority of the papers do not verify their methods nor include input and output parameters. As a result, most methods are only suitable for one-time use and cannot be further developed. Thus, it appears that the manufacturing industry has similar challenges to ship design. Psarommatis and May (2022) propose a flowchart of the design decisions needed before the DT can be developed (Figure 23). This targets shortcomings in the current literature that the maritime industry also encounters. These steps are general and can be integrated into the ship design process with minor modifications, depending on the intended application.

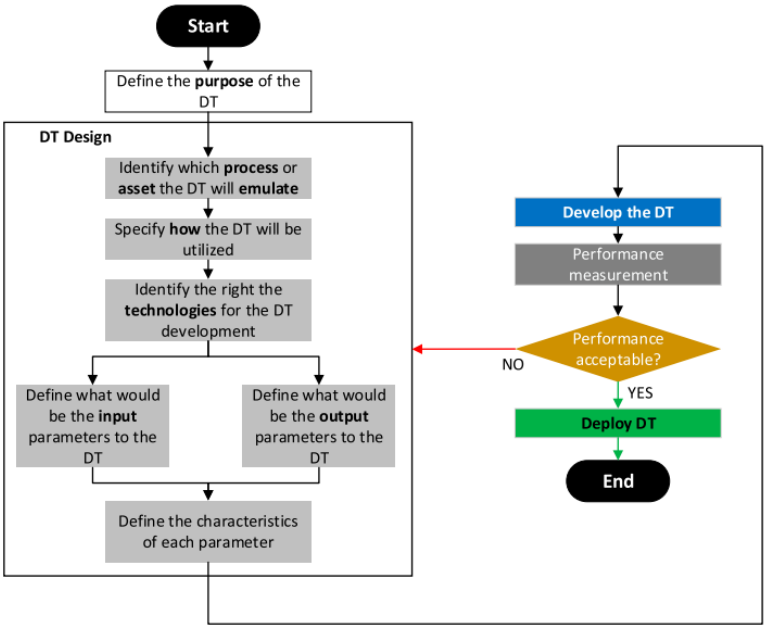

Figure 23: Proposed DT-based design method by Psarommatis and May (2022)

Finally, the aerospace industry has more experience in the application of DTs and proven effectiveness in quality improvement. NASA is working on the integration of model-based systems engineering (MBSE) and DT design (Weiland, 2021) which has also been explored in the shipping industry (NAVAIS, 2022). MBSE enables the inclusion of contributors and stakeholders, facilitating collaboration throughout the product life cycle, and resulting in more efficient data exchange and shared model information compared to traditional methods (Lopez and Akundi (2022). MBSE can also handle fast changes, and improve the collaboration of engineers and digital machines by providing knowledge-sharing infrastructure, automating designs, and simulating system behaviour (Weiland, 2021). This paper thus argues for additional research effort within the ship design community in the application of formal MBSE to support DT-based design and retrofit as it provides a promising framework to develop a virtual space in which digital twins can be developed for different types of ships.

Digital Twin Modelling for Ship Design and Retrofit

This section provides a high-level DT modelling process that can support DT-based design. It is designed to be generic and thus also be coherent with the application of MBSE stated above. Before starting the process, the objective of a DT must be determined which covers the composition and modelling process of the DT. The DT objective will indicate which virtual models are required for the DT. The DT output is based on performing simulations, using available operational data. The composition of the virtual part of the DT depends on this data, as this will determine the feasibility of modelling certain parts within the DT, and thus drives the modelling process (Giering & Dyck, 2021). By investigating the available data, the virtual models which are feasible to construct are identified. Finally, the overlap between the required models (derived from the DT objective) and the feasible models (derived from the available data) provides the models to be selected for the final DT (see Figure 24).

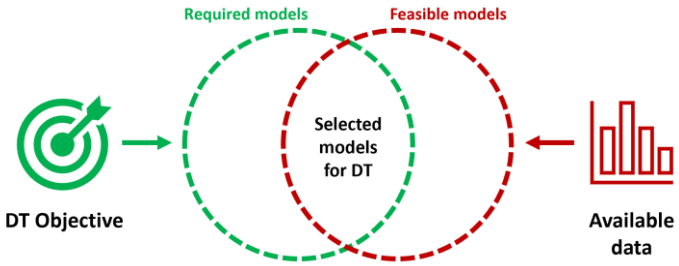

Figure 24: Selection process for DT models (Hermans, 2024)

After establishing the DT's objective and the model selection process, the modelling phase involves the following general steps:

1. **Set-up the data acquisition**: To acquire the data for the DT, a data acquisition system needs to be established, which collects the information required to model the DT, and functions as a collector for the bi-directional data connection.
2. **Establish a data pre-processing framework:** The data needs to be pre-processed in order to be of use as input for the virtual models. García et al (2016) discuss key data preprocessing techniques in the field of computer science, which can also be leveraged for DT modelling, such as data cleaning and normalization. A preprocessing framework depends on the chosen modelling approach, and consequently on the type of data. By establishing an effective framework, redundancies are reduced regarding connected features within the DT (Autiosalo et al., 2019).
3. **Choose modelling approaches for virtual models:** The three different modelling approaches adopted in standard data-science literature are: black-box, white-box, and grey-box. Black-box models are digital models purely based on statistical techniques in order to find relationships between a set of empirical input data and a set of desired output data. White-box models are the exact opposite, and are constructed based on physical principles, theoretically derived set of equations and experimental-derived data. A grey-box model aims to achieve the advantages of both model types by combining the analytically and experimental-driven methods of a white-box model to achieve physical accuracy, and the statistical techniques of a black-box model to identify patterns (Ehmer & Khan, 2012).
4. **Perform model training in case of statistical-based models:** Through training, the model is calibrated in order to achieve the acceptable accuracy. Model training is required for black-box models.
5. **Verify and validate (V&V) the virtual models:** When the chosen models are constructed, and trained in case of applying a black-box or grey-box approach, they need to be verified and validated to ensure the accuracy and reliability of the chosen modelling approaches
6. **Integrate the virtual part with the physical part:** After the models have been verified and validated, they can be integrated into the DT infrastructure. Following the DT definition by Grieves (2014), the output of the virtual models needs to be connected in an automated way to the physical ship. As it is related to the physical vessel, this output can directly be received and used by the respective vessel. In the case of a DT for retrofit purposes, the output will relate to recommendations regarding design decisions. It is considered that the output of the models will drive the retrofit design, and after the retrofit has successfully been performed, the virtual models will represent the modified vessel. Thus, after the retrofitting occurs, the virtual-physical integration can take place. With the integration completed, the DT is established and can be used for operational purposes, such as performance monitoring.

Figure 25 shows a schematic representation of the transition towards a DT for retrofitting. The integration step is performed at the end and can occur simultaneously with the completion of the retrofit (step 5). The final retrofit DT originates from a digital model which represents the ship (step 1), and which is further investigated for possible retrofit options (step 2). The chosen retrofit design (step 3) will then be used for the actual retrofitting of the respective vessel (step 4).

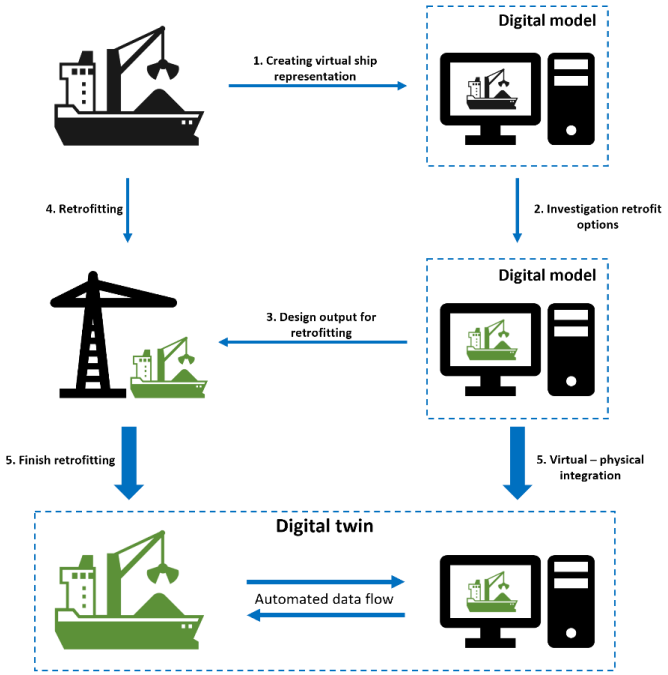

Figure 25: The development of the digital twin for retrofitting (Hermans, 2024)

ARTIFICIAL INTELLIGENCE

Erikstad and Lagemann (2022) have already addressed the introduction of artificial intelligence (AI) in ship design in their IMDC 2022 State-of-the-Art report. However, it was a few months later that the world was astonished by the release of OpenAI's Chat Generative Pre-trained Transformer (ChatGPT) at the end of November 2022 (Wikipedia, 2024). Since then, the research on the potential benefits, limitations and challenges of the application of AI in the ship design field has intensified.

According to the definition adopted by the European Commission in 2018 (Boucher, 2020) "*AI refers to systems that display intelligent behaviour by analysing their environment and taking action – with some degree of autonomy – to achieve specific goals*". There are many attempts to classify the key technologies that are associated with AI. According to Boucher (2020) for EC there are three main stages of development. The first was the symbolic AI (or Rule-Based AI) that included expert systems, Artificial Neural Networks (ANN), deep learning and fuzzy logic. The second stage includes the introduction of machine learning (ML) algorithms such as surrogate models and data-driven intelligence. The third wave includes 'strong' or 'general' AI (AGI) that shows intelligence in a wide range of problem spaces. This includes Natural Language Processing (NLP) algorithms and in the future artificial superintelligence (ASI).

Huang et al. (2022) have attempted a review of the research addressing ML's application in sustainable ship design and operation. Their classification of ML models was inspired by Sarker (2021).

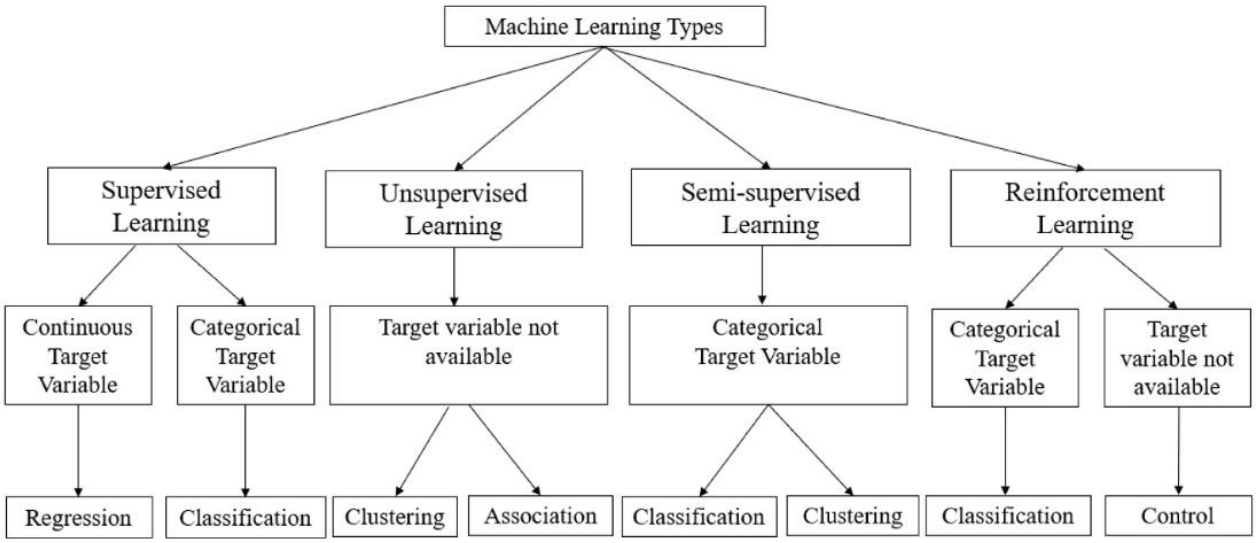

Figure 26: Classification of Machine Learning according to Huang et al. (2022) inspired by Sarker (2021)

AI accelerating applications in ship design provide solutions to several challenging problems. These include hull optimisation, performance prediction, holistic design optimisation; accelerated structural analysis and material selection; energy efficiency, decarbonisation and environmental impact; safety analysis and compliance with the applicable rules and regulations; and prognostics and diagnostics for predictive maintenance.

Hullform optimisation

Yu and Wang (2018) introduced a Principal Component Analysis (PCA) methodology to compress the geometric representation of a group of existing vessels. The resulting principal scores are used to generate many derived hull forms, which are evaluated computationally for their calm-water performances. A Simple-Source Panel Method (SPM) based on potential flow theory was used to calculate the wave resistance, accelerated by a Graphic Processing Unit (GPU). The results were used to train a Deep Neural Network (DNN) establishing the performances of the different hull forms. Based on the DNN's evaluation, a large-scale search for optimal hull forms is performed very quickly and with increased flexibility. However, the authors note that the pool of parent hulls should be expanded and CFD and EFD results should be included in the training to increase the accuracy of the DNN predictions. Additional performances should be evaluated to establish a more comprehensive optimization process.

Panchal et al. (2019) in their guest editorial for the special issue on ML for Engineering Design, argue that machine learning algorithms have an evolutionary impact on mechanical design, uncovering hidden patterns in data and developing autonomous systems. DNN and other modern ML techniques are enabling progress in AI. Examples include ANN, Gaussian processes,

clustering techniques, and Natural Language Processing. They also point out that engineering design research has more recently benefited from the introduction of deep learning techniques such as convolutional neural networks (CNNs) and generative adversarial networks (GANs). The research they present in the special issue introduces a first taxonomy of the area: (i) ML techniques to support surrogate modelling, design exploration, and optimization, (ii) ML-supported design synthesis, (iii) extraction of human preferences and design strategies utilizing ML, and (iv) ML-informed comparative studies and research platforms from design researchers support. The editorial team recognizes that ML has already applications in modelling human decision-making, market system design, human or surrounding environment interactions with products , design for reliability, informing the design using of real-time data from products (design-for-X),where a particular aspect of the lifecycle or across several aspects of the lifecycle are benefit for the analysis of data gathered. Security, privacy, cyber-resilience, trustworthiness and other non-traditional design challenges in engineering design, arising from smart products and systems, present emerging opportunities for the use of ML.

Grigoropoulos et al. (2021) presented a mixed-fidelity method to optimise hullforms combining genetic algorithms (GA), hydrodynamics potential flow numerical codes and a surrogate model based on ANN to account for the viscous effects. The ML tool is trained to capture the impact of viscosity on the flow around the stern of the vessel by analysing the results of a series of Design-of-Experiment (DoE) runs with a Reynolds-Average Navier-Stokes (RANS) solver. The approach accelerates the evaluation of the calm water resistance of the various designs and reduces the computational time required to reach an optimal hull design. The final design was evaluated with the RANS solver and the accuracy was satisfactory. The authors note that the exact number of neurons in the network are less important than the quality and quantity of the input data used for training the ANN. However, they recon that full-scale simulations at large Reynolds numbers are still challenging.

Ao et al. (2022) presented a data-driven multiple-input neural network (MINN) model to predict the total resistance of the ship's hull with the objective of avoiding inconsistencies from input parameters. It utilised three Fully Connected Neural Networks (FCNNs). The authors argue that the developed AI-based ML algorithm can assist the ship hull design process in real time by accurately providing the total resistance. They validated their results against a potential flow resistance prediction method. Through their validation studies, the authors have shown that a well-trained ANN can accurately estimate the hydrodynamic performances of a hull based on its geometry modification parameters. Therefore, the authors claim that the approach gives an accurate and fast AI-based method that provides optimum estimation accuracy in the entire design space.

Bagazinski and Ahmed (2023a) proposed a generative AI model based on a guided diffusion algorithm for parametric ship hull generation. They used a denoising diffusion probabilistic model (DDPM) that created the tabular design vectors of a ship hull. The model managed to improve performance through guidance. It utilised the dataset of 30,000 parametrised hull forms called Ship-D (Bagazinski and Ahmed, 2023b). Utilising 45 hull parameters and 49 algebraic feasibility constraints and guidance from performance prediction models, the algorithm was able to generate high-performance designs with only information learned from the low-performing hulls in the dataset. However, the significant reductions in wave drag were calculated using Michell's integral and they were not confirmed by more precise tools (e.g. VOF CFD) and the impact of other design changes (e.g. increased displacement) was not compensated by changes to other design parameters such as lightship, deadweight, stability etc.

Khan et al. (2023) introduced the generic parametric modeller ShipHullGAN. Deep convolutional generative adversarial networks (GANs) were used for an adaptive representation and generation of ship hulls. The model is trained on a dataset of more than fifty-two thousand physically validated designs. They included a variety of different ship types, such as bulkcarriers, tankers, container ships, crew supply vessels and tugboats. All training designs are converted into a common geometric representation using a shape extraction and representation strategy. They have the same resolution, as typically GANs can only accept vectors of fixed dimension as input. Right after the generator component, a space-filling layer was placed. Its purpose was to confirm that the trained generator could cover all design classes. The designs are provided in the form of a shape-signature tensor (SST) during training. It harnesses the compact geometric representation using geometric moments that further enable the cost-effective integration of physics-informed components in ship design. The authors argue that comparative studies and optimisation cases have shown that ShipHullGAN was capable of producing designs a broad spectrum of designs, both traditional and innovative, with geometrically sound and practically viable configurations.

Sharma et al. (2023) review Physics-informed Machine Learning (PIML) and how it integrates ML with domain knowledge. The authors suggest that higher data efficiency and more stable predictions can be achieved. Therefore, high-fidelity numerical simulations of complex turbulent flows can be augmented or even replaced. The authors categorise ML into unsupervised, supervised, and semi-supervised. Unsupervised learning refers to algorithms that learn from unlabelled data, This is opposed to supervised learning where algorithms recognise patterns of input–output relationships from labelled data. In semi-supervised learning, algorithms contain characteristics of both unsupervised and supervised learning. Regression and classification problems are typical applications of supervised learning. The PIMLs are the most recent step in the evolution of ML towards their applicability in fluid mechanics problems as they combine ML techniques with physics knowledge, and model loss

functions as can be seen in Figure **27: Methods for incorporating knowledge from physics into supervised learning framework models (Sharma et al., 2023)**

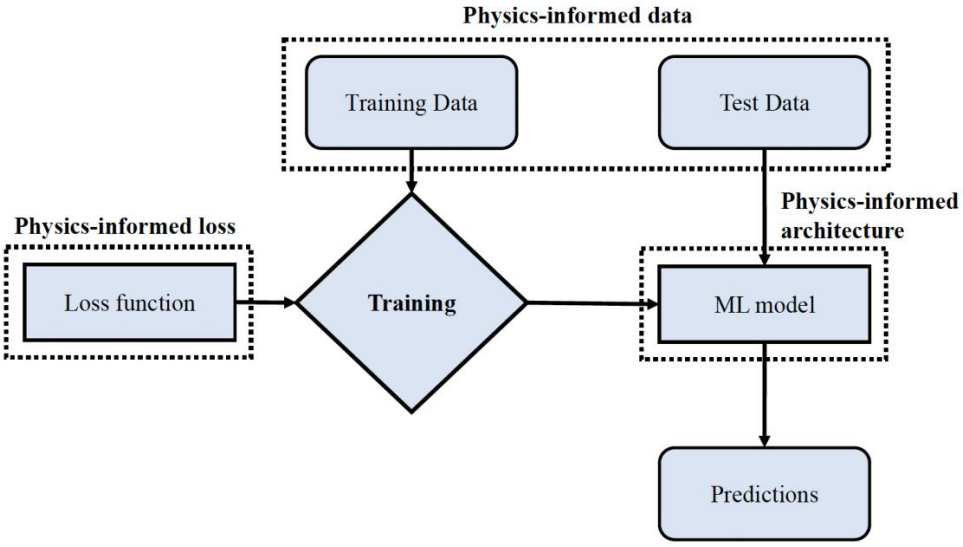

Figure 27: Methods for incorporating knowledge from physics into supervised learning framework models (Sharma et al., 2023)

Majnarić et al. (2024) investigated the use of ML-based determination of a containership's main particulars at the early design stage. They applied a synthetic data generation technique for generating a large amount of synthetic data points regarding container ships' main particulars, utilising a multilayer perceptron (MLP) regressor on both original and synthetic data mixed with original data points. The models were validated based on real data showing very good agreement.

Performance Prediction

Wang et al. (2022) present a deep neural network (DNN)-based approach to convert hull designs to condensed representations, generate innovative designs, and based on their hydrodynamic performance, optimize the synthetic design. The DNN-based 3D ship hull encoding and optimisation framework is shown in Figure 28**:** 8. It consists of three components integrated with CFD simulations: ship data augmentation and parameterization, VAE, and design optimization with virtual screening.

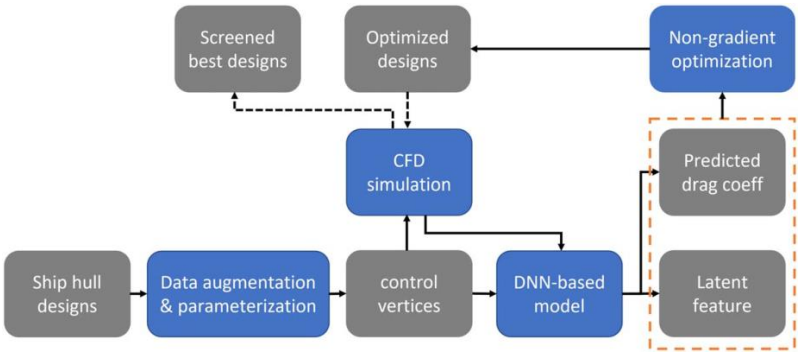

Figure 28: Overview of the data-driven ship 3D hull encoding and optimization framework (Wang et al., 2022)

A variational autoencoder (VAE) equipped with a hydro-predictor has been developed to reconstruct the geometry of hulls by reconstructing the Laplacian parameterized hulls. It also encodes the CFD-simulated resistance. Perlin noise mapping and free-form deformation (FFD) data augmentation algorithms generate the training set from a parent hull. This VAE model is then used to search efficiently through a vast array of generated hulls to identify those with minimum resistance. The most promising hulls are verified using CFD calculations. Numerical experiments verify the ability of the framework to reconstruct the input geometries and predict their resistance accurately using a convolutional neural network (CNN). The authors note that it has

produced new hull designs showcasing a 35% resistance reduction compared to the parent design. However, despite its adeptness, it is limited to intraclass ship design as the VAE reconstruction network is highly model-specific.

Hodges et al. (2022) utilized Siemens' NX CAD software to parametrize the hull form of MV Regal with 12 independent geometrical variables. They determined the powering requirements of the designs using the CFD solver Simcenter STAR-CCM+. Then, utilizing the results, they created in Simcenter ROM Builder and Monolith surrogate models. The workflow of the methodology is shown in Figure 29. The outputs of the models include torque, total resistance, powering, and propulsion metrics. These were then supplemented with additional ML CFD predictions for local field results including the wake fraction at the propeller, the generated wake, and the shear and pressure loads on the hull. The authors depict the capabilities of ML models to predict accurately the local field (see Figure 30), and their potential of enhancing the hull optimization pipeline.

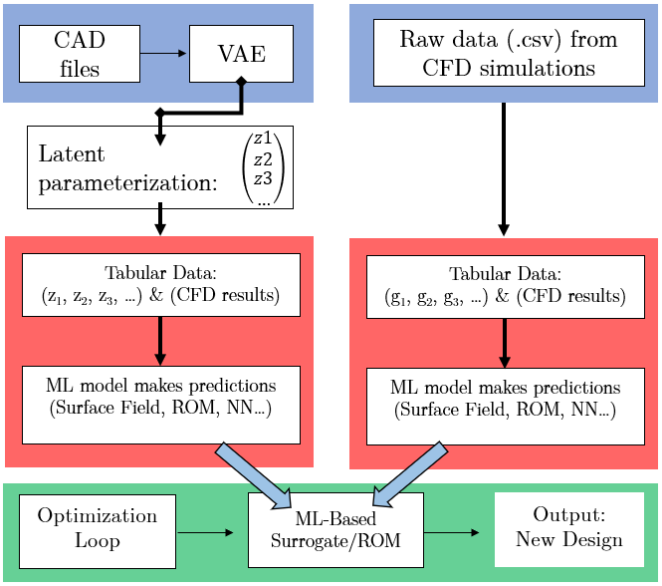

Figure 29: The different workflows used by Hodges et al. (2022)

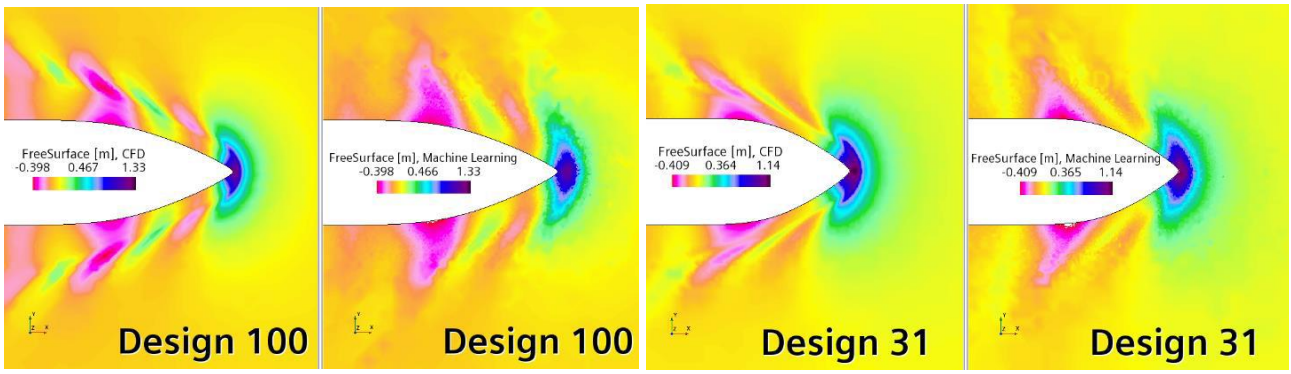

Figure 30: Free surface elevation comparisons between CFD simulation and ML model predictions (Hodges et al., 2022)

Safety Analysis

Louvros et.al. (2023) described a novel approach that introduces a fast decision support tool which can provide information regarding the ongoing damage stability casualty utilizing prior knowledge gained from simulations. Case-based reasoning and Machine Learning methods are used, providing real-time predictions based on "analyzing" a dataset of pre-run damage scenarios. In this way, the lengthy and costly computations that describe the actual flooding phenomena can be bypassed. Case studies simulating realistic scenarios are presented to showcase the performance and practical application of the methodology.

Holistic Design Optimisation

Nazemian et al. (2024) presented a Machine Learning (ML) tool for calm water resistance prediction and used it to develop a systematic series for battery-driven catamaran hullforms. Furthermore, they employed the ML predictor for design optimization using a GA. For the dataset training, three regression models were tested, namely, Regression Trees (RTs); Support Vector Machines (SVMs); and Artificial Neural Network (ANN). The authors use the framework for the optimization of several catamarans, including dimensional and hull coefficient parameters based on resistance, structural weight reduction, and battery performance improvement. Lackenby transformation is initially used to explore the design space, and then, a novel self-blending method generates new hullforms based on two-parent blending. Finally, the generated data of the case study are encoded in an ML model. The ANN algorithm has shown a good correlation with the expected resistance. Accordingly, by choosing any new design based on owner requirements, GA optimization obtained the final optimum design by using an ML fast resistance calculator. The design of a 40 m passenger catamaran vessel was optimised in a showcased study. The framework achieved a 9.5% improvement proving that combining ML and GA optimization may accelerate significantly the ship design process.

Energy efficiency, decarbonisation and environmental impact

Nikolopoulos and Boulougouris (2023) presented a Robust Holistic Ship Design Approach (RHODA) using voyage simulation and surrogate models. The authors deployed the framework for the optimization of Zero-Emission Ships. They implemented the simulation-driven optimization in the case study of an NH3-fulled Large Bulk Carrier. The framework was adapted to cover the ship and fuel-specific aspects of the design of the Zero-Emission ship configuration

Zhang et al. (2024) utilize a deep learning method for the prediction of ship fuel consumption. Their approach makes use of big data from sensors, voyage reporting and hydrometeorological data, summing up to a total of 266 variables. Their model is trained based on results from sea trials of a Kamsarmax bulk carrier. Using a Decision Tree (DT), patterns are recognized within the available dataset. Implementing a deep learning model, the influence of variables such as sailing speed, heading, displacement/draft, trim, weather, sea conditions, etc. on ship fuel consumption (SFC) is established. This is achieved by incorporating a DLM based on Bi-LSTM with an attention mechanism. The methodology is validated using k-fold cross-validation and implemented in a case study. The author concluded that the method could be useful in the context of a decision-support system for environmentally friendly operations, subject to further testing and validation.

Other areas

Mikulić and Parunov (2019) presented an overview of the AI and ML state-of-the-art in different areas of the maritime industry. This included design, structures, hydrodynamics, forecast of environmental factors, corrosion, production, and machinery. The authors concluded with recommendations for potential implementations.

AI and ML algorithms have also found their way into the integration of ship design and ship production in the form of the recently started Horizon Europe Project ESY (2024), where digital tools will support sustainable shipbuilding practices.

CONCLUSIONS AND WAY AHEAD

Conclusions

In today's era of smart digitalization in the frame of Industry 4.0, recently introduced digital/software tools and systems have increased the efficiency and quality of the life-cycle ship design process. Parametric optimisation and simulation-driven design, product lifecycle management, digital twins and artificial intelligence are nowadays frequently used by the maritime industry during the commissioning/quality control activities and in the various phases of ship design, ship operation and ship production.

Classical and novel concepts of ship design and the assessment of life-cycle operation are nowadays implemented in versatile, integrated design platforms, offering the user a vast variety of options for the efficient development of alternative ship designs by use of tools for their analysis and parametric, multi-objective optimisation with respect to all relevant (ship) design disciplines, as well as virtual prototyping. Some design software systems (e.g., as developed in HOLISHIP) adopt an open architecture that allows for the continuous adaptation to current and emerging design and simulation needs, flexibly setting up dedicated synthesis models for different application cases. The exploration of the huge design space is enabled by the use of automated parametric models of significant depth, which are processed with reduced lead time.

Simulation-driven ship design has become an important part of today's design teams and the authors believe that it will play an even more decisive role in the future. As presented in sections *Parametric Ship Design Optimization*, *Simulation-driven*

Ship Design and *Artificial Intelligence* the trend is to address more complex design tasks while doing so with higher efficacy. SDD campaigns increasingly accommodate more objectives and several disciplines. This is because competition continues to be high, calling for better products, while the need for sustainable shipping has become evident as is now also reflected in recent legislation. Furthermore, the environment in which design teams need to make decisions has become more complicated over the last years. Potential solutions for energy-efficient shipping are developing more rapidly – with some that are just emerging – while the prediction of available fuels, trade patterns and retrofits for ships in service is presently rather difficult, adding uncertainty and calling for flexibility as elaborated in section *Ship Production and Lifecycle Management*.

We believe lifecycle aspects of marine systems design will become even more important in the coming years. Our common ambitious goals for net zero 2050 will be the main driver. Business-as-usual is not an option. Nor are currently available technology, energy carriers, concepts of operations and regulatory framework sufficient to solve this problem. Thus, innovative and even radical measures are needed – but what this will turn out to be is not yet known. For the maritime industry, this is a severe risk for most, but also an opportunity for those who are able to make and implement the best lifecycle strategies for business development, fleet renewal, retrofits, and operations. For the marine systems design community, it poses a challenge for the years ahead to develop the necessary models, methods and tools to foster change built on a holistic, lifecycle perspective.

A review of the state-of-the-art of digital twins in the design and retrofit of ships concludes that there is currently no standardized design method or approach for DT-based design or retrofit within the ship design industry, or even in other relevant industries. Thus, this state-of-the-art report argues for four points. First, ship design literature should be consistent with their terminology when researching and applying DTs. This paper argues for the DT definitions proposed by Grieves (2014), and Kritzinger et al. (2018). Second, the development of a standardized DT-enabled framework, applicable to both new-builds and retrofits, which is flexible, reusable, and verifiable, and includes, among others, specific methods, input data, output data and reliability of the design would help with the research and innovation in this domain. This should be done to support the development of a virtual space in which DTs can be developed for different types of ships. Third, additional research and application focus should be placed on the use of formal MBSE to support DT-based ship design and retrofits. Finally, additional research focus should be placed on DTs in the operational phase specifically to support retrofitting to extend the lifetime of a ship, increase its energy-efficiency and improve its operation.

The integration of AI in ship design is set to accelerate, expanding from the conceptual phase where its benefits are already evident. AI's role is expected to grow across all stages of design, including hull optimization, performance prediction, and structural and safety analysis. Despite these advancements, engineers face challenges such as ensuring the transparency and verification of AI-generated results, as AI learning is ongoing. Additionally, the impact on the training and employability of future engineers is a concern. The adoption of these tools could significantly reduce task completion times, but there is scepticism about their potential negative effects on job availability in the sector. Naval architects and marine engineers must adapt to leverage AI's advantages while mitigating its challenges.

Way Ahead

The complexity of solving multi-objective and even multi-disciplinary design tasks is intrinsically high since many free variables are involved and many high-fidelity simulations are needed. Surrogates and ML have been proposed to cope with high complexity and to more easily capture mutual influences. In order to provide the necessary training data Design-of-Experiments are utilized. There currently are several approaches to reduce the number of variants that need to be run along with the computational effort that has to be spent: (i) The reduction of the number of free variables by dimensionality reduction, see for instance Diez et al (2015), (ii) the mixture of simulations of different fidelity, see for instance Pellegrini et al (2022), and (iii) the adaptive sampling of design spaces, see for instance Serani et al (2019).

The abundance of data produced during SDD campaigns should and could be utilized more intelligently and more systematically in the future, see section Digital Twins in the Design and Retrofit of Ships. The various levels of digital representation (i.e., model, shadow and twin) can certainly benefit from design data and vice versa. Here, one challenge lies in ship hydrodynamics where full-scale simulations by means of CFD are very resource-intensive and, unfortunately, are difficult to verify by means of reliable measurements while sailing in accurately known weather conditions. Here, the industry at large appears to be still at the beginning of developments.

There are naturally several trends that have not been discussed in this paper so as to deliberately limit its scope. Yet, some of them should be briefly mentioned as they may influence the not-too-distant future in ship design: (i) Cloud solutions, even though still looked at with a certain skepticism when it comes to sensitive data, (i) web-based applications and micro-services that could help increase access to more design teams and “democratize” the usage of high-fidelity simulations at acceptable costs while ensuring results of high quality.

Last, but not least: the complexity of the employed design methods, software tools and design platforms has created an increased demand for proper training of users of software platforms in information technology and beyond traditional naval architecture. This calls for an urgent adaptation of the curricula of university education in naval architecture and marine technology. Ship design is a synthetic, multi-disciplinary field and only properly trained naval architects will be able to assess the validity of results of simulation tools/design software platforms and take proper decisions on the way ahead in stages of the ship design process.

CONTRIBUTION STATEMENT

Author 1: Conceptualization; supervision; writing introduction and chapter on parametric ship design optimisation; paper consolidation; review and editing. **Author 2:** conceptualization; writing chapter on Artificial Intelligence – review and editing. **Author 3**: conceptualization; writing chapter on Life Cycle Management– review and editing. **Author 4:** conceptualization; writing chapter on Simulation-driven Ship Design – review and editing. **Author 5**: conceptualization; writing chapter on Digital Twins - review and editing.

ACKNOWLEDGEMENTS

The support of the presented research by the European Union's Horizon research and innovation program, Projects HOLISHIP (Grant Agreement No 689074), TrAM (Grant Agreement No 769303), Orcelle (Grant No 101096673) and DT4GS (Grant Agreement No 101056799), is acknowledged.

Dr. Harries has been partially supported by the Horizon Europe project "RETROFIT55 – Retrofit solutions to achieve 55% GHG reduction by 2030", grant agreement 101096068 (see https://www.retrofit55.eu/).

Prof. Boulougouris has been partially supported by the Horizon Europe project "ESY-EcoShipYard", grant agreement 101138730. He also acknowledges the support from RCG and DNV, sponsors of the Maritime Safety Research Centre at the University of Strathclyde. The opinions expressed herein are those of the author and does not reflect the views of EC, DNV or RCG.

The authors would like to acknowledge Julien Hermans (Hermans, 2024) and Isabel van Noesel (van Noesel, 2023) of Delft University of Technology who provided significant contributions to the digital twin section of this paper. The authors are also grateful to Mrs. Aimilia Alissafaki (NTUA), for her support in edition of the paper.

REFERENCES

ABS (2023). American Bureau of Shipping, Explore Data and Digitalization, online access (8-12-2023) https://ww2.eagle.org/en/innovation-and-technology/data-and-digitalization.html

Ahmed, O., Harries, S., Lohse, J. and Salecker, S.-E. (2023). *Parametric Modelling, CFD Simulations, DoE and Machine Learning for the Design of a Planing Boat*, Conference on Computer Applications and Information Technology in the Maritime Industries (COMPIT 2023), Kloster Drübeck, Germany.

Andrews, D., Papanikolaou, A. and Singer, D. (2012). Design for X., Proc. 11th International Marine Design Conference, IMDC 2012, Glasgow, Scotland.

Andrews, D. and Erikstad, S-O (2015). State of the art report on design methodology, Proc. 12th International Marine Design Conference, IMDC 2015, Tokyo, Japan.

Andrews, D., Kana, A., Hopman, J. and Romanoff, J. (2018). State of the art report on design methodology, Proc. 13th International Marine Design Conference, IMDC 2018, Helsinki, Finland.

Ao, Y., Li, Y., Gong, J. and Li, S., (2022). Artificial Intelligence Design for Ship Structures: A Variant Multiple-Input Neural Network-Based Ship Resistance Prediction. Journal of Mechanical Design. 144. 1-18. 10.1115/1.4053816.

Arrichiello, V. and Gualeni, P. (2020). Systems engineering and digital twin: A vision for the future of cruise ships design, production and operations. *International Journal on Interactive Design and Manufacturing (IJIDeM), 14*.

Autiosalo, J., Vepsäläinen, J., Viitala, R. and Tammi, K. (2019). A feature-based framework for structuring industrial digital twins. *IEEE Access, 8.*

Bagazinski, N.J. and Ahmed, F. (2023a). ShipGen: A Diffusion Model for Parametric Ship Hull Generation with Multiple Objectives and Constraints. J. Mar. Sci. Eng. 2023, 11, 2215. https://doi.org/10.3390/jmse11122215.

Bagazinski, N.J. and Ahmed, F. (2023b). Ship-D: Ship Hull Dataset for Design Optimization using Machine Learning. In Proceedings of the International Design Engineering Technical Conferences and Computers and Information in Engineering Conference, Boston, MA, USA, 20–23 August 2023; American Society of Mechanical Engineers: New York, NY, USA.

BEST+ Project (2011-2012). Better Economics with Safer Tankers, Tri-lateral NTUA-FSS-GL project; Funding: Germanischer Lloyd, Duration: 2011-2012 .

Boulougouris, V., Papanikolaou, A., Zaraphonitis, G. (2004). Optimization of Arrangements of Ro-Ro Passenger Ships with Genetic Algorithms. Journal Ship Technology Research, Vol. 51, No. 3.

Boucher, P. (2020). Artificial intelligence: How does it work, why does it matter, and what can we do about it?. Scientific Foresight Unit (STOA), Directorate-General for Parliamentary Research Services (EPRS) of the Secretariat of the European Parliament. ISBN: 978-92-846-6770-3, doi: 10.2861/44572.

Brett, P. O., & Ulstein, T. (2015). *What is a better ship? It all depends ...* Proceedings IMDC 2015 International Marine Design Conference 2015, Tokyo, Japan.

Bureau Veritas (2023). The Future of Marine and Offshore Classification, online access (8-12-2023) https://www.bureauveritas.gr/digital-innovation

Celik, C., Özsayan, S., Köksal, C.S., Danışman, D.B., Korkut, E. and Gören, Ö. (2022). *On the Full-Scale Powering Extrapolation of Ships with Gate Rudder System (GRS)*, A. Yücel Odabaşı Colloquium Series, 4th Int. Meeting - Ship Design & Optimization and Energy Efficient Devices for Fuel Economy, 15th–16th December 2022, Istanbul, Turkey.

ClassNK (2023). ClassNK Digital Grand Design 2030: Creating innovation for a blue economy, online access (8-12-2023) https://www.classnk.or.jp/hp/en/activities/techservices/dgd2030/index.html

Dassault Systemes, 3ds (2023). Digital and sustainable: The next milestone in shipbuilding transformation, online access (8-12-2023) https://www.3ds.com/insights/corporate-reports/digital-and-sustainable-next-milestone-shipbuilding-transformation

Deb, K., Pratap, A., Agarwal, S. and Meyarivan, T. A. M. T. (2002). A fast and elitist multiobjective genetic algorithm: NSGA-II. IEEE transactions on evolutionary computation, *6*(2), 182-197.

Diaz R., Smitha K., Bertagnab S. and Vittorio B. (2023). Digital Transformation, Applications, and Vulnerabilities in Maritime and Shipbuilding Ecosystems , International Conference on Industry 4.0 and Smart Manufacturing , Procedia Computer Science 217 (2023) 1396–1405 , https://doi.org/10.1016/j.procs.2022.12.338 , online access (8-12-2023) https://www.sciencedirect.com/science/article/pii/S1877050922024231

Diez M., Campana, E.F. and Stern, F. (2015). Design-space dimensionality reduction in shape optimization by Karhunen–Loève expansion. Computer Methods in Applied Mechanics and Engineering, 283, pp 1525–1544. https://doi.org/10.1016/j.cma.2014.10.042

DNV (2023). Det Norske Veritas ,Digitalization in the maritime industry, online access (8-12-2023) https://www.dnv.com/maritime/insights/topics/digitalization-in-the-maritime-industry/index.html

DNV (2023). Energy Transition Outlook 2023: Maritime Forecast to 2050, https://www.dnv.com/energy-transition-outlook

DT4GS (2024). DT4GS: The digital twin for green shipping. Horizon Europe project. https://dt4gs.eu/

ESY (2024). *EcoShipYard*, Horizon Europe Project, Grant Agreement No. 101138730.

Ehmer, M., and Khan, F. (2012). A comparative study of white box, black box and grey box testing techniques. *International Journal of Advanced Computer Science and Applications, 3*(6).

Erikstad, S. O. (2019). Designing Ship Digital Services. In V. Bertram (Ed.), COMPIT´19 - 18th Conference on Computer and IT Applications in the Maritime Industries. Tullamore, Ireland.Erikstad, S.-O. (2017). Merging physics, big data analytics and simulation for the next-generation digital twins. *High-Performance Marine Vehicle (HIPER)*. Zevenwacht, South-Africa.

Erikstad, S.-O. and Lagemann, B. (2022). Design Methodology – State of the Art Report, Proc. 14th Int. Marine Design Conference, Vancouver, June 2022, DOI: 10.5957/IMDC-2022-301.

Fonseca, Í.A. and Gaspar, H.M. (2020). Challenges when creating a cohesive digital twin ship: a data modelling perspective. *Ship Technology Research, 68*(2).

Funke, C. and Jonsson, D. (2019). *A Framework for Implementing Simulation-Driven Design*, KTH Royal Institute of Technology, School of Industrial Technology & Management, KTH, TRITA ITM-EX-2019:146

García, S., Ramírez-Gallego, S., Luengo, J., Benítez, J.M. and Herrera, F. (2016). Big data preprocessing: Methods and prospects. *Big Data Analytics*, *1*(1).

Gaspar, H., Ross, A. M., & Erikstad, S. O. (2012). Handling temporal complexity in the design of non-transport ships using epoch-era analysis. International Journal for Maritime Engineering (RINA Transactions Part A), (AP).

Giering, J.-E., & Dyck, A. (2021). Maritime digital twin architecture: A concept for holistic digital twin application for shipbuilding and shipping. *at-Automatisierungstechnik*, *69*(12).

Grieves, M. (2014). Digital twin: Manufacturing excellence through virtual factory replication. White paper, 1–7.

Grieves, M. (2015). Digital Twin: Manufacturing Excellence through Virtual Factory Replication, https://www.researchgate.net/publication/275211047

Grigoropoulos, G., Bakirtzoglou, C., Papadakis, G. and Ntouras, D. (2021). Mixed-Fidelity Design Optimization of Hull Form Using CFD and Potential Flow Solvers. Journal of Marine Science and Engineering. https://doi.org/10.3390/jmse9111234.

Gürkan, A.Y, Ünal, U.O., Aktaş, B. and Atlar, M. (2023). *An investigation into the gate rudder system design for propulsive performance using design of experiment method*, Ship Technology Research, DOI: 10.1080/09377255.2023.2248721

Hagen, A. and Grimstad, A. (2010). The Extension of System Boundaries in Ship Design. *International Journal of Maritime Engineering, 152*, pp.17-28, http://dx.doi.org10.3940/rina.ijme.2010.a1.167

Harries S (1998). Parametric design and hydrodynamic optimization of ship hull forms. Ph.D. Thesis, Technical University Berlin, Mensch & Buch Verlag, ISBN 3-933346-24-X

Harries, S. (2020). *Practical Shape Optimization using CFD – State-of-the-art in Industry and Selected Trends*, Conference on Computer Applications and Information Technology in the Maritime Industries (COMPIT 2020), Pontignano, Italy

Harries, S. and Abt, C. (2019). *Faster Turn-around Times for the Design and Optimization of Functional Surfaces*, Ocean Engineering 193 (2019) 106470, Elsevier

Harries, S. and Abt, C. (2019). *The HOLISHIP Platform for Process Integration and Design Optimization*, published by A. Papanikolaou (Ed.) in *A Holistic Approach to Ship Design – Vol. 1: Optimisation of Ship Design and Operation for Life Cycle*, Springer 978-3-030-02809-1

Harries, S., Abt, C. and Brenner, M. (2015). *Upfront CAD – Parametric Modelling Techniques for Shape Optimization*, Int. Conf. on Evolutionary and Deterministic Methods for Design, Optimization and Control with Applications to Industrial and Societal Problems (EUROGEN 2015), published in 2018 by E. Minisci et al. (Eds.) in Advances in Evolutionary and

Deterministic Methods for Design, Optimization and Control in Engineering and Sciences, Springer 978-3-319-89986-2, Glasgow, UK

Harries, S., Ahmed, O. and Uharek, S. (2024). *Simulation-driven Design of a fast Monohull*, Ship Technology Research, DOI: 10.1080/09377255.2024.2305540

Harries, S., Brunswig, J., Gatchell, S., Hauschulz, S., Schuhmache, A., Thies, F. and Marzi, J. (2023). *The Need for Sufficiently Accurate Geometrical Representations of Ship Hull Forms for Digital Twins for Performance Prediction*, 8th Int. Symposium on Ship Operations, Management & Economics (SOME), Athens, Greece

Hermans, J. (2024). Retrofit modelling for green ships A data-driven design approach for emission reduction using bunker delivery notes. MSc thesis. Delft University of Technology.

HOLISHIP (2016-2020) Holistic Optimisation of Ship Design and Operation for Life Cycle. Project funded by the European Commission, H2020- DG Research, Grant Agreement 689074, http://www.holiship.eu

Hodges, J., Wheeler, M., Belhocine, M. and Henry, J. (2022). AI/ML Applications for Ship Design, International Conference on Control, Automation and Systems, 2022.

Huang, L., Pena, B., Liu, Y. and Anderlini, E. (2022). Machine learning in sustainable ship design and operation: A review, Ocean Engineering, Volume 266, Part 2, 112907, ISSN 0029-8018, https://doi.org/10.1016/j.oceaneng.2022.112907.

Ibrion, M., Paltrinieri, N. and Nejad, A.R. (2019). On Risk of Digital Twin Implementation in Marine Industry: Learning from Aviation Industry. *Journal of Physics: Conference Series*, *1357.*

Ichimura Y., Dalaklis D., Kitada, M., Christodoulou A. (2022). Shipping in the era of digitalization: Mapping the future strategic plans of major maritime commercial actors, Digital Business, Volume 2, Issue 1, 2022, 100022, ISSN 2666-9544, https://doi.org/10.1016/j.digbus.2022.100022 (https://www.sciencedirect.com/science/article/pii/S2666954422000023)

Ishii, K. (1995). Life-Cycle Engineering Design. *Journal of Mechanical Design, 117*(B), 42-47. doi:10.1115/1.2836469

Klaveness, https://www.klaveness.com/sustainability, Visited 05/02/2024

Kritzinger, W., Karner, M., Traar, G., Henjes, J. and Sihn, W. (2018). Digital twin in manufacturing: A categorical literature review and classification. *16th IFAC Symposium on Information Control Problems in Manufacturing INCOM 2018, 51*(11).

Kusaka Y., Nakamura H. and Kunitake, Y. (1980). Hull form design of the semi-submerged catamaran vessel, Proceedings 13th Symposium on Naval Hydrodynamics, Tokyo, Japan, pp.555-568.

Lagemann, B., Lagouvardou, S., Lindstad, E., Fagerholt, K., Psaraftis, H. N., & Erikstad, S. O. (2023). Optimal ship lifetime fuel and power system selection under uncertainty. *Transportation Research Part D: Transport and Environment, 119*. doi:10.1016/j.trd.2023.103748

Lagemann, B., Lindstad, E., Fagerholt, K., Rialland, A. and Ove Erikstad, S. (2022). Optimal ship lifetime fuel and power system selection. *Transportation Research Part D: Transport and Environment, 102*, 103145. doi:https://doi.org/10.1016/j.trd.2021.103145

Lagouvardou, S., Lagemann, B., Psaraftis, H. N., Lindstad, E. and Erikstad, S. O. (2023). Marginal abatement cost of alternative marine fuels and the role of market-based measures. *Nature Energy*. doi:10.1038/s41560-023-01334-4

Lindstad, E., Gamlem, G., Rialland, A. and Valland, A. (2021). *Assessment of Alternative Fuels and Engine Technologies to Reduce GHG.* Paper presented at the SNAME Maritime Convention.

Lloyds Register, LR: Foo J. (2023). Lloyd's Register Digitalisation driving change in shipbuilding, online access (8-12-2023) https://www.lr.org/en/knowledge/insights-articles/digitalisation-driving-change-in-shipbuilding/

Lopez, V. and Akundi, A.(2022) A Conceptual Model-based Systems Engineering (MBSE) approach to develop Digital Twins. *International Systems Conference*. Montreal.

Louvros P., Stefanidis F., Boulougouris E., Komianos A. and Vassalos D. (2023). Machine Learning and Case-Based Reasoning for Real-Time Onboard Prediction of the Survivability of Ships. Journal of Marine Science and Engineering. 2023; 11(5):890. https://doi.org/10.3390/jmse11050890.

Maersk (2024). https://www.maersk.com/sustainability/our-approach/strategy, Visited 05/02/2024

Maggioncalda, M., Gualeni, P., Notaro, C., Cau, C., Bonazountas, M., andStamatis, S. (2019). Life Cycle Performance Assessment (LCPA) Tools. In A. Papanikolaou (Ed.), A Holistic Approach to Ship Design: Volume 1: Optimisation of Ship Design and Operation for Life Cycle (pp. 383-412). Cham: Springer International Publishing.

Massobrio, A. (2023). *What is Simulation-Driven Design? Main Benefits Explained*, https://www.neuralconcept.com/post, accessed on December 18, 2023

Mauro, F. and Kana, A. (2023). Digital twin for ship life-cycle: A critical systematic review. *Ocean Engineering*, 269.

Majnarić, D., Baressi Šegota, S., Anđelić, N. and Andrić, J. (2024). "Improvement of Machine Learning-Based Modelling of Container Ship's Main Particulars with Synthetic Data". J. Mar. Sci. Eng. 12, 273 https://doi.org/10.3390/jmse12020273 .

Mikulić, A. and Parunov J. (2019). "A review of artificial intelligence applications in ship structures". In "Trends in the Analysis and Design of Marine Structures: Proceedings of the 7th International Conference on Marine Structures", Guedes Soares, C. and Parunov, J. (Eds.). (MARSTRUCT 2019, Dubrovnik, Croatia, 6-8 May 2019) (1st ed.). CRC Press. https://doi.org/10.1201/9780429298875 .

Mouzakitis, S., Kontzinos, C., Tsapelas, J., Kanellou, I., Kormpakis, G., Kapsalis, P. and Askounis, D. (2023). Enabling maritime digitalization by extreme-scale analytics, AI and digital twins: The vesselai architecture. *Intelligent Systems and Applications. IntelliSys, 544*

NAPA (2023). Software solutions for ship design, online access (8-12-2023) https://www.napa.fi/software-and-services/ship-design/?utm_source=google_ads&utm_medium=search&utm_campaign=design&gad_source=1&gclid=CjwKCAiA1MCrBhAoEiwAC2d64TBAeXTYz5aVwPMgvX5UgZ-4aiVtiIZcGRjJR_F_cyGxm6d3znsaRhoCcAEQAvD_BwE

Mauro, F. and Kana, A. (2023). Digital twin for ship life-cycle: A critical systematic review, Ocean Engineering, Vol. 269, Elsevier, https://doi.org/10.1016/j.oceaneng.2022.113479.

Marzi, J., Harries, S., Schwarz, B., Scharf, M., Demmich, K. and Pontius, M. (2024). MariData – Digital Twin for Optimal Vessel Operations Impacting Ship Design. Proc. 15th International Marine Design Conference, IMDC2024 (to be published).

NAVAIS (2017). NAVAIS: New advanced value added innovation in ship building. European Horizon 2020 project. https://www.navais.eu/.

Nazemian A., Boulougouris E. and Aung MZ. Utilizing Machine Learning Tools for Calm Water Resistance Prediction and Design Optimization of a Fast Catamaran Ferry. Journal of Marine Science and Engineering. 2024; 12(2):216. https://doi.org/10.3390/jmse12020216.

de Neufville, R. and Scholtes, S. (2011). *Flexibility in Engineering Design*. The MIT Press, ISBN electronic: 9780262303569, doi: https://doi.org/10.7551/mitpress/8292.001.0001

Newrzella, S.R., Franklin, D.W. and Haider, S. (2022). Methodology for Digital Twin Use Cases: Definition, Prioritization, and Implementation. *IEEE Access, 10.*

Nikolopoulos, L. and Boulougouris, E. (2020). A novel method for the holistic, simulation driven ship design optimization under uncertainty in the big data era. *Ocean Engineering, 218*.

Nikolopoulos L. and Boulougouris E. (2023). Simulation-Driven Robust Optimization of the Design of Zero Emission Vessels. Energies. 2023; 16(12):4731. https://doi.org/10.3390/en16124731

van Noesel, I. (2023). Advancements in Digital Twin-Based Approaches for Ship Design and Production: A Comprehensive Literature Review. Independent research project report, Delft University of Technology.

Nowacki, H., Brusis, F. and Swift, P.M. (1970). Tanker Preliminary Design - An Optimization Problem with Constraints. Trans SNAME. Volume 78.

Murphy, R., Sabat, D. and Taylor, R. (1965). Least Cost Ship Characteristics by Computer Techniques, Marine Technology, SNAME, April 1965.

Papanikolaou, A. (ed), et al (2019). A Holistic Approach to Ship Design, Vol. 1: Optimisation of Ship Design and Operation for Life Cycle, Springer International Publishing, ISBN 978-3-030-02809-1, https://doi.org/10.1007/978-3-030-02810-7

Papanikolaou, A. (ed), et al (2021). A Holistic Approach to Ship Design, Vol. 2: Application Case Studies, Springer International Publishing, ISBN 978-3-030-71090-3, June 2021, https://doi.org/10.1007/978-3-030-71091-0

Papanikolaou, A. (2010). Holistic Ship Design Optimization. *Computer-Aided Design*, vol. 42, no. 11, Elsevier, 2010, pp. 1028–1044, https://doi.org/https://doi.org/10.1016/j.cad.2009.07.002.

Papanikolaou, A., Andersen, P., Kristensen, H.-O., Levander K., Riska, K., Singer, D. andVassalos, D. (2009). State of the Art Report on Design for X., Proc. 10th International Marine Design Conference, Vol. 2, IMDC2009, pp. 577–621.

Papanikolaou, A., Nowacki, H., Androulakakis, M. and Zaraphonitis, G. (1989). Concept Design and Optimization of a SWATH Passenger/Car Ferry, Proc. IMAS-89 Int. Conf. on Applications of New Technology in Shipping, Athens, May 1989.

Papanikolaou, A. and Androulakakis, M. (1991). Hydrodynamic Optimization of High-Speed SWATH. In: Proc. of 1st FAST '91 Conf., Trondheim.

Papanikolaou, A., Kaklis, P., Koskinas, C. and Spanos, D. (1996). Hydrodynamic Optimization of Fast Displacement Catamarans. In: Proc. 2lst Int. Symposium on Naval Hydrodynamics, ONR' 96, Trondheim.

Papanikolaou, A., Harries, S., Hooijmans, P., Marzi, J., Le Nena, R., Torben, S., Yrjänäinen, A. and Boden, B. (2022). A Holistic Approach to Ship Design: Tools and Applications, Journal of Ship Research 25-53, Vol. 66, Issue 1, March 2022, https://doi.org/10.5957/JOSR.12190070

Papanikolaou, A., Xing-Kaeding, Y., Strobel, H., Kanellopoulou, A., Zaraphonitis, G., Tolo, E. (2020). Numerical and Experimental Optimization Study on a Fast, Zero Emission Catamaran, Journal of Marine Science and Engineering, MDPI, 2020, 8, 657; doi:10.3390/jmse8090657

Papanikolaou, A. (2022). Holistic Approach to Ship Design, J. Mar. Sci. Eng. 2022, 10(11), 1717; https://doi.org/10.3390/jmse10111717 (registering DOI) - 10 Nov 2022

Papanikolaou, A. (2024). On parametric modelling, digital siblings and ship design optimization, Journal Ship Technology Research (Schiffstehnik), Special issue of Ship Technology Research on 'Simulation-Driven Design of Maritime Systems' in Honor of Prof. Dr.-Ing. Dr. h. c. Horst Nowacki, https://doi.org/10.1080/09377255.2024.2312307, Taylor & Francis.

Panchal, J.H., Fuge, M., Liu, Y., Missoum, S. and Tucker, C. (2019). Guest Editorial, Special Issue: Machine Learning for Engineering Design, Journal of Mechanical Design, ASME, NOVEMBER 2019, Vol. 141 / 110301-1.

Pellegrini R., Serani A., Liuzzi G., Rinaldi F., Lucidi S. and Diez M. (2022). A Derivative-Free Line-Search Algorithm for Simulation-Driven Design Optimization Using Multi-Fidelity Computations. Mathematics 10(3), 481. https://doi.org/10.3390/math10030481

Pérez Fernández, R. (2021). What the shipbuilding future holds in terms of CAD/CAM/CIM systems. *7th International Symposium on Ship Operations, Management and Economics (SNAME-SOME).* Virtual, April.

Ponkratov, D. (2023). *JoRes Joint Research Project - the Largest Global Community Developing Benchmark for Ship Scale CFD*, 25th Num. Towing Tank Symposium (NuTTS), Ericeira, Portugal

Psarommatis, F. and May, G. (2022). A literature review and design methodology for digital twins in the era of zero defect manufacturing. *International Journal of Production Research, 61*(5).

RETROFIT55 (2024): Retrofit Solutions to achieve 55% GHG Reduction by 2030. Horizon Europe project. https://www.retrofit55.eu/

Sarker, I.H. (2021). Machine learning: algorithms, real-world applications and research directions. SN Comput. Sci. 2, 1–21.

Salvesen, N., Kerczek, C. V. and Scragg, C. (1985). Hydro-Numeric Design of SWATH ships, Transactions of the Society of Naval Architects and Marine Engineers.

Sharma, A., Kosasih, E., Zhang, Y., Brintrup, A. and Calinescu, A. (2022). Digital Twins: State of the Art Theory and Practice, Challenges, and Open Research Questions, Journal of Industrial Information Integration, 100383.

Sharma, P., Chung, WT., Akoush, B. and Ihme, M. A. (2023). Review of Physics-Informed Machine Learning in Fluid Mechanics. Energies, 16, 2343. https://doi.org/10.3390/.

Siemens (2023). Towards Maritime 4.0: Let us guide you, online access (8-12-2023) https://www.sw.siemens.com/de-DE/marine-digital-thread-executive-briefs/

Kusaka, Y., Nakamura, H., Kunitake, Y. (1980). Hull Form Design of the Semi-submersed Catamaran Vessel, Proc. 13th ONR Symposium of Naval Hydrodynamics, Tokyo, 1980.

Rehn, C. F., Pettersen, S. S., Agis, J. J. G., Brett, P. O., Erikstad, S. O., Asbjørnslett, B. E. And Rhodes, D. H. (2018). Quantification of changeability level for engineering systems. Systems Engineering (July 2018). doi:10.1002/sys.21472

Rehn, C. F., Agis, J. J. G., Erikstad, S. O. andNeufville, R. d. (2018). Versatility vs. retrofittability tradeoff in design of non-transport vessels. Ocean Engineering (November 2018). doi:10.1016/j.oceaneng.2018.08.057

RINA. (2020). What does it mean to be a retrofit ship of the future? *The Naval Architect*, Jul/Aug.

Serani A., Pellegrini R., Wackers J., Jeanson C.-E., Queutey P., Visonneau M. and Diez, M. (2019). Adaptive multi-fidelity sampling for CFD-based optimisation via radial basis function metamodels. International Journal of Computational Fluid Dynamics 33(6-7), 237–255. https://doi.org/10.1080/10618562.2019.1683164

Stachowski, T. and Kjeilen, H. (2017). Holistic ship design – how to utilise a digital twin in concept design through basic and detailed design. *International Conference on Computer Applications in Shipbuilding (ICCAS).* 26-28 September, Singapore.

Tao, F., Zhang, H., Liu, A. and Nee, A.Y.C. (2019). Digital twin in industry: state-of-the-art. *IEEE Transactions on Industrial Informatics*, *15*(4).

TrAM project (2018-2023) Transport: Advanced and Modular, Funded by the European Union's Horizon2020 Research and Innovation programme, Grant Agreement 769303, https://tramproject.eu/

Tuzcu, C., Dinsdale, C., Hawkins, J., Zaraphonitis, G. and Papadopoulos, F. (2021). RoPax Design Revisited—Evolution or Revolution? In A Holistic Approach to Ship Design, Vol. 2: Application Cases, SPRINGER Publ.s, 978-3030710903, June 2021 (Papanikolaou, A., ed.)

Zaraphonitis, G, Papanikolaou, A. and Mourkoyiannis, D. (2003). Hull Form Optimization of High-Speed Vessels with Respect to Wash and Powering. In: Proc. 8th International marine Design Conference (IMDC), Athens, 5-8 May 2003.

Zaraphonitis G., Skoupas S., Papanikolaou A. and Cardinale M. (2012). Multi-objective optimization of watertight subdivision of RoPAX Ships considering the SOLAS 2009 and GOALDS s factor formulations. In: Proceedings of 11th International Conference on the Stability of Ships and Ocean Vehicles

Zwaginga, J., Stroo, K. and Kana, A. (2021). Exploring market uncertainty in early ship design. *International Journal of Naval Architecture and Ocean Engineering, 13*, 352-366. doi:https://doi.org/10.1016/j.ijnaoe.2021.04.003

Wang, J., Xiao, Z., Wu, T. (2022). Construction and Application of Digital Twin for Propulsion System in New Energy Ships. *International Conference on New Materials, Machinery and Vehicle Engineering, (22)*. Virtual, March.

Wang, Y., Joseph, J., Aniruddhan Unni, T. P., Yamakawa, S., Barati Farimani, A. and Shimada, K. (2022). Three-Dimensional Ship Hull Encoding and Optimization via Deep Neural Networks, ASME. J. Mech. Des. October 2022; 144(10): 101701. https://doi.org/10.1115/1.4054494.

Weiland, K. (2021). Future Model-Based Systems Engineering Vision and Strategy Bridge for NASA. Technical report.

Wikipedia (2024), ChatGPT, https://en.wikipedia.org/wiki/ChatGPT , accessed on 11 Feb 2024.

Xiao, W., He, M., Wei, Z. and Wang, N. (2022). SWLC-DT: An architecture for ship whole life cycle digital twin based on vertical–horizontal design. *Machines, 10*(11).

Xing-Kaeding, Y. and Papanikolaou, A. (2021). Optimisation of the propulsive efficiency of a fast catamaran. Journal of Marine Science and Engineering, MDPI, 2021, 9, 492, https://doi.org/10.3390/jmse9050492.

Yu, D. and Wang, L. (2018), Hull Form Optimization with Principal Component Analysis and Deep Neural Network, ArXiv Preprint, ArXiv:1810.11701v1.

Zhang, H., Li, G., Hatledal, L.I., Chu, Y., Ellefsen, A., Han, P., Major, P., Skulstad, R., Wang, T. and Hildre, H.P. (2022). A digital twin of the research vessel Gunnerus for lifecycle services: Outlining key technologies. *IEEE Robotics Automation Magazine, 30*(3).

Zhang, M., Tsoulakos N., Kujala P. and Hirdaris S. (2024). A deep learning method for the prediction of ship fuel consumption in real operational conditions, Engineering Applications of Artificial Intelligence, Volume 130, 107425, ISSN 0952-1976, https://doi.org/10.1016/j.engappai.2023.107425

THE EXPANDING SCOPE OF SHIP DESIGN PRACTICE

Professor David Andrews[1,*]

ABSTRACT

As the former International Chair of IMDC, the initiator of the continuing series of IMDC State of Art (SoA) Reports and the lead author of most IMDC SoA Reports on design methodology from 1997 to 2018, the author has both pioneered and observed an increasingly broader scope in the practice of the design of particularly complex vessels.

The paper commences with reviewing some key publications, not just to recent IMDCs, that have tracked the manner in which "ship design" (in the broadest sense) has become more sophisticated – especially in the crucial early stages of design. The diversity of ship design practice, not just due to computer-based methods, is readily observable. Moreover, the impact of computer aided design in ship design has not just been to better analyse ship performance (e. g. in hydrodynamics, strength and ship infrastructure systems behaviour) but also in the increasing use of graphical tools and design methods to enable "better ship design". In a growing number of, mainly, academic centres, but also in some government agencies and design consultancies, there is a clear desire to better understand how to design "ships" and to manage the ship design process, especially for the most complex and novel classes of vessels. In particular, the objectives being sought when conceptualising and synthesising a range of ship options (as part of the requirement elucidation approach) in an ever-increasing scoping of the relevant issues, amounts to developing a more holistic approach. This is not just due to an increasingly complex ship acquisition and ownership environment, but also due to environmental and socio-economic (especially system safety) concerns. Overlaying all this are the opportunities or the spectre of Artificial Intelligence (or perhaps more immediately those of Machine Learning) and its likely impact on engineering practice as well as those other professions in the "marine design enterprise". The paper concludes by emphasising that while ship design has distinct differences, when compared with most other large scale engineering design practice, the lead ship design profession of the naval architect has somehow to deal with this expanding scope in the practice of "ship design". This means the education and on the job development thrust must broaden if the ship design profession is not to be side-lined into acting as mere hull engineers. It is argued, such a specific role will be more vulnerable in an increasingly Machine Learning dominated future, than the holistic ship creating and systems architectural alternative. Finally an ambitious vision for future ship designers is given alongside a summary of the specific main contributions by the author to ship design methodology.

***(Creativity is) "The production of new knowledge from already existing knowledge and – accomplished by problem solving"** Arthur I Miller: "The Artist in the Machine: The World of AI Powered Creativity", M.I.T. Press, Cambridge, MA 2019.*

***"No theory, no ideology, no set of rules can deal with human complexity, human sensitivity or vulnerability"** Sir Ove Arup: "What I believe" undated in "Ove Arup: Philosophy of Design", (Ed. N Tonks, Prestel, London, 2012)*

KEY WORDS

Ship Design Process; Ship Design Practice; Computer Aided Ship Design; AI; Machine Learning.

[1] Design Research Centre, Marine Research Group, Department of Mechanical Engineering, University College London, UK

* Corresponding Author: d.andrews@ucl.ac.uk

Submitted: 19 January 2024, Revised: 15 April 2024, Accepted: 1 May 2024, Published: 26 May 2024

Conference paper, DOI: https://doi.org/10.59490/imdc.2024.905 e-ISSN: 3050-4864

1. INTRODUCTION

1.1 Preamble

It is the opinion of the author, from a close involvement in the triannual IMDC conferences for more than the last two decades, that the scope of the practice of ship design has expanded in recent years. This is investigated by looking back even beyond this timeframe to the commencement of such considerations, which could be said to have been initiated by Stian Erichsen, the first chair of what was first designated as the International Marine Systems Design Conference series from the inaugural IMSDC 1982 conference in London. This conference resulted from a precursor symposium in 1979, called by Erichsen in Trondheim, with contributions from twelve eminent practitioners in the field of "marine design" (Erichsen,1979). After the initiation of the IMSDC series, the first conference followed a similar pattern to that of 1979 with eleven invited authors to present their versions of the state of the art in, essentially, ship design, which was seen as the essence of "marine systems design practice". The term 'marine systems" reflected Erichsen's particular view that the bulk of merchant shipping can be seen to be part of larger transportation systems, for bulk goods, like petroleum products, or containerised manufactured items. The conference title also reflected a wider engineering design paradigm, that of systems engineering, which was first adopted to manage large military programmes (including submarines and surface vessels) in the post Korean War NATO-Warsaw Pact conflict. A similar paradigm may shortly arise with the design practice for complex systems due to current rapid developments in Artificial Intelligence (AI) or at least Machine Learning (ML) and so it seems necessary to address the expanding scope of marine design at this point.

IMDC conferences have been a good (if not perfect) mixture of input from industry as well as from academia involved in "marine design' and with a focus on the ship design process and practice. Thus, we should take Erichsen's "whole systems" stance as a broad measure and also go beyond classic naval architectural views of ship design. The current author introduced the distinct conference feature of State of Art (SoA) reports into the 1997 IMDC, under the IMDC chairmanship of Erichsen's successor, the late Pratyuch Sen. The SoA reports were seen as a way of reflecting, not just rapid advances in computer aided design but also scoping the increasing diversity of "ship" types (including floating offshore structures) and many design approaches being introduced, including a realisation of the widening scope of what "ship design" should encompass. This broadening scope came from a view by the author, who having had two short (four years each) "secondments from the UK Ministry of Defence (MoD)" to academia, which included authoring a ground-breaking PhD (Andrews, 1984), while teaching at UCL, returned permanently to UCL in 2000 after a career of three decades in naval construction in the UK Ministry of Defence (MoD).

Thus, the author also presented at IMDC conferences over more than two decades several IMDC Keynote papers, including one in 2012 asking "Is Marine Design now a mature Discipline?" This issue of the emerging discipline in naval architecture of ship design was in part behind the initiation of the wider SoA Reports and specifically those on Design Methodology. Two years before that 2012 Keynote, I reviewed for the RINA Anniversary "150 Years of Ship Design". Both perspectives drew on 35 years designing a very wide range of vessels for the British Royal Navy followed by over two decades leading research on an innovative "inside-out" approach to the design of complex vessels, which culminated in 2018 with writing a Special Edition of the RINA Transactions (Andrews, 2018a). This was uniquely commended by the RINA Council and still provides the basis for me to argue that not only have the types of marine vessels continued to become ever more diverse, but also the practice of "ship design" has expanded well beyond traditional (apparently simple) approaches to ship synthesis, such as the ubiquitous "design spiral" that I have criticised as being simplistic and misleading.

While naval ship design might seem to be a rather specialised experience of "marine design" (especially when that includes the highly demanding and specific domain of nuclear submarine design), in terms of the types of designs undertaken, it can be seen to be highly diverse. This is because those "ship" types range across naval combatants, submarines, specialist large naval vessels, naval auxiliaries (with tanker and cargo carrier characteristics) and novel vessels, such as a royal yacht and procuring the first ocean going trimaran ship. My "naval ship" design experience also encompassed all phases of ship design "from cradle to grave", including being the Design Authority for a large part of the Royal Navy's surface fleet (SAOS, 2020). This range of experience is summarised in Appendix A at Table A1, where my role for each of 18 separate designs for the Royal Navy is identified and gives my view as to "what drove each design" and the "key lessons learnt from each of those design involvements". The latter set of summary statements was produced to reinforce the message that such ship design practice is already highly diverse in scope.

I was able to undertake relatively early research in CASD (1980-84), when still practicing "ship design", while a permanent move to academia in 2000 enabled more extensive research to be conducted into ship design methods, types of ship design and design issues, many of which have been presented at IMDC conferences over the last two decades. This research is briefly summarised, with appropriate detailed references in the major monograph on the early-stage design of complex vessels

produced as a Special Edition of IJME/RINA Transactions in October 2018 (see Sections 6.2 and 6.3 of Andrews (2018a) for example UCL projects). A further justification for the current paper focusing on the expanding scope of ship design is due to the likely impact of the advent of the specific form of Artificial Intelligence (AI), namely, Machine Learning (ML). The implications for the practice of managing the design and build of Physically Large and Complex Systems (PL&C) Systems has already been outlined for the architectural profession (Bernstein, 2022). Possible implications for the design and project management of acquiring complex vessels are addressed later in the paper, where the future practice of ship design is considered once the nature of the postulated expansion of ship design practice has been explored.

1.2 Lessons from IMDC State of Art Reports

Having persuaded the IMDC chair to introduce the SoA Reports, the first set of reports in the VI IMDC (Andrews et al., 1997) was clearly scene setting and of an overall reviewing nature. Consequently, the process was not revisited until the IXth IMDC (Andrews et al., 2006), and since then, there have been SoA Reports at each IMDC (Andrews et al., 2009; Andrews et al., 2012; Andrews and Erikstad, 2015; Andrews et al., 2018; Erikstad and Lagemann, 2022). The first SoA Report on Design Methodology (DM) consisted of ten separate sections in two halves: the first five could be considered generic (e.g., general design theory, systems engineering, preliminary ship design methods, safety) while the remainder covered the design of specific vessels, from passenger ships, unconventional vessels, offshore structures, to naval ships and submarines). Notably, the latter sections did not include sections on bulk carriers and container ship design, despite that being the original intent. Subsequent SoA reports covered "ship design methodology" as well as specific ship design issues that were usually on topics of particular interest to the maritime sector of the hosting country (e.g., Offshore Engineering for the USA in 2006, Artic Design for Finland in 2018). The introductions to the 2015 and 2018 SoA reports on design methodology provide more detailed summaries of the various previous SoA reports, each of which included copious lists of key publications.

Before passing on from the IMDC SoA (DM) reports and the extensive source they provide on marine design practice and how it has expanded in scope over recent decades, it is worth recalling the nine issues that the first SoA DM report raised when presented. These were in brief: -

- (*There are) "*Different models of the (*ship*) design process;
- Models of design/design practice (*are*) too academic;
- Concept tools too often ignore context;
- Design on the *(computer)* screen needs traceability;
- Concept design (is) vital, noting (*the*) role of decision-making methods;
- Concept *(Phase)* in commercial ship design is too short;
- Method vs. methodology needs defining;
- *(It is wise to)* look at the Science of Design, elsewhere;
- A formal taxonomy (*would help*), while avoiding rigid design procedures."

This set of concerns can be contrasted with the last SoA report (Erikstad and Lagemann, 2022), which saw four "main evolutionary tracks" in marine systems design methodology: a holistic optimisation strategy; a systems engineering based approach; a set-based strategy; and configuration based design. Each of these tracks were then allocated to 34 PhDs in "marine design" completed from 2016 to 2022 in nine universities in Europe and USA. Erikstad and Lagemann's four tracks are revisited below, as are the nine bulleted issues above, at the end of the paper, to see if they cover the extent to which it is surmised that the scope of marine design has truly expanded.

1.3 Is Marine Design now a Mature Design Discipline?

A paper with this title was presented by the author to the XIth IMDC (Andrews, 2012a) after thirty years of IMDC and some fifteen SoA reports. This keynote started by asking "why this question needs to be posed, both as a general issue and at this time at IMDC", furthermore, asking "haven't ship designers been perfectly happy designing ship for centuries?" This was addressed (through reviewing key IMDC papers and certain other selected publications) by answering the following points: -

a. What actually is marine design?
b. Has three decades of consideration (in the tri-annual IMDCs) established marine design as a coherent and accepted body of work and practice, vis a vis the other two naval architectural sub-disciplines (those of ship structures and ship hydrodynamics – *with their own regular international conferences*)?
c. If ship design is a mature discipline, is there a clear route towards marine design's future development with the assumed aim of providing "better ship designs" undertaken by "better ship designers"?"

In fact, the last issue has been more recently addressed in a more satisfactorily manner, at least for naval vessels, in Andrews (2022) which followed on from the last IMDC. A summary of the 2022 discussion of "good ship design" is covered in Section 4.3.

The 2012 IMDC paper on whether marine design was now "mature" reviewed IMDC conferences, not just from the State of Art reports, but also considering several keynote papers, such as Andreasen's (2003) vision of design methodology which he spelt out as threefold: -

- "By what methods do we design?
- What are the theories, and
- Scientific basis for this?"

Also, the 2012 IMDC paper drew attention to Nowachi's (2009) IMDC Keynote on "Marine Design Methodology -: Roots, Results and Future Trends" from over five decades of involvement, to which it seems appropriate to return, when this paper ends by consideration of the future of ship design. The 2012 keynote also discussed several publications that had been recently produced that were seen to be highly pertinent to the already wide scope of ship design practice. Two of those were lecture texts made available to the ship design fraternity (Lamb (2004a) and Yang (2004)). Both provided extensive lists of "key references" and can still be seen to be useful in parallel with the IMDC SoA reports and their copious references. The first of these sets of lecture notes were by the editor of the two volume multi-authored SNAME book "Ship Design and Construction" (Lamb, 2003, 2004b), which also addresses some fundamental design issues, while Yang's presentation gives a historic timeline (reproduced in Andrews (2012a) IMDC keynote at Figure 5) of "Design Theory" on the "practical design of ships". This starts with Baker (dated 1942) and ends at 1995, which now poses the question as to whether we need an up-date. Finally, mention should be made of the 26 "models of the Ship Design Process" collected in the X IMDC SoA DM Report (Andrews et al., 2009).

1.4 What can be learnt from "150 Years of Ship Design"

The above title refers to a RINA Transactions paper (Andrews, 2010a), which (as part of RINA's 150th anniversary) reviewed 150 years of ship design published in the longest series of naval architectural articles. This review pointed out that there had been immense changes in ship design in that period. This was ably reinforced by the companion paper by Buxton (2011) entitled "Enabling Technology and the Naval Architect 1860-2010". Notably papers in the first 100 years of that review were seen to be largely descriptive of the many technological advances of the day, however there was seen to be a distinct broadening of considerations of ship design in more recent years. Thus, in the latter part of that 2010 review it was seen as sensible to draw a distinction between the earlier and more recent papers on ship design – not least due to the radical change in ship design practice arising from the advent of electronic computers. Six specific categories were thus adopted to review the progress of ship design in the last five decades (up to 2010): -

i. General design reviews, where developments across a range of ship types were undertaken, such as naval reviews (e.g., Purvis 1974) to the evolution of the modern cruise ship (e.g., Payne 1990, 1998);
ii. Specific merchant ship designs, with probably the most notable being Meek's series (1964, 1969, 1970, 1972) outlining, through four series of designs, the epoch-making transition from his "ultimate cargo liner" to the modern container ship;
iii. Specific naval designs ranging from the first GRP MineCounterMeasures Vessels (Harris, 1980) to submarines (Wrobel, 1985), new aircraft carriers (Honnor & Andrews, 1982) and the Danish Fishery Protection Vessel (Watson & Fritis, 1992);
iv. Novel ship types, showing the explosion in types of marine vehicles from LNG vessels (MacGregor et al., 2006) to a wide range of unconventional hull forms (e.g., Semi-Submersible Drill ships (Winters et al., 2001));
v. Specific design issues, ranging from economics (e.g., Goss, 1965 and Rawson, 1973) to accommodation (e.g., Cain and Hatfield, 1979 and Andrews et al., 2008) and the impact of electronics (e.g., Gates & Rusling, 1982);
vi. Design methods and practice, which given the stance of this paper, deserves more extensive consideration here and can be seen as a direct consequence of the computer's ubiquitous impact on ship design practice and (in recent years) the parallel need, or desire, to better understand the ship design process.

While these six categories are useful to see the expanded scope of ship designing over recent decades, in design methodological terms it is the last of these that is now considered. The early consideration of CASD was noticeable for considerable discussion from the RINA membership of each development. From 1977 (almost commensurate with IMDC's origins), papers on ship design methods and design approaches were in the RINA Transactions: notable on the merchant ship side was Watson and Gilfillan's (1977) "Some Ship Design Methods" to be seen in contrast with both Canadian and British naval originated papers, including the author's early 'configurationally/inside-out" synthesis proposals (Andrews, 1981, 1986, 2003a). There were also

papers on thematic design, such as Brown's (1993) "History as a Design Tool" and Woods' (2008) yacht design paper. Also worth mentioning are the seminal papers by van Griethuysen (1992, 1994), on "monohull warship geometry" and the most detailed presentation of the early-stage design of a specific naval combatant option, using the UCL Design Building Block (DBB) approach (Andrews and Pawling, 2008), which also provided an extensive bibliography of preliminary ship design methods. The final group of papers on the practice of ship design cover the years 1993 through to 2009 and are mainly on naval ship design practice internationally but also includes one on maritime rescue craft (UK RNLI paper: Cripps et al., 2005).

The brief outline above, with a few selected examples from the fuller listing in the 2012 paper, is seen as further justifying the immense scope to be encompassed by any consideration of the nature of marine design as currently practiced and, by implication, the difficulty in arriving at any clear understanding of marine design methodological assessments. It needs to be said there are other summary articles that also provide similar reviews of ship design to that in the 2010 RINA review, such as Benford (1993) (see also TransSNAME 1993 Vol.101 for various Centenary papers, not just on ship design) and Nowachi's (2010) paper in a general CAD publication. However, as the rest of this current exposition suggests, there is no reason why common themes should not be identified, if we are to look forward to future needs and developments in our discipline, as suggested by the third of the issues identified in Section 1.3.

1.5 Initial conclusions on the expanding scope of ship design practice

Even before the main disposition in the rest of this keynote, it is possible to discern the degree to which ship design methods and practice have already expanded greatly from the traditional design approaches used by shipping companies (and then shipyards), for merchant shipping, and by navies and naval yards for warships, even prior to the immense changes in very recent decades. However, there still seem to be some constants in the maritime sector, that may or may not finally change. I have in mind the fact (aside from some very few radical designs touch upon in the fourth category in the previous sub-section) that the following are still relevant: -

i. The implications in not resorting to full-scale prototypes, unlike automobiles and aircraft design and manufacture, though some might argue that the advent of the Digital Twin facility means we now have virtual prototyping?
ii. The lack of investment in ship design, when compared to the development of naval combat systems and even general ship equipment (especially for recent main machinery developments driven by carbon reduction pressures);
iii. Both of the above points can be seen to be consequences of ship design being characterised by risk adverse shipbuilders, who undertake the bulk of ship design, if this is to be judged (perhaps questionably?) by the extent of engineering construction resources deployed. This applies across the ship design domain and has been made worse in the naval sector by the adoption of Prime Contractorship (Andrews, 2018b). While there has been some signs, such as the adoption of alliances (as for the UK Queen Elisabeth Class aircraft carriers (Coles, 2007)), it is the case the merchant shipping sector has not adopted the Cost Reduction in the New Era (CRINE) strategy (Cox and Newland, 2000), that the UK Offshore Industry introduced over two decades ago, to reduce cost risk margins being accumulated down the sub-contracting ladder, which had led to such projects becoming unaffordable.

1.6 Outline of the rest of paper

This consists of five main sections, each divided into several sub-sections: -

- Diversity of ship design and impact of computers and CAD;
- Trying to understand ship design and the ship design process;
- Seeing the objectives in ship design as holistic;
- The future impact of AI on design;
- Conclusions – four main topics with two appendices.

2. DIVERSITY OF SHIP DESIGN AND IMPACT OF COMPUTERS AND CAD

2.1 Types of "ship" roles

One reason why ship design has continued to increase in scope is the ever-expanding types of "ships" (or better marine vehicles/vessels/structures). As ever we are presented with a typological challenge. Erichsen (1998) talked of marine systems design, and this was right in so far that all marine entities (ships) are part of some larger marine system (such as bulk cargo transportation or naval fleets). But when it comes to designing, our focus (hopefully with a growing awareness beyond – because that is part of the expansion in the scope of ship design) is largely on the 'ship". It is clearly a floating vessel (and not

a platform – see argument in Andrews (2022)) and could be a (mobile) vehicle from a systems perspective, 'though hardly to be seen as similar to much smaller land and air supported vehicles. The latter two types of vehicles have comparatively limited endurance and sustainability, while offshore structures have limited mobility, but they do float and so are not civil engineered fixed structures, even if "planted in an inhospitable seaway".

"Ships" are often divided up into consideration on the basis of their owners' motivation for such a large investment in money and human resources. Thus, bulk carriers, container carriers, passenger carriers (blurred by the difference between essentially acquired for entertainment or ferrying) are about delivering "a cargo" ocean wide through ports, while other ships (including the highly diverse set of very expensive naval vessels (see Table A1)) are designed to provide a service "at sea". That "service" is often motivated by a need to deal readily with unpredictable events, be those supporting offshore floating/fixed facilities or the extremes of disasters ashore/policing at sea/outright warfare. Thus, in simple terms there are ships which are designed to be part of a larger transportation system and those (often more highly diverse and without clear measures of merit to guide design choices) which are essentially service vessels, where the design problem could be said to be more "wicked" (see Section 3.3).

This very wide range of "roles" has expanded over recent decades to deal with new markets and needs, by largely newly emerging national and commercial imperatives. It is likely with growing world trade, challenges of environmental change and political upheavals, that further discrete "ship types" will emerge. Not least, ship design is driven by the current search to mitigate the effects of carbon (and other environmental impacts), while there remains the general motivation (with the somewhat bizarre exception of mega yacht owners) to maximise the capability (however that is defined – see Section 4) for the expenditure able to be provided in order to acquire and operate new vessels.

2.2 Types of "ship" forms

Having said there are many roles that ships undertake, which perhaps justifies the need for a better understanding of ship design, there is an aspect of ship design, which can be said to add to the complexity of the ship designer's challenge. It can be argued that few other designers of complex systems seem to have, alongside general engineering design demands, the level of choice that the ship designer has in the form of their mobile floating structure. It needed an engineering design theorist, with no marine design background, to reveal this explicitly at the second IMSDC. The late Stuart Pugh, author of many publications on "Total Design" (Pugh, 1996), presented a paper entitled "Systematic Design Procedures and their Application in the Marine Field" (Pugh, 1985), which is still worth reading, however I particularly want to quote his view that for some industries "true conceptual design in totality is no longer necessary". Such designs are what Pugh called conceptually "static" and this applies to the design of automobiles and aircraft but, much to Pugh admitted surprise, this is not the case for ships.

Why this investigation of the "dynamic choice" of form is not done as a matter of course in most ship design is worth debating and in my seminal monograph of 2018 (Andrews, 2018a) I strongly suggest the Concept Phase for complex vessels should, as a matter of course, explore the solution space and do so much more widely than is usually the practice. It should also, in so doing, recognise that different conceptual options require different approaches to obtaining the first balanced "ship" concepts. Thus, clearly there is no single ship design process, if we are talking of synthesising a ship solution that may be subsequently developed. This is discussed further in the next sub-sections.

2.3 Types of "ship design" practice

Depending on who wants/funds a new "ship" and who undertakes the design process and whether they are involved through-out the subsequent ship design process, including the build/assembly of the completed vessel and maybe even through in-service to disposal, it seems clear that ship design practice varies greatly. Furthermore, the appropriate ship design practice in each new ship acquisition is fundamentally dependent on the intent behind the acquisition process for each design considered.

In the IX IMDC State of Art Report (Andrews et al., 2006), of the 26 models of the ship design process already mentioned, there were six versions of the Design Spiral. When it comes to most textbooks on naval architecture dealing with the initial design of a new ship, they resort to the "Design Spiral", as do many designers writing of ship design. This is in a way odd in that its originator, Harvey Evans, was an American ship structural academic and presented, in what he edited as a text launching the modern (probabilistic) approach to ship structural design (Evans, 1975a), a figure, which is <u>no</u>t of the ship design process but a ship structural design process, which he showed as a spiral. Evans had already produced a wider ship design spiral seeing "structural design itself is but a part of a larger whole made up of spirals within spirals" (Evans, 1975b). So, the structural spiral is just one of many? That this was taken up by designers of whole ships and applied as a single spiral to not just initial ship design but often the whole ship design process through to build, without much obvious debate, seems a little odd to this author (see Pawling, et al., 2016) and to other actual design practitioners, given actual ship design is nothing like that.

The attraction of the Ship Design Spiral seemed to be that a spiral shows the observed iterative steps undertaken, apparently in a sequential manner, in order to size a new design option through balancing weight and buoyancy, powering and resistance, and, probably, just initial intact stability. Thus, the spiral implied a fixed sequence, one that at best was strictly only applicable to certain conventional monohulls, took no account of any external activities, including inputs (or even decisions) from various stakeholders (including sub system designers), and proceeded in a fixed sequential manner without any decisions or changes to the proscribed sequence. All of which is clearly unrepresentative of real ship design practice – certainly at the more sophisticated end of the spectrum of "ship design". This highly simplistic view of ship design will be compared with both the author's decision-based strategic process and a more holistic human centred process originating from the author's more philosophically based vision of ship design (i.e., Requirement Elucidation driven and "inside-out" focused (Andrews, 2018a)).

2.4 The Impact of computers on designing "ships"

It was an eminent Dutch naval architectural academic Gallin (1973) who quite early on said "ship design without computers is no longer conceivable". I take it that he was referring to the fact that most engineering analysis, which I, like most engineers of that ilk in my earliest "calculating posts" (see Table A1), learnt to do engineering analysis using mechanical calculators. However, this century old practice rapidly transitioned when the author acquired the UK MoD's first hand-held "pocket calculator" (using Reversed Polish notation). This enabled me to carry out the necessary calculations on site while conducting the Trim and Inclined Experiments on submarines coming out of major refits, an evolution that almost rebuilt each vessel's internal outfit. Just a few years later, we were using large "main frame" computers to undertake finite element analysis (FEA) of whole ship structures (Honnor and Andrews, 1982), while still hampered by the lack of pre-processors and post-processors to facilitate the management of what then seemed to be a vast amount of data. Clearly, engineering analysis has come on by leaps and bounds and has fundamentally changed how we do the analytical side of engineering design.

One issue concerning modern presentation of results of what can seem to be "black box" analyses, is the apparent plausibility of superb results presentations, that leaves the designer with the need to understand the veracity of their modelling of reality. Furthermore, there is the question as to whether the specific sophisticated analysis undertaken is appropriate to the investigation of that design for the likely environmental behaviour, to which the overall ship system will be subjected when in service. When it comes to the specifics of, say, designing a hull form and checking that form is right for the likely response of the whole system (rather than just specific strength concerns addressed by (say) FEA) we can, for example, now impose the likely statical stability response at the press of a keyboard button. While the geometry of the underwater form is now easily modelled, the assumption (until quite late in a design) as to where the mass centroid of the complete vessel lies (particularly vertically), remains a "guess" by the human designer, a typical example of ship design uncertainty.

2.5 The impact of computer-aided ship design on "ship design"

I have observed through my career, as firstly a designer of naval vessels (see Table A1) and latterly as an academic engineering researcher and design philosophiser, that the advent of computer graphics, linked with the appropriate mathematics and physics applied to each design, has enabled the designer to open up the ship design process. However, this immense capability will only work to produce "better" designs if we resist the misapprehension that CAD doesn't mean the computer does design but rather it **Aids** the designer. Thus, the naval architecturally aware designer has to provide the creative input into the design evolution of a new whole ship design and do so from a true position of understanding the ship as a whole. To do so means other players in the ship design process must accept that the ship design experienced naval architects is **the** designer, being the one who makes most of the crucial ship design decisions. Those key design decisions at a generic level have been spelt out several times through extensive appendices in the author's key papers (Andrews, 2012b, 2018a).

Given a broad view of the development of ship design since the advent of CAD, and the increasingly ubiquitous implications of Data Driven Design (D3) (Gaspar 2018) with the further implication of using Machine Learning tools, this future needs to be debated. This D3 view was made as one of the published responses to my major exposition by on the sophistication of early-stage ship design (ESSD) (Andrews 2018a). The effect of CAD and project management techniques (such as systems engineering) on how ships are designed have not been broadly debated. A clear exception to this is in the naval ship design field where the series of papers (in SNAME Transactions and US Naval Engineers Journal) over several decades by Keane and his colleagues (Keane et al., 2009, Keane and Tibbitts, 2015, 2018) have addressed US naval ship design practice. To a degree, this has been matched by various (largely RINA) papers by the current author looking at the procurement practice for UK naval vessels (Andrews, 1993, 1994, 2016, 2018b). Both sets of publications on this topic were drawn on in a recent SNAME SMC paper (Andrews, 2022) and some of the relevant arguments are also addressed in the current exposition.

It is provisionally concluded from this opening review of the current state of ship design, that ships and their design should be seen as a highly diverse set of engineering endeavours, and furthermore that the diversity of product and process is becoming ever greater. So, are there lessons to be learnt as to how we, as ship design practitioners and researchers in pushing the

boundaries of these endeavours, might better understand what we do and thus how it can be made more resilient to cope with future challenges?

3. TRYING TO UNDERSTAND SHIP DESIGN AND THE SHIP DESIGN PROCESS

3.1 Ship Design is part of Engineering Design which is part of wider Design Practice

Seeing marine design in a broader design context has been part of the IMDC approach since 1997, when State of Art Reports were introduced, and particularly the Design Methodology series, which has included consideration of developments in the wider design community. This was consistent with earlier IMDCs inviting theoreticians in engineering design to present their broader perspectives (see Pugh (1985), mentioned in Section 2.2, and Andreasen (2003)). Such wider design visions were also reflected in my first methodological paper (Andrews, 1981), which looked at a range of design tools and techniques as part of a "creative approach" to future ship design. Thus issues, such as design thinking (Engholm, 2020), or which see design as a creative process (Nelson and Stolterman, 2012) and design philosophy, beyond marine design, are considered worth keeping an eye on. This is not just in case some insights from designers in other challenging domains could provide insights but also that (given this paper's theme) the likely developments in general computer aided design will have impact on our design practice.

This all comes under the umbrella of "Design Methodology", where the use of the term methodology is not the adoption of a fancy word for a new method but "the science of method in scientific procedure" (Chambers, 1971), which means consideration of such methods at a meta-level. Given many engineering design practitioners "just want to get on with designing" and thus too readily adopt the first convenient model (e.g., the ship design spiral), there has been some questioning of this broader view of design methodology. As a view from two eminent engineering thinkers, I have previously presented Finklestein and Finklestein's (1983) four specific rebuttals to those objecting to this intent to raise the intellectual and philosophical vision of engineering design. This I presented to IMDC 2012 (Andrews, 2012a) with my response addressing the relevance of these issues to ship design, and is reproduced as Table 1 in order to discuss it further in the light of the theme of the current paper and the major changes expected to engineering (and architectural) design practice from AI related developments.

Table 1: Finklestein and Finklestein (1983) Justifying Design Methodology and Andrews (2012a) Comments

	Objections to Design Methodology	Finklesteins' Answers	Relevance to Ship Design
1.	Design is intuitive and creative any methodology stifles creativity.	Design not purely intuitive, it is amenable to understanding.	Good ship designers often intuitive but have clear approach – a Methodology.
2.	Methodology constrains the designer.	Methods are sets of rules and alter the context.	Rules are used but awareness is important.
3.	All methodologies have inherent value systems.	Value systems are inherent the important thing is to be aware (of their influence).	Value systems lead to different design solutions by different designers.
4.	No evidence of applicability of design methodology.	There is a wide number of design methods used in different fields.	Ship designers still naval architecture dominated (S^4) and need ship architecture.

Taking each point in Table 1 in turn: -

1. While a good ship designer (however that might be defined and determined - see next section) can be intuitive (probably enhanced by experience), they need to adopt a clear approach, which ought to be based on methodological awareness. This becomes harder given changes to both the constraints (see Table 2 of Andrews (2018a)) and to the practice of ship design, which is seen to be happening ever more rapidly;
2. Ship design "rules" have been used, especially when new projects have significant uncertainty. While databases are increasingly available, they also introduce dependencies on "black box" tools and on databases with likely opaqueness. Awareness by designers of such issues becomes more essential and hence it seems even more necessary to adopt my decision-making strategy, which is summarised by Figure 1 at Section 3.2.
3. So as ever, value systems (inculcated by each designer's culture and education, which need to be seen in the widest sense, not just in university degrees obtained) mean there is a distinct "style" (which is discussed in the next item) implicit in each design solution, or, at a minimum, the (unquestioned?) adoption of a default style and practice.

4. Currently ship designers approaches to a new ship design are, for very good historic reasons (i.e., both of safety and a designer's limits to understanding), still dominated by the traditional naval architectural sub-disciplines (i.e., the first four of Brown and Andrews "S^5" issues - see Figure 1 in Brown and Andrews (1980)). However, a significant portion of this is becoming highly amenable to Machine Learning (see Section 5) and therefore the less ML amenable internal architectural drivers will become a greater focus for the ship designer. The growing need to put the ship internal configuration together more coherently, further justifies my advocacy of an "inside-out" approach (Andrews, 2018a). This is not just to achieve a better design synthesis but also to guide the development of the subsequent design's full definition.

Previous IMDC SoA design methodology reports have reported on what seems key wider design discussions beyond the maritime domain to provide potential insights, as the scope of ship design continues to broaden. Beyond such insights also lies the unease motivating this author regarding the understanding of the nature of ship design by the broader stakeholders (Andrews, 2022). That is to say that few of the other players in the ship design process seem to comprehend the unique nature of ship design. In part this may be due to the vast bulk of ship design (especially in the commercial field of transportation vessels – see the distinction made in Section 2.1) just following a basic evolutionary or even a "type ship" based approach. However, it could be argued that not just "service vessels" but ships in general will have to be designed in a more questioning and responsive manner to cope with the likely complexity of the future "market" and design environment (see also Section 4.3).

Thus, further design methodologic insights of a philosophical stance will arise beyond those brought to recent IMDC DM presentations, such as by Love (2000) (see Andrews et al., (2006) for discussion) and Nelson and Stolterman (2012) and even critiques of questionable views, such as those due to the philosopher Parsons (2016), who in his "philosophy of design" excludes engineering design entirely from consideration. Both of the last contrasting texts were reviewed in the IMDC 2018 DM report (Andrews and Erikstad, 2018) as it was considered discussing such different views serves to counter narrow understandings of design as well as to where ship design sits, both in wider engineering design practice (Andrews, 2010b) and with regard to similar design fields, such as architecture. This is not just due to the need to look to the human factors' component in ship designs and the nature of the ship design process, especially now AI developments are "around the corner", but also because the architecture of ships has parallels with (and clear distinctions from) the architectural design of "bespoke" buildings. Finally, it is worth mentioning, alongside the quantum physicist, Rovelli's (2018) defence of thinking philosophically (see Andrews 2022), an eminent design engineer, Ove Arup. Arup, interestingly went from studying philosophy to becoming the greatest structural engineer of the late 20th Century, in complete contrast to Ludwig Wittgenstein's opposite journey (Sterrett, 2006)), thus Arup wrote strongly about his philosophy of (engineering) design (Arup et al., 2012) which he saw as holistic.

3.2 Ship design issues

In their excellent IMDC 2022 Design Methodology State of Art report, Erikstad and Lagemann considered there to be four "evolutionary tracks" typifying strategic approaches to characterise the "high level plan(s)" that are adopted to organise the ship design process. Despite also criticising the ship design spiral's limitations (as in Section 2.3 above) they see it as the origin of the four tracks: model-based systems engineering; set-based strategy; configuration-based approach; and an optimisation strategy. One or more of these tracts were used by them to identify the design strategy used by each of 34 PhDs produced in 2016 to 2022 from the 10 universities, which can be said to be the centres of academic research in "marine systems design".

As the originator (Andrews, 1981, 1984) of the "configuration based" (or inside-out/architectural) approach to ship synthesis, I would question whether these four "tracks" are all comparable as approaches to ship design or even strategic in the same sense. The difficulty as I see it is that (as Erikstad and Lagemann acknowledge) there cannot be a "one-size-fits-all" model of ship design (Andrews, 2018a) and the four "tracks" together don't necessarily address the same level of ship design process. Rather than the configuration-based approach being "strategic", I see it as a more sophisticated approach to ship synthesis (than just a simple numeric balance sometimes called "point-based design (Singer et al., 2009)) that can be chosen instead of a purely numeric (weight and space balance) or even a fixed sequential one (as implied in the design spiral). This is particularly appropriate to "complex and novel mono and multihull forms" (including naval submarines and configuration driven surface vessels), especially where the internal configuration is complex and actually drives the sizing of the vessel (see Sections 6.1 and 8.1 to 8.4 of Andrews (2018a)).

Is also worth, when considering possible ship design "tracks", comparing both Andrews seven types of ship design for increasing design novelty (Andrews, (2018a) Table 3 and Section 5) with Papanikolaou's (1997) four types of "fundamental initial ship sizing methods" or ship synthesis: -

- The parent ship "by interpolation but un-innovative" i.e., "type ship";

- Regression data "averaging empirical values for specific ship types" i.e., akin to design lanes and "evolutionary design";
- Density approach "empirical coefficients – "crude" formulae for payload fraction, vessel density and weight coefficients" i.e., akin to a numeric synthesis (item 4 of Andrews (2018a) Table 3) built into student design exercises and many spread sheet approaches (Hyde and Andrews, 1992);
- Parametric variation "first principles "versatile" CASD algorithms for innovative designs".

However, I would argue that for true innovative design outcomes, just varying hullform coefficients and dimension parameters (even with CASD driven algorithms) without being combined with an inside-out (DBB) approach (Item 5 of Table 5 in Andrews (2018a)) results in a configuration, constrained by possibly inappropriate choices and, even, by algorithms (invisible to the CASD user), that is hard to layout and hard to work up to meet modern multi-dimensional design aims and constraints.

The strategic track appropriate to such "configuration-based synthesis" can draw on system-based, or optimisation techniques and even set-based design process strategies. However, I prefer a higher-level strategic approach to (complex) ship design, by which I mean the concept designer should follow a clear decision-making strategy, that is knowingly making significant choices about each of several design options, rather than all too often "just doing what we did last time". I have simplified this strategic decision-making process for a single design option – in a wider solution space (see Figure 4 of Andrews (2018a), with each step spelt out in that paper's Appendix A and reproduced here as Figure 1). A version, appropriate to tackling multiple design options, using the decision-making overview/strategy is given by the "rich picture" representation (with, in that case, showing just four concept options) by Andrews and Andrews (2021), which was reproduced as Figure 13 at the end of the 2022 DM SoA Report (Erikstad and Lagemann, 2022) and also is here as Figure 2, presented at the end of Section 4.

There could be said to be related ship design issues associated with one other of Erikstad and Lagemann (2022) design methodological "strategic tracks" – that which comes under the umbrella of "optimisation". While this can be seen as a design strategy appropriate to the marine sector, as it is for example the basis for Papanikalou (2022) EU HOLISHIP project, optimisation has also proved attractive at a ship sub-system design level, particularly applied to structural weight minimisation. To me, the latter is seen as a common error often used in much of engineering analysis, where optimisation poses as a design approach, thereby exhibiting the flaw that "we have a good technique" (meaning highly mathematically amenable) "so let's use it here". This is too often done and called "optimisation" or an optimised solution, when at best (in whole ship terms – or even more so regarding a whole maritime transportation system) it is minimising a sub-system (say, steel weight). As such it is a classic version of sub-optimisation of the intent of the ship or worse the fleet or wider business system.

The argument for optimisation can have even worst implications if applied to designing service vessels, where both the wider system is likely to be ill-defined and, often, the ship's purpose is to deal with the unexpected (e.g., Offshore Support Vessels (OSVs) or naval vessels – see the discussion on what is a "good (ship) design" in Andrews (2022) and summarised in Section 4.3 below, where both Brown's (2000) analysis of the performance of the British Navy ship designs in World War II is covered and the quite different approach to designing OSVs by Ulstein and Brett (2015). In fact, these two cases can both be seen to be facing up to the subtilties that most optimisation approaches don't properly address. I think it would be of concern if AI/ML enhanced ship design was to go down a "black box optimisation" path rather than be used to help address the key decisions flagged up by Figure 4 and the associated exposition in Andrews (2018a), which Figure 1 summarises.

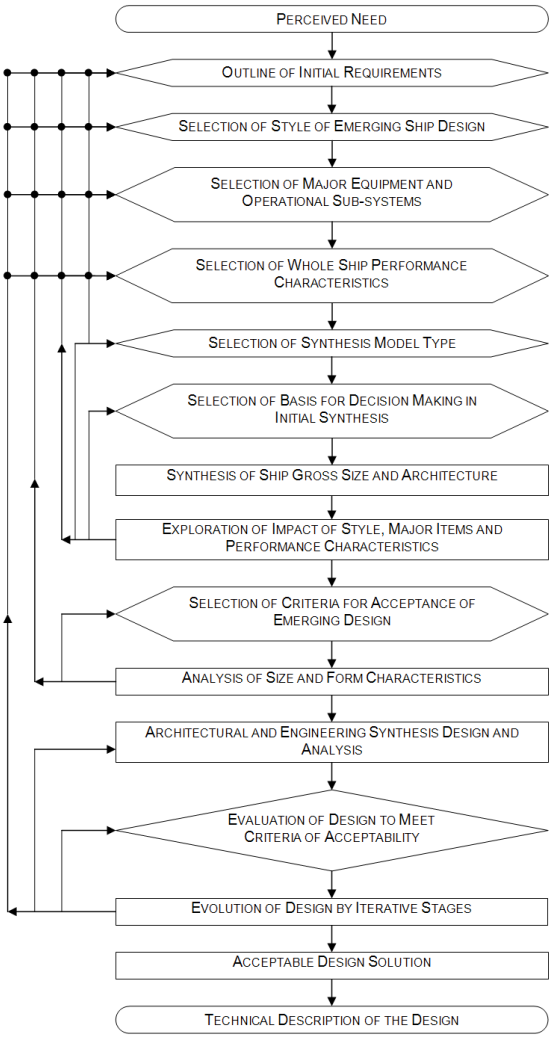

Figure 1: A Representation of the Overall Design Process for PL&C Systems Emphasising Key Decisions (see Andrews (2018a) including its Appendix A that describes each step, in detail)

3.3 Ship Design is Decision-making

Although the characteristic that is seen to typify ship design – that of making major or key decision(s) has already been highlighted (and emphasised in my key publications, including IMDC design methodology SoA reports) this section specifically addresses this. This is because this was seen as the key message of the 2018 Special Edition (Andrews 2018a), where the heart of the message of that extensive publication is at its Section 3. This section, which was entitled "The fact that the concept phase is unlike the rest of design", can be summarised: -

1. There are many views of early stage/concept phase ship design: This suggests that each study is different and searching for a set approach (even for different options of the same concept) in a concept process is questionable?
2. For the design of physically large and complex (PL&C) systems the design practice of wider engineering and other sophisticated design fields (like architecture) provide insights but also raise distinct issues of their own.
3. The concept phase is different to the subsequent phases of design – as it is about big decision-making: While all design involves making decisions (see Ferguson's (1992) "dozens of small decisions and hundreds of tiny one's"), those, often made by default or without question, in the Concept Phase are almost always the most important and hard to go back on beyond that phase.
4. Different (ship) design processes are distinguished by the nature of each potential option's novelty as shown by the table of increasing novelty (Andrews (2018a) Table 3) where each type is spelt out in that paper's Section 5.
5. The motivation for the concept phase is to undertake Requirement Elucidation (because of the nature of the design issue is that it is a "wicked problem" (see Rittel & Webber (1973) and full comparison of this urban design term with ship design practice is in Appendix B of Andrews (2018a). Again, it is necessary here to point out the term "wicked"

does not mean such design is complex, but rather the "wickedness" lies in determining what is actually the objective or set of balanced objectives that the new design is intended to meet through a Requirements Elucidation activity.

6. Why the concept phase (particularly for complex vessels) has a different design motivation/objective to all subsequent phases, which are focused on working up a chosen and initially balanced ship design to construct, assemble, set to work, operate, maintain, and to be disposed. So, the concept phase does not have the same design focus but rather a meta-design stance, that leads post-concept to what many seem to see (falsely) as "design proper" i.e., engineering analysis of the progressively worked up solution and build description.

The above list, apart from reinforcing the 2018 paper's assertion of the sophistication of ESSD for (certainly) complex vessels, also should have demonstrated that the design spiral is a simplistic and inaccurate summary of such sophistication and is no more than a reminder (sort of) of the iterative nature of much of design, which is used to achieve and maintain ship design balance. But, with the expanding scope of design tools and methods, not to mention CASD's ability (already the case before further AI advances) to inform the sophistication spelt out in the summary above, leaves both CASD developers and users with the responsibility to question those design decisions. These range from the strategical to the myriad (see Ferguson, 1992) and their potential impact on each design option being explored. The range of options covers both those being further pursued and those, perhaps, rejected with insufficient further consideration. The latter approach remains all too common a procedure, due to the pressure to "get through concept" and "get commitment" to work up the (crudely in design exploration terms) chosen concept design, which is then taken into feasibility and subsequent detailed design and build.

The author, in several of the examples of his "real" (as opposed academic) design projects (see Table A1 for top level summaries of each project's distinct design drivers, constraints and outcomes), was forced to revisit the chosen and developing concept-based design, not just in the subsequent feasibility phase but very late in the contractual phase or even in detailed design. Sometimes this was due to a design "flaw" emerging, but more often it was due to "the need to reduce initial build cost" (below that best costed in concept design) or to cases of late major changes that the "end customer" declared were "more important to incorporate than keeping the ship (usually the first of class, sometimes seen as a sort of prototype) to the contracted programme and cost". This might not often occur outside the very resource intense and politically charged (meaning politics in both senses) naval "ship" procurement environment, but I would hazard that when this does occur elsewhere this is due to commercial pressures to proceed to build, despite it often being obvious that a "better" design could have been worked up with emerging hindsight?

I have already criticised use of the design spiral and, given the theme of this paper that the scope of the ship design process is ever expanding, this critique also relates to an all-too-common view that design is merely "working up the specification". To some extent this is the approach in architecture and civil engineering for complex "one-offs" – once an architect's concept has been selected (after, say, an architectural competition). Of course, the question is "who writes the spec?". I would argue much that is covered in the outline of a sophisticated concept phase in the six points in the first paragraph of this sub-section (summarising Section 3 of Andrews (2018a)) needs to be well addressed and should underpin any coherent specification. This would still be the case even if the decision is to select an "as previous/type ship" option, if that has been coherently arrived at through proper Requirements Elucidation (Andrews, 2011).

Certainly, any properly evolved concept phase should follow the process undertaken for most service type vessels and, I hazard to guess, that in the uncertain future for the design environment in which many more commercial ships may emerge, that their acquisition is likely to be more exposed to such decision-making implied by my six points above. I would contrast the exposition in Andrews (2018a) to that of, say, Watson's (1998) detailed and informative "practical ship design" text. Watson's exposition of commencing ship design with a detailed specification and then working up a clear (specification detailed) concept, is contrasted with commencing much earlier in the design process with a true *ab initio* ship design, as called for and outlined in Andrews (2018a). So, the former will more likely end up with an incoherent concept than one following Andrews (2018a) outline. This is discussed further in the next main section addressing the changing nature of the objectives in ship design practice.

3.4 The Ship Design Process is a human endeavour

As the design tools and data driven design (D3) becomes ever more capable, what remains then of the role of the human designer? This begs the question that we can define a measure of design system capability, when for many designs we cannot define an adequate measure of performance in comparing each design solution, particularly through its life in an uncertain future. If we believe that designing a PL&C system, such as a complex vessel, remains a human driven process then how do we ensure that control and decision making is not subsumed by ML/AI capabilities that are likely to come on stream, as is considered in Section 5?

It is a fundamental belief that a properly sophisticated approach to ship design (especially in ESSD) for complex vessels, requires full human engagement, such that using CAD systems as assistance to the designer, can be followed through despite more advanced methods increasingly drawing on the data mining and analysis of what is called Artificial Intelligence. The description of the ship design process I favour is one that is a series of high-level decisions addressing the basis behind that design process with as wide a sense of the full practice being undertaken. This must cover exploring widely, not just the solution space but questioning the sequence of design investigations and the basis for design decision making (see Figure 1). It must also question, or at least acknowledge, that any design approach is biased by the design education and experience of the ship design team, the methods, tools and data they choose (or are constrained to use) to adopt on each design study, or possibly each individual design option, they select to populate the solution space. This selection should be motivated by being part of a Requirements Elucidation (RE) philosophy (Andrews, 2003b, 2011) and should lead to insights into each particular design's main design driver or drivers, which then focus the subsequent design evolution.

This RE approach includes the major decision for each significant option of the style of that design leading to the appropriate design synthesis type dependant on the novelty of each option, as is spelt out in Section 5 (and Table 4) of Andrews (2018a). That this can be seen as a very human process has been humorously captured by the 'Rich Picture" by Andrews and Andrews (2021) of the naval SDP example in Figure 2. This human endeavour is further emphasised by the need for the ship design naval architect/ship design manager to lead the decision-making, that only they (or in a worst-case practice, the CASD synthesis system/creator) can holistically direct in arriving at a balanced concept design and a coherent set of requirements to take forward through the requirements elucidation dialogue. This ought to involve all the necessary stakeholders – but more likely just the ship owner or requirements owner. Relevant to this is the insight of those software engineers that based their systems approach, known as Systems Architecture (Maier, 1998), on what they perceived was the creative, balanced and integrative approach to the whole design, from initiation through to acceptance (and even in-service), by the "first systems architects", that Maier calls naval architects (see Andrews, 2015).

The exercise of this "system architecting" to maintain the coherence of the original concept design has been seen in major defence projects as the task of that project's named individual chief engineer, acting as "the Design Authority". (See Gates (2005) for argument for the UK Type 45 Destroyer contracted project exercising Design Authority and Betts (2006) and Andrews (2006b) arguments against that case study's viability.) This further shows the very "fuzzy' nature of the endeavour of designing and procuring such complex vessels. In reality, that endeavour is achieved by an initially small group of individuals, but for most of the design process, then undertaken by a large number of detailed designers in discrete (contracted) teams, hopefully united by the project intent. This is a social and human endeavour, with all the psychological complexities of such activities, hinted at in Figure 2 and reflected in histories, such as Hughes (1998) for four major US technological projects and Johnstone-Bryden (2018), on the origins of the UK Post-Falklands War's Amphibious Replacement Fleet. In the latter case, Johnstone-Bryden records the current author's pivotal early role in ensuring the project for the new assault ships survived its early progress against "administrative animosity".

3.5 Conclusion on Ship Design & the Ship Design Process

In spelling out the nature of ship design and the process at the most complex levels it is practiced, I now argue that this also means (given the theme of this article) that the task of better understanding what a new ship design is intended to achieve and how all those involved might best be engaged, needs to be debated. Another aspect of the expanding scope of this practice is the extent of those involved, namely, intended users (i.e., sailors); owners (be that government or shipping operators); the other disciplines, beyond our focus on the whole ship designers; the wider set of stakeholders, which goes beyond the shipbuilder and a host of systems and equipment vendors to include commercial, insurance, classification and consultancy sectors and, often, wider society and if things "go wrong" both public and media involvement (see Yule & Woolner, (2008) on the Australian Collins Class Submarines).

The other immediate conclusion is that this involvement of a growing set of organisations, is changing the process. This then suggests that any consideration of ship design and the SDP must recognise the need for multiple levels and types of dialogue, especially in the crucial earliest stages in the most sensitive ship programmes. I have long argued that any such dialogues are better facilitated by architecturally based descriptions or sketches of potential design solutions. This is part of seeing the concept phase as drawing on the right set of tools, given the object in the concept phase is not doing better "classical naval architecture" (i.e., S^4) but undertaking: -

- a better exploration of the solution space (see Figure 8 of Andrews (2018a));
- questioning requirement assumptions in the light of design implications;
- and (initially) searching for unknown synergies (such as a Trimaran combatant solution being better at facilitating enhanced organic aviation assets with less total ship impact than a monohulled "equivalent").

This need for wider exploration at concept led the author to question CASD tools that "provide faster concept design" (de Winter, 2018). I said this because "faster concept design' would be at the price of coming out of the concept phase with apparent insights that appear to give solutions with "better naval architectural definition" but lacking a robust exploration of the solution space and of a demonstrated coherence between design and requirement (Andrews, 2019).

4. SEEING THE OBJECTIVES IN SHIP DESIGN AS HOLISTIC

4.1 The Issue of Human Factors in Ship Design

The traditional view of what is wanted in exploring the role(s)/ performance/cost of even the most complex service vessels, such as naval combatants, has emphasised the operational needs in terms of incorporating into the design equipment (e.g., weapons/sensors/command and control (for a combatant) or towing capacity/manoeuvrability (for an Offshore Support Vessel)) or providing facilities onboard (e.g., a flight deck and organic hangar (combatant) or stowage of rig supplies or spare wind turbine blades (OSV)). However, this leaves out consideration one significant aspect of the total "system of systems" (Andrews, 2022) that can be said to constitute a complex vessel, which is that of adequately integrating into the ship design the personnel onboard. This is a challenge as the personnel, who work the vessel, also live on the completely constructed and mobile environment, which is something that is not replicated in the designing of onshore architecture or urban constructions.

Despite the fact that RINA, as the major international institution for the profession that leads ship design, has for several decades held specific conferences to address 'Human Factors' (or ergonomics) in regard to ship operations and hence ship design (RINA, 2023a), little progress seems to have been made in putting this key aspect of the "system of systems" into the design process as an integrated part of designing ships. When the contents of such regular HF conferences are inspected, one finds many papers by ergonomists, that are relevant to ship design, bemoaning the fact that their emphasis on a scientific approach to designing ships so the crew can work onboard efficiently and also live for long periods on the vessels which are effectively their homes, is poorly considered in the ship design process (Cook, 2017; Schumacher and Banks, 2019). The reasons for this, like much of how ship design has been taught to naval architects and practiced in detailed design (where ergonomic relevant issues have largely been addressed, if at all), usually in the shipyard drawing offices, lie in the origins of modern ship design and procurement practice. When ships are compared with (say) aircraft, the maritime approach has been one of "cheap and quick" initial design combined with the highly significant absence of prototypes or extensive production runs, in favour "bespoke acquisition". This has led, since the beginning of time, to nearly all ship owners to both directly influence "their" ship's design and any consideration of ergonomics in it. Thus that consideration has been regarded as secondary by all involved except engaged Human Factors experts and those directly concerned with the welfare of the sailors onboard.

I was asked by the UK Nautical Institute, as the professional institution for mariners, to contribute to their most recent publication entitled "Improving Ship Operational Design" (The Nautical Institute, 2015), which was said to be primarily addressed to the naval architect "to improve your design". Thus, I spoke for the ship designer in two introductory sections: on the evolution of a ship design through to its final design (using a naval vessel as a very complex case study with high density of personnel onboard); and on the general (ship) design process, including the role of the naval architect. So, I sought to disabuse the HF experts as to why ship designs largely fail to be ergonomically designed. There are of course exceptions, particularly modern ship bridges and machinery control rooms in most ships and high intensity combat compartments (such as the Operations Room/Combat Information Center (CIC)) in naval vessels. However, the vast bulk of the spaces in a ship inboard (such as the key main passageways) and on most of the upper weather decks, where physically demanding operations are largely carried out, are not subjected to intense ergonomically driven design. This is because the scale of the product, the lack of a full-scale prototype (to iron out poor ergonomic design), and the manner in which shipyards win contracts (by the lowest price bid). Thus, at the level of detailed design, the focus is primarily on production aspects to meet contracted cost and time. So it must be admitted (as my section in the Nautical Institute 2015 publication tried to explain to the disappointed HF experts), detailed ergonomic concerns come low down in priority when compared to those aspects that have dominated ship design, which remain the naval architects' primary concerns. The latter have to ensure the ship design (as agreed at the end of the concept phase/bid acceptance) remains balanced and stable, structurally intact, achieves contracted power/speed/endurance, and (maybe) is appropriately seaworthy. So traditionally, any detailed ergonomically good features are addressed by the detailed designers with appropriate inspections, but only if "an expensive" acquisition process has been contracted. Otherwise, anything more than "usual practice" is unlikely and also to be low on the naval architects' priorities, needless to say, this has been (rightly) ill received by HF experts.

If we assume both greater levels of automation in future vessels and fewer highly trained personnel at sea, then perhaps (outside exceptions, such as the US Navy's Zumwalt Class combatants with extensive automation to reduce ship's complement (Feege, and Truver, 2016)) more attention ought to be paid to HF, as yet another sub-discipline for the naval architect to master. This was the question I posed at the 2018 IMDC: "Does the future ship designer need to be a human factors expert?" (Andrews,

2018c). There is some useful guidance (beyond the papers in the RINA HF conferences already mentioned) by authorities such as Sherwood-Jones (2005) and Cook (2017) as well as the contributions from several authors in the Nautical Institute (2015) publication. One can even look at urban design, where terrestrial architects have long given attention (at least in the best designed buildings) to the needs of their human occupants. A comprehensive example of this was summarised in my (2018c) paper, namely Broadbent's (1988) seminal text which "places (the role of) the psychological and cultural aspects" at the centre of building design. Thus some 21 human sciences (from Anatomy to Sociology) are outlined for architects, some of which Broadbent considered provide useful information to designers. While it might be argued (as indeed I largely did in Andrews (2018c)) that there is little scope in a naval architect's current education for acquiring in-depth ergonomic skills, some might see AI as about to readily "assist" by performing much of the naval architect's traditional "engineering" computational role. This could then leave room for more creative and "human centred design" capabilities? Once more, the author's emphasis on a graphically and architecturally centred "inside-out" ship synthesis approach (Andrews, 2018a) provides the scope to foster a holistic HF consideration more readily, right from the initiation of any ship design study.

4.2 Broadening the set of Ship Design Objectives

Beyond the likely increased scope in ship design for HF aspects, there have already been quite a few approaches over recent decades to essentially broaden what has been traditionally seen as ship design objectives. This broadening can be seen as a wider mix of specific objectives, in terms of improving performance against cost. Defence procurement organisations in democracies, where the underlying objective can be seen to be achieving the best capability or set of performance characteristics for an acceptable impact on the defence or national budget, might be considered a basis for making procurement decisions for specific major (naval vessel) programmes. However actual practice is far from that straight-forward and is probably an explanation as to why major naval acquisitions are so politically sensitive. Thus, the placement of orders for individual vessels for a nation that has several comparable shipyards (a diminishing situation for even major naval powers) can result in the allocation of a batch of vessels between several yards for political reasons, despite usually being economically less efficient. Or a major feature in a design can be imposed to sustain a specific national industrial capability. (A clear example of this was the French Government's insistence that the CHARLES DE GAULLE aircraft carrier be fitted with two nuclear power plant to maintain that production line for the French Navy's nuclear submarine fleet. Such pragmatism, beyond the individual procurement of that vessel, also occurred when the build duration of the same vessel was deliberately stretched because the government facility, in which it was built (Brest naval yard), did not increase the workforce but "built more slowly" to keep continuity of labour force demand. This meant that individual programme's total procurement cost was greater but the "cost" to the national budget was more efficient year on year and the wider national naval shipbuilding capacity (in continuous build and constant workforce) better maintained.)

That wholistic French approach, outlined in the above paragraph, can be contrasted with somewhat parallel UK programmes in which I have been involved, where a project "silo mentality" of just considering "your project", was demanded of individual ship projects at the risk to a coherent national industrial capability. Such examples justify my view that the constraints on such sensitive national programmes need to be recognised for their potential impact on key early design decisions (see Figure 3 and Table 2 in Andrews (2018a) for further discussion on the importance of the three types of constraints on the ship design process). So, while there can be sophisticated ways of compounding a set of detailed objectives for a new design (such as multi-criteria approaches (see IMDC DM reports Andrews et al., 1997, and Andrews et al., 2006), cost effective presentations (see Hockberger's (1993) critique) and Pareto Front presentations (see Purton, 2015 and Burger and Horner, 2011)), such methods are best used to provide insights, reveal broad trends and to be seen as advisory, rather than obeyed without question when making design choices (Andrews, 2021a).

A non-naval and government driven practice, that faces up to the broadening scope of assessing the basis for judging the right mix of capabilities to achieve the best design choices for multi-role service vessels in an unpredictable market, has been produced by the research of Gaspar (2013) and the associated investigations reported by Ulstein and Brett to the 2015 IMDC. Both Gaspar's adoption of the M.I.T. Epoch Era approach and Ulstein and Brett's (2015) division of the aspects that a complex vessel design needs to address, have been proposed in preference to simplistic summing of performance metrics weighted against build or, even, predicted through life costings, which are inevitably high risk. Thus, the latter authors' three elements of ship design objectives consist : -

1. Design for Efficiency: namely, Technical (over the design's life cycle); Operational (for different missions); and Commercial (systems influencing valuation, preferences and exploitation regarding Return On Investment (ROI);
2. Design for Effectiveness: namely, Safer, Smarter, Greener;
3. Design for Efficacy: namely, Flexibility, Robustness, Agility.

In many respect one can see this more comprehensive basis for assessing a "better ship design", as comparable to the current author's separation of the purely technical (historic ship design) issues, summarised by "S^4" (Brown and Andrews, 1980) from

the more holistic issues under the 5th term "Style". (See Table 1 in Andrews (2018a) for the case of a naval combatant, Table 1 in Andrews, (2021a) for the "Style" items of a submarine and Table 1 in Andrews (2018d), comparing Style issues for a combatant with the Style breakdown for an Offshore Support Vessel, the latter being a comparable example with Ulstein and Brett's typical shipyard products.)

Many of the "qualities/issues/capabilities" identified in Ulstein and Brett's (2015) Design for Efficacy also occur in Andrews (2018a, 2021a, 2018d) style tables. Thus, Flexibility in a design is a measure of being adaptable to new conditions, and hence the Style term Adaptability (see also Andrews, 2001) is comparable – in fact I prefer the latter term as from a structural design stance I don't want excessively flexible ship structures. Robustness is identified by Ulstein and Brett as being better able to resist failure modes or to accommodate changes in operating contexts and is repeated in my Design Style listing. (A classic example of responding to experience was the case of a "highly efficient" modern structural design found wanting when in the UK-Iceland "Cod Wars" in the 1970s, very expensive British frigates were damaged by "robust" Icelandic gunboats. Thus, the next class of UK frigates were specifically structurally beefed-up around their bows.) Agility was defined for a design as being more readily modified through life, whereas the Design Style listing assumed this was part of a wider definition of Adaptability. Achieving the latter often comes down to providing adequate (weight, space, and stability) margins, beyond the design margins. The latter reflect the designers' need to provide sufficient allowances from the start of a design through to its completion to accommodate design uncertainties, in a manner that these margins are progressively absorbed in the budgets up to completion (Gale, 1975). The margins provided for mission changes and significant equipment additions through life are often excluded, against the ship designers' advice, in attempts to "keep the design tight". An example of this is the UK Type 42 Destroyers discussed in the next section.

4.3 What is Good Design?

It could be seen, for such complex service vessels as those focused upon above, that this clear broadening of scope in current ship design practice, is just making ever more demanding that complex decision process (such as that seen strategically by the author's main SDP representation, which has been provided in many papers - see Figure 1). Another way of looking at this is to take Ulstein and Brett's (2015) paper's title question and see it in terms of identifying what is a "Good" design. This I see best done through the design of naval vessels, the justification being that (as Table A1 shows) these are many and varied, both in their several sub-types (e.g., combatants; amphibious vessels and craft; submarines and auxiliaries and even a royal yacht) and their different ship configurations, from Trimarans to nominally "commercial/utility" styled warships.

One way to investigate the nature of good design is to draw comparisons between broadly similar completed ships produced in a similar timescale. This was done by Brown and Andrews (1980) for a set of British warships produced over the last century. These five pairs of design comparisons were each of a "first-rate" design compared to one deliberately "second-rate", in terms of comparable capability, the apparent logic being that more cheaper hulls could then be afforded. In every comparison the (relatively) marginal extra procurement cost for the "first-rate" was found to be better value for money, both in added performance and in longevity of service, the latter being seen as a measure of successful design. Specific design comparisons have been discussed in earlier papers (Andrews, 2022 and 2017b) thus the UK Type 42 (Air Defence) Destroyers have been compared to the "first-rate" Type 22 (Anti-Submarine) Frigates produced shortly after. The T42 was a tightly packed design to reduce procurement build cost, but this meant necessary up-grades through life of that class of ship became a very expensive exercise, leaving the ships' overall performance significantly degraded. In contrast the T22s, having been designed with decent design and future up-grade margins, which initially led to accusations by operators that they were inadequately "armed", were both more easily maintained through life and the design easily "stretched" twice to produce very successful further batches of the class. This suggests that if a more holistic approach to design choices had been adopted the British Navy might have lessened the shrinkage of its fleet, even before the end of the Cold War and the subsequent (premature) taking of a "peace-dividend". The second example is of the UK and US comparable submarine designs, which revealed an interesting holistic insight into submarine design. Thus, the case of the UK SWIFTSURE Class when compared with the US THRESHER/LOS ANGELES Classes, as is debated in Andrews (2017b), where it was questioned as to whether the latter seemed to have been "sub-optimised" for high top speed rather than the more resilient and noise reduction configured SWIFTSUREs and their second batch TRAFALGAR Class?

Considering the good naval vessels design debate above, alongside the offshore support vessels that were the focus of Ulstein and Brett (2015), then the clearest naval ship design analysis was by the naval ship designer and technical historian, David Brown (2000), who went back to the last extensive wartime example, that of WWII. Andrews (2022) summarises Brown's analysis which concluded the (British) fleet's overall design performance was "probably the best that was achievable within the UK's marine industries capability to deliver". Brown remarks that the best design according to "some naval architects *(is the design)* that meets the *(formal)* requirement at a reasonable price" but Brown disputed that, as being far too narrow a definition. He proposed a better definition lay in that by the 1842 UK Parliamentary Committee on naval ship design which

ends: "...to endeavour to produce the best effects with given means". Thus, the basis of what is "good design" is consistent with the "Fleet" arguments in the following sub-section and sensibly leaves the issue qualitative and reflects my belief that ship design remains a subtle and sophisticated multi-facetted and, therefore, human directed process.

4.4 Properly incorporating Readiness/Sustainability/Availability

One of the measures of a good design achieved by focusing on "design style" issues (see in the last column of Table 1 of Andrews (2018a)) would be a better recognition that the process is one of designing several complex vessels, which usually consist of a class design providing a "fleet capability". This might be for a naval force or providing support to the growing number of large-scale offshore facilities (i.e., by OSVs), and therefore to move away from a traditional "good design" approach focused on an individual ship. Rather, the measure in such cases should be directly focused on a significant number (say six hulls) of units and their total fleet availability. This focus has only recently achieved prominence in the open organs for discussing naval ship design, such as the RINA annual "Warships Conferences". At the latest of these devoted to submarine design, Availability was headlined (RINA, 2023b).

The reason for this emphasis on availability could be said to have arisen due to the extensive press coverage in Australia and the publication by the Australian Government of several reports on the very poor operational availability of their six COLLINS Class conventional submarines (Coles, 2012). This then led to the topic for the 2023 RINA Submarine conference (RINA, 2023b), namely "Capability and Availability in Submarine Design". I took that title and turned it into a question (Andrews, 2023) and concluded, from reviewing some four decades of papers on submarine design in such conferences, that most submarine design presentations have been on how the design of these unique vessels is different to that of the most complex surface ships. Thus Andrews (2017b) is entitled "Submarine Design is not Ship Design" and like many of those papers is on the design of both non-nuclear and nuclear-powered submarines (the latter being the most important and costly distinction in submarine capability and design), and it does so largely in terms of the design of an individual vessel. Whereas, Coles and his team in investigating for the Australian Government why their "current level of availability ..*is*…poor" (both absolutely and relatively to comparable submarine fleets), provided some five main issues and 25 recommendations to achieve better fleet availability than those of comparable forces. Most of these identified improvements came down, not to the direct submarine design aspects but the wider management by three sets of participants:-

- "At a national level combining the main government responsibilities (such as funding and overall ownership authority);
- The Australian Navy and wider Defence organisation.
- The related submarine industry, especially the designer and builder (the Australian Submarine Corporation)."

Andrews (2023) saw this expanded scope of "submarine design", which ought to focus on sustainability/availability/readiness of a whole class/fleet to achieve through life performance for the number of "available hulls" to the Fleet Commander, to be a paradigm shift (to use Kuhn's (1962) term for scientific revolutions) in the design of such complex products. This clearly is a major expansion of the way in which design of such complex vessels is addressed, namely, by focusing on designing such vessels and seeing the capability sought from a class/fleet perspective, rather than just producing a good technical solution for a single vessel. Thus, the traditional approach has the danger of failing to give sufficient attention to through life (TL) availability of the whole enterprise. So, it is necessary to design for "support" from the start and, once again, an "inside-out" synthesis can best encourage this from the concept phase.

The above term, enterprise, was adopted in recent conference paper by Macdonald and Nicholl (2022) entitled "Nuclear Submarines – the most complex endeavour in defence" and directly addresses the Australian intent to acquire a fleet of SSNs, with the active involvement of the USA and UK. These authors argue, from their experience as senior UK MoD engineers and in subsequent leading roles in the naval acquisition industry, that the wider aspects are what make the design and acquisition and through life (TL) ownership of nuclear submarines such a demanding and unique activity. This complexity is seen to be the joint involvement of players from: industry; finance; military; societal; legal and regulatory; and political, and they highlight that "not everyone understands all this". Looking to the nuclear submarine endeavour that the Commonwealth of Australia is commencing to embark upon, they identify three critical success factors:

- "The right mindset;
- An enterprise approach;
- Continuous investment, indefinitely."

While not arguing with their strategic analysis, acquiring such a broader whole system understanding from those involved in submarine design also requires this national commitment. Thus, as a designer, teacher and researcher in submarine design and

bearing in mind the insights from the analysis in my 2023 paper that the key capability of Fleet availability needs greater prominence, I consider Macdonald and Nicholl's paper should also have had a greater emphasis on the unique demands required of submarine designers when designing such a demanding system of systems. Given specifically, that military submarines have to operate for extensive periods in extreme physical environments, this requires submarine designers, in addition to all that "normal" naval ship designers need to appreciate, to further understand two unique sub-specialisms regarding the physics of these large and relatively fast vehicles, that are not necessarily obvious from the wider ship S^4 issues (see Section 3.1 Item 4 above): -

- the physics of pressure hull collapse (see Faulkner, (1983) for an overview and key references), and,
- manoeuvring at speed in three dimensions, which is more akin to modelling aircraft behaviour than that of a ship (see Chapter 8 of Burcher and Rydill (1994)).

I have taught both these subjects, at master's level, from first principles. When this extra understanding is added to general naval architectural principles and the skill of integrating the many sub-systems (from nuclear power plant through combat systems to the many fluid service systems in a densely packed and finely balanced vehicle of several thousands of tonnes (see Mukti, 2022), which is also home to some hundred or so highly trained sailors, then this truly can be seen as a pinnacle of engineering design. This specifically requires producing and sustaining an engineering cadre, with that submarine naval architectural knowledge and experience, if this "indefinite" endeavour is to be successfully pursued at a national defence level of capability. So at least for the most complex of maritime vessels, the scope of "ship design" practice now has been recognised as a further expansion of ship design endeavour. Furthermore, this expansion might become more of the norm for general ship design practice, given the growing complexity to be expected of future of maritime endeavours plus the added question of what this might mean in an AI impacted future, which is explored in the next main section.

4.5 Incorporating a Better Systems Awareness

Given that a systems approach was the fourth of Erikstad and Lagemann's (2022) strategic tasks used to identify recent academic research in "marine design" when considering the broadening scope of ship design (see Section 3.2), it is sensible to consider both why a systems approach has been seen to be attractive in ship design practice and how that also has become a less purely technical management "philosophy" in recent years. Erichsen's systems approach has already been referred to in a formative approach to consideration of marine design. Alongside this consideration of the maritime transport "system", in Andrews (2022) I recently challenged the ship design applicability of systems engineering (S.E.) to an American (and largely naval) audience that has a long history of considering defence procurement as systems engineering and even synonymous with "naval ship design". Specifically, Andrews (2022) questioned whether, for complex ship design, S.E. is more of a management philosophy or even just a systematic procedure for managing such acquisition, rather than actually a method of ship design.

The latter question, regarding S.E. as ship design management practice, was argued in Andrews (2022), by referring back to van Griethuysen's (2000) IMDC paper and to an even earlier systematic rebuttal of S.E. as the solution to future ship design by Rydill (1978). The specific UK MoD obsession with the false "god" of Requirements Engineering was first rebutted in the 2003 IMDC (Andrews, 2003b – see also Andrews, 2011) by proposing a more open approach, namely that of design centred "Requirement Elucidation" (item 5 of Section 3.2) and drew on support provided by a strong argument against solution-less based Requirements Engineering by the systems engineering expert John (2000). Rather than repeat the argument for requirements elucidation, which I am pleased to observe is now common thinking, at least in marine design academia, I draw attention to my IMDC 2015 strong call for "Systems Architecture" (S.A.) as a better reflection of the systems philosophy. This has recently been further broadened and "softened" by ICOSE's new initiative (RAEng, 2021) under the banner of "Elegant Design" (see Andrews (2022) summary). This return to Checkland's (1981) "soft systems" approach can be said to better reflect the needs of managing a more complex world than the very technocratic "hard systems" vision of the past and seems a more general version of Ultstein and Brett's (2015) holistic design approach for OSVs. That S.A. also includes focusing on human factors, both from designing for people to be fully accommodated through making new systems for them and, separately, recognising the human nature of the design process (see Figure 2). It can also be seen to be more consistent with concerns regarding the engineering discipline's response to the potential impact of AI developments on future engineering design practice.

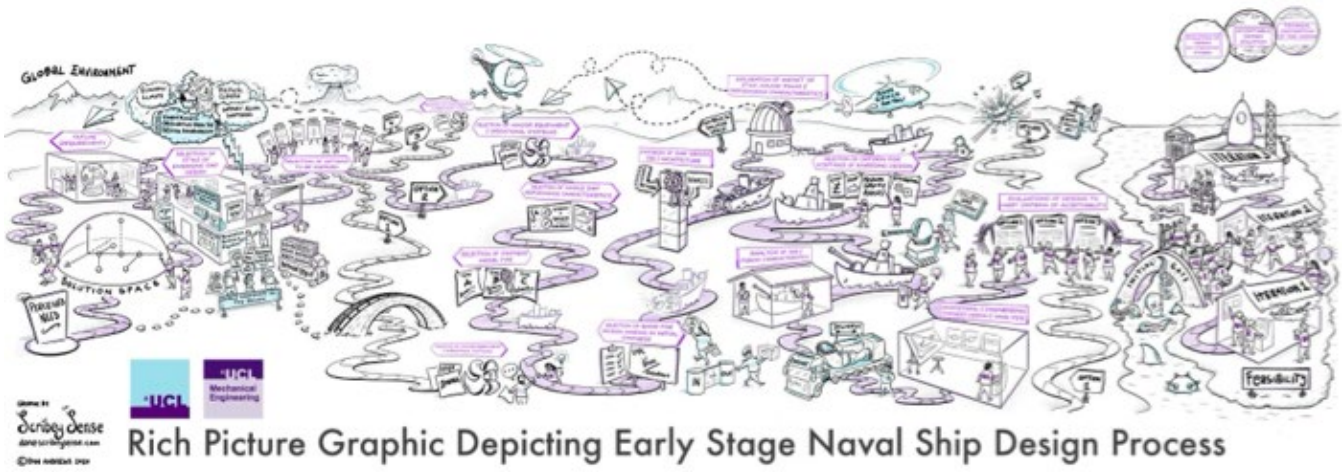

Figure 2: Rich Picture Graphic of a Typical Naval Ship Design Process (Andrews & Andrews 2021)

Finally, from a systems stance, which I consider to be a strategic management philosophy rather than a direct ship design approach, I remarked in Andrews (2022) that the US Navy, as the largest procurer of naval vessels, had concluded that it needed to take back control of ship design and construction, as a reflection of the complexity of such activities (Winter, 2008). This then had implications for how naval ship design is to be undertaken and how the engineers who will do this are educated and career managed (see also that this is one of the example significant constraints on how ships are designed, as listed in Table 2 of Andrews (2018a): "Specialisation and training of design team"). The best summary of how the US Navy's ship designers are addressing this is given in the pithily entitled paper: "Ready to Design a Naval Ship? - Prove It!" (Keane et al., 2009), which presents three tables summarising the skill set and career experiences seen to be required by future Ship Design Managers. That this should be appropriately read across to all ship designers to meet the challenging future for ship design, I consider irrefutable.

5. THE FUTURE IMPACT OF AI ON MARINE DESIGN

5.1 Current state of art

While AI seems to be the current preoccupation for many involved in the design of technological products, it is not that design, since the advent of electronic computation and then CAD systems, has not been, with the continued existence of Moore's Law, trying to cope with the changes to design practice that have been "assaulting" us for over half a century. It is worth tracking recent indications that suggest what might be the issues with the Machine Learning (ML) systems already upon us and furthermore how future AI developments will possibly impact on the more creative/human capabilities used to control complex design activities.

Data driven design (D3) was the response by Gaspar (2018) to my lengthy exposition on the sophistication of ESSD (Andrews 2018a), which the current paper on the expanding scope of ship design practice has heavily drawn upon. Thus, in Gaspar's "technical paper" he proposes a D3 approach to "extract information and knowledge", which sounds very like current ML proposals. He connects sophistication and complexity to Rowley's (2007) identification of: data; information; knowledge; and wisdom (DIKW) and lists a common set of processes reflecting the description of the design of complex vessels (as outlined in Andrews (2018a)). He concludes with six key topics taken from Andrews (2018a), which Gaspar considers provides the challenge to implementing a D3 future: -

- "Quantifying Style;
- Comprehensive Synthesis;
- Success Factor for Ship Design;
- Design as a Learning Process;
- Aided versus Automatic;
- Architecturally Driven Data."

All these issues and Gaspar's related concerns, need to be seen alongside Bernstein's (2022) ML analysis for urban architectural practice and Ruiz et al., (2023) similar view for the maritime industry, that are compared and contrasted in the next sub-section.

Before the ML comparison between urban and naval architecture is made, mention of Gaspar's (2023) paper on the "Past, Present and Future of CASD" is seen as pertinent. It is left to readers to go through Gaspar's excellent survey of the past and present and just briefly highlight his categories summarising the points relevant to the future of CASD: -

- "Hopes – problems that should be solved soon;
- Worries – problems that we may not solve;
- Fear – problems that we do not know that exist;
- Proposal for an optimistic future – A bias for data Driven Methods".

I am happy to note Gaspar calls for Andrews (2018a), as a comprehensive outline for ESSD, "to be implemented in design offices". This goes beyond the RINA Council's already unique commendation of Andrews (2018a) Special Edition publication as "a seminal paper, which sets the benchmark …considered to be essential reading for all naval architects and marine engineers, and not just those working in concept design." I would be delighted if this were so but six years on from the Special Edition (which includes the five eminent contributions to its discussion) being published in the RINA Transactions, I doubt it. Gaspar concludes by quoting my post-PhD paper to RINA (Andrews, 1986) with its call for "The more sophisticated design description *(from adopting the inside-out synthesis approach) …* makes the designer consciously address, as early as possible, many of the less tangible design issues. …. to provide an open, responsive, and 'softer' approach to CAD", which ML and, hopefully, AI developments will also foster. But this will only be the case if the profession rises to this (ultimate?) challenge as a response to the ever-expanding scope of ship design practice?

5.2 Insights regarding Machine Learning from Architecture and Maritime Engineering

Phil Bernstein (a professor at the prestigious Yale School of Architecture and previously a Vice President at Autodesk) was asked by RIBA to write a book "about the implications of AI for the architecture profession", which he (interestingly) called "Machine Learning: Architecture in the Age of AI" (Bernstein, 2022). The book is comprehensive with many insightful diagrams summarising AI and architectural practice (seen as a business undertaken by the profession of architecture and by other stakeholders), rather than a detailed speculation on the actual design process. Thus, ML is seen as already involved in architectural practice, such that there are chapters under Part 2 (Relationships) that consider the "fuzzy parts" of architectural practice (in a manner akin to Andrews (2022) response to Keane's (2018) comments to Andrews (2018a) Special Edition's holistic but more design specific outline of ESSD). So, Bernstein covers economics and value/laws, policy and risk/professionalism/education, where he sees ML having a profound impact. Rather than try to summarise his detailed analysis, which includes comparing US and UK architectural processes and issues, I want to just pick out some pertinent comments in that book before turning to our own profession.

Bernstein opens with a professional strategy that recognises a "preponderance of intelligent machines in every dimension of design, construction and built asset operation" and then asks what then is the "proper role for humans". He quotes Daniel Susskind (2020) pointing out "computers are increasingly becoming capable of tasks as opposed to entire jobs" and then hopefully proposes "a more intelligent route" where "computers assist in the critical, but more mundane, aspects of practice: those that drive project delivery, technical precision and performative predictability" (Bernstein, 2022). All this sounds sensible and should be able to be read across to complex maritime "jobs". It also re-inforces my strong emphasis on managing the SDP though strategic decision-making (i.e., Figure 1's process which is informed by human intervention, as is indicated by cartoon like examples in Figure 2). There is much that is worth pondering in Bernstein's thoughtful and informed proposal, including an AI taxonomy to cut through a lot of popular hype and a pertinent question thrown up by the AI challenge, which he considers to be: "what is professional knowledge?" The latter question is also one to be addressed by any engineering discipline, such as those undertaking ship design and construction (through life).

Turning to a recent maritime article that also addresses the implications of ML, this is by three authors from ETSIN at the University Polytechnique of Madrid (Ruiz et al., 2023). One of the co-authors is Professor Perez Fernandez, who gave the 2023 RINA President's Lecture (Perez Fernandez, 2023) entitled "Artificial Intelligence vs. Engineering Intelligence" with some pertinent conclusions for all maritime engineers, to be read directly across to ship designers. Firstly, the ESTIN authored article usefully gives detail on some nine ML algorithms, some of which are already used in the maritime sector and their Figure 8 breaks these down into three categories regarding their use. This scheme is then applied to analysing predictions for the propulsion system of a 9500 TEU container ship, addressing: Brake Power; Propeller Diameter; and material classification. Unfortunately, this seems a little prosaic alongside Bernstein's holistic review concerning architectural practice or possible ML applications with similar broad scope to whole ship design practice. Perez Fernandez RINA lecture was more of a grand overview and concluded, while software engineers may well be an "AI threatened species", naval architects and marine engineers were far less threatened, as the nature of their tasks and responsibilities were much more diffuse and he considered "the threat of AI is overblown". The latter was justified by Perez Fernandes because he considers that AI requires the human on top and he felt AI was a sub-set of "Engineering Intelligence". More likely AI might give engineeringly creative professions

(particularly in the complex and diverse maritime sector) more time to achieve "better ship designs"? However, given a more radical response to ML by Bernstein (2022) on behalf of the holistically design focused architectural profession, Perez Fernandez view could leave the ship design fraternity exposed, if we are too relaxed?

6. CONCLUSIONS

6.1 Why Ship Design is different to so much of Engineering Design

The first conclusion on the expanding scope of ship design is that even before this paper addressed the topic, the nature of ship design, when compared to most engineering design and other forms of large-scale design, such as architecture, is different, not just in the product (ships) but also the process. Both are particular and quite diverse across the maritime domain. There are other physically and large products/systems, as outlined before (Andrews, 1998), but both the ever-changing ocean environment and the mobile, long endurance, inhabitable entities we design, challenge many aspects of engineering analysis, construction and the design process. So, there is a need to train ship designers in naval architecture, not just on the traditional fundamentals (i.e., Brown and Andrews' (1980) "S^4") but also the 5th "S" of Style issues. Furthermore, that knowledge has expanded and, while covering the fundamentals, advanced topics (like the examples given by the third set of bullets at Section 4.4) have to be formally understood from first principles. This is so that the over-arching ship designer can both quiz the growing bands of different deep specialists and ensure their inputs are incorporated appropriately within the whole ship design context. Reference has already been made to the issue of Design Authority (see Section 3.4 - third paragraph), which for ships can only sensibly be executed by a naval architect, not a generic systems engineer or domain knowledge limited manager. Thus, it is ethically wrong for ship safety certification to be signed off by senior (unqualified) personnel, as it is the senior most naval architect in a ship project with whom realistically the buck stops on most of whole ship safety (Andrews, 2021b).

Beyond the "S^4" NA issues, there is the whole ship design (with Style issues summarising much of where the ship designer leads) covered by the six items listed in Section 3.3 and the three bullets of Section 3.5. If in addition the nine issues raised by the very first IMDC SoA report and listed at Section 1.2 are revisited, almost three decades later, it can be seen that many have been responded to over that time, not least in the subsequent conferences. Not all are resolved but most have been progressed and the remaining issues are appropriate (even with ML and current AI upon us) for future IMDCs to take forward. It was interesting that in the year's delay to the XIV IMDC at Vancouver, due to Covid-19, the International Committee rejected a virtual conference in 2021. It was not just felt that a full physical conference was nice to have but rather it was essential for the next generation of new researchers in ship design to present in person and openly discuss their ongoing research with the marine design community.

6.2 The Future of Ship Design Practice

Although I have both called for a clear, if creative and non-prescriptive, approach to the manner in which ship design should be undertaken and, in this paper, which has discussed the growing diversity of ship/marine design, this is now considered in the forward-looking conclusion of this wide ranging and summary review. Thus, it is considered worthwhile to also list some of the questions I have proposed over the last decade in addressing future ship design and its practice. This is done in Table 2, which poses these questions, all of which are directly the titles for a set of recent design methodological papers. I leave it to the next IMDC in June 2027 to take up any or all of these questions, where my initial response to each question posed is given in the initial publication referenced.

Table 2: Questions for the Future of Ship Design

	Andrews' suggestions as to Ship Design Methodology Issues still needing to be addressed.	Initial/Key Andrews Reference
1.	Is there "Art and Science in the Design of Physically Large & Complex Systems"?	Proc.Roy Soc London, Part A, April 2012.
2.	What are the "Philosophical Issues in the Practice of Engineering Design"?	Phil Eng, Vol.1 of Proc, RAEng, June 2010.
3.	"The Nature of Requirements Elucidation?"	IJME/TRINA, Vol.153, Part A, 2011.
4.	"Is Marine Design a Mature Discipline?"	Proc XI IMDC, June 2012.
5.	What is the "True nature of Ship Concept Design?"	Proc COMPIT, May 2013.

6.	Do "Ship Project Managers need to be Systems Architects, not Systems Engineers?"	RINA Conf. Maritime Project Management, Feb. 2016.
7.	"Does one size fit all or do different designs require different Ship Design Processes?"	RINA Warship Conf. June 2016.
8.	"The Key Design Decision: Choosing the Style of a specific ship design option"?	IJME/TRINA Part A4, Vol. 159, Oct 2017.
9.	"Do future Ship Designers need to be Human Factors Experts?"	Proc COMPIT, May 2018.
10.	"Is a NA an atypical Designer or just a Hull Engineer?"	Proc XII IMDC, June 2018.
11.	What is "The conflict between Ship Design and procurement policy?"	RINA Warship Conf. Sept 2018.
12.	Is "ESSD for Complex Vessels really Sophisticated?"	IJME/TRINA Spec Ed. Vol.160, Oct 2018.
13.	How important is the "Fuzzy Half of Ship Design?"	SNAME, SMC, Houston, 2022.
14.	"Is there an Expanding Scope of Submarine Design?"	Submitted 2024.

6.3 An ambitious vision of Where Ship Design may Lead

One future vision for a better and more holistic approach to ship design, based on the issues raised in this paper, would be to apply the future ship design practice called for to future "physically large and complex systems". The obvious maritime extension is to "inner space" or subsea habitats (Divemagazine, 2024). Perhaps not so obvious, unless my architecturally based approach to early stage design synthesis is seen as applicable beyond marine vessels to other PL&C systems, is future space "ships", where the latter word is of course "a giveaway". In fact, the architecturally DBB SURFCON module in QinetiQ's Paramarine SD suite (Qinetiq, 2019) has been used in UCL student projects to design both a low terrestrial orbiting "Space hotel" (Bowditch, 2011) and an interplanetary "Spaceship" (Downton, 2023). It is argued that these large vessels are like many complex marine vessels, sensibly designed from "inside out" in a similar manner, and where achieving the naval architectural balance of the DBB "Master Building Block" (Andrews, 2018a) is replaced by the demands of the physics of terrestrial orbiting or interplanetary travel, respectively. The point being this is an extension of ship design methods and practice, which is more applicable than the aeronautical design approach (e.g., Mavris et al., 1998) used for current space "craft' (i.e., small vehicles for few people for short journeys). The ship type issues of no full-scale prototypes and bespoke design on a large scale, reinforce this analogy.

To round off this look at future ship design practice, I go back to my first formal publication on ship design, which led to my 1984 PhD thesis (Andrews, 1984), and was boldly entitled "Creative Ship Design" (Andrews, 1981). I would argue that the point behind that paper is more than ever relevant, given the "threat" of AI/ML. Thus, the routine approach to much of the practice of ship design would seem to be likely to be subsumed by tools driven by ML (and then AI) and the issues identified by Bernstein (2022) for urban architecture and planning will totally alter the human-machine design relationship. What will (hopefully) be left with the human ship designer will be the "creative" aspects of designing complex entities, hence the referral back to the 1981 "Creative Ship Design" paper, which originally argued for an architectural design synthesis (the inside-out approach) and thus to expand the ship synthesis from sizing, just to achieve "naval architectural balance" (i.e., S^4), into the harder challenge of the wider (e.g., HF driven) design needs. This challenge has been (at best) left by ship designers until too late in most current designs, namely well after the concept phase and thus when only highly constrained options are then practicable. Underlying this early creative call was a desire to make the design of ships better recognised (by the profession, our stakeholders and wider society) as one of the most sophisticated endeavours done by designers of complex systems and for that to be done to its best, requires a creative and open mind set.

6.4 Author's contribution to Expanding Ship Design Practice

I am conscious that a new reader to this paper's exposition of many previous voicings, of its messages on ship design, may consider there is too much presented of this author's many ship design publications. However, I consider these are best encapsulated in the 2018 major statement (Andrews, 2018a) that permeates much of the current paper. As the originator of not just the architectural approach to ship synthesis (Andrews, 1981, 1984) but a strong believer in the fascination (Andrews, 2006a) and creativity (Andrews (1981, 2003a, 2012)) in the design of "ships" (of all types – so maybe vessels or marine design is a better term?), I attach at Appendix B a summary (Table B1) of my specific main contributions to the field of ship design

methodology. This tabulation is presented as it summarises the innovations originated in a career in ship design, covering practice (Table A1), teaching and research (Table B1). As such this paper may well be my last IMDC contribution. It should, therefore, be seen as making the argument for the expanding scope likely for future ship design practice, and as such leaves a clear challenge to my current colleagues and future successors.

Given I have always considered that a good designer ought to look to those beyond their own ilk, I have attached two prescient quotes above my Introduction, which ought to be taken to heart, regardless of the future posed by ML and AI for our profession.

ACKNOWLEDGEMENT

As already mentioned, this is likely to be the author's last major contribution to an IMDC, having been a contributor since the VI IMDC, member of the International Committee from then, initiator and lead editor for the SoA reports from 1997 to 2018 and International Chair from 2015 to 2022. So, I want to thank my past and present colleagues on the International Committee, past chairs of the Local Organising Committee of each of those nine wonderful conferences and, not least, the very many contributing authors, who efforts made each conference a success, and finally all the other attendees, who gave life to each conference and sustained we believers in the magic that is ship and marine design, in which I feel privileged to have spent my professional life, and met so many committed colleagues.

REFERENCES

Andreasen, M.M., (2003), Design Methodology – Design Synthesis, Proc. IMDC2003, Athens, May 2003.
Andrews, D.J., (1981), Creative Ship Design, TransRINA, Vol.123, 1981.
Andrews, D.J., (1984), *Synthesis in Ship Design*, PhD Thesis, University of London, 1984.
Andrews, D.J., (1986), An Integrated Approach to Ship Synthesis, TransRINA, Vol.128, 1986.
Andrews, D.J., (1998), A Comprehensive Methodology for the Design of Ships (and Other Complex Systems), Proceedings of the Royal Society, Series A(1998), Vol.454, Jan 1998.
Andrews, D.J., (1993), The Management of Warship Design, TransRINA, Vol.135, 1993.
Andrews, D.J., (1994), Preliminary Warship Design, TransRINA, Vol.136, 1994.
Andrews, D.J., (2001), Adaptability – the Key to Modern Warship Design, RINA Warship Conference, London, June 2001.
Andrews, D.J., (2003a), A Creative Approach to Ship Architecture, TransRINA, Vol.145, 2003.
Andrews, D.J., (2003b), Marine Design – Requirement Elucidation rather than Requirement Engineering, IMDC 2003, Athens, May 2003.
Andrews, D.J., (2006a), The Fascination of Ship Design, Keynote Paper IMDC06 Ann Arbor MN May 2006.
Andrews, D.J., (2006b), Discussion to "Design Authority of the DARING Class Destroyers" By: Gates, PJ, TransRINA/IJME, Vol.147, Discussion Vol.148, 2006.
Andrews, D.J., (2010a), A 150 Years of Ship Design, IJME, Vol.152, Part A1, 2010. Discussion and Author's reply IJME, Vol.153 Part A1, 2011.
Andrews, D.J., (2010b), Philosophical Issues in the Practice of Engineering Design, Philosophy of Engineering, Vol 1 of Proceedings, The Royal Academy of Engineering, London, June 2010.
Andrews, D.J., (2011), Marine Requirements Elucidation and the Nature of Preliminary Ship Design, IJME Vol.153 Part A1, 2011.
Andrews, D.J. (2012a), Is Marine Design now a Mature Discipline? Keynote Paper, Proceedings 11th IMDC, Strathclyde University, Glasgow, June 2012.
Andrews, D.J., (2012b), Art and Science in the Design of Physically Large and Complex Systems, *Proc. Roy. Soc. Lond*. A (2012) Vol.468, April 2012.
Andrews, D.J., (2015), Systems Architecture is Systems Practice in Early Stage Ship Design, IMDC 2015, Tokyo Univ, May 2015.
Andrews, D.J., (2016), Does one size fit all? Or do different warship designs require different ship design methods? Warship 2016: Advanced Technologies in Naval Design, RINA, Bath, UK, June 2016.
Andrews, D.J., (2017a), Choosing the Style of a new design: The Key Ship Design Decision, TransRINA Vol 159, Part A4, IJME, Oct-Dec 2017.
Andrews, D.J., (2017b), Submarine Design Is Not Ship Design, RINA Warship Conference: Naval Submarines & UUV's, 16. Bath, UK. 2017.
Andrews, D. J., (2018a), "The Sophistication of Early Stage Design for Complex Vessels." TransRINA, IJME Special Edition including Written Discussion and Author's Response, Oct 2018.
Andrews, D.J., (2018b), The Conflict between Ship Design and Procurement Policies, RINA Warships Conference 2018, London, Sept 2018.
Andrews, D.J., (2018c), Does the future ship designer need to be a Human Factors expert? COMPIT 2018, Castello di Pavone, Italy, May 2018.

Andrews, D.J., (2018d), Is a naval architect an atypical designer – or just a hull engineer? IMDC 2018, Aalto Univ., Helsinki, June 2018.
Andrews, D.J., (2019), A quizzical response to 'accelerated concept design', Letter to the Editor *The Naval Architect*, Jan 2019.
Andrews, D.J., (2021a), Who says there are no real choices in Submarine Design? RINA Warship 21: Naval Submarines, RINA On-line conference, June 2021.
Andrews, D.J., (2021b), Design Errors in Ship Design, JMSE Special Edition on Maritime and Ship Design, Vol.9, 2021.
Andrews, D.J., (2022), Babies, Bathwater and Balance – the Fuzzy half of Ship Design and Recognising its Importance, SNAME Maritime Convention 2022, Houston, TX, Sept 2022.
Andrews, D.J., (2023), Capability versus Availability in Submarine Design? Warship 2023 RINA Conference Delivering Submarine Capability and Availability with Agility and Pace, Bath, UK, June 2023.
Andrews, D.J. and Andrews, D.A.W., (2021), A New Way to Visualise the Design Process of Complex Vessels, *The Naval Architect*, Jan 2021.
Andrews, D.J. and Erikstad, S-O., (2015), State of the Art Report on Design Methodology, IMDC2015, Tokyo, June 2015.
Andrews, D.J. and Pawling, R.J., (2008), A Case Study in Preliminary Ship Design", IJME, 150, Part A3, 2008. Discussion and Authors' reply IJME, 151, Part A1, 2009.
Andrews, D.J. et al., (1997), IMDC State of the Art Report on Design Methods, Proceedings of IMDC 1997, Vol.2, University of Newcastle, UK, 1997.
Andrews, D.J. et al., (2006), IMDC State of the Art Report on Design Methodology", Proceedings of IMDC 2006, University of Michigan, Ann Arbor, MI, June 2006.
Andrews, D.J. et al., (2008), Integrating Personnel Movement Simulation in Preliminary Ship Design, TransRINA, Vol.151, 2008.
Andrews, D.J. et al., (2009), IMDC State of the Art Report on Design Methodology, Proceedings of IMDC 2009, Trondheim, Norway. 2009.
Andrews, D.J. et al., (2012), Design for X, State of Art Report presented at IMDC2012, Strathclyde University, Glasgow, June 2012.
Andrews, D.J. et al., (2018), State of the Art Report on Design Methodology, IMDC2018, Aalto University, Helsinki, June 2018.
Arup, O., (2012), What I believe, undated in Ove Arup: Philosophy of Design, Ed. N Tonks, Prestel, London, 2012.
Arup, O. et al., (2012), *Philosophy of Design – Essays 1942-1981*, (Ed N.Tonks), Prestel Verlag, Munich, 2012.
Benford, H., (1993), A Half Century of Maritime Technology 1943-1993, TransSNAME, Jersey City NJ, 1993.
Bernstein, P., (2022), *Machine Learning: Architecture in the Age of Artificial Intelligence*, RIBA, London, 2022.
Betts, C.V., (2006), Discussion to "Design Authority of the DARING Class Destroyers" By: Gates, PJ, TransRINA/IJME, Vol.147, Discussion Vol.148. 2006.
Bowditch, A., (2011), Use of the SURFCON Ship Design Tool to design a Large Space Station, UCL Mechanical Engineering MEng 3rd Year Project, April 2011.
Broadbent, G., (1988), *Design in Architecture: Architecture and the Human Sciences*. London: D. Fulton. 1988.
Brown, D.K., (1993), History as a Design Tool, TransRINA, Vol.134, 1993.
Brown, D.K., (2000), *Nelson to Vanguard- Warship Design and Development 1923-1945*, Seaforth Publishing, Barnsley, Yorkshire, 2000.
Brown, D.K. and Andrews, D.J., (1980), The Design of Cheap Warships, Proc. of International Naval Technology Expo 80, Rotterdam, Netherlands, 1980.
Burcher, R. and Rydill, L.J., (1994), *Concepts in Submarine Design*, Cambridge UP*,* 1994.
Burger, D. and Horner, D., (2011), The Use of Paramarine and ModeFRONTIER for Ship Design Space Exploration." 10th International Conference on Computer and IT Applications in the Maritime Industries. Berlin. 2011.
Buxton, I., (2011), Enabling Technology and the Naval Architect 1860-2010, TransRINA Vol.153, 2011.
Cain, J. and Hatfield, M., (1979), New Concepts in Design of Shipboard Accommodation & Working Spaces, TransRINA, Vol.121, !979.
Chambers, (1971), *Chambers' twentieth century dictionary*, (Ed W. Geddie) W & R Chambers, Edinburgh. 1971.
Checkland, P.B., (1981), *Systems Thinking, Systems Practice.* John Wiley & Sons, Chichester, UK, 1981.
Coles, J.D., (2007), The Future Aircraft Carrier – the engineering and technical challenges of designing and building the largest ever warship for the Royal Navy, Lecture to Royal Academy of Engineering, London, 20th March 2007.
Coles, J.D., (2012), Study into the Business of Sustaining Australia's Strategic COLLINS Class Submarine *Capability,* Commonwealth of Australia, Russell Offices, R1-G-C052, Canberra*,* Nov 2012.
Cook, M.J., (2017), Tempis Fugit: But where does it Go, RINA Submarines & UUVs Conference, Bath, June 2017.
Cox, J. and Newland, N., (2000), UK Warship Building Capacity Study, Report No.35048/R3375, BMT DSL, Bath UK, Feb 2000.
Cripps, R. et al., (2005), Development of Integrated Design Procedures for Lifeboats, TransRINA, Vol.148, 2005.
de Winter, R., (2018), Accelerated Concept Design, article in *The Naval Architect,* October 2018.

Divemagazine, (2024), Https://divemagazine.com/scuba-diving-news/new-deep-sea-underwater-habitat-announced (Accessed: 2 Jan 2024)
Downton, W.J., (2023), Can Ship Design be a guide to designing Large Inhabited Space Complex? UCL MSc Naval Architecture Project, Aug 2023.
Engholm, I., (2020), *Quick guide to design thinking*, Danish design series Strandberg Publishing, Copenhagen, 2020.
Erichsen, S., (1979), Advances in Marine Technology, (Ed), NTNU, Trondheim, Norway, 1979.
Erichsen, S., (1998), *Management of Marine Design*, Butterworths, London, 1998.
Erikstad, S-O. and Lagemann, B., (2022), Design Methodology State of the Art Report, IMDC2022, UBC Vancouver, June 2022.
Evans, J.H., (1975a), Ship structural design concepts, SSC Report, Cornell Maritime Press, 1975.
Evans, J.H., (1975b), Basic design concepts, ASNE Journal, 1975.
Faulkner, D., (1983), The Collapse Strength and Design of Submarines, RINA Warship '83, Naval Submarines, London, 1983.
Feege, E. and Truver, S.C., (2016), We are going to cut our teeth on DDG-1001! The ZUMWALT-Class Destroyer, N.E.J, Dec 2016, No.128-4.
Ferguson, E.S., (1992), *Engineering and the Mind's Eye*. M.I.T Press. Cambridge, MA, 1992
Finklestein L. and Finklestein, A.C.W., (1983), Review of Design Methodology, IEE Proceedings Vol.130 PtA, No.4, June 1983.
Gale, P., (1975), Margins in Naval Surface Ship Design, US Naval Engineers Journal, April 1975.
Gallin, C., (1973), Which way computer-aided preliminary ship design and optimisation? Proc.ICCAS, Tokyo, Sept. 1973.
Gaspar, H.M., (2013), *Handling Aspects of Complexity in Conceptual Ship Design*. Ph.D. NTNU, Trondheim, Norway. 2013.
Gaspar, H.M., (2018), Data-Driven Methods to Handle Complexity and Enable Sophistication during Ship Design, Comments submitted as paper to written discussion to Andrews (2018a), Special Edition in Transactions RINA, Oct 2018.
Gaspar, H.M., (2023), A Perspective on the Past, Present and Future of Computer-Aided Ship Design, COMPIT 2023, May 2023.
Gates, P.J. and Rusling, S.C., (1982), Impact of Weapon Electronics on Surface Warship Design, TransRINA, Vol.124, 1982.
Gates, P.J., (2005), Design Authority of The Daring Class Destroyers, TransRINA/IJME, Vol.147, 2005.
Goss, R., (1965), Economics Criteria for Optimal Ship Design, TransRINA, Vol.107, 1965.
Harris, A.J., (1980), HUNT Class MCM Vessels, TransRINA, Vol.122, 1980.
Hockberger, W.A., (1993), Cost and Operational Effectiveness Analysis (COEA) in Naval Ship Design, SNAME Chesapeake Section, May 1993.
Honnor, A.F. and Andrews, D.J., (1982), HMS Invincible - The First of a New Genus of AircraftCarrying Ships, Trans. RINA, Vol.123, 1982.
Hughes, T.P., (1998), *Rescuing Prometheus: Four Monumental Projects that Changed the Modern World*, Vintage Books, NY, NY, 1998.
Hyde, M. and Andrews, D.J., (1992), CONDES - A Preliminary Design Tool to Aid Customer Decision Making, PRADS 92, Newcastle University, May 1992.
John, P., (2000), Acquiring Capability through solution independent requirements – a help or a hinderance ?" Defence Capability Analysis Conference, RMCS Shrivenham, April 2002.
Johnstone-Bryden, R., (2018), *HMS Bulwark (VII): Second of Class, Second to None*, Royal Navy De Decommissioning/Commissioning Books, London, 2018.
Keane, R.G. and Tibbitts, B.F., (2015), The Fallacy of Using A Parent Design: "The Design is Mature", TSNAME , Vol.121, Jan 2015.
Keane, R. G., and Tibbitts, B.F., (2018), The Goldilocks Effect in Naval Ship Design: Too Little, Too Much, Just Right, TSNAME, Vol.124, 2018.
Keane, R., Fireman, H., Hough, J., Helgerson, D., and Whitcomb, C., (2009), Ready to Design a Naval Ship? - Prove It! Journal of Ship Production, Vol.25. (01), 2009.
Kuhn, T.S., (1962), *The Structure of Scientific Revolutions*, University of Chicago Press, Chicago, IL, 1962.
Lamb, T., (2003), *Ship Design and Construction* Vol.1, (Ed), SNAME, New Jersey, NJ, 2003.
Lamb, T., (2004a), Ship Design methods, Lecture to Australian Branches of RINA/IMarEST, Sydney, 4th August 2004.
Lamb, T., (2004b), *Ship Design and Construction* Vol.2, (Ed), SNAME, New Jersey, NJ, 2004.
Love, T., (2000), Philosophy of design: a meta-theoretical structure for design theory, Design Studies Vol.21 No. 3, 2000.
Macdonald, M. and Nicholl, A., (2022), Nuclear Submarines – the most complex endeavour in defence', SIA Biennial Conference, Australia, Nov 2022.
MacGregor, P. et al., (2006), Some Aspects in the Design of Compressed Natural Gas Ships, TransRINA, Vol.149, 2006.
Maier, M.W., (1998), Architecting Principles for Systems-of-Systems, *Systems Engineering,* 1 (4), 1998.

Mavris, D. et al., (1998), A stochastic approach to multidisciplinary aircraft analysis and design, Proceedings AIAA 98-0912, 1998.
Meek, M., (1964), Glenlyon Class – Design and Operation of High-Powered Cargo Liners, TransRINA, Vol.106, 1964.
Meek, M. and Adams, R., (1969), "Priam" Class Cargo Liners – Design and Operation, TransRINA, Vol.101, 1969.
Meek, M., (1970), Encounter Bays – First OCL Container Ships, Trans RINA, Vol.112, 1970.
Meek, M., (1972), Structural Design of the OCL Container Ships, Trans RINA, Vol.114, 1972.
Miller, A.I., (2019), *The Artist in the Machine: The World of AI Powered Creativity*, M.I.T. Press, Cambridge, MA, 2019.
Mukti, M.H., (2022), *A Network-Based Design Synthesis of Distributed Ship Services Systems for Non-Nuclear Powered Submarines in Early Stage Design,* Ph.D. Thesis, University College London, 2022.
Nelson, H.G. and Stolterman, E., (2012), *The design way*, 2nd Edition, M.I.T. Press, Cambridge, MA, 2012.
Nowachi, H., (2009), Developments in Marine Design Methodology: Roots, Results and Future Trends, Keynote Paper, Proc. IMDC 2009, (Ed. S O Erikstad), NTNU, Trondheim, June 2009.
Nowachi, H., (2010), Five decades of Computer-Aided Ship Design, Computer-Aided Design, Vol.42 (11), 2010.
Papanikolaou, A., (1997), Methodology for Small Craft Design, 25th WEGEMT Grad School, NTNU Athens, Oc. 1997.
Papanikalou, A., (2022), Holistic Approach to Ship Design, JMarSciEng, Vol.10(11), Nov 2022.
Parsons, G., (2016), *The Philosophy of Design*, Polity Press, Cambridge, 2016
Pawling, R.J., Percival, V. and Andrews, D.J., (2016), A Study into the Validity of the Ship Design Spiral in Early Stage Ship Design, Journal of Ship Production and Design, Vol32 No.3, Aug 2016.
Payne, S., (1990), Evolution of the Modern Cruise Ship, TransRINA, Vol.132, 1990.
Payne, S., (1998), From *Tropicale* to *Fantasy*: A Decade of Cruise Ship Development, TransRINA, Vol.140, 1998.
Perez Fernandes, R., (2023), Artifical Intelligence versus Engineering Intelligence, 2023 President's Invitation Lecture, RINA London, 1st Nov. 2023.
Pugh, S., (1985), Systematic Design Procedures and their Application in the Marine Field: An Outsider's View" IMSDC, Lyngby, Denmark, 1985.
Pugh, S., (1996), *Creating Innovative Products Using Total Design* – The Living Legacy of Stuart Pugh, (Ed. Clausing and Andreade), Addison-Wesley Pub Co, Reading MA, 1996.
Purton, I., (2015), *Concept Exploration for a Novel Submarine Concept Using Innovative Computer-Based Research Approaches and Tools*. Ph.D. thesis, University College London.
Purvis, K., (1974), RN Post-war Frigate and Destroyer Designs, TransRINA, Vol.116, 1974.
Qinetiq, (2019), https://paramarine.qinetiq.com/products/paramarine/index.aspx (Accessed: 8 July 2019)
RAEng, (2021), 2021 On-line Insight Event: "A Model for Transdisciplinary Design", Royal Academy of Engineering, 23 Nov 2021.
Rawson, K.J., (1973), Towards Economic Warship Acquisition & Ownership, TransRINA, Vol.115, 1973.
RINA, (2023a), RINA Conference on Human Factors, RINA, London, 2023,
RINA, (2023b), Warship 2023 Conference Delivering Submarine Capability and Availability with Agility and Pace, Bath, UK, June 2023.
Rittel, H.W.J. and Webber, M.M., (1973), Dilemmas in a General Theory of Planning, Policy Sciences Vol.4 (2), 1973.
Rovelli, C., (2016), Brexit won because those who opposed it did not address its core philosophy, The Guardian, 23rd Sep 2016.
Rowley, J., (2007), The wisdom hierarchy: representations of the DIKW hierarchy, Journal of Information Science, Vol.33 (2), 2007.
Ruiz M.A.G. et al., (2023), Application of Machine Learning Techniques to the Maritime Industry, JMSE, Sept 2023.
Rydill, L.J., (1978), No, the future of Corps is not in Systems Engineering, *RCNC Journal,* MoD, Bath, 1966.
SAOS, (2020), SOAS Pioneers Series, 2020, A Pioneer in Naval Ship Design, SOAS Hall of Fame, Doi/10.1080/17445302.2020.1787590 2020.
Schumacher, P. and Banks, S., (2019), A human centred approach to optimise human performance in complex marine environments and habitable spaces, IMC 2019, Pacific Int Maritime Conference, Adelaide, South Australia, 2019.
Sherwood-Jones, B.M., (2005), Twenty Years on the wrong heading dead ahead, Conference on Human Factors in Ship Design, Safety & Operation, RINA London, 2005.
Singer, D.J. et al., (2009), What is Set-Based Design? Naval Engineers Journal, Vol.121 No.4, 2009.
Sterrett, S.G., (2006), *Wittgenstein Flies a Kite*, Pi Press, NY, NY, 2006.
Susskind, D., (2020), *A World without Work: Technology, Automation and How we should Respond*, Metropolitan Books/Henry Holt and Company, NY, NY, 2020.
The Nautical Institute, (2015), *Improving Ship Operational Design.* NI, London, 2015.
Ulstein, T. and Brett, P.O., (2015), 2015, "What is a better ship? – It all depends…," IMDC 2015, Tokyo, June 2015.
van Griethuysen, W.J., (1992), On the Variety of Monohull Warship Geometry, TransRINA, Vol.133, 1992.
van Griethuysen, W.J., (1994), On the Choice of Monohull Warship Geometry, TransRINA, Vol.135. 1994.
van Griethuysen, W.J., (2000), Marine Design - Can Systems Engineering Cope? IMDC2000, Kyongju, Korea, June 2000.
Watson, D.G.M., (1998), *Practical Ship Design*, Elsevier, Oxford, 1998.

Watson, D.M. and Fritis, A., (1992), A New Danish Fishery Inspection Ship Type, TransRINA, Vol.133, 1992.
Watson, D.M. and Gilfillan, A., (1977), Some Ship Design Methods, TransRINA, Vol.119, 1977.
Winter, D.C., (2008), Getting Shipbuilding Right, US Naval Institute Proceedings, June 2007.
Winters, D. et al., (2001), *Borgland Dolphin*- Creation of a Modern Semi Submersible Drilling Ship, TransRINA, Vol.144, 2001.
Woods, B., (2008), Role of Ambiguity in the Art & Science of Yacht Design, TransRINA, Vol.151, 2008
Wrobel, P.G., (1985), Design of the Type 2400 Patrol Class Submarine, Trans RINA, Vol.127,1985..
Yang, Y-S., (2004), Marine Design Applications of Design Theory and Methodology, Int. Conference on Axiomatic Design (ICAD) 2004, Seoul, Korea, June 2004.
Yule, P. and Woolner, D., (2008), *The Collins Class Submarine Story,* Cambridge UP, 2008.

APPENDIX A

Table A1: A Summary of the Author's Involvement in Major UK Warship Designs as a Naval Constructor (1972-2000) (see Section 2.1 of Andrews (2018a) for further detail on most listed designs)

UK Warship Project	Time span of Author's Involvement	Role played by Author	What Drove that design	Key lesson from design/project
SWIFTSURE SSN	1973-75	Assistant Constructor –Structural design + Cold Bent Frame Investigation	Combating Soviet SSNs – Acoustic Performance	Even the best designs can have critically unforeseen problems (e.g., Cold bent frames (Faulkner, (1983)) Building in generous margins can reap major benefits beyond that design
SSNOY (Became TRAFALGAR Class SSN)	1974-75	Assistant Constructor-Structural new design + lead calculator	Step change from SWIFTSURE Class – New sonar + new reactor	Ended up too ambitious, so replaced by very successful Batch 2 Swiftsure Class (Trafalgar Class); Could be seen as akin to USN SEAWOLF experience – but UK Changed to Batch 2 Swiftsure.
INVINCIBLE Class CVS	1975-78	Constructor (Air and Weapons integration)	Initially ASW helo carrier with provision for a few STOVL	Modern light but medium sized carrier; First all Gas Turbine propelled major warship saved 30% crew; FBNW STOVL modified while building to take new FRS Sea Harrier (author led on fit to CVS)
Type 23 Frigate	1978-80	Lead Concept Designer (TA Tug with CODLAG)	To provide GRIUK Barrier + Merlin Helicopter	Do not design to precise OA scenario (ISD 1989 – End of Cold War) Ships then became GP with gun and PDMS. Lacked margins for adaptation or enough accommodation
FORT Class AOR	1978-80	Lead Concept Designer (one stop logistics support to Type 23 in GRIUK gap	Commodities + 4 Merlin Helicopters full Support	Became main fleet support when Cold War role collapsed. Trying to mix a warship capable AOR with RFA standards meant cost excessive.
SANDOWN Class SRMH	1978-80	Lead ship concept design	Cheaper version of Hunt MCMVs	Example where shipbuilders' competition led to real build innovation by Vosper Thornycroft Shipbuilders
Various Frigate/CV Studies	1978-80	Lead Concept Designer (series of Hilo mix studies)	Square the circle of affordability +Exportability	Need to explore options widely to provide better basis for naval decision making on future ships and ship Research & Development.
VANGUARD Class SSBN	1984-86	Head of Hydrodynamics + Structural Design	Provide national Nuclear deterrent Submarines.	Assembled "A Team" to do the design in-house with top priority to deliver fully to time, within cost, meeting national capability
LPD (Replacement) Class	1986-90	Warship Project Manager for Replacement Amphibious Fleet	Concept studies on up lift capability ro-ro LCUs	Key Amphibious Units. Author forced to adopt Proc Strategy (build to specification by 3 industry teams) that then failed as MoD needed to lead design. Reverted to MoD led design.

UK Warship Project	Time span of Author's Involvement	Role played by Author	What Drove that design	Key lesson from design/project
ASS/LPH OCEAN	1986-90	Warship Project Manager for Replacement Amphibious Fleet	Cheap helicopter carrier Thought possible without costed studies by senior naval staff	Flawed concept by non-ship designers without concept/feasib design. Proc strategy: fixed price even non-naval standards unaffordable. Got un-survivable High Value Unit (12 Helos + 800 Marines +vehicles) not sensible (Andrews 2018b).
RFA ARGUS ATS	1986-90	WPM to "get out of shipyard" (major conversion)	Ro-ro Container ship converted to helicopter training	Example of how not to procure a warship (see Andrews (2018b)) even on an apparent Fixed Price contract. Used by senior staff to explore Hands-off, so Major cost hike.
HMRY Replacement	1988-89	WPM conduct one-year Special Design Study for Head of State	Replacement of HMRY for No.10 and Head of State	Find cost of Replacement to modern standards – electric power/reduced crew/enhanced Public Spaces/helicopter landing/modern comms & security
Wave Class AO	1990-91	Head of Concept Design	Replace existing Fleet Oilers	Staff (OPNAV equivalent) "awaiting Fleet Studies" so author produced concept design; first navy double hulled tanker. Do not need OA when in a hurry to replace fleet assets.
Future Surface Combatant - became Type 26	1990-93 and 1998-2000	Head of Concept Design then Project Director	Main ASW Escort + general combatant	Not driven by major weapon but Adaptability – which MoD system found hard to model/approve; MoD approval system built on weapon capability not TL adaptable naval presence.
FCV (became QE Class Carriers)	1991-93	Head of Concept Design	Strike carrier STOVL/ CTOL	Needed to get large carrier adaptable to STOVL or CTOL. Basis of internecine RN-RAF " warfare". Navy finally got capability by Carrier Alliance of MoD with main shipbuilders.
CNGF (became the T45 Destroyer Class)	1991-92	Head of Concept Design as Member of Anglo-French Steering Group	Fleet AAD-PAAMS escort	Example of single weapon system (PAAMS) dominating design. But major Machinery and Accommodation needs also drove size. Collaboration (UK/FR/IT) not easy, so reverted to Type 45.
FASM (became FSSN)	1990-92	Head of Concept Design	New SSN: post-Cold War	Need to change design approach (SUBCON based on author's Building Block approach) to explore solution space widely.
RV TRITON First Trimaran Ship	1990-93 and 1998-2000	Head of Concept Design then Project Director for acquisition	2/3rd scale Prototype Trimaran Destroyer	Needed prototype (on cheap) to explore novel hull form (with steel structural design) and "win hearts and minds" of operators – successful but through USN LCS programme.

List of Acronyms in Table A1 (in order of first usage in Table A1)

SSN – Nuclear powered submarine
SSNOY – OY was second class of "new" SSNs to follow the 1970s Swiftsure Class (SSNOX)
USN – United States Navy
CVS – (Aircraft) Carrier (Support) – not Fleet (Attack) carrier
ASW – Anti-Submarine Warfare
STOVL – Short Take-Off and Vertical Landing Carrier Aircraft
FBNW – For But Not With – Ship designed to receive (weapon) fit but not installed on build
FRS – Fighter, Reconnaissance and Strike – designation of the UK Sea Harrier STOVL Aircraft
TA – Towed Array – Passive Sonar Array for ASW
CODLAG – Combined Diesel Electric And Gas(Turbine) ship propulsion fit
GRIUK – Greenland, Iceland and UK Gap – Cold War ASW choke point
OA – Operational Analysis
1SD – In-Service Date – for naval vessels Acceptance into the Fleet

GP – General Purpose – Designation for combatants with all-round capabilities
PDMS - Point Defence Missile System – last ditch AAD against missile attack
AOR – Auxiliary Oiler Replacement – One stop fleet replenishment vessel
SRMH – Single Role Minehunter – MCMV with single (detection) role
MCMVs – Mine Counter Measurers Vessels – broad MCM designation
CV – (Aircraft) Carrier
SSBN – Ballistic Missile delivery nuclear powered submarine – Nuclear Deterrent armed
LPD - Landing "Platform" (Dock) – Amphibious Warfare (LCU delivery) vessel and Force Command
Ro-ro LCUs – Roll on/Roll off Landing Craft (Utility) – new LCU concept for 1980s RN LPD
ASS/LPH – Aviation Support Ship became Landing "Platform" (Helicopters) – Amphibious Vessel
RFA – UK Royal Fleet Auxiliary – RN ships operated by Merchant ship "company" rules
ATS – Aviation Training Ship – RFA to train helicopter operations at sea
AO – Auxiliary Oiler – Fleet support tankers for underway replenishment
FCV – Future (Aircraft) Carrier
QE Class – Queen Elisabeth Class UK Attack Carrier Class
TL – Through Life
CTOL – Conventional Take-Off and Landing (Aircraft operated from Carriers with catapults and arrestors
CNGF – Common New Generation Frigate – designation of Anglo-French 1990s AAD combatant project
RN-RAF – UK Royal Navy and Royal Air Force
T45 – Type 45 – designation of RN AAD Destroyer class replacing earlier Type 42
ADD-PAAMS – Anti-Aircraft/Air Defence- Principal AA Missile System – fitted to Type 45
UK/FR/IT – UK France and Italy combined project for AAD (PAAMS) combatants – became T45 (UK) and Horizon (FR/IT)
FASM - Future Attack Submarine – UK replacement for current ASTUTE Class SSNs
FSSN – Future SSN – later designation for FASM (1990s/2000s)
SUBCON – SUBmarine CONcept - concept design tool developed by UK MoD/BMT Icons in 1990s using UCL DBB approach (BMT Icons– British Maritime Technology – Icons formerly BSRA now Aveva)

APPENDIX B

Table B1: Andrews Specific major contributions to Ship Design Methodology

	Andrews' contributions to Ship Design Methodology	Initial Reference	Subsequent verification in Ship Design
1.	Inside-out approach to ship design synthesis.	Andrews (1981)	Andrews (1984)/(1986)/(1987)
2.	DBB realisation of inside-out ship synthesis	Andrews & Dicks (1997)	Andrews (2018a), Andrews&Pawling (2003, 2008)
3.	The importance of constraints on SDP	Andrews (1981)	Andrews (2018a)
4.	The importance of Style in going from function to form	Andrews (2012b)	Andrews (2017, 2018a)
5.	Requirement Elucidation NOT Requirements Engineering is aim of the Concept Phase	Andrews (2003a)	Andrews (2011, 2022)
6.	Proposing a 3-D ship solution space	Andrews (1993)	Andrews (2012b, 2018a)
7.	Identifying that the level of Novelty requires different design approaches/methods/tools	Andrews (2012b)	Andrews (2016a, 2016b, 2018)
8.	Showing the fuzzy "half" of ship design is a human driven decision process	Andrews (2012b)	Andrews (2012, 2018a, 2018b, 2018c, 2018d, 2022, 2023), Andrews & Andrews (2021)

Proceedings of 15th International Marine Design Conference (IMDC-2024)
June 2-6, 2024
Amsterdam, the Netherlands

The Impact of Maritime Decarbonization on Ship Design: State-of-the-Art-Report

Thomas A. McKenney[1,*]

ABSTRACT

The maritime industry faces a critical challenge to decarbonize and meet the ambitious goal of net-zero emissions by 2050. This transition requires innovative ship design strategies to address the increasing complexity and multiplicity of technical solutions amidst dynamic regulatory, geopolitical, and market uncertainties. This paper examines the maritime decarbonization challenge's impact on ship design and decision-making under uncertainty, highlighting the necessity for collaboration between researchers and practitioners to tackle this emerging challenge. To navigate the uncertainty, stakeholders can integrate advanced design methods and decision-making processes considering the full lifecycle and fleet-level implications. This paper promotes taking a holistic approach that incorporates regulatory compliance, technological advancements, and commercial considerations, as well as a blend of methods to manage decision-making under uncertainty. Continued research in specific areas is essential to develop and refine frameworks that optimize design and operation for the industry's sustainable future.

KEY WORDS

Ship design; sustainability; maritime decarbonization; energy efficiency; alternative fuels

INTRODUCTION

Sustainability has become a pressing concern in various industries, especially in maritime. The urgency stems from the ongoing climate crisis, highlighted in July 2023 at the International Maritime Organization (IMO) Marine Environmental Protection Committee (MEPC) 80 meeting where its greenhouse gas (GHG) strategy was revised, aiming for net-zero emissions by 2050, setting interim targets, and proposing measures. Further discussions at the MEPC 81 meeting in March 2024 confirmed the direction while discussing existing and mid-term measures needed to achieve the revised targets.

Maritime decarbonization is a complex challenge with no one-size-fits-all solution. Numerous alternative fuels and ship technologies, both existing and under development, complicate the landscape. Industry stakeholders also grapple with uncertainties and dynamics such as shifting regulations and geopolitical events.

The need for immediate action, coupled with numerous options and evolving conditions, requires a substantial shift in the approach of industry players, including ship designers. It is important to stay up to date on the latest maritime decarbonization developments and consider whether the maritime decarbonization challenge presents the need to think differently about how commercial ship design is conducted. This paper offers ship designers a comprehensive overview, combining industry advancements driving decarbonization and recent academic research on sustainable ship design.

Multiple industry reports are regularly updated and readily available on maritime decarbonization topics such as energy efficiency (EE) and alternative fuels as well as industry-level analysis on how the industry can achieve decarbonization by 2050 (MMMCZCS, 2022a; ABS, 2022; DNV, 2023). General decarbonization pathways are provided, and proposed scenarios can be presented to understand broad industry directions. Key stakeholders interested in this type of analysis are mainly regulators from the IMO, regions like the European Union (EU), and countries. This type of information is helpful background for ship designers and ship owners/operators but lacks specific or actionable direction.

At the same time, there is an increasing number of academic research in the areas of sustainability, decarbonization, and, most importantly, design methods, decision-making, and support (Trivyza et al., 2022; Mansouri, Lee, and Aluko, 2015). Most research on ship design is related to "complex ship design" that includes naval vessels, submarines, and specialist commercial vessels like cruise ships. Andrews (2022) describes complex ship design as a "wicked problem," where the

[1] Associate Professor of Engineering Practice, Department of Naval Architecture and Marine Engineering, University of Michigan, USA; ORCID: 0009-0008-7910-8482
* Corresponding Author: tmckenne@umich.edu

Submitted: 22 February 2024, Revised: 9 April 2024, Accepted: 1 May 2024, Published: 26 May 2024

Conference paper, DOI: https://doi.org/10.59490/imdc.2024.907 e-ISSN: 3050-4864

challenge is not only in the ship's inherent complexity, but in determining what is really wanted (i.e., defining the requirements). Andrews (2022) continues by identifying two types of ships: "those that are part of a wider transportation system and those that go to sea to do something." With the introduction of the maritime decarbonization challenge, ships like container ships, bulk carriers, and tankers are becoming more complex and difficult to define requirements.

With so much uncertainty and changes in how the industry operates, the energy transition presents a case for placing more emphasis on the early stages of design of even simpler ships. The decarbonization challenge also demands a broader perspective than a single vessel design to account for full life cycle impacts and fleet-level considerations affecting future regulatory compliance. This paper is intended to strengthen the collaborative bridge between research and industry by evaluating the need from industry for ship design and operational decision-support, what methods and tools already exist today, and why they are needed now more than ever to help achieve full decarbonization of the maritime industry.

This paper caters to both researchers and practitioners, providing actionable insights for their daily work. For researchers, industry developments are moving quickly, and help is needed to bring relevant use cases and ensure they are addressing the right challenges and applying their research in the most effective way possible to maximize impact. This includes clearly identifying the best applications for given methods available or under development. For practitioners, there is a need to bring ship design methods and decision-making processes into the normal way of working to best handle the inherent uncertainties and dynamics associated with the maritime decarbonization challenge.

THE MARITIME DECARBONIZATION CHALLENGE

This paper focuses on the environmental sustainability challenge of reducing the maritime industry's GHG emissions and how this impacts ship design. In addition to maritime decarbonization, sustainability broadly covers social sustainability and governance for sustainability as well as other environmental sustainability topics such as air pollution and impacts on marine life. Ship designers should not overlook these other topics or how they relate to maritime decarbonization considerations and decisions. Some examples include:

- Reducing nitrogen oxides (NO_X) emissions, which are an air pollutant, from an internal combustion engine usually requires an increase in fuel consumption, leading to increased carbon dioxide (CO_2) emissions, a GHG impacting the climate.
- Black carbon is a type of particulate matter (PM), typically regarded as an air pollutant, that also can have regional short-term global warming potential.
- While ammonia as a fuel has no carbon, which can lead to low GHG emissions, its toxicity can potentially harm marine ecosystems if discharged into water.

Focusing on the maritime decarbonization challenge, projections indicate that emissions will continue to increase if we rely on current decarbonization efforts. Shipping has the least emissions intensity for freight transported, but the maritime industry's enormous scale makes it a noticeable contributor (approximately 3%) to global emissions (IMO, 2020). Moreover, maritime is a hard-to-abate sector. If maritime emissions are not reduced, the sector may be responsible for a greater share of global emissions by 2050, as other sectors decarbonize at a faster pace (e.g., power and road transport). Three segments - bulk, tanker, and container - account for around two-thirds of emissions, making them the key focus areas for future emission reduction pathways (IMO, 2020). Without additional decarbonization efforts, emissions will remain far from the Paris Agreement's 1.5-degree trajectory or science-based targets (MMMCZCS, 2021). It is crucial to act this decade to bend the curve and set the course for the 2030s and beyond.

Historically, the industry has been slow to change and has not dealt with major technological or regulatory disruptions. It remains the most cost- and emission-efficient mode of transportation, which creates limited incentives for competition with other industries. In the early 1900s, the internal combustion engine was introduced with heavy fuel oil (HFO) used for propulsion. HFO is now the dominant fuel with worldwide availability, and the two-stroke diesel engine remains the prime mover of choice for most vessels. There have been some disruptions and innovations, such as the introduction of liquefied natural gas (LNG) as a fuel and regulations including ballast water treatment and the 2020 sulfur cap. However, these have not significantly changed the industry's operations.

As shipping is globally regulated by the IMO, part of the United Nations (UN), decisions are made by consensus, which tends to result in slow decision-making. The initial IMO GHG strategy was only introduced in 2018, but ambition is now increasing. This has led to a regulatory disruption that significantly affects the industry, impacting both fuel and technology use. At the MEPC 80 meeting in July 2023, the IMO’s GHG strategy was revised, aiming for net-zero emissions by 2050 and setting interim targets and proposed measures. Additionally, regional regulations, particularly from the EU, are driving significant regulatory compliance and financial risks for maritime stakeholders. Ships also have a long lifespan of 20-25 years or more in certain segments, meaning decisions made today will determine the industry's makeup in 2050.

There are at least five candidate groups for future wide-use alternative fuels, including hydrogen, ammonia, methane, methanol, and liquid biofuels such as e-diesel and bio-oils. Each group, in turn, contains different types of fuels,

distinguished depending on feedstock and fuel production processes. In addition, alternative energies include wind, electricity (energy storage), and nuclear.

Meeting the energy demands and optimizing EE onboard ships can be achieved through a diversity of methods. Every vessel has distinct performance needs dictated by its type, size, and operations. To satisfy these specific needs, there are numerous solution pathways for vessels, encompassing a variety of energy and fuel configurations, onboard technologies, initiatives for enhancing EE, and concepts for power and propulsion systems.

Key stakeholders, such as policymakers, technology developers, fuel suppliers, and ship owners/operators, must make decisions under uncertainty, including interdependencies across stakeholder groups. Uncertainty encompasses fuel/technology availability and cost, willingness to pay/finance, and policy and regulation. Dynamics result from politics, consumer behavior, disruptive innovations, and geopolitical events. The war in Ukraine is an example of an event that has significantly impacted the energy market and led to an acceleration of policy support and investment in renewables within Europe (IEA, 2022).

Vessel owners/operators must evaluate options and decide what they believe is best for their vessel. In addition to the standard newbuild vessel design, vessels can be designed to be adaptable for other fuels or retrofitted with different or new technologies throughout their lifespan. This adds another layer of decision-making complexity, especially with high uncertainty regarding the main future fuels.

In summary, the industry's decarbonization challenge is captured in three main statements:

- First, we need to act now in an industry that is not easy to change.
- Second, there are many options, most of which are not fully mature.
- And third, key stakeholders must handle uncertainty and dynamic conditions.

The need for immediate action, along with numerous options and evolving conditions, necessitates a substantial shift in the approach of industry players, including ship designers. Keeping abreast of the latest maritime decarbonization developments and their impacts on ship design is crucial.

The solutions to the decarbonization challenge are multifaceted and require development in three main areas: regulation, technical, and commercial. Psaraftis (2019) stated that the main obstacles are not technical or economic in nature but political, manifesting in regulations at global, regional, and local levels. Although the maritime industry has achieved significant EE improvements over the past decade, EE alone will not be sufficient to decarbonize (Cullinane & Yang, 2022). With EE falling short, the industry is turning to alternative fuels to bridge the remaining gap to zero. The number of publications related to alternative fuels in the maritime sector has surged since 2018, with a significant increase starting in 2020 (dos Santos et al., 2022). This heightened attention within academic research is promising and welcomed, but it must now be translated and applied within the industry.

REGULATIONS

There are two main types of maritime decarbonization regulations impacting ship design: EE and emissions. Safety regulations associated with the introduction of new technical solutions to support maritime decarbonization should also be considered in parallel. Environmental sustainability rules and regulations affecting ship design and operation can be at the global, regional, or local levels, depending on where the vessel is intended to operate. This review will focus on global and select regional considerations, mainly related to the EU. An example of an impactful local regulation is provided; however, such local regulations should be considered on a case-by-case basis, depending on expected operations.

At the international level, the 2023 IMO Strategy for the Reduction of GHG Emissions from Ships is driving updates and the introduction of EE and emissions regulations (MMMCZCS, 2023a). The levels of ambition, on a well-to-wake (WTW) GHG emissions basis, include:

- A decline in the carbon intensity of the ship through further improvement of the EE for new ships,
- A 40% carbon intensity reduction by 2030, compared to 2008,
- The uptake of zero or near-zero GHG emission technologies, fuels, and/or energy sources to constitute at least 5%, striving for 10%, of the energy used by 2030, and
- Net-zero GHG emissions by or around 2050 (IMO, 2023).

Indicative checkpoints to reach net-zero absolute GHG emissions include striving for a 20% reduction in 2030 and aiming for a 70% reduction by 2040. Figure 1 provides an overview of the latest IMO efforts related to achieving the ambitions of the 2023 strategy. The IMO has already implemented short-term measures to reduce carbon intensity, including the introduction of the Energy Efficiency Design Index (EEDI) in 2013 and, more recently, the Energy Efficiency Existing Ships Index (EEXI) and Carbon Intensity Indicator (CII). These short-term measures will be revised in 2026. Mid-term measures, such as carbon pricing and a GHG fuel standard, are currently under consideration and are expected to be adopted in 2026, with enforcement planned for 2027.

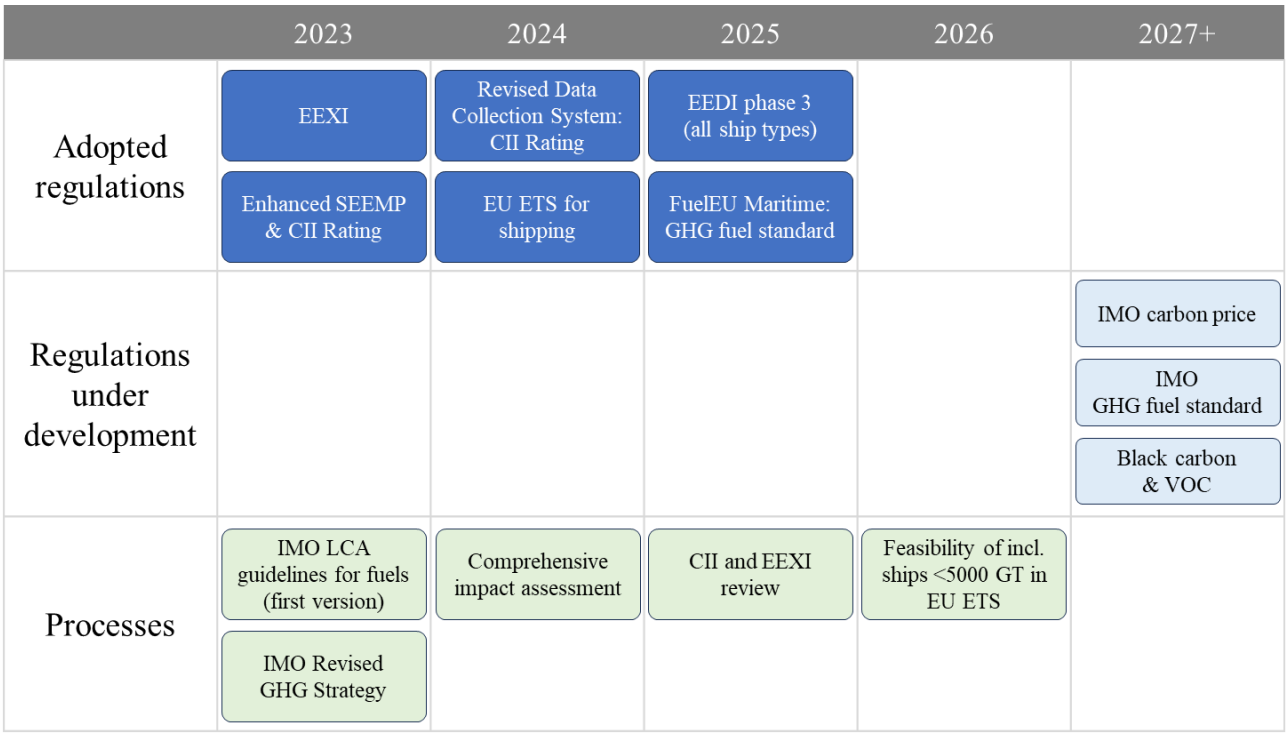

Figure 1: GHG regulatory timeline, adapted from DNV (2023)

This section does not aim to provide detailed descriptions of each regulation and how they function for the various ship types and sizes. It will present the increasing regulatory pressure placed on the maritime industry, necessitating further emphasis within existing areas and the introduction of new solutions, including design for efficient operations, the introduction of alternative energies and solutions, and financial considerations like carbon pricing.

Table 1 provides an overview of the main regulations, their current design impacts, and potential future design impacts. This summary is described in more detail in the following sections.

Energy Efficiency Regulations

This section will highlight the main ship design impacts already identified for each main EE regulation, as well as project what potential impacts could be as these regulations are updated in the future to align with IMO's revised GHG reduction strategy.

EEDI

The EEDI is a design-related hard regulation that is the one-time responsibility of the ship designer or shipyard to prove compliance. The EEDI formula either drives a reduction in CO_2 emissions or an increase in transport work, which mainly relates to the classic ship-engine-propeller matching process (Ren et al., 2019) and involves a balance between ship capacity, power, speed, minimum fuel consumption, and the smallest quantity of CO_2 emitted into the atmosphere (Constantin and Amoraritei, 2019). Optimization of main dimensions can also improve EEDI values (Calisal et al., 2022).

A working group at the Mærsk Mc-Kinney Møller Center for Zero Carbon Shipping (MMMCZCS) recently published findings (MMMCZCS, 2023b) related to EEDI compliance, stating, "The combination of derating and propeller diameter changes delivers increased efficiency by aligning the optimal operational point of the propulsive system more closely with the vessel's actual usage. Feedback from working group participants indicates that compliance with the EEDI can be achieved through power reduction alone, without implementing other EE gains (through engine efficiency, retrofits, etc.)".

While evolutionary improvements in hull forms and power generation efficiency have mainly contributed to EEDI compliance, the introduction of energy-saving devices (ESDs) on newbuilds has proven beneficial for business and the environment (Kenney & Palmejar, 2023). Most adopted ESDs are hydrodynamic improvements (e.g., twisted rudders, rudder bulbs/fins, pre-swirl stators, propeller boss cap fins) or engine-related (e.g., waste heat recovery, shaft generators) (EC, 2021). Members of the MMMCZCS working group attribute their introduction mainly to the risk of poor sea trial results.

Table 1: List of regulations, current, and potential future design impacts

Regulation	Type / Responsible	Current Design Impact	Potential Future Design Impact	References
EEDI	Design, Hard for New Vessels Ship designer, shipyard	Evolutionary improvement of hydrodynamics, propulsion and power generation on newbuilds. Introduction of new ESDs. • Ship-engine-propeller: Derated engines (linked to slow steaming trends) + increase propeller diameter, streamlined hullforms • Energy saving devices: Mostly hydrodynamic improvements (increased speed at fixed power to ensure sea trial results) or engine-related (WHRS, shaft generator) • Introduction of LNG • Increased capacity	Could change metric from CO_2-centric to a power or energy basis or enlarge the scope of emissions. Increased reduction rates. Updating of reference lines to include newer (and usually larger ships). • Incorporation of more innovative ESD technologies including air lubrication and wind-assisted propulsion • Introduction of new main energy converters including hybrid arrangements, all-electric with batteries and fuel cells	Ren et al. (2019), Constantin and Amoraritei (2019), Calisal et al. (2022), MMMCZCS (2023b), Kenney & Palmejar (2023), EC (2021)
EEXI	Design, Hard for Existing Vessels Ship owner	Limited to no design impacts on existing vessels with limited operational (mostly speed) limitations. • Adoption of power limitation that reduces maximum allowable engine power output • Limited to no introduction of new ESDs unless already planned	Older (less efficient) vessels impacted more by power limitation could lead to increased scrapping. Updating of EEDI can lead to updates of EEXI limits if additional phases are introduced or another metric is introduced.	MMMCZCS (2023b)
CII/SEEMP Part III	Operational, Soft (until 2026) Ship owner, technical manager	Higher impact on operations, however, improved designs lead to more operational freedom. • Vessel monitoring system requirement • More efficient designs are able to comply with CII more easily	First operational measures will be exhausted. Then consideration for advanced technologies. Newbuilds to be more energy efficient to give further operational flexibility. Design for efficient operation emphasized. Speeds will generally go down. Wind-assisted propulsion, air lubrication, waste heat recovery systems, shaft generators, and hybridization of the engine room (e.g., using batteries or fuel cells).	MMMCZCS (2023b), Sun et al. (2023)
Fuel Standards (IMO Mid-term Measure, FuelEU)	Operational, Hard Ship owner, technical manager	Major impact for new vessels with expected lifetime of 20+ years as readiness for alternative fuels needs to be considered. Due to small short-term reductions, limited impact for existing vessels with benefits seen from introduction of LNG as a fuel and small modifications required to use liquid biofuels. Use of fossil-based LNG provides compliance window up to at least 2030. Small modifications required for biofuels (to be discussed in next section).	With the anticipated increased reductions upcoming, all new vessels need to address this compliance challenge based on the solutions available (to be discussed in next section). Fleet considerations like FuelEU pooling requires designers to think at vessel and fleet level.	EU (2023), MMMCZCS (2022d)
MBMs (IMO Mid-term Measure, EU ETS)	Operational, Hard Ship owner, technical manager	Unclear as in short term it is a relatively small added cost of operation. Emphasized efficient operation and reducing absolute emissions from vessel.	MBMs more closely linking economic incentives and penalties to the technical description of the vessel. Cost of GHG emissions could become major driver of design decisions (techno-economic analysis).	IMO (2024), Hansson et al. (2023)

The introduction of LNG dual-fuel vessels has also contributed to lower EEDI ratings (around a 20% reduction) due to the tank-to-wake (TTW) carbon factor used to calculate CO_2 emissions. It is important to note that the EEDI formula only considers direct vessel emissions and excludes other GHGs, such as methane. While the primary decision to design a dual-fuel LNG vessel has most likely not been for EEDI compliance alone, it has shown to be an easy way to comply with the latest EEDI Phase 3 requirements. Another method to improve EEDI values is to increase capacity while keeping power low. A good example of this is raising the wheelhouse height on container vessels to accommodate more twenty-foot equivalent units (TEUs) without impairing visibility.

The implementation of EEDI, especially under favorable market conditions, has increased focus on EE and led to more efficient ship designs, including the introduction of ESDs (MMMCZCS, 2023b). However, the EEDI attained values of recent newbuild vessels have plateaued (EC, 2021), and its future is not clear, with discussions on Phase 4 postponed to later in this decade. The IMO is now discussing the development of mid-term measures focused on reducing absolute emissions, which could render aspects of the existing EEDI calculation redundant (MMMCZCS, 2023b). The MMMCZCS working group suggests that the metric could be changed from CO_2-centric to a power or energy basis or expand the scope of emissions. This would coincide with increased reduction rates and the updating of reference lines to include newer (and

usually larger) ships. It could lead to wider adoption of more innovative ESD technologies such as air lubrication and wind-assisted propulsion, as well as the introduction of new main energy converters, including hybrid arrangements, all-electric with batteries, and fuel cells.

EEXI

The EEXI is a design-related hard regulation that is the one-time responsibility of the ship owner to prove compliance starting from January 1, 2023. It is based on EEDI reference lines and can be considered as an extension of EEDI to cover existing vessels in addition to newbuilds. Due to the limited time ship owners had to prepare for the introduction of EEXI regulations and the small periods of time vessels operate at higher engine loads, most vessels have adopted a power limitation, which reduces the maximum allowable output of the engine (MMMCZCS, 2023b).

Data suggests that vessels can achieve EEXI compliance with minimal impact on operations. However, EEXI imposes a technical limit if vessels are incentivized to go faster, such as under certain market conditions or when catching up on a schedule (MMMCZCS, 2023b). While having a more significant impact on existing and mostly older vessels, EEXI compliance confirms a trend towards lower installed power and slower speeds as a major EE measure contributing to an overall reduction in GHG emissions. EEXI is an initial example of why operational factors have become more important for ship designers to pay attention to and consider as part of the design process, especially when projecting throughout the lifetime of a vessel.

CII

CII is an operational EE regulation based on annual operational data. It came into effect on January 1, 2023, and will be effective until at least 2030, with a review planned in 2026. CII reduction factors relative to 2019 start at 5% in 2023 and increase to 11% by 2026. If a vessel has low CII ratings for periods of time, corrective actions need to be agreed upon and taken (MMMCZCS, 2023b).

Along with the CII, Part III of the existing Ship Energy Efficiency Management Plan (SEEMP) was introduced in 2023 to ensure proper documentation of each vessel's implementation plan to obtain the required CII ratings. As part of the SEEMP Part III, the recognized organization, often a classification society, needs to verify its implementation plan, including the use of a vessel monitoring system (MMMCZCS, 2023b).

While intended to improve the operational EE of a vessel, studies have shown that a more efficient ship design can provide additional operational flexibility and higher CII ratings (MMMCZCS, 2023b). Design can be a differentiating factor for operational EE regulatory compliance, placing more emphasis on energy-efficient designs going forward. It is also expected that CII modeling during the design phase will be requested, and an understanding of the impact of EE technologies and operational measures on CII rating will be needed during this phase. This is a new consideration for ship designers and shipyards that previously only had to ensure compliance with EEDI. Subsequently, this raises more awareness of operational considerations and the operational part of the ship's lifecycle during the design phase, which should further improve the EE of newbuilds.

However, delivering an energy-efficient vessel does not guarantee good CII ratings, as operational conditions mainly drive the final rating, over which the ship owner typically has little control. Very efficient ships can have poor CII ratings. In addition to a focus on vessel efficiency, vessel, port, and canal operations, as well as commercial considerations, can significantly impact a CII rating (MMMCZCS, 2023b). While the ship designer has control over designing an energy-efficient vessel, they should not overlook the other drivers and their relationship to a ship's design. This includes considerations like expected speed, cargo utilization, and deployment.

How do ship owners intend to achieve CII compliance? Owners expect to first implement as many operational measures as possible, such as performance monitoring. Once operational measures are exhausted, owners must consider introducing advanced technologies like wind-assisted propulsion, air lubrication, waste heat recovery systems, shaft generators, and engine room hybridization, such as using batteries or fuel cells (MMMCZCS, 2023b). Additionally, speed becomes an important parameter for CII compliance, understanding that commercial aspects also need to be considered (Sun et al., 2023).

Emissions Regulations

Emissions regulations are essential for designers to understand, as they can be fulfilled in different ways, including through design and operational solutions. This further integrates the designer into the operational environment where the owner's requirements, including operational profiles and conditions, should now be more deeply explored in an environment of impactful regulatory and economic considerations.

Fuel Standards

GHG fuel standards are expected at the international level through IMO mid-term measures (with enforcement starting in 2027) and regionally in the EU with FuelEU for Maritime, starting enforcement in 2025. The main purpose of fuel standards is to promote the use of sustainable fuels. The measure, which is based on GHG emissions per unit energy on a WTW

basis, is independent of the vessel's EE, as a reduction in GHG emissions will also lead to lower energy consumption. As such, this measure requires the introduction of more sustainable fuels.

FuelEU for Maritime required reduction levels start at 2% in 2025 compared to 2020 levels and will increase to 6% in 2030, 31% around 2040, and 80% around 2050 (EU, 2023). FuelEU for Maritime also introduces the concept of pooling, which allows a company to compensate for non-compliant reductions with over-compliant reductions across multiple ships in their fleet for the same time period. This concept changes the focus from single vessel compliance to fleet compliance, granting shipping companies greater flexibility in developing their compliance plans. This also introduces a new consideration for ship designers when defining newbuild design requirements that will join a company's larger fleet. Instead of designing for expected reduction trajectories, designers can introduce near-zero or zero-emission vessels that can help offset emissions from multiple sister vessels within a fleet.

The IMO's GHG fuel standard, considered a mid-term measure, is expected to follow a similar structure as FuelEU for Maritime. However, it is not confirmed, and there will likely be some differences as the IMO targets its revised GHG reduction strategy levels.

While alternative fuels will be discussed further in the next section, it is crucial to highlight that existing vessels either need to introduce biofuel blending or benefit from pooling (as described above). Owners who have introduced alternative-fueled newbuilds, including LNG and methanol dual-fuel vessels, can benefit from the use of compatible fossil and sustainable fuels. Recent studies have shown that LNG-fueled vessels operating on fossil-based LNG can remain compliant with FuelEU for Maritime regulations at least until 2030, based on the regulation's current setup (MMMCZCS, 2022d).

Nonetheless, these fuel standards are effectively compelling owners to introduce alternative-fueled vessels, which are now an essential part of a designer's considerations, especially early in the design process when the vessel's requirements are defined.

Market-Based Measures

Market-based measures (MBMs) put a price on GHG emissions to provide an economic incentive to reduce emissions through ship design and operation. The EU has recently included the maritime industry in its Emissions Trading System (ETS), a cap-and-trade system. The IMO is considering a list of potential MBMs as part of their mid-term measures, ranging from contribution schemes for GHG emissions through an ETS to schemes based on actual ship efficiency by design and operation (IMO, 2024). Each of the ten proposed MBMs for the IMO's mid-term measure either requires a direct cost per amount of fuel consumed or emissions, the purchase of related allowances, or sets strict EE standards with associated penalties (IMO, 2024). How any collected revenue from such measures will be used or distributed is yet to be determined.

MBMs are fuel- and technology-agnostic and provide flexibility to designers and operators when selecting solutions to minimize financial impact. Cost-effectiveness and abatement become critical metrics when evaluating solutions. With the expected cost of EU ETS emissions allowances in the short to mid-term, the least-cost measures like increased EE of ship designs and EE operational measures are likely to be implemented first as these abatement costs are typically negative due to fuel savings (Hansson et al., 2023). With higher abatement costs, alternative fuels and technologies would require greater costs associated with a MBM. Lagouvardou et. al. (2023) studied the marginal abatement cost of alternative marine fuels to demonstrate the role of MBMs in helping bridge the price gap between the fossil-based fuels of today and the more expensive alternative fuels of tomorrow. Revenues from MBMs can also be used to fund scaling of alternative fuel production as fuel availability can become a major constraint in the uptake of alternative fuels (Lagouvardou et. al., 2023).

MBMs now link economic incentives and penalties more closely to the technical description of the vessel beyond typical metrics such as the required freight rate (RFR). Techno-economic assessments are now intrinsically linked to the ship design process, and will be in the future, even if MBMs will potentially have an outsized impact on technical decisions compared to typical RFR measures.

Local Emissions Regulations

A pertinent example of an impactful local regulation is the zero-emissions requirement for cruise ships, tourist boats, and ferries in the Norwegian World Heritage fjords by 2026 (NMA, 2023). In response to this upcoming regulation, Norwegian shipowners and designers have developed power solutions to allow large cruise ships to operate emissions-free for up to 12 hours and have conceived zero-emission cruise ship designs (Business Norway, 2024).

Non-Regulatory Drivers/First Movers

Although regulatory compliance is the minimum requirement for an existing or future ship design, some companies prefer to be first movers setting more ambitious targets, including substantial investments in advanced technologies and alternative fuels. First movers seek competitive advantages, such as strong brand recognition, technology leadership, and resource control, while also taking on increased financial, technical, and operational risks (Esau & Bentham, 2023).

These pioneering companies are trying to capitalize on current and expected future demand for "green" transportation. While the demand is currently low, it exists and is growing. While regulations will be the primary driver of the eventual decarbonization of the industry, first movers responding to the market demand for clean transportation have been the start of solution investigation. In addition, various organizations publish guidelines or best practices to be considered. For a ship designer, understanding the motivation and objectives as part of the ship requirements definition is critical.

TECHNICAL SOLUTIONS

Technical solutions are available and under development to help achieve regulatory compliance or to meet individual company decarbonization targets. This section will focus specifically on solutions that impact ship design. Pure operational measures, for example, will not be covered; however, operational measures are in most cases the easiest to implement and should be considered, especially for existing vessels.

While most operational measures are purely operational or behavioral in nature, ship designers still need to understand what operations are expected and if any operational measure impacts ship design, or if the ship design can be optimized to maximize the impact of targeted operational measures. This section will briefly cover some of these operational measures to ensure proper coverage of solutions and ship design-related considerations.

Technical decarbonization solutions can be divided into three main categories:

1. Energy efficiency technologies,
2. Alternative energies and fuels, and
3. Emission reduction technologies.

These solutions will be introduced, but not discussed in detail, as there are plenty of good sources that provide more detail and will be referenced in the associated sections.

This section will provide evidence of a general increase in ship design complexity and more design challenges with the introduction of maritime decarbonization technical solutions. While some solutions can maintain complexity levels (e.g., a newer, more efficient engine), most introduce additional complexities and interdependencies with other systems onboard. This increase in complexity and a high-level identification of the main ship design impacts with examples will be presented and discussed.

Design complexity discussed in this section is focused on the design product, not the design problem or process. Complexity of a design product can be described by the product's structure, such as the physical arrangement, its function like the number and connectivity of systems, and its behavior, such as predictability (Ameri et al., 2008). When discussing the technical solutions in this section, increased complexity is demonstrated by the addition of systems and their connection or relationship to other systems and overall vessel performance. Cost can also be used as a complexity metric and will be indicated where possible in parallel with technical complexity descriptions. Systems with higher complexity generally have higher lifecycle costs (Ameri et al., 2008) and failure rates (Jones, 2021).

Energy Efficiency Technologies

Energy efficiency technologies (EETs) reduce the vessel's energy consumption. MEPC.1/Circ.815 provides guidance on how EETs can be treated for EEDI calculation and verification, including categorization (IMO, 2013):

- “Technologies that shift the power curve, resulting in a change of combination of propulsion power and speed.
- Technologies that reduce the propulsion power but do not generate electricity, leading to increased propulsion efficiency.
- Technologies that generate electricity, leading to saved energy, typically in the form of reduced auxiliary power.”

From a ship design impact perspective, three general categories of EETs can be defined:

1. Standard Practice: Low ship design impact baseline technologies that are (or should be) incorporated into any newbuild vessel.
2. Moderate Effects: Medium ship design impact technologies that might cost more and require integration but can be managed without significant design or performance impacts.
3. Systematic Integration: High ship design impact technologies that cost more, have larger systems and interconnections, and implications for the overall ship design and performance.

Table 2 provides an overview of the main EETs, their maturity level, cost and complexity, and ship design impacts. It also includes specific examples of ship designs operating with EETs onboard.

While general technology categories can be grouped by ship design impact level, any novel or new technology within any category might require a more systematic integration study and should be evaluated on a case-by-case basis. A good example of such a case is the novel gate rudder system (Tacar et al., 2020). While within the propulsive loss reduction category that is typically low design impact, being a new and novel system, a more thorough assessment is needed.

Table 2: List of energy efficiency technologies, maturity level, cost, technical complexity, main ship design impacts

Impact Category	Technology Category	EET Type	Maturity Level / Cost ($)	Design Impact & Technical Complexity	Examples / References
Low-Standard Practice	Hullform design	Dimensions, hull, openings optimization, asymmetric stern, skeg shape training edge, twin skeg. Use of model-based simulations.	Mature <500k	Part of normal design process. Enhanced through advanced CFD simulations.	
	Structural design	Superstructure optimization (wind resistance), lightweight reduction. Use of model-based simulations.	Mature <500k	Part of normal design process. Enhanced through advanced CFD simulations.	
	Hull drag reduction	Low friction coating, heating, surface texturing, additives	Low friction coatings well-established (mature), new technologies under development. <1M	Minimal. Can be retrofitted. Part of normal drydocking schedule. Coatings have low impact. Any active system would require additional supporting systems.	
	Propulsive loss reduction	Controllable pitch, contra-rotating, tip raked propellers, propeller nozzle/duct, pre swirl stators, post swirl fins/stators, rudder bulb, thrust fin, twisted rudder, ducktail waterline extension, gate rudder	Mature <1M	Impact on ship performance, both from a propulsion efficiency perspective, but also other important aspects such as reliability, maneuvering, structural fatigue. Can be retrofitted. Usually requires drydocking. Loss of efficiency by designing for an existing hullform. Usually well-known and demonstrated. Part of normal design process. New propulsion devices and rudders such as gate rudders requires integration studies (supporting systems, structural integration) with increased complexity.	Novel Gate Rudder system includes two asymmetric rudders at each side of the propeller (Tacar et. al., 2020).
	Machinery efficiency	Engine design	Mature	Part of normal design process. Improved fuel consumption while maintaining NO_X compliance and other emission targets (e.g., low methane slip)	
Medium-Moderate Effects	Shaft generator	Power take-off (PTO), power take-in (PTI), front-end/aft-end, on-engine, on tank-top, shaft mounted, geared/direct	Mature <1M	Space is a consideration when placed aft of the main engine (could effect hullform), requires switchboard integration. Retrofit can be challenging due to space limitations. Additional system needs to be integrated close to engine, frequency converter and couplings, electrical integration	
	Waste heat recovery	Beyond exhaust gas boilers incl. steam turbine, power turbine, organic rankine cycle	Semi-Mature. Demonstrated onboard vessels. 1-5M (more if combined)	Space/weight requirements, piping, switchboard integration. Retrofit can be challenging due to space limitations. Additional system, piping, electrical integration	
	Solar panels	Solar panels	Not mature. Limited demonstrations <500k	Large amount of deck space needed. Only applicable to certain vessel types (e.g., car carriers). Can be retrofitted. Additional system that requires large area. Electrical integration.	K-Line's Drive Green Highway car carrier installs large solar energy system (Haun, 2016)
	Energy storage/ batteries	Peak load shaving	Semi-mature 1M	Additional system, requires space, electrical integration. Retrofit can be challenging due to space limitations. Space requirements, control and automation integration, fire safety	
	Cold ironing/ shore power	Cold ironing/shore power	Semi-Mature <1M	Additional system that requires space, access, high-voltage cabling, electrical integration. Can be retrofitted. Space requirements and outside access/interface, switchboard integration. Containerized options exist.	
High-Systematic Integration	Air lubrication system (ALS)	Bubble drag reduction, air layer drag reduction, partial air cavity drag reduction	Semi-mature. Demonstrated onboard various vessel types. 1-5M	Interconnected with hullform design, additional support systems such as compressors requiring additional energy demand, piping. Can be retrofitted. Requires drydocking. Loss of efficiency by designing for an existing hullform. Hullform and ALS system designed together - performance dependent on good match (e.g., location of air cavities). Additional power demand and space for supporting systems such as compressors. Risk of air bubble interactions with propeller and sea chests. More suitable for certain types of ships (e.g., draft considerations).	Kim & Steen (2023)
	Wind assisted ship propulsion (WASP)	Wingsails or rigid sails, square rig sail systems, towing kites, flettner rotor	Not mature. Demonstrated onboard a few vessel types. 1-5M	Additional system that has additional weight, requires deck space, supporting systems, structural integration. Can be retrofitted. Current share of retrofits is significant (EMSA, 2023). Air draft restrictions (e.g., bridges), stability, change in operations (wind-based route optimization), visibility.	Pyxis Ocean bulk carrier (operated by Cargill) was retrofitted with two rigid sails (WindWings) (Neuman, 2023), EMSA (2023), Khan et al. (2021)

The EETs with the highest complexity are also the ones with the highest potential. Two good examples are the air lubrication system (ALS) and wind-assisted ship propulsion (WASP). Potential net power savings of ALS technologies can range from 2-22% (Kim & Steen, 2023), while WASP can provide up to 30% savings (EMSA, 2023).

ALS technologies are considered semi-mature and have been demonstrated onboard various vessel types. With high initial capital expenditure (CAPEX) of around $1-5 million (M), ensuring sufficient savings to justify the investment is critical. Additionally, the ALS is interconnected with the hull form design, and performance will depend on a good match (e.g., location of air cavities). Additional power demand and space for supporting systems such as compressors are also required. The risk of air bubble interactions with the propeller and inlets like sea chests also needs to be managed.

WASP technologies are not considered mature yet, but demonstrators are currently onboard a few vessel types. Like ALS, WASP has high CAPEX ($1-5M), and ensuring maximum savings is critical. With multiple WASP systems added to a ship design, the additional weight and deck space can be limiting factors. Structural reinforcement is also required (Khan et al., 2021). Air draft restrictions (e.g., bridges), stability with large weights on deck, and visibility need evaluation. WASP performance will also depend on operations, creating an important link between design and operations. For example, the vessel can deviate from the shortest route if additional WASP savings can be achieved.

ALS and WASP provide two examples of high-impact ship design considerations that require systematic integration. While "low-hanging fruit" with low to moderate impact do exist, significant savings will usually require acceptance of increased cost and complexity.

Alternative Energies and Fuels

While significant EE improvements can and should be made due to their favorable emission abatement economics, EE alone is not enough. This has been highlighted by recent fuel standards being implemented or developed, as well as continued trade growth projections that will only lead to increased emissions without the introduction of other solutions (Cullinane & Yang, 2022).

To reduce the emissions per unit of energy required by ships, alternative energies and fuels have been proposed and introduced in the maritime industry to replace fossil fuels like HFO, diesel, and LNG. Along with the introduction and development of alternative energies and fuels, new and modified energy converters such as dual-fuel internal combustion engines and fuel cells are being developed.

The main energies and fuels currently under consideration within the maritime industry are listed in Table 3 and include wind, electricity, liquid biofuels (including biodiesel and bio-oils), methane, methanol, ammonia, and hydrogen. These energies and fuels can be produced or provided in different ways. Renewable energy is used to produce e-fuels, fossil feedstocks are used as a basis to produce blue fuels, while bio-diesel and bio-oils include a range of techniques that convert biological material into an oil-like substance. Depending on the feedstock and production process, each pathway has a certain level of WTW emissions relative to fuel oil. A WTW methodology that includes the emissions from fuel production and onboard the vessel is needed to unlock carbon-based fuel pathways like methane and methanol.

While the molecular makeup of fuels can be identical, their emission intensities can vary. From a ship design perspective, the integration of "green ammonia" versus "blue ammonia" is identical; however, it's important to properly account for the source and production method when calculating lifecycle emissions (on a WTW basis).

The main energies and fuels have different maturity levels and commercial readiness levels, as seen in the number of alternative-fueled vessels delivered or on order. Based on DNV's Alternative Fuels Insight (as of April 9, 2024), with over 1,000 vessels in operation and on order, methane-based vessel designs are the most prevalent, with only 16 ammonia-fueled vessels on order.

While technical complexity generally increases with the introduction of alternative energies and fuels, this is not always the case. Most of the design complexity for fuels such as methane, ammonia, and hydrogen come from their storage requirements and proper management of liquefied gases onboard the vessel. They also require dual-fuel engines with two fuel supply systems and additional support systems and spaces, such as ventilation, double-walled piping, and fuel preparation rooms. Methanol is more easily stored but still requires additional systems like inerting and dual-fuel engines. In addition to the typical NO_X reduction after-treatment technologies that are required, ammonia-fueled vessels may require additional systems to mitigate ammonia slip and nitrous oxide (N_2O) emissions, as well as ammonia release mitigation systems due to its toxicity.

Table 3: List of alternative energies/fuels, maturity levels, technical design complexity, main ship design impacts

Energy/ Fuel	Maturity Level	Design Impacts	Technical Complexity		
			Port Interface	Energy Storage	Energy Conversion & After-Treatment
VLSFO	Mature	-	Standard bunkering	Integrated tank	Mono-fuel engine. NO_X reduction (EGR/SCR).
Wind	For more than EE, majority of energy demand to be met. Not yet mature for this application.	Class guidelines and incorporation into EEDI/EEXI calculations available. Potential change in operations such as speed (wind-based route optimization). Deck space, air draft restrictions (e.g., bridges), stability, visibility.	-	-	-
Electricity	Semi-Mature	Class guidelines available, risk-based approval process. Relationship between endurance, energy density and space requirements.	Power connection	Battery	-
Bio-Diesel/ Bio-oils	Mature	Minor modifications potentially needed.	Standard bunkering.	Integrated tank. Small modifications potentially needed.	Mono-fuel engine. Small modifications potentially needed. NO_X reduction (EGR/SCR).
Methane	Mature	Prescriptive rules in IGF Code. Well-established design considerations. Additional storage volume requires an evaluation of endurance and cargo loss. Locating key spaces like the tank connection space, fuel preparation room and vent mast important for arrangement.	Liquified bunkering requires additional systems including vapor return line, safety measures, operational procedures.	Liquified at -163 deg C, requires independent prismatic (Type A/B), cylindrical (Type C) or membrane tanks, stainless steel, aluminum or nickel steel, tank aeration, tank connection space, inerting, vent mast and piping, boil-off gas management (e.g., reliquification).	Dual-fuel engine. Two fuel supply systems. Fuel preparation room. Fuel heating. Ventilation. Double-walled piping. Pilot fuel consumption. NO_X reduction (EGR/SCR).
Methanol	Semi-Mature	IMO Interim Guidelines with risk-based approval. Integrated tanks require cofferdams that impacts required space in addition to energy density difference. Alternative designs can be proposed to reduce the impact of the cofferdam requirement.	Usually requires additional bunker lines (due to higher quantities for same amount of energy), vapor return, safety measures, operational procedures.	Integrated tank with proper coating. Liquid under ambient conditions. Inerting. Vent mast and piping.	Dual-fuel engine. Two fuel supply systems. Fuel preparation room. Ventilation. Pilot fuel consumption. NO_X reduction (EGR/ SCR/ water injection).
Ammonia	Not Mature	Class guidelines available, risk-based alternative design required. Gas dispersion and quantitative risk assessment analyses recommended. Additional storage volume requires an evaluation of endurance and cargo loss. Locating key spaces like the tank connection space, fuel preparation room and vent mast important for arrangement. Additional integration of emissions and safety systems to achieve equivalent safety levels to methane and meet emissions regulations.	Requires additional bunker lines (due to higher quantities for same amount of energy), vapor return(s), safety measures, operational procedures.	Liquified at -34 deg C or 18 bar pressure, requires independent prismatic (Type A/B) or cylindrical (Type C) tank. Low temperature or high tensile steel. Tank aeration, Tank connection space, inerting, vent mast and piping, boil-off gas management (e.g., reliquification).	Dual-fuel engine. Two fuel supply systems. Fuel preparation room. Fuel heating. Ventilation. Double-walled piping. Pilot fuel consumption. NO_X reduction (EGR/SCR), potential need to reduce ammonia slip and nitrous oxide (N_2O) via additional catalyst. Ammonia release mitigation system.
Hydrogen	Not Mature	Class guidelines available, risk-based alternative design required. Additional storage volume can pose a significant design challenge that requires an evaluation of endurance and cargo loss. Locating key spaces like the tank connection space, fuel preparation room and vent mast important for arrangement.	Requires additional bunker lines (due to higher quantities for same amount of energy), vapor return(s), safety measures, operational procedures.	Liquified at -253 deg C or compressed at above 200-300 bar, requires usually a well-insulated cylindrical (Type C) tank. Special low-temperature material that avoids embrittlement. Tank connection space, inerting, vent mast and piping, boil-off gas management (e.g., reliquification).	Large two-stroke engines not currently being developed. Most likely converter for direct hydrogen use is fuel cells. NO_X reduction (EGR/SCR) if burned in an engine.

Main ship design impacts with the introduction of alternative energies and fuels include increased fuel storage volumes, additional space for fuel management and safety systems, as well as key integration challenges such as placement of vent masts and routing of fuel piping. Ship performance is usually impacted, and compromises need to be made in terms of endurance, speed, and/or cargo capacity. Typically, alternative-fueled vessels will not have the same endurance as their conventional-fueled counterparts, where fuel capacity is not as constrained. Methanol-fueled vessels have their own integration challenges, including the need for additional space around the fuel tanks for cofferdams. However, alternative designs can be proposed to reduce the impact of the cofferdam requirement.

Hydrogen-fueled vessels have significant ship design challenges, including the lack of internal combustion engine development and the need for large storage volumes (Ustolin et al., 2022). There has yet to be a large hydrogen-fueled deep-sea oceangoing vessel developed. Hydrogen as a fuel has been successfully implemented on smaller vessels, though (Comyn et al., 2022). All-electric solutions have been implemented for smaller vessels, while batteries are mostly considered an EET on larger vessels. Industry and academic studies have indicated the advantage of using batteries for smaller short-sea vessels such as ferries, like hydrogen (Wang et al., 2022).

Nuclear propulsion has also gained renewed interest with the development of advanced nuclear reactor technologies, including small modular reactors and microreactors. Benefits of nuclear-based technology and applications include a zero-emission, base-load power source with more predictable financials compared to other alternative fuels that struggle with both availability and high price concerns. While commercial nuclear for maritime applications shows promise, there are several concerns and barriers to implementation that would need to be addressed. In addition to the well-known concerns of non-proliferation, nuclear accidents, and public perception, there are barriers associated with maturing the technologies for maritime application, merging nuclear and maritime regulations to form a viable regulatory framework and pathways, as well as the need to rethink how risks are calculated. The broader societal and industry impacts of such applications can also not be forgotten.

While the technical design complexity discussion has mostly revolved around the use of internal combustion engines as the main energy converter of today and will likely remain well into the future, alternative energy converters such as fuel cells are under development and show promise for use with alternative fuels. The use of hydrogen directly in fuel cells or the use of a cracker or reformer with fuels like ammonia, methanol, and methane can provide increased conversion efficiencies compared to internal combustion engines (Herdzik, 2021). While fuel cell technologies and their applications onboard vessels are not fully mature, their ship design implications should be considered and can, in most cases, lead to a less complex design compared to an alternative-fueled internal combustion engine design.

The introduction of new alternative energies and fuels has also raised safety concerns and the need to rethink how risk assessments and risk-based approvals are done. Comparing alternative fuels with different characteristics, such as flammability, explosiveness, and toxicity, that can impact safety can be challenging and requires new types of analyses and updated risk-based frameworks.

Emission Reduction Technologies

Emission reduction technologies or after-treatment technologies have been used within the maritime industry to address mainly air pollutant emissions but are now also being considered to reduce GHGs and other alternative fuel-related emissions. Figure 2 provides a high-level overview of the emission risks for the main fuels and potential solutions to mitigate these risks, originally introduced by MMMCZCS (2022b).

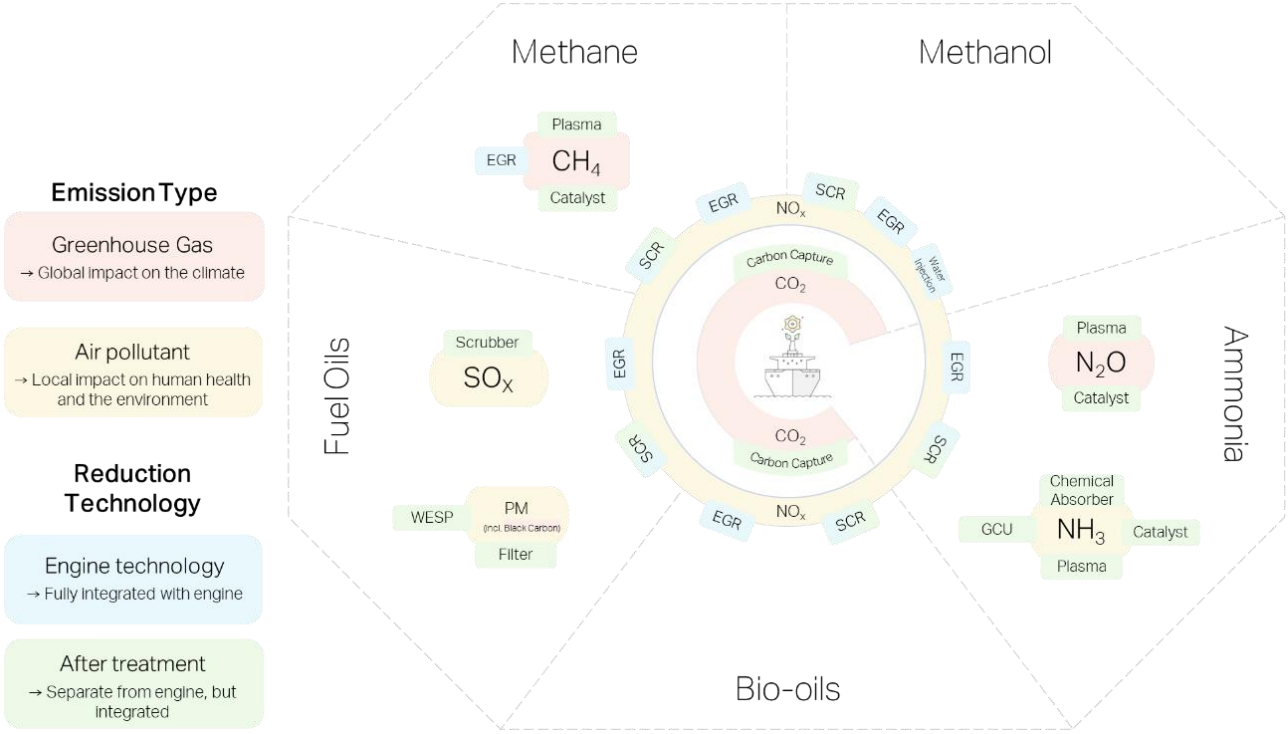

Figure 2: Highlighting emission risks for main fuels, reprinted with permission from MMMCZCS (2022b)

The most notable technologies used today include exhaust gas recirculation (EGR) and selective catalytic reduction (SCR) systems to reduce NO_X and exhaust gas cleaning systems (commonly known as scrubbers) to reduce sulfur oxides (SO_X) and PM from engine exhausts.

EGRs and SCRs are not going anywhere, as NO_X compliance will still be required with the use of alternative fuels, and most of the fuels under consideration require after-treatment. SO_X scrubbers will become a technology of the past as HFO use will decrease as the first fossil fuel impacted by upcoming regulations. HFO is also not expected to be used as a pilot fuel for alternative fueled vessels in the long term.

One of the main emission reduction technologies currently under development for maritime applications are shipboard carbon capture (SCC) systems that can, most commonly, capture CO_2 from engine exhaust onboard a vessel. There are different types of SCC systems, and each has its own integration challenges and considerations. More extensive studies have been completed on amine-based absorption systems, as they are the most mature and are already used onshore. While studies have shown SCC to be technically feasible, there are high energy requirements, significant CAPEX investment, and integration challenges on certain vessel types due to the space requirements for the capture system, liquefaction, and CO_2 storage (MMMCZCS, 2022c).

Finally, with the introduction of alternative fuels including methane, methanol, and ammonia, emission reduction technologies either need to be applied and developed to ensure compliance with air pollutant emissions while limiting other GHG emissions in addition to CO_2, such as methane and N_2O. Special regional considerations for emissions like black carbon (BC) should also be considered (MMMCZCS, 2022b).

UNCERTAINTY AND DYNAMICS

With the understanding that future regulations will be stricter and that there are many technical solutions that can help fulfill these regulatory requirements, commercial decisions will ultimately be driven by economics. In addition to economics, the added complexity due to adoption of new technical solutions presents an integration challenge, especially as regulations develop and evolve. While techno-economic assessments can be completed, the ability to capture the broad and varying types of uncertainties and dynamics can be challenging.

Uncertainty exists due to upcoming policy and regulation, technology and alternative fuel advancements (Trivyza et al., 2022), fuel specifications and standards, customer demand, and finance sector mobilization (MMMCZCS, 2022a). Conditions are constantly changing as more knowledge is gained about potential solutions being developed and policy decisions are made, in addition to the occurrence of disruptive innovations like advanced nuclear reactor technologies or geopolitical events such as the war in Ukraine or Houthi attacks on ships in the Red Sea. Uncertainty levels are also higher because maritime decarbonization is a long-term challenge that is at least 25 years from its achievement and the regulatory, technical, and commercial solutions are not yet in place today (Erikstad & Lagemann, 2022).

Key decision-makers include policymakers, technology developers, fuel suppliers, ports, ship owners, operators, charterers, and cargo owners. Each decision-maker has its own objectives but must consider decisions being made by all others along the value chain and across the industry. A good example is the relationship between alternative fuel producers and ship owners/operators. Fuel producers might not be able to proceed with the financial investment of building a new fuel production plant without long-term off-take agreements from shipowners/operators, who are in turn reluctant to lock in high prices not knowing future market dynamics. This example highlights the uncertainty associated with customer willingness to pay the additional costs to decarbonize and the uncertainty regarding how the additional investments will be supported by the financial sector.

Questions that now need to be addressed include:

- What decarbonization targets can be realistically achieved, and by when?
- Which alternative fuels will be available, by when, and at what price?
- What can I do with my current fleet to accelerate decarbonization?
- Should I ensure my newbuilds are generically "future fuel-ready," or should I focus on specific fuels?
- What roadmap should I follow to implement the transition of my vessel or fleet?

The link between company strategy and understanding the various uncertainties and dynamics becomes more important than ever. One of the main alternative-fueled design considerations is the evaluation of optionality and conversion potential related to preparing a vessel to be converted to an alternative fuel later in the vessel's lifetime. This is mainly driven by the uncertainty around when and at what price alternative fuels will be available in the future, combined with the uncertainty around future regulations. For ammonia, it is also due to the onboard technologies not being commercially available yet, such as the engine.

Future alternative fuel availability, and associated pricing, for the maritime industry continues to be one of the main uncertainties that stakeholders need to understand and manage. To a large extent, the development of alternative fuel availability and pricing within the maritime industry will be externally driven as multiple sectors compete for a limited

supply of renewables. With renewables being a scarce resource over the next decades, Lindstad et al. (2023) suggests renewable energy should first be prioritized for replacing coal fired electricity production then to electrify road transport. Hard-to-abate sectors including shipping and aviation would be expected to continue fossil fuel use until more renewable energy becomes available.

The decisions do not stop once the vessel is delivered and is in operation, which is both a positive in the sense that there are options to mitigate any uncertainty or dynamics, but also options mean you need to constantly evaluate them and select the best for your current situation. Based on a selected baseline fuel pathway, you have options to use fuels directly onboard or decide to convert your vessel to change from one pathway to another. Especially with such long lifetimes and the aggressive industry-level targets being set, replacing newbuilds with alternative-fueled vessels will not be enough. This means that fuel conversions will need to play a role in maritime decarbonization.

One example is starting with the LNG/methane fuel pathway, you can use fossil liquid fuels like HFO, low-sulfur fuel oil, marine gas oil, use liquid biofuels like biodiesel or bio-oils, fossil-based LNG, or bio- or e-methane. Additionally, you can decide to convert to the ammonia pathway, for example. This optionality, even in operation, demonstrates the requirement to take a holistic lifecycle approach to ship design that can consider changes in operations and operational decisions (Erikstad & Lagemann, 2022).

With the tightening of EE regulations and the introduction of fuel standards like FuelEU Maritime that provides the flexibility to consider fleet-level operations and compliance, ship design will take on another dimension: fleet design. A larger system perspective that considers a fleet of vessels versus a single ship will become even more important (Erikstad & Lagemann, 2022).

When attempting to capture the main maritime decarbonization regulatory, technical and economic drivers related to ship design, the following uncertainties and dynamics should be considered:

- Timing and levels of global, regional, and local regulatory requirements related to EE, fuel standards, and market-based measures.
- Technical maturity, commercial availability, and pricing of alternative energies, fuels, and technologies.
- Customer demand and finance sector mobilization.

In addition, two key macro trends have been identified that need to be captured when attempting to better understand and model these uncertainties and dynamics:

- A holistic lifecycle approach including design and operation,
- Concepts of optionality and flexibility/changeability, and
- Fleet-level design, operations, and perspectives.

DECISION-MAKING UNDER UNCERTAINTY

Decision-making under uncertainty and dynamics is a broad and thoroughly studied research area, as well as an activity most organizations engage in regularly. With the urgency to act in an industry not easy to change, combined with many technical solutions and the introduction of various uncertainties and dynamics, the obvious next question is, how should key stakeholders make decisions?

Zwaginga & Pruyn (2022) highlight the deep uncertainties of the maritime energy transition and that, while uncertainty is not uncommon in ship design, the maritime decarbonization challenge introduces such high levels of uncertainty that new methods to deal with them are needed.

In their 2022 *Design Methodology State-of-the-Art Report*, Erikstad and Lagemann (2022) present four main design strategies that have emerged from the design spiral model: optimization, set-based, system-based, and configuration-based. While this paper is not intended to be a complete review of all ship design approaches and their applicability to the maritime decarbonization challenge, a central theme is that ships like container ships, bulk carriers, and tankers are becoming more complex and difficult to define requirements for. Transitioning from the classic design spiral to more advanced design strategies as presented by Erikstad and Lagemann (2022) can be beneficial and this section will describe some of these along with other strategic approaches that can be taken to manage uncertainty with specific examples relevant to ship design and the maritime decarbonization challenge.

Garcia Agis (2020) provides a good structure that defines four types of strategic approaches, each with several methods that can be applied: ignore (not the preferred option if the uncertainties are known), delay, reduce/control, and accept/protect. The "ignore" approach will not be covered in detail in this section as the main argument of this paper is that the use of deterministic models and approaches is not sufficient. This section will cover each of the remaining three strategic approaches (delay, reduce/control, accept/protect). The final part of this section will briefly discuss further development areas related to maritime decarbonization and environmentally sustainable ship design decision-making under uncertainty.

Delay

Delaying decisions while gaining knowledge can be a helpful approach, especially during ship design. Applicable methods include concurrent engineering, set-based design, or real options (Garcia Agis, 2020). Most uncertainties and dynamics will not go away during the design process and will continue into a vessel's operation. This is why delay methods can capture decision-making throughout the vessel's lifetime.

Pomaska & Acciaro (2022) propose a real option analysis approach to hydrogen as an alternative fuel. The analysis demonstrated the value of deferring investment decisions to get a better understanding of regulation, fuel price, and technology developments while benefiting from potentially decreased hydrogen prices in the mid-term future. Metzger (2022) presents the use of the fuzzy pay-off method for real options analysis to better understand the impact of market-based measures on the valuation of greening technologies. The potential level and timing of a price on carbon are one of the main uncertainties key stakeholders must consider. While set-based design has been proven within the ship design context, its principles could be extended to apply to a full lifecycle perspective where set convergence could continue after the delivery of a vessel on certain design and operational aspects.

Reduce/Control

Reducing or controlling uncertainty by gaining more information and increasing communication involves using scenario planning integrated into a strategic decision-making framework, data analytics, simulation, and optimization (Garcia Agis, 2020). When attempting to understand and model decision-making under uncertainty, the main goal is to increase knowledge so that uncertainties can be reduced or controlled as best as possible. Two main approaches that have been applied to the maritime decarbonization challenge are the use of scenario thinking and simulation and optimization with sensitivity analysis.

Scenario Thinking

Scenario thinking evaluates changes in specific values or metrics under different scenarios. For this type of analysis, specific scenarios need to be defined that include different values for defined variables. This could be a baseline scenario, a best-case scenario, and a worst-case scenario, for example. Scenario analysis promotes a holistic big-picture perspective that can focus efforts on important and relevant areas.

Scenario thinking is a tool that helps manage uncertainty by looking into the future and building a structure used to assign priorities (Bentham, 2023a). A good starting point for an individual stakeholder or company is to adapt broad scenario definitions such as those by Lehmacher & Lind (2022) to their specific decision-making situation and circumstances:

- "Storms: A world of nationalism, geopolitical conflicts, and a worsening climate crisis. Both the Paris climate goals and the IMO 2018 decarbonization ambitions are missed.
- Swells: Initially, businesses and governments concentrate on growth and decarbonization advances slowly. Then, as the climate crisis intensifies and disrupts shipping services and ports, quick, abrupt changes are needed and finally initiated. These are costly and cause significant disruptions. Accelerated decarbonization is late but eventually meets the Paris goals…
- Clear Sky: Politicians, business leaders, citizens, and investors worldwide align to meet the Paris climate goals..."

Mestemaker et al. (2020) presented a scenario-based life cycle assessment (LCA) method that incorporated variable fuel prices and emission costs. Scenario thinking has also been associated with improving a business's competitive advantage by acting earlier (Bentham, 2023b).

Simulation and Optimization

Multi-objective optimization and multi-criteria approaches, decision-support systems, and simulation models have been studied but have not fully addressed the need to move from deterministic to stochastic modeling while managing the increased complexity of the decarbonization problem (Mansouri et al., 2015; Frangopoulos, 2020; Frangopoulos, 2018; Trivyza et al., 2022). Methods like LCA can be used to quantify the environmental impact of a fuel or ship over its lifetime (Trivyza et al., 2022); however, LCA is a deterministic method that does not capture inherent uncertainties, for example, fuel specifications and standards. Typically, LCA is used to calculate the climate impact (in terms of GHG emissions) of an alternative fuel over its lifetime (i.e., WTW emissions).

Various decision-support tools have been developed to help evaluate and compare technologies and their impact on ship design (Robertson et al., 2022). Wei & Liu (2022) proposed a multi-objective optimization method based on a parametric ship model to reduce the negative impact of regulatory uncertainty that identified, in some cases, a ship design can be too eco-friendly based on a given regulatory scheme.

When using optimization methods and simulation models, it is important to incorporate uncertainty either by conducting sensitivity analysis or considering uncertainties during the optimization (Trivyza et al., 2022). Lagemann, Lindstad, et al. (2022) developed a deterministic model to optimize a ship's lifetime fuel and power system but identified that there is significant uncertainty related to the fuel prices and retrofit costs assumed. This highlights the need for sensitivity analysis when utilizing optimization within a decision-making framework. Lagemann et al. (2023) followed up this work with a

two-stage stochastic optimization model that considers uncertain fuel and carbon emission prices while also capturing the ability to convert to other fuels during a vessel's lifetime.

Accept/Protect

Another approach is to accept the uncertainty and develop strategies that can handle uncertainties, including adaptive control, use of margins, resilience, robust design, optimization under uncertainty, Markov Decision Process (MDP), and fuzzy decision support (Garcia Agis, 2020).

Ship design concepts of flexibility/changeability, modularity, and robustness have been studied extensively and demonstrated to be effective under uncertain lifetime conditions (Rehn et al., 2018; Choi et al., 2018; Schank et al., 2016). Lagemann, Erikstad, et al. (2022) describe the introduction of agility as a parameter for fuel-flexible ships, including preparing vessels to be converted later in life. Agility, a characteristic of flexibility and changeability, can help mitigate future unpredictability and uncertainty, for example, related to emission regulation compliance. Niese (2012) introduced a ship-centric MDP (SC-MDP) that can improve early-stage design decisions related to uncertain environmental policy and non-technical disturbances. SC-MDPs are now used in long-term strategic decision-making and can help better understand key decisions (Garcia Agis, 2020). Kana & Harrison (2017) presented a Monte Carlo approach to SC-MDP to analyze whether a containership should convert to LNG to comply with Emission Control Area regulations. The results demonstrated how variations in uncertainties can significantly impact optimal decision strategies.

While most previous case studies have been applied to ballast water treatment and air pollutant emissions like SO_X and NO_X, the same methodologies are applicable to the maritime decarbonization challenges today. A good example of this approach is the introduction of dual-fuel internal combustion engines that can utilize a mix of conventional liquid fossil-based fuels as well as alternative fuels like LNG, methanol, and ammonia. While the push for dual-fuel capability is rooted in the need for a pilot fuel for alternative fuels, it provides fuel flexibility that allows the owner to maintain the use of conventional fuels until they want or are required to use alternative fuels.

Further Development Areas

As part of a state-of-the-art review of decision support methods for sustainable ship energy systems, Trivyza et al. (2022) identified eight areas for future research, including uncertainty & stochasticity and the expansion of borders: holistic ship design and supply chain analysis. Trivyza et al. (2022) conclude their paper by noting that the maritime industry faces huge challenges due to the explosion in technological developments, the complexity of marine systems, and its conservatism, all while operating within an environment that is becoming increasingly sensitive and demanding.

While basic frameworks exist to consider maritime decarbonization decision-making under uncertainty, the latest research has also shown a need for further research in certain areas, particularly what decision-making strategies for managing uncertainty should be used for the maritime decarbonization challenge or, more likely, what strategies should be used for certain aspects of the overall challenge and how do they all connect to form an overall strategy. A comprehensive evaluation of ship design strategies and methodologies as they relate to the maritime decarbonization challenge is needed.

The methods identified above are usually best used to manage decision-making under certain types of uncertainty. This leads to the belief that there will not be one solution that fits all the challenges of the maritime decarbonization problem, but a collection of multiple strategies under an overarching framework. With increased pressure to change the way we have done things for a long time, combined with the increased complexity of the available solutions and the increased uncertainty they bring, there is a need to expand existing design strategies, approaches, methods and decision-support tools to a wider segment of the maritime industry where in the past design has not been a distinguishing or competitive advantage (most focus on producibility). This is a call to action for ship designers, and especially shipyards, to adapt their way of designing commercial vessels.

CONCLUSIONS

Responding effectively to the maritime industry's decarbonization challenge is necessitated by the urgent need to reduce GHG emissions and meet global climate targets, such as the Paris Agreement and the IMO's revised GHG strategy aiming for net-zero emissions by 2050. The maritime industry, traditionally slow to change, must undergo a substantial shift in approach due to the proliferation of alternative fuels and technological options, as well as evolving regulatory, geopolitical, and market conditions.

Figure 3 provides a summary of the maritime decarbonization cause-and-effect chain that can be used to describe the overall challenge and the knock-on effects of maritime decarbonization on ship design. Industry stakeholders, including ship designers and owners, can enhance their methods and decision-making support for ship design and operation, incorporating considerations for a change in emphasis and new focus areas, including design for efficient operation, reduced emissions per unit of energy, and carbon pricing. EETs, alternative energies and fuels, and emission reduction technologies are available or are being developed to help achieve maritime decarbonization; however, they come with emerging economic and technical considerations.

These considerations include increased ship costs and complexity, the need to rethink safety, risk assessments, and reliability, increased uncertainty, the need for a lifecycle approach, and a fleet-level perspective. The significance of emerging economic and technical considerations for shipping segments such as container ships, bulk carriers, and tankers is creating a gap that needs to be filled; a gap that academic research already has the tools to support from experience with more complex ship design activities and decision-making under uncertainty.

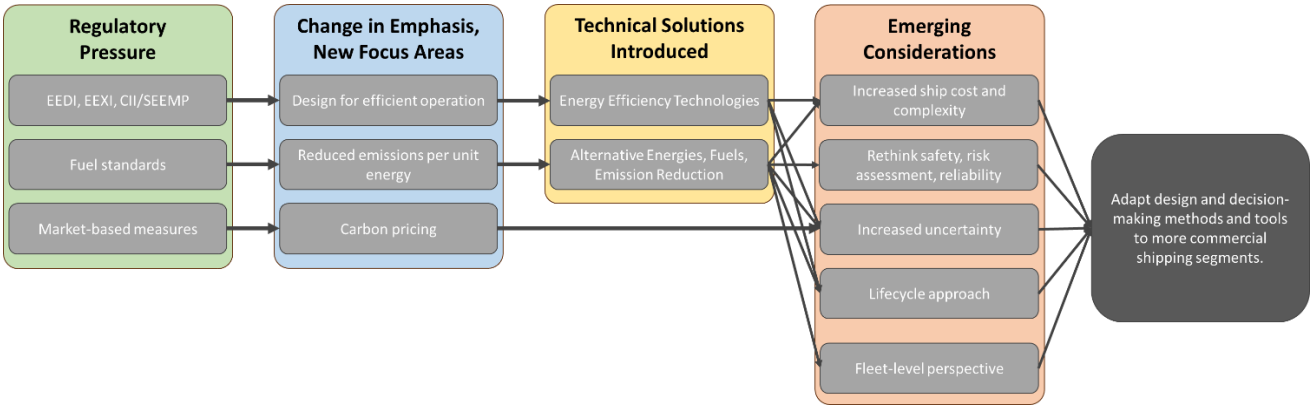

Figure 3: Maritime decarbonization ship design cause-and-effect chain

To tackle the complexities and uncertainties involved, researchers and industry practitioners must strengthen their collaboration, with each having the ability to provide valuable contributions. Researchers are called upon to ensure applications are addressing the right challenges and utilizing relevant use cases to maximize impact. Practitioners are advised to integrate advanced ship design methods and decision-making processes into their standard operations to manage uncertainties effectively.

Ultimately, there is an imperative for immediate action, suggesting that a combination of regulatory compliance, technical progress, and innovative commercial strategies is essential to decarbonize the maritime industry. Decision-making under uncertainty is an important aspect that requires new strategies, tools, and a holistic approach that includes design, operation, and fleet-level perspectives.

Considering the complexity and dynamic nature of the decarbonization challenge, the maritime industry should employ a blend of strategic approaches to manage uncertainties. It is necessary to continue research in specific areas related to decision-making under uncertainty to better support the industry in reaching its ambitious decarbonization goals.

REFERENCES

Ameri, F., Summers, J. D., Mocko, G. M., & Porter, M. (2008). Engineering design complexity: An investigation of methods and measures. *Research in Engineering Design*, *19*(2), 161–179. https://doi.org/10.1007/s00163-008-0053-2

American Bureau of Shipping (ABS) (2022), *Setting the Course to Low Carbon Shipping*. https://ww2.eagle.org/en/publication-flip/zero-carbon-outlook.html

Andrews, D. (2022, June 26). *100 Things (or so) a Ship Designer Needs to Know*. SNAME 14th International Marine Design Conference. https://doi.org/10.5957/IMDC-2022-230

Bentham, J. B. (2023a). Scenario Thinking and Its Place in Maritime Decarbonization. In M. Lind, W. Lehmacher, & R. Ward (Eds.), *Maritime Decarbonization: Practical Tools, Case Studies and Decarbonization Enablers* (pp. 71–77). Springer Nature Switzerland. https://doi.org/10.1007/978-3-031-39936-7_5

Bentham, J. B. (2023b). Scenario Thinking To Build Business Advantages That Accelerate Decarbonization. In M. Lind, W. Lehmacher, & R. Ward (Eds.), *Maritime Decarbonization: Practical Tools, Case Studies and Decarbonization Enablers* (pp. 129–140). Springer Nature Switzerland. https://doi.org/10.1007/978-3-031-39936-7_10

Business Insurance (2024). *Alternative ship fuels raise safety concerns*. Retrieved February 19, 2024, from https://www.businessinsurance.com/article/20230601/NEWS06/912357612/Alternative-ship-fuels-raise-safety-concerns.

Business Norway (2024). *Green cruising: Norway's World Heritage fjords are becoming emission free*. Retrieved February 20, 2024, from https://businessnorway.com/articles/green-cruising-norway-world-heritage-fjords-becoming-emission-free.

Calisal, S., Yurdakul, O., Kucuksu, G., & Saydam, Z. (2022, June 26). *A Decision Making Process for the Selection of Better Ship Main Dimensions with the Fuel EEDI Requirements*. SNAME 14th International Marine Design Conference. https://doi.org/10.5957/IMDC-2022-226

Choi, M., Erikstad, S. O., & Chung, H. (2018). Operation platform design for modular adaptable ships: Towards the configure-to-order strategy. *Ocean Engineering*, *163*, 85–93. https://doi.org/10.1016/j.oceaneng.2018.05.046

Comyn, G., Bruns, A., Dobie, N., Mulder, C., MacNearney, D., Gene, B., & Degirmenci, J. (2022, June 26). *H2Ocean: Design of a Hydrogen Fuel Cell Propelled Passenger Vessel*. SNAME 14th International Marine Design Conference. https://doi.org/10.5957/IMDC-2022-498

Cullinane, K., & Yang, J. (2022). Evaluating the Costs of Decarbonizing the Shipping Industry: A Review of the Literature. *Journal of Marine Science and Engineering*, *10*(7), Article 7. https://doi.org/10.3390/jmse10070946

DNV (2023), *Energy Transition Outlook 2023: Maritime Forecast to 2050, A Deep Dive into Shipping's Decarbonization Journey*. https://www.dnv.com/maritime/publications/maritime-forecast-2023/index.html

dos Santos, V. A., Pereira da Silva, P., & Serrano, L. M. V. (2022). The Maritime Sector and Its Problematic Decarbonization: A Systematic Review of the Contribution of Alternative Fuels. *Energies*, *15*(10), Article 10. https://doi.org/10.3390/en15103571

Erikstad, S., & Lagemann, B. (2022, June 23). *Design Methodology State-of-the-Art Report*. https://doi.org/10.5957/IMDC-2022-301

Esau, S., & Bentham, J. B. (2023). Decarbonization Action by Energy Companies. In M. Lind, W. Lehmacher, & R. Ward (Eds.), *Maritime Decarbonization: Practical Tools, Case Studies and Decarbonization Enablers* (pp. 387–402). Springer Nature Switzerland. https://doi.org/10.1007/978-3-031-39936-7_28

European Commission (EC) (2021). *Decarbonisation of shipping: Technical Study on the future of the Ship Energy Efficiency Design Index*. https://op.europa.eu/en/publication-detail/-/publication/207b7ff4-b3c0-11ec-9d96-01aa75ed71a1/language-en

European Maritime Safety Agency (EMSA) (2023). *Potential of Wind-Assisted Propulsion for Shipping*. https://www.emsa.europa.eu/publications/item/5078-potential-of-wind-assisted-propulsion-for-shipping.html#:~:text=Among%20the%20broad%20spectrum%20of,(GHG)%20and%20other%20emissions.

European Union (EU) (2023). *Regulation (EU) 2023/1805 of the European Parliament and of the Council of 13 September 2023 on the use of renewable and low-carbon fuels in maritime transport, and amending Directive 2009/16/EC*. https://eur-lex.europa.eu/eli/reg/2023/1805/oj

Frangopoulos, C. A. (2018). Recent developments and trends in optimization of energy systems. *Energy*, *164*, 1011–1020. https://doi.org/10.1016/j.energy.2018.08.218

Frangopoulos, C. A. (2020). Developments, Trends, and Challenges in Optimization of Ship Energy Systems. *Applied Sciences*, *10*(13), Article 13. https://doi.org/10.3390/app10134639

Garcia Agis, J. J. (2020). *Effectiveness in Decision-Making in Ship Design Under Uncertainty*.

Hansson, J., Zetterberg, L., Rootzén, J., Parsmo, R., Fridell, E., Flodén, J., Woxenius, J., Raza, Z., Christodoulou, A., Dimitrios, D., & Ölcer, A. (2023). *Impact of including maritime transport in the EU ETS*.

Herdzik, J. (2021). Decarbonization of Marine Fuels—The Future of Shipping. *Energies*, *14*(14), Article 14. https://doi.org/10.3390/en14144311

IEA (2022), *Renewables 2022,* Paris https://www.iea.org/reports/renewables-2022, Licence: CC BY 4.0

International Maritime Organization (IMO) (2013), *2013 GUIDANCE ON TREATMENT OF INNOVATIVE ENERGY EFFICIENCY TECHNOLOGIES FOR CALCULATION AND VERIFICATION OF THE ATTAINED EEDI*. https://wwwcdn.imo.org/localresources/en/OurWork/Environment/Documents/Circ-815.pdf.

International Maritime Organization (IMO) (2020), *Fourth IMO Greenhouse Gas Study*. https://www.imo.org/en/ourwork/Environment/Pages/Fourth-IMO-Greenhouse-Gas-Study-2020.aspx

International Maritime Organization (IMO) (2023), *Strategy on Reduction of GHG Emissions from Ships*. (2023). International Maritime Organization. https://wwwcdn.imo.org/localresources/en/OurWork/Environment/Documents/annex/MEPC%2080/Annex%2015.pdf

International Maritime Organization (IMO) (2024), *Market-Based Measures*. Retrieved January 25, 2024, from https://www.imo.org/en/OurWork/Environment/Pages/Market-Based-Measures.aspx

Jones, H. W. (2021). The System Complexity Metric (SCM) Explains Systems Design and is Correlated with Cost and Failure Rate. In *ASCEND 2021*. American Institute of Aeronautics and Astronautics. https://doi.org/10.2514/6.2021-4029

Kana, A., & Harrison, B. (2017). A Monte Carlo approach to the ship-centric Markov decision process for analyzing decisions over converting a containership to LNG power. *Ocean Engineering*, *130*, 40–48. https://doi.org/10.1016/j.oceaneng.2016.11.042

Kenney, M., & Palmejar, E. (2023). *DECARBONISATION TOOLKIT: A PRACTICAL GUIDE FOR DECARBONISING THE MARITIME INDUSTRY FOR A BETTER, GREENER FUTURE.* Thetius & inmarsat.

Khan, L., Macklin, J., Peck, B., Morton, O., & Souppez, J.-B. (2021, September 15). *A Review of Wind-Assisted Ship Propulsion for Sustainable Commercial Shipping: Latest Developments and Future Stakes*. Wind Propulsion 2021. https://doi.org/10.3940/rina.win.2021.05

Kim, Y.-R., & Steen, S. (2023). Potential energy savings of air lubrication technology on merchant ships. *International Journal of Naval Architecture and Ocean Engineering*, *15*, 100530. https://doi.org/10.1016/j.ijnaoe.2023.100530

Lagemann, B., Erikstad, S. O., Brett, P. O., & Garcia Agis, J. J. (2022, June 26). *Understanding Agility as a Parameter for Fuel-Flexible Ships*. SNAME 14th International Marine Design Conference. https://doi.org/10.5957/IMDC-2022-259

Lagemann, B., Lagouvardou, S., Lindstad, E., Fagerholt, K., Psaraftis, H. N., & Erikstad, S. O. (2023). Optimal ship lifetime fuel and power system selection under uncertainty. *Transportation Research Part D: Transport and Environment*, *119*, 103748. https://doi.org/10.1016/j.trd.2023.103748

Lagemann, B., Lindstad, E., Fagerholt, K., Rialland, A., & Ove Erikstad, S. (2022). Optimal ship lifetime fuel and power system selection. *Transportation Research Part D: Transport and Environment*, *102*, 103145. https://doi.org/10.1016/j.trd.2021.103145

Lagouvardou, S., Lagemann, B., Psaraftis, H.N. et al. (2023). Marginal abatement cost of alternative marine fuels and the role of market-based measures. *Nat Energy* 8, 1417. https://doi.org/10.1038/s41560-023-01360-2

Lehmacher, W., & Lind, M. (2022). *Practical playbook for maritime decarbonisation*. Nordic West Office. https://www.nordicwestoffice.com/s/NWO_Maritime_decarbonisation_final-wbxc.pdf

Lindstad, E., Ask, T. Ø., Cariou, P., Eskeland, G. S., & Rialland, A. (2023). Wise use of renewable energy in transport. *Transportation Research Part D: Transport and Environment*, 119, 103713. https://doi.org/10.1016/j.trd.2023.103713

Mansouri, S. A., Lee, H., & Aluko, O. (2015). Multi-objective decision support to enhance environmental sustainability in maritime shipping: A review and future directions. *Transportation Research Part E: Logistics and Transportation Review*, *78*, 3–18. https://doi.org/10.1016/j.tre.2015.01.012

Mærsk Mc-Kinney Møller Center for Zero Carbon Shipping (MMMCZCS) (2021), *Industry Transition Strategy*. https://www.zerocarbonshipping.com/industry-transition-strategy-report-2021/

Mærsk Mc-Kinney Møller Center for Zero Carbon Shipping (MMMCZCS) (2022a), *Maritime Decarbonization Strategy 2022: A decade of change*. https://www.zerocarbonshipping.com/publications/maritime-decarbonization-strategy/

Mærsk Mc-Kinney Møller Center for Zero Carbon Shipping (MMMCZCS) (2022b), *Determining the Impact and Role of Onboard Vessel Emission Reduction*. https://cms.zerocarbonshipping.com/media/uploads/documents/MMMC_ERA.Intro.Paper_FINAL.pdf-1.pdf

Mærsk Mc-Kinney Møller Center for Zero Carbon Shipping (MMMCZCS) (2022c). *The role of onboard carbon capture in maritime decarbonization*. https://cms.zerocarbonshipping.com/media/uploads/publications/The-role-of-onboard-carbon-capture-in-martime-decarbonization.pdf

Mærsk Mc-Kinney Møller Center for Zero Carbon Shipping (MMMCZCS) (2022d). *Reducing methane emissions onboard vessels*. Mærsk Mc-Kinney Møller Center for Zero Carbon Shipping. https://cms.zerocarbonshipping.com/media/uploads/publications/Reducing-methane-emissions-onboard-vessels.pdf

Mærsk Mc-Kinney Møller Center for Zero Carbon Shipping (MMMCZCS) (2023a). *Setting Sail on a Sustainable Course: Implications of the 2023 IMO GHG Strategy for the Shipping Industry*. https://www.zerocarbonshipping.com/publications/implications-of-the-2023-imo-ghg-strategy-for-the-shipping-industry/

Mærsk Mc-Kinney Møller Center for Zero Carbon Shipping (MMMCZCS) (2023b). *The role of energy efficiency regulations*. https://cms.zerocarbonshipping.com/media/uploads/documents/Energy_Efficiency_v9.pdf
Mestemaker, B., van den Heuvel, H., & Castro, B. (2020). Designing the zero emission vessels of the future: Technologic, economic and environmental aspects. *International Shipbuilding Progress*, *67*, 5–31. https://doi.org/10.3233/ISP-190276
Metzger, D. (2022). Market-based measures and their impact on green shipping technologies. *WMU Journal of Maritime Affairs*, *21*(1), 3–23. https://doi.org/10.1007/s13437-021-00258-8
Niese, N. D. (2012). *Life Cycle Evaluation under Uncertain Environmental Policies Using a Ship-Centric Markov Decision Process Framework.* [Thesis]. http://deepblue.lib.umich.edu/handle/2027.42/96130
Norwegian Maritime Authority (NMA) (2023). *Zero emissions in the world heritage fjords by 2026*. https://www.sdir.no/en/shipping/vessels/environment/prevention-of-pollution-from-ships/zero-emissions-in-the-world-heritage-fjords-by-2026/
Pomaska, L., & Acciaro, M. (2022). Bridging the Maritime-Hydrogen Cost-Gap: Real options analysis of policy alternatives. *Transportation Research Part D: Transport and Environment*, *107*, 103283. https://doi.org/10.1016/j.trd.2022.103283
Psaraftis, H. N. (2019). Decarbonization of maritime transport: To be or not to be? *Maritime Economics & Logistics*, *21*(3), 353–371. https://doi.org/10.1057/s41278-018-0098-8
Rehn, C. F., Garcia Agis, J. J., Erikstad, S. O., & de Neufville, R. (2018). Versatility vs. Retrofittability tradeoff in design of non-transport vessels. *Ocean Engineering*, *167*, 229–238. https://doi.org/10.1016/j.oceaneng.2018.08.057
Ren, H., Ding, Y., & Sui, C. (2019). Influence of EEDI (Energy Efficiency Design Index) on Ship–Engine–Propeller Matching. *Journal of Marine Science and Engineering*, *7*(12), Article 12. https://doi.org/10.3390/jmse7120425
Robertson, N., McNabb, J., Balchanos, M., Sudol, A., & Mavris, D. (2022, June 26). *A Design Decision-Support Environment for Evaluating the Impact of Ship Technologies*. SNAME 14th International Marine Design Conference. https://doi.org/10.5957/IMDC-2022-353
Schank, J. F., Savitz, S., Munson, K., Perkinson, B., McGee, J., & Sollinger, J. M. (2016). *Designing Adaptable Ships: Modularity and Flexibility in Future Ship Designs*. RAND Corporation. https://www.rand.org/pubs/research_reports/RR696.html
Sun, L., Wang, X., Lu, Y., & Hu, Z. (2023). Assessment of ship speed, operational carbon intensity indicator penalty and charterer profit of time charter ships. *Heliyon*, *9*(10), e20719. https://doi.org/10.1016/j.heliyon.2023.e20719
Tacar, Z., Sasaki, N., Atlar, M., & Korkut, E. (2020). An investigation into effects of Gate Rudder® system on ship performance as a novel energy-saving and manoeuvring device. *Ocean Engineering*, *218*, 108250. https://doi.org/10.1016/j.oceaneng.2020.108250
Trivyza, N. L., Rentizelas, A., Theotokatos, G., & Boulougouris, E. (2022). Decision support methods for sustainable ship energy systems: A state-of-the-art review. *Energy*, *239*, 122288. https://doi.org/10.1016/j.energy.2021.122288
Ustolin, F., Campari, A., & Taccani, R. (2022). An Extensive Review of Liquid Hydrogen in Transportation with Focus on the Maritime Sector. *Journal of Marine Science and Engineering*, *10*(9), Article 9. https://doi.org/10.3390/jmse10091222
Wang, H., Trivyza, N., Boulougouris, E., & Mylonopoulos, F. (2022, June 26). *Comparison of decarbonisation solutions for shipping: SNAME 14th International Marine Design Conference*. https://doi.org/10.5957/imdc-2022-297
Wei, Q., & Liu, Y. (2022, June 26). *Ship Design Optimization Framework Considering Future Uncertain Carbon Emission Regulations*. SNAME 14th International Marine Design Conference. https://doi.org/10.5957/IMDC-2022-232
Zwaginga, J. J., & Pruyn, J. F. J. (2022, June 26). *An Evaluation of Suitable Methods to Deal with Deep Uncertainty Caused by the Energy Transition in Ship Design*. SNAME 14th International Marine Design Conference. https://doi.org/10.5957/IMDC-2022-252

Part 2:
DESIGN METHODOLOGY

Proceedings of 15th International Marine Design Conference (IMDC-2024)
June 2-6, 2024
Amsterdam, the Netherlands

SATISFACTION OF PASSENGERS – PROCESS COMPARISON BETWEEN TWO CRUISE SHIP CLASSES

Sabina Akter[1,*] and Jani Romanoff[2]

ABSTRACT

In cruise ship design, a ship designer often focuses on the ship's function, while a cruise operator's focus is on the creation of a comfortable and enjoyable cruise experience for passengers. Today, these two viewpoints are strongly connected, and thus, the way the inside of a ship is designed can impact how satisfied passengers are on their cruise journey. Thus, we need to figure out the best way to design a passenger ship from the perspective of the passengers themselves. In this paper, we analyse the differences in the combination passenger ship environmental elements and overall consumer satisfaction in two different cruise ship classes from the same ship operator, but from different eras. First, we present a theoretical framework and model for the cruise ship environment that consist of ambient, layout/design, social, product/service and onboard enjoyment factors. Then, by using data collected from the public domain, we compare two types of cruise ships using open-source data (N=755). This allows us to identify the factors contributing to the discrepancy in expectations across cruise guests. Based on this limited data, we create several linear regression models which indicates a favourable and statistically significant link between environmental elements and passengers' conduct while on board. Information processed this manner can be utilised to make informed decisions on cruise ship layout and amenities. In addition, the developed innovative KPI proved instrumental in influencing decision-making processes related to cruise ship designs and operations. Therefore, the findings from our research show a positive link between the onboard environment and the overall happiness of passengers.

KEY WORDS

Cruise class comparison; Process comparison; Onboard environmental factors; Customer Satisfaction; Cruise experience.

INTRODUCTION

Ships design is determined by their intended purpose or mission. Levander (2004) says that we start making a passenger ship by first understanding the customer's needs or the ship mission. When putting together a ship, different people might focus on different aspects. For instance, a naval architect might concentrate on the cost and how the ship works, while an interior designer might want to make the inside of the ship as pleasant as possible. Thus, we need to fully understand how best to design a passenger ship from a passenger's viewpoint.

Cruise ships are complex and their performance is not measured only by technical key-performance indicators (KPI), but also by cruise travellers' experience. The technical KPIs for cruise ships are well-documented; for example, in the chapter by Levander (2004) in the Ship Design and Construction. These include factors like GT/pax and crew/pax, which directly indicate the quality in terms of volume of the ship per passenger and service per passenger. However, this information is often

[1] Sabina Akter (Department of Mechanical Engineering, Aalto University, Espoo, Finland); ORCID: 0000-0003-3331-907X
[2] Jani Romanoff (Department of Mechanical Engineering, Aalto University, Espoo, Finland); ORCID: 0000-0002-4642-0225
* Corresponding Author: sabina.akter@aalto.fi

Submitted: 5 February 2024, Revised: 17 April 2024, Accepted: 1 May 2024, Published: 24 May 2024

Conference paper, DOI: https://doi.org/10.59490/imdc.2024.892 e-ISSN: 3050-486

too general to provide a descriptive understanding of cruise experience itself and the effect of ship and cruise designs on the overall satisfaction of the passengers.

In recent tourism studies, tourist satisfaction has become the core concept of tourist behavioural studies (Huang et al., 2015). Therefore, cruise passengers, who are a pivotal group in the cruise industry, play a crucial role in the cruise purchasing cycle and thus their behaviour must be better understood. They make purchasing decisions periodically, but from the cruise industry's perspective, it is challenging to track and understand these decision-making processes and identify which aspects no longer satisfy the passengers' needs and expectations. On the other hand, building and maintaining clear lines of communication and transparency within the organization is pivotal to spotting and solving potential problems before they escalate. Routine reporting is advocated to promptly identify and correct performance issues, increasing visibility and accountability throughout project management. Collaboration between experts and customers is crucial for enhancing project outcomes. Ongoing customer feedback is instrumental in refining product quality and meeting customer expectations.

Individuals responsible for decision-making often tend to favour certain evaluative criteria over others. This bias is generally represented through the differential weighting assigned to each criterion. Upon deriving an initial ranking of decisions, these individuals might find it necessary to re-evaluate and adjust their original preferences. The discipline of multiple-criteria decision-making primarily deals with identifying and selecting the best possible choices (Gou et al., 2016). Businesses employ data mining, regression analysis and KPI techniques to discern consumer purchasing behaviours, enabling them to tailor their sales strategies and provide personalised customer services. Data-driven clustering methods are used to truly understand customer behaviour or tendencies. A significant obstacle in this area is the obfuscation of critical information due to its dispersal across the Internet and elsewhere. The exhaustive search for pertinent data is not only time-intensive and resource-consuming but is also frequently unsuccessful due to the vast amounts of irrelevant information. In many advanced organisations, the current strategic focus is on enabling dynamic decision-making. This requires consideration of several key aspects: acquiring and analysing real-time data, understanding the interconnectedness of data sets, and engaging users with data-driven strategic approaches. Analysing consumer behaviour is critical for generating system-driven recommendations in consumer-centric decisions.

Executives must quickly interpret this data, as timely and updated insights are crucial for adapting organizational strategies to meet market demands. Multi-attribute decision-making (MADM) involves selecting the most satisfying option from a range of alternatives, each characterised by specific attributes, a process inherent in human activities (Xu & Zhang, 2013). Therefore, ineffective data communication can lead to an organization's inability to fulfil customer expectations. Sustaining an organization in the contemporary market requires continual evolution and adaptation aimed at customer satisfaction, which necessitates a thorough assessment of organizational processes for effectiveness and efficiency. The present process is highlighted due to its complexity and propensity for errors. Simplifying and streamlining these processes is essential so all stakeholders understand the required actions clearly. An optimised process is anticipated to enhance efficiency, reduce customer complaints, and increase satisfaction for both customers and executives.

The cruise industry requires a systematic approach for continuous improvement, especially concerning passenger decision-making processes and the onboard environment including layout, ambience, service, and social features (see Akter et al. 2021 a and b), see Figure 1. In Figure 1, the entire circle represents overall satisfaction, which is essentially the overall rating of the cruise. The individual segments of the circle represent different aspects of the onboard experience, including ambient conditions, layout and design, social interactions, quality of products and services, and the overall enjoyment. These factors are regarded as independent variables that can influence overall satisfaction, which is considered the dependent variable in this context. Furthermore, it's important to note that the independent variables may vary in their impact based on different scenarios and circumstances (Tsiotsou, R. H., & Wirtz, J. 2015; Akter et al., 2021 a).

Currently, the cruise industry heavily relies on the knowledge and skills of senior coordinators of ship design and building, and cruise operations, who process the information, make decisions, and pass on information and expertise to less experienced staff. The cruise experience environmental performance metrics are neither measured nor communicated between the stakeholders and real-time monitoring systems for establishing necessary Key Performance Indicators (KPIs) are not in place. Customer feedback, irregular and potentially biased, serves as the sole source of performance data, offering a view that may be disproportionately positive, neutral, or negative. Identifying customer issues is essential for continuous improvement of the cruise ships. Thus, this study introduces the cruise environment model proposed by Akter et al. (2021 a and b), which encompasses critical components such as ambient, layout/design, social engagement, product/service quality, and onboard enjoyment factors. This paper specifically emphasises the explanation of various environmental elements and the correlation between onboard environmental factors and an evolved Key Performance Indicator (KPI) is determined based on the absolute net score of the customer feedback measured with Likert scale. The computation of the KPI is automated using a standard procedure that processes customer reviews.

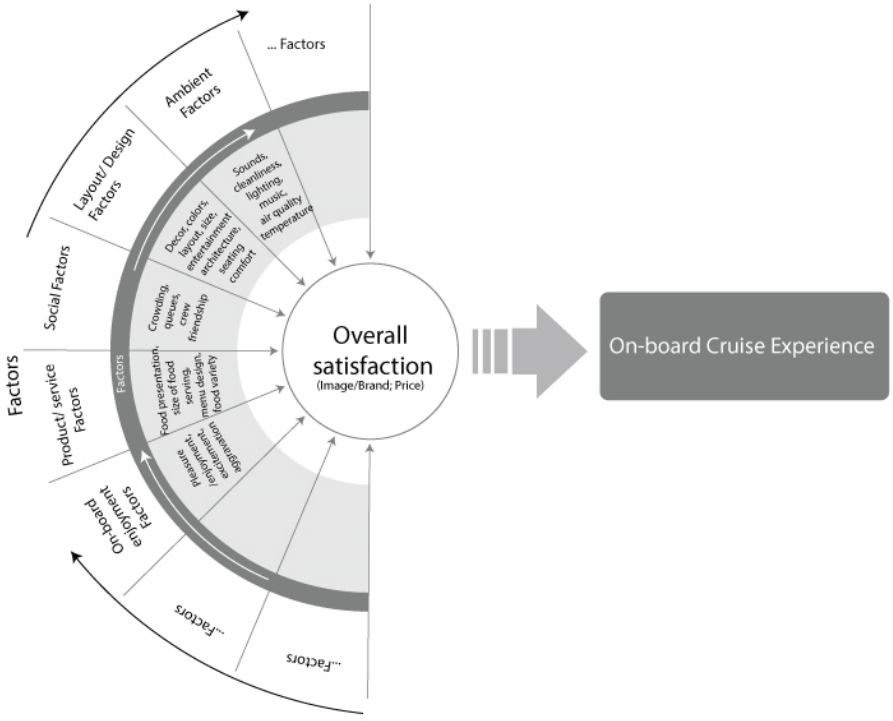

Figure 1: approach to describe onboard environmental factors affecting the onboard experience of cruise passengers'(Akter et al., 2021 a)

THEORETICAL BACKGROUND

Process and Key Performance Indicators (KPIs)

Key Performance Indicators (KPIs) are set to track and measure the performance of any advanced system. Establishing robust communication and transparency within the organization addresses the challenge of poor information flow, facilitating early problem detection. It is advisable to utilise daily reports to identify and address performance discrepancies quickly. This practice enhances visibility and accountability throughout project implementation. Establishing solid collaboration between experts and customers is crucial. In an organization such as the cruise industry, it is practical for supervisors to regularly update or auto-update projects. A steady flow of customer updates can improve production quality and meet customer demands effectively. Employing Key Performance Indicators (KPIs) is essential for tracking performance metrics. The challenge in cruise ship application is that the performance in service can be changed during and between the cruises, while issues related to the layout can be only significantly changed during ship conversions or dockings. Thus, the KPI developed must account for this bias in implementing corrective measures.

Services should be viewed as processes rather than mere outputs. The three-stage service usage model suggests that customers experience three key phases when using services: pre-purchase, service encounter, and post-encounter (Lovelock and Wirtz 2011; Tsiotsou and Wirtz 2012; Tsiotsou and Wirtz, 2015). Studies have explored each stage to understand their key factors, influences (both direct and indirect), processes, and results (Tsiotsou and Wirtz, 2015).

The pre-purchase stage: The pre-purchase phase in service decision-making is notably more intricate than that for products due to a broader range of factors and actions (Fisk 1981; Tsiotsou and Wirtz, 2015). Consumers are active participants in creating the service, so their decision-making process is longer and more complex. Consumer expertise, knowledge, and perceived risk are significant during this initial phase (Tsiotsou and Wirtz, 2015). Services, characterised by their experiential and credence attributes, are typically more challenging for consumers to evaluate before purchase (Mattila and Wirtz 2002; Zeithaml 1981; Tsiotsou and Wirtz, 2015).

The service encounter stage: Customers interact with the service provider during the service encounter stage. At this point, customers are not just buyers but active participants, helping to shape their own experiences and the final service delivered while assessing the service quality (Tsiotsou and Wirtz, 2015). Consumer engagement involves actions that show support or criticism of a service, such as giving positive feedback, recommending services to others, assisting fellow customers, blogging, posting reviews, or even taking legal actions (van Doorn et al. 2010). Recent studies highlight that consumer engagement is multifaceted, involving thinking (like being fully absorbed), feeling (such as commitment), and doing (such as energetic participation and interactions) (Brodie et al. 2011; Tsiotsou and Wirtz, 2015). Service encounters offer opportunities

for customers to develop and either positively or negatively enhance their engagement with a service provider (Tsiotsou and Wirtz, 2015). These encounters are intricate, involving customer interactions and the setting influencing consumer expectations, contentment, loyalty, intentions to repurchase, and the likelihood of recommending the service to others (Tsiotsou and Wirtz, 2015).

The post-encounter stage: The final phase of service consumption is the post-encounter stage, which encompasses consumers' behavioural and attitudinal reactions to the service experience. Research in this stage has predominantly focused on consumer satisfaction and perceived service quality due to their significant impact on business performance (Brady and Robertson 2001; Tsiotsou and Wirtz, 2015). However, satisfied consumers with high perceptions of service quality may only sometimes become repeat customers or continue using the same service provider (Keiningham and Vavra 2001; Tsiotsou and Wirtz, 2015). Therefore, recent consumer research has shifted its focus to other crucial post-purchase outcomes, including perceived service value, consumer delight, how consumers respond to service failures (e.g., complaints and switching behaviour), and how they react to service recovery efforts. This perspective is supported by Tsiotsou and Wirtz (2015).

Onboard Environment Factors

The servicescape of a cruise company encompasses a range of physical and social factors. As Bitner (1992) identified, the physical dimensions include ambient conditions, spatial layout, and functionalities, all enriched by various signs, symbols, and artistic elements. Beyond the tangible aspects, the social environment and the sense of enjoyment on board, generated by the interactions of those present on the ship, also play a vital role. Akter et al. (2021 a and b) proposed a categorization that expands this concept to include ambiance, layout/design, social dynamics, product/service quality, onboard enjoyment factors, and the overall satisfaction. These aspects are detailed in Table 1. The ambient conditions, highlighted by Jeon and Jeong (2009), consist of sensory elements such as temperature, colour, lighting, noise, music, and scent. These elements shape customers' perceptions of the cruise service environment.

Functional components such as architectural design, spatial layout, and functionality are essential in-service environments. They dictate the placement and interrelation of items like furniture, equipment, and service areas crucial for exhibitors to deliver services effectively. Such arrangements directly impact customer comfort and their emotional reactions. The physical environment's design, including ambiance, layout, and functionality, significantly influences consumer behaviour toward a service or business. Functionality specifically pertains to the enhancement of the service process and customer experience. Creating a user-friendly setting is crucial for customer satisfaction, as detailed by Rosenbaum and Massiah (2011).

In addition to the physical environment, a customer's decision-making process is also swayed by social elements and the service or product quality (Andersson, 2013). The servicescape model posits that the collective emotions within a service setting are mirrored by the interactions among employees, customers, and the venue's social density (Dad et al., 2016). It has been observed that several product and service dimensions, namely the culinary experience, presentation of dishes, size of servings, menu creativity, diversity of cuisine, and calibre of service, are critical to customer satisfaction (Akter et al., 2021a and b). The factors contributing to pleasure while onboard are linked to emotional states such as happiness, joy, excitement, and overall engagement. It has been further noted that a customer's comprehensive satisfaction correlates with aspects including the nation of service, the establishment's brand image, pricing, symbolic elements, artefacts, and the experience of value for money (Akter et al., 2021a and b), see Table 1.

Table 1: Attributes of onboard environmental factors and overall satisfaction (extended from Akter et al., 2021a and b)

Ambient Factors		
	Dimensions	**Attributes**
	sounds	music /sound effects; audio (music, noise); favourite sounds; auditory cues /elements. (e.g. music, noise; non-musical sound; music/sound effects; background music; both a quiet and loud disco, piano music acoustics, noise/ noise (level, pitch)
	cleanliness	cleanliness (scent, air quality, fragrance); cleanliness: coins, ashtrays, ceiling, machine screens, employees appearance, overall cleanliness; aesthetic cleanliness
	lighting/ light	visual aesthetic (lighting)
	air quality	air quality e.g. temperature, humidity, circulation /ventilation; ambient (temperature)
	odour	aroma/scents; olfactory cues (scent, air quality, fragrance)
	taste/smells	sensory component: seeing, hearing, smelling, touching, tasting; textures
	comfort and discomfort	seating comfort, seating comfort: seat back, elbow room, distance from table, overall comfortableness, easy in and out, comfortable furniture uncomfortable chairs, comfortable workspace
	color	colors used; color schemes; visual aesthetic
	atmosphere	atmosphere refers specifically to relaxing, having fun, home- and country-specific
	visual attractiveness	quality photos, animation effects, virtual tour; visual (e.g. lighting, colors, brightness, shapes visual aesthetic (shapes); materials sensory elements e.g. color, light, texture; variety, uniqueness, quality
Layout/design factors		
	Dimensions	**Attributes**
	style of décor	interior décor; design; interior design e.g. layout/ store layout/layout accessibility/overall structure/layout; design characteristics e.g. form, size, texture, animation; décor e.g., furniture, fixtures, artifact; the design of the outdoor areas, and a calm experience; separate design area for all age groups; classical and stylish restaurants; interior (design, equipment, furniture, layout); design factors: floor and carpet, aisle width, wall composition, paint and wallpaper, ceiling composition, merchandise, layout, drink placement, bar placement, cash register placement, waiting areas, waiting rooms, dance floor locations, traffic flow, queues, furniture, point of purchase displays, signs and cards, wall decoration, license and certificates, artwork, product displays, price displays, entrances; furniture; arrangement of furniture equipment; interior décor: background colors, electric signs design, wall treatment design, floor treatment design, overall design attractiveness; the design of the outdoor areas, and a calm experience; exterior factors: exterior signs, display windows, surrounding stores, address and location, architectural style, surrounding area, parking, exterior walls; luxuriously styled areas such as large windows provide a unique and beautiful panoramic view of the sea; ocean-view balconies; perceived services cape for exterior (external) variables e.g. entrance, parking, architecture, design, exterior design, surrounding area location and so on; landscape, architecture, parking; design and arrangement of buildings
	colours/ style of décor (incl. colour)	architecture, color; aesthetic e.g. color, style; aesthetic e.g.materials décor
	scale/size	shape, room/cabin size, spacious, modern and comfortable cabins; aesthetic e.g. scale shape: spacious, modern and comfortable cabins; space/function; shapes, symbols; signs, symbols and artefacts e.g. signage/ directional signage; informational signage, interpretational signage; personal artifacts
	architectural entertainment	product/service: room, restaurant, ball room, fitness center, kids center, uniqueness/hotel, resort, boutiques, and galleries; bathroom: bath, shower; basic amenities; considerations: non-smoking, swimming pool, high speed internet, fitness center, pet

Submitted: 5 February 2024, Revised: 17 April 2024, Accepted: 1 May 2024, Published: 24 May 2024

Conference paper, DOI: https://doi.org/10.59490/imdc.2024.892 e-ISSN: 3050-486

		allowance, promenade and comfort; object-based authenticity: architecture impression, peculiarities of interior design, attractive historical town, heritage information; architecture; aesthetic e.g. architecture
	comfort or arrangement of seating	uncomfortable chairs, comfortable workspace
	space/function/layout and quality	layout e.g. easy to move, convenience; overall structure; traffic flow; way finding; quality of product: form, quality of performance, durability, design; assortment e.g. variety, uniqueness, quality; more single seating, more group seating , separate design area for all age groups; aesthetic e.g. texture, pattern; product display; overall structure/layout, navigation, way finding, the nine-story atrium, direct access to the spa, ocean-view balconies; use of space, space/function; need enough workspace; alternative space solutions; space/function consists of layout, equipment and furnishing; accessories-functional e.g., layout, comfort, signage, accessories
	product/furniture/displays	product display; furnishings; product assortment; amenities (tools, IT, equipment); equipment/ electric equipment and display/dining equipment; equipment, space/function: lounge (socializing), kitchen, toilet/shower, equipment (XX); furnishings, spatial crowding
Social factors		
	Dimensions	**Attributes**
	crowding	the level of crowd, the type of crowd; lack of privacy
	queues	front desk/check in
	friendliness of the crew	staff: attitude, enthusiasm, politeness, courteous, commitment, friendliness, staff quality; staff behaviour: customer orientation credibility; suitable behaviour; friendly staff, helpful staff, personalized, always there employee response: enjoy working and helping guests, feel happy; the nature of interactions; personal service; crew members' language skills and communication
	embarkation experience (employee-customer support, customer-to-customer interaction)	crew members' communication; friendly, helpful, happy, always look happy, cozy and welcoming atmosphere, homelike, security; privacy; personal service; crew members' language skills and communication; customer: being friendly with other guests; number, type and behaviour of customers and employees; customers: customer types, number, appearance; employees: service, personal, number, appearance, uniforms; customers' image, employees' image; social interactions between and among customers and employees; employees, customers, social density, displayed emotions of others; verbal interaction; interaction with others; reference groups, reviews ; seeing others as motivation, others as distraction ; social scape: social relationship; displayed emotions of others (emotional contagion); service relationship ; in between salespeople relationship quality, salespeople store manager relationship quality; surroundings: couple-friendly, children-friendly; maintenance standard; employees' good/bad lookin; employees: service, personal, number, appearance, uniforms , physical appearance, both casual and formal attire with some preferring more casual dress; staff image: competence physical attractiveness, in addition, personal service: both casual and formal attire with some preferring more casual dress
Product/service factors		
	Dimensions	**Attributes**
	food quality	food and service experience refer specifically to food quality: delicious food and beverages
	food variety	food variety: in culinary terms such as offering many choices, cuisine offering almost all tastes, offering a '50s-style diner, American fast food, serving a variety of coffees, offering Italian food with five different restaurants, 12-13 bars with a wide variety of beverages
	food presentation	food presentation: providing different possibilities for enjoying food, providing the panoramic views through the meter-high glass; the size of food servings, menu design, the variety of food, food experience, variety, uniqueness,
	service experience	offers personal, friendly, professional and 24-hour free cabin service, etc. ;service interface: service person (customer room service), technological support, call center, service guarantee, facility, security; service experience of expenses on-board refer specifically to the cost of a bottle of wine around 22 USD and above ; passengers need to pay 11 and 12 USD as a service charge per day ; additional charge for a table reservation, private experience, and private chef facilities ; a service charge added to the

		drink prices ; whereas no additional charge for a pizzeria or sea view café ; an extra charge for breakfast in the cabin, and so on ; product/product characteristics: convenience vs. specialty, durable vs. nondurable; mattress, pillow comfort; complementary product, material; price (expensive, discounted, or affordable); additional charge; Environment -approval, others e.g. customer service, window display
	serviceability factor	convenience in layout, privacy, communication, w/staff wayfinding, cleanliness.
	Service encounter	service encounter- product quality e.g. variety /choice; value for money
	perceived serviceability	way finding, privacy protection, comfortable furniture, conduciveness to communication with staff, convenient layout
On-board enjoyment factors		
	Dimensions	**Attributes**
	pleasure or enjoyment; entertainment/emotional experience	entertainment experience activity includes a surf simulator; a romp in the aqua park; bathing in two whirlpools that hang XX metres above the sea; a sky pad virtual reality experience; a glow-in-the-dark laser tag facility; the "perfect storm" waterslide trio for all water lovers aboard; wall climbing; swimming pool; long water slide; sauna; mini-golf; enjoying fascinating shows; a 4d cinema; escape room; musical evenings, musical evenings; musical evenings; big casino; a disco; many bars; art auctions and has around XX paintings and sculptures; classic bingo games and lectures; various shops to avoid boredom, and so on; excitement, aggravation; consumer attitudes: innovativeness; variety, uniqueness, quality
	sports, fitness, and wellness	entertainment experience activity includes sports, fitness, and wellness refer specifically to sports and leisure activities for people of all age groups, or mostly focuses on younger groups of people; inside and outside the sports court; fitness gyms; a spa offering many different treatments for fees; a spacious fitness area with a splendid ocean view; a pool with a relaxation area; fitness centre and courses, XX square metres of facilities for wellness and relaxation; a large samsara spa and treatments, and so on
Overall satisfaction		
	Dimensions	**Attributes**
	country image or brand	cruise brands (an American or an Italian or other); includes a brand with an incredible history; the image of the country of its builders (Finland, German, Italy, other etc.); preferably focusing on all age groups or a mostly younger group of people; family-friendly ships; largest cruise ship; utility: market value brand, term and conditions, location convenience, price range, reputation, overall quality, risk management, trust, security
	price/ cost experience	price: discount, price conformity to product quality; cost experience; such as a good return on value for money, ticket price; choice: comparison, star-ratings, pictures, sorting facility, reviews, offers; in details, price e.g. loyalty program, member card, events program, advertisement; in details, promotion e.g. advertisement, sales promotion, personal selling, public relation; customer relationship: loyalty program, previous usage experience; consumer attitudes (e.g., price sensitivity, involvement, innovativeness)
	sign, symbol and artefacts	such as a slow cruise, a real adventure; often feeling as if the passengers are on board a floating city; physical clues; maps and painting; search aids & slogans: keywords, meta-tag, slogans
	approach/avoidance	switching behaviour, switching intent; customers e.g. individual response - approach e.g. affiliation, exploration, stay longer, commitment, carry out plan avoid

MODEL AND RESEARCH METHODOLOGY

To examine the environmental factors affecting the onboard customer experience, Akter et al., (2021a and b) have identified following key factors: ambient, layout/design, social, product/service, and onboard enjoyment factors that result in overall satisfaction. To connect the passenger overall satisfaction to these elements of design, we have sorted the questions of one openly available website Cruisecritic according to these dimensions. The questions used on the website are about cabin quality, public rooms, family, embarkation, dining, service, value for money, entertainment, fitness and recreation and overall satisfaction. The questionnaire is divided into six sections. The questions of the first factor are related to *ambient factors* such as sounds, cleanliness, lighting, music, temperature, air quality, odour, etc., which impact the question related to, for instance, the cabin and public rooms. On the other hand, the *layout/design* factors of the cruise consisted of interior design, entertainment architecture, etc., which in turn impact questions about cabin, public rooms, family. Moreover, the *social factors* of the cruise consist of crowding, queues, crew friendship, embarkation experience, etc., influence questions about embarkation procedures and family interactions. *Product/service* factors of the cruise involve food experience, service experience, etc., which refer to questions regarding dining, service, and value for money. *Onboard enjoyment* factors of the cruise lie in pleasure or enjoyment, excitement, aggravation, entertainment experience, etc., referring to the questions regarding entertainment and fitness and recreation. In addition, factors contributing to *overall customer* satisfaction include the country image or brand and price, etc., impacting questions regarding questions about overall satisfaction and value for money. Respondents were requested to provide their agreement level of each item on a five-point Likert scale, where 1 is considered "strongly disagree," and 5 is "strongly agree. The answers were weighted as arithmetic means of the scores of the sub questions." The overall passengers' satisfaction is modelled with a regression model:

$$Ys = \beta o + \beta 1X1 + \beta 2X2 + \beta 3X3 + \beta 4X4 + \beta 5X5 + e \quad [1]$$

where Ys = tourists' overall level of satisfaction, βo = constant (coefficient of intercept), X1 = ambient; X2 = layout/design; X3 = social; X4 = product/service and X5 = onboard enjoyment factors; β1,..., β5 = regression coefficients and e = error term. We use the data from two ship classes from Royal Caribbean Cruise Lines: Freedom (3 ships, built 2006-2008) and Radiance class ships (4 ships, built 2001-2004). The ships present different eras of design and sizes, see for technical details and KPI's (crew to passenger, GT to passenger and stateroom to passenger -ratio) Table 3.

Table 2: Onboard environmental factors for cruise- Freedom and Radiance class effects on the onboard cruise experience

Factors	Dimensions	Case company's elements	Questions number
Ambient Factors	Sounds, cleanliness, lighting, music, temperature, air quality, odour, and so on	cabin, public rooms	1A, 1B
Layout/ design Factors	Style of décor, colours, size, architectural entertainment, the comfort or the arrangement of seating	cabin, public rooms, family	2A, 2B, 2C
Social Factors	Crowding, queues, the friendliness of the crew, embarkation experience	embarkation, family	3A, 3B
Product/ service Factors	Food presentation, the size of food servings, menu design, food variety, food experience and food quality; service, service experience provided by companies	dining, service, value for money	4A, 4B, 4C
Onboard enjoyment Factors	Pleasure or enjoyment, excitement, aggravation, emotional response, emotional experience, entertainment experience	entertainment, fitness and recreation	5A, 5B
Overall satisfaction	Country image or brand, sign, symbol and artefacts; price, cost experience	overall, value for money	6A, 6B

Submitted: 5 February 2024, Revised: 17 April 2024, Accepted: 1 May 2024, Published: 24 May 2024

Conference paper, DOI: https://doi.org/10.59490/imdc.2024.892 e-ISSN: 3050-486

Table 3: Ship Facts

Ship Facts	**Royal Caribbean International - Freedom-class cruise ships** • The Freedom of the Seas • The Liberty of the Seas • The Independence of the Seas			**Royal Caribbean International - Radiance- class cruise ships** • The Radiance of the Seas • The Brilliance of the Seas • The Serenade of the Seas • The Jewel of the Seas			
Cruise name	**The Freedom of the Seas Facts**	**The Liberty of the Seas Facts**	**The Independence of the Seas Facts**	**The Radiance of the Seas Facts**	**The Brilliance of the Seas Facts**	**The Serenade of the Seas Facts**	**The Jewel of the Seas Facts**
Built in	2006; renovated 2015	2007	2008; renovated 2018	2001; last renovated 2016	2002; last renovated 2013	2003; last renovated 2012	2004; last renovated 2016
Builder	Kvaerner Masa-yards, Turku Finland			Meyer Werft yard, Papenburg, Germany			
Tonnage	156,271 GT	154,407 GT		90,090 GT			
Length	1,112 ft			962 ft		965 ft	962 ft
Wide/ beam/width	185 ft	185 ft	185 ft	106 ft	106 ft	106 ft	106 ft
Draft/ draught	29.5 ft	28 ft	28 ft	28 ft	28 ft	28 ft	28 ft
Speed	21.6 knots	21 knots	21.6 knots	25 knots			
Guest capacity	3,934 (double occupancy); 4,553 (total)	3,798 (double occupancy), 4,960 (total)	3,858 (double occupancy), 4,560 (total)	2,143 (double occupancy), 2,466 (total)	2,142 (double occupancy), 2,543 (total)	2,146 (double occupancy), 2,476 (total)	2,191 (double occupancy); 2,702 (total)
Decks	14 guest, 15 total, 14 passenger elevators			12 guest, 13 total, 9 guest elevators			
Crew	1,447 (internationa)	1,360 (internationa)	1,440 (internationa)	894 (international)	848 (international)	848 (international)	852 (international)
Staterooms	1,967	1,899	1,929	1,071	1,070	1,073	1,097
GT/pax	34.32	31.13	33.86	36.53	35.43	36.39	33.34
Crew/pax	0.32	0.27	0.32	0.36	0.33	0.34	0.32
Stateroom/pax	0.43	0.38	0.42	0.43	0.42	0.43	0.41

Sources: (Extended from Akter et al., 2021b)

Submitted: 5 February 2024, Revised: 17 April 2024, Accepted: 1 May 2024, Published: 24 May 2024

Conference paper, DOI: https://doi.org/10.59490/imdc.2024.892 e-ISSN: 3050-486

DATA ANALYSIS AND DISCUSSION

Freedom class had 385 respondents (Freedom of the Seas 105, Liberty of the Seas 127, Independence of the Seas 153), and Radiance class, 370 respondents (Radiance of the Seas 62, Brilliance of the Seas 72, Serenade of the Seas 115, Jewel of the Seas 121), from the Cruisecritic website covering the period from January 1st 2019 to October 26th 2022 (total 773 respondents). The cruise company pays close attention to various aspects of the onboard cruise experience, such as cabin quality, public rooms, family, embarkation, dining, service, value for money, entertainment, fitness and recreation, and overall satisfaction. While some of questions may be related and interconnected, they are crucial for evaluating different aspects of the cruise experience and the overall process satisfaction. The post-travel experience per onboard environmental factors is summarised in Appendix and Figure 2. The regression model parameters are summarised in see Table 4.

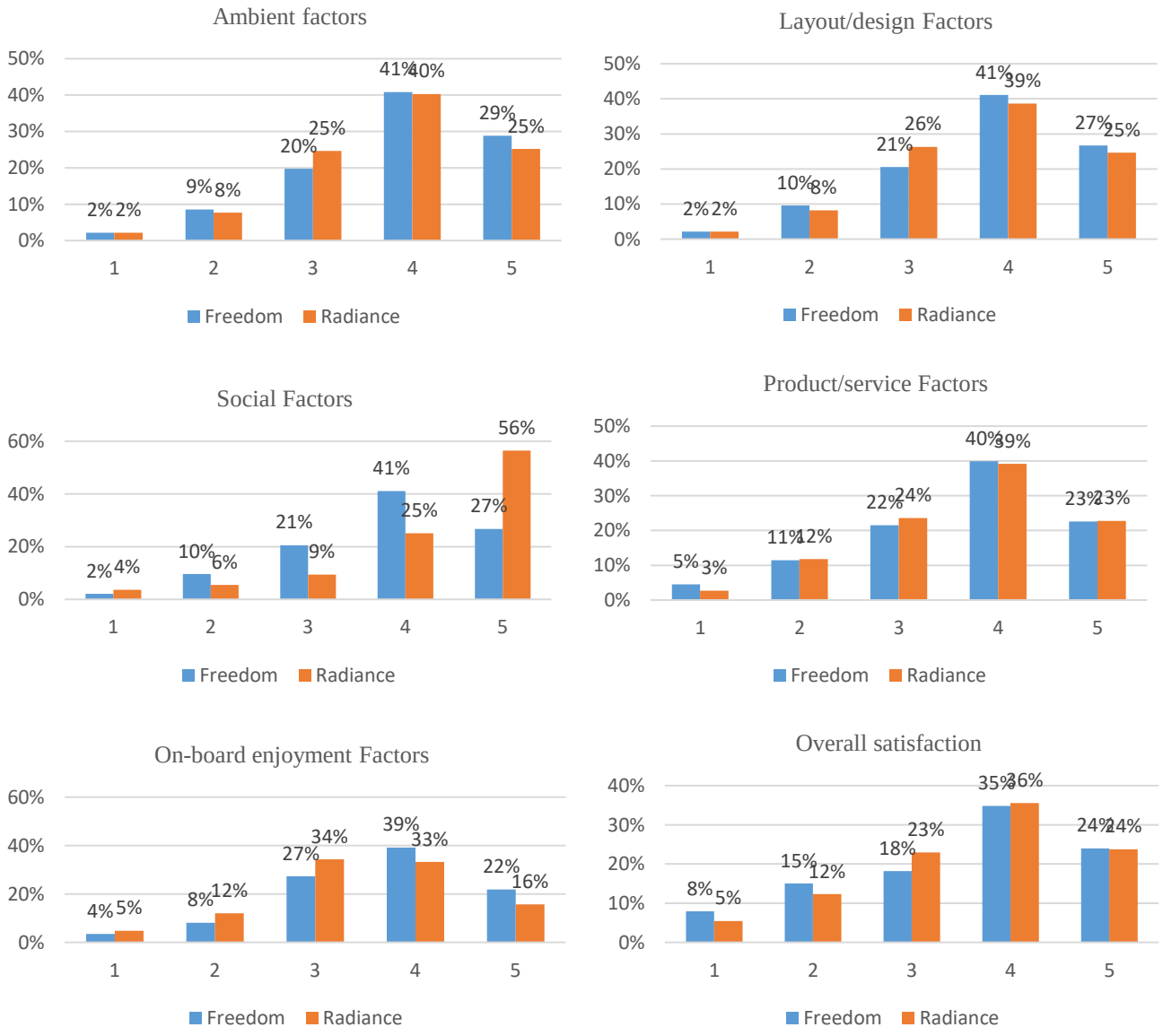

Figure 2: summary the post-cruise experience data observed in the two case ships' classes

In the category of **"ambient factors,"** it is apparent that the, older and in terms of size smaller, Radiance class ships received slightly lower customer satisfaction scores than those of the Freedom class at the scale of between 5 and 4. Notably,

Submitted: 5 February 2024, Revised: 17 April 2024, Accepted: 1 May 2024, Published: 24 May 2024

Conference paper, DOI: https://doi.org/10.59490/imdc.2024.892 e-ISSN: 3050-486

the number of passengers rating their satisfaction at the higher end of the scale (5) increased for both the Freedom and Radiance classes, with a larger concentration of Radiance class customers assigning a rating of 3 compared to Freedom class. Conversely, both ship classes recorded a substantial tally of lower-end scores, between 1 and 2, signalling customer dissatisfaction.

The newer Freedom class ships outperformed, with a notable 41% of respondents rating their satisfaction with **"layout/design"** at level 4. The Radiance class, while also receiving a significant positive response, peaked at 39% respondents giving a score of 4. However, the Freedom class ships were marked by a larger proportion, 10%, of responses at the lower satisfaction level 2, signifying a measure of discontent. Across both classes, there was a pronounced trend of passenger opinions favouring the higher end of the satisfaction scale (5).

From the gathered data, it is evident that **"social aspects"** were highly rated, with the Radiance class receiving a peak of 56% responses at the highest satisfaction level 5, followed by the Freedom-class with 27% respondents also giving a score of 5. Moreover, the distribution of responses shows a noticeable number of low-end ratings, suggesting some passengers experienced dissatisfaction. Notably, when considering the mid-range satisfaction level 3, passengers in the Freedom class exhibited a marginally higher contentment than those in the Radiance class.

Regarding **"product/service"** factors, the scores are more equal, with 40% and 39% passengers rating their experience at the satisfaction level 4 and equal scores of 23% at the highest level of 5. This indicates that the crew operations are almost equal and thus the age and size of the ship seems not to correlate with the ratings. Despite this, the Freedom class ships observed a larger share of lower ratings, specifically level 1, suggesting higher dissatisfaction among its passengers than those on the Radiance class ships.

In terms of **"onboard enjoyment"** factors, analysis reveals that the Freedom class ships receive, as a newer ship, many positive responses, with 39% of guests rating their satisfaction at level 4 and 22% on the level 5. The Radiance class also attained a robust satisfaction score, with 33% of guests granting a level 4 rating. Additionally, the Freedom class ships recorded fewer low-end ratings, between 1 and 2, indicating a generally satisfactory experience among its passengers.

Finally, the element of "**overall satisfaction**": Regarding "overall satisfaction," the figures reveal that the Radiance class notched up 36% high-level satisfaction responses (scores of 4), while the Freedom class had a corresponding value of 35%. Both classes recorded a notable cluster of responses at the satisfactory level of 5, which amounted 24%. Comparatively, the Radiance class had fewer low-end ratings, indicative of a more satisfying passenger experience than the Freedom class, which displayed greater dissatisfaction overall (see Appendix).

Table 4: Implementation of the Equations

Freedom class, Model: Overall satisfaction = -1.114 + 0.42 Layout/design factors +0.59 product/service factors +0.21 onboard enjoyment factors +error.	Shares of Contributing Environmental Factors +59%, in product/service factors (e.g., dining, service) +42% layout/design factors (e.g., cabin, public rooms) +21%, onboard enjoyment factors (e.g., entertainment)
Radiance class, Model: Overall satisfaction = -0.758 + 0.32 Layout/design factors +0.68 product/service factors +0.16 onboard enjoyment factors +error.	+68%, in product/service factors (e.g., dining, service) +32% layout/design factors (e.g., cabin, public rooms) +16%, onboard enjoyment factors (e.g., entertainment)
Freedom and Radiance class together, Model: Overall satisfaction = -1,005 + 0.35 Layout/design factors + 0.06 social factors + 0.61product/service factors + 0.19 onboard enjoyment factors +error.	+61%, in product/service factors (e.g., dining, service) +35% layout/design factors (e.g., cabin, public rooms) +19%, onboard enjoyment factors (e.g., entertainment) +6%, social factors (e.g., embarkation, family)

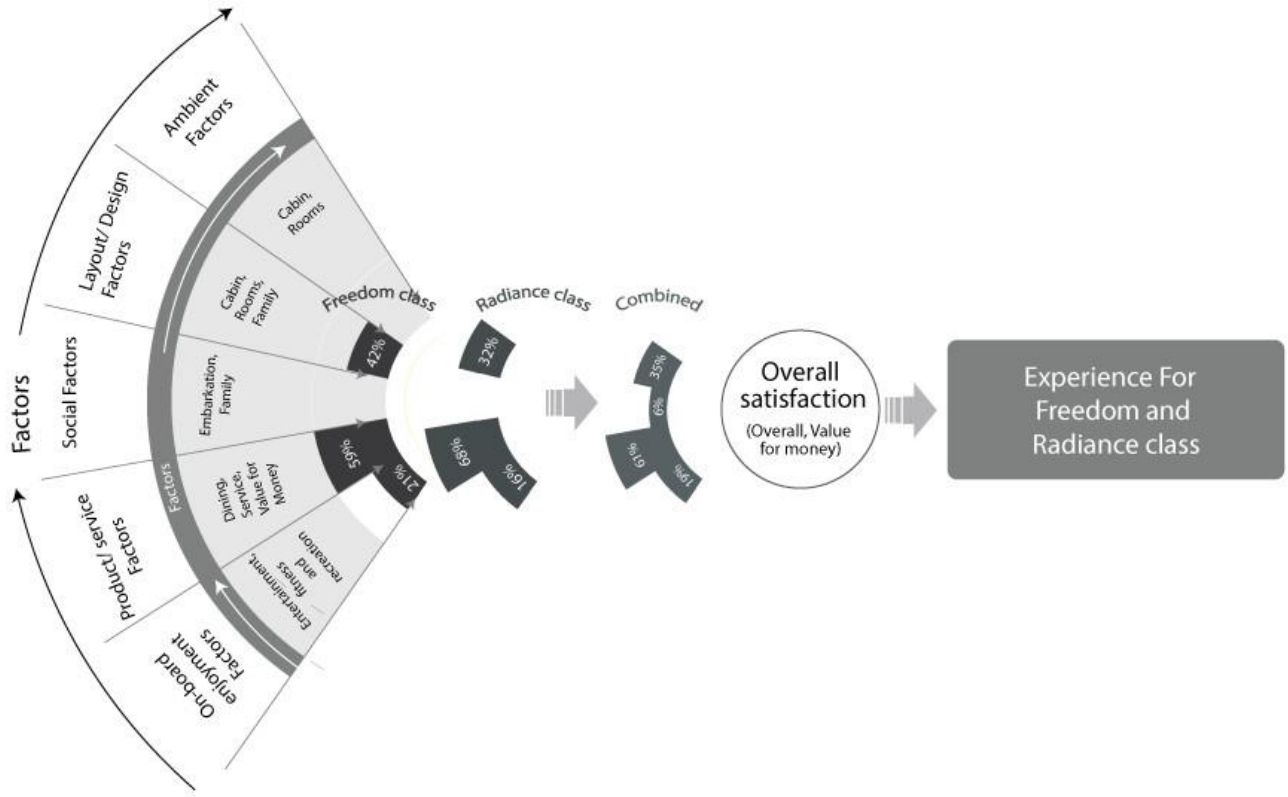

Figure 3: A proposed model of user motion to describe factors affecting the onboard experience in "Freedom and Radiance class".

As Table 4 indicates, the proposed environmental framework, and resulting regression model can be used to describe the ratio of ambient, layout/design, social, product/service, and onboard enjoyment factors on the overall satisfaction, see Figure 3 for Freedom and Radiance class separately and together. In Freedom class, 59% is the factor for the product/service factors, 42% for the layout/design factors, and 21% for the onboard enjoyment factors respectively; neglecting the effects of ambience and social factors completely. On the other hand, in Radiance class 68% is the factor for the product/service factors, 32% for the layout/design factors, and 16% for the onboard enjoyment factors; again neglecting the effects of ambience and social factors. In contrast, when the two ship classes, Freedom and Radiance are considered together, the resulting factors are 61% in product/service factors, 35% in layout/design factors, 19% in onboard enjoyment factors, and 6% in social factors respectively; this time only ambience neglected in the regression model. When using the model, comparing performance before and after making improvements and conversion in the layout, service etc is essential to evaluate how effective these improvements are in practice. Thus, the regression model proposed needs updates and new data after improvements. Here, Key Performance Indicators (KPIs) Tables 1 and 2 are set up for the purpose of continuous enhancement and commitment to quality. Employing KPIs is crucial for tracking performance, increasing productivity, and ensuring that operations align with the organization's larger goals. Based on these critical success factors' affected ratio, decision-makers can focus on further development and acquiring more information, continuing this analysis to determine areas for improvement.

CONCLUSIONS

There has been a growing need for data mining and knowledge management (KPI) techniques to uncover and utilise the insights hidden within large volumes of stored data. This study investigated how different onboard environmental factors, including the ambient, layout/design, social elements, products/services, and entertainment, relate to overall passenger satisfaction after the cruise. The Key Performance Indicators (KPIs) were derived based on these elements. Based on the data from a public website, a simple regression model was derived for two cruise ship classes from the same operator. The resulting regression models were found to be different when ship classes were treated separately or together. In the newer ship class, the layout/design and onboard enjoyment factors dominated the overall satisfaction, while in the older ship class, product/service factors dominated. This indicates that the operators should change their strategy in securing customers' overall satisfaction as new ship classes enter their fleet. In both cases, the ambient and social factors were less significant contributors to overall satisfaction; in the

case where the ship classes were combined social factors became somewhat important. When the data changes, this conclusion can naturally change.

To discover customer behaviour or tendencies, data-driven regression methods should be exposed to large data sets from public and company databases. However, the data set used in this paper shows the potential of the proposed model in helping the decision-makers plan their actions related to the ship design, conversions/maintenance, and operations. Implementing the proposed model to larger data sets is left for future work, which should be done in the industry rather than academia due to sensitive source information.

REFERENCES

Huang, S., Weiler, B., & Assaker, G. (2015). Effects of interpretive guiding outcomes on tourist satisfaction and behavioral intention. Journal of Travel Research, 54(3), 344-358.

Gou, X., Xu, Z., & Liao, H. (2016). Alternative queuing method for multiple criteria decision making with hybrid fuzzy and ranking information. Information Sciences, 357, 144-160.

Xu, Z., & Zhang, X. (2013). Hesitant fuzzy multi-attribute decision making based on TOPSIS with incomplete weight information. Knowledge-Based Systems, 52, 53-64.

Tsiotsou, R. H., & Wirtz, J. (2015). The three-stage model of service consumption. The Handbook of Service Business: Management, Marketing, Innovation and Internationalisation, by Bryson, JR and Daniels, PW (eds.) Cheltenham: Edward Elgar, United Kingdom, 105-128.

Levander, K. 2004. Passenger ships. In T. Lamp (Ed.), Ship Design and Construction (pp. 1-39). New York: Society of Naval Architects and Marine Engineers.

Lovelock, C. and J. Wirtz (2011), Services Marketing: People, Technology, Strategy (7th edn), Upper Saddle River, NJ: Prentice Hall

Tsiotsou, Rodoula H. and Jochen Wirtz (2012), 'Consumer behavior in a service context', in V. Wells and G. Foxall (eds), Handbook of Developments in Consumer Behavior, Cheltenham and Northampton, MA: Edward Elgar, pp. 147–201.

Fisk, Raymond P. (1981), 'Toward a consumption/evaluation process model for services', in J.H. Donnelly and W.R. George (eds), Marketing of Services, Chicago, IL: American Marketing Association, pp.191–195.

Mattila, A.S. and J. Wirtz (2002), 'The impact of knowledge types on the consumer search process: An investigation in the context of credence services', International Journal of Service Industry Management, 13 (3), 214–230.

Zeithaml, V.A. (1981), 'How consumer evaluation processes differ between goods and services', in J.A. Donnelly and W.R. George (eds), Marketing of Services, Chicago, IL: American Marketing Association, pp.186–190.

van Doorn, J., K.N. Lemon, V. Mittal, S. Nass, D. Pick, P. Pimer and P.C. Verhoef (2010), 'Customer engagement behavior: Theoretical foundations and research directions', Journal of Service Research, 13 (3), 253–266

Brodie, R.J., L.D. Hollebeek, B. Juric and A. Ilic (2011), 'Customer engagement: Conceptual domain, fundamental propositions and implications for research', Journal of Service Research, 14 (3), 252–27

Brady, M.K. and C.J. Robertson (2001), 'Searching for a consensus on the antecedent role of service quality and satisfaction: An exploratory cross-national study', Journal of Business Research, 51 (1), 53–60.

Keiningham, T.L. and T.G. Vavra (eds) (2001), The Customer Delight Principle: Exceeding Customers' Expectations for Bottom-Line Success, New York: McGraw-Hill

Akter, S., Valdez Banda, O., Kujala, P., & Romanoff, J. (2021). Understanding Cruise Passengers' On-board Experience throughout the Customer Decision Journey. World Academy of Science, Engineering and Technology, 15(4), 429-435.

Akter, S., Banda, O.V., Kujala, P. and Romanoff, J. (2021) 'The gap between cruise passengers' expectations and the on-board experience through on-board environmental factors and overall satisfaction', Int. J. Tourism Policy, Vol. 11, No. 4,pp.371–400.

Bitner, MJ. (1992). Servicescapes: The Impact of Physical Surrounding on Customers and Employees. Journal of marketing, 56 (2), 57-71.

Rosenbaum, M. S., & Massiah, C. (2011). An expanded servicescape perspective. Journal of Service Management.

Andersson, K. (2013). Changing the servicescape: The influence of music and self-disclosure on approach-avoidance behavior (Doctoral dissertation, Karlstads universitet).

Dad, A. M., Davies, B. J., & Rehman, A. A. (2016). 3D servicescape model: Atmospheric qualities of virtual reality retailing. International Journal of Advanced Computer Science and Applications, 7(2).

Jeon, M. M., & Jeong, M. (2009). A conceptual framework to measure e-servicescape on a B&B website.

cruisecritic (2022). Royal Caribbean Oasis of the Seas Cruise Reviews. Retrieved December 12, 2022, from https://www.cruisecritic.com/

APPENDIX

The research utilised SPSS software for a five-step data analysis process involving reliability testing, exploratory factor analysis for data validity, correlation, and regression analysis. The basic information is given in Tables 5 to 7.

Table 5: Overall satisfaction coefficient regression model. Freedom Class (N=360).

Predictor variable	**Outcome variable**	**Global *F* (*p*-value)**	**Intercept / Constant**	**Unstandardized Coefficients B**	**R^2**	**Adjusted R^2**	**Result**
Ambient factors	Overall satisfaction	>0.001		-0.212	0.788	0.787	Not Supported
Layout/design factors	**Overall satisfaction**	**<0.001**	**-1.114**	**0.417**	**0.788**	**0.787**	**Supported**
Social factors	Overall satisfaction	>0.001		0.050	0.788	0.787	Not Supported
Product/Service factors	**Overall satisfaction**	**<0.001**	**-1.114**	**0.594**	**0.788**	**0.787**	**Supported**
On-board enjoyment factors	**Overall satisfaction**	**<0.001**	**-1.114**	**0.210**	**0.788**	**0.787**	**Supported**

Table 6: Overall satisfaction coefficient regression model. Radiance Class (N=337).

Predictor variable	**Outcome variable**	**Global *F* (*p*-value)**	**Intercept / Constant**	**Unstandardized Coefficients B**	**R^2**	**Adjusted R^2**	**Result**
Ambient factors	Overall satisfaction	>0.001		-0.034	0.830	0.828	Not Supported
Layout/design factors	**Overall satisfaction**	**<0.001**	**-0.758**	**0.316**	**0.830**	**0.828**	**Supported**
Social factors	Overall satisfaction	>0.001		0.024	0.830	0.828	Not Supported
Product/Service factors	**Overall satisfaction**	**<0.001**	**-0.758**	**0.683**	**0.830**	**0.828**	**Supported**
On-board enjoyment factors	**Overall satisfaction**	**<0.001**	**-0.758**	**0.159**	**0.830**	**0.828**	**Supported**

Table 7: Overall satisfaction coefficient regression model. Freedom and Radiance Class (Together N=716).

Predictor variable	**Outcome variable**	**Global *F* (*p*-value)**	**Intercept / Constant**	**Unstandardized Coefficients B**	**R^2**	**Adjusted R^2**	**Result**
Ambient factors	Overall satisfaction	>0.001		-0.161	0.806	0.805	Not Supported
Layout/design factors	**Overall satisfaction**	**<0.001**	**-1,005**	**0.348**	**0.806**	**0.805**	**Supported**
Social factors	**Overall satisfaction**	**>0.001**	**-1,005**	**0.061**	**0.806**	**0.805**	**Supported**
Product/Service factors	**Overall satisfaction**	**<0.001**	**-1,005**	**0.609**	**0.806**	**0.805**	**Supported**
On-board enjoyment factors	**Overall satisfaction**	**<0.001**	**-1,005**	**0.188**	**0.806**	**0.805**	**Supported**

Proceedings of 15th International Marine Design Conference (IMDC-2024)
June 2-6, 2024
Amsterdam, the Netherlands

An Overview of Digital Engineering Methods for Platform Integration of Power and Energy Systems

Robert M. Ames[1], Dr. Norbert H. Doerry[1], Madeleine M. Koerner[1] and Dr. **Mark A. Parsons[2,*]**

ABSTRACT

US Navy ships, and combatant ships in particular, have requirements for integrated systems that are designed and configured for operational efficiency, redundancy, and survivability. Mission systems today and in the future will not always come with their own energy and many may, at times, require extreme pulse power loads. In addition, the migration away from fossil fuels to hybrid systems with energy storage, or the requirements for autonomous platforms, is challenging our ability to design platforms for these systems. Understanding the interdependencies between components, the systems they support, and the energy domains they are member of is a critical ontological design requirement. This paper will address how we applied digital engineering principles and computer science to the design of ontologies that allow for the modeling of complex operational systems riding on the same shipboard energy network. This system network must support varying levels of detail needed during design while at the same time understanding the impacts of that design on ship system operations and their energy loads over time.

KEY WORDS

Design, Power, Energy, Ontology, System

DEFINITIONS

Capability - The ability to achieve a desired effect under specified performance standards and conditions through combinations of ways and means [activities and resources] to perform a set of activities. Capabilities are only described in the abstract and does not specify how a capability is to be implemented. A Capability is structured as a hierarchy of Capabilities, with the most general at the root and most specific at the leaves. At the leaf-level, Capabilities may have a measure specified, along with an environmental condition for the measure.

Component – A Component class represents objects that can be thought of as parts of a Concept. They may be connected in ways that provide function and capability. Components can be thought of as any part of a ship that represents something physical and as discrete as a radar or engine, or as abstract as proxy for something temporal or needing further refinement. A Component is in many ways just a small Concept, but it is modeled as something a Concept owns. A Component does not have their own Systems, but Components do have most of everything a Concept does.

Concept - A class that defines the attributes, the Systems, the Components and the views of geometry that represents a product in design or under study. It is generic to all things engineered, but is used here to define platforms such as a ship, submarine, aircraft, or other engineered product.

Connection - The Connection class provides information on how the contained Component, System, Node, and Connection objects are connected (i). Connections are logical relationship between connection members (Component, System, Node, and other Connections).

Diagram - The Diagram class provides the schematic information that defines a connected graph or network. Diagrams can define a connected network between Components, within a Component, and a Connection between Components and Concept structure.

Domain Network– A Domain Network is a domain specific subset of the total Energy Network. Domain Networks facilitate the distribution of energy specific to its domain type. Domain types include, but are not limited to, electric, fluid, thermal, chemical, magnetic, structural, and mechanical. Each Domain Network is capable of energy transfer (work) within the Energy Network. Components may participate in zero or more Domain Networks. A Component can be both a Domain Source and a Domain Sink (e.g. battery). The Domain Network does not formalize energy flow, it only defines its possible boundaries.

[1] Naval Architecture and Engineering, Naval Surface Warfare Center Carderock, Bethesda, MD, USA
[2] Surface Ship Design and Systems Engineering, Naval Sea Systems Command, Washington DC, USA

Submitted: 23 February 2024, Revised: 29 February 2024, Accepted: 1 May 2024, Published: 29 May 2024

Conference paper, DOI: https://doi.org/10.59490/imdc.2024.916 e-ISSN: 3050-4864

Domain Sink – A Domain Sink is defined as a domain terminus. The Domain Sink is the last Component specific to a domain that is exclusive of any energy process outside of the sink Component. If the domain is electric, then a radar, light, or motor could be examples of Domain Sinks.

Domain Source – A Domain Source is defined as the source of energy specific to a particular domain. The Domain Source is the first Component specific to that domain that is exclusive of any energy transfer process outside of the Component. For example, if the domain is electric then a generator, solar panel, or fuel cell may be the Domain Source.

Energy Network – A Diagram defining an interconnected network of Components and Energy Resources that facilitate the distribution of energy throughout the Concept. Energy Networks are bounded by Primary Energy Resources at one end and the Natural Environment on the other. Within the network, energy is transferred from sources (Primary Energy Network) to sinks (Operational Energy Sink). Energy Networks are defined as Connections between Concept and Component via their respective Connections.

Energy Resource – An Energy Resource is something that can produce electricity, move objects, generate heat, and power and sustain life. Most shipboard energy today is matter stored energy from the Natural Environment. Forms of Energy Resources include, but are not limited to, fossil fuel, nuclear (fusion or solar, fission), energy stored in chemical bonds used in Components like fuel cells, and biomass.

Manmade Energy Resource – Manmade Energy Resources are Components that exist by design as sources of energy. They are not natural. Examples include, but are not limited to, batteries, capacitors, and flywheels. Manmade Energy Resources can be either primary or secondary resources depending on their configuration in the Energy Network and their intended use.

Natural Energy Resource – Natural Energy Resources are resources used in the conversion of energy and are extracted from the environment. They may be stored on the platform (e.g. fuel) or extracted from the environment during operation (e.g. solar). They include, but are not limited to, fossil fuels, wind, solar, natural gas, oxygen, uranium, and hydrogen.

Natural Energy Resource Storage - Some Natural Energy Resources are stored and consumed by the Concept (e.g. fuel, natural gas, uranium, hydrogen). This does not include Natural Energy Resources that are available through the environment (e.g. oxygen, wind, solar). In some cases, this storage exists within a Component and other cases it is stored in a compartment of space of a vessel.

Natural Environment – The Natural Environment is everything that is not owned by the Concept and is not an engineered physical thing. In contrast to the Natural Environment is the build environment. For a vessel operating in the real world, the Natural Environment includes everything that is in nature. This includes people. All elements of the Natural Environment are temporal. They can pass through and around Systems and Components within a Concept (e.g. crew, water, air, light, etc.) and can be stored, consumed, and replenished (e.g. potable water, fossil fuel, etc.) Note: Chemical and biological engineering cross the boundary between natural and man-made. Fossil fuel is a good example. Within this ontology, chemically engineered products like fuel or the generation of potable water from seawater are considered part of the Natural Environment.

Node - The Node class represents a location in space either relative to the Concept or relative to a Component. Nodes can be defined in Cartesian space, or they can be defined as a location in relative space (meaning, a Node can be defined as a location on a surface or curve of another object). The surface or curve can be owned by a Concept or a Component.

Non-Operational Energy Sink – A Non-Operational Energy Sink is like an Operational Energy Sink but it does not provide an Operational Capability. Non-Operational Energy Sinks include, but are not limited to, Components that reject significant amounts of energy like waste heat to the environment. An exhaust uptake is a good example. Since most Components transfer heat into the environment, Non-Operational Energy Sinks are differentiated by the need to network certain Components to the Energy Network for design reasons and simulate the transfer of energy to the environment through these Components. They are significant to the ship design and are therefore significant to the definition of the Energy Network. In theory, all Components store or transmit energy in some capacity and can participate as passive energy emitters into the Natural Environment (e.g. a Component's thermal energy emitted to a compartment). For purposes in modeling efficiency, not all non-operational energy emitters need to be designated as a Non-Operational Energy Sink. Only the ones that have significant impact at that stage of design.

Operational Capability - An Operational Capability is a Capability of a System to perform a mission, operation, or function in the intended environment. An Operational Capability is a specific type of Capability.

Operational Energy Sink – An Operational Energy Sink is a Component that transforms' energy for the purpose of providing one or more Operational Capabilities. One or more Operational Sink Components can have direct or indirect relationships with Operational Capabilities through System Function Actions. An Operational Sink can be as complex as a weapon or sensor, or as simple as a light fixture. For example, a radar is an Operational Energy Sink that provides detection through the conversion of electrical and thermal energy into heat and radio waves. This energy is transmitted off the platform and is therefore considered an energy sink. A multi-function radar can also provide communications and Electronic Warfare (EW) functions. Because this Component is multi-functional, it has multiple System Function Actions which provide multiple Operational Capabilities. It is the System Function Action that provides the functions and properties that describe and define how the Operational Energy Sink(s) behave as needed to provide an Operational Capability.

Primary Energy Resources – Primary Energy Resources are the sole originating source of energy for the platform. Primary Energy Resources may be a Natural Energy Resource or a Manmade Energy Resource.

Secondary Energy Resources - Secondary Energy Resources are Manmade Energy Resources that provide energy to the Energy Network but are replenished from some Primary Energy Resource. Examples include, but are not limited to, an electric battery, flywheel, or capacitor Components.

System – A collection of connected Components and Energy Resources that support one or more Operational Capabilities. Systems are defined as the aggregation of all Components that are involved in providing energy to Operational Energy Sinks. Systems are bounded at one end by Operational and Non-Operational Energy Sink Components and all Primary Energy Resources necessary for the System to function at the other end. Systems interact and operate along Energy Networks and may involve one or more Energy Domains.

System Domain: A System Domain is defined as all the Components of a System in a Domain Network for a particular System. It is a subset of the Energy Domain specific to a System. The electric Energy Domain of a propulsion System is an example. The mechanical Energy Domain for the same System is another.

System Information Networks: A System Information Network communicates data for the purpose of System monitoring and control. This network may be a subset of a larger network that serves additional capabilities outside of System control. An Information Network includes all the Components necessary to generate information and move that information from the information sources to the information sinks. In many cases, information sources and information sinks could be associated with the same component – (an HMI, engine order telegraph, telephone for example); or they could only be an information source (a sensor) or an information sink (an actuator or display). The System Information Network influences how the Components of the Energy Network operate, and thus should be modeled to some degree. In some cases, the System Information Network includes properties of the energy – voltage level at the bus for reactive power sharing …. Frequency for real power sharing, I2t for circuit protection coordination, etc.) Connections within System Information Networks are logical and from a modeling perspective do not include the transfer of energy; the law of energy conservation does not apply.

System Function Action - A System Function Action defines the action of an Operational Energy Sink needed to support an Operational Capability.

INTRODUCTION

Electric cars, renewable energy, autonomous vehicles, and consumer electronics are evidence that a new power and energy future is emerging in the civilian and military worlds. In the naval world, recent developments in weapon systems have delivered the next-generation in defense capability, and these systems are challenging existing ship design practices, theory, and engineering tools. Like hybrid or all-electric cars, Navy ships are moving to a new paradigm where electric power and energy supply are directly related to ship performance (Ames, R., 2016). In non-military applications, Yara Birkeland, developed by Yara International, is an autonomous, fully electric-powered container ship. She has a 7MWh battery, charged by Norwegian hydropower. In today's environment, everyone wants high-power density, energy-efficient systems, speed, control, survivability, and upgradeability—all at an affordable price in a functional package. For naval applications, the promise of these new systems is so compelling that it will set the stage for warships for the next 50 years and push naval design toward a future centered around high levels of power and energy that can be directed wherever it is needed, whenever it is required.

This new future will require power architectures that include energy storage, thermal management, and specialized power converters. For any future ship design activity, engineers, and the tools they use to design these Energy Networks, must understand the boundaries of what defines a system, how systems use energy, and how that energy is transferred and transformed (Ames, R. et al., 2018).

Ontologies are crucial for software applications as they provide a common vocabulary and relational structure to ensure a shared understanding of information structures. In the case of naval ships, it becomes even more critical to understand the interdependencies between ship Components, the Systems they support, and the Energy Domains they belong to. This understanding is necessary due to the complexity and diversity of the missions naval ships must support. Precise and sophisticated design and analysis are required at an early stage of design to ensure that ship designs meet their naval requirements.

To support these analyses, a comprehensive data model is needed to understand each ship System, its functionality, capabilities, and dependency within the full ship Energy Network. This necessitates an understanding of energy within a Component, between Components, and within a Energy Network of connected Components. Controlling this energy is vital to providing Operational Capabilities and meeting survivability requirements.

This paper will address how we applied digital engineering principles and computer science to designing ontologies that allow for the modeling of complex operational systems riding on the same shipboard Energy Network. This Energy Network must support varying levels of detail needed during design while at the same time giving insight into the impacts of that design on ship system operations and their energy loads over time.

An ontology precisely describes how Concepts can be decomposed into Systems and Components and how those Systems and Components are connected as part of networks. Well-defined ontologies are important to enable multiple design tools to unambiguously have a common understanding of a share Concept data model. See Noy and McGuinness 2001 for a complete description of ontologies and the ontology development process. The ontology described in this paper is being implemented through evolving the class structures of the Leading Edge Architecture for Prototyping Systems (LEAPS) in support of FOCUS. FOCUS is the US Navy-managed ship-specific ontology shared among multiple ship design tools. It is also an acronym for Formal Object Classification for Understanding Ships.

The bulk of the work in ontology building is to make sure that the definitions are sound. In some ways, the true output of this paper is the definitions. It is suggested that the reader refer to the definitions section often as they progress through the paper. Capitalized words in this document indicate that they are being used according their respective definitions.

SYSTEMS AND ENERGY NETWORKS

The relationship between Capabilities, Energy Networks, and operational Systems forms the foundation of the developed ontology. Wikipedia defines a System as; "... a group of interacting or interrelated elements that act according to a set of rules to form a unified whole. A System, surrounded and influenced by its environment, is described by its boundaries, structure, and purpose and is expressed in its functioning." In our ontology, a ship System represents a collection of interconnected Components and subsystems that work together to perform a specific function or set of functions that provide Operational Capabilities. We define a Capability as the ability to achieve a desired effect under specified performance standards and conditions through combinations of ways and means [activities and resources] to perform a set of activities. The boundaries of a ship System are expressed by the System's Capabilities to the operator at one end, and the energy source needed to function on the other. A System uses an Energy Network.

Illustrated in Figures 1 through 4 are simple schematic representations of an IPS propulsion System that spans three Energy Domains: electrical, mechanical, and fluid. We define a System, such as this propulsion System, as a collection of Components and Energy Resources that support one or more Operational Capabilities. An Operational Capability is the Capability of a System to perform a mission, operation, or function in the intended environment. In the case of our propulsion system below, the Capability supported is mobility – power is provided to the propellers and forward pod such that the ship can move from point A to point B.

Systems are bounded at one end by Operational Energy Sinks and on the other end by the Energy Resources necessary for the System to function. Energy sinks are Components that transfer energy into the Natural Environment. Operational Energy Sinks transform energy to provide one or more Operational Capabilities. Non-Operational Energy Sinks transfer significant amounts of energy to the Natural Environment but do not provide an Operational Capability. The seawater cooling outlets in Figure 4 are examples of Non-Operational Energy Sinks; they reject energy as waste heat into the environment. The propellers and the pod in Figure 2 are Operational Energy Sinks. The generator sets in Figure 1 are Electrical Domain Energy Sources. A Domain Source is the energy source specific to a particular Energy Domain. The Domain Source is the first Component specific to that domain that is exclusive of any energy transfer process outside the Component. A Domain Sink is defined as a domain terminus. The Domain Sink is the last Component specific to a domain exclusive to any energy process outside of the sink Component. Each propeller in Figure 2 is an example of a mechanical Domain Sink.

The Primary Energy Resource for the System is the fuel in the tank (Figure 3). An Energy Resource can produce electricity, move objects, generate heat, and power and sustain life. Most shipboard energy today is in the form of Natural Energy Resources. Natural Energy Resources are resources used to convert energy and are extracted from the

Natural Environment. They may be stored on the platform (e.g., fuel) or extracted from the environment during operation (e.g., solar). They include, but are not limited to, fossil fuels, wind, solar, natural gas, oxygen, uranium, and hydrogen. Manmade Energy Resources are Components that exist by design as sources of energy. Energy resources can also be categorized as either primary or secondary. Primary Energy Resources are the sole originating source of energy for the platform and may be natural or manmade. Secondary Energy Resources are Manmade Energy Resources that provide energy to the Energy Network but are replenished from some Primary Energy Resource. Examples include, but are not limited to, an electric battery, flywheel, or capacitor Components.

Each System is part of a larger Energy Network that defines the network of Components and Energy Resources that facilitate the distribution of energy throughout the Concept. Energy Networks are bounded by Primary Energy Resources at one end and the Natural Environment on the other. Within the Energy Network, energy is transferred from source to sink. Energy Networks consist of all of the Connections between concept and Components, between Components, and within Components.

A Domain Network is a domain specific subset of the total Energy Network. Domain Networks facilitate the distribution of energy specific to its domain type. Domain types include, but are not limited to, electric, fluid, thermal, chemical, magnetic, structural, and mechanical. A System Domain is defined as all the Components and Connections of a System in a Domain Network for a particular System. Figure 1 depicts the electrical System Domain for the propulsion System. Figure 2 shows the mechanical System Domain. Figure 3 and Figure 4 show the system in the fluid Domain.

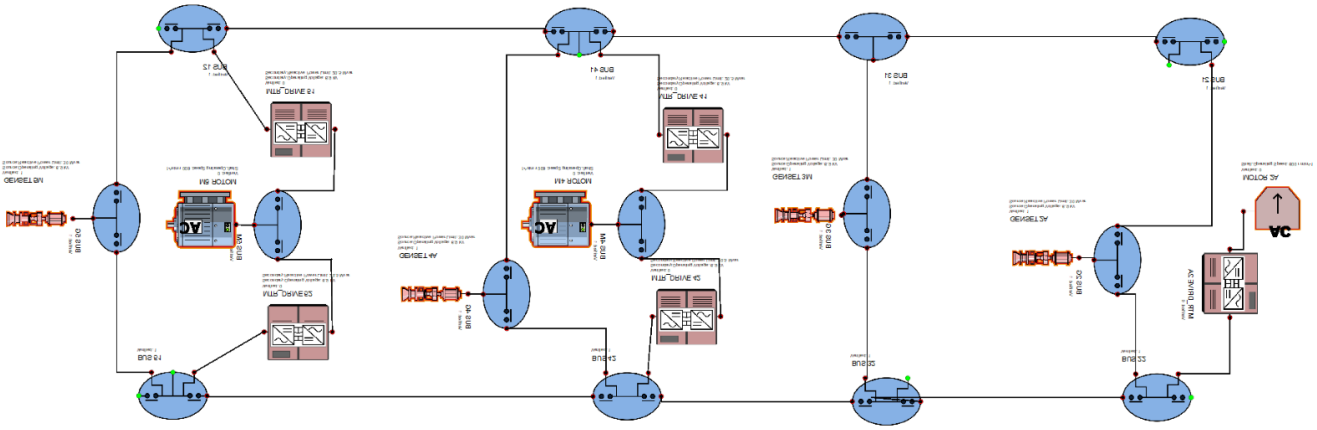

Figure 1- Example IPS propulsion System, electrical domain view

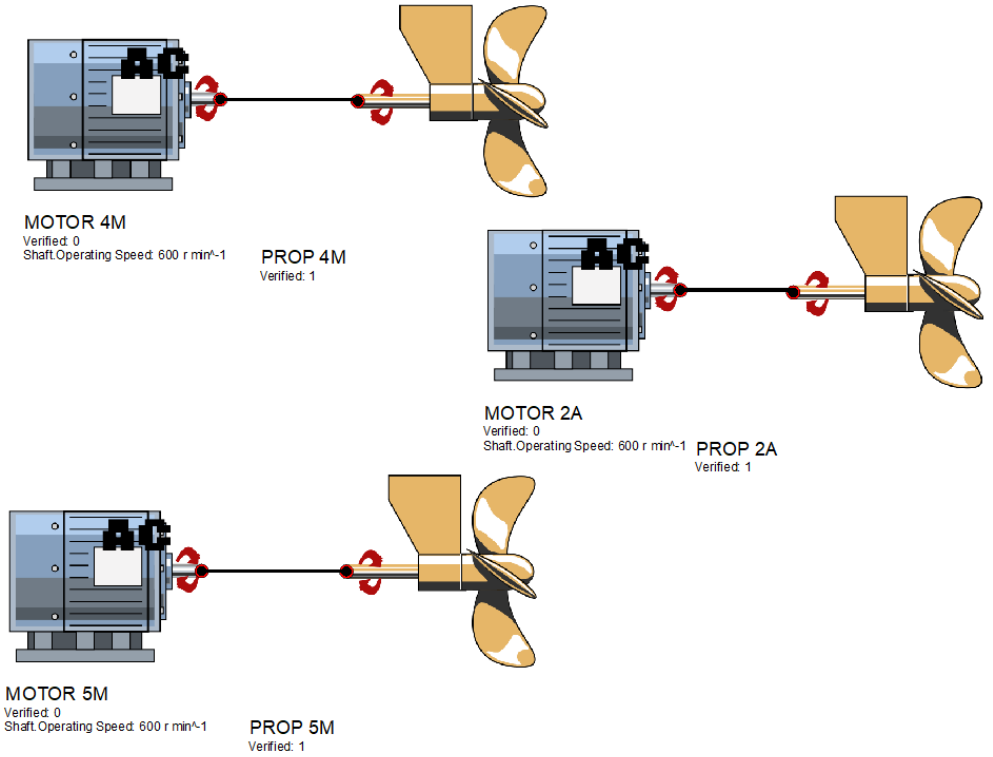

Figure 2- Example IPS propulsion system, mechanical domain view

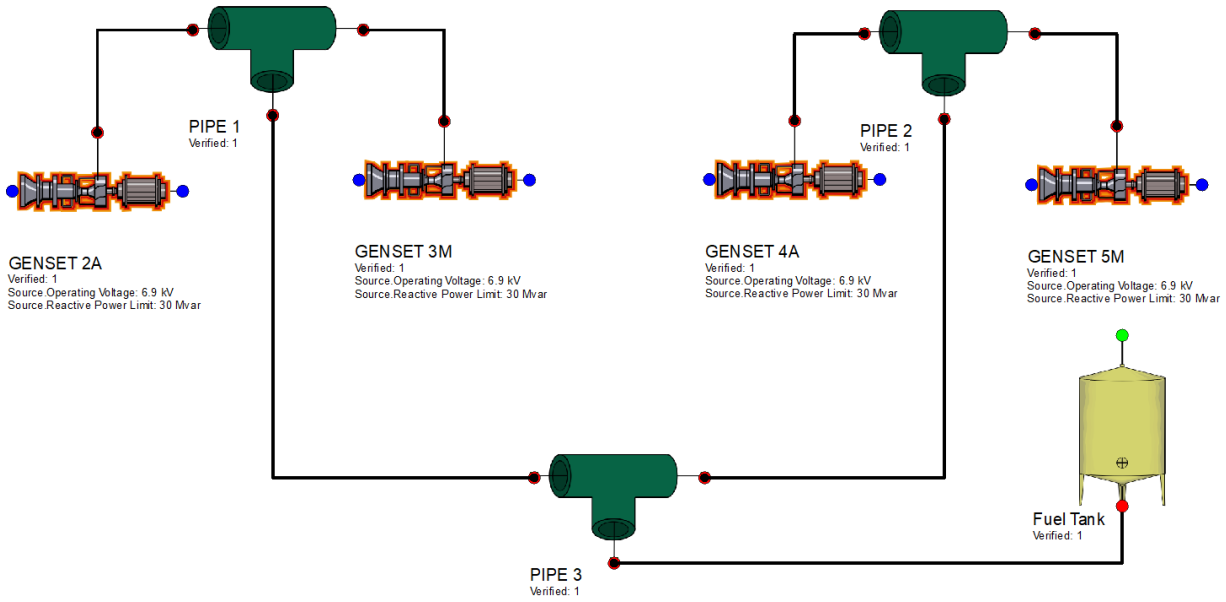

Figure 3- Example IPS propulsion System, fuel proxy, fluid domain

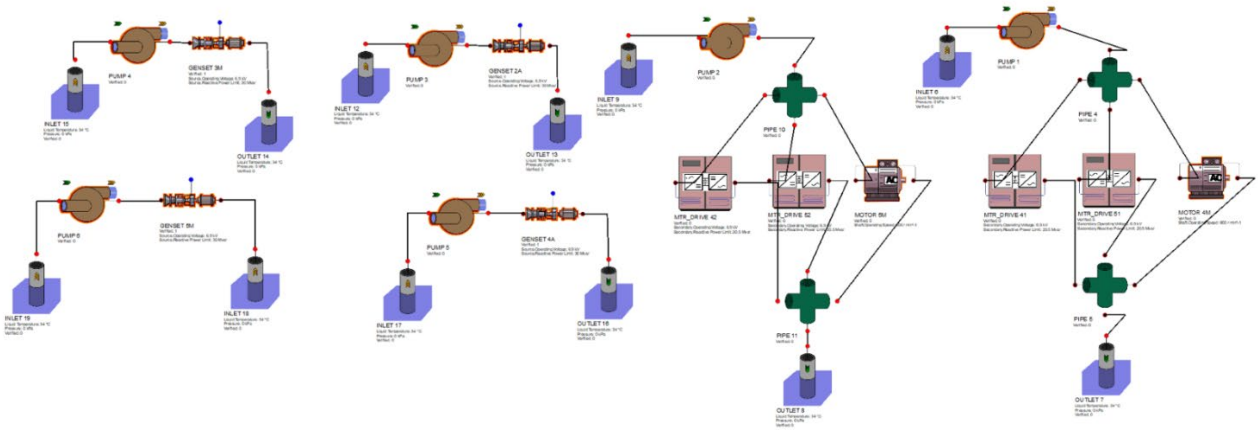

Figure 4- Example IPS propulsion System, seawater cooling, fluid domain

We should not design and engineer Systems independently, but rather we should design and engineer Energy Networks that provide and transport energy through these Systems. The differentiation between Systems and Energy Networks is foundational to any modeling requirement used during the design process. For example, the sizing of generators, chillers, and load centers, and the design of zonal architectures are done to support multiple ship Systems. In this way, a ship design objective is to engineer an Energy Network that supports the operational requirements of all ship Systems; and to discover the interdependence between these Systems and the Components that they share. The challenge becomes designing an Energy Network while at the same time meeting System requirements.

Designing Energy Networks and analyzing System performance cannot be properly executed without appropriate tools. These tools must be able to model and analyze the design; the design analyzed should be based on a commonly understood definition of the Concept's design. This requires a data model or ontology that can capture the complexity of the network/system relationship while dealing with the various levels of knowledge about the design as it matures along an acquisition process.

An Energy Network can be thought of as a graph defining how Components and Energy Resources are connected to distribute energy throughout the ship. Within the Energy Network, energy moves from one or more primary Energy Resources, like oxygen and fuel, through connected Components and terminates at Operational Energy Sinks where the energy provides an action necessary for an Operational Capability to exist. The actions of these terminus Components transfer that energy to the natural environment. Once the understanding of energy flow and conversion is gained, building an ontology model that represents this Energy Network and the Systems riding on it becomes the challenge.

The modeling philosophy that was applied makes the following assumptions.

1. Through the law of energy conservation, energy is a conserved quantity that cannot be created or destroyed but is instead converted in form.
2. Energy resources are part of the Energy Network. For example, if a ship runs out of stored fuel, or the batteries of a fully electric ship are depleted, and the ship is dead in the water, then energy was converted, is now in the environment, and is no longer onboard and available for use.
3. Energy is distributed, controlled, and converted along one or more distinct Energy Networks to support required Operational Capabilities.
4. Energy Networks have multiple Energy Domains. These include but are not limited to electrical, mechanical, and fluid (gas and liquid).
5. Humans are not part of the Energy Network. They are operators and are part of the Natural Environment.

Most engineers will logically think of Energy Networks in the context of a network of connected Components. Engineers model these Components and networks within modeling and simulation tools/applications appropriate to answer specific questions. The ontology used by these modeling and simulation applications must provide the mechanism to define and simulate these Components and networks unambiguously; the definitions must be understood the same way among multiple applications.

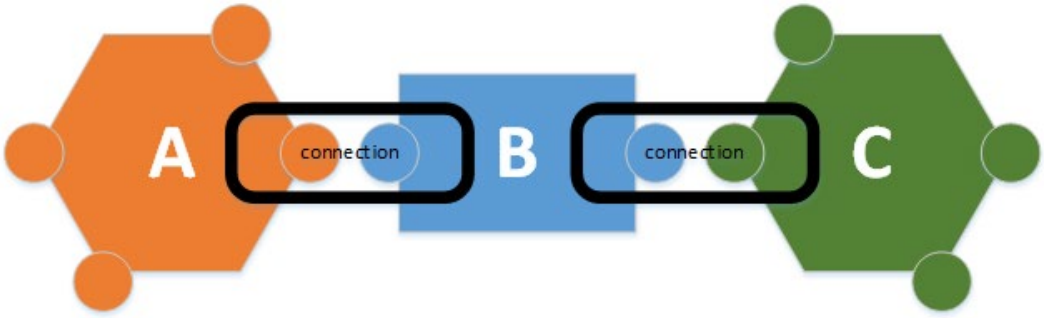

Figure 5- Connected Components

In Figure 5 we have three connected Components, but we know nothing about A, B, and C individually; we know only that they are connected. Concerning their Connections, we may have information about the Ports on each Component, the Energy Domains, properties, and possibly even the physical interface of each Port. We can formalize the Connection object, which can have properties. But at this level of modeling, we do not know what happens inside each Component or how it behaves in relation to its connected neighbors. For all Components of an Energy Network to simulate, applications would need to know specific details about each Component's behavior and its ports. Each Component needs to be defined, formalized, unique, and have associated code modeling its behavior.

A simplistic example of these Energy Networks might include an engine connected to a generator by way of a shaft (Figure 6). A cable is connected to a generator that powers some electrical device, like a radar, through a switchboard and/or load center.

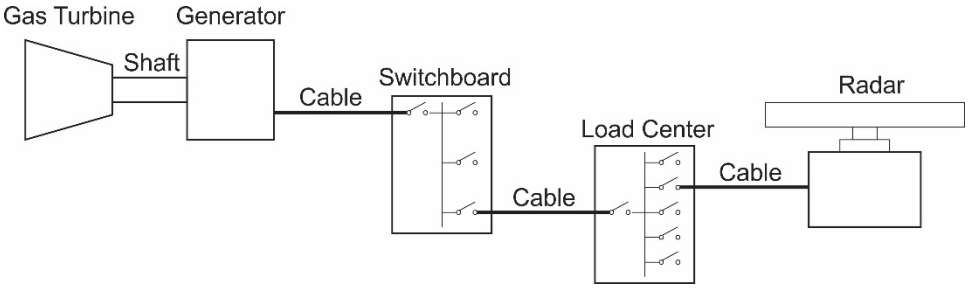

Figure 6-Simple Engine and Electric Load

In the model shown in Figure 6, the network is incomplete as an energy model. It is incapable of being simulated without additional modeling assumptions. It could exist as a pattern or subnetwork for reuse, but it is incapable of an end-to-end energy simulation as no energy can be generated for use in one or more Systems; there is no energy source or resource. The model also does not include dependent Components like chilled water that are required for it to function. This increased level of detail is depicted in Figure 7. Like the generic model depicted in Figure 5, to perform an end-to-

end energy simulation, the constituent parts of this model, including their Connections, must be formalized and connected to an energy source. For early stage design, this level of detail is limited but may be sufficient in most use cases with adequately formalized and modeled Components and Energy Networks.

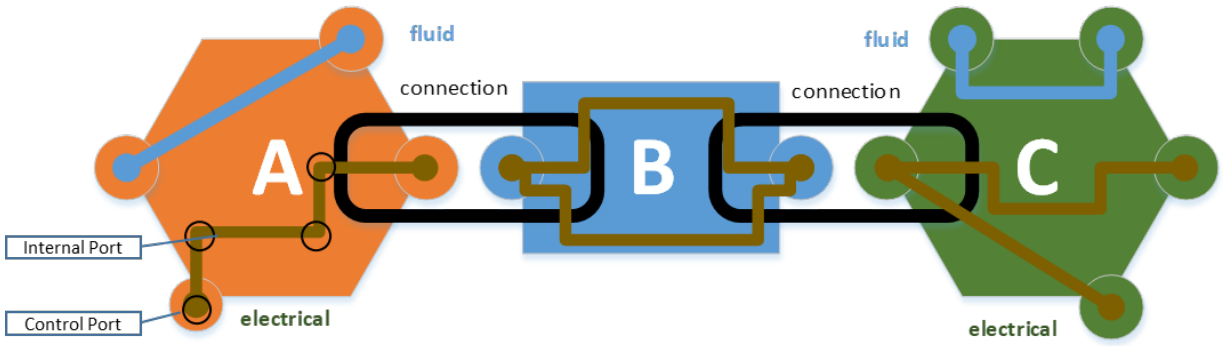

Figure 7 - Components with Internal Connectivity

When the level of detail increases and the definition of the behavior and control of Components operating in an Energy Network becomes critical to answering design questions, the ontology model must allow for the refinement of Components. These refinements include, but are not limited to, Energy Network paths within each Component. This also affords multiple configurations of the same Component type. Switchboards, computers, and cables are examples of standard Components that may have many different numbers of Ports and internal conductors or fluid paths, but functionally belong to the same family of Components.

If we consider again the model in Figure 6 as a use case, we can see how this Energy Network meets the requirements of a single System supporting a single radar and its Operational Capabilities. We also know that many of these Components will serve more than this single System function within the larger context of the ship design. This simple example can quickly get complicated when the fuel necessary to power the engine is stored in a compartment in the ship, and we add additional Components needed to support additional capabilities like ship propulsion (Figure 8).

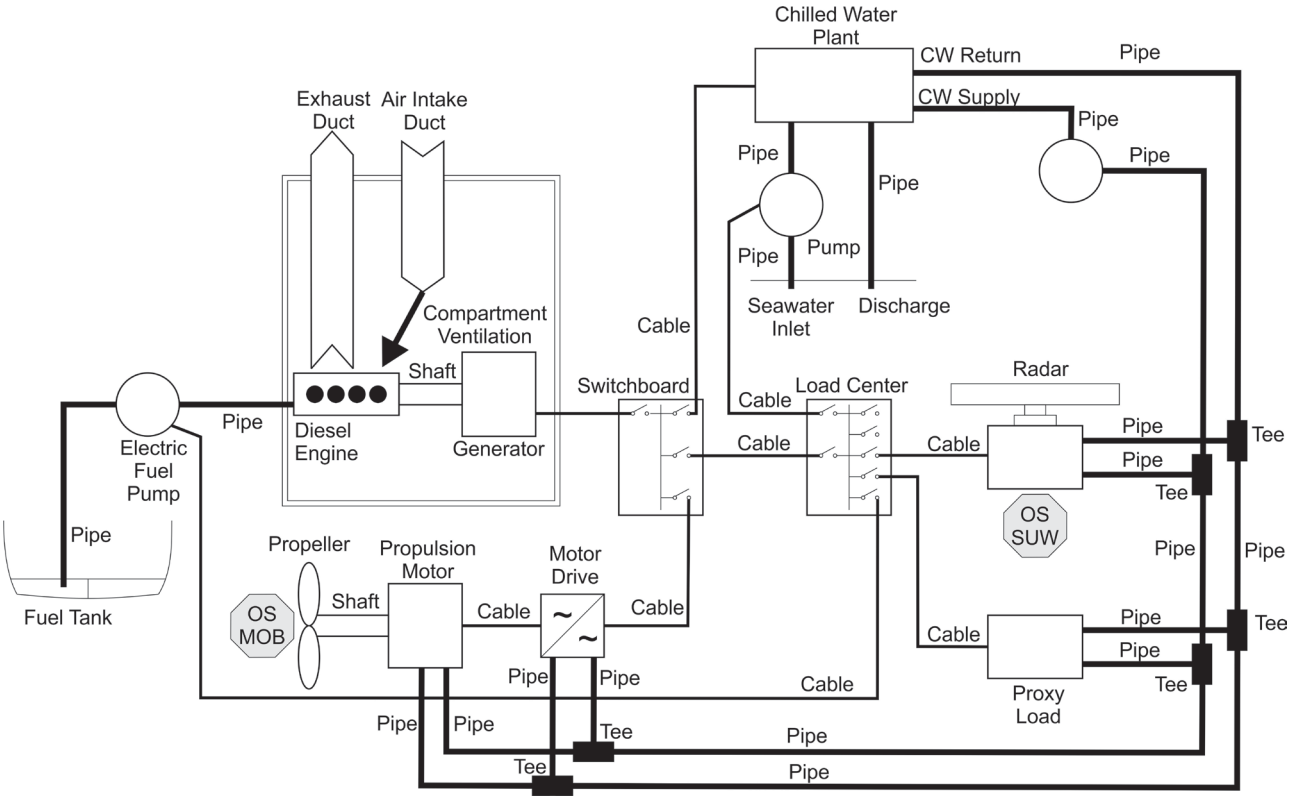

Figure 8- Simplified Notional Energy Network

Now, there are two ship functions that share some, but not all, of the Energy Network Components. Both are dependent on fuel and oxygen to provide energy to the network and, therefore, to each system. The ontological relationships between Energy Network Components are critical. Note that the capacity of the tank is directly related to the design of the ship and space available for fuel storage and, therefore, defines the operational limits of ship Systems. Two Components of Figure 8, the radar and the propeller are the Operational Sinks for two Operational Capabilities; these two Operational Capabilities are implemented through two interconnected Energy Networks. During their operation, these two Energy Networks consume Energy Resources and act as an energy sink to transfer energy off the Energy Network through some action. This relationship breaks down into well-defined model objects that ultimately define each of the two Systems (the propulsion system and the air radar sensing system.)

In the example shown in Figure 8, the air in this naturally aspirated combustion engine comes from air within a compartment. The compartment air is serviced by an air intake duct via a ventilation System that terminates at a Domain Source. This Source Port has a Connection to a Natural Energy Resource which is oxygen from outside air. Likewise, the engine is cooled by seawater; without cooling, the engine will fail. This figure also illustrates the multiple domains of the Energy Network: electrical, mechanical, and fluid.

Figure 9 shows a 3D view of the Compartment/air relationship. The HVAC duct serves to both cool the Compartment and to ensure that air is provided to the engines. Since the Compartment doors can be closed, a dedicated external air source is required. In the event the HVAC fans fail, or the intake air is blocked, the Compartment doors can offer a redundant air source. An Energy Network should be able to model this relationship. While not shown in the figure, a System Information Network could be used to sense whether the HVAC fan fails and to cause the Compartment door to be opened, either manually or automatically. In this example, the exhaust duct would be an example of a Non-Operational Energy Sink.

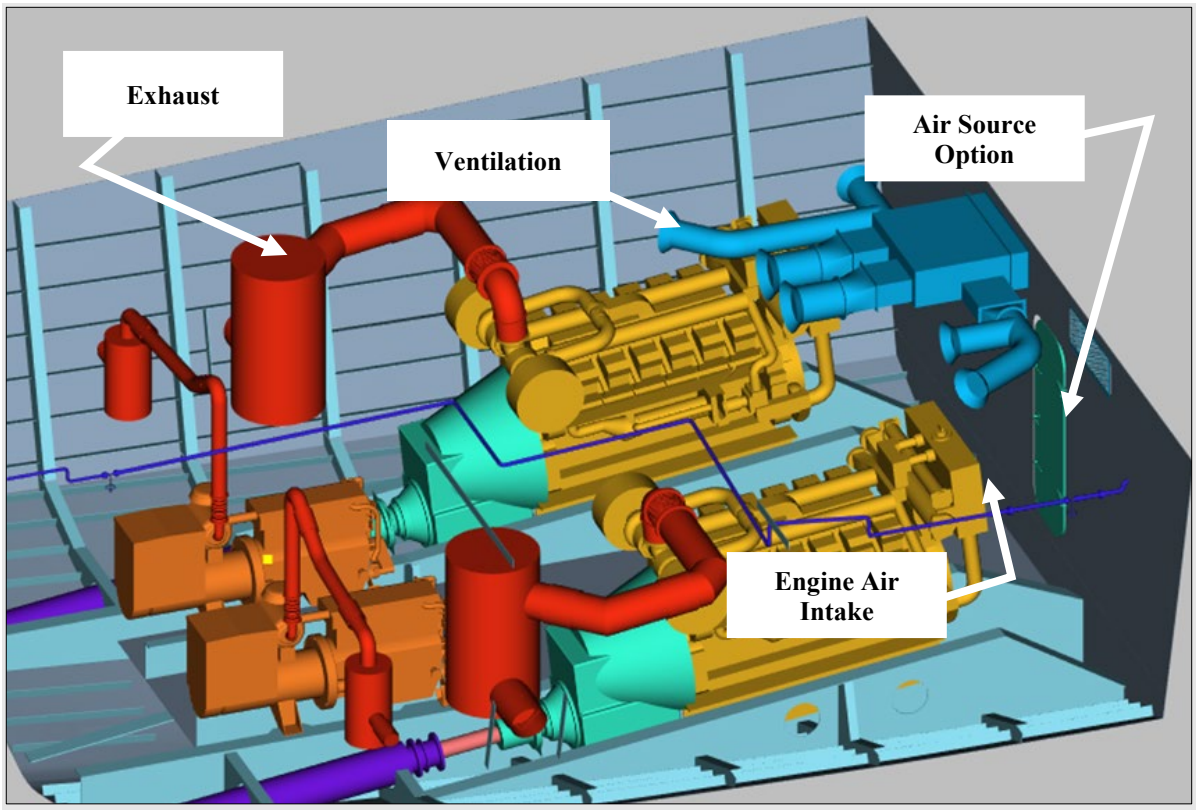

Figure 9 - Notional Machinery Room

DEVELOPMENT OF NETWORK ONTOLOGY

The requirements and use cases that drive the modeling of an Energy Network should be identified prior to ontology development. The objective is to enable Component and platform sizing, technology fusion, and operational measures of performance during early stages of design. However, the strategy of ontology design and development follows a philosophy of supporting all stakeholders of data at all stages of design. The ontology model must be rich in information related to connectivity, properties, and operational state. The energy flow model must be able to understand this ontology, analyze energy flow, and be able to change the state of Components. The ontology model must be able to characterize behaviors between Components, within Components, and between Components and Concept space (e.g. arrangements).

In ship design it is easy to ignore the complexity of some standard ship Components simply because there are so many of them, and modeling everything at all levels of detail is not possible or desirable. To the engineer worried about the performance of some of those Components, however, these details matter. Ontology development should not care what you choose to model, or how much detail you provide or require, only that you can provide the data necessary to model the problem. This leaves the detail of details to the application generating or using the data.
The following are some of the decisions that were made about ontology development given the requirements we established.

From a data modeling standpoint,

1. Capabilities correspond to a hierarchy of required Operational Capabilities. Capabilities are only described in the abstract and does not specify how a capability is to be implemented. A Capability is structured as a hierarchy of Capabilities, with the most general at the root and most specific at the leaves. At the leaf-level, Capabilities may have a measure specified, along with an environmental condition for the measure.
2. An Operational Capability is the last Capability in the hierarchy related to a System Function Action.
3. A System Function Action defines the action of an Operational Energy Sink needed to support an Operational Capability. An Operational Sink is the Component, or Components, providing the System Function Action that transfers the energy off platform.
4. Operational Sinks define the function of a System and are the terminus of the System boundary.
5. Systems are defined as all connected Components of the Energy Network required to provide energy to the System Function Action that enables the Operational Capability of the System. This includes Components required to maintain operational integrity that do not necessarily provide energy to the System. (e.g. cooling).

Table 1 provides examples of Operational Capabilities and how they are implemented through Systems, Operational Sinks, and System Function Action.

Table 1: Example of linkages among Capability, Systems, Operational Sinks, and System Function Actions.

Mission	Capability	Operational Capability	System	Operational Sink	System Function Action
MOB	MOB 1.7-Transit at high speed.	Move	Propulsion Prime Mover System	propeller(s)	generate thrust
MOB	MOB 7.3- Get Underway/Moor	Hoist	Mooring System	windlass (s)	rotate
AW	AW 6.7- Detect, classify, track	track	Surface Surveillance Radar System	radar antenna(s)	Transmit-Receive-Rotate
AW	AW 6.7- Detect, classify, track	track	Surface Surveillance Radar System	display monitor (s)	emit

LEAPS, FOCUS, and UML

The system ontology developed is generic in its approach and was modeled using the Unified Modeling Language (UML). The UML model was built as part of the Leading Edge Architecture for Prototyping Systems (LEAPS) software development framework. Two software products, the Rapid Ship Design Environment (RSDE) and the Smart Ship Systems Design (S3D) tool (Rigterink,et al, 2016) are both leveraging this ontology model as part of design tool integration. RSDE is a 3D ship design tool that is having its Machinery Module modified to support Energy Networks and System analysis, and S3D will be a plugin within RSDE that will provide for multi-domain Energy Network modeling, energy flow, and System discovery. Once completed, these tools and others will be able to support the integration of operational requirements, Energy Network design, System discovery, and operational analysis like Electric Plant Load Analysis (EPLA). As described by Snyder et al. (2019), LEAPS and FOCUS are also being used to integrate other ship design tools.

The LEAPS MetaModel is part of the LEAPS framework. The LEAPS MetaModel is a class structure - a set of classes and the relationships between them. It is designed to be flexible enough to represent any engineered system or structure. The current version, LEAPS 6, was upgraded to facilitate the work described in this paper. A few key classes are introduced below.

Concept class - A class that defines the attributes, the Systems, the Components and the views of geometry that represents a product in design or under study. It is generic to all things engineered, but is used here to define platforms such as a ship, submarine, aircraft, or other engineered product.

Component class – represents physical objects that can be thought of as parts of a Concept. They may be connected in ways that provide function and capability. Components can be thought of as any part of a ship that represents something as discrete as a radar or engine, but also includes parts like stiffeners, plates, foundations, and mounts. A Component in many ways acts as a small Concept, but it is modeled as something a Concept owns. Components do not have their own Systems, but Components do have most of everything a Concept does.

Node class – can be owned by either a concept or a Component. Used to connect Component interfaces to either a concept interface or another Component interface. Can also be used to represent physical location or as a container for domain specific properties. Ex: Component location Nodes, ports

Diagram class - The Diagram class provides the schematic information that defines a connected graph or network. Diagrams can define a connected network between Components, within a Component, and a Connection between Components and Concept structure.

Connection class – can be owned by either a concept or a Component. Used to represent logical relationships, such as energy flow, both within a Component and across a concept. Used to connect Components to each other and the concept. Ex: interface Connections, conductors

System class – can have both diagrams and Components. The system class allows us the flexibility to model both physical and logical relationships. Ex: assemblies – collection of Components that are in physical proximity that also have a logical relationship. Ex: System, Energy Network, Domain Networks

All of these classes inherit properties. The relationships among these classes is depicted in Figure 10.

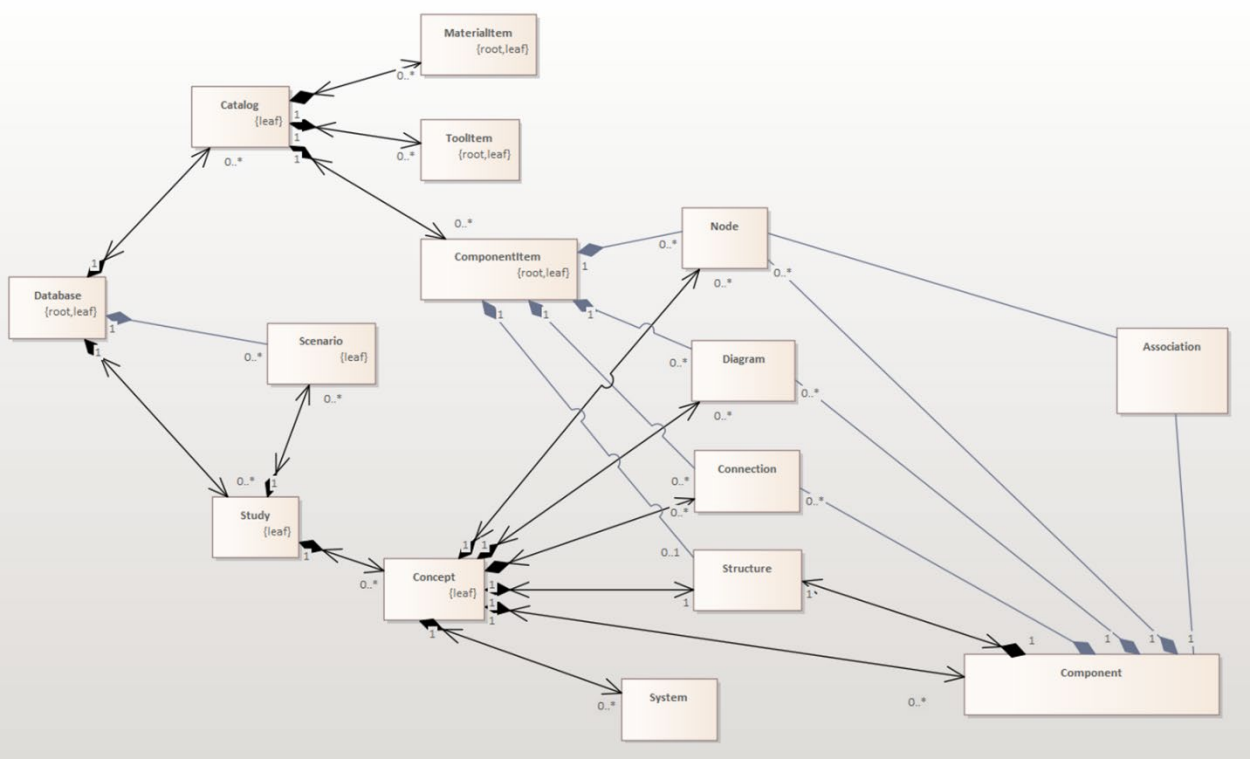

Figure 10 - LEAPS Meta Model (high level view)

Our data model is formalized at the object level. A product meta model (PMM) is an object metamodel that represents the structure and behavior of a product, such as a ship. It takes a data centric approach to integration as opposed to a data driven design (McComb, 2018). The PMM is composed of objects of the LEAPS metamodel classes and the relationships between them. It is at this level where we begin to formalize products as objects with recognizable names, such as ship Concepts, energy storage Components, etc.

Once we understand the class structure, we can look at how we use instance objects in our models. As we have mentioned earlier, one of the more challenging modeling requirements involves the ontology modeling of Components.

Component Ontology Modeling

There are varying levels of abstraction when it comes to modeling the internal workings of a Component. At the lowest level of abstraction, Figure 5, we need to look at energy flow into and out of a Component, any network relationships (Port Connections) that are necessary for a Component to function (e.g., air and fuel for combustion), and what Energy Domains a Component participates in by way of its Ports.

At a higher level of abstraction, a Component can be modeled with more detail and that detail may vary for each Energy Domain. This modeling can involve detailed internal Component networks when controls and interacting behaviors must

be simulated. The gas turbine in Figure 11 supports an explanation of Energy Network Diagrams as they relate to the behavior of a Component.

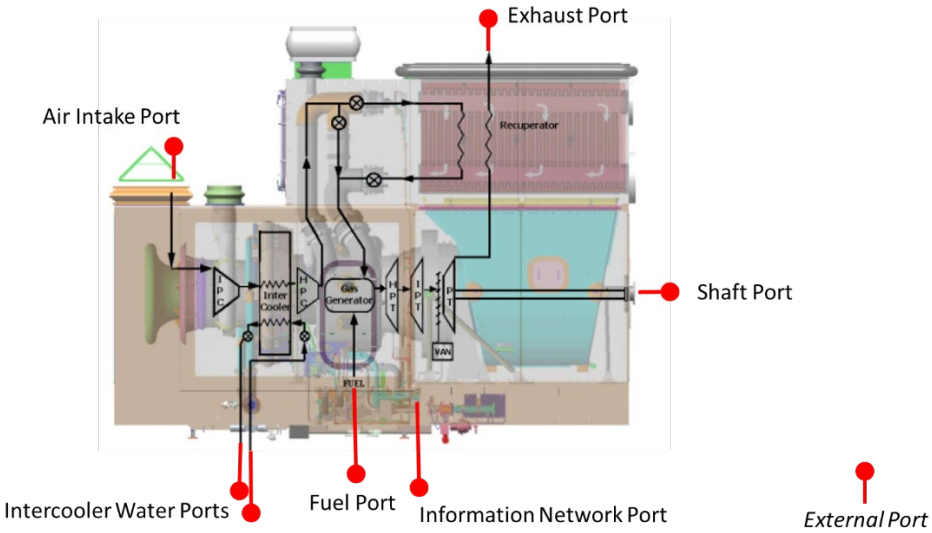

Figure 11-External Ports for Gas Turbine Diagram

In this example, the gas turbine has internal Component energy transformation as well as external Port Connections to Energy Domains like fluid-HVAC via intake and uptake ducts. Energy Domains within Components may have interacting behaviors. Consider a Component fluid domain designed to cool the electrical domain or mechanical domain – these domains will have a direct dependency on each other's behavior. It is the responsibility of the Component to capture the dependency/behavior relationship between Energy Domains interacting with each other within a Component. In the gas turbine example, when connected into the Energy Network, the HVAC ducting Components will impact the gas turbine's performance based on losses from their routing or the ambient intake air temperature. Figure 12 illustrates this relationship. In this case, pressure losses for the design of the intake duct (fluid domain Port) and the exhaust duct (fluid domain Port) are affecting rated output power at the shaft (mechanical domain Port).

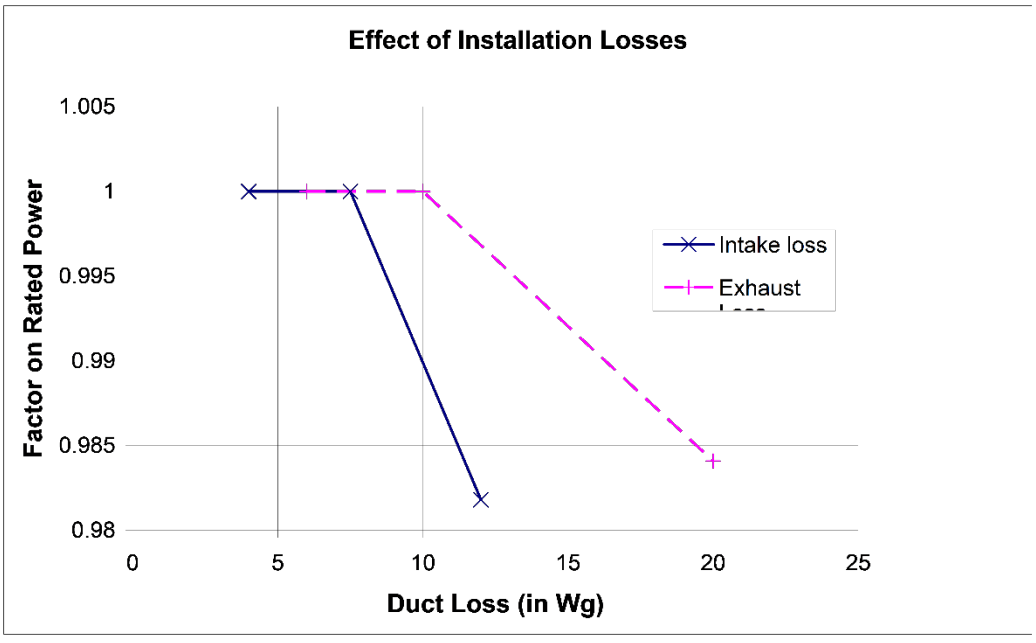

Figure 12- Port and Component Dependency

This use case requirement for Components to have internal network Diagrams demonstrates that Components can model a complexity level usually associated with Concepts, and that they have their own operational states, performance, and controls, just as a Concept does.

Ultimately the Energy Network is a graph composed of both Concept and Component networked objects. Components can have varying levels of configuration in addition to varying levels of modeling detail. Configurable Components add significant complexity when differentiating one from another. A computer Component is a perfect example. Because

Concepts and Components can have any number of Diagrams having any number of Ports (Nodes) and Port Connections, the ability to formalize something like a computer at the instance level is possible. Both the tablet and the blade server can be modeled. The challenge is in the building of specific computer instances that represent an actual Component. What will differentiate one from the other will be the Component's Diagrams. Defining these internal Energy Networks will take time and effort. As such, the need for a library of available Components with their respective Diagrams is essential.

Logical and Physical Views

The ontology follows a data centric approach. This means that the data model is designed to represent reality rather than the data requirements of any software application. In a data centric strategy, all tools see the same data even if the application is limited and specific in its use of that data. If we look at 2D schematic flow solvers like S3D, we recognize that these tools perform analysis on a logical view of the Energy Network. Applications like RSDE are more 3D driven, requiring accurate weight and volume analysis that the logical tools do not need or use. Both S3D and RSDE need to model the same Energy Network and understand the Systems represented in the design. Logical and physical views of a single data representation are possible and desirable in a data centric model, but the data must be synchronized as each application makes changes to the shared data. Consider the arrangement of Components within a Concept in the example shown in Figure 13. The purpose of the example is not to demonstrate a realistic Energy Network, but rather to show the logical and physical relationship between a cable and two connected and arranged Components. In a data centric model, there is only one cable, one laser, and one energy storage device. A very plausible use case may suggest that the logical data like Ports and Connections of the three Components may exist first. It is very likely that these logical designs will exist as patterns or collections of sub-networks persisted for reuse by tools like RSDE or S3D across different designs.

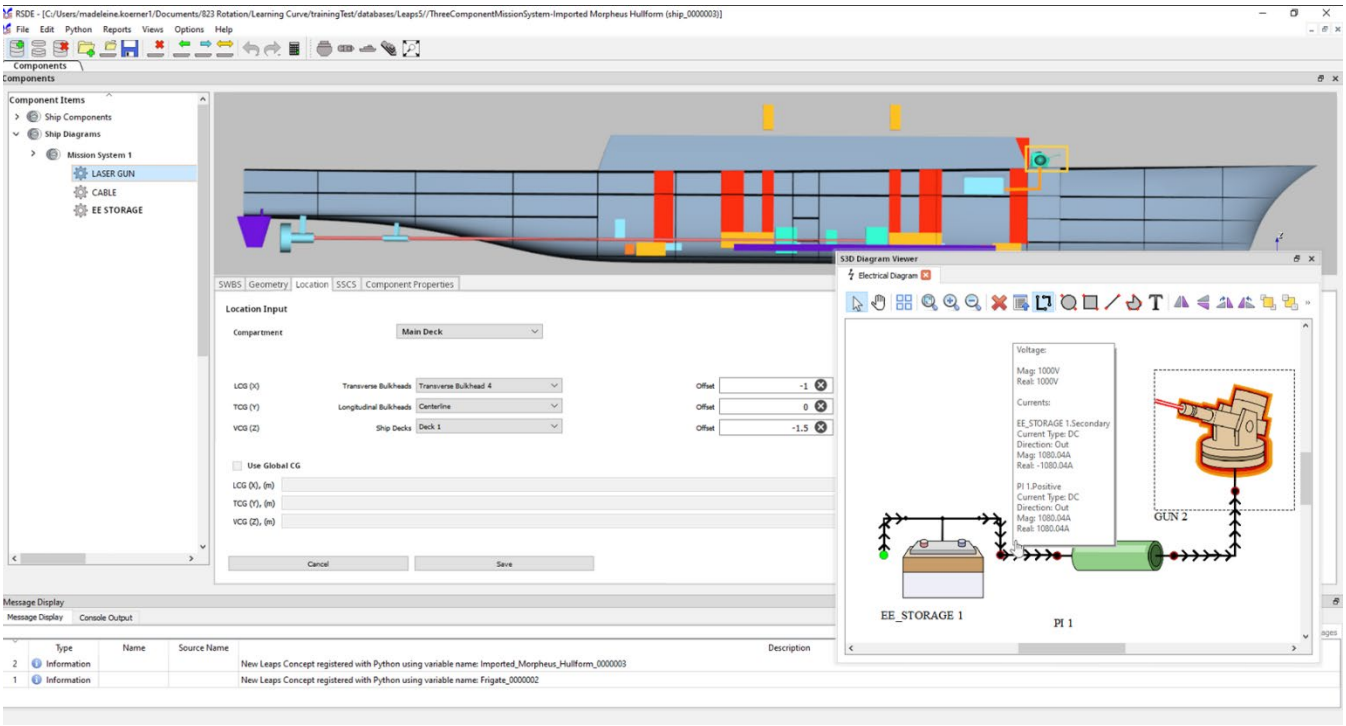

Figure 13- RSDE (physical) and S3D (logical) views of the same data

RSDE may need to add this pattern and rearrange either the battery Component or the laser Component. Within RSDE the cable would need to be routed and the resultant cable length updated in the database. The logical connectivity between the three Components remains unchanged.

The relationship between the electricCable Component and the electricalCableLength Property in the UML model is depicted in *Figure 14*. The cable owns this length property, but it is the responsibility of the applications to ensure that as a cable changes, its data is updated.

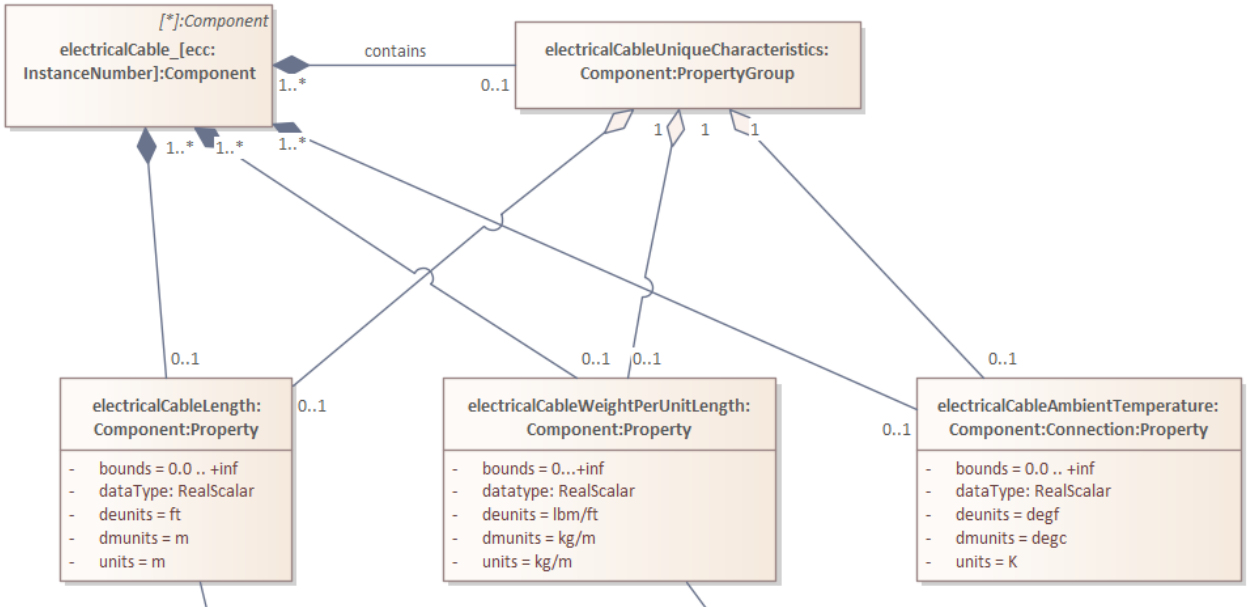

Figure 14- Electrical Cable properties

The electrical resistance of the cable provides another example of the interdependency between the Concept and the Component. This property will change based on the temperature of the compartments that the cable is routed through. The powerflow simulation is therefore affected by the Concept even if the simulation is unaware the Concept exists. Ship design software like RSDE define and update Component Property data, such as cable length, during arrangements. Analysis software such as S3D use these Component property data to analyze and simulate the Concept.

Proxy Components

During early stages of the design process, not every Component will necessarily be modeled. Compartment lighting is a good example. It is not feasible during concept design to model every light and electrical cable and switch on the ship so estimates of the lighting load are used. These estimates are captured in Proxy Components.

Currently tools like RSDE estimate the lighting load based off of the arrangeable area of compartment spaces in the ship. A Proxy Component should have both a knowledge of the Concept it belongs to and a method to solve for its load independent of the power flow simulation. For the lighting example, the proxy lighting Component (or an external application) would get the space volume data from the Concept and would include the equation that relates the volume to the properties, such as requestedElectricalPower, necessary for the power flow simulation. Proxy Components can also be used to simulate a portion, or sub-network, of an overall Energy Network by providing substitute sources and loads. As depicted in Figure 15, the proxy Components provide or sink the energy at the boundary interfaces of the sub-network under study; they establish the sub-network boundary conditions.

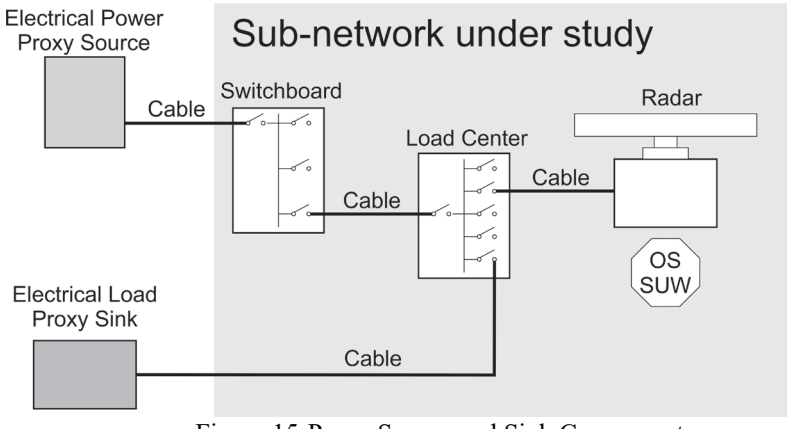

Figure 15-Proxy Source and Sink Components

Ports

As depicted in Figure 16, Component Ports can be of multiple Port types:

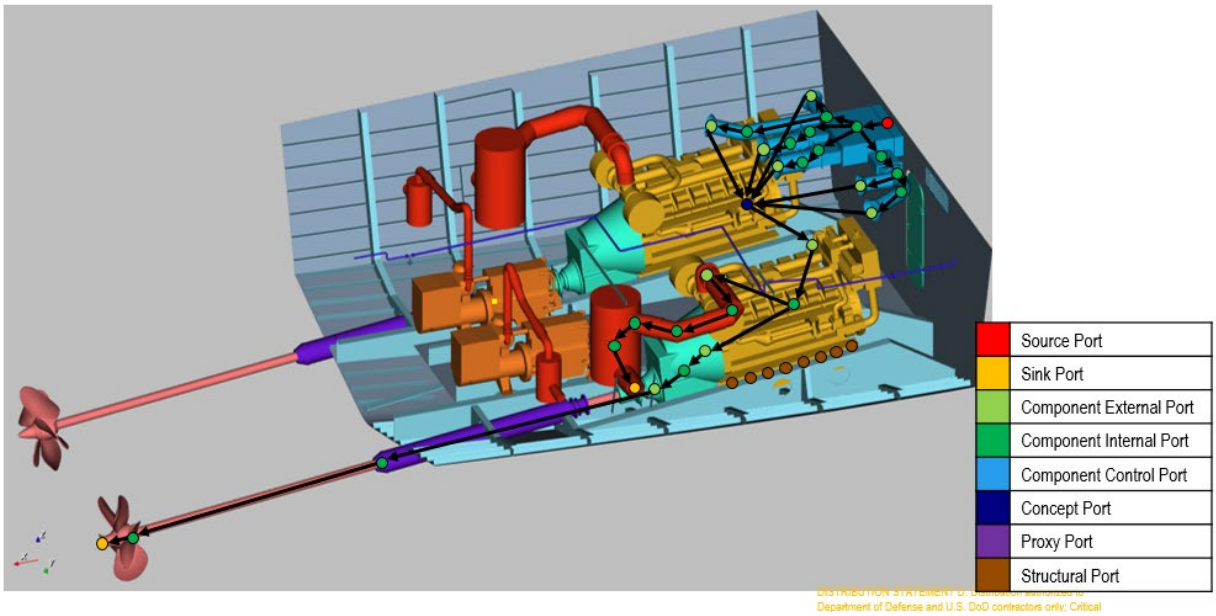

Figure 16- Port examples

Component External Ports

External Ports are Ports that allow for input and output into and out of a Component, and provide Connection to other Components via their external ports. For example, the gas turbine from Figure 11 will have multiple external ports. There will be input external ports for fuel and air, there will be output external ports such as power out and exhaust out. These ports have attributes such as Connection type, ratings for inputs such as flowrate for fluids and power ratings for electrical ports. External ports can also be bi-directional.

Component Internal Ports

Internal ports are used to define any changes within a Component that provide necessary information for a simulation. An example of an internal Port is a T-Pipe. Unlike a straight pipe, a T-Pipe will have a single input and two outputs (or vice versa.) At the intersection point of the T, an internal Port will be used to inform the fluid flow simulation that the flow is splitting at this location and to calculate the necessary flowrates for all inputs and outputs.

Component Control Ports

Component Control Ports are ports on a Component that describe controllable attributes or measured quantities for simulations. A simple example of a control Port could be a ball valve actuator handle. See Figure 17. The Port would not have an effect on the physical representation of the Component but would contain the information needed for analysis in simulation tools.

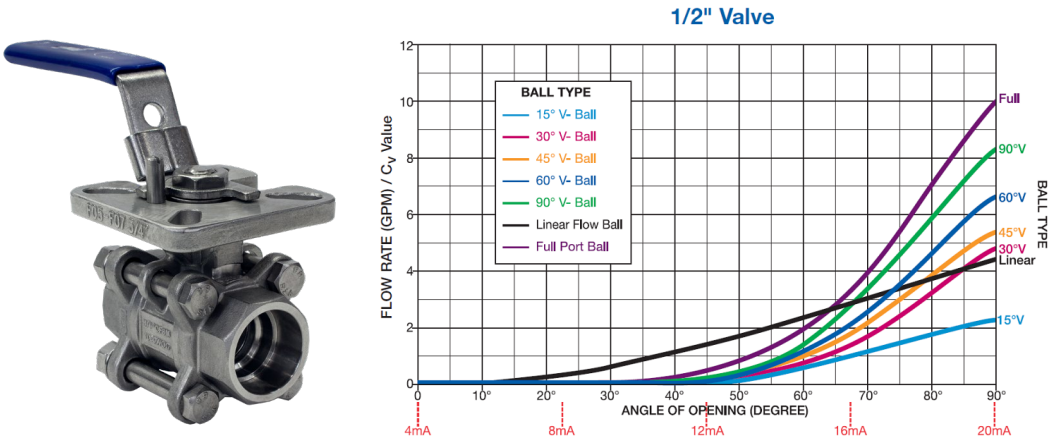

Figure 17: Component Control Port example

Source Ports

A Source Port will be the entry point of an Energy Network where an Energy Resource (Natural or Manmade) enters the network from the concept or the environment. An example of this type of Port is the inlet to a fuel line or an air intake to a gas turbine. See Figure 18. A space in the ship used to store fuel is not a Component, but the fuel contained there is a

natural Energy Resource. The external Port of an inlet pipe should connect with and understand that is it connected to a fuel tank if the Energy Network is to connect sources to sinks. It may need to understand the tank's capacity.

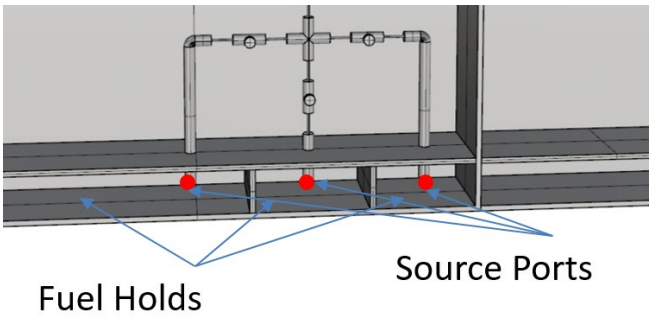

Figure 18- Source Port Example

Sink Ports

A Sink Port is the last point of an Energy Network where energy is discharged to the Natural Environment. The propellers of a ship would have Sink Ports (Figure 18) where the energy from Fuel and Air for Combustion Sources is finally discharged to the environment to "Move" the ship. (A lot of the energy is also discharged through the exhaust pipes – but not all of the energy discharged through the exhaust pipes is attributable to a given Energy Network)

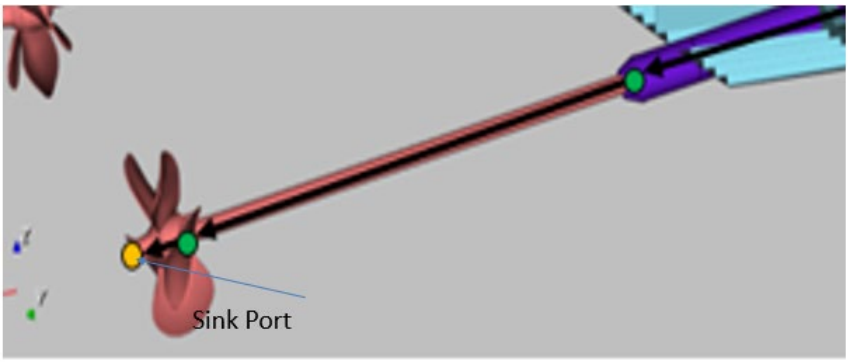

Figure 18: Sink Port Example

Concept Ports

Concept ports are the subset of Component Ports that connect to the environment at the boundaries of the Concept but are neither Source Ports nor Sink Ports. In LEAPS, openings can have properties that define them as doorways, hatches, ducts, and other open boundaries in the ship's geometry where the knowledge of that opening is important. Knowing a compartment has an opening with a door associated with it allows for the opening to have a state (open, closed).
Concept Ports also provide for energy transfer between Components that are not physically connected.

ONGOING WORK

This paper has described the ontological work completed to date. We are currently exploring the incorporation of Elements, Patterns, and Templates into the ontology.

An Element (Figure 19) is a type of Interface that provides for a specific and possibly formalized function. Elements are composed of other Interfaces that provide logical Connections to proxy Components, Component Blocks, Patterns, or other Elements. Elements can be owned by either the Concept, Component, or Catalog Component Item.

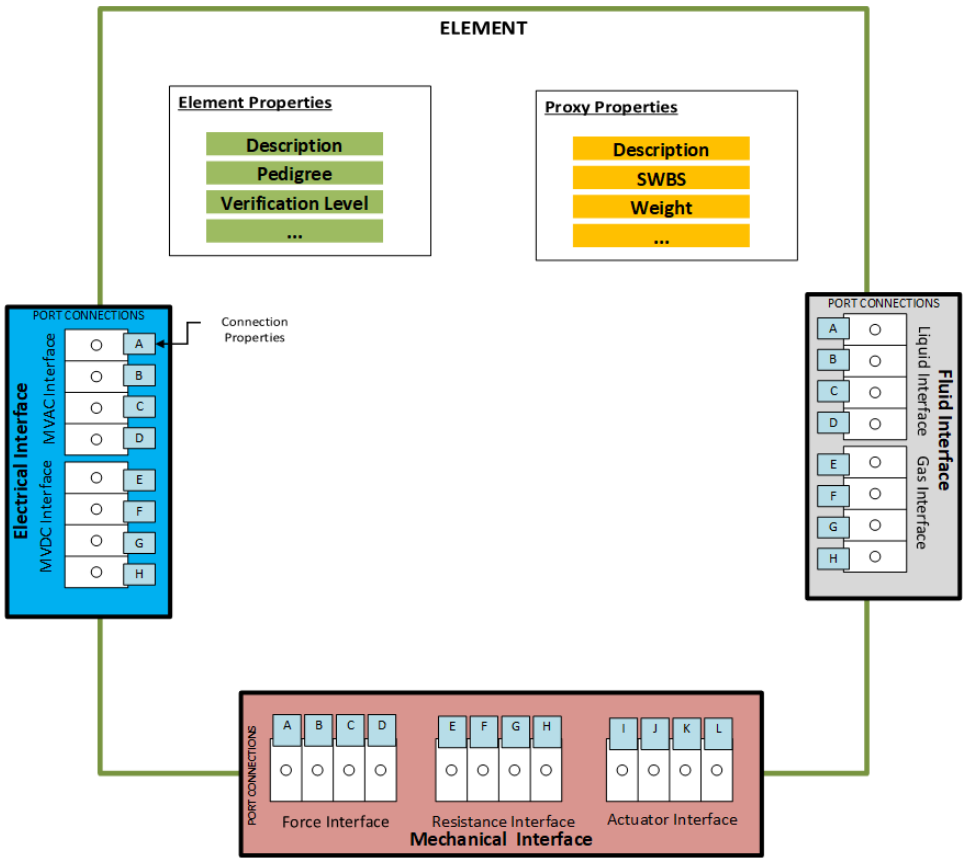

Figure 19: Element example

Elements can have many applications. The initial application of interest is the ability to represent a single interface from which multiple Components, Component Blocks, and Patterns can be substituted during design and analysis. As a design matures, the Element remains as an architectural feature of the network, but the model structure connecting its interfaces can become more detailed as required. Figure 20 depicts an Element where the contained Component evolves from a proxy Component to a diagram of Components. Ongoing work is determining how to represent elements within the ontology.

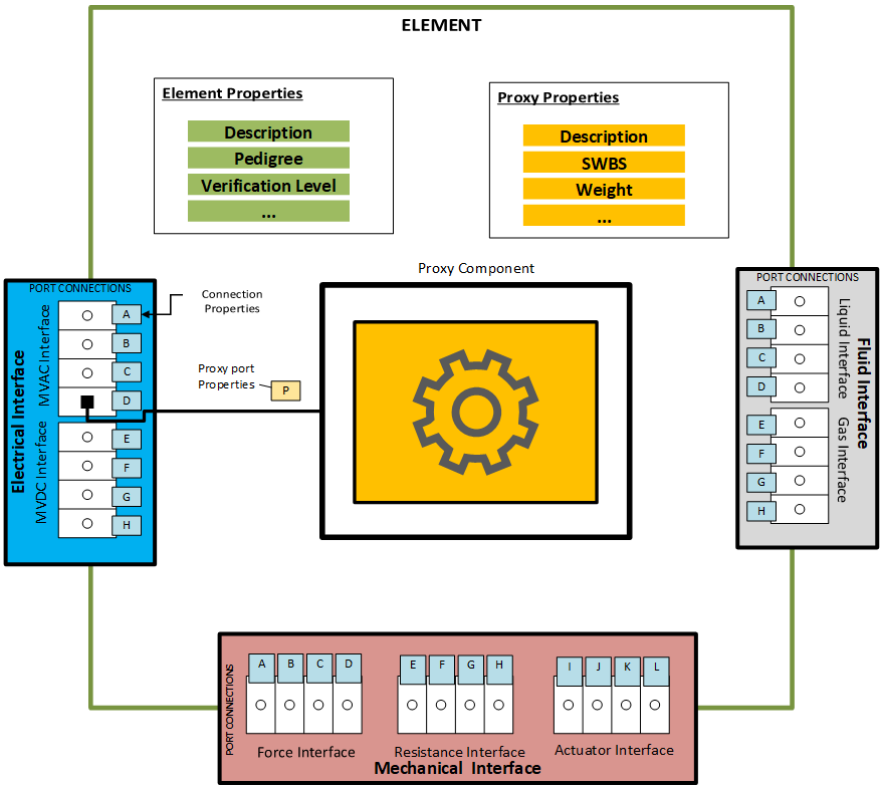

(a)-

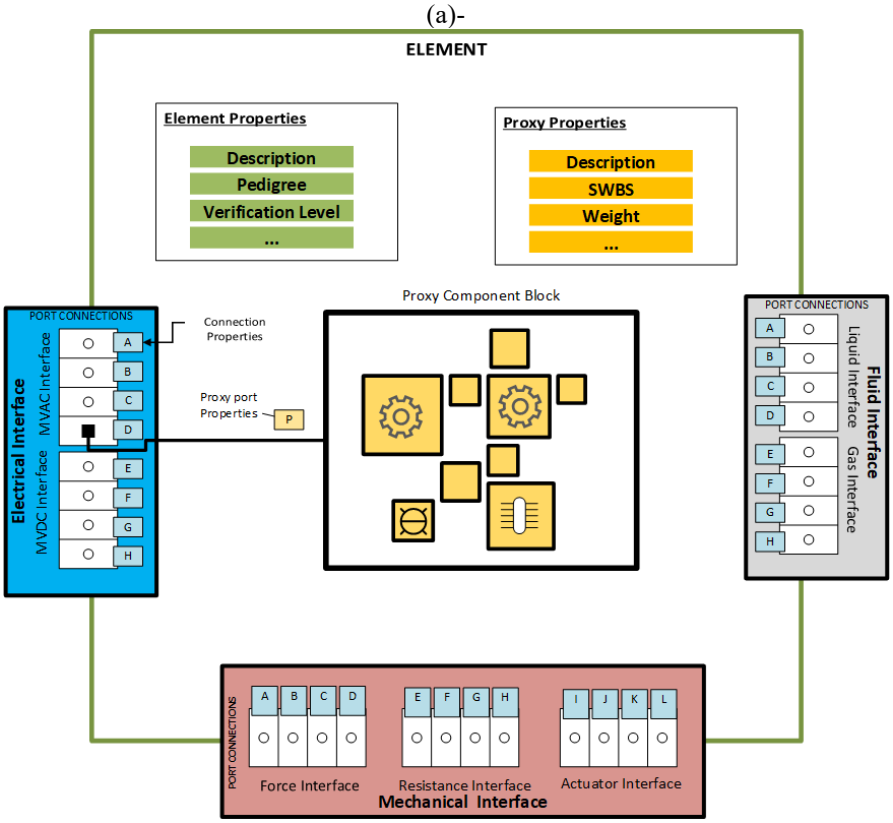

(b)

Figure 20: Element evolution (a) early stages of design (b) later stages of design

As described by Rigterink et al. 2016, Chalfant and C. Chryssostomidis 2017, and Chalfant et al. 2019, patterns are diagrams of sub-networks or networks where the Component properties are set at default values. Patterns enable reuse of architectures across multiple designs; the Components serve as functional entities. A template is a pattern where the Component properties have been defined to represent a specific concept and sufficient sources and sinks (perhaps proxy sources and sinks) are incorporated to conduct a simulation to answer a specific question. Ongoing work is identifying how to represent patterns and templates within the ontology.

CONCLUSION

A well-defined and extendable ontology is a key enabler for integrating multiple ship design and analysis tools. This paper focuses on describing ongoing efforts to define such an ontology to support ship design and the analysis of Energy Networks. This ontology is being implemented in LEAPS and FOCUS to enable interoperability of RSDE and S3D in the near term. More tools are anticipated to be integrated in the future.

REFERENCES

Ames, R., (Fall 2016). *Shifting Ship Design into High Gear: A New Power and Energy Future Is Coming*, Naval Science and Technology, Future Force Magazine,

Ames, R., & Cooper, K., (2018). *A Perspective on US Navy Early Stage Design Tools and Future Challenges*, SNAME SMC

Chalfant J., & Chryssostomidis,C. (Aug 2017) *Application of templates to early stage ship design*," IEEE Electric Ship Technologies Symposium (ESTS), pp. 111–117.

Chalfant, J., Z. Wang, M. & Triantafyllou M., (August 14-16, 2019). *Expanding the Design Space Explored by S3D*, presented at IEEE Electric Ship Technologies Symposium 2019, Westin Crystal City Hotel, Arlington VA,

Fowler, M., (September 15, 2003). *UML Distilled: A Brief Guide to the Standard Object Modeling* Language (3rd), ISBN 9780321193681

McComb, D., (2018) *Software Wasteland and The Data-Centric Revolution*

Noy, N. F. & McGuinness, D.L. (2001). *Ontology Development 101: A Guide to Creating Your First Ontology*, Retrieved from URL https://protege.stanford.edu/publications/ontology_development/ontology101.pdf

Rigterink, Dr. D. T., Ames, R., Gray, Dr. A., & Doerry, Dr. N. (May 25-26, 2016*). Early-Stage Assessment of the Impacts of Next Generation Combat Power and Energy Systems on Navy Ships*, ASNE Advanced Machinery Technology Symposium, Villanova University Connelly Center, PA,

Rumbaugh, James, Jacobson, Ivar, Gooch, & Grady, *The Unified Modeling Language Reference Manual*", ISBN 0-321-24562-8

Snyder, D. J., Parsons, M, Brown, Dr. A., & Chalfant, J., (August 14-16, 2019). *Network Architecture Framework Applications with FOCUS-Compliant Ship Designs*. IEEE Electric Ship Technologies Symposium 2019, Westin Crystal City Hotel, Arlington VA,.

Unified Modeling Language Specification, (Jan. 2005). Version 1.4.2. ISO/IEC 19501:2005(E), formal/05-04-01, Retrieved from URL https://www.iso.org/standard/32620.html

Proceedings of 15th International Marine Design Conference (IMDC-2024)
June 2-6, 2024
Amsterdam, the Netherlands

Hydrodynamics of an Underwater Vehicle Near the Sea Surface

Mavrakos S. Anargyros[1,2], Konispoliatis N. Dimitrios[2*], Rossides George[3], Mavrakos A. Spyridon[2]

ABSTRACT

The primary goal of this study is to evaluate the hydrodynamic characteristics and the wave exciting forces on a shallowly submerged vehicle. A thin, rigid plate, which is completely submerged beneath the free surface in waters of finite depth is considered herein. The examined body is similar to an unmanned vehicle which is developed in Cyprus Marine and Maritime Institute for ocean science applications. From the present analysis the phenomenon of negative added mass and rapid variations of the added mass and damping coefficients is verified due to the free surface effect which is explained in terms of near-resonant standing waves above the submerged body.

KEY WORDS

Hydrodynamics; Exciting Forces; Added Mass; Damping Coefficient; Submerged Structure.

1. INTRODUCTION

Studying the hydrodynamic characteristics of bodies submerged near to the sea surface is especially crucial for specific scenarios in ocean engineering. Specifically, the maneuverability and control of unmanned underwater vessels when they interact with the sea surface become critical for safe operations, requiring accurate prediction of hydrodynamic loading and vessel motion characteristics. However, motion maneuvering analysis is traditionally focused on surface vessels and submerged bodies floating far away from the free surface. On the other hand, little analysis is available on the case where a vessel is floating near the free surface.

As early as 1960s Ogilvie (1963) presented a two-dimensional analysis concerning horizontal cylindrical bodies with circular or square cross sections submerged near the free water surface, concluding to a negative hydrodynamic (added) mass occurrence. In addition, Chung (1977) conducted experiments on a two-dimensional submerged circular or square cross section which was forced to oscillate in sway and heave directions for several submergences below free water surface. He illustrated negative added mass values for a square section when the submergence was on quarter of the semi-width. Newman et al. (1984) explained the occurrence of negative added mass values, along with rapid variations in the damping and added mass coefficients for certain frequency ranges, based on the resonant free surface motion observed in the fluid region above a submerged body. Similar physical argumentation was applied by Mavrakos (1993) in order to explain the negative added mass and sharp peaks of the force coefficients and the hydrodynamic characteristics of groups of interacting axisymmetric submerged bodies near the free surface or the seabed. Recently, a self-regulating fuzzy depth control method was developed by Shao et al. (2012) in order to maintain a cylindrical submerged structure at a specific depth below the free water surface, under free surface disturbances.

Fully submerged objects moving near the free surface deform the water surface and create propagating waves that carry away energy. This dissipation of energy leads to a resisting force known as wave drag force. The problem was theoretically treated by Michell (1898) and Havelock (1917, 1931) for spheres and spheroids, whereas Chepelianskii et al. (2010) addressed the

[1] Inlecom Group, Brussels, Belgium; 0000-0002-8290-9861
[2] Laboratory for Floating Structures and Mooring Systems. Division of Marine Structures, School of Naval Architecture and Marine Engineering, National Technical University of Athens, Athens, Greece; 0000-0001-7256-513X; 0000-0002-7250-9581
[3] Cyprus Marine and Maritime Institute, Larnaca, Cyprus; 0000-0003-0522-812X
* Corresponding Author: *dkonisp@naval.ntua.gr*

Submitted: 16 February 2024, Revised: 17 April 2024, Accepted: 1 May 2024, Published: 21 May 2024

Conference paper, DOI: https://doi.org/10.59490/imdc.2024.861 e-ISSN: 3050-4864

influence of an immersed cylinder on wave propagation based on the analysis on submerged spheres. Also, Benusiglio et al. (2015) used fully submerged spheres to study the effect of the wave drag near the free surface. It was emphasized that the wave drag was comparable in magnitude to the hydrodynamic drag when the top of the sphere was at less than one sphere radius from the surface.

Although little analysis is available on submerged axisymmetric cylindrical/spherical bodies near the free surface, the movement of submarines in a near-surface water environment has been the subject of many studies in the literature. Submarines descend to periscope or snorkeling depth for target exploration or battery recharging. In such scenarios environmental loads like waves, currents, resistance and suction forces are imposed on the submerged structure (Arentzen and Mandel, 1960; Burcher and Rydill, 1995). Several studies have been presented in the literature investigating the impact of the free water surface on an underwater vehicle through both numerical and experimental methods. Indicatives are Jagadeesh et al., 2009; Manssorzadeh and Javanmard, 2014; Nematollahi et al., 2015; Conway et al. 2018; Amiri et al., 2018, 2019a, 2019b, 2020; Lambert et al. 2020; Sudharsun et al. 2022; Ling et al. 2023. Furthermore, since the imposed forces on a submerged structure are different from those in large water depths, submarines are required to keep the necessary navigating pose (depth, roll angle and trim angle). Consequently, numerous research activities on depth control have been performed. Specifically, Hao et al. (2004) developed a two-step depth fuzzy controller to produce stern angle to counteract the second-order exciting wave forces on a submarine, whereas Choi et al. (2006, 2008) proposed a mathematical model for the evaluation of the wave exciting forces on a submerged structure and performed depth control simulations using the proportional-integral-derivative method. Rezazadegan et al. (2015) proposed a novel adaptive trajectory tracking control of an autonomous underwater vehicle in six-degree of freedom. In addition, Park et al. (2016) elaborated an adaptive control technique utilizing a neural network and a proportional-integral-derivative controller to regulate the depth of a submerged body in close proximity to free water surface. At the same time, the case of the water surface being covered with ice has also been considered. Zemlyak et al. (2021, 2023) studied theoretically and experimentally the motions of a submerged body near the free water surface when the latter was covered by ice. Here a sink-source model was applied, and the ice cover was simulated as a thin elastic plate floating on the water surface, whereas the experiments were performed in an ice tank. It was concluded that the variation of the relative submergence of a body moving at a shallow submergence attained non negligible values.

The main objective of this investigation is to evaluate the hydrodynamic characteristics and the wave exciting forces on a shallowly submerged vehicle. A thin, rigid plate, which is completely submerged beneath the free surface in waters of finite depth is considered herein. The examined body is similar to an unmanned vehicle which is developed in Cyprus Marine and Maritime Institute (CMMI) for ocean science applications. In the present analysis a semi-theoretical formulation is described by properly composing the solutions of the diffraction and the motion radiation problems around the floating structure within the framework of linear potential theory. This is done under the assumption of an incompressible and inviscid fluid and an irrotational flow. In addition, two numerical simulation tools, ANSYS Aqwa and HAQi software, are also implemented to compare the numerical results with the theoretical ones.

The rest of this paper is structured as follows. In Section 2 the geometric model of the underwater vehicle is introduced. Section 3 presents the developed theoretical formulation within the domain of linear potential theory, whereas focus is also given to the applied numerical models. Section 4 is dedicated to the presentation of the outcomes of the two applied formulations whereas conclusions of the work are drawn in Section 5.

2. DESCRIPTION OF THE CONSIDERED AUTONOMOUS UNDERWATER VEHICLE

Underwater gliders are autonomous vehicles that move through the water by changing their buoyancy and pitch (Javaid et al., 2014), which makes them more energy-efficient than other types of autonomous marine vehicles (AMVs) while minimizing their acoustic signature. This makes them ideal for many oceanic surveying applications, including long-term environmental monitoring, marine animal tracking and oceanographic surveying (Javaid et al., 2014). Additionally, gliders are relatively low-cost and can be deployed for extended periods.

The traditional torpedo-shaped underwater gliders are limited by their slow speed and restricted maneuverability, which can make them unsuitable for some applications (Javaid et al., 2014). To address some of these limitations, Disk-Type Underwater Gliders (DTUG) emerged (Nakamura et al., 2007, 2008; Yu et al., 2017; Zhou et al., 2020). Unlike torpedo-shaped gliders, DTUGs have omnidirectional motion capabilities, which make them more maneuverable and better suited for navigating complex underwater environments, such as near islands or inside narrow channels. An important example of such a marine environment is the Aegean Sea, where the existence and close proximity of large and small islands and rocky islets as well as the dense marine traffic (both for commercial and leisure purposes), require autonomous vehicles that operate in this region to have high-manoeuvrability capabilities. The Cyprus Marine and Maritime Institute is exploring the DTUG trend through the design and implementation of its own DTUG prototype, which has diameter of 5.2m and overall height of 0.86m, as shown in Figure 1, specifically for use in the Aegean Sea and eastern Mediterranean regions.

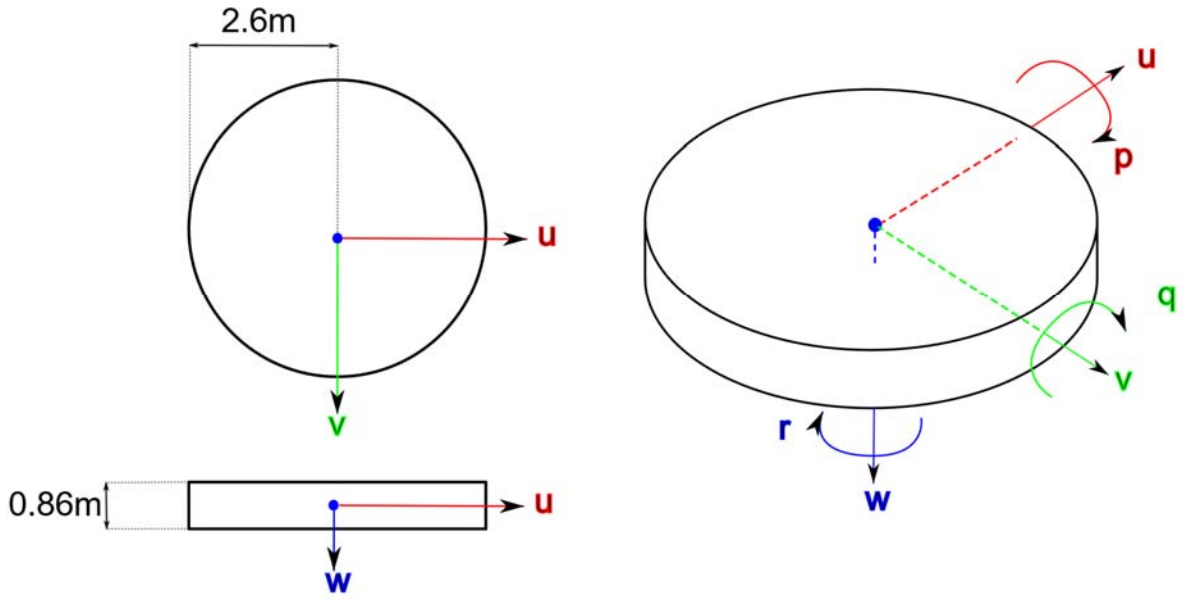

Figure 1: Schematic representation of the examined Disk-Type Underwater Glider

The large size of the DTUG enables it to carry high-volume buoyancy engines, which in turn allow it to navigate while carrying large payloads of more than 200kg, including components of energy harvesting technologies that can enhance its overall power autonomy. Additionally, its flat and wide structure offers stealth capabilities when the DTUG lies on the ocean surface, since it can become nearly invisible to both underwater and above surface detection methods (e.g., underwater sonar and above-surface radar).

The existence of negative hydrodynamic (added) mass and excitation forces that can occur near the ocean surface can enable the DTUG to maintain its shallow depth without the need for additional consumption of energy. At the same time, to achieve full submersion away from the ocean surface, these hydrodynamic effects need to be overcome. The creation of a comprehensive autonomous controller that can properly utilize or overcome these hydrodynamic effects depending on the mission needs of the DTUG, requires the proper understanding of the magnitude and occurrence of these effects under different situations.

According to Fossen (2011), from a maneuvering theory perspective, the 6 DOF motion model of an underwater vehicle is given by:

$$\boldsymbol{M\dot{v} + C(v)v + D(v)v + g(x) = \tau + \tau_{wave},} \quad (1)$$

where $\boldsymbol{v} = [u, v, w, p, q, r]$ is the glider's velocity vector in the body frame, as shown in Figure 1, while $\boldsymbol{x} = [x, y, z, \varphi, \theta, \psi]$ is the glider's position and orientation vector in the inertial frame. $\boldsymbol{M = M_{RB} + M_A} \in \mathbb{R}^{6x6}$ is the system inertia matrix, $\boldsymbol{C(v)} \in \mathbb{R}^{6x6}$ is a skew-symmetric matrix describing the Coriolis and centripetal effects due to the motion of the glider and $\boldsymbol{D(v) = D_P + D_V + D_n(v)} \in \mathbb{R}^{6x6}$ is a positive-semidefinite symmetric matrix denoting the (potential, linear and quadratic) damping forces. It should be noted that quadratic damping forces (described by the $\boldsymbol{D_n(v)}$ matrix) are largely excluded from the motion model of underwater gliders, due to the very low maximum speeds that they can reach. Additionally, forces occurring by Coriolis and centripetal effects (described by the $\boldsymbol{C(v)}$ matrix) can be also assumed to be negligible due to the low maximum speeds of the vehicle. These simplification assumptions are further strengthened in the case of DTUGs, where their omnidirectional motion characteristics allow for small deviations between the actual motion of the DTUG and its modelled behaviour, caused by such forces, to be easily corrected as soon as they occur.

The vector $\boldsymbol{g(x)} \in \mathbb{R}^6$ describes the gravitational/buoyancy forces and moments acting on the underwater vehicle, while the vector $\boldsymbol{\tau} \in \mathbb{R}^6$ describes its actuation forces and moments. In the case of underwater gliders, the actuation of the vehicle occurs through the manipulation of its gravitational/buoyancy forces and moments and thus the two terms can be merged. Lastly, the vector $\boldsymbol{\tau_{wave}} \in \mathbb{R}^6$ describes the excitation forces acting on the glider when it operates at water depths close to the ocean surface, inside the wave-affected zone. Therefore, the simplified motion model of the DTUG takes the form:

$$\boldsymbol{[M_{RB} + M_A]\dot{v} + [D_P + D_V]v + g(x) = \tau_{wave}} \quad (2)$$

$\boldsymbol{M_{RB}}$ represents the rigid body mass and inertia and assuming that the centre of gravity (CG) of the vehicle is at the origin of its body frame, it is given by:

$$\boldsymbol{M_{RB}} = \begin{bmatrix} m & 0 & 0 & & & \\ 0 & m & 0 & & 0 & \\ 0 & 0 & m & & & \\ & & & I_x & -I_{xy} & -I_{xz} \\ & 0 & & -I_{yx} & I_y & -I_{yz} \\ & & & -I_{zx} & -I_{zy} & I_z \end{bmatrix} \tag{3}$$

$\boldsymbol{M_A}$ is the hydrodynamic (added) mass matrix which can be approximated using the potential coefficients $\boldsymbol{A}(\omega)$ by:

$$\boldsymbol{M_A} \approx \begin{bmatrix} A_{11}(0) & 0 & & \cdots & & 0 \\ 0 & A_{22}(0) & & & & A_{26}(0) \\ & & A_{33}(\omega_{heave}) & 0 & 0 & \\ & \vdots & 0 & A_{44}(\omega_{roll}) & 0 & \vdots \\ & & 0 & 0 & A_{55}(\omega_{pitch}) & \\ 0 & A_{62}(0) & & \cdots & & A_{66}(0) \end{bmatrix} \tag{4}$$

where the natural frequencies ω_{heave}, ω_{roll} and ω_{pitch} depend on the hydrostatic characteristics of the vehicle in the centre of flotation (CF) (Fossen, 2011). Due to the actuation characteristics of underwater gliders, their CF may be continuously varying throughout their operation. Describing the internal configuration of the actuation elements of the studied DTUG is beyond the scope of this paper and therefore, further analysis on how the aforementioned natural frequencies can be obtained will not be presented.

Like $\boldsymbol{M_A}$, the potential damping matrix $\boldsymbol{D_P}$ can be approximated using the potential coefficients $\boldsymbol{B}(\omega)$ by:

$$\boldsymbol{D_P} \approx \begin{bmatrix} 0 & 0 & & \cdots & & 0 \\ 0 & 0 & & & & 0 \\ & & B_{33}(\omega_{heave}) & 0 & 0 & \\ \vdots & & 0 & B_{44}(\omega_{roll}) & 0 & \vdots \\ & & 0 & 0 & B_{55}(\omega_{pitch}) & \\ 0 & 0 & & \cdots & & 0 \end{bmatrix} \tag{5}$$

On the other hand, the linear viscous damping matrix $\boldsymbol{D_V}$ is usually approximated by a diagonal matrix:

$$\boldsymbol{D_V} \approx \text{diag}\{B_{11v}, B_{22v}, B_{33v}, B_{44v}, B_{55v}, B_{66v}\} \tag{6}$$

where the elements B_{iiv} $(i = 1, \dots 6)$ depend on the potential coefficients $\boldsymbol{A}(\omega)$ and can be computed from the time constants and natural periods of the vehicle (Fossen, 2011). Once again, further elaboration on the methods used to obtain the time constants and natural periods of the vehicle, requires a description of its internal actuation elements, which lies beyond the scope of this paper.

The presented manoeuvering theory applies to vehicles operating at water depths below the wave-affected zone and it results in reduced model complexity to enable real-time motion prediction and control. To achieve this reduced complexity, the theory assumes no coupling between the surge, heave-roll-pitch and the sway-yaw subsystems, which in turn excludes the use of the potential coefficients $A_{15}, A_{51}, A_{24}, A_{42}, B_{15}, B_{51}, B_{24}$ and B_{42} from Equations (4) and (5).

Conversely, motion control near the sea surface is limited due to the way of actuation of DTUGs and it primarily involves motion along their heave-roll-pitch degrees of freedom (i.e., using the potential coefficients $A_{33}, A_{44}, A_{55}, B_{33}, B_{44}, B_{55}$) while also considering possible wave-excitation forces. That said, the calculation of other significant potential coefficients ($A_{15}, A_{51}, A_{24}, A_{42}, B_{15}, B_{51}, B_{24}$ and B_{42}) can enable further DTUG functionalities to be developed in the future. More specifically, using advanced parameter-estimation algorithms along with a more detailed motion model, it is expected that the vehicle will be able to accurately estimate the current sea-state, based on its past motion, both for oceanographic surveying applications and in order to be able to submerge itself in unfavourable weather conditions. To this end, the rest of this paper will focus on the study of all significant potential coefficients $\boldsymbol{A}(\omega)$ and $\boldsymbol{B}(\omega)$ for the studied DTUG.

3. FORMULATION OF THE PROBLEM

3.1 Theoretical Formulation

We consider a cylindrical submerged disk with vertical axis of symmetry, similar to the above DTUG, which is exposed to the action of regular waves propagating in water depth *d* with frequency *ω*. A cylindrical co-ordinate system (*r, θ, z*) is defined with origin on the sea bottom and its vertical axis Oz directed upwards (Figure 2). Let the linear translation and rotational

vector of the body's motion be denoted by $\boldsymbol{\xi} = (\xi_1, \xi_2, \xi_3)$ and $\boldsymbol{\theta} = (\xi_4, \xi_5, \xi_6)$, respectively. Their components correspond to the surge (j = 1), sway (j =2), heave (j =3), roll (j = 4), pitch (j = 5) and yaw (j =6) modes of motion. Under the assumption of a symmetrical mass distribution, a vertical cylindrical body undergoes three-degree of freedom motion in the wave propagation plane under the influence of a regular wave train, i.e. two translations (surge, ξ_1; heave, ξ_3) and one rotation (pitch, ξ_5).

Assuming further that the viscous effects are negligible, the fluid is incompressible, and the displacements of the body and the wave height are small, classical linearized water wave theory can be employed. The fluid flow can be delineated by the potential function:

$$\Phi(r, \theta, z; t) = Re[\varphi(r, \theta, z).\, e^{-i\omega t}] \tag{7}$$

where the complex potential function $\varphi(r, \theta, z)$ can be expressed, on the basis of linear modelling, as a superposition of the incident, φ_0, scattered, φ_7, and radiated wave fields due to the motion of the body, i.e.

$$\varphi = \varphi_0 + \varphi_7 + \sum_{j=1,3,5} \dot{\xi}_{j0}\, \varphi_j = \varphi_D + \sum_{j=1,3,5} \dot{\xi}_{j0}\, \varphi_j \tag{8}$$

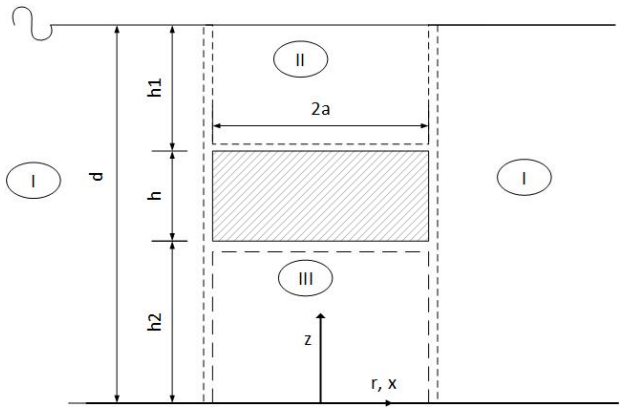

Figure 2: Submerged disk. Definitions and discretization of the flow field around the body.

Here, φ_j denotes the potential of the wave field due to the forced oscillation of the body in the *j* th mode of motion with unit velocity amplitude $\dot{\xi}_{j0}$. Moreover, all contributions to the total potential φ must be solutions of the Laplace's equation in the entire fluid domain and must meet the following boundary conditions:

$$\omega^2 \varphi_D - g\, \frac{\partial \varphi_D}{\partial z} = \omega^2 \varphi_j - g\, \frac{\partial \varphi_j}{\partial z} = 0, \quad z = d, \quad j = 1, 3, 5 \tag{9}$$

$$\frac{\partial \varphi_D}{\partial z} = \frac{\partial \varphi_j}{\partial z} = 0, \quad z = 0, \quad j = 1, 3, 5 \tag{10}$$

$$\frac{\partial \varphi_D}{\partial \boldsymbol{n}} = 0, \quad on\ S \tag{11}$$

$$\frac{\partial \varphi_j}{\partial \boldsymbol{n}} = n_j, \quad on\ S, \quad j = 1, 3, 5 \tag{12}$$

Where $\partial(\ )/\partial \boldsymbol{n}$ stands for the derivative in the direction of the outward unit normal vector $\boldsymbol{n}$ to the mean wetted surface *S* of the body and n_j are its generalized normal components specified by:

$$\boldsymbol{n} = (n_1, n_2, n_3), \quad \boldsymbol{r} \times \boldsymbol{n} = (n_4, n_5, n_6) \tag{13}$$

$\boldsymbol{r}$ is the position vector of a point on *S* with respect to the body's reference point of motion expressed in the co-ordinate system (*r, θ, z*). Finally, a radiation condition must be enforced stipulating that propagating disturbances must be outgoing.

The velocity potential of the undisturbed incident wave system, φ_0 propagating along the positive x – axis can be described in the cylindrical co-ordinate system (*r, θ, z*) as follows:

$$\varphi_0(r,\theta,z) = -i\omega A \frac{Z_0(z)}{Z_0'(d)} \sum_{m=0}^{\infty} \varepsilon_m i^m J_m(kr)\cos(m\theta) \tag{14}$$

In Equation (14), A denotes the wave amplitude, ε_m is the Neumann's symbol (i.e., $\varepsilon_0 = 1;\ \varepsilon_m = 2$ for $m > 0$), J_m is the mth order Bessel function of first kind, Z_0 equals to:

$$Z_0(z) = N_0^{-1/2}\cosh(kz) = \left[\frac{1}{2}\left[1 + \frac{\sinh(2kd)}{2kd}\right]\right]^{-\frac{1}{2}}\cosh(kz) \tag{15}$$

and $Z_0'(d)$ denotes Z_0 derivative at $z = d$. The wave number k is associated with the wave frequency ω by the dispersion equation: $\omega^2 = kg\tanh(kd)$.

For solving the diffraction and radiation problems, the method of matched axisymmetric eigenfunction expansions will be utilized. As per the method, the flow around the submerged cylinder is subdivided into cylinder - shaped fluid regions, denoted by I, II, III (see Figure 2), where appropriate series representations of the fluid's velocity potential in cylindrical co-ordinates will be established.

In accordance with the series representation of the undisturbed incident wave potential, eq. (14), the diffraction potential at each fluid region $\ell = I, II, III$ is anticipated to:

$$\varphi_D^l(r,\theta,z) = -i\omega A \sum_{m=0}^{\infty} \varepsilon_m i^m \Psi_{Dm}^{\ell}(r,z)\cos(m\theta) \tag{16}$$

while for the radiation velocity potential φ_j^p at each fluid domain, ℓ, yields:

$$\varphi_j^l(r,\theta,z) = \sum_{m=0}^{\infty} \Psi_{jm}^{\ell}(r,z)\cos(m\theta)\,,\ j = 1,3,5 \tag{17}$$

In the unknown functions Ψ_{jm}^{ℓ} (see Equations (16) and (17)), the first subscript $j = D, 1, 3, 5$ signifies the representative boundary value problem being considered, while the second subscript the m values that need to be taken into account. It is worth noting that the fluid flow resulting from the forced oscillation of the cylinder in still water, is symmetric about $\theta = 0$ - plane and antisymmetric about $\theta = \frac{\pi}{2}$ -plane for surge (j = 1) and pitch (j = 5) mode of motions, whereas it is symmetric with respect to both these planes for heave mode, (j = 3). Hence, Equation (17) can be rewritten as:

$$\varphi_j^l(r,\theta,z) = \Psi_{j1}^{\ell}(r,z)\cos(\theta),\ j = 1{,}5 \tag{18}$$

$$\varphi_3^l(r,\theta,z) = \Psi_{30}^{\ell}(r,z),\ j = 3 \tag{19}$$

To evaluate the unknown functions Ψ_{jm}^{ℓ} the method of separation of variables for the Laplace differential equation is employed. Consequently, suitable series representations of the functions $\Psi_{jm}^{\ell}, j = D, 1, 3, 5;\ \ell = I, II, III$ in each fluid domain around the submerged disk can be established (Kokkinowrachos, et al, 1986; Mavrakos, 1985, 1988, 2004)

(a) Outer fluid domain I $(r \geq a, 0 \leq z \leq d)$

$$\frac{1}{\delta_j}\Psi_{jm}^{I}(r,z) = g_{jm}^{I}(r,z) + \sum_{n=0}^{\infty} F_{jmn}^{I} \frac{K_m(a_n r)}{K_m(a_n a)} Z_n(z) \qquad \text{for } j=D,\ 1,\ 3,\ 5; \tag{20}$$

where:

$$g_{Dm}^{I}(r,z) = \left\{J_m(kr) - \frac{J_m(ka)}{H_m(ka)}H_m(kr)\right\}\frac{Z_0(z)}{d\dot{Z}_0(d)}\ ; \qquad g_{11}^{I}(r,z) = g_{30}^{I}(r,z) = g_{51}^{I}(r,z) = 0 \tag{21}$$

and $\delta_D = \delta_1 = \delta_2 = \delta_3 = d,\ \delta_4 = \delta_5 = d^2$; H_m, K_m are the m-th order Hankel function of first kind and the modified Bessel function of second kind, respectively. Also, F_{jmn}^{I} are the unknown Fourier coefficients to be established by the solution process. Moreover,

$$Z_n(z) = \left[\frac{1}{2}\left[1 + \frac{\sin(2a_n d)}{2a_n d}\right]\right]^{-1/2} \cos(a_n z), n \geq 1 \tag{22}$$

The eigenvalues a_n are roots of the transcendental equation: $\omega^2 + g a_n \tan(a_n d) = 0$, which possesses one imaginary, $a_0 = -ik, k > 0$ and infinite number of real roots.

(b) For the fluid domain of type *II* ($0 \leq r \leq a, h_2 + h \leq z \leq d$

$$\frac{1}{\delta_j}\Psi_{jm}^{II}(r,z) = g_{jm}^{II}(r,z) + \sum_{q=0}^{\infty} F_{jmq}^{II} \frac{I_m(a_q r)}{I_m(a_q a)} Z_q(z) \qquad \text{for } j = \text{D, 1, 3, 5} \tag{23}$$

where:

$$g_{Dm}^{II}(r,z) = g_{11}^{II}(r,z) = 0; \quad g_{30}^{II}(r,z) = \frac{z}{d} - 1 + \frac{g}{d\omega^2}; \quad g_{51}^{III}(r,z) = -\frac{r}{d^2}\left[(z-d) + \frac{g}{\omega^2}\right] \tag{24}$$

and $\delta_D = \delta_1 = \delta_2 = \delta_3 = d$, $\delta_4 = \delta_5 = d^2$; I_m , the *m*-th order modified Bessel function of first kind. Here F_{jmq}^{II} denote the unknown Fourier coefficients to be determined by the solution process. Additionally,

$$Z_q(z) = \left[\frac{1}{2}\left[1 + \frac{\sin(2a_q(d-(h+h_2)))}{2a_q(d-(h+h_2))}\right]\right]^{-1/2} \cos\left[a_q\left(z - (h + h_2)\right)\right], q \geq 1 \tag{25}$$

The eigenvalues a_q are roots of the transcendental equation: $\omega^2 + g a_q \tan\left[a_q\left(z - (h + h_2)\right)\right] = 0$, which possesses one imaginary, $a_0 = -ik_{II}$, $k_{II} > 0$ and infinite number of real roots.

(c) For the fluid domain of type *III*

$$\frac{1}{\delta_j}\Psi_{jm}^{III}(r,z) = g_{jm}^{III}(r,z) + \sum_{p=0}^{\infty} \varepsilon_p F_{jmp}^{III} \frac{I_m\left(\frac{p\pi r}{h_2}\right)}{I_m\left(\frac{p\pi a}{h_2}\right)} cos\left(\frac{p\pi z}{h_2}\right) \tag{26}$$

where:

$$g_{Dm}^{III}(r,z) = g_{11}^{III}(r,z) = 0; \; g_{30}^{III}(r,z) = \frac{z^2 - (\frac{1}{2})r^2}{2h_2 d}; \; g_{51}^{III}(r,z) = -\frac{r\left[z^2 - (\frac{1}{4})r^2\right]}{2h_2 d^2} \tag{27}$$

δ_j, $j = D, 1, 3, 5$, is defined above and ε_p is the Newmann's symbol, see eq. (8); F_{jmp}^{III} are the unknown Fourier coefficients to be determined through the solution process. In Equations (20), (23) and (26), $g_{jm}^{l}(r,z)$, l = *I, II, III* and j =1, 3, 5 represent particular solutions for the different mode of motions, which satisfy the respective kinematic conditions on the horizontal boundaries of the fluid domains of types *I, II* and *III.* The same is valid for the homogeneous parts of the series expansions of the velocity potential representations, see Equations (20), (23) and (26), which are properly selected so that the kinematic boundary conditions on the horizontal walls of the cylindrical body, the linearized dynamic condition on the free surface, see Equation (9), and the kinematic one on the seabed, see Equation (10), are satisfied beforehand. Employing Galerkin's method the potential solutions are aligned by ensuring continuity of hydrodynamic pressure and radial velocity at the vertical boundaries of adjacent fluid regions. Additionally, kinematic conditions on the bodies' wetted surfaces are satisfied. The methodology has been thoroughly detailed in prior publications for both the diffraction and the radiation problems (Kokkinowrachos, et al, 1986; Mavrakos, 1985, 1988, 2004) and thus, it will be no further elaborated in the present study.

Considering the extreme positions of the cylindrical disk near the free surface, i.e. $h_1 \to 0$, special attention has to be paid as the respective arguments of the Bessel functions involved in the series representation (23) become too large. To circumvent the difficulty, asymptotic expressions for the Bessel functions for large arguments are introduced (Abramowitz and Stegun, 1970) and the corresponding expression for the velocity potential representation in the second fluid domain, i.e. j = *II*, is recast as follows:

$$\frac{1}{\delta_j}\Psi_{jm}^{II}(r,z) = g_{jm}^{II}(r,z) + \sum_{q=0}^{\infty} F_{jmq}^{II} \sqrt{\frac{a}{r}} \frac{e^{a_q r}}{e^{a_q a}} \frac{f_1(a_q r)}{f_1(a_q a)} Z_q(z) \qquad \text{for } j = \text{D, 1, 3, 5} \tag{28}$$

with

$$f_1(z) = 1 - \frac{\mu-1}{8z} + \frac{(\mu-1)(\mu-9)}{2!(8z)^2} - \frac{(\mu-1)(\mu-9)(\mu-25)}{3!(8z)^3} + \cdots. \quad (29)$$

where $\mu = 4m^2$; the rest of the symbols and functions involved in Equation (28) have been defined previously.

3.2 Numerical Formulation

Concerning the numerical formulations, two simulation tools, ANSYS Aqwa and HAQi software, are implemented. ANSYS AQWA is part of ANSYS Mechanical Enterprise suite which performs diffraction and radiation analysis based on potential theory (ANSYS AQWA theory manual, 2015). The physics of AQWA are applicable for finite depth waters and are solved under the frequency domain framework. The version that is used in the present work is the 2021R1. The central processing unit (CPU) time required to achieve the numerical simulation using 17208 wetted elements is about a quarter of a minute for each wave frequency. Figure 3 depicts the element discretization of the examined submerged body.

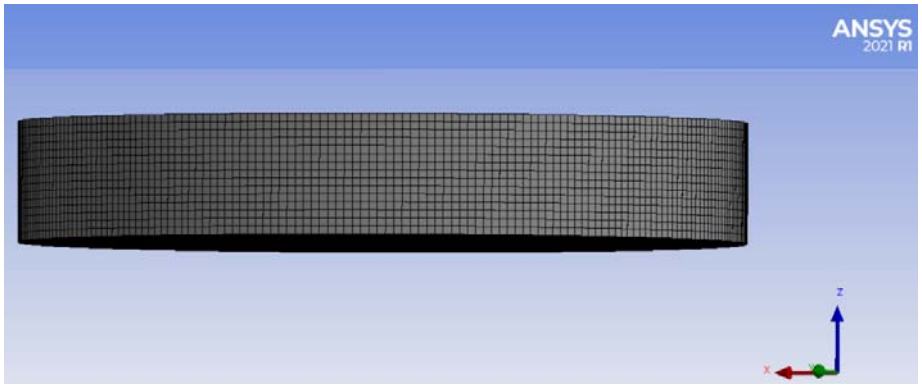

Figure 3: Mesh overview of the examined submerged body for ANSYS AQWA.

HAQi is an in-house developed numerical panel code (Bardis and Mavrakos, 1988) using the sink source technique. Specifically, the velocity potential at every point in the field is derived as the superposition of potentials arising from pulsating singularities (sources) distributed across the wetted surface of the body. Consequently, the fluid potential $\Phi_j, j = 1, \ldots, 6, 7$, around the submerged structure, can be expressed as:

$$\Phi_j(x,y,z) = \frac{1}{4\pi} \iint_{S_0} Q_j(\xi,\eta,\zeta)\, G(x,y,z,\xi,\eta,\zeta) dS\,, j = 1,2,\ldots,6,7 \quad (30)$$

Here $Q_j(\xi,\eta,\zeta)$ is the strength (i.e. density) of the singularity at (ξ,η,ζ); the $G(x,y,z,\xi,\eta,\zeta)$ is the Green function for finite water depth as given in Wehausen and Laitone (1960); $x, y, z, \xi, \eta, \zeta$ are rectangular coordinates, and S_0 is the submerged body's mean wetted surface.

The Laplace differential and the proper boundary conditions are automatically satisfied (see Section 3.1). Hence, the following integral equation can be derived for the diffraction ($j = 7$) and the radiation problems ($j = 1,2, \ldots, 6$), respectively:

$$\frac{1}{2} Q_j(x,y,z) + \frac{1}{4\pi} \iint_{S_0} Q_j(\xi,\eta,\zeta) \frac{\partial G(x,y,z,\xi,\eta,\zeta)}{\partial n} dS = \begin{cases} -\frac{\partial \varphi_0}{\partial n} \text{ for j} = 7 \\ n_i \text{ for j} = 1,2,\ldots,6 \end{cases} \quad (31)$$

Here n_i denote the generalized normal components.

Equation (31) is addressed by subdividing S_0 into plane quadrilateral or triangular elements with singularities positioned at the geometrical center of each element. The integral in Equation (31) is approximated by a finite series of P terms, where P represents the number of plane elements. Consequently, a linear system of P equations is formulated, which is then solved with respect to the source's strengths $Q_j(\xi,\eta,\zeta), j = 1,2,\ldots.,6$. Once $Q_j(\xi,\eta,\zeta)$ has been computed for each element the flow potential can be readily determined from Equation (30). The theoretical framework of this three-dimensional method is extensively described in Wehausen and Laitone (1960); Garrison (1974, 1975); Mavrakos and Bardis (1984), thus it is no further elaborated herein.

The computational workload of the sink-sources formulation can be decreased for bodies with a symmetry plane. Specifically, in the examined case one half of the immerged surface is subdivided. Hence, a total of 266 elements have been considered for the discretization of the half body's wetted surface as can be seen in Figure 4, whereas the CPU time required is about less than a min for each wave frequency.

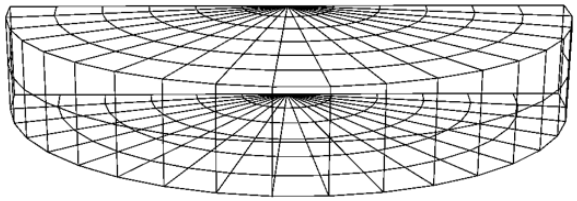

Figure 4: Panel discretization of the examined submerged body for HAQi.

4. NUMERICAL RESULTS

This section compares and discusses the outcomes of the three presented formulations on the hydrodynamics of the submerged unmanned vehicle. The precision of the theoretical modelling is influenced by the evaluation procedure of the Fourier coefficients within each fluid domain surrounding the body. In the present calculations 80 terms are utilized for the series expansions of the velocity potential in the outer I, and upper II, fluid domain, whereas 150 terms are retained for the velocity representation in the lower type III. The theoretical results are acquired using an in-house computer software (Mavrakos, 1995) in FORTRAN programming language. The CPU time is set to less than a second for each analyzed wave frequency.

The geometric characteristics of the considered submerged body are: height of the body h, radius of the body $a = 3.023h$, whereas the water depth $d = 290.7h$. These dimensions have been properly selected based on the geometry of the underwater vehicle developed by the CMMI (see Section 2). Initially, the body is assumed to be floating at $0.116h$ below the free water surface. In Figure 5 the Response Amplitude Operator (RAO) of the exciting wave forces and moments on the submerged vehicle are presented. The depicted results are evaluated by the theoretical formulation and the numerical software.

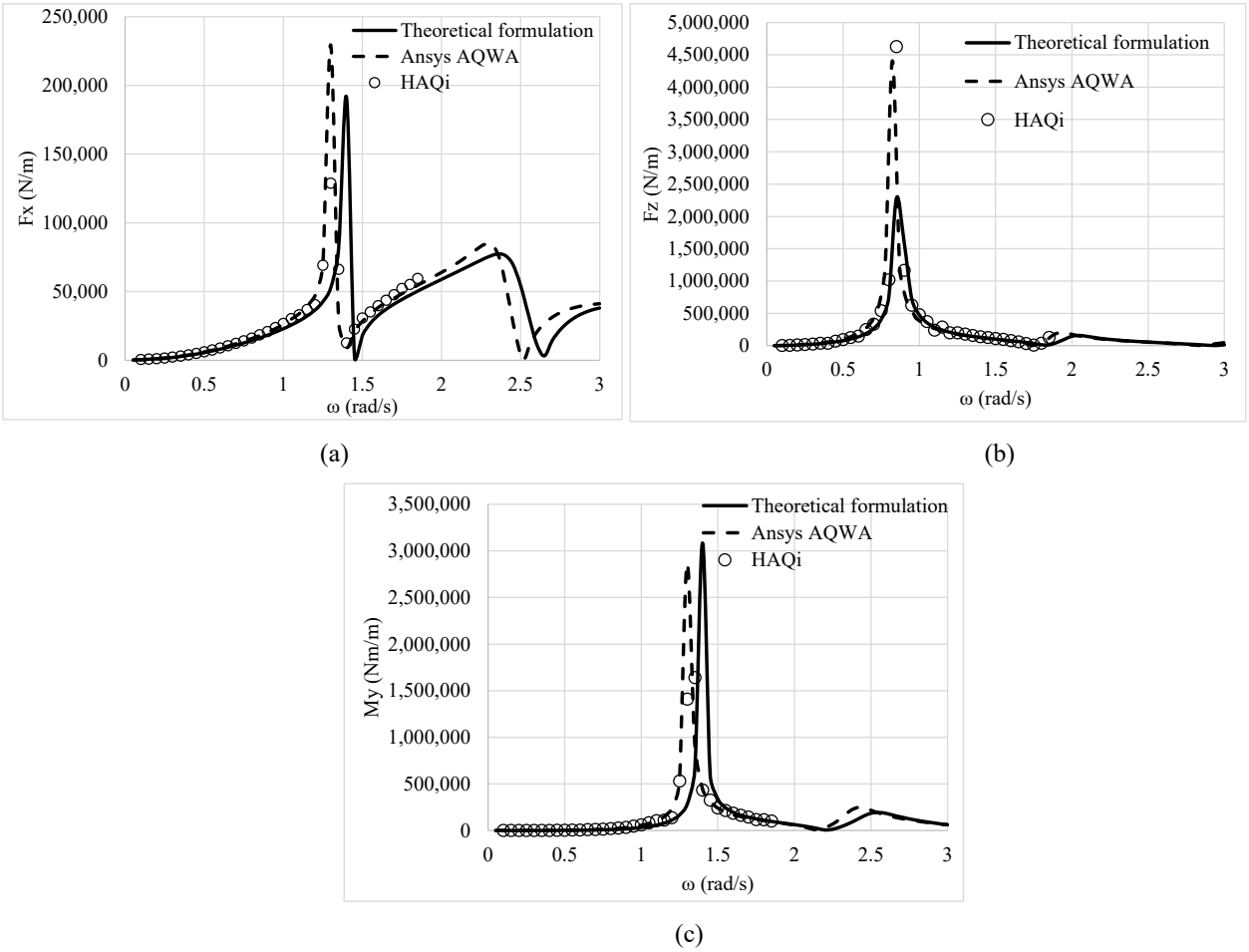

Figure 5: RAO of the exciting forces and moments on the submerged body: (a) horizontal forces; (b) vertical forces; (c) horizontal moments

It is evident from Figure 5a that the horizontal exciting forces show an oscillatory behavior. Specifically in the vicinity of $\omega = 1.3$rad/s the forces depict a quite rapid increase, while a rapid decrease follows leading to a local minimum at $\omega = 1.4$rad/s. The values of F_x exhibit a similar pattern of variation also in the vicinity of $\omega = 2.3$ rad/s and $\omega = 2.4$ rad/s, with a smoother, however, increase and decrease, respectively. It can be also seen from Figure 5c that similar to the surge exciting forces, the sharp peaks observed in horizontal moments are presented at the same wave frequencies. Regarding, the heave exciting forces (see Figure 5b) a smooth variation pattern is depicted with a peak at the neighborhood of $\omega = 0.85$rad/s. As far as the comparisons of the applied methodologies are concerned it can be seen that the results from the numerical software HAQi correlate excellently to the outcomes of AQWA. It is worth noting that certain differences between the results of the theoretical and numerical methods, particularly at wave numbers where the exciting forces reach peaks, can be deemed negligible. This is because the theoretical results are perfectly aligned with the variation pattern observed in the outcomes derived from the numerical formulation.

Figure 6 illustrates the comparison of the added mass coefficients, $A_{11}, A_{33}, A_{55}, A_{15}$ between the theoretical and the numerical models. A strong frequency dependance on the hydrodynamic mass is depicted. The latter is accompanied by sharp peaks at certain frequency ranges. It should be noted that the variation of A_{11} is marked by the occurrence of distinct peaks at the same wave frequencies in which F_x attains maximum and minimum values (see Figure 6a). The same applies to the concerned wave frequency range, where resonance phenomena occur in A_{33} (see Figure 6b). Specifically, A_{33} shows an oscillatory variation pattern at the neighborhood of $\omega = 0.85$rad/s, where the heave exciting forces also attain a peak. Additionally, it is important to note that negative values of the added mass coefficients A_{11}, A_{33}, are depicted near the resonant frequencies. Ogilvie (1963) also observed a similar phenomenon. Regarding the comparisons between the applied methodologies, it can be obtained that the two numerical approaches attain similar results. However, discrepancies between the results of the numerical and the theoretical methods are notable, especially at the vicinity of the resonant frequencies.

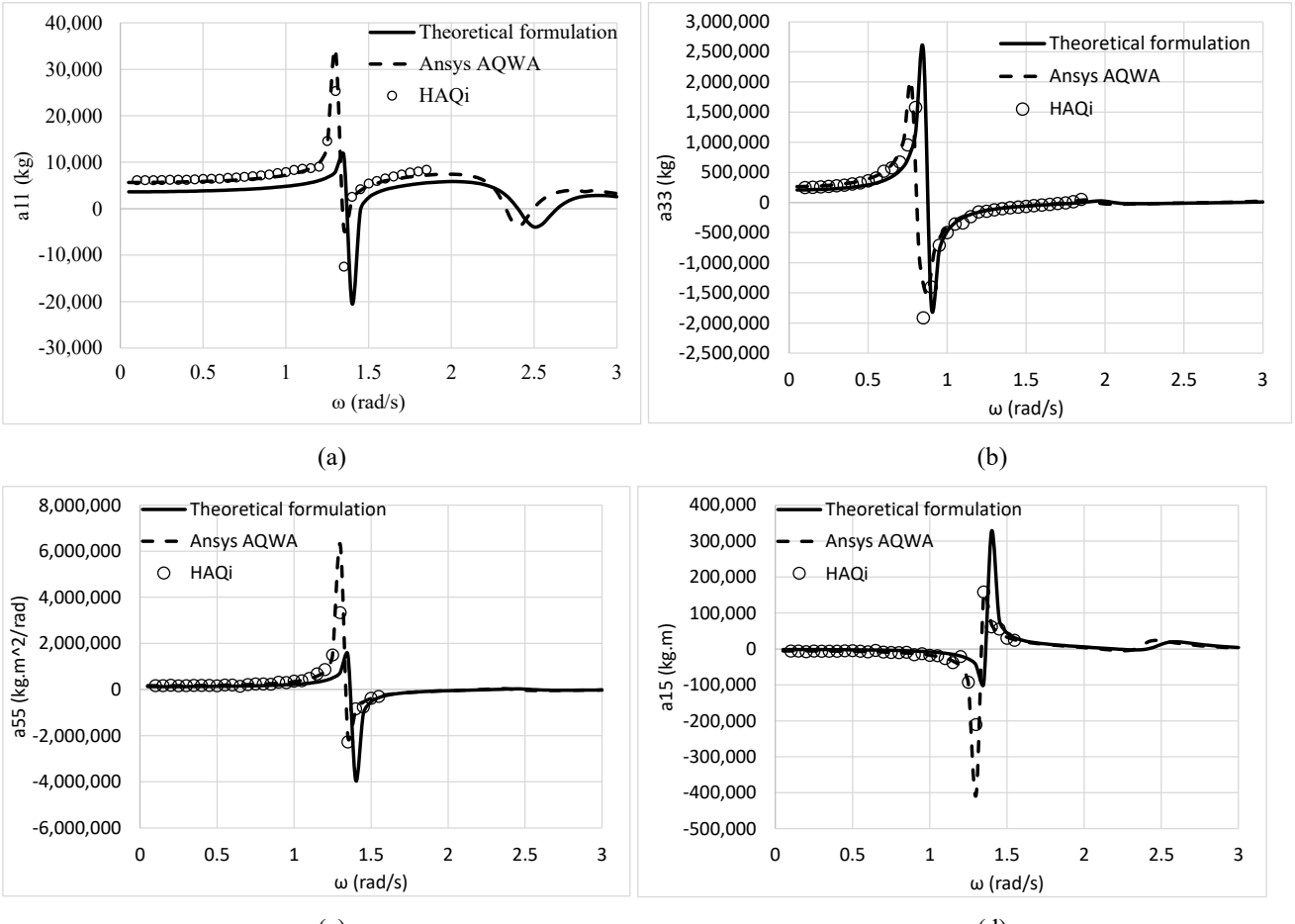

Figure 6: Hydrodynamic mass of the submerged body: (a) at the surge direction due to its forced oscillation in surge; (b) at the heave direction due to its forced oscillation in heave; (c) at the pitch direction due to its forced rotation in pitch; (d) at the surge direction due to its forced rotation in pitch

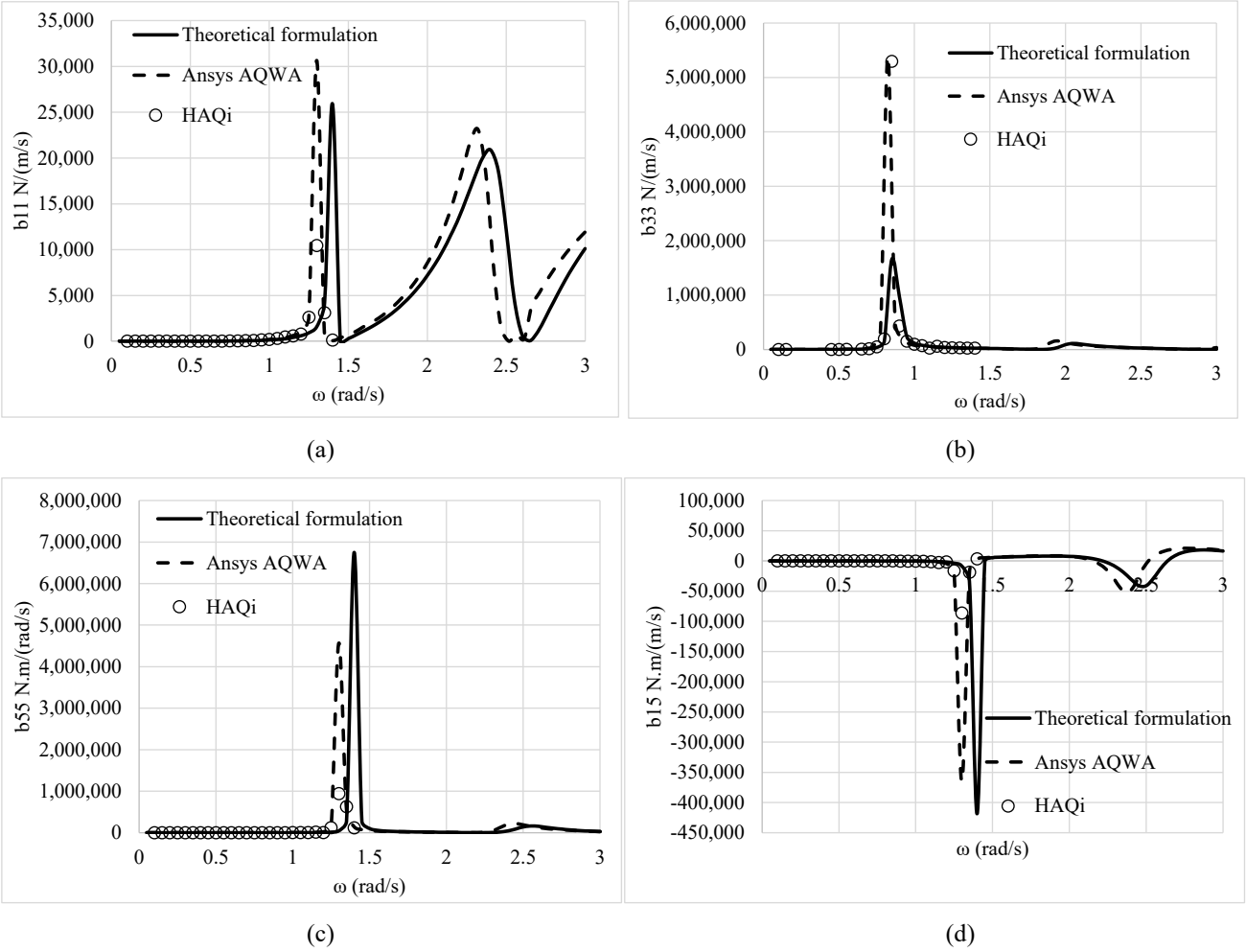

Figure 7: Damping coefficient of the submerged body: (a) at the surge direction due to its forced oscillation in surge; (b) at the heave direction due to its forced oscillation in heave; (c) at the pitch direction due to its forced rotation in pitch; (d) at the surge direction due to its forced rotation in pitch

Figure 7 illustrates the comparison of the damping coefficients $B_{11}, B_{33}, B_{55}, B_{15}$ among the three considered formulations. It is evident that B_{11}, B_{33} follow, in general, the variation pattern of the surge and heave exciting forces, characterized by peaks occurring in the neighborhood of $\omega = 1.3$rad/s and $\omega = 0.85$rad/s, respectively. It is worthwhile to note that the damping coefficients express positive values in the examined wave frequency range. Concerning the comparison between theoretical and numerical methods, it can be concluded that both numerical methods achieve comparable outcomes, whereas the theoretical analysis predicts the resonant locations at slightly higher values of wave frequencies. Nevertheless, these discrepancies are limited only near the resonant frequencies, whilst the theoretical formulation can describe accurately the hydrodynamic characteristics in the remain wave frequencies.

In Figure 8 the horizontal and vertical motions, as well as the horizontal rotations of the submerged vehicle are plotted. It can be seen that the values of x_1 decrease as the wave frequencies increase. On the other hand, x_3 begins its variation from a baseline value of one (at $\omega = 0.05$rad/s), and it increases up to $\omega = 1.7$ rad/s, where a local maximum of x_3 is attained. A smooth decrease follows leading to a local minimum of x_3 at $\omega = 1.8$ rad/s. Regarding x_5 a sharp increase is depicted in the neighborhood of $\omega = 2$ rad/s, which is followed by a prompt decrease at $\omega = 2.2$ rad/s. Furthermore, it should be noted that both the numerical models and the theoretical formulation attain similar results for the body's motions and rotations.

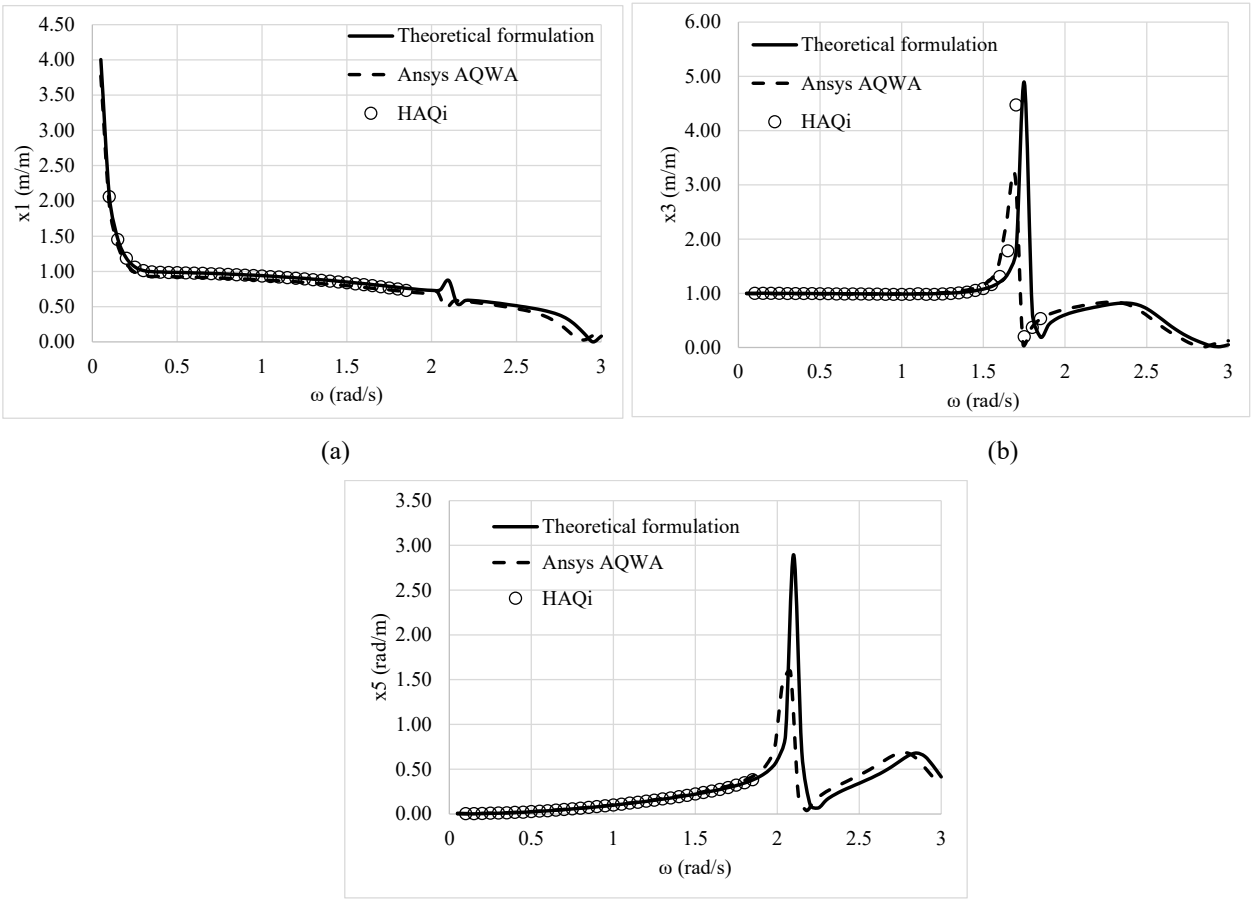

Figure 8: Motions and rotations of the submerged body: (a) horizontal motion $x_1/(H/2)$; (b) vertical motion $x_3/(H/2)$; (c) horizontal rotation $x_5/(kH/2)$

Subsequently, several submergences below free water surface are examined. Specifically, the submerged vehicle is assumed to be floating at $1h, 2h, 3h, 4h,$ below the free water surface, whereas the geometrical characteristics of the body and the water depth are remained constant. Here the outcomes are derived by the theoretical formulation, whereas the AQWA software is applied for comparative purposes for a submergence of $0h$, i.e., there exists no gap between the body's upper surface and the free water surface.

Figure 9 depicts the exciting forces and moments on the body for the various considered submergences. It can be seen that the oscillatory behavior of F_x, F_z, M_y for the $0.116h$ case is not present for higher submergences and for the scenario where the body is floating at the free surface. Furthermore, it is depicted that the exciting forces and moments decrease as the submergence increases.

Figure 10 displays the hydrodynamic coefficients of the submerged body for different levels of submergence considered. The figure illustrates that the closer to the free surface the submerged body is, the stronger the frequency dependence of the hydrodynamic parameters is. The latter is described by the decrease of sharp peaks at certain frequency ranges as the submergences increase. This also holds true for the body floating on the free surface in which no sharp peaks are presented. Therefore, it can be concluded that the hydrodynamic characteristics of the submerged cylinder undergo considerable influence by the position which is closest to the free surface. Based on McIver and Evans (1984) this can be attributed to near-standing waves which are occurred at certain wave frequencies above the submerged body at small submergence distances compared to the body's diameter.

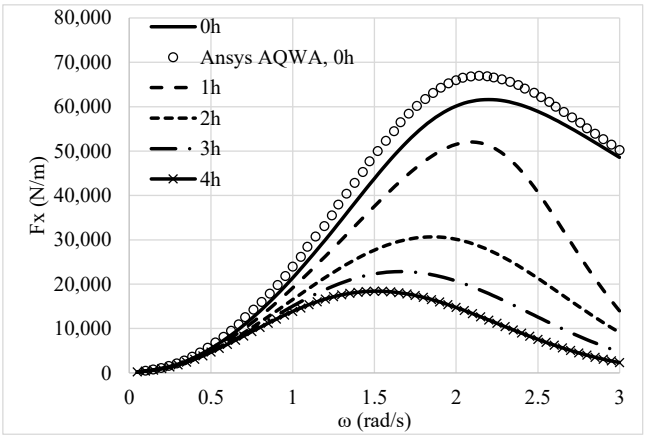

(a)

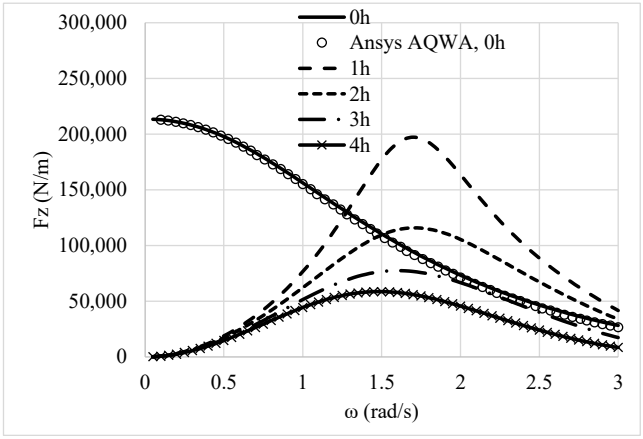

(b)

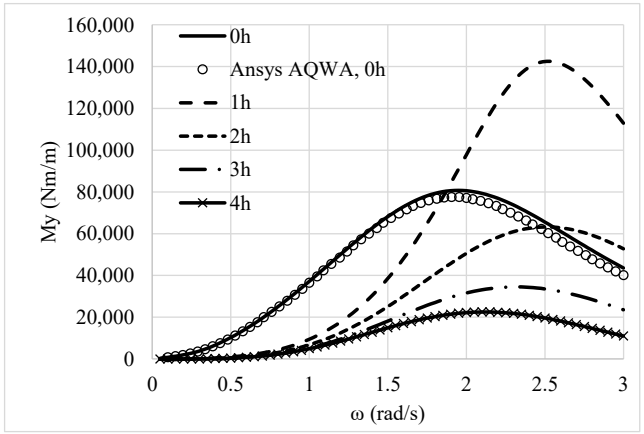

(c)

Figure 9: RAO of the exciting forces and moments on the submerged body for various submergences: (a) horizontal forces; (b) vertical forces; (c) horizontal moments

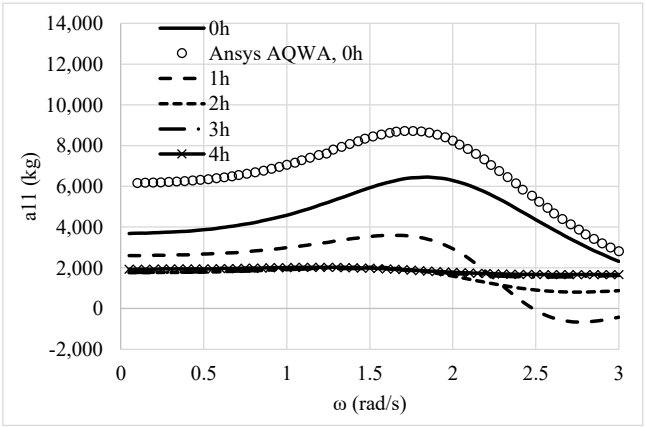

(a)

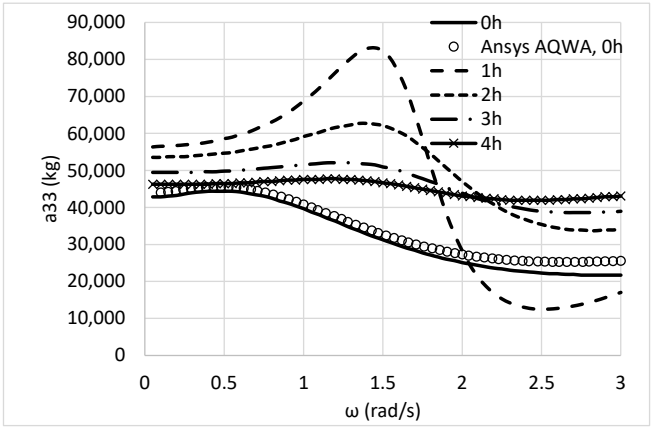

(b)

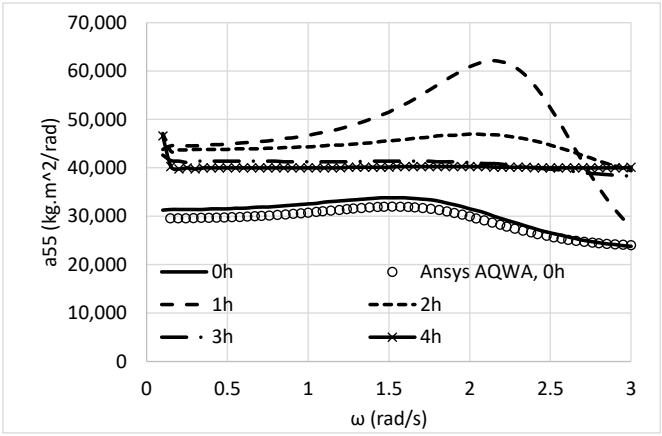

(c)

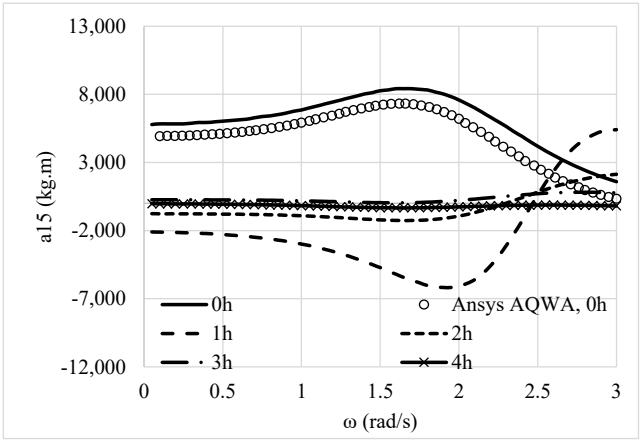

(d)

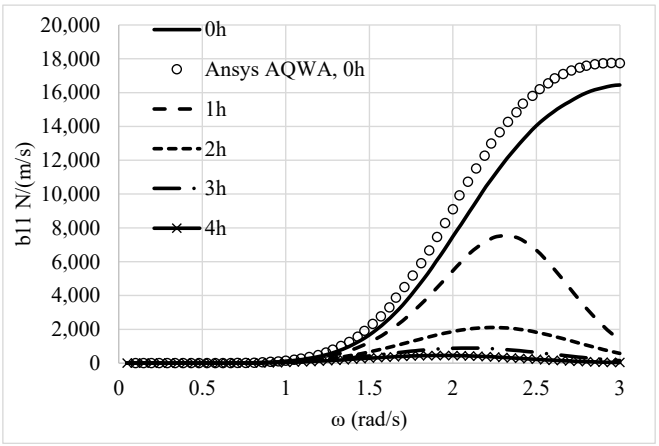

(e)

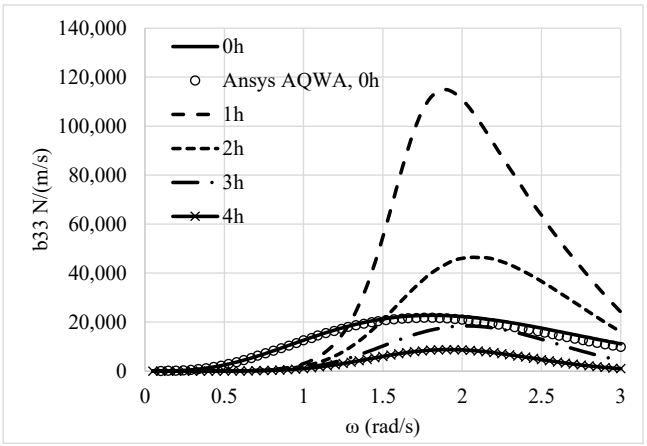

(f)

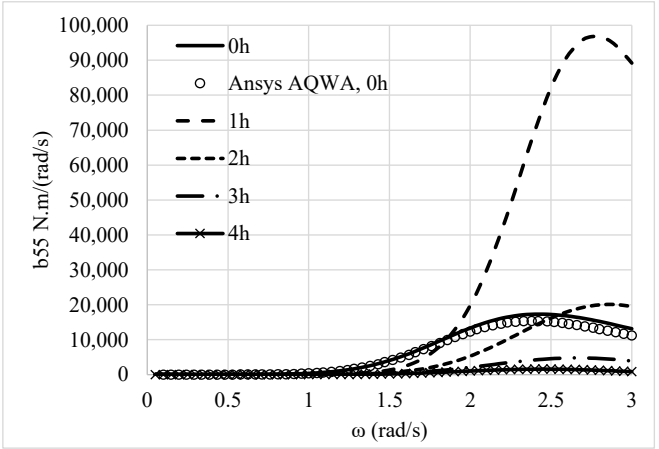

(g)

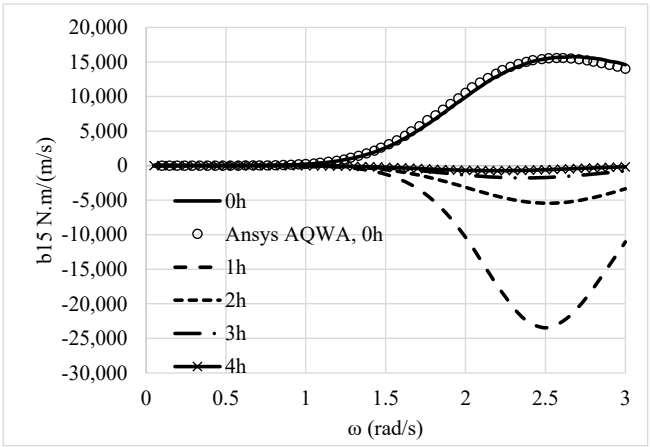

(h)

Figure 10: Hydrodynamic coefficients of the submerged body: (a) added mass at the surge direction due to its forced oscillation in surge; (b) added mass at the heave direction due to its forced oscillation in heave; (c) added mass at the pitch direction due to its forced rotation in pitch; (d) added mass at the pitch direction due to its forced oscillation in surge; (e) damping coefficient at the surge direction due to its forced oscillation in surge; (f) damping coefficient at the heave direction due to its forced oscillation in heave; (g) damping coefficient at the pitch direction due to its forced rotation in pitch; (h) damping coefficient at the pitch direction due to its forced oscillation in surge

5. CONCLUSIONS

In this paper, the effect of submergence on the hydrodynamics of an unmanned cylindrical vehicle floating below the free water surface is investigated. Three different methodologies, one theoretical and two numerical, are described and compared for various submergence distances between the body and the sea surface. The main conclusions of this study are as follows:

- the hydrodynamics of the submerged cylinder are significantly affected by the submergence of the body below the free water surface. Specifically, for small distances between the body and the free water surface sharp peaks are attained on the vehicle's hydrodynamics,
- the added mass coefficients express negative values at specific wave frequencies are noted for small submergence, which are eliminated as the body-free surface distances increase. Nevertheless, the damping coefficients express positive values in the examined wave frequency range, regardless the submergence values,
- regarding the applied methodologies, the in-house numerical software HAQi attains similar outcomes with the commercial AQWA software. Furthermore, the results from the developed theoretical formulation are perfectly aligned with the variation pattern of the outcomes from the numerical methods. However, deviations do exist at wave frequencies in which the body's hydrodynamics attain peaks.
- The findings of this analysis suggest that in near-surface operations (i.e., for a submergence depth lower than the radius of the submerged body), wave motion primarily consists of a standing wave, leading to swift alterations in both added mass and damping coefficients. Therefore, when designing submerged bodies, it's crucial to carefully consider the geometric attributes in relation to the wave characteristics since unexpected forces on the hull may be introduced increasing the inertia of the body and affecting its acceleration.

This inquiry could be expanded to explore the effect of the distance between a submerged body and the seabed on the body's hydrodynamics. Furthermore, the analysis could be further developed on the effect of various submergence distances between the free water surface and a random shaped body on the latter hydrodynamics.

DATA ACCESS STATEMENT

The data that support the findings of this study are available from the corresponding author upon reasonable request.

CONTRIBUTION STATEMENT

Mavrakos, A.: Conceptualization; methodology; writing – original draft. **Konispoliatis, D.:** Software; visualization; validation; writing – original draft, **Rossides, G.:** Visualization; writing – original draft, **Mavrakos, S.:** Methodology; software; supervision; writing – review and editing.

ACKNOWLEDGEMENTS

The DTUG prototype on which this research is based, as well as parts of this research (specifically the work performed by Dr G. Rossides), were funded by CMMI Cyprus Marine and Maritime Institute. CMMI was established by the CMMI/MaRITeC-X project as a "Center of Excellence in Marine and Maritime Research, Innovation and Technology Development" and has received funding from the European Union's Horizon 2020 research and innovation program under grant agreement No. 857586 and matching funding from the Government of the Republic of Cyprus.

REFERENCES

Abramowitz, M., Stegun, I. 1970. Handbook of Mathematical Functions, Dover Publications, Inc., New York
Amiri, M.M.; Esperana, P.; Vitola, M.A.; Sphaier, S.H. (2018). How does the free surface affect the hydrodynamics of a shallowly submerged submarine? Applied Ocean Research 76, 34-50. https://doi.org/10.1016/j.apor.2018.04.008
Amiri, M.M.; Esperana, P.; Vitola, M.A.; Sphaier, S.H. (2019a). An initial evaluation of the free surface effect on the maneuverability of underwater vehicles. Ocean Engineering 196, 106851. https://doi.org/10.1016/j.oceaneng.2019.106851
Amiri, M.M.; Esperana, P.; Vitola, M.A.; Sphaier, S.H. (2019b). Investigation into the wave system of a generic submarine moving along a straight path beneath the free surface. European Journal of Mechanics – B/Fluids 76, 98-114. https://doi.org/10.1016/j.euromechflu.2019.02.006
Amiri, M.M.; Esperana, P.; Vitola, M.A.; Sphaier, S.H. (2020). Viscosity effect on an underwater vehicle-free surface

hydrodynamic interaction. Applied Ocean Research 104, 102365. https://doi.org/10.1016/j.apor.2020.102365
ANSYS AQWA Theory Manual, 2015. ANSYS Inc. Southpointe 2600 ANSYS Drive Canonsburg, PA 15317
Arentzen, E.S.; Mandel, P. (1960). Naval architectural aspects of submarine design. The Society of Naval Architects and Marine Engineers
Bardis, L.; Mavrakos, S. (1988). User's manual for the computer code HAQ. Laboratory for Floating Bodies and Mooring Systems, National Technical University of Athens
Benusiglio, A.; Chevy, F.; Raphael, E.; Clanet, C. (2015). Wave drag on a submerged sphere. Physics of Fluids 27, 07210. https://doi.org/10.1063/1.4923454
Burcher, R.; Rydill, L.J. (1995). Concepts in submarine design. Cambridge University Press. https://doi.org/10.1017/CBO9781107050211
Chepelianskii, A.; Schindler, M.; Chevy, F.; Raphael, E. (2010). Self-consistent theory of capillary–gravity-wave generation by small moving objects. Physical Review E, 81, 016306. https://doi.org/10.1103/PhysRevE.81.016306
Chung, J.S. (1977). Forces on submerged cylinders oscillating near free surface. Journal of Hydronautics, 11(3), 100-106. https://doi.org/10.2514/3.63081
Choi, J.H.; Yeo, D.J.; Rhee, K.P.; Park, J.Y. (2006). On the vertical plane dynamics modeling and depth control of a submerged body moving beneath free surface. Journal of the Society of Naval Architects of Korea 43(6), 647-655. https://doi.org/10.3744/SNAK.2006.43.6.647
Choi, J.H.; Rhee, K.P.; Ann, S.P.; Lee, S.K. (2008). Mathematical model of wave forces and moments for the depth control of a submerged body. Proceedings of the Annual Spring Meeting of the Society of Naval Architects of Korea, 1228-1235
Conway, A.S.T.; Valentinis, F.; Seil, G. (2018). Characterization of suction effects on a submarine body operating near the free surface. Proceedings of the 21st Australian Fluid Mechanics Conference, 10-13 November, Adelaide, Australia.
Fossen, T. I. (2011). Handbook of Marine Craft Hydrodynamics and Motion Control. John Wiley & Sons, Ltd. https://doi.org/https://doi.org/10.1002/9781119994138.ch2
Garrison, C.J. (1974). Hydrodynamics of large objects in the sea. Part I: Hydrodynamic analysis. Journal of Hydronautics 8, 5-12. https://doi.org/10.2514/3.62970
Garrison, C.J. (1975). Hydrodynamics of large objects in the sea. Part II: Motion of free floating bodies. Journal of Hydronautics 9, 58-63. https://doi.org/10.2514/3.63020
Hao, Y.; Shen, D.; Xiong, Z. (2004). Design of submarine near-surface depth controller. Proceedings of the 5th World Congress on Intelligent Control and Automation, 15-19 June, Hangzhou, China. https://doi.org/10.1109/WCICA.2004.1342374
Havelock, T.H. (1917). Some cases of wave motion due to a submerged obstacle. Proceedings of the Royal Society A 93, 520-532. http://doi.org/10.1098/rspa.1917.0036
Havelock, T.H. (1931). The wave resistance of a spheroid. Proceedings of the Royal Society A 131, 275-285. http://doi.org/10.1098/rspa.1931.0052
Jagadeesh, P.; Murali, K.; Idichandy, V.G. (2009). Experimental investigation of hydrodynamic force coefficients over AUV hull form. Ocean Engineering 36, 113-118. https://doi.org/10.1016/j.oceaneng.2008.11.008
Javaid, M. Y., Ovinis, M., Nagarajan, T., & Hashim, F. B. M. (2014). Underwater Gliders: A Review. MATEC Web of Conferences, 13, 2020. https://doi.org/10.1051/matecconf/20141302020
Lambert, W.; Brizzolara, S. (2020). On the effect of non-linear boundary conditions on the wave disturbance and hydrodynamic forces of underwater vehicles travelling near the free-surface. Proceedings of the 39th International Conference on Ocean, Offshore and Arctic Engineering, The American Society of Mechanical Engineers, 3-7 August, Fort Lauderdale, FL, USA
Ling, X.; Leong, Z.Q.; Duffy, J. (2023). Effects of pitch angle on a near free surface underwater vehicle. Ocean Engineering 286, 115611. https://doi.org/10.1016/j.oceaneng.2023.115611
Kokkinowrachos, K.; Mavrakos, S.; Asorakos, S. (1986). Behavior of vertical bodies of revolution in waves. Ocean Engineering 13, 505 – 538.
Mansoorzadeh, S.; Javanmard, E. (2014). An investigation of free surface effects on drag and lift coefficients of an autonomous underwater vehicle (AUV) using computational and experimental fluid dynamics methods. Journal of Fluids and Structures 51, 161-171. https://doi.org/10.1016/j.jfluidstructs.2014.09.001
Mavrakos, S.A.; Bardis, L. (1984). Hydrodynamic characteristics of large offshore units. Proceedings of the 3rd International Congress on Marine Technology (IMAM), 28 May – 1 June, Athens, Greece
Mavrakos, S.A. (1985). Wave loads on a stationary floating bottomless cylindrical body with finite wall thickness. Applied Ocean Research 7(4), 213 – 224. https://doi.org/10.1016/0141-1187(85)90028-8
Mavrakos, S.A. (1988). Hydrodynamic coefficients for a thick-walled bottomless cylindrical body floating in water of finite depth. Ocean Engineering, 15(3), 213 – 229. https://doi.org/10.1016/0029-8018(88)90040-6
Mavrakos, S.A. (1993). Hydrodynamic characteristics for groups of interacting axisymmetric bodies submerged near the sea surface or the sea bed. Proceedings of the 3rd International Offshore and Polar Engineering Conference, 6-11 June, Singapore
Mavrakos, S.A. (1995). Users manual for the software HAMVAB. School of Naval Architecture and Marine Engineering, Laboratory for Floating Structures and Mooring Systems, Athens, Greece
Mavrakos, S.A. (2004). Hydrodynamic coefficients in heave of two concentric surface-piercing truncated circular cylinders. Applied Ocean Research 26(3–4), 84–97. https://doi.org/10.1016/j.apor.2005.03.002

McIver, P., Evans, D.V. (1984). The occurrence of negative added mass in free-surface problems involving submerged oscillating bodies. Journal of Engineering Mathematics 18, 7–22
Michell, J.H. (1898). The wave-resistance of a ship. The London, Edinburgh, and Dublin Philosophical Magazine and Journal of Science, 45:272, 106-123, http://dx.doi.org/10.1080/14786449808621111
Nakamura, M., Hyodo, T., & Koterayama, W. (2007). "LUNA" Testbed Vehicle For Virtual Mooring. All Days.
Nakamura, M., Koterayama, W., Inada, M., Marubayashi, K., Hyodo, T., Yoshimura, H., & Morii, Y. (2008). Disk Type Underwater Glider For Virtual Mooring And Field Experiment. All Days.
Nematollahi, A.; Dadvand, A.; Dawoodian, M. (2015). An axisymmetric underwater vehicle-free surface interaction: a numerical study. Ocean Engineering 96, 205-214. http://dx.doi.org/10.1016/j.oceaneng.2014.12.028
Newman, J.N.; Sortland, B.; Vinje, T. (1984). Added mass and damping of rectangular bodies close to the free surface. Journal of Ship Research 28(4), 219-225. https://doi.org/10.5957/jsr.1984.28.4.219
Ogilvie, T.F. (1963). First- and second- order forces on a cylinder submerged under a free surface. Journal of Fluid Mechanics, 16(3), 451-472. https://doi.org/10.1017/S0022112063000896
Park, J.Y.; Kim, N.; Yoon, H.K.; Cho, H. (2016). Adaptive depth controller design for a submerged body moving near free surface. Applied Ocean Research 58, 83-94. http://dx.doi.org/10.1016/j.apor.2016.04.001
Rezazadegan, F.; Shojaei, K.; Sheikholeslam, F.; Chatraei, A. (2015). A novel approach to 6-DOF adaptive trajectory tracking control of an AUV in the presence of parameter uncertainties. Ocean Engineering 107, 246-258. http://dx.doi.org/10.1016/j.oceaneng.2015.07.040
Shao, Z.; Chen, Y.; Fang, D.; Feng, S. (2012). Fuzzy depth control of small cylindrical object navigating near free-surface. Applied Mechanics and Materials 128(129), 886-889. https://doi.org/10.4028/www.scientific.net/AMM.128-129.886
Sudharsun, G.; Ali, A.; Mitra, A.; Jaiswal, A.; Naresh, P.; Warrior, H.V. (2022). Free surface features of submarines moving underwater: study of Bernoulli Hump. Ocean Engineering 249, 110792. https://doi.org/10.1016/j.oceaneng.2022.110792
Wehausen, J.V.; Laitone, E.V. (1960). Surface Waves. In Encyclopedia of Physics; Springer: Berlin/Heidelberg, Germany, Volume 9
Yu, P., Wang, T., Zhou, H., & Shen, C. (2017). Dynamic modeling and three-dimensional motion simulation of a disk type underwater glider. International Journal of Naval Architecture and Ocean Engineering, 10. https://doi.org/10.1016/j.ijnaoe.2017.08.002
Zemlyak, V.; Pogorelova, A.; Kozin, V. (2022). Motion of a submerged body in a near-surface water environment. International Journal of Naval Architecture and Ocean Engineering 14, 100433. https://doi.org/10.1016/j.ijnaoe.2021.100433
Zemlyak, V.; Pogorelova, A.; Kozin, V. (2023). Motion of a submerged body under a free surface and an ice cover in finite water depth conditions. Ocean Engineering 288, 116161. https://doi.org/10.1016/j.oceaneng.2023.116161
Zhou, H., Yu, P., Jin, X., & Wang, T. (2020). Analysis of the In Situ Steering Motion Characteristics and Sensitivity of Disc-Type Underwater Gliders. Journal of Marine Science and Engineering, 8, 663. https://doi.org/10.3390/jmse8090663

Proceedings of 15th International Marine Design Conference (IMDC-2024)
June 2-6, 2024
Amsterdam, the Netherlands

The Importance of Ontological Commitment and Linguistics in Relation to the Elucidation of Design Requirements

Connor W. Arrigan[1,*], Morgan C. Parker[1], and David J. Singer[1]

ABSTRACT

One of the design process's earliest and most critical stages is establishing and determining requirements. Design requirements are often expressed through language, whether in written documents, diagrams, or verbal discussions in terms of the client's "wants" and "needs" or balancing what they can "afford." Designers use of quotes around "wants," "needs," and "afford" signals ambiguity or doubt in the meaning of the terms. The language used during early discourse is crucial for expressing and translating these ambiguous terms into specific unambiguous design requirements, which significantly shape and constrain possible solutions. In philosophy, this concept is known as ontological commitment. Embedded language in requirements documents, expressed through constraints, objectives, and functions, establish the ontological commitment to a specific solution space. Prior marine design research has focused on the wicked problem of requirements elucidation, with the goal visualizing potential solutions derived from language, and a more direct link to ontological commitment was developed by Andrews in the concept of style Duchateau (2016) van Ores (2011) Andrews (2012). However, the role and impact of linguistics in translating and interpreting uncertain or ambiguous terms into specific design requirements has been largely overlooked. This paper presents modern direct examples of ontological commitment from requirements development for the Littoral Combat Ship.

KEY WORDS

Design Requirements, Ontological Commitment, Naval Vessel Design, Linguistics, Early-Stage Concept Design

INTRODUCTION

The process of engineering design is a complex, highly entangled, and multifaceted endeavor, that commences with concept design and the establishment of design requirements. At this formative stage, the articulation of design needs, goals, and constraints are often conveyed through language, be it in written documents, visual diagrams, or verbal interactions. An intriguing phenomenon within this domain is the use of scare quotes by designers to underscore terms such as "wants," "needs," and "afford," signifying an element of doubt or ambiguity surrounding these crucial design aspects. Numerous examples of scare quotes can be found for in the design language for both military and commercial ships. A recent defense example can be seen through the development of the Landing Ship Medium. An article announced the "Draft Proposal for 'Affordable' Medium Landing Ship" Lagrone (2023). The scare quote around the word affordable signal the uncertainty with the cost of the vessel being designed. Further, some of the initial desired features for the ship state the want for

[1] Department of Naval Architecture and Marine Engineering, University of Michigan, Ann Arbor, MI, USA; ORCID: 0009-0002-8243-9086 (CWA), ORCID: 0000-0002-5293-6236 (DJS)
[*] Corresponding Author: arriganc@umich.edu

Submitted: 23 Febraruy 2024, Revised: 22 April 2024, Accepted: 1 May 2024, Published: 26 May 2024

Conference paper, DOI: https://doi.org/10.59490/imdc.2024.910 e-ISSN: 3050-4864

“a “modest” suite of C4I equipment” or “a “Tier 2+” plus level of survivability” O’Rourke (2023). In both of these cases there is a level of ambiguity in how one would define modest or the level of survivability. These scare quotes, which typically serve to express uncertainty, are emblematic of the intricate interplay between language and the design process. One commercial example from the cruise ship industry can be seen through the idea used by Royal Caribbean of “above and beyond compliance” Royal Caribbean Group (2020). Primarily, this scare quote is concerning safety and environmental concerns, although they weren’t initially specified requirements at the onset of the design process in terms of what “above” compliance means in relation to additional capability needed. Throughout the design process ideas evolved into innovative concepts such as the Safety Command Center Royal Caribbean Group (2024). Initially undefined, this concept emerged and matured during the design process, guided by the philosophy of surpassing mere compliance to embrace a higher standard of safety. Additionally, one can argue that there is a large amount of uncertainty with what “above” compliance really means.

Language, with its capacity to express the nuanced aspects of “wants” and “needs,” plays a pivotal role in translating abstract desires into precise, unambiguous design requirements. The manner in which these requirements are framed through embedded language significantly influences and constrains the realm of possible design concepts and solutions, a concept analogous to the philosophical notion of ontological commitment. In philosophy, ontological commitment explores the connection between statements of existence and specific entities or types of entities, and in the context of design, the language embedded in requirements documents as well as design approaches, methods, processes, and tools establishes an ontological commitment to a predicated solution space Jubien (1998). The purpose of this paper is to present ontological principles within the framework of marine design, elucidating their impact on and ability to clarify design results.

Philosophy in Marine Design

Engineering, as a discipline, is often perceived as a realm of technical knowledge and practical applications. However, “overlying every technical or civil system is a social system that provides purpose, goals, and decision criteria” Miles and California Institute of Technology (1973). All engineering activities, including the language used in requirements or the logical reasoning behind decisions, are grounded in humanity based fields like cognitive psychology or philosophy. Looking back, Aristotle believed there were many reasons philosophy was practically important, “the analysis of foundational philosophical concepts cannot but influence science” Rovelli (2016) Andrews (2018b). Additionally, in his discussion on the philosophy of design, Galle argues that philosophy “serves the end of helping, guiding, suggesting how the [designer] comes to understand what he is doing, and not simply how he comes to do what he is doing.” This coming to understand what one is doing, rather than just understanding how to do it is an insight about design... [that] can only be pursued by philosophical means ” Galle (2002) Andrews (2018b). Philosophy enhances conceptual clarity in engineering. It helps engineers define and refine abstract concepts, such as efficiency, sustainability, affordability, and risk, to ensure that they are well-understood and can be effectively implemented in the design and evaluation of engineering systems.

Andrews’ exploration of Style in many works largely aims to introduce philosophy into the domain of ship design and requirements elucidation Andrews (2018a). Andrews states that “the style to be adopted in a specific design option is seen to be the key design decision for that option and so is the first design decision...” Andrews (2018b). Additionally, Andrews argues that “style can make a substantial difference to the final outcome of a design, so their relative impact ought, in the case of a complex ship, to emerge from a proper dialogue between designer and client ...” Andrews (2018a). Keane and Tibbits similarly argue that “the way ahead for a successful ship design starts with establishing the initial design philosophy...” Keane and Tibbits (2013). A design philosophy sets the tone for an entire program, such as “Design/Build” for the U.S. Navy’s Virginia class attack submarine, which signaled major changes to organizations, contracts, and processes relative to past Navy programs.

The setting of a design philosophy or Style is an ontological commitment, in how ontological commitment directly establishes relations to a predicated solution space. A direct justification of the need for Style in design lies within the concepts of ontology. The intent of this paper is to introduce ontological concepts in the context of marine design, and how they can influence and explain design outcomes.

IMPORTANT PHILOSOPHICAL AND ONTOLOGICAL CONCEPTS IN ENGINEERING DESIGN

The following section introduces and defines multiple philosophical and ontological concepts that are relevant to engineering design and in elucidating design requirements. The case study presented later in this manuscript largely utilizes and investigates the concepts of a universe of discourse, an ontological anchor, and ontological conflict (anguish). However, the other concepts introduced below are to help provide a more compressive understanding.

The Notion of a Universe of Discourse

A universe of discourse establishes the scope or domain of a statement or argument, indicating what is relevant and applicable to the discussion at hand. A universe of discourse is implied or defined, clarifying the boundaries of the discussion and ensuring that statements or arguments are meaningful within the specified context. Certain types of objects or concepts will be included, while others will be excluded. The universe of discourse is particularly important in relation to the elucidation of design requirements as this is a key point in the design process when domains to be included in a design are set and ranges on design variables are specified. Returning to Style, selecting a certain Style directly influences the universe of discourse of a design. For example when designing a container ship one may consider the styles of robustness, commercial quality, operational serviceability, or producability, but would probably not include lethality. On the other hand if one were designing a naval vessel by nature one would need to include lethality, while excluding commercially unique concepts. In general terms, a universe of discourse is an inclusive class of entities that is implied or defined relative to a statement or theory.

The Notion of Ontological Commitment

Ontological commitment is defined "to be a relation that holds between persons or existence assertions, on the one hand, and specific entities or kinds of entities, on the other" Jubien (1998). This implies that "assertions of the existence of specific entities or kinds of entities are the intuitive source of the notion of an ontological commitment" Jubien (1998). In more basic terms, the concept of ontological commitment represents the acknowledgment that one assigns value to something through inference of belief within an existing domain or context, and the ontological commitment is only valid when it is connected to some conception of past existence. There are many examples that exist of ontological commitments. For example, some of the ontological commitments of physics include atoms, quarks, and space-time. To further this example, physics theory is ontologically committed to the concept of electrons. This means that the truth of physics requires that electrons exist and behave in certain ways.

Another way to think about ontological commitment is through the idea that ontological commitment reveals the "demands imposed on the world" Rayo (2007). Explicit and implicit ontological commitment are two of the more recent concepts that have been introduced. The concepts are directly a byproduct from the modern efforts to try to quantify all entities involved in a commitment and were originally present by Peacock and Krämer and expanded upon by Österblom Peacock (2011) Krämer (2014) Österblom (2017). Explicit ontological commitments are defined by the entities that are claimed to exist that are directly stated in the statement of a theory or statement Peacock (2011) Österblom (2017). In other more simple terms "a theory is explicitly ontologically committed [to an entity] if it contains some sentence that means there are X" Krämer (2014) Österblom (2017). Explicit ontological commitment is a pretty clear notion and really covers any direct statement of existence. In common language, explicit commitment refer to relations, statements, or entities that are clearly stated and actually understood by individuals. To cover the commitments that are not directly stated or directly related to a theory or statement there is implicit ontological commitment. Implicit ontological commitment are defined by two criteria. The first of the criteria for determine implicit ontological commitments is "the theory could not be true unless X existed," and the second is "the theory is committed to X and not explicitly committed to X" Peacock (2011) Österblom (2017). In more common language implicit commitments refer to relations, statements, or entities that either classify as believed to be understood or that fall into the category of unknown-unknowns. In relation to the case study presented later in this manuscript,

this work does not directly attempt to use ontological commitment from philosophy but is inspired and investigates commitments relative to design requirements and decisions.

The Notion of Ontological Cost

Ontological cost was introduced by Peacock and furthered by Österblom and it is meant to look at the preconditions of an ontological commitment and reckon what cost is imposed by making that commitment Österblom (2017) Peacock (2011). The "ontological cost of a theory is to ask what is given that it must be true. It is to ask what entities or kinds of entities are needed or required for the truth of the theory" Österblom (2017). In other words this is essentially to ask what explicit and implicit commitments are needed to make a given ontological commitment. In relation to the case study presented later in this manuscript, ontological cost can be physically interpreted and measured by the cost implications of a specific design requirement, ontological commitment, or design change or decision.

The Notion of an Ontological Anchor

A novel, critical concept to introduce that is directly related to the concept of ontological commitment is the concept of an ontological anchor. The term ontological anchor is not defined in the field of philosophy, but is rather inspired from philosophy. The term was coined in a conversation with a retired U.S. Navy Captain. The term ontological anchor refers to a stronger concept than ontological commitment. An ontological anchor refers to the fastening of one's view of the universe of discourse or belief system to a specific assertion or assertions. While at first ontological commitment and ontological anchors may seem the same, there are some important subtle differences. An important note on ontological commitment is that in evaluating relations the universe of discourse and truth are static. There is also a dependence that the universe of discourse and truth statement need to be aligned in ontological commitment. In this context a truth statement is defined by a proposition or sentence that is considered to accurately represent reality. It is a statement that is true or perceived true, meaning it corresponds to the facts or the way things really are or how things are perceived. However, with an ontological anchor, truth is independent of the universe of discourse. Thus, the largest and most important difference between ontological commitment versus ontological anchors is truth versus untruth. Ontological anchors hold in situations with false truth statements as one either creates a universe of discourse to justify the incorrect truth statement or ignores the universe of discourse all together. Organizational bias can be seen as a strong example of an ontological anchor. Ontological anchors can also be supported from concepts from organizational theory. Two concepts from organizational theory that help support the concept of an ontological anchor are the anchoring effect and the concept of strategic misrepresentation. The idea of the anchoring effect is that "an individual's judgements or decisions are influenced by a reference point or "anchor" which can be completely irrelevant" Wikipedia (2023). Strategic misrepresentation is the concept that "decisions are based solely on the optimism of benefits and projected accordingly to management or leadership" The Strategy Institute (2023). In both of these theories the root influence or reference represent an ontological anchor.

Cognitive dissonance theory suggests that individuals experience discomfort or tension when holding conflicting beliefs, attitudes, or values. When someone is presented with information that contradicts their existing beliefs, they may experience cognitive dissonance and attempt to resolve it by reinforcing their existing beliefs rather than changing them Festinger (1957). Thus, direct truth or facts cannot be used since the individual is anchored to a universe of discourse that justifies their views. In more common language the ontological anchor occurs when people or designers know what they are doing is bad or incorrect, but they proceed to do it anyway even though they know better.

To introduce an analogy as an example of an ontological anchor one can consider a game of Sudoku. In Sudoku a number of the squares depending on the difficulty are already filled in with numbers. These numbers can be considered one's ontological anchors. When playing Sudoku one must account for the pre-filled in numbers in their solution and if the pre-filled in numbers are moved or changed, the predicated solution changes or may become infeasible. This same behavior can be seen with design and complex engineering problems.

Two interesting examples of ontological anchors during design are illustrated through the SR-71 Blackbird Program. With

the SR-71, the U.S. Air Force insisted on having its insignia painted on the wings and fuselage, “even though no one would ever see it at eighty-five thousand feet” Rich and Janos (1994). This anchor of needing insignia painted even on a spy aircraft caused for major ontological costs, actual costs, and development. They even had to use pink paint instead of white to try to limit detection Rich and Janos (1994). Another example of an ontological anchor during the program was how the U.S. Air Force also mandated the aircraft could pass a dust test for low altitude flight over the desert even though the aircraft would be flying at altitudes of over 16 miles Rich and Janos (1994). These can be seen as ontological anchors as they directly show the fastening of the U.S. Air Force’s view on the design of an aircraft.

The Notion of Ontological Conflict (Anguish)

Ontological conflict (anguish) is an important concept to define prior to delving into the presented case study. Ontological conflict or anguish is not defined in the field of philosophy, but is rather inspired from philosophy. In philosophy the existential concept of anguish, as articulated by philosophers like Jean-Paul Sartre and Søren Kierkegaard, plays a significant role in the context of decision-making. This concept is rooted in the idea that human existence is characterized by a fundamental sense of anxiety and anguish, which arises from our freedom and responsibility to make choices. Existential anguish, also known as existential dread or anxiety, is considered a fundamental aspect of the human condition. It emerges from the realization that human beings are free to make choices, and with this freedom comes the burden of responsibility for those choices. The act of making choices in this context becomes a source of anguish. When individuals confront a decision, they experience existential anguish as they grapple with the uncertainty of outcomes and the weight of their choices. This anguish is not merely a psychological condition but an inherent part of the human experience. This can directly apply to the decision making one faces as a designer or an engineer. In relation to ontological commitment, when a design decision is made that causes for a misalignment of “truth,” universe of discourse, or another ontological commitment, there exits ontological conflict (anguish) associated with the decision. This will be shown later in the investigated case study. Practical examples of ontological anguish can be seen through computation fluid dynamics (CFD) replacing towing tanks or one’s struggle in developing new methods that disprove prior methods.

The Philosophical Concept of Discourse Ontology

In philosophy, discourse ontology refers to the study or analysis of existence and reality as expressed through language and discourse. It involves examining how our understanding of being and the nature of reality is shaped, conveyed, and constructed through language and communication. Discourse ontology explores the relationship between language and our understanding of reality. It considers how language structures and influences our perception of being and existence. Tombras defines discourse ontology formally as “an ontology—in so far as it concerns being, i.e. the open space where a world can present itself as intelligible to the human being—with the designation “discourse” denoting the source of this intelligibility” Tombras (2019). One should note that by combining discourse ontologies one is able to form a universe of discourse. This process involves bringing together various discourses or ways of talking about existence to create a broader and more inclusive context for investigation and inquiry.

Introducing Philosophy to Engineering Design

Navigating the intricate realm of design requires a nuanced understanding of its complexities and entanglements. Entanglement in this case refers to the concept that one cannot look at certain aspects or concepts in isolation but rather as a whole in terms of both macroscopic and microscopic impacts. As begins the elucidation process of defining requirements and initiating the design process, the philosophical and ontological concepts introduced above each wield a substantial influence on the process. Among these, the notions of universe of discourse, ontological commitment, ontological cost, ontological anchor, ontological anguish, and discourse ontology play a profound role in shaping the trajectory of design endeavors. By delving into real-world examples, one can unravel the intricate interplay of these ontological considerations and appreciate their substantial impact on engineering design. To underscore their significance, it is insightful to examine the challenges

encountered by naval vessel design programs, as they represent long duration design projects, and many have significant amounts of publicly available information. The following sections will look at public information from the Littoral Combat Ship (LCS) program to illustrate philosophical and ontological aspects in design and the elucidation of design requirements.

AN INTRODUCTION TO U.S. NAVY SURFACE SHIP DESIGN

The design of U.S. Navy ships involves several key entities including the Office of the Chief of Naval Operations (OPNAV), Naval Sea Systems Command (NAVSEA), Program Executive Office Ships (PEO Ships), and shipbuilders. For ship design, OPNAV establishes strategic and operational requirements and is responsible for resource allocation. PEO Ships manages the design, construction, and delivery of ships, ensuring that ships meet operational, schedule, and budget requirements. PEO Ships is affiliated with NAVSEA, and NAVSEA engineering directorates are the principal authority for design and engineering. NAVSEA defines and manages technical requirements including adherence to safety, environmental, and performance standards. Shipbuilders and industry play a pivotal role in the actualization of naval ship designs, translating design specifications into detailed designs and ultimately construction and delivery. The process for the acquisition of a ship is complicated and bureaucratic, involving the development of binding design requirements, specifications, and contract documents.

THE LITTORAL COMBAT SHIP (LCS) AS A CASE STUDY

One of the U.S. Navy's more recent ship design programs was the development of the Littoral Combat Ship (LCS). The design of LCS proves to be an insightful study as there is an atypically large volume of publicly available literature showing a change in perception of the design. Perception has ranged from being what the Navy needed as a "streetfighter" during concept development, to derision as "The Navy's Very Expensive Mistake" when several ships in the class were decommissioned early Barbaro and Lipton (2023). This case study looks to explain that change in perception through a philosophical and ontological analysis of the design challenges and requirements development.

It is the authors' premise that top level truth statement(s) for an organization must hold true for a design to be successful, acting as ontological anchors. These anchors can be considered a Style, or design philosophy. If the motives or narrative for a design or design decision are in line with the ontological anchors, the process can move ahead smoothly. However, if entities are working toward false anchors or the design becomes misaligned with the true ontological anchors, this will result in design churn or re-work until the design either aligns or fails. Recognizing and accounting for the discourses, ontological commitments, and ontological anchors is critical for a successful design program. In the case of LCS, the change in perception about the program may be explained using the premise that a global universe of discourse with shared ontological anchors did not exist. Once the true anchors became clear and were commonly held, the pull toward alignment came in the form of changes to the program.

Three aspects of the LCS program will be presented as two cases: changes in vessel rules during the bidding and design process, changes in the evaluation of survivability over the design process, and changes in vessel lethality over the design process and introduction to the fleet.

Case 1: The Ontological Anchors of a Commercial Parent, Commercial Rules, and Survivability

The LCS program was originally conceived as part of a surface combatant family of ships. LCS was envisioned to be the small and low cost ship that could be built in larger numbers, in part relying on the broader force network for effectiveness and survivability Work (2014). Attempting to meet affordability targets meant designing LCS to a commercial parent, with reduced survivability, and to commercial standards. Each of these ontological anchors is examined in turn.

The first ontological anchor was to use a commercial parent hull form and industry partnered vessel rules. Based on the initial stipulations for LCS, industry designs were based on high speed ferries. “The philosophy of the two industry design teams was to leverage technical advances and risk-reducing lessons learned in these high-speed commercial ferry designs, while integrating features and design approaches that are unique to a U.S. Navy Combatant” Keane and Tibbits (2013) However, “the incorrect framing assumption was that these commercial vessels were appropriate parents upon which to base an appreciably different warship” Keane and Tibbits (2013). While at the time this may have seemed like a good idea, this represents a major ontological commitment. By using commercial ferry designs as a parent hull, the industry design teams greatly predicated, influenced, and committed the universe of discourse for the design and translation of requirements for LCS. During this process however, “grumblings from the surface warfare community, which was highly skeptical of warship based on commercially derived designs,” started to cause a shift in requirements Work (2014). This shift is an example of ontological conflict resulting from a false ontological anchor. In this case, the design started to be pulled away from the false ontological anchor (commercial parent) and begin aligning with the underlying true ontological anchor (warship).

The next ontological anchor is that industry partnered rules were sufficient for a warship. When initially setting out the bid for LCS, “the Navy initially asked for ship designs using American Bureau of Shipping (ABS) High Speed Naval Craft Rules, which were essentially commercial standards” Work (2014). In 2003, a partnership was developed between the U.S. Navy and ABS. The partnership was intended to help develop the Naval Vessel Rules (NVR), a set of rules meant to update military general specifications and develop rules in collaboration with industry. LCS was the first vessel where NVR would be implemented. It should be noted that the “implementation of new Naval Vessel Rules (design guidelines) further complicated the Navy’s concurrent design-build strategy for LCS. These rules required program officials to redesign major elements of each LCS design to meet enhanced survivability requirements, even after construction had begun on the first ship” United States Government Accountability Office (2007). The switch from ABS High Speed Naval Craft Rules to the NVR occurred after the contract for the vessel was awarded.

In testimony before Congress at the time, NAVSEA stated the partnership with ABS was “to write a new set of rules to take the best of the old and some of the good commercial practice from ABS and blend them together in a set of Naval Vessel Rules for the ship. A problem is that we did that throughout–concurrently throughout the time when the bidders were bidding on the ship and the ship that we bid and the ship that we costed out is not the same ship that we are buying today because of the parallel development of those rules” U.S. Government Printing Office (2007). The development of the rules in parallel with the design of the ship caused for numerous late stage design changes. This can directly be seen through how NAVSEA stated in the testimony that “the ship that was bid did not include many of the provisions of the Naval Vessel Rules because it was based on a commercial design and in getting the ship design from the commercial design to meet the rules that we need to keep our sailors safe” U.S. Government Printing Office (2007). The ontological anguish of this can also be seen on the shipbuilder side from the same hearing from testimony by the president of Lockheed Martin at the time, “we bid, as [NAVSEA] said, a commercial ship. ABS class ship was our bid. The Navy decided, for good reasons, to make this ship a surface combatant which would be very survivable, which it is. And that caused a lot of change” U.S. Government Printing Office (2007).

The final anchor, alluded to above, was the acceptability of a less survivable warship. At the outset, LCS was designed to a “Level 1+ survivability standard, which is greater than the Level I standard to which the Navy’s current patrol craft and mine warfare ships were designed, but less than the Level II standard to which the Navy’s current Oliver Hazard Perry (FFG-7) class frigates were designed” O’Rourke (2012). However, hitting this requirement with a commercial parent and commercial based standards proved a challenge, “...designers simply did not believe they could hit the LCS cost targets... Consequently, early program documents established “crew survivability” as the minimal design standard” Work (2014). Even then, this meant changes relative to commercial rules, including shock hardening of systems, additional water-tight compartmentalization, and redundant firefighting systems. The yards selected for the ship did not initially have the capability needed to build the ship to the increased level of survivability, and it had to be built up. Even with all of the design churn, the Director, Operational Test and Evaluation did not expect LCS “...to be survivable in a hostile combat environment. This assessment is based primarily on a review of LCS design requirements, which do not require the inclusion of the survivability features necessary to conduct sustained operations in its expected combat environment” O’Rourke (2012).

The public record and abundance of published opinions about LCS survivability are evidence the ontological anchor was

false Lagrone (2013) Hilger (2016). Remembering that an ontological anchor is the fastening of one's view of the universe of discourse to a specific assertion, the LCS survivability anchor was false because the assertion that Level 1+ survivability was sufficient was based on a false perception of the Navy's universe of discourse on survivability. The true universe of discourse was around traditional warship surivivability. This is evidenced by the 2014 Secretary of Defense directive for the Navy to submit more frigate like survivable alternatives to LCS.

Case 2: The Ontological Anchor of Lethality

The LCS was designed to be lethal against asymmetric near coastal threats, emphasizing prosecution of small boats, mine warfare, and littoral anti-submarine warfare, enabling other forces to focus on primary missions Defense Acquisition Management Information Retrieval (2004). This ontological anchor for lethality was fastened to a universe of discourse in the context of a "...a new security agenda that addresses contemporary threats such as the proliferation of nuclear, chemical and biological weapons, terrorism, and international crime" The White House (2000). Over the course of the program the universe of discourse shifted, "inter-state strategic competition, not terrorism, is now the primary concern in U.S. national security, " but the original ontological anchor for lethality had already been actualized via design, construction, and delivery of ships and was still reflected in program reports U.S. Department of Defense (2018) Defense Acquisition Management Information Retrieval (2018). The ontological anchor for lethality was true for the original universe of discourse, but became a false anchor as the universe of discourse shifted. Attempts to align the two did occur. Efforts to change the ontological anchor to align with the shifting universe of discourse started in 2014 when the Secretary of Defense directed the Navy to "...submit alternative proposals to identify and procure a more lethal and survivable small surface combatant, with capabilities generally consistent with those of a frigate" U.S. Department of Defense (2014). Attempts to change the universe of discourse to better align with original anchor also occurred, "to compensate for any gaps in the ship's survivability and lethality capabilities, the Navy continues to redefine the concept of operations (CONOPS) for LCS" United States Government Accountability Office (2015) .

The misalignment over time between anchor (lethality) and universe of discourse (threat) has ultimately resulted in early decommissioning of several ships, and cancellation of key portions of the program, including the Anti-Submarine Warfare (ASW) mission package. The explanation was that "those requirements for that ASW package for LCS were developed back in 2008 against a diesel [submarine] threat in the littorals. And then our minds shifted to we'll be using these things in the deep blue ocean" Ong (2022). However, what is intuitive retrospectively (significant changes in requirements means rework and consequent cost and schedule impacts) can be difficult to see in the present. Ontological and philosophical concepts provide a more general, structured and rigorous way to identify and understand as a designer what one is doing, rather than just understanding how to do it.

DISCUSSION

One of the most important concepts that can be gleaned from the presented case study is that requirements elucidation is really just working to resolve one's ontological anchor (true or perceived). Work to resolve the ontological anchor is supported by low fidelity engineering, for example, concept design activities. Once the ontological anchor or anchors are resolved, the process moves into the design phase where the anchors are considered to be set. To implement the anchor, one conducts design activities so that design knowledge can be generated over time. If an anchor changes, an anchor is found to be false, or a new anchor emerges, this causes for design rework or for the design to fail.

In regards to the LCS program, this can be clearly seen through how in the Work report it is stated that "perhaps the most serious objection to LCS is that the Navy charged into series production without having a clear idea of how the ship would be used" Work (2014). This sentiment is directly connected to the idea of not properly resolving one's ontological anchor.

One of the reasons for the larger amount of rework and failures seen with naval design is the time scale. The duration of Navy design programs are very long, some upwards of 20 years. Given the long time scale of naval design, the probability

of an ontological anchor or universe of discourse changing is very high. This means if the anchor changes the prior engineering work may no longer supports the new anchor. The high probability of an ontological anchor changing can also be partially attributed to changes in personnel over the course of a design program or evolving threats.

The case on survivability hints that even if entities try to do things differently, an organization will be pulled toward its cultural anchors. Cultural and societal based ontological anchors can be enduring, whereas anchors based on an individual's vision are comparably unstable and short. Thus, in an organization with long-time scale projects and staff turnover, things are likely to revert to more enduring cultural or societal anchors. This could directly be seen with LCS in how the initial vision for a commercially based less survivable ship was pulled toward the more culturally accepted idea of a frigate. The pull away from anchors for commercial parents, standards, and reduced lethality and survivability toward more traditional anchors is not unique in warship design.

CONCLUSIONS

In conclusion, the elucidation of requirements is foundational in the early stages of the engineering design process. In the realm of design, language serves as a crucial medium for articulating desires and necessities, which then transform into explicit and unambiguous design requirements. This transformation, facilitated by embedded language in various design documents and tools, contributes significantly to shaping and constraining potential solutions, encapsulated in the philosophical concept of ontological commitment.

However, the translation of uncertain or ambiguous language into concrete design requirements has been overlooked from a linguistic standpoint. The true implications of design requirements and their ontological commitments and anchors, often only become fully apparent later in the design process. The real-world examples presented from the Littoral Combat Ship program underscore the tangible impact of ontological and philosophical concepts in the requirements process. These examples serve as a modern lens through which to examine how language, through the articulation of requirements, shapes and guides the trajectory of design solutions. As the design process evolves, it becomes increasingly evident that the linguistic choices made in the early stages exert a profound influence on the ontological commitments and anchors that underpin the final design outcomes. While the presented case may seem specific the concepts and method introduced are largely and generally applicable to marine design and other design disciplines.

A few important concepts can be taken from the case study presented in this manuscript. One important realization is that universe of discourse and truth statements can be relative to an individual or group. This is akin to the idea that "beauty is in the eyes of the beholder." This concept does not work in naval design. Given this, in design it is important to try to find a universe of discourse that is generally global and robust. The other critical realization is that requirements elucidation is really just working to resolve and properly account for one's ontological anchor. This is critical to try to get right from the early stage of the design process to try to prevent design churn, re-work, or failure.

Looking to the future, concurrent engineering approaches may address the challenges facing current and future design programs, based on the presented theory. Concurrent engineering approaches, including close interaction between stakeholder organizations, may be able to avoid silo effects and better identify enduring ontological anchors and form a global universe of discourse. In any event, ontological anchors and commitments will need to be accounted for and properly resolved.

CONTRIBUTION STATEMENT

CWA: Conceptualization; investigation, methodology; writing – original draft. **MCP:** conceptualization; methodology; writing – review and editing **DJS:** conceptualization; supervision; writing – review and editing.

ACKNOWLEDGEMENTS

We would like to thank Dr. Jessica Dibelka from the Office of Naval Research for providing support for this project. This work was funded under grant number N00014-21-1-2795, Data Model Fusion: Design, Experiments, and Frameworks for Surface Platforms. Additionally, this work received Government support awarded by the Department of Defense, Office of Naval Research, National Defense Science and Engineering Graduate (NDSEG) Fellowship, 32 CFR 168a.

REFERENCES

Andrews, D. (2018a). Choosing the style of a new design - the key ship design decision. *International Journal of Maritime Engineering*.

Andrews, D. (2018b). The sophistication of early stage design for complex vessels. *International Journal of Maritime Engineering*.

Andrews, D. J. (2012). Arts and science in the design of physically large and complex systems. *Proceedings of the Royal Society A: Mathematical, Physical and Engineering Sciences*, 468(2139):891–912.

Barbaro, M. and Lipton, E. (2023). The navy's very expensive mistake. Available at `https://www.nytimes.com/2023/02/13/podcasts/the-daily/navy-littoral-combat-ships.html`.

Defense Acquisition Management Information Retrieval (2004). *Selected Acquisition Report (SAR) Littoral Combat Ship (LCS)*.

Defense Acquisition Management Information Retrieval (2018). *Selected Acquisition Report (SAR) Littoral Combat Ship (LCS)*.

Duchateau, E. (2016). *Interactive Evolutionary Concept Exploration in Preliminary Ship Design*. PhD thesis, Technical University Delft.

Festinger, L. (1957). *A Theory of Cognitive Dissonance*.

Galle, P. (2002). Philosophy of design: an editorial introduction. *Design Studies*, 23(3):211–218. Philosophy of Design, Available at `https://www.sciencedirect.com/science/article/pii/S0142694X01000345`.

Hilger, L. R. (2016). *Rethinking Survivability*. Available at `https://www.usni.org/magazines/proceedings/2016/january/rethinking-survivability`.

Jubien, M. (1998). Ontological commitment. In Taylor and Francis, editors, *The Routledge Encyclopedia of Philosophy*. Accessed 22 June 2022.

Keane, R. and Tibbits, B. (2013). The fallacy of using a parent design: "the design is mature". *Trans. SNAME*, 121.

Krämer, S. (2014). *On What There is For Things To Be: Ontological Commitment and Second-Order Quantification*. Vittorio Klostermann, Frankfurt Am Main.

Lagrone, S. (2013). *Navy Responds to Pentagon LCS Survivability Claims*.

Lagrone, S. (2023). *Draft Proposal for 'Affordable' Medium Landing Ship Out to Shipbuilders*.

Miles, R. and California Institute of Technology (1973). *Systems Concepts: Lectures on Contemporary Approaches to Systems*. A Wiley Interscience Publication. J. Wiley.

Ong, P. (2022). *Admiral Gilday Explains LCS ASW And MCM Module Decisions*. Available at `https://www.navalnews.com/naval-news/2022/05/admiral-gilday-explains-lcs-asw-and-mcm-module-decisions/`.

O'Rourke, R. (2012). Navy littoral combat ship (lcs) program: Background and issues for congress. Technical report, Congressional Research Service.

O'Rourke, R. (2023). *Navy Medium Landing Ship (LSM) (Previously Light Amphibious Warship [LAW]) Program: Background and Issues for Congress*. Congressional Research Service.

Peacock, H. (2011). Two kinds of ontological commitment. *The Philosophical Quarterly (1950*, 61(242):79–104.

Rayo, A. (2007). Ontological commitment.

Rich, B. R. and Janos, L. (1994). *Skunk Works: A Personal Memoir of My Years at Lockheed*.

Rovelli, C. (2016). Brexit won because those who opposed it did not address its core philosophy. Available at `https://www.theguardian.com/books/2016/sep/23/philosophy-dead-brexit-carlo-rovelli`.

Royal Caribbean Group (2020). *Code of Business Conduct and Ethics*.

Royal Caribbean Group (2024). *Inside Anthem of the Seas' Safety Command Center: Royal Caribbean Implements Award-Winning Technology*.

The Strategy Institute (2023). Organizational bias: The curse and the cure. Available at `https://www.thestrategyinstitute.org/insights/organizational-bias-the-curse-and-the-cure`.

The White House (2000). *A National Security Strategy For a Global Age*.

Tombras, C. (2019). *Discourse Ontology: Body and the Construction of a World, From Heidegger Through Lacan*. Springer Verlag.

United States Government Accountability Office (2007). *Testimony Before the Subcommittee on Seapower and Expeditionary Forces, Committee on Armed Services, House of Representatives, Defense Acquisitions: Realistic Business Cases Needed to Execute Navy Shipbuilding Programs*. United States Government Accountability Office. Available at `https://www.gao.gov/assets/gao-07-943t.pdf`.

United States Government Accountability Office (2015). *Report to Congressional Committees, Littoral Combat Ship: Knowledge of Survivability and Lethality Capabilities Needed Prior to Making Major Funding Decisions*. United States Government Accountability Office. Available at `https://www.gao.gov/assets/gao-16-201.pdf`.

U.S. Department of Defense (2014). *Statement by Secretary Hagel on the Littoral Combat Ship*.

U.S. Department of Defense (2018). *Summary of the 2018 National Defense Strategy of the United States of America: Sharpening the American Military's Competitive Edge*.

U.S. Government Printing Office (2007). *H.A.S.C. No. 110-114 Acquisition Oversight of the U.S. Navy's Littoral Combat System: Hearing Before the Seapower and Expeditionary Forces Subcommittee of the Committee on Armed Servies*. U.S. Government Printing Office.

van Ores, B. (2011). *A Packing Approach for the Early Stage Design of Service Vessels*. PhD thesis, Technical University Delft.

Wikipedia (2023). Anchoring effect. Available at `https://en.wikipedia.org/wiki/Anchoring_effect`.

Work, R. O. (2014). *The Littoral Combat Ship: How We Got Here, and Why*. United States Government and Office of the Undersecretary of the Navy.

Österblom, F. (2017). What is a neutral criterion of ontological commitment?

Proceedings of 15th International Marine Design Conference (IMDC-2024)
June 2-6, 2024
Amsterdam, the Netherlands

Practical implementation of configuration management in the context of concept ship design – first lessons

S. Bedert[1,*], R. Hoogenboom[2]

ABSTRACT

The implementation of configuration management (CM) in support of concept design activities at the Products and Proposals department of Damen Naval has put forward a number of challenges that seem to be unique to the shipbuilding industry and the process of concept development therein, that traditional enterprise-level product lifecycle management software and processes are unable to tackle. Information fluidity, an uneven and fast evolving tooling landscape and limited team sizes have driven us to pursue dedicated software implementations in support of CM during concept design. From the first attempts of doing so, we have seen that a number of performance requirements for the software that were completely under the radar are now driving factors for further selection (mostly related to speed and agility of the tool), while some others even impact our way of working and organizational structure as a whole, requiring us to carry system responsibility per discipline, instead of only functional responsibility.

KEY WORDS

Configuration Management; concept design; contract design; database; shipbuilding; ship design;

INTRODUCTION

This paper aims to describe the lessons learned derived from our initial attempts to introduce configuration management and the associated tooling in our concept design workflow at the Proposals department of Damen Naval. Given that the number of theoretical papers on the subject, and descriptions on cross-industry abstraction levels are widespread, the explicit premise of this report is to stay as practical and 'down-to-earth' as possible, noting and highlighting primarily the challenges faced within the context of our own department, and the naval shipbuilding industry by extension, as far as the processes and organizational structures applied are comparable with those of Damen Naval (which cannot be verified by the author).

The paper starts by defining configuration management (CM) as applied in the context in this paper and the reasons why this is deemed 'special' in the context of ship concept design. In a second part, the paper shortly touches the rules of play of configuration management (CM) as laid out at Damen Naval and describes two initiatives rolled out for the introduction of configuration management software.
In the final part, the actual lessons learned from these initiatives are described, with a possible outlook for further work.

SCOPE DEFINITION

This chapter defines (and restricts) the scope of the term Configuration Management to that part relevant in the context of this paper and the concept design department of Damen Naval and describes why this is deemed to be a special case of implementation compared to more widespread descriptions, definitions and uses of the concept warranting custom implementation.

[1] Manager Marine Engineering at Damen Naval B.V. (Dept. Proposals; Vlissingen, Netherlands);
[2] Manager Product Development & Innovation at Damen Naval B.V. (Dept. RD&I, Vlissingen, Netherlands);
* Corresponding Author: s.bedert@damennaval.com

Submitted: 15 January, Revised: 29 April 2024, Accepted: 1 May 2024, Published: 23 May 2024

Conference paper, DOI: https://doi.org/10.59490/imdc.2024.887 e-ISSN: 3050-4864

Configuration Management

Since Configuration Management is a multifaceted concept, it is essential to establish precise boundaries for its application in the context of this paper.

The fundamental goal of the work done is/was to create a centralized repository for information related to the physical components and systems that constitute a ship, especially suitable for use during concept- and tender design phases in a ships lifecycle. This information, especially the aspects which holds cross-disciplinary importance, such as size, weight, and electrical power requirements, will be managed by the relevant specialists. The objective is to maintain this information as a constantly available and up-to-date snapshot over time. In simpler terms, we are focusing on managing the ship's system configuration, rather than the concept design project configuration, which primarily involves document and requirement management and has not been considered in this context.

The overall aim is to allow the different systems in the ship to be developed in accordance with their own largely unaligned, albeit overlapping, timelines, without having to wait for a full design cycle on all systems before an updated snapshot is made available, as long as all the data available is the ‘latest status available at that time’ in any given snapshot.

Once the initial idea was proposed, we structured it into an internally peer-reviewed 'master' functional specification (the concept was dubbed Krypton at the time, a name which persists to this day within our company for anything related to the concept). With this functional specification in hand, we pursued the following implementation routes:

a. We invited software vendors to offer solutions that align with the specification.
b. We developed software in-house from scratch that matches the specification.
c. We sought partnerships to explore and enhance an existing system based on this specification.

Over time, steps (a) through (c) have been carried out in overlapping cascade, with (a) now completed, (b) nearly finished/scrapped, and (c) in a start-up phase. As a result, this paper focuses on the lessons learned during steps (a) and (b), which are of course also being considered in the execution of step (c).

Concept Development/Contract Design vs Engineering

It is to be noted that configuration management both in terms of document control and technical data management are well established within the (ship) engineering and building processes. In support of these, many well-established (Product Lifecycle Management; PLM) software suites are available, both on an enterprise and small business level.

So, what makes ship concept design activities so much different from production activities that we claim we need special software to do it? The reasons for that as we have identified them within our company are the following:

- Data persistence rigidity: Concept design is largely a matter of design space exploration and solution generation. Configuration items are generated, changed and deleted again on the fly on every level of detail throughout the process. In opposition, data is created in a PLM environment once, and is made there to stay, because the underlying hard- or software is being procured, built or created in real life. In essence, a concept design is all about defining a solution and all (building) budgets related to it, while a production phase is about realizing a (pre-)defined solution from definition to reality as quickly and efficiently as possible.
- Interfacing to tools/availability of software functionality: The PLM packages in use are targeted for interfacing with the existing engineering and building tool suites (CAD/CAM packages etc.). Just as the PLM package itself, however, the intrinsic overhead of that tool suite is in almost all cases too high for use in concept design, and much simpler alternatives are used.
- Procedural overhead vs. project throughput times: the speed at which tenders, and concept development projects are started, scrapped, and renewed is not compatible with the application management overhead of traditional PLM packages. Traditionally, it can take up to 4 to 8 weeks to setup a project in our PLM environments, involving at least three different departments at an average of two people per department.

IMPLEMENTATION INITIATIVES

This chapter describes two implementation initiatives taken to introduce configuration management in our department, corresponding to cases (a) (implementation through external vendor software) and (b) (implementation through own software development) from the scope definition described above.

In each of these cases, the practical goal was to have:

- A collaborative piece of software that allowed multiple users to work simultaneously.
- Gather, per discipline, lists of equipment that contained sufficient data to support the three main ships balances (weight, electrical load and heat load) in a single database.
- Get all relevant data out of the database in a format that allowed updating of the balance sheets.

Although the goal seems quite simple, from a database point of view this proved to be quite the feat, as in practice, this implied the system had to be capable to manage a Product Breakdown Structure, a ship's space list with associated data and a ship's equipment list, and the allocation between those data concepts (e.g. a piece of equipment is always part of one or more parts in the PBS structure, and always allocated to a space).
Beyond that basic goal, ambitions where set even higher on a few functionalities. For example, we expected the data fields to be managed to be flexible (user-managed) and values to be flexible on unit of measurement. Furthermore, we wanted to be able to compare ship configurations (since it is applied during concept design), which meant we wanted to 'disable' part of the database temporarily in favor of an alternative (i.e. support for trade-off from within the tool analysis).

External Software (Case (a))

For the first pilot attempt, we selected a closed but flexible platform from a software vendor that offered a 'configured to spec' version of their software. The software had a principally closed architecture, with interfacing created especially for us to be able to implement data I/O using an excel interface. At the time of delivery, the software implemented approx. 80% of the original Krypton functional specification.

After initial testing of the software using parts of a fictional ship concept and a limited dataset, the application was deployed for use in the most recent large contract design project ran by the Damen Naval Proposal department to keep track of ship (system) configuration. The software was used over the full period of the project (p/m two years) and served as configuration management tool for disciplines Propulsion, Electrical, Auxiliaries and Automation.

Success criteria for the pilot execution did not constitute numerical KPI's as such. The sole, practical pass criterion was that the tool would enable multiple engineers to input data of equipment in their disciplinary scope and in accordance with their discipline's applicable timelines, and that data could be exported again in support of a weight calculation and electrical load balance, which it did to successful extent.

However, after careful review, it was still decided to discontinue its use, primarily due to the lessons learned *Adaptability* and *software performance*/*scaling challenges* as described below (even if these were not part of the pilot's original success criteria). The web portal providing the user interface, for example, became unmanageably slow due to the server capacity reserved for the proof-of-concept once the pilot project contained its 'full' list of equipment, spaces and PBS elements. As a further example, we were unable to change the data views ourselves for the most basic use cases (for example, showing the space number to which a piece of equipment was allocated in the tabular equipment overview was impossible without outside consultancy).

In-house Development (Case (b))

To implement the initial lessons learned concerning openness of interfaces to unlock data (refer to below), mostly instigated by server capacity limitations and a need for more customizability, we swung almost stereotypically to the opposite extreme of the spectrum and started building our own version of what Krypton should be, as opposed to an externally sourced, closed architecture software package. In that attempt, we built a rudimentary piece of software that implemented the core functionalities of the Krypton spec, using SQL (SQLite) databases and a Django framework with web front-end.

This software was never developed further than a proof-of-concept. It was never used in production, nor was it put through serious 'malicious' testing. Success criteria for this test were also not defined as numerical KPI's. The practical pass criterion here was to have a 'configurable' data model available (adaptable to different types of equipment and systems), in which we could define data and later extract it again, and in that goal, the software succeeded again without fail.

Although it could be considered a successful 'start', the work was never finished because we saw that the work involved would require us to venture too far off from our core competences, as described in the *Software Support* lesson learned described.

LESSONS LEARNED

The lessons learned from using the third-party software (case (a)) and programming our own tool(s) (case (b)), roughly fall into the following categories:

1. Software functionality and performance
2. Modelling conventions
3. Organizational structure
4. Obvious/novice mistakes

Firstly, we are not above admitting that some very basic mistakes were made in all this (category 4). As we do not buy, create, or configure software every day, we obviously fell into pitfalls which may be marked as stereotypical. To get them out of the way, the most notable:

- We grossly overestimated the percentage-ready associated with a proof-of-concept at approx. 80% instead of the 30% it deserved. As you will see from all the lessons learned below, we still have a lot to figure out. This applies independently to both implementation case (a) and (b) as some of the main lessons learned relate directly to business rules, and not software implementation itself.
- We underestimated the effect of computational speed and performance on useability and user satisfaction in our on-premise implementation, lapsing too far from well-established 0.1/1/10 norms posed by (Miller, 1968).

It is worthwhile to notice that the second point is directly related to the concept design challenges described in the Scope Definition chapter before. Given that data values are more fluid in concept design, the software speed associated to data manipulation should be an order of magnitude faster that what we have seen in the past in traditional PLM packages (where our company has more experience and a more widespread frame of reference). So software speed is a unique aspect in which we will expect more instead of less when compared to traditional PLM packages.

Software functionality and performance

Batch editing
In drafting the functional Krypton specification, the use of batch creation and editing was posed as a nice-to-have. However, in use of both Krypton implementations, this proved to be a more than essential feature. In hindsight, this is a perfectly logical conclusion provided that in reality, most of the data is created and/or updated in batches from parts of the design process (e.g. a space list is (re)generated from a CAD source in one go for all spaces in a ship; or an equipment list for a full system is defined by a specialist or generated by a subcontractor in one go). As such, the majority of interactions with users with the software will be batch related, and the functionalities provided thereto should be on-point.

Adaptability
Tooling in support of configuration management is not the only part of our working environment that is undergoing changes. With the launching of the Krypton concept, we also inspired a wave of initiatives that aim to disclose information between software tools, calculation sheets and 3D models regardless of what we come up with on the configuration management side (e.g. transporting the information from a 2D general arrangement to a 3D model for further evaluation).
With that, a whole new set of data and related data formats come into play that could also be relevant for plugging in to a CM database, signifying the importance of adaptability of the Krypton implementation, as the tools surrounding the CM platform will, with a high chance, evolve faster than the platform itself. This in turn poses a requirement for any Krypton platform to be highly adaptable, not only regarding input and output formats, but data visualization within the tool itself.

Scaling challenges
As the products we build are large in absolute scale by themselves, the number of elements within them that contribute significantly to their design balances is equally so. Consequently, the number of elements to be considered for CM is also large. Both of our implementation cases have shown that these numbers can cause problems in the tested software packages, which both rely on server-side processing for data integrity checks on each Create, Read, Update or Delete (CRUD) action on the data, when server-side processing capacity is not duly considered.

Apart from server-side computational power limitations, it has also been remarked that the lists and tabular data representations used on both our implementations started to become cumbersome to work with (with endless scrolling, and just-not-there-yet

filtering capabilities). Without knowing what to look for exactly for improvements in further experimentation, this is a point that deserves attention.

Modelling conventions

In a conceptual design phase, team sizes are notably smaller compared to a production environment, where an extensive group of engineers and CM professionals collaborate on ship configuration maintenance. In a 'typical' conceptual design team, each discipline is represented a single individual or a handful of people. These team members primarily engage in primary design activities, next to ensuring that the configuration management effort remains commensurate with the phase of development.

To prevent CM activities to dominate design work, it is essential to tailor the level of abstraction in the information provided to the specific requirements of the design phase. Consider a main engine as an illustrative example. The scope of delivery for a main engine extends beyond the engine itself. It encompasses a long list of associated elements, each with dedicated specifications regarding weight, dimensions, etc. (e.g., a preheater, a local control panel, or external coolers). However, during the conceptual design phase, the primary interest often only lies in confirming the presence of a main engine installation rather than scrutinizing the particulars of its constituent parts. Yet, if inexperienced engineers receive the instruction to model solely the main engine, there is a risk that they may overlook the associated components, inadvertently underestimating the overall system's weight. Nevertheless, it is impractical to model and maintain each of these individual components separately. Doing so would introduce superfluous data into the configuration, resulting in excessive effort and the potential loss of 'belongs-to' relationships among these objects.
Hence, it is imperative to permit aggregation of a configuration to the appropriate level, alleviating the burden of model maintenance while retaining sufficient details to instill confidence in users and model auditors regarding completeness and the preservation of 'belongs-to' relationships. For instance, one approach may involve modeling large items with three distinct weight values: one for the primary hardware, one for associated hardware fluids, and one for all auxiliary components.

However, as you can image, the aggregation level that is acceptable is not uniform over all the different systems in a ship, nor, if you are truly honest, across projects. Inevitably so, finding the correct aggregation level is a matter of getting a ‘feeling’, or more extensive experience in using such models. In the end, it is not unimaginable for this experience to end up in some sort of data modelling guideline.

Development time

Given the considerations mentioned, achieving proficiency in data aggregation, and identifying suitable data views requires substantial practice and experience. Given the rapid pace of concept design projects and their heavy workload, expecting rapid mastery is unrealistic.

It is important to leverage the flexibility inherent in any chosen tool and remain open to iterative adjustments. Nevertheless, crafting an effective working method will take considerable time, potentially spanning years. Therefore, exercising patience is crucial, particularly when encountering user complaints during the initial implementation phase.
However, it's essential to recognize that despite potential challenges, benefits from implementing configuration management in concept design can still be observed from the outset, even if perfection isn't immediately attainable.

Organisational Structure

Data Ownership

The introduction of configuration management has brought to surface a fundamental aspect in the organizational structure of various disciplines within our department, that requires attention and improvement to fully realize the potential of this initiative.

At our department, knowledge, responsibilities, and people are organized in traditional shipbuilding-related disciplines (naval architects, structures, propulsion, electrical…). That division in disciplines is, as the pilots done in the context of this paper have clearly shown however, purely on functional level, meaning that a specialist is held responsible for defining what is necessary of an item to perform its primary function, but not directly for any secondary information that is a direct consequence of that decision. For example, a mechanical engineer is responsible for defining the correct flow and pressure requirement for a main firefighting pump, but he is not held responsible or accountable for the weight and dimensions of these pumps.

That functional subdivision is a problem in terms of configuration management, as this requires, in practice, ownership of all item properties within a single owner, if only from an efficiency point-of-view. That is because, as you can imagine, the data source for information pertaining to a configuration item is concentrated at one place (for example, technical manual of a pump contains the QH-curve as well as a dimensional drawing). So, it would only be logical for a specialist to own all data related to that pump. Even more so, when considering that all that 'secondary' information will only change when the primary specialist makes a design change.

This requirement for workflow alignment entails that specialists within the department should start acting as general system owners instead of purely functional owners, whereby their responsibilities lie in all system parameters, not just the functional ones. This transition further demands a reevaluation of incentives to encourage specialists to take ownership across all system parameters. Finding the right motivators will be pivotal in driving this change, enabling a more efficient and cohesive configuration management approach.

Software Support Workload

Implementation case (b) has clearly highlighted the distinction between our expertise as shipbuilders and that of professional software developers. Our excursion into creating a proof-of-concept provided invaluable insights into the intricate dynamics of software development, and especially software maintenance.

Upon venturing into programming software intended for a broader user community, software that surpasses the complexities of typical online programming tutorials, we encountered the many challenges that software developers will surely recognize, such as outdated third-party source code packages, evolving library versions, deprecated functionalities, and the continual need for adaptation within our source code. Programming for a larger user base also highlighted the increased need for meticulous software documentation and ditto reliability. This underscored the necessity for extensive source code documentation to ensure sustained functionality, irrespective of the original creator.

In the end, it became apparent that continuing this trajectory would necessitate the establishment and ongoing maintenance of dedicated resources to support the tool we developed. This signified the integration of software development into the core activities of our department, which was, in hindsight never the intention.

CONCLUSIONS

Our first exercises with third-party and our own (attempt to create) software in support of configuration management has taught us that the road ahead of us to find that sweet spot where tools are at their peak of added value is going to be a long one still. Within a landscape where the tooling surrounding such attempts is also evolving rapidly, it is unavoidable that any attempt to build something sustainable will require a high level of flexibility and future adaptability to new interfaces.

Given that data sources are very dispersed during concept design, data entry will remain a matter of manual labor for the foreseeable future. As such, software performance in terms of speed and responsiveness is a key requirement for successful implementation of such.

Furthermore, the use of a configuration management concept has shown us that we can no longer rely on traditional functional ownership of systems across disciplines. Instead, we need to change our attitude towards data correctness to systemwide ownership, where specialists no longer care only for the functional performance of the systems they design, but also for every consequential aspect associated therewith.

Although the goals set before implementation cases (a) and (b) where largely met, the lessons learned described in this document have shown that continuing those paths is not preferable, yet the premise of configuration management for concept design does warrant further exploration.

Implementation case (c) as described above is the next iteration being considered. The views depicted in this paper will serve in a large part as additional boundary conditions, goals and requirements in that project. Implementation case (c) is seen as a hybrid between cases (a) and (b), whereby the aim will be to find a piece of software which is developed and managed by an external partner on the one hand (avoiding the maintenance burden of software identified in implementation case (b)), but which is, by design, sufficiently open to allow flexible data access and visualization (for example, one which provides a full-access external API that allows manipulating, importing and/or exporting or reading data using small scripts, or maybe a strong interface to MS Excel). At the time of writing this paper, implementation case (c) was in the initial start-up phase. Feedback from that case was thus not yet available for further evaluation.

DECLARATION OF GENERATIVE AI AND AI-ASSISTED TECHNOLOGIES IN WRTITING

During the preparation of this work the author(s) used ChatGPT 3.5 to improve grammar and overall conciseness of writing style. After using this tool/service, the author(s) reviewed and edited the content as needed and take(s) full responsibility for the content of the publication.

CONTRIBUTION STATEMENT

S. Bedert: Conceptualization; writing – original draft. **R. Hoogenboom**: Supervision; writing – review & editing

ACKNOWLEDGEMENTS

First and foremost, the author would like to acknowledge Claassen, J.P. for his continued support in the exploration and implementation of this work within his department and the projects under his care. Further acknowledgement is made to the pilot user group for their patience and valuable user feedback for implementation scenario A; (de Jong, F.; Den Engelsman, J.; Ferea, V.; Lukasse, R.; Van de Voorde, L), as well as Schouten, G. for providing enthusiastic external feedback, proving that we are on (the right) track with the concepts we came up with. Further thanks goes out to N. Gheorghe for her hard work in programming our own efforts for CM as scenario B.

REFERENCES

Miller, R. (1968). Response time in man-compute conversational transactions. Proc. AFIPS Fall Joint Computer Conference Vol. 33, 267-277

Proceedings of 15th International Marine Design Conference (IMDC-2024)
June 2-6, 2024
Amsterdam, the Netherlands

Naval Wargaming as a Requirements Elucidation Tool for Warship Design Teams

Nick Bradbeer[1,*] and David Manley[2]

ABSTRACT

This paper discusses some of the challenges of setting the requirements for a future warship program and how manual naval wargaming might be employed to make the process more efficient and structured. It goes on to describe some case studies where UCL's wargame "A Balanced Fleet" was applied to requirements-phase problems, in particular the ASW Barrier wargame conducted for the NATO Specialist Team on Naval Ship Systems Engineering. The paper concludes that wargaming is a useful tool in the requirements phase, in particular for helping to direct subsequent and more detailed operations analysis work.

KEY WORDS

Operations Analysis; Requirements; Wargaming; Warship Design

INTRODUCTION

In 2016 a series of wargames conducted in the UK and focussed on low intensity naval operations demonstrated the initial value of wargaming as a concept assessment tool. In this case, wargaming was used to explore facts of Mission Modularity when applied to a naval force, comparing its effectiveness with a force comprising more traditionally designed ships. The games involved members of the NATO Specialist Team on Naval Ship Systems Engineering (ST/NSSE) who sought to formalise the use of wargaming in their suite of concept assessment and analysis tools.

The work was initiated due to concerns in ST/NSSE, that project teams were launching into expensive and time consuming Operations Analysis (OA) without having conducted their own pre-analysis work aimed at refining the OA questions they were posing. This has the potential to allow the OA to unintentionally stray away from prime areas of interest. ST/NSSE's previous exposure to wargaming as a tool to demonstrate and investigate aspects of Mission Modularity gave rise to the thought that it could be broadly applied by projects at an early stage in concept development to test hypotheses and concepts, and thus allow follow on, comprehensive OA, to be better focussed.

Over the same period, UCL has developed a series of naval wargames as teaching tools for use in its MSc-level warship design programmes. One of these wargames, "A Balanced Fleet" has been further developed from a teaching tool into one suitable for application to requirements elucidation problems and was used in support of ST/NSSE's ongoing research.

This paper outlines the challenges that face a warship design team in the requirements elucidation phase, before going on to describe the development of ABF and how it has been used in several case study applications, including a week-long game series run for ST/NSSE. The paper concludes with the conclusions drawn from these series, indicating that wargaming may be a useful tool to assist requirements elucidation, and highlighting features which are desirable in such a wargame.

[1] Affiliation (Mechanical Engineering, UCL, London, UK); ORCID: 0000-0001-7938-1990 [2] Affiliation (Mechanical Engineering, UCL, London, UK); ORCID: 0009-0003-1756-622X
* Corresponding Author: email n.bradbeer@ucl.ac.uk

Submitted: 23 February 2024, Revised: 4 April 2024, Accepted: 1 May 2024, Published: 23 May 2024

Conference paper, DOI: https://doi.org/10.59490/imdc.2024.878 e-ISSN: 3050-486

THE REQUIREMENTS ELUCIDATION PROBLEM

Defining the requirements for a new type of a warship is a challenging task. It is oft said in design circles that "the customer doesn't know what they want"; this is meant as no slight on the customer, who usually has to juggle a large set of mutually interacting mission goals while constrained by funding. This is often a complex problem with opaque interactions and synergies between mission goals, to the point where it is often impossible to understand what a sensible compromise design would look like until some design work has been done. The process of setting the requirement is therefore often called Requirements Elucidation since it is less a process of deciding what desired requirement is, and more a process of gaining understanding about how the different requirements interact and what would produce a harmonious compromise that falls within budget.

If using a Systems Engineering framework, requirements are usually initially defined in a User Requirements Document (URD) in terms of Measures of Effectiveness (MoE) - statements of capability which can be expressed numerically and which relate directly to how capable the ship is at completing mission tasks. A MoE might be phrased as "defend a High Value Unit against an attack by X missiles of Y type, with at least Z probability of defeating all missiles." In order to relate these values to things that a ship designer can easily quantify, Measures of Performance (MoP) are defined, being quantities which can be numerically expressed and measured or estimated directly from the design – quantities like top speed, radar horizon, or number of vertical-launch system cells. To relate the MoEs that the customer cares about to the MoPs that engineers can readily provide some kind of model is required. This is usually the domain of Operations Analysis (OA), which can provide mathematical models which take MoPs as inputs and deliver predicted values of MoEs that result.

OA is a powerful field, but the complexity of the problems mean that it is usually reliant on making assumptions, which in turn are reliant on correctly framing the scenario to be modelled. How to frame these scenarios is the first problem of Requirements Elucidation.

The second problem is the complex nature of the interaction between different MoEs and MoPs. A warship will usually have a range of quite disparate missions, the relative importance of which is difficult to define. Different capabilities on the ship will usually contribute, in different degrees, to more than one mission. There may be synergies – an ASW helicopter also provides very useful maritime surveillance, liaison, and resupply capabilities at no additional cost. There may be capabilities which both contribute to a mission but do not synergise well – high ship speed and onboard aviation for a surface search mission, for example. Understanding the interplay of these capabilities is challenging, and typically customers rely on the judgement and experience of subject matter experts (SMEs). SME judgement offers good utility for relatively low cost but can have limitations; bias in favour of systems or approaches the SME is personally familiar with can often be observed, and novel systems can present a problem if there is nobody with experience in operating that kind of system.

An important tool in squaring the Requirements Elucidation circle is the Concept of Employment (CONEMP.) This is a document which outlines the missions that the ship is expected to undertake, and how it will undertake them. As with the requirement set, deciding the CONEMP is not straightforward; it is sensitive to cost/capability trade-offs and interactions between capabilities, and like the requirement set can usually not be pinned down until some exploratory design work has been done to understand the relationship between various Measures of Performance, the relevant Measures of Effectiveness, and procurement cost. The CONEMP should therefore be a living document subject to revision during the early stages of design.

Two potential pitfalls arise when defining the CONEMP. First, that it does not describe the whole of the mission and skips past some mission phase which turns out to be a vital driver of capability. (This may be most likely to occur around "boring" mission phases like deployment or extraction rather than the more kinetic central phases of the mission.) Second, it is very important to ensure that the entire design team share the same vision of the CONEMP and easy to get this wrong, especially if the CONEMP is a living document, of which several revised versions have existed.

Finally, humans are in general bad at visualising speeds, distances and times when expressed numerically, and these factor centrally into most CONEMPS. Allowing the team to properly understand the position and movement of the new design, relative to allied and enemy units, is a vital part of ensuring the CONEMP is workable.

WHAT IS WARGAMING

Wargaming is a term for which there is no single agreed definition within the community of practice. For the purposes of this work, the authors have used the definition used in the UK Wargaming Handbook (Ministry of Defence, 2017):

> *"A scenario-based warfare model in which the outcome and sequence of events affect, and are affected by, the decisions made by the players."*

Wargaming may use a computer model or may use a more manual approach with physical maps, pieces representing ship and other units, and a set of rules to adjudicate the outcome of uncertain events. These rules may be based on expert judgement to adjudicate each situation (open mechanics) or the generation of a probabilistic model and generation of random numbers (rigid mechanics.) The wargames described in this paper all used a manual approach, using paper maps, wooden blocks or models to represent ships, and a rigid ruleset. Some subjective adjudication was required, usually to decide edge cases outside the core areas the game rules represented.

The boundaries between wargaming and operational analysis are somewhat blurred, and different definitions draw their boundaries in slightly different places. Operational analysis seeks to provide numerical outputs to inform decision making, which can be obtained through a wide range of analytical approaches. Wargaming exists on a spectrum from very analytical games which seek to provide numerical data, through to very non-mathematical games modelling human interaction, especially in politics, where only very subjective data gathering can occur. Naval wargames used for requirements elucidation tend to fall somewhere between these extremes; the technology-centric nature of naval warfare means that some degree of rigid numerical rule mechanics is required, but the problem space tends to be too poorly defined to allow very analytical wargaming.

"A BALANCED FLEET" – A FAMILY OF WARGAMES

ABF as a Teaching Tool

A Balanced Fleet is a naval wargame which started life a teaching tool for use on UCL's Naval Architecture and Marine Engineering MSc courses (Bradbeer 2022), (Manley 2023). Initially named "A Simple UCL Wargame", or ASUW, it was developed to help student ship designers who often lacked background domain knowledge, to understand the engineering factors which make for a good or bad fighting ship. Initially delivered as a whole-class extra-curricular wargame running through an afternoon and evening, it was soon integrated into the teaching curriculum to meet three objectives:

- Develop students' understanding of the modern naval warfare context
- Allow students to rapidly explore possible design options for their capstone ship design exercise (SDX)
- Allow students to informally assess the effectiveness of their SDX ships at the end of the exercise.

To meet these objectives, a game would need to reflect the impact of design engineering choices on capability, in as transparent and granular a way as possible. It would also have to support a robust and transparent workflow for characterising an arbitrary (and often quite unconventional) student design. Finally, it would have to support between two and twenty-four players, to allow for small group design explorations and whole-class capstone games. A search for a suitable commercially available game turned up nothing, so ABF was developed internally.

The teaching incarnation of the game focussed on missile combat in deep water between surface ships with their organic aviation, with very limited modelling of gunnery combat, land units, land-based aircraft and submarines. Game scale was adjusted over time, but settled on turns representing one hour of time, map hexes representing 10 nautical miles of space, and opposing forces comprising between one and ten ships each. Large games were found to take approximately six hours to play.

Parts of the game were necessarily complex in order to represent the impact of design choices in a meaningful way. To preserve enough simplicity to be playable, other parts of the game were deliberately kept simple. For example, the representation of the ship's layout was kept very detailed, resulting in a complicated control sheet for each ship (Fig. 1), while all anti-ship missiles were considered as one of only three types: lightweight subsonic, subsonic, or supersonic.

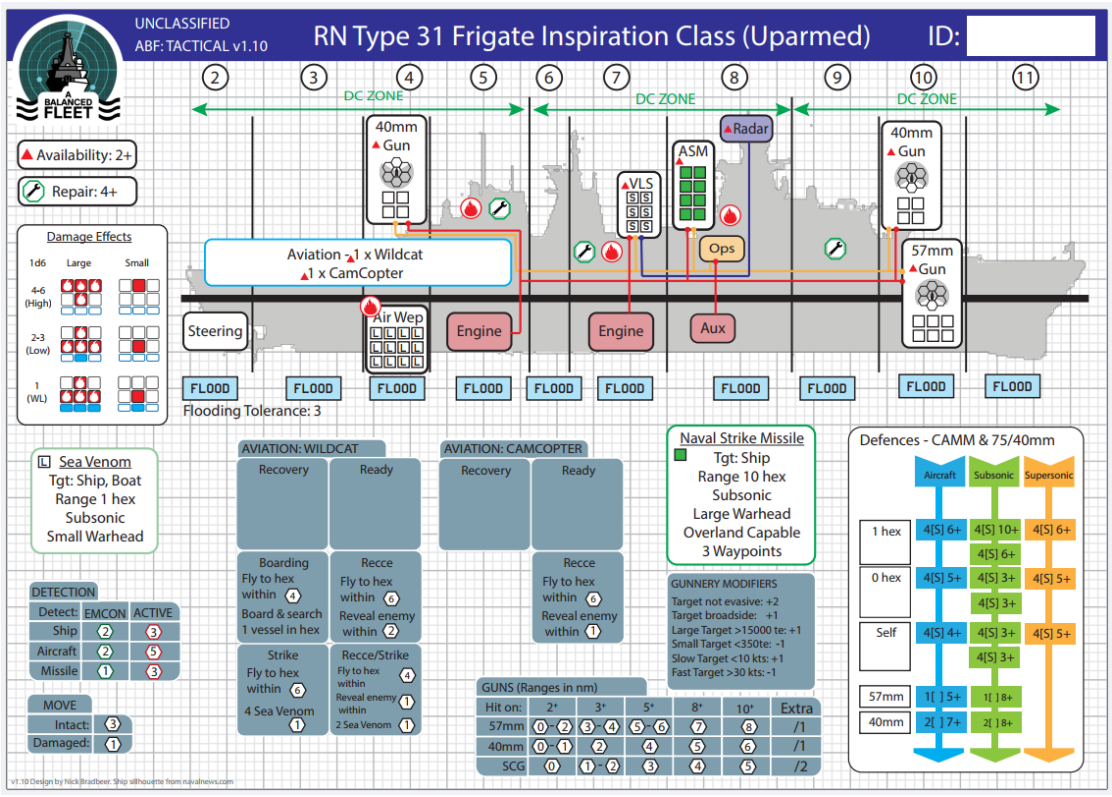

Figure 1: A ship record sheet from ABF: Tactical.

The game was designed with a modular architecture (Fig. 2); the game mechanics themselves were simple models designed to reasonably well match the outputs of more complex OA models, which themselves drew on a database of information about various units and their performance. This structure allowed for transparency in showing why the various game mechanics worked the way they did, as well as allowing the game to be adapted readily, either by changing out an OA model for a different one or by using a different database. This allowed the game to be incrementally improved since, for example, gunnery combat could be improved as better OA models were available, without impacting other parts of the game. While the game was developed around an unclassified database of open-source information, in principle it would be straightforward to substitute a database containing proprietary or classified data if required. (Every incarnation of the game described in this report used the unclassified database, keeping all the games unclassified.)

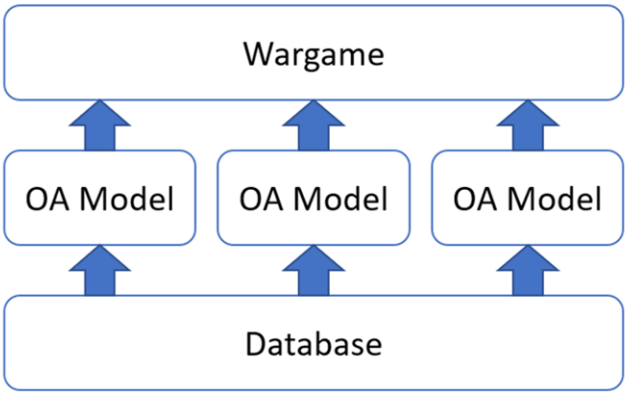

Figure 2: Architectural structure of ABF

Developing ABF Into a Requirements Elucidation Tool

Since 2022, ABF has been developed further to broaden its applicability, including a focus on making it a more useful tool for Requirements Elucidation.

The first major change was in expanding the range of game scales both upwards and downwards from the tactical scale originally chosen. The use of 8-hour game turns and 40 nautical mile hexes allows for play on an operational scale, with task forces in place of individual ships. This expanded scope allows for changes in weather, for ships to return to port after action to rearm, and for logistics chains to matter. Conversely, the use of 6-minute game turns and 1 nautical mile hexes allows for tactical ASW to be modelled in detail. Procedures exist to allow telescoping time scales, allowing operational level games to pause the action elsewhere and zoom in to resolve a tactical ASW engagement.

Secondly, the game was adapted to support a play-redesign-play cycle. This was originally adopted because repetition of scenarios is good practice to support learning, and because the ability of students to make changes to their ships and see the effects of those changes was useful. The first approach taken was to pre-prepare a set of baseline ships and then a set of (usually 3) variant designs which improved some feature. Players would play once with the baseline ships and then use their experience from the first game to select a mix of variants to play again. This was useful but felt limiting and players tended to want to express their own design choices instead. An interim approach was to play the first game, conduct a groupwide brainstorming session to suggest options, apply estimated costs to each option and then allow each team to select options up to a budget limit. Baseline ship sheets would then be modified (rapidly, by hand, using Sharpie markers) and the game replayed. The loss of production value was considered worth the gain in versatility.

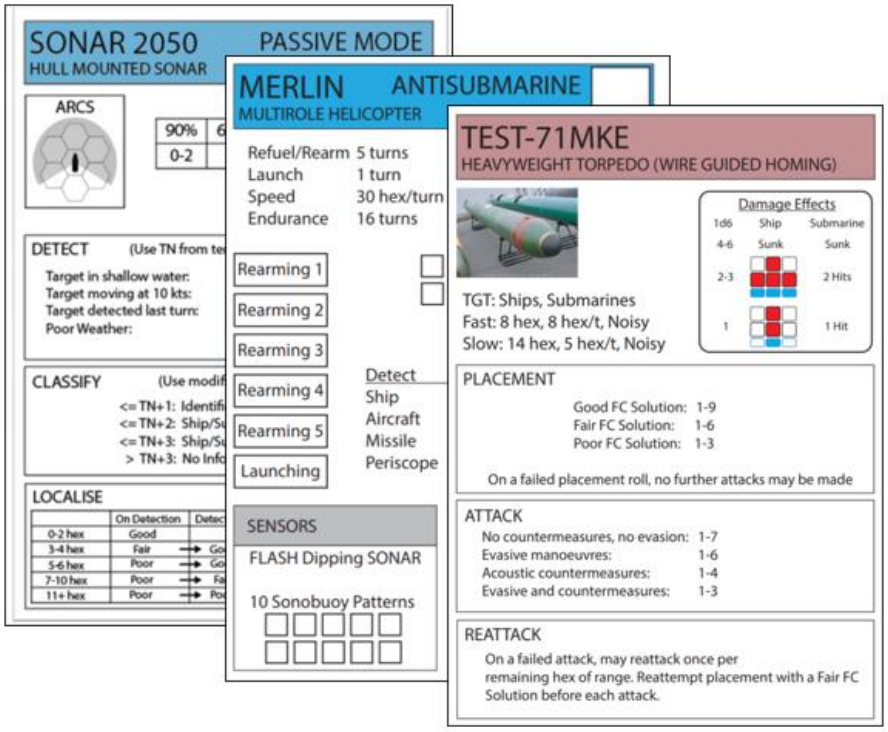

Figure 3: ABF Capability Cards

The most recent iteration of the game disconnects individual capabilities from the ship design. Originally the ship control sheet contained all the data needed to operate the ship, including detection ranges, performance of offensive missiles and the ship's air defence system. These have since been removed from the ship record sheets onto individual capability cards (Fig 3), so a baseline ship might be accompanied by cards for a particular radar and sonar, a particular offensive missile system, helicopter and air defence system. Creating a variant with a different combat system is then just a process of selecting a different combination of payload capability cards. (Within the bounds of practicality, of course.) Variations in layout or subdivision still require adjustment to the ship control sheet, but the use of capability cards certainly simplifies the adoption of different sensor and weapon systems, not to mention increasing legibility over performance numbers scrawled in Sharpie.

The third major change made to the game was to develop rules for additional unit types and operations, to broaden the range of missions ABF could model. The most significant addition was the creation of rules for submarines and ASW, requiring a detection model for sonars, rules for ASW weapons, acoustic signatures and the impact of water depth and weather on ASW detection. Sonar detection is inherently a very complicated process with many important variables, and the game's ASW model is still considerably more involved than the missile combat model, but it does allow for the simulation of tactical ASW engagements in a reasonable time frame.

In part driven by the need to model ASW systems and in part by the demands of a game with 6-minute game turns, a model for persistent aircraft was developed, in contrast to the original ABF model which considered air missions to be essentially instantaneous events. This allowed for helicopters to conduct lengthy ASW search missions, as well as Airborne Warning & Control missions.

Finally, a (very simplified) system for land/amphibious operations was developed, centring on amphibious transport capacity and logistics rather than units' land combat capabilities.

CASE STUDY GAMES

ABF has been applied to a number of problems in the requirements space for a variety of client organisations across several nations. With the exception of the week-long game run for the NATO Specialist Team on Naval Ship Systems Engineering described in the next section, client confidentiality means that only limited detail can be presented about each of these, but they serve to illustrate the range of ways in which wargaming can be employed by design teams in the early stages of specifying a new ship.

Game 1 – Team Building

The authors delivered an event for a shipyard who design and build naval ships. The shipyard was standing up a new team to develop a warship from the outline design provided by their government customer, into a detailed design suitable for building. The team comprised mostly early-career engineers who were specialists in a particular area of ship design.

The wargame event had two functions; first to serve as a teambuilding event, and second to introduce the specialist engineers to the whole-ship design considerations that drive cross-cutting capability areas like survivability. ABF as-designed already had a number of features to support that objective; the centrality of layout and zoning to the ships' representation in the game and how those factors affect survivability required no alteration to the game.

This was the first time that the Play-Redesign-Play cycle was explicitly used in ABF. The sixteen players were divided into four groups of four and each group played the introductory ABF scenario "Shell Game", based around a Board, Inspection, Search & Seizure (BISS) operation in the Western Pacific. Shell Game pits a multinational force of three frigates attempting to find a contraband shipment against three frigates attempting to prevent them. The game used the basic ABF Tactical ruleset (1 hour turns, 10 nautical mile hexes) and took roughly two hours to play through.

After the first playthrough, when the players had a feel for how the game worked and the relative strengths and weaknesses of their ships, they were given the opportunity to replace each ship with one of three pre-prepared variant designs; each variant improving some aspect, generally either offensive weapons, defensive weapons or vulnerability reduction features. Teams were then shuffled so each pair of players had a new opponent, and the scenario was replayed. Increased familiarity with the game meant the second playthrough took roughly one hour, and it was in fact possible to fit three games into the day.

Aside from working well as a teambuilding experience, the game proved to be a useful way to give system specialists an overview of whole-ship considerations like layout and subdivision. In particular, participants said it helped them understand the reasons for some of the demanding naval standards they had to comply with. The event was considered successful and a follow-up event has been requested.

Game 2 – CONEMP Exploration

The authors developed and delivered a wargame for a government warship design project. The project was in a preliminary stage and working on a ship with a relatively novel mission set and incorporating new technologies with which the customer

had limited experience. Lacking experienced personnel who could make informed judgements, the team looked to other approaches to help explore the CONEMP.

The purpose of the game was twofold; to allow an initial workthrough of the CONEMP with the whole team, and to evaluate whether wargaming was a worthwhile tool to apply to the problem.

This game used the basic ABF Tactical ruleset, although a new scenario was developed around the candidate ship's CONEMP. The one-day event contained a briefing in the morning followed by 2v2 playthroughs of the introductory "Shell Game" scenario to give the participants familiarity with the game rules. This was followed after lunch by a playthrough of the CONEMP scenario, with the group divided between four simultaneous games.

While there was no repeated play of the CONEMP scenario, the outcomes of the four games were fed back in a hot washup discussion. While this sort of wargaming should never be considered predictive, the fact that several of the games identified the same difficulties with certain parts of the CONEMP was useful, directing focus and further analysis onto those parts. The event was considered successful in meeting both its objectives; participants reported an increased understanding of their CONEMP and the team's design goals, and a more formal follow-up program of analytical wargaming was initiated.

Game 3 – Force Development

A third client was a national defence research agency interested in conducting exploratory force development experimentation with a view to shaping the requirements of future platforms procured across the sea, air and littoral/land domains. The objective of this game was primarily to explore how useful wargaming could be to assist with these force development planning activities.

The ABF Tactical ruleset was modified slightly for this game to include maps of the desired areas of operation and current platforms for the client and potential adversary forces. A scenario was designed to model a typical operation of interest to the customer. The wargame could then be used to play that scenario through with existing platforms and weapon systems, then replayed using potential future force mix options, to better understand how the capabilities offered by each option contributed to the mission, against current and expected future adversary forces.

At the time of writing, this project was still ongoing, so no conclusions can be reported.

ST/NSSE WARGAME CASE STUDY

The NATO Specialist Team on Naval Ship Systems Engineering (ST/NSSE) requested a wargame to explore whether wargaming could form a useful part the concept assessment and requirements elucidation process, specifically whether it could help give shape and structure to the initial stages of operational analysis, saving time and cost in the programme. The team were of the opinion that wargaming could be used as a "precursor" event, allowing projects to conduct initial evaluation of the value of their developing concepts, allowing initially attractive but unfeasible options to be discounted, whilst more credible options were refined and developed. This would allow for a more targeted approach to the conduct of formal OA, making more effective use of OA resource and enabling savings and efficiency in the use of research budgets. The outcome of these considerations was the proposal of a wargaming element within ST/NSSE's programme of work (Manley & Logtmeijer 2023).

In order to maximise the benefit of the work it was felt that any wargames conducted should be based on areas of interest to the NATO maritime community, although it was accepted that, at this stage, any work would need to be conducted at an unclassified level. This would create an atmosphere of familiarity with the subject when calling for support and discussing outputs with seniors. It was decided to use Anti Submarine Warfare (ASW) as the subject for study, and more specifically the conduct of ASW using uncrewed offboard systems in place of or supporting more traditional ASW assets. This is an area of considerable current interest, with a dedicated NATO Strategic Defence Initiative (SDI) project in place as well as several independent national studies being undertaken. It was hoped that, as well as demonstrating the validity or otherwise of wargaming in the intended role, that the outputs could inform, albeit at low classification, these various work streams.

UCL's ABF wargame formed the core of the wargaming engine, but this required significant development to cover some of the specialist areas required for the ASW-focussed games. These included the mechanics, sensors, weapons and tactics of ASW itself as well as a more detailed consideration of the management of uncrewed systems, in particular launch and

recovery. Environmental aspects were felt to have a more significant impact on smaller uncrewed assets hence a meteorological model was required to be developed.

NSSE Case Study Scenario

The specific operation chosen as the subject for the wargames was the use of an ASW barrier protecting a naval force against potentially hostile submarines and mine warfare forces. The series of games to be played would test the deployment, sustain and eventual recovery of the ASW assets through a number of stages of a mission.

Two forces would be considered, a “future force” comprising vessels designed specifically to operate uncrewed assets, and a “legacy force” made up of vessels broadly comparable to vessels currently in service. This would allow a direct comparison of the relative effectiveness of the new approach and the old. The future force was allowed to iterate, in that lessons identified in one game could give rise to mitigations that were then implemented in following games. The scope of improvements was moderated by the game management team to keep developments within realistic scopes in terms of cost and performance (the sudden development of “wonder weapons” was not allowed).

The overall campaign scenario selected was a Non-combatant Evacuation Operation (NEO) conducted in an environment where there was a potentially hostile submarine threat (surface threats were also considered as these could have an effect on the ASW assets, but the primary focus was the enemy’s submarines. The wargame campaign was set in the fictional countries of Florin and Guilder (it was felt that assigning names to countries and locations would create a deeper player engagement). Florin was a nation in the grip of both a civil war and the outbreak of a deadly epidemic. Meanwhile, Guilder was a nation seeking to benefit from florin’s misfortunes up to and including the use of military force to force territorial gains. “Blue Force”, the ASW-focussed side, was asked with conducting an evacuation of NATO citizens from a port in Florin, protecting the evacuation force from the threat of Guilder’s submarines (which constituted “Red Force”)

Blue Force was required to escort the high value units (HVUs) conducting the NEO to the area, protect them for five days of operations, and then depart. This provided a particular challenge for handling time throughout the scenario since the game would have to cover a week, but ASW operations have a decision cycle measured in minutes. This required a new “telescopic” approach to managing game turns, where time would be stepped through in units of 8 hours, 1 hour or 6 minutes depending on how much detail was required at any given moment. During phases where Red was waiting for a weather window to attack, large timesteps were used, stepping down to smaller ones as submarines manoeuvred into position and smaller again at time when there was a risk of detection and ASW combat.

Figure 4: Playing area and pieces for the NATO ASW Wargame

Game Management

The game's players were divided into three teams, broadly in accordance with normal professional wargaming practice. The teams, or "cells" comprised the Blue Team (ASW team), Red Team (Guilder's submarine force) and the White Team, where the game management staff and controllers sat. Each cell was located in a different room in the building so that they could not overlook each other's playing areas. Red and Blue cell players were restricted to their rooms, White cell were able to roam if needed to confirm their view and knowledge of the game state of play if necessary.

The White Cell was made up of the following participants:

- The Game Controller – responsible for maintaining the overall running of the game, timekeeping, turn flow, etc. They were also responsible for managing "injects" – specific events that both sides would need to react to, and for resolving any ambiguous or conflicting situations that may arise, often by drawing on the judgement and experience of SMEs.
- Green Cell Controller: controlling the actions of civilian units in the area, "background noise" and the friction of war. The Green Cell controller was necessary to turn the battlespace from a sterile environment containing only Red and Blue units into a more realistic situation where units could hide among everyday activity.
- The Adjudicators, or "Team Runners". At least one and ideally two members were allocated to act in this role as the link between the White Cell and Blue and Red Cells. They collected orders and other information from the cells and resolved the outcome of those on the White Cell map. They then fed back the results of their adjudications to their respective cells. Their roles became quite demanding when interaction between Red and Blue occurred, for example when Red was conducting a torpedo attack, or Blue ASW assets had detected and were prosecuting one of Red's submarines.

Red and Blue Cell participants comprised two to three players dedicated solely to the actions of their side in the game.

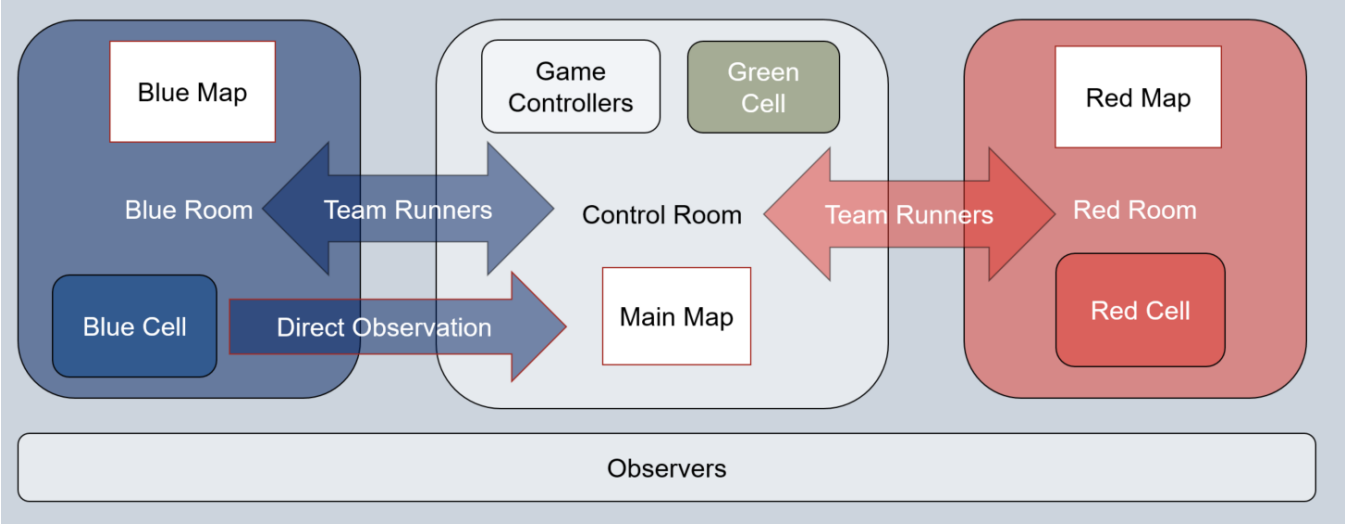

Figure 5: ASW Game Team/Cell Organisation

Game Execution

The wargame campaign was executed over a three-day period, with a fourth day set aside for evaluation, analysis and planning the next steps. Each playing day was made up of two sessions, one in the morning, the second in the afternoon, with a "wash up" taking place after each session.

A session was made up of the following events:

- A briefing for all players at the White Cell map, explaining the broad outline of the scenario. On completion all participants withdrew to their respective cells.

- Mission Planning; teams developed plans for their assets including locations, courses, speeds, and action to be taken in the event of a contact with enemy forces.
- Mission Execution; Adjudicators would then compare plans in the White Cell to determine where encounters occurred and would then begin resolution of those events, feeding back to Red and Blue as necessary and receiving updates orders or reactions to events. Missions were played to their conclusion, i.e. to the point where either Red or Blue had successfully completed their mission, or where mission completion was clearly not achievable.
- Recording – during each element of the games, players would record the rationale for their actions and decisions. This would form a key element of post-game analysis.
- Post game wash up; all cells were brought together at the White Cell map where the Game Controller briefed on what had actually in the game. This was also the opportunity for feedback, consideration of concept details and consideration for amendments. Again, this was recorded for post-game analysis.

Six game scenarios were planned as follows:

- Game 0 – A simple training game for all participants to give them familiarity with the game mechanisms. This game was not part of the formal concept assessment and hence was not recorded
- Game 1 – Approach Phase- Blue Force, using the conventional fleet construct, enters the Operational Area (OA) and clears the evacuation point and approaches of any Red submarines.
- Game 1a – a repeat of Game 1 but Blue Force uses the new modular force employing offboard systems.
- Game 2 – Evacuation Phase – Blue uses the conventional force to establish and maintain its ASW Barrier whilst Red submarines attempt to penetrate and interrupt the ongoing NEO.
- Game 3 – Evacuation Phase – a repeat of Game 2 but with Blue using the modular offboard-enabled force.
- Game 4 – Evacuation Phase – a modified version of game 3, with Blue able to amend its force mix based on experience from Game 3
- Game 5 - Exfiltration phase – Blue uses its evolved force from Game 4 and tempts to bring the evacuation force away from shore to safety.

It was originally intended to run each game once, but the players quickly became familiar with the rules and game execution so it was decided to tun two parallel instances of games 2 to 5 in order to increase experience, evidence and learning opportunities

At the end of each day a more extensive “hot wash” discussion was carried out to consider learning points for the day and to consider whether any changes were required for the following day’s games, including the inclusion of any new capabilities. An example of this was a deployable seabed sonar array (based loosely on a system advertised by Sonardyne), and a mobile hard kill anti torpedo system for defence of the evacuation anchorage (which was named “Palisade”). In both cases relevant SMEs were consulted for likely performance parameters and these were converted into game parameters overnight.

Capabilities Investigated

Blue Force was initially made up of conventional anti-submarine frigates, analogous to UK Type 23 or the Canadian Halifax class. They were equipped with towed array and hull mounted sonars and a capable ASW helicopter. After the initial games these were replaced with frigates using mission modularity concepts to embark offboard systems as well as their integral sensors. The offboard capabilities examined included:

- Uncrewed Undersea Vehicles (UUV). These were equipped with thin line towed array sonars. They were able to operate at the same depths as the threat submarines, but being small they were unable to process their own data. As a result they were required to go to periscope depth at preset intervals to transmit their recorded data back to their motherships for processing. This introduced inevitable data latency into the ASW problem. Being small and slow, however, meant they were extremely quiet and difficult to detect so a threat submarine was unlikely to be aware of their presence.

- Uncrewed Surface Vehicles (USV). These were small (8-11m) fast craft using the same thin line towed arrays as the UUVs. Again, due to their small size and lack of power they were unable to process their own

sonar data, but as they were operating on the sea surface they were able to transmit data back for processing on a continual basis.

- Uncrewed Aerial Vehicles (UAV). Large quadcopters or small helicopter-style aircraft capable of embarking and deploying up to four sonobuoys or a single lightweight torpedo. Their speed and endurance was limited whilst carrying heavy payloads such as torpedoes, but they were able to stay in flight for long periods of time and could work effectively in concert with each other or supplementing larger manned helicopters (the latter being Blue's preferred mode of use).

As mentioned earlier, lessons identified in the games led to proposals for new capabilities to be fielded. These included:

- Deployable seabed sonar system – a "spoke and hub" design was suggested featuring six passive hydrophone arrays ("spokes") radiating from a central buoy ("hub|) that maintained communications with command and control assets such as the modular frigates where signal data processing could take place. The system parameters set by the White Cell proved to be too effective, forming an impenetrable screen (although this did demonstrate the considerable benefit should such a high capability system be developed). The system was cumbersome and took time to deploy and recover, hence the Blue Team abandoned many of their arrays during the final scenario as recovering them would have left the force exposed for a significant time.
- USV-based torpedo defence system. In early games Blue was required to position its ASW frigates some distance from the evacuation port in order to be able to react quickly to submarine detections. Unfortunately this left the evacuation anchorage undefended and if a submarine could get within torpedo range there was nothing available to protect the evacuation ships. The frigates were already able to select a modular torpedo hard kill system so it was suggested that such a system could also be deployed in an 11m surface craft to provide local protection.
- Seabed communications network – a portable sonar based undersea communications network was discussed during the game but not fielded as it was felt this was more appropriate for use in a fixed location, such as a friendly harbour and its approaches, rather than in an expeditionary scenario as the campaign presented. If it had been used then the data latency issues of the UUVs could be mitigated.

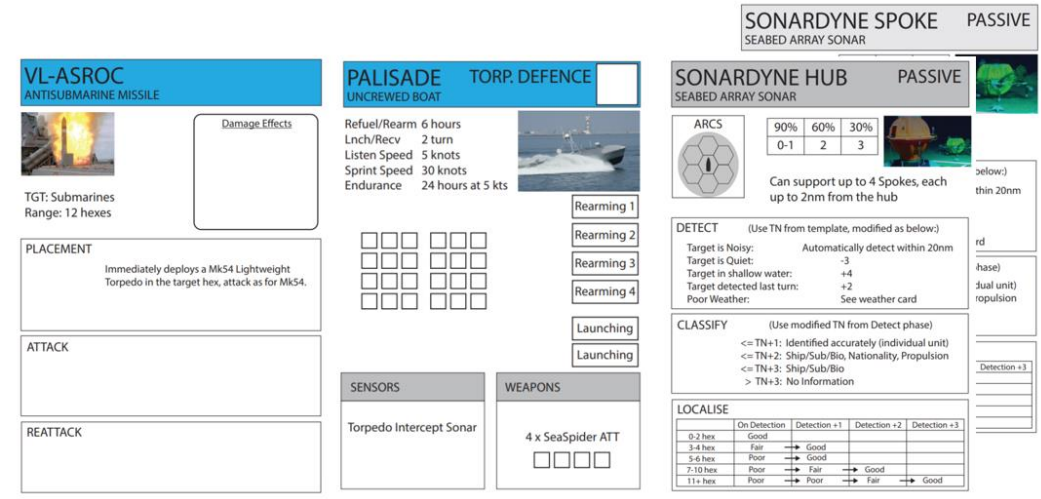

Figure 6: Examples of Capability cards created during the games

Results and Conclusions from the NSSE Wargame

At the end of the three days of gaming it was concluded that the game system worked effectively and had given realistic results. Several ASW SMEs were in attendance and confirmed that the events in the game and various conclusions drawn were in accord with their own understandings. This was considered by some to be quite remarkable given the unclassified nature of the games.

On day 4 the UCL wargaming team and the game's NSSE sponsors conducted a deeper review of the various lessons identified during each game. The NSSE team's view was unanimous; the wargames had successfully allowed a range of ASW and force mix options to be considered, evaluated and developed in such a way that a hypothetical OA study could begin from a more focussed staring point. From the NATO customer's perspective the applicability to the concept phase of project was clear (NATO 2023).

It was noted that, as well as achieving the stated aim, wargaming brought with it a number of other benefits. System designers and stakeholders were able to observe how elements of the various concepts interacted with each other, allowing synergies (and issues) to be identified. SMEs were able to see how their particular areas of expertise fitted into the overall ASW system, providing essential operational context that they had been previously unaware of. The multi-faceted makeup of the players involved – wargamers, operators, designers and deep experts - meant that each had an opportunity for interaction with their fellow players from different backgrounds, promoting learning and development. These were seen as essential elements over and above the primary objectives of the event. In its summing up of the event the NATO team was satisfied that wargaming had been shown to be capable of being used effectively as a concept analysis and elucidation tool whilst also delivering the potential for wider benefit. As a result, ST/NSSE is now moving working to include wargaming as an essential domain-specific activity in its new naval ship design NATO standard. As an additional spinoff the UCL team has been in discussion with other UK and NATO project teams on the possibility of using ABF and other tools for "real world" project analysis.

Noting that ST/NSSE's primary objective was to demonstrate and explore the role of wargames the outcome from the games and the discussions that surrounded them and the game process were (within the restrictions imposed by the unclassified nature of the event) felt to have shown:

- the potential for an effective anti-submarine barrier using offboard assets compared with a traditional arrangement when used in a defensive posture;
- benefits and drawbacks of the component elements of the system as proposed;
- capability gaps that existed in the ASW system as well as some in wider maritime operations, along with possible mitigations and solutions;
- the power of wargaming as a method for investigating the criticality or otherwise of components and characteristics of a system;
- how complex element such as sensor interaction, data processing and reliable communications are likely to impact the viability of a solution;

It was also demonstrated that:

- wargaming requires support from experienced wargamers to ensure that the learning points, including those arising from negative experiences, are relevant,
- wargaming and modelling and simulation (M&S) serve distinct and different purposes: wargaming considers the "big picture" and therefore should not be used for the study of extensive variations of the operational problem (it would take far too much time); M&S can be used to study an operational problem in great detail with many variations, with a much smaller problem scope compared with wargaming,
- the results of modelling and simulation can be condensed into game artifacts and used to develop the wargaming model.

CONCLUSIONS

The case studies described in this paper show four examples of ways that technically-focused manual naval wargaming has been applied to practical problems facing design teams in the requirements elucidation phase of ship design. The authors and clients have concluded that wargaming offers significant utility as a tool in this phase, in particular:

- Wargaming can help a design team understand which areas of performance will be most critical to ensuring mission success, helping to allocate subsequent and more in-depth operations analysis effort more efficiently.
- Wargaming can be an effective tool for exploring a warship's CONEMP, as well as ensuring that the CONEMP is fully understood by the whole team. Wargaming can be used as a form of active learning, which has shown to be more effective for communicating complex subjects than reading written material.
- Wargaming allows low-level technical models of novel systems to be integrated into higher level tactical or operational models, allowing assessment of those systems' effectiveness without access to prior operational experience.
- Wargaming allows the interactions between subsystems to be explored and better understood (in conjunction with subject matter experts, who remain a vitally useful resource).
- Wargaming allows the rapid exploration of the "arms race" of countermeasures and counter-countermeasures to a novel system, which can help to anticipate the future operational environment.

Some common useful features have been identified for wargames intended for use in requirements elucidation:

- Transparency about how game statistics are derived from real-world measures of performance.
- The ability to rapidly incorporate new systems and capabilities into the game.
- The ability to readily adjust the game mechanics to model different scenarios of interest.
- Credibility allowing faith in the results – most easily obtained by involvement of subject matter experts, historical data and OA models in creation and adjudication of the game.
- The ability to rapidly play the same scenario multiple times.

CONTRIBUTION STATEMENT

Nick Bradbeer: Conceptualization, investigation, resources, writing – original draft, writing – review & editing.

David Manley: Conceptualization, investigation, writing – original draft, writing – review & editing

REFERENCES

Bradbeer, N. (2022) Naval wargaming as a teaching tool for warship design engineers. Vancouver, Canada. International Marine Design Conference.

Ministry of Defence (2017). UK Wargaming Handbook. Shrivenham, UK. Defence Concepts and Doctrine Centre (DCDC). https://www.gov.uk/government/publications/defence-wargaming-handbook

Manley, D. (2023) Wargaming as a design and concept analysis tool at UCL. Bristol, UK. Defence Simulation Education & Training.

Manley, D & Logtmeijer, R. (2023) The use of wargaming as a naval concept exploration tool. Sydney, Australia. International Maritime Conference. https://paxsims.files.wordpress.com/2023/11/session-19-david-manley-fp.pdf

NATO ST/NSSE. (2023) NATO UXV ASW Barrier Wargaming – Game Report, Issue 1.0. Utrecht, Netherlands. NATO ST/NSSE.

Proceedings of 15th International Marine Design Conference (IMDC-2024)
June 2-6, 2024
Amsterdam, the Netherlands

Development of a Novel Codesign Method for Use in Early-Stage High-Performance Craft Design

Evan J. Branson[1,*] Arend Vyn[2,] Kevin Maki[1,] and David J. Singer[1]

ABSTRACT

The performance requirements of modern vessels have increased significantly over time, introducing unique challenges in design and analysis. Driven by competition, such as in the case of racing craft, new high-performance vessels require design spaces that push the envelope of hydrodynamic technology. This optimization knowledge resides in the experience of racing experts and hasn't yet been translated into a naval architecture taxonomy. This paper seeks to bridge the knowledge gap between experienced race manufacturers and naval architects, and in doing so, delineate a design methodology. Modeling risk as a function of vessel speed, as well as coupling the design of the control system in conjunction with its physical design embodiment, allows the overall system to reach a greater point of optimality than what can be accomplished by traditional iterative design processes alone. The approach will be demonstrated utilizing the design of a University of Michigan student-led undergraduate high-speed, electric boat competition team design. The team's goal is to develop a vessel that has a top speed of 135 mph. The paper will discuss how the team used marine design methodologies integrated with a novel codesign method to create the design that is currently under construction for professional racing use by the team.

KEY WORDS

Codesign; Design Theory; High-Performance Craft; Racing; Speedboat.

INTRODUCTION

Powerboating and marine racing, also known as offshore powerboat racing, trace their origins back to the early 20th century, born from the desire to push the limits of marine engineering and hull design. The major modern competitors in powerboating include both manufacturers and private teams that specialize in the design, construction, and operation of these high-performance vessels. Prominent brands in the field include Cigarette Racing, Mystic Powerboats, Skater, and MTI (Marine Technology Inc.), which have developed reputations for their racing prowess and technological innovations. In terms of racing teams, organizations MCON Racing (pictured in Figure 1) have been very successful in international competitions such as Class 1 World Powerboat Championship. The marine racing industry has also grown to accommodate a variety of classes and different types of powerboats, from outboard engines to multi-engine offshore powerboats capable of reaching speeds exceeding 200 mph.

[1] Department of Naval Architecture & Marine Engineering, University of Michigan, Ann Arbor, United States;
[2] Department of Mechanical Engineering, University of Michigan, Ann Arbor, United States;
[*] Corresponding Author: ebranson@umich.edu

Submitted: 24 February 2024, Revised: 1 May 2024, Accepted: 3 May 2024, Published: 20 May 2024

Conference paper, DOI: https://doi.org/10.59490/imdc.2024.847 e-ISSN: 3050-4864

Figure 1: Class 1 Offshore Race Boat ”Monster Energy MCON”; Source: mconracing.com (2023)

The advent of electric power in the marine racing industry has marked a major evolution, echoing the shift toward sustainability seen in automotive racing with series like Formula E. This rise of electric racing boats is propelled by the increasing global emphasis on reducing carbon emissions and harnessing renewable energy sources. Initiatives like the UIM E1 World Electric Powerboat Series showcase the potential of battery-powered craft, which offer a powerful yet environmentally friendly alternative to traditional internal combustion engines. As battery technology has advanced, with improvements in energy density, efficiency, and charging speeds, electric racing boats have become more competitive, promising high speeds, lower noise levels, and zero emissions.

A new addition to this transition toward electric racing craft is University of Michigan Electric Boat (UMEB), a team of students attempting to break the electric water speed record. UMEB was founded in September 2019 by a small group of undergraduate Aerospace and Naval Engineers to further develop battery-electric vessel technology. As the team developed, it became apparent that the limited budget, resources, and experience in a student project meant that designing and operating like a professional powerboat manufacturer was not feasible. Instead, the characteristics of the team’s operation more closely matched those of the wicked problems associated with large vessel and platform design. Thus, UMEB was presented with the following problem: translating the knowledge, best practices, and design elements developed from decades of experience of team contacts in the marine racing industry into a novel marine design methodology.

This paper delineates the methodology employed by UMEB in crafting a competitively adept racing vessel through the lens of naval architecture principles.

CHANGING LENSES

The Tragedy of *Snowfinkle*

The realization that UMEB needed to integrate naval architecture principles and methodologies into the design of speedboats was not immediate, and only years of failure taught the team to change. These failures began in 2021 with the team’s first true attempt at a performance vessel: *Snowfinkle*.

Before the design process even began, there were reductions in the design space in that the vessel’s hull form was limited to the 17-foot sailing catamaran that was donated to the team in the previous year. This meant that a successful craft would have to match the characteristics of a sailboat, which was designed purely to act in a displacement capacity and not able to plane. Electric battery systems have an inherent drawback in their low power density, which is somewhat incompatible with the dynamics of a very lightweight sailing craft. Navigating this problem is where the team made its first critical mistake in failing to assess the root cause of these problems and instead attacking the surface-level design incompatibilities. The team looked to the marine industry to find solutions, and seeing as industry offerings for battery-electric craft almost exclusively utilized hydrofoils to meet their operational requirements, the team embraced hydrofoils as a potential saving grace to the emergent design challenges. What should have been a question of what would create the best craft that met the re-

quirements quickly turned into a question of how to make hydrofoils work. Consequently, the team followed a point-based design approach, with the initial conditions being the hull form and the hydrofoils. Due to 'walls' being put up between the propulsion, battery, hydrofoils, and structures teams to divide the work, systems integration became a major obstacle. This manifested throughout *Snowfinkle*, emerging most obviously between the physical junction of the hydrofoils and the rest of the craft, as well as the propulsion system. The team also stumbled into an endless need for weight distribution adjustments due to the poor balance characteristics of *Snowfinkle* while foiling, leading to consistent changes in general arrangement. As the team continued following the spiral, progressively more changes needed to be made, often compromising the overall vessel mass and the functionality of the vessel's control system. These changes often occurred after major portions of *Snowfinkle* had already been built, which further complicated the problem. No matter the decisions made, the initial conditions of the design meant that we could not converge to a point of optimality, let alone acceptability.

Figure 2: *Snowfinkle*

The methodology used on *Snowfinkle* illustrated a failure to execute proper marine design on many levels. With a bit more design space exploration, it would have become evident that the low drag characteristics of the hull meant that the craft could have easily met its design requirements with an 80-horsepower propulsion unit and no further changes to the hydrodynamics of the hull, thus the resultant design space would have greatly differed. Even had UMEB used spiral-based design (which might have been a necessity given a new and inexperienced team with limited resources) to generate *Snowfinkle*, delaying critical decisions would have led to a greater understanding of the driving variables with which the team worked, which might have had the potential to generate better initial conditions and eventually an acceptable convergence.

In the end, *Snowfinkle* experienced a complete and total system breakdown after nearly every interface had been reworked, then reworked again to no avail. The team decided that the countless hours spent fixing the unsolvable issues was not worth their effort, and instead began focusing on eliminating the issues with *Snowfinkle* through a much more mature approach to boat design.

A Step in the Right Direction

As the *Snowfinkle* was sunset, a new chapter began for UMEB. The team had grown significantly over two years both in number and in expertise, especially regarding battery, control, and propulsion systems. A growing team presence at the University of Michigan and the local community had opened up many doors in terms of resources, additions of physical workspace, and bargaining power with the school administration. Most importantly, however, the team's leadership changed: this time with a much greater focus on designing for high-performance.

Considering the new leaders were many of the people who experienced firsthand the failures of *Snowfinkle*, there was an early push to truly understand the design errors at a fundamental level. The team first identified that a marine design ap-

proach was needed, something the aerospace students who previously ran the team did not completely recognize or understand, and therefore could not execute successfully. In other words, a much more methodical and strategic process would be needed to avoid making premature decisions that would force the team into undesirable designs. Additionally, the walls put up across subteams needed to be broken down and instead replaced with collaborative systems thinking, with a much greater emphasis on cross-functional work to ensure interfaces were accounted for.

While the new leaders understood the issues with the poor design strategy correlated with *Snowfinkle*, the team identified that there were still significant gaps in our understanding of successful marine design processes. To address these gaps, team leadership began meeting with professors in the University of Michigan Naval Architecture and Marine Engineering department, especially Professor David J. Singer.

Requirements Elucidation

The first step UMEB took in improving its design methodology was working to better understand the speedboat design space. Due to the limited budget, timeline, and experience present in the project, there was a major need to derisk this design space and guarantee that whatever design elements were chosen would not result in emergent design failures that would compromise the project, much like what happened with *Snowfinkle*. To address this knowledge gap, UMEB performed a functional decomposition based on the team's overarching goal to travel at 100 knots for 5 nautical miles (See Figure 3). The goal of this process was to develop a knowledge structure that could guide our end embodiment and the decisions we made along the way, following the taxonomy presented by Goodrum (2020).

To perform this functional decomposition, we employed a Andrews (2021)-style requirement elucidation process. Within this process, we started at the overarching goal of our design, and from there worked our way down through design variables with the help of taxonomies, not to reach a feasible design, but more to learn about the complex interactions within the design space and discover requirements as we went.

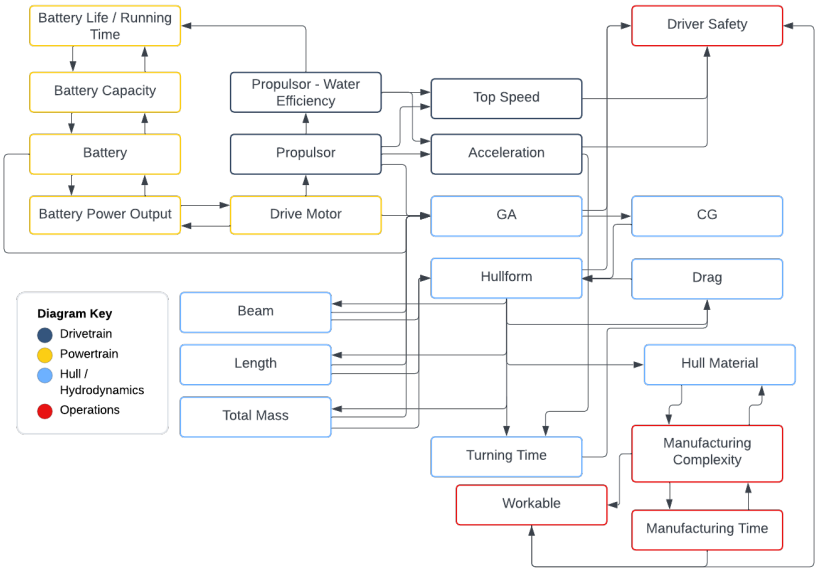

Figure 3: UMEB Functional Decomposition

One example of this was how we grew to understand lift within our design space. We knew from industry experts that lift was going to be a major part of being able to go fast efficiently, but breaking down the actual factors that drove that proved difficult. At this point, we were introduced to the sustension cube (See Figure 10) as explained by McKesson (2009), which provided us with a taxonomy to classify how different vessels produce lift. From here, we could analyze how other high-performance crafts fit onto the sustension cube. We found that the fastest craft we knew of had high passive aerodynamic and hydrodynamic lift characteristics, thus discovering the requirement that our vessel should structure its lift characteristics similarly. More specifically, we discovered the requirement that our vessel needed to have some sort of surface, be that wings, tunnels, or hull form, that would pressurize air beneath the craft and that the geometry touching the water needed to plane efficiently.

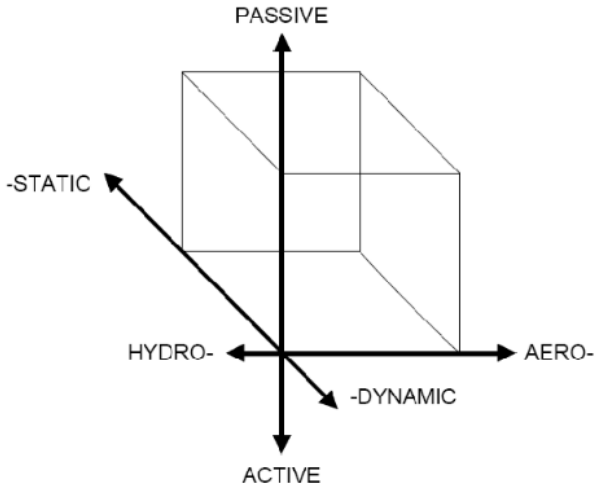

Figure 4: McKesson's Sustension Cube

IDENTIFYING DISCREPANCIES

As UMEB continued the process of functional decomposition, informing our new discoveries with the knowledge gained through previous design space explorations, team members would often talk to UMEB's industry partners, especially Skater and the American Powerboating Association (APBA), using their knowledge and experience as a feasibility check for the discovered requirements and design elements. The team discovered in this process that there were discrepancies in the way that the racing professionals analyzed the design space and how naval architects would do the same. To address our findings, the team contacted the best high-speed hydrodynamics experts they could find to further explore this. Specifically, UMEB explored the missing pieces of the problem through detailed analysis with Dr. Kevin Maki and Dr. Armin Troesch. In discussions with both, a similar conclusion could be drawn, best encapsulated in the following quote from Dr. Troesch: "Even the best naval architect can only design a 90% boat; it takes a different type of knowledge to get the last 10%". When the team brought up this issue with Peter Hledin, the owner of Skater and one of the most respected offshore catamaran designers in the world, he responded with the following (albeit heavily paraphrased due to the use of expletives): "[Naval Architects] know what the boat will do, but I also know what the driver will do and I know what the APBA will let me run". Quite simply, this explanation illustrated a framework for what design tools were missing.

Codesign

"I know what the driver will do"

With a little bit of abstraction, the role of the driver can be viewed as an active controller for the physical plant of the craft. When analyzing through this lens, there are many evident similarities to high-performance aircraft design, which uses a knowledge structure where design elements physical plant and design elements of its control system simultaneously inform each other. This aerospace concept is more colloquially referred to as codesign.

Codesign in Aerospace

Codesign has been a major tenet of aircraft design since the 1970s, specifically concerning projects within the US military black budget. Much of modern stealth fighter technology would not have proven viable had it not been for early-stage design exploration illustrating that an airframe with poor flight characteristics due to the requirement of a small radar cross-section could still be effective by combining pilot input with highly responsive flight computers according to Aronstein and Piccirillo (1997). The effectiveness of this design methodology is evident in its continued use in the defense industry despite nearly half a century of technological progress as evidenced by continued aerospace research on the topic from academic works such as Abedini et al. (2022). It should be noted that there exists very little academic research from a design theory perspective on this topic as the aerospace industry views codesign more as a strategy to address instabilities and less so as an overall methodology; the further complexity of the marine design space demands a more comprehensive approach.

Codesign in Marine Research

The use of codesign is not a foreign idea in the marine academic sphere; it should be noted that the most complete mathematical example comes from Castro-Feliciano (2016). This paper illustrates the potential benefits of coupling an active control system to the design of a planing craft, specifically concerning dimensional and numeric figures such as the longitudinal center of gravity. It can be argued that the math used by the authors is limited in scope to implementation in planing craft with very geometrically simple hull forms, as is standard. This becomes a problem within the research scope of this paper as many, if not all, of the racing vehicles that make use of advanced control surfaces, also make use of extremely complex hull forms with the addition of features like steps, multiple hard chines, and rear strakes according to Yun and Bliault (2012), not to mention multiple hulls. The highest-speed racing craft are further complicated with hull forms that in addition to planing also make use of the ground effect (often referred to in the industry as “packing air”) through the use of tunnels, Venturi tubes, and wing surfaces. The greatest benefit of Castro-Feliciano’s version of codesign concerning racing craft comes from his point that control systems can take advantage of traditionally undesirable dynamic nonlinearities and instead use them to increase vessel performance. Take porpoising, for instance. Without a control system, porpoising can lead to significant inefficiencies due to a change in lift characteristics and drag, which sharply limits the top speed of a vessel, or in more extreme cases, can lead to a crash. Despite the aggregate effect of porpoising being negative in terms of vessel performance, there is a point in the oscillation in which the craft is further out of the water and has lower overall drag than achievable without dynamic instability: this is where well-integrated control surfaces come in. If a control surface can provide lift during the periods when porpoising would force the craft downward, then the net effect of this controlled nonlinearity is less drag and therefore greater top speed. One problem with this approach is that it requires a working understanding of exactly what function a control surface will perform, which is sometimes not possible to derive in early-stage design. This approach can be reversed, however; by defining a control surface in terms of the function it must perform, which thus can generate design knowledge without reducing the design space.

Codesign in Marine Racing

Given that competition drives a need for designs to perform as optimally as possible, as many feasible designs as possible need to be considered when determining dominance. We can visually represent how codesign can be useful for expanding the set of feasible designs using Figure 5, which illustrates a hypothetical feasible set within an imaginary design space. Note that there exists a boundary where designs exit the realm of feasibility due to failure to meet a requirement.

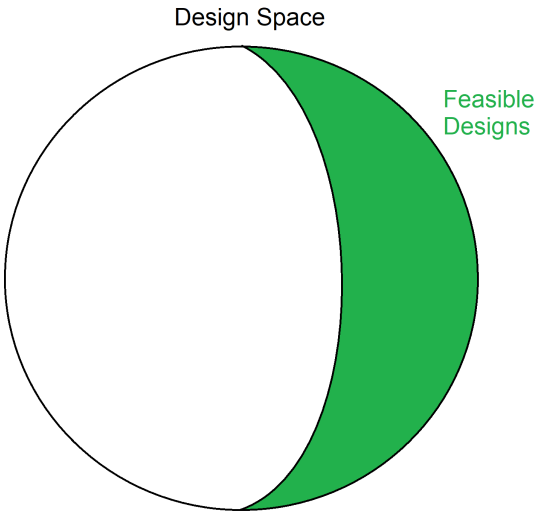

Figure 5: Hypothetical Design Space Example

This becomes problematic when we start comparing these designs, as there exist spaces in which the most dominant designs lie on the boundary due to a requirement acting as an active constraint. This can be visualized in Figure 6, where we can see the most optimal designs lying nearest to the boundary.

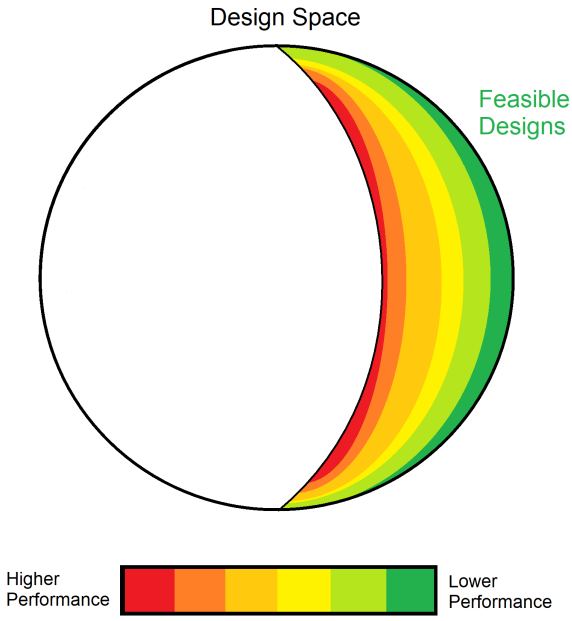

Figure 6: Design Space Dominance Example

With this in mind, there becomes a vested interest in expanding this boundary of feasibility to reach a higher performance but satisfactory design. This is where codesign can provide some advantages in the racing sphere. By taking advantage of designs that might not be conventionally feasible due to factors such as poor stability and then pairing them with a control

system (be that a computer or a human driver) that can address this, a certain previously infeasible set of designs can once again enter the realm of feasibility. Following the other presented figures, Figure 7 illustrates the inclusion of more designs into the feasible set.

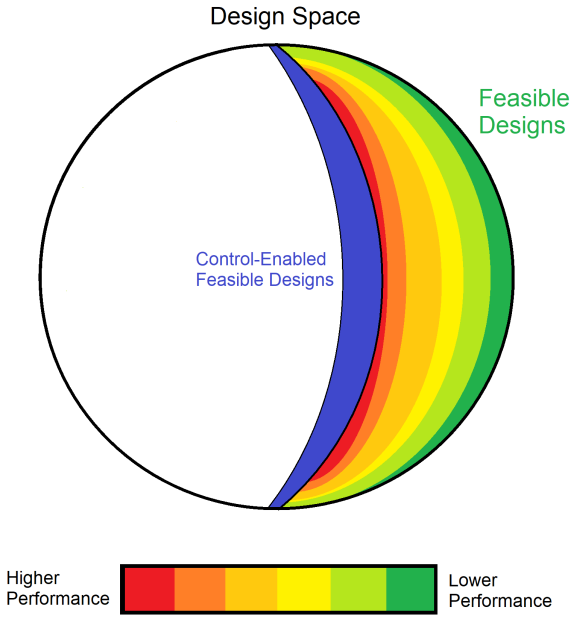

Figure 7: Feasibility Boundary Expansion Example

It should be noted that while controls can solve some level of instability, control authority is a design variable in itself and there are countless instances where the control requirements to reach stability are infeasible in themselves. To determine the feasibility of a control system, further modeling with the dynamics of the rest of the vessel is needed, thus requiring a mathematical model for codesign. This will be further explored in the implementation section of this paper.

The Risk Model

"I know what the APBA will let me run"

The second missing piece of the racing design problem comes from the inherent need for a craft to be competitive. In order to win, a racing craft must be pushed to its absolute performance limits. Simultaneously, an ideal racing craft should completely disintegrate as it crosses the finish line, which means that every component is being designed to be just robust enough to finish a race. This creates several problems, as pushing a craft to these performance limits with limited knowledge can be very irresponsible, given that the line between winning and dying can be very thin. This problem is well documented; according to Atwal (2024), seven of the thirteen people who have attempted to break the water speed record have died during their attempts.

Because of this, managing risk within the vessel's engineering becomes the designer's responsibility. Like any risk model, such as a HazID (see ABS (2020)), we can identify threats to the vessel with both their likelihood to occur and the associated consequences if they do. As a vessel has to exert greater performance, the consequences of failure as well as the likelihood of failure increase, thus coupling these two factors. Consequently, vessels operating with lower performance targets can exhibit fewer mitigation and prevention measures, often contextualized as safety features. For instance, the APBA (2022) states that cockpits on boats designed to travel faster than 150 miles per hour require a cockpit structural strength of

8,000 Newtons whereas cockpits designed for lower speed boats only require 2,000 Newtons. In conclusion, as a vessel's performance requirements increase, the degree of risk that can be taken significantly decreases.

One system that we have developed to understand and track this risk-based design space is a tool we call a Vessel Integrity - Vessel Speed (VI-VS) plot. Vessel speed, in this context, is a broad term that describes the inherent performance metric that a racing craft is trying to meet; for an endurance craft, this might be vessel velocity at range, for a circuit track craft, this might be velocity maintained through a turn, and for a drag boat, this might be acceleration over short distances. The other component of this relationship is vessel integrity; this is a measure of how likely the vessel is to experience an extreme event that would prevent it from continuing normal operation, "blowing over" or an engine failure for example. This plot helps a designer characterize both designs and requirements simultaneously. One critical piece of using a VI-VS plot to its full advantage is plotting a curve that represents the acceptable risk associated with a craft as it relates to increasing performance, or, in context, vessel speed. This is written as the minimum allowed the integrity of a design at a given "speed". As discussed previously, these minimum requirements almost always increase with speed, but the exact quantization and form of this relationship often come from competition rules, careful design consideration, and the quality of the relationship between the craft owners and their insurance companies. Once placed on the VI-VS plot, we refer to the relationship as the Acceptable Design Risk (ADR) curve. An example of a VI-VS curve with a sample ADR curve is shown in Figure 8. Further definition of how these plots are generated will be illustrated in UMEB's implementation of this concept.

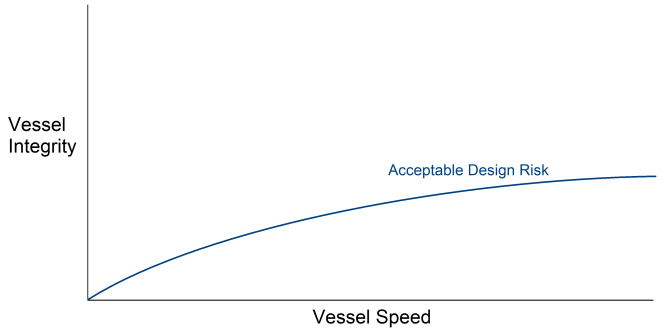

Figure 8: VI-VS Curve Plot (Acceptable Design Risk Only)

IMPLEMENTING NEW DESIGN TOOLS

With a greater understanding of what needed to be done to develop an optimal craft, UMEB moved forward in their design process, using a set-based design process based on Singer et al. (2010) including a novel codesign component to derisk the design and ensure the team would not experience another system-level failure. Improving on the walls of the past, UMEB used its subteams - powertrain (batteries), drivetrain (power transmission), and structures (safety and hydrodynamics) - as specialties to base our set conversion.

Expanding Feasible Design Sets through Codesign

UMEB used a very basic initial pass of designs using top-speed estimations based on Gerr (2001); afterward, the analysis became much more complex. While examining designs, UMEB focused extensively on seakeeping, as finding designs that wouldn't destabilize and flip over or crash proven to be the main limitation on feasibility. Because of this, the team first implemented codesign within a general stability equation. Given that the scope of the project is limited to racing craft that would only travel across extremely clean water (Sea State 1.5 or less), a linearized approach should suffice given that hydrodynamic disturbances due to waves will be minimal. With that information, Equation 1 defines a fairly accurate model of the dynamic relationships across the design space of vessels UMEB explored.

$$[m]\ddot{x} + [c]\dot{x} + [k]x = 0 \tag{1}$$

We will further expand this definition with Equation 2, Equation 3 and Equation 4. Note that this expansion includes all 6 degrees of freedom.

$$[m]\ddot{x} = \begin{bmatrix} m_{xx} & m_{xy} & m_{xz} & m_{xk} & m_{xm} & m_{xn} \\ m_{yx} & m_{yy} & m_{yz} & m_{yk} & m_{ym} & m_{yn} \\ m_{zx} & m_{zy} & m_{zz} & m_{zk} & m_{zm} & m_{zn} \\ m_{kx} & m_{ky} & m_{kz} & m_{kk} & m_{km} & m_{kn} \\ m_{mx} & m_{my} & m_{mz} & m_{mk} & m_{mm} & m_{mn} \\ m_{nx} & m_{ny} & m_{nz} & m_{nk} & m_{nm} & m_{nn} \end{bmatrix} \begin{bmatrix} \ddot{x} \\ \ddot{y} \\ \ddot{z} \\ \ddot{\phi} \\ \ddot{\theta} \\ \ddot{\psi} \end{bmatrix} \tag{2}$$

$$[c]\dot{x} = \begin{bmatrix} c_{uu} & c_{uv} & c_{uw} & c_{up} & c_{uq} & c_{ur} \\ c_{vu} & c_{vv} & c_{vw} & c_{vp} & c_{vq} & c_{vr} \\ c_{wu} & c_{wv} & c_{ww} & c_{wp} & c_{wq} & c_{wr} \\ c_{pu} & c_{pv} & c_{pw} & c_{pp} & c_{pq} & c_{qw} \\ c_{qu} & c_{qv} & c_{qw} & c_{qp} & c_{qq} & c_{qr} \\ c_{ru} & c_{rv} & c_{rw} & c_{rp} & c_{rq} & c_{rr} \end{bmatrix} \begin{bmatrix} \dot{x} \\ \dot{y} \\ \dot{z} \\ \dot{\phi} \\ \dot{\theta} \\ \dot{\psi} \end{bmatrix} \tag{3}$$

$$[k]x = \begin{bmatrix} k_{xx} & k_{xy} & k_{xz} & k_{x\phi} & k_{x\theta} & k_{x\psi} \\ k_{yx} & k_{yy} & k_{yz} & k_{y\phi} & k_{y\theta} & k_{y\psi} \\ k_{zx} & k_{zy} & k_{zz} & k_{z\phi} & k_{z\theta} & k_{z\psi} \\ k_{\phi x} & k_{\phi y} & k_{\phi z} & k_{\phi\phi} & k_{\phi\theta} & k_{\phi\psi} \\ k_{\theta x} & k_{\theta y} & k_{\theta z} & k_{\theta\phi} & k_{\theta\theta} & k_{\theta\psi} \\ k_{\psi x} & k_{\psi y} & k_{\psi z} & k_{\psi\phi} & k_{\psi\theta} & k_{\psi\psi} \end{bmatrix} \begin{bmatrix} x \\ y \\ z \\ \phi \\ \theta \\ \psi \end{bmatrix} \tag{4}$$

The terms inside of the matrices presented were gathered through computer simulation and estimation of existing hull forms; an example of one of the forms tested by this model can be shown in Figure 9.

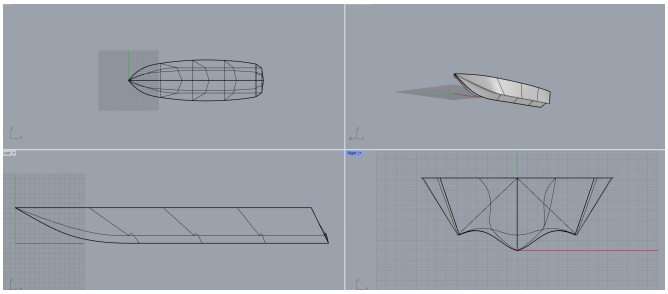

Figure 9: Example Hull Form

Given that the operational requirements given by the team were incredibly limited, the straight-line speed at the range of the vessel proved far more important than factors such as maneuvering and endurance. Because of this, the seakeeping equation can be reduced to only include trim, roll, and heave, shown in Equation 5. This reduction grants us sufficient knowledge to make design decisions while reducing the computational cost to simulate large numbers of design options; however, it should be noted that a more complex physics simulation is necessary when developing the final control system.

$$\begin{bmatrix} m_{zz} & m_{z\phi} & m_{z\theta} \\ m_{\phi z} & m_{\phi\phi} & m_{z\phi} \\ m_{\theta z} & m_{\theta\phi} & m_{\theta\theta} \end{bmatrix} \begin{bmatrix} \ddot{z} \\ \ddot{\phi} \\ \ddot{\theta} \end{bmatrix} + \begin{bmatrix} c_{zz} & c_{z\phi} & c_{z\theta} \\ c_{\phi z} & c_{\phi\phi} & c_{z\phi} \\ c_{\theta z} & c_{\theta\phi} & c_{\theta\theta} \end{bmatrix} \begin{bmatrix} \dot{z} \\ \dot{\phi} \\ \dot{\theta} \end{bmatrix} + \begin{bmatrix} k_{zz} & k_{z\phi} & k_{z\theta} \\ k_{\phi z} & k_{\phi\phi} & k_{z\phi} \\ k_{\theta z} & k_{\theta\phi} & k_{\theta\theta} \end{bmatrix} \begin{bmatrix} z \\ \phi \\ \theta \end{bmatrix} = 0 \tag{5}$$

The reality of the design space when discussing the craft of extreme speed regimes is that instability is near guaranteed at some point, thus there is a point at which the seakeeping dynamics of the craft do not converge to zero as they do in Equation 5. There are many reasons for this occurring, but often this has a lot to do with the hull form characteristics changing across different dynamic domains at different speeds. Mathematically, an error term appears in the equation to model how small disturbances while in a high planing state can propagate into instabilities or extreme events. This emergence of instability generates Equation 6.

$$\begin{bmatrix} m_{zz} & m_{z\phi} & m_{z\theta} \\ m_{\phi z} & m_{\phi\phi} & m_{z\phi} \\ m_{\theta z} & m_{\theta\phi} & m_{\theta\theta} \end{bmatrix} \begin{bmatrix} \ddot{z} \\ \ddot{\phi} \\ \ddot{\theta} \end{bmatrix} + \begin{bmatrix} c_{zz} & c_{z\phi} & c_{z\theta} \\ c_{\phi z} & c_{\phi\phi} & c_{z\phi} \\ c_{\theta z} & c_{\theta\phi} & c_{\theta\theta} \end{bmatrix} \begin{bmatrix} \dot{z} \\ \dot{\phi} \\ \dot{\theta} \end{bmatrix} + \begin{bmatrix} k_{zz} & k_{z\phi} & k_{z\theta} \\ k_{\phi z} & k_{\phi\phi} & k_{z\phi} \\ k_{\theta z} & k_{\theta\phi} & k_{\theta\theta} \end{bmatrix} \begin{bmatrix} z \\ \phi \\ \theta \end{bmatrix} = e(t) \tag{6}$$

Given the idea that a control surface can provide a certain degree of authority to force a system into stability, this error term can sometimes be a surmountable obstacle. To determine if the vessel can reach stability through controls, a term can be added to the seakeeping equation to represent the required effort of a control system to maintain stability through changing dynamic domains. This action is illustrated in Equation 7 and Equation 8.

$$\begin{bmatrix} m_{zz} & m_{z\phi} & m_{z\theta} \\ m_{\phi z} & m_{\phi\phi} & m_{z\phi} \\ m_{\theta z} & m_{\theta\phi} & m_{\theta\theta} \end{bmatrix} \begin{bmatrix} \ddot{z} \\ \ddot{\phi} \\ \ddot{\theta} \end{bmatrix} + \begin{bmatrix} c_{zz} & c_{z\phi} & c_{z\theta} \\ c_{\phi z} & c_{\phi\phi} & c_{z\phi} \\ c_{\theta z} & c_{\theta\phi} & c_{\theta\theta} \end{bmatrix} \begin{bmatrix} \dot{z} \\ \dot{\phi} \\ \dot{\theta} \end{bmatrix} + \begin{bmatrix} k_{zz} & k_{z\phi} & k_{z\theta} \\ k_{\phi z} & k_{\phi\phi} & k_{z\phi} \\ k_{\theta z} & k_{\theta\phi} & k_{\theta\theta} \end{bmatrix} \begin{bmatrix} z \\ \phi \\ \theta \end{bmatrix} = e(t) - C(t) = 0 \tag{7}$$

$$\begin{bmatrix} m_{zz} & m_{z\phi} & m_{z\theta} \\ m_{\phi z} & m_{\phi\phi} & m_{z\phi} \\ m_{\theta z} & m_{\theta\phi} & m_{\theta\theta} \end{bmatrix} \begin{bmatrix} \ddot{z} \\ \ddot{\phi} \\ \ddot{\theta} \end{bmatrix} + \begin{bmatrix} c_{zz} & c_{z\phi} & c_{z\theta} \\ c_{\phi z} & c_{\phi\phi} & c_{z\phi} \\ c_{\theta z} & c_{\theta\phi} & c_{\theta\theta} \end{bmatrix} \begin{bmatrix} \dot{z} \\ \dot{\phi} \\ \dot{\theta} \end{bmatrix} + \begin{bmatrix} k_{zz} & k_{z\phi} & k_{z\theta} \\ k_{\phi z} & k_{\phi\phi} & k_{z\phi} \\ k_{\theta z} & k_{\theta\phi} & k_{\theta\theta} \end{bmatrix} \begin{bmatrix} z \\ \phi \\ \theta \end{bmatrix} + C(t) = e'(t) = 0 \tag{8}$$

Distilling Control Requirements from C(t)

$C(t)$, as defined in the previous section, is at its core a measure of the error between desired and actual dynamic characteristics. To pull more specific information out of $C(t)$, it needs to be decomposed into error terms in each direction, which is shown in Equation 9. These functions can be fairly easily picked apart using a linear regression model using data points from the simulation.

$$C(t) = e_z(t) \begin{bmatrix} 1 \\ 0 \\ 0 \end{bmatrix} + e_\phi(t) \begin{bmatrix} 0 \\ 1 \\ 0 \end{bmatrix} + e_\theta(t) \begin{bmatrix} 0 \\ 0 \\ 1 \end{bmatrix} \tag{9}$$

From this point, two key pieces of information are needed to determine the feasibility of the control system: the first of these is the required effort of the control system. This can be found by finding the maximum value of $|e_z(t)|$, $|e_\phi(t)|$, and $|e_\theta(t)|$ across the selected time domain. For instance, $max(|e_z(t)|)$ might return a value of 2000 Newtons, which tells us that our control system must be able to produce 2000 Newtons of lift when all surfaces are fully extended. This does not necessarily mean one control surface has to do this, but the aggregate effect of the control surfaces must produce that effect.

From here, the reactivity of that control system must be determined, or in other words, the speed at which the control sys-

tem must fight a disturbance. the first step of determining this information is taking the derivative of the error functions, returning $e'_z(t)$, $|e'_\phi(t)|$, and $e'_\theta(t)$. From there, the maximum magnitude of the derivative of the error function should be found, $max(|e'_z(t)|)$ for instance. The last step is to determine the time domain in which controls must be able to engage. Generalized control reactivity values in the context of the reduction used by UMEB can be found in Equation 10, 11 and 12.

$$t_z = \frac{max(|e_z(t)|)}{max(|e'_z(t)|)} \tag{10}$$

$$t_\phi = \frac{max(|e_\phi(t)|)}{max(|e'_\phi(t)|)} \tag{11}$$

$$t_\theta = \frac{max(|e_\theta(t)|)}{max(|e'_\theta(t)|)} \tag{12}$$

This process during simulation should give enough information to determine the feasibility of a control-enabled design and avoid its loss to set reduction. Following this process, UMEB was left with a feasible set of designs that included the effect of control surfaces on vehicle dynamics.

Dominance through Risk Modeling

Once UMEB had a clearly defined range of design variables that was deemed to produce feasible results, the question of execution became increasingly more important. While the team had grown both in personnel and resources significantly, there were still limitations. The greatest block in the design process was that there were many components that the team knew were going to be impossible to manufacture in-house, which meant we had to purchase them; specifically, the hull and primary drive motor were both components that had to be purchased and not designed, thus creating anchors within the design space. There were a limited number of commercially available hull forms and drive motors that fell within the realm of feasibility, which discretized some of the design variables. Additionally, while all of these designs were feasible, UMEB wanted to pick the most competitive design possible in order to increase our chances of winning the electric boat arms race. Because of this, UMEB realized that comparison and dominance would have to be achieved through a method beyond set-based design. The team settled on the usage of Pugh's method of controlled convergence, shown in Figure **??**, to develop this knowledge, first laying out all of the commercially available hull forms and motor options that fell within the feasible set. To determine the dominance of designs, an evaluation criteria had to be used, which is where the VI-VS risk model became useful.

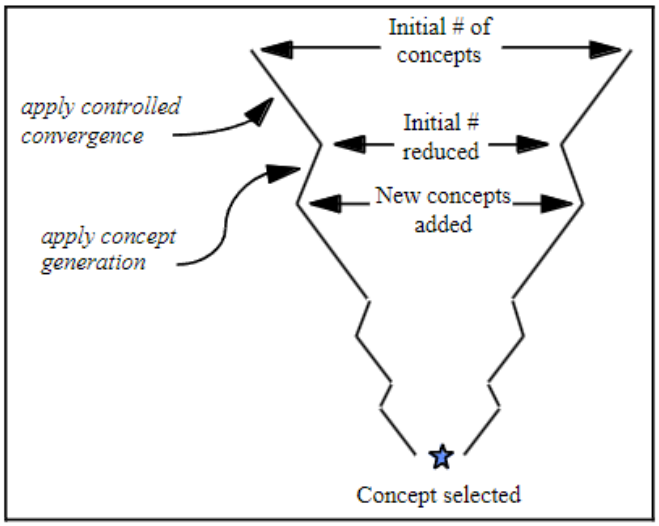

Figure 10: Visual for Method of Controlled Convergence from Bernstein (1998)

Quantifying VI-VS

As discussed earlier, Vessel Integrity and Vessel Speed both represent composite functions of many factors that contribute to safety and performance respectively. The team determined these functions in a manner very similar to AHP, where they subjectively categorized how important each element of each criterion was over another. Following this, they generated the comparison matrices found in Table 1 and Table 2.

Table 1: Preference Matrix for Vessel Integrity

	Trim Stability	Roll Stability	Driver Capsule Strength	Powertrain Stress (C-rate)
Trim Stability	1	7	4	3
Roll Stability	1/7	1	1/3	1/5
Driver Capsule Strength	1/4	3	1	3
Powertrain Stress (C-rate)	1/3	5	1/3	1

Table 2: Preference Matrix for Vessel Speed

	Top Speed	Turning Radius	Acceleration	Range
Top Speed	1	7	4	3
Turning Radius	1/7	1	1/5	1/6
Acceleration	1/4	5	1	1/3
Range	1/3	6	3	1

From here, the team took the eigenvectors of these matrices to determine a weight vector, with results shown in Equation 13 and Equation 14.

$$w_{VI} = \begin{bmatrix} 0.88 \\ 0.09 \\ 0.38 \\ 0.26 \end{bmatrix} \tag{13}$$

$$w_{VI} = \begin{bmatrix} 0.86 \\ 0.07 \\ 0.23 \\ 0.44 \end{bmatrix} \tag{14}$$

Similar to TOPSIS as defined by Sen and Yang (1998), the designers identified an upper and lower bound for each of these metrics; by normalizing these values throughout the process, a nondimensionalized measure is gained for both vessel speed and vessel integrity which can each be plotted as single variables.

Comparison with VI-VS

From this point, it became necessary to define an acceptable design risk curve that would act as the optimization goal. The team agreed that due to the policies of the University of Michigan, there was a baseline level of Vessel Integrity that was independent of Vessel Speed. There was also agreement that as Vessel Speed increased beyond around 0.500, there was no reason to increase the required Vessel Integrity much further as an extreme event at that level of performance would spell disaster regardless of the mitigation, prevention, and safety measures in place. For this reason, the team decided that the best way to model this behavior was through a square root relationship. Plotting this on the VI-VS curve generates Figure 11.

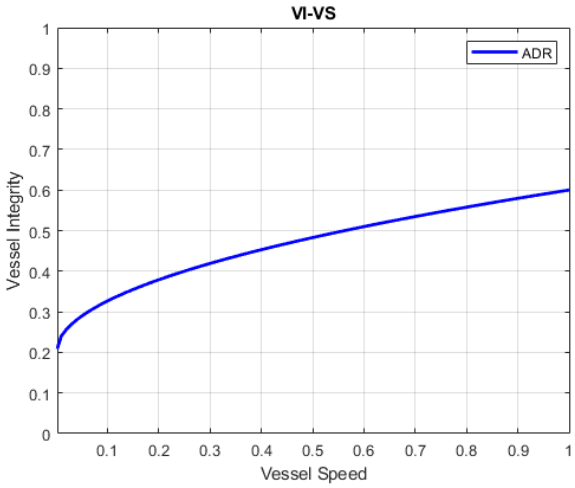

Figure 11: Decided ADR Curve

Once an ADR was established, the team moved onto using the VI-VS curve to analyze the dominance of individual designs by characterizing how Vessel Integrity changed across the domain of Vessel Speeds. Much of this was done subjectively or using simple curve fits from known points. Once a surrogate model had been established, dominance was determined based on the intersection between a design's VI-VS curve and the ADR curve. Take *Snowfinkle* for instance; due to the anhedral hydrofoils and poor weight distribution, *Snowfinkle*'s stability degraded quickly with increased performance, generating Figure 12.

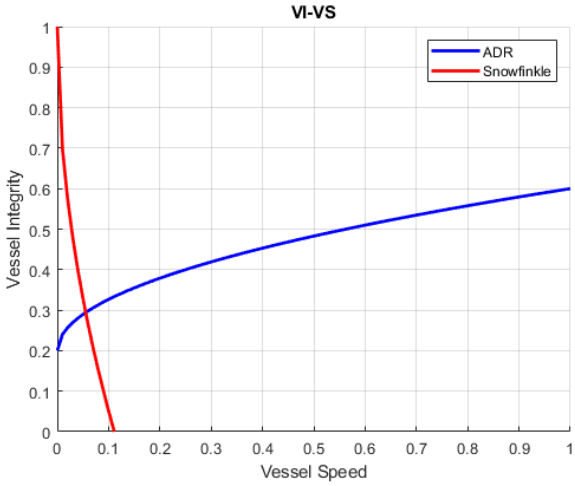

Figure 12: *Snowfinkle* VI-VS Plot

This can be extrapolated further by looking at the VI-VS curves for further designs in Figure 13. By analyzing the problem through this lens, one can determine that "Design Alternative 2" dominates the others, as it can extract the most performance without an unacceptable risk of an extreme event occurring.

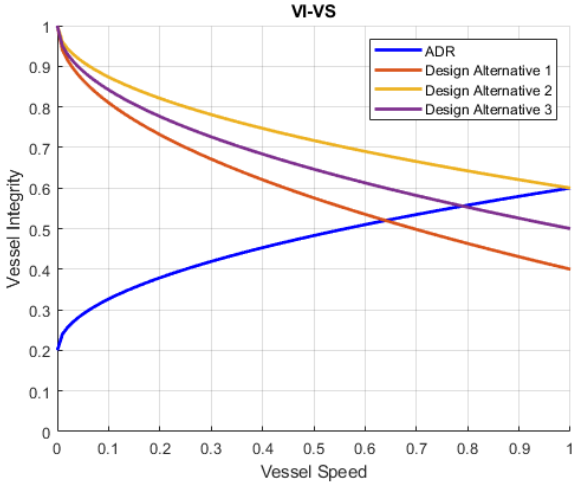

Figure 13: Sample VI-VS Plots

This kind of analysis drove the remainder of the early-stage design process for UMEB, and the team was left with a set of design elements that they were confident were strong enough to be competitive. Thus came the second, and much more entertaining, problem: how to take the chosen design from a spreadsheet to a working boat.

EXECUTION

First began the monumental task of figuring out how to pay for a 24-foot race boat. Due to the frontloading of the design work, UMEB had a very clear vision of what our end product was going to be; this was advantageous as it was much eas-

ier to illustrate this vision to potential sponsors comapred to past UMEB projects. Through building connections and sharing the plan, the team built more and more allies: powerboat builders, electric vehicle manufacturers, consulting firms, and software companies to name a few; UMEB's net worth passed a million US dollars within six months of starting fundraising.

With financial resources unlocked, the team experienced a shift in November 2023, as the time had arrived to start physically putting together the parts of the craft. This was kicked off by the arrival of the hull, which the team had to travel to pick up from a sponsor across the country. As the new craft was pulled into the team workspace, the team announced to the world the name of the project: *TiDE*. As the project progressed and grew in physical scale, more external eyes found the craft UMEB had created. Working with the resources and technical support of Skater Powerboats, the team was able to complete a structural canopy that met the required APBA rules. At the same time, UMEB worked with a Slovenian hypercar manufacturer to source a motor powerful enough to drive the craft.

Figure 14: *TiDE* in UMEB's Workshop

The team continued building and making component-level decisions, eventually leading to the creation of three patentable technologies, specifically concerning the extremely advanced battery system developed to address mass requirements. In less than a year, better leadership and design methodologies had turned around the trajectory of the team, pivoting from its greatest failure to its greatest success thus far. Most of these successes can be attributed to the extensive work done early on to characterize *TiDE*'s design space, unlock a broader range of feasible designs through advanced control theory, and use a careful process to lock in a final design. UMEB is a testament to the application of Naval Architecture and Marine Engineering to the racing world.

CONCLUSIONS

It is an understatement to say that there are a lot of gaps between how marine designers and high-performance racing teams create craft. Viewing racing through an academic lens has the potential to open a lot of doors in the realm of optimization, marine control theory, and uncrewed applications. Translating their methods into a space understood by naval architects,

with concepts like risk management and codesign, we can better analyze extremely high-performance systems and learn from them. Additionally, developing a framework to marine design methods, like set-based design, opens the door for more optimal racing craft to emerge. An understanding of the bridge between these two worlds is important in furthering advanced marine technologies.

CONTRIBUTION STATEMENT

EJB: conceptualization, lead designer for UMEB, methodology; writing – original draft. **AMV:** conceptualization; methodology; writing – review and editing. **KM:** Conceptualization; **DJM:** conceptualization; supervision; writing – review and editing.

ACKNOWLEDGEMENTS

An immense amount of gratitude should be extended to Dr. Norbert Doerry, Dr. Armin Troesch, Dr. Jonathan Page, and Dr. Thomas McKenney. Without their assistance, many of the concepts of codesign and risk identification used in this document would not have become evident or defined well within the context of marine design. A point of recognition is extended to our friends at Skater Powerboats, Peter Hledin and Robert Bloom, who have acted as guides and mentors in the realm of powerboating. The authors would also like to thank their team members on University of Michigan Electric Boat for allowing us to use their project as a platform for the proof of concept of our novel design methodology.

REFERENCES

Abedini, A., Bataleblu, A. A., and Roshanian, J. (2022). Co-design optimization of a novel multi-identity drone helicopter (micopter). *Journal of Intelligent & Robotic Systems*.

ABS (2020). Risk assessment applications for the marine and offshore industries.

Andrews, D. (2021). Marine requirements elucidation and the nature of preliminary ship design. *International Journal of Maritime Engineering*.

APBA (2022). Section i - cockpit related safety rules.

Aronstein, D. C. and Piccirillo, A. C. (1997). *Have Blue and the F-117A: Evolution of the Stealth Fighter*. American Institute of Aeronautics and Astronautics.

Atwal, S. (2024). The deadly history of the water speed world record.

Bernstein, J. I. (1998). Design methods in the aerospace industry: Looking for evidence ofset-based practices.

Castro-Feliciano, E. (2016). *Co-Design of Planing Craft and Active Control Systems*. PhD thesis, University of Michigan.

Gerr, D. (2001). *The Propeller Handbook*. International Marine.

Goodrum, C. J. (2020). *Conceptually Robust Knowledge Generation in Early Stage Complex Design*. PhD thesis, The University of Michigan.

McKesson, C. B. (2009). *The Practical Design of Advanced Marine Vehicles*. University of New Orleans College of Engineering.

Sen, P. and Yang, J.-B. (1998). *Multiple Criteria Decision Support in Engineering Design*. Springer.

Singer, D., Doerry, N., and Buckley, M. (2010). What is set-based design? *Naval Engineers Journal*.

Yun, L. and Bliault, A. (2012). *High Performance Marine Vessels*. Springer.

Proceedings of 15th International Marine Design Conference (IMDC-2024)
June 2-6, 2024
Amsterdam, the Netherlands

Data Models in Ship Design and Construction - Insights from 4D BIM

Janica A. Bronson[1,*], Ícaro A. Fonseca[2], Henrique M. Gaspar[3], and Fernando H. P. Luz[4]

ABSTRACT

The lack of a cohesive understanding of a ship product data model, from design to operations, is currently a limiting factor in realizing more efficient ship lifecycle management and design processes. The paper sheds light on the history and gaps in realizing an integrated, interoperable, and multi-domain ship product data model. It also explores practices from BIM (Building Information Modelling) as an inspiration for solutions to overcome challenges related to information modeling, integrated design environment, and 4D engineering and planning.

KEY WORDS

Ship product data model, Building Information Management (BIM), Lifecycle Management

THE IMPORTANCE OF COHESIVE PRODUCT DATA MODEL

Accurately representing a product's data across its lifecycle is a challenge most industries face today. For engineer-to-order (ETO) sectors that handle the design and production (or construction) of multi-functional assets, such as manufacturing, construction, and shipbuilding, competitiveness depends on how well the product data is maintained physically and digitally (Wyman et al., 1997). Proper management enables process and operational efficiency and decreases the likelihood of technical errors that become more expensive to reconcile as the product matures (Rigterink, 2014).

Today, various international standards provide an understanding of how the data of multi-functional assets can be represented appropriately and communicated across highly dispersed teams via a product data model (ISO, 2022; DNV AS, 2023; ISO, 2004b, 2024). A product data model is a way to organize or structure relevant product data. Other terms equivalent to this concept are Common Reference Information Models (RIM) (ISO, 2022) or Asset Information Models (AIM), which are a 'collated set of information gathered from multiple sources' encompassing the structure and relationships of the data in these sources and or databases (DNV AS, 2023). Where there is no cohesive product data model, companies risk lacking the capacity for (1) efficient product lifecycle management (PLM) and (2) challenges in the integration and interoperability of asset data (Wyman et al., 1997).

The shipbuilding industry currently does not have a standard solution to tackle these gaps, as a complete view of a ship's data (from design to operations) has yet to be realized. A ship is a complex system, and both the built physical asset and digital representations of a ship are often developed in a highly modular and concurrent fashion (Koenig et al., 1997; Pal, 2015). Only upon delivery for construction is an integrated view of a ship's design realized; however, this integrated view

[1]IHB, NTNU, Ålesund, Norway; ORCID: 0009-0002-4259-2246
[2]IHB, NTNU, Ålesund, Norway; ORCID: 0000-0003-0189-2576
[3]IHB, NTNU, Ålesund, Norway; ORCID: 0000-0003-4286-5304
[4]IHB, NTNU, Ålesund, Norway; ORCID: 0009-0005-2735-433X
[*] Corresponding Author: janica.echavez@ntnu.no, fernando.luz@ntnu.no

Submitted: 23 February 2024, Revised: 1 May 2024, Accepted: 3 May 2024, Published: 19 May 2024

Conference paper, DOI: https://doi.org/10.59490/imdc.2024.842 e-ISSN: 3050-4864

is often only partially complete. In managing and operating the ship, multiple stakeholders may have incomplete interpretations of the ship as a whole due to its scale and numerous onboard systems.

Other ETO industries have also developed their own solutions to tackle these challenges. For example, in the aerospace and manufacturing industries, the use of 'digital mock-ups' (DMUs) (Oh et al., 2008) and generic AIMS (ISO, 2004b) as the equivalent of product data models is well-established.

Despite facing similar challenges related to high regulatory intervention, multi-organization, and customization (Emblemsvåg, 2014), the architecture, engineering, and construction (AEC) industry has seen significant digitalization in design and construction practices thanks to the introduction of the Building Information Model (BIM). BIM has helped solve these interoperability issues and continues to help advance the AEC industry's digitalization efforts (Azhar et al., 2008).

In light of the benefits of BIM, this paper aims to explore what the shipbuilding industry can learn from the AEC industry, focused on understanding potential improvements related to (1) data modeling and (2) collaborative design practices, including a temporal understanding of the system. In addition, this paper explores previous and current ship product data modeling attempts and proposes possible solutions that the shipbuilding industry can consider.

CURRENT PRACTICES IN SHIP DESIGN AND PLANNING

Today's ship lifecycle involves disparate processes, tools, and needs for each phase. These phases, covering upstream design to downstream operations and maintenance, differ in the generation, usage, and transformation of information related to a ship's product data model (Andritsos and Perez-Prat, 2000; Whitfield et al., 2003). Currently, product data models in shipbuilding are not similarly developed as an AIM according to ISO unless integrated platforms such as CADMATIC Wave and Siemens Teamcenter are used. When these tools are not used, a ship's design data is dispersed, involving a combination of a 3D model, drawings, and digital documents. Issues related to version control and change management are common, especially when multiple instances of these files are copied, modified, and not incorporated with other drawings. These practices perpetuate 'information silos' and decision-making with incomplete information (Stachowski and Kjielen, 2017). These gaps are most apparent in early design stages, where design uncertainty is high, but the most expensive decisions are made (Love and Sing, 2013; Mavris and Delaurentis, 2000).

While the lack of product information is the critical risk faced in early design, manual data integration is the concern in detail engineering. In detailed engineering, technical information is rapidly received from multiple cross-disciplinary sources, often in various file types and formats, as the focus shifts to technical evaluation and increasing design granularity. Where file formats are incompatible, manual exchange or conversion is expected. Dedicated integration engineers are often hired to ensure that all relevant drawings, documents, and models are consistent and incorporated into a technical package for delivery to a client or yard (NAVSEA, 2012; Gale, 2003).

Meanwhile, during construction, a shipyard's shopfloor planners are mainly concerned with developing transitional work packages that suit available resources, people, and time. Hence, the concern is not related to integration but to the translation and reorientation of design data into process data. Developing a bill of materials (BOM) and bill of processes (BOP), along with work packages, further leads to a ballooning of information that now incorporates planning and operations details (Pal, 2015). Post-commissioning, ship information must still be maintained in the downstream value chain to track the health of ship systems. All of this information remains in disparate onboard equipment and physical or digital copies managed by ship operators. Unfortunately, this type of data typically never goes back to ship designers to improve product information.

The differences in data management needs across a ship's lifecycle have led to the development of highly distinct and specialized software tools addressing particular ship design and planning functions, as shown in Figure 1 (Andritsos and Perez-Prat, 2000). However, this has also led to a paradoxical problem where, while there is now a greater range of ship design tools, the methods for exchanging data between these tools are outdated. It is not uncommon for these tools to have their own model and representation of a ship that remains isolated and spread organizationally or globally, with different levels

of detail (LOD) (Erikstad and Fathi, 1999; Whitfield et al., 2003). The separation of ship data domains, continually being persisted by these disparate software, has led to a business culture where technical data development can be detached from the management and operations of such development process.

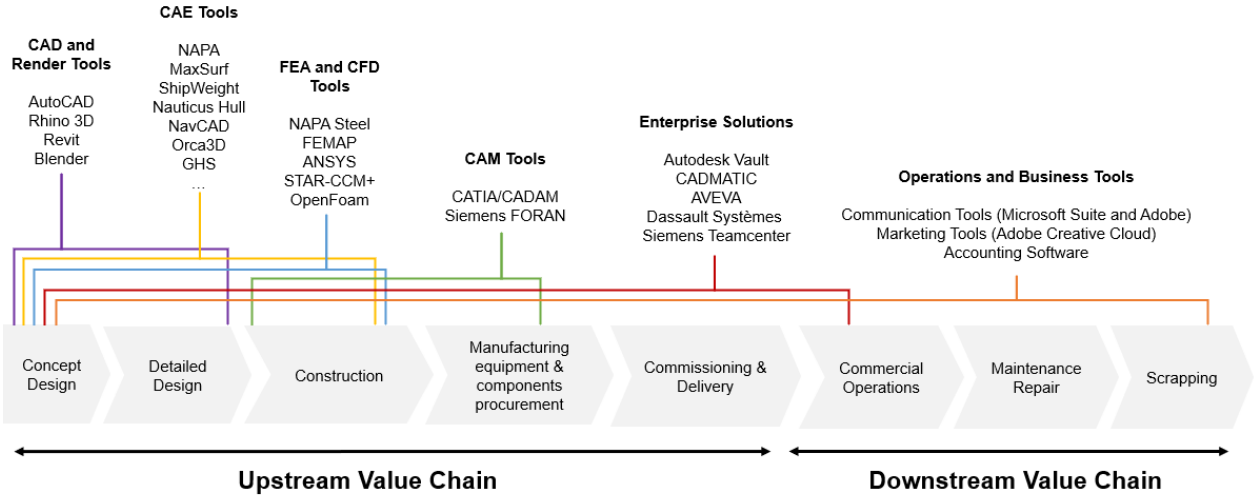

Figure 1: Disparate Tools with Overlapping Use Across the Shipbuilding Lifecycle

Integrating disparate ship data to produce a unified ship model is a highly complicated task. Before delving into the history of shipbuilding attempts, it is essential to note the following concepts on data exchange and management that shed light on the complexity of maintaining a product data model.

- ***Data Modeling*** – Data modeling focuses on how information is structured and how data relationships are represented (ISO, 2023, 2003). Typically, these relationships can be defined with human-readable diagrams, including IDEF, NIAM, etc.(Wyman et al., 1997), but they can also be represented in schemas such as relational database schemas and graphical database schemas (Härder, 2005) that are codified in implementation languages such as Basic, FORTRAN, C, C++, Java and EXPRESS. Several standards exist to help define what these schemas are, including the Knowledge Interchange Format (KIF), Web Ontology Language (OWL), and Resource Description Framework (RDF), which provide reasoning over how information can be represented in that domain (Rachuri et al., 2008). Concerns related to data modeling are typically focused on ensuring that product data models capture most of the information. Therefore, integrating information and managing increasing granularity or data fidelity are important considerations. This can cover product or even full enterprise integration, incorporating company and other resource planning data (Whitfield et al., 2003).
- ***Data Exchange*** – Data exchange is focused on the transfer of data across different applications and programs. To enable this, machine-interpretable syntax (defined in data formats) must be used to encode and share data digitally (Edelman et al., 2018) or direct translators are used when data formats are incompatible across software (Whitfield et al., 2003). The use of neutral file formats that can be interpreted by different software, as opposed to native file formats that are designed to be usable for only specific software, is therefore advisable. These neutral data formats for storage use extensions that vary based on the data contents, whether graphical (.IGES and .STL) or otherwise (.XML and .STP). When discussing data exchange, the concerns typically revolve around enabling interoperability. Hence, well-defined and formalized data models that can be used across industries ultimately help with interoperability. Hence, Open standards are typically related to data exchange, as are concepts pertaining to centralized or distributed data architectures. While there are plenty of neutral file formats, including XML and JSON, the ISO-certified format for interoperability is STEP, which uses the EXPRESS programming language (ISO, 2004a).
- ***Data Management*** – Data management relates to operations, systems, or tools that enable consistent and reliable data quality, security, and trustworthiness. Facilitating the use of data models and enabling data exchange is, therefore, just one of the few functions that efficient data management systems can help with (Samonas and Coss, 2014).

ISO 15926-1 defines data models relative to 3-layer database management (DBMS) architecture, emphasizing that data models should not be interpreted in isolation (ISO, 2003). The above elements can, therefore, be understood in terms of where they stack in this 3-layer architecture. Data models typically reside in the conceptual schema, data exchange is related to the dictionary and or interpreters for the conceptual schema, and data management is the infrastructure related to the database and applications or front-facing user interfaces.

DESIGN AND PLANNING REPRESENTATIONS USED IN SHIPBUILDING

Classification and Coding Systems

While there are now more widely accepted definitions of a product data model, it is essential to recognize the unique history of data modeling and shipbuilding. The challenge to arrive at a coherent product data model is not new; attempts have been made since the 1970s, starting with dimensional coding systems.

Ship classification and coding systems are still some of the most popular means of presenting ship data today. These systems were developed partly due to the popularity of modularity as a means to increase industrial competitiveness in the 1970s. These were heavily popularized by companies such as Boeing, who developed proprietary codes such as BUCCS-3 (Boeing Uniform Classification and Coding System) to streamline manufacturing processes. These classification and coding systems, also interchangeably called product structures, are hierarchical representations of an asset. These hierarchical product structures and modularity modernized shipbuilding, changing how shipyards were designed such that equipment and materials were laid out to enable the efficient execution of similar work types (NSRP, 1986). Coding systems are still widely used today (Oh et al., 2008) due to the relative simplicity and reliability of being used since the onset of modern shipbuilding practices.

Ship and Product Work Breakdown Structures. The Ship Work Breakdown Structure (SWBS) is one of the most widely used coding systems in North America. The SBWS, first developed by the United States (US) Navy in 1977, uses a 3-digit function-based code with main group divisions including hull structure, propulsion and electrical plants, outfitting and furnishings, integration engineering, and ship assembly and support. SWBS codes can be used to organize drawing schedules, material catalogs, work planning, work orders, craft labor, and cost collection. Unfortunately, while SWBS provided a means of organizing work, it could not capture the most effective information for accomplishing work, especially when complicated work packages are involved. Addressing these limitations led to the development of the Product Work Breakdown Structure (PWBS), which included work type, manufacturing level, zone type, problem area, and stage (Koenig et al., 1997; NSRP, 1986). The development of the PWBS classification system introduced additional domains as dimensions to SWBS representation based on cost, function, and tasks – leading to a three-dimensional understanding of a ship product as shown in Figure 2. However, the implementation of this dimensional coding system was time-consuming. Without automation capabilities, the PWBS codes were generated and retrieved manually via a massive PWBS Classification and Coding book that served as a dictionary for translating these three domains. Various attempts were made to digitize this process and manage coding systems using computers. One such example is the Decision and Classification Information System (DCLASS) from Brigham Young University. This generic tree processor proved to cut 95 percent of the time for data retrieval in cost estimation exercises.

Skipsteknisk Forskningsinstitutt (SFI) Coding System. In Europe, the widely-used alternative to the SWBS is the SFI Code, named after the Norwegian Skipsteknisk Forskningsinstitutt (SFI) that developed it. The SFI Code or System has a comprehensive product structure covering various aspects of ship and offshore specifications. SFI Code uses a 3-digit decimal code system to classify all ship and rig operation functions into ten main groups from 0 to 9 that cover the hull, equipment for cargo, and ship equipment, among others (Xantic, 2001). Officially launched in 1972 in Norway, the SFI Group was developed by a joint consortium of industry partners to establish a unilateral coding system that could be used unanimously among different shipyards and design stakeholders. The SFI Code was intentionally designed to be simple, applicable to all ships, and capable of future expansion. It was also intended to be a functional-oriented system for adaptability in design and production (Manchinu and McConnell, 1977).

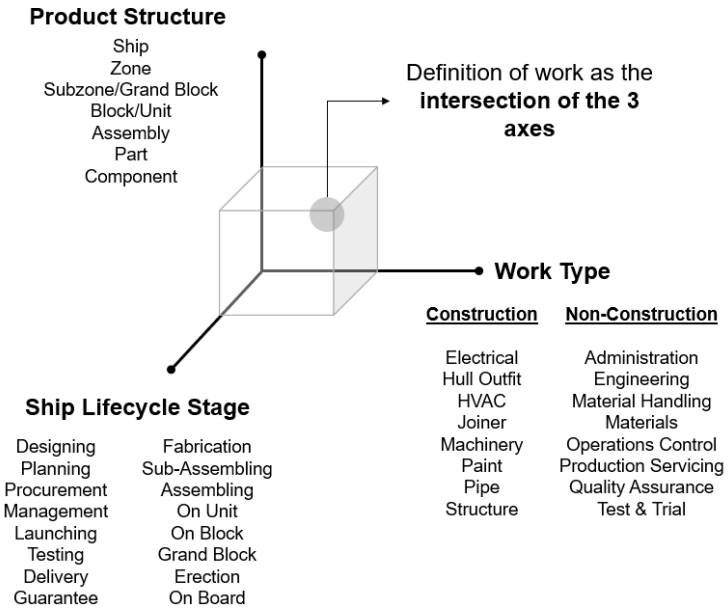

Figure 2: Dimensions in Generic Product Work Breakdown Structure (GPWS). Adopted from Koenig et al. (1997)

Ship Product Data Models

Product structures, especially with expanded domains and dimensions related to planning, faced hurdles in implementation due to the need and lack of tools to automate their usage. With the onset of computer-aided design (CAD), computer-aided engineering (CAE), and computer-aided manufacturing (CAM) in the 1980s, ship designers and yards quickly picked up on the potential of these tools in improving technical design processes, which led to the natural integration of coding systems with modeling and 3D graphics. CAD/CAE/CAM enabled the transformation from coding systems to 3D graphical product-oriented information databases (Murphy, 1992). As such, what was involved in a digital product representation of a ship was relatively malleable from the 1970s to 1990s while both shipbuilding and software engineering were evolving rapidly (Ross, 1997; Gischner et al., 1997).

One of the earliest definitions of a ship product data model comes from Martin (1980), who described it as a 'logically structured, product-oriented database' that supports the analysis and informational needs for a ship's engineering, design, construction, and maintenance (Whitfield et al., 2003; Ross, 1997, 2003). The use of the term 'common model' was ubiquitous, as multiple ship representations with varying embellishments across different departments were typical. Hence, a ship product data model was understood to support a certain degree of information integration, which can include enterprise data. Computer-integrated manufacturing (CIM) is an example of an enterprise integration concept, enabling testing, production, and control, all within a shared database.

These growing integration needs also led to interoperability issues that called for a serious assessment of digital information exchange standards (Gischner, 2006). International Standards Organization's (ISO) STEP (STandard for the Exchange of Product Model Data), more formally known as ISO 10303, was launched in 1986 to solve cross-platform and cross-application development issues by producing a system-independent data representation (including geometry, topology, and functionality) of design artifacts (NSRP ASE, 2007). Its development was inspired by the Product Data Exchange Program (PDES), which tried to arrive at a consensus of a data exchange standard for industrial automation (Kelly, 1985). STEP largely followed traditional Database Management System (DBMS) Architecture at this time, which included a 3-schema architecture (as shown in Figure 3a) covering External Schema with user-facing applications, a Conceptual or Logical Schema for the translation of data via mapping or other logical representations of the system of interest, and the Physical Schema which involves the physical representation of the data as stored in a database (McDermid, 2013; Kelly, 1985). In

this architecture, STEP was most concerned with the standardization of the components in the Conceptual Schema, which over time took the moniker of a data model as understood in software engineering today and as defined in ISO 15926 (ISO, 2003). The Conceptual Schema or Conceptual Model represents the view of the data negotiated between end-users and the databases, covering the meaning and the relationships of the data with each other. To facilitate this, the EXPRESS data modeling language was developed explicitly for STEP (Whitfield et al., 2003). This program prompted multiple initiatives for various industries to formalize their standards with ISO STEP in mind. In ship design and shipbuilding, the notable ones include NIDDESC and ISE from the US and NEUTRABAS from Europe.

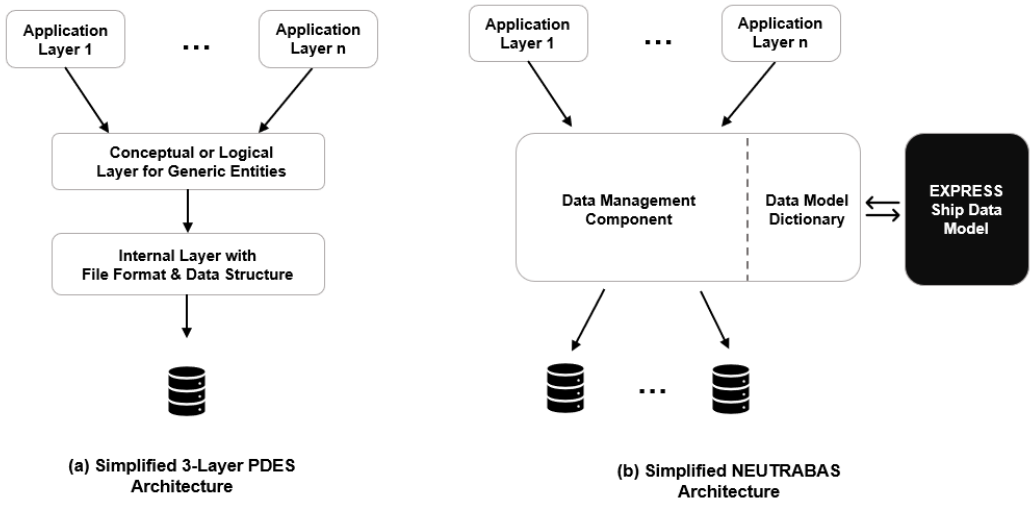

Figure 3: Simplified DBMS Architecture for PDES and NEUTRABAS. Adopted from Kelly (1985) and Nowacki (1995)

NIDDESC, 1986. The Navy/Industry Digital Data Exchange Standards Committee (NIDDESC) was developed in 1986 as a joint effort of the US Navy (NAVSEA) and the National Shipbuilding Research Program (NSRP), which focused on creating an industry consensus on the definition of product data and ensuring that these requirements were incorporated into national and international data exchange standards. The program's result was identifying product data model content for the marine industry and developing documentation for a neutral file format that incorporates IGES' specifications with the emerging STEP standards of that time. The developed documents were known as Application Protocols (APs) that defined the requirements for a ship's product information or Conceptual Schema for a specific domain. They converged to six APs submitted for inclusion into the STEP standards covering Piping, HVAC, Electrical Distribution and Wireways, Structural Systems, Outfit and Furnishing, and Standard Parts. These APs have been further refined into AP 215 for Ship Arrangements, AP 216 for Ship Moulded Forms, and AP 218 for Ship Structures, which are still usable today (Gischner et al., 1997; Murphy, 1992; Whitfield et al., 2003).

NEUTRABAS, 1989. NEUTRABAS is an EU ESPRIT-funded project to develop a neutral product understanding for ships and similar large multi-functional products. The NEUTRABAS project worked collaboratively with the NIDDESC program, which preceded it two years earlier. The project aimed to meet the following: (1) a formal definition of a ship product information model, (2) specifications for a neutral database technology, (3) implementation of a neutral database, and (4) the development of a prototype for pre and post-processors for neutral data exchange. (Welsch et al., 1991; Nowacki, 1995). The ship product data model they developed was written in EXPRESS and required a bespoke data management component (DMC) to facilitate communication between one system-specific format and any other system, as seen in Figure 3b. The NEUTRABAS effort was, therefore, one of the first to describe how a neutral model can be implemented outside purely providing recommendations on the Conceptual Schema. Regarding the model itself, NEUTRABAS and NIDDESC were similar and focused on the development of reference models but differed in the degree of integration between their reference models. While NIDDESC developed multiple models for different functional domains with discrete APs for piping, structures, etc., NEUTRABAS adopted the position that integrating all current and future shipbuilding APs required the standardization of a single comprehensive and high-level Ship Application Reference model. They deemed this a prerequi-

site to the interoperability of all APs (Nowacki, 1995; Welsch et al., 1991). This position helped to make a significant point about the importance of assessing the data structure to effectively manage the exchange of information across various complex and heterogeneous ship development applications.

ISE, 1999. The Integrated Shipbuilding Environment Consortium (ISEC) was established in 1999 with a group of shipyards and CAD vendors. It aimed to develop information interoperability solutions for US Naval shipbuilding in a series of NSRP initiatives called the Integrated Shipbuilding Environment (ISE) projects (Gischner, 2006). Specifically, the goal was to develop the next-generation Integrated Product Development Environment (IPDE). This open architecture information system supports the delivery of integrated acquisition, engineering, and logistics products for the naval ship lifecycle (Oh et al., 2008). It is understood to be the family of systems that maintains the digital product data model. With the growing popularity of enterprise software such as Product Data Management (PDM) and Product Lifecycle Management (PLM), these tools were naturally considered as implements to enable the IPDE capability.

Latest Initiatives (Early 2000s-Current)

The realization of a product data model with capabilities related to integration, interoperability, and data exchange remains a challenging task that is continually being addressed today. Central to this problem is the need for more clarity in defining how ship data should be presented and what domains of ship data should be incorporated (Gischner, 2006). These shifts are presented in Figure 4. Data modeling practices and paradigms have also grown and developed much faster than they could be formally implemented in this context. The evolution of data modeling paradigms is also presented in Figure 4 adopted from Patni et al. (2021).

STEP's EXPRESS language follows a hierarchical and entity-relationship-based paradigm, which requires rigid, well-defined relationships. For this reason, adapting and expanding the ship product data model with definitions based on AP 215 (for Ship Arrangement), 216 (for Ship Moulded Forms), and 218 (for Ship Structures) was a cumbersome process (Whitfield et al., 2003; Gischner, 2006; Kramer et al., 1992; Rando, 2001). Gischner (2006) states that it takes, on average, about 3 to 5 years to implement STEP. These STEP APs, in addition to needing plenty of information and time to implement, also required a constant effort to finalize and update to 'avoid stagnation and improve general uptake across the industry' (Whitfield et al., 2003). Ross and Garcia (1998) describe that multiple special-purpose tools are needed for STEP, one of the main inhibitors for broad acceptance into the industry. These challenges were recognized by ISO themselves, as reflected by the multiple changes done on the APs - from isolated guidelines to plug-and-play modules - to make them easier to adopt.

XML or eXtensible Markup Language was determined to be a credible alternative to the STEP EXPRESS language due to its broader support in the IT industry and more noticeable structure and hierarchy. However, while XML has more advanced data-sharing operations, such as enabling persistent storage of ship data from application to application, it is constrained by the amount of storage space it requires (Rando, 2001). This is a limitation with the massive amount of digital data involved in most ship design and shipbuilding programs today. A modern commercial vessel may be expected to have an associated product data model of 2 to 10 gigabytes in size, depending on its complexity (Whitfield et al., 2003).

Outside XML, extensive industry-led work has been done to define a standard exchange format, with the inception of the OCX (Open Class 3D Exchange) Consortium in 2021. OCX as a format was developed in 2016 by the APPROVED Industry project involving partners such as Aveva, Hexagon, Siemens, and NAPA aimed towards defining a format that can address the unique data exchange needs amongst classification societies and shipbuilders. Although some additional work is still required to support the use of OCX, the consortium is actively promoting its use with the aim of industry-wide adoption (Zerbst, 2023).

Along with these developments, interest has also risen in the concept of digital twins applied in maritime systems over the past decade. Digital twins are virtual prototypes of physical assets that have garnered attention for their ability to enable remote operations and co-simulation (Grieves, 2022; DNV AS, 2023). As of 2023, DNV published DNV-RP-A204, which provides best practices for implementing, assessing, and maintaining the functional elements (FE) toward realizing a digi-

tal twin. At the heart of the digital twin is a consolidated AIM, which incorporates multiple data domains per ISO 81346's class libraries. Along with the definition of the desired AIM, they also stipulate advanced change management processes (MOC+) to ensure the trustworthiness of the ship AIM throughout its usage. While they do not present specifics on the software side, this latest development recognizes the regulatory and class societies' perspectives on best practices to arrive at a cohesive model. Additional understanding and research on the challenges of digital twin implementation from a data modeling perspective, specifically in data fragmentation stemming from the transition from upstream to downstream lifecycle, are also studied deeper in Bronson et al. (2024).

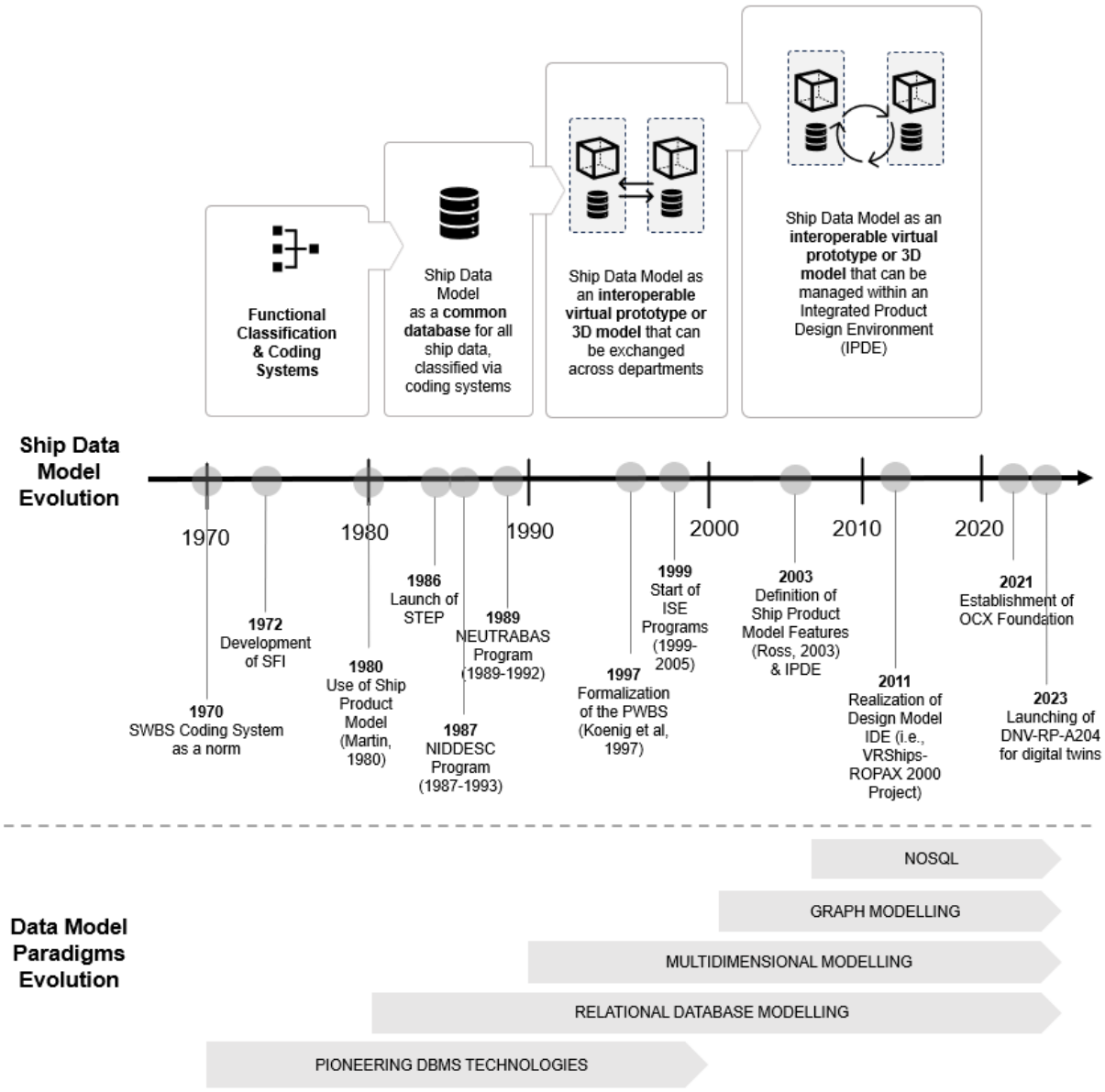

Figure 4: Evolution of Ship Data Concept

BUILDING INFORMATION MODELING (BIM)

Today, there is no tangible equivalent for the definition of a ship AIM except for that described by DNV for digital twins. In the AEC industry, the equivalent full building product data model is that of BIM. Like shipbuilding, the AEC industry had a notoriously long history of tackling data integration and interoperability issues, as shown in Figure 5.

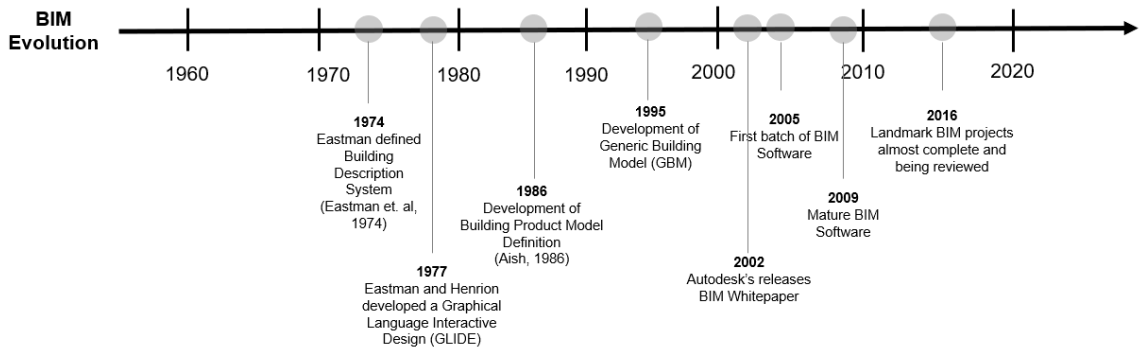

Figure 5: History of BIM, Adopted from Sinoh et al. (2020)

In a study by the US National Institute of Standards and Technology (NIST) in 2004, up to about USD 15.8 billion was lost annually due to 'the highly fragmented nature of the industry, the industry's continued paper-based business practices, a lack of standardization, and inconsistent technology adoption among stakeholders' (Gallaher et al., 2004). Although the knowledge of a cohesive building description system has been well-understood since the 1970s (Eastman et al., 1974), its formal implementation is a recent phenomenon. The original definition of BIM included three main elements: the structuring of design data, a digital model, and other non-graphical data, which were realized by bespoke tools such as RUCAPS in the 1970s (Aish, 1986). The implementation and broad commercialization of BIM as it is understood today were pioneered by commercial software companies such as GraphiSOFT, Bentley Systems, Autodesk, and Nemetschek AG (Autodesk, 2002; Wierzbicki et al., 2011). Autodesk's 2002 Whitepaper on BIM was one of the first to formalize a software strategy to implement digital databases, change management functions, and abilities to reuse information. In addition to formalizing a strategy, Autodesk also led the formation of IAI (Industry Alliance for Interoperability), now buildingSMART to understand the industry's take on data classes that can support integrated application development. This led to the development of IFC, in partial response to the slow adoption of STEP, as a neutral AEC product data model catered to the industry. Laakso and Kiviniemi (2012) describes this as one of the most ambitious standardization efforts in IT at that time. In addition to this formalization, the wide dissemination of BIM's practical uses has also influenced its success. As Azhar et al. (2008) cited, several case studies continue to encourage the use of BIM. Along with the iterative implementation and continued improvement of BIM came the modern understanding of it today as both a process and a tool.

According to the ISE (2021), BIM is a collaborative process enabled by technology, covering the whole lifecycle, from design and construction to asset operations. As a process, BIM allows the cohesive understanding of building data and fosters inter and intra-disciplinary collaboration. As a tool, BIM facilitates building data management across different lifecycle stages. Azhar et al. (2008) suggests the following benefits of BIM: (1) visualization, (2) fabrication and shop drawing support, (3) code reviews, (4) cost estimating, (5) construction sequencing, (6) conflict and collision detection, (7) forensic analysis, (8) facilities management, (9) quality take-off, (10) model-based estimating, (11) feasibility analysis, (12) alternative development, and (13) environmental analysis.

As there are different use cases for the application of BIM throughout a building's lifecycle, the qualitative and quantitative impacts of BIM overall are challenging to assess. However, in his study, Azhar et al. (2008) was able to share various scenarios where BIM has helped reduce costs in building projects. For example, the Atlanta Aquarium Hilton Garden Inn used BIM to plan the clash and collision detection. It identified about 55 clashes, resulting in a cost avoidance of over 124,500 USD. Similarly, BIM was used by the Emory Psychology Building for sustainability analysis, particularly in determining

the most suitable building orientation, skin option, and position. In all these cases, BIM provided relative cost savings due to the ability to view and rapidly simulate different design possibilities.

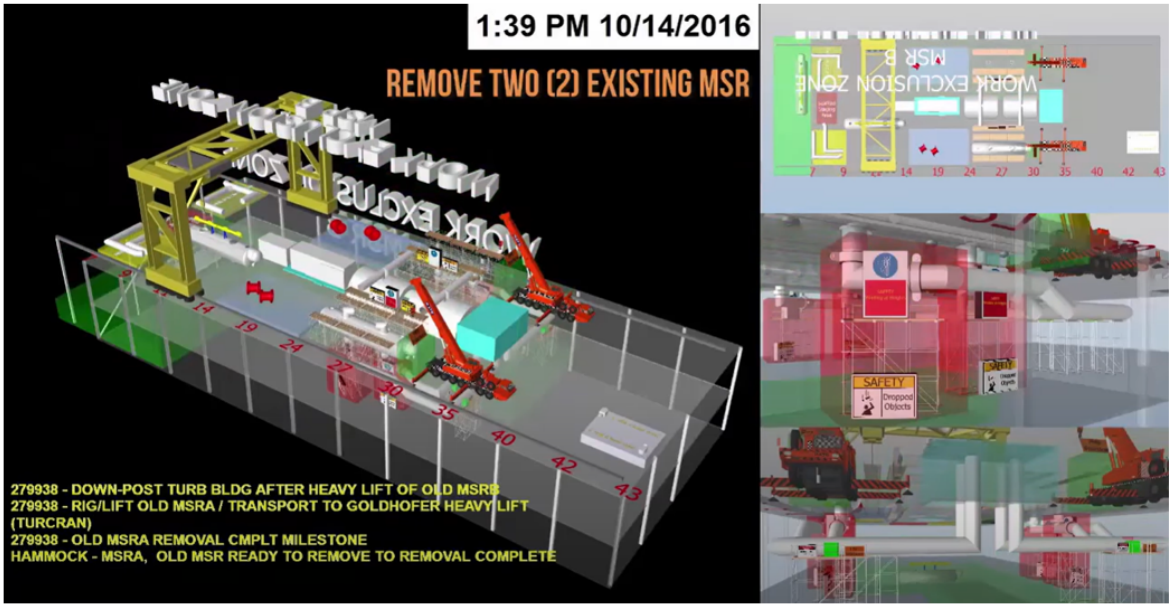

(a) Synchro4D Combining Physical Model with Functional legend, task codes, and time simulations

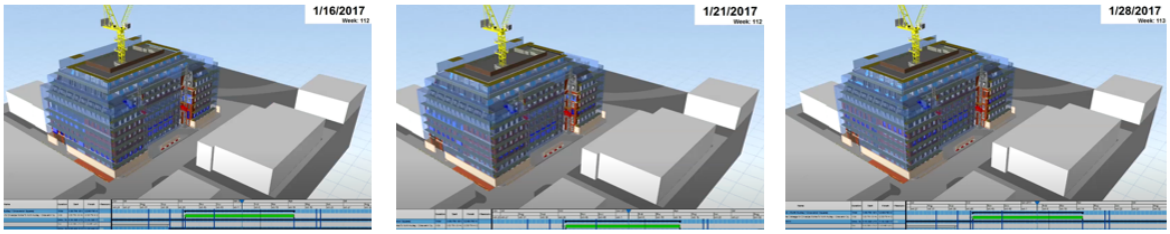

(b) Time-frames from Synchro4D displaying time simulation and Gantt Chart

Figure 6: Synchro4D Project Simulations (SYNCHRO, 2017)

The overall trajectory of BIM development is focused on complete lifecycle management, as suggested by BIM dimensionality or ND modeling. This philosophy assigns informational dimensions of data to the building information model based on purpose. The current dimensions are accepted as 3D (for two spatial dimensions), 4D (for the inclusion of time), 5D (the inclusion of costs), and 6D (the inclusion of facilities management) (ISE, 2021). Although there is ambiguity surrounding BIM beyond the 4D version, it has piqued interest due to its potential to integrate scheduling data. The capabilities of 4D BIM, which enable simulated planning, is one of the most attractive features marketed by most BIM software today. For instance, Synchro4D, shown in Figure 6, displays the potential of viewing the physical model with task codes and time simulations from design to production (SYNCHRO, 2017). The advantages of 4D BIM have been realized in some projects to date, including the planning of Peachtree Mansion in Atlanta, Georgia. Determining how all resources should be coordinated and how the construction sequence can be optimized was highly beneficial (Azhar et al., 2008). This simulated design and planning is a functionality that other industries are not yet able to realize today, including the ship design and shipbuilding industry.

The following section goes through the critical features of BIM in terms of the product data model it uses and the collaborative processes surrounding the maintenance of such a model.

Features of BIM

Collaboration Mandated by BIM. BIM relies heavily on collaboration, which is well-established with BIM's definition of Levels of Maturity (LOM). BIM's LOM is defined as 'measures of how well each party's information is structured for use in the federation by a collaborator without requiring significant remodeling for their purpose' (ISE, 2021). There are currently three levels of BIM based on LOMs: Level 0 is unstructured, Level 1 is partially structured unfederated data, Level 2 is a structured federated information model, and Level 3 is a server-based object information model hosted on a queryable database. To meet Level 2 standards, which is the stage mandated in the UK for public projects (Cotter, 2023), data needs to be available for contractual client demands and stored in information-rich and federated 3D models. Other non-graphical formats should also be agreed upon, along with an execution plan to use and exchange data with such formats. Acceptable file formats include COBIe or Construction Operations Building Information Exchange (for exchanging meta-data) and other native data formats as long as they are specified in the BIM Execution Plans (BEPs) (ISE, 2021).

Structured and Federated Information Models. To cater to the specific needs of the construction industry, the IFC-neutral data schema was developed by IAI (currently buildingSMART) as a framework for the exchange of building information. IFC consists of multiple entities organized into an object-based inheritance hierarchy. The implementation of IFC into BIM solutions comes in the form of defining attributes for building components already present for the user in a BIM software. The benefit of using IFC is that the substantial number of these descriptive entities can enable a comprehensive view of building information. The IFC contains four conceptual layers in its building model: domain, interoperability, core, and resource. These layers follow a strict referencing hierarchy or ladder to ensure that the information is complete and easily maintainable (buildingSMART, b; ISE, 2021). Compared to STEP's AP 225, which is STEP's product model definition for building construction, IFC is also considered to have more representation possibilities (Chen, 2012; Burkett and Yang, 1995).

The latest version of IFC is the IFC4, which includes a definition of construction scheduling task via the ifcTask (buildingSMART, a). This entity enables the linking of building elements to the task of a construction schedule for simulation, as shown in Figure 7. Other entities in IFC4 include ifcresourcetime, which captures the time-related information about a construction resource, further linking time data with planning information. These definitions are the backbone of 4D BIM functionalities, as shown in Figure 6.

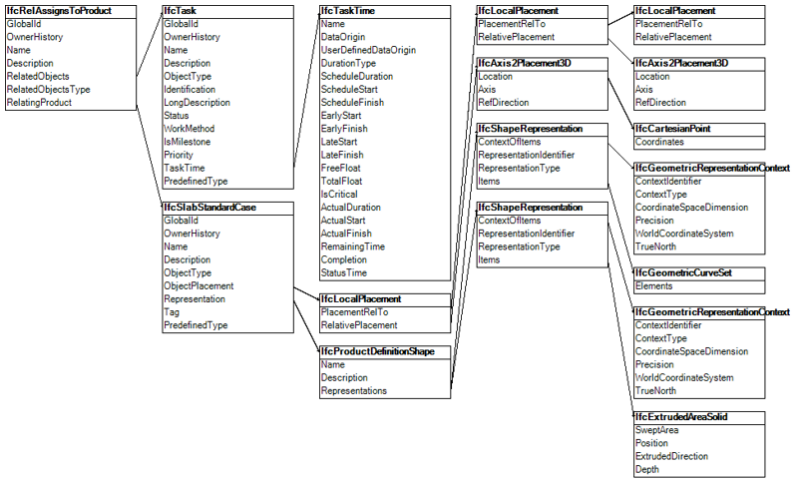

Figure 7: Definition of a IFC4 - ifctask Entity (buildingSMART, a)

Defined Process for Implementation and Maintenance. It is crucial for companies implementing BIM to have a well-defined pipeline that encourages collaboration and ensures compliance with BIM mandates. Without the use of BIM workflow, the benefits of BIM would not be realized. Several documents are necessary for implementation – including the Exchange Information Requirements (EIR) and BEPs. Hence, in trying to execute BIM, companies must ensure that (1) a clear articulation of what information is required from each participant is contained in the EIR document and (2) a defini-

tion of how each participant will provide such information is written in the BEPs. Defining goals, project milestones, and procedures for data exchange is therefore crucial in the BIM process (ISE, 2021).

To help facilitate these processes, a shared data environment called Common Data Environment (CDE), as shown in Figure 8, is used. In BIM, a CDE is a centralized system that compiles, manages, and distributes all project documentation. CDE also defines the states for developing and sharing a version of the design before it is handed over to the client. Without proper enforcement of these procedures, the risk still exists of creating isolated islands of information and outdated versions of the building model in the process (ISE, 2021; Borrmann et al., 2018).

Due to the availability of platforms that enable a seamless adoption of BIM today, BIM has become a standard practice in countries like Finland, Singapore, South Korea, and the US. BIM is mandatory for government projects in some countries, such as the UK (Cotter, 2023). Client demands and regulations have led to a vast proliferation and development of tools that deliver BIM capabilities, which today include Autodesk Revit, Autodesk Navisworks, GraphiSOFT ArchiCAD, Bentley Arch, and TEKLA, among others (Rice, 2010).

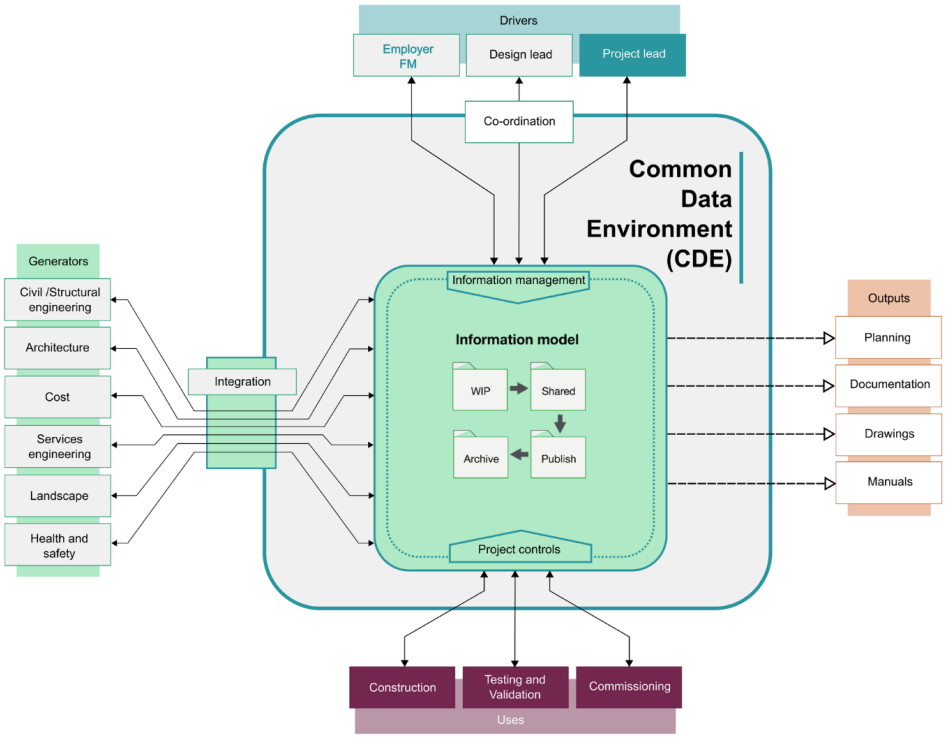

Figure 8: BIM Common Design Environment (ISE, 2021)

DISCUSSION AND COMPARISON

This paper has so far highlighted the ongoing efforts of both shipbuilding and AEC industries to improve asset information management. While the AEC industry has made significant progress with the use of BIM, the shipbuilding industry still needs to catch up in developing and adopting a standardized ship product data model. While both industries are unique, there is potential for cross-industry learning, especially from the shipbuilding side.

In both AEC and shipbuilding, the definition of the product data model is more or less analogous to each other. The differences mainly lie in the development and maintenance of such product data models. While current efforts, as with DNV-RP-A204's adoption guidelines (DNV AS, 2023), provide policies and aspirational procedures for addressing these gaps, the

actual implementation has not been fully realized. We converge to four gaps in the adoption of a cohesive ship product data model, including an assessment of where BIM's solutions stack in addressing these gaps:

1. Undefined ship product data model representation that is unable to incorporate multi-domain ship data incorporating time, process, and functional information
2. The lack of industry-wide data exchange standards impeding interoperability
3. The lack of an IPDE that impedes collaboration
4. The lack of data management protocols to support the IPDE, modeling standards, and exchange standards

Inflexible Ship Model Representation and undefined exchange standards. Current data modeling standards are outdated to suit the shipbuilding industry's needs. The rigid representations defined in ISO standards, unfortunately, impose the following challenges: (1) they are not easy to customize for the wide range of shipyards today, and (2) they are not flexible for the diversity of projects (proposals vs. detailed) in a single company that has varying LODs. The latter also applies to the variety of customers ship designers may need to cater to, whether commercial or government clients. Customizing a product data model, as it is structured today based on ISO standards, to suit these diverse needs is infeasible, and the reuse of a ship product data model as a template is not practical unless ship systems are entirely transferable (Oh et al., 2008). The amount of disclosure that is possible based on client preferences or security protocols also impedes the transfer or reuse of design templates. Pollini and Meland, in a 1997 paper where they developed a bespoke Smart Product Model (SPM) for a shipyard, expressed that creating a product modeling system bespoke to a yard took an enormous amount of effort, where 'over 30,000 methods and object-oriented databases on the order of 2.5 gigabytes of data' were generated (Whitfield et al., 2003).

Well-defined product data models that are widely accepted help enable interoperability. Consistency in expressing data increases the successful exchange of information. Currently, the standardization required for information exchange remains vague, and ISO ship APs are limited to their respective domains, so there is limited focus on a comprehensive and holistic view of ship design information.

BIM manages the balance between collaboration and information security by utilizing tools and standards to create detailed and robust building information. In addition, it requires parties to define the extent of collaboration and agree upon neutral or native formats to use in the project through the use of BEPs and EIRs. BIM does not enforce a single solution but is flexible enough in implementation to suit the needs of the parties involved, whether these parties themselves have strict data security protocols or otherwise. This flexibility is reflected in the degrees of LOMs that clients can choose from. A similar framework can be applied to the shipping industry, whereby the level of federation in the data model and the degree of interoperability can vary to suit the diversity in the project types and client preferences. This can also cover various diverse LODs within a ship design company so that a lower level of federation can be applied for designs or early concepts with minimal design granularity. For more mature designs involving multiple parties, a high level of federation could be applied.

While this flexibility exists, BIM is still able to provide reliable and robust means to generate a comprehensive view of the building data via the IFC model. To compensate for the challenges of manually defining the model, IFC is intended to be used complementary with BIM software where .ifc files can be generated easily. This software can be used at various stages of maturity of a design, such that it is compatible with designs with low and high data fidelity.

Lack of Data Management Protocols and Integrated Development Environment (IPDE). Provided formats exist to enable data exchange, an environment that allows and facilitates this exchange can only be fostered with collaboration. Enabling this environment is not yet well understood in commercial and large-scale contexts in shipbuilding, as open standards are not the norm and shipbuilding stakeholders are heavily dispersed. Luming and Singh (2015) cites that the shipbuilding's position in collaboration can best be described with the One-CAD Solution, which is a mentality focused on using the same CAD tools to reduce interoperability and communication issues. This mentality, however, locks shipyards to specific proprietary software.

BIM addresses these issues by primarily focusing on collaboration. The success of BIM implementation relies heavily on two factors - the availability of BIM tools and the shared ownership of the BIM process among the technical team and management. These BIM tools are intended to provide a secure and common design environment or CDE, covering the database and data management components. The shared ownership of the BIM process incentivizes the disciplined use of these tools to make the most of their capabilities.

NOTES FOR DEVELOPERS

Shipbuilding has a long history of attempts to handle dense technical and planning databases. This has presented an ironic dilemma where the industry has a good understanding of the challenges that come with big data but needs to have updated data management solutions. This paper converges to reevaluating what is possible with technology-driven and culture-driven changes related to product data management. Specifically, highlighting the following considerations for future developers:

1. Implementation of industry-acceptable data modeling and data exchange standards custom to shipbuilding needs
2. Development of an IPDE environment for managing custom ship product data models

A BIM-like solution that incorporates multi-domain product data models specific to the industry and managed within a collaborative IPDE environment can help realize 4D Shipbuilding akin to 4D BIM. Despite the challenges that already exist in the definition of a ship product data model, as listed in the previous section, investing in the potential of a BIM-like solution is still worthwhile, provided the aspirational capabilities this model can provide, as summarized in Figure 9.

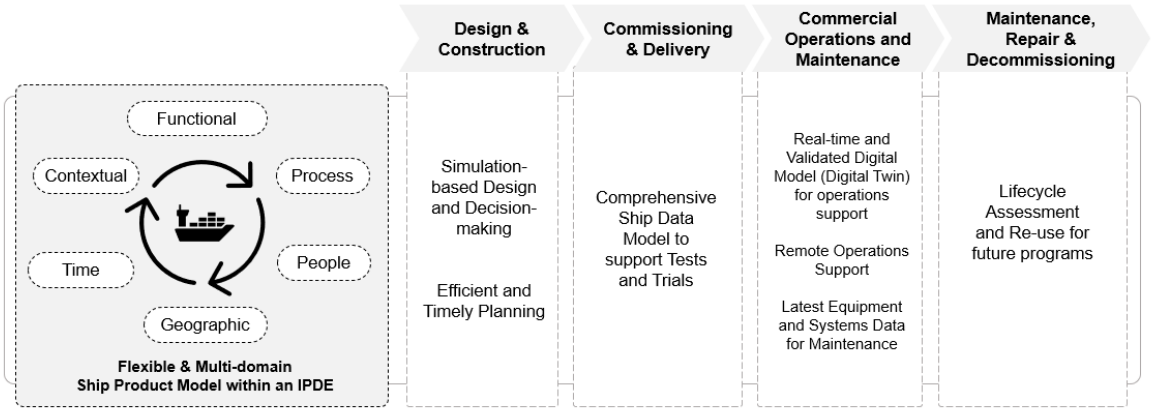

Figure 9: A Multi-domain and Federated Ship product data model to support various lifecycle phases

Today, no single tool has transformed the ship design and shipbuilding industry like BIM. An ongoing project that aims to fill this gap is the EU HORIZON SEUS Project, addressing inefficiencies in ship design and operations using computational tools (Gaspar et al., 2023). Gleaming into software practices, the project aims to tackle the challenges of defining, using, and managing a ship product data model throughout its entire lifecycle to reduce the time of ship production by 20 to 30 percent.

A current paradigm the project is investigating is graph data modeling. By investigating a more flexible data modeling paradigm, as opposed to the existing rigid entity-relationship models commonly used today, it may be possible to establish connections across multiple data domains with minimal effort. In addition to investigating ways to develop a multi-domain

ship product data model, the project aims to understand interoperability solutions and create a PLM software to encourage collaboration among various stakeholders. Other considerations it aims to note include data quality and security of the model, noting risks that may be posed by lack of data accuracy and cyber security. These developments are done with close industry and academic collaboration, hoping to explore solutions that can realize the same impacts BIM has had in the AEC industry.

CONCLUSION

This paper reviewed the history of initiatives related to adopting and understanding a cohesive ship product data model. It was found that despite shipbuilding's long history of tackling interoperability issues, actual solutions to address these problems remain limited. The inflexibility of ship product data models, the lack of technology enabling an integrated design environment (IPDE), and the absence of data exchange standards in the industry were consistently determined to be limiting factors in the realization of ship product data models.

BIM, especially the concept of 4D BIM from the AEC industry, poses a refreshing take on solutions to address these issues in their sector. It demonstrates the importance of standards related to product data modeling. BIM's CDE, a digital centralized platform for developing and sharing building design and operations data, can be a template for shipbuilding's IPDE concept. Additionally, IFC, as BIM's modeling schema that currently encapsulates not only geometrical data but also time data, proves the possibility of a multi-domain product data model that can be used to integrate planning and design domains. Future developers can take inspiration from these elements to create a platform, bespoke for shipbuilding, that addresses interoperability in today's software practices. The success of BIM, not only as a tool but also as a process, may also encourage ship design and shipbuilding managers to incorporate technology-enabled collaboration for more efficient ship design and operations.

CONTRIBUTION STATEMENT

Author 1: Writing – original draft; conceptualization; data curation; visualization
Author 2: Conceptualization; supervision
Author 3: Conceptualization; supervision; project administration
Author 3: Writing – original draft; conceptualization; data curation

REFERENCES

Aish, R. (1986). Building Modelling: The Key to Integrated Construction CAD. *CIB 1986: International Symposium on the Use of Computers for Environmental Engineering Related to Buildings*.

Andritsos, F. and Perez-Prat, J. (2000). The Automation and Integration of Production Processes in Shipbuilding 2000. Technical report.

Autodesk (2002). Building Information Modeling (Whitepaper). Technical report.

Azhar, S., Nadeem, A., Mok, J. Y. N., and Leung, B. H. Y. (2008). Advancing and Integrating Construction Education, Research & Practice.

Borrmann, A., Beetz, J., Koch, C., Liebich, T., and Muhic, S. (2018). Industry foundation classes: A standardized data model for the vendor-neutral exchange of digital building models. In *Building Information Modeling: Technology Foundations and Industry Practice*, pages 81–126. Springer International Publishing.

Bronson, J. A., Fonseca, I. A., and Gaspar, H. M. (2024). Challenges Towards an Integrated Digital Twin Platform for Maritime Systems: Tackling Shifts in Data Ownership. [Manuscript accepted for publication].

buildingSMART. E.13.1 Construction scheduling task. Retreived from https://standards.buildingsmart.org/.

buildingSMART. Standards Introduction. Retrieved from https://standards.buildingsmart.org/.

Burkett, W. C. and Yang, Y. (1995). *The STEP Integration Information Architecture*, volume 11, pages 136–144. Springer-Verlag London Limited.

Chen, D. (2012). *Information Management for Factory Planning and Design*. PhD thesis.

Cotter, K. (2023). How Building Information Modelling (BIM) is transforming the construction industry. Retrieved from https://www.hsbcad.com/news/how-building-information-modelling-bim-is-transforming-the-construction-industry.

DNV AS (2023). DNV-RP-A204 RECOMMENDED PRACTICE: Assurance of Digital Twins. Technical report.

Eastman, C., Fisher, D., Lafue, G., Lividini, J., Stoker, D., and Yessios, C. (1974). An Outline of the Building Description System. Technical report.

Edelman, J., Lowe, S., and Oswalt, M. (2018). *Network Programmability and Automation*. O'Reilly Media.

Emblemsvåg, J. (2014). Lean project planning in shipbuilding. *Journal of Ship Production and Design*, 30(2):79–88.

Erikstad, S. O. and Fathi, D. E. (1999). Applying the STEP Shipbuilding Protocols as a Basis for Integrating Existing In-House Ship Design Applications.

Gale, P. (2003). THE SHIP DESIGN PROCESS. In Lamb, T., editor, *Ship Design and Construction*, volume I. Jersey.

Gallaher, M. P., O'Connor, A. C., Dettbarn, Jr., J. L., and Gilday, L. T. (2004). Cost Analysis of Inadequate Interoperability in the U.S. Capital Facilities Industry. Technical report.

Gaspar, H., Seppäla, L., Koelman, H., and Jorge Garcia Agis, J. (2023). Can European Shipyards be Smarter? A Proposal from the SEUS Project. *Computer and IT Applications in Marine Industries 2023*.

Gischner, B. (2006). Integrated Shipbulding Environment Consortium (ISEC): ISE-4 Final Report. Technical report.

Gischner, B., Bongiorni, B., Howell, J., Kassel, B., Lazo, P., Lovdahl, R., Vogtner, G., and Wilson, A. (1997). STEP Implementation for US Shipbuilding - MariSTEP Progress Report. Technical report, The Society of Naval Architects and Marine Engineers, Jersey City.

Grieves, M. (2022). Intelligent digital twins and the development and management of complex systems. *Digital Twin*, 2:8.

Härder, T. (2005). DBMS Architecture-the Layer Model and its Evolution. Technical report. Retreived from https://api.semanticscholar.org/CorpusID:16418586.

ISE (2021). An Introduction to Building Information Modelling (BIM). Technical report, London.

ISO (2003). ISO 15926-2 Industrial automation systems and integration-Integration of life-cycle data for process plants including oil and gas production facilities-Part 2: Data model. Technical report.

ISO (2004a). ISO 10303-11 Description methods: The EXPRESS language reference manual. Technical report.

ISO (2004b). ISO 15926-1 Industrial automation systems and integration-Integration of life-cycle data for process plants including oil and gas production facilities-Part 1: Overview and fundamental principles. Technical report.

ISO (2022). IEC 81326-1 Industrial systems, installations and equipment and industrial products - Structuring principles and reference designations - Part 1: Basic rules. Technical report.

ISO (2023). ISO 10303-2 Industrial automation systems and integration-Product data representation and exchange-Part 2: Vocabulary. Technical report.

ISO (2024). ISO 10303-1 Industrial automation systems and integration-Product data representation and exchange-Part 1: Overview and fundamental principles. Technical report.

Kelly, J. (1985). The Product Data Exchange Standard (PDES). Technical report.

Koenig, P., MacDonald, P., Lamb, T., and Dougherty, J. (1997). Towards a Generic Product-Oriented Work Breakdown Structure For Shipbuilding. In *1997 Ship Production Symposium*, Louisiana.

Kramer, T. R., Palmer, M. E., Feeney, A. B., Mosbacher, R. A., and Lyons, J. W. (1992). Issues and Recommendations for STEP Application Protocol Framework. Technical report.

Laakso, M. and Kiviniemi, A. (2012). The IFC Standard - A Review of History, Development, and Standardization. *Journal of Information Technology in Construction (ITcon)*, 17:134–161.

Love, P. E. and Sing, C. P. (2013). Determining the probability distribution of rework costs in construction and engineering projects. *Structure and Infrastructure Engineering*, 9(11):1136–1148.

Luming, R. and Singh, V. (2015). Comparing BIM in Construction with 3D Modeling in Shipbuilding Industries: Is the Grass Greener on the Other Side? In *12th IFIP International Conference on Product Lifecycle Management (PLM)*, pages 193–202. Doha.

Manchinu, A. and McConnell, F. (1977). The SFI Coding and Classification System for Ship Information. In *REAPS Technical Symposium*, Louisiana.

Mavris, D. N. and Delaurentis, D. (2000). METHODOLOGY FOR EXAMINING THE SIMULTANEOUS IMPACT OF REQUIREMENTS, VEHICLE CHARACTERISTICS, AND TECHNOLOGIES ON MILITARY AIRCRAFT DESIGN. *ICAS 2000 CONGRRESS*, 144(1).

McDermid, J. (2013). *Software Engineer's Reference Book*. Butterworth-Heinemann.

Murphy, J. (1992). NIDDESC-Enabling Product Data Exchange for Marine Industry. In *Ship Production Symposium*. Louisiana.

NAVSEA (2012). SHIP DESIGN MANAGER (SDM) AND SYSTEMS INTEGRATION MANAGER (SIM) MANUAL. Technical report.

Nowacki, H. (1995). *NEUTRABAS - A Neutral Product Definition Database for Large Multifunctional Systems*. Springer.

NSRP (1986). Product Work Classification and Coding (Prepared by TODD Shipyard Corporation). Technical report, Seattle.

NSRP ASE (2007). NSRP Systems Technology Panel Final Report. Technical report.

Oh, D. K., Jeong, Y. H., Kim, Y. G., Shin, J. G., Yeo, Y. H., and Ryu, C. (2008). Development of product model management system for naval shipbuilding. *Journal of Ship Production*, 24(2):82–91.

Pal, M. (2015). SHIP WORK BREAKDOWN STRUCTURES THROUGH DIFFERENT SHIP LIFECYCLE STAGES. *International Conference on Computer Applications in Shipbuilding*.

Patni, J. C., Sharma, H. K., Tomar, R., and Katal, A. (2021). *Database Management System*. Chapman and Hall/CRC, Boca Raton.

Rachuri, S., Subrahmanian, E., Bouras, A., Fenves, S. J., Foufou, S., and Sriram, R. D. (2008). Information sharing and exchange in the context of product lifecycle management: Role of standards. *CAD Computer Aided Design*, 40(7):789–800.

Rando, T. C. (2001). XML-Based Interoperability in the Integrated Shipbuilding Environment (ISE). *Journal of Ship Production*, 17(02):69–75.

Rice, S. (2010). The Perceived Value of Building Information Modeling in the U.S. Building Industry. *Journal of Information Technology in Construction*, 15:185–201.

Rigterink, D. (2014). *Methods for Analyzing Early Stage Naval Distributed Systems Designs, Employing Simplex, Multislice, and Multiplex Networks*. PhD thesis.

Ross, J. (1997). Evaluation of Shipbuilding CAD/CAM/CIM Systems-Phase II (Requirements for Future Systems). Technical report.

Ross, J. (2003). Computer-based Tools. In Thomas Lamb, editor, *Ship Design and Construction*, volume I, chapter 13. Society of Naval Architects and Marine Engineers, Jersey City.

Ross, J. M. and Garcia, L. (1998). Making the Jump to Product Model Technology. *Journal of Ship Production*, 14(01):15–26.

Samonas, S. and Coss, D. (2014). THE CIA STRIKES BACK: REDEFINING CONFIDENTIALITY, INTEGRITY AND AVAILABILITY IN SECURITY. *Journal of Information System Security*, 10(2).

Sinoh, S. S., Ibrahim, Z., Othman, F., and Muhammad, N. L. N. (2020). Review of BIM literature and government initiatives to promote BIM in Malaysia. *IOP Conference Series: Materials Science and Engineering*, 943(1):012057.

Stachowski, T.-H. and Kjielen, H. (2017). HOLISTIC SHIP DESIGN - HOW TO UTILISE A DIGITAL TWIN IN CONCEPT DESIGN THROUGH BASIC AND DETAILED DESIGN. *International Conference on Computer Applications in Shipbuilding*, pages 26–28.

SYNCHRO (2017). SYNCHRO 4D BIM/VDC Construction Project Management. Retrieved from https://www.youtube.com/watch?v=sX0NUKDJ3b4.

Welsch, M., Lynch, J., and Brun, P. (1991). A Data Model for the Integration of the Pre-commissioning Life-cycle Stages of the Shipbuilding Product. Technical report, The Society of Naval Architects and Marine Engineers, Jersey City.

Whitfield, R. I., Duffy, A. H., Meehan, J., and Wu, Z. (2003). Ship Product Modeling.

Wierzbicki, M., De Silva, C. W., and Krug, D. H. (2011). BIM-HISTORY and TRENDS. *International Conference on Construction Applications of Virtual Reality*.

Wyman, J., Wooley, D., Gischner, B., and Howell, J. (1997). Development of STEP Ship Model Database and Translators for Data Exchange Between Shipyards. *Journal of Ship Production*, 13(2):111–124.

Xantic (2001). SFI® Group System-Product Description. Technical report.

Zerbst, C. (2023). OCX on the Way from Research to Industry Practice. *Computer and IT Applications in the Maritime Industries 2023*, pages 127–133.

Proceedings of 15th International Marine Design Conference (IMDC-2024)
June 2-6, 2024
Amsterdam, the Netherlands

Modular Ship Design: Rapid Prototyping and Enhancing Efficiency through Design Modules

Minjoo Choi[1,*] and Jaekyeong Lee[1]

ABSTRACT

In this paper, we introduce a modular approach to ship design, utilizing design modules to streamline the initial design phases. Ships are conceived as combinations of a primary 'ship module' and various 'design modules' tailored for specific spaces. These modules encompass predefined geometries, layouts, and equipment configurations. We introduce an optimization model that integrates decision variables for ship attributes and configuration variables for module selection. Through this framework, we aim to simplify design complexities, accelerate the production of detailed drawings, and foster innovation in ship design methodologies.

KEY WORDS

Modularity, Configure-to-order, Ship module, Design module, Modular ship.

INTRODUCTION

Modularity, as elucidated by Baldwin and Clark (2000), embodies a structured design framework wherein parameters and tasks intricately interconnect within modules, while retaining independence across them. These modules act as discrete units within a system, facilitating integration or separation through standardized interfaces, thereby offering manifold advantages across the lifecycle of modular ships.

In the realm of ship design, modularity emerges as a pivotal approach fostering innovation and efficiency. It enables designers to capitalize on previous designs and streamline representations within modules to effectively navigate the inherent complexities of maritime vessels (Papanikolaou, 2010). This simplification is paramount given the multitude of subsystems and diverse stakeholder requirements inherent in comprehensive ship designs. Moreover, principles underlying design building blocks (Andrews, 2011) and the packing approach (Van Oers, 2011), which employ independent design elements termed 'blocks' and 'objects', respectively, closely align with the concept of modularity.

Furthermore, modularity significantly influences ship production processes. By enabling parallel manufacturing and testing of modules, it reduces production timelines and enhances the efficiency of dry dock operations, a vital resource for shipyards. Additionally, standardized interfaces foster expanded outsourcing opportunities, further streamlining production processes.

In the operational phase, modularity facilitates concepts like ‘evolutionary acquisition’ and ‘mission flexibility,’ as delineated by Abbott et al. (2003). Unlike conventional ship acquisition processes, evolutionary acquisition defers investment decisions for modules until more information becomes available, aligning investment decisions with operational needs.

The SIMOSYS project from 2014 to 2018, spearheaded by Erikstad and Choi, proposed optimization models for the design of modular ships, leveraging modularity to navigate uncertainties in the operational phase, dubbing such ships as modular

[1] Division of Naval Architecture and Ocean Systems Engineering, Korea Maritime and Ocean University, Busan, Republic of Korea; ORCID: 0000-0001-6797-0210 (Minjoo Choi)

* Corresponding Author: minjoo.choi@g.kmou.ac.kr

Submitted: 24 February 2024, Revised: 2 May 2024, Accepted: 3 May 2024, Published: 7 May 2024

Conference paper, DOI: https://doi.org/10.59490/imdc.2024.765 e-ISSN: 3050-4864

adaptable ships (MASs). However, in the design of MASs, complexity may arise in valuating flexibility due to their dynamic nature in responding to contextual changes. Addressing this challenge, Choi and Erikstad (2017) and Choi et al. (2017) present optimization models combining module configuration and valuation problems of MASs. Additionally, Choi et al. (2018) propose an optimization model for the design of the platform module of MASs, which serves as the basis accommodating various mission-related modules.

This paper is in alignment with the objectives set forth by the SIMOSYS project, placing a significant emphasis on enhancing module configuration and valuation methods while taking into account the layout, geometry, and scalability of modules. Scalability plays a pivotal role in augmenting the reusability of modules to effectively address the diverse requirements of stakeholders. As a result of addressing these optimization challenges, the overall design layout can be derived, facilitating a comprehensive solution to the design problem at hand.

DESIGN PROCESS OF MODULAR SHIPS

According to Ulrich (1995), modularity can be categorized into different types based on interface diversity and the presence of a main body. These types include sectional, bus, and slot modularity. Salvador et al. (2002) further elaborate on slot-type modularity, distinguishing between combinatorial modularity and component-swapping modularity. For the design of MASs, component-swapping modularity is often suitable, as the hull serves as the main body accommodating various module configurations. Unlike bus modularity, component-swapping modularity does not necessitate identical interfaces, making it a more versatile option. Figure 1 provides a visual representation of these four types of modularity.

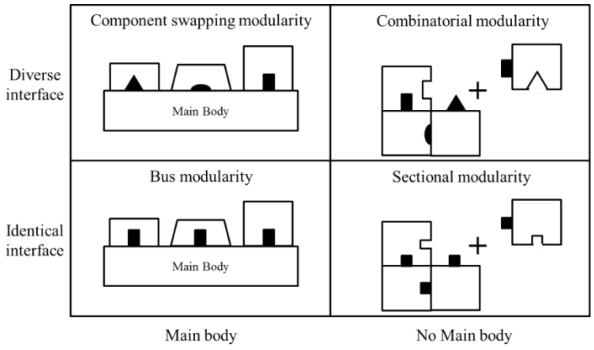

Figure 1: Four Types of Modularity Defined by Salvador et al. (2002).

The traditional ship design process follows a top-down approach, where designers refine options for a benchmark ship iteratively, ultimately reaching a finalized design. This aligns with a 'build-to-order' strategy, aiming to deliver customized products to each customer. Conversely, the module-based design process operates bottom-up. Here, design alternatives are generated by configuring predeveloped modules, indirectly determining design characteristics through module configuration. This facilitates the 'configure-to-order (CTO)' strategy, where multiple design projects utilize standard modules developed prior to confirmed orders, based on demand forecasts. Implementing the CTO process allows design teams to reduce development time and costs while enhancing design reliability with tested technologies. Additionally, rapid prototyping enhances customer communication, crucial for defining appropriate key performance indicators for design projects. Figure 2 depicts ship design projects employing the CTO process.

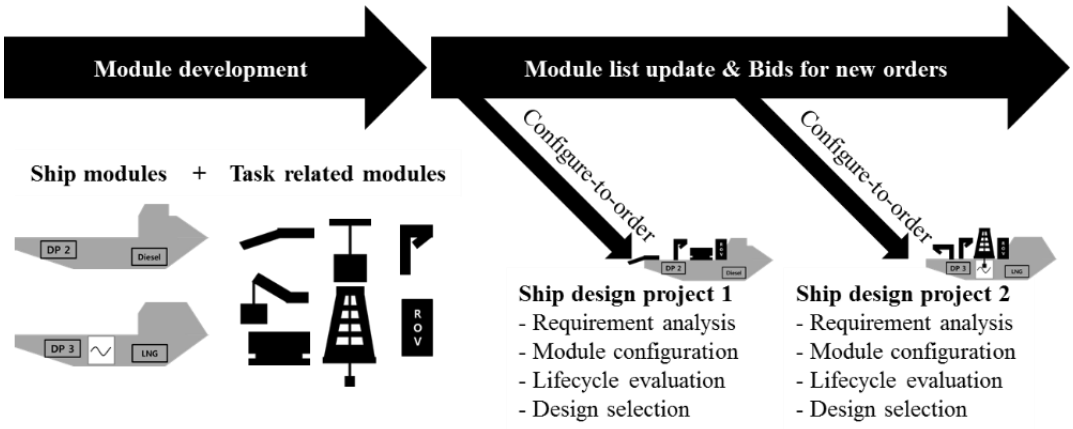

Figure 2: Ship Design Projects Based on the Configure-To-Order Strategy (Choi and Erikstad, 2017).

While Figure 2 offers valuable insight into the CTO process for modular ships, a deeper exploration is warranted to elucidate the intricate steps involved in obtaining detailed designs, such as general arrangements, through this method.

SHIP MODULES

Ship modules are the main body of modular ships in the component swapping modularity. In an optimization point of view, ship modules can be represented by decision variables and parameters, in which the decision variables indicate the attributes the value of which needs to be determined in the design problem, and the parameters indicate constant attributes the value of which are given. The choice of which design variables and constants to use to represent a ship module depends on the intended use of the ship module.

A ship module has its own properties but also spaces that are relatively high-level topology and geometry information acting as interfaces with other modules. Figure 3 describes an example of the ship module, in which the ship module has 7 spaces: steering gear room, main deck, store, stern deck, deck house, bow deck, and deck house up.

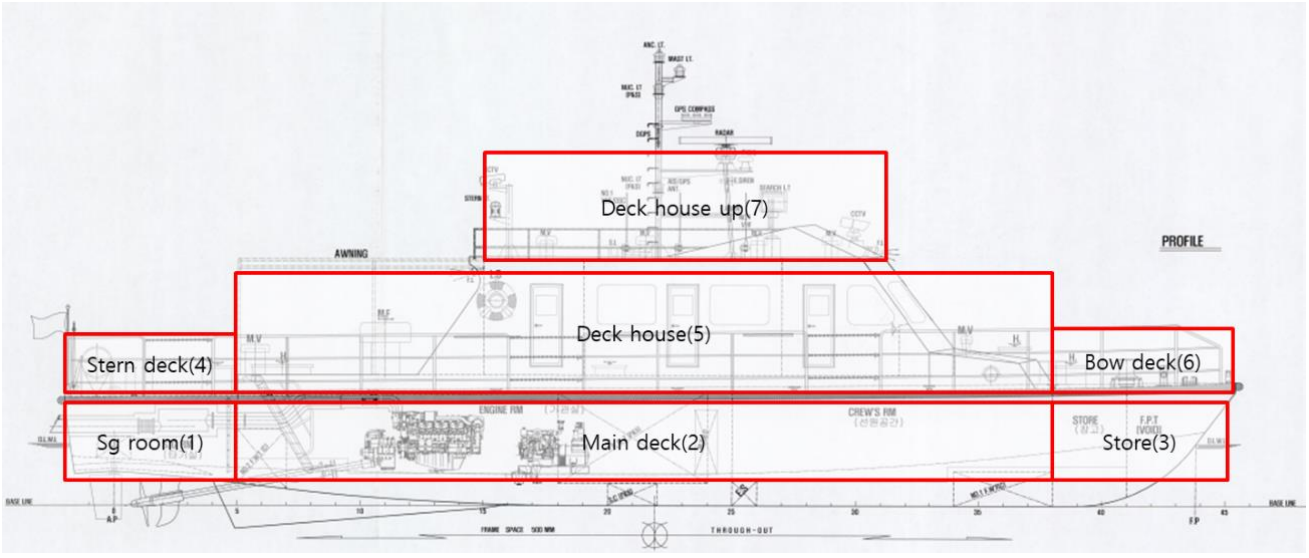

Figure 3: An Example of a Ship Module.

DESIGN MODULES

Because spaces in a ship module have only their boundary shape, the spaces need to be divided into more smaller subspaces. This is a highly complex problem that requires simultaneous consideration of geometry and topology. As the complexity of the

problem increases from an optimization perspective, finding good solutions becomes increasingly challenging. Therefore, this study introduces the concept of design modules to reduce the complexity of the problem.

The design modules are predeveloped partial designs which comprise subspaces. Each subspace has its geometry information and could have a set of equipment and its lower-level subspaces. Figure 4 describes examples of design modules of main deck and Figure 5 presents the schematic diagram that illustrates the relations between ship module, space, design module, subspace.

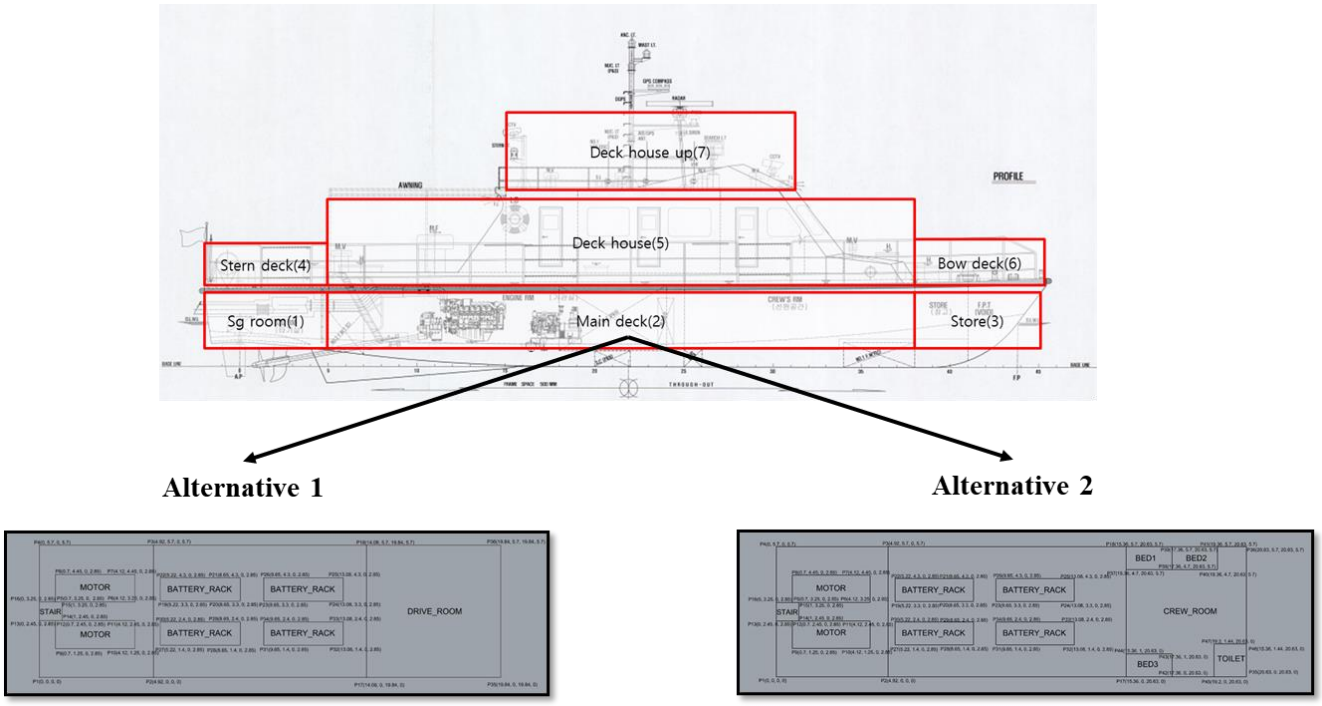

Figure 4: Two Design Module Alternatives of the Main Deck Space.

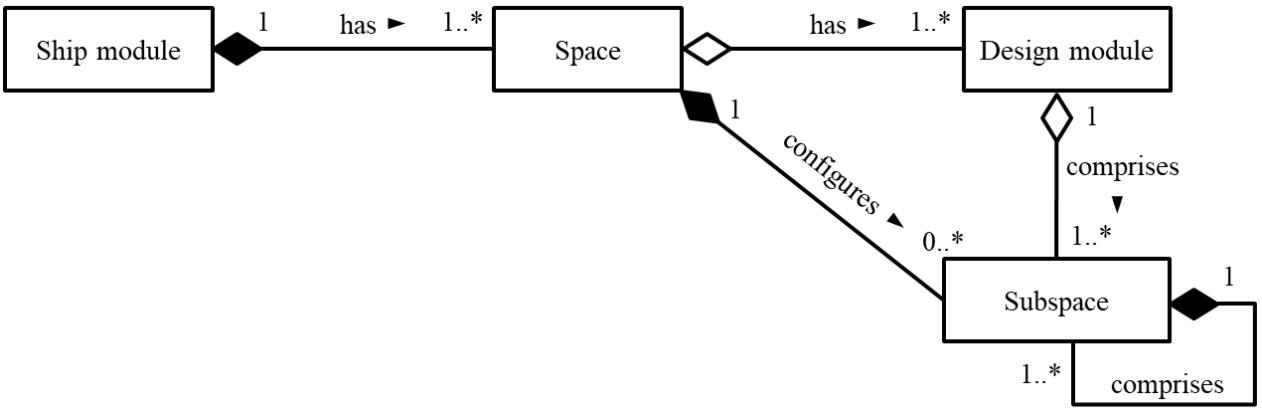

Figure 5: Schematic Diagram Between Ship Module, Space, Design Module, and Subspace.

Let's delve deeper into these alternatives. Figures 6 and 7 depict alternative 1 and 2, respectively, of the main deck space. A notable distinction between these alternatives lies in the presence or absence of the drive room and accommodation space. The selection of each module can vary depending on the specific accommodation requirements for the main deck space.

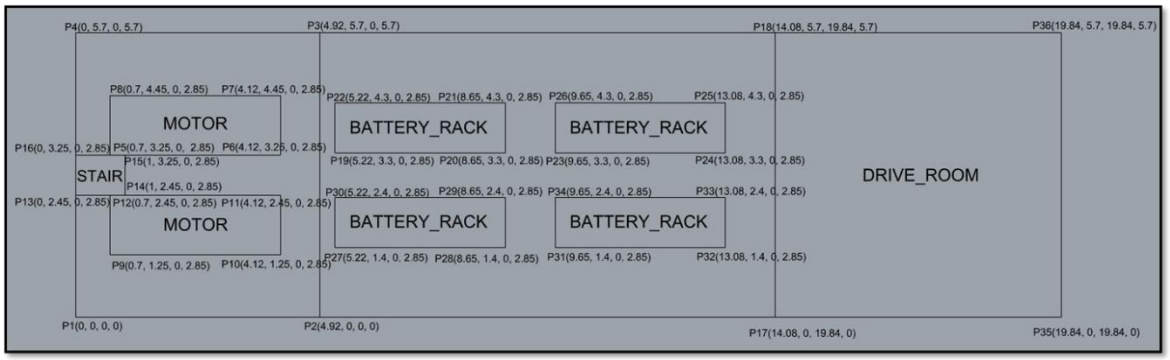

Figure 6: Design Module Alternative 1 of the Main Deck Space.

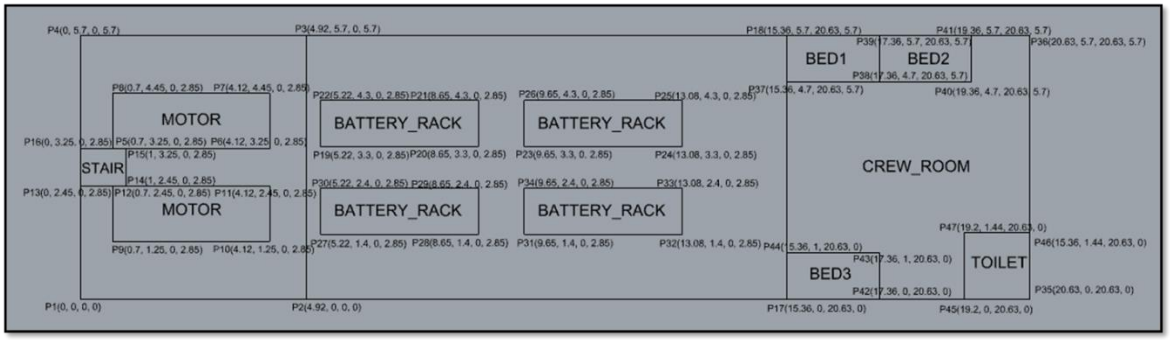

Figure 7: Design Module Alternative 2 of the Main Deck Space.

Because the design modules are predeveloped designs, the scale of the design modules needs to be adjusted to fit to the space where the design modules are assigned. Design modules are developed with scalability in mind to compensate for differences in basic form and allocated space size. The vertices of the detailed compartments constituting the design module are comprised of four pairs of values (x, y, a, b), where each value sequentially represents the x-coordinate, y-coordinate, x-scale factor, and y-scale factor. Here, the x and y coordinates denote the coordinates in the basic form, while the scale factors a and b are used to define the scalability of the design module, determining the new coordinates of the vertices through Equations 1 and 2.

$$\text{New } x = x + (\text{length of space along x-axis} / \text{length of ship module along x-axis} - 1) * a \quad [1]$$

$$\text{New } y = y + (\text{length of space along y-axis} / \text{length of ship module along y-axis} - 1) * b \quad [2]$$

Let's examine a more detailed example. In Figure 5, the design module includes spaces for a galley, toilet, and meeting room. The galley's shape can expand or contract based on the length of the allocated space along the y-axis, causing P6 and P7 to move vertically. However, its dimensions along the x-axis remain constant regardless of the allocated space's length in that direction. Conversely, alterations in the allocated space's dimensions along both the x and y axes do not affect the shape of the toilet. However, adjustments in both the x and y axes of the allocated space impact the configuration of the meeting room. Specifically, changes along the x-axis cause P8 and P9 to shift horizontally, while variations along the y-axis prompt vertical movements of P6 and P9. Notably, P2, P3, and P5 remain unaffected by adjustments in the dimensions along both axes of the allocated space.

Figure 8 illustrates the geometric alterations observed in the toilet. The x-scale factor and y-scale factor values for the toilet's vertices are set to 0, signifying that vertex coordinates remain constant regardless of the design module's allocation to different spatial configurations. Determining the scale factor values allows design module creators to accurately convey their design intentions.

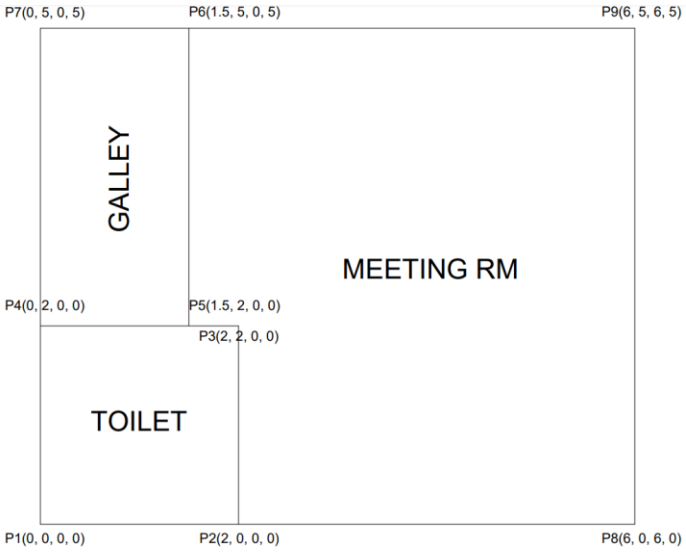

Figure 8: An Example of a Design Module That Comprises a Galley, Toilet, and Meeting Room.

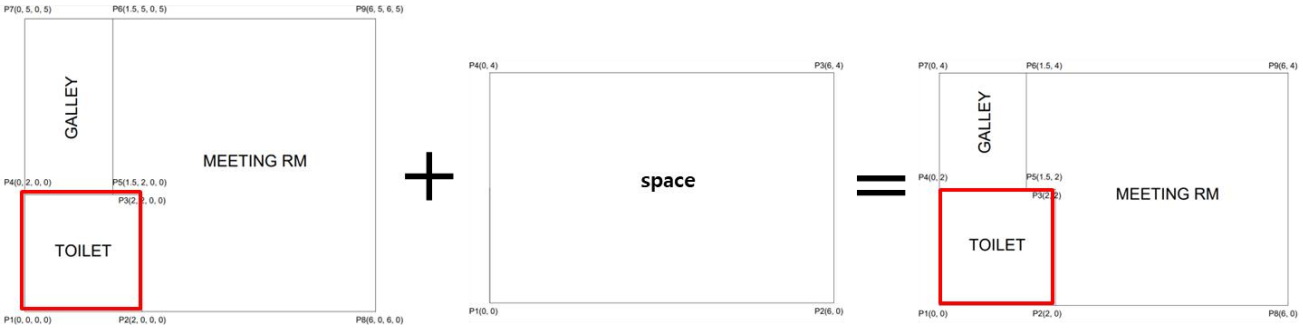

Figure 9: Geometry Changes When the Design Module Is Combined with a Space.

MATHEMATICAL MODEL FOR MODULAR SHIP DESIGN USING DESIGN MODULES

In this section, we introduce an optimization model tailored specifically for addressing design challenges inherent in modularity through the utilization of design modules. It is important to note that our approach assumes a static design problem, wherein dynamic changes occurring during the operational phase are not explicitly accounted for.

Sets:

$\boldsymbol{S}$	Set of spaces, indexed by s
$\boldsymbol{M_s}$	Set of design modules of space s, indexed by m
$\boldsymbol{P}$	Set of capabilities, indexed by p
$\boldsymbol{P^{MAX}}$	Subset of capabilities that need to be maximized, indexed by p
$\boldsymbol{P^{MIN}}$	Subset of capabilities that need to be minimized, indexed by p
$\boldsymbol{P^{GOAL}}$	Subset of capabilities that have a goal value, indexed by p
x	Set of ship variables, indexed by x_i
y	Set of module selection variables, indexed by y_{sm}

Parameters:

R_p^{MIN}	Minimum requirement of capability p
R_p^{MAX}	Maximum requirement of capability p
L_i^X	Lower boundary of basic variable x_i
U_i^X	Upper boundary of basic variable x_i
W_p	Weight of capability p
W_p^-	Weight of negative deviation of capability p
W_p^+	Weight of positive deviation of capability p

Variables:

x_i	i-th ship variable
y_{sm}	1 if design module m is selected for space s, 0 otherwise

Model:

$$\text{Min} \quad \sum_{p \in \boldsymbol{P^{MIN}}} W_p f_p(\mathbf{x},\mathbf{y}) - \sum_{p \in \boldsymbol{P^{MAX}}} W_p f_p(\mathbf{x},\mathbf{y}) + \sum_{p \in \boldsymbol{P^{GOAL}}} W_p^- d_p^- + W_p^+ d_p^+ \qquad [3]$$

$$\text{s.t.} \quad \sum_{m \in M_s} y_{sm} = 1 \qquad s \in \boldsymbol{S} \qquad [4]$$

$$f_p(\mathbf{x},\mathbf{y}) + d_p^- - d_p^+ = G_p \qquad p \in \boldsymbol{P^{GOAL}} \qquad [5]$$

$$d_p^-, d_p^+ \geq 0 \qquad p \in \boldsymbol{P^{GOAL}} \qquad [6]$$

$$R_p^{MIN} \leq f_p(\mathbf{x},\mathbf{y}) \qquad p \in \boldsymbol{P^{MIN}} \qquad [7]$$

$$f_p(\mathbf{x},\mathbf{y}) \leq R_p^{MAX} \qquad p \in \boldsymbol{P^{MAX}} \qquad [8]$$

$$x_i \in \{0,1\} \quad \text{if } x_i \text{ is a binary variable,}$$
$$L_i^X \leq x_i \leq U_i^X \quad \text{otherwise,} \qquad i \in \{1,\ldots,|\mathbf{x}|\} \qquad [9]$$

$$y_{sm} \in \{0,1\}. \qquad s \in \boldsymbol{S}, \mathrm{m} \in \boldsymbol{M}_s \qquad [10]$$

Equation [3] serves as the objective function, encompassing the overarching goals of the design process. It balances the minimization and maximization of various capabilities essential for the ship's performance while ensuring convergence towards a desirable outcome. Equation [4] guarantees the integrity of the design by stipulating that only one design module can be selected for each space, preventing redundancies or conflicting configurations. Equation [5] establishes a connection between the desired goals for specific capabilities and their actual achievement, employing negative and positive deviation variables to quantify the extent of any discrepancies. Equation [6] enforces the non-negativity constraint on the deviation variables, ensuring that any deviations from the desired goals are expressed as positive values, reflecting a proactive approach to addressing deficiencies. Equations [7] and [8] set the boundaries for the minimum and maximum requirements of each capability, respectively, ensuring that the design satisfies essential performance thresholds while avoiding over-specification. Equations [9] and [10] define the feasible ranges for the ship and module selection variables, allowing for binary decisions regarding the inclusion or exclusion of specific design elements within the overall configuration.

CONCLUSIONS

The modular approach presented in this paper offers several notable advantages in ship design methodologies. By employing design modules and optimization models, the design process is streamlined, leading to enhanced efficiency and innovation. Here, we discuss the implications and potential future directions stemming from this research.

Firstly, the use of modular design significantly simplifies the initial design phases. Instead of starting from scratch for each new ship design, designers can leverage predeveloped design modules, saving time and resources. This streamlined process accelerates the production of detailed drawings and prototypes, facilitating rapid prototyping and iteration cycles.

Secondly, the optimization model introduced in this paper enables optimal selection and configuration of design modules based on specific ship requirements. By considering both ship attributes and module configurations simultaneously, the model ensures that design decisions are made with the overarching goals of the ship's performance in mind.

Furthermore, the scalability of design modules enhances their reusability across different ship designs and types. This scalability not only improves design efficiency but also fosters innovation by allowing designers to experiment with different configurations and arrangements to meet diverse stakeholder needs.

However, it is important to acknowledge the limitations of the proposed approach, particularly in the context of 3D design. While the optimization model and design modules offer significant benefits in 2D design spaces, translating these concepts into three-dimensional environments poses challenges. Future studies could explore methodologies for extending the modular approach to 3D design, addressing issues such as spatial constraints, interface complexities, and computational requirements.

In conclusion, the modular ship design framework presented in this paper offers a promising pathway towards more efficient and innovative ship design methodologies. By simplifying design complexities, accelerating prototyping processes, and fostering innovation, this approach holds the potential to revolutionize the way ships are conceptualized and developed. Future research could focus on further refining optimization models, expanding the range of design modules, and addressing the challenges of 3D design integration.

CONTRIBUTION STATEMENT

Minjoo Choi: Conceptualization; data curation; methodology; software; writing – original draft; writing – review and editing; supervision; project administration; funding acquisition. **Jaekyeong Lee**: Data curation; methodology; validation; software; visualization.

ACKNOWLEDGEMENTS

This work received partial support from the Ministry of Trade, Industry & Energy of Korea. Firstly, through the HRD program for industrial innovation, specifically the 'Smart Yard Professional Human Resources Training Project' (P0017006), and secondly, via the project (20018667) focusing on 'Development of an Integrated Ship Design System for Hull, Compartment, Basic Calculation, and Loading Guidance Using Artificial Intelligence Technology.'

REFERENCES

Abbott, J., Devries, R., Schoenster, W., Vasilakos, J., Firebaugh, M., Malchiodi, A., & Goddard, C. (2003). The impact of evolutionary acquisition on naval ship design. Transactions Society of Naval Architects and Marine Engineers (SNAME), 111, 259-286.

Andrews, D. J. (2011). Marine requirements elucidation and the nature of preliminary ship design. Transactions Royal Institution of Naval Architects (RINA), Vol 153, Part A1, International Journal Maritime Engineering (IJME), Jan-Mar 2011.

Baldwin, C. Y., & Clark, K. B. (2000). Design rules: The power of modularity (Vol. 1). Cambridge: MIT press.

Choi, M., & Erikstad, S. O. (2017). A module configuration and valuation model for operational flexibility in ship design using contract scenarios. Ships and Offshore Structures, 12(8), 1127-1135.

Choi, M., Rehn, C. F., & Erikstad, S. O. (2018). A hybrid method for a module configuration problem in modular adaptable ship design. Ships and Offshore Structures, 13(4), 343-351.

Choi, M., Erikstad, S. O., & Chung, H. (2018). Operation platform design for modular adaptable ships: Towards the configure-to-order strategy. Ocean Engineering, 163, 85-93.

Papanikolaou, A. (2010). Holistic ship design optimization. Computer-Aided Design, 42(11), 1028-1044.

Salvador, F., Forza, C., & Rungtusanatham, M. (2002). Modularity, product variety, production volume, and component sourcing: theorizing beyond generic prescriptions. Journal of Operations Management, 20(5), 549-575.

Van Oers, B. J. (2011). A packing approach for the early stage design of service vessels. PhD Thesis, TU Delft.

Proceedings of 15th International Marine Design Conference (IMDC-2024)
June 2-6, 2024
Amsterdam, the Netherlands

Characterizing Three-Dimensional General Arrangements and Distributed System Configurations Utilizing an Architecturally Normalized Current Representation

Matthew Dowling[1], Willis Tarn[2], Alexander D. Monahar[1], Connor W. Arrigan[1], and David J. Singer[1, *]

ABSTRACT

Designing ships involves intricate layouts and multifaceted systems—ranging from mechanical to operational—that must be interdependent and thus precisely arranged. Traditional automated tools, though effective, are often too resource-intensive to be feasibly employed during the critical early stages of design. This paper builds on prior work that introduced an innovative solution: a network-based, architecturally normalized current representation, which offers a computational method to predict system arrangements in two dimensions without generating detailed vessel models. Our method's advantage lies in its ability to guide early-stage design decisions, thereby optimizing the use of subsequent, more resource-intensive design tools. This study extends the method to a three-dimensional framework, capturing more nuanced system-to-system interactions and yielding more realistic ship arrangements. A methodology was proposed to support this three-dimensional extension and demonstrate its applicability through a case study focused on the conceptual design of a naval frigate.

KEY WORDS

Early-Stage Design; Complex Systems; General Arrangements; Distribution Systems; Design Network Analysis.

INTRODUCTION

The advent of three-dimensional (3D) modeling in naval architecture heralds a transformative era in ship design, one that transcends the conventional two-dimensional (2D) paradigms and unlocks a new dimension of possibilities. This paper critically extends the 2D network-based approach by Shields et al. (2018), tailored for ship design, into a more sophisticated and spatially comprehensive 3D framework. The methodology by Shields et al. (2018), notable for its computational approach to guide early-stage design decisions, established a novel approach in naval architecture by simplifying the multifaceted interplay of ship layouts and systems. However, STERN et al. (2015) highlights an inherent complexity of modern naval vessels, with their intricate spatial configurations and interdependent systems, which then necessitates a shift to a 3D perspective that can encapsulate these complexities with greater fidelity.

The objective of this study is thus twofold: to validate the feasibility of transitioning to a 3D network-based ship design algorithm and demonstrate its efficacy in addressing the spatial dynamics integral to modern ship design. The transition from

[1] Department of Naval Architecture and Marine Engineering, University of Michigan, Ann Arbor, MI, USA; ORCID: 0009-0000-5924-5887 (ADM), ORCID: 0009-0002-8243-9086 (CWA), ORCID: 0000-0002-5293-6236 (DJS)
[2] Republic of Singapore Navy, Singapore
[*] Corresponding Author: djsinger@umich.edu

Submitted: 11 March 2024, Revised: 2 May 2024, Accepted: 3 May 2024, Published: 19 May 2024

Conference paper, DOI: https://doi.org/10.59490/imdc.2024.836 e-ISSN: 3050-4864

2D to 3D is not just an incremental step but offers a different approach to naval architecture, one that captures the knowledge without necessarily going into high-fidelity models, which has inherent challenges as proposed by Jeong et al. (2017). This methodology is particularly advantageous in the early stages of design, where the flexibility to explore a set of configurations and their implications on the overall design is paramount.

To elucidate the practical application and efficacy of this 3D algorithm, this paper presents a proof-of-concept study centered on the conceptual design of a naval frigate. This case study, chosen for its complexity and relevance, serves as a testbed to underscore the algorithm's potential in navigating the intricate landscape of naval vessel design. By demonstrating the algorithm's utility in a real-world scenario, the authors aim to establish its role as a pivotal tool in the modern naval architect's toolkit, contributing significantly to the evolution of ship design practices.

The migration to 3D design in naval architecture represents not just an advancement in design techniques but a paradigm shift in conceptualizing and actualizing naval vessels. Brefort et al. (2018) also highlights the need to offer the ability to preempt and address design challenges in early-stage design, and provide a knowledge-based view of the vessel's architecture. By conducting a proof-of-concept with a naval frigate design, this study aims to demonstrate how 3D modeling can enhance early-stage design decisions, offering a more comprehensive and flexible approach to naval architecture. This incremental transition offers a greater understanding into a vessel's operational and structural inter-dependencies, necessary for a design to consider during early-stage design.

BACKGROUND

A network-based approach may utilize two types of centrality within its algorithm: betweenness centrality and eigenvector centrality, as highlighted in Shields et al. (2018)'s work. Newman (2010) defines betweenness centrality as the number of times a node acts as a bridge along the shortest path between two other nodes. A node with high betweenness centrality in a naval design network might represent a critical component or design feature that connects various subsystems or design areas, highlighting its influence on information or workflow across the design process. Eigenvector centrality considers not only the number of connections a node has but also the quality of those connections. A node connected to other highly connected nodes has high eigenvector centrality. In naval design, this could identify key components or systems that are not only well-connected but also linked to other central elements, amplifying their influence.

Eigenvector Centrality

Eigenvector centrality $C_E(v)$ assigns relative scores to all nodes in the network based on the principle that connections to high-scoring nodes contribute more to the score of the node in question than equal connections to low-scoring nodes. The eigenvector centrality of node v is defined as:

$$C_E(v) = \frac{1}{\lambda} \sum_{t \in M(v)} A_{vt} C_E(t) \tag{1}$$

where:

1. $M(v)$ denotes the set of neighbors of v
2. A_{vt} is an element of the adjacency matrix A of the network, which is 1 if v and t are connected and 0 otherwise
3. λ is a constant (specifically, the largest eigenvalue of A)

This can be represented in a more compact form using the eigenvector equation:

$$A\vec{x} = \lambda\vec{x} \tag{2}$$

where $\vec{x}$ is the eigenvector corresponding to the largest eigenvalue λ, and the components of $\vec{x}$ are the eigenvector centralities of the nodes.

In naval design, nodes (design elements of systems) with high eigenvector centrality are those that are not only well-connected but also connected to other well-connected nodes, indicating their strategic importance in the design's overall effectiveness and efficiency.

Betweenness Centrality

Betweenness centrality $C_B(v)$ of a node v quantifies the extent to which v lies on the shortest paths between other nodes. It is defined as:

$$C_B(v) = \sum_{s \neq v \neq t} \frac{\sigma_{st}(v)}{\sigma_{st}} \tag{3}$$

where:

1. σ_{st} is the total number of shortest paths from node s to node t
2. $\sigma_{st}(v)$ is the number of those paths that pass through v

This metric highlights nodes that serve as critical connectors or bridges within the network, which in the context of naval design, could represent elements or systems critical to the integration or interoperability of different components.

Impact on Centrality Metrics

Changing requirements within the network impacts the centrality metrics in different ways.

For betweenness centrality, changing a requirement may affect the betweenness centrality of certain nodes by altering the shortest paths through the network. Newman (2005) proposes that nodes that previously acted as critical bridges between different parts of the design might see their betweenness centrality decrease if the change bypasses them, highlighting alternative pathways or components that have become more critical. Conversely, the introduction of new requirements or the modification of existing ones could elevate the strategic importance of previously peripheral nodes, as they become pivotal in connecting various components of the design.

For eigenvector centrality, the eigenvector centrality of a node reflects its connection to other influential nodes. As highlighted by Newman (2006), changing a node, hence requirement, could shift the network's structure of influence, affecting which nodes are considered central. A requirement change could make certain nodes more central if they are now more directly connected to or dependent on other highly central nodes. This shift can reveal which elements of the design are gaining or losing importance in the context of the overall system architecture and where design efforts may need to be concentrated.

These changes to centralities inform the designer mathematically in 4 ways:

1. **Identifying Critical Components:** By tracking the percentage-value changes in centrality measures, designers can identify which components have become more or less critical to the design's functionality. This can guide resource allocation, highlighting where additional analysis or robustness might be necessary in the design.
2. **Understanding System Interdependencies:** Changes in centrality can also reveal previously unnoticed interdependencies between components. Designers can use this insight to anticipate potential cascading effects of changes throughout the system, leading to more resilient designs.

3. **Highlighting Opportunities for Optimization:** Significant changes in the network's structure, as reflected by centrality measures, can uncover opportunities for optimizing the design. For instance, reducing the betweenness centrality of overloaded nodes can lead to a more balanced and efficient design.
4. **Informing Design Iteration:** By quantitatively assessing how a single requirement change affects the network, Shields (2017) suggests that designers can make more informed decisions about subsequent iterations, potentially exploring alternative solutions that balance centrality across the network more effectively.

Ultimately, the iteration of designs in the representation of a network, with changing requirements, provides a dynamic tool for designers to quantitatively assess and optimize the design process. This approach not only aids in making informed decisions but also enhances the overall design by understanding and leveraging the complex interplay of its components, also concurred by Shields (2017).

To define the impact on the centrality metrics mathematically:

1. $G = (V, E)$ as the graph representing the design network, where V is the set of nodes (including requirements, components, and systems) and E is the set of edges (representing relationships or dependencies between these elements)
2. $C_B(v)$ as the betweenness centrality of node v
3. $C_E(v)$ as the eigenvector centrality of node v
4. v_r as the node representing a specific requirement that is being changed
5. $G' = (V', E')$ as the modified graph after changing v_r

The change in betweenness centrality $\Delta C_B(v)$ for a node v due to the modification of v_r can be represented as:

$$\Delta C_B(v) = C'_B(v) - C_B(v) \tag{4}$$

where $C'_B(v)$ is the betweenness centrality of v in the modified network G'.

Similarly, the change in eigenvector centrality $\Delta C_E(v)$ for a node v due to the modification of v_r can be calculated as:

$$\Delta C_E(v) = C'_E(v) - C_E(v) \tag{5}$$

where $C'_E(v)$ is the eigenvector centrality of v in the modified network G'.

Informing the Designer

The impact of changing a requirement on the network can be further analyzed by examining the aggregate changes in centrality across all nodes. For example, the average change in betweenness centrality can be computed to understand how the design's connectivity or integration points shift. Similarly, examining the distribution of changes in eigenvector centrality can reveal how the overall influence landscape of the design has been altered.

Quantitatively, a designer can use these percentage-based changes to make better-informed decisions:

1. **Prioritization of Components:** If $\Delta C_B(v)$ or $\Delta C_E(v)$ significantly increases for certain nodes, those components may require additional focus or resources.
2. **Reevaluation of Dependencies:** Large percentage changes in centrality measures might trigger the need to perform a reevaluation of dependencies and relationships within the design to optimize performance or resilience.

3. **Iterative Optimization:** By systematically modifying requirements and analyzing the resulting changes in centrality, designers can explore the design space more thoroughly and identify different configurations, and their associated trade-offs.

The mathematical representation allows designers to illuminate and quantify the impact of requirement changes in the design network, providing a basis for better-informed decision-making and optimization throughout the design process.

METHODOLOGY

In this exploration into the three-dimensional realm, the approach was multifaceted, encompassing both theoretical development and practical application. At the heart of this methodology is the expansion of Shields et al. (2018)' two-dimensional network-based approach, reengineered to consider the complexities and spatial intricacies of 3D ship design. This progression was not a straightforward task; it required a deep understanding of both the established principles of naval architecture with three-dimensional modeling in the form of a network.

The primary challenge was to develop an algorithm capable of accurately representing a ship's layout and systems in three dimensions. This required a significant enhancement of the original 2D model, integrating vertical spatial dynamics alongside the conventional horizontal plane. The 3D model had to account for factors such as vertical access routes, stack effects, and the vertical distribution of weight, which are crucial in naval architecture but were not considerations in the 2D approach.

A crucial aspect of the methodology was the incorporation of spatial dynamics within the 3D model. This included understanding how different spaces within a ship interact, how systems are routed through these spaces, and how these aspects impact the ship's overall functionality and performance. The model needed to be sensitive to the nuances of distribution, ensuring that every probability was accounted for and computed.

To demonstrate the practical applicability of the 3D model, the conceptual design of a naval frigate was chosen as a case study. This choice was driven by the inherent complexity in frigates, which offered a fine balance between weaponry, propulsion, living quarters, and other critical systems. The case study aimed to show how the 3D model could be used to explore various design configurations, assess their feasibility, and optimize the layout for operational efficiency and effectiveness.

A key focus of the methodology was its application in the early stages of design. The ability to visualize and manipulate a ship's design in three dimensions from the outset allows for a more informed decision-making process. It opens up new avenues for exploring design options, foreseeing potential issues, and making strategic decisions that significantly impact the final design.

The final phase of the methodology involved analyzing the results obtained from the naval frigate case study. This analysis aimed to determine the effectiveness of the 3D model, its impact on early-stage design decisions, and its potential role in future naval architecture practices. The discussion also highlights the limitations of the current model and suggests areas for future research and development.

DEVELOPMENT OF PROOF-OF-CONCEPT

In transforming the theoretical aspects of the three-dimensional naval architecture model for real-life applications, the approach was centered around developing a robust proof-of-concept. This phase was crucial to demonstrate not just the technical feasibility but the practical utility of the model in real-world scenarios. The focus was on the intricate process of translating complex naval architectural concepts into a functional and interactive 3D model, in the form of a naval frigate.

Pivotal to the development strategy was the use of centrality matrices. These matrices were employed as a means to mea-

sure ”decision influence” within the ship design. Essentially, these ”decision influence” matrices allowed the authors to quantify the impact of each design decision on the overall layout and functionality of the ship. By analyzing the centrality of various components and spaces within the ship, designers could understand how changes in one area might ripple through to others, thereby influencing the entire design network.

Another significant area of the development process involved the integration of 3D dynamics into the model. This was a step from the 2D scope of naval architecture, which focused more on the side layout. The aim was to fully utilize the three-dimensional space to elucidate how 3D elements such as the combination of horizontal and vertical weight distribution affect the ship's overall design and performance.

For the proof-of-concept, the naval frigate presented a sufficiently comprehensive challenge, offering a broad spectrum of variables to test the model's capabilities. The model, built upon Shield's previous work, was simulated with a design scenario to assess the design feasibility over multiple configurations and predict the operational efficacy.

The simulation process involved iterative runs to test various configurations and layouts. The model was repeatedly fine-tuned to adapt to the dynamic requirements of naval frigates, incorporating feedback loops that allowed for continuous improvement of the design process. The changes to centrality matrices were tracked and normalized in these simulations, providing quantitative data that informed the decision-making process at every step.

RESULTS

The methodology, detailed in the earlier section, quantifies the resultant shifts in the network's dynamics, particularly focusing on the betweenness and eigenvector centralities of pivotal components such as the bridge, VLS, and supporting pipes. This investigation illuminates the intricate interdependencies within naval systems, showcasing how alterations in a single design element can precipitate significant reconfigurations across the network, also seen in Shields (2017) work. The enhanced roles of specific components, underscored by their changes in centralities, highlight their critical importance in maintaining operational efficiency and design integrity. This nuanced understanding of design element interplay advances our capability to navigate the complex landscape of naval architecture, fostering more informed decision-making and innovation in naval design practices.

Mathematically, Shields et al. (2018) proposes that a shift in centralities reflects a re-evaluation of the importance of certain nodes (such as the bridge, VLS, and supporting pipes) within the network. This change indicates how central a node is in the context of the entire network, taking into account not just the number of connections, but also the significance of those connections. High centrality values post-removal of the naval gun imply these components play a more crucial role in maintaining the network's functionality, highlighting their increased influence on the ship's design and operational efficiency.

By quantifying the shifts in centralities of critical components, the method offers insights into these elements' enhanced roles. This approach highlights the interdependencies within naval systems and guides more informed decision-making for future design strategies, emphasizing the importance of considering component significance and system-wide impacts in naval architecture, which is detailed in the following sub-sections. The results will first discuss the impact of design changes through eigenvector centralities, which will highlight components which has a greater influence on operations. The study will then discuss components that require greater consideration, discussion, or impact to support the design through betweenness centralities. Finally, the study will investigate the impact of fidelity on eigenvector centralities by expanding the 3-D space.

Eigenvector Centralities as a measure of influence and importance

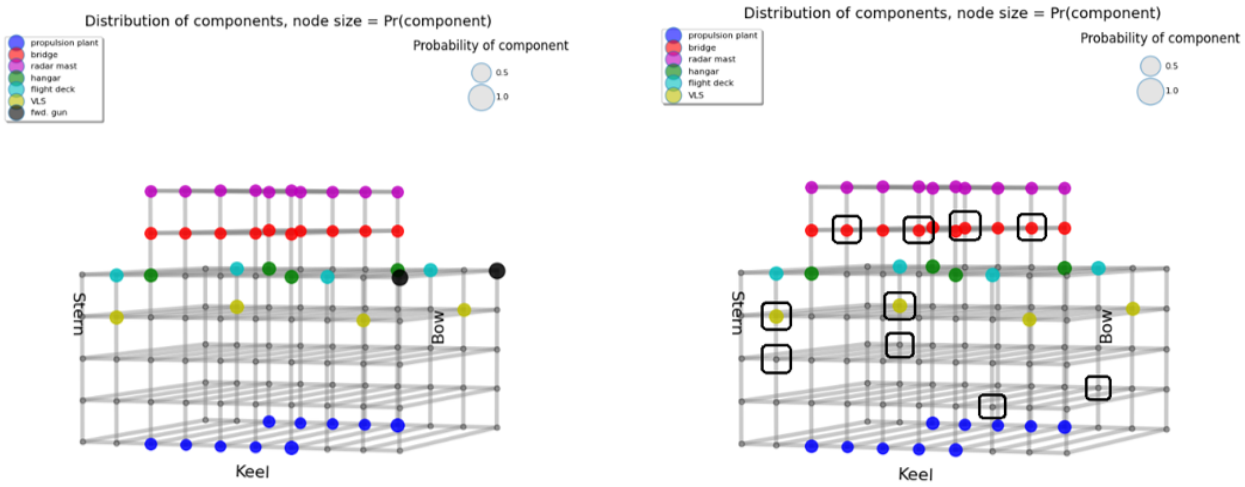

(a) gun **(b)** no gun

Figure 1: gun in the general arrangement vs no gun (eigenvector centrality)

In Figure 1(a), the presence of the gun is illustrated by a network where the gun node possesses a size proportional to its centrality. Surrounding components display varying degrees of centrality, suggesting a more dispersed distribution of influence across the network. The network appears balanced, indicating that the removal of any single component—while impactful—would not drastically destabilize the system or design.

Contrastingly, Figure 1(b) reveals the aftermath of the gun's removal. Notably, the bridge, VLS, and supporting pipes emerge with significant changes to their eigenvector centralities, signified by their "highlighted" node representations. This highlights a shift towards a more centralized network architecture, where the influence is now concentrated among fewer components. Referencing Newman (2005), the resultant configuration suggests that these elements have assumed more critical operational roles in the absence of the naval gun, potentially becoming new focal points for maintaining the vessel's functionality.

The changes in centralities within the naval design network provide critical insights for designers. The changes in eigenvector centralities for key components like the bridge, VLS, and supporting pipes following the gun's removal indicate these elements have become more crucial in the network's functionality. This shift towards a more centralized network structure informs designers about potential new focal points in ship functionality, meaning:

1. **Resource Allocation:** The design team may need to prioritize the bridge, VLS and supporting pipes for further development and robustness checks, ensuring they are capable of handling their critical roles effectively.
2. **System Redesigns:** The bridge, VLS, and supporting pipes might need to add redundancy to enhance the resilience of these parts to mitigate risks associated with potential failures.

The 3D model provides a more nuanced view of system interdependencies compared to traditional 2D models, which tend to simplify complex relationships. In 3D, the spatial configuration and the relative placement of components are captured, revealing how changes in one part of the system can affect others in a way that flat representations cannot. This validation of our hypothesis underscores the importance of considering three-dimensional interactions in naval design to fully understand and anticipate the impacts of alterations within the ship's architecture. The increased centralities observed in the 3D model after the removal of the naval gun reflect this depth of analysis, validating the hypothesis that certain components will grow in operational significance when a major system is removed.

Betweenness Centralities as a measure of criticality

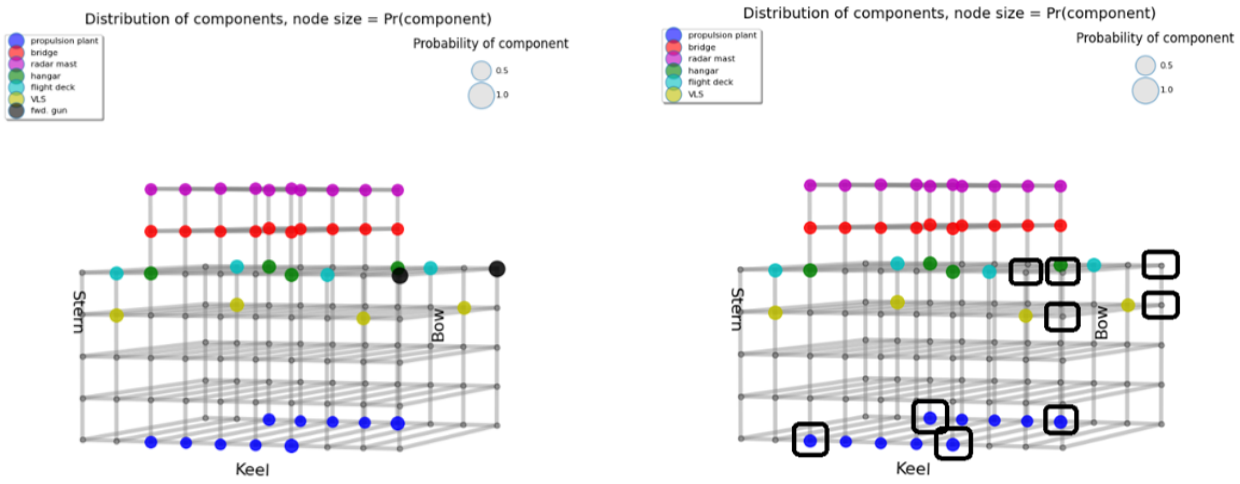

(a) gun **(b)** no gun

Figure 2: gun in the general arrangement vs no gun (betweeness centrality)

Figure 2's graphical sub-section presents a visualization of betweenness centrality within the naval ship's design network, with two distinct configurations: one with the gun (a) and one without (b). The combination of Newman (2010)'s definition and Shields et al. (2018) research could then define betweenness centrality as a measure of a component's role as a conduit or bridge within the network—its importance in connecting different parts of the ship. The graphical comparison powerfully illustrates the redistribution of this measure among the ship's components.

In configuration (a), with the gun present, the betweenness centrality is relatively evenly distributed across the network, suggesting a balanced design with multiple pathways for operational flow and no single point of over-reliance. The hangar, propulsion plant, and supporting pipes exhibit centralities indicative of their role but are not overly dominant.

Configuration (b), however, tells a different story. Here, the removal of the naval gun has led to a significant change in the betweenness centrality of the hangar and propulsion plant, with supporting pipes towards the front also becoming more prominent. This shift points to a reconfiguration of operational pathways, now heavily reliant on these components. The increased centrality of the hangar and propulsion plant suggests they are now key nodes, critical for the ship's performance and structural integrity.

The betweenness centrality information can be utilized by naval designers in several practical ways:

1. **Identifying Key Components:** Designers can prioritize the hangar and propulsion plant for enhanced robustness and reliability in design specifications.
2. **Redesigning Flow Paths:** The hangar and propulsion plant are major conduits, which means the design team needs to ensure efficient flow paths and reduce potential bottlenecks in ship operations through these conduits.
3. **Improving Operational Resilience:** By reinforcing the hangar and propulsion either through redundancies or armoring, designers can improve the overall resilience of the ship, ensuring it remains operational even if key components are compromised.
4. **Strategic Modifications:** Designers can strategically plan mid-life upgrades to the hangar and propulsion plant, which could have significant impacts on the ship's functionality.

The variations between these two configurations reveal the adaptable nature of naval design networks. Referencing Newman (2005)'s research, the variations demonstrate how the removal of a single component can lead to a redistribution of functional importance across the network, necessitating a reassessment of design priorities. This validates the hypothesis that naval design is a dynamic and interdependent system, where changes in individual elements can have far-reaching impacts. By providing a quantifiable measure of component significance, the betweenness centrality analysis offers designers a powerful tool for assessing potential modifications and their ramifications. It underpins the need for comprehensive simulations and modeling in naval architecture to ensure that designs are both robust and flexible, capable of accommodating changes while understanding the trade-offs on operational effectiveness.

Extending the 3D layers

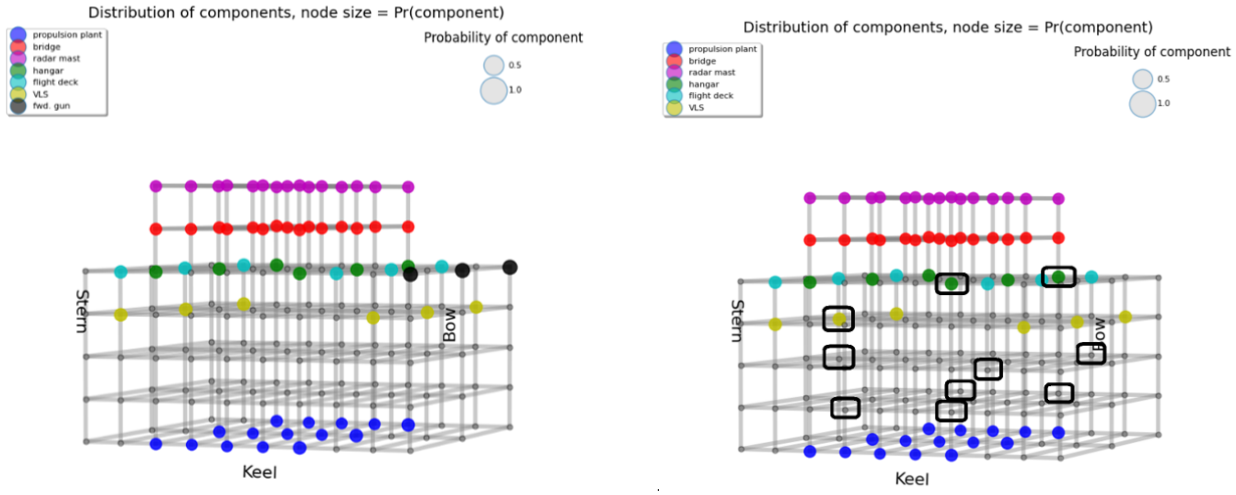

(a) gun **(b)** no gun

Figure 3: 3 guns, eigenvector centrality gun vs no gun comparison (eigenvector centrality)

As the study extends the fidelity of the model in the analysis of eigenvector centralities depicted in Figure 3, three potential positions for the guns in the ship's design are compared against a configuration without any guns. The three-layered representation of nodes offers a different understanding of the influence exerted by the supporting pipes within the ship's network, highlighting a significant change in their centrality in the absence of the gun. This reinforces the point on the need for the design team to consider adding redundancies within the supporting pipes network, highlighted in the earlier sub-section.

This extension of an additional layer within the network underscores the heightened impact that supporting structures have in the absence of key offensive components, offering critical insights for future design considerations where Knight et al. (2015) highlights the need for flexibility and adaptability may be required for subsequent downstream upgrades.

The comparison between Figures 1 and 3, which illustrate the eigenvector centralities in two different configurations of naval ship design, reveals the nuanced shifts in the ship's structural network. In Figure 1, the removal of the naval gun impacts the centrality of the bridge, VLS, and supporting pipes, demonstrating their increased operational significance. In contrast, Figure 3 expands this analysis to a three-layer node view, uncovering the broader influence of supporting pipes throughout the ship's design, especially in the gun's absence. This expansion provides a deeper understanding of the role that the pipes play in the ship's resilience and design adaptability.

The information from the analysis can be used by naval designers in several ways:

1. **Prioritizing Component Enhancement:** By identifying which components like the supporting pipes gain in central-

ity, designers can prioritize these for enhancements, ensuring they are robust enough to handle increased responsibilities.

2. **Redesigning for Resilience:** Recognizing components that become more central to the ship's functionality allows designers to focus on redesigning these elements to enhance the overall resilience of the ship.
3. **Risk Management:** The analysis helps in assessing potential risks associated with the removal or modification of major components and planning mitigations accordingly.

In the context of naval design, the comparison between Figure 1 and Figure 3 suggests a shift in the functional significance of the ship's components when the naval gun is removed. Specifically, the three-layer eigenvector centrality analysis in Figure 3 emphasizes that the supporting pipes increase in importance, indicating they may take on a more central role in maintaining the structural and operational integrity of the ship. This suggests that in the absence of the gun, the ship's design compensates by relying more on other elements to maintain its performance capabilities.

DISCUSSION

The comprehensive analysis of the naval ship design network in the absence of the gun, as demonstrated by the shift in centralities, offers an insightful perspective into the future of naval architecture. This paradigmatic observation in network behavior, where supporting infrastructural components like pipes accrue shifts in centrality, necessitates a reconsideration of their role within the structural integrity and operational efficiency of naval vessels.

From a mathematical viewpoint, Newman (2001) definition suggests that eigenvector centrality could elucidate the relative influence of a node within the network. As presented in the earlier section, as the supporting pipes gain prominence in the absence of the gun, it indicates that these components have now become instrumental nodes through which significant portions of the network's operational pathways are mediated. This increase in centrality suggests that the design's resilience is now more heavily reliant on the robustness of these elements, which may not have been primary factors in the initial design considerations.

The implications for future ship design are substantial. The conventional approach to naval architecture, as described by Pawling et al. (2017), which is generally characterized by a siloed focus on individual components rather than their interactions, may no longer be sufficient. Instead, Shields (2017)'s proposal of a holistic view that embraces the interconnectivity of all ship elements and their contributions to the overall network is required. This shift towards an integrated network perspective will enable naval architects to create designs that are inherently adaptable, and capable of withstanding the removal or malfunction of critical components without significant loss of functionality.

Moreover, the study's findings highlight Knight et al. (2015)'s point on the importance of modularity in design, where components can be removed or replaced with minimal disruption to the broader system. In the context of rapidly evolving military technologies and strategies, such modularity becomes indispensable. It ensures that ships can be upgraded or reconfigured in response to emerging threats and operational requirements without necessitating complete redesigns, thus extending the vessels' operational lifespans and enhancing their return on investment.

Furthermore, the network-centric approach to design implicates the potential impact of these findings on naval architecture education and practice. The current training may need to evolve to incorporate principles of network science and systems thinking, equipping the next generation of naval architects with the tools and perspectives necessary to design the resilient and responsive vessels required for future maritime challenges.

In conducting a detailed analysis of ship design using network science methodologies, the authors confronted significant challenges while implementing a component arrangement algorithm. The desired outcome was to programmatically determine an optimal design where specific components, such as the flight deck and forward gun, were preferentially distanced. Utilizing Newman (2005)'s random walk betweenness centrality measure, the algorithm inadvertently amplified the central-

ity scores of nodes adjacent to crucial components, regardless of the targeted arrangement. This unexpected result presented a quandary: how to penalize configurations where the flight deck was undesirably positioned near the forward gun.

The challenges were compounded by the algorithm's nature, which globally enhanced centrality scores based on proximity to key nodes, influencing unrelated calculations. A simplistic solution like removing front flight deck nodes to refocus the algorithm on aft sections contradicted the objective of establishing a proof of concept. The essence of the endeavor was to reduce manual labor in developing more efficient designs—options that are not immediately apparent to designers.

Addressing this challenge necessitated a reevaluation of the algorithmic approach. The study nuanced adjustments to the algorithm, accounting for these centrality distortions. Potential solutions involved introducing penalty factors within the centrality calculations or developing a multi-criteria optimization framework that could simultaneously consider proximity preferences alongside other design requirements.

These adjustments had to be carefully balanced to not undermine the overall integrity of the ship's network. The intricacies of the design elements' interplay needed meticulous consideration to ensure that operational efficiencies were not sacrificed. The insights derived from these explorations are vital for naval architecture, pointing towards a future where computational algorithms can significantly augment human expertise in early-stage design, leading to innovative naval vessels engineered for optimal performance and resilience.

The integration of such algorithmic solutions holds the potential impact on naval architecture. By automating complex design decisions, this approach could significantly streamline the design process, allowing for rapid prototyping and testing of various configurations. This would not only save time and resources but also enable the exploration of a broader design space, potentially unveiling novel configurations that human designers may not intuitively consider.

CONCLUSION

Our research revealed a fundamental reconfiguration of the naval ship design network when key components such as the naval gun are altered. The significant increase in the eigenvector centralities for supporting structures like pipes upon the gun's removal indicates a shift towards a design that compensates for the loss by redistributing functional importance across the network. This insight is vital for future naval designs, where resilience and adaptability must be engineered into the vessel from the outset. It suggests that naval architecture is entering a phase where flexibility and robustness are not merely desired but required, laying the groundwork for innovative approaches in ship design. These findings pave the way for future research to develop algorithms that can more effectively navigate the complex trade-offs between design intuitiveness and computational optimization.

The advances in network-centric naval architecture presented in our study hint at transformative possibilities for future ship design. Pioneering research can progress towards developing advanced algorithms that not only predict but also adaptively recalibrate the ship's design network in response to changes in component configurations. There is potential for creating intelligent design systems that can autonomously optimize layouts for operational efficacy, considering factors such as spatial constraints and mission-specific requirements. Additionally, investigations into the resilience of these networks against unforeseen failures could lead to the evolution of ships with unprecedented structural robustness. Future research directions are poised to harness machine learning to predict and propose optimal designs, significantly reducing the iterative cycle of design and testing, and to employ virtual reality for immersive design evaluation, which could revolutionize the conceptualization phase of naval engineering.

CONTRIBUTION STATEMENT

MD: Conceptualization; data curation, methodology; software; writing – original draft. **WT:** Conceptualization; data curation, methodology; software; writing – original draft. **ADM:** conceptualization; supervision; writing – review and editing

CWA: supervision; writing – review and editing **DJS:** supervision; writing – review and editing.

ACKNOWLEDGEMENTS

We would like to thank Captain Lynn Petersen from the Office of Naval Research for providing support for this project. This work was funded under grant number N00014-23-S-B001.

REFERENCES

Brefort, D., Shields, C., Habben Jansen, A., Duchateau, E., Pawling, R., Droste, K., Jasper, T., Sypniewski, M., Goodrum, C., Parsons, M. A., Kara, M. Y., Roth, M., Singer, D. J., Andrews, D., Hopman, H., Brown, A., and Kana, A. A. (2018). An architectural framework for distributed naval ship systems. *Ocean Engineering*, 147:375–385.

Jeong, D.-H., Roh, M.-I., Ham, S.-H., and Lee, C.-Y. (2017). Performance analyses of naval ships based on engineering level of simulation at the initial design stage. *International Journal of Naval Architecture and Ocean Engineering*, 9(4):446–459.

Knight, J., Collette, M., and Singer, D. (2015). Design for flexibility: Evaluating the option to extend service life in preliminary structural design. *Ocean Engineering*, 96.

Newman, M. (2006). Finding community structure in networks using the eigenvectors of matrices. *Physical review. E, Statistical, nonlinear, and soft matter physics*, 74:036104.

Newman, M. E. J. (2001). Scientific collaboration networks. ii. shortest paths, weighted networks, and centrality. *Phys. Rev. E*, 64:016132.

Newman, M. E. J. (2010). 168Measures and metrics: An introduction to some standard measures and metrics for quantifying network structure, many of which were introduced first in the study of social networks, although they are now in wide use in many other areas. In *Networks: An Introduction*. Oxford University Press.

Newman, M. J. (2005). A measure of betweenness centrality based on random walks. *Social Networks*, 27(1):39–54.

Pawling, R., Percival, V., and Andrews, D. (2017). A study into the validity of the ship design spiral in early stage ship design. *Journal of Ship Production and Design*, 33:81–100.

Shields, C. (2017). *Investigating Emergent Design Failures Using a Knowledge-Action-Decision Framework*. PhD thesis.

Shields, C., Sypniewski, M., and Singer, D. (2018). Characterizing general arrangements and distributed system configurations in early-stage ship design. *Ocean Engineering*, 163:107–114.

STERN, F., WANG, Z., YANG, J., SADAT-HOSSEINI, H., MOUSAVIRAAD, M., BHUSHAN, S., DIEZ, M., YOON, S.-H., WU, P.-C., YEON, S. M., DOGAN, T., KIM, D.-H., VOLPI, S., CONGER, M., MICHAEL, T., XING, T., THODAL, R. S., and GRENESTEDT, J. L. (2015). Recent progress in cfd for naval architecture and ocean engineering. *Journal of Hydrodynamics, Ser. B*, 27(1):1–23.

Proceedings of 15th International Marine Design Conference (IMDC-2024)
June 2-6, 2024
Amsterdam, the Netherlands

Improving Ship Response Estimation with Neural Networks

Samuel J. Edwards[1,*] **and Michael Levine**[1]

ABSTRACT

The feasibility of a data-adaptive multi-fidelity seakeeping model is assessed for use in early stage design in this study. Data adaptive tuning (or correction) of lower-fidelity model predictions are implemented based on training with higher fidelity ship motion response data. Long Short-Term Memory (LSTM) neural networks are incorporated as part of a multi-fidelity approach for prediction of 6 degree of freedom (6-DOF) ship motion responses in waves. LSTM networks are trained and tested with Large Amplitude Motion Program (LAMP) simulations as a target, and SimpleCode simulations and wave time-series as inputs. LSTM networks improve the fidelity of SimpleCode seakeeping predictions relative to LAMP, while retaining the computational efficiency of a lower-fidelity simulation tool.

KEY WORDS

Neural Networks; Seakeeping; Extreme Events.

INTRODUCTION

To understand how a ship will respond in different environmental conditions is vital in early stage design. Consideration of the operating conditions can be made in the form of a developing a database that covers a comprehensive set of ocean wave conditions. Within the database is a collection of ship response statistics as a function of ship heading, speed, and wave conditions. Operational limits are determined based on relationships between these statistics and maximum allowable responses. Generating large databases containing many possible combinations of ship headings, speeds and wave conditions allows for more robust operational guidance ability.

To identify and compare against operational limits, extreme event analysis must be performed. The most straightforward approach to estimating extreme ship response characteristics is through Monte Carlo simulations. However, for most tools of reasonable fidelity, the computational cost is far too expensive when considering potential extreme events for longer return periods and simulation run times on the order of real time. Extrapolation methods, generally based on Weibull distributions, can be explored with a limited dataset. However, this approach requires prior knowledge of the response distribution with particular focus on the tail of the distribution.

Other methods to identify extreme behavior efficiently without overextending assumptions have been developed. One such method is the Design Loads Generator (DLG) (Alford 2008, Kim 2012). DLG was initially developed for linear systems with stochastic Gaussian input, and drew from modified phase distributions based on Extreme Value Theory to generate ensembles of extreme realizations for a given return period.

Another method that has been explored is a lower-fidelity simulation tool that retains major nonlinearities to identify extreme conditions, and then running the identified conditions with a higher-fidelity simulation tool (Reed 2021). In this framework, a surrogate model does not need to be identified but requires a high level of correlation of the peaks between the two simulation tools employed.

An approach with Long Short-Term Memory (LSTM) to correct lower-fidelity ship response data to the level of higher fidelity ship response data was developed in Levine et al. (2024). In the paper, statistics generated by two different training methods were compared between the LSTM and the higher fidelity responses with good results. However, only three degrees-of-freedom (3-DOF) were applied in the ship simulation software solvers.

[1] Naval Surface Warfare Center – Carderock Division, West Bethesda, MD, USA; ORCID: 0000-0002-7512-1742
Author: samuel.j.edwards33.civ@us.navy.mil

Submitted: 20 February 2024, Revised: 19 April 2024, Accepted: 1 May 2024, Published: 21 May 2024

Conference paper, DOI: https://doi.org/10.59490/imdc.2024.864 e-ISSN: 3050-4864

In this paper, the method outlined in Levine et al. (2024) is further refined to produce predictions with 6 degrees-of-freedom (6-DOF) simulations. The method applies two seakeeping simulation tools of lower and higher fidelity, which are SimpleCode (Weems and Wundrow 2013) and the Large Amplitude Motion Program or LAMP (Shin et al. 2003), respectively. By running the lower fidelity code (SimpleCode) under the same conditions as the higher fidelity code (LAMP), the motions predicted by SimpleCode can be improved to approximate those from LAMP though a Long Short-Term Memory (LSTM) neural network. However, the forces in the 6-DOF simulations acting on the SimpleCode-simulated ship differ from the LAMP-simulated ship and the simulated ships diverge in space over time. To account for the difference in experienced conditions under the same seaway, a first stage LSTM neural network is introduced to learn the ship path of the LAMP model with the SimpleCode simulation as input. In this approach, all ship motion degrees-of-freedom are considered in the hydrodynamic solvers and are used in the training of the neural networks. After training the LSTM networks, many LAMP-quality ship simulation realizations can be generated with LSTM-corrected SimpleCode results in a much more computationally efficient manner.

In the following sections, the network architecture for training a framework of LSTM networks with SimpleCode as input and LAMP as a target is described. Then, a case study with the David Taylor Model Basin (DTMB) Model 5415 (Moelgaard, 2000) is described and results from the application of the framework are presented.

METHODOLOGY

SimpleCode and LAMP

SimpleCode is a reduced-order seakeeping code that can quickly produce acceptable results (Smith 2019). One of the key simplifications is in the local variation of wave pressure, where the hydrostatic and Froude-Krylov equations can instead use volume integrals rather than integrating over the surface of the ship (Weems and Wundrow 2013). With pre-computed Bonjean curves, the instantaneous submerged volume and geometric center; therefore, sectional hydrostatic and Froude-Krylov forces can be calculated quickly.

LAMP is a higher fidelity code that considers all forces and moments acting on the ship in the time-domain within a 6-DOF, 4th order Runge-Kutta solver (Shin et al. 2003). Central to the code is the solution of the 3-D wave-body interaction problem. Within LAMP, the complexity of this solution can be altered. LAMP-3 is utilized in the current work, where the pertubation velocity potential is solved over the mean wetted hull surface and the hydrostatic and Froude-Krylov forces are solved over the instantaneous wetted hull surface. Additionally, LAMP-3 allows for large lateral motions and forces. LAMP has effectively estimated motions comparable to model tests (Lin and Yue 1991) but is, of course, much more computationally expensive than a lower-fidelity code like SimpleCode. Through some parameters e.g., number of wave frequency components, free surface panel definition, hull offsets, can be altered, LAMP-3 runs at nearly real time i.e., 30 minutes of wall-clock time is required to generate 30 minutes of simulated data. In the same 30 minutes and the same number of frequency components, SimpleCode can produce upwards of 5,000 independent realizations of 30 minutes.

SimpleCode can produce an approximation of LAMP, especially with tuned radiation and diffraction forces included (Weems and Belenky 2018, Pipiras et al. 2022). However, a fidelity gap exists, especially when considering a bimodal wave spectrum. In this study, the 6-DOF implementations of SimpleCode and LAMP were both used. Using the 6-DOF solvers in both SimpleCode and LAMP provides a more accurate representation of the pertinent degrees of freedom as the simulated ship is allowed to move more realistically and the forces act on the ship accordingly. However, only the three vertical degrees of freedom (heave, roll, and pitch) were for comparison. These degrees of freedom have the greatest applicability to the evaluation of typical design criteria.

Long Short-Term Memory (LSTM)

One of the major drivers of the presented method is the Long Short-Term Memory (LSTM) neural network (Hochreiter and Schmidhuber 1997). An LSTM neural network is a recurrent neural network that incorporates both long- and short-term effects that are learned and developed during the training process. These memory effects are stored in weight matrices where they, along with other operations, transform input matrices to the target output matrices. The causal nature of marine dynamics and inclusion of memory effects make LSTM networks particularly well suited for the presented problem.The following set of equations describe the operations that occur in an LSTM layer.

$$f_1 = \sigma\left(W_{f_1} x^{[t]} + U_{f_1} h^{[t-1]} + b_{f_1}\right) \quad [1]$$

$$f_2 = \sigma\left(W_{f_2} x^{[t]} + U_{f_2} h^{[t-1]} + b_{f_2}\right) \quad [2]$$

$$f_3 = \tanh\left(W_{f_3} x^{[t]} + U_{f_3} h^{[t-1]} + b_{f_3}\right) \quad [3]$$

$$f_4 = \sigma\left(W_{f_4} x^{[t]} + U_{f_4} h^{[t-1]} + b_{f_4}\right) \quad [4]$$

$$c^{[t]} = f_1 \odot c^{[t-1]} + f_2 \odot f_3 \quad [5]$$

$$h^{[t]} = f_4 \odot \tanh\left(c^{[t]}\right) \quad [6]$$

where W and U are weight matrixes, b are the bias vectors, $x^{[t]}$ is the input vector, standardized by the respective standard deviations and means for each input channel, by the respective at time t, $h^{[t]}$ is the hidden state vector at time t, $c^{[t]}$ is the cell state vector at time t, σ is the sigmoid function, tanh() is the hyperbolic tangent function, and $\odot$ represents the Hadamard product. The output or target at time t is equal to the hidden state vector at time t, $h^{[t]}$. The weight matrices and bias vectors are progressively learned during the training process to minimize the specified loss between the training data and the test data. The present work employes the mean-squared error in Equation 7 to quantify the error between the training and test sets.

$$MSE = \frac{1}{N}\sum_{i=1}^{N}\left(y_T(t_i) - y_L(t_i)\right)^2 \quad [7]$$

where N is the number of points in the time series, y is the response matrix which contains the time series of heave, roll, and pitch, subscript T is the target time series, subscript L is the LSTM produced time series, and t_i is the *i-th* time instant in the time series.

In Levine et al. (2024), the 3-DOF SimpleCode and LAMP simulations were well correlated and the motions and wave elevation time series derived from the SimpleCode simulations could be input into the LSTM with the LAMP heave, roll, and pitch time series as the targets. However, the difference in realized forces acting on the simulated ships in 6-DOF simulations results in a difference in the global position between the SimpleCode and LAMP models. The result is a reduction in correlation between the input and output time series. To account for this lower correlation, a two-step LSTM model is introduced. First, an LSTM framework is trained to transform the 6-DOF SimpleCode motions and wave elevation time series derived from SimpleCode to the surge and sway of the LAMP simulations. These surge and sway time series are combined with the wave spectrum and phases from the given realization to estimate the wave elevation at the center of gravity of the LAMP model. In Levine et al. (2024), an LSTM framework is capable of estimating LAMP motions through a data-driven approach with only the wave elevation as input ("LSTM-Waves"). A similar effort comprises the second step of the LSTM architecture where the wave elevation generated from the estimated LAMP surge and sway are inputs into an LSTM network trained to estimate 6-DOF LAMP heave, roll, and pitch from LAMP-generated wave elevation time series. The framework is illustrated in Figure 1.

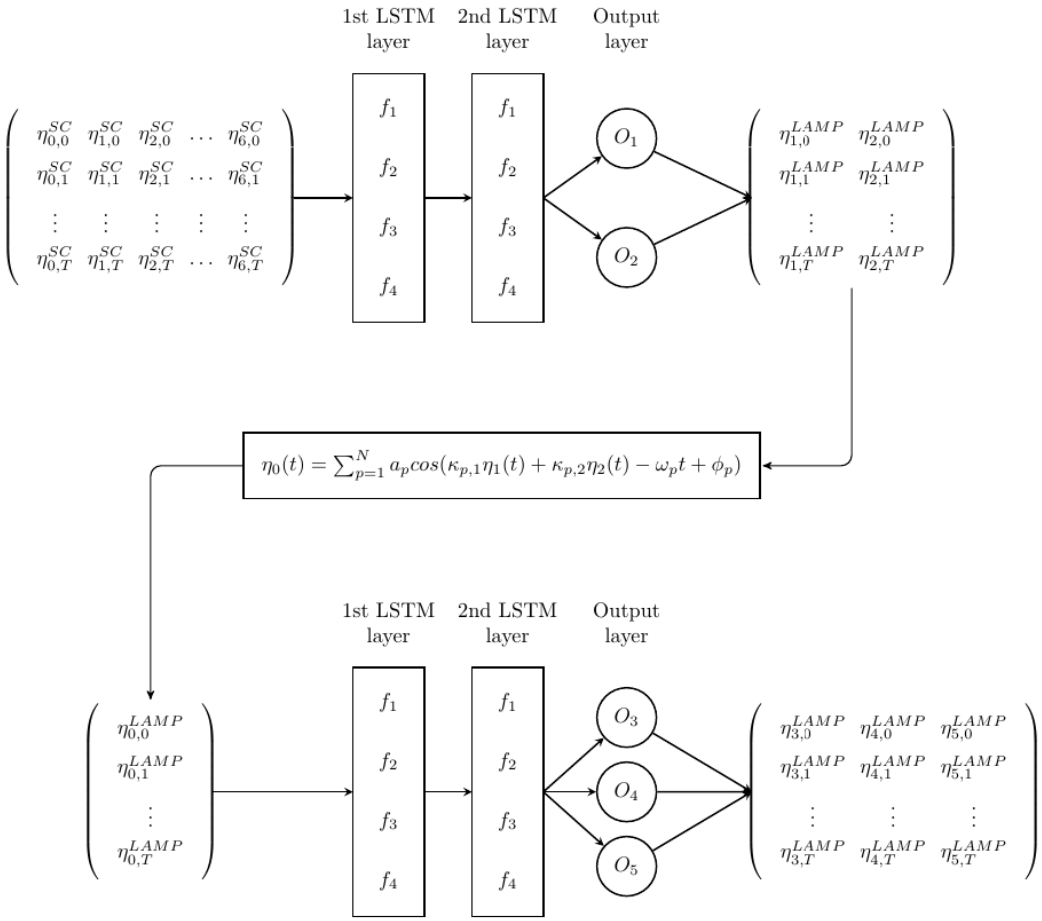

Figure 1: LSTM Two-Step Framework Architecture

Each LSTM architecture consisted of two layers of size 50. The characters and symbols outlined in Figure 1 are described in Table 1. Additionally, superscripts *SC* and *LAMP* indicate that the corresponding time series elements were sourced from SimpleCode or LAMP, respectively. Furthermore, Figure 1 lays out the *training* structure. In testing, the LAMP time series are effectively replaced by LSTM generated time series.

Table 1: LSTM Architecture Parameter Definitions

Parameter Definition	**Variable**
Input wave at time-step j	$\eta_{o,j}$
Total number time steps	T
i^{th} degree-of-freedom at time-step j	$\eta_{i,j}$
k^{th}gate for LSTM layer	f_k
Number of LSTM units per layer	n
Output layer cell for DOF m	O_m
Number of frequencies in spectrum	N
Wave amplitude for frequency p	a_p
Wave number r for frequency p	$\kappa_{p,r}$
Frequency p	ω_p
Phase for frequency p	ϕ_p

Numerical Experimental Setup

The model hullform for this study was the David Taylor Model Basin (DTMB) Model 5415 (Moelgaard 2000). Figure 2 is a rendering of the DTMB Model 5415 and Table 2 provides the particulars for the vessel.

Figure 2: Rendering of DTMB Model 5415

Table 2: Particulars for DTMB Model 5415

Particular	Symbol	Value
Length between perpendiculars	L_{PP}	142.0 m
Beam	B	19.1 m
Draft	T	6.2 m
Radius of gyration about X-axis	k_{xx}	7.1 m
Radius of gyration about Y-axis	k_{yy}	35.5 m
Vertical center of gravity (w.r.t baseline)	KG	7.5 m
Longitudinal center of gravity (w.r.t midships)	L_{cg}	-0.9 m
Displacement mass	Δ_m	8424.4 t

For this case study, a primary International Towing Tank (ITTC) spectrum (ITTC 2002) characterizing wind-generated waves was applied with $H_{\mathrm{s}} = 4.0$ m and $T_{\mathrm{p}} = 15.0$ s (standard Sea State 5 and most probable modal period) and the relative wave heading set to bow-quartering seas (135°). Additionally, the primary ship speed was set to 10.0 knots. Proportional-integral-derivative (PID) controllers maintained speed and "soft springs" maintained heading in both the SimpleCode and LAMP models.

A total of 50 realizations each 30 minutes in duration were generated in LAMP and SimpleCode. The first stage of the framework to estimate the surge and sway was trained with 30 realizations and validated with 10 realizations. The second stage of the framework to predict the 6-DOF motions was trained with 30 realizations, validated with 10 realizations, and tested with 10 realizations. There was not any testing performed during the first stage as only the output of second stage was compared.

The average standard deviations and time series correlation coefficient for heave, roll, and pitch from the 10 test realizations generated using SimpleCode, LAMP, and the LSTM framework were compared. Equation 8 is the formula for the correlation coefficient.

$$\rho = \frac{\mathrm{cov}(x, y)}{\sigma_x \sigma_y} \tag{8}$$

The correlation coefficient is the ratio between the covariance of two random processes, *x* and *y*, and the product of the respective standard deviations σ_x and σ_y. To further capture the reliance on strong correlation with LAMP, the relative motion at the starboard bow was also compared. In addition, the absolute relative error was a comparison metric for SimpleCode and the LSTM method to LAMP. The equation for absolute percentage error is as follows:

$$\epsilon = 100\% * \frac{|\hat{X}_L - \hat{X}_E|}{\hat{X}_L} \tag{9}$$

where $\hat{X}_L$ represents the standard deviation of LAMP data and $\hat{X}_E$ represents the standard deviation of the LSTM estimate or SimpleCode.

In addition to the standard deviation statistic, the estimations of peaks between mean up-crossings were compared. The peaks between mean up-crossings from each of the test SimpleCode, LAMP, and LSTM time series were tabulated and probability distribution functions (PDFs) were generated.

RESULTS

Framework Training

To benefit from the neural network framework, it is important to retain computational efficiency along with accuracy compared to the target. Table 3 shows the time necessary to train the network along with time necessary to generate the data. The network training was performed using a NVIDIA Quadro T2000 GPU with 4 GB of memory,the LAMP simulations were performed on a computing cluster using 8 cores each containing 192 GB of memory, and the SimpleCode runs were generated locally on a 32 GB CPU.

Table 3: Computation Time for Data Generation and Network Framework Training

Process	Stage	Computation Time [s]
Data Generation	SimpleCode	37
	LAMP	9,142
Network Training	Surge-Sway Prediction NN	234
	Heave-Roll-Pitch Prediction NN	705

Table 3 shows that the bulk of the process is generating the higher-fidelity LAMP data. After completing the sunk cost of training the framework, much more LAMP-quality data can be generated with the framework and the small cost of producing additional SimpleCode data.

Statistical Comparison

To evaluate the LSTM method relative to LAMP and SimpleCode, the standard deviation from each degree of freedom was estimated from the 10 test realizations. The absolute relative error of the standard deviation compared to LAMP was also calculated to provide a quantitative comparison. Table 4 provides the standard deviation and relative absolute error between LAMP, LSTM, and SimpleCode.

Table 4: Standard Deviation and Absolute Percentage Error to LAMP for Heave, Roll, Pitch, and Starboard Bow Relative Motion

DOF	LAMP	LSTM	LSTM ϵ	SimpleCode	SimpleCode ϵ
Heave [m]	0.472	0.462	2.1%	0.507	7.5%
Roll [deg]	1.397	1.322	5.3%	3.464	147.9%
Pitch [deg]	1.154	1.142	1.0%	1.108	3.9%
Stbd. Bow Relative Motion [m]	1.567	1.547	1.3%	1.887	20.4%

The LSTM method provided an improvement in standard deviation estimate relative to LAMP for each degree-of-freedom. While SimpleCode provides a reasonable estimate in heave and pitch, the roll prediction is significantly over-estimated, which also affects the calculation of the starboard bow relative motion.

While SimpleCode was able to capture generally the heave and pitch statistics, the SimpleCode model diverges spatially in the wave field relative to the LAMP model. As a result, the ship responses between SimpleCode and LAMP are uncorrelated. Table 5 lists the average correlation coefficients for heave, roll, pitch, and the relative motion of the starboard bow between LAMP, LSTM method and SimpleCode.

Table 5: Correlation Coefficients between LAMP, LSTM and SimpleCode for Each Degree of Freedom

DOF	LSTM ρ	SimpleCode ρ
Heave	0.945	0.000
Roll	0.967	0.001
Pitch	0.980	0.001
Stbd. Bow RM	0.964	0.003

The LSTM method shares a very high level of correlation with LAMP across all degrees of freedom. The high level of correlation is imperative in the estimation and identification of extremes or large peak values. In the following section, the peak and time series maxima behavior are investigated.

Peak Behavior

To investigate the behavior of the peaks for LAMP, LSTM, and SimpleCode, the maxima between zero-up-crossings were tabulated across each test realization for each degree of freedom. Figure 3 provides the kernel density estimates of the PDFs for heave, roll, pitch, and relative motion of the starboard bow for LAMP, LSTM, and SimpleCode (SC).

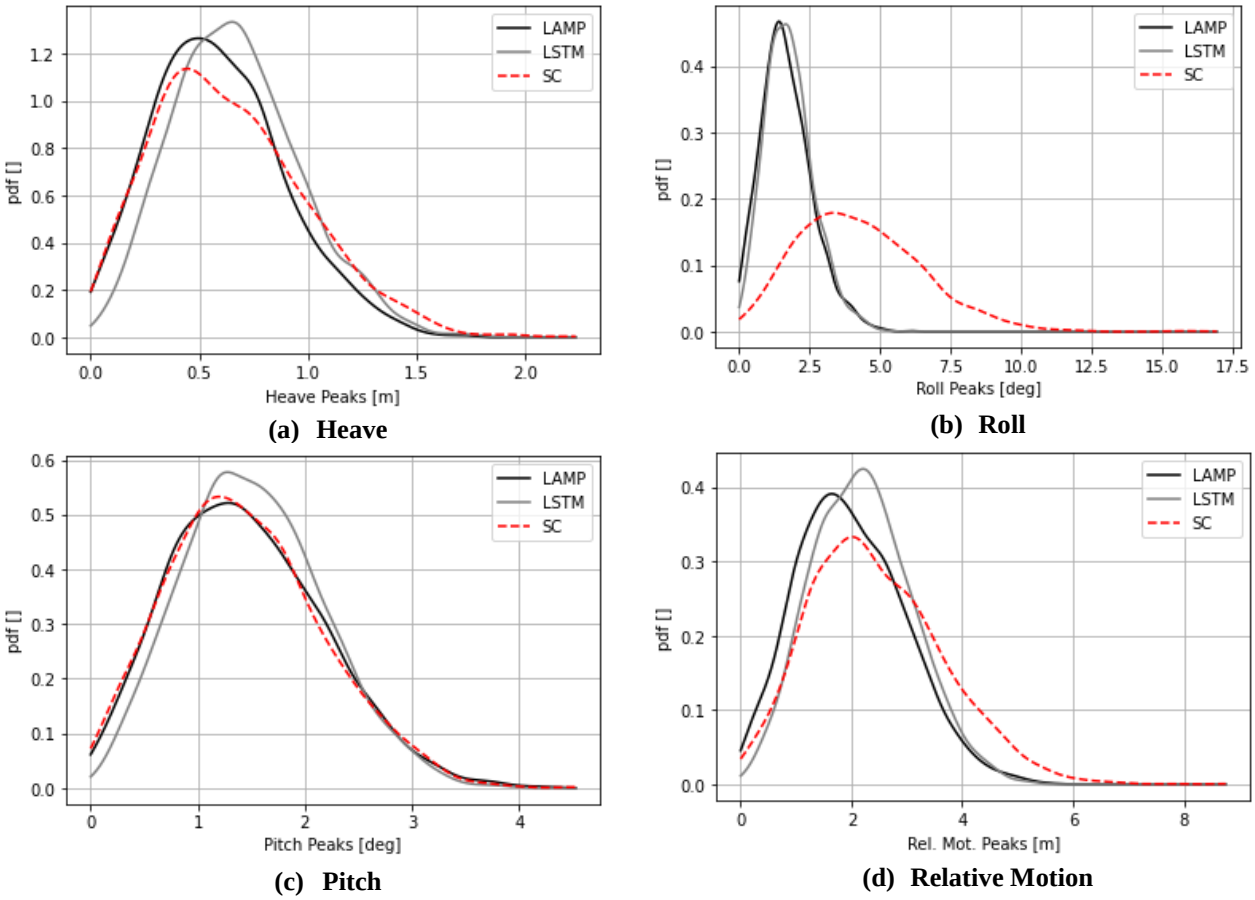

(a) Heave **(b) Roll**

(c) Pitch **(d) Relative Motion**

Figure 3: Peak PDF Comparison for LAMP, the LSTM, and SimpleCode

The most probable peak magnitude (MPPM) and 95th percentile values estimated from each PDF in Figure 3 are summarized in Table 6.

Table 6: PDF Characteristic Comparison between LAMP, LSTM, and SimpleCode

DOF	LAMP MPPM	LAMP 95th	LSTM MPPM	LSTM 95th	SimpleCode MPPM	SimpleCode 95th
Heave [m]	0.50	1.14	0.65	1.22	0.44	1.28
Roll [deg]	1.41	3.36	1.65	3.37	3.35	8.22
Pitch [deg]	1.28	2.72	1.28	2.76	1.20	2.73
Stbd. Bow RM [m]	1.65	3.70	2.21	3.77	2.01	4.62

In general, the LSTM method over-estimates the most probable peak magnitude but generally captures the tail behavior produced by the LAMP simulations. The over-estimation of the moderate peaks is likely a result of a high-frequency modulation that was generated in one of the LSTM networks. An example of the modulation is in the pitch time series section in Figure 4.

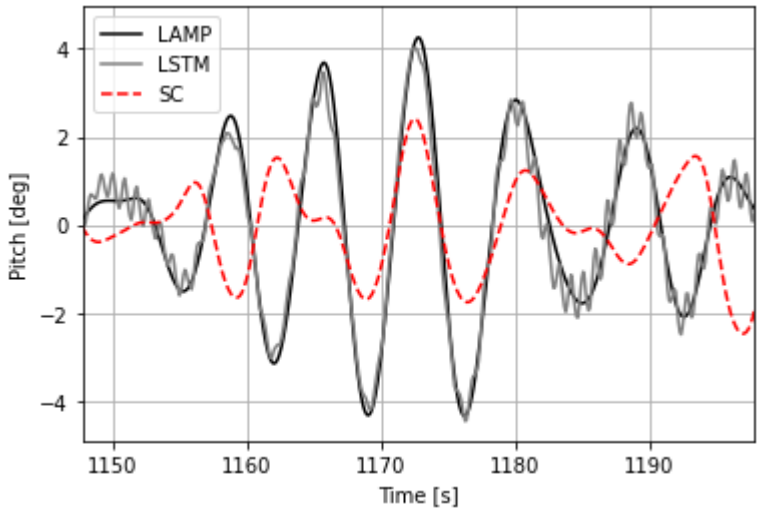

Figure 4: Pitch Time Series of LAMP, the LSTM, and SimpleCode (SC)

The modulation in Figure 4 near the moderate peaks could likely be attenuated with a low-pass filter. Still, the LSTM method is a good estimator of the peaks, particularly in the tail of the distribution. SimpleCode again is a reliable estimator of heave and pitch. However, the SimpleCode peaks are completely uncorrelated to the LAMP peaks and are not necessarily good predictors for a given realization. To test the predictions across realizations, the time series minima and maxima were gathered from the 10 test realizations for each degree of freedom in SimpleCode and the LSTM and compared directly to the corresponding LAMP time series maxima and minima for the given realization. Figures 5 and 6 show the maxima and minima comparisons for each degree of freedom along with the root mean squared error relative to LAMP.

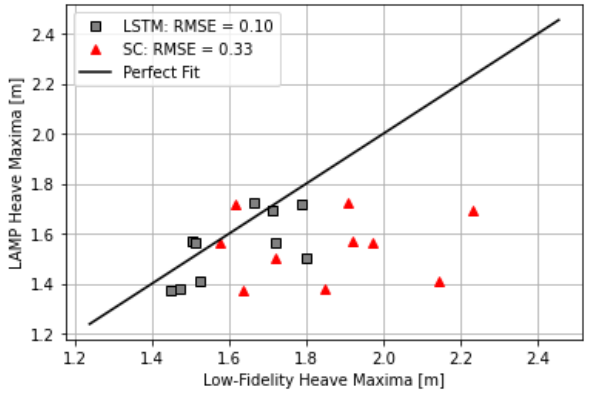

(a) Heave

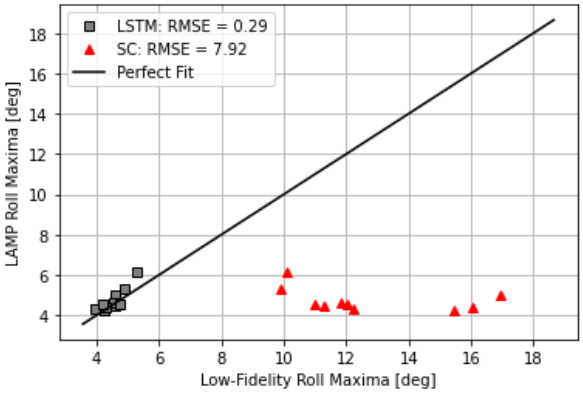

(b) Roll

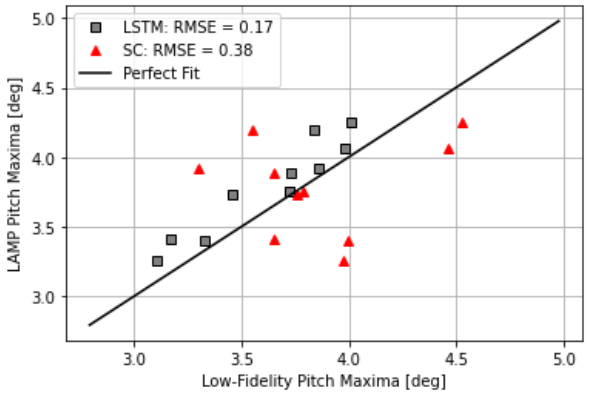

(c) Pitch

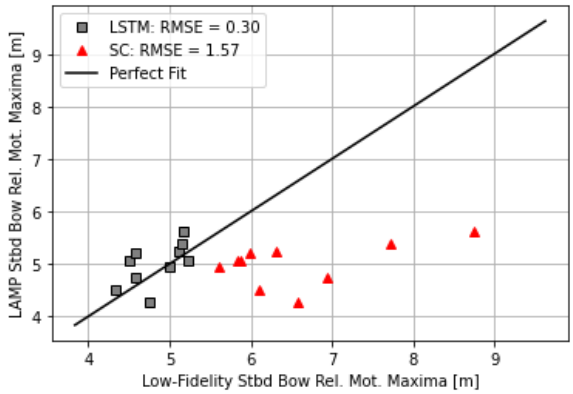

(d) Relative Motion

Figure 5: Time Series Maxima Comparisons

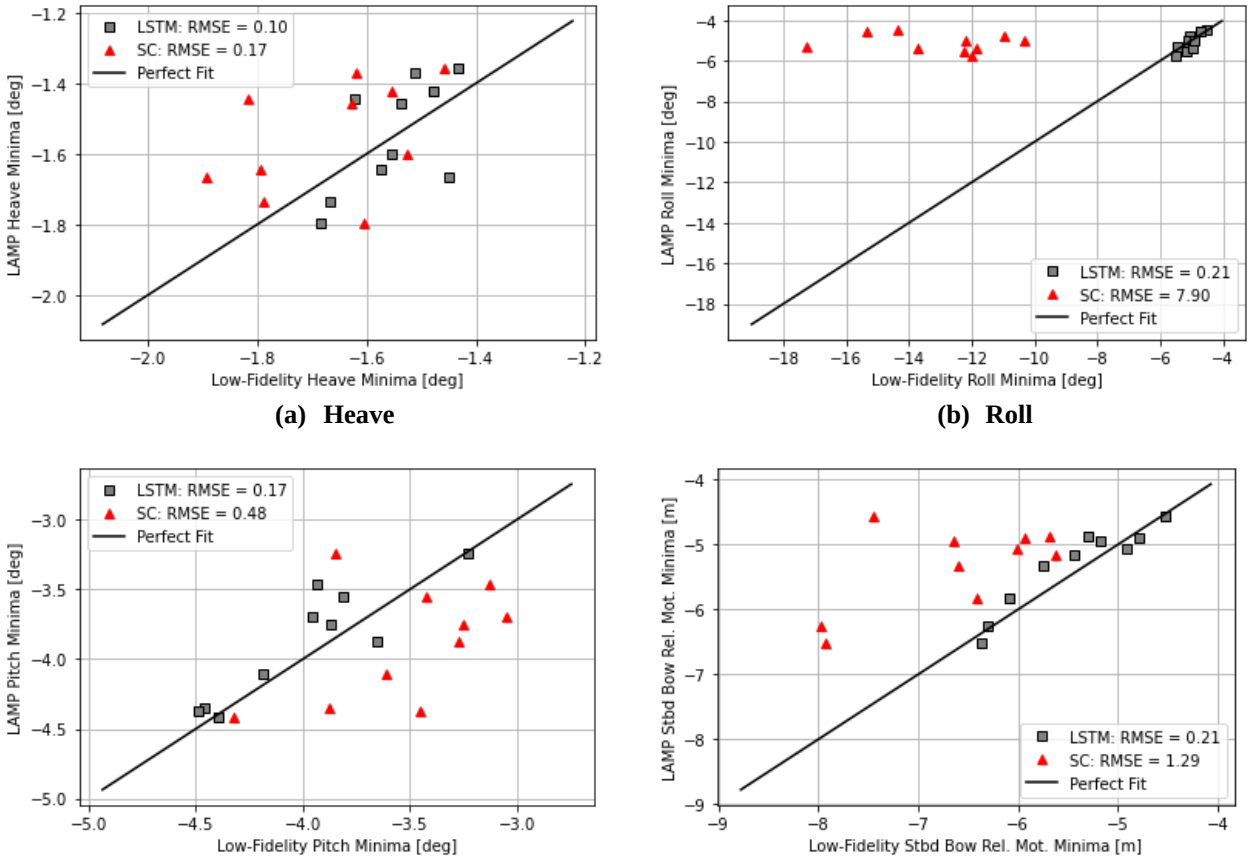

(a) Heave **(b) Roll**

(c) Pitch **(d) Relative Motion**

Figure 6: Time Series Minima Comparisons

An important quality of a good qualitative predictor would be for the largest value in the predictor set to line up with the largest value in the test set. The wave realization that produced the largest magnitude LAMP value should also produce the largest LSTM/SimpleCode value. An absolute conclusion cannot necessarily be made with a small dataset of 10 values but the general trend of behaviors can start to be identified. In general, the largest magnitude LSTM events line up with the largest magnitude LAMP events. While the wave field in SimpleCode was produced with the exact same phases, the global position of the SimpleCode model diverges from that of LAMP; therefore, the time series maxima and minima statistics do not necessarily align with that of LAMP. To be able to identify the largest LAMP time series maxima is very important because as the sea state increases, more non-linear effects are included and SimpleCode no longer is a good quantitative estimator of LAMP. Without the ability to estimate the quantitative extremes or identify qualitative extremes, SimpleCode alone cannot reliably identify extreme conditions in early stage design. However, with the LSTM approach, the issue of identifying the qualitative extremes is addressed but further testing must be done in higher sea states for the quantitative extreme estimates.

CONCLUSIONS

An objective of this study was to assess the potential feasibility of a data-adaptive multi-fidelity seakeeping model for use in early stage design. Data adaptive tuning (or correction) of reduced-order model predictions have been implemented based on training with higher fidelity ship motion response data. From these initial results, this approach provides a plausible means for improving the performance of a reduced-order model for ship response estimation.

LSTM neural networks have been incorporated as part of a multi-fidelity approach for prediction of 6-DOF ship motion responses in waves. LSTM networks were trained and tested with LAMP simulations as a target, and SimpleCode simulations and wave time-series as inputs. LSTM networks improve the fidelity of SimpleCode seakeeping predictions relative to LAMP while retaining the computational efficiency of a lower-fidelity simulation tool.

The LSTM neural networks trained through a hybrid approach comprised of a physics-based model and data-adaptive stage. The results indicate that the LSTM architecture is an improved predictor of the LAMP time-series maxima and first-order statistics compared with SimpleCode.

In practice, an entire matrix of condition combinations would be run through the seakeeping software to determine an operating envelope for each sea state. To account for the many combinations of conditions, especially in the early design stage, to obtain accurate but rapid estimates of these statistics is vital. The LSTM method provides a basis for addressing this problem in reducing the time to produce many realizations of different conditions quickly with a level of fidelity approaching a higher-fidelity code like LAMP. Of course, to be feasible, the method must demonstrate extensibility to other sea states, relative wave headings, and ship speeds to effectively reduce the computational effort. Still, even with training and testing on a single environmental and operating condition, the LSTM method could produce many higher-fidelity realizations in a relatively short period of time, which would be valuable for estimating extreme characteristics.

Based on the results of this study, the two-stage LSTM architecture trained to correct SimpleCode global positioning is a suitable candidate for further investigation and application to extreme event predictions.

Potential future work includes:

- For prediction structural loads, accelerations, and resistance.
- Extending assessment to cover a range of wave parameters including significant wave heights, modal periods, ship speeds, and relative wave directions.
- Application to other hull form geometries.
- Evaluation of LSTM network configurations in terms of hyperparameters and prediction performance.
- Investigation into Bayesian LSTM networks to include uncertainty in time series predictions

ACKNOWLEDGEMENTS

The authors would like to thank the SMART SEED Grant for providing the funding necessary for this study.

CONTRIBUTION STATEMENT

Samuel J. Edwards: Conceptualization; software; data curation; methodology; formal analysis; visualization; writing – original draft. **Michael Levine:** conceptualization; writing – review and editing.

DATA ACCESS STATEMENT

No publicly accessible dataset was used in this paper.

REFERENCES

Alford, L. (2008). Estimating Extreme Responses Using a Non-Uniform Phase Distribution. Doctoral dissertation. Ann Arbor, Michigan, USA: University of Michigan

Hochreiter, S. and Schmidhuber, J. (1997). Long Short-Term Memory. *Neural Computation*, *9*(11), 1735-1780

International Tow Tank Conference (ITTC). (2002). The Specialist Committee on Waves – Final Report and Recommendations for the 23rd ITTC. *Proceedings of the 23rd International Tow Tank Conference*. Venice, Italy

Kim, D. (2012). Design Loads Generator: Estimation of Extreme Environmental Loadings for Ship and Offshore Applications. Doctoral dissertation. Ann Arbor, Michigan, USA: University of Michigan

Levine, M.,Edwards, S. J., Howard, D., Weems, K., Pipiras, V., and Sapsis, T. (2024). Multi-Fidelity Data-Adaptive Autonomous Seakeeping. *Ocean Engineering, 292*

Lin, W. and Yue, D. (1991). Numerical Solutions for Large Amplitude Ship Motions in the Time-Domain. *Proceedings of the 18th Symposium on Naval Hydrodynamics.* Ann Arbor, Michigan, USA.

Moelgaard, A. (2000). PMM-tests with a Model of a Frigate Class DDG-51. Report 2000071, No 1. Brandy, Denmark: Danish Maritime Institute, now Force Technology

Pipiras, V., Howard, D., Belenky, V., Weems, K., Sapsis, T. (2022). Multi-Fidelity Uncertainty Quantification and Reduced-Order Modeling for Extreme Ship Motions and Loads. *Proceedings of the 34th Symposium of Naval Hydrodynamics.* Washington, D.C., USA

Reed, A.M. (2021). Predicting Extreme Loads and the Processes for Predicting Them Efficiently. *Proceedings of the 1st International Conference on the Stability and Safety of Ships and Ocean Vehicles.* Glasgow, UK

Shin, Y.S., Belenky, V., Lin, W., Weems, K. (2003). Nonlinear Time Domain Simulation Technology for Seakeeping and Wave-Load Analysis for Modern Ship Design. *SNAME Transactions, 111*, 557-589

Smith, T. (2019). Validation Approach for Statistical Extrapolation. In: V. Belenky, M. Neves, K. Spyrou, N. Umeda, F. van Walree (Eds.), *Contemporary Ideas on Ship Stability, Risk of Capsizing* (pp 573-589). Springer

Weems, K. and Belenky, V. (2018). Hybrid Models for the Fast Time-Domain Simulation of Stability Failures in Irregular Waves with Volume based Calculations for Froude-Krylov and Hydrostatic Forces. *Proceedings of the 13th International Conference on Stabiltiy of Ships and Ocean Vehicles.* Kobe, Japan

Weems, K. M., and Wundrow, D. (2013). Hybrid Models for the Fast Time-Domain Simulation of Stability Failures in Irregular Waves with Volume based Calculations for Froude-Krylov and Hydrostatic Forces. *Proceedings of the 13th International Ship Stability Workshop*. Brest, France

Proceedings of 15th International Marine Design Conference (IMDC-2024)
June 2-6, 2024
Amsterdam, the Netherlands

Digital Shipbuilding – Needs, Challenges, and Opportunities

Jose Jorge Garcia Agis[1,*] and Per Olaf Brett[2]

ABSTRACT

Ship design firms, shipyards, and ship equipment manufacturers – the shipbuilding industry or just shipbuilding, must adapt their products and services' deliverables to the steadily evolving expectations of the stakeholders in the market.

Digitalization and the use of computational tools have been suggested as the effective means to meet such challenges. However, many anecdotal statements and industry recognitions have expressed concern that such efforts have proven less effective than should be expected and promised, and opposite to what many application suppliers advertise. It is argued by this paper that such a situation is experienced because of, among other explanatory factors, incompatibility, lack of proper protocols for information sharing and isolated implementation efforts in single departments rather than a holistic organizational approach. The lack of full understanding of the ship designer's role and responsibility as the main facilitator of such a change process is also recognized as a clear weakness in the effort of successful digitalization of shipbuilding. It is argued that such a vital transformation process cannot be left alone to the software application providers, despite their size and dominance.

This paper explains and discusses why this situation is experienced and indicates what improvement measures could be introduced to counteract the opportunity loss. The article addresses five potential digital service deliverables that could complement the existing service delivery of shipbuilding operations and thereby increase competitiveness and market attractiveness. These services include a) vessel support and control centres, b) performance monitoring, c) maintenance management, d) spare part handling, and e) life cycle assessment (LCA). The article also reflects on what implications and consequences this development has on the ship designers' work and their firm's adaptation to new services' demand in the shipbuilding market. The paper concludes with some reflections on the actual implementation of these services, highlighting challenges and further opportunities.

KEY WORDS

Digital; digitalization; shipbuilding; ship design; opportunity search

NOMENCLATURE

PLM – Product Lifecycle Management, ERP – Enterprise Resource Planning,

INTRODUCTION

Ship design firms, shipyards, and ship equipment manufacturers – the shipbuilding industry or just shipbuilding, must adapt their data-based deliverables to the steadily evolving expectations of the stakeholders in the market, and adjust their value chain positions and interrelationship with relevant project stakeholders to achieve maximum value creation and competitiveness. This will require going beyond traditional and existing ship design and shipbuilding activities and tools. This is much in line with

[1] Ulstein International AS (Ulsteinvik, Norway); ORCID: 0000-0001-6610-1136
[2] Ulstein International AS (Ulsteinvik, Norway), Norwegian University of Science and Technology (Department of Marine Technology, Trondheim, Norway); ORCID: 0000-0002-8767-5494
* Corresponding Author: jose.jorge.agis@ulstein.com

Submitted: 24 February 2024, Revised: 16 April 2024, Accepted: 1 May 2024, Published: 20 May 2024

Conference paper, DOI: https://doi.org/10.59490/imdc.2024.849 e-ISSN: 3050-4864

our recent observations that market expectations are quickly moving towards a more integrated demand and supply situation for products and services. Such services are: - environmental performance of vessel; - performance-based and predictive maintenance; -autonomous operations; - sustainability reporting; - green loans, - emission regulations; - real-time performance evaluation and optimization; - recycling of vessels; - reuse of materials, equipment, systems equipment, vessel and fleet traffic and port operations and their complementary product tools. Efficient communication and information exchange channels must be set up between these downstream services and upstream ship design solution work activities to provide continual feedback and feed-forwarding to secure effective operational decision-making support. Hence, the complexity and uncertainty of such decision-making related to shipbuilding – ship design and erection, and ships-in-operation will continue increasing (Brett et al., 2022; Ebrahimi, 2022; Garcia, 2020).

The interrelationships among stakeholders involved in shipbuilding projects, manufacturers, other service providers, work processes and tasks performed by each engaged actor, have become a "spider-web"- type network of information exchanges and transaction-oriented situations to support the identification, collection, collation, storage, and dispersion of such information and or data. Value chain communication needs and appropriate exchange channels, tools, and formats have, therefore, grown considerably – in scope, extent, and use. A worldwide shipbuilding activity exists out there, where owners and financiers can be in one region, the ship designer in another region, the shipyard and equipment supplier in a third or fourth region, and other stakeholders like flag state, class society, and charterers (cargo owners) being in an "opposite direction of the world". There is no doubt that such a dispersed network of project actors and information exchange model could not easily function without the internet and other efficient satellite-based communication facilitating channels.

What a few decades ago was a simplistic discussion between two actors in the value chain about what engine size and type to install onboard – a choice among 2 to 3 relevant options, has today, become a much more complicated and cumbersome multi-stakeholder involved decision-making process where fundamentally different energies (fuels), energy converters (engines, fuel cells), energy storage and transfer systems came into place. Further, varying expectations and regulations as to energy usage and emissions are making the selection of the power plan of a vessel a dynamic, rather than static choice. Most of the vessels being designed today will have to make modifications to their power systems during their operational lifecycle. Similarly, the expectations of the end users of the vessels are changing, requesting much more transparency about the vessels and their operations. Emission reporting has already become a requirement for many vessels. Financial institutions, charterers, and cargo owners frequently request information about the markets within which the vessels are operating, the stature or physical condition of the assets in use, and the economic situation for the vessel and owner - and the list of information users continues. More than ever, operational and performance data and information exchange relating to capabilities and functionality have become a central element of vessels' design, ship erection, and operation, and must be well planned to maximize the benefits.

In shipbuilding, we, therefore, see a rapidly growing tendency of increased interaction among stakeholders in the maritime value chain and the need for improved information exchange. Digital connectivity increases in most organizations due to the pressure outside by customers and other stakeholders. But also, internal needs relating to work process harmonization and enhanced value creation employing new products and services are growing. Looking from a multi-modularity and interdisciplinary point of view, it is crucial to understand how to make seamless exchange interphases and data transfer protocols from one stakeholder to the other and between ship designers, shipbuilders, and system suppliers. Yet, the authors suggest that today, shipbuilding organizations should think about their digital connectivity around the system they are or represent and the new added value activities to be created step-by-step. This will mean that ship designers in their preparation of a ship design solution and the shipyard, must take into consideration these new challenges and promising digital solutions. The appreciation of current data availability, storage capacity and increasing capabilities of software applications are key drivers in opening new business opportunities, and the emergence of big data analyses and artificial intelligence (AI and generative AI) bring them further capabilities that will undoubtedly enhance our understanding of the extended potential. The way we perform design work or ship construction work today, and how we treat and store information, will enable (or constrain) the potential services that shipbuilding companies can perform in the future.

Figure 1 depicts an overall situation of shipbuilding activities, which need to be interconnected and as seamlessly as possible ensure that critical information is relayed among the elements of the digital business model or value chain elements for shipbuilding.

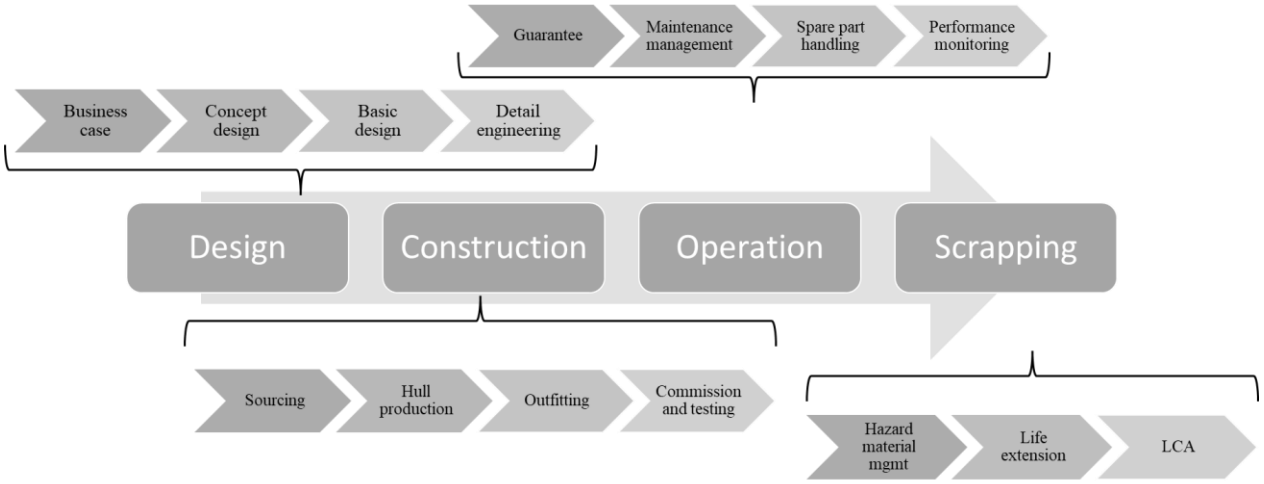

Figure 1. A digital business model for shipbuilding.

Unfortunately, there is no general framework or architecture for digital connectivity or data description to be easily enabled and implemented. Such a broader digital generic connectivity system is missing. Shipbuilding is a small and special industry, requiring specific architectures that, due to limited volume sales potential, few are interested in developing. Requiring, therefore, a strong collaboration between ship design software providers, data and document management providers and shipbuilders (Gaspar et al., 2023). Such lack of digital architecture for shipbuilding delimits the overall understanding and opportunity search for the full exploitation of digital ecosystems and their virtual interoperability. An example is the application of virtual reality (VR) tools in early concept ship design, which have been claimed to potentially provide efficiency improvements to the overall process (Schiavon et al., 2019). The author's previous recent research has concluded that the use of VR in conceptual ship design has revealed that very often its application is time-consuming and user-case limited, resulting in an extensive "nice-to-have" feature, and not a means to improve efficiency (Garcia et al., 2020). In the future data economy, the question is, therefore, not anymore who has the monopoly of the data. The question then becomes how to make the organizations interoperable and build new capabilities to exchange the data/information with the domain of their business interoperability (Arola, 2018; Keane et al., 2017).

This article briefly discusses aspects of such a new complex business situation. Certain interoperability aspects mentioned above are deliberately left out of the discussion of reasons for the consequent length and comprehensiveness of the article. This article, therefore, focuses primarily on some of the lifelong data exchange and service opportunities and reflects what implications such new business interoperability can have on the ship designer and the shipyard operations – other aspects of digitalization in shipbuilding are left out in this article. At the same time, it is fully appreciated that the development and implementation of such new technologies will be challenged by high cost, and human-resources consumption, since the industry is characterized by having a fairly short time horizon for their investments, and are deeply conservative when it comes to new ways of doing things (Keane et al., 2017). Considering these premises and difficulties of directly connecting technological developments to growth in revenue and profits - competitiveness, historically it has taken time for such improvement efforts to become realized and derivative effects to come to fruition.

From vessel to "system of systems"- thinking

Given this new situation, it is tempting to make a parallel to what contemporary systems thinkers claim: " that the whole is more than the sum of its parts and that everything is interconnected" (Jackson, 2019). They suggest that you must always start with the whole system because you need to know everything to know anything. Further, unless you know the whole system, you cannot justify acting because you can never anticipate the results. When it comes to digitization of shipbuilding, it is argued in this article that, a similar systemic approach is necessary to reveal as many of the drivers and enablers elements and causal factors influencing.

Hence, expectations and demands from shipping companies as to the delivery of a vessel and the services related to it are also changing. This requires going beyond traditional ship design approaches and traditional shipyard activities and the maintenance and repair work during the lifecycle of the vessel. Market expectations are developing towards a more integrated delivery where aspects such as environmental reporting (environmental footprint in design, production, operation, and recycling phases),

performance- and predictive-based maintenance, autonomous/remote operations, etc. A traditional basic design drawings package with complementary outline specifications and supporting analysis reports is simply not sufficient any more as transaction and information documentation between the service provider and buyer. Such needs for increased information exchange and life cycle follow-up possibilities of assets or services being provided over time, must be catered for within the delivery of the vessel in the future, either by the ship designer, the shipyard, equipment supplier and or other third parties or all of them together.

Thus, what is delivered is no longer just a vessel design solution or a manufactured ship, it is a three-level information or data-producing repository: level 1 – the ship as a twin, level II - the ship when in operation and at level III, the ship in operation within the broader shipbuilding values chain model – a system of systems.

What does digital mean?

Digital is a broad term. It is sometimes uncritically used as a badge to represent anything new. Often it is applied to distinguish from other practices, behaviours or products that are simply older (Fletcher & Adolphus, 2021). "A wider appreciation of the increasing scale and wide-ranging impact of digital technology in contemporary economic and social activity leads directly to an acknowledgement of the importance of developing and maintaining a digital presence", they conclude (Dörner & Edelman, 2015) On the other hand, argue for digital to be seen less as a thing and more as a way of doing things. In this way, they argue, "digital is an enabler for action, not a goal in itself". Examples of this interpretation are digital marketing, digital business; e-commerce; or even email. In this article, we address digital as various actions to accomplish improved competitiveness and attractiveness – making a preferred supplier in line with the Dörner and Edelman (2015) interpretation. Thus, we discuss in the further of this article, digital shipbuilding, web-based ship design, and digital ships-in-operation.

Digitalization – a deeper view

What is digitalization? The use of digital technologies to change an organization's business model to provide new revenue and higher value-producing opportunities – the process of moving to a digital business (*Digitalization*, 2024).

It is already well recognized and argued by many that digitalization has and will have a profound impact on how to execute shipbuilding business and create sustainable ship design-related products and services in the future. But it is important to notice that digitalization transforms products from physical goods into tangible services, in many cases into manipulated data and data analyses results as the "product or service". It supports the increased speed at which products and services are being produced and implemented using digital processes, data, and communication channels. Digitalization efforts support viewing work processes, products, and services as a source to generate and collect more information - leading to increased value creation.

There are 12 critical elements of successful digital transformation:1. End-to-end connectivity, 2. Data and work process management, 3. Configuration management, 5. Model-based application structures, 6. A digital thread, 7. Digital twins, 8. IOT and PLM platforms in place, 9. Changing views of product – into servitization, 10. Big data analytics, 11. Data governance and security, and 12. Digital expertise and skills transformation (MacKrell, 2024).

Among the 12 digitalization enablers, the digital thread (6) is looked upon as the most important because it relates to the communication framework that allows a connected data flow and integrated holistic view of the value chain and business concept throughout the products and or the services' delivered lifecycle across traditionally siloed functional perspectives.

Furthermore, digitalization has three powerful implications for product and service development and lifecycle management: - ensuring that all stakeholders and transformation processes are fully accessible with access to all data, - reversion of data files (documents) into data records to unlock them and reducing them as typical stumbling blocks, because nobody remembers where to find them. Finally, big data is at the heart of digitalization.

Digitalization has no "borders"

The pivotal digital technology for realizing all these opportunities is the internet and satellite communication. Without this well-established, open, and global network of computing working under the same protocols and processes, what we now label digital would simply not work. Increasingly the purpose of computers, laptops, tablets, and mobile phones is to have physical touchpoints on the internet (Fletcher & Adolphus, 2021; Gaspar et al., 2014). "Exploiting the unique characteristics of the internet is at the heart of understanding how to create and capture value through a digital presence", Fletcher and Adolphus (2022) state.

This digital mindset must go beyond the traditional digitalization of design and production processes; however, it is here where it should start. The information generated during the design and production phases of the vessel should lay the foundation for the future of digital shipbuilding operations. History, however, shows us that digitalization and the use of computational tools for analysis and drawing production have proven to be less effective than should be expected and promised. It is argued by this paper that such a situation is experienced because of incompatibility and lack of proper protocols for information sharing. The authors of this paper are convinced that digitalization has been performed in silos, one activity at a time, and without an overall holistic plan. Furthermore, overambitious software application development – one system (suites) for all purposes and needs, rather than building up a step-by-step functionality and allowing a robust platform infrastructure. Also, underestimation of the time of populating these new applications and costs of training and start-to-use initiatives have among other factors contributed to the digitalization disappointment, so far. This does not mean gains cannot be met or arrived at, but it will take time, extra costs, and pain to get there.

The toolbox of shipbuilders (incl. ship design companies) typically consists of system platforms, 3rd party special applications, and internal proprietary bespoke software applications. Such systems are normally not developed with effective connection protocols for the exchange of design and production information with external receiving applications. This situation creates significant extra work and costs, deteriorating the competitiveness of the industry. Alternatively, shipbuilders can go in with a full software system supplier delivering all the tools, becoming too dependent on the single software supplier.

This paper explains, discusses, and suggests improvement measures for how to enhance the effectiveness and efficiency of these information exchange processes. Enhancements are closely linked to a better understanding of how the information stream flows among all relevant stakeholders with an emphasis on addressing commercial, operational, and technical matters.
This article discusses the overall competitiveness challenge the shipbuilding industry is exposed to and the need for change to meet present and future opportunities. The availability and use of current computational tools are limiting shipbuilders in expanding their business due to this fact. This article builds on the foundation that the European-funded SEUS project (Gaspar et al., 2023) is building, and will explore complementary digital business opportunities for shipbuilding companies.

Digitalization - "raison d'etre"

This article highligths the importance of making connections and building relationships through digital channels is part of the purpose of creating a worldwide presence as a part of competitiveness building, also it emphasizes a mindset of sharing, openness, and transparency so vital for ESG recognition. Digitalization should help us to a) improve profit margins of design, engineering, fabrication and assembly (traditional shipbuilding deliverables), and b) exploit opportunities within aftermarket activities and early design.

Figure 2 shows how the estimated average performance yield of different activities of the shipbuilding value chain for two different periods for a selection of Norwegian firms. The results for 2006/12 are the performance yield during "good market" conditions and the 2016/22 results represent "bad market". There is a significant level difference among the main value chain activities – typically, the upstream ship design-focused business produces acceptable, but low-profit margins, ship erection or hull production notoriously low partly unacceptable profit margins, and downstream "aftermarket" or life cycle-oriented services produce profit margins at encouraging and attractable high levels. When we know that the downstream value chain activities yearly and over the lifetime of the vessel, typically 20 to 30 years, bring in such high-profit margins successfully positioning oneself in that part of the shipbuilding value chain is a "no-brainer", if possible, when, and for how long.

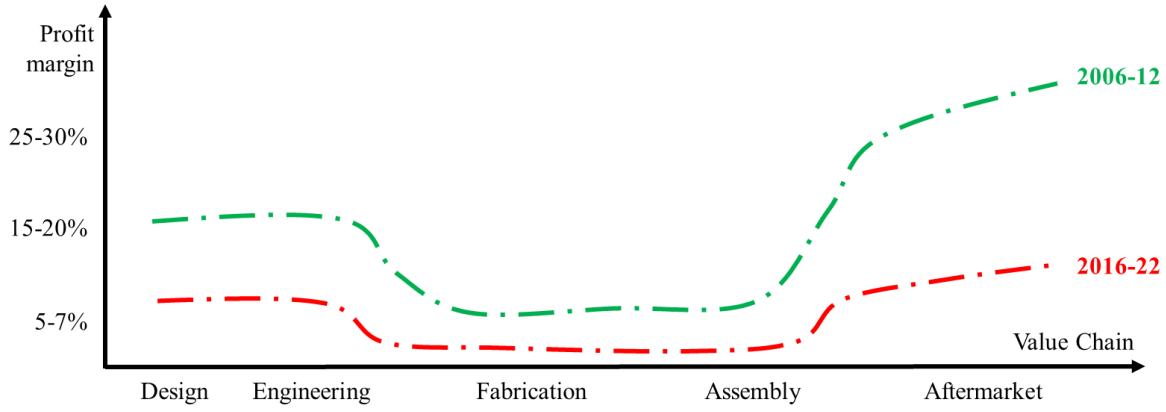

Figure 2. Profit margin of different activities in the shipbuilding value chain.

Many shipbuilding companies are currently in transition wrt to what future avenues to take: i) status quo – stick to what you already are and try to make the best out of it, or ii) adapt to the new demands and transition to digital shipbuilding – develop, expertise and skills to handle a new digital service portfolio. Such a transition will require a fundamental change for most shipbuilders. A new "digital mindset" (Leonardi & Neeley, 2022) must be established to understand how data, information, and digital solutions can enhance the existing business model or completely revamp it.

A DIGITAL FOUNDATION FOR SHIPBUILDING

Product lifecycle management (PLM) is the process of managing product-related design, production, and maintenance information. PLM integrates people, data, processes, and business systems and provides a product information backbone for companies and their extended enterprises. The word PLM is not new in the maritime industry, but to date, its implementation is scarce and to some degree not successful (Recio Rubio et al., 2023). A strong reason for the limited implementation and success is that in most cases a standard PLM structure has been pressed into a ship design and shipbuilding process. Hence, pushing ship designers and builders to change the way they were working, rather than adapting the PLM software to the peculiarities of the industry.

An internal survey among employees of a Norwegian shipbuilding firm identified some key challenges that employees considered as the anchors for further improvements in productivity and process efficiency (NA, 2018). These challenges include: i) product and design data are not organized – because every project has its peculiarities, the same information is not available for all the projects, and if so, it might have a different name or be stored in a different folder; ii) company knowledge is residing in people's heads. The experience and knowledge developed at ship design firms are primarily tacit, hence difficult to store and retain isolated; iii) very limited reuse partly because required information is hard to find. For early concept development, when a project is finished without a shipbuilding contract, the documentation is rarely reviewed and categorized. Thus, the re-use of this information is limited, as people might not be aware of it, or don't have contextual information about the project or the status of the documentation; and finally, iv) multiple specialized software packages model the product from different viewpoints, making difficult and time-consuming the synchronization of design changes. Different areas of a ship design firm and shipyard have their specialized software, which requires either a strong connectivity between software solutions, or manual work to ensure correct product definitions. The structural department might use a different hull definition than hydrodynamics, and the general arrangement might be drawn based on hull lines from the 3D rendering tool. Hence, three hull designs need to be synchronized and calibrated to secure mirror definitions.

A summary of the main challenges identified in the survey is depicted in Figure 3 below.

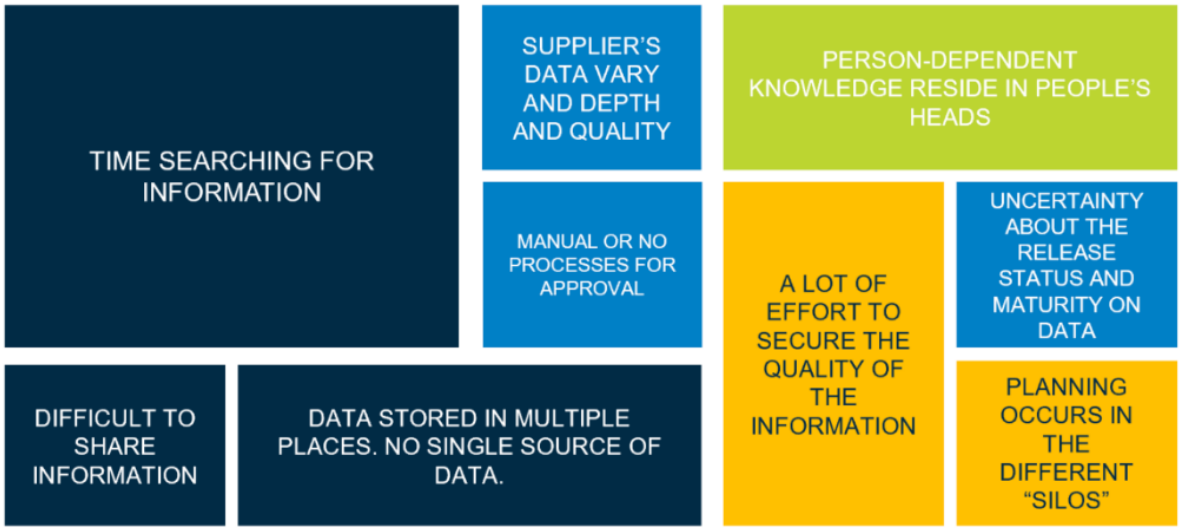

Figure 3. Challenges identified on current data and project management practices at Ulstein.

Interconnectivity among software utilized in ship design and shipbuilding activities is essential to secure a smooth and effective implementation of PLM. Figure 4 reflects the complexity of software integration. The overview does not include all the functions or software used by a ship design firm or a shipbuilding company, but the most critical ones. The integration of systems/software needs to follow a stepwise approach. Each stage of the implementation process pursues covering one of the expectations and goals defined.

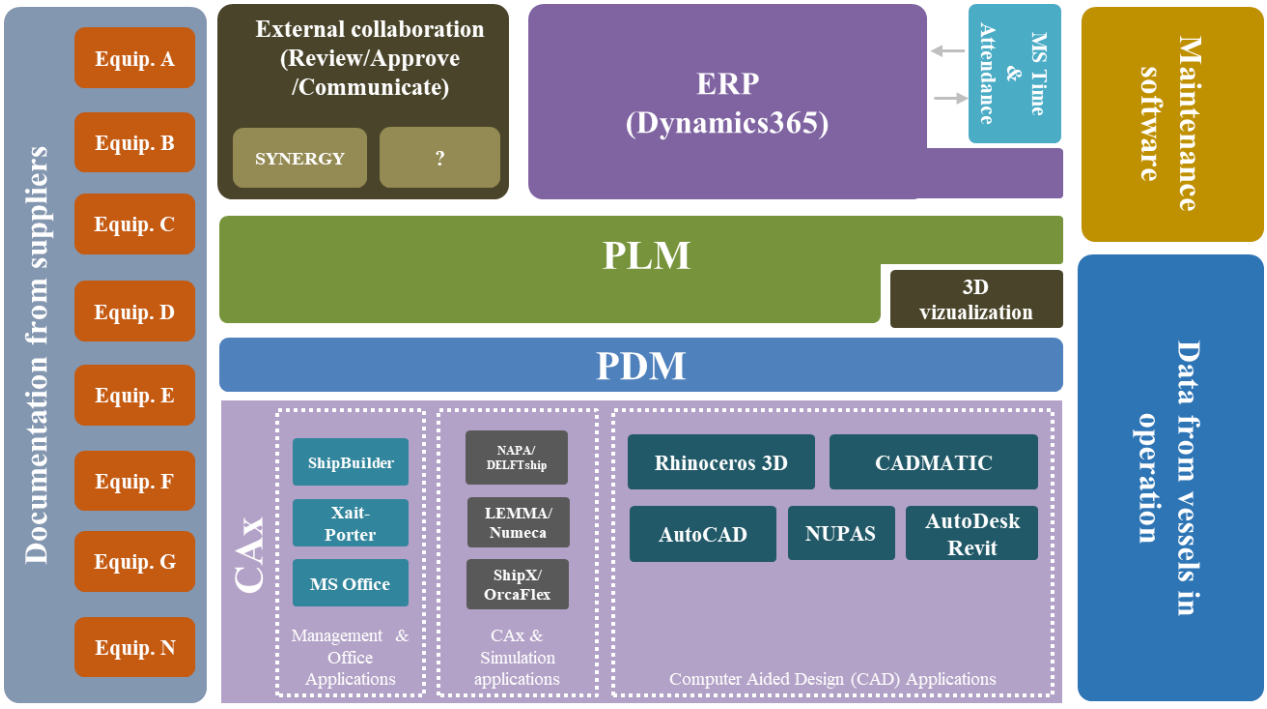

Figure 4. Software integration and complexity of shipbuilding projects.

The partners in the European-funded SEUS project are working on establishing this platform, integrating a well-established project and data management tool (Contact Software) into a well-established design tool (Cadmatic) (Gaspar et al., 2023). Connecting these two central elements of shipbuilding projects, the consortium targets 30%-time savings in engineering activities and 20% in production and assembly. Achieved by architecting and developing an integrated platform for a combined and open solution incorporating CAE, CAD, CAM, and PDM software and testing it at shipyards. The new platform solution will be built with the best European shipbuilding expertise provided by academic and industrial partners. Figure 5 organizes the value chain activities, indicates from estimates the savings potential in time saved, and suggests by what means these accomplishments will be achieved (Gaspar et al., 2023).

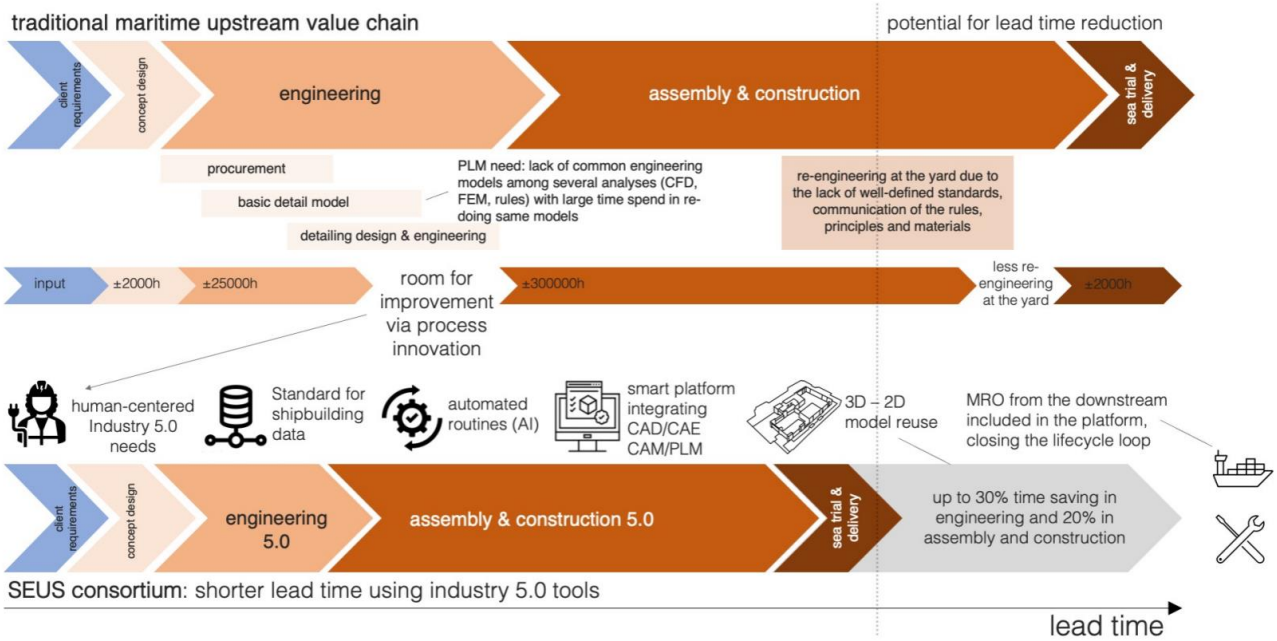

Figure 5. Potential for lead time reduction predicted by SEUS project (Gaspar et al., 2023).

But when all that data information has been generated, captured, structured, and stored during the design and building phases, is there any potential for further value creation during the operational and scrapping phases? What can be done with such information, and who will do it? It is argued in this article that such achievements can be obtained by carefully planning, developing, and stepwise implementing a digital business model for shipbuilding representing the digital thread or electronic communication structure necessary to integrate both upstream and downstream shipbuilding value chain activities.

A DIGITAL BUSINESS MODEL FOR SHIPBUILDING

Business models describe the design or architecture of the value creation, in other words, describe how a firm plans to deliver value to its customers and be left in a position to perform such businesses sustainably, including, but not limited to economic and financial performance (Teece, 2010). The business model of ship design firms relies on the provision of ship design drawings and calculations (Lagemann et al., 2024), while the shipyard focuses on the construction of vessels and integration of vessel systems. As the ship owner takes control of a vessel after delivery, the state of the vessel traditionally transforms information-wise from "as built" to "as is". Thus, from the moment a change is made onboard when the ship is in operation – either by the crew, equipment supplier or by a third-party shipyard, the documentation of the vessel and its systems become quickly incorrect or at worst, obsolete. Hence, as the "ownership" of the "ship description"- specification, drawings and complementary vessel records/reports, changes hands in the value chain, the information and interrelationship interphases are challenged wrt what, when, and which formats shall be used and who is responsible for making the transactions take place. Who is responsible for the updates, collection, and safe and secure storage of this information? During the lifetime of the vessel, typically, this information transfer process can take place several times, when the ships are shifting ownership hands. Over time, it has been experienced that it is difficult if not impossible to start working on the upgrading of the vessels from a re-designing and refit standpoint without updated and "as is" past and present condition status documentation of the ship.

Traditionally, such downstream activities have been carried out by "any ship designer and shipyard" available with the capacity to handle such a particular vessel – not necessarily the ship designer and or shipyard that originally built the ship. Such situations represent very often a major hassle to the shipowner in terms of providing needed original – "as built" documentation of the vessel to be shared with the repair yard. Far too often has the vessel that has been subject to alterations underway – in some cases larger upgrades or conversions have taken place, in other circumstances has the vessel been subject to minor changes of which in many cases, the complementary documentation of these changes is non-existent or at best poorly described and supplied. No doubt, therefore, it is critical to the owner and repair yard that upgrading the information history of the vessel is well documented and preferably can be supplied electronically and efficiently shared with relevant stakeholders. To counteract this lack of "as is" information, many repair yards, and consultants have had to 3D scan the whole ship or relevant parts of it and reproduce 3D work drawings for progressing in the task at hand. Such expensive and time-consuming extra work would be unnecessary if proper digitalization of shipbuilding was in place.

Yet, these "anyone" shipbuilding outfits have no original deep understanding and appreciation as to how and why the vessel was designed, constructed, and equipped the way it was and what are the accompanying operational premisses or/and restrictions. The original ship design firms, designers, and shipyard building the ship, are, therefore, in a much better and partly unique position to take a central role in this integration exercise and required digitization development. They are the ones who know best the original vessels and most likely are best prepared to make changes to the vessel within recognized knowledge boundaries. They know what equipment is onboard, why, how, and where it is installed, and the performance expected of them. This alternative approach can contribute to the development of a successful digital business model (Teece, 2010, Lagemann et.al 2024), since only the designer and builder have this information in their possession, and thereby represent barriers to entry for other competitors. A change in the shipbuilding value chain as suggested, could, therefore, make life easier for most relevant stakeholders in the value chain. This does not mean that the ship owner has to re-position their ships to another place in the world to get the downstream repair work done, but using a properly planned administration of the lifelong maintenance of the vessels and a digital business model for shipbuilding in place, the owner should be able to trigger the original manufacturers of the design and ship, as they do with equipment suppliers today, set up a trusted digital communication and information channel among the original manufacturers and system suppliers, the chosen "any ship designer and shipyard", the classification society and other relevant stakeholders, if any, and the owner himself in a seamless way. Eventually, "everybody" will be a subscriber and supplier to a sort of a new "Open Vessel Description (OVD-DSP)" facilitating and encouraging an all-in-one open system approach. May be very optimistic, but an ideal goal to be reached, by the few or the many…

Ship owners and other value chain stakeholders are dramatically changing and increasing their expectations towards ship designers and shipbuilding companies, as they are required to operate in a more dynamic environment where information flows are increasing and operational information demands growing. Environmental regulations require shipping companies to report their emissions, to qualify the fuels and technologies they use. What is the vessel prepared for… and how future rule-proof is it? Investors require information regarding level 1, 2, and 3 emissions of the vessel – including its production, operation, and scrapping. Charterers demand real-time information on the operations of the vessel. Vessel managers need robust and reliable

information about the state of health of the vessel, its systems, and equipment. So, if all this information is required, who will enable it and who will take benefit of it and generate value out of it? Figure 6 depicts a conceptual idea of Ulstein when it comes to what an evolving digital business model for shipbuilding could look like.

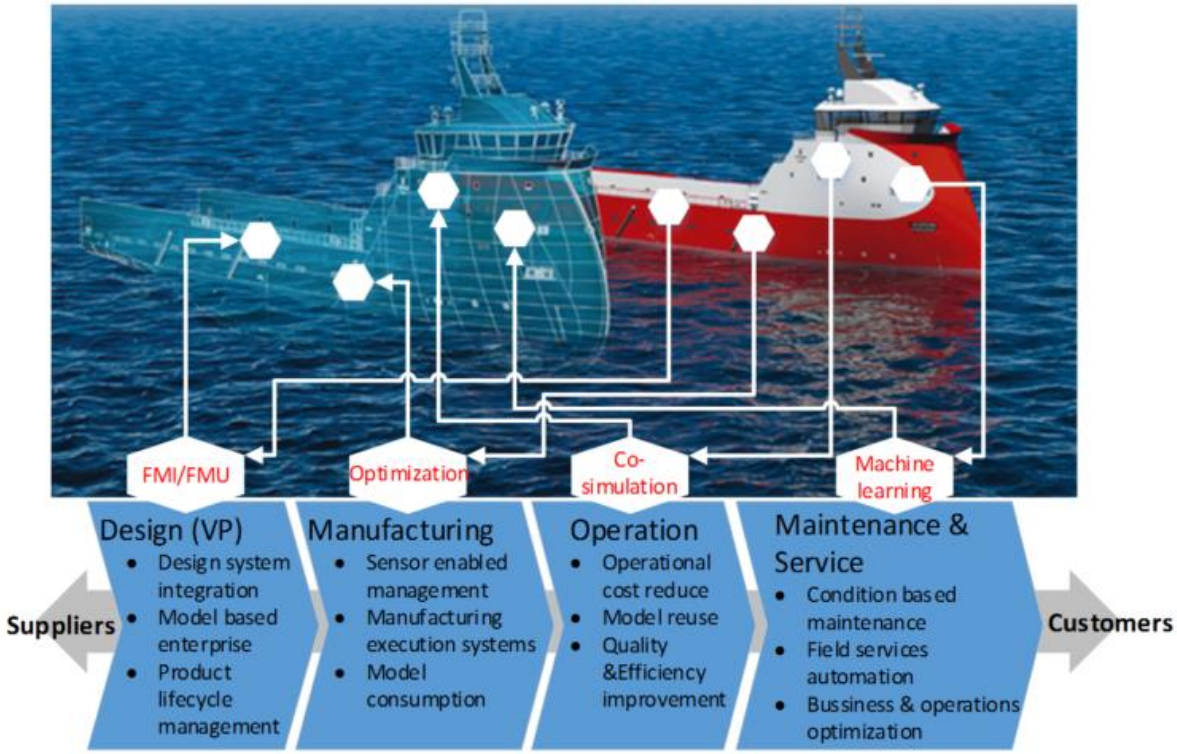

Figure 6: The conceptual idea of Ulstein's digital business model for shipbuilding.

At present, it is experienced by many that there are expectations and deliverables gaps in the way we operate, communicate and exchange information with each other. Some of them are listed here for the sake of good order and make up a list of future "work orders" for the big OVD-DSP initiative – "be aware before you start factors": suppliers will not agree to a single delivery platform being the single source of information. Stakeholders are not able to agree upon an exchange format standard; interphase and systems' architecture standardization is going slow or not there in the first place, initiative-wise; ship design business and work process, as well as ship production workflows, are inherently complex, processes with intricate details, and very often varies depending upon the new building project at hand; different work processes require different software tools and application adaptations – and triggers the "chicken and egg" problem of what comes first – the established work process or the software application way of doing it; different operations have and require different set of tools, machines, facilities, amenities; location, people, knowledge, expertise and skills; domain logic, etc.

Digital shipbuilding is, therefore, all about connectivity – not just the physical and digital ship design and shipyard operations, but also with and among all relevant value chain stakeholders – the future interrelationship "spider-web".

In the following paragraphs, we have summarized and briefly described some of the downstream digital business model initiatives. In this article, we will not repeat some of the upstream digital business model initiatives relating to the existing vessel concept design phase challenges, because these have been revealed and discussed in previous IMDC papers to the extent thought necessary to capture the total digital idea (Brett et al., 2022; Brett et al., 2018; Keane et al., 2017; Ulstein & Brett, 2012, 2015). However, it is stressed that certainly do these upstream and downstream digital model initiatives belong together and should be considered as a whole – the overall digital thread of shipbuilding.

TYPICAL DOWNSTREAM DIGITAL BUSINESS MODEL DEVELOPMENT ACTIVITIES

A: - Vessel support and control centre (VSCC)

The focus on the development of autonomous vessels addresses aspects such as reducing operating costs – primarily linked to manning, but also maritime incidents linked to human error. Partly or fully autonomous ships have attracted a long debate across shipping, with several projects implemented recently to integrate them into commercial operations. However, the slow

regulatory framework will likely not allow fully autonomous ships to mature and be integrated into commercial maritime operations for at least another 10 years. Even if we are technology-wise there, we won't be there regulation-wise, as regulation needs to be harmonized all over the world.

Autonomy will follow a step-wise implementation in the shipping industry, and as such, the value chain needs to develop services that support such a development process. Figure 7 shows a plan for how vessel autonomy can be stepwise developed building on the foundations of vessel monitoring and remote control. Such a plan builds on IMO's four degrees of autonomy. Degree one represents the first three stages: availability, monitoring, and decision support, degrees two and three relate to remote control, and degree four for full autonomy. In other words, before we see fully autonomous vessels, we will see a wide range of vessel support and control centres.

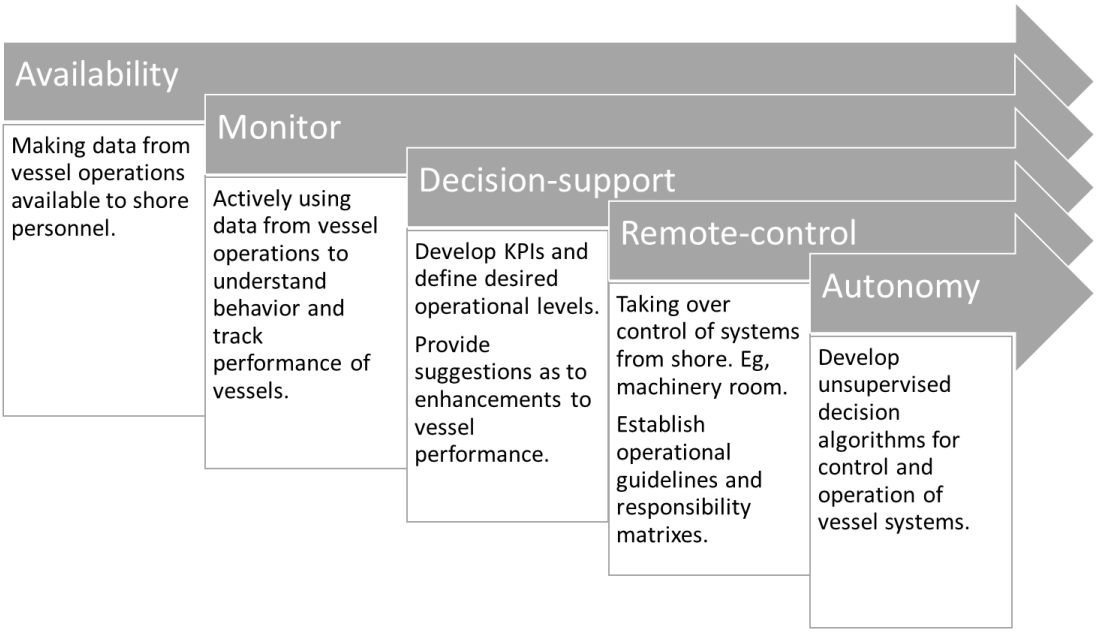

Figure 7. A stepwise implementation of remote-control and autonomy services.

Remote support and control of ships (as a stage towards full autonomy) is growingly becoming a reality. Remote control technology is increasingly seen as a game changer for moving some crew onshore, rather than developing a completely unmanned ship, and at the same time, increasing the visibility of vessel operations. Intelligent software systems and enhanced ship-to-shore connectivity have laid the groundwork for the growth of remote solutions and autonomy in shipping. These control centers have as natural first step the machinery systems of the vessel. In other words, the establishment of the engine control room of a vessel ashore. This will require changes in maintenance procedures, as maintenance of systems might be performed only when the vessel is ashore.

B: - Performance monitoring

Vessel performance monitoring is the process of collecting and analyzing data related to the operation of a vessel. The data collected typically includes information on fuel consumption, engine performance, navigation, and other factors that affect the vessel's efficiency and environmental impact. The type of data and the factors that are relevant to monitor will change from case to case, strongly driven by the type of operation the vessel is designed to perform. For a work vessel, it will typically, include power generation, propulsion, environmental forces, and control system dynamics. With these insights, the performance monitoring system helps operators to achieve reductions in resources and materials consumption, fuel, emission, and maintenance costs, without compromising vessel redundancy margin or operating efficiency. Based on analyses, operational advice is provided to managers, and officers onboard and onshore on what work processes or machinery can be stopped to run the ship operations more efficiently. This type of advisory service is dynamic – if a change in the production level falls or w*eat*her conditions, power plant system, or DP system settings are detected, the performance monitoring system recommendations will change accordingly.

Performance monitoring involves the measurement of performance over time against index indicators of performance or key performance indicators (KPIs). Thus, it helps in identifying performance gaps and therefore be used to improve performance on a continual and or continuous basis. It provides an opportunity to exploit the full potential of optimizing the commercial,

and technical operation of and the navigation and control of the vessels when at sea. Monitoring the performance helps the organization and ship in providing accurate, objective, and balanced feedback to the ships, management and anyone involved with the upping of operational performance.

Performance monitoring is often broken down into five basic steps: i) Definition of performance objectives (or KPIs), ii) communication of objectives with vessel crew, iii) planning and defining operational guidelines, iv) monitoring operations and work progress, and v) correcting or rewarding performance.

C: - Maintenance management

Vessel maintenance ensures the safety of the vessel, its crew, passengers, and cargo. Regular inspections and upkeep prevent accidents and mitigate risks at sea, minimizing the potential for undesirable events. Furthermore, vessel maintenance is vital for operational efficiency, but also the development of the 2nd hand value of the vessels in case a sales and purchase situation should pop up.

In the maritime world, a well-maintained ship is a happy ship - and a happy ship makes a successful business! Ensuring that vessels are in top condition isn't keeping them afloat; it's about safety, efficiency, and, of course, profitability. A well-maintained ship is a safe ship. Efficient ship operations depend on well-functioning systems and machinery. Routine maintenance checks and timely repairs help prevent breakdowns and reduce the risk of costly delays. After all, time is money in the maritime industry, and every day spent at the quayside or dock instead of at sea can have significant financial implications. With the growing emphasis on environmental sustainability, effective ship maintenance plays a crucial role in minimizing a vessel's ecological footprint. A well-maintained ship is a comfortable and enjoyable workplace for the crew. Good living and working conditions on board can boost morale, leading to better productivity and crew retention rates. A ship is a significant investment, and proper maintenance helps protect its value. So, how to ensure that a vessel is well maintained without overinvesting in preventive maintenance? How to ensure a homogeneous maintenance plan across a fleet of vessels? And how to evaluate what is good enough when considering a maintenance plan?

Preventive, predictive, and corrective maintenance are the 3 main forms of maintenance strategies of which time-based, condition-based, or health monitoring philosophies are derivatives of preventive or predictive maintenance. Time-based preventive maintenance is a method relying on fixed intervals maintenance intervals. This can either be related to time (days, months, or years), or cycles (system starts, running hours, accumulated cycles). Intervals are typically defined by the original equipment manufacturer (OEM), or defined in the guidelines of the shipping company. Most of these intervals are defined based on very risk-averse profiles. In other words, they suggest maintenance or replacement of components way before the system degradation would otherwise require. This approach is the most common in the industry. Condition-based maintenance is a further development of preventive approaches where maintenance periods are driven by the condition of a system. This requires the definition of performance factors and thresholds to which maintenance is required. An example is RAM and CPU utilization (%) for computers onboard.

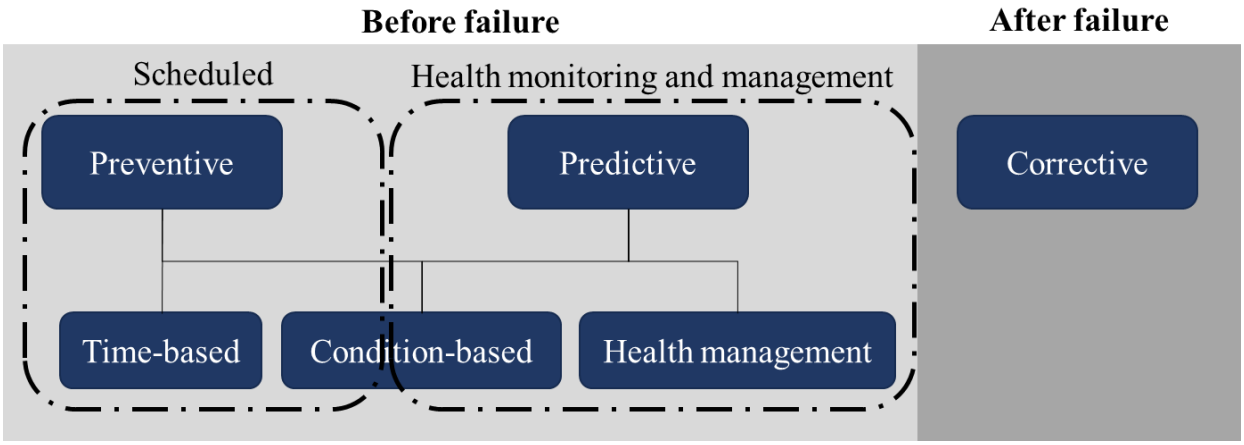

Figure 8. Classification of maintenance strategies. Adapted from (Montero Jimenez et al., 2020).

Predictive maintenance is a further development of condition-based maintenance involving systematic measuring, monitoring, and evaluation of equipment conditions across time. The condition evaluation that results allows for the forecast of the remaining life for components. Predictive maintenance is applied when mechanics or software can be examined for the health of equipment before it breaks down, this is also called proactive maintenance. Health management is a variant of predictive approaches

focusing on the performance of the vessel and its systems as a totality, and not on single-equipment isolated. Corrective maintenance, on the other hand, is introduced when the upkeep is relatively straightforward. When anything goes wrong the mechanic, software or hardware needs to be repaired. Figure 8 describes the various maintenance strategies commonly practised in shipbuilding.

Real-time data available from vessel operations measuring events, such as running hours for engines, or start-ups for pumps, are a first step for health monitoring that can enable efficient predictive maintenance practices. Fatigue measurement is a natural next step, which involves the measurement of vibrations in critical components such as propulsion lines or electrical motors. Operational data from the vessel coupled with performance thresholds defined during the design or production phase (sea trials) are also meant to evaluate the health of components and to consider maintenance actions. In any case, health monitoring requires the definition of a threshold and the association of a vessel component or system. To monitor the health of a main engine, for example, it is required to have access to detailed data from the engine and to have a deep understanding of when a component of the engine starts deteriorating and risk increases for breakage. Such information needs to be identified and structured during the design and construction phase, so it can be used during the operational phase and the final recirculation of the vessel. Without a data structure of vessel components and their characteristics, the shipbuilding industry will not be able to go beyond traditional preventive or corrective maintenance.

D: Spare parts handling

Vessels need to replace some of their components over their lifecycle. This includes everything, from critical components such as electrical motors, anchors and chains, or switchboards, to minor components such as doors, tables, or TVs. What seems an easy task can become very complex when relevant information about the system to be replaced is not available or has become obsolete.

For shipping companies handling components that need to be replaced onboard can represent a significant load of work. Identifying the component and its characteristics, identifying and requesting quotations from relevant suppliers, evaluating quotations and technical feasibility, purchasing, coordinating shipping, reception and installation. It sounds like the day-to-day job of a purchasing department at a shipyard, rather than a shipping company. So, why aren't shipyards offering this service to their customers? Is it because they lack an information system to manage vessel components after the delivery of the vessel? Shipyards could make available a list of all the components installed on their vessels, with characteristics, and contact details to the supplier. Hence, when needed, a new component could be ordered "almost" automatically. And probably at a better price than what the ship owner could, as the yard will probably buy larger volumes.

E: Life cycle assessment

Life cycle assessment (LCA) is an approach and very often complementary analysis tool to assess potential environmental impacts throughout a product's life cycle, i.e., from natural resource acquisition, via production and use stage to waste management (including disposal and recycling). New national and international regulations require shipping companies a detailed report of emissions related to their operations. Investors and charterers go, in many cases, one step further, requiring Level 1, 2, and 3 emissions. In other words, emissions relating to the entire lifecycle of the vessel involve production, operation, and scrapping.

The emissions related to a vessel start with its production. The production of steel as raw material, its manipulation and integration in a complete hull. The production of pipes, cables, pumps, isolation, and other materials runs in parallel with the production of the hull. All need to be transported to the outfitting yard and integrated into the vessel. So sea trials and the operational life of the vessel start. Here is primarily energy consumption and the emissions related to it. Figure 9 showcases an LCA evaluation for a commissioning service operation vessel (CSOV).

Sooner than later, lifecycle emissions will impact the selection of a vessel design and the location where it will be built. For ship designers and builders, this means that LCA methodology needs to be integrated as part of their design decision-making toolbox. For us is still unclear how and when LCA should be integrated in the design process, but what is clear is that it needs to be integrated somehow.

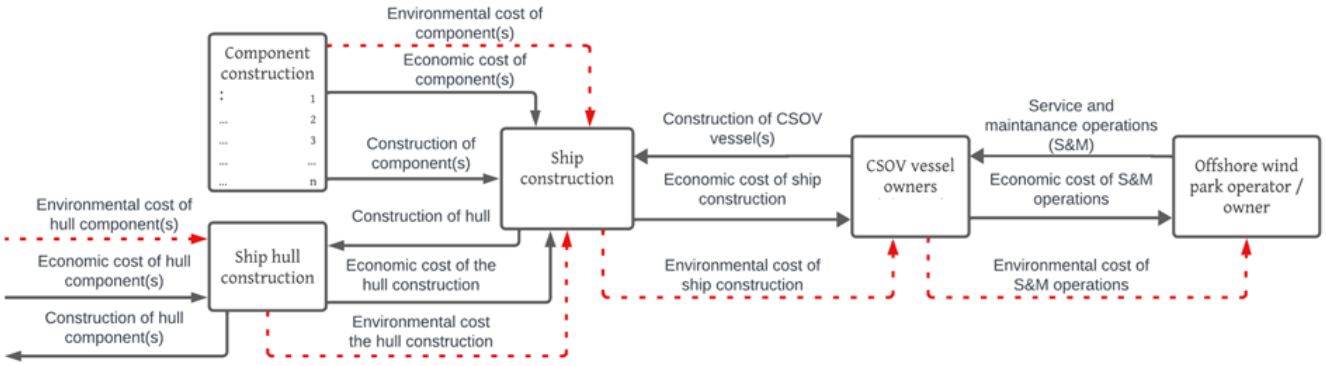

Figure 9. Example of an LCA evaluation for a CSOV vessel.

IMPLICATIONS TO MARINE SYSTEM DESIGN

For various reasons being addressed in this article, information, and data sharing from and between all these downstream services and their need to receive correct information from the upstream digital thread activities (ship design and ship production and equipment systems' integration) needs to be managed efficiently. It is obvious to the authors that all this intra- and inter-activity communication is simply not possible without a new overarching vessel digital business model for shipbuilding. Without it, necessary fidelity, and accuracy in providing better and robust management and operator support will suffer. It is, therefore, timely and important to address and start a sincere discussion as to how we can proceed from here.

The implementation of a digital business model like the one discussed and proposed in this paper has significant implications for the expertise, the processes, the tasks, and the activities carried out by ship design firms. Extracting the value of data and information collected during the design process, construction and operation of vessels will require a mix of mathematical and statistical knowledge, programming skills and ship design expertise. The latter is abundant in ship design firms, but the former are scarce and need to be recruited or trained. New processes need to be defined for the additional deliverables, and existing processes, related to traditional ship design and ship production activities, must be revised. As an example, the delivery of maintenance procedures – preventive or predictive – will require the definition of maintenance periods or performance levels. Today this information is not collected in design processes nor during the construction of the vessel. Rather, it is available on user manuals provided by equipment suppliers. Thus, new processes must reflect activities where such information is identified, collected from suppliers, and integrated into the PLM system. A similar example is the delivery of life cycle assessments for vessels, reflecting the emissions related to the design, production, operation and scrapping phase. Such deliverables, which are already being requested by shipping companies operating in the offshore wind market, will include an additional optimization goal, a Design-for-X (Papanikolaou et al., 2009). Targeting low emissions during the overall lifecycle of the vessel, as opposed to during the operational phase alone, will add a complexity layer for ship designers. But will also require the identification, capture and storage of emission information related to the production of equipment, systems, and vessels.

CONCLUSION

This article argues that digitally linking data and processes streamlines shipbuilding activities, and can bring ship designers and shipyards back into a more central position in the coordination of the overall digitalization efforts of the marine industry. However, to take on such a challenging endeavour will require determination, financial strength, patience, expertise, collaboration and a bit of luck to become successful. Competition about the position-taking in the shipbuilding value chain is unavoidable, but, everyone can participate in contributing proportionally to the digital thread and establish themselves within the overall vessel digital business model for shipbuilding in an open and orderly fashion thereby creating a "win for all" situation ahead.

In this way, tedious and manual operations can be partly eliminated and sometimes minimized to those that add specific value. Business relationships can become more sustainable by removing ambiguity and misinterpretation, compliance assurance, and allowing controlled changes and better handling of business operation dynamics over time. Flexibility in digitalization systems' building is a must and should allow process variation, without having to use extra resources to manage and operate digital infrastructure. So far, the experience is that well documented, and controlled digitalization business processes are easier to sustain. It is expected that upstream digital twins of products, production, and downstream services will eventually lead to new value-creation opportunities. Digitalization efforts, so far, have shown potential for improving collaboration and innovation throughout the ship's lifecycle and should be further motivated. Fragmented and experimental digitalizing has anecdotally,

proven beneficial to ship designers, shipyards, suppliers, and owner/stakeholders and improving their overall chain value. Particularly digital twins and various integrated and partly disjointed digital thread elements in operation have been documented to positively impact ship-lifecycle performance. In Ulstein, we have also found increased digitalization to contribute to more sustainable product and service development and more transparent administration of shipbuilding projects. But, so far, not as a surprise to us, for uncertain reasons, more qualitative gains are registered, than quantitative ones, like for example economic results of our operation.

While agility and innovation are key to success in a rapidly changing business landscape, there is no excuse for not preparing your organization. Digitalization helps achieve agility, innovation, and new business developments. The march of technology, digitalization included, is widely recognized as unstoppable. Today we see only the beginnings of the connectivity that will be required and imposed by competitors. Digitalization is a journey – where to go and what roadmap to follow.

The marine industry is conservative – tend to be late followers in all things digital except for automation and navigation. The adoption of CAD has been focused on being followed by PDM and gradually PLM. Paper drawings do still have a central role – especially in production. Although urgency is written all over digital shipbuilding advancement, we expect this digitization transformation still to take years or decades before full adoption of evolving digital technology is in place and full competitiveness power benefits from it.

It is also concluded that a new effective digital business model for shipbuilding is strongly needed to more efficiently be able to administer the rapidly growing information exchange among stakeholders in the shipbuilding value chain. It is argued that an effective digital business model for shipbuilding development can only take place if all the prime actors in the value chain are participating in the development sufficient data handling rigour is secured, and at the same time, flexibility is allowed in the development process to include the existing, but only compatible myriad of applications, out there. Yet, it is important not to exclude new ship design, ship construction, vessel automation and control and logistics-related, and other business administration-oriented applications. Proper interfacing protocols must be developed internationally and discipline amongst the developers of useful applications must be motivated. At present, it is primarily, the larger ship equipment manufacturers and suppliers, and classification societies that have taken on the spearhead position for these developments. Many smaller and less powerful application outfits, like software provers of administrative software for shipping and independent consultancy firms, are also a part of the group of new business adventurers. So far, these small actors are struggling to establish a critical mass in the market and are notoriously searching for extra funding for their initiatives. Only to a small extent have ship design firms and shipyards seen their natural expanded value chain position opportunity and prioritized sufficient time, money, and expertise to support such a strategic initiative. Not, diminishing the importance of the efforts already realized in building up a full complete digital shipbuilding platform, that goes far beyond today's "ship twin" and "remote inspection" experiments, it is paramount to the authors and argued herein the need for a reorganization of who should take the lead for this development in the future. Although their stature (economics, expertise and recognition) is not an encouraging one, compared to the well-established large and rich equipment manufacturers and classification societies, still will, collaboration and smartness can get them there…

There might be natural and unfortunate reasons for this asymmetry in the lead position of the development and the very late involvement of shipbuilding. If we go back to Figure 2 of this article, it is a fact that shipbuilding is the value chain element actors that have over a long time, yielded the least performance, and thereby have put themselves in a bad position financially, geographically, and expertise-wise to take a lead position in the digitalization project. On the other hand, we can observe that the shipbuilding downstream actors –equipment manufacturers and suppliers have been and are in a different positive and more appropriate position to take on larger and demanding digitalization efforts…

The efficiency of the new "Open Vessel Description (OVD)" digital platform is secured if the ship owner and shipbuilder take the lead together in such a bold endeavour. We recommend that the ship designer – the new naval architect and marine engineer - the business developer, must lead such an effort with the firm and looser inclusion of all relevant suppliers and information takers (users). Since this means that much of the present initiatives and firms' involvement will be challenged a broader type of interest group must come together to coordinate both the standardization work and guidelines for the individual complementary partial software application work. The digitalization efforts will cost money and resources…

CONTRIBUTION STATEMENT

Jose Jorge Garcia Agis: Conceptualization; data curation, methodology; writing – original draft.
Per Olaf Brett: Conceptualization; structure and argumentation; supervision; writing – review and editing.

ACKNOWLEDGEMENTS

We acknowledge the funding support from the Horizon Europe Framework Programme (HORIZON) under grant agreement No 101096224.

REFERENCES

Arola, T. (2018). Towards Maritime Data Economy Using Digital Maritime Architecture. *Proceedings of the 13th International Marine Design Conference*.

Brett, O., Garcia, J. J., Ebrahimi, A., Erikstad, S. O., & Asbjørnslett, B. E. (2022). A Rational Approach to Handle Uncertainty and Complexity in Marine Systems Design. *14th International Marine Design Conference*.

Brett, P. O., Gaspar, H. M., Ebrahimi, A., & Garcia, J. J. (2018). Disruptive Market Conditions require New Direction for Vessel Design Practices and Tools Application. *International Marine Design Conference (IMDC)*.

Digitalization. (2024). Gartner.

Dörner, K., & Edelman, D. (2015). What 'Digital' Really Means. *McKinsey & Company*.

Ebrahimi, A. (2022). *Handling Ship Design Complexity to Enhance Competitiveness in Ship Design* [PhD Thesis]. Norwegian University of Science and Technology.

Fletcher, G., & Adolphus, N. (2021). *Creating a Successful Digital Presence: Objectives, Strategies and Tactics*. Taylor & Francis Ltd.

Garcia, J. J. (2020). *Effectiveness in Decision-Making in Ship Design under Uncertainty* [PhD Thesis]. Norwegian University of Science and Technology (NTNU).

Garcia, J. J., Brett, P. O., Ebrahimi, A., & Kramel, D. (2020). The Potential of Virtual Reality (VR) Tool and Its Application in Conceptual Ship Design. *Conference on Computer Applications and Information Technology in the Maritime Industries*.

Gaspar, H. M., Brett, P. O., Ebrahimi, A., & Keane, A. (2014). Data-Driven Documents (D3) applied to Conceptual Ship Design Knowledge. *Conference on Computer Applications and Information Technology in the Maritime Industries*, *May*.

Gaspar, H., Sepalla, L., Koelman, H., & Garcia Agis, J. J. (2023). Can European Shipyards be Smarter? A Proposal from the SEUS Project. *22 Nd Conference on Computer and IT Applications in the Maritime Industries*, 406–416.

Jackson, M. C. (2019). *Critical Systems Thinking and the Management of Complexity*. John Wiley & Sons Inc.

Keane, A., Brett, P. O., Ebrahimi, A., Gaspar, H. M., & Garcia, J. J. (2017). Preparing for a Digital Future - Experiences and Implications from a Maritime Domain Perspective. *International Conference on Computer Applications and Information Technology in the Maritime Industries*.

Lagemann, B., Lunnan, R., Brett, P. O., Garcia Agis, J. J., Solheim, A. V., & Erikstad, S. O. (2024). What is a ship design firm, really? *Proceedings of 15th International Marine Design Conference* .

Leonardi, P., & Neeley, T. (2022). *The Digital Mindset: What It Really Takes to Thrive in the Age of Data, Algorithms, and AI*. Harvard Business Review.

Montero Jimenez, J. J., Schwartz, S., Vingerhoeds, R., Grabot, B., & Salaün, M. (2020). Towards multi-model approaches to predictive maintenance: A systematic literature survey on diagnostics and prognostics. *Journal of Manufacturing Systems*, *56*, 539–557. https://doi.org/10.1016/j.jmsy.2020.07.008

NA. (2018). *Internal PLM Survey at Ulstein*.

Papanikolaou, A., Andersen, P., Kristensen, H. O., Levander, K., Riska, K., Singer, D. J., McKenney, T. A., & Vassalos, D. (2009). State of the Art Report on Design for X. *International Marine Design Conference (IMDC)*.

Recio Rubio, L., Martin Mariscal, A., Peralta Alvarez, E., & Mas, F. (2023). A Process-Oriented Approach for Shipbuilding Industrial Design Using Advanced PLM Tools. *IF19th IP International Conference on Product Lifecycle Management*, 144–154.

Schiavon, M., Keber, M., Cossutta, A., Zini, A., Jez, M., & Ambrosio, L. (2019). Virtual Reality in Shipbuilding: Three use Cases in a Cruise Ship Design Process. *International Conference on Computer Applications in Shipbuilding*.

Teece, D. J. (2010). Business Models, Business Strategy and Innovation. *Long Range Planning*, *43*, 172–194.

Ulstein, T., & Brett, P. O. (2012). Critical Systems Thinking in Ship Design Approaches. *International Marine Design Conference (IMDC)*.

Ulstein, T., & Brett, P. O. (2015). What is a Better Ship? – It all depends …. *International Marine Design Conference (IMDC)*.

Proceedings of 15th International Marine Design Conference (IMDC-2024)
June 2-6, 2024
Amsterdam, the Netherlands

Wither now the Design Building Block (DBB) Approach

Henrique M. Gaspar[1], Ícaro A. Fonseca[1], David Andrews[2]

ABSTRACT

A description of the Design Building Block approach (DBB) was first published at IMDC1997, followed by a practical realisation presented at IMDC2003, both emphasised 3D as a key element of dialogue and creativity in early ship design. The current article celebrates, at the 15th IMDC, this architecturally driven ship synthesis approach with an overview of its fundamentals, followed by a suggestion for an open, collaborative and web-based implementation, and then provides examples that can be used when teaching the approach in ship design. The paper's first part covers the basics of this UCL-developed method, with an overview of the processes, terminology, flow of ship design information, key analyses and key examples published in the literature. The second part focus on an initial attempt to compile a version of this method that can be adapted and implemented in other academic environments, outside the original scope, which was focused on the early stage design of a range of innovative naval vessels. This part of the paper includes an extension of the current taxonomy to commercial vessels, as well as an adapted approach that can be used for ship design teaching and research. Additionally, a compilation of open online stepwise examples is presented, using the NTNU-developed web-based library Vessel.js. These examples cover the basic steps to teach the use of and to readily modify DBB for environments outside the constraints more applicable to multirole naval vessels. The paper concludes with a summary of its main intentions, emphasising the current gap that it is seen to fulfil by compiling the key DBB derived information in a single document. This is then followed by open and online examples that can be readily accessed, modified and expanded.

KEY WORDS

Computer aided ship design (CASD); Design Building Block (DBB) approach; Early Stage Ship Design (ESSD) of service vessels; 2D and 3D modelling; Teaching Ship Design.

A (NOT SO) SHORT STORY OF THE DESIGN BUILDING BLOCK METHOD – WHY IT FOSTERS INNOVATION

Introduction

DBB has been explained in many previous papers, here at IMDC and pretty much most of other important maritime conferences and journals, by our preeminent co-author, David. J. Andrews, or by one of his colleagues and students. When the first author proposed the idea of this paper to the third, the core objective was to extract the key elements that makes the DBB one of the few ship design approaches able to produce real innovative designs from the start. DBB has at its core facilitating creative innovation in the *inside-out* conception and so was proposed with future CASD features in mind. In other words, DBB starts with a colour coded, visual and hands-on approach. It starts with the architectural mindset. Consequently, the validation and evaluation of the goodness of the design are part of the intent as was the fact that the ship model could be readily changed.

From the requirements elucidation, (Andrews, 2003a; 2011), overall sketches and formalisation of design margins via the, DBB approach pushes the designer to draw conceptual assemblies which, with modern 3D tools, can be *Lego-like* to

[1] Dept. of Ocean Operations and Civil Engineering – Norw. Univ. of Science and Technology (NTNU), Ålesund, Norway
[2] Dept of Mechanical Engineering – University College London (UCL), London, UK

Submitted: 7 March 2024, Revised: 2 May 2024, Accepted: 3 May 2024, Published: 27 May 2024

Conference paper, DOI: https://doi.org/10.59490/imdc.2024.915 e-ISSN: 3050-4864

explore the infinite space of ship arrangements. One may argue that this can be risky, as by stepping out of the traditional reliable evolutionary zone of designs, we are incorporating uncertainty and less knowledge, which may be true. But by having a new ship with at best incremental changes from previous designs, we also have made a stylistic choice in being constrained by the limitations from decisions made decades ago, and thus stagnating the field of ship design. Stagnation, imitation, replication thus oppose any possible Innovation.

It is thus a matter of style (5^{th} of the S^5 the traditional focus of the naval architect on the aspects of Speed, Seakeeping, Stability, Strength and additionally that of Style - see Figure 1 and Table 1 in Andrews, 2017) in trading off innovation (and risk) against stagnation (and reliability) during ESSD. At one end of the spectrum, we can skip innovation and just copy the last ship, and we will possibly end up with a reliable, functional and cheap, and existing design. It might (if we are lucky) perform the mission, through the outdated solutions and limitations of the chosen previous design. This *shelf to order* (StO) solution is the bread and butter of ship design, since the majority of commercial ships are designed with functionality and reliability in mind, not innovation.

In this sense, most of the ship design methods taught need to cover the last approach, as starting from a Type Ship/reference ship and making incremental changes to it, which is a useful way to introduce the students to the terminology, trade-offs and challenges of the ship design task. This, however, hinders innovation and, in our personal opinion, removes also the joy of our craft. A young student that chooses naval architecture in her earlier years is attracted by the challenge of constructing large and unique artificial systems, including the freedom to draw, create and explore. We teachers, however, quite soon put aside all of it, pushing the students to rules, regressions, spreadsheets. In many cases the drawing, sometimes only a General Arrangements (GA), is done only at the end, only after all the tabular approach that is proposed in so many books and compendia is finished and approved. A ship design course may force a student to spend more time on complying with rules and criteria, typing these into a spreadsheet, than the real designs tasks involving decision making (see Figure 4, Andrews 2018).

The DBB approach does not jump into the design decomposition so rapidly, rather, it spends more time on providing the basis for elucidating the requirements and establishing limits for each requirement, in the shall / should manner. The functional decomposition, at first, is also less detailed than in traditional approaches (Rawson and Tupper, 2001), as it rarely covers more than twelve functions in the first approach. Each of these functions are indeed connected to Super Building Blocks (SBB), which, by adding a visual representation, improve on the tabular approach. It does, however, require the blocks, and moreover, it gets the designer to assign specific set colours (i.e. Blue, Red, Yellow and Green) to each of the four functional groups (i.e., Float, Move, Fight/Operation and Infrastructure - see Andrews 2018), thus bringing in the visual element right from the start. The design is then made by parsing these blocks into modern CASD software, connecting it to a certain space definition (e.g., taxonomy, such as cargo, weapons, etc.), geometric definition (main dimensions, decks, compartments, etc.), hullform (enveloping the blocks) and consequently the information consequently necessary for the initial naval architectural calculations, such as weights, centres and materials.

The approach to ship synthesis, prior to the use of computers in initial design, was initially continued using computers to speed up the iterative, weight and space, and (intact stability and power estimating) balancing process. This was followed by the computational facility, to explore a wider range of alternative design inputs and hull form relationships, which had been previously limited by manual methods. However, this early stage exploration was still one of a largely evolutionary nature, with weight group balancing by naval architects and draughtspersons drawing profiles and, occasionally, also deck plans. In 1980 the third author presented a paper to RINA entitled 'Creative Ship Design' (Andrews, 1981). The intention in choosing that title was not to imply that ship design as then practised was not capable of being innovative, but rather to make the point that, if naval architects were to fully utilise the benefits becoming available through the veritable explosion in design methods and creative techniques for dealing with complexity, they would then be better enabled to design even more creatively than hitherto. That early paper suggested that designers should focus more intensely, at the initial design stages, on ship architecture – both internally and on the topsides – than was possible before the advent of computer aids. Even that long ago rudimentary computerised graphics were becoming available to designers, and subsequently advances in computer graphics made such possibilities even more achievable, consequently a 2003 paper

entitled: *A Creative Approach to Ship Architecture*, presented a fully achievable architectural emphasis to early stage ship design (Andrews, 2003b).

The Evolution of the Design Building Block approach

The arguments advanced in the 1981 paper led to a research programme into ship design methodology (Andrews, 1984: 1986; 1987; Andrews and Dicks, 1997) and naval ship design and acquisition (Andrews, 1993; 1994; 2013). It was perceived that the evolutionary approach to ship design, typified by so much of existing design approach and built into most design tools, has become progressively less appropriate. The latter aspect can be illustrated by the following observations made in the 2003 paper:

a) Dependence on an evolutionary approach is less likely to lead to the production of designs responsive to the accelerating rate of change (Andrews, 2001a), whereas a creative design approach enables exploration of responsive and adaptable design options (Andrews, 2001b);
b) Potentially better solutions, such as the Trimaran configuration (Andrews, 2004), are unlikely to be considered in an evolutionary approach, while many of the techniques now available are conducive to the search for and development of novel solutions;
c) These new techniques, in conjunction with a creative approach, are practically indispensable for adequately coping with what has been termed the 'wicked problem' (Rittel and Webber, 1973). This arises in requirement elucidation when designing complex ships (i.e., requirement formulation and design responses are in a circular relationship).

While a research version of what was denoted as a 'Design Building Block' approach to the design of physically large and complex entities had been demonstrated in the 1998 paper, this was written (Andrews 1998) based on a breadboard demonstration using the developments in computer graphics when presented to the 1997 IMDC by Andrews and Dicks (1997). Already a working version had been produced in the form of a classified system, specifically for naval submarine concept design (SUBCON - Andrews et al., 1996), but it was not until 2001 with Andrews final return to UCL that a more general working system was produced and made openly available. It was then possible to demonstrate the approach could be applied to actual (rather than research) design problems (Andrews and Pawling, 2003, 2008). Since it has now become possible to demonstrate that the DBB approach has matured and can be applied to a large range of design studies *for real* (see Sections 6.2 and 6.3 in Andrews (2018) for outlines of published UCL studies). Moreover, regarding ship design as an example of Design on the Grand Scale, this graphical way of proceeding “inside-out” could provide insights relevant to a more general understanding of design philosophy and design methodology.

Before proceeding with the main body of the paper, it is appropriate to acknowledge that there has been a distinct bias towards naval ships in the examples used to illustrate the DBB based themes. This tendency arises from the third author’s career as a naval architect working for the UK Ministry of Defence up to 2000, where he was largely engaged in the design of surface warships and submarines for the Royal Navy. We believe that warship design can be said to have made significant contributions to the discipline as a whole (see Andrews, 2010). This assertion is made even though the timescales and very significant resources, invested in the course of many warship designs, dwarf those invested in even the largest and most complex merchant ships.

While it could be argued that a design procedure capable of addressing such a level of complexity in the most complex of naval vessels should be scalable to suit less complex ship design processes, it is open to debate whether the naval ship design environment is disproportionately “over the top” and so makes the procedure – and the associated design philosophy – inappropriate for application to even the most sophisticated commercial vessels. On the contrary it is considered that all ship design is increasing in complexity and that there are growing synergies between naval and commercial ship design approaches, as instanced by the moves to apply naval ship rules and codes of engineering practice to be managed by the commercial classification societies (Gibbons, 1984). Therefore it has been argued that the creative ship design approach advocated, centred on an architectural schema, has a wider applicability to marine design in general.

As stated in the introduction, the 1980 paper concluded that creativity in ship design would be fostered by an approach to the initial ship synthesis which placed greater emphasis on the physical description of the ship's layout. A subsequent justification for this approach to initial ship sizing was reported in a 1986 RINA paper that followed the third author's PhD (Andrews, 1984), an early naval architecture thesis on ship design methodology.

In the 1984 PhD thesis, entitled "Synthesis in Ship Design", the third author contrasted the sequential process of gross ship sizing, followed by hull parameter determination and then architectural and engineering development with the *all in one* or integrated synthesis. This was subsequently confirmed by development of the Design Building Block approach, firstly in the UK MoD's developed SUBCON CASD tool (Andrews *et al.,* 1996) and then the UCL sponsored SURFCON module in the Paramarine CASD system (Munoz and Forrest, 2002). This combination of the ship architectural and naval architectural balanced numerical description served to provide an ability for the ship designer to develop *ab initio* design options, which could consider many of the main ship requirement drivers from the start of a new design study.

FEATURES OF THE UCL DESIGN BUILDING BLOCK APPROACH

The manner in which the SURFCON tool is structured was described at the 7th IMDC following its beta testing by Andrews and Pawling (2003). Two features are considered worthy of note:

a) A functional breakdown of the design building blocks adopted for ship description. The categories of the building blocks (i.e., float, move, fight/operational and infrastructure) can be distinguished by their four characteristic colours, plus purple for the main access routes (as a subset of the Float function, highlighted because it is seen as key to the ship's internal layout). This breakdown of the Design Building Blocks was introduced to foster the exploration of more innovative configurations as part of Requirements Elucidation (Andrews, 2003a, 2011), where choice of style is the key to synthesising a new ship option.

b) Use of the term Master Building Block to indicate how the overall aggregated attributes of the DBBs would be brought together, to provide the numerical description of the resultant "appropriately balanced" ship design. The audited building block attributes assembled within the Master Building Block (constituting the top-level whole ship description) could be used directly by the Paramarine analytical modules, thereby enabling the necessary naval architectural calculations to be performed to ascertain the balance, or otherwise, of the whole ship configuration being derived by the designer.

Each design building block, as the fundamental component of the SURFCON approach, can be regarded as an object in the design space and as a "placeholder" or "folder" containing all the information relating to a particular function within the functional hierarchy. Importantly the "block definition" object permits the designer to add whole ship margins and characteristics, such as accommodation demands, once the "block summary" object has summarised all the information in the top-level block in the building block hierarchy – this is the Master Building Block object. The "design audit" object then allows the design description to be audited for any of the characteristics selected for monitoring, which typically will include style aspects alongside primary naval architectural capabilities. Results can be displayed using the functional group hierarchy; this "design audit" object is assessed for a range of design infringements, by other objects in the design space, and for the balance of the overall ship design from the whole ship characteristics listed in the Master Building Block.

After the SURFCON initiative finished, the exploration of ship internal configuration has been taken further by the Marine Group at UCL, specially the third author and his UCL colleague Dr. R. Pawling (see Section 6 in Andrews 2018). Firstly, in the exposition of the integration of configuration in ship design (Andrews, 2003b) and subsequently by expounding this approach to the design of ships (and other complex systems) to a wider scientific and technical audience (Andrews, 2012). This led to the realisation of the UCL Design Building Block approach, an integrated approach to ship synthesis, at the commencement of the design process, accomplished by using computer graphics to build up the ship's internal architecture, which can then be used to feed the traditional numerical sizing synthesis. Illustrations of the graphics output, linked to the PARAMARINE balanced numerical ship definition, exemplified the UCL DBB approach and taken from the extensive presentation of the architectural approach to early stage design of complex vessels (Andrews, 2018), are given in Figure 1.

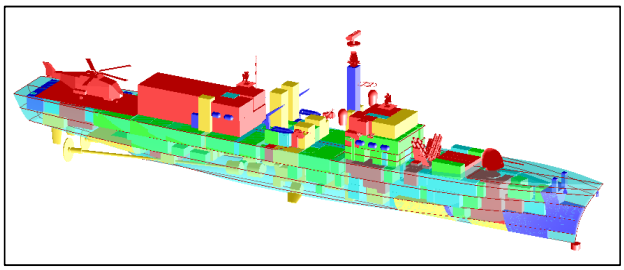

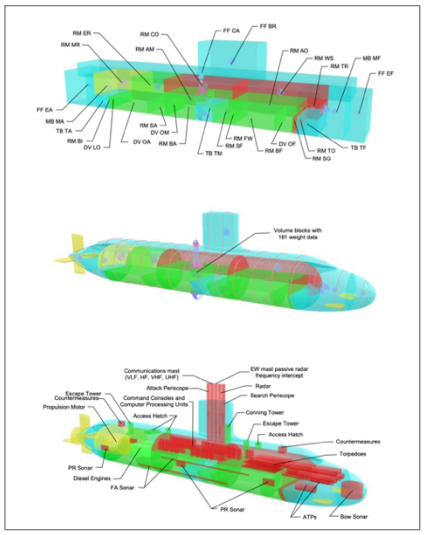

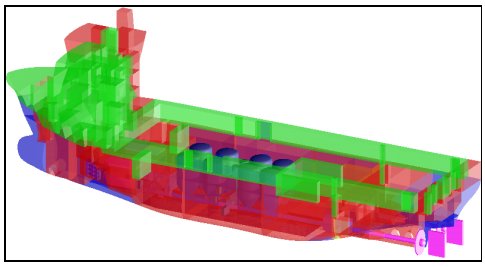

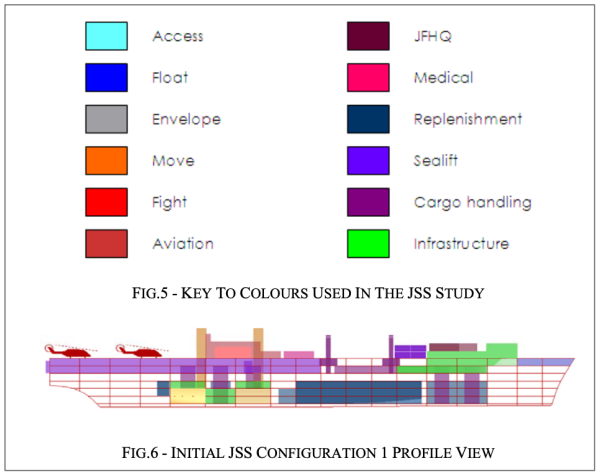

FIG.5 - KEY TO COLOURS USED IN THE JSS STUDY

FIG.6 - INITIAL JSS CONFIGURATION 1 PROFILE VIEW

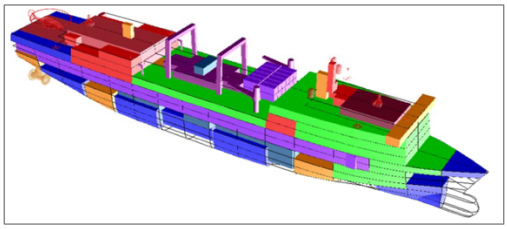

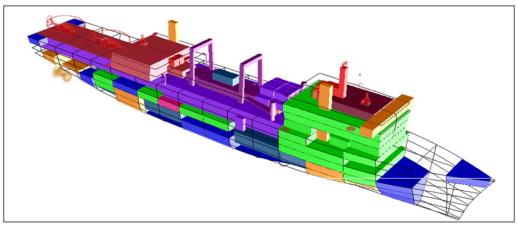

Figure 1 – Examples of Designs made by UCL using DBB method (compiled in Andrews, 2018)

With an architecturally based description at the early stages of a design, it becomes possible to explore many of the issues which are of direct interest to the client/owner and stakeholders. Such issues - ranging from those concerned with naval vessel's fighting capabilities or the service ship's crew evolutions on board, to the sustainability and supportability of the vessel conducting tasks at sea - are best investigated for their impact on the overall design at the earliest exploratory stages of the design. Thus, for example, layout for weapons effectiveness is a function of topside disposition (Gharib, *et al.*, 2016) and also of internal arrangement and zone logic (Piperakis and Andrews, 2014), both of which are more readily explored through the ship's architecture. Zoning is also relevant to survivability concerns and to the logic adopted for routeing ship systems (Mukti, 2022), and these in turn interact with considerations on producibility and constructional building block arrangements. The initial design can also, with this approach, meet the aspirations of concurrent engineering (Keane, 2018) because the initial configuration is able to reflect not just the traditional focus of the naval architectural aspects of the S^4 as performance drivers but also producibility and even through life supportability considerations.

One clear reason why a 3D *inside-out* approach should be adopted in early stage ship design is that many issues that really ought to be addressed, early in design, can then be more easily considered. Given many of the practicalities of major interest to the client/stakeholders are best revealed by the upper decks/internal configuration definitions, then integrating the architecture into initial concepts must be preferable to the somewhat one-dimensional numeric exploration. However, this would counter the evolutionary set of steps in the initial design development and also the ability of the approach to produce, relatively quickly, an architecturally, numerically and analytically balanced design. Thus, an initial crude internal arrangement can be very useful in grasping the major "blocks" of operational, mobility and infrastructure categories and avoids being distracted by too much detail too early. With respect to the time taken to achieve design

balance appropriate to concept definition, Figure 1 shows four distinct configurations (plus three variants) for a heavy lift LCS Mothership concept, all with some 200 DBBs and balanced in space, weight, stability and powering (Andrews and Pawling, 2004).

We realise that the DBB approach can be used to discuss the *goodness* of a design in many ways, here summarized (from Andrews, 2022):

a) ***Cost***: By better understanding what is wanted and how it might be achieved, the partners in the process are more likely to understand, early in the process, where are the *knees in the cost-capability curves* and how they can be efficiently exploited, and how ships can be cheaper to construct and or operate in preference toadopting the *smallest* (less effective) design.
b) ***Sophistication***: A more sophisticated initial design approach would be able to both feed the marine design research and development and respond better to research innovation coming the other way, often hard to be revealed by tradition numeric concept design outputs. Quite unlike the aerospace industry, for too long the naval ship design community have accepted that it was possible, and therefore justifiable, to not adequately resource the R&D associated with ship design often reflecting commercial ship acquisition practice (Andrews, 2024). In the sophisticated offshore market (Ulstein and Brett, 2015) and cruise ship practice (Levander, 2015) this has become much more nuanced.
c) ***Holistic implications***: An enhanced DBB type of design approach might then help to recover the ship designer's role as *prime interpares* in the ship design process. This is not trying to recover lost glory but recognition of the naval architect's inherent stance that *everyone else's problems are also the naval architect's, and they can best appreciate the whole ship implications* (Andrews, 2022).

ADAPTING THE DBB APPROACH

As the DBB approach has been mostly taught at UCL, and most of the examples publicly available are naval service vessels, although these include not just combatants and carriers but also naval auxiliaries which are more like commercial tankers and cargo vessels, (e.g., Littoral mothership, Canadian Navy Joint Support Ship see Andrews, 2018), in the rest of this work we took on the challenge of adapting some its core elements to commercial ship design, both service and transportation vessels. In this context, traditional ship design disciplines like stability, resistance, strength and seakeeping (S^4) can be taken out of the scope here, given that these calculations are necessary for any kind of ship, no matter the approach behind its design. Additionally, a better assessment of the ship's centroid, through a DBB description, should improve the initial stability assessment, as indeed would use of DBBs to allocate specific space and weight margins, furthermore, the DBB approach can be used to emphasise stylistic choices. The rest of this paper, thus, focuses on the use of design blocks, that is, this abstract and colourful construction that is the essence of the DBB approach.

We emphasize here some of the elements from the DBB approach that are connected to the fostering of innovative designs. It is important to note that this is a simplification, with the intention of identify the reasoning that leads towards achieving an innovative design culture. For a more detailed description, see references from the previous section.

Table 1 uses the terminology described in IMDC 1997 by Andrews and Dicks, adapted to a more generic description of the ship. In this case, phases like *Weapons and Sensor Placement* becomes *Task Related Equipment Placement*, and *Aircraft Systems Sizing & Placement* is changed to *Payload Systems Sizing and Placement*. Similarly, the block category FIGHT becomes OPERATE. This thus accommodates service vessels, such as Anchor Handling and Towing (winch) and heavy lift (crane), as well as cargo / transport vessel features, such as tanks and cargo areas. The explanation is based on the work of Pawling (2007) and Andrews (2012).

Table 1 – Adapted DBB Stages to ship types beyond naval vessels (preliminary, first attempt)

Adapted DBB Design Stages		Purpose	Output
1	**Design Preparation**		
1.1	Selection of Design Style and Capabilities	- Select type of design in terms of novelty, namely: second (stretched) batch, simple type ship,	Design Framework, containing sketches and sufficient data to start

		evolutionary, simple (numerical) synthesis, architectural synthesis, radical configuration and radical technology (Andrews 2018, Table 3). - Select major style aspects, such as hullform topology and technical design standards. - Key design drivers (e.g. mission and operational profiles) - Identify capabilities required, such as speed, range (autonomy), tasks (mission), payload, crew.	the iterative design process, such as weight and space grouping systems, equipment and subsystems data and validate existing design data. Main design drivers and interactions.
2	**Topside and Major Feature Design Phase**		
2.1	Design Space Creation	- Populating the library of blocks, with geometry and volume definitions, that is, digitalizing the design framework. - Selection of the blocks taxonomy (e.g. FLOAT, MOVE, FIGHT /OPERATION, INFRASTRUCTRE) - Super Building Blocks (SBB) to develop overall layout and spatial style of the design. - Design margins and options - Study of alternative layout styles (parallel development)	Library of SBBS according to the taxonomy. First design definition (layout style) Shall / Should Requirements
2.2	Task Related Equipment Placement	Estimation of size and weight of equipment related to key tasks of the ship (and support crew, if necessary)	SBB blocks for tasks (e.g. FIGHT, OPERATION)
2.3	Engine and Machinery Compartment Placement	Gross machinery size, based on style, type of fuel, estimated resistance and autonomy.	SBB blocks for machinery (e.g. MOVE, propulsion system)
2.4	Payload Systems Sizing and Placement	Gross estimation of payload, like tanks, cargo areas, deck areas	SBB blocks for payload (e.g. FLOAT)
2.5	Superstructure Sizing and Placement	Gross estimation of superstructure size (bridge, accommodation)	SBB for infrastructure and accommodation (e.g. INFRASTRUCTURE)
3	**Super Building Block Based Design Phase (10-20 SBBs)**		
3.1	Composition of Functional Super Building Blocks	Prepare an initial layout according to the taxonomy.	Initial estimation of overall vessel size and displacement Initial hulform (topology) and resistance
3.2	Selection of Design Algorithms	Algorithms, constraints and criteria for preliminary analyses (S4 – stability, speed, strength and seakeeping) Scaling and morphing algorithms (hull)	Models for assessment of S4 criteria
3.3	Assessment of Margin Requirements	Procedure to check if the design with SBBs is within the margin requirement (e.g. shall/should), criteria and constraints.	Procedure for evaluation / auditing
3.4	Placement of Super Building Blocks	Placement of SBBs and creating a layout. Checking for necessary additional spaces (e.g. fuel tanks, auxiliary machinery, ballast tanks). Preliminary (parametric) hullform	Vessel estimation with improved topology, subdivision, and high-level functional zoning. Hullform aspect detailed.
3.5	Design Balance & Audit	Iteration to numerical balance: adjusting current design iteration towards balance and evaluation of the requirements	Balanced design, assessed within the criteria, margins and constraints.
3.6	Initial Performance Analysis for Master B.B.	Limited analyses of S4 performance indicator. Weight and volume demand trade-off and iteration.	Preliminary design, rough layout, Main design drivers revealed. Volume and weight estimated, iterated to satisfy gross margins.
4	**Building Block Based Design Phase (100 - 500DBBs)**		

4.1	Decomposition of Super Building Blocks by function	Decomposition of SBBs into DBBs. Refinement of design into a level of detail that satisfies the designer as to assess the performance within safe assumption of the margins. Volume and/or weight definition and geometry	Design Building Blocks (volume, weight, description).
4.2	Selection of Design Algorithms	Approaches to detail the procedures, constraints and criteria for preliminary analyses (S4 – stability, speed, strength and seakeeping). Algorithms for hullform tunning.	Models for analyse DBBs layout
4.3	Assessment of Margins and Access Policy	Procedure to check if the design with DBBs is within the margin requirement (e.g. shall/should), criteria and constraints.	Procedure for evaluation / auditing
4.4	Placement of Building Blocks	Iterative process of design development, manual and routines. Detailed study of hullform shape.	Vessel estimation with subdivisions and spaces, and low-level functional zoning (pre-GA). Hullform shape detailed
4.5	Design Balance & Audit	Iteration to numerical balance: adjusting current design iteration towards balance and evaluation of the requirements with DBBs	Iteration towards balanced design, with main and support related systems (spaces)
4.6	Further Performance Analysis for Master B.B.	Performance analyses according to the mission and taxonomy (e.g. FLOAT, MOVE, OPERATIONS, FIGHT, INFRA filtered systems)	Detailed analyses of the vessel systems and functions according to the requirements, margins, criteria and constraints.
5	**General Arrangement Phase**		
5.1	Drawing Preparation	Parsing DBB layout (3D) intro traditional 2D GA and lines plan. Detail of DBB into modern 3D GA software	GA, linesplan, 3D rendering

DEVELOPING DBB IN AN OPEN AND COLLABORATIVE WEB-ENVIRONMENT

2D IMPLEMENTATION (2016 / 2019)

Since 2016 an online a simplified 2D design tool inspired by the DBB has been available as a joint collaboration from the first and third author. The first version of the tool was developed at UCL and can be accessed at http://dbb.ucl.im/2016 (Figure 2a, Piperakis and Gaspar, 2016). An extended version was developed by Kramel in 2019 at NTNU, including a more comprehensive resistance analyses as well as closed-form functions for seakeeping (vertical movement, acceleration and roll), observed in Figure 2b (http://dbb.ucl.im, Kramel, 2019). This tool was based on an incipient work from 2015, published last IMDC, attempting to quantifying interfaces in general arrangements (Gaspar and Andrews, 2022).

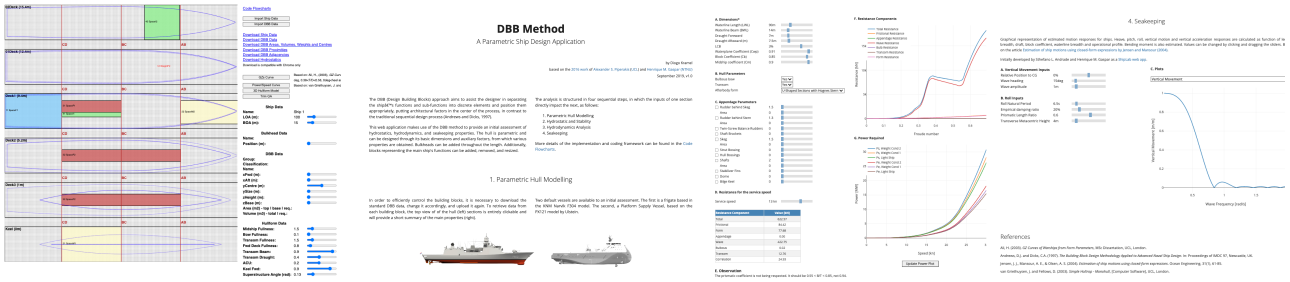

Figure 2 – 2D web-application of DBB by Piperakis and Gaspar (2016) and Kramel (2019)

Kouriampalis et al., (2021) uses this simple (and to be honest not user friendly) prototype DBB design tool to model the operational effects of deploying and retrieving a fleet of uninhabited vehicles (UXVs) in naval surface ships. The design revolves around the innovative idea of a mother vessel capable of transporting and deploying UXVs. The 2016 tool was

used to play around with the blocks, allowing the creation, visualisation and manipulation of the ship's GA. After a layout was preliminary established, the numerical sizing was made in Excel, with detail in traditional CASD software (e.g., Paramarine). Figure 3 exemplifies this work, depicting two different internal arrangements made with this simple and 2D ship layout design tool.

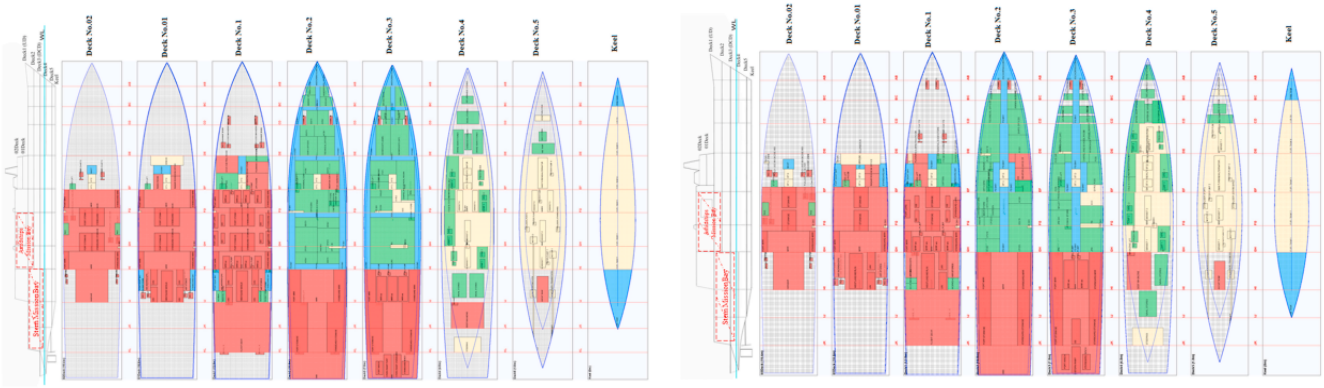

Figure 3 – Internal arrangements for two design variants of motherships made by Kouriampalis *et al.,* (2021), using the 2D web-application of DBB from Piperakis and Gaspar (2016)

3D IMPLEMENTATION – ADAPTING VESSEL.JS: OBJECTS AS BLOCKS

Vessel.js is an open-source library with tools and methods for Early-Stage Ship Design. The library has been described in more detail in previous IMDCs (Gaspar, 2018, 2022). In short, its main characteristics are being developed in JavaScript and employing an object-oriented approach to modelling of digital ship designs. In the same manner as the 2D DBB implementations, the choice for JavaScript stems from its usage in development of web-based applications and user interfaces. This makes it suitable for creation of interactive apps with graphics, such as charts and 3D rendering. All these come in handy when designing a ship, as they provide immediate understanding of architectural implications of a building block, such as its size relative to the other blocks and its interaction with the hull. Other advantages of web applications are their geographic availability with low threshold to use. Users can access apps on any web browsers installed on modern devices without additional installations. This allows students to promptly access developed examples and start playing with them in the classroom. As the source is open, they might eventually inspect the code to understand the logic underlying the analyses, modify it with different functionalities, or reuse it when creating new applications.

Vessel.js' object-orientation means it resorts to the computational concept of an "object" to represent vessel components and even modules used to run design analyses or render 3D visualisations. An object is a variable or data structure which contains values, functions, and methods, usually combined to encapsulate a significant aspect of computation in a single construct. Object-oriented paradigms support inheritance mechanisms, allowing the creation of several object instances, possibly containing different internal values, from a single blueprint, which might be defined as a "class" or "prototype", depending on the implementation. Figure 4 shows Vessel.js' overall structure, containing ship-related objects in blue, design analyses in red, and supporting functionalities in white.

A ship model in Vessel.js comprises a hull, major structural elements, or dividers (decks and bulkheads), and internal systems placed into the ship. Those systems are represented with generic objects, named "base" and "derived" objects. These constructs were created to provide the flexibility when addressing different types of vessel components. A vessel object includes weight and spatial definition about an equipment or compartment, possibly with a 3D model to be loaded in its place (if no 3D model is provided, a bounding box is used instead). A derived object defines a specific placement of a base object, allowing its replication in multiple locations inside the vessel. Base and derived objects are not prescriptive as to whether the element being modelled is a tank, compartment, machinery, equipment, or other component. They simply provide a mechanism to define spatial and weight characteristics and replicate them with a 3D visualisation in the design. These functionalities yield an adequate framework to handle the DBB approach, as a base object might also be created to represent a Super Building Block or smaller Building Blocks, depending on the design stage.

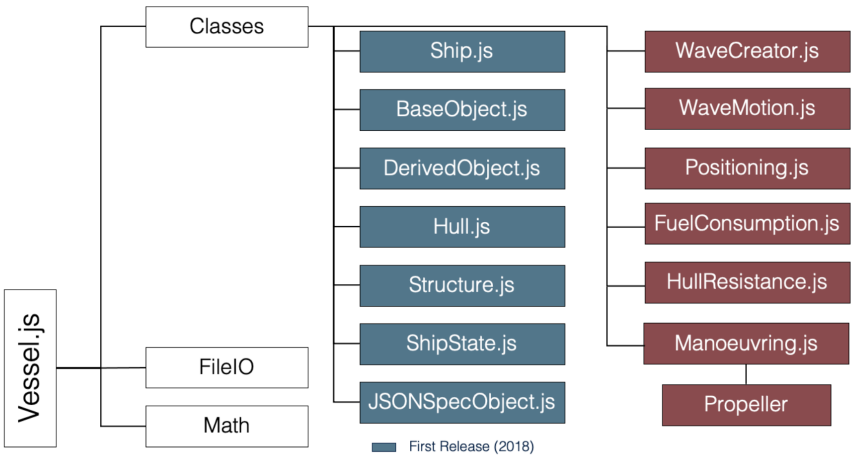

Figure 4 – Vessel.JS structure, with core *classes, fileIO* and *math (Gaspar 2018; 2022).*

In addition, the web-based architecture allows the vessel as blocks to be combined with more realistic descriptions, such as 3D rendered models from gaming and animation. Such models do not incorporate the mathematical modelling but are important to communicate the idea that blocks (early design) and final drawings (with details, colours and texture) are part of the same process. Figure 5 presents cases with both representations. On the left, the blocks, during conceptual design, can be used for the evaluation of the S4 performance, while on the right is the artistic representation, from 3D art and based on sketches. Additional elements like sea or ocean can be added to aid the communication of the final product.

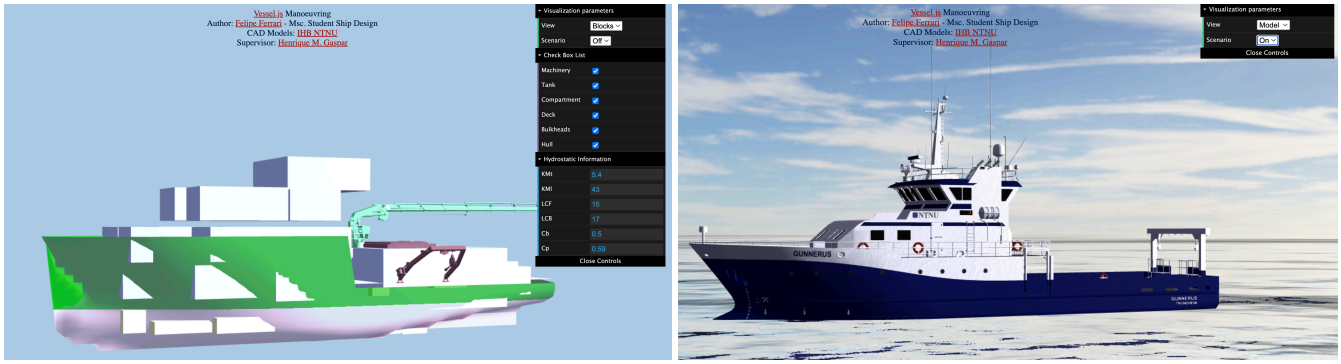

Figure 5 – Vessel.JS architecture blending early design, with blocks and a rough hull (left), used for calculating hydrostatic (right side menu) and the conceptual art in 3D of the same design, with a sea and sky scenario.

A PLATFORM SUPPORT VESSEL (PSV) DBB CASE

Design Preparation, Topside and Major Feature Design Stage

A simplified case study is presented to illustrate the DBB approach using the 3D implementation. The design style was chosen to be that of a modern commercial PSV, an offshore support vessel aimed at transporting supplies between onshore and offshore installations. In that design style, superstructure and engines are placed forward on the vessel, leaving the midship and aft available for carrying cargo, either inside tanks (e.g., for drilling fluids), or on an extensive open deck. Propulsion usually supports Dynamic Positioning (DP) to allow for precise control of the vessel's position in relation to the installation being supplied, which is commonly an oil rig. The design in this case study is inspired by the PX121, a PSV designed and built by Ulstein (Ulstein, 2014).

The taxonomy of building blocks includes the functional group:

- FLOAT: trim and ballast tanks.
- MOVE: propulsion machinery, thrusters and containing spaces, fuel and lube oil tanks, exhaust openings, navigation rooms and equipment.
- FIGHT/OPERATE: cargo decks (open, covered) and tanks.

- INFRASTRUCTURE: accommodation, ship's stores and provisions, auxiliary machinery spaces and systems.

The functional groups are not prescriptive and can be chosen by the designer, to better support their activities. Additional categories such as ACCESS might be adopted in more detailed cases and are suppressed here for simplification.

The design characteristics are situated within a range delimited by a common list of equipment and minimum cargo runs and by mobile temporary storage capacity. Shall and Should requirements elucidation are adapted from the 2015 IMDC case (Gaspar *et al.,* 2015), transformed into feasible combinations. In this exercise, it was decided to constrain the overall size (GT) of the vessel, therefore assuming a new feature (e.g., Ice Class) would mean a smaller capability in another feature of the vessel (e.g., cargo size). Also, not all equipment is compatible, for instance *Towing and Salvage* equipment cannot be installed if a full *Fire-Fighting* capability is necessary, and vice-versa. At the end, Table 2 present the feasible combinations considered during the design preparation phase, with seven missions and five PX121 market options.

Table 2 - Missions, market options and compatibility for PX121

Vessel missions and use	PX121 Mrk1	PX121 Mrk2	PX121 Mrk3	PX121 Mrk4	PX121 Mrk5
Cargo Runs	V	V	V	V	V
Mobile Temporary Storage	V	V	V	V	V
Oil Recovery and Stand by			V	V	
Light Well and Extra Accomodation					V
Towing and Salvage		V	V		
Fire-Fighting				V	
Ice Class	*	*	*	*	*

* - Optional at extra CAPEX

Super Building Block Based Design Stage

The design was first modelled with "Super Blocks", meaning major building blocks, which could have been further decomposed into more detailed Building Blocks. This reduced the threshold to modifying the early-stage design proposal and exploring alternative configurations by reducing the number of blocks to be arranged and provided a higher-level view of space utilisation inside the ship. Figure 6 shows the PSV early design modelled in superblocks. Green superblocks represent INFRASTRUCTURE, yellow superblocks are MOVE, and red superblocks are OPERATE.

Two algorithms for preliminary analyses were selected and applied to the design Constrained Linear Scaling (Figure 7) and Block Configuration Editor (Figure 8)

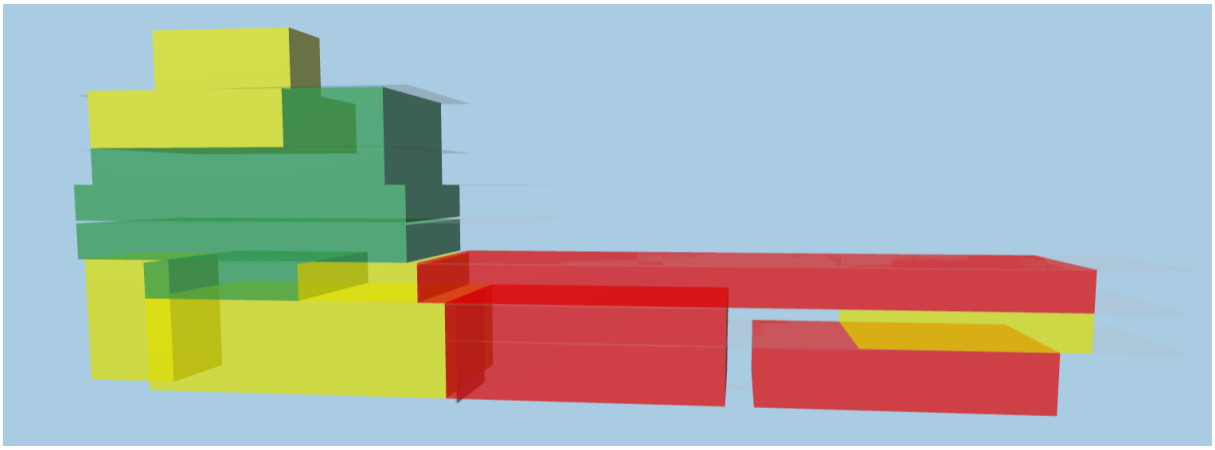

Figure 6 – PSV SBB Representation

Constrained Linear Scaling. The first algorithm allows changing blocks' dimensions while maintaining their sizes and positions in relation to each other constants. The algorithm constrains the total volume of blocks to a fixed number but allows the designer to "stretch" the design's main dimensions: Length, Beam, and Depth. This was developed with a web application where the user can use a slider to scale one of the linear dimensions. Say for instance, that increase Length is investigated, then Beam and Depth will then be automatically adjusted by the algorithm to keep overall volume constant. The user might also decide to lock one of the dimensions to a fixed value, say Depth. This will allow them to resize the Length while the Beam is automatically adjusted to compensate for the modification (and vice-versa). The changes in block and hull sizes are rendered in real time. This algorithm allows quick prototyping of design alternatives with different deck areas and identical volumetric capacities, while keeping an overall arrangement with the same relative positions among blocks.

For example: SBB1 must have 40m3 (criteria x). It can be 2x4x5; 2x2x10. So for each arrangement, L/B/D could be varied, from the smallest L that is acceptable until the largest, seeing real time consequences in B and D. Same with B, and D, with six variations in total, each of them one maximum or minimum, for the same arrangement. One of the dimensions (e.g., L) could be fixed and the others played with (D and B). Each option will then have different tank and deck sizes. If design speed is changed, then the whole design is adapted to it (e.g., larger or smaller propulsion), then the process starts over again.

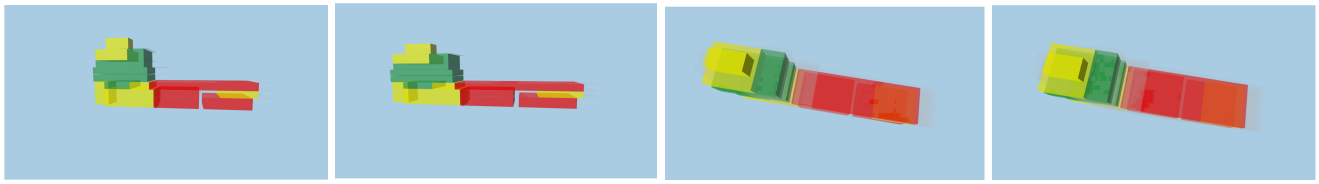

Figure 7 – Variations pf the SBB PSV design by *stretching* and *squeezing* blocks, maintaining the volume SBBs criteria, while *playing* with *LxBxD*

Block Configuration Editor. An alternative algorithm within the DBB approach, involves changing relative placement of the blocks by manipulating them akin to *Lego pieces*. This allows the designer to obtain and evaluate multiple arrangements before further detailing any of such alternatives. Vessel.js' "3D block editor" application allow users to modify design configurations with intuitive manual controls like drag and drop. This expedient can of course be interchanged with the previous one, so that first the designer defines block placement, then adjust dimensions, or vice-versa.

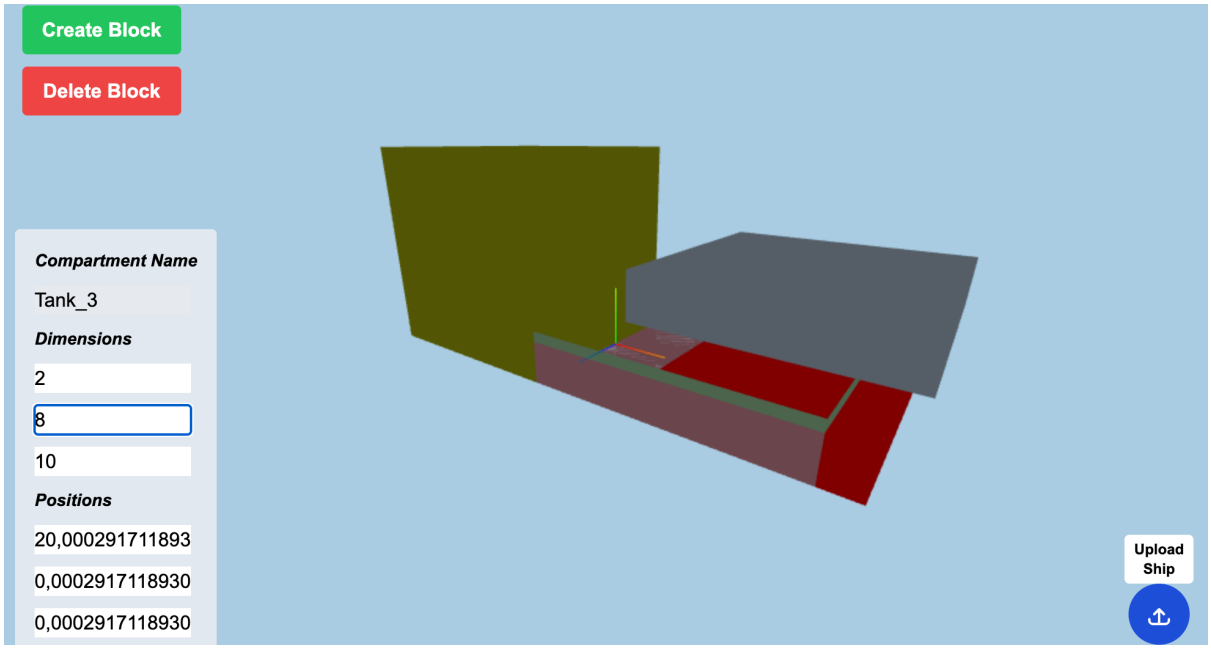

Figure 8 – Preliminary block-editor, able to decompose SBBs into DBBs

Building Block Based Design Stage

Once design balance is reached, the design is refined by decomposing the Super Building Blocks into smaller building blocks corresponding to the position of specific vessel systems. Figure 9 illustrates the PSV design after being refined with 106 building blocks. Similar *stretching* and *squeezing* was performed, to test 441 different variations of the design according to the criteria.

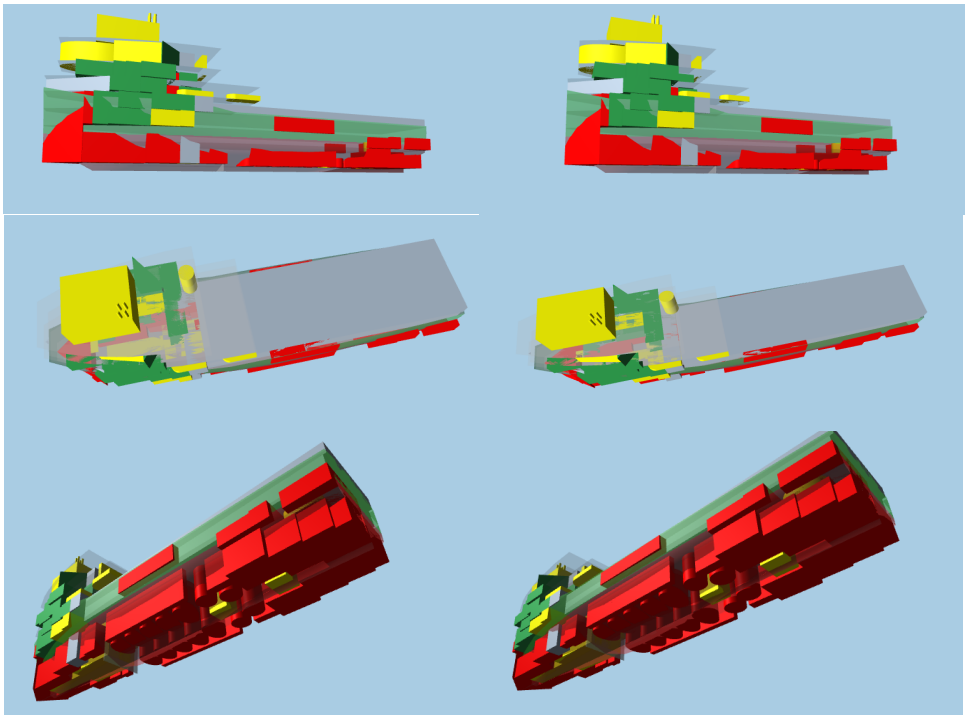

Figure 9 – 441 solutions were developed, with 106 DBBs, maintaining the fixed GT constraint.

At this stage, a more refined evaluation of design weight, hydrostatics and stability balance is carried. An existing Vessel.js app receives the digital ship definition in JSON format and plots a report containing the list of blocks, with positions and weights, and a summary of hydrostatic parameters for that design (Figure 10).

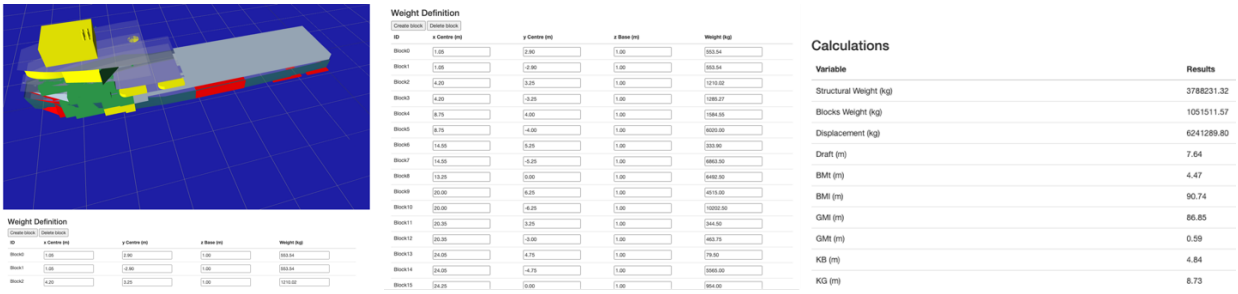

Figure 10 – PSV DBB hydrostatic data using vessel.js library.

General Arrangement Stage

Resorting to a combination of a 3D-first design approach and tools allows a simple General Arrangement to be automatically generated as a by-product of the 3D visualisation created during the previous steps, instead of having it being drawn manually as a separate document. A specific Vessel.js web app renders top views of the ship model on each deck, resulting in the General Arrangement depicted in Figure 11 As the PSV design was detailed, building blocks were gradually substituted by 3D models of parts and equipment. The GA was consequently updated toward a detailed version adequate to upcoming design stages.

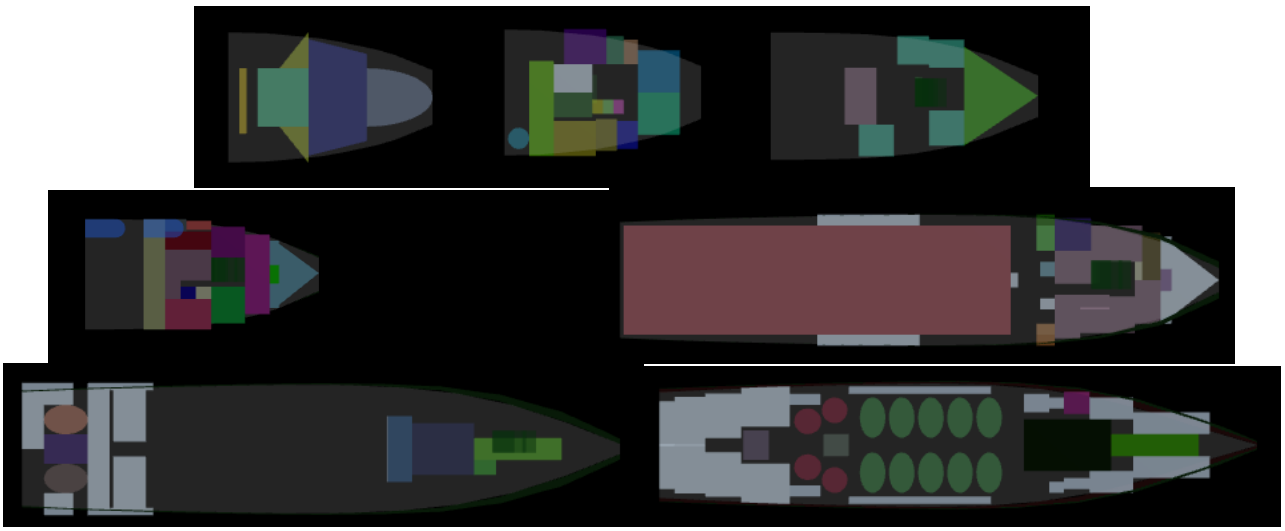

Figure 11 – Simple GA from blocks, adjusting the camera from the web-based render.

DBB USE IN BSc STUDIES – INNOVATION IN THE SPECTRUM OF SHIP DESIGN METHODS

Since 2017 the second author has attempted to introduced DBB method in his *SKID2300 Ship Design III - Design Methods* in combination with other methods, in his NTNU modules (Gaspar, 2023). The course is offered in the 5th semester of the BSc in Naval Architecture (Ship Design Course), in Ålesund, Norway. The students at that stage have already learnt the fundamentals of S4 (Andrews, 2018), so they are sure that they can calculate stability, resistance, design a safe hull, comply with regulations and classification, and understanding a (basic) dynamic response of the vessel (seakeeping / dynamic stability). It is one of the objectives of this last course, thus, to present to the students a compilation of more modern and realistic ship design methods. This is given theoretically by the second author, and in practice, by Øyvind Kamsvåg, Head of Design at Ulstein Group (Kamsvåg, 2018). Importantly, this course was designed with the intention of rekindling the students' desire to be creative, that the two previous years of analyses had supressed. The logic of the course is the following:

1) Self-evaluation from the previous design exercises: The student has to explain their previous designs, and is challenged with critical thinking questions, specially connected to *Why X and not Y*. It is no surprise that the usual answer *is because I copied from Z, and they used it*. It is also in this phase that the student realise that their previous attempts are addressing the learning of an analytical skill (e.g. *stability or resistance*) rather than designing skills.

2) Mission Matrix and Requirements Elucidation: This phase presents two basics taxonomies to the students. First, that vessels operate in a spectrum of *Service and Transport*, and that they can be designed to maximise *Weight or Volume*. This is a starting point to point to expose the limitations of the basic design spiral, as well as that their previous attempts, which addressed analytic skills, can now reveal that to produce a new design requires a stylistic choice on their part (Andrews, 2018). In other words, it's a stylistic decision from the designer to place the design more towards one or other side of this *spectrum*. Requirements Elucidation are tackled with the Shall / Should approach, and so communicate expectations. Figure 12 presents a collage from student's reports: in the left the *Mission Matrix* and in the right *a Shall / Should* example for a PSV.

3) Top-Down Methods (Reference Ship / Catalogue / StO): Top-Down is here used to describe ship design methods that have a starting point data from formulas, regressions, previous designs and parametric studies based on existing solutions, such as the one commented in Parsons (2011), most of Watson and Gilfillan (1976) and Roh and Lee (2018). Such top-down approaches to collecting data, usually find a practical and consensual solution in a short time and cost but lacks innovation and carries on the bias and out of date insights from previous designs. At this step is important to go into the detail of the design of a reference ship, understanding the design and stylistic choices that the designer of that ship has

made. In this stage the Systems Based Ship Design (SBSD) Taxonomy from Levander (2006) is also introduced, asking as a core exercise that the student decompose the ship into a functional breakdown, such as *Ship Systems* and *Payload Systems*.

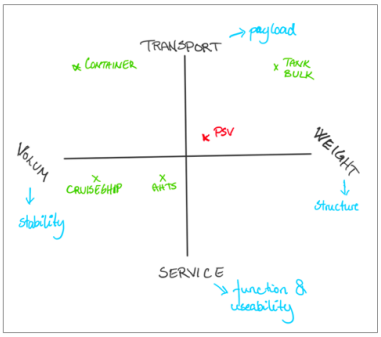

a)

Requirements	Shall	Should
Payload		
Baseoil, m^3	200	250
Drill water, m^3	1000	1500
Brine, m^3	800	1000
Methanol, m^3	150	250
Mud, m^3	1000	1500
Deck capacity, *tons*	2750	3000
Dry bulk, m^3	250	400
Fresh water, m^3	1000	1250

Performance		
Economical speed, *knts*	10	12
Max speed, *knts*	14	15
Accomodation		
Crewspace	25	25
Dimensions		
T, m	6	7
D, m	7.5	8.5
LOA, m	85	90
B, m	20	20

b)

Figure 12 – a) Mission Domain Matrix (*Service x Transport / Volume x Weight*); b) *Shall / Should* description of requirements

4) Bottom-Up (Design Inside Out, SBSD++, proto-DBB): Bottom-up methods are here understood as starting the design from specific key elements and subsystems that directly affect the mission of the ship. Bottom-up data presents different taxonomies or different vessel descriptions and understanding them, such as in SBSD and DBB. Bottom-up data is the starting point for innovative and technological break-through designs, but may suffer from the lack of knowledge connected to the uncertainty of one-of-a-kind projects. A key change to the traditional SBSD method, is to introduce the concept of DBBs, with the addition of distinct colours to identify the functional breakdown. Figure 13 presents this exercise made for a RoPax Ferry (left, in Norwegian) and a Factory stern trawler (right).

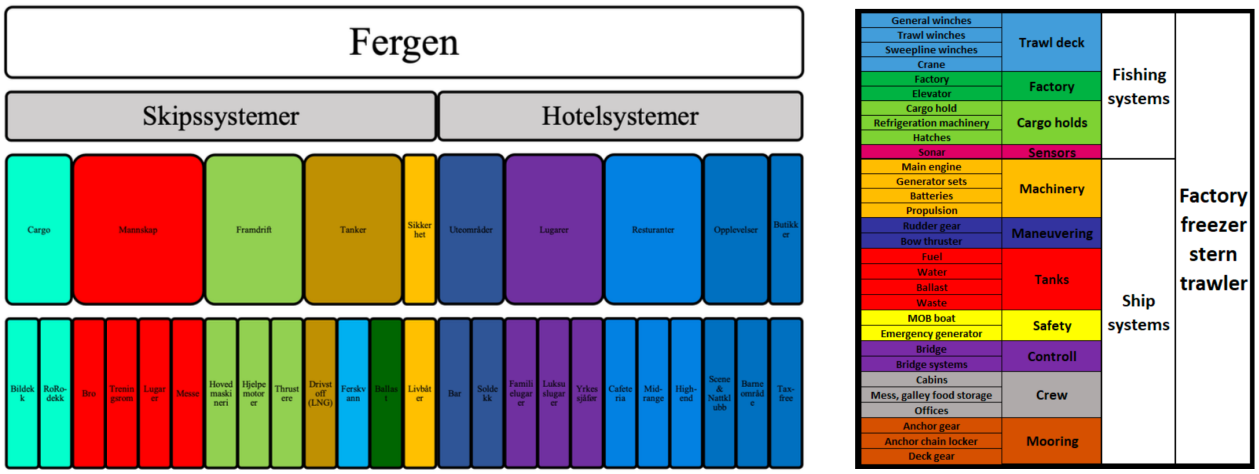

Figure 13 – From functionalities break-down to colours - initial step to connect SBSD and DBB

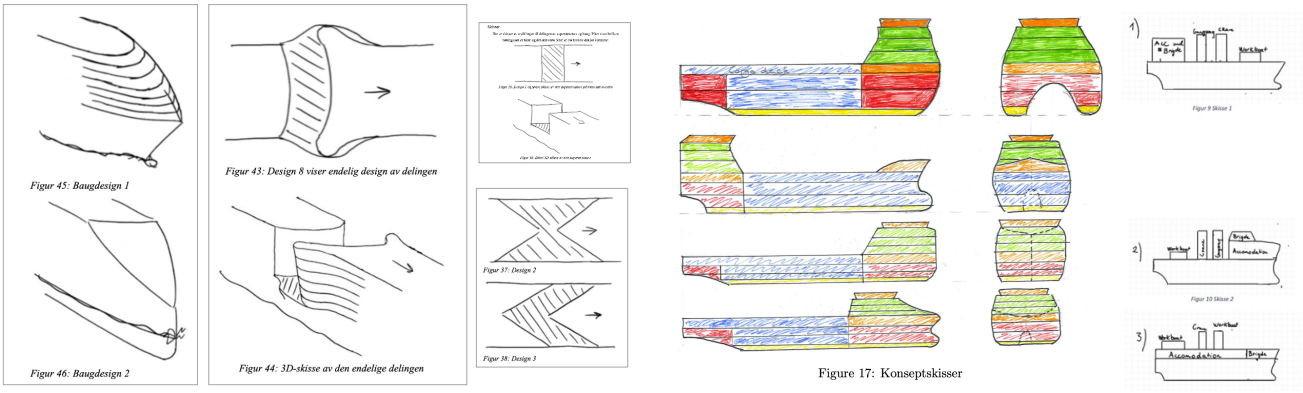

Figure 14 – Sketches to foster innovative solution in BSc student designs.

5) Sketching and design space exploration: This step is crucial, as the students have a class in the middle of the course to pause the dense theoretical approach and sketch, freehand, the innovative and key elements that are the core of its mission. Is it emphasised that artistic qualities are not being judged, but this is rather an exercise to explore solutions out of the box. Figure 14 presents a collage of sketches from the students.

6) Proto-DBB Exercise: This stage gets the students to implement some of the DBBs methods to explore their innovative ideas. The functional breakdown from Step 3 is used to create a simple library of SBBs, mostly visual, that is, not necessarily provided in ship design software. The core of this phases is not the comprehensive validation of a concept, but the use of 2D and 3D tools to *play around* with the newly sketched ideas. That said, the *weapon of choice* is for the student to select. Some use traditional naval architecture software, like Maxsurf (Passenger Ferry Design, Figure 15a), others use drawing tools like AutoCad or Sketch-Up (Cruise Ship, Figure 15b). The important thing is for them to explore the design space.

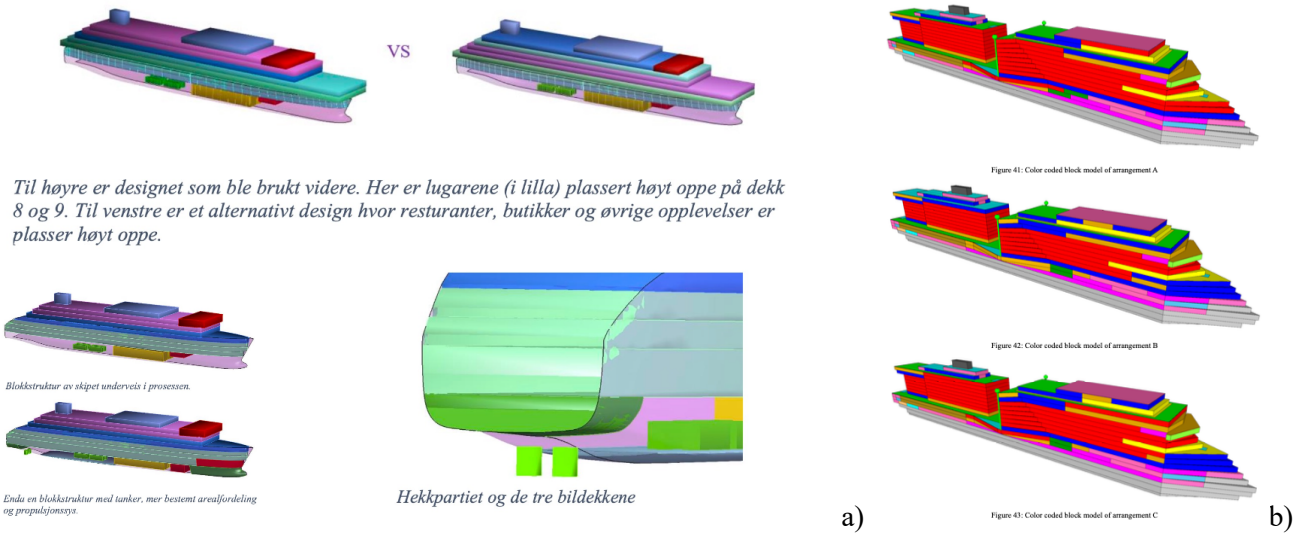

Figure 15 – proto-DBB exploration of a passenger Ferry (a) and Cruise Ship (b)

7) Tabular Summary and GA: Parsing the blocks and assembly into useful information is the next step. The student thus converts the blocks into volumes, areas, weights and centres, in a way to quickly input the data in the existing S⁴ tools. A GA is also created, documenting the innovative design in the proper manner. Figure 16 exemplifies this step.

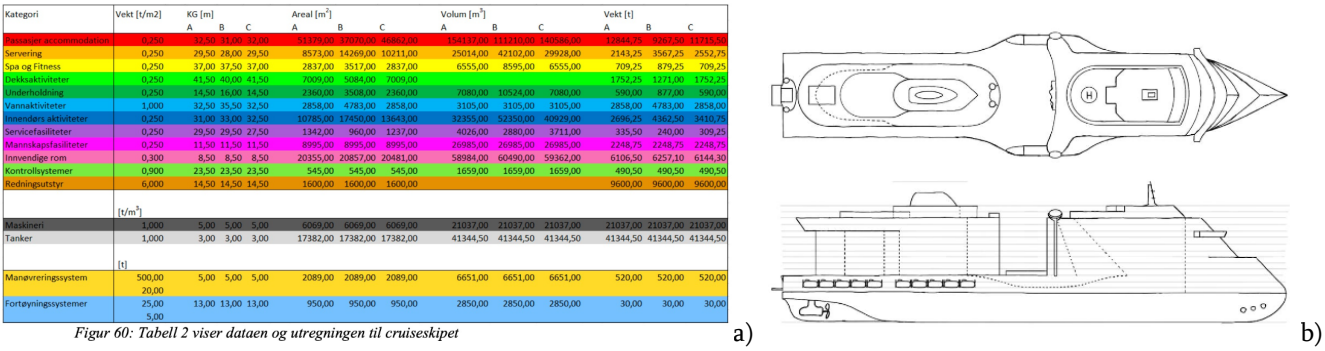

Kategori	Vekt [t/m2]	KG [m]			Areal [m²]			Volum [m³]			Vekt [t]		
		A	B	C	A	B	C	A	B	C	A	B	C
Passasjer accommodation	0,250	32,50	31,00	32,00	51379,00	37070,00	46862,00	154137,00	111210,00	140586,00	12844,75	9267,50	11715,50
Servering	0,250	29,50	28,00	29,50	8573,00	14269,00	10211,00	25014,00	42102,00	29928,00	2143,25	3567,25	2552,75
Spa og Fitness	0,250	37,00	37,50	37,00	2837,00	3517,00	2837,00	6555,00	8595,00	6555,00	709,25	879,25	709,25
Dekksaktiviteter	0,250	41,50	40,00	41,50	7009,00	5084,00	7009,00				1752,25	1271,00	1752,25
Underholdning	0,250	14,50	16,00	14,50	2360,00	3508,00	2360,00	7080,00	10524,00	7080,00	590,00	877,00	590,00
Vannaktiviteter	1,000	32,50	35,50	32,50	2858,00	4783,00	2858,00	3105,00	3105,00	3105,00	2858,00	4783,00	2858,00
Innendørs aktiviteter	0,250	31,00	33,00	32,50	10785,00	17450,00	13643,00	32355,00	52350,00	40929,00	2696,25	4362,50	3410,75
Servicefasiliteter	0,250	29,50	29,50	27,50	1342,00	960,00	1237,00	4026,00	2880,00	3711,00	335,50	240,00	309,25
Mannskapsfasiliteter	0,250	11,50	11,50	11,50	8995,00	8995,00	8995,00	26985,00	26985,00	26985,00	2248,75	2248,75	2248,75
Innvendige rom	0,300	8,50	8,50	8,50	20355,00	20857,00	20481,00	58984,00	60490,00	59362,00	6106,50	6257,10	6144,30
Kontrollsystemer	0,900	23,50	23,50	23,50	545,00	545,00	545,00	1659,00	1659,00	1659,00	490,50	490,50	490,50
Redningsutstyr	6,000	14,50	14,50	14,50	1600,00	1600,00	1600,00				9600,00	9600,00	9600,00
	[t/m³]												
Maskineri	1,000	5,00	5,00	5,00	6069,00	6069,00	6069,00	21037,00	21037,00	21037,00	21037,00	21037,00	21037,00
Tanker	1,000	3,00	3,00	3,00	17382,00	17382,00	17382,00	41344,50	41344,50	41344,50	41344,50	41344,50	41344,50
	[t]												
Manøvreringssystem	500,00 20,00	5,00	5,00	5,00	2089,00	2089,00	2089,00	6651,00	6651,00	6651,00	520,00	520,00	520,00
Fortøyningssystemer	25,00 5,00	13,00	13,00	13,00	950,00	950,00	950,00	2850,00	2850,00	2850,00	30,00	30,00	30,00

Figur 60: Tabell 2 viser dataen og utregningen til cruiseskipet

a) b)

Figure 16 – Tabular conversion of blocks into weight, centres, volumes and areas (a) and final design drawings (b)

WITHER NOW THE DBB: ADVANTAGES, LIMITATIONS AND PROMISES WHEN BORDERS ARE EXTENDED

The first two authors share similar experiences from the ship design approach taught during their graduation years. It was aimed at vessels for commodity transports and relied on methods heavily reliant on previous designs, such as use of regressions and of previous general arrangements for vessels of comparable size and capacity. From the commercial

perspective, this might be a suitable combination for transport vessels as they are often designed to similar (if not identical) requirements and might as well be standardised for reproducible manufacturing in shipyards. From the educational perspective, it might be useful to have students have their first design experience with that a non-original set ups for two good reasons. First, it gives them some confidence that their design decisions are at least plausible, by providing external references. Second, it provides them with the opportunity to practice basic design analyses (e.g., stability assessment, propulsion sizing, structural dimensioning) in an exercise environment where the solution is roughly known beforehand. This means propulsion will be comparable to that of other Suezmax vessels and so will adopt the same compartmentation and similar aspects.

The disadvantage of such regression-based methods is that once students and practitioners are familiar with the knowledge needed for addressing common design aspects, the process tends to become mechanistic and repetitive, as a direct consequence of design reuse. In that sense, the DBB approach puts higher emphasis on holistic and architectural design concerns. It assumes the ship designer already has sound knowledge (and maybe even intuition) of fundamental trade-offs incurred by key design decisions and, for that reason, is able to focus on space use and arrangement without losing sight of the ship as a whole system. As already pointed, this gives the designer greater autonomy to explore design alternatives (and thus innovate) by not resorting to prescribed templates. It also reduces the threshold to iteration in early design by giving a set of elements (building blocks) that can be directly manipulated to consider and evaluate different alternatives without committing to any in detail. As a result, it can be said that the overall process becomes more engaging as it gives the naval architect space to explore the design problem with a creative mindset, instead of being limited to being the professional who ensures a previously chosen design sticks (without questioning) to applicable rules and standards by class, IMO, or others.

The attempts to extend the boundaries of the DBB discussed here are far from finalised, and many shortcuts were taken. The 2D and 3D online tools are in an incipient stage of development, given the lack of commercial support. The example from the BSc course is limited by the scope of the course, as well as the strong connection that the campus from NTNU in Ålesund has with the local ship design companies. In this sense, elements from DBB are adapted and merged with other methods. It is important to reiterate, however, that the proto-DBB exercise is one of the highlights of the course, resulting in engaged and motivated students. We invite the readers, naval architects working for the industry or academia, to dig into the references and adapt for their cases, DBB elements, especially if the aim is to explore innovative designs.

Given that, before the research and teaching at NTNU described in the latter part of this paper, the only research and educational use of the UCL Design Building Block approach to synthesising complete descriptions of ESSD were those in the Design Research Group team under the third author at UCL, it is worth ending this *Whither* paper by considering whether the DBB approach in an age of "advanced CASD", with AI and ML implications, can be adopted more widely. This needs to be considered from both a teaching/academic research perspective and actual ESSD "in the real world". It is the case that the specific Paramarine applications of the UCL DBB approach (facilitated by the SURFCON module incorporated in the Paramarine suite (Monez and Forrest, 2002)) have been used "for real ship design" by ship design agencies, including non-naval ship designers (www.paramarine.qinetiq.com).

It is hoped this academic and wider usage will be undertaken in a manner consistent with the intent that the current paper's introductory remarks re-iterated. As part of considering how this might be taken forward the following remarks are offered:

- There are clear different types of ship design approaches due to its very diverse nature. Andrews (2018) spelt this out in Table 3 and Section 5, covering the range of design novelty undertaken with specific extra sections: Sections 8.1 (configurationally driven designs); 8.2 & 8.3 (examples of unconventional hullforms) and "the very special case of submarine design (Section 8.4). All of the latter can only be sensibly synthesised by a DBB like architectural approach, while the conventional monohull also ought (especially if "novel" to any noticeable degree) to be designed "inside-out" (i.e., a DBB like approach).
- Accepting a requirements elucidation approach (see Section 3 of Andrews, 2018) even the conventional monohulled service vessel when synthesised "inside-out", can (and normally should) be explored for different

internal configurations to see what is "best" as part of requirements elucidation. (A quite old but very comprehensive presentation of different configurations explored as part of the design of a major new class of combatant was provided by Leopold and Reuter (1971) - see Figure 7.) The message of a DBB type approach is that different internal configurations can be readily explored and tied to the numerical balance (through the Paramarine NA suite) so that the whole outer hull (and the superstructure) can be readily adjusted to accommodate "better" internal (DBB) configurations. This is creative ship design.

- A final set of SD educational remarks: Teaching ship design, both progressively to undergrads and to more general engineering graduate entrants (at NA masters level) can be done in steps and using an architectural/sketching approach (see Pawling and Andrews, 2011); the higher level of PhD and post-doctoral SD research is best fostered by a DBB type approach (see Andrews (2018) Sections 6.2 and 6.3 for UCL examples of new ship designs and researching specific ship design issues for whole ship implications); Sketching needs to be fostered as part of inside-out/architectural/DBB exploitation – to both encourage creativity and to not be limited by specific tools. This further encourages innovation and the necessary dialogue with design stakeholders (especially requirements owners/operators/funding bodies).

CONTRIBUTION STATEMENT

All Authors Equally: Conceptualization; data curation, methodology; writing.

ACKNOWLEDGEMENTS

To Dr. Pawling (UCL), who did the bulk of the Beta Test of the Paramarine realisation of the DBB approach and subsequent research students that used the approach to design innovative vessels and wider aspects of ship design behaviour; To the former NTNU students, and now naval architects, Magnus Weidemann, Hans Jørgen Sveen, Lars Vestnes and Sivert Rosø for sharing part of their exercises. The online tools presented in this work are available at https://vesseljs.org/. This research is part of the Ship Design and Operation Lab at NTNU (https://www.ntnu.edu/ihb/ship-lab) and UCL Marine Research Group (https://www.ucl.ac.uk/mechanical-engineering/research/marine) ongoing collaboration since 2016.

REFERENCES

ANDREWS, D. J. (1981), Creative Ship Design, Trans RINA Vol. 123, 1981.

ANDREWS, D. (1984) Synthesis in Ship Design, PhD, University of London

ANDREWS, D.J. (1986), An Integrated Approach to Ship Synthesis, RINA Transactions, Vol. 128, 1986

ANDREWS, D (1987), Exploration into the Nature of Frigate Preliminary Design, RINA Symposium on Anti-Submarine Warfare, May 1987.

ANDREWS, D.J. (1998), A Comprehensive Methodology for the Design of Ships (and Other Complex Systems), Proc. of the Royal Society, Series A (1998) 454, p.187-211, Jan 1998.

ANDREWS, D. (2001a), Adaptability – the Key to Modern Warship Design, RINA Warships 2001, London, June 2001.

ANDREWS, D. (2001b), Trends in Future Warship Design, Naval Platform Technology Seminar 2001, IMDEX Asia 2001, Singapore, May 2001.

ANDREWS, D.J. (2003a), Marine Design – Requirement Elucidation rather than Requirement Engineering, IMDC 03 Athens, May 2003.

ANDREWS, D.J. (2003b), A Creative Approach to Ship Architecture, RINA IJME, Sept 2003, Discussion and Author's response IJME Sept 2004, Trans RINA Vol. 145, 146, 2003, 2004.

ANDREWS, D. (2004), Multi-Hulled Vessels, Chapter 46 of Ship Design and Construction, Lamb T (Ed): SNAME, New Jersey, Vol. 2. Summer 2004.

ANDREWS, D.J. (2010), A 150 Years of Ship Design, IJME, Vol. 152, Part A1, 2010. Discussion and Author's reply IJME Vol. 153 Part A1 2011.

ANDREWS, D. J. (2011), Marine Requirements Elucidation and the Nature of Preliminary Ship Design, IJME Vol.153 Part A1, 2011.

ANDREWS, D.J. (2012), Art and science in the design of physically large and complex systems, Proc. Roy. Soc. Lond. A (2012) Vol. 468.

ANDREWS, D.J. (2017), The Key Ship Design Decision – Choosing the Style of a New Design, COMPIT 2017, Cardiff, May 2017.

ANDREWS, D. (2018), The Sophistication of Early Stage Design of Complex Vessels, Trans RINA, Special Edition, Intl J Maritime Eng, 2018

ANDREWS, D. (2022), Babies, Bathwater and Balance – the Fuzzy half of Ship Design and Recognising its Importance, SNAME Maritime Convention 2022, Houston, TX, Sept 2022.

ANDREWS, D AND DICKS, C (1997), The Building Block Design Methodology Applied to Advanced Naval Ship Design, IMDC 1997, Newcastle University, June 1997.

ANDREWS, D.J. & PAWLING, R. (2003). SURFCON – A 21st Century Ship Design Tool,

IMDC 03, Athens, May 2003.

ANDREWS, D.J. & PAWLING, R. (2004), Fast Motherships - A Design Challenge, International Conference 'Warship 2004:Littoral Warfare & the Expeditionary Force', RINA, London, June 2004.

ANDREWS, D.J. & PAWLING, R., (2008), A case study in preliminary ship design, Int. J. Maritime Engineering, 150/A3

GHARIB ET AL., (2016), GHARIB, A., ANDREWS, D. & GRIFFITHS, H. (2016), Prediction of Topside Electromagnetic Compatibility in Concept Phase Ship Design, Transactions on Electromagnetic Compatibility, IEEE, 2016.

GASPAR, H. M., BRETT, P. O., ERIKSTAD, S. O. AND ROSS, A. M. (2015). Quantifying robustness of OSV designs taking into consideration medium to long term stakeholders' expectations 12th Int. Marine Design Conf. (IMDC), Tokyo.

GASPAR, H.M. (2018), Vessel.js: an open and collaborative ship design object-oriented library, 13th Int. Marine Design Conf. (IMDC), Helsinki

GASPAR, H. M. (2022). Current State Of The Vessel.Js Library: A Web- Based Toolbox For Maritime Simulations. 14th Int. Marine Design Conf. (IMDC), Vancouver, B.C.

GASPAR, H. M. & ANDREWS, D. (2022) Quantifying Interfaces in General Arrangement Drawings. 14th Int. Marine Design Conf. (IMDC), Vancouver, B.C.

GASPAR, H. M. (2023) Ship Design III – Design Methods Lecture Notes (NTNU, Ålesund)

KAMSVÅG, Ø. (2018) Ship Design Lecture Notes (NTNU, Ålesund)

KEANE, R.J. (2018), Written Discussion to Andrews, D. (2018), The Sophistication of Early Stage Design of Complex Vessels, Trans RINA, Special Edition, Intl J Maritime Eng, 2018

KOURIAMPALIS, N., PAWLING, R. J., ANDREWS, D. J. (2019) Modelling the operational effects of deploying and retrieving a fleet of uninhabited vehicles on the design of dedicated naval surface ships. Ocean Engineering 219 (2021) 108274

KRAMEL, D. 2019 DBB web application. http://dbb.ucl.im/

LEOPOLD, R. & REUTER, W. (1971) Three Winning Designs – FDL, LHA, DD963 Methods and Selected Features, Trans SNAME, 1971.

PAWLING, R. (2007) The Application of the Design Building Block Approach to Innovative Ship Design. PhD Thesis, UCL, London

PAWLING, R., & ANDREWS, D. (2011). Design Sketching for Computer Aided Preliminary Ship Design. Ship Technology Research, 58(3), 182–194. https://doi.org/10.1179/str.2011.58.3.006

PIPERAKIS, A., GASPAR, H.M. 2016.DBB Method – A Web-based App http://dbb.ucl.im/2016

RAWSON, K.J. & TUPPER, E.C. (2001), Basic Ship Theory, (5th Edition), Longmans, London, 2001.

RITTEL, H.M.J, & WEBBER, M.W. (1973), Dilemmas in the general theory of planning policy sciences, Policy sciences, Vol. 4, 1973.

PIPERAKIS, A & ANDREWS, D (2014), A comprehensive approach to survivability assessment in naval ship concept design, Int. J. Maritime Engineering, Vol.156/A4.

ULSTEIN (2014) Platform Supply Vessel, PX121 Blue Ship Invest Catalogue (Ulstein Group ASA)

Proceedings of 15th International Marine Design Conference (IMDC-2024)
June 2-6, 2024
Amsterdam, the Netherlands

Seeing a Sea of Ships - Exploring the Ship Design Space in the Digital Domain

Henrique M. Gaspar[1,*], Yasuo Ichinose[2] and Kazuo Nishimoto[3]

ABSTRACT

We tackle in this work aspects of the ship design space in the digital domain, with an overview of the current status and opportunities to shift from fixed arrangements towards open technologies, proposing a mix of open and proprietary databases. The discussion is focused on the visual domain and digital thread in ship design. Literature examples from the Brazilian case and the visualization of the ocean space are presented (Numerical Offshore Tank - TPN), followed by the Japanese services to design and optimize hull for specific missions (NMRI), and lastly the current open ship design library developed in Norway (Vessel.js, NTNU). We present the argument that seeing a sea of ships, that is, visualizing the behavior of many options is already a reality, accessible from a portable device, without the need a large cluster as in the past, exemplified by web-based cases. Our conclusion is that computer graphics approaches to Ship Design should be considered open and exchangeable. Naval architects should focus on what they do best: creating, analyzing, refining, storing and populating the database of the know-how from the institution (e.g. university, research institute or company).

KEY WORDS

Virtual Prototype; Web-based simulation; Hull simulation; Digitalization.

SEEING THE DESIGN OF A SHIP

The Visual Domain in Maritime – Towards a Coherent Digital Thread

Bertram (2023) uses an analogy with DNA and its four simple elements to express the ship design process when highlighted by computer. His CAVE acronym stands for Creation, Analyses, Visualization and Enlightenment, and the use of these terms are used to remind us that creation remains in the realm of the human (centric or driven), but that the computer (created by us) accelerates and improves the final result of the design, that is, the ship. We explore in the rest of this work this idea, that the *tool* computer, when properly used, is essential to CAVE, and exploring the ship design space is, in essence, exploring the opportunities that the computer gives us to CAVE when the abstract idea and physical existence of a ship are parsed to the digital domain.

A great practical example of this whole loop is presented by Ulstein Group in a 3m11s video about the vessel SX121 Island Performer, a subsea (RLWI/IMR) vessel delivered in 2015 (https://www.youtube.com/watch?v=I9YGFm2AzTo). This short piece of visual information can cover in its small duration the power of the CAVE analogy. The hundreds of thousands of hours that humans used to design, analyze, and construct that vessel are summarized in this brilliant piece of advertise. Figure 1 presents a collage of this vide, highlighting the human activities in the design, engineering,

[1] Norwegian University of Science and Technology, Ålesund, Norway; ORCID: 0000-0003-2128-2863 [2] National Maritime Research Institute, Tokyo, Japan; ORCID: 0000-0003-1566-913X
[3] University of São Paulo, São Paulo, Brazil; ORCID: 0000-0003-2008-8524
* Corresponding Author: henrique.gaspar@ntnu.no

Submitted: 23 February 2024, Revised: 2 May 2024, Accepted: 3 May 2024, Published: 24 May 2024

Conference paper, DOI: https://doi.org/10.59490/imdc.2024.893 e-ISSN: 3050-486

construction and sea trial of the ship. Such video enlightens us on the nature of the ship upstream value chain (Brett and Ulstein, 2012).

Figure 1: Ship design as a human-centric and human driven activity – collage from Ulstein Island Performer video

The one of a kind nature of the maritime domain, thus, bring two additional assumptions when watching the video: i) innumerous designs and analyses were explored and discarded for Island Performer exists as it is; and ii) the ship existed first in the digital world, decomposed in thousands of files, bits and bytes of text, drawings, functions and tables.

The older generation of ship designers is still proud to remember how the maritime industry was pioneer in adopting CAD (or computer aided ship design, CASD) in the 70s and 80s (Gaspar, 2019). CASD thus appeared as the future step to document, copy, reuse and detail the design, a digital alternative for the blueprint firstly, and a drastic way to change the engineering and yard offices lately. The equivalent process of doing each of the parts, assemblies, blocks and other drawings were firstly mimicked in the new CAD systems, one digital file for each required drawing, and multiple copies of parts due to individual storage of each drawing in a unique.

The old school may argue (with reason) that the high dependency on CASD for all the calculations may remove the student from the tactile knowledge of a ship, since the abstraction required for a 3D drawing of a hull is different than decomposing it on the 2D surfaces that are cut to physically assembly the hull from frames and plates. But undoubtedly the screens, computers, keyboards and mouse are responsible for:

- 2D/3D design processes quicker; designers can create new concepts in short time.
- Reliable documentation of the whole ship design process, from early design to construction and maintenance.
- Exploration of a large number of options during early stages, smartly copying, pasting and adapting past design into new ones
- Exchange and exporting drawings and descriptions between formats, as well as filtering level of detailing.
- Connect design (creation) with performance (analysis), and visually understanding cause and consequence of changes in internal (e.g. geometry) and external (e.g. environment) parameters, enlightening the decision-making process.

Not all promises from the last decades, however, are fully concretized. Take the hype idea of *integrated model,* and *3D as basis* for all models. Ideally, the 3D concept developed during the tender package could be the start point to feed the next phases, like 2D general arrangements, and detailed engineering .Very little, however, of the original 3D file is really used in the next phases of engineering analysis and detailing, with each of the design groups, such as hydrodynamic, structures and cargo systems to name few, redoing and redrawing the hull and GA over and over again in each of their specific software – a task *fancily* called *manual flow* in the flowcharts.

Additionally, traceability is not a strong point when multiple software is used, and usually a major change in the design implies a large time of re-work and precious engineering time in correcting each of the non-connected engineering models.

The same lack of integration is observed in the subsequent phases, with multiple proprietary databases, sometimes inside the same company. Observing the development of the systems from the past, five reasons can be commented, namely: proprietary formats, lack of integration, licensing and profitability of the tool, high cost to training and a deviation from the principle of parsimony (Gaspar, 2018).

The commercial aspect of modern CASD software also keeps an unnecessary level of paperwork and licensing *contortionism* with outdated technology from the 90s, a political approach that yet requires a dedicated server which checks a license for each of the computers that are using the software. While this seemed a good solution to avoid piracy and gain control from the side of the creators on the past, this looks extremely counter-productive in face of the modern online tools, apps and pay per use technologies that we have available in non CASD computer software. On the top of it, count the hours that IT technicians use to install the software in each machine, a long process configuring client and server due to antiquate anti-piracy policies. We dare to speculate that the ship design developers would benefit of providing as open as possible solutions to install and use their software in order to gain terrain in the market share (Fonseca *et al.*, 2023).

We present in the rest of this paper three developments towards a coherent digital thread, shifting from fixed and closed platforms towards open technologies and the choice of open and/or proprietary databases. The next section presents an example from University of São Paulo (USP, Brazil) developed more than two decades ago, which still holds valid and feels *modern.* This is followed by the developments at the National Maritime Research Institute (NMRI – Japan), in hydrodynamic simulation, combining processing demanding CFD of a hull with efficient machine learning (ML) techniques to quickly obtain the hydrodynamic response of a set of hulls, developed by the Japanese in the last decade. Lastly, it gives an update on the open ship design library developed at the Norwegian University of Science and Technology (NTNU-Norway), with a web-based proof of concept able to generate and simulate 10 000 designs in time-domain analyses in real time, using validated surrogate models.

SPACE AND BEHAVIOR - VIRTUAL TOWING TANK

The numerical offshore model basin, TPN-USP (Nishimoto et al., 2003, Gaspar *et al.,* 2009), is a 20+ year old ongoing initiative between a collaboration of Brazilian universities, research institute, and the oil company PETROBRAS. Its utilization was initially focused on analyses and verification of the design of complex offshore systems that normally requires even more complex tests in physical model basins. Today, it also included a physical basin calibrator and simulators for crew training and operational assessment.

TPN was created as a time domain simulator that encompasses several methods and algorithms in a single tool. The main characteristic of the simulator was the possibility of carrying out a coupled analysis of the lines with the bodies. The lines are modeled with Finite Element Method that demanded great computational power two decades ago. Its procedure followed the trend of the time, with pre and pos processing or the analyses in separate instants (Figure 2).

Parallelization of the code was the key innovation at the time (Luz *et al.,* 2009). The distribution of process was linear among processors. First the cases processes were processed and in sequence the bodies and lines processes. The communication among the processes occurred as: 1) Before initializing the simulation, main process import the data file and distributes it among other processes. 2) In each time step of simulation, the body process receives the force that each line process computes, sums the other loads and computes the acceleration, velocity and position of body, sending this data to the case process that it belongs. The case process replenishes its body's processes whit this data and the line forces that attach the bodies (linking lines) for the calculus of next time step. Simultaneously, it gives directly to the lines processes the position of corresponding body, since the calculation of force acting in the line depends only upon its upper ending coordinates. A common bottleneck was the the number of processes being superior than available CPUs, which required some sort of multiprocessing parallel Interface to distribute automatically the extra load homogeneously among CPUs.

TPN had its architecture based mostly in open software (e.g. Linux, OpenFOAM), and used proprietary commercial program when necessary (e.g. WAMIT). The same idea was applied to its database of solutions. Some of them were based on open data, from non-proprietary calibration and simulation, which could be shared; others, were based on analyses developed for its main partner (PETROBRAS), and were proprietary, not to be shared outside the laboratory, but nevertheless contributing to increase the expertise of the team.

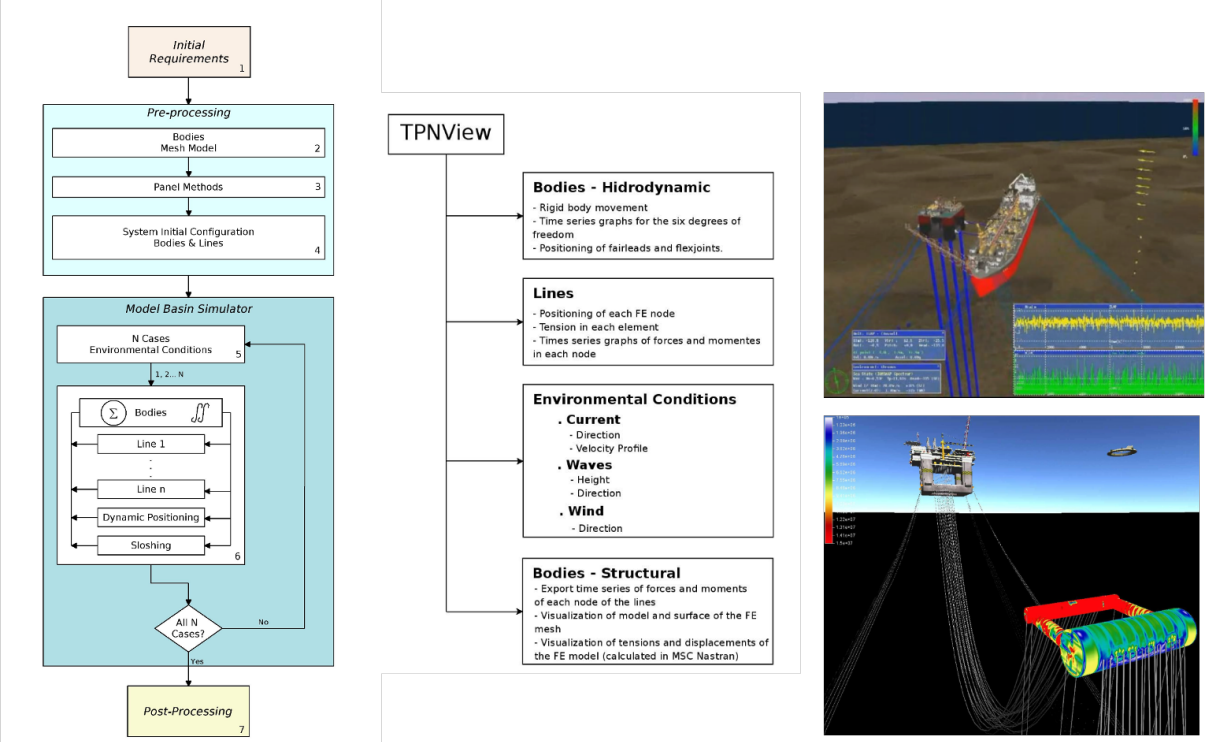

Figure 2: A time domain simulator encompasses several method and algorithms in a single tools in TPN

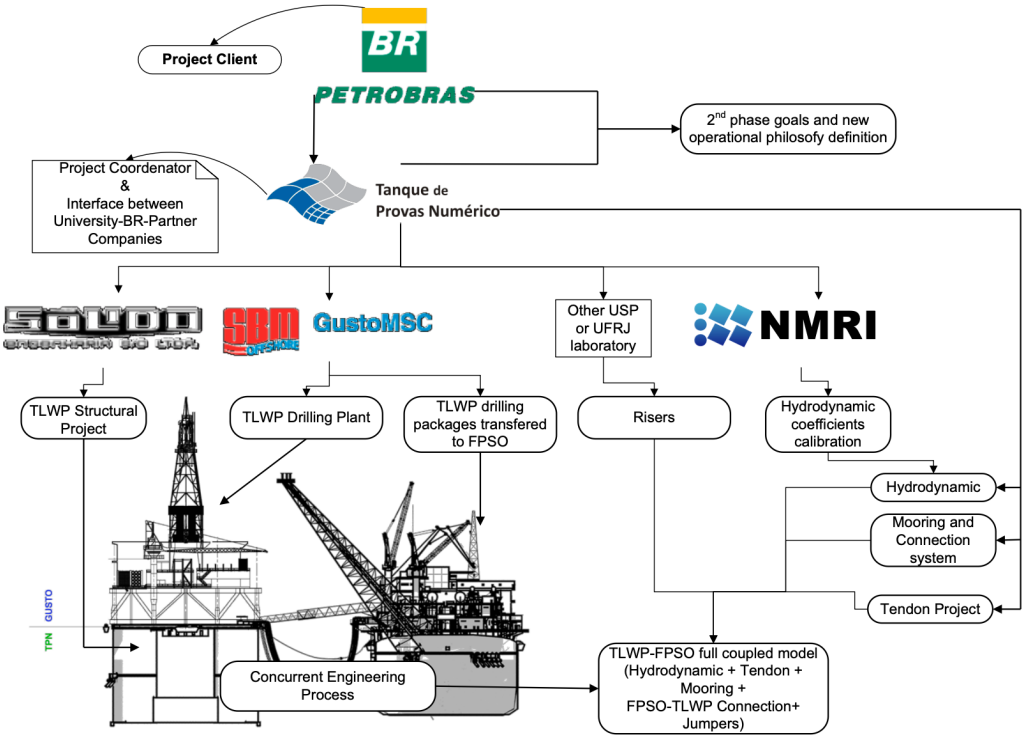

Figure 3: System Dimensioning Integration of TPN Simulator (Rampazzo et al., 2010)

The initiative was very successful, both national, boosting the offshore innovation in Brazil, and international, placing TPN as a key provider of simulation and visualization solutions for evaluation the design of vessels and multi-bodies operations. Other research institutes, such as Marin (NL), Marintek (NO) and NMRI (JP) developed at the same time complementary initiatives, and in few years the new ideas from early 2000s, like realistic graphics and hybrid methods combining physics based with surrogate models were implemented in most maritime research institutes. Figure 3 exemplify this synergy, in a collaboration from 2010 between TPN, Petrobras, engineering companies and the NMRI, for the development of a conceptual design of a FPSO + TLWP coupled system.

HULL AND SEA - SIMULATION AND OPTIMIZATION

In certain Ship Design *niches,* especially the ones connected to the high-sea transport of heavy cargo, the field of simulation-based design has become a prominent approach for shaping hull forms since the early 2000s, with the promise that CFD could *scrap* few percentages in efficiency, which could materialize in huge fuel savings over long trip. Such specialized analyses become thus a service offered by few, firstly in research institutes, and later by (some) software companies (Bertram, 2014).

Even with many advancements, ensuring design optimality under diverse operational scenarios yet remains a challenge. Researchers have explored stochastic shape optimization and visualizing design space to enhance robustness. Stochastic optimization studies have focused on minimizing total resistance and improving operability across different ship speeds. Visualizing the design space aids decision-making by elucidating effective parameter limits (Ichinose, 2022). Recent research has delved into using machine learning (ML) methods to analyze propulsive performance. Artificial neural network (ANN) models have been developed to estimate total resistance, trim conditions, and added resistance. Despite their efficacy, these automated design methods often lack transparency, posing challenges for designers. Efforts to develop explainable artificial intelligence or organizing hull-form databases for deeper understanding are underway.

Integrating visualization methods into machine learning-based hull design methodologies can be useful for effective decision-making and consensus-building among stakeholders involved in ship design. Visualizing and analyzing hull form performance requires a structured approach to organize and parameterize their database. Unlike propellers, which can be defined through factors like pitch and skew, hull forms present a challenge due to their complex 3D shapes. While various parameterization methods have been explored, no single standard has been universally adopted.

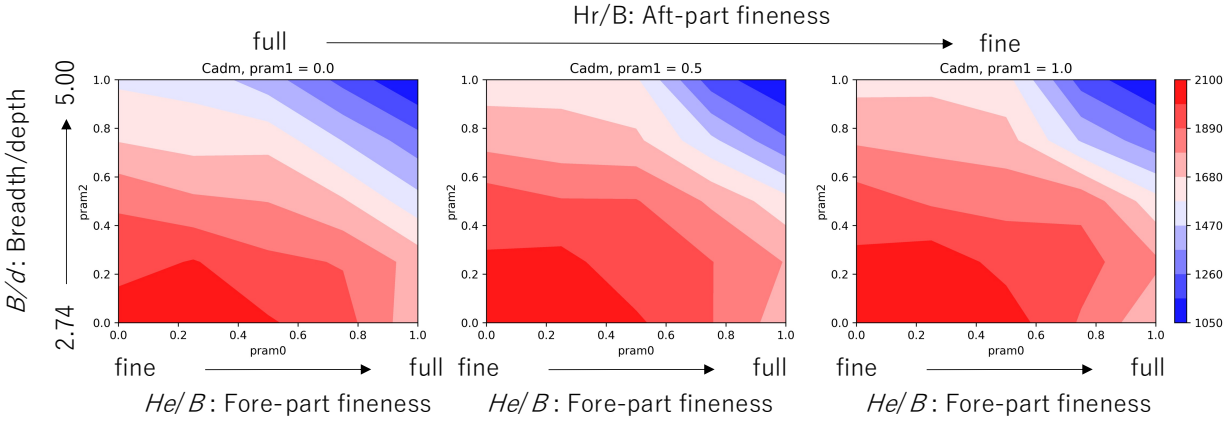

Figure 4: Distribution of admiralty coefficient (C_{ADM}) isolating the fineness factor in the aft part (Hr/B) (Ichinose, 2022).

In recent years, computer graphics techniques have been integrated into hull form deformation processes (Ichinose, 2022) Concurrently, shape morphing, originally developed for satellite image transformation, has found utility in ship design, preserving detailed shape information and facilitating better understanding of results. However, the practical application of shape morphing is hindered by its limited degrees of deformation, typically restricted to mixing two or three hull forms due to visualization challenges. Addressing this limitation, Ichinose has extended the morphing method into a multi-

dimensional context and proposed a Hull-form coordinate system that defines each ship type. Figure 4 is an example of visualizing the design space of ship forms using the Hull-form coordinate system. Here, the admiralty coefficient (C_{ADM}) in the figure is a performance coefficient representing transport efficiency, which is widely prevalent in the naval architecture field. Observing this performance distribution, it is evident that there are areas where performance remains stable despite slight changes in shape parameters and areas where performance is unstable in response to shape deformation.

In designing within the Digital Domain, particular attention must be paid to simulation errors and variance. That is, the optimal point obtained in numerous optimization simulations may not necessarily be the shape to be adopted in an actual construction project. We require a iteration of CAVE, from creation to enlightenment. Therefore, instead of a single optimal shape in the domain, it is necessary to adopt a group of candidate shapes, including the second and third viable options, in the design. Visualizing thus a design space that indicates a stable performance domain is a crucial technological element in engineering projects.

Furthermore, in engineering projects, efforts to improve physical interpretability through visualization are also essential for consensus formation and decision-making among designers and stakeholders in the Digital Domain. Figure 5 illustrates another example of visualizing a large set of simulations at once, presenting how the distribution of waves changes with the deformation of the hull form. We observe that, when the forepart becomes a full body, the generated wave height increases sharply (Figure 5, red perimeter). Thus, by optimizing the design space with physical interpretability, it is possible to achieve designs with high robustness.

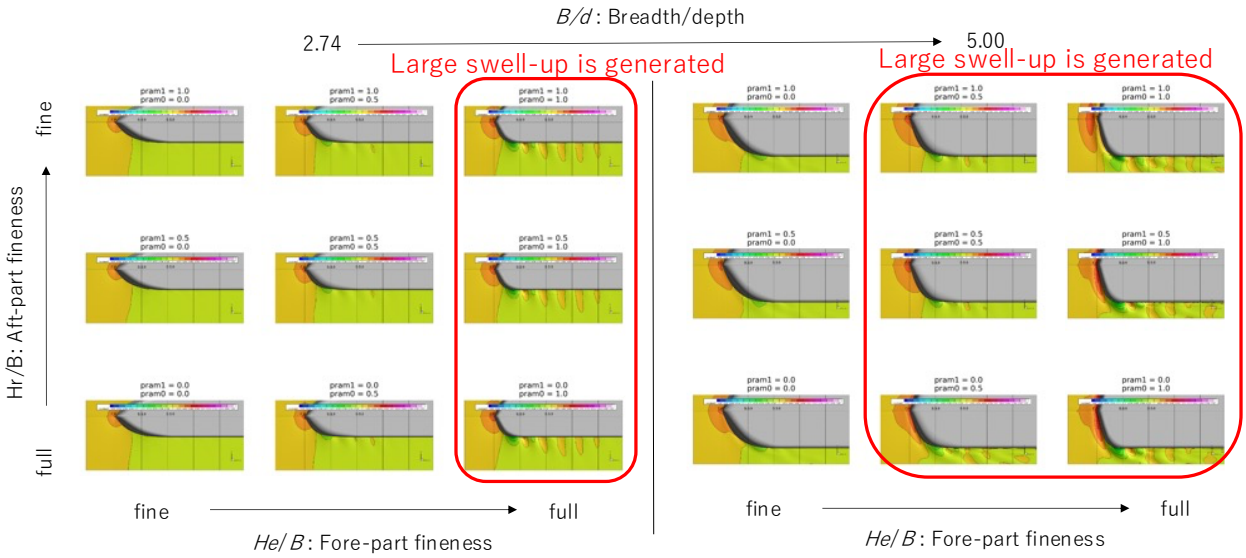

Figure 5: Listed figures of wave patterns in fore parts isolated by breadth-to-depth ratio (B/d) (Ichinose, 2022).

A bottleneck in adopting design methodologies that explore and visualize the entire design space is the time-consuming nature of simulations. Especially since the Navier-Stokes equations, which are the governing equations of fluid dynamics, are nonlinear and require numerical discretization to be solved, numerical analysis demands extensive time for grid generation. As an alternative to such numerical calculations, design charts have traditionally been used. However, there is a recent trend towards replacing design charts with machine learning methods. For this, a database with a large number of validated hydrodynamic simulations is needed. This database does not need necessarily to be open. The methods, however, need (and are), given that merging ML and surrogate models is a task beyond the ship design domain. In response to this, research is being conducted in ship design to visualize pressure distributions on hull surfaces and flow fields using machine learning surrogate models, traditionally performed with CFD simulations (Ichinose & Gaspar, 2023). Utilizing such surrogate models for CFD, it is possible to visualize thousands of cases in a matter of seconds as shown in Figure 6. This represents an evolution in the application of machine learning in ship design that goes beyond merely replacing

traditional design charts and highlights the anticipated growth in design development through using the existing validated databases.

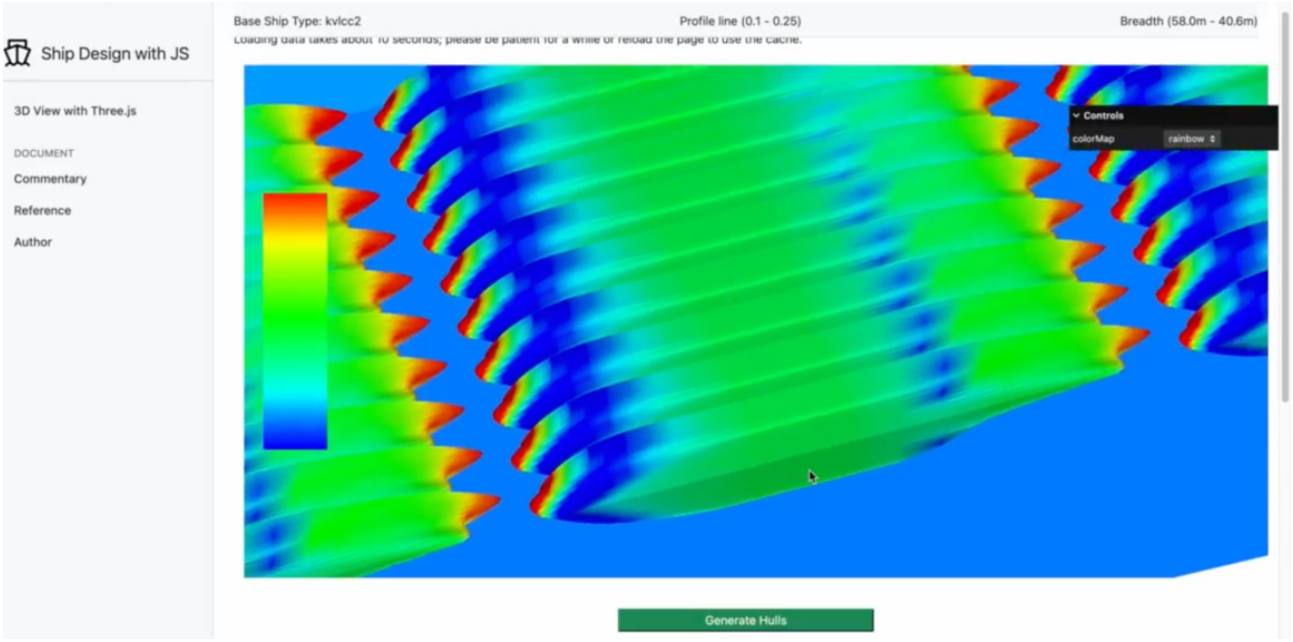

Figure 6: Example of Visualizing Pressure Distribution Across Thousands of Cases in Seconds Using a Machine Learning Surrogate Model for CFD, extended from Ichinose and Gaspar (2023)

A (DIGITAL) SEA OF SHIPS - THE ARGUMENT FOR WEB-BASED TECHNOLOGIES

Open digital methods allow us today to simulate and visualize in real-time 100s, 1 000s or even 10 000s of hull designs using a laptop. Actually, as the technology is web-based, probably with a modern mobile or tablet, using as example the open Vessel.js (https://vesseljs.org/) library. As introduced in earlier IMDCs (Gaspar 2018; 2022), this open ship design development is aimed at the design and simulation of maritime entities, combining ship design thinking within a JavaScript-based object-oriented approach. As the library is web-based, all examples and codes discussed there are available to be accessed, modified, and re-used by a community. The data and methods there are therefore transparent and can be tested and scrutinized.

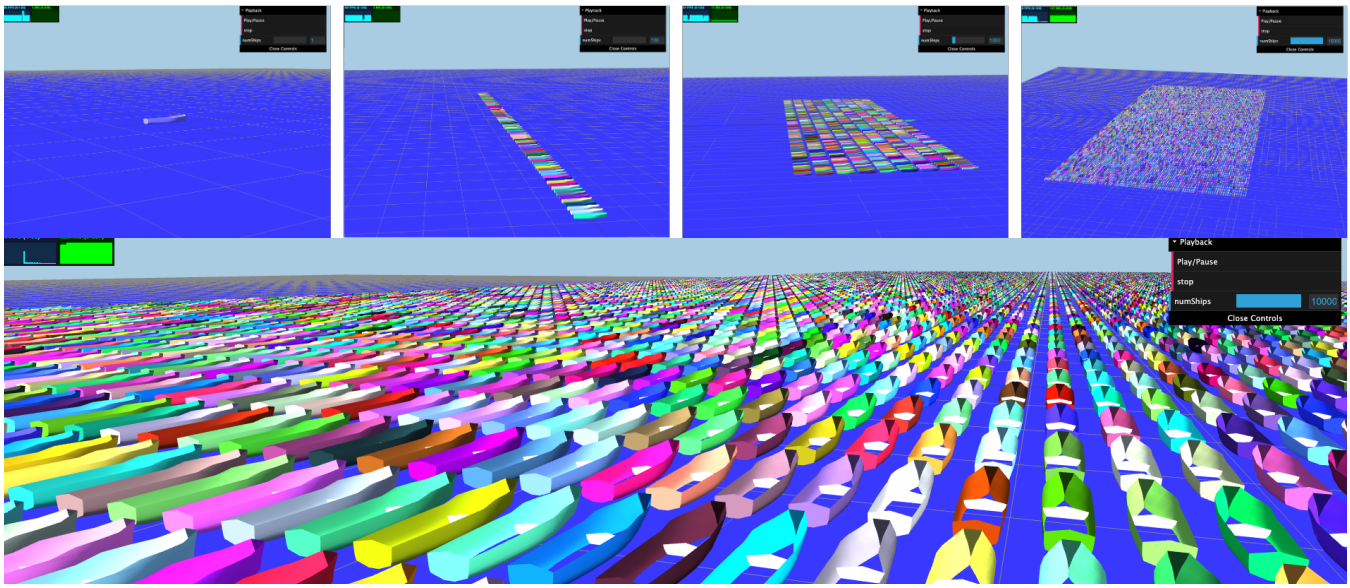

Figure 7: Visualization of 1, 100, 1000 and 10 000 hull in a fixed 4km x 4km virtual square.

Figure 7 presents the *Sea of Ships* currently implemented in the examples sections of the library (Ferrari and Gaspar, 2024). It presents a proof of concept able to load a database of many hulls, varying in real time from 1 to 10 000. As this was tested using a normal personal computer, we believe that a gamer PC, aimed at fast 3D rendering could jump this number to even one order of magnitude higher.

To exemplify open simulation, the described static representation is then connected to the seakeeping simulator described in Chaves and Gaspar (2016). It uses validated closed-form expressions from Jensen *et al. (2004)* to estimate wave-induced motion for mono-hull vessels. These expressions require only vessel main dimensions and basic hull form coefficients, being especially relevant for conceptual design, where little information about the hull form is available. The approach allows the designer to vary amplitude (A), period (T), direction (θ), phase (ϕ), and quickly assess their influence on the wave-induced motion. The case from 2016 was the first to present in an open web-based version the response of a vessel. Now, we implement it to the *Sea of Ships*, simulating seakeeping for 1, 100, 1 000 and 3 000 hulls in the same environment, in real time (Figure 8).

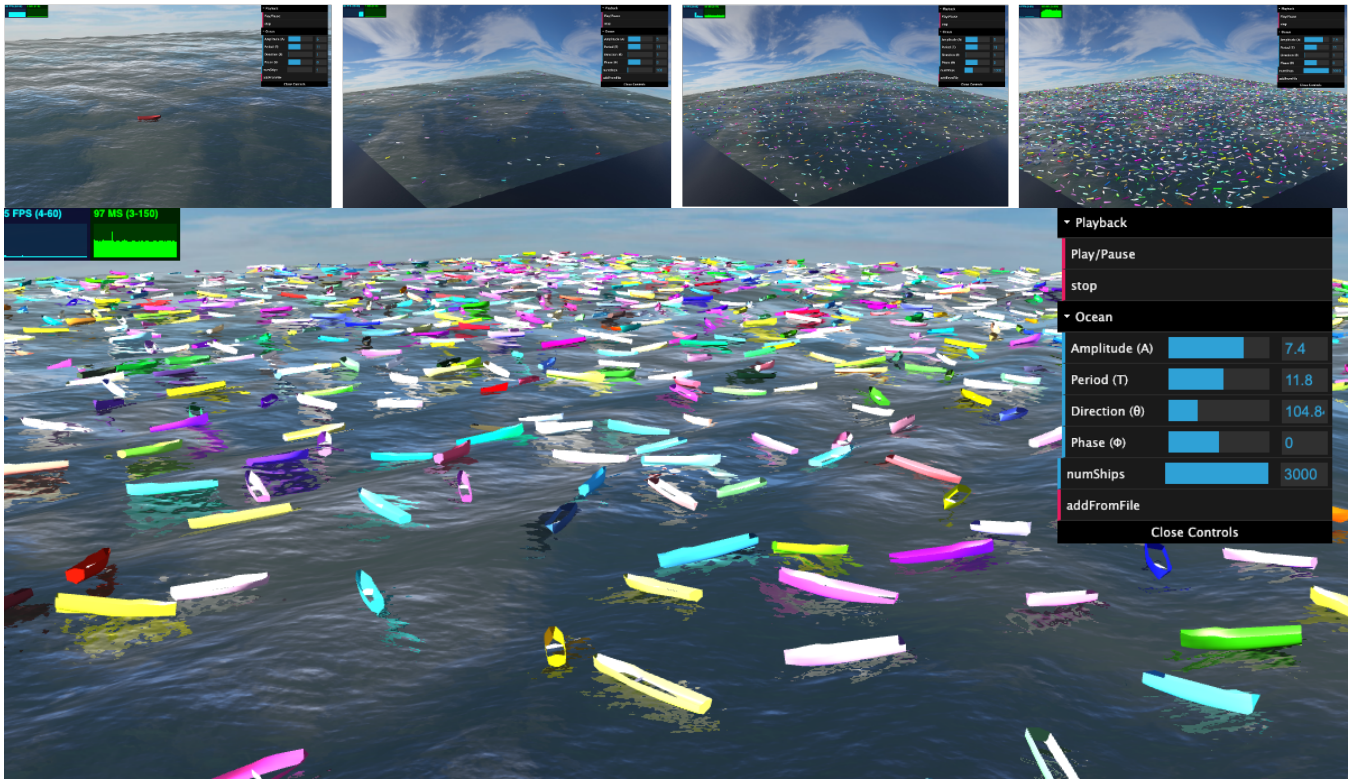

Figure 8: Simulating the seakeeping behavior of 1, 100, 1000 and 3 000 hulls using closed-form functions, in a virtual 4km x 4km ocean with virtual waves.

Compared to traditional engineering programming environments, web technologies provide more options and freedom for the creation of sophisticated user interfaces. The developer of a web application may use sliders, text fields and buttons to gather inputs from the user – exemplified in Figure 8 by the sliders to modify the simulation parameters. Results can be presented as formatted text, tables, plots or interactive visualizations, either 2D or 3D. Multiple textual and graphic elements can be combined in dashboards to present a cohesive experience to the user, allowing them to vary inputs and observe the effects of the variation on the results in real-time.

It is important to note that the possibility of assessing in real time such sea of ships is not a common feature in the majority of commercial software. The usability of this exercise is being tested also outside the boundaries of NTNU. Similar to the case discussed at TPN, collaboration between research institutes to check the validation and usability of open web-based technologies is increasing (Q.E.D. this article). The attempt made by NTNU seem in Figure 8 inspired a Japanese version,

result from the recent MoU signed between NTNU and NMRI. Diverse implementations of the method were combined with existing initiatives at NMRI (Figure 9).

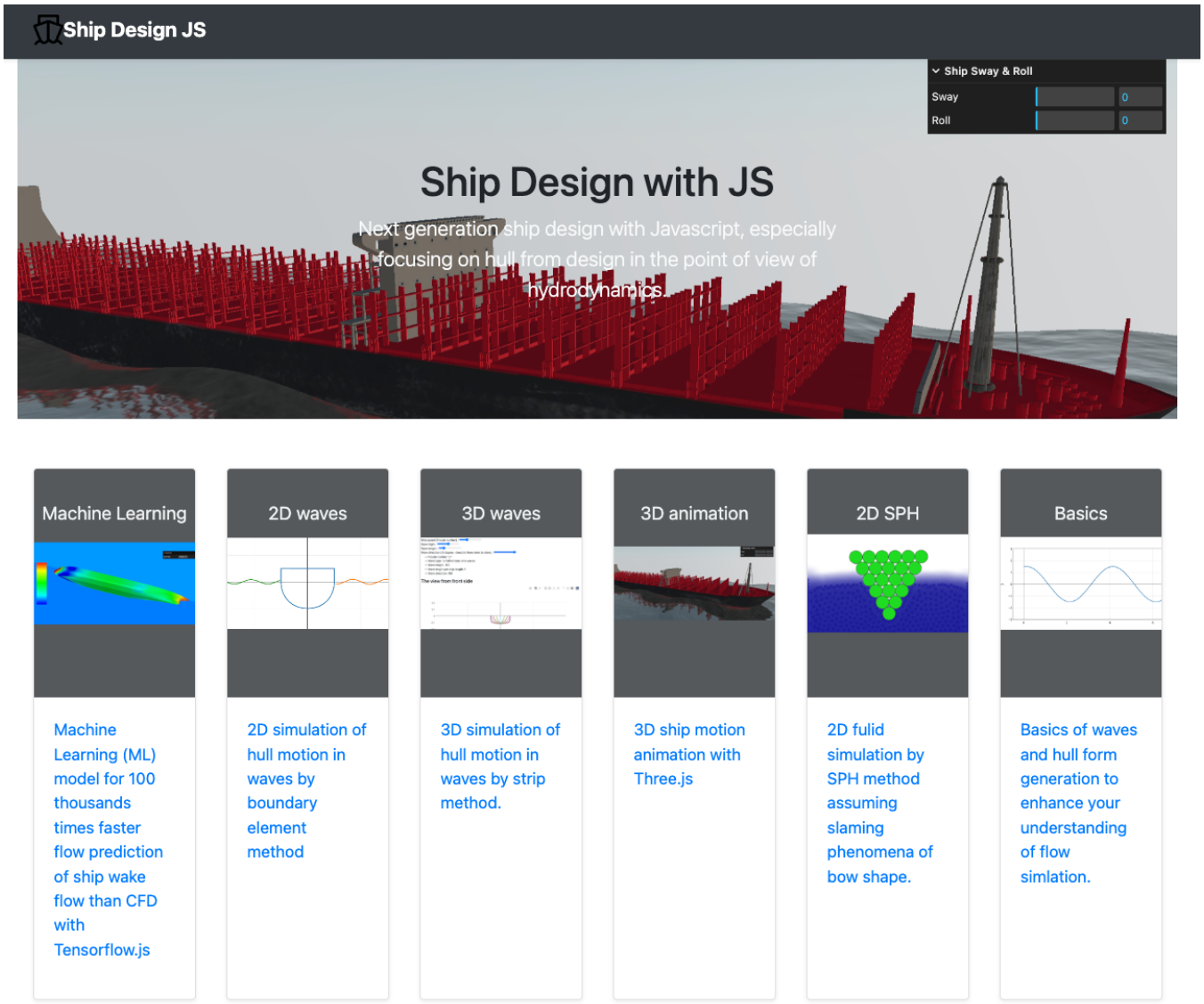

Figure 9: NMRI Research on Web-based Hydrodynamics, based on a joint initiative with NTNU from 2023.

FINAL NOTES: THE OPEN AND COLLABORATIVE APPROACH

We close this paper with a call for colleagues and students to consider trying develop their own version of a *A Sea of Ships.* The code and examples to replicate the examples in Figure 8 are open and available. We believe that by implementing open and collaborative methods in the everyday design tasks, both at academic and industrial environments, will foster innovation. Simple practices for versioning, tagging and library concepts are recommended (Gaspar, 2018). A Github page for a project – either public or private (paid) is also an experience highly recommended. As this is used to manage large software projects, it has functions like allocating tasks, discussions a traceability in pair (or even better) than most of PDM/PLM solutions. Giving up proprietary data-files in exchange of a standard among all tools seems to be a feasible (and lucrative) path.

The open initiatives here discussed are a working in process, and much of the libraries and methods intends to be improved in the years to come. The main point defended in this paper is that technology is not a bottleneck any longer, and a development that in 2003 would require a cluster of computers and proprietary software, can be done nowadays using a

laptop and downloading from an open repository. The real value lies in the humans working with ship design, and their ability to access and filter the open and proprietary databases. In other words, how efficient ship design data is able to be transferred from books and experience to useful reusable models. As for the development of real ship design engineering in an open library, we recognize the value of current engineering tools and PLM suites; no doubt, they are responsive for the visible gain in productivity that the maritime industry faced in the last decade. Industry 5.0, with an open digital thread that all actors may follow is thus the next step (Sepalla *et al.,* 2023).

As a final call, we believe that a large part of the digital tools for Ship Design should be considered open and exchangeable. Naval architects should focus on what they do best: creating, analyzing, refining, storing and populating the database of the know-how from the institution (e.g. university, research institute or company). Learning from modern software companies shows that the gain nowadays, both technological and commercial, seems to be in efficiently handling digitally the intrinsic ship design knowledge (databases), providing services from the know-how rather than a more powerful computer, a mesh more refined or a cluster with *n+1* CPUs. Seeing is a reality one click away.

ACKNOWLEDGEMENTS

To Olivia Chaves, Elias Hasle and Felipe Ferrari (NTNU). The first two, for developing the first version of the *sea of ships* at the Ship Design and Operations Lab at NTNU, back in 2016. The second, to improve and build on this version years later, creating the recent online interactive version presented in Figures 7 and 8 and available online for scrutiny at vesseljs.org.

REFERENCES

Aragão Fonseca, Í., Ferrari De Oliveira, F., & Murilo Gaspar, H. (2023). Open Framework for Digital Twin Ship Data: Case Studies on Handling of Multiple Taxonomies And Navigation Simulation. International Journal of Maritime Engineering, 165(A1), 23–42. https://doi.org/10.5750/ijme.v165iA1.813.

Bertram, V. (2014), Computational methods for seakeeping and added resistance in waves, 13th Conf. Computer and IT Applications to the Maritime Industries (COMPIT), Redworth, pp.8-16

Bertram, V. (2023). CAE Matrix, Proceedings of 22nd International Conference on Computer and IT Applications in Shipbuilding - COMPIT 2023, 23-25 May 2023, Drübeck, Germany.

Brett, P.O; Ulstein, T. Critical systems thinking in ship design approaches. IMDC 2012, Glasgow. Proceedings, 11-14

Chaves, O., and Gaspar, H. M. (2016). A Web Based Real-Time 3D Simulator for Ship Design Virtual Prototype and Motion Prediction. In International Conference on Computer Applications in the Maritime Industries, Lecce, Italy, 410–19.

Luz, F. H. P., Gaspar, H. M., & Nishimoto, K. (2009). System Architecture of a Numerical Model Basin Simulator.

Ferrari, F. O. And Gaspar, H. M. Sea of Ships *in vesseljs.org*
https://shiplab.github.io/ vesseljs/examples/Many_ships_performance_verification.html.

Gaspar, H. M., Fucatu, C., & Nishimoto, K. (2009). Design of Conceptual Offshore Systems based on Numerical Model-Basin Simulations. Proceedings of the 10th International Marine Design Conference.

Gaspar, H. M. (2018). Vessel.js: An open and collaborative ship design object-oriented library. Marine Design XIII, Volume 1, Proceedings of the 13th International Marine Design Conference (IMDC 2018), June 10-14, 2018, Helsinki, Finland.

Gaspar, H. M., (2019). A perspective on the past, present and future of computer-aided ship design". In 18th Conference on Computer and IT Applications in the Maritime Industries (COMPIT'19), pp. 485–499.

Gaspar, H. (2022). Current State of the Vessel.JS Library: A Web-Based Toolbox for Maritime Simulations. Day 3 Tue, June 28, 2022, D031S007R003. https://doi.org/10.5957/IMDC-2022-271

Ichinose, Y. (2022). Method involving shape-morphing of multiple hull forms aimed at organizing and visualizing the propulsive performance of optimal ship designs. Ocean Engineering, 263, 112355. https://doi.org/10.1016/j.oceaneng.2022.112355

Ichinose, Y., & Gaspar, H. M. (2023). Interactive Ship Flow Simulation Enhanced by Neural Network Model in a Web Environment. ECMS 2023 Proceedings Edited by Enrico Vicario, Romeo Bandinelli, Virginia Fani, Michele Mastroianni, 155–161. https://doi.org/10.7148/2023-0155.

Jensen, J.J.; Mansour, A.E.; Olsen, A.S. (2004), Estimation of ship motions using closed-form expressions, Ocean Engineering 31/1, pp.61-85. https://doi.org/10.1016/S0029-8018(03)00108-2.

Nishimoto, K., Ferreira, M. D., Martins, M. R., Masseti, I. Q., Martins, C. A., Jacob, B. P., Russo, A., Caldo, J. R., & Silveira, E. S. S. (2003). Numerical Offshore Tank: Development of Numerical Offshore Tank for Ultra Deep Water Oil Production Systems. Volume 1: Offshore Technology; Ocean Space Utilization, 575–584. https://doi.org/10.1115/OMAE2003-37381

Rampazzo, F. P., Watai, R. A., Matsumoto, F. T., Vilameá, E. M., Bronneberg, J., & Nishimoto, K. (2010). Development of a Conceptual Design of a FPSO+TLWP Coupled System Through University & Companies Interaction, Proceedings of Rio Oil & Gas Expo and Conference 2010, September 2010, Rio de Janeiro, Brazil.

Seppälä, L. Integrated Shipbuilding Data Management. 2023. 22nd COMPIT Drübeck *et al.,* (2023).

Proceedings of 15th International Marine Design Conference (IMDC-2024)
June 2-6, 2024
Amsterdam, the Netherlands

On empirical methods to predict the rolling period of ships

Rob Grin[1,*]

ABSTRACT

A reliable prediction of the roll period is crucial, as it forms the basis of the calculation of the roll motion and transverse accelerations. Both are extremely important for the comfort and safety of passengers and crew as well as the loads on the cargo and their lashings. At present, some prediction methods are quite unreliable, with sometimes errors in the predicted roll period of 5 to 10 s. This paper describes and compares eight methods. It shows that the four best performing methods have a mean absolute error of less than 1.4 s for the three validation cases evaluated, making them considerably more reliable than some of the other methods used in the industry.

KEY WORDS

Rolling period; Radii of inertia; Stability; Seakeeping; Ship motions

NOMENCLATURE

$A_{lateral}$	[m^2]	Projected side area of ship	H	[m]	Effective depth of ship
a_{xx}	[m]	Roll added mass radius of gyration	h	[m]	Height of item
B	[m]	Beam of ship	h_{tank}	[m]	Water height in tank
b	[m]	Width of item	I_{44}	[ton·m^2]	Roll inertia including added mass
β	[-]	Roll inertia factor	I_{fluid}	[ton·m^2]	Roll inertia of fluid cargo
b_{tank}	[m]	Width of tank	I_{xx}	[ton·m^2]	Roll inertia
C	[-]	Roll coefficient	k	[-]	Roll factor
C_b	[-]	Block coefficient	k_{spring}	[kN/m]	Spring stiffness
C_u	[-]	Waterline coefficient of the main deck	k_{xx}	[m]	Roll radius of gyration
D	[m]	Depth of ship	L_{pp}	[m]	Length between perpendiculars
Δ	[ton]	Displacement	m	[ton]	Mass
δ	[-]	Prefix denoting uncertainty e.g. δGM_t	MAE	[%]	Mean absolute error
δI_{xx}	[ton·m^2]	Roll added mass inertia	T	[m]	Draft at midship
FSC	[m]	Free surface correction	T_a, T_f	[m]	Draft at stern and bow
g	[m·s^{-2}]	Gravitational acceleration (9.81 m/s^2)	T_ϕ	[s]	Natural period of roll
GM_t	[m]	Transverse metacentric height	VCG	[m]	Vertical centre of gravity

INTRODUCTION

The rolling period has a large influence on the ship roll motion and accelerations of ships, not only for resonant roll but also for parametric roll. Both are extremely important for the comfort and safety of passengers and crew as well as the loads on the cargo and their lashings. As part of the design verification, seakeeping assessments (either numerical or experimental) are performed. However, when the real roll period is not known, incorrect estimates are made, and the predicted ship

[1] Maritime Research Institute Netherlands (MARIN), The Netherlands
* r.grin@marin.nl

Submitted: 14 March 2024, Revised: 25 April 2024, Accepted: 1 May 2024, Published: 23 May 2024

Conference paper, DOI: https://doi.org/10.59490/imdc.2024.881 e-ISSN: 3050-486

performance might be misleading. This is also the case when applied to vulnerability criteria within the second generation of intact stability code. At present, many prediction methods are quite unreliable, with errors in the predicted roll period of more than 10% regularly occurring. This paper will give guidelines for the required accuracy that will ensure that the changes in roll behaviour are marginal. Various estimation methods are compared for a range of illustrative ship types. For each of the methods, advantages and disadvantages will be discussed and a practical estimation method will be proposed that can be used both in the ship design phase and in operation.

ROLL PERIOD AND UNCERTAINTY

The natural frequency (ω_0) of an undamped mass spring system is given by equation 1, where k_{spring} is the spring stiffness and m the mass. Assuming that the roll is lightly damped this equation can be used to calculate the roll natural period, see equation 2, in which the roll inertia I_{44} consists of the total roll inertia including added mass and the spring term C_{44} is the roll restoring coefficient. This can be rewritten and further simplified to equation 3 as $\pi/\sqrt{g}$ is around one. In this equation k_{xx} is the roll radius of inertia, a_{xx} the roll added mass radius of gyration and GM_t the transverse stability (see also the chapter on transverse stability if that should be the dry or wet GM_t).

$$\omega_0 = \sqrt{\frac{k_{spring}}{m}} \quad [1]$$

$$T_\varphi = 2\pi\sqrt{\frac{I_{44}}{C_{44}}} = 2\pi\sqrt{\frac{I_{xx} + \delta I_{xx}}{g\Delta GM_t}} \quad [2]$$

$$T_\varphi = 2\pi\sqrt{\frac{\Delta k_{xx}{}^2 + \Delta a_{xx}{}^2}{g\Delta GM_t}} \approx 2\sqrt{\frac{k_{xx}{}^2 + a_{xx}{}^2}{GM_t}} \quad [3]$$

$$\text{with} \quad k_{xx} = \sqrt{\frac{I_{xx}}{\Delta}} \quad \text{and} \quad a_{xx} = \sqrt{\frac{\delta I_{xx}}{\Delta}} \quad [4]$$

The uncertainty (error) in the rolling period can be estimated if the uncertainties δk_{xx}, δa_{xx} and δGM_t are known and have a normal distribution (Coleman and Steele, 1999). From equation 3 and after some math, equation 5 gives the total uncertainty in the rolling period. It shows that the δk_{xx} and δa_{xx} make a bigger contribution than the δGM_t, as the uncertainty in GM_t has a cube root of the GM_t in the denominator. As the k_{xx} is typically about twice as large as the a_{xx} the δk_{xx} is typically bigger than the δa_{xx}. It can therefore be argued that for a small uncertainty in the rolling period (δT_ϕ), the uncertainty in the k_{xx} prediction should be reduced as much as possible. This can be illustrated by taking the 77,500 DWT bulk carrier loaded with grain as example (see Appendix A, ship ④). When an uncertainty of 10% is assumed for all 3 input parameters, the roll period is 16.0±1.8 s. If the δk_{xx} is reduced to 5% the uncertainty in the rolling period reduces to 1.3 s, whereas it only reduces to 1.7 s or 1.6 s when the uncertainty of the a_{xx} or GM_t reduces to 5%. It is therefore important to get a good prediction of k_{xx} as it makes the biggest contribution to the rolling period.

$$\delta T_\varphi = \sqrt{\frac{4}{GM_t}\left(\delta k_{xx}{}^2 + \delta a_{xx}{}^2\right) + \frac{k_{xx}{}^2 + a_{xx}{}^2}{\sqrt[3]{GM_t}}\delta GM_t{}^2} \quad [5]$$

EXISTING APPROXIMATION METHODS

Many of the existing methods for monohull vessels use equation 3 as starting point but do not split the roll radius of inertia and the roll added mass. They typically provide the total roll radius inertia as a fraction of the beam of the vessel B (see equation 6). This factor is called the roll factor k. Note that in most formulations the factor 2 is contained in the roll factor, causing twice as large a roll factor. Some other formulations use a constant bigger than 2, accounting for the roll added mass. For comparison reasons these variations are not applied in the present work.

$$T_\varphi = 2\frac{kB}{\sqrt{GM_t}} \quad [6]$$

Some examples for the roll factor are given in Table 1. It is shown that it ranges from 0.33 up to 0.52 and on average 0.42. There seems to be no clear trend; for instance, bulk carriers can be both well below average (BV) or well above (IACS).

Table 1: List of roll factors

Source	Ship type	Roll factor k	Remarks
LR, 2022	Container	0.41	
DNV, 2023	All Tanker, ballast	0.45 0.40	Except bulk and ore carriers
ABS, 2019	Container	0.40	
ClassNK, 2023	All	0.40	
BV, 2014	All Bulk carriers	0.39 0.33	 Ore carrier
Lewis, 1989	All	0.36	Range: 0.29 – 0.43
IACS , 2012	Bulk carriers	0.40 0.48 0.52 0.46	Homogeneous full load Steel coil Ballast Heavy ballast

Instead of a fixed value, a slightly more complicated estimation of roll factor was proposed by the Shipbuilding Research Association of Japan, JSRA (1982) and IMO (2024). This method is adopted within several IMO documents, for instance the intact stability code (IMO, 2008) and the interim guidelines on second generation intact stability criteria code (IMO, 2020). As shown in equation 7, it increases with the beam over depth ratio (B/D) and decreases with ship length. For small vessels this gave satisfactory results, however for large vessels it gives a considerable underestimation of the roll period. For this reason, JSRA made an alternative fit only depending on B/D-ratio (equation 8). Figure 1 shows the reproduced cross plots of JSRA, with on the x-axis the k-factor recalculated from the measured rolling period of in total 70 vessels and on the y-axis the estimated k-factor according equation 7 and 8. Both fits give fairly equal but considerable scatter, with an r^2 of 0.59 versus 0.43 without ship length dependency.

$$k = 0.373 + 0.023\frac{B}{D} - 0.043\frac{L_{wl}}{100} \quad [7]$$

$$k = 0.3437 + 0.024\frac{B}{D} \quad [8]$$

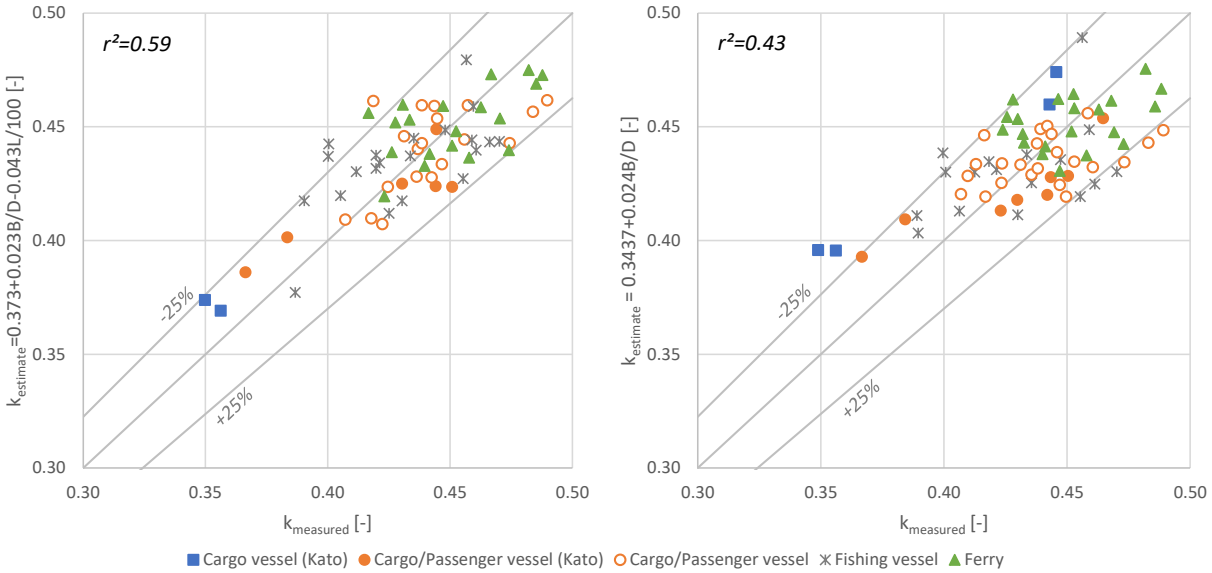

Figure 1: Reproduced scatter plots according to Shipbuilding Research Association of Japan (1982)

Much longer ago, Doyere (1927) proposed equation 9 with a ship dependent *c*-factor. The formula shows that the rolling period increases with increasing beam and vertical centre of gravity (VCG). According to Doyere, the average *c*-factor is 0.29. Doyere provided a table with five naval vessels with multiple loading conditions where *c* varied between 0.26 and 0.32.

$$T_\varphi = c\sqrt{\frac{B^2 + 4VCG^2}{GM_t}} \qquad [9]$$

Kato, 1956 proposed equation 10 in which T is the draft of the vessel, C_u is the waterline coefficient of the main deck and H the effective depth (defined as the lateral area divided by the ship length). The factor 0.125 is valid for passenger and cargo vessels. For tankers a value 0.133 was suggested and for navy ships 0.172. It shows that larger C_b and larger H/B ratio give a larger roll factor. The C_u is often close to 1.0 for modern ships; for this reason the middle term is in most cases small compared to the C_bC_u term and the $(H/B)^2$ term. It can even become slightly negative.

$$k = \sqrt{0.125\left(C_bC_u + 1.10C_u(1 - C_u)\left(\frac{H}{T} - 2.20\right) + \frac{H^2}{B^2}\right)} \qquad [10]$$

Lehmann, 1940, Laurenson, 1949 and Vossers, 1962 assumed that k_{xx} should be between a solid homogeneous rectangular beam (equation 12) and a rectangular tube with wall thickness of 0.025B. The second is practically identical to a rectangular tube with infinitely thin walls (equation 13). By combining equation 4 and equation 12 and replacing the term $\sqrt{1/12}$ by coefficient *c*, equation 11 is obtained. It results in a *c*-value of 0.289 ($\sqrt{1/12}$) and 0.397, respectively. These factors only include the roll mass inertia and not the roll added mass. Laurenson proposed a *c* ranging between 0.33 and 0.39, which is very similar to Peach, 1987 suggesting a factor *c* of 0.30. Both include the roll added mass. It has to be noted that for ships with heavy cargo concentrated around the centre of gravity (like loaded bulk carriers and tankers), *c*-values of less than 0.289 are possible.

Figure 2 shows the resulting curves for Lehmann and Vossers (blue lines), Laurenson (red lines) and the homogeneous rectangular beam and the tube with infinitely thin walls (black lines). Note that for Vossers and Lehmann the line for the empty ship ① is equal to the rectangular tube.

$$kB = c\sqrt{B^2 + D^2} \qquad [11]$$

$$\textit{Homogeneous rectangular beam: } I_{xx} = \frac{1}{12}m(b^2 + h^2) \qquad [12]$$

$$\textit{Rectangular tube with infinitely thin walls: } I_{xx} = \frac{1}{12}m(b + h)^2 \qquad [13]$$

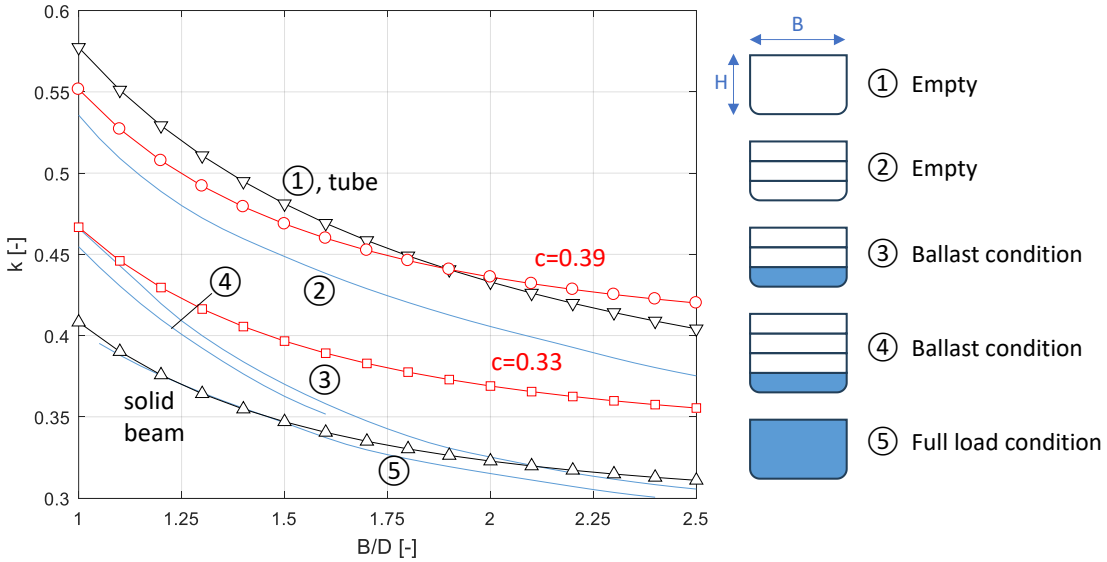

Figure 2: c-factors as function of B/D ratio

ROLL RADIUS OF INERTIA

The aforementioned methods estimate the roll factor, which combines the roll radius of inertia and the roll added mass. As there are methods to calculate or estimate the roll added mass (see next section), it would be good to separately calculate or estimate the roll radius of inertia. Preferably, detailed weight calculations are used; however, they are often not available, despite all state of the art CAD tools and software to calculate stability.

Estimation of the k_{xx} can be done for instance with ITTC, 2017. In equation 14 it is shown that the ITTC formula weights the rectangular tube (first term in the equation) and the solid beam (second term). The last term is a measure for the vertical offset for a half-submerged homogeneous beam (in that case the last term is zero).

$$k_{xx} = \sqrt{\frac{1}{12}\left(0.4(B+D)^2 + 0.6(B^2+D^2) - \left(2T - \frac{D}{2} - VCG\right)^2\right)} \quad [14]$$

Another estimation method was proposed by Grin et al., 2016, shown in equation 15. This method is based on detailed weight calculations for 9 vessels and in total 16 loading conditions. It also consists of 3 terms. The first term is solid beam with factor β being ship type and loading condition dependent (and 12 for a solid beam, see also equation 12). The second term is accounting for the offset between the real VCG and the VCG for a solid beam (H/2). The last term gives a correction in case of fluid cargo. In this case part of the roll inertia of the fluid should be subtracted from k_{xx}. This is done by the c_{fluid} factor, which varies between 1 for solid cargo and 0 for fluid cargo in a cylindrical tank (Grin et al, 2016). The suggested β-factors are 9.8 for ships in (near) ballast condition, 11 for ships in loaded condition with a more or less homogeneous mass distribution and relatively high stowage factors and 14.7 for ships carrying cargos with low stowage factor or a large portion of the mass close to centre of gravity.

$$k_{xx} = \sqrt{\frac{B^2+H^2}{\beta} + \left(\frac{H}{2} - VCG\right)^2 + (c_{fluid} - 1)\frac{I_{fluid}}{\Delta}} \quad [15]$$

ROLL ADDED MASS

It is recommended to calculate the roll added mass a_{xx} by means of potential flow strip-theory or panel codes. This gives the most reliable estimate accounting for the hull shape, speed of the vessel and roll period. Note that the roll added mass is also dependent on water depth and presence of side walls (e.g. the quay). In the case of restricted water, the a_{xx} increases and thereby the rolling period.

In the case of deep water, a first rough estimate can be made using equation 16. This is based on the recalculated a_{xx} from MARIN model tests of 228 different monohull vessels, varying from small patrol boats to large tankers and container vessels. This estimate assumes that the a_{xx}/B increases linearly with the B/T ratio. Figure 3 shows a cross plot of the measured and predicted roll added mass. It shows that correlation is fair, with an r^2 of 0.46.

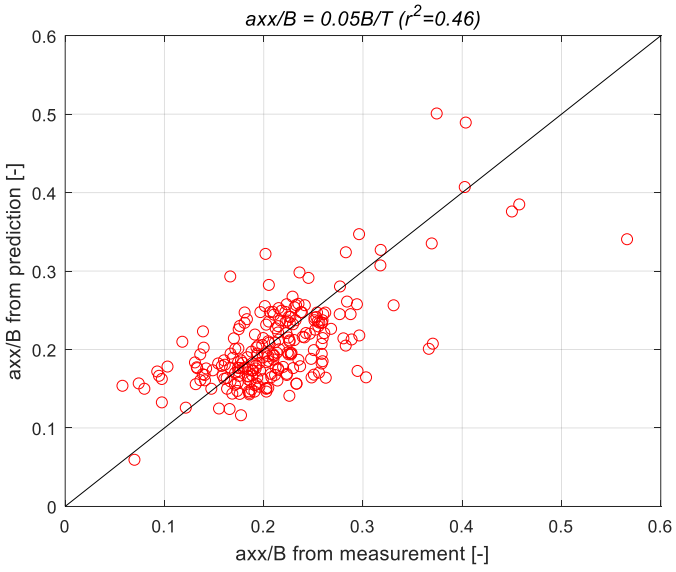

Figure 3: Predicted against measured roll added mass

$$a_{xx} = 0.05\frac{B^2}{T} \quad [16]$$

TRANSVERSE STABILITY

The transverse stability is in the denominator of the rolling period equation: the higher the transverse stability (GM_t) the lower the rolling period of the vessel (a stiff ship). In most publications it is not clearly stated if the dry GM_t or the wet GM_t (including the free surface correction, FSC) should be taken. In IMO, 2020 (SGISC) it is recommended to use the dry GM_t for excessive accelerations and for the other modes the wet GM_t. This is considered a conservative estimate by IMO.

Using the wet GM_t assumes that the fluid in the tanks is always in phase with the roll motion and consequently always at the lee side. For many tank geometries this is indeed true. With equation 17 the natural period of a rectangular tank can be predicted. This further simplifies to equation 18 in shallow water. In this equation b_{tank} is the width of the tank and h_{tank} the water level.

$$T_{tank} = \frac{2\pi}{\sqrt{\frac{\pi g}{b_{tank}} tanh\left(\frac{\pi h_{tank}}{b_{tank}}\right)}} \quad [17]$$

$$T_{tank} = \frac{2b_{tank}}{\sqrt{g h_{tank}}} \quad [18]$$

For example, the natural period is only 1.6 s for a side tank of 2.0 m wide and 7.5 m height and 20% filled with water. Assuming a rectangular double bottom tank with a width of 12.5 m, a height of 2.0 m and also 20% full, this increases to 12.6 s. However, that assumes that there are no obstructions in the tank. In reality, a double bottom tank has many obstructions like longitudinal frames and girders. In Figure 4 an example is shown of the typical double bottom construction of a large container ship. These ships have a girder for each stack of containers, leading to a girder spacing of around 2.5 m. These girders have typically only a few manholes, for instance every 3.5 m one manhole of 700x500 mm and only a few small discharge holes at the bottom of the girders. In the case of a static heel angle the water (or fuel) eventually flows to the lee side. This is why the free surface correction of a double bottom tank is significantly larger than for a side tank. However, in the case of a rolling motion of say 20 to 30 s, the water does not have sufficient time to flow to the lee side and will move mostly in between two girders, and at low water levels maybe even in between two longitudinal frames. It is therefore not realistic to account for the full FSC of these double bottom tanks for the calculation of the roll period. In the previous example of the 12.5 m wide double bottom tank the FSC decreases by a factor 25 if the water moves between girders. In practice this means that for many ships the FSC can be disregarded and the dry GM_t can be taken in the calculation of the rolling period. However, caution should be taken in the case of for instance large fluid cargo tanks, LNG fuel tanks and other tanks with only few internal obstructions. For these cases the FSC should be included in the calculation of the rolling period. A special case are anti-rolling tanks; these tanks are designed to reduce the roll motion and therefore the water is moving in counterphase of roll motion. For this reason, the FSC of these tanks should be disregarded.

Note that the GM_t could also be speed dependent. When ships with a flat transom sail at forward speed, the steady wave pattern, trim and sinkage typically increase the waterline area at the stern. This increases the BM and thereby the GM_t. As a result, the roll period could decrease somewhat at forward speed.

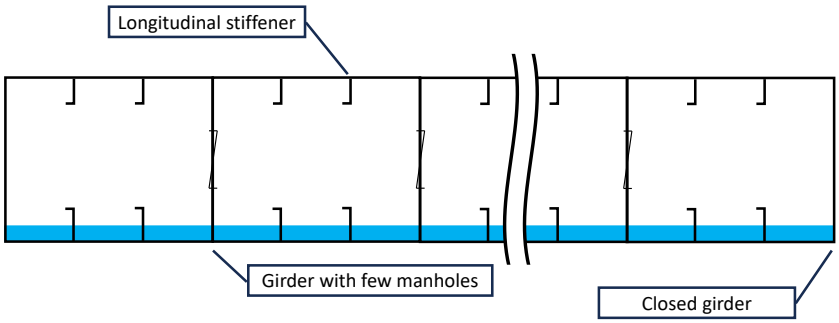

Figure 4: Typical cross section of double bottom tank of a large container ship

VALIDATION

Two statistical quantities are used for the three validation cases mentioned below: the well-known correlation coefficient (r^2) and the mean absolute error (MAE). The first one is a good measure for the scatter but does not show bias, whereas the second one also accounts for bias. Cross plots are presented in which the measured or calculated values are shown on the x-

axis and the predicted values on the *y*-axis. With a perfect correlation (an r^2 of 1 and an MAE of 0) all points will be on the diagonal.

Case 1, detailed weight calculations

For the first validation case, detailed weight calculations were done for 9 ships and 16 loading conditions (Grin et al., 2015 and Grin et al., 2016). A variety of ship types were used: 2 general cargo vessels, 2 tankers (LNG and LPG), 2 bulk carriers, a container vessel, a cruise ship and a frigate. The main particulars, stability data and roll coefficients are given in Appendix A. The previous publications focused on the detailed weight calculation and the prediction of the roll, pitch and yaw radius of gyration. For this work, strip-theory calculations were done to predict the roll added mass a_{xx} and on the basis of the given dry GM_t and the k_{xx} from the weight calculations, the roll period was calculated.

The cross plots in Figure 5 shows the eight different prediction methods. It is shown that most methods give a fair to good prediction. Even a straightforward method like the roll coefficient method with a fixed value of 0.40 has an r^2 of 0.96 and an MAE of 2.0 s. JSRA (as used by IS2008 and SGICS), Kato and ITTC and are the methods that have the smallest r^2 and highest MAE. On the other hand, the JSRA without the ship length in the empiric formula performs quite well (3rd place) with an r^2 of 0.98 and an MAE of 1.4 s. The roll coefficient method (with k=0.40), Doyere (with c=0.34) and the beam method (with c=0.36) fall in the middle. Grin has the best performance, with an r^2 of 0.998 and an MAE of only 0.7 s. It has to be noted that this is logical as the method is based on these ships.

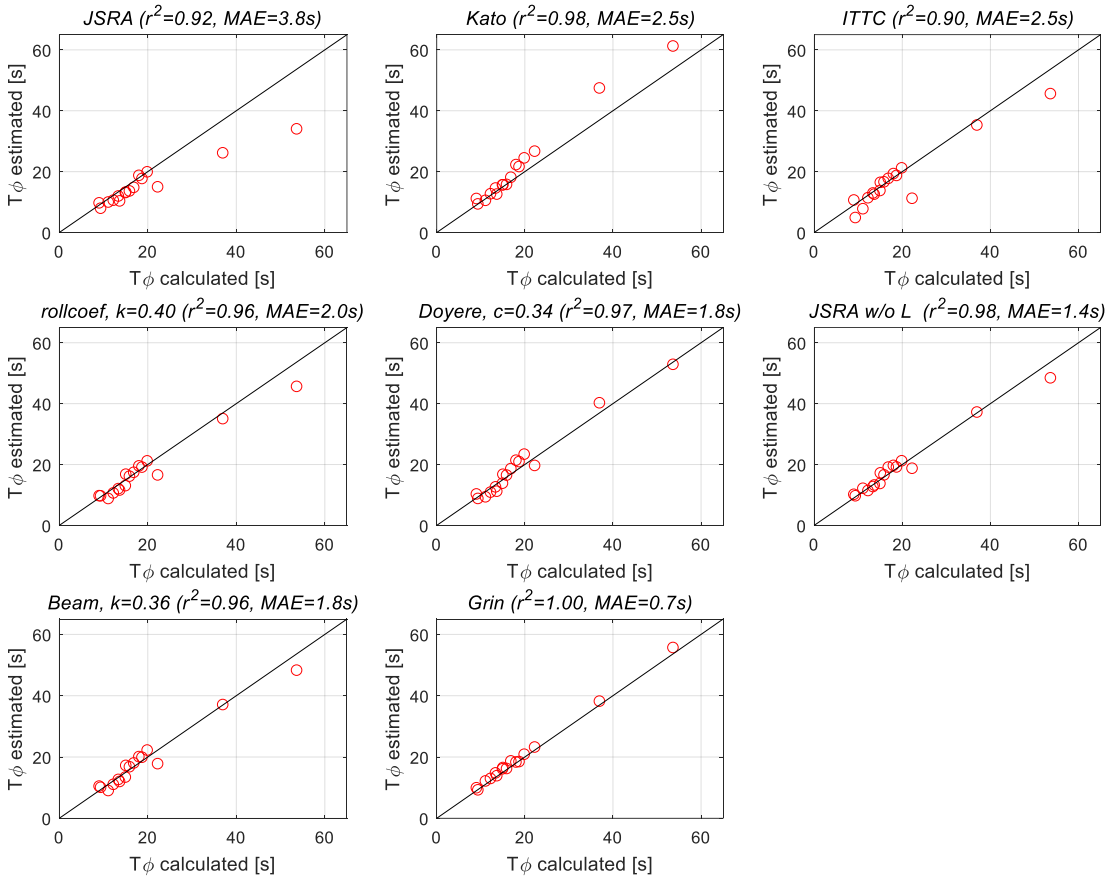

Figure 5: Cross plots of calculated and estimated rolling period of 9 vessels (16 loading conditions)

Case 2, full scale measurement data on a 9200 TEU container vessel

Full scale measurements on a 9200 TEU container vessel were re-analysed within the TopTier joint industry project. This project aims at a significant reduction of containers lost at sea (Koning et al, 2022). A proper estimation of the roll period is very important as it is used in the lashing software to determine if lashing loads are within limits as well as for determining the risk of large roll motions during the voyage. The main dimensions of the vessel are given in Table 2 and Figure 6 shows the side view for one of the voyages including the calculation of the effective depth H (total lateral area divided by L_{pp}).

The measurements were done for a long period of time and for part of this period also the loading conditions for each voyage were stored. In total 114 voyages contained both measurements as well as the loading condition. As shown in Table 2, the variation in loading conditions is large, ranging from (near) ballast conditions to full load condition at almost scantling draft. Also, the GM range was large, from relatively low stability of 1.2 m up to 13.2 m in very light load coastal voyages in Asia. Note that the effective depth is dependent on the arrangement of deck containers and is variable as well.

Table 2: Main dimensions of the 9200 TEU container vessel

		min	max
Lpp	[m]	333.0	
B	[m]	42.8	
D	[m]	27.3	
H	[m]	30.2	49.6
Ta	[m]	7.3	14.8
Tf	[m]	4.9	14.7
Δ	[ton]	47,000	143,000
VCG	[m]	13.3	19.4
GM	[m]	1.2	13.2
FSC	[m]	0.1	1.2
Tϕ	[s]	11	34.5
β	[-]	14.7	
Cu	[-]	0.89	

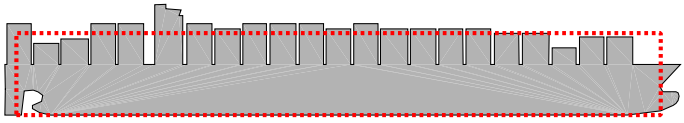

Figure 6: Side view of the 9200 TEU container vessel

From all the measurements only the roll motion is used. The sample rate was 20 Hz and data was stored in 1-hour datafiles. The roll period was obtained by a spectral analysis (Welch method) of these 1-hour measurements. A small frequency step of 0.002 rad/s was used to get enough resolution. The drawback is that the spectrum is quite spiky. The peak frequency of the spectrum was stored and if the same peak frequency is measured 10 times, it is considered to be the roll natural period. This procedure is needed as a ship is not necessarily rolling at its natural roll period: this could be easily 5% longer or shorter. This is clearly illustrated in Figure 7. The upper plot shows one 1-hour timestep of the roll motion within one of the voyages. The accompanying roll spectrum is shown in the lower left plot with the largest peak at 0.242 rad/s, resulting in a roll period of 26.0 s in that timestep. After 52 timesteps, the same roll period was found 10 times, being 26.2 s. The histogram shows all 52 roll periods found; they show a considerable spread, from 20.9 s to 32.1 s. It is probably possible to find a more efficient procedure to accurately measure the roll period, but these results illustrate that simply timing 10 roll oscillations is not sufficient for an accurate assessment.

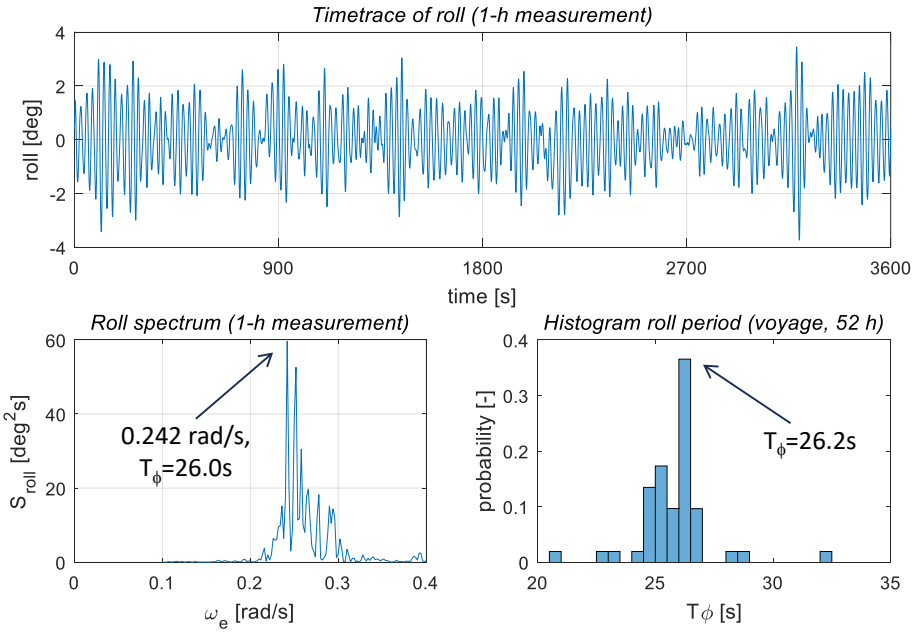

Figure 7: Example of 1-h time trace, roll spectrum and resulting roll period for the complete voyage

Similar to the previous case, cross plots are made with the measured roll period against the estimated roll period, see Figure 8. The score is more or less the same, with JSRA and Kato being the worst. The ITTC and the roll coefficient method are in the middle. The top 4 consists of Doyere, JSRA without the length, Grin and the beam method. All 4 methods perform equally well with an MAE of around 0.9 s. Note that the scatter in these plots comes not only from an imperfect fit, but also from uncertainty in GM_t, as the actual weight and position of the stowed containers might be different from the provided one.

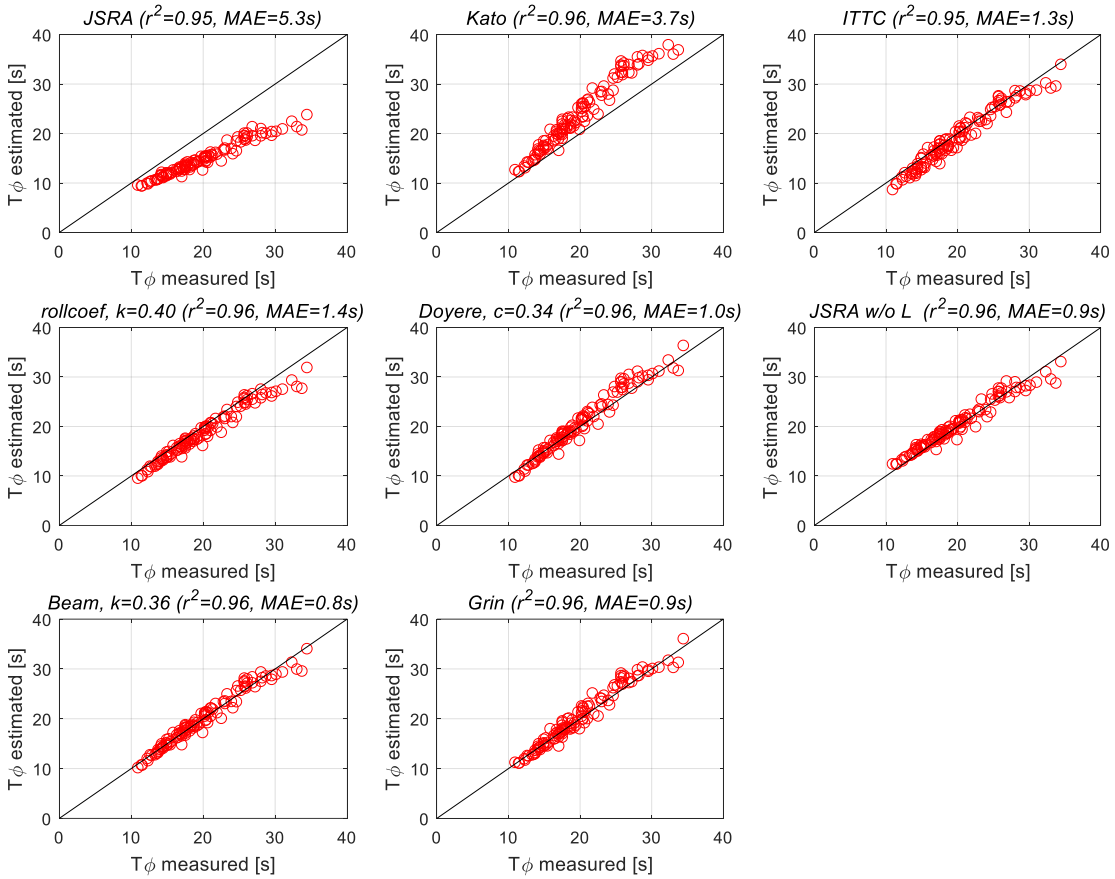

Figure 8: Cross plots of measured and estimated roll period of 114 voyages of a 9300 TEU container vessel

Case 3, full scale measurement data of a 14,000 TEU container vessel

Within the Toptier joint industry project, full scale measurements are ongoing on 3 large container vessels. For the 14,000 TEU vessel part of the measurements are already analysed, resulting in the roll period for 45 voyages. Table 3 shows the main particulars and loading conditions of the vessel. In this case the stow positions of the deck containers was not available. Consequently, the effective depth (D) was not calculated per voyage, but an average was taken assuming an average of five high cube containers stowed on deck. As shown in the previous benchmark case the effective depth could vary considerably and this affects to some extend the results of Kato and Grin as both use the effective depth. The roll period is determined using the same analysis procedure as for validation case 2.

Table 3: Main dimensions of the 14,000 TEU container vessel

		min	max
Lpp	[m]	340.5	
B	[m]	53.5	
D	[m]	29.9	
H	[m]	47.9	
Ta	[m]	10.8	16.5
Tf	[m]	9.4	16.3
Δ	[ton]	119,000	215,000
VCG	[m]	16.5	23
GM	[m]	2.3	10.4
FSC	[m]	0.2	1.0
Tϕ	[s]	14.8	37.9
β	[-]	14.7	
Cu	[-]	0.96	

Figure 9 shows the resulting cross plots. It is shown that the correlation coefficient is somewhat lower than previous two benchmark cases, mainly caused by a few outliers (whereas the MAE is comparable). After checking these outliers, no reason was found to disregard these voyages. The prediction methods give again similar results, with JSRA and Kato having the largest MAE, ITTC, JSRA without length and the roll coefficient method ending in the middle and Doyere, Grin and the beam method as 3 best performing methods.

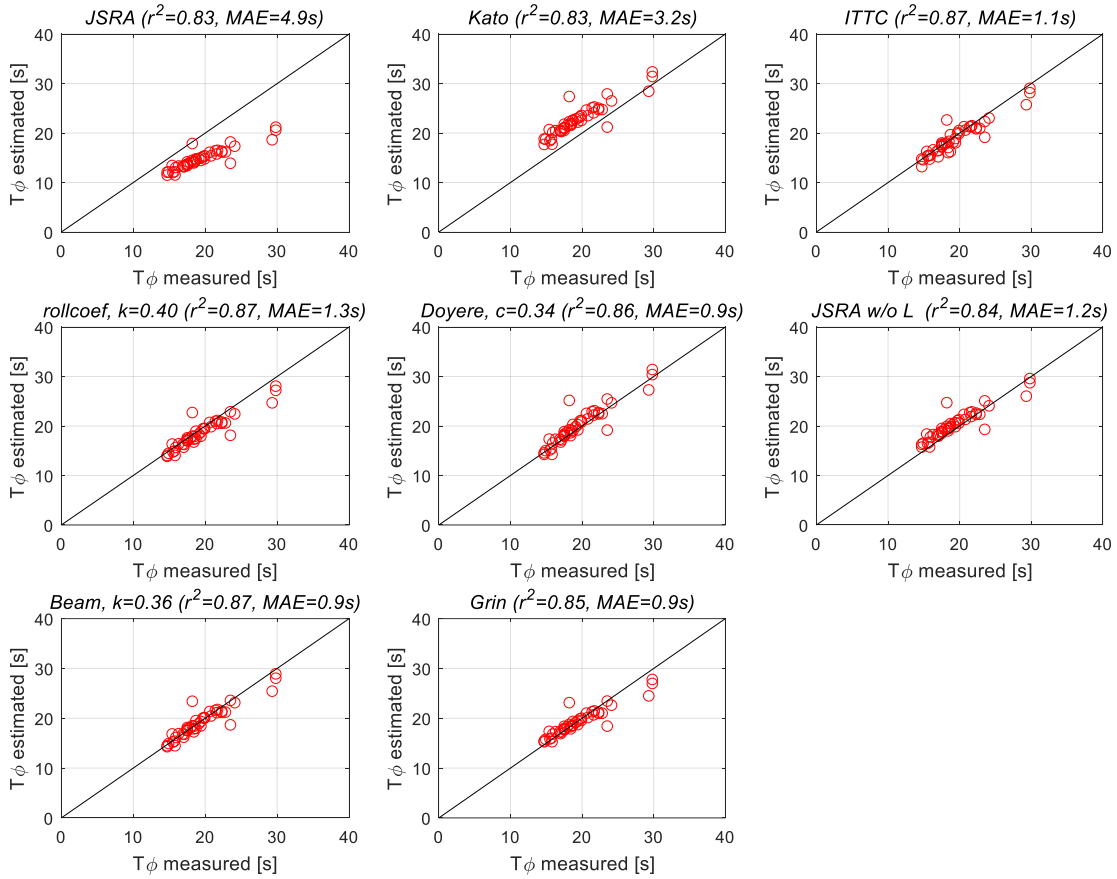

Figure 9: Cross plots of measured and estimated roll period of 45 voyages of a 14,000 TEU container vessel

CONCLUSIONS

A reliable prediction of the roll period is crucial, as it forms the basis of the calculation of the roll motion and transverse accelerations. If the roll period and underlying parameters k_{xx}, a_{xx} and GM_t are wrong all subsequent calculations are wrong as well. This could have large consequences and might even affect safety when passenger, crew and cargo are exposed to large, unexpected roll motion e.g. due to parametric roll. Within this paper eight methods are evaluated and compared. Based on the present work, the following conclusions can be drawn:

- The uncertainty in roll period comes in large part from the uncertainty in k_{xx}. The uncertainty in a_{xx} and GM_t have roughly equal contribution. In order to reduce the uncertainty in roll period it is best to reduce the uncertainty in k_{xx}. The difficulty is that k_{xx} is not as readily available as for instance the GM_t.
- The a_{xx} can easily and reliably be calculated with any frequency domain seakeeping code. The a_{xx} is dependent on hull shape, roll period and water depth. In shallow water the a_{xx} increases and thereby the roll period. For this reason, onboard measurement of the roll period should take place in deep water. As the a_{xx} dependency is not very sensitive to loading condition, a fairly small a_{xx} database with as variables draft and GM_t would be sufficient and intermediate values can be interpolated from this database. If direct calculation or interpolation from a database is not possible, a rough estimate can be made with equation 16.
- For the prediction of the roll period, the dry GM_t (without FSC) is typically the best choice. This is because for many ships the FSC mainly originates from the double bottom tanks in which the water ballast or fuel cannot move freely when exposed to rolling because of the internal structure. Also, for anti-rolling tanks the FSC should not be included. The remaining tanks typically have a small FSC which can be included in the rolling period calculation, but if disregarded the error is fairly small. Only in the case of wide tanks without a lot of internal structure like e.g. cargo tanks and LNG fuel tanks, should the FSC be accounted for.
- Eight roll period prediction methods were evaluated. All of them essentially predict the k_{xx} and except two (ITTC and Grin), all of them include the a_{xx}. These methods have been compared to three validation cases: 1) detailed weight calculations and strip-theory calculations of 9 different ships with 16 loading conditions in total; 2) full-scale

measurements on a 9200 TEU container vessel consisting of 114 voyages and 3) full-scale measurements on a 14,000 TEU container vessel consisting of 45 voyages.

- Based on these 3 cases it is shown that JSRA (as used in IS2008 and SGICS) and Kato have relatively large errors, with a MAE of 2.5 s up to 5.3 s. All other methods give a fair to good estimate with a MAE of 0.7 s to 2.5 s. The four best performing methods are listed in the table below.

Table 4: Best performing methods to predict roll period

Method	r^2, case			MAE [s], case			Pro (+) / cons (-)
	1	2	3	1	2	3	
Doyere, c=0.34	0.97	0.96	0.86	1.4	0.9	0.9	Only B and VCG needed (+), physics based (+), added mass in c-factor (-)
JSRA w/o L	0.98	0.96	0.84	1.4	0.9	1.2	Only B and D needed (+), not based on physics (-), added mass in c-factor (-)
Beam, k=0.36	0.96	0.96	0.87	1.2	0.8	0.9	Only B and D needed (+), physics based (+), added mass in k-factor (-)
Grin	1.00*	0.96	0.85	0.7*	0.9	0.9	Require effective depth H (-), physics based (+), added mass separated (+)

** It has to be noted that the first validation case is also used within the development of Grin, it is therefore logical that it performs best there.*

FURTHER WORK

Ship stability software has potentially the capability and information (weight, position and geometry of all deadweight mass) to accurately calculate the k_{xx}. It only requires the radii of inertia of the light ship. This would make estimation methods obsolete; only roll added mass needs to be calculated or predicted.

It is advised to do onboard measurement of the rolling period. This can be used for onboard advice to reduce the risk of large roll motions but also to tune roll factors for the specific ship, and if needed, loading conditions. It is however not straightforward to accurately derive the rolling period from measurements. Guidelines on how to do this should be developed.

The three validation cases showed almost the same four best performing roll period predictors. Within TopTier full scale measurement campaigns on another 2 large containers vessels are ongoing. These will be used to further validate these methods for container vessels. It is recommended to do some further validation work for other ship types as well. After validation, it is suggested to update the roll period formulas in IMO, ITTC and Class to (one of) these four methods.

ACKNOWLEDGEMENTS

The author would like to acknowledge the participants of the TopTier joint industry project who made this research possible. A second acknowledge goes to the Shipbuilding Research Association of Japan who supplied background information on the alternative JSRA fit without length.

REFERENCES

ABS (2019), *"The Assessment of Parametric Roll Resonance in the Design of Container Carriers"*, Section 2.4 p23

BV (2014), "*Rules for the Classification of Steel Ships*", Section 3, 2.4.1

ClassNK (2023), *"Guidelines on preventive measures against parametric roll (Edition 1.0)"*, Appendix 2, p12

Coleman, H. W., and Steele, W. G. (1999), *"Experimentation and Uncertainty Analysis for Engineers"*, 2nd Edition, USA

Doyere (1927), *"Théorie du navire"*, p334-337

DNV (2023), *"Rules for classification, Ships",* Part 3, Chapter 4, Section 3 2.1.1, p28

Grin, R. and Fernandez Ruano, S. (2015). *"On the prediction of Radii of Inertia and their Effect on Seakeeping"* 12th International Marine Design Conference Vol 3, pp 189-203

Grin, R., Fernandez Ruano, S., Bradbeer, N. and Koelman, H. (2016). *"On the prediction of Radii of Inertia and their Effect on Seakeeping",* PRADS2016 Copenhagen

IACS (2012), "*Common structural rules for bulk carriers*", Chapter 4, Section 2.1.1

IMO (2008), "*International Code on Intact Stability, 2008*", ISBN 978-92-801-17202

IMO (2020), "*Interim Guidelines On The Second Generation Intact Stability Criteria*", MSC.1-Circ.1627

IMO (2024), *"Alternative roll period formula to be used for the second generation intact stability criteria"*, MSC 108/INF.7

Koning, J., Grin, R. and Pauw, W. (2022), *"TopTier, seakeeping and container cargo securing safety"*, 18th International Ship Stability Workshop, Polland

ITTC (2017), *"Numerical simulation of capsize behaviour of damaged ships in irregular seas"*, 75-02-07-044 p7

Laurenson, R. (1949), "*Ship rolling constants*" Marine Engineering and shipping review p49

Lewis, E. V. (1989), *"Principles of Naval Architecture, 2nd Revision, Volume 3, Motions in Waves and Controllability",* SNAME

LR (2022), *"Rules and Regulations for the Classification of Ships"*, Part 3, Section 14 1.7.1, p563

Kato, H. (1956), *"Approximate Methods of Calculating the Period of Roll of Ships"*, Journal of the ZOSEN KYOKAI (Society Naval Architects of Japan), Vol.89, pp.59-64.

Shipbuilding Research Association of Japan (1982), No.114R, *"IMCO research to new stability rules"*, RR24 Research Panel Report, p6

Vossers, G. (1962), "*Behaviour of ships in waves*", Ships and marine engines, volume II C p240

APPENDIX A – MAIN DIMENSIONS AND ROLL PERIOD OF REFERENCE SHIPS

		① ② 6,000 m3 LPG Carrier		③ ④ 77,500 DWT Bulk Carrier		⑤ ⑥ 12,500 DWT general cargo		⑦ ⑧ 8,000 DWT general cargo		⑨ Frigate	⑩ ⑪ 183,000 DWT Bulk Carrier		⑫ ⑬ 13,000 TEU Container Ship		⑭ ⑮ 173,000 m3 LNG Carrier		⑯ 100,000 GT Cruise Ship
		Full load	Ballast	Full load Iron Ore	Full load Grain	Full load homog.	Ballast	Full load homog.	Ballast	Full load	Grain	Ballast	8T/TEU	12T/TEU	Full load	Ballast	Full load
Lpp	[m]	107.0		233.7		134.0		120.0		106.2	282.9		355.3		291.7		271.2
B	[m]	17.6		32.2		18.95		16.6		13.1	45.8		48.92		46.44		36.4
D	[m]	9.8		18.7		11.0		10.0		8.6	25.1		30.3		26.3		23.8
H	[m]	17.1	17.1	22.0	22.0	17.2	17.2	15.8	15.8	12.1	28.9	28.9	52.8	52.8	35.0	35.0	46.4
Ta	[m]	7.2	6.5	13.9	12.4	8.6	5.6	7.6	5.4	4.2	17.4	7.3	14.8	15.1	11.6	9.8	8.0
Tf	[m]	6.9	4.3	13.3	10.6	7.3	4.9	6.4	4.7	4.2	15.5	3.1	14.2	13.9	11.6	9.8	8.0
Δ	[ton]	10,100	7,400	88,900	74,400	17,000	10,500	11,500	7,900	3,100	180,000	53,200	184,000	165,500	115,700	100,400	55,200
VCG	[m]	7.2	6.6	6.1	10.7	7.7	6.4	6.9	6.0	4.9	14.1	17.3	22.7	22.3	17.7	12.6	17.8
GM_t	[m]	0.5	1.2	7.3	2.6	0.6	2.1	0.4	1.3	1.2	4.9	18.0	0.7	1.3	4.6	10.6	3.2
FSC	[m]	0.06	0.02	0.05	0.09	0.13	0.19	0.02	0.04	0.12	0.08	0.00	0.11	0.74	1.01	1.07	0.00
k_{xx}	[m]	5.9	7.7	11.3	11.7	7.1	8.5	5.9	7.2	4.6	14.8	19.4	21.3	18.5	15.8	20.1	18.1
a_{xx}	[m]	3.0	3.1	6.1	5.39	2.5	2.8	2.2	2.2	2.0	7.9	13.7	9.09	9.5	9.1	10.0	8.3
Tϕ	[s]	18.1	15.1	9.5	16.0	18.8	12.4	20.0	13.5	9.1	15.2	11.2	53.8	37.1	17.0	13.8	22.4
I_{fluid}	[ton m²]	6.76E+04	0	0	0	0	0	0	0	0	0	0	0	0	8.38E+05	0	0
β	[-]	14.7	9.8	14.7	11.0	14.7	9.8	14.7	9.8	14.7	14.7	9.8	11.0	11.0	11.0	9.8	11.0
C_u	[-]	0.89	0.89	0.93	0.93	0.98	0.98	0.98	0.98	0.94	0.93	0.93	0.99	0.99	0.85	0.85	0.92
Tϕ JSRA	[s]	18.6	12.9	7.8	13.5	17.5	10.4	19.7	11.8	9.5	13.1	9.8	33.9	26.0	14.6	10.2	14.8
Tϕ Kato	[s]	22.1	15.5	9.2	15.6	21.5	12.5	24.3	14.4	11.0	15.5	10.4	61.1	47.3	17.9	12.4	26.5
Tϕ Doyere (c=0.34)	[s]	21.2	13.7	8.7	16.3	20.8	10.7	23.2	12.5	10.1	16.6	9.2	52.7	40.1	18.4	11.0	19.5
Tϕ Rollcoef (k=0.4)	[s]	19.3	12.9	9.5	16.0	19.0	10.5	21.0	11.9	9.6	16.6	8.6	45.5	34.9	17.2	11.4	16.4
Tϕ ITTC	[s]	19.2	13.6	4.7	16.5	18.5	11.2	21.0	12.8	10.5	16.3	7.6	45.4	35.1	17.6	12.4	11.1
Tϕ Grin	[s]	18.2	15.9	9.1	16.0	18.3	12.8	20.7	14.6	9.8	16.4	12.0	55.5	38.0	18.5	13.7	23.0
Tϕ JSRA w/o L	[s]	19.5	13.6	9.5	16.4	19.0	11.3	21.0	12.6	10.0	17.1	12.0	48.3	37.0	19.0	13.1	18.6
Tϕ Beam (k=0.36)	[s]	18.8	14.0	9.9	16.6	18.6	11.5	20.8	13.2	9.7	17.1	9.3	50.8	36.9	17.8	12.5	18.6

Proceedings of 15th International Marine Design Conference (IMDC-2024)
June 2-6, 2024
Amsterdam, the Netherlands

An Automated Method for Pipe Routing in Ship Unit Modules

Jisang Ha[1], Myung-Il Roh[2,*], Min-Chul Kong[3], Mijin Kim[4], Jeoungyoun Kim[3,4], Nam-Kug Ku[5]

ABSTRACT

This study addresses challenges in ship arrangement design by proposing an automated pipe routing method in ship unit modules. Currently, designers rely on experience, lacking quantitative assessments and causing difficulties for non-experts. The proposed method incorporates expert knowledge and design rules into an expert system, evaluating expertise and adherence to rules. The system's evaluation result was used as the objective function of an optimization problem formulated for pipe routing in conjunction with metrics such as total pipe length, the number of bends, and space availability. Through validation by comparing actual unit module designs, it is demonstrated that the proposed method suggested improved pipe routing design while adhering to expert knowledge.

KEY WORDS

Ship Unit Module; Pipe Routing; Expert System; Arrangement Design; Optimization

INTRODUCTION

The equipment in the ship is installed by connecting a ship's unit modules, each individually manufactured. These unit modules consist of the equipment with similar functions and pipes connecting them. This is a frequently used method because it can reduce production and installation costs by considering the similarity of the equipment or piping systems that comprise the modules and performing the arrangement through modularization (Gunawan et al., 2021). However, when doing the design for these modules, designers must consider the locations of the installed equipment and pipes when they perform pipe routing. However, the current approach to pipe routing in unit modules relies heavily on the designers' experience and lacks quantitative assessments. Consequently, non-experts have difficulty understanding the characteristics of unit modules and performing pipe routing. Moreover, the design review of pipe routing is time-consuming and challenging due to intricate pipe patterns and the absence of quantitative evaluation. To address these issues, this study proposed a method that analyzes pipe patterns and automates pipe routing in unit modules while incorporating expert knowledge and design rules. For this, an expert system was developed to assess the expertise of pipe routing experts and their adherence to design rules. The result of evaluating the system, the feasibility index, was used as one of the objective functions of an optimization problem formulated for pipe routing in conjunction with metrics such as total pipe length, the number of bends, and space availability. An effective pathfinding algorithm was used to solve the optimization problem. The designs of actual unit modules were compared to the results obtained using the proposed method to validate its effectiveness. The comparative analysis with manual designs demonstrated that the proposed method finds better alternatives for pipe routing while adhering to expert knowledge.

[1] Department of Ocean Operations and Civil Engineering, NTNU, Ålesund, Norway; ORCID: 0000-0002-6235-0829
[2] Department of Naval Architecture and Ocean Engineering, and Research Institute of Marine Systems Engineering, Seoul National University, Seoul, Republic of Korea; ORCID: 0000-0001-7972-6848
* Corresponding Author: miroh@snu.ac.kr
[3] Department of Naval Architecture and Ocean Engineering, Seoul National University, Seoul, Republic of Korea; ORCID: 0000-0002-0976-2621
[4] HD Korea Shipbuilding & Offshore Engineering Co., Ltd., Seongnam-si, Gyeonggi-do, Republic of Korea.
[5] Department of Naval Architecture and Marine Systems Engineering, Pukyong National University, Busan, Republic of Korea

Submitted: 23 February 2024, Revised: 3 May 2024, Accepted: 3 May 2024, Published: 18 May 2024

Conference paper, DOI: https://doi.org/10.59490/imdc.2024.830 e-ISSN: 3050-4864

Related Works

Since automating pipe routing in ships has the benefit of reducing design and review costs, there have been several studies on automated pipe routing and optimal pipe routing to achieve better results. Kimura and Ikehira (2009) and Furuholmen et al. (2010) tried to optimize piping cost by using optimization algorithms such as genetic algorithm and ant colony algorithm to optimize pipe routing. Ando and Kimura (2011), Lee et al. (2019), and Gunawan et al. (2022) utilized pathfinding algorithms to perform automated pipe routing. Also, research has been done in the form of using a combination of pathfinding and optimization algorithms, such as the work of Dong and Bian (2020). More recently, research has been conducted on pipe routing using reinforcement learning (Shin et al., 2020; Y. Kim, Lee, Nam, & Han, 2023). In this study, one of the heuristic pathfinding algorithms was chosen to perform automated pipe routing for faster route finding. A summary of studies related to pipe routing and this study is in Table 1.

Table 1. A summary of related studies on pipe routing and this study

Study	Method for pipe routing	Considerations
Kimura and Ikehira (2009)	Optimization algorithm (Genetic algorithm)	Piping cost and valve operationality
Furuholmen et al. (2010)	Optimization algorithm (Genetic algorithm)	Pipe length and number of bends
Ando and Kimura (2011)	Pathfinding algorithm (Dijkstra algorithm)	Pipe length and number of bends
Jiang et al. (2015)	Optimization algorithm (Ant colony algorithm)	Space availability
Lee et al. (2019)	Pathfinding algorithm (Dijkstra algorithm)	Pipe length, number of bends, and space availability
Shin et al. (2020)	Reinforcement learning	Pipe length, number of bends, and space availability
Dong and Bian (2020)	A*–GA Router algorithm	Pipe length, number of bends, space availability, and sharing racks
Gunawan et al. (2022)	Pathfinding algorithm (Dijkstra algorithm)	Piping cost and design procedure
Kim et al. (2023)	Reinforcement learning	Pipe length and number of bends
This study	Heuristic pathfinding algorithm	Pipe length, number of bends, space availability, and feasibility index

THEORETICAL BACKGROUND

The pipe routing target of this study, the ship unit module, refers to a set of equipment, piping, etc., that are typically grouped together within a particular system. Each piece of equipment and pipe that constitutes a module has input and output points, and they are complexly connected. Therefore, a detailed analysis of the characteristics of the connection relationship between equipment and pipes is required, and this study performs pipe routing of existing or new equipment based on the patterns already analyzed. The information analyzed includes the equipment's location, orientation, and bounding box information. Nozzle information was obtained by considering the pipes at the point of contact with the bounding box as the input/output point. We also utilized the pipes and equipment information, which includes pipe type, diameter, length, and coordinates.

Expert System for Pipe Routing in Ship Unit Modules

Many parts of pipe routing design are based on the data of previous ships or the know-how of experts. In order to apply the data of previous ships or the know-how of experts, this study uses an expert system to evaluate the results of pipe routing design and utilize them as objective functions or constraints (Kendal & Creen, 2007; Kim et al., 2015; Kim and Roh, 2016; Kim et al., 2017; Jung et al., 2018). The expert system utilized in this study consists of an Arrangement Template Model and an Arrangement Evaluation Model. They are described in the following sub-sections.

Arrangement Template Model

An Arrangement Template Model is a data structure for storing information about an arrangement target. The main value of the information of each "Node" that constitutes the "Pipe" that is most utilized in this study is stored in the "Pipe." For example, the "Max. Serial straight nodes" property value (maximum intuition length) is utilized in the Arrangement Evaluation Model by selecting the largest value among the "Serial straight nodes" values for each "Node."

Arrangement Evaluation Model

An Arrangement Evaluation Model consists of an ID, a target object, an attribute, and a target value (K. S. Kim et al., 2015). A target object and a subjective object are the objects that specify information. An attribute means the attribute of the object, such as the distance between objects whether they are connected. A target value is a value that the attribute should have. Object information refers to expert knowledge about the requirements related to the properties of a particular object, and relationship information refers to expert knowledge about the relationships between objects.
The American Bureau of Shipping (ABS) recommended arranging items that need to be precise, frequently used, or used for emergency purposes at a height of 860 to 1,350 mm from the floor (American Bureau of Shipping, 2018) as shown in Figure 1.

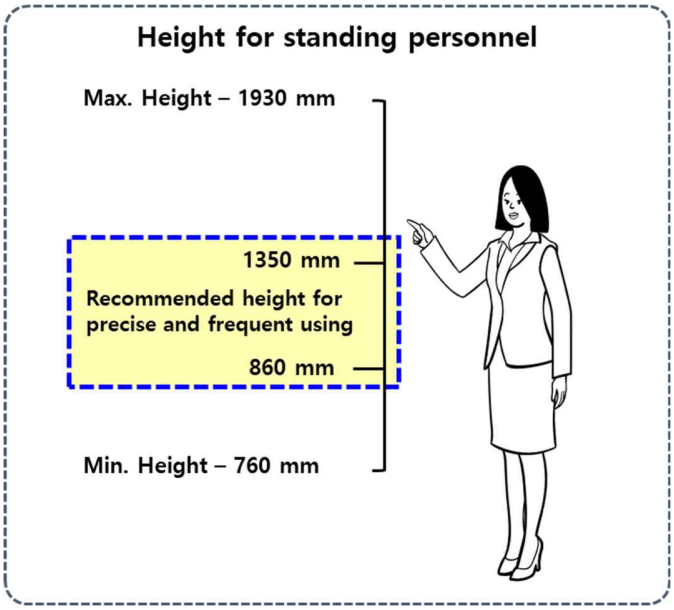

Figure 1: Recommended height for standing personnel

Expert knowledge can be expressed in the IF/THEN rule and used in the Arrangement Evaluation Model (rule-based expert system). If the corresponding expert knowledge is not essential, a continuous feasibility index can be calculated. An example of this categorized expert knowledge is shown in Table 2.

Table 2: Examples of expert knowledge in the Arrangement Evaluation Model

ID	Target object	Attribute	Target value	Knowledge expression	Priority
A001	All nodes	Node z coordinate	860_MIN_mm	IF node z coordinate ≥ 860 mm THEN 100 ELSE 0	3
A002	All nodes	Node z coordinate	1350_MAX_mm	IF Node z coordinate < 1350 mm THEN 100 ELSE 0	3

In Table 1, ID refers to the ID that classifies the relevant expert knowledge. The target object refers to the target to which the expert knowledge is applied. Attribute refers to the property of an object to which expert knowledge is applied. Target value refers to the value that an attribute must achieve to satisfy expert knowledge. Knowledge expression is content expressing the relevant expert knowledge using IF/THEN rules. If expert knowledge is satisfied, a feasibility index of 100 is obtained; otherwise, a feasibility index of 0 is obtained. The total feasibility index is used as the third objective function. Priority refers to the level of priority of that expert's knowledge. This is determined through interviews with experts and is an integer between 0 and 3. 0 is the most essential expert knowledge that must be satisfied, and 3 is the least important.

Pipe Routing for Ship Unit Modules

Design Variables

For design variables, we set the positions of nodes constituting each pipe as design variables. For objective functions in pipe routing, we calculate values based on the information of each node constituting the pipe p_i. Figure 2 shows an example of a pipe with nodes. For example, the pipe p_1 in Figure 2 consists of four nodes (n_1, n_2, n_3, n_4).

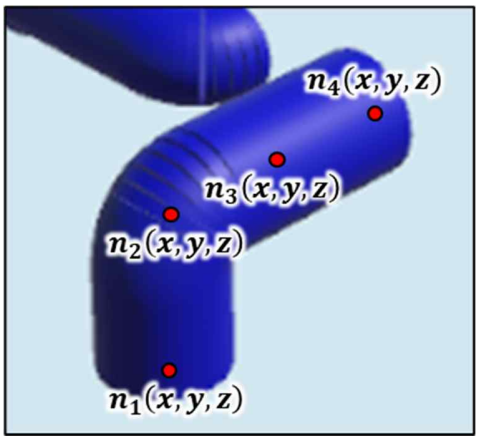

Figure 2: An example of nodes of the pipe p_1

Objective Functions

The 1st objective function $F_1 = L(p_i)$ is calculated as the sum of the distances between nodes constituting p_i. In Figure 2, the sum of the length between nodes (n_1, n_2, n_3, n_4) is $L(p_1)$. In the 2nd objective function, the total number of bends F_2 is calculated by the number of bends in pipe $B(p_i)$. In Figure 2, the number of bends $B(p_1) = 1$ can be calculated from the information of nodes (n_1, n_2, n_3, n_4). To consider the workability and cost of pipe installation and maintenance, The smaller the total length of pipes (F_1) and the number of bends (F_2), the better the pipe routing. F_1 and F_2 were commonly utilized as objective functions for pipe routing in various related works, including Furuholmen et al. (2010), Ando and Kimura (2011), and Lee et al. (2019). For the 3rd objective function, the space availability of pipes F_3 is used. It is a value of how efficiently the pipe is utilizing the space. In this study, space availability is a measurement of how efficiently the piping is arranged in a given design space. When piping is co-located with other equipment, the arrangement of supports and space availability should be considered. While there are previous studies that have considered space availability, this study used the space availability metric of the study of Lee et al. (2019). They calculated the distance from the wall or obstacle to where the piping is installed and used this as an indicator of space availability. The lower this value is, the closer the piping is located to the wall and the better the space is utilized. Minimizing this value was defined as the 3rd objective function F_3. As the final objective function F_4, we used the sum of the feasibility index, the output of the Arrangement Evaluation Model.

Constraints

For constraints, we check pipe routing to prevent collisions with obstacles and deviations from the pipe installation area.

Pipe Routing Method

For generating routes for pipes, the Jump Point Search (Harabor & Grastien, 2011; Min, Ruy, & Park, 2020) algorithm is used. To improve the computational speed of pipe routing, we utilized a grid with a dynamic size. By defining a grid that changes dynamically according to the complexity around the grid space, it is designed to use a grid of a different size depending on the situation (Ha, Roh, Kim, & Kim, 2023). Let d be the distance from where the node is located to the closest obstacle, and if $d \leqq$ *grid space*, smaller grid spaces are created for considering the distance to the nearest obstacle/ bulkhead. In this study, the maximum grid space is 200 mm, and the minimum grid space is 10 mm.

APPLICATIONS

In this study, pipe routing was performed using the proposed method for a ship's on-deck unit modules. A comparison of the objective function with the results of a manual design is shown in the following figures and tables. In this study, manual design refers to pipe routing results that are designed by experts according to design rules and manuals. Figure 3 and Table 3 show the pipe routing results for the first module.

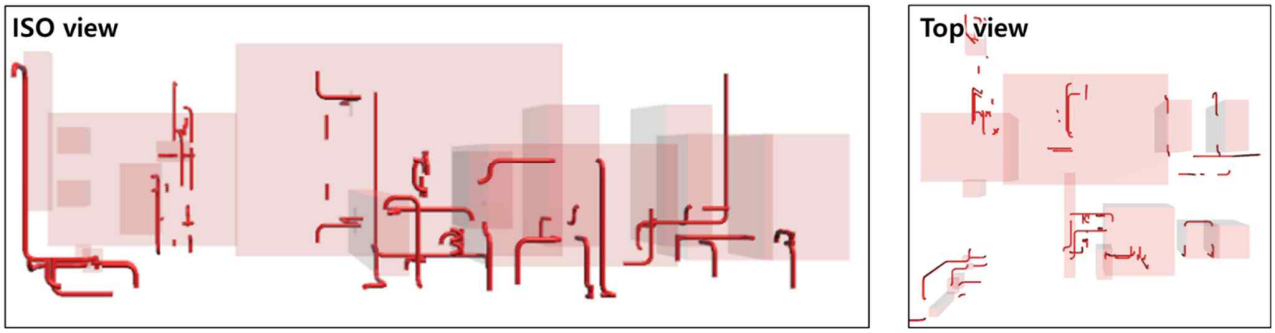

Figure 3: The result of pipe routing for Module 1

Table 3: The objective functions of pipe routing for Module 1

Case	Total length of pipes (F_1, Min) [m]	Total number of bends (F_2, Min)	Avg. space availability of pipes (F_3, Max)	Feasibility index of pipes (F_4, Max)	Calc. time [Sec]
Module 1 (Manual)	74.87 (100%)	183 (100%)	8,166.5 (100%)	483 (100%)	-
Module 1 (Proposed)	**58.50 (78.1%)**	**112 (61.2%)**	**10,274.4 (125.8%)**	**483 (100%)**	**64.21**

For Module 1, the total length of pipes (F_1) was reduced by 21.9%, and the total number of bends (F_2) was reduced by 38.8%. The space availability of pipes (F_3) improved by 25.8%, and the routing results satisfied all expert knowledge (F_4). The pipe routing results for Module 2 are shown in Figure 4 and Table 4.

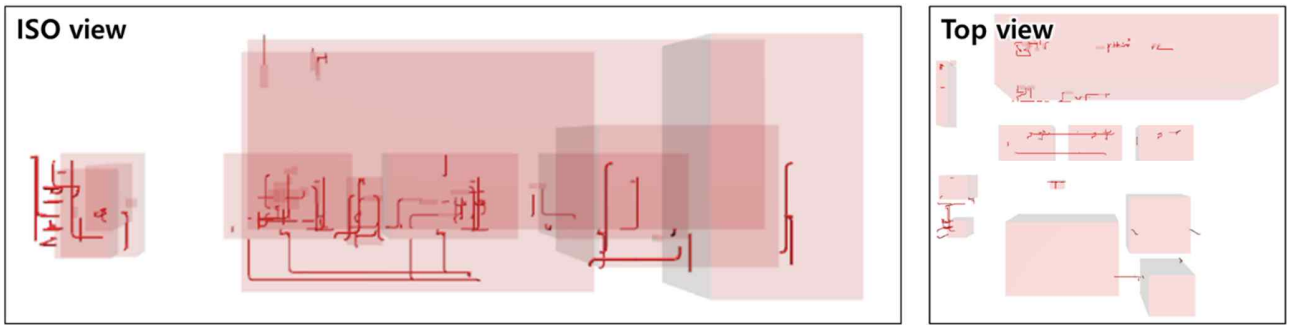

Figure 4: The result of pipe routing for Module 2

Table 4: The objective functions of pipe routing for Module 2

Case	Total length of pipes (F_1, Min) [m]	Total number of bends (F_2, Min)	Avg. space availability of pipes (F_3, Max)	Feasibility index of pipes (F_4, Max)	Calc. time [Sec]
Module 2 (Manual)	111.89 (100%)	204 (100%)	8,255 (100%)	952 (100%)	-
Module 2 (Proposed)	**97.20 (86.9%)**	**185 (90.7%)**	**10,022.6 (121.4%)**	**952 (100%)**	**89.7**

For Module 2, the total length of pipes (F_1) was reduced by 13.1%, and the total number of bends (F_2) was reduced by 9.3%. Space availability of pipes (F_3) improved by 21.4%, and the routing results satisfied all expert knowledge (F_4). The pipe routing results for all on-deck modules are shown in Figure 5 and Table 5.

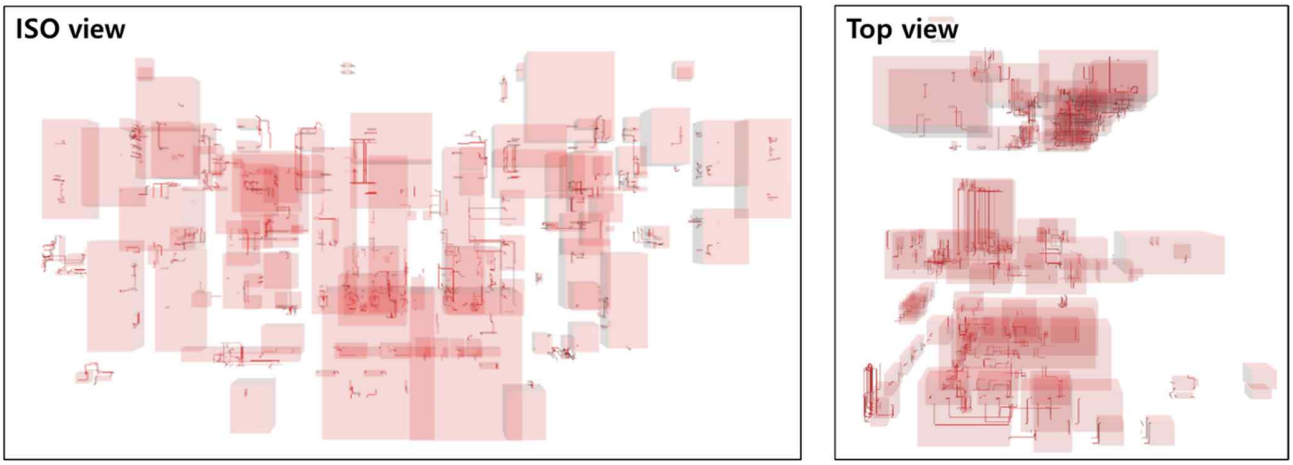

Figure 5: The result of pipe routing for all on-deck modules

Table 5: The objective functions of pipe routing for all on-deck modules

Case	Total length of pipes (F_1, Min) [m]	Total number of bends (F_2, Min)	Avg. space availability of pipes (F_3, Max)	Feasibility index of pipes (F_4, Max)
All on-deck modules (Manual)	4,887 (100%)	1,439 (100%)	10,640.2 (100%)	15,006 (100%)
All on-deck modules (Manual)	4,843 (99.1%)	1,236 (85.9%)	11,778.2 (110.7%)	15,006 (100%)

After performing pipe routing, we can see that all the objective functions improved compared to the original results of the manual design. F_1 improved by 0.9%, F_2 by 14.1%, and F_3 by 10.7%, and the feasibility index for expert knowledge was the same as the manual design given by the expert. The routing results satisfied every expert knowledge.

CONCLUSIONS

This study performs successful pipe routing by utilizing the given information about the unit modules of a ship and the interrelations between pipes. The pipe routing results obtained in this study show a significant improvement over manual designs, achieving a reduction of up to 21.9% in the total length of pipes (F_1) and up to 38.8% in the number of bends (F_2). Space availability in the piping was improved by up to 25.8%, and the feasibility index for expert knowledge was evaluated, and all expert knowledge was satisfied. Leveraging the method proposed in this research, we developed a prototype for an automated program dedicated to the pipe routing of ship unit modules.

The accurate start and end points of the pipes are defined based on the connection information of the pipes, ensuring precision in the pipe routing process. Since the pipe routing in this study is targeted at the initial design stage, there is a limitation that prior research is needed to extract the information required for pipe routing from P&IDs at this stage. Additionally, we will include a review of potential improvements in pipe routing to meet the requirements of additional expert knowledge in this field.

ACKNOWLEDGEMENTS

This study is an extension of our previous study (Ha et al., 2023) and was partially supported by (a) HD Korea Shipbuilding & Offshore Engineering Co., Ltd., Republic of Korea, (b) BK21 Plus, Education & Research Center for Offshore Plant Engineers (COPE) of Seoul National University, Republic of Korea, and (c) Research Institute of Marine Systems Engineering of Seoul National University, Republic of Korea.

REFERENCES

American Bureau of Shipping. (2018). Guidance Notes on the Application of Ergonomics to Marine Systems.

Ando, Y., & Kimura, H. (2011). An Automatic Piping Algorithm Including Elbows and Bends. *Proceedings of the International Conference on Computer Applications in Shipbuilding*, 3, 153–158.

Furuholmen, M., Glette, K., Hovin, M., & Torresen, J. (2010). Evolutionary Approaches to the Three-dimensional Multi-pipe Routing Problem: A Comparative Study Using Direct Encodings (pp. 71–82). Springer, Berlin, Heidelberg. https://doi.org/10.1007/978-3-642-12139-5_7

Gunawan, G., Utomo, A.S.A., Hamada, K., Ouchi, K., Yamamoto, H., & Sueshige, Y. (2021). Optimization of Module Arrangement in Ship Engine Room. *Journal of Ship Production and Design*, 37(01), 54–66. https://doi.org/10.5957/jspd.12190066

Ha, J., Roh, M.I., Kim, K.S., & Kim, J.H. (2023). Method for Pipe Routing Using the Expert System and the Heuristic Pathfinding Algorithm in Shipbuilding. *International Journal of Naval Architecture and Ocean Engineering*, 15, 100533. https://doi.org/10.1016/J.IJNAOE.2023.100533

Harabor, D., & Grastien, A. (2011). Online Graph Pruning for Pathfinding On Grid Maps. *Proceedings of the AAAI Conference on Artificial Intelligence*, 25(1), 1114–1119. https://doi.org/10.1609/AAAI.V25I1.7994

Jung, S. K., Roh, M. Il, & Kim, K. S. (2018). Arrangement Method of a Naval Surface Ship Considering Stability, Operability, and Survivability. *Ocean Engineering*, 152, 316–333. https://doi.org/10.1016/J.OCEANENG.2018.01.058

Kendal, S. ., & Creen, M. (2007). *An Introduction to Knowledge Engineering*. London: Spring.

Kim, K.S., & Roh, M.I. (2016). A Submarine Arrangement Design Program Based on the Expert System and the Multistage Optimization. *Advances in Engineering Software*, 98, 97–111. https://doi.org/10.1016/J.ADVENGSOFT.2016.04.008

Kim, K.S., Roh, M.I., & Ha, S. (2015). Expert System based on the Arrangement Evaluation Model for the Arrangement Design of a Submarine. *Expert Systems with Applications*, 42(22), 8731–8744. https://doi.org/10.1016/J.ESWA.2015.07.026

Kim, S.K., Roh, M.I., & Kim, K.S. (2017). Evaluation of Feasibility Index in the Arrangement Design of an Offshore Topside Based on the Automatic Transformation of Experts' Knowledge and the Fuzzy Logic. *Ocean Engineering*, 130, 284–299. https://doi.org/10.1016/J.OCEANENG.2016.11.057

Kim, Y., Lee, K., Nam, B., & Han, Y. (2023). Application of Reinforcement Learning Based on Curriculum Learning for the Pipe Auto-routing of Ships. *Journal of Computational Design and Engineering*, 10(1), 318–328. https://doi.org/10.1093/JCDE/QWAD001

Kimura, H., & Ikehira, S. (2009). Automatic Design for Pipe Arrangement Considering Valve. *Proceedings of the International Conference on Computer Applications in Shipbuilding*, Shanghai, China.

Lee, J. B., Roh, M.I., & Oh, M.J. (2019). Pipe Routing of Offshore Structure Considering Space Availability. *Korean Journal of Computational Design and Engineering*, *24*(3), 280–288. https://doi.org/10.7315/cde.2019.280

Min, J.G., Ruy, W.S., & Park, C. S. (2020). Faster Pipe Auto-routing Using Improved Jump Point Search. *International Journal of Naval Architecture and Ocean Engineering*, *12*, 596–604. https://doi.org/10.1016/J.IJNAOE.2020.07.004

Shin, D., Park, B., Lim, C., Oh, S., Kim, G., & Shin, S. (2020). Pipe Routing using Reinforcement Learning on Initial Design Stage. *Journal of the Society of Naval Architects of Korea*, *57*(4), 191–197. https://doi.org/10.3744/SNAK.2020.57.4.191

Proceedings of 15th International Marine Design Conference (IMDC-2024)
June 2-6, 2024
Amsterdam, the Netherlands

Defining a Framework for Implementing the Circular Economy Principles into Ship Design

Elise Hoffmann[1,*] and Jeroen Pruyn[2]

ABSTRACT

This research addresses the importance of sustainability in shipping beyond fuel selection, stressing the need for responsible material usage in vessel construction and maintenance. Transitioning to a circular economy is crucial for sustainable waste management in the industry, yet current ship design neglects circularity considerations, prioritising functionality and cost. The research evaluates frameworks such as the butterfly diagram, Cradle-to-Cradle, 10R, and ReSOLVE to integrate circularity into ship design. Combining the 10R framework with the Material Circularity Indicator method, this study offers practical insights for circularity in ship design. Challenges include integrating these methods into standard design processes, which are mitigated by fusing 10R strategies with systems engineering. A case study on wheelhouse redesign demonstrates the effects of this approach, highlighting the importance of supplier collaboration for circularity enhancement.

KEY WORDS

Circular Economy, Systems Engineering, Ship Design, Sustainability

INTRODUCTION

In 2015, 193 world leaders have agreed to 17 global goals to end extreme poverty, inequality and climate change by 2030. Goal number 12 states: ”Responsible consumption and production” (The Global Goals, 2015). The aim of this goal is to ensure sustainable consumption and production patterns. To achieve this goal eleven targets have been set to create action. One of them also being: ”Substantially reduce waste generation”. By 2030, the aim is to substantially reduce waste generation through prevention, reduction, recycling and reuse.
In the maritime sector, currently virgin materials are used for the construction of vessels which all have to be taken care of again at the end of a ship’s life. Ships are broken down at ship recycling yards, where steel is recycled, but often with disregard for the environment (Mikelis, 2019). In 2018, 90.4% of the ships (measured in the gross tonnage) were recycled by shipbreaking and recycling industries in Bangladesh, India, and Pakistan. These are popular countries because of the absence of strict environmental regulations (Alam et al., 2019). Also, recycling is a valid option but when looking at retaining value, recycling is not the best way and other methods such as reuse or refurbishment are preferred (Cramer, 2020). Not only at the end of a ship’s life, during demolition, the materials need to be processed but also during the ship’s lifetime of approximately 25 years, components on board are replaced, creating a lot of waste. Additionally, little is known about how all other parts except for the steel of the hull are handled, such as electronic systems or furniture.

[1] Department of Maritime and Transport Technology, Delft University of Technology, Delft, The Netherlands
[2] Department of Maritime and Transport Technology, Delft University of Technology, Delft, The Netherlands; CoE HRTech, Rotterdam University of Applied Science, Rotterdam, The Netherlands; ORCID: 0000-0002-4496-4544
[*] Corresponding Author: elisehoffmann@hotmail.com

Submitted: 14 February 2024, Revised: 1 May 2024, Accepted: 3 May 2024, Published: 19 May 2024

Conference paper, DOI: https://doi.org/10.59490/imdc.2024.843 e-ISSN: 3050-4864

At the moment shipbuilding is not considering the reuse of materials at the input and output side of the process. As a result, circular economy would offer many opportunities for improvement and could increase the sustainability of this key sector. In a circular economy there is no waste since waste is seen as a raw material for new products (Stahel, 2016). Currently, vessels are designed with a focus on functionality, cost and operability. Next to that, designers mainly reuse existing knowledge to establish assumptions and probability to deal with uncertainty. This makes it difficult to take higher levels of uncertainty into account, whilst due to the ongoing energy transition there is uncertainty about the required refits and updates of systems in the future (Zwaginga and Pruyn, 2022). Taking into account the circularity of products when designing a vessel could reduce waste and improve the sustainability of vessels since up to 80% of a product's environmental impact is determined already in the design phase (European Commission, 2020a). The circular economy principles, also known as cradle-to-cradle, are therefore seen as a sustainable strategy.

This paper explores a method of implementing the circular economy principles into the ship design approach. Where circularity is considered to be any process that improves the reuse of equipment, components, parts and materials, where the maintenance of value is a key priority. This is achieved by first assessing the current state of circularity in the shipping industry. Next, there is a selection of a definition of circularity and a way to measure it. After that, the goal is to identify important system properties that enable identifying the level of circularity that is currently prioritised in the design of the system by looking at these system properties. Combining these topics, a framework will be drafted to guide future ship designers in also taking circularity into account alongside the current design drivers such as functionality, cost and operability. As a case study, the framework will be tested on the wheelhouse of a Damen RSD2513 tug. In the case study, different system levels will be examined on their current circularity level and improvements to increase the circularity level will be proposed.

THEORY

In this section, the current state of circularity in the shipping industry is researched to determine the potential of applying (more) circularity in the sector. After that, the theory behind the circular economy will be elaborated upon. Lastly, approaches for both circular design and ship design will be discussed to look for opportunities of combining these two approaches.

Circularity in Shipping

Literature research on the topic of circularity in the shipping industry was done by the use of the databases of Scopus, WorldCat, the TU Delft repository and Google Scholar. To achieve relevant results, search terms were determined in advance. The keywords such as ”Circular*”, ”Ship Design”, ”Ship recycling”, ”Ship repair”, ”Systems Engineering”, and any combination of these words were used. This research revealed no scientific resources on the topic and by use of Google and the same keywords, an understanding of the circularity in shipbuilding was obtained.

Sustainable Shipping Initiative and 2BHonest (2021) state that the shipping industry is already applying reuse, repair and recycling, which are all circular principles. However, the circular economy is more than those three principles and the current practice is primarily cost-driven, so other principles of the circular economy have great potential to be implemented in the shipping industry as well. To ensure this, more and more rules and regulations such as the Hong Kong Convention (IMO, 2015), EU Ship Recycling Regulation (European Commission, 2020b), the Circular Economy Action Plan, The European Sustainability Reporting Standard (EFRAG, 2022) and ISO standards are put into place (Balder, 2021). During the process of this research, the requirements to put the Hong Kong Convention into force were met and on June 26th 2025, the convention will enter into force (IMO, 2023). However, the fact that the HKC took almost 14 years to be signed by enough states, shows that many states are not very eager to comply with the regulations that would improve circularity, most likely because of the cost and extra work that will come with it. If the maritime sector wishes to become more circular and more sustainable, all stakeholders in a vessel's lifetime need to be on board. How circularity can be achieved will be researched in the next section.

The Theory of the Circular Economy

The current 'take-make-dispose' economy is called a linear model (Di Maio and Rem, 2015) (Bocken et al., 2016). Di Maio and Rem (2015) state that in Circular Economy (CE) models, products maintain their added value for as long as possible and minimise waste. The aim is to keep resources within the economy when products no longer serve their functions so that materials can be used again and therefore generate more value. Thus circular business models create more value from each unit of resource than traditional linear models. Stahel (2016) describes the linear economy as a flowing river, whilst the circular economy can be seen as a lake, where the goods and materials are reprocessed.

The World Business Council for Sustainable Development (WBCSD) concludes that the concept of the circular economy is relatively vague and amorphous, resulting in companies moulding and defining circularity in ways that are most relevant to their core business (wbcsd, 2018). As a result of this, most companies have their own approaches for the implementation of the circular economy. Popular approaches are Cradle-to-Cradle, 10R, the butterfly diagram and ReSOLVE. Even though the frameworks differ in name and exact approach, there are many overlapping principles. First of all the main takeaway for every circular framework is to have as little waste as possible and ideally never throw any materials away by closing the loop. But also the way materials are kept in the loop shows some overlapping principles within the frameworks; words such as reuse, refurbish, recycle etc are in the butterfly diagram of the Ellen McArthur Foundation (2019) but also in the 10R framework. The environmental impact besides material circularity is not part of these frameworks. This was also defined in the scope, to not look at other environmental impacts but purely circularity in terms of material reuse and using as little material as possible. The 10R framework is widely cited and shows clear steps for the circularity level of a product/material in every stage of the life cycle of a product; from design until the end of life (in its current function). The different R-levels are Refuse, Reduce, Redesign, Reuse, Repair, Refurbish, Remanufacture, Repurpose, Recycle and Recover. Additionally, even though R0 until R8 can all be seen as circular, it is important to make a clear distinction between the levels of circularity, something that other frameworks have a less clear definition of. Therefore, to continue this project, the 10R framework will be chosen to work with (Cramer, 2020). In Figure 1 the order of the 10R's is shown together with their applicability in the lifetime of a system.

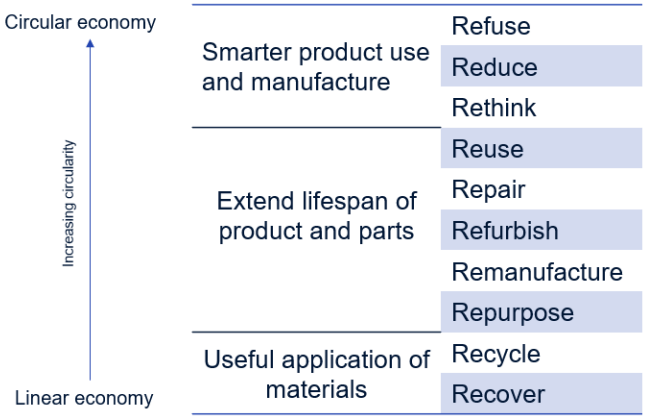

Figure 1: The 10R framework from Refuse (R0) to Recover (R9) based on Cramer (2020)

This framework does not have a clear way of measuring on which step of the circularity ladder a system is currently functioning, but to measure how circular products are, again multiple frameworks and methods exist. To measure circularity, the Material Circularity Indicator (MCI) method is selected (Goddin et al., 2019). This is because it makes a clear distinction between the different circularity levels of the 10R method, the formulas are clear and open access, and the focus is on the product level. The method calculates circularity by taking the average of the circular inflow, which can be a combination of recycled, refurbished or remanufactured materials flows, and the circular outflow, which can be a combination of recycling, refurbishing, remanufacturing or repurposing, measured in percentage of mass. During the lifetime, the utility is calculated based on the lifetime and intensity of use of the system compared to the industry averages of similar systems. The different material flows are visualised in Figure 2.

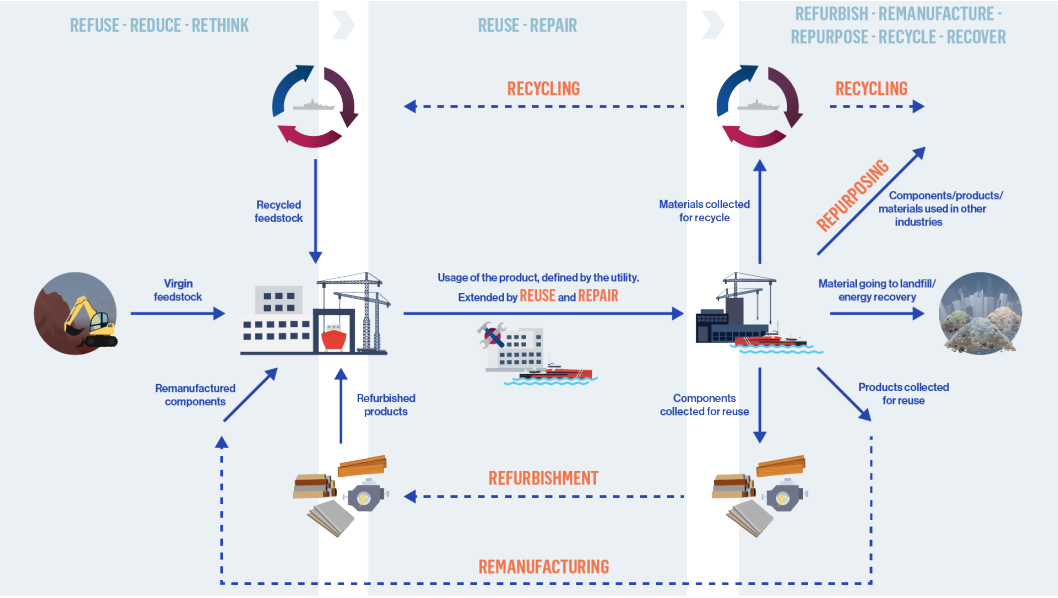

Figure 2: Visual of the material flows when combining the 10R framework with the MCI tool

Design Approaches

Looking at design approaches, two types of design approaches will be discussed in this section; Ship design approaches and circular design approaches.

Ship Design

In ship design, four classes of high-level design strategies are often distinguished; Point-based design, Set-based design, System-based design and Optimisation-based design. Of the four presented design approaches, system-based design, also known as systems engineering, is the preferred method for this research because it defines the customer needs and required functionality early in the development cycle, focuses on documenting requirements and after that proceeds with design synthesis and system validation while considering the complete problem. Kossiakoff et al. (2011) states that ”The function of systems engineering is to guide the engineering of complex systems”. Where a system is seen as ”a set of interrelated components working together toward some common objective” ((Kossiakoff et al., 2011)). In systems engineering, a system can be broken down into systems, sub-systems, components, sub-components, and parts (Hopman, 2021). Systems engineering solves some of the problems that occur in the other methods such as the point-based design where the design spiral is often used and the starting point is so important that it is hard to implement innovations. Next to that, the method considers both business and technical needs of all customers in order to provide a quality product that meets the user’s needs. The fact that the system is broken down in a modular way also helps in including circularity, where modularity plays a big role in the circularity of a system. Modular products can be divided into different modules and each module can be repaired/replaced separately ((Kimura et al., 2001)). The determination of size and content of each module is complicated to decide and are determined by multiple factors such as cost, functional independence, standardisation, ease of maintenance, etc.

Within systems engineering, an application of the theory is the Requirement-Functional-Logical-Physical model (RFLP). The complexity of systems is not only determine by the amount of connected physical components, but also the functional interdependencies play a huge role (Li et al., 2020). By working together, various systems can achieve one function. This so-called functional integration is associated with the different power sources and information flow between the systems. The requirements need to be validated against the higher level of requirements and user needs, therefore there are horizontal validation rules.

None of the four design approaches for ship design takes circularity into account. This can be because circularity is hard to express in terms of an optimisation code or functional requirement. Therefore there is a need to explore design approaches for a circular product since circular design is already quite common for consumer goods.

Circular Design

For circular design, there is no step-by-step guide on how to apply the circular economy principles to the design process. However, for every R-value, one or multiple design focuses can be identified. Many of the current circular design strategies are focused on consumer goods and are not yet applied in technical fields. The first three; refuse, reduce and reuse, focus on the cut down on raw material usage by use of design for reduction of resource consumption (Cramer, 2020)(Bocken et al., 2016). The design focus for the strategies Reuse, Repair, Refurbish, Remanufacture and Repurpose focuses on product life extension. For Recycle and Recover, the focus is mostly on designing for resource recovery or using materials for multiple cycles.

Combining the Approaches into Circular Ship Design

According to Ashby and Johnson (2003), there is a difference between engineering design, under which the art of ship design could be seen, and industrial design which involves the design of consumer goods. First of all, engineering is systematic; it follows well-established and commonly accepted procedures, whilst industrial design does not. Industrial design is strongly influenced by fashion and advertising. Industrial design is less about functionality and efficiency, but the focus is more on qualities such as form, style, and texture; the ones that cannot be measured. Engineering designers often use formal guidelines such as ISO standards whilst industrial designers have representations which are imprecise, ill-defined and less established (Pei et al., 2011). Pei et al. (2011) also states that engineering design is more about associating models with engineering principles, production issues, and functional mechanisms, whilst appearance and usability are the most important focus points for industrial design. The need for clear guidelines and standards is also bigger when looking at ship design since a vessel is way larger and more complex than consumer goods. Inside a ship, many systems, sub-systems, components and parts are present, whilst consumer goods such as chairs and tables, often consist of significantly fewer parts and components.

To include circularity, the systems engineering method has to be combined with the ten design methods complying with the 10R framework. Because systems engineering follows a clear step-by-step approach, circular design principles are best to be included in the steps of systems engineering. To include these principles, the differences between the design methods should be kept in mind and where possible the circular principles should be added in every step of systems engineering.

METHOD

Now that the definition of circularity is clear, the circularity measurement method is chosen and the different design approaches have been reviewed, the next step of combining all this into a framework on how to design a vessel whilst applying the circular economy principles can be made. The framework consists of six steps that will all be separately elaborated upon in this section. The framework is visualised in Figure 3. The first step is to identify an overall goal the system needs to achieve, after which the system is broken down using the RFLP-approach in step 2. After this, in step 3, the MCI score of a comparable, existing design will be determined. After this, the system's life cycle and associated stakeholders will be identified. Finally, in step 5 the system is (re)designed by use of the RFLP approach and the use of circular principles, after which the new design will be validated in step 6. Looking at the method and comparing it to the "classic" V-diagram which is often used to visualise the RFLP approach, it becomes clear that the new method adds a few steps. The steps that differ from the classic approach are highlighted by the orange blocks.

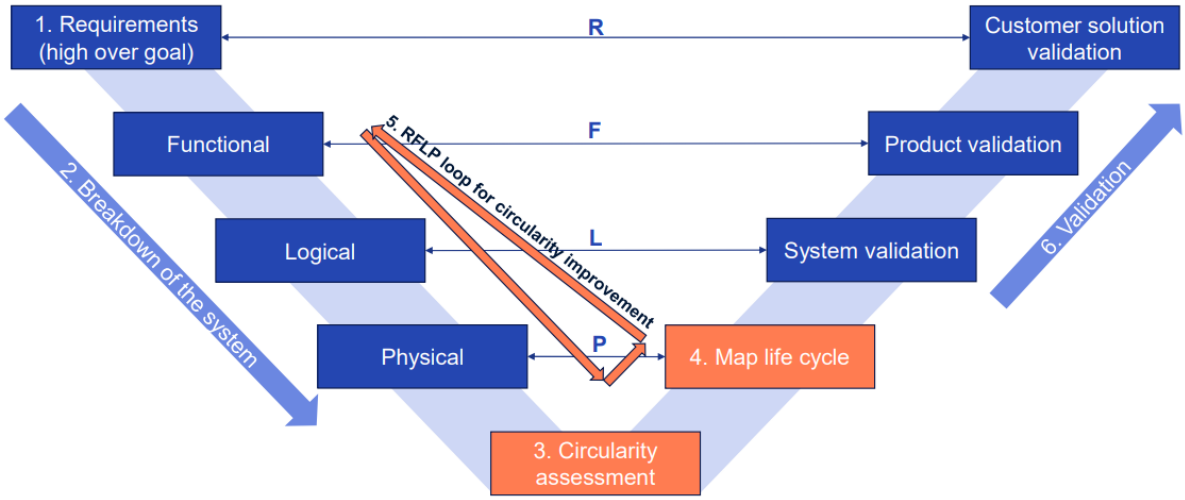

Figure 3: Visual of the framework for including the circular economy principles the classical V-diagram visualisation of the RFLP approach

Step 1: Identify the Goal and Overall Mission

In systems engineering, the first step is a needs analysis. During the needs analysis, the goal is to show clearly and convincingly that there is a valid operational need for a new system or an update of an existing design. To do this, it needs to be assessed whether or not a system already exists that is meeting the needs or whether a (re)new(ed) system is required. The general or main requirements are often dominated by three main parties; customers, production and regulations (B. Vink, Personal Communication, June 28, 2023). Where, in identifying the high-over mission, the customer often has the biggest say. Requirements are, in non-circular design strategies, often operational and functional requirements. However, when looking at the circular design, there should also be a circular goal from the start. Not only do circular aspects have to be a part of the performance and physical requirements, but also general things such as the quality of the product can be performance and physical requirements. Ideally, the goal might be to have one hundred per cent circular systems, but this might not always be achievable. For the general circular requirements, it would be wise to specify this wish into different material streams. Examples of this would be to set a requirement that ninety per cent of the inflow of materials needs to be non-virgin, or at least ten per cent of the outflow of materials should be used in remanufacturing.

Based on the set requirements there are three possible scenarios:

1) A system exists that fulfils the high over requirements
2) A system exists that fulfils the operational requirements but not the circularity requirements
3) No system at all exists that fulfils the operational nor circular requirements

In case a system already exists that fulfils all requirements (scenario 1), no need exists to design a (re)new(ed) system. In case a system exists that fulfils the operational requirements but not the circularity requirements (scenario 2), step two of the framework should be carried out. In case no system at all exists that can fulfil any requirements (scenario 3), steps two and three of the framework can be skipped and step four of the framework should be carried out.

Step 2: Identify and Breakdown System, Sub-System, Components, Sub-Components, and Parts

As mentioned before, the theory of systems engineering divides systems into sub-systems, components, sub-components and parts. According to Kossiakoff et al. (2011), the term ”system” should only be used ”for entities that 1) possess the properties of an engineered system, and 2) perform a significant useful service only with the aid of human operators and standard infrastructures” (Kossiakoff et al., 2011). How far a system can be broken down for analysis is very dependent on the information provided; if no information is there on the structure of the system because, for example, the system is designed by a separate company, this is hard to break down further. Next to breaking the system down, it is also important to identify the boundaries of a system to define what is inside the system, and what is outside. Several criteria can be used to help determine whether an entity is part of a system or not; Development control, operational control, functional control and unity of purpose. For every criterion, questions can be asked such as; ”Does the system developer have control over the entity’s development?” and ”In the functional definition of the system, is the systems engineer ”allowed” to allocate functions to the entity?” (Kossiakoff et al., 2011). Additionally, entities that are not part of the system, will still interact with it. Once the boundaries have been set and the system has been broken down, the connections within the system can be analysed. The interactions on multiple levels of a system can be evaluated by the use of architectures. Architectures help to capture the relationship between the different elements of a system. There are functional, logical and physical architectures, all visualised in Figure 4.

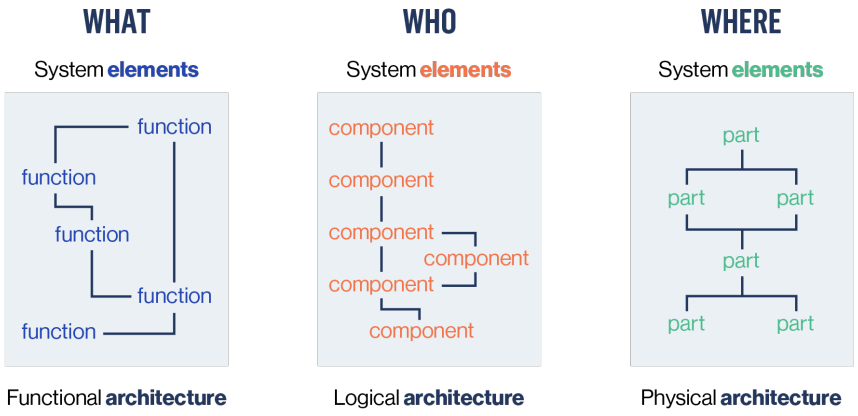

Figure 4: Visualisation of a functional, logical and physical architecture, based on The Mathworks (2020)

After all these theoretical boundaries and frameworks on how to identify the system, practice might prove to be different. In reality, one needs to work with the information available. This information could be retrieved from drawings of systems, material lists or other documentation. The level of detail per system might differ since some systems might be designed and built by the company performing the analysis whilst others might be designed and built by suppliers. Since the circularity of the systems is measured based on weight, resulting in the heaviest components or parts having the biggest influence on the total circularity level of a system. Thus selecting a heavy system when having the choice between multiple systems to assess is an effective way to increase the circularity level.

Step 3: Determine the Current Level of Circularity of Existing Design

To have a baseline and be able to measure improvement in terms of circularity after redesigning it, the previously selected MCI method will be applied. During the assessment of a system on its current level of circularity, mostly material choice, modularity, reliability and cost play an important role. For the outflow, the material should allow for a certain level of circularity, the modularity should be high enough to allow for easy dismantling and the cost of the value retaining steps should not too high, otherwise system will be disposed of.

For the determination of the input and output values of the MCI method, the key indicators identified can be used. For every input, multiple questions can be asked in order to determine the contribution of the input. For the inflow of materials, the key indicator of material choice is the most important. The most important question here is; have non-virgin materials been used, and are these materials reused or recycled materials? The inflow is often controlled by designers and suppliers. Therefore this is where this research can have the most impact. A very important aspect here is good communication with suppliers to get information about used materials, but also to ensure the reuse of non-virgin materials in the future.

The same type of questions can be asked about the utility and end-of-life of the product: Is the product reliable enough to reuse? Is the product built modular so it can be dismantled into different materials? Does the material choice allow for recycling? Since the MCI calculation is based on weight, the mass of the product also needs to be determined, preferably split out all the way to the part level. To acquire all this information, contact with the supplier of the system and its materials needs to be established. If the resource of the materials is unknown, industry averages can be used based on a material database such as Ansys Granta Edupack (Ansys Granta Edupack, 2006).

Based on the circularity calculation, it needs to be verified that a valid need exists to (re)design a system that fulfils the overall goal and mission.

Step 4: Map the System's life cycle and Associated Stakeholders

To know which stakeholders need to be involved in the (re)design process, the life cycle of the system and its associated stakeholders need to be mapped. The first step is to map the life cycle, which encompasses all the necessary steps involved in taking a product in service from its initial idea stage through the various stages of production (including physical transformation and the involvement of different producer services), delivery to end consumers, and ultimate disposal after use (Kaplinsky and Morris, 2000). General example life cycle steps for a vessel are engineering, manufacturing, commissioning, operation and decommissioning. To help guide a designer in mapping the life cycle, Kossiakoff et al. (2011) suggests mapping or modelling at least the following circumstances:

1. storage of the system and/or its components,
2. transportation of the system to its operational site,
3. assembly and readying the system for operation,
4. extended deployment in the field,
5. operation of the system,
6. routine and emergency maintenance,
7. system modification and upgrading, and
8. system disposition.

Once the life cycle has been mapped, stakeholders in each step of the life cycle can be identified. For the mapping of the stakeholders, not every stakeholder is of equal importance. Additionally, often the needs that different stakeholders have are in conflict. Stakeholders can be divided into the direct beneficiary and several indirect beneficiaries (Erikstad, 2018). When looking at stakeholders and their needs with regard to circularity, often an outside incentive is required. Here, the regulations that were mentioned in the theory section can be the main driver. For every stakeholder, a different regulation will be of the appliance. A strategy to reach more circularity within companies is to set goals on company-wide goals that are measured by indicators; Key Performance Indicators (KPIs) (Coalition circular accounting, 2023). These indicators can help stakeholders in guiding them in defining requirements they have with regard to circularity. In case a company does not have KPIs on circularity yet, it is recommended to first draft these before setting needs for a specific system.

Step 5: (Re)design the System by use of the RFLP method, Applying Circularity Principles

The selected RFLP method uses requirements to define functions, which are connected by logic and then put into a physical form. It is essential for every step that the level of detail of the previous step is sufficient to make the next step.

The first step of creating a (re)new(ed) system is to set up the requirements the system has to comply with. These requirements are determined by the stakeholders as identified in Step 4. There are different types of requirements; operational, functional, performance and physical requirements (Kossiakoff et al., 2011). To check requirements, a requirements analysis can be executed. Requirements need to have certain characteristics; they should for example be feasible and verifiable. In addition to the currently common practice of operational and performance requirement defining, circular requirements should be defined. These can be seen as operational, performance and physical requirements. For circular design, there is a higher urge to reach a higher level of detail in the requirements. During ”normal” design it might be enough to specify the need for, for example, a pipe with a certain length and diameter. In the case of circular design, it is important to also specify the material the pipe needs to consist of and in which way it should be attached to other parts of the system.

Once the requirements have been identified, the next step in defining the system is to define the functions. A function often consists of a verb and a noun/object (The Mathworks, 2020) and the in and outflow of a function is information, energy and/or material (Hopman, 2021). So it is a task or activity that must be performed to achieve a desired outcome. Functions are mostly the result of operational requirements. Because functions describe an action that needs to be performed, circularity is hard to capture in terms of functions. This means, that the influence of the circular requirements is minimised in this step of the systems engineering because the operational requirements, such as ”lift objects and materials” say nothing about circularity.

Once the requirements and functions have become clear, logic comes into place to see where logical connections can be made. However, this is also a step that needs feedback, because in the next step, the physical components will be defined based on requirements and functions. When multiple components can be combined into a logical module, this step needs to be repeated to enable that. Applying logic to the design is something that comes back in the key indicator of modularity; if systems or parts are connected in a certain way, they will be or not be suitable for repair, remanufacturing, recycling, etc. This means that in the phase where the components, which then again consist of parts, are identified, these components need to be connected in a modular way that allows for these actions.

By use of the identified requirements, functions and logical connections, physical elements for the system can be selected. There is no clear step-by-step process on how to do this, but it is an iterative process where the level of detail gets more and more clear with every step. A way to explore the options and make a decision between different possibilities is a morphological chart as presented by Zwicky (1969). The goal of the Morphological chart is to provide a structured approach to concept generation to widen the area of search for solutions to a defined design problem (University of Cambridge, 2016). To visualise this, the functions are listed in the first column, and the possible solutions are listed in the rows.

Every time the requirements, functional and logical structure have been defined, the market or in-house availability of a physical element should be checked that meets the RFL structure. In case it is not available, the RFL structure should be brought to a deeper level of detail. In case there is no further level of detail possible then it should be checked if multiple parts or components can be combined into a logical module. This stresses the need to constantly make the connection between the physical and logical analysis.

Step 6: Validate the (re)design

As a way of checking whether or not the physical (sub-)system fulfils the desired functions, and whether these functions meet the requirements, a validation matrix can be filled in and to check the circular requirements the level of circularity can be measured. The validation is also known as a Product Management Map (PMM) and is shown in Figure 5. The PMM consists of four matrices where requirements are checked to functions (QFD), requirements to physical solutions (RTM), functions to physical solutions (DPM), and one where the interfacial connection is mapped between physical solutions. The

colour of the dot indicates the strength of the relationship between the requirements, functions and physical solutions. The darker the dot, the stronger the relationship. After the PMM has been filled out, the designer can see whether the physical solutions match all functions and requirements and if this is not the case, the designer can adjust the design or the requirements/functions.

To see whether or not a system meets the requirements in terms of circularity, the level of circularity needs to be measured throughout the design process and at the end of the design process. This can be done following the same procedure as described in Step 3. However, an advantage is that during the design a good overview of the whole system and its connections is already available. This makes it ”easier” to make the breakdown of systems, sub-systems, components, etc. For this step, it is very important that, in case the circularity was also measured in step 3 an existing system, the same level of detail for the measurement is taken. Otherwise, the comparison is not fair and can result in an unreliable outcome. In case the outcome of the circularity measurement is not sufficient to meet the requirements, the design is not finished and there is a need for a designer to continue making alterations until all requirements are met.

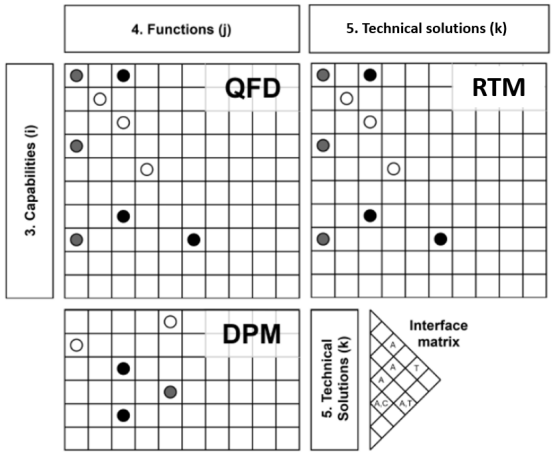

(a) Product Management Map

QFD/DPM	MIM	Score	Symbol
Strong relationship	High impact	9	●
Moderate relationship	Medium impact	3	◉
Weak relationship	Low impact	1	○
No relationship	No impact	0	

(b) Legend of the product management map

Figure 5: The Product Management Map and the meaning of its connections (Kana, 2021)

CASE STUDY

To test the suggested framework, a case study is executed. This case study will focus on the wheelhouse of a vessel. The choice for the vessel and the wheelhouse will be first elaborated upon and after this all steps of the framework will be completed.

Step 1: Identify the goal and overall mission

This goal and mission are often defined by a client that has a need for a (re)new(ed) system or is caused by a change in regulations which makes the existing system obsolete. In this case, Damen Shipyards wishes to create a new design for a wheelhouse. The chosen goal for the system is; To create a space from where the crew can operate and control the complete vessel. The choice for this goal is consistent with the capabilities of a current wheelhouse.

Regarding circularity, the overall mission and goal is to design and build the systems in the most circular way possible whilst following the 10R principles

Figure 6: Visual of the RSD Tug 2513 (Damen Shipyards, 2023)

for a circular economy. This does not mean that the goal is to make a 100% circular product or system, but that the system should be as circular as possible with the current technologies whilst also meeting the general requirements.

Damen Shipyards made a new, graphic design for a wheelhouse of a tug in 2019. Because the design of the ”new” wheelhouse is in line with the design of the current tug boat type RSD Tug 2513, this is the vessel type that will be assessed. It can be concluded that there is a system present on the RSD Tug 2513 that meets the general goal but does not meet the circular goal (scenario 2). Therefore the current wheelhouse will be assessed in Step 2 and 3 of the case study.

Step 2: Identify and breakdown system, sub-system, components, sub-components, and parts

The wheelhouse is seen as the main system here and will consist of sub-systems. These sub-systems are identified by the information available at Damen Shipyards To limit the physical boundaries of the wheelhouse, it has been chosen to view the wheelhouse as everything inside (and including) the superstructure of the wheelhouse until the floor of the bridge deck. it is almost impossible to discuss every component in the wheelhouse and after that every part since there are so many components and parts. Therefore it has been chosen to select five sub-systems and examine them further. The sub-systems' names might sound like they are components or parts but sub-systems consist of multiple components and these components again out of parts.

- The captain's chair
- The consoles
- The windows
- The superstructures
- The floor

As an example, the breakdown of the floor will be shown. Similar steps have been taken to analyse the other four sub-systems. The floor that will be assessed is not the floor presented in the RSD Tug 2513 at this moment, but the floor present in the ASD Tug 2312. This is because the floor in the RSD Tug 2513 is supplied by an ”old” supplier, whilst Damen Shipyards is shifting toward the new supplier for their standardisation of the tug. This new standard is already present on the ASD Tug 2312 and this vessel has dimensions comparable to the RSD Tug 2513, therefore the floor on this vessel will be analysed. All the components and parts are identified and shown in Figure 7a

Sub-system	Components	Parts
Floors	Floating floor	Two-component polyurethane cast floor
		Two-component epoxy primer
		Electro galvanized steel plate (2mm)
		Bonding adhesive
		Electro galvanized steel plate (3mm)
		Steel strip
		Insulation
		Self-levelling mortar
		Primer
		Visco Elastic Mortar (2mm)
		Glue
	Floor covering	Two-component seal layer
		Coating, Coloured chips
		Two-component seal layer
		Two-component decorative resin
		Synthetic floor covering

(a) Breakdown of the components and parts of the sub-system ”Floor”.

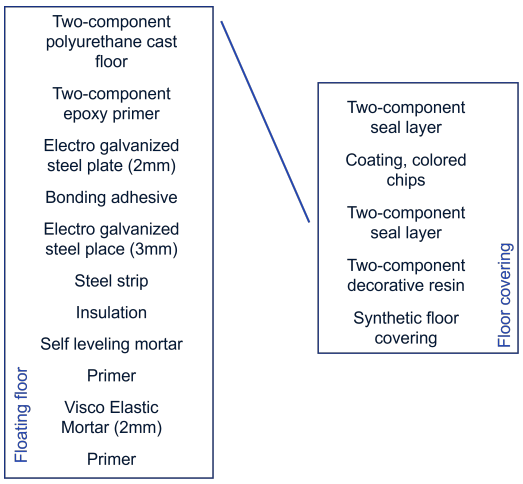

(b) Logical and Physical architecture of the floor

Figure 7: The breakdown into components and parts on the sub-system ”Floor”

As can be seen in the breakdown, the floor consists of sixteen layers made from a lot of different materials. The layers are glued together and quite some layers are cast. The floor is made of primers, followed by isolation, covered with steel plates, and on top of that cast floor covering. The physical and logical architecture of the floor are shown in Figure 7b.

Step 3: Determine the current level of circularity of existing design

The circularity level of current sub-systems will be analysed to show the need for a redesign when the circularity level does not meet the requirement. To measure the circularity of the five sub-systems, the weights need to be known, but also information about the key indicators needs to be acquired. To acquire the weight of different sub-systems, the ”weight calculation” of the whole vessel can be used. In the weight calculation, the weights of all systems in the vessel are listed per system code. The system codes are specific for Damen Shipyards and divide the vessel into sections. To gather information about the key indicators, multiple paths have been explored. For the inflow, the most important indicator is the material choice. Information about the material of the components and parts can be often found on the bill of material of the sub-systems. However, the process of figuring out exactly what part of the material inflow which is stated on the bill of material is circular, is very hard. To determine the source of the material that is used in the four different sub-systems, the suppliers of the parts were contacted. Where data about the type of inflow was unavailable, use was made of the material database of Ansys Granta Edupack (2006). The lifetime of the sub-systems that were selected is therefore very likely to be equal to the industry average because they set the industry average. For this reason, it was chosen to not use the calculation of the utility (X) in the calculation of the MCI because the value for the utility will be equal to 1. Because the systems that are analysed are not yet at the end of their lifetime, the outflow is not 100% sure. However, looking at the key indicators we can make an estimation or determine the potential regarding the destiny of the sub-systems at the end of life. For the outflow of materials, no standardised database exists and common practices were researched that will be discussed per sub-system

Finally, the calculated circularity of every sub-system is divided into circular inflow, outflow and the total circularity. The results are shown in Table 1.

Table 1: Results of the circularity assessment of the five sub-systems

	Inflow	**Outflow**	**Total MCI**
The Captain’s chair	64%	94%	79%
The Consoles	19%	100%	59%
The Windows	14%	97%	57%
The Superstructure	35%	93%	67%
The Floor	19%	0%	9.6%

The combined circularity of these systems comes to 60%. This is mostly due to the superstructure’s significant influence caused by its weight. Out of the five sub-systems, the floor has the lowest MCI mostly due to the lack of modularity and material choices in this sub-system. Due to the lack of modularity and the use of glue, the materials are not separable at the end of life, resulting in a circular outflow of zero per cent. Looking at the weight of the five sub-systems that were selected in comparison to the total weight of the vessel, the systems represent a small fraction of 2.62% of the total vessel weight.

It is important to note that the percentages show the potential circularity and not the actual circularity since the systems are still operable and have not been shifted towards the end-of-life phase. Recycling is at this moment the most commonly used method to keep materials in the loop. However, recycling should be a last option when looking at the 10R principles and therefore the application of refurbishment, remanufacturing and repurposing should be considered more often. To do this, companies need to communicate with their supplier to explore the options of taking back products by the suppliers but also contact with other organisations that can help enable these strategies. Because the floor has the lowest MCI score and there is room for improvement, the floor will be worked out in more detail in the next steps. The low circularity of the floor is a result of the lack of non-virgin materials in the inflow and the low modularity, making it hard to separate materials for recycling/reuse/refurbishment at the outflow. Step four will still look at the life cycle of all five systems with an additional

focus on the floor, and steps 5 and 6 will only be completed for the floor.

Step 4: Map the system life cycle and associated stakeholders

The life cycle of the five presented sub-systems is different. This is because the chair is designed once and then manufactured many times because it is a universal product made by an ”independent” supplier. This is contrary to the superstructure and windows, which are specifically designed for the RSD Tug 2513. The consoles are a bit in between the two since they are also used on other vessels but are still quite specifically designed for vessels built by Damen Shipyards. The floors have a standard design but are tailor-made in size for the application on the RSD Tug 2513. The Damen RSD Tug 2513s are not so-called ”one-off” vessels so this means that there will not be a specific design for every new vessel that is requested but will be sold multiple times based on the same design. It can be concluded that the chosen sub-systems can be divided into two categories; Unique products and Multi-user products. A Unique product is identified as a product that is designed specifically for this vessel type and which cannot be used on other vessels, an example being the windows and superstructure. A multi-user product is a product that is usable in multiple vessel types or maybe even other types of systems, an example being the captain’s chair and the floor. These two products have different life cycles because the design and manufacturing process is not the same. Multi-user products can be built in stock whilst unique products are built once the product has been sold.

Looking at the current floor, the design process was done in close collaboration with Damen Shipyards’ Research and Development department. The most prominent stakeholders in this process were thus the development departments of both the supplier and Damen Shipyards, but also other suppliers of the floor were involved to see what the physical options were that met the requirements. Next to that, a classification was involved with the RSD Tug 2513 design to get the vessel class approved. At this moment, the floor is quite a linear product following the flow that is presented in Figure 8 with associated stakeholders.

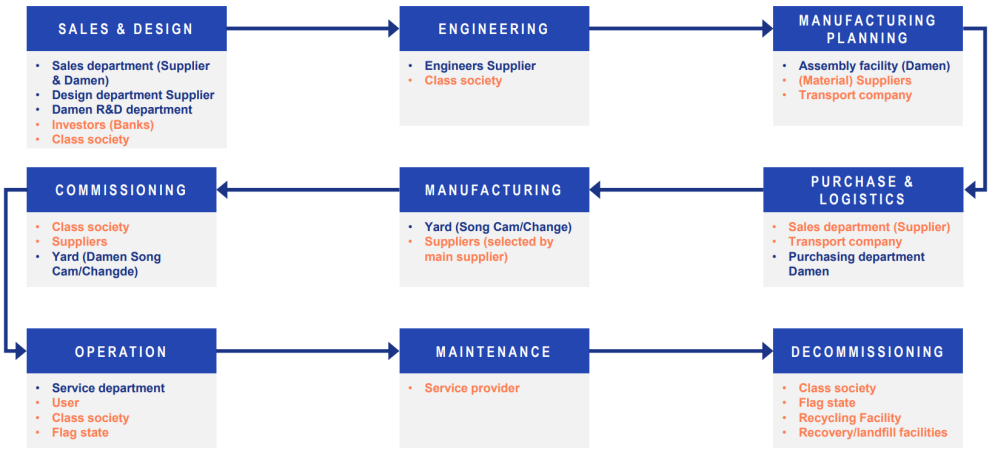

Figure 8: The life cycle and associated stakeholders for the current, linear floor

The figures show the current situation, but to shift to a circular approach, the flows will also have to shift from linear to circular loops. The circular loop is shown in Figure 9. In this shift, the connection needs to be made between the end-of-life stage and the design stage. This connection is not necessarily a material flow connection but needs to be a knowledge connection. Also, other flows start playing a role. Maintenance is extended with repair, refurbishment and remanufacturing and will loop back to the purchasing and logistics. Decommissioning is extended with recycling and will also loop back to purchasing and logistics It is convenient for a client such as Damen Shipyards if the suppliers have a take-back process to repair, refurbish and remanufacture their systems. The role of suppliers in a circular material flow can be way more important than in a linear flow. Ideally, the supplier is willing to take back their supplied system at any time so in case of obsolescence of any kind the system can still come to good use. However, this means that a repair, refurbishment, remanufacturing

or even recycling process needs to be set up by the supplier. This supplier might in itself also be dependent on suppliers and so on. This means that to get the re-looping cycles in place a new supply chain needs to be set up where decommissioning parties, suppliers, purchasing and logistics and all circularity-enabling companies play a role.

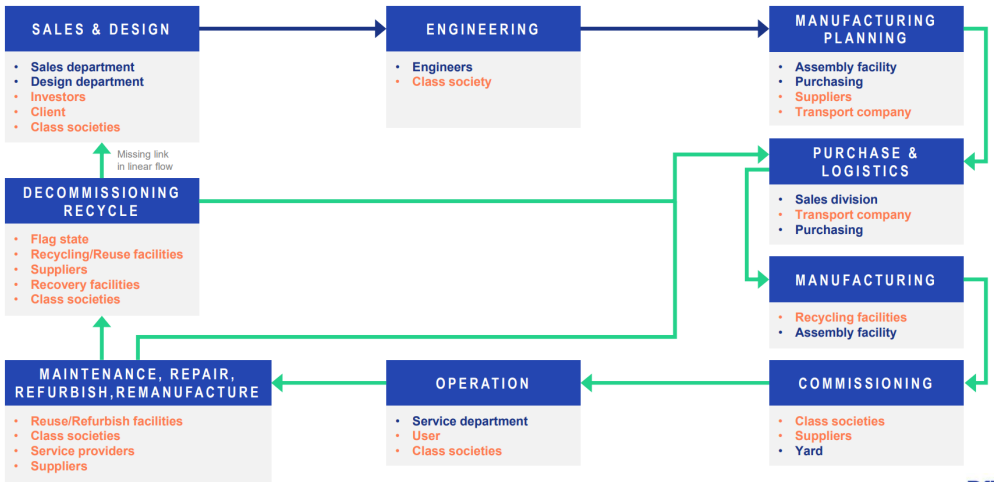

Figure 9: The life cycle and associated stakeholders for a circular floor

Step 5: (Re)design the system by use of the RFLP method, applying circularity principles

With all stakeholders identified, their requirements can be analysed. After that, these requirements translate into functions, these functions into a logical structure and in the end into a physical system. It is important to note that the goal is not to design the best floor technically, but the goal is to test the framework and show ways in which circular design strategies can be used for maritime systems.

During the design phase, there are three main stakeholders having a say: The design department of the supplier, the client (Damen) and class societies. Where the design department has to implement the requirements of the client and class societies. The eventual overview of requirements has been visualised in a breakdown shown in Figure 10.

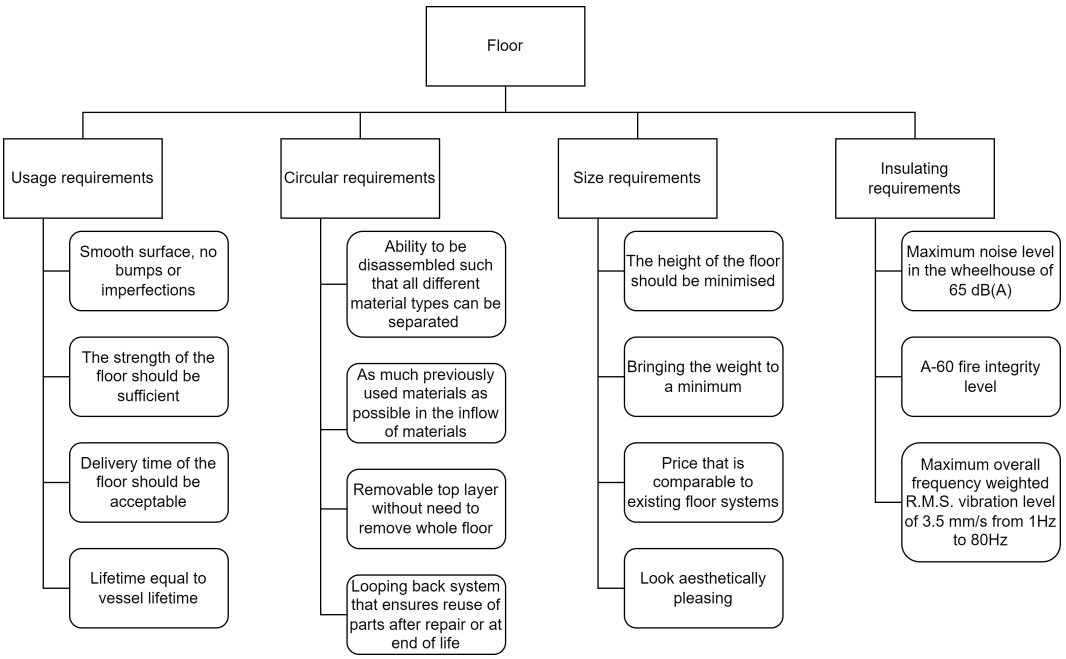

Figure 10: Requirement breakdown structure for the floor in a wheelhouse

The main function of a floor is to be an isolating layer whilst providing a standing surface. The requirements can also be translated into more detailed functions. These functions can again be visualised in a breakdown structure. This is done in Figure 11. It can be concluded that quite some requirements cannot be translated to a function, but are more performance and physical requirements. The circular requirements also can be categorised as this type of requirement and are therefore not translated into functions.

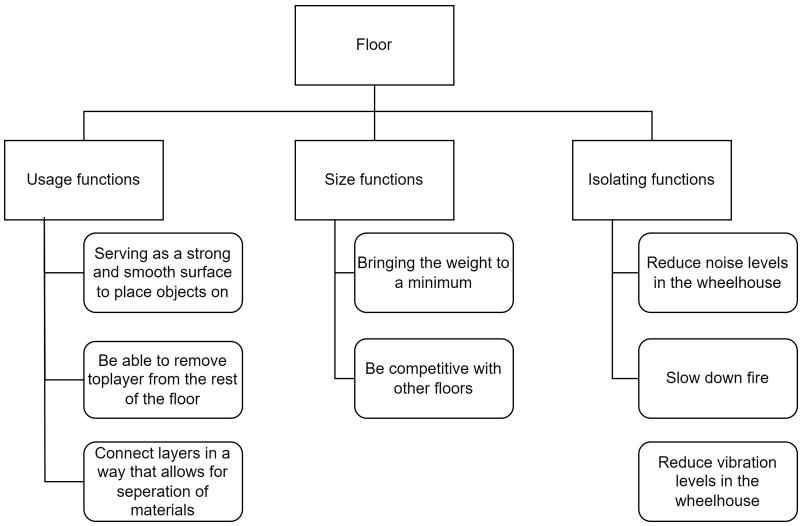

Figure 11: Functions breakdown for the floor

In the logical phase, the focus should be on the composition of the system and the connections between the different components and parts. Common sense plays a role here in making logical connections between parts to combine them into components and in the end combine the components into systems. Some of these connections have already been made by cate-

gorising the requirements and functions into different subjects.

To come from the RFL overview to a physical solution, all possible options have to be considered. This is by use of a morphological chart. For the functions, multiple viable solutions have to be researched. This is done by literature research into materials, shapes, forms and other solution types that can fulfil the set functions. A morphological overview of the solutions linked to the functions is shown in Table 2. In the morphological overview, several lines have been drawn that show the best solutions in terms of price, weight, circularity and height. This way, several combinations of options can be explored.

Table 2: Morphological overview of the physical solutions matches with the functions

Function	Solution 1	Solution 2	Solution 3	Solution 4	Solution 5	Solution 6	Solution 7
Smooth surface	Synthetic cast floor	Carpet	Laminate	Steel plates	Vinyl	PVC	Carbon fibre
Removable top layer	Carpet	Laminate	Vinyl	PVC			
Strong surface	Galvanized steel	Carbon fibre	Aluminium	Cement			
Connecting two layers	Primer	Glue	Welding	Bolds and nuts	Magnets	Robe	Staple
Reduction of noise levels	Isover isolation	Visco-elastic mortar	Self leveling mortar	Stonewool	Cement	Steel plates	
Slowing down fire	Steel plates	Fire resistant glass	Concrete	Fire-retardend treated wool	Iron		
Reduction of vibration levels	Stonewool	Isover isolation	Visco-elastic mortar	Cement	Steel plates		

Cheap
Lightweight
Circular

After looking at the circularity of the current floor, it can be concluded that even though the lower four layers of the current floor might not be the most circular option for isolation, they are the best solution in terms of functionality and it is not technically possible to find another, more circular solution that still fulfils all functions. However, the primer can be made with a higher recycled content. The isolating layer will be further complemented with recycled isolation material and two steel plates made of recycled content. On top of the steel, many options are possible and the best option might be to let the client buying the vessel choose the surface as long as it is not a cast floor. For recycling purposes, PVC is the best option preferably in the form of planks that can be clicked together. If preferred, a sub-floor can be added but in terms of noise or vibrations, this should not be necessary. A visual of the redesigned floor is shown in Figure 12. However, to ensure a long lifetime and a good purpose for the materials at the end of the floor's life, agreements need to be made between different stakeholders. Agreements such as the stone wool supplier taking back the wool for recycling or the supplier of the PVC laminate to reuse the laminate again on other vessels.

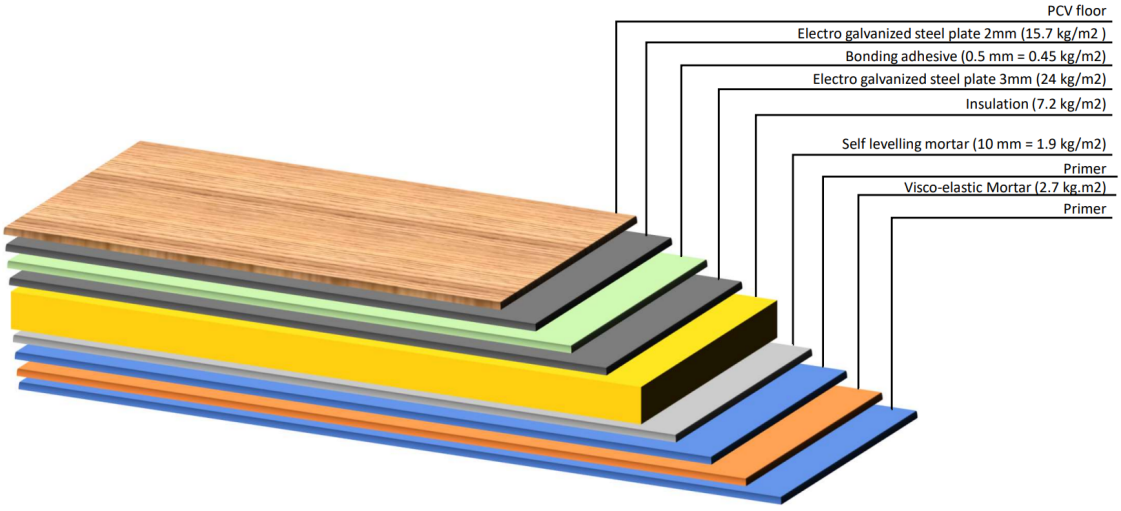

Figure 12: Visual of the redesigned floor

Step 6: Validate the (re)design

As a final step of the framework, the redesign will be tested to the set requirements and functions, but will also be tested on the new circularity level. After this, it can be concluded whether or not the proposed solution is an improvement compared to the existing system.
In Table 3, the PMM is filled out for the redesigned floor. It can be seen that all requirements are matched to functions and the other way around. Additionally, all requirements and functions are translated into physical solutions. Therefore it can be concluded that, in terms of requirements and functions, the redesign is a viable replacement of the current design. However, for some requirements, there is only a weak relationship matched to a function or physical solution. So in case a new design is made, these requirements are where improvements can be made.

To further validate the design, once again, the circularity of the system will be measured. To compare the ”old” floor and the redesigned floor, the circularity level of the ”old” floor will also be calculated at the same level of detail as the new floor is built up. It can be seen that with the higher level of detail, the circularity of the ”old” floor has increased a bit. However, comparing it to the new floor, the redesign shows a way higher circularity outcome. The table with the calculation is shown in Table 4.

The circularity of the floor has gone up from 15% to 90.5%. The biggest difference can be spotted in the outflow of the materials. For the ”old” floor, there is no potential to win back materials due to the construction of the floor, but also due to the lack of agreements between stakeholders. For the redesign, all stakeholders will have to be on board to be able to keep the parts and materials in the circular loop. This means that with every supplier, agreements have to be made for taking back materials, or a separate stakeholder needs to be found that will reuse the materials. As an extra in-depth analysis, also alternative scenarios were researched where different requirements were left out.

Table 3: Filled in Product Management Map for the redesigned floor

		Functions								Physical solution			
		Serving as a strong and smooth surface to place objects on	Be able to remove toplayer from the rest of the floor	Connect layers in a way that allows for separation of materials	Bringing the weight to a minimum	Be competitive with other floors	Reduce noise levels in the wheelhouse	Slow down fire	Reduce vibration levels in the wheelhouse	Combination of Primer, VEM and Self leveling mortar	Isolation wool	Steel plates with bonding adhesive	PVC floor covering
Requirements	Smooth surface, no bumps or imperfections	●	○	○			○					◍	●
	The strength of the floor should be sufficient	●	◍		○		○	○	○			●	
	Delivery time of the floor should be acceptable					○				○	○	○	○
	Lifetime equal to vessel lifetime	○	○	○						○	○	○	○
	Ability to be disassembled such that all different material types can be separated		◍	●	○	○	○			○	●	○	●
	As much previously used materials as possible in the inflow of materials				○	○				○	●	◍	●
	Removable top layer without need to remove whole floor	○	●	○		○						◍	●
	Looping back system that ensures reuse of parts after repair or at end of life		○		◍	○					●	◍	◍
	The height of the floor should be minimised				○	○	○	○	○	◍	◍	◍	◍
	Bringing the weight to a minimum				●					◍	○	◍	◍
	Price that is comparable to existing floor systems		○			●				◍	◍	◍	◍
	Look aesthetically pleasing	◍				○				○	○	○	●
	Maximum noise level in the wheelhouse of 65 dB(A)						●		○	●	●	●	
	A-60 fire integrity level							●			◍	●	
	Maximum overall frequency weighted R.M.S. vibration of 3.5 mm/s from 1Hz to 80Hz						◍		●	●	●	●	
Physical solution	Combination of Primer, VEM and Self leveling mortar				○	○	●	○	●				
	Isolation wool		◍	◍	◍	○	●	◍	◍	C,S			
	Steel plates with bonding adhesive	●	●	○	○	○	●	◍	●	S	C,S		
	PVC floor covering	●	●	●	○	◍				S	S	C,S	

The goal was to design three alternatives for the floor by leaving out requirements, compared to the previous sections. Since this research is about increasing circularity, the circular requirements were not left out. Looking at the influence of requirements on the design, it can be concluded that there is a big difference between the influence of the requirements on the design. The requirement to reduce the noise and vibration levels has by far the biggest influence. Since it is a requirement also by class to have a maximum noise and vibration level in the wheelhouse, this is not a requirement that is likely to be dropped, but one that might change with the ongoing developments regarding alternative propulsion options. To increase circularity, it could be seen that giving in on weight and cost can contribute in a positive way.

Next to that, this case study focused only on a few sub-systems in the wheelhouse, whilst when a whole vessel has to be designed, this will be a more time-consuming process, with more stakeholders and more agreements to be made. Also from this point of view, it is important that stakeholders assess their own process on the topic of circularity to make of designing circular vessels possible for the design and shipbuilding companies. Additionally, agreements have to be made with the owner of the vessel to actually use the supplier agreements to keep the materials in the loop.

Table 4: Comparison in MCI level of the ”old” and ”new” floor design

System	Parts	Mass	Inflow		Outflow					MCI	
		Mass [kg]	Virgin	Recycled	Refurbishment	Remanufacturing	Repurposing	Recycling	Recovery	MCI	Total MCI
Redesigned floor	PVC laminate	63,84	0,00%	100,00%	100,00%	0,00%	0,00%	0,00%	0,00%	1	0.905
	Steel plate	125,286	0,00%	100,00%	0,00%	100,00%	0,00%	0,00%	0,00%	1	
	Bonding adhesive	3,591	100,00%	0,00%	0,00%	0,00%	0,00%	100,00%	0,00%	0,5	
	Steel plate	191,52	0,00%	100,00%	0,00%	100,00%	0,00%	0,00%	0,00%	1	
	Insulation	57,456	50,00%	50,00%	0,00%	0,00%	100,00%	0,00%	0,00%	0,75	
	Self leveling mortar	15,162	100,00%	0,00%	0,00%	0,00%	0,00%	100,00%	0,00%	0,5	
	primer	0,1	70,00%	30,00%	0,00%	0,00%	0,00%	100,00%	0,00%	0,65	
	Visco elastic mortar	21,546	100,00%	0,00%	0,00%	0,00%	0,00%	0,00%	100,00%	0	
	Primer	0,1	70,00%	30,00%	0,00%	0,00%	0,00%	100,00%	0,00%	0,65	
Original floor	Two-component seal layer	1,1172	100,00%	0,00%	0,00%	0,00%	0,00%	0,00%	100,00%	0	0.149
	Coating, Coloured chips	0,399	100,00%	0,00%	0,00%	0,00%	0,00%	0,00%	100,00%	0	
	Two-component seal layer	1,1172	100,00%	0,00%	0,00%	0,00%	0,00%	0,00%	100,00%	0	
	Two-component decorative resin	19,152	100,00%	0,00%	0,00%	0,00%	0,00%	0,00%	100,00%	0	
	Synthetic floor covering	0,27132	100,00%	0,00%	0,00%	0,00%	0,00%	0,00%	100,00%	0	
	Two-component polyurethane cast floor	16,758	100,00%	0,00%	0,00%	0,00%	0,00%	0,00%	100,00%	0	
	Two-component epoxy primer	0,1	100,00%	0,00%	0,00%	0,00%	0,00%	0,00%	100,00%	0	
	Steel plate	125,286	62,50%	37,50%	0,00%	0,00%	0,00%	0,00%	100,00%	0,1875	
	Bonding adhesive	3,591	100,00%	0,00%	0,00%	0,00%	0,00%	0,00%	100,00%	0	
	Steel plate	191,52	62,50%	37,50%	0,00%	0,00%	0,00%	0,00%	100,00%	0,1875	
	Steel strip	57,456	62,50%	37,50%	0,00%	0,00%	0,00%	0,00%	100,00%	0,1875	
	Insulation	18,8328	100,00%	0,00%	0,00%	0,00%	0,00%	0,00%	100,00%	0	
	Self leveling mortar	15,162	100,00%	0,00%	0,00%	0,00%	0,00%	0,00%	100,00%	0	
	Primer	0,1	100,00%	0,00%	0,00%	0,00%	0,00%	0,00%	100,00%	0	
	Visco Elastic Mortar	21,546	100,00%	0,00%	0,00%	0,00%	0,00%	0,00%	100,00%	0	
	Primer	0,1	100,00%	0,00%	0,00%	0,00%	0,00%	0,00%	100,00%	0	

DISCUSSION

This study has shown that circularity can be implemented in ship design, with relative simple process adjustment. After testing this framework by a case study where the wheelhouse of an RSD Tug 2513 was subjected to the framework, it became clear that the framework has multiple limitations:

- The analysis/optimisation only looks at the inflow and outflow of materials in the end product, not at the materials used during the production or dismantling process, nor does it look at recycling efficiencies.
- The MCI calculation is based on weight, whilst hazardous and rare materials should also be considered an essential factor during the design phase.
- It is hard to compare a system’s lifetime and use frequency to industry averages because the systems that are analysed set the average.
- The level of detail of the framework is highly dependent on the information available from suppliers, often resulting in an estimation based on industry averages with general weights.
- The use of industry averages is not a representative way of calculating the circularity level of a product.

Looking at all these limitations, it can be concluded that the provided framework is a concrete step in the right direction but further extensions can be made to solve these limitations. However, to implement the framework several steps are required.

First of all, a universal definition of circularity needs to be set to make sure all stakeholders are on the same page. After this, all stakeholders need to assess their own part of the supply chain in order to map the current status of the systems and set a circular baseline. Starting with the material extraction and ending with the final product going to the recycling facility, or even better, being reused, remanufactured, refurbished or repurposed. After successfully inventorying the current status of the circular economy in the ship design process, KPIs can be set for companies to determine a vision and future goals with regard to circularity. These KPIs can help a company with designing a new system or selecting (new) suppliers. After all this, the framework can be used. Since, in the ideal case, all stakeholders have already mapped their progress in terms of circularity, designers can now optimise their design based on all requirements, functions and logical structures set based on the needs in terms of general and circular demands.

For all this to work, incentives should be there for designers, such as the design department of Damen Shipyards, to start designing vessels with circularity in mind. Incentives can be government regulations and rules, but also clients asking for this. Additionally, the new CSR reporting requirements will help to give a push in the right direction for companies to start thinking about their circularity.

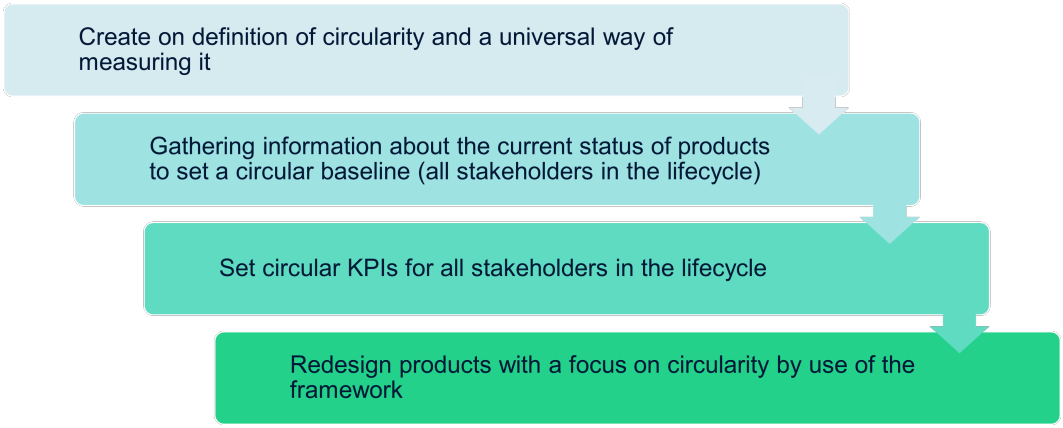

Figure 13: Steps for the implementation of the framework

Additionally, to continue research on the topic of circular ship design, multiple recommendations are formulated:

- When performing an analysis of the environmental impact of a system, often only the CO_2 emissions are taken into account (Heijungs and Suh, 2002). It would be preferable to have a method that performs a life cycle analysis that takes both the ”general” environmental impact and the circularity of the system into account. This way, trade-offs can be made between different systems whilst having a complete image of the possibilities.
- At this moment, circularity does not have a value that is expressible in a number. This results in companies having a conservative view towards circularity, often assuming it is more expensive than systems that follow a linear lifetime. Therefore it would be wise to perform a study into the reduction of the environmental impact a fully circular product makes, but also review the reduction or increase of the cost and lead time of a circular product and compare this to a non-circular product.
- The goal of a shipbuilding company such as Damen Shipyards can be to become 100% circular, but the process to get there involves many stakeholders. To start with implementing more circular components in the end product, a start could be to perform research similar to this research at an equipment manufacturer to see the more practical potential and also have the potential to change the business model of this manufacturer towards one where used products are taken back and directly reused in the production process to (re)new(ed) products.

- To help organise the available information on a system with regard to circularity, it would be helpful to set up an (international) system that captures all relevant information in a document (Circularise, 2023). This document could then be used during the lifetime and at the end of the life of a system to see the potential of all materials used in the system. This way, a client will also be able to compare products on their circularity level.

CONCLUSION

To include circularity in the ship design process multiple principles and frameworks were combined. First of all, for the definition and ranking of circularity, the 10R framework was deemed the most appropriate, in combination with the adjusted MCI method for the calculation of the circularity level. With the 10R framework also come 10 design strategies for consumer goods that have been compared to the ship design approach of systems engineering. As a last theoretical step, key indicators were identified that influence the circularity of a system. After all this, the 10R framework for the definition of circularity, the corresponding circular design strategies, the method of systems engineering, and several key indicators were combined into a framework that represents a step-by-step guide on how to design a circular system. The main purpose of the framework is to prove there is a valid need for a (re)new(ed) system and starting at the beginning with the design process is to fully focus on a system's function instead of trying to improve an existing system that might not be the optimal solution for the function it needs to fulfil. To make the framework work, contact with the suppliers is a very important aspect since the information required to fill out the steps has to come from them. Next to that, changes to make products more circular will also require suppliers to change with regard to design and be more involved during the whole life cycle of a system to ensure that materials are kept in the circular loop.

REFERENCES

Alam, I., Barua, S., Ishii, K., Mizutani, S., Hossain, M. M., Rahman, I. M., and Hasegawa, H. (2019). Assessment of health risks associated with potentially toxic element contamination of soil by end-of-life ship dismantling in Bangladesh. *Environmental Science and Pollution Research*, 26(23):24162–24175.

Ansys Granta Edupack (2006). Eco properties: recycling and disposal.

Ashby, M. and Johnson, K. (2003). The art of materials selection.

Balder, M. (2021). Ontwikkeling ISO-normen voor circulaire economie.

Bocken, N. M., de Pauw, I., Bakker, C., and van der Grinten, B. (2016). Product design and business model strategies for a circular economy. *Journal of Industrial and Production Engineering*, 33(5):308–320.

Circularise (2023). Take control of your supply chain with digital product passports.

Coalition circular accounting (2023). Leveraging corporate sustainability reporting for circular transformation.

Cramer, J. (2020). *How Network Governance Powers the Circular Economy Ten Guiding Principles for Building a Circular Economy, Based on Dutch Experiences*.

Damen Shipyards (2023). RSD Tug 2513.

Di Maio, F. and Rem, P. C. (2015). A Robust Indicator for Promoting Circular Economy through Recycling. *Journal of Environmental Protection*, 06(10):1095–1104.

EFRAG (2022). Draft European Sustainability Reporting Standards.

Ellen McArthur Foundation (2019). Circular economy systems diagram.

Erikstad, S. O. (2018). Design Methods for Ocean Engineering Systems: Developing requirements.

European Commission (2020a). A new Circular Economy Action Plan For a cleaner and more competitive Europe.

European Commission (2020b). Shipbreaking: Updated list of European ship recycling facilities to include seven new yards.

Goddin, J., Marshall, K., Pereira, A., Design, G., Herrmann, S., Ds, S., Sam, J., Dupont, T., Krieger, C., Lenges, E., Ben, C., Pierce, J., Susan, E., Gispen, I.-J., Veenendaal, R., Per, I., Natureworks, S., Ford, L., Goodman, T., Vetere, M., Graichen, F., Anu, S., Tetrapak, N., and Cockburn, D. (2019). Circularity Indicators: An Approach to Measuring Circularity.

Heijungs, R. and Suh, S. (2002). *Development of LCA software for ships and LCI Analysis based on actual shipbuilding and operation*. Kluwer Academic Publishers.

Hopman, H. (2021). From Evans Design Spiral to Systems Engineering MT44035 Design of Complex Specials.

IMO (2015). Recycling of ships.

Kana, A. (2021). Introduction to modular ship platforms.

Kaplinsky, R. and Morris, M. (2000). A Handbook for Value Chain Research.

Kimura, F., Kato, S., Hata, T., and Masuda, T. (2001). Product Modularization for Parts Reuse in Inverse Manufacturing.

Kossiakoff, A., Sweet, W. N., Seymour, S. J., and Biemer, S. M. (2011). *Systems Engineering Principles and Practice*. 2 edition.

Li, T., Lockett, H., and Lawson, C. (2020). Using requirement-functional-logical-physical models to support early assembly process planning for complex aircraft systems integration. *Journal of Manufacturing Systems*, 54:242–257.

Mikelis, N. (2019). Ship recycling. In *Sustainable Shipping: A Cross-Disciplinary View*, pages 203–248. Springer International Publishing.

Pei, E., Campbell, I., and Evans, M. (2011). A taxonomic classification of visual design representations used by industrial designers and engineering designers. *Design Journal*, 14(1):64–91.

Stahel, W. R. (2016). Circular economy: A new relation with our goods and materials would save resources and energy and create jobs.

Sustainable Shipping Initiative and 2BHonest (2021). Exploring shipping's transition to a circular industry.

The Global Goals (2015). Goal 12: Responsible consumption and production.

The Mathworks, I. (2020). The Benefits of Functional Architectures | Systems Engineering, Part 3.

University of Cambridge (2016). Morphological charts.

wbcsd (2018). Circular Metrics Landscape Analysis.

Zwaginga, J. J. and Pruyn, J. F. J. (2022). An evaluation of suitable methods to deal with deep uncertainty caused by the energy transition in ship design.

Zwicky, F. (1969). Discovery, Invention, Research through the Morphological Approach. *Macmillan*.

Proceedings of 15th International Marine Design Conference (IMDC-2024)
June 2-6, 2024
Amsterdam, the Netherlands

Early Risk Quantification Strategy for Design Space Reduction Decisions in Set-Based Design

J.B. Van Houten[1,*], A.A. Kana[2], D.J. Singer[1] and M.D. Collette[1]

ABSTRACT

Perceptions of feasibility in design spaces are susceptible to change if new and conflicting information becomes available later. Design space reduction decisions made in set-based design can amplify vulnerability to new information if remaining design spaces and present perceptions are unable to adapt. This paper considers different ways new information can alter perceptions of feasibility for complex design problems and introduces an early, probabilistic strategy for quantifying the risk of eliminating potential design solutions based on the vulnerability of remaining design spaces to new information. Emergent designs of a set-based design process gauging this risk are evaluated against one neglecting it for an analogous design problem. Early results indicate that the probabilistic model is able to effectively delay design decisions and prevent lock-in while design space understanding is still growing.

KEY WORDS

Set-based design; Space reductions; Information; Fragility; Risk quantification.

INTRODUCTION

Design decisions made within the web of interdependencies and requirements ingrained in the marine design process produce complex knowledge structures. While different methods have been proposed to characterize the knowledge generation accompanying these decisions (Braha and Reich, 2003; Hatchuel and Weil, 2009; Shields, 2017; Goodrum, 2020), each one seeks to track and better understand the emergence of (or lack thereof) design solutions. Decisions made in set-based design (SBD) build up these knowledge structures gradually, but they also leave design spaces vulnerable to emergent design failures if the information supporting them changes. Providing designers with a tool to understand the potential impacts of new information on a reduced design space after eliminating potential design solutions from consideration would assist them in making more informed space reduction decisions.

Using iteration to make decisions and generate knowledge is an understood reality of many complex design problems (Wynn and Eckert, 2017). Different studies have investigated how enhancing the allocation of resources (Smith and Eppinger, 1997) or communicative pathways (Mihm and Loch, 2006; Parraguez et al., 2015) between iterative tasks can promote more efficient information flow. As these strategies are improved upon to assist with iterative design decisions, they can fixate a designer's knowledge on one decision path, restricting the solutions that can be attained through others (Page, 2006). Examples of this fixation are shown in Van Houten et al. (2022) where viable solutions within a discipline's design space are significantly limited by the path chosen. In some cases, designers can lose influence if a finite set of absorbing paths constrain the knowledge structures generated from these temporal decision processes (Niese et al., 2015; Kana, 2017).

[1] Naval Architecture and Marine Engineering, University of Michigan, Ann Arbor, USA
[2] Maritime Transport and Technology, Delft University of Technology, Delft, the Netherlands; ORCID: 0000-0002-9600-8669
[*] Corresponding Author: joeyvan@umich.edu; ORCID: 0000-0001-6569-8524

Submitted: 19 February 2024, Revised: 15 April 2024, Accepted: 1 May 2024, Published: 20 May 2024

Conference paper, DOI: https://doi.org/10.59490/imdc.2024.852 e-ISSN: 3050-4864

A consequence of becoming overly fixated on a particular decision path is leaving a design susceptible to emergent design failures. Dong (2017) discusses the prevalence of this problem in product development when companies introduce innovative technologies into their product's existing functional architecture. He argues that integration issues arise before the establishment of their product's physical architecture and should instead be attributed to the solution principles the design team committed to during development. He and others (Shields and Singer, 2017; Goodrum, 2020) insist that understanding emergent design failures requires a shift in viewing them from a product-centric to a knowledge-centric perspective. As Goodrum (2020) explains, a design decision is a commitment to a knowledge structure, and how those decisions affect future design activities will vary depending on how new knowledge integrates with existing knowledge.

Set-based design (SBD) protects against emergent design failures stemming from path fixation by having design decisions focus on eliminating undesirable regions rather than making premature commitments to hard-set characteristics. By delaying commitments and keeping variable sets open, SBD decisions create low-risk knowledge structures (Shields and Singer, 2017) and allow designers to maintain influence over the design problem while their understanding of it grows (Bernstein, 1998; Singer et al., 2009). Advantages of SBD include basing the earliest and most critical design decisions on acquired data, promoting institutional learning within the design environment, encouraging concurrence in the design and manufacturing process, and supporting a search for more globally optimal designs (Ward et al., 1995). These advantages have fueled US Navy interest in making ship design and analysis tools compatible with SBD methods (Doerry, 2012) and applying SBD to various projects such as the Ship to Shore Connector (Mebane et al., 2011), Amphibious Combat Vehicle (Burrow et al., 2014), and Small Surface Combatant (Garner et al., 2015). Despite the advantages, it is still either infrequently applied to problems in industry or generally confined to introductory design stages (Toche et al., 2020). Singer et al. (2009) claim SBD's biggest obstacle in naval design coincides with current government acquisition policies conforming to point-based methodologies. Other hurdles are summarized in McKenney and Singer (2014) and Gumina (2019) and involve having to manage misconceptions *about implementation* and lacking a regimented process *for implementation*.

The SBD implementation process is multifaceted and has disciplines individually explore areas of their design spaces to accumulate information, form perceptions of preferred and nonpreferred areas from this information, and propose space reductions from these perceptions (Bernstein, 1998). A representation of an example design space is depicted in Figure 8 of Andrews (2018) where *space reductions* refer to reducing the range of potential design solutions being left open. A Design Integration Manager (DIM) will then consider the space reductions proposed and the information supporting them to finalize a conceptually robust set of space reductions across all disciplines (Singer et al., 2009). Each of these later steps are directly tied to the information gathered at the beginning, so effective decision-making in SBD necessitates robust information. Gembarski et al. (2021) evaluates the robustness of information in decision-making by using Bayesian probabilities to model uncertainties that originate from a scarcity of information. Sypniewski (2019) takes a different approach and assesses how the inherent biases of information that has already been gathered can lead to inadequate characterization of a design space and misinformed decisions. As the robustness of information pertains to decisions made during SBD specifically, research is limited. Doerry (2015) presents a method for measuring the diversity of information in a design space to increase the likelihood of viable solutions being found later; however, this method intends to insure reduction decisions against uncertain information rather than understand the uncertainty permissible for those decisions to remain advisable.

The purpose of this paper is to present a new approach for quantifying the risk of design space reduction decisions in SBD by considering the potential for new information to alter perceptions of feasibility and incite emergent design failures. Although in a much broader sense, the aim of this research is to assess how future information can undo the foundation of knowledge already established through previous design decisions. In the following sections, a brief background on SBD and a design space's fragility (or its vulnerability to new and conflicting information) will first be provided. Next, details of a SBD simulation will be presented for proposing reasonable space reductions. After explaining how the simulation works, an early framework built for assessing the fragility of design spaces and quantifying the risk of space reduction decisions will be explained. The developed fragility framework plugs in at the very end of the space reduction process. Finally, emergent design spaces for simulations performed on a problem analogous to complex design with and without the framework will be observed and discussed.

SET-BASED DESIGN

SBD is a convergent design approach that seeks a final solution through the gradual elimination of design spaces rather than cycles of rework and refinement synonymous with most iterative approaches. Bernstein (1998) describes the *ideal* way SBD should be performed with illustrative help from Figure 1 developed by Dr. William Finch. In the early stages of SBD, disciplines individually explore areas of their design spaces and expand their ranges of potential design solutions. From a marine design perspective, these disciplines may consist of (but not be limited to) a weights division negotiating lightship and deadweight tonnage allotments along with center of gravity positioning, a stability division considering allowable beam and vertical center of gravity pairings, and a structural division contemplating various plate thickness and stiffener sizing schemes. As potential solution spaces are identified by each discipline, they work together to identify areas of overlap between their interdependent design spaces that satisfy all requirements of the design problem. For example, the weights division may have its own displacement and trim requirements to satisfy, but the vertical center of gravity of a load case cannot prevent the stability division from satisfying intact or damage stability requirements, and the lightship allotment must be sufficient for the structural division to satisfy material yielding requirements within a specific safety factor. As a solid understanding of potential design solutions and trade-offs is formed, nonpreferred areas of each discipline's design space are eliminated until a final solution remains.

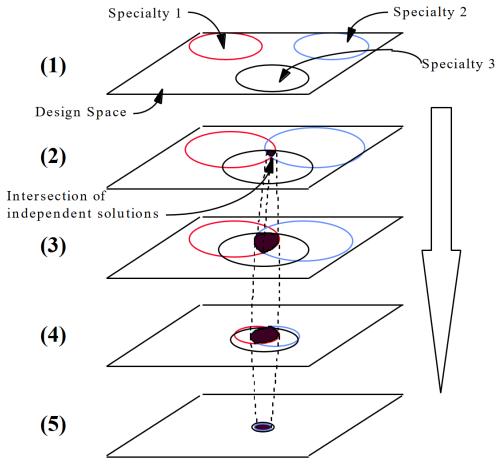

Figure 1: Ideal convergence of the SBD process through gradual elimination of nonpreferred areas (Bernstein, 1998)

Through this process, a major principle of SBD is delaying decisions until the consequences of those decisions are understood (Ward et al., 1995; Singer et al., 2009). During discussions with managers utilizing "set-based concurrent engineering" at Toyota, Ward et al. (1995) learned that a critical aspect of their job is to discourage engineers from making important design decisions too soon. They believe it is necessary to delay decisions to ensure all the requirements of the customer are met while also ensuring that the design is manufacturable. Bernstein (1998) and Singer et al. (2009) discuss the benefits of delaying design decisions from the perspectives of accrued knowledge, committed costs, and stakeholder influence. They explain that knowledge of a design is gathered with time as designers run analyses to build their understanding of the characteristics and requirements driving the process. By delaying decisions through a set-based approach, designers can increase the influence maintained and decrease the costs incurred until the information and existing knowledge supporting these decisions is more robust.

The difficulty of eventually making these reduction decisions is that design spaces cannot be understood absolutely. Different disciplines often manage large design spaces that cannot be explored completely while tolerating analyses with varying degrees of uncertainty. Moreover, it is common for changes in design requirements as well as the fidelity or underlying assumptions of analyses to be introduced throughout the design process that shift preferred and nonpreferred areas. Shields and Singer (2017) assert that space reduction decisions create low-risk knowledge structures while also acknowledging that SBD relies on considerable knowledge generation and decision-making to work effectively. In their words, "Only making decisions when the supporting knowledge is well-understood and is unlikely to change leaves stable knowledge to be

further developed" (Shields and Singer, 2017). Each space reduction decision in SBD is supported by information that is incomplete, uncertain, and susceptible to change. If designers do not account for this uncertainty of information, their reduction decisions may lead to exceedingly fragile design spaces, or design spaces whose perceived feasibility is vulnerable to new and conflicting information. In instances when new information exposes fragile design spaces, designers using a SBD approach cannot simply rely on backtracking and reopening design spaces either, because their design timelines are limited by the considerable time already spent exploring those design spaces in the first place.

Design Space Fragility and Reduction Decisions

To help visualize a design space's fragility, Figure 2 has been created to mirror the third layer in Bernstein's explanation of SBD. In Figure 2, the perceived feasible regions of each discipline are located within the red, blue, and black circles. The green regions signify perceived feasible areas of the design space for one discipline, the yellow regions signify the same perceived feasibility for two regions, and the orange region signifies the same perceived feasibility for all three regions. Suppose the fragility is being assessed from the red discipline's perspective. One source of fragility is attributed to learning new information that alters the perceived feasible space of the red discipline itself, as depicted by the dashed red circle in Figure 3. As it pertains to the red discipline, the pink region captures newly perceived feasible space, and the grey region captures newly perceived infeasible space. If new information shifts the perceived feasible space of the red discipline such that the grey region outweighs the pink region, then that originally perceived design space would have been very vulnerable to the new information. Another source of fragility is attributed to learning new information that alters the perceived feasible space of an interdependent discipline, as depicted by the dashed blue circle in Figure 4. As it pertains to the blue discipline, the pink region captures newly perceived, shared feasible space, and the grey region captures newly perceived, shared infeasible space. If new information shifts the shared feasible space such that the grey region outweighs the pink region, then that originally perceived design space would have also been very vulnerable to the new information. In both scenarios, new information's effect on perceived feasibility is determinant of a design space's fragility.

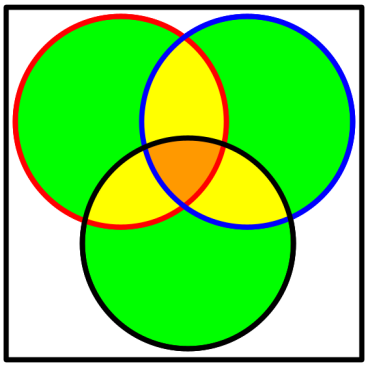

Figure 2: Overlapping regions of perceived feasible spaces for three disciplines of a design problem

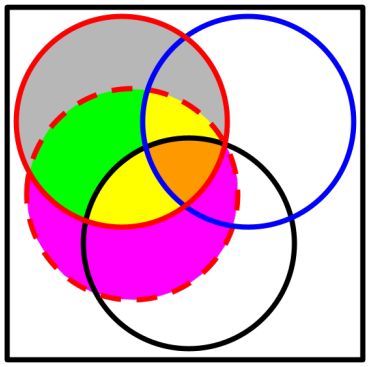

Figure 3: Fragility attributed to design change of main discipline

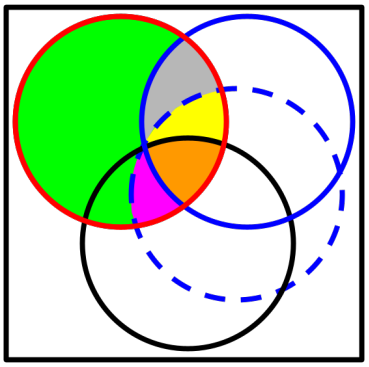

Figure 4: Fragility attributed to design change of interdependent discipline

While a design space's fragility directly corresponds to its vulnerability to new information, that vulnerability can be amplified by the particular space reductions that have previously been made. In both Figure 3 and Figure 4, the DIM may have already decided to eliminate portions of the pink region. If that is the case, disciplines would be left without newly perceived feasible space, meaning that the grey region would further outweigh the pink region. Designers want to avoid space reduction decisions that lead to exceedingly fragile design spaces, yet they must make reductions to keep the design process moving. At each space reduction cycle, every design space is susceptible to increases in design space fragility that can be further exacerbated by previous reductions. And even though the figures have portrayed instances of increasing fragility in the context of new information and previous space reductions, the size of a feasible design space alone does not dictate its fragility. For example, if a multidimensional design space is very large, but one of its input variables only has two feasible values, then that design space is vulnerable to new information from its own discipline and/or other disciplines finding

those two values to be infeasible. By effect, there are varying levels of risk for space reduction decisions due to the varying levels of fragility that result from prior reductions and new information.

Originating Sources of New Information

In the development of solutions to complex design problems, designers are compelled to explore and gain an understanding of their own discipline's design space, integrate the understanding and preferences of designers from interdependent disciplines with their own, and endure changing design requirements and maturing analyses throughout the entire process. Bearing each of these challenges in mind, three different sources of new information are worth considering when characterizing the fragility of a design space: (1) newly explored design points of a directly affected discipline, (2) newly explored design points of an interdependent discipline, and (3) new or updated design requirements or analyses. In this work, only the first originator for new information will be considered, but it is important to keep the other two in mind for future improvements to the fragility assessment process.

To observe how new information originating from newly explored design points of a directly affected discipline can impact perceptions of design space behavior, consider Figures 5 to 6. In these figures, green points represent tested designs that are feasible, red points represent tested designs that are infeasible, green regions represent perceived feasible spaces, red regions represent perceived infeasible spaces, and yellow regions represent spaces of mixed feasibility. With the information from design points presently available in Figure 5, clear regions of feasibility have been formed for the discipline; designers of *this discipline* are perceiving smaller values of *Variable 1* to be feasible and larger values of *Variable 1* to be infeasible. However, those perceptions shift in Figure 6 when new information originating from newly tested design points becomes available. Larger values of *Variable 1* are still perceived as infeasible, but designers have also learned they may have less area to work with for smaller values of *Variable 1* than they previously thought. Before learning this new information, suppose the decision is made to eliminate some of the smallest values of *Variable 1* because, in contrast to this discipline, other disciplines prefer large values of *Variable 1* to small values. Designers of this discipline may be inclined to approve the space reduction thinking they still have plenty of feasible space with which to work. Later, they would regret to learn that the space reduction decision has limited far more feasible solutions remaining for them than they originally anticipated.

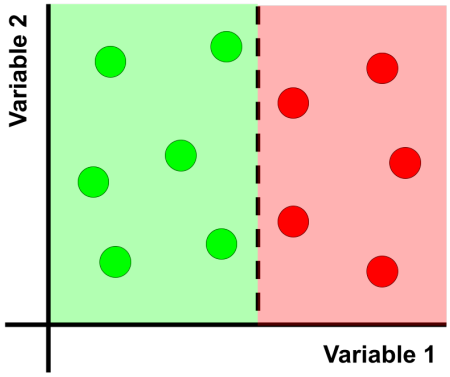

Figure 5: Perceptions of feasibility before sampling new points within primary design space

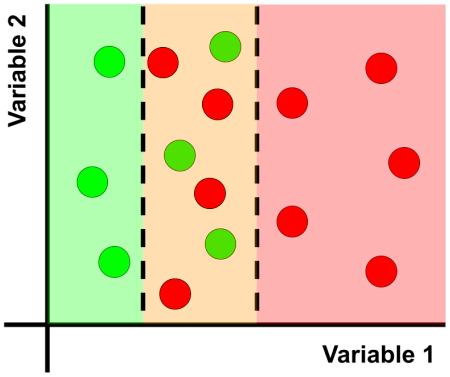

Figure 6: Perceptions of feasibility after sampling new points within primary design space

The intent of a fragility framework will be to protect design spaces against scenarios like the one described. DIMs may be capable of taking proposed space reductions from disciplines and carefully assessing the impact those reductions would have on other disciplines with the information *at hand*, but they lack a tool for understanding the consequences of those reductions if the perceptions formed from that information *changes*. Before introducing an early strategy for quantifying this space reduction risk, a SBD simulation to which a fragility framework can tie in must to be developed.

CREATING A SBD SIMULATION

Before discussing the logic behind a framework intended to evaluate the fragility of design spaces, a SBD simulation that proposes reasonable space reductions is needed. With the simulation, experiments can be run that compare emergent design spaces when there are fragility checks in place compared to when there are not. The decision was made to automate the simulation for a couple of reasons. For one, automating the simulation removes the impact that human inconsistencies would have on the emergent design spaces by ensuring the same criteria are used to explore design spaces and propose space reductions every time. Additionally, automating the simulation speeds up the process and cuts back on the time it would take for a DIM to evaluate the present state of the data and formulate their next exploration or reduction decision. The simulation is not meant to be a perfect replication of how SBD activities are performed and reductions are made because SBD is fundamentally a human-centric process that is driven by knowledgeable designers. A simplified depiction of how the SBD simulation works is shown in Figure 7, while a more detailed depiction of the simulation and the actual Python code can be viewed via the link in the Data Access Statement at the end of this paper. Different parts of the simulation fall under the groupings of problem setup, exploration, or space reduction.

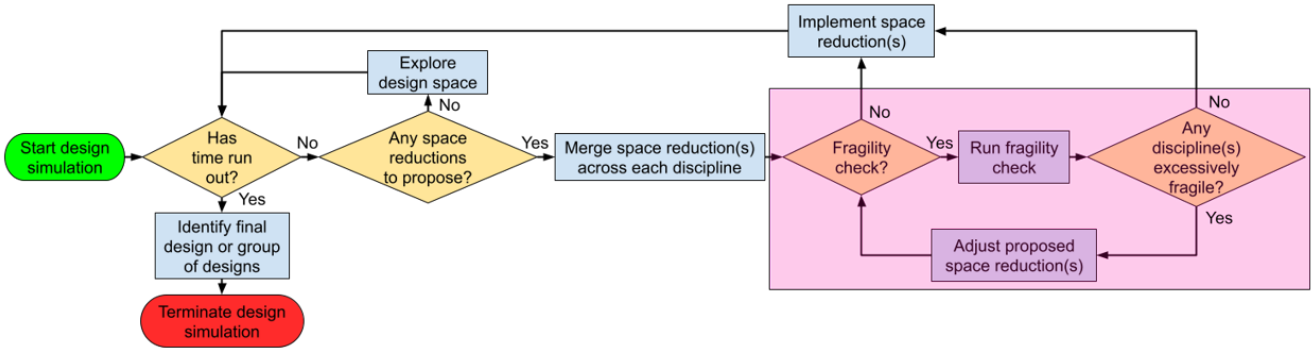

Figure 7: Simplified flowchart of the automated SBD simulation with a fragility framework plug-in

Problem Setup

The problem setup portion initializes the design problem and prepares various aspects of the code for the time-based simulation. The user has the option to set certain user inputs that dictate characteristics of the design problem, exploration tendencies of the algorithm, and space reduction tendencies of the algorithm. The code is intended to work for any design problem as long as the user defines the input variables, output variables, initial input rules, initial output rules, and analyses of each discipline. To ensure exploration does not continue indefinitely, a bounded timeline is established, and the user must define how long the analyses of each discipline take to run during exploration. This portion of the code also sets an exponential-based function that encourages a minimum amount of each discipline's design space to be reduced relative to the time elapsed. An exponential function was chosen to promote exploration without required space reductions early on while saving more of the required space reductions for later once more information has been gathered. In an actual SBD process, there usually is not any sort of timeline established to keep space reductions on pace. However, for an automated SBD process without human involvement, it is important to ensure all of the space reductions are not delayed until the end.

Exploration

The exploration portion is where each discipline is free to sample designs within their remaining design space. Exploration occurs whenever there is time remaining, there are no space reductions being proposed by any discipline, and there are no space reductions being forced because of the time that has elapsed compared to the size of each discipline's remaining design space. Based on guidelines set by the user in advance of the simulation, a specific amount of time will be dedicated to

sampling new points at each exploration cycle. The location of new points chosen for sampling are randomized throughout each discipline's remaining design space. Each discipline will then calculate the output values of the new points according to their specific analyses and check whether the calculated output values satisfy the current set of output requirements. Design time is only reduced during exploration as it is assumed that the time to run analyses is significantly greater than the time to propose space reductions or evaluate fragility.

For infeasible points, the algorithm is programmed to determine the extent to which each point fails. This failure calculation finds the difference between the calculated amount and the nearest threshold amount of each failing requirement (normalizing the difference to ensure no one requirement bears more influence on the failure amount than the others), and then calculates the root-mean-square deviation of the normalized differences. After going through this process, each infeasible point will have a failure amount assigned to it where values closer to zero indicate that the point is right on the threshold of passing, while larger values indicate that the point is very far off from passing. These calculated failure amounts come in handy when the SBD simulation goes through its space reduction and fragility assessment processes. Equation 1 shows an example calculation of the failure amount (FA) involving three different requirements ($y_1 > 0.2, 0.3 < y_2 < 0.6$, $y_1 + y_2 < 0.8$), three different calculated amounts ($y_1 = 0.1$, $y_2 = 0.25$, $y_1 + y_2 = 0.35$), and three different ranges of output values ($y_1 \in [0.05, 1.2]$, $y_2 \in [0, 0.9]$, $y_1 + y_2 \in [0.05, 2.1]$).

$$FA = \sqrt{\frac{\left(\frac{0.1-0.2}{1.2-0.05}\right)^2 + \left(\frac{0.25-0.3}{0.9-0}\right)^2 + \left(\frac{0}{2.1-0.05}\right)^2}{3}} = 0.103 \tag{1}$$

For feasible points, the algorithm is programmed to determine the extent to which each point passes. This passing calculation is done in a similar process to that of the failure calculation with a couple of slight modifications. First off, the difference is now taken between the calculated output amount and the nearest threshold amount of each *passing* requirement. Secondly, rather than taking the root mean square of each requirement's normalized difference between the calculated value and threshold, the passing calculation simply takes the minimum normalized difference to gauge how close an output value is to failing the nearest requirement. By effect, passing amount values closer to zero indicate that the point is right on the threshold of failing, while larger values indicate that the point is very far off from failing. These calculated passing amounts also come in handy when the SBD simulation goes through its space reduction and fragility assessment processes. Equation 2 shows an example calculation of the passing amount (PA) involving the same three requirements ($y_1 > 0.2, 0.3 < y_2 < 0.6, y_1 + y_2 < 0.8$), three new calculated amounts ($y_1 = 0.4$, $y_2 = 0.35$, $y_1 + y_2 = 0.75$), and the same ranges of output values ($y_1 \in [0.05, 1.2]$, $y_2 \in [0, 0.9]$, $y_1 + y_2 \in [0.05, 2.1]$).

$$PA = \min\left(\frac{|0.4-0.2|}{1.2-0.05}, \frac{|0.35-0.3|}{0.9-0}, \frac{|0.75-0.8|}{2.1-0.05}\right) = 0.024 \tag{2}$$

Space Reduction

The space reduction portion is where each discipline can propose new input rule(s) that reduce design spaces if adopted by the DIM. The process each discipline goes through to propose these rule(s) involves a series of steps. It starts out by sorting all the failure amounts of previously explored points remaining in a discipline's available design space by magnitude. The algorithm then labels a percentage of the points with the highest failure amounts as "bad" while all of the remaining points are labeled as "good". Next, a decision tree classifier (DTC) is built in the design space based on these "good" and "bad" points. The goal of the DTC is to create boundaries within the design space such that all the "good" and "bad" points are grouped together as succinctly as possible. After the decision tree is formed, the boundaries of the decision tree grouping the highest fraction of "bad" points together are extracted to act as the threshold of a newly proposed input rule. A benefit of the decision tree is that each one of its boundaries are defined by a first-order equation only involving one input variable. This benefit reflects what is often seen in actual SBD as human designers tend to define simple rules for elimination rather than complicated equations cutting through the design space. The new input rule is finally checked against a set of user-

defined criteria to ensure it is supported by adequate information before a discipline can formally propose it.

If no rules are proposed by any discipline, then the simulation will ask whether a reduction should be forced for any discipline. If the answer to that question is yes (due to substantial space remaining relative to time remaining), then one of the user-defined criterion will be relaxed, and the disciplines will reassess if they have any reductions to propose. If the answer to that question is no, then the algorithm will continue to the exploration part of the simulation.

If one or more disciplines do have a new rule to propose, then the DIM becomes responsible for thoughtfully merging these requests based on available information and the impact each rule would have on other disciplines. This is a difficult part of the SBD process to reproduce because a preferred reduction for one discipline may not be preferred by another; human DIMs must often think critically when finalizing requests based on infeasibility and dominance. In the simulation, this merging process is handled by having each discipline directly affected by the input rule form an opinion on it that is represented by a value between 0 and 1 (where a value of 0 indicates the discipline is completely opposed to the rule, while a value of 1 indicates the discipline is completely in favor of the rule.) The opinions are quantified through each discipline's answers to two different questions:

1. Is the proposed space reduction removing clearly infeasible designs in your discipline's design space?
2. If the proposed space reduction is enacted, how less likely is it that feasible designs exist in your discipline's remaining design space?

To answer the first question, the area of the remaining design space that the space reduction would remove (the *eliminated design space*) is assessed. This area of the design space is discretized, and then a Gaussian process regressor (GPR) is trained with the available data from all of the explored points. The x-training data of the GPR are the input locations of the explored points, while the y-training data are the difference between each point's passing and failing amount. The trained GPR is then used to predict the difference between the passing and failing amounts at each discretized (unexplored) point in the eliminated design space. A negative value indicates the discretized point is predicted to be infeasible, while a positive value indicates the discretized point is predicted to be feasible. As the question is concerned with discerning *clearly infeasible* areas of the eliminated design space, the predicted difference between the passing and failing amounts is permitted to fluctuate between three standard deviations. The fraction of this range staying *below* zero for each discretized point is calculated, and the average value of those fractions acts as the metric answering the first question. Large values of this metric reflect *assuredness* that the eliminated design space is clearly infeasible.

The answer to this first question may be sufficient for validating proposed spaces reductions early in the SBD process when designers are purposefully delaying commitments to hard-set specifications and working with large infeasible spaces. If the answer to this question is a resounding yes for all disciplines involved, then the DIM can move forward with the space reduction for the universally infeasible design space. However, later on in the SBD process when these infeasible spaces have diminished, dominance-based decisions may be required that consequentially cut away at some of the feasible spaces of various disciplines. In these cases, the second question becomes more important to ask to ensure that a dominance-based reduction decision does not end up severely limiting any one discipline from producing a feasible design.

To answer the second question, the area of the design space that would remain after the space reduction (the *reduced design space*) is assessed in relation to the original design space before the space reduction (the *non-reduced* design space). The same trained GPR is now used to predict the difference between the passing and failing amounts at each discretized (unexplored) point in the reduced and non-reduced design spaces. However, now the question is concerned with discerning *likely feasible* spaces to ensure the space reduction does not significantly reduce the potential of finding a feasible design. In this case, the normal distribution about each discretized point's predicted value is determined, and the average fraction of those distributions falling *above* zero is calculated for both the reduced and non-reduced design spaces. The ratio of the reduced average to the non-reduced average acts as the metric answering the second question, where large values reflect *little reduction* in the *likeliness* of finding feasible designs in the reduced design space.

With metrics produced that quantify a discipline's answers to both questions, the influence that each metric should have on a discipline's overall opinion of a space reduction can be determined. Equation 3 is used to quantify this opinion (OP)

where m_1 and m_2 are the metrics for the first and second question, and w_1 and w_2 are the weights assigned to each metric. Because the second question only comes into play if the answer to the first question is not a resounding yes, the weight of the second metric is dictated by the value of the first metric. If m_1 is high because clearly infeasible spaces would be eliminated, then w_2 should be low because those spaces are not needed regardless. On the other hand, if m_1 is low because clearly infeasible spaces are *not* being eliminated, then w_2 should be high to account for how much the space reduction would actually hinder the remaining space in the opinion formulation. To reflect this behavior while not limiting the relationship between w_2 and m_1 to a linearly inverse correlation, a user-specified quadratic Bezier curve between the two variables is adopted. Once w_2 is determined, w_1 is calculated through the equation $w_1 = 1 - w_2$ to ensure the overall value on the opinion stays between 0 and 1.

$$OP = w_1 * m_1 + w_2 * m_2 \tag{3}$$

Once the opinions are formed, the DIM can finally decide how much influence each opinion should have when finalizing the universal set of input rule(s) for the newest space reduction. In the simulation, this decision is made by establishing a threshold which permits a discipline to veto an input rule based on the value of their opinion in relation to the opinion of the discipline proposing the new input rule(s). Early on in the SBD process when space reductions do not necessarily need to be forced by the DIM, this threshold is low to allow for more vetoing of rules and less dominance-based reduction decisions. Later on in the SBD process when space reductions are becoming more forced by the DIM, this threshold is high to prevent more vetoing of rules and allow for more dominance-based reduction decisions.

At the end of this space reduction process, the DIM will have decided on a universal set of space reductions by which all disciplines must abide. Again, it is not meant to be a perfect representation of how space reduction decisions are made in SBD. Rather, it is meant to consistently produce reasonable space reductions for both infeasibility and dominance-based decisions so that the fragility of those decisions can be studied.

FRAGILITY FRAMEWORK

Traditionally in SBD, the space reduction decision process ends with the universal set of reductions instituted by the DIM. At this point, designers have explored their own design spaces to form perceptions and propose space reductions, and the DIM has merged them together with the information available through infeasibility or dominance. As discussed though, this process, which only considers present information, leaves reduced design spaces vulnerable to new information.

The intent of a fragility framework is to gauge the vulnerabilities of each discipline's design space to new information before committing to any space reductions. To accomplish this goal, a developed framework will require components that address various complexities inherent to the space reduction process. Table 1 summarizes those space reduction complexities and corresponding fragility framework requirements. In this work, a Probabilistic Fragility Model (PFM) is introduced for fragility assessment. The PFM is still a work in progress and does not address every framework requirement outlined in the table. Still, it addresses many complexities inherent to SBD's space reduction process and has the potential to be expanded further in future work. After discussing the underlying logic behind the PFM, it is incorporated as the final step in the SBD simulation's space reduction process.

Probabilistic Fragility Model

The main idea behind the PFM is to characterize a discipline's present understanding of a design space with straightforward probabilities of feasibility and infeasibility and then to quantify its vulnerability based on how likely that understanding is to change. There are three main parts to the PFM which include forming perceptions of feasibility in the design spaces, determining potentials for regret and windfall from those perceptions, and using metrics to compare those potentials between the reduced and non-reduced design spaces.

In the first step, designers need to form perceptions of feasibility throughout their design space by leveraging data from their explored points thus far. To meet this requirement, the same GPR from the space reduction process is used to predict the difference between the passing and failing amounts (pass-fail) for all unexplored areas of the design space. With these predictions, designers can form perceptions for feasible and infeasible areas depending on if the pass-fail value is positive or negative. Designers will also have an idea of how much different areas are passing or failing depending on its magnitude. Figure 8 depicts this process for the remaining areas of a design space involving two input variables (x_1 and x_2). On the left-hand side of the figure, pass-fail amounts are formed for three explored points. Data from those explored points train a GPR, and then the trained GPR forms predictions for the discretized areas of the design space.

Table 1: Complexities that exist when making space reduction decisions with uncertain information and the corresponding fragility framework requirements addressing these complexities

Space Reduction Complexity	**Framework Requirement**
Space reductions are focused on eliminating undesirable solutions from a ranging design space. The desirability of solutions are rooted in perceptions of feasibility formed by running *discrete* design points through the analyses established by each discipline.	The framework needs to form initial perceptions of feasibility with presently available information. A technique for converting information from explored points and their output values into perceptions of feasibility *throughout* each discipline's design space is required.
Perceptions of feasibility are uncertain because they are formed with incomplete information within a discipline's design space. Information from newly analyzed design points *within a design space* could alter perceptions.	Formed perceptions of feasibility for unexplored areas of the design space are not definitive. The framework should account for the possibility of new design points being tested with feasibility that is contradictory to expectations.
Perceptions of feasibility are uncertain because of the *interdependencies* that exist through shared variables between disciplines. Vulnerabilities of one design space to new information could directly or indirectly amplify the vulnerabilities of other design spaces.	The framework must include a cross-discipline component that ties the individualistic fragilities of each discipline together such that the vulnerabilities tracked across interconnected design spaces are representative of their dependencies on each other.
Perceptions of feasibility are uncertain because they are formed with output information that is susceptible to change. New information originating from *changes to design requirements or analyses* could alter perceptions.	The location of calculated output values within the objective space must not be treated as definitive. Instead, the framework should account for the possibility of output values and requirements shifting in relation to each other.
A design space may be fragile when considering all input variables together (i.e. x_1, x_2, x_3) and when considering various *combinations* of input variables (i.e. x_1, x_2).	The framework cannot only measure the fragility of a design space as a whole. It must be flexible enough to also identify component-based fragilities.
The number of ways new information can alter perceptions of feasibility within a design space is *unbounded and unknown* until the information is made available. The risk of a space reduction in context of itself is unlimited.	Comparing the fragility of a reduced design space to a non-reduced design space and determining what new information a discipline *can* handle rather than it would *have to* handle will narrow the DIM's scope and allow space reduction risk to be quantified.

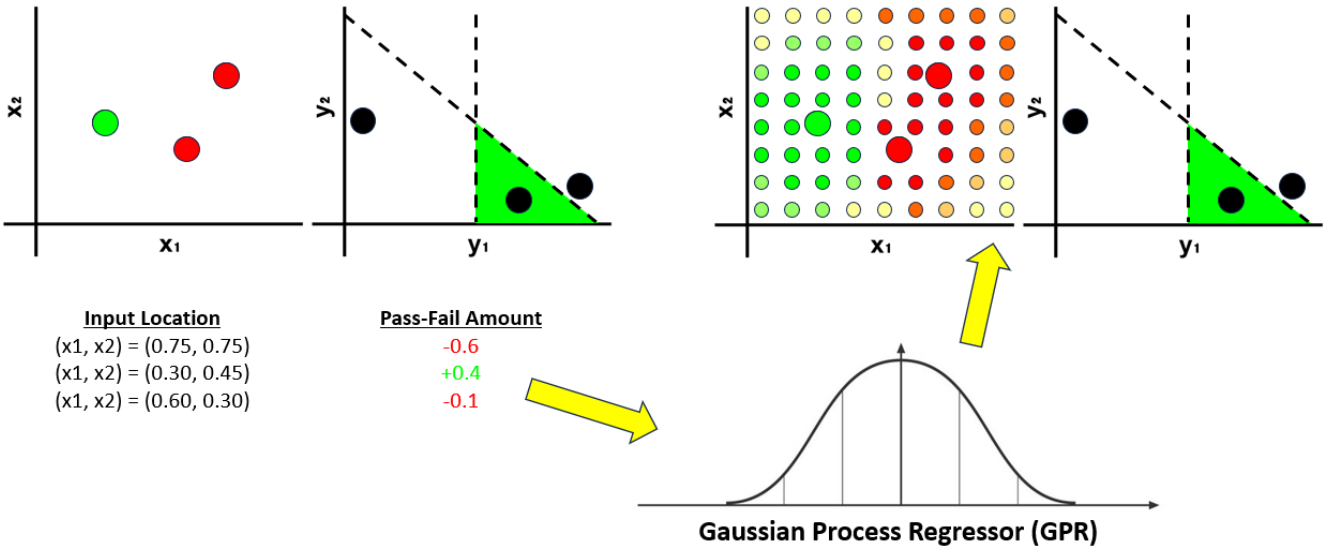

Figure 8: Forming perceptions of feasibility for unexplored areas of the design space

In the next step, designers need to consider the consequences of their formed perceptions of feasibility being incorrect. This requirement leads to the introduction of regret and windfall in a design space. Suppose the sampled design space in Figure 9 is considering the space reduction depicted by the black box. The space reduction would eliminate portions of the design space perceived as feasible (top-left) as well as portions of the design space perceived as infeasible (top-right). Now suppose new information comes along that throws off those perceptions of feasibility as depicted by the left-hand design space in Figure 10. This new information would cause designers to regret the space reduction if they are left *with infeasible* space that was expected to be feasible or left *without feasible* space that was expected to be infeasible (instances of regret). In contrast, the new information would benefit designers if they are left *with feasible* space that was expected to be infeasible or left *without infeasible* space that was expected to be feasible (instances of windfall). Before committing to a space reduction, the PFM considers these *potentials* for windfall and regret for the reduced design space in context of the non-reduced design space (right-hand side of Figure 10). This logic allows designers to consider the consequences of moving forward with a space reduction compared to forgoing the space reduction.

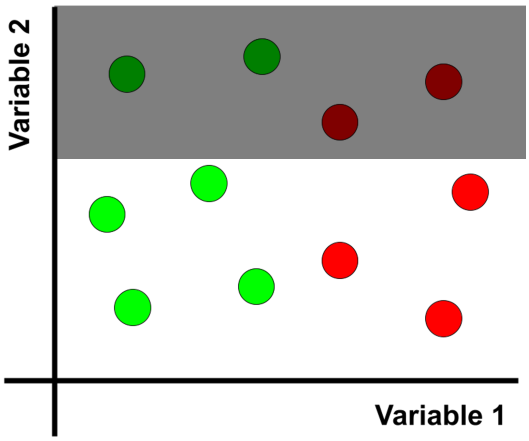

Figure 9: Design space considering a proposed space reduction (signified by the grey box)

Considering the consequences of a space reduction alone is not enough as there are different likelihoods of these consequences actually coming to fruition. Fortunately, probabilities of feasibility can be calculated from the predicted pass-fail values of the GPR to account for the regret and windfall likelihoods. Figure 11 depicts this process for the PFM. Once all

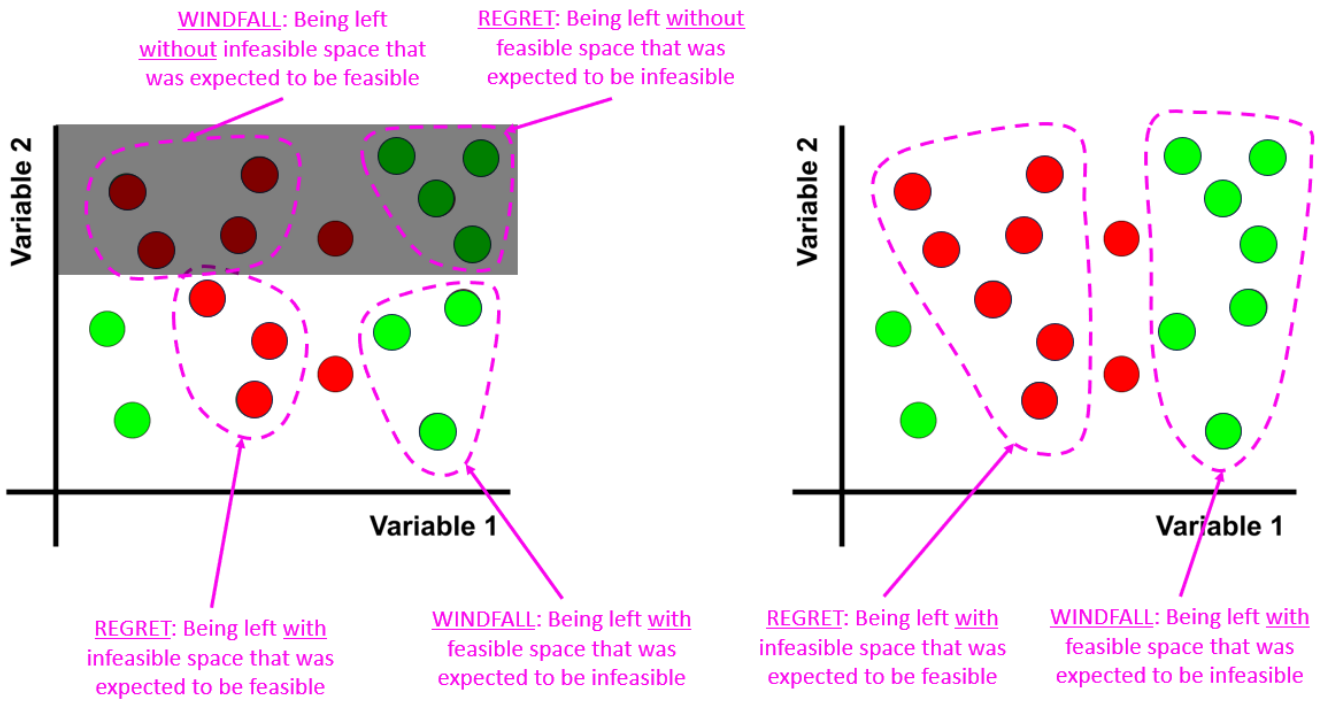

Figure 10: Instances of regret and windfall for the reduced design space (left) and non-reduced design space (right)

discretized areas of the design spaces are labeled as feasible or infeasible based on their predicted pass-fail value, the value itself and the accompanying standard deviation are used to create a normalized probability distribution on each prediction. The probability of feasibility or infeasibility is determined based on the portion of a point's probability distribution maintaining the predicted positive or negative pass-fail value. Finally, the potentials for regret or windfall are taken from the complementary probabilities of feasibility for each discretized point. Whether the complementary probability results in a potential for regret or windfall will depend on where the discretized point falls in the non-reduced or reduced design space.

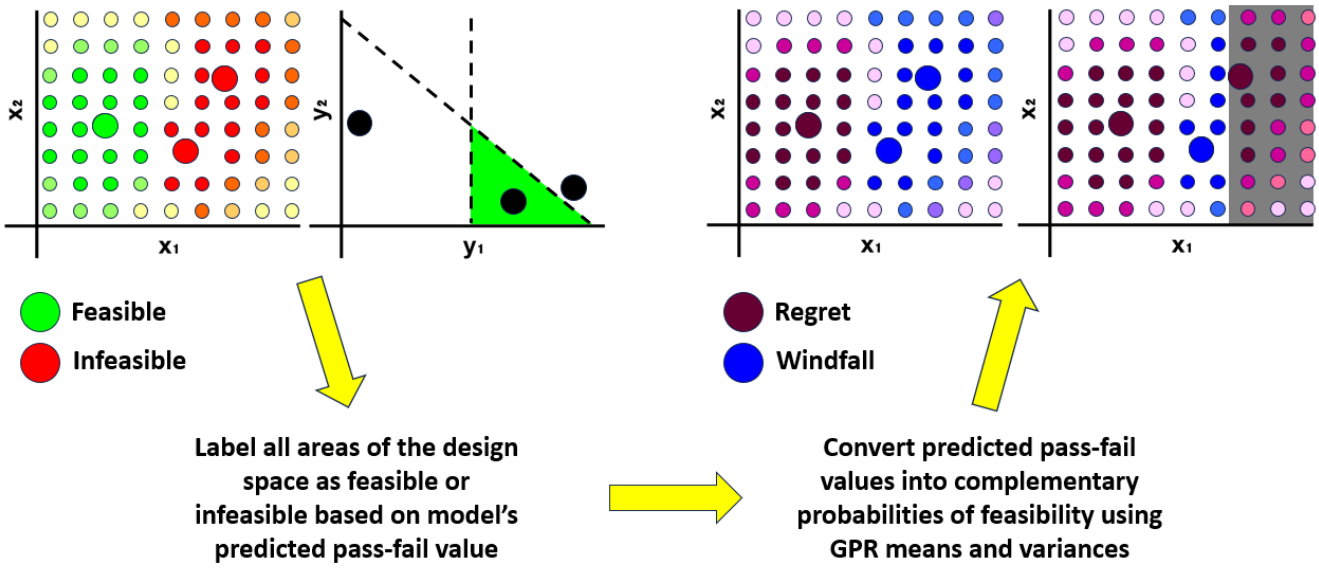

Figure 11: Converting perceptions of feasibility into potentials for regret and windfall for a non-reduced and reduced design space

The last step in the PFM involves gauging regret and windfall potential for the entirety of the reduced design space from each discretized point. A straightforward method to do so is summing up each discretized point's regret and windfall potentials. However, to actually understand the *risk* of a space reduction from these potentials, further context is needed. This context is provided by calculating the same summation for the non-reduced design space as is done for the reduced design space and then calculating the *added* potentials for regret and windfall (shown in equations 4 and 5). Working with these added potentials for regret and windfall allow a DIM to understand the risk of moving forward with a space reduction in context of leaving the design space untouched. High risk space reductions correspond to large positive values of added potential for regret and large negative values of added potential for windfall, which would reflect a reduced design space taking on more potential for regret and giving up potential for windfall. In equations 4 and 5, Δ_{reg} and Δ_{wind} are the added potentials for regret and windfall, $p_{reg,red}$ and $p_{wind,red}$ are a discretized point's probability of regret and windfall in the reduced design space, and $p_{reg,nonred}$ and $p_{wind,nonred}$ are the same probabilities for the non-reduced design space.

$$\Delta_{reg} = \frac{\sum_{i=1}^{n} p_{reg,red}(x)}{\sum_{i=1}^{n} p_{reg,nonred}(x)} - 1 \tag{4}$$

$$\Delta_{wind} = \frac{\sum_{i=1}^{n} p_{wind,red}(x)}{\sum_{i=1}^{n} p_{wind,nonred}(x)} - 1 \tag{5}$$

Incorporating Fragility in SBD Simulation

In the SBD simulation, fragility checks occur immediately after the DIM has merged proposed space reductions into a universal set, as depicted by the red box in Figure 7. Up to this point in the simulation, all space-reduction-related decisions are solely supported by present information that is assumed not to change. The fragility framework intends to protect design spaces against this assumption and consider the effect that the space reductions would have on the remaining design spaces if new information were to alter the perceptions formed.

After calculating the added potential for regret and added potential for windfall, the amount of risk a DIM is willing to take on must be determined. In this work, a maximum risk threshold that increases exponentially with project time is established. The idea behind choosing an exponential threshold is to undertake little risk in space reduction decisions early on when conflicting information can be more common and influential on design space perceptions, and to increase the amount of risk endured later when conflicting information is less common and design spaces are more locked in.

With the exponential risk threshold set, the actual risk experienced from a space reduction in the simulation is set as the added potential for regret subtracted by the added potential for windfall. This risk setup allows the DIM to weigh each discipline's shift in potential to be hurt and helped by new information following a space reduction. In any given space reduction cycle, disciplines are permitted to keep proposing space reductions that can be added by the DIM as long as the risk does not exceed the threshold for any one discipline. If the threshold is exceeded, the input rule that put the risk over the limit is temporarily banned from being proposed again until design spaces have been explored further.

With that, the SBD simulation is established with the option to include a probabilistic fragility check before fully committing to each space reduction decision. After first validating the pre-fragility portion of the simulation with a simple SBD problem, emergent design spaces of the design problem with and without the PFM are ready to be observed.

VALIDATING SIMULATION WITH A SBD PROBLEM

Investigating the impact of this new fragility framework on emergent design spaces requires a simple design problem. Testing the framework on a simple problem directs focus on the framework and makes interpretation of results in its early stages

more straightforward. After first describing the problem, it will be used to validate the efficacy of the SBD simulation without yet incorporating the PFM. Once the simulation is validated, it will then be used to assess the vulnerabilities of emergent design spaces for SBD simulations with and without the PFM.

SBD Problem

A design problem has been created for testing the developed fragility framework. As shown in Figure 12, the design problem involves three different disciplines having some shared input variables and unique output variables. The input variables are analogous to the different ship characteristics that a discipline has influence over, while the output variables are analogous to the different ship performance characteristics with which a discipline is concerned. Circling back to the marine design disciplines used as an example in the *SET-BASED DESIGN* section, Discipline 1 could represent the Weights division, Discipline 2 could represent the Stability division, and Discipline 3 could represent the Structural division. It is important to note that only a simple design problem is being investigated right now, and there are numerous other disciplines and subdisciplines (e.g. arrangements, powering, seakeeping, maneuvering) that would tie into more complex problems.

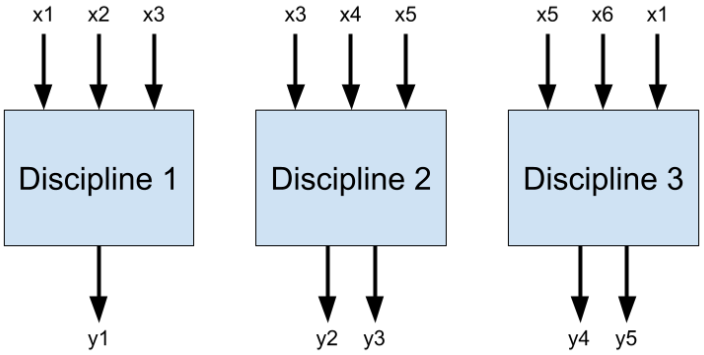

Figure 12: Input and output variables for three disciplines of SBD problem

Each one of these disciplines have analyses that calculate the output variables from the input variables to provide insight on how a potential design solution will perform. For this design problem, arbitrary mathematical equations act as the analyses for each discipline as shown in equations 6 to 10. These equations are analogous to the different parametric models or design programs used to evaluate performance metrics of a potential design solution.

Discipline 1:

$$y_1 = 0.8x_1^2 + 2x_2^2 - x_3 \tag{6}$$

Discipline 2:

$$y_2 = 1.25x_5 - 12.5x_3^3 + 6.25x_3^2 \tag{7}$$

$$y_3 = \left(x_4^3 + x_5\right)^2 \tag{8}$$

Discipline 3:

$$y_4 = 2x_5 + 0.2\sin\left(25x_6\right) - x_1^{\frac{1}{5}} \tag{9}$$

$$y_5 = x_1^{\frac{1}{3}} - \cos\left(3x_5\right) \tag{10}$$

Each of the input and output variables have requirements that must be satisfied. The bounds on all the input variables are normalized such that they must fall between 0 and 1. The bounds on the output variables are unique and described as follows: $0 \leq y_1 \leq 0.4$ or $1.2 \leq y_1 \leq 1.6, 0.5 \leq y_2 \leq 0.7, 0.2 \leq y_3 \leq 0.5, 0 \leq y_4 \leq 0.5, 0.8 \leq y_5 \leq 1.6$. These

requirements are analogous to the different stakeholder or industry-set design requirements that the design must satisfy. In marine design, the bounds on the input variables could be normalized length, beam, depth, etc. ranges, while the bounds on the output variables could be standardized displacement, wind-righting arm, yielding stress, etc. ranges.

The equations and required bounds of the design problem produce the feasible spaces depicted in Figures 13 to 15. In each of the figures, red points represent discrete design solutions not meeting output requirements, while green points represent discrete design solutions meeting output requirements. The feasible boundaries are unknown to the designers of each discipline, so they must form their perceptions of these feasible boundaries solely from the discrete points they decide to test. The equations and bounds are formulated in such a way that the feasible spaces have complex boundaries for designers of the SBD simulation to learn.

Validating SBD Simulation Approach

The code simulating SBD decisions needs to be validated to ensure reasonable space reductions are being proposed from the present information. The aim of the fragility framework is to evaluate the suitability of a space reduction decision based on the potential for perceptions of feasibility to be altered by *new information* rather than present information. Even so, if unreasonable space reductions that neglect infeasible areas and surround feasible areas are proposed, then new information could not make perceptions any worse, and the framework would never find a reduced design space to be fragile.

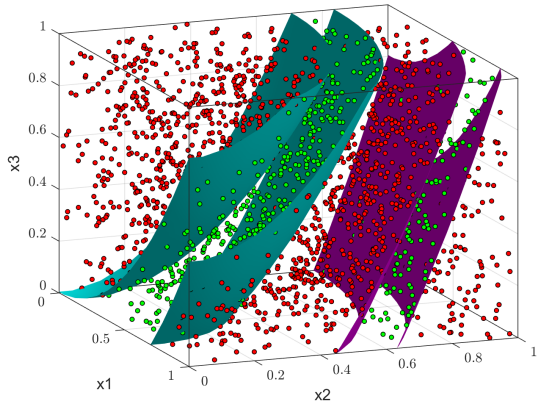

Figure 13: Feasible bounds of Discipline 1 depicted with 2,000 sampled points

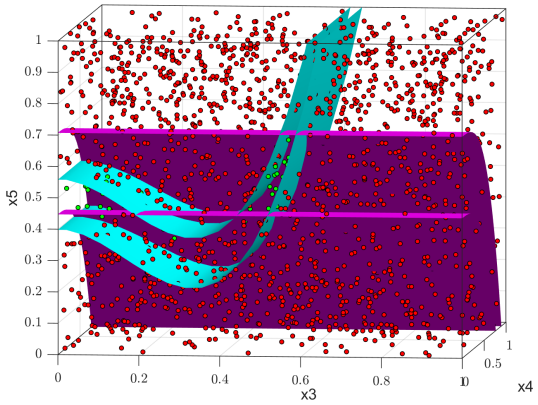

Figure 14: Feasible bounds of Discipline 2 depicted with 2,000 sampled points

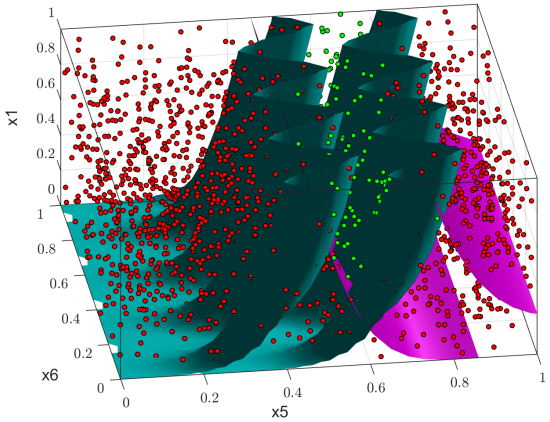

Figure 15: Feasible bounds of Discipline 3 depicted with 2,000 sampled points

To validate the SBD code, 200 runs of the SBD problem without the fragility framework were executed. Table A1 shows all of the user inputs selected for these simulations. Short analysis run times ([2, 3, 4] iterations) relative to a long project timeline (1000 iterations) were chosen to ensure ample time is given to build up information for proposing reasonable space reductions. Each discipline was also given the goal of reducing their designs space's down to at least 5% of their initial size.

Figures 16 to 18 show locations of remaining solutions in each discipline's design space at the end of all 200 runs with the tan-colored points. The more opaque points show where remaining designs are most commonly found in each discipline at the end of a run, while the more transparent points show where remaining designs are less commonly found or not found at all. The surfaces show the feasible bounds of the design problem unknown to designers in the simulation. As can be seen in each figure, the remaining solutions are most commonly found within or around each discipline's feasible areas. This finding shows that remaining designs are being narrowed down to these feasible areas without actual knowledge of them, indicating that the SBD code is proposing reasonable space reductions.

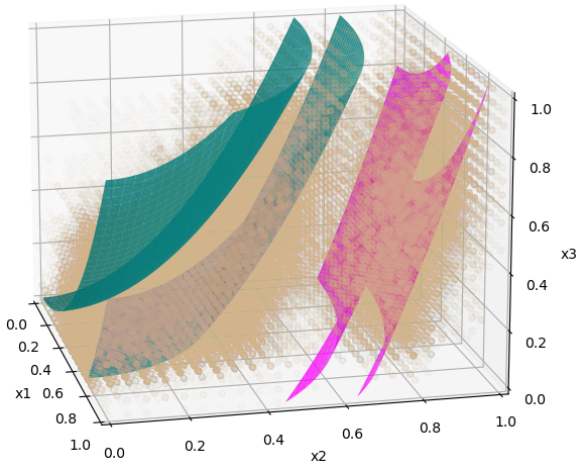

Figure 16: Locations of remaining design solutions for Discipline 1 at the end of the simulation

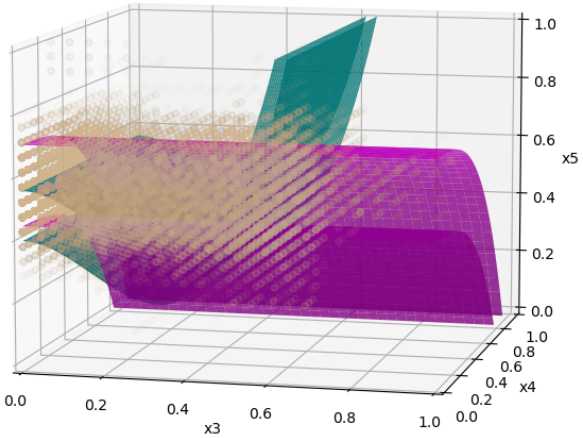

Figure 17: Locations of remaining design solutions for Discipline 2 at the end of the simulation

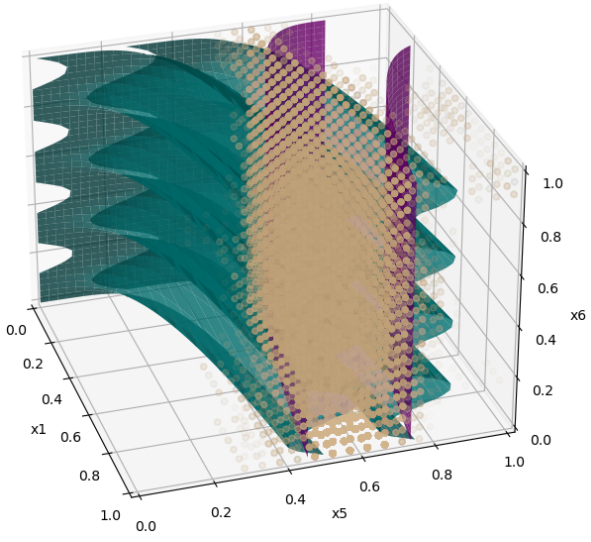

Figure 18: Locations of remaining design solutions for Discipline 3 at the end of the simulation

ASSESSING FRAGILITY IN SBD PROBLEM

With the SBD code validated, experiments can be run comparing the emergent design spaces of SBD simulations including the PFM to those that do not. As the proposed method does not yet consider the potential of analyses or requirements to change, random design changes do not need to be introduced to the simulation. The PFM currently only considers the impact that new information arising from newly tested design points in a primary discipline would have on a remaining design space. The results focus on evaluating the fragility of design spaces following space reductions by tracking remaining designs as the simulation progresses.

Experimental Setup

Experiments are run for two different scenarios. In the first scenario, emergent design spaces with and without the PFM are compared to each other when a large amount of time has been allotted to the design problem relative to analysis run times. These test cases will have more time to generate information and presumably form more stable perceptions of design space behavior before proposing various space reductions. In the second scenario, emergent design spaces with and without the PFM are compared to each other when little time has been allotted to the design problem relative to analysis run times. These test cases will have less time to generate information and presumably form less stable perceptions of design space behavior before proposing various space reductions.

Table 2 highlights the differences made in the simulation between these two scenarios, while all other design parameters selected for the simulations match up with those shown in Table A1. The first and third test cases do not include any sort of fragility checks, but the second and fourth test cases include the PFM. Each test case is executed over 200 runs, and the averages of those runs are observed when examining the emergent design spaces.

Table 2: Independent variables for various test cases of the SBD simulation

Design Parameter	User Input	Test Case 1	Test Case 2	Test Case 3	Test Case 4
Project timeline (iterations)	iters_max	200	200	1000	1000
Fragility check	fragility	False	True	False	True
Starting Fragility Threshold	fragility_shift	0.0	0.2	0.0	0.2

Results and Discussion

While executing the runs of each test case, the total design space remaining and the remaining number of feasible solutions are tracked across each discipline. Figures 19 to 21 display these results as various percentages. In each figure, the “Total Space” curves show the average percentage of the remaining design space, the “Feasible Space” curves show the average percentage of the remaining feasible designs, and the “Feasible-to-Remaining” curves show the ratio of the remaining feasible designs to the remaining design space, all over the elapsed project time.

One immediate takeaway from each of the figures is that including fragility checks with the PFM does not result in a higher ratio of feasible designs to space remaining by the end of the simulations. When comparing test cases of the same project timeline in each figure, the ratio of feasible-to-remaining designs is generally the same or slightly higher for test cases that do not include fragility checks. For Test Case 1 and Test Case 2 in Discipline 3, the ratio of feasible-to-remaining designs is much higher (roughly 25%) for simulations without the PFM. While these results may seem deterring, one explanation for them is there being more total space remaining at the end of the simulations with the fragility checks. In Discipline 3 specifically, there is on average about 10% more designs remaining in Test Case 2 at the end of the simulations than every other test case. More test cases remaining can result in a lower ratio of feasible-to-remaining designs. This occurrence is confirmed by the fact that despite its much lower ratio, Test Case 2 has more remaining feasible designs than Test Case 1 at

the end of the simulation for Discipline 3. Regardless, the behavior this work is more concerned with studying occurs for the emergent design spaces rather than the final design spaces.

Another takeaway is that having more time to explore each discipline's design space does lead to a higher understanding of the space. Across each discipline, Test Cases 1 and 2 (having an 80% shorter project time) consistently retain fewer feasible designs than Test Cases 3 and 4. As Test Cases 3 and 4 have more time to explore areas of their design space before proposing space reductions, they can be more careful about eliminating feasible solutions. It is worth noting that the feasible-to-remaining design space ratio of Test Case 1 does rapidly catch back up to Test Cases 3 and 4 towards the end of the simulations. While it would require further investigation to confirm this explanation, the smaller dispersion of designs in Figure 18 than Figure 16 and Figure 17 hints that this behavior may be attributed to the actual equations and requirements established for Discipline 3 in the SBD problem. The feasible solutions for Discipline 3 can vary over the entire range of its unique variable (x_6) but has distinct feasible regions for its shared variables (x_1 and x_5). This coincidence gives designers of Discipline 3 some more freedom to still find feasible designs in their design space whether or not any sort of premature design lock-in has occurred for its shared variables.

Circling back to the fragility aspect of the simulations, the total space remaining results show that simulations including the PFM support a more gradual reduction of design spaces with less lock-in than simulations neglecting fragility checks. For most of Discipline 1's reduction time and for all of Discipline 2 and 3's reduction time, simulations including fragility checks maintain a larger remaining design space than simulations without them. The PFM is effectively delaying the space reduction process and forcing disciplines to really consider the potential consequences of a space reduction before they commit to it. Those consequences are being realized at the "notches" in Test Case 1 and 3's total space curves just past the 40% elapsed timeline, primarily in Disciplines 2 and 3.

The rapid decline in total space remaining and apparent change in pace at each notch suggests the disciplines are eliminating infeasible areas of their design spaces without much hesitation and then finding themselves locked in on the design solutions that remain. While design changes are not introduced in the experiments conducted for this work, the design spaces of Test Cases 1 and 3 find themselves very vulnerable at this point to new information stemming from slight changes to requirements or analyses. Whereas the design spaces of Test Cases 2 and 4, who do consider the consequences stemming from new and conflicting information, are more prepared to handle design changes. Test Case 4 in Discipline 2 does see a similar notch in its total space remaining curve at the same elapsed project time. However, it tries to correct for this rapid space reduction to a greater extent than Test Cases 1 and 3, almost to the point of meeting back up with the total space remaining curve of Test Case 2 at 70% of its elapsed timeline. For what Test Case 2 sacrifices in extra space retained at the end of SBD process, it makes up for in flexibility to handle new information.

As a whole, the results are encouraging and support introducing a step for fragility assessment to support DIMs making space reduction decisions. Using the PFM to make these fragility checks is a promising first attempt, but it is by no means perfect. The PFM meets many of the framework requirements laid out in Table 1, but it is still lacking in a few areas. Namely, the PFM has no such network component that considers vulnerabilities of interdependent disciplines, it does not account for the possibility of calculated output values or design requirements shifting, and it is not yet built to identify any component-based fragilities. Furthermore, the PFM has only been tested for space reduction decisions of a simple design problem involving just three interconnected disciplines. To really justify the PFM's incorporation into the space reduction process, it needs to be proven against more comprehensive design problems while tracking metrics such as the diversity of remaining design spaces to better substantiate claims of rapid convergence and lock-in. Future work will focus on addressing each of these shortcomings.

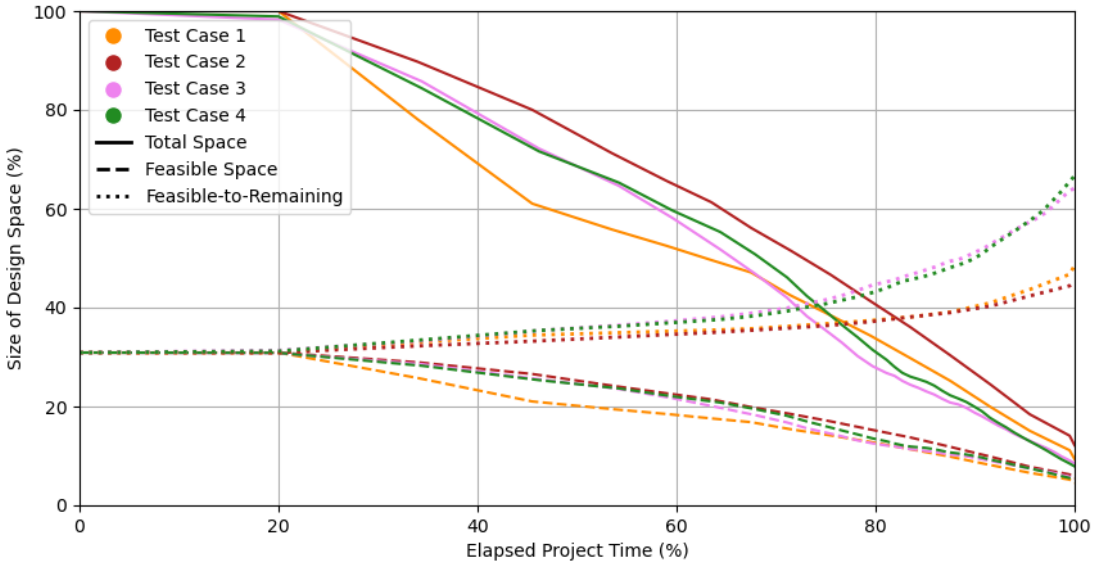

Figure 19: Size of Discipline 1's total design space, feasible design space, and feasible design space relative to remaining design space over the elapsed project time

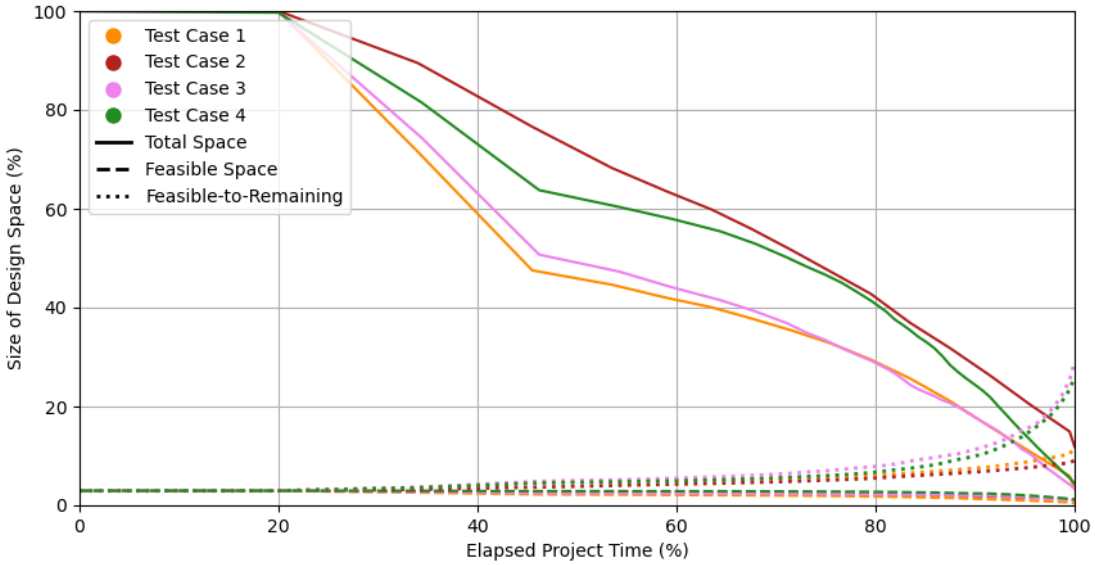

Figure 20: Size of Discipline 2's total design space, feasible design space, and feasible design space relative to remaining design space over the elapsed project time

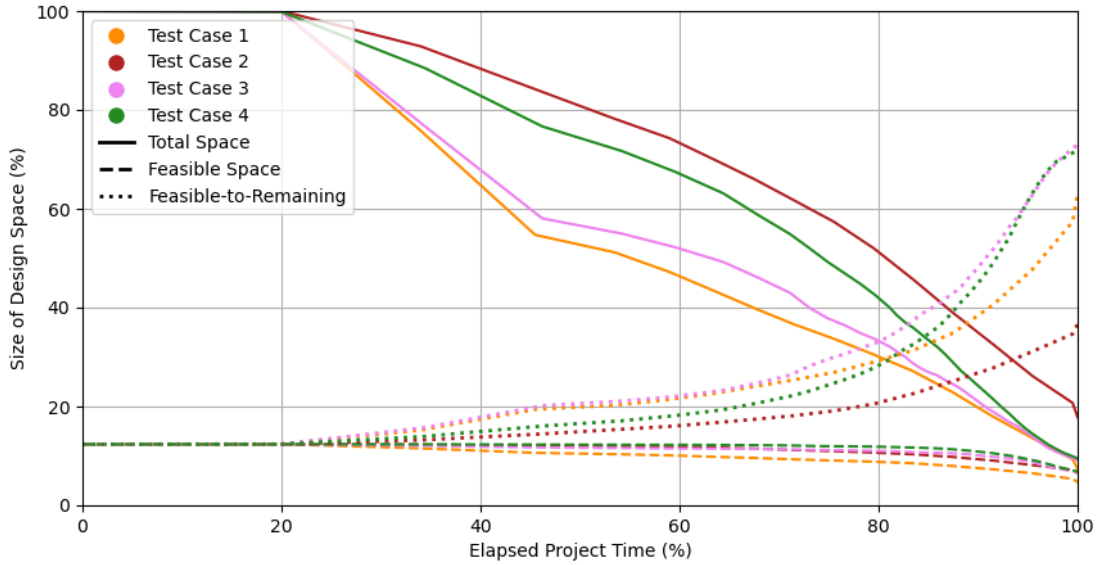

Figure 21: Size of Discipline 3's total design space, feasible design space, and feasible design space relative to remaining design space over the elapsed project time

CONCLUSIONS

The intent of this work is to introduce a framework to help DIMs make more informed space reduction decisions in SBD by considering the vulnerabilities of remaining design spaces to new information. The framework, or Probabilistic Fragility Model (PFM), uses present perceptions of feasibility formed from sampled points in a design space to gauge the potential and likelihood for those perceptions to be altered by new information. An automated SBD simulation is built to observe the emergent design spaces of a space reduction process including the PFM against one that does not for a simple design problem involving three interdependent disciplines. When tracking their emergent design spaces, initial results indicate that the framework could be a useful tool for delaying space reduction decisions and preventing designers from fixating on certain design solutions while new knowledge is still integrating with existing knowledge. Such a framework could become a critical final step to ensuring space reduction decisions are made with both present and future information in mind.

DATA ACCESS STATEMENT

All code for the SBD simulation and fragility framework along with data for each of the test cases can be publicly accessed at `https://github.com/Marine-Structures-Design-Lab/DesignSpace_Fragility/releases/tag/IMDC_2024`.

CONTRIBUTION STATEMENT

J.B. Van Houten: Conceptualization, Methodology, Software, Investigation, Data curation, Writing – original draft, Visualization, Funding acquisition. **A.A. Kana:** Conceptualization, Resources, Writing - review and editing, Supervision. **D.J. Singer:** Conceptualization, Resources, Writing - review and editing. **M.D. Collette:** Conceptualization, Methodology, Resources, Writing - review and editing, Supervision.

ACKNOWLEDGEMENTS

This work is primarily supported through the Department of Defense (DoD) National Defense Science and Engineering Graduate (NDSEG) Fellowship Program. The program's continued support is greatly appreciated. This work is also supported by the University of Michigan's Rackham Conference Travel Grant.

REFERENCES

Andrews, D. (2018). The Sophistication of Early Stage Design for Complex Vessels. *International Journal of Maritime Engineering*, Vol 160(SE 18).

Bernstein, J. I. (1998). Design Methods in the Aerospace Industry: Looking for Evidence of Set-Based Practices. Master's thesis, Massachusetts Institute of Technology, Cambridge, MA, USA.

Braha, D. and Reich, Y. (2003). Topological structures for modeling engineering design processes. *Research in Engineering Design*, 14(4):185–199.

Burrow, J., Doerry, N., Earnesty, M., Was, J., Myers, J., Banko, J., McConnell, J., Pepper, J., and Tafolla, T. (2014). Concept Exploration of the Amphibious Combat Vehicle. In *SNAME Maritime Convention*, Houston, Texas, USA. SNAME.

Doerry, N. (2012). A Vision for Ship Design and Analysis Tools. *SNAME (mt) Marine Technology*, pages 8–9.

Doerry, N. (2015). Measuring Diversity in Set-Based Design. In *ASNE Day*, pages 1–14, Arlington, VA, USA.

Dong, A. (2017). Functional lock-in and the problem of design transformation. *Research in Engineering Design*, 28(2):203–221.

Garner, M., Doerry, N., MacKenna, A., Pearce, F., Bassler, C., Hannapel, S., and McCauley, P. (2015). Concept Exploration Methods for the Small Surface Combatant. In *World Maritime Technology Conference*, page D021S004R005, Providence, Rhode Island, USA. SNAME.

Gembarski, P. C., Plappert, S., and Lachmayer, R. (2021). Making design decisions under uncertainties: probabilistic reasoning and robust product design. *Journal of Intelligent Information Systems*, 57(3):563–581.

Goodrum, C. J. (2020). *Conceptually Robust Knowledge Generation in Early Stage Complex Design*. PhD thesis, University of Michigan, Ann Arbor, MI, USA.

Gumina, J. M. (2019). *A Set-Based Approach to Systems Design*. PhD thesis, Naval Postgraduate School, Monterey, CA, USA.

Hatchuel, A. and Weil, B. (2009). C-K design theory: an advanced formulation. *Research in Engineering Design*, 19(4):181–192.

Kana, A. A. (2017). Forecasting design and decision paths in ship design using the ship-centric Markov decision process model. *Ocean Engineering*, 137:328–337.

McKenney, T. and Singer, D. (2014). Set-Based: A concurrent engineering approach with particular application to complex marine products. *SNAME (mt) Marine Technology*, pages 51–55.

Mebane, W. L., Carlson, C. M., Dowd, C., Singer, D. J., and Buckley, M. E. (2011). Set-Based Design and the Ship to Shore Connector. *Naval Engineers Journal*, 123(3):79–92.

Mihm, J. and Loch, C. H. (2006). Spiraling out of Control: Problem-Solving Dynamics in Complex Distributed Engineering Projects. In Braha, D., Minai, A. A., and Bar-Yam, Y., editors, *Complex Engineered Systems*, pages 141–157. Springer Berlin Heidelberg, Berlin, Heidelberg. Series Title: Understanding Complex Systems.

Niese, N. D., Kana, A. A., and Singer, D. J. (2015). Ship design evaluation subject to carbon emission policymaking using a Markov decision process framework. *Ocean Engineering*, 106:371–385.

Page, S. E. (2006). Path Dependence. *Quarterly Journal of Political Science*, 1(1):87–115.

Parraguez, P., Eppinger, S. D., and Maier, A. M. (2015). Information Flow Through Stages of Complex Engineering Design Projects: A Dynamic Network Analysis Approach. *IEEE Transactions on Engineering Management*, 62(4):604–617.

Shields, C. P. F. (2017). *Investigating Emergent Design Failures Using a Knowledge-Action-Decision Framework*. PhD thesis, University of Michigan, Ann Arbor, MI, USA.

Shields, C. P. F. and Singer, D. J. (2017). Naval Design, Knowledge-Based Complexity, and Emergent Design Failures. *Naval Engineers Journal*, 129(4):75–86.

Singer, D. J., Doerry, N., and Buckley, M. E. (2009). What Is Set-Based Design? *Naval Engineers Journal*, 121(4):31–43.

Smith, R. P. and Eppinger, S. D. (1997). Identifying Controlling Features of Engineering Design Iteration. *Management Science*, 43(3):276–293.

Sypniewski, M. J. (2019). *A Novel Analysis Framework for Evaluating Predisposition of Design Solutions through the Creation of Hereditary-Amelioration Networks Derived from the Dynamics within an Evolutionary Optimizer*. PhD thesis, University of Michigan, Ann Arbor, MI, USA.

Toche, B., Pellerin, R., and Fortin, C. (2020). Set-based design: a review and new directions. *Design Science*, 6:1–41.

Van Houten, J., Singer, D., and Collette, M. (2022). Balancing Designer Influence with Rework for Design Paths of a Simple Polynomial Model. In *Practical Design of Ships and Other Floating Structures*, volume 1, pages 508–527, Dubrovnik, Croatia.

Ward, A., Liker, J. K., Cristiano, J. J., and Sobek II, D. K. (1995). The second Toyota paradox: how delaying decisions can make better cars faster. *Sloan Management Review*, 36(3):43–61.

Wynn, D. C. and Eckert, C. M. (2017). Perspectives on iteration in design and development. *Research in Engineering Design*, 28(2):153–184.

APPENDIX A

Table A1: User Inputs established in Python for validating SBD simulation

Simulation Parameters	Parameter Values
problem_name	‘SBD1’
iters_max	1000
sample	‘uniform’
search_factor	100
total_points	10000
run_time	[2, 3, 4]
exp_parameters	array([0.2, 2.2, 1.0, 0.95])
part_params	{‘cdf_crit’: [0.1, 0.1], ‘fail_crit’: [0.0, 0.05], ‘dist_crit’: [0.2, 0.1], ‘disc_crit’: [0.2, 0.1]}
dtc_kwargs	{‘max_depth’: 2}
gpr_params	{‘length_scale_bounds’: (1e-2, 1e3), ‘alpha’: 0.00001}
bez_point	{‘P0’: (0.0, 1.0), ‘P1’: (0.5, 0.8), ‘P2’: (1.0, 0.0)}

Proceedings of 15th International Marine Design Conference (IMDC-2024)
June 2-6, 2024
Amsterdam, the Netherlands

Enhancing Hull Form Design for Robust Efficiency: A Data-Enhanced Simulation-Based Design Approach

Yasuo Ichinose[1,*] and Tomoyuki Taniguchi[2]

ABSTRACT

This paper presents a design approach that integrates machine learning techniques with traditional physics-based simulations/models to enhance the ship design process with robust efficiency. While generative machine learning methods, which can directly produce design outputs such as the 3D hull form, have the potential to transform the design strategy, ship design inherently involves a decision-making process that requires consensus among stakeholders based on a foundation in physics-based simulations/models. This paper proposes a practical design strategy that positions physics-based simulations/models at the core of the design process, augmented by data-driven models. The paper first classifies hybrid types of the two models and integrates them into a practical design process. Finally, it demonstrates the effectiveness of the proposed design approach by showcasing the impact of data circulation, which accumulates and reinforces data in day-to-day design operations, on improving design outcomes.

KEY WORDS

Ship Design Methodology, Simulation-Based Design, Data-driven Model, Physics-based Model, Hybrid Model

INTRODUCTION

Until now, the application of machine learning in hull form design has primarily involved using parameters that surrogate the hull form, such as principal dimensions, instead of directly dealing with the detailed 3D hull shapes. However, recent developments have begun to propose methods that handle the detailed 3D shapes directly as design outputs. Khan has proposed a machine learning model that uses a deep convolutional generative model to produce multiple 3D hull shapes from a latent input vector (Khan et al., 2023). Similarly, Ichinose has proposed a surrogate model for viscous Computational Fluid Dynamics (CFD) that uses a Convolutional Neural Network (CNN) to estimate the hull resistance, surface pressure distribution, and wake flow distribution at the propeller plane (Ichinose & Taniguchi, 2022) in real-time on a web browser, following to changes in the hull form (Ichinose & Gaspar, 2023). The significant difference between machine learning methods traditionally presented at naval architecture conferences and those proposed more recently lies not in predicting scalar values such as horsepower, which are one of the evaluation values but not the design products themselves, but in the use of decoder models represented by image-generating AI to handle 2D and 3D data, namely the design outputs themselves, including hull shapes and pressure distributions.

The emergence of data-driven approaches capable of directly outputting design products has been impacting ship design strategies. Erikstad has classified Marine system design methodology at the strategy level into four categories:

[1] Fluids Engineering & Hull Design Department, National Maritime Research Institute, Tokyo, Japan; ORCID: 0000-0003-1566-913X

[2] Structural and Industrial System Engineering Department, National Maritime Research Institute, Tokyo, Japan
* Corresponding Author: ichinose@m.mpat.go.jp

Submitted: 13 February 2024, Revised: 26 April 2024, Accepted: 1 May 2024, Published: 21 May 2024

Conference paper, DOI: https://doi.org/10.59490/imdc.2024.856 e-ISSN: 3050-4864

Optimization, Set-based, System-based, and Configuration-based, as an evolution from conventional design spiral methods (Erikstad & Lagemann, 2022). Each method has its advantages and disadvantages, and the choice among them is significantly influenced by design time constraints dictated by commercial practices. Bulk carriers, tankers, and container ships, which are predominantly built in East Asia, are often designed under strict time constraints due to negotiations with shipowners, making it difficult to move away from Design spiral methods. Papanikolaou, in the HOLISHIP project (Papanikolaou, 2022) aimed at Optimization, is constructing surrogate models for CFD calculations, which have been a bottleneck in multidisciplinary optimization due to their time dominance. Additionally, in adopting a system-based strategy, efforts are being made to optimize the entire process using a fast-responsive simulator known as 1D CFD (Perabo et al., 2020). In hull form design, which addresses the highly nonlinear flow around the hull, fast and accurate surrogate models for CFD are essential for designing environmentally friendly ships. Energy Saving Devices (ESDs), installed either before or after the propeller, are adapted on most ships to reduce the environmental impact of their operations. Viscous CFD calculations are the only way to design ESDs while considering the interaction effects between the hull form and the propeller. Integrated design of a hull form, a propeller, and ESDs can improve propulsive performance by a few percentage points compared to the sequential design method(Ichinose & Tahara, 2019). Aiming to enhance the integrated design of a ship's propulsive performance, accurately modeling time-dominant viscous CFD calculations becomes a key technology for adopting next-generation ship design strategies.

Physics-informed machine learning (ML) is one approach to accelerate time-consuming CFD calculations using ML. Raissi has estimated the flow field around a 2D cylinder by applying the Navier-Stokes equations as the loss function during Neural Network training (Raissi et al., 2018). A significant benefit of Physics-informed machine learning is that it eliminates the need for time-consuming mesh generation, which still requires some expert's techniques. Furthermore, "Physics-informed neural networks can seamlessly integrate multi-fidelity/multi-modality experimental data with various Navier–Stokes formulations for incompressible flows" (Cai et al., 2021). Multi-fidelity CFD, a combination of potential-based and RANS-based CFD, has been developed for hull form optimization to expand the exploration space in designing hull forms(Peri & Campana, 2005). Physics-informed neural networks have the potential to smoothly combine these multi-fidelity physics models, which could significantly alleviate the bottleneck in the overall optimization of ships by integrating one-dimensional and three-dimensional CFD methodologies.

On the other hand, ship design is an integral component of larger engineering projects and necessitates a comprehensive design methodology that accommodates the decision-making process, including achieving consensus among stakeholders. While machine learning models and generative AI can offer significant advantages, one of their notable drawbacks is the potential to produce misleading information. Therefore, to facilitate consensus-building and ensure robust decision-making, it is crucial to strategically combine these models with physics-based simulations. Employing machine learning models in a controlled setting, integrated with reliable simulation techniques, is essential for enhancing the accuracy and reliability of ship design processes.

This study discusses how to integrate data-driven approaches with physical model simulation design from a practical perspective. After organizing the structural challenges of current Simulation-Based Design, this paper proposes a practical data-driven method that integrates traditional simulation design with a data-enhanced, rationale-based design approach to overcome these challenges. Finally, demonstrating the proposed method shows its effectiveness. The core of our proposed design strategy is the effective circulation of data, which accumulates and is reinforced through day-to-day design operations. This paper partially showcases the impact of this data circulation, providing partial evidence of the efficacy of our approach.

CHALLENGES IN SIMULATION-BASED DESIGN ARCHITECTURE

First, this paper discuss about challenges in the conventional Physics-Simulation-Based Design architecture. The design of hull form has benefited from the adoption of Simulation-Based Design since around the year 2000 (ex. Matsumura & Ura, 1997). This led to have reduced the number of model tests and contributing to the reduction of design costs. Moreover, flow field information such as the pressure distribution on the hull surface and the wave height distribution provided by CFD outputs has deepened researchers' and designers' understanding of physical phenomena. However, the current architecture of Simulation-Based Design is described as a closed system that combines performance evaluation tools, shape

deformation tools, and optimization tools (Tahara et al., 2003). Nevertheless, this architecture has the following practical challenges:

1. Limited Design Space: The time-consuming CFD forces to constrain the design space to exploration in the optimization process.
2. Lack of Information for Robust Efficiency: Decision-making suffers due to a lack of information during the design process.
3. Lack of Design Reusability: Designs can't be reused for similar projects.

Figure 1 illustrates the configuration of the Simulation-Based Design (SBD) architecture and its three challenges. The SBD architecture consists of three components: a Performance Evaluator, which estimates performance using methods such as CFD; a Geometry Manipulator, which performs shape modifications; and an Optimizer, which optimizes these components. This study proceeds with discussions based on this architecture.

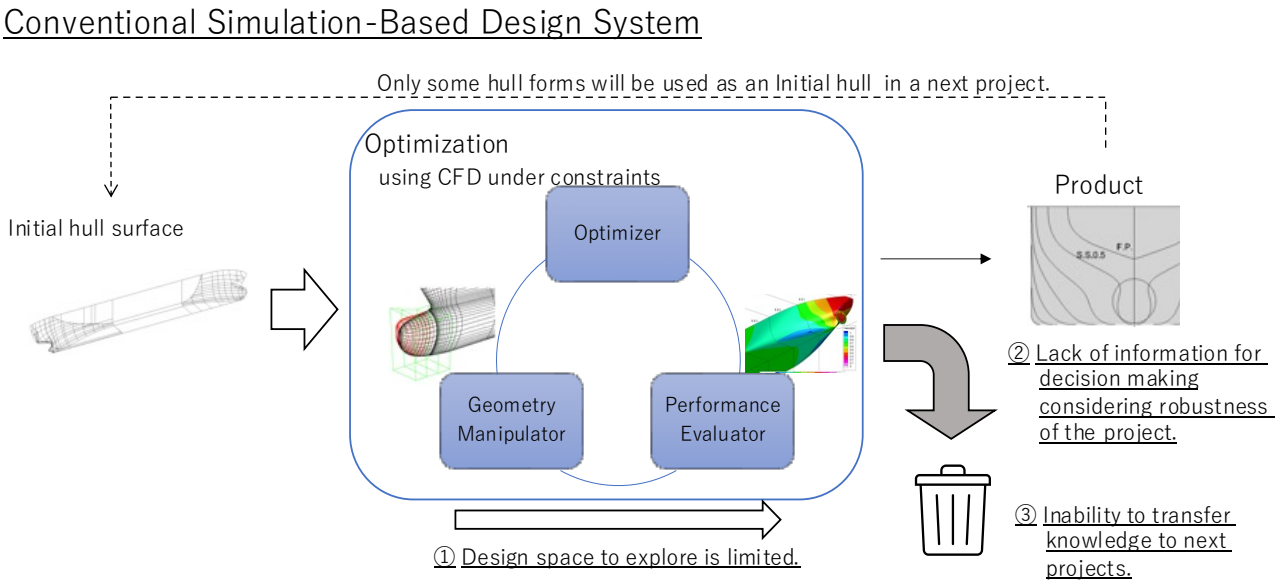

Figure 1: Challenges of Conventional Simulation-Based Design System.

The first challenge in conventional SBD architecture is that time-consuming CFD calculations, especially those solving the Reynolds-averaged Navier-Stokes (RaNS) equations through direct discretization, restrict the design space that can be explored. As a result, a broader exploration beyond basic hull parameters is often left to the designer's tacit knowledge, not covered by the design system. To address this issue, Kandasamy has proposed a method to explore a wider space by combining potential flow calculations with RaNS-based CFD in a multi-fidelity optimization approach (Kandasamy et al., 2010). Furthermore, Diez have suggested a method for dimensionality reduction of the design space through eigenvalue analysis of hull form deformation parameters (Diez et al., 2015). Indeed, these methods accelerate CFD calculations. However, they do not address the challenges of high-dimensional spaces encountered with the parametric hull form deformation methods currently used as Geometry Manipulators. As a solution to these high-dimensional challenges, Ichinose has proposed the use of machine learning to analyze a hull form database through the Hull-form Coordination System (Ichinose, 2022).

The second challenge is that the output of the SBD system is insufficient for design decisions such as determining the hull form, which is the main objective of ship design. The system lacks integration of information on simulation uncertainties, as well as information on other evaluative factors affecting the hull form that are not related to simulation, such as stability, structure, productivity, and propulsive performance. Factors like CFD calculations, scale effects of actual ships, and wave conditions have high uncertainties not currently considered in the SBD architecture. To address this, Tahara have proposed a method that theoretically handles variations in sea conditions and other factors using reliability optimization

theory (Tahara et al., 2014) . Meanwhile, Ichinose and others have suggested visualization of the design space, which is compatible with data-driven approaches (Ichinose, 2022).
The third challenge is the lack of a mechanism within the SBD architecture to reuse data obtained from SBD in subsequent projects, necessitating almost starting from scratch for each redesign. This issue stems from the absence of an information feedback mechanism within the architecture, suggesting that a solution could potentially be found through Data-driven approaches.

FOUR HYBRID MODELING APPROACHES COMBINING PHYSICS-BASED MODEL/SIMULATION AND DATA-DRIVEN MODEL

In ship design, the integration of physical simulations and data-driven methods is not actually a new concept. Ship design has long utilized design charts and empirical formulas from past data as data-driven tools. The direction of integrating physical simulation and data-driven approaches in this study involves replacing these design charts with machine learning models that are more accurate or advanced, and these models will be combined with physical simulations. Especially, the physical explain ability and reliability of the final design outputs based on physical simulations are particularly important considerations. On the other hand, introducing machine learning requires building mechanisms different from before. These include methods of databasing and data visualization, which become new considerations necessary for handling large-scale data.

Kanazawa has classified the enhancement methods of a ship dynamic model for ship motion prediction into four modes (update mode, convert mode, serial mode, parallel mode) while using a physics-based model as the foundation model to ensure physical explain ability and reliability (Kanazawa, 2023). These classifications, which include methods of correcting physics-based simulations and ways of applying machine learning loss functions, aim to increase the reliability of physics-based simulation results.

Moreover, design is a series of processes, and the integration methods of data-driven models with physics-based simulations are not solely for the purpose of improving reliability. That is, in the challenge of how to efficiently and robustly explore the design space to produce the optimal design output, several integration methods of data-driven models and physics-based simulations can be considered.

This study classifies and discusses the integration relationship between physics-based models and simulations and data-driven models in the ship form design process into four models, as shown in Figure 2.

A) Surrogate Model: The purpose of this model is to speed up time-consuming physics-based simulations. This integration method is particularly effective in multi-disciplinary optimization for overall optimization across various fields.
B) Complementary Model: This model is used in the process of narrowing down the design space. Currently, the design space is narrowed down using design databases and design charts based on key hull parameters, and detailed shape design is performed within this narrowed range using physics-based models such as physics-based simulations and model tests.
C) Correction Model: This model corrects the results of simulations or model tests using a design database. It is the most commonly used method in engineering, including scale effect correction of model test results for actual ships and data assimilation.
D) Constrained Model: This model involves setting design conditions and operational scenarios from operational data and designing with physics-based models. In the aviation field, Kim has proposed a model where machine learning models based on flight data set the simulation's flight phases and constraints(Kim et al., 2022).

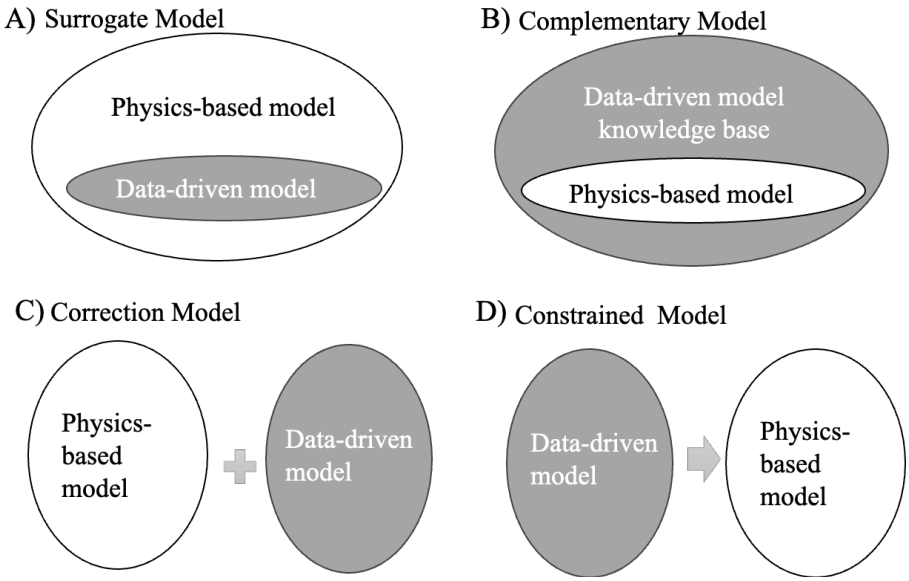

Figure 2: Schematic Representations of Four Hybrid Modeling Approaches Combining Physics-Based Model/Simulation and Data-driven Model

The hybrid models of physics-based models/simulations and data-driven models in the design process can be organized into four categories. However, as these hybrid models are incorporated into the design process, there may be instances where each model is sequentially combined or nested in accordance with the level of detail in the design deliberations. Therefore, when integrating physics-based models and simulations with data-driven models throughout the entire hull design process, it is necessary to appropriately apply these four models to each area of the design process. The next section will discuss how to practically construct a process that integrates physics-based models/simulations with data-driven models.

DATA-ENHANCED SBD ARCHITECTURE

This section discusses how to practically implement the hybrid models explained in the previous section into a practical design process.

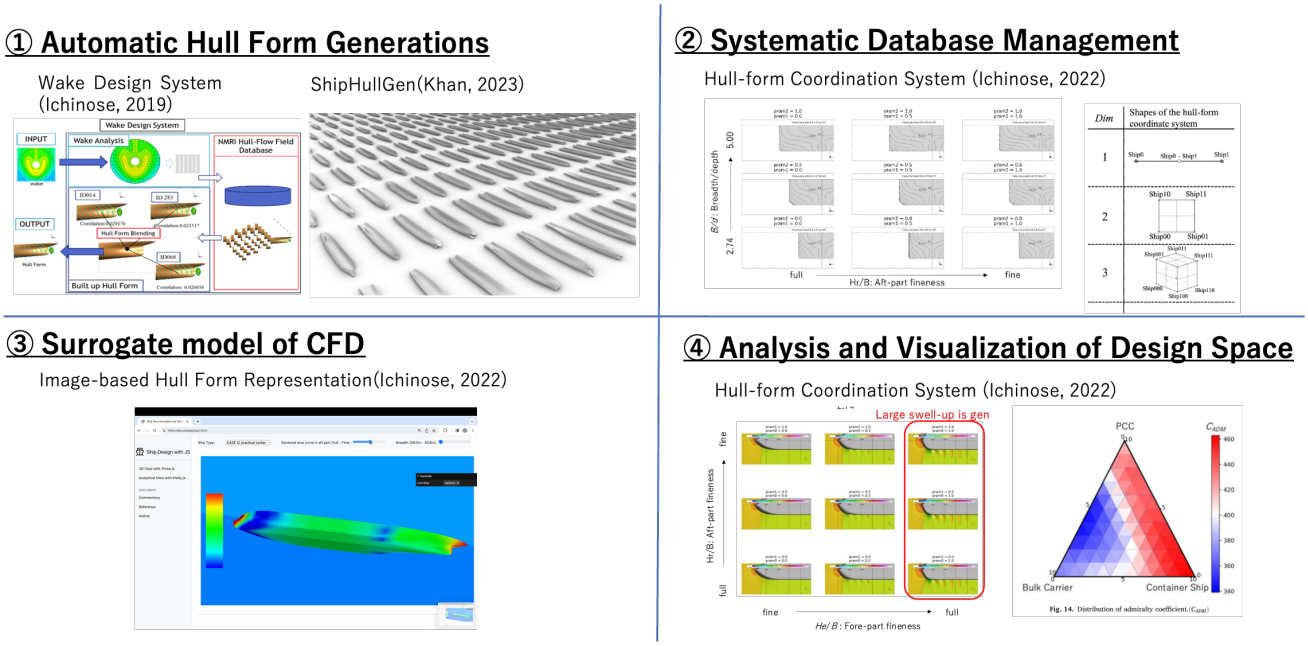

Figure 3: Component Technologies for Integration into Data-Enhanced Simulation-Based Design.

Figure 3 shows four data-driven design technologies that are considered capable of overcoming the challenges of the traditional Simulation-Based Design architecture discussed in the previous section. The first is an automatic hull-form generation tool. A hull design tool that automatically generates multiple design candidates from latent vectors (Khan et al., 2023) or past linear databases (Ichinose & Tahara, 2019) is one of the most critical technologies in the hull design process utilizing data-driven methods. Many conventional formulaic hull representations and parametric hull deformation methods are used for local hull modifications, but not extensively for entire design processes. This is because it is challenging to encapsulate the tacit knowledge of past designs, an asset of shipyards or experienced designers, into formulaic or parametric expressions with limited hull parameters. The second method, the Hull-form Coordination System (Ichinose, 2022), has potential to overcome this difficulty. It uses assets of past design project as basis vectors, allowing systematic expansion (interpolation) of hull form which was unable to express in conventional formulation. The purpose of interpolating hull form to increase database density is to create a CFD Surrogate model. For example, expanding the database with the Hull-form Coordination System by dividing 15 basic hull forms into four parts can automatically generate 15,504 ($=_{15+(4+1)}\ C_{15}$) hull forms. With a system that constantly runs CFD calculations in the background for these hull forms, the database and CFD Surrogate model (Ichinose & Taniguchi, 2022) continuously update based on accumulating day-to-day design work. Naturally, this database can also include data generated by traditional parametric hull representations and deformation methods. The last of the four is the method for analyzing and visualizing the database. Nonlinear optimization methods for designing hull forms within specific constraints often result in local optimal designs with uncertainties questioning their robustness. This necessitates further investigation by designers before deciding on the final design of a ship. The method for analyzing and visualizing the database enhances the robustness of these designs by allowing for analysis and visualization of the design space surrounding the optimal solution.

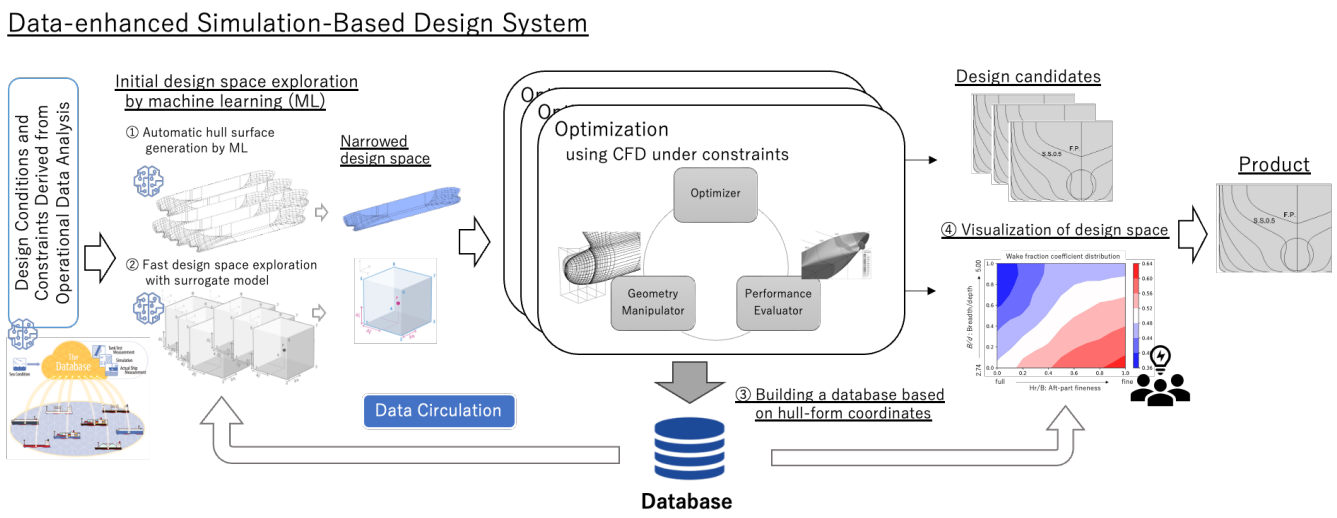

Figure 4: Overview of Data-Enhanced Simulation-Based Design system.

Considering the ways of integrating models discussed in the previous sections, this paper proposes the Data-enhanced Simulation-Based Design method illustrated in Figure 4. Here, based on the observation that the decision-making of the design process is always carried out based on physics-based model and simulation such as CFD and towing tank tests, the term "Data-enhanced" is used to explicitly denote the enhancement of processes using data, signifying the symbiotic relationship between data-driven methods and physics-based simulation.

As shown in Figure 4, the foundational Simulation-Based Design architecture is incorporated within the proposed method, enveloping it with the application of hull form databases and machine learning methods to overcome the three challenges of traditional SBD. First, regarding challenge 1 – limitation of the design space, the proposed method features initial hull form recommendations using the hull form database (1 in Figure 1) and narrowing down the design space with a CFD calculation Surrogate model by machine learning (2 in Figure 1). Next, for challenge 2, the proposed method addresses this challenge through two methods: proposing robust hull form selection using the Visualization method of the design space shown in 4 in Figure 4 (Ichinose, 2022), and multi-objective optimization considering general arrangement, stability, structure, and productivity (Papanikolaou, 2022). Lastly, for challenge 3, the proposed method enables data reuse in similar projects by

creating a database of all CFD calculation results and hull information, including performance evaluation results of hull forms discarded during optimization calculations, by databasing them based on the Hull-form Coordinate System treating each hull shape like a gene, thereby creating a cycle of data.

DEMONSTRATION OF THE PROPOSED METHOD

This section demonstrates the effectiveness of the proposed Data-enriched Simulation-Based Design method through a partial demonstration.

This paper takes as an example the design database shown in Table 1, which simulates an asset in a shipyard. Generally, shipyards tend to build ships with similar principal dimensions which they have built in the past, due to factors like crane capacity and dock size. The designs of these previously built ships are saved as CAD data along with CFD calculation data. These data have not been able to be organized by a set of hull parameters, making it difficult to database them. The Image-based Hull Form Representation method (Ichinose & Taniguchi, 2022) holds the hull form as the surface data of CFD structural grids, saving this data in a format similar to image data, which is more manageable for machine learning methods, thus allowing for databasing. This makes it possible to database nearly all hull forms that can be represented by structural grids.

Furthermore, the Hull-form Coordination System can generate new hull forms from this database. This method allows for the automatic expansion of a denser hull form database suitable for machine learning. The 20,952 data points shown in Table 1 are from a hull form database expanded from 20 basis hull forms using the Hull-form Coordination System. This expanded database is utilized as a surrogate model for CFD calculations by a Convolutional Neural Network (CNN) model.

Table 1: Overview of Database for the Demonstration

Ship Type	Container Ship, Pure Car Carrier, Bulk Carrier, Chemical Tanker, Oil Tanker, Mathematical Hull Form with Buttock Flow Stern
Basis Ships	20
Total Number of Ships	20,952
Length/Breadth	5.00 – 7.50
Breadth/Draft	2.0 – 3.60
Blockage Coefficient	0.47 – 0.88

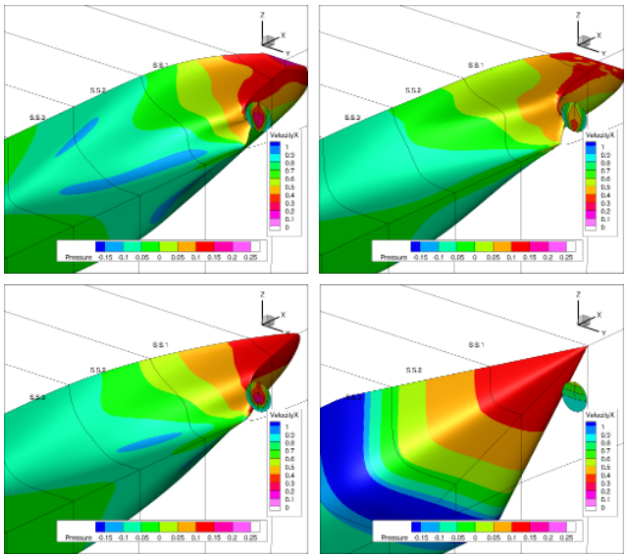

Figure 5: An Examples of Hull Forms and on the Database generated by Basic Ships

A feature of this proposed method is that the items related to estimated propulsive performance are not limited to integrated values such as resistance values, which have traditionally been estimated by design charts. By incorporating a Decoder model

into the Neural Network architecture, as shown in Figure 6, it is possible to present information useful for designers to understand physical background and deepen the insight, such as the pressure field on the hull surface and the wake flow distribution on the propeller surface. The Decoder model is a type of generative AI model used for creating images. Historically, the application of machine learning in ship design has been confined to tasks such as classification and scalar value inference. While scalar values, such as main engine output, are essential estimations for design, they do not provide guidance on which specific parts of the hull form could be improved. In contrast, models utilizing the Decoder model can estimate the pressure distribution on the hull surface and the wake distribution behind the propeller. This capability marks a significant shift as it offers detailed guidelines on how to modify the hull form for design improvements, providing much-needed directional insights for enhancing overall ship design.

Moreover, the estimation time for this surrogate model by machine learning is less than 0.1 seconds, significantly faster than the hours it takes for one case of RaNS-based CFD. Although the design space that can be covered by machine learning is limited in this example, in actual operation in shipyards, it is assumed that the design exploration range of this surrogate model is almost equivalent to the entire expected design space due to the abundance of conventional databases and the ability to semi-automatically construct a large amount of hull form data using Hull Form blending methods or FFD methods.

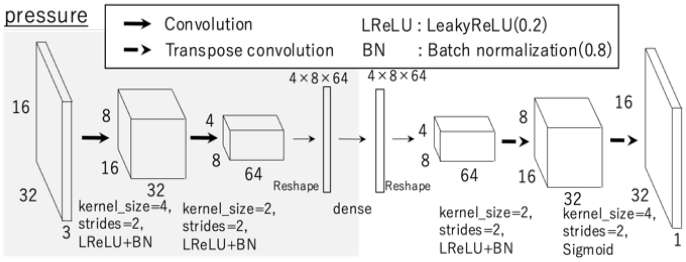

Figure 6: Architecture of neural network for prediction of pressure distribution

Figure 7 shows the difference between the resistance coefficient predicted by the CNN model and the true value (CFD calculation value). The dataset shown has not been used in the machine learning training. The results in Figure 7 confirms that the resistance values are estimated within ±5% accuracy that is sufficient for practical design across a wide range of ship types and principal dimensions. This estimation is intended for narrowing down options in the preliminary phase of traditional design.

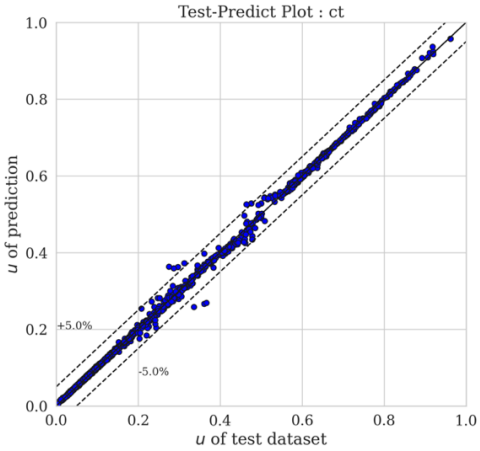

Figure 7: Comparison of prediction and grand truth of resistance coefficient

Next, Figure 8 compares the predicted and true values of the pressure distribution on the hull surface by the CNN model. The figure shows the pressure distribution from the bow to the stern from left to right, and from the bottom to the water surface in the girth direction from bottom to top, accurately reproducing the island-like shape of the pressure distribution that creates the adverse pressure gradient significant for resistance at the stern bilge. Such information is necessary for designers to physically understand why resistance has increased. Even while using an estimation method that can easily become a "black box" like machine learning, providing a means to understand physical phenomena is one advantage of the proposed method.

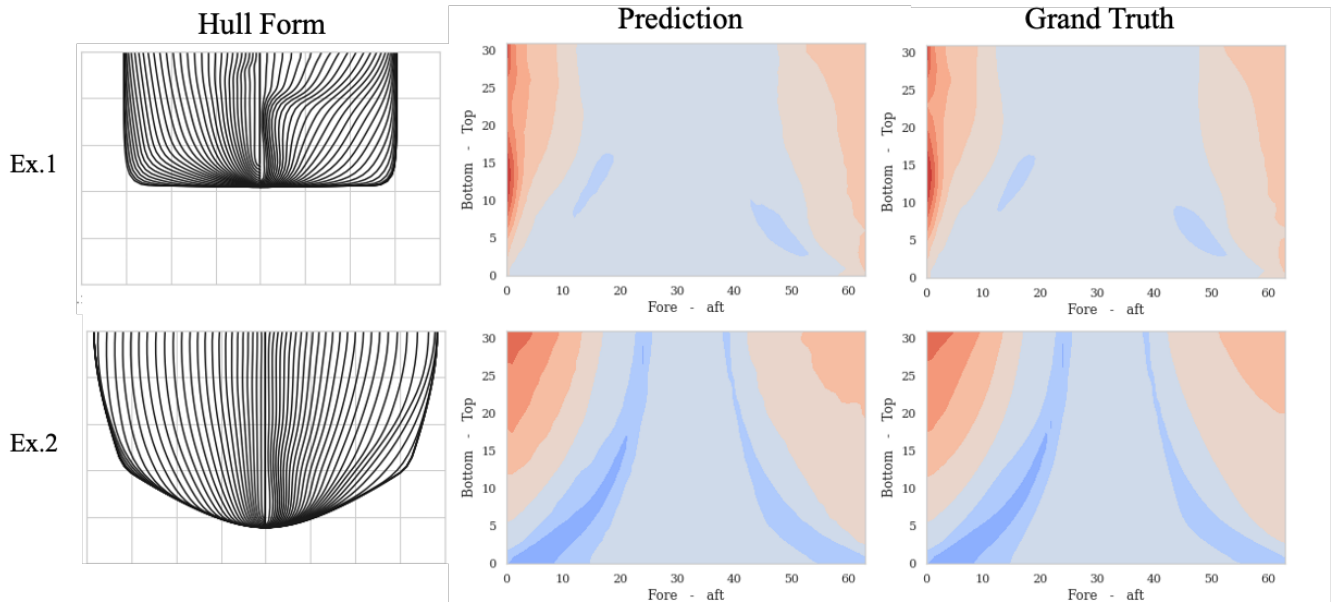

Figure 8: Comparison of prediction and grand truth in pressure prediction

CONCLUSIONS

In conclusion, this paper has explored the transformative potential of machine learning techniques for directly producing design outputs, such as the 3D shape and pressure distribution of hull forms, within the realm of ship design. However, it also underscores the critical importance of achieving consensus among stakeholders in the inherently complex decision-making process of ship design, a process deeply rooted in physics-based simulations/models. This paper proposes a design strategy that leverages the strengths of both physics-based and data-driven models, positioning the former at the core of the design process while enhancing it with the latter.

This paper has systematically outlined a method for hybridizing two model types and demonstrated their effective integration into a practical design process. This approach not only adheres to the traditional reliance on physics-based models but also leverages the efficiency gains provided by machine learning. The demonstration confirms that the CNN model, serving as a tool for initial exploration across a wide design space, can predict resistance performance with an accuracy of ±5%, which is sufficient for practical design across a broad range of ship types and principal dimensions. Additionally, this machine learning model is capable of estimating pressure distribution in viscous flow with high Reynolds number within 1 second, thereby enabling designers to incorporate physics-based insights to achieve robust efficiency.

CONTRIBUTION STATEMENT

Yasuo Ichinose: Conceptualization; data curation, investigation; methodology; software, validation; visualization; writing – original draft. **Tomoyuki Taniguchi:** Formal analysis; software; writing – review and editing.

ACKNOWLEDGEMENTS

This work was partially supported by JSPS KAKENHI Grant Number 20K04954.

REFERENCES

Cai, S., Mao, Z., Wang, Z., Yin, M., & Karniadakis, G. E. (2021). Physics-informed neural networks (PINNs) for fluid mechanics: A review. *Acta Mechanica Sinica*, *37*(12), 1727–1738. https://doi.org/10.1007/s10409-021-01148-1

Diez, M., Campana, E. F., & Stern, F. (2015). Design-space dimensionality reduction in shape optimization by Karhunen-Loève expansion. *Computer Methods in Applied Mechanics and Engineering*, *283*, 1525–1544. Scopus. https://doi.org/10.1016/j.cma.2014.10.042

Erikstad, S., & Lagemann, B. (2022). *Design Methodology State-of-the-Art Report*. https://doi.org/10.5957/IMDC-2022-301
Ichinose, Y. (2022). Method involving shape-morphing of multiple hull forms aimed at organizing and visualizing the propulsive performance of optimal ship designs. *Ocean Engineering*, *263*, 112355. https://doi.org/10.1016/j.oceaneng.2022.112355
Ichinose, Y., & Gaspar, H. M. (2023). Interactive Ship Flow Simulation Enhanced By Neural Network Model In A Web Environment. *ECMS 2023 Proceedings Edited by Enrico Vicario, Romeo Bandinelli, Virginia Fani, Michele Mastroianni*, 155–161. https://doi.org/10.7148/2023-0155
Ichinose, Y., & Tahara, Y. (2019). A wake field design system utilizing a database analysis to enhance the performance of energy saving devices and propeller. *Journal of Marine Science and Technology*, *24*(4), 1119–1133. https://doi.org/10.1007/s00773-018-0611-x
Ichinose, Y., & Taniguchi, T. (2022). A curved surface representation method for convolutional neural network of wake field prediction. *Journal of Marine Science and Technology*, *27*(1), 637–647. https://doi.org/10.1007/s00773-021-00857-3
Kanazawa, M. (2023). *Data-driven enhancement to ship dynamic model for motion prediction* [Doctoral thesis, NTNU]. https://ntnuopen.ntnu.no/ntnu-xmlui/handle/11250/3088275
Kandasamy, M., Ooi, S. K., Carrica, P., & Stern, F. (2010). Integral Force/Moment Waterjet Model for CFD Simulations. *Journal of Fluids Engineering*, *132*(10). https://doi.org/10.1115/1.4002573
Khan, S., Goucher-Lambert, K., Kostas, K., & Kaklis, P. (2023). ShipHullGAN: A generic parametric modeller for ship hull design using deep convolutional generative model. *Computer Methods in Applied Mechanics and Engineering*, *411*, 116051. https://doi.org/10.1016/j.cma.2023.116051
Kim, D., Seth, A., & Liem, R. P. (2022). Data-enhanced dynamic flight simulations for flight performance analysis. *Aerospace Science and Technology*, *121*, 107357. https://doi.org/10.1016/j.ast.2022.107357
Matsumura, T., & Ura, T. (1997). Preliminary Estimation Tool of Propulsive Performance for High Speed Craft based onArtificial Neural Networks. *Journal of the Society of Naval Architects of Japan*, *1997*(181), 221–232. https://doi.org/10.2534/jjasnaoe1968.1997.221
Papanikolaou, A. D. (2022). Holistic Approach to Ship Design. *Journal of Marine Science and Engineering*, *10*(11), Article 11. https://doi.org/10.3390/jmse10111717
Perabo, F., Park, D., Zadeh, M. K., Smogeli, Ø., & Jamt, L. (2020). Digital Twin Modelling of Ship Power and Propulsion Systems: Application of the Open Simulation Platform (OSP). *2020 IEEE 29th International Symposium on Industrial Electronics (ISIE)*, 1265–1270. https://doi.org/10.1109/ISIE45063.2020.9152218
Peri, D., & Campana, E. F. (2005). High-Fidelity Models and Multiobjective Global Optimization Algorithms in Simulation-Based Design. *Journal of Ship Research*, *49*(03), 159–175. https://doi.org/10.5957/jsr.2005.49.3.159
Raissi, M., Yazdani, A., & Karniadakis, G. E. (2018). *Hidden Fluid Mechanics: A Navier-Stokes Informed Deep Learning Framework for Assimilating Flow Visualization Data* (arXiv:1808.04327). arXiv. https://doi.org/10.48550/arXiv.1808.04327
Tahara, Y., Diez, M., Volpi, S., Chen, X., Campana, E., & Stern, F. (2014). CFD-Based Multiobjective Stochastic Optimization of a Waterjet Propelled High Speed Ship. *Proceedings of 30th Symposium on Naval Hydrodynamics*, 21.
Tahara, Y., Sugimoto, S., Murayama, S., Katsui, T., & Himeno, Y. (2003). Development of CAD/CFD/Optimizer-Integrated Hull-Form Design System. *Proceedings of the Kansai Society of Naval Architects*, *20*, 1–5.

Proceedings of 15th International Marine Design Conference (IMDC-2024)
June 2-6, 2024
Amsterdam, the Netherlands

The Method to Navigate the Forward and Backward Path of a Towing Tractor for Transporting Aircraft

Ki-Su Kim[1], Kwang-Phil Park[2,*] and Sang-Hun Kang[3]

ABSTRACT

Aircraft carriers are the backbone of the Navy. They are equipped with aircraft, and their ability to take off and land aircraft quickly and efficiently determines their performance. Therefore, the number of aircraft is a key consideration in the design of an aircraft carrier and ensuring that they can be operated in the space of the aircraft carrier is an important factor in the arrangement design as well. On the other hands, towing tractors are used to move aircraft around. Towing tractors must safely move aircraft in open spaces while avoiding multiple obstacles, which requires skilled operators. In this study, we propose a method to automate the path of a towing tractor and then follow it. First, we studied the kinematics of the towing tractor and aircraft carrier, considering the wheel movement and steering angle. Then, we calculated the optimal path of the tractor and aircraft considering both forward and backward motion. Finally, we applied dynamics to verify that the towing tractor and aircraft carrier could follow the calculated path. We tested the proposed method in a field with various obstacles and in a narrow area such as a parking lot and confirmed that it was effective.

KEY WORDS

Aircraft carrier; Towing tractor; Navigation; Optimal path; Dynamics.

INTRODUCTION

Traditionally, aircraft carriers are the main power of major powers as well as the navy. (Ryan et al., 2011) Aircraft are typically equipped in aircraft carriers, and how many and how fast they can take-off and land determine the performance of aircraft carriers. In general, for preparing the take-off and landing sequence of aircraft, a towing tractor is used. On land, this work can be carried out smoothly like airplane at general airports along guidance lines and work instructions. However, as described above, since this process must be performed in limited space in an aircraft carrier lined with many aircraft and equipment, the time and efficiency of moving aircraft depend on the proficiency of the towing tractor operator. Therefore, it is necessary to automate the path of the towing tractor and follow it. this study proposes a method of optimizing and following the path of the towing tractor in the aircraft carrier.

Various methods have been proposed for utilizing towing tractors to determine and track the optimal path for aircraft carriers. Gomez-Brabo et al. (2005) proposed a method for planning the path of a tractor-trailer, predicting the path based on the kinematics and restricted maneuvering modeling of the tractor-trailer's motion. They then utilized fuzzy system inverse mapping to generate the optimal path for movement. Similarly, Elhassan (2015) performed modeling to predict the path of the connected vehicle and then used the rapidly exploring random tree (RRT) method to generate the optimal path. This was then applied to the docking task. In addition to the aforementioned studies, our research has explored various methods for generating and tracking the optimal path for aircraft and towing tractors.

[1] Ki-Su Kim (School of Naval Architecture and Ocean Engineering, University of Ulsan, Ulsan, Republic of Korea); ORCID: 0000-0003-3058-8661

[2,*] Kwang-Phil Park (Department of Autonomous Vehicle System Engineering, Chungnam National University, Daejeon, Republic of Korea); ORCID: 0000-0002-5196-5537

[4] Sang-Hun Kang (School of Naval Architecture and Ocean Engineering, University of Ulsan, Ulsan, Republic of Korea)
* Corresponding Author: kppark@cnu.ac.kr

Submitted: 13 Febraruy 2024, Revised: 17 April 2024, Accepted: 1 May 2024, Published: 27 May 2024

Conference paper, DOI: https://doi.org/10.59490/imdc.2024.911 e-ISSN: 3050-4864

KINEMATICS

When moving aircraft in a hanger or deck on aircraft carrier, it does not move by itself with propulsion, but uses a tractor to tow the ship. Therefore, the tractor fixes the nose wheel and then tow it to move aircraft. This movement becomes very similar to the movement of a general tractor-trailer, which is expressed in figure 1. And if kinematics is derived for this, it can be expressed as equation 1.

$$\frac{d}{dt}\begin{bmatrix} x_1 \\ y_1 \\ \theta_{CA} \\ \theta_T \end{bmatrix} = \begin{bmatrix} v_T \cos\beta_{CA} \cos\theta_{CA} \\ v_T \cos\beta_{CA} \sin\theta_{CA} \\ \dfrac{v_T \cos\beta_{CA} \tan\beta_{CA}}{L_{CA}} \\ \dfrac{v_T \tan\beta_T}{L_T} \end{bmatrix} \quad [1]$$

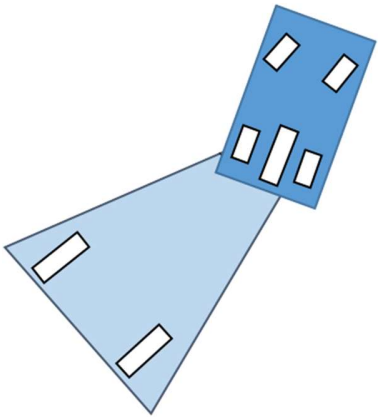

Figure 1. Schematic of towing tractor and aircraft

There are two wheels, an axis, and a nose wheel in front of the rear wheel. And the distance between the axes of the loader is called L_{CA}, and θ_{CA} is the angle of the loader based on the fixed coordinate system. And β_{CA} is the angle between the nose wheel and the central axis of the loader, and x_1 and y_1 are the absolute coordinates of the center of the rear wheel shaft of the loader. The distance between the axes of the turning tractor is L_T, and the rotation angle and steering angle of the tractor are θ_T and β_T, respectively. And the speed of the tractor is set to be v_T.

HYBRID A*

In general, Dijkstra's method (Dijkstra, 1959) or A* method (Russell, 2018) is used for path search. However, in the case of this method, as a method designed for graph search, a graph is generally constructed based on grid and used to find a path. Therefore, there is a great disadvantage that the search area is limited due to grid. Hybrid A* method was designed to apply dynamics or kinematic to the A* method. If the existing A* method moved within a predefined grid, the hybrid A* method is a big difference in that the node for search is not the center of the grid or a point based on the grid, but a point considering the kinematic model at the current node. Therefore, it is possible to construct a node in consideration of dynamics that could not be considered in the existing grid-based method. Path search scheme using hybrid A* for towing tractor and aircraft can be expressed as figure2.

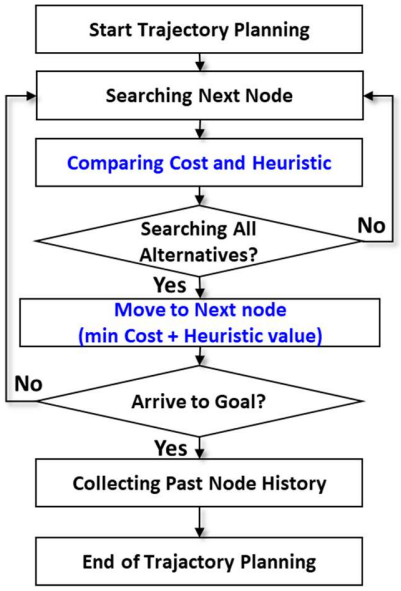

Figure 2. Path search scheme for towing tractor and aircraft using Hybrid A*

The cost function is a function representing the cost required to proceed to the node, and in general, the distance is often used as a cost value for the shortest distance search. In the case of our problem, the distance between the two nodes was considered as a cost because the shortest distance had to be considered basically. And in the case of backward movement, an additional cost was added because it is a relatively more difficult path than forward movement. In addition, in the same way, an additional cost was added when the direction was changed from forward to backward or from backward to forward. Here, the additional cost was selected in consideration of the interval between nodes and configured to be changed according to the needs of the user.

APPLICATION

In this study, a user program based on the kinematics and hybrid A* described above was implemented. The program can generate simple fields and examples for the towing tractor and aircraft. The program was developed in a .Net environment using the C# language, and a GUI was implemented using the MVVM pattern. The GUI configuration is shown in figure 3.

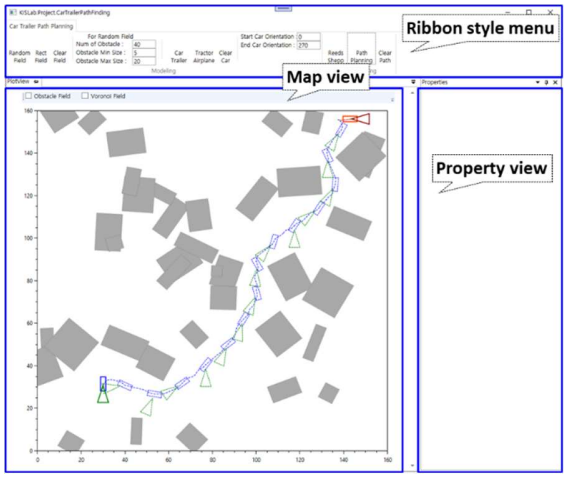

Figure 3. Configuration of in-house program for applications

The hangar of the aircraft carrier is very crowded with aircraft and equipment. Therefore, assuming the situation, two examples were carried out under the assumption that the aircraft is carried from a narrow field to a tuning tractor as follows.
The first example is how to get the aircraft back to its destination after the turning of the towing tractor. This requires very precise transportation, and of course, the backward movement must be carefully performed in consideration of the jack-knifing.

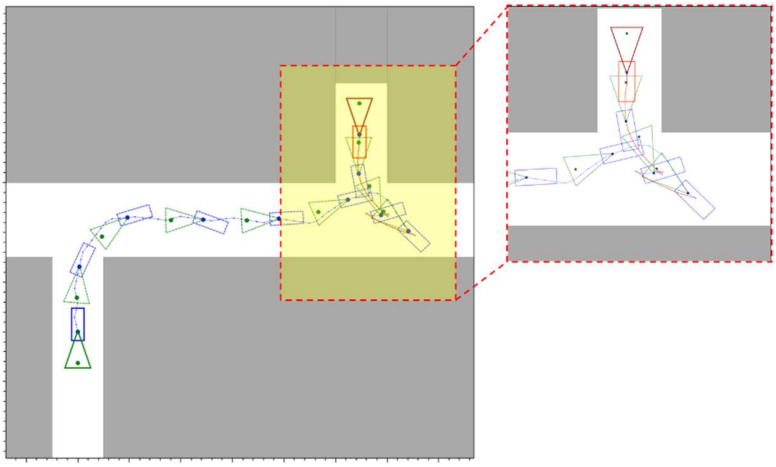

Figure 4. Path planning for backward movement

As can be seen in figure 4, while considering kinematics, it is important to pay attention to collisions with the surrounding environment when reversing. The blue path is forward movement and red path is backward movement. The following path was shown that forward and backward movement were harmonically used as a skilled operator and it can be seen that the path is found smoothly.

The second example is for parallel parking. Since the aircraft acts like a cargo of a truck, parallel parking is a much more difficult maneuver than normal parking. Figure 5 shows a path of parallel parking of an aircraft in a very narrow environment. As can be seen in figure 5, the towing tractor is rotated, and parallel parking is performed smoothly as operators driving pattern.

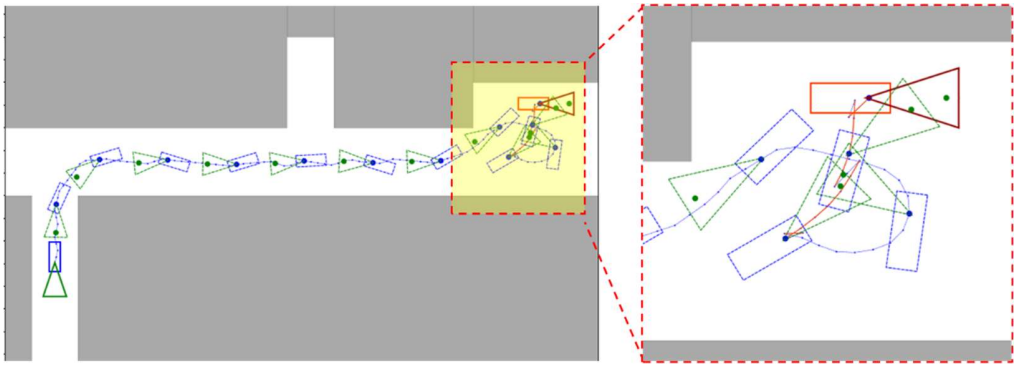

Figure 5. Path planning for parallel parking

CONCLUSIONS AND FUTURE WORKS

In this study, we proposed a method to find a path that can effectively transport an aircraft in the aircraft carrier, which is a limited space for the towing tractor. This method is based on the kinematics for the towing tractor and aircraft. And using this, hybrid A* method was used to find the path considering forward and backward movement. For implementing this, in-house program was developed and applied to two cases. Two cases were modeled after frequently performed operations in aircraft carriers. The results show that generated path for towing was acceptable and similar to real operations.

The proposed method in this study is a path planning method that considers the connection between a aircraft and a tractor. However, it can also be applied to path planning for large ships being towed by tugboats in narrow coastal waters. Therefore, in the future, we plan to expand this method to towing problems for large ships in coastal area. In this case, the ship's equations of motion will be mainly used, and the ship's optimal fuel consumption and time will be considered accordingly.

CONTRIBUTION STATEMENT

Ki-Su Kim[1]: conceptualization; methodology; implementation; writing – original draft, **Kwang-Phil Park**[2,*]**:** conceptualization; supervision; writing – review and editing **and Sang-Hun Kang**[3]**:** research assistance.

ACKNOWLEDGEMENTS

This result was partially supported by "Regional Innovation Strategy (RIS)" through the National Research Foundation of Korea(NRF) funded by the Ministry of Education(MOE)(2021RIS-003), and Korea Institute for Advancement of Technology (KIAT) grant funded by the Korea Government (MOTIE) (P0017006, HRD Program for Industrial Innovation).

REFERENCES

Gomez-Bravo, F., Cuesta, F. & Ollero, A. (2015) Autonomous tractor-trailer back-up manoeuvering based on changing trailer orientation, 16th Triennial World Congress, Grague, Czech Republic.
Elhassan A., (2015) Autonomous driving system for reversing an articulated vehicle, Mater Thesis, School of Electrical Engineering, Department of Automatic Control, The Royal Institute of Technology.
Ryan, J.C., Cummings, M.L., Roy, N., Banerjee, A., & Schulte, A. (2011). Designing an interactive local and global decision support system for aircraft carrier deck scheduling. AIAA Infotech at Aerospace Conference and Exhibit 2011.
Dijkstra, E.W. (1959). A note on two problems in connexion with graphs, Numerische Mathematik, 1, 269–271.
Russell, S.J. (2018). Artificial intelligence a modern approach. Norvig, Peter (4th ed.). Boston: Pearson.

Proceedings of 15th International Marine Design Conference (IMDC-2024)
June 2-6, 2024
Amsterdam, the Netherlands

A Service Blueprint Approach in Shipbuilding Activity Mapping

Yong Se Kim[1,*] Junsong He[2,] Ludmila Seppälä[3]

ABSTRACT

In the evolving landscape of shipbuilding, the confluence of innovative methodologies and advanced technologies is reshaping paradigms in ship design and production. The industry's quest for multidisciplinary methods that elaborate representing diverse ship building activities and boost efficiency in managing these activities has unveiled the potential of the service blueprint, a tool used in service design, which addresses design of activities and determining who does what activities when in collaboration with whom.

Our proposition centres on the structured activity mapping representation, a novel activity map that utilizes service blueprint with detailed description of activities with rich and structured representation of context. The framework offers a comprehensive perspective, illuminating intricate processes such as concept design, detailed design and production stages as well as service and operation stages. This mapping would ensure alignment of each activity with overarching project objectives, encapsulating values, interactions, collaborations. This paper illustrates the approach of service blueprint in representing ship building activities with discussion on improvement potential of current activity mapping through the service blueprint approach as being conducted in the SEUS EU Horizon project.

Key Words

Shipbuilding Process Methodology, Human-Centricity, Activity Mapping, Service Blueprint

Introduction

The European shipbuilding industry is currently navigating a complex landscape with challenges, including intensified competition from thriving Asian counterparts, economic volatility, and a growing demand for environmentally sustainable and technically advanced vessels (Seppälä et al., 2023). This paper examines these challenges as the industry stands at the intersection of addressing current impediments, redefining its competitive strategies for the future, and embracing the shift into a more human-centric paradigm. This paper is based on research conducted within the Smart European Shipbuilding (SEUS) project.

One of the primary challenges faced by European shipyards is the rising competition from Asian nations such as South Korea, China, India, and Vietnam. These competitors have progressively expanded their market share, driven by factors like robust economic growth, substantial government support, reduced production costs, and technological advancements (ECORYS, 2009). To ensure a sustainable competitive advantage, European shipyards may make a prudent decision by placing greater emphasis on the concept design phase. It is asserted that a substantial 80% of the total life-cycle costs of a product are determined during the design and planning stages. Therefore, the concept design holds a crucial role in the overall process of product development (Ohtomi, 2005). A typical commercial ship takes about two to three years to build (Payne & Chokshi,

[1] Turku Design Studio, University of Turku, Turku, Finland; ORCID: 0000-0001-7320-7772

[2] Turku Design Studio,University of Turku, Turku, Finland; ORCID: 0009-0006-3405-9109

[3] Marine Industry Business Development, CADMATIC, Turku, Finland;

* Corresponding Author: email yskim83395@gmail.com

Submitted: 23 February 2024, Revised: 13 April 2024, Accepted: 1 May 2024, Published: 18 May 2024

Conference paper, DOI: https://doi.org/10.59490/imdc.2024.827 e-ISSN: 3050-4864

2020). A well-conceived concept design, characterized by a comprehensive integration of emerging technologies, business prospects, and human ingenuity, would bring a competitive advantage (Agis, 2020). In this context, the question arises: How can we foster innovation by adopting more comprehensive and advanced perspectives?

In shipbuilding industry, needs, functions and structures of typical design issues are applied in the concept design phase of shipbuilding to enhance resilience by considering latent capabilities (Pettersen, 2018). It emerges that value considerations should be articulated early in the design process to enhance the concept design phase. This will empower designers to make informed decisions and integrate values into technological innovations, leading to responsible and accountable design outcomes (Van Den Hoven et al., 2015). Thus, the value issues should be addressed in the concept design phase because it helps to empower the design process by ensuring that the project aligns with the organization's diverse values and goals. By considering the value perspective, the design team can ensure that the project is not only technically feasible and efficient but also aligns with the organization's mission, vision, and culture. Shipbuilding activities vary across different shipyards due to different contexts (Strandhagen et al., 2020). Various shipyards may prioritize distinct values, such as a commitment to environmental sustainability, and may emphasize the transition towards advanced technologies (Oloruntobi et al., 2023). Furthermore, it is important to acknowledge that there are additional values that could be considered in the decision-making process.

Now the research issue is to develop a methodology with a proper tool to enable considerations of diverse value perspectives in an integrated manner to encompass the overall shipbuilding process including concept design, detail design, production, and operation and use stages at a high-level so that value issues of diverse stakeholders are reflected. This paper presents an approach to address this research issue as being developed at the SEUS project. Specifically, this is done with overall shipbuilding planning and management with human-centric representation and management of shipbuilding activities and interaction and collaboration of various shipbuilding actors including ship owners, operators, and service providers as well as users and passengers.

The paper first reviews of service design and a method with a tool used in service design so that activities of diverse stakeholders are designed and represented. Service design results are typically represented as service blueprints. Shipbuilding activity mapping is briefly reviewed. Then a service blueprint approach of activity mapping is sketched as this would allow planning and management shipbuilding activities with emphasis on human-centric perspectives. The next section summarizes findings on current practices of activity mapping in two shipyards including their unmet needs and expectations. In the following section, a structured activity mapping framework is proposed with detailed explanations including a sketchy utility of the proposed framework in enabling comprehensive integration of shipbuilding process including concept design, detail design, production, and operation and use stages for the next-generation shipbuilding competitiveness. The paper is concluded with discussions on novel characteristics of the proposed activity mapping framework as well as future work.

Service Blueprint Approach in Activity Mapping

Service Design and Service Blueprint

A service blueprint has been used in designing services (Shostack, 1982), and is a visual representation of the process involved in delivering a service, specifying the linkages between different activities and the roles of different actors involved in service delivery (Patrício et al., 2011). The service blueprint prioritizes roles and activities of actors over individual tasks. Utilizing service blueprints, the process of shipbuilding activity mapping can place a greater emphasis on human-centered perspectives.

Service design and service blueprint are receiving greater attention because they play critical roles in creating new forms of values co-created with customers, organizations, and experts, and service innovation involves a new process or service offering that creates value for one or more actors in a service network through a human-centred and holistic thinking approach (Patrício et al., 2018). In simpler terms, service blueprints prioritize human-centric issues such as customers, service providers and other stakeholders within the entire system of value chain. The real virtue of service design has been verified with cases in various industries, particularly in the context of experience-centric services (Zomerdijk & Voss, 2010). Moreover, the emphasis on human-centricity in manufacturing-oriented industries through service integration has been in a growing trend in Product-Service System (PSS) development (Goedkoop et al., 1999; Costa et al., 2018). Note that a PSS is a system of products, services, supporting networks and infrastructure that is designed to satisfy customer needs and to generate values (Goedkoop et al., 1999; Tukker, 2015). Note that, in recent view of human-centered PSS design perspective, values are elucidated by activities and experiences that human stakeholders make using product artefacts in collaboration with other stakeholders of the ecosystem, rather than directly from artefacts (Kim, 2023).

In essence, service design is the process of designing human activities of service provider and service receivers. A service blueprint is a visual representation of all activities in the entire system, which helps to identify which stakeholder is engaged in which activities, in relation to which other stakeholders and in interaction with which other stakeholders. That is, a service

blueprint, a tool used in service design, addresses design of activities and determining *who does what activities when in collaboration with whom.*

Shipbuilding Activity Mapping

Bruce (2021) explains what shipbuilding activity mapping in detail as follows. Shipbuilding activity mapping refers to the process of creating an overview of ship production, outlining the stages of a ship project and the major functions within a shipyard. Shipbuilding activity addresses a set of tasks, processes, or events related to a particular project. Shipbuilding activity can include financial planning, schedule planning, design work planning, design team organization, reporting, staff meetings, action items, master calendars, security classification and document marking. According to our interviews with two shipyards participating in the SEUS project, as summarized in the third section, current shipbuilding activity mapping practices concentrate on tasks and schedules. This current approach supports in planning, tracking, and monitoring all ongoing tasks and resources, ensuring timely delivery to ship owners.

Toward Human-Centric Shipbuilding Activity Mapping

There are extensive and diverse range of stakeholders and subcontractors involved in shipbuilding activities. They may include ship owners, government agency representatives, port engineers, ship supervisors and risk insurers; designers, naval architects, inspectors, marine engineers, and estimators; shipyard personnel, major vendors, major subcontractors, consultants, contract preparers; project managers, project planners, superintendents, maintenance supervisors (Bruce, 2021). It is important to recognize that these individuals are active actors with intent, motivation, expertise and relationships with other actors. Human-centricity issues are significant as reflected in Industry 5.0 (Xu et al., 2021).

Conventional shipbuilding activity mapping primarily centers on tasks. That is, activity mapping addresses how tasks are assigned considering resources and when tasks are done. Tasks are shown vertically with timeline progresses as in Figure 1 (a). By incorporating the service blueprint approach, actor-centered considerations including relationships among actors can be addressed with primary focus. In this approach, on the other hand, actors are shown vertically with horizontal timeline as in Figure 1 (b). Moreover, diverse values can be specifically associated with activities by utilizing the context-based activity modeling (CBAM) method. Please note that the CBAM method has been devised to represent activities in service design field with a formal and rich representation together with context elements (Kim et al., 2020) as briefly reviewed in a later section.

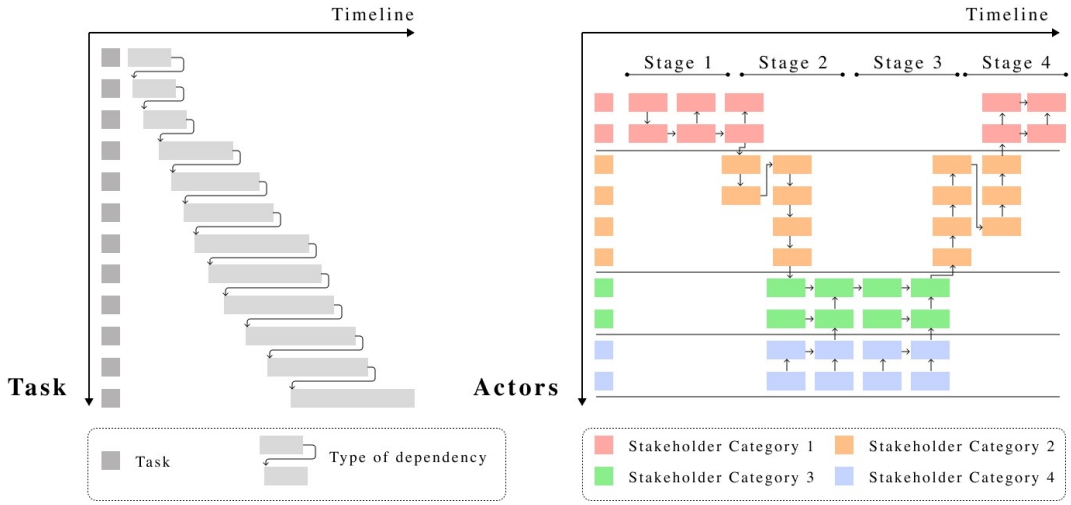

(a) Task-focused Approach (b) Service Blueprint Approach

Figure 1: Shipbuilding Activity Mapping Approaches

Emerging Demands in Activity Mapping Practices: Cases of Two Shipyards

The current practices of two shipyards, Shipyard A in Spain and Shipyard B in Norway, in their activity mapping have been investigated through semi-structured interviews. Three kinds of questions were made on how their activity mapping practices are done currently, on their unmet needs and expectations, and on their visions on the next-generation activity mapping. Key contents of the interviews have been summarized in Table 1. Their approaches to planning and managing shipbuilding projects have been understood and some insights were obtained.

Activity Mapping	*Shipyard A*	*Shipyard B*
How shipyard maps the activity nowadays	Microsoft Project serves as the primary software for activity mapping. The primary emphasis lies in scheduling functions, encompassing coordination of tasks and monitoring project progress.	Microsoft Project is employed currently. There is a lack of dedicated software for facilitating communication with suppliers. No software exists to help manage resources and retain their knowledge and experience.
Needs and expectations	A strong interest and need in the integration and analysis of data to derive actionable insights, generate reports, and establish benchmarks.	A desire for collaborative tools to engage with ship owners and to boost collaboration among supervisors and team members. The expectation of data integration across design, production, sourcing, and engineering.
Vision of next generation activity mapping	A high level planning of high of task, resource, allocation, schedule, and team. The detailed activity information about "who does what activities when in collaboration with whom"	The emphasis is on thorough planning, covering major milestones, dependencies, and confirmations. Extension to detailed activity information, specifying task ownership, collaboration with others and understanding the relationships between different activities.

Table 1: Interview Results of Two Shipyards

As shown in table 1, regarding the current practices employed by both shipyards in mapping project activities, it is discerned that software tools are integral to their methodologies. Notably, Microsoft *Project* serves as the primary software for activity mapping in Shipyard A, with a predominant focus on scheduling functionalities. Shipyard B also uses *Project*. Shipyard B would want collaborative tools to engage with shipowners and to boost collaboration among project supervisors and team members. Shipyard A expressed interest in the integration and analysis of data to derive actionable insights, generate reports, and establish benchmarks. Similarly, Shipyard B would like data integration. Both shipyards desire hierarchical and structured activity representation tools which support high-level planning capability encompassing tasks, resource allocation, schedules, and team coordination, as well as a detailed activity information system specifying the who, what, when, and collaborative engagements involved in the shipbuilding process.

Proposed Structured Activity Mapping Representation Framework

A structured activity mapping representation is proposed in this section. In contrast to shipbuilding activity mapping currently used as in (Bruce, 2021), the stages addressed in activity mapping can be expanded to include maintenance, operation and use by reflecting PSS concept as shown in the activity mapping framework of Figure 2. Within this framework, activities conducted by various stakeholders in the shipbuilding process are organized across these stages so that activities of stakeholders are described horizontally in corresponding lanes of actors with stakeholders as used in service blueprints. Activity mapping can be represented with specific value dimensions highlighted in corresponding value layers as shown on the right part of Figure 2. A layer with values for human-centric issues, PSS, and knowledge management is shown on top. Layers with each of these three value viewpoints are shown below respectively. The incorporation of value layers can help quick and efficient identification and attention of relevant activities associated with specific values.

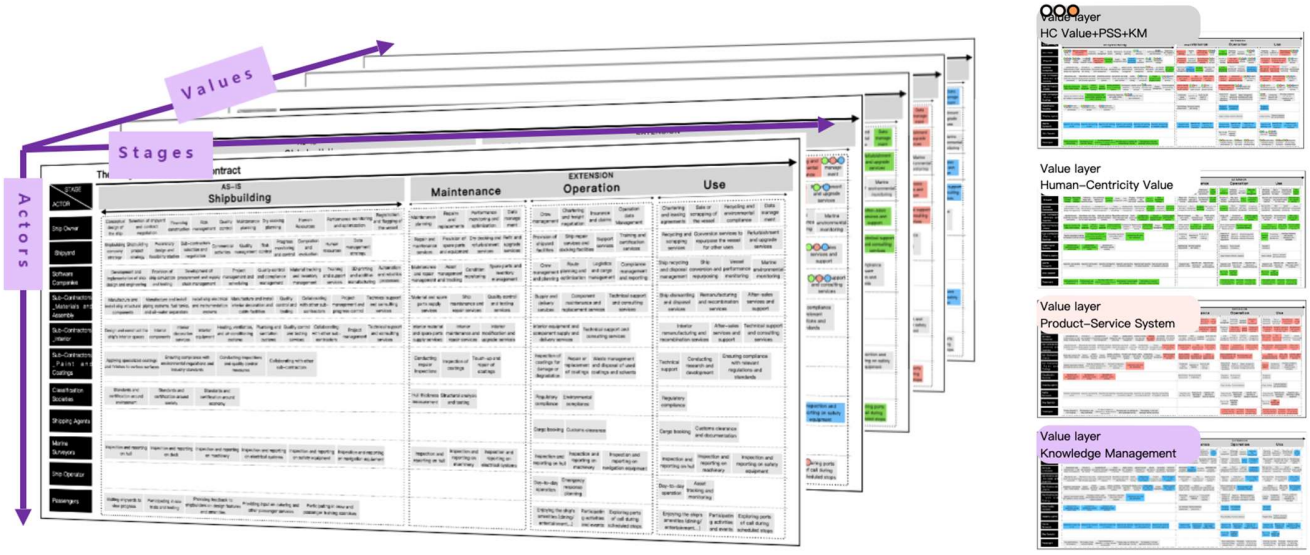

Figure 2: The Activity Mapping Representation Framework

Stages

Taking a cruise ship as an example, the duration required to construct such vessels may vary, typically ranging two to three years. For instance, the construction of the *Icon of the Seas*, the world's largest ship, spanned a period of about 29 months. In contrast, the operational lifespan of a cruise ship commonly exceeds 20 years. Comparing the 20-year operational span with the construction period of two to three years, it becomes evident that the operational and usage phases are significantly longer, implying ample opportunities for value creation and business development in the post-construction phases reflecting the PSS perspective. In Figure 3, we broaden the perspective beyond the current emphasis solely on the construction phase. We extend this perspective to include maintenance, operation, and usage phases.

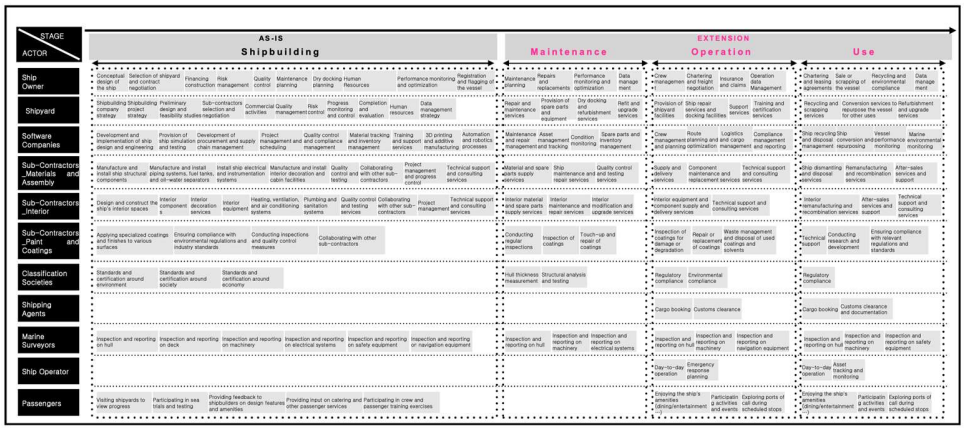

Figure 3: The Activity Mapping Representation Framework: Stages

Actors

There are extensive and diverse range of stakeholders and subcontractors involved in shipbuilding activities as Bruce (2021) highlighted. Stakeholders, also referred to as actors, play crucial roles. Service blueprint representation of activities of a project allows actor focused representation of the process of a project as shown in Figure 4. The service blueprint of Figure 4 illustrates how a PSS development project is represented so that how activities of different stakeholders interact and how stakeholders collaborate can be represented and interrogated in a structured manner (Kim and Lee, 2021). In this representation, stakeholders are presented vertically, emphasizing their central role, while arrows show the interrelations between different activities. Each individual box represents a high-level PSS development activity conducted by specific stakeholders. Three top lanes in blue

show activities of a company with different responsibilities. The PSS design team activities are shown with two lanes in light yellow. Activities of other relevant stakeholders are represented as well. The second column shows that the CEO of the company and the leader of PSS design team collaboratively determined the servitization strategy of PSS development. This is then followed by the activity of servitization direction decision collaboratively conducted by three stakeholders from three organizations as shown in the next progress step. In this way, the service blueprint representation of PSS development process shows *who does what activities when in collaboration with whom.* Our objective is to develop a comprehensive, human-centric representation and management framework for shipbuilding, fostering interaction and collaboration among diverse stakeholders, including shipowners, operators, service providers, users, and passengers. Central to our approach is the emphasis on stakeholders and their respective activities, facilitating clarity regarding roles, responsibilities, and collaborative dynamics.

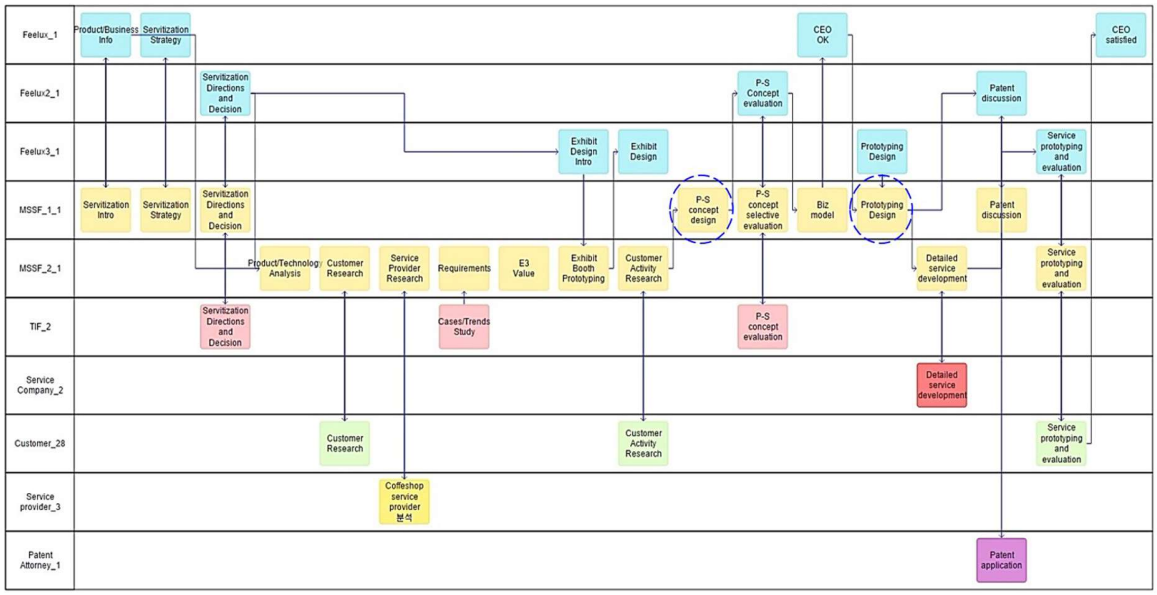

Figure 4: Service Blueprint Representation of a PSS Development Process (from (Kim and Lee, 2021))

Values

Different shipyards and shipowners may prioritize distinct values based on their individual contexts. As depicted in Figure 5, the integration of value layers enables the emphasis of activities associated with specific values. For instance, if the value of *human-centricity* is emphasized, corresponding activities will be highlighted in green. Similarly, activities linked to *PSS* or *knowledge management* will be highlighted in red or in blue respectively if those values are prioritized. In cases where multiple values are emphasized, all relevant activities will be highlighted accordingly.

Figure 5: The Activity Mapping Representation Framework: Values

Context-Based Activity Modeling

Human activities have been the object of designing services, and detailed representation of activities has been achieved through the CBAM method (Kim et al., 2020). Note that activities in a service blueprint would be represented by CBAM specifically. The CBAM method of modeling activities is illustrated in Figure 6. The activity description is centered around the action verb. The object of the action is specified as the *object* element of the activity. The *active actor* is the subject stakeholder of the activity who performs the action. In some cases, the *passive actor* and/or the *third-party actor* are specified as well. The *tool* of the activity is specified when a tool is used in the action. Another element of the activity in CBAM is the *context*, which is in turn described by the following 4 context elements: the *goal context*, the *relevant structures*, the *physical context*, and the *psychological context*.

Note that the goal context can be either other activities which the current activity supports or value themes derived by the current activity. The relevant structures are the entities associated with the object element in the action. Note that the relevant structure context represents various entities related to the object in this specific activity. This allows representation of relations of the object with various specific structure components. The physical contexts such as location and time are specified. The psychological context such as emotional states and motivation level can be associated. CBAM offers systematic and rich representation of context information of an activity. The psychological context includes sub-fields like social context, motivation context and emotional experiences, and can contain specific placeholders for specific value themes and their elucidated levels. In this way, CBAM enables specific association of various value items to activities.

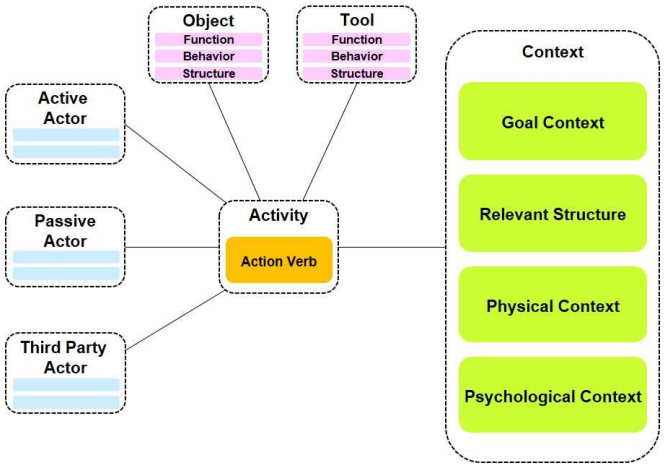

Figure 6: Context-Based Activity Modeling (from (Kim et al., 2020))

Toward the Next Generation Shipbuilding with Comprehensive Integration

With the proposed structured activity mapping framework, comprehensive integration of shipbuilding over stages and over a longer span of shipbuilding business can be envisioned with a smart PSS perspective supported by data-driven approaches. Considering cruise shipbuilding cases, as exemplified in Figure 7, the following three pivotal situations can be postulated: (1) the completion of building a cruise ship several years ago, (2) the ongoing building of a new cruise ship, and (3) the early planning of building of a later cruise ship. These situations correspond to distinct phases of *operation and use*, *building*, and *design*, respectively. The cruise ship built earlier, now in operation, presents abundant opportunities for gathering insights and addressing needs by comprehensively analyzing data from various stakeholders involved, including end users, shipowners, operators, service providers, and related communities. The building of a new cruise ship provides another avenue for identifying needs and insights, involving stakeholders such as ship builders, architects/engineers, construction contractors, subcontractors, regulatory authorities, and suppliers. Through data from an operating ship, production of a new ship can be improved. Furthermore, insights obtained from an operating ship and current ship production as well as various stakeholders can even improve designing of a future ship.

By integrating insights and opportunities across these three situations and engaging stakeholders in collaborative efforts, competitive advantages can be harnessed. With the proposed activity mapping framework and repository of activity maps of diverse ships and various shipyards, the next-generation shipbuilding can be postulated with data-driven ship design and building encompassing design data, production data and use data. Beyond utilizing design data in production planning and shipbuilding, shipbuilding activity information can support maintenance and operation. Moreover, various use and experience data from use, operation and service can support design of future ships.

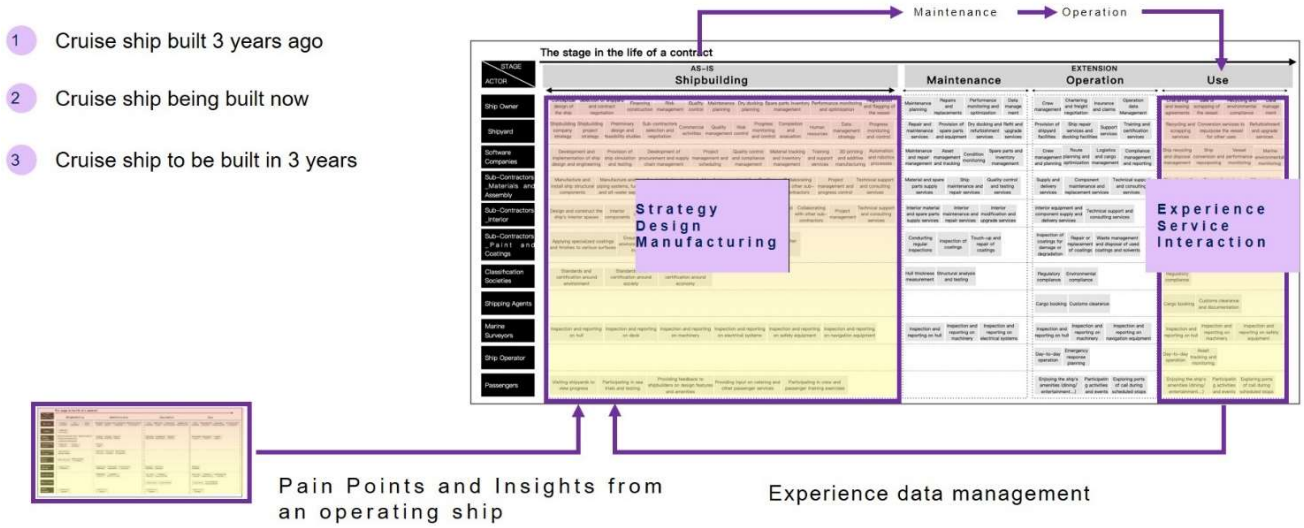

Figure 7: Integration of Design, Production, Service, Operation and Use Stages

Discussions and Conclusion

The objective of the SEUS project is to create a framework for European shipyards by architecting and developing an integrated platform for data-driven shipbuilding, with a focus on human-centricity, smart technology, digitalization, and cyber-physical systems, to improve efficiency, reduce engineering time, and provide a competitive advantage through cost- and time-saving innovations (Seppälä et al., 2023). Within the SEUS framework, our research centers on representing shipbuilding activities with a focus on prioritizing human-centric approaches. This paper contributes to that overarching goal.

Specifically, in this paper, the human-centric approach in shipbuilding with a structured activity mapping framework was described as proposed in the SEUS project. The service blueprint representation of shipbuilding activities inherently focuses stakeholders as the activities are arranged for stakeholders, not for tasks. This is a significant improvement over the perspective where people are regarded as resources like in the case of Bruce (2021). Furthermore, specific values can be associated to activities through the detailed and rich representation of activities by utilizing the CBAM method. This human-centric approach with detailed value association enabled by the proposed structured activity mapping framework would be comprehensively applicable whether activities are about ship production or about customer involvement.

Furthermore, interaction and collaboration of actors are the most important part of activity management whether the activities are about strategies and contracts or about production and test. Representation and management of collaboration and coordination of diverse shipbuilding stakeholders are particularly important for human-centricity in the era of digital transformation. Note that *smartness* can be assessed based on how rich co-creative activities were done in various parts of shipbuilding activities. For example, shipbuilding activity staging, that is, determining which actors are involved in what phase in collaboration with which other actors should be effectively supported in the proposed activity mapping framework.

Moreover, to address after-sales services, such a human-centric approach is very important. Considering the use stage, various stakeholder experience data can be obtained as well as diverse artefact data so that truly data-driven ship experience design could be realized as explained in (Kim, 2023). We believe people aspects are getting more and more important as digital technologies are utilized in more and more parts of ship design, production, operation and use stages. The proposed activity mapping framework would work as a major enabler for smart data-driven ship design and ship experience design as a high-level planning tool addressing vast range of ship design and building stages and as a detailed information provider for activities. In this way, the activity mapping with service blueprint representation would make a significant next-generation shipbuilding competitiveness management tool.

Future work on this activity mapping research would include the following tasks. Efforts will be made to accommodate different shipbuilding contexts and shipyard characteristics in a structured manner in shipbuilding activity maps. This will allow repositories of diverse ship design and building cases so that smart data-driven ship design and building can be supported. Immediate future work will address systematic development of cases. This will entail selecting and combining scenarios from

various shipyards, each with distinctive priorities and contexts. This will be structured with four main aspects: shipyard activities for planning and building phases, strategic mapping of activities during design phase, defining ship owner activities related to customer experience during operation and use stage, and scenarios focusing on systematic considerations guided by diverse data-driven methods. How specific collaborations were done in previous shipbuilding cases can be captured and represented as knowledge so that future shipbuilding cases will exploit this. With digital technologies, collaborations are happening with wider partnership and these kinds of knowledge would be important as closer feedback from various stakeholders are enabled in such a collaboration.

CONTRIBUTION STATEMENT

Author 1: Conceptualization; methodology; supervision; writing – original draft, review and editing.
Author 2: Conceptualization; data curation; investigation; visualization; writing – original draft, review and editing.
Author 3: Conceptualization; writing – review and editing.

ACKNOWLEDGEMENTS

This research has been supported by the Smart European Shipbuilding (SEUS) project. The SEUS project has received funding from the Horizon Europe Framework Programme (HORIZON) EU program under grant agreement No 101096224. Info is updated at http://seus-project.eu/. This article reflects only the authors' views, and the European Commission is not responsible for any use that may be made of the information it contains.

REFERENCES

Agis, J. J. G. (2020). *Effectiveness in Decision-Making in Ship Design under Uncertainty*. Doctoral Thesis. Norwegian University of Science and Technology.

Bruce, G. (2021). An Activity Map of the Shipbuilding Process. In G. Bruce, *Shipbuilding Management* (pp. 9–21). Springer Singapore. https://doi.org/10.1007/978-981-15-8975-1_2

Costa, N., Patrício, L., Morelli, N., & Magee, C. L. (2018). Bringing Service Design to manufacturing companies: Integrating PSS and Service Design approaches. *Design Studies*, 55, 112–145. https://doi.org/10.1016/j.destud.2017.09.002

ECORYS. (2009). *Study on competitiveness of the European shipbuilding industry.pdf* (Within the Framework Contract of Sectoral Competitiveness Studies – ENTR/06/054) [Final Report]. ECORYS Research and Consulting.

Goedkoop, M.J., van Halen, C.J.G., te Riele, H.R.M. & Rommens, P.J.M. (1999). P*roduct Service Systems, Ecological and Economic Basics*, the Dutch ministries of Environment and Economic Affairs. Hague, The Netherlands.

Kim, Y. S. (2023). Customer Experience Design for Smart Product-Service Systems Based on the Iterations of Experience – Evaluate – Engage Using Customer Experience Data, *Sustainability*, 15 (1).

Kim, Y. S., & Lee, H. (2021). Process Characteristics of Product-Service Systems Development: Comparison of Seven Manufacturing Company Cases. *Journal of Cleaner Production*, Vol.286.

Kim, Y. S., Jeong, J. Y., Hong, Y. K., & Hong, S. J. (2020). A Schema for Systematic Service Imagining: Context-Based Activity Modeling. *Sustainability*, 12(22).

Ohtomi, K. (2005). Importance of upstream design in product development and its methodology. *EuroSimE 2005. Proceedings of the 6th International Conference on Thermal, Mechanial and Multi-Physics Simulation and Experiments in Micro-Electronics and Micro-Systems, 2005.*, 17–18. https://doi.org/10.1109/ESIME.2005.1502763

Oloruntobi, O., Mokhtar, K., Gohari, A., Asif, S., & Chuah, L. F. (2023). Sustainable transition towards greener and cleaner seaborne shipping industry: Challenges and opportunities. *Cleaner Engineering and Technology*, 13, 100628. https://doi.org/10.1016/j.clet.2023.100628

Patrício, L., Fisk, R. P., Falcão E Cunha, J., & Constantine, L. (2011). Multilevel Service Design: From Customer Value Constellation to Service Experience Blueprinting. *Journal of Service Research*, 14(2), 180–200. https://doi.org/10.1177/1094670511401901

Patrício, L., Gustafsson, A., & Fisk, R. (2018). Upframing Service Design and Innovation for Research Impact. *Journal of Service Research*, 21(1), 3–16. https://doi.org/10.1177/1094670517746780

Payne, C., & Chokshi, N. (2020, June 17). How Giant Ships Are Built. *The New York Times*. https://www.nytimes.com/interactive/2020/06/17/business/economy/how-container-ships-are-built.html

Pettersen, S. S. (2018). *Resilience by Latent Capabilities in Marine Systems.* Doctoral Thesis. Norwegian University of Science and Technology.

Seppälä, L., Gaspar, H., Koelman, H., & Agis, J. J. G. (2023). *Can European Shipyards be Smarter? A Proposal from the SEUS Project / Articles / Resources*. http://www.cadmatic.com/en/resources/articles/can-european-shipyards-be-smarter/

Shostack, G. L. (1982). How to Design a Service. *European Journal of Marketing*, 16(1), 49–63.

Strandhagen, J. W., Jeong, Y., Woo, J. H., Semini, M., Wiktorsson, M., Strandhagen, J. O., & Alfnes, E. (2020). Factors Affecting Shipyard Operations and Logistics: A Framework and Comparison of Shipbuilding Approaches. In B. Lalic, V. Majstorovic, U. Marjanovic, G. Von Cieminski, & D. Romero (Eds.), *Advances in Production Management Systems. Towards Smart and Digital Manufacturing* (Vol. 592, pp. 529–537). Springer.

Tukker, A. (2015). Product services for a resource-efficient and circular economy–A review. *Journal of Cleaner Production*, Vol.97, 76–91.

Van Den Hoven, J., Vermaas, P. E., & Van De Poel, I. (Eds.). (2015). *Handbook of Ethics, Values, and Technological Design: Sources, Theory, Values and Application Domains*. Springer Netherlands. https://doi.org/10.1007/978-94-007-6970-0

Xu, X., Lu, Y., Vogel-Heuser, B., & Wang, L. (2021). Industry 4.0 and Industry 5.0—Inception, conception and perception. *Journal of Manufacturing Systems*. 61, 530–535

Yitmen, I., Almusaed, A., & Alizadehsalehi, S. (2023). Investigating the Causal Relationships among Enablers of the Construction 5.0 Paradigm: Integration of Operator 5.0 and Society 5.0 with Human-Centricity, Sustainability, and Resilience. *Sustainability*, 15(11), 9105. https://doi.org/10.3390/su15119105

Zomerdijk, L. G., & Voss, C. A. (2010). Service Design for Experience-Centric Services. *Journal of Service Research*, 13(1), 67–82. https://doi.org/10.1177/1094670509351960

Proceedings of 15th International Marine Design Conference (IMDC-2024)
June 2-6, 2024
Amsterdam, the Netherlands

Piping Layout Integrated in Ship Design and Stability Assessment

Herbert J. Koelman[1,*]

ABSTRACT

Damage stability assessment in ship design is a well-established area of our trade. However, where originally only a limited number of aspects were involved, gradually more details are included. Notably compartment connections by pipes and ducts etcetera. Combined with a high number of damage cases, in practice this results in a set of computations which is not complex as such, yet complicated by its sheer size. Although in the PIAS ship design software suite quite some dedicated tools are available, those have never been designed to support the requirements from today. In this light the software has been extended with a new system to fully define shape and topology of compartments and their connections. This paper reports on the system design, its application in damage scenarios, and on complications.

KEY WORDS

Damage stability; Piping; Time-domain; Ship design.

INTRODUCTION

If a compartment is damaged in such a way that it is open to the sea, then it will obviously be flooded, which can also extend further into the vessel through all kinds of openings or connections between compartments. In stability regulations, the word *progressive flooding* is mostly used for this, but we rather avoid that because it suggests that the flooding continues until it is fatal, which is not necessarily the case. The ship design and stability suite PIAS accommodates this phenomenon, by a sub-system *complex intermediate stages of flooding*, which dates back to the nineties. This works on the basis of non-uniform filling percentages per compartment, where necessary supplemented by virtual compartment connections. Although this has served the program users well over the past decades, it has some limitations:

- It supports only *virtual* connections between compartments. That means that a point in 3D space can be assigned as being 'the connection location', without any physical object connected to that point.
- Only one single location is supported as connection point between two tanks.
- Data input and output only in text.
- Supports computation of time to equalization. Yet only a) for a single compartment connected to the sea, and b) as disconnected calculation, not integrated in the stability computation and assessment.

Although as such it works well and is widely used, this system has never been conceived for intensive usage. While on the other hand we can witness an ever-increasing attention to effects of filling and flooding through holes, openings, ducts and pipes. Which is caused by stringent rules, increasing scrutiny by authorities and classification societies, hence increasing awareness of ship designers and shipyards, and finally increasingly complex vessels (from the layout design point-of-view). So, in order to satisfy this market demand, it was about time for a new PIAS subsystem for next-level damage stability assessments, including major effects of internal flooding and its progression.

In the set of rules and regulations on ships and shipping literally dozens of places can be identified where aspects of openings, internal connections and damage to piping systems are addressed. Although it is not the intention to provide a full overview here, some examples will be presented. For example, in IACS Unified Interpretations, notably No. 110, on tankers, chemical

[1] SARC, Bussum, The Netherlands
* H.J.Koelman@sarc.nl

Submitted: 7 February 2024, Revised: 9 April 2024, Accepted: 1 May 2024, Published: 23 May 2024

Conference paper, DOI: https://doi.org/10.59490/imdc.2024.886 e-ISSN: 3050-486

tankers and gas carriers: “Progressive flooding through internal pipes: In case of damage of an internal pipe which is connected to an undamaged compartment, the undamaged compartment should also be flooded, unless arrangements are fitted (e.g. check valves or valves with remote means of control), which can prevent further flooding of the undamaged compartment”. Another example, taken from IMO (2020), on Probabilistic Damage Stability: “The factor s_i is to be taken as zero in those cases where the final waterline immerses the lower edge of openings through which progressive flooding may take place and such flooding is not accounted for in the calculation of factor s_i. Such openings shall include air pipes, ventilations and openings which are closed by means of weathertight doors or hatch covers”. Finally, MSC (2020) links consequences to equalization times by cross-flooding arrangements (which are constructed to reduce the heel in the final equilibrium condition), with thresholds of one and ten minutes.

Until now, we have discussed the realm of requirements. Now we will briefly revisit recent related advances in modelling of algorithms on internal flooding after damage. Both Vermeer et al. (1994) and Ruponen (2007) researched in detail flooding scenarios after collision damage. Although this has created valuable insights, the applications were quite detailed and focused on specific specimens. Ruponen et al. (2012) have compared cross-flooding times as derived with different methods, and concluded amongst others that the simplified formula from IMO resolution MSC.245(83) satisfies well in case of small pressure variations, however, this conclusion may not be extended to different flooding cases. In Kariolus et al. (2019) a probabilistic assessment of progressive flooding has been proposed which takes into account the probability of opening internal watertight doors etcetera. In Braidotti & Mauro (2019), a fast method for the calculation of progressive flooding is presented, based on an analytical solution of the linearized system of differential equations.

THE NEW PIPING-BASED SYSTEM

Although from the viewpoints of regulations and science on the models and scenarios of flooding and related residual stability the last word has not been said, our aim in the development of the new system was not on advancing the latest theoretical insights. Instead, our contribution lies in helping our software users by taking one step forward from the conventional, while still maintaining an understandable and traceable modelling and computation method. With this background a design specification has been drafted, which was circulated under PIAS’ customer base. Some replied with valuable remarks or ideas, which have been processed in the specification and the subsequent implementation.

In the remainder of this section, we will discuss the modelling methods, followed by an overview of the computational approach, and finish with a few core computational details.

Topology And Geometry of Openings, Pipes and Ducts

A foundational choice for the new system was to build the data entities and mutual relationships onto a specific standard for a sector which is — as a matter of speaking — littered by pipes and their purpose: the process plant industry, ISO (2019). However, this ISO 15926 standard is conceived for a wide range of industries and applications, so unavoidably quite broad, and yet unfocussed. Fortunately, for the process industry this has been further detailed by the DEXPI association, DEXPI (2019). From this extended standard five entities have been used which are sufficient to model a shipboard piping system for our purposes:

- **Equipment**, which is a thing, not being a compartment, connected to a pipe line but not part of it. Such as an engine or a chiller. Equipment play no role in computations, it is just defined for the completeness of definition and drawings.
- A piping **system**, which is an administrative collection of pipes of the same type, for example ‘ballast’ or ‘Methanol’.
- A piping **network**, which is one closed system of connected pipes, which belongs to a piping system. This is the core of the piping data structure.
- A piping **segment**, which is one branch of a piping network, and extends between two points without sub-branching in between.
- A piping **connection**, which is a part located at the extremities of a piping segment. These come in six types:
    - Branch, where multiple piping segments meet.
    - Unprotected opening, external (so, to the outside of the ship).
    - Opening + Weathertight Air Pipe Closing Device (WAPCD) a.k.a. vent check valve.
    - Terminator, which closes a dead-end segment.
    - Compartment, or, more precisely, a connection to a tank or compartment at a certain location. So, a compartment may have multiple connections. The representation method of compartments will not further be discussed here, that has been elaborated in De Koningh et al. (2011).
    - Equipment, or, more precisely, a connection to a piece of equipment at a certain location.

- A piping **component**, which is a part located in a piping segment. This can be a waypoint, elbow, valve, pressure relief valve, reducer, check valve, internal WAPCD or a straight pipe section.

A schematic example of a piping system, including these entities and their relationships, is sketched in Figure 1, while an(other) example of the PIAS GUI implementation is reproduced in Figure 2. Space does not allow here to discuss all tools and features of this GUI, so we suffice here with this link to the manual.

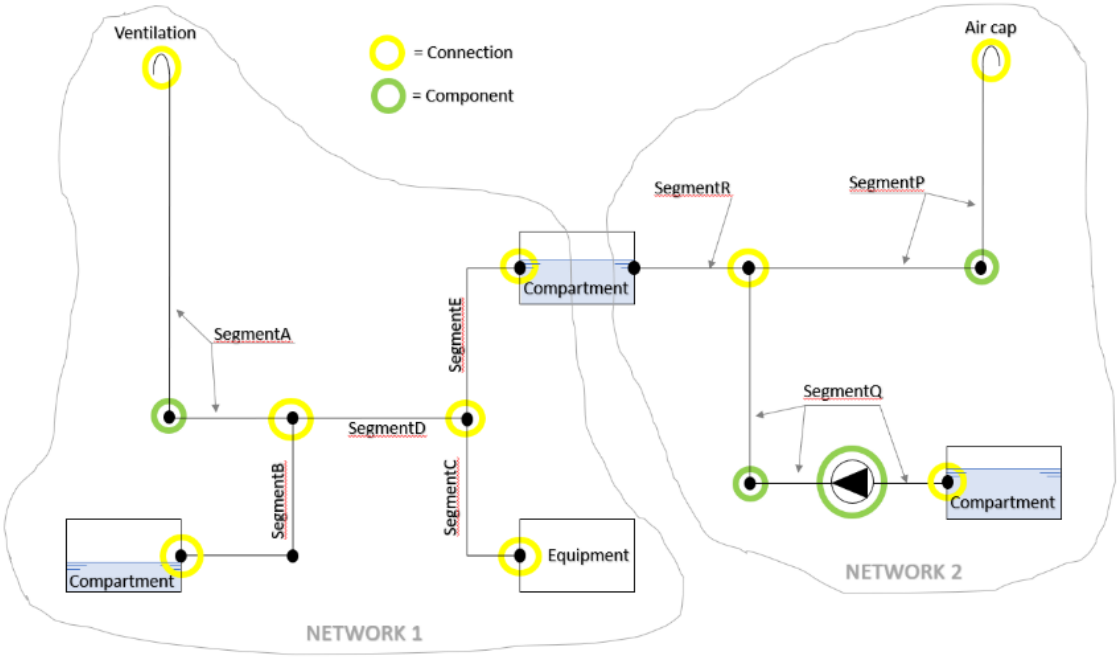

Figure 1: Schematic example of a two piping networks

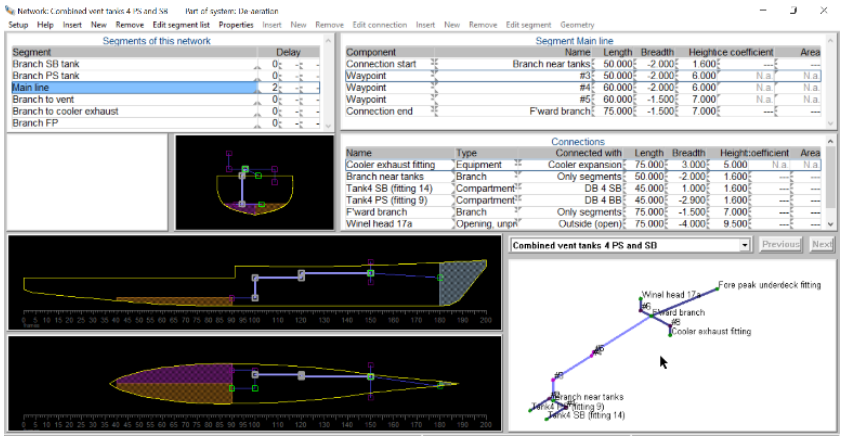

Figure 2: GUI implementation, showing a single network including connected compartments

Two Categories of (Damage) Stability Computations Including Pipes and Ducts

As elaborated in the introduction, the aim of our developments has been to create a framework for next-level damage stability assessments, which is a) suitable for large-scale application, b) efficient from the viewpoint of human effort and c) understandable by the commonly trained naval architect. The presented piping networks, combined with existing representations of loading conditions, hull shape and compartments, open the way to a twofold of such applications:

- A time-domain analysis. For the reasons that a) this has a clear physical meaning, so b) it represents reality an order better than conventional 'intermediate stages of flooding', while c) time as such plays a role in some stability criteria and time-to-capsize assessments.

- Something that resembles ‘stages of flooding’. For the mere fact that such stages are anchored in tradition, and hence in textbooks and regulations.

Combined, the new system, which embraces these two calculation types, is called *Consecutive Flooding*.

We start the discussion with **time domain** because its physical background makes it easy to grab. In line with the premise to create a practically useful system, the simplifications which are common in stability assessment have been applied here as well. These concern the omission of inertia of ship and fluids, temperature effects and the impulse of the inflowing water. Furthermore, the following assumptions apply:

- Ultimately, in fully damaged condition all initial damaged tank content is lost and fully replaced by sea water.
- Fluids mix instantaneously and fully, so there is no density gradient. For a damaged tank with intact fluid this implies that a stage at 99% of total flooding time will contain a mixture of intact and ingressed fluid, which introduces a discontinuity with the previous bullet. This is addressed by the computation of two variants at the moment of total flooding, the first with a mixture of fluids and the second with sea water. The first represents the condition directly after full flooding, the second at a long time after that.
- Non-damaged tanks, which are filled through connections with other tanks, receive a new density which is the proportional mix between original and ingressed densities. So, the intact content is never fully replaced (unless it flows out through another pipe connection), regardless the size of the connection.
- The volumes of the connecting pipes are neglected.
- Components have a single resistance coefficient, so there is no transition between laminar and turbulent flow.

With the latter simplification, the effort comes down to applying Bernoulli's equation in discrete time steps. In Ruponen (2006) this numerical differential equation was solved by a second-order scheme, which is more efficient than linear. However, it also requires that discontinuities (in flow vs. time) are identified, which is easy to do with time-based events (e.g. opening a valve) but less easy to identify in case of geometric effects (e.g. a large discontinuity in the shape of a tank). For that reason we have chosen first-order Euler integration. In each integration step the following actions are performed:

- Set the positions of pressure relief valves.
- Extending pipe openings with an outflow above a fluid surface with an additional, artificial pipe perpendicular to that surface. For the reason that pipe flow theories are based on pipes and reservoirs, and don’t support waterfalls.
- Converting this piping network into a (mathematical) graph.
- Identifying closed loops in this graph, with a method for finding Fundamental Cycles.
- Applying Kirchhoff's laws around these loops and all nodes, as illustrated in Figure 6.25 from White & Xue (2021). This leads to a system with N equations and N unknowns.
- The resulting flow multiplied by the time step gives the fluid quantities per tank. These are capped if that leads to overfilling (>100%) or underfilling (<0%) of a tank in that time step.

With the second system the flooding is modelled with **intermediate stages of flooding**, so without explicit time. This implementation was conceptualized given two facts:

- Standard stability regulations apply the concept of ‘intermediates stages of floodings’ of fixed percentages, i.e. 25%, 50%, 75% and 100%.
- Not all compartments are always flooded with the same percentages, i.e. with small connections between compartments the flooding of the connected compartments may lag behind the flooding of the ruptured compartment.

Our system maintains the notion of ‘percentual stage of flooding’, because a) this is a fundamental concept in present damage stability regulations, b) therefore this concept is familiar to authorities and classification societies and c) the concept is easy to understand. To have a shorthand word for this concept it was labelled *fractional*, because essentially it fills compartments by ‘fractions’ of the final volume. Additionally, an integer *delay* is available to specify a lagging in time. All in all, this is a simple system, supporting conventional intermediate stages and a bit beyond. Those interested in examples are directed to this section in the manual.

Core Computational Details

Besides the core of the computation, some additional facilities and choices are of interest. The first is the **WAPCD** (Weathertight Air Pipe Closing Device), which besides its common modus operandi according to IMO/SOLAS interpretation, in our implementation also supports an additional *safety distance*, hence accommodating European Inland Waterway tanker regulations ES-TRIN, CESNI (2019).

Frictional resistance by pipes is in the essence a complex issue. In practice, however, a number of practical methods and parameters exist, some of which have been implemented:

- The (cross-sectional) shape. Choice of round or square, the most common shapes.
- The cross-sectional dimension. If round then diameter, if square then edge length.
- The (dimensionless) resistance coefficient, for which three common methods are available:
    - According to IMO resolution MSC.362(92), where the frictional resistance per meter length is 0.02 ÷ hydraulic diameter.
    - With a user-specified Darcy-Weisbach coefficient, where the frictional resistance per meter of length is that coefficient ÷ hydraulic diameter.
    - With a user-specified resistance coefficient per meter of length.

A second issue is the energy loss due to **fluid outflow from a pipe**. For flow resistance of pipes and components, IMO has adopted a family of resolutions, namely A.266 1973, MSC.245(83) 2007 and MSC.362(92) 2013. To support the stability assessment of elder vessels, our system supports all three. A central element in these resolutions is the so-called 'reduction of speed', F, which is directly related to component resistance coefficients. A confusing factor is that in the three resolutions the equations for F are similar, but not equal, because two of the three have a factor *one* in the denominator, which the other lacks. This factor is to account for the energy loss due to outflow from the end of a pipe, Söding (2002). In order to harmonize these regulations, as well as to accommodate more than a single pipe outlet, the user can choose between implicit (= with the *one* in the denominator) or explicit (= user-defined) outflow energy loss. By the way, in the mentioned IMO resolutions the underlying outflow differential equation is (after some simplifications) solved analytically, which leads to a closed-form expression of equalization time. Instead of that expression, in our approach the flow resistance factors from these resolutions are used directly during the numerical integration of the differential equation.

Finally, the issue of **larger angle stability**, the computation of the GZ curve. From the viewpoint of consistency this is a bit of a strange phenomenon, because it is artificial. In the physically based time domain computation, no force or moment exists that forces the ship to heel. And there is not sufficient time to heel, because the next unheeled time step is ready to commence. This is solved by a) computing GZ without time effects, while b) omit possibly ingressed or shifted fluid *during heel* in the next time step. Still, there is an open question on how to determine whether fluid is transferred through pipes or openings during heel. In case of a small diameter pipe it is obvious that the roll period is not sufficiently large to allow for significant fluid transfer during heel. While a half-height bulkhead allows a waterfall over the bulkhead edge during heel (possibly without backflow when heeling to the other side). To differentiate between the two cases, a user can specify a 'minimum cross-sectional area for instantaneous fluid passage', which gives the program a handle to either allow flow through pipes and openings (if the actual area is larger than this minimum) or block the flow (if the actual area is less).
For all intermediate stages a GZ curve will be computed and assessed. In time domain for each time step full stability could be computed as well, however, this would lead to a large number of computations without much added values. For this reason, the program has a few switches to balance the amount of GZ evaluations. Anyway, for each time step draft, trim, heel and fluid quantities are available.

CHOICES AND OBSTACLES

Although the basic functionality and procedures are rather straightforward, completing it into a computer program usable in day-to-day ship design practice requires quite some deliberations and choices, in which we also encountered an unexpected obstacle here and there, which will be discussed in this section.

Permeabilities

There is this famous Monty Python sketch about an accountant, Herbert Anchovy, who gets bored of the dullness of his work. Well, our profession equally knows a Herbert who also has that feeling, about a small detail that has haunted him for more than four decades; the permeability of a tank. We all know that for the computation of tank tables a 2% reduction on volume is a common estimation to account for internal construction of steel vessels. Hence, a permeability of 98%, while all damage stability regulations impose a 95% permeability for tanks containing liquids. As such it is silly to apply different permeabilities for the same space; suppose a double bottom (DB) is fully filled with sea water. When it becomes damaged, due to some magical intervention from above suddenly 3% of the content is assumed to vaporize. And suppose the ship has separated SB and PS DB tanks, with the SB tank damaged and PS intact. Then, due to this loss of weight at SB, the vessel will slightly heel over to PS. While in reality nothing happens.

In the 1980s, for PIAS the choice has been made to interpolate permeabilities based on the stage of flooding, in order to achieve continuity at 0% stage = intact, and 100% stage= fully damaged. But now, with pipe connections, the situation is even more confusing, Take, for instance, a tank which is not ruptured but nevertheless flooded by seawater through a pipe, which is on its

turn connected to a second, damaged, tank. What should then be the permeability of the first tank, damaged or intact? Consulting the regulations does not provide a unison answer, for IMO (2016) provides a different choice than IMO (2020). So, a program setting was created for this, including a paragraph in the manual with some more details.

Later in this paper the verification process will be discussed, and it can already be revealed that on many occasions we thought to be looking at wrong results, which later turned out to be correct. Had permeability again played tricks on us.

Intermediate stages of flooding

The whole assumption behind the idea of a *fraction* (a generalization of an intermediate stage of flooding) is that the immediately affected compartments will be flooded through a small damage. After all, if the damage were large, the ingressed water would spread rapidly, and the intermediate stage would be so short that it would have no effect on ship's position and stability. So, then the intermediate stage would actually not exist. Based on this physics-based reasoning, a distinction is made between large and small damages.

To assess stability in damaged condition, the worst-case scenario will have to be considered and since it is not known in advance how large the damage will be, cases with both a large and small damage are calculated. In the event of large damage, seawater can flow freely in and out of the damaged compartments, so that even during roll the water level in those compartments is equal to the sea water level. Because this all happens so quickly, intermediate stages do not actually emerge. In the case of a small damage, on the other hand, the water flows through the hole so slowly that the intermediate stages can take a long time, and thus should be considered in separate consideration. However, if the water flows slowly, then during rolling it does not have time to flow in or out significantly. So, in this case the volume of water in a compartment can be assumed to be constant for all heeling angles. Suppose intermediate stages of 25, 50 and 75% are specified by the user, the complete damage stability evaluation will consist of:

Table 1: Damage stability assessment stages.

Damage	Stage	Water in compartment	Verification against stability criteria for
Large	Final	Freely flowing in and out	Final stage
Small	Final	Constant, as at equilibrium heel (call that W)	Final stage
Small	Intermediate	75% of W	Intermediate stages
Small	Intermediate	50% of W	Intermediate stages
Small	Intermediate	25% of W	Intermediate stages

Damage stability criteria

Table 1 already shows which criteria for final or intermediate stages of flooding are applied. For the time domain computation, for (user-configurable) time intervals a full stability calculation can be made and verified against criteria. The question whether to apply criteria for final or for intermediate stages can be derived if a time limit is given, for example the 10 minutes from MSC (2020).

Another dilemma with stability assessment is the displacement through which the uprighting moment is divided, in order to obtain uprighting lever. Intact displacement or damaged displacement? Quite often, in literature this aspect is related to the lost buoyancy vs. added weight issue, but that is utterly confusing, for this issue is related to two separate *computation methods*, while our dilemma is just the choice of a denominator in an arithmetic division. Even in my favorite textbook on stability, Biran & Lopez-Pulido (2014), the method (lost buoyancy) is confused with the denominator equaling the intact displacement (which is called *constant displacement* in some stability regulations). Because different stability regulations dictate different denominators, our program has, reluctantly, been equipped with a setting where the user can specify the applicable choice. *Constant displacement* has been the program's default since the 1980s, a choice that has recently conveniently been formulated by eq. 3 of Ruponen et al. (2018).

Program settings

In the ideal world, where everything is equal, a computer program needs no settings. In reality, preferences, traditions, ships and regulations differ, so there is a compelling need for settings in a program or app. Quite some settings have already been discussed in this paper, while some additional remarkable settings will be elaborated in this section.

The whole idea of a time domain calculation is to calculate the **time in which the fluids equalize**. The flooding process is finished when the whole system of vessel and fluids have come to rest. However, towards the end of the process the fluids start to flow slower and slower; after all, the level differences get smaller, and hence the pressures and the flow velocities and flow rates. In essence, it is an asymptotic process (in particular exponential, see Braidotti & Mauro (2019)) where after, so to speak, many hours, milliliters are still flowing through the pipelines and openings. Indeed, in theory, equalization time will always be infinite. In practice, a certain tolerance can be set, so that if e.g. the difference in draft between two consecutive time steps is less than a mm or 1/10 mm, that is considered as 'rest'. However, that is an arbitrary tolerance that unintentionally has a large outcome on the final answer; at 1/10 mm, the equalization time can easily be twice as long as at 1 mm.
One might think of implementing a practical limit; after all, we are interested in the tons flowing through the system in the early time, and not so much in the milliliters in the last seconds. With that idea, a criterion can be formulated that is related to the transferred weight. For example 'if 98% of the total, final, fluid weight has flown through then I consider the system at rest'. The default percentage used in PIAS is indeed 98%, but this setting allows the users to adjust it as they see fit.

Another aspect is the concept of **equalization time** itself. In MSC (2020) this appears to be a strong issue, although the concept is not crystal clear. We assume that the idea is that an asymmetric damage is equalized by fluid flowing through a cross-flooding device, to the other side of the ship. And that, in the ideal world, this process comes to an end when symmetry has been achieved. But what when the geometry as such is not purely symmetrical, when, for instance, the tank at the other side is slightly smaller than the ruptured tank? Then a symmetrical condition will never be reached, and hence it will never be equalized? Unless MSC (2020) is augmented with explanatory notes, this will be an issue for subjective preferences by ship designer or inspection body. Hence, a cause for a setting.

Finally, **conflicting settings** may exist in our program. As such, this does not raise an alarm, it is just a matter of choices, some of which were made decades ago. Quite some of these conflicts are not fundamental, it is just that we don't consider it to be economical to allow for a certain combination of features, such as *heeling angles larger dan 90 degrees* (which exists in PIAS since 1982, and has been used a few dozen times) combined with this new *Consecutive Flooding* system. Others are intrinsic, such as that this advanced *Consecutive Flooding* cannot be combined with the approximative method of accounting free liquid surfaces by only their transverse moment of inertia. That is fundamentally impossible. Anyway, when conflicting options have been set, the conflicts are reported in a matrix in a popup box to the user, so he or she can make an appropriate choice. We realize that such messages are always a bit annoying when popping up, but they are inevitable given the sheer size of computation options in PIAS. An alternative would be to discard elder options, but we never know who in the customer base will still want to use such a legacy feature, for whatever reason, one day.

Effects of internal openings on the GZ curve

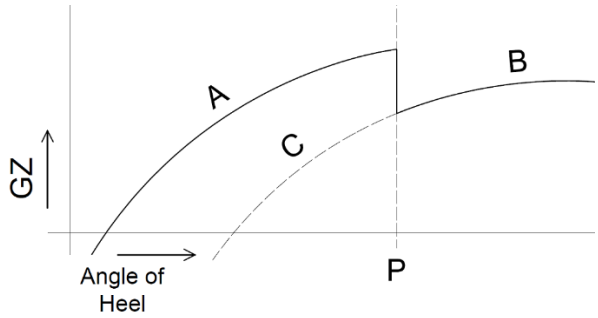

Figure 3: GZ curve with internal opening submerged at angle P

How does our program deal with an internal threshold or pipe which is submerged, and consequently allows transfer of water, at an angle of heel which is beyond the static equilibrium? Take for example the GZ curve from Figure 3, where at angle P the upper edge of a partial bulkhead overflows, leading to the filling of an adjacent compartment and therefore a deteriorated stability. It will be undebatable that the GZ will initially follow curve A, until angle P is reached, where a greater amount of

ingressed water will lead to reduced curve B. However, the question is what happens on the "way back", i.e. with decreasing angle of heel? The water will not fully flow back over the bulkhead, so a curve as indicated by C can be expected. And the subsequent question is which curve to use for the verification of GZ against stability criteria, A+B or C+B?

In PIAS, the past decades A+B has always been used — numerous calculations have been issued at classification societies and shipping inspections, and approved — based on the reasoning that the notion "way back" is never properly addressed, neither in literature nor in regulations. A few more arguments can be made in favor of this choice:

- The example above is expressive, but counter examples also exist. Take the GZ curve from Figure 4, with the partial bulkhead now immersed at an angle P which is much larger now. If the vessel is subject to IMO's Intact Stability Code then the maximum heel for criteria evaluation is 50° — the weather criterion — while angle P is much larger than 50°. So, this loading condition meets all stability criteria long before P is reached, and a reduced C-branch will not be applicable.
- Will 50° then be the determining angle? In many cases not, because dynamic stability equality (area A=B from the weather criterion) may have been reached at a much smaller angle. So, the possible branching of the GZ curve should be related to the applicable stability criteria, one way or another.
- Assume now that at the same large angle P not an internal opening spills over, but an external opening (e.g. a ventilation inlet), which sinks the ship. Then beyond P, the GZ curve will vanish, so also branch B. If one would argue that with an internal opening branch C should be taken, then the same reasoning should be applied to external ones. However, with branch B also C has vanished, so using this branch will render the whole GZ curve non-existent. Nobody — user, researcher, authority nor classification society — has ever suggested such a 'solution', because it would be unrealistic.

Supported by these arguments, it was chosen to keep the computation method for this subject in PIAS as it always has been. This is an implementation choice, not the irrevocable result of the modelling method. So, alternative choices could be made, if there would be a generic reason, such as clear and unambiguous guidance by rules or regulations, or unified regulations from institutions, such as IMO, IACS or national authorities.

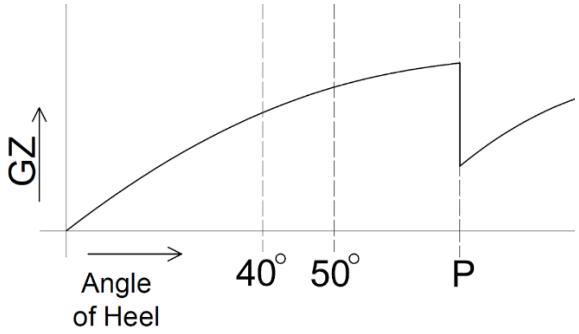

Figure 4: GZ curve with internal opening submerged at a large angle

VERIFICATION AND ACCEPTANCE

The whole idea behind this software is that it satisfies user demands, for which it needs to be practically usable, efficient, and reliable. The first two aspects have permanently been in the background, in the discussion of the software design so far. Anyway, all three issues will be addressed in this section.

Manufacturer's verification

For verification of the proper functioning of software, the first impulse is mostly to maintain a few test cases on file, which can be used to verify the outcome at regular intervals. Although this is as such a feasible approach, it has a few drawbacks:

- In practice it is not easy to keep the test cases stable. If, for example, for a specific test or demonstration somebody changes something in the ship data, or even in a setting, some outcomes may change. But not necessarily all outcomes, which makes the change sometimes hard to notice.
- If multiple settings should be tested, then multiple instances of the same test cases are required. If, subsequently, something changes in the test case then that change should be (manually?) copies to the other instances.
- Automated comparisons are not feasible without special provisions. Each and every change in a piece of static text in the output (a word, a unit) leads to a difference. Indeed, all outputs are different anyway, because of different times and dates!

So, for the piping-based computations a different approach is used. The basis is still some pre-defined data in PIAS format, although only from shape of hull and compartments. All other elements are added by a specific test program, which generates

variations in openings, pipes, connections, loading and program settings. In that way the consistency of the test cases is guaranteed because the variations are not stored, but re-generated when necessary. This test program — which is actually very short, and relies for all computations on the same libraries as the regular program — redirects the computational results to a plain text file, without pages, dates or much text. These text files are fit for automatic comparison on a regular basis. Obviously, the output of the end-user's program should still correspond with these text files, which requires a manual verification. However, if later undeliberate program modification destroys some output then it will be quickly apparent. The consequences of an unintended change in computation is much more dangerous, because it is not always visible. And that has been covered by the test program.

The test program generates some 50 independent test cases, with varying levels of complexity. All these cases are in separate documents compared with independent verifications, which are as such quite basic, for example by spreadsheet or by comparing with other PIAS output (such as that the 0% intermediate stage of flooding should equal the intact loading condition). Obviously, verifying all computation steps would be too labor intensive, so e.g. in a time domain computation of 800 time steps, a few samples have been verified manually.

These verification documents form a part of our IP, and will not reach the public domain. Although one or two of the test cases will be commented and released, to serve as example for others to do similar exercises. Because the underlying calculation steps are so elementary, with a simple test ship, tables of (inclined) hydrostatics & tank volumes and workable knowledge of Bernoulli's equation, every naval architect should be able to verify (samples of) these calculations with spreadsheet or calculator. That is not the prerogative of SARC.

Anticipated embracement by users

Inspired by literature on engineering design, in particular Horváth (2007) and Gero & Kannengiesser (2004), for new software functionality we apply a stepwise process, including a number of feedback loops. The steps comprise 1) Establishing the need, 2) Analysis of task, 3) Conceptual design, 4) Embodiment design, 5) Detailed design and 6) Implementation and dispatchment. Usually, a written specification of the first four steps is drawn, while the last two steps are set during implementation or short pre-implementation tests. For the software under consideration, such a specification of the first four steps, with an outlook to the fifth, has been reviewed by (some) program users, so a thorough design document was available at the start of the implementation.

Although this specification was very much aimed at the *solution* — the data structure and visual appearance of the new system — the *fundamental reason* for change was also addressed, and recognized by the reviewers. So, in principle we have no reason to doubt a warm reception by the community of PIAS users, although we always have to wait and see how the market reacts when such a plan is actually put into software form, including a price tag (no matter how modest). A possible reluctance could be caused by the concern that calculation times may increase, because where previously a few intermediate stages of flooding were considered to be sufficient, today, in time domain mode, some hundreds of time steps will be calculated. Indeed, here and there processing time may increase, although some counterarguments can be made as well:

- Determining (temporary) equilibrium in each time step requires iterations, and hence computing time. However, each iteration starts with as initial condition the previous time step, which in general will not differ much from the final condition in that step. So, the number of iterations *per step* will be less than with conventional stages of flooding.
- For a ship with a device that acts for cross-flooding, the time to equalization should be determined anyhow. That used to be done in a separate assessment, with the outcome to be processed manually. So we can ask the user what he or she prefers; spending manual time or let the computer do the work?
- In PIAS many intensive computation tasks are spread over multiple cores or threads. That will also become available for these *Consecutive Flooding* computations, so up to a maximum of (today) twenty damage stability computations can be performed simultaneously.
- Experiments have indicated that total computation time on one core of a single time domain computation consisting of roughly 1000 time steps takes some 5-20 seconds, depending on level of detail of hull form and compartments. Concentrating on Probabilistic Damage Stability, in combination with an efficient method for determining the probability of damage p_i —such as by *Numerical Integration*, Koelman (2006), a variant of what is nowadays called the *Monte Carlo Method* — this delivers a good balance between accuracy and processing time.
- Indeed, Braidotti & Mauro (2019) proposed a computational more efficient method for progressive flooding, at the cost of increased algorithmic complexity. If computational costs of the internal flooding in time domain would become an issue, such a method could be investigated. If..would..could, because a sensible adage in software development is to only solve real problems.

Appraisal by national authorities and classification societies

It could have been an option to distribute mentioned specification to inspection bodies as well, for their comments or advices. However, the question is what we would have gained by this. Because it's been quite a few years now, when SARC developed another new piece of software, on heeling and stability around an arbitrary axis. Similarly, we had drawn up a rather detailed elucidation of the proposed computational approach, including algorithms and references to specific and high-level literature, such as Pawlowski (2016). For comments we had sent that to a few inspection bodies, from whom most did not reply, while one wrote a short email reading “we use computer program ABC, and if your software provides the same results as ABC then we agree”. Although multiple normative, administrative and practical comments can be made regarding this statement, this particular paper is not the place for that. Let it suffice that we trust the reader appreciates that we lost appetite for this path.

Fortunately, the design of our piping software, and its underlying algorithms, data structures and choices are rather well documented, by its specification document, this paper and a bit more extensively in the manual. Additionally, on request some more design considerations or sketches from the implementation records can be made available. That should enable inspection bodies to perform their independent verification of the proper functioning of the software. A reassuring idea, incidentally, is that a time domain calculation is explicitly supported by regulations such as MSC (2020).

Concerning the ship design verification (i.e. the appraisal of damage stability computations), the obviousness of the ship model will only improve. Where with elder PIAS’ compartment connection facility the physical reality was to be translated into tables with numbers from virtual ‘connection’, now the basis is a topological and geometrical model which is easy to verify, as demonstrated by the report of the input from Figure 5.

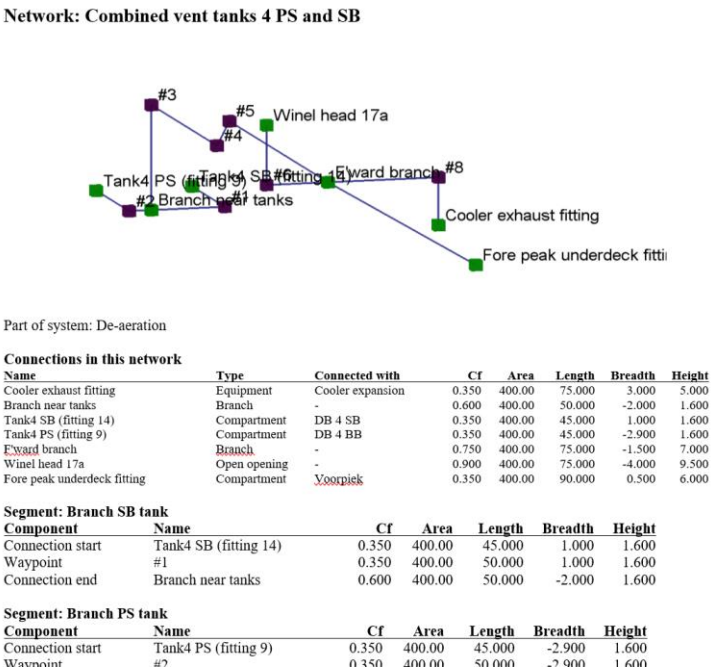

Figure 5: Small part from program output of a piping network

FURTHER DEVELOPMENTS

The software system as described offers these advantages:

- Physics-based computations on basis of a model which includes topology, geometry and true features of the piping system. So, no artificial notions or concepts; WYSIWYG (What You See Is What You Get).
- Intuitive definition of compartment connections, by just adding shape and types of pipes and their components.
- As a result, interfacing with other CAD/CAE software is in principle doable, as the same concepts (pipe shape and connections) form their basis.
- Both conventional (stages of flooding) and time domain damage stability computations.
- Easy generation of complicated stages of flooding.

The next developments of this system will comprise:

- Time domain computations *integrated* in Probabilistic Damage Stability. So, the effect of exceeding maximum allowable equalization time (for example 10 minutes, for SOLAS 2020) can automatically be determined, and incorporated in the table of results of damage cases and their *a* probabilities, and ultimately in the Attained Subdivision Index.
- With damage *to* pipes. For example, in PIAS' Probabilistic Damage Stability module the damage cases are presently generated on the basis of compartment boundaries. This will be extended to include piping edges and corners as well.

These are internal developments, which can be realized at SARC, independent of others. It is different when exchanging data with other CAD/CAE software. Ideally, this would be elaborated on the basis of a common data standard, which includes geometry, connectivity as well as functionality (e.g. the opening pressure of a pressure relief valve), while still being easy to manage and not too elaborate. Preliminary investigations have indicated that such a standard is not available, at least not widely used in the maritime domain. So, finding a solution is a challenge, which is at present being undertaken within a consortium where shipyards, universities and software suppliers are collaborating to develop a next-generation maritime software framework, SEUS (2023). In that context, lately we have been experimenting with a Graph Database, see Koelman et al. (2024), which most probably offers the flexibility to represent the piping data structure as described in this paper. This flexibility goes so far that, in addition to database capacity for pipe geometry, components and connections, there is also capacity for other facets of the pipeline system, such as its requirements and functions, as well as the design validation. This opens the door to a representation of the piping system which is extended with concepts of Systems Engineering — functional definition, physical definition, design validation (see Kossiakoff et al. (2011) — and hence support for a Model-Based Systems Engineering framework.

Where our computation method for the modelling of the flooding process will be adequate for many practical applications — and offers the advantage of traceability — it is not at the technological cutting edge. As SARC does not have the ambition to extend to more enhanced computation methods —such as a 6-DOF motion analysis, or the effects of waves, ship's inertia and the momentum and sloshing of the ingressed water — there lies an opportunity for interfacing with specialized third-party computational analysis software that covers this area.

CONCLUSION

In this paper a new system for modelling geometry and connectivity of pipes, ducts and openings is presented, including the application of these data in damage stability analyses. The status is that this is fully implemented in PIAS' deterministic and probabilistic damage stability modules, including the corresponding manual pages. After a small addition (consisting of some more intermediate results) it will be ready to be distributed for production use. That will be the first independently usable and useful release of PIAS' *Consecutive Flooding* system, including both the systems of delay factors (an extension of stages of flooding) and time domain. On this basis, more extensions will follow, either on the computational side, such as time domain integrated in Probabilistic Damage Stability, or on interfacing with external software. From the user's perspective this new software tool will come with some uncertainties —such as how to determine a crisp equalization time in the asymptotic flooding process, or how to cope with differing permeabilities for the same space — as elaborated in this paper. However, one must realize that these ambiguities have always existed and are now surfacing through the use of sophisticated software. The hope and expectation is that regulators will eventually make responsible choices here.

Occasionally we are asked to indicate the effect of this new software on a particular ship design, however, the prime motive for this new development lies in the process, not in optimizing the computational result. Having said that, it may be expected that by not considering all flooding as a priori progressive, the conclusion of some computations may switch from 'capsized or sunk' to 'survived'. In any case, combined with an efficient non-zonal computation method to determine the probability of damage p_i, results of the probabilistic damage stability assessment will be more in line with reality.

Perhaps, some day after the mentioned extensions have been implemented, we could make some comparative computations with and without Consecutive Flooding, with realistic specimen of ship designs. On the other hand, that would be mere examples, with little generic value. Just examples, while contemporary literature in our profession is already littered with examples of specific computations applied to specific ships. The new software presented in this paper is so easy to use that users will be able to create their own examples.

REFERENCES

Biran, A. & Lopez-Pulido, R. (2014). Ship Hydrostatics and Stability, 2nd ed. Butterworth-Heinemann.

Braidotti, L. & Mauro, F. (2019). A new calculation technique for onboard progressive flooding simulation, Ship Technology Research, 66(3), 150-162.

CESNI (2019). European Standard laying down Technical Requirements for Inland Navigation vessels (ES-TRIN). European Committee for drawing up Standards in the field of Inland Navigation (CESNI).

De Koningh, D., Koelman, H.J. & Hopman, J.J (2011). A Novel Ship Subdivision Method and its Application in Constraint Management of Ship Layout Design. Journal of Ship Production and Design, 27(3), 137-145.

Dexpi (2019). DEXPI P&ID Specification Version 1.3. https://dexpi.org/wp-content/uploads/2020/09/DEXPI-PID-Specification-1.3.pdf.

Gero, J. S., & Kannengiesser, U. (2004). The situated function–behaviour–structure framework. Design Studies, 25(4), 373–391.

Horváth, I. (2007). Comparison of Three Methodological Approaches of Design Research. International Conference on Engineering Design. ICED 07, (7), 28–31.

IMO (2016). International Code for the Construction and Equipment of Ships carrying Dangerous Chemicals in Bulk. International Maritime organization.

IMO (2020). SOLAS Consolidated Edition, chapter II-1, part B. International Maritime organization.

ISO (2019). Industrial automation systems and integration – Integration of lifecycle data for process plants including oil and gas production facilities – Part 4: Initial reference data, ISO/TS 15926-4.

Karolius, K.B., Cichowicz, J. & Vassalos, D. (2019). Modelling of compartment connectivity and probabilistic assessment of progressive flooding stages for a damaged ship. 17th International Ship Stability Workshop.

Koelman, H.J. (2006). A new method and Program for Probabilistic Damage Stability. Ship Technology Research 53:183–193.

Koelman, H.J., Veelo, B.N., Seppälä, L. & Filius, P. (2024). Closing the Gap between Early and Detailed Ship Design Models. 15th International Marine Design Conference (IMDC), Amsterdam, Netherlands, June 3-6.

Kossiakoff, A., Sweet, W.N., Seymour, S.J. & Biemer, S.M. (2011). Systems Engineering Principles and Practice. John Wiley & Sons, New Jersey, USA.

MSC (2020). Resolution MSC.429(98)/rev.1: revised explanatory notes to the SOLAS chapter II-1 subdivision and damage stability regulations.

Pawlowski, M. (2016). The Stability of a Freely Floating Ship. Polish Register of Shipping, Technical Report 72. www.prs.pl/uploads/tr_no_72.pdf.

Ruponen, P. (2006). Pressure-Correction Method for Simulation of Progressive Flooding and Internal Air Flows. Ship Technology Research, 53, No.2, 63-73.

Ruponen, P. (2007). Progressive flooding of a damaged passenger ship. Doctoral dissertation. Helsinki University of Technology.

Ruponen, P., Queutey, P., Kraskowski, M., Jalonen, R. & Guilmineau, E. (2012). On the calculation of cross-flooding time. Ocean Engineering, 40, 27-39.

Ruponen, P., Manderbacka, T. & Lindroth, D. (2018). On the calculation of the righting lever curve for a damaged ship. Ocean Engineering, 149, 313-324.

SEUS (2023). Smart European Shipbuilding. Horizon Europe Framework Programme. www.ntnu.edu/seus.

Söding, H. (2002). Flow computations for ship safety problems. Ocean Engineering (20), 7, 721-738.

Vermeer, H., Vredeveldt, A.W. & Journée, J.M.J. (1994). Mathematical modelling of motions and damaged stability of ro-ro ships in the intermediate stages of flooding, STAB'94 Conference, Melbourne, USA, Nov. 7-11.

White, F.M. & Xue, H. (2021). Fluid mechanics. 9th ed. Mcgraw-Hill.

Proceedings of 15th International Marine Design Conference (IMDC-2024)
June 2-6, 2024
Amsterdam, the Netherlands

Closing the Gap between Early and Detailed Ship Design Models

Herbert J. Koelman[1,*], Bastiaan N. Veelo[1], Ludmila Seppälä[2] and Paul Filius[2]

ABSTRACT

Conventionally, ship design and engineering are segregated activities, carried out with different software packages that thus each have their own place, qualities and tools. And consequently, a different data model. As a report on ongoing work to bridge that gap, this paper first explores existing neutral data models and standards employed or considered in maritime applications and concludes that none of these is directly applicable. It continues with describing the requirements and derived abstract data model of the SEUS project and its design and engineering applications. A graph database is identified as a potentially useful tool for SEUS data modelling, and a hands-on experiment confirms this presumption.

KEY WORDS

Ship design methodology; Data models; Digital transition.

INTRODUCTION

In the ship design process, the transition from early conceptualisation to detailed design marks a critical juncture — a "tipping point" that involves a change of stakeholders. Early design models emphasize the vessel's fundamental characteristics, naval architectural and functional aspects. Detailed design and production design delve into the intricacies of layout and deal with the generation of production and construction data. This dichotomy in focus leads to disparities in the tools employed and necessitates the alignment of data models.

This paper explores data standards in maritime applications, data models of two particular software systems — PIAS (by SARC) and CADMATIC — and the direction for integrating these models in the SEUS[3] project. SEUS aims at creating a high Technological Readiness Level solution to provide a set of computational tools for shipbuilding, incorporating data flows while the design matures and providing a comprehensive toolset for different stakeholders of the overall shipbuilding process, with access to a single source of true data. However, conventional neutral models or industry standards have not generally demonstrated their suitability for this task, so the research question addressed in this paper is to find a data model for shipbuilding which provides coherence of the data generated along the life cycle. Critical for SEUS are its anticipated impacts — such as a) platform solution for PLM, b) facilitation of digital transformation and c) integration of early design into the overall design process, see Gaspar et al. (2023) —many of which require software integration between design and engineering. However, it is not the first time in the history of mankind that such an endeavor is undertaken, so in the next section the applicability of existing maritime product data standards is investigated.

DATA STANDARDS FOR MARITIME APPLICATION

The authors share a combined 100^{+} years of experience in developing maritime software, where aspects of interfacing and (software) collaboration have played an important role, from time to time. In that context, we have regularly been surprised

[1] SARC, Bussum, The Netherlands.
[2] CADMATIC, Turku, Finland.
* H.J.Koelman@sarc.nl.

[3] See acknowledgement at the end of this paper for SEUS project details.

Submitted: 13 February 2024, Revised: 8 April 2024, Accepted: 1 May 2024, Published: 19 May 2024

Conference paper, DOI: https://doi.org/10.59490/imdc.2024.837 e-ISSN: 3050-4864

by the surprise of others when we have been asked why we don't just use one of the many existing data exchange standards. By way of a (late) response, this will be addressed later in this section. First, however, a brief overview of potentially applicable standards is given, without seeking to be complete.

An Outline of Potentially Applicable Neutral Models and Data Standards

The obvious idea of a neutral model is demonstrated in Figure 1, where without specific provisions the eight independent computer programs A..H need 8 x 7 = 56 interfaces to share their data, while some kind of centralized format only requires eight interfaces.

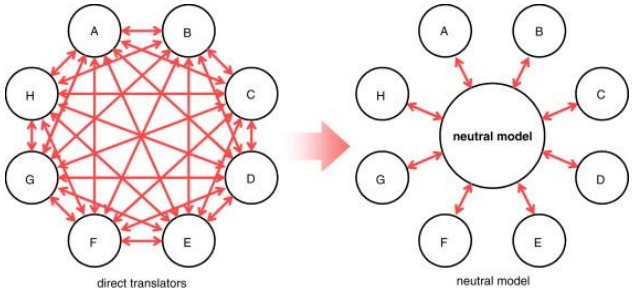

Figure 1: The neutral model saves on interfaces (from Gielingh (2008)).

The paradigm of the neutral model is reflected in several neutral file formats which are used for this purpose. The search for a recent overview of the popularity of the various (file) standards for product information did not yield anything, so we fall back on the survey in Srinivasan (2008). The most frequently used data exchange standards appear to be DXF, IGES and ISO 10303 — commonly known as STEP, STandard for the Exchange of Product model data — with a combined utilization of 60%. The remaining 40% cannot be considered to be suitable for generic exchange of 3D data, for example PDF is listed, very useful, but 'just' a document format. Although quite widely used for data transfer, DXF is merely a drawing exchange and not specifically suitable for the exchange of product model data. IGES dates back to 1980, and, as its name suggests — Initial Graphics Exchange Specification — is more aimed at the exchange of 3D shape than of a product model. Although e.g. in Kirkwood and Sherwood (2020) STEP is recommended above IGES, the latter is still widely in use, for example for exchanging the shape of a ship hull in IGES types 126 or 128, which encode for NURBS curve or surface representation. This demonstrates a phenomenon that shall be encountered in a broader sense later: IGES contains a wide range of some hundred types, for all kinds of mathematical representations of shape, such as lines, curves, planes, surfaces and solids. So, the producer of a computer program that produces an IGES file is free to choose a few favorite representations, there is no need to support all (actually, nobody does).

This leaves STEP as perhaps the most viable alternative for product data exchange, a conclusion which is drawn in many papers, e.g. Kim et al. (2008) where it is proposed to use STEP not only for the exchange of 3D shapes, but to extend it to design intent (e.g. parameters, features, constraints and history). Furthermore, STEP specializes in specific areas of industry for so-called Application Protocols (APs), with maritime application AP215 (Ship Arrangement, see ISO (2004a)), AP216 (Ship Moulded Form, ISO (2003)) and AP218 (Ship Structures, ISO (2004b). Incidentally, there is a short related anecdote to tell: when we ordered the STEP standard from the Netherlands Standardization Institute, a whole package arrived, but without AP215, 216 and 218. On enquiry, they maintained that these had since expired. Fortunately, the purchase could be made at ISO in Switzerland, but the exact status is now not entirely clear to us. Anyway, multiple researchers have formulated a preference for STEP for maritime application, e.g. Whitfield et al. (2011) and Shiplys (2019). Qin et al. (2017) report on some shortcomings of STEP, and they propose some improvement by combining it with Web Ontology Language (OWL) methods.

All these standards aim at a model for shape, with some ambition to grow towards product modelling. They have evolved into extensive books covering all kinds of pre-considered variations, more or less like a dictionary of a human language. Some considered that too limited, because life-cycle support, explicit semantics and relationships between entities are missing. This awareness has gradually led to a new standard, ISO-15926, see ISO (2005), from which a readable overview is presented on https://15926.blog/. The latter reports a twofold goal, a) global semantic interoperability and b) archiving, collecting and integrating plant life-cycle information. This terminology already reveals that this standard is leaning towards process plants, which might limit the applicability in the ship design area. Nevertheless, in the ship-borne integrated piping system as reported in Koelman (2024) the underlying data structure was inspired by ISO 15926. Another maritime

connection is that in a Dutch maritime research program from a decade ago, “Integraal Samenwerken”, a pilot with ISO 15926-11 (see ISO (2023)), was commenced — with the keywords “triple” and “Gellish” — but that did not proceed.

Another interesting industrial standard that has a wider scope than just the product and its shape, is ISO 81346, see ISO (2022). Here the multifacetedness of a product is addressed by assigning different *aspects* to a product, where each aspect can have its own hierarchy and taxonomy. An example is given in Figure 2, which shows three aspects: a) the constructional relations with the components, b) the functional relations and c) the spatial relations (e.g. the location). The application is not limited to these three; other aspects may also be considered, such as financial or logistical. As argued in Leclerc et al. (2022), this framework fits very well with a Systems Engineering approach, a method that is expected to enhance the productivity of the maritime sector (see the acronym *MBSE* in Maritiem Masterplan (2023)).

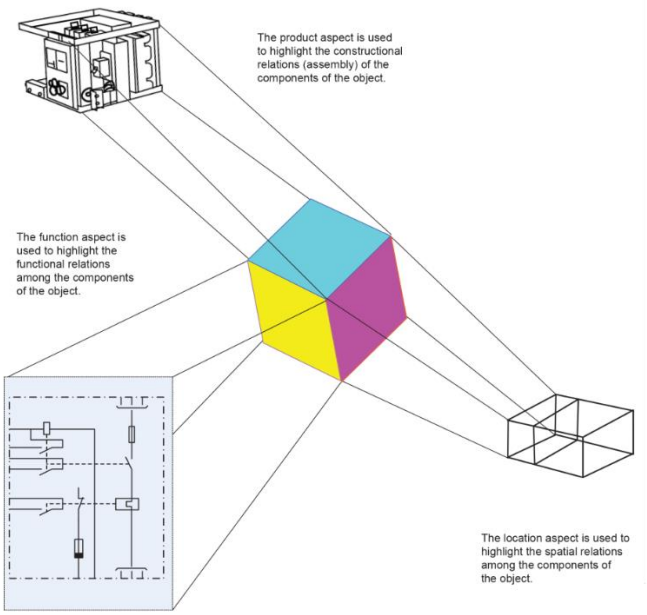

Figure 2: Different aspects of an object (from ISO (2020)).

The discussed standards relate to properties of a product in the design and construction phase. An emerging field is to include operational data as well, where a significant contribution is delivered by sensor data. This application is targeted by ISO 19848 (see ISO (2023)), which has been used by Fonseca et al. (2022) for an experiment with a digital twin of a scale model of a ship. Another emerging standard is the XML-based Open Class 3D Exchange (OCX) (see Zerbst (2023)), however, this is at the edge of our area of applicability, as expressed on https://3docx.org/: “The OCX is a vessel-specific standard addressing the information needs by the classification society”.

This ends a somewhat impressionistic overview of data standards and neutral data formats. A follow-up section discusses applicability and pitfalls, but first the data flow in a typical maritime project is outlined.

Data Flow and Growth in a Typical Maritime Project

Kirkwood and Sherwood (2021) contains an interesting approach to simplify the sustained integration between CAD and CAE. This is motivated by the CAE application being a FEM analysis, and indeed such a representation may contain somewhat less detail than the original CAD model. However, in the maritime world CAE is predominantly seen as the precursor to production, which implies that data is becoming both more detailed and richer. For example, a watertight transverse bulkhead in a ship. In the first instance, this is just a line on a GA plan (or a plane in a 3D CAD model) with the intrinsic property that it is watertight, so it could act as a separator between tanks or compartments. This limited information is sufficient for producing tank capacity tables and damage stability computations. Later in the design process, this bulkhead data is extended with details of plate thicknesses, panels, beams, stiffeners, and perhaps paint details or manufacturing logistics; augmented with data that can be *derived*, such as weight, centroids and cost. And this all belongs to the bulkhead that started as a line in a GA plan. Consequently, when in a design update the bulkhead is shifted one frame position, some of

these properties have to change correspondingly. In a sense this issue is an instantiation of Figure 2, because functional, constructional, financial and logistical aspects are included, each with their own taxonomy and/or codification system. But it is also a matter of Level Of Detail (LOD), for example when at the stage of the General Construction Plan only the main structural elements are included, which are extended with brackets and welds in the final production preparation stage. If one would have the desire to shape such a system in a third generation (3G) programming language — only in RAM, without considering permanent storage and interfacing — a structure with arrays, classes and pointers connecting the different entities, could do the job. This is depicted in Figure 3, where:

- The bulkhead is part of subsystem "bulkheads" (which in turn could be part of the system "hull structure").
- Each bulkhead contains a GUID[4]/UUID[5], which acts as unique and permanent identifier (what is called a Virtual Persistent Identifier in Kirkwood and Sherwood (2021)). A unique identifier from another source (e.g. from a supporting data management system) might be an alternative for the GUID.
- Each bulkhead contains three types of subclassed information:
    1. Topology and geometry.
    2. References to compartments on both sides (in the system "compartments").
    3. List of panels.
- The CAD system manages 1 and 2, never "sees" 3.
- The CAE system uses 1 and 2 and manages 3.

Please understand that this 3G solution is only presented to elucidate the process around and with the data. Practical considerations, such as the lack of a common 3G programming language, prevent its actual implementation.

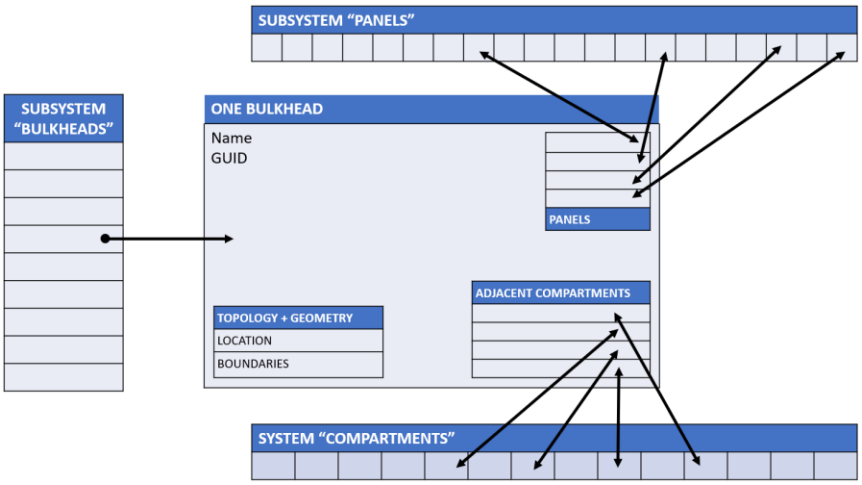

Figure 3: A class-based example of a data structure around a bulkhead, suitable for integrated CAD and CAE

This example illustrates the continuously increasing completeness of information over the whole design and engineering process. This observation is somewhat contrary to the notion of design phases — concept, preliminary, contract and detail — of which it was once useful to distinguish between. The demise of the notion of distinct phases can be witnessed in practice, for example the typical 'preliminary design' requirement of sufficient damage stability is greatly influenced by the presence and position of pipes, valves and ventilation openings; details that are typically addressed in later moments of the design process. Also in literature this trend can be observed, for example a recent state-of-the-art report on ship's design methodology, Erikstad and Lagemann (2022), counts zero entries of the words "design stage". Yet, the title of the present paper addresses a gap, which is not a gap between design phases, but between models. The early design model is a bit more holistic — including non-material aspects such as simulation results — but smaller in size than the detailed model. Bridging the gap between models does imply that the connected tools should be unified for all design activities, indeed the objectives in the earliest stage of the ship design will differ from the later stages, as eloquently motivated in Andrews (2018).

Finally, there is the issue of bidirectional vs. unidirectional flow of data traffic. The ideal with a neutral model has always been that all connected applications are able to read and write from the central storage, as depicted by the bidirectional arrows in Figure 1, at the right. If the information involved is simple, such as an isolated number, then bidirectionality is easy to achieve. However, if complex logic or functionality is involved, then it can happen that not all applications are able to perform modelling changes. For example, the duality between compartments and bulkheads & decks can be managed by one

[4] https://en.wiktionary.org/wiki/GUID
[5] https://en.wikipedia.org/wiki/Universally_unique_identifier

application only, while others can read and use that information without the need for specific tools to address that duality. Another example is hull shape modelling, where one parent application has the specific modelling tools, acting upon a parent representation, while other representations — such as STL, VRML, X3D and 3D-wireframe — at each design change are instantaneously derived and stored in neutral form. Ready to be used by other applications, without them having the tools for shape changes. If different applications are geographically dispersed then unidirectionality might be a bit awkward, but when two applications are open in two windows on the same monitor then it is neither unnatural nor time consuming that only one of the two can be used to make hull shape changes. It might even offer an advantage when an HVAC engineer is not able to change the shape of the bulbous bow.

Applicability of Neutral Models and Data Standards in Ship Design and Engineering

At this point, the paper suffers from self-plagiarism, because what follows is an anecdote that one of the authors surely must have told hundreds of times over the past 20 years. As reported by Owen (1997), STEP has aimed at 'completeness', which led inevitably to 'conversion'. This is illustrated by nine different representations of a circular arc in 2D, e.g. a) centre + radius + start angle + finish angle, b) center, radius, start point, end point, or c) polyline. If an application should want to support all these representations, and it uses one of them internally, then that implies eight conversion algorithms being required. From which item a) can be done with simple math, but item c) already requires some numerical analysis, which may result in round-off errors.
A similar example can be found in STEP AP 216, Ship Moulded Form, which supports three alternative representations: offset table, wireframe and surface. So, if a computer program internally applies a NURBS surface representation, and it receives a STEP file in offset tables, then it should be able to convert. Which is no trivial task in this example, see Koelman and Veelo (2013).

These are examples of the 'variation in representations', which are also addressed in the seminal paper by Gielingh (2008). There it is concluded that while we aimed for the nirvana of Figure 1, due to the large variation in representations, in practice only a subset is supported, leading to a situation of all kinds of ad hoc representation conversions, as depicted in Figure 4, regardless whether these representations are stored or communicated by DXF, IGES or STEP. This is the fate of any neutral model. One way or another underlying representations have to be converted, unless the world (or a workable subset of the world) decides to use a single representation for each and every entity.

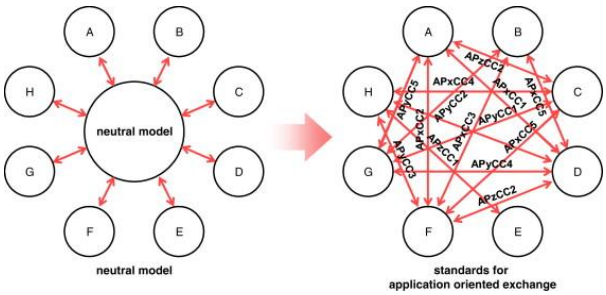

Figure 4: From theory (left) to practice (right); the neutral model doesn't really exist, from Gielingh (2008).

Another issue with standards, such as IGES, DXF and conventional STEP, is that each only contains geometric data as stated by Qin et al. (2017): "A well-known problem of STEP AP 203/AP 214 neutral file-based exchange method is that this method is limited to exchange geometric data, where those nongeometric data related to design intent, such as construction history, parameter, constraint, and features, are completely lost after the exchange". A practical issue of conventional neutral formats is that it does not always work properly, so that their usage may lead to errors and information loss, see Gielingh (2008) on STEP files read into an application and subsequently identified: "significant differences between these files were found: some entities disappeared, others appeared, and others were changed". This observation was confirmed recently in Kurylo et al. (2023).

In particular STEP AP 215 is quite extensive, but still does not cover everything:

- It supports a single permeability per compartment, while in practice intact and damaged permeabilities will differ.
- Three types of block coefficients are specified, but not the one based on the design waterline length, as required for Holtrop's resistance prediction. It is questioned why include such *derived* information as the block coefficient in a standard? Each application should be capable of dividing a volume by length, breadth and draught, specifically in the variant that is relevant for that particular application.

- The height of the sounding pipe is included, but not its shape.
- A tank total volume and corresponding Center of Gravity is included, but not its free surface or a complete tank table provided. Again, here the question is why is easily derivable information stored?
- Although some relationships between entities are supported, there is no generic support for explicit dependencies and relationships between entities.

So, it can be concluded that STEP AP 215 is on the one hand too extensive, while on the other hand not complete. Probably, that will be the fate of any global neutral model. Furthermore, it can considered to be a dictionary, not an ontology. Nevertheless, a lot of effort has been put into developing this standard, and many parameters and entities have been given a name and meaning, so why not use it, at least as inspiration?

The attractive feature of ISO 81346 (ISO, 2022) is that it addresses the multifacetedness of an object explicitly, but it defines a framework more than that it provides an implementable solution. Furthermore, it includes a standard on the coding of the location of objects, however, this is tailored to modeling buildings and is not directly applicable to ships.

Building Information Modelling (BIM) standards have not been discussed in the section on neutral models, because of the large volume, complexity and diversity of standards, national and international. The authors have not studied BIM in detail, yet BIM ISO standards 23386 and 19650 appear to be quite high-level, providing more of the general structure than relevant details. It seems that for many different fields of application this is further elaborated on a national or regional scale, (see www.etim-international.com/, which contains article codings, for example: electrotechnical, HVAC and plumbing components). Although these components are vital in the ship's outfitting phase, their relationship with the design and engineering activities is relatively limited.

TOWARDS THE SEUS DATA MODEL

At this point the conclusion is that of all the existing models and standards, none is directly usable for our purposes. Although, precise purposes have not so far been explicitly formulated, and thus this is addressed in the next subsection.

Requirements for the SEUS Purpose

Minimum requirements can be derived from the analysis and discussion above, and consist of:

- A dictionary of the names and implicit relationships between entities. Although it is perhaps a bit premature to mention a solution at this stage, STEP AP215 provides a useful basis for this, without necessarily needing to adopt everything in it, and with the knowledge that it will need to be extended here and there.
- Support for explicit relationships between entities.
- Support for variations in representations. Since these are uni-directional an object may be defined by one parent application, which derives from each design change other child representations, which are read-only for the other applications of the system.
- Support for multifacetedness, so an entity can be part of multiple taxonomies or other data structures.

Furthermore, there is a feature that, very strictly speaking, is not minimally required, but which could be extremely useful in practice: that of support for *functions*, in addition to *data*. A function is a procedure, a subroutine, a piece of processing software that can be called by all connected applications, implemented as DLL, API or Remote Procedure Call (RPC[6]). The advantage of such a tool has been discussed in Koelman et al. (2015), under the name "request/reply".

Finally, there are some desirable features that are not strictly necessary, but could prove to be useful:

- A tool for documenting the essence and properties of entities and relations. This may be done in a common text editor, typically Word, however, that is not the most user-friendly tool, and for the tabular and reference work at hand, its usefulness is even less. Preferably, the documentation tool is integrated with the data management tool because they both deal with data, structures and relations, either to be understood by a human or by the computer.
- Explicit support for data integrity and authorisation.
- Aspects of system performance, such as processing speed and limits in data sizes. However, this is considered to be self-evident, and it is a bit premature to start quantifying it at this point, but it should not be forgotten in the end.

The ambition of the SEUS project extends beyond the design and engineering phases, which means another similar endeavour to find the data model links for operational data and engineering. This phase is not included in the present paper

[6] https://en.wikipedia.org/wiki/Remote_procedure_call

although the approach can be applied to it in later stages of the project. In PDM terms, the focus of this paper extends to linking “as designed” and “as engineered” data models, with a potential to extend to “as build” and “as in operation”. Hence focusing now on the data models links, means applying later on a similar approach to digital twin platform solutions where different applications can form digital threads.

A First Experiment with Graph Databases

Although it is possible to implement a shared data format that can represent the relations depicted in Figure 3 on the basis of XML or JSON, that would be a laborious undertaking, because every element would need its own GUID and relations would need to be expressed in those terms. It would require a lot of cooperation, extensive formal specifications as well as data validation. The resulting text files would be very substantial and difficult to interpret by human designers, so the advantage of it being in natural language text would diminish. An alternative to sharing data in files is to share a database.

A traditional relational database consists of tables of rows and columns, where each row represents one data entry, and each property of that entry sits in its dedicated column. This enforces the need for the data to be structured: each column contains only data of a particular type and meaning, and each entry in the table has the same number and types of properties. Relations between entries are encoded as a property containing a reference to another row, possibly in another table; this is called a foreign key. An example would be a table of users and a table of orders, where each order has a reference to a user that placed the order. This encodes a “one to many” relation, where a user can place multiple orders. To collect all orders that were placed by a particular user, the entire column must be searched for matches with the user’s key. Because foreign keys are subjected to the rigid structure of this database format, relational databases aren’t very well suited to model systems with many relations or arbitrary relations, such as social networks and financial systems.

A different type of database has emerged that allows modeling completely unstructured data, the so-called graph databases. Different approaches exist, but common to them all is that a graph database describes nodes of information and how various nodes connect to each other. As such, the term “graph” refers to topology and discrete mathematics, not graphics. Depending on the application, a graph database can yield higher performance than can a relational database, it can be easier to query and it gives more freedom in conceptualising a system. Another aspect that is gaining relevance is that a graph may be easier to train using AI than a collection of tables, because semantics are expressed more clearly.

It is important to note that in the end there it is not necessary to use a graph database. A graph database gives the freedom and flexibility that is important for solution exploration. If the experiment is successful, this will to some extent demonstrate that it is implementable. Preferably, there is a concept that can be filled in by the PLM software of the SEUS consortium partner Contact Software.

In early 2024, the popularity ranking site db-engines.com had 41 graph database management systems (graph DBMS) in its ranking, and 13 additional DBMS capable of representing graphs as secondary model. Many of these build on open-source implementations, with some of them offering additional commercial services, which are seen to be more attractive than purely commercial solutions. Without the desire or need to do an exhaustive evaluation of all of these, the following graph DBMS have been considered: Neo4j, NebulaGraph, Memgraph, ArangoDB, Redis, GraphDB and Virtuoso. We have installed and programmed against both Neo4j and ArangoDB, after which the latter came out as the more appropriate DBMS. ArangoDB is performance oriented with features that allow some structuring of the data where that is desired. Nodes and edges in the graph are functionally equivalent to JSON documents, which can include arrays. Relations between nodes can be encoded as edges, which are just like nodes but with mandatory “from” and “to” properties containing node identifications. Edges allow the application of typical graph algorithms such as “shortest path” and facilitate validity guarantees that prevent dangling edges. Alternatively, relations may be encoded by having references as a property of the nodes themselves. In this way, ArangoDB offers a mix between graph database and document store.

Thus, an experiment has commenced representing the case depicted in Figure 3, using ArangoDB. The source code of the experiment is publicly available on GitHub[7]. Communication between the DBMS and the client program happens over HTTP. This allows the database and the client to be at different geographical locations, which is how the experiment was developed. Also included is an option to run the experiment in a Docker container, which simplifies reproduction and demonstrates that network overhead can be reduced when everything runs on the same hardware. In this case the reduction was 60 milliseconds, to under ten milliseconds per query. Evaluation of processing speed at scale is not part of this initial

[7] https://github.com/seus-project/graphexperiment

experiment, but increasing the size of the graph to one million nodes meant the slowdown was measurable but not significant. The VelocyPack binary transport[8] was not utilised, which has the potential to increase throughput.

The main question that this experiment tried to address is how the data of the design model can be sensibly organised in a graph database. It was noted that not all required functionality had to be covered by the database as such, because rules and logic in the governing applications can guarantee database consistency. As the database was not filled directly by an unauthorized system or human, nonsensical relations should in practice be prevented. Similarly, aspects of authorization can be handled by applications.

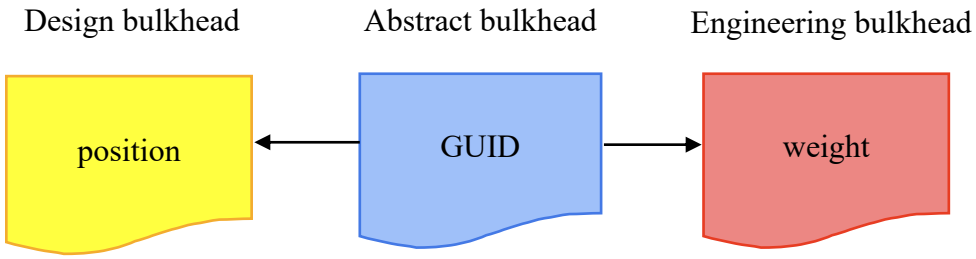

Figure 5: Bulkhead representation.

Considering the viewpoint of the applications, the ship model can be simplified by only considering bulkheads. For design software, a bulkhead primarily defines the partition of space and thereby determines the volumes of compartments. For engineering software, a bulkhead is primarily a structural object. The objective of the experiment was to allow both design and engineering software to work on the same bulkheads without getting in the way of each other. The approach that this experiment took (Figure 5) is to start with a node that represents the abstract concept of a bulkhead, by only containing its identity. Connected to it are separate nodes that represent specializations for design and engineering. This principle is scalable to additional systems, such as cost estimation, construction process logistics and maintenance.

Each specialisation contains properties that are specific to that specialization and can also extend the graph with nodes that are specific for that representation, as is shown in Figure 6.

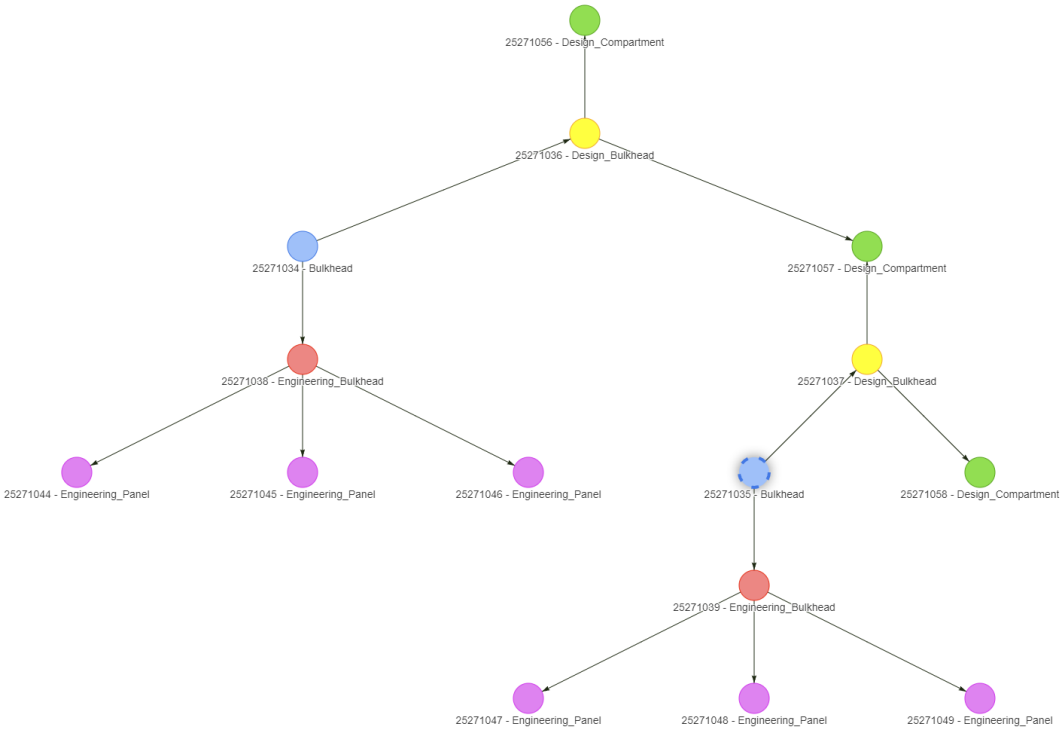

Figure 6: Automatically generated plot of a graph database with two bulkheads and three panels per bulkhead.

[8] https://github.com/arangodb/velocystream

The source code for the experiment contained a procedure[9] that synthetically generated data for a given number of bulkheads, where each bulkhead consists of a given number of panels on the engineering side of the graph, and on the design side of the graph the boundaries of compartments are defined. Figure 6 shows the nodes and connections for two bulkheads, three compartments and six panels. The connections are directional, but they can be traversed in any direction. The following lines of ArangoDB Query Language (AQL) are an excerpt of the source code that traverses the graph and lists the compartment names together with the positions of their bounding bulkheads:

```
FOR c IN Design_Compartment
    FOR db IN INBOUND c Design_BulkheadAdjacentCompartment
        RETURN [ c.name, db.position ]
```

The experiment demonstrated how the output changed when one of the bulkheads was moved to a new position.

In practice, the possibilities of extending the graph with additional information are endless. The design software could include constraints from the constraint management system (see De Koningh et al. (2011)), and any other model data that is currently stored in separate files. The engineering software can store the panel data, such as identification number, dimensions, and position in relation to the appropriate local coordinate system, and connections to other nodes representing other parts and production details. Even versioning can be implemented as part of the graph, where properties of nodes aren't simply updated, but a new version of the complete node is pushed on top of a stack of node versions, where edges between the versions contain the date of the change, approval by superior, etcetera.

In principle, the complete graph is traversable by both engineering client and design client. For example, when the engineering software needs the position of a bulkhead, it could locate the abstract bulkhead, traverse to the corresponding design bulkhead, and read out the position from there. But this requires the engineering software to have knowledge of the topology of the design side of the graph, and it also means that the developers of the design software cannot change their side of the graph without coordinating this with the developers of the engineering software. Interestingly, ArangoDB allows for the installation of so-called Foxx microservices, that can be used to provide a stable API for querying potentially dynamic subgraphs. A Foxx microservice is essentially a snippet of JavaScript that can be uploaded to the graph DBMS after which it can be accessed at a specific URL. When a client accesses that URL, the code in the microservice is executed inside of the DBMS, and the resulting data is returned. Among other things, a microservice can perform a graph query. This way, the developers of a particular system are free to change the layout of their side of the graph if they adapt their microservices accordingly, and other systems can continue using them without change, coordination, or synchronisation.

The experiment demonstrates that with 22 lines of JavaScript[10], a microservice can be implemented by which the position of a bulkhead can be queried by name: thus, `http://localhost:8529/_db/seus/bulkhead_position/B1` produces the output `[10]`. ArangoDB's HTTP API follows the OpenAPI specification and is integrated with Swagger 2.0, meaning that the database server serves its own API documentation together with a web form where the API can be tested interactively. This functionality also covers the microservices. So, the microservice can include documentation that the returned value is the longitudinal distance in metres between the aft surface of the bulkhead and the aft perpendicular, with positive values meaning forward, and negative values aft, of the aft perpendicular.

A microservice can also contain additional logic. Thus the weight of a bulkhead does not need to be a discrete property stored in the engineering representation of a bulkhead, but a value that is determined dynamically, by a microservice. In an early stage of the design, the structure of a bulkhead might still be undetermined, meaning that there are no nodes connected to it that represent panels and stiffeners. In that case, the microservice could return an estimated weight, possibly with a low level of confidence. But as soon as panels have been defined, the plate thickness and dimensions known, the material known, and the stiffeners have been defined, then the weight can be calculated with a high level of confidence. When the weight of a module is requested, the microservice can recurse into all the parts that make up the module and accumulate the weights of the parts.

What is concluded from this experiment is that a graph database has great potential in the implementation of a shared data model. Flexibility and scalability is offered by a graph database, and the extensibility with microservices addresses to some degree the need for documentation (taxonomy) and RPCs. Whether the ship design department and the engineering department are working on the same model in different geographical locations, or all systems are run on the same computer, the HTTP interface of the DBMS means that it is applicable in either situation.

[9] https://github.com/seus-project/graphexperiment/blob/v0.1.0/source/app.d#L150
[10] https://github.com/seus-project/graphexperiment/blob/v0.1.0/foxx/bulkhead_position.js

SEUS' DATA MODELS

The purpose of this section is to conceptualise the model of data, relations and services from SEUS. Prior to that the existing data models of the design and engineering software suites are sketched out.

The pre-existing data model of the design software

The basis of the ship design data model is formed by the hull shape, which can have two representations. The most complete is a solid model with closed curved surfaces, in proprietary H-Rep representation, see Koelman (2003). Another contains a wireframe, i.e. cross sections and stem/stern & deck contours, which is sufficient for all computations. The solid/surface model is convertible to PIAS' wireframe, and to IGES, NURBS surface and IGES/DXF 3D curves. The wireframe model can be converted to solid/surface, albeit with human assistance.

The space inside the hull is filled with constituting planes (bulkheads and decks) and compartments (tanks and other spaces), which form a duality: planes shape compartments, while spaces are bounded by planes. This duality is modelled by a proprietary method (see De Koningh et al. (2011)), which is based on Binary Space Partitioning (BSP). These constituting planes divide the internal of the ship hull into convex spaces, which are called subcompartments. Multiple subcompartments can be assigned to be part of a compartment. In this structure the spaces are 'logical' building blocks, while the compartments are physical, i.e. they are watertight. A finer subdivision may be obtained when non-constituting planes are also taken into account; these are not explicitly modelled, however their presence can be effectuated by modelling subcompartments by their corner vertices, typically, but not limited to, eight. These two compartment modelling methods can be mixed, and an average PIAS user applies the plane-based method for larger, systemic, subdivision planes, and the vertices-based method for smaller tanks or voids. Regardless which of the two modelling methods has been used, the final compartment shape is computed by an intersection with the ship's hull. Although this shape is the core property of a compartment, other properties are also stored, such as its name, permeability, design density, location and type of external openings, and location and shape of the sounding pipe(s).
From the viewpoint of hydrostatic and (damage) stability the connections from and to compartments — such as by pipes, internal openings and ducts — are as equally important as their shapes. This forms an integral part of PIAS' data model, but as this is already a topic of another paper on this conference, Koelman (2024), it is not discussed further here.

This comprises more or less the geometrical and topological ship design data, which are shared in many stages of design and engineering. However, an accurate prediction of all kinds of technical properties — such as draught, cargo capacity, power consumption, stability and strength — also depends on the ship's weight and its distribution. Obviously, PIAS supports this, basically with a long list of numbers of components, their weights, three spatial coordinates, and their aft and forward boundaries.

The 'design' software is not only applied during the ship design phase, but also to produce simulation and delivery documents. These include tables of tank capacity, assessment of (damage) stability, longitudinal strength and maneuvering characteristics. Such reports are currently exported to ASCII, XML or Word formats, although many of these computations can be offered in an RPC fashion.

Furthermore, all entities can be equipped with a Virtual Persistent Identifier, possibly a GUID, a concept that has attracted our attention before. This uniquely and permanently identifies an object, which facilitates tracking and processing changes.

The pre-existing data model of the engineering software

The data model of CADMATIC Hull is based on relationships, which directly support the requirement that any change in shape or position will directly affect another element and provide a chain reaction to others. In addition, standards such as end shapes, holes, cutouts, lugs are included as a feature and not as their shape; and its form is recorded in a referenced library. The body and thickness directions are also assigned as a parameter of the object and therefore the CL and reversed frame have a direct influence on the final 2D and 3D presentations. A group of elements (plates and profiles) are recorded as a whole in a sub-database and this part is linked to a parameterised grid definition which also indicates the x, y and z directions or a plane definition defined as a surface. The whole (the ship) is a collection of these sub-databases, which can be flexibly exchanged, this approach facilitates simultaneous work in large models and possibility to replicate database of the project for several physical servers to provide seamless experience for remote work teams and users. This is the basis of the Hull application, from which all presentations are derived, such as 2D cross-sections, 3D views, derived information, such as

weight, length and material, and production data, such as cutting, robot and bending data. All objects have their unique GUIDs, which are used as a link for all relationships.

The CADMATIC applications are Hull, P&ID, Plant Modeller and Piping Isometrics & Spools. All the components, parts, symbols, and design instructions are stored and managed in Library & Project Databases. These databases also include the format control for sheets, listings, and reports. All applications use the same database, ensuring the information remains the same throughout the design project. Access is governed by the COS (CADMATIC Object Storage, see Figure 7) environment, where data is protected from being modified at multiple sites at the same time. Therefore, remote design teams can work in distributed projects using a common model database without conflicts. Projects are split into blocks, general project data, hull line subsets and 2D symbols, and these can all be saved to the COS server separately. In P&ID, the designer describes the process schematically in 2D format using predefined symbols and metadata information. In Plant Modeller and Piping Isometrics & Spools the process diagram is rebuilt in a 3D format to describe the ship in a realistic way using pipes, fittings, equipment, structural components, etc.
While different applications work in a slightly different way, depending on the discipline they serve, the overall project data is consolidated in the COS database. CADMATIC represents so called "intent-driven" CAD solution, which focuses primarily on the shipbuilding nature of the designer's work, see Dush et al. (2017). Each application has their own API to serve the needs of particular integrations for design disciplines, while COS Web API serves the needs of integration with overall project data.

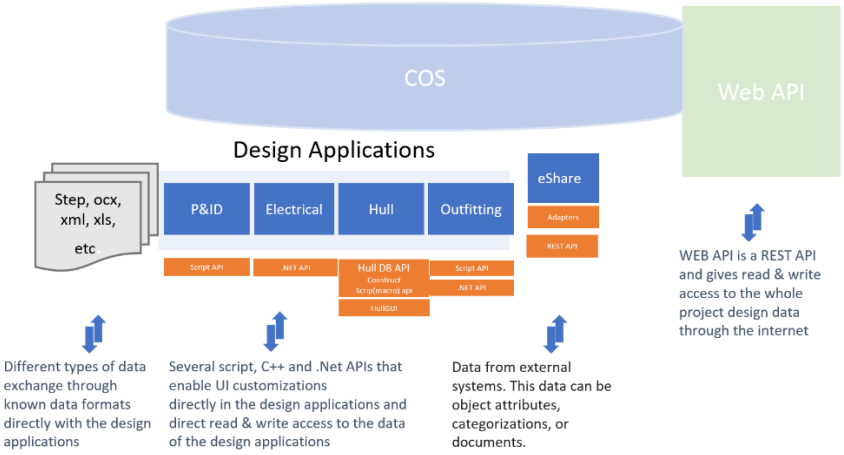

Figure 7: CADMATIC Object Storage structure.

A sketch of the SEUS service warehouse

As a learned lesson, it is worth reflecting on a prior CADMATIC – PIAS interface, see Koelman et al. (2015), which comprised a) direct communication over TCP/IP instead of a shared database, b) data synchronisation on demand, rather than continuously and c) exchange of high-level data entities, based on STEP semantics, which means that in essence the deepest data representations were not shared. For example, both systems had a notion of *deck*, which was shared, while the underlying representation differed quite radically. As such, that software collaboration was impressive to see; with two windows open, showing the same model in the two distinct applications, with one press of a button the changes from one was transferred to the other. Nevertheless, the direct TCP/IP communication had one drawback: the lack of a central permanent storage; if one of the applications was not connected the *synchronisation actions* from the other vaporized. This conclusion, combined with the other analyses and experiments in this paper, led to an envisioned SEUS warehouse with the following functions and services:

1. Storage of data and their relationships are extendable, offering varying Levels of Detail, and multiple facets (i.e. the entities can be part of multiple taxonomies, each of a different kind and with a different purpose).
2. With data semantics based on the maritime STEP application protocols, extended where required.
3. Should this come down to a dictionary, then preferably some integrated documentation system for human use is required.
4. There is easy communication by API or RPC with this storage system, including systems of varying types, such as high-level programming languages and scripting tools.
5. It is extended with a set of system-wide services, among which there is conversion of data representations.
6. Control of access of the data is possible.

To underline that this is not limited to data, this is called a *service warehouse*, in analogy with a physical warehouse, where services are also provided, with or around the goods.

However, the world is littered with abstract plans and grand designs from the past, so how can the feasibility of this SEUS service warehouse be assessed? The first two items combined have been a bottleneck for many years, but the experiment described in this paper suggests that solutions exist. It is now time to sharpen this choice by also involving considerations around SEUS project strategy, involved effort, costs and other aspects of licencing of supporting software. At present how existing software solutions can satisfy the third and fourth requirement is being investigated.

Finally, a word on the *modus operandi* with this service warehouse. It will be obvious that the design and engineering programmes will not be using the service warehouse, so synchronisation between the internal representations and the service warehouse will be required from time to time. The question as to whether this is done automatically (at certain time intervals), or at the instigation of the user, or even restricted to authorised users, is a practical one that it is considered can be answered later. There may be a setting for this if necessary.

CONCLUSIONS

In this paper the background, requirements and desires for the integration of design and engineering shipbuilding program suites have been sketched. After a survey of maritime data standards, it was concluded that none of these are directly applicable for our purposes, mainly because they do not support the inherent multifacetedness of the design and engineering data. The recently emerged category of *graph databases* might perhaps fill this gap, and as a first investigation a practical implementation with a set of bulkheads and compartments has been created and evaluated. The results look quite promising, although non-technical aspects, such as licensing and costs, have not yet been considered. Anyway, these experiments, combined with an analysis of the existing data models of SEUS' design and engineering applications, led to a sketch design of SEUS' central *service warehouse.* The considerations and experiments have shown that viable tools and methods exist to solve significant software integration aspects. Future steps in the SEUS development are intended to be:

- Exploration of attractive alternatives for the functionality offered by graph databases.
- Addressing the integrated support for RPCs.
- The management of the (STEP-based) dictionary, or, alternatively, the integration of dictionary and warehouse software implementation.
- The development of a second demonstration case, with piping, associated components and their connections to equipment and compartments.

CONTRIBUTION STATEMENT

Author 1: Conceptualization; conclusions; sketch of the warehouse; literature review; PIAS background; writing. **Author 2:** Graph databases research and writing; review and editing. **Author 3**: Conceptualization; conclusions; sketch of the warehouse; CADMATIC background; writing. **Author 4**: CADMATIC background.

ACKNOWLEDGEMENTS

The SEUS project has received funding from the Horizon Europe Framework Programme (HORIZON) EU program under grant agreement No 101096224. Info is updated at http://seus-project.eu/. This article reflects only the authors' views, and the European Commission is not responsible for any use that may be made of the information it contains.

REFERENCES

Andrews, D. (2018). The Sophistication of Early Stage Design for Complex Vessels. Trans RINA, Special Edition, IJME, 160, (SE 18).

De Koningh, D., Koelman, H.J. & Hopman, J.J (2011). A Novel Ship Subdivision Method and its Application in Constraint Management of Ship Layout Design. Journal of Ship Production and Design, 27(3), 137-145.

Dusch, T., Franke, B., Grau, M. & Zerbst, C. (2017), Intent-driven CAD vs. Mechanical CAD in Shipbuilding – A review and Solution Outline, ICCAS 2017.

Erikstad, S.O. & Lagemann, B (2022). Design Methodology State-of-the-Art Report. 14th International Marine Design Conference (IMDC), Vancouver, Canada, June 28.

Fonseca, Í.A., Gaspar, H.M., de Mello, P.C. & Sasaki, H.A.U. (2022). A Standards-Based Digital Twin of an Experiment with a Scale Model Ship. Computer-Aided Design, 145, 103191.

Gaspar, H.M., Seppälä, L, Koelman, H.J. & Agis, J.J.G. (2023). Can European Shipyards be Smarter? A Proposal from the SEUS Project. COMPIT'23. Drübeck, Germany, May 23-25.

Gielingh, W. (2008). An assessment of the current state of product data technologies. Computer-Aided Design, 40(7), pp. 750-759.

ISO (2003). ISO 10303. Industrial Automation Systems and Integration: Product Data Representation and Exchange. Part 215: Application Protocol: Ship Moulded Form.

ISO (2004a). ISO 10303. Industrial Automation Systems and Integration: Product Data Representation and Exchange. Part 215: Application Protocol: Ship Arrangement.

ISO (2004b). ISO 10303. Industrial Automation Systems and Integration: Product Data Representation and Exchange. Part 218: Application Protocol: Ship Structures.

ISO (2005). ISO-15926-1. Industrial Automation Systems and Integration - Integration of Life-Cycle Data For Process Plants Including Oil and Gas Production Facilities - Part 1: Overview and Fundamental Principles.

ISO (2018). ISO 19848. Ships and marine technology - Standard data for shipboard machinery and equipment.

ISO (2022). ISO/IEC 81346-1. Industrial Systems, Installations and Equipment and Industrial Products - Structuring Principles and Reference Designations - Part 1: Basic Rules.

ISO (2023). ISO-15926-11. Industrial Automation Systems and Integration - Integration of Life-Cycle Data for Process Plants Including Oil and Gas Production Facilities - Part 11: Simplified Industrial Usage of Reference Data Based on RDFS Methodology.

Kahn, M.T.H. & Rezwana, S. (2021). A review of CAD to CAE integration with a hierarchical data format (HDF)-based solution. Journal of King Saud University - Engineering Sciences, Vol 33 (4). pp 248-258,

Kim, J., Pratt, M.J., Iyer, R.G. & Sriram, R.D. Standardized Data Exchange of CAD Models with Design Intent. . Computer-Aided Design, 40(7), pp. 760-777.

Kirkwood, R. & Sherwood, J.A. (2021). Sustained CAD/CAE Application Integration: Supporting Simplified Models. J. Comput. Inf. Sci. Eng. 21(1).

Koelman, H.J. (2003). Application of the H-rep Ship Hull Modelling Concept. Ship Technology Research. 50 (4), pp. 172-181.

Koelman, H.J. (2024). Piping Layout Integrated in Ship Design and Stability Assessment. 15th International Marine Design Conference (IMDC), Amsterdam, Netherlands, June 3-6.

Koelman, H.J., van de Zee, J. & de Jonge, T. (2015). A Virtual Single Ship-Design System Composed of Multiple Independent Components. COMPIT'15. Ulrichshusen, Germany, May 11-13.

Koelman, H.J. & Veelo, B.N. (2013). A technical note on the geometric representation of a ship hull form, Computer-Aided Design 45(11), pp. 1378-1381,

Kuryło, P., Frankovský, P., Malinowski, M., Maciejewski, T., Varga, J., Kostka, J., Adrian, Ł., Szufa, S. & Rusnáková, S. Data Exchange with Support for the Neutral Processing of Formats in Computer-Aided Design/Computer-Aided Manufacturing Systems. Appl. Sci. 2023, 13, 9811.

Leclerc, J-C., Keraron, Y., Fauconnet, C., Chauvat, N. & Zelm, M. (2022). New ways of using standards for semantic interoperability towards integration of data and models in industry. 11th International Conference on Interoperability for Enterprise Systems and Applications (I-ESA 2022), Valencia, Spain, March 23-25.

Maritiem Masterplan (2023). Aanvraag nationaal groeifonds (in Dutch). maritiemmasterplan.nl/wp-content/uploads/sites/3/2023/10/230203_Maritiem-Masterplan_Verkorte-versie-zonder-appendices.pdf

Owen, J. (1997). STEP, an introduction. Information geometeers, Winchester, UK.

Qin, Y., Lu, W., Qi, Q., Liu, X., Zhong, Y., Scott, P. & Jiang, X.. (2017). Status, Comparison, and Issues of Computer-Aided Design Model Data Exchange Methods Based on Standardized Neutral Files and Web Ontology Language File. Journal of Computing and Information Science in Engineering. 17.

Shiplys (2019). Ship Lifecycle Software Solutions (SHIPLYS). D9.7 SHIPLYS Software and its Functionality in Relation to Existing Standards and Potential for Inputs to Future Standards. www.shiplys.com/library/deliverables/d97-shiplys-software-and-its-functionality-in-relation-to-existing-standards-and-potential-for-inputs-to-future-standards/

Srinivasan, V. (2008). Standardizing the specification, verification, and exchange of product geometry: Research, status and trends, Computer-Aided Design 40(7), pp. 738-749.

Whitfield, R., Duffy, A., York, P., Vassalos, D. & Kaklis, P. (2011). Managing the Exchange of Engineering Product Data to Support Through Life Ship Design. Computer-Aided Design 43(5), pp. 516-532.

Zerbst, C. (2023). OCX on the Way from Research to Industry Practice. COMPIT'23. Drübeck, Germany, May 23-25.

Proceedings of 15th International Marine Design Conference (IMDC-2024)
June 2-6, 2024
Amsterdam, the Netherlands

Methods for Graph Conversion and Pattern Recognition for P&IDs

Min-Chul Kong[1], Myung-Il Roh[2,*], In-Chang Yeo[3], In-Su Han[4], Dongki Min[5], Dongguen Jeong[6]

ABSTRACT

In this study, we developed a method to simplify the analysis of complex Piping and Instrumentation Diagrams (P&IDs) on ships. By converting P&IDs into a graph format, we extracted lines and symbols from the original DXF files, enabling easier identification of connections between ship systems. Utilizing the graph, we can intuitively understand complex P&ID and easily apply it to research such as pipe routing optimization. This approach enhances the understanding of ship systems and has potential applications in recommending similar systems within existing ships, streamlining the design and analysis process.

KEY WORDS

P&ID; Pattern Recognition; Deep Learning; Arrangement Design; Connection relationships Analysis

INTRODUCTION

A piping and instrumentation diagram (P&ID) is a drawing that uses simple symbols to represent the connections of equipment and piping within systems on a ship. Understanding the connections within the P&ID is important for designers to comprehend the systems on the ship. However, this process is difficult because various systems on the ship are complexly connected. In addition, since the P&ID represents the connection relationships as a line, it is inconvenient to find and follow the connection lines between the equipment among many complex lines. Therefore, we proposed a method to analyze the existing P&ID by converting it into a graph. Lines and strings were extracted from the original P&ID in DXF (Drawing eXchange Format), and symbols were recognized using the connections between the extracted lines. We could identify their connections with the extracted lines and the recognized symbols and convert them into a graph. The converted graph can represent the complex connection relationships of P&ID in a simplified form. Using this, we can obtain connection relationships between equipment and utilize it for the pipe auto-routing. With the method proposed in this study, P&IDs can be automatically converted into a graph and utilized for various applications. This graph format is specialized for representing connection relationships; it can help with topological analysis, such as recommending similar systems within existing ships.

THEORETICAL BACKGROUND

The P&ID targeted for recognition in this study has the form shown in Figure 1. There are various objects in a P&ID, such as pumps, valves, and instruments. Objects in the drawing are represented by symbols that briefly represent the characteristics of the equipment. These symbols are composed of basic elements such as lines and are difficult to recognize because they are relatively small compared to the large size of the drawing. Additionally, because the types of objects are very diverse and mixed

[1] Department of Naval Architecture and Ocean Engineering, Seoul National University, Seoul, Republic of Korea; ORCID: 0000-0002-0976-2621

[2] Department of Naval Architecture and Ocean Engineering, and Research Institute of Marine Systems Engineering, Seoul National University; ORCID: 0000-0001-7972-6848

[3] Department of Naval Architecture and Ocean Engineering, Seoul National University, Seoul, Republic of Korea; ORCID: 0000-0003-3940-2093

[4] Department of Naval Architecture and Ocean Engineering, Seoul National University, Seoul, Republic of Korea; ORCID: 0009-0009-0014-6978

[5] HD Korea Shipbuilding & Offshore Engineering Co., Ltd., Seongnam, Republic of Korea

[6] HD Korea Shipbuilding & Offshore Engineering Co., Ltd., Seongnam, Republic of Korea

* Corresponding Author: miroh@snu.ac.kr

Submitted: 23 February 2024, Revised: 5 April 2024, Accepted: 1 May 2024, Published: 21 May 2024

Conference paper, DOI: https://doi.org/10.59490/imdc.2024.876 e-ISSN: 3050-4864

with strings containing information about the objects, it is not easy even for experts to check them. Therefore, research on recognizing or extracting specific objects from P&ID is being conducted in many fields. Table 1 shows a summary of related studies for recognizing various elements in drawings such as P&ID and the method proposed in this study.

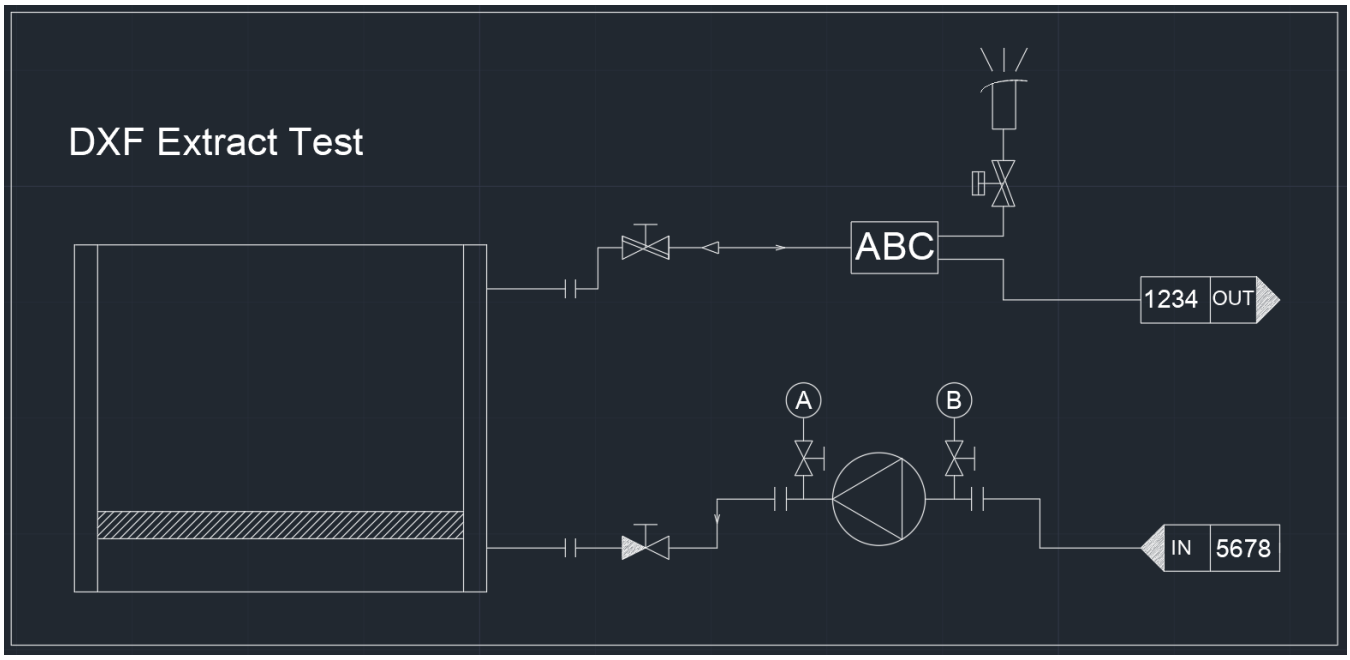

Figure 1: Example of P&ID (expressed briefly for security reasons)

Table 1: Summary of the related studies and comparison with this study

Studies	Application field	Recognition algorithms/model	Recognition target
Luo & Liu (2003)	Schematic	X	Schematic symbol
Yu et al. (2019)	P&ID	CNN (modified AlexNet)	P&ID symbol
Rahul et al. (2019)	P&ID	CPTN & FCN	P&ID symbol, text
WAN et al. (2019)	Mathematical formula	CNN	Math symbol
Kim et al. (2022)	P&ID	GFL, Tesseract	P&ID symbol, text
Moon et al. (2023)	P&ID	Modified hough transform	Line
This study	P&ID	Cascade R-CNN, DXF extraction tool	P&ID symbol, text, line, connection relation

As we can see from the table, there are two main ways to recognize objects in P&ID. The first method is to extract elements from a drawing and specify objects from their relationships. This method has the advantage of being able to accurately find an object under the condition that the drawing contains various information and can be extracted. Luo & Liu (2003) used a case-based recognition method to specify symbols from relationships such as points and lines. Additionally, Moon et al. (2023) used an image-based line recognition algorithm to find connecting lines in P&ID. Conversely, if the drawing is not created accurately and the creator makes a mistake when drawing some objects, there is a disadvantage in that the corresponding part cannot be found. In addition, the work process is complicated because users have to specify what the object looks like and find the corresponding characteristics.

The second method is a deep learning-based recognition method that has been popular recently. Convert the drawing into an image, and users directly label the objects they want to learn within the image. Afterward, a deep learning model for object recognition is built and trained to find objects in the image. Yu et al. (2019) and WAN et al. (2019) used a convolutional neural network (CNN) to recognize symbols in images. CNN is the most basic model among deep learning models for image recognition and is used to extract and classify image features using 2D images as input. Rahul et al. (2019) were able to extract more detailed features of equipment within P&ID by combining two deep learning-based object recognition models and text recognition models. In this method, because the deep learning model itself learns the characteristics of the object, there is a possibility of finding it well, even if there are slight errors or variations in the drawing. However, the disadvantage is that learning a deep learning model requires a large amount of data, and the user must label it. Therefore, it is crucial to understand the advantages and disadvantages of the two methods for recognizing objects within drawings in order to utilize them

appropriately. For example, Kim et al. (2022) were able to achieve more accurate recognition results by leveraging the strengths of both the Tesseract (Smith, 2007) model, which recognizes characters from extracted images in drawings, and a deep learning-based image recognition model. Therefore, in this study, these two methods were appropriately combined to select the optimal recognition method suited to the characteristics of objects in the drawing.

Another important piece of information that P&ID contains is the connection relationships. Objects in the drawing represent equipment, and the pipes connecting them are expressed as lines. Therefore, the user can check this and know how the equipment is connected by referring to the drawing. Humans can easily understand connections by following lines, but in order to automate this process, lines must be recognized accurately. There are many elements in a drawing that make it difficult to construct a recognition algorithm, such as lines representing objects and lines representing pipes being mixed and intersecting, with one line being cut off in the middle. In this study, information was extracted from a common drawing format called drawing interchange format (DXF), and connection lines were recognized through a preprocessing process.

If the equipment and connection relationships in the drawing are extracted through the above process, this information can be used to analyze the characteristics of the P&ID. In this study, the recognition results were converted into data using the concept of a graph. As shown in Figure 2, the graph is composed of nodes and edges, with nodes expressed as points and edges expressed as lines. We converted P&ID into a graph by representing equipment as nodes and connection relationships as edges. The converted graph is easy to analyze topology and connectivity because it excludes unnecessary elements and only has connections. Therefore, we proposed a method to convert P&ID into a graph automatically. As a result, this graph can be used for research, such as creating piping routes or analyzing similar systems.

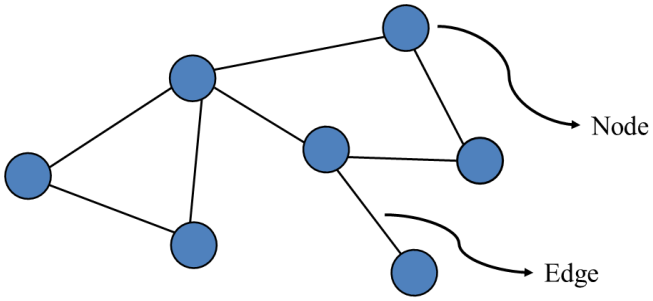

Figure 2: Components of a graph

APPLICATIONS

We used a deep learning model to recognize objects in P&ID. Deep learning allows us to find objects in drawings quickly; it is suitable for large-sized P&IDs. However, deep learning models require a large amount of training data. Because P&ID is large and contains various types of objects, the labeling process takes much time and labor. Therefore, we designed a model that can automatically generate training data. First, select an image that will become the background. At this time, several noises were added to the base image to increase the diversity of training data. Next, various objects are placed in random positions on the base. We called the placed objects as material. Material also went through the process of adding noise, such as rotation and scaling, to ensure diversity in the training data. The drawing created by this method is shown in Figure 3. Since we know where the materials are placed, we can automatically generate labeled data. Using this, we were able to generate a large amount of training data and train a deep-learning model for object recognition.

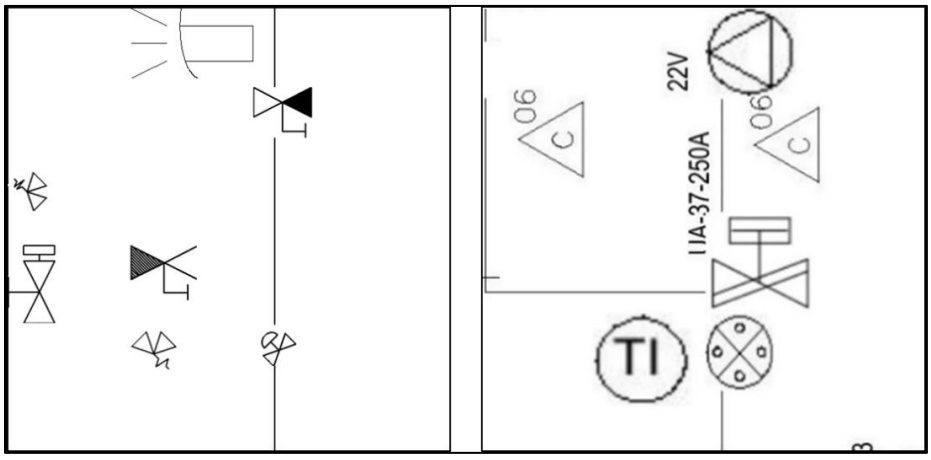

Figure 3: Example of the generated training data

Two-stage models generally showed better accuracy than one-stage models when recognizing objects in drawings (Kong et al., 2022). In this study, we used a two-stage CNN model called Cascade R-CNN (Cai & Vasconcelos, 2018) as a deep learning model to recognize objects. This model is known to have a high recognition rate for multiple overlapping objects. As shown in Table 2, we trained several two-stage models to find 26 types of objects and measured recognition accuracy on 11 actual drawings. Each model was trained using the same 120,000 pieces of virtually generated data. We trained the models using RTX 4070 Ti in a Windows 10 environment, and each parameter used the default values of each model. As a result, Cascade R-CNN showed the best performance among them. It took an average of 90 seconds to recognize each drawing, and most objects were recognized with F1-score=0.9863. Figure 4 shows some of the results of object recognition with the Cascade R-CNN model. We confirmed that the types, sizes, and locations of objects in the P&ID were accurately recognized.

Table 2: Accuracy analysis between the detection models

	Cascade R-CNN	Faster R-CNN	Sparse R-CNN
Elapsed time (s)	90	89	94
Precision (%)	99.29	97.19	96.06
Recall (%)	97.99	98.63	45.83
F1-score (%)	98.63	97.88	58.11

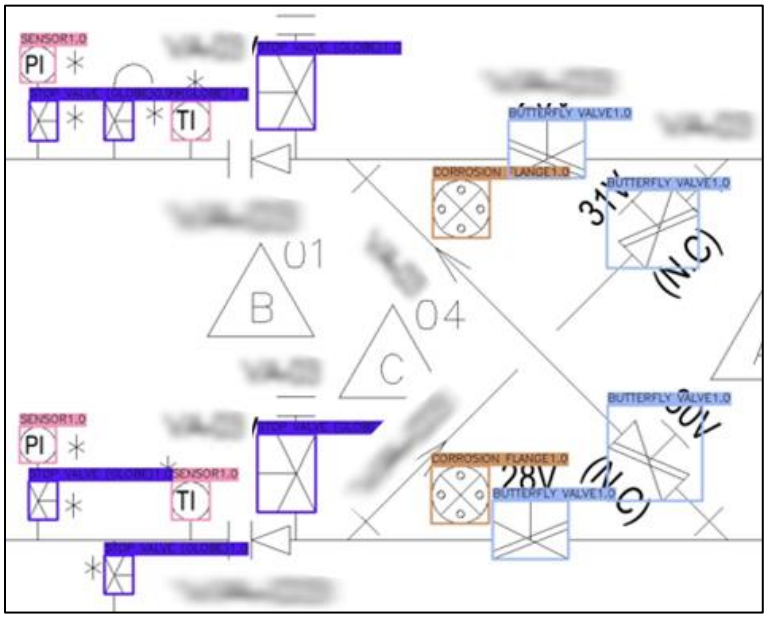

Figure 4: Example of P&ID recognition results with Cascade R-CNN model (text blurred for security reasons)

Deep learning models have the advantage of recognizing objects with distinct features, but they are known to have relative difficulty in recognizing simple elements such as lines. Therefore, we devised a method to extract lines directly from the drawing and preprocess them to find connecting lines between objects.

The DXF format converts drawings created with a computer-aided design (CAD) program into a highly compatible format. Elements that can be extracted from the DXF format include lines and strings. Figure 5 shows the types of elements that can be extracted from the DXF format. We analyzed the extractable elements and extracted only the lines representing the connecting lines. Lines extracted from the DXF format have both their start and end points. By using these, line elements in the object recognition results can be removed.

Furthermore, by sequentially linking the end points from the line connected to the object, a connecting line can be identified (Figure 6). Combining this result with the object recognition result is shown in Figure 7 (a). Since each extracted line has a starting point and an ending point, connecting lines between objects can be found by continuously extracting adjacent lines based on these points. As a result, it is possible to find all connections within the drawing, shown in Figure 7 (b). This result can again be expressed in graph form, as shown in Figure 7 (c).

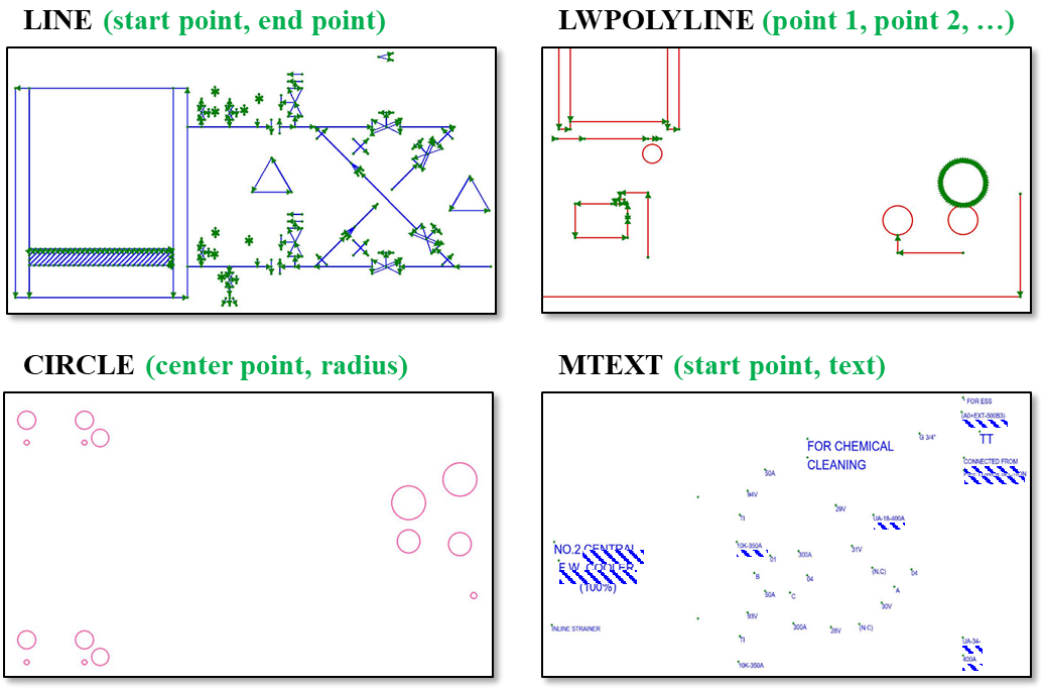

Figure 5: Examples of elements that can be extracted from files in the DXF format (text blurred for security reasons)

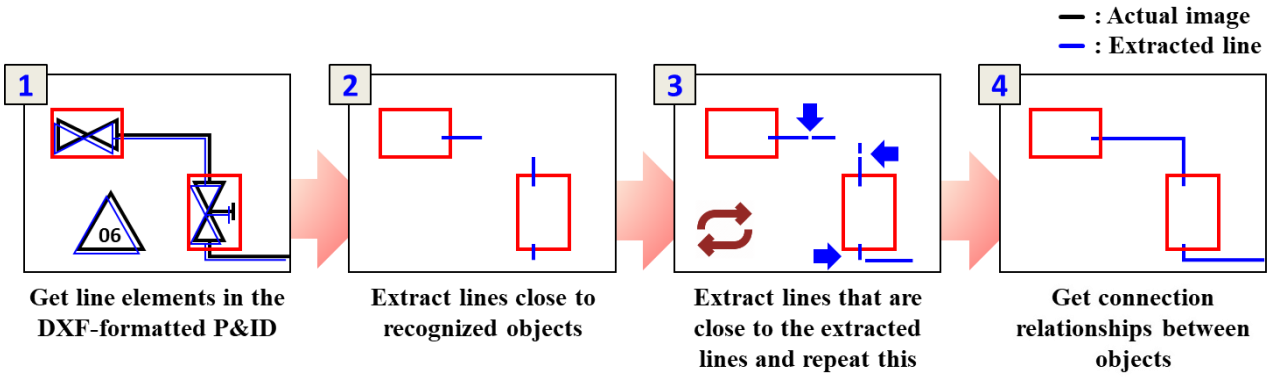

Figure 6: Process of obtaining connection relationships between objects using extracted line elements

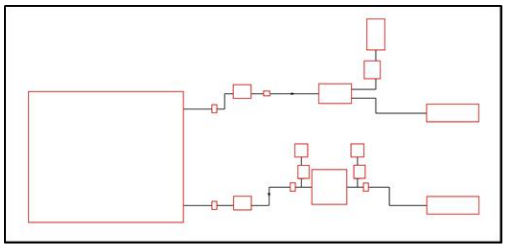

(a) Pre-processed elements

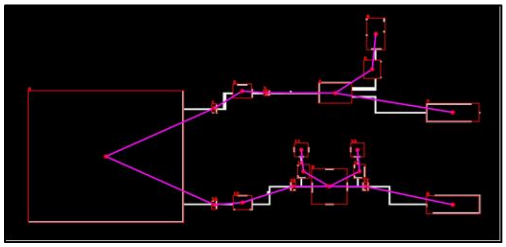

(b) Defined connectivity

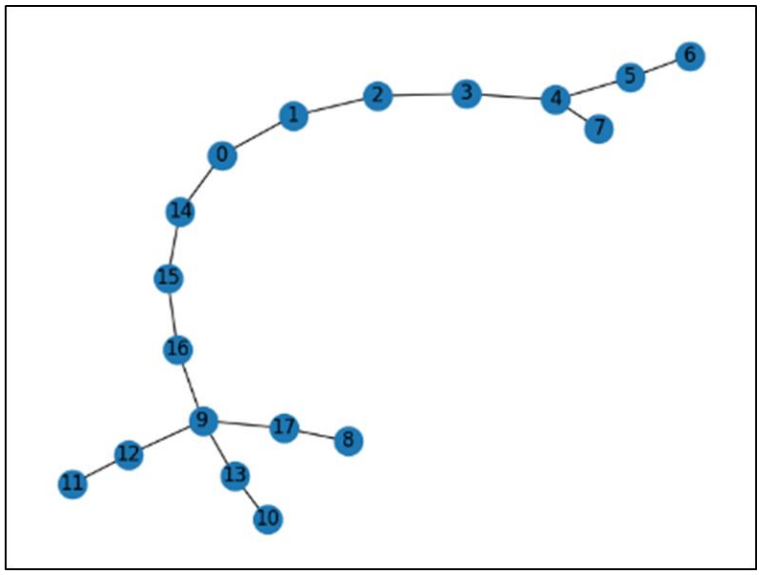

(c) Converted to a graph

Figure 7: Conversion process of the P&ID to a graph (expressed briefly for security reasons)

As mentioned above, P&ID represents the connection relationships between equipment in the form of a line. When the P&ID is converted into a graph form, we can use the connection relationships of the graph to check how the pipe is connected between each equipment. Each piece of equipment has a specific location for the part connected to the pipe, that is, the nozzle. Therefore, if we only determine the location of each equipment, we can automatically create pipes utilizing the graph. Even if they look like different P&IDs, if the recognized graph (so-called pattern) is the same, they can be considered the same system.
Ha et al. (2023) established measures for evaluating layouts of pipe by quantifying the expertise of professionals and, based on this, devised an algorithm to generate the optimal pipe routes. Utilizing this study, we designed a method that automatically creates pipes from the connection relationships of each piece of equipment. Figure 8 shows the results of creating pipe routes by adding the locations of equipment based on the graph extracted from P&ID. In the eyes of humans, the two results may appear as different systems, but from a graph perspective, they represent the same system. Therefore, an analysis from a graph perspective is necessary to recognize the patterns inherent in P&IDs.

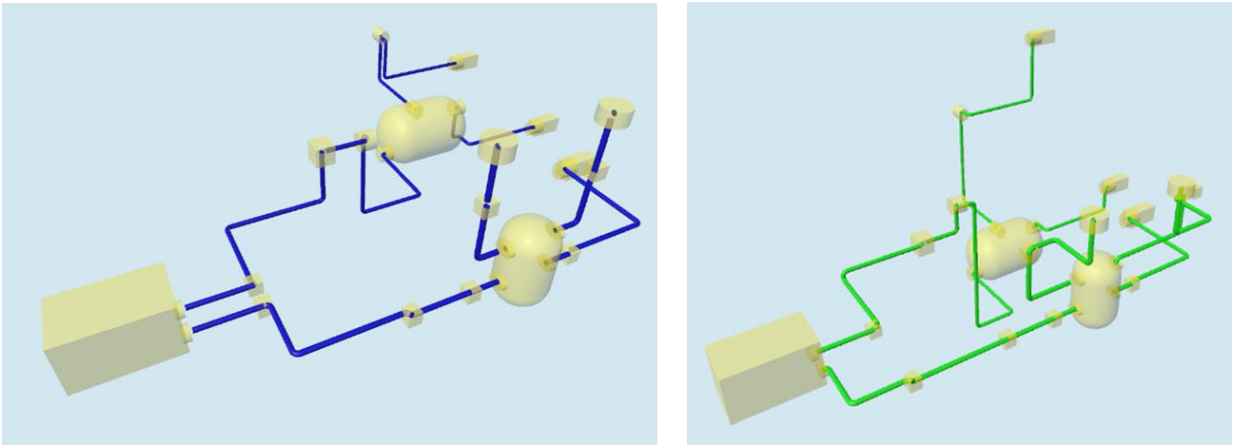

Figure 8: Results of creating different pipe routes from the same P&ID

Moreover, through the proposed process, we can convert many P&IDs into a graph form and train a deep learning model on the graph structure itself. In the future, we can train a deep learning model with a graph neural net (GNN; Scarselli et al., 2009) structure and create a model that classifies which system the input graph is similar to the database. As a result, we plan to build an automated process that takes P&ID as input, finds objects, interprets connection relationships, converts them into a graph, and recommends the one most similar to the existing system.

CONCLUSIONS

This study proposed an automated process for object recognition and connection relationships analysis targeting P&ID. P&ID consists of various objects such as pumps, valves, and instruments. So, precisely recognizing them is a difficult task. We trained the two-stage based CNN model with virtual images generated with our algorithm and were able to recognize objects in the drawing with high accuracy. Additionally, we extracted elements like lines or circles in the DXF format and obtained connection relationships between the recognized objects. We represented the results in a graph format. As a result, the proposed process could build an automated system. It receives P&ID as input, finds objects, and interprets the connection relationships. Then, it converts them into a graph and can be utilized in various studies. We applied the converted graph to the study for pipe auto-routing. Consequently, we confirmed that we could automatically place pipes by extracting the connection relationships between equipment from the P&ID. Due to the use of deep learning models and innovative application of training data generation methods, most objects were able to be recognized, and the characteristics of the system were successfully inferred through graph analysis.

We plan to convert more P&IDs into graphs and analyze additional features that can be learned from them. To confirm the practicality of the method proposed in this study, we must verify it on more diverse data. Additionally, the features of the converted graph must be labeled to train deep learning models in the future. We plan to research ways to create virtual data in DXF format, just as we created virtual data for object recognition. There are also many ways to utilize the graph, such as embedding the characteristics of each node and edge in addition to the characteristics of the structure itself used in this study. Therefore, we plan to investigate various possibilities that can be applied using the above process.

ACKNOWLEDGEMENTS

This study is an extension of our previous study (Kong et al., 2023) and was partially supported by (a) HD Korea Shipbuilding & Offshore Engineering Co., Ltd., Republic of Korea, (b) BK21 Plus, Education & Research Center for Offshore Plant Engineers (COPE) of Seoul National University, Republic of Korea, and (c) Research Institute of Marine Systems Engineering of Seoul National University, Republic of Korea.

REFERENCES

Cai, Z., & Vasconcelos, N. (2018). Cascade R-CNN: Delving into High Quality Object Detection. *Proceedings of the IEEE Computer Society Conference on Computer Vision and Pattern Recognition*. https://doi.org/10.1109/CVPR.2018.00644

Ha, J., Roh, M. Il, Kim, K. S., & Kim, J. H. (2023). Method for pipe routing using the expert system and the heuristic pathfinding algorithm in shipbuilding. *International Journal of Naval Architecture and Ocean Engineering*, *15*. https://doi.org/10.1016/j.ijnaoe.2023.100533

Kim, B. C., Kim, H., Moon, Y., Lee, G., & Mun, D. (2022). End-to-end digitization of image format piping and instrumentation diagrams at an industrially applicable level. *Journal of Computational Design and Engineering*, *9*(4), 1298–1326. https://doi.org/10.1093/jcde/qwac056

Kong, M. C., Roh, M. Il, Ha, J., Kim, M., & Kim, J. (2023). A Method for the Pattern Recognition and Analysis in P&IDs Based On GNN. *Proceedings of the Society of Naval Architects of Korea, SNAK*, 108.

Kong, M. C., Roh, M. Il, Kim, K. S., Lee, J., Kim, J., & Lee, G. (2022). Object detection method for ship safety plans using deep learning. *Ocean Engineering*, *246*. https://doi.org/10.1016/j.oceaneng.2022.110587

Luo, Y., & Liu, W. (2003). Engineering drawings recognition using a case-based approach. *Proceedings of the International Conference on Document Analysis and Recognition, ICDAR*. https://doi.org/10.1109/ICDAR.2003.1227657

Moon, Y., Han, S. T., Lee, J., & Mun, D. (2023). Extraction of line objects from piping and instrumentation diagrams using an improved continuous line detection algorithm. *Journal of Mechanical Science and Technology*, *37*(4). https://doi.org/10.1007/s12206-023-0333-9

Rahul, R., Paliwal, S., Sharma, M., & Vig, L. (2019). Automatic information extraction from piping and instrumentation diagrams. *ICPRAM 2019 - Proceedings of the 8th International Conference on Pattern Recognition Applications and Methods*. https://doi.org/10.5220/0007376401630172

Scarselli, F., Gori, M., Tsoi, A. C., Hagenbuchner, M., & Monfardini, G. (2009). The graph neural network model. *IEEE Transactions on Neural Networks*, *20*(1). https://doi.org/10.1109/TNN.2008.2005605

Smith, R. (2007). An overview of the tesseract OCR engine. *Proceedings of the International Conference on Document Analysis and Recognition, ICDAR*, *2*. https://doi.org/10.1109/ICDAR.2007.4376991

WAN, Z., FAN, K., WANG, Q., & ZHANG, S. (2019). Recognition of Printed Mathematical Formula Symbols Based on Convolutional Neural Network. *DEStech Transactions on Computer Science and Engineering*, *ica*, 80–85. https://doi.org/10.12783/dtcse/ica2019/30711

Yu, E. S., Cha, J. M., Lee, T., Kim, J., & Mun, D. (2019). Features recognition from piping and instrumentation diagrams in image format using a deep learning network. *Energies*. https://doi.org/10.3390/en12234425

Proceedings of 15th International Marine Design Conference (IMDC-2024)
June 2-6, 2024
Amsterdam, the Netherlands

System level simulation of the winter navigation in the Baltic Sea

Kujala Pentti[1,2], Kulkarni Ketki[1,3], Kondratenko Aleksandr[1], Lu Liangliang[1], Winberg Casper[1], Li Fang[4] , and Musharraf Mashrura[1]

ABSTRACT

Efficient winter navigation has crucial importance for Finland as all Finnish harbors are icebound every winter. A winter navigation system level simulation tool has been developed to analyse the marine traffic in wintertime and to analyse the present and future need of icebreakers when both marine traffic patterns, ice-going ship characteristics and ice conditions will change. This paper summarises the basic principle of the tool and presents some recent applications together with the conducted verification and validation. The tool has been applied both in the northern part of the Baltic Sea and in the south to study the winter navigation system: on the Bay of Bothnia for Finnish marine traffic and the Gulf of Finland for Estonian marine traffic.

KEY WORDS

Maritime; Winter navigation; Simulation; System level; Icebreaking

INTRODUCTION

The Baltic Sea holds significant socio-economic importance for the surrounding nations such as Finland, Estonia, and Sweden. It serves as a vital transportation route for goods, services, and passengers, while also supporting essential ecological systems. Ensuring the reliability and efficiency of maritime operations in this region is crucial. Particularly challenging is the winter season, when substantial portions of the northern Baltic Sea are covered with ice, a phenomenon that varies greatly from year to year in terms of extent. In response to these challenges and to facilitate safe and efficient navigation throughout the year, the Finnish-Swedish Winter Navigation System (FSWNS) has been implemented (Kulkarni et al., 2022, Trafi 2022).

Finland has more than 150 years' experience of winter navigation. The FSWNS system has been developed to guarantee safe and reliable shipping throughout the winter even though many of the Finnish harbours are ice-covered each winter. The system consists of three elements: ice-strengthened ships, icebreaker assistance, and traffic restrictions. The traffic restrictions ensure that only ships with some minimum size and ice class will get icebreaker assistance on the winter period and the harder the ice conditions the stricter will be the traffic restrictions. This is to guarantee that the icebreaker fleet is capable of offering the service required to keep the winter navigation operations safe and aiming for minimum waiting time for the merchant vessels. In order to ensure ships possess the necessary ice-going capabilities for safe and efficient operations, adherence to the Finnish–Swedish Ice Class Rules (FSICR) is imperative. (Trafi, 2022).

We have developed during the last 10 years a simulation tool to study the system level performance of the winter navigations in Finland (Lindeberg et al., 2015, 2018, Kulkarni et al., 2022a, Kulkarni et al., 2022b). The main aim of the tool development

[1] Mechanical Engineering Department, School of Engineering, Aalto University, Espoo, Finland
[2] Estonian Maritime Academy, Tallinn University of Technology, Tallinn, Estonia
[3] HUMLOG Institute, Supply Chain Management and Social Responsibility, Hanken School of Economics, Helsinki, Finland
[4] School of Naval Architecture, Ocean and Civil Engineering, Shanghai Jiao Tong University, Shanghai, China
* Corresponding Author: pentti.kujala@aalto.fi

Submitted: 28 January 2024, Revised: 15 April 2024, Accepted: 1 May 2024, Published: 26 May 2024

Conference paper, DOI: https://doi.org/10.59490/imdc.2024.902 e-ISSN: 3050-4864

has been to obtain a research-based prototype and decision-making aide that can be used to simulate the need of icebreakers as well as socio-economical and environmental impacts related to FSWNS in the future when both ice conditions, maritime traffic and characteristics of ice-strengthened ships will be under dynamic change. Climate change will affect the ice conditions so that the maximum ice thickness might decrease but the annual variations will be high and the ice movements can increase causing other type of challenges for the winter navigation system. Ship's size seems to increase and at the same time the new strict environment regulations will decrease the used engine power on ships. In efforts to curb Greenhouse Gas emissions from ships, the International Maritime Organization implemented the Energy Efficiency Design Index (EEDI) regulations in 2011 (EEDI, 2022). These regulations are geared towards promoting the adoption of highly energy-efficient solutions in maritime operations. While the focus is on reducing GHG emissions, the technical specifications of these regulations restrict the maximum propulsion power installed on ships and encourage the use of hull forms optimized for open water conditions. This will decrease dramatically the ice-going capabilities of these ships. All these aspects are included in the simulation tool.

The aim of this paper is to shortly describe the current status of the simulation tool. The main structure and elements of the tool will be described. In addition, some recent case studies with the tool will be summarized to demonstrate the extent of its application: a) Validation of the tool, b) Optimization of icebreaker assistance for sustainable shipping and c) Analysis of the icebreaker needs in Estonia.

DESCRIPTION OF THE TOOL

General description of the tool

The objective of the tool remains as described above: to simulate the FSWNS performance across a range of potential operating scenarios, aiding decision-making regarding its operation and development, including considerations like icebreaking resources and ice class regulations. To achieve this, the tool is designed to replicate winter traffic patterns under various operating conditions, incorporating elements such as icebreaker scheduling and directed pathway adjustments. Icebreaker scheduling involves determining the number of icebreakers available each day, their initial positions, and their designated operational areas. Additionally, mathematical modeling is employed at the ship level to capture individual vessel interactions with ice conditions and their impact on overall traffic flow. Vessel speeds under different ice conditions, such as convoys and towing, are calculated using closed-form expressions. The proposed tool enables users to assess how the FSWNS would perform under different hypothetical scenarios, enhancing understanding of the system's behavior. This project aims to combine the strengths of simulation modeling with the expertise of maritime professionals. Figure 1 illustrates a schematic block diagram of the simulation tool. (Kulkarni et al., 2022a)

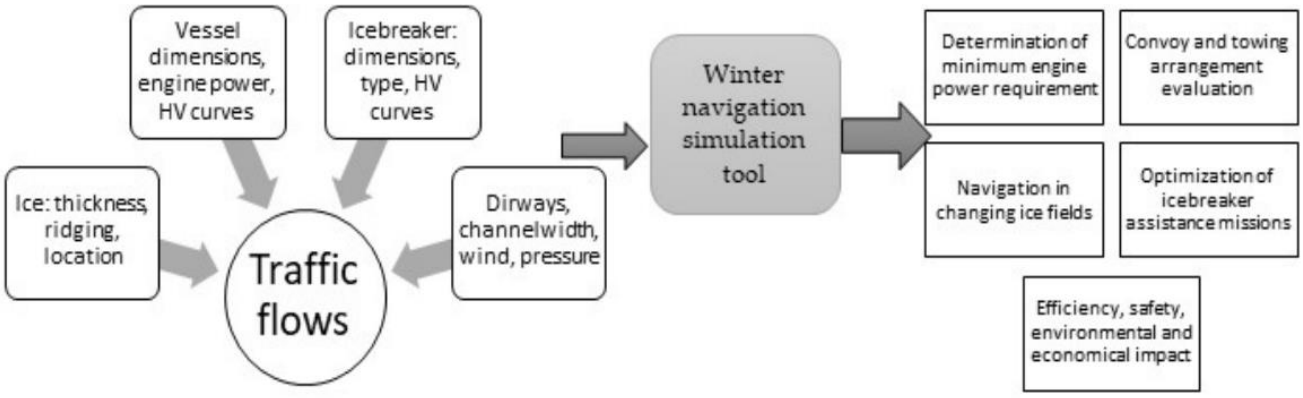

Figure 1: Simulation tool structure (Kulkarni et al., 2022a)

The simulation tool incorporates a hybrid approach, utilizing discrete-event and agent-based simulation techniques along with process flow modeling. This selection of modeling methodologies enables the visualization of simulation processes and outcomes, as well as the integration of stochastic elements. Individual components within the FSWNS, e.g., merchant ships, icebreakers, and ports, are represented using an agent-based framework, which includes detailed decision-making processes. Each component, whether a merchant ships or icebreaker, faces numerous decisions throughout the winter season, responding to changing situations. The decision process for each component is governed by a series of rules presented in an if-then-else format, dictating adjustments to direction, speed, and operational mode according to system parameters. Moreover, an optimization logic is employed for icebreakers to determine the most effective ways for assisting vessels. (Kulkarni et al, 2022a).

The tool is designed to be utilized by domain experts, serving as a complement to their expertise rather than functioning as a standalone solution. Experts provide crucial details regarding resource availability (such as the available icebreakers and operational ports on a specific day) and other scenario specifics not available from existing data sources. The model inputs encompass vessel particulars, including dimensions of ships and coefficients of hv curve (abbreviation for the ice thickness vs ship's speed), traffic patterns, and ice conditions. The inputs are processed to derive formula for vessel and icebreaker speed variations, trip parameters (origin, destination, departure time), daily ice conditions, and dirway locations (dirway defines the ship path through ice). Traffic data are obtained through the processing of AIS (Automatic Identification System) data, which serves as essential input to the simulation model. At its core, the simulation engine incorporates agent-based models to replicate entity behaviors, discrete-event models to emulate both scheduled and random occurrences, and process flow models to depict the movements of vessels and icebreakers at sea and within ports. It also includes visualization functionalities, such as a color-coded scheme that illustrates different ice thicknesses, with darker hues of blue representing thicker ice layers. The primary simulation output is a visualization of traffic flows illustrating vessel movements across evolving dirways towards destinations see Figure 2. Vessel speeds adjust according to ice conditions along their routes, while icebreakers are observed assisting vessels unable to maintain speeds above a specified threshold. Following the simulation's completion, a Key Performance Index (KPI) referred to as the average waiting time is generated. These results are then presented to the domain expert, who serves as the decision-maker, for potential adjustments to future configurations. Subsequently, the expert offers feedback to enhance the simulation tool iteratively. (Kulkarni et al., 2022a).

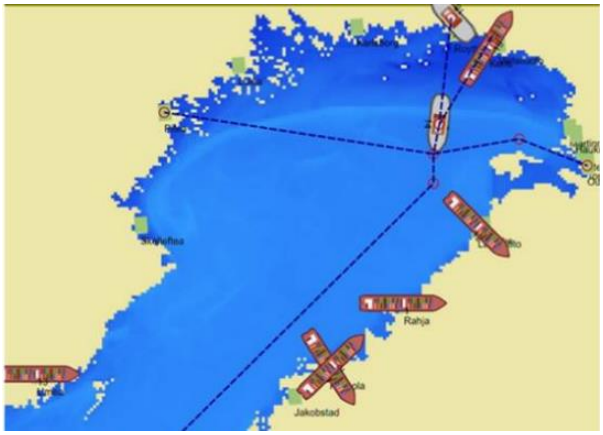

Figure 2: Visualization of ice fields, dirways and ships on the Bay of Bothnia (Kulkarni et al., 2022a)

Definition of ice conditions

To accurately depict the complexities of winter navigation, it is crucial to include ice conditions with precision. Ice data encompasses various aspects like thickness, concentration, and topography, typically sourced from Finnish Meteorological Institute (FMI) ice charts. However, this data originates from diverse sources, necessitating the integration of multiple file formats to compile a comprehensive view of ice conditions. Furthermore, ice data is dynamic, with updates available hourly for each geographical grid. To facilitate integration into the model, this information undergoes suitable aggregation to balance detail with computational efficiency.

In the simulation, vessels must be responsive to these dynamic ice conditions, adjusting speeds or halting. This necessitates that vessels can continually understand ice information and adapt behavior throughout a journey. To achieve this, concepts like equivalent ice thickness and HV curves are employed. Equivalent ice thickness utilizes a mathematical formula to derive a single value representing ice thickness, incorporating factors such as concentration, thickness, and topography. This approach enables vessels in the simulation to effectively gauge and respond to changing ice conditions as they navigate. The formula given by Lindeberg et al. (2018) is used in the model for obtaining the equivalent ice thickness (Kulkarni et al., 2022a).

Given that ice conditions can vary daily, they can significantly impact routing decisions. Actual ice data is employed to compute the equivalent ice thickness, which is derived from averaging the ice volume within a grid. These ice data sets are updated on a daily basis, but the frequency of updates can be adjusted as needed. The equivalent ice thickness definition may vary depending on the available ice data. In this study, equivalent ice thickness is calculated as the product of concentration and thickness to maintain volume equivalence based on NetCDF data (Milakovic et al., 2020). The equations are similar to those used in Lindberg et al. (2018). For more information, readers are pointed to Sormunen et al. (2018).

Evaluation of ship performance in ice

The vessels simulated in the model must be responsive to fluctuations in ice conditions, adjusting their speeds accordingly or even halting when necessary. Each vessel is assigned an hv curve profile tailored to its dimensions, with Aker Arctic having developed numerous such curves for typical ice-capable ships as part of project Winmos I/Winmos II (2021). These hv curves are incorporated into the model as entity attributes, governing speed adjustments based on equivalent ice thickness. Each vessel is assigned an hv curve code. This code allows the vessel to reference the pertinent hv curve information during simulation runs. The expressions in level ice (v_1) and in the convoy (travel at a distance following an icebreaker) condition (v_d) to obtain ship speeds are provided in equations (1) and (2):

$$v_l = a_l h^3 + b_l h^2 + c_l h + v_{ow} \quad [1]$$
$$v_d = a_d h^3 + b_d h^2 + c_d h + v_{ow} \quad [2]$$

In the given equations, the symbol h represents the equivalent ice thickness, while the coefficients a, b, and c denote the parameters defining the relevant ship speed in the ice condition, and w signifies the speed in open water. Table 1 illustrates a standard array of coefficients for an hv curve.

Table 1: Example of hv curve coefficients

Hv_Ship	v_{ow} [kn]	a_l	b_l	c_l	a_d	b_d	c_d
Example	15	-199.84	210.24	-87.997	-0.1658	1.5976	-7.4582

The polynomial expressions of two representative hv curves are depicted in Figure 3. It is notable from both plots that the open water speed is maintained at 15 kn. In Figure 3A, it is evident that the speed decreases swiftly with escalating ice thickness, approaching nearly 0 kn at approximately 0.4 m. Conversely, Figure 3B illustrates that speeds can be sustained up to 9 kn for ice thicknesses ranging from 0.4 m to 1 m when in convoy.

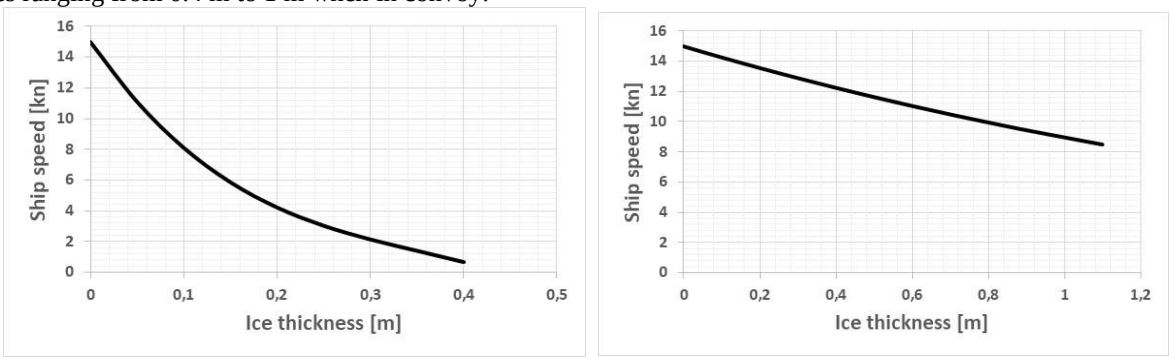

A B

Figure 3: Example of h-v curves. (A) Vessel in level ice; (B) Vessel in convoy. (Kulkarni et al., 2022a)

The equivalent level ice thickness approach is used to make the simulation tool development systematic and easy to adapt. However, determination of equivalent level ice thickness is not straight forward process as various ice conditions require totally different approaches, as reviewed by Milakovi'c et al., (2020). For ridged ice, one approach used is to estimate the relative increase of level ice thickness based on the density of the ridges. The values used in the model are as follows: rafted ice + 7.5%, slightly ridged ice + 22.5%, ridged ice + 60%, and heavily ridged ice + 105% increase (Lindeberg et al., 2018). For floe ice with varying concentration no good methods exist so far to determine the equivalent level ice thickness.

In Aalto University, the latest development has been related to the topic: how to evaluate the ship resistance and hv curves on two different important cases: 1) The effect of vessel breadth on the resistance during escort and 2) The effect of closing channel and compressive ice on the resistance. Li et al. (2021) conducted thorough investigations on the characteristics of the hv curves in what is termed a 'narrow ice channel.' In scenarios involving escort and convoy operations, an icebreaker creates a passageway while accompanying ships trail along this designated path. However, if the width of the assisted ship exceeds that of the channel formed by the icebreaker, the created pathway becomes insufficient for the assisted ship. Consequently, the assisted ship must independently break through some ice. This situation is denoted as navigation in a 'narrow ice channel.' To address this, a model-scale test was initially carried out, simulating a ship navigating through ice channels with varying widths

and ice thicknesses. Subsequently, numerical simulations of the model test scenarios were executed using an in-house simulation program specifically designed for ship operations in icy conditions. The simulation accurately captured the primary aspects of changes in ship resistance relative to channel width, validating its efficacy as a simulation tool. Further numerical simulations were then conducted with various other ships to gain comprehensive insights into ship performance in narrow ice channels. Emphasis was placed on evaluating the impact of channel width on ships' encountered resistance and achievable speed in icy conditions. Figure 4 illustrates an example of the obtained curves, with the parameter γ representing the relative breadth of the channel compared to the ship breadth. For instance, γ=0.25 indicates that the channel width is 25% of the vessel breadth. When γ=0, the scenario corresponds to breaking level ice, and with γ=1.0, the ship navigates in a channel with a width equal to the ship's breadth. An illustrative example is the Agulhas II, a ship with ice class PC 5, constructed in RMC for South Africa to operate in Antarctica's icy conditions.

The other case stated above, i.e. the closing channel due to the moving ice, has been studied by Lu et al., (2023). The moving ice will close the channel in front of the ship causing increased resistance mainly due to increase of frictional forces at the straight midship part of the vessel. This will cause dramatic decrease of ship speed in ice, as shown in Figure 5. The curves represent various compressive ice conditions (different ice drift speeds). There are mainly three clusters. The first cluster follows the original level ice h-v trend. The second cluster is the ones drops quickest. The third is the ones between the two clusters. They show the transitions from no compression to compressive ice conditions, which can also be defined as ‘critical ice speed’. After the ‘critical ice speed’ curve, the ship will totally follow the compressive ice clusters. In the critical ice speed, h-v curve also demonstrate ‘up and down’ feature which is affected by relative relationship between the broken ice cusps and ship speed. The ice movement is caused by the high wind and therefore the wind speed and direction on the navigation area should also be known before this can be included in our simulation tool and that development is still on-going.

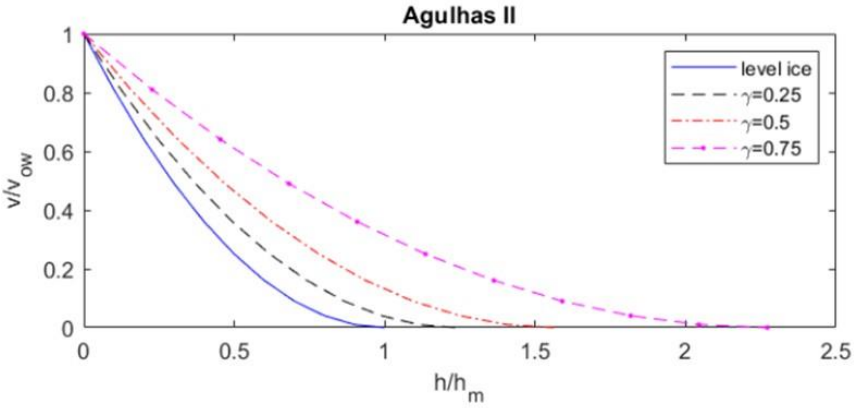

Figure 4: Example of h-v curves for narrow channel. Ice thickness is made non-dimensional by dividing it with the maximum level icebreaking capability of the ship and ship speed is relative to the open water speed. (Li et al. (2021)

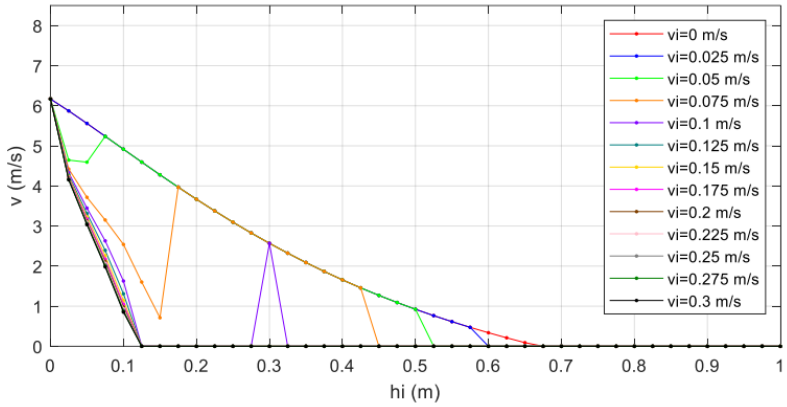

Figure 5: Example of h-v curves for closing channel for MS Envik. Ship initial speed is 5 kn and v_i is the speed on the ice movement transversal to the ship movement. (Lu et al. (2023)

Icebreaker decision making

The pathways navigated by vessels, termed dirways, constitute an integral part of the model. Dirways are established by icebreakers in ice-laden regions and are susceptible to alterations due to factors like wind, pressure, and evolving ice conditions. Another critical consideration involves the transition between dirways. As vessels traverse ongoing journeys on existing dirways, new journeys are concurrently scheduled on updated dirways. Icebreakers must effectively coordinate between the two sets of dirways until all traffic seamlessly transitions to the new routes. This dynamic process also impacts convoy formation and can influence system waiting times.

Vessel speeds fluctuate in alignment with their respective hv curves. If a vessel's speed falls below a predefined threshold, icebreaker assistance is solicited. Depending on the vessel's location, an appropriate icebreaker from the available fleet is selected. Convoys may form when multiple vessels require assistance in the same direction. The simulation concludes once all vessels have completed their scheduled journeys within the specified time frame. The operational area is divided into distinct operating zones, delineated based on prevailing ice conditions, which may evolve dynamically throughout the simulation. Each zone is ensured to have at least one icebreaker available. Icebreakers possess specific ice-going capabilities, modeled using hv curves akin to those employed for assisted ships (refer to Figure 3), with examples of icebreaker hv curves provided by Lindberg et al. (2018).

Despite being assigned specific zones, icebreakers frequently collaborate to make sure the safe and efficient operation of the entire system. Vessels often require assistance across different zones. Usually, one icebreaker leads a vessel through its designated operating zone, leaving the vessel at a secure stopping point known as a waypoint. The next icebreaker assumes responsibility for guiding the vessel further along its journey from there. However, icebreakers have the flexibility to operate beyond their designated zones to alleviate traffic congestion or assist larger vessels requiring dual icebreaker support. Icebreakers must dynamically make decisions regarding prioritizing vessel assistance, coordinating with other icebreakers, selecting paths, and organizing convoys. When a vessel becomes stopped in ice, it sends a distress signal to the icebreaker control unit, which may consist of an icebreaker with a coordinating captain or a decision-making unit on land. A free IB can also "predict that point. The different merchant vessel threshold speed to start the assistance is an input parameter in the tool. The responsible icebreaker calculates the vessel's potential route based on its current position and destination, identifying one or more icebreaker zones through which the vessel must navigate to reach its destination. A schedule is then devised for the vessel, updated each time it completes a zone. The initial icebreaker assigned to assist the vessel is dispatched to guide it to the end of its assigned zone or port if the port falls within the zone. At the conclusion of each zone, the vessel's route is reassessed as necessary, and the subsequent icebreaker is tasked with guiding it onward. A comprehensive list of requests for each icebreaker is maintained and updated as the vessel progresses from one zone to another. Once the vessel reaches a port, it is removed from all lists. This coordinated approach ensures the efficient movement of vessels through ice-covered waters. More detail description of the IB decision making can be found from Kulkarni et al. (2022a, 2022b).

VERIFICATION AND VALIDATION OF THE TOOL

To ensure the model reliability and instill confidence in its functionalities, both verification and validation processes are essential. Verification entails assessing whether the model behavior reflect the conceptual description and specifications. On the other hand, validation assesses the extent to which the modelling represent the real world from the perspective of end users. Essentially, verification addresses the question: " Is the model right?", while validation addresses the question: " Is this the right model?". Both processes can be conducted at both the individual ship level and the system level, as elaborated below.

Several challenges exist in the validation of this simulation tool. Firstly, despite the extensive AIS dataset, organizing and processing the data to suit the simulation is a complex task that demands dedicated attention. Secondly, the majority of data originate from a single common source, which was utilized to construct the model. Therefore, there are presently no additional data available solely for testing purposes. Thirdly, conducting trials of the tool alongside existing icebreaker management methods necessitates obtaining extensive permissions, undergoing checks, and adhering to regulations. Consequently, various validation approaches have been adopted for the simulation tool, detailed in the subsequent validation sections.

Verification

Field experts attended the demonstrations where the model was operated at a discernible pace. The KPIs included in this case are summarised next. They monitored vessel speeds across a localized area characterized by high ice variability to ensure their adaptation to changing ice conditions. Dirway alterations were also closely observed, with an expectation of changes occurring weekly throughout the runtime. Experts also examined waiting time averages at various ports and for all vessels collectively. Some of these experts had prior involvement in field assistance during the same timeframe. They corroborated that the Key

Performance Indicators (KPIs) obtained fell within acceptable ranges for the winter season, meaning less than 10% deviations. Moreover, the assistance numbers provided by each icebreaker was recorded and compared with reality (Kulkarni et al., 2022a).

Validation on a ship level

The validation on a ship level has been done by Sormunen et al. (2018). The main idea of the validation was to compare the speed variation on varying ice conditions for the Bay of Bothnia for one ice breaker and for the Gulf of Finland for one Ro-Ro vessel during winter 2010. The voyage length was few hours for both cases. The results indicate that the difference between AIS data and simulation model was less for the icebreaker (varying from -31 % to 41 %) than for the Ro-Ro (varying from -71 % to 61 %).

In a recent study by Kulkarni et al. (2024), a comprehensive approach to ship performance modeling is introduced, encompassing various parameters including ice conditions, power variations, and icebreaker assistance. This approach undergoes validation against real ship voyages. The h-v curves delineate the breaking capabilities of candidate ships against level ice, with the paper summarizing the methodologies employed for handling ice ridges, variable ice concentration, and ice floe sizes. Real-world ice fields often exhibit greater complexity than level ice, with variations in ice floe size and ice field concentration, as well as the formation of ice ridges under pressure. Equivalent ice thickness serves as a convenient means to streamline intricate ice fields into a single level-ice thickness, facilitating speed determination via the corresponding h-v curve. To validate the approach of ship performance modeling, real ship voyages documented by Kujala and Sundel (1991) are utilized as validation cases. These voyages were logged onboard corresponding ships during their visits to Finnish ports. Various parameters, like actual ship speed and power, are recorded, while ice parameters including level ice thickness, ice concentration, ridge sail height, and floe size are obtained by visual observation. Additionally, the operation modes (e.g., independent operation or assistance) are noted. This comprehensive dataset offers insights into the actual voyages, enabling ship speed estimations using the proposed approach, which can then be compared against the actual speeds observed during the voyages. In total, 12 ship voyages are included with 10 different vessels, with the typical duration of each voyage spanning a few hours. Comparing the average speed form the simulation tool and from the real observations, the relative difference is varying from – 47,5 % to + 7,2%.

Validation of the traffic system

For the traffic system in the simulation model, three different types of validations have been conducted:

1) Ship waiting times,
2) Ship arrival times,
3) Time used for each voyage.

These are described in future details next. Ship waiting time was validated by Lindberg et al. (2018) using the previous version of the tool, a deterministic simulation tool developed to analyze the performance of the FSWNS regarding the cumulative waiting time for icebreaker assistance under predefined operating conditions. Validation of the tool using real-world data suggests its reasonable accuracy. One month period from 15 January to 15 February on winter 2011 was used for the validation. A 1.7% margin was obtained to the average real life port waiting times based on AIS data.

Kulkarni et al. (2022a) validated the ship arrival times including winter traffic from 15 January 2018 to 15 February 2018 on the Bay of Bothnia. A total of 115 vessels were incorporated into the study, and a total of 249 trips were analyzed. Only level ice thickness was used to define the prevailing ice conditions for the used hv curves. These vessels were categorized into 18 vessel types with similar hv curves. The historical dataset comprises arrival and departure timestamps at various ports, along with the duration of stay at each port. Port departure times are integrated into the model as inputs. The arrival of a vessel at its designated destination port hinges on several factors, including ice conditions, dirways, icebreaker availability, and the prioritization logic employed by icebreakers when handling assistance requests from multiple vessels. One approach to validating the model involves comparing the scheduled arrival times of vessels at different ports with their historical counterparts. Typically, the arrival times were within few hours error margins but also few exceptional cases were found with the error of several days showing the sensitivity of system on a number of parameters, which require further analysis.

The latest validation was done by Winberg (2023) in his master's thesis. Rather than validating for one winter, the model was studied on trip-level using three different historical winters, being 2011, 2018, and 2020 on the Bay of Bothnia. These represent the three different winter types of mild, average, and severe, classified by the Finnish Ice Service. One month period i.e. from mid-January to mid-February was used as the studied period. For the study, a trip-level validation is performed for the different winter classes (mild, average, severe). Trip-level validation is preferred, since that allows the individual trips

to be studied, and thus help find the root cause for the errors more easily than using a broader system-level overview. Therefore, comparing the trip durations from real-life to the results provided by the simulation, are chosen as the main method of the validation. Winberg (2023) made detail study of the AIS data and filtered out a remarkable number of voyages due to the errors on the data and thereafter the data resulted in 232, 599 and 408 trips for the winters of 2011, 2018 and 2020, respectively. In the study, 45 reference vessel hv curves were used for the studied ships, and only level ice thickness was used to define the prevailing ice conditions for the used hv curves. Vessel speed threshold to start assistance was 3kn and convoy maximum speed 6 kn. The trip distance was from the Northern Quark strait to the harbour on the Bay of Bothnia, so typical voyage length is from few hours to few days. The average difference between the trip durations was 72.7 %, -90.1 % and 40.2 % for the winters of 2011, 2018 and 2020, respectively. This is naturally a remarkable scatter as the results obtained from the three winters are very diverse. Winberg (2023) summarises on his conclusions the following possible error sources:

- There is possibility of errors in the AIS data
- The waypoints used by vessels for navigation in the area do not correspond to the routes used in real-life
- Icebreaker decision making is not optimized and do not follow the real-life procedures
- Winds and currents impact on the ice movement are not included
- The optimized utilization of ice channels is not included
- Only one speed threshold for the icebreaker assistance is included
- Inaccuracies may be present on the used h-v curves

OPTIMIZATION OF ICEBREAKER ASSISTANCE FOR SUSTAINABLE SHIPPING

Kondratenko et al. (2023) employed the simulation tool to introduce a novel approach for decarbonizing shipping in icy conditions. This proposed method optimizes icebreaker support with a focus on both ecological and cost efficiency, thereby facilitating the implementation of more sustainable icebreaking strategies. While the fee of icebreaker assistance is not directly remitted to Finnish and Swedish organizations who provide such assistance, it is encompassed within the fairway fee collected by the government. This fee is contingent upon the ice class (only applicable to Finnish authorities) and the vessel size. As reported by Baltic Icebreaking Management (2020), the average total operational cost of one icebreaker during the 2019–2020 navigation season amounted to 4.91 million euros per month, with approximately 11 percent allocated to fuel expenses. The total amount of fuel needed by the assisted ships in ice is now known, but the simulation tool can be used to approximate this. The main research question is then what is the optimum number of icebreakers so that the total amount of fuel and emissions on the air can be minimized on the winter navigation system level. In other words, can we use some other KPIs as average waiting time in future, to account for both ecological and cost efficiency KPIs, supporting sustainable shipping in ice.

Kondratenko et al. (2023) expanded the model to incorporate an eco-efficiency Key Performance Indicator (KPI) by estimating the total CO2 emissions (in tons) of the FSWNS encompassing all transport vessels and icebreakers simulated in the analysis. While port emissions are negligible and remain unaffected by icebreaking assistance, they are thus not factored into the calculations. The total CO2 emissions are determined for the scheduled voyages of transport vessels and all simulated assistance operations conducted by the icebreakers. This can be done as the simulation tool knows the used engine power and voyage time and length for both icebreakers and assisted ships. Using standard approaches the fuel consumption as a function of engine power can be determined and conversion factor between fuel consumption and CO2 emission exists as well. The fuel cost can then also be determined once we know the total amount of fuel. The other economic costs in the model are included using the time charter rate (USD/hour) of a transport vessel or an icebreaker. More details of the approach used can be found from the paper by Kondratenko et al. (2023).

The case studies are established based on historical AIS traffic data and ice data during an average winter from traffic and ice perspective (15 Jan - 15 Feb 2018). Freight rates for each vessel are estimated based on publicly available data, taking into account the vessel's purpose and capacity (measured in deadweight (DW) or twenty-foot equivalent unit (TEU)). Estimated daily freight rates vary significantly, ranging from 4900 USD/day for small transport vessels to 43,000 USD/day for large vehicle carriers, and 60,000 USD/day for icebreakers. The study systematically varies the number and size of icebreakers, determining CO2 emissions and costs using the simulation tool. Findings indicate that current practices are close to optimal, but alternative operational strategies could potentially reduce greenhouse gas emissions by up to 7% or lower costs by up to 14.2%. Results suggest that the proposed approach holds promise in offering recommendations for environmental and economic policies aimed at decarbonizing Finnish-Swedish icebreaking assistance. Naturally, this is the first attempt to evaluate the other KPIs than average waiting time and the model needs improvements, but the study shows the strength of the tool to study also other KPIs.

ANALYSIS OF THE ICEBREAKER NEEDS IN ESTONIA

The latest application of the developed simulation tools has been the evaluation of icebreaker needs for Estonia until the year 2025 (Tapaninen at al., 2023). Figure 6 shows the developed model layout for Estonian maritime traffic. The main objective of the study was to simulate the Estonian wintertime traffic and analyse how many icebreakers Estonia will need as described next in further detail.

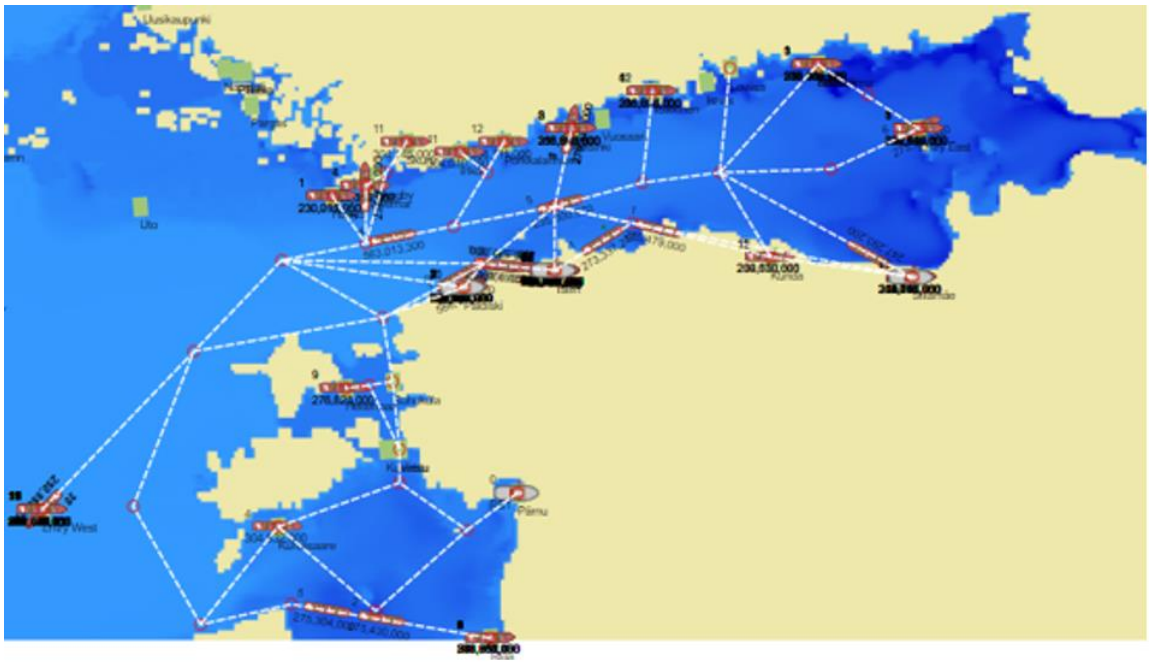

Figure 6: A demonstration of the Estonian Winter Navigation System model (Tapaninen et al., 2023)

Evaluation of ice conditions

The ice conditions on the Estonian water were analysed by Taltech, Department of Marine Systems. Figure 7 illustrates the mean and maximum ice thickness on Estonian waters based on the long-term data. As can be seen that there are winters with very minor amount of ice, but also hard winters with extensive ice coverage on Estonian harbours. Over the years 1993–2022 about 20% winters have been sever, 60% have been average, and 20% have been mild winters. As temperatures are projected to increase in climate scenarios, a rise in occurrence of average and mild winters is anticipated. Consequently, severe winters are expected to become significantly less frequent. Nevertheless, under extreme weather conditions in warmer climate scenarios, there remains a possibility for severe winters to occur. Consequently, the simulation tool was used to analyse the winter navigation system on a mild, average, and hard winter.

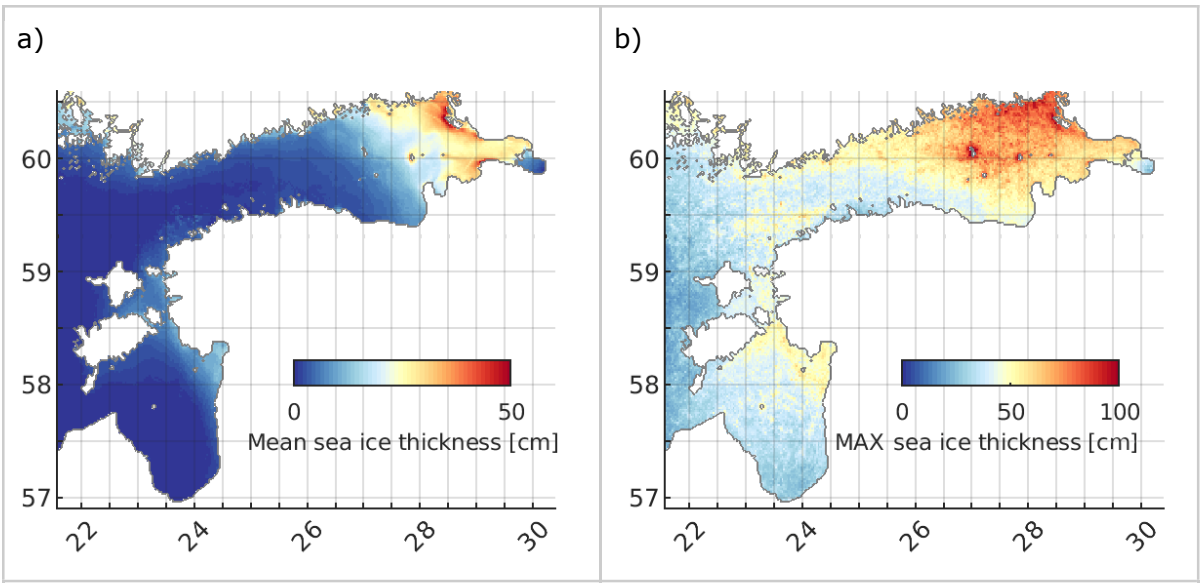

Figure 7: (a) Mean and (b) maximum of ice thickness. The values are retrieved from data between 1993 and 2021 (Tapaninen et al., 2023)

Simulated scenarios

In order to simulate the effects of the different combinations of icebreakers (IB), the scenarios given in Table 2 are used. Three of the used icebreakers are delegated to Gulf of Finland (GUF) and one to Gulf of Riga (GUR). IB scenario 1 includes two icebreakers, i.e. one in both areas and scenario 2 have three icebreakers, i.e. one in GUR and 2 in GUF, and scenario 3 activates all four icebreakers, i.e. one in GUR and 3 in GUF.

Table 2: Icebreaker scenarios studied (Tapaninen et al., 2023)

Icebreakers	Main Engine power [kW]	Shaft power [kW]	IB scenario 1	IB scenario 2	IB scenario 3
GUF, Primary IB	13000	10000	+	+	+
GUF, Secondary IB	9100	7000		+	+
GUF, Third IB	6250	5000			+
GUR, IB	5500	4400	+	+	+

Obtained results

In the conducted simulation, the level of maritime traffic flows are kept same using historical AIS traffic data from 2018 Jan 15th to Feb 15th. The studied scenarios are given in Table 2. One of main KPIs for icebreaker assistance is average waiting time for each assisted ship, i.e., how much time is needed for merchant ships to wait for icebreaker assistance. Therefore, this will be one of the main outcomes. In addition to this, the icebreaker operation time used in winter navigation system and corresponding fuel consumption are also outputs from the modelling. Table 3 summarises the obtained results for the average waiting time KPI, indicating that on mild winter scenario 1 is satisfactory, on average winter scenario 2 is satisfactory and on hard winter scenario 3 is satisfactory when the average waiting time is kept less than 4 hours (240 mins).

Although the simulation results show reasonable trend for the scenarios, the modeling of the Estonian winter navigation system still has many limitations and simplifications comparing to the practical working system. The absolute values of the waiting time need to be referred to carefully. The icebreaker assistance logic still needs improvements, and the practical icebreaker assistance is affected number of additional parameters. The average waiting time is likely to decrease if the optimal home port or waiting location for IBs can be identified in further detail. Especially in IB Scenario 1, with only one icebreaker in Gulf of Finlaand and Gulf of Riiga respectively, the waiting time is likely to reduce dramatically. In addition, near the coastline, there are possibilities for icebreaking assistance from tugs and channels can also be left open by other ships, which are not able to be

included in the simulation. These will also reduce the waiting time in practice. In general, further validation and comparisons with the practical cases are planned in future research for improving the accuracy and resilience of the model.

Table 3: Summary of the main KPI-average waiting time (mins) for all scenarios (Tapaninen et al., 2023)

Scenarios	Mild winter	Average winter	Severe winter
1	130	500	1000+
2	110	160	400
3	110	140	150

DISCUSSION

The developed simulation tool aims to capture all the main elements of the winter navigations system: ice-going ships, icebreakers, varying ice conditions and varying situations for assisting ships in ice. All these elements are challenging to simulate. Ice conditions are dynamic with great variations even for one day. In addition, the idea of using the equivalent level ice thickness to describe various ice conditions with one value aiming to simulate reliably the ship average speed on these ice condition causes a number of challenges. This is due to the fact that evaluation of the equivalent ice thickness needs accurate physics-based models to determine ship performance in varying ice conditions. Historically, ship performance in level ice has been the dominating research area to develop analytical formulation for ship resistance. The other ice conditions, such as ridges, dynamic moving ice, and ice floes with varying concentrations have obtained less attention. Consequently, the methods used to evaluate the equivalent ice thickness for these ice conditions needs further research as well how to link the equivalent ice thickness calculation methods to the main particulars of the ice-going ships.

Another important area for further development is how to simulate the decision-making process of icebreaker captains coordinating the whole maritime operations during wintertime. This has crucial effect on the efficiency of the winter navigation system. This decision-making process should include knowledge of a number of parameters like: summary of the ships and their ice-going performance being or approaching the studied area, most probable development ice conditions in near future, available ice-breakers on the area and their location and duties in near future etc. On the present form the tool is using mainly the maximum waiting time for ice-going ships as the main decision-making criteria, which is naturally too simple.

However, the first results of applying the system level simulation tool are promising even though of the prevailing challenges describe above. This is unique tool worldwide trying to simulate all the main elements of the winter navigation system. On system level the average waiting time for ships have been obtained with less than 10 % accuracy. Comparing the ship arrival time to harbors the scatter has been much wider caused mainly by the limitations on the factors: Icebreaker decision making, winds and currents impact on the ice movement not included, optimized utilization of ice channels not included, only one speed threshold for the icebreaker assistance is included and inaccuracies on the used hv curves. All these topics will need further development in near future.

CONCLUSIONS

We have developed during the last 10 years a simulation tool to study in the system level the performance of our winter navigation activities. The main aim of the tool development has been to develop a research-based prototype that can be used to simulate the need of icebreakers in the future when both ice conditions, maritime traffic and characteristics of ice-strengthened ships will be under dynamic change. In this paper, the current status of the simulation tool is shortly described together with the main structure and elements of the tool. Some recent case studies with the tool are also summarised: Validation of the tool, optimization of icebreaker assistance for sustainable shipping and analysis of the icebreaker needs in Estonia.

The tool has been applied with success to analyse the wintertime marine traffic both on the Bay of Bothnia for Finnish marine transport and for Gulf of Finland for Estonian marine transport. On system level the accuracy (e.g., the average waiting time of ice-going ships) has been found adequate, but create variation can take place on the voyage based comparisons. The validation of the simulation tool with AIS data to determine the arrival times to harbors shows extensive scatter as the used methods to determine equivalent ice thickness with a reliable link to the used hv curves as well the ice-breaker decision making needs further development.

CONTRIBUTION STATEMENT

Kujala, P.: Conceptualization; methodology; writing – original draft. **Kulkarni, K.:** simulation tool development, review and editing, **Kondratenko, A.:** sustainable shipping part development review and editing, **Lu, L.:** dynamic ice part development, review and editing., **Winberg, C.**: validation part development, **Li, F.:** hv curve development, review and editing, **Musharraf, M.**: supervision, review and editing.

ACKNOWLEDGEMENTS

The research was supported by the Winter Navigation Research Board – a Finnish-Swedish cooperation co-funded by the Finnish Transport and Communications Agency, the Finnish Transport Infrastructure Agency, the Swedish Maritime Administration, and the Swedish Transport Agency under the projects WinterSim and W22-1 SIMNAV. The research also receives funding from the Finnish Transport Infrastructure Agency through the project 'Development of winter navigation simulation model' (agreement No. 2022.2379.1). In additions, Estonian Transport Administration funded the study: Analysis of alternatives for providing icebreaking services in Estonia. The authors would like to thank all the other participants of the project "Analysis of Alternatives for Providing Icebreaking Services in Estonia." – Tapaninen, U. P., Palu, R., Uiboupin, R., Rikka, S., Maljutenko, I., Hunt, T., Mylly, M., Ojala, L., Heinonen, T., Suojanen, R-A.
Author 1 was also supported by the Academy of Finland project: Towards human-centered intelligent ships for winter navigation (Decision number: 351491). The 2nd author was supported by Science and Technology Commission of Shanghai Municipality Project (23YF1419900). In addition, the authors would like to thank Aker Arctic Technology Inc for providing the sample ship database containing established h-v curves.

REFERENCES

Baltic Icebreaking Management. (2021). Baltic Sea Icebreaking Report 2020-2021. https://baltice.org/app/static/pdf/BIM%20Report%202020-2021.pdf.
EEDI. (2022). Energy Efficiency Measures. Available online: https://www.imo.org/en/OurWork/Environment/Pages/Technical-andOperational-Measures.aspx (accessed on 17 March 2022).
JCOMM Expert Team on Sea Ice. (2014). SIGRID-3: A Vector Archive Format for Sea Ice Georeferenced Information and Data. Version 3.0.;WMO & IOC: Geneva, Switzerland, 2014.
Kondratenko A., A., Kulkarni K., Li F., Musharraf M., Hirdaris S., Kujala, P. (2023).Decarbonizing shipping in ice by intelligent icebreaking assistance: A case study of the Finnish-Swedish winter navigation system. Ocean Engineering 286 (2023) 115652
Kujala, P. & Sundell, T. (1991). Performance of ice-strengthened ships in the northern Baltic Sea in winter 1991. Report M-117, Helsinki University of Technology.
Kulkarni, K., Kujala, P., Musharraf, M., Rainio, I. (2022a). Simulation tool for winter navigation decision support in the Baltic Sea. Appl. Sci. 12, 7568. https://doi.org/ 10.3390/app12157568.
Kulkarni, K., Li, F., Liu, C., Musharraf, M., Kujala, P. (2022b). System-level simulation of maritime traffic in northern Baltic Sea. In: Pedrielli, G., Peng, Y., Shashaani, S., Song, E., Corlu, C.G., Lee, L.H., Lendermann, P. (Eds.), Proceedings of the 2022 Winter Simulation Conference B. Feng.
Kulkarni, K., Li, F., Kondratenko, A., Kujala, P. (2024). A voyage-level ship performance modelling approach for the simulation of the Finnish-Swedish winter navigation system. Paper under review process.
Li, F., Goerlandt, F., Kujala, P. (2020). Numerical simulation of ship performance in level ice: a framework and a model. Appl. Ocean Res. 102, 102288 https://doi.org/ 10.1016/j.apor.2020.102288.
Li, F., Suominen, M., Kujala, P. (2021). Ship performance in ice channels narrower than ship beam: Model test and numerical investigation. Ocean Engineering 240 (2021) 109922.
Lindeberg, M., Kujala, P., Toivola, J., Niemelä, H. (2015). Real-time winter traffic simulation tool – based on a deterministic model. Sci. J. Marit. Univ. Szczec. 42 (114), 118–124.
Lindeberg, M., Kujala, P., Sormunen, O.-V., Karjalainen, M., Toivola, J (2018). Simulation model of the Finnish winter navigation system. In: Marine Design XIII. CRC Press, Boca Raton, FL, USA.
Milakovic, A.-S, Li, F., Polach, R.U.F.v.u., Ehlers, S. (2020). Equivalent ice thickness in ship ice transit simulations: Overview of existing definitions and proposition of an improved one. Ship Technol. Res. 2020, 67, 84–100.
Lu, L., Kujala, P., Toivola, J., Orädd, H., Kuikka, S. (2023). New approach to determine equivalent ice thickness for ships in dynamic compressive ice. Proceedings of the 27th International Conference on Port and Ocean Engineering under Arctic Conditions, 12-16 June 2023, Glasgow, United Kingdom.

Sormunen, O.V., Berglund, R., Lensu, M., Kuuliala, L., Li, F, Bergström, M., Kujala, P. (2018). Comparison of vessel theoretical ice speeds against AIS data in the Baltic Sea. In Marine Design XIII; CRC Press: Boca Raton, FL, USA, 2018.
Tapaninen, U. P., Palu, R., Kujala, P., Uiboupin, R., Rikka, S., Maljutenko, I., Hunt, T., Musharraf, M., Kondratenko, A., Lu, L., Mylly, M., Ojala, L., Heinonen, T., Suojanen, R-A. (2023) Analysis of Alternatives for Providing Icebreaking Services in Estonia. Final Report. Tallinna Tehnikaülikool, Aker Arctic Technology Inc, logscale oy, Saaresalu OÜ (Unpublished).
Trafi, 2022. F.T.S.A. "Ice Class Regulations and the Application Thereof," Finnish Transport Safety Agency, Helsinki.
Winberg, C. (2023). Validation of a Computational Simulation Model of the Finnish-Swedish Winter Navigation System. Master thesis. Aalto University, School of Engineering.
Winmos II (2021). Developing the Maritime Winter Navigation Systems, Winmos II. Available online: http://www.winmos.eu/ (accessed on 4 October 2021).

Proceedings of 15th International Marine Design Conference (IMDC-2024)
June 2-6, 2024
Amsterdam, the Netherlands

What is a ship design firm, really?

Benjamin Lagemann[1,*] and Randi Lunnan[3] and Per Olaf Brett[3] and Jose Jorge Garcia Agis[4] and Astrid Vamråk Solheim[5] and Stein Ove Erikstad[6]

ABSTRACT

Ship design is a creative process serving a defined objective. This is normally an iterative process with the design being corrected and adjusted many times until it satisfies this objective. Ship design is taking place in a broader business context consisting of stakeholders providing necessary resources and information to enable the realization of a vessel newbuilding project. Activities performed by different actors, such as customers, suppliers and brokers, are organized by and integrated into a ship design firm. This paper addresses and discusses different ways of organizing integrated design-related activities to deliver on the firm´s value proposition. A value proposition denotes the promised value to a selected customer, and through its value proposition, a ship design firm provides "superior" solutions to a customer's needs. To enable this solution, a design firm draws on its current resources, including its past knowledge and experiences, and uses these resources in different types of processes, and – in different ways of collaborating with internal and external actors and specialists.

In this paper, we draw on approaches from the field of business strategy to understand implications and trade-offs in different logics of value creation processes, how they can be applied in ship design firms, and their implications.

KEY WORDS

Ship design; firm strategy; resource organization; value activity analysis

[1] Department of Marine Technology, Norwegian University of Science and Technology (NTNU), Trondheim, Norway and SINTEF Ocean, Trondheim, Norway; ORCID: 0000-0002-6106-0280

[2] Department of Strategy and Entrepreneurship, BI Norwegian Business School, Oslo, Norway; ORCID: 0000-0002-5624-4464

[3] Ulstein International AS, Ulsteinvik, Norway and Department of Marine Technology, Norwegian University of Science and Technology (NTNU), Trondheim, Norway; ORCID: 0000-0002-8767-5494

[4] Ulstein International AS, Ulsteinvik, Norway; ORCID: 0000-0001-6610-1136

[5] Department of Marine Technology, Norwegian University of Science and Technology (NTNU), Trondheim, Norway; ORCID: 0000-0002-6142-1015

[6] Department of Marine Technology, Norwegian University of Science and Technology (NTNU), Trondheim, Norway; ORCID: 0000-0001-7323-6901

* Corresponding author: benjamin.lagemann@ntnu.no

Submitted: 16 February 2024, Revised: 24 April 2024, Accepted: 1 May 2024, Published: 27 May 2024

Conference paper, DOI: https://doi.org/10.59490/imdc.2024.914 e-ISSN: 3050-4864

1 INTRODUCTION

Ship design has traditionally been executed by naval architects and marine engineers (Andrews, 2010) with an integrating role for specific disciplines involved in the process. In the past, this activity was mostly done by integrated shipyards, while more recently the ship design role – particularly during the vessel concept ship design phase – has been decoupled from yards and, in the merchant shipping world, is done mostly by firms that are specialized in ship design activities (Semini, Sjøbakk, & Alfnes, 2013; Semini, et al., 2023).

Shipbuilding is still considered, by most parties, as comprising the design of the vessels, the erection of the ships, and finally, the production of all main systems and equipment onboard to eventually constitute an operable floating ship. Shipbuilding, including ship design activities, is a highly competitive global industry. Over the past decades, European shipyards have lost a considerable part of their market share to East-Asian shipyards, especially within the conventional and high-volume cargo-carrying segments, such as tankers, bulkers, and container vessels. In these segments, European shipyards now play a marginal role – a market share of less than 10% of the worldwide annual orderbook (Brett, Gaspar, Ebrahimi, & Garcia Agis, 2018; Semini, et al., 2023). In Europe, and Norway in particular, shipyards and their affiliated or independent ship design firms have focused on a limited set of specialized vessels, but still stand for a good portion of the worldwide orderbook value within passenger vessels, fishing and aquaculture vessels, service vessels, including both the offshore oil & gas service vessels as well as ships for the offshore wind industry. Yet, for most of the European ship design firms the European shipbuilding market is not sufficient, and they also provide ship design services to other international yards. Projects with the European shipyards are typically one-of-a-kind rather than series of ships, which is the case in the Far East. Typically, European ship design firms deliver few, but novel design packages with high degree of innovation – complex and expensive designs.

With the past and current low levels of demand and ordering of ships, yards and ship design firms have been and still are struggling to make sufficient profit margins out of meager order books and falling market shares. Competitiveness is dwindling too. To regain competitiveness – despite other parts of the world benefitting from lower wages, lower material costs, more favorable financial support, more lenient laws, and regulations – there is a critical need for European shipbuilders and independent ship design firms to improve their understanding of why this long-term market trend is happening, what affects their performances and how it can be improved. It is argued by this article that for regaining competitiveness in the ship design firm business segment, a much deeper and broader insight into how value creation and extra profits can be achieved is paramount. Further, it is argued that competitiveness is among other factors, particularly interlinked to the choice and application of strategy models for value creation in that business segment. Therefore, this article looks for ways to improve competitiveness by better understanding the basis for applying one or a mix of the generic strategy models for effective value creation (Fjeldstad & Lunnan, 2022).

This paper is rooted in the DREAMS research project, which has researched these challenges for a couple of years with the goal of improving the competitiveness of Norwegian ship design companies. The project was introduced to the IMDC participants at the Vancouver IMDC 2022 conference (Brett, Asbjørnslett, Garcia Agis, & Erikstad, 2022). In this paper, we would like to share and discuss some of the preliminary findings. The study and this paper take a broader view, stressing that such a study must take a comprehensive approach to competitiveness – with the purpose of the ship design activity to make money and not only produce better and innovative design solutions.

Previous papers at IMDC have discussed many technical aspects and considerations around the ship design process as well as design methodologies (Andrews, et al., 1997; Andrews, Keane, Lamb, Sen, & Vassalos, 2006; Andrews, Papanikolaou, Erichsen, & Vasudevan, 2009; Ulstein & Brett, 2012; Andrews & Erikstad, 2015; Andrews, Kana, Hopman, & Romanoff, 2018; Erikstad & Lagemann, 2022). Little emphasis has been placed on the organization of human resources in performing design activities. However, in several IMDC papers it has been stated that naval architects and marine engineers as well as ship design firms must expand their knowledge, expertise, and skills to be able to handle future ship design challenges from a commercial, operational, and technological standpoint (Ulstein & Brett, 2012; Brett, Garcia Agis, Ebrahimi, Erikstad, & Asbjørnslett, 2022).

This paper discusses ship design activities from an organizational and business perspective by discussing strategic aspects around the design team composition. We hope this opens a relevant discussion on how ship design is performed in practice and how a ship design firm can create value for its customers. This has important implications for the type of people employed, their competence and skills and consequently also demands for academic education (Asbjørnslett, Erikstad, Lagemann, & Brett, 2022).

Our paper is structured as follows: Subsections 1.1 to 1.3 introduce the topic and important concepts and definitions. Section 2 presents four strategic models for value creation. Section 3 describes how the two most common strategic models can be applied

to ship design firms, supplemented by two empirical cases. Section 4 compares and discusses the two models, and Section 5 concludes the paper.

1.1 Definition of a ship design firm

Design is a decision-making process that results in the specification of an artifact (Goel & Pirolli, 1989; Simon, 1996). The ship design process can be categorized as a special variant of the design of physically large and complex systems (Andrews, 1998; Garcia Agis, et al., 2019; Ebrahimi, Brett, & Garcia Agis, 2018). The ship design process is typically executed by a team of naval architects and marine engineers, with support and expertise from various other disciplines such as sales, interior design, electrical engineering, and suppliers. If this team is part of a business entity[1], can this organization be termed a 'ship design firm'? In other words, are all organizations that conduct some ship design activities called a 'ship design firm'? To our understanding, the answer to this question is 'no'.

Figure 1 indicates the general ship design process timeline and several relevant stakeholders involved. Each of these stakeholders may employ naval architects, marine engineers, and other experts, and each may engage in the ship design process in one way or another. Yet, we would not call all of these stakeholders 'ship design firms'. Instead, for this paper, we suggest the definition of a ship design firm as 'a business entity where ship design constitutes the primary value activity and where a significant integration effort takes place'. To be more precise, we consider only firms that sell the specification and drawings of a ship to be a ship design firm. In other words: If you cannot buy a ship design from it (i.e., a specification, class-approved drawing package and supporting analyses), that firm does not count as a ship design firm for the purpose of this paper. This definition aligns with the idea that systems architecture is at the core of early-stage ship design (Andrews, 2003; Andrews, 2015).

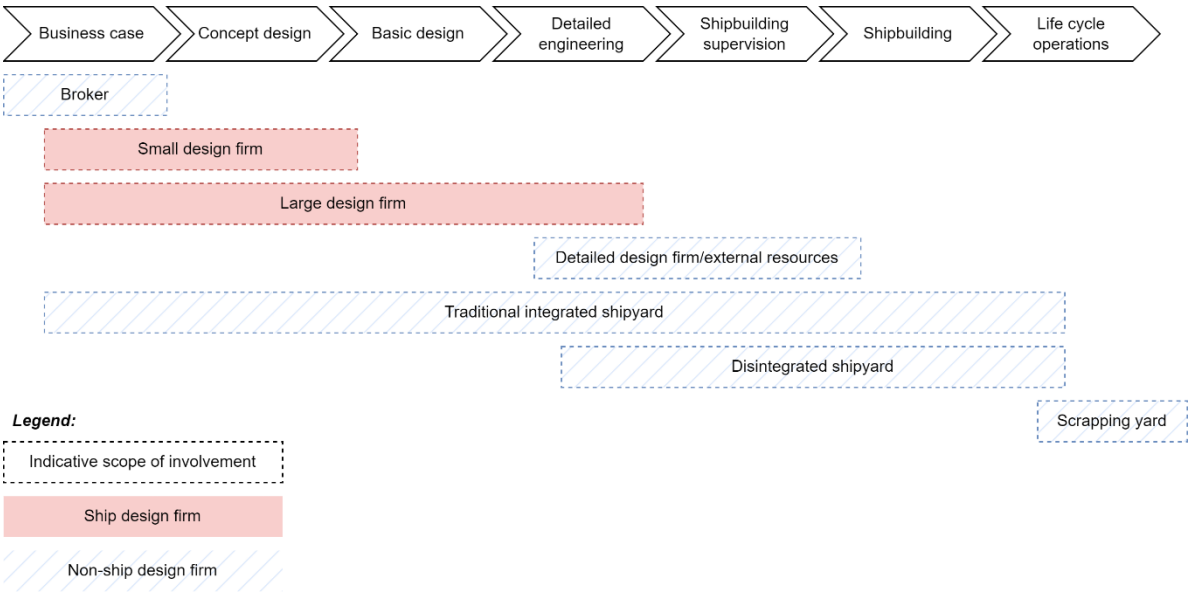

Figure 1: Different actors in the ship life cycle

It should be noted that formerly, ship design was mainly executed at what is here called 'traditional integrated shipyards', spanning the whole value chain from early-stage ship design to shipbuilding, maintenance and repair of ships. While this is still common practice in some instances and many countries (Cho & Porter, 1986), diversification and specialization have taken place in many locations. More firms are entering the market that focus their main activities on ship design. These firms' main activities are design, not shipbuilding. This is especially true for the Norwegian market, where yard activities and market share have been declining over many years (Menon Economics, 2023), but we see independent ship design companies are generally growing by number, revenue and employees – albeit growth was halted after 2015 (inhouse compilation based on data from Proff (2023)). While the Norwegian ship design firms' global market share is around 3 to 5%, ship designers provide important design and integration competence to Norwegian yards, the maritime cluster (Menon Economics, 2022), and to customers (owners, operators, and yards) abroad. The labels 'small design firm' and 'large design firm' in Figure 1 relate to the firms' scope of involvement (concept, basic or detail) in the design process, not directly to their size in terms of turnover or employees

[1] The Oxford English Dictionary (2023) defines a firm as "generally: a commercial enterprise, business, or company".

as such. A 'disintegrated shipyard' (ship factory), in this paper, shall denote a yard that does not undertake substantial design activities itself, but instead focuses on ship production and repair.

1.2 Standardized and customized design and market interaction strategies

Shipyards typically follow different product portfolio strategies with respect to standardization and customization and sometimes a mix of the two. In most cases, customer strategies are then linked to market interaction strategies and the value creation strategy of the company. Ship designers may certainly, also employ such different strategies. One element of this strategy concerns activities covered and their customization. Semini et al. (2014) discuss four different approaches. First, make-to-stock, where products are manufactured to and sold from stock. Second, assemble-to-order, with components produced to stock and awaiting the final assembly to an order. Third, make-to-order, with all components and assembly waiting until an order is placed. Fourth, engineer-to-order (EtO), where the design is completely customized to an order. The four different approaches and their relation to the customer order decoupling point (CODP) are illustrated in Figure 2. The choice of approach has profound implications for what a ship design firm is, its organization, and how it operates.

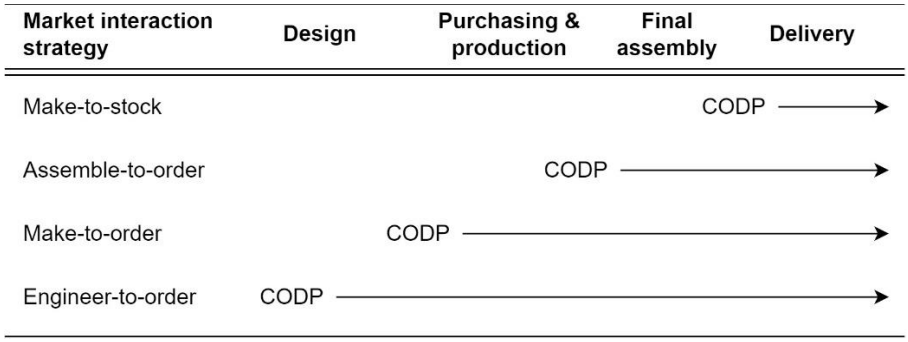

Figure 2: Market interaction strategies and customer order decoupling point (CODP), adapted from Semini et al. (2014) and based on Olhager (2003).

The make-to-order (customize existing design concepts) and engineer-to-order (design solution from scratch) strategies are the most relevant in this context, as they involve design activities as opposed to production and assembly activities (shipbuilding) only. On the surface, there may seem to be a certain overlap with Andrews' (1986) different degrees of novelty in ship design, i.e., adapting existing designs versus developing radically new technology and system solutions. The difference between the two is that a market interaction strategy describes a designer's approach towards a customer, whereas Andrews' degrees of novelty describe the following internal design processes. In this paper, we explore the importance of a fit between a market strategy towards the customer, the novelty of the design solution, and the organization of the ship design process and the role of the team.

1.3 Different types of customer interactions

Closely linked to the market interaction strategies, different types of customer interactions exist. In Table 1, we outline five customer interaction types that are commonly exercised in commercial merchant ship design processes.

Table 1: Customer interaction types

#	Customer interaction	Archetypical request	Typically initiated by	Solution response strategy	Competition
1	Customer design inquiry	"I want to have this ship"	Ship owner	New/existing	Unknown
2	Broker inquiry	"Do you have a solution that can do...?"	Broker or ship owner	Existing	Unknown
3	Tender inquiry	"Can you help us respond to this tender?"	Ship owner	New/existing	Usually known
4	Customer project inquiry	"Can we develop this together with your expertise/knowledge?"	Various	New	None
5	Project-making	"We have an interesting business proposition to offer you - do you want to be part of the initiative?"	Ship designer	New/existing	None

The market interaction strategies are closely linked through the 'solution response strategy' indicated in Table 1. A 'project-making' customer approach is normally combined with a standardize-to-order market interaction strategy. Thus, a standardized technical solution (StO) is developed, most often, without a customer involvement in the early phases of the project, but one or more takers (customers) may be involved at a later stage in the finalization of the new building project realization. While this inquiry approach is not so common, more often make-to-order strategies (configuration-based design or variant design; CtO) are experienced in the interrelationship with the customers. Interesting to note for our discussion are the differences between re-using existing designs, simple adaptations of these, and designing a complete novel ship from scratch.

In addition to the customer interaction strategy chosen, the overall value creation activities in a ship design firm, i.e., the ship design activities and resources' organization, may be arranged and performed according to a set of different value creating logics. It is argued in this article, therefore, that these logics have profound implications on the way activities are organized and executed, and what people, knowledge, experience, and tools are needed. The next section presents and analyzes ship design activities considering these models. We will particularly focus on two strategic models for value chain creation: the 'value chain' and the 'value shop'.

2 STRATEGIC MODELS FOR VALUE CREATION

A firm's strategy can be described as a plan or pattern to attain overall goals (Nag, Hambrick, & Chen, 2007). Reaching strategic decisions, the firm must make three consistent choices (Miles & Snow, 2003):

i) What products and services to deliver in which markets;
ii) What activities and resources to utilize to deliver these products and services;
iii) How to acquire, develop and organize these resources and activities to balance efficient operations and innovation.

These choices are partly interdependent. That is, to offer a low-priced product or service, for example, the firm must pursue low-cost resources and activities, whereas costly technology development may be needed for novel and unique designs. It should also be noted that the competitive advantage is only temporal (McGrath, 2013) and a firm needs to continuously monitor and critically evaluate its choices with respect to aspects i) to iii).

To examine, study, and understand activity systems and the drivers of cost and customer value, Porter (1985) introduced the value chain, outlining a "manufacturing" logic, focusing on economies of scale, capacity utilization, and activity linkages as core cost and value drivers. This configuration framework was later expanded by Stabell and Fjeldstad (1998), introducing the "value shop" and the "value network", building on the long-linked, intensive, and mediating technologies topology by Thompson (1967). Furthermore, Fjeldstad & Lunnan (2022) introduce "value access" as a fourth value creation model. Value access means appropriating value by offering customers access to shared resources, e.g., cloud computing or "management for hire". Each of these models focuses on different sets of activities, different dynamics between these, and different drivers of cost and value. Table 2 provides an overview and comparison of the different value creation models.

Table 2: Value creation models

	Value chain	Value shop	Value network	Value access
Business problem[1]	Transforming inputs into products (production-based)[1]	(Re)solving customer problems (Problem solving-based)[1]	Linking customers directly and indirectly (Network-based)[1]	Providing access to resources[3]
Deliverables created[1]	Products[1]	Solutions[1]	Services[1]	Access to resources[3]
Business-logic method[1]	Sequential[1]	Cyclical, spiraling[1]	Simultaneous, parallel[1]	Continuous[3]
Value creation strategy[1]	Achieve scale and focus on efficient linkages between activities[1]	Make optimal use of human capital and reputation[1]	Create superior connectivity and ability to carry products and services[1]	Secure resources and their quality[3]
Activities[1]	Inbound logistics Operations Outbound logistics Sales and marketing Service[1]	Problem finding Problem solving Solution choice Execution Control/evaluation[1]	Network promotion Contract management Service provisioning Network infrastructure[1]	Acquiring resources Managing resources Manage customer interface[3]
Frequent activity tradeoffs[2]	Differentiation vs. cost leadership Integration our outsourcing[2]	Knowledge depth and scope[2]	Open source vs. walled garden. Broad vs. specialized[2]	Focused vs. Specialized[3]

Sources:
[1] Sjåvåg (2022), Table 3.1
[2] Fjeldstad & Haanæs (2001)
[3] This paper

In ship design activities, the 'value chain' and 'value shop' appear to be the most common value creation models and will be examined and exemplified in the following section. The 'value network' and 'value access' configurations are less common as explicit and individual strategies for ship design activities as such, but for some appear as complimentary value creation strategies for supporting, additional products and service deliveries. Maritime examples for these two models do exist, however: Broker activities are typical instances of a 'value network' configuration. DNV's Veracity platform (DNV, 2023) may be seen as an example of 'value access', with elements of a 'value network' as it enables third-party app developers to link with customers. Moreover, a 'project-making' type of customer interaction in ship design shares many elements with a 'value network' logic.

3 VALUE CHAIN AND VALUE SHOP EXAMPLES OF DESIGN FIRM STRATEGIES

In this section, we will first outline the two value configuration logics of a 'value chain' and a 'value shop' and illustrate these two logics with examples from two different ship design firms. One of the ship design firms more often uses the logic of a 'value chain', whereas the other one uses the logic of a 'value shop'. The description of the illustrative cases is based on a total of 17 interviews with employees from the two firms. The semi-structured interview setup covered a pre-defined set of topics, while giving the interviewees the opportunity to elaborate. The interviews were conducted mostly by one interviewer, who asked questions and simultaneously took notes to document the interviewees answers. After the interview, the answers were analyzed and condensed by the interviewer into one summarizing document.

The activities of firm A and B can to some extent be described by one of the two value creation logics. In practice, however, both firms do adapt and mix the logics to a certain extent, dependent upon the type of customer inquiry received. Such a mix can be observed within and across projects. That is, within one project, a firm may predominantly follow a 'value chain' logic for instance, while still employing elements of the 'value shop' logic to a limited extent. Across projects, the firms may also switch between strategic approaches and in that sense adapt their value creation logic to the nature of the project and customer inquiry and thereby, mix the two whenever meaningful.

3.1 Design firm A – example of the applied value chain logic

In a typical value chain framework, the ship design firm follows a sequential logic, which often relies on standardization. The design processes can be portrayed as a chain of interlinked and linearly organized activities, where the work performed in one activity builds on the work done in the prior activity. The work is done by separate units, and specialized. In principle, there should be no need for feedback loops, the process is one-directional. This type of design firm is akin to an assembly line and is therefore also called a 'project factory' approach, in this paper.

At the initiation of each project, the project manager divides the project into specific parts identified by discipline. The project manager oversees the combination and coordination – the linkages between – these parts and information exchange. Ideally, the boundaries between disciplines are as clear-cut and as specific as possible, following a seamless handover between different disciplines. Each discipline is handled by a group of specialists, who do not necessarily need to know what other specialists do, if the interfaces between the parts of the design are clear, well-specified, and structured. The design process can follow a sequential and established logic, where each part is done according to allocated time and clear specifications. The customer, normally, takes no part in the execution of the design work processes, as the various tasks are clear and well understood by the naval architects, marine engineers and other specialists involved. Therefore, this process only works well if the project-specific expectations and requirements are clearly defined, documented, communicated, and understood prior to the design process execution and the naval architects and marine engineers are well trained and experienced in their work disciplines.

This logic can be illustrated by design firm A. Design firm A employs about 40 people directly engaged in the design activities, many of them with a specific discipline training and experience and/or shop floor background from a shipyard. The firm engages normally in projects with a concept and basic design scope. To engage in the latter one, a "winning" or an accepted customer concept design is a prerequisite. For both design phases – concept and basic – the firm's activities can be described with a value chain logic (similar to a project factory): In concept design, the project team usually consists of seven people with different roles. Two out of seven have an integrating function, and five out of seven work within their specific discipline. Each discipline uses its own specialized set of tools. Although employees are located on the same floor, they typically have separate offices combined with separate meeting rooms and more informal social areas. In the basic design phase, the design team is typically enlarged, and each discipline follows its own pre-defined and specific workflow. This work process triggers a lot of coordination meetings and mini seminars.

Design firm A has a long tradition in the design of complex vessels of medium size. Most of these vessels can be classified as service vessels. Examples in the most recent past are service offshore wind vessels (SOV), expedition cruise vessels, fishing and aquaculture vessels, or cable laying vessels. Common for all these vessels is that they have complex operational patterns and systems to integrate on a small to medium-sized vessel, typically up to 160m. The vessels are typically built as one-offs or in small series. Design firm A makes use of all five types of customer interactions (Table 1). Over time, a considerable design portfolio has been built up. The firm proactively develops this portfolio/catalog, both to strengthen inhouse knowledge and to be able to offer standardized, but customizable solutions to certain customers, such as for customer approach #2 (Broker inquiry: "Do you have a solution that can do...?"). To cut response time in a tender process, catalog solutions may serve as a starting point for most customization or adaptation work.

3.2 Design firm B – Example of the applied value shop logic

In a typical value shop framework, the design firm follows a logic of problem-solving. The design a customer demands is unique and does not currently exist. Every new project starts a creative process, where the main idea is to match customer preferences with the design in a novel way. Customers may have non-standard requests that cause ripple effects among different disciplines involved in design, and initially, the main elements of these must be identified. At times, the customer may not be clear on her exact demands and needs to explore the feasibility of these together with the design firm. The interaction between the customer and the design firm is normally handled by the most senior experts in the firm. These seniors have deep and broad knowledge of the major disciplines and have skills in customer communication. In this process, important stakeholders, such as customers and major suppliers are involved in early discussions and in offering comments to early design suggestions, promoting an interactive (as opposed to the sequential value chain logic) value creation logic. The process is characterized by feedback loops and trials until the main elements of the design are settled. Then, the detailed work may be handed over to specific disciplines and sometimes junior engineers (yet, with deep knowledge in one discipline). In such a value creation logic strategy, it is important to stop the process and revert back to start if surmountable problems occur and incorporate more deliberate customer and expert feedback along the way.

Design firm B consists of about 20 people directly engaged in design activities. Most of these have a master-level education in naval architecture, resulting in a workforce with consistently high and homogenous academic training. All naval architects are trained on a small set of tools. These tools partly consist of commercial software, and partly of special in-house developments.

In concept design, the project team typically consists of three to five people in total, with one senior naval architect as a project leader. Due to their relatively homogenous skills, one person can have different roles in different projects. To promote and further develop this versatile and homogeneous skillset, it is common practice to rotate the roles among employees over time. All people work on the same floor and in open plan office facilities.

Firm B is an established designer for large, offshore energy vessels applied in segments such as wind turbine installation vessels (WTIVs) or foundation installation vessels (FIVs), and heavy lift and other specialized vessels (HLVs) for the offshore oil & gas industry. These vessels are typically somewhat larger in size, more expensive and tailor-made one-offs. Firm B is usually contacted by customers to develop tailor-made solutions. While the firm also maintains its own design portfolio, the firm's target segment is characterized by tailor-made, one-off solutions as opposed to potentially small series. Vessels in this segment are, on average, more expensive and the engineering hours – particularly concept design hours – amount to a smaller proportion of the overall costs of the vessel.

4 DISCUSSION

The two value creation logics we have outlined may both provide competitive value propositions to customers. A 'project factory' model is normally more cost- and time-efficient on known designs and when market conditions are good – many inquiries that need quick turnaround time for response – much dependence on continual high production throughputs, whereas the 'value shop' model offers highly customized designs for special missions and is less sensitive to consequences of good and bad market conditions. The project factory approach is also less demanding w.r.t the qualifications of the engineers involved – a few well-seasoned naval architects can handle several less trained engineers. On the other hand, it requires more organizational structure and management – more formalism. The value shop model requires more experienced and fuller-fledged naval architects and marine engineers, i.e., project managers being capable of both handling the upstream sales interaction and the downstream managing the project efforts until delivery of the design package.

If we consider our two examples of solutions (firm A and B), both operate on a project basis. That is, a temporary project team is assembled individually for each project – whether paid for or not, and whether a concept or basic design scope – from the pool of available employees within each company (relatively constant over time). The skillset and composition of this human resource pool differs between the two design firms, and this is reflected in the project team composition. Firm A employs specialists in each discipline that focus on a specific part of the design process. For firm A, it is vital to have a clear overview of the design project, and design the interfaces where activities are handed over to the next discipline. Firm B's work force is less discipline-specific and has a more versatile background. Their skillsets, tools, and collaborative shared workspace facilitate a more problem-oriented working style in line with the value shop logic.

The main challenge of a 'value shop' type of logic is to as quickly as possible come up with a concept design solution that is agreeable to the customer and feasible for all other stakeholders. This implies that the initiation of a value shop project is crucial, and that handling and coordinating initiatives from all stakeholders finding a solution is the key (Brett, Gaspar, Ebrahimi, & Garcia Agis, 2018; Garcia Agis, et al., 2019). Our illustrative example shows that firm B has succeeded with this collaborative and less streamlined working style in the conceptual phase, reporting good experience and high satisfaction with this value configuration logic. Firm A's more streamlined 'project factory', in turn, showed more variety in terms resource consumption and deviated more often from its original plan in the conceptual design phase. A possible explanation for this is that the conceptual design phase can be more successfully approached by 'architecting' (Brooks, 1995; Maier, 1996; Maier & Rechtin, 2000; Andrews, 2012; Andrews, 2018) instead of a streamlined 'engineering' approach, as the V-model and others suggest.

Fjeldstad & Lunnan (2022) suggest that the chosen value creation model must fit the other strategic choices, e.g., resources and market positioning, of a firm, in addition to factors such as culture and practice. This is also suggested by Porter (1996) as the notion of "strategic fit" between different activities. Thus, when discussing the two firms' value creation logics in the conceptual design phase, the relation and fit to its other activities, its market positioning (target segment and customer interaction types), and its resources must not be neglected. Neither should general time-dependent circumstances be forgotten: In periods with high market activity, firm A reported good experience with the 'project factory' value creation logic. This was possibly due to a high level of similarity between different designs and high project turnaround, which enabled an efficient utilization of personnel and expertise. In this situation it was much easier to divide tasks and standardize interfaces, simply based on prior experiences. Thus, there was much less need for an initial consultation with the customer because the task was assumed clear. In periods with lower market activity and higher demand for unique designs, firm A has been forced to expand into other market segments in order to keep the business going and utilize its personnel. Under such circumstances, the firm lacks the experience needed to standardize the workflow and may also enter projects where the customer wants a unique design. In this situation, the 'project factory' is more problematic.

5 CONCLUSIONS

In this paper, we have characterized a 'ship design firm' as 'a business entity where ship design constitutes the primary value activity and where a significant integration effort takes place'. By this definition, the ship design firm is thus fundamentally different to a shipyard, where ship erection constitutes the primary value generation activity. We have shown that the difference between the two can – in certain cases – also be seen in the value creation logic, i.e., the internal configuration of the firm's activities and personnel: The value creation logic at a shipyard, with relatively well-defined and sequential tasks, can almost always be described as a 'value chain' logic. In contrast, ship design firms – in particular in the concept phase – often operate with less streamlined, iterative problem-solving activities that can be described as a 'value shop' logic. Our two example firms have shown that a seemingly streamlined 'value chain' logic creates friction in the conceptual design phase. A likely reason is that the nature of the problem (Andrews (2011) "wicked"; Pettersen et al. (2018) "ill-structured") conflicts with well-defined and streamlined processes in a 'value chain'. The 'value chain' does, however, work well in ship design when project turnover is high, as it enables an efficient utilization of resources. To exploit these scale effects, it seems to be necessary to have well-defined tasks with clear interfaces. This can be achieved by strategically focusing on projects with a high similarity in the conceptual design phase, or by a higher share of activities in the more well-defined basic design phase.

Our illustrative examples and the discussion are based on the comparison of only two firms. To strengthen or discard our illustrations, a larger number of case studies as well as a quantitative study would seem useful. Moreover, our analysis has primarily focused on the conceptual design phase in both firms. For both firms, a successful concept design is seen as necessary to win projects with a basic design scope. Both firms adapt their value creation logic to the different demand of such projects. However, successfully employing different value creation logics within the same firm and with potentially the same people may pose challenges. The explicit switch between the two logics within the same firm should therefore be further investigated. Finally, we have described the 'as-is' state of two design firms as examples of the two most common value creation logics. In order to improve competitiveness and develop 'to-be' states, the application of the remaining logics 'value network' and 'value access' should be critically examined (Sjåvåg, 2022).

ACKNOWLEDGMENTS

We would like to thank all interviewees for their willingness and openness to share information with the DREAMS project. Moreover, we acknowledge the funding support from the Research Council of Norway under the KSP DREAMS, project number 327047.

CONTRIBUTION STATEMENT

Benjamin Lagemann: Conceptualization; formal analysis; investigation; resources; data curation; writing – original draft; visualization. **Randi Lunnan**: Conceptualization; methodology; writing – original draft; supervision; funding acquisition. **Per Olaf Brett**: Conceptualization; methodology; validation; writing – original draft; supervision; funding acquisition. **Jose Jorge Garcia Agis**: Conceptualization; validation; resources; writing – review & editing; supervision; funding acquisition. **Astrid Vamråk Solheim**: Investigation; writing – review & editing. **Stein Ove Erikstad**: Conceptualization; writing – review & editing; supervision; project administration; funding acquisition.

REFERENCES

Andrews, D. J. (1986). An Integrated Approach to Ship Synthesis. *Transactions of the Royal Institution of Naval Architects*, 73–102.

Andrews, D. J. (1998). A comprehensive methodology for the design of ships (and other complex systems). *Proceedings of the Royal Society of London. Series A: Mathematical, Physical and Engineering Sciences, 454*, 187–211. doi:10.1098/rspa.1998.0154

Andrews, D. J. (2003). Marine design - requirements elucidation rather than requirement engineering. *IMDC 2003: the Eight[h] International Marine Design Conference. 1*, pp. 3–20. Athens: National Technical University of Athens, School of Naval Architecture & Marine Engineering.

Andrews, D. J. (2010). A 150 years of ship design. *International Journal of Maritime Engineering, 152*, A61–A70.

Andrews, D. J. (2011). Marine Requirements Elucidation and the Nature of Preliminary Ship Design. *International Journal Of Maritime Engineering, 153*, 23–39.

Andrews, D. J. (2012). Art and science in the design of physically large and complex systems. *Proceedings: Mathematical, Physical and Engineering Sciences, 468*, 891–912. Retrieved from http://www.jstor.org/stable/41345944

Andrews, D. J. (2015). Systems Architecture is Systems Practice for Early Stage Ship Design. *IMDC 2015: proceedings of the 12th International Marine Design Conference*, *3*, pp. 14–30. Tokyo.

Andrews, D. J. (2018). The Sophistication of Early Stage Design for Complex Vessels. *International Journal of Maritime Engineering, 160*, 1–72. doi:10.3940/rina.ijme.2018.SE.472

Andrews, D. J., & Erikstad, S. O. (2015). State of the Art Report on Design Methodology. *IMDC 2015: proceedings of the 12th International Marine Design Conference*, *1*, pp. 89–105. Tokyo.

Andrews, D. J., Atlar, M., Drake, K., Gee, N., Levander, K., Sen, P., & Snaith, G. R. (1997). IMDC State of the Art Report on Design Methodology. *IMDC'97: the Sixth International Marine Design Conference. 2*, pp. 137–187. Newcastle: Penshaw Press.

Andrews, D. J., Kana, A., Hopman, H., & Romanoff, J. (2018). State of the art report on design methodology. *Marine design XIII: proceedings of the 13th International Marine Design Conference (IMDC 2018). 1*, pp. 3–16. Espoo: Taylor & Francis Group.

Andrews, D. J., Keane, R. G., Lamb, T., Sen, P., & Vassalos, D. (2006). IMDC 2006 State of the Art Report: Design Methodology. *IMDC 2006: the Ninth International Marine Design Conference*, *1*, pp. 77–103. Ann.

Andrews, D. J., Papanikolaou, A., Erichsen, S., & Vasudevan, S. (2009). State of the Art Report on Design Methodology. *IMDC 2009: 10th International Marine Design Conference*, *2*, pp. 537–576. Trondheim.

Asbjørnslett, B. E., Erikstad, S. O., Lagemann, B., & Brett, P. O. (2022). Educating the next generation marine system design engineer – the NTNU perspective. Vancouver. doi:10.5957/IMDC-2022-267

Brett, P. O., Asbjørnslett, B. E., Garcia Agis, J. J., & Erikstad, S. O. (2022). Design Re-Engineering and Automation for Marine Systems. Vancouver. doi:10.5957/IMDC-2022-263

Brett, P. O., Garcia Agis, J. J., Ebrahimi, A., Erikstad, S. O., & Asbjørnslett, B. E. (2022). A rational approach to handle uncertainty and complexity in marine systems design. Vancouver. doi:10.5957/IMDC-2022-270

Brett, P. O., Gaspar, H. M., Ebrahimi, A., & Garcia Agis, J. J. (2018). Disruptive market conditions require new direction for vessel design practices and tools application. *Marine design XIII: proceedings of the 13th International Marine Design Conference (IMDC 2018). 1*, pp. 31–47. Espoo: Taylor & Francis Group. Retrieved from https://www.researchgate.net/publication/325797375_Disruptive_market_conditions_require_new_direction_for_vessel_design_practices_and_tools_application

Brooks, F. P. (1995). *The mythical man-month: essays on software engineering* (Anniversary ed. ed.). Reading, Mass: Addison-Wesley.

Cho, D. S., & Porter, M. E. (1986). Changing Global Industry Leadership: The Case of Shipbuilding. In M. E. Porter (Ed.), *Competition in Global Industries.* Cambridge, Massachusetts: Harvard Business School. Retrieved January 29, 2024, from https://www.academia.edu/2918008/Changing_global_industry_leadership_the_case_of_shipbuilding

Das, T., & Teng, B.-S. (2000). Instabilities of Strategic Alliances: An Internal Tensions Perspective. *Organization Science, 11*(1), 77-101. Retrieved from https://www.jstor.org/stable/2640406

DNV. (2023, 09 11). *Veracity by DNV's Integrated Partner program grows its reach to 35 000 vessels*. Retrieved from DNV: https://www.dnv.com/news/veracity-by-dnv-s-integrated-partner-program-grows-its-reach-to-35-000-vessels-246939

Ebrahimi, A., Brett, P., & Garcia Agis, J. J. (2018). Managing complexity in concept design development of cruise-exploration ships. *Marine design XIII: proceedings of the 13th International Marine Design Conference (IMDC 2018). 1*, pp. 569–577. Espoo: Taylor & Francis Group.

Erikstad, S. O., & Lagemann, B. (2022). Design methodology state-of-the-art report. Vancouver. doi:10.5957/IMDC-2022-301

Fjeldstad, Ø. D., & Haanæs, K. (2001). Strategy Tradeoffs in the Knowledge and Network Economy. *Business Strategy Review, 12*, 1–10. doi:10.1111/1467-8616.00160

Fjeldstad, Ø. D., & Lunnan, R. (2022). *Strategi* (3 ed.). Fagbokforlaget.

Garcia Agis, J. J., Pettersen, S. S., Rehn, C., Erikstad, S. O., Brett, P., & Asbjørnslett, B. E. (2019). Overspecified vessel design solutions in multi-stakeholder design problems. *Research in Engineering Design, 30*(4), 473–487. doi:10.1007/s00163-019-00319-3

Goel, V., & Pirolli, P. (1989). Motivating the Notion of Generic Design within Information-Processing Theory: The Design Problem Space. *AI Magazine, 10*, 19–36. doi:10.1609/aimag.v10i1.726

Maier, M. W. (1996, February). Systems architecting: an emergent discipline? *1996 IEEE Aerospace Applications Conference. Proceedings*, *3*, pp. 231–245. doi:10.1109/AERO.1996.496066

Maier, M. W., & Rechtin, E. (2000). *The art of systems architecting* (2 ed.). CRC Press LLC. Retrieved from https://sdincose.org/wp-content/uploads/2017/10/TheArtOfSystemsEngineering_inaugural.pdf

McGrath, R. G. (2013). *The End of Competitive Advantage: How to Keep Your Strategy Moving as Fast as Your Business.* Boston, Massachusetts: Harvard Business Review Press.

Menon Economics. (2022). *Maritim verdiskapningsrapport 2022.* Retrieved from https://www.menon.no/wp-content/uploads/2022-10-Maritim-verdiskapingsrapport-2022.pdf

Menon Economics. (2023). *Maritim verdiskapningsrapport 2023.* Retrieved from https://www.menon.no/wp-content/uploads/2023-6-Maritim-verdiskapingsrapport.pdf

Miles, R. E., & Snow, C. C. (2003). *Organizational Strategy, Structure, and Process.* Stanford: Stanford University Press.

Nag, R., Hambrick, D. C., & Chen, M.-J. (2007). What is strategic management, really? Inductive derivation of a consensus definition of the field. *Strategic Management Journal, 28*, 935–955. doi:10.1002/smj.615

Olhager, J. (2003). Strategic positioning of the order penetration point. *International Journal of Production Economics, 85*(3), 319-329. doi:10.1016/S0925-5273(03)00119-1

Oxford English Dictionary. (2023). Meaning & use of "firm". Retrieved 1 14, 2023, from https://www.oed.com/dictionary/firm_n2?tab=meaning_and_use#4241186

Pettersen, S. S., Rehn, C. F., Garcia Agis, J. J., Erikstad, S. O., Brett, P. O., Asbjørnslett, B. E., . . . Rhodes, D. H. (2018). Ill-structured commercial ship design problems: The responsive system comparison method on an offshore vessel case. *Journal of Ship Production and Design, 34*, 72–83. doi:10.5957/JSPD.170012

Porter, M. E. (1985). *Competitive Advantage: Creating and Sustaining Superior Performance.* New York, United States: Thre Free Press. Retrieved from http://resource.1st.ir/PortalImageDb/ScientificContent/182225f9-188a-4f24-ad2a-05b1d8944668/Competitive Advantage.pdf

Porter, M. E. (1996). What Is Strategy? *Harvard Business Review*, 37–55. Retrieved October 21, 2023, from https://hbr.org/1996/11/what-is-strategy

Proff. (2023). Retrieved from Proff – The Business Finder: www.proff.no

Semini, M., Gotteberg Haartveit, D. E., Alfnes, E., Arica, E., Brett, P. O., & Strandhagen, J. O. (2014). Strategies for customized shipbuilding with different customer order decoupling points. *Journal of Engineering for the Maritime Environment (Part M), 228*(4), 361–372. doi:10.1177/1475090213493770

Semini, M., Patek, C., Brett, P. O., Agis, J. J., Strandhagen, J. O., & Vatn, J. (2023). Some relationships between build strategy and shipbuilding time in European shipbuilding. *Proceedings of the Institution of Mechanical Engineers, Part M: Journal of Engineering for the Maritime Environment*. doi:10.1177/14750902221141749

Semini, M., Sjøbakk, B., & Alfnes, E. (2013). What to Offshore, What to Produce at Home? A Methodology. In C. Emmanouilidis, M. Taisch, & D. Kiritsis (Ed.), *Advances in Production Management Systems. Competitive Manufacturing for Innovative Products and Services* (pp. 479–486). Berlin: Springer Berlin Heidelberg. Retrieved from https://link.springer.com/chapter/10.1007/978-3-642-40361-3_61

Simon, H. A. (1996). *The sciences of the artificial* (3 ed.). Cambridge, Massachusetts: MIT Press. doi:10.7551/mitpress/12107.001.0001

Sjåvåg, L. (2022). *Considering Alternative Strategies to Improve Synergies between Shipbroker and Ship Designer in Upstream Shipbuilding Activities.* mathesis, Norwegian University of Science and Technology, Trondheim. Retrieved from https://hdl.handle.net/11250/3025987

Stabell, C. B., & Fjeldstad, Ø. D. (1998). Configuring value for competitive advantage: on chains, shops, and networks. *Strategic Management Journal, 19*, 413–437. doi:10.1002/(SICI)1097-0266(199805)19:5<413::AID-SMJ946>3.0.CO;2-C

Thompson, J. (1967). *Organizations in Action: Social Science Bases of Administrative Theory.* New York: Routlege.

Ulstein, T., & Brett, P. O. (2012). Critical systems thinking in ship design approaches. *IMDC 2012: 11th International Marine Design Conference*, *1*, pp. 365–383. Glasgow.

Proceedings of 15th International Marine Design Conference (IMDC-2024)
June 2-6, 2024
Amsterdam, the Netherlands

Sailing through uncertainty: ship pipe routing and the energy transition

B.T. Markhorst[1,*], J. Berkhout[2], A. Zocca[3], J.F.J. Pruyn[45] and R.D. van der Mei[6]

ABSTRACT

The energy transition from fossil fuels to sustainable alternatives makes the design of future-proof ships even more important. In the design phase of a ship, it is uncertain how many and which fuels it will use in the future due to many external factors. In fact, a ship typically sails for decades, increasing the likelihood that it will use different fuels during its lifetime. Pipe route design is expensive and time-consuming, mainly done by hand. Motivated by this, in previous research, we have proposed a mathematical optimization framework for automatic pipe routing under uncertainty of the energy transition. In this paper, we build on the state-of-the-art by implementing design constraints in mathematical models based on discussions with maritime design experts. Additionally, we apply these models to realistic, complex situations of a commercial ship design company. Our experiments show that location-dependent installation costs, which reflect reality, increase the usefulness of stochastic optimization compared to deterministic and robust optimization. Additionally, to prepare for a possible transition to more sustainable fuels, we recommend installing suitable pipes near the engine room upfront to prevent expensive retrofits in the future.

KEY WORDS

Pipe routing; Ship design; Mathematical optimization; Energy transition; Design automation

INTRODUCTION

The maritime industry is responsible for 2-3% of global carbon emissions (International Maritime Organization, 2020). Therefore, new regulations from the IMO and UN state that net zero should be reached by 2050 (International Maritime Organization, 2023). Consequently, ship designers want to consider these measures when designing a new ship. However, Pruyn (2017) states that this is not the case, as most ship owners optimize their ships for the economic situation at the beginning of construction. As a result, ships are not future-proof upon delivery, leading to expensive retrofits in the future.

For sustainability and financial reasons, ship designers must consider future alternative fuels already in the design phase to prevent these retrofits. Using a new fuel typically impacts three essential aspects of a ship: the engine (or the prime mover), the fuel storage, and the pipe routes between them. Although the academic literature elaborately describes the first two aspects (Lindstad et al., 2021; Zwaginga and Pruyn, 2022), the role of pipe routing is not often considered in the academic literature according to Blokland et al. (2023). Automated pipe routing can save time and costs as it is done mainly manually and, consequently, requires over half of the total detail-design labor hours (Park and Storch, 2002). This effort is expected to increase as pipe routing constraints largely depend on the fuel used (Lloyd's Register, 2023).

[1] Stochastics department CWI; Mathematics department VU, Amsterdam, The Netherlands; ORCID: 0000-0002-3383-6862 [2] Mathematics department VU, Amsterdam, The Netherlands; ORCID: 0000-0001-5883-9683
[3] Mathematics department VU, Amsterdam, The Netherlands; ORCID: 0000-0001-6585-4785
[4] Department of Maritime and Transport Technology TU Delft, Delft, The Netherlands; ORCID: 0000-0002-4496-4544
[5] CoE HRTech, Rotterdam University of Applied Science, Rotterdam, The Netherlands
[6] Stochastics department CWI; Mathematics department VU, Amsterdam, The Netherlands; ORCID: 0000-0002-5685-5310 * Corresponding Author: berend.markhorst@cwi.nl

Submitted: 22 February 2024, Revised: 18 April 2024, Accepted: 1 May 2024, Published: 23 May 2024

Conference paper, DOI: https://doi.org/10.59490/imdc.2024.891 e-ISSN: 3050-486

In Markhorst et al. (2023), we have proposed a mathematical optimization framework consisting of three models: deterministic, robust, and stochastic optimization. These models route pipes such that they minimize the sum of the installation and retrofit costs while adhering to (some of) the pipe routing rules from Lloyd's Register (2023). In the following, we explain how we have built these models on the current state-of-the-art and what our academic and practical contributions are.

Literature Two extensive works extensively describe the literature on pipe routing (Asmara, 2013; Blokland et al., 2023). They almost exclusively mention works that do not consider any form of uncertainty. More specifically, in their conclusion, Blokland et al. (2023) suggests to include the energy transition uncertainty in pipe routing models. For this, we can model the problem of connecting multiple tank(s) and engine room(s) in a ship as a Steiner Tree Problem (STP); see Ljubić (2021) for a survey. A stochastic version of this problem is called the Stochastic Steiner Tree Problem (SSTP), for which Bomze et al. (2010); Zey (2016); Leitner et al. (2018) have elaborately described exact solution methods. In Markhorst et al. (2023), we consider a generalization of the SSTP called the Stochastic Steiner Forest Problem (SSFP), which connects multiple independent groups of terminals (i.e., tanks and engine rooms). We have built on Schmidt et al. (2021), who describe exact solution methods for the Steiner Forest Problem (SFP).

Our contributions In this work, we build on the state-of-the-art by implementing design constraints in mathematical models based on discussions with maritime design experts. One of the main conclusions from discussions with these experts is that installation costs largely depend on the location in the ship. We apply the models to realistic, complex situations of a commercial ship design company and study different versions of location-dependent costs, which reflect reality, and their impact on the pipe routes and costs. This work aims to show the power of mathematical optimization in the maritime pipe routing domain.

Outline The rest of this paper is structured as follows. First, we describe the three different models using an illustrative example. Then, we describe the data, the experiments, and the corresponding results. Finally, we formulate our conclusions and sketch directions for future research.

METHODOLOGY

In this section, we formally describe the deterministic and stochastic problem formulation of our pipe routing problem in mathematical terms. To this end, we start with an example that will later show the characteristics of the different models. Then, we continue with the deterministic optimization model and explain why this is a naive benchmark. Finally, we elaborate on the value of adding uncertainty to our models, after which the robust and stochastic optimization models follow. We only sketch the general idea behind the models and refer to Markhorst et al. (2023) for further details.

The translation from maritime design to mathematics

For this work, we consider a ship that sails on diesel but *could* transition to methanol in the future. In the following simplistic example, we assume that the methanol and diesel tanks are placed on the starboard side of the ship and that the engine room is placed on the port side. Schematically, we represent this ship, where each room may contain one or more engines or fuel tanks, as a graph; see Figure 1. For simplicity, we only consider rooms A, B, C, and D in the corresponding graph representation. Additionally, we assume that installing a pipe between adjacent rooms costs €1, except for the connection between room A and E, which costs €0.5, hence an installation cost of €1.5 for the connection between A and D. The undirected graph $G = (\mathcal{V}, \mathcal{E})$ consists of a set of vertices $\mathcal{V}$ (the rooms in a ship) and a set of edges $\mathcal{E}$ (the possible connections between the rooms). Later, we will assume that the ship's graph representation G remains the same when considering future scenarios.

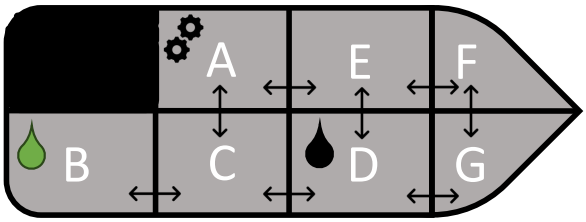

(a) Simplistic top-down view of a ship.

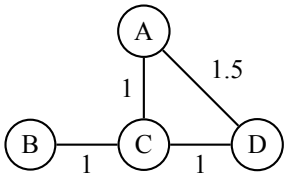

(b) Graph with the first stage installation costs.

Figure 1: Example of the mathematical representation of a ship with 8 rooms. The icons in Figure 1a indicate the function of a room: A denotes the engine room, while C, E, F, and G represent voids, and vertices B and D denote the methanol and diesel tanks, respectively. For simplicity, we only consider rooms A, B, C, and D in the graph representation. The arrows indicate possible pipes and the black square denotes a room through which we cannot route any pipes.

In our problem, we want to connect the fuel tank(s) with the engine room(s). Because we consider different fuel types, we must route according to different rules for pipe routing. For example, diesel pipes cannot be routed through rooms adjacent to water due to regulations from, for example, Lloyd's Register (2023). Consequently, we consider two different terminal groups. One group corresponds to diesel, whereas the other corresponds to methanol. For now, we assume that we only need to connect the diesel tank with the engine room. To do so, we can use a set of types $\mathcal{P}$ denoting the set of feasible pipes for diesel, which are single and double walled pipes in this case. Introducing these sets of pipes allows us to consider different fuel types in the future. The installation cost of a pipe p at a particular edge (u, v) is given by $\gamma_{puv} > 0$.

Due to regulations from Lloyd's Register (2023), we cannot route some dangerous fuel types through certain areas in a ship. For instance, we cannot route diesel through rooms adjacent to the waterside. To model this, we introduce the set of admissible edges, which contains the edges that can be used for the installation of pipes to connect the tank(s) and engine room(s) for the fuel type under consideration. This model choice enables us to consider different fuel types in the future.

Our problem consists of three components: (i) a graph consisting of vertices and (feasible) edges; (ii) a set of (feasible) pipes, which depends on the fuel type under consideration; and (iii) the cost parameters for the installation of a pipe on an edge. A feasible solution connects each terminal group's tank(s) and engine room(s), only uses feasible pipes and edges, and can install pipes in advance that might be redundant for now but may become useful in the future.

Deterministic optimization: a naive benchmark model

Deterministic optimization aims to connect the terminal group's tanks(s) and engine room(s) while only using feasible pipes and edges with as little installation costs as possible. Mathematically, we can formulate the deterministic mathematical optimization problem as

$$\textbf{(DO)} \qquad \min_{\mathbf{S}\in\mathcal{M}(I)} F(I, \mathbf{S}_0, \mathbf{S}) = \min_{\mathbf{S}\in\mathcal{M}(I)} \sum_{(p,(u,v))\in\mathbf{S}\setminus\mathbf{S}_0} \gamma_{puv}. \tag{1}$$

We denote our problem by I and the set of all feasible solutions by $\mathcal{M}(I)$. We introduce the set $\mathbf{S}_0$ of pipe-edge pairs that describe which pipes already exist on which edge to consider previous stages in time. For example, $(p, (u, v)) \in \mathbf{S}_0$ represents pipe p which is installed at edge (u, v). We denote the cost of solution $\mathbf{S} \in \mathcal{M}(I)$ for instance I when pipe-edge pairs $\mathbf{S}_0$ are present by $F(I, \mathbf{S}_0, \mathbf{S})$. In (1), we find the feasible solution with the lowest installation costs that are required to connect each terminal group's tank(s) with the engine room(s). We compute these costs per feasible solution by summing the installation costs of all the pipe-edge pairs that we have to install except for the ones that are already "pre-installed". For deterministic optimization, it holds that $\mathbf{S}_0 = \emptyset$ as no pipes have been pre-installed.

We cannot directly solve the problem described in (1) with (commercial) solvers, but we need the corresponding Integer

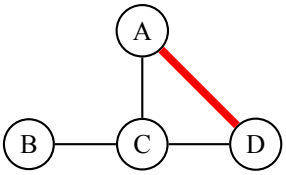

(a) Deterministic optimization.

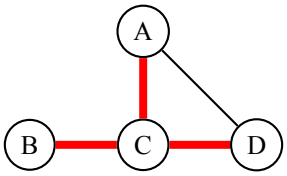

(b) Robust optimization.

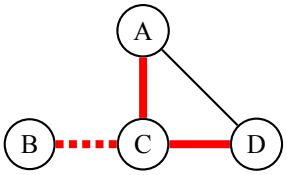

(c) Stochastic optimization for $p_2 = 0.4$.

Figure 2: Optimal pipe routes for Figure 1b according to the three mathematical models. The red solid and dotted lines represent the pipes we installed in the first and second stages, respectively. Note that for simplicity, we have not yet distinguished between single- and double-walled pipes. In Figure 2c, p_2 denotes the probability that the methanol tank must be connected to the engine room. We will discuss these probabilities later.

Linear Optimization (ILO) model. If we apply this model to the pipe routing problem sketched in Figure 1b, we install a pipe on the edge between vertices A and D, as shown in Figure 2a. However, a possible retrofit to methanol would be expensive, especially when installation costs increase, which is typically the case in the maritime industry. Our deterministic optimization model is naive as it does not consider any other (future) scenario than the present. Throughout the rest of this work, this model will mainly serve as a benchmark to compare with the other two models, which will be explained in the following section.

Adding uncertainty is useful for future-proof design

Pruyn (2017) states that ship owners typically design their ships for the current economic situation, leading to future suboptimality. Retrofitting a ship is not preferable as it comes with considerable costs due to its downtime and complex maintenance. To prevent these high costs, ship designers must consider alternative fuels in the design phase.

In practice, however, we do not yet know which alternative fuel will be used in the future as this depends on external factors, such as technology improvements, availability, and future costs (Prussi et al., 2021). To capture this uncertainty over time, we consider two time periods in our framework: the present (i.e., first stage) and the future (i.e., second stage). Figure 3 shows these two stages, of which we know the possible outcomes. For instance, we know the fuel a ship will sail on in the present, typically diesel. However, in the future, this could change to a sustainable alternative, such as green methanol, which has different pipe route requirements than diesel. For instance, it can be routed through rooms next to the waterside and requires double-walled pipes. At each stage, we can install pipes to connect the engine room(s) and the fuel tank(s). Unfortunately, the future outcome is unknown due to uncertainty, adding another layer of complexity to the problem.

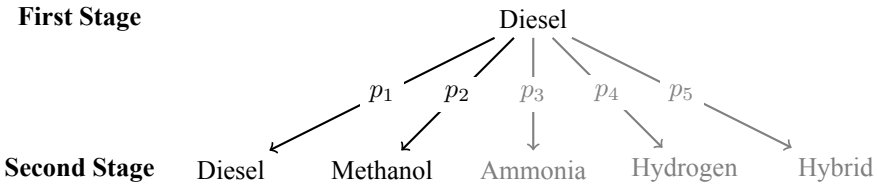

Figure 3: Two-stage scenario tree which describes our problem setting: we start with the diesel scenario in the present, but it is unknown which scenario will take place in the future. We assume that we can install pipes in the first- and second-stage and that we know the probabilities of each future scenario, i.e., p_1 corresponds to the probability of a future diesel scenario. This work only considers two future scenarios, diesel and methanol, which are colored black in the scenario tree. The other scenarios are not studied in this work and are therefore colored gray.

To illustrate the value of considering future scenarios, we use the example from Figures 1 and 2. In the first stage, the ship sails on diesel, whereas in the second stage, it is uncertain whether a transition to methanol is required. As Figure 2a shows, the deterministic optimization model suggests installing a pipe on the edge between the diesel tank (vertex A) and the en-

gine room (vertex D), leading to high second-stage costs in case a transition to methanol takes place. To prevent this situation, we can prepare for the transition by connecting both the diesel and methanol tank (vertices B and D) to the engine room (vertex A), as shown in Figure 2b. We call this way of modeling robust optimization, which is rather expensive and might yield redundant pipes. The route in Figure 2c lies between deterministic and robust optimization. The pipe installation between the void (vertex C) and the methanol tank depends on the probability of the methanol scenario and the installation costs on that edge. This way of modeling is a form of the stochastic optimization model. Although this route seems inefficient for the diesel scenario, it prepares the ship for a possible transition to methanol in the future and balances current and (expected) future costs.

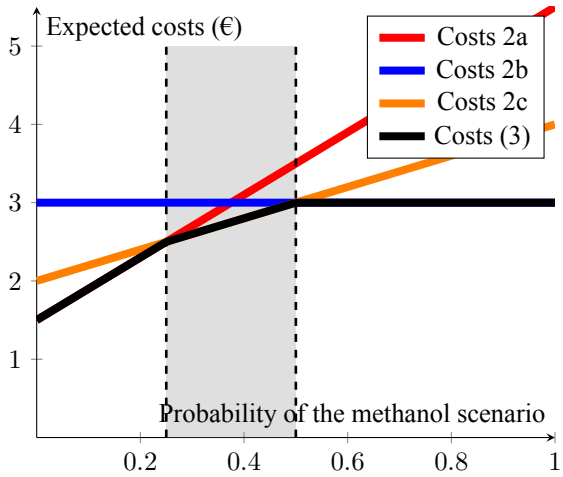

Figure 4: Expected costs of the three routes shown in Figure 2 and the stochastic optimization model (3). As (3) considers the probabilities of the future scenarios, it follows the minimum of the expected costs of the three routes shown in Figure 2.

Figure 4 shows the expected costs of the three pipe routing options for our example on the y-axis and the probability of the methanol scenario on the x-axis. Here, we assume that installing a pipe on an edge in the second stage is twice as expensive as the corresponding first-stage costs. Hence, we can compute the route costs shown in Figure 2a with $1.5 + 4p_2$ where $p_2 \in [0, 1]$ represents the probability of the methanol scenario. In contrast, the robust route costs shown in Figure 2b yield a horizontal line at €3 as the costs do not depend on any probability. Finally, we can compute the costs from the route of Figure 2c with $2 + 2p_2$. The grey dashed area indicates where stochastic optimization outperforms deterministic and robust optimization. Hence, this toy example illustrates that the only way to make the best pipe routing decisions is to explicitly include uncertainty in our mathematical models.

Extending the deterministic model: robust and stochastic optimization

As discussed, we want to include uncertainty in our models. Stochastic optimization (SO) and robust optimization (RO) consider uncertainties and variability in real-world optimization problems, but each follows a different approach. While SO requires distribution information and, in our case, optimizes the *average* case, RO uses the support of the uncertain parameters and optimizes the *worst* case. We refer the reader to Birge and Louveaux (2011); Klein Haneveld et al. (2020) and Ben-Tal et al. (2009); Gorissen et al. (2015) for extensive discussions on SO and RO, respectively. Their application in the context of ship pipe routing is novel.

To model different future scenarios, we introduce a set of second-stage scenarios $s \in \mathcal{S}$, where each scenario corresponds to one fuel type. We can almost exactly reuse the notation for the deterministic optimization model: we only introduce a superscript (s) for scenario s. For example, $I^{(s)}$ denotes a pipe routing problem in scenario s and $\mathbf{S}^{(s)}$ represents the decisions taken in scenario s. The installation costs of a pipe p at a particular edge (u, v) is given by $\gamma^{(s)}_{puv} = \gamma_{puv} \cdot \nu_{uv}$ where $\nu_{uv} \geq 1$ is the increase rate.

Robust Optimization We formulate the robust optimization model in which we anticipate the *worst-case* future scenario as follows:

(RO)

$$\min_{\mathbf{S}\in\mathcal{M}(I)} \left(F(I,\emptyset,\mathbf{S}) + \max_{s\in\mathcal{S}} \min_{\mathbf{S}^{(s)}\in\mathcal{M}(I^{(s)})} \left(F(I^{(s)},\mathbf{S},\mathbf{S}^{(s)}) \right) \right) \tag{2a}$$

$$= \min_{\mathbf{S}\in\mathcal{M}(I)} \Big(\underbrace{\sum_{(p,(u,v))\in\mathbf{S}\setminus\mathbf{S}_0} \gamma_{puv}}_{\text{First stage costs}} + \underbrace{\max_{s\in\mathcal{S}} \min_{\mathbf{S}^{(s)}\in\mathcal{M}(I^{(s)})} \sum_{(p,(u,v))\in\mathbf{S}^{(s)}\setminus\mathbf{S}} \gamma^{(s)}_{puv}}_{\text{Second stage (retrofit) costs}} \Big). \tag{2b}$$

The minimization in (2b) depends on the first- and second-stage costs. For the first-stage costs, we do not have to consider the pipe-edge pairs from the set $\mathbf{S}_0$ as these are pre-installed. For the second-stage costs, we minimize the total installation costs of the worst-case scenario, hence the combination of minimization and maximization. The pipe-edge pairs installed in the first stage can be considered as "pre-installed" in the second stage and do not have to be considered when computing the second-stage costs.

Stochastic Optimization The stochastic optimization problem (SO), which aims to minimize the *sum of expected costs*, can be formulated as:

(SO)

$$\min_{\mathbf{S}\in\mathcal{M}(I)} \left(F(I,\emptyset,\mathbf{S}) + \mathbb{E}_{\mathbb{S}} \left[\min_{\mathbf{S}'\in\mathcal{M}(I^{\mathbb{S}})} \left(F(I^{\mathbb{S}},\mathbf{S},\mathbf{S}') \right) \right] \right) \tag{3a}$$

$$= \min_{\mathbf{S}\in\mathcal{M}(I)} \Big(\underbrace{\sum_{(p,(u,v))\in\mathbf{S}\setminus\mathbf{S}_0} \gamma_{puv}}_{\text{First stage costs}} + \underbrace{\mathbb{E}_{\mathbb{S}} \Big[\min_{\mathbf{S}'\in\mathcal{M}(I^{\mathbb{S}})} \sum_{(p,(u,v))\in\mathbf{S}^{(s)}\setminus\mathbf{S}} \gamma^{(s)}_{puv} \Big]}_{\text{Second stage (retrofit) costs}} \Big), \tag{3b}$$

where $\mathbb{E}$ denotes the expectation and $\mathbb{S}$ represents a discrete random variable for the future scenario with a known distribution, i.e., $\Pr(\mathbb{S} = s)$ is known for all $s \in \mathcal{S}$. The minimization from (3b) differs from (2b) in the second-stage costs. Instead of minimizing the costs of the worst-case scenario, the expected costs over the future scenarios are computed.

RESULTS

We concluded from discussions with maritime experts that pipe installation costs largely depend on the location in the ship. Therefore, we study the impact of a location-dependent cost increase on the pipe route and the corresponding costs. In the following, we elaborate on the used data and then explain the experimental setup. After this, we provide the results of our numerical experiments, including a discussion and analysis of the value for considering uncertainty. To solve the models from (1), (2), and (3) with (commercial) solvers, we use the corresponding ILO formulations.

Ship modelling and data

For this work, we have collaborated with a commercial shipyard company that provided us with data from a state-of-the-art ship consisting of four decks. As it is not trivial to visualize the original data, a 3D network of 75 compartments on the ship and 156 edges, we use four 2D graphs. Figure 5 shows the result, where the vertex colors indicate whether a room contains an engine, a fuel tank, or a void. We have data on the location of diesel and methanol tanks due to the work of Minderhoud (2023). We chose this specific ship as it contains a moonpool, which makes pipe routing more complex as it restricts routes.

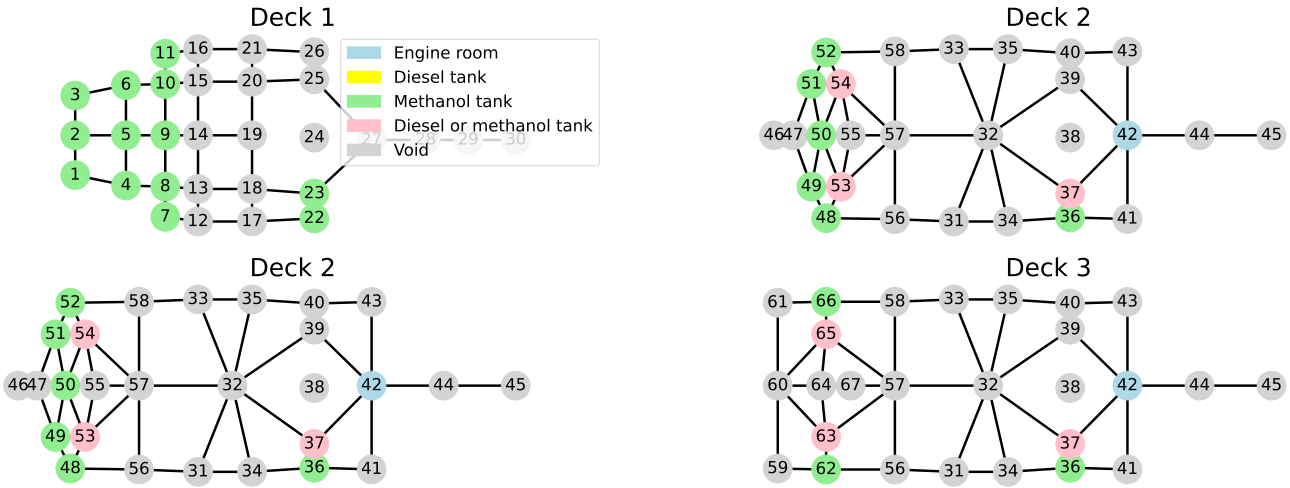

Figure 5: Four 2D graphs representing the data we obtained from the shipyard and Minderhoud (2023). The vertex colors indicate whether a room contains an engine or tank or can be seen as a void, and indicate that there are rooms that can be both diesel and methanol tanks. Note that there are no rooms that can only contain diesel (and no methanol) tanks, hence no vertex is colored yellow. The lines indicate the edges on which we can install pipes. Vertices 24, 38, and 70 correspond to the moonpool.

Similarly to the example in Figure 2, we assume that we start with diesel in the first stage and might transition to diesel or methanol in the second stage. The locations of the diesel and methanol tanks and the engine room are shown in Figure 5. We cannot route diesel pipes through the double bottom or rooms adjacent to the water. Furthermore, we can use single- or double-walled pipes for diesel, but only double-walled pipes for methanol.

Experimental setup

We carried out numerical experiments to study the impact of the cost increase from single- to double-walled pipes (η) and the cost increase from first to second stage (ν_{uv}) on the pipe route and the corresponding costs. First, we use the Manhattan distance between the vertices for the costs γ_{1uv} of installing a single-walled pipe in the first stage, or mathematically: $\gamma_{1uv} = d(u, v)$, where $d(u, v)$ denotes the Manhattan distance between the vertices u and v. We chose this distance measure because it reflects the natural distance a pipe travels. Next, we assume that double-walled pipes are more expensive than single-walled:

$$\gamma_{2uv} = \eta \cdot \gamma_{1uv},$$

where typically $\eta = 2$. However, in our experiments, we will study the impact of η on the pipe route and its corresponding costs. We introduce ν_{uv}, which is the increase rate from first- to second-stage costs for installing a pipe on edge $(u, v) \in \mathcal{E}$:

$$\gamma^{(s)}_{puv} = \nu_{uv} \cdot \gamma_{puv}.$$

The simplest parameter definition for ν_{uv} is a homogeneous cost increase rate, which we assume to be equal to 2 for now

$$\nu_{uv} = 2, \forall (u, v) \in \mathcal{E}, \tag{4}$$

In other words, the increase rate from the first- to the second-stage costs is the same for each pipe-edge pair. As suggested by the maritime experts, it is more realistic to make ν_{uv} dependent on the location in the ship. For example, they suggested that retrofitting the pipe network might be more expensive in rooms adjacent to the engine room or tanks than in a void.

We have incorporated this intuition into two parameter definitions, one only depends on the distance to the engine room whereas the other depends on the function of the rooms. We chose these definitions to study the difference in impact on pipe routes and the costs. First definition looks as follows

$$\nu_{uv} = \frac{\max_{(a,b)\in\mathcal{E}}\{d(a,\mathrm{ER}) + d(b,\mathrm{ER})\}}{d(u,\mathrm{ER}) + d(v,\mathrm{ER})}, \tag{5}$$

where ER denotes the vertex representing the engine room. In (5), the value of ν_{uv} decreases as the distance between ER and the vertices u and v increases. Note that ν_{uv} is always bigger than or equal to 1 for all edges. The intuition behind (5) is that the further an edge lies from the engine room, the lower the complexity of the retrofit and hence the lower the increase rate for the second stage costs. The second definition for ν_{uv} looks as follows:

$$\nu_{uv} = \begin{cases} 6 & \text{if } u \text{ or } v \text{ is ER,} \\ 3 & \text{if } u \text{ or } v \text{ is a tank,} \\ 2 & \text{otherwise.} \end{cases} \tag{6}$$

The intuition behind (6) is that retrofits near the engine room are the most expensive, as many essential elements of the ship are close to each other in a narrow space. Additionally, retrofitting through a tank is expensive as additional safety measures are required for the pipe routing. Finally, routing through a void is cheaper but still relatively expensive, as we should consider the costs of not sailing and the complexity of the installation.

Finally, all experiments are executed on a laptop with four cores and CPU 1.2GHz using the Gurobi solver Gurobi Optimization, LLC (2023) for our Python code, which is available upon request.

Numerical experiments: studying the impact of two cost increase rates (ν_{uv} and η)

In the following, we will divide our numerical experiments, which consist of a parameter study, into two parts: the impact of ν_{uv} and η on the pipe route and the corresponding costs.

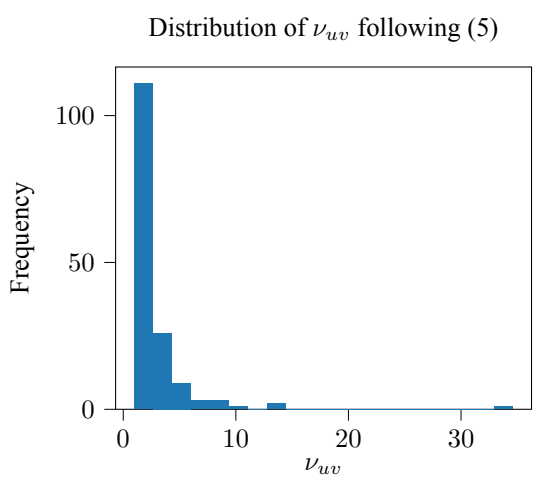

(a) Distribution of ν_{uv} following (5). We see that most edges yield relatively low increase rates, and one extreme value corresponds to the edge (27, 42).

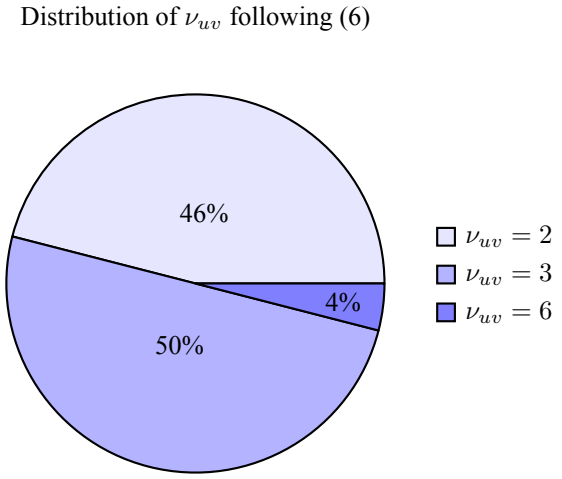

(b) Distribution of ν_{uv} following (6). We see a minority of the edges connected to the engine room and the majority to a fuel tank.

Figure 6: Distribution of the ν_{uv}-values under the two parameter defintions (5) and (6).

Increase rate from first- to second-stage costs (ν_{uv}) The two proposed parameter definitions (5) and (6) yield considerably different distributions for ν_{uv} as shown in Figure 6. In Figure 6a, which displays the values of ν_{uv} on the x-axis and the frequency on the y-axis, we see a skewed distribution, which indicates that most edges have relatively low increase rates, whereas only a few yield extreme values. In Figure 6b, which is a pie chart of the ν_{uv}-values, we see a small number of edges connected to the engine room and many edges connected to a fuel tank.

Recall that we use three parameter definitions for ν_{uv}: (4), (5), and (6). A consequence of these different definitions is a difference in expected costs between the mathematical models as shown in Figure 7, where $\eta = 2$. The three figures display the probability of the methanol scenario on the x-axis, the expected costs on the y-axis, and the three mathematical models colored by different colors. Figure 7a shows that the stochastic optimization model slightly outperforms the deterministic and robust optimization model in a small range of probability values. This gap becomes larger in Figure 7c and even larger in Figure 7b, which shows that the heterogeneity of ν_{uv} yields more cost efficiencies for the stochastic optimization models than for the deterministic and robust optimization models. Hence, we conclude that the value of stochastic optimization is enhanced by heterogeneous cost increase rates.

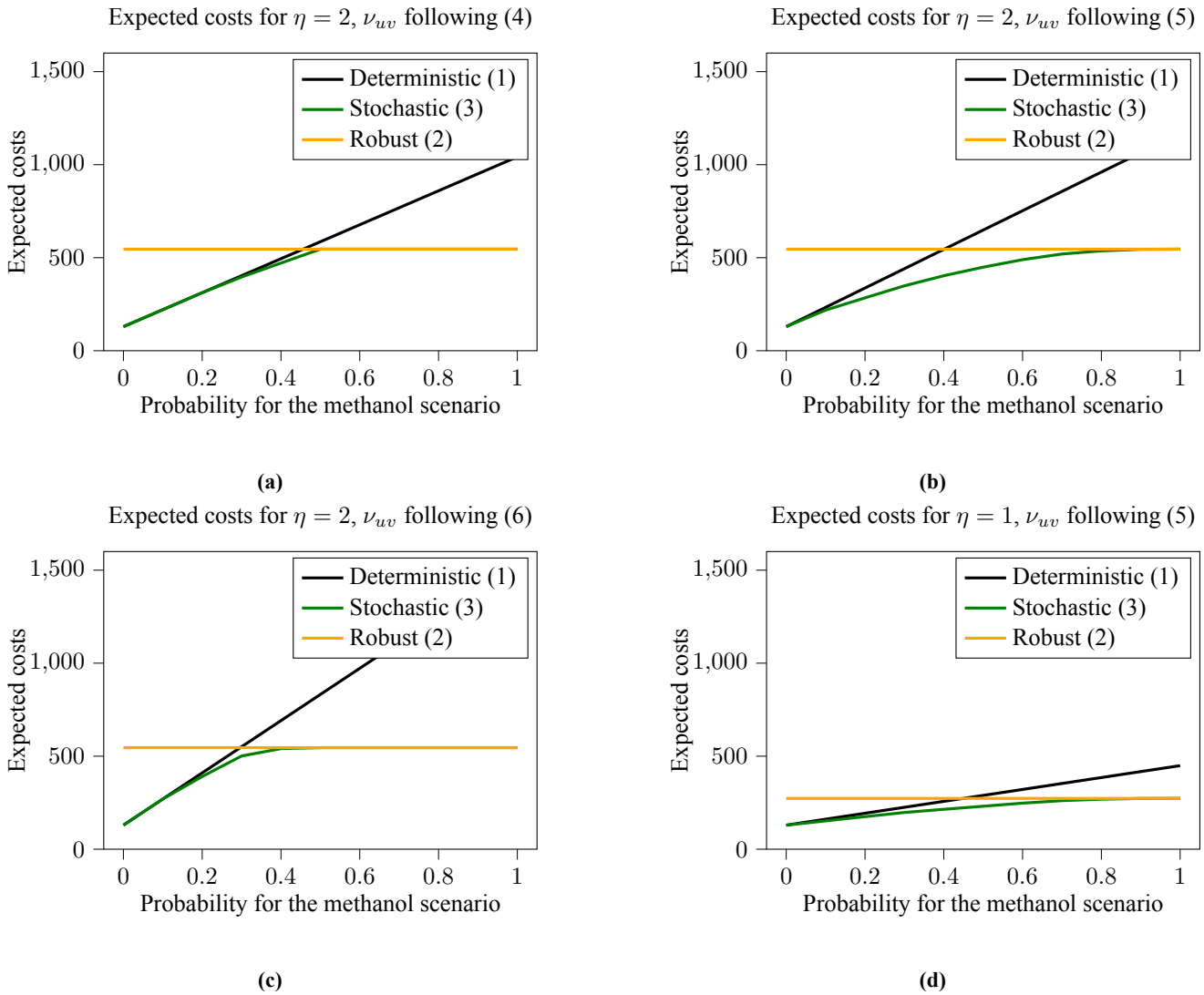

Figure 7: Expected costs of the three mathematical models under different parameter settings. It shows that more heterogeneous cost rates lead to more cost efficiencies for the stochastic optimization models than the deterministic and robust optimization models.

Besides the expected costs of the three models, we are also interested in how the corresponding optimal pipe route looks. Figure 8 shows the result of stochastic optimization with equal probabilities for each future scenario using the parameter settings $\eta = 2$ and ν_{uv} according to (4), (5), and (6). The blue and red lines indicate an installation of a single- or double-walled pipe on the corresponding edge, respectively. The vertex colors tell if a vertex is connected to a lower and/or upper deck via a pipe. We see that the pipes go via the ship's starboard side due to rooms 22, 23, 36, and 37 that contain fuel tanks. We make two observations in Figure 8. First, Figure 8a contains the least pipes and second, does not contain many double-walled pipes. On the other hand, Figure 8c contains the most pipes and already installs double-walled pipes in the double-bottom to prepare for the methanol scenario. In other words, we see that Figure 8b and Figure 8c prepare better for a possible methanol scenario than Figure 8a as shown in the first decks. As Figure 8a is based on homogeneous cost increase rates, they do not differ between edges based on their location in the ship. We already installed double-walled pipes between vertices 17, 22, and 23 in Figure 8b as these are close to the engine room and are relatively expensive to install in the second stage. Additionally, we see a difference in the pipe routes between Figure 8b and Figure 8c. We explain this result using the difference between Figure 6a and Figure 6b, where (5) mostly yields considerably smaller values for ν_{uv} than (6) despite the fact that the outliers from (5) are considerably higher than the highest value for ν_{uv} in (6). Consequently, the second stage becomes more expensive for (6), and stochastic optimization will install more pipes in the first stage to prevent expensive retrofits.

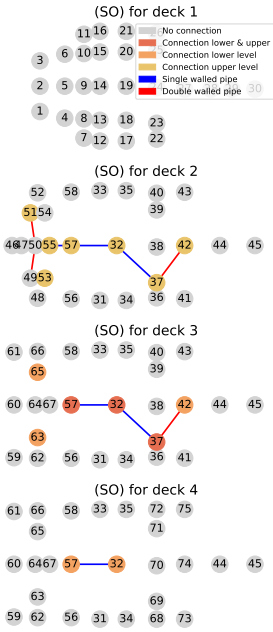

(a) Optimal pipe route when $\eta = 2$ and ν_{uv} follows (4).

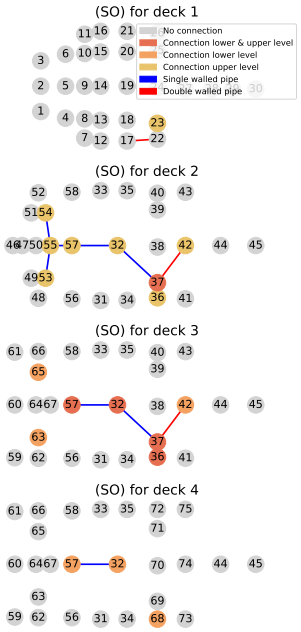

(b) Optimal pipe route when $\eta = 2$ and ν_{uv} follows (5).

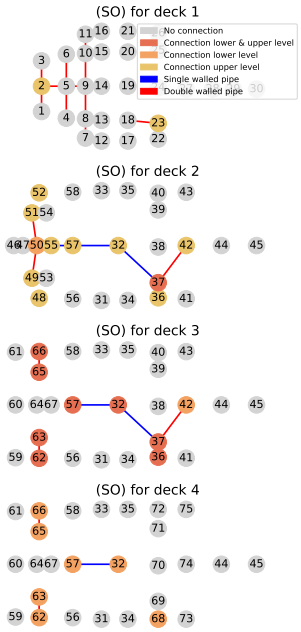

(c) Optimal pipe route when $\eta = 2$ and ν_{uv} follows (6).

Figure 8: Optimal pipe routes based on (3) under different parameter settings with equal probabilities for the two future scenarios. Figure 8a contains the least pipes, whereas Figure 8c contains the most.

Increase rate from single- to double walled pipes (η) To illustrate the findings of the numerical experiments, we compare Figures 7b and 7d, which correspond to ν_{uv} following (5) with $\eta = 2$ and $\eta = 1$, respectively. These values were chosen for simplicity reasons. We see that η positively correlates with the expected costs because it directly impacts both first- and second-stage costs. For example, the costs for robust optimization are considerably higher for $\eta = 2$ in Figure 7b

than for $\eta = 1$ in Figure 7b. Additionally, η influences the relative cost behavior: stochastic optimization still outperforms deterministic and robust optimization, but the range of probabilities under which this happens changes with η. Figures 7b and 7d a larger probability range for $\eta = 1$ than for $\eta = 2$. In other words, when the installation costs of double- and single-walled pipes become more similar, which is realistic, the stochastic solution becomes more powerful compared to deterministic and robust optimization.

CONCLUSION

Motivated by ship pipe routing under the uncertainty of the energy transition, we have applied the mathematical framework to realistic, complex situations of realistic ship data from a commercial ship designer. In collaboration with maritime design experts we have implemented design constraints in these models: deterministic, robust, and stochastic optimization models. Using these models, we analyzed the impact of realistic location-dependent costs for installing pipes on the pipe route and the corresponding costs. For a more elaborate overview of the different models, we refer the reader to Markhorst et al. (2023).

We find that realistic, heterogeneous cost increase rates depending on the location in the ship enforce the usefulness of stochastic optimization compared to deterministic and robust optimization. More specifically, in our experiments, this effect also depends on the relation between double- and single-walled pipe costs. We see this difference in the corresponding optimal pipe routes as well because the rooms containing an engine or tank get considerably more expensive for retrofits in the future. Consequently, we install most pipes near these sensitive areas in the first stage. Our results show the value of considering uncertainty in ship pipe routing for which our models can be used. Discussions with the maritime experts show that our methods can lead to cost reduction and decreased (financial) risk for ship owners. Additionally, our methods allow the engineers to consider various degrees of preparation for the energy transition with limited effort in the early design stage.

Future research could focus on methods that solve larger instances of the SSFP, which enable ship designers to include even more details in the (graph-)data. Furthermore, we could include more constraints from Lloyd's Register (2023), allow multiple fuel types (i.e., hybrid solutions) in one scenario, and include multiple decision stages over time to make the models more realistic. Finally, we could add other piping and cable infrastructure that may interact with the fuel piping system to our optimization models, to further reduce both costs and risks.

CONTRIBUTION STATEMENT

B.T. Markhorst Conceptualization; Methodology; Software; Formal analysis; Investigation; Data Curation; Writing - Original Draft; Visualization **J. Berkhout** Validation; Writing - Original Draft; Writing - Review & Editing supervision; Supervision. **A. Zocca** Writing - Review & Editing; Supervision. **J.F.J. Pruyn** Resources; Writing - Review & Editing; Supervision; Project administration; Funding acquisition. **R.D. van der Mei** Resources; Writing - Review & Editing; Supervision; Project administration; Funding acquisition.

ACKNOWLEDGEMENTS

We thank Jesper Zwaginga, Joris Slootweg, and Ruurd Buijs for their insights and help during this research. Additionally, we thank Henrik van den Heuvel from Royal IHC for his feedback during the project. This publication is part of the project READINESS with project number TWM.BL.019.002 of the research program *Topsector Water & Maritime: the Blue route* which is partially funded by the Dutch Research Council (NWO).

REFERENCES

Asmara, A. (2013). *Pipe routing framework for detailed ship design*. VSSD, Delft. OCLC: 864752777.

Ben-Tal, A., El Ghaoui, L., and Nemirovski, A. (2009). *Robust Optimization*. Princeton University Press.

Birge, J. R. and Louveaux, F. (2011). *Introduction to Stochastic Programming*. Springer Series in Operations Research and Financial Engineering. Springer New York, New York, NY.

Blokland, M., van der Mei, R. D., Pruyn, J. F. J., and Berkhout, J. (2023). Literature Survey on Automatic Pipe Routing. *Operations Research Forum*, 4(2):35.

Bomze, I., Chimani, M., Jünger, M., Ljubić, I., Mutzel, P., and Zey, B. (2010). Solving Two-Stage Stochastic Steiner Tree Problems by Two-Stage Branch-and-Cut. In Cheong, O., Chwa, K.-Y., and Park, K., editors, *Algorithms and Computation*, volume 6506, pages 427–439. Springer Berlin Heidelberg, Berlin, Heidelberg. Series Title: Lecture Notes in Computer Science.

Gorissen, B. L., Yanikoglu, I., and Den Hertog, D. (2015). A practical guide to robust optimization. *Omega*, 53:124–137.

Gurobi Optimization, LLC (2023). Gurobi Optimizer Reference Manual.

International Maritime Organization (2020). Fourth IMO Greenhouse Gas Study. url: https://www.imo.org/en/OurWork/Environment/Pages/Fourth-IMO-Greenhouse-Gas-Study-2020.aspx.

International Maritime Organization (2023). IMO Strategy on reduction of GHG emissions from ships. url: https://wwwcdn.imo.org/localresources/en/MediaCentre/PressBriefings/Documents/Resolution%20MEPC.377%2880%29.pdf.

Klein Haneveld, W. K., Vlerk, M. H. v. d., and Romeijnders, W. (2020). *Stochastic programming: modeling decision problems under uncertainty*. Graduate texts in operations research. Springer.

Leitner, M., Ljubić, I., Luipersbeck, M., and Sinnl, M. (2018). Decomposition methods for the two-stage stochastic Steiner tree problem. *Computational Optimization and Applications*, 69(3):713–752.

Lindstad, E., Lagemann, B., Rialland, A., Gamlem, G. M., and Valland, A. (2021). Reduction of maritime GHG emissions and the potential role of E-fuels. *Transportation Research Part D: Transport and Environment*, 101:103075.

Ljubić, I. (2021). Solving Steiner trees: Recent advances, challenges, and perspectives. *Networks*, 77(2):177–204.

Lloyd's Register (2023). Rules and Regulations for the Classification of Ships. url: https://www.lr.org/en/knowledge/lloyds-register-rules/.

Markhorst, B. T., Berkhout, J., Zocca, A., Pruyn, J. F. J., and van der Mei, R. D. (2023). Robust ship pipe routing: navigating the energy transition. Publisher: arXiv Version Number: 1 DOI: 10.48550/ARXIV.2312.09088.

Minderhoud, M. (2023). A Real Options Approach to determine the Value of Design-for-Conversion under Uncertainty.

Park, J.-H. and Storch, R. L. (2002). Pipe-routing algorithm development: case study of a ship engine room design. *Expert Systems with Applications*, 23(3):299–309.

Prussi, M., Scarlat, N., Acciaro, M., and Kosmas, V. (2021). Potential and limiting factors in the use of alternative fuels in the European maritime sector. *Journal of Cleaner Production*, 291:125849.

Pruyn, J. (2017). Are the new fuel-efficient bulkers a threat to the old fleet? *Maritime Business Review*, 2(3):224–246.

Schmidt, D., Zey, B., and Margot, F. (2021). Stronger MIP formulations for the Steiner forest problem. *Mathematical Programming*, 186(1-2):373–407.

Zey, B. (2016). ILP formulations for the two-stage stochastic Steiner tree problem. arXiv:1611.04324 [cs].

Zwaginga, J. J. and Pruyn, J. F. J. (2022). An Evaluation of Suitable Methods to Deal with Deep Uncertainty Caused by the Energy Transition in Ship Design. In *Day 2 Mon, June 27, 2022*, page D021S003R002, Vancouver, Canada. SNAME.

Proceedings of 15th International Marine Design Conference (IMDC-2024)
June 2-6, 2024
Amsterdam, the Netherlands

The effect of main dimensions on the preliminary design of motor yachts

Francesco Mauro[1,*], Ermina Begovic[2], Enrico Della Valentina[3], Antonino Dell'Acqua[3], Barbara Rinauro[2], Gennaro Rosano[2] and Roberto Tonelli[3]

ABSTRACT

The design process of motor yachts mainly relies on the experience of designers, who have confidence in the knowledge acquired from designing units with similar hull-form characteristics. However, once a new concept needs to be developed, the acquired experience on a standard platform is no longer sufficient to achieve in a short time a successful design. The design of a motor yacht implies considering multiple aspects of ship hydrodynamics: resistance, propulsion, seakeeping, and manoeuvring. Such factors have been widely discussed individually on different kinds of ships, but an appropriate joint investigation of hulls like motor yachts is missing in the open literature. Therefore, the present paper intends to cover this gap, providing guidelines for the design of motor yachts in a length range between 20 and 40 meters. As a preliminary study, a series of 15 yacht hulls has been developed, starting from a reference hull form. Seakeeping, manoeuvring, and propulsive performances have been evaluated at a reference environmental condition and speeds according to the ISO 22834:2022 guidelines. Such calculations allow for developing response surfaces of the hydrodynamic properties for the series of yachts as a function of the hull's main dimensions. As a final result, the obtained responses allow for identifying the best compromise solutions for the main dimension selection of a new motor yacht in the length range of 20-40 meters.

KEY WORDS

Large-yacht; ship design; multi-attribute design; hydrodynamic performances

INTRODUCTION

Designing a motor yacht involves several key considerations, including the size of the yacht, its intended use, materials, propulsion system, interior layout, and aesthetic features. More precisely, it is necessary to identify since the beginning of the project the primary use of the vessel (cruising, entertaining, fishing or a combination of them) to evaluate the operative profile of the large yacht, the estimation of crew and passengers and a preliminary definition of the internal spaces (number of cabins, living rooms, etc.). Afterwards, a crucial part of the design process concerns the estimation of the vessel's size and style. The sizing focuses on the selection of the main dimensions of the unit (length, breadth, draught, and a preliminary estimate of displacement), the style is the design theme of the yacht, which means, as an example, if it is a conventional bow, vertical bow, a sport yacht or an explorer unit (Ansaloni et al, 2024). Subsequently, all the decisions concerning the propulsion system (conventional, podded or hybrid electric solutions) and the definitive hull design need to be taken, before considering the definitive internal layout and the aesthetic of the external shape and interiors (Mancuso & Tumino, 2022, Mauro et al. 2021a). However, for the specific case of concept design, the most essential part is to determine the sizing of the vessel, which means choosing the best combination of hull dimensions leading to a given displacement and granting the achievement of some performance criteria concerning relevant attributes for the vessel (Papanikolaou, 2014, Papanikolaou et al., 2022).

[1] Sharjah Maritime Academy, 180018, Khorfakkan, Sharjah, UAE; ORCID: 0000-0003-3471-9411
[2] Department of Industrial Engineering, University of Naples Federico II, Naples, 80125, Italy
[3] Maritime Research Institute of the Netherlands (MARIN), Haagsteg 2, 6708 PM, Wageningen, the Netherlands.
* Corresponding Author: Francesco.Mauro@sma.ac.ae

Submitted: 23 February 2024, Revised: 2 April 2024, Accepted: 1 May 2024, Published: 26 May 2024

Conference paper, DOI: https://doi.org/10.59490/imdc.2024.904 e-ISSN: 3050-4864

The design is generally based on the designers' confidence in the knowledge acquired from the design of units with the same hull-form characteristics. This approach is worthy once sister units must be built but is not advisable for the development of a new concept. Therefore, general guidelines are needed to achieve a successful new design in a short time.
The design of a motor yacht implies considering multiple aspects of ship hydrodynamics: resistance, propulsion, seakeeping, and manoeuvring, respectively. Such factors have been widely discussed individually on different kinds of ships (Tonelli et al., 2015), but an appropriate joint investigation of small hulls like motor yachts is missing in the open literature. The only guidelines available in the recent literature concern solely the vertical motions in waves (Ivanova & Gyurov, 2022, Begovic et al. 2023a, Begovic et al. 2020) or dedicated studies on the hybrid-electric propulsion (Geertsma et al., 2017, Bucci et al. 2020, Coppola et al. 2022, Begovic et al. 2022) or dynamic positioning of such units (Mauro et al. 2021b). A comprehensive analysis of the effect of different hull forms on the overall hydrodynamic performances of a motor yacht is not yet available, also considering that the relations between hull form parameters and hydrodynamic performance may lead to counteracting solutions while considering, as an example, propulsion or seakeeping characteristics.
To fill the gap between designers' needs and what the actual literature offers, this work presents a preliminary investigation of the effect of main dimensions on the hydrodynamic performance of a motor yacht. The study covers the estimation of some peculiar hydrodynamic attributes of a motor yacht, concerning resistance, seakeeping and manoeuvring characteristics. To this end, it is necessary to build a design space, starting from a reference hull and changing parametrically the main dimensions; here the variations are limited to the length, the breadth and the immersion, keeping, the hull form coefficients constant. With this approach, a design space has been built with the design of experiment techniques, applying a central composite design. From the process, 14 hulls have been derived from the initial hull form, by systematically changing the length, the breadth and the draught. For all hulls, resistance, seakeeping and manoeuvring calculations have been carried out for speed and heading conditions derived from the ISO 22834:2022 guidelines. More precisely, resistance parameters have been calculated with viscous flow CFD calculations. Seakeeping performances have been assessed with a linear 2D strip theory code and manoeuvring performances with rigid-body time domain simulations. The results formed a database of hydrodynamic attributes that can be analysed with multiple linear regression techniques and finally regressions of the attributes as exclusive functions of the main dimension of the vessel have been performed.
The present paper describes in the first section the definition of the design space. Section 2 describes the hydrodynamic calculations performed on the 15 hulls composing the design space. Section 3 reports the multiple linear regression analysis and, finally, section 4 reports an example of the applicability of the obtained regression to identify the effect of hull forms on the hydrodynamic performances of the large-yacht.
The results reported in this paper are promising for the definition of hydrodynamic performances in the early design stage of a motor yacht and encourage future studies on a wider range of hull form variations, including also hull form coefficients.

THE DESIGN SPACE

The present study investigates the hydrodynamic performances of motor yachts for optimal dimension investigations during the concept design phase of a new unit. To this end, it is necessary to develop mathematical instruments, like response surfaces, for capturing the variations of relevant hydrodynamic quantities with the vessels' main dimensions. In this sense, it is necessary to select a reference vessel and a set of geometrical transformations for the main parameters (applying the design of experiments) to form a design space suitable for regression analyses. In the following sections, the reference hull form is described, together with the parametric variations leading to the definition of the 15 hull forms composing the database.

Parent hull form

The reference hull form has been designed specifically for the present study. The main dimensions of the parent hull have been determined based on a preliminary analysis of the yacht database available at MARIN. The main particulars of the hull are listed in Table 1, while the transversal sections of the vessel are given in Figure 1.

Table 1: Reference hull main particulars

Quantity	Value	Quantity	Value
Length between perpendiculars (m)	30.00	Block coefficient (-)	0.563
Length on waterline (m)	29.99	Midship coefficient (-)	0.846
Breadth (m)	7.5	Prismatic coefficient (-)	0.665
Draught (m)	1.625	Waterline coefficient (-)	0.817
Volume (m^3)	205.768	Vertical prismatic coefficient (-)	0.689

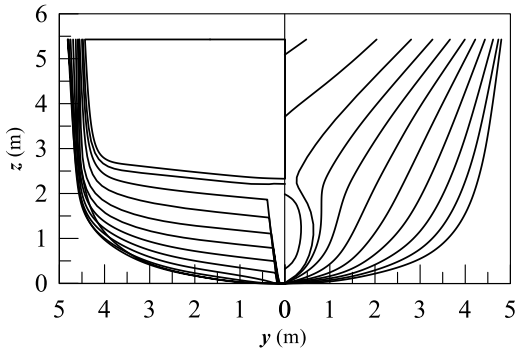

Figure 1: Body sections of the reference hull form.

Table 2: Hull form variations starting from the original hull form.

Hull Number	L_{BP} (m)	B (m)	T (m)	*Volume* (m^3)
HULL 1	20.0	6.0	1.250	84.418
HULL 2	20.0	6.0	2.000	135.068
HULL 3	20.0	9.0	1.250	126.626
HULL 4	20.0	9.0	2.000	202.602
HULL 5	40.0	6.0	1.250	168.835
HULL 6	40.0	6.0	2.000	270.137
HULL 7	40.0	9.0	1.250	253.253
HULL 8	40.0	9.0	2.000	405.205
HULL 9	20.0	7.5	1.625	137.179
HULL 10	40.0	7.5	1.625	274.357
HULL 11	30.0	6.0	1.625	164.614
HULL 12	30.0	9.0	1.625	246.922
HULL 13	30.0	7.5	1.250	158.283
HULL 14	30.0	7.5	2.000	253.253
HULL 15 (original)	30.0	7.5	1.625	205.768

The initial hull represents an example of a yacht that can be used to study parametric variations of the main dimensions ranging from a length of 20 to 40 metres. In the following section, more details are given about the ranges and transformations performed on the reference hull form.

Hull form variations

Starting from the parent hull form, a set of 15 hull forms has been developed by systematically changing the main dimensions. As a simplification, the hull form coefficients have been kept constant and equal to the parent hull, as reported in Table 1. Then, by applying the design of experiment techniques (DoE) (Chang, 2008, Myers et al. 2008), a Central Composite Design (CCD) has been chosen to represent the 15 design variations (Beaver et al, 1977, Montgomery, 2009). The main dimensions of the resulting matrix of hull forms are reported in Table 2 and in Figure 2. The variations performed on the original hull forms led to the following range of main dimensions:

$$\begin{aligned} 20.0 < L_{BP} < 40.0 \\ 6.0 < B < 9.0 \\ 1.25 < T < 2.00 \end{aligned} \qquad [1]$$

This is an approximation that may affect the final results, as coefficients may influence the hydrodynamic performances. From a manoeuvring point of view, the choice of keeping the coefficients constant is in line with typical preliminary studies, as for instance, Clarke's diagram (1977) that shows the dynamic stability boundaries per block coefficient as a function of the length

to breadth L/B and breadth to draught B/T ratio. However, this is a starting point to develop a methodology for the preliminary design stage that may be improved with time by adding more hull form variations considering also changes in the hull form coefficients.

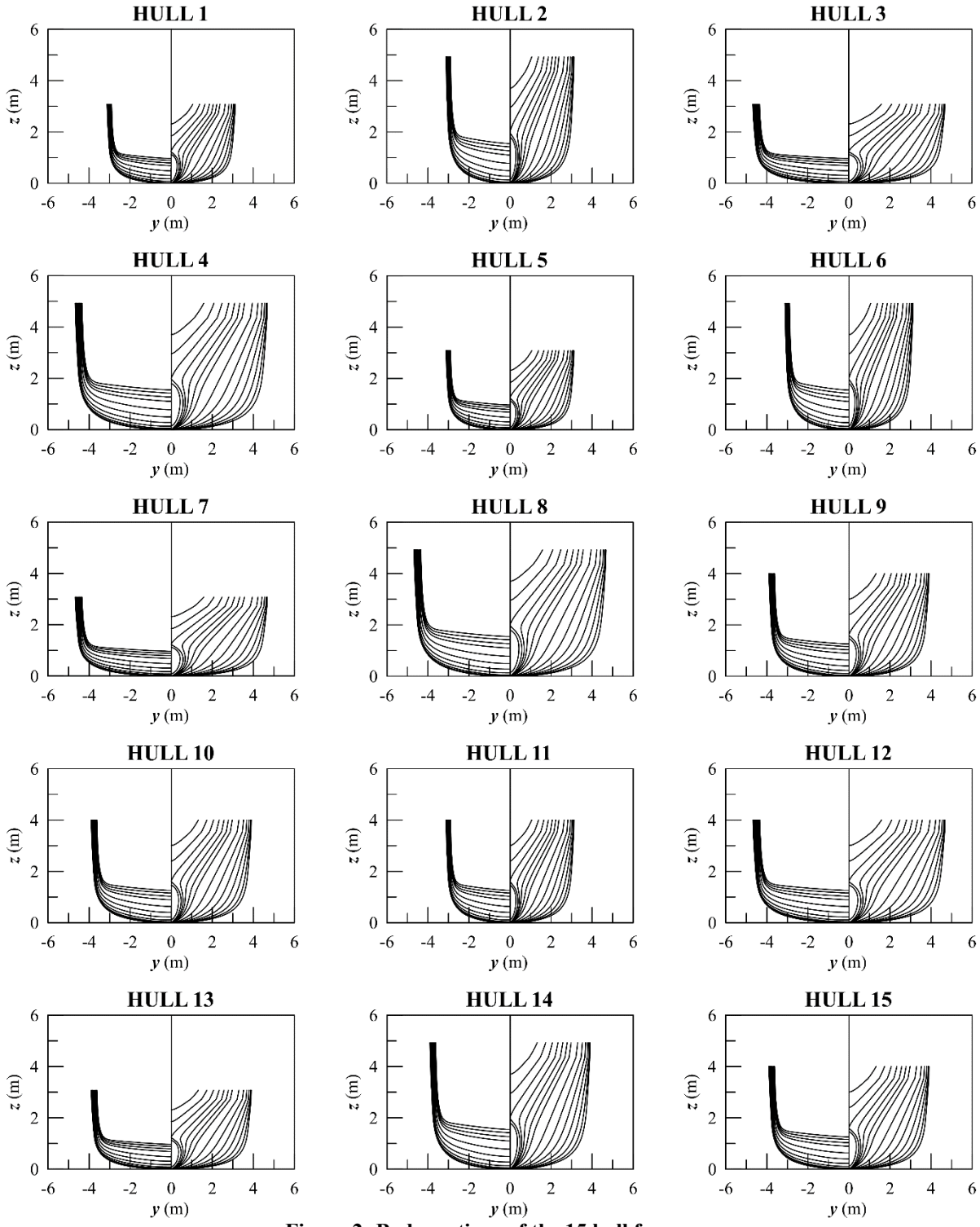

Figure 2: Body sections of the 15 hull forms.

The choice of a CCD design has a consequence on the type of analysis that can be carried out on the resulting hull series. In fact, any attribute relevant to a single hull can be described with at most a full quadratic model. Therefore, having in mind to derive multiple linear regressions on the resulting datasets, such a limitation should be taken into strict consideration as a bound for the research.

HYDRODYNAMIC CALCULATIONS

The crucial part of building design instruments for the preliminary design of a new vessel concerns the reliability of the initial dataset used to form the tools themselves. As such, the modern methodologies employed for the numerical estimation of hydrodynamic performances grant reaching high level of reliability, enhancing the accuracy of initial prediction. In the open literature, it is not common to find methods aiming at preliminary design relying on first-principle calculations
The main aspects to focus on for this study, concerning the hydrodynamics of large yachts, relate to the behaviour of the vessel while sailing in calm water, in waves and during a manoeuvre. Different tools have been used to evaluate the hydrodynamic performances for the specific characteristics needed to describe the behaviour of the vessel. In the specific, for the behaviour in calm water, i.e. resistance and dynamic trim, viscous flow CFD (Computational Fluid Dynamics) calculations have been performed. The behaviour of the vessel in waves has been assessed through strip-theory calculations, with a focus on the comfort characteristics of the yacht. Concerning the manoeuvring, time-domain simulations have been carried out to determine the yaw, checking turning ability of the vessel. In the following sections, a more detailed description of the performed calculations is given together with the parameters selected as principal attributes for the hydrodynamic description of a yacht.

Resistance Calculations

Resistance calculations have been carried out with the MARIN's in-house CFD (package ReFRESCO (https://www.marin.nl/en/facilities-and-tools/software/refresco).ReFRESCO is a community-based, open-access CFD code for the maritime sector. It solves multiphase unsteady incompressible viscous flows using the Navier-Stokes equations, complemented with turbulence models, and volume-fraction transport equations for different phases. The equations are discretised using a finite-volume approach with cell-centred collocated variables. A pressure-correction equation based on the SIMPLE algorithm is used to ensure mass conservation. Time integration is performed implicitly with second-order backward schemes. ReFRESCO is currently being developed, verified and its several applications validated at MARIN in collaboration with several worldwide known non-profit organisations.
The computational grids used in this study were generated using the software Hexpress. Surface refinements were used on the ship hull itself to provide space resolution to resolve the near-wall flow. The surface refinement was then complemented with three groups of boxes, defined to further improve space resolution in the near and far-field flow. The computations were performed at full scale and the computational domain size was chosen sufficiently large to ensure that the influence of the boundary conditions on the flow solution was negligible
For the specific case study, CFD simulations have been carried out in calm water, at a speed of 12 knots and results are presented in terms of total resistance (Larson and Raven, 2010) and dynamic trim. Resistance results include a correlation allowance (C_A) which incorporates the drag due to hull roughness, still-air drag of the hull and superstructures. For the dynamic trim, positive values indicate a bow-down trim, while negative values indicate a stern-down trim.

Seakeeping Calculations

To evaluate the seakeeping characteristics of the developed series of yachts, the new regulation ISO 22834:2022 has been applied to estimate the global comfort level. ISO 22834:2022 considers the Effective Gravity Angle (EGA) and the Motion Sickness Incidence (MSI) as key performance indicators for global comfort, which is afterwards translated into a star rating system ranging from one star (poor) to five stars (excellent). The assessment is performed by evaluating the EGA and MSI, at a reference heading of 135 deg and for speeds of 0 and 12 knots, across five locations along the yacht: the beach club (BC), the crew area (CA), the dining area (DA), the owners' cabin (OC), and the wheelhouse (WH).
The coordinates of the locations onboard the 15 vessels have been assumed according to the reference used by the authors in previous publications (Begovic, et al. 2023a, Mauro et al 2021). Table 3 reports the coordinates used for the calculation in non-dimensional form, as a function of the length between perpendicular L_{BP}, the breadth B and the draught T.

Table 3: Nondimensional coordinates for considered locations.

	BC	CA	DA	OC	WH
x/L$_{BP}$	0.06	0.90	0.43	0.83	0.73
y/B	0.00	0.00	0.00	0.00	-0.23
z/T	1.81	1.09	2.54	3.26	3.99

For all the hulls, the longitudinal position of the centre of gravity has been set to have a zero-trim condition at rest. The vertical position of the centre of gravity has been calculated by taking the transverse metacentric height equal to 10% of the breadth at the waterline, to guarantee a uniform application of seakeeping calculations.
The evaluation of EGA and MSI for each location and speed requires knowledge of the Response Amplitude Operators (RAOs) of the ship motions for the 5 locations at a heading of 135 deg and the speeds of 0 and 12 knots. For this purpose, use has been made of the software ShipX, based on the strip theory as developed by Salvesen et al. (1970).
For each vessel the comfort level has been evaluated according to a number from 0 to 100, reflecting the percentage scale of the star system reported in the ISO rules. The final level of comfort is then assessed with the following weighted sum:

$$ISO_{TOT} = \sum_{i=1}^{2} \sum_{j=1}^{N_l} \sum_{k=1}^{N_{T_z}} w_{v_i} w_{lj} w_{T_{z_k}} I_{ijk} \quad [2]$$

Where w_v, w_l and w_{Tz} are the weights for speed, locations and wave periods, respectively. I is the functional that accounts for the satisfaction of the criteria imposed by ISO 22834:2022. The functional is equal to 1 when both EGA and MSI are under the given thresholds (2 deg for EGA and 10% in one hour of exposure time for MSI). The functional is equal to 0 if at least one criterion is not fulfilled.
To have a more detailed description of the trends in EGA and MSI in different locations, the assessment can be performed also at a local level, considering each location individually and for each sea state, reducing equation (2) to just a summation of the weights for the reference wave periods. Alternatively, the comfort can be assessed globally per each speed, reducing equation (2) to the some of weights for locations and wave periods.
In this study, the global evaluation of comfort given by equation (2) has been considered for the calculations.

Manoeuvring Calculations

To predict the dynamic variation of the motion of a ship, specific manoeuvring simulations have been carried out employing the software ANYSIM XMF. The software computes the motion of a ship resulting from non-linear hydrodynamic and mechanic loading. Ship-specific results from model-test, semi-empirical methods (such as slender body and cross-flow drag theory), and linear frequency domain tools are used for modelling hydrodynamics. Other elements such as rudders, propellers, thrusters, etc. are modelled in the time domain. The equations of motion are integrated through a fourth-order Runge-Kutta method with a fixed time step of 0.1 s. Such a time step is sufficient to have a converged solution. The software can handle the use of both propellers and rudder or pod for the manoeuvring of the vessel.
The simulations need the definition of a linearised stiffness matrix composed of terms derived by the hydrostatics of each one of the 15 hull forms. Besides, the simulations require the definition of a resistance curve or in general a resistance value for the speed of interest. For the specific case of this study, the speed of 12 knots is the target speed for the simulation and the resistance used for the simulation derives directly from the ReFRESCO simulations described in the previous sections. Hydrodynamic forces (damping and added mass) are then computed according to the sectional approach employed in the slender body theory and cross-flow drag theory (Toxopeus, 2006, Hooft, 1994).
The propeller model is based on the B-series, employing for all the hulls the same wake fraction (w=0.05) and thrust deduction (t=0.15). This is a reasonable approximation for the determination of general guidelines for the preliminary design stage.
Simulations performed include speed runs, zig-zag manoeuvres (both 10-10 and 20-20, i.e. the steering-yaw checking angles) and turning circles. The simulation process has been performed in two steps, employing a tuning process for the yaw moment calculated by the slender body theory. The tuning process employs empirical coefficients derived from the correlation between simulations, model tests and sea trials available at MARIN.
From manoeuvring simulations, there are a lot of parameters that can be used as a main attribute for ship design purposes. Between them, particular attention should be given to the initial turning ability and the yaw checking ability. The initial turning ability, also called course-changing ability, describes the responsiveness of the ship to initiate a turn with a moderate helm. The yaw-checking ability is a measure of the ship reaction to counter steering. It is identified by the response delay when reversing the helm angle of a turning ship. The most relevant manoeuvring characteristics related to these abilities are the overshoot angles and the initial turning distance. The overshoot angle is the heading deviation from the moment the steering device is

reversed to the moment the heading rate of turn is zero. The initial turning distance is the distance travelled in the direction of the original course by the ship from the moment the first steering order of, e.g., 20° is given (first execute) to the moment the heading has changed 20° from its original course.

Parameter Selection

The simulations performed to determine the hydrodynamic characteristics of the hulls can define multiple attributes as an output of the simulations. However, to proceed with the definition of the design guidelines for the large-yacht in the preliminary design stage, it has been decided to select a reduced number of attributes. Such a decision aims to give a more focused overview of global attributes for the preliminary design, instead of going too much into capillary details in a phase where most of the final details of the project are not defined yet. In any case, the procedure that will be shown in the next section can be applied to all possible attributes derived from hydrodynamic analyses.
The following attributes have been then selected to proceed with the multiple linear regression analysis:

- Resistance at 12 knots, (kN)
- Trim at 12 knots, (deg)
- Global ISO_{TOT} index for comfort, (-)
- Initial turning ability (from a 20-20 zig-zag manoeuvre), (-)
- Yaw checking ability (from a 20-20 zig-zag manoeuvre), (-)

This set of preliminary attributes grants a comprehensive vision of the operational profile of a motor yacht of small dimensions, capturing issues related to resistance, comfort and manoeuvring. Therefore, the regression analysis has been conducted on the sets of data describing such attributes, by employing a process that will be described in the following section.

MULTIPLE LINEAR REGRESSION ANALYSIS

In the field of engineering, the Design Of Experiments (DoE) is frequently used to analyse the response of a certain variable as a function of others by reducing the number of observations necessary to describe the variations. This results in a lower effort for experimentation or calculation work. In parallel, Response Surface Methodology (RSM) quantifies the relationship between the controllable input parameters and the obtained response variables. To this end, the following working principle should be pursued:

- Design a set of experiments for an adequate and reliable measurement of the analysed response.
- Develop a mathematical model of the response surface by applying a best-fitting technique.
- Represent the direct and interactive effects of processed parameters through multidimensional plots.

The first step has been already tackled by the definition of the design space of the motor yachts, which is choosing a CCD design for the 15 hulls developed in this study. Therefore, it is necessary to better define the mathematical models employed to identify the response surface for the selected parameters for the hydrodynamic properties of the yachts.
A response surface of a generally measurable variable can be identified by the following equation:

$$y = f\left(x_1, \cdots, x_n\right) \tag{3}$$

where y is the output of the process and x_i are the n variables of the problem to describe. Under the assumption that the independent variables are continuous and adherent to experiments with negligible errors, a suitable approximation for the relationship between the independent and the independent variables should be found. Adopting a CCD design, it is possible to use a complete second-order model to describe the surface response, following the subsequent general regression model:

$$y = \beta_{0,0} + \sum_{i=1}^{n} \beta_{i,0} x_i + \sum_{i=1}^{n-1} \sum_{j=i+1}^{n} \beta_{i,j} x_i x_j + \sum_{i=1}^{n} \beta_{i,i} x_i^2 + \varepsilon \tag{4}$$

Where $\beta_{i,j}$ are the unknown parameters and ε is the regression error. In the literature, there are several methods available to evaluate the unknown parameters. However, in the specific case of relatively simple models, it is convenient to employ a least square method. Then, equation (4) can be written in the following matrix form:

$$\mathbf{Y} = \mathbf{bX} + \varepsilon \tag{5}$$

Where **Y** is the matrix of the measured values and **X** is the matrix of the independent values. The matrix of independent variables includes not only the variables themselves but also their combinations up to the second order. The matrices **b** and ε

are the regression coefficients and the errors, respectively. Adopting this matrix formulation, the coefficients matrix can be determined by applying the least square method technique, deriving in the following expression:

$$\mathbf{b} = \left(\mathbf{X}^T\mathbf{X}\right)^{-1}\mathbf{X}^T\mathbf{Y} \quad [6]$$

Where $\mathbf{X}^T$ is the transpose matrix of $\mathbf{X}$ and $(\mathbf{X}^T\mathbf{X})^{-1}$ is the inverse matrix of $\mathbf{X}^T\mathbf{X}$.
For performing the multiple linear regression analysis on the selected dataset of hydrodynamic parameters, use has been made of a stepwise selection process (Harrell, 2001). In the initial step, all the variables are included in the complete second-order model. Afterwards, at each step, a different variable is removed from the equation changing its status (from removed to inserted and vice-versa). For each variable whose status changes, the change in the sum of squared error (SSE) is evaluated and the variable is consequently removed or added to the final model. The process continues automatically until there is no more variable changing the SSE over a given threshold. Moreover, to keep the same threshold in SSE throughout the study, all the dependent and independent variables have been normalised in [-1,1] before starting the regression procedure. Then the threshold is set to 0.06. To judge the quality of the regression, a key performance indicator has to be selected. Here use has been made of the determination coefficient R^2 and the adjusted determination coefficient R^2_{adj}. The coefficients are defined as:

$$R^2 = 1 - \frac{SSE}{SS_{tot}} \quad [7]$$

$$R^2_{adj} = 1 - \left(1 - R^2\right)\frac{n-1}{n-p-1} \quad [8]$$

where n is the number of points to fit, p is the number of variables included in the model (after executing the stepwise procedure) and:

$$SSE = \sum_{i=1}^{n}\left(y_i - y_i^*\right)^2 \quad [9]$$

$$SS_{tot} = \sum_{i=1}^{n}\left(y_i - y_M\right)^2 \quad [10]$$

Being y_i the datapoint to fit, y_M the mean value of datapoint and y_i^* the fitted values derived from the application of regressions. The following section reports in graphical and tabular form the regression performed on the hydrodynamic attributes according to the process that has been here described.

Surface responses

The procedure for determining multiple linear regression and the associated surface responses described in the previous section has been applied to the data processing of the main attributes defined beforehand.
Table 4 reports the results of the regression analysis, reporting the coefficients together with the quality of the regression assessed through the performance indicators described by equations (7) and (8).
From the results reported in Table 4, it is evident that the general quality of the regression is high. All the values for the R^2 are above 0.9 and the unbiased estimator of R^2, the R^2_{adj}, is also high except for the dynamic trim regression. It is interesting to observe that none of the final regressions employ all the estimators of a full quadratic model. Such a matter is the effect of the stepwise iterative procedure used to develop the regression models, which automatically excludes the non-significant terms.
Analysing in detail the individual regressions, for the resistance, it is interesting to observe that the dependence from the vessel length is only linear, no significant higher order, coupled terms are present. Higher order dependency is observed only for the breadth and draught. For the dynamic trim, coupled terms became significant for the length, but still, the higher order is not present. Changing hydrodynamic quantity and going for the analysis of comfort, the regression for the ISO comfort considers all the coupled terms but is missing higher order terms for the length and breadth. The same situation is for the initial turning ability, while for the yawing ability the coupled term between breadth and draught is missing together with all the higher order terms. Such a trend in the significant coefficients does not have a direct explanation for the resulting hydrodynamic properties as the selection of coefficients is purely associated with the automatic selection procedure described in the previous section. It could be possible that with a different dataset as an input to the process, the resulting coefficients would be different, resulting in other conclusions. In fact, even though the multiple linear regression analysis can be classified as a white-box model, the relationship between the data remains difficult to directly analyse the effect of main dimensions on the hydrodynamic properties.

Table 4: Regression coefficients for the hydrodynamic attributes.

	RT	***Trim***	***ISO $_{TOT}$***	***Init_20***	***Yaw_20***
	(kN)	***(deg)***	***(-)***	***(-)***	***(-)***
	Coefficients				
Intercept	5.702E+03	-1.588E+02	5.006E+02	2.718E+00	5.551E+00
L	-1.193E+00	1.061E-01	5.241E+00	1.112E-01	-1.183E-01
B	-1.541E+03	4.122E+01	-5.793E+01	-1.194E-01	-2.756E-01
T	-7.175E+03	1.943E+02	-6.244E+02	-1.327E+00	1.341E+00
LB	-	-7.850E-03	-7.461E-01	-3.208E-03	7.975E-03
LT	-	-2.293E-02	-3.747E+00	-3.443E-02	-2.157E-02
BT	1.954E+03	-5.101E+01	8.821E+01	7.889E-02	-
L^2	-	-	-	-	-
B^2	1.030E+02	-2.667E+00	-	-	-
T^2	2.223E+03	-5.932E+01	1.998E+02	4.459E-01	-
R^2	**0.9526**	**0.9353**	**0.9669**	**0.9687**	**0.9661**
R^2_{adj}	**0.9052**	**0.8189**	**0.9228**	**0.9269**	**0.9407**

On the other hand, having an instrument like the regressions allows for visualising the behaviour of the dependent variables (i.e. the attributes) as a function of the dependent ones (i.e. the ship's main dimensions). Therefore, a particular set of diagrams can be derived to observe the variations of the attributes for a particular set of hull forms. The design space considers hull form variations that keep the coefficients constant. Then, all the hulls having the same volume can be plotted as a single surface in a diagram having *L*, *B* and *T* as principal axes. On this surface, it is possible to visualize in the form of a contour plot the value of a single attribute, highlighting the areas where the main dimensions have a good value for the reference attribute or not. Here, these graphs have been reported for the 5 main hydrodynamic attributes selected for the analysis, using as a reference a project constraint that imposes a reference volume of 225 m^3. The selection of this volume is purely arbitrary and is just a value that allows a good visualisation of the variations of the hydrodynamic properties along with the vessel main dimensions. The response surfaces are reported in Figures from 3 to 7. Figure 3 shows the response surface for the resistance, highlighting the area most favourable for hulls having main dimensions with a length of around 40 metres, breadth of 6.0 metres and draughts ranging between 1.6 and 1.8 metres. Such a combination of values is expected as the slender the ship is the lower is resistance. Figure 4 shows the behaviour of the dynamic trim. Here the behaviour of the data is different compared to the case of resistance, as not only one minimum or maximum are identified. In any case, for the trim the most preferable value for designers is the achievement of a neutral trim; therefore, for the reported surface, the best combinations refer to the saddle points populating the central part of the surface.

Figure 5 shows the response surface for the ISO_{TOT} comfort index. In this case, a maximum of the function is clearly identifiable for combinations of L, B and T around 30-35, 8.5-9.0 and 1.2-1.5 metres, respectively. This area is different compared to the area of minimum for the resistance, confirming that attributes for hydrodynamic characteristics are sometimes antithetic between each other.

Figure 6 highlights the variations of the initial turning ability. Also in this case the most favourable is for the attribute to be clearly identifiable, with a maximum for long and slender ships and a minimum for short slender ships. Such a behaviour is totally opposite to the description of the yaw-checking ability shown in Figure 7. It is interesting to notice that the two attributes related to manoeuvring have antithetic behaviour, that in both cases do not match between optimal regions for resistance or comfort. This would apply even to the turning ability from the turning circle test. This is in fact most likely antithetic to the yaw-checking ability from zig-zag manoeuvres

From this qualitative analysis, it is evident that a designer can make his decisions based on empiricism by just interpreting the graphs with the associated surfaces. However, the adoption of more advanced mathematical techniques can give more quantitative help to designers. In fact, the obtained surfaces can be employed to feed a Multi-Attribute Decision Method (MADM) in order to find the best compromise solution between the given attributes, providing also weightings according to the desiderata of the designer. The following section reports the description and the application of this technique on a reference yacht size.

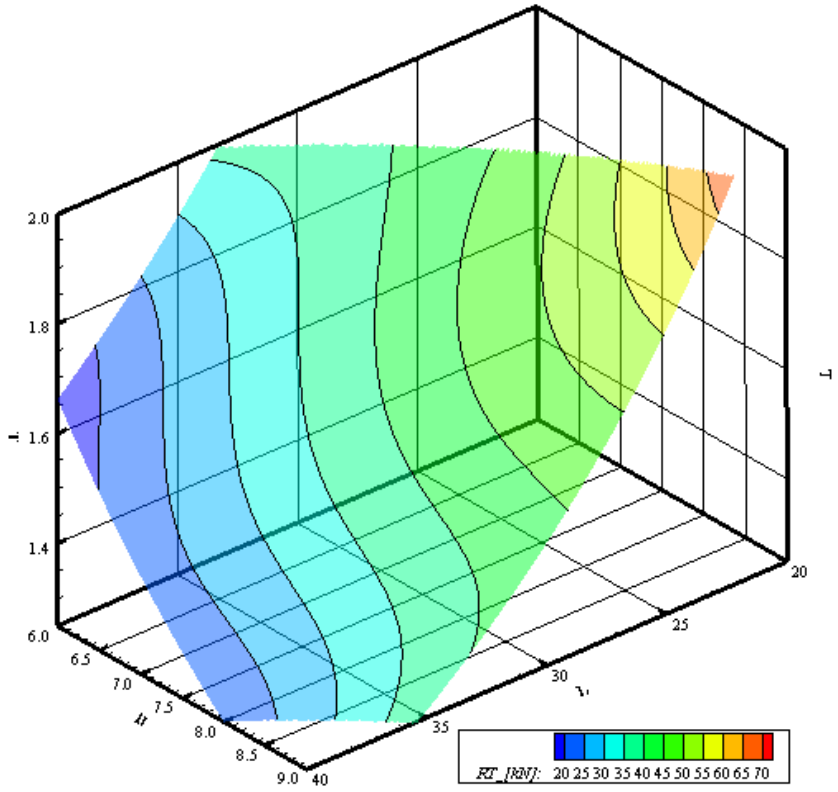

Figure 3: Response surface for the resistance at 12 knots for a hull of 225 m3 of displacement.

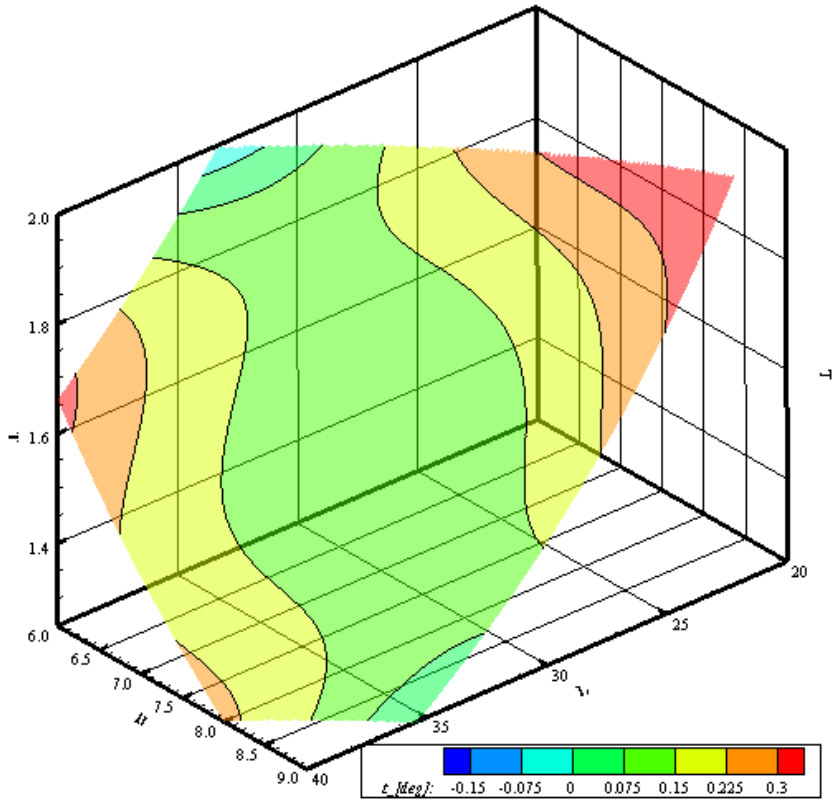

Figure 4: Response surface for the dynamic trim at 12 knots for a hull of 225 m3 of displacement.

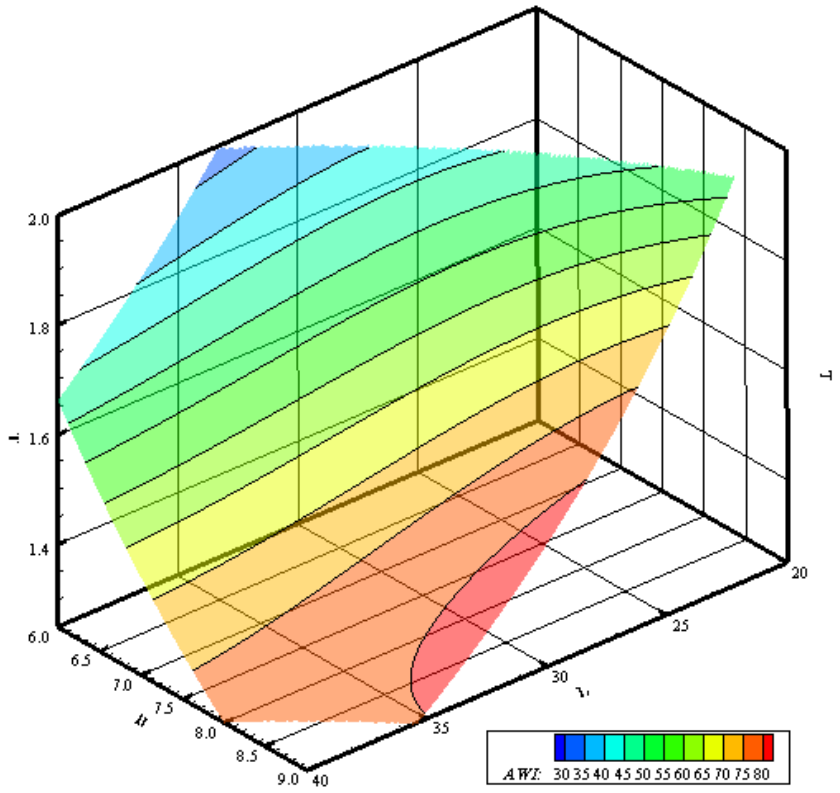

Figure 5: Response surface for the ISO comfort for a hull of 225 m3 of displacement.

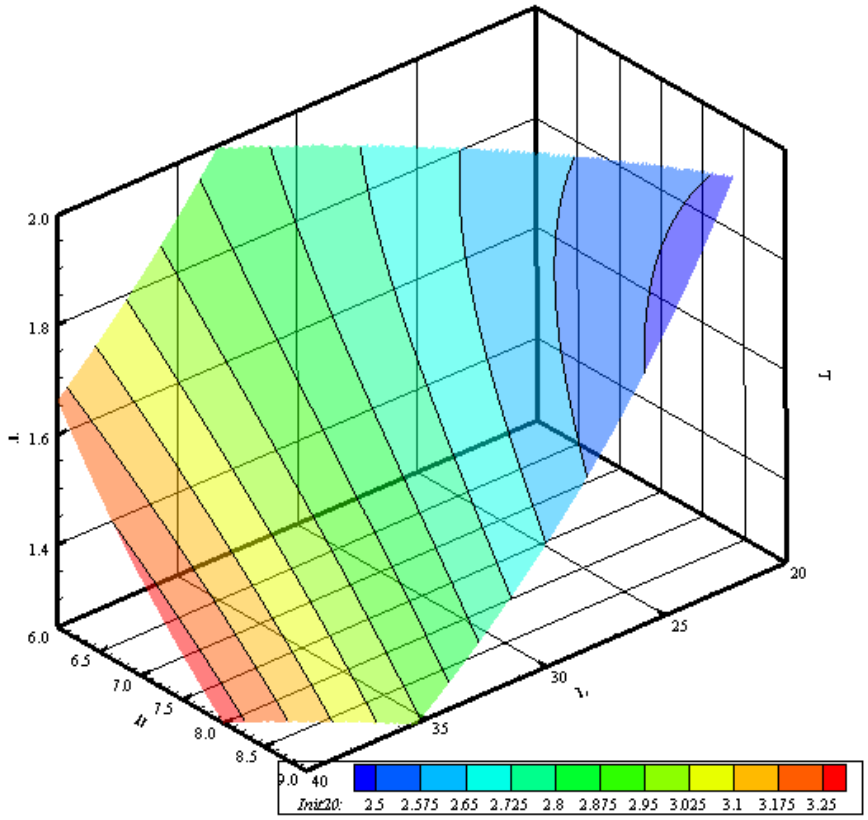

Figure 6: Response surface for the Initial turning ability for a hull of 225 m3 of displacement.

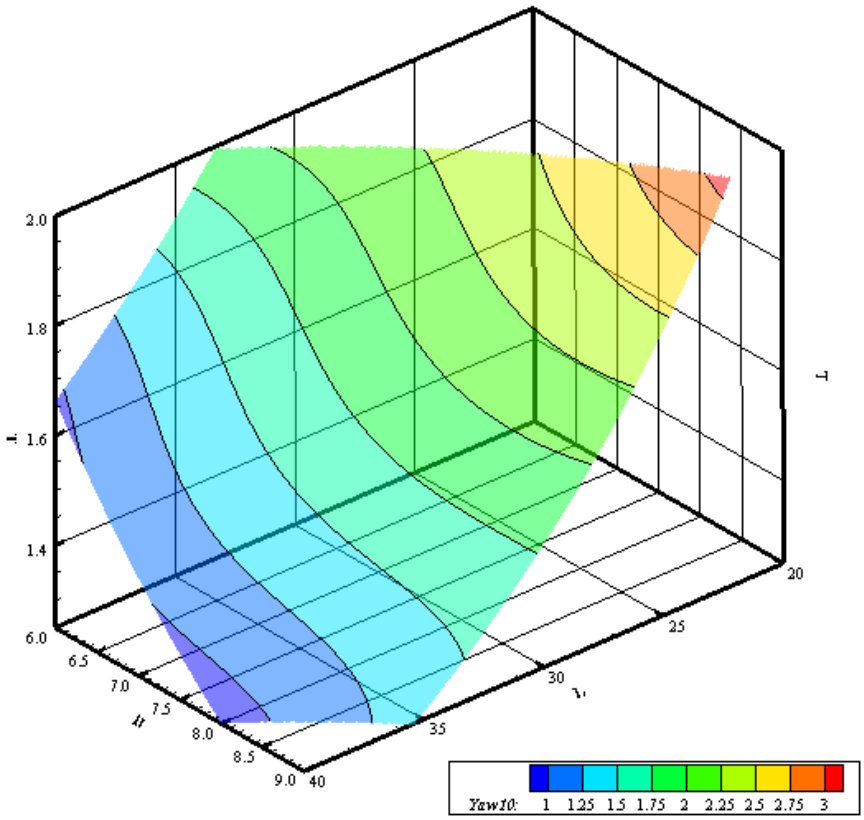

Figure 7: Response surface for the Yaw ability for a hull of 225 m3 of displacement.

APPLICATION TO CONCEPT DESIGN

The concept design of a new vessel implies the handling of different knowledge in Naval Architecture and Marine Engineering, ranging from resistance determination up to the estimation of the structural loads on a ship. As such, the designer should face a multi-criteria environment to find a proper design solution. Due to the complexity of the environment, a proper methodology needs to be applied in the early stages of design. In this respect, Multi-Attribute Decision Making (MADM) stands as an valuable tool for decision-makers facing complex and multifaced choices (Trincas, 2001, Kumar, 2010). In fact, by systematically considering multiple criteria and employing rigorous analysis techniques, MADM enhances the decision-making process, leading to more informed and effective choices in a complex environment as the design of a vessel.

Several methodologies can be employed to select the weighting attribute criteria, the decision matrix and the scoring of the best solutions. The Technique for Order of Preference by Similarity to Ideal Solution (TOPSIS) is one of the possible methodologies that can be applied to the early design of ships as it has been recognised to be simple and effective for the problem (Behzadian et al. 2012).

TOPSIS is based on the concept that the best alternative is the one closest to the positive best ideal solution and the farthest from the negative ideal solution; where the maximum positive represents the best quality for all criteria and the negative the lowest quality. By calculating the proximity of these alternatives to the ideal solutions, TOPSIS assigns a score to each alternative, providing a rank among different solutions. To proficiently work, the TOPSIS procedure needs to go through the following steps:

1. Attribute definition: identifying the project attributes relevant to the design process.
2. Weight assignment: assign relative weights to each attribute according to the designer's preference.
3. Determination of Decision Matrix: normalise all the attributes and multiply them according to the given weights.
4. Determine the Positive and Negative ideal: find the best and worst case according to given weights
5. Rank the solutions: identify through Euclidean distance the closeness of each solution to the ideal and rank the solution accordingly.

The process is quite straightforward and allows for easily determining the rank among different solutions with sufficient flexibility for incorporating the desiderata weights for each attribute in a complex scenario.

While MADM offers valuable insights into complex decision scenarios, it has also a large number of challenges. These may include the data uncertainties, the susceptibility in criteria weighting, and the difficulties in capturing the dynamic nature of the decision environments. Therefore, also the application of these techniques requires an iterative approach and training before defining and refining the best decision model.
The adoption of first-principle tools for the definition of the main hydrodynamic attributes aims at reducing the uncertainties due to the methods employed to generate the initial database. However, even though the regressions show a high accuracy level, the resulting responses are still an approximation of the process and, therefore, the results should be interpreted by the designers with caution. Nonetheless, the implementation of the calculation process, automating the calculations and providing a graphical representation of the output help in streamlining the decision-making process and consequently enhance the efficiency.
In the present section, the TOPSIS process is applied to the example of the large yachts, employing the response surfaces described in the previous sections as an input to generate multiple design solutions for a given design space. For demonstration purposes, the design target is a large yacht with a displacement of 225 m^3. According to the definition of the TOPSIS process, it is necessary to assign weights to the different attributes, to incorporate designers' preferences into the project. For this initial calculation, the weights have been hypothesised to be evenly distributed among the attributes, afterwards they have been arbitrarily changed to reflect different kinds of design strategies. Table 5 reports the weights employed and the results for the main dimension obtained by applying the TOPSIS procedure on a dataset of 10,000 randomly generated projects.

Table 5: Example of TOPSIS procedure for different weighting factors.

Project	Weights [R_T, τ, ISO_{TOT},Init,Yaw]	L [m]	B [m]	T [m]
P1	[0.20;0.20;0.20;0.20;0.20]	39.446	7.857	1.303
P2	[0.20;0.10;0.50;0.10;0.10]	32.107	7.609	1.678
P3	[0.50;0.10;0.20;0.10;0.10]	30.161	7.645	1.725
P4	[0.10;0.10;0.10;0.35;0.35]	37.053	7.007	1.503
P5	[0.60;0.10;0.10;0.10;0.10]	33.595	6.003	1.968

From Table 5, it is evident how different weights identify different main dimensions for the same target displacement of the yacht. It has to be underlined that weights are arbitrary and do not reflect any design strategy derived from yacht designers but they have been used to reflect possible design strategies that favour more attributes related to resistance, comfort or manoeuvrability.
Even though the present method considers only the main dimensions of the yacht, the methodology proposed allows potential designers to make decisions on the main dimensions of a new project intrinsically considering attributes related to resistance, comfort and manoeuvring. Therefore, by adding further hull form variations to the initial dataset it would be possible to increase the flexibility of the current set of regression, by including also hull form parameters variations. In manoeuvring and seakeeping, only the main dimensions are often looked at, considering moreover large variations, and local modifications to the hull are often considered negligible. However, local modifications on the hull lines in the stern could produce different manoeuvring performance. Future studies as described in this paper could bring better insight.

CONCLUSIONS

The present study investigates the possibility of generating response surfaces for ship design purposes on a set of large-yacht hulls. An initial database of 15 hulls has been generated by parametrically changing the main dimensions in a specific range of values and by keeping constant the hull form coefficients. The changes have been performed according to a CCD design. On the resulting set of hull forms, CFD resistance calculations, strip theory seakeeping calculations and time-domain manoeuvring simulations have been carried out to evaluate the hydrodynamic performances of the yachts. Afterwards, multiple linear regression analyses were performed to determine the surface responses of all the hydrodynamic characteristics previously derived by first-principles calculations. Thanks to this process, the resulting responses can be employed in a MADM approach to find the best combination of main dimensions for a yacht having a predetermined target displacement, considering the weighting of attributes.
The resulting response surfaces from the first-principles calculations show the behaviour of the hydrodynamic attributes along with the changes in the main dimension, highlighting the antithetical nature of certain attributes. The developed graphs including the variations of hull form parameters for specific hull displacements could provide help to designers, in identifying the areas where the best solutions for each attribute are located. Besides, the development of response surfaces allows the application of such instruments to the selection process of main parameters through the application of MADM approaches. This allows for identifying the best tuple of dimensions taking into account also different weights among the attributes.

The process developed in this study is just a starting point for subsequent developments, since modifying only the main dimension is not sufficient to have a thorough understanding of the changes of hull forms on the hydrodynamic performances. The hull form coefficients strongly influence the hydrodynamic performances, and, in this case, they are kept constant as a preliminary assumption. Furthermore, progress can be made in the methodologies applied for the determination of the hydrodynamic coefficients, which means applying CFD also for manoeuvring purposes and 3D diffraction codes for seakeeping. Nonetheless, the methodology developed for this study can easily be implemented to a wider dataset that may become available by increasing the number of changes in the hull form generation.
In any case, the findings of this study are the first step to initiate a series of studies oriented to identifying response surface for the hydrodynamic performances of small and large yachts, taking finally into consideration all the aspects of ship hydrodynamics (i.e. resistance/propulsion, seakeeping and manoeuvring) plus additional attributes that are nowadays not included at all in the preliminary design of yachts like the Dynamic Positioning. The present work shows that this path can be pursued by employing the tools and methods described in the paper, ensuring promising results for the following research.

CONTRIBUTION STATEMENT

F. Mauro: Conceptualization; data curation, methodology; calculations, software, supervision, writing – original draft, writing – review and editing. **E. Begovic:** calculations; data curation, supervision; writing – review and editing. **E. Della Valentina:** Supervision **A. Dell'Acqua:** calculations, data curation, writing – review and editing. **B. Rinauro**: calculations, writing – review and editing. **G. Rosano**: calculations, data curation, writing review and editing. **R. Tonelli**: calculations, data curation, writing review and editing.

ACKNOWLEDGEMENTS

The research by MARIN was partially funded by the Ministry of Economic Affairs.

REFERENCES

Ansaloni, G.M.M., Bionda, A., Ratti, A. (2024). The Evolution of Yacht: From Status-Symbol to Values' Source. In: Zanella, F., et al. Multidisciplinary Aspects of Design. Design! OPEN 2022. Springer Series in Design and Innovation , vol 37. Springer, Cham.
Beaver, R., Montgomery, D. (1977). Design and Analysis of experiments. Biometrics, 33, 273-283.
Begovic, E., Della Valentina, E., Mauro, F., Nabergoj, R., Rinauro, B. (2023a), The impact of different bow shapes on large yacht comfort.
Begovic E., Bertorello C., Fasano E., Rinauro B., Rosano G. (2023b) Application of ISO 22834 for Comfort Assessment on a Large Yacht, Progress in Marine Science and Technology, 7, 223–232
Begovic, E., Bertorello, C., Cakici, F., Kahramanoglu, E., Rinauro, B. (2020), Vertical motions prediction in irregular waves using a time domain approach for hard chine displacement hull, Journal of Marine Science and Engineering, 2020, 8(5), 33
Begovic, E., Bertorello, C., De Luca, F., Rinauro, B. (2022), KISS (Keep It Sustainable and Smart): A Research and Development Program for a Zero-Emission Small Crafts, *Journal of Marine Science and Engineering*, 2022, 10(1), 16
Behzadian, M, Otaghsara, S.K., Yazdani, M., Ignatius, J. (2012), A state-of-the-art survey of TOPSIS applications. Expert systems with applications, 39, 13051-13069.
Bucci, V., Mauro, F., Vicenzutti, A., Bosich, D., Sulligoi, G. (2020). Hybrid-electric solutions for the propulsion of a luxury sailing yacht. 2nd IEEE International Conference on Industrial Electronics for Sustainable Energy Systems (IESES).
Chang, H. (2008). A data mining approach to dynamic multiple responses in Taguchi experimental design. Expert Syst. Appl., 35, 1095-1103.
Clark, D. (1977). Consideration of shiphandling in hull design. Conference on Shiphandling. Plymouth, UK. November 1977
Coppola, T., Micoli, L. Russo, R. (2022). Concept design and feasibility study of propulsion system for yacht: innovative hybrid propulsion system fuelled by methanol. International symposium on Power electronics, Electrical Drives, Automation and Motion (SPEEDAM), Sorrento, Italy. 683-688.
Geertsma, R.D., Negenborn, R.R., Visser, K., Hopman J.J. (2017) Design and control of hybrid power and propulsion systems for smart ships. A review of developments. Applied Energy 194, 30-54.
Kumar, D.N. (2010) Multicriterion analysis in engineering and management. PHI Learning Pvt. Ltd.
Harrel, F. (2009). Regression modelling strategies with application to linear models, logistic regression and survival analyses. Springer, New York, NY, USA.

Hooft, J.P. (1994) The cross flow drag on a manoeuvring ship. Ocean Engineering, 21(3), 329-342.
ISO 22834:2022(E) (2022), Large yachts – Quality assessment of life onboard – Stabilization and sea seakeeping.Ivanova, G., Gyurov, G. (2022). Assessment of energy efficiency of a motor yacht depending on routes and sailing area. IOP Conf. Ser.: Mater. Sci. Eng. 1216 012004
Larson, L., Raven, H. (2010). Ship resistance and flow, The Principles of Naval Architecture, Transactions SNAME.
Mancuso A, Tumino D. (2022). Advanced Techniques for Design and Manufacturing in Marine Engineering. Journal of Marine Science and Engineering; 10(2):122.
Mauro F, Ghigliossi E, Bucci V, Marinó A. (2021a). Design of Hybrid-Electric Megayachts: The Impact of Operative Profile and Smart Berthing Infrastructures. Journal of Marine Science and Engineering; 9(2):186.
Mauro, F., Benci, A., Ferrari, V., Della Valentina, E. (2021b). Dynamic Positioning analysis and comfort assessment for the early design stage of large yachts. International shipbuilding Progress, 68, 33-60.
Myers, R., Montgomery, D., Anderson-Cook, C. (2008). Response Surface Methodology-Process and Product optimisation using designed experiments. 3rd edition, Wiley &Sons, Hoboken, NJ, USA.
Montgomery, D. (2009) Design & Analysis of Experiments. 7th edition. J. Wiley and Sons, Hooboken, NJ, USA.
Papanikolaou, A. (2014). Ship Design-Methodologies of Preliminary Design. 1st edition, Springer Dordrecht.
Papanikolaou, A., Harries, S., Hooijmans, P., Marzi, J., Nena, R., Torben, S., Yrjan, A., Boden, B. (2022). A Holistic approach to ship design: tools and applications. Journal of Ship Research, 66, 25-63.
Salvesen N., Tuck E. O., Faltinsen O. (1970), Ship Motions and Sea Loads, Transactions of the Society of Naval Architects and Marine Engineers 78, pp. 250–287.
Tonelli, R., Della Valentina, E., Quadvlieg, F. (2015). Prediction tool for preliminary design assessment of manoeuvring characteristics of a twin screw displacement yacht. 18th International Conference on Ships and Shipping Research, NAV 2015. Lecco, Italy.
Toxopeus, S.L. (2006) Validation of slender-body method for prediction of linear manoeuvring coefficients using experiments and viscous flow calculations. In 7th ICHD International conference of Hydrodynamics, Ischia, Italy, 589-598.
Trincas, G. (2001). Survey of design methods and illustration of multiattributes decision making system for concept ship design. Proceedings of the MARIND 2001, Varna, Bulgaria.

Proceedings of 15th International Marine Design Conference (IMDC-2024)
June 2-6, 2024
Amsterdam, the Netherlands

Operational Matrix Framework for Energy Balance Analysis for Early Stage Design of Complex Vessels

M. H. Mukti[1,*] R. J. Pawling[1], D. J. Andrews[1]

ABSTRACT

Considering vital ship systems or distributed ship service systems at the early stage of complex vessels is a challenging task. The recent UCL Network Block Approach aimed to enable ship designer to address ship systems design synthesis simultaneously as a logical network using MATLAB with a CPLEX Toolbox in MATLAB and representative piping, cabling, and trunking routings on the physical description of the ship using a proven CASD tool PARAMARINE-SURFCON. This was possible due to adopting a set of frameworks, as part of this comprehensive approach. The paper presents one of the frameworks: the Operational Matrix, to formulate distributed ship service systems network in the early stage design of complex vessels. The application of the framework could take on many forms and can be manipulated to suit a specific distributed ship service system's design. In this paper, a tutorial is given, leading from the simplest application of the Operational Matrix Framework to an example of a complex Operational Matrix application for the 3D multiplex submarine systems problem. The use of the proposed Operational Matrix Framework is shown to reveal the relationship between objective functions, constraints, bounds, and solutions of that linear programming formulation. The Operational Matrix Framework can enable the solvers (CPLEX Toolbox in MATLAB) to be very efficient in advancing early stage ship design applications. The Framework could be developed further for investigating the analysis of energy balances for new systems to achieve net zero energy demands for future naval vessels.

KEY WORDS

Distributed Ship Service Systems, Network Theory, Early Stage Ship Design.

NOMENCLATURE

Symbol	Description
α	Coefficient of the objective function for a cable type A
a	The set of all arcs
β	Coefficient of the objective function for a cable type B
b_i	Specific amount of commodity at a node i
$c_{i,j}$	Generic "cost" coefficient in an objective function
$\delta_{i,j}$	Binary variable of an arc i,j
e	Energy coefficient
γ_h	Power flow produced by a hub/path/intermediate node
γ_s	Power flow produced by a source node
γ_t	Power flow produced by a sink/target node
H_{sub}	Hotel load submerged for a submerged submarine
$i \in n$	A node i as a subset of a set of nodes n
$(i,j) \in a$	An arc i,j as a subset of a set of arcs a
$j \in n$	A node n as a subset of a set of nodes n
$k \in K$	An operating scenario index k as a subset of scenarios K
$\lambda_{i,j}$	Power to volume ratio of an arc i,j

[1]Marine Research Group, Department of Mechanical Engineering, University College London, London, UK; ORCID: 0000-0003-3047-1543

* Corresponding Author: hary.mukti@ucl.ac.uk

Submitted: 16 February 2024, Revised: 30 April 2024, Accepted: 1 May 2024, Published: 23 May 2024

Conference paper, DOI: https://doi.org/10.59490/imdc.2024.883 e-ISSN: 3050-486

Symbol	Description
$L(i,j)$	Distance between nodes i and j
$\mu_{i,j}$	Coefficient of the objective function of an arc i,j
$m \in M$	Indexed damage scenario m as a subset of scenarios M
$k \in K$	Indexed operating condition k as a subset of scenarios K
n	The set of all nodes
$OF_{i,j}$	Objective function value of an arc i,j
$P_{i,j}$	Power of an arc i,j
$u_{i,j}$	Flow capacity/variable of an arc i,j
$U_{i,j}$	Flow capacity of an arc i,j
$x_{i,j}/x_{j,i}$	Flowpath or flow variable of an arc i,j or arc j,i
$x_{i,n}$	Flow variable from a node i to node n
$x_{n,j}$	Flow variable from a node n to node j
Y_s	Power flow capacity of a source node
Y_t	Power flow capacity of a target node

1. INTRODUCTION

In the initial sizing of complex vessels, where recourse to type ship design can be overly restrictive, the estimation of the weight and space demands of vital distributed ship service systems has traditionally been poorly addressed (Andrews, 2018). The UCL Network Block Approach (Mukti, 2022) can help the concept designer to consider the impact of different configurations for the distributed ship systems in concept design with more inputs than a parametric approach but fewer assumptions than detailed systems design. This is possible because the UCL Network Block approach combines the use of an architecturally driven ship synthesis approach (Andrews, 2018), and the use of network tool called SUB/RFLOW: SUBFLOW for submarine (Mukti et al., 2021) or SURFLOW for surface ships (Mukti et al., 2024).

SUB/RFLOW was originally derived from the Architecture Flow Optimisation (AFO) (Brown, 2020) and Non-Simultaneous Multi Commodity Flow (NSMCF) (Trapp, 2015). Compared to this previous research, the SUB/RFLOW process is integrated with a 3D CASD tool (Paramarine (Qinetiq, 2019)) for designing ship systems both in terms of the network (logical representation) and the physical representation of piping, cabling, or trunking routings incorporated in the ship. The SUB/RFLOW tool uses network theory and linear programming, with nodes and arcs modelled as a set of linear programming optimisation formulations. These formulations mainly consist of constraints that define the physics of the problem and the objective function to focus the solver to maximise or minimise the solution of the problem (e.g., the multiplication between “cost” and the commodity flow) (Trapp, 2015).

The tools to solve the optimisation can use the standalone CPLEX software (IBM, 2014) or CPLEX toolbox in MATLAB (2019). The use of CPLEX toolbox in MATLAB streamlines the network analysis to be done fully in MATLAB, which allows the use of matrices for defining network properties to be read sequentially and visualised instantaneously in MATLAB. Most importantly, the use of the CPLEX toolbox in MATLAB enables the naval architect to intervene in the network formulation code for CPLEX using a MATLAB programming language (i.e., use of matrix-based computation). This, in turn, can minimise any black-box tendencies in a linear programming formulation as it reveals the interaction between the objective function, constraints, and bounds in the form of several matrices which can be themselves a single matrix, depending on the size of the network problem. Such a matrix is referred to as the Operational Matrix framework in the UCL Network Block Approach (Mukti, 2022). That framework is the focus of this paper and has been proposed to assist the designer by formulating a linear programming description, able to reflect simplified steady state temporal relationship of ship systems and the operating conditions, which has been described as the operational architecture of the ship (Brefort et al., 2018). Also, the Operational Matrix framework could be seen as a subset of the logical architecture, which interacts with a specific operating condition (e.g., loads during sprint submerged and snorting) and a discrete system’s response (i.e., the simplified steady state response of specific distributed ship service systems during those particular operating conditions).

The next section of the paper provides an introduction to the proposed Operational Matrix Framework drawing on network theory. This is followed by design examples and applications of the framework to different Network Flow Optimisation setups. The Operational Matrix for the UCL Network Block Approach is then outlined. Lastly, the paper presents the advantages and limitation of the proposed framework approach and summaries what is novel in the approach through a high level comparison with previous research in the field of ship systems design.

2. THE BASIC FORM OF THE OPERATIONAL MATRIX FRAMEWORK

A network description is a set of points called nodes that are connected by lines called arcs or edges (Newman, 2010) while Network Flow Optimisation (NFO), in its basic form, is a method using linear programming that finds the lowest cost of the flow of a specific distributed commodity from a set of sources to a set of sinks (loads) through a network containing various flows (Trapp, 2015). In the case of the distributed ship service systems, the commodity can be anything that can be modelled in terms of flows, such as electrical power (energy) and data (Brown, 2020), or fluid (gas or liquid) (Trapp, 2015).

In the formulation of the linear programming of the NFO, a prescribed objective function (also called the "cost" function, which is not always the actual currency) is minimised (or maximised) by the solver, subject to constraints. The constraints define the physics of the distributed ship service systems problem in the form of equality and inequality constraints which mathematically define supply and demand limits considerations relevant to the appropriate distributed ship service systems. Thus, the units of the flow are determined and the equations describing the continuity at various supply, demand and distribution or hub nodes are derived to achieve a feasible NFO solution.

Consider a simplistic example of a NFO problem in Figure 1. This system consists of a source node, two distribution (or hub/intermediate) nodes, and a target (or sink/user) node. Described generally, an arc or edge which allows one-way flow from node i to node j is described by (i, j). Let a be the set of all arcs. Each arc (i, j) is limited to $u_{i,j}$ units of flow. There is a "cost" $c_{i,j}$ (not always currency) associated with the rate of flow in each arc of the network. Let n be the set of all nodes. Each node provides a supply or a demand of b_i units of flow. For distribution nodes, $b_i = 0$. For a supply node, $b_i > 0$ and for a demand node $b_i < 0$. The task of the solver is to find the minimum cost flow for the network such that (all) required demand is met. To do this, the solver must minimise total cost of transport over the arcs while accounting for the variation in cost for each arc (see the linear programming formulations in Table 1). To formulate as a linear programming problem, flow variables $x_{i,j}$ are used, where the annotated flow is in arc (i, j). Before there is no flow in the network, the arcs in Figure 1 are shown as thin lines. Lastly, the equation under each node represents the continuity of each node in the system as the set of constraints for the formulation.

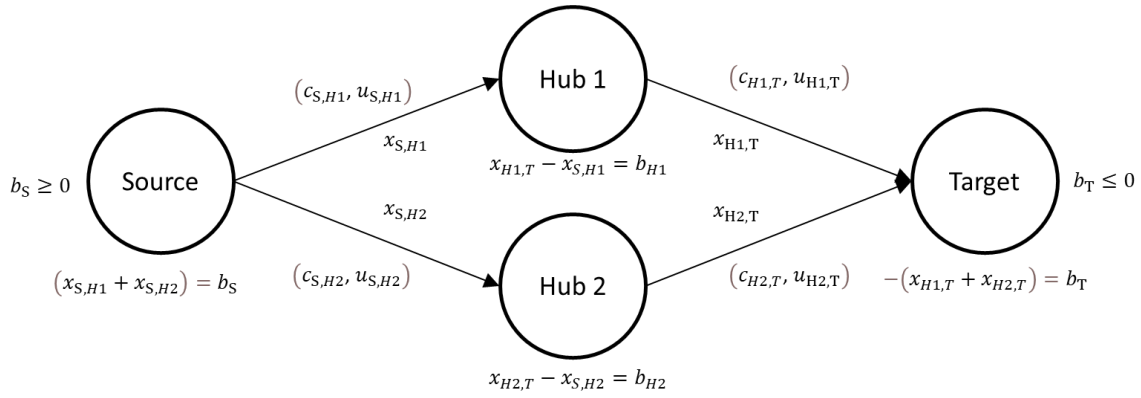

Figure 1: Simple network flow problem

Table 1: Linear programming formulations of Figure 1

Linear Programming Formulation	Mathematical Notation	Realisation
Objective Function	$min. \sum_{(i,j)\in a} c_{i,j}x_{i,j}$	$c_{S,H1}x_{S,H1} + c_{H1,T}x_{H1,T} + c_{S,H2}x_{S,H2} + c_{H2,T}x_{H2,T}$
Subject To:		
Continuity	$\sum_{(i,j)\in a} x_{i,j} - \sum_{(i,j)\in a} x_{j,i} = b_i$	$x_{S,H1} + x_{S,H2} = b_S$ $\quad x_{H1,T} - x_{S,H1} = b_{H1}$ $-x_{H1,T} - x_{H2,T} = b_T$ $\quad x_{H2,T} - x_{S,H2} = b_{H2}$
Bounds	$0 < x_{i,j} \leq u_{i,j}$	$0 < x_{S,H1} \leq u_{S,H1}$ $\quad 0 < x_{H1,T} \leq u_{H1,T}$ $0 < x_{S,H2} \leq u_{S,H2}$ $\quad 0 < x_{H2,T} \leq u_{H2,T}$
Operating Scenario	b_i	$b_S \geq 0$ $\quad b_{H1} = 0$ $\quad b_{H2} = 0$ $\quad b_T \leq 0$
Indices	$(i,j) \in a$	$(S,H1) \in a$ …. $(H2,T) \in a$
	$i \in n$	$S, \dots, T \in n$

Fundamentally, the operational matrix is used to compile all variables in the linear programming formulations into a set of rows and columns of a matrix. The matrix is called "operational" when it is specifically applied to distributed ship service systems subject to appropriate operating conditions, i.e., temporal relationships (as is demonstrated later in this paper). Thus, the operational matrix for the example in Figure 1 is shown in Table 2. The number of columns in Table 2 is given by the quantity of arcs and nodes in the network. Each row provides the "coefficients" in the linear programming formulation. In this example, it consists of the objective function or the cost function (to be minimised), the equality constraint for the continuity (i.e., all flow into and out of the node must equal the supply or demand b_i unit flow at each node), and the bounds limiting the flow to given arc capacities $u_{i,j}$ and ensuring that the flow is unidirectional. The flowpaths or flow variables $x_{i,j}$ are referred to as the set of decision variables. The solver then determines what value each of the variables in $x_{i,j}$ should take in order to minimise (or maximise, whichever is specified) the cost function. The variables in brackets for the equality constraints are not in the actual Operational Matrix. They are there to aid the ship designer's understanding of the framework.

Table 2: A simplistic example of an Operational Matrix Framework

Formulation	Arc 1	Arc 2	Arc 3	Arc 4	Source	Hub 1	Hub 2	Target
Objective function	$c_{S,H1}$	$c_{H1,T}$	$c_{S,H2}$	$c_{H2,T}$	0	0	0	0
Constraints (Equality)	$1(x_{S,H1})$	0	$1(x_{S,H2})$	0	$-1(b_S)$	0	0	0
	$-1(x_{S,H1})$	$1(x_{H1,T})$	0	0	0	$-1(b_{H1})$	0	0
	0	0	$-1(x_{S,H2})$	$1(x_{H2,T})$	0	0	$-1(b_{H2})$	0
	0	$-1(x_{H1,T})$	0	$-1(x_{H2,T})$	0	0	0	$-1(b_T)$
Lower bound	0	0	0	0	0	0	0	0
Upper bound	$u_{S,H1}$	$u_{H1,T}$	$u_{S,H2}$	$u_{H2,T}$	∞	0	0	$-\infty$

As an example, let the node and arc properties are known as summarised in Table 3 and Table 4. The network demands a 10-unit flow at the target node, so each arc is limited to 10-unit flow. For a minimisation problem, flowing through Hub 2 would be more "costly" than Hub1.

Table 3: Node properties of Figure 1

Node	Unit Flow Supply/Hub/Demand b_i	b_i value/bounds
Source	b_S	≥ 0
Hub 1	b_{H1}	0
Hub 2	b_{H2}	0
Target	b_T	-10

Table 4: Arc properties of Figure 1

Arc (i,j)	Cost $c_{i,j}$	Cost $c_{i,j}$ Value	Capacity $u_{i,j}$	Capacity $u_{i,j}$ Value
$(S,H1)$	$c_{S,H1}$	1	$u_{S,H1}$	10
$(H1,T)$	$c_{H1,T}$	1	$u_{H1,T}$	10
$(S,H2)$	$c_{S,H2}$	2	$u_{S,H2}$	10
$(H2,T)$	$c_{H2,T}$	2	$u_{H2,T}$	10

To solve the problem above, the following steps need to be undertaken:

- Generate a network matrix using an adjacency matrix or an adjacency list in MATLAB (see Table 5).
- Plug the numbers outlined in Table 3 and Table 4 into that network matrix (i.e., as network properties in MATLAB), following the format of the Operational Matrix Framework outlined in Table 2.
- The Operational Matrix can then be fed into a solver in MATLAB.
- Once the solver produces a set of flow solutions, this can be stored back in the Operational Matrix in MATLAB (see Table 6).
- Using that Operational Matrix, the system network with the network flow solution can be visualised using MATLAB.

Table 5: The adjacency matrix (left) and the adjacency list (right) of Figure 1

$$\begin{bmatrix} Node & S & H1 & H2 & T \\ S & 0 & 1 & 1 & 0 \\ H1 & 0 & 0 & 0 & 1 \\ H2 & 0 & 0 & 0 & 1 \\ T & 0 & 0 & 0 & 0 \end{bmatrix} \qquad \begin{pmatrix} i & j \\ Source & Hub1 \\ Source & Hub2 \\ Hub1 & Target \\ Hub2 & Target \end{pmatrix}$$

The network flow solution for the problem above is shown in Figure 2.

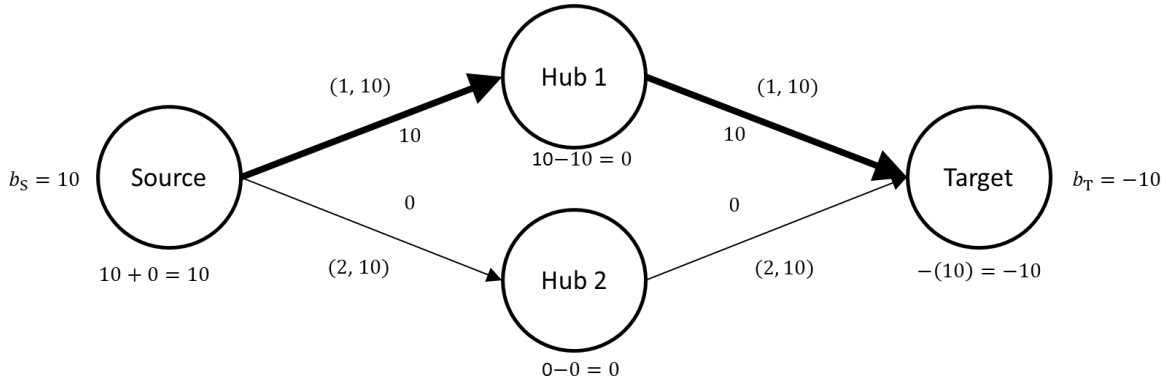

Figure 2: Simple network flow problem solution

As expected, the solver chose Hub 1 since it gives the lowest objective function value. This is 20, rather than 40, which would be the case for flowing through Hub 2. At the Source node, 10 unit flow is produced and leaving the node via arc $(S, H1)$. The continuity can be seen at the Hub 1, where 10 unit flow is entering from $(S, H1)$ and leaving the node to arc $(H1, T)$. Finally, the 10 unit flow commodity is received by the Target node from arc $(H1, T)$. The solutions satisfied the objective function (the lowest value), constraints, and the bounds. This is summarised in Table 6 using the Operational Matrix Framework (see Appendix A for the MATLAB code for this example).

Table 6: Operational Matrix Framework solution of Figure 2

Formulation	Arc 1	Arc 2	Arc 3	Arc 4	Source	Hub 1	Hub 2	Target	=
Objective function	$1(10)$	$1(10)$	$2(0)$	$2(0)$	0	0	0	0	20
Constraints (Equality)	$1(10)$	0	$1(0)$	0	$-1(10)$	0	0	0	0
	$-1(10)$	$1(10)$	0	0	0	$-1(0)$	0	0	0
	0	0	$-1(0)$	$1(0)$	0	0	$-1(0)$	0	0
	0	$-1(10)$	0	$-1(0)$	0	0	0	$-1(-10)$	0
Lower bound	0	0	0	0	0	0	0	-10	0
Upper bound	10	10	10	10	∞	0	0	-10	0

From the simple example above, the general template of the Operational Matrix Framework is given in Table 7. By using the Operational Matrix Framework, the formulation of the Network Flow Optimisation can be manipulated easily by changing the coefficients in the matrix. Understanding the use of the Operational Matrix Framework is essential before modelling, formulating, and dealing with a much larger network that could represent a large number of distributed ship service systems equipment on a vessel (Mukti, 2022). Thus, the next section provides more comprehensive examples and applications of the Operational Matrix Framework.

Table 7: The general template of the Operational Matrix framework

Formulation	Number of Arcs	Number of Nodes
Objective function	Coefficients associated with the LP formulation	
Constraints, such as equality, inequality, and bounds		

3. APPLICATIONS OF THE OPERATIONAL MATRIX FRAMEWORK

To better understand the proposed Operational Matrix Framework, this section presents three examples: the application of the Operational Matrix Framework to a simple "transportation" Non-Simultaneous Multi Commodity Flow (NSMCF) problem (Trapp, 2015); the application of the Operational Matrix Framework to a simplified Power and Propulsion Systems (PPS) submarine (SSK) problem (Mukti et al., 2021); and lastly, the application of the Operational Matrix Framework for a high-level SSK problem (Mukti, 2022).

3.1 Operational Matrix for a simple NSMCF problem

In this section, the use of an operational matrix framework for a simple NSMCF problem is presented. This is given in Figure 3 and the properties of the nodes and arcs in Table 8 and Table 9, respectively. In this example, there are two source nodes (A and E in green); two hub or intermediate nodes (C and D in black); and two user nodes (B and F in red). The top part of Figure 3 shows that the objective function result "OF" is equal to zero, as there is no flow yet in the network. Each arc has objective function "cost" $c_{i,j}$ and flow capacity $u_{i,j}$ in a form of $c_{i,j} * u_{i,j} = OF_{i,j}$. Thus, Figure 3 shows the value of $u_{i,j}$ at each arc is zero before the solver is used.

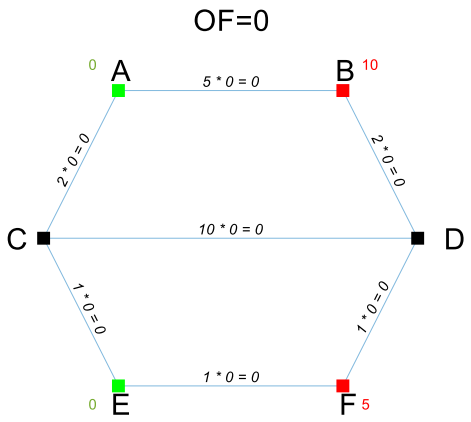

Figure 3: A simple NSMCF network problem(Trapp, 2015) coloured and revisited using the Operational Matrix framework before the NFO solver has been applied in this network

Table 8: Node properties of a simple NSCMF problem in Figure 3 so derived from Trapp (2015) node labelling, node type, and data type were added

Node n	Type	Data	Notation	b_i value/bounds
A or 1	Source	Output	b_A	≥ 0
B or 2	Target	Input	b_B	**10**
C or 3	Hub	Input	b_C	0
D or 4	Hub	Input	b_D	0
E or 5	Source	Output	b_E	≥ 0
F or 6	Target	Input	b_F	**5**

Table 9: Arc properties of the NSCMF network problem in Figure 3 connecting node i to node j outlined in Table 8 so derived from Trapp (2015)

Arc (i,j)	Cost $c_{i,j}$	Cost $c_{i,j}$ Value	Capacity $u_{i,j}$	Capacity $u_{i,j}$ Value
(A,B)	$c_{A,B}$	5	$u_{A,B}$	15
(A,C)	$c_{A,C}$	2	$u_{A,C}$	10
(B,D)	$c_{B,D}$	2	$u_{B,D}$	10
(C,D)	$c_{C,D}$	10	$u_{C,D}$	10
(C,E)	$c_{C,E}$	1	$u_{C,E}$	10
(D,F)	$c_{D,F}$	1	$u_{D,F}$	10
(E,F)	$c_{E,F}$	1	$u_{E,F}$	15

The objective function of this linear programming was to minimise the total value of the multiplication between the objective function coefficient $c_{i,j}$ and arc flow capacity $u_{i,j}$. Compared to the simple Network Flow Optimisation in Figure 1, the flowpath in this problem can be bidirectional, i.e., it can change direction (but only one direction/ non-simultaneous) in an operating condition. This means the flow variable $x_{i,j}$ can be positive or negative. Thus, inequality constraints, known as the 'capacity roll-up' (Trapp, 2015), were required to ensure the flow capacity $u_{i,j}$ is always positive as does the multiplication between the objective function coefficient $c_{i,j}$ and arc flow capacity $u_{i,j}$ regardless the sign (direction) of the flow variable $x_{i,j}$. Such a formulation is summarised in Table 10.

Table 10: The linear programming formulation and the realisation of the simple "transportation" NSMCF problem (Trapp, 2015) are presented in a table form with colour added for the application of the proposed Operational Matrix framework (see Table 11)

Linear Programming Formulation	Mathematical Notation	Realisation		
Objective Function Subject To:	$min. \sum_{(i,j)\in a} c_{i,j}u_{i,j}$	$c_{A,B}U_{A,B} + c_{A,C}U_{A,C} + c_{B,D}U_{B,D} + c_{C,D}U_{C,D} + c_{C,E}U_{C,E} + c_{D,F}U_{D,F} + c_{E,F}U_{E,F}$		
Continuity	$\sum_{(i,j)\in a} x_{i,j} - \sum_{(i,j)\in a} x_{j,i} = b_i$	$1x_{A,B} + 1x_{A,C} = 1b_A$ $-1x_{B,D} - 1x_{C,D} + 1x_{D,F} = 1b_D$	$-1x_{A,B} + 1x_{B,D} = 1b_B$ $-1x_{C,E} + 1x_{E,F} = 1b_E$	$-1x_{A,C} + 1x_{C,D} + 1x_{C,E} = 1b_C$ $-1x_{D,F} - 1x_{E,F} = 1b_F$
Capacity Rollup	$\lvert x_{i,j}\rvert \leq U_{i,j}$	$\lvert x_{A,B}\rvert \leq U_{A,B}$	$\lvert x_{A,C}\rvert \leq U_{A,C}$	$\lvert x_{B,D}\rvert \leq U_{B,D}$
		$\lvert x_{C,D}\rvert \leq U_{C,D}$	$\lvert x_{C,E}\rvert \leq U_{C,E}$	$\lvert x_{D,F}\rvert \leq U_{D,F}$
			$\lvert x_{E,F}\rvert \leq U_{E,F}$	
Bounds	$-\infty \leq x_{i,j} \leq \infty$	$-\infty \leq x_{A,B} \leq \infty$	$-\infty \leq x_{A,C} \leq \infty$	$-\infty \leq x_{B,D} \leq \infty$
		$-\infty \leq x_{C,D} \leq \infty$	$-\infty \leq x_{C,E} \leq \infty$	$-\infty \leq x_{D,F} \leq \infty$
			$-\infty \leq x_{E,F} \leq \infty$	
	$0 \leq U_{i,j} \leq u_{i,j}$	$0 \leq U_{A,B} \leq u_{A,B}$	$0 \leq U_{A,C} \leq u_{A,C}$	$0 \leq U_{B,D} \leq u_{B,D}$
		$0 \leq U_{C,D} \leq u_{C,D}$	$0 \leq U_{C,E} \leq u_{C,E}$	$0 \leq U_{D,F} \leq u_{D,F}$
			$0 \leq U_{E,F} \leq u_{E,F}$	
Operating Scenario	b_i	$b_A \geq 0$	$\mathbf{b_B = 10}$	$b_C = 0$
		$b_D = 0$	$b_E \geq 0$	$\mathbf{b_F = 5}$
Indices	$(i,j) \in a$	$(A,B) \in a \ldots (E,F) \in a$		
	$i \in n$	$A, \ldots, F \in n$		

Using the same procedure as outlined in Section 3.1, the linear programming formulation in Table 10 is then presented as a $[23 \times 21]$ Operational Matrix and outlined in Table 11. The network solution is also included in brackets to understand the relationship between the objective function and the constraints of the linear programming formulation.

The network solution, which consists of values in brackets in the matrix, were divided into three groups based on the number of columns in Table 10. The first seven columns (black) give the flow capacity $U_{i,j}$ values, whereas the second seven columns (blue) give the flow variable $x_{i,j}$ values. The remainder values, which are in columns 15 to 20 (green or red), give the amount of supply or demand of the commodity b_i. The supply values (green) are part of the output while the demand values are part of the predefined input as shown in Table 8.

The first row of the matrix gives the objective function. The values, that are not in the bracket in the first seven columns in this row, provide coefficients $\mu_{i,j}$ for the objective function, and the remaining columns (8 to 20) were set to zero because the flow capacity $U_{i,j}$ (black) was the variable that was minimised, not the flow variable $x_{i,j}$ (blue), nor the commodity b_i (green and red).

Values at rows 2 to 7 and the first seven columns are zero because these rows were given by continuity constraints. Continuity is given by the equality constraints matrix, which consists of rows 2 to 7 and columns 8 to 21 to model six continuity constraints in Table 10. Values +1 and -1 in purple represent coefficients of continuity constraints. The realisation of 'capacity roll-up' (Trapp, 2015) that connects the flow variable $x_{i,j}$ (blue) and the flow capacity $U_{i,j}$ was applied in the inequality constraints matrix located at rows 8 to 23 and columns 1 to 14 and 21. Values -1 (dark orange) in this region indicate coefficients for the capacity roll-up (Trapp, 2015). As this formulation was applied to arcs instead of nodes, the remaining values were seen for the inequality constraints matrix, situated at rows 8 to 21 and columns 15 to 21.

Rows 22 to 23 and columns 1 to 14 show the lower bounds and the upper bounds for the flow capacity $U_{i,j}$ (black) and the flow variable $x_{i,j}$ (blue), respectively. The flow capacity $U_{i,j}$ could be used to limit the possible maximum flow capacity at each arc. However, such a formulation was not used and thus the flow capacity $U_{i,j}$ could be any positive values. Lower bounds and upper bounds that define the supply or demand amount of commodity b_i are located in the same row but in different columns, which are 15 to 20.

Arrows were added to reveal the relationship between various values and coefficients of the linear programming formulation in the matrix. Although all elements (i.e., those without bracket) in the Operational Matrix provide the input of the linear programming formulation, bounds (situated at rows 22 to 23 and columns 15 to 20) are key inputs in this formulation. Therefore, the arrows are originated from this input, which directly constrains the commodity b_i, the flow variable $x_{i,j}$, and then the flow capacity $U_{i,j}$ solutions. The flow capacity $U_{i,j}$ and the flow variable $x_{i,j}$ solutions are also constrained by bounds located at rows 22 to 23 and columns 1 to 14.

Table 11: The Operational Matrix of the basic NSCMF example, showing the simple "transportation" NSMCF example (Trapp, 2015) is presented using the proposed Operational Matrix framework with arrows showing relationships of constraints (see Table 10)

	NO	1	2	3	4	5	6	7	8	9	10	11	12	13	14	15	16	17	18	19	20	21
	1	5 (0)	2 (0)	2 (10)	10 (0)	1 (0)	1 (**10**)	1 (**15**)	0	0	0	0	0	0	0	0	0	0	0	0	0	
					Arcs							Arcs						Nodes				
Objective Function		$\mu_{A,B}U_{A,B}$	$\mu_{A,C}U_{A,C}$	$\mu_{B,D}U_{B,D}$	$\mu_{C,D}U_{C,D}$ $\sum_{(i,j)\in a}\mu_{i,j}U_{i,j}$	$\mu_{C,E}U_{C,E}$	$\mu_{D,F}U_{D,F}$	$\mu_{E,F}U_{E,F}$	$x_{A,B}$	$x_{A,C}$	$x_{B,D}$	$x_{C,D}$	$x_{C,E}$	$x_{D,F}$	$x_{E,F}$	b_A	b_B	b_C	b_D	b_E	b_F	
											$\sum_{(i,j)\in a}x_{i,j}-\sum_{(i,j)\in a}x_{j,i}$							$-b_i$				= 0
Equality constraints matrix for continuity	2	0	0	0	0	0	0	0	1 (0)	1 (0)	0	0	0	0	0	-1 (0)	0	0	0	0	0	0
	3	0	0	0	0	0	0	0	-1 (0)	0	1 (-10)	0	0	0	0	0	-1 (-10)	0	0	0	0	0
	4	0	0	0	0	0	0	0	0	1 (0)	0	-1 (0)	-1 (0)	0	0	0	0	0	0	0	0	0
	5	0	0	0	0	0	0	0	0	0	-1 (-10)	1 (0)	0	1 (-10)	0	0	0	0	0	0	0	0
	6	0	0	0	0	0	0	0	0	0	0	0	-1 (0)	0	1 (15)	0	0	0	0	-1 (15)	0	0
	7	0	0	0	0	0	0	0	0	0	0	0	0	-1 (**-10**)	-1 (**15**)	0	0	0	0	0	-1 (**-5**)	0
								$-1U_{i,j}-1x_{i,j}$														≤ 0
Inequality constraints matrix for bidirectionality	8	-1 (0)	0	0	0	0	0	0	-1 (0)	0	0	0	0	0	0	0	0	0	0	0	0	0
	9	0	-1 (0)	0	0	0	0	0	0	-1 (0)	0	0	0	0	0	0	0	0	0	0	0	0
	10	0	0	-1 (10)	0	0	0	0	0	0	-1 (-10)	0	0	0	0	0	0	0	0	0	0	0
	11	0	0	0	-1 (0)	0	0	0	0	0	0	-1 (0)	0	0	0	0	0	0	0	0	0	0
	12	0	0	0	0	-1 (0)	0	0	0	0	0	0	-1 (0)	0	0	0	0	0	0	0	0	0
	13	0	0	0	0	0	-1 (**10**)	0	0	0	0	0	0	-1 (**-10**)	0	0	0	0	0	0	0	0
	14	0	0	0	0	0	0	-1 (**15**)	0	0	0	0	0	0	-1 (**15**)	0	0	0	0	0	0	0
	15	-1 (0)	0	0	0	0	0	0	1 (0)	0	0	0	0	0	0	0	0	0	0	0	0	0
	16	0	-1 (0)	0	0	0	0	0	0	1 (0)	0	0	0	0	0	0	0	0	0	0	0	0
	17	0	0	-1 (10)	0	0	0	0	0	0	1 (-10)	0	0	0	0	0	0	0	0	0	0	0
	18	0	0	0	-1 (0)	0	0	0	0	0	0	1 (0)	0	0	0	0	0	0	0	0	0	0
	19	0	0	0	0	-1 (0)	0	0	0	0	0	0	1 (0)	0	0	0	0	0	0	0	0	0
	20	0	0	0	0	0	-1 (**10**)	0	0	0	0	0	0	1 (**-10**)	0	0	0	0	0	0	0	0
	21	0	0	0	0	0	0	-1 (**15**)	0	0	0	0	0	0	1 (**15**)	0	0	0	0	0	0	0
								$-1U_{i,j}+1x_{i,j}$														≤ 0
Lower bounds matrix	22	0	0	0	0	0	0	0	$-\infty$	$-\infty$	$-\infty$	$-\infty$	$-\infty$	$-\infty$	$-\infty$	0	-10	0	0	0	-5	
Upper bounds matrix	23	15	10	10	10	10	10	15	∞	∞	∞	∞	∞	∞	∞	∞	-10	0	0	∞	-5	
					$0 \le U_{i,j} \le u_{i,j}$							$-\infty \le x_{i,j} \le \infty$						b_i				

The Operational Matrix solution is visualised as a network. As shown in Figure 4, the multiplication between the "cost" coefficient $c_{i,j}$ and the flow capacity $U_{i,j}$ solution is shown as the label for each arc. Consistent with the Operational Matrix in Table 11, at the top part of Figure 4 the total objective function (OF) value is 45 (i.e., 15 from Arc (E,F) + 10 from Arc (D,F) +20 from Arc (B,D) =45).

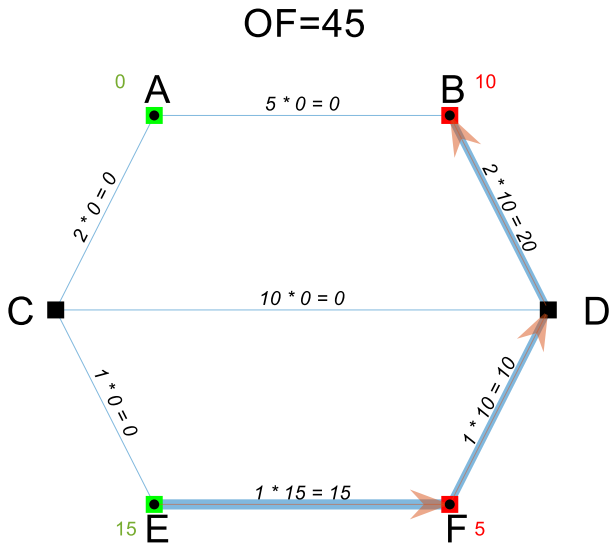

Figure 4: The network flow solution for a simple "transportation" NSMCF network problem from Trapp (2015), revisited using the proposed Operational Matrix framework

The solution shown in Figure 4 would have been different if, for example, Arc (B,D) is unavailable or damaged. This has been referred to as the minus one (M-1) survivability, which guarantees the specified demands in the network can be met with a minimum '"cost" flow although an arc is assumed to be lost (i.e., flow variable $x_{i,j}$ = 0) in a given loss scenario (Trapp, 2015). Thus, if there are seven arcs, as in this example, there are seven arc loss scenarios in the linear programming formulations. Once those formulations are solved, the 'aggregate' solution, which is a term introduced by Robinson (2018), then captures maximum capacity flows in those loss scenarios i.e., an arc from the aggregate solution is sized to accommodate all possible arc flow capacities ($U_{i,j}$) in those loss scenarios. The application of such formulations in the Operational Matrix is now discussed.

To simulate arc loss scenarios for this simple "transportation" NSMCF example, the formulation becomes multicommodity or multiflow conditions (i.e., not just one flow condition as in Figure 4). Thus, more than one set of constraints could be considered where each set of constraints represents an arc loss scenario and would be incorporated in a 'global' objective function (Trapp, 2015). This means the implementation of multiflow conditions would result in a large number of constraints in the Operational Matrix, e.g., rows 7 to 23 and columns 8 to 21 of Table 11 will expand seven fold (i.e., necessary in this example for seven arc loss scenarios). Since this expansion depends on the number of arcs a and number of nodes n in a network problem, theoretically, it can be mathematically described as a $[a^2 \times (a+n)^2]$ matrix. Hence, the scalability of the Operational Matrix for a network with (say) 100 arcs and 50 nodes would be about 10,000 rows and 22,000 columns, which would increase both the designer's workload and the solver computational resources.

Rather than expanding the Operational Matrix from that shown in Table 11, the optimisation was solved individually in each flow situation, using a loop in MATLAB. Thus, the Operational Matrix was repeated seven times (as many as the number of arcs in the network) with a flow variable $x_{i,j} = 0$ for each arc loss scenario. This can be referred to as a "single" flow formulation rather than "multi-commodity" flow formulation. The results are presented in Table 12 for each pair of networks such that the aim (left) are compared with the results of multicommodity formulation from Trapp (2015), which is given in Table 12 (right). In this comparison, some differences were found, more specifically, the flow path of scenarios (a), (c), (e), and (f), which are marked with an asterisk (*) in Table 12. These flow path discrepancies reveal that in those arc loss scenarios, the single flow formulation always gives a local minimum, i.e., the multicommodity formulation in some cases results in a higher objective function (OF) value than the single flow formulation.

Table 12: Results comparison of a simple "transportation" NSCMF network problem between single flow formulation and multicommodity formulation, the results due to single flow formulation in the proposed Operational Matrix framework are given in the left part of each cell, while the multicommodity solution from Trapp (2015) is presented in the right part of each cell with the OF value added by the candidate at the top part of each cell (nodes A, B, C, D, E, F are equivalent to nodes 1, 2, 3, 4, 5, 6)

(a) No loss*		(b) Loss of arc A,B	
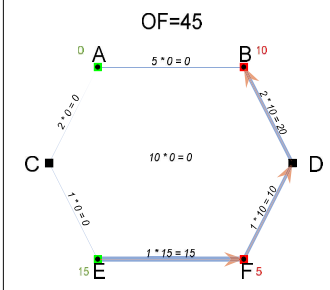	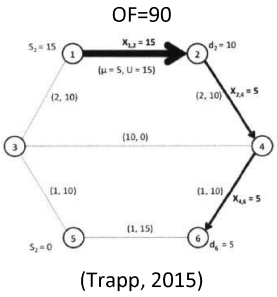	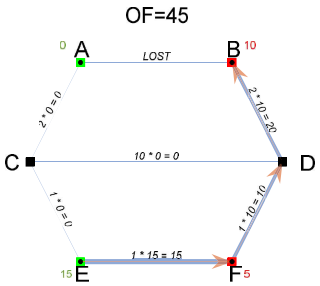	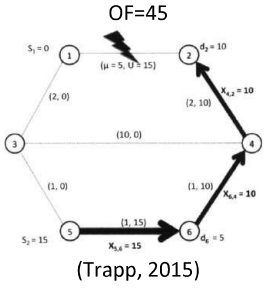
(c) Loss of arc A,C*		**(d) Loss of arc B,D**	
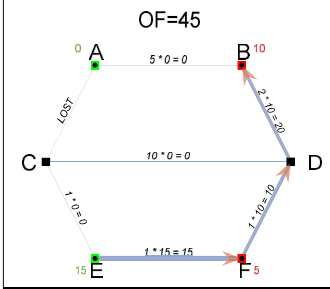	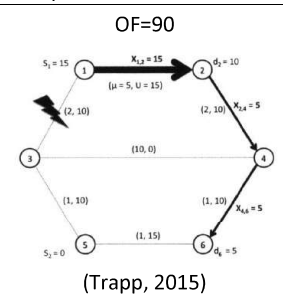	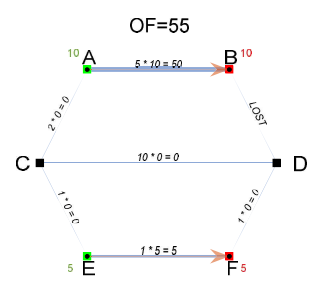	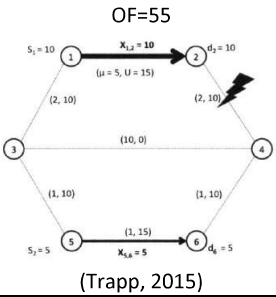
(e) Loss of arc C,D*		**(f) Loss of arc C,E***	
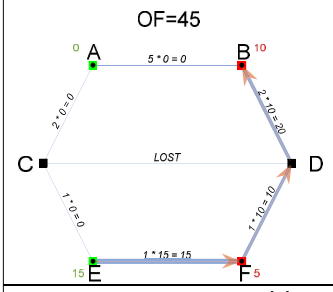	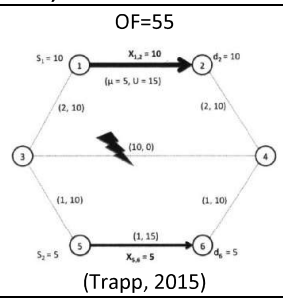	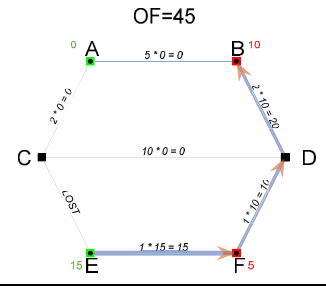	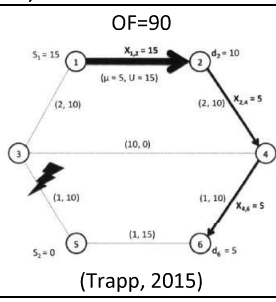
(g) Loss of arc D,F		**(h) Loss of arc E,F**	
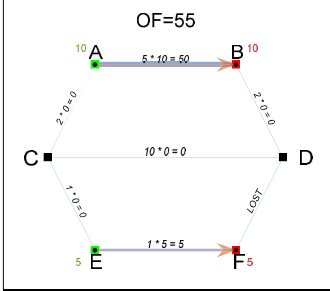	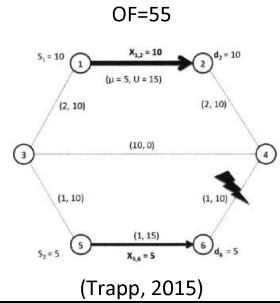	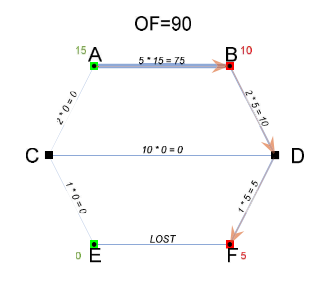	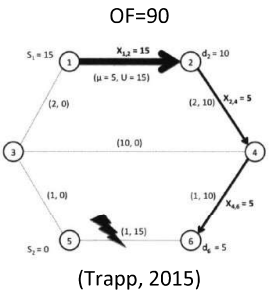
Aggregate solution			
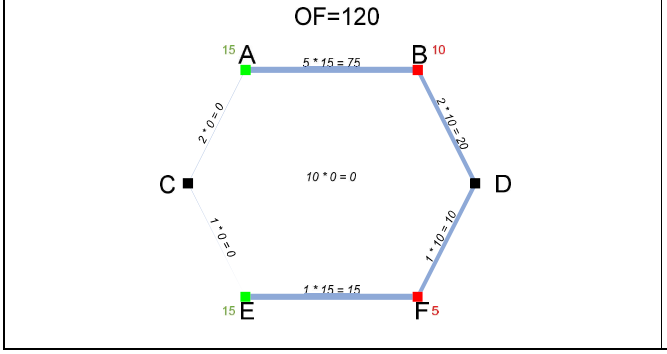		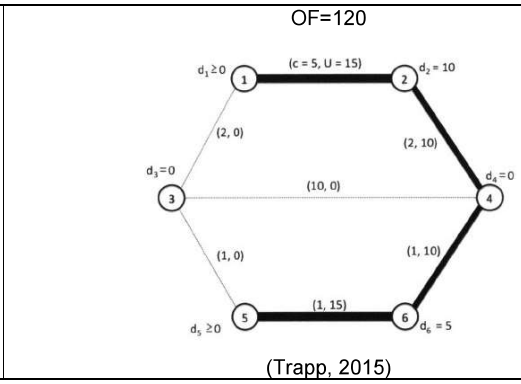	

Despite the difference in terms of the local minima, the single flow formulation gives the same aggregate result as the multicommodity formulation (see the aggregate solution at the bottom part of Table 12). This confirms that the same aggregate solution in this specific NSMCF example can be obtained more efficiently with fewer constraints without the need to include all arc loss scenarios in the global objective function. Therefore, this example suggests that by using the proposed Operational Matrix Framework, the input required for the NFO could potentially be easily manipulated and reduced. This would be more efficient for quick distributed ship service systems sizing focused investigations and thus more appropriate for early-stage ship design applications.

The next section provides the application of the Operational Matrix Framework to simplified power and propulsion systems in a diesel-powered submarine.

3.2 The Operational Matrix applied to simplified submarine power and propulsion systems

This section describes the Operational Matrix Framework used to solve a simplified power and propulsion systems (PPS) SUBFLOW problem outlined in (Mukti et al., 2021). In the SUBFLOW formulation, there are only two broad types of nodes: terminal nodes and hub nodes (Mukti, 2022). Terminal nodes were used to model sources or sinks at the extremities of the flow. The extremities in the network were identified by the number of in-degree and out-degree flows. If a terminal node has only one or multiple out-degree flows (diverging), that node was taken to be a source. Conversely, if the flow(s) were converging and there were no out-degree flow(s), that node would have been considered as a sink/ target. Figure 5 shows the PPS configuration of a diesel-powered submarine (SSK) study, which was taken from a 3D Paramarine-SURFCON synthesis process (Mukti et al., 2021).

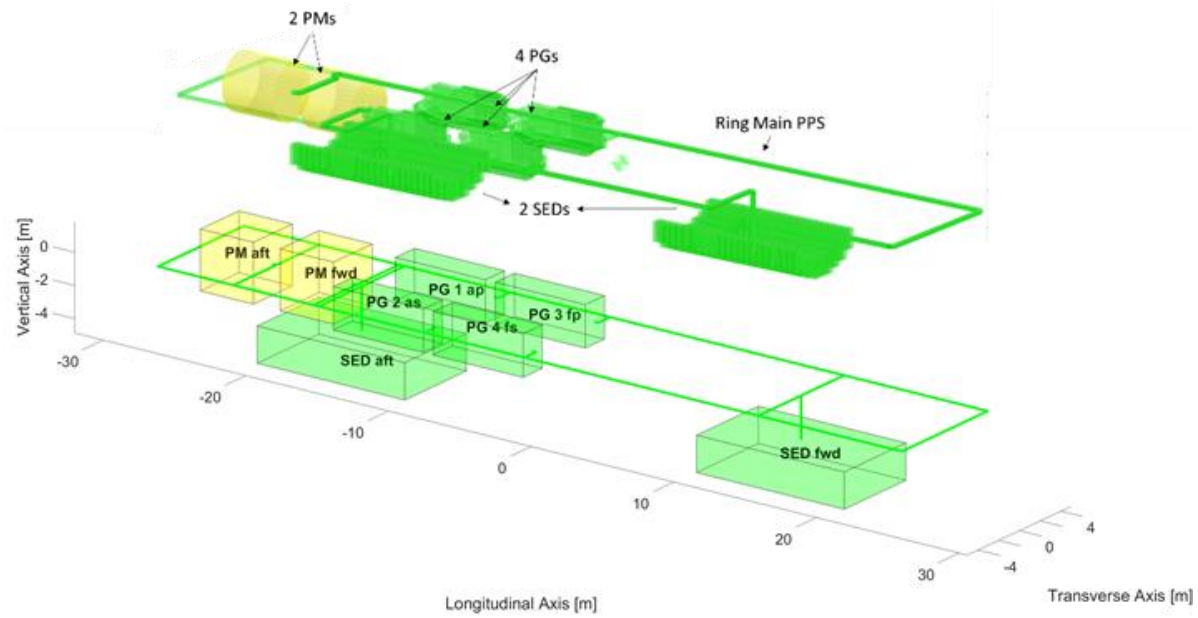

Figure 5: A simplified PPS architecture displayed in Paramarine-SURFCON (top) translated into MATLAB model for the SUBFLOW analysis (bottom) on the SSK Case Study

The simplified PPS 3D model above was then taken as a basis for the logical network as shown in Figure 6 with the network properties in Table 13. Figure 6 shows the PPS ring-main configuration network consists of 32 nodes and 36 arcs. There are two Propulsion Motors (PMs) as target (user) nodes, four Power Generations (PGs) as source nodes, and two electrical Stored Energy Devices (SEDs). The SED nodes can be the demand nodes during a snorting operating condition and can be supply nodes during a submerged operating condition. The rest of the nodes in the PPS network are hub or junction nodes. The nodes properties in Table 13 had to be defined from design requirements, i.e., the demanded power was based on the baseline SSK design (Mukti et al., 2021).

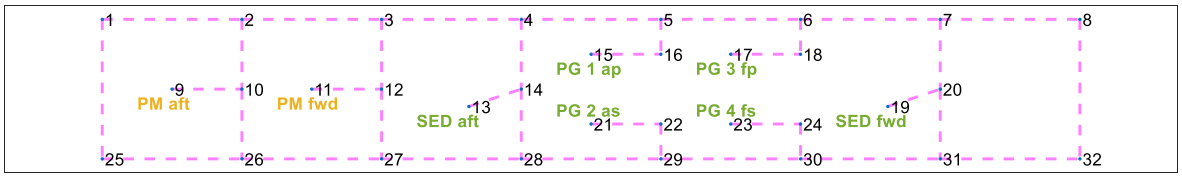

Figure 6: Nodes labelling to the PPS architecturen MATLAB (not to scale)

Table 13: The summary of the power commodity in snorting and transit

System Component	Supply Y_s (kW)	Demand Y_t (kW)	Node ID (Figure 6)
PM aft	-	346	9
PM fwd	-		11
PG 1 ap	1600 (max)	-	15
PG 2 as	1600 (max)	-	21
PG 3 fp	1600 (max)	-	17
PG 4 fs	1600 (max)	-	23
SED aft	-	2930	13
SED fwd	-	2930	19

As an early development of SUBFLOW formulation as outlined in Table 14, this PPS example was kept simple (i.e., it does not represent myriad components in the actual submarine PPS). The equations are now briefly described in turn, the reasonings for the formulation are addressed in detail in (Mukti et al., 2021).

Table 14: Linear programming formulation and realisation of a simplified PPS SUBFLOW problem

Linear Programming Formulation	Mathematical Notation	Realisation
Objective Function:	$\sum_{(i,j)\in a} (\alpha\,\delta_{i,j} + \beta\,\delta_{i,j} + \lambda_{i,j}\,P_{i,j})$	$(\alpha\,\delta_{1,2} + \beta\,\delta_{1,2} + \lambda_{1,2}\,P_{1,2}) + \cdots$ $(\alpha\,\delta_{31,32} + \beta\,\delta_{31,32} + \lambda_{31,32}\,P_{31,32})$
Subject To		
Continuity	$\sum_{(i,j)\in a}^{k} x_{i,j}^{k} - \sum_{(i,j)\in a}^{k} x_{j.i}^{k} = \gamma_i^k$	$x_{1,2}^{k} - x_{25,1}^{k} = \gamma_1^k \ldots$ $x_{32,8}^{k} - x_{31,32}^{k} = \gamma_{32}^k$
Capacity Rollup	$\lvert x_{ij}^{k}\rvert \le P_{ij}^{k}$	$\lvert x_{1,2}^{k}\rvert \le P_{1,2}^{k} \ldots$ $\lvert x_{31,32}^{k}\rvert \le P_{31,32}^{k}$
Inequality constraints	$\gamma_s^k \le Y_s^k$	$\gamma_{15}^k \le Y_{15}^k \ldots \gamma_{23}^k \le Y_{23}^k$
Bounds	$\gamma_h^k = 0$	$\gamma_h^k = 0$
	$\sum_{(t)\in n}^{k} \gamma_t^k = Y_t^k$ $\gamma_t^k = Y_t^k$	$\gamma_9^k + \gamma_{11}^k = Y_{PM}^k$ $\gamma_{13}^k = Y_{13}^k$ $\gamma_{19}^k = Y_{19}^k$
	$P_{i,j}^{k} \ge 0$	$P_{1,2}^{k} \ge 0 \ldots P_{31,32}^{k} \ge 0$
Operating Scenario	$P_{i,j}^{k,m} = 0$	$P_{1,2}^{k,m} = 0 \ldots P_{31,32}^{k,m} = 0$
Indices	$\delta(i,j) \in \{0,1\}$	$\delta(i,j) \in \{0,1\}$
Capturing aggregate solution	$P_{i,j} = \max_{(k,m)\in K,M} (P_{i,j}^{k,m})$	$P_{1,2} = \max_{(k,m)\in K,M} (P_{1,2}^{k,m}) \ldots$ $P_{31,32} = \max_{(k,m)\in K,M} (P_{31,32}^{k,m})$

In this example, the SUBFLOW formulation adopts the M-1 survivability (Trapp, 2015) by looping a 144×176 Operational Matrix (see Table 16) as many as the quantity of arcs in the PPS network, i.e., 32 arcs. The objective function for the PPS study, which is given in Table 14, is in the first row and columns 1 to 108 in the Operational Matrix (see Table 16). To define variables α and β in (located in the first row and the first 72 columns) there were two assumed 'standard' edge components.

In this formulation, the network solution can be used into two different ways. The first one was termed as the 'binary variables' method that minimised the space taken by PPS connections using coefficients α and β. These coefficients categorised arcs in the PPS network to a certain standard edge component via binary decisions $\delta_{i,j}$. The second one was the 'integer variables' method, which also minimised the value of multiplication between the power to volume ratio $\lambda_{i,j}$ and the power $P_{i,j}$. The power to volume ratio $\lambda_{i,j}$ quantifies the power $P_{i,j}$ for each set of arcs connecting a node i and a node j into a discrete volume. By assuming some variables related to the PPS cabling specifications, the power to volume ratio $\lambda_{i,j}$ was obtained. Since there were unique x, y, z locations for each node from the DBB synthesis, the distance between nodes $L(i,j)$ could be calculated (see Table 15).

Table 15: Assumed variables in the PPS study

Variable	Description	Value
α	Binary coefficient of first category for cable sizing via the binary variables in the objective function	1.4 MW
β	Binary coefficient of second category for cable sizing via the binary variables in the objective function	4.8 MW
$\lambda_{i,j}$	Power to volume ratio for sizing via the integer variables in th objective function	$\frac{1.043 \times 10^{-5} m^2}{kW} L_{ij}$

In this case study, SUBFLOW did not just seek the minimum space for PPS cabling but also satisfied several constraints. These constraints were developed to show the distinctive SSK PPS operating conditions. In these constraints, k is an indexed scenario within a set of operating conditions K to represent various operating conditions, such as snorting and submerged conditions. In this PPS study, only the snorting (and transit) condition was considered, where the SEDs become the highest load in the PPS network, letting operating condition $k = 1$. The continuity formulation ensures the flow variable or flow path x entering and leaving a node n from a node i or j within a set of nodes n is equal to the amount of commodity γ at that node n and is preserved throughout the arcs A, except at relevant sources and targets. This equation is indicated in rows 2 to 33 and columns 109 to 176 in the Operational Matrix (Table 16).

For bidirectionality, the flow variable $x_{i,j}$ was 'rolled up' (Trapp, 2015) and converted to power capacity flow $P_{i,j}$ as the decision variables in SUBFLOW. Thus, the required power P_{ij}, as the decision variables in the SUBFLOW formulation, is always positive. This formulation is located in two parts in the Operational Matrix (see Table 16): rows 35 to 106 and columns 72 to 144; rows 143 to 144 and columns 109 to 144. The bounds in the formulation define the amount of power source and demand Y in the PPS network. The source nodes in the PPS study were the PGs, i.e., nodes 15, 17, 21, and 23 (see Table 16). This equation is assigned at rows 143 to 144 and columns 145 to 176 in the Operational Matrix framework. The bounds for hub nodes were set to zero. The examples of hub nodes in the PPS study were nodes 1, 2, 3, etc (see Figure 6). This equation is assigned at rows 143 to 144 and columns 145 to 176 in the Operational Matrix.

For applying the M-1 survivability by Trapp (2015) in this PPS network problem, each operating condition k is associated with an edge loss scenario m (the flow was set to zero) within a set of damaged scenarios M. This equation was applied by setting the upper bound of a power capacity flow $P_{i,j}$ to zero in the Operational Matrix, which is located at row 144 and columns 72 to 108. This setup forced the solver to be unable to use that arc and then search for an alternative set of flowpaths in the network.

Table 16: The Operational Matrix of the simplified PPS study, which is developed based on the formulation in Table 14

		Formulation for arcs				Formulation for nodes		
		36	36	36	36	32		
	No	**1-36**	**37-72**	**72-108**	**109-144**	**145-176**		**177**
Objective Function	**1**	$\boldsymbol{\alpha\ \delta_{i,j}}$	$\boldsymbol{\beta\ \delta_{i,j}}$	$\boldsymbol{\lambda_{i,j}\ P_{i,j}}$	$\sum_{(i,j)\in E} x_{i,n} - \sum_{(i,j)\in E} x_{n,j}$	$-\gamma_n$	=	0
Equality constraints matrix for continuity	**2**	0	0	0	+1	+1		
	.	0	0	0	or	or		
	.	0	0	0	-1	-1		0
	.	.	.	.	.	.		
	.	.	.	.	.	.		
	33	.	.	.	.	.		
	34					See LP Formulation for the PPS study		
					$-P_{i,j} \pm x_{i,j}$		≤	0
Inequality constraints matrix for bidirectionality and binary variables	**35**	0	0	-1	-1	0		
	.	0	0	-1	-1	0		
	.	0	0	-1	-1	0		
	.	.	.	.	.	.		
	.	.	.	.	.	.		0
	70	.	.	.	.	.		
	71	0	0	-1	+1	0		
	.	0	0	-1	+1	0		
	.	0	0	-1	+1	0		
	.	.	.	.	.	.		
	.	.	.	.	.	.		
	106	.	.	.	.	.		
		$\boldsymbol{\alpha\ \delta_{i,j}}$	$\boldsymbol{\alpha\ \delta_{i,j}}$	$P_{i,j}$			≤	0
	107	$\boldsymbol{-\alpha}$	$\boldsymbol{-\beta}$	**1**	0	0		
	.	$\boldsymbol{-\alpha}$	$\boldsymbol{-\beta}$	**1**	0	0		
	.	$\boldsymbol{-\alpha}$	$\boldsymbol{-\beta}$	**1**	0	0		0
	.	.	.	.	.	.		
	.	.	.	.	.	.		
	142	.	.	.	.	.		
Lower bounds matrix	**143**	. . . 0 . . .	. . . 0 . . .	**. . . 0 . . .**	. . . –inf . . .	See LP Formulation for the PPS study		
Upper bounds matrix	**144**	. . . 1 . . .	. . . 1 . . .	**. . . inf . . .**	. . . inf . . .			
		$\boldsymbol{\delta(i,j) \in \{0,1\}}$		$\boldsymbol{P_{i,j}^k \geq 0}$	$\boldsymbol{\left\lvert x_{ij}^k \right\rvert \leq P_{ij}^k}$			

The δ in Equation in Table 16 serves as the binary decision to classify a capacity of an edge i to j to achieve certain standards for an edge component (type α and β). This equation is assigned at rows 143 to 144 and columns 1 to 72 in the Operational Matrix (see Table 16).

The redundant Propulsion Motors (PM)s were set as user nodes, but the solver could only select one PM to be online in an operating condition k. Other user nodes in the same operating condition (snorting) were set as the hard constraints. These are the batteries (SED) charging demands. Therefore, in the PPS study, the user nodes t were PMs and SEDs (nodes 9, 11, 13 and 19 in Table 14). These equations are shown in rows 34 and 143 to 144 and columns 145 to 176 in the Operational Matrix (see Table 16). Finally, the network solutions from the solver, which consisted of numerical data in a matrix, were presented in Table 17. This used the last equation in Table 14.

Using the Operational Matrix framework, the solver was able to find the solutions. Table 17 shows three different set of network solutions. The first solution is referred to as a "conservative" solution as it was obtained by selecting the maximum possible power flow in the PPS problem, i.e., maximum power available from the four PGs. The second and third solutions were based on the Objective Function of the SUBFLOW PPS explained above. The three solutions can be used as a basis for sizing the PPS cabling although it was recognised that the aft part of the PPS network would have required further operating scenarios k to be considered beyond snorting and transit (e.g., sprint condition). In this simple PPS example, there were found to be three possible options, the designer was able to choose between a smaller space solution (3 m^3 and 5 m^3) or the conservative solution (10 m^3) for the PPS cable sizing. Another example is provided and thus the next section outlines another version of SUBFLOW formulation for an SSK power load network at a high level.

3.3 Applying the Operational Matrix using high-level submarine power sizing variables

Network can also be used to represent the constants, coefficients, and variables within the concept design model as opposed to the items of the distributed ship service systems. This means the nodes are not directly representing the actual distributed ship service systems equipment unlike the previous examples. Therefore, a mathematical relationship for diesel power (P_{DIES}) sizing was used, which is given in Figure 7 (top) (Burcher and Rydill, 1994). This algorithm expresses that the power output that a diesel engine fit must be able to satisfy the electric service demand for charging batteries, propulsion load, and hotel load, as well as the likely inefficiencies and margins required to accomplish snorting operations.

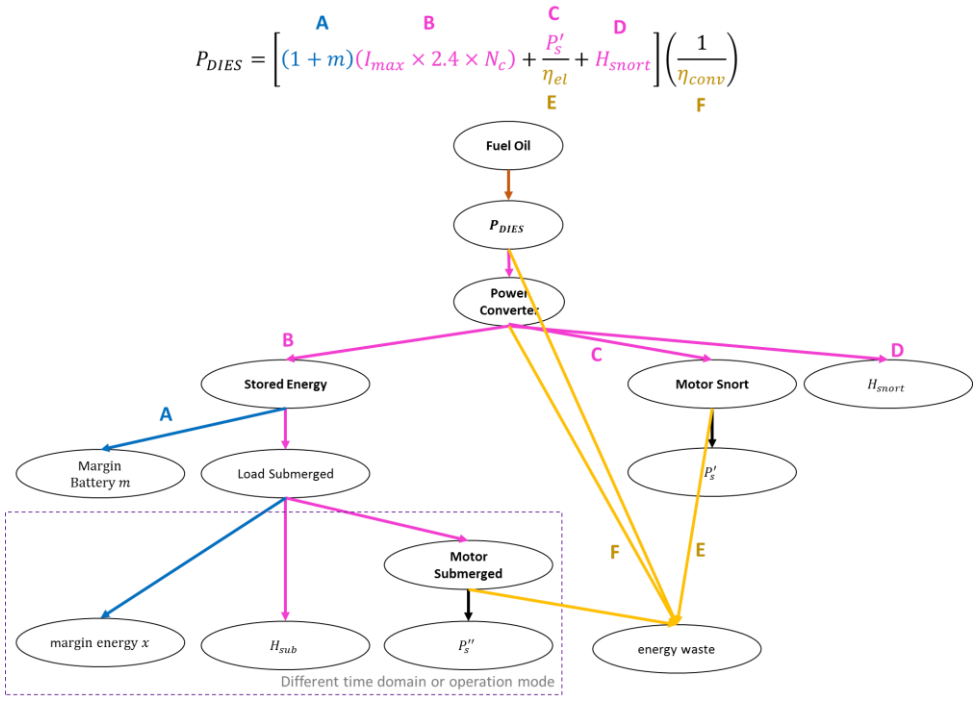

Figure 7: A high level SSK power system problem based on to the power sizing algorithm due to Burcher & Rydill (1994)

Table 17: Sizing results of the Power and Propulsion Systems (PPS) study

Arc No	Node		Power to volume ratio $\lambda_{i,j}$ (m³/kW)	Conservative Result		Integer Variables Result		Binary Variables Result			
	i	j		Power $P_{i,j}$ (kW)	Volume $V_{i,j}$ (m³)	Power $P_{i,j}$ (kW)	Volume $V_{i,j}$ (m³)	Alpha α	Beta β	Power $P_{i,j}$ (kW)	Volume $V_{i,j}$ (m³)
1	1	2	5.52E-05	6291	0.347	0	0.000	-	-	0	0.000
2	1	25	8.68E-05	6291	0.546	0	0.000	-	-	0	0.000
3	2	3	5.84E-05	6291	0.367	346	0.020	yes	-	1400	0.082
4	2	10	4.31E-05	6291	0.271	346	0.015	yes	-	1400	0.060
5	3	4	4.02E-06	6291	0.025	1401	0.006	yes	-	1400	0.006
6	3	12	4.31E-05	6291	0.271	1401	0.060	yes	-	1400	0.060
7	4	5	7.72E-05	6291	0.486	3280	0.253	-	yes	4890	0.378
8	4	14	4.31E-05	6291	0.271	2934	0.127	-	yes	4890	0.211
9	5	6	7.30E-05	6291	0.459	1680	0.123	-	yes	4890	0.357
10	5	16	1.18E-05	6291	0.074	1600	0.019	-	yes	4890	0.058
11	6	7	1.71E-04	6291	1.076	3014	0.515	-	yes	4890	0.836
12	6	18	1.18E-05	6291	0.074	1600	0.019	-	yes	4890	0.058
13	7	8	1.05E-04	6291	0.660	0	0.000	-	-	0	0.147
14	7	20	4.31E-05	6291	0.271	3014	0.130	-	yes	4890	0.211
15	8	32	8.68E-05	6291	0.546	0	0.000	-	-	0	0.121
16	9	10	2.61E-06	6291	0.016	346	0.001	yes	-	1400	0.004
17	10	26	4.36E-05	6291	0.275	0	0.000	-	-	0	0.000
18	11	12	2.61E-06	6291	0.016	346	0.001	yes	-	1400	0.004
19	12	27	4.36E-05	6291	0.275	1401	0.061	yes	-	1400	0.061
20	13	14	2.74E-05	6291	0.172	2934	0.080	-	yes	4890	0.134
21	14	28	4.36E-05	6291	0.275	2934	0.128	-	yes	4890	0.213
22	15	16	2.61E-06	6291	0.016	1600	0.004	-	yes	4890	0.013
23	17	18	2.61E-06	6291	0.016	1600	0.004	-	yes	4890	0.013
24	19	20	2.74E-05	6291	0.172	2934	0.080	-	yes	4890	0.134
25	20	31	4.36E-05	6291	0.275	3014	0.132	-	yes	4890	0.213
26	21	22	2.61E-06	6291	0.016	1600	0.004	-	yes	4890	0.013
27	22	29	1.24E-05	6291	0.078	1600	0.020	-	yes	4890	0.060
28	23	24	2.61E-06	6291	0.016	1600	0.004	-	yes	4890	0.013
29	24	30	1.24E-05	6291	0.078	1600	0.020	-	yes	4890	0.060
30	25	26	5.52E-05	6291	0.347	0	0.000	-	-	0	0.000
31	26	27	5.84E-05	6291	0.367	0	0.000	-	-	0	0.000
32	27	28	4.02E-06	6291	0.025	1401	0.006	yes	-	1400	0.006
33	28	29	7.72E-05	6291	0.486	3280	0.253	-	yes	4890	0.378
34	29	30	7.30E-05	6291	0.459	1680	0.123	-	yes	4890	0.357
35	30	31	1.71E-04	6291	1.076	3014	0.515	-	yes	4890	0.836
36	31	32	1.05E-04	6291	0.660	0	0.000	-	-	0	0.147
Total Volume					**10.865**		**2.723**				**5.243**

The network in Figure 7 shows the hierarchal sources and sinks of a SSK power system with several nodes starting from the fuel (oil) tankage node as the source of energy followed by the diesel generator node (quantified by P_{DIES}), which converts the fuel is chemical energy (brown) to electric energy. The electrical energy is then converted and distributed by a power converter node to the three main electric loads which are coloured in magenta: the energy storage or battery charging for fully submerged operation (B); the hotel load in the snorting operation (D); and the propulsion load in snorting operations (C). Further nodes have been modelled to represent margins (coloured in blue) for battery charging (A) and submerged energy (B), as well as efficiencies (F and E) coloured in yellow, which contribute to energy waste or power loss. The detailed heat due to battery charging and hotel load in the snorting operation was not considered in this modelling.

The properties of the nodes shown in Figure 7 are given in Table 18. The source node in this study was the Fuel Oil (FO) node, while the rest of the terminal nodes were sinks and between the terminal nodes, there were hub nodes. Unlike terminal nodes, hub nodes have to have at least one in-degree and one out-degree flow. The hub nodes shown in Table 18 are the Diesel Generator (DG), the Power Converter (PC), the Stored Energy (SE), the Margin Battery (MM), the Load Submerged (LS), Motor Submerged (MS), and Motor Snort (MT). Compared to the AFO approach (Brown, 2020), each arc in the SUBFLOW network also focuses on one commodity, which is energy (chemical, electrics, mechanical, or heat loss). However, in the AFO approach, there could be a non-energy flow, such as data flow (carrying binary 0 and 1 numerical data), as the 'parallel' commodity in the AFO formulation (Robinson, 2018). Reducing the number of commodities within the SUBFLOW then reduced the number of inputs and the complication in the network formulation, making the SUBFLOW more appropriate to be applied early in the design process, as in the implementation shown in Table 18. The energy storage was also explicitly modelled as the Load Submerged (LS) node in this network.

Table 18: Nodes properties for an SSK power system network in Figure 7

Node Name	Relevant Variable	Node Identification	SUBFLOW Setup	Node Type	Data
Fuel Oil	P_{Fuel}	FO	$P_{FO} \geq 0$	Terminal	(Output)
Diesel Generator	P_{Dies}	DG	$P_{DG} \geq 0$	Hub	(Output)
Power Converter	P_{Conv}	PC	$P_{PC} \geq 0$	Hub	(Output)
Stored Energy	P_{Batt}	SE	$P_{SE} \geq 0$	Hub	(Output)
Margin Battery	m	MM	$P_{MM} \geq 0$	Hub	(Output)
Load Submerged	-	LS	$P_{LS} \geq 0$	Hub	(Output)
Margin Energy	x	MX	$P_{MX} \geq 0$	Terminal	(Output)
Hotel Submerged	H_{sub}	HS	$\boldsymbol{P_{HS} = H_{sub}}$	Terminal	280 kW
Motor Submerged	P''_{Motor}	MS	$P_{MS} \geq 0$	Hub	(Output)
Velocity Submerged	P''_s	VS	$\boldsymbol{P_{VS} = P''_s}$	Terminal	68 kW
Motor Snort	P'_{Motor}	MT	$P_{MT} \geq 0$	Hub	(Output)
Velocity Snort	P'_s	VT	$P_{VT} = P'_s$	Terminal	(Output)
Hotel Snort	H_{snort}	HT	$P_{HT} = H_{snort}$	Terminal	224 kW
Heat Loss	-	HE	$P_{HE} \geq 0$	Terminal	(Output)

In this example, a formulation used in the AFO approach (Robinson, 2018) was applied to continuity constraints and to define how much energy could come in and out of a hub node, denoted as an energy coefficient e_i in this SUBFLOW simulation (see Table 19 and the continuity in Table 21). For example, at the Diesel Generator (DG) node, 100% of the incoming energy flow from the Fuel Oil (FO) node would be converted to the Power Converter (PC) node as the electric energy (48%) and Heat Loss (HE) node (52%). This split could be said to be similar to the Sankey diagram that can be used to breaking down energy inputs and outputs (Kennedy and Sankey, 1898). Thus, all hub nodes' energy coefficients e_i in this SUBFLOW network (Figure 7) are provided in Table 19.

Table 19: Arcs properties for an SSK power system network in Figure 7

Arc (i,j)	Energy	Colour Code	SUBFLOW Setup $\sum_{(i,j)\in E} P_{i,j} - e_i P_i = 0$
(FO,DG)	Chemical	Brown	$P_{FO,DG} = P_{FO}$
(DG,PC)	Electrical	Magenta	$P_{DG,PC} = 48\%\ P_{DG}$
(DG,HE)	Heat	Yellow	$P_{DG,HE} = 52\%\ P_{DG}$
(PC,SE)	Electrical	Magenta	$P_{PC,SE} = 98\%\ P_{PC} - P_{PC,MT} - P_{PC,HT}$
(PC,MT)	Electrical	Magenta	$P_{PC,MT} = 98\%\ P_{PC} - P_{PC,SE} - P_{PC,HT}$
(PC,HT)	Electrical	Magenta	$P_{PC,HT} = 98\%\ P_{PC} - P_{PC,SE} - P_{PC,MT}$
(PC,HE)	Heat	Yellow	$P_{PC,HE} = 2\%\ P_{DG}$
(SE,MM)	Electrical	Blue	$P_{SE,MM} = 4.8\%\ P_{SE}$
(SE,LS)	Electrical	Magenta	$P_{SE,LS} = 95.2\%\ P_{SE}$
(MT,HE)	Heat	Yellow	$P_{MT,HE} = 3\%\ P_{MT}$
(MT,VT)	Mechanical	Black	$P_{MT,VT} = 97\%\ P_{MT}$
(LS,MS)	Electrical	Magenta	$P_{LS.MS} = 64\%\ P_{LS} - P_{LS.HS}$
(LS,HS)	Electrical	Magenta	$P_{LS,HS} = 64\%\ P_{LS} - P_{LS.MS}$
(LS,MX)	Electrical	Blue	$P_{LS,MX} = 36\%\ P_{LS}$
(MS,HE)	Heat	Yellow	$P_{MS,HE} = 3\%\ P_{MS}$
(MS,VS)	Mechanical	Black	$P_{MS,VS} = 97\%\ P_{MS}$

All arcs in the network were not capped and thus it can be any positive values $0 \leq P_{i,j} \leq \infty$ (or Inf). This will also be the case for the supply node, the Fuel Oil (FO) γ_s, all hub nodes γ_h, and some target nodes γ_t, such as the Margin Energy (MX), the Motor Submerged (MS), the Motor Snort (MT), and the Heat Loss (HE) (see the bounds in Table 14. The capacities of the user nodes γ_t in the network then need to be calculated, which are dependent on the operating scenarios (see Table 14). They are the Hotel Submerged (HS), the Velocity Submerged (VS), the Velocity Snort (VT), and the Hotel Snort (HT). Finally, the coefficients of the objective function coefficient $c_{i,j}$ in this SUBFLOW example were set to zero (see Objective Function equation in Table 14), because the aim of this optimisation example was not to cost the distributed ship service systems configuration, as in the case of Trapp's (2015) NSMCF investigation or Robinson's (2018) AFO study (including its variants (Parsons et al., 2020)). In this study, SUBFLOW was used to solve the energy balance, through a linear programming, set of equations. This ensured that the total energy demand on the submarine would be equal to the total energy available, indicating an initial systems design balance. Thus, in this SUBFLOW example, the network styles were proposed on the basis of prior expert knowledge and were deliberately not validated by analysis in early stage of ship design. Nonetheless, the SUBFLOW network created could have provided a suitable basis for further analyses in subsequent design phases, if required.

Table 20: Linear programming formulation and realisation of an SSK power system network in Figure 7

Linear Programming Formulation	Mathematical Notation	Realisation
Objective Function:	$min. \sum_{(i,j)\in a} c_{i,j} P_{i,j}$ where $c_{i,j} = 0$	$c_{FO,DG} P_{FO,DG} + \ldots + c_{MS,VS} P_{MS,VS}$

Subject To		
Linear Programming Formulation	**Mathematical Notation**	**Realisation**
Continuity	$\sum_{(i,j)\in E} P_{i,j} - e_i P_i = 0$	$P_{FO,DG} - e_{FO}P_{FO} = 0 \ldots$ $P_{DG,HE} + P_{PC,HE} + P_{MT,HE} + P_{MS,HE} - e_{HE}P_{HE} = 0$
Bounds	$0 \le P_{i,j} \le \infty$ (or Inf)	$0 \le P_{FO,DG} \le \infty \ldots$ $0 \le P_{MS,VS} \le \infty$
	$0 \le \gamma_s \le \infty$ (or Inf)	$0 \le P_{FO} \le \infty$
	$0 \le \gamma_h \le \infty$ (or Inf)	$0 \le P_{DG} \le \infty, 0 \le P_{PC} \le \infty, 0 \le P_{SE} \le \infty,$ $0 \le P_{MM} \le \infty, 0 \le P_{LS} \le \infty, 0 \le P_{MS} \le \infty,$ $0 \le P_{MT} \le \infty$
	$0 \le \gamma_t \le \infty$ (or Inf)	$0 \le P_{MX} \le \infty$ *and* $0 \le P_{HE} \le \infty$
Investigated Operating Scenarios	$\gamma_t = Y_t$	$\gamma_{HT} = Y_{HT}, \gamma_{VT} = Y_{VT}, \gamma_{VS} = Y_{VS}, \gamma_{HS} = Y_{HS}$

The Operational Matrix for this particular SUBFLOW example is outlined in Table 21. Since undirected network or bidirectional network contains more information than an undirected network (Mukti, 2022), the size of the Operational Matrix would have become quite large if bidirectionality had had to be considered (i.e., a $[61 \times 47]$ matrix). Nonetheless, in this case, bidirectionality was not necessary as there had to be no backward flow from the target to the source nodes and thus the Operational Matrix has only 29 rows and 31 columns. Compared to the Operational Matrix for Sections 3.1 and 3.2, the Operational Matrix in this example shows how to arrange the energy coefficient from the AFO approach (Parsons et al., 2020) in the matrix, which is reflected as the coefficient e_i for the continuity constraints (rows 2 to 27 and columns 17 to 30).

By using the Operational Matrix in Table 21, the solver can provide the network solution as shown in Figure 8. Figure 8 shows 5.7 MW of power is transferred from the Fuel Oil node to the Diesel Generator node. The Diesel Generator node then converted the 5.7 MW of the fuel flow to 2.7 MW to Power Converter node (as electrical flow shown in magenta) and 2.9 MW to Heat Loss node (as waste heat shown in yellow). At the Power Converter node, the 2.7 MW of electrical flow was divided into 2.3 MW electrical flow for Stored Energy node, 166 kW for Motor Snort node, 224 kW to Hotel Snort node, and 55 kW to Heat Loss node. For the Stored Energy various flows simulate how much energy is needed during the submerged operating condition, i.e., a different time domain from the snorting operating condition. All of the flows shown in Figure 8 satisfied the SUBFLOW constraints given in Table 21.

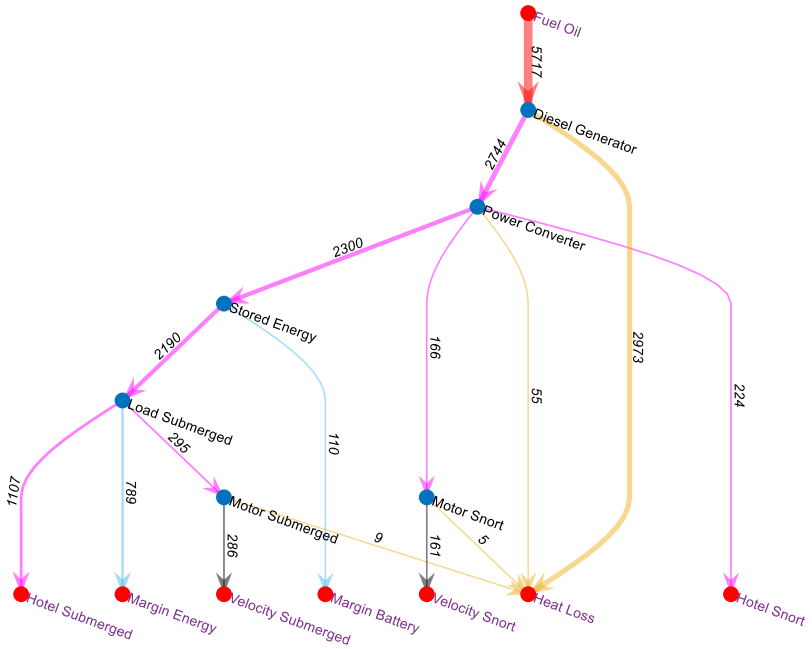

Figure 8: SUBFLOW solution for an SSK power system

Table 21: The Operational Matrix of a high level SSK power system in Figure 7, which is developed based on the formulation in Table 20.

	No	1	2	3	4	5	6	7	8	9	10	11	12	13	14	15	16	17	18	19	20	21	22	23	24	25	26	27	28	29	30	31
Objective Function	1	0	0	0	0	0	0	0	0	0	0	0	0	0	0	0	0	0	0	0	0	0	0	0	0	0	0	0	0	0	0	
		Arcs																Nodes															
		$\sum_{(i,j)\in E} P_{i,j}$																$-e_i P_i$														= 0
		$P_{FO,DG}$	$P_{DG,PC}$	$P_{DG,HE}$	$P_{PC,SE}$	$P_{PC,MT}$	$P_{PC,HT}$	$P_{PC,HE}$	$P_{SE,MM}$	$P_{SE,LS}$	$P_{MT,HE}$	$P_{MT,VT}$	$P_{LS,MS}$	$P_{LS,HS}$	$P_{LS,MX}$	$P_{MS,HE}$	$P_{MS,VS}$	P_{FO}	P_{DG}	P_{PC}	P_{SE}	P_{MM}	P_{MT}	P_{HT}	P_{HE}	P_{VT}	P_{LS}	P_{MS}	P_{VS}	P_{HS}	P_{MX}	
Equality constraints matrix for continuity	2	1	0	0	0	0	0	0	0	0	0	0	0	0	0	0	0	-1	0	0	0	0	0	0	0	0	0	0	0	0	0	0
	3	1	0	0	0	0	0	0	0	0	0	0	0	0	0	0	0	0	-1	0	0	0	0	0	0	0	0	0	0	0	0	0
	4	0	1	0	0	0	0	0	0	0	0	0	0	0	0	0	0	0	-0.48	0	0	0	0	0	0	0	0	0	0	0	0	0
	5	0	0	1	0	0	0	0	0	0	0	0	0	0	0	0	0	0	-0.52	0	0	0	0	0	0	0	0	0	0	0	0	0
	6	0	1	0	0	0	0	0	0	0	0	0	0	0	0	0	0	0	0	-1	0	0	0	0	0	0	0	0	0	0	0	0
	7	0	0	0	1	1	1	0	0	0	0	0	0	0	0	0	0	0	0	-0.98	0	0	0	0	0	0	0	0	0	0	0	0
	8	0	0	0	0	0	0	1	0	0	0	0	0	0	0	0	0	0	0	-0.02	0	0	0	0	0	0	0	0	0	0	0	0
	9	0	0	0	1	0	0	0	0	0	0	0	0	0	0	0	0	0	0	0	-1	0	0	0	0	0	0	0	0	0	0	0
	10	0	0	0	0	0	0	0	0	1	0	0	0	0	0	0	0	0	0	0	-0.952	0	0	0	0	0	0	0	0	0	0	0
	11	0	0	0	0	0	0	0	1	0	0	0	0	0	0	0	0	0	0	0	-0.048	0	0	0	0	0	0	0	0	0	0	0
	12	0	0	0	0	0	0	0	1	0	0	0	0	0	0	0	0	0	0	0	0	-1	0	0	0	0	0	0	0	0	0	0
	13	0	0	0	0	0	0	0	0	1	0	0	0	0	0	0	0	0	0	0	0	0	0	0	0	0	-1	0	0	0	0	0
	14	0	0	0	0	0	0	0	0	0	0	0	1	1	0	0	0	0	0	0	0	0	0	0	0	0	-0.64	0	0	0	0	0
	15	0	0	0	0	0	0	0	0	0	0	0	0	0	1	0	0	0	0	0	0	0	0	0	0	0	-0.36	0	0	0	0	0
	16	0	0	0	0	0	0	0	0	0	0	0	0	0	1	0	0	0	0	0	0	0	0	0	0	0	0	0	0	0	-1	0
	17	0	0	0	0	0	0	0	0	0	0	0	0	1	0	0	0	0	0	0	0	0	0	0	0	0	0	0	0	-1	0	0
	18	0	0	0	0	0	0	0	0	0	0	0	1	0	0	0	0	0	0	0	0	0	0	0	0	0	0	-1	0	0	0	0
	19	0	0	0	0	0	0	0	0	0	0	0	0	0	0	0	1	0	0	0	0	0	0	0	0	0	0	-0.970	0	0	0	0
	20	0	0	0	0	0	0	0	0	0	0	0	0	0	0	1	0	0	0	0	0	0	0	0	0	0	0	-0.030	0	0	0	0
	21	0	0	0	0	0	0	0	0	0	0	0	0	0	0	0	1	0	0	0	0	0	0	0	0	0	0	0	-1	0	0	0
	22	0	0	0	0	1	0	0	0	0	0	0	0	0	0	0	0	0	0	0	0	0	-1	0	0	0	0	0	0	0	0	0
	23	0	0	0	0	0	0	0	0	0	0	1	0	0	0	0	0	0	0	0	0	0	-0.970	0	0	0	0	0	0	0	0	0
	24	0	0	0	0	0	0	0	0	0	1	0	0	0	0	0	0	0	0	0	0	0	-0.030	0	0	0	0	0	0	0	0	0
	25	0	0	0	0	0	0	0	0	0	0	1	0	0	0	0	0	0	0	0	0	0	0	0	0	-1	0	0	0	0	0	0
	26	0	0	0	0	0	1	0	0	0	0	0	0	0	0	0	0	0	0	0	0	0	0	-1	0	0	0	0	0	0	0	0
	27	0	0	1	0	0	0	1	0	0	1	0	0	0	0	1	0	0	0	0	0	0	0	0	-1	0	0	0	0	0	0	0
Lower bounds matrix	28	0	0	0	0	0	0	0	0	0	0	0	0	0	0	0	0	0	0	0	0	0	0	**224**	0	**160**	0	0	**285**	**1107**	0	
Upper bounds matrix	29	Inf	Inf	Inf	Inf	Inf	Inf	Inf	Inf	Inf	Inf	Inf	Inf	Inf	Inf	Inf	Inf	Inf	Inf	Inf	Inf	Inf	Inf	**224**	Inf	**160**	Inf	Inf	**285**	**1107**	Inf	
		$0 \le P_{i,j} \le \infty$																Investigated operating conditions/scenarios (see Table 20)															

4. THE OPERATIONAL MATRIX FRAMEWORK APPLIED TO THE UCL NETWORK BLOCK APPROACH

Section 3 addresses how the Operational Matrix Framework can be used to assess different types of network flow formulations. This section presents the setup of the Operational Matrix Framework that has been adopted in the UCL Network Block Approach (Mukti, 2022). Unlike the previous examples, the SUBFLOW formulation in the UCL Network Block Approach was devised to be ship design efficient, yet without losing the advantages of capturing the complexity of distributed ship service systems using a range of applicable network tools. In the UCL Network Block Approach, spreadsheet-based tools are used to define the ship design and its distributed ship service systems (Mukti et al., 2022). The tools specific for defining the network configuration and SUBFLOW inputs for the distributed ship service systems are the Component Granularity Program (CGP) and System Connection Program (SCP) (see (Mukti et al., 2022)).

Table 22 shows the example of the CGP inputs: the type of components (nodes), which were either terminal or hub nodes; the equipment load demand or maximum capacity was used to define the lower and upper bounds for the SUBFLOW in various operating conditions, for example, snort or sprint submerged); the objective function coefficient, which was set to zero; the energy coefficients e of each component up to 15 different types of distributed ship service systems commodities; and the logical layout (x, y, z coordinates) to create a "logical" multiplex network.

The energy coefficients e of each component node in Table 22 are defined as follows:

- The energy that enters a node is expelled 100% outside the node (IN=-1). This option was used for terminal source nodes, such as fuel, or terminal sink nodes, such as propulsion load.

- The energy that enters a node is dispersed to different types of energy in a form of some fraction (IN=fractional OUT). This reflects the Sankey Diagram practice and could have been used for electrical consumer nodes, including energy storage.

- The energy that enters a node is determined by the proportion of the energy from at least two different nodes in different systems. This option could have been used for modelling the fuel-air (energy) ratio of the diesel generator.

- The energy that might have entered a node could have been specified as a fraction of the total heat received at the node and that fraction of energy that has not been forwarded beyond that node (fractional IN=OUT). This choice could be used to describe the 'coefficient of performance' of cooling systems components.

- A 'child' node could receive 100% energy from two parent nodes from different systems and then store 100% energy output to that child node. This could have been used to model sink nodes on the vessel, for example, a seawater node.

Table 22: Example of the CGP inputs for performing SUBFLOW

Node	Name	Description	Terminal/Hub	Energy (kW)	FO		EL		ME		HVIN		HVHE		HVEX		LO		CW		FW/SW		SW HE	
			Type	lb	IN	OUT	IN	OUT	IN	OUT	IN	OUT	IN	OUT	IN	OUT	IN	OUT	IN	OUT	IN	OUT	IN	OUT
1	BB_DB_DT_CO_SS_f	distribution fwd	terminal	10.000	-	0.000	IN	-1.000	-	0.000	-	0.000	-	0.000	-	0.000	-	0.000	-	0.000	-	0.000	-	0.000
2	BB_DB_DT_CO_SS_m	distribution mid	terminal	10.000	-	0.000	IN	-1.000	-	0.000	-	0.000	-	0.000	-	0.000	-	0.000	-	0.000	-	0.000	-	0.000
3	BB_DB_DT_CO_SS_a	distribution aft	terminal	10.000	-	0.000	IN	-1.000	-	0.000	-	0.000	-	0.000	-	0.000	-	0.000	-	0.000	-	0.000	-	0.000
4	BB_DB_DT_MA_CO	main command CCS 80 etc	terminal	20.000	-	0.000	IN	-1.000	-	0.000	-	0.000	-	0.000	-	0.000	-	0.000	-	0.000	-	0.000	-	0.000
5	BB_DB_FO_SE_TK_p	settling tank port	terminal	0.000	IN	-1.000	-	0.000	-	0.000	-	0.000	-	0.000	-	0.000	-	0.000	-	0.000	-	0.000	-	0.000
6	BB_DB_FO_SE_TK_s	settling tank stbd	terminal	0.000	IN	-1.000	-	0.000	-	0.000	-	0.000	-	0.000	-	0.000	-	0.000	-	0.000	-	0.000	-	0.000
7	BB_DB_FO_CE_PU_p	centrifugal purifier port	hub	0.000	OUT	-1.000	0.010	0.000	-	0.000	-	0.000	-	0.000	-	0.000	-	0.000	-	0.000	-	0.000	-	0.000
8	BB_DB_FO_CE_PU_s	centrifugal purifier stbd	hub	0.000	OUT	-1.000	0.010	0.000	-	0.000	-	0.000	-	0.000	-	0.000	-	0.000	-	0.000	-	0.000	-	0.000
9	**BB_DB_EL_GT_EN_p**	Gas turbine generator set	hub	0.000	0.064	0.000	-	-0.480	-	0.000	0.936	0.000	-	0.000	-	-0.439	-	-0.081	-	0.000	-	0.000	-	0.000
16	**BB_DB_EL_GT_EN_s**	Gas turbine generator set	hub	0.000	0.064	0.000	-	-0.480	-	0.000	0.936	0.000	-	0.000	-	-0.439	-	-0.081	-	0.000	-	0.000	-	0.000
10	BB_DB_EL_PD_AL	power distribution aft load	hub	0.000	-	0.000	IN	-0.900	-	0.000	-	0.000	-	-0.100	-	0.000	-	0.000	-	0.000	-	0.000	-	0.000
11	BB_DB_EL_PD_ML	power distribution mid load	hub	0.000	-	0.000	IN	-0.900	-	0.000	-	0.000	-	-0.100	-	0.000	-	0.000	-	0.000	-	0.000	-	0.000
12	BB_DB_EL_PD_FL	power distribution forward load	hub	0.000	-	0.000	IN	-0.900	-	0.000	-	0.000	-	-0.100	-	0.000	-	0.000	-	0.000	-	0.000	-	0.000
13	BB_DB_ME_PM_MO_p	propulsion module port	hub	0.000	-	0.000	IN	0.000	-	-0.900	-	0.000	-	-0.100	-	0.000	-	0.000	-	0.000	-	0.000	-	0.000
14	BB_DB_ME_TT_BE_p	thrust block port	hub	0.000	-	0.000	-	0.000	IN	-0.900	-	0.000	-	0.000	-	0.000	-	-0.001	-	0.000	-	0.000	-	0.000
15	BB_DB_ME_PR_NE_p	propeller port	terminal	18500.000	-	0.000	-	0.000	IN	-1.000	-	0.000	-	0.000	-	0.000	-	0.000	-	0.000	-	0.000	-	0.000
17	BB_DB_ME_PM_MO_s	propulsion module stbd	hub	0.000	-	0.000	IN	0.000	-	-0.900	-	0.000	-	-0.100	-	0.000	-	0.000	-	0.000	-	0.000	-	0.000
18	BB_DB_ME_TT_BE_s	thrust block stbd	hub	0.000	-	0.000	-	0.000	IN	-0.900	-	0.000	-	0.000	-	0.000	-	-0.001	-	0.000	-	0.000	-	0.000
19	BB_DB_ME_PR_NE_s	proeller stbd	terminal	18500.000	-	0.000	-	0.000	IN	-1.000	-	0.000	-	0.000	-	0.000	-	0.000	-	0.000	-	0.000	-	0.000
20	BB_DB_HV_IN_BP_p	inlett bypass doors port	terminal	0.000	-	0.000	-	0.000	-	0.000	IN	-1.000	-	0.000	-	0.000	-	0.000	-	0.000	-	0.000	-	0.000
21	BB_DB_HV_IN_SI_p	intake silencing splitters port	hub	0.000	-	0.000	-	0.000	-	0.000	IN	-1.000	-	0.000	-	0.000	-	0.000	-	0.000	-	0.000	-	0.000
22	BB_DB_HV_IN_BP_s	inlett bypass doors stbd	terminal	0.000	-	0.000	-	0.000	-	0.000	IN	-1.000	-	0.000	-	0.000	-	0.000	-	0.000	-	0.000	-	0.000
23	BB_DB_HV_IN_SI_s	intake silencing splitters stbd	hub	0.000	-	0.000	-	0.000	-	0.000	IN	-1.000	-	0.000	-	0.000	-	0.000	-	0.000	-	0.000	-	0.000
24	BB_DB_HV_HE_ZA	heat zone aft	hub	0.000	-	0.000	-	0.000	-	0.000	-	0.000	IN	-1.000	-	0.000	-	0.000	-	0.000	-	0.000	-	0.000
25	BB_DB_HV_HE_ZM	heat zone mid	hub	0.000	-	0.000	-	0.000	-	0.000	-	0.000	IN	-1.000	-	0.000	-	0.000	-	0.000	-	0.000	-	0.000
26	BB_DB_HV_HE_ZF	heat zone fwd	hub	0.000	-	0.000	-	0.000	-	0.000	-	0.000	IN	-1.000	-	0.000	-	0.000	-	0.000	-	0.000	-	0.000
27	BB_DB_HV_HE_AT_a	ATU aft	hub	0.000	-	0.000	0.020	0.000	-	0.000	-	0.000	OUT	0.000	-	0.000	-	0.000	-	-1.000	-	0.000	-	0.000
28	BB_DB_HV_HE_AT_m	ATU mid	hub	0.000	-	0.000	0.020	0.000	-	0.000	-	0.000	OUT	0.000	-	0.000	-	0.000	-	-1.000	-	0.000	-	0.000
29	BB_DB_HV_HE_AT_f	ATU forward	hub	0.000	-	0.000	0.020	0.000	-	0.000	-	0.000	OUT	0.000	-	0.000	-	0.000	-	-1.000	-	0.000	-	0.000
31	BB_DB_HV_EX_EJ_p	exhasust por	terminal	0.000	-	0.000	-	0.000	-	0.000	-	0.000	-	0.000	IN	-1.000	-	0.000	-	0.000	-	0.000	-	0.000
30	BB_DB_HV_EX_SI_p	silincing splitter port	hub	0.000	-	0.000	-	0.000	-	0.000	-	0.000	-	0.000	IN	-1.000	-	0.000	-	0.000	-	0.000	-	0.000
33	BB_DB_HV_EX_EJ_s	exhaust stbd	terminal	0.000	-	0.000	-	0.000	-	0.000	-	0.000	-	0.000	IN	-1.000	-	0.000	-	0.000	-	0.000	-	0.000
32	BB_DB_HV_EX_SI_s	silincing splitter stbd	hub	0.000	-	0.000	-	0.000	-	0.000	-	0.000	-	0.000	IN	-1.000	-	0.000	-	0.000	-	0.000	-	0.000
34	BB_DB_LO_HX_PT	LO HX	hub	0.000	-	0.000	0.070	0.000	-	0.000	-	0.000	-	0.000	-	0.000	OUT	0.000	-	0.000	-	-1.000	-	0.000
35	BB_DB_CW_HX_PT	CW HX	hub	0.000	-	0.000	0.061	0.000	-	0.000	-	0.000	-	0.000	-	0.000	-	0.000	OUT	0.000	-	-1.000	-	0.000
36	BB_DB_FW_SW_HX	FW/SW HX	hub	0.000	-	0.000	0.006	0.000	-	0.000	-	0.000	-	0.000	-	0.000	-	0.000	-	0.000	OUT	0.000	-	-1.000
37	BB_DB_SW_EX_EN	sea chest	terminal	0.000	-	0.000	-	0.000	-	0.000	-	0.000	-	0.000	-	0.000	-	0.000	-	0.000	-	0.000	IN	-1.000

Like the CGP, the System Connection Program (SCP) also provides necessary inputs for the SUBFLOW formulation, particularly for the connections/arcs. As shown in Table 23, the input consists of the identification of distributed ship service systems commodity/ technology (e.g., DT for data, EL for electrics), the minimum and maximum capacity of the connection based on a given scenario (e.g., snort or sprint submerged for submarine case), and the objective function coefficient, which was also set to zero.

Table 23: Example of the SCP inputs for performing SUB/RFLOW

ID	Medium (m	PL ID	lb	ub snort	ub sprint	ub sub	OFF	OFV
1	DT_1	PL0	0	1.00E+99	1.00E+99	1.00E+99	0	0
2	DT_2	PL0	0	1.00E+99	1.00E+99	1.00E+99	0	0
3	DT_3	PL0	0	1.00E+99	1.00E+99	1.00E+99	0	0
4	DT_4	PL0	0	1.00E+99	1.00E+99	1.00E+99	0	0
5	DT_5	PL0	0	1.00E+99	1.00E+99	1.00E+99	0	0
6	DT_6	PL0	0	1.00E+99	1.00E+99	1.00E+99	0	0
7	DT_7	PL0	0	1.00E+99	1.00E+99	1.00E+99	0	0
8	DT_8	PL0	0	1.00E+99	1.00E+99	1.00E+99	0	0
9	DT_9	PL0	0	1.00E+99	1.00E+99	1.00E+99	0	0
10	DT_10	PL0	0	1.00E+99	1.00E+99	1.00E+99	0	0
11	DT_11	PL0	0	1.00E+99	1.00E+99	1.00E+99	0	0
12	DT_12	PL0	0	1.00E+99	1.00E+99	1.00E+99	0	0
13	DT_13	PL0	0	1.00E+99	1.00E+99	1.00E+99	0	0
14	DT_14	PL0	0	1.00E+99	1.00E+99	1.00E+99	0	0
15	DT_15	PL0	0	1.00E+99	1.00E+99	1.00E+99	0	0
16	DT_16	PL0	0	1.00E+99	1.00E+99	1.00E+99	0	0
17	DT_17	PL0	0	1.00E+99	1.00E+99	1.00E+99	0	0
18	DT_18	PL0	0	1.00E+99	1.00E+99	1.00E+99	0	0
19	DT_19	PL0	0	1.00E+99	1.00E+99	1.00E+99	0	0
20	DT_20	PL0	0	1.00E+99	1.00E+99	1.00E+99	0	0
21	DT_21	PL0	0	1.00E+99	1.00E+99	1.00E+99	0	0
22	DT_22	PL0	0	1.00E+99	1.00E+99	1.00E+99	0	0
23	DT_23	PL0	0	1.00E+99	1.00E+99	1.00E+99	0	0
24	DT_24	PL0	0	1.00E+99	1.00E+99	1.00E+99	0	0
25	DT_25	PL0	0	1.00E+99	1.00E+99	1.00E+99	0	0
26	DT_26	PL0	0	1.00E+99	1.00E+99	1.00E+99	0	0

Once these inputs had been defined, the inputs above (captured in CGP and SCP) needed to be converted into an Operational Matrix format so that the solver in MATLAB could produce the SUBFLOW network solution. The generation of the Operational Matrix format can be demanding in the early stage of ship design if it was not automated as there can be thousands of rows and columns for defining a network of distributed ship service systems SUBFLOW problem. Thus, to make SUBFLOW as efficient as possible, the generation of the Operational Matrix need to be automated (see Figure 9).

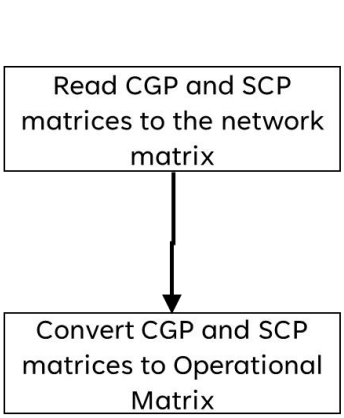

Table 22

Table 23

Formulation	Number of Arcs	Number of Nodes
Objective function	Coefficients associated with the LP formulation	
Constraints, such as equality, inequality, and bounds		

Figure 9: Automatic generation of the Operational Matrix from CGP and SCP inputs

To make an automated generation of the Operational Matrix possible, a MATLAB script was developed. Figure 10 shows the process including reading the CGP and SCP inputs and storing them into the network matrix in MATLAB. The SUBFLOW formulation is next converted into the Operational Matrix format and the Operational Matrix is fed into a solver in MATLAB to find the SUBFLOW solution. If the solver fails to find a set of feasible solutions, the CGP and SCP inputs need to be evaluated and altered. Once the SUBFLOW solution is found, the data is stored back in the network matrix in MATLAB.

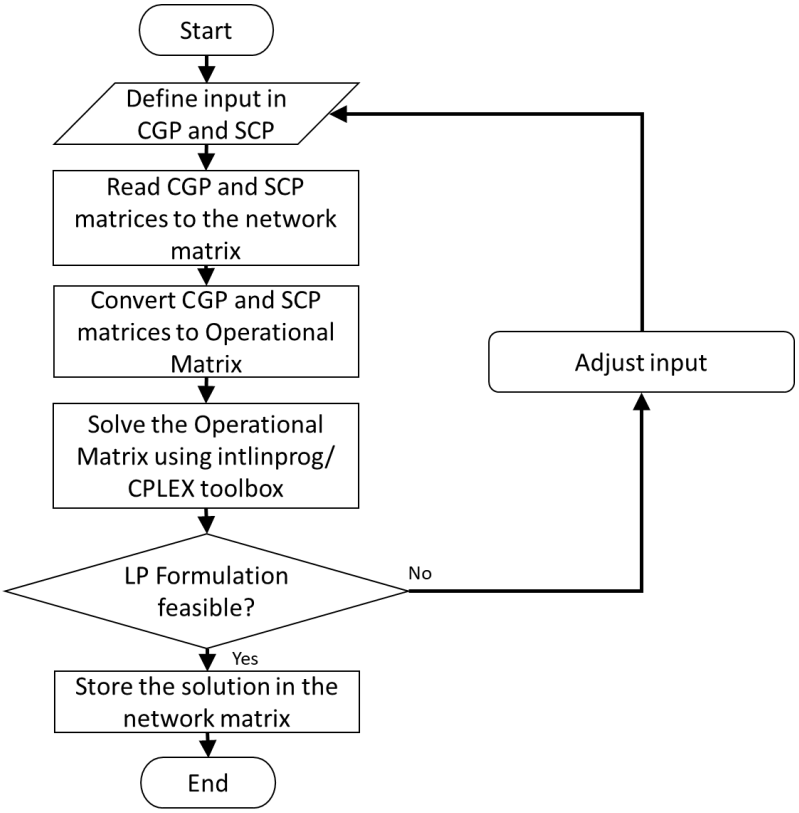

Figure 10: The procedure for automatic Operational Matrix generation

The pattern of the Operational Matrix for the UCL Network Block Approach is given in Table 24. The number of columns of the Operational Matrix depends on the number of arcs in the SUBFLOW network. This matrix is divided into several groups of boxes in rows. The first box of the matrix in Table 24 gives the objective function coefficients, which is set to zero to obtain the energy balance. The second box is allocated to continuity as well as the energy coefficient e for each node, which can be positive or negative. The third box contains the inequality constraints and the last two boxes consists of the lower bounds and the upper bounds. The lower and upper bounds are where the 'operational' aspect is defined, i.e., the supply or demand of a commodity of a node in each operating condition. Therefore, a different operating condition (e.g., snort and sprint submerged) requires a different Operational Matrix, which can be treated as a loop in MATLAB (see Figure 11).

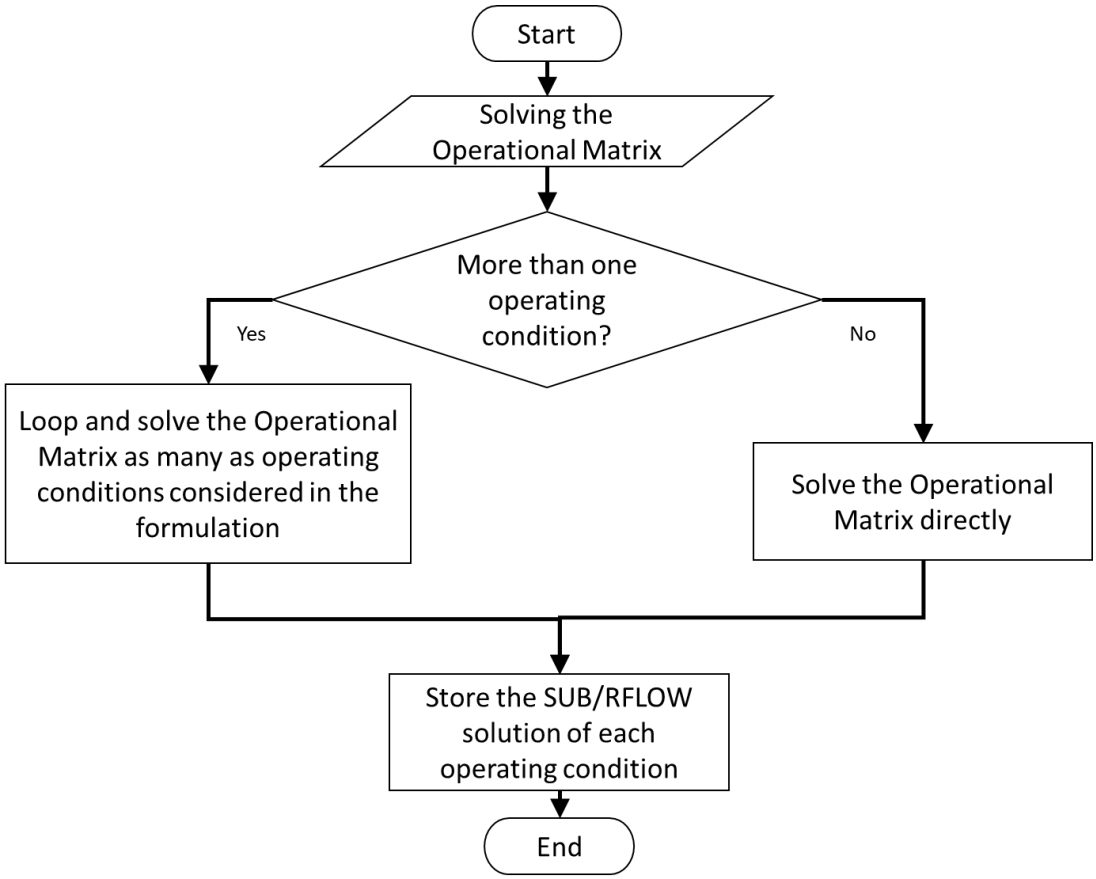

Figure 11: Solving the Operational Matrix based on operating condition(s)

Compared to example Operational Matrices in the previous section, the matrix in Table 24, is scalable and simpler. This was to reduce the extent of the SUBFLOW analysis to be commensurate with early stage ship design. SUBFLOW was used to perform a steady state simulation of power flow in a distributed ship service systems network. SUBFLOW was employed to provide early estimates of the distributed ship service systems space and weight input as well as to explore distributed ship service systems options as part of the Requirement Elucidation process (Andrews, 2018).

The continuity constraints in the SUBFLOW network for the UCL Network Block Approach were hardcoded, i.e., automatically generated. However, the rest of the mathematical model for SUBFLOW formulation could be adjusted/ defined in the Component Granularity Program (CGP) and the System Connection Program (SCP). The formulation process was iterative and substantial to achieve a feasible network solution, i.e., if the formulation is incorrect, the solver will not be able to find the linear programming network solution (see Figure 10). Still, the SUBFLOW required more engineering and inputs than parametric approach, such as the configuration of the distributed ship service systems, also specifying its properties, and creating mathematical models for the energy balance analysis.

The SUBFLOW in the UCL Network Block Approach allows the style (Andrews, 2018) of distributed ship systems to be captured and can aid the designer to understand how a given system functions. Most importantly, when combined with the whole ship UCL Design Building Block approach (Andrews and Pawling, 2003), it enabled a more realistic distributed ship service systems synthesis to be undertaken. This was thus not just numeric but also addressed spatial/architectural aspects which a parametric approach lacking. However, it is not as detailed as collaborative analysis tools which are more appropriate to detailed design of such distributed ship service systems. Figure 12 shows an example of modelling a range of submarine systems: fuel (FO); electrical (EL); data (DT); mechanical (ME); hydraulics (HY); trim and ballast (TB); saltwater (SW); high-pressure air (HP); low-pressure air (LP); ventilation (HVIN/HE/EX); chilled water (CW); lubricating oil (LO); fresh water (FW) cooling systems (see (Mukti, 2022) for details).

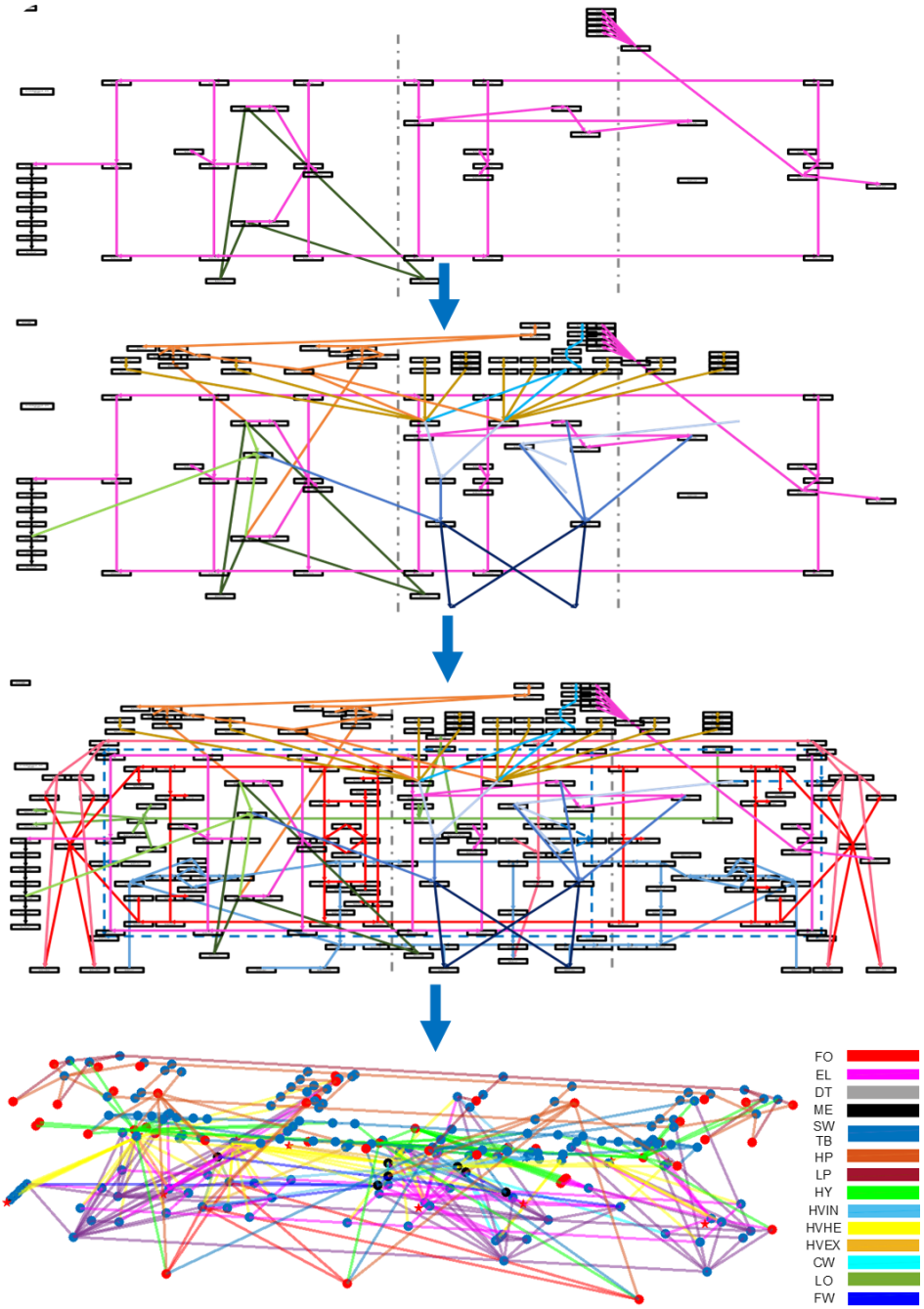

Figure 12: An example of SUBFLOW network development and solution in the UCL Network Block Approach (Mukti, 2022), showing energy flows in various distributed ship service systems

Table 24: The pseudo-Operational Matrix of SUB/RFLOW in the UCL Network Block Approach

	1, 2, … number of arcs	1, 2, … number of arcs	1, 2, … number of arcs	1
Objective Function	0 . . .	0 . . .	0 . . .	0
Equality constraints matrix for continuity	0 0 . . . 0 . . .	$+e$ or . . . $-e$ . . .	$+e$ or . . . $-e$ . . .	0
Inequality constraints matrix for bidirectionality	-1 -1 . . . -1 . . . -1 -1 . . . -1 . . .	-1 -1 . . . -1 . . +1 +1 . . . +1 . . .	0 0 . . . 0 . . 0 0 . . . 0 . . .	0
Lower bounds matrix	. . . 0 . . .	. . . -inf . . .	Based on input provided in the Component Granularity Program (CGP) and the System Connection Program (SCP)	
Upper bounds matrix	. . . inf . . .	. . . inf . . .		

5. CONCLUSION AND FUTURE WORK

There are several possible applications of the Operational Matrix Framework, such that it could be employed to suit several specific network flow formulations. Table 25 shows the high-level comparison between various Network Flow Optimisation setups. Generally, the SUB/RFLOW excludes the survivability analysis to allow enhancement in several aspects, such as the incorporation of a colour-coded 3D multiplex network with the labels showing how much energy flowing from system to system (Figure 12). The Operational Matrix Framework approach has enabled the solvers to be very efficient compared to millions of lines of CPLEX scripts (Brown, 2020). Most importantly, SUB/RFLOW enabled the incorporation of the 3D rich architecturally centred approach, the UCL DBB approach, which shows the potential benefits in assessing wholeship impact of a new (style) of distributed ship service systems design (Mukti, 2022). However, as aforementioned, the design data in the UCL Network Block Approach could have provided a suitable basis for further (survivability) analyses in subsequent design phases, if required.

Table 25: General comparison between different types of Network Flow Optimisation setup for naval ships applications

Formulation	**Network Flow Optimisation for Ship Systems Application**		
	NSMCF (Trapp, 2015)	**AFO** (Brown, 2020)	**SUBFLOW** (Mukti, 2022)
Objective Function	Procurement and installation cost	Procurement and installation cost	None ("constraints only" approach to find energy balance)
Solver	CPLEX	CPLEX	CPLEX toolbox (or *linprog*) in MATLAB
Software interface/ Programming language	MATLAB script to CPLEX script	MATLAB script to CPLEX script	Fully in MATLAB using Operational Matrix Framework
Survivability analysis	Yes	Yes	No
Can be used for sizing distributed systems	No	Yes	Yes
Application	Integrated Engineering Propulsion (IEP) plant	Surface ship systems	Submarine/ Surface ship systems (Mukti et al., 2024)
Using energy coefficient	No	Yes	Yes
Using flow capacity	Yes	Yes	No
Hot and cool model	Yes	Yes	No/Simplified
Multilayer network/ all arcs visible to inspect the energy flow between systems	No	No	Yes, using SUB/RFLOW Multiplex Framework
Support 3D rich ship architecture definition (e.g., equipment arrangement and routings)	No	No	Yes, via Paramarine-SURFCON

In this paper, studies range from the simplest application of Operational Matrix Framework to an example of one of the more complex Operational Matrix applications to the 3D multiplex submarine systems problem in the last section. The use of the proposed Operational Matrix Framework can reveal the relationship between objective functions, constraints, bounds, and solutions of that linear programming formulation. This is demonstrated particularly by the arrows in Table 11, which shows that the network formulation is driven by the constraints at the user nodes, i.e., the lower and upper bounds for the user nodes. These values first influence the equality constraints and subsequently the inequality constraints (these are defined earlier in the paper). The set of solutions in the inequality constraints is directly influenced by the lower and upper bounds for the inequality

constraints. Ultimately, the solver ensures that the objective function produces the possible minimum value for the network solution (see the values in the bracket in the first seven columns in the first row of Table 11).

By mapping the coefficients of the linear programming formulation and the network solution in a manner of the Operational Matrix Framework, coefficients that drive the network solution could be identified before incorporating more extensive cost/survivability coefficients as part of meeting an objective function and responding to further constraints. This gave the ship designer awareness, clarity, and confidence in understanding the logical reasoning behind why the solver produces such a network solution. Without the Operational Matrix Framework, the linear programming in the UCL Network Block Approach would not have been sufficiently simplified for early-stage ship systems sizing applications. An overcomplicated network formulation could distract the designer from the main focus of requirement elucidation: to understand the impact of distributed ship service systems (DS3) choices on the overall submarine design, which could have consequences for the vessel's overall architecture. Thus, the Operational Matrix Framework can be seen to reduce the "black box" nature when using the linear programming tool to explore DS3 choices in early stage of ship design.

One of the main areas of future work is to consider whether the existing execution time of the MATLAB script could be further improved by incorporating a new solver other than CPLEX toolbox (e.g., MATLAB *linprog*) to ensure a designer could perform the many iterations required to formulate SUB/RFLOW. Another area would be to expand the application of the Operational Framework to other complex vessels, including but not limited to various surface warships or oil and gas service vessels (Floating Production Storage and Offloading (FPSO) ship, OSVs, drilling ship, etc). This includes expanding the consideration of aspects of maintenance, and supportability for evaluating various submarine systems style choices. The Operational Matrix Framework could also be developed further for investigating the analysis of energy balances for new systems to achieve net zero energy demands for future naval vessels.

CONTRIBUTION STATEMENT

Author 1: conceptualisation, data curation, formal analysis, methodology, writing – original draft. **Author 2:** funding acquisition, supervision. **Author 3:** funding acquisition, writing – review and editing.

ACKNOWLEDGEMENT

This research stems out of a multinational university collaboration involving: University of Michigan, Delft University of Technology, University College London, and Virginia Tech. These partners gratefully acknowledge the funding of this Naval International Cooperative Opportunities in Science and Technology Program (NICOP) contract number N00014-15-1-2752, sponsored by Ms. Kelly Cooper of the US Navy Office of Naval Research, which is a follow-on of a previously successful collaboration. That was undertaken by the first three universities exploring ship layout in early stage of ship design (Andrews et al., 2012). The original work was focused on studying methods for generating and analysing general arrangements in early-stage ship design (Andrews et al., 2012). The second NICOP extended that layout work to study the relationship between distributed system design and general arrangements, in the context of ship survivability (Brefort et al., 2018). The current study could be seen to build on both NICOP projects activities in early stage of ship design research and the current outcome acknowledges the insights from both collaborative endeavours.

DISCLAIMER

The work presented in this paper is part of the thesis of the first author (Mukti, 2022), which in part has been presented in several other papers also referenced in this paper. However, the Operational Matrix focus of this paper has not been presented directly beyond the thesis.

REFERENCES

Andrews, D.J. (2018) The Sophistication of Early Stage Design for Complex Vessels. RINA IJME Special Edition, vol 160 Part A. doi:10.3940/rina.ijme.2018.SE. Oct 2018.

Andrews, D.J., Duchateau, E., Gillespe, J.W., et al. (2012) IMDC State of the Art Report: Design for Layout. 11th International Marine Design Conference (IMDC), Glasgow, UK, 11-14 June, 2012. Available at: http://resolver.tudelft.nl/uuid:f53cb8ba-1174-4975-b12a-c89242027c82 (Accessed: 12 July 2018).

Andrews, D.J. and Pawling, R.J. (2003) "SURFCON A 21st Century Ship Design Tool." In The 8th International Marine Design Conference. Athens, Greece, May 2003. IMDC.

Brefort, D., Shields, C., Habben Jansen, A., et al. (2018) An architectural framework for distributed naval ship systems. Ocean Engineering, Vol 147: 375–385. doi:10.1016/j.oceaneng.2017.10.028.

Brown, A.J. (2020) Design of marine engineering systems in ship concept design. Parsons, M.G. (ed.). Alexandria, VA: The Society of Naval Architects and Marine Engineers. Alexandra, VA. 2020.
Burcher, R. and Rydill, L. (1994) Concepts in Submarine Design. Cambridge ocean technology series. Cambridge [England]: Cambridge University Press. 1994.
IBM, C. (2014) IBM Knowledge Center. Available at: https://www.ibm.com/support/knowledgecenter/SSSA5P_12.5.0/ilog.odms.cplex.help/CPLEX/MATLAB/topics/cplex_matlab_overview.html (Accessed: 29 June 2019).
Kennedy, A.B.W. and Sankey, H.R. (1898) The Thermal Efficiency of Steam Engines. Report of The Committee Appointed to The Council Upon the Subject of The Definition of a Standard or Standards of Thermal Efficiency for Steam Engines: With an Introductory Note. (Including Appendixes and Plate at Back of Volume). Minutes of the Proceedings of the Institution of Civil Engineers, 134 (1898): 278–312. doi:10.1680/imotp.1898.19100.
MATLAB (2019) MATLAB - MathWorks. Available at: https://uk.mathworks.com/products/matlab.html (Accessed: 8 July 2019).
Mukti, M., Pawling, R. and Andrews, D. (2024) Computer Aided Sketching in The Early-Stage Design of Complex Vessels. Ocean Engineering. To be Published
Mukti, M.H. (2022) A Network-Based Design Synthesis of Distributed Ship Services Systems for a Non Nuclear Powered Submarine in Early Stage Design. Ph.D. thesis, UCL (University College London). Available at: https://discovery.ucl.ac.uk/id/eprint/10147800/ (Accessed: 21 November 2022).
Mukti, M.H., Pawling, R.J. and Andrews, D.J. (2021) Distributed Ship Service Systems Architecture in The Early Stages of Designing Physically Large and Complex Vessels: The Submarine Case. IJME, Vol 163. doi:https://doi.org/10.5750/ijme.v163iA2.755. 2021.
Mukti, M.H., Pawling, R.J. and Andrews, D.J. (2022) “Development of an Early-Stage Design Tool for Rapid of Distributed Ship Service Systems Modelling in Paramarine – a Submarine Case Study.” In 21th Conference on Computer Applications and Information Technology in the Maritime Industries. Pontignano, Italy, June 2022.
Mukti, M.H., Pawling, R.J. and Andrews, D.J. (2024) Computer Aided Sketching in The Early-Stage Design of Complex Vessels. Ocean Engineering Journal. To be Published.
Newman, M. (2010) Networks: An Introduction. Oxford University Press. Available at: http://www.oxfordscholarship.com/view/10.1093/acprof:oso/9780199206650.001.0001/acprof-9780199206650 (Downloaded: 22 November 2018).
Parsons, M.A., Kara, M.Y., Robinson, K.M., et al. (2020) Early-Stage Naval Ship Distributed System Design Using Architecture Flow Optimization. Journal of Ship Production and Design, 37: 1–19. doi:10.5957/JSPD.10190058. 2020.
Qinetiq (2019) Paramarine. Available at: https://paramarine.qinetiq.com/products/paramarine/index.aspx (Accessed: 8 July 2019).
Robinson, K.M. (2018) Modeling Distributed Naval Ship Systems Using Architecture Flow Optimization. Master’s thesis, Virginia Tech. 2018.
Trapp, A. (2015) Shipboard Integrated Engineering Plant Survivable Network Optimization. Ph.D. thesis, Massachusetts Institute of Technology. 2015.

APPENDIX A

```
G = digraph([0 1 1 0; 0 0 0 1; 0 0 0 1; 0 0 0 0]);
G.Nodes.Name = {'Source' 'Hub1' 'Hub2' 'Target'}';

ops_mtx=[1 1 2 2 0 0 0 0;
        1 0 1 0 -1 0 0 0;
        -1 1 0 0 0 -1 0 0;
        0 0 -1 1 0 0 -1 0;
        0 -1 0 -1 0 0 0 -1;
        0 0 0 0 0 0 0 -10;
        10 10 10 10 inf 0 0 -10];
x=linprog(ops_mtx(1,:),[],[],ops_mtx(2:5,:),zeros(4,1),ops_mtx(6,:),ops_mtx(7,:));

G.Edges.Weight(1) = x(1,1);
G.Edges.Weight(2) = x(3,1);
G.Edges.Weight(3) = x(2,1);
G.Edges.Weight(4) = x(4,1);

G.Edges.LWidths = 7*G.Edges.Weight/max(G.Edges.Weight)+1; p=plot(G); p.LineWidth =
G.Edges.LWidths;
```

Proceedings of 15th International Marine Design Conference (IMDC-2024)
June 2-6, 2024
Amsterdam, the Netherlands

Static hydroelastic study of composite T-foils with beam and lifting line models

Galen W. Ng[1,*], Eirikur Jonsson[2], Yingqian Liao[3], Sicheng He[4], Joaquim R.R.A. Martins[5]

ABSTRACT

Well-designed hydrofoils improve ship resistance and seakeeping by lifting the hull above the water. With greater speeds come greater loads, and the two-way interaction of structural deflections of lifting surfaces on the hydrodynamics must be considered. Tailored structural anisotropy can improve hydrodynamic and structural efficiency of lifting surfaces compared to rigid counterparts by exploiting the layup of composite materials. Structural efficiency here means reduced risk of structural failure for a given amount of material, and hydrodynamic efficiency means lower drag. A T-foil is a prototypical multi-component appendage, consisting of the foil wing and the strut, which we investigate in this work. We use simple composite beam and lifting line theory to explore the static fluid-structure interaction of a composite T-foil for a variety of fiber angles ($\theta_f = 0°, \pm 15°$). We apply a simple approximation on lift coefficient at infinite Froude number (Fn) to model the free-surface effects, which is valid at high depth-based Froude numbers ($Fn_h > 10\sqrt{h/c}$) when C_L is independent of Fn_h and the inertial effects dominate. Results for the moth rudder T-foil geometry studied here indicate that aligning composite fibers towards the leading edge results in a more hydrostructurally efficient foil and that free-surface effects are minor because of the large submergence for this flow condition.

KEY WORDS

Hydrodynamics; Composite structures; Hydrofoil; Hydroelasticity; Fluid-structure interaction

INTRODUCTION

T-foils are prototypical lifting surface configurations commonly used to lift a vessel above the free surface. Flying above the water improves seakeeping performance because of the reduced waterplane area. Foiling also removes any resistance associated with hullborne operation: hull wetted skin friction drag, hull form drag, hull wave making drag, wave added resistance, etcetera. For a fixed amount of total resistance, a foiling vessel can sail much faster than a hullborne one since drag force scales with speed squared. In other words, foilborne vessels have better energy efficiency than hullborne vessels in higher speed regimes, which was investigated by Godø and Steen (2023a). However, faster vessels come with concerns for cavitation and ventilation phenomena on the foils. Additionally, loads on the structure approach yield limits, and the two-way coupled effect of the deformed state of the foils on the hydrodynamic loads must also be considered. Hydroelastic analysis is thus critical for the accurate assessment of higher speed vessels.

[1] Ph.D. Candidate (University of Michigan, Ann Arbor, USA); ORCID: 0000-0001-7980-9483
[2] Post-doctoral research fellow (University of Michigan, Ann Arbor, USA); ORCID: 0000-0002-5166-3889
[3] Post-doctoral research fellow (University of Michigan, Ann Arbor, USA); ORCID: 0000-0001-6904-8844
[4] Assistant Professor (University of Tennessee, Knoxville, USA); ORCID: 0000-0003-1307-4909
[5] Pauline M. Sherman Collegiate Professor (University of Michigan, Ann Arbor, USA); ORCID: 0000-0003-2143-1478
[*] Corresponding Author: Galen W. Ng nggw@umich.edu

Submitted: 20 February 2024, Revised: 28 April 2024, Accepted: 1 May 2024, Published: 26 May 2024

Conference paper, DOI: https://doi.org/10.59490/imdc.2024.900 e-ISSN: 3050-4864

More recently, composite materials have gained the interest of foil designers because of hydroelastic tailoring, which improves the hydrodynamic and structural performance of these devices in off-design conditions. Directional stiffness, or *material anisotropy* opens up the potential for passive, load-dependent, shape-adaptative marine structures. A more structurally efficient foil can be realized because deflections under fluid load can be designed to avoid critical stresses and deflections, and hence material failure. Flow-induced vibrations and noise can also be designed away through tuning of plies and structural sizing variables (Ng et al., 2022; Mulcahy et al., 2014; Groo et al., 2019). These structurally efficient foils require less material to achieve a given objective. Composites also improve hydrodynamic efficiency through lower drag designs because the load-dependent deflections favorably reduce subcavitating drag as demonstrated by Liao et al. (2021).

The composite structure can be modeled with varying fidelity to capture quantities of interest. For example, Faye et al. (2024) used low-fidelity composite beam elements to model material bend-twist coupling for a deflecting hydrofoil. Beam theory is cheap, but it can miss some material failure mechanisms. In contrast, Liao et al. (2023) modeled grouped layers of composite laminates with brick finite element models of a hydrofoil to more accurately capture through-thickness stresses and deformations that can then be used in more rigorous material failure criteria. Maung et al. (2023) went further with their composite hydrofoil optimization using a detailed finite element model of a hydrofoil with curved fibers that also captured ply drops.

For lifting surfaces operating near the free surface, one must additionally consider the effects of free-surface proximity on the loads and local pressures on the appendage to accurately optimize a design. The first-order effects of the free surface boundary on hydrodynamic loads can mostly be captured with potential flow methods and a linearized free-surface boundary condition. A numerical lifting line method is the lowest order potential flow model appropriate for loads on a hydrofoil wing. Godø and Steen (2023b) present one example of a lifting line method for determining the hydrodynamic loads on a hydrofoil with linearized free-surface effects computed through a Green's function, which avoids the need to mesh the free surface boundary. Nicolas et al. (2023) used the linearized free-surface boundary condition as well but modeled the hydrofoil with panels on the body, which captures thickness and lifting effects more accurately than a lifting line method. Beck and Reed (2001, Fig. 1) presents an overview of numerical methods for handling free surface effects from inviscid potential flow to viscous direct numerical simulation. The latter is too costly for preliminary design and analysis, which is the area of focus for this work.

At low speeds, the free surface behaves like a rigid wall boundary, whereas at high speeds, it acts as pressure relief because the perturbations forces of the moving body overcome the gravity of the water that maintains the rigid wall behavior at low speeds (Faltinsen, 2006, Ch. 6). The non-dimensional number that best characterizes these regimes of free-surface effects is the *Froude number*, which is the ratio of inertial to gravitational forces. The chord-based (c) and depth-based (h) Froude numbers are given by

$$Fn_c = \frac{U_\infty}{\sqrt{gc}}, \qquad Fn_h = \frac{U_\infty}{\sqrt{gh}}. \tag{1}$$

Faltinsen (2006, Ch. 6) presents approximations to the hydrodynamics loads in the Froude number limits used in this work.

The choice of hydrodynamic and structural model fidelity depends on the balance between computational speed and required accuracy of the physics to assess a candidate design. This work deals with preliminary hydroelastic design of foils so we deem lifting line and composite beam theories as adequate. First, we discuss the theoretical background and the case setup of our hydro-structural model in the Dynamic Composite Foil (DCFoil.jl) program. Then, we present and discuss the static hydroelastic behavior of a moth T-foil rudder for various material configurations with the free-surface effect turned on and off. We conclude with overall insights based on our results and suggestions for future work.

METHODOLOGY

The following sections describe the basic background of the static analysis mode of the Dynamic Composite Foil (DCFoil.jl) program. DCFoil.jl was originally developed considering second-order dynamical system analysis in the mass-

spring-dashpot sense of $\mathbf{M_s}\ddot{\mathbf{u}} + \mathbf{C_s}\dot{\mathbf{u}} + \mathbf{K_s}\mathbf{u} = \mathbf{f_{hydro}}$ (Ng et al., 2023), but we remove time derivative terms for static analysis. The governing discrete equation for static analysis is

$$\mathbf{K_s}\mathbf{u} = \underbrace{\mathbf{f}_{\text{hydro}}(\mathbf{u})}_{=-(\mathbf{K_f})\mathbf{u}} \tag{2}$$

where $\mathbf{u}$ are the structural states, $\mathbf{K_s}$ is the structural stiffness matrix, and $\mathbf{K_f}$ is the hydrodynamic stiffness matrix. We solve this equation for $\mathbf{u}$ using a Newton-Raphson scheme. The next section describes the computation of $\mathbf{K_s}$; the following, $\mathbf{K_f}$. The global coordinate system, shown in Figure 1, is x streamwise, y to starboard, and z up.

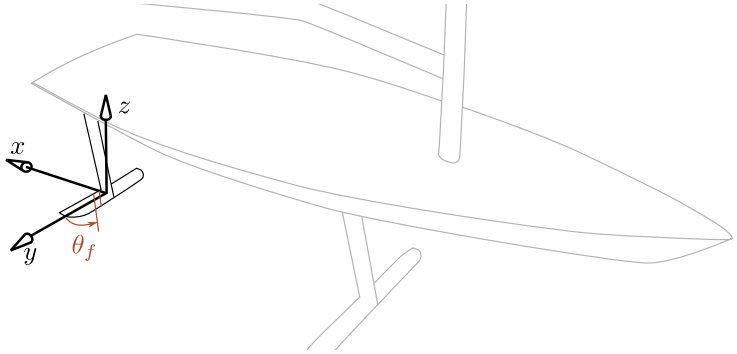

Figure 1: Global coordinate system for the composite T-foil with positive fiber angle convention.

Composite beam finite element model

The composite beam model has been previously developed and validated against a composite plate model in ABAQUS (Ng et al., 2023). The beam finite element has two nodes with nine degrees of freedom at each node to account for structural warping. The only noteworthy new extension to the implementation is the mesh generation routine for a T-foil. Previously, we only studied cantilevered beams (half-wing). We updated the routine for generating meshing and element connectivity to handle three "half-wings": two port-starboard (P/S) symmetric wings and one strut. Figure 2 shows the stick model.

As for structural properties, we specify only two sets of parameters for the half-wing and strut, since the wings are P/S symmetric. For example, a fiber angle of $\theta_f = 15^\circ$ on the starboard wing (aligned towards the leading edge) is mirrored on the port wing. We assume the elastic axis (locus of shear centers) is along the midchord.

Hydrodynamic lifting line model

The basic lifting line model builds on our previous work (Ng et al., 2022, 2023) that follows Glauert's method (Glauert, 1983, Ch. 11) for the static lifting line of a hydrofoil of arbitrary planform. We assume a Fourier sine series expansion for the spanwise vorticity $\gamma(y)$ and solve a linear system for the Fourier coefficients using relations for the spanwise downwash and vorticity. Because the strut interrupts the wing at the centerline, the spanwise vorticity is zeroed out at the junction collocation node. Then we compute the spanwise lift slope $c_{\ell_\alpha}(y)$ to populate the $\mathbf{K_f}$ matrix. The center of lift is at $c/4$ for each section, which is an inviscid thin-airfoil assumption. Note, the quarter-chord center of pressure assumption does lose validity at higher angles of attack because of flow separation that causes the center of pressure to migrate towards the midchord.

In steady-state potential flow, the *negative image method* is appropriate for representing the free surface in the high Froude number limit. Conversely, the *positive image method* is for low Froude number flows. The *linearized*[1] *free-surface bound-*

[1] Assuming small wave slopes and removing higher order velocity terms

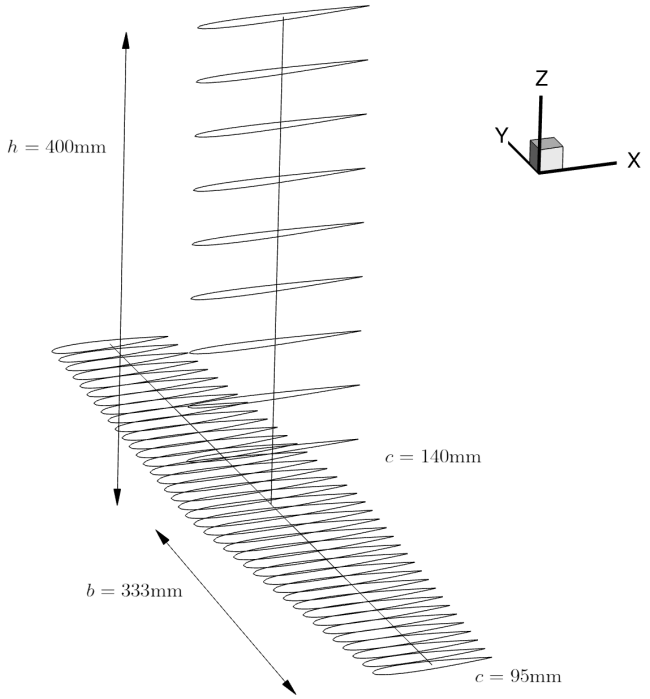

Figure 2: Stick model of a T-foil with overall dimensions labeled. Airfoil slices are drawn at node locations to aid with visualization.

ary condition, which can be derived from combining a dynamic and kinematic boundary condition (Newman, 2018, Sec. 6.1), is

$$U_\infty^2 \frac{\partial^2 \varphi}{\partial x^2} + g \frac{\partial \varphi}{\partial z} = 0 \quad \text{for } z = 0, \tag{3}$$

where $z = 0$ is the mean free surface and φ is the perturbation potential of the lifting body. The total potential is $\Phi = U_\infty x + \varphi$. Equation 3 tells us the first term vanishes for low Fn, and the second term vanishes for high Fn. For high Froude numbers, $\varphi = 0$ on $z = 0$ is a solution to the boundary condition equation 3. Putting negative images of source and vortex singularities equal distances from the free surface as the actual body satisfies this. Approximations to the asymptotical behavior of lift and drag at high Froude numbers exist that facilitate rapid analysis for submerged lifting surfaces. Faltinsen (2006) gives this 2D lift relation accounting for free-surface effect

$$c_\ell \left(\frac{h}{c} \right) = c_\ell \left(\frac{h}{c} = \infty \right) \cdot \left[\frac{1 + 16(h/c(y))^2}{2 + 16(h/c(y))^2} \right] \quad \text{for } Fn_h > 10/\sqrt{h/c}, \tag{4}$$

where the bracketed term is a "corrective" factor accounting for the negative image vortex. The extension to a 3D foil follows as a correction on the spanwise vorticity. The spanwise vorticity, is a decomposition of circulation in 2D and downwash-induced circulation from neighboring vortex elements

$$\gamma(y) = \underbrace{\gamma_{2D}}_{\text{airfoil}} \underbrace{-\pi c(y) w_i(y)}_{\text{downwash effect}}. \tag{5}$$

The correction applies to the airfoil vorticity

$$\gamma_{2D}\left(y, \frac{h}{c}\right) = \underbrace{-U_\infty c(y)\pi\alpha}_{\gamma_{2D}\left(y, \frac{h}{c}=\infty\right)} \left[\frac{1+16(h/c)^2}{2+16(h/c)^2}\right]. \tag{6}$$

We compute the total spanwise vortex strength $\gamma(y)$ from Glauert's method so we simply subtract the γ_{2D} with no free-surface effect and add back the circulation with free-surface effect (Equation 6).

CASE SETUP

The T-foil model is based on the moth rudder T-foil studied by Liao et al. (2022); Ashworth Briggs (2018); Binns et al. (2008). The foil has a 0.4 m strut with a NACA0015 section. The wings are NACA0012 sections with a $b = 0.333$ m semi-span, a root chord of 0.14 m, and a tip chord of 0.095 m. The stick model showing the dimensions is given in Figure 2. We use 19 elements for each half wing and nine for the strut. The planform area of a half-wing is 0.039m^2, and the area we use in nondimensionalization of forces in the next section is twice that value ($A = 0.078\text{m}^2$).

The material properties are for uni-directional (UD) carbon fiber-reinforced plastic (CFRP) given in Table 1. In reality, the foil would be made of a laminate with several plies of different angles embedded in a resin matrix to avoid crack propagation, but for the purposes of exploring anisotropy effects, these mechanical properties are adequate.

Table 1: Subscript 1 is along the fiber, 2 is in-plane, and 3 is out-of-plane.

Variable	Symbol	CFRP	Units
Solid density	ρ_s	1,590	kg/m^3
Elastic moduli	E_1	117.8	GPa
—	$E_2 = E_3$	13.4	GPa
Shear moduli	$G_{12} = G_{23}$	3.9	GPa
Poisson's ratio	$\nu_{12} = \nu_{13}$	0.25	—

For the flow setup, we consider one speed of $U_\infty = 18$ m/s (≈ 35 kts), which corresponds to the top speed analyzed by Liao et al. (2022) and is consistent with typical hull speeds sailorscan achieve during races. The depth Froude number is then $Fn_h = 9.09$, which is greater than the highest limiting value of $10/\sqrt{h/c} = 5.92$ at the root chord, so the negative image method applies. Fluid density is $\rho_f = 1025$ kg/m^3 for seawater. We assume no yaw angle or leeway effects, so flow comes head on and the strut produces no load. The wing has a base rake angle of $\alpha_r = 2^\circ$.

We look at three hydrofoils with varying fiber angles on the wing. The first is $\theta_f = 0^\circ$ and the next two are $\pm 15^\circ$. The strut fiber angle stays at $\theta_f = 0^\circ$ because there will be no side loads in these cases. We also divide the results further into the ones with a deeply submerged assumption (no correction to $\gamma(y)$) and ones with the free surface model as explained prior. The foils will not all produce the same lift, so at the end, we run a polar varying α_r.

RESULTS

The following section first discusses the case setup and then presents the results.

Static hydroelasticity of the T-foils

Lifting forces and deflections

In Table 2, we see the lift generated by the various foils. As one would expect, as fiber angle goes from negative to positive (trailing edge to leading edge), the total lift decreases because of an increased de-pitching effect to which the material anisotropy contributes. Furthermore, the lift between no free surface model and the free surface model decreases marginally because of the reduction in circulation caused by proximity to the free surface at high Fn_h. The reduction is minor because depth-to-chord ratio (h/c) is high. The depth-to-chord ratio is squared in Equation (6) and thus brings the correction factor close to unity. The reduction in forces is also less pronounced when less lift is produced.

Table 2: Lift of the various foils with percent difference from no free surface model.

	$\theta_f = -15^\circ$		$\theta_f = 0^\circ$		$\theta_f = 15^\circ$	
	L [N]	C_L	L [N]	C_L	L [N]	C_L
No free surface model	5738.7	0.442	2469	0.190	1787	0.138
Free surface model	5527.9 (-3.7%)	0.425	2444 (-1.0%)	0.188	1776 (-0.6%)	0.137

Table 3 presents the moments about the midchord where positive is nose-up. Consistent with the lift trend, the moments also decrease as the fiber angle goes from negative to positive angle alignment. The percentage difference between free surface and no free surface model are also consistent with lift trends, since the differences are smaller for more lightly loaded foils. The overall moments remain positive because the center of lift (assumed $1/4$ chord) are all upstream of the midchord location. Moments decrease because there is less lift applied.

Table 3: Moment about midchord line of the various foils.

	$\theta_f = -15^\circ$		$\theta_f = 0^\circ$		$\theta_f = 15^\circ$	
	M_y [N-m]	C_{My}	M_y [N-m]	C_{My}	M_y [N-m]	C_{My}
No free surface model	165.1	0.108	73.2	0.048	54.0	0.035
Free surface model	159.2 (-3.6%)	0.104	72.5 (-1.0%)	0.047	53.7 (-0.6%)	0.035

The total lift loads and coefficients are consistent with Reynolds-averaged Navier-Stokes (RANS) simulations by Liao et al. (2022) as these foils are also around $C_L = 0.2$ except for the $\theta_f = -15^\circ$ foil, which produces much more lift. We would not expect identical loads since the foils are not identical to Liao et al. (2022), and we have structural compliance in the current study. Furthermore, Liao et al. (2022) used a symmetry boundary condition, which is analogous to the positive image method, so we would expect their results to have slightly more lift than the present study if everything else were the same.

The deflected states of the hydrofoils with no free-surface effect are visualized in Figure 3. The deflections are scaled by two to better visualize the differences between the different fiber angle foils. The $\theta_f = -15^\circ$ T-foil experiences significantly more deflection.

Figure 4 shows the half-wing spanwise loading and deflections for the three fiber angles with no free-surface effect in solid lines and with free-surface effect in dashed lines. There are minor differences, which makes sense because this is a relatively high h/c. At lower submersion depths (smaller h/c), we expect there to be a greater reduction in lift and moments because of free-surface proximity, and thus, the wings would deflect less. The spanwise loads and deflections here illustrate the minor impact the free surface proximity has on the foils.

An implication of these lift and deflection studies is on susceptibility to cavitation and ventilation. Cavitation depends on local pressure dropping below the saturated vapor pressure of water (Brennen, 2014). Ventilation depends on proximity to the free surface, the existence of flow separation, and going above a critical lift threshold (Damley-Strnad et al., 2019;

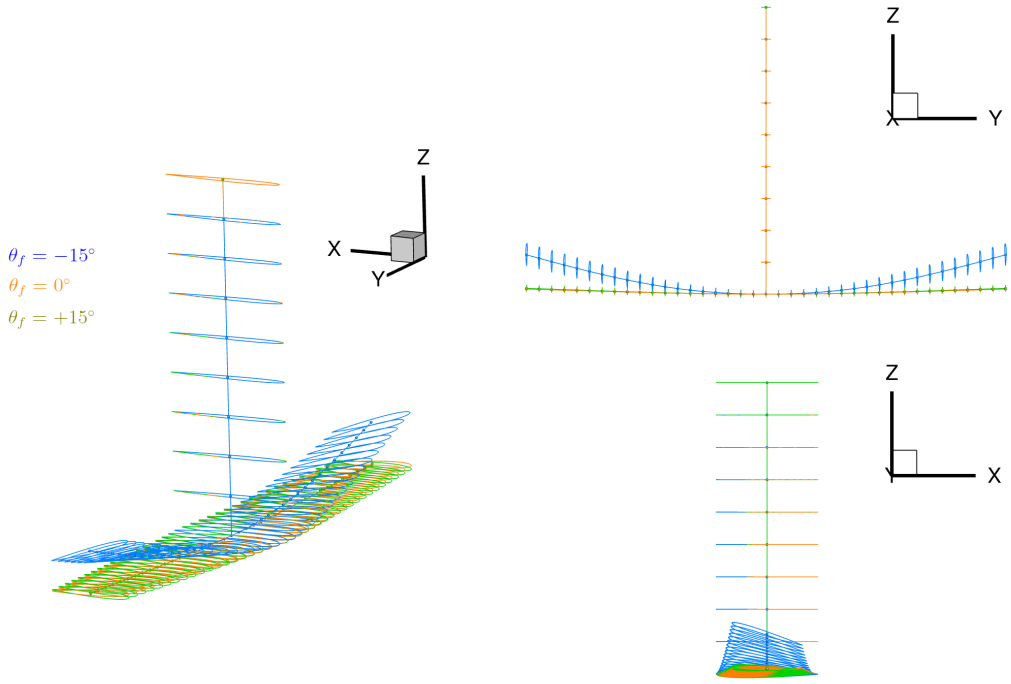

Figure 3: 3D views of the deflected hydrofoil. Deflections scaled by two for visualization purposes.

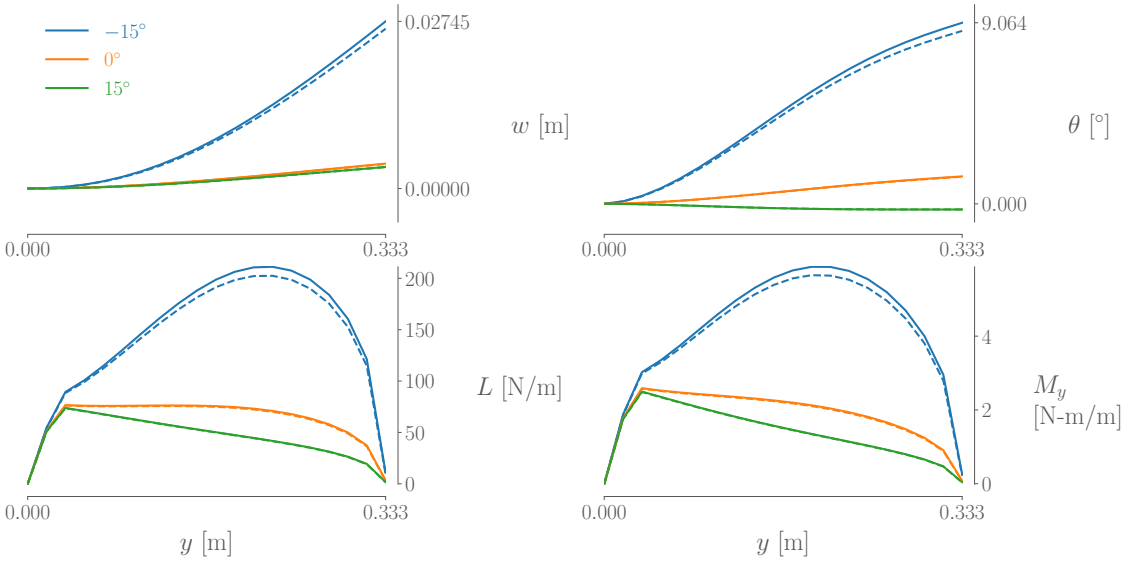

Figure 4: Spanwise vertical bending, twisting, lift, and moment distributions for the different fiber angle T-foils using the deeply submerged assumption (solid) and infinite Froude number free surface effect (dashed).

Young et al., 2017). Based on this intuition, one could deduce that the $\theta_f = -15°$ composite T-foil would have many issues. It produces more lift at the tip than the other foils at this rake angle. The tip twist is around $\theta_{\text{tip}} + \alpha_r = 9° + 2° = 11°$, which when coupled with any variations in angle of attack due to waves or vessel motions could create a strong tip vortex and stall the tip. A strong tip vortex has a low-pressure core, which can result in undesired tip vortex cavitation. Cavitation can be particularly damaging to composite structures (Yamatogi et al., 2009), and it also creates noise and vibrations that

are harmful to the vessel operation. In addition to the cavitation problems, the stalled tip could create a low-energy flow area that is a pathway for air to be sucked down onto the foil. It is also possible for tip vortex cavitation to promote tip ventilation. Collapse of vaporous bubbles induces local velocities towards the body, which break the surface seal earlier than without cavitation. Another effect is that the buoyancy of a cavitating tip vortex is greater than that of a subcavitating tip vortex (Young et al., 2017, Sec. 4.1.4). Sudden ventilation would be detrimental to overall vessel performance and controllability since lift would suddenly drop by about half.

Furthermore, the overall deflections of the $\theta_f = -15^\circ$ hydrofoil are quite high (about 8% of semispan) and structural failure may also be a concern. In contrast, the 0° and 15° are more well-behaved and safer candidate designs for further exploration because they do not have as high a risk of static structural failure or ventilation. There appears to be little merit to aligning fibers towards the trailing edge unless there were some aileron-like surface outboard, in which case, the controllability of the foiling vessel would be improved. Any dynamic hydroelastic failure mechanisms, such as flutter, remain to be explored.

Drag build-up

A steady-state drag build-up model must consider parasitic drag (D_p) and drag due to lift. Drag due to lift is not the same as lift-induced drag (Kroo, 2001). In equation form, total drag (not considering multiphase flow) is

$$D = D_p + \underbrace{\frac{L^2}{q\pi b^2 e}}_{\text{drag due to lift}} \qquad \text{where } D_\text{p} = D_\text{fric} + D_\text{form} + D_\text{w} + D_\text{int} + D_\text{spray}, \tag{7}$$

and e is the Oswald efficiency factor. For this hydrofoil assuming single-phase flow, the parasitic drag (everything that is not drag due to lift) consists of interference (D_int), spray (D_spray), wave-pattern (D_w assumed zero), skin friction (D_fric), and form drag (D_form). To supplement the equation form of total drag, Figure 5 hierarchically categorizes the drag components and typical nomenclature used to describe calm-water drag.

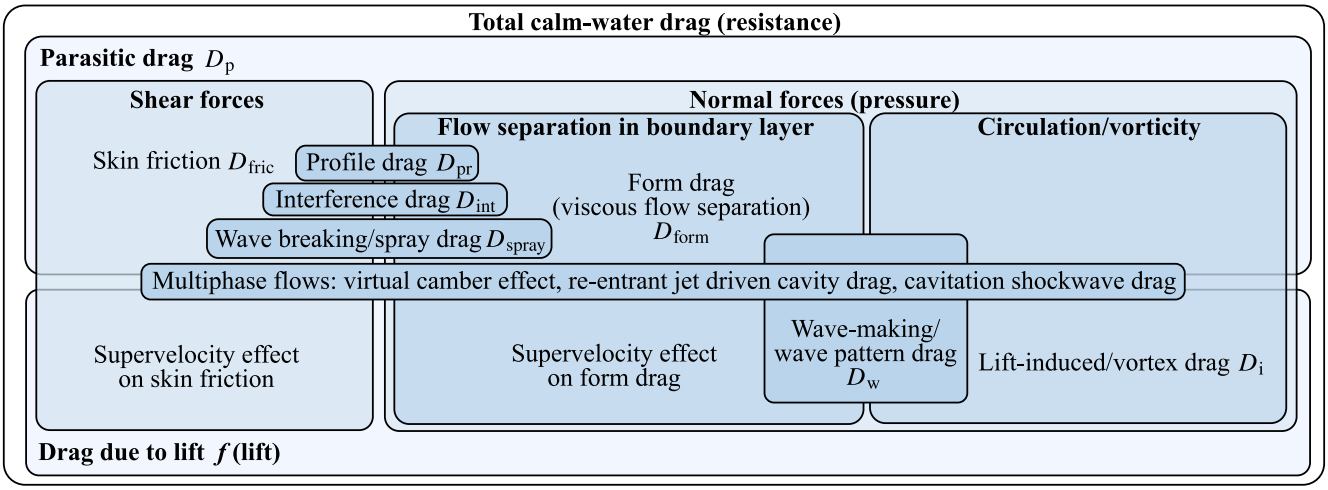

Figure 5: Sources of hydrodynamic drag

A model for the lift-induced drag is based on the spanwise vorticity and downwash. The total induced drag is computed via

$$F_x = -\rho \int_{-b}^{b} \gamma(y) w_i(y) dy \approx -\rho \sum_{n=1}^{\text{nstrips}} \gamma_n(y) w_{i,n}(y) dy_n. \tag{8}$$

The empirical relation for interference drag for a strut junction with no fairing from Hoerner (1965, Ch. 8) is

$$C_{D,\mathrm{j}} = \frac{D_{\mathrm{int}}}{qt^2} = 17\left(\frac{\bar{t}}{c}\right)^2 - 0.05, \tag{9}$$

where $\bar{t}$ is the mean thickness of the strut and wing near the junction and $q = \frac{1}{2}\rho_f U_\infty^2$ is the dynamic pressure. In reality, junction drag depends on much more than the thickness-chord ratio, such as the bluntness of the nose that affects the strength of the necklace vortex (Simpson, 2001).

Due to lifting and thickness effects, the foil generates surface waves, which adds a component called wave drag. The lifting effect on the generated waves tends to be more important. In 2D, wave drag goes to zero at very high Fn_h (Faltinsen, 2006, Ch. 6) and hence we assume it to be zero. In the case of 3D flow, the aforementioned behavior is that of the transverse waves. The divergent waves still contribute to wave drag regardless of how high Fn_h is. It behaves asymptotically at high enough Fn_h, so it would be a constant offset in our results. Nevertheless, we neglect this component due to time constraints, but Faltinsen (2006, Eq. 6.167) gives the relation.

Hoerner (1965, Ch. 10) gave an empirical relation for the spray drag caused by water piling up on the forebody and shooting into the air as $C_{D,\mathrm{s}} = D_{\mathrm{spray}}/\left(qt_{\mathrm{strut}}^2\right) = 0.24$, which applies to $Fn_c > 3$. However, this does not consider some details of the strut form, so we use the spray drag relation from Chapman (1971)

$$C_{D,\mathrm{s}} = \frac{D_{\mathrm{spray}}}{qc_{\mathrm{strut}}t_{\mathrm{strut}}} = 0.009 + 0.013\left(\frac{t}{c}\right)_{\mathrm{strut}}, \tag{10}$$

where the location of maximum thickness $(x/c)_{\mathrm{max}}$ is around 35%.

The profile drag (skin friction plus form) at hydrofoil sections assumes a flat-plate estimate with form factor corrections. The friction drag is estimated via the ITTC 1957 line

$$C_f = \frac{D_{\mathrm{fric}}}{q\mathrm{WSA}} = \frac{0.075}{\left(\log_{10}\left(Re\right) - 2.0\right)^2}, \tag{11}$$

where WSA is wetted surface area. The equation is an empirical formula for skin friction of naked ship hulls assuming turbulent flow (Carlton, 2018). The empirical form factor $(1 + k)$ is determined from Torenbeek (1990) for a subsonic wing

$$1 + k = 1 + 2.7\left(\frac{t}{c}\right) + 100\left(\frac{t}{c}\right)^4, \tag{12}$$

where the first term with thickness captures the increased skin friction from thickness effects and the quartic term accounts for flow separation drag. This equation misses the angle of attack effects on the profile drag, sometimes referred to as a supervelocity effect (Raymer, 2012, Sec. 12.5.5), which increases the skin friction and form drag. Full profile drag is then just $D_{\mathrm{pr}} = (1 + k)D_{\mathrm{fric}}$.

The total drag of the foils at $\alpha_r = 2^\circ$ are in Table 4. Since the foils are not all at the same lift condition, the lift-induced

Table 4: Total drag of the various foils.

	$\theta_f = -15^\circ$		$\theta_f = 0^\circ$		$\theta_f = 15^\circ$	
	D [N]	C_D	D [N]	C_D	D [N]	C_D
No free surface model	605.7	0.0468	387.3	0.0299	369.4	0.0285
Free surface model	585.2 (-3.4%)	0.0452	386.7 (-0.2%)	0.0299	369.3 (-0.03%)	0.0285

drag plays the biggest role in the differences. The spray and junction drag relations do not depend on lift, so they are identical between the foils. The drag is highest for $\theta_f = -15^\circ$ and decreases for more positive fiber angle since the foils produce less lift. The drag is also reduced when adding free-surface effects because of the reduction in lift. Figure 6 shows the drag build-up for the runs. The results tell the same message that lift-induced drag is the largest contributor to drag differences

between the various foil configurations. Figure 6 also shows that the free surface influences the lift-induced drag calculation for all foils, but the effect is greatest for the foil that produces the most lift ($\theta_f = -15°$). The drag build-up also tells us that profile drag and spray drag are significant portions of total drag that dominate the drag at low C_L conditions; however, this finding is not novel, at least for rigid hydrofoils research. Godø and Steen (2023b) found that strut-related drag, comprised of profile and spray, were large components in total drag (around a quarter of total drag, similar to here).

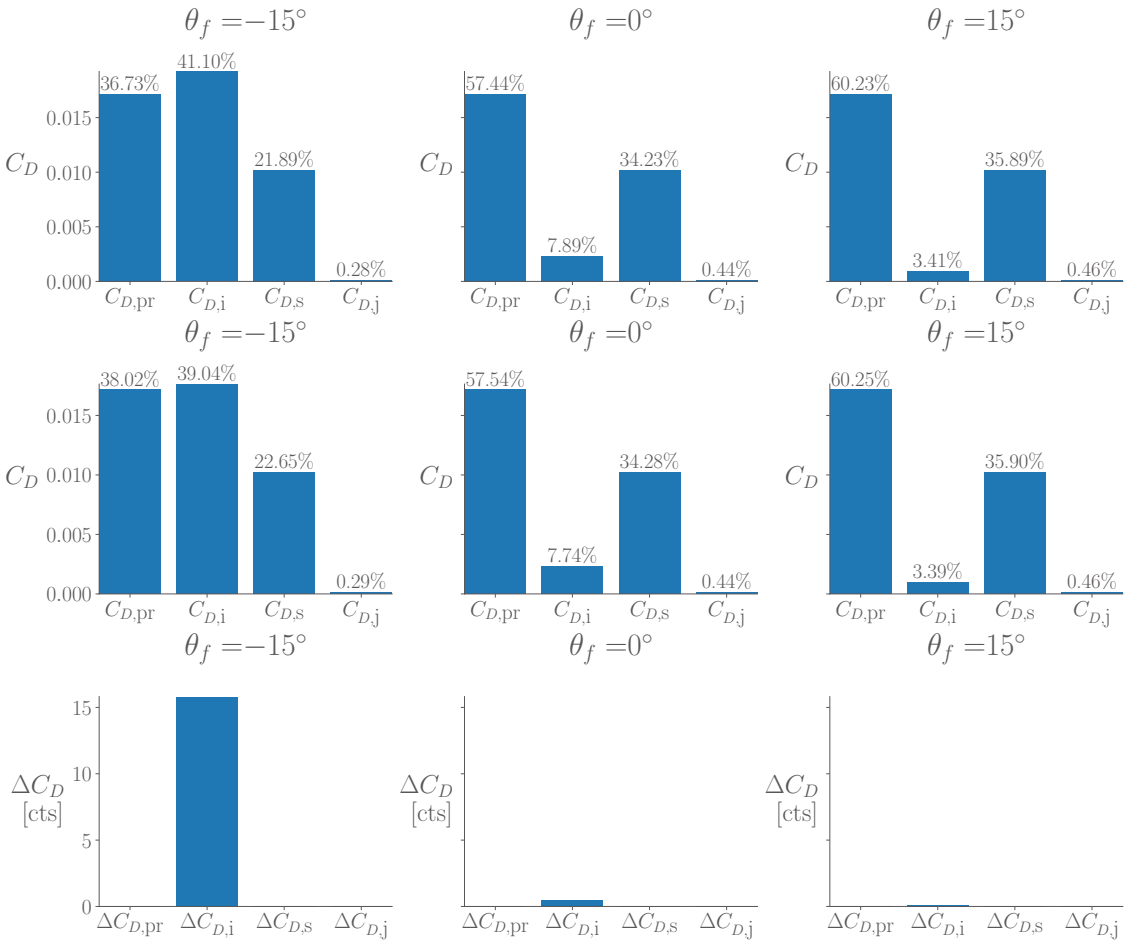

Figure 6: Drag build-up for different fiber angles with no free-surface effect (top row) and with free-surface effect (middle) at $U_\infty = 18$ m/s. Drag deltas between no free-surface and free-surface given in drag counts (bottom).

As a final exploration into the performance, we run polars by varying the wing mounting rake α_r from $-5°$ to $15°$ in $0.5°$ steps. This could correspond to a rake control mechanism or a designer choice. The polars are in Figure 7 where dashed lines are with the free surface model. We add a rigid hydrofoil case as well to see if tailored flexibility offers performance gains. There are some experimental results from Ashworth Briggs (2018, Sec. 6.4.1) for a pitching polar (not wing mounting rake) at $Re = 0.48 \times 10^6$ and $U_\infty = 4$ m/s, which is a very different flow condition; however, we plot them as a comparison to have a general idea of the polar trends. The overall bucket shape comparisons will not be entirely fair because (1) the simulations are at a high enough speed where structural deflections occur and influence drag, whereas the experiment can be assumed to have mostly rigid T-foil hydrodynamics, (2) the angle of attack here is base rake whereas the experiment varied overall pitch, and (3) laminar flow existed in the experiment but our empirical model assumes fully turbulent flow. Nevertheless, we can look at the $\alpha = 0°$ cases between experiment and simulation and draw some parallels.

As expected, the simulated polars are symmetric about $C_L = 0$ and $\alpha_r = 0°$ because of the uncambered hydrofoil section. All T-foils have the same $C_{D,\mathrm{min}} = 275$ drag counts at the $C_L = 0$ condition corresponding to the same parasitic drag. The

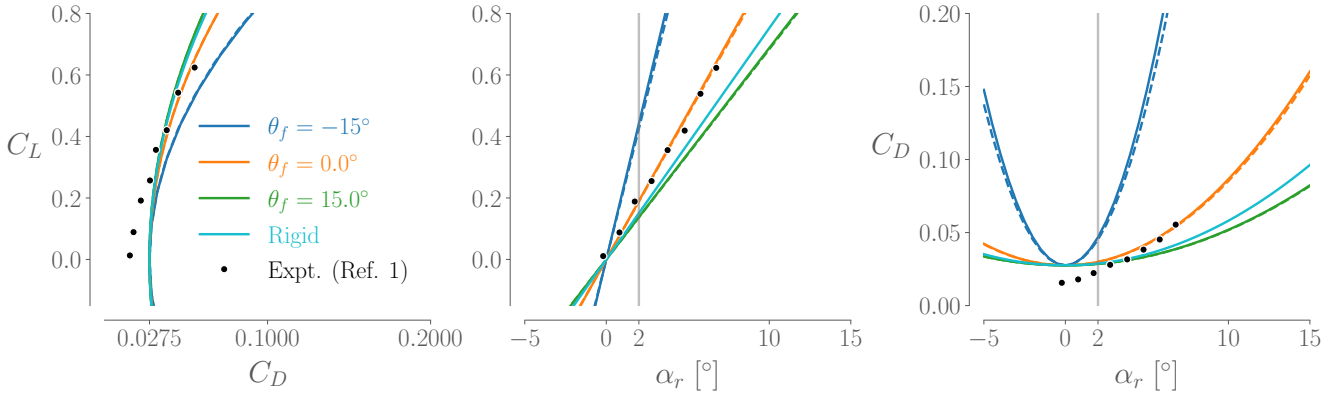

Figure 7: Performance polars of T-foils for $U_\infty = 18$ m/s varying base rake. Solid lines are no free surface and dashed are with the free surface model. The experimental results varied strut rake.

$C_L = 0$ drag value is slightly higher than the experimental $C_{D,\text{min}}$, but this could be a combined effect of inaccurate spray drag, junction intersection drag, and skin friction drag because of the mismatched Reynolds and Froude numbers between experiment and simulation. The experiment had laminar flow at low angles of attack (Binns et al., 2008) while we assumed turbulent flow in the ITTC 1957 line. Future work may warrant an improved parasitic drag model accounting for these effects to accurately assess drag trades.

The more positive fiber angle foils have wider drag buckets, indicating that the max L/D would be best for the $\theta_f = 15°$ T-foil. This would suggest that the $\theta_f = 15°$ T-foil is able to maintain a spanwise lift distribution closer to elliptical across angles of attack and thus reduce the lift-induced drag. This hydrofoil even outperforms the rigid hydrofoil, though not noticeably until much higher C_L and α_r. The polar makes sense because the $\theta_f = 0°$ has positive tip twist (see Figure 4) with increasing lift, but the $\theta_f = 15°$ has washout at the tips from the nose-down bend-twist coupling. The $\theta_f = 0°$ T-foil would therefore have too much load outboard. Lastly, since the lifting line model is potential flow, we do not capture the stalling effect at higher α_r so we should actually see a precipitous drop-off in C_L in the polars at higher angles. Based on these results, the $\theta_f = 15°$ seems to be the best-performing T-foil of the studied configurations, indicating that a designer should look in the direction of more positive fiber angle composite T-foils that promote washout at higher lift.

CONCLUSIONS

Through simple structural and hydrodynamic models, we explored the influence of free-surface effects and material anisotropy on the static hydroelastic response of a composite T-foil. We explored the hydrostructural performance of three composite T-foils, each with different fiber angles.

Negative fiber angles produce more outboard lift and moment, resulting in more outboard deflections with nose-up tip twist. This behavior is bad for both hydrodynamics and structures because of increased cavitation, ventilation, and tip stall susceptibility as well as material failure risk. Zero or positive fiber angles are better for load alleviation because there is more tendency towards washout via nose-down bend-twist coupling. The more positive fiber angle T-foils had better drag polars because of the lower lift-induced drag. We deduce that these types of composite T-foils tend to be hydrodynamically and structurally better, at least for the given initial geometry.

The free surface model used here assumes infinite Froude number and reduced all lift and moments (and hence deflections) on the T-foils. In the cases studied, lift-induced drag dominated, so the free surface also reduced drag because of the reduced lift. The effect was minor because of low depth-to-chord ratio, though further studies into heel or cant angle would be interesting to see the asymmetric loading effect on the flexible composite structure.

In a more sophisticated hydrodynamics lifting line model, finite Froude number effects would more accurately model the bound vorticity (γ) on the foil than the infinite Froude number assumption. This would then enable more accurate lift-induced drag and wave drag estimates that depend on vorticity. The accuracy across finite Froude numbers will be important for higher fidelity design optimizations that may tune submergence depth and chord of hydrofoils if they were design variables, which both affect Froude number. A possible future avenue for considering free-surface effects that balances accuracy and cost is the desingularized Rankine-source panel method with a body-exact, linearized free-surface condition (Cao et al., 1991).

Overall, material anisotropy offers potential for customized spanwise loading of T-foils, which is important for control surface effectiveness, hydrodynamic efficiency through lower drag, and structural efficiency through less/more effective material usage. The models presented here are a computationally cheap way to evaluate preliminary composite foil designs whilst capturing the necessary fluid-structure interactions present in high-speed surface craft design. Our results also show expected and consistent trends with previous numerical and experimental work that verifies the current toolset for rapid, conceptual, design space exploration of more complicated marine appendage geometries. Future work could consider a Froude number-dependent free surface model, coupling of T-foil deflections to vessel dynamics, or unsteady analyses to capture the vessel response in waves.

CONTRIBUTION STATEMENT

Galen W. Ng: Methodology, Software, Formal analysis, Conceptualization, Data curation, Writing – original draft. **Eirikur Jonsson:** Supervision, Methodology, Writing – review and editing. **Yingqian Liao:** Supervision, Methodology, Writing – review and editing. **Sicheng He:** Supervision, Methodology, Writing – review and editing. **Joaquim R.R.A. Martins:** Supervision, Resources, Writing – review and editing.

ACKNOWLEDGEMENTS

Financial support for this research was provided by the U.S. Office of Naval Research (ONR) under Contract N00014-18-1-2333 managed by Dr. Robert Brizzolara. Galen Ng's graduate education is supported by the National Defense Science and Engineering Graduate (NDSEG) Fellowship. The first author acknowledges helpful discussions with Hugo Nicolas in formulating the drag build-up.

REFERENCES

Ashworth Briggs, A. J. E. (2018). *Free surface interaction of a ' T-foil ' hydrofoil*. PhD thesis, University of Tasmania.

Beck, R. F. and Reed, A. M. (2001). Modern computational methods for ships in a seaway. *Transactions of Society of Naval Architects and Marine Engineers*, 109:1–51.

Binns, J. R., Brandner, P. A., and Plouhinec, J. (2008). The effect of heel angle and free-surface proximity on the performance and strut wake of a moth sailing dinghy rudder T-foil. In *Proceedings of the 3rd High Performance Yacht Design Conference*, Auckland, NZ.

Brennen, C. E., editor (2014). *Cavitation and bubble dynamics*. Cambridge University Press.

Cao, Y., Schultz, W. W., and Beck, R. F. (1991). Three-dimensional desingularized boundary integral methods for potential problems. *International Journal for Numerical Methods in Fluids*, 12(8):785–803.

Carlton, J. (2018). *Marine Propellers and Propulsion*. Butterworth-Heinemann.

Chapman, R. B. (1971). *Spray drag of surface-piercing struts*, volume 251. Naval Undersea Research and Development Center.

Damley-Strnad, A., Harwood, C. M., and Young, Y. L. (2019). Hydrodynamic performance and hysteresis response of hydrofoils in ventilated flows. In *Sixth International Symposium on Marine Propulsors*, Rome, Italy.

Faltinsen, O. M. (2006). *Hydrodynamics of high-speed marine vehicles*. Cambridge University Press.

Faye, A., Perali, P., Augier, B., Sacher, M., Leroux, J.-B., Nême, A., and Astolfi, J.-A. (2024). Fluid-structure interactions response of a composite hydrofoil modelled with 1d beam finite elements. *Journal of Sailing Technology*, 9(01):19–41.

Glauert, H. (1983). *The Elements of Aerofoil and Airscrew Theory*. Cambridge Science Classics. Cambridge University Press.

Godø, J. M. K. and Steen, S. (2023a). A comparative study of the energy efficiency of hydrofoil vessels and slender catamarans. In *HSMV 2023: Proceedings of the 13th Symposium on High Speed Marine Vehicles*, volume 7, pages 159–171.

Godø, J. M. K. and Steen, S. (2023b). An efficient method for unsteady hydrofoil simulations, based on non-linear dynamic lifting line theory. *Ocean Engineering*, 288:116001.

Groo, L., Steinke, K., Inman, D. J., and Sodano, H. A. (2019). Vibration damping mechanism of fiber-reinforced composites with integrated piezoelectric nanowires. *ACS Applied Materials and Interfaces*, 11(50):47373–47381.

Hoerner, S. F. (1965). *Fluid-Dynamic Drag*. Hoerner Fluid Dynamics, Bakersfield, CA.

Kroo, I. M. (2001). Drag due to lift: Concepts for prediction and reduction. *Annual Review of Fluid Mechanics*, 33:587–617.

Liao, Y., Martins, J. R. R. A., and Young, Y. L. (2021). 3-D high-fidelity hydrostructural optimization of cavitation-free composite lifting surfaces. *Composite Structures*, 268:113937.

Liao, Y., Martins, J. R. R. A., and Young, Y. L. (2023). Hydrostructural optimization of single-layer and multi-layer composite lifting surfaces. *Composite Structures*, 307:116650.

Liao, Y., Yildirim, A., Martins, J. R. R. A., and Young, Y. L. (2022). RANS-based optimization of a T-shaped hydrofoil considering junction design. *Ocean Engineering*, 262:112051.

Maung, P. T., Prusty, B. G., Donough, M. J., Oromiehie, E., Phillips, A. W., and St John, N. A. (2023). Automated manufacture of optimised shape-adaptive composite hydrofoils with curvilinear fibre paths for improved bend-twist performance. *Marine Structures*, 87:103327.

Mulcahy, M. L., Croaker, P., McGuckin, D. G., Brandner, P. A., and Kississoglou, N. (2014). Optimisation applied to composite marine propeller noise. In *INTER-NOISE and NOISE-CON Congress and Conference Proceedings*, volume 249, pages 4012–4019. Institute of Noise Control Engineering.

Newman, J. N. (2018). *Marine hydrodynamics*. The MIT press.

Ng, G. W., Jonsson, E., He, S., and Martins, J. R. R. A. (2023). Coupled strip theory and finite element method for stability analysis of composite hydrofoils. In *Proceedings of the 6th International Conference on Innovation in High Performance Sailing Yachts and Wind-Assisted Ships*, Lorient, France.

Ng, G. W., Martins, J. R. R. A., and Young, Y. L. (2022). Optimizing steady and dynamic hydroelastic performance of composite foils with low-order models. *Composite Structures*, 301:116101.

Nicolas, H., Perali, P., Sacher, M., and Bot, P. (2023). Boundary element method analysis of 3d effects and free-surface proximity on hydrofoil lift and drag coefficients in varied operating conditions. *Journal of Sailing Technology*, 8(01):183–199.

Raymer, D. P. (2012). *Aircraft Design: A Conceptual Approach*. AIAA, Reston, VA, 5th edition.

Simpson, R. L. (2001). Junction flows. *Annual Review of Fluid Mechanics*.

Torenbeek, E. (1990). *Synthesis of Subsonic Airplane Design*. Delft University Press and Kluwer Academic Publishers, 6th edition.

Yamatogi, T., Murayama, H., Uzawa, K., Kageyama, K., and Watanabe, N. (2009). Study on cavitation erosion of composite materials for marine propeller. In *The 17th International Conference on Composites (ICCM-17)*, Edinburgh, UK.

Young, Y. L., Harwood, C. M., Montero, M. F., Ward, J. C., and Ceccio, S. L. (2017). Ventilation of lifting bodies: Review of the physics and discussion of scaling effects. *Applied Mechanics Reviews*, 69(1):010801.

Proceedings of 15th International Marine Design Conference (IMDC-2024)
June 2-6, 2024
Amsterdam, the Netherlands

Improve Ship Design Success by Utilising Proactive Elicitation to Enhance Communication Among Diverse Stakeholders

Chengfeng Ou [1], David Trodden [2], and Serkan Turkmen [3]

ABSTRACT

Ships serve as crucial tools for maritime transportation and account for over 80% of global trade. However, the boundary between naval architecture and the maritime industry has existed for 150 years since the first Industrial Revolution. Despite the current ship design processes ensuring compliance with standards, a significant gap exists in effectively communicating and incorporating diverse stakeholders' expectations and desires during the ship design process. This communication gap may lead to a potential risk for incidents and compromise safety. To tackle this issue, this paper proposes to use proactive elicitation as a means to enhance the communication between various stakeholders and naval architects. To verify the impact of proactive elicitation on ship design success, discrete event models were developed in the study to simulate the ship design process. The simulation results demonstrated that the earlier the proactive elicitation is applied to ship design, the higher the level of design success can be achieved. In the short term, this approach can assist shipyards in the timely delivery of ships, while in the long term, it fosters improved compatibility between stakeholders and ships, enabling effective adaptation to future complex design conditions.

KEY WORDS

Ship design; Conceptual design; Tender phase; Elicitation; and Whole ship design

INTRODUCTION

In the current ship design practice, Ships are often tailor-made and designed to meet the specific expectations of the stakeholders. So, the design brief is provided by stakeholders at the beginning of the ship design process. Then naval architects utilise their knowledge and engineering expertise to plan, formulate and design the ship according to the stakeholders' design brief. According to the statistics of the ship design flaws observed from 1545 to 2006 (Andrews, 2020), misunderstanding, poor communication, and overconfidence are the primary causes of ship design flaws in the commercial shipping sector. To minimise these flaws, international organisations established standards and regulations for design criteria that stakeholders and naval architects should adhere to. However, eliminating ship design flaws has not been entirely achieved today, which poses a potential risk of operational accidents.

Long-term marine accident investigation data reveals that approximately 80% of accidents are attributed to human error, with 30% specifically resulting from human failure to take evasive action (Baker & Seah, 2004). The remaining 70% of accidents happened when no one was aware that something was happening (Bafang & Chen, 2021). Nevertheless, the majority of reports persistently attribute human error as the primary cause of accidents, thereby placing a disproportionate burden on seafarers.

[1] Marine, Offshore and Subsea Technology Group, Newcastle University, Newcastle upon Tyne, UK
c.ou1@newcastle.ac.uk

[2] Marine, Offshore and Subsea Technology Group, Newcastle University, Newcastle upon Tyne, UK
david.trodden@newcastle.ac.uk

[3] Marine, Offshore and Subsea Technology Group, Newcastle University, Newcastle upon Tyne, UK
serkan.turkmen@newcastle.ac.uk

Submitted: 23 January 2024, Revised: 19 April 2024, Accepted: 1 May 2024, Published: 21 May 2024

Conference paper, DOI: https://doi.org/10.59490/imdc.2024.863 e-ISSN: 3050-4864

However, among the maritime incidents widely cited as being caused by human error, it is worth noting that 80% of them lack substantial supporting evidence (Wróbel, 2021). One potential contributing factor to these accidents is flaws resulting from a ‘communication gap’ between various stakeholders during the ship design process.

In the current era of highly advanced information and communication technology, the ‘communication gap’ between diverse stakeholders arises mainly from the assumption on each side that the other will actively familiarise themselves with their respective knowledge rather than a lack of willingness to communicate. For example, sailing, navigation, and naval architecture are all interconnected with ships. However, they represent distinct fields. Seafarers may assume that naval architects will naturally incorporate user-friendly features into ship designs, while naval architects may assume that seafarers will provide explicit guidance on the need for such features. If seafarers did not provide clear requirements for these features, naval architects may assume that these features are not necessary. On the other hand, management personnel focus more on integrating the entire ship design plan, providing comprehensive solutions, and demonstrating and communicating the overall ship design concept and capabilities to customers during the early ship system design (ESSD) (Andrews, 2018). Consequently, these differing understandings among the parties naturally lead to discrepancies.

In the past, some efforts have been made to address the barriers within the maritime and shipbuilding industry. For instance, the Nautical Institute (1998) conducted a study examining the relationship between ship design and operation, especially focusing on incorporating the input of seafarers. In the study, the institute distributed a survey questionnaire to seafarers, generating 185 comments. The study concluded that enhancing naval architects' understanding of nautical knowledge is crucial for improving communication with stakeholders and ensuring that the design meets stakeholders' needs. Hughes (1989) categorised operational problems into ten topics, with dedicated sections on equipment and management. The study advocated for the use of precise standards as guidelines for naval architects to facilitate communication with stakeholders during ship design. Those studies highlight the importance of communication between naval architects and stakeholders in ship design. Additionally, several studies have highlighted the significance of incorporating stakeholders' requirements across various aspects of ship design, particularly during the conceptual stage. For instance, Heather (1993) and Graham (1996) emphasised the aspect of 'Requirement' Andrews (1985) and Tibbitts et al. (1993) focused on 'Functional Requirement' Andrews (1985) and Burcher & Rydill (1995) considered 'Operational requirements' Rawson (1986) explored 'Reliability, Maintainability, availability, and logistics' Andrews (1985) delved into 'Systems operating and upkeep philosophies' Andrew (1985) considered the aspect of 'Performing need analysis' and Andrew & Dicks (1997) considered the aspect of 'Functional hierarchical decomposition', and so on. However, how to implement such a recognition in the actual ship design process remains an issue today. Moreover, as the issue evolves and the range of stakeholders may expand under increasingly complex design conditions, incorporating diverse stakeholders’ requirements and desires into ship design becomes more challenging. This motivates the research of this paper, which aims to improve ship design success by utilising proactive elicitation as a means to bridge the ‘communication gap’ among diverse stakeholders.

STUDY FOR GAINING INSIGHTS INTO THE ‘COMMUNICATION GAP’

To facilitate the study, a preliminary survey was conducted, and the stakeholders’ backgrounds covered ship owners, ship managers, equipment suppliers, shipyard naval architects, ship design firm naval architects, seafarers, and academics. A total of 20 people participated in this survey. The first part of this survey was conducted to gain insights into the ‘communication gap’ between stakeholders and naval architects. A questionnaire was thoughtfully designed based on 12 keywords. The survey results are illustrated in Fig.1. During the survey, the 12 keywords were classified into two distinct groups: i.e. ‘concrete’ and ‘cogitation’. The former, indicated by the colour orange, signifies data and standards. Meanwhile, the latter, indicated by the colour blue, highlights the need for exploration and research. In each group, subcategories are distinguished using different shades of the colours. Lighter shades represent aspects that have already been integrated into existing ship design practices, while darker shades indicate areas that require improvement in the future. The degree of concern indicates the areas within ship design to which three distinct stakeholder groups attach importance.

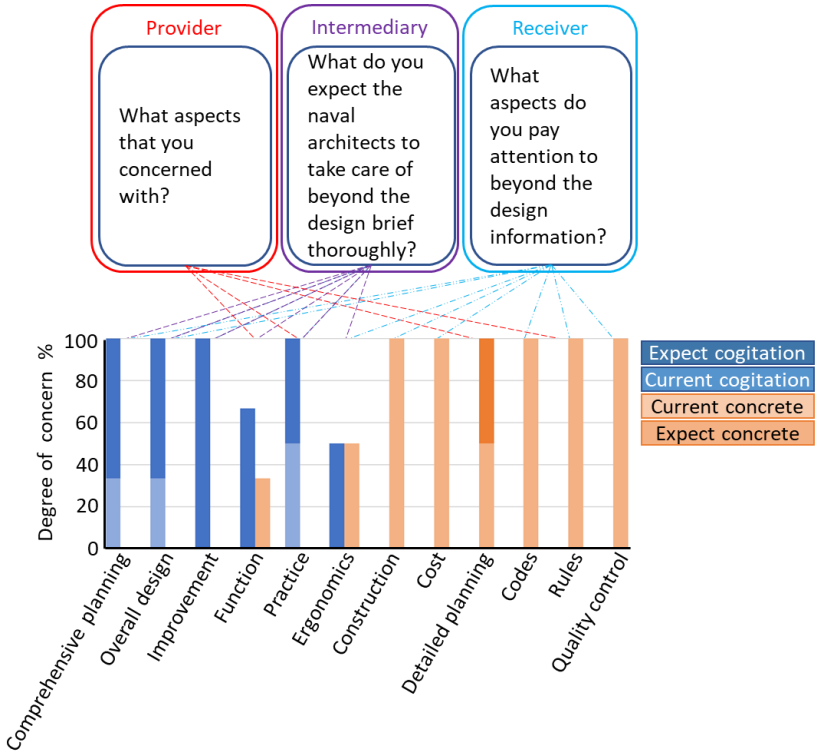

Figure 1 Results of the preliminary survey

Based on the insights depicted in Figure 1, the elements along the horizontal axis are arranged chronologically from the comprehensive planning to the quality control of the shipbuilding production process. It is evident that information providers exhibit greater concerns before the "construction" stage. They prioritise the integration and enhancement of their ideas with lofty expectations. By contrast, information recipients, primarily naval architects, express concerns at every stage and tend to emphasise practical considerations over abstract thinking. This disparity between stakeholders and naval architects highlights the need for additional sources to complement the information provided, as stakeholders' expectations might not be explicitly outlined in the design brief.

Subsequently, a further survey was conducted to investigate the additional sources the naval architects tend to favour. These information sources are categorised into primary (first-hand) and secondary (second-hand), and the findings of the survey are presented in Figure 2. In the figure, the primary sources are depicted on the left side, while the secondary sources are shown on the right. The vertical axis of the chart displays the degree of preference. The results in Figure 2 highlight that naval architects predominantly rely on secondary sources to supplement the design information, with a higher proportion leaning towards indirect means. This observation suggests that naval architects demonstrate a preference for sources that acquire information through intermediaries or administrative procedures, thereby aiding in the reduction of design risks.

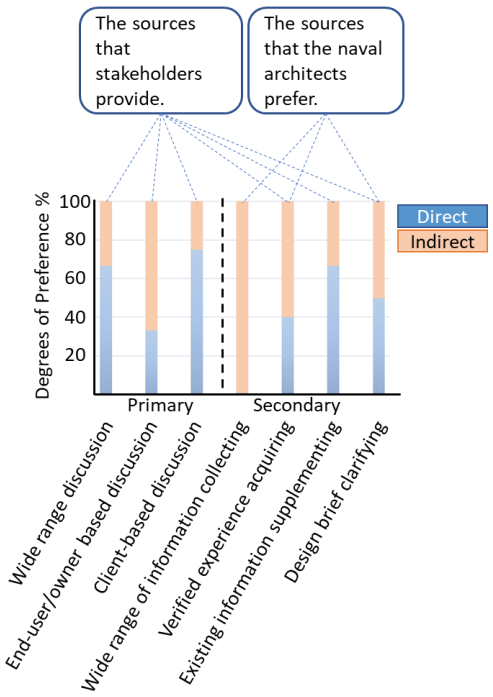

Figure 2: Survey results of information sources.

IMPACT OF COMMUNICATION ON SHIPBUILDING PROJECTS

From 2017 to 2020, a shipyard implemented an experimental policy aimed at successfully delivering 11 shipbuilding projects, as outlined in Table 1. It was discovered that proactive engagement with stakeholders and the broadening of design information sources by naval architects, coupled with an active approach to integrating diverse requirements during the concept design stage, led to a notable enhancement in design success. To assess the implications of this policy, an on-site investigation was conducted at the shipyard, employing a readily understandable market indicator known as the 'on-time delivery rate' of ships. This indicator signifies the ratio between the scheduled and actual building time, offering insights into the efficiency of project management within the organisation. The on-time delivery rate contributes to the effective utilisation of resources, including manpower, materials, and time, while also aiding in waste reduction. Moreover, the 'on-time delivery rate' serves as a measure of the cognitive gap between stakeholders and naval architects throughout the entire project execution process. This cognitive gap represents the additional time required to explore solutions. By successfully completing a project on time, it can be inferred that the surplus time spent on the project is relatively minimised. Thus, the on-time delivery rate serves as a tangible representation of the effectiveness of the experimental policy.

Table 1. Ship projects are being observed.

Project No.	Size and function	Hull type
1	16m Patrol Boat	Monohull
2	17m Attack boat	Monohull
3	18.5m Rapid Response boat	Monohull
4	19m Patrol Boat	Monohull
5	41m Utility craft	Monohull
6	28m Missile boat	Catamaran
7	35m Firefighting boat	Catamaran
8	65m Patrol craft	Catamaran
9	25m Crew Transfer Vessel	SWATH
10	25m Hydrographic vessel	SWATH
11	25m Crew Transfer Vessel	SWATH

In 2018, the shipyard faced two significant challenges that had notable impacts on its operations. Firstly, during the bi-annual audit inspection for ISO 9001 compliance, the International Standard Organization (ISO) identified deficiencies in the shipyard's handling of comment replies, particularly regarding the ISO 9001 8.2.1 Customer Satisfaction standard. Secondly, clients raised complaints asserting that comments on drawings or inspections were not adequately addressed, leading to delays in delivery. These incidents directly affected the shipyard's production quality and design management. To address these issues, the shipyard issued the following directives to all naval architects:

(1) All naval architects and marine engineers must comprehensively understand the requirements and criteria before initiating any schematic drawings.
(2) Issues, comments, and conflicts should be resolved through consensus and approved by both parties prior to considering them as completed.
(3) When explicit instructions are unavailable from the client, it is advisable to seek guidance from individuals possessing relevant expertise. If required, contractual adjustments should be considered.
(4) Should a proposed solution deviate from established rules, regulations, practical engineering handbooks, previous references, or contractual documents, it is imperative to initiate immediate discussions. Design work should not commence without a viable solution.
(5) All outstanding issues must be resolved prior to the commencement of production.

The objective of this observation is to assess the number and percentage of comments that have been formally addressed and accepted, as well as to compare the on-time delivery rates across various ship projects. Figure 3a provides an overview of the approximate number of comments received (indicated by the blue bar) and replied comments (indicated by the orange bar) for 11 projects. Figure 3b illustrates the degree of reply. In both charts, the diamond shape stands for the project that is applied to the new policies.

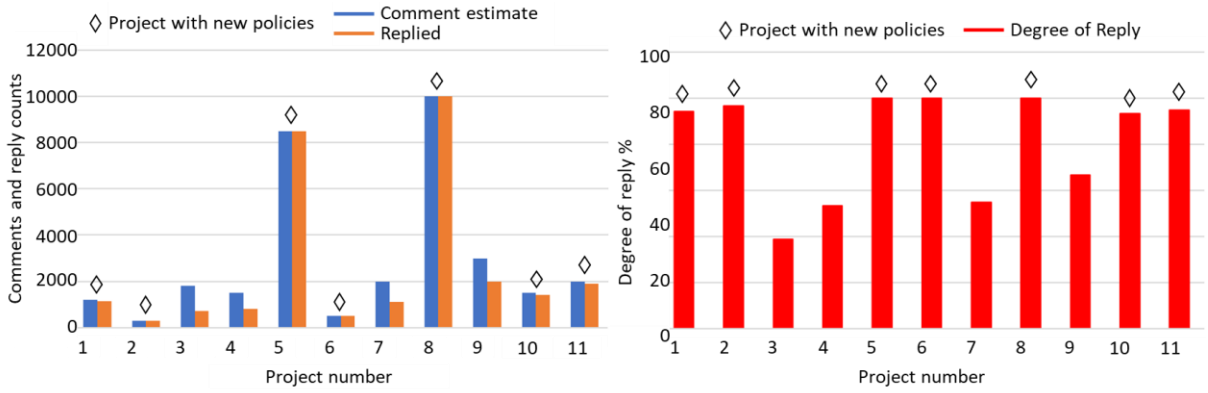

(a) Comments and reply counts estimate **(b) Rate of reply degree**

Figure 3. Comments and replies count corresponding to the Rate of reply degree.

The bar chart in Figure 3b shows a significant increase in the number of comment replies within projects that have been applied with the new policies. This observation highlights a noticeable shift in the behaviour of naval architects, who previously prioritised substantive design tasks (Andrews, 2015) over administrative paperwork. Prior to the enforcement of the new policy, naval architects may have viewed the process of addressing comments as burdensome, potentially hindering the progress of design work and causing distractions and disruptions. Imposing a mere requirement of a 100% response rate to comments may result in counterproductive outcomes resembling a checkbox approach. Such an approach fails to address the fundamental issue of precision in ship design. Consequently, three different approaches have been revealed between conventional design philosophy and new policies. These disparities serve to underline critical areas for improvement, and these two aspects are related to the idea of elicitation:

(1) Under the new policies, the project places a strong emphasis on completing the design phase to ensure alignment among stakeholders and the shipyard, even if it results in a delay to the construction schedule.
(2) In situations where the contract, specifications, and design brief are not adequately defined, the shipyard engages in collaborative efforts with stakeholders to enhance and augment these elements, identifying potential solutions that effectively align with the established criteria.

Figure 4 illustrates the on-time delivery of each project, represented by the blue dimonds or circle, along with their respective reply rates, indicated by the red dimonds or circles. Notably, projects 1 and 2 remain on schedule despite a lower reply rate. Nevertheless, the overall trend demonstrates that the implementation of new policies has played a significant role in ensuring adherence to the established project schedule. In the figure, two additional bars are also presented, i.e. ‘Eliciting from client’

represented by the grey bar and 'Eliciting beyond client' represented by the yellow bar. These bars reflect the efforts of naval architects in expanding their search for additional sources of information, which has contributed to the timely delivery of ships.

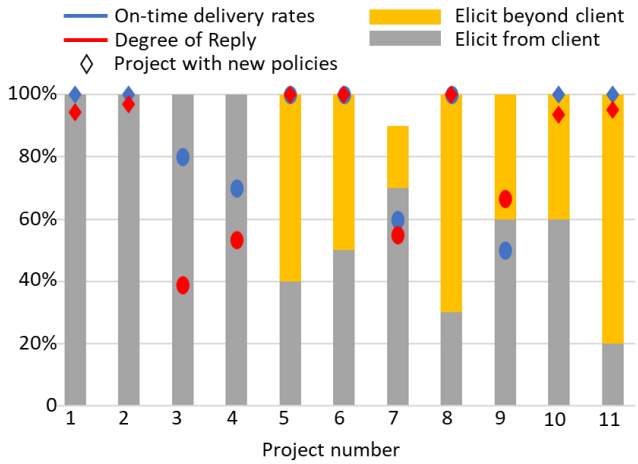

Figure 4. Comments replied corresponding to on-time delivered rate and elicitation source.

In Figure 4, projects 1 and 2 stand out as exceptions to the general trend due to their status as repeat projects. Many of the challenges faced in these projects have already been addressed based on feedback from previous batches, resulting in a consensus between the shipyard and clients. Consequently, most potential conflicts have already been anticipated, and corresponding solutions are readily available.

THE CONCEPT OF PROACTIVE ELICITATION

The aforementioned study unearths a notion of 'elicitation', which emphasises proactive information-seeking and problem-solving approaches (Delicado, 2019). 'Elicitation' extends its focus beyond the customer and includes a wide range of stakeholders, placing a strong emphasis on establishing comprehensive requirements through a rigorous and independent process. It is worth noting that elicitation is not limited by design briefs. Since elicitation focuses on capturing the essence of diverse stakeholders' desires, it can be used as a means to gather information for decision-making and bridge the gap between stakeholders and the 'real design' (Andrews, 2021).

In this study, proactive elicitation endeavours to gather comprehensive information during the initial or concept stage of ship design. Conflicts between stakeholders' expectations and the design brief can be resolved by proactively seeking additional information beyond design briefs. The timing of applying proactive elicitation can significantly impact its effectiveness in improving ship design accuracy. To facilitate understanding, Figure 5 illustrates an area between the curves of Commitment Technology (represented by the orange curve) and System-Specific Knowledge (represented by the red curve). This area between the two curves is referred to as 'design freedom'.

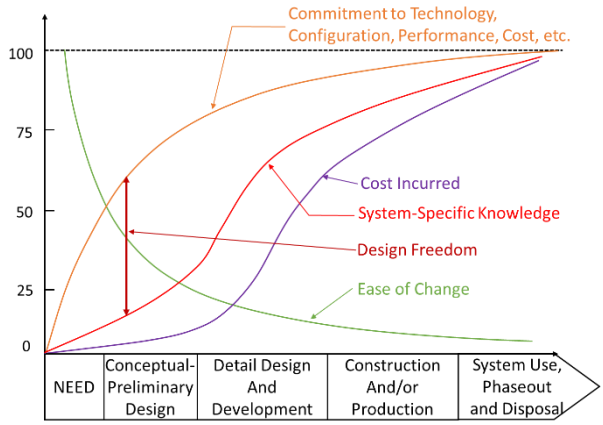

Figure 5. Illustration of project phases and design freedom (Malmgren & Ulfvarson, 2006).

During the conceptual design phase, naval architects will explore various design options in a variety of ways, with the goal of minimising 'design freedom' while meeting the stakeholder's requirements. To fully harness the advantages of proactive elicitation, it is imperative to establish it as a systematic workflow. Therefore, an extensive survey, called the full survey in this paper, was conducted, encompassing stakeholders at various management levels in the shipbuilding industry. The aim was to investigate the essential tasks involved in this workflow. In the survey, the stakeholders were divided into two groups. The first group are stakeholders who contribute design information or standards to naval architects. They responded favourably when questioned about their capacity to integrate their requirements and actively identify potential needs. This signifies that they recognise and appreciate the willingness of naval architects to enhance the design of their products. Another group of stakeholders consists of naval architects responsible for driving the ship design process and overseeing it at a supervisory level. They also expressed a positive inclination towards proactively considering potential requirements beyond the initial design brief. This underscores the naval architects' awareness of their pivotal role in shaping ship design and the significance of adopting a proactive approach to overcome constraints. The keywords adopted in the open-end questionnaires are categorised into 12 stages throughout the design process, concrete and cogitation aspects and current/expectation concepts. The survey results are shown in Figure 6. The degree of concern indicates the areas within ship design to which two distinct stakeholder groups attach importance.

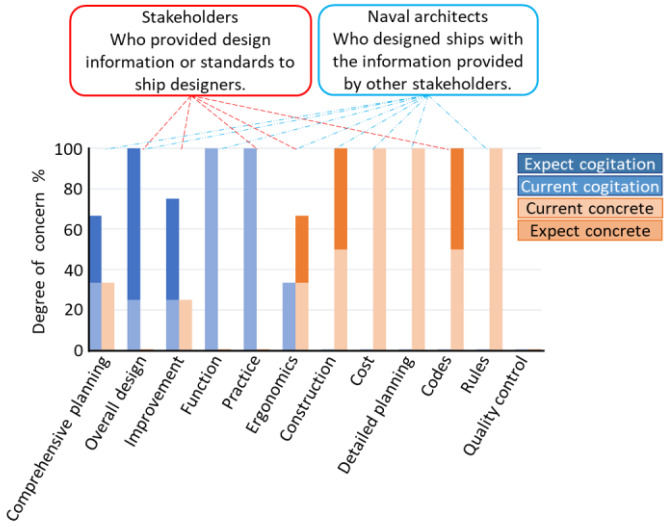

Figure 6. Results of the full survey.

Figure 6 indicates a significant emphasis by both groups of stakeholders on the cogitative and expectation aspects of the design process, particularly in the pre-construction phase. The survey results suggest that all stakeholders hold high expectations and demonstrate a strong desire to explore the design's potential. However, as the design progresses towards the detailed and construction plan stage, both groups of stakeholders tend to prioritise preserving a particular style while solidifying their ideas, aiming to minimise potential risks. This approach is justifiable as it ensures that the design plan is well-defined and carries minimal risk upon completion. Additionally, the survey results also suggest that stakeholders require additional information to meet their design expectations during the ESSD stage. It is evident that stakeholders' concerns encompass two distinct aspects: concrete and cogitation. To establish proactive elicitation as a self-contained process and seamlessly integrate it into the current ship design process, a potential implementation approach is depicted in Figure 7.

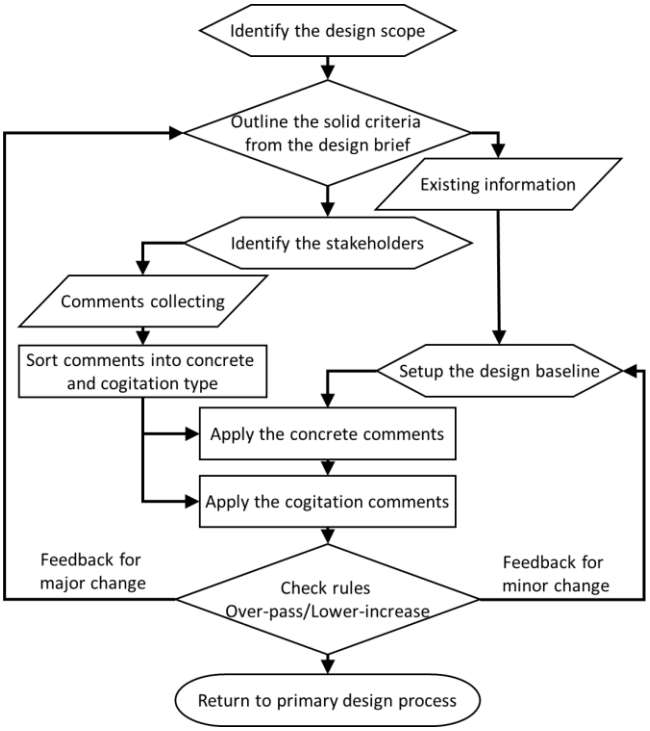

Figure 7. Implementation approach of proactive elicitation.

The proactive elicitation implementation approach depicted in Figure 7 originates from numerous shipbuilding projects. Through extensive trial and error, it has been observed that design issues can generally be classified into two principal categories: concrete issues, which can be resolved through specific information such as rules, regulations, or quantitative analysis, and cogitation aspects, which necessitate thoughtful deliberation or brainstorming for resolution. This approach can be incorporated at any stage of ship design to acquire additional information. To be specific, at the initial stage of ship design, there is a lot of room for design freedom, which needs to be decreased in subsequent stages. The process commences by utilising existing information to establish a design baseline, serving as a reference point. Subsequently, stakeholders are identified, and their concrete and cognitive comments are extracted for application. The final stage involves evaluating the design against concrete criteria, such as industry rules and regulations. If the design meets the specified criteria, it can proceed. Otherwise, adjustments are made to ensure compliance, or it may be sent back to the appropriate stage for reevaluation.

Development of discrete event models

To assess the efficacy of proactive elicitation in improving the success of ship design, two discrete event models were constructed in Simulink in the following. The agent-based discrete event model is appropriate for tracing the agent that travels through the model to study the interactions between agents and events. The agent-based model is built with a series of events as a loop according to individual agents (stands for accuracy and elicitation accuracy in this paper) assigned certain attributes and could be processed by each event. These models were designed to simulate real bureaucratic systems, aiming to provide a realistic representation of the workflow of ship design. The first model serves as a generic bureaucratic system model, simulating design-related tasks, while the second model is specifically tailored to implement and incorporate proactive elicitation in the ship design process.

The general bureaucratic system model for design work was derived from an on-site investigation and transformed into a series of discrete events. These events are scheduled over time, with sequential processing events representing the progress of the design tasks. This event-driven simulated model effectively captures the characteristics commonly found in bureaucratic systems. However, it should be noted that each design team have its own unique bureaucratic culture. This discrete event model cannot fully represent a specific design team or serve as a standard process for the overall design system. Nonetheless, the model serves as a valuable testing platform, allowing the simulation of specific work nodes within the design process. Simulation enables the examination of the impact and effectiveness of these nodes. The proactive elicitation model is built upon the proactive elicitation process depicted in Figure 7. It comprises a series of events aligned with the specific tasks outlined in the flowchart. This model serves as a modular component that can be seamlessly integrated at any stage within the generic bureaucratic system model. When simulating real-world systems using these two discrete event models, certain assumptions

must be made, and relevant variables need to be accounted for. The assumptions considered in this study are outlined below, and the variables are listed in Table 2.

- The ‘agent’ is named as the accuracy for the general bureaucratic system model and elicitation accuracy for the proactive elicitation model. Both stand for the level of the design that could reflect the stakeholders’ expectations and desires. Both units are in %.
- The agent going through the design/feedback node will decrease by multiplying the design performance when going through the split node, which results in the split rate. This stands for the agent portion going to feedback or sharing. The agent from feedback or sharing will add to the agent in the mainstream.
- In the model, the term ‘Time’ represents a specific phase in the design process. It does not refer to the duration or length of time.
- The ‘model’ represents the entire design process, which means the process is complete once the agent reaches the last node.

Table 2. Variables.

Types	Variables
Explanatory Variables	1. Design parameters. 2. Split parameters. 3. Sharing parameters. 4. Criteria for the design check.
Controlled Variable	1. Total design time. 2. Feedback time. 3. Information exchange time. 4. ‘Dream’ represents 100% accuracy.
Dependent Variable	Accuracy (%)

Figure 8 depicts the generic bureaucratic system model, which serves to simulate the activities carried out by a single team at each event node. In the figure, the nodes are represented by black font, while the activities are indicated using red font.

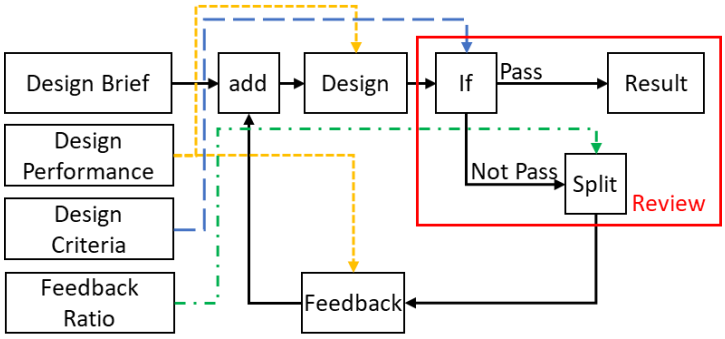

Figure 8. Generic bureaucratic system model for simulating the activities of a single team.

In Figure 8, the term "Design Performance" refers to how well the design team interprets the Design Brief throughout the design process. A higher value indicates a stronger alignment between the design outcomes and the expectations outlined in the Design Brief. On the other hand, "Design Criteria" represents the set of standards utilised to assess the design outcomes during the review process. If the outcomes meet these criteria, they are considered satisfactory; otherwise, feedback is provided to the design team for improvement. The "Feedback Ratio" illustrates the proportion of outcomes that require feedback and subsequent redesign. All these values are expressed in percentages (%), and their specific values depend on the particular design environments being considered. Regarding the "Design Brief," it is also expressed as a percentage (%), with its value indicating the accuracy of the Design Brief in conveying stakeholders' requirements and expectations. A value of 100% signifies a Design Brief that perfectly and completely reflects the needs of the stakeholders. It is important to note that the accuracy of this parameter depends on the initial stage of the design process. If the design process starts with direct stakeholder engagement, the accuracy of the Design Brief may be close to 100%. However, during the Concept Design phase, the Design Brief might be derived from contractual documents, resulting in a lower accuracy level (e.g., 80%). As listed in Table 3, all the aforementioned parameters will be assigned fixed values in subsequent simulations to ensure consistent simulation conditions.

Table 3. Values of model parameters.

Parameters	Value	Remark
Design Brief	80%	Design Brief at the ESSD represents stakeholders' expectations and requirements with 80%.
Design Performance	70%	The design team has comprehension of up to 70%.
Design Criteria	70%	The approval criteria of the Review is 70%.
Feedback Ratio	20%	Assuming that 20% of the design needs to be rechecked when the design is not approved.

The model depicted in Figure 8 can be easily extended to incorporate the activities of multiple design teams, thus enhancing its flexibility and applicability. In order to provide a clearer representation, Figure 9 presents an illustration of the model specifically tailored to simulate the activities of two design teams.

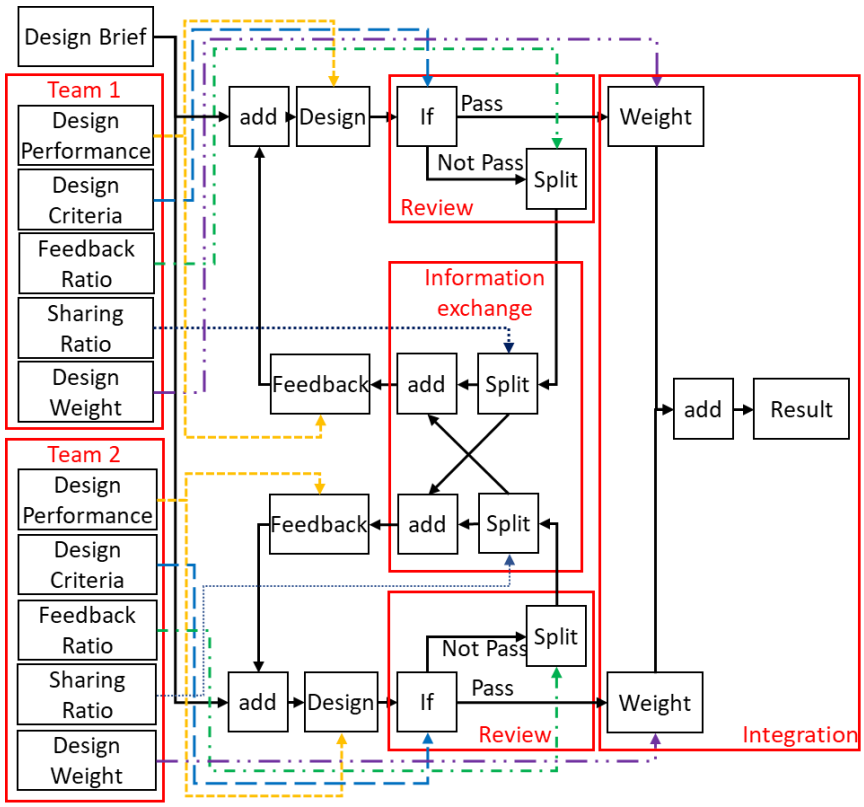

Figure 9. Generic bureaucratic system model for simulating the activities of two teams.

From Figure 9, it is seen that the model has been expanded to include additional event nodes, facilitating the exchange of information between different design teams and enabling the integration of design outcomes. The 'Sharing Ratio' parameter has been introduced to account for the cross-team collaboration within a specific team. Furthermore, individual design teams are assigned different design weights, which capture their specific characteristics and account for the variations arising from their respective design responsibilities within the overall design process.

In the simulations conducted for this study, the focus was on a scenario involving two design teams. While maintaining the unified simulation conditions with Design Brief and Design Criteria set respectively at 80% and 70%, the remaining parameter

values are provided in Table 4. It is necessary to note that these parameter designs were based on the relationship between a Structure Design Team (Team 1) and a Propulsion Design Team (Team 2) in a real ship design office. However, different ship design offices may have their own unique cultures and systems in place. Therefore, this particular case serves as only a reference for parameter configuration and should not be considered an absolute standard.

Table 4. Model parameter values for a two-team model.

Team 1 (Structure)		Team 2 (Propulsion)		Remark
Parameters	**Value**	**Parameters**	**Value**	
Design Performance	70%	Design Performance	40%	Team 1 has more personnel than Team 2, with higher performance.
Feedback Ratio	10%	Feedback Ratio	50%	The structure is concrete knowledge, so the propulsion is more flexible with a higher value.
Sharing Ratio	10%	Sharing Ratio	50%	Team 1's sharing range is the engineering section, but Team 2 needs to share all information to help Team 1.
Design Weight	70%	Design Weight	30%	The range of Team 1 in the design is more than that of Team 2.

Overall, these two models serve as testing platforms to validate the effectiveness of the proactive elicitation model. The single-team model is suitable for representing a comprehensive organisation, such as a shipyard, design firm, or similar entity, where the precise breakdown of work information may not be available. In such cases, the single-team model can be utilised, with each node in the model representing the overall performance of similar teams. On the other hand, the multi-team model allows for the incorporation of efficiency parameters specific to individual teams within the organisation. This enables a more in-depth analysis of team efficiency and provides a more detailed understanding of organisational performance. The functionality of this model accurately reflects the operational performance of a particular organisational structure, offering insights into how different teams interact and contribute to the overall success of the organisation. The proactive elicitation model is depicted in Figure 10, which is developed based on the flowchart illustrated in Figure 7. The agent of this model is referred to as 'elicitation accuracy'. It is independent of the accuracy of the design process.

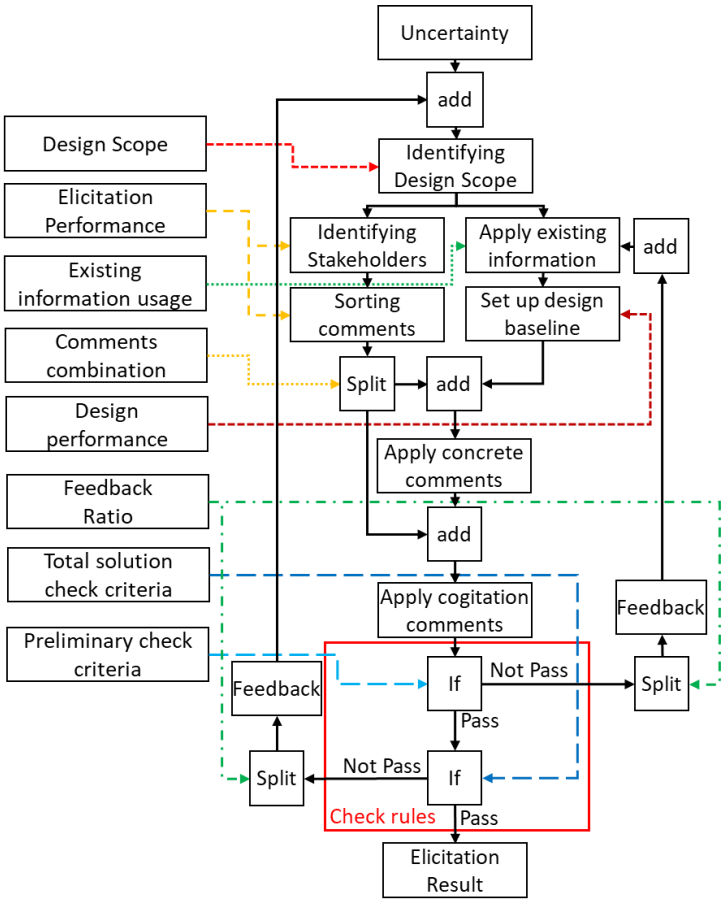

Figure 10. Proactive elicitation model.

In this proactive elicitation model, a total of eight parameters are configured based on the simulation conditions. They are explained in Table 5. In Figure 10, the term 'Uncertainty' represents the flexibility of proactive elicitation in addressing issues during the design process. Generally, as the design progresses and achieves higher completion, the value of Uncertainty tends to decrease. The term 'Design Scope' indicates the design freedom in the design process. A higher value indicates greater design freedom, and it is typically higher at the initial stages of the design process, gradually decreasing as the design progresses.

Table 5. Parameter values in the proactive elicitation model.

Parameters	Value	Remark
Elicitation performance	80%	This team has 80% performance in identifying the stakeholders and understanding their comments.
Existing information usage	40%	The design brief could provide information with 40% accuracy.
Design performance	80%	This design team has comprehension of up to 80%.
Comments combination	80%	This design team has 80% accuracy in sorting the comments into correct categories.
Feedback ratio	50%	50% of the information must be reviewed if it does not meet the criteria.
Preliminary check criteria	20%	The criteria of the preliminary check are 20% accuracy.
Total solution check criteria	50%	The criteria of the Total solution check is 20% accuracy.

CASE STUDY

The case study in this section comprises simulations involving both single-team and multiple-team scenarios, focusing on investigating the influence of the intervention stage of proactive elicitation. The objective is to find which stage at which the implementation of proactive elicitation can yield the highest effectiveness. Figures 11 and 12 show the nodes that represent the three different intervention points of proactive elicitation in the simulations of each model. Table 6 presents the values of Uncertainty and Design Scope when proactive elicitation is incorporated in different stages of ship design. In the table, Case 0 is designated as the control group, where no proactive elicitation intervention is applied. This case serves as a baseline for comparison with the other three cases that incorporate proactive elicitation.

Table 6. Uncertainty and Design scope in different cases.

Parameters	Case 0	Case 1	Case 2	Case 3
	control group	Before the design stage	During the design stage	After the design stage
Uncertainty	0	100%	75%	50%
Design scope	0	80%	60%	40%

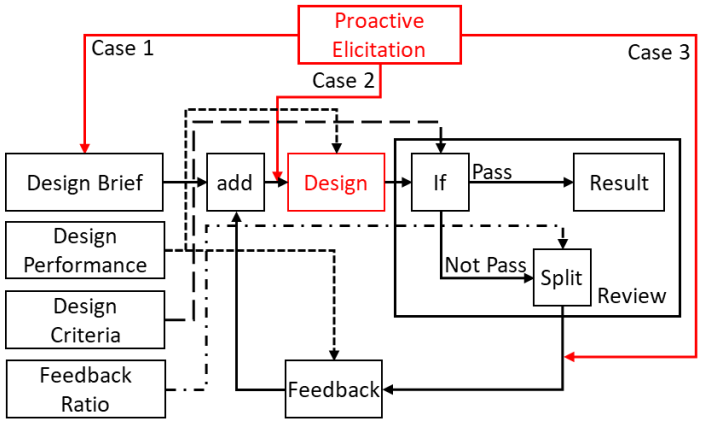

Figure 11. Intervention on the single-team generic bureaucratic system model.

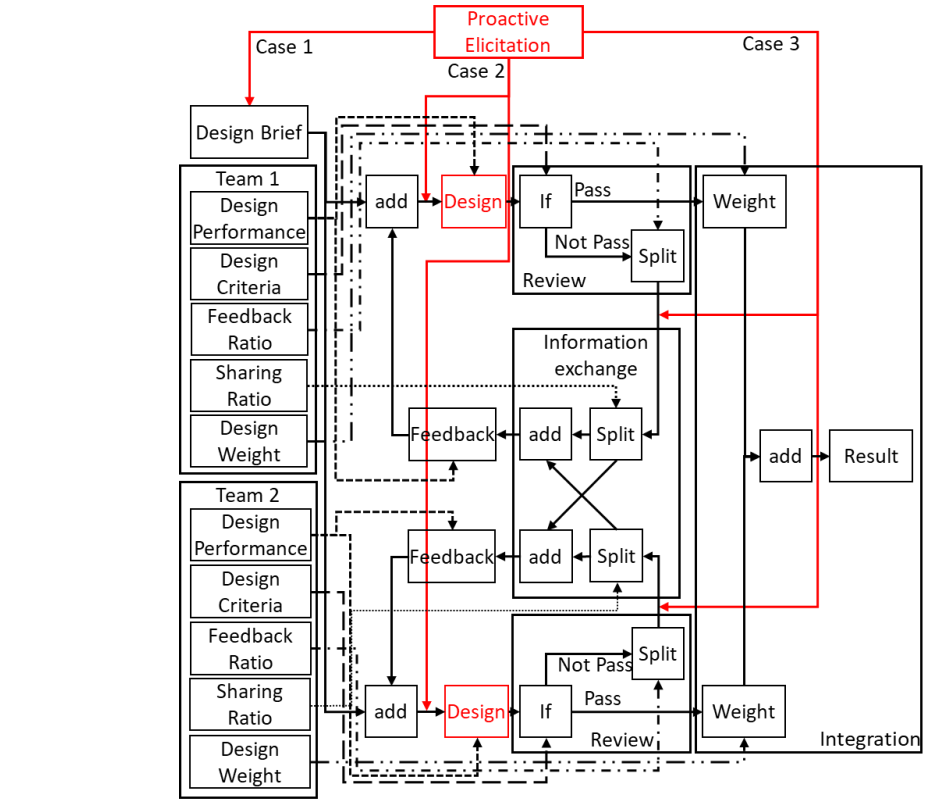

Figure 12. Intervention on two-team generic bureaucratic system model.

The simulation results for the single-team generic bureaucratic system are presented in Figure 13. Figure 13a depicts the proactive elicitation to assess the level of understanding through elicitation accuracy. In the four different cases, CASE 0 serves as the control group, where the elicitation accuracy is 0. On the other hand, CASE 1-3 presents the elicitation accuracy levels of proactive elicitation under varying conditions of different stages. Similarly, Figure 13b illustrates the accuracy of the design result, which serves as an indicator of the level of understanding in the design brief through the design process of a single-team generic bureaucratic system. CASE 0 represents the control group without proactive elicitation intervention, thus reflecting the design result accuracy achievable under the design brief. CASE 1-3 demonstrate the design result accuracy achieved by incorporating proactive elicitation at different intervention points and considering the associated elicitation accuracy. The simulation results for the two-team generic bureaucratic system are presented in Figure 14. As shown in Table 4, different parameters are assigned to each team in the simulation to highlight the differences between the two teams. In Figure 14, the curve indicated by 'total' represents the overall design outcome.

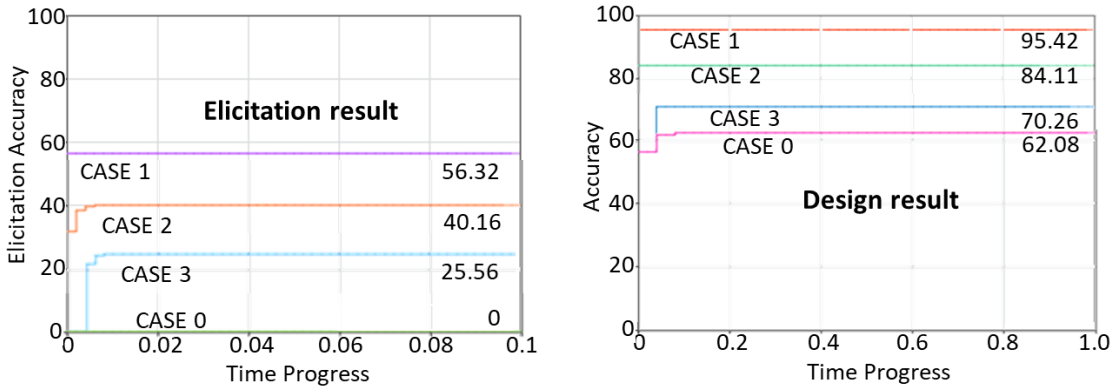

(a) Accuracy of elicitation result **(b) Accuracy of design result**

Figure 13. Impact of proactive elicitation on a single-team generic bureaucratic system.

From Figure 13b, it is seen that in Case 0, the design information enters the design process through the design brief. However, due to imperfect understanding, the comprehension of the design brief is not flawless, leading to a result that the efficiency of understanding is not as high as 100%. For this reason, the efficiency of understanding will decline gradually over time in the

simulation. However, by employing the ‘review process’, any components of the agent that fail to meet the design criteria will be fed back to the design stage. They are then redesigned and incorporated into the original design, resulting in an iterative process. Consequently, the overall trajectory of the process remains upward. Nevertheless, as the design accuracy improves, the instances where design outcomes fail to meet the criteria and are returned to the design stage will progressively diminish. As a result, the rate at which the process is increasing will continuously decelerate until it eventually approaches zero and stabilises at a certain level.

In contrast to the outcomes observed in Case 0, which does not incorporate proactive elicitation, the results obtained in Cases 1, 2, and 3 show the impact of employing proactive elicitation at different stages of ship design. These results reveal that proactive elicitation indeed enhances design effectiveness, regardless of when it is implemented. The underlying rationale behind this phenomenon can be attributed to the design process itself. When supplementary information is provided, the agent's 'accuracy' achieved through proactive elicitation is integrated with the existing accuracy. This process mirrors real-world scenarios, where the inclusion of new information enriches the comprehensiveness of design outcomes. In other words, by considering additional information through proactive elicitation, the design process becomes more comprehensive, thereby leading to improved design effectiveness. However, the effectiveness of proactive elicitation varies across the three intervention points, with Case 1 demonstrating the highest impact, followed by Case 2 and Case 3. This implies that the earlier the proactive elicitation is introduced, the greater benefits will be yielded.

In Figure 14, in addition to the intervention of proactive elicitation prior to the design stage, which resembles the operations in the single-team model, the two teams also engage in proactive elicitation during and after the design stage. As a result, the information presented in Figure 14 is more abundant compared to the results shown in Figure 13. From Figure 14, it is noticed that the outcomes of Case 1 and Case 2 show an 'accuracy' exceeding 100%. In real-world terms, this situation can be interpreted as heightened stakeholder involvement and the incorporation of a broader range of information, which can lead to designs that surpass the expectations outlined in the design brief. This phenomenon can also be understood as the generation of superior alternative solutions based on the design brief.

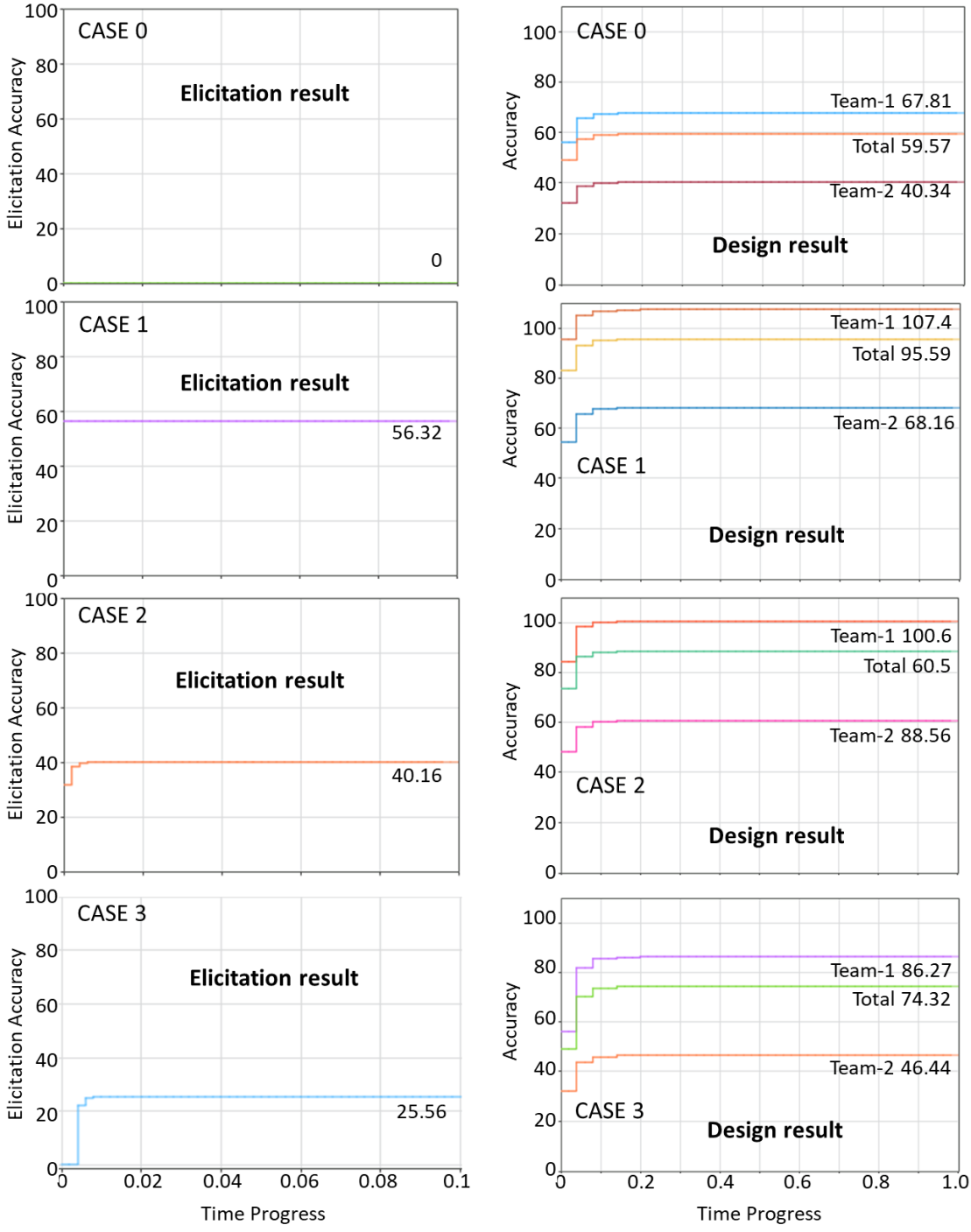

Figure 14. Impact of proactive elicitation on a two-team generic bureaucratic system.

By summarising the simulation results depicted in Figures 13 and 14, it can be inferred that:

- Proactive elicitation functions as a self-contained module unaffected by the quality of the design brief. The information generated through this independent process is directly incorporated into the "accuracy" of specific stages within the design process, leading to an additive effect. Consequently, irrespective of the accuracy of the design process or proactive elicitation, any enhancement in accuracy contributes to an overall improvement in the success of the design results.
- It is evident that proactive elicitation yields the greatest benefits when applied 'before the design stage'. This particular stage presents a direct opportunity to enhance the quality of the design brief. Moreover, during this stage, proactive elicitation exhibits the widest ranges in terms of 'uncertainty' and 'design scope'. These aspects indicate that the initial design stage offers the most significant potential for exploring improved design solutions. However, as the design progresses towards

completion, the scope for modifications diminishes. That will limit the effectiveness of proactive elicitation within the constraints of the existing design.

CONCLUDING REMARK

This paper focuses on studying proactive elicitation and its effectiveness in enhancing ship design success. It is important to reiterate that proactive elicitation transforms naval architects from passive information receivers into active information seekers. It is not a management tool or organisational standard. Instead, it represents an attitude and philosophy towards design embraced by naval architects. Therefore, implementing proactive elicitation involves training personnel in this mindset or utilising policies to encourage naval architects to strengthen their collaboration and communication with stakeholders.
The simulation results demonstrate that the timing of applying proactive elicitation has an impact on the attainment of design success (higher design accuracy in the model). This suggests that individual factors can also contribute to enhancing the design process. Therefore, enhancing the design process or proactive elicitation is meaningful.

Future research on proactive elicitation will emphasise interdisciplinary integration and its influence on education and training for naval architects. This study advocates for naval architects to proactively explore design information. However, it raises the question of whether naval architects possess the ability to understand and effectively apply such information. Observations suggest naval architects rely on accumulated experience but lack comprehensive understanding and application of design information. Therefore, adjustments to education and training are needed to cultivate naval architects who can effectively apply proactive elicitation during the initial design phase.

CONTRIBUTION STATEMENT

Cheng Feng Ou Conceptualised the study and chose the Methodology. Cheng Feng Ou performed Data curation, Investigation, Formal analysis, and original draft and manuscript Writing. David Trodden and Serkan Turkmen contributed to Supervision, Resource provision, Reviewing the draft, and Editing the manuscript.

REFERENCES

Andrews D., and Stein Ove Erikstad. State of the Art Report on Design Methodology. University College of London, London, UK, 2015.

Andrews, D. (2020) 'Design Errors in Ship Design.' Journal of Marine Science and Engineering, 9, pp. 34.

Andrews, D. ‘The sophistication of early-stage design for complex vessel.’ RINA, Special Edition, International Journal Maritime Engineering. (2018): 1-54.

Andrews, D. ‘Is a naval architect a typical designer – or just a hull engineer?’ International Marine Design Conference, Marine Design XIII, (2018): 55-76.

Andrews, D. 2021. WHAT MAKES THE EARLY-STAGE DESIGN OF COMPLEX VESSELS SOPHISTICATED? London, UK: Royal Institution of Naval Architects.

Andrews, D. (2022) ‘What makes the early-stage design of complex vessel sophisticate.’ PowerPoint lecture RINA AGM 2022, Royal Institution of Naval Architects, London, 12th May.

Baker, C. C. and Seah, A. K. (2004) 'Maritime Accidents and Human Performance: The Statistical Trail.', ABS TECHNICAL PAPERS, pp. 225-229.

Bernardo A. Delicado (2019). ‘Introduction to System Engineering’ [PowerPoint presentation]. Awareness Seminar SESGE-AEIS/INCOSE. Available at:
https://www.aeis-incose.org/wp-content/uploads/2019/05/INCOSE_SESGE_29_5_2019.pdf (Accessed: 20 January 2022).

Bafang, C.-H. and Chen, S.-T. (2021) 'A Brief Analysis of the Core Essence of Ship Safety Management (ISM)', Journal of Taiwan Maritime Safety and Security Studies, 12, pp. 28.

Hughes, C. N. (1989) Shipboard operational problems. London: London: Lloyd's of London.

Improving ship operational design / compiled by the Nautical Institute. (1998) London: Nautical Institute.

Juan, S., Student, P., Malmgren, I. and Ulfvarson, A. (2006) 'Systems Engineering in Ship Design Education-is this the answer to changed industry demands?'.

Wróbel, K. (2021). "Searching for the origins of the myth: 80% human error impact on maritime safety." Reliability Engineering & System Safety 216: 107942.

Proceedings of 15th International Marine Design Conference (IMDC-2024)
June 2-6, 2024
Amsterdam, the Netherlands

New Conventions: Intentional Implementation of Set-Based Design Leveraging Point-Based Approaches

Jonathan E Page[1,*], Warren P Seering[2], Christopher J Higgins[3], and Drake M Platenberg[3]

ABSTRACT

This article communicates a practical application of Set-Based Design (SBD) during its adoption within the U.S. Navy's latest surface ship design processes. It highlights how the team harnessed SBD to explore the vast design space and make critical decisions. Intriguingly, the article explores the design team's use of point-based designs (PBD), a counterintuitive approach within the context of SBD. It delves into the rationale behind their implementation and the diverse purposes they serve in bridging knowledge gaps such as prototyping, integration, and evaluation of set interfaces. Furthermore, the article presents a preliminary ontology outlining various use cases for these PBDs. A key focus of this article is understanding how these PBDs coexist within the larger set-based construct while recognizing their inherent differences. The article examines the utility and boundaries of this approach, shedding light on the pragmatic interplay.

KEY WORDS

Set-based design; point design; risk management; ship design

INTRODUCTION

This article shares some observations made through action research while designing the U.S. Navy's next class of destroyers, currently designated DDG(X). The article first reviews some principles of point- and set-based design methods. These reviews intend to ground the reader in the methods and lead to a comparison of the two. Next, the article introduces the design effort for DDG(X), including excerpts of the fundamental philosophical, organizational, and methodological principles. Finally, the article reveals the authors' use of point-based designs and methods within their set-based design construct. It instigates an important observation that the two methods are not necessarily mutually exclusive and can be complimentary or necessary.

POINT-BASED DESIGN AND THE TRADITIONAL DESIGN SPIRAL

Gale (2003) documented the known point-based design (PBD) methods for ships that had been developed and refined over decades. Figure 1 presents a typical formulation of that process. Despite the appearance of a spiral, the process is linear. Each discipline performs its tasks in succession and passes its products to the subsequent discipline. Each loop through the spiral includes changes invoked by previous stages and adds fidelity to the design in their domain. This process iterates through these steps and spirals until the design converges to the final solution.

Ship design methods evolved to this over time because of the complexity of the undertaking; there is no simple or finite set of equations that define a ship. Instead, each discipline involved in ship design has unique equations and relationships dependent on the other disciplines. This method may suffice with a competent and practiced workforce because their initial educated guesses for the ship's parameters are well-informed. That situation dictates minimal rework and refinement as the design converges. Therefore, as the name suggests, this method creates and analyses one point in a basically infinite plane of possible ship designs. If any parameter changes substantially (an ill-defined modifier), a new point in that design space must be explored because it drives a different balance through the various parameters of the various disciplines.

[1] University of Michigan (Naval Architecture and Marine Engineering, Ann Arbor, United States); ORCID: 0000-0001-7779-4169

[2] Massachusetts Institute of Technology (Mechanical Engineering, Cambridge, United States); ORCID: 0000-0001-8846-4851

[3] United States Navy (Naval Sea Systems Command, Washington, DC, United States)
* Corresponding Author: jonpage@umich.edu

Submitted: 3 March 2024, Revised: 1 May 2024, Accepted: 3 May 2024, Published: 23 May 2024

Conference paper, DOI: https://doi.org/10.59490/imdc.2024.879 e-ISSN: 3050-486

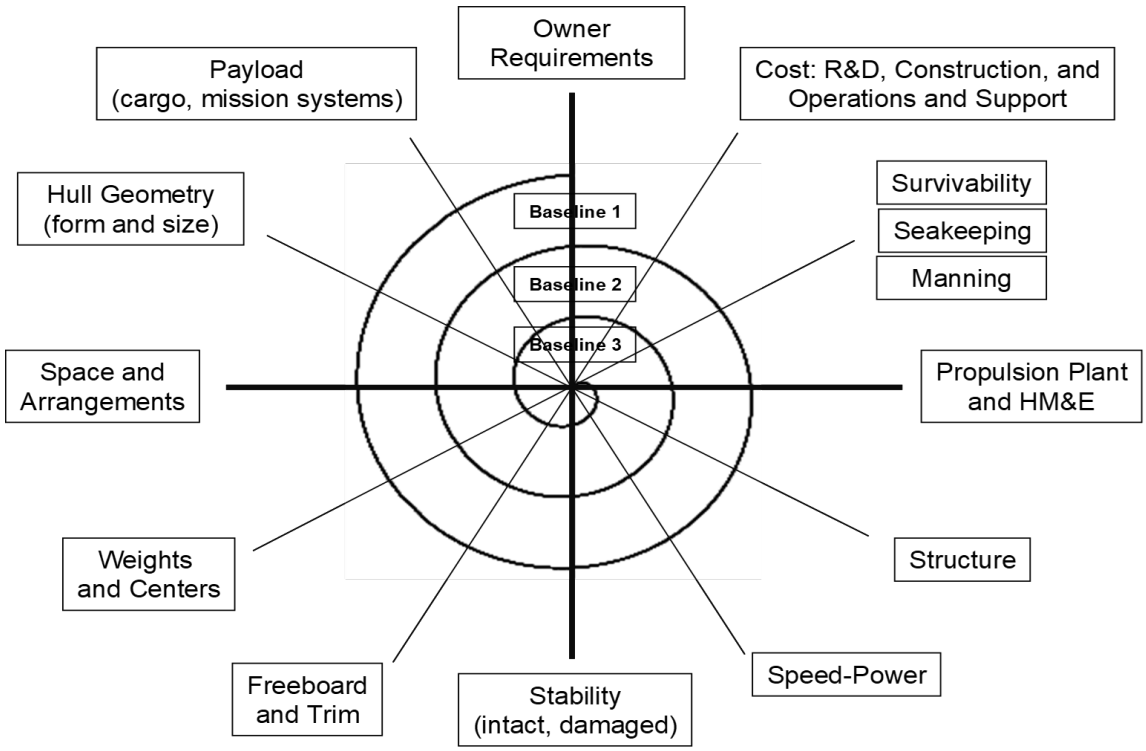

Figure 1: The Design Spiral in Point-Based Design *(Gale, 2003)*

A point-based method may be appropriate when the requirements present a well-understood design problem with known technologies. In this case, the characteristics and values within the disciplines can be easily determined or derived from a parent design with similar requirements. Even if one or two parameters change, for instance, a new propulsion engine to meet emissions standards and a new mission system topside, the boundaries of the new design space may only require minimal expansion from existing knowledge. Once again, point-based methods can be used effectively in these conditions. Similarly, suppose the requirements call for optimization within the design along one or two parameters, such as speed and survivability. In that case, point-based methods may be appropriate since other disciplines will acquiesce to optimizing those parameters.

Outside those example conditions, point-based design methods can present risk. The highest risk of PBD is forfeiting the globally optimal design. Because the method is generally a refinement of initial rough parameters, many more designs and design parameters are -*not*- considered compared to the single point that -*is*- considered, refined, and analyzed. Another risk is that of rework. Suppose the initial estimates of parameters are not accurate enough. In that case, subsequent efforts through the spirals rework those parameters instead of refining them because there may be initial divergence instead of convergence of the parameters into a balanced design. The risk of significant rework is exceptionally high if the requirements change, as is often the case for naval vessels.

SET-BASED DESIGN AND ITS TENETS

On the contrary, set-based design (SBD) is a method that considers sets of variables in the design space instead of a single point. The method considers more than one viable option for variables of interest and, depending on the design requirements, potentially for most variables. Ideally, the options evaluated are also diverse (Doerry, 2015), allowing the opportunity for refinement and avoiding analysis that is similar across variables and potentially duplicative and inefficient. Ward and Seering (1993) introduced the engineering design community to SBD and started formalizing this teachable doctrine and methodology in addressing design needs (Simon, 2019). Since that time, several publications have extended its tenets from those origins of detailed design to concept development, preliminary design, and contract design activities across a variety of platforms and industries, most notably with its alignment to Toyota's design processes (Burrow et al., 2014; Garner et al., 2015; Raudberget, 2010; Sobek II et al., 1999). During those studies, SBD was also called set-based concurrent engineering (Sobek, 1996). The recent publication by Toche et al. (2020) provides an extensive review of research on SBD. It concludes that few complete examples of SBD exist regarding large complex systems like naval vessels. Dullen et al. (2021) also provide a review of relevant research, especially relevant to quantitative methods within an SBD construct. Shallcross et al. (2020) assess the state-of-the-

practice of SBD. Each article presents that the SBD method incorporates distinguishable tenets, principles, and practices (D. Singer et al., 2017; D. J. Singer et al., 2009).

First, SBD has philosophical tenets worth understanding. The name derives from the primary tenet: consider a range or group of alternatives – a set. A set for a variable or solution should consist of all viable and diverse options. Further, none of these options should be eliminated from further consideration unless there is a logical reason for doing so. That logic ought to be robust such that no new information will likely reverse the elimination of the option(s). That tenet discloses a tangential philosophical point; the method operates by removing infeasible and dominated solutions from the set instead of selecting one that seems dominant or preferred. Therefore, one arrives at decisions by systematically removing the "worst" answer(s) instead of trying to select the "best" or "right" one. The sets exist at every perceivable level of abstraction in the design space, from fully synthesized and converged artifacts to subcomponents several levels down in the design structure. This abstraction range means a design team can create non-traditional sets for trade-space exploration and decisions, such as sets encompassing entire power and propulsion architectures. Such approaches allow comparison and analysis at those abstraction levels instead of component or sub-component levels, a necessary condition for enabling decisions from the limited data and knowledge that is available in the earlier stages of a complex design process. An important implication of this method is that the design manager decides to keep or remove portions of the design space based on data instead of intuition. Therefore, this technique forces important and recurring conversations regarding what type and amount of data is sufficient to support any given decision. Design team leadership, in conjunction with the team, continues to refine the measures of effectiveness and measures of performance that constitute "adequacy." Another tenet of the method is that these decisions are made at the last responsible moment, often leading to delayed decisions and a process in which a design manager keeps more of the trade space open longer. This is difficult for engineers, leadership, and program managers alike since, under the historically used measures of team performance, it may appear the team is not making progress on the design. One last tenet is improved communication because concurrent engineering approaches necessitate this.

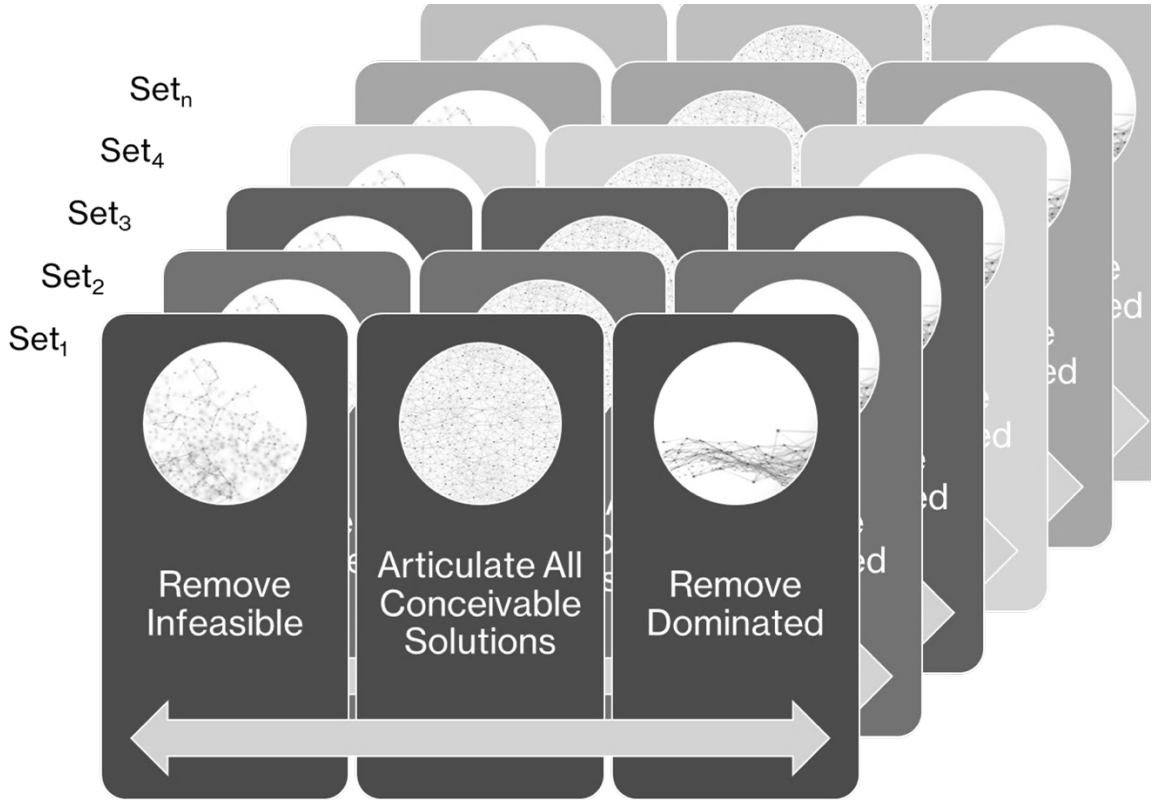

Figure 2: Conceptual Structure of SBD Method *(Page & Seering, 2023)*

Figure 2 shares a new conceptual structure of SBD that utilizes and moves away from the usual cited construct from Bernstein (1998). The figure first relates that several sets are in consideration at once, labeled Set_1 through Set_n. The "points" within each set represent the different options within that Set space, thus the Figure labels the middle portion in each Set with "Articulate All Conceivable Solutions." The other portions of a Set space represent analyses that remove portions of the fully articulated Set due to either infeasibility or dominance. The different approaches to removing portions of the fully articulated trade space are neither linear nor sequential. The removals result from analyses that close knowledge gaps in the space.

Additionally, each Set represented may have intersections to the other Sets along shared dimensions. For instance, each point in Set_1 could have a connection with one or several points in Set_2 and one or several points in Set_n. This creates an intricate tapestry of connections between solutions in each space with each other, invoking concepts related to Hilbert spaces to bring multi-dimensional relationships into lower-dimension arithmetic.

Second, Sobek et al. (1999) suggest several fundamental principles of SBD, which have withstood significant modification (Ghosh & Seering, 2014). First, they discuss mapping the design space, which includes defining feasible regions for the parameters under evaluation, exploring trade-offs within that region using multiple alternatives, and communicating those sets of possibilities. Their next principle suggests that the design combines and integrates the feasible and non-dominated regions of the various parameters by intersection – a difficult principle with the tightly coupled and complex design of a ship where thousands of parameters exist to intersect with each other in numerous primary and secondary ways. This principle expects imposing minimum constraints for these intersections to avoid unnecessarily deciding on parameters before the time is right and potentially invoking rework. This principle also seeks conceptual robustness, meaning designs will work regardless of the various parameters' outcomes. Invoking conceptual robustness in design decisions requires a process that supports the knowledge structures of the decisions in a way that enables this. The last principle is establishing feasibility before commitment. This principle starts with gradually narrowing sets while increasing detail. Doing so saves the computationally expensive analyses for the smallest number of solutions. It eliminates more significant swaths of the design space using first-principle and computationally inexpensive analyses at the beginning of the process. This principle also means that once the design manager decides to remove a portion of the design space, the team must stay within the boundaries of the new design space once committed. The team addresses uncertainty around these commitments at gate reviews with appropriate criteria, data, and experience communicated.

Third, following these tenets and principles reveals practices common to SBD (Ghosh & Seering, 2014). One practice is that SBD emphasizes frequent, low-fidelity prototyping to gain new knowledge on the design space and its integration. While Toyota executed this practice physically with clay models and complete prototypes, the practice does not preclude virtual prototyping and invites an intersection between SBD and model-based systems engineering. Another practice with SBD is under-defined system specifications; the method is tolerant to this condition. If the design manager deems one characteristic infeasible, then every design that uses that characteristic is also infeasible. The SBD method instills better communication practices among subsystem teams when executed properly. Another critical SBD practice emphasizes documenting lessons learned and new knowledge. This documentation allows the design teams to reapply the knowledge in other projects and understand decisions for the life cycle of the artifact. SBD enables decentralized leadership and distributed teams through concurrent engineering and improved communication practices. SBD also allows suppliers and subsystems to explore their versions of optimality within the communicated boundaries instead of attempting optimality at the system-of-systems level for a complex product like a naval vessel. Lastly, the SBD method promotes flow-up knowledge creation from the various disciplines' engineers and creators involved instead of flow-down decisions from design management.

Altogether, the tenets, principles, and practices provide a view of SBD and how the method manages complexity, uncertainty, communication, decision-making, and design space exploration. SBD presents a natural step forward in managing these aspects of a complex system design, but it may only sometimes be appropriate. Therefore, the two methods deserve a comparison and contrast.

COMPARISON

The preceding sections revealed aspects of PBD and SBD that allow one to compare and contrast the methods. Both are methods developed to manage the complexity of a tightly coupled design, in this case, that of a naval vessel. Both start with relatively little information and low-fidelity analyses for the first decisions. The similarities quickly end, however. Singer et al. (2009) provide a good accounting of the differences between the two methods, including the points made here and derived from Bernstein (1998).

In the face of little information and low fidelity, a PBD method selects one point in the design space to iterate around and refine with increasing levels of fidelity. In contrast, SBD uses the information to decide what areas of the design space to stop exploring but keeps many options open for longer. This difference generates a key divergence in the performance of the methods. PBD commits to cost with selection decisions early in the process, with less available information and fewer completed analyses, thus making rework more likely and expensive. Put another way, SBD encourages management to make the right decision the first time by delaying until the appropriate information is available and shifting their influence and cost obligations later in the process.

Another point of comparison between the two methods considers the number of variables involved. With PBD, only a few design space parameters should be independent variables. The method still analyzes, refines, and adjusts all necessary

parameters. However, most are dependent variables adjusted due to decisions made and optimizations elsewhere in the design space. This condition applies at both system and subsystem levels. The dependent parameters are known, specific technologies that are well understood and only require refinement instead of exploration. Alternatively, SBD encourages variations and independent variables to explore a broader solution set across more parameters. Both methods recognize tightly coupled parameters, but PBD controls variation through early decisions, while SBD encourages variation and global optima exploration across several parameters. Therefore, SBD is better suited to design challenges where requirements conflict or the technology or design challenge still needs to be better understood.

Additionally, the two methods differ based on idea generation. PBD methods generate ideas from the tacit knowledge of the individuals involved, typically derived from previous work experience. To reach a solution, the design team iterates around this point solution. Suppose the solution does not and cannot converge. In that case, the team may invoke brainstorming techniques to determine the rework necessary in the design, whether a new technology solution or changing a previously dependent variable to an independent one. Alternatively, SBD defines a feasible space with boundary conditions and systematically reduces it by removing infeasible or dominated regions. Thus, the SBD method promotes ideation up front so that the team considers more solutions and possibilities from the outset.

The two methods also take alternate approaches to optimization. PBD uses known optimization techniques with fitness functions and preferences and applies them when suitable. They are applied against a single point to refine and optimize given parameters, which will likely sacrifice the performance of the other parameters. On the other hand, SBD creates alternatives and tests multiple parameters in parallel, eliminating infeasible and dominated solutions from further consideration. This approach considers a more global consideration to optimization, striking a different balance in the design space with the interaction of the coupled parameters. To enable this, SBD uses minimum control specifications and constraints to allow the intersections of parameters to create this global optimum and mutual adjustment. PBD, alternatively, imposes maximum constraint early in the process, attempting to ensure functionality and interface compatibility. The constraints in PBD also lead to the behavior that invokes margins and allowances around specific parameters and constraints to account for uncertainty and give design teams "budgets" to stay within. These margins developed empirically over time and are potentially fraught with the same risks as other parameters regarding the educated estimates that create these values early in the process. Alternately, SBD allows the knowledge to develop with time, reducing the uncertainty as much as possible before committing to a design decision.

Within those constraints and uncertainty, a team using PBD methods integrates by using synthesis methods, typically conducted using software codes. If a particular discipline cannot stay within its budgets and constraints, leadership must reallocate or reapportion the risk and budget to another domain. At the end, a prototype may be built for testing and validation purposes, including virtually. However, SBD integrates by intersection. Suppose two elements of two sets do not intersect along a common parameter. In that case, there is clear data to remove those portions of the design space from further consideration, validating the minimal-constraint approach: the design space naturally culls itself as more information becomes available without transferring risk throughout the team. SBD encourages prototyping along the way to generate knowledge that can flow up to higher levels of abstractions and sets in the system of systems. These prototypes tend to invoke lower-cost tests that prove the infeasibility or dominance of a select portion of the design space versus the converged artifact as a whole.

Lastly, the two methods differ regarding risk management. SBD engenders a decentralized risk management approach. Each discipline establishes feasibility before commitment. All disciplines pursue their options in parallel. They have a charter to find solutions robust to physical, logical, market, and design variations. Once the design manager commits to a choice, the team stays within the sets and manages uncertainty at least as often as process gates. PBD requires centrally managed feedback channels with high frequency. The disciplines must respond quickly to changes due to analysis in other disciplines or decisions by management. Table 1 provides a summary of these comparison points. Singer et al. (2009) first developed a similar table.

Table 1: Summary Comparison of PBD and SBD

Characteristic	Point-Based Design	Set-Based Design
Variables	Very few independent variables, many dependent variables	Many with tight coupling. Most are treated as independent
Requirements Stability	Known, stable, thoroughly documented	Uncertain; flexibility and trades are required or desired
Initial Knowledge	Well-understood technologies and design challenges; less uncertainty	Many knowledge gaps regarding technology, integration, and the design challenge
Finding Solutions	Iterate an existing design based on previous work or educated estimates, modifying it to achieve objectives and improve performance. If necessary, brainstorm new ideas.	Define a feasible design space, then reduce it by removing regions where solutions are proven infeasible or dominated.
Communication	Frequent, latest iteration of the “best” idea	Less frequent; sets of possibilities; broadcast knowledge for the team vice the next step
Integration	Synthesis and convergence through iteration. Disciplines given budgets and constraints, which can be reallocated to other disciplines	Intersections of sets along matching parameters
Selection	Select the "best one" based on a developed decision scheme. Prototype at the end to confirm the working solution.	Concurrent engineering. Eliminate inferior choices. Conduct low-cost tests along the way to generate flow-up knowledge that supports choices.
Optimization	Typical methods with fitness functions and preferences are invoked at any level of abstraction in the design. Typically, one or two parameters dominate the function.	Alternatives and disciplines design in parallel. Infeasibility and intersections drive global optimization.
Constraints	Maximize constraints in specifications to ensure functionality and interface fit.	Use minimum control specifications to allow optimization and mutual adjustment. Design decisions create constraints and requirements for subsequent analyses.
Risk	Centralized and managed with budgets and constraints.	Decentralized, everyone establishes feasibility before commitment, seeks robust solutions, and honors commitments and choices.

DDG(X) SBD METHOD AND SCALE

In 2018, the U.S. Navy took action to begin the development of a new class of combatant ships to address uncertainty in future needs and accommodate potential future missions above and beyond those of the current DDG-51 and CG-47 classes (O’Rourke, 2023). A Requirements Evaluation Team analyzed suitable initial parameters. Then, it delivered them to the inaugural design team led by Higgins and Page as the Senior Ship Design Manager (SSDM) and Deputy Ship Design Manager (DSDM), respectively. Their initial charter was to further explore cost-capability trades and concept designs to inform the Capability Development Document. We decided that a set-based method was appropriate to manage the complexity and complicatedness of this undertaking in line with previous Navy efforts (Burrow et al., 2014; Garner et al., 2015). Excerpts from Page (2022) and Page et al. (2022) follow to provide the context for the organization, philosophy, and methodology created.

Organization

Organizationally, the team used a hub-and-spoke model. This structure balanced the distributed nature of the U.S. Navy's ship design organizations and our initial chosen sets. The SSDM and DSDM designated seven Functional Area Leads for systems engineering, naval architecture, marine engineering, warfare systems, survivability, flexibility, and affordability, as seen in Figure 3. Those leads were responsible for designated sets in their domains. Leadership planned to co-locate the team at a

design site for high-frequency communications and collaboration, but resources prevented that initially, and then COVID-19 precluded co-location. So, the set teams operated from their designated work sites in Pennsylvania, Maryland, Virginia, and Washington, DC, with little opportunity for face-to-face interaction. This lack of co-location presented an unanticipated opportunity to demonstrate the concurrent engineering aspects of Set-Based Design.

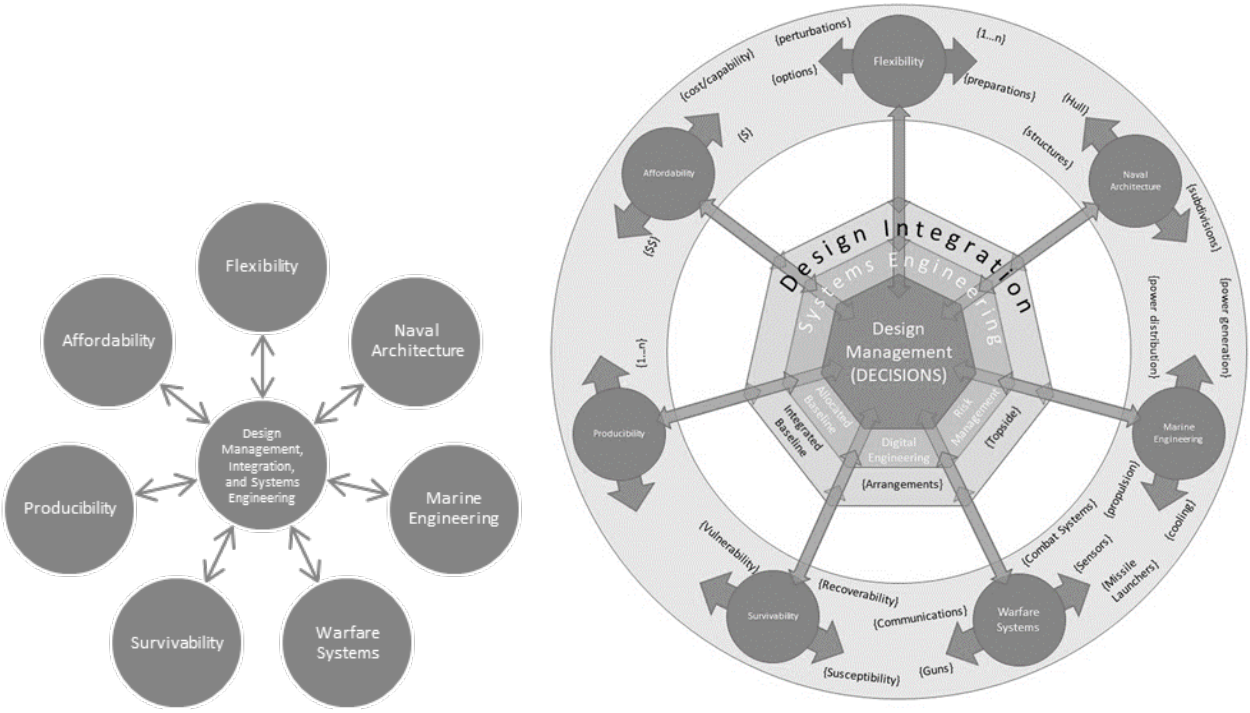

Figure 3: Initial Design Team Organization and Scaled Design Team Organization

With time, the team expanded, explored more sets, and the organization and process scaled. Figure 3 also reveals the scaled structure of the organization, which retains much of the foundational framework. The hub expanded and discretized the systems engineering and design integration functions distinct from design management. The spokes of the framework are now connected, forming a wheel representing the communications and negotiations delegated to the domains from the hub.

Philosophy

The SSDM and DSDM created a design philosophy and promulgated it through a series of Design Guidance Memoranda (DGM). There were initially seven, but that has expanded to include many more. The topics include meeting minutes, routing processes, digital engineering strategy, testing and test objectives, margin management, team training, critical systems, and, of course, how to implement the set-based method for DDG(X). Fundamentally, the philosophy was to manage the risk inherent to the ship and the ship design process while delivering the attributes and characteristics of an affordable and flexible combatant that would serve the Navy for the next 60 to 80 years. The SSDM and DSDM perceived risk with knowledge capture, configuration control, an overly constrained design space, design rework, team communication, and a method unfamiliar to many within the Navy organization. These DGMs addressed those risks and others by instituting practices and providing foundational knowledge and desired behaviors.

The second DGM in the series was especially important because it communicated the SBD philosophy and process to the team. It promulgated the policy that every team member was empowered to retain a valuable portion of their trade space, and only the SSDM (or his delegate) could remove a portion of the design space from further consideration. It also included a requirement to document assumptions within the process and have them approved by the SSDM to avoid the risk of artificially limiting a region of the design space. The assumptions served as placeholders for data not yet known or available to the teams, and they had a potential to affect the boundaries and constraints of the analysis. It established the guiding principle to explore the various domains and sets using appropriate methods. It dictated that sets ought to be no bigger than necessary to analyze an appropriate level of abstraction to close a knowledge gap. The SSDM and DSDM also required the team to think through the metrics and criteria they would use in their analyses to drive to the next decision to avoid the risks of needless investigations that did not close a knowledge gap or extended studies that did not reach conclusions on time. The DGM also included a glossary of the

new terms representing this new way of thinking. It established the concept of a Set Review with the desired outcome of the Reviews being these decisions and approvals.

Method

The next step in executing SBD with the DDG(X) design team was to meet with the functional area leads depicted in Figure 3 and their set team leads to discuss how to apply this method in their set. These meetings served several purposes, including training, calibration, brainstorming, and just plain storming (from the ubiquitous form-storm-norm-perform model of team dynamics). The group would discuss the first knowledge gaps to address in the design germane to their domain and move forward with agreement on the proper analysis to resolve that knowledge gap, the assumptions necessary to accomplish that analysis, and the metrics and criteria appropriate for the analysis. Reaching mutual understanding often required several meetings with leadership and set teams.

These meetings served as the basis for what became Set Reviews. The Set Review was a structured meeting that provided consistency to the presentation of information to the SSDM for decisions. The Review served other purposes, too. It reinforced training and developed the team's familiarity with our SBD process. Eventually, it was the forum where the design team discussed integration and the intersection of overlapping parameters across domains. For each Set Review, team leadership expects a set team to review eight fundamental elements. The DGM on SBD directed these elements to the team and provided a case example for them to follow.

Each Set Review started with the purpose of the study (i.e., which knowledge gap the team is addressing) and of the Set Review (e.g., interim review, approve assumptions, decision review, set reduction). Next, the Set Review shared the team's approach to closing the knowledge gap. Next, the Set Team briefed the assumptions necessary to use that approach. Subsequently, they communicated the criteria for developing their findings, conclusions, decisions, or recommendations. Then, with that background in place, the team could share the analysis and results followed by the outcomes (e.g., findings, conclusions, recommendations, and decisions to remove portions of the design space). After that, the team shared any uncertainty about the outcomes that may influence the outcomes or future analysis. Finally, the Set Review ended with the anticipated next steps, including further analysis within the current set, recommendations for the following knowledge gap or set to explore, or others.

To document the useable, and hopefully re-useable, knowledge, a successful Set Review culminated in a Design Decision Memorandum (DDM). These DDMs are critically important because they record the team's progress, capture the team's work, and record the outcomes of the Set Reviews for posterity. They were widely available to the team and the community of stakeholders surrounding this effort, including resource sponsors, requirement generators, subject matter experts outside the design team, and acquisition professionals. Of course, not every Set Review generated a DDM as the team instantiated this SBD process: through the first year, there were 66 Set Reviews and 26 DDMS (39%); through the second year, there were 139 Set Reviews and 75 DDMs (54%), and through the third year there were 156 Set Reviews and 86 DDMs (55%). In addition to the increase in successful outcomes with time, another important metric related to the process was a decrease in the time to achieve the first DDM, lowering from about 49 days in the first year to about eight days by the third year. In other words, when the team first presented a new set or analysis, it used to take almost two months of rework and adjustments to reach a satisfactory level of information for a successful outcome. However, by the third year, the Set Reviews were more productive as the team learned from each other and leadership the standards necessary for a successful Set Review.

Risk and the First Sets

While the DGMs addressed many risks and set policies in place that answered many questions of the growing team, there was one other philosophical question to answer that did not necessarily belong in a DGM: Where do we start? In other words, what are the first sets? Do we start with every possibility in every set? The answer to this last question is emphatically "no." A naval vessel is sufficiently complex that doing so is impossible. The answer to the other questions, generalized to any naval vessel, is that it depends. Generally, the requirements will drive the answer. An aircraft carrier will have a different start than an amphibious vessel, which will have a different start than a submarine, which will have a different start than a combatant. Also, generally speaking, the answer is outside the Work Breakdown structure of the vessel. Instead, *knowledge gaps* are a vital concept that helps determine the first sets and subsequent sets. The SSDM and DSDM used the requirements, known risks, critical path analysis, external sources, and our judgment and experience with previous projects to derive knowledge gaps and thus the first sets.

One example of requirements dictating the first sets derives from the combat systems domain. The requirement stated that the ship would use the latest variant of the AEGIS combat system but incorporate a service life allowance to change and expand in the future (LaGrone, 2022). One might think there was little work left and few knowledge gaps; however, although that requirement defined some of the material solutions, the team still needed to determine the placement of the sensors in the suite

and define what service life allowance for the system in terms of computing power, space and volume, weight, arrangements, electrical power, and cooling. Of course, the initial placement of sensors depends on superstructure geometry, so this drove another of the initial set explorations due to the tight coupling between these parameters, which were equally undefined at the start. Therefore, warfare systems and combat systems were one of the first sets, and teams formed in this domain to explore these knowledge gaps.

An example of the critical path dictating one of the first sets is with the hull. Despite the fidelity of modeling tools available for hydrostatics and hydrodynamics of a vessel, the U.S. Navy still conducts model tests of hull forms at the Naval Surface Warfare Center, Carderock Division, to explore performance ranges, reduce risk, and confirm the expected performance under various conditions. This test requires building a properly scaled model (which takes time) based on the hull form's final dimensions, which requires analysis of many other coupled parameters throughout the rest of the ship design (and, therefore, also takes time). The testing takes time, as does analyzing the data and many other activities in this process. Knowing this, the hull form definition and testing was a critical path item and, therefore, one of the first sets explored.

Judgment and experience with previous projects led the SSDM and DSDM to include boat handling (the launch and recovery of the ship's boats) as one of the first sets. One may think this discipline should not entertain the same regard as the hull form, combat system placements, or power and propulsion architecture. However, in this case, experience from a previous ship class where boat handling systems had proven difficult and caused significant and expensive rework informed this process of the breadth of potential solution space and the varying degrees of impact on hull form and other major systems, revealing the potential risk that warranted early consideration of the boat handling subsystem. After all, the team had not yet ruled out any parameters with the hull form, arrangements, or other domains that may have removed the risky solution. Further, SBD allowed exploration in this domain for solutions that may have precluded the issues that developed in the previous class.

The SSDM and DSDM chose eleven initial sets and their constituent knowledge gaps. They were:

1. **Hull form** began by exploring three basic shaping choices that affected **survivability**. **Hull form** was also on the critical path because of model testing.
2. **Survivability** began with certain **susceptibility** studies and the gathering of attributes for **vulnerability**. This is a risk area for every naval vessel.
3. **Propulsion** began with the architecture: mechanical, hybrid, or integrated power. **propulsion** was also a risky area with the potential to be on the critical path due to land-based testing.
4. **Power distribution** began with its architecture, i.e., ring bus, zonal, and a few characteristics like voltage and power quality standards.
5. **Power generation** began with the type (gas turbine vs. diesel vs. combinations).
6. **Boat handling** started with the launch location of the ship's boats: side, astern, or both. This was a risk area from previous projects.
7. **Warfare system** began and tracked various characteristics of the delivered combat system (the Flight III combat system) and alternate future combat system characteristics that could be envisioned and added, such as directed energy weapons, new sensors, and new computing.
8. **Topside** began by exploring rough deckhouse size, shape, and location measures.
9. **Flexibility** began by establishing a framework for analysis and developing **uncertainty** to start the framework. It was a critical enabler of the ship and the design. This was the first time anyone had holistically and quantifiably analyzed it, so we felt strongly that it needed to be one of the first **sets** and that it should be its own **set**.
10. **Affordability** had eleven distinct studies informed by other sets and included cost specialists that helped quantify some of the cost-capability trades.
11. **Ships** was a set that represented balanced concepts. We used them to validate and integrate other **sets**.

This final set, the **ship** set, is particularly interesting because it is a set of synthesized, converged, and balanced designs. In other words, it is a set full of point designs.

DDG(X) USE OF POINTS WITHIN THE SBD CONSTRUCT

The use of PBD within SBD may seem counterintuitive. After all, the summary comparison of the two methods presents a case in which the two have few similarities and many differences. That comparison and this article - so far - imply that the two methods are mutually exclusive. This section aims to dispel that thinking. When one carefully crafts the interactions of the two methods, they are complementary. Integrating the two methods requires mindful development of the point designs to fulfill the closure of particular knowledge gaps in a given set in a calculated way, similar to any other analysis a set team may conduct.

The team's discovery of this interaction was both reluctant and serendipitous. It emerged as a discovery due to the final two listed sets of our initial effort: **affordability** and **ships**. Early in the timeline of the design effort, the team's charter was to

explore cost-capability trades, which initiated the **affordability** set. In line with the process, discussions ensued to determine the proper analysis, metrics, criteria, assumptions, and approach to resolve the knowledge gaps and inform requirements regarding affordability. The team quickly realized that affordability, like many other emergent properties of a vessel, is a system-level attribute that is difficult to allocate cleanly to subsystems, but the team needed to evaluate cost and affordability at both discrete and integrated levels of abstraction. Many affordability attributes are tightly coupled with other design aspects, often non-linearly, such as speed, engines, and hull form that have cubic behaviors with resistance and discrete increases in cost due to engine sizing. This abundance of attributes certainly invoked SBD but created the conundrum of understanding affordability at the system (vessel) level to include the secondary and tertiary effects to cost that changing certain parameters and analyzing them may have. At this point, when trying to stand up an SBD method, creating point designs to understand cost and affordability seemed paradoxical. Reluctantly, the team moved forward with this approach, understanding that these points would be more tightly controlled and require faster creation than in previous efforts. The emphasis of the points was on realistic representation of the open design space across all domains while isolating a particular set or characteristic of interest.

Before this effort, including in the Requirements Evaluation Team, the Navy created point-based designs with a few exceptions (Burrow et al., 2014; Garner et al., 2015; Mebane et al., 2011). The Navy has a tool that synthesizes the various parameters of a vessel's design into a feasible solution or tells the user why the vessel will not synthesize. They also have a companion tool to change parameters within boundaries and constraints to produce many point designs rapidly and allow comparisons. It can produce 1,000-2,000 point designs per hour if run on high-power computers. This toolset enables a design space exploration based on boundaries at the moment in time coupled with the programmed code, but does not necessarily create new knowledge. The Requirements Evaluation Team generated 25,000 points during its exploration similar to the **ship** set the affordability team created, but none of those points were used in subsequent design phases with the DDG(X) team.

The DDG(X) effort did not require thousands of designs, though; it required carefully curated point designs that could be compared in all-else-equal techniques to generate knowledge that informed affordability measures. Therefore, each analysis required a unique study guide, a document usually a dozen pages or less that defined benchmark vessels, excursions from that benchmark, and what parameters were allowed to vary from one to the next. The combination of the benchmark vessel and the parameters varied as part of the study created the excursion that generated new knowledge of the design within the boundaries and constraints of the excursion. These study guides listed the approved assumptions and boundary conditions for each point design in the analysis. Collectively, all of these point designs constitute the **ship** set.

The **ship** set contains a few variations of point designs. One variation is called a benchmark. A benchmark vessel represents a synthesized vessel that incorporates decisions and outcomes from Set Reviews up to a certain point. Put another way; a benchmark incorporates the knowledge created and decisions made into a representative point design. Due to this approach, only known and approved knowledge structures (or known and approved assumptions) created new product structures. This limitation helped keep rework loops small and ensured that knowledge built upon itself as the process revealed the design. Depending on the knowledge sought in the open trade space, the process may require several related benchmarks. For instance, when exploring the major power and propulsion architecture, the team created one benchmark with a mechanical architecture, another with a hybrid architecture, and another with an integrated electric architecture so that knowledge creation happened across these architectures until the SDM made a down-select decision. That introduces the final variation of the **ship** set, an excursion. This type of point design allowed specific parameters to vary in controlled ways to help analyze the ship-wide impacts of these changing variables.

Another variation of the approach is that a benchmark vessel represents a synthesized vessel that reflects a portion of the ship set trade space, whereas a few benchmarks are developed and maintained to represent the total ship set trade space. Over time, these benchmarks are updated to incorporate decisions and outcomes from Set Reviews. When decisions and outcomes have not been completed (e.g., warfare system selection), different benchmarks will vary the sets they are designed with to ensure representation of the ship trade space. These benchmarks are then utilized to support the determination of the metrics that can only be determined from a synthesized vessel. When a particular set needs to understand total ship affordability or other metrics for comparisons within the set space being examined (e.g., power generation type – gas turbine or diesel), excursion concepts will be developed from the benchmarks that vary one set (e.g., diesel power generation set in an excursion from a gas turbine benchmark). The differences from the excursion concept to the benchmark represent the impact of the set variation, and that difference becomes the finding for that set's impact across the ship trade space. (e.g., diesel generators are much less power dense but more fuel efficient than gas turbines, increasing ship size to accommodate the diesel generators but reducing ship size on fuel demand; benchmark/excursion comparisons will identify the overall impact on affordability).

A practical example helps to illustrate these points and understand the different variations of point designs. Two of the cost-capability trades requiring more knowledge at the beginning were the top speed of the vessel and the architecture of the power and propulsion plant, specifically mechanical, hybrid, or integrated-electric. Naval engineers ought to recognize that 1) changing the propulsion plant architecture is not trivial, 2) changing speed changes costs in non-linear ways, and 3) the change

in cost for the change in speed will depend on the architecture. Therefore, the team created a coupled design study that varied each parameter to close this knowledge gap for the team and our stakeholders. At the time, the team had three benchmarks for each propulsion architecture within a common hull form with a common combat system and topside arrangement. Those benchmarks became the standard from which two excursion ships varied in their top speed (six new point designs total). These benchmarks and excursions are still only representatives of the open trade space: the team selected specific power generation and propulsion components that had not been locked in with design decisions, and the synthesized models included inherent assumptions on how to best trade hydrodynamics against installed power since that decision space was also still open. The results allowed the team and our stakeholders to compare three cost curves across variations in propulsion plant and top speed. The team could determine and report which plants were more affordable at which speeds. They could also reveal which plants were more sensitive to speed changes – an essential measure of uncertainty at this design stage. The team could couple this information with others like risk and technology readiness to help in the decisions regarding speed, cost, architecture, and others moving forward from that scenario. The speed and propulsion architecture decisions were made within the next year, resulting in a new benchmark that incorporated those decisions and others into a new synthesized and balanced reference vessel, finishing this practical example.

These benchmark and excursion point designs serve many vital purposes. First, one use case for these point designs within SBD is as a risk reduction measure. There are scenarios when schedules accelerate or time runs out for a given design phase. The benchmarks provide a balanced and synthesized design that *could* proceed to subsequent phases at any time since the benchmark presents a representative point that should meet all the requirements. The number of knowledge gaps unanswered dictates the uncertainty and risk in moving forward. The benchmarks also validate the requirements by showing one possible solution of many.

A second use case is in performing ship-wide comparisons and analyses when only select variables change. This purpose allows the design team to tease out second and third-order effects through the design and their cost implications. This case is essential in designing a naval vessel because of the tight coupling of the design parameters.

A third use case relates to the second: knowledge generation. When carefully curated and analyzed, the point designs generate knowledge on a ship scale to understand requirements and cost impacts. In the vein of knowledge generation, they also provide a means by which a design team can match their knowledge structure with the product structure, at least within the boundaries of the synthesis code, in this case. Further, the point designs allow a design team to test the boundaries of the design space. DDG(X) terms these tests “diversity of thought” exercises. When leadership or the team wants to challenge a requirement, assumption, or technology solution, the use of point designs in the manner relayed here provides a structure to conduct those tests, generate new knowledge, and potentially stretch the boundaries of the design space.

In essence, these point designs act as virtual prototypes, a purpose SBD encourages. However, while Toyota can afford to (and does) build physical prototypes of cars and subsystems, it makes less sense for the Navy or another ship owner to follow the same practice. Virtual prototyping allows the Navy to “build” a ship and create a digital engineering underpinning for the effort, with digital threads that can carry through into production and sustainment. The value of the prototype is limited in the same way as any model used is: one must understand the assumptions, code, and fidelity of the information involved.

One last case to note is that the point designs help transition SBD from theory to practice. The U.S. Navy had limited exposure to SBD, especially on a large scale for a combatant. Some stakeholders perceived a considerable risk in using SBD on such an important project without more of a track record for the method. These point designs grounded SBD by providing a sense of familiarity. At the risk of speaking for those stakeholders, they appreciated this approach and, for the first time in their careers, saw (literally seeing in the charts and data graphs presented) the effects requirements and assumptions had on cost and the other coupled parameters of the design. This approach was able to visualize a trade space for decision-makers that transparently presented the capabilities, limitations, and assumptions of the data and outcomes. The design team leadership had to carefully remind stakeholders, when appropriate, that these point designs were for knowledge regarding possibilities and causal relationships of parameters and results that lead to decisions but are not necessarily - *the* - solution (notwithstanding the first use case communicated above).

CONCLUSIONS

While it may seem counterintuitive to use PBD within SBD, the two methods complement each other when constructed in ways that enable their interaction. For complex design challenges like naval vessels, using point design within SBD to generate knowledge and understand causal relationships in the tightly coupled and non-linear trade space benefits the effort. These point designs help reduce risk, act as virtual prototypes, and enable analysis of ship-wide impacts when only a few parameters change. DDG(X) created a preliminary ontology of point designs that suited the team’s purpose: benchmarks and excursions. These basic variations facilitated the team's knowledge generation and matched their knowledge structure to the product structure in

repeatable and valuable ways. Though the DDG(X) team was reluctant to create point solutions as part of their SBD implementation, it proved a valuable practice worth repeating, with well over two hundred point designs created to explore the space, create knowledge, and reduce risk. The two methods are not mutually exclusive, and this approach can generalize to apply to any complex design undertaking.

CONTRIBUTION STATEMENT

Page: Conceptualization, investigation, methodology, visualization, writing - original draft. **Seering:** Conceptualization, methodology, project administration, supervision, writing – review and editing. **Higgins:** Conceptualization, investigation, methodology, project administration, supervision, writing – review and editing. **Platenberg:** Data curation, formal analysis, investigation, visualization, writing – review and editing.

REFERENCES

Bernstein, J. I. (Joshua I. (1998). *Design methods in the aerospace industry: Looking for evidence of set-based practices* [Thesis, Massachusetts Institute of Technology]. https://dspace.mit.edu/handle/1721.1/82675

Burrow, J., Doerry, N., Earnesty, M., Was, J., Myers, J., Banko, J., McConnell, J., Pepper, J., & Tafolla, T. (2014). Concept Exploration of the Amphibious Combat Vehicle. *Day 1 Wed, October 22, 2014*, D011S001R007. https://doi.org/10.5957/SMC-2014-T19

Doerry, D. N. (2015). Measuring Diversity in Set-Based Design. *Proceedings of ASNE Day*, 14.

Dullen, S., Verma, D., Blackburn, M., & Whitcomb, C. (2021). Survey on set-based design (SBD) quantitative methods. *Systems Engineering*, *24*(5), 269–292. https://doi.org/10.1002/sys.21580

Gale, P. (2003). The Ship Design Process. In T. Lamb & Society of Naval Architects and Marine Engineers (Eds.), *Ship design and construction. Vol. 1* (Vol. 1, pp. 5–1 to 5–38). Society of Naval Architects and Marine Engineers.

Garner, M., Doerry, D. N., MacKenna, A., Pearce, F., Bassler, D. C., Hannapel, D. S., & McCauley, P. (2015). *Concept Exploration Methods for the Small Surface Combatant*. 10.

Ghosh, S., & Seering, W. (2014). Set-Based Thinking in the Engineering Design Community and Beyond. *Volume 7: 2nd Biennial International Conference on Dynamics for Design; 26th International Conference on Design Theory and Methodology*, V007T07A040. https://doi.org/10.1115/DETC2014-35597

LaGrone, S. (2022, January 12). Navy Unveils Next-Generation DDG(X) Warship Concept with Hypersonic Missiles, Lasers. *USNI News*. https://news.usni.org/2022/01/12/navy-unveils-next-generation-ddgx-warship-concept-with-hypersonic-missiles-lasers

Mebane, W. L., Carlson, C. M., Dowd, C., Singer, D. J., & Buckley, M. E. (2011). Set-Based Design and the Ship to Shore Connector: Set-Based Design. *Naval Engineers Journal*, *123*(3), 79–92. https://doi.org/10.1111/j.1559-3584.2011.00332.x

O'Rourke, R. (2023). *Navy DDG(X) Next-Generation Destroyer Program: Background and Issues for Congress* (IF-11679; In Focus, p. 3). Congressional Research Service. https://crsreports.congress.gov/product/pdf/IF/IF11679

Page, J. E. (2022). *A Model for Set-Based Design at the System-of-Systems Scale with Approaches for Emergent Properties*. Massachusetts Institute of Technology.

Page, J. E., Higgins, C. J., & Seering, W. P. (2022). Starting and Scaling a Set-Based Design Method for a Maritime System of Systems: Designing a Modern Warship. *Proceedings of the Design Society*, *2*, 2503–2512. https://doi.org/10.1017/pds.2022.253

Page, J., & Seering, W. (2023, August 20). Steps Toward Development of a Comprehensive Set-Based Design Process Model: A Case Study. *IDETC-CIE2023*. https://doi.org/10.1115/DETC2023-115315

Raudberget, D. (2010). THE DECISION PROCESS IN SET-BASED CONCURRENT ENGINEERING - AN INDUSTRIAL CASE STUDY. *Proceedings of the International Design Conference*, 10.

Shallcross, N., Parnell, G. S., Pohl, E., & Specking, E. (2020). Set-based design: The state-of-practice and research opportunities. *Systems Engineering*, *23*(5), 557–578. https://doi.org/10.1002/sys.21549

Simon, H. A. ; L., John E. (2019). *The sciences of the artificial*. The MIT Press; U-M Articles Search. https://doi.org/10.7551/mitpress/12107.001.0001

Singer, D. J., Doerry, N., & Buckley, M. E. (2009). What Is Set-Based Design? *Naval Engineers Journal*, *121*(4), 31–43. https://doi.org/10.1111/j.1559-3584.2009.00226.x

Singer, D., Strickland, J., Doerry, N., McKenney, T., & Whitcomb, C. (2017). *SNAME T&R Bulletin 7-12 Set-Based Design*. The Society of Naval Architects and Marine Engineers.

Sobek, D. K. (1996, July). A set-based model of design. *Mechanical Engineering*, *118*(7), 78.

Sobek II, D. K., Ward, A. C., & Liker, J. K. (1999). Toyota's principles of set-based concurrent engineering. *Sloan Management Review*, *40*(2), 67–83. bth.

Toche, B., Pellerin, R., & Fortin, C. (2020). Set-based design: A review and new directions. *Design Science*, *6*, e18. https://doi.org/10.1017/dsj.2020.16

Ward, A., & Seering, W. (1993). Quantitative Inference in a Mechanical Design 'Compiler.' *Journal of Mechanical Design (1990)*, *115*(1). U-M Articles Search. https://doi.org/10.1115/1.2919320

Proceedings of 15th International Marine Design Conference (IMDC-2024)
June 2-6, 2024
Amsterdam, the Netherlands

Beyond Jack-Ups: A Moonshot for Future Offshore Wind Turbine Installation Vessels for an Uncertain Market

J.J. de Ridder[1,2,*], J.D. Stroo[2], and A.A. Kana[3]

ABSTRACT

This paper addresses the growing offshore wind market's demand for larger turbines in deeper waters by highlighting limitations in existing installation solutions and proposing a new concept with a floating monohull, named Moonshot, which will thus be different than traditional jack-up or semi-submersible crane installation vessel options. This paper discusses the design process, which combines Ulstein Rotterdam's Controlled Innovation and Blended Design to develop the concept. This process is used to explore various market scenarios to determine optimal vessel parameters. Results demonstrate how optimizing for financial performance or seakeeping behavior impacts the design. Moonshot's initial parameters are established, and its performance is compared to existing installation solutions.

KEY WORDS

Early-stage design; Complex design methods, Design space exploration; Offshore wind turbine installation; Seakeeping.

INTRODUCTION

Today's society faces growing concern over climate change, which is primarily caused by the release of greenhouse gases and other hazardous emissions. Generating electricity and heat by burning fossils fuels causes a large part of global emissions (United Nations n.d.). To help mitigate the impacts of climate change, it is crucial to reduce the reliance on fossil fuels and transition to cleaner, renewable energy sources. One of those sources is offshore wind energy. As a result, offshore wind energy is a rapidly growing industry. The global wind market has experienced significant growth in recent years, with the total installed capacity increasing from zero in the 1990s to over 40 GW in 2020. This growth is expected to continue towards 630 GW in 2050 (Kuhn, et al 2023).

Due to the improvement in offshore wind energy and growing demand, the landscape of the offshore wind turbines is also changing. Analysis of 4C Offshore wind farm data (February 24, 2023) has been performed, revealing three major trends. The first is the increasing capacity of turbines. The turbine capacity has significantly increased over the last years and is expected to continue to increase. With the increasing capacity of turbines, the physical size of turbines also increases, making them larger and heavier. The second is the increasing distance from shore to the offshore wind farms (OWFs). The main reason for this is that available location near the coast, especially in the North Sea, are getting scarce (WindEurope 2020). Also, wind speeds are higher and thus more favorable (Nikitas, et al 2020). From 2011 to 2023, the average distance from land to OWF has more than doubled (NORWEP 2022). The third is the increase in water depths at OWF locations. The analysis showed that water depth was not more than 20 meters in 2010, while nowadays the water depth is almost 40 meters. The wind farm data showed that this number is expected to increase in the future.

Currently, wind turbine and foundation transportation and installation (T&I) is done by the same vessels. However, due to the increasing weight and size of foundations, which are growing faster than turbines, foundation installation work is shifting to purpose-built foundation installation vessels (FIVs) (Foxwell 2022). Wind turbine installation will therefore soon be done by dedicated wind turbine installation vessels (WTIVs). This research is thus focused on the process of wind turbine installation. Other research focused on understanding the driving factors behind offshore wind installation vessels includes van Lynden et al (2020). There are various ways of T&I for offshore wind turbines. Seven distinctive methods were identified for offshore wind turbine installation with vessels, as shown in Figure 1.

[1] Department of Maritime and Transport Technology, Delft University of Technology, Delft, The Netherlands
[2] Ulstein Design and Solutions B.V., Rotterdam, The Netherlands
[3] Department of Maritime and Transport Technology, Delft University of Technology, Delft, the Netherlands; ORCID: 0000-0002-9600-8669
* Corresponding Author: jesse.deridder@ulstein.com

Submitted: 23 February 2024, Revised: 25 April 2024, Accepted: 1 May 2024, Published: 18 May 2024

Conference paper, DOI: https://doi.org/10.59490/imdc.2024.834 e-ISSN: 3050-4864

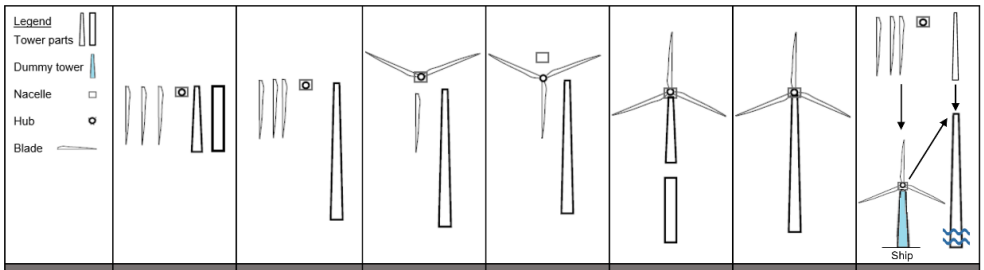

Method	1	2	3	4	5	6	7
Name	Single-blade	Single-blade with preassembled tower	Bunny ears	Star assembly	Fully preassembled with split tower	Fully preassembled	RNA method
Number of offshore lifts	6	5	3 or 4	3 or 4	2	1	**6**
Of which overboard	6	5	3 or 4	3 or 4	2	1	**2**

Figure 1: Overview of common methods for offshore wind turbine installation, based on (Jiang 2021, Richmond et al 2018, EnergyFacts.eu 2019)

The methods mainly differ on the number of onshore preassembled components and subsequently the number of required lifts. The method and degree of preassembly influences the number of offshore lifts. Since offshore lifts are risky and susceptible to delay or damage due to wind conditions, the preference is to minimize offshore assembly (Kaiser, et al 2011; Iberdrola n.d.). Also, from a cost perspective it is beneficial to reduce the number of lifts offshore. For example, (Robinson, et al 2022) state that if construction costs would be $1 onshore, it is $2 in port, and $10 offshore. Despite, most offshore wind turbines are currently installed using method 2 – single blade with preassembled tower - (Asgarpour, 2016) because components can be transported more easily and deck space is used most-efficiently, reducing the number of required roundtrips (Kaiser, et al 2011). Method 7 is a novel installation method which combines the advantages of method 2 and method 6, ensuring efficient use of deck space, while also keeping the number of overboard offshore lifts as low as possible. The rotor nacelle assembly (RNA) is assembled on board of the vessel in a controlled environment with a dummy tower.

Regarding transportation of turbine components, there are two options. The first option is all-in-one, in which the installation vessel both transports and installs the turbine components. The vessel loads at the marshalling port and sails to the installation site. There, the components are installed by the same vessel. When empty, the vessel returns to the marshalling port, repeating the cycle (Vis, et al 2016). The second option is a feeder system, in which the WTIV stays at the OWF location and is supplied by feeder barges or vessels that shuttle between the marshalling port and OWF to be loaded and unloaded with turbine components. An advantage of this strategy is that installation vessel's productivity could be higher because it does not have to sail. However, lifting from another vessel at sea, which is moving due to waves, could be very risky (Vis, et al 2016), potentially damaging the fragile turbine components (Asgarpour 2016).

Currently, mostly jack-up vessels are used for wind turbine T&I (Asgarpour 2016). These vessels can elevate themselves above the sea surface with their legs to provide a stable (Nørkaer Sørensen, 1984) base for lifting operations and eliminate vessel and crane displacements due to waves and surges (Streatfeild, et al 2013; Attari, et al 2014). Analysis of the existing fleet of jack-up vessels used for wind turbine T&I with the 4C Offshore wind vessel database (March 10, 2023), showed that they will not be able to lift the next-generation turbines. Furthermore, the increasing water depths are a negative progression for jack-ups. The leg length of these vessel dictates the maximum working depth (Attari, et al 2014). In addition, because of their interaction with the seabed, they are dependent on soil conditions. A seabed survey must be done beforehand, requiring other vessels (Riviera Newsletters 2010), and these vessels cannot be deployed at all locations. In addition, lowering and raising the legs takes up a considerable amount of time (Uraz 2011), especially considering that this must be done at every turbine location and in port. This makes jack-ups very inefficient.

Alternatively, floating solutions are also sometimes used for wind turbine installation, such as semi-submersible crane vessels (SSCVs). A major drawback of these vessels is that their day rates are very high (Jiang 2021) and their capabilities exceed what is needed for offshore wind turbine installation (Kaiser, et al 2011), making them cost-inefficient. In addition, these vessels require a feeder system, despite having a substantial deck area. This is because SSCVs have a transit draft of 10 to 12 meters. Their maximum draft, during lifting operations, ranges from 25 to 32 meters (Saipem n.d.; Heerema Marine Contractors 2020), while the water depth at marshalling ports is typically not larger than 9 to 13 meters (Parkinson, et al 2022). As a result, SSCVs are not able to enter the marshalling ports to load turbine components, requiring a feeder system with all risks associated.

Multiple ways to address the gap between the existing wind turbine installation fleet and the market demands were investigated. Vessels currently on order or being built were found to be just larger jack-ups. Existing jack-ups are being retrofitted with larger cranes to be able to install the next-generation turbines. However, these approaches do not address the installation bottlenecks associated with jacking. In addition, several new concepts for future wind turbine installation were researched. These concepts were found to be mostly floating installation solution, relying on fully preassembled

installation methods, reducing the number of offshore overboard lifts. However, there are stability and seakeeping risks when sailing with a fully preassembled turbine (Herman 2002; Díaz, et al 2023). Most of the concepts were found to still have installation bottlenecks, such as the jacking or the need for a feeder system. Also, most concepts were found to have complex hull types, such as semi-submersibles or catamarans, which are expensive to build, leading to higher day rates (Djupevåg Eri 2015). Additionally, operational costs are generally higher for these hull types (Schouten 2018).

Based on the market, concept analysis, and previous development with industry partners, it was concluded that there is a need for a new cost-effective and efficient solution. This research proposes a new floating monohull vessel concept, called Moonshot, to address the gap between future market demand and current and near-term solutions. Monohulls generally have a large open deck area and are therefore capable of carrying a lot of cargo. Also, day rates are lower than for the other types of WTIVs (Jiang 2021). Also, they are capable of higher transit speeds than, for example, jack-ups and SSCVs (Djupevåg Eri 2015). But most of all, this vessel type would not have any of the mentioned installation bottlenecks. However, a floating monohull would be more susceptible to motions because of waves during the installation of the turbines, which is important to consider.

The aim of this research is to explore the feasibility of Moonshot and to investigate how it can be developed into a viable concept. Because of the unpredictable nature of the market it will operate in, it is important to explore the design space of Moonshot and elucidate optimal design parameters for both financial performance and seakeeping performance. The main research question of this paper is: "What should optimal design parameters be for the innovative Moonshot concept, a floating monohull vessel for offshore wind turbine installation, taking into account financial and seakeeping performance, while considering the uncertainties and evolving requirements of the offshore wind market?"

DEVELOPING MOONSHOT

To design Moonshot, it is important to choose a suitable design strategy. Multiple design strategies were investigated. These included: point-based design, set-based design, systems engineering, systems-based design, and optimization-based design. Each of these design strategies were evaluated on several aspects that are important for the development of Moonshot, including: (1) applicability in ship design, (2) the degree of innovation the strategy enables, (3) optimization with a parametric ship model, and (4) flexibility in dealing with changing requirement and market uncertainty. None of the design strategies was found to meet all requirements. In response to this, two strategies developed by Ulstein Design & Solutions B.V. (UDSBV) were introduced: Controlled Innovation (CI) and Blended Design. When investigating these strategies, it was found that they are amalgamations of the main state-of-the-art design strategies.

CI was originally developed by Van Bruinessen (2016) as part of his PhD dissertation and is a strategy to evaluate functions and design aspects in the ship design process. The application of development packages for high-risk design aspects allows for knowledge generation and often results in new solutions and an improved design. Therefore, this method proves to be very useful when innovating in the realm of ship design. Blended Design was developed by Zwaginga (2020), Zwaginga et al (2021) and allows for multi-parameter optimization for many variations of a parent ship design within different (market) scenarios, while considering the lifetime financial performance.

The two strategies have been combined into one design strategy, suitable for the development of Moonshot. CI is used to determine the functions of Moonshot, as well as to establish the underlying design aspects. These design aspects are then evaluated to identify which ones require additional focus or extra knowledge. It is then important to differentiate between the design aspects that should be addressed in the development packages of the CI process and those that can be handled through Blended Design. The results obtained from the development packages will eventually serve as input or boundaries for Blended Design. The adopted design strategy for this research is shown in Figure 2 and described in more detail below.

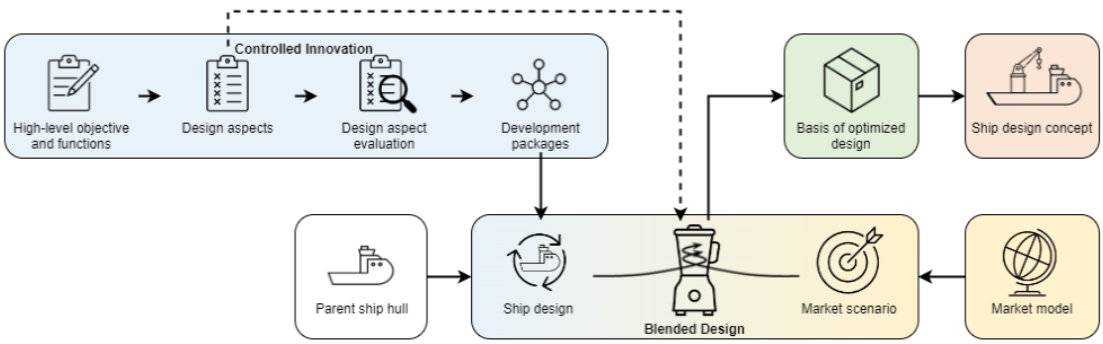

Figure 2: Schematic of the adopted design strategy for this research.

High-level objective, Functions, and Design aspects

Following the CI process, first the high-level objective of Moonshot was determined, which is that the design should aim to be competitive in the offshore wind market and be efficient. Secondly, the functions to reach the objective were established, which are: hull shape requirements, mission equipment for wind turbine installation, payload, station keeping, motion performance, mobility, and accommodation. Then, the associated design aspects to these functions were determined. The identified design aspects are shown in the first column of Table 1. Arranging the design aspects revealed that there were a lot of unknowns for the design aspects, including requirements for ship particulars, type of lifting equipment, and the number of turbines Moonshot should carry per roundtrip. Also, properties of the cargo are unknown.

Design aspects evaluation

Table 1 shows the design aspect evaluation, in which all design aspects are ranked. The first step involves assessing the level of the uncertainty of each requirement of a design aspects. Uncertainty in this context refers to the likelihood of changes in the requirements. Thereafter, the expected impact of an aspect on the ship design is determined. The two scores are then multiplied. Design aspects with higher scores indicate greater risks to the ship design. To decrease these risks, it is crucial to reduce uncertainty of the high-scoring design aspects and generate more knowledge to establish the right requirements with more certainty. Following CI, these high-risk design aspects are covered in detail in development packages. However, not all aspects will be covered solely in the development packages, as some will be addressed through Blended Design. The table shows the evaluation of the identified design aspects and indicates whether the path of development packages or Blended Design is proposed for high-scoring design aspects.

Table 1: Evaluation of the design aspects.

	Uncertainty 1 = certain 5 = uncertain	Consequence Design 1 = low impact 5 = high impact	Score Design Aspect U x C x 0.2	Assigned solution
Hull shape requirements				
Hull type	1	5	1.0	
Main dimensions	5	5	5.0	Blended design
Mission equipment wind turbine installation				
Installation method	2	5	2.0	
Lifting equipment	5	5	5.0	**Development package**
Lifting capacity	5	5	5.0	Blended design
Payload				
Type	1	4	0.8	
Size, mass and CoG of components	5	4	4.0	**Development package** and Blended design
Amount of turbines	5	5	5.0	Blended design
Deck cargo layout	4	4	3.2	**Development package**
Station keeping				
DP capability	2	4	1.6	
Operational area	1	3	0.6	
Motion performance				
Motion limits	5	3	3.0	
Workability	5	5	5.0	Blended design
Mobility				
Speed	4	5	4.0	Blended design
Mission	1	5	1.0	
Accommodation				
People on board	3	3	1.8	

Development packages

Three design aspects were identified that should be covered in development packages to generate more knowledge, or before they can be incorporated in Blended Design, namely: the lifting equipment; the size, mass and CoG of components, and optimal deck layout.

Development package 1: Lifting equipment

Since Moonshot will be a monohull and will install the turbine while floating, it will be susceptible to wave-induced motions. Therefore, the number of overboard lifts should be as low as possible to minimize risk. Therefore, the decision has been made to combine two installation methods to combine the benefits of those methods. The idea is to transport the turbine components separately, to allow for efficient use of deck space, and when at the installation location, assemble the turbine on board of the vessel. Then, the assembled turbine will be lifted overboard and installed on the turbine foundation. The right lifting equipment should be selected for this purpose. When looking at existing wind turbine installation vessels and future concepts, two types of vertical lifting mechanisms can be identified, free-hanging and guided (Figure 3).

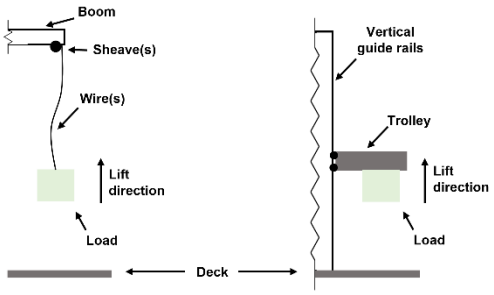

Figure 3: Visualization of lifting mechanisms: free-hanging lift (left) and guided lift (right).

The two mechanisms have been evaluated on the five aspects in Table 2. The main advantage of a guided lift mechanism would be to prevent swinging loads, minimizing the risk of damage to the turbine components. However, the main drawback of this mechanism would be that it would not be flexible and could not be used for other lifting purposes, because the working area of a guided lift system would be very small. Therefore, a hybrid solution between the two lifting mechanisms is preferred, a crane that can do both, such as the Zephyr crane by Huisman. Therefore, this lifting solution is adopted on the concept for Moonshot.

Table 2: Assessment of the different lifting mechanisms, including a hybrid solution.

	Free-hanging lift	Guided lift	Hybrid solution
Sufficient lifting capacity			
Prevention of swinging loads			
Stored position during transport			
Flexible			
Acceptable			

Development package 2: Size, mass, and CoG of components

Information about the properties of next-generation offshore wind turbines is not available, resulting in uncertainty regarding the size, mass, and CoG of turbine components. To overcome this, an analysis into the properties of turbines has been conducted. A database was created with properties of 16 commercially available offshore turbine models of different sizes, and 7 generic reference offshore wind turbine models provided by research institutions. Spearman's rank correlation was used to determine the correlation between the various size and mass properties of the turbines. This showed that there is a strong correlation between all properties. The design of a wind turbine depends on the rated power, which is in turn linked to the squared rotor diameter (D). To understand the mass and size properties of turbines would scale with increased turbine capacity, scaling laws have been established with D as the independent variable. Two approaches, as described by (Sergiienko, et al 2022), were employed:

1) **Heuristic engineering fit** with $y=cx^d+f$, where x is the independent variable, and the exponent d is constant and based on expected geometric upscaling from physical laws or literature. Coefficients c and f are unknown, and f is non-zero for linear scaling;
2) **Best power fit** with $y=ax^b$, where coefficients a and b are unknown.

The coefficients were obtained by fitting curves, following the two approaches, through the data points from the wind turbine database. Then, the coefficient of determination (R^2) was calculated to indicate how well the resulting curves fit the data. Eventually, the best fitting scaling law for each of the wind turbine properties has been established. These are shown in Table 3. When extrapolated, these can subsequently be used in Blended Design to estimate the size and mass of future turbine components. The center of gravity (CoG) location of the turbine components was estimated using literature and assumed for towers to be at 41% of the height (Quancard, et al 2019). The CoG of blades is located 35% from the blade root (Sørensen 1984) and for nacelles and hubs at the center of the components.

Table 3: Scaling laws for each parameter based on a heuristic engineering approach and best power fit, based on the database with 23 offshore wind turbine models.

Parameter	Heuristic engineering fit	R^2	Best power fit	R^2
P_{rated}	-	-	-	-
D_{rotor}	$5.98 \times 10^{1} \cdot P_{rated}^{0.5}$	0.913	$6.02 \times 10^{1} \cdot P_{rated}^{0.497}$	0.913
L_{blade}	$4.86 \times 10^{-1} \cdot D^{1} + 0.113$	1.000	$4.89 \times 10^{-1} \cdot D^{0.999}$	1.000
M_{blade}	$1.16 \times 10^{-3} \cdot D^{2}$	0.903	$5.58 \times 10^{-3} \cdot D^{1.707}$	0.929
$L_{nacelle} + L_{hub}*$	$8.23 \times 10^{-2} \cdot D^{1} + 2.112$	0.819	$1.66 \times 10^{-1} \cdot D^{0.890}$	0.815
$B_{nacelle}*$	$7.03 \times 10^{-2} \cdot D^{1} - 4.433$	0.834	$1.47 \times 10^{-3} \cdot D^{1.658}$	0.882
$H_{nacelle}$	$6.13 \times 10^{-2} \cdot D^{1} - 2.136$	0.719	$1.98 \times 10^{-2} \cdot D^{1.175}$	0.703
$M_{nacelle}$	$1.20 \times 10^{-2} \cdot D^{2}$	0.866	$1.59 \times 10^{-2} \cdot D^{1.947}$	0.867
M_{hub}	$2.76 \times 10^{-3} \cdot D^{2}$	0.584	$1.08 \times 10^{-3} \cdot D^{2.174}$	0.588
L_{tower}	$3.80 \times 10^{-1} \cdot D^{1} + 39.328$	0.730	$4.27 \times 10^{0} \cdot D^{0.622}$	0.735
D_{tower}	$3.89 \times 10^{-2} \cdot D^{1} + 0.766$	0.888	$6.38 \times 10^{-2} \cdot D^{0.924}$	0.885
M_{tower}	$3.07 \times 10^{-2} \cdot D^{2}$	0.624	$5.89 \times 10^{-2} \cdot D^{1.880}$	0.626
H_{hub}	$4.68 \times 10^{-1} \cdot D^{1} + 32.540$	0.822	$2.56 \times 10^{0} \cdot D^{0.737}$	0.822

*Only the direct and semi-direct drive turbines were used for this parameter.

Development package 3: Deck layout

To investigate the optimal deck layout for Moonshot, eighteen different deck layouts were manually drawn with components for 15 MW turbines. The deck layouts differed with respect to crane, assembly, and installation location, as well as placement of the components on deck. Subsequently, all deck layouts were evaluated on the following aspects:

- Port logistics and transit
  - Loading
  - Transit
- Offshore operations
  - Tower lifting
  - Nacelle lifting
  - Blade lifting
  - Assembly lifting
- Capacity
  - Number of turbines
  - Efficient use of deck space
- Motion behavior
  - Assembly location
  - Installation location

An analysis was performed to establish local motions in the nacelle for two different loading conditions and at two different locations. The analysis was done for a case in the North Sea with a JONSWAP spectrum with γ=3.3 at a significant wave height of 2.5 meters. The vessel was allowed to weathervane. For the analysis, software SESAM package by DNV was used. GeniE was used for creating a panel model, HydroD for modeling the environment and perform the hydrodynamic analysis in the frequency domain, using WADAM as a hydrodynamic solver.

All deck layouts were evaluated and scores on the various aspects were assigned. After evaluation, it was concluded that the best deck layout and crane position for Moonshot would be as shown in Figure 4.

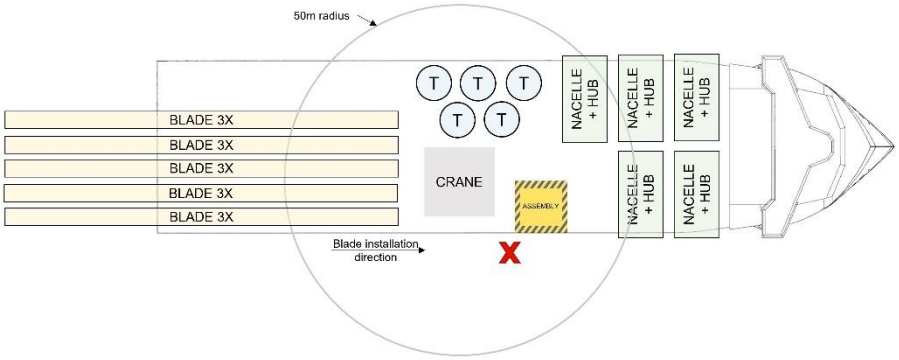

Figure 4: The selected optimal deck layout for Moonshot.

BLENDED DESIGN FOR MOONSHOT

Blended Design is used to explore the design space of Moonshot and to elucidate the ship parameters based on financial and seakeeping performance. The existing model, as developed by Zwaginga (2020), Zwaginga et al (2021) generates a large number of unique design variations on a parent ship design by varying naval architectural parameters. For each of those design configurations, the lifetime financial performance is calculated within a simulated market environment. The model incorporates market uncertainty and different market scenarios can be considered to identify the optimal vessel size for evolving markets while balancing short- and long-term competitiveness. The current model could not directly be applied for the purpose of Moonshot as it cannot take into account seakeeping behavior and was originally designed for different vessel types, specifically heavy transport vessels (HTVs) and FIVs for monopile and jacket foundation T&I. In order to

adapt Blended Design for Moonshot, existing assumptions and functions needed to be updated or modified. Furthermore, new functionalities were added. Figure 5 visualizes the different parts of Blended Design and the connection between different functions of the entire model. The colors indicate what parts are added (green), unused (red), modified (blue), and left unchanged (white).

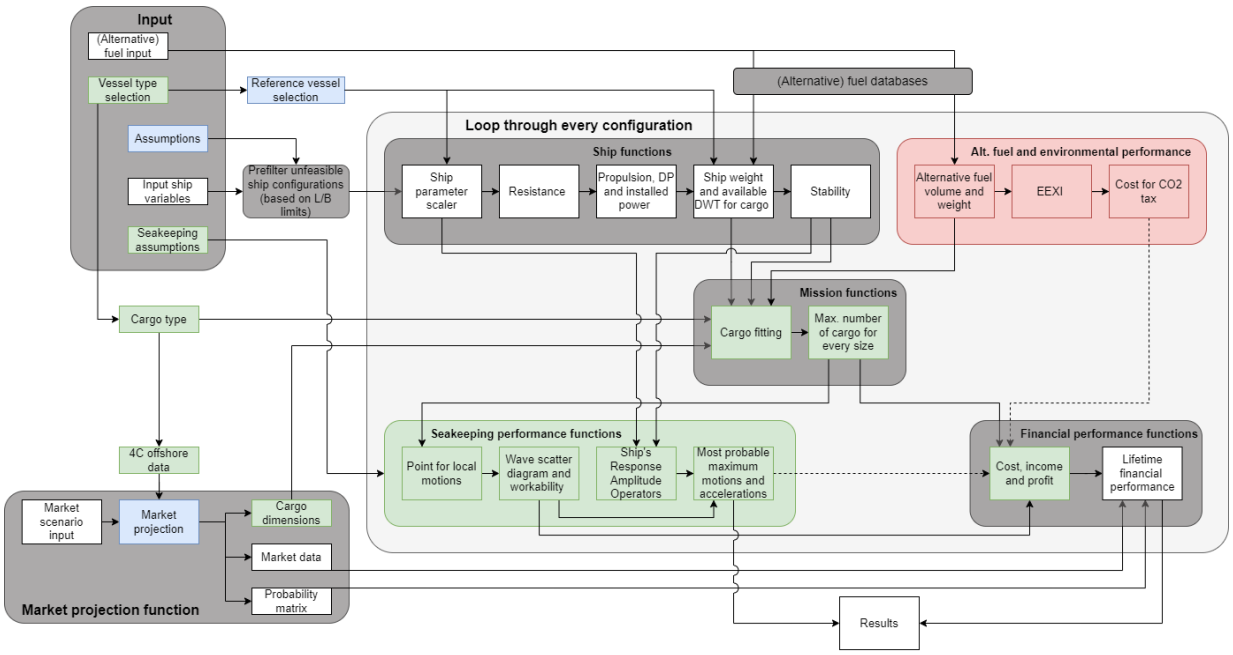

Figure 5: Integration of functions for Moonshot in Blended Design.

The biggest modifications to the model are the addition of the seakeeping performance functions and the mission functions for wind turbine components.

Method for seakeeping analysis

Figure 6 presents the adopted approach for determining the seakeeping performance of every ship configuration in the design space. The output of this approach aims to provide the most probable maximum responses for the most-occurring sea state within the operational range of a vessel configuration. The operational range can be specified as input for Blended Design by setting a desired significant wave height (H_s) limit. Based on the findings from the literature and market research, this limit was set to 2.5 meters for Moonshot.

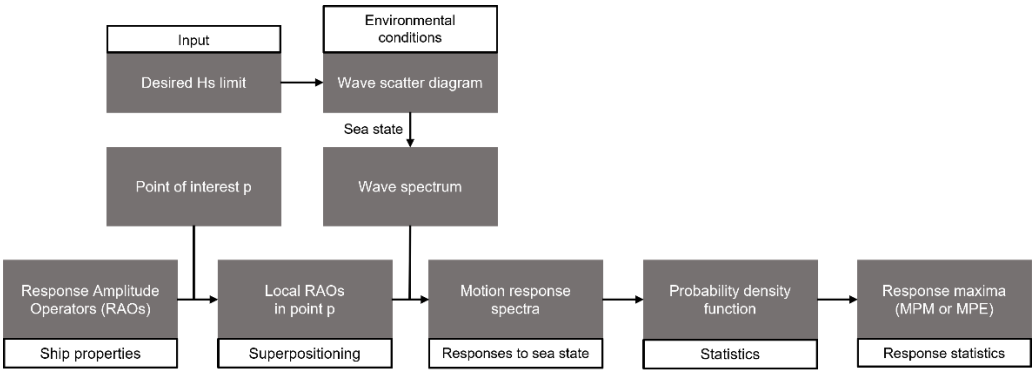

Figure 6: The approach to determine seakeeping behavior.

Response Amplitude Operators

The main challenge with the approach is to determine the Response Amplitude Operators (RAOs) for all ship configurations within the design space. 2D Strip theory and 3D boundary element methods would not be applicable for the purpose of Blended Design, because these calculation methods would take too much time when calculating the RAOs for hundreds of thousands ship configurations. Furthermore, these methods require a hull-form geometry. However, this specific information is not available during the early-stage design and, as a result, not included in Blended Design. Therefore, a simpler method which only relies on ship parameters is needed. The paper by (Jensen, et al 2004) presents closed-form expressions (CFEs) to estimate the heave, roll, and pitch RAOs of a homogeneously loaded box by applying linear strip theory. To validate the method, RAOs were calculated for an UDSBV design of which RAOs computed with hydrodynamic analysis software (HAS) were available. The RAOs for different wave headings from the two methods were then compared. The visual validation revealed that the RAOs for the three motions, as calculated using the CFEs, appeared to be remarkably

similar. The trajectory of the RAOs calculated with the CFEs aligned with the behavior of the RAOs from HAS. The amplitudes of the motion RAOs appear to be around the same angular wave frequency, and the order of magnitude of the RAOs falls within the same range. Additionally, the area under each RAO curve was calculated and compared. The area is a measure of the transferred energy. This comparison is shown in Table 4.

Table 4: Comparison of the areas under RAO curves for results from HAS and CFEs.

			Wave heading angle										
	Method		0°	15°	30°	45°	60°	90°	120°	135°	150°	165°	180°
Heave	HAS	[s^{-1}]	0.41	0.42	0.44	0.48	0.57	0.93	0.61	0.51	0.46	0.43	0.42
	CFE	[s^{-1}]	0.38	0.39	0.41	0.47	0.57	1.13	0.57	0.47	0.41	0.39	0.38
	Error		**-9%**	**-8%**	**-5%**	**-3%**	**1%**	**21%**	**-6%**	**-8%**	**-10%**	**-11%**	**-11%**
Roll	HAS	[deg/ms]	0.00	0.24	0.49	0.72	0.93	1.11	0.90	0.70	0.48	0.24	0.00
	CFE	[deg/ms]	0.00	0.19	0.41	0.66	0.97	2.04	0.97	0.66	0.41	0.19	0.00
	Error		**0%**	**-21%**	**-16%**	**-9%**	**4%**	**84%**	**8%**	**-5%**	**-14%**	**-20%**	**0%**
Pitch	HAS	[deg/ms]	0.47	0.47	0.47	0.49	0.51	0.04	0.52	0.48	0.44	0.42	0.41
	CFE	[deg/ms]	0.33	0.33	0.35	0.39	0.45	0.00	0.45	0.39	0.35	0.33	0.33
	Error		**-30%**	**-29%**	**-25%**	**-20%**	**-12%**	**-100%**	**-13%**	**-19%**	**-20%**	**-20%**	**-21%**

As displayed, the CFEs tend to underestimate the area under the RAO curves in comparison to the RAOs obtained from HAS. This implies that there is a difference in the total transferred energy across the entire range angular wave frequencies. The disparities between the two methods are most pronounced in beam seas. Also, a validation has been performed with another way to validate the RAOs from CFEs is to compare the standard deviation (σ) of the resulting response spectra. This is because the distribution of the area under the RAO curves is also important to consider. Therefore, the differences in transferred energy do not provide the complete picture. To incorporate the distribution into the validation, response spectra were calculated for all RAOs in three different sea states with different wave peak periods (T_p). A comparison for one of the periods is shown in Table 5.

Table 5: Comparison of the standard deviation (σ) of the response spectra at Tp = 7s, calculated using the RAOs from HAS and CFEs.

			Wave heading angle										
	Method		0°	15°	30°	45°	60°	90°	120°	135°	150°	165°	180°
Heave	HAS	[m]	$5.8{\cdot}10^{-2}$	$5.7{\cdot}10^{-2}$	$5.9{\cdot}10^{-2}$	$6.8{\cdot}10^{-2}$	$8.0{\cdot}10^{-2}$	$3.9{\cdot}10^{-1}$	$1.1{\cdot}10^{-1}$	$8.8{\cdot}10^{-2}$	$7.3{\cdot}10^{-2}$	$6.5{\cdot}10^{-2}$	$6.3{\cdot}10^{-2}$
	CFE	[m]	$4.2{\cdot}10^{-2}$	$4.4{\cdot}10^{-2}$	$4.9{\cdot}10^{-2}$	$7.2{\cdot}10^{-2}$	$8.4{\cdot}10^{-2}$	$5.7{\cdot}10^{-1}$	$8.4{\cdot}10^{-2}$	$7.2{\cdot}10^{-2}$	$4.9{\cdot}10^{-2}$	$4.4{\cdot}10^{-2}$	$4.2{\cdot}10^{-2}$
	Error		**-26%**	**-23%**	**-16%**	**7%**	**5%**	**46%**	**-21%**	**-18%**	**-32%**	**-32%**	**-32%**
Roll	HAS	[deg]	0.0	$7.7{\cdot}10^{-4}$	$1.4{\cdot}10^{-3}$	$2.0{\cdot}10^{-3}$	$2.4{\cdot}10^{-3}$	$1.3{\cdot}10^{-3}$	$2.0{\cdot}10^{-3}$	$2.0{\cdot}10^{-3}$	$1.5{\cdot}10^{-3}$	$8.5{\cdot}10^{-4}$	0.0
	CFE	[deg]	0.0	$3.2{\cdot}10^{-4}$	$7.2{\cdot}10^{-4}$	$1.2{\cdot}10^{-3}$	$2.0{\cdot}10^{-3}$	$1.1{\cdot}10^{-2}$	$2.0{\cdot}10^{-3}$	$1.2{\cdot}10^{-3}$	$7.2{\cdot}10^{-4}$	$3.2{\cdot}10^{-4}$	0.0
	Error		**0%**	**-59%**	**-49%**	**-38%**	**-17%**	**735%**	**-1%**	**-36%**	**-51%**	**-62%**	**0%**
Pitch	HAS	[deg]	$2.5{\cdot}10^{-3}$	$2.5{\cdot}10^{-3}$	$2.6{\cdot}10^{-3}$	$3.0{\cdot}10^{-3}$	$5.0{\cdot}10^{-3}$	$4.7{\cdot}10^{-4}$	$5.1{\cdot}10^{-3}$	$2.9{\cdot}10^{-3}$	$2.3{\cdot}10^{-3}$	$2.0{\cdot}10^{-3}$	$1.9{\cdot}10^{-3}$
	CFE	[deg]	$1.3{\cdot}10^{-3}$	$1.4{\cdot}10^{-3}$	$1.8{\cdot}10^{-3}$	$2.1{\cdot}10^{-3}$	$4.2{\cdot}10^{-3}$	0.0	$4.2{\cdot}10^{-3}$	$2.1{\cdot}10^{-3}$	$1.8{\cdot}10^{-3}$	$1.4{\cdot}10^{-3}$	$1.3{\cdot}10^{-3}$
	Error		**-46%**	**-42%**	**-32%**	**-29%**	**-15%**	**-100%**	**-17%**	**-27%**	**-22%**	**-28%**	**-30%**

The comparison showed that the error in the variances decreases as wave periods increase, or wave frequencies decrease. Overall, the variances from CFEs were lower than from HAS, but in the correct order of magnitude. Also, it is important to keep in mind the primary purpose of the method for determining the RAOs, which is to assess seakeeping behavior within Blended Design and predict the relative merits of various ship configurations. In this context, the method appears to be applicable. However, absolute results obtained from this method should be interpreted with caution.

Local RAOs

RAOs are calculated in the CoG of a vessel. When linearizing for small motions, the independent RAOs can be translated to local motions in a point P through superposition. The phase angles of the RAOs are not known, so it is assumed for this research that the phases of all motions are such that the maximum motions occur at the same instance. This approach would yield the most conservative results. The resulting RAO in each of the three directions is then the sum of the associated RAOs in combination with the coordinates of point P with respect to the origin of the coordinate system, located at the CoG of the ship. For this project, point P will be located at the hub height in its installation position of the largest turbine every ship configuration can potentially carry in its lifetime in a specific market. This is visualized in Figure 7.

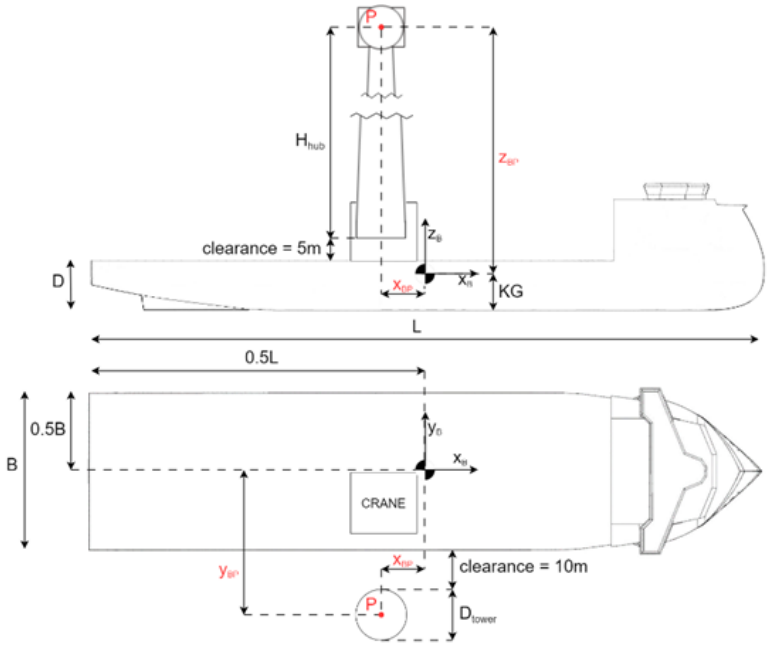

Figure 7: Schematic of the location of point P for local motions.

Wave scatter diagram

A wave scatter diagram represents the join probability of significant wave height (H_s) and wave zero-up-crossing period (T_z). The wave scatter diagram can be calculated for different worldwide locations and depends on multiple parameters. The values for those parameters have been derived using measurements and can be obtained from DNV-RP-C205 Environmental Conditions and Environmental Loads (Det Norske Veritas AS 2017). The seakeeping module is programmed such that different wave scatter diagrams can be considered, based on the input. For this research, zone 11 is used. The corresponding wave scatter diagram is presented in Figure 8.

When designing a vessel, it is common practice to aim for a certain workability or to set the limits up to which it can operate. Based on market research, it was decided that Moonshot should be able to operate up to H_s of 2.5 meters. This is highlighted by a black outline in the figure above and corresponds to a workability of more than 75 percent, which is acceptable. Of the sea states with a H_s of 2.5 meters, a T_z of 6.5 seconds is most occurring. For this research, this sea state (outlined in red) will be the sea state of interest.

Percent occurrence	Tz [s] 0.5	1.5	2.5	3.5	4.5	5.5	6.5	7.5	8.5	9.5	10.5	11.5	12.5	13.5	14.5	15.5	Sum
0.5			0.467%	8.780%	14.052%	7.111%	1.972%	0.392%	0.064%	0.010%	0.001%						32.85%
1.5			0.009%	1.083%	6.704%	9.701%	6.324%	2.576%	0.786%	0.200%	0.045%	0.010%	0.002%				27.44%
2.5				0.133%	1.868%	5.036%	5.401%	3.321%	1.436%	0.493%	0.145%	0.039%	0.010%	0.002%	0.001%		17.89%
3.5				0.017%	0.447%	1.954%	3.071%	2.580%	1.449%	0.623%	0.223%	0.070%	0.020%	0.006%	0.001%		10.46%
4.5				0.002%	0.098%	0.650%	1.413%	1.544%	1.078%	0.557%	0.234%	0.085%	0.028%	0.008%	0.002%	0.001%	5.70%
5.5					0.020%	0.195%	0.567%	0.782%	0.662%	0.402%	0.194%	0.079%	0.029%	0.010%	0.003%	0.001%	2.94%
6.5					0.004%	0.054%	0.206%	0.352%	0.355%	0.250%	0.136%	0.062%	0.025%	0.009%	0.003%	0.001%	1.46%
7.5					0.001%	0.014%	0.069%	0.144%	0.172%	0.138%	0.085%	0.042%	0.018%	0.007%	0.003%	0.001%	0.69%
8.5						0.003%	0.022%	0.055%	0.076%	0.070%	0.048%	0.026%	0.012%	0.005%	0.002%	0.001%	0.32%
9.5						0.001%	0.006%	0.019%	0.032%	0.033%	0.025%	0.015%	0.008%	0.003%	0.001%		0.14%
10.5							0.002%	0.007%	0.012%	0.014%	0.012%	0.008%	0.004%	0.002%	0.001%		0.06%
11.5								0.002%	0.005%	0.006%	0.006%	0.004%	0.002%	0.001%	0.001%		0.03%
12.5								0.001%	0.002%	0.002%	0.002%	0.002%	0.001%	0.001%			0.01%
13.5									0.001%	0.001%	0.001%	0.001%	0.001%				0.00%
14.5																	0.00%
15.5																	0.00%
Sum	0.00%	0.00%	0.48%	10.02%	23.19%	24.72%	19.05%	11.77%	6.13%	2.80%	1.16%	0.44%	0.16%	0.05%	0.02%	0.00%	100%

Hs [m]

Figure 8: Wave scatter diagram calculated for zone 11 (North Sea).

Wave and response spectra

For this research, a JONSWAP wave spectrum will be used with a peak enhancement factor (γ) of 3.3. The wave spectrum will be calculated for the sea state of interest for the specified zone in Blended Design, as explained earlier. After the wave spectrum is determined, the response spectra for each of the motion directions and wave headings can be established. The motion response spectrum describes the response to waves of a floating body at different wave frequencies.

Response maxima

To assess the seakeeping characteristics of the ship configurations, it is important to predict the highest response value within an irregular sea state within a certain time. This is done with probability distributions. A good approximation for the distribution of response maxima can be obtained using a Rice distribution function. This probability distribution depends on the variance (σ_s) of the response spectrum and spectral width parameter (ε). When the ε=0, the Rice distribution reduces to the Rayleigh distribution. For $\varepsilon \leq 0.9$, the most probable largest value in n observations of a random process, as given in (Bhattacharya 1973), is calculated by Equation 1 and 2.

$$n = \frac{T}{T_z} \quad [1]$$

$$\eta_n = \sigma_S \left[2 \ln \left(\frac{2\sqrt{1-\epsilon^2}}{1+\sqrt{1+\epsilon^2}} \cdot \frac{n}{\alpha} \right) \right]^{1/2} \quad [2]$$

The most probable largest value η_n depends on a risk factor α. This factor is the probability that the extreme value will exceed η_n. For example, for α=1, the most probable maximum (MPM) value is calculated. This is the most-likely maximum response that will occur within the specified time interval T. This interval is commonly 3 hours. The MPM response value typically has a 63 percent probability of being exceeded. On the other hand, with α=0.01, the exceedance probability is only 1 percent, which is often referred to as the most probable extreme (MPE) response. An example of a probability density function (PDF) and cumulative distribution function (CDF) for n response observations is depicted in Figure 9. Also, the MPM and MPE values with an α of respectively 1.0 and 0.01 are shown.

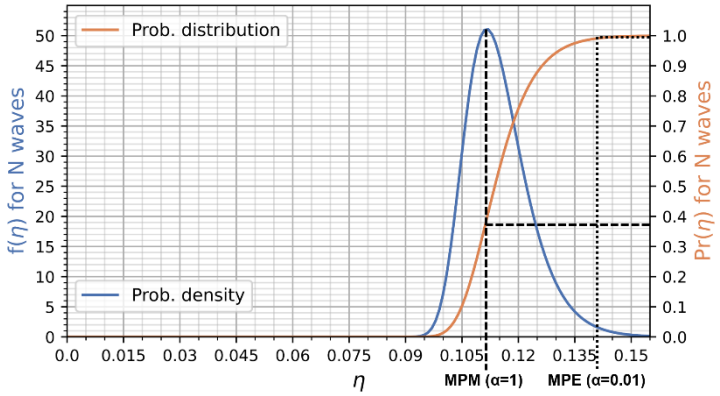

Figure 9: Rayleigh PDF and CDF (ε = 0) for $m_0 = 8.02 \cdot 10^{-4}$ and n=2,207 waves (Tp =5.5s).

The decision of the value for α depends on the acceptable risks and designer's decision. When looking at the MPM and MPE responses of the CDF above, it stands out that the difference between the two values is relatively low, respectively 0.114 and 0.142 meters. This depends on the steepness of the CDF and is thus directly related to the properties of the response spectrum. It should be noted that the response spectrum will be different for every wave heading, ship motion direction, and sea state. Therefore, the MPM and MPE values of other cases might be further apart, and when interpreting the results, it is important to keep in mind that the results are based on statistics and larger responses could occur. Thus, for this research, the decision was made to calculate the MPE (α = 0.01) responses, representing a more conservative approach. The calculation of MPE response values is executed for every wave heading. Ultimately, the MPE responses across the three directions (x,y,z) for all wave headings are determined. With these results, the worst MPE responses across the longitudinal, transverse, and vertical direction can be determined for every ship configuration.

Validation of the module

To validate the output of the seakeeping module, the worst local MPE motion responses were calculated for an UDSBV design. These results were compared to the results from HAS under the same conditions as used in the module. The results were calculated for two different loading conditions, at both the assembly and installation position of the turbines, and for different sea states. Also, the validation was conducted for both a weathervaning and omnidirectional condition. The results demonstrated that the local MPE displacement of the two methods are comparable and within the same order of magnitude in the weathervaning condition. One of the validations, for T_p=6.2s is shown in Table 6.

Table 6: Validation of weathervaning MPE motion-induced displacements from the seakeeping analysis module (SAM) with hydrodynamic analysis software (HAS).

		Most probable extreme					
		Fully-loaded			Lifting last turbine		
Position	Method	Long. disp. [m]	Trans. disp. [m]	Vert. disp. [m]	Long. disp. [m]	Trans. disp. [m]	Vert. disp. [m]
Assembly location	HAS	0.77	0.15	0.26	0.94	0.25	0.32
	SAM	0.74	0.22	0.21	0.74	0.27	0.21
	Error	**-4%**	**44%**	**-21%**	**-21%**	**10%**	**-33%**
Installation location	HAS	0.84	0.15	0.27	1.01	0.25	0.32
	SAM	0.74	0.22	0.23	0.74	0.27	0.25
	Error	**-11%**	**44%**	**-14%**	**-26%**	**10%**	**-24%**

However, minor differences were observed, especially in longitudinal motion direction. This is likely because the simplified method does not consider coupling effects between motions and probably the omission of three of the six RAOs

does play a minor role. However, for the purpose of this research, the outcomes of the new module are considered acceptable. The validation of the omnidirectional condition showed that this method cannot be used for this type of environment. This is mainly a result of the large discrepancies in the RAOs in beam seas.

Wind turbine mission module

The wind turbine mission module connects the wind turbine market within Blended Design with the ship configurations. The module determines the feasible number of turbines that can be transported and installed by each ship configurations. Given the diversity of turbine sizes in a market, this calculation is performed for every possible turbine size. The number of turbines is dependent on multiple constraints. The module calculates the number of turbines a ship configuration can carry for each of the constraints and then identifies the limiting factor that yields the smallest number of turbines that can be transported and installed. This procedure is depicted in Equation 3.

$$N = \min\{N_{CC}, N_A, N_{DWT}, N_{tot,tr}, N_{tot,lift}\} \quad [3]$$

Crane capacity constraint

The crane capacity of a ship configuration determines the maximum turbine weight that can be lifted, (see Equation 4).

$$N_{cc} = \begin{cases} \infty, & if\ m_{WTG} < crane\ capacity \\ 0, & else \end{cases} \quad [4]$$

Deck area constraint

The number of turbines for different sizes, that could fit in the free deck space of a configuration is calculated. For the analysis, the deck area is divided into two parts (see Figure 10). It is assumed that the green area will be reserved for towers and nacelles with hubs. The yellow area, behind the crane, is designated for blade storage. White areas cannot be used.

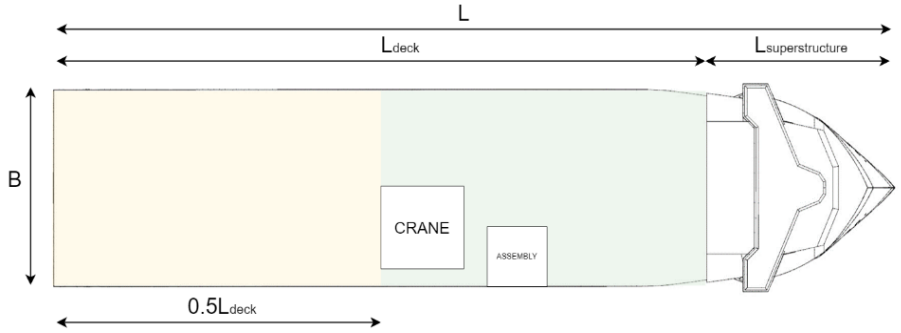

Figure 10: Division of deck area.

The dimensions originate from the results from development package 2. To account for seafastening and ensure sufficient spacing, a margin of 1 meter around the nacelles is assumed. For towers, a square footprint of the tower diameter with an offset of 1 meter on each side is assumed. To account for unused space, a margin of 90 percent is adopted. The number of turbines, with this margin included, was found to better match realistic deck layouts. The number of turbines, based on towers and nacelles fitting in the green area is calculated according to Equation 5.

$$N_{A,1} = 0.9 \cdot A_{deck,green} / [(L_{nacelle} + 2) \cdot (B_{nacelle} + 2) + (D_{tower} + 2)^2] \quad [5]$$

Afterwards, the number of blades that fit within the width of the yellow part is calculated. Blades are assumed to be stacked in blade racks in pairs of three. The algorithm checks whether the width of all blade stacks does not exceed the breadth of the vessel and automatically adjusts the number of turbines if that is the cae. This is depicted in Equation 6.

$$N_{A,2} = \begin{cases} B/(B_{blade} + 2), & if\ N_{A,1} \cdot (B_{blade} + 2) > B \\ N_{A,1}, & else \end{cases} \quad [6]$$

Based on the deck layout, blades are assumed to extend over the aft of the vessel. The estimated length that should fit on the length of the yellow part of the deck is set at 60 percent of the total blade length. A check is performed to verify if this requirement is satisfied. A margin of 5 meters between the aft of the crane and blade racks is assumed (Equation 7).

$$N_A = \begin{cases} N_{A,2}, & if\ 0.5L_{deck} - 5\ \geq 0.6L_{blade} \\ 0, & else \end{cases} \quad [7]$$

Deadweight constraint

The third limiting factor is associated with the deadweight available for cargo. The algorithm calculates the maximum number of turbines that can be accommodated within the vessel's deadweight. This calculation assumes that there is no ballast water used. The total mass of a single turbine is defined in Equation 8.

$$m_{WTG} = m_{tower} + m_{nacelle} + m_{hub} + 3 \cdot m_{blade} \quad [8]$$

The number of turbines is calculated using Equation 9. An allowance of 10 percent is assumed for the mass of seafastening.

$$N_{DWT} = DWT/(1.1 \cdot m_{WTG}) \quad [9]$$

Transit and lifting stability constraints

Blended Design calculates the maximum allowable KG value for both transit and lifting conditions of all ship configurations. Within the turbine mission module, the vertical center of gravity (VCG) for an increasing number of wind turbines of every size in the market simulation is calculated. It then checks if the VCG of the turbines is still below the allowable KG. If not, the vessel will be unstable and not be able to carry that number of wind turbines. The algorithm eventually finds the maximum number of wind turbines for which the KG value is still positive. Ballast water is incorporated in both cases. The VCG of ballast water is a fixed ratio of the depth. The mass of ballast water is calculated following Equation 10.

$$m_{bal} = DWT - N_{WTG} \cdot m_{WTG} \quad [10]$$

The VCG of the turbine components corresponds with the findings from development package 2. To determine the resulting VCG of these components, when they are in storage position on deck during transit, Equation 11 is used.

$$VCG_{comp} = D + \frac{3m_{blade} \cdot 0.5 \cdot 3h_{blade} + m_{tower} \cdot VCG_{tower} + (m_{nacelle} + m_{hub}) \cdot VCG_{nacelle}}{m_{turbine}} \quad [11]$$

The VCG of the deck cargo in transit and lifting condition is then calculated with the following Equations 12 and 13.

$$VCG_{tr} = \frac{VCG_{LSW} \cdot LSW + N_{tot,tr} \cdot VCG_{comp} \cdot m_{WTG} + VCG_{bal} \cdot D \cdot m_{bal,tr}}{\Delta_{tr}} \quad [12]$$

$$VCG_{lift} = \frac{VCG_{LSW} \cdot LSW + \left(N_{tot,lift} - 1\right) \cdot VCG_{comp} \cdot m_{WTG} + VCG_{bal} \cdot D \cdot m_{bal,lift} + z_{load} * m_{WTG}}{\Delta_{lift}} \quad [13]$$

Validation

The module has been validated using a reference vessel from UDSBV. Validation has been performed for 8, 15, and 20 MW turbines. Deck layout drawings were made, and calculations were done to check whether the calculated number of turbines for every constraint for the different turbine sizes matches. The results were found to be the same, so it is assumed that the wind turbine mission module produces sensible results.

EVALUATING THE PERFORMANCE OF MOONSHOT

After the new modules were created and adaptations to Blended Design were made, the design space is explored to evaluate the performance of different ship configurations and to elucidate optimal design parameters for next phases of the design. Firstly, a design space was created by varying ship parameters. In total, the design space consisted of 158,340 unique ship configurations, as displayed in Table 7.

Table 7: The created design space in Blended Design.

Particular		Start	End	Step size	#
Length	[m]	140.0	280.0	5.0	29
Breadth	[m]	36.0	72.0	3.0	13
Depth	[m]	10.0	19.0	1.0	10
Sailing speed	[kn]	10.0	15.0	1.0	6
Crane capacity	[t]	1,000	7,000	1,000	7
Block coefficient	[-]	0.77	-	-	1
Unique configurations					**158,340**

The output from Blended Design is visualized in graphs that show the performance of all configurations for a specific ship parameter. A Pareto front is drawn through the best-performing configurations for every parameter. Figure 11 depicts the visualization of the how the resulting graph is constructed and how to interpret it. The optimal range is user-defined and is set to 2.5 percent for this research.

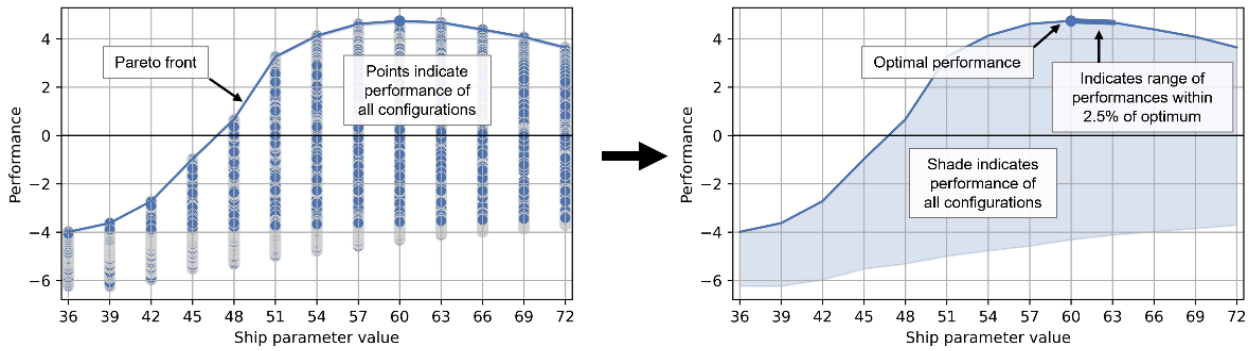

Figure 11: Visual guide on how to interpret the result plots.

Firstly, the results from the financial performance analysis of all configurations within the design space is discussed. Secondly, the seakeeping performance will be presented.

Financial performance

The influence of ship parameters on the financial performance has been investigated. Different scenarios have been incorporated in the analysis and optimal design ranges have been determined. The financial performance is measured in return on investment (ROI), which is the ratio between the net profit over the lifetime and the investment costs. The revenue of each ship configuration consists of an installation reward per installed MW. Thus, every vessel will be rewarded for the number of turbines and size of turbines it installs.

Performance in different market scenarios

Figure 12 presents the financial performance in four different future markets. The unbound market assumes that the turbine growth is not limited. The 16MW bound market assumes that the turbines will not grow beyond the maximum turbine capacity of all offshore wind projects currently in operation, planned or within the Procurement, Construction, and Installation (EPCI) phase. The 1,000 feet bound market assumes that the growth of turbines is restricted to a tip height of 1,000 feet. This scenario has recently been proposed by the Netherlands Wind Energy Association (NWEA) (Rijntalder 2023). The maximum rotor diameter in this case would be around 280 meters (Netherlands Wind Energy Association 2023), which would correspond to a 22MW turbine. Once this capacity is reached, the size of turbine components is assumed to not further increase. Uncertainty in the mass of components is only considered in the third scenario. In the fourth scenario, the market would be bound to 22MW, but uncertainty in both the size and mass properties is considered. The difference in optimal design parameters for different market scenarios is clearly visible.

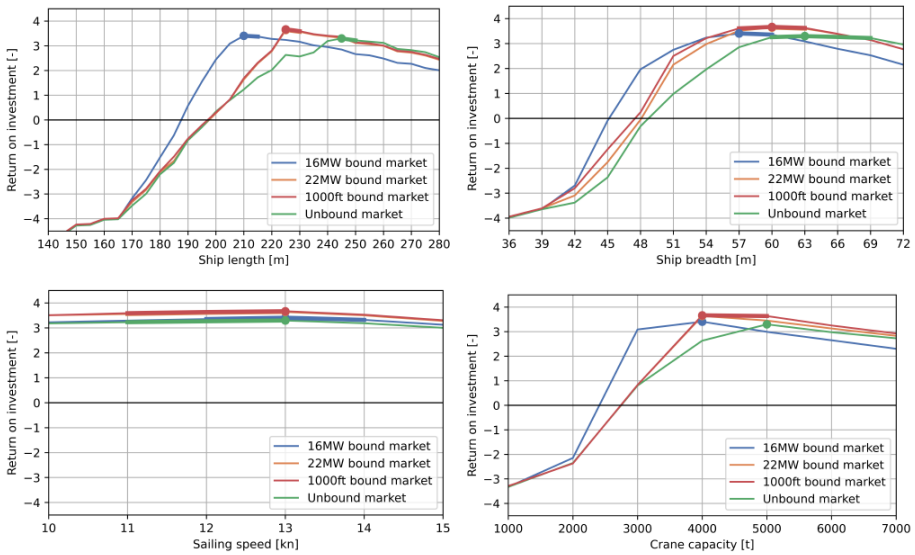

Figure 12: Visualization of the results for the four market scenarios.

Influence of distance to port

Figure 13 presents the financial results for different distances between the OWFs and marshalling ports. The calculations for the different market scenarios were conducted with a distance of 140 nautical miles (NM). This distance was selected based on insights from literature, as it corresponds to the anticipated maximum distance to shore for future OWFs in 2026 (NORWEP 2022). To explore the impact of varying distance ranges, both shorter and longer distances were included. The short distance of 35 NM is based on current global maximum distances from (NORWEP 2022). The long distance is ten times that distance. The distance to port effects the ROI of different configurations. This is mainly due to the increasing

sailing distance, decreasing the number of turbines that can be installed. Larger vessels perform better as distance increases, which can be attributed to the increased cargo capacity, ensuring that they can take more turbines per roundtrip. The optimal sailing speed is the same for all distances, but the optimal range narrows down as distances increase, favoring faster configurations at large sailing distances.

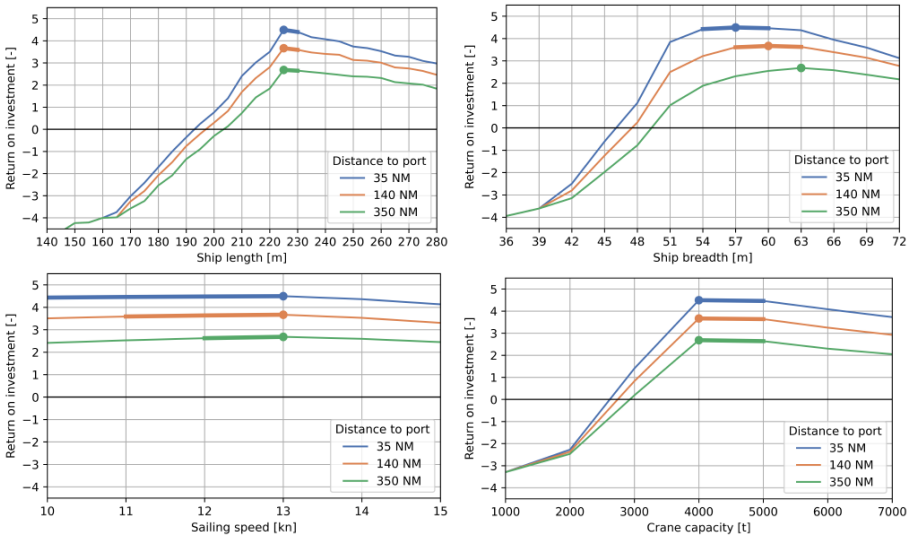

Figure 13: Visualization of the results of a 1,000ft bound market with three distances to port.

Influence of splitting the turbine towers

The turbine towers are assumed to be transported vertically and as one part. The towers are very heavy and tall, resulting in high VCGs. The number of turbines a ship configuration can transport and install could be constrained by five different limiting factors, including stability. Therefore, an analysis was conducted on the distribution of limiting factors across all feasible ship configuration, to gain insight in what drives the carrying capacity. Figure 14 presents a breakdown of the limiting factors for all feasible ship configuration and a distribution with distinction per turbine size.

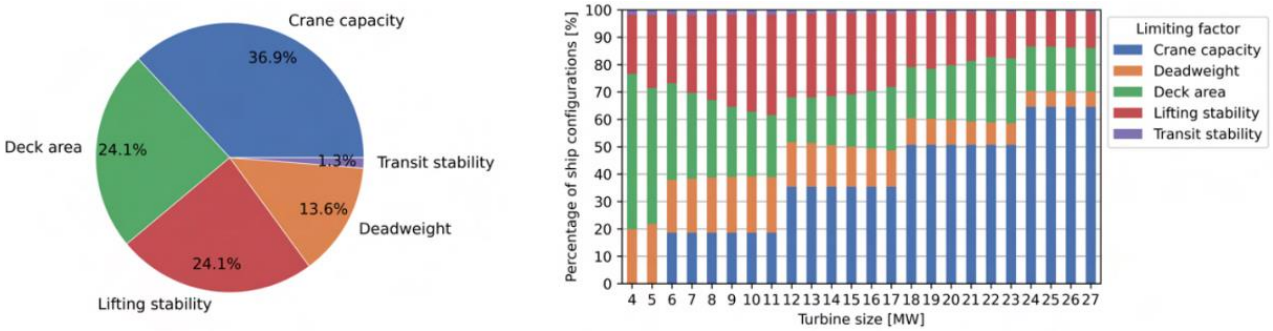

Figure 14: Distribution of limiting factors for ship configurations (left) and aggregated per turbine size (right).

In most ship configurations, the limiting factor is the crane capacity. This is because the design space consists of configurations with crane capacities ranging from 1,000 to 7,000. As turbine size increases, crane capacity becomes more limiting. After that, deck area and lifting stability are the most limiting constraints. The fact that many configurations is limited by lifting stability, indicates that the deck area or deadweight, and thus the full potential of a lot of ship configurations is not completely used. The main reason why lifting stability is limiting in a lot of configurations is because of the high VCG of the turbine towers.

This led to investigating the effects of transporting the turbine towers as two smaller parts, rather than one large components. Splitting the towers in two parts would benefit the overall VCG of the turbine components. On the other hand, more deck area would be needed to transport one tower and more lifts would have to be performed when loading and installing the towers, doubling loading and installation times for tower parts. Figure 15 depicts how the limiting factors are distributed across the carrying capacity of all feasible ship configurations when the towers are transported as two parts.

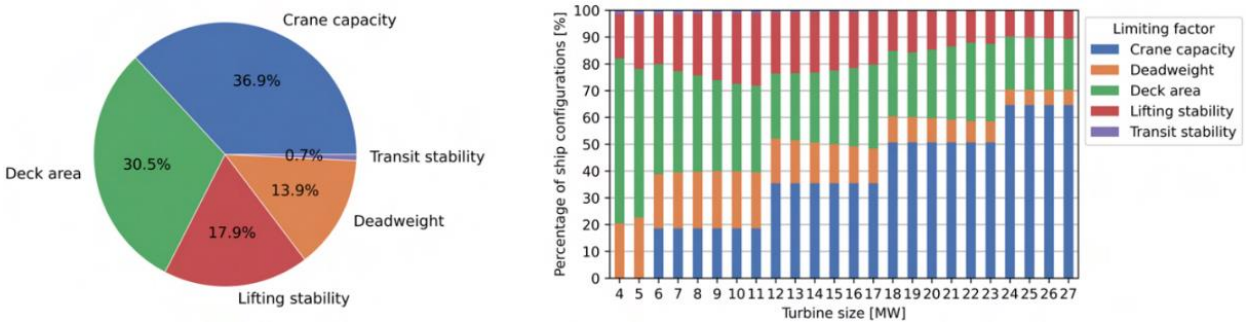

Figure 15: Distribution of limiting factors for ship configurations (left) and aggregated per turbine size (right) with towers transported as two parts.

As shown in the figures above, the lifting stability constraint is a less dominant limiting factor for the carrying capacity of wind turbines. The share of the deck area limiting factor among all configurations has significantly been increased. This shift suggests that the carrying capacity of the ships is used more efficiently. The difference in carrying capacity when the tower is divided into two parts, for one of the configurations in the design space is visualized in Figure 16. The two plots depict the number of turbines that can be transported according to the five constraints for every turbine size. It also shows the main limiting factor for every turbine size and the resulting capacity.

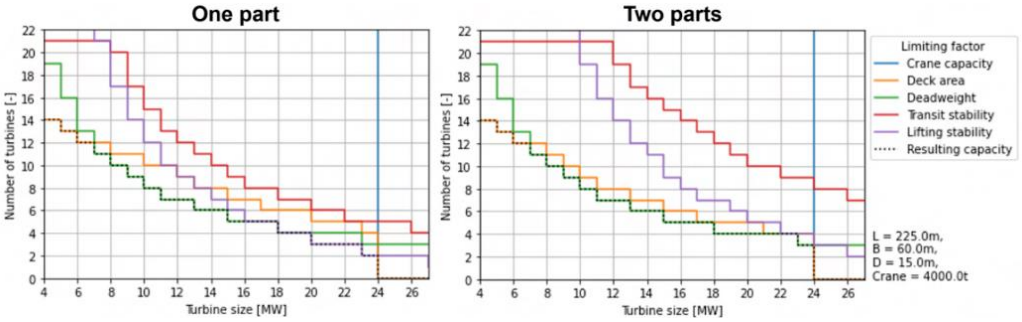

Figure 16: Visualization of limiting factors and number of turbines for the two tower strategies.

To assess the benefits of the transportation strategy, a financial performance analysis was conducted. The goal is to determine whether the advantages of transporting the towers as two parts outweighs the negative consequences. The financial performance is depicted in Figure 17. As visible, the ROI of all configurations is lower when the towers are divided into two parts instead of being transported as single components with a high VCG. Therefore, it can be concluded that there is no financial benefit in carrying the towers as two parts.

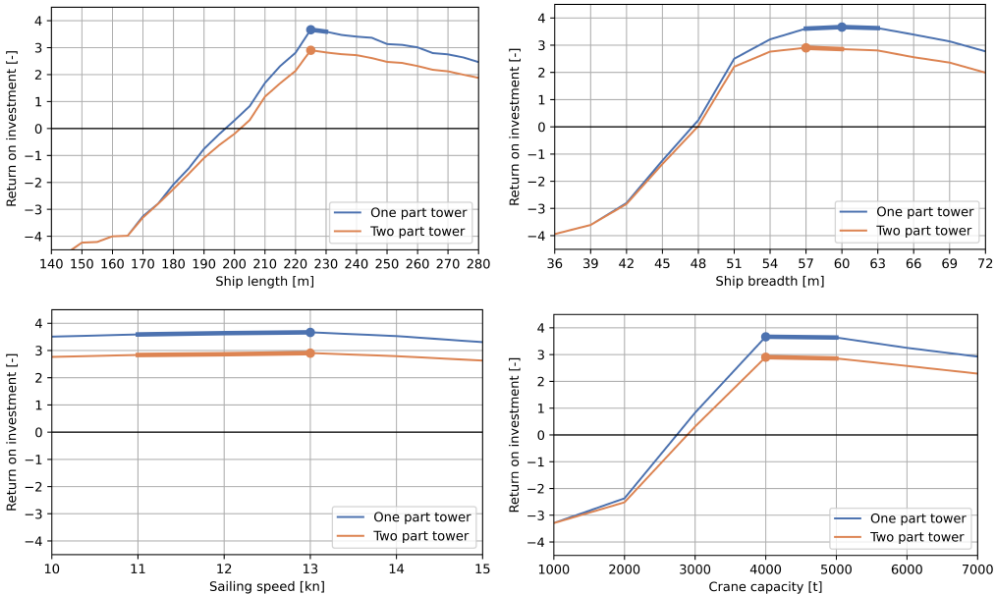

Figure 17: Visualization of the results for two different tower transportation strategies in a 1,000ft bound market. The distance to port is 140 NM.

Seakeeping performance

The influence of various ship parameters will be investigated, and optimal design configurations will be determined for best seakeeping performance. The calculations have been performed for a significant wave height of 2.5 meters. The performance is measured in local MPE responses, as explained earlier. The lower the responses, the better. The local responses are calculated at the hub height of the largest turbine a ship configuration can possibly transport and install during its lifetime. This is during offshore operations, so when the vessel is station keeping. The ship is assumed to weathervane, meaning that it is allowed to align the bow with the incoming environment. This improves seakeeping and reduces the power required for dynamic positioning. While weathervaning, the environment is assumed to be at 180 degrees with an offset of 30 degrees to both sides, as visualized in Figure 18.

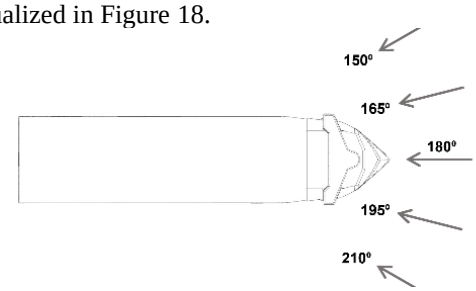

Figure 18: Wave headings during weathervaning with an allowed offset of +-30 degrees.

Weathervaning displacements

Figure 19 shows the MPE motion-induced displacements in each of the three motion directions for different ship parameters. The results reveal that the longitudinal motion response is most dominant. This can be attributed to the environment while weathervaning, where waves are primarily coming in at the bow of the vessel. The main contributor to the longitudinal response is the pitch motion, which is lower for increasing ship lengths. Increasing the breadth does not really influence the MPE motion responses. In transverse direction, the main contributor to the motion displacement is the roll motion. However, roll motion is quite low due to the weathervaning and the used method for determining the RAOs. The used method neglects coupling effect between motions, disregarding for example roll motion due to pitch. Regarding vertical direction, the foremost contributor to the motion displacement is the heave motion in combination with pitch and roll. The results show that the vertical motion decreases for longer ships. This could be because the heave motion RAO shift to lower wave frequencies for longer ship. This results in lower RAO values at the same wave frequency for longer ships. When looking at breadth, relatively constant lines are observed. This is because heave motion is not significantly influenced by ship breadth with the used calculation method. In addition, due to decoupled motions and the weathervaning, the roll motion is also very little influenced by increased breadth.

The influence of depth on the motion behavior of configurations is not straightforward. As depth increases, so does the maximum draft of a configuration, leading to an increase in displacement, which affects the motion behavior. However, an increase in draft leads to a decrease in sectional hydrodynamic damping (A) and the Smith correction factor (κ) in the method from (Jensen, et al 2004), influencing the forcing functions for heave (F_3) and pitch (F_5), subsequently affecting heave and pitch RAOs. Additionally, increasing depth and draft affect stability in several ways. Draft affects the GM_T value of a ship configuration, impacting stability and the behavior of the roll RAO. An increase in depth at the same breadth reduces the B/D ratio, crucial for establishing the GZ curve, which determines the transverse stability. Stability influences the maximum turbine size the configurations can transport and install and, consequently, dictating point P in which local responses are calculated. In general, increasing depth results in decreased MPE motion displacement in all directions, as reflected in Figure 19.

Crane capacity has limited influence on motion behavior. The lines for all three directions remain relatively constant because the best ship configurations with optimal motion behavior are independent of crane capacity. For instance, the 'best' configurations for longitudinal motions have low to moderate breadth and the highest depth, providing the best motion behavior in the longitudinal direction. But due to their low B/D ratio resulting from the combination of breadth and depth, their stability is typically poorer, limiting their ability to handle larger turbine sizes in the market. For these smaller sizes, the point P where motions are calculated is closer to the CoG of the vessel, resulting in lower longitudinal motions.

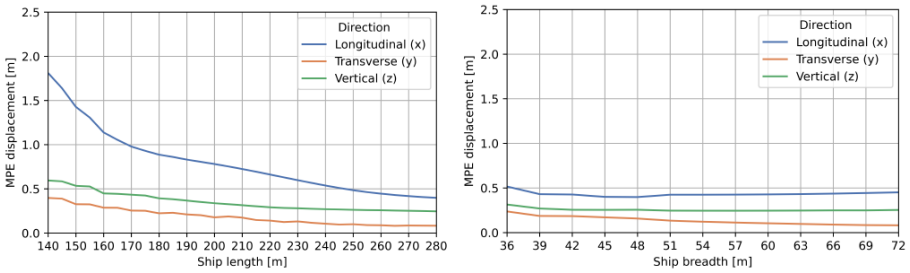

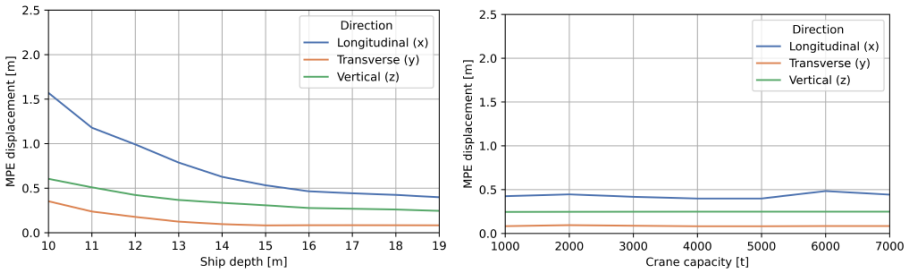

Figure 19: Wave headings during weathervaning with an allowed offset of +-30 degrees.

The model behavior explained above is not the most elegant way to design a vessel, but the model does achieve the objective of findings the configurations with the best seakeeping behavior. This model behavior, while effective, can be considered undesired and should be considered when evaluating motion behavior or optimizing a vessel on motion performance.

Figure 20 presents a parallel coordinates plot of the motion performance. The plot shows all possible configurations with their MPE motion responses in all three directions. Three combinations of ship parameters have been highlighted. These three configurations would have the lowest MPE displacement for one of the three directions. These three optimal ships would be very large, with the smallest crane possible. The model selects these configurations as the best one, because it can only lift the smallest turbines, with point P for motion calculation closest to the CoG of the vessel. Considering the findings from financial performance and the best configuration in terms of motion performance, a large gap between the best ship configuration for Moonshot is found. This gap will be addressed later.

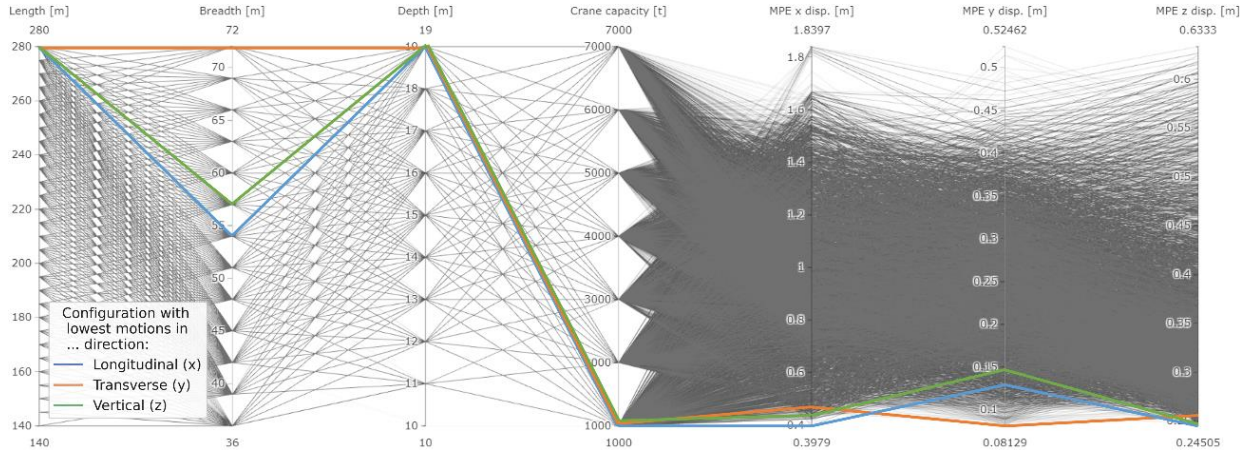

Figure 20: Parallel coordinates plot of motion performance.

Weathervaning accelerations

The accelerations during weathervaning have also been evaluated. Just as the MPE displacements, the MPE accelerations were also calculated in point P for the three directions. These three components were then translated to a resultant MPE acceleration vector using Equation 14.

$$MPE\ \boldsymbol{a} = \sqrt{(MPE\ \boldsymbol{a}_x)^2 + \left(MPE\ \boldsymbol{a}_y\right)^2 + (MPE\ \boldsymbol{a}_z)^2} \qquad [14]$$

Figure 21 depicts the resulting MPE acceleration vector in relation to displacement of all configurations. To prevent damage to wind turbines, suppliers prescribe limits on acceleration in the nacelle during T&I. The acceleration limit is typically 0.5g (~4.9 m/s²) (BVG Associates 2019). As demonstrated in the figure, the local MPE acceleration for all configurations remains well below this specified limit. Consequently, accelerations in the nacelle are not deemed to be a major concern.

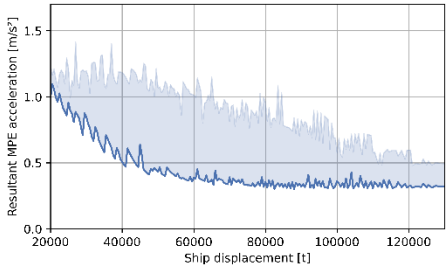

Figure 21: Visualization of the MPE acceleration vector results.

Combining seakeeping and financial performance

As previously highlighted, conflicting optimal ship configurations emerge when optimizing for either financial performance or seakeeping performance. To reconcile this discrepancy between the two objectives, a financial penalty will be imposed on configurations exhibiting inferior seakeeping behavior. This penalty will be in the form of an added cost for motion compensation, which is a supplement to the base cost for the main crane. The unit of this metric is €/(t.m), encompassing both the crane capacity and the cumulative MPE displacement in longitudinal, transverse, and vertical direction, measured in meters. While the metric might not be documented in existing literature, it aligns well with practical considerations. It is reasonable to expect that cost of lifting equipment would increase with increasing motion compensation requirements. Moreover, the inclusion of crane capacity in the metric is also logical, as a motion compensation system for higher crane capacity would likely be more complex and larger, inherently being more expensive.

As this metric is not documented in existing literature, there is no reference for quantifying the cost of motion compensation. Consequently, a range with different cost levels has been assumed. This range spans from €0 to €10,000/(t.m). The resulting ROI for these different cost levels is depicted for different ship parameters in Figure 22. As displayed, the ROI decreases for increasing cost levels for motion compensation. What stands out, is that the optimum for length shifts to longer configurations. This indicates that at a certain point, the higher cost of investing in and operating a longer ship surpasses the increased cost for motion compensation of shorter vessels.

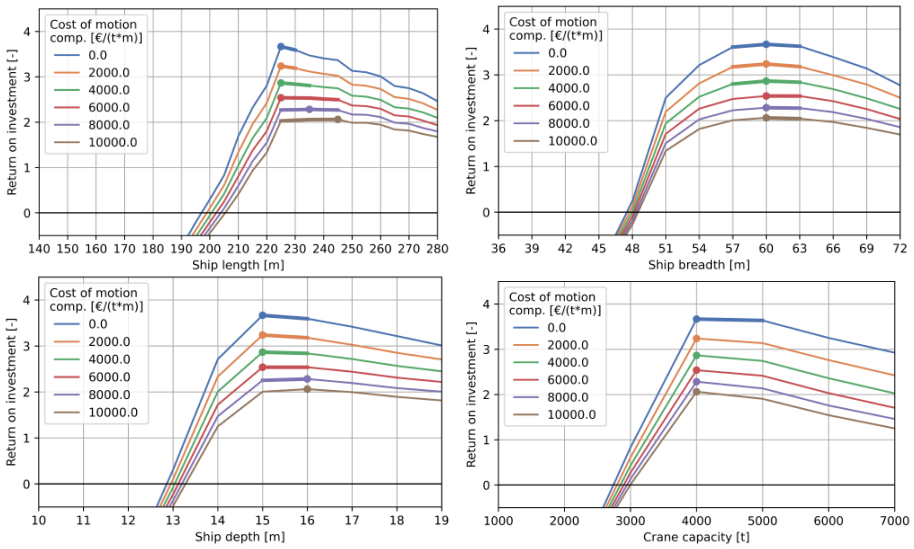

Figure 22: Visualization of the financial results with motion performance penalty in a 1,000ft bound market with an operational H_s limit of 2.5 meters.

Optimal design ranges for Moonshot

Considering all findings, optimum design ranges for the ship have been established. These findings for different scenarios are summarized in Table 8. The initial design parameters can be chosen according to client preferences or based on a designer's perspective. The initial design parameters, as chosen by the author, are displayed in the last row of the table.

Table 8: Summary of optimal design parameters for Moonshot.

Scenario	Length [m]	Breadth [m]	Depth [m]	Sailing speed [kn]	Crane capacity [t]
Financial performance					
16MW bound market	210-215	57-60	14-15	12-14	4,000
22MW bound market	225-230	60-63	15	11-13	4,000
1,000ft bound market	225-230	57-63	15-16	11-13	4,000-5,000
Unbound market	245-250	60-69	16-17	11-13	5,000
Distance to port[+]					
35 NM	225-230	54-60	15	10-13	4,000-5,000
140 NM	225-230	57-63	15-16	11-13	4,000-5,000
350 NM	225-230	63	16	12-13	4,000-5,000
Seakeeping performance[+,°]					
Weathervaning x-displacement	280	54	19	11-13	1,000
Weathervaning y-displacement	280	72	19	11-13	1,000
Weathervaning z-displacement	280	57	19	11-13	1,000
Motion compensation[*,°]					
€2,000/(t·m)	225-230	57-63	15-16	11-13	4,000
€6,000/(t·m)	225-245	60-63	15-16	11-13	4,000
€10,000/(t·m)	225-245	60-63	16	11-13	4,000
Initial design parameters	**230**	**63**	**16**	**12**	**4,000**

[*] in a 1,000ft bound market with a 140 NM distance between port and OWF. [°] for a maximum significant wave height of 2.5 meters. [+] in a 1,000ft bound market scenario.

BENCHMARKING THE DESIGN

Previous results indicate that the Moonshot could be a viable alternative for offshore wind turbine installation. However, the question arises whether it measures up against existing technologies. To benchmark, a version of Moonshot has been designed to directly compete with the largest jack-up design in the market, the NG-20000X (GustoMSC n.d.). This jack-up has a capacity of four 20 MW turbines (4C Offshore n.d.). Blended Design has been used to explore the design space and determine the ship parameters for the direct competitor, the 20MW Moonshot. This Moonshot concept is designed to operate in a market with only 20 MW turbines for only one year. 1,532,160 ship configurations were investigated. Firstly, optimal design ranges were determined with cost for motion compensation levels of €0 to €10,000/(t·m). The actual cost would probably be somewhere in that range. The results are shown in Figure 23.

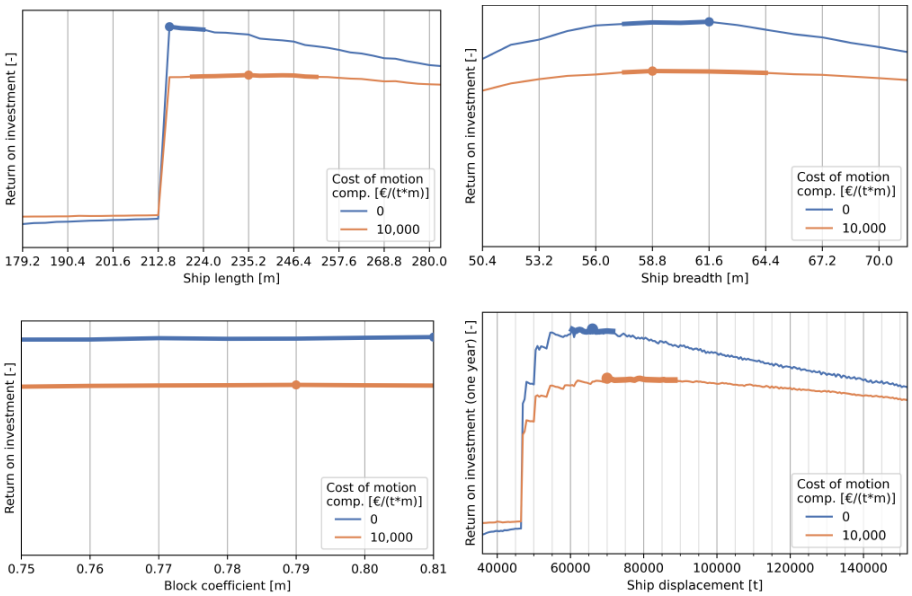

Figure 23: Visualization of the financial performance results for the 20MW Moonshot.

The optimal design ranges reveal an overlap when looking at the two different cost levels. An optimal displacement for both cost levels can be found around 70,000 tonnes. Following a slightly different approach then earlier, the displacement will be fixed at this value to find the optimal ship parameters for best seakeeping performance within this displacement. The results from this analysis are shown in Figure 24. Based on the results from both the financial and seakeeping performance, an optimal configuration can be selected.

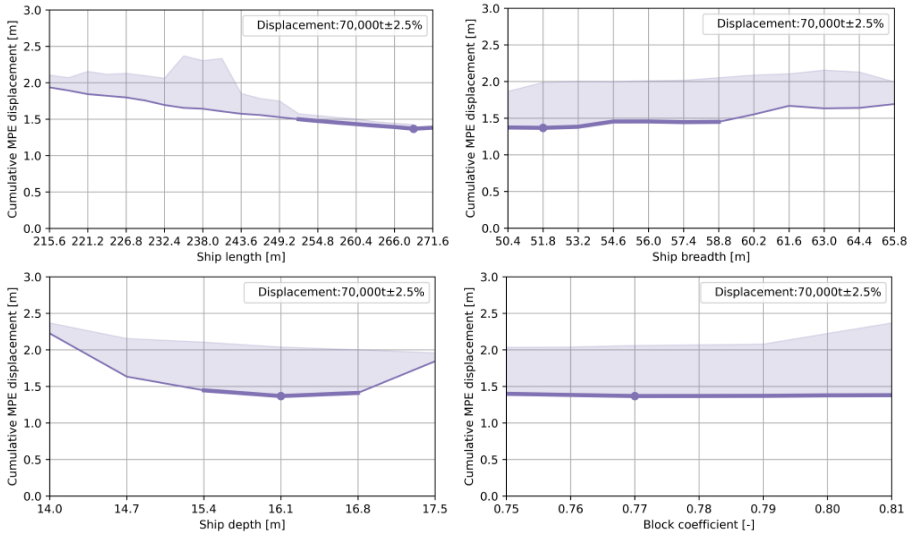

Figure 24: Visualization of the seakeeping performance results for the 20MW Moonshot with a fixed displacement.

After selecting the optimal configuration for the 20MW Moonshot, the day rate, number of installed turbines per year, and the cost per installed MW were extracted from Blended Design. The same metrics were calculated for the NG-20000X jack up, an SSCV, and Huisman's windfarm installation vessel concept. The number of turbines installed per year for those

solutions was determined based on estimated cycle times of the operational cycles. With an assumed day rate, derived from literature or internal knowledge at UDSBV, the cost per installed MW was calculated. These values were then compared to the installation cost per MW of the 20 MW Moonshot.

Table 9: Comparison of different installation solutions to benchmark Moonshot.

Parameter		NG-20000X	SSCV	Huisman's WIV concept	20 MW Moonshot
Sailing speed	[kn]	11	10	12	13
Cargo capacity (20 MW turbines)	[-]	4	-	-	5
Workability	[-]	0.6	0.6[+]	0.6[+]	0.78
Day rate installation vessel	[€/day]	375,000	750,000	750,000	260,000[*]
Day rate feeder vessels	[€/day]	-	2x 50,000	2x 50,000	-
Day rate harbour crane	[€/day]	-	32,000	32,000	-
Installed turbines per year	[-]	110	165	179	180
Cost per installed MW	**[€/MW]**	**50,900**	**80,100**	**73,900**	**21,500***

[*] Profit margins are not reflected in the day rates and installation cost per MW of Moonshot, whereas in the others it is included.
[+] Actual workability of the installation vessels is higher. However, it is assumed that the workability is dictated by the offshore transfer from the feeder barges or vessels.

The benchmarking revealed that Moonshot is a more efficient and cost-effective solution, capable of installing a larger number of turbines per year at a considerably lower cost per MW compared to other solutions. The results of the benchmarking show the potential of Moonshot in comparison to other solutions as a competitive and cost-efficient offshore wind turbine installation solution. Above all, since Moonshot is a floating solution and has no interaction with the seabed, it would remain feasible in areas where jack-up vessels might no longer be feasible in the future. Overall, these findings underscore the cost-effectiveness and competitive advantage of the Moonshot concept in the offshore wind industry, positioning it as a promising solution for the evolving demands of the sector.

CONCLUSIONS

This paper introduced a novel installation solution for offshore wind turbine installation, named Moonshot. The development process involved a combination of UDSBV's Controlled Innovation and Blended Design. With Controlled Innovation functions and design aspects were identified. An evaluation of design aspects revealed the ones that required special attention. These included the choice of lifting equipment, size and mass properties of wind turbine components, and the deck layout. Since Moonshot is a monohull solution that will install turbines while afloat, it would be more susceptible to waves than other existing WTIVs. Therefore, seakeeping assessment is deemed to be important. Modifications to the Blended Design model were made to accommodate Moonshot's unique characteristics and to assess seakeeping performance. With Blended Design, different scenarios were analyzed on both financial and seakeeping performance to explore the design space of Moonshot and elucidate optimal design parameters. The results revealed a disparity when optimizing for financial or seakeeping performance. To balance these factors, a penalty mechanism was introduced, resulting in new optimal ship configurations. Furthermore, Moonshot was benchmarked against other wind turbine solutions, such as jack-ups and SSCVs. Blended Design was used to determine optimal design parameters for a direct competitor. Then, the cost per MW of the other solutions was compared to the optimal 20 MW Moonshot. The comparison showed that Moonshot could be a viable alternative in the offshore wind turbine installation sector.

CONTRIBUTION STATEMENT

J.J. de Ridder: Conceptualization; formal analysis; investigation; methodology; project administration; validation; visualization; writing – original draft. **J.D. Stroo:** Conceptualization; resources; supervision; writing – review and editing. **A.A. Kana:** Conceptualization; supervision; writing – review and editing.

ACKNOLEDGEMENTS

This work was performed as part of the MSc thesis for the lead author, (de Ridder 2023). The thesis was performed in Marine Technology at Delft University of Technology and the authors would like to acknowledge both Delft University of Technology and Ulstein Design and Solutions B.V. for their support of this research.

REFERENCES

4C Offshore. (n.d.). *NG-20000X*. Retrieved from https://www.4coffshore.com/vessels/vessel-ng-20000x-vid2304.html

Asgarpour, M. (2016). Chapter 17 - Assembly, transportation, installation and commissioning if offshore wind farms. In C. Ng, & L. Ran, *Offshore Wind Farms - Technologies, Design & Operation* (pp. 527-541). Woodhead Publishing. doi:10.1016/B978-0-08-100779-2.00017-9

Attari, A., Olayinka Okuyemi, G., Goormachtigh, J., Møller Christensen, J., Tang Kristensen, J., Koch Nielsen, J., . . . Rolland, Y. (2014). *3.1 - WP Framework/Industry Challenges Report – Novel vessels and equipment.* LEANWIND - Logistic Efficiencies And Naval architecture for Wind Installations with Novel Developments.

Bhattacharya, R. (1973). *Dynamics of Marine Vehicles.* John Wiley & Sons Ltd.

BVG Associates. (2019). *Guide to an offshore wind farm - Updated and extended.* The Crown Estate and the Offshore Renewable Energy Catapult.

de Ridder, J. J. (2023). *Beyond Jack-Ups: A Moonshot for Future Offshore Wind Turbine Installation Vessels for an Uncertain Market.* Delft, The Netherlands: Delft University of Technology.

Det Norske Veritas AS. (2017). *DNV-RP-C205: Recommended practice: Environmental Conditions and Environmental Loads.* Høvik, Norway.

Díaz , H., & Guedes Soares, C. (2023). Approach for Installation and Logistics of a Floating Offshore Wind Farm. *Journal of Marine Science and Engineering*. doi:10.3390/jmse11010053

Djupevåg Eri, S. (2015). *Analysis of Operability in Installing Heavy Subsea Modules.* Stavanger, Norway: University of Stavanger.

EnergyFacts.eu. (2019). *Revolutionary Construction Methodology for Arcadis Ost 1 Offshore Wind Farm*. Retrieved from https://www.energyfacts.eu/revolutionary-construction-methodology-for-arcadis-ost-1-offshore-wind-farm/

Foxwell, D. (2022). *Warning issued that offshore wind won't have enough foundation installation*. Retrieved from Riviera: https://www.rivieramm.com/news-content-hub/news-content-hub/warning-issued-that-offshore-wind-sector-wont-have-enough-foundation-installation-vessels-71561

GustoMSC. (n.d.). *NG-20000X brochure*. Retrieved from https://www.nov.com/-/media/nov/files/products/rig/marine-and-construction/ng-20000x/ng-20000x-brochure.pdf

Heerema Marine Contractors. (2020). *Sleipnir*. Retrieved from https://www.heerema.com/heerema-marine-contractors/fleet/sleipnir

Herman, S. A. (2002). *Offshore Wind Farms - Analysis of Transport and Installation Costs.* TNO.

Iberdrola. (n.d.). *Wikinger Offshore Wind Farm*. Retrieved from https://www.iberdrola.com/about-us/what-we-do/offshore-wind-energy/wikinger-offshore-wind-farm

Jensen, J. J., Mansour, A. E., & Olsen, A. S. (2004). Estimation of ship motions using closed-form expressions. *Ocean Engineering*, 61-85. doi:10.1016/S0029-8018(03)00108-2

Jiang, Z. (2021). Installation of offshore wind turbines: A technical review. *Renewable and Sustainable Energy Reviews*, 1364-0321. doi:10.1016/j.rser.2020.110576.

Kaiser, M. J., & Snyder, B. (2011). *Offshore Wind Energy Installation and Decommissioning Cost Estimation in the U.S. Outer Continental Shelf.* Herndon, VA: U.S. Dept. of the Interior, Bureau of Ocean Energy Management, Regulation and Enforcement.

Kuhn, F., Liebach, F., Matthey, T., Schlosser, A., & Zivansky, J. (2023). *How to succeed in the expanding offshore wind market.* McKinsey & Company.

Matsui, S., Shinomoto, K., Sugimoto, K., & Ashida, S. (2021). Development of Simplified Formula for Froude-Krylov Force of 6-DOFs Acting on Monohull Ship. *Journal of the Japan Society of Naval Architects and Ocean Engineers*, 9-19. doi:10.2534/jjasnaoe.32.9

Netherlands Wind Energy Association. (2023). *(Dutch) Windmolens op zee niet hoger dan 1000 voet*. Retrieved from https://www.nwea.nl/windmolens-op-zee-niet-hoger-dan-1000-voet/

Nikitas, G., Bhattacharya, S., & Vimalan, N. (2020). Chapter 16 - Wind Energy. In T. Letcher, *Future Energy (third edition)* (pp. 331-355). Elsevier.

Nørkaer Sørensen, J. (1984). On the Calculation of Trajectories for Blades Detached from Horizontal Axis Wind Turbines. *Wind Engineering*, 160-175. doi:https://www.jstor.org/stable/43749983

NORWEP. (2022). *Global Offshore Wind: Annual Market Report 2022.* OSLO: Renewable Consulting Group .

Parkinson, S. B., & Kempton, W. (2022). Marshaling ports required to meet US policy targets for offshore power. *Energy Policy*. doi:10.1016/j.enpol.2022.112817

Quancard, R., Girandier, C., & Robic, H. (2019). *D.4.2 – Design Brief: Specifications of a generic wind turbine.* INNOSEA (INS).

Richmond, M., Balaam, T., Causon, P., Leimeister, M., Kolios, A., & Brennan, F. (2018). Multi-Criteria Decision Analysis for Benchmarking Human-Free Lifting Solutions in the Offshore Wind Energy Environment. *Energies*. doi:10.3390/en11051175.

Rijntalder, H. (2023). *Recommended maximum height for offshore windturbines*. Retrieved from Pondera consult: https://ponderaconsult.com/en/ponderacontent/recommended_maximum_height_for_offshore_windturbines/#:~:text=A%20workgroup%20on%20the%20issue,the%20developments%20of%20wind%20turbines.

Riviera Newsletters. (2010). *Interview with Nick Wessels (Ulstein Design & Solutions BV) in Concept quickens installation of offshore turbines*. Retrieved from https://www.rivieramm.com/news-content-hub/news-content-hub/concept-quickens-installation-of-offshore-turbines-45123

Robinson, R., & Futado, I. (2022). Alternatives to Conventional Offshore Fixed Wind Installation. *Offshore Technology Conference.* Houstan, TX. doi:10.4043/31986-MS

Saipem. (n.d.). *Hywind*. Retrieved from https://www.saipem.com/en/saipem-worldwide-projects/hywind-floating-wind-turbines

Schouten, E. (2018). *Monohull versus Semi-submersible for offshore heavy lift crane operations.* Delft, The Netherlands: Delft University of Technology.

Sen, D. T., & Vinh, T. C. (2016). Determination of Added Mass and Inertia Moment of Marine Ships Moving in 6 Degrees of Freedom. *International Journal of Transportation Engineering and Technology*, 8-14. doi:10.11648/j.ijtet.20160201.12

Sergiienko, N. Y., da Silva, L. S., Bachynski-Polić, E. E., Cazzolato, B. S., Arjomandi, M., & Ding, B. (2022). Review of scaling laws applied to floating offshore wind turbines. *Renewable and Sustainable Energy Reviews*, 160-175. doi:10.1016/j.rser.2022.112477

Streatfeild, C., Hoyle, M., Edwards, D., Hodged , B., Osborne, J., Mallett, C., . . . Frampton, M. (2013). *Guidelines for the Selection and Operation of Jack-ups in the Marine Renewable Energy Industry.* London, UK: RenewableUK.

Ulstein. (2023). *ULSTEIN U-STERN - smart monopile installation on DP*. Retrieved from https://ulstein.com/news/ulstein-u-stern-smart-monopile-installation-on-dp

United Nations. (n.d.). *Causes and Effects of Climate Change*. Retrieved 2023, from https://www.un.org/en/climatechange/science/causes-effects-climate-change

Uraz, E. (2011). *Offshore Wind Turbine Transportation & Installation Analyses. Planning Optimal Marine Operations for Offshore Wind Projects.* Gotland University. Visby, Sweden: Offshore Energy.

van Bruinessen, T. M. (2016). *Towards controlled innovation of complex projects. A social-technological approach to describing ship design.* Delft, The Netherlands: Delft University of Technology.

Van Lynden, C., van Winsen, I., Westland, C. N., & Kana, A. A. (2022). Offshore wind installation vessels: Generating insight about the driving factors behind the future design. *International Journal of Maritime Engineering, 164*(A2). doi:10.5750/ijme.v164iA2.1175

Vis, I. F., & Ursavas, E. (2016). Assessment approaches to logistics for offshore wind energy installation. *Sustainable Energy Technologies and Assessments*, 80-91. doi:10.1016/j.seta.2016.02.001

WindEurope. (2020). *Offshore wind in Europe*. Retrieved from https://windeurope.org/wp-content/uploads/files/aboutwind/statistics/WindEurope-Annual-Offshore-Statistics-2019.pdf

Zwaginga, J. J. (2020). *Exploring Market Uncertainty in Early Ship Design.* Delft, The Netherlands: Delft University of Technology.

Zwaginga, J. J., Stroo, J. D., & Kana, A. A. (2021). Exploring market uncertainty in early ship design. *International Journal of Naval Architecture and Ocean Engineering, 13*, 352-366. doi:10.1016/j.ijnaoe.2021.04.003.

Proceedings of 15th International Marine Design Conference (IMDC-2024)
June 2-6, 2024
Amsterdam, the Netherlands

Digital Sailmate: Enhancing Safety through Low-Cost Stability Monitoring in Artisanal Fishing

Nathan Manojlovic Smith[1*], Priscila Melo[1] and Simon Benson[1]

ABSTRACT

Despite overall mortality decreasing, offshore fishing remains one of the riskiest work-based activities worldwide. For example, fishing communities in East Africa have a 43-fold higher rate of drowning than the general population. A lack of safety culture and knowledge around vessel stability contributes to this issue. Formal safety measures can be difficult to enforce, especially in small scale and subsistence fishing activities dominated by small artisanal boats. Digital technologies hold potential to effectively improve fishing safety. A digital safety device based on commonly held and relatively low-cost consumer products such as smartphones can provide increasing information to fishers enabling more informed safety decisions to be taken during vessel use. This paper proposes the algorithms for a prototype device to monitor stability of fishing vessels, with focus on the capabilities of low-fidelity data in stability assessment. The findings of experimental results at model and full scale are presented. The research indicates that an inclining test can be carried out with minimal training or knowledge base to allow an adequate stability assessment of a vessel before departure on a fishing trip. This baseline measure can then be used to track stability whilst underway as vessel motion is recorded and processed continually updating the stability assessment.

KEY WORDS

Safety; Fishing vessels; Digital Technology; Stability; Accessibility.

INTRODUCTION

Globally, offshore fishing remains one of the most dangerous occupations (Jensen et al., 2014; Roberts et al., 2021; Womack, 2003) and is especially hazardous for artisanal fishers in low- and middle-income countries (LMICs). Willis et al. (2023) estimate the global mortality rate at over 100,000 fishers a year. Insufficient vessel stability, leading to capsize, is a key aspect of this safety crisis. This research proposes that providing more information about the stability condition of a vessel enables fishers to make more informed decisions on operational safety. This information can be collected, analysed, and then communicated to fishers via a low-cost digital device that measures and monitors vessel stability.

The paper links the problem of fishing boat safety due to loss in stability to the opportunity that low-cost consumer level digital technology provides. The premise of this research is that low fidelity data may be used for stability assessment in a low-cost system. The focus of the paper is the initial testing of a prototype device with the ability to both measure stability in a controlled procedure and monitor vessel stability during normal operations.

The case study for this project investigates artisanal fishing vessels in East Africa. Tests are carried out in two environments, model scale testing in laboratory wave tanks and a full-scale pilot study on a fishing boat in a harbour. The model scale tests demonstrate some of the difficulties in applying a sensor to measure the underlying natural roll period of a vessel in a discrete frequency wave train such as is generated in a smaller wave tank. The full-scale study demonstrates improved results from real wave environments and suggests the applicability of the approach to develop a full featured safety application.

[1] Newcastle University (School of Engineering, Newcastle upon Tyne, UK); ORCID: 0009-0000-3274-5152
* Corresponding Author: n.smith11@newcastle.ac.uk

Submitted: 18 February 2024, Revised: 30 April 2024, Accepted: 1 May 2024, Published: 20 May 2024

Conference paper, DOI: https://doi.org/10.59490/imdc.2024.848 e-ISSN: 3050-4864

BACKGROUND

Fishing Boat Safety

In high-income countries (HICs) mortality rates of fishers are over 100 per 100,000 fisher-years (Sindall et al., 2022). Mortality rates in low- and middle-income countries (LMICs) are not as well documented and are estimated to range from 2 to 5 times more than the mortality in HICs (Sindall et al., 2022). Regardless of the economic development of the country, in both LMICs and HICs most deaths are associated with capsizing of boats, due to bad weather conditions or economic pressures resulting in fishers overloading vessels or going out in conditions unsuitable for their vessels (Sindall et al., 2022).

This study focuses on Kenya as a case study location. The fishing industry in Kenya employs over 60,000 fishers directly and 1.2 million indirectly through fishing, production, and supply chains. The areas of fish production in Kenya are the coast and open sea, freshwater lakes, such as Lake Victoria, rivers, and man-made dams. Across the country, use of traditional canoes, small dhows (*mashua*) and outriggers dominates, with less than 10% of these being motorised (Kimani et al., 2018). Examples of these vessels can be seen in Figure 1.

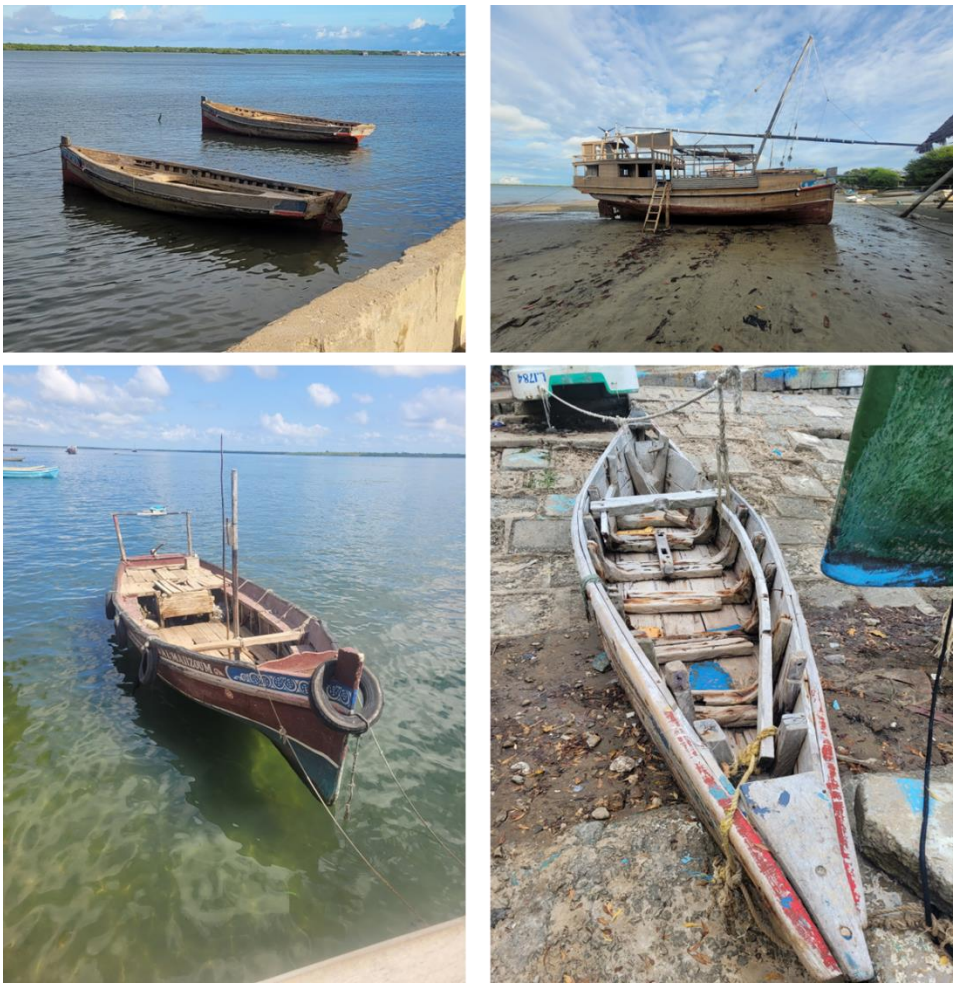

Figure 1: Typical Artisanal Vessels. Mid-size dhows (top left, bottom left), large sailing dhow (top right), small canoe (bottom right)

There is a lack of data on drowning fatalities in East Africa, especially among coastal communities with many studies based around Lake Victoria. There have been several studies into the epidemiology of drowning around Lake Victoria, using techniques such as verbal autopsies (Opemo et al., 2014). Such techniques can be difficult to scale up from communities to a regional level and there remains a lack of official figures. Fishing communities in East Africa were found to be at a higher risk of drowning with a 43-fold higher incidence of drowning than in the general population (Whitworth et al., 2019), which was mostly associated to the lack of safety equipment such as life jackets (97% of cases) and the inability to swim. Many of these cases were likely initiated by a capsizing or other stability driven event.

The annual estimated number of deaths on Lake Victoria has been reducing from between 3000 and 5000 in 2014 (International Federation of Red Cross and Red Crescent Societies, 2014) to around 1500 in 2020 (Watkiss et al., 2020).

The reduction was mostly attributed to greater use of life jackets and a trend for larger boats. Although it is not known how many boats capsize due to loss of stability, around two thirds of drowning deaths a year can be attributed to the weather conditions (Watkiss et al., 2020).

Stability Challenges

The risks within fishing which can lead to drowning include combinations of human and physical factors. One fundamental risk is that the boat is compromised during fishing operations through capsize or damage, thereby putting the crew at risk of entering the water. Stability can change quickly during onboarding of a catch bringing extra weight into the boat and moving the centre of gravity upwards. Associated risks around swimming ability and the lack of personal flotation devices means that capsize is a significant risk factor for drowning. Measures to improve the stability characteristics of fishing vessels can therefore reduce drowning risks.

Stability related accidents have the most causalities as they often happen suddenly meaning crew cannot access safety devices such as lifejackets. For this reason, it is important that vessels have their stability conditions assessed before coming up against potentially dangerous conditions. Vessels under 24 metres have a much higher rate of accidents caused by stability conditions than larger vessels which are generally better equipped to deal with adverse conditions due to the size of the vessel and crew training. Although crews of small and medium vessels can assess the stability of the vessel, this is in most cases based off previous experience and it may be difficult to assess a reduction in stability (Míguez González et al., 2012).

The most common issues on fishing vessels that lead to stability problems are changes in weight distribution, operational situations, weather situations and dynamic instabilities (Míguez González et al., 2012).

- **Changes in weight distribution** leading to change of location of centre of gravity. This can be from changes in structure, equipment or the use of spaces that are not tracked and recalculated leading to potentially dangerous loading conditions. This may include changes in ballasting and any modifications made to vessels.
- **Operational situations** such as inappropriate or overloading the vessel, raising the centre of gravity. Additionally suspended loads or fishing gear may change stability conditions particularly in the case of nets grounding the will cause loss of stern freeboard.
- **Weather situations** such as water intake in heavy rains – especially relevant on small open vessels. Breaking waves are particularly dangerous in beam seas, and high winds will create greater heel angles which in both cases vessels with a reduced stability condition will be more susceptible to capsize.
- **Dynamic instabilities** related to the interaction of the vessel underway and waves such as parametric resonance where the vessel will experience high amplitude rolling motions, losses of stability or steering capacity due to sailing in following seas or quartering seas.

Digital Safety Devices

Digital devices with safety features for personal use are becoming increasingly prevalent, such as sensors in smartwatches able to contact emergency services after a fall is detected. Decreasing cost and increasing sophistication has allowed development of technologies integrating into workplaces and everyday life. Access to technology such as smartphones is now prevalent in LMICs and presents opportunities to develop safety features useful for hazardous activities such as fishing.

Access to mobile phones is increasing in Kenya, with 94.6% of the population owning or having access to a SIM card, (Van Hove & Dubus, 2019). The use of smartphones is lower, with 33.9% of the phone owning population having smartphones and 52.8% owning basic phones (text and call features only) (Jelassi & Martínez-López, 2020; Krell et al., 2021; Van Hove & Dubus, 2019). This statistic is likely to increase rapidly as smartphone technology becomes further accepted, especially amongst younger people.

There are several existing technologies to estimate a boat's stability based on gyroscopic motion and baseline information about a vessel. The SKIPPER software gives updating stability condition with risk level for vessel and the maximum recommended wave height. To use the software information about the hull form, tanks and holds, flooding points, decks, minimum freeboard, lightweight and other ship particulars need to be inputted (Míguez González et al., 2012). This makes the makes it effective on industrialised vessels where a stability matrix as seen in Womack (2003) would become too large and complex. Needing a large amount of data about the vessel makes the software more difficult to set up on traditional fishing boats where much of the data needed is unlikely to be known. Building from this paper, the Kora Kora mobile application uses a similar concept focusing on Indonesian fishing vessels (Grech La Rosa et al., 2022). This uses an app to measure roll period to collect data which can be used to provide a measure of vessel stability which is then presented in a traffic light system.

Another study proposed a device to monitor draft and stability from a vessel rolling motion, this found the current waterline of the vessel through the roll motion then made use of the displacement-draught curve to find total displacement. When a given limit is reached the device detects this and alert the crew (Sakib, 2015). This method requires a displacement -draught curve for the vessel which is not a realistic prerequisite for artisanal vessels in LMICs. The existence of these technologies show the potential for linking the issue of fishing boat safety due to the loss in stability with the opportunity presented by low-cost consumer level digital technology.

METHODOLOGY

Approach

The core principle of this research is that a vessel's roll motion, measured by a gyroscope, can be directly linked to vessel stability through the estimation of the metacentric height. This link, which is an established naval architecture technique, is explained in the following subsections. The novelty within this research is to apply this technique using a low-cost consumer device such as a smartphone, single board microcontroller or computer, and without the direct intervention of a stability expert. The device will give fishers an insight into the stability condition of the vessel allowing them to visualise significant changes in stability and make more informed decisions during operations.

The device requires capability to monitor motions for three types of tests:

- Inclining Test: A well established and widely used method for finding vessel metacentric height (GM). Found by moving weights to create heel angles and recording the angle change.
- Roll Test: Commonly only used on smaller vessels such as fishing vessels. A heel angle is created, and the vessel then allowed to oscillate. Generally considered less accurate than the inclining test but can be more accessible in a practical environment.
- Continuous Monitoring: Using the same principles as the roll test, a device can continuously measure the roll period and provide an immediate estimate of a vessel's stability condition.

In this paper a device, detailed below, is tested at two scales and locations. Firstly, a series of model scale wave tank tests using a 1 metre length model of an artisanal fishing boat, and secondly a full-scale pilot test in a harbour using a 5 metre length open deck fishing boat. Further tests will be undertaken on typical artisanal fishing boats in Kenya but are not reported in this paper.

Stability Tests

Principles.

The metacentric height, GM, is a measure of static stability on a floating object. It defines the distance between the object's centre of gravity and the stability position known as the metacentre. When GM is greater than zero a boat is considered stable, meaning it will return to its upright equilibrium position. Maintaining sufficient positive GM, also to account for dynamic effects, is an important criterion for vessel safety. For larger ships GM is part of a regulated stability assessment which accounts for different loading conditions, damage, dynamic effects, and additional aspects such as wind loading. For smaller boats, especially in LMIC settings, assessing GM may not be a regulatory requirement, but it still provides a fundamental practical measure of stability and motion behaviour.

A larger GM gives more initial stability but also a shorter roll period (Biran, 2003), commonly known as being stiff. Conversely a lower GM causes the vessel to roll more slowly, known as being tender. For a vessel to be considered safe the GM needs to be positive with margins depending on boat type and operational area. The requirements for measuring GM depend on the boat type and the country it is operating in.

For example, the Maritime and Coastguard Agency in the United Kingdom issue guidance for fishing vessels under 15 metres registered length. The guidance advises exciting the vessel externally using a rope, once the vessel is rolling sufficiently the motion is allowed to decay and the average time of each oscillation is taken and is compared to the beam of the vessel to determine its safety (Maritime & Coastguard Agency, 2022).

Inclining test.

The inclining test is a well-established and widely used method to find GM for a vessel in its 'as built' condition and whilst in service. This is essential for ships to meet regulatory stability criteria. The test is conducted by moving known weights a given distance across the ship to create a small angle of heel. The angle of heel is found by recording the position of a pendulum or angle meter before and after the weight is moved. This can then be fed into an equation to find GM for small

angles of heel. This method will be used to find GM using the inclining test feature of the device. The GM can then be used to validate results and compare accuracy during further testing.

Roll test.

The roll period stability test is performed by creating a heel angle on a vessel and allowing oscillation at the natural roll frequency. On small vessels this is done by the crew moving to one side of the vessel to induce the heel angle and then moving back to the centre line to allow the vessel to oscillate or by using a rope to induce a roll motion. From this the roll period is measured and GM can be estimated. This is generally a less accurate measure of GM than the inclining experiment due to the estimation of the roll radius of gyration. However, it is a more accessible method with simpler analysis required to produce a result. For this reason, it is often used for small vessels, particularly fishing vessels (Maritime and Coastguard Agency, 2009).

The Weiss formula (Weiß, 1953, as cited in Kobylinski & Kastner, 2003; Santiago Caamaño et al., 2022; Grech La Rosa et al., 2022) as shown in Equation 1 can be used to find the natural roll frequency, ω_0 :

$$\omega_0 = \frac{\sqrt{g * GM}}{k_{xx}} \quad [1]$$

Where k_{xx} = the total roll radius of gyration in meters [m], GM = metacentric height in meters [m] and g = acceleration due to gravity $\left[\frac{m}{s^2}\right]$.

As seen in Santiago Caamaño et al. (2019) and Grech La Rosa et al. (2022), the roll radius of gyration can be estimated as:

$$k_{xx} = 0.4 * B \quad [2]$$

Where $B =$ vessel beam in meters [m]. By rearranging for the metacentric height this method enables an immediate estimate of vessel stability in uncontrolled environmental conditions. Therefore, it can potentially be used to predict progressive changes in different settings, such as during operations where the vessel loading condition may change or weather-related instabilities. This technique will form the basis of the prototype algorithm.

Continuous monitoring.

The continuous monitoring function uses the same principles as the roll tests but requires a more elaborate data processing approach. As the vessel carries out normal operations the device monitors the roll motion of the vessel. As shown in this study, the estimation of natural roll period from a continuous signal is challenging. It requires an algorithm to find consistent peak frequencies through signal analysis such as Fast Fourier Transform (FFT). The tracking of these peak frequencies over time can then be used to detect significant changes that may occur due to a shift of the centre of gravity, for example in the case of loading a vessel with a catch of fish when out at sea. It is important to detect these changes quickly as when the vessel is suddenly put in adverse conditions the change in stability can rapidly lead to capsize.

Experimental Flow

Figure 2 describes the experimental flow of the prototype device for all three types of stability test (inclining test, roll test and continuous monitoring). The first step is to first ensure the vessel is loaded in its normal operating condition prior to testing. Then the appropriate measurements of the vessel are taken to estimate displacement. The prototype is securely fastened to the vessel on a flat surface with the gyroscope appropriately aligned to the centreline of the vessel. The vessel is allowed to settle before testing begins and ideally weather conditions should be calm. Baseline motion data is collected to allow the device to calibrate itself. One or more of the three tests is then performed. The output can then be immediately used, for example to provide an alert. It is also saved for later analysis.

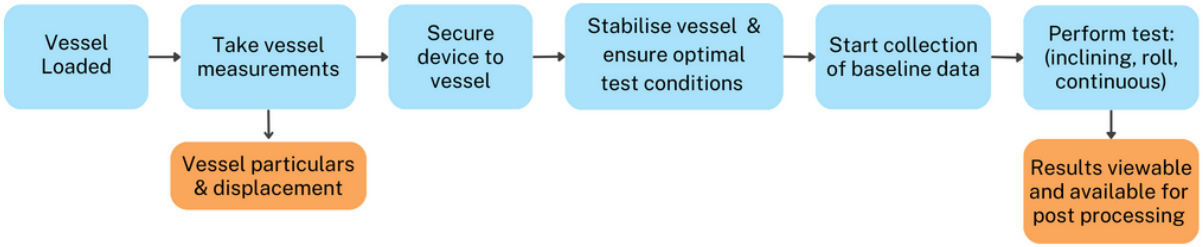

Figure 2: Experimental Flowchart

The Device

To measure roll motion on a vessel using a low-cost system operated by the fisher, a device with the following criteria is needed (Table 1):

Table 1: Device Requirements and Capabilities

Requirement Description	Requirement value	Prototype Device Specification
Measurements	Gyroscope to measure roll motion	MPU-6050 Accelerometer and Gyroscope
Cost	Low	Approx. £70 - £150, dependant on setup (addition of screen, fans etc.)
Power	< 10W	Variable, with a maximum draw of 6W
Sample rate	Adjustable, with capability of at least 100 Hz sample rate.	Sample rate set in algorithm. Capable of 1kHz sample rate.
Timescales	Storage capacity for several days of continuous measurement	32GB SD card capable of storing raw data for over 100 days of continuous running.
Size	Portable and small. Larger devices should have a carry case with handle.	157 x 82 x 41 mm in case without screen (no handle) 270 x 246 x 124 mm in case with screen (with handle)
Scale	Suitable for both model and full-scale measurements.	Yes
Environmental protection	Waterproof case	Hard, buoyant, waterproof case
Battery	Sufficient for 1 day operation on a single charge	2 x 5000mAh will power Pi for up to 19 hours

The ambition of the present study is to apply the experimental flow on a cross platform smartphone app. However, this adds layers of unnecessary complexity in the initial prototyping stages. Therefore the prototype device is based on a Raspberry Pi single board microcomputer. The advantages to choosing this device are that it is easily accessible, simple to use, robust and low cost. Additionally, it is capable of both collecting and processing large datasets on the same device. It comes set up with an operating system (OS) and graphical user interface (GUI) making the initial set up of the device simple.

The Raspberry Pi is coupled with an MPU-6050 accelerometer and gyroscope unit, a low-cost sensor capable of measuring angular acceleration and rotation around 6 axes. The MPU-6050 is a Micro-Electro-Mechanical Systems (MEMS) module, the angle data produced by the unit may be considered low fidelity data, similar to that produced by a mobile phone. The Raspberry Pi is fixed within a waterproof case with the gyroscope fixed to the Pi alongside a battery and a charging cable.

To complete the experimental flow, shown in Figure 2, data is collected from the device and converted into degrees, then is filtered to remove noise and extreme values. The clean data is then ready for Fast Fourier Transform (FFT) analysis of the signal. The Fourier transform converts a signal from the time domain to the frequency domain enabling detection of the underlying natural roll period of the vessel.

Model Tests

Initial testing of the device was applied on a model scale fishing boat. It was considered important to test on a model relevant to the case study in East Africa so that the algorithm can be better tuned to the characteristics for these hull shapes. Vessels in the case study are noticeably different in style to many HIC settings in terms of the hull form shape, the powering (sails, motors etc) and the type of fishing operations (trawling vs line fishing).

The model used was a 20th scale model of a proposed 21 metre traditional Kenyan fishing dhow designed by the Flipflopi project (Flipflopi Project, 2017). The model was 3D printed enabling a lower cost yet accurate representation for stability and motion experiments. The model has a waterline length of 1.064 metres and is ballasted using metal weights fixed to the hull and deck. The vessel particulars are shown below in Table 2.

Table 2: Model and full-scale particulars

Vessel Particular	Full-scale	Model-scale
Water Line Length [metres]	21.38	1.064
Beam [metres]	6.75	0.338
Draught Amidships [metres]	2.50	0.125
Volume of Displacement [$metres^3$]	17.66	0.017

The model has one full wooden deck and a second partial deck at midships to allow for a standardised vertical movement of weights to simulate multiple loading conditions across different tests. Figure 3 shows the 3 different loading conditions relative to each other:

- Low Position: Weight on vessel deck (baseline)
- Mid Position: Weight on top of foam blocks on vessel deck (decreasing value of GM by 2.4%)
- High Position: Weight on top of second deck (decreasing value of GM by 20%)

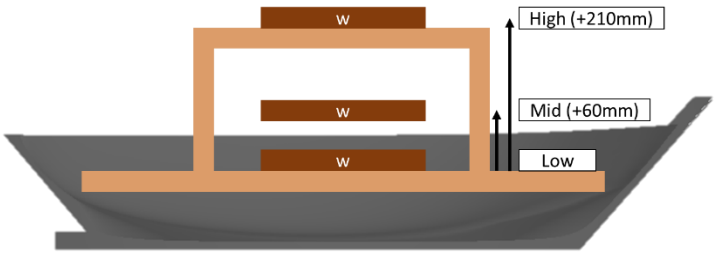

Figure 3: Model weight positions: Low (baseline), Mid (+60mm), High (+210mm)

For each inclining test, it was ensured that the model was in the correct loading condition and all weights were securely fixed. The inclining weights were placed on the deck with the prototype device and an inclinometer. To validate results from the prototype device the inclining tests were initially run both through the prototype and manually using the inclinometer.

Model testing was carried out at Newcastle University across the Wind Wave Current Tank (WWCT) and the Towing Tank (TT) shown in Figure 4, which have the dimensions shown in Table 3:

Table 3: Testing facilities main parameters.

Parameter	Towing Tank	Wind Wave Current Tank
Length [metres]	37	11
Width [metres]	3.7	1.8
Water Depth [metres]	1.25	1.0
Wave Period [seconds]	0.5-2.0	0.8-4.0
Wave Height [metres] (period dependant)	0.02-0.12	0.02-0.2

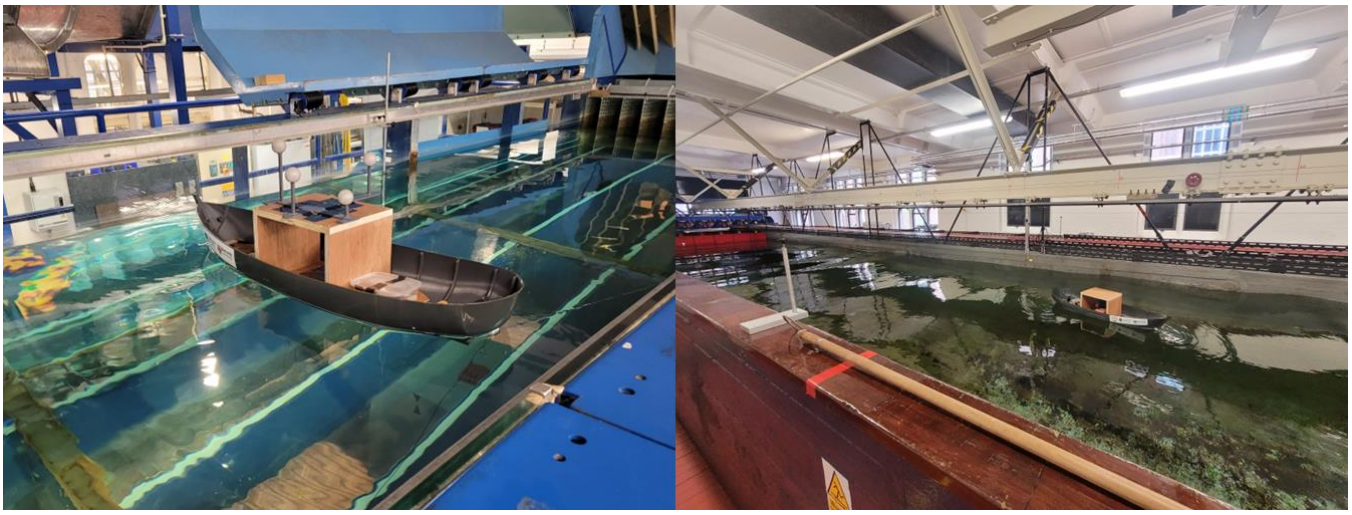

Figure 4: Model in Testing Facilities, Newcastle University. Wind Wave Current Tank (left), Towing Tank (right)

Full-Scale Tests

The vessel used for the full-scale pilot study was an Arran 16 displacement hulled boat, as seen in Figure 5 with particulars shown in Table 4 (Arran Boats, 2023).

Table 4: Arran 16 Particulars

Vessel Particular	Value
Length [metres]	4.88
Beam [metres]	1.98
Draft [metres]	0.30

Figure 5: Arran 16 used for full scale testing.

The full-scale tests were completed in Beadnell Harbour, Northumberland, UK in August 2023. The vessel was moored at bow and stern. The weather conditions were mild with a gentle breeze and small waves, as can be observed in Figure 5. The tide was continuously coming in during the tests. The boat was set up for deployment of marker buoys and contained several inflatables and anchors. The outboard engine was not fitted.

RESULTS AND DISCUSSION

The first stage of testing was to complete inclining and roll decay tests for the model in the 3 different loading conditions. This allowed validation for the results from wave testing. The inclining tests and roll tests were repeated before further phases of testing to ensure consistency of positions throughout. The model testing was divided into 2 phases, the first phase tested the device in regular waves using a commercial motion tracking system (Qualisys) as a baseline to investigate the accuracy of motion data collected from the device. The second phase tested the device in irregular waves with the aim of highlighting the natural roll frequency of the model. The final stage of testing presented is a full-scale pilot study, showing the validity of the methodology at full scale.

Model Scale Inclining Tests

Inclining tests were completed in a small basin using a standard approach. The model was loaded in the three different weight positions as described previously (Figure 3). Four small inclining weights of 200 grams were added and 5 repeats were carried out for each position. The device was used alongside a separate digital inclinometer for validation. The average GM was calculated and is shown in Table 5. The radius of gyration, k_{xx} , was estimated at 0.135 metres using Equation 2. The values for GM and k_{xx} were used in Equation 1 to estimate the roll frequency for each weight position.

Table 5: Inclining Tests and Roll Period

Weight Position	Displacement [kg]	k_{xx} [mm]	GM from Inclining Test [mm]	Roll Frequency (Estimated) [Hz]	Roll Frequency (Measured) [Hz]
Low	17.8	135.2	85*	1.08	1.10
Mid	17.8	135.2	83	1.06	1.04
High	17.8	135.2	68	0.96	0.98

*The models low position GM value was slightly changed from the WWCT tests (WWCT: 0.086m, TT: 0.085m) due to changes to the device setup, namely a new battery and case however the positioning of the weights was the same.

Roll decay tests were completed by exciting the model from the port side by pushing down, when the roll was sufficient, data collection was started, and the roll motion was allowed to decay. This was repeated 5 times ensuring that each decay test produced 5 complete oscillations. The data was collected using the device to record the roll periods and verified with a stopwatch. The device then produced an FFT plot and the roll frequency presented as the 'Roll Frequency (Measured)' in Table 5. An example of one of the roll period tests with plots of the roll angle and FFT is shown in Figure 6.

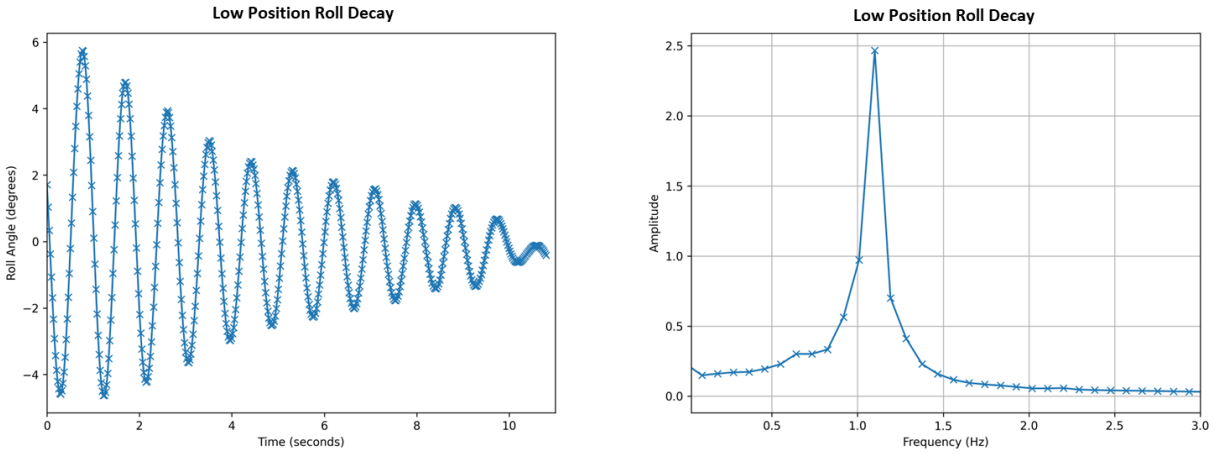

Figure 6: Roll Decay Test Results for Low Position. Roll angle (left) and FFT plot showing roll frequency of 1.10Hz (right)

The results of the inclining and roll tests show that the measured roll frequency is within a window of the estimated roll frequency and the device can pick up changes of GM in model scale. As seen in Figure 3, the difference between the Low and Mid positions is 60mm, under a third of that between the Low and High (210mm) representing a 2.4% and 20.0% reduction of GM respectively. For the change between the Low and the Mid positions the device did not produce a clean enough signal to say with certainty that the device could pick up slight changes of GM. However, the difference between the Low and High positions was clear and the measured roll periods reflected the estimated roll period and showed an evident change in the stability condition of the vessel.

Model Scale Wave Tests: Phase 1

The purpose of Phase 1 was to investigate the accuracy of data capture from the device in comparison to a commercial system. The Wind Wave Current Tank (WWCT) at Newcastle University was selected for this first phase of testing. This allows testing in a wide range of regular waves. The WWCT has a commercial motion capture system, Qualisys, that records the vessel motion through the tracking of 4 reflective spherical targets using 2 cameras set at either end of the test area.

The vessel was placed in 'Low' position and moored in the tank as shown in Figure 7. The GM was calculated at 0.086m from inclining tests conducted at the beginning of testing. The expected roll frequency for this setup was 1.08Hz.

The model used is of a vessel designed for use on the Kenyan coast and for ocean-going trips, so it is likely to encounter a range of operating conditions from calm inshore waters into the Indian Ocean and subject to heavy seas. A test matrix made up of 9 regular waves was selected and is shown in Table 6. These waves were chosen to represent a scaled representation of the wave heights and frequencies that the full-scale vessel is likely to encounter. All the waves tested are shown in Table 6 with the ratios of wavelength over the model water line length and breadth of the model. The wave lengths were measured in the centre of the tank test area where the model was located. The results of 3 of these tests (indicated by *) are presented in Figure 8 with the nominal waves.

Table 6: Phase 1 Test Matrix showing nominal wave frequency and height alongside ratios of wave length to model waterline length and breadth

	Wave Frequency [Hz]	Wave Height [m]	Wave Length/L_{WL_model}	Wave Length/B_{model}
*	0.8	0.01	2.69	8.46
	0.8	0.02	2.49	7.83
	0.8	0.03	2.39	7.53
	1.0	0.01	1.48	4.64
*	1.0	0.02	1.55	4.87
	1.0	0.03	1.69	5.33
	1.25	0.01	0.98	3.10
	1.25	0.02	1.02	3.19
*	1.25	0.03	1.05	3.29

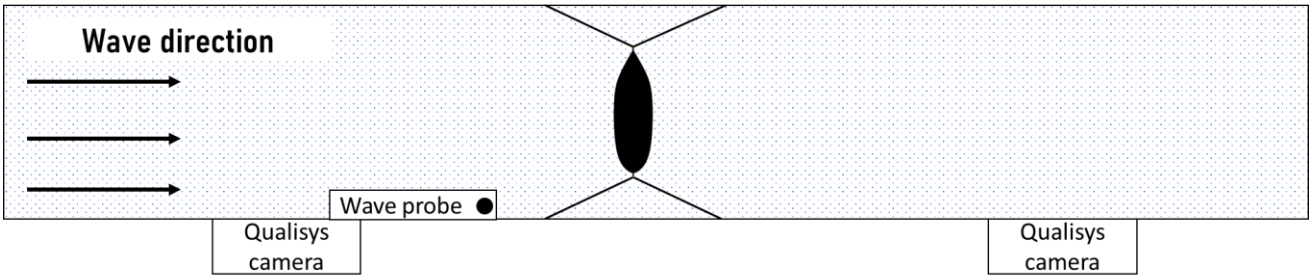

Figure 7: Scaled plan view of the test setup in the Wind Wave Current Tank.

The vessel was placed at beam seas and moored from the bow and stern to 4 points on the tank. The sampling rate of the device was set to 33Hz and the data collection was started remotely through a VNC server to start it simultaneously with Qualisys and the wave probe.

FFT analysis was carried out on the data collected by both the device and Qualisys. The peak frequencies for the tests are shown in Figure 8. The model's motion was entirely dominated by the wave frequency. As can be seen in Figure 8 there was no significant difference between the nominal wave frequency and the recorded peak frequency for both the device and Qualisys, with the peak nominal wave frequencies being 0.8 Hertz (8a, 8d), 1.0 Hertz (8b, 8e) and 1.25 Hertz (8c, 8f). For each of these, the vessel roll frequency is the same as the wave frequency.

Most notably, Figure 8 shows the alignment of the two data acquisition methods, with the device showing peaks at the same frequency and with comparable clarity to Qualisys. The data from the device has greater amounts of noise surrounding the peaks, however this noise is remains low relative to the amplitude of the peak. This noise is due to several factors: lower fidelity raw data from the device, the effect of electrical noise from the environment, greater amount of processing of raw device data and lower sampling rate of the device in comparison to Qualisys. These factors are likely the cause of the lower peak amplitude seen in the FFT from data collected by the device. The effect of the reduced sampling frequency

should be diminished at full scale due to the longer roll periods resulting in a higher number of data points per roll period giving greater definition then at model scale.

Overall, the results from the WWCT show there is no significant difference between the two acquisition methods with both detecting the same peak frequencies. The signal using lower fidelity data produces lower amplitude peaks with more noise however the effect of this is minimal as the peaks are easily identifiable, showing the validity of the device methodology. The first phse of the model scale testing ensured the accuracy of the data produced by the device, the second phase builds upon this to identify the natural roll period using irregular waves and more complex wave spectra.

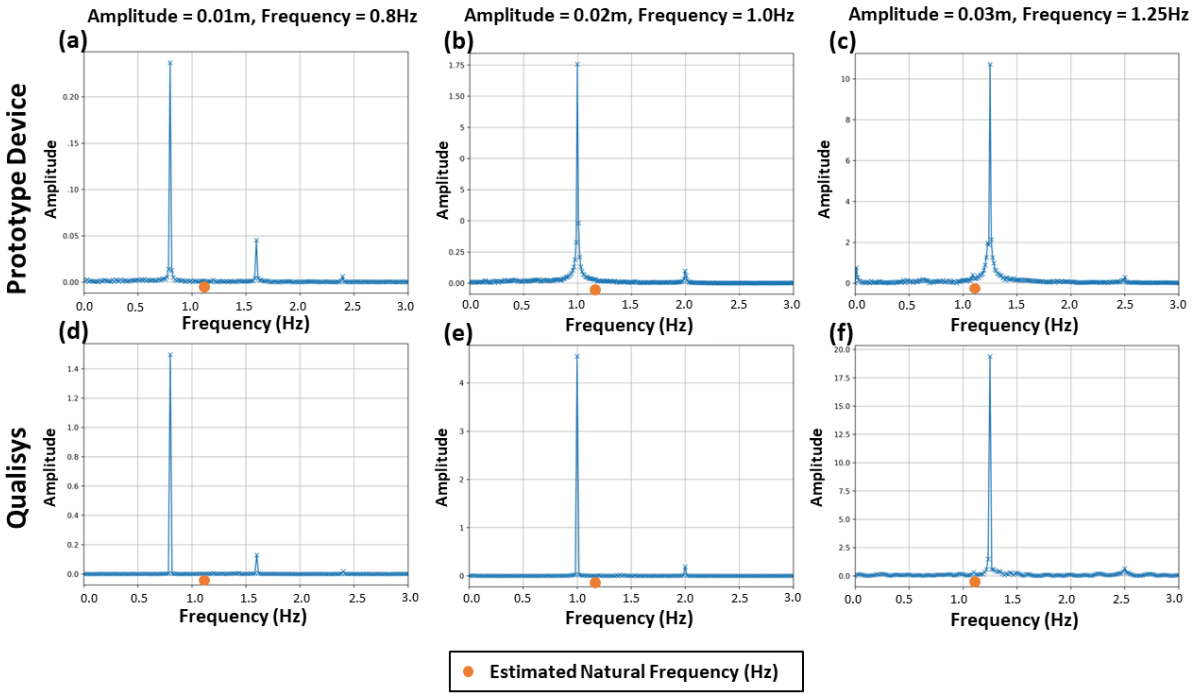

Figure 8: Comparison of FFT graphs for the two acquisition methods, the prototype device (a, b, c) and Qualisys (d, e, f) for a sample of 3 nominal sine waves described in Table 7. The estimated natural frequency is denoted by the orange dot above the x axis for each subplot.

Table 7: Nominal and Recorded Wave Data

Nominal Wave		Average Recorded Wave Probe Data		Subplots in Fig.8
Amplitude [m]	Frequency [Hz]	Amplitude [m]	Frequency [Hz]	-
0.010	0.800	0.010	0.800	a, d
0.020	1.000	0.013	1.000	b, e
0.030	1.250	0.039	1.249	c, f

Model Scale Wave Tests: Phase 2

The Towing Tank at Newcastle University was selected for the second phase of model testing due to the greater length and breadth of the test area. Initially, the model was moored first in 4-point mooring in beam seas as in the WWCT and regular waves were used. As these results were consistent with the WWCT it could be said that the difference made by the tank size was minimal. The vessel was then modelled as being 'at anchor' using a mooring line attached to a lead weight at the bottom of the towing tank, this mooring line was measured to ensure that the model vessel would not be able to make contact with the sides of the towing tank, the set up can be seen in Figure 9.

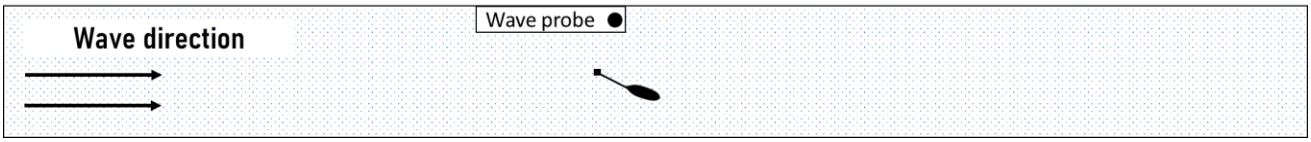

Figure 9: Scaled plan view of the test setup in the Towing Tank.

The intention in the second phase was to create more complex wave forms and allow waves to disperse over the tank length and mix, for this reason the test duration was also extended to 20 minutes. Two quasi wave spectra were created using combinations of wave fronts, sine waves, modified JONSWAP spectra and white noise, and are presented below in Figure 10a, &10b, denoted by Wave 1 and Wave 2.

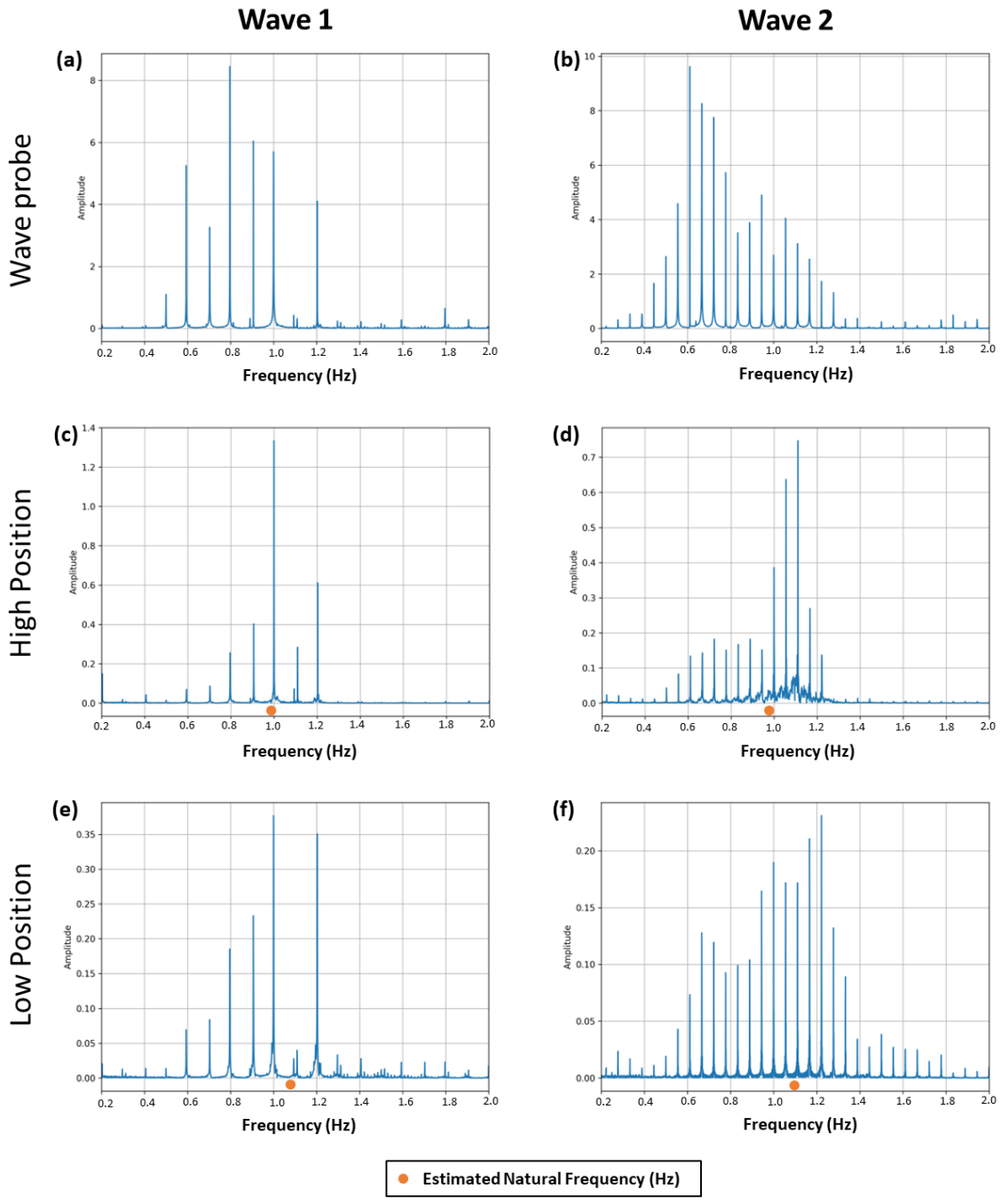

Figure 10: FFT results from Phase 2 testing. The 2 quasi wave spectra: Wave 1 (a) and Wave 2 (b) are shown with the vessel motion for each Wave 1 (c, e) and Wave 2 (d, f). The estimated natural frequency is denoted by the orange dot above the x axis for each subplot.

The model setup remained the same as in Phase 1of model testing and the model was tested in 2 of the loading conditions shown in Figure 3:

- Low Position: Weight on vessel deck (GM: 85mm, estimated roll frequency: 1.08Hz)
- High Position: Weight on top of second deck (GM: 68mm, estimated roll frequency: 0.96 Hz)

Figure 10 shows the FFT analysis of the model roll motion analysis data for the 2 loading conditions; high (10c, d) and low (10e, f) for 2 wave spectra; Wave 1 (10a, c, e) and Wave 2 (10b, d, f). The FFT plots for the vessel roll motion (10c-f) are shown alongside the FFT plots for the wave probe data (10a, b). The estimated natural roll frequencies for each position are denoted by the orange dot above the x axis.

Looking at the data from Wave 1 (Figure 10, left), initially it appears the natural roll frequency has been picked up for the high position, as there is a clear peak at 1.0Hz and roll frequency estimated at 0.96Hz and measured at 0.98 Hz from roll decay tests. However, as the same frequency of 1.0Hz is also the peak frequency in the low position it is clear this is a vessel response to the wave frequency.

For the more complex wave, Wave 2 (Figure 10, right) again the natural frequency of the vessel is not clear. The highest amplitudes seen are around 1.1Hz for the High position and 1.2 Hz for the Low position, around 0.1 Hz higher than the estimated roll frequency. The data recorded on the device across all tests has a negative skew whereas both waves have a positive skew. This shows general shift away from vessel motion being dominated by the wave frequencies in the Towing Tank in comparison to the Wind Wave Current Tank. Although the peak frequencies had moved away from the wave frequencies the two could not be said to be independent of each other, this is more evident in the more complex wave, W2.

Across all 4 tests the FFT plots have a more similar shape for each wave rather than each position suggesting the wave frequencies have far greater affect in the model than the weight position. This suggests the results from the towing tank show a continuation of issues faced in the Wind Wave Current Tank, with the natural roll frequency not being seen in continuous monitoring of the vessel motion. As this may be due to unrepresentative conditions using unidirectional waves a small pilot study was conducted.

Full Scale Tests

A pilot study was conducted at full scale using a vessel in the local area to investigate whether issues present in model scale would still present at full scale. To test this a series of tests were conducted, each with a duration of 5 minutes, allowing different loading conditions to be assessed. The vessel used was a 4.88 metre Arran 16, described previously in Table 4. The vessel was moored on a beach at bow and stern in a similar fashion to the mooring lines used in first phase of model testing. During the testing the tide was continually coming in and there were slight changes in the wind and waves during the time of testing, but both remained calm.

The peak frequency over time graphs are shown for the following tests in Figure 11:

- Test 1: 2 people in vessel (Added Weight: 130kg), walking around vessel randomly.
- Test 2: 2 people in vessel (Added Weight: 130kg), rocking vessel to create constant roll motion.
- Test 3: Vessel empty, vessel allowed to roll freely.
- Test 4: Vessel empty, constant roll motion induced externally.

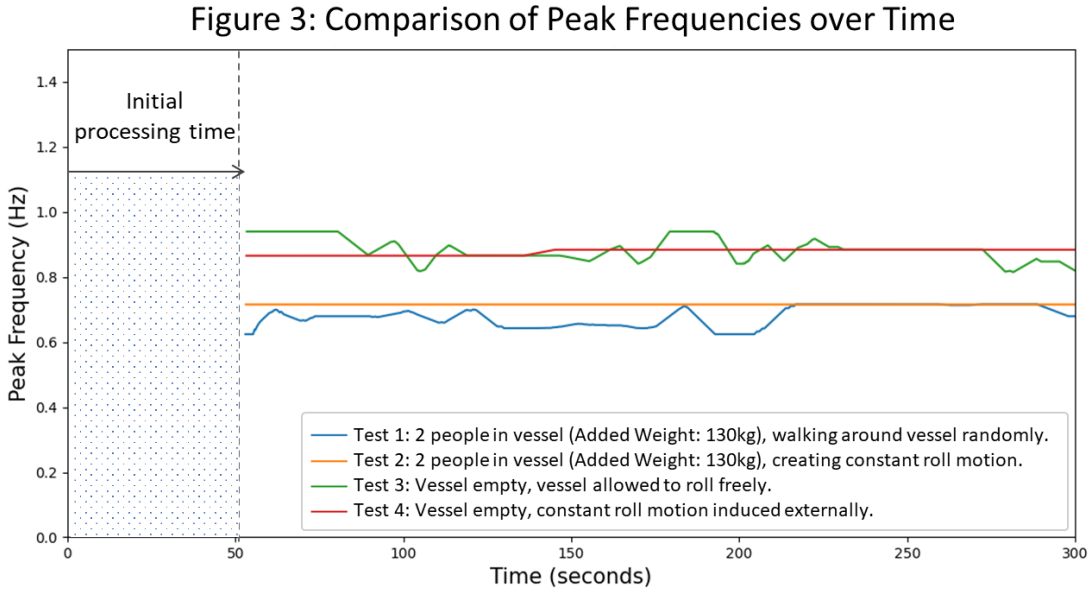

Figure 11: Comparison of peak frequencies over time for 4 test conditions.

The peak frequency found from the FFT analysis is plotted against time in Figure 11, with the FFT using a 50 second 'window' of data, updating itself every 10 seconds. No significant change in peak frequency within each test was expected to be seen as test conditions remained stable and no change in the position of the centre of gravity, G, was made. Although there is variation in the peak frequency detected, there remains a clear difference between the two loading conditions, with

Tests 1 and 2 having a roll frequency of around 0.7 Hz and Tests 3 and 4 around 0.9 Hz. As can be expected the Tests 2 and 4, where roll motion was constant, had almost no change in recorded roll frequency. For Tests 1 and 3 there is expected to be a greater effect of environmental conditions such as wind and waves and this is reflected in Figure 11, where both tests have more variation of recorded peak frequency in comparison to Tests 2 and 4. The results from these tests showed a clear difference between peak frequencies for the 2 loading conditions and the device was able to pick up differences between these, as well as pick up peak frequencies clearly out of laboratory conditions dealing with the effects of waves, wind and tidal currents.
This pilot study showed that the device could collect and process roll data for a full-scale vessel to a sufficient level of accuracy. Therefore, the device shows potential for use on fishing vessels in small scale and subsistence fishing, where there is a need for lower cost devices.

CONCLUSIONS

This project has laid the foundations for further work investigating how low-cost digital technology can be used to assess the stability of fishing vessels in artisanal settings. The results of a prototype device have been presented from both model and full-scale testing.

The first phase of model testing has shown that low fidelity data can be used to measure roll motion in a comparable fashion to a commercial system. However, in regular waves unrepresentative of ocean waves the natural roll frequency of the model was not detected. The second phase of model testing aimed to create more realistic waves through quasi wave spectra, the vessel motion here was a clear response to the waves rather than simply reflecting the wave frequencies however this still did not allow the natural roll frequency to be detected.

The full-scale pilot study was successful in detecting the natural roll frequencies of the vessel and detecting changes in the roll frequency and therefore the vessel GM. Although work to refine the model scale testing remains, the results from full-scale tests are promising, demonstrating real-life applications. While further development is needed to make a full functioning device for everyday use, this study has effectively demonstrated proof of concept.

FUTURE WORK

Further work into model testing should take place to resolve issues around wave frequency domination and investigation into the minimum value of GM before the stability condition of the vessel becomes dangerous should be carried out to determine alert levels for the device.

Full-scale testing is planned to take place on a traditional East African fishing boats and complete stability testing will also be carried out. This will include an inclining test and full lines plan. Alongside this the device should be used in its inclining test feature and then using the roll test to investigate error margins between a comprehensive stability test and this device.

Further development of the prototype device with a more user-friendly Graphical User Interface (GUI) will take place, whilst also investigating the potential to integrate the proposed technology and algorithms into regular smartphones. These are increasingly owned and used by fishers, and provide an opportunity to efficiently implement the technology. However, there are anticipated difficulties in the use of a smartphone which may include the robustness of the sensor architecture and setting a steady sampling speed, especially when the phone's processor is completing background operations.

Additionally, the creation of a vessel database to aid understanding of East African fishing boat forms will improve the device algorithms and support improve estimation of key parameters such as displacement and ensure the estimated radius of gyration is suitable.

CONTRIBUTION STATEMENT

Nathan Manojlovic Smith: conceptualization; methodology; investigation; visualisation; writing – original draft. **Priscila Melo:** supervision; visualisation; writing – review and editing. **Simon Benson**: conceptualization; project administration; supervision; writing – review and editing.

ACKNOWLEDGEMENTS
The research is funded by the John Prime Foundation and the Willis Fund. The authors thank the Flipflopi Project in Lamu Kenya for providing the dhow model and inspiring the project.

REFERENCES

Arran Boats. (2023, September, 09). *Price list for arran 16 and components*. Retrieved from: https://www.arranboats.co.uk/price-list/

Biran, A. (2003). *Ship Hydrostatics and Stability*. Oxford, United Kingdom: Butterworth-Heinemann

Flipflopi Project. (2017). *The Flipflopi Story*. Retrieved from: https://www.theflipflopi.com/our-story

Grech La Rosa, A., Ryan, C., Thomas, G., Huang, L., Hetharia, W., Riyadi, S., Setyawan, D., & Utama, I. (2022, September 13-15). *Design of a Mobile Application To Assess the Stability of Small Fishing Boats.* International Conference on Computer Applications in Shipbuilding *2022*, Yokohama, Japan, 121–136. doi.org/10.3940/rina.iccas.2022.11

International Federation of Red Cross and Red Crescent Societies. (2014). *World Disasters Report: Focus on culture and risk*. Retrieved from: https://www.ifrc.org/document/world-disasters-report-2014

Jelassi, T., & Martínez-López, F. J. (2020). *Digital Business Transformation in Silicon Savannah: How M-PESA Changed Safaricom. In* T, Jelassi & F.J, Martínez-López. *Strategies for e-Business* (pp. 633–658). Retrieved from: doi.org/10.1007/978-3-030-48950-2_23

Jensen, O. C., Petursdottir, G., Holmen, I. M., Abrahamsen, A., & Lincoln, J. (2014). A review of fatal accident incidence rate trends in fishing. *International Maritime Health*, *65*(2), 47–52. doi.org/10.5603/IMH.2014.0011

Kimani, E., Okemwa, G., & Aura, C. (2018). *The Status of Kenya Fisheries: Towards Sustainable Exploitation of Fisheries Resources for Food Security and Economic Development.* Mombasa, Kenya: Kenya Marine and Fisheries Research Institute (KMFRI)

Kobylinski, L. K., & Kastner, S. (2003). *Stability and Safety of Ships* (1st ed.). Oxford, United Kingdom: Elsevier

Krell, N. T., Giroux, S. A., Guido, Z., Hannah, C., Lopus, S. E., Caylor, K. K., & Evans, T. P. (2021). Smallholder farmers' use of mobile phone services in central Kenya. *Climate and Development*, *13*(3), 215–227. doi.org/10.1080/17565529.2020.1748847

Maritime & Coastguard Agency. (2022). *Procedure for Carrying out Small Fishing Vessel Stability Tests* (MGN 503 Amendment No. 1 (F)). U.K. Department for Transport. Retrieved from: https://assets.publishing.service.gov.uk/government/uploads/system/uploads/attachment_data/file/1106738/MGN503_Amendment_1.pdf

Maritime & Coastguard Agency. (2009). *Procedure for Carrying out a Roll or Heel Test to Assess Stability for Fishing Vessel Owners and Skippers* (MGN XXX (F)). U.K. Department for Transport. Retrieved from: https://assets.publishing.service.gov.uk/government/uploads/system/uploads/attachment_data/file/561857/MGN_503.pdf

Míguez González, M., Sobrino, P. C., Álvarez, R. T., Casás, V. D., López, A. M., & Peña, F. L. (2012). Fishing vessel stability assessment system. *Ocean Engineering*, *41*, 67–78. https://doi.org/10.1016/j.oceaneng.2011.12.021

Opemo, D., Aloo, P. A., Arudo, J. A., & Mbithi, J. N. (2014). A study of common causes of mortality among Fishermen in Lake Victoria, Kenya. *African Journal of Health Sciences*, *27*(1), 19–29. Retrieved from: www.researchgate.net/publication/328630291

Roberts, S. E., Carter, T., Smith, H. D., John, A., & Williams, J. G. (2021). Forgotten fatalities: British military, mining and maritime accidents since 1900. *Occupational Medicine*, *71*(6–7), 277–283. doi.org/10.1093/occmed/kqab108

Sakib, S. (2015, May 21-23). *A novel device for dynamic loading and stability measurement of inland vessels based on its rolling motion*. 2nd International Conference on Electrical Engineering and Information and Communication Technology, Savar, Bangladesh. doi.org/10.1109/ICEEICT.2015.7307480

Santiago Caamaño, L., Galeazzi, R., Nielsen, U. D., Míguez González, M., & Díaz Casás, V. (2019). Real-time detection of transverse stability changes in fishing vessels. *Ocean Engineering*, *189*, 106369. doi.org/10.1016/j.oceaneng.2019.106369

Santiago Caamaño, L., Míguez González, M., Allegue García, S., & Díaz Casás, V. (2022). Evaluation of onboard stability assessment techniques under real operational conditions. *Ocean Engineering*, *258*, 1–9. doi.org/10.1016/j.oceaneng.2022.111841

Sindall, R., Mecrow, T., Catarina Queiroga, A., Boyer, C., Koon, W., Peden, A. E., & Environment, G. (2022). Drowning risk and climate change: a state-of-the-art review. *Injury Prevention*, *28*, 185–191. doi.org/10.1136/injuryprev-2021-044486

Van Hove, L., & Dubus, A. (2019). M-PESA and financial inclusion in Kenya: Of paying comes saving? *Sustainability, 11(3)*. doi.org/10.3390/su11030568

Watkiss, P., Powell, R., Hunt, A., & Cimato, F. (2020). *The Socio-Economic Benefits of the HIGHWAY project*. WISER. Retrieved from: https://www.eol.ucar.edu/publication/socio-economic-benefits-highway-project

Weiß, G. (1953). Erfahrungen mit der Stabilitätsprüfung durch Roll versuche. *Hansa*, *90*.

Whitworth, H. S., Pando, J., Hansen, C., Howard, N., Moshi, A., Rocky, O., Mahanga, H., Jabbar, M., Ayieko, P., Kapiga, S., Grosskurth, H., & Watson-Jones, D. (2019). Drowning among fishing communities on the Tanzanian shore of lake Victoria: A mixed-methods study to examine incidence, risk factors and socioeconomic impact. *BMJ Open*, *9*(12). doi.org/10.1136/bmjopen-2019-032428

Willis, S., Bygvraa, D. A., Hoque, M. S., Klein, E. S., Kucukyildiz, C., Westwood-Booth, J., & Holliday, E. (2023). The human cost of global fishing. *Marine Policy*, *148*(December 2022), 105440. doi.org/10.1016/j.marpol.2022.105440

Womack, J. (2003). Small commercial fishing vessel stability analysis: Where are we now? Where are we going? *Marine Technology and SNAME News*, *40*(4), 296–302. doi.org/10.5957/mt1.2003.40.4.296

Proceedings of 15th International Marine Design Conference (IMDC-2024)
June 2-6, 2024
Amsterdam, the Netherlands

Leveraging a Small Dataset to Predict Nonlinear Global Loads

Kyle E. Marlantes* **and Kevin J. Maki**

ABSTRACT

In this work, a hybrid machine learning method, which uses ML strategies to model high-order force components within a low-order equation of motion, is considered in the context of the global wave-induced loads of a ship in irregular waves. It is shown that the method can make predictions in a range of wave conditions even when the training data set only includes a single seaway. The proposed method offers a data-leveraging technique which may be useful in the design space, where a small data set derived from a high-fidelity source can be leveraged to make similar fidelity predictions in a larger number of wave conditions.

KEY WORDS

Wave-induced; global loads; shear forces; bending moments; hybrid machine learning

INTRODUCTION

Global wave-induced loads are an important consideration in the design of ship structures. Often, shear forces and bending moments are estimated using rules-based distributions or simplified quasi-static methods (Payer and Schellin, 2013). Though practical for early-stage design, research has shown that real-world measurements can exceed rules-based predictions (Andersen and Jensen, 2014). In many cases, linear frequency-domain hydrodynamic tools such as strip theory are used (Payer and Schellin, 2013). However, it is well-known that such low-fidelity methods can underpredict the maximum bending moment (Wu and Hermundstad, 2002), (Rajendran et al., 2016), (Gaspar et al., 2016), sometimes by as much as 32% when considering long-term responses (Parunov et al., 2022a), and compensating with large safety margins may lead to an over-designed structure (Parunov et al., 2022b).

Nonlinear global loads are predominantly a second-order effect (Juncher and Terndrup, 1979), (Marlantes and Taravella, 2019) and strongly related to the body-nonlinear hydrodynamic forces, so it is necessary to use nonlinear numerical models. However, high-fidelity computational hydrodynamic tools, such as Reynolds Averaged Navier-Stokes (RANS) CFD methods or nonlinear potential flow methods, especially if coupled to a structural solver, suffer from a high computational cost, making it impractical to evaluate a large number of wave conditions (Hirdaris et al., 2014), (Temarel et al., 2016). As a result, body-nonlinear methods, which model the Froude-Krylov and hydrostatic restoring forces nonlinearly, are popular tools, as the nonlinearity from these forces capture much of the difference between hogging and sagging bending moments (Guedes Soares, 1991), which is especially evident in ships with large flare (Rajendran et al., 2016). One promising approach for high-fidelity methods is to use design waves, such as the Design Loads Generator proposed in Alford (2008) and

Department of Naval Architecture and Marine Engineering, University of Michigan, Ann Arbor, USA
* Corresponding Author: kylemarl@umich.edu

Submitted: 22 February 2024, Revised: 29 April 2024, Accepted: 1 May 2024, Published: 21 May 2024

Conference paper, DOI: https://doi.org/10.59490/imdc.2024.873 e-ISSN: 3050-4864

Alford et al. (2011) or the Critical Wave Groups method in Anastopoulos and Spyrou (2016), which greatly reduce the simulation time required. The role of simulators in design is enticing, but without the ability to identify "edges" in the design space, their usefulness is reduced (Schellin et al., 2015). Developing new computational methods which preserve nonlinearity, but are inexpensive to evaluate in a large number of wave conditions, is important to advancing simulation-based design (Hirdaris et al., 2014).

In recent years, machine learning (ML) methods have been explored to reduce the computational cost of predictions, but the accuracy of most ML methods is reduced when making predictions in wave conditions which differ from the original training dataset, and most data-only methods require a large amount of training data (Portillo Juan and Negro Valdecantos, 2022). Hybrid machine learning methods, which combine physics with ML techniques, have been shown to reduce the training data requirements (Willard et al., 2020). However, few examples of hybrid machine learning methods applied to global wave-induced loads are found in the literature. Several examples of data-only methods, such as the work of Moreira and Soares (2020), Hou et al. (2024), and Kwon et al. (2022) have been given, and a recent, and novel, approach in Wang and Ti (2024) which considers the wave-induced loads on bridge structures with arbitrary shapes. Several studies also take a probabilistic approach, such as the Bayesian models described in Zhu and Collette (2017). However, most studies focus on structural health monitoring in real-time, fatigue monitoring, or structural event detection. Moreover, most of these studies considered in-situ applications where data is plentiful, which often precludes their use in a design or analysis scenario, especially for unusual designs.

In this work, the hybrid machine learning method of Marlantes and Maki (2022) is considered in the context of the global wave-induced loads problem. The method relates a high-fidelity and low-fidelity model by a force correction that is modeled using an artificial neural network. To illustrate, Eq. (1) is the high-fidelity model, indicated by the superscript (h), and the solution to this differential equation is the high-fidelity state $\ddot{z}^{(h)}$. This model might be a RANS-CFD simulation or a fully-nonlinear three-dimensional panel method, but in general, the high-fidelity model is assumed to be both more accurate and signficantly more expensive to evaluate. Eq. (2) is the low-fidelity model–a model that is inexpensive to solve but lacks accuracy–indicated by superscript (l), where the solution to the equation is the low-fidelity state $\ddot{z}^{(l)}$.

$$m\ddot{z}^{(h)} = f^{(h)} \tag{1}$$

$$m\ddot{z}^{(l)} = f^{(l)} \tag{2}$$

Adding and subtracting the low-fidelity force model $f^{(l)}$ from Eq. (2) from the right-hand-side of Eq. (1) results in a force correction term δ, as shown by Eq. (4).

$$m\ddot{z}^{(h)} = f^{(l)} + f^{(h)} - f^{(l)} \tag{3}$$

$$m\ddot{z}^{(h)} = f^{(l)} + \delta \tag{4}$$

An analytical model for δ may not be available, so it is modeled using an artificial neural network, which introduces an error $\epsilon = \delta - \delta^*$, where δ^* is the approximate force correction obtained by the trained model. Considering this error, Eq. (4) becomes Eq. (5). A solution to Eq. (5) will yield an approximate high-fidelity state $\ddot{z}^*$ which will approach $\ddot{z}^{(h)}$ as $\epsilon \to 0$.

$$m\ddot{z}^* = f^{(l)} + \delta^* \tag{5}$$

Both recurrent neural networks like Long Short-Term Memory (LSTM) and simpler feed-forward densely-connected multilayer networks have been used to model δ, but it is found in Marlantes et al. (2023) that relatively small, simple networks are sufficient for ship hydrodynamics problems, with the added benefit that they are inexpensive to train and evaluate. The

primary consideration when designing the network is to accomodate numerical integration of Eq. (5). To this end, δ is modeled as a function of k-length discrete sequences of prior state $\{z\}_{n-k-1}^{n}$, $\{\dot{z}\}_{n-k-1}^{n}$, $\{\ddot{z}\}_{n-k-1}^{n}$ and the wave elevation $\{\eta\}_{n-k-1}^{n}$, where the current time is t^n. Therefore, the state and wave elevation comprise the input features of the neural network and the output is simply $\delta^{*,n+1}$.

In this paper, Eq. (5) is extended to the global loads problem by means of classical rigid beam theory. Of specific interest is how well the method performs in wave conditions which differ from the training dataset, and the role that the low-fidelity forcing model $f^{(l)}$ plays in this behavior. This property, known as generalizability, is critical to using data-driven simulation methods in a design scenario, where limited data is the norm. The ability to train a model of δ on a small, initial dataset, and then make predictions of wave-induced loads at similar fidelity in many additional wave conditions could provide considerable insight into the performance of a design.

THEORY

The classical model of global shear forces and bending moments assumes the hull behaves as a single rigid beam, as shown in Figure 1. While this model is greatly simplified, it will be used as the basis for this work as it encompasses the essential physics. The total length of the beam L is taken as the principle length of the vessel under consideration. We restrict the hull girder to move only in the vertical direction, z, such as in the heaving motion of a vessel in a seaway, reducing the problem to a single degree-of-freedom (DOF) system. As a consequence, any effect pitch motion may have on the nonlinear shear and bending moment is not considered. This simplifies the formulation of the hydrodynamic forces as they will depend only on heave motion and wave elevation, and will not have any coupling into rotation, which may alter the amplitude, frequency, or phase of the response.

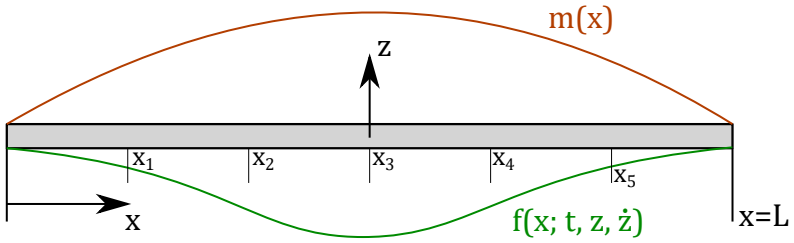

Figure 1: Hull girder as a rigid beam. The physical mass distribution $m(x)$ is time-invariant. The hydrodynamic force distribution $f(x;t,z,\dot{z})$ is shown at an instant in time t.

The dynamics of the rigid hull girder shown in Figure 1 follow Eq. (6), where the total physical mass M is the integral of the longitudinal mass distribution $m(x)$ and is assumed to be time-invariant. The total hydrodynamic force $F(t;z,\dot{z})$ varies with time t and is nonlinear with respect to the state variables z, $\dot{z}$ and is found by integrating the sectional hydrodynamic forces $f(x;t,z,\dot{z})$ over the length of the hull. Note that because the beam is rigid and moving only in heave, the vertical acceleration $\ddot{z}$ is pulled out of the integral on the left-hand-side of Eq. (7).

$$M\ddot{z} = F(t,z,\dot{z}) \tag{6}$$

$$\ddot{z}\int_0^L m(x)\,dx = \int_0^L f(x;t,z,\dot{z})\,dx \tag{7}$$

The total force $F(t;z,\dot{z})$ is nonlinear, high-fidelity, and assumed to be exact. Following the method outlined in the introduction, the high-fidelity total force $F(t,z,\dot{z})$ can be expressed in terms of a force correction $\Delta(t,z,\dot{z})$ to some inexpensive and low-order forcing model $F^{(l)}(t,z,\dot{z})$, given by Eq. (8). Similarly, the low-order total force $F^{(l)}$ and force correction Δ are the integral of their sectional counterparts $f^{(l)}$ and δ, respectively.

$$F(t,z,\dot{z}) = F^{(l)}(t,z,\dot{z}) + \Delta(t,z,\dot{z}) \tag{8}$$

$$= \int_0^L f^{(l)}(x;t,z,\dot{z})\,dx + \int_0^L \delta(x;t,z,\dot{z})\,dx \tag{9}$$

The instantaneous vertical shear force V at time t at a section $x = s$ balances the difference between the inertial forces I and hydrodynamic forces F acting on the hull girder up to s, as given by Eq. (10). The internal bending moment is found by a nearly identical process after including the lever-arm $(x - s)$ in the integrand, so for brevity it will not be presented here. We extend the same force-correction approach from Eq. (8) to the vertical shear force and bending moment. The resulting expression for shear is given by Eq. (12).

$$V(s;t) = I(s;t) - F(s;t,z,\dot{z}) \tag{10}$$

$$= \ddot{z}\int_0^s m(x)\,dx - \int_0^s f(x;t,z,\dot{z})\,dx \tag{11}$$

$$= \ddot{z}\int_0^s m(x)\,dx - \int_0^s \left[f^{(l)}(x;t,z,\dot{z}) + \delta(x;t,z,\dot{z})\right]\,dx \tag{12}$$

The sectional low-fidelity forcing model $f^{(l)}(x;t,z,\dot{z})$ and force correction $\delta(x;t,z,\dot{z})$ in Eq. (12) are the same terms as in Eq. (9). Therefore, we restrict our focus to the sectional forces at $x = s$, and express the dynamics of a section as Eq. (14), which is simply the two-dimensional version of Eq. (6). If the sectional forces $f^{(l)}$ and δ are modeled, the shear force and bending moment will follow.

$$m(s)\ddot{z}_s = f(s;t,z_s,\dot{z}_s) \tag{13}$$

$$= f^{(l)}(s;t,z_s,\dot{z}_s) + \delta(s;t,z_s,\dot{z}_s) \tag{14}$$

While a solution of Eq. (14) will yield a $\ddot{z}_s$ that is indeed different than $\ddot{z}$, due to the rigid body assumption, it differs by only a constant factor equal to L. Therefore, a solution to Eq. (14) captures the same underlying dynamics of the global problem and an investigation of Eq. (14) will allow us to make conclusions about Eq. (10). In the remainder of this work, we will focus primarily on Eq. (14), as it is the fundamental building block of the global loads problem.

Duffing Equation

To investigate the choice of $f^{(l)}$ on the performance of the method, a forced Duffing equation is used as a theoretical model of the sectional hydrodynamic force $f(s;t,z_s,\dot{z}_s)$, as it captures the salient features of the nonlinear hydrodynamics problem of a ship in waves. The Duffing equation model is given by Eq. (15), where c_1 and c_3 are the linear and cubic hydrostatic restoring coefficients, b_1 and b_2 are the linear and quadratic hydrodynamic damping coefficients, and the wave excitation forcing due to irregular waves is expressed as a summation of harmonic wave components. The wave excitation is made nonlinear by including the state z_s in the amplitude, modified by a coefficient α.

$$m(s)\ddot{z}_s = \sum_i (\zeta_i - \alpha z_s)\cos(k_i s + \omega_i t + \phi_i) - c_1 z_s - c_3 z_s^3 - b_1\dot{z}_s - b_2\dot{z}_s^2 \tag{15}$$

The wave component amplitudes ζ_i, wave numbers k_i, and angular frequencies ω_i are sampled from a generic wave energy spectrum $S(\omega)$ given by Eq. (16), where H_s is the significant wave height and ω_p is the peak frequency. The component phase angles ϕ_i are selected randomly from the range $[-2\pi : 2\pi]$.

$$S(\omega) = H_s^2 \frac{5}{3} \frac{\omega_p^4}{\omega^5} \exp\left(-\frac{5}{4}\left(\frac{\omega_p}{\omega}\right)^4\right) \tag{16}$$

To cast Eq. (15) in the form of Eq. (14), we must choose a model for $f^{(l)}(s; t, z_s, \dot{z}_s)$. This choice will determine the physics that are solved directly versus what must be learned by the ML model for δ_s. Five different low-fidelity forcing models are proposed, given by Eqs. (17)-(21), with Eq. (17) having the most physics retained (and consequently the least physics that must be learned in δ_s). In Eq. (21), the entire forcing function must be learned by the ML model.

Model A: $$f_A^{(l)}(s; t, z_s, \dot{z}_s) = \sum_i \zeta_i \cos(k_i s + \omega_i t + \phi_i) - c_1 z_s - b_1 \dot{z}_s \tag{17}$$

B: $$f_B^{(l)}(s; t, z_s, \dot{z}_s) = -c_1 z_s - b_1 \dot{z}_s \tag{18}$$

C: $$f_C^{(l)}(s; t, z_s, \dot{z}_s) = -c_1 z_s \tag{19}$$

D: $$f_D^{(l)}(s; t, z_s, \dot{z}_s) = \sum_i \zeta_i \cos(k_i s + \omega_i t + \phi_i) - c_1 z_s \tag{20}$$

E: $$f_E^{(l)}(s; t, z_s, \dot{z}_s) = 0 \tag{21}$$

To further illustrate the differences in the low-fidelity forcing models, Table 1 shows the force contributions that are modeled analytically and those that are data-driven for each choice of forcing model $f^{(l)}(s; t, z_s, \dot{z}_s)$.

Table 1: Forces retained as physics (P) in $f^{(l)}(s; t, z_s, \dot{z}_s)$ or learned by ML in δ_s

		Forcing Model				
Force Description	Term	A	B	C	D	E
Linear Restoring	$c_1 z_s$	**P**	**P**	**P**	**P**	ML
Nonlinear Restoring	$c_3 z_s^3$	ML	ML	ML	ML	ML
Linear Damping	$b_1 \dot{z}_s$	**P**	**P**	ML	ML	ML
Nonlinear Damping	$b_2 \dot{z}_s^2$	ML	ML	ML	ML	ML
Linear Excitation	$\sum_i \zeta_i \cos(..)$	**P**	ML	ML	**P**	ML
Nonlinear Excitation	$\sum_i -\alpha z_s \cos(..)$	ML	ML	ML	ML	ML

RESULTS

The Duffing equation is configured using $m(s) = 1.0$, $c_1 = 1.0$, $c_3 = 0.01$, $b_1 = 0.1$, $b_2 = \alpha = 0$ so that the only nonlinear term is the cubic restoring force. For a given significant wave height H_s and peak frequency ω_p, the wave elevation η_s, and time series of nonlinear state z_s, $\dot{z}_s$, $\ddot{z}_s$ and force correction δ_s, are generated by solving Eq. (15) numerically. This is done to generate training data which are used to train the ML model for δ_s. In addition, testing data are also generated, but these data are used to verify the performance of the trained models and are not used during the training process, as is discussed later in this section.

Throughout the study, each of the five low-fidelity forcing models given in Table 1 are considered. In all time series, a time step of $\Delta t = 0.1$ s is used. Also, when sampling the wave spectrum to create η_s, the sample frequency bandwidth is taken

such that the repeat period of the resulting summation is equal to the length of the time series.

An ML model consisting of a feed-forward, densely-connected neural network with 2 hidden layers, 30 nodes per layer, and ReLU activation functions is trained for each δ_s corresponding to each low-fidelity forcing model $f_s^{(l)}$. In this work, a stencil length k = 5 is used, per the recommendations outlined in Marlantes et al. (2023). The reason a small k is effective in this case is because the nonlinear force components are functions only of the instantaneous state variables z_s and $\dot{z}_s$. Each model is trained for a total of 1000 epochs until the training loss no longer improves, however, only the weights from the epoch with the lowest loss are retained as final weights. The training time for each model is approximately 1 minute on a modest computing platform.

The average L_2 error, L_∞ error, given by Eqs. (22) and (23), respectively, are used to evaluate the accuracy of the time series predictions in terms of RMS and extreme values.

$$L_2 = \sqrt{\frac{\sum_i^N (\hat{x} - x)^2}{N}} \tag{22}$$

$$L_\infty = \max(|\hat{x} - x|) \tag{23}$$

However, such measures are sensitive to small phase errors. As a more powerful measure of performance, the Jensen-Shannon divergence (JSD), as given by Eq. (24), is used to estimate the entropy of the predicted response pdf relative to a known reference pdf. P is the reference distribution and Q is the model distribution, both being pdfs, and M is the mixture. The Jensen-Shannon divergence is based on the Kullback-Leibler divergence D, given by Eq. (25), which is a measure of the relative entropy between the model distribution K and the reference distribution M, both defined over the domain χ. It can be thought of as a measure of information loss, or expected surprise, if a certain distribution is used to model a reference distribution. A lower JSD means the model is closer to the reference, with a divergence of zero meaning the two distributions are identical.

$$JSD(P\|Q) = \frac{1}{2}D(P\|M) + \frac{1}{2}D(Q\|M) \tag{24}$$

$$M = \frac{1}{2}(P + Q)$$

$$D(K\|M) = \sum_{x \in \chi} K(x) \log\left(\frac{K(x)}{M(x)}\right) \tag{25}$$

The L_2, L_∞, and JSD metrics will be evaluated on predictions of the sectional acceleration $\ddot{z}_s$ as it captures both the accuracy of the force integral on the right-hand-side of Eq. (9), as well as the inertial force of the entire beam to a constant factor.

Training Data Size

We wish to use the smallest training dataset possible, so the influence of training dataset size on prediction accuracy is first investigated. Using a significant wave height H_s = 1.0 and a peak frequency of ω_p = 1.0, irregular wave records of η_s ranging in total length of 10 s up to 1000 s are generated, and the corresponding responses z_s, $\dot{z}_s$, $\ddot{z}_s$, and the force correction δ_s are computed. Using this data, an ML model is trained for each low-fidelity forcing model in Table 1. The trained models are used to make predictions of the response in 1000 s of irregular waves with the same H_s = 1.0 and ω_p = 1.0, but with different random phase angles. For each model, the L_2, L_∞, and JSD are computed. Figure 2 shows the prediction errors vs

training dataset size for each low-fidelity forcing model. Note that the training dataset size is given as the number of Zero-Up-Crossings (ZUCs) in the wave record, as this is a more meaningful measure of response encounters than time alone.

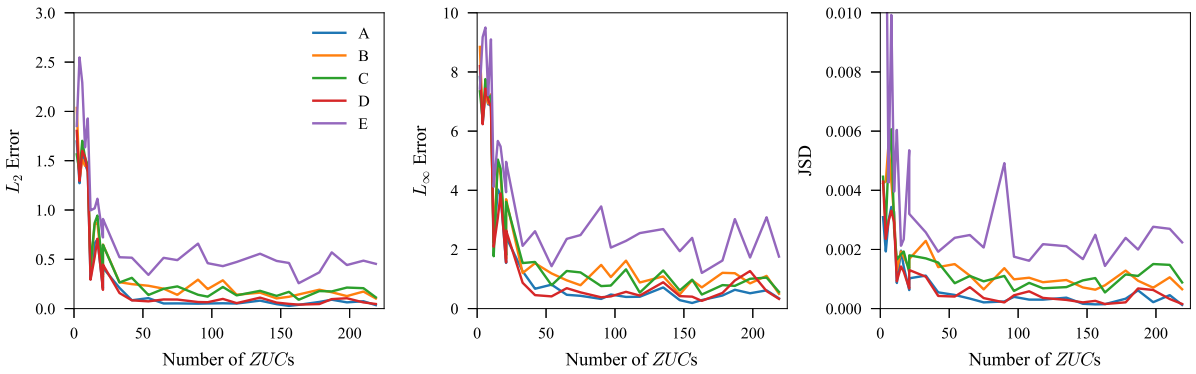

Figure 2: L_2, L_∞, and JSD prediction errors for each low-fidelity forcing model over increasing training data size measured in wave record Zero-Up-Crossings (ZUCs). Predictions are in irregular waves $H_s = 1.0$, $\omega_p = 1.0$, with random phase angles that differ from the training dataset.

Figure 2 shows that prediction errors of the five different models converge at roughly the same rate relative to the size of the training dataset. Datasets of approximately 50 ZUCs and larger yield similar prediction errors, with the exception of model E, which requires at least 100 ZUCs.

Generalizability in H_s

Training data is generated for two different significant wave heights, $H_s = 0.7$ and $H_s = 1.0$, at a peak frequency of $\omega_p = 1.0$ for a total time series lenth of 500 s, or about 108 ZUCs to correspond with the findings in Figure 2. The time series for the state variables z_s, $\dot{z}_s$, $\ddot{z}_s$, and wave elevation η_s are shown in Figure 3.

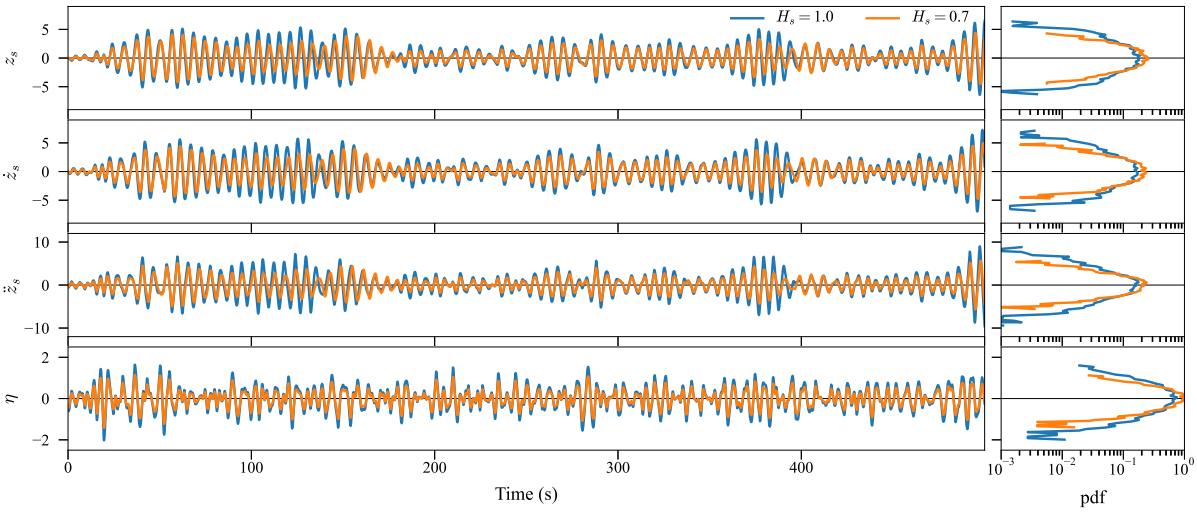

Figure 3: Training data time series for Duffing equation: $m(s) = 1.0$, $c_1 = 1.0$, $c_3 = 0.01$, $b_1 = 0.1$, $b_2 = \alpha = 0$, in irregular waves: $H_s = 0.7$ and $H_s = 1.0$, $\omega_p = 1.0$.

Figure 4 shows the corresponding δ_s for each low-fidelity forcing model for the training data case $H_s = 1.0$ and $\omega_p = 1.0$. Note the difference in magnitude of δ_s between the models, where $\delta_{E,s}$ encompasses all of the hydrodynamic forces.

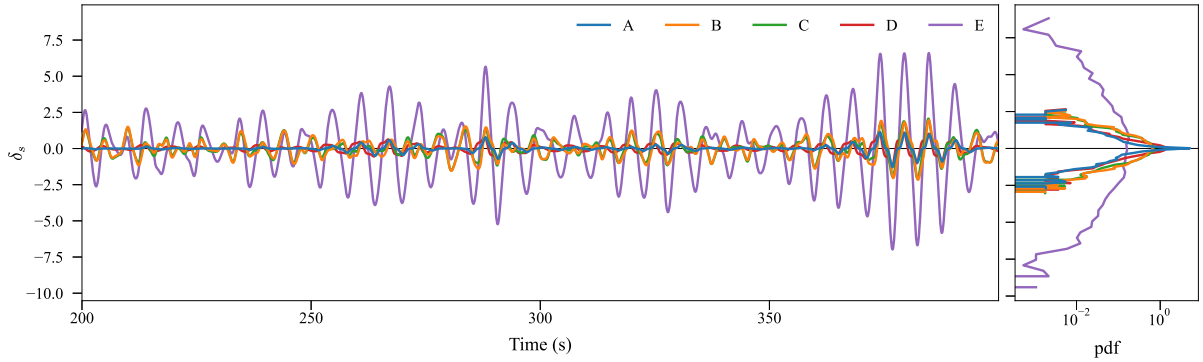

Figure 4: Training data for force correction δ_s for the five different low-fidelity forcing models $f_j^{(l)}$, $j = A, B, C, D, E$ in irregular waves: $H_s = 1.0$, $\omega_p = 1.0$. The time series is given only from 200 s to 400 s so that the difference between the models is easier to distinguish, however, the pdfs are generated from the entire 500 s time series.

Training data for two different H_s are shown in Figure 3, however, only one realization will be used for training at one time. This represents the minimum useful training dataset: 100 ZUCs in a single H_s. ML models for each of the five low-fidelity forcing models are trained at each wave height, to investigate any difference the training H_s may have on the performance of the models when making predictions.

As a benchmark, a Long Short-Term Memory (LSTM) neural network is also trained using a sequence-to-sequence paradigm, where the entire wave elevation η_s is used as the input to the network, and the output is the corresponding responses z_s, $\dot{z}_s$, and $\ddot{z}_s$. LSTM networks and their variants are widely used in literature on data-driven modeling of marine dynamics (Xu et al., 2021), (Silva and Maki, 2022), and may be the predominant data-driven model for time series modeling. Due to its popularity, the LSTM is chosen for comparison. The network is composed of 4 hidden layers with 50 cells per layer to mimic the models used in Xu (2020). The model is trained for 200 epochs, until the loss plateaus at a value less than 1%. The best weights during the training process are restored at the end of the training process. The training time for the LSTM network using the data in Figure 3 is approximately 2 hours on a modest computing platform.

A testing dataset is generated for a range of significant wave heights H_s from 0.01 to 1.5 and a peak frequency $\omega_p = 1.0$ over 1000 s of time. The component phase angles ϕ_i are selected randomly to differ from the phase angles used in the training dataset. Each trained ML model is used to make predictions of the responses in each H_s from the testing dataset. Using Eqs. (22) through (24), the L_2, L_∞, and JSD metrics for the predictions are computed over the last 900 s of time series, omitting the first 100 s as it is a transient region. Figure 5 shows the performance metrics for each low-fidelity forcing model, the LSTM predictions, and a benchmark linear model, over the range of test significant wave heights. The wave height that was used for training is marked by a vertical line in each figure.

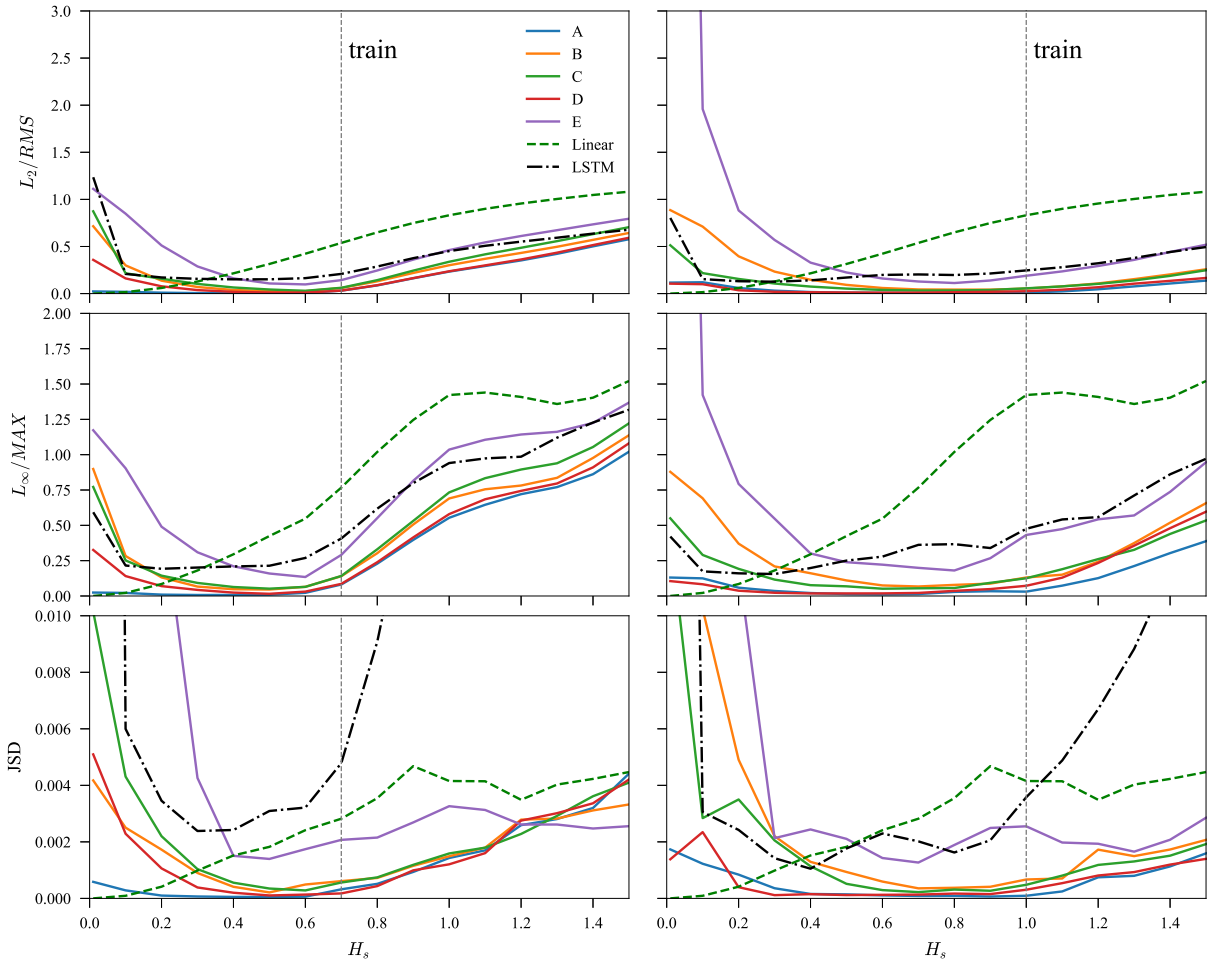

Figure 5: L_2, L_∞, and JSD error metrics for predictions of $\ddot{z}_s$ for different low-fidelity forcing models over a range of H_s. The left panels correspond to models trained using H_s = 0.7, and the right panels H_s = 1.0. Results from the LSTM predictions are also shown for comparison. The linear model is also included to show how the linear error decreases to zero in the limit of small significant wave heights.

Figure 5 shows model A–the model that retains the most physics–performs better than the other models, and the LSTM benchmark, in nearly all wave conditions. This suggests that the more physics that are retained as analytical terms in the model, i.e. not data-driven, the generalizability of the model is improved. This is especially evident at low wave heights, where the low-fidelity physics enforce the correct dynamics at the linear limit. The L_2 and L_∞ errors from the LSTM predictions are roughly in line with model E, which is perhaps intuitive as it is almost a purely data-driven model as well. Training in larger H_s seems to reduce prediction errors in larger H_s, while slightly increasing prediction errors at low-H_s. However, this difference is greatly reduced in models which retain more physics.

To emphasize the performance of model A further, Figures 6 and 7 give the time series and pdfs of the predictions for each forcing model and the LSTM benchmark at the smallest H_s = 0.01 and the largest H_s = 1.5 significant wave heights. It is shown that the LSTM model struggles in both extremes, especially to predict the tails of the distribution. In comparison, models A and D perform well for both cases. Model E performs the worst, greatly over-predicting the response in small H_s, appearing as rapid, but stable, oscillations. Consider the pdf for model A at H_s = 0.01 in Figure 6 and note the sensitivity of the JSD to small errors in the predicted distributions, as this proposed model fits qualitatively well to the reference distribution, but the small errors in the tails are magnified in Figure 5.

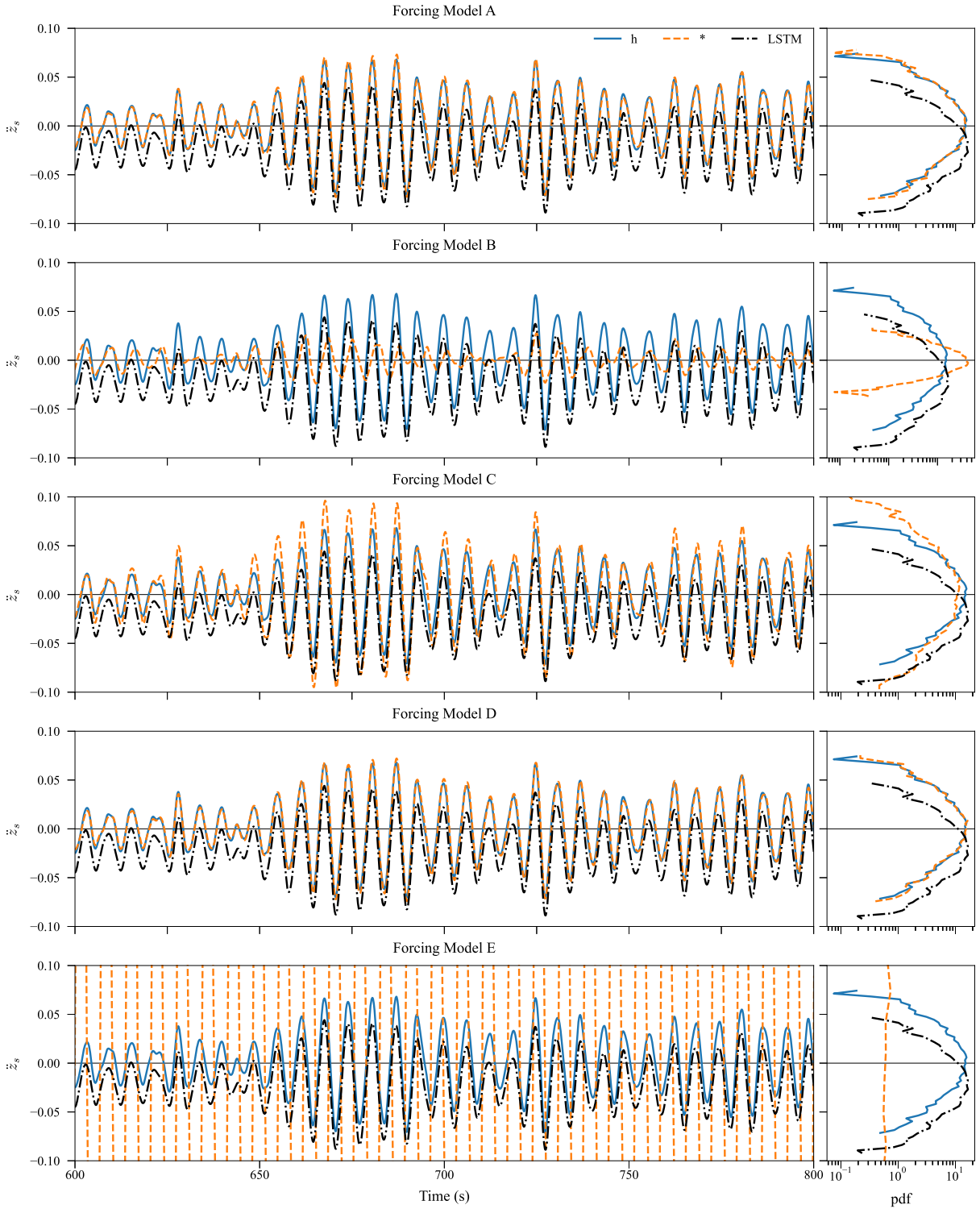

Figure 6: Predictions of $\ddot{z}_s$ in irregular waves $H_s = 0.01$, $\omega_p = 1.0$ using the proposed method with different low-fidelity forcing models. Each model is trained in irregular waves with $H_s = 1.0$, $\omega_p = 1.0$. Results from an LSTM prediction are also shown for comparison. Only 200 s of response is shown for clarity, however, the distributions encompass the entire 1000 s time series.

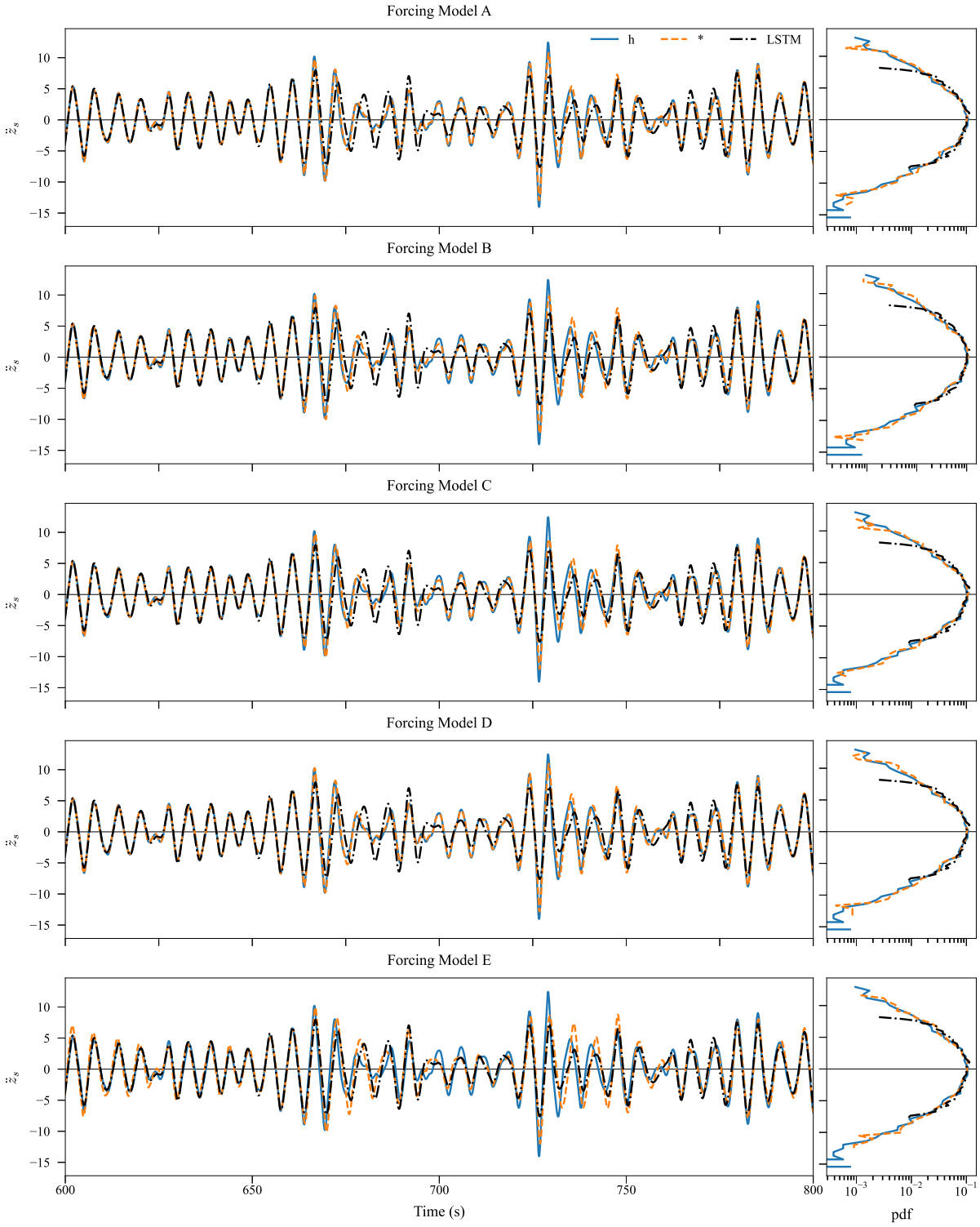

Figure 7: Predictions of $\ddot{z}_s$ in irregular waves $H_s = 1.5, \omega_p = 1.0$ using the proposed method with different low-fidelity forcing models. Each model is trained in irregular waves: $H_s = 1.0, \omega_p = 1.0$. Results from an LSTM prediction are also shown for comparison. Only 200 s of response is shown for clarity, however, the distributions encompass the entire 1000 s time series.

CONCLUSIONS

The results of this study show that the neural-corrector method of Marlantes and Maki (2022) can be extended to the global loads problem and provide predictions in a range of irregular wave conditions that differ from the original training dataset. It is also found that retaining low-fidelity physics greatly improves the generalizability of the model. The accuracy of the predictions exceeds that of an LSTM benchmark when trained on an equivalent training dataset, especially in preserving the tails of the response distributions. The fact that a simple, feed-forward neural network as used in the proposed method offers improved performance over a typical LSTM model is largely due to the inclusion of low-fidelity physics in the formulation. A well-tuned linear model intrinsically captures much of the important dynamics of the problem, so that the ML correction must learn only higher-order terms, as shown in Marlantes and Maki (2022), such that a much simpler network is adequate. Finally, the proposed method, when including the most physics in the low-fidelity forcing model, requires a dataset of responses encompassing only 50 - 100 irregular wave encounters.

This work considered the responses of only a single section of the global loads problem. To implement multiple sections in unison, there are two possibilities: training a single model with multiple output nodes corresponding to a spatial discretization of $\delta(x; t, z, \dot{z})$ at different longitudinal locations; or, training multiple models with single node outputs–such as done in this paper. In the former case, the output nodes must respect the integral on the right-hand-side of Eq. (9), which could be enforced in the loss function during training.

CONTRIBUTION STATEMENT

Kyle E. Marlantes: Conceptualization; data curation; formal analysis; software; visualization; methodology; writing – original draft. **Kevin J. Maki:** Conceptualization; supervision; methodology; writing – review and editing.

ACKNOWLEDGEMENTS

This work was supported financially by grants from the US Office of Naval Research (ONR).

REFERENCES

Alford, L. K. (2008). *Estimating Extreme Responses Using a Non-Uniform Phase Distribution.* PhD thesis.

Alford, L. K., Kim, D.-H., and Troesch, A. W. (2011). Estimation of extreme slamming pressures using the non-uniform fourier phase distributions of a design loads generator. *Ocean Engineering*, 38(5):748–762.

Anastopoulos, P. A. and Spyrou, K. J. (2016). Ship dynamic stability assessment based on realistic wave group excitations. *Ocean Engineering*, 120:256–263.

Andersen, I. M. V. and Jensen, J. J. (2014). Measurements in a container ship of wave-induced hull girder stresses in excess of design values. *Marine Structures*, 37:54–85.

Gaspar, B., Teixeira, A., and Guedes Soares, C. (2016). Effect of the nonlinear vertical wave-induced bending moments on the ship hull girder reliability. *Ocean Engineering*, 119:193–207.

Guedes Soares, C. (1991). Effect of transfer function uncertainty on short-term ship responses. *Ocean Engineering*, 18(4):329–362.

Hirdaris, S., Bai, W., Dessi, D., Ergin, A., Gu, X., Hermundstad, O., Huijsmans, R., Iijima, K., Nielsen, U., Parunov, J., Fonseca, N., Papanikolaou, A., Argyriadis, K., and Incecik, A. (2014). Loads for use in the design of ships and offshore structures. *Ocean Engineering*, 78:131–174.

Hou, C., Wang, W., Li, Y., Wang, X., Zhang, H., and Hu, Z. (2024). A predicting method for the mechanical property response of the marine riser based on the simulation and data-driven models. *Ocean Engineering*, 293:116612.

Juncher, J. and Terndrup, P. (1979). Wave induced bending moments in ships–a quadratic theory.

Kwon, D.-S., Jin, C., and Kim, M. (2022). Prediction of dynamic and structural responses of submerged floating tunnel using artificial neural network and minimum sensors. *Ocean Engineering*, 244:110402.

Marlantes, K. E., Bandyk, P. J., and Maki, K. J. (2023). Investigating nonlinear forces in ship dynamics using machine learning. In *Proceedings of the 10th International Conference on Computational Methods in Marine Engineering (MARINE), Madrid, Spain*.

Marlantes, K. E. and Maki, K. J. (2022). A neural-corrector method for prediction of the vertical motions of a high-speed craft. *Ocean Engineering*, 262:112300.

Marlantes, K. E. and Taravella, B. M. (2019). A fully-coupled quadratic strip theory/finite element method for predicting global ship structure response in head seas. *Ocean Engineering*, 187:106189.

Moreira, L. and Soares, C. G. (2020). Neural network model for estimation of hull bending moment and shear force of ships in waves. *Ocean Engineering*, 206:107347.

Parunov, J., Guedes Soares, C., Hirdaris, S., Iijima, K., Wang, X., Brizzolara, S., Qiu, W., Mikulić, A., Wang, S., and Abdelwahab, H. (2022a). Benchmark study of global linear wave loads on a container ship with forward speed. *Marine Structures*, 84:103162.

Parunov, J., Guedes Soares, C., Hirdaris, S., and Wang, X. (2022b). Uncertainties in modelling the low-frequency wave-induced global loads in ships. *Marine Structures*, 86:103307.

Payer, H. G. and Schellin, T. E. (2013). A class society's view on rationally based ship structural design. *Ships and Offshore Structures*, 8(3-4):319–336.

Portillo Juan, N. and Negro Valdecantos, V. (2022). Review of the application of artificial neural networks in ocean engineering. *Ocean Engineering*, 259:111947.

Rajendran, S., Fonseca, N., and Soares, C. G. (2016). Prediction of extreme motions and vertical bending moments on a cruise ship and comparison with experimental data. *Ocean Engineering*, 127:368–386.

Schellin, T. E., Shigunov, V., Troesch, A. W., Kim, D.-H., and Maki, K. (2015). Prediction of loads for ship structural design. *Naval Engineers Journal*, 127(1):103–134.

Silva, K. M. and Maki, K. J. (2022). Data-driven system identification of 6-dof ship motion in waves with neural networks. *Applied Ocean Research*, 125:103222.

Temarel, P., Bai, W., Bruns, A., Derbanne, Q., Dessi, D., Dhavalikar, S., Fonseca, N., Fukasawa, T., Gu, X., Nestegård, A., Papanikolaou, A., Parunov, J., Song, K., and Wang, S. (2016). Prediction of wave-induced loads on ships: Progress and challenges. *Ocean Engineering*, 119:274–308.

Wang, H. and Ti, Z. (2024). Wave force prediction on truncated cylinders with arbitrary symmetric cross-sections using machine learning. *Ocean Engineering*, page 116716.

Willard, J., Jia, X., Xu, S., Steinbach, M., and Kumar, V. (2020). Integrating physics-based modeling with machine learning: A survey.

Wu, M. and Hermundstad, O. A. (2002). Time-domain simulation of wave-induced nonlinear motions and loads and its applications in ship design. *Marine Structures*, 15(6):561–597.

Xu, W. (2020). *A Machine Learning Framework to Model Extreme Events for Nonlinear Marine Dynamics*. PhD thesis, University of Michigan, Ann Arbor, MI.

Xu, W., Maki, K. J., and Silva, K. M. (2021). A data-driven model for nonlinear marine dynamics. *Ocean Engineering*, 236:109469.

Zhu, J. and Collette, M. (2017). A bayesian approach for shipboard lifetime wave load spectrum updating. *Structure and Infrastructure Engineering*, 13(2):298–312.

Proceedings of 15th International Marine Design Conference (IMDC-2024)
June 2-6, 2024
Amsterdam, the Netherlands

Supplementing Industry-Specific Dynamic Positioning Requirements to Network Theory

E.L. Scheffers[1*] and P. de Vos[1]

ABSTRACT

The trend towards fully autonomous navigation or reduced manning concepts, coupled with increased integration and interdependence of onboard systems due to the shift towards sustainable fuels and ever-increasing electrification and automation, has stressed the significance of ship systems' reliability. These developments reinforce the demand for a clear assessment of the robustness of main and auxiliary systems in early-stage ship design. Network theory offers a promising approach to address this demand. However, current graph measures do not align with industry-specific requirements for improving system robustness. This study aims to augment robustness evaluation components, such as modularity (independent subsystems), redundancy and reconfigurability, with additional considerations specific to Dynamic Positioning (DP) applications in the maritime industry. The enhanced robustness evaluation components are translated into graph measures. By employing these graph measures, different systems can be compared with respect to robustness, enabling informed decision-making in the trade-offs typical to early stages of the design process (e.g., cost versus redundancy). The proposed methodology combines the principles of network theory and industry-specific DP requirements to provide a comprehensive framework for evaluating the robustness of ship systems. System reliability can be assessed by integrating the identified robustness components and incorporating them into the graph measures. The early findings of this study show the potential to improve ship design processes by providing a systematic and quantifiable approach to enhance robustness.

KEY WORDS

Onboard Distribution Systems; Dynamic Positioning Regulations; Ship Design; Network Theory; Robustness; Reliability; Design Heuristics

INTRODUCTION

Safety and reliability are two of the most essential aspects in the process of ship design, as becomes particularly clear in the regulations for ships with Dynamic Positioning (DP) capability. A common way to express different levels of reliability for DP systems is by specifying the so-called "DP class" of the vessel. A Dynamic Positioned Vessel (DP Vessel) is:

> *A unit or a vessel which automatically maintains its position and/or heading (fixed location, relative location or predetermined track) by means of thruster force (ABS (2021))*.

The DP class regulations are subsequently based on increasing degrees of redundancy within the system. The high and

[1] Department of Maritime and Transport Technology, Delft University of Technology, Delft, the Netherlands
[*] Corresponding Author: E.L.Scheffers@tudelft.nl

Submitted: 7 March 2024, Revised: 8 May 2024, Accepted: 9 May 2024, Published: 14 May 2024

Conference paper, DOI: https://doi.org/10.59490/imdc.2024.820 e-ISSN: 3050-4864

well-defined redundancy facilitating maintaining a position is essential in the continuous operation of, for example, wind-turbine installation vessels, crew supply vessels and other offshore operations vessels because it increases the availability of the ships in more challenging conditions.

The first step of a theoretical DP system approach is to define the underlying principles of the system requirements. All requirements share a common goal: to increase the system's overall reliability. The number of definitions in this study, especially due to its interdisciplinary character, is high; the aim is to be explicit in the meaning of discussed concepts. Therefore, Table 1 provides an overview of reliability-related concepts from a marine engineering perspective. In Table 2, the right column contains the assumed working principle related to the system requirement. Most requirements are based on "component redundancy", whilst the aspects "distribution redundancy" and "independent subsystems" are both applied once.

The DP System is the complete installation necessary for dynamically positioning a vessel including, but not limited to the power system, thruster system, DP control system and independent joystick system (ABS (2021)). Regulations encompassing DP subsystems have been explicitly defined by IMO since 1994. The IMO acknowledges equipment class 1,2 and 3. The ABS levels of class notation, DPS-1, DPS-2 and DPS-3 are in line with the IMO classes and are stricter with regard to robustness requirements with an increasing level of DP class notation. Table 2 shows an overview of DP system requirements by subsystem and DP level (Clavijo et al. (2022)). The right column shows the related reliability principles, explained hereafter. In the development of these rules, experience and expert advice have been of leading influence. Therefore, we can consider the DP rules to be mainly based on empirical evidence, i.e. a posteriori knowledge. If we can design a framework in which we can understand the theoretical concepts behind the regulations, we can develop a priori knowledge with theoretical evidence. This understanding could aid in increasing the design space and possibly safer systems. The interdisciplinary scientific study of networks enables the use of tools or metrics based on graph theory. Network theory combines ideas from e.g. mathematics, physics and computer science to understand networks better. These networks can represent the system topology of the aforementioned DP subsystems. Using a network representation allows for system analysis in early design stages since the network can be defined using very limited To the authors' knowledge, no prior studies exist on the comparison between empirical DP regulations and theoretical network metrics.

Table 1: Robustness and Reliability Concepts

Concept	Definition
Robustness	The ability of distribution systems on board of (war)ships to withstand perturbations during system operation (Vos de & Stapersma (2018))
Reliability	The ability of a system to function as required without fault under given conditions during the given period quantified as the probability that a system will not fail or malfunction (Makoto ITO (2022))
Resilience	The ability of a system to withstand failure and to continue operations following failure (ABS (2021))
Redundancy	Ability of a component or system to maintain or restore its function when a single fault has occurred (ABS (2021)) The extent of degradation the structure can suffer without losing some specified elements of its functionality (Kanno & Ben-Haim (2011))
Component Redundancy	Achieved by the installation of multiple components (ABS (2021))
Distribution Redundancy	The presence of "independent alternative paths between source and demand nodes which can be used to satisfy supply requirements during disruption or failure of the main paths" (Goulter (1987))
Independent subsystems	Two or more component groups, each of which is capable of individually and independently performing a specific function (ABS (2021))

Paper Outlook

A comparison between empirical DP regulations and theoretical network metrics is a new approach. Therefore, the focus of this paper is 1) to provide a clear outline of the assumptions made to enable the comparison, 2) to introduce a selection

Table 2: Subsystem requirements (Clavijo et al. (2022)) and the corresponding reliability principles

Subsystem (Item)	**Minimum system requirements**			**Reliability Principle**
	Class 1	**Class 2**	**Class 3**	
Power subsystem				
Generators and prime movers	Non-redundant	Redundant	Redundant	Component redundancy
Switchboard	1	1 with bus-tie 1 with coupler	2 with bus-tie in separate compartments 1 with coupler	Distribution redundancy
Bus-tie breaker	No	1 (open or closed)	2 (open)	Independent subsystems
Power management	No 1	Yes 2	Yes 3	
Thruster subsystem				
Rudders	Non-redundant	Redundant	Redundant	Component redundancy
Thruster	Non-redundant	Redundant	Redundant	Component redundancy
Single lever for each thruster at main DP-control center	Yes	Yes	Yes	Component redundancy
Control subsystem				
Position reference system (PRS)	2	3	2 + 1 backup	Component redundancy
Vertical reference sensor (VRS)	1	3	2 + 1 backup	Component redundancy
Wind	2 2	3 3	2 + 1 backup 3	Component redundancy
Gyro	2 1	3 3	2 + 1 backup 3	Component redundancy
Uninterruptible power supply (UPS)	1 1	2 2	2 + 1 backup 3	Component redundancy
Independent joystick system (IJS)	Yes	Yes	Yes	Independent subsystems
Computer system: number of control computers	1 1	2 2	2 + 1 backup 3	Component redundancy
Consequence analyzer	No	Yes	Yes	
Backup control station	No	No	Yes	Backup

of network metrics and their working principles, and 3) to discuss the comparison and future research directions. The paper starts with the ”translation” from system diagrams to networks and the related assumptions (Section ”Method: Network Definition”). The next Section introduces a selection of reliability network metrics, classified using the theoretical reliability principles which are deduced from the DP regulations (Section ”Method: Network Reliability Metrics”). The method, consisting of the network definition and reliability metrics, is applied to a case study of two DP systems (Section ”Case Study”). Concluding this paper, we will discuss the results, reflect on the approach and draw final conclusions (Section ”Conclusion”)

METHOD: NETWORK DEFINITION

The DP System is the complete installation necessary for dynamically positioning a vessel (ABS (2021)). The following components or machines are always present in a DP system: electric power generation components such as engine-generator sets, multiple levels of electric power distribution via switchboards and distribution boards, electric converters, electric motors driving thrusters, a control system and finally, non-propulsion-related electric power consumers. When a comparable level of detail is maintained, most steps in translating a system to a network topology are straightforward. In each graph representation G of a network, components like generators, thrusters and converters are represented as nodes or vertices V; pipes, shafts and cables are represented as links or edges E so that a network becomes a combination of nodes and edges $G(V, E)$. The networks are assumed to be simple undirected, unweighted connected graphs, meaning that the network 1) does not contain two or more connections between a pair of nodes, there are no self-loops (connections starting and ending at the same node), 2) the edges are undirected (the start point and end point can be considered interchangeably), 3) all edges have weight 1, and 4) all nodes are connected via one or more paths (Newman (2010)). The first three of these network properties result in a simplified network representation, only considering the network properties present in the logical architecture representation as defined by Brefort et al. (2018). The edges are undirected because edge direction is considered a temporal aspect and, therefore, part of the operational architecture. Certain aspects, however, are more subjective in their representation approach. Therefore, they are explained separately in the following sections.

Distribution system components

The switchboard is a less straightforward component within the translation from system diagram to network topology. A switchboard as part of an electric system diagram is often represented as a (double) line or bar with different connecting lines entering and exiting this bar. The two extreme approaches to modelling a switchboard are shown in Figure 1a and Figure 1b respectively: the entire switchboard as a single point of failure. Meaning that, if something fails within the switchboard, in the model this is approached by a failure of the entire switchboard. The other extreme is disregarding the switchboard altogether and connecting the supplier nodes directly to all possible user nodes, as if the system is a complete bipartite graph (Newman (2010)). A failure within the switchboard influences a certain connection between this supplier and user but does not influence any of the other connections. Other approaches are, in terms of reliability, found between these extremes.

In this study, the switchboards are an essential part of the analysis since they are explicitly mentioned in the regulation overview in Table 2. Therefore, they must be included in the network. Considering switchboards as nodes within the network is in line with the node differentiation approach by Vos de (2018), who considered converter nodes (like generators) and hub nodes (like switchboards). This is approached by having the switchboards present as nodes connected to other nodes that represent the switchboard input and output ports. Whenever a switchboard is split by a switch or a bus-tie, a second node is added to the switchboard.

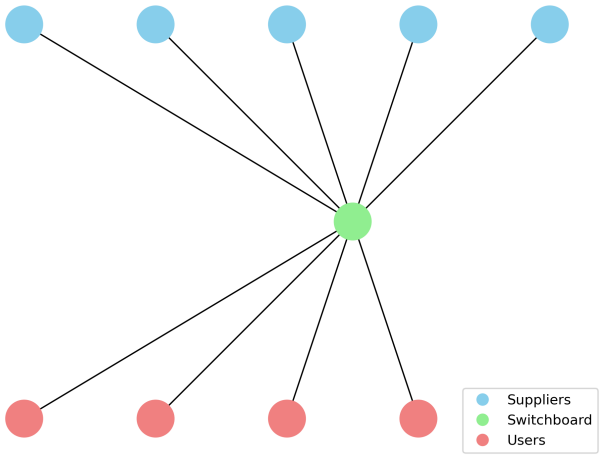

(a) Complete switchboard represented as single node → single point of failure

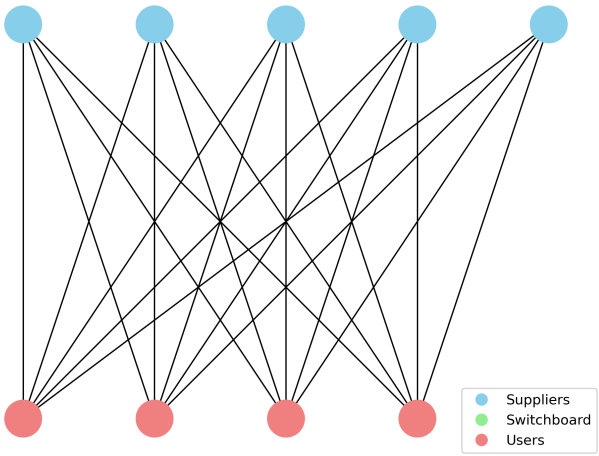

(b) Complete switchboard overlooked by directly connecting all supplier nodes to user nodes

Figure 1: Extremes of distribution component network representations

Control system

The control system is taken into consideration separately as part of simplifying the network representation. The control system is an essential part of the network; however, it is of such a different nature that it cannot automatically be compared using the same tools as the physical system components and connections. Moreover, the design freedom to determine the topology of the control system is so significant that the subjective choices made influence the network too significantly. This case study considers values of the network including and excluding the control system.

Spatial considerations

An important part of improving resilience is by placing redundant components in separate compartments. This spatial aspect is, within this study, only taken into consideration when it is explicitly present in the system diagram. This differentiation between spatial system design and logical system design is in line with Brefort et al. (2018) and his division between functional architecture, logical architecture and physical architecture in the analysis of onboard systems.

METHOD: NETWORK RELIABILITY METRICS

Component Redundancy

This reliability aspect refers to redundancy achieved by the installation of multiple components performing a certain function (ABS (2021)). In this study, we do not apply system diversification (using different yet functionally similar components) to prevent common cause failures from happening. The following two network metrics have been selected to be a proxy measure for component redundancy: effective resistance (Ellens & Kooij (2013)) and maximum flow (Newman & Girvan (2004)).

Effective Graph Resistance

Following the approach of (Ellens & Kooij (2013)), component redundancy facilitates parallel paths within a network and, therefore, increases with decreasing graph resistance. The effective graph resistance is based on the number of paths (parallel) and the length of paths (series) between different sets of nodes, which indicates the vulnerability of the connection between those nodes Ellens et al. (2011). In line with electrical resistance, a lower value suggests an "easier" flow between nodes. Therefore, we assume that the component redundancy increases with a decreasing graph resistance. Moreover, the effective graph resistance strictly decreases when an edge is added (Ellens & Kooij (2013)). The resistance between two nodes can be calculated using standard series and parallel resistance calculations. If each edge has a resistance $r = 1$ Ohm, two nodes (a and b) connected by a single path of length 2 have a resistance of

$$r_{a\to c} = r_{a\to b} + r_{b\to c} = 1 + 1 = 2 \text{ Ohm} \tag{1}$$

Where$r_{a\to c}$ is called the effective resistance or resistance distance between node a and b. Adding an extra path between these respective nodes of length 3 gives

$$\begin{aligned} \tfrac{1}{r_{a\to c}} &= \tfrac{1}{r_{a\to b}+r_{b\to c}} + \tfrac{1}{r_{a\to d}+r_{d\to e}+r_{e\to c}} = \tfrac{1}{2} + \tfrac{1}{3} = \tfrac{5}{6} \\ r_{a\to c} &= \tfrac{6}{5} \text{ Ohm} \end{aligned} \tag{2}$$

The effective graph resistance R_G or Kirchhoff index is the sum over all pairs i, j of nodes. And can be calculated as (Ellens & Kooij (2013))

$$R_G = \sum_{1\le i\le j\le N} R_{ij} = N \sum_{i=2}^{N} \frac{1}{\lambda_i} \tag{3}$$

Here, N is the number of nodes in the network and λ_i is the i-th eigenvalue of the Laplacian matrix L, which is defined as $L = D - A$. The degree matrix $D_{N\times N}$ contains the degree (number of edges connected a node) on the diagonal so $D_{i,i} =$ degree of node i. The adjacency matrix $A_{N\times N}$ has, generally speaking, non-zero values where nodes are adjacent (connected by an edge). In this study, we assume the networks to be undirected, unweighted graphs, thus $A_{i,j} = A_{j,i} = 1$ if node i and j are connected. Since we assume the networks to be connected as well, only the first Laplacian eigenvalue $\lambda_1 = 0$. Therefore, the sum of the eigenvalues starts at the second eigenvalue λ_2.

Note that effective graph resistance as an indicator of component redundancy is currently still subject to active academic discussion. This statement is in fact applicable to all graph metrics discussed here and their corresponding maritime reliability principles, as this is part of ongoing research.

Maximum Flow

The idea of component redundancy is to avoid single points of failure in the system. This translates to 'bottlenecks' when the system is considered as a flow network. These bottlenecks can be calculated using cut sets: a set of nodes or edges whose removal will disconnect a specified pair of nodes (Newman (2010)). The weight of each edge can physically be interpreted as the length or the capacity of that edge. Here, the capacity of each edge is set to 1 since we assumed the network to be unweighted; the primary reason for this assumption is the fact that length or capacity of the connections are unknown (as will very often be the case in early stages of ship/system design). This gives us the following definition for maximum flow: the maximum flow between a given pair of nodes in a network is equal to the sum of the capacity of the edges of the minimum edge cut set that separates the same two nodes (Newman (2010)). Calculating the maximum flow of a given network is an NP-hard problem; its value is approached using an algorithm. Algorithm 1 shows a basic greedy algorithm in order to explain an approach to $f_{textmax}$. In this study, maximum flow as approached by the push-relabel algorithm (Goldbergt & Tarjan (n.d.)), which is further explained in (Roughgarden (2016b)) but will not be detailed here. Most DP systems are required to have more than one source node (e.g., the generator sets) and more than one sink node (e.g. thrusters). Therefore, a synthetic source and sink node are added in the calculation of this metric, respectively connected to all "actual" source nodes and all "actual" sink nodes.

Algorithm 1 Greedy approach to Maximum Flow (Roughgarden (2016a))

Input: G, V, E, c_e, ▷ network, nodes, edges, edge capacity
Output: $f_{\max,G}$ ▷ maximum flow between source node s and sink node t

$f_e \leftarrow 0$ for all $e \in E$ ▷ initialise edge flow as all-zero flow
repeat ▷ path P is a walk with no nodes repeated
  find $s-t$ path P such that $f_e < c_e$ for every $e \in P$ ▷ edge flow f_e can never be larger than capacity c_e
  if no such path **then** halt with current flow $\{f_e\}_{e \in E}$
  else
    $\Delta \leftarrow \min_{e \in P}(c_e - f_e)$ ▷ Calculate available capacity of edges on path P
    for all edges e **do**
      $f_e \leftarrow f_e + \Delta$
    end for
  end if
until $f_e \leftarrow f_{\max}$

Distribution Redundancy

Distribution redundancy refers to how well the redundant components can be utilised within the network. This aspect borders on reconfigurability: if a connection fails, can we still reach all relevant components via a different path? Therefore, the focus in selecting an appropriate metric for this aspect is on measures that express cycles, triangles and other cyclic topologies. The first metric we considered was the meshedness coefficient (Yazdani & Jeffrey (2012); Buhl et al. (2006)), which is the fraction between the total and maximum number of independent loops in a planar graph. This is a metric that has been applied to, i.a., water distribution networks (Yazdani & Jeffrey (2012)) and urban road networks (Buhl et al. (2006)). However, since onboard systems are designed within a three-dimensional space, we cannot guarantee that all networks are planar (can be drawn on a plane without having any edges cross (Newman (2010))). Therefore, the meshedness coefficient cannot be applied to onboard systems. Two other measures, however, can be applied to undirected non-planar networks: the clustering coefficient and the cycle basis.

Clustering Coefficient

In real-world networks, two properties are often found: a high clustering coefficient and robustness to random node failures. This clustering refers to the idea that "my friends are likely to be friends"; an expression for the triangle density within the network. Triangles facilitate two ways of reaching a certain point within the network, which we consider as distribution redundancy. Thus, the local clustering coefficient c_i of node i is defined as the number of edges among neighbours of i divided by the possible number of edges among its neighbours (Ellens & Kooij (2013)). The global clustering coefficient (over the complete network) is either expressed as the average of the local clustering coefficients or as six times the number of triangles divided by the number of triples (three connected nodes). In this study, we have chosen to apply the second definition for its focus on the complete network:

$$\tilde{c}_G = \frac{6 \times triangles_G}{N_2 - W_2} = \frac{trace(A^3)}{\sum_{i=1}^{N} d_i(d_i - 1)} \tag{4}$$

Where $\tilde{c}_G$ is the global clustering coefficient of network G, N_2 is the number of walks of length 2 (all sets of three connected nodes: $e_{a \to b}, e_{b \to c}$), W_2 is the number of closed walks (same begin and end node), A the adjacency matrix and d_i the degree of node i.

Circuit Rank

The second proxy for distribution redundancy is an extension of the clustering coefficient: the circuit rank or cyclomatic number Berge (2001). This metric provides the number of closed loops in the network that provide the base for all loops present and is equal to the number of independent cycles. The rank indicates a minimum number of edges to be removed to lose all cycles within the network and can therefore be considered as a minimum redundancy boundary. The circuit rank r_G is calculated as

$$r_G = E - V + C \tag{5}$$

Where E is the total number of edges in G, N the number of nodes and C the number of connected components, which $C = 1$ in case of a connected network.

Independent Subsystems

The last reliability aspect is perhaps most directly related to network metrics. Having two or more component groups capable of individually and independently performing a specific function can be seen as a specific network partitioning with additional requirements. Network partitioning is the grouping of nodes in communities or partitions. The quality of this network division can be expressed as modularity (Newman & Girvan (2004)). To maximise modularity is to maximise the difference between the actual number of edges in a community and the expected number of such edges (Traag et al. (2019)). Again, we need an algorithm to approach the optimal network division. The Leiden algorithm is applied to partition the network (Traag et al. (2019)). The main disadvantage of this current network-based modularity approach is that the different functions of the components are not taken into account when determining the communities.

CASE STUDY

The case study consists of two Dynamic Positioning Systems of class level 2 and 3. The systems are defined by Clavijo et al. (2022) and initially used to perform a Reliability, Availability and Maintainability (RAM) analysis. This is a theoretically defined system based on literature and system knowledge. In future work the authors aim to apply the network analysis to real-world systems. Figure 2 shows the two considered systems, each consisting of a power subsystem (red), thruster subsystem (yellow), and control subsystem (green).

As mentioned in Section ”Control system”, the control system is regarded separately in this work. Figure 3 presents the corresponding network representation of the complete DP2 system. This figure shows the difference in structure between the power and thruster subsystems versus the control subsystem; the degree distribution is clearly completely different. Due to this difference in nature, the DP system is analysed both including and excluding the control system components.

In line with the assumptions made in Section Method: Network Definition, we have constructed the DP2 and DP3 systems as shown in Figure 4. Based on a visual inspection of the networks, the DP3 system clearly has three main components in its main switchboard, whereas the DP2 system has two components. However, the connections between the transformers in DP2 seem to add to the overall reliability. Lastly, the double connection to one of the computer system components in DP3 creates an additional loop. This is expected to add to the distribution redundancy estimation.

Table 3 shows the different calculated network metrics (of subsystems) of the DP2 and DP3 systems. The first two networks show the metrics of the complete DP systems as shown in Figures 2 and 3. The last two columns contain the metrics of the simplified DP systems as shown in Figure 4. The bold green values indicate a ”higher reliability”, which is not for all metrics a positive correlation. First, the table is inconclusive in indicating the most reliable system based on the selected network metrics. The component redundancy, estimated using effective graph resistance and maximum flow, contradicts itself. This is also the case for the distribution redundancy metrics global clustering and circuit rank. However, the independent subsystem defined using network modularity is higher for the two DP3 network representations.

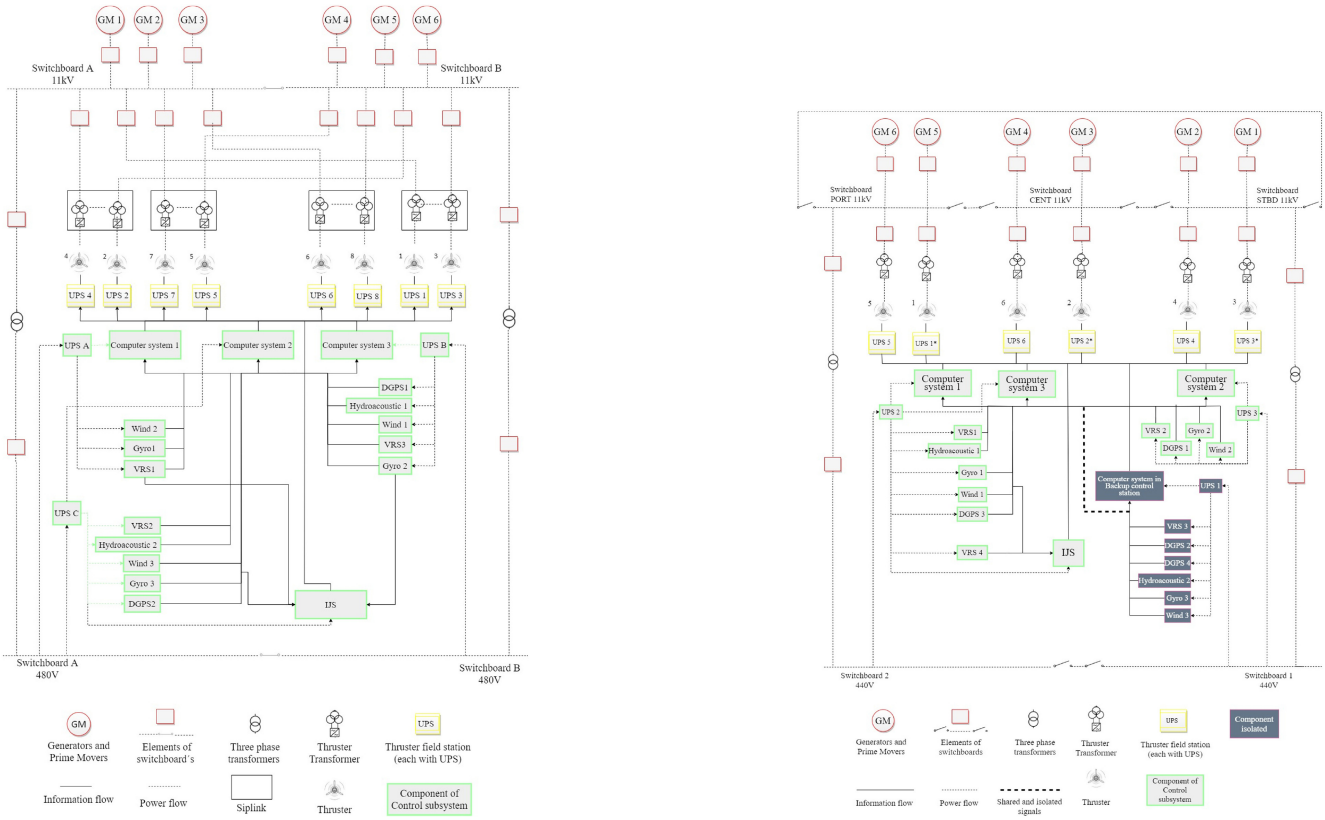

(a) DP2 System Diagram (Clavijo et al. (2022))

(b) DP3 System Diagram (Clavijo et al. (2022))

Figure 2: Dynamic Positioning System Diagram with the following Subsystems: Computer System (COMP), Generator/Prime Mover (GM), Main Switchboard (MSWB), Switchboard (SWB), Transformers (TF), Uninterrupted Power Supply (UPS)

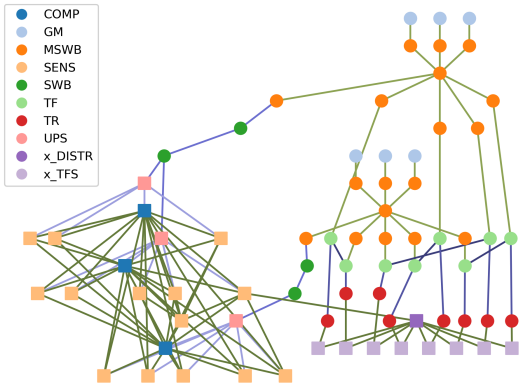

Figure 3: DP2 Network Representation with the following Subsystems: Computer System (COMP), Generator/Prime Mover (GM), Main Switchboard (MSWB), Sensors (SENS), Switchboard (SWB), Transformers (TF), Thrusters (TR), Uninterrupted Power Supply (UPS), Control System Components (x_DISTR and x_TFS). The square nodes are part of the control system and are separately considered.

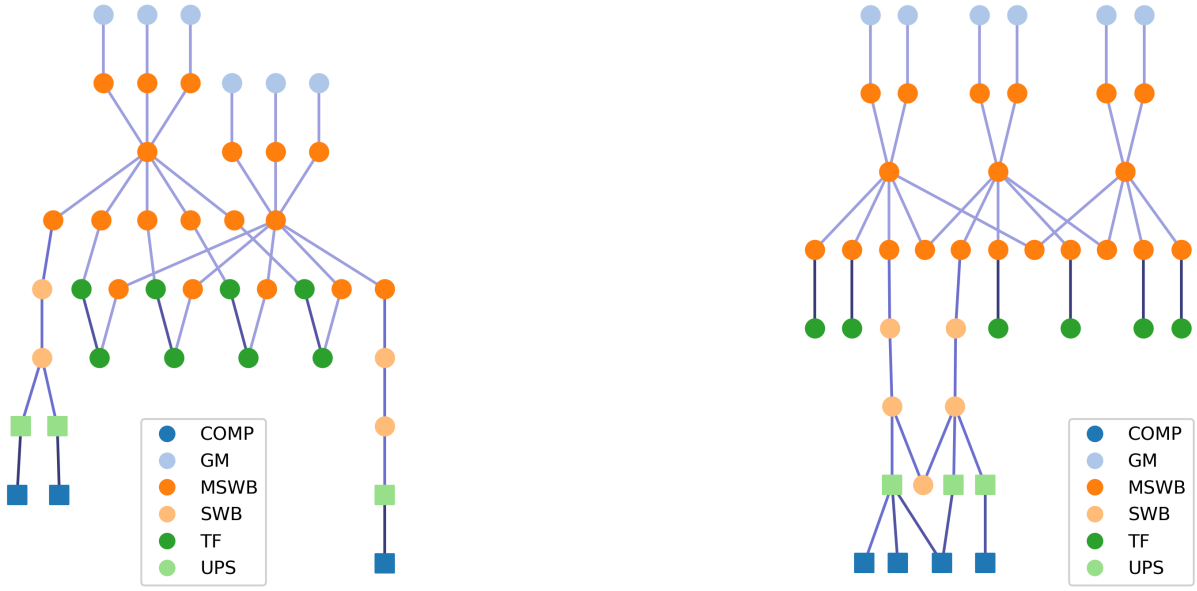

(a) Network Representation of DP2 System

(b) Network Representation of DP3 System

Figure 4: Dynamic Positioning Network Representation with the following Subsystems: Computer System (COMP), Generator/Prime Mover (GM), Main Switchboard (MSWB), Switchboard (SWB), Transformers (TF), Uninterrupted Power Supply (UPS). This representation mainly shows the nodes not part of the control system (round nodes) whilst a few control system components (square nodes) have been included to show where they are connected to the other system components

Table 3: Network Metrics for the full DP Systems and for the Power and Thruster Subsystem; metrics sorted by Component Redundancy (1,2), Distribution Redundancy (3,4), Independent Subsystems (5) and General Network Metrics (6,7) and the value implicating ”higher reliability” in **bold green**

	DP2 (incl control)	DP3 (incl control)	DP2 (excl control)	DP3 (excl control)
1) Effective Graph Resistance	**5043**	5498	**3203**	3257
2) Maximum Flow	3	**5**	1	**1,25**
3) Global Clustering	0,072	**0,163**	0	0
4) Circuit Rank	**58**	53	3	3
5) Modularity	0,480	**0,493**	0,496	**0,520**
6) Number of Nodes	73	74	42	44
7) Number of Edges	130	126	44	46

CONCLUSION

The goal of this study was to compare empirical DP regulations and theoretical network metrics. This was approached by 1) providing a clear outline of the assumptions made to enable the comparison, 2) introducing a selection of network metrics and their working principles, and 3) discussing the comparison and future research directions. We have translated two dynamic positioning systems into network representations and analysed these networks using selected network metrics. This selection was based on the assumed working principles behind the regulations in Table 2.

The resulting comparison shows that the selected network metrics do not affirm the working principles. The DP3 systems have a higher modularity and maximum flow indicating higher component redundancy, however, the higher effective graph resistance indicates the opposite conclusion. No conclusions can be drawn about the DP2 and DP3 power and thruster subsystems distribution redundancy since the networks contain no triangles (global clustering coefficient is 0) and the same number of closed loops (3).

Discussion and Outlook

This study has been an initial attempt to express regulations for dynamic positioning systems as network metrics. Despite the inconclusive results, we believe that a future framework based on network theory can aid ship designers and marine engineers in designing safer onboard systems. However, we like to emphasize that additional research is essential before completing such a framework:

- This case study used two DP systems based on literature. Having actual networks (complete systems or subsystems) to compare would be a major step in making the network metrics more applicable to real-world systems. In future research, we aim to study systems with a higher number of components. This might reduce the arbitrariness in defining the network and could therefore yield more reliable results.
- The research approach of this study contained a series of assumptions: definition of reliability principles $\rightarrow$ matching these principles with regulations $\rightarrow$ selecting network metrics as a proxy for the reliability principles. We have been aware of possible bias in these steps, however, a formal framework to make these steps would be recommended for future research. This framework should also contain a very good and very bad example of a DP system to facilitate bench-marking the studied networks and the corresponding metrics.
- The translation of the DP systems to networks included a number of assumptions as well. Whilst most of them have been described in Section ”Method: Network Definition ”, a significant assumption has been disregarded so far: the difference in network size between the DP2 and DP3 systems. The authors are aware that it is no common practice in network science to compare networks with different number of nodes (components). This size difference is, however, a network aspect that is inherent to systems onboard ships. Therefore, a comprehensive approach to this sizing problem and related normalisation concepts is recommended as future research.
- The aspect that makes the analysis of DP system regulations interesting, the fact that it sets requirements on different aspects of the integrated system, also makes it challenging to study. The DP systems often show a variety of components and connections. We consider the different components and connections to be a multilayer network: nodes and edges are part of a certain “layer” based on their respective type of flow. Interdonato et al. (2020) shows a range of possible approaches to simplify a multilayer network, motivated by reducing system “noise”, being able to use already existing monoplex analysis methods, improved computational performance. The case study is presented as a multilayer network in Figure 5. The multilayer aspect is further disregarded in line with the motivations provided by Interdonato et al. (2020).

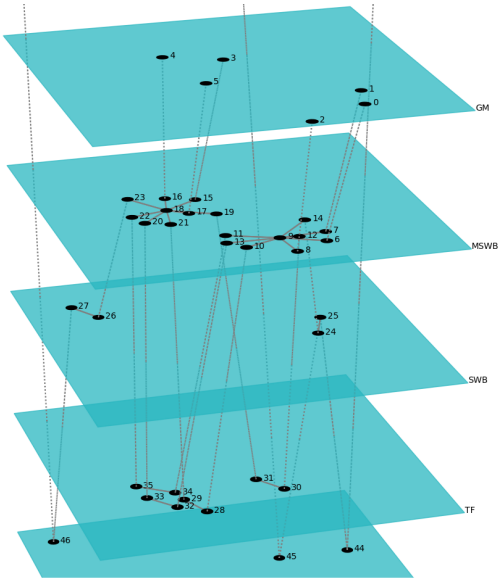

Figure 5: DP2 Multilayer Network Representation (close-up) showing the subsystems in different layers (blue ”levels”): Generator/Prime Mover (GM), Main Switchboard (MSWB), Switchboard (SWB), Transformers (TF), Thrusters (TR)

CONTRIBUTION STATEMENT

E.L. Scheffers: Conceptualization; data curation, methodology; writing – original draft. **P. de Vos:** conceptualization; supervision; writing – review and editing.

ACKNOWLEDGEMENTS

This work is part of the project RODIN (Robust Onboard Distribution Networks), which has received funding from the Delft University of Technology, Department of Maritime and Transport Technology.

REFERENCES

ABS. (2021). Guide for Dynamic Positioning Systems 2021.

Berge, C. (2001). *The theory of graphs*. Courier Corporation.

Brefort, D., Shields, C., Habben Jansen, A., Duchateau, E., Pawling, R., Droste, K., … Kana, A. A. (2018, January). An architectural framework for distributed naval ship systems. *Ocean Engineering*, *147*, 375–385. doi: 10.1016/j.oceaneng.2017.10.028

Buhl, J., Gautrais, J., Reeves, N., Solé, R. V., Valverde, S., Kuntz, P., & Theraulaz, G. (2006, February). Topological patterns in street networks ofself-organized urban settlements. *The European Physical Journal B - Condensed Matter and Complex Systems*, *49*(4), 513–522. doi: 10.1140/epjb/e2006-00085-1

Clavijo, M. V., Schleder, A. M., Droguett, E. L., & Martins, M. R. (2022, December). RAM analysis of dynamic positioning system: An approach taking into account uncertainties and criticality equipment ratings. *Proceedings of the Institution of Mechanical Engineers, Part O: Journal of Risk and Reliability*, *236*(6), 1104–1134. doi: 10.1177/1748006X211051805

Ellens, W., & Kooij, R. E. (2013, November). Graph measures and network robustness. doi: 10.48550/arXiv.1311.5064

Ellens, W., Spieksma, F., Van Mieghem, P., Jamakovic, A., & Kooij, R. (2011, November). Effective graph resistance. *Linear Algebra and its Applications*, *435*(10), 2491–2506. doi: 10.1016/j.laa.2011.02.024

Goldbergt, A. K., & Tarjan, R. E. (n.d.). A New Approach to the Maximum Flow Problem.

Goulter, I. C. (1987, December). Current and future use of systems analysis in water distribution network design. *Civil Engineering Systems*, *4*(4), 175–184. doi: 10.1080/02630258708970484

Interdonato, R., Magnani, M., Perna, D., Tagarelli, A., & Vega, D. (2020, May). Multilayer network simplification: Approaches, models and methods. *Computer Science Review*, *36*, 100246. doi: 10.1016/j.cosrev.2020.100246

Kanno, Y., & Ben-Haim, Y. (2011, September). Redundancy and Robustness, or When Is Redundancy Redundant? *Journal of Structural Engineering*, *137*(9), 935–945. doi: 10.1061/(ASCE)ST.1943-541X.0000416

Makoto ITO. (2022). Fundamentals and applications for risk-based design. *ClassNK Technical Journal*.

Newman, M. E. J. (2010). *Networks: An introduction*. Oxford ; New York: Oxford University Press.

Newman, M. E. J., & Girvan, M. (2004, February). Finding and evaluating community structure in networks. *Physical Review E*, *69*(2), 026113. doi: 10.1103/PhysRevE.69.026113

Roughgarden, T. (2016a). CS261: A Second Course in Algorithms Lecture #1: Course Goals and Introduction to Maximum Flow.

Roughgarden, T. (2016b). CS261: A Second Course in Algorithms Lecture #3: The Push-Relabel Algorithm for Maximum Flow.

Traag, V. A., Waltman, L., & Van Eck, N. J. (2019, March). From Louvain to Leiden: Guaranteeing well-connected communities. *Scientific Reports*, *9*(1), 5233. doi: 10.1038/s41598-019-41695-z

Vos de, P. (2018). *On early-stage design of vital distribution systems on board ships* (Doctoral dissertation, Delft University of technology). doi: 10.4233/UUID:EB604971-30B7-4668-ACE0-4C4B60CD61BD

Vos de, P., & Stapersma, D. (2018, December). Automatic topology generation for early design of on-board energy distribution systems. *Ocean Engineering*, *170*, 55–73. doi: 10.1016/j.oceaneng.2018.09.023

Yazdani, A., & Jeffrey, P. (2012, March). Applying Network Theory to Quantify the Redundancy and Structural Robustness of Water Distribution Systems. *Journal of Water Resources Planning and Management*, *138*(2), 153–161. doi: 10.1061/(ASCE)WR.1943-5452.0000159

Proceedings of 15th International Marine Design Conference (IMDC-2024)
June 2-6, 2024
Amsterdam, the Netherlands

Integration of the methanol power propulsion and energy systems' temporal uncertainties in a Markov decision process framework

Apostolos S. Souflis - Rigas[1a,*], Jeroen F.J. Pruyn[1,2] and Austin A. Kana [1b]

ABSTRACT

The ongoing technological development of methanol energy converters (EC) towards decarbonization means that their dimensions and performance characteristics will be continually updated during the lifecycle of vessels currently designed. These advancements influence the ease of EC integration within the general arrangement of the vessel. The decision to switch from an internal combustion engine to a fuel cell or a hybrid configuration depends both (1) the technology adoption costs (i.e. CAPEX, OPEX) of the EC and (2) on the effect of EC on the actual engine room layout. The state-of-the-art literature has typically addressed these two challenges separately. This study proposes a design method to bridge these two fields by combining the use of (1) Markov decision processes to assess uncertain future methanol EC developments during the vessel lifecycle and (2) a generative probabilistic layout algorithm to quantify the risks associated with the EC systems layout integration. The case study identifies the drivers behind the EC technology choice during the lifecycle of a notional yacht vessel.

KEY WORDS

Ship Design; Methanol; Uncertainty propagation; Markov Decision Process; Maritime energy transition; Layout integration

INTRODUCTION

Background

Greenhouse gas (GHG) emissions produced from the maritime industry have increased by 9,6 % between 2012 and 2018, in spite of operational measures regarding the speed of the vessel being imposed (IMO, 2021). Forecasting studies have shown that emissions may increase between 90 % to 130 % compared to 2008 levels (IMO, 2021). Chen et al. (2019) demonstrated that the targets of International Maritime Organisation (IMO) cannot be met with the current measures in place. In 2023, IMO (2023) introduced the revised target of net zero GHG emissions in 2050 matching the goals of European Commission policy (EU, 2023), which are more strict in comparison to the standards in the study of Chen et al. (2019). Aakko-Saksa et al. (2023) and Lindstad et al. (2021) found that adoption of carbon neutral fuels is key towards reaching the ambitious and challenging emissions mitigation targets. Several energy converter (EC) technologies are available to facilitate the transition towards carbon neutrality. A large proportion of existing fleet are using diesel internal combustion engines (ICE) (2-stroke or 4 -stroke) that when using conventional diesel contribute to emissions generation (Gray et al., 2021).

[1a] Maritime Trasport & Technology, Delft University of Technology, Delft, Netherlands; ORCID: 0009-0000-7637-5683
[1b] Maritime Trasport & Technology, Delft University of Technology, Delft, Netherlands; ORCID:0000-0002-9600-8669
[2] CoE HRTech, Maritime Innovation, Hogeschool Rotterdam, Rotterdam, Netherlands; ORCID:0000-0002-4496-4544
[*] Corresponding Author: a.s.r.souflis-rigas@tudelft.nl

Submitted: 25 February 2024, Revised: 2 May 2024, Accepted: 3 May 2024, Published: 21 May 2024

Conference paper, DOI: https://doi.org/10.59490/imdc.2024.868 e-ISSN: 3050-4864

Retrofitting of these vessels is a necessary measure towards decarbonization (Gray et al., 2021) and the dual fuel engines have proven popular option (Tadros et al., 2023). Methanol has emerged as one of the prime candidates, being the 4th most widespread fuel (IMO, 2021), because it is in a liquid state and has properties resembling more closely to diesel in comparison to other alternative fuels (Zincir and Deniz, 2021; Harmsen, 2021). Methanol is thought to require minor modifications to be integrated within a vessel (Korberg et al., 2021; Zincir and Deniz, 2021). However, when considering the technologies available to be integrated within the power, propulsion and energy systems (PPE) (i.e. fuel cells (FC), batteries) as well as safety requirements for the fuel Zincir et al. (2023) and redundancy for vessel operation, the modifications will likely prove to be more than minor and thus more investigation is necessary. Souflis Rigas et al. (2023) showed that a large estimation discrepancy exists when attempting to compute the effect on the overall size of the vessel, pointing out the need for further research.

This study aims to compare different methanol energy converters on a lifecycle scope, while factoring in the challenge of layout modifications required for methanol EC technology adoption. A common trend in recent studies so far is to compare the alternative technologies and fuels based on financial and emission objectives (Zwaginga and Pruyn, 2022; Lindstad et al., 2022; Lagemann et al., 2022, 2023). However, these evaluation approaches have traditionally overlooked the challenges of the energy converters integration. Korberg et al. (2021) studied the feasibility of alternative fuels and propulsion configuration based on the total cost of ownership (TCO) and found methanol an advantageous choice, pointing out that FCs would need efficiency enhancement and capital cost reduction to become competitive. Similarly Lagemann et al. (2023) considered the most appropriate propulsion configurations based on uncertain emission regulations and pricing of fuel and carbon emissions and found methanol and LNG as strong candidates, but did not have a clear conclusion on which energy converter (FC or ICE) to use. Assessing the ease of implementing the proposed configuration is crucial before reaching a conclusion about the optimal choice. Lagemann et al. (2022) pointed out that technical and safety challenges may influence the solution outcome. This study aims to consider at a conceptual level the factors affecting the integration of the systems by integrating a probabilistic layout generation tool developed by Souflis Rigas et al. (2023) and Poullis (2022) to compute the probability of shifting to another energy converter during the lifecycle of a vessel, within a Markov decision process (MDP) employed for lifecycle modelling.

Energy converter uncertainties

ICEs, FCs, or a hybrid configuration can be selected for the methanol adoption. FCs are still under development, meaning their specific power density (volumetric and gravimetric) and efficiency rate remain uncertain van Biert et al. (2016); Van Veldhuizen et al. (2023). Elkafas et al. (2022); van Biert et al. (2016); Van Veldhuizen et al. (2023) highlighted that the efficiency rates and the power densities (volumetric and gravimetric) remain highly uncertain, as shown in Table 1. FCs are still a technology under development (EMSA and DNV, 2021), and it is fair to assume that their volumetric power density is far from becoming a deterministic value. Even, methanol internal combustion engines are still under development with their volumetric power density and efficiency rate improvements being part of ongoing research (Juho Repo et al., 2023). Additionally, Table 1 presents the uncertainty in estimating the cost of acquiring the main energy converter. This study focuses on interpreting the uncertainty in volumetric power density via Equation 1 (Torabi and Ahmadi (2020)) into physical dimensions uncertainty that is an input parameter for the probabilistic layout tool.

Table 1: Energy converters uncertainties considered (data derived from Elkafas et al. (2022); Zwaginga and Pruyn (2022); MARIN (2024); Wartsila (2024); MAN (2024))

Energy Converter	Volumetric Power Density (kW/m³)	Capex (€/kW)	Efficiency Rate
PEM - Fuel Cell (PEM-FC)	45-500	500-1680	47%-65%
ICE 4-Stroke	120-290	451-677	30% - 45%

$$P_{volumetric} = \frac{Power_{installed}}{L \cdot B \cdot H} \tag{1}$$

in which:

- $Power_{installed}$: installed power of the component
- L: length of the component
- B: width of the component
- H: height of the component

Review of studies on alternative fuels adoption -shaping of the research gap

Besides the studies focused on EC technology development, there are comparative studies for alternative fuels that consider the challenge of adopting alternative fuels in the form of additional space, volume, or weight objectives within an optimization framework. Ritari et al. (2023) investigated several ways to configure the PPE systems within the lifecycle period of a vessel using a total cost of ownership (TCO) minimization framework, but did not consider uncertainties in the dimensions or the performance of the components described. The properties of the potential PPE components were deterministic. Similarly, Zhang et al. (2023) evaluated different PPE configurations for a cruise vessel based on emissions and costs. Zhang et al. (2023) estimated the additional space demand in proportion to the size of the prime energy converters (EC): meaning that the engine room is assumed 5 times larger than the size of an internal combustion engine (ICE) and fuel cells are set to 2.5 times bigger than the fuel cell (FC) volume. Additionally, the conclusions of this study, through time, proved highly sensitive to the carbon pricing variation. Rivarolo et al. (2021) implemented a tool that evaluated various energy converters for a cruise ship based on volume, weight, costs and emissions and calculated volume and weight based on empirical equations derived from market data. The computed volume remains mostly focused on the additional fuel storage, disregarding possible alterations because of the PPEs uncertainties. These studies highlight that the space requirement is a decision influencing factor when comparing alternative fuels and energy converters. Additionally, the development of the EC technologies and their related sizing uncertainties have been totally overlooked. Higher fidelity in the layout modelling can generate more insightful information regarding the actual integratability of the EC within the engine room space.

Table 2 presents the elements that constitute relevant studies on lifecycle analysis and evaluation of suitable main EC (energy converter) technologies. Two elements are not sufficiently adressed:

- Space requirement for alternatively fuelled components integration: has been calculated based on volume requirement for additional fuel storage based on empirical equations or data trendlines and overlooks PPE configuration complexity Rivarolo et al. (2021); Lagemann et al. (2023); Ritari et al. (2023)
- The performance of the components under development (FCs, batteries, ICEs) and their *uncertainty* in terms of *volumetric, gravimetric power density and efficiency rates* as presented on Table 1

Table 2: Overview of objectives of studies focused on alternative fuels

Financial uncertainties	Emission uncertainties	Components performance uncertainties	Space requirements	Determinstic values	Reference
✓	✓	✗	✓/✗	✗	Lagemann et al. (2023)
✓	✓	✗	✓/ ✗	✗	Zwaginga and Pruyn (2022)
✗	✗	✗	✓	✓	Rivarolo et al. (2021)
✓	✓	✗	✓	✓	Zhang et al. (2023)
✓	✗	✗	✓	✓	Ritari et al. (2023)
✗	✗	✗	✗	✓	Korberg et al. (2021)
✓	✓	✗	✗	✗	Kana et al. (2015)
✗	✗	✓	✓	✗	Souflis Rigas et al. (2023)

Table 2 in combination with the overlooked discrepancy estimations in the size effect of the alternative fuelled PPE components integration Souflis Rigas et al. (2023) and the uncertainties in the performance evolution of energy converters - see Table 1, shapes the need to integrate the 4 objectives considered within Table 2. This paper developed a method that combines elements of the studies of Kana et al. (2015) and Souflis Rigas et al. (2023) to take a step further in the accuracy of the lifecycle evaluation and integrate the uncertainty aspects described.

State of the Art of Markov decision process in ship design

Markov decision process has been selected to quantifiably propagate the technical uncertainties of the ECs through time. Kana et al. (2015) highlighted that MDPs are beneficial because they integrate quantified uncertainties related to policy application, reflect the net present value per epoch via the rewards and provide the optimal decision per epoch (*epoch: refers to the executed time steps*). Kana and Harrison (2017) pointed out that MDPs generate an understanding of the decisions made within a time dynamic framework rather than provide one optimized solution on a specific time static case.

Kana et al. (2015); Kana and Harrison (2017) demonstrated through a case study regarding the conversion of a containership vessel to LNG fuel, that the emission regulation advancement uncertainties and supply chain risk uncertainties can be captured within an MDP to generate insight on the conversion choices through time. Niese (2012) developed an MDP framework that accounts for policy to generate a strategic maintenance plan for a ballast water treatment system and showcased the effect of uncertain regulation requirements on the maintenance decisions of deteriorating components. Niese et al. (2015) applied ship centric Markov decision process (SC - MDP) to evaluate the effect of alternative technologies, alternative fuels and operational measures adoption (e.g. engine derating) to the design choices (e.g. principal ship dimensions) being made as well as the rewards generated throughout lifecycle. The design space of the alternative vessels' was produced via low-fidelity modeling. However, this study outlined the potential of MDPs to compare and evaluate the influence of various technologies on the design and the economic viability of a vessel. Overall MDP, provide a reliable method to capture stochastic temporal uncertainties caused by regulation, policy, costs, and technology alterations.

Research contribution

As shown in Table 1 and using equation 1, the uncertainty of volumetric power density can be matched to the uncertainty of the physical dimensions of the component. The focus remains on propagating the uncertainty of the physical systems dimensions throughout the vessel's lifecycle and thus accounting for uncertainties overlooked by previous research. The main goal of this work is to compare the potential ECs through the vessel lifecycle while using the probabilistic layout tool output to define the transition probabilities and see which are the influential factors to the outcome.

METHOD

MDPs are designed to capture and solve a sequential decision-making problem that deals with time dynamic uncertainties in the state space (Kana et al., 2015; Russell et al., 2010).

The key components to define an MDP are:

- states (s): representing a set of states that the agent may be in through time
- actions (a): a finite set of actions that can be selected
- Transition Probabilities ($T(s'|s, a)$): expresses the probability upon choosing action a, the agent in state s will move to state s' in the upcoming epoch.

- Rewards (R): is the reward given after moving to a new state s' by selecting action a

Note: agent represents the entity that selects the action to be implemented based on the solution followed for the MDP.

Solving MDPs produces a sequence of states through time that are selected based on the optimal value per epoch. The algorithm selected to solve the MDP is the value iteration algorithm using the Bellman equation (see Equation 2), which is typical for solving a stochastic dynamic programming problem Bethke and How (2009). Equation 2 is used to compute the utility for each state per epoch. The sequence of actions selected using Equation 3 compiles the policy of actions to be made per state throughout the defined time horizon. The optimal policy in this case is considered the one that yields the highest expected value.

$$U(s) = R(s,a) + \gamma \max_a \sum_{s'} T(s,a,s')U(s') \tag{2}$$

$$\pi(s) = \arg\max_a \sum_{s'} T(s,a,s')U(s') \tag{3}$$

Russell et al. (2010) described the value iteration algorithm as: *a way to propagate the information through the state space by means of local updates, which provides a way for uncertainty percolation through time*. The selected MDP has a finite time horizon and features non-stationary dynamics, where both the probability and reward vectors evolve over time. Kana et al. (2015) pointed out that the changes in the probability and reward vectors can be caused by degradation, regulatory shifts and logistics risks. In this case study the non- stationary property is derived from the changeable performance properties and technology acquisition/ adoption costs of the ECs.

Novel Transition probabilities definition

The transition probability in a MDP represents the probability of moving from state B at epoch n (B_n) to state A at epoch n+1 (A_{n+1}) (see Equation 4), depending on the decision-action that is selected per time step Sheskin (2010). However, if the states are considered independent, the probability is equal to the probability of event A, according to Equation 4. For this study, the states are considered independent and probabilities are defined applying Equation 5.

$$P(A_{n+1}|B_n) = \frac{P(A_{n+1} \cap B_n)}{P(B_n)} = \frac{P(A_{n+1}) \cdot P(B_n)}{P(B_n)} = P(A_{n+1}) \tag{4}$$

Probability can be defined by using the relative frequency approach Gebali (2015), as shown in Equation 5. This means that an experiment is conducted N times and based on the N_a times that the selected outcome occurs, a probability is defined.

$$P(A) = \lim_{N \to \infty} \frac{N_a}{N} \tag{5}$$

Connecting this approach to the framing of this study's problem, the probabilistic layout tool by Souflis Rigas et al. (2023) conducts a Monte Carlo simulation (MCS) on the dimensions of components to be fitted in a simplified engine room layout based on various system architectures and generates distributions of engine room length (see Fig. 1). Souflis Rigas et al. (2023) showed there is inconsistency between the input dimensions and the output of the overall engine room size, which is the foundation for using a layout modeling tool to incorporate the dimension uncertainties rather than empirical trendlines. Using the distribution of the engine room length against a specified requirement for the length, Equation 5 can provide the probability of a PPE configuration with uncertain dimensions to fit within the required length. The uncertain dimensions can be derived from the volumetric power density uncertainty underlined in Table 1. Souflis Rigas et al. (2023) therefore

highlighted that there is a struggle with available space when existing vessels convert to methanol. A threshold of a required length reflects the requirement of fitting the equipment for the retrofit of an existing vessel from ICEs to using FCs as prime energy converter. The requirement and testing of specific $Length_{\text{engine room}}$ reflects on a potential length threshold that leads to moving a bulkhead and triggering extra conversion costs.

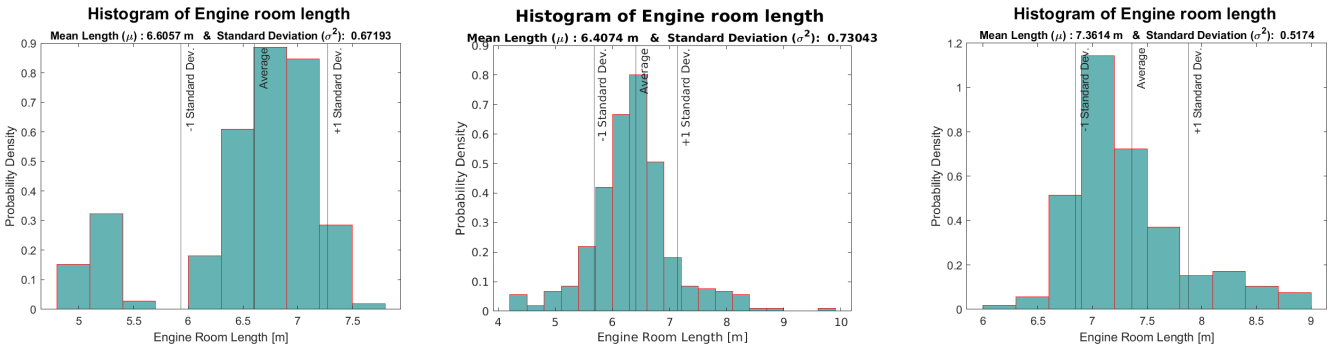

(a) ICE case **(b) FC case** **(c) Hybrid case**

Figure 1: Representatinve engine room length distribution per epoch per energy converter

Framework for Energy Converters case study

The current model framework is based off of a modified ship centric markov decision process (SC - MDP). Figure 2 shows that the model starts by generating the necessary inputs for the MDP - transition probabilities and rewards matrices. Firstly, it uses the uncertainty analysis in the physical space of an engine room that is conducted with the probabilistic layout tool Souflis Rigas et al. (2023) for transition probabilities definition. By computing the fuel consumption for every EC on a yearly basis, the OPEX is calculated. Using the CAPEX values on Table 1, CAPEX is calculated, and based on the action, the reward over time is computed. Rewards are considered to be changing every 4 years until the 12th year. In this case study 1 year equals 1 epoch. The MDP in this case study consists of:

- **states:**
  - Energy converters that can be selected during the lifecycle of the vessel: ICE, FC, Hybrid.
  - Substates have been defined to be able to apply extra maintenance costs after 4 years for Hybrid and FC states. Dall'Armi et al. (2022) showed that the performance of PEMFCs deteriorates after 2 years. Additionally, the lifetime of FCs shows a variation between 5000 and 10000 hours Elkafas et al. (2022). Considering the estimation variation, an extra operational is incurred every 4 years. Substates that would lead to extra maintenance were defined for the FC and the hybrid state. When entering the state of a brand new EC, it is considered that the model will transition until the year the extra maintenance cost is applied.
  - Combination of states and substates generates 9 states in total that can be accessed from the agent, 1 for ICE and 4 for FC and hybrid respectively.
- **actions:**
  - Switch Energy Converter: is the action of switching to an energy converter (e.g. ICE).
  - Use Energy Converter: keep using the same energy converter for the next epoch.
  - There are 6 actions in total, 2 for each energy converter.

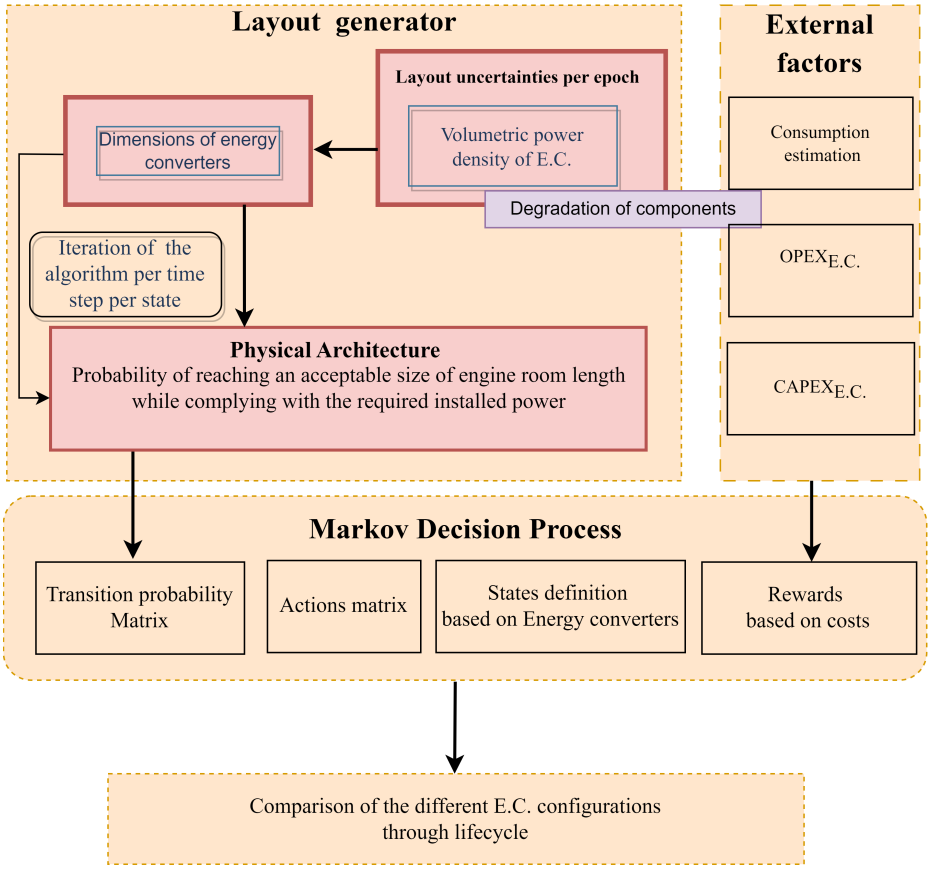

Figure 2: Architecture of modelling framework

- **Transition probabilities**

$$\mathbf{T} = \begin{array}{c} \\ \text{ICE} \\ \text{FC} \\ \text{Hybrid} \end{array} \begin{array}{c} \begin{array}{ccc} \text{ICE'} & \text{FC'} & \text{Hybrid'} \end{array} \\ \left\| \begin{array}{ccc} p_{\text{ICE}} & 1 - p_{\text{ICE}} & 0 \\ 0 & 1 & 0 \\ 0 & 1 - p_{\text{Hyb}} & p_{\text{Hyb}} \end{array} \right\| \end{array} \tag{6}$$

$$p_{ICE} = \frac{\sum_{n=1}^{N_{\text{eff}}} \text{ICE layouts reaching the required length}}{\sum_{n=1}^{N} \text{ICE layouts}} \tag{7}$$

$$p_{Hyb} = \frac{\sum_{n=1}^{N_{\text{eff}}} \text{Hyb layouts reaching the required length}}{\sum_{n=1}^{N} \text{Hyb layouts}} \tag{8}$$

N_{eff}: defines the amount of produced layouts that reach the engine room length requirement.

– Probabilities: are dependent on the action selected. Using Equation 5, the probability of an EC configuration attaining the required $Length_{\text{engine room}}$ is computed. These probabilities change per 4 years (see Figure: 5a), as volumetric power density improvement for each EC is considered (see Figure 4). An example of the transition probabilty matrix definition for the action *Use FC* is given in Equation 6. For the FC state, it is set to stay in

the same state and thus a probability value of 1. For ICE, the probability of switching to FC is the remainder of the stochastic row of the p_{ICE}. Similarly, probabilities for the hybrid state are defined. To make the definition of p_{ICE} and p_{Hyb} more elaborate, Equations 7 and 8 are provided respectively. p_{ICE} and p_{Hyb} represent the amount of generated layouts per EC that reached the set Length threshold. The transition probabilities matrices are parametric and dependent on the probability distributions generated by the layout algorithm (see Eq. 4). The transition probability matrices have been kept the same both for the *Use actions* and *Swtich actions* per EC.

  - Probabilities for EC degradation: the probability is assumed 1 that the agent will switch to the degrading sub-states, until the extra maintenance cost (for replacing stacks of the FC) occurs.

- **Rewards:** are dependent on the action selected and the initial state, see Table 3 and the calculation of CAPEX, OPEX is done based on Table 4. For FC and hybrid, an additional maintenance cost was calculated based on CAPEX. This is set 4% of the CAPEX according to Elkafas et al. (2022) and trial and error. The $OPEX_{maintenance}$ is applied only to FC, hybrid states when it is selected to keep using the same EC.

Table 3: Reward definition per action

Use Energy Converter	Switch to Energy Converter
$OPEX_{EC}$	$CAPEX_{EC} + OPEX_{EC}$

- **discount factor(γ)**: is calculated with Equation 9 (Sheskin, 2010), and in this case study interest rate is assumed: i = 7%

$$\gamma = \frac{1}{1+i} \tag{9}$$

Table 4: Parameters of each computed cost

$OPEX_{\text{EC}}$	f(fuel consumption$_{\text{EC}}$ [tons/year], fuel cost [€/ton], EC)
$OPEX_{\text{maintenance FC}}$	4% $CAPEX_{\text{FC}}$
$CAPEX_{\text{EC}}$	f($CAPEX_{\text{EC}}$ [€/kW], $P_{\text{installed}}$[kW], EC)

It is worth noting that MDP is memoryless, meaning that the optimal action per time step is selected regardless of the path that the agent followed to reach that state. Based on the solution of the EC decision-making problem, an analysis is conducted of the financial risks of each main Energy converter configuration choice to determine methodological insights and influential parameters to the solution trends.

CASE STUDY

A simplified yacht engine room was selected based on the studies of Poullis (2022), and Souflis Rigas et al. (2023). Table 5 presents the components configurations that were selected to be tested per case and Figure 3 presents indicative layouts for each state, that are generated per scenario in the layout simulation. The operational profile of the vessel was set up based on a master thesis studying a yacht similar to our conceptual vessel (L. Menano de Figueiredo, 2018).

Table 5: Engine room configurations represented per state

ICE	FC	Hybrid(ICE + FC)
Methanol supply	Methanol supply	Methanol supply
ICE	Generator	ICE
Generator	Swtichboard	Generator
Swtichboard	FCs	Swtichboard
	Reformer	FCs

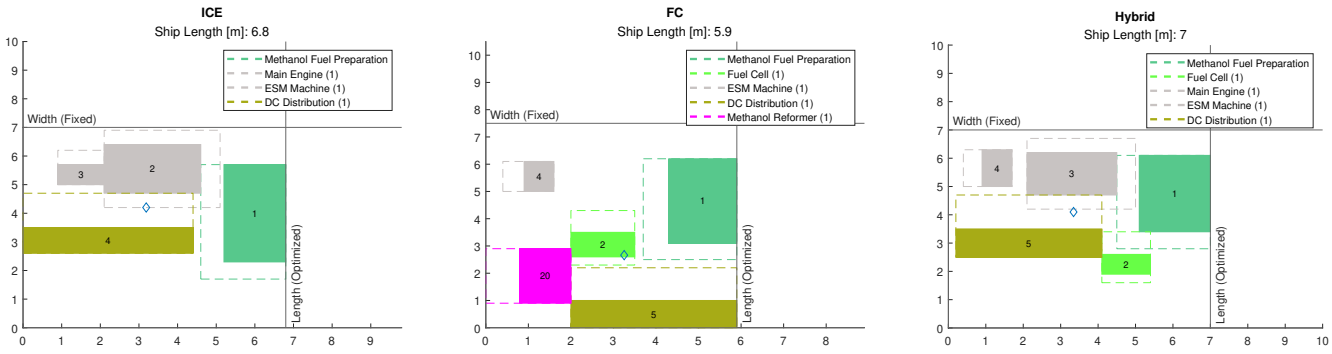

(a) ICE layout **(b)** FC layout **(c)** Hybrid Layout

Figure 3: Indicative layouts per Energy converter

Operational Profile and EC sizing

Based on the maximum required power found in Table 6 the installed power of the ECs was determined. Table 7 presents the installed power selected for each EC state. In hybrid state, FC was sized to be able to meet the power demand during maneuvering and anchor loads (see Table 6).

The consumption was calculated using Equation 10 and the values referred in Table 8. In the hybrid state, the loads below 250 kW are assumed to be satisfied by the FC and the loads above 250 kW by the ICE.

$$\text{fuel consumption} = \begin{cases} \eta_{\text{FC}} \cdot \eta_{Reformer} \cdot Energy_{demand} & ,FC \\ SFC \cdot Energy_{demand} \cdot \frac{LHV_{diesel}}{LHV_{methanol}} & ,ICE \end{cases} \quad (10)$$

where:

- SFC [g/kWh]: specific fuel consumption
- LHV [MJ/Kg]: Lower heating value
- $Energy_{demand}$ [kWh]
- η: efficiency rate of a component

Table 6: Operational profile and yearly consumption per configuration

Load State	Power demand	Frequency	Yearly Energy Demand [kWh]	Methanol ICE Consumption [tons]	PEMFC Consumption [tons]	Hybrid [tons]
Cruising	473	13.8%	1,248,720	549.3	475	549.3
Max Speed	800	7.1%	2,112,000	929	803.3	929
Crossing	562	13.2%	1,483,680	652.6	564.4	652.6
Anchor	155	63.9%	409,200	180	155.7	155.7
Maneuvering	238	2.13%	628,320	276.4	239	239

Table 7: Installed Power per state

Energy converter	$P_{installed}$ [kW]
ICE	840
FC	840
Hybrid	600 (ICE) + 250 (FC)

Table 8: Values assumed for consumption caclculation

Unit	Value]	Reference
sfc [g/kWh]	205	(Warsila, 2024)
η_{FC}	0.58	(Elkafas et al., 2022)
$\eta_{Reformer}$	0.82	(RIX, 2024)
$LHV_{methanol}$ [MJ/kg]	19.9	(Harmsen, 2021)
LHV_{diesel} [MJ/kg]	42.7	(Trancossi, 2015)
$sailing_{time,year}$ [h]	2600	(L. Menano de Figueiredo, 2018)

Considering the uncertainties in volumetric power density of the main ECs (see Table 1), the length and width of the ECs were sampled in the probabilistic layout tool with steadily reducing uncertainty margins changing every 4 years as shown in Table 9. The uncertainty margin is reduced to account for the potential technology development during the lifecycle of the vessel. Figure 4 illustrates the actual distribution of volumetric power densities ranging from 5% to 40% depending on the epoch and the technology. 40 % FC means that there was a 40 % uncertainty range for the width and length of the FC system.

Table 9: Dimension uncertainty margins per epoch per EC

Year	ICE [%]	FC [%]
0	30	40
4	20	30
8	10	20
12	5	10

To derive the dimensions of the ECs, a PEMFC model of Ballard (2024) was selected as a reference case, and a 4 stroke high-speed engine by Warsila (2024) for the ICE. Their dimensions are shown in Table 10. ICE is assumed to be a methanol-only ICE, and the FC a PEMFC. Dimensions for the additional layout components are shown in Table 11. By fixing the EC height and installed power, the volumetric power density uncertainty is matched to uncertainty margins in the EC's width and length. Using the probabilistic layout tool developed to better understand its effect on the overall size of a simplified engine room, this uncertainty can be integrated within the MDP as a factor reflecting on technical uncertainty and systems integration challenges.

Table 10: Reference dimensions for energy converters

Energy Converter	L [m]	W [m]	H [m]	Power [kW]	Power Density [W m^{-3}]	Reference
FC	1.20	0.87	0.51	100	189.52	Ballard (2024)
ICE	2.3	1.4	1.8	865	149.24	Warsila (2024)

Table 11: Auxiliary systems dimensions ranges

Building Block	Length [m]	Width [m]
Methanol Fuel Preparation	2.6 - 3.5	1.6 - 2.1
ESM Machine	1.1 - 1.4	0.6 - 0.9
DC Distribution	3.8 - 5.1	0.8 - 1.1
Reformer	2-2.4	1-1.2

MDP implementation

The MDP time horizon is set to 20 years to observe how the actions are converging. From year 0 until year 12, there is an update of the probabilities per state, the CAPEX and the OPEX, as shown in Figure 5. The inputs are kept constant to evaluate the convergence of the MDP solution.

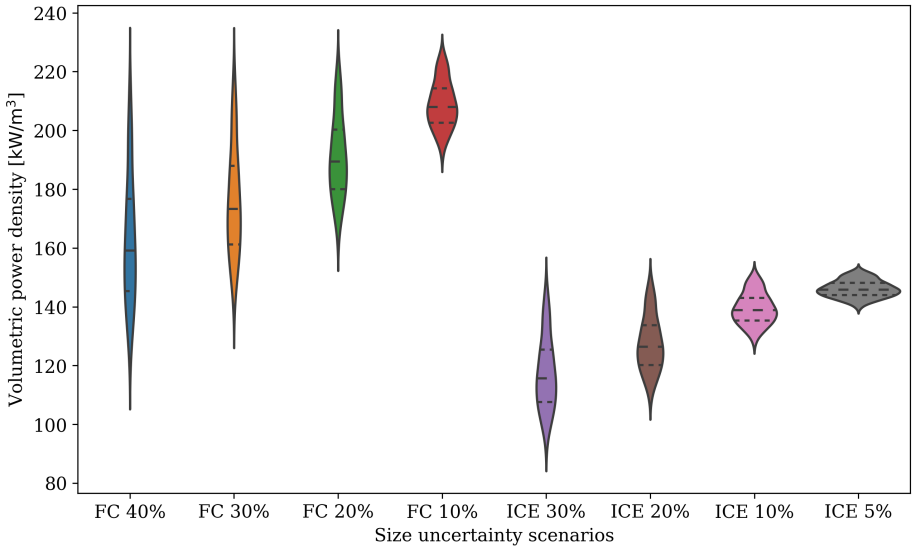

Figure 4: Comparative plot of EC volumetric power densities distribution per epoch

Figure 4 illustrates that ICE has a smaller power density variation than the FCs, which is in accordance with the uncertainty margins found on Table1. The required engine room length is set to 6.52 m based on the mean engine room length of the 30 % ICE case. The computed probabilities for each EC are shown in Table 12 and Figure 5a. Similar volumetric power densities were used for the Hybrid state calculations. It is clear that the FC state displays the highest probabilities and these probabilities depict a similar trend to the trends of volumetric power densities in Figure 4.

Table 12: Probabilities per state per epoch

Energy converter	Yeat 0	Year 4	Year 8	Year 12
ICE	0.382	0.389	0.458	0.534
FC	0.756	0.779	0.699	0.751
Hybrid	0.023	0.037	0.080	0.080

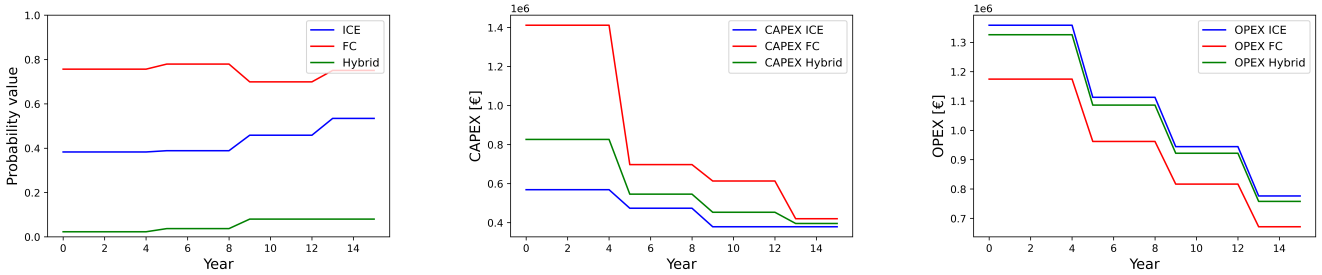

(a) Probabilities per epoch **(b) CAPEX per EC** **(c) OPEX per EC**

Figure 5: Inputs for finite horizon Markov decision process

Figure 4 illustrates the evolution assumed in the volumetric power density of the ECs according to the tightening dimension uncertainty margins selected per time step (Table 9). Volumetric power density is calculated with Equation 1, by fixing the height of the EC and using the installed Power per state (Table 7) and using the variable length and width of the ECs per scenario (see Table 9). To make the layout solution comparable, it was assumed that FCs can be stacked on top of each other, meaning an overall height H = 3 m. Similarly, the reformer in the hybrid configuration is considered packed within the FC unit. ICE height was set to H = 1.8 m according to the reference engine (Table 10).

Table 12 and sub-Figure 5a illustrate that FC has the relatively highest probability of integration in accordance with the higher volumetric power density displayed in Figure 4. From a methodological point of view, the interest lies on observing which kind of actions are selected depending on the newly proposed way of defining the transition probabilities according to Equation 5. The state FC that had more increased power densities presented the highest probabilities of layout integration through time, and the switch to that state was selected on several consecutive steps from the hybrid state, in spite of the extra maintenance cost per 4 years. Additionally, state ICE displays a period of 4 years potentially switching to FC, but selects again *Action:* Use ICE because of the extra maintenance cost.

CAPEX and OPEX for each technology were calculated using Equations 11 and 12. Methanol cost is assumed to be constantly decreasing from 525 [€/ton] in year 0 to 300 [€/ton] by year 12 (MARIN, 2024). The specific CAPEX is set according to the values on Table 1. The trend of the CAPEX and OPEX cost are presented on Figures 5b and 5c.

$$CAPEX_{year,EC} = CAPEX_{EC} \cdot P_{installed} \tag{11}$$

$$OPEX_{year,EC} = fuelconsumption_{year,EC} \cdot fuelcost \tag{12}$$

Figure 6 provides an action pathway for each state of the MDP. In this case, 2 extra states (FC0.25 and hybrid0.25)are plotted to reflect the degradation of *FC and Hybrid states*. In these states, the extra maintenance cost is applied, and because of that, a switch to another EC may occur. Figure 6 shows that the switch to FC is the optimal decision for the *Hybrid state* in several years, which is explained both by the lower OPEX costs that FC offers in comparison to hybrid as well as the much lower probabilities of hybrid layout fitting - see Figure 5. Additionally, the action switch to FC becomes optimal after year 12 for state ICE, which is explained by the convergence of the CAPEX costs for the technology adoption (see Figure 5b). Lastly, a switch action is not selected at all for *FC state*, which is justified by the highest probability of reaching the required engine room length and the relatively low OPEX.

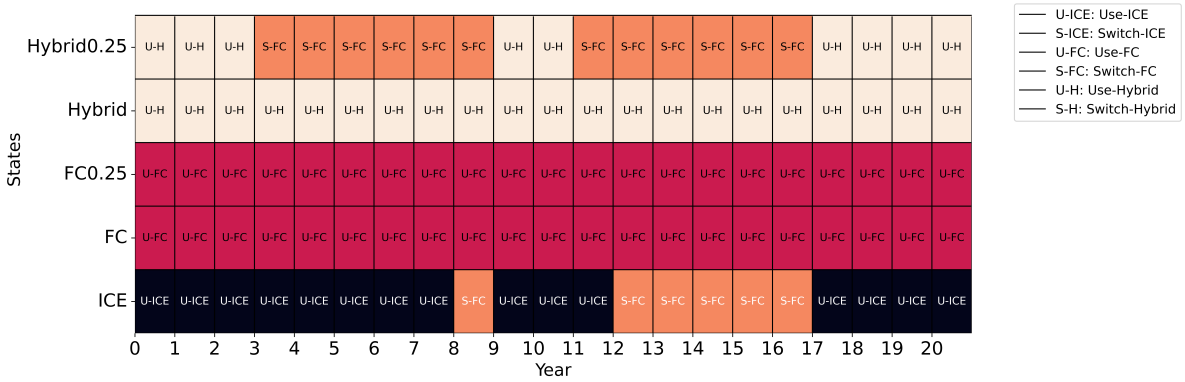

Figure 6: Policy map indicating optimal action per state and per year

Complementary to Figure 6 that prescribes an action path for each state per year, Figures 7, 8, 9 represent the optimal state accessed based on following the actions derived from the MDP policy pathway. This metric was developed based on Kana et al. (2015) and provides the optimal state to select, given a starting state.The colorscale on the side indicates the probability of being in that state,with red meaning 100 % chance and blue meaning 0 % chance. In Figure 7, ICE was selected as the starting state and shows that FC starts being the optimal state after year 12, which is in agreement with the policy of Figure 6. When selecting FC as the initial state, Figure 8 illustrates that FC is the optimal state to be selected. Lastly, Figure 9 demonstrates that for hybrid as the initial state, the switch to FC becomes the optimal after year 4 after completing the degradation phase that is modeled with substates hybrid0.75 to hybrid0.25. This result is in accordance with the policy map produced by the MDP in Figure 6. Figures 6, 7, 8 and 9 prove that both the high layout fitting probabilities, as well as competitive actions rewards, are necessary for a *switch action* to take place. For the ICE initial scenario, the FC state becomes optimal after the interval between the states' CAPEX cost has been zeroed.

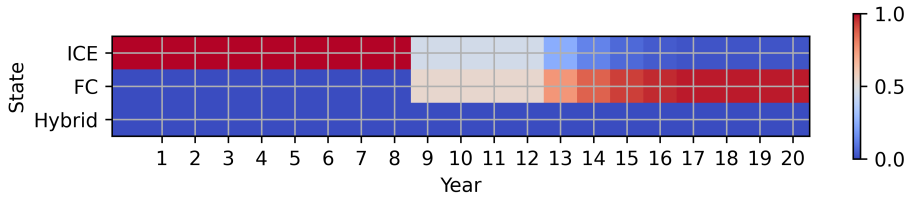

Figure 7: Optimal state accessed per action using ICE as initial state

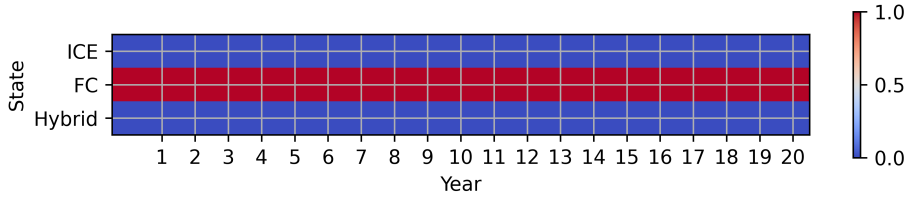

Figure 8: Optimal state accessed per action using FC as initial state

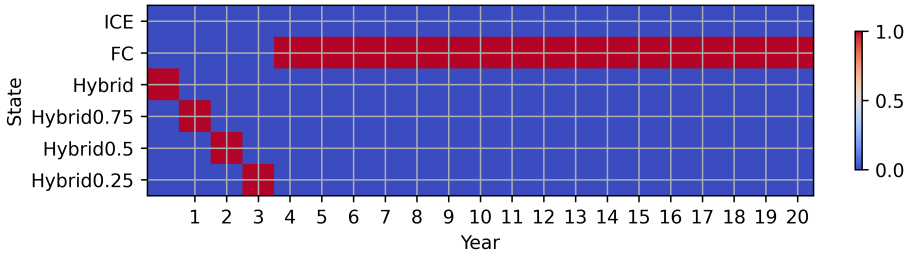

Figure 9: Optimal state accessed per action using hybrid as initial state

Figure 10 is used to plot the cumulative expenses that arise per state if the agent follows the policy proposed per epoch in accordance with Figure 6. To make a reasonable comparison, the most degraded substates of hybrid (Hybrid0.25) and FC (FC0.25) were plotted, in which the $OPEX_{maintenance}$ was applied. Figure 10 shows that FC has the lowest cost, in spite of the extra maintenance cost introduced every 4 years. Also, the cumulative cost deviation between the different states remains around 100.000 €, which is relatively small for a 20-year period. The relative cost convergence can be explained by the selection of *actions: Use EC* and not having to switch to other ECs. To have more robust outputs, the need for more detailed rewards calculation arises.

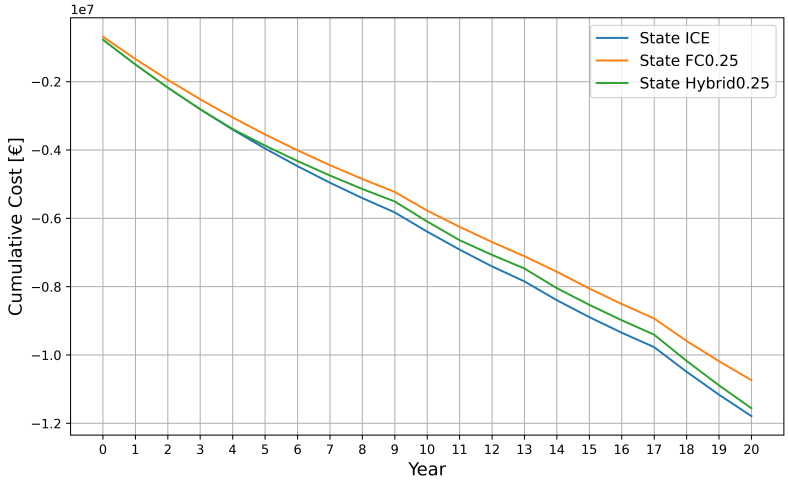

Figure 10: Cumulative cost for each EC option, when adopting the policy of the MDP decision matrix

DISCUSSION

The method presented is an attempt to integrate within a MDP framework, the technical uncertainties that are overlooked in lifecycle studies evaluating alternative configurations for a decarbonized vessel. The probabilities that reflected the integration challenges proved influential as the energy converter (FC) with the highest probability was the only one that the other two states may switch to in the future. Decisions are highly impacted by the reward vectors set for each action, meaning that the bigger differences in Capex costs for technology adoption during the first years of the case study prevented the switch action from being selected for ICE. The extra maintenance cost accounting for FC degradation did not prove triggering enough to cause a switch action and should be modeled in more detail. For more insightful results, a model of higher accuracy for the consumption costs should be applied that can integrate variable EC efficiency rate parameters and compute costs based on produced emissions per EC. Additionally, the selected type of vessels and its power profile influence the OPEX per technology and thus it is valuable to investigate the policy that would come out for alternative operational

profiles. Complementary to that, the probabilistic layout tool can be further advanced to handle scenarios with more components and possible system architectures, to increase the reliability of the predicted probabilities. Keeping in mind that this paper focused on applying a novel methodology to combine two normally disassociated tools - a lifecycle model and a probabilistic layout modeling tool, the core idea has proved to function successfully when applied to a proof of concept.

CONCLUSIONS

This paper outlined a way to further advance the lifecycle evaluation of the alternative fuelled PPEs by accounting for ECs' technical uncertainties that have traditionally been disregarded by the state-of-the-art research. The uncertainty quantification of systems layout integration challenges combined with the constant evolution of ECs technologies, led to the proposed method which has advantages worth highlighting. Markov Decision processes offer a very clear structure in which inputs from other models can be integrated and generate insights into decision pathways of PPE configurations towards a decarbonized ship design. The transition probability matrix, relating to selected actions, offers a clear structure to model the stochastic probability of the decision to switch or use a PPE technology based on its fitting to the layout. The reward vector can reflect on costs arising for the adoption of each technology. The MDP produces insight to the evolution of decisions within the lifecycle of the vessel. The coupling of MDPs with the probabilistic layout tool is a method that can account for technical, environmental, and financial uncertainties. The EC case study demonstrated that the probabilities defined for each EC based on their layout, paired with the computed EC costs, strongly influence the optimal decision pathway. The presented method sets the base for further development of both the probabilistic layout tool and the MDP, as well as their coupling, to produce insights for design pathways to be selected towards decarbonization with alternative fuels.

CONTRIBUTION STATEMENT

Apostolos S. Souflis - Rigas: Conceptualization; Methodology; Data Curation; Software; Visualisation; Writing – Original Draft.
Jeroen F.J. Pruyn: Supervision; Writing - Review & Editing
Austin A. Kana: Conceptualization; Software; Supervision; Writing - Review & Editing

ACKNOWLEDGEMENTS

This work is part of the MENENS project, funded by the Netherlands Enterprise Agency (RVO) under the grant number MOB21012.

REFERENCES

Aakko-Saksa, P. T., Lehtoranta, K., Kuittinen, N., Jarvinen, A., Jalkanen, J.-P., Johnson, K., Jung, H., Ntziachristos, L., Gagne, S., Takahashi, C., Karjalainen, P., Ronkko, T., and Timonen, H. (2023). Reduction in greenhouse gas and other emissions from ship engines: Current trends and future options. *Progress in Energy and Combustion Science*, 94:101055. Place: Oxford Publisher: Pergamon-Elsevier Science Ltd WOS:000901511200001.

Ballard (2024). Fuel Cell Power Module for Heavy Duty Motive Applications.

Bethke, B. and How, J. P. (2009). Approximate dynamic programming using Bellman residual elimination and Gaussian process regression. In *2009 American Control Conference*, pages 745–750, St. Louis, MO, USA. IEEE.

Chen, J., Fei, Y., and Wan, Z. (2019). The relationship between the development of global maritime fleets and GHG emission from shipping. *Journal of Environmental Management*, 242:31–39.

Dall'Armi, C., Pivetta, D., and Taccani, R. (2022). Uncertainty analysis of the optimal health-conscious operation of a hybrid PEMFC coastal ferry. *International Journal of Hydrogen Energy*, 47(21):11428–11440.

Elkafas, A. G., Rivarolo, M., Gadducci, E., Magistri, L., and Massardo, A. F. (2022). Fuel Cell Systems for Maritime: A Review of Research Development, Commercial Products, Applications, and Perspectives. *Processes*, 11(1):97.

EMSA and DNV (2021). Study on Electrical Energy Storage for Ships. Technical report, EMSA.

EU (2023). Press releases - Fuel EU Maritime.

Gebali, F. (2015). *Analysis of Computer Networks*. Springer International Publishing, Cham.

Gray, N., McDonagh, S., O'Shea, R., Smyth, B., and Murphy, J. D. (2021). Decarbonising ships, planes and trucks: An analysis of suitable low-carbon fuels for the maritime, aviation and haulage sectors. *Advances in Applied Energy*, 1. Publisher: Elsevier Ltd.

Harmsen, J. (2021). Green Maritime Methanol. Towards a zero emission shipping industry. Technical report, Green Maritime Methanol Consortium. Publisher: TNO.

IMO (2021). Fourth Greenhouse Gas Study 2020 International Maritime Organisation. Technical report, IMO.

IMO (2023). UN body adopts climate change strategy for shipping.

Juho Repo, Martin Axelsson, and Viktor Heir (2023). Methanol combustion concept alternatives for new build and retrofit of 4-stroke medium speed engines. In *30th CIMAC World Congress 2023*.

Kana, A., Knight, J. T., Sypniewski, M. J., and Singer, D. J. (2015). A Markov Decision Process Framework for Analyzing LNG as Fuel in the Face of Uncertainty. In *12th International Marine Design Conference*. Publisher: Unpublished.

Kana, A. A. and Harrison, B. M. (2017). A Monte Carlo approach to the ship-centric Markov decision process for analyzing decisions over converting a containership to LNG power. *Ocean Engineering*, 130.

Korberg, A. D., Brynolf, S., Grahn, M., and Skov, I. R. (2021). Techno-economic assessment of advanced fuels and propulsion systems in future fossil-free ships. *Renewable and Sustainable Energy Reviews*, 142. Publisher: Elsevier Ltd.

L. Menano de Figueiredo (2018). The_yacht_of_2030. Master's thesis, Delft University of Technology.

Lagemann, B., Lagouvardou, S., Lindstad, E., Fagerholt, K., Psaraftis, H. N., and Erikstad, S. O. (2023). Optimal Ship Lifetime Fuel and Power System Selection Under Uncertainty.

Lagemann, B., Lindstad, E., Fagerholt, K., Rialland, A., and Ove Erikstad, S. (2022). Optimal ship lifetime fuel and power system selection. *Transportation Research Part D: Transport and Environment*, 102:103145.

Lindstad, E., Lagemann, B., Rialland, A., Gamlem, G. M., and Valland, A. (2021). Reduction of maritime GHG emissions and the potential role of E-fuels. *Transportation Research Part D: Transport and Environment*, 101:103075.

Lindstad, E., Polić, D., Rialland, A., Sandaas, I., and Stokke, T. (2022). Decarbonizing bulk shipping combining ship design and alternative power. *Ocean Engineering*, 266:112798.

MAN (2024). MAN V12-2000 | MAN Engines.

MARIN (2024). Sustainable Power @ MARIN.

Niese, N. D. (2012). *Life Cycle Evaluation under Uncertain Environmental Policies Using a Ship-Centric Markov Decision Process Framework.* Thesis. Accepted: 2013-02-04T18:06:05Z.

Niese, N. D., Kana, A. A., and Singer, D. J. (2015). Ship design evaluation subject to carbon emission policymaking using a Markov decision process framework. *Ocean Engineering*, 106:371–385.

Poullis, I. (2022). Application of Model Based System Engineering (MBSE) with Ship Design Arrangement Tool of advanced zero emissions Power, Propulsion and Energy Systems in Maritime Technology. Master's thesis, Delft University of Technology.

Ritari, A., Huotari, J., and Tammi, K. (2023). Marine vessel powertrain design optimization: Multiperiod modeling considering retrofits and alternative fuels. *Proceedings of the Institution of Mechanical Engineers, Part M: Journal of Engineering for the Maritime Environment*, page 14750902221145747. Publisher: SAGE Publications.

Rivarolo, M., Rattazzi, D., Magistri, L., and Massardo, A. F. (2021). Multi-criteria comparison of power generation and fuel storage solutions for maritime application. *Energy Conversion and Management*, 244:114506.

RIX (2024). Hydrogen Power Generator Systems.

Russell, S. J., Norvig, P., and Davis, E. (2010). *Artificial intelligence: a modern approach*. Prentice Hall series in artificial intelligence. Prentice Hall, Upper Saddle River, 3rd ed edition.

Sheskin, T. J. (2010). *Markov Chains and Decision Processes for Engineers and Managers*. Taylor & Francis Inc, Boca Raton, FL, eerste editie edition.

Souflis Rigas, A., Pruyn, J., and Kana, A. (2023). Establishing the Influence of Methanol Fuelled Power Propulsion and Energy Systems on Ship Design. *Modelling and Optimisation of Ship Energy Systems 2023*.

Tadros, M., Ventura, M., and Soares, C. G. (2023). Review of current regulations, available technologies, and future trends in the green shipping industry. *Ocean Engineering*, 280:114670.

Torabi, F. and Ahmadi, P. (2020). Chapter 1 - Battery technologies. In Torabi, F. and Ahmadi, P., editors, *Simulation of Battery Systems*, pages 1–54. Academic Press.

Trancossi, M. (2015). What price of speed? A critical revision through constructal optimization of transport modes. *International Journal of Energy and Environmental Engineering*, 7.

van Biert, L., Godjevac, M., Visser, K., and Aravind, P. V. (2016). A review of fuel cell systems for maritime applications. *Journal of Power Sources*, 327:345–364. Publisher: Elsevier.

Van Veldhuizen, B., Van Biert, L., Aravind, P. V., and Visser, K. (2023). Solid Oxide Fuel Cells for Marine Applications. *International Journal of Energy Research*, 2023:1–35.

Warsila (2024). Wärtsilä 14 high-speed engine.

Wartsila (2024). Wärtsilä 31 - the most efficient 4-stroke marine engine.

Zhang, W., He, Y., Wu, N., Zhang, F., Lu, D., Liu, Z., Jing, R., and Zhao, Y. (2023). Assessment of cruise ship decarbonization potential with alternative fuels based on MILP model and cabin space limitation. *Journal of Cleaner Production*, 425:138667.

Zincir, B. and Deniz, C. (2021). Methanol as a Fuel for Marine Diesel Engines. In *Energy, Environment, and Sustainability*, pages 45–85. Springer Nature. ISSN: 25228374.

Zincir, B., Shukla, P. C., and Agarwal, A. K., editors (2023). *Decarbonization of Maritime Transport*. Energy, Environment, and Sustainability. Springer Nature, Singapore.

Zwaginga, J. J. and Pruyn, J. F. J. (2022). An evaluation of suitable methods to deal with deep uncertainty in ship design caused by the energy transition.

Proceedings of 15th International Marine Design Conference (IMDC-2024)
June 2-6, 2024
Amsterdam, the Netherlands

An Evaluation of System Modularity and Interface Standards as a Means for Continued Platform Level Relevance

Jason D Strickland, PhD, PE, FSNAME[1,*]

ABSTRACT

This paper will develop a descriptive working definition of modularity regarding ship systems. An effort will be made to expose the underlying motivation and attractiveness of modularity in naval vessels utilizing economic salvage value and continued operational relevancy. A survey of 50 years of modern system development in support of modularity will be supported by a historical case study. The historical analogy will focus on the concurrent development of platforms and weapon systems during the age of sail. Specific focus will be given to platform developments and the advent of marine artillery and their associated technological development. The insight developed will then be applied to two modern naval corollaries.

KEY WORDS

Modularity, Naval Design, Weapons Systems, System Design, Decoupled Architecture

MOTIVATION

The first section of this paper will develop a descriptive definition of modularity along six continuums: 1) Componentization, 2) Architecture, 3) Configurability, 4) Flexibility, 5) Interface Points, and 6) Allocation. An effort will be made to expose the underlying motivation and attractiveness of modularity in naval vessels utilizing economic salvage value and a less tangible ship effectiveness. Finally, the first section concludes with a look at investment duration by project for the last five decades relating to the development of architectural standards and why many modern modularity efforts have failed to produce the envisioned results.

The second and third section of this paper develop a historical analogy and review modern corollaries, respectively. The historical analogy will focus on the concurrent development of platforms and weapon systems during the age of sail. Specific focus will be given to platform developments and the advent of marine artillery and their associated technological development. The final section presents two modern modularized naval vessels and will assess their success of integrating modularization, considering these historical lessons learned.
It is the goal of this paper to illuminate several critical factors in determining the success or failure of a modularization effort on the scale of a modern naval vessel. To this end, this discourse is driven by four motivational questions:

1. What is the allure of system level modularity for ships?
2. How does an architectural standard develop to support sustained modularity?
3. Why have modularity efforts failed to date?
4. What can we learn from historical implementations of modular system architectures in the marine environment?

1 STRICKLY SHIPS, LLC (Gatihersburg, Maryland, United States)

* stricklyships@gmail.com

Submitted: 29 March 2024, Revised: 2 May 2024, Accepted: 3 May 2024, Published: 18 May 2024

Conference paper, DOI: https://doi.org/10.59490/imdc.2024.831 e-ISSN: 3050-4864

MODULARITY DEFINITION

Let's begin our analysis of system level modularity and impact that it potentially may have on a modern naval vessel with a standardized definition set. What exactly is modularity? We will double back to the guiding questions outlined in the motivation once we establish a baseline vernacular. To begin with modularity is an imprecise term. As such it has a multitude of meanings dependent upon the context of the discussion. (Kubota et al., 2017; Schank et al., 2016) For the purposes of this discussion, I would like to define modularity along six continuums: 1) Componentization, 2) Architecture, 3) Configurability, 4) Flexibility, 5) Interface Points, and 6) Allocation. While several of these concepts are potentially understood I will expand upon each to maintain clarity.

1. Componentization is the degree to which the end unit system is comprised of segregable subunits. This concept is the underpinning of modern software development approaches, define a self-contained reusable block of code that is insulated from changes in the rest of the stack. (Baresi & Miraz, 2011) For this discussion which is focused upon hardware systems componentization will range from *sparse* to *prevalent*.
2. Architecture is the degree to which new components can be integrated into the overall system. (Elmenreich, 2007) An architecture can assume values between *closed* to *open*. Theoretically in a completely open architecture any new component could be easily incorporated into the existing system. This does have some limitation in application.
3. Configurability is the degree to which subsystems and components can be dynamically arranged. (Balka & Wagner, 2006) Configurability can be scored on the continuum from *unconfigurable* to *adaptive*. It is important to note that each new configuration needs to function for an intended purpose.
4. Flexibility can be considered the number of functional uses for a single component or subsystem. (Lafou et al., 2016) Flexibility is scored between *limited* to *versatile*. While higher levels of flexibility are typically a good thing, the versatility of an object typically comes at the expense of another system attribute.
5. Interface points are either *customized* or *standardized*. One might be wondering what the gradation between these end points. An example of an interface point that is partial standardized and partially customized would cell phone chargers or USB 2/3 A-plugs. While the form factor is the same the power and data rates vary greatly depending on the standard that is being employed.
6. The final continuum definition has to do with the system level allocation or more specifically the requirement that is being addressed with this subsystem, this value can be assessed between *single use* to *multipurpose*.

While this six-vector scoring system is not likely to incorporate all the features that a designer would be concerned about during the integration of a complex system, it does begin to outline some of the major factors for the consideration of modularity and the influence of that modularity upon the rest of the ultimate system. Some notable exceptions would be system level mission effectiveness, space and weight considerations, and ultimately total system level cost. Now that a vernacular has been developed let's revisit the motivation and explore some recent efforts in sustaining system level modularity.

WHAT IS THE ALLURE OF SYSTEM LEVEL MODULARITY FOR SHIPS?

As highlighted in the prior example the cost versus capability of an upgrade in context with the service life of the total system creates the trade space for a modularity reasonableness assessment. If you consider the traditional economic concept of salvage value in conjunction with the fact that a ship is not a singular end system but truly a system-of-systems, the modularity of the subsystems becomes an imperative for continued operation.

First let's address the concept of asset depreciation and salvage value. The basic formula for calculating salvage value of an asset can be found in any engineering economics textbook or various other sources. (Eschenbach, 2011) Equation 1, below represents a simple declining balance depreciation approach.

$$S = P(1 - i)^y \quad [1]$$

The salvage value, S, is the product of the present value of the asset, P, and value retention rate, $(1 - i)$, raised to the number of years, y. If one begins with a present value of \$1B and applies a constant depreciation schedule (DBD) of 10% annually (*TR 2021/3*, 2021) the salvage value is approximately \$42M at the end of 30 years or 4.2% of the initial value. However, if one applies a compounding custom schedule depreciation (CSD) behaving similar to Moore's Law that doubles every decade, the salvage value is nearly \$200K or 0.02% of the initial value.

The custom schedule depicted in CSD data presented in Figure 1, applies a 10% depreciation for the first decade, a 20% depreciation for the second decade, and a 40% depreciation for the third decade. This acceleration in depreciation can be largely attributed to vessel wear and tear and system level obsolescence. The accelerated rate of obsolescence and depreciation is particularly applicable to military vessels, a bulk carrier would not be as dramatically affected by technology modernization.

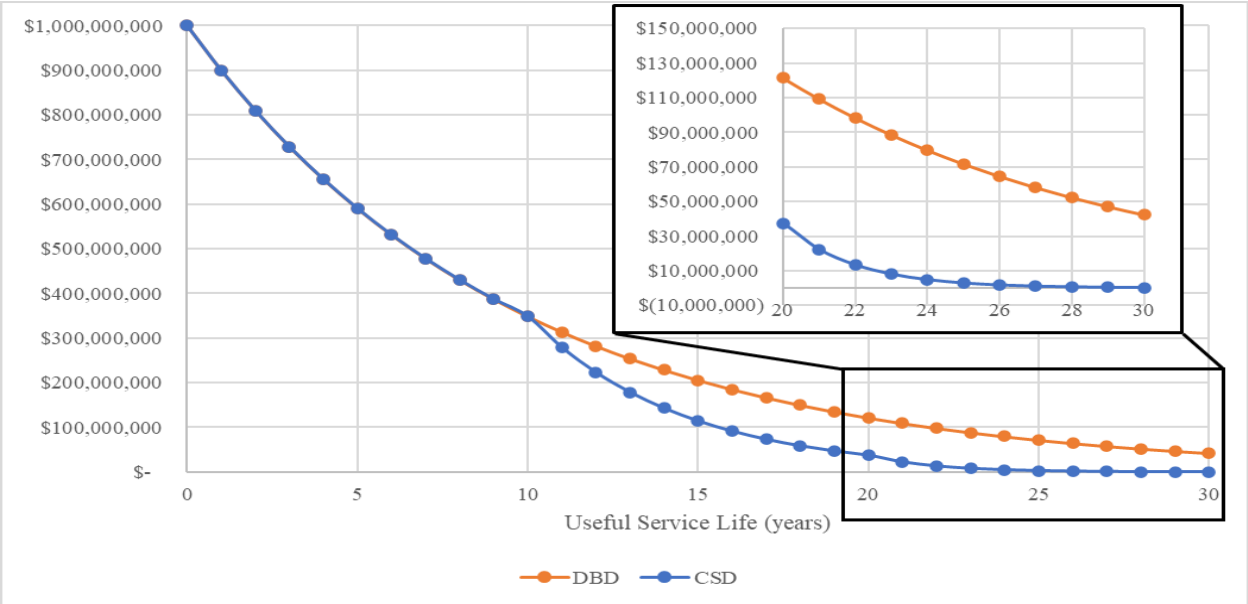

Figure 1 - Salvage Value with Respect to Time

While this is only part of the picture it does start to bring into the focus the financial side of the discussion. In short how much will the proposed upgrade cost versus the cost of the vessel. This starts to drive at a fundamental question that should be asked before a system upgrade commences. Is it worth the expense given the current value of the asset? It is acknowledged that salvage value is an artifice of economics, just because an asset has zero value on the books doesn't mean that it has no capability. Specifically in the context of working ships and military vessels capability is often the point. So, if the upgrade passes the initial cost-based litmus test, then the conversation returns to cost versus capability. While this gets more subjective there are some basic ground rules that should be employed. Consider a 4x4 grid with Additional Capability on the horizontal axis and Impact of Addition on the vertical axis. Then each block would roughly represent quartiles. The low end of the Additional Capability scale would be replacement in kind systems or software upgrades. The high end of this scale would be wholly new capabilities such as new weapons systems, launch and recovery systems, or automation approaches. The low end of the Impact of Addition could be bolt on systems that do not require an availability in a shipyard. The high end of this scale is a multi-year yard period with a complex or total overhaul. With these end posts, Quadrant 1 would represent high installation impact for a minimal capability increase. This is largely an area to be avoided for maximizing end product capability. Quadrant 2 would represent high installation impact but the addition of a potentially game-changing new capability. Quadrant 3 has low installation impact with a minimal capability increase. This leaves Quadrant 4; low installation impact and significant capability increase. Quadrant 4 is the optimist's corner, high payoff with low cost. Upgrades that fall into this area should be executed once they pass the previous financial screening. Figure 2 below summarizes this construct.

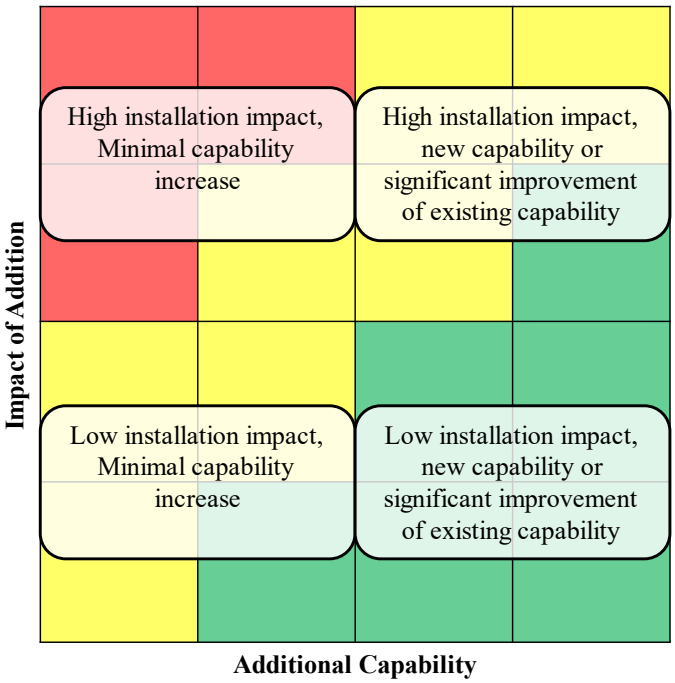

Figure 2 - Capability - Impact Scoring

"Note that while there has been considerable progress in maturing technology, no single technology has successfully met all the criteria for being institutionalized." (Doerry, 2014) In Figure 3 it can be seen how the total ship effectiveness is maintained and augmented by individual system additions across a span of 25 years. In this case since the design interface standard was locked to a MK41 Vertical Launch System incremental improvement was possible as technology matured across the complete system. However, if there was not a definitive standard such as the MK41 this story may have been much less compelling, this is also supported by historical development.

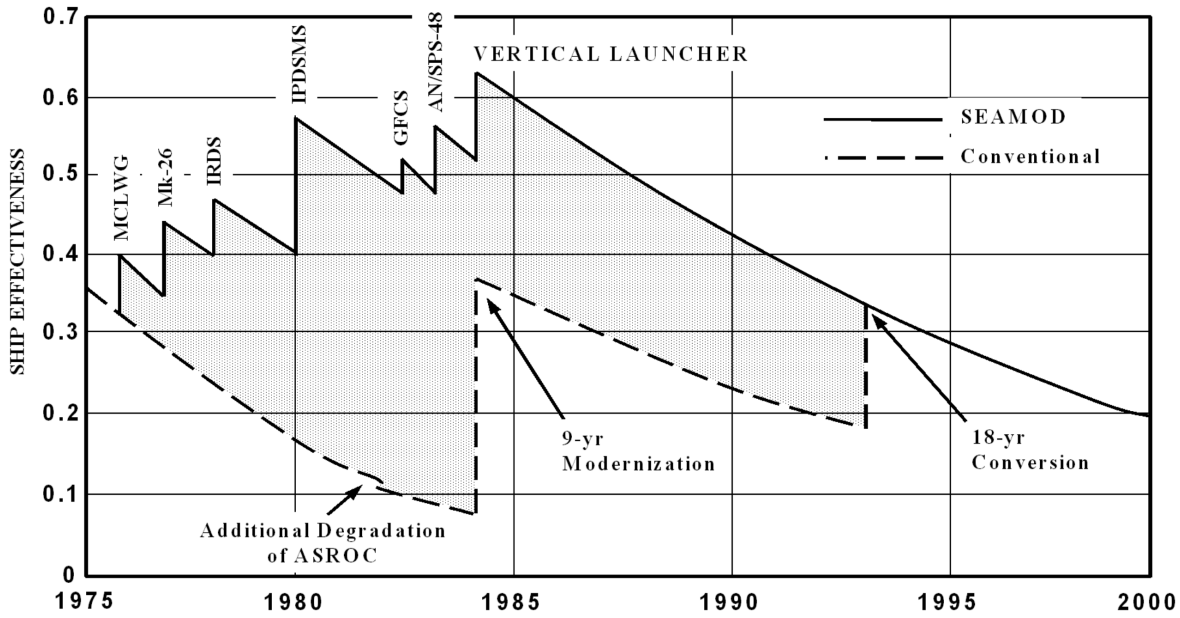

Figure 3 - Ship Effectiveness: SEAMOD vs Conventional (Abbott, 2006)

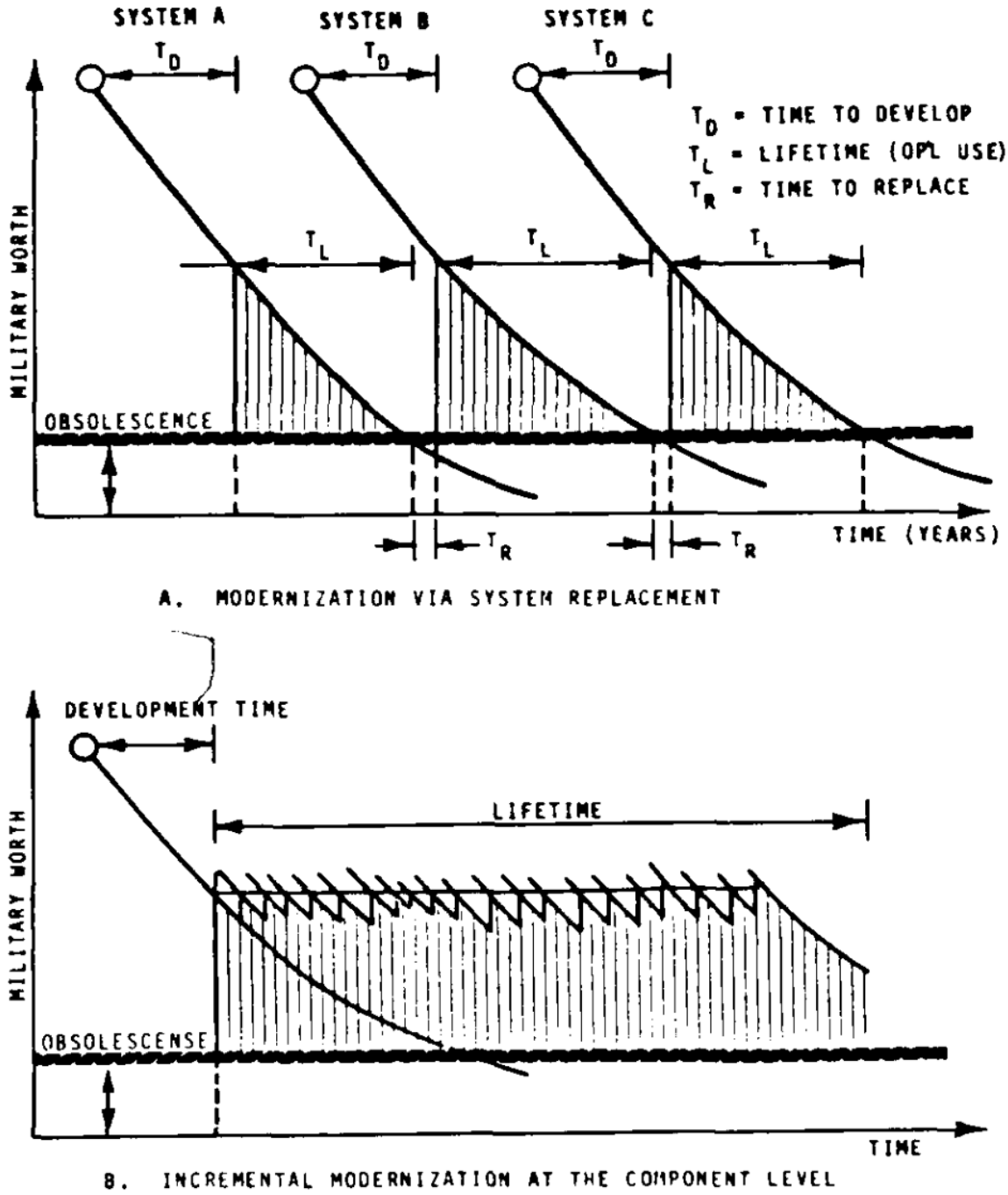

Figure 4 - Incremental Modernization Prior to Systems Obsolescence (DREWRY, 1975)

Figure 4 - Incremental Modernization Prior to Systems Obsolescence (DREWRY, 1975) illustrates an idealized scenario in which "incremental modernization at the component level" are made on a consistent basis to maintain the overall "military worth" of the vessel across the service life of the ship. This is proposed in contrast to the "modernization via system replacement" approach. The challenge with this approach is it requires an immense amount of consistency across the life of the class, and it assumes a linear technology growth path. Both are potentially flawed assumptions.

This section has looked at what system modifications should be entertained based upon the capability enhancement and the impact of installation, what are the alternative fielding strategies for modifications, and an example of incremental upgrades in a fielded system. This sets up the next discussion point.

HOW DOES AN ARCHITECTURAL STANDARD DEVELOP TO SUPPORT SUSTAINED MODULARITY?

The US Navy has had sporadic efforts related system level modularity in naval vessels since 1972. (Schank et al., 2016) The following bullets provide a synopsis of US Navy efforts in the establishment of a modular architectural standard.

- 1972 – 1978: Sea Systems Modification and Modernization by Modularity (SEAMOD)
  - Focused on modularized combat systems
  - Results were encouraging but required an overhaul of business and design practices
  - DD963 (com. 1975) and FFG7 (com. 1977) baseline ships under evaluation
- 1980 – 1985: Ship Systems Engineering Standards (SSES)
  - Focused on interface standards and variable payload systems
  - DDG51 (com. 1991) was the baseline for this effort
- 1992 – 2003: Affordability Through Commonality (ATC)
  - Focused on the reduction of acquisition and life cycle cost
  - Fleetwide implementation vice specific baseline
- 1994 – 2004: Open Systems Joint Task force (OSJTF)
- 1998 – 2003: Total Ship Open systems Architecture (TOSA)
- 2003: Open Architecture Computing Environment (OACE)
- 2003 – 2015: Architectures, Interfaces, and Modular Systems (AIMS)
  - Focused on a future implementation of modularity vice a backfit scenario

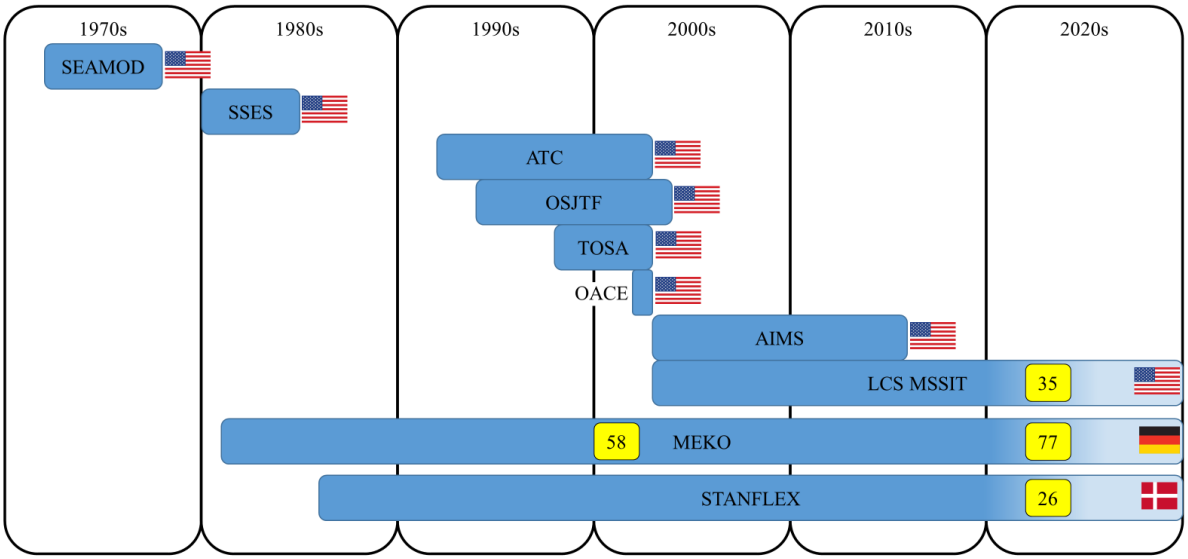

Figure 5 - Global Modular System Efforts (Strickland, 2023)

"The DDG 51 Class, which was supposed to be limited to 8,300 tons full load to show it was smaller than the preceding CG 47 cruiser class, was not fitted with extensive modularity for that reason. Only the 2 VLS weapons were built to Ship Systems Engineering Standards (SSES) Interfaces." (Garver et al., 2011)

Figure 5 illustrates to scale, the time span of efforts of the US Navy, Thyssen Krupp Marine Systems (TKMS) Mehrzweck-Kombination (MEKO) (Thyssen Krupp Marine Systems, n.d.), and Royal Danish Navy (RDN) Standard Flex (STANFLEX) (Harboc-Hansen, 1992), while this does not represent the total volume of funding expended it does begin to illustrate two key points. The first is that a steady state development absent of temporal breaks produces better results in terms of number of full systems delivered. The second is that there is not a single approach. Both the US Navy and the RDN have subscribed to an encapsulated subsystem that can be removed and replaced depending on the platform mission set and the need at present. This contrasts with the TKMS MEKO system that has less overall flexibility but creates standardized "sections" to produce vessels in support of customer requirements. This approach of modularized sections has been well received on the global market with 2-3 times the number of ships produced above encapsulated subsystems. The numbers in the yellow boxes on Figure 5, represent the total number of vessels delivered with these inherit features. This is somewhat misleading because the MEKO vessels are full systems complete with associated combat systems, and in some cases for the US Navy and RDN vessels the combat systems is dependent upon the installation of a mission module governed

by a separate procurement. (Piñeros Bello & Segovia Forero, 2020) This construct of decoupled weapon systems and vessel design is not novel. The basic premise of allowing each to progress along a desired development path and then integrate them also brings a series of opportunities and challenges.

WHY HAVE MODULARITY EFFORTS FAILED TO DATE?

It is hard to discuss system level modularity without being drawn to the IT sector. In order to illuminate this critical question, I will begin this section with a personal anecdote. When I first started buying my own computers in the late 1990s, I realized that the rate of development and change was hard to keep pace with and there was the balancing act of being a cash strapped college student. As such I chose a tower chassis that had several expansion slots for additional RAM and PCI cards. In turn I continued to upgrade that machine utilizing the system level "modularity" of the PC market. After a RAM upgrade, a HDD, a sound card, a video card, and a modem, I reached the functional limit of the machine. While the process of upgrading a machine was gratifying, after the fact I still needed to replace it. While I continued to increase the relevance of the machine over time the cost of the upgrades was clearly in excess of the total cost of a machine that had these upgrades at the beginning. Further once you factor in the personal time in trouble shooting software compatibility issues it was far cheaper to purchase the end product at the beginning. This is the first axiom of modular systems. The cost over time of the end item is greater utilizing modular upgrades than the initial purchase cost of an upgraded system.

But there was a larger failed premise underlying this learning exercise. The machine was going to continue to be relevant even after all possible upgrades had been made. While the interface standards remained consistent during the personal example above, and many of those standards are still in use almost 30 years later the incremental upgrades could not keep pace with the component rate of change. I believe that this is one of the fundamental sources of failure in total system level modularity.

While interface standardization and commitment are necessary conditions, they are not fully sufficient for successful implementation on modularized systems. Even with the necessary conditions met one needs to balance the cost vs the capability of the system upgrade. Back to the PC example, if it is determined that the service life of the machine is five years, this adds a context to support the tradeoff of cost versus capability. With the addition of Moore's Law, it can be shown that within the five-year service life of the machine, the industry standard computing power quadrupled. So, the question becomes is the cost of the upgrade going to increase the relevance of the total system to a point that is on par with the current industrial standard. The answer is unfortunately no. While the modular upgrade may add a new capability or even improve an existing capability it will not be competitive with the current market standard.

This brings us to the second axiom of modular system failure; piece meal system acquisition will never keep pace with the developmental capability of new production. The computer growth issue highlighted by Moore's Law is just one component of total system level capability maturation scheme. This axiom has transcended computer systems into mechanical systems at this point. The automobile industry is a great example of the last point. New vehicles have hundreds of processors and are incapable of operation if the Electronic Control Unit is offline. (Charette, 2021)

HISTORICAL ANALOGY: AGE OF SAIL AND MARINE ARTILLERY

During this 400-year period of history it is the height of European colonialism, a great power competition, and a technological development race. The renewed focus on scientific pursuits from the Renaissance and the Great Enlightenment ultimately culminated in the Industrial Revolution. This is the backdrop for the historical analogy. See Figure 6 - Timeline of key developmental events.

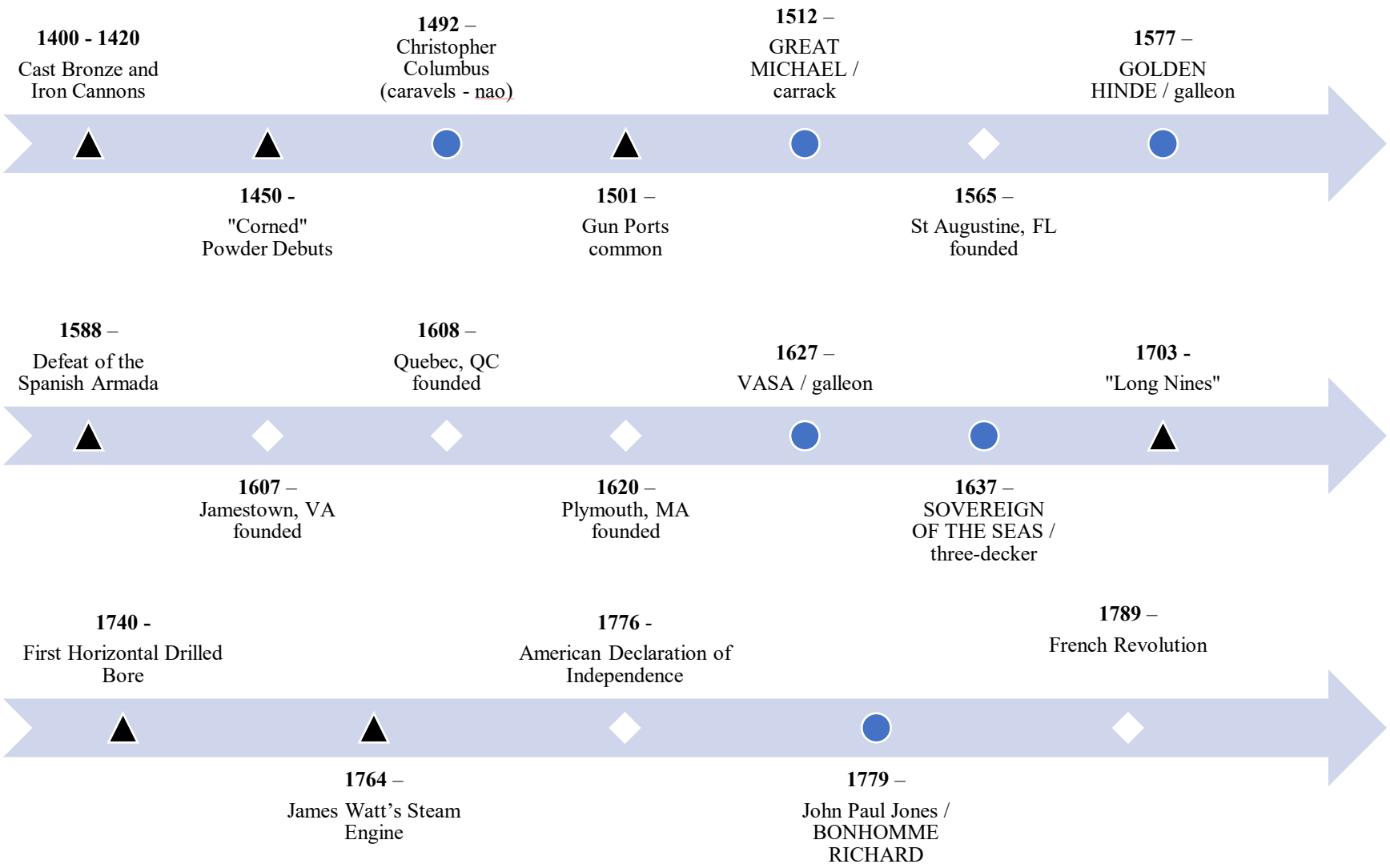

Figure 6 - Timeline of key developmental events; In the above figure entry symbols represent the following: ▲ technological advancements that influenced maritime system development; ● significant vessels discussed within the context of this paper; ◇ major geopolitical events that impacted naval systems and maritime system development

European Colonialism

For this discussion the colonialization of North America is representative of the broader world stage. On Figure 6 there are six events represented by a diamond. The first four of these events represents the establishment of permanent settlements in North America by the Spanish, English, and French. St Augustine (Spanish) (*Our History | St. Augustine, FL*, 2023), Jamestown (English) (US National Park Service, 2022), and Quebec (French) (Mendel, 2022) were the new focal points in a struggle between these three countries that dated back hundreds of years at this point. The founding of Plymouth, MA is interesting for several reasons. First the MAYFLOWER was a hired transit, while they did need permission to build a colony it was not strengthen the position of the European Monarchs via trade routes and raw materials. The final two diamonds are the American and French Revolutions. These resulted in massive changes to the geo-political fabric of the time and helped to fuel the great power competition underway by destabilizing the established order.

Technological Development Race

To continue to support the competitive nature and massive expansionism, new technologies were being developed and fielded almost constantly. Any advantage or technological edge could make an enduring difference in the power race. From a naval perspective two technology trends need to be discussed, the advancement of sailing ships and marine artillery. These technology milestones are marked by circles or triangles respectively, see Figure 6.

"During the Hundred Years' War (1339-1453) cannons came into general use. Those early pieces were very small, made of iron or cast bronze, and fired lead or iron balls. They were laid directly on the ground, with muzzles elevated by mounding up the earth. Being cumbrous and inefficient, they played little part in battle, but were quite useful in a siege." (Manucy, 1949) In the early part of the 15th century artillery manufacturing obtained a critical breakthrough, casting of iron and bronze of ever increasing size. (Dana, 1911) In this same timeframe the transition from a ground-based siege weapon to a naval weapon was well underway. (Devries, 1990) In fact by the turn of the 15th century, most English ships of any size were equipped with powder fired weapons. (Devries, 1990) It should be noted that these weapons were mounted on the topsides of the vessels and cannon/gun ports do not become prevalent until vessel construction moves away from clinker type hulls. The technological advance of casting muzzle loading cannons is met with the development of corned powder, "corned powder develops its propulsive force far more quickly than a tightly packed charge of dry-mixed, or serpentine, powder" (Guilmartin, 2007) This massive increase in the effectiveness and consistency of gunpowder allowed for greater range and control of the combustion in support of artillery operations.

On the timeline this brings us to Columbus' voyage to North America, possibly one of the most fortuitous mistakes of history. But the focus for this discussion is on the three vessels utilized in the 1492 crossing. The Nina, Pinta, and Santa Maria were two caravels and a carrack / nao, respectively. The caravel class of vessel began to use carvel construction approach vice the previous clinker type hulls. These smoother hulls proved durable, agile, and faster than their rougher predecessors. This is largely why the caravel became a popular platform for exploration and trade. Figure 7 illustrates a model of a caravel likely in a typical rigging pattern. The caravel's prominence was supplanted by the larger carrack. Larger in every dimension the carrack was like a caravel in construction with the addition of a focsle. Figure 8 illustrates the squared rigged sails forward with the prominent focsle. These vessels maintained the aft lateen sail.

Figure 7 - Three masted caravel with lateen rigged sails (Deutsches Historisches Museum, n.d.-a)

Figure 8 - Three masted carrack / nao with square rigged sails forward and lateen sail aft

With carvel construction as the dominating European approach, smooth hulls with carefully carved butt joints between planks affixed over a series of deep frames, the stage was set for the next advancement in naval artillery. The relocation of guns from the topside is largely due to the advent of gun ports. By the early 1500's gun ports were a predominant feature in naval designs. (Skaarup, 2021) The GREAT MICHAEL (Newhaven Heritage Centre, n.d.) and the MARY ROSE (Mary Rose Trust, 2023), both launched 1511, featured extensive armament via gunports below the weather deck.

As the GREAT MICHAEL and the MARY ROSE began to maximize the capacity of the carrack, the next evolutionary step was devised in the platform. The galleon's length was increased to support an additional mast and provide better seakeeping and resistance characteristics without a reduction in cargo fraction. (Deutsches Historisches Museum, n.d.-b; Mariners' Museum and Park, 2023). These vessels were specifically designed to support military operations and open ocean transits. "The Golden Hind, an English galleon launched in 1577 and best known for her privateering circumnavigation of the globe between 1577 and 1580, captained by Sir Francis Drake" (National Historic Ships UK, 2023) is a great example of this design marriage. The purpose of Golden Hind was to sail the oceans and raid Spanish settlements further supporting the building international competition to colonize the globe. Upon Drake's return tensions between the English and Spanish were at an all-time high. These tensions culminated with the English defeat of the Spanish Armada. This historical milestone was not solely predicated on technological advancements but on the employment of innovative new tactics. "In 1588, Spain's King Philip II ordered a naval invasion of England. Philip's Spanish Armada of 124 ships, 27,000 men, and 1,100 guns departed from Lisbon on May 30, 1588. England meanwhile, led by Queen Elizabeth I, readied a counterforce of 197 vessels, 16,000 men, and 2,000 guns." (Adams, n.d.) The English had the advantage of numbers in ships, but they were smaller and more agile than the landing force galleons employed by Spain. A fundamental shift in tactics made all the difference in the outcome. "To the Spanish, ships were floating fortresses to be grappled and taken at sword's point, but to the English, they were fast and maneuverable gun platforms." (Niderost, 2007) This new style of naval combat, maintaining a standoff and pummeling your opponent with gun fire, remains a prevalent tactic. We have however just increased the standoff distance and engagement speed with missiles. This decisive victory cemented the cannon's place in naval artillery as a ship-to-ship weapon not just a tool for shore bombardment.

The first half of the 17th century is marked by another expansion of platforms to support naval artillery and longer sailing distances at speed. The ship of the line had become the preferred battle tactic and quite often the vessel with the most guns won. Most vessels in this role during this time were galleons with one or more full gun decks. Let's look quickly at two such ships in the pivotal time. The VASA was a galleon, with a traditional design and a single gun deck. The original design was to carry thirty-two 24-pound guns. (Fairley, n.d.) During the construction revisions to the design added a second deck and another thirty-two 24-pounders (5,600 lb. / cannon). (Kessler et al., 2001) This

raised her effective center of gravity. Further ships were a symbol of national pride and as such they were extremely ornate. This also created an increase in the center of gravity. The vessel's maiden voyage lasted 1,300 meters, before capsizing in 1628. The SOVEREIGN OF THE SEAS was a three-decker, meaning she carried three full gun decks. She had very similar ornate decorations and an increased capacity from her predecessors. The SOVEREIGN OF THE SEAS served in multiple campaigns from 1637-1696. (Holmes, 2010) Table 1 allows one to compare the principal characteristics of the VASA to the SOVEREIGN OF THE SEAS. One should note that there is only a decade between the launch dates of these vessels. Further the VASA would have been one of the most aggressively armed vessels of the time, although the SOVEREIGN OF THE SEAS had a 55% increase in the total number of cannons with a modest increase in total displacement. Finally, if the cannon designations seem confusing, it is because they are nonstandard. Every country at this time forged their own barrels and mass standardization of barrel length, bore diameter, shot weight, and other key attributes of marine artillery were not standardized until the middle of the 18th century. (Berkowitz & Dumez, 2016; Henry, 2009; Manucy, 1949) The end of the 18th century effectively marks the end of the golden age of sail. With the advent of the steam engine, and the further geopolitical unrest the stage was set for the next major development modification of platforms. This conjoined development process of weapon systems and platforms continues to this day. While there are almost endless volumes of historical examples that could be evaluated. Let's use the balance of the discussion to examine a few select modern corollaries considering this context.

Table 1 - Comparison of VASA to SOVEREIGN OF THE SEAS (Holmes, 2010; The Vasa Museum, 2015)

	Vasa	Sovereign of the Seas
LOA	155.8 ft	167 ft
Beam	38.4 ft	48.3 ft
Depth	63.3 ft	76 ft
Displacement	1210 tons	1683 tons
Armament	Lower Deck 28 x cannons (24 pdrs) Upper Deck 22 x cannons (24 pdrs) Weather Deck 2 x cannons (1 pdrs) 8 x cannons (3 pdrs) 6 x cannons (6 pdrs) Total 66	Lower deck 20 × cannon drakes (42-pdrs) 4 × demi-cannon drakes (32-pdrs) 2 × demi-cannon drakes (32-pdrs) 2 × demi-cannon drakes (32-pdrs) Middle deck 22 × culverin drakes (18-pdrs) 2 × demi-culverin drakes (9-pdrs) 4 × culverins (18-pdrs) 2 × culverins (18-pdrs) Upper deck 22 × demi-culverin drakes (9-pdrs) 2 × demi-culverins (9-pdrs) 2 × demi-culverins (9-pdrs) Quarter deck 6 × demi-culverin drakes (9-pdrs) Poop deck 2 × demi-culverin drakes (9-pdrs) Forecastle 8 × demi-culverin drakes (9-pdrs) 2 × culverin drakes (18-pdrs) Total 102

MODERN COROLLARIES

This section will discuss the development of two of the three modern modularity exercise highlighted in Figure 5. Specifically, the Littoral Combat Ship (LCS) and the Standard Flex (STANFLEX) efforts will be analysis for similarities and difference. The previous historical case study will be utilized for contextualization. The MEKO approach has been omitted from this conversation since the approach is dramatically different than that employed by

the US and Danish Navies. Global componentization in construction should be further evaluated and the MEKO would be a beneficial case study in that endeavor.

Littoral Combat Ship

The Littoral Combat Ships was envisioned to be a high speed, inexpensive platform with a modular mission system that could be dynamically assigned in theater. "Rather than being a fully multimission ship like the Navy's larger surface combatants, the LCS is to be a focused mission ship, meaning a ship equipped to perform one primary mission at any given time. The ship's primary mission orientation can be changed by changing out its mission package, although under the Navy's latest plans for operating LCSs, that might not happen very frequently, or at all, for a given LCS." (O'Rourke, 2019) One potential performance issue with the disaggregated development and acquisition of the LCS Mission Packages was the fact that each Mission Package consisted of multiple Mission Modules. (Asst Secretary of Navy, Research, Development, and Acquisition, 2018) These Mission Modules had different developers and integrators. This is further confounded by the development and testing timeline associated with each Module at the sub-Package level. The result was "the total initial mission package operational capability has been delayed by about 9 years (from 2011 to 2020) and the Navy has lowered the level of performance needed to achieve the initial capability for two packages". (Francis, 2016) Further, "Changes in the LCS concept of operations are largely the consequence of less than expected lethality and survivability, which remain mostly unproven 7 years after delivery of the lead ships". (Francis, 2016) this brings us to the current scenario with 35 hulls being awarded in various stages of construction with two distinct variants. Despite the lapse of 21 years since program initiation, and almost 3 dozen ships, the reality of a hot swapable flexible combat system has fallen dramatically short of the initial vision.

Why did this effort fall so short of initial expectations? It is my feeling that there are two fundamental underlying contributors to these results. First, a lack of established standards. This total system acquisition effort undertook the development effort of two distinct sea frames, three mission packages, and the development of modular interfaces. This effort would have been challenging enough with a single sea frame, mission package, and associated interface standards. This challenge coupled with aggressive requirements created a scenario for the much-publicized difficulties of the LCS Program. Unlike the historical scenario above there was not a clear shipboard interface for independent development of modularized systems. The gun port, albeit simplistic, allowed for independent development of platforms and weapons and further facilitated the integration of these systems without major retrofits. The complexity of integrating a modern cannon or missile system is not lost here, however the point is that the interface standards did not exist prior to program initiation and these newly developed standards created in stride with the program development needed to accommodate a range of modules further increasing the total system complexity. Regarding system complexity this brings us to the second contributor, the hierarchical mission package – mission module – mission system construct adds a tremendous amount of requirement interdependency and thus increases the overall risk to execution. With three distinct Mission Packages each comprised of multiple modules and sub systems all being coincidentally independently developed by a variety of vendors the opportunity to encapsulated schedule risk and hedge performance characteristics is virtually nonexistent. A performance or developmental failure in a lower tier system would lead to cascading failures. This was realized with Surface-to-Surface Missile Module (SSMM), Remote Multi-Mission Vehicle (RMMV), and Dual-mode Array Transmitter (DART).

The SSMM was designed and tested with the AGM-114L Longbow Hellfire missile. This missile variant was actively produced until 2005 and is scheduled to be replaced with the AGM-179 Joint Air-to-Ground Missile (JAGM). Meanwhile the first successful land attack exercise was conducted with the Longbow Hellfire on 12MAY2022. (Hardgrove, 2022) While this is not a failure in the development of the SSMM it will mean the need to retest and potentially delay operational use of the module as it is being certified for the launch of another missile platform. The RMMV was somewhat operationally successful but unreliable. (Remote Minehunting System (RMS), 2016) After ship integration issues due to launch and recovery (FY15 Navy Programs - Remote Minehunting System (RMS), n.d.), two Nunn-McCurdy programmatic breaches (2009, 2015) (Eckstein, 2015), and failure to progress after a dedicated reliability improvement effort (FY15 Navy Programs - Remote Minehunting System (RMS), n.d.) the RMMV was officially canceled in 2016 (Remote Minehunting System (RMS), 2016). This realized failure in a critical system within the Mine Countermeasures (MCM) Mission Package required that the entire package be refactored and rearchitected. As such years of delay were experienced, in fact the MCM Mission Package just obtained its Initial Operational Capability in early 2023. (Shelbourne, 2023) The DART was optimized for weight considerations and

modular employment within the LCS waterborne systems area of the mission bay. The prototypes were initially accepted in 2018 and then development was subsequently canceled in 2022. This cancelation was due to SONAR performance and reliability. (Abott, 2022; *Navy Canceled Raytheon's DART Sonar Due to High Risk | InsideDefense.Com*, n.d.) Given the above one can begin to see how the inability to encapsulate schedule and performance risks during the development created a realized risk in each of the Mission Packages for the 35 LCS sea frames.

STANFLEX

"The driver for StanFlex was money—the Royal Danish Navy needed to replace 22 warships of three classes, but it could not afford to do so on a one-for-one basis, so it came up with the idea of building 16 multirole modular vessels (later cut to 14)." (*Beware the Allure of Mission Modularity*, 2023) The basic assumption behind the STANFLEX concept was that "logistic standardization and operational flexibility can be achieved by use of rapidly exchangeable, modular systems matching a variety of roles" (Harboc-Hansen, 1992) Does this sound familiar? It should, it is the exact same justification that was utilized for the LCS program. So, the ultimate question becomes why the STANFLEX experience is considered successful and the LCS experience is considered painful. Maybe it is the scale of the effort, the complexity of the end system, or acquisition approach.

The first vessels to be outfitted with the STANFLEX modules were the Surface Auxiliary Vessel (Harboc-Hansen, 1992) later designated as the Flyvefisken Class (SF 300) ("Flyvefisken Class (SF 300)," n.d.). These composite vessels were of a size and complexity that supported a multitude of roles from MCM to environmental support and provided a perfect opportunity to work out the bugs associated with fielding a modular combat system. The length of the Flyvefisken is 54m, with four STANFLEX slots accounting for 12m of the vessels weather deck. In this initial case of modularization, the RDN allocated a smaller vessel than the LCS with a much higher percentage of modularization. The total scale of the initial effort is drastically different, but it allows for the required learning by the government and industry. The complexity of the ultimate end system and desired mission effectiveness could be the next key to success. Again, like the LCS the RDN had originally envisioned surveillance, combat, offensive mining, anti-pollution, anti-submarine warfare, and MCM mission packages composed of distinct modules. The biggest difference is that each of the modules all conformed to the same structural envelope and utilized standardized connections. This self-encapsulated module approach helps to mitigate performance and schedule risk associated with the concurrent development of the mission packages. Finally this brings us to an acquisition approach, Naval Team Denmark (*Https*, n.d.) is an industry and regulatory consortium that develops, and delivers the STANFLEX modules. It does make one wonder if the top 20 naval defense agencies in the US was to form a design and fabrication consortium that would have sufficiently altered the LCS experience. In this case the parallels to the historical case are enlightening. The RDN had a definitive fixed standard for modularized systems that was trialed on a small case and then eventually expanded to all following classes. This allows for consistent spiral development and compatibility. The ultimate complexity was managed starting with the least taxing cases and eventually evolving and increasing capability to account for more challenging configurations. And finally, this became a point of national pride. Much like the capital sailing vessels the defense conglomerate that was empowered around the STANFLEX project pulled the best from the industrial base to develop a successful program and new naval standard.

SUMMING UP

During the first section of this paper a more descriptive definition of modularity has been developed. This definition describes modularity along six continuums: 1) Componentization, 2) Architecture, 3) Configurability, 4) Flexibility, 5) Interface Points, and 6) Allocation. While the treatment of this definition is subjective in this document a more objective mechanism has been developed and is under evaluation at this time. An effort has been made to expose the underlying motivation and attractiveness of modularity in naval vessels utilizing economic salvage value and a less tangible ship effectiveness. Finally, the first section concludes with a look at investment duration by project for the last five decades relating to the development of architectural standards and why many modern modularity efforts have failed to produce the envisioned results. Culminating in two axioms of modular system failure: 1) the cost over time of the end item is greater utilizing modular upgrades than the initial purchase cost of an upgraded system, and 2) piece meal system acquisition will never keep pace with the developmental capability of new production.

The second and third section of this paper develop a historical analogy and review modern corollaries, respectively. Specifically with respect to the historical section the decoupling of platform and weapons system development allowed for gains in both systems since the interface point was a loose constraint. This concept of independent development allowed for each system to evolve based on technological limits and the application of new techniques. The maintenance of a loose interface standard allowed for frequent upgrades and modifications to occur on a timeline that made the most sense for system fielding. Additionally, developmental and schedule risk was encapsulated thus minimizing the total acquisition impact. The final section presented two modern modularized naval vessels considering these historical lessons learned. One program fell far short of it envision capability due to the lack of established standards, and a tremendous amount of requirements interdependency. While the second controlled the scale of the effort, the complexity of the end system, and applied a community-style acquisition approach. Even though the initial case of modularization was assigned to a much smaller vessel than the previous example, there was a much higher percentage of modularization.

While this is a quick survey of 50 years of modern system development spanning countless millions of dollars, supported by a case study that spans almost 300 years, the principal key to success in modular systems is the adoption and commitment to an interface standard that is not overly constrained. Historically the gun port allowed for the development of platform and weapon technology to be decoupled and developed independently. Similarly, the STANFEX fixed a geometric interface and has allowed for the iterative development of new combat and support systems to be developed and successively deployed across new classes. Modularity will continue to be attractive to naval vessels but to realize the potential of this modularity, a definitive standard must be adopted and employed uniformly across multiple classes.

SOURCES CITED

Abbott, J. W. (2006, April 27). *The History of Modular Payload Ships:*

Abott, R. (2022, September 1). *Navy Cites Reasons For Ditching DART Sonar For LCS, Frigate*. Defense Daily. https://www.defensedaily.com/navy-explains-challenges-of-canceled-dart-lcs-frigate-sonar/navy-usmc/

Adams, R. (n.d.). *The Spanish Armada, 1588*. Gilder Lehrman Institute of American History. Retrieved August 29, 2023, from https://www.gilderlehrman.org/history-resources/spotlight-primary-source/spanish-armada-1588

Asst Secretary of Navy, Research, Development, and Acquisition. (2018). *Report to Congress for the Littoral Combat Ship Mission Modules Program—Annual Report* (4–5617062). US Navy. https://news.usni.org/2018/04/03/littoral-combat-ship-mission-package-annual-report

ATO Depreciation Rates 2021 • Vessel. (2021, July 1). Australian Taxation Office (ATO) Depreciation Rates 2021. https://www.depreciationrates.net.au/vessel

Balka, E., & Wagner, I. (2006). Making things work: Dimensions of configurability as appropriation work. *Proceedings of the 2006 20th Anniversary Conference on Computer Supported Cooperative Work*, 229–238. https://doi.org/10.1145/1180875.1180912

Baresi, L., & Miraz, M. (2011). A Component-Oriented Metamodel for the Modernization of Software Applications. *2011 16th IEEE International Conference on Engineering of Complex Computer Systems*, 179–187. https://doi.org/10.1109/ICECCS.2011.25

Berkowitz, H., & Dumez, H. (2016). The Gribeauval system, or the issue of standardization in the 18th century. *GÉRER & COMPRENDRE - ENGLISH LANGUAGE ONLINE SELECTION*, *125*. https://www.annales.org/gc/GC-english-language-online-edition/2016/BERKOWITZ-DUMEZ.pdf

Beware the Allure of Mission Modularity. (2023, May 1). U.S. Naval Institute. https://www.usni.org/magazines/proceedings/2023/may/beware-allure-mission-modularity

Charette, R. (2021, June 7). *How Software Is Eating the Car—IEEE Spectrum*. https://spectrum.ieee.org/software-eating-car

Dana, C. E. (1911). Notes on Cannon-Fourteenth and Fifteenth Centuries. *Proceedings of the American Philosophical Society*, *50*(199). https://www.jstor.org/stable/984031

Deutsches Historisches Museum. (n.d.-a). *Caravel*. Retrieved August 28, 2023, from https://www.dhm.de/mediathek/en/ship-types/milestones-in-the-history-of-european-shipbuilding/05-caravel/?backlinkAnchor=content-127

Deutsches Historisches Museum. (n.d.-b). *Galleon*. Retrieved August 28, 2023, from https://www.dhm.de/mediathek/en/ship-types/milestones-in-the-history-of-european-shipbuilding/08-galleon/

Devries, K. R. (1990). A 1445 Reference to Shipboard Artillery. *Technology and Culture*, *31*(4), 818–829.

Doerry, N. (2014). Institutionalizing Modular Adaptable Ship Technologies. *Journal of Ship Production and Design*, *30*. https://doi.org/10.5957/JSPD.30.3.130038

DREWRY, J. T. (1975). MODULARITY: MAXIMIZING THE RETURN ON THE NAVY'S INVESTMENT. *Naval Engineers Journal*, *87*(2), 198–214. https://doi.org/10.1111/j.1559-3584.1975.tb03730.x

Eckstein, M. (2015, October 13). UPDATED: Navy Launches Independent Review of Littoral Combat Ship Remote Minehunting System. *USNI News*. https://news.usni.org/2015/10/13/navy-launches-independent-review-of-littoral-combat-ship-remote-minehunting-system-new-look-could-cause-more-testing-delays

Elmenreich, W. (2007). A Review on System Architectures for Sensor Fusion Applications. In R. Obermaisser, Y. Nah, P. Puschner, & F. J. Rammig (Eds.), *Software Technologies for Embedded and Ubiquitous Systems* (pp. 547–559). Springer. https://doi.org/10.1007/978-3-540-75664-4_57

Eschenbach, T. (2011). *Engineering Economy: Applying Theory to Practice* (3rd ed.). Oxford University Press. https://global.oup.com/us/companion.websites/9780199772766/student/pdf/Chapter12E2010.pdf

Fairley, R. (n.d.). *Why The Vasa Sank: 10 Lessons Learned*. Retrieved February 13, 2023, from https://faculty.up.edu/lulay/failure/vasacasestudy.pdf

Flyvefisken Class (SF 300). (n.d.). *Naval Technology*. Retrieved September 25, 2023, from https://www.naval-technology.com/projects/fly/

Francis, P. (2016). *Littoral Combat Ship and Frigate—Congress Faced with Critical Acquisition Decisions* (GAO-17-262T). Government Accountability Office. https://www.gao.gov/assets/gao-17-262t.pdf

FY15 Navy Programs—Remote Minehunting System (RMS). (n.d.). Director, Operational Test and Evaluation. https://www.dote.osd.mil/Portals/97/pub/reports/FY2015/navy/2015rms.pdf?ver=2019-08-22-105645-710

Garver, S., Marcantonio, R., & Sims, P. (2011). *Modular Adaptable Ship (MAS) Total Ship Design Guide for Surface Combatants.pdf*. NAVSEA.

Guilmartin, J. F. (2007). The Earliest Shipboard Gunpowder Ordnance: An Analysis of Its Technical Parameters and Tactical Capabilities. *The Journal of Military History*, *71*(3), 649–669.

Harboc-Hansen, H. (Ed.). (1992). *Standard Flex 300*. Danyard. http://www.marinehist.dk/orlogsbib/h/StanFlex.pdf

Hardgrove, S. (2022, May 12). *LCS Successfully Completes First Land Attack Missile Exercise*. Naval Surface Force, U.S. Pacific Fleet. https://www.surfpac.navy.mil/Media/News/Article/3033364/lcs-successfully-completes-first-land-attack-missile-exercise/http%3A%2F%2Fwww.surfpac.navy.mil%2FMedia%2FNews%2FArticle%2F3033364%2Flcs-successfully-completes-first-land-attack-missile-exercise%2F

Henry, N. C. (2009). *Analysis of Armament from Shipwreck 31CR314: Queen Anne's Revenge Site* (QAR-B-09-01). Department of Cultural Resources, State of North Carolina. www.qaronline.org

Holmes, G. (2010). *Ancient and Modern Ships. Part 1. Wooden Sailing Ships*.

Https://navalteam.dk/members/. (n.d.). Retrieved September 25, 2023, from https://navalteam.dk/members/

Kessler, E., Bierly, P., & Gopalakrishnan, S. (2001). Vasa syndrome: Insights from a 17th-century new-product disaster. *Academy of Management Executive*, *15*(3), 80–91.

Kubota, F. I., Hsuan, J., & Cauchick-Miguel, P. A. (2017). Theoretical analysis of the relationships between modularity in design and modularity in production. *The International Journal of Advanced Manufacturing Technology*, *89*(5), 1943–1958. https://doi.org/10.1007/s00170-016-9238-4

Lafou, M., Mathieu, L., Pois, S., & Alochet, M. (2016). Manufacturing System Flexibility: Product Flexibility Assessment. *Procedia CIRP*, *41*, 99–104. https://doi.org/10.1016/j.procir.2015.12.046

Manucy, A. (1949). Artillery Through the Ages: A Short Illustrated History of Cannon, Emphasizing Types Used in America. *National Park Service Interpretive Series*, *3*. http://npshistory.com/series/interpretive/3/is3toc.htm

Mariners' Museum and Park. (2023). *Galleon—Ages of Exploration*. https://exploration.marinersmuseum.org/watercraft/galleon/

Mary Rose Trust. (2023). *The History of the Mary Rose: 1510-1545*. The Mary Rose. https://maryrose.org/the-history-of-the-mary-rose/

Mendel, D. (2022, April 19). *History of Québec City | Visit Québec City*. https://www.quebec-cite.com/en/quebec-city/history-quebec

National Historic Ships UK. (2023). *The Golden Hinde*. National Historic Ships. https://www.nationalhistoricships.org.uk/page/golden-hinde-london

Navy canceled Raytheon's DART sonar due to high risk | InsideDefense.com. (n.d.). Retrieved September 25, 2023, from https://insidedefense.com/insider/navy-canceled-raytheons-dart-sonar-due-high-risk

Newhaven Heritage Centre. (n.d.). *The Great Michael*. Newhaven : A Stravaig through Time. Retrieved August 28, 2023, from https://www.newhavenstravaigs.scot/locations/19-andrew-wood-court/the-great-michael/

Niderost, E. (2007, June). Defeat of the Spanish Armada. *Military Heritage*, *8*(6), 60–67.

O'Rourke, R. (2019). *Navy Littoral Combat Ship (LCS) Program: Background and Issues for Congress* (RL33741). Congressional Research Service. https://crsreports.congress.gov/product/pdf/RL/RL33741/257

Our History | St. Augustine, FL. (2023). City of St Augustine. https://www.citystaug.com/693/Our-History

Piñeros Bello, L. A., & Segovia Forero, C. E. (2020). Evolution and Present of Modularity in Warships. In V. A. J. E. Carreño Moreno, A. Vega Saenz, L. Carral Couce, & J. Saravia Arenas (Eds.), *Proceeding of the VI International Ship Design & Naval Engineering Congress (CIDIN) and XXVI Pan-American Congress of Naval Engineering, Maritime Transportation and Port Engineering (COPINAVAL)* (pp. 201–210). Springer International Publishing. https://doi.org/10.1007/978-3-030-35963-8_17

Remote Minehunting System (RMS) (DD-A&T(Q&A)823-286; Selected Acquisition Report (SAR)). (2016). Defense Acquisition Management Information Retrieval. https://www.esd.whs.mil/Portals/54/Documents/FOID/Reading%20Room/Selected_Acquisition_Reports/FY_2015_SARS/16-F-0402_DOC_75_RMS_DEC_2015_SAR.pdf

Schank, J., Savitz, S., Munson, K., Perkinson, B., McGee, J., & Sollinger, J. (2016). *Designing Adaptable Ships: Modularity and Flexibility in Future Ship Designs*. RAND Corporation. https://doi.org/10.7249/RR696

Shelbourne, M. (2023, May 12). Navy Talks Details on LCS Mine Countermeasures Mission Package. *USNI News*. https://news.usni.org/2023/05/12/navy-talks-details-on-lcs-mine-countermeaures-mission-package

Skaarup, H. (2021). *Artillery in Portugal: Lisbon, Museu Militar de Lisboa (Portuguese Army Military Museum of Lisbon) 1*. https://silverhawkauthor.com/post/artillery-in-portugal-lisbon-museu-militar-de-lisboa-portuguese-army-military-museum-of-lisbon-1

Strickland, J. D. (2023). Design Considerations for Unmanned Surface Vessels in Naval Service. *Journal of Ship Production and Design*, 1–11. https://doi.org/10.5957/JSPD.10220025

The Vasa Museum. (2015, October 17). *Vasa in numbers*. https://web.archive.org/web/20151017033410/http://www.vasamuseet.se/en/The-Ship/Vasa-in-numbers/

Thyssen Krupp Marine Systems. (n.d.). *Our Surface Vessels*. Retrieved August 21, 2023, from https://www.thyssenkrupp-marinesystems.com/en/products-services/surface-vessels

US National Park Service. (2022, September 16). *A Short History of Jamestown—Historic Jamestowne Part of Colonial National Historical Park*. https://www.nps.gov/jame/learn/historyculture/a-short-history-of-jamestown.htm

Proceedings of 15th International Marine Design Conference (IMDC-2024)
June 2-6, 2024
Amsterdam, the Netherlands

Statistical Reliability Analysis of Marine Systems with varied Levels of Redundancy

Andreya Ware[1,*] and Matthew Collette[2]

ABSTRACT

In designing autonomous vessels for long-duration independent operation, maintaining the performance of machinery systems without human intervention is a key challenge. Designers are faced with a range of potential system architecture choices but have little guidance on which will be optimal. Working only with high-reliability components can increase the probability of completing a voyage successfully, though the availability of such components may be limited. Alternatively, designers can select a redundant architecture to provide options for reconfiguration if a component fails during a voyage, such architectures typically have weight, space, and cost implications. This work presents a parametric exploration of the probability of system failures over time under different architectures. The reliability of individual components is expressed through exponential probability distributions and the weight of each component is approximated. Two systems are presented and the effectiveness of various architectures for both systems is compared. A simple design penalty function is also tracked to capture the different architectures' weight and implication number of components. From this study optimal architectures for long-term autonomous missions are proposed.

KEY WORDS

Reliability; Redundancy; Series-Parallel Configuration; Marine Systems; Fuel Oil System; Cooling System.

INTRODUCTION

Ship systems are highly sophisticated systems, being comprised of many subsystems and numerous components. Components in these systems are often placed in parallel configuration on-board ships as a safeguard against catastrophic system failures. Ensuring spare parts are on-board and readily available during emergency is vital to performance of the ship and the ensured safety of the crew. This point is reinforced by classification societies, such as American Bureau of Shipping (ABS, 2018), Lloyds Register of Shipping (Lloyds Registrar of Shipping, 2013) and also International Marine Organization (IMO, 2002), which all have established guidelines for redundancy levels in critical systems, such as main propulsion. Guidelines on system redundancy exist for both main engine systems and their supporting systems, such as engine cooling water, fuel oil, and lube oil systems (Liberacki, 2007). Generally, societies require systems to have secondary pumps and valves in major systems because these parts are known to have high rates of failure. While parallel configuration of components may mitigate system failures, the precise balance required for optimal operation and reliability over a desired period remains ambiguous, prompting the need for a more data driven approach. This approach toward including reliability in systems has not proven to prevent critical failures of systems or unexpected maintenance being necessary. The existing redundancy rules also assume humans are on-board the vessel, which means the systems must be reliable and safe enough to mitigate risk to human life. Assuming a crewed vessel also implies that there will be human intervention if a system malfunction or failure is found by the crew, happening in the form of maintenance, reduction in the operating state of the vessel, or a return to port. For a crewless vessel however, their may be a higher risk profile that is acceptable since there are no human lives at stake.

As the maritime industry progresses toward autonomous operations, reliance on human intervention for system monitoring diminishes, deepening the importance of accurate predictive maintenance strategies. Traditional methods such as scheduled inspection and condition-based monitoring will become more heavily influenced by the predictive models that leverage component reliability data for failure predictions. Accuracy of such predictions requires historical data, which is scarce in the maritime sector due to limited sharing of failure statistics. Data sharing in this industry is driven by mutual benefit, often

[1] Naval Architecture and Marine Engineering, University of Michigan, Ann Arbor, USA; ORCID: 0009-0008-0688-2936
[2] Naval Architecture and Marine Engineering, University of Michigan, Ann Arbor, USA; ORCID: 0000-0002-8380-675X
* Corresponding Author: adware@umich.edu

Submitted: 21 February 2024, Revised: 2 May 2024, Accepted: 3 May 2024, Published: 26 May 2024

Conference paper, DOI: https://doi.org/10.59490/imdc.2024.901 e-ISSN: 3050-4864

resulting in retention of vessel and component data deeming it to be confidential (Teijl, 2014). Despite this, recent reports can be found which utilize confidential data and present their limited findings (Knežević et al., 2022). Additional information may be gathered from reports which interview crew members and vessel maintenance workers, many of which mention that preventative maintenance and avoiding machinery failures are a major concern in mission planning (Sulkowski et al., 2022). Reports such as these can be leveraged in statistical investigations and predictive modelling approaches such as the one presented here.

Current redundancy standards lack statistical foundation proving the level of redundancy can lead to overall improvements in system reliability. Predictive modelling approaches also lack consideration concerning factors such as component weight and cost. Addressing this gap, this work aims to quantify the trade-offs between high-reliability components and redundancy through simulations, assessing various configurations for their redundancy levels, reliability, and weight. The systems that have been analyzed include the engine cooling water and fuel oil systems. Results from the study conducted here may offer insights into optimal system configurations and informing future standards in naval system design practices.

First, the metrics defining system reliability are presented. Next, assumptions made to estimate weights of components are detailed. An overview of the initial models for both systems is given and the results of testing various configurations of these systems with differing levels of redundancy are presented. Finally, conclusions are drawn from observed trends.

MODELLING ASSUMPTIONS

Reliability Metrics

Reliability of a component has long been defined as "the probability that a component will be able to perform a required function for a given operational period and stated conditions" (MIL-STD-721C, 1981). Various metrics have been used to quantify a components reliability. The chosen metrics for analysis in this paper are average failure rate and mean time between failures for each component tested. A component or systems rate of failure (Equation [1]) and mean time between failures (Equation [2]) are defined as:

$$Failure\ Rate\ (\lambda) = \frac{total\ number\ of\ failures}{operational\ time} \quad [1]$$

$$Mean\ Time\ Between\ Failure\ (MTBF) = \frac{operational\ time}{\lambda} = t_f - t_0 \quad [2]$$

These definitions assume a fixed operational time. Failure rate is given in units of failures per million operating hours, so a operational time of 1 million hours has been assumed. Mean time between failures may also be defined in terms of a difference between the time related to a component's maximum reliability, the initial operation start time, t_0, and the components time of failure, t_f. This modelling approach will assume no maintenance interventions or environmental affects. All components are modelled individually with distinct average lifetimes and average rates of failure. The python *SciPy* package was utilized for creating exponential random variate distributions of failure times for each component. From each distribution 1000 random failure times were selected.

Reliability metrics for this study were taken from multiple sources with all components designated supporting an approximately 17,000kW 6-cylinder Diesel Engine (MAN, 2009). For the high-pressure pumps, metrics come from a study investigating the optimal maintenance plan for high pressure fuel systems (Knežević et al., 2022). Metrics for the low-pressure pumps, heat exchanger, and cross tie valves are sourced from a study optimizing maintenance of heat exchange systems for submersibles (Zhang, 2021). SciPy random exponential function is defined by a variance of failure and not a failure rate, therefore the variance of failure is set so that each parts exhibits the failure pattern described by the failure rates gathered.

Table 1: Reliability Metrics for Components Considered

Component	Mean Time Between Failure (MTBF) (Years)	Variance of Failure Used in Simulation (Years)	Failure Rate (λ) (fails/10^6 Hrs.)
Low-Pressure Pumps	1.97	0.30	56.88
High-Pressure Pumps	0.54	0.08	208.69
Heat Exchangers	6.85	1.65	16.36
Valves	27.52	4.48	4.07

SYSTEM MODELS

Two marine propulsion support systems are included in this paper: the fuel oil system and the cooling water system. A failure of either system can lead to malfunction or failure of propulsion systems which would be a critical failure. Both system configurations are based initially on the schematics of the Marine Design Laboratory, a propulsion simulator at the University of Michigan which emulates shipboard machinery systems using six coupled systems (Marine Engineering Laboratory, 2022). Of the existing ship systems in the simulator, the cooling and fuel oil systems feature redundancy of cooling lines and fuel injection lines, as well as simulation valves for clogs and leaks. In this paper, the initial system configurations only included in-series layout of components with high rates of failure, such as pumps, valves, and heat exchangers will be considered. Clogs and leak simulator valves were removed and other components of the systems with lower rates of failure were also ignored. Additionally excluded components include oil service tanks and cooling water tanks as they are not prone to failure and are low risks components of these systems.

Engine Cooling System

The cooling water system consists of 6 total components, which were divided into two groups. The first group consisted of a single cooling pump and three valves, valve #1, #2, and valve #3 respectively. The cooling pump was considered as a centrifugal pump, assuming the reliability and weight of a low-pressure pump. The second group consisted of a heat exchanger and a final valve, valve #4. Components were considered in two groups so that parallel lines for cooling pumps or parallel heat exchangers could be implemented in testing various configurations. The initial layout of the cooling system is seen below with the component of highest failure rate highlighted in red in Figure 1. In this initial configuration, it was determined that the low-pressure cooling water pump causes cooling system failure most often.

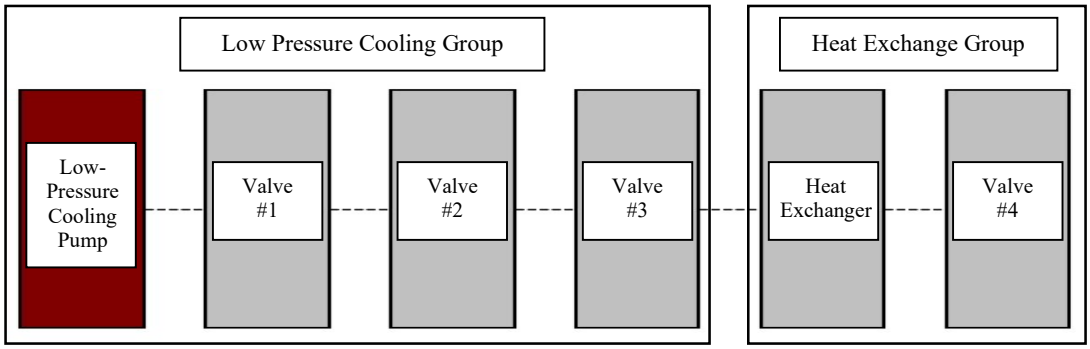

Figure 1: Initial Engine Cooling System Model

For this initial system layout, a reliability over time curve was generated as seen below, over a period of 100,000 operating hours. The system reliability followed the lowest reliability of all parts in the system at each time step, which happened to be the low-pressure cooling pump at all times tested. The four valves have similar reliability curves to each other as expected and showed slightly higher reliability at each time step compared to the cooling pump. The reliability of the heat exchanger far exceeds the reliability of the low-pressure cooling pump and valves. Due to this observation, most tested configurations of this system will investigate adding cooling pump groups in parallel, rather than parallel heat exchange groups in order to improve overall system reliability.

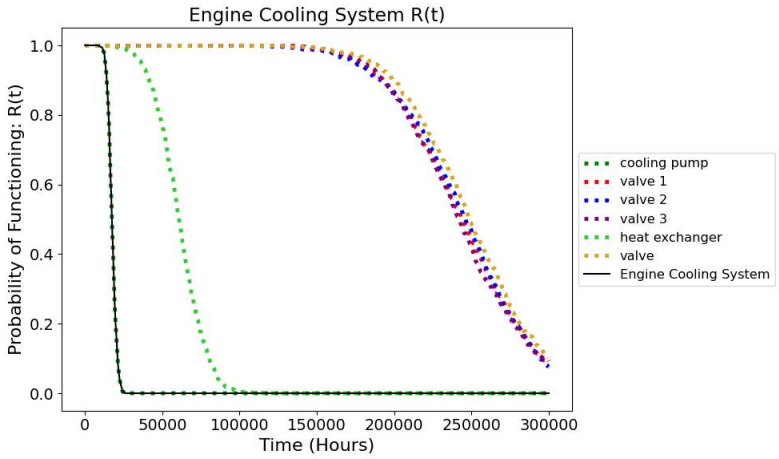

Figure 2: Initial Engine Cooling R(t), Reliability over 100,000 operating Hours

Fuel System

The fuel oil system consisted of 7 components total. These components were again split into two distinct groups. Starting with the cooling pump, valve #1 and valve #2 they were referred to as the fuel cooling group. The fuel injection group was comprised of a high-pressure fuel injection pump and valves #3, #4, and #5. This grouping allows for investigation of parallel lines of fuel cooling or fuel injection during testing. For this system, the fuel injection pump was the component with the highest failure rate, highlighted in red in Figure 3, and caused most of simulated fuel oil system failures.

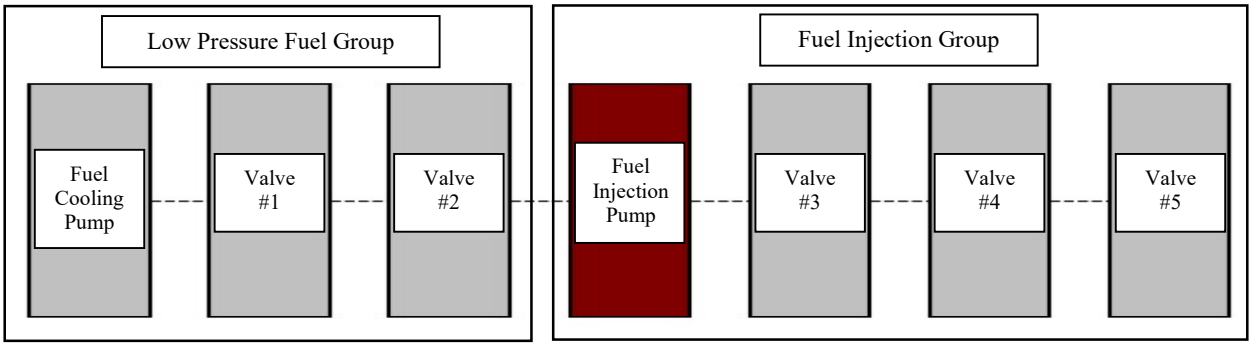

Figure 3: Initial Fuel Oil System Model

The reliability curve for the system was generated using the metrics for low pressure cooling pumps, high pressure fuel injection pumps and valves presented in the previous section. For this system the high-pressure cooling pump was the lowest reliability component in the system at each time step and was therefore equal to the system reliability over time. In testing, many configurations adding parallel redundancy of the cooling pump group for improving system reliability were tested.

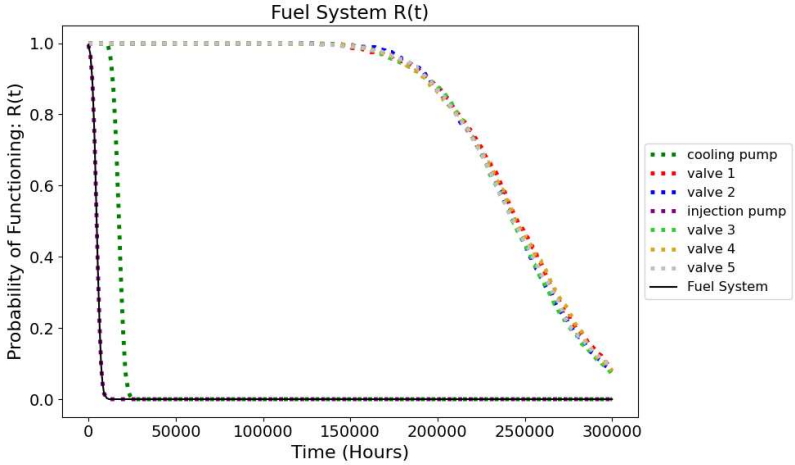

Figure 4: Initial Fuel Oil System R(t), Reliability over 100,000 operating Hours

System Weight Estimation

The components selected for the fuel oil and cooling systems were intended to support a 6-cylinder slow-speed diesel engine, MAN 6S70MC-C, with a maximum continuous rating of 16,780 kW operating at 91 RPM (MAN, 2009). This engine is a frequent choice for tankers and bulk carriers (Žan, 2009). The total weight of both two auxiliary systems combined was assumed to be 5% of the main engine weight. For the 550-ton engine this yields a total weight of 27.5 tons split between the total components in each system. To distribute this weight amongst the individual component's, catalogues were reviewed to determine a weight ratio between parts. The resultant total weight was then distributed amongst the individual components as seen in Table 2. The weight presented assuming inclusion of all necessary piping and fittings for each component, for example, high pressure fuel injection pumps may be double walled, so the casing and pipes and other subcomponents of the assembly were included in the estimated weight.

Table 2: Distribution of Total Auxiliary System Weight Between Components

Component	Quantity in Initial Systems	Individual Component Weight (tons)	Fraction of Total Initial Systems Weight (%)
Cooling Pump	2	5.64	41.07
Injection Pump	1	13.30	47.41
Heat Exchanger	1	2.70	9.82
Valves	8	0.05	1.70
Total Auxiliary Systems	12	27.50	100

From the calculated individual weights of components, the total weight of each proposed system was found. The total weight of the initial engine cooling system and fuel systems are presented in Tables 4 and 5 below.

Table 4: Distribution of Total Cooling System Weight

Component	Quantity in Cooling System	Individual Component Weight (tons)
Cooling Pump	1	5.64
Heat Exchanger	1	2.70
Valves	4	0.05
Cooling System	6	8.44

Table 5: Distribution of Total Fuel Oil System Weight

Component	Quantity in Fuel System	Individual Component Weight (tons)
Cooling Pump	1	5.64
Injection Pump	1	13.30
Valves	5	0.05
Fuel System	7	19.19

The next section explains parallel configurations required a component for switching between parallel lines. A cross-tie valve was placed between groups for this purpose. The fixed weight of this valve was 0.07 tons and was found using factors determined from marine valve manufacturer catalogues. This additional weight was factored into tested configurations having increased levels of redundancy. The reliability of the cross-tie valve is assumed to be the same as that utilized for all other valves.

TESTING PARALLEL CONFIGURATIONS

Redundancy in Testing

For testing the reliability of increased levels of redundancy, the groups were configured in different ways to determine the improvements to system reliability that could be gained from parallel component groups. For Tables 6 and 7, Test #0 outlines a system with no redundancy which was presented in section 2 of this report as the initial systems. For comparison, these systems are included as in tables and graphs in this section. Test #0 was the only configuration with no cross-tie valves. In the event of parallel groups, a cross tie valve is also added to the system between groups to allow for switching between lines. For all tested parallel configurations, the weight of the cross tie was also be added to the total system weight. An example configuration of the engine cooling system with parallel cooling groups, a singular heat exchange group, and a single cross tie is seen in Figure 5. This example is the same as Test #1, conducted for the fuel cooling system.

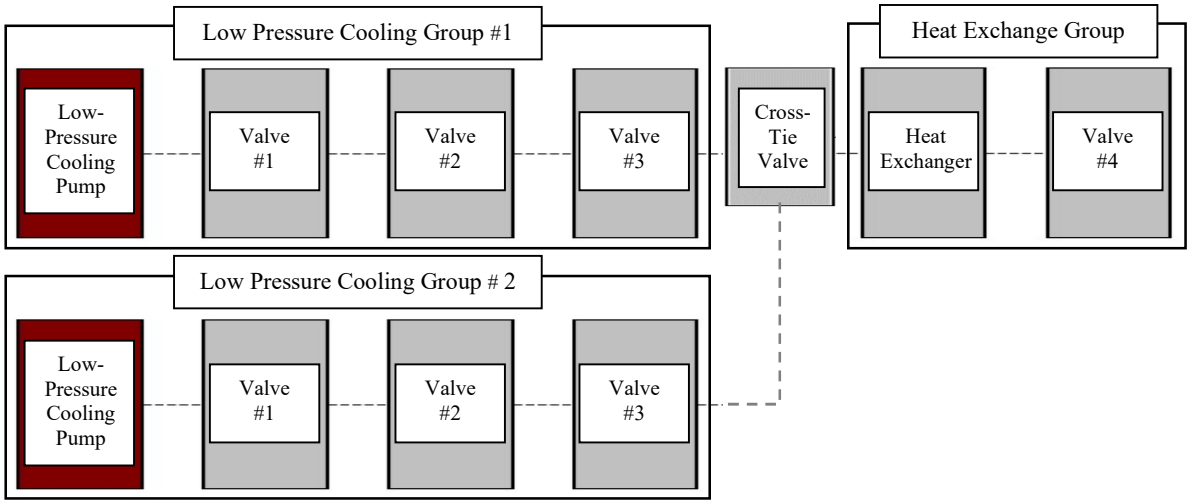

Figure 5: Test #1 of Engine Cooling System with Parallel Redundancy, 2 Cooling Groups, 1 Cross Tie Valve and 1 Heat Exchange Group

Cooling System Tests

For the engine cooling system, a total of 30 tests were conducted, with 12 presented in Table 6 below. Many of the test focus on increasing the number of cooling groups since the cooling pump is the most frequent cause of failure within the system. The tests presented within Table 6 highlight the general trends observed from simulations. Test #0-3 shows a single heat exchange group, Test #4-8 shows two heat exchange groups in parallel and Tests #9-12 shows 3 heat exchange groups in parallel. The number of parallel cooling groups is increased until the system failure is no longer completely determined by the cooling group. System weight was also limited to be less than 50 metric tons.

Table 6: Results from Cooling System Configurations Tested

Test #	# of Cooling Groups	# of Cross Ties	# of Heat Exchange Groups	Total Count of Components	System Weight (metric tons)	MTTF (Years)	Failure Rate (fails/MH)
0	1	0	1	6	8.54	3.02	11.94
1	1	1	2	11	14.40	6.04	10.14
2	1	1	3	15	20.19	9.05	7.95
3	1	1	4	19	25.98	11.81	6.64
4	2	1	3	17	22.94	8.95	7.07
5	2	1	4	21	28.73	12.07	5.99
6	2	1	5	25	34.52	15.09	5.20
7	2	1	6	29	40.31	17.91	4.86
8	2	1	7	33	46.10	21.03	4.68
9	3	1	4	23	31.48	11.97	5.43
10	3	1	5	27	37.27	14.89	4.73
11	3	1	6	31	43.06	18.01	4.41
12	3	1	7	35	48.85	21.03	4.11

As more cooling groups were added, the mean time between failure of each system increased, allowing for more operational time before the system would need maintenance services. The overall failure rate of the various configurations also decreased with the inclusion of multiple cooling groups. This which reflects higher reliability of the system caused by higher levels of redundancy, with mean time between failures increased by about 3 years per cooling group added in parallel. The tradeoff of this improved reliability is a much heavier system with a system weight increase of 60 % of the initial weight per cooling group in parallel.

For single heat exchange system configurations, Tests #0 – 4, the reliability of system was improved each time a cooling group was added to the parallel configuration. The reliability plot for Test #0, seen in the top left of Figure 6, shows the cooling group (blue curve) has a lower reliability at every time step then the heat exchanger group (red curve) and is the first group in the system to fail. In tests 1 to 4, the number of cooling groups in parallel increased by one each test. This additional redundancy moves the reliability curve the cooling groups to the right, indicating a longer time of high reliability and an extended mean time to failure of the grouping. Test 2 shows the system reliability is only partially determined by the 3 cooling groups in parallel, whilst in test #4 the system is no longer dependent on the failures of the cooling pumps at all, but instead on the heat exchanger group.

Investigating a system with two heat exchanger groups a similar trend persisted. The system reliability over time curve, R(t), was completely dependent on the cooling group reliability curve in Test #4, with only four cooling groups in parallel, whilst in Test #8, the addition of seven cooling groups in parallel pushed the reliability of the cooling group to be greater than that of two heat exchange groups.

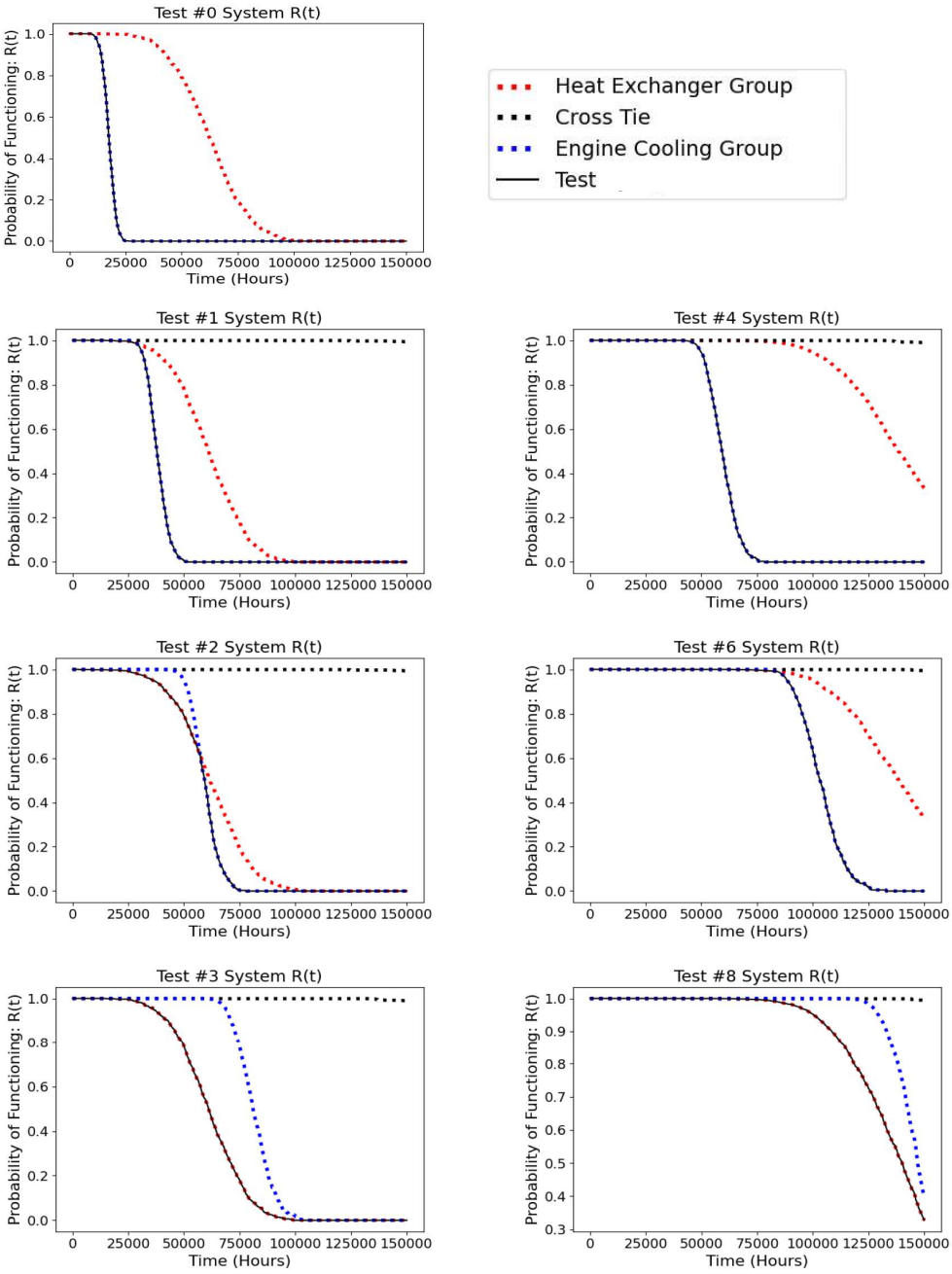

Figure 6: Engine Cooling System Single Heat Exchanger Tests #0, 1, 2, 3 (left), and Double Heat Exchanger Tests #4, 6, 8 (right)

Fuel System Tests

For the fuel system similar simulations were conducted. Fuel injection groups were added in parallel until the system reliability was no longer entirely dependent on failure of the fuel injection group. Test #0-7 considered single cooling group with varied numbers of redundant injection groups. Test #8-10 investigated system configurations with 2 cooling groups, and tests #11 was the only simulated test configuration including triple cooling groups. The fuel injection pump was the heaviest part considered in this report, so the system weight was found to be increasing even more rapidly than the previously tested cooling system, when adding more fuel injection groups. A total of 30 systems were investigated in simulation but only the systems weighing less than 100 metric tons in total are presented in Table 7.

Table 7: Results from Fuel System Configurations Tested

Test #	# of Cooling Groups	# of Cross Ties	# of Injection Groups	Total Count of Components	System Weight (tons)	MTTF (Years)	Failure Rate (fails/MH)
0	1	0	1	7.00	19.19	0.79	30.29
1	1	1	1	8.00	19.26	0.77	22.19
2	1	1	2	12.00	32.71	1.53	27.32
3	1	1	3	16.00	46.16	2.34	18.66
4	1	1	4	20.00	59.61	3.12	14.83
5	1	1	5	24.00	73.06	3.86	12.54
6	1	1	6	28.00	86.51	4.64	10.92
7	1	1	7	32.00	99.96	5.46	9.55
8	2	1	4	23.00	65.35	3.11	14.47
9	2	1	5	27.00	78.80	3.94	11.78
10	2	1	6	31.00	92.25	4.70	10.57
11	3	1	6	34.00	97.99	4.65	10.01

As of the fuel injection groups, the group with the lowest reliability components, were added in parallel the mean time between failure of the system increased while failure rate reduced. This is desirable as the system will be more likely function over extended periods of time. The weight increase cost for this increased system reliability was approximately 70 % the original system weight per injection group added in parallel. This weight cost in many cases might not be justified by the minimal increases in mean time between failures and reductions in failure rate for some applications, so an optimum configuration would be based on a desired the operational time. Applicability of these results is discussed more in the next section.

Observing the reliability over time plots of the tests presented these trends can be better understood visually. The low variance of the fuel injection failures results in an almost vertical reliability curve, this corresponds to components whose failures occurred at approximately the same time every time it fails. The high variance of failures of the cooling groups leads to a much more spread reliability curve. Presented in Figure 7, the right side shows reliability curves for a singular cooling group and two, four and seven parallel injection groups considered in Test #0, #1, #4 and #7. The right side of Figure 7 shows reliability over time for Tests #8, #9, and #10, which considered two cooling groups and four, five, and six parallel injection groups.

For both sets of tests, the addition of parallel injection groups shifts the reliability curve for these groups minimally and corresponded to a small increase in mean time between system failures. Looking specifically at the right column of figure 7 we see per injection groups added, the reliability curve moved right about 12,000 hrs., this corresponded to an increase mean time to failure of less than 1.5 years. The weight of three injection groups however is more than 30 tons. Addition of such a heavy group, for a low tradeoff in increased reliability over time is not justifiable in for any design where being lightweight is desired. This is more important for vessel which operate at high speeds or in shallow waters and seems to be less relevant for heavy vessels such as bulk carriers and tankers.

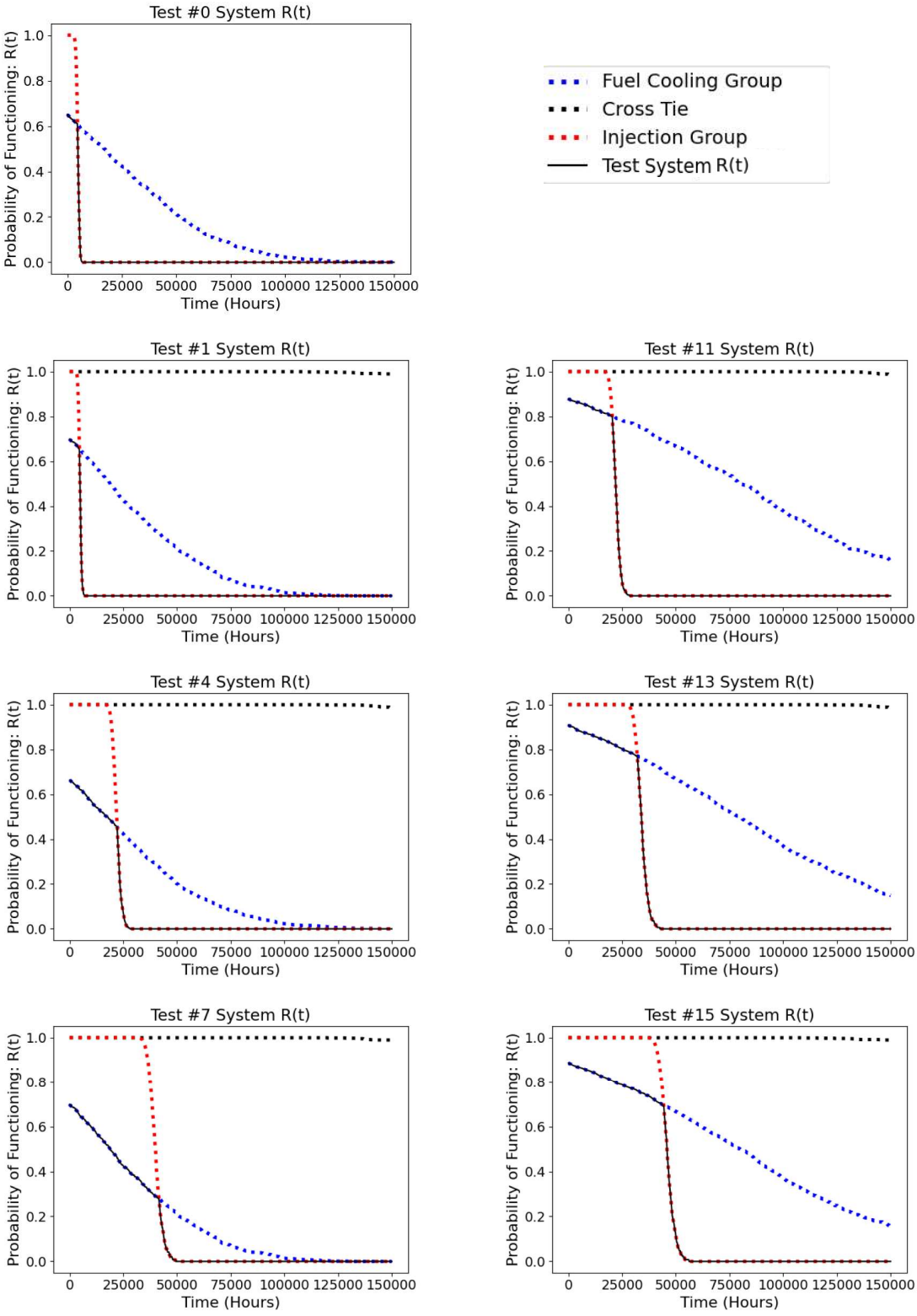

Figure 7: Fuel System with Single Cooling Group, Tests #0, 1, 4, and 7 (left), and Double Cooling Groups Tests #11, 13, 15 (right),

APPLICATION OF TEST RESULTS

From the resulting reliability metrics of various system architectures tested, a level of redundancy needed for desired performance can be quickly decided for a specified mission lengths. The few crewless vessels existing today have a maximum operational range is 2000Nm at 16 Knots (Ziajka-Poznańska & Montewka, 2021). This application of autonomous vessels corresponds to only 125 hours of autonomous operations. A long-term goal could be to have the vessel operate autonomously for months to years at a time with no on-board human interference. This goal will only be achieved if a highly reliable machinery system is implemented. Using the results from the test cases, an optimal configuration for the cooling and fuel oil systems can be selected for an autonomous vessel operating for 1, 2 ,3, 4, and 5 years at a time. The optimal system was selected with emphasis on reliability of at least 30% probability of functioning until the end of each desired mission length, as well as minimizing the weight of the system.

Table 8: Cooling System Performance of Optional Configurations over Various Mission Lengths

Mission Length (years)	# of Cooling Groups	# of Cross Ties	# of Heat Exchange Groups	Total Count of Components	System Weight (tons)	System Reliability at the end of the Mission Length
1	1	0	1	6	8.54	99.9 %
2	1	0	1	6	8.54	53.8 %
3	1	1	3	15	20.19	99.5 %
4	1	1	3	15	20.19	96.5 %
5	1	1	3	15	20.19	88.6 %

The cooling system, at the beginning of its operation would highly reliable because of its higher reliability components compared to the fuel oil system. As seen in the curves present previously, most components in this system do not fail until about 25,000 Hrs. which is after approximately 3 years. This being known, the initial configuration is optimal for mission lengths on 1 or 2 years but for 3-5 years of operation, a more redundant configuration would be the more optimal choice for reliable system performance. The fuel system on the other hand was shown to fail much earlier than the cooling system in its initial configuration and this leads to a much more diverse selection of optimal architecture dependent on increasing mission lengths as seen below.

Table 9: Fuel System Performance of Optional Configurations over Various Mission Lengths

Mission Length (years)	# of Cooling Groups	# of Cross Ties	# of Heat Exchange Groups	Total Count of Components	System Weight (tons)	System Reliability at the end of the Mission Length
1	1	1	2	12	32.71	62.9 %
2	1	1	4	20	59.61	49.3 %
3	1	1	5	24	73.06	40.8 %
4	1	1	6	28	86.51	34.8 %
5	2	1	8	39	119.15	70.5 %

The goals presented here are assuming complete autonomy of the vessel and continuous operation, but in practice would require a consideration of scheduled inspections for maintaining the vessel, as well as stops to prevent overloading or over heating of equipment. These considerations are not made in this paper but would be needed for a real-life implementation.

CONCLUSIONS

This paper has presented the tradeoffs between increased reliability through parallel configurations at the expense of increase system total weight. Investigations showed that low reliability components should be the focus of parallel options if reductions in system failure rate and increases to mean time between failures are desired. Simulated results for multiple configurations of cooling and fuel oil system have been presented. Pumps proved to be the most common failing components investigated in both systems, cooling water pumps in the cooling system and fuel injection pumps in the fuel oil system.

Testing of parallel configurations revealed a considerable increase in system weight for improvements in system reliability. The necessity of these improvements in reliability should be determined by the application specific needs, whether that be a desire to remain highly reliable or lightweight. These results were tested and normalized over various mission lengths to find optimal configurations for 1, 2, 4, and 10 years of system operation. The results from this investigation reaffirm that the selected level of redundancy should be based on specific mission criteria required rather than classification society rules to

result in highly reliable autonomous operations. Future studies may investigate lighter weight or higher reliability components for increases to system reliability over time for a lower increase in system weight. Additional parameters such as cost of components should be considered in future work if they are available.

The majority of this work was completed using estimated values but for companies and organizations that have similar data available to them, this statistical analysis approach could be utilized. Methods for estimating reliability metrics and system weights presented here are repeatable and using this information, various configurations could be simulated and compared. Following such simulations, a predetermined mission length can be used to decide and the most reliable configuration for this requirement.

CONTRIBUTION STATEMENT

Andreya Ware: Conceptualization; Software; Investigation; Writing – original draft.
Matthew Collette: Conceptualization; Supervision; Writing – review and editing.

REFERENCES

[1] American Bureau of Shipping (August 2018). Part 4, Vessel Systems and Machinery. *ABS, "Rules for Building and Classing."*

[2] Lloyd's Register of Shipping (2013) Part 5: Main and auxiliary machinery". *Lloyd's Register, "Rules and regulations for the Classification of Ships".*

[3] (2002) International Maritime Organization, Guidelines for Formal Safety Assessment (FSA) for Use in the IMO Rule – Making Process, MSC/Circ.1023 MEPC/Circ.392.

[4] Liberacki, R. (2007). Influence of Redundancy and Ship Machinery Crew Manning on Reliability of Lubricating Oil System for the MC-Type Diesel Engine.

[5] Knežević, V., Stazić, L., Orović, J., & Pavin, Z. (2022). Optimisation of Reliability and Maintenance Plan of the High-Pressure Fuel Pump System on Marine Engine. Polish Maritime Research, 29(4), 97–104. https://doi.org/10.2478/pomr-2022-0047

[7] Teijl, T. (December 2014). *Innovating in The Maritime Cluster.* (Master's Thesis). Delft University of Technology.

[8] Sulkowski, B., Magistro, A., Houten, J. V., & Collette, M. (2022). *Long-Term Voyage Decision Making for Crewless Platforms.*

[9] Moon, J.H. and Kim, J. R. (2007) An Estimation on Two Stroke Low Speed Diesel Engines' Shaft Fatigue Strength due to Torsional Vibrations in Time Domain.

[10] MAN. (January 2009). MAN B&W S70MC6 Project Guide.

[11] MIL-STD-721C. (1981). Military Standard Definition of Terms for Reliability and Maintainability, Department of Defence, United States of America

[12] O'Connor P. D.T. (1981). Practical Reliability Engineering, John Wiley & Sons, New York, United States of America.

[13] Žan, V. (2009). Multiattibute Decision Making Methodology in the Concept Design of Tankers and Bulk Carriers

[14] Zhang, K., & Cao, H. (2021). Reliability analysis of heat exchanging system of deep-sea manned submersibles using Markov model. Quality Engineering, 33(3), 487–496. https://doi.org/10.1080/08982112.2021.1907407

[15] Marine Engineering Laboratory. (2022). https://mel.engin.umich.edu/

[16] Ziajka-Poznańska, E., & Montewka, J. (2021). Costs and Benefits of Autonomous Shipping—A Literature Review. Applied Sciences, 11(10). https://doi.org/10.3390/app11104553

Proceedings of 15th International Marine Design Conference (IMDC-2024)
June 2-6, 2024
Amsterdam, the Netherlands

Application of Sampling Methods for Constrained Space in Hull Form Optimization

HOU Wen-long[1,2]，CHANG Hai-chao[1,2,*]，FENG Bai-wei[1,2]，LIU Zu-yuan[1,2]，ZHAN Cheng-sheng[1,2], CHENG Xi-de[1,2]

ABSTRACT

Use of approximation models instead of direct application of CFD tools plays a crucial role in hull form optimization to enhance efficiency. The selection of sample points directly impacts the accuracy and cost of approximation models, and the effectiveness of hull form optimization. This paper presents a sampling method based on constrained space. The distribution pattern of the constrained space is initially analyzed, and its boundary is subsequently extracted by the Support Vector Machine (SVM), providing guidance for the subsequent sample selection. To ensure effective sampling within the constrained space, the maximum minimum distance criterion is employed. The proposed methodology is validated via a case study involving a 13,000DWT inland twin-screw bulk carrier. The Kriging approximation model is constructed to optimize the hull form while adhering to specific constraint conditions, thereby demonstrating the feasibility and efficacy of the proposed approach.

KEY WORDS

Hull Form Optimization; Constrained Space; Support Vector Machine; Maximum Minimum Distance Criterion.

INTRODUCTION

At present, ship shape optimization based on approximate model has garnered significant attention. Utilizing an approximation model, instead of a higher-accuracy simulation model, during the ship optimization process serves to reduce computational complexity and enhance optimization efficiency. Wang et al. (2018) introduced the Kriging approximation model in the multi-objective fast optimization process of container ship (KCS) and combined it with the non-dominated genetic algorithm (NSGA-II) to complete the resistance optimization objective for KCS ship under design draft and service speed, and at the same time, improve the ship's wave resistance and optimization efficiency. Liu et al. (2022) constructed a multi-fidelity Co-Kriging agent model, and illustrated the advantages of multi-fidelity Co-Kriging agent model compared with single-fidelity Kriging agent model in terms of fidelity and efficiency through a series of numerical examples. Finally, the ship shape optimization design for the total hull drag of DTMB-5415 at the design speed is given. Chen et al. (2015) optimized the hull shape of a high-speed Delft catamaran to reduce the drag based on the idea of dimensionality reduction in the design space and geometrical variability assessment by means of the Karhunen-Loève unfolding, approximate modeling, and deterministic Particle Swarm Optimization (PSO), compared with the previous optimization process Compared with the previous optimization process, the computational cost is reduced by 90% and the drag is further reduced by 6.6%. Bonfiglio et al. (2018) used multi-fidelity gaussian process regression (MF-GPR) to build a probabilistic approximation model and explored the 35-dimensional SWATH hull-shape optimization and 17-dimensional underwater wing-shape optimization, respectively, which greatly reduced the optimization and computational workload. In order to further improve the accuracy of the approximation model, Hochkirch et al. (2013) studied the Hybrid Model (HM).

[1] School of Naval Architecture, Ocean and Energy Power Engineering, Wuhan University of Technology, Wuhan 430063, China
[2] Key Laboratory of High Performance Ship Technology (Wuhan University of Technology), Ministry of Education, Wuhan 430063, China
[*] Correspondence: 361169473@163.com

Submitted: 12 February 2024, Revised: 13 April 2024, Accepted: 1 May 2024, Published: 18 May 2024

Conference paper, DOI: https://doi.org/10.59490/imdc.2024.832 e-ISSN: 3050-4864

Before constructing the approximation model, a certain number of sample points need to be selected in the design space for CFD calculation, and subsequently they will be used as the training set for constructing the approximation model. Currently, the common sampling methods used in ship optimization are as follows: orthogonal design, Latin square design, uniform design, sobol random sampling and so on. On the basis of these commonly used methods, many scholars have conducted a large number of detailed studies. Ouyang et al. (2022) proposed a maximum entropy adaptive sampling method based on uniform experimental design. By comparing with the incremental Latin hypercube-based method, the adaptive sample distribution obtained by the proposed method is more uniform and the global approximation model is more accurate. Chang et al. (2021) proposed a dynamic sampling method (DSM) to improve the accuracy and efficiency of the approximation model by taking into account the effect of sample quality measurements in the input and output parameter spaces. The proposed method is compared with the conventional sampling method, and it is proved that the DSM outperforms the static sampling method. Wang et al. (2021) comparatively analyzed the hydrodynamic performance of a smooth boat in the mono-hull state (MFS) and the three-hull state (TFS), and the optimal range of the sideboard arrangement is given by using the full factorial design space sampling method, which is verified on the scale of a real boat. Based on the LHD sampling method, Wang et al. (2021) analyzed the prediction accuracy of the SVR model with different sample set sizes, and completed the multi-objective optimization of drag and companion flow of offshore aquaculture vessels. Feng et al. (2018) also optimized the hull profile and jet conduit shape of a water-jet propelled trimaran based on the LHD sampling method.

The above studies on approximate modeling and sampling methods seek to make the samples fill the entire design space uniformly, while the limitations of the constraints are not considered. This means that the sample set we obtain through the above sampling methods will contain both sample ship types that satisfy the constraints and sample ship types that do not satisfy the constraints, leading to a decrease in the accuracy of the model forecasts. Therefore, if the constraints can be considered at the sampling stage, and the sample point sets satisfying the constraints can be obtained directly through the sampling method, avoiding the mixing of sample ship types satisfying the constraints and those not satisfying the constraints to the maximum extent, it will be conducive to the construction of the subsequent approximate model and optimization algorithms, which will improve the forecast accuracy of the approximate model and at the same time, save the time cost of optimization.

This paper focuses on a 13,000DWT inland twin-screw bulk carrier, considering the total ship resistance as the optimization objective. The paper employs the constraint-space oriented sampling method proposed herein to construct a Kriging approximation model. A comparative study is conducted on the optimization of the ship type under specified constraint conditions.

SAMPLE POINT SELECTION METHOD FOR CONSTRAINT SPACE

To incorporate constraints into the sampling stage and achieve the goal of directly obtaining a set of sample points that satisfy the constraints through sampling, this paper introduces a sample point selection method based on the support vector machine in the constraint space. The workflow is illustrated in Figure 1. The specific process is as follows:

(1) The range of variation of the variables is first determined to form the initial design space;

(2) Sampling in Design Space;

(3) The constraints on the sample points are calculated to complete the data preparation for partitioning the initial design space;

(4) The initial design space is partitioned using the support vector machine method to obtain the space we need to satisfy the constraints;

(5) If the number of sample points in the feasible space that satisfies the constraints is sufficient, these sample points can be used for the construction of the approximation model, otherwise, new sample points have to be co-opted in the feasible space that satisfies the constraints until the requirement of the number of sample points for the construction of the approximation model is met.

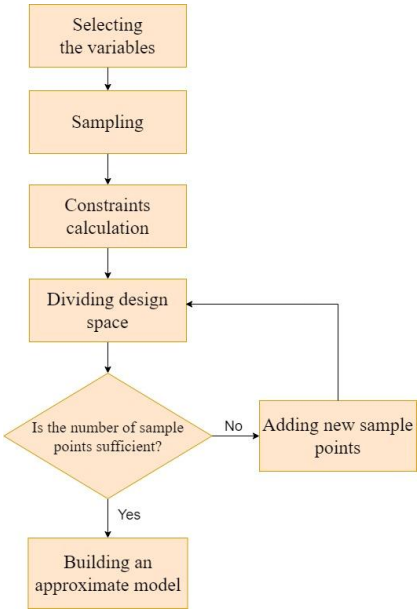

Figure 1: Constraint space oriented approximation model construction process.

As can be seen, the core of the method is the delineation of the design space and the selection of subsequent sample points, which are described below respectively.

Support Vector Machine Algorithm Principles

The SVM algorithm is a machine learning method based on statistical learning theory, which aims to find the "optimal hyperplane" that can effectively classify the training samples. In most cases, this "optimal hyperplane" should have the best robustness to local perturbations in the training samples, while having the smallest classification error and the strongest ability to generalize to unseen examples.

Suppose that for a given training set is as follows:

$$\{(x_1, y_1), (x_2, y_2), \cdots, (x_n, y_n)\}, \quad x \in R^n, y \in \{1, -1\} \tag{1}$$

The hyperplane can be expressed as $\omega^T x + b = 0$, where $\omega = (\omega_1; \omega_2; \ldots; \omega_d)$ is the normal vector and b is the displacement term. It can be found that the normal vector ω and the displacement b determine a hyperplane, so we can denote a definite hyperplane as (ω, b). In order for a hyperplane to classify all training samples correctly and have a classification interval, it is required to satisfy the following constraints:

$$y_i[(\omega^T \cdot x_i) + b] \geq 1 \quad i = 1, 2, \cdots, n \tag{2}$$

As shown in the Figure 2., the closest sample points to the hyperplane such that the equality sign of the constraints holds are the "support vectors", and the sum of the distances of the two dissimilar support vectors to the hyperplane is

$$\gamma = \frac{2}{\|\omega\|} \tag{3}$$

γ is also referred to as the classification interval. In order to maximize the classification interval, the problem of constructing an optimal hyperplane can be transformed into solving the following equation under constraints:

$$\begin{cases} \min\limits_{\omega,b} \dfrac{1}{2}\|\omega\| \\ s.t.\ y_i[(\omega^T \cdot x_i)+b] \geq 1 \end{cases} \quad [4]$$

Using the Lagrange factorization method and the dyadic principle, the above equation can again be transformed into the following optimal classification function problem:

$$f(x) = sign[\sum_{i=1}^{n} \alpha_i y_i \langle x_i, x \rangle + b] \quad [5]$$

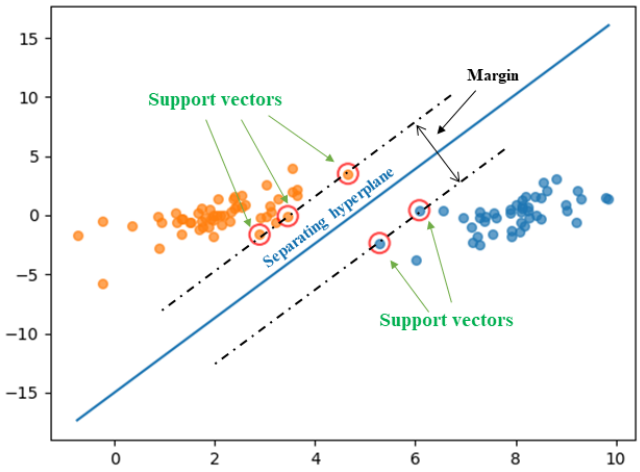

Figure 2: Optimally separating hyperplane and support vectors.

If the data are nonlinearly differentiable, SVM first maps the input space to a high-dimensional linearly differentiable space through the kernel function, and then classifies in the new space. In addition, the outliers in the data will seriously affect the classification performance of SVM, in order to make the model more robust, the soft interval and penalty term are introduced, and the improved SVM objective function is as follows:

$$\begin{cases} \dfrac{2}{\|\omega\|} \min\limits_{\omega,b} \dfrac{1}{2}\|\omega\| + C\sum\limits_{i=1}^{n} \xi_i \\ s.t.\ y_i(\omega^T x_i + b) \geq 1-\xi,\ \ \xi_i \geq 0,\ C \geq 0 \quad i = 1, 2, \cdots n \end{cases} \quad [6]$$

In the above equation, C is the penalty coefficient to control the misclassification of outliers, the larger C means the stricter, the lower tolerance for outliers; on the contrary, it means the more lenient, the higher tolerance for outliers. The classification function of SVM in the case of kernel mapping is:

$$f(x) = sign[\sum_{i=0}^{n} a_i y_i K\langle x_i, x \rangle + b] \quad [7]$$

In the above equation, $K\langle x_i, x \rangle$ is the kernel function. The commonly used kernel functions are polynomial kernel function, Gaussian radial basis kernel function and Sigmoid kernel function.

Dividing the Design Space

In this paper, SVM method is utilized to divide the design space to get the corresponding form of constraint space, the basic division process is shown in Figure 3., and the specific division process is as follows:

Step 1: The sample point set that completes the calculation of constraints is filtered and divided into samples that satisfy the constraints and samples that violate the constraints, forming the sample point set respectively. And then the whole sample set is divided into training set and testing set according to a certain proportion.

Step 2: Preliminarily, the penalty coefficient C and other related parameters of the SVM model are selected, the Gaussian kernel function is selected as the kernel function of the SVM, and the kernel function parameters, which will affect the number of support vectors and the dispersion of the sample features.

Step 3: The training samples are classified and the relevant parameters of the SVM are adjusted appropriately according to the accuracy of the classification.

Step 4: Finish training the SVM model and save the model output.

With the SVM algorithm, it is possible to divide the region occupied by feasible and infeasible sample points to obtain a new feasible space that satisfies the constraints, providing a guide for subsequent sampling in the feasible space.

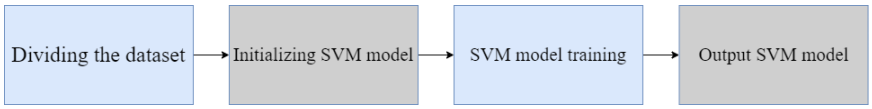

Figure 3: Process of dividing the design space.

Sample Points Selection Method

After dividing the design space by SVM method, we get the feasible space and infeasible space. If the number of sample points in the feasible space is not enough for constructing the approximate model, then we need to select new sample points in the feasible space. The following briefly describes the sample point selection strategy in the feasible space:

First, the existing sample points in the feasible space are formed into a sample point set, and then, starting from the selection of the first point, it is necessary to satisfy the maximization of the minimum distance from each newly selected sample point to the existing sample points. According to the following rule, the sample points are selected sequentially until the number of sample points in the point set meets the required number of inputs (Teng et al., 2018). Denote the minimum distance between any two points as the Euclidean distance:

$$d(x,y)=\|x-y\|_2 \tag{8}$$

The first n sample points that have been selected are $s_1, s_2, \cdots, s_n$, then the set of points is

$$S_n=\{s_1, s_2, \cdots, s_n\} \tag{9}$$

The distance from any sample point x to the set of points S_n is

$$d(x,S_n)=\min\{d(x,s_i)\} \tag{10}$$

The next sample point to be selected is

$$s_{n+1}=\arg\max\{d(x,S_n)\} \tag{11}$$

All sample points in the final point set are widely and uniformly distributed in the feasible space.

Taking the two-dimensional constraint space constituted by inequality [12] as an example, the effect of sample point selection is shown in Figure 4. Where the region constituted by the blue points is the constraint space region, and the red points are the sample points obtained by sampling.

$$\begin{cases} 0\le x\le 10 \\ 0\le y\le 10 \\ x+y\le 10 \end{cases} \tag{12}$$

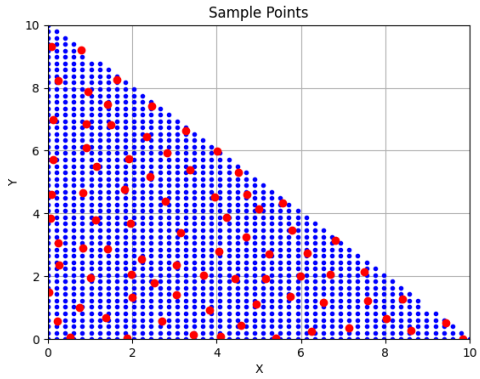

Figure 4: Sample point selection oriented to the constraint space

EXAMPLE

The Optimization Model

Taking the 13,000DWT inland bulk carrier as an example, a three-dimensional parametric model of the ship was constructed in the fully parametric modeling software CAESES, with a scaling ratio of 1:25 (e.g. Figure 5), and its main parameters are shown in Table 1. Three variables to be optimized for the design were selected as b_B, y_b, and area_ratio, and their specific meanings and ranges of variations are shown in Table 2.

Figure 5: 13,000DWT inland waterway twin-screw bulk carrier

Table 1: Main parameters of model ship

L_{pp}	L_{cb}	B	T	C_b	∇	S_{wet}
5.08 *m*	2.564 *m*	0.872 *m*	0.22 *m*	0.86	0.836 m^3	6.018 m^2

Table 2: Design parameters

Design Variables	Design Variable Meaning	Initial Value	Lower Bound	Upper Bound
b_B	Stern Axis Distance Breadth Ratio	0.5287	0.5	0.55
y_b	Bobtail Medial Fullness	0.4162	0.1	0.6
area_ratio	Design Below-Waterline Fullness	0.8356	0.75	0.9

Minimizing the total resistance R of the model ship at the draft of T=0.22m and F_r=0.1457 is taken as the optimization objective.

$$\min f_{obj} = R \quad T=0.22m \quad F_r = 0.1457 \qquad [13]$$

The constraints are listed below:

(1) The optimized displacement must not be less than that of the mother ship, and this constraint is shown in Equation [14]:

$$\frac{\nabla_{opt} - \nabla}{\nabla} \geq 0 \quad [14]$$

(2) The optimized longitudinal position of the buoyant center of gravity of the corresponding structure must not exceed the midship position at 0.55% towards the bow, and this constraint is shown in Equation [15]:

$$\frac{L_{cb} - L_{pp}/2}{L_{pp}} \leq 0.55\% \quad [15]$$

Analysis of the Design Space

According to the upper and lower limits of the three design parameters, 500 sample points are sampled in the design space using the uniform design sampling method, and these 500 sample points correspond to 500 different sample ship types. The hydrostatic calculation module of CAESES is used to calculate the hydrostatic data for these 500 sample points, and the calculated results are compared with the optimized performance constraints of the ship types. The 500 sample points are classified into two categories based on the comparison results: 1. feasible sample points that satisfy the constraints; 2. infeasible sample points that do not satisfy the constraints. Visualize this 3D design space as shown in Figure 6.

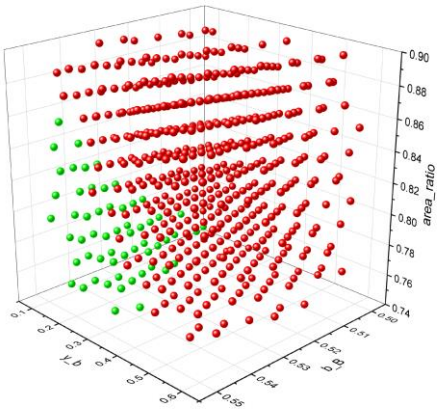

Figure 6: Three-dimensional design space

The red points in Figure 5 indicate infeasible sample points that do not satisfy the constraints, and the green points indicate feasible sample points that satisfy the constraints. From the figure, it can be seen that most of the sample points obtained after sampling according to the original design parameter variation range do not satisfy the performance constraints, and only a small number of feasible sample points satisfy the performance constraints and are distributed in the corner of the design space, so constructing an approximation model based on the whole set of sample points will cause a big trouble to the optimization work.

Optimization Strategies

Optimization Processes

After obtaining the feasible space, the number of sample points distributed within it is 71 in total, which does not meet the demand for the number of samples for constructing the approximation model, and it is necessary to increase the number of sample points in the feasible space to 80, and use the sample point selection method based on the maximum-minimum distance to increase the sample points by 9 sample points in the feasible space. Some of the selected sample points are shown in Table 3 below:

Table 3: Selected sample points co-opted in the feasible space

Number	b_B	y_b	area_ratio
1	0.5500	0.1256	0.8154
2	0.5423	0.1641	0.7500
3	0.5500	0.3051	0.7731
4	0.5436	0.1128	0.7615
5	0.5498	0.2154	0.8000
6	0.5449	0.1641	0.7962
7	0.5487	0.2026	0.7615
8	0.5346	0.2795	0.7500
9	0.5415	0.1256	0.7885

And then the total resistance of these 80 sample ship types is calculated by STAR-CCM+ software to get the sample set for training the approximation model. Then the Kriging approximation model is constructed and the optimization solver is set up, and the genetic algorithm is chosen for optimization. Finally, the study on the hydrodynamic performance line optimization of this ship is completed.

The constraint space-oriented sampling method proposed in this paper and the traditional method based on uniform test design are simultaneously applied to optimize the hull profile, and the optimization effects of the two methods are compared, and the basic flow of the two methods is shown in Figure 7.

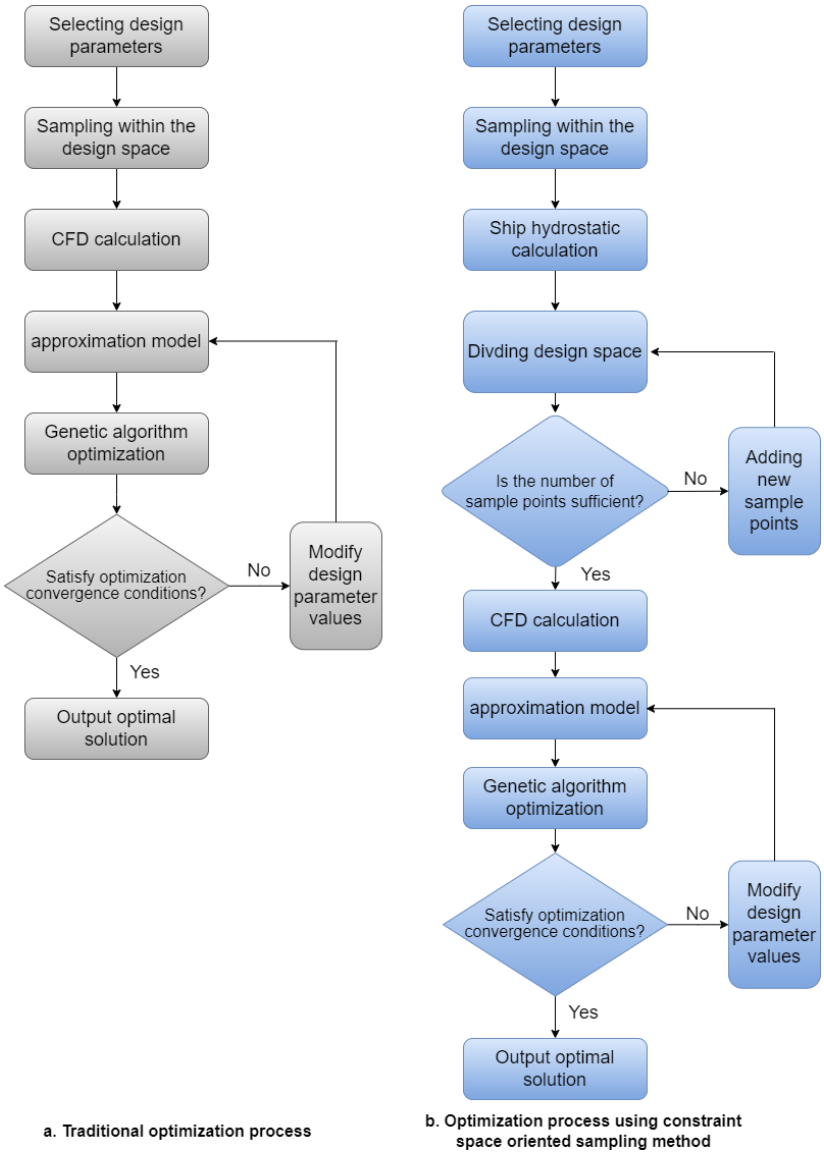

Figure 7: Optimization process

In order to compare the accuracy of the approximate models constructed by the two methods, five sample points are re-selected in the feasible space using the Latin hypercubic sampling method, and the total resistance value is calculated for each sample ship type using the STAR-CCM+ software as the corresponding prediction sample set, and these samples are shown in Table 4. The prediction sample set was forecasted using the Kriging approximation model constructed through two different methods. Finally, the forecasting results of the approximate models constructed by the two methods are evaluated using the root mean square error (RMSE), and the evaluation results are shown in Table 5.

Table 4: Sample points used for assessment

b_B	y_b	area_ratio	Traditional optimization method	Constraint space-oriented optimization method	CFD calculation results
0.5465	0.215	0.7875	14.003 N	13.964 N	13.974 N
0.5395	0.175	0.7815	13.802 N	13.835 N	13.826 N
0.5405	0.125	0.7785	13.873 N	13.832 N	13.793 N
0.5375	0.235	0.7575	13.793 N	13.801 N	13.806 N
0.5415	0.295	0.7725	14.015 N	14.027 N	14.039 N

Optimization Results Analysis

Taking the CFD calculation result as the real drag value of the ship model, the prediction error of the drag and the computational cost of the approximate models constructed by the two methods are compared as shown in Table 5. From the table, it can be seen that the prediction error of the constructed Kriging approximation model is smaller and the prediction accuracy is higher compared with the traditional optimization process after using the method proposed in this paper. This is because the optimization process based on the constraint-space oriented sampling method excludes the sample points that do not satisfy the constraints in the process of constructing the approximation model, which improves the forecast accuracy; On the other hand, using the method proposed in this paper has a lower CFD computational cost, i.e., the number of training samples required to achieve the same accuracy of the approximation model as the traditional method is lower, which is also due to the fact that we only select the sample points that satisfy the constraints to perform the CFD computation and construct the approximation model.

Table 5: Comparison of the accuracy and computational cost

	RMSE	RMSE Comparison	The number of samples for modeling that need to be calculated by CFD
Uniform Design	0.0414	——	500
Constrained Space Sampling Optimization	0.0193	-53.4%	80

Comparison of the bow and stern profiles of the optimized ship and the initial ship obtained after optimization using the two methods can be seen in Figure 8, and it can be seen that some of the ship's profiles have changed to different degrees before and after optimization. As can be seen from the waveforms in Figure 9, the amplitude of the rising wave of both optimized ships is reduced to some extent after optimization compared with the initial ship.

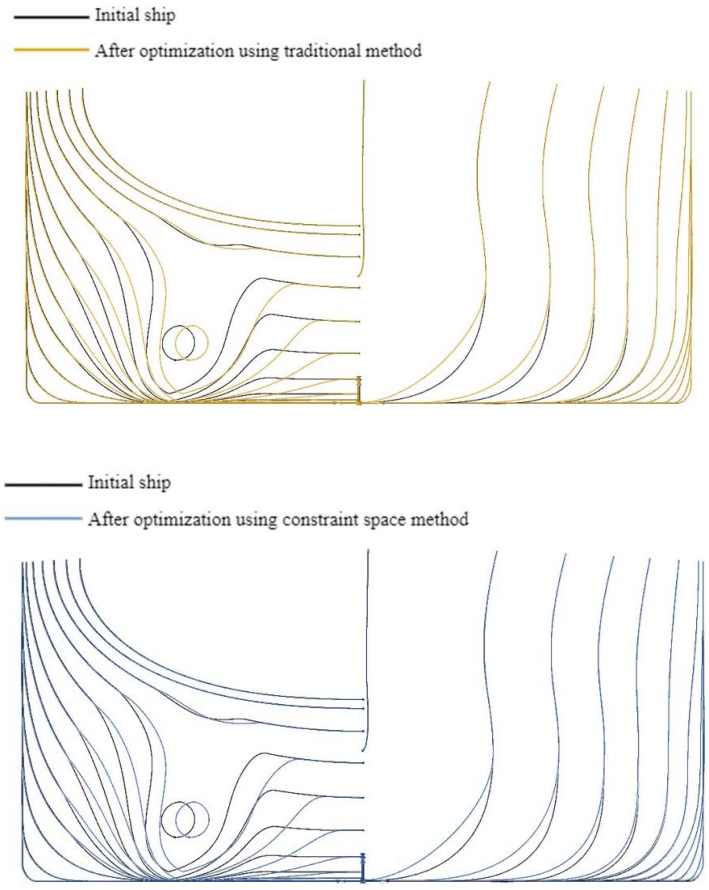

Figure 8: Comparison diagram of the hull lines

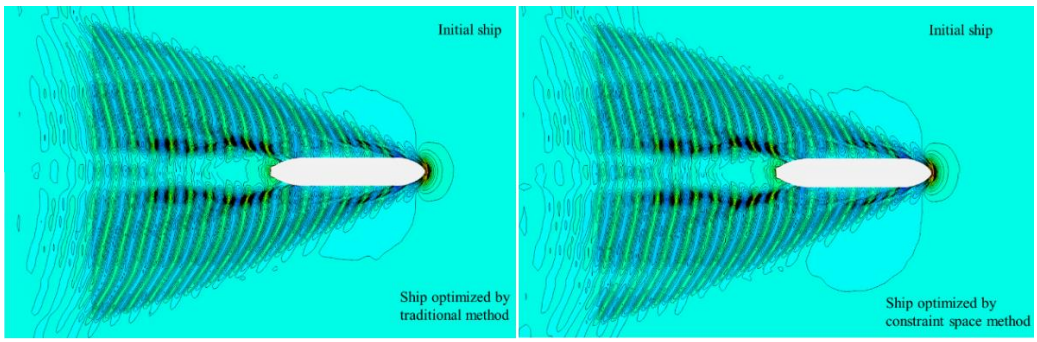

Figure 9: Comparison of waveforms

Comparison of the hydrostatic data of the ship model optimized by the two methods is shown in Table 6. From the hydrostatic data, the displacement volume of the ship model optimized for constraint-oriented spatial sampling increases by 0.23% compared to the initial ship. The longitudinal position of the center of gravity is shifted to the stern direction by 0.001 m compared with the initial ship, and its wet surface area is reduced by 0.75% compared with the initial ship. The drainage volume of the optimized ship model sampled by the traditional uniform design method increased by 0.39% compared to the initial ship, the longitudinal position of the center of buoyancy shifted by 0.003m in the aft direction compared to the initial ship, and the wet surface area decreased by 0.50% compared to the initial ship. It indicates that the frictional resistance of the ship models optimized using both methods has been reduced to different degrees.

The comparison of the drag optimization results of the two methods is shown in Table 7. The total drag of the ship model optimized by the constraint-oriented spatial sampling method is 13.778 N, which is a decrease of 3.35% in the total drag compared with the initial ship, and the error of the approximate model forecast is 0.36%; the total drag of the ship model optimized by the traditional uniform design method is 13.876 N, which is a decrease of 2.66% in the total drag compared with the initial ship, and the error of the approximate model forecast is 0.36%. The approximate model prediction error is 0.36%. Through comparison, it can be found that the approximate model constructed by the constraint space-oriented sampling method proposed in this paper has higher optimization accuracy and better optimization effect.

Table 6: Hydrostatic data

	Drainage volume ∇ (Percentage change)	Longitudinal position of the floating center L_{cb} (Magnitude of change)	Wetted surface area S_{wet} (Percentage change)
Mother ship	0.836 m^3	2.564 m	6.018 m^2
Uniform Design	0.8393 m^3 (+0.39%)	2.561 m (-0.003m)	5.988 m^2 (-0.50%)
Constrained Space Sampling Optimization	0.838 m^3 (+0.23%)	2.563 m (-0.001 m)	5.973 m^2 (-0.75%)

Table 7: Ship model drag optimization results

	Approximate model forecast values	CFD calculated values	Resistance reduction ratio
Mother ship		14.225 N	
Uniform Design Optimization	13.613 N	13.876 N	-2.66%
Error	1.90%		
Constrained Space Sampling Optimization	13.728 N	13.778 N	-3.35%
Error	0.36%		

CONCLUSIONS

This paper proposes a constraint space oriented sampling method in ship shape optimization, taking an inland river 13,000-ton double-tailed bulk carrier as the optimization object, using the method to select the sample points meeting the constraints to construct the approximation model, and using the optimization algorithm to search for the optimal in the feasible space, and finally completing the research on the application of the constraint space oriented sample point selection method in the line shape optimization of this ship. The conclusions are as follows:

(1) The constraint space-oriented sampling method proposed in this paper can improve the forecasting accuracy of the constructed approximate model and save the time cost of calculation.

(2) The application of the constraint space-oriented sampling method to the hydrodynamic performance line shape optimization study of an inland double-tailed bulk carrier, and the comparison with the optimized ship obtained by using the uniform experimental design optimization, shows that the application of this method to the ship shape optimization is feasible.

List of abbreviations

Abbreviations	Explanations
SVM	Support Vector Machine
DWT	Dead Weight Tonnage
L_{pp}	The length between perpendiculars
L_{cb}	The longitudinal center of buoyancy
B	The ship's breadth
T	The ship's draught
C_b	The block coefficient
∇	The volume of displacement
S_{wet}	The wetted surface area
Fr	Froude number
R	The total resistance

CONTRIBUTION STATEMENT

HOU Wen-long: conceptualization, methodology, validation, formal analysis, data curation; **CHANG Hai-chao:** conceptualization, methodology, validation, formal analysis; **FENG Bai-wei:** software; **LIU Zu-yuan:** conceptualization, methodology, formal analysis; **ZHAN Cheng-sheng:** software; **CHENG Xi-de:** software. All authors have read and agreed to the published version of the manuscript.

ACKNOWLEDGEMENTS

This research was funded by the Equipment research Joint Fund of Ministry of Education (Young Talents) project [8091B032201], National Natural Science Foundation of China [grant Numbers 51979211, 52271327, 52271330], 111 Project (BP0820028), to which the authors are most grateful.

REFERENCES

Bonfiglio L, Perdikaris P, Vernengo G, et al. Improving swath seakeeping performance using multi-fidelity Gaussian process and Bayesian optimization[J]. Journal of Ship Research, 2018, 62(04): 223-240.

Chang H, Zhan C, Liu Z, et al. Dynamic sampling method for ship resistance performance optimisation based on approximated model[J]. Ships and Offshore Structures, 2021, 16(4): 386-396.

Chen X, Diez M, Kandasamy M, et al. High-fidelity global optimization of shape design by dimensionality reduction, metamodels and deterministic particle swarm[J]. Engineering Optimization, 2015, 47(4): 473-494.

Feng Y, Chen Z, Dai Y, et al. Multidisciplinary optimization of an offshore aquaculture vessel hull form based on the support vector regression surrogate model[J]. Ocean Engineering, 2018, 166: 145-158.

Guo J, Zhang Y, Chen Z, et al. CFD-based multi-objective optimization of a waterjet-propelled trimaran[J]. Ocean Engineering, 2020, 195: 106755.

Hochkirch K, Mallol B. On the importance of full-scale CFD simulations for ships[C]//11th International conference on computer and IT applications in the maritime industries, COMPIT. 2013.

Liu X, Zhao W, Wan D. Multi-fidelity Co-Kriging surrogate model for ship hull form optimization[J]. Ocean Engineering, 2022, 243: 110239.

Ouyang Xuyu, Chang Haichao, Liu zuyuan, et al. Application of Adaptive Sampling Method in Hull Form Optimization[J].Journal of Shanghai Jiao Tong University, 2022,56(07):937-943.
Teng Yiyang, Wu Yun, Xiong Shifeng, et al. A space-filling property of sequential maximin distance designs[J]. Journal of University of Chinese Academy of Sciences,2018,35(06):731-734.
Wang Gangcheng, Ma Ning, Gu Xiechong. Fast Collaborative Multi-Objective Optimization for Hydrodynamic Based on Kriging Surrogate Model[J].Journal of Shanghai Jiao Tong University, 2018,(6): 666-673.
Wang Jiandong, Zhuang Jiayuan, Su Yumin, et al. Inhibition and hydrodynamic analysis of twin side-hulls on the porpoising instability of planing boats(Article)[J].Journal of Marine Science and Engineering, 2021,9(1): 1-26.

Part 3:
NOVEL CONCEPTS

Proceedings of 15th International Marine Design Conference (IMDC-2024)
June 2-6, 2024
Amsterdam, the Netherlands

Flipflopi: Circular economy design inspiration from a recycled plastic sailing dhow

Simon Benson[12]*, Ali Skanda[1], Hassan Shafii[1], Katharina Elleke[13], Simon Scott-Harden[4], Nathan Smith[2], Richard Birmingham[2] and Dipesh Pabari[1]

ABSTRACT

Flipflopi is an East African organisation with a mission to end single use plastic, driving this agenda using circular economy principles applied to the design and build of fully recycled plastic sailing dhows from their boatyard in Lamu Kenya. Flipflopi has achieved measurable global impact by showcasing the world's first ocean going recycled sailing boat, Ndogo, a 9 metre long, lateen rigged dhow which has sailed the East African coastline and across Lake Victoria. Flipflopi is now aiming to build a much larger ocean-going dhow, named Kubwa, which presents further technical challenges from a marine design perspective. To meet these challenges. Flipflopi are utilising a combination of generational heritage boatbuilding expertise in Lamu; specific design experience from building and sailing Ndogo; technological progress driven by other recycled plastic projects; and more formalised naval architecture and engineering design approaches. This paper introduces the context within which Flipflopi is centred, the links to circular economy design principles and the specific design challenges from working with recycled plastic as a boatbuilding material.

KEY WORDS

Plastic; Recycling; Circular Economy; Boatbuilding; Flipflopi.

INTRODUCTION

In this paper we consider a circular economy approach to the design, construction, and operation of marine craft through a broad overview of current achievements and challenges from Flipflopi, an organisation which has launched three sailing dhows made almost completely from recycled plastic waste and now plans to build a larger 24 metre ocean going sailing dhow. We also share some of the practical challenges and continuing design questions from using recycled plastic as a boat building material.

Flipflopi is an East African organisation, based in Lamu Kenya, with a stated mission to end single use plastic, ensure all other plastics are part of a circular economy and promote environmental solutions to the plastic waste crisis. The organisation is centred around the construction and operation of fully recycled sailing dhows. Flipflopi works with communities to "close the loop" on waste plastics, collecting and recycling waste to produce boats and products rooted in indigenous heritage. They also harness appropriate high technology techniques to meet the unique design demands from using recycled plastic as a construction material.

Flipflopi has demonstrated global impact from their campaigning work, perhaps most significantly by showcasing the world's first ocean going recycled sailing boat, Ndogo (small in Swahili), a 9 metre long, lateen rigged dhow with lines typical of Lamu heritage designs (Figure 1). Ndogo has completed several voyages around the East African coast and on Lake Victoria, which stretches across the borders of Kenya, Uganda, and Tanzania. These voyages aimed to promote messages to end plastic

[1] The FlipFlopi Project Foundation, Kenya

[2] Newcastle University (School of Engineering, Newcastle upon Tyne, UK); ORCID: 0000-0002-8476-8687

[3] Precious Plastic

[4] Northumbria University (School of Design, Newcastle upon Tyne, UK)

Submitted: 23 February 2024, Revised: 30 April 2024, Accepted: 1 May 2024, Published: 21 May 2024

Conference paper, DOI: https://doi.org/10.59490/imdc.2024.857 e-ISSN: 3050-4864

pollution, bring awareness to the issue, engage East Africans in alternative ways to use existing waste plastic and demand legislative action to ban single-use plastics. The impact is evidenced in several end of year organisation reports (Flipflopi 2021; 2022; 2023).

Since building Ndogo, Flipflopi have designed and built several smaller boats, including a canoe and a 7-metre taxi dhow that will carry passengers and light cargo within the Lamu archipelago. A training centre has been established at the Flipflopi boatyard, which has so far taught 30 people from the Kenyan Coast traditional boat building techniques in combination with circular economy practices.

A central ambition for Flipflopi is to launch a substantially bigger dhow, Kubwa (large, in Swahili), which will be about 24 metres long. The design of Kubwa aims to integrate the knowledge generated from Ndogo. There are also new challenges inherent in a larger and more complex boat.

This paper first introduces the context within which Flipflopi is centred – the plastic waste crisis that is especially problematic in LMIC settings such as East Africa. The principles of circular economy design are then introduced, starting from a broad overview and then focusing in on the open-loop recycling system followed by Flipflopi. The application of circular economy principles in other areas of marine design are briefly considered. The paper then focuses on the specific design principles and challenges from working with recycled plastic as a boatbuilding material: developing hull lines, structural design, material properties and joining techniques. The linked challenge of sustainable propulsion is also summarised.

Figure 1: A Flipflopi "closing the loop" poster with dhow Ndogo sailing in the Lamu archipelago (left), an impression of Kubwa sailing alongside Ndogo (right)

PLASTIC WASTE AND POLLUTION

Over 8 billion tonnes of virgin plastics have been produced up to 2021 (Geyer et al. 2017). Around 80% of this total has been discarded, demonstrating a loss of valuable resources and the origin of an environmental disaster (Bucknall 2020). The most visible consequence of this is the huge volume of plastic that ends up in the ocean, which has become a maritime crisis. Lau et al. (2020) shows that 78% of the plastic pollution problem could be solved by 2040 but only if all the possible reduction pathways are followed: that means reducing consumption, increasing reuse, improving waste collection and recycling, and accelerating innovation in the plastic value chain.

Plastic pollution strongly affects coastal communities and their natural environment. These communities, particularly in rural and lower economy regions, face sometimes overwhelming quantities of plastics on beaches and in fishing waters (Phelan et al. 2020). Negative consequences to the coastal environment include entanglement in plastic by megafauna, ingestion of plastic by fish, microplastic ingestion by invertebrates, ghost fishing by abandoned nets, algae growth in plastic debris, contaminated fisheries and reduced natural health of beaches littered with plastic (Thushari & Senevirathna 2020).

The focus of this paper is Amu Island, which is part of the Lamu Archipelago on the Kenyan coast with a population of around 30,000. The community generates about 14 tonnes of waste daily, of which about 2.5 tonnes is plastic waste (Moejes 2023a). The quantity of washed-up ocean plastic is not quantified, but by illustration a single community beach clean-up on a 10-km stretch of beach (see Figure 2) typically collects 35 to 40 tonnes of plastic waste (Scott Harden et al. 2020; Moejes 2023b). To exacerbate the problem, there is only one waste disposal site on Amu Island. This area has no separation facilities and waste is left to pile up, blow across the island into the ocean and in many instances is burnt openly.

A community survey in Lamu, completed as part of a plastic waste mapping study by Flipflopi in 2022, found that 98% of respondents viewed plastic waste as a problem. They also found significant interest in not only learning about the environment and pollution, but also taking part in innovative solutions, such as boat building with recycled plastic, as a practical way of tackling the growing plastic waste problem (Flipflopi 2022).

Figure 2: A beach cleanup on Shela beach, Amu Island (Flipflopi 2022)

CIRCULAR ECONOMY DESIGN PRINCIPLES

Definition

Circular economy is a model of production and consumption which centres on the reuse and recycling of materials. There are many definitions of circular economy and an extensive body of literature that discusses, applies and critiques the concept. We only provide a summary of some well-established circular economy definitions, for the purpose of contextualising the Flipflopi approach. We use circular economy from a practitioner-led perspective, and do not take a detailed theoretical position or critique of the concept in this paper.

Velenturf and Purnell (2021) summarise the circular economy as "a technology-focused concept that can generate economic gains while alleviating pressure on the environment". It involves "circularity of resource flow by preventing loss of material out of the system" (Bucknall 2020). It aims to make "better" use of resources, although "better" is sometimes difficult to define. For plastics this goes well beyond recycling, incorporating the pillars of sustainability – economic, social and environmental. In this way a product design incorporates life cycle aspects such as durability, reuse, repair, remanufacture alongside beneficial economic activity such as employment and enterprise, environmentally driven considerations of energy consumption and social considerations of ownership costs and community benefits.

The Ellen Macarthur Foundation, inspired by the founder's solo sailing circumnavigation of the globe, is a leading advocate of circular economy approaches. They base the circular economy on three principles driven by design (Macarthur 2019):

1. Eliminate waste and pollution
2. Circulate products and materials (at their highest value)
3. Regenerate nature

The Plastic Circular Economy

The plastic circular economy, shown in Figure 3, prevents linear economy waste such as landfill, incineration and environmental pollution. Circularity is enabled at several levels, including (Bucknall 2020):

- Reuse of plastic products for their original purpose, such as a reusable water bottle, or for new purposes, such as using a water bottle as a plant pot.
- Open-loop recycling, where the plastic is recycled into a new product or use, such as recycling water bottles into polyester clothing.
- Closed-loop recycling, where the plastic is recycled back to its original purpose, such as recycling used water bottles into new water bottles.

Open and closed loop recycling are typically characterised as remote industrial processes. Waste plastic is collected and removed from a community to a large-scale processing plant. It will then re-enter a different community economy as a raw material or a newly recycled product. Whilst this process may meet the "three principles" definition, there is less community engagement in the complete economic model. This misses opportunities to "better" the sustainability at a local level. For example, despite high awareness of recycling in the UK population, there continues to be pitifully low rates of acceptably separated plastic waste collection from the kerbside (Burgess et al. 2021).

Alternative circular models, such as that advocated by Precious Plastic (Spekkink et al. 2022), promote local engagement throughout the recycling-remanufacture process. This includes developing small scale recycling spaces to process plastic waste and demonstrating innovative manufacturing methods for recycled product designs that benefit the communities that collected the waste. Scott-Harden et al. (2022) discusses the design challenges of locally recycled products. Recycled material can be used to manufacture a diverse range of high precision, durable products where tolerances are high such as sunglass frames, plug sockets and jewellery. However, the processing of larger quantities of locally recycled plastic is often better suited to less refined large-scale structures such as furniture, window frames, bricks and fencing. Traditionally built dhows, and therefore many other wooden boat types, can be included in this category. With proper consideration of the material properties and consistency, boatbuilders can use recycled plastic lumber with established carpentry techniques in very much the same way as wood (Scott-Harden et al. 2022).

As will be shown, Flipflopi is an exemplar of a community centred approach to open loop recycling. The flow of plastic from waste to a new product is entirely within the community, and the products themselves contribute to and promote further recycling and awareness of the plastic pollution crisis. The success of Flipflopi suggests that alternative circular models hold an important and powerful role for building sustainability into the circular economy.

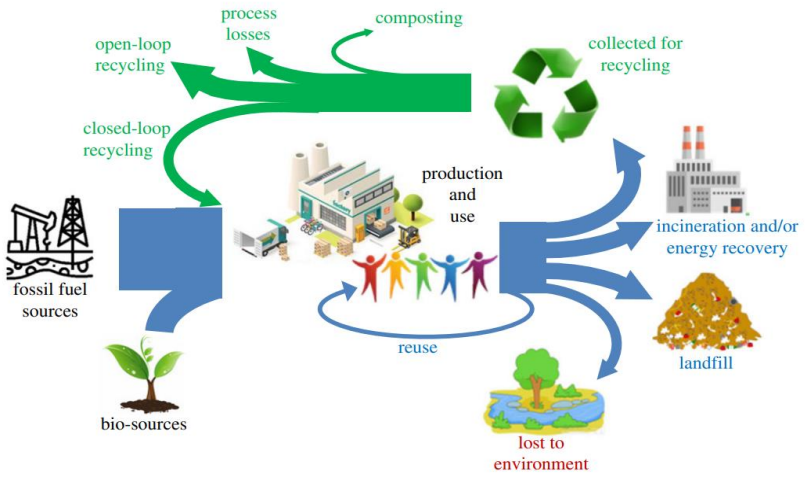

Figure 3: The lifecycle of plastics, including linear and circular economy principles (Bucknall 2020)

The Flipflopi Approach

Flipflopi uses an open-loop recycling system coupled to an alternative circular economy model to turn locally generated plastic waste into carpentry products for the community including dhows, furniture and decorative products. The system steps (Figure 4) are:

1. Household, small-scale industrial and washed-up plastic waste from the sea is gathered and macro sorted by people within the Lamu archipelago. At present only some plastic types can be recycled.
2. The waste is collected from various stations or brought to the Flipflopi boatyard on special collection days. It is weighed and a collection payment is made.
3. The waste is then further sorted into polymer type and colour. Some polymers, such as PET, are sent away to industrial recycling centres. Polymers that Flipflopi can effectively recycle, such as HDPE, continue through the recycling space.
4. The plastic is crushed into shreds, thoroughly washed, and then moulded or extruded into construction materials including planks, beams and special mouldings. New processes such as sheet pressing are being developed.
5. The construction materials are used in several carpentry and boatbuilding spaces within the yard, including a workshop for craft products and furniture, a skills training centre and the boatbuilding sheds.
6. Smaller carpentry products are commissioned and sold, mostly in the local community and often as high value items.
7. The dhows continue to be operated by Flipflopi as prototype demonstrators and are the focus of their broader campaign work to end single-use plastic. The smaller boats are also planned to be used for enterprise, such as passenger transport, and for plastic collection.
8. At end of life, the thermoplastics embodied in Flipflopi products can be looped back into the recycling process.

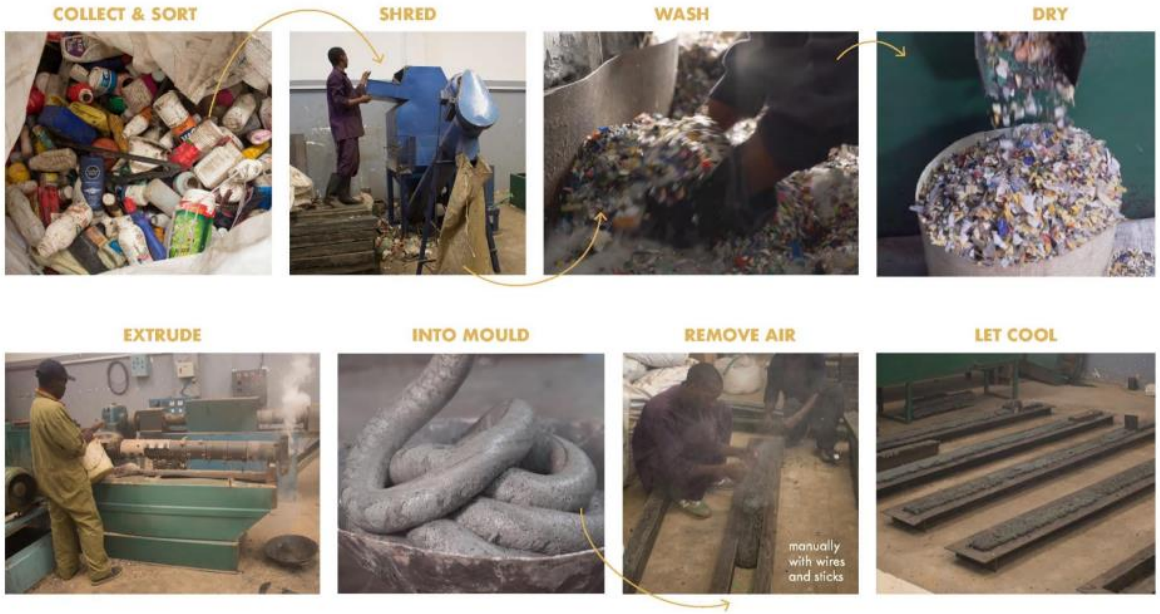

Figure 4: The Flipflopi recycling centre process, in this case showing a moulding technique to produce plastic lumber

Flipflopi operates a full systems approach to their organisation strategy, which they define as "the combination of education leading to behavioural change, innovation within the circular economy, and campaigning to influence legislative change to end single-use plastics" (Flipflopi 2022). This is applied through a strategy integrating education, innovation and influence. For example:

- Education is directly delivered via a heritage boatbuilding training centre, which piloted a 12-week vocational course in 2022. Broader educational programmes to change behaviour around plastic consumption is delivered via community-based partners and artivists across East Africa, with diverse contributions including storytelling, scientific research and projects to advance the role of women in waste management and boatbuilding.
- Innovation is driven broadly to include systems from recovery to upcycling and is applied directly to overcome the practical challenges of building larger boats such as Kubwa from recycled plastic, as outlined in the Design Challenges section of this paper.
- Influence is underpinned by the education and innovation activities, which provide a backdrop for Flipflopi to effectively lobby for regional consensus to ban unnecessary single use plastics in East Africa.

The Flipflopi approach meets the "three principles" of circular economy. The full systems approach creates added benefit to the design capabilities and philosophy that "betters" the overall sustainability of the process:

- Eliminate waste and pollution: Flipflopi now collects over 12 tonnes of plastic every month, has become the de-facto recovery and recycling centre for Lamu, and is now extending operations across the entire archipelago. About 30% of the collected plastic cannot be processed on site, and whilst the onward chain to larger recycling centres in Kenya is established it is not yet economical. Whilst this presents space and capacity challenges for the Flipflopi boatyard, it

has also driven considerable design innovations to find new ways to use more of the waste plastic. For example, to investigate the use of polypropylene sacks, a common waste product from the food and construction sectors, to provide strength in sheet materials produced in a bespoke press machine. The envisaged outcome is large format sheets suitable for a new range of construction products such as stud walls and doors.

- Circulate products and materials (at their highest value): Flipflopi has proven that circulated plastic waste can be used to produce new products at high value. Apart from the dhows, the most notable high value product is the 'King's Throne' presented to the British monarch on a visit to Kenya in 2023 (Figure 5). However, the range of polymer types, quality, suitability for re-manufacture and subsequent consistency has challenged the design process. Whilst the plastic lumber can be worked in a similar way to wood, it does not have similar material properties. Flipflopi are now quantifying material behaviour by adapting established material testing methods and linking to formalised boat design codes (see Design Challenges section).
- Regenerate nature: Using recycled plastic as a building material potentially places less pressure on wood sourced from local forests. Flipflopi also contribute to regeneration of nature through their influence in better managing the local environment, for example by replanting mangroves, and campaigning for an end to single use plastic. The eco-design philosophy enables further innovation in additional benefits to other environmental issues. For example those hinging around the use of fossil fuels, including reducing carbon emissions from boats, building renewable energy capacity, improving local air quality, and preventing pollution from unburnt and spilled petrol. The potential of electric propulsion, discussed in the Design Challenges section, is an example of this added benefit.

Flipflopi also meets the three pillars of sustainability. An example is the impact on people engaged with the organisation in different ways. Flipflopi employs 30 people directly, 46% of whom are women, and has 9 skilled artisans on contract. The vocational course has trained 30 people in plastic carpentry techniques. The recycling process engages with over 700 local people, 50% of whom are women, from lower income communities. They collect waste and generate income from this, currently representing a cash injection of about $24,000 in direct payments to date. The employment and education activity therefore has economic benefit by promoting local enterprise. The high percentage employment of women promotes societal benefit, especially within a local maritime economy which is traditionally dominated by men. All the people involved in Flipflopi are engaged and contributing to the environmental benefit from recycling and reusing plastic waste.

Figure 5: High Value Recycled Plastic Products: the "Kings Throne" presented to King Charles III, November 2023 (left), a traditional Swahili chair (right). Left photo © British Embassy in Kenya

Circular Economy in Marine Design

Flipflopi is centred in heritage boatbuilding and maritime activities. It holds potential for direct application in many other coastal communities, particularly those where more traditional boat use is still prevalent. Whilst this constitutes a majority of the total marine craft across the globe, it is a small fraction of the total tonnage, which is dominated by large cargo vessels. What does the circular economy mean for this wider shipping industry and the marine design that underpins it?

Agarwala (2023) argues that the maritime industry continues to find it difficult to adopt full circular economy approaches to design. Aspects such as shipbreaking-reuse of materials (Rahman 2021) and decarbonization (Gilbert et al. 2014) can fulfil the "three principles" of circular economy, but currently suffer sustainability failings. For example, Dewan and Sibilia (2023) describe those exposed to toxic pollution from shipbreaking as suffering a form of structural violence in the maritime economy. Decarbonization, the most prominent current challenge for the maritime industry, suffers from "woefully insufficient progress in vessel designing with alternative fuels in mind, as well as in securing alternative fuel supply chains" (Tomos et al. 2024).

Despite the tiny-scale of Flipflopi within the global maritime industry, the project provides questions for marine design to more widely integrate full circular economy. For example, we briefly consider the two "grand challenges" for the marine industry summarised above: decarbonization and shipbreaking.

- Decarbonization: The media attention for Flipflopi demonstrates the social power of iconic boat design to capture public imagination and more crucially to promote engagement. Coastal communities across the world hold powerful cultural identity to maritime (Alegret & Carbonell 2014), from tangible activities like shipbuilding and fishing through to intangible feelings of ethos and identity. These communities also suffer some of the worst effects of climate change including erosion, extreme weather events and sea level rise. Can marine designers work better with coastal communities - the builders, users and witnesses of maritime activity - to better capture their imagination through iconic, locally centred ship designs, and through this engage community power to drive a more rapid change to decarbonization and zero emissions in the maritime industry?
- Shipbreaking: Flipflopi has made a real impact in their local community to reduce plastic pollution, whilst also inspiring action for zero plastic waste policy in Kenya and internationally. For example, Flipflopi and legal partners have drafted a Bill to ban unnecessary single use plastics across all seven countries in the East African Community (EAC). Over 16,000 people have signed a public petition and 22 legislators representing the EAC unanimously agreed to a regional approach to tackle plastic pollution. The Bill is now being considered for tabling at the East African Legislative Assembly. How can this impactful model – where the marine designers are also the campaigners - be transferred to improve the localised human and environmental costs associated with shipbreaking in countries such as Bangladesh, whilst highlighting the responsibility of the entire maritime sector to focus on stopping unsustainable scrapping practices?

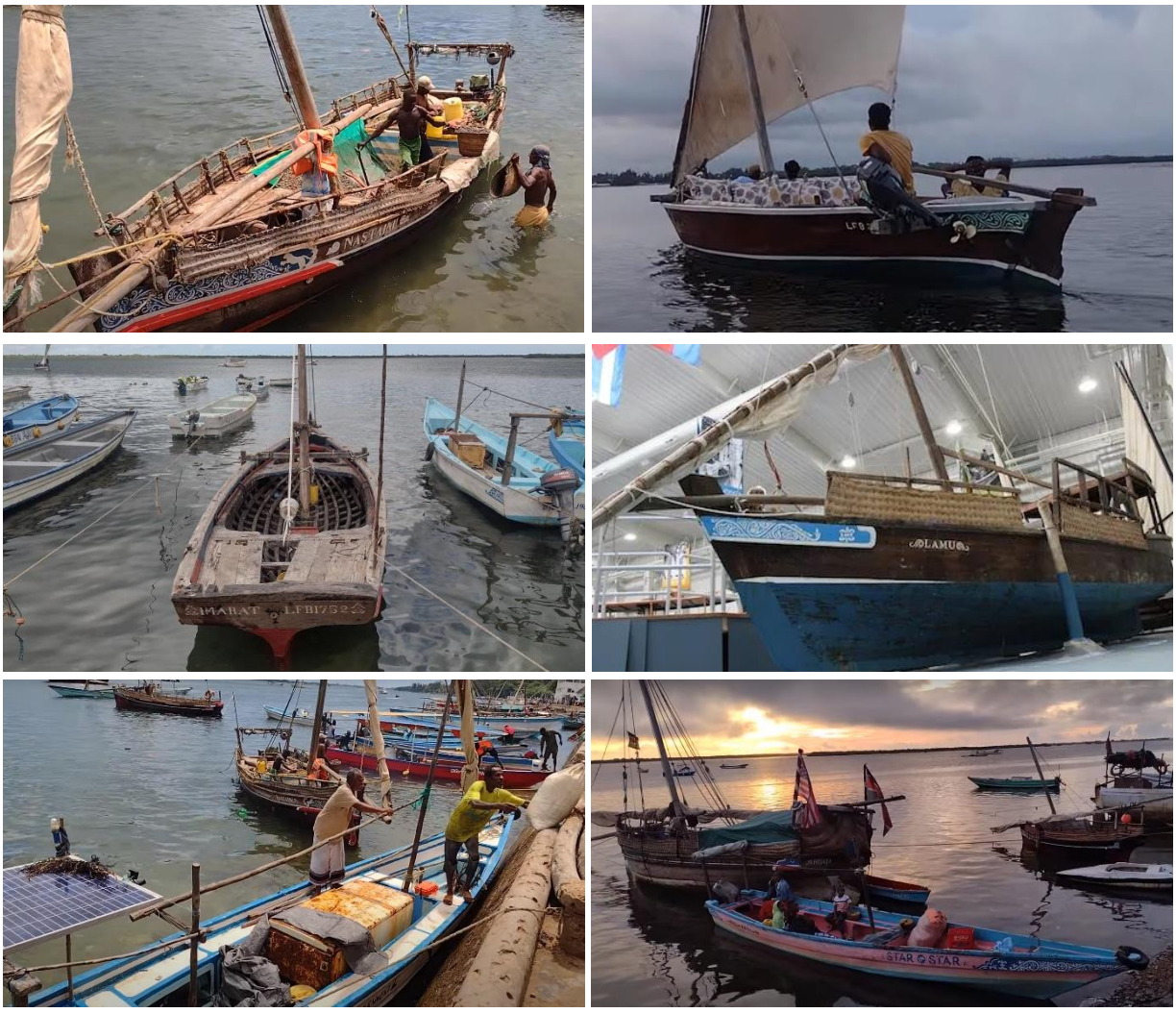

Figure 6: A wooden dhow offloading cargo (top left), a fibreglass Mozambique dhow on a tourist cruise (top right), a racing mashua (middle left), Ali Skanda's Lamu dhow in the International Small Craft Center, USA (middle right), a fibreglass dhow loading ice for a fishing trip (bottom left), a daily scheduled morning passenger dhow (bottom right)

DHOWS IN THE LAMU ARCHIPELAGO

Dhow Types, Construction Methods and Uses in Lamu

Boats and the maritime economy are woven into the fabric of Lamu's culture and daily life. This means there are many uses of boats including: local passenger transport within the archipelago; cargo transport from the mainland and between island villages; coastal goods transport stretching between Somalia and Tanzania; inshore and offshore fishing; a variety of tourist activities such as cruises, fishing, diving and expeditions; and a dynamic culture of competitive dhow racing.

Figure 7: Construction Methods. A new wooden build (top left), an older dhow, Utamaduni, prior to renewal (top right), fibreglass taxiboat moulds (bottom left), "Almas" – a fibreglass dhow under construction (bottom right)

Dhows with traditional aesthetics and construction arrangements are still prevalent, with examples shown in Figure 6. The Jahazi, with a standing bow stem and a flat transom, is the unique Lamu traditional design. The Jahazi is a recognized cultural icon, and is included in international heritage boat collections. The transom is notably different to the stereotypical boom stern of Arabic dhows. The shape is thought to give easier loading and added comfort. Increasingly popular, especially for tourism, are the wider beam Mozambique dhows. These may still be built from hardwood but are now increasingly using fibreglass which needs less skill to produce and reduces the challenges of boat maintenance.

Mashuas, also called taxi dhows, are the most common way of getting around the Lamu archipelago and are also used for fishing and cargo transport. These are slender flat bottom hulls 6-12 metres long and typically powered by a 15hp outboard. In recent years traditional wooden taxi dhows have been increasingly replaced by fibreglass boats.

There is an active boatbuilding, repair and maintenance industry concentrated in Lamu town and several other villages within the archipelago including Matandoni. Construction methods, also shown in Figure 7, include:

- New wooden "artisanal" construction of dhows. These are mostly for tourism;
- Renewal / refurbishment of existing wooden dhows, such as Utamaduni, a 20 metre dhow also pictured in Figure 15;
- Hand layup fibreglass construction of smaller boats using purpose built moulds, with a mashua shown in Figure 7;

- Fibreglass construction of larger boats, also using concrete and aggregates for keels and stems. These may use end of life wooden dhows as plugs, such as mashua Almas, pictured during construction in Figure 7.

The Flipflopi Fleet

Flipflopi have designed, constructed and launched three sailing dhows: Dau la Mwao (Canoe), a small mashua (Water Taxi) and the custom designed expedition mashua dhow Ndogo (see Figure 8 and Table 1).

Figure 8: Dau la Mwao / Canoe (left), Taxi (middle) and Ndogo (right) all sailing in the Lamu archipelago

Table 1: Main Particulars

	Dau la Mwao	Water Taxi	Dhow Ndogo	Dhow Kubwa
Length (m)	6	7.4	9	24
Beam (m)	1.4	2.4	4.0	7.5
Draft (m)	0.3	0.6	1.0	1.8
Approx. Displacement (tonnes)	0.7	1.1	7.25	115
Propulsion System	Sail	Sail and 15hp engine	Sail and 15hp engine	Sails and engine

Dhow Ndogo (Figure 9) was conceived in 2016 by Ben Morrison and Dipesh Pabari as a campaigning tool to spread the message about plastic waste. In Lamu they met master dhow fundi (boatbuilder) Ali Skanda who comes from a generational family of expert carpenters and boatbuilders. Ali accepted the challenge and construction started in 2016. Ndogo was conceived as a prototype to learn boat building methods using recycled plastic. The knowledge from this process was captured through different media resources including a boat building "toolkit" that can be downloaded from the Flipflopi website. All recycled plastic boat parts were first sourced from external recycling companies in Kenya before the in-house plastic recycling facility took over production later on, enabling a better control over quality. The keel, ribs and structural elements of Ndogo are all made from recycled HDPE (mostly found in jerry cans or other containers for liquids, like shampoo bottles). HDPE has favourable properties (buoyancy and flexibility) and is easily available to be collected in sorted and relatively clean form.

Figure 9: The elements of Ndogo – frames (left), planks (middle) and covering (right)

Dau la Mwao is a small canoe built entirely from HDPE recycled plastic by students on the first Flipflopi heritage boatbuilding course. The design follows a traditional fishing canoe (Figure 10) in shape and construction method, enabling the boatbuilders to use their traditional approach and maintain their boatbuilding heritage. The frames were extruded through custom moulds. The build then followed traditional techniques and was completed over a 6 week period. A complete build process is documented by Flipflopi in collaboration with Precious Plastic (Flipflopi 2023).

Figure 10: The basis fishing boat (left), placing the mataruma/ribs (centre), the completed canoe (right)

The Taxi dhow is the latest boat built by Flipflopi. It is a bespoke design sized for potential commercial use and to establish a market for recycled boats to compete with equivalent fibreglass designs now dominating in Lamu. The size is suitable for transporting goods and people across the archipelago, and also offering leisure and tourism trips. The build has also enabled Flipflopi to stress test new types of plastic lumber from the recycling centre, along with new construction and sealing techniques including plastic welding as shown in Figure 11.

Figure 11: Mould for a type of rib (left), welding planks (centre), view from transom showing welded transom (right)

The proposed large Jahazi dhow (Kubwa) will bring together the knowledge, techniques and experience gained from the previous boat builds. The size and subsequent design complexity of Kubwa presents new challenges, which are summarised in later sections of this paper.

DESIGN AND BUILD PRINCIPLES

The construction of the traditional dhows of Lamu are easily recognisable as similar to the wooden boat building techniques found in Europe and North America and would be described as carvel planking on sawn frames. However the procedure followed by the dhow builders is not the same as that usually followed elsewhere, being more akin to the method employed in clinker (called lapstrake in North America) boatbuilding. Once the keel, stem and transom have been set up, so defining the overall dimensions, temporary moulds are inserted to guide the shape of the planking. These moulds are continually adjusted by the builder who, using an experienced eye, continually makes minor adjustments to the shape. Once the planking is complete the frames are cut to shape and fastened inside the hull. The timber used has the required curve to the grain, however on larger dhows the entire frame has to be made in two parts (futtocks). These are simply butted together, without doubling pieces for continuity of the structure, however strength is maintained by moving the position of the butt joint in adjacent frames, with the frames themselves being closely spaced. For Ndogo the same traditional procedure was followed, but with plastic timber planks, and the curved plastic frames being made in individual custom steel moulds. This process is illustrated in Figure 12 and documented in the Flipflopi boatbuilding toolkit. While the wooden dhows are typically coated with antifouling paint externally, and with linseed oil and turpentine internally, the plastic dhow Ndogo was coated with the instantly recognisable pattern of recycled flip flop sheets.

From the description above the traditional dhows of Lamu are not ‘designed’ in the current sense of the word. The builder is responsible for the shape and scantlings, and this is based on inherited knowledge, experience, and several ‘rules of thumb’ to decide on scantlings. There is also an ongoing element of innovation as the builder responds to personal views of what would be an improvement, feedback from the operators of previous designs, and customer or market requirements. As a result, an evolution in the designs, or styles, can be observed in the multitude of dhows observable in Lamu harbour and the adjoining channels. Abandoned on the beaches can be seen old and decaying wooden vessels, with other similar solid working boats still working, their lateen sails furled while they offload cargos of coral stone bricks, timber, and sack of grain, or land fish at the town jetty. Alongside these are water taxis or small passenger ferries, with slender and sharp overhanging bows, driven by outboard motors. In amongst all these working boats are the latest evolution in the design of the traditional dhow: graceful sailing vessels with high aspect lateen rigs, and a finish that is of a similar standard to that found on many yachts. These are the tourist sailing dhows, taking guests to the reefs for snorkelling, or on sunset cruises in the channels of the estuary. The current peak of the evolution of this traditional craft is manifest in the design of racing dhows, developments in their shape, rig and construction material contributing to the success of this popular and highly competitive sport.

In this context the development of dhows whose shape echoes the traditional vessels in Lamu harbour, and whose construction is based on the heritage skills of the Lamu boatbuilders is in keeping with other influences on the evolution of these vessels. However as more ambitious vessels are planned the need for a more formalised approach to the refinement of the shape, and the scantlings of the structure, becomes increasingly important.

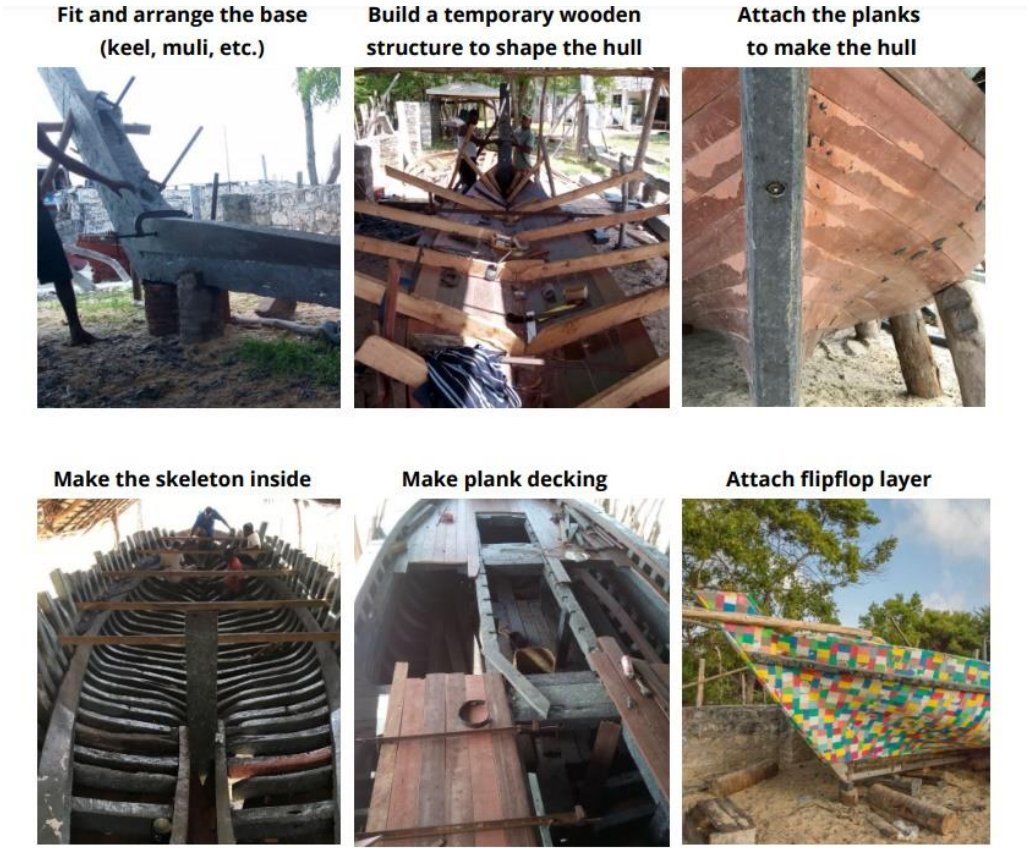

Figure 12: Design and construction process of Ndogo

DESIGN CHALLENGES

Flipflopi has encountered and overcome many design challenges since the first preliminary ideas were kindled for a recycled plastic boat building project in 2016. These range from very broad production challenges in the local recycling of plastic into structural materials, through to very specific challenges of a particularly difficult joint in the stern stem of the boat. Therefore, this section is not exhaustive, but instead focuses on five challenges which we have found to be important and specific to the design and construction of the dhow itself.

Hull Lines

In a new dhow design following traditional methods, the hull lines are developed during planking from the fundi/boatbuilder's knowledge and experience of previous dhows. In other cases, such as Utamaduni pictured in Figures 7 and 13, older dhows are renewed to maintain their shape and characteristics whilst almost the entire structure is replaced.

This process is challenged when replacing wood with plastic, because there needs to be some prior knowledge of shape to efficiently form the frames, rather than selecting and shaping appropriate lumber. In addition, the change in material properties and subsequent scantling weight needs to be more properly considered.

To assist with this, marine design software including Rhino and Maxsurf have been introduced to the Flipflopi design process by bringing together a team including the boatbuilding fundis, naval architects and industrial designers. Working together, the team were able to transfer the traditional lines and design philosophy of the fundi into a digital model, with an example shown in Figure 14. This included measuring and digitising an existing dhow (Utamaduni) in Rhino and using this to conceptualise then fair the features for the new design in Maxsurf. The Maxsurf model was then used to give confidence with new features introduced by the fundi into the design, such as the unique rounded stern. This was checked in terms of buoyancy distribution, stability, and the shape of key hull lines known to influence resistance such as at the bilge diagonal. These efforts were effectively communicated back to the Flipflopi team through several webinars and online discussions. These were also incorporated into lectures for the heritage boatbuilding course.

The digital model also enabled a scale model of the dhow to be manufactured for towing tank and stability experiments at Newcastle University (Figure 15). A physical model provides a practical and effective way to communicate key naval architectural concepts to the Flipflopi team, including the methods to measure stability, the effects of free surface and the hydrodynamic performance.

Figure 13: The original ribs of Utamaduni in the Flipflopi boatyard (left) and the renewed structure (right)

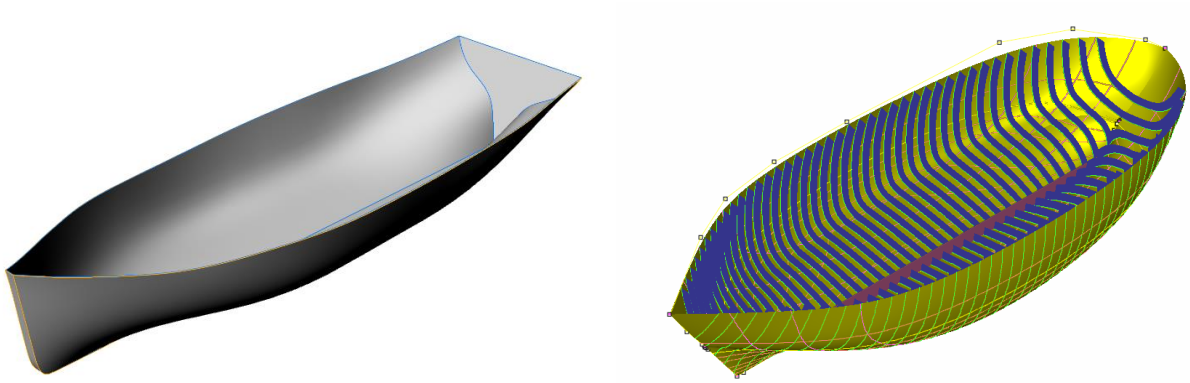

Figure 14: Rhino model of Utamaduni generated from a hull survey (left), Maxsurf model of an early iteration Kubwa design including ribs and keel for structural analysis (right)

Figure 15: A 1/16th 3D print model of Kubwa: preparation (left), inclining experiment (centre), resistance test (right)

Structural Design Principles

Traditional dhows are predominantly built from generational knowledge and expertise, which drives structural design principles including:

- The sizing of scantlings such as the keel, planking, frames, knees and brackets
- The sourcing of appropriate wood, locally and imported. Planks may be imported whilst frames are still sought locally and directly from the forest by the boatbuilder, selecting logs with the right shape for the curved frames.
- Joining methods include nailing, stitching and caulking.
- Dhows need to be heavy, to minimise the need for comparatively expensive ballast. Therefore, the scantlings are likely to be much larger than would be specified in a design driven by lightweighting.

We are unaware of any formal structural design guides, codes or calculations used for dhow construction. Provisions for traditional wood construction in design codes such as ISO12215 and Seafish, or empirical design approaches driven by the scantling number (Sn) such as by Gerr (2000) could probably be applied, but the success across generations of dhows sailing in Lamu probably precludes the need for this in typical wood construction projects.

Changing the material from hardwood to recycled plastic beams and planks must rely on the trusted knowledge of heritage designs. This is also essential for local acceptance of the design with factors including perceived seaworthiness, safety and aesthetics (Birmingham and Wibawa 2018). However, the significant change in material properties must be carefully investigated to ensure the boat remains stiff, strong and robust for a long sailing life.

For the smaller boats, including Ndogo, the Flipflopi team made incremental judgements on the structural design principles based on immediate observations of material quality and strength. This iterated with the production processes, with the eventual structure in Ndogo showing improvements during the build process. For example, the first laid planks were bought from external recycling suppliers, and were found to be poor for joining and strength. In response, the Flipflopi team developed better production processes and new equipment to produce their own higher quality planks. The relatively small scale of Ndogo also meant the structural spacing and sizing could mostly replicate equivalent wood.

The larger scale of Kubwa, with an envisaged length of 24 metres, further challenges the inherent structural design principles. The photo of the similar length Utamaduni in Figure 7 illustrates the typical magnitudes of wooden beams and planks in a large dhow. It is likely that stiffness, as much as strength, becomes critical for the equivalent recycled plastic structure. The boat will be ocean going, and needs to be prepared for significant wave loads. A judicious use of design codes is therefore being used, accounting for their limitations and boundaries when dealing with a completely different material. This is appropriate for some aspects, for example calculating maximum design hull pressures. But in other cases use of codes can be inappropriate and misleading, especially where they are bounded by material type (such as Seafish rules that are restricted to wooden construction).

This is an ongoing design challenge for Flipflopi. For example, ISO12215 can be applied to determine the hull pressure loading, which is independent of material type. ISO12215 provides an appropriate method to calculate bottom, side and deck design pressures (Nabi 2023). Using the provisional dimensions of Kubwa (Table 1), the calculated design pressures are shown in Table 2.

Table 2: Maximum Design Hull Pressures

	Value (kPa)
Bottom Pressure	50.3
Side Pressure	17.3
Deck Pressure	17.3

This enables first principles calculations to design and compare plastic scantlings as a replacement for wood. For example, the influence of frame spacing on the bending stress and deflection of different plank thicknesses under a design pressure of 50.3kPa is shown graphically in Figure 16. These provisional results indicate that doubling the plastic plank thickness compared to wood produces similar deflections under the design hull pressure loads whilst also keep bending stresses below typical strength limits for LDPE (note that these limits are literature values, and not necessarily equivalent to the actual strength of the recycled plastic planks).

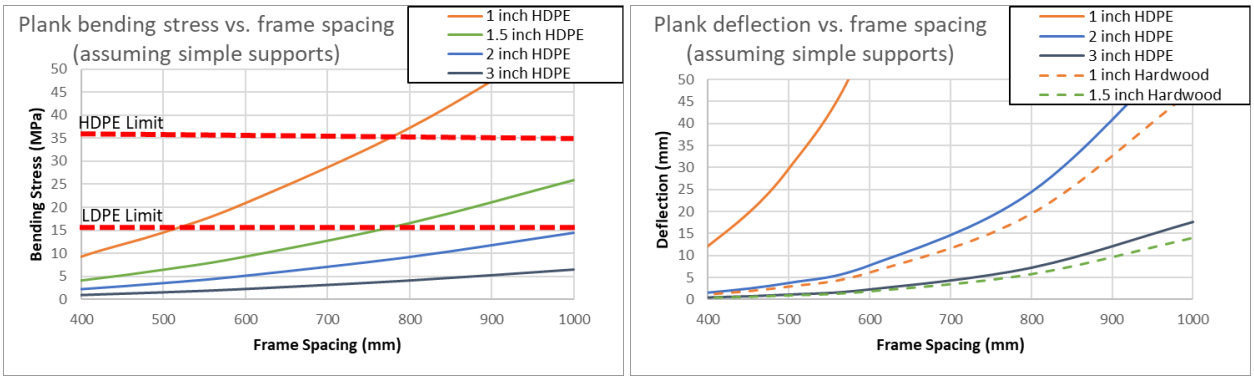

Figure 16: Provisional design charts to determine plank thickness as a function of frame spacing

Moulding, Welding, Bending and Laminating

The traditional construction of the dhows in Lamu required the need for large timber sections for the internal ribs and structural components. Flipflopi have developed low tech closed moulds which uses existing extrusion machinery to produce large complex forms that can then be used in the construction (Figure 17).

Figure 17: Large mould production using closed mould extrusion techniques

Traditionally sailing dhows in Lamu and from further afield have been secured together using rope, bolts, screws, and nails. Whilst these fixing methods are superb for use in wood, they present difficulties when applied to equivalent plastic joints. The flexibility and stress concentration around the screw causes them to easily become loosened cause stress concentration points within the plastic that can lead to cracking and failure. This led the team to identify plastic welding as a fabrication process, Figure 18 shows how the welded section removed the stress concentration that led to cracking and failure in the screwed section.

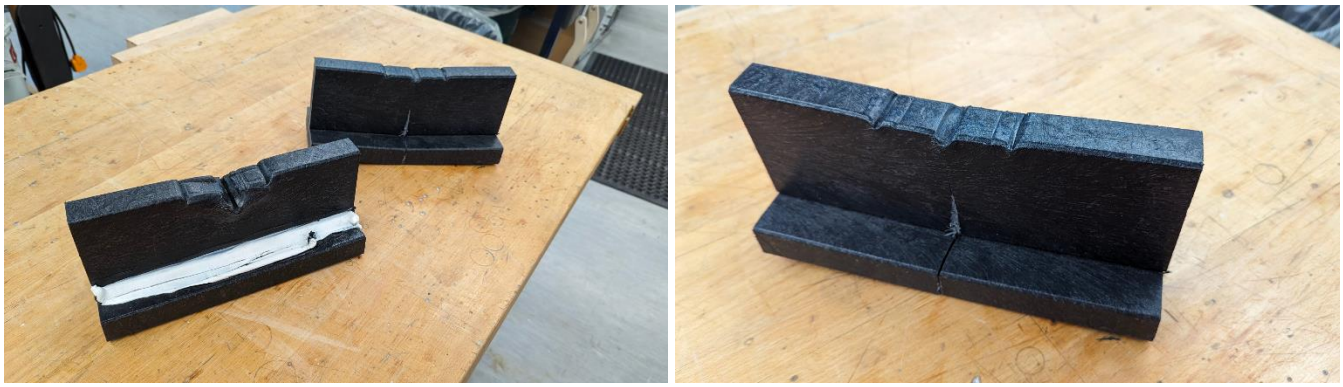

Figure 18: Testing of (left) screwed versus (right) welded sections of plastic lumber, the welded sections removed the stress concentration that led to cracking and failure.

Secondary uses (Figure 19) for the welding have yielded other benefits, welding the planks allows the vessels to be watertight, the HDPE planks do not expand when submerged in water so welding is used instead of the traditional methods of caulking. The production facility can also only produce planks successfully up to 4.80m long, to achieve longer profiles the welding can be utilised to join the planks together using the traditional scarf jointing methods already used in traditional timber construction.

Figure 19: Traditional timber scarf joint (left) and HDPE welding and scarf plank joining system (middle and right)

Figure 20 illustrates a further application for the welding process in the production of more complex shapes that are produced through post production heat bending and lamination of the planks into larger sections. The planks are re-heated using conventional steam bending used traditionally in timber fabrication, the sections can then be bent into their desired shape and then welded holding them together in their desired final shape.

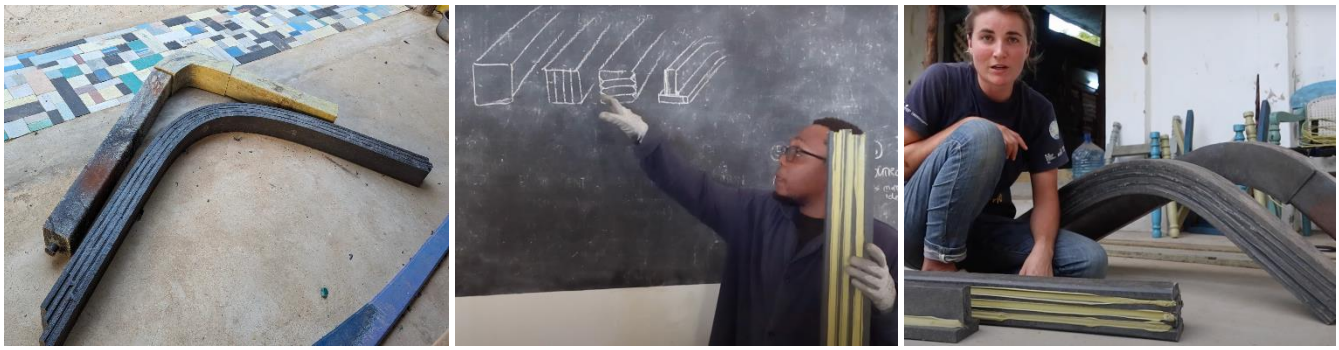

Figure 20: Heat bending and welding planks together creating laminated sections

Material Properties

Common polymer plastics have material properties less favourable to large boat construction when compared to wood, metals and polymer composites (the “big three” boat building materials). Creating construction materials from recycled plastics present additional challenges in terms of quality and consistency, initial materials produced was of low quality and with significant defects in the material, early testing in 2017 at Northumbria University, UK, yielded poor results. Applying plastic recycling techniques in a relatively low resourced setting furthers this challenge.

Figure 21: Materials bend testing (left) and materials (middle and right) May 2017.

Significant innovations in production methods have been developed to improve the material consistency, the principal influences on the material properties and structural behaviour of recycled plastic lumber include sorting appropriate plastics, washing, drying and applying a consistent production processes; appropriate use of moulds or extrusions; monolithic or laminated beam fabrications; the use of complex shapes; methods to bend beams into shapes; the colour; and joining and welding methods.

HDPE is the predominant polymer used in the Flipflopi recycling process. Typical material properties for virgin HDPE are 10-30MPa tensile strength and around 1000MPa modulus of elasticity. This means 10% the stiffness and 10-40% the strength of a typical hardwood (depending on the type, treatment and load direction of the wood). Flipflopi have completed several efforts to quantify material properties of recycled plastic using established research lab techniques. Figure 22 shows example results from 3-point bend tests on 4" x 1" planking samples conducted in Northumbria University, UK. These tests showed that the recycled HDPE maintained similar properties to equivalent virgin product, but only at this relatively small sample level, which didn't fully account for the manufacturing and environmental variations inherent in the processes used at the Flipflopi recycling centre. It has also proven difficult to transfer samples appropriately from Lamu to test facilities within Kenya and internationally.

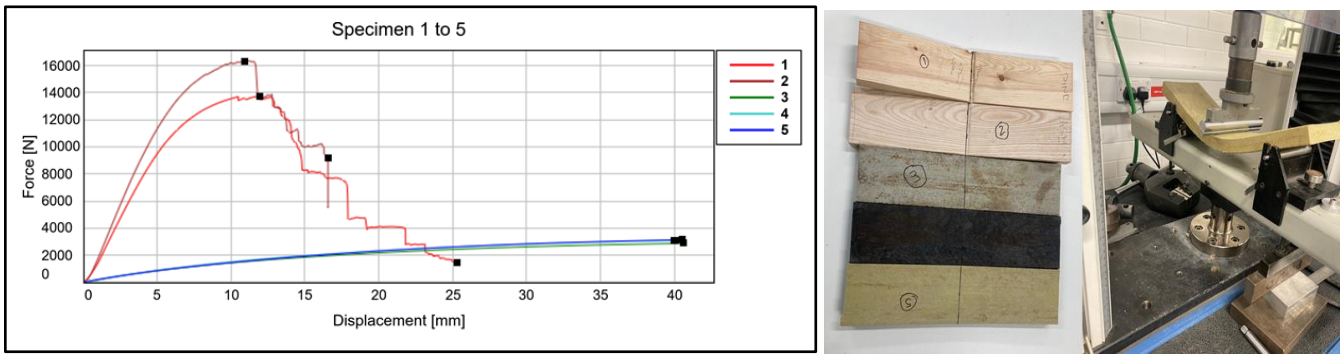

Figure 22: Bend test comparison results for Pine (1), Ash (2), White HDPE (3), Black HDPE (4) and Yellow HDPE (5)

To overcome these challenges an "on the ground" approach was required to test the structural properties of the recycled plastic in-situ and provide further confidence to the boat build. A bespoke 3-point bending test rig was therefore designed and fabricated at the boatyard as shown in Figure 23. This enables beams and planks about 1.45m long to be tested under 3-point bending. The test rig is manually operated and doesn't require an electricity supply. The central load is applied via a hand-turned winch (meaning tests can continue with intermittent power supply) and deflections are measured using a dial indicator.

First results show reasonably linear load-deflection at relatively small loads (Figure 24). The tests are ongoing, so only provisional findings are reported here. These indicate that:

- The recycled plastic has a stiffness about 10% of locally available boatbuilding hardwood
- The Young's modulus is about 800MPa, which is slightly lower than the reported values for new HDPE in literature but within acceptable boundaries.
- Tests are in relatively high temperatures, which has a greater detrimental effect on plastic than wood. Initial tests at lower temperatures, using ice packed around the test specimens, show slightly improved stiffness.

Figure 23: The 3-point structural test rig (left), a 4" x 4" HDPE laminated beam (right)

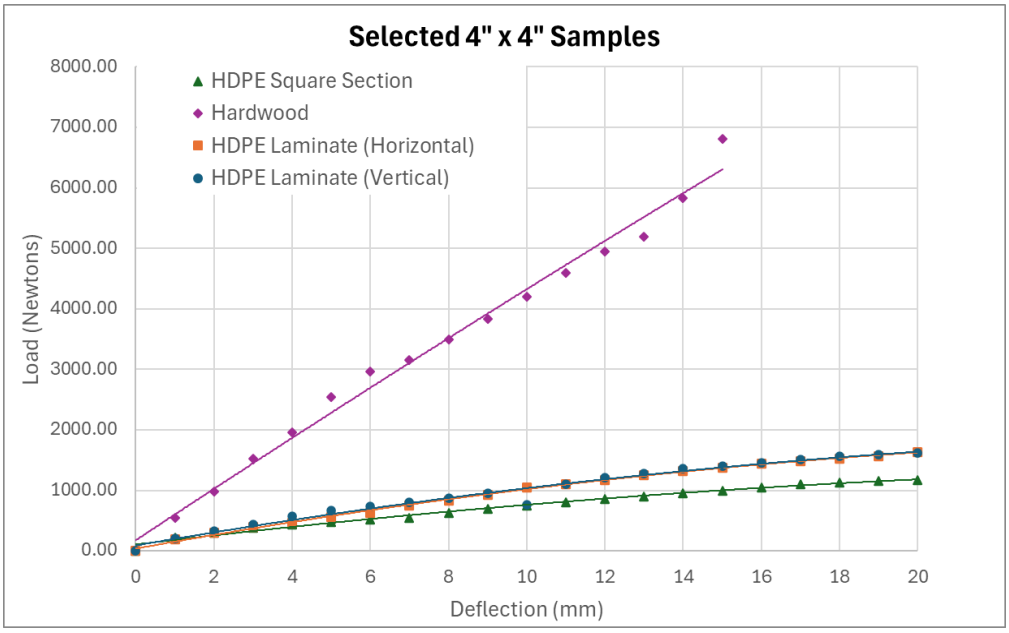

Figure 24: Selected Load-Deflection Test Results of 4" x 4" sections with different materials and constructions

Propulsion

Whilst the focus of Flipflopi is the use of recycled plastic as a construction material for boatbuilding and other carpentry products, the project opens up broader environmental and sustainability considerations. A specific and important challenge identified in the local Lamu maritime community is the cost, availability and distribution of fuel for inboard and outboard engines on almost all boats. Boat fuel in Lamu currently costs about 250 Kenyan Shilling ($1.50) per litre, the price of which has reportedly more than doubled within a year. This is putting significant pressure on local maritime activities, especially fishing and local transport. Added to this, distribution of fuel is via open poured jerrycans, outboard engines are often old and noisy, and there is notable pollution in waterways also used for swimming and agriculture. Examples of conventional outboard use are shown in Figure 25. This local challenge is likely repeated in many other LMIC coastal communities. This also intersects with the global challenge of fossil fuel use and the impacts of this on the climate emergency.

Flipflopi are addressing this challenge by trialling the use of a 6kW battery-electric outboard coupled to a solar panel charging system as a complete independent power system for their recycled plastic water taxi (Figure 26). The advantages of the water taxi as a use case for solar power is the size and arrangement of the boat, and the relatively short journeys. The 8kWh outboard battery provides sufficient power for an estimated 10 km at normal cruising speeds on a single charge. A canopy will be installed in the stern area of the boat to house 1-2kW of solar panels, which will be tested to determine whether the acquired charge power is sufficient to maintain 100% operability without resorting to mains charging.

Figure 25: Typical water taxi with 15hp Yamaha outboard and sun canopy (top left), jerrycan refilling of petrol from floating station (top right), fishing dhow with auxiliary sail used to save fuel (bottom left), A Lamu style and Mozambique style dhow on a sunset cruise with tourists – sail propulsion but outboards in reserve (bottom right)

Figure 26: The Flipflopi water taxi equipped with a 6kW battery-electric outboard

CONCLUSIONS

Flipflopi shows the synergistic power of imagination, passion, capability, creativity and practicality in a marine design context. The paper shows that novel marine design approaches, such as implementing a circular economy approach at a local scale, is effective in responding to global environmental crises such as plastic pollution. In the Flipflopi approach, waste has become a precious resource. It is collected, processed and remade into a valuable product that retains heritage whilst embedding innovative cutting-edge technologies. Whilst this process can be used for replacing timber in many applications, the iconic design of a traditional sailing dhow is a powerful tool that impacts on community, enterprise and engagement for environmental sustainability. Looking to the future, Flipflopi has plans to build a larger sailing dhow, which is hoped will circumnavigate the world taking the message of plastic pollution and local circular economy to coastal communities everywhere. Closer to home, the aspiration is to export this knowhow and technology to other communities in East Africa and eventually further afield.

CONTRIBUTION STATEMENT

Simon Benson: Conceptualization; investigation; visualisation; writing – original draft. **Ali Skanda:** conceptualization; methodology; project administration; supervision; writing – review and editing. **Hassan Shafi:** methodology; supervision. **Katharina Elleke:** conceptualization; methodology; visualisation; project administration; writing – review and editing. **Simon Scott-Harden:** methodology; writing – original draft; funding acquisition. **Nathan Smith:** writing – review and editing. **Richard Birmingham:** supervision; writing – review and editing. **Dipesh Pabari:** conceptualization; methodology; project administration; supervision; writing – review and editing; funding acquisition.

ACKNOWLEDGEMENTS

Funders (Newcastle University): The John Prime Foundation Endowment Fund. The Willis Endowment Fund. International Science Partnerships Fund (for the propulsion system).

Funders (Flipflopi): UK Foreign Commonwealth and Development Office, UN Environment Programme, Africa Legal Network, Agence Française de Développement, Embassy of France, Embassy of Portugal in Kenya and many individuals who have donated and enabled the build of Ndogo

People (Newcastle University): Aftab Nabi (structural calcs ISO12215), Georgia Richardson, Harry Syllantavos and Rebecca Stokes (summer 2021 model testing)

People (Northumbria University): Johnny Hayes, Phil Hackney and Simon Neville (production design, development and testing)

People (Flipflopi): The entire Flipflopi team and community (see https://www.theflipflopi.com/our-team)

REFERENCES

Alegret, J. L. & Carbonell, E. (2018). Introduction. Revisiting the coast: new practices in maritime heritage. Ed. Tejero, JLA, & Camós, EC (Vol. 11).

Birmingham, R. W., & Wibawa, I. P. A. (2018). The role of aesthetics in engineering design—insights gained from cross-cultural research into traditional fishing vessels in Indonesia. In Marine Design XIII, Volume 1 (pp. 275-284). CRC Press.

Bucknall, D. G. (2020). Plastics as a materials system in a circular economy. Philosophical Transactions of the Royal Society A, 378(2176), 20190268.

Burgess, M., Holmes, H., Sharmina, M., & Shaver, M. P. (2021). The future of UK plastics recycling: one bin to rule them all. Resources, Conservation and Recycling, 164, 105191.

Dewan, C., & Sibilia, E. A. (2023). Global containments and local leakages: Structural violence and the toxic flows of shipbreaking. Environment and Planning C: Politics and Space, 23996544231208202.

Flipflopi (2021, 2022, 2023). Annual Reports. https://www.theflipflopi.com/on-expeditions

Gerr, D. (2000). The Elements of Boat Strength: for builders, designers, and owners (p. 352). International Marine/McGraw-Hill.

Geyer, R., Jambeck, J. R., & Law, K. L. (2017). Production, use, and fate of all plastics ever made. Science advances, 3(7), e1700782.

Gilbert, P., Bows-Larkin, A., Mander, S., & Walsh, C. (2014). Technologies for the high seas: Meeting the climate challenge. Carbon Management, 5(4), 447-461.

Lau, W. W., Shiran, Y., Bailey, R. M., Cook, E., Stuchtey, M. R., Koskella, J., ... & Palardy, J. E. (2020). Evaluating scenarios toward zero plastic pollution. Science, 369(6510), 1455-1461.

MacArthur, E. (2019). The virtuous circle (Volume 7). European Investment Bank.

Moejes, K. (2023). Impact of recycling interventions on waste composition of dumpsites in Lamu, Kenya. Sustainable Manufacturing and Environmental Pollution (SMEP) Programme.

Moejes, K. (2023). A Survey of Marine Macro-Litter Accumulation at Selected Sites across the Lamu Archipelago. Sustainable Manufacturing and Environmental Pollution (SMEP) Programme.

Nabi, M. A. (2023). A study of structural design and analysis of recycled plastic in small craft for safe and efficient performance. MSc Thesis. Newcastle University.

Phelan, A. A., Ross, H., Setianto, N. A., Fielding, K., & Pradipta, L. (2020). Ocean plastic crisis—Mental models of plastic pollution from remote Indonesian coastal communities. PLoS One, 15(7), e0236149.

Precious Plastic (2023). Build a Fishing Canoe. https://community.preciousplastic.com/how-to/build-a-fishing-canoe

Rahman, S. M., & Kim, J. (2020). Circular economy, proximity, and shipbreaking: A material flow and environmental impact analysis. Journal of Cleaner Production, 259, 120681.

Scott-Harden, S., English, S., Skanda, A., Schurg, L., Elleke, K., & Morison, B. (2020). Unblocking the Circular Economy. In International Association of Societies of Design Research Conference 2019: Design Revolutions (pp. 296-309). Manchester Metropolitan University Press.

Spekkink, W., Rödl, M., & Charter, M. (2022). Repair Cafés and Precious Plastic as translocal networks for the circular economy. Journal of Cleaner Production, 380, 135125.

Thushari, G. G. N., & Senevirathna, J. D. M. (2020). Plastic pollution in the marine environment. Heliyon, 6(8).

Tomos, B. A. D., Stamford, L., Welfle, A., & Larkin, A. (2024). Decarbonising international shipping–A life cycle perspective on alternative fuel options. Energy Conversion and Management, 299, 117848.

Velenturf, A. P., & Purnell, P. (2021). Principles for a sustainable circular economy. Sustainable Production and Consumption, 27, 1437-1457.

Proceedings of 15th International Marine Design Conference (IMDC-2024)
June 2-6, 2024
Amsterdam, the Netherlands

Early Marine Systems' Design – Cracking the wicked problem - The case of a novel biomass harvesting vessel.

Per Olaf Brett[1,*], Jose Jorge Garcia Agis[2] and Benjamin Lagemann[3]

ABSTRACT

Several IMDC contributions have argued for a better approach to capture stakeholders' expectations in vessel newbuilding projects' execution. The appropriate processes of requirements elucidation are, however, often forgotten or insufficiently handled in traditional ship design and customer-designer settings. Such situations most often reveal a situation in which both "tamed" and "wicked" problems are addressed and must be dealt with properly and effectively at the earliest stage of the process. This paper shows how such problems can be addressed by using the existing multidisciplinary methodology. A practical approach consisting of a set of methods, tools, and work processes integrated into the Accelerated Business Development (ABD) approach is applied to a specific use case, a next-generation factory stern trawler development.

A detailed step-by-step story of the early vessel design process – requirements elucidation in parallel with concept design solution development – is outlined following a narrative approach. The process being described covers how necessary support information, stakeholders' expectations identification, business-related analyses, specific design layout, onboard comfort, and fish process handling and storage are dealt with effectively and efficiently. This case study exemplifies specific solutions to better handle particularly wicked problem situations, but also tamed problems are addressed systemically.

The paper concludes by showing how a final ship design solution can look like and consequently be prepared for and to be built. The handover process and documentation from requirements capture and concept design solution development to further basic design activities are highlighted. The case vessel at hand won the prestigious "ship-of-the-year" award in Norway in 2023. The paper critically discusses what are likely to be the most important factors leading to this outcome.

KEY WORDS

Ship Concept Design; Vessels Design Solutions; Stakeholder Requirement Elucidation; Accelerated Business Development; Novel Stern Trawler Design

INTRODUCTION

Loopholes still exist in early ship design processes…

Over the years, several previous IMDC papers (Ebrahimi et al., 2018; Ulstein & Brett, 2009, 2012, 2015) have discussed the topic of how to improve the customer-ship designer requirements elucidation process and project realization dialogue. Improved understanding of the issue, methodology, theory, and practical approaches have been developed, introduced, and partly applied in what we can call piloting initiatives, but few discuss their full-scale application. Many of the useful

[1] Ulstein International AS (Ulsteinvik, Norway), Norwegian University of Science and Technology (Department of Marine Technology, Trondheim, Norway); ORCID: 0000-0002-8767-5494

[2] Ulstein International AS (Ulsteinvik, Norway); ORCID: 0000-0001-6610-1136

3 Norwegian University of Science and Technology (Department of Marine Technology, Trondheim, Norway); ORCID: 0000-0002-6106-0280

* Corresponding Author

Submitted: 15 February 2024, Revised: 16 April 2024, Accepted: 1 May 2024, Published: 20 May 2024

Conference paper, DOI: https://doi.org/10.59490/imdc.2024.850 e-ISSN: 3050-4864

contributions still treat this early phase of ship design very superficially and new methods to improve the situation have proven to be very "toyish" in the sense that they are mere conceptual ideas, initial and very generic and generalized examples of applications, at best, providing relative indication values because of simplistic analyses or simulations with "dummy" variables applied. Some of them are, however, well documented in open sources and available for experience capture and repeat studies, but their real-life applications are scarce (Curry et al., 2017; Garcia et al., 2019; Pettersen et al., 2018; Rehn et al., 2016).

Introducing a novel work process in a conservative business environment represented by the mainstream naval architecture and marine engineering fraternity can be a long and bumpy road to pave. Thus, it should be of no surprise to anybody that progress in the refinement of the current naval architecture and marine engineering discipline, is a gradual and step-by-step process, much influenced by different cultural and regional practices, and specific shipping sector and industry segment preferences. Frequently, it has been indicated that a proper customer–ship designer interaction process is partly neglected, or simply missing altogether (Ulstein & Brett, 2009, 2012, 2015). It is argued by some, that this discrepancy is due because such interaction is being considered too complex or too intrusive to effectively capture the vital and critical information elements of a new building project. Consequently, the outcome of such vital processes, so far, has proven to be meagre, and the following concept and basic design work correspondingly uncertain, risky, and costly. Despite these pledges to the ship design community to pay more attention to this early part of the ship design process, recent industry experiences have not shown significant improvements, according to the authors' observations. There are exceptions though. One of these exceptions is the story being told in this article – explaining in more detail and chronological order how novel systemic-based requirement elucidation and new building project information solicitation can be carried out successfully. The reason for addressing this topic one more time is the belief that practical applications of novel approaches in ship design, like the accelerated business development approach of Ulstein, might bring more understanding to the benefits of approaching tame and wicked problem-solving holistically and as early as possible in the concept vessel design process. The paper shows what is going on in practice, who are the actors, what is the program, what are the interphases and interrelations in the process, what are critical inputs, control functions, resources, transformations, outputs and finally, outcomes of the communication and information sharing efforts. How can this comprehensive and collaborative setup enhance and progress future early concept ship design, and thus the quality of the basic design and detailed engineering downstream initiatives, finally leading to better ships are elaborated upon in this article and specific results documented and discussed.

Furthermore, this article shares reflections on commercial, operational, and technical aspects relating to early conceptual ship design and the requirement elucidation process between the customer and the ship designer. It contrasts how theory and practice can go "hand in hand" with significant real-life process achievements as a result. When following a new building project initiative over a longer period and trying to describe in more detail what is happening along the way, it is hopefully obvious to the reader that such a longitudinal study (Huber & Van de Ven, 1995) presented in a 20-page article cannot go into all details about the events and happenings. The authors of the article have, therefore, taken the liberty to condense the actual process that took place in the early phase of the project, trying to focus on what turned out to be the most important events, discussions and under way conclusions, and leaving out minor details.

This article addresses the challenge of the naval architecture and marine engineering community about the fact that, although many authors and scholars on the subject promise early-stage ship design improvements, most of them end up starting their storytelling with the "pre-defined" box of design requirements. That is, presumably all relevant and critical requirements have already been identified and documented, ready for the designer to work on, without any further checks and balances. This can be seen as a quick way to avoid or escape wicked problem aspects. Nevertheless, the authors of this paper experience that not going through these early extra rounds of clarifications has in some cases led to catastrophic or at least substantial project development failures. We try to show how such ineffective ship design processes can be avoided and original expectations be met.

This story begins - customer inquiry…

The telephone is ringing: "Hello, Brett speaking." – "…Mr. Brett, I have been asking around already, talking to three ship designers and they have not been interested in exploring my ideas about a novel next-generation factory stern trawler. They want to sell me their existing designs, which are the best on the market, they say and are not interested in spending time and money on exploring our new ideas. - That's not what we want, I told them, Mr. Brett. My customers want a novel vessel solution that can secure high-quality catch and make sure the fish products are being presented at the counter of the fish mongers on the Continent, such that I can achieve extra profits compared to the other trawler fishermen out there. Honestly speaking, I don't think they understand our ideas and expectations in the first place, but we have some ideas worked out already based on our best knowledge and experience from many years of trawling. … Are you guys willing to help us explore these ideas and develop a new vessel concept that can meet our overall expectations?" – "…Yes, we are. When can we get together and start

the development process? We think we have the right apparatus, skills, and experience to assist you... You are more than welcome to see us quickly."

Project milestones – how did it go…

Seven years later, the novel factory stern trawler is just about to be launched and put into service. After six months of structured, facilitated, and continual documentation of business concept development, market, and business performance yield evaluations, onboard studies, idea exploration workshops, functional modelling and simulation, and vessel concept development, the stakeholders' expectations and requirements' elucidation were considered fully captured and a feasibility study concluded. Hence, a vessel concept design documentation package could be delivered to the naval architects and marine engineers to start their basic design process and later a detailed engineering process.

One more year was spent developing the basic design of the vessel together with the exploration of the novel fish catching and handling system at the stern, combined with the new fish processing factory solutions. Another year was used to engineer the whole vessel system in detail and be ready for contracting and construction at the yard. Yet another year was, however, consumed to identify, negotiate, and placing the new building order at agreed upon price, finalise financing, and secure the right suppliers for the extensive equipment systems development and delivery.

This article concentrates on the very early phases of a marine systems design process and particularly outlines how well-documented facilitation techniques can be used to master tamed and wicked problems, which almost always are present in various ways in vessel new building projects to be carried out. The rest is history and not part of this article's story. Figure 1 shows the macro activity of the use case study indicating the timing and resources consumption of the key events of the process.

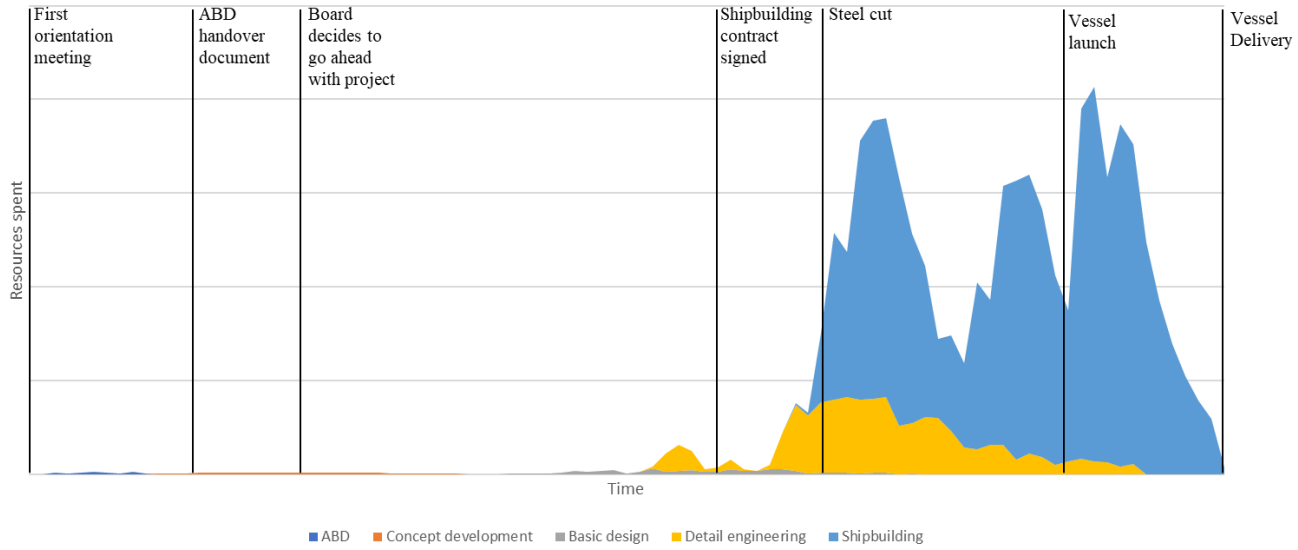

Figure 1: Key events in the project development and equivalent resource consumption.

The "tame" and "wicked" problems – how do we go about them…

Solving "tame" problems in early marine systems design is typically handled traditionally by addressing the problem at hand with one part of the problem that can be isolated and fixed by simply eliminating the problem, treating or mitigating the problem, transferring the problem (to a collaborating partner or insuring the latent risk involved), and or finally tolerating that the problem exists, but might not after all mean a lot of risk to the project realization process (Head, 2022). Typically, the process starts with a given, not necessarily verified requirement list and specific input as to the gross size of the vessel, its functionality, and special features desires. Relevant and preferred suppliers are identified and listed for later contact and project dealings. Then a traditional "circular" or iterative basic design approach in line with the design spiral (Garcia, 2020; Ebrahimi, 2021) is carried out producing one or more comparative vessel design solutions, within a set of pre-defined target specifications. A final decision about the preferable design solution is taken and the project is ready for launch.

Typically, our traditional and well-proven approaches to naval architecture and marine engineering's role are proven to be efficient in solving such linear and analogue problems. Many articles over the years have confirmed this observation (Andrews, 2018).

"Wicked" problems, however, represent issues that are different - emergent and systemic - and thus require changes in multiple systems or development logic constituting the problem at hand. Systemic, in the sense that you can't fix them by fixing the parts, you can only try to change the system of systems to dissolve them (Rittel & Webber, 1973; Head, 2022). You must change your approach from fixing parts to trying to re-organize the system(s) functionally, utility, capacities and space allocation, technologically – new equipment and their integration, commercially – a new business setting and performance yield offering, and or operationally – for example, higher operability, because no amount of increasing or improving the parts makes an integrated whole, which results in the emergence of new levels of improvement. It is only by improving the organization of the parts or sub-systems that you can increase and grow the integrity of the whole ship as a system and get the emergence of the system's overall performance, i.e. regeneration of the vessel solution as an integrated system.

One way to effectively map and handle the wicked problem situation is, therefore, to begin with a process of discovery or elucidation (Adi & Stoeckle, 2022). Begin with the current, observable facts and ask "why" – going backwards in time to create a chain of causality – causal maps exploration – what is related to what and how. Remember, each cause also has an effect in such circumstances. The next step is to predict what will happen going forward in time and ask, "what if" and "what next". By asking what next and if and continuing the chain of events, we can get sets of ongoing future consequences – causal maps of the situation at hand including, but not limited to the already known domino effect of our present decisions and actions (Sarkar & Kotler, 2018).

"Are these challenges one problem or several problems to handle, and is it at all possible to expect a rational and elucidated handling of the nature of such a wicked problem situation?" (Andrews, 2003). Andrews continues: “Identifying what is the nature of the problem is the main problem, and that attempting to do so without recourse to potential material solutions verges on making a difficult operation impossible”. The wicked problem is, therefore, much more than identifying all the expectations, requirements, and needs of the ship owner and or close by stakeholders – it is truly about identifying what is the nature of the greater problem, what is the main problem. The nature of the greater problem is an all-encompassing feature including the life-cycle aspects of the vessel concept design solution, and we are, therefore, of the opinion that also such features as the market situation, the economic situation in general and the involved firms' condition – desires, qualities, capacities, capabilities, experience, and robustness, play a significant part in the overall nature and dynamics of the “wicked problem” identification and description challenge.

It is still a limiting consideration and an interpretation of the original “wicked problem” concept (Rittel & Webber, 1973), which prevails in the ship design world among naval architects and the like (Brett, Carneiro, et al., 2006; Ulstein & Brett, 2009, 2012, 2015). This is demonstrated by the repeated rationalization of the solution space: Setting strict and limiting boundaries to the solution space, taking for granted that the functional expectations and requirement description of the customer are properly documented, and validated, and that the parametric set of ship dimensions are well balanced and verified, thereby, partly avoiding the complexity and uncertainty aspects of the new building project at hand. It is also seldom understood and practised that the solution space will change over time because of good and bad times (Epoch-Era) and other unforeseen events (Gaspar et al., 2012; Keane et al., 2015) influencing the life cycle performance of the vessel designed. Thus, future projects require an identification and mapping of the likely life cycle use of the vessel design solution and its utility functionality. Only in a few use cases known to the authors, have the overall medium to long-term market situation, commercial use, and corresponding built-in utility functions of the vessel design solution been explicitly handled as a decisive factor defining the final life-long solution space. More recently, the decarbonization of the shipping fleet has emerged as yet another extremely difficult problem to solve and entails a life cycle dilemma for the actors involved in the project development discussions and decision-making.

The paper is structured as follows: First, the premisses for the article are outlined - is it possible to handle tamed and wicked problems after all, arising in concept ship design contexts and if so, by which method(s) and approach(es)? Second, the story of a real design project is told. We conclude and discuss why the applied process is a preferable way of performing ship design solution work in the future.

One approach doesn’t fit all situations…

Yet, it is the opinion and experience of the authors that effective early-stage ship design process approaches must be aligned with the nature of the customer inquiry to the naval architect and marine engineer, and tuned to the specific context or business situation the inquiry is generated from.

The StO, CtO, and EtO terms are archetype design and production approaches being described in complementary design literature (Semini et.al, 2014). Their interpretations are StO or MtS – Standardize to Order or Make to Stock, CtO or AtO – Customize to Order or Assemble to Order, and finally, EtO – Engineer to Order, with StO being the most downstream position and EtO the most upstream position in the ship design value chain. The basic idea behind these terms is to understand the

characteristics and attributes of the final ship products being produced and offered. These terms are used in te next paragraphs to categorized and describe different customer-designer (C-D) relationships.

The more specialized the product, the more flexibility is needed, and the more the customer or the relevant stakeholders must be involved in the development process. The more standard the ship design solution, the more downstream and little involvement of the customer is necessary, yet existing and in-depth market and product knowledge and expertise is very high – you get what we offer you. Typically, the downstream-oriented processes lead to shorter lead times, higher delivery reliability, and lower costs; in contrast, the upstream-oriented approaches allow a higher degree of customization, increased reliance on customer participation and continual decision-making, longer lead time, higher costs – the solution is developed as you go.

Over the years, the authors have experienced many different customer-designer relationships and types of inquiries, which probably can be categorized into five different archetypes (Lageman, et.al, 2024):

- C-Ds1: "I want this particular vessel; can you design it for me?" – triggers normally an EtO vessel design solution process…
- C-Ds2: "Do you have a solution that can do..." – this triggers normally a CtO vessel design solution process…
- C-Ds3: "Can you help us respond to this tender" – this triggers normally a StO vessel design solution process…
- C-Ds4: "I have a promising idea about a new vessel design we would like to order; can you develop it for us" – triggers normally an EtO vessel design solution process… and finally,
- C-Ds5: "We have an interesting business proposition to offer you – do you want to be part of the project-making initiative" – triggers normally an StO (CtO) vessel design solution process…

These five C-D archetypes of inquiries, typically, require or dictate a different dialogue with the customer and the follow-up process of the project initiated by the inquiry. Since the dialogue and the follow-up process of the project are different, we are of the opinion that also the overall approach of the dealings of the projects must follow different approaches concerning – what information to identify, collect, collate, and store, who are the most important stakeholders involved and what decision-making processes will most likely take place or should take place, how far is the customer willing to stretch when it comes to costs and price, what are the premises for the project realization, involved presumptions and assumptions – the project boundaries for defining the ship design solution space. Unconventional situations require alternative responses. Hence, the naval architect and marine engineer must develop sufficiently flexible and adaptive behaviours to master such a variety of customer-designer settings. Fast adoption of new work processes and use of novel design tools, including generative artificial intelligence, become a must. So is also real-time handling of big data and statistics – multi-variate regression analysis (MVRA), analytical hierarchical process (AHP), neural network (NN) techniques, and the like.

The use case to follow aims to show how such flexibility, adaptability, and adaptation capabilities are used to make successful early concept ship design projects come to fruition.

But some approaches for improvement are better than others…

Knowledge about the project requirements and or expectations is normally spread over many actors being involved in realizing the ship design initiative. The actors in such processes are ship owners, operators, charterers, brokers, investors, designers, consultants, ship equipment suppliers, classification societies, flag states, and other more peripheral stakeholders in the value chain. None of these parties has alone or isolated the full picture and specific knowledge on assessing a ship's commercial, operational, and technical performance in a broader business concept realized. Culture, traditions, and specialization over many years among actors in the overall realization value chain are most likely to blame for not bringing these actors closer together and making them more effective in communicating with each other. Historically, separate documents like outlines, contracts and/or building specifications and drawings have constituted the communicational instrument and transactional document among the players in the overall decision-making process. Owners' specifications are typically formulated based mainly on their experience in ship operations. Ships are in operation all the time, but new building projects commonly take place only every 5 to 7 years period with that ship type and capability. Expanding on what is, or has been, the experience of the past is more typical than what it is that we need. Designers, on the other hand, typically optimize a vessel concerning preferred engineering criteria, such as installed engine power, speed, or lane meters, and not infrequently their production facilities. If more specific and complimentary project information is necessary, ad-hoc inquiry sessions are typically held with different information sources both firsthand and secondhand type. More often than is admitted, solutions developed along these lines are presented as best practice and state-of-the-art, without really meeting preferred requirements following a sound set of rationales and scientific reasoning. Too often it is forgotten to ask the wicked problem solver questions – why, what if, and what next? As such, they are not grounded on proper explanatory theory and methodology capturing the total complexity and broader context of a true business idea realization. Quite typically, the business development process, fleet and/or ship design integration and their respective decision-making processes are separate and fragmented with little interaction across the stakeholders' boundaries. Furthermore, existing embedded design processes with yards and ship design firms and logistics performance

cannot normally be directly compared against operational performance parameters, which work against the pre-conditions for the achievement of effective design and marine systems' service solutions. Additionally, the nature of ad-hoc solutions is that they must be elaborated under the pressure of time, and therefore these solutions themselves very often contribute to deficient designs and extra costs.

All stakeholders' expectations must be integrated into the overall development and decision-making process. The required elements for effective decision-making are not always quantifiable and many of them are purely qualitative considerations, highly subjected to personal perception and appreciation of things and stories. This paper, again, suggests that an integrated and complementary analysis tools package should exist as part of an overall systemic approach to handle this complexity. This can support more effective decision-making in marine systems and concept ship design developments.

The way forward – the ABD-approach as mitigating methodology…

The ABD approach is both a communicational and a decision-making support methodology to be used among all the actors in the total decision-making process of a marine system realization. Its role is to record and guide the complex information-gathering and decision-making process when a new building project takes place, particularly in the early phases of such project execution. Expectations, requirements, assumptions, presuppositions, limitations, and project boundary restrictions are described and kept readily available for further and later interpretation of the results of the feasibility analyses being carried out, and finally benchmark what is a better vessel design solution (Ulstein & Brett, 2015). Various influences among system variables are identified and measured concerning their interrelationship strength or correlations. Sensitivities are also estimated and studied. The ABD approach is the structure (process guide) within which the various methods, analysis techniques, supporting default values, preliminary design tools and work procedures are found and elaborated upon. Over time, an experienced database is built up to be used as a benchmark, as well as a best practice repository for faster business development-oriented concept ship design solutions (Brett et al., 2018a).

The owner-designer interaction is often complicated by the owner's focus on previous solutions and gradual improvements thereof. Designers, on the other hand, tend to optimize the design towards specific technical Key Performance Indicators (KPIs) and their production facilities. The ABD approach counteracts these discrepancies and inefficiencies and secures holistic management of complex data in the form of analysis metrics, models, maps, film/video, statistics, sensor signals and the like. In short, the ABD approach is a methodology that is developed to structure the process of turning a business idea and vessel design concept into reality, which includes a concept ship design solution or a smaller portfolio of promising solutions, which can easily be turned into a comprehensive detailing of a ship description and specification. Thus, ABD provides a structure to the process of identifying promising ship solutions that fit into the commercial and operational context in which they shall operate.

The ABD approach is organized as a guideline consisting of 9 modules ensuring a comprehensive and structured approach for capturing the commercial, operational, and technical context of the ship design(s). Using the method contributes to reducing uncertainties in marine business development projects. Figure 2 shows the structure of the ABD approach as it is practised today and in this use case study, highlighting in blue the modules described in this paper. A more detailed description about the different modules can be found in previous IMDC papers (Brett et al., 2006 & 2018; Garcia, 2020; Pettersen et al., 2018). In this paper, the practical application of it about a specific concept ship design project is elaborated upon.

The approach advocates that a new or improved marine solution system, where the ship plays a significant role, shall fulfil the needs and expectations of all the involved stakeholders in the best possible way. We have carried out more than 20 such ABD processes over the last 15 years, on our development projects (C-Ds5) and together with customers (C-Ds4). Comprehensive data analytics processes, field studies, statistical regression studies, AIS observations and recordings of vessel types to understand their real-life operational patterns over time have been carried out as typical complementary fact-finding in such ABD approaches. In addition, it has been necessary to expand the ABD toolbox with a Fast Track Concept Design Approach (FTCDA) (Ebrahimi et al., 2018). This simulation tool combines multivariate statistics, network data resources ship design expertise and classic naval architecture and marine engineering methods from all disciplines to accelerate effective decision-making in vessel design. The FTDCA is an integration tool which gathers information elements from the ABD approach and uses these inputs to balance one or more ship design solutions applied in Module 5 of the ABD methodology. These concept design solutions are then benchmarked by a performance yield indexing matrix with relevant existing peer vessel alternatives. Hence, the concept design solution is validated, and vessel features verified such that the overall performance of the vessel can be rectified if inferior or undesirable performance yield is the result. Typically, final vessel design solutions are to be spotted and selected in the vicinity of relevant performance-based Pareto fronts' knuckle points (points of diminishing returns). A more detailed explanation of the FTDCA is to be found in other IMDC papers (Ulstein & Brett, 2012). All this work is done before any principal drawings are carried out for the vessel.

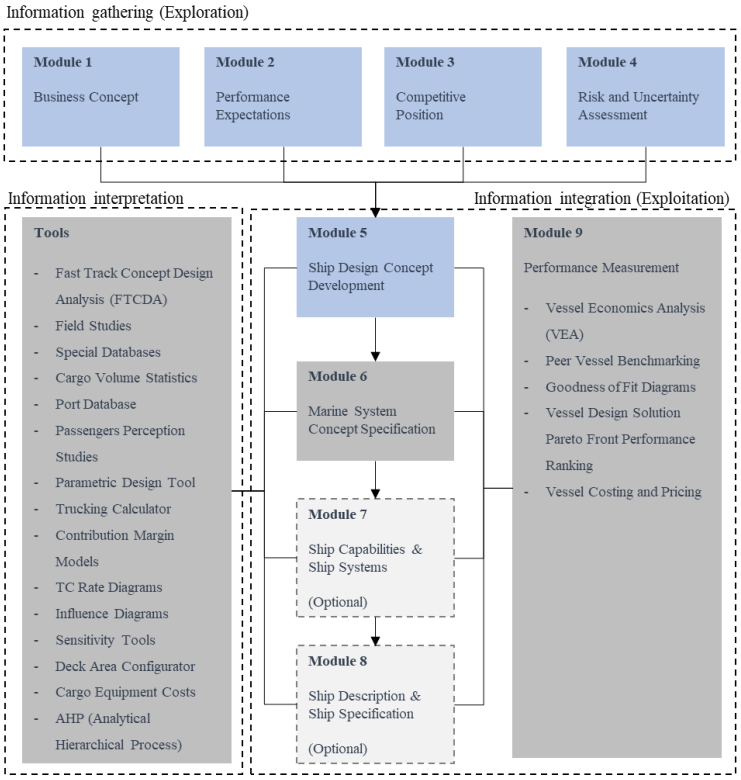

Figure 2: The ABD approach structure of activities.

The implementation of an ABD approach in early design phases has demonstrated three principal advantages: more robust decisions, and higher quality vessel design solutions - due to the availability of additional information at an early stage of the concept design process. Other achievements include a significant reduction in response time and committed resources and the capability of evaluating (visually and analytically) multiple design solutions. In addition, it brings the possibility of performing sensitivity analyses of cost, capacities, and capabilities towards specific design parameters. Complementary use of the FTCDA, ABD and other data-driven analytics tools allows us to validate and verify promising solutions very quickly. This again, has dramatically reduced the response time with customers at the concept design solution stage.

Apply structure and formats with care and pragmatism…

Yet, when an ABD approach is carried out in real life, adaptations and practical adjustments when applying the facilitated methodology are necessary. With more than 15 years of experience in performing such project-customized approaches, it is clear that a few very important principles and practices still apply for the methodology or approach to function the way it is developed. These principles and practices are:

i) Be loyal to the holistic or systemic principles of systems theory and management – the whole is more important than the details of the individual parts…

ii) Be sure you cover the intent of the 1 to 8 modules – a structured approach for information gathering and step-by-step decision-making with as little room for reconsidering previous decisions as possible – a red thread of decision-making logic should be visible as the overall process progresses. Module 9 is only a "toolbox" of different analysis tools and techniques to support the effective decision-making process feeding in and out of the other 1 to 8 Modules.

iii) Always apply the wicked problem solver: the why's-, the what ifs-, and the what-next questionnaire…

iv) Record and document everything that is said and decided…

v) Be sure there is progression in all workshops…even if important challenges must be left behind – you can always go back when your info box or repository is expanded to the extent necessary

vi) Be sure you perform the ABD process in an appropriate setting… - room for everyone to think, read, discuss, and write as well and electronic multi-display facilities are readily available.

vii) Relevant executive management of the customer firm must be present – In addition, support personnel and or specialists could be present.

viii) Educated pragmatism should be applied – when the development process takes a new direction be sure you let go about the structure but not intent, and only to the extent that serves the purpose of arriving at the goal of the project.
ix) Identify critical "white spots" – areas of interest where information is lacking partly or completely and search for improved knowledge in these areas that can have a vital effect on the final decision-making in the project.
x) Develop and expand causal maps of obvious and not-so-obvious causal relationships among project output and outcome-sensitive factors.
xi) All agreed-upon project activities and information sharing must be carried out on a "free will" basis when the direction and intent of development is agreed.
xii) Customers should be willing to share, normally considered proprietary and partly confidential commercial information.
xiii) Agree upon deliverables throughout the ABD process and be sure mutual project performance expectations are adjusted and balanced.
xiv) Make sure you can justify the project partnership and execution from a policy, strategic, expertise, experience, and economic sustainability perspective.

In addition to these principles, several practices have proven to work well and support the ABD approach. It is important that:

1. Sketches of ideas are made along the way.
2. A design protocol is established and kept up to date during the process to document all underway decisions.
3. A consistent presence in workshops of executive decision-makers and their invited specialists.
4. Preparation between workshops and regular exchange of preliminary project material developed.
5. Continual documentation of discussion of options, limitations, and reservations' - flipcharts and operative marker pens are crucial – tape-recording can be used for safeguarding information – and to avoid unnecessary repetition in consecutive workshops.
6. Workshops are held to the convenience of the customer, but preferably not more than two to a maximum of three weeks in between workshops – they can be half a day or a full day session.
7. Arrange as many workshops as found necessary to capture all important information and make customers/stakeholders comfortable about the information robustness and methodological rigour, but not more – once every month over a three to six-month period is feasible, sometimes more often when arriving faster at promising solutions.
8. Typically, it can be useful to discuss and agree upon various exit possibilities along the way of project execution, to be triggered if one of the parties becomes uncomfortable in the process or for other reasons the project has to be brought to a stop.
9. Bring along as much relevant background information and documented experiences as you can think of – electronically or on paper.
10. Identify, make available and test relevant data sources.
11. Look for opportunities to make pre-studies of known or identifiable information about typical issues, problems, and accidents – "learning" events relating to the vessel segment to be studied and critically scrutinized.
12. Investigate opportunities if it is possible to arrange for shorter or longer site field trips onboard similar or related vessels to better reveal facts about the vessel's operation and "life onboard".
13. Behave like a professional process consultant – be sure your attitude and behaviour vis-à-vis the customer are proper and will motivate the customer to continue the process. Provide useful information elements, critically analyse and diagnose the information shared, ensure effective support for ideas development and make the process a comfortable one. Recommend alternative solutions and discuss how they can be realized – a process consultation does not assume that the customer knows what is wrong what the challenges or problems are, what is needed to mend the situation, or what the consultant or customer should do to improve the situation. Let the common diagnosis and suggestions for improvement – the intent, help the project to plan how to achieve the goals of the project initiative and improve the situation (Schein, 1988).
14. Perform as many relevant pre-analyses of the data repository as found useful for the coming study at hand – too much is better than too little.
15. For new market segment entry make an extra effort to study the macro and micro commercial, operational and technical aspects of the segment and behaviours over at least 10 years and preferably 30 years overview can be quite useful.
16. Be sure you make a thorough update of the customers' existing fleet, operations, technical preferences, and commercial performance.

It is also important to adopt and adjust the use of analysis tools and simulations as necessary and useful. Minor to moderate changes also must be made to the process of documentation of process progress. Typically, more formal report formats of the MS-Word-type have been exchanged with the use of MS-PowerPoint as the prime communication tool. The whole process

must be carried out with a high degree of pragmatism. In the use case story being presented in the following, these principles and practices are largely followed.

As previously mentioned, the ABD approach is not a universal tool for any ship design requirement capture or elucidation situation. It is particularly valuable, in customer-designer situations C-Ds4 and C-Ds5, described more in detail in paragraph "One approach doesn't fit all situations…" (page 6) of this article. Typically, the first category is generated by a customer project inquiry and not a customer design inquiry (C-Ds1, a broker inquiry (C-Ds2) or a vessel tender inquiry (C-Ds3). These latter three categories from experience do not require the full ABD approach to be handled properly. They can in most cases be carried out with an ABD-light methodology application – by specialised questionnaires and requirements checklists, for example. The C_Ds5 situation, on the other hand, is what in more recent times has been described as project making activity and will almost always require a full ABD process to be performed, documented, and used for the promotion of the initiative of a promising marine system business proposition and its corresponding ship design solution(s).

The use case reviewed and discussed in this article is typically, a C-D4 (EtO) situation. Before starting to elaborate on the C-D4 (EtO) use case, we review the broader ABD-based pre-analysed business environment for the Factory Stern Trawler market segment.

The context and subject – why a factory stern trawler focus and what are we up against…

It is expected that aquaculture and ocean fisheries will have to cover a major portion of the growth in seafood demand in the future, as it is said to have less effects on the reduction of fish stocks, but ocean fisheries are also expected to contribute. Firstly, by improvements in the exploitation of current fish biomass (using fish oil, fish meal and other products), and secondary by exploitation of biomass species (mesopelagic). Both factors could contribute to the growth of biomass food produced from the sea while maintaining the level of capture and reproduction of resources. (Garcia et.al, 2018)

The need for more effective vessels producing higher quality biomass motivates a renovation and renewal of the fleet – a fifth generation of factory trawlers. This new generation should be characterized by fishing efficiency, with a focus on fish product quality and better exploitation of fishing captures, flexibility from the number of products, species and waters or regions, and the best possible quota utilization.

Another factor spurring a fleet renovation is the poor energy efficiency and environmental footprint of the current trawler fleet, as compared to more modern pelagic trawlers or purse seiners (Ziegler et al., 2013). The replacement of environmentally harmless refrigerants, used by many of the vessels in the current fleet, could reduce the carbon footprint of factory trawlers by up to 30% (Ziegler et al., 2013).

History and introduction to factory trawlers – what to be prepared for…

The Food and Agriculture Organization in the United Nations (FAO) identifies 11 types of fishing vessels (Thermes et al., 2023). Of these, there are three that represent most of the fleet and represent the three principal fishing techniques: seiners, trawlers and liners. Figure 3 includes a short description of these three categories represented by the most popular vessel type under them. The type of fish or protein to catch, the area of operations, and the quota assigned are the main drivers in the selection of what vessel type to go for. Hence, seiners are used primarily for pelagic species, while trawlers and liners are used for mesopelagic and demersal species.

a. Seiners - Purse seiner/pelagic trawler:

- This combination of fishing gear requires that the deck arrangement and equipment be planned for dual use. As the power requirement for trawling is higher the vessel is usually designed as a trawler with a suitable combination winch for both methods

b. Trawlers - Stern trawler:

- On stern trawlers the trawl is set and hauled over the stern. These vessels are fitted with trawl winches and equipment necessary to haul the net on board and lift the cod-end over the deck. Freezer trawlers are outfitted with refrigerating plants and freezing equipment. The holds are insulated and refrigerated

1. Beam trawlers
2. Otter trawlers
3. Pair trawlers
4. Side trawlers
5. Stern trawlers
6. Outrigger trawlers
7. Freezer trawlers
8. Wet-fish trawlers

c. Liners - Longliner:

- The number of hooks and lines handled depends on the size of the vessel, the degree of mechanization, and crew size
- The wheelhouse can be situated aft or forward, but on larger vessels, the bridge is generally placed aft. In most cases the gear is hauled from the bow or the side with a mechanical or hydraulic line hauler and the lines are set over the stern

Figure 3: Main categories of fishing vessels and sub-categories of trawlers.

Due to their catching efficiency, stern trawlers are among the most populated vessel types. Ranging from smaller vessels focused on coastal operations and with cargo holding keeping fish on ice, to large units equipped with factories capable of processing the capture and freezing it. This fleet has evolved significantly since the first units were built in the 50's, characterized by the combination of a stern ramp and onboard processing. The vessels built after 2010 are considered the fourth generation of factory stern trawlers. With a focus on fuel efficiency, the vessels of the fourth generation have engines with up to 20% lower specific fuel oil consumption than those of the third generation (Fernandez et al., 2014), representing a major improvement in the vessel's economics and emission footprint. According to (CRISP, 2015), the newer tonnage is 50% more efficient in terms of unit fuel consumption used per kilo captured fish/biomass and resulting in a fishing business which is 5-15% more profitable. The same article highlights some of the improvements from this generation, such as hull shape design and factory processes, including robotized freezers and storage. However, methods for fish handling are still poor and little evolution has taken place over the past 60 years (CRISP, 2015), resulting in more than 15% dead fish before the fish can be processed.

We advocate, therefore, that the design of the next generation of factory stern trawlers, the fifth generation, should focus on fishing efficiency, looking for maximizing revenue and profit through improved quality of the end biomass product by flexibility dictated by the number of products, species, and waters (regions) to be explored and a best possible quota utilization. It requires therefore to integrate technical, operational, and commercial perspectives, and a better collaboration of the different stakeholders in the early stages of the ship design process. It is our proposition, that a shipowner will not invest in a new vessel if he or she cannot see an economic benefit from it. Hence, our approach must ensure that such an intent must be met.

USE CASE STUDY

The use case in this paper is a written description of how the customer-ship designer setting works in real life in a new building project context. It outlines, from the users' point of view, the realization of an ABD approach in developing a concept vessel design solution within a given business concept framework. This use case is represented as a sequence of simplistic steps, beginning with exploring the ABD module one to eight guidance and ending with a proper business concept description and the handover documentation of a fit-to-purpose ship design solution, ready for detailed design and finally a new building project realized at a yard.

Project initiative background…

Inquiry from customer: "Do you want to participate in a joint industry project to develop the next generation factory stern trawler with novel fish catching and process treatment equipment and ship factory arrangement?" - As previously stated, we quickly responded to the customer and accepted their invitation. There were three main reasons for this fast response. Firstly, we had for some time seen that the market demand for larger fishing boats was expanding – so the market potential looked promising, and we needed an additional new ship segment to be consolidated into our existing, but declining product and

service portfolio of existing ships. Secondly, we love innovation challenges and could see a fine possibility to grab this chance to develop something novel and groundbreaking and demonstrate our vision – "turning visions into reality". Thirdly, re-vitalize and leverage our strong fishing vessel newbuilding project delivery history, totalling 63 vessels, including trawlers, longliners and purse seiners.

Our project involvement strategy was, however, accepted under one very important premise: The FST concept design solution had to represent something completely new – just making a copy of the most recent FST design solutions of our competitors was not an option. If we should go along with this customer inquiry and offer to run a full ABD process on a no-cure-no-pay basis, we should also retain the rights to the design solution for repeat sales, either on our own or together with the customer. Perhaps we could even use the customer to promote the eventual successful and attractive design.

The customer insisted that we listen carefully to their ideas and expand upon those ideas for the realization of the project. Then, whatever additional ideas we might have to enhance their ideas and conceptual thinking was much welcomed.

Both parties accepted the preliminary terms and mutual project exit possibilities were agreed upon. Consequently, a Memorandum of Understanding, a Cooperation Agreement, and a Concept Design Agreement were agreed upon and signed. When the Basic Design work started an additional Agreement for Front-End Engineering and Design contract was also signed.

The project initiative was started, and 6 consecutive ABD workshops were carried out within half a year, to identify, collect and collate relevant vessel concept design solution project data. Two field study trips were carried out – one visit to an FST in port alongside the quay and one three-day trip offshore at a fishing site to acquaint with the FST operations and test new ideas from people onboard FSTs.

Preparations for the kick-off meeting…

Less than a week after our two telephone discussions, a project kick-off meeting was agreed upon and held at the ABD facility room of the designer. Four executives from the customer and 6 representatives from the designer firm met to clarify the project terms, a presentation of the customer business idea and proposition was given, and a quick review of the ABD approach was performed.

Within the next 4 weeks, a first full-day ABD workshop at the designer premises was arranged to primarily find out: What is the project idea? What is the project background? Who will be the permanent participants (decision-makers)? Who will participate in what, when, and in what way? What relevant skills, expertise, and knowledge are available for problem-solving challenges? What is the project schedule? What could be the project milestone plan forward? How much time can be spent and the time availability of key decision-makers? What is the project funding capability of the project initiative? Who are the relevant and preferred suppliers to work with, when do we introduce them to the project initiative, and who will contact them? What do we know about the project challenge at hand? Where can we find relevant and useful problem-solving background material? How do we involve our people – experts, specialists, and facilitators (consultants)?

Agreed upon information exchange, collection, collation and storage of the various background documents, analyses reports, drawings, miscellaneous illustrations, and other materials were carried out and a common project development Sharepoint site was established.

ABD Module 1, 2, 3, and 4 work – a brief synopsis…

Module 1 sets out to develop a realistic and well-thought-through description of the business concept, a clear statement as to what is the business proposition that the customer wants to pursue. Critically assess the realism and feasibility of the business concept and proposition by answering key questions about the various aspects surrounding the business concept. In Module 2, the objective is to identify all important project stakeholders that are affected and/or involved in the overall project to be realized and assess their individual and collective expectations towards the concept vessel design solution to be developed. Also identifying the competitive position and context of the proposed project business concept is important and is handled by the guidelines of Module 3. Assess what the potential is for the business concept to be successful, given the competition it will face. Identify competitive issues and aspects that will influence the development of the vessel concept design solution. Module 4 assists the ship design process by identifying important aspects that represent a risk for the project to be realized. A risk aspect in this context is any element that poses a threat to the successful development and execution of the vessel concept design solution. Module 5 identifies and assesses different and promising vessel concept design solutions utilizing relevant specialized and proprietary ship design tools listed in Module 9 of the ABD methodology in addition to "standard" naval architecture and marine engineering methods (Papanikolaou, 2019).

Modules 1, 2, 3, and 4 are critical to the follow-up work to be carried out in Modules 5 to 8. In this use case, only project work related to Modules 1 to 5 is presented and reflected in the article discussion. Fragments of the overall approach relating to these 5 modules are primarily depicted to give association to the more detailed work taking place in the real-life set of ABD workshops carried out. Brief comments have been inserted where found necessary and useful to link the various tableaus and make a continuous use case story.

ABD Module 1, 2, 3, and 4 work – results…

Firstly, we had to define the scope of the project. The fishing company had experience, and quotes, for ownership and operation of factory stern trawlers targeting white fish (cod, pollock, haddock) and shrimp. In line with the ABD procedure, the customer presented their original business idea and project intent. Very clearly, they stated and documented, what the direction of the innovation should take: To develop a new factory stern trawler vessel concept different from a traditional stern trawler concept into a new biomass production platform/floating factory to secure a differentiated biomass product from a quality standpoint. Furthermore, to secure full biomass utilization of any catch and increased utilization of more sustainable species' catch including new technology and novel catch processing and handling equipment – restitution tanks for live fish catch, hydrolysis of enchilada, CO_2 freeze, filleting and separation, and a protected shrimp factory. Additionally, the vessel solution should be optimized from an energy consumption standpoint and alternative decarbonized fuel solutions should be considered. Maximum safe operational robustness should also be achieved.

The business proposition for the development of the 5th generation factory stern trawlers extracted from Module 1 was then framed as follows:

"Maximizing revenue and profit through improved quality of the end product by flexibility from nos. of products, species and waters and a best possible quota utilization."

The business proposition relies on three main opportunities identified in the wild fish market segment:

1. 100% resource utilization of the raw material currently being extracted from sustainable Norwegian marine resources.
2. Producing high-quality and differentiated products in the catch line.
3. Increase in the exploitation of sustainable stocks that are lower in the marine food chain (mesopelagic).

That, together with the market situation (rising fish prices, relaxation of fuel prices and political willingness) and the stagnation of the fleet and vessel design developments, had motivated a rising interest in a renewal of the factory stern trawler fleet in the coming years.

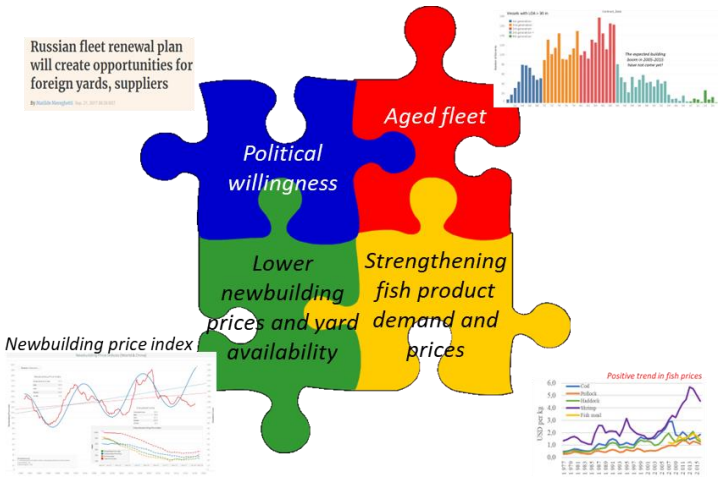

Figure 4. Contextual factors supporting the robustness of the business idea.

The business proposition came hand in hand with a set of expectations for the vessel design. The expectations were captured during the initial ABD workshops. Firstly, with an unstructured brainstorming to capture important expectations from the different stakeholders and actors involved (captain, chief, financial manager, end consumer of fish, etc). The different expectations were thereafter structured and further described by items that could related to the systems, functions, and performance elements of the vessel, as described in Figure 5.

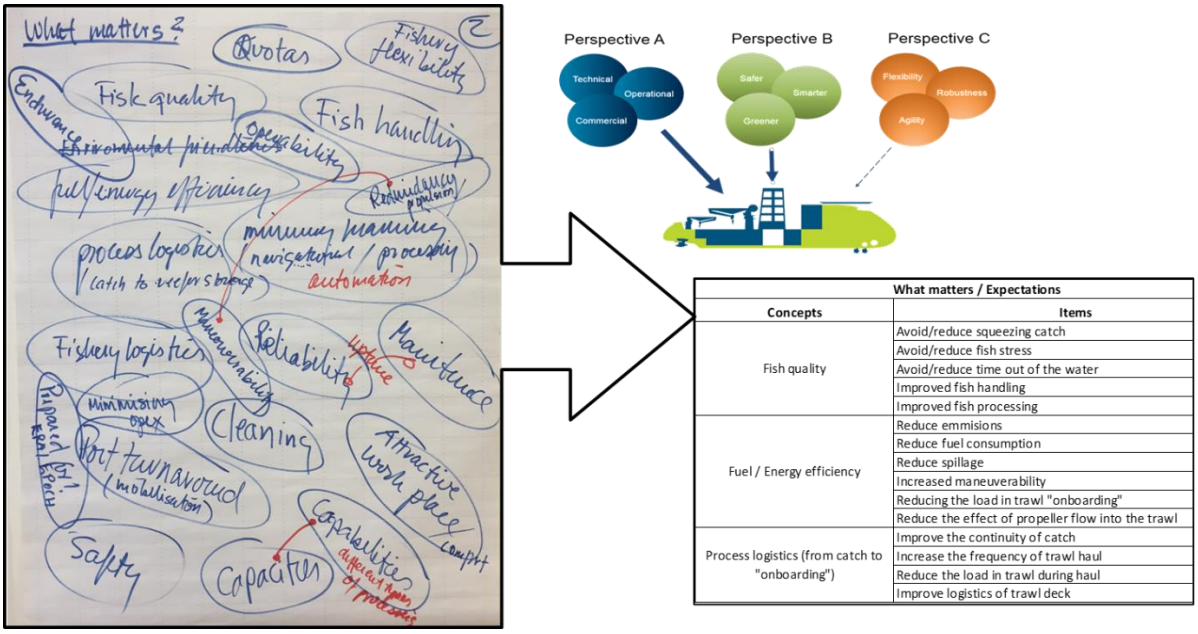

What matters / Expectations	
Concepts	**Items**
Fish quality	Avoid/reduce squeezing catch
	Avoid/reduce fish stress
	Avoid/reduce time out of the water
	Improved fish handling
	Improved fish processing
Fuel / Energy efficiency	Reduce emmisions
	Reduce fuel consumption
	Reduce spillage
	Increased maneuverability
	Reducing the load in trawl "onboarding"
	Reduce the effect of propeller flow into the trawl
Process logistics (from catch to "onboarding")	Improve the continuity of catch
	Increase the frequency of trawl haul
	Reduce the load in trawl during haul
	Improve logistics of trawl deck

Figure 5: Identification of stakeholder expectations for a 5th generation type FST.

Ahead of initiating a design development process, the ABD process involves a familiarization with the existing vessel operations and the context in which they are carried out, including commercial, operational, and technical aspects. Figure 6 exemplifies some of the support documentation extracted for project challenge identification and broadening the elucidation of the project solution space and later important vessel concept design solution development decision-making. Some of the analyses included an analysis of vessel operations and the development of operational profiles, a study of the quota system and expectations on quota developments, and fish price developments. Furthermore, it was clarified what to fish and where to fish. Similarly, analysis work was performed to identify a complex fish quota (Norwegian) arrangement, which was found to have a major impact on the FST vessel design solution. Figure 6 is a collage of the module 5 analyses.

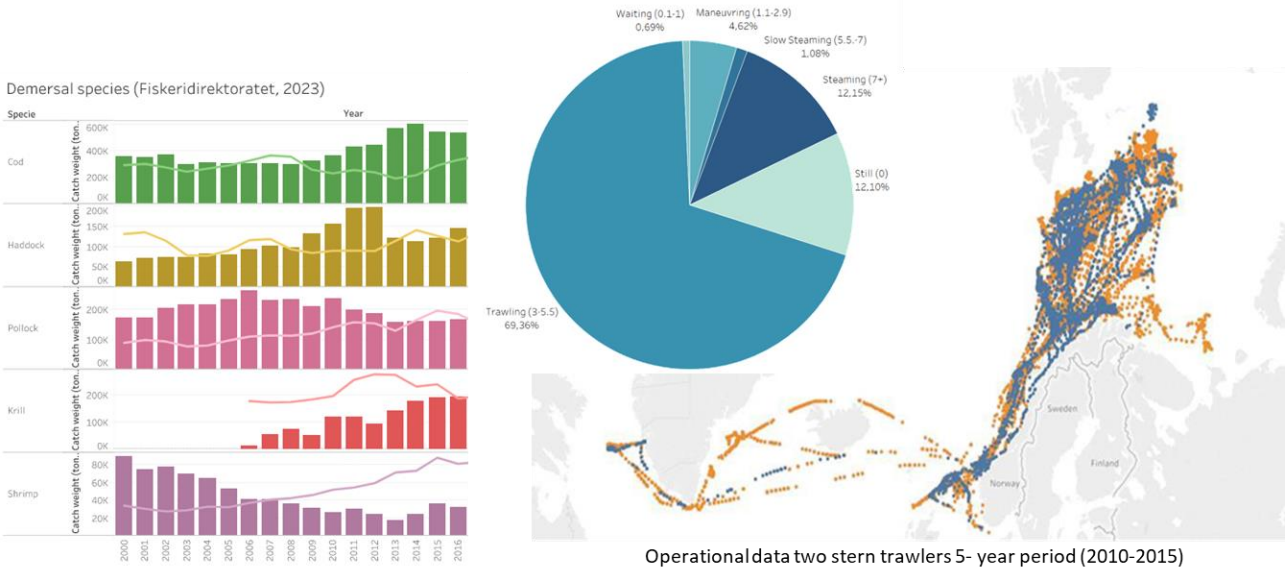

Figure 6: Collage of analyses performed during the ABD process.

The understanding of the market was strengthened by an analysis of the market competition performed as part of Module 3. For this purpose, the project performed a deep analysis of the existing fleet, including analysis of trends on main vessel parameters (length, beam, cargo hold capacity, etc), a clustering of the factory stern trawler fleet (Figure 7), and a review of competing designers and relevant building yards.

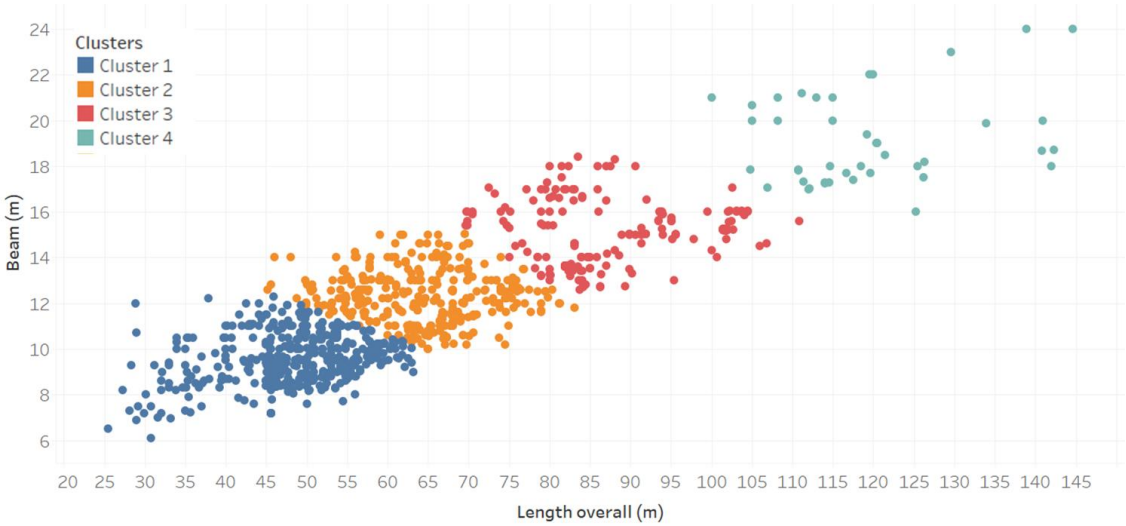

Figure 7: Overview of the stern trawler fleet categorized in clusters by length overall and beam.

A vital aspect of developing such a novel vessel design solution is to map the causal models of revenue and cost drivers and enablers. Figure 8 depicts the two causal maps for revenue-making and cost-driving factors of the FST model. The different factors contributing to revenue generation and vessel expenses are categorized by the degree to which the project can influence them – high (green), medium (orange), and low (red) influence.

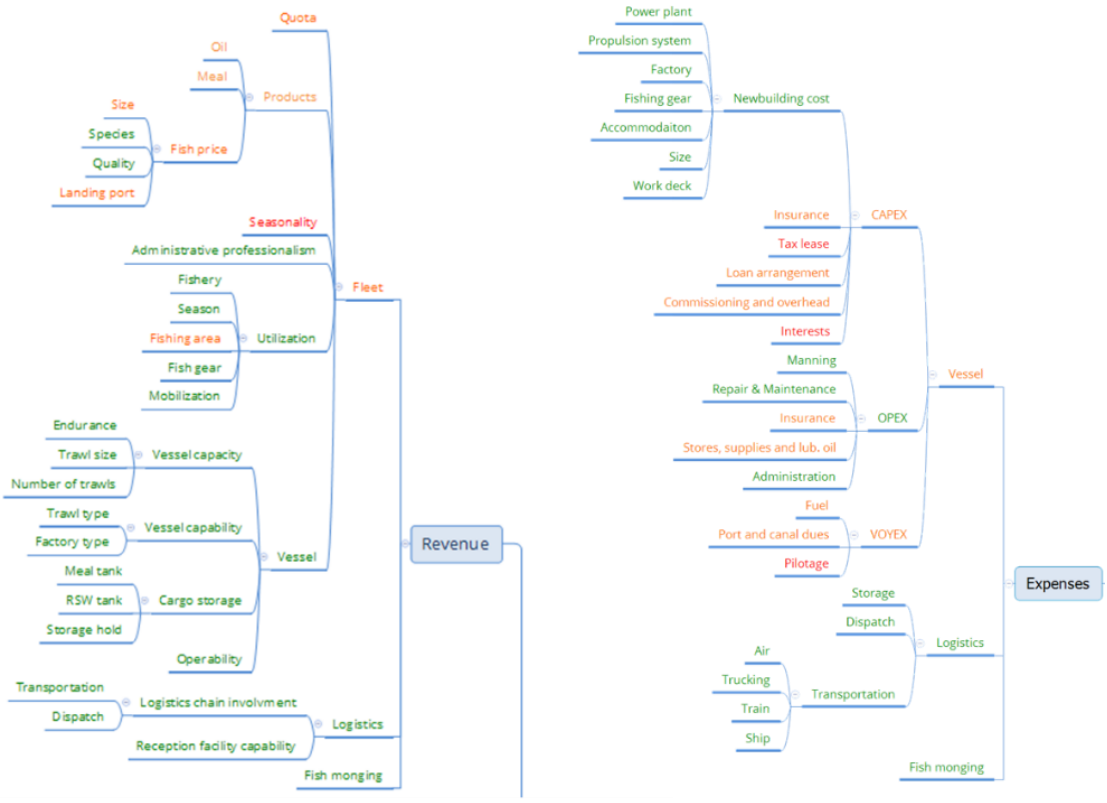

Figure 8: FST vessel revenue-making and cost-generation models.

The project carried out an onboard field study to establish a broad and deep understanding of the FST operation and feedback on vital operational vessel design features for improvement. Field studies are a structured process to capture "hands-on" information from vessel operations. The methodology is well documented in previous literature (Gernez et al., 2014; Lurås & Nordby, 2014) hence, it is not detailed described in this article. Figure 9 summarizes special aspects and design features relating to the bridge, accommodation, fish handling, fish factory, fish equipment deck, and finally, the trawl concept and reception facility, to be carefully looked at and improved as part of developing the novel 5th generation FST.

Figure 9: Main evaluation areas during the field trip.

The project also carried out an evaluation of risk and uncertainties (Module 4) related to the vessel business case. This process has been previously described in an IMDC publication (Garcia et al., 2018). The evaluation included the development of a simulation model to explore the impact of externalities on the cash flow of the vessel while in operation.

There is only one last element required before the traditional design work (naval architecture and marine engineering calculations) starts: defining a design strategy and tactics that cater for the achievement of the business proposition and guide the designers during the conceptualization and detailing of the vessel design solution. Figure 10 exemplifies the breakdown of our design strategy and tactics related to enhancing the quality of the fish product.

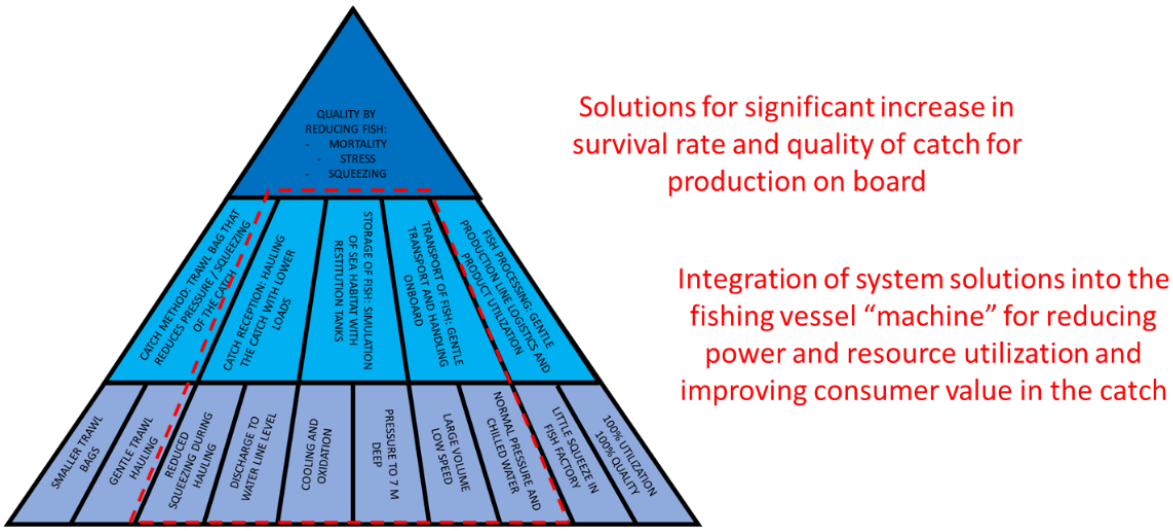

Figure 10: Design strategy and tastings for enhancing fish quality.

ABD Module 5 work – a promising vessel concept design solution is emerging…

The objective of Module 5 work of the ABD approach is to describe, supported by conceptual drawings and supporting analyses, different but promising solutions meeting the initial and underway stated expectations and requirements and assess these solutions by a set of specific, pre-defined criteria. These criteria are metric interpretations of all the expectations and requirements available and are relevant for proper and robust decision-making as to what is the better ship concept solution of the ones proposed. In this way, the main attributes, unique features, and performance yield can be compared and benchmarked in a micro and macro contextual way.

The design development (Module 5) started by framing the business proposition on tangible needs and expectations, that are thereafter elucidated in design parameters that define the boundaries of the design solution. Figure 11 exemplifies this process as a mind map leading from performance expectations (extracted in Module 2) into a vessel design definition. This process also requires identifying critical functions of the vessel platform. The project also depicted the early ship function diagram of the main and most critical functions of the novel vessel design to be explored (Figure 11 – right) and concluded as a part of the vessel concept design solution configuration.

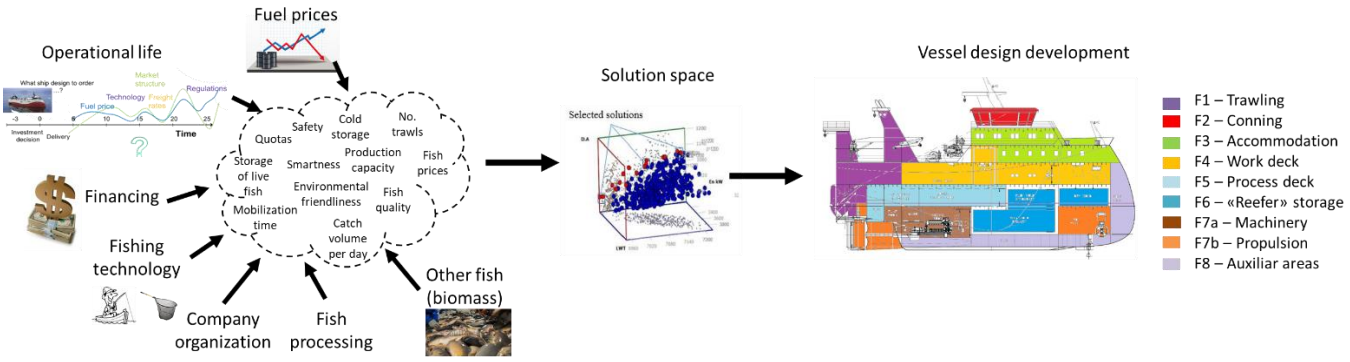

Figure 11: Mind map of the wicked problem leading towards a solution space and the vessel functional design development.

Here is where the identification and selection of technical solutions start. The project carried out a detailed evaluation and review of different technologies and technological solutions for the different functions of the vessel. Different alternatives were proposed and discussed during the workshops, involving expertise from the ship design company, shipyard, equipment suppliers and not least the vessel operators. Figure 12 briefly documents the process of testing new ideas in introducing new functional ideas to the FST and their configuration consequences and implications. It shows how various alternatives (A, B, C, D, etc) are considered, evaluated, and finally decided as to what seems to be the most promising solution and arrangement. From the illustrations, it is indicated by a big cross what solutions were disqualified in the workshop-based decision-making processes. The various functional areas (F1 to F8) are considered one by one with various solution options.

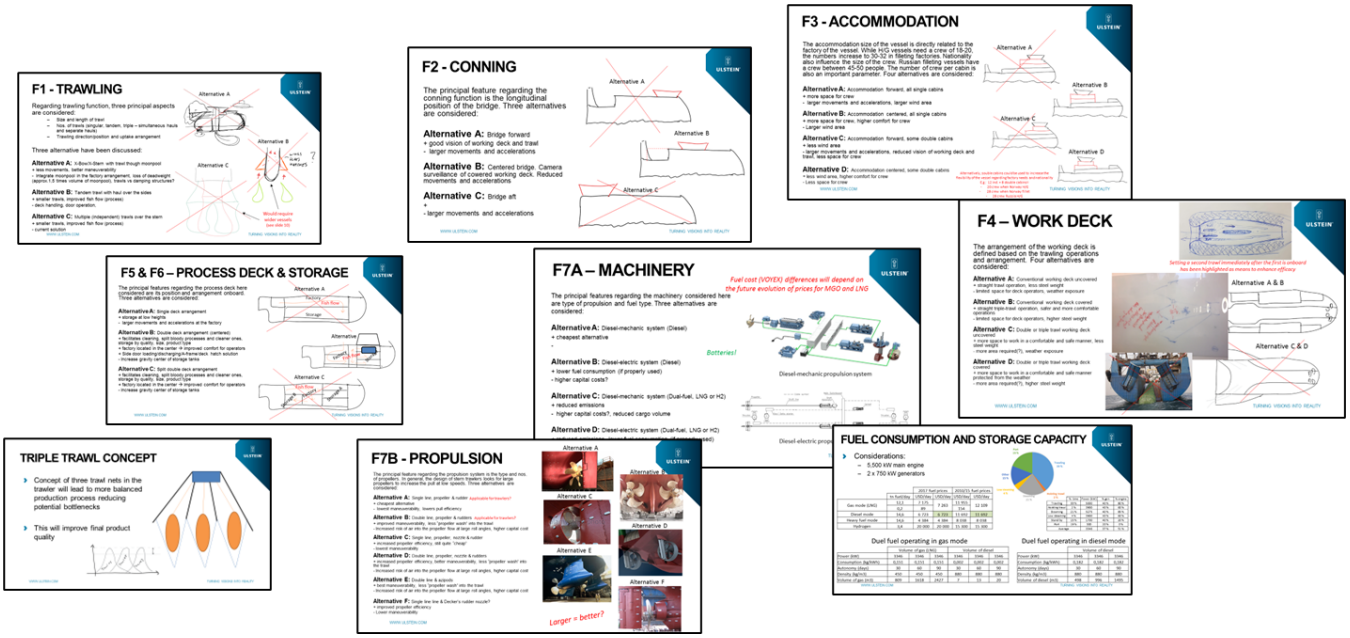

Figure 12: Examples of workshop configuration exercises summarized.

No ABD-scrutinized project can be finalized without a proper measure of merit benchmarking process. In Module 9, different performance yield indexed benchmarking methods are suggested and recommended for use. The project developed a set of key performance indicators (KPI) and a goodness-of-fit (GOF) matrix that were used in the ABD approach to distinguish what is a better FST vessel concept design solution among alternatives developed and existing trawlers in operation . The "-" sign in the KPI definitions represents the average value for the fleet, i.e., the KPIs are non-dimensional. Figure 13 presents the relative performance yield of different concept design solutions compared against each other and a full Goodness-of-Fit (GOF, with expectations and requirements') index satisfaction (Brett, Boulougouris, et al., 2006; Brett et al., 2018b; Ebrahimi et al., 2018).

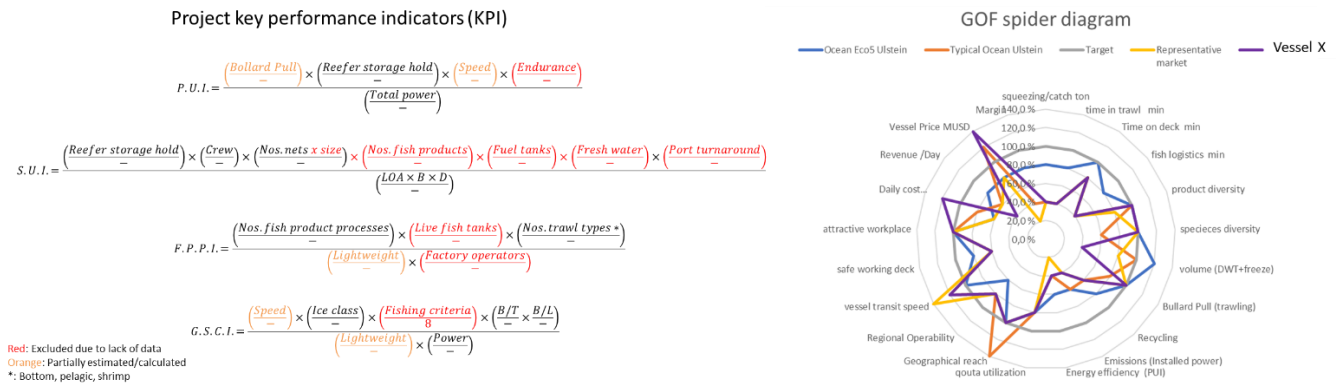

Figure 13: Evaluation of key performance indicators and goodness-of-fit.

Figure 14 represents an excerpt of ABD approach documentation, outlining and displaying the findings of the ABD process and effort.

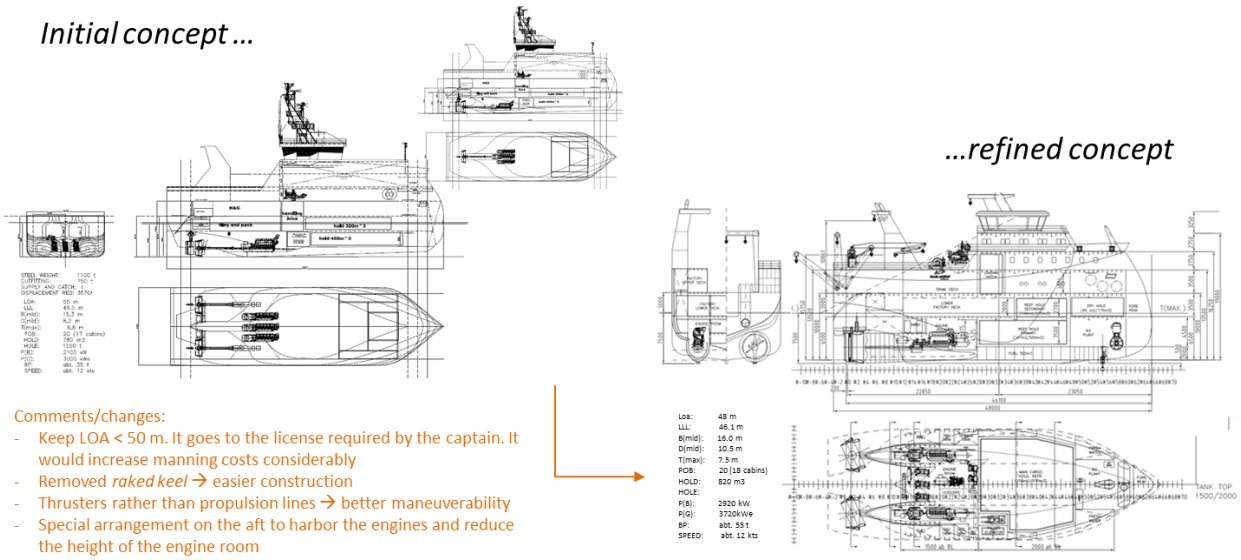

Figure 14: Stages of the vessel concept design solution development including the novel catch reception system.

Figure 15 presents the final 3D rendering of the FST vessel concept design solution in its natural environment – at sea. The project has been recognized with the "Innovation Award" at Nor-Fishing in 2022 and named "Ship of the Year" at Nor-Shipping in 2023.

Figure 15: a 3D rendering of the final FST vessel concept design solution.

Figure 16 displays the cover page of the vessel concept design handover document summing up the ABD approach undertaken and sent to our basic design naval architects and marine engineers for the final realization of the design project and preparing for contractual work and yard detailed engineering and production planning. The document was complemented by all the preliminary analysis reports and MS.ppt series of vessel concept design solution descriptions.

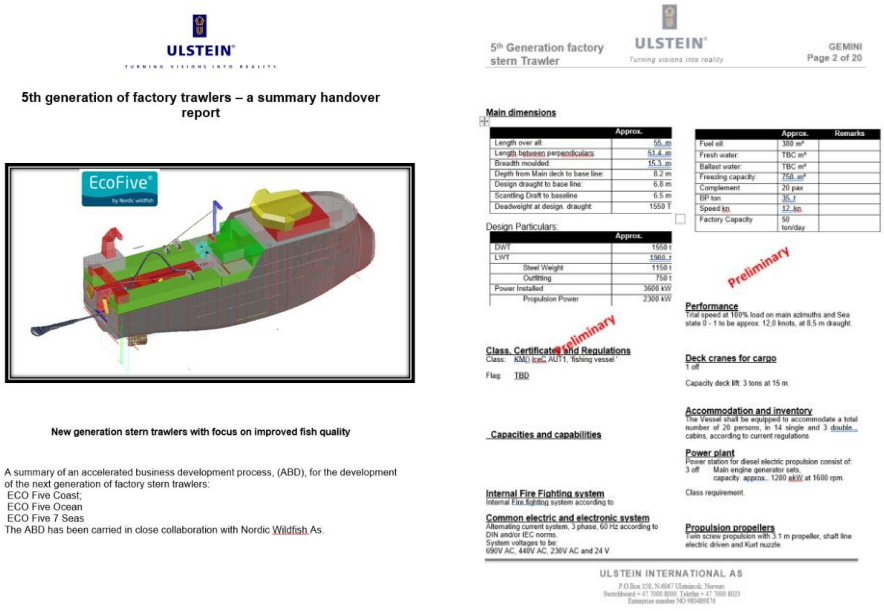

Figure 16: an example of the information handover document and appendixes exchanged between concept and basic design development teams.

The ABD use case aftermath…

Seeing the opportunity to launch a new ship segment in the Ulstein portfolio of services and designs it was decided to immediately expand the ABD approach findings into a suite of FSTs based on the ABD work process findings. Three different sizes were explored and parametrically adapted – Coast, Ocean, and 7SEAS. In addition, three different branding concepts were introduced – high, medium, and low-standard outfitting solutions. The unique features of the novel 5th generation FST portfolio, including all three versions of the novel FST concept, were extracted and made into strong selling points. Figures 17 and 18 present these ideas in a pictorial format.

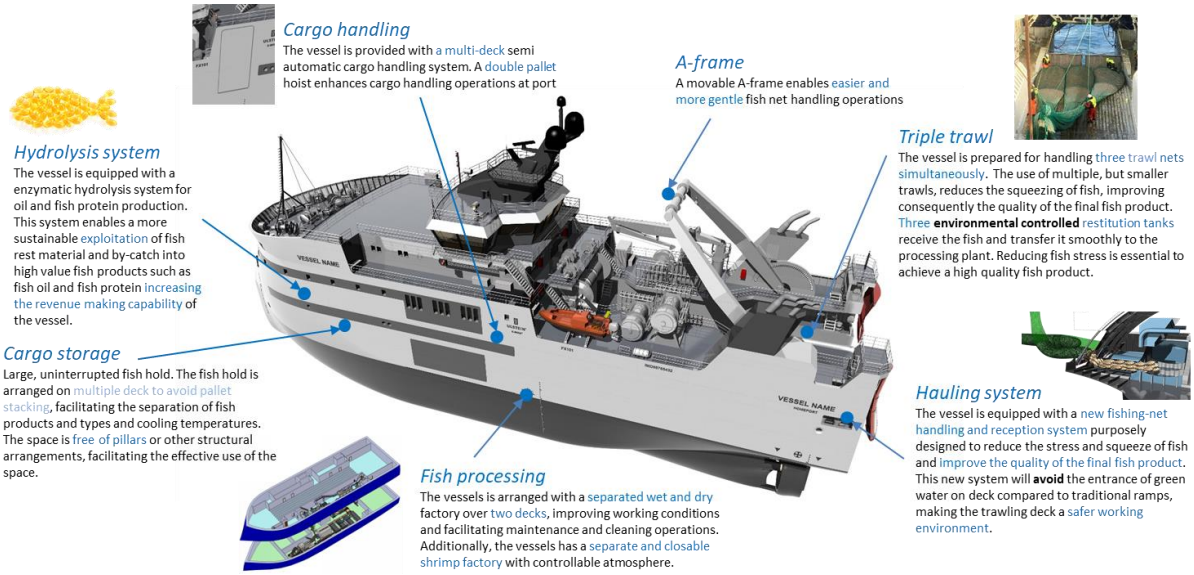

Figure 17: An overview (I) of the unique features of the novel FST developed.

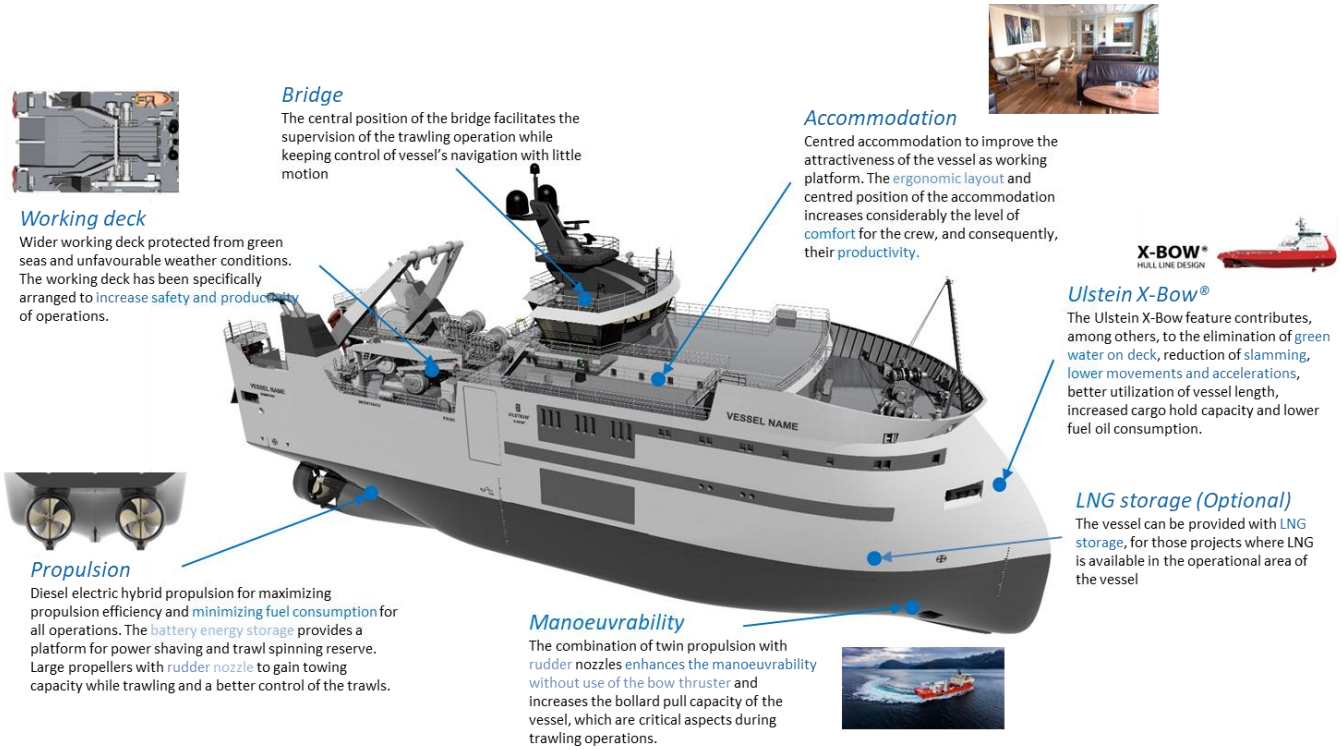

Figure 18: An overview (II) of the unique features of the novel FST developed.

CONCLUSION

This paper summarizes and describes a real-life ABD-guided development of a "family" of FST vessel concept design solution(s). The paper shows how a final ship design solution on a conceptual level, can look like, and consequently be built. This comprehensive and rather laborious article is developed with the principle of "seeing is believing" in mind. Over the years, so many interesting and most likely useful ship design approaches have been introduced and argued for as a must-have to state-of-the-art naval architecture and marine engineering practices. However, many of these methods are still only fragmentary. They tend to address only parts of the whole ship design process, rather than trying to deal with the full work process – concept, basic design, and detailed engineering. Many of the contributions are also very "toyish" in the sense that they have only been tested out as pilots and quite frequently user simulations have been based on "dummy" variables and the like. Practical real-life applications are scarce and therefore, custodians of the marine community have only to some extent, included them in their naval architecture and marine engineering toolboxes and daily ship design practice. For this paper, we felt it was important to share and demonstrate that in some cases, some of these novel approaches can be used in real-life situations. Yet, with the danger of exceeding the paper limit for IMDC papers, it was still considered useful to share pictorially, real project development experiences with the ship design community. We have shown in an anecdotal way, how the ABD approach can be executed, and findings meaningfully be used to produce successful vessel concept design solutions.

The paper starts with a recapitulation of what is still missing, or which loopholes still exist in the early ship design process. The tame and wicked problem aspects are addressed, and the authors argue that with the introduction and application of the much-referred and reviewed ABD approach in several IMDC papers, it is practically possible to master both tame and wicked ship design problems. A particular real-life use case of an ABD approach application has been introduced and reviewed in the paper. How it all started and how the process was continued are briefly documented and commented on.

The paper commences with a discussion about the fact that not all approaches fit all situations. Likely reasons for this are elaborated upon. The comprehensive (and successful) demonstration of the ABD approach in this paper makes a case for holistic design methodologies that explicitly address customer interaction and requirements elucidation as well as technical, operational, and commercial aspects in one go.

Practical implications to ship designers…

Although this particular use case study realization took a very long time, such an observation is, to our experience, uncorrelated with the ABD approach application. The ABD-approach-assisted novel vessel concept design solution development took place

well within the timeframe experienced in other ABD projects we have arranged and performed – typically 4 to 6 months. Also, the separate basic design job was carried out within normal time limits. The extreme project time spent was primarily due to project externalities, such as customer firm upheaval, sickness, tightening market conditions and extreme price increases with corresponding slow and costly financing opportunities and other matters outside the control of the project. The authors argue that the ABD process went very smoothly and the customer in question was an ideal partner "playing by the ABD rules". They were highly motivated to pursue the goals and intent of the project. They were very patient and receptive to new approaches. Even when this was the first time, they tried to follow the systematic procedure. They were very disciplined with the process, open-minded and willing to go with the flow of the ABD approach regimen. An enormous amount of information sharing took place, resulting in a wider educational business operation both on the customer's side and the designer's side. Hence, it can be concluded that the ADB approach to the project was an effective one. It is also a learning process that more vessel innovation projects could benefit from a similarly facilitated ABD approach. As stated earlier in the paper, it is typically C-Ds4 and C-Ds5 customer-ship designer settings that easily lend themselves to ABD approach applications and where extraordinary ship design process effectiveness could be expected. In other situations, the ABD approach might be found too time-consuming or resource-demanding, and the customer or project owner might not be willing to adapt to the new way of doing things.

The example described in this paper, together with the authors' experience, suggests that this type of ABD-based project can be suggested and carried out in many more new building situations with substantial gains to all parties involved. Although the ABD approach has not yet been applied in a Navy vessel situation, to the knowledge of the authors, it is strongly recommended that such a new application test is initiated and reported. The more real-life projects being carried out and reported, the faster and more qualified ABD-approach "facilitator-pilots" are developed for the renewal and enhancement of the ship designer community.

Again, we can see the role of the naval architect and marine engineer being strengthened as an integrator of the ship design project – administering the new building project development on behalf of the customer, but at the same time, the architect must also develop stronger interpersonal and social expertise and skills to better facilitate these complex and uncertain development processes. That is, more naval architects and marine engineers need to expand their multi-disciplinary expertise and skills to better support such new development of the discipline, topic, and related subjects, not at the expense of deep discipline knowledge – but in addition. More than ever, it is suggested strongly that "the ship designer of the future" must master equivalent expertise and knowledge within the fields of commercial, operational, and technical challenges related to a new building project realization. Thus, a new type of competent naval architects and marine engineering candidates must be developed through academic training and put into practice in situations different from the past (Asbjørnslett et al., 2022).

It becomes clearer to the authors that the traditional transaction-based ship design approach, where two parties deal with each other via a negotiation-based information-sharing process, does not work very efficiently – particularly not where and when novel innovations are to be developed and realized. Consequently, the traditional information exchange formats in ship design settings need to be improved or completely substituted. The same applies to the contractual formats being applied today. Finally, but not least, various new forms for "open book" partnerships can or must be established between project parties – open book means full trust between parties, no hidden agenda or desires and free information sharing even of traditionally considered confidential information.

Implications to academia…

Academia should, therefore, extend or establish and offer multi-disciplinary training courses and marine technology educational programs with content and learning objectives to match this new situation. Some Naval Architecture and Marine Engineering schools are already trying out such multi-disciplinary educational programs with course syllabus including own and cross-institutional/faculty complimentary courses and students' participation. The suggested change in design practice is likely most effectively achieved through the influx of freshly educated, multi-disciplinary designers who are trained in ABD-like design approaches.

What are some personal experiences to share…

While the overall ABD approach has worked very well and successfully in the described project, there are always things that can be improved on. In the opinion of the authors, establishing the facilitator and complete ship design team as early as possible in the process and earlier than was practised in this project would have helped. Thus, the ABD team from the ship designer side should be fixed and be a fixed group along the way. Also, more in-house, multi-skilled and experienced naval architects and marine engineers would have helped the process carried out. It is not very productive to involve basic design engineers now and then – they should be a permanent part of the ABD team and participate in the process from the very beginning and all along the way. If the customer is lean, the ABD team should follow the project into the premises and internal discussions of

the customer and partly become their permanent project support – avoid retaining a two-avenue process with transactional negotiations taking place between the customer and ship designer as the basic design and detailed engineering stages take place.

CONTRIBUTION STATEMENT

Per Olaf Brett: Conceptualization; data curation; structure and argumentation; methodology; writing – original draft.
Jose Jorge Garcia Agis: Conceptualization; data curation, writing – review.
Benjamin Lagemann: writing – a review.

ACKNOWLEDGEMENTS

This work reports on advances made in the Ulstein Group ASA and its affiliated companies as to how to modernize and enhance existing vessel concept design theory and practices, activities normally, performed together with customers. A sincere thank you to all of you. Much of the theoretical and methodological foundation and the exploration of improved vessel concept design is based on previous developments much of it being presented and discussed in previous IMDC 2006, 2009, 2012, 2015, 2018, and 2022 proceedings. This time the authors have intended to share first and foremost some practical experiences with applying novel naval architecture and marine engineering methods, theory, and approaches to demonstrate their applicability. Without the opportunity to consult with and exchange ideas around the topic, with colleagues at the Department of Marine Technology, NTNU Trondheim this study and article summary wouldn't be possible.

This paper reflects and presents the authors' viewpoints about the integrated customer-ship designer setting study taking place for a unique real-life ABD approach application in which both authors participated as facilitators and analysts. A sincere appreciation of contributions from several customers and their executives and experts is also conveyed hereby.

REFERENCES

Adi, A., & Stoeckle, T. (2022). Public relations as responsible persuasion: Activism and social change. In *The Routledge Companion to Public Relations* (1st edition, pp. 302–314). Routledge.

Andrews, D. J. (2003). Marine Design - Requirement Elucidation rather than Requirement Engineering. *International Marine Design Conference (IMDC)*.

Andrews, D. J. (2018). Choosing the Style of a New Design - The Key Ship Design Decision. *International Journal Maritime Engineering*, *160*(Part A1). https://doi.org/10.3940/rina.ijme.2018.a1.457

Asbjørnslett, B. E., Brett, P. O., Lagemann, B., & Erikstad, S. O. (2022). Educating the Next Generation Marine Systems Design Engineer – The NTNU Perspective. *14th International Marine Design Conference*.

Brett, P. O., Boulougouris, E., Horgen, R., Konovessis, D., Oestvik, I., Mermiris, G., Papanikolaou, A., & Vassalos, D. (2006). A Methodology for Logistics-Based Ship Design. *International Marine Design Conference (IMDC)*.

Brett, P. O., Carneiro, G., Horgen, R., Konovessis, D., Oestvik, I., & Tellkamp, J. (2006). LOGBASED: Logistics-Based Ship Design. *International Marine Design Conference (IMDC)*.

Brett, P. O., Gaspar, H. M., Ebrahimi, A., & Garcia, J. J. (2018a). Disruptive Market Conditions require New Direction for Vessel Design Practices and Tools Application. *International Marine Design Conference (IMDC)*.

Brett, P. O., Gaspar, H. M., Ebrahimi, A., & Garcia, J. J. (2018b). Disruptive Market Conditions require New Direction for Vessel Design Practices and Tools Application. *International Marine Design Conference (IMDC)*.

CRISP. (2015). Quality improvement. *Crisp Annual Report*.

Curry, M. D., Rehn, C. F., Ross, A. M., & Rhodes, D. H. (2017). Designing for System Value Sustainment using Interactive Epoch-Era Analysis : A Case Study from Commercial Offshore Ships. *Conference on System of Systems Engineering Research*, 1–10.

Ebrahimi, A., Brett, P. O., & Garcia, J. J. (2018). Fast-Track Vessel Concept Design Analysis (FTCDA). *International Conference on Computer Applications and Information Technology in the Maritime Industries*.

Fernandez, A. S., Toulemonde, V. R., Fuentes, A. J., Rodriquez, D. R., Iturrioz, A. J., Rey, J. R., Acevedo, O. F., Castro, J. I., Carceller, P., & Gandoy, J. D. (2014). ARALFUTUR PROJECT: Energy Efficiency of Deep Sea Trawlers for South Atlantic Fisheries. *Third International Symposium on Fishing Vessel Energy Efficiency E-Fishing*, *May*.

Garcia, J. J. (2020). *Effectiveness in Decision-Making in Ship Design under Uncertainty* [PhD Thesis]. Norwegian University of Science and Technology (NTNU).

Garcia, J. J., Brett, P. O., Ebrahimi, A., & Keane, A. (2018). Quantifying the Effects of Uncertainty in Vessel Design Performance - A Case Study on Factory Stern Trawlers. *International Marine Design Conference (IMDC)*.

Garcia, J. J., Pettersen, S. S., Rehn, C. F., Erikstad, S. O., Brett, P. O., & Asbjørnslett, B. E. (2019). Overspecified Vessel Design Solutions in Multi-Stakeholder Design Problems. *Research in Engineering Design*, *30*(4), 473–474. https://doi.org/10.1007/s00163-019-00319-3

Gaspar, H. M., Erikstad, S. O., & Ross, A. M. (2012). Handling Temporal Complexity in the Design of Non-Transport Ships Using Epoch-Era Analysis. *Transactions of the Royal Institution of Naval Architects Part A: International Journal of Maritime Engineering*, *154*(3), 109–120. https://doi.org/0.3940/rina.ijme.2012.a3.230

Gernez, E., Nordby, K., & Sevaldson, B. (2014). Enabling a service design perspective on ship design. *RINA Marine Design Conference*.

Huber, G. P., & Van de Ven, A. H. (1995). *Longitudinal Field Research Methods, Studying Process Patterns of Organizational Change*. Thousand Oaks.

Keane, A., Gaspar, H. M., & Brett, P. O. (2015). Epoch Era Analysis in the Design of the Next Generation Offshore Subsea Construction Vessels. *Annual System of Systems Engineering Conference*.

Lurås, S., & Nordby, K. (2014). Field Studies Informing Ship's Bridge Design at the Ocean Industries Concept Lab. *International Conference on Human Factors in Ship Design & Operation*.

Pettersen, S. S., Rehn, C. F., Garcia, J. J., Erikstad, S. O., Brett, P. O., Asbjørnslett, B. E., Ross, A. M., & Rhodes, D. H. (2018). Ill-Structured Commercial Ship Design Problems: The Responsive System Comparison Method on an Offshore Vessel Case. *Journal of Ship Production and Design*, *34*(1), 72–83. https://doi.org/https://doi.org/10.5957/JSPD.170012

Rehn, C. F., Pettersen, S. S., Erikstad, S. O., & Asbjørnslett, B. E. (2016). Investigating Feasibility of Flexible Ship Concepts using Tradespace Network Formulations. *International Symposium on Ships and Other Floating Structures*, *September*.

Rittel, H. W. J., & Webber, M. M. (1973). Dilemmas in a General Theory of Planning. *Policy Sciences*, *4*(2), 155–169. https://doi.org/10.1007/BF01405730

Sarkar, C., & Kotler, P. (2018). *Brand Activism: From Purpose to Action*. Idea Bite Press.

Thermes, S., van Anrooy, R., Gudmundsson, A., & Davy, D. (2023). *Classification and Definition of Fishing Vessel Types* (267).

Ulstein, T., & Brett, P. O. (2009). Seen Whats is Next in Design Solutions: Developing the Capability to develop a Commercial Growth Engine in Marine Design. *International Marine Design Conference (IMDC)*.

Ulstein, T., & Brett, P. O. (2012). Critical Systems Thinking in Ship Design Approaches. *International Marine Design Conference (IMDC)*.

Ulstein, T., & Brett, P. O. (2015). What is a Better Ship? – It all depends …. *International Marine Design Conference (IMDC)*.

Ziegler, F., Winther, U., Hognes, E. S., Emanuelsson, A., Sund, V., & Ellingsen, H. (2013). The Carbon Footprint of Norwegian Seafood Products on the Global Seafood Market. *Journal of Industrial Ecology*, *17*(1), 103–116. https://doi.org/10.1111/j.1530-9290.2012.00485.x

Proceedings of 15th International Marine Design Conference (IMDC-2024)
June 2-6, 2024
Amsterdam, the Netherlands

Capability driven vulnerability analysis of a naval combatant

Czop, Michal[1,*]; Megen, Demi van[1]; Droste, Koen[1]

ABSTRACT

This paper presents a fine-tuned approach to vulnerability assessment, focusing on protecting capabilities instead of individual systems and their components. The foundation of this method is a system model which uses functional chains to identify the contribution of individual systems towards to fulfilment of the ships capabilities. The key advantage of using functional chains is that by showing that individual functions can still be fulfilled, it is demonstrated that the vital capability containing those functions remains available. This paper first explains the theory behind the methodology and then demonstrates its working principles using a generalized case study for a single capability.

KEY WORDS

ship vulnerability; ship survivability; model-based system engineering; functional chains; naval design.

INTRODUCTION

In naval design, survivability is a set of measures aimed at reducing the likelihood of being hit by a hostile effector and limiting the consequences of such damage. It can be divided into two sub-disciplines: susceptibility and vulnerability. The former includes managing the asset's signatures (radar, infra-red, acoustic, etc.) to prevent detection, confusing the weapon's homing systems (for example using decoys), or ultimately destroying the incoming threat. The latter i.e., vulnerability reduction, which is the focus of this paper, includes the measures which reduce weapon effects with the assumption that the vessel has already been hit.

There are multiple reasons to implement the vulnerability aspect in a modern naval combatant design. The overarching goal is to reduce the potential death toll amongst the crew, following the philosophy that while ships are replaceable, people are not. However, replaceable does not equal disposable, thus the second objective is to limit the extent of damage and decrease the risk of the loss of the asset. An additional benefit is that reduced vulnerability increases the availability of ship's systems in a damaged state, thus improving the prospects of completing mission objectives. It is worth noting, that the approach discussed in this paper is only relevant to threats on or above the waterline, resulting in kinetic damage, blast, and fragments emission. The underwater threats, such as mines and torpedoes, usually lead to a shock event affecting the entire vessel, which requires a fundamentally different approach.

ESTABLISHED APPROACH TO VULNERABILITY REDUCTION

Physical protection measures

Vulnerability reduction includes multiple distinct solutions which need to be considered at consecutive design stages. In the age of battleships, for the most part, this objective was fulfilled by heavily armouring the ships, which made them more resistant to (naval) gunfire. However, the technological landscape has completely changed; modern, more powerful weapons have

[1] Damen Naval (Vlissingen, Netherlands)
* Corresponding Author: m.czop@damennaval.com

Submitted: 14 February 2024, Revised: 1 May 2024, Accepted: 3 May 2024, Published: 19 May 2024

Conference paper, DOI: https://doi.org/10.59490/imdc.2024.835 e-ISSN: 3050-4864

rendered this strategy ineffective and impractical. Additionally, the heavy armour comes with a major penalty to other design aspects, primarily signatures, weight, and space, thus increasing cost of construction and operation (due to increased fuel requirement). Nonetheless, certain impact protection measures continue to play a key role in limiting the extent of damage to the ship. Blast-, Fragment and/or fire retaining bulkheads and reinforced decks are applied in strategic locations to contain the effects of a hit to a limited part of the vessel. With increasing prevalence of asymmetric scenarios, it is becoming more common to additionally protect high value and/or heavily manned compartments with the aim of stopping the penetration of the ship's hull by smaller weapons fire. Similarly, sections of reinforced bulwarks as well as bulletproof vests serve to protect the personnel on the open decks against small-calibre gunfire.

System architecture measures

In addition to shielding and containment, system architecture measures are implemented to improve resilience of the vital systems of the ship. This strategy drives the arrangement of systems by acknowledging that they may be partially damaged, therefore single points of failure must be avoided to reduce the impact of weapon effects. The established approach to this issue is designating a set of ship's systems as vital and ensuring there are multiple instances of each in the vessel with sufficient physical separation. This is the key distinction between availability and vulnerability analysis – two systems located in the same compartment are redundant from the availability standpoint, however they can be damaged by a single weapon hit. When selecting the locations of the vulnerability-redundant systems, longitudinal separation is preferred over vertical. This is not only because ships are usually longer than they are tall, but also due to the fact that that bulkheads tend to offer more resistance to blast effects than decks do. For most support systems (providing consumables, control, cooling, etc.) the distribution infrastructure must also follow a redundant design to be able to service the dependent vital systems outside of the damaged section. This is achieved either by routing the main line through compartments well under the waterline with riser pipes extending upwards or by developing a ring arrangement for cabling and piping. Switchboards and valves are placed at selected boundaries allowing to isolate the damaged section and continue servicing the remainder of the vessel.

A ship contains multiple interconnected systems, very few of which are capable of functioning fully independently. The measures described above are effective at providing redundancy of individual systems, however on their own they fail to capture the interdependencies amongst them. For example, let us assume a vessel with a redundant electric propulsion system, powered by a ring-shaped distribution network with two generator sets in different areas of the ship. These generator sets have independent cooling circuits, which require uninterrupted supply of freshwater, delivered from either of two pumps located in a single machinery space, halfway between the generator rooms. In this case a single weapon hit can damage both pumps, not only indirectly disabling the propulsion system but also leading to a complete blackout. This is only an illustrative example – in complex naval platforms these interdependencies are often obscured by the sheer amount of complexity and interconnectivity of all systems on board.

Based on the arguments above, simply doubling and separating all the systems on the vessel may seem like the optimal solution, however the redundancy measures come with a severe penalty to weight, space, and cost. Consequently, a more in-depth analysis is needed to accurately select the systems and components to protect and develop a resilient design without compromising other design aspects.

CAPABILITY DRIVEN APPROACH

The defining feature of capability-driven approach is that it shifts the focus of the analysis from protecting individual system components to protecting high-level (vital) capabilities of the ship. This chapter explains how these capabilities are described in a system model and mapped to the relevant systems, followed by the assumptions of the analysis and the principles of evaluating system performance.

System model as the foundation of analysis

This paper presents an approach to the issues described above by basing vulnerability analysis on functional chains created with ARCADIA – a model-based systems engineering method developed by THALES (Voirin, 2017). The system model describes the capabilities of the vessel represented using functional chains. A functional chain consists of several functions which interact with each other, in essence describing the sequence of events/actions which need to happen in order to achieve a given desired capability. These functions are then assigned to (or allocated to) systems which execute them. This makes the interactions between functions become a representation of interactions (or interfaces) between systems. These interfaces are modelled as functional exchanges, showing both the functional and physical interdependencies between systems (Roques, 2017). This approach makes it possible to analyse the systems one-by-one and ensure a functionally resilient design regardless

of its complexity. The fundamental assumption is that if all functions in the relevant chain can be fulfilled, the capability in question is secured.

The vulnerability analysis is focused on the overall design philosophy of a system and location of components. The system model is constructed on an even higher level where each system as a black box with allocated functions. Generic representation of systems, functions, and functional exchanges is shown in Figure 1. In this diagram the crew is modelled as a logical actor (external to the system but interacting with it), whereas the ship is acting as a container for the systems being analysed. Both the logical actors and systems have functions allocated to them and interact with each other by the means of functional exchanges (shown as arrows), which represent an interaction (e.g., exchange of matter or information) between two functions.

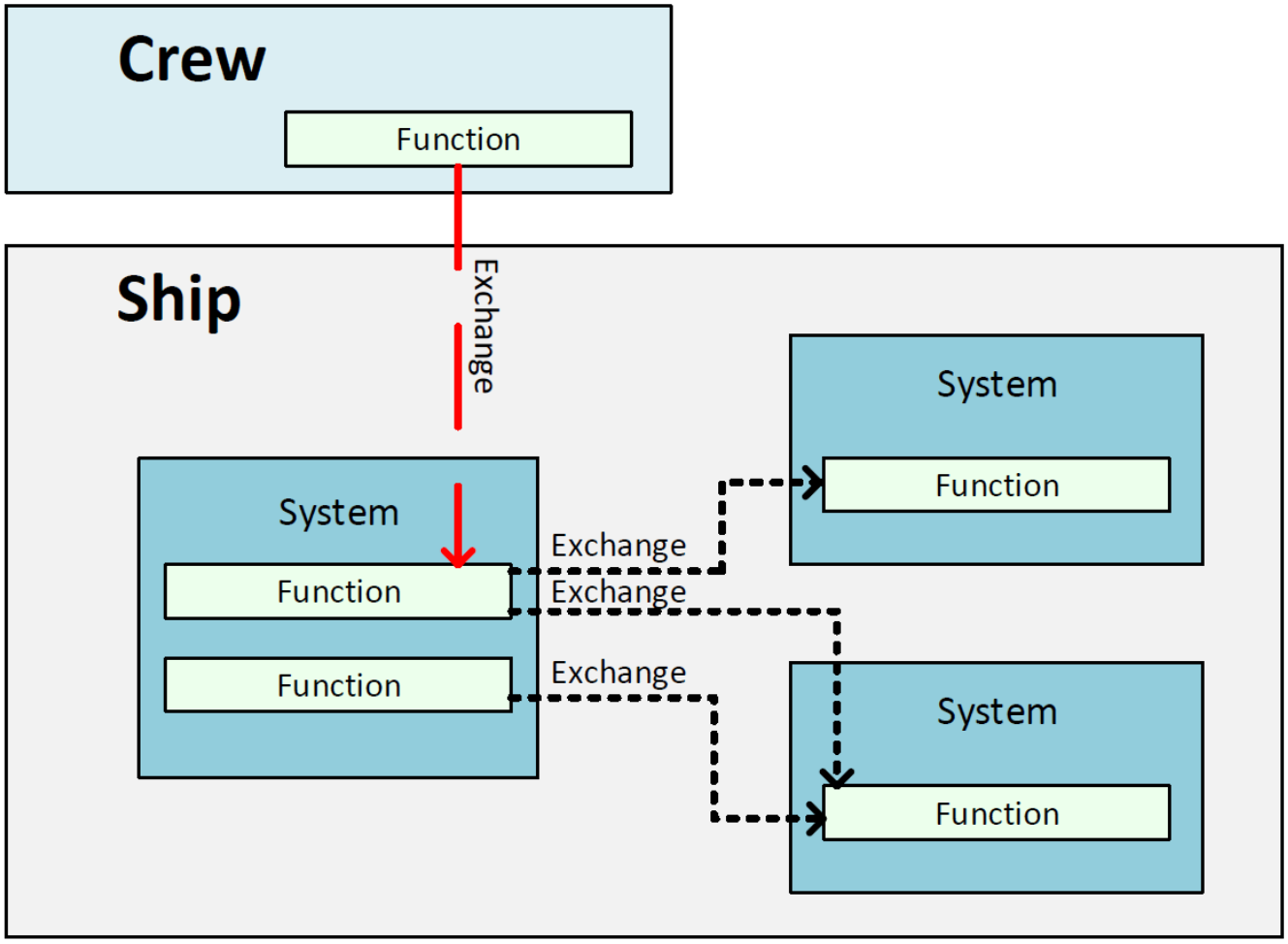

Figure 1. Generic representation of systems, functions, and functional exchanges

Definition of residual capability

It can be expected a damaged ship will not have the same capabilities as an intact one. Thus, vulnerability reduction effort should start by defining the minimum required residual capabilities after a damage event. These residual capabilities describe which functionalities of the vessel must remain available even after sustaining damage. Normally, several capability levels will be specified, with fewer functionalities required for increasing severity of damage. In this paper, two levels will be used, corresponding to arbitrarily defined small hit and large hit. The assumptions relating to threats are discussed in the next section.

Based on the system model, the functional chains contributing to the specified residual capabilities are evaluated and the functions which need to be preserved are classified as vital. By extension, the systems fulfilling these functions are also classified as fully or partially vital, i.e., only the parts of the systems supporting the residual capabilities are considered vital. The degree to which a system can fulfil its function after damage (in degraded state) is referred to as residual performance.

At the initial design stages, the residual capability may be stated as simply as “The vessel shall be able to propel itself and control its heading after a small hit”. As the design matures and trade-offs are better understood, more precise level of residual performance can be specified, e.g., that the speed of 5kn must still be achievable after a small hit. As such, the capability-driven approach does not force a specific arrangement, instead giving system designers freedom to choose the best solution. As long as the residual capability objective can be met in the damaged state, the outcome of the analysis would be considered satisfactory.

Assumptions of damage effects

As mentioned in the previous section, the residual capability levels correspond to threat levels, i.e., the assumed weapon threats from which the ship needs to be protected. The selection of these design threats and calculation of their effects is beyond the scope of this paper. To demonstrate the following stages of the analysis, two threat levels are specified: a small hit is defined as damage to one compartment (volume between two consecutive decks and two consecutive watertight bulkheads), whereas a large hit includes multiple compartments. The weapon impact can occur in any location above the waterline, resulting in an array of damage cases to be calculated and evaluated in the analysis.

Due to inherently unpredictable nature of explosions, it is infeasible to predict, which equipment in the damaged compartments will be affected. While there are methods which can provide a finer estimate of failure, they are overly time-consuming to be applied for every investigated damage scenario. Therefore, a conservative assumption is that all the equipment, cabling, and piping located in these spaces may be destroyed, reflecting the worst-case scenario. It is worth noting that less pessimistic assumptions can be made for small-calibre ballistic threats, but these are not considered in this paper.

Effects of damage on residual capability

The damage effect analysis is used to determine the residual performance of the ship after battle damage and, if it is not satisfactory, the measures required to increase the survivability of the ship. All the vital systems are individually analysed for the impact of each damage case. Two types of system degradation are considered after battle damage: through direct damage, when system components are located in an affected compartment, or degradation following a failure of a support system (providing an essential consumable or control to the system in question). The indirect cases are mentioned during an analysis, but mostly function as a quality check, since they will also be identified when the damage effects on the relevant system are evaluated. In certain cases, the loss of a function might be acceptable as long as it can be compensated by another system, thus avoiding a complete loss of the vital capability, since there is a functional back-up.

Vulnerability analysis generally focuses on the worst-case scenario for each system. In practice, residual performance after a hit is likely to be higher than the guaranteed minimum. Besides proving that the minimum required performance is met, the capability-driven approach gives the designer and the user comprehensive understanding of the consequences of damage in various areas and the potential impact on damage control and residual capability. To demonstrate the practical implications of this theory, the next part illustrates the strategies and principles listed above in a case study.

GENERIC CASE STUDY – FIRE FIGHTING

This example shows the analysis of a simplified firefighting case on a fictitious ship. The goal of the analysis performed in this case study is to demonstrate that the residual capability of firefighting remains available after battle damage by proving that all functions contributing to this capability can still be sufficiently fulfilled. A large hit damage case was chosen, as it affects a wider range of systems, therefore making the vulnerability analysis more complex. Both the damage case and the functional chain describing the capability are provided as an input and their development is not discussed in detail.
The following sub-sections correspond to the three steps of the process: functional chain analysis, damage extent analysis, and damage effect analysis.

Functional chain analysis

The functional chain analysis breaks down the process of firefighting into the contributions of the different systems and/or actors. Following the specification of residual performance level required, the system model describing the normal operation is adapted to only contain the functions required after battle damage. Figure 2 shows the functional chain describing firefighting during normal operation, with different line styles corresponding to different exchange media. The interactions between the crew and the functions assigned to the crew are outside of the scope of this paper and are therefore modelled in a

very simplistic manner. The detailed explanation of contributing systems and functions if provided in the subsequent paragraphs.

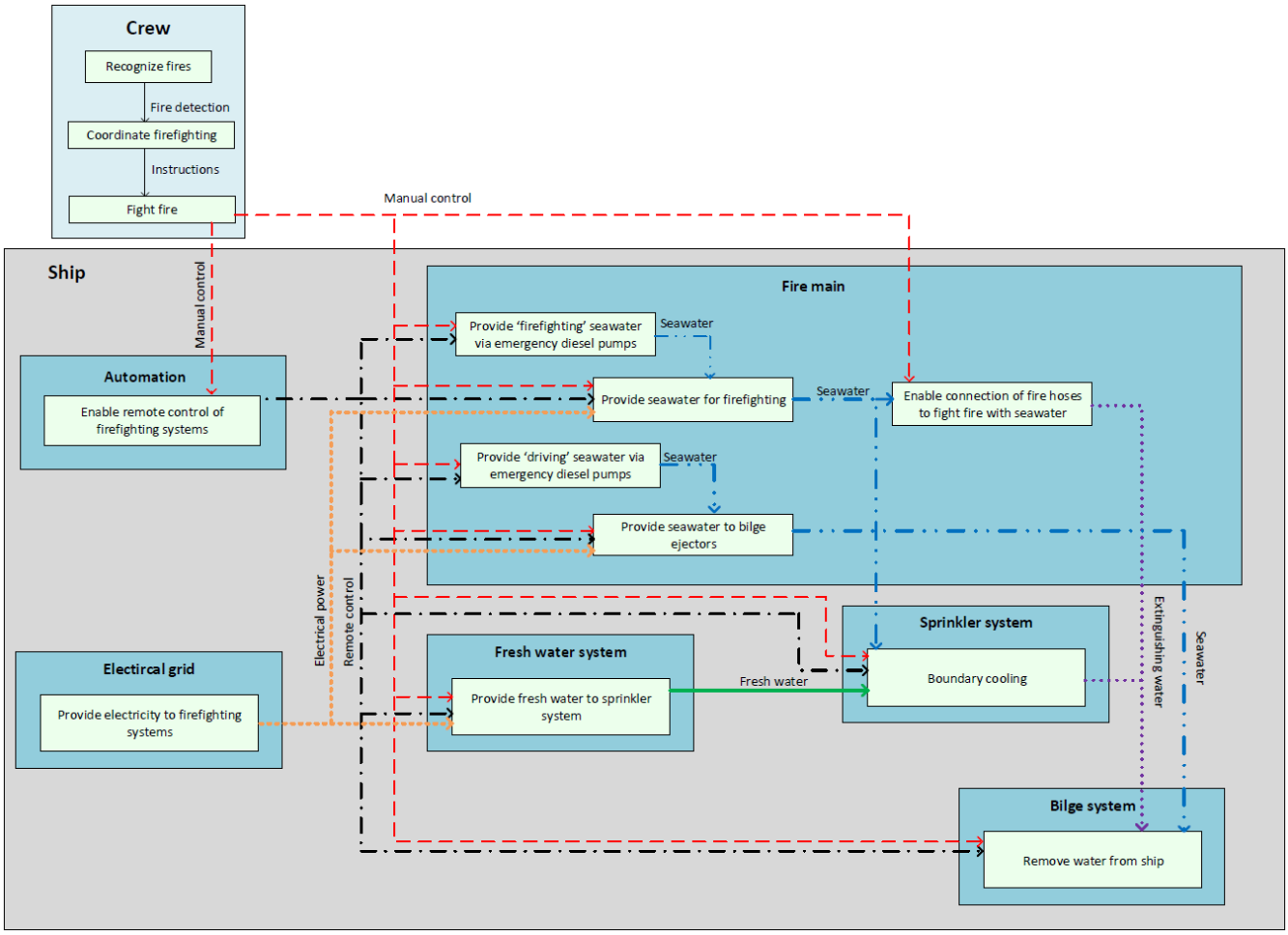

Figure 2. Simplified diagram of functional chain Firefighting

Firefighting during normal operation

In this scenario, the ship is sailing through friendly waters on the way to a deployment area. It is a quiet night and most of the crew are resting, except those on watch. During a routine patrol of the vessel, a petty officer smells a hint of smoke in the passageway and follows the scent to find that a fire had broken out inside an unmanned machinery space. The fire is clearly too big to put out with a fire extinguisher, so he immediately reports this to his superior officer. The alarm is raised and the officer gathers a firefighting team, coordinates a response strategy, and the crew promptly start firefighting using the onboard systems.

On this ship, fire hoses serve as the primary means of firefighting. The crew will normally use the hydrant located in the affected compartment or, if inaccessible, connect the fire hoses to the hydrants in adjacent compartments. The fire hoses are sufficiently long to span multiple compartments.

If fire is present in a compartment adjacent to an ammunition store, the store will require boundary cooling as a safety precaution to prevent an explosion. This is achieved with a sprinkler system which can cool the room using the fresh water supply or seawater as an emergency backup solution. Activation of the system is done either from one of the command spaces via the automation systems or by a local panel.

The build-up of extinguishing water, from both firefighting and boundary cooling, is removed from the ship via ejectors which are part of the bilge system. These bilge ejectors utilize the Venturi effect to enable the intake of water. To do so a driving medium is required, which in this case is seawater provided by the fire main.

During normal operation, the crew will activate all the electric pumps required for water supply via the integrated platform management system (IPMS), or alternatively every system can also be manually activated on the location. Two diesel-driven seawater pumps are available in case of a power outage.
Coming back to the firefighting crew, with all systems are available and functioning correctly, it only takes a few minutes for the personnel to take control and safely extinguish the fire. None of the crew suffered any injuries, but the damage is significant enough that the vessel will need to stop for emergency repairs at a friendly port. After a few weeks, she will be able to sail again and resume deployment.

Firefighting with a ship damaged in battle

Following the unscheduled maintenance due to the previous fire, the ship is back to full availability and continues the mission: protecting a vital trade route from pirates and other armed groups. Not long after the vessel and the crew arrive in the area, one of key countries in the region is shaken by a coup-d'état putting a hostile military dictatorship in power. The immediate collapse of diplomatic relations and escalation of the political conflict leads to something that would have been unthinkable just weeks prior. The hostile regime sends a barrage of anti-ship missiles towards the vessel. Three missiles are tracked and eliminated by the self-defence systems, but one gets through – the ship is hit.

After the initial impact, the crew promptly assess the severity of the situation. Again, a petty officer sees a fire inside the affected compartments and reports it to his superior. Clearly the blast has damaged most components, cabling, and piping in the affected compartments, so the performance of firefighting systems is now degraded. The question arises: will the crew be able to control and extinguish the fire?

To ensure that the vessel can fulfil the vital residual capability of firefighting, the relevant functions must be identified. They can be defined based on the normal operation, by determining which functions are considered essential after battle damage and, as such, require protective measures. This rationale causes several functions (from the 'normal' functional chain) to be labelled as non-essential. In this case, the loss of electrical power is acceptable thanks to the diesel-driven back-up for the electrical fire pumps. Similarly, remote control (provided by IPMS) is not essential since all required equipment can also be controlled manually.

The freshwater system has also been marked as non-vital, but for a different reason. The preferred medium for boundary cooling is indeed freshwater as it is less corrosive than seawater. Freshwater is however considered a limited resource as it takes time and energy to produce it, therefore the sprinkler system is also connected to the fire main as a backup, since seawater can be supplied virtually indefinitely. Marking the freshwater system as a vital system would imply that protective measures need to be provided to the system. This would likely entail either a redundant system layout or local protection. Both options would come with severe penalty to weight and space. The fire main is already designated as a vital system due to the seawater requirement of the hydrants and of the bilge system. Adding another consumer to the list will not result in a dramatic increase of the weight of the ship nor will it take significant space within. The preferred solution is to prioritize protection of one system instead of two.

All systems that are allocated a vital function are now considered vital systems. Therefore, the vital systems are the fire main, the sprinkler system and the bilge system. The remaining functions are considered required for the residual capability and are summarized (together with the systems they are assigned to) in Table 1.

Table 1. Functions forming the residual capability Firefighting

Vital System	Function
Fire main	Provide 'firefighting' seawater via emergency diesel pumps
Fire main	Provide seawater for firefighting
Fire main	Enable connection of the fire hoses to fight fire with seawater
Fire main	Provide 'driving' seawater via emergency diesel pumps
Fire main	Provide seawater to bilge ejectors
Sprinkler system	Room cooling
Bilge system	Remove water from ship

Damage extent analysis

During the damage extent analysis, the areas that are affected by weapon impact are determined, based on the specified design threat, vessel arrangement, and a set of assumptions. Only one battle damage event is considered at a time and the secondary effects, in this case fire, will only affect the damaged area.

In the scenario being analysed, a single damage case is evaluated; a missile hit in compartment C IV. This is considered a large hit affecting multiple compartments. The damaged area of the fictitious ship used in this case study is shown in Figure 3.

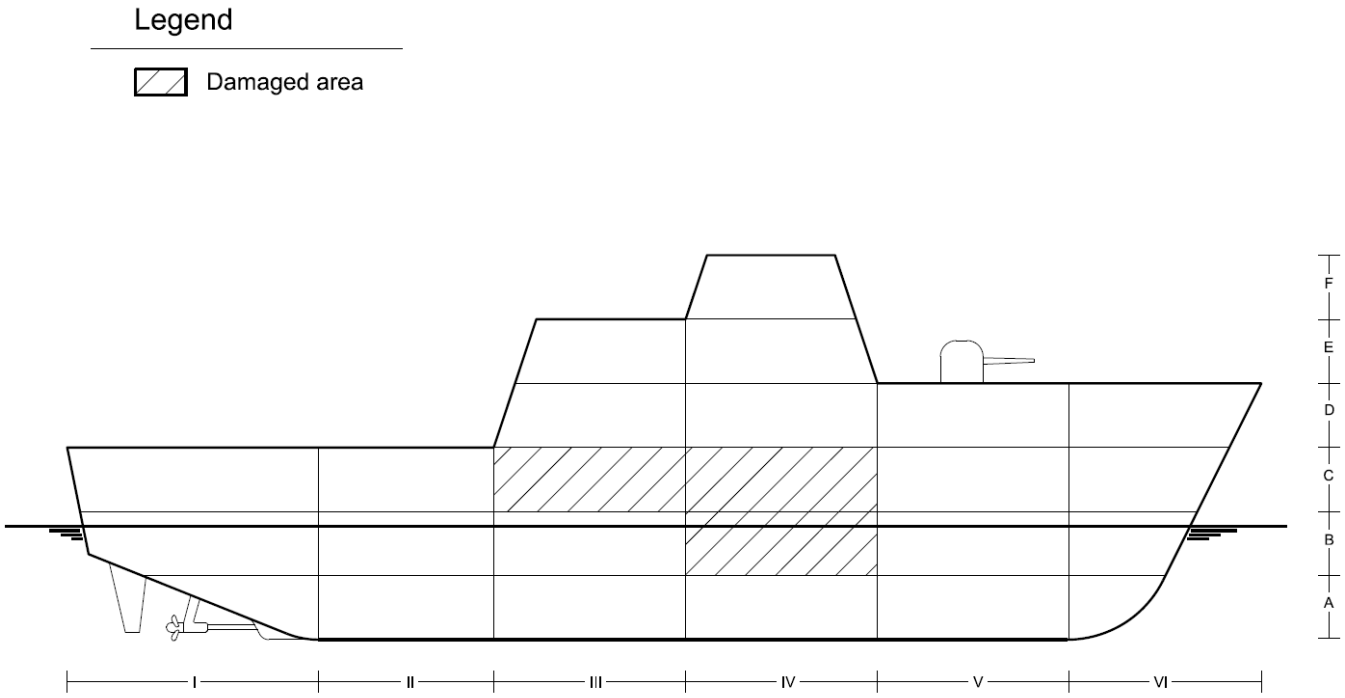

Figure 3. Side view of a vessel showing large hit damage

Damage effect analysis

All the vital systems are individually analysed for the selected damage case. Firstly, a brief description of the functions allocated to the system and the minimum expected performance of the system is provided, followed by description of the system layout and dependencies, and lastly performance after damage is discussed. The systems are discussed in the order of increasing complexity and the number of dependent systems: the sprinkler and the bilge systems are analysed first, followed by the evaluation of the supporting system fire main.

Sprinkler system

The sprinkler system only has one function which is to cool the ammunition room in case of fire in an adjacent space. This is also considered to be the minimum required functionality.
The layout of the system is given in Figure 4. To fulfil this function the system consists of branches with open nozzles (modelled as black bulbs) within the ammunition store. A valve is opened to allow seawater to enter the branches from the fire main (red flag).

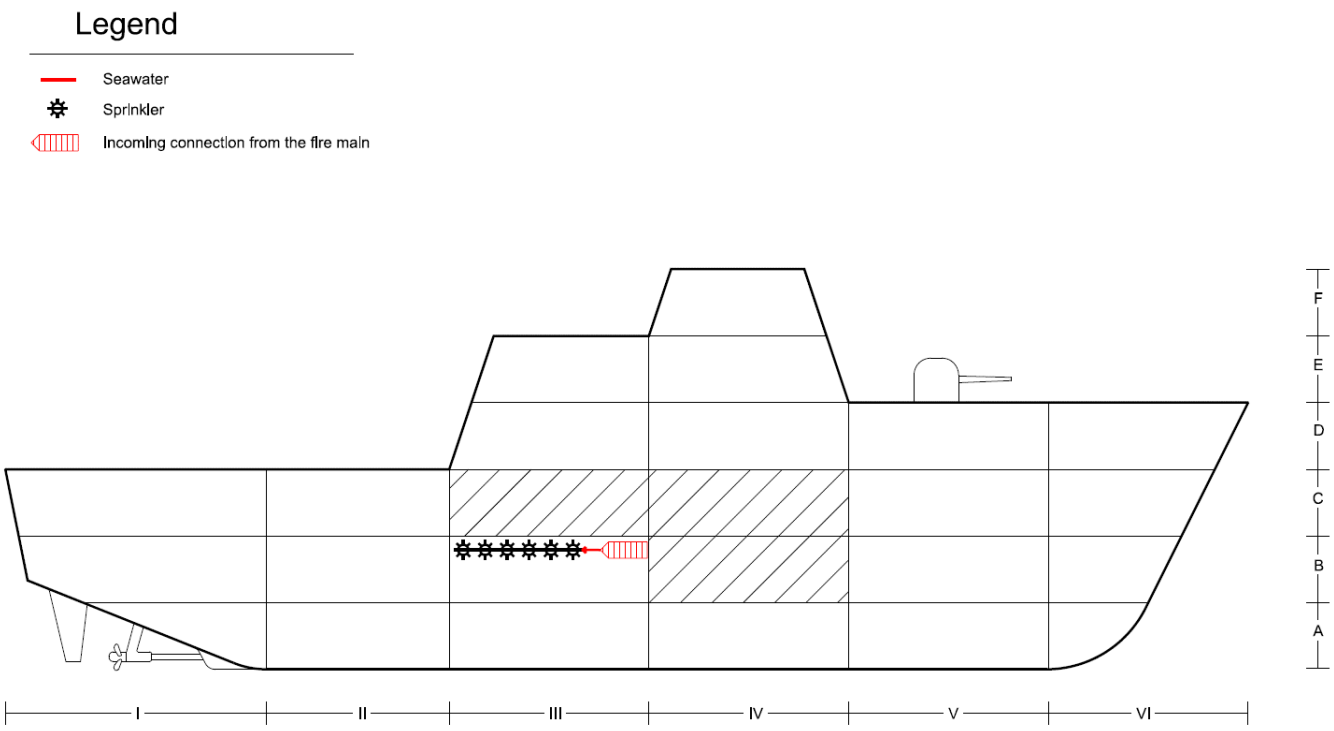

Figure 4. Layout of the sprinkler system

According to the system model, the sprinkler system is dependent on the crew, the automation system, the freshwater system, and the fire main. The sprinkler system requires the crew to activate the system and the fire main to provide a cooling medium to function properly. Automation, the electrical grid, and the freshwater system have been marked as non-vital and thus should be assumed to no longer provide any support towards the sprinkler system, i.e., full degradation is allowed. The dependencies of the system have been summarized in Table 2.

Table 2. Dependencies of the sprinkler system on other systems

System	Provision towards the sprinkler system	Allowable degradation	Effect of full degradation
IPMS (Automation)	Means of starting/stopping the boundary cooling.	Full degradation allowed	The crew will have to start and stop the system locally.
Crew	Means of starting/stopping the boundary cooling.	No degradation allowed	No means of starting or stopping the system.
Freshwater system	Provision of fresh water as a cooling medium.	Full degradation allowed	The sprinkler system will use seawater as a cooling medium.
Fire main	Provision of seawater as a cooling medium.	No degradation allowed	The sprinkler system no longer receives a cooling medium.

The system itself is located outside of the damaged area and therefore remains intact. This damage case does not prevent the system from fulfilling its function and therefore the performance is sufficient.

Bilge system

According to the system model, the bilge system is required to remove the water that has collected on A-deck from the ship. After battle damage, the source of this water will be from both boundary cooling and firefighting. The minimal required performance after any damage case is the ability to remove water from every watertight zone. The system layout of the bilge system is shown in Figure 5.

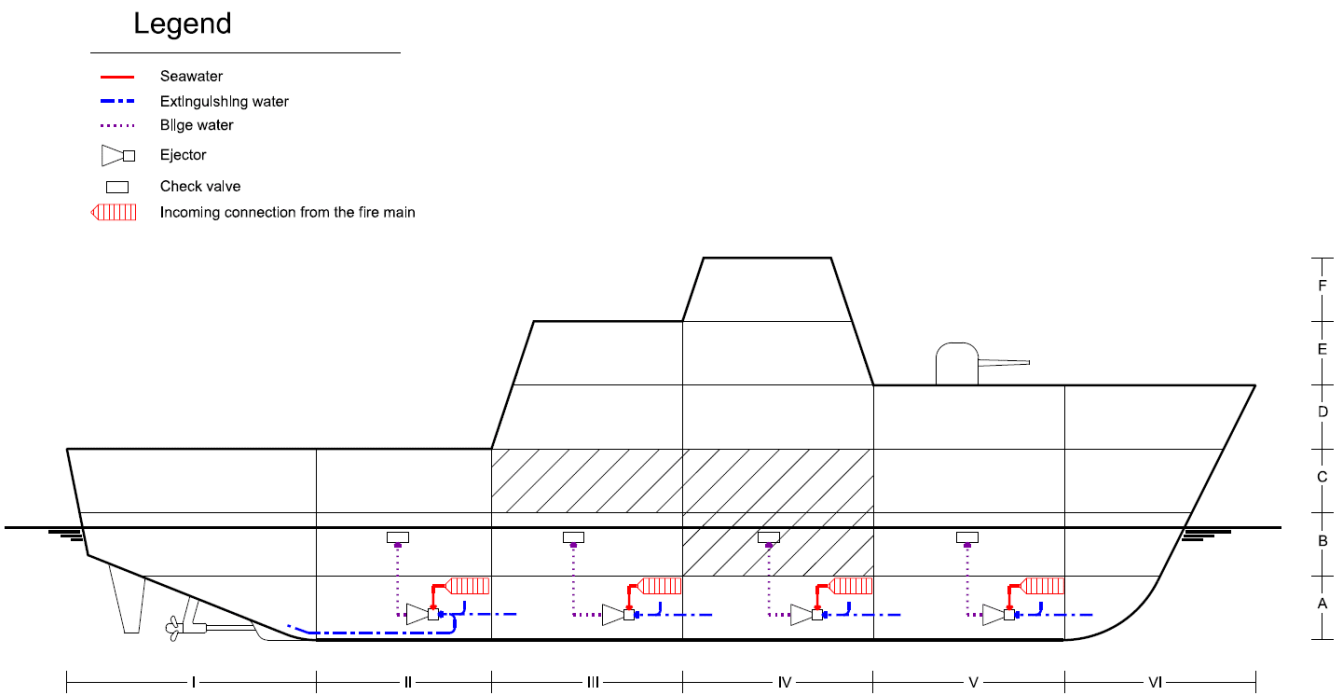

Figure 5. Layout of the bilge system

The system consists of four bilge ejectors which remove water from their corresponding compartment via suction lines (marked blue). Additionally, each ejector can drain the adjacent compartment forwards of the one it is placed in via an emergency suction line. The ejector located in compartment A II also has a suction line connecting to the aftmost compartment. When a valve is opened, the driving seawater (marked red) flows through the bilge ejector which starts removing water from the compartment. The mix of removed and driving water (marked purple) is then ejected from the ship via check valves in the decks directly above the bilge ejectors.

The bilge system depends on the crew to activate the system and on the fire main to provide a driving medium. Similarly to the sprinkler system, the IPMS is not required thanks to the back-up local control. Table 3 gives an overview of the system dependencies.

Table 3. Dependencies of the bilge system on other systems

System	Provision towards the sprinkler system	Allowable degradation	Effect of full degradation
Automation	Means of starting/stopping the bilge system.	Full degradation allowed	The crew will have to start and stop the system locally.
Crew	Means of starting/stopping the bilge system.	No degradation allowed	No means of starting or stopping the system.
Fire main	Provision of seawater as a driving medium.	No degradation allowed	The bilge system will not be able to remove water without a driving medium.

One of the check valves and its connected piping is damaged in this example. Thus, water cannot be removed via that compartment. However, the emergency connection is still available to remove water from compartment A IV.

The system can still remove water from every watertight compartment. The minimum performance is thus met, and the degraded state is considered acceptable.

Fire main

Most functions for this residual capability are assigned to the fire main. These functions can be summarized as providing seawater to the firefighting systems and allowing the connection of fire hoses. The minimum performance of this system is more complicated than the previous two systems as the fire main is a support system. The layout of the fire main is shown in Figure 6.

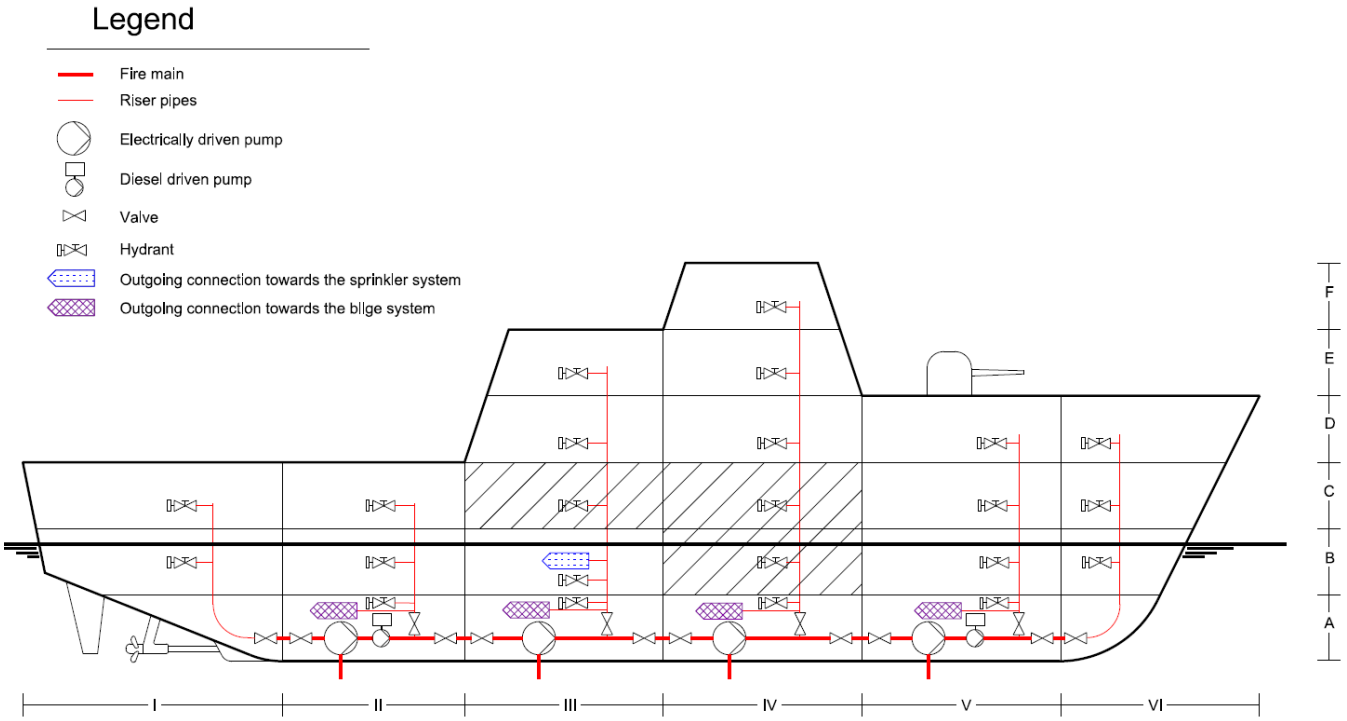

Figure 6. Layout of the fire main

Fire hoses are the primary means of firefighting, the minimum performance for the fire main is therefore the availability of a functioning fire hydrant in at least one compartment adjacent to every damaged compartment.

The bilge system needs a driving medium and is required to remove water from every zone, however that does not imply that seawater must be available in all zones. For this damage case, the minimum performance of the fire main is the availability of seawater in zone II, III, and V, so that water can be removed from every zone. Lastly, the minimum requirement derived from the sprinkler system is the availability of seawater in compartment B III.

The system consists of four electrically driven pumps and two emergency diesel driven pumps. To fight fire, boundary cool one room, and remove water from the ship, a single pump (electrically or diesel-driven) is required.
A valve is provided whenever the fire main penetrates a bulkhead and all riser pipes are fitted with a valve at A-deck. A little flag is added to signify when a riser pipe is connected to a different system. Hydrants are provided in every compartment. Table 4 gives an overview of the dependencies of the fire main.

Table 4. Dependencies of the fire main on other systems

System	Provision towards the sprinkler system	Allowable degradation	Effect of full degradation
Automation	Means of starting/stopping the (emergency) pumps.	Full degradation allowed	The crew will have to start and stop the system locally.
Crew	Means of starting/stopping the (emergency) pumps.	No degradation allowed	No means of starting or stopping the system.
Crew	Manual connection of the fire hoses and firefighting.	No degradation allowed	No means of fighting fire.
Electrical grid	Provision of power towards electrical firefighting pumps.	Full degradation allowed	Emergency diesel driven pumps will provide seawater for firefighting.

The system requires electrical power for its four main pumps. The generation of power is not guaranteed as it is not marked as a vital system for firefighting, as such it should be assumed that the main pumps are not available. The crew will therefore activate the emergency diesel-powered pumps.

Two riser pipes are located in the damaged area, so these riser pipes will be closed off to isolate the damaged part of the system. The function to fight fire with hoses remains available as the compartments adjacent to the damaged area are equipped with working hydrants that can provide seawater. However, seawater cannot be supplied to the sprinkler system in compartment B III or the bilge system in compartments A III & A IV, since they are connected to the closed-off riser pipe. The functions "Provide seawater to bilge ejectors" and "Provide seawater for firefighting" are not fulfilled. This is not an acceptable performance, thus adjustments to the system are required to improve the availability of seawater.

The supply of seawater towards the bilge system must be evaluated. As discussed before, part of the bilge system is located in the damaged area, therefore the bilge ejector located in compartment A IV will remain unavailable even if seawater is supplied. However, the ejector located in compartment A III has an emergency suction line to compartment IV. Both compartments A III and A IV can thus be emptied if the bilge ejector in compartment A III is supplied with seawater. An additional valve could increase the availability of the seawater supply.

The supply of seawater to the sprinkler system must not be compromised. A solution could be either a second pipeline routed to the sprinkler system or smart placement of an additional valve. The pipeline is not the preferred solution as it adds additional weight, takes up space and further adds to the complexity of the system. The recommended solution would be placing an additional valve in the riser pipe located in compartment B III above the connection to the sprinkler system, as shown in Figure 7. This would ensure the availability of seawater to both the bilge system and the sprinkler system. With the additional valve implemented all functions assigned to the fire main can be fulfilled to an acceptable standard.

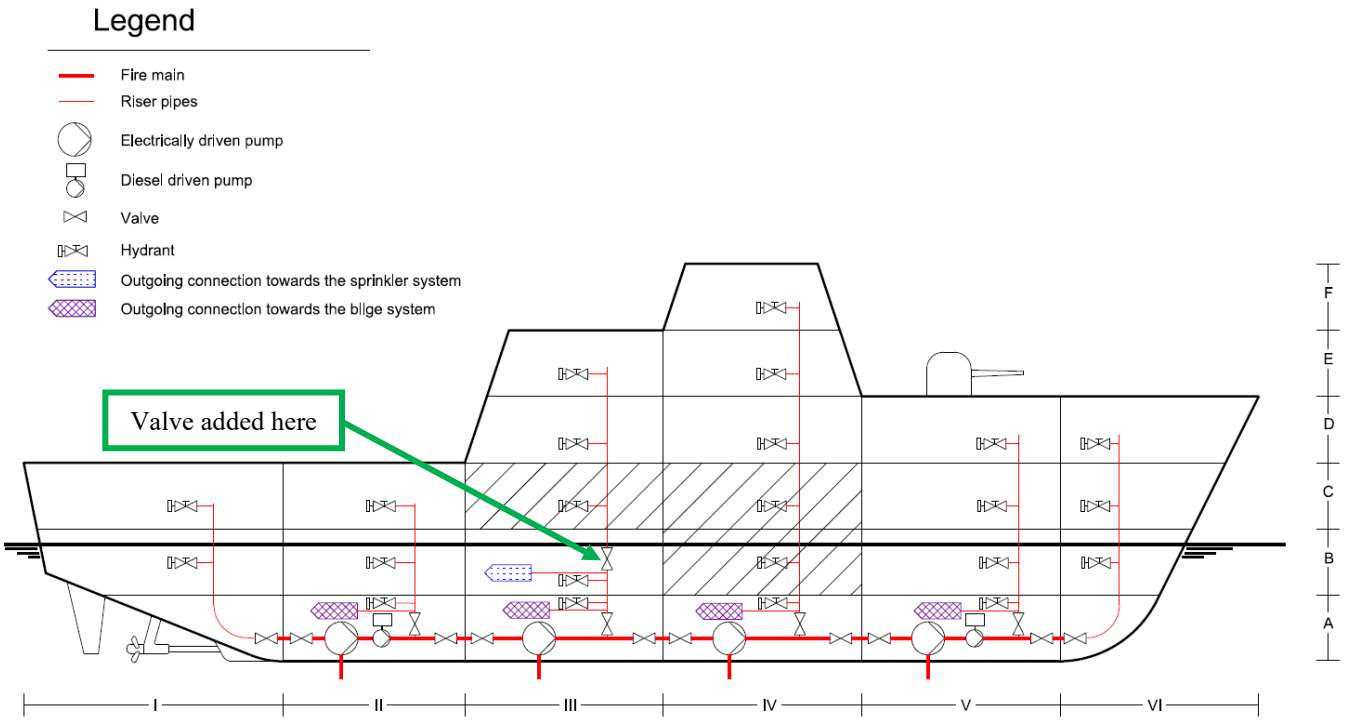

Figure 7. Placement of the additional valve based on vulnerability analysis

Firefighting after battle damage

Luckily for the crew, this comprehensive system vulnerability assessment had been completed on the design stage and the additional valve is present. The commanding officer leading the firefighting operation is well-aware of the design of the vessel and the damage control response required to ensure the performance of the firefighting systems.
The officer orders one of his crewmates to close the valve in the riser pipe located in compartment B III and open the valve connected to the sprinkler system located in the same compartment. He directs another crewmate to open the valve connected

to the bilge ejector located in A III. Two people are sent to start the diesel-powered pumps and the remaining firefighting crew are set to fight the fire within the compartment using the fire hoses. Even with fewer systems available, the crew are able to extinguish the fire successfully, keeping the ammunition store intact.

Since the ship sustained severe structural damage from the missile impact, she will require major repairs before returning to service. The important thing is that the platform was salvaged and the crew members are able to make it home safe and sound and live to sail another day.

CONCLUSIONS

The example showed that with minimal changes to the design, the survivability of the ship could be significantly increased, whilst avoiding unnecessary penalties to other design aspects. It is worth stressing, that the example only considers one capability, a small selection of systems and a single damage case. Naturally, the complexity of the analysis increases as more vital capabilities, systems, and damage cases are included. Nonetheless, by employing the approach presented in this paper, it is possible to break up the analysis into manageable parts and evaluate ship's resilience in a logical and structured manner. The functional model serves as an excellent tool to determine how degradation of individual functions is detrimental to the required residual capability. Overlaying this information with the calculated damage extents results in an analysis that focuses on the protecting the functionality of the ship rather than individual components. This fine-tuned approach to vulnerability analysis makes it possible to deliver more resilient and better optimised designs in a cost-efficient manner.

CONTRIBUTION STATEMENT

Michal Czop: investigation; methodology; writing – original draft; writing – review and editing.
Demi van Megen: conceptualization; investigation; methodology; writing – original draft; visualisation.
Koen Droste: conceptualization; investigation; methodology; supervision.

ACKNOWLEDGEMENTS

We extend our heartfelt gratitude to the following colleagues who played pivotal roles in the development and success of this work:

Jitte van Dijk and **Marijn Hage**: Their invaluable expertise in system modelling elevated the quality of the theoretical foundations of the paper. Furthermore, their dedication and insightful feedback significantly contributed to the overall quality of the work.

Rob de Gaaij and **Sander Allefs**: On the discipline front, Rob and Sander provided encouragement, guidance, and institutional support which made the creation of this paper possible. We appreciate their commitment to our shared vision.

Additionally, we would like to recognise **Damen Naval** for providing the time and resources necessary to complete and present this work to the IMDC.

REFERENCES

Voirin, J.-L. (2017). Model-based System and Architecture Engineering with the Arcadia Method. Elsevier.

Roques, P. (2017). Systems Architecture Modeling with the Arcadia Method: A Practical Guide to Capella. ISTE Press.

Proceedings of 15th International Marine Design Conference (IMDC-2024)
June 2-6, 2024
Amsterdam, the Netherlands

A comparative analysis of side and stern installation of a monopile lifting operation using a heavy lift crane vessel

A.M. Elzinga [1,2,*], J.D. Stroo [2], and A.A. Kana [3]

ABSTRACT

This paper compares two 2XL monopile installation methods: at the leeward side of the heavy lift crane vessel and in the recess at the stern of the vessel. The multi-body system of the vessel, monopile, crane, and mission equipment induces interaction and resonance behaviour. Operational limits are assessed at the crane tip and pile gripper during upending and lowering of the monopile. Stern installation provides a larger operability window during upending compared to side installation. During the lowering stage, the operability depends on the monopile submergence: side and stern installation provide a comparable operability. Considering both stages, stern installation shows promising results.

KEY WORDS

Heavy lift vessel; monopile; installation method; allowable sea states; time-domain simulation

INTRODUCTION

The offshore wind energy sector is rapidly growing with an increase in the capacity of offshore wind turbines (OWT). This implies an increase in size and weight of OWTs. Additionally, there is a tendency to locate offshore wind farm sites further offshore. More consistent wind speeds, and therefore better quality wind resources, and more space are available further offshore. Sites with a water depth of less than 70 metres are suitable for OWT-fixed bottom foundations. The increasing capacity and greater water depth at OWF locations result in increasing OWT, and therefore also the foundation of the OWT (Ulstein, 2019). A commonly applied fixed-bottom foundation is the monopile. 65% of the fixed-bottom foundations worldwide are monopiles (MP). In the planning phase, 88% of the fixed-bottom foundations are monopiles, due to their simplicity, ease of installation, and relatively low costs (Inernational Energy Agency, 2019; Liu, 2021; Ramírez et al., 2020). Over the past years, the diameter of an MP, an indicator for its size and weight, increased from an average of 5 metres to 10-12 metres. Monopiles are categorised into L, XL, XXL (2XL), and XXXL (3XL) monopiles. 2XL monopiles have an average diameter of 10 metres and a weight of around 2500 tonnes (Stroo, 2023a).

Monopiles are typically installed from jack-up vessels, which provide a stable platform. However, these vessels are limited in terms of water depth, seabed conditions, and crane capacity. The ever-growing monopiles need to be installed from floating vessels, such as a heavy lift crane vessel (HLV). Heavy lift crane vessels are not dependent on the water depth, seabed conditions, or the crane capacity due to the absence of the extendable legs of a jack-up vessel. During installation, the heavy lift crane vessel forms a multi-body system with the crane and monopile, inducing coupled dynamic behaviour. Pendulum effects of the monopile might occur. The current method to install an MP from a heavy lift crane vessel is at the

[1] Department of Maritime and Transport Technology, Delft University of Technology, Delft, The Netherlands
[2] Ulstein Design & Solutions B.V., Rotterdam, The Netherlands
[3] Department of Maritime and Transport Technology, Delft University of Technology, Delft, The Nederlands; ORCID: 0000-0002-9600-8669
[*] Corresponding Author: anke.marij.elzinga@ulstein.com

Submitted: 8 March 2024, Revised: 27 April 2024, Accepted: 3 May 2024, Published: 16 May 2024

Conference paper, DOI: https://doi.org/10.59490/imdc.2024.822 e-ISSN: 3050-4864

leeward side of the vessel. The monopile is placed transversely on deck and upended to a vertical position at the starboard side of the vessel, after which it is lowered towards the seabed. The vessel creates a shielding effect. This method is called side installation. A new development is stern installation (Stroo, 2023b). The MP is placed longitudinally on deck and is upended in the centre line of the vessel. The lowering of the MP takes place in a recess at the stern of the vessel, creating a shielded environment. This principle can be compared to the installation concept of pipe layers.

The lowering stage of the monopile installation is considered as a critical event (Li et al., 2015; Guachamin-Acero et al., 2016; Chen et al., 2022). The multi-body system of the vessel, monopile, crane, and mission equipment induces interaction and resonance behaviour might occur. Therefore, it is important to assess the operational limits. Moreover, it is required to assess these limits during marine operations in the planning phase. The purpose of this paper is to present a comparison between side and stern installation using a heavy lift crane vessel during upending and lowering of an XXL monopile (2XL MP) in terms of operational limits.

METHOD & TOOLS

A general evaluation method is defined to establish the operational limits of an installation method, which can be applied parallel to multiple installation methods. Two different installation methods are evaluated for the same vessel and mission equipment. The design of the hull and mission equipment, such as the crane and pile gripper, are not a part of this study. Therefore, this evaluation method focuses on the effects of different installation methods on the dynamic behaviour of the coupled HLV-MP system.

The installation sequence of the method needs to be defined, where after the key positions of the sequence are established. The loading condition of every key position is calculated and the loading conditions are applied. The floating equilibrium needs to be found for every loading conditions. If realistic, the hydrodynamic properties of the loading condition are generated. The response at the relevant positions, obtained by numerical simulations, is analysed of which then the key critical positions are identified. The most critical positions may be reviewed again in more detail. The operational limits are obtained from the response, leading to a comparison between the two monopile installation methods. The method is presented in a flowchart in Figure 1. The loading conditions are based on existing loading conditions, generated in DELFTship. The applied loading conditions are calculated in Excel, which is also used for pre- and post-processing the results. HydroD, a diffraction programme, is used to calculate the load and displacement RAOs, added mass and damping matrices. The numerical time-domain simulations are performed in OrcaFlex, a package for dynamic analysis of offshore marine systems.

CASE STUDY

Hornsea Offshore Wind Farm on the North Sea is used as a reference project. Monopiles are installed at a water depth of 68 metres, the largest known water depth for MP installation, based on 4C Offshore data (2022). The environmental data is based on the wind and wave characteristics of the North Sea. The JONSWAP spectrum is applied as wave spectrum. For the wind speed spectrum, the NPD wind speed spectrum is applied. For side installation, the wave direction is 210° to create a shielding effect, according to the angle definition as defined in Figure 2. For stern installation, the wave direction is 180°. Wave spreading and current are excluded. Significant wave height, H_s, values of 2 and 3 metres are chosen. Figure 3 shows the seasonal mean H_s, with the upper red dot representing Hornsea Wind Farm. During spring and summer, a mean H_s of 1.5 metres is observed. During autumn and winter a mean H_s of 2.5 metres is observed.

The spectral peak period T_p is varied between 5.0 and 15.0 seconds, as presented in Table 1. This range is chosen based on wave scatter diagram, as presented in Figure 4, and the hindcast data of Hornsea Wind Farm. The shorter wave periods around 5.0 to 8.0 seconds occur more frequently on the North Sea, due to the relatively small water depth. However, the larger wave periods are included in the case study to assess the dynamic behaviour for these environmental conditions and to put the results of the shorter wave periods into perspective. Additionally, by simulating these larger wave periods on purpose, the critical conditions can be assessed.

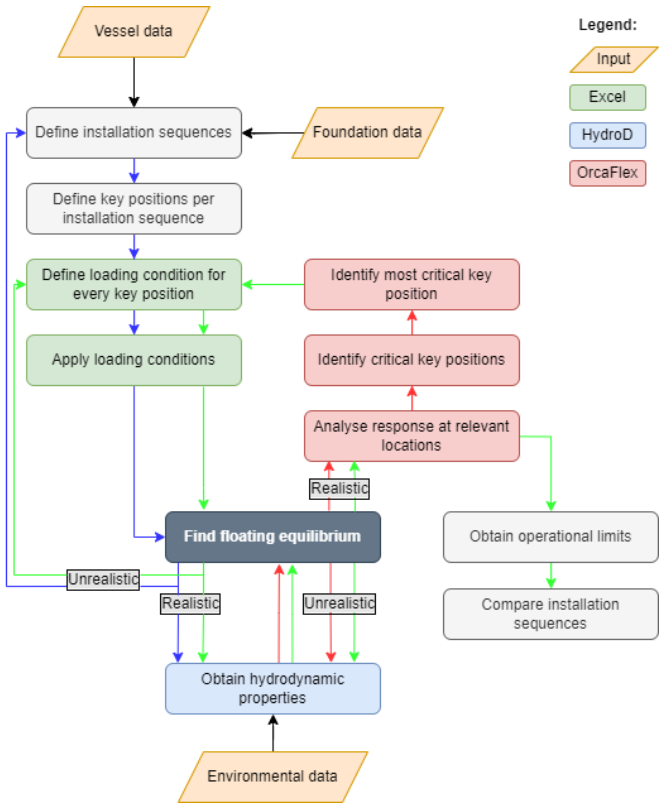

Figure 1: Flowchart of the applied method to establish the operational limits: from definition of installation sequences and loading conditions to analysis of responses at relevant locations and comparison of installation sequences.

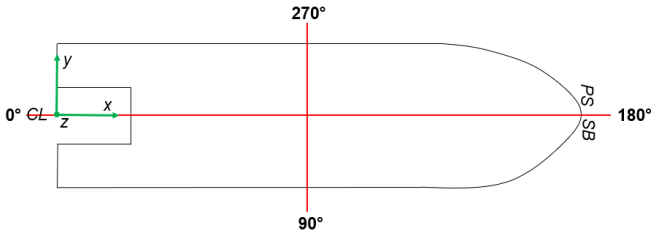

Figure 2: Angle definition for wave direction and slewing angle for the crane boom

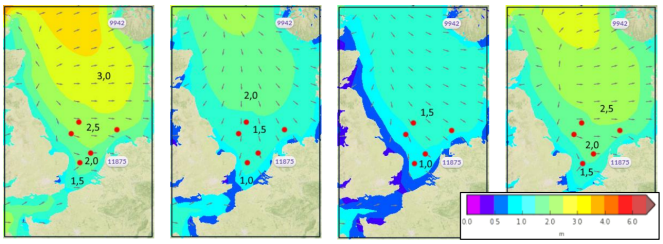

Figure 3: Seasonal mean H_s [m] in January - April - July - October on the North Sea with MetOcean View Hindcast (Brans et al., 2021; MetOcean Solutions, 2020)

Table 1: Range of simulated spectral peak period T_p [s]

T_p [s]	5.0	6.1	7.2	8.3	9.4	10.6	11.7	12.8	15.0

Percentage [%] of occurrence of joint significant wave height and zero up-crossing period for North Sea (zone 11)

Tp [s]	5,0	6,1	7,2	8,3	9,4	10,6	11,7	12,8	15,0	
Tz [s]	3,9	4,7	5,6	6,5	7,3	8,2	9,1	10,0	11,7	Sum [%]
0	0,00	0,00	0,00	0,00	0,00	0,00	0,00	0,00	0,00	0,00
1	6,69	12,65	10,53	5,37	2,01	0,55	0,15	0,04	0,00	37,98
2	1,23	5,05	7,86	6,76	3,95	1,65	0,62	0,21	0,02	27,35
3	0,21	1,48	3,59	4,44	3,53	1,97	0,93	0,38	0,05	16,57
4	0,03	0,38	1,33	2,21	2,25	1,58	0,89	0,43	0,07	9,16
5	0,01	0,09	0,43	0,93	1,18	1,00	0,66	0,36	0,07	4,74
6	0,00	0,02	0,13	0,35	0,54	0,55	0,42	0,26	0,06	2,32
7	0,00	0,00	0,04	0,12	0,22	0,27	0,23	0,16	0,05	1,09
8	0,00	0,00	0,01	0,04	0,08	0,12	0,12	0,09	0,03	0,49
9	0,00	0,00	0,00	0,01	0,03	0,05	0,05	0,05	0,02	0,21
10	0,00	0,00	0,00	0,00	0,01	0,02	0,02	0,02	0,01	0,09
Sum [%]	8,17	19,67	23,92	20,22	13,81	7,75	4,08	1,98	0,39	100,00

Hs [m]

Figure 4: Wave scatter diagram based on empirical data of the North Sea (zone 11) (DNV, 2021a)

The multi-body system consists of a vessel, monopile, crane, and pile gripper ring. The reference vessel is a heavy lift crane vessel developed by Ulstein, HX118, with a recess in the stern for both side and stern installation. The characteristics are presented in Table 2. The monopile is a 2XL monopile (Table 3). The mission equipment consists of a crane and a pile gripper ring, which is acting as a hinge. The mass moments of inertia of the crane boom and pile gripper ring are calculated using thick-walled theory of a cylinder. This complete multi-body system is visualised in Figure 5.

Table 2: Characteristics of heavy lift crane vessel

Characteristics	*HX118*
Length [m]	215.60
Beam [m]	57.40
Depth [m]	16.80
Max. deadweight [tonnes]	40000

Table 3: 2XL monopile characteristics

Characteristics	*2XL MP*
Length [m]	100
Diameter [m]	11
Mass [tonnes]	2300

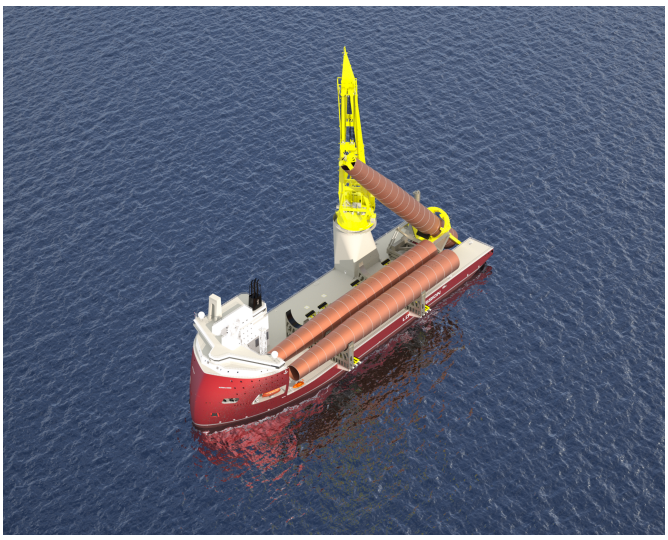

Figure 5: HX118 upending an MP in the stern

MODELLING OF COUPLED HLV-MP SYSTEM

This section discusses the modelling of the case study. The loading conditions for both installation methods are covered. Additionally, the modelling of the input data in OrcaFlex is presented, together with the used simulation approach.

Installation sequence

The upending and lowering process for side installation is schematically represented in Figure 6. Five loading conditions are set up: the monopile in horizontal position, the monopile 45° upended, a fully upended monopile, the monopile halfway the water depth (35 metres of submergence), and finally the monopile 3 metres above seabed (65 metres of submergence). The upper part of the monopile is guided by the crane. The lower end of the monopile is placed into the pile gripper, which acts as a hinge, and upending frame. The upending frame prevents the monopile from sliding through the gripper. After upending, the upending frame is removed by rotating 90°. When the monopile is fully upended, the monopile is still in the frame of the pile gripper ring. This results in a level of submergence of 5.56 metres. The pile gripper is lowered towards the water surface, the bottom support is opened and then the monopile is lowered.

The loading conditions corresponding to each stage of the installation sequence are established and are presented for side and stern installation in Table 4. The loading condition depends on the position of the monopile, and is defined for the stages depicted in Figure 6. The coding *GE-03-80%* stands for general departure empty, consumable tanks filled at 80%. *LI* implies a lifting condition with the main crane. The load is 2300 tonnes, at a certain radius from the centre of rotation of the crane in the horizontal plane. The lightship weight and deadweight are based on the loading conditions of the reference vessel HX118. The inertia terms are simplified by only taking the Steiner terms into account. The buoyancy of the partly submerged monopile is also excluded. The luffing and slewing angle are calculated based on the angle convention as depicted in Figure 2. The transverse centre of gravity (TCG) and longitudinal centre of gravity (LCG) are set to have zero list and trim by using a nonlinear solver varying the water ballast (and anti-heeling tanks). This nonlinear solver is a Generalised Reduced algorithm, which is an extension of the simplex method for linear programming (Lasdon et al., 1978). The corresponding vertical centre of gravity (VCG) and free surface moment (FSM) are calculated, based on International Maritime Organization (IMO) rules (International Maritime Organization, 2022).

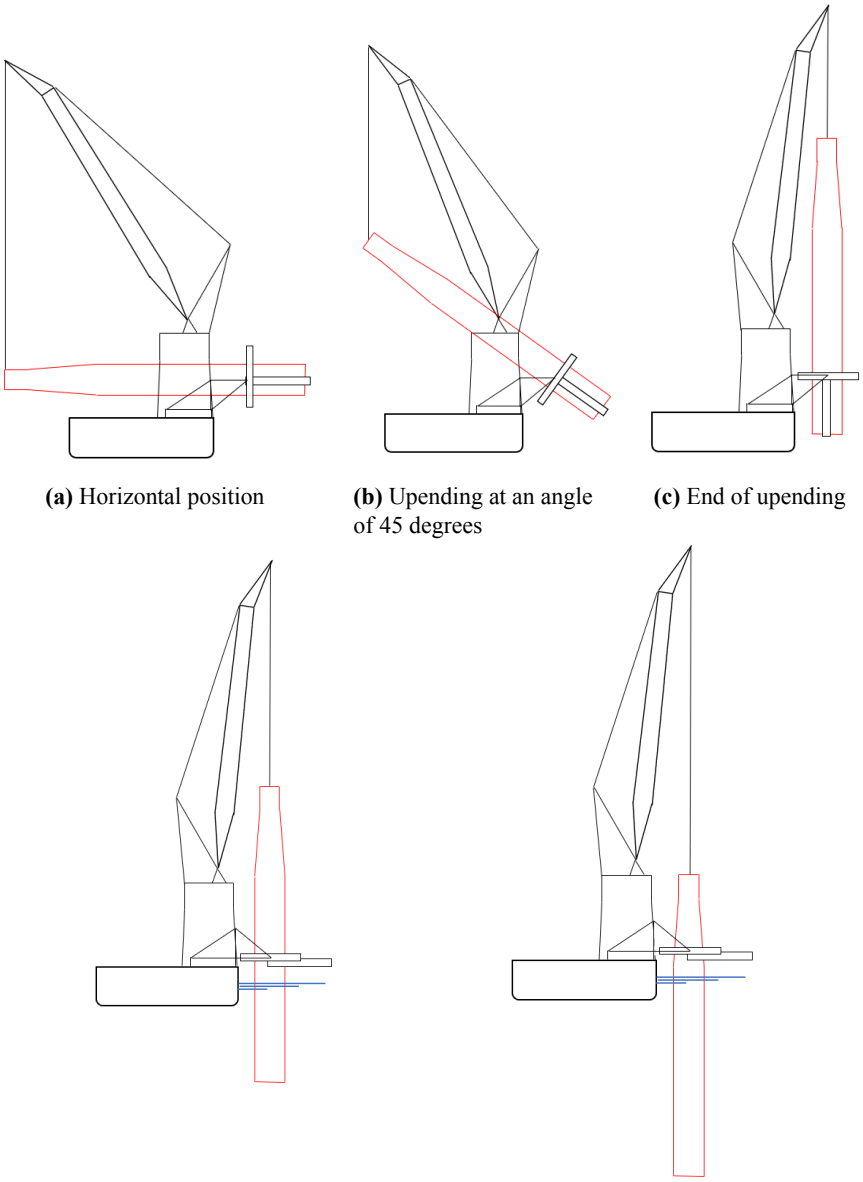

(a) Horizontal position

(b) Upending at an angle of 45 degrees

(c) End of upending

(d) 35 metres of submergence

(e) 65 metres of submergence

Figure 6: Stages of upending and lowering of a monopile towards the seabed for side installation

The installation sequence of stern installation is similar to side installation. The schematic representation of stern installation is depicted in Figure 7. The crane is at the same position as for the side installation. The pile gripper is placed at the centre line of the vessel in front of the recess. The monopile is upended in the centre line of the vessel in a similar way as pipe-laying vessels. Stern installation provides a sheltered installation position. The loading conditions for stern installation (Table 4) are established similarly to the loading conditions of side installation.

Table 4: Loading conditions for side and stern installation

	Position MP	Side installation	Stern installation
1	Horizontal position	GE-03-80%-LI: 2300t@63.8m, 243°	GE-03-80%-LI: 2300t@63.8m, 221°
2	45° upended	GE-03-80%-LI: 2300t@50.7m, 235°	GE-03-80%-LI: 2300t@27.9m, 247°
3	Fully upended	GE-03-80%-LI: 2300t@31.6m, 159°	GE-03-80%-LI:2300t@47.8m, 303°
4	Halfway water depth	GE-03-80%-LI: 2300t@31.6m, 159°	GE-03-80%-LI:2300t@47.8m, 303°
5	3 metres above seabed	GE-03-80%-LI: 2300t@31.6m, 159°	GE-03-80%-LI:2300t@47.8m, 303°

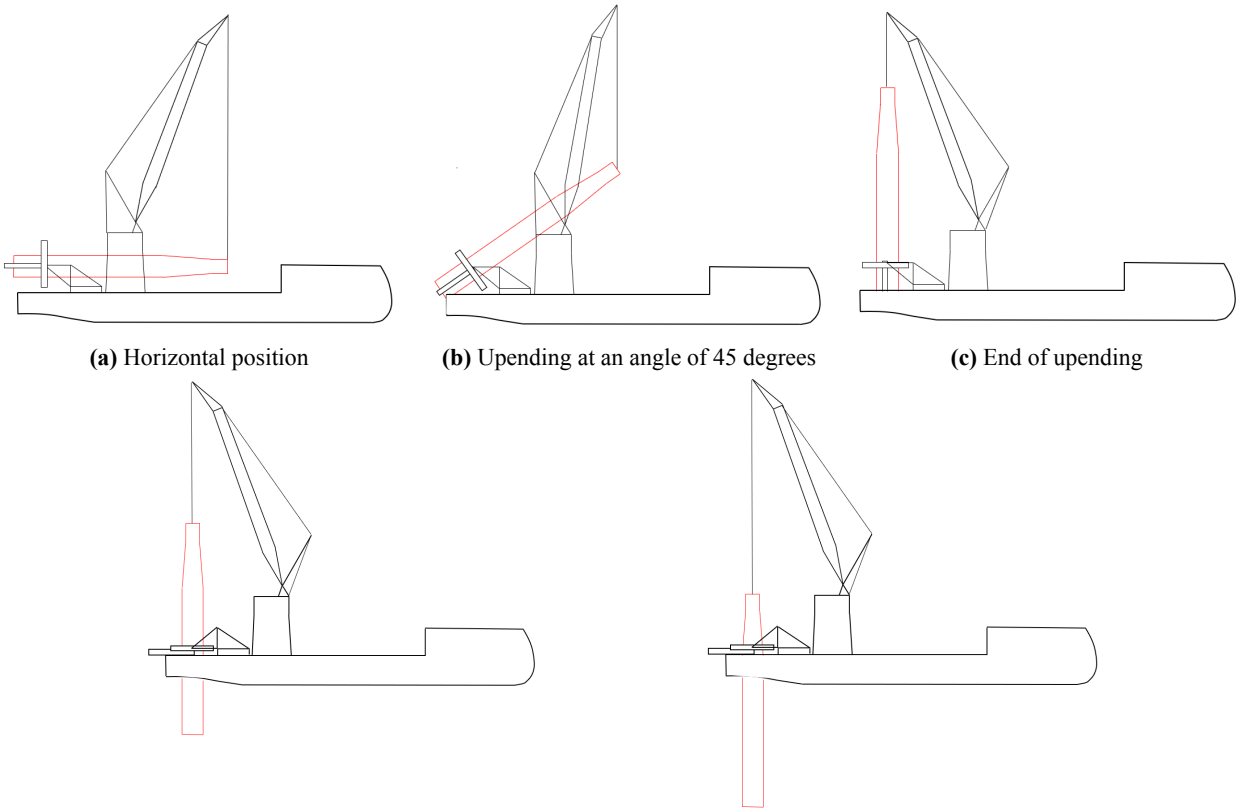

(a) Horizontal position **(b)** Upending at an angle of 45 degrees **(c)** End of upending

(d) 35 metres of submergence **(e)** 65 metres of submergence

Figure 7: Stages of upending and lowering of a monopile towards the seabed for stern installation

OrcaFlex model

The installation sequences including the generated hydrodynamic properties are set up in OrcaFlex. The multi-body system is modelled identically for side and stern installation except for the location of the monopile and pile gripper ring. The properties of the vessel, mission equipment and monopile are identical as well. This section describes the important modelling choices regarding the monopile, mission equipment, wave shielding, and simulation approach. Based on this model set-up, time-domain simulations are performed.

Monopile

Depending on the position of the MP, the MP is modelled differently to incorporate all the relevant hydrodynamic information. When the MP does not have any water contact, the monopile is modelled as a line object, as presented in Figure 8. A line is a flexible linear element in OrcaFlex which can be used for ropes, chains, but monopiles as well. The chosen line type is a general pipe with the inner and outer diameter and structural properties inserted as defined in Table 3. When the MP is (partly) submerged, the monopile is modelled as a hybrid buoy-vessel-line object. The spar buoy accounts for the viscous drag and inertia regime, while the vessel accounts for the diffraction regime. The vessel object also includes the tip vortex damping derived from model tests and CFD tests in a cooperation with Ulstein Design & Solutions, Huisman Equipment and Heerema. The vessel object is part of a multi-body group, together with the vessel itself. This multi-body group allows interaction between these two objects, such as wave shielding. Additionally, the multi-body group defines properties such as the frequency dependent added mass and damping matrices of the monopile and the vessel, and the hydrostatic stiffness are also defined in this multi-body group. The line object acts as a sleeve and models the contact with the pile gripper ring. The vessel and line object are rigidly connected to the 6 DoF spar buoy. The hybrid modelling for the submerged monopile is shown in Figure 9.

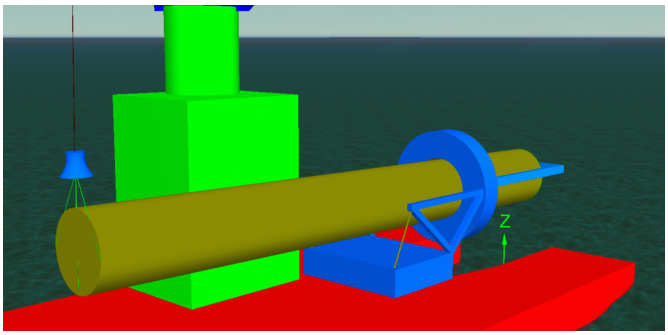

Figure 8: Modelling of monopile in OrcaFlex as line object for horizontal and upended monopile

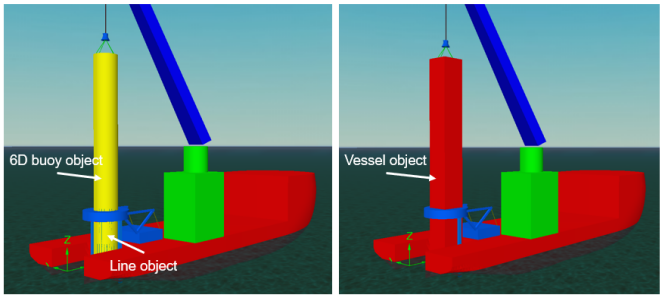

Figure 9: Modelling of monopile in OrcaFlex as hybrid buoy-vessel-line object for partly submerged monopile

The spar buoy creates the possibility to include the corresponding drag coefficient, added mass, slamming coefficients, and more accurately the buoyancy force. The spar buoy is discretised into multiple cylinders to better control the buoyancy force. The hydrodynamic loads on spar buoys are calculated with Morison's equation (Morison et al., 1950). The added mass and drag forces are applied on the submerged parts. When the object is partly submerged, the forces are scaled to the proportion of cylinder volume of the submerged buoy. The interaction effects on the fluid forces between the vessel and the monopile are imported from HydroD. A special multi-body group is created to take these effects into account.

The Morison equation for a fixed object in an oscillatory flow is shown in Equation 1. The first addend represents the fluid inertia force, related to the water particle acceleration, while the second addend represents the drag force, related to the water particle velocity. For a cylinder with a diameter D Equation 1 is rewritten to Equation 2.

$$F = \rho \cdot C_m \cdot V \cdot \dot{u} + \frac{1}{2} \cdot \rho \cdot C_d \cdot A \cdot u \cdot |u| \tag{1}$$

$$F = \rho \cdot C_m \cdot \frac{\pi}{4} \cdot D^2 \cdot \dot{u} + \frac{1}{2} \cdot \rho \cdot C_d \cdot D \cdot u \cdot |u| \tag{2}$$

When the object itself also moves with a velocity $v(t)$, the Morison equation is rewritten to an equation with three addends. (Equation 3): respectively the Froude-Krylov force, which is proportional to the fluid acceleration relative to the earth, the hydrodynamic added mass force, which is proportional to the fluid acceleration relative to the body, and lastly the drag force:

$$F = \rho \cdot V \cdot \dot{u} + \rho \cdot C_a \cdot V \cdot (\dot{u} - \dot{v}) + \frac{1}{2} \cdot \rho \cdot C_d \cdot A \cdot (u - v)|u - v| \tag{3}$$

Mission equipment

The crane consists of a slewing column and a crane boom. The slewing column rotates, however the vertical position remains identical. Therefore, the slewing column is not separately modelled in terms of mass and mass moment of inertia, but included in the vessels mass and inertia. The crane boom however changes in the x, y, and z direction which affects the mass moment of inertia and the loading condition. The crane boom and crane hook are separately modelled. The crane hook is connected to the monopile with 4 springs. The crane hook has 6 degrees of freedom to model the behaviour of the crane hook as realistic as possible.

Wave shielding

Wave shielding is a phenomenon of diffraction of the incoming waves by the presence of a hull or object. For side installation, the monopile is lowered at the leeward side of the vessel. For stern installation, the monopile is lowered in the recess of the stern. The position and behaviour of the monopile is influenced by the presence of the vessel. The wave shielding reduces the overall dynamic forces that act on the subsea asset when it is lowered due to the decrease of the displacement, velocity and acceleration of the waves (Li et al., 2014; Amer et al., 2022). It is modelled in OrcaFlex by sea state RAOs defined for vessel objects in multi-body groups. These RAOs depend on the wave direction, wave frequency, velocity potential and velocity potential gradient, and are generated in HydroD. Shorter waves are more affected by shielding, because the vessel tends to follow the motion for longer waves. The hull of the vessel and the vessel object of the monopile are modelled in a multi-body group which allows to account for the interaction between these two objects, and therefore for wave shielding.

A comparison of the monopile force is made between CFD tests and the OrcaFlex simulations. The CFD tests are performed internally at Ulstein, for a wave height of 4.65 metres, corresponding with the highest wave height for H_s of 3 metres, and a wave period of 7.0 seconds, using Airy wave theory (Stroo, 2022). The water depth is 50 metres and the monopile of 100 metres is fixed at the seabed. The wave direction is 210° for side installation. For stern installation, the wave direction is 165°. The MP force for side and stern installation is divided by the MP force without the presence of a vessel. The wave height, wave period and wave direction of the CFD tests are implemented in the OrcaFlex files to enable a comparison. The loading condition of the monopile 3 metres above seabed is used as a basis. Between the CFD and OrcaFlex are multiple modelling differences: the position of the monopile is slightly different for side and stern installation, the loading conditions are not identical, and diameter of the MP is 10 metres for the CFD tests and 11 metres for the OrcaFlex simulations. The results between the two methods are presented in Table 5.

Table 5: Comparison between maximum horizontal force for CFD tests and OrcaFlex simulations for side and stern installation, with a wave direction of respectively 210° and 165° with a wave height of 4.65 metres and wave period of 7 seconds

	CFD	OrcaFlex
$\frac{F_{MP_{stern}}}{F_{MP}}$ [%]	24%	31%
$\frac{F_{MP_{side}}}{F_{MP}}$ [%]	33%	35%
$\frac{F_{MP_{stern}}}{F_{MP_{side}}}$ [%]	74 %	89 %

The results for side installation for the CFD tests and OrcaFlex correspond, with a difference of 2 %. The differences in results for stern installation are larger, due to difference in modelling the recess for the CFD tests and OrcaFlex. The sea state RAOs of OrcaFlex are generated in HydroD, which cannot deal with the sides of the recess. This leads to the difference in MP forces for stern installation. A more accurate modelling of the recess in HydroD will probably provide a larger reduction in MP force and larger shielding effect for the OrcaFlex simulations.

Simulation approach

The upending and lowering of a monopile is a nonstationary process. Two approaches to simulate nonstationary processes are proposed by Sandvik (2012):

1. Steady-state simulations in irregular waves of the most critical vertical positions of the object.
2. Simulations of a repeated nonstationary lowering process with different irregular wave realisations and for every simulation an analysis of the extreme response.

It was shown that the second approach, to have a repeated nonstationary lowering process, results in more realistic results compared to the steady-state simulations. The first approach creates a build-up of oscillation which is not observed in reality. However, steady-state simulations in the time domain are applied due its relatively fast, effective and simple way of modelling an installation sequence, compared to modelling a nonstationary version of the same installation sequence. By simulating different loading conditions of the installation sequence for various environmental conditions, the critical situations for different T_p and H_s can still be distinguished. For further research, setting up simulations with a nonstationary lowering process are recommended and interesting to analyse differences between the steady-state simulations and repeated nonstationary lowering processes.

The duration of the simulation is set at 1800 seconds, which is found to be a sufficient representative of a sea state reference period, which is 3 hours. Besides the actual simulation time of 1800 seconds, a build-up period of 50 seconds is applied, which provides a smooth build-up of sea conditions to avoid transients when the simulation starts.

Due to the stability, the implicit time integration method is applied with a constant time step. A time step sensitivity analysis is conducted for 0.01, 0.10, and 1.00 seconds, as presented in Figure 10a, Figure 10b, and Figure 10c. A trade-off between capturing all the relevant effects and the computational time led to a time step of 0.1 seconds. A larger time step results in less computational time, however the difference in results between 0.01 and 0.10 seconds is found to be small enough. Therefore, a time step of 0.1 seconds is found to be sufficient.

A sea state reference period takes 3 hours. For the numerical simulations a simulation time of 1800 seconds is set. In Figure 11a, Figure 11b, and Figure 11c, a comparison between a simulation time of 1800 seconds and 3 hours are displayed for the loading condition where the MP is submerged for 5.56 metres, with a H_s of 2 metres and a T_p of 12.8 seconds. The total energy of the 3 hours run seems slightly higher for the dynamic x and y than for the 1800 seconds run. In addition, for the dynamic x and y, there are some differences in the curve of the graph due to possibly more scatter of waves, which are

or are not in the simulation. For the dynamic y, the natural frequency of the MP seems more dominant, which explains the better correspondence compared to the dynamic x. In conclusion, the differences in spectral density are found to be negligible enough to continue with the 1800 seconds simulation time while also taking into account the longer computational time which is needed for 3 hours simulations.

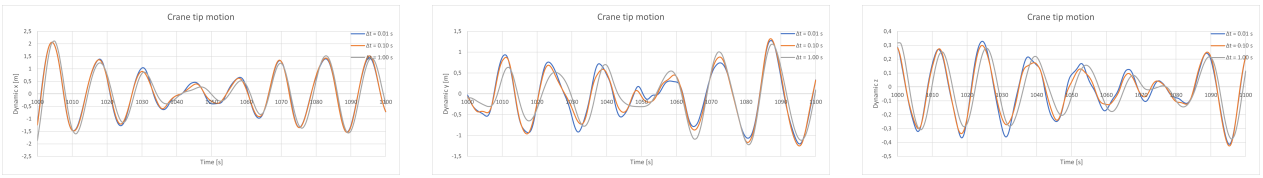

(a) Dynamic x [m] **(b)** Dynamic y [m] **(c)** Dynamic z [m]

Figure 10: Dynamic x, y, and z at the crane tip [m]

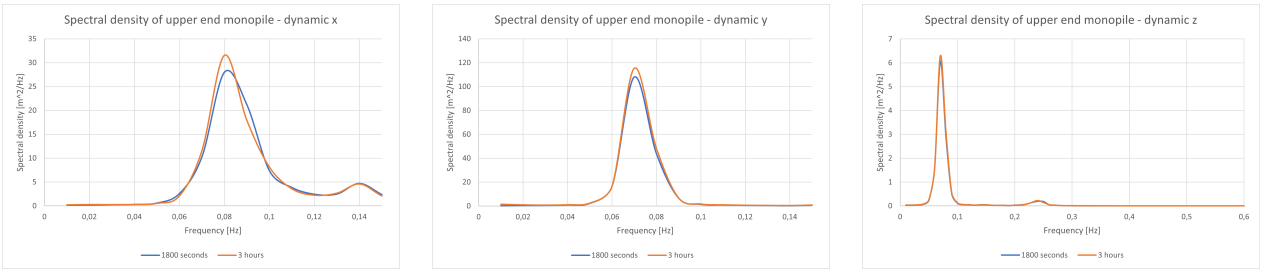

(a) Dynamic x [m] **(b)** Dynamic y [m] **(c)** Dynamic z [m]

Figure 11: Dynamic x, y, and z at the monopile tip [m]

DOUBLE PENDULUM CALCULATIONS

The multi-body behaviour of the crane boom with the monopile, rigging and crane hook results in resonance behaviour when the peak period of the wave coincides with the natural periods of system. The eigenfrequencies are determined to explain behaviour observed in the results. The natural periods are analytically derived for a double pendulum. The double pendulum includes the characteristics of the falls, crane hook, and 2XL monopile, but neglects the presence of the pile gripper ring. A schematic representation is presented in Figure 12.

For the double pendulum, there are two angles of inclination, θ_1 and θ_2. The small angle approximation is also applied for the double pendulum. The equation of motion is solved with the assumption that the solution is a sine-function. This results in Equation 4, which is an eigenvalue problem with two degrees of freedom.

$$\mathbf{K} \cdot \mathbf{x} = \lambda \mathbf{M} \cdot \mathbf{x} \tag{4}$$

The natural periods are calculated for multiple levels of MP submergence and graphically displayed in Figure 13. The two natural periods of the monopile do not coincide between 0 and 65 metres of MP submergence. The first and second natural period flip between 15 and 20 metres of submergence, because the natural period of the falls and the monopile, and therefore the rotation point, change over a different submergence levels. The difference between the natural periods increases when the monopile is more submerged.

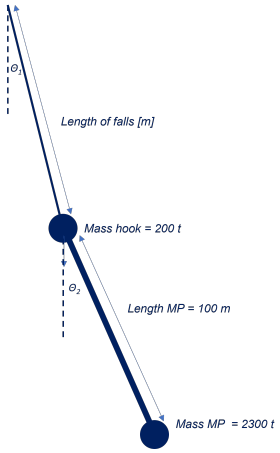

Figure 12: Schematic representation of the double pendulum with the characteristics of the falls, the crane hook, and the 2XL MP without the pile gripper ring

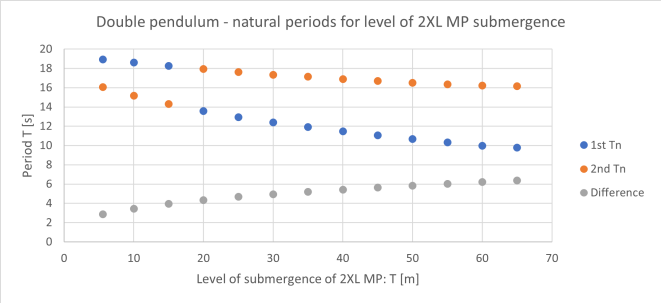

Figure 13: Natural periods for multiple levels of submergence of the monopile

The double pendulum calculations include the added mass. When the monopile is more submerged, the added mass is larger. The rotation point shifts downwards, and the added mass shifts upwards over the length of the monopile (Dam, 2018). These shifts reduce the distance between these two points and therefore reduces the inertia moment. The influence of the reduced arm is larger than the increase in added mass, since the length is squared. Therefore, the mass matrix reduces, resulting in a decrease in natural period. This effect corresponds with the results of the double pendulum calculation.

NATURAL PERIODS HLV & MP

The natural periods of the vessel and the monopile are relevant for the analysis of the operational limits. The natural periods for the vessel for heave, roll, and pitch for side and stern installation are presented in Table 6. These periods are obtained from the vessel RAOs generated in HydroD. The natural periods for the MP for sway, heave, and roll are shown in Table 7.

Table 6: Natural periods of the vessel for side and stern installation, based on vessel RAOs depending on corresponding wave direction

HLV	**Heave**	**Roll**	**Pitch**
Side installation	13 s	13 s	13 s
Stern installation	14 s	-	14 s

Table 7: Natural periods of MP, based on MP RAOs, for fully upended MP

MP	Sway	Heave	Roll
	6 s	6 s	6 s

OPERATIONAL LIMITS

The operational limits are considered for the mission equipment, and are based on the following key indicators:

- Off- and sidelead at the crane tip in vessel x- and y-direction
- Dynamic amplification factor of the crane
- Dynamic utilisation factor of the crane
- Dynamic utilisation factor of the interface loads at the pile gripper ring in global x- and y-direction

The results for side and stern installation expressed in terms of these key indicators.

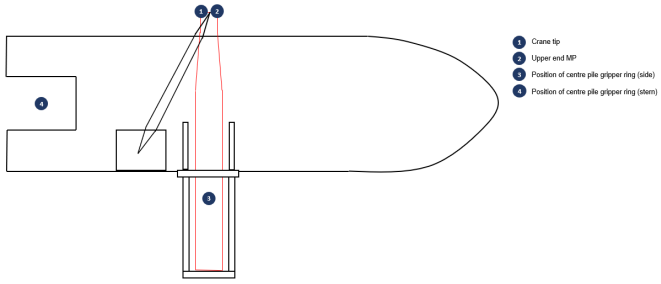

Figure 14: Locations for response analysis with the position of the pile gripper ring at starboard of the vessel for side installation and at the recess for stern installation

Crane tip forces

The crane tip forces in x, y-, and z-direction in the global coordinate system are necessary to obtain the operational limits in terms of a off- and sidelead at the crane tip, and the dynamic amplification factor (DAF) and dynamic utilisation factor (DUF) of the crane tip. The off- and sidelead are calculated with respectively F_x and F_y of the global coordinate system. The DAF and DUF are assessed using F_z of the global coordinate system.

Off- and sidelead

The sidelead (ϕ_{crane}) and offlead (θ_{crane}) at the crane tip are the maximum allowable angles when hoisting or lifting a load, and are defined based on the global coordinate system of the vessel. The maximum values of the off- and sidelead are provided by the manufacturer of the crane.

The sidelead of a crane consists of a static and dynamic part. The static sidelead is the heeling of the crane. The dynamic part of the sidelead is the dynamic angle between the vertical and the hoist tackle, resulting from swinging of the lifted load due to slewing and/ or drift-off of the vessel (Huisman, 2021).

Similarly the offlead consists of a static and dynamic part. The static offlead is the trim of the crane. It is the angle between the crane slewing axis and vertical, as a result of the static inclination of the vessel, and is in plane of the boom. The dynamic offlead is the dynamic angle between the vertical and the hoist tackle, as a result of swinging of the lifted load due to slewing and/or drift-off of the vessel, which is in plane of the boom (Huisman, 2021).

For the crane with a maximum capacity of 5000 tonnes at a radius of 36 metres in horizontal plane, used in this case study, both the off- and sidelead have a maximum angle of 3.5°, including a maximum of 1° from the crane heel or trim, as provided by the crane manufacturer. For this crane capacity condition, the off- and sidelead are equal. Therefore, the maximum off- and sidelead at the crane tip are also set to 3.5°.

From the F_x and F_y of the crane tip, the off- and sidelead are calculated to check whether the maximum limit is exceeded as presented in Equation 5 and Equation 6.

$$\phi_{crane} = \arctan(\frac{F_y}{(M_{MP} + M_{rigging}) \cdot g}) \tag{5}$$

$$\theta_{crane} = \arctan(\frac{F_x}{(M_{MP} + M_{rigging}) \cdot g}) \tag{6}$$

Dynamic Amplification Factor (DAF)

The DAF is a dimensionless ratio representing the dynamic hook load at the crane tip to its static hook force as described in Equation 7 and Equation 8.

$$DAF = \frac{Dynamic\ hook\ load}{Static\ hook\ load} \tag{7}$$

$$Static\ hook\ load = (M_{MP} + M_{rigging}) \cdot g \tag{8}$$

DAF is used for lifting operations to account for global dynamic effects (DNV, 2021b). This DAF should be determined by either specific analysis of the operation or by model testing. Depending on the location of the operation and the static hook load (SHL), the factor varies: offshore operations require higher DAFs compared to inshore or onshore, and for larger static hook loads the DAF becomes less. For this offshore marine operation with a 2XL MP, the maximum DAF is 1.15 based on the regulations of DNV (DNV, 2021b).

Dynamic Utilisation Factor (DUF)

The DUF is the dimensionless ratio between the dynamic vertical force on the crane tip and the maximum crane capacity as presented in Equation 9. This factor is introduced due to cases when the mass of the lifted load is relatively low compared to the crane capacity, but the DAF is already close to its maximum allowable limit. The DUF derived from the vertical dynamic crane tip force needs to be less than 1.00. The DUF is internally used at Ulstein and not described in literature.

$$DUF = \frac{Dynamic\ hook\ load}{Crane\ capacity \cdot g} \tag{9}$$

Pile gripper interface loads

The interface loads between the monopile and the pile gripper ring are considered as well. The pile gripper ring used for heavy lift crane vessels is specialised construction equipment. Therefore, there are no explicit regulations according to a class society like DNV. A DUF for the pile gripper ring is introduced in Equation 10 and Equation 11 to assess the lateral forces on the pile gripper ring. This DUF is the dimensionless ratio between the lateral force in the global coordinate system and the working load limit (WLL) in global x- and y-direction. The WLL for the pile gripper ring is not provided by the manufacturer for this case study, but a value is chosen based on the industry experience of Ulstein for global x- and y-direction.

$$DUF_{pile\ gripper\ ring\ x} = \frac{F_x}{WLL} \tag{10}$$

$$DUF_{pile\ gripper\ ring\ y} = \frac{F_y}{WLL} \tag{11}$$

The DUF for the pile gripper is only applied when the MP is lowered. During the upending of the monopile, the pile gripper ring is not acting as a gripper. The mass of the MP is then divided between the crane and a steel cradle with a rubber pad on which the MP partly rests. This implies the DUF to be irrelevant for the loading conditions during the upending of the monopiles.

RESULTS

The results are presented per key indicator and H_s. The key indicators are calculated based on crane tip forces and pile gripper contact forces, which are the Most Probable Maximum (MPM) for each T_p. The MPM is an extreme value statistic, based on the Rayleigh distribution. In Table 9, Table 8, and Table 10 an overview is presented for which loading conditions the maximum allowable limits are exceeded.

Side installation

In Table 8 and Table 9 an overview of the operability per loading condition of the upended and lowered MP is presented for side installation for a range of T_p between 5.0 and 15.0 seconds. A checkmark implies that that specific operational limit based on the MPM of the crane tip force or pile gripper force is not exceeded for the entire range of simulated T_p. When the allowable limit is exceeded, the corresponding spectral peak period is mentioned.

In Table 8 the operability check for the upending stage is presented, solely for the crane tip, for the horizontal position of the MP and the MP $45°$ upended for side installation. The offlead is limiting for side installation for the horizontally placed and $45°$ upended 2XL MP. For the horizontally placed MP, the vessel RAOs experience a maximum around the range of $12 - 15$ seconds. These maxima correspond with the maxima of the responses of the offlead. For the 45° upended MP, the sidelead is additionally exceeded at 15.0 seconds for side installation.

Based on Table 9, it is observed that the offlead, θ_{crane}, is limiting the operability. For the fully upended MP, the limits for the offlead is only exceeded at a T_p of 7.2 and 8.3 seconds. For the MP halfway the water depth, the offlead is first limiting and afterwards the pile gripper loads in x-direction, the DAF of the crane tip and finally the sidelead for H_s = 3 m. For T_p of 15.0 seconds for H_s of 3 metres, the DUF of the pile gripper in y-direction is exceeded. When the MP is 3 metres above the seabed, the allowable limits are not exceeded.

Table 8: Operability with a maximum off- and sidelead of 3.5 °, maximum crane tip DAF of 1.15, and crane tip DUF of 1 for range of T_p between 5.0 and 15.0 seconds for a horizontal placed and 45° upended 2XL MP for side installation and stern installation

Crane tip	H_s = 2 m	H_s = 3 m	H_s = 2 m	H_s = 3 m	H_s = 2 m	H_s = 3 m	H_s = 2 m	H_s = 3 m
	Side installation		*Side installation*		*Stern installation*		*Stern installation*	
	Horizontal position		*45° upended*		*Horizontal position*		*45° upended*	
Sidelead [°]	✓	✓	At 15.0 s	At 15.0 s	✓	✓	✓	At 12.8 s
Offlead [°]	>10.6 s	>10.6 s	>11.7 s	>10.6 s	✓	✓	✓	✓
DAF [-]	✓	✓	✓	✓	✓	✓	✓	✓
DUF [-]	✓	✓	✓	✓	✓	✓	✓	✓

For the fully upended monopile, the natural periods of the double pendulum calculation of Figure 13 are approximately 16 and 19 seconds. These values do not correspond with the displacement RAOs of the vessel for heave, pitch, and roll which peak around the 13 seconds. The MP halfway the water depth experiences the largest responses for peak periods larger than 8.3 with in general a maximum response at 12.8 or 15.0 seconds. This corresponds with the natural period based on the double pendulum calculations in Figure 13, based on the level of submergence of the 2XL MP. In addition, the displacement RAOs of the vessel for heave, pitch, and roll peak around the period of 12.8 seconds. The RAOs and the natural period of the double pendulum reinforce the responses, thus the analysed forces, which eventually result in a peak in the operational limits. Lastly, it is important to consider that these long waves do not occur regularly on the North Sea based on the wave scatter diagram in Figure 4. When the monopile is almost at the seabed, the responses are below the allowable limits. The natural periods of the double pendulum of the rigging and 2XL MP are outside the range of the peak of the displacement RAOs of the vessel. The motion behaviour of the monopile is damped by the wave loads. The responses due to behaviour of the multi-body system do not exceed the operational limits.

Table 9: Operability with a maximum off- and sidelead of 3.5°, maximum crane tip DAF of 1.15, crane tip DUF of 1 and pile gripper DUF for x- and y-direction of 1 for range of T_p between 5.0 and 15.0 seconds for a fully upended 2XL MP, a 2XL MP halfway the water depth, and 2XL MP 3 metres above seabed for side installation

Side installation		H_s = 2 m	H_s = 3 m	H_s = 2 m	H_s = 3 m	H_s = 2 m	H_s = 3 m
		Fully upended		*Halfway water depth*		*3 m above seabed*	
Crane tip	Sidelead [°]	✓	✓	At 12.8 s	> 10.6 s	✓	✓
	Offlead [°]	✓	At 7.2, 8.3 s	> 9.4 s	> 8.3 s	✓	✓
	DAF [-]	✓	✓	✓	≥ 10.6 s	✓	✓
	DUF [-]	✓	✓	✓	✓	✓	✓
Pile gripper	DUF_x [-]	✓	✓	> 10.6 s	> 9.4 s	✓	✓
	DUF_y [-]	✓	✓	✓	At 15.0 s	✓	✓

Stern installation

Table 8 also includes the operability for horizontal placed MP and the 45° upended monopile for stern installation. The offlead is not limiting the operability for stern installation for the horizontal placed MP and the MP 45° upended. The allowable limit for sidelead is exceeded at 12.8 seconds, for H_s of 3 metres, in case of the 45° upended monopile.

The operability overview of the lowering of the MP for stern installation is shown in Table 10. The allowable limits are similar to side installation. The offlead is governing the allowable limits for the lowering stage as it is first exceeded for a fully upended MP and the MP halfway the water depth. For the fully upended MP, only the maximum offlead is exceeded, and only at the spectral peak period of 7.2 seconds. A peak in the displacement and load RAOs of the MP is visible around 6 seconds (Table 7), which explains the increase in response for the smaller T_p in the range of $5.0 - 7.2$ seconds. For the MP halfway the water depth, the offlead is limiting at first, after that the sidelead, and finally the DUF for the pile gripper and the DAF for the crane tip. The displacement and loads RAOs of the monopile are the largest in the range of $12 - 15$

seconds, which explains the increase in response at these larger spectral peak periods. The MP 3 metres above seabed does not exceed the operational limits, similarly to the side installation. The load and displacement RAOs of the monopile are at a maximum around 21 seconds, which is outside the range of the spectral peak periods.

It is observed that similarly to the side installation sequence, the MP halfway the water depth exceeds the most limits, but only for larger T_p. This observation corresponds with the natural period of the double pendulum of 12.8 seconds in combination with the peak of RAOs of the MP and the displacement RAOs of the vessel for heave and pitch (Table 6). The vessel RAO is negligible for roll for head waves, which is the case for stern installation.

The operational limits during upending are presented in Table 8. Only the sidelead is exceeded at 12.8 seconds, which is the only case without a limiting the offlead. For stern installation, the offlead is restricted due to the position of pile gripper ring and the MP placed longitudinally in the centre line. However, a sidelead is possible, which explains the exceedence for the largest simulated H_s for the upended MP. The loading condition with the horizontally placed MP complies for every key indicator.

Table 10: Operability with a maximum off- and sidelead of 3.5°, maximum crane tip DAF of 1.15, crane tip DUF of 1 and pile gripper DUF for x- and y-direction of 1 for range of T_p between 5.0 and 15.0 seconds for a fully upended 2XL MP, a 2XL MP halfway the water depth, and 2XL MP 3 metres above seabed for stern installation

Stern installation		H_s = 2 m	H_s = 3 m	H_s = 2 m	H_s = 3 m	H_s = 2 m	H_s = 3 m
		Fully upended		*Halfway water depth*		*3 m above seabed*	
Crane tip	Sidelead [°]	✓	✓	>9.4 s	>9.4 s	✓	✓
	Offlead [°]	✓	At 7.2 s	>8.3 s	>8.3 s	✓	✓
	DAF [-]	✓	✓	✓	At 11.7, 12.8 s	✓	✓
	DUF [-]	✓	✓	✓	✓	✓	✓
Pile gripper	DUF_x [-]	✓	✓	> 10.6 s	> 9.4 s	✓	✓
	DUF_y [-]	✓	✓	✓	>11.7 s	✓	✓

Comparison side and stern installation

The 5 loading conditions of side and stern installation differ from the wave direction and the position of the monopile compared to the vessel. Other than that, the loading conditions are analogous and this is particularly visible during the lowering stage, for instance for the fully upended MP and the MP halfway the water depth for the offlead as shown in Figure 15. However, the responses during the upending stage show differences due to the change in position of the pile gripper ring and the monopile.

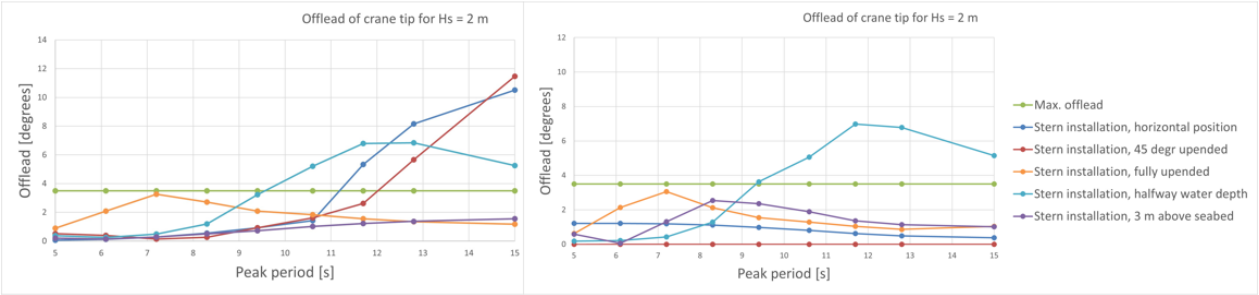

Figure 15: Offlead [°] for H_s = 2 metres for respectively side and stern installation with a maximum allowable limit of 3.5 °

Upending stage: The off- and sidelead are the key indicators that are exceeding the maximum allowable limits during upending. The DAF and DUF of the crane tip are not exceeding limits for both installation methods, since the monopile also partly rests on a cradle. During upending the offlead is not exceeding the allowable offlead, however for the side installation it happens. For stern installation, the monopile is placed in the centre line of the vessel. The pile gripper constrains the

behaviour of the monopile so the offlead for stern installation is smaller during upending than for side installation. During side installation, chaotic double pendulum behaviour occurs when the monopile is in horizontal position, when the spectral peak period corresponds with natural period of the vessel.

Lowering stage: During the lowering stage, the offlead is governing for every loading condition. The case with the fully upended MP does not exceed the allowable limits for H_s = 2 metres. In addition, the offlead is only exceeded at 7.2 and 8.3 seconds for H_s = 3 metres. The RAOs of the monopile are at its maximum in the range of $5.0 - 8.0$ seconds. The case with the MP halfway the water depth exceeds most limits compared to the other 2 loading conditions during lowering, starting from a T_p of 8.3 seconds for both side and stern installation. The natural frequency of the double pendulum coincides with the RAOs of the vessel and the spectral peak period, resulting in exceedence of operational limits in the range of $12 - 15$ seconds. The sidelead for the MP halfway the water depth is exceeded for a smaller T_p compared to side installation. For both installation methods, the DUF of the pile gripper in x- and y-direction is exceeded. The case with the MP 3 metres above seabed does not exceed the allowable limits for both installation methods. The RAOs of the MP are outside the range of the T_p and the RAOs of the vessel. However, for stern installation, there is a maximum in response for the off- and sidelead visible at 8.3 seconds, and corresponding to that for the DUF of the pile gripper in x- and y-direction. This is still underneath the allowable limits, however, in the vessel RAOs graphs for this loading condition there is a local maximum visible.

DISCUSSION

The results of side and stern installation show a difference in operability during upending: stern installation provides a larger operability window than side installation. The lowering phase shows a comparable operability window for both installation methods. Based on the results, for these applied allowable limits a comparison between two methods during upending and lowering can be made. Additionally, differences in responses between T_p and H_s can be observed from the results. This provides an insight into the performance of different methods and helps to gain understanding of the installation of 2XL monopiles. The operability, however, can change based on maximum allowable limits. This paper only zooms in on the operability of the mission equipment during upending and lowering. Current, directional wave spreading, and slamming are not included in the model. More accurate modelling of the recess in HydroD will provide a more realistic shielding effect for stern installation. Steady-state time-domain simulations are performed, which imply an unrealistic build-up of oscillation. For further research, it is recommended to include current, wave spreading, and slamming to have a more realistic model. Moreover, performing nonstationary simulations of both installation methods would provide a valuable and more realistic insight. Simulations of the monopile hook-up could provide further insight into the operational comparison between side and stern installation methods. Lastly, sudden loss of hook load scenarios are interesting to study in more detail. It is expected that stern installation provides advantages compared to side installation. For stern installation, the vessel will not experience any roll-back since the lifting operation is done at the centre line. For side installation, the roll-back can be severe because of the large amount of anti-heeling ballast.

CONCLUSIONS

Concluding, the offlead is generally governing the operational limits for both side and stern installation except during the upending of the monopile with stern installation. For stern installation, during upending, the sidelead can be governing, due to the longitudinal position of the monopile. During upending, the differences in operational limits between side and stern installation are clearly visible: the offlead is limiting the operation only for side installation and not for stern installation. The operability during upending is larger for stern installation. However, during the lowering stage, both installation sequences show a similar course in the key indicators plotted against the spectral peak periods.

For the fully upended MP, the shorter spectral peak periods are critical due to the maximum in RAOs of the monopile. These periods coincide with the spectral peak periods that have a larger chance of occurring on the North Sea. However, the most critical loading condition is the MP halfway the water depth, the operational limits are most exceeded for both in-

stallation sequences, for T_p in the range of $12.0 - 15.0$ seconds. The spectral peak period coincides with the natural period of the double pendulum system of the crane hook and the monopile, and in addition with the natural period of the vessel for heave, pitch, and roll. On the other hand, these operational limits are exceeded for T_p in the range of $12.0 - 15.0$ seconds, which are long waves which do not occur frequently on the North Sea. When the monopile is almost at the seabed, the operational limits are not limiting the operation for both side and stern installation. The natural period of the monopile is then outside of the range of the spectral peak period and the natural period of the vessel.

Stern installation shows a larger operability window during upending compared to side installation. During the lowering stage, the operability differs per loading condition. For the fully upended monopile, stern installation has a larger operability window based on these allowable limits. The results for the monopile 3 metres above seabed are underneath the allowable limits for both side and stern installation. Considering both the upending and lowering phase of 2XL monopiles from heavy lift crane vessel, stern installation shows promising results in terms of operability.

CONTRIBUTION STATEMENT

A.M. Elzinga: Conceptualization; formal analysis; investigation methodology; project administration; validation; visualization; writing – original draft. **J.D. Stroo:** Conceptualization; resources; supervision; writing - review and editing. **A.A. Kana:** Conceptualization; supervision; writing - review and editing.

ACKNOWLEDGEMENTS

This work was performed as part of the MSc thesis for the lead author (Elzinga, 2024). The thesis was performed in Marine Technology at Delft University of Technology and the authors would like to acknowledge both Delft University of Technology and Ulstein Design and Solutions B.V. for their support of this research.

REFERENCES

Amer, A., Li, L., and Zhu, X. (2022). Dynamic analysis of splash-zone crossing operation for a subsea template. *Sustainable Marine Structures*, 4(2):18–39.

Brans, S., Rinne, A., and Kana, A. (2021). Applying a needs analysis to promote daughter craft for year-round access to far-offshore wind turbines. *High-Performance Marine Vehicles (HIPER '21)*, pages 71–87. September 13-15: Tullamore, Ireland.

Chen, M., Yuan, G., Li, C., Zhang, X., and Li, L. (2022). Dynamic analysis and extreme response evaluation of lifting operation of the offshore wind turbine jacket foundation using a floating crane vessel. *Journal of Marine Science and Engineering*, 10(12).

Dam, M. (2018). Monopile installation assessment: a critical assessment of an oscillating monopile during offshore installation. Master's thesis, Delft University of Technology.

DNV (2021a). *Environmental conditions and environmental loads*. Det Norske Vertias AS, Høvik, Norway.

DNV (2021b). *ST-N001: Marine operations and marine warranty*. Det Norske Veritas AS, Høvik, Norway.

Elzinga, A. (2024). Operational limits of 2xl monopile installation: a comparative analysis between side and stern installation. Master's thesis, Delft University of Technology.

Guachamin-Acero, W., Li, L., Gao, Z., and Moan, T. (2016). Methodology for assessment of the operational limits and operability of marine operations. *Ocean Engineering*, 125:308–327.

Huisman (2021). Technical specification - tmc 270000-5000. Technical report, Huisman Equipment BV.

Inernational Energy Agency (2019). Offshore wind outlook 2019. Technical report, International Energy Agency.

International Maritime Organization (2022). *Code on Intact Stability for all Types of Ships covered by IMO Instruments*. IMO, London, United Kingdom.

Lasdon, L., Waren, A., Jain, A., and Ratner, M. (1978). Design and testing of a generalized reduced gradient code for non-linear programming. *ACM Transactions on Mathematical Software*, 4(1):34–50.

Li, L., Gao, Z., and Moan, T. (2015). Response analysis of a nonstationary lowering operation for an offshore wind turine monopile substructure. *Journal of Offshore Mechanics and Arctic Engineering*, 137(5).

Li, L., Gao, Z., Moan, T., and Ormberg, H. (2014). Analysis of lifting operation of a monopile for an offshore wind turbine considering vessel shielding effects. *Marine Structures*, 39:287–314.

Liu, Y. (2021). Monopile forever: Overcoming the technical boundaries of monopile foundations in deep waters. Master's thesis, Delft University of Technology.

MetOcean Solutions (2020). Mean significant wave height. Avalaible at: https://app.metoceanview.com/hindcast/.

Morison, J., O'Brien, M., Johnson, J., and Schaaf, S. (1950). The force exerted by surface waves on piles. *Journal of Petroleum Technology*, 5:149–154.

Ramírez, L., Fraile, D., Brindley, G., and O'Sullivan, R. (2020). Offshore wind in europe. Technical report, WindEurope.

Sandvik, P. C. (2012). Estimation of extreme response from operations involving transients. *Proceedings of the 2nd Marine Operations Specialty Symposium (MOSS '12)*. August 6-8: Singapore.

Stroo, J. (2022). U-stern cfd in waves rev 04. Presentation, Ulstein Design and Solutions B.V.

Stroo, J. (2023a). Ulstein u-stern foundation installation vessel. Technical report, Ulstein Design and Solutions B.V.

Stroo, J. (2023b). A vessel and method configured to install a foundation structure: Wo 2023/001493 a1.

Ulstein (2019). Future trends offshore wind - rev 2.3. Technical report, Ulstein Design and Solutions B.V.

Proceedings of 15th International Marine Design Conference (IMDC-2024)
June 2-6, 2024
Amsterdam, the Netherlands

Design of Floating Installation Vessel for Offshore Installation of Floating Offshore Wind Turbines

Karl H. Halse[1,*], Sunghun Hong[2], Behfar Ataei[3], Ting Liu[4], Shuai Yuan[5], and Hans P. Hildre[6]

ABSTRACT

The installation of the present wind farms Hywind Scotland and Hywind Tampen are both carried out by towing the fully assembled wind turbine from the assembly site in the Norwegian fjords to the final offshore site. In the present study an alternative installation method is proposed where the fully assembled tower is transported to the site on the installation vessel and mounted onto the preinstalled floating substructure (a spar buoy). The paper presents a brief outline of the design process for the proposed concept and gives an overview of the work done to evaluate variations of the installation vessel and the proposed lifting mechanism. The paper is a summary of the results obtained by a project team in SFI MOVE addressing marine operations related to installation of floating offshore wind turbines.

KEY WORDS

Offshore installation; Wind turbines; Novel marine design concept; Wave-induced motion; Co-simulation.

INTRODUCTION

Offshore Wind Turbines (OWTs) can be categorized into bottom-fixed and floating OWTs based on the type of foundation for the wind tower. Traditionally, the installation of bottom-fixed offshore wind turbines has been carried out using jack-up vessels with large cranes. As the offshore wind industry move to deeper waters, the bottom-fixed turbines gradually become less attractive and floating OWTs become the only possible alternative. The installation of floating OWTs can no longer be carried out by bottom-fixed jack-up vessels. The preferred installation method for floating OWTs has been to complete the assembly of the wind turbine in sheltered waters and tow it to the installation site. However, for offshore wind farms far from a coastline where the OWT assembly can take place, alternative installation methods are desired. As a part of the research project SFI MOVE (NTNU, 2024), a team of researchers has proposed an alternative installation process by designing an installation vessel which is capable of mounting the fully assembled wind turbine onto a floating substructure at the offshore installation site. This paper is a summary of the work carried out by the project team from SFI MOVE.

Floating OWTs needs to have sufficient buoyancy to carry the weight of the turbines and some kind of mooring system to facilitate station-keeping of the floating system. Figure 1 illustrates three typical floating OWT concepts which all have been built. The spar-shaped substructure is the one with most industrial application so far, and the work in SFI MOVE has used this concept to assess the feasibility of performing an offshore installation of a floating offshore wind turbine.

[1] NTNU (Dep. of Ocean Operations and Civil Engineering, Ålesund, Norway); ORCID: 0000-0002-0563-5115. [2] Moreld Apply (Front End & Green Solutions, Stavanger, Norway); ORCID: 0000-0003-2543-879X.

[3] CDynamics (Kristiansand, Norway); ORCID: 0000-0002-4942-1506.
[4] DNV (Risers and cables, Renewable energy, Oslo, Norway).
[5] DNV (Dep. of Subsea, Risers and Pipelines, Oslo, Norway); ORCID: 0000-0001-7679-2428.
[6] NTNU (Dep. of Ocean Operations and Civil Engineering, Ålesund, Norway).
* Corresponding Author: karl.h.halse@ntnu.no

Submitted: 23 February 2024, Revised: 30 April 2024, Accepted: 1 May 2024, Published: 20 May 2024

Conference paper, DOI: https://doi.org/10.59490/imdc.2024.845 e-ISSN: 3050-4864

The fundamental principle in the concept is to follow a procedure like this:

1. Tow-out of substructure – Horizontal towing of the spar-shaped substructures.
2. Upending and Mooring – Upending and mooring of the spar-shaped structures.
3. Assembly of OWT – Inshore assembly of the Offshore wind turbine (OWT) (tower, nacelle and blades).
4. Transport of OWT to site – Installation vessel to carry 3-4 fully assembled OWTs to the site.
5. Mounting of OWT – Installation vessel mounting the OWTs onto the moored substructure using a low-height lifting mechanism.

The work presented in this paper focusses on the last part of this procedure.

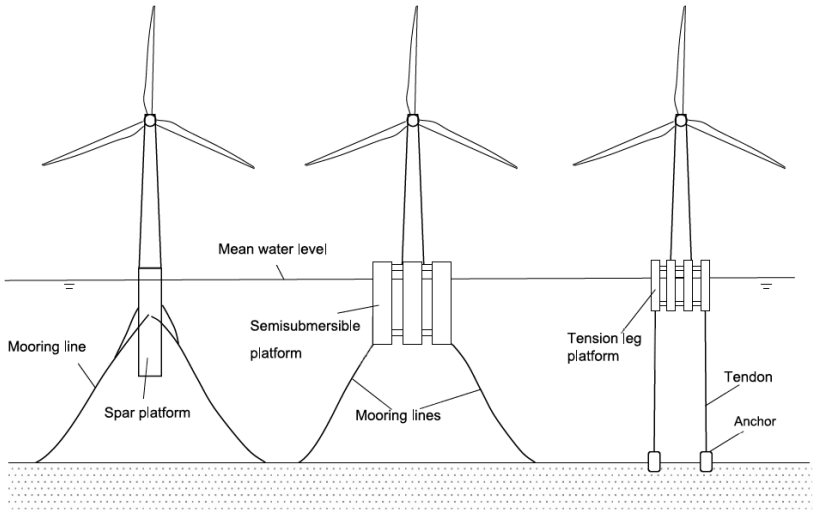

Figure 1. Schematic of various floating offshore wind turbine concepts (From Jiang, (2021)).

The paper is organized as follows: First an outline of how the design process evolved from the original idea to the development of the concept and the presentation of the final concept. The most important modelling issues and the critical response parameters are also described. Then the system modelling, and the various computer models are described. This includes how the relative motion between the two floating bodies are evaluated, how the dynamics of the lifted object influences the relative motion, and several other aspects which have been studied by the project team. The SFI MOVE project was an 8-year research project, and the various parts of the work have already been published. However, since the project lasted such a long period, and has resulted in several publications, the purpose of the present paper is to give an overall summary of the work done in the project. The new contribution from this paper is that it conveys the design strategy and concept idea in a condensed and more readable way, compared to the original and individual publications.

DESIGN OUTLINE

Original Idea

The underlying idea for the development of an installation vessel for floating wind turbines was to keep investment costs down. Hence, a relatively small vessel was proposed. To save time during installation, the idea of carrying more than one fully assembled wind turbine from the onshore assembly site and to the offshore was followed. Therefore, a vessel with sufficient weight-carrying capacity and sufficient stability characteristics was needed. To be able to perform the installation at the offshore site it is important to keep the relative motion between the lifted OWT and the floating substructure within some limitations. Consequently, we want to minimise the relative motions between the two floating structures, and we want to control the motion of the lifted OWT. Both improved stability characteristics and reduced vessel motions will presumably be achieved by increasing the vessel size. However, this alternative will come at an increased cost. The optimal ratio of vessel cost vs. vessel size is not investigated in this study.

The design of the proposed installation vessel was partly motivated by other recent studies by Huisman (Bereznitski, 2011) and Ulstein (Skipsrevyen, 2011), see Figure 2. In Huisman's concept a relatively small installation vessel is proposed and to ensure sufficient stability the vessel needs a large width which is achieved by using a catamaran hull. Ulstein has proposed a novel idea of carrying several wind turbines which can be installed from the same vessel. The concept proposed by SFI

MOVE builds on both these ideas and includes a catamaran hull to obtain sufficient stability with a relatively large deck area to cover 3-4 wind turbines.

(a) (b)

Figure 2. Huisman (a) and Ulstein (b) have both proposed concepts for installing fully assembled wind turbines onto floating substructures.

(a) (b)

Figure 3. Huisman (a) and Offshoretronic (b) introduce different crane systems to handle the installation of wind turbines onto floating substructures.

To lift the fully assembled tower from the installation vessel and onto the floating platform, some kind of lifting arrangement is needed. Again, the project found inspiration in existing solutions. Figure 3 shows two proposed alternatives from Huisman (2009) and Offshoretronic (2020). In the traditional lifting crane (like the one proposed by Huisman), the crane tip must be above the top of the tower. With the turbines gradually increasing in size, this leads to higher and higher cranes, which becomes more and more challenging from a stability perspective. In Offshoretronic's solution, the weight of the tower is carried by wires which are attached to a collar in the lower end of the tower. In this way, the lifting structure can be designed to avoid the extreme heights, thereby reducing the negative effect on the stability of the vessel. To avoid the extreme height of the lifting arrangement the proposed concept has a similar idea as the one proposed by Offshoretronic.

Concept Development

An initial design of a floating installation vessel together with an initial design of a low-height lifting mechanism was proposed by Hatledal et al. (2017), see Figure 4. The concept included a catamaran hull as the installation vessel; with a dynamic position system for station-keeping. The low-height lifting mechanism included a gripper mechanism to reduce the relative motion between the floating installation vessel and the moored floating substructure (a spar buoy) and a hydraulically controlled lifting mechanism (see Figure 5).

Compared with traditional methods using jack-up vessels, this concept avoids the use of high and heavy offshore cranes and can transport and install the pre-assembled OWT's in an efficient manner. Consequently, the operational time has the potential of being reduced from "a few days" to "a few hours". A more comprehensive work on the same concept was carried out by Jiang et al. (2018). In this work the technical feasibility of the concept in terms of acceptable relative motions between the lifted OWT and the spar buoy was confirmed, but again rather high contact forces were found in the sliding gripper which connects the installation vessel to the spar-shaped substructure. The contact forces were too high in both the gripper mechanism and the lifting mechanism.

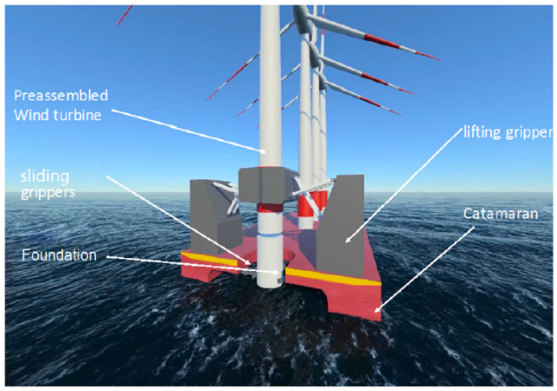

Figure 4. Initial design of the offshore installation vessel (from Hatledal et al (2017)).

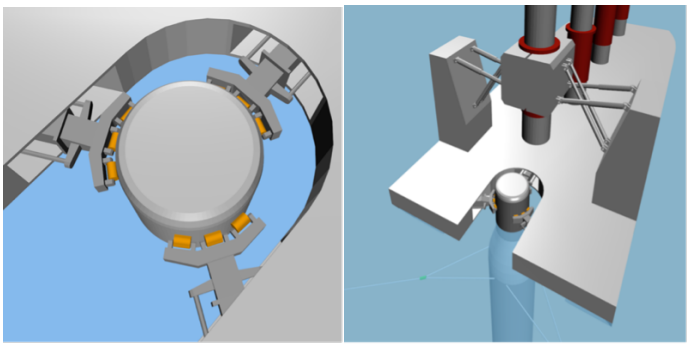

Figure 5. Illustrations of the gripper design and the lifting mechanism (From Hatledal et al (2017)).

An improved concept was proposed to reduce the relative motion between the OWT and the Spar substructure. The lifting mechanism was updated and mounted on a motion-compensated platform which was designed to follow the wave-induced motions of the Spar buoy, see Figure 6. Following this approach, the concept evolved to an alternative where the low-height lifting gripper mechanism was replaced by a set of lifting wires in a low-height truss-frame structure and balanced by a set of stabilizing wires, as shown in Figure 7 (left).

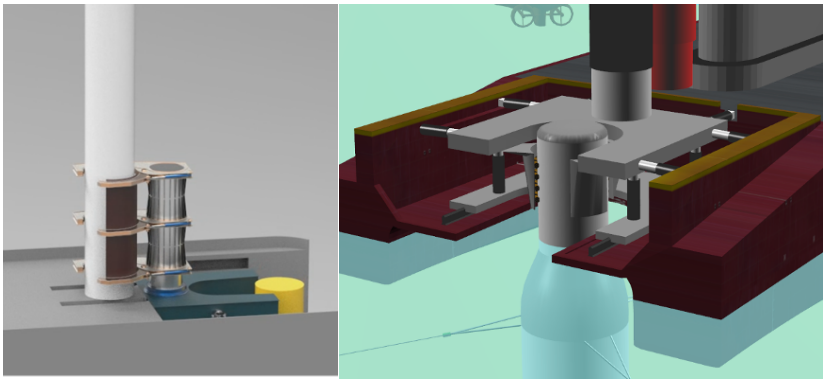

Figure 6. Illustrations of the modified gripper design and the motion-compensated platform.

The relative motion is controlled by active winch control. Vågnes et al. (2020) studied the effect of including a preliminary active heave compensation (AHC) system based on a PID controller to control the relative vertical displacement between the mating points. The main conclusion to be drawn from that study was that by introducing the AHC system, the relative displacement was reduced by approximately 50% at the resonant periods. Xu et al. (2020) proposed a simple but more general 6DOF active compensation control algorithm for the system. This study confirmed the findings from the study by Vågnes et al. (2020) which was limited to control of the vertical motions only. Ren et al. (2021a) developed a control algorithm using singular perturbation theory to minimize the relative heave motions between the mating points of the OWT and the floating spar foundation.

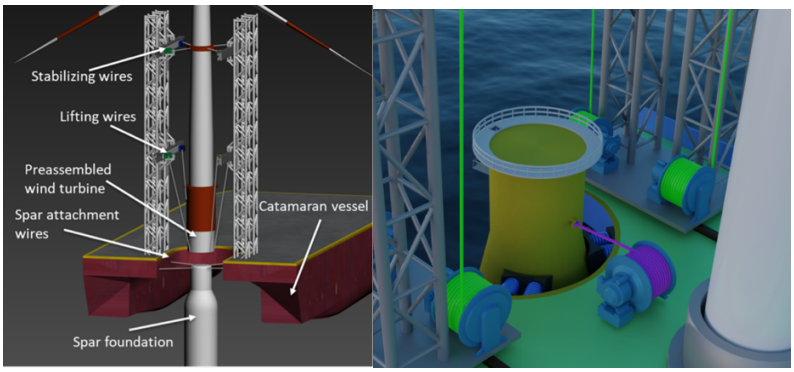

Figure 7. Improved concept with separate lifting and stabilising wires (left; from Vågnes et al (2020)) and the mechanical damping device between the catamaran and the SPAR (right; from Hong et al. (2022)).

The idea of the SFI MOVE concept is that the installation vessel can carry fully assembled wind turbines to the site and that an offshore installation operation is carried out on site. A detailed procedure of the steps involved in this offshore marine operation is described in Hong et al. (2022). A short summary of the involved steps is given below.

1. **Mobilization.** Assembled offshore wind turbines (OWTs) are loaded onto the installation vessel.
2. **Transportation.** The installation vessel transports the OWTs to the operation site.
3. **DP activation.** The dynamic position (DP) system is activated for station-keeping of the installation vessel.
4. **Mechanical coupling on.** The mechanical coupling system connects the installation vessel to the spar buoy.
5. **Lifting and hovering.** One of the OWTs is lifted and hovers on top of the spar buoy. Active motion compensation is activated.
6. **Lowering and mating.** The lifted OWT is lowered and mated onto the spar.
7. **Mechanical coupling off.** The assembled OWT is now connected to the spar and the floating OWT is disconnected from the installation vessel.
8. **Next location.** The installation vessel moves to the next installation location.

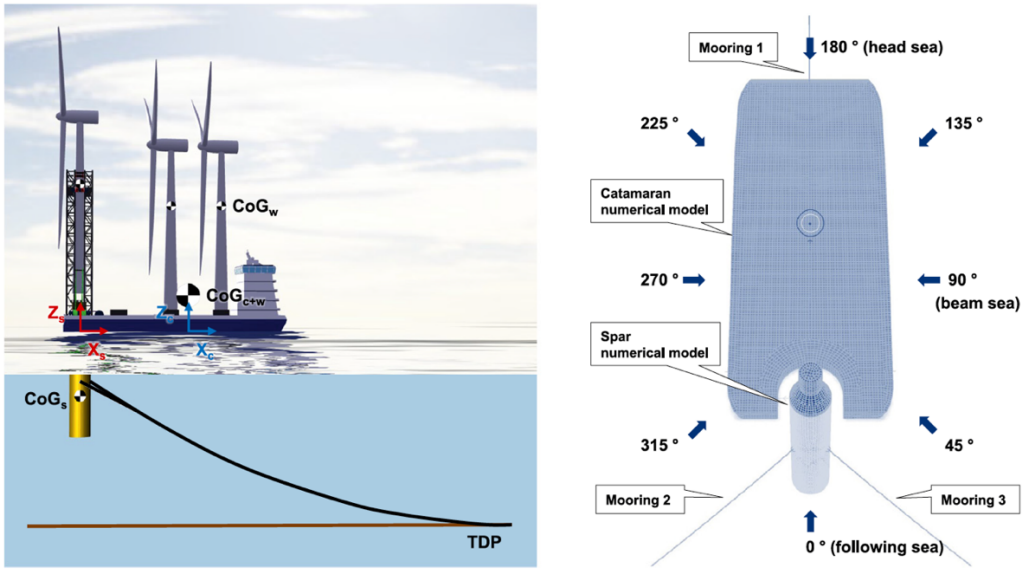

(a) Side view

(b) Numerical models and orientation of wave headings

Figure 8. Side view (a) and Top view (b) of the catamaran installation vessel and the wave directions (from Hong et al. (2023b).

An illustration of the concept is shown in Figure 8. The concept allows the floating substructure (the spar buoy) to be preinstalled and moored at the installation site. The work presented in this study is limited to step no. 5 “Lifting and Hovering”.

The main dimensions of the installation vessel, the spar buoy and the wind turbine are given in Table 1.

Table 1. Design parameters of the wind turbine, catamaran and spar (data from Hong et al, 2022).

Parameter		Wind turbine	Catamaran	Spar
Rated power	[MW]	10	-	-
Hub height	[m]	119	-	
Rotor diameter	[m]	178.3	-	
Length over all	[m]	-	153	90
Width over all	[m]	-	60	14
Draft	[m]	-	8	70
Fairlead position	[m]	-	-	35
Body origin in global coordinate system	[m]	-	(63, 0, 0)	(0,0,0)
Center of Gravity (CoG)	[m]	(-0.3, 0, 84.2)	(-0.1, 0, 21.2)	(0, 0, -51.1)
Displacement	[ton]	1 302	18 309	12 642
Radius of gyration about CoG (Roll)	[m]	41.85	48.12	20.10
Radius of gyration about CoG (Pitch)	[m]	41.85	58.75	20.10
Radius of gyration about CoG (Yaw)	[m]	4.79	42.52	5.69
Roll-pitch inertia about CoG	[t m^2]	0	-76.4	0
Roll-yaw inertia about CoG	[t m^2]	-1.55 E4	-6.46 E6	0
Pitch-yaw inertia about CoG	[t m^2]	0	6.75	0

Modelling Issues

The evaluation of the various concepts was based on modelling the complex dynamic system and a subsequent simulation of the dynamic behaviour of the system. Hence, the main part of this work has been to establish proper computer models of the various parts of the system. In the following the modelling of the main parts of the concept are discussed. Figure 9 illustrates how the main parts of the system can be isolated and modelled separately.

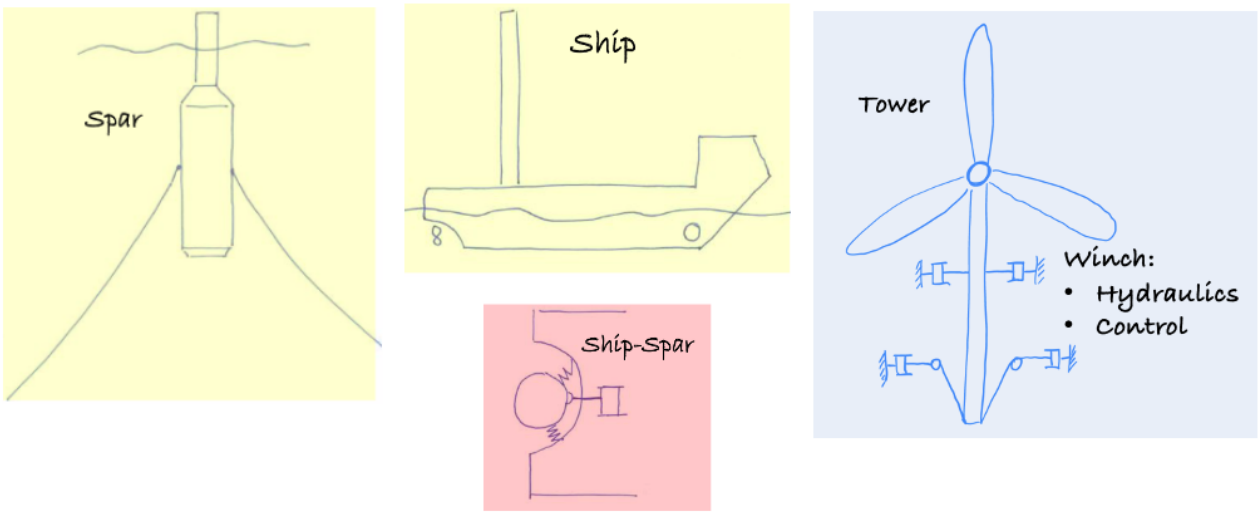

Figure 9. The system is comprised of two floating rigid bodies (ship and spar), a complex payload (wind tower) which is lifted and balanced by a set of wires all hydraulically controlled from several winches, and a mechanical connection system between the ship and the spar to reduce the relative motion between these.

In establishing reliable computer models of the total system, there are at least three main areas which needs to be addressed:

1. **Hydrodynamic modelling.** The hydrodynamic properties of two floating bodies (the ship and the spar buoy) needs to be established. To calculate the proper hydrodynamic loading for two rigid bodies floating close to each other, the hydrodynamic interaction between them needs to be accounted for. Furthermore, the sloshing mode between the two hulls of the catamaran must be included in the analyses and for the small water plane area of the spar buoy, the second order hydrodynamic loading may be important. In addition, the viscous effects of both the catamaran and the spar buoy should be accounted for in the modelling.
2. **Structural modelling.** The system may be modelled as two rigid floating bodies and one rigid lifted complex payload (the wind tower). The mechanical connections between the catamaran and the spar as well as the lifting arrangement connecting the catamaran and the wind tower need to be carefully modelled. In addition, the influence of the flexibility of the lifting mechanism should be considered. It is important to establish the eigenmodes of the complex system and thus to understand the dynamic characteristics of the system.
3. **Modelling of the control system.** There are several control systems which needs to be properly modelled. For the station-keeping of the installation vessel a dynamic positioning (DP) system needs to be modelled. During the mating phase, a proper winch control system needs to be modelled to reduce the relative motion between the spar motion and the lifted tower. Furthermore, it may be necessary to include an active control scheme to the mechanical connection between the catamaran and the spar buoy to reduce the relative motion between the two floating objects (thus reducing the relative motion of the mating points at the lifted tower and the spar).

For the modelling and analysis of complex multi-domain systems like this, several general-purpose simulation platforms exist like MATLAB/Simulink, Dymola, Algoryx, 20-Sim etc. On the other hand, there are also tailor-made time-domain simulation software to handle marine operations in the design phase. These software tools can handle hydrodynamic effects, structural dynamics, as well as hydraulic and control systems to some extent. However, none of these monolithic integrated solutions can handle high-fidelity and efficiency in a flexible way (Yuan et al. 2022).

Co-simulation with FMI/FMU

It would be better if the whole system could be distributed to separate domain solvers, and then recollecting the various connecting parameters in a common general simulation. A practical problem with this idea is that there can be compatibility issues between the different simulator environments. To solve all of this, a co-simulation approach has been developed along with an interface standard called Functional Mock-up Interface (FMI). In an FMI-based co-simulation, the individual local domain models are compiled as Functional Mock-up Units (FMU). This approach also allows to protect the intellectual properties of individual models as the different FMUs only needs to share and exchange a limited set of parameters.

In Yuan et al. (2022) a framework to analyse the proposed installation concept using co-simulation following the FMI/FMU approach was presented, see Figure 10.

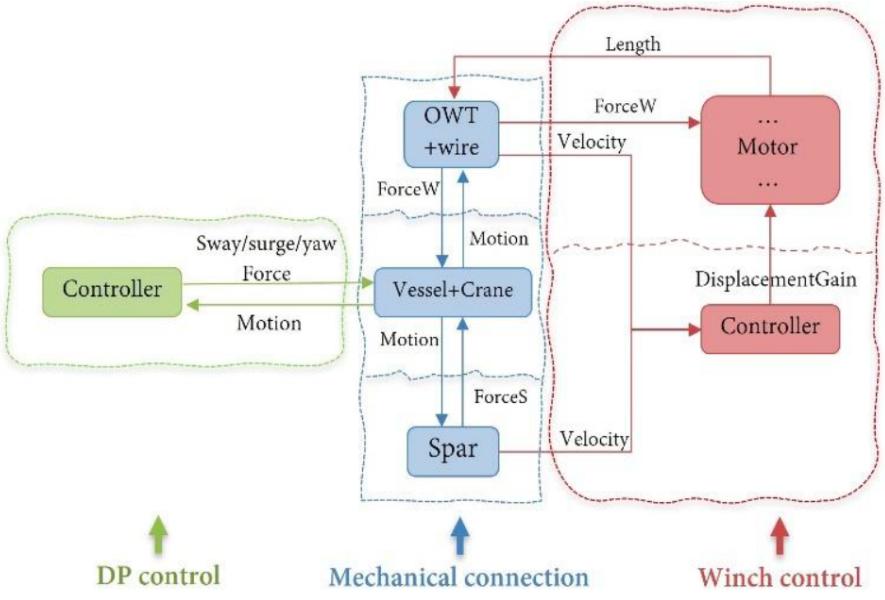

Figure 10. A framework for an FMI-based co-simulation of the installation concept (Yuan et al. 2022).

SYSTEM MODELLING AND COMPUTER MODELS

Several studies have been conducted to evaluate the proposed concept, the methods used have some unique variations and are described in more detail in each of the studies, but the overall method is the same and is briefly described in the following. The critical response for performing a successful mating operation of the OWT onto the floating spar buoy is the relative motion between the bottom of the OWT and the top of the spar. The underlying processes for this relative motion are formed by the motion of the two floating bodies: the catamaran and the spar buoy. Hence, to get a thorough understanding of the dynamic responses of the concept, the fist attempts were to study the relative motion between the stern of the catamaran (as if the lifted OWT was a rigid part of the catamaran) and the top of the spar buoy, see e.g. Hong et al. (2023b). In the next type of analysis, the OWT was a separate dynamic object hanging in a set of lifting wires, this adds complexity to the dynamic processes and the need to include a control strategy to the concept was recognised, see Ren et al. (2021b). It was also realised that with the high and slender crane structure lifting the OWT one could expect some dynamics from the crane structure. A study which compared the importance of including flexibility of the lifting crane structure was carried out by Ataei et al. (2023). And finally, as the dynamics of the lifting structure is one of the underlying dynamic processes dictating the relative motion between the OWT and the spar buoy, a study to compare the influence of using a different installation vessel was conducted. In Liu et al. (2023b) the relative motion between the OWT and the spar buoy when using a SWATH installation vessel was compared with the original catamaran installation vessel. The different scenarios are illustrated in Figure 11.

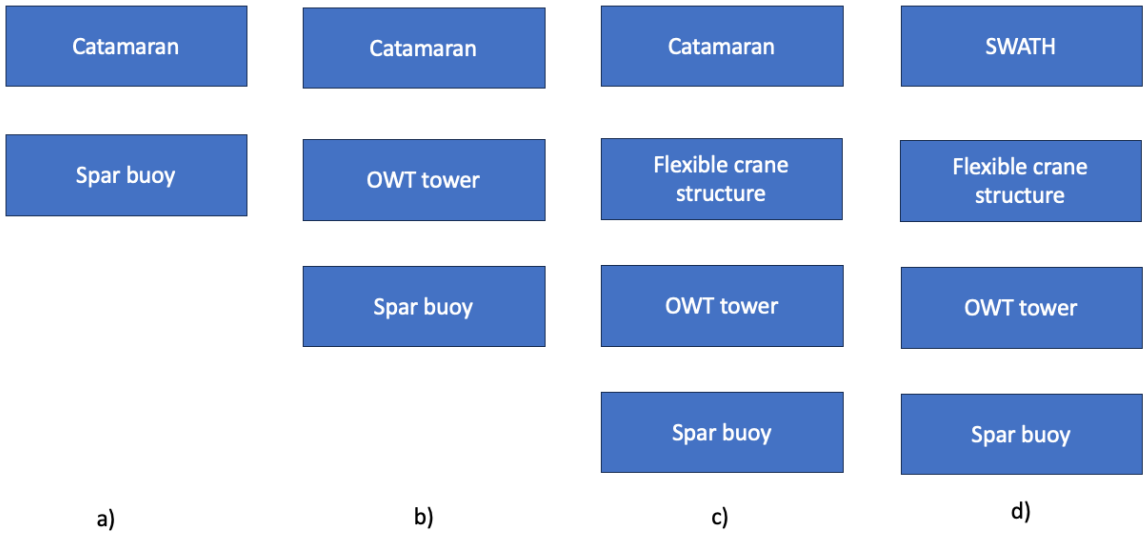

Figure 11. The study includes analyses with various level of sophistication of the computer models.

The proposed concept has primarily been studied by modelling and analysing the system using the features available in SIMO (MARINTEK, 2016). In Hong et al. (2023a) the modelling and analysis capabilities of SIMO were compared with the Orcaflex software (Orcina, 2024). The modelling capabilities in Orcaflex are slightly different than in SIMO but follows the same overall structure and the resulting response analyses gave no different conclusions than obtained from the SIMO analyses. SIMO is a time-domain simulation program for simulating motions and station-keeping of multibody systems. The installation vessel and the floating substructure (the spar buoy) were modelled as two rigid bodies connected by mechanical couplings. Thrusters and mooring system were added to the installation vessel and the floating substructure, respectively. The hydrodynamic properties including interaction effects were calculated using the Sesam module HydroD (DNV, 2024b). Wind coefficients have been estimated using the HAWC2 software (Larsen & Hansen, 2007). The panel models used in HydroD were established using the Sesam module Genie (DNV, 2024a).

Relative Motion Between Installation Vessel and Floating Substructure

The first attempts to study the dynamic behaviour of the concept simplified the analysis model by assuming the lifted OWT to be a rigid part of the installation vessel. The idea was to study the relative motion between the two floating bodies.

Base Case – Stern Installation. The present work is focusing on step 5 **Lifting and hovering** defined above, and analyses were carried out (e.g. by Hong et al. 2022) to understand the dynamic behaviour of the concept and to evaluate the installation criteria to be used. The main critical response which has been studied in detail is the relative motion between the lifted OWT and the floating spar buoy. Figure 12 illustrates how the relative motion is defined and how it can be split into a horizontal displacement, a vertical displacement and an angular component. Comprehensive analyses have been carried out to study the relative motion between the bottom of the lifted OWT and the top of the floating spar buoy. As the underlying mechanisms for the relative motion are the wave-induced motion of the two floating structures (the installation vessel and the spar buoy), the initial efforts were to study the relative motion between the two mating points indicated in Figure 12 (a) between the OWT rigidly connected to the installation vessel and the spar buoy.

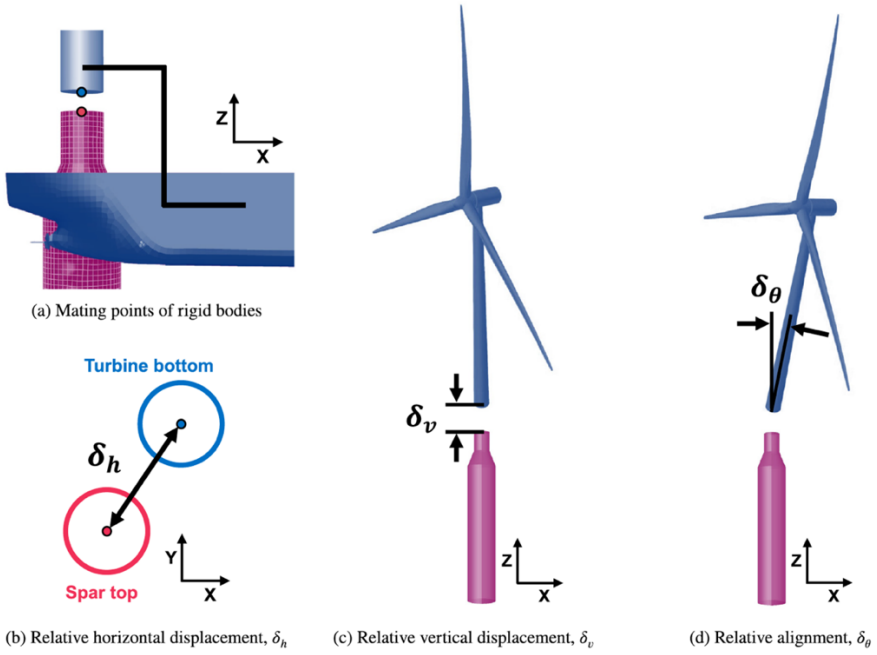

Figure 12. The definition of the main critical response parameter; the relative motion between OWT and spar buoy (From Hong et al (2022)).

In Figure 13 we see the footprints of a 1-hour simulation of the system. In the upper part of the figure, we see the heave and surge motion and in the lower part of the figure we see the roll and pitch motion. The wave direction is head sea. The pitch motion of both the catamaran and the spar buoy clearly dominates the response pattern. Since the mating point is located at the stern of the catamaran, the response at the mating point also has a significant pitch-induced heave component. For the relative motion at the mating point this results in quite severe motions both in the horizontal (surge) and the vertical (heave) directions.

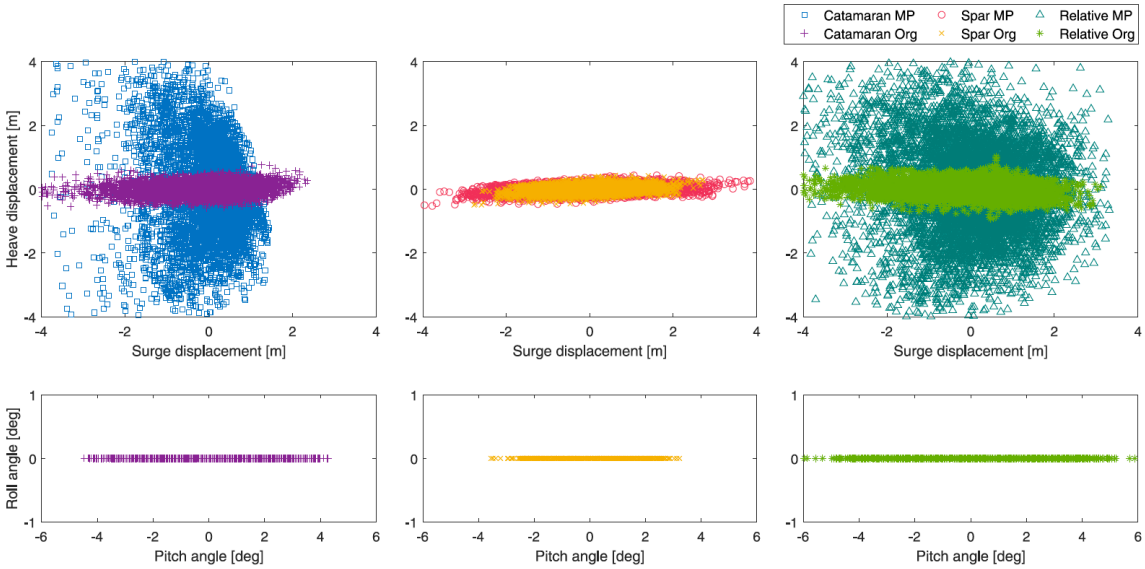

Figure 13. Footprints of 1-h simulations for body responses at the mating points and the body origin of the catamaran and the spar as well as the relative motion between the two mating points. The results are shown without any mechanical coupling between catamaran and spar ($\theta = 180°, H_s = 2\ m, T_p = 11\ s$). (From Hong et al. 2022).

The main challenge for the proposed concept was to reduce the relative motion between the lifted OWT tower and the floating substructure (the SPAR buoy). Figure 14 illustrates how the mating part of the operation can be carried out. In Figure 14 (a) we see how the mechanical coupling is defined, Figure 14 (b) shows the phase which is analysed in detail in this work and Figure 14 (c) shows how the OWT is mated on top of the floating spar buoy.

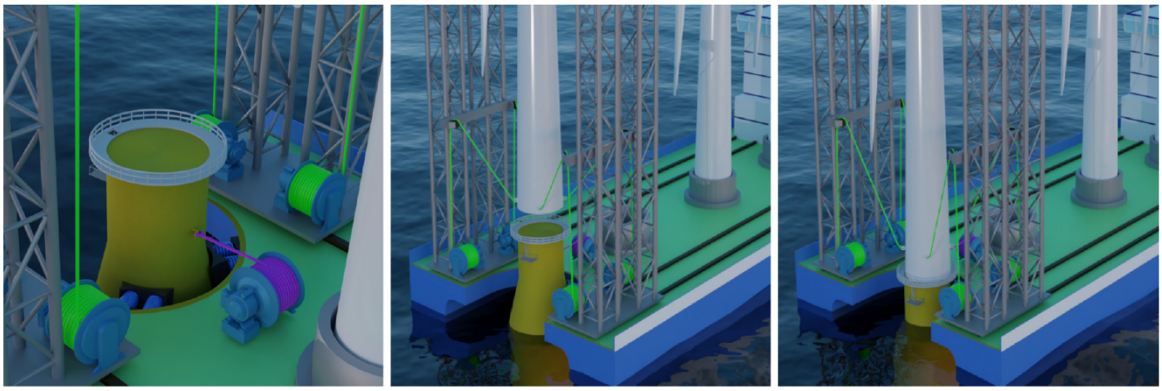

(a) Step 4: mechanical coupling connection (b) Step 5: lifting and hovering (c) Step 6: lowering and mating

Figure 14. Illustration of the main steps during the installation phase, (from Hong et al. (2022)).

Effect of Mechanical Coupling. To reduce the relative motion at the mating point, Hong et al. (2021, 2022) introduced a mechanical coupling connection between the catamaran and the spar buoy, see Figure 14(a). The mechanical coupling system consists of fenders and pre-tensioned wires designed to create a condition where the two floating bodies remain in close contact, reducing the relative motions between the moored floating spar buoy and the DP-controlled floating installation vessel. Figure 15 provides a visual representation of the 1-hour simulation for different pretension levels in the wire system, with the blue squares and red circles representing the footprint of the catamaran and spar mating points, respectively, and the green triangles representing the footprints of the corresponding relative motion between them. Figure 16 further compares the standard deviation of the relative surge, heave and pitch motions for different pretension levels and wave conditions, highlighting the system's effectiveness in reducing relative motions.

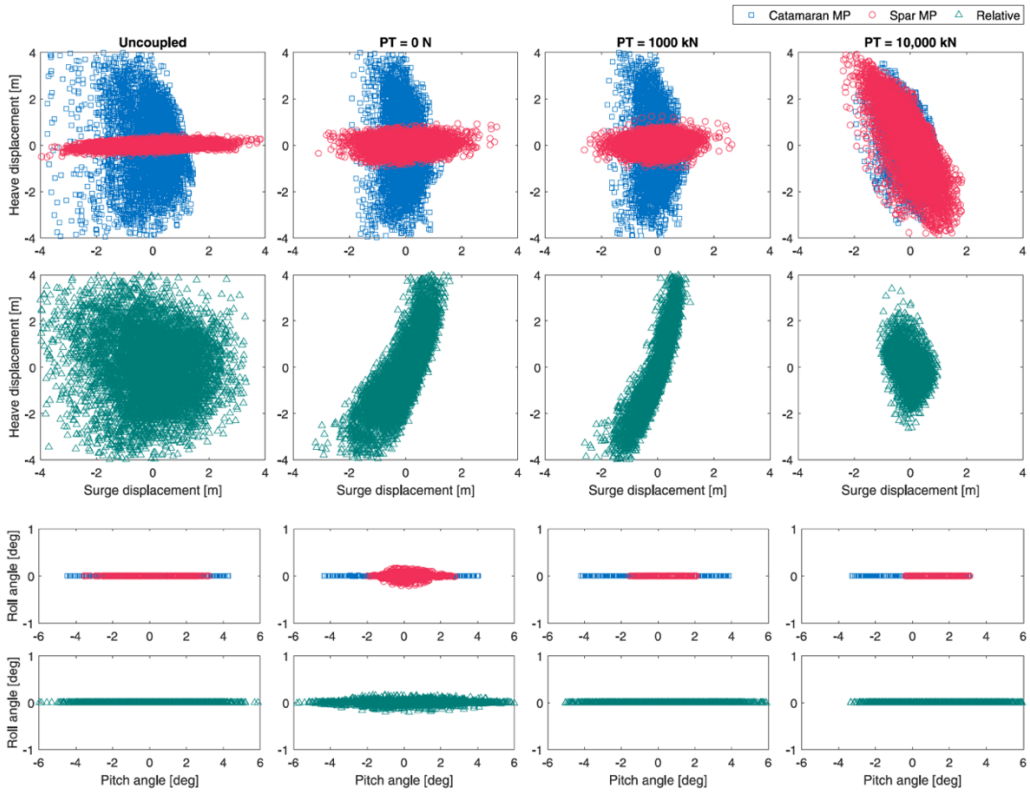

Figure 15. Footprints of 1-h simulations of the mating points with different mechanical coupling conditions ($\theta = 180°, H_s = 2\ m, T_p = 11\ s$). (From Hong et al. 2022).

The simulation results provide clear insights into what effect the mechanical coupling has on reducing the relative motions. The introduction of the system significantly reduces relative horizontal motion, even in the absence of pretension, with a 60-83% reduction in the standard deviation of the relative surge motion depending on the wave condition and pretension. However, the pretension needs to be increased beyond a certain level to reduce the relative vertical motion. When the pretension is increased to 10,000 kN, the relative vertical motion is affected and reduced, and the standard deviation is reduced by 55-72%, depending on the wave condition. This reduction is due to the frictional force of the fender system, emphasizing the need for evaluation and development for durability and reliability. The relative pitch motion was less affected by introducing the mechanical coupling as can be seen from the bottom row of Figure 16.

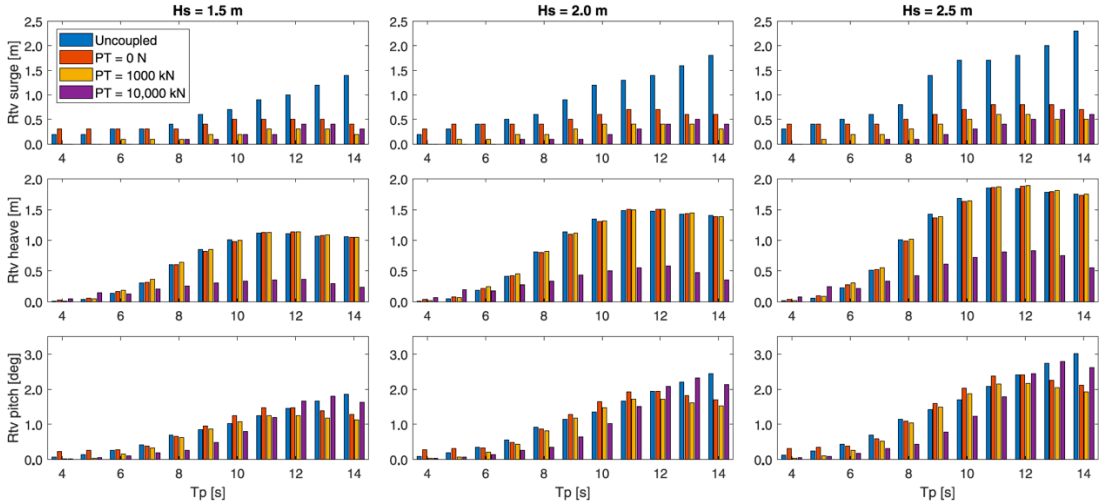

Figure 16. Comparison of standard deviation of the relative motions under varying pretension levels and wave conditions ($\theta = 180°, H_s = 1.5 - 2.5\ m, T_p = 4 - 14\ s$). Top row – surge; middle row – heave; bottom row – pitch, (From Hong et al. 2022).

Effect of Moving the Mating Location from Stern to Side. The pitch motion of both the installation vessel and the spar buoy has proven to dominate the resulting relative motion between the OWT and the spar. To reduce the relative motion between the OWT and the spar buoy, this motivated a study of moving the mating location to the mid ship of the installation vessel. In Figure 17 (Hong et al., 2024) three different installation systems are shown: a) The initial stern installation, b) The side installation, c) The side installation with a mechanical damping system.

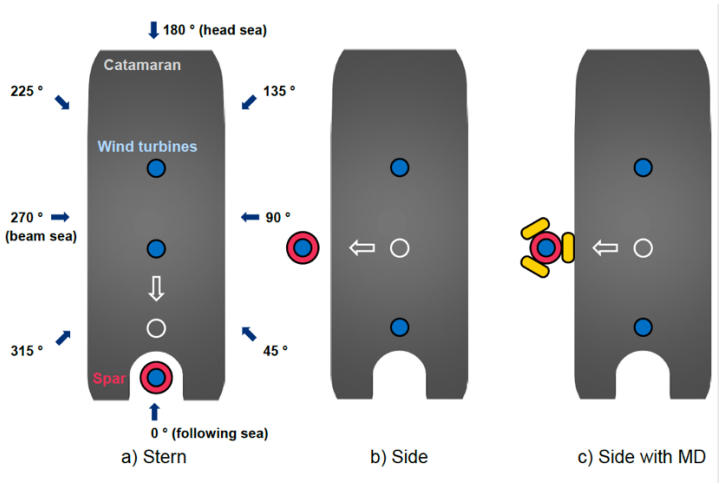

Figure 17. An overview of the three alternative installation systems which are compared (from Hong et al. (2024)).

In Figure 18 the relative responses (mean + st.dev.) for the three different installation systems are compared. From these results, we see that the relative vertical responses are clearly reduced when the mating location is moved from the stern to the side. However, the in-plane relative responses are not reduced simply by moving the mating location to the midship of the installation vessel. By including a mechanical damping system, the in-plane relative response is reduced significantly. Hong et al. (2024) have shown that the side installation alternative with a mechanical damping system has reduced the relative motion by 70-90% compared to the base case stern installation.

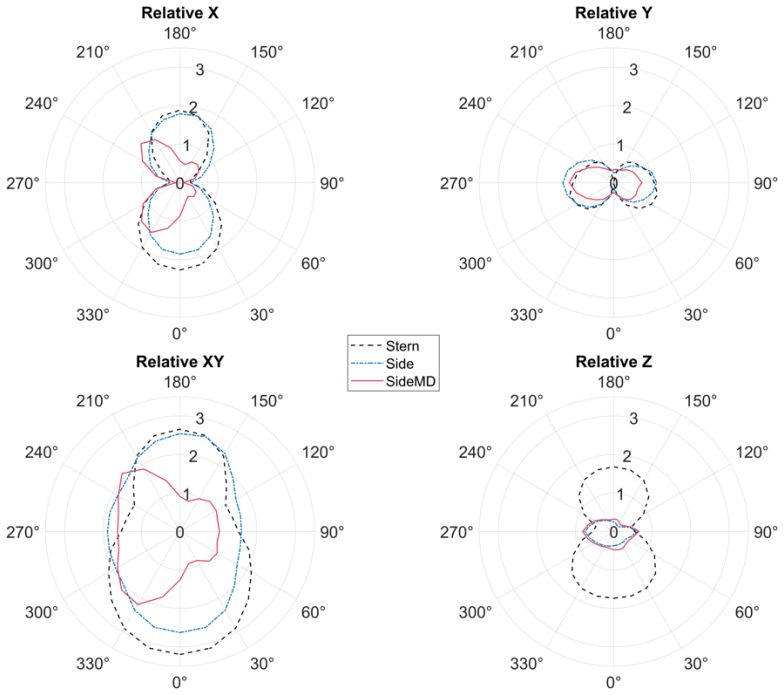

Figure 18. Comparison of the relative response (mean + st.dev.) for the three different installation systems ($H_s = 2.5\ m, T_p = 10\ s, \theta = 0 - 360°$ in steps of 15 degrees)

Relative Motion Between Lifted Object and Floating Substructure

The lifted OWT forms a third moving body with its own dynamic characteristics. In Vågnes et al (2020) a study of the complete system including the dynamics of the lifted OWT was carried out. This was an initial analysis and not all design parameters were fixed. It was observed that the natural periods of the lifted OWT was clearly below the range of wave excitation, but it complicated the dynamic response pattern. An active heave compensation model was introduced in the analyses which reduced the relative motion significantly but to the price of increased tension in the lifting wires. The results were still promising, and it was decided to proceed with more detailed studies on the motion of the floating bodies as well as with the modelling of the lifting structure.

An active heave compensation control alternative was also studied by Ren et al. (2021a) and they confirmed the importance of reducing the relative motion between the OWT and the spar buoy by some kind of active control. In Ren et al. (2021b) an anti-swing control model of a fully assembled wind turbine lifted by several lifting wires from a floating installation vessel, was proposed. In this approach, the control scheme also manages to control the in-plane motion. The control scheme is based on the knowledge of inverse dynamics and range-based localization. It has a simple form without considering state-space equations but can effectively reduce the pendular payload motion without detailed system configuration.

Effect of Including Flexibility in the Crane Structure. In Ataei et al. (2023), the effect of including the flexibility of the lifting crane was studied. Compared to the case where the crane was assumed as a part of the rigid body vessel motion, the flexibility introduced increased responses and shifted the resonance frequencies considerably. In this work the truss-framed crane structure was simplified with a simple beam structure with equivalent constant cross-section properties. The principle is illustrated in Figure 19. The conclusion from this investigation was that the flexibility increased the relative response between the lifted OWT and the spar buoy. In particular, the relative alignment between the OWT tower and the floating spar buoy is increased when the flexibility of the lifting arrangement is considered. Furthermore, it is observed that the standard deviation of the forces in the lifting wires increases when the flexibility is accounted for.

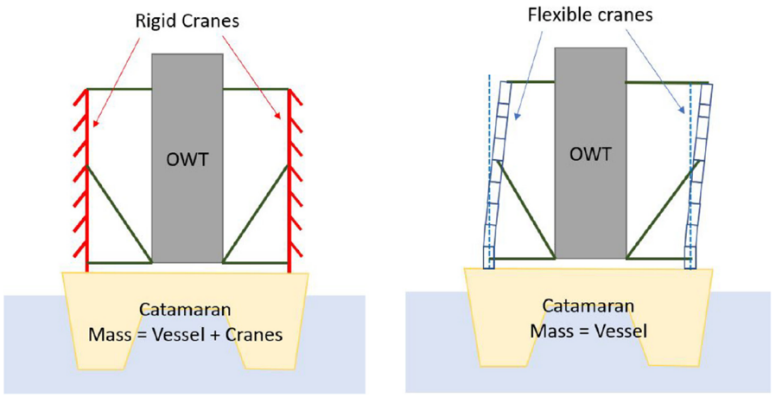

(a) Model 1: Rigid cranes (b) Model 2: Flexible cranes

Figure 19. Modelling the flexibility of the high truss-shaped structures used to lift the OWT (Ataei et al., 2023).

The behaviour of the truss-shaped crane structure was further studied by Gao et al. (2023). In their work the individual truss members were defined as illustrated in Figure 20. An additional observation from this work was that a particular concern should be raised about possible buckling failure of the lower truss members.

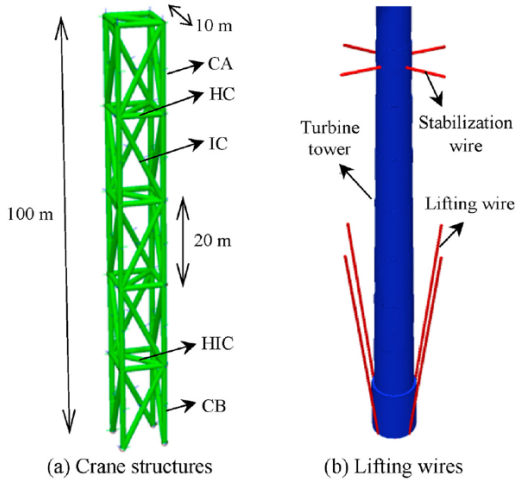

Figure 20. Crane structure and wire systems

Design of Quick Connection Device – Impact Issues

To succeed with an offshore installation of fully assembled OWTs onto floating substructures, the connection between the two objects needs to be optimized. The current solution with grouted or bolted connections has inherent difficulties which needs to be improved if an offshore installation should be possible. Grouted connections are unsuitable as the grout needs substantial time to harden. Bolted connections require very low tolerances during the mating process, which can be challenging during offshore operations. Ateai et al. (2024) presents a concept where two conic cross-sections are forced into each other, and the load is carried by friction forces. Figure 21 illustrates the various phases during the mating operation.

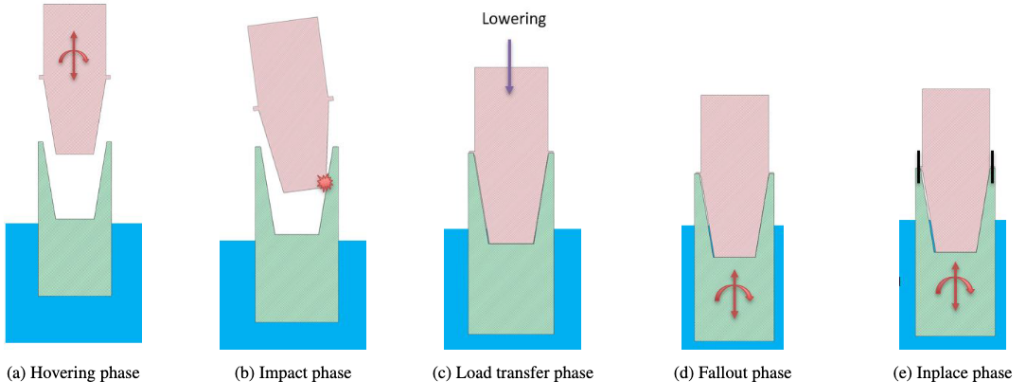

Figure 21. Overview of the mating operation stages.

In Ataei et al. (2024) both global analyses to establish the relative motion between the two objects and local analyses to study the possible impacts and structural damage to the objects are performed.

Effect of Introducing an Alternative Installation Vessel

The critical response parameter for using the proposed installation concept is to minimize the relative motion between the lifted OWT and the floating spar buoy. Since the wave-induced motion of both the installation vessel (the catamaran) and the spar buoy determines the relative motion between the OWT and the spar buoy, the idea of using an installation vessel less susceptible to wave effects than a catamaran, was attractive. The Small Waterplane Area Twin Hull (SWATH) concept was designed to bring the vessels natural periods out of the typical wave frequencies. Huisman Equipment B.V. proposed in 2011 to use a SWATH as an installation vessel for fully assembled OWTs (Bereznitski, 2011). Later this concept was reinvestigated and modified by Lee at al. (2020). However, none of these studies included the floating substructure of the OWT or the mating process in the analysis work.

In the SFI MOVE program we have performed several studies to address the mating process. Liu et al. (2023a) studied the hydrodynamic performance of the SWATH and the response analysis of the coupled SWATH-spar system. A numerical model of a SWATH including second order difference frequency force effect and damping forces was established and compared with experimental data for a SWATH of comparable dimensions. The numerical model was modified to satisfy the criteria of weight-carrying capacity and hydrostatic stability for the proposed concept. Furthermore, a multibody numerical model for the SWATH-spar system was developed, where also the hydrodynamic interaction between the two floating bodies was included.

In Gao et al. (2023) the numerical model was developed further to include a structural model of the low-height lifting mechanism and a model of the lifted OWT. The environmental conditions were varied over a range of sea states also including wind loads in some cases, (see Table 2). The study was limited to wind and waves coming from the same direction (head seas).

Table 2: Loading conditions (LC) applied in the study by Gao et al. (2023).

LC	U_w (m/s)	T_I (%)	H_s (m)	T_p (s)
LC1	7.0	24.8	-	-
LC2	-	-	1.0	7.3
LC3	7.0	24.8	1.0	7.3
LC4	5.6	28.0	0.5	6.8
LC5	8.3	22.9	1.5	7.7
LC6	7.0	24.8	1.0	[5,6,7,8,9,10]

Global dynamic response of both the OWT mating point motion, the lifting wire tension, and the strength of the lifting structure were studied. Both the wave and the wind spectra provide low frequency excitation forces to the system, and this study revealed that the wind-induced low-frequency motions of the lifted tower caused the SWATH to respond with low-frequent surge motions. In Figure 22, the displacement spectrum of the motion at the OWT tower mating point is presented, and for LC2, (without wind), the low-frequency response in x-direction is almost negligible.

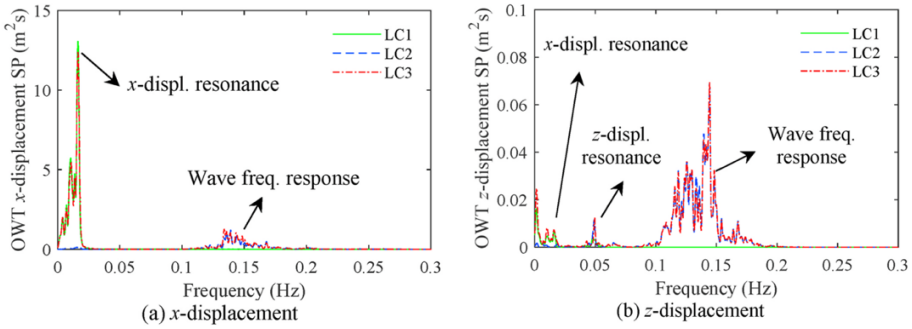

Figure 22. OWT tower mating point displacement spectrum. LC1 – wind only; LC2 – wave only; LC3 – both wind and waves included (from Gao et al., 2023).

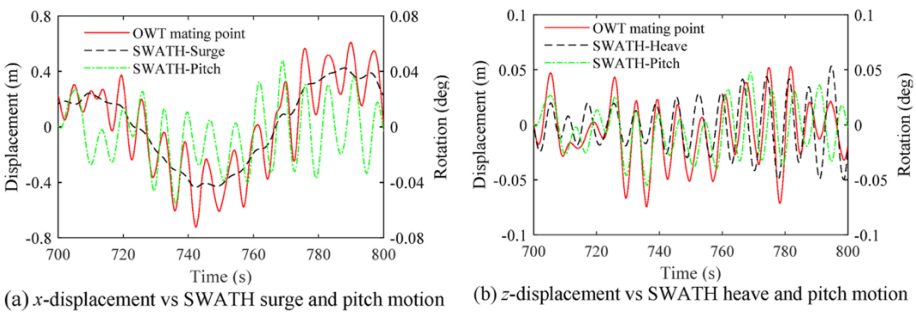

Figure 23. Mating point displacement vs SWATH motion (LC3)

Figure 23 show time series of both the mating point displacement and the SWATH motion. Here, we clearly see that the SWATH motion follows the low-frequent response of the lifted OWT tower. Although there also was a clear low-frequent response of the SWATH in surge due to waves only, this response was much smaller and did not cause a significant response of the OWT tower (see Figure 22).

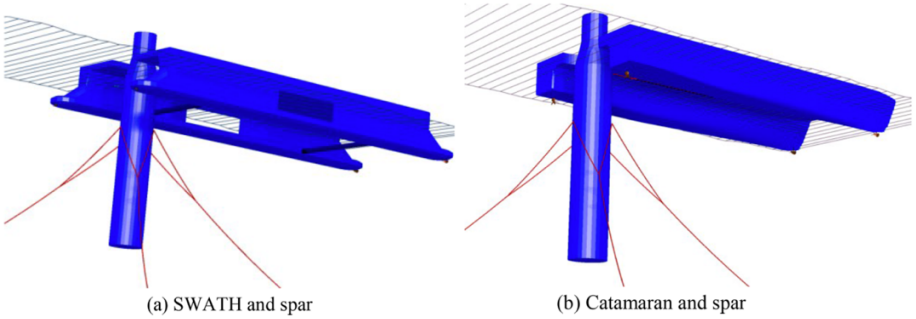

Figure 24. Numerical model of the installation vessels and the spar buoy, (Liu et al. 2023b).

Liu et al. (2023b) have compared the relative response of the two mating points by using the SWATH installation vessel with the relative response by using the catamaran. The numerical model of the two cases is shown in Figure 24. Figure 25 clearly illustrates the different behaviour of the two installation vessels. We see that he natural period for the SWATH in pitch is around 18 s and consequently outside the most typical wave periods.

The critical response parameter for the success of the proposed concept is the relative motion between the mating point at the spar top and the mating point at the bottom of the OWT. The motion RAOs for the vertical displacement of the mating points are shown in Figure 26.

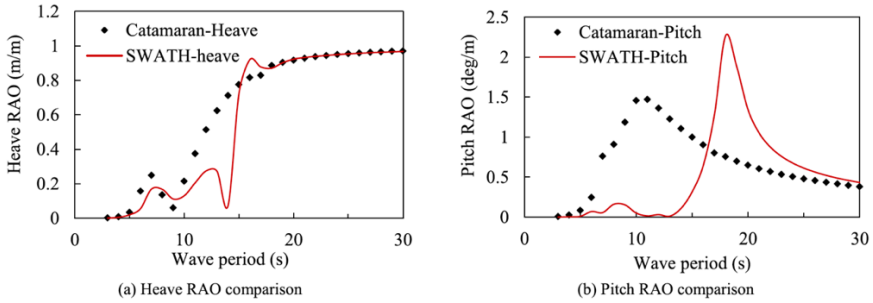

Figure 25. Motion RAO comparison of the SWATH and the catamaran installation vessels, (Liu et al. 2023b).

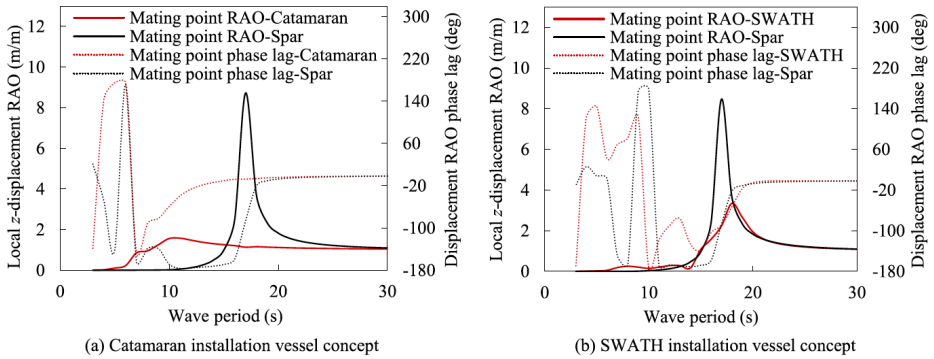

Figure 26. Transfer functions for the vertical displacements of the mating points in the installation (Liu et al. 2023b)

Considering a typical sea state with H_s = 2 m and T_p = 9 s, Liu et al. (2023b) studied the relative motion for the head sea condition. Figure 27 shows the resulting motion in terms of motion spectra for surge, heave and pitch responses both with and without a mechanical coupling between the installation vessel and the spar buoy.

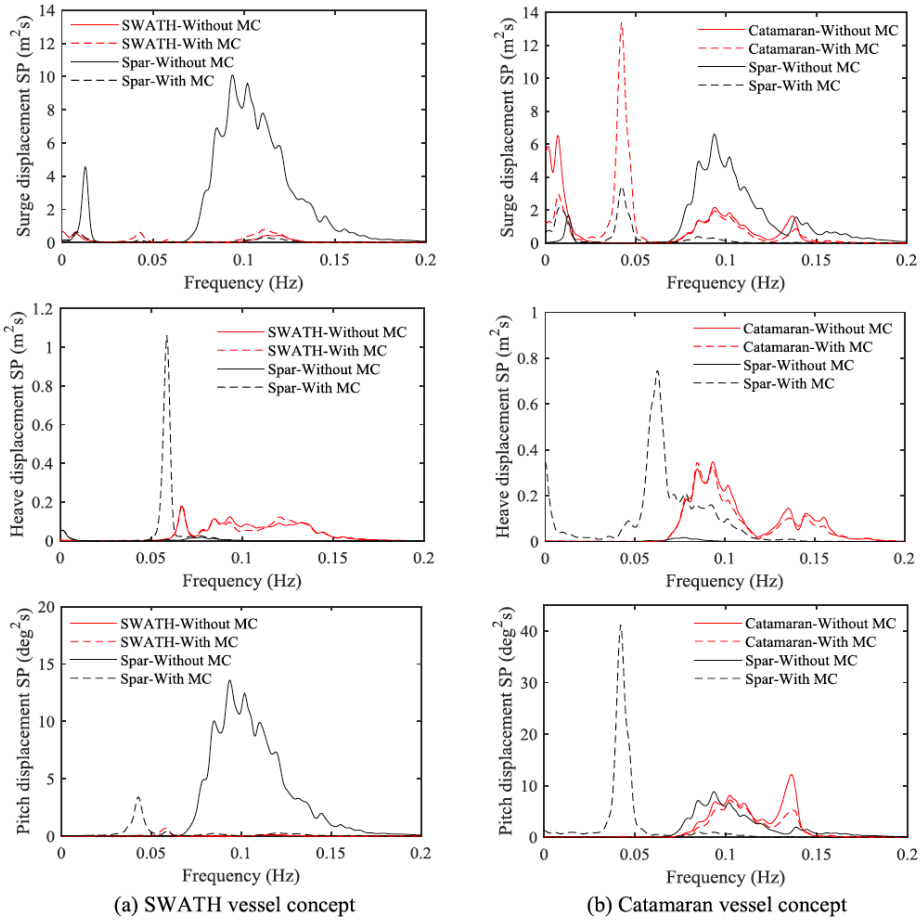

Figure 27. Motion spectra for the vessel and the spar with and without mechanical coupling (MC), head sea condition, H_s = 2m, T_p = 9s, (from Liu et al. 2023b).

To improve the understanding of the differences of using the two different installation vessels as well as the importance of including a mechanical coupling between the installation vessel and the floating spar buoy, a series of loading conditions (LCs) were analysed in Liu et al. (2023b). The significant wave height was assumed to be constant in all cases (H_s = 2m) and the peak period was varied over five periods (T_p = 5s, 7s, 9s, 11s and 13s). The different loading conditions are numbered LC1-LC5. The standard deviations of the relative x- and z-displacement for the mating points are given in Figure 28 for both installation vessels and with/without the mechanical coupling.

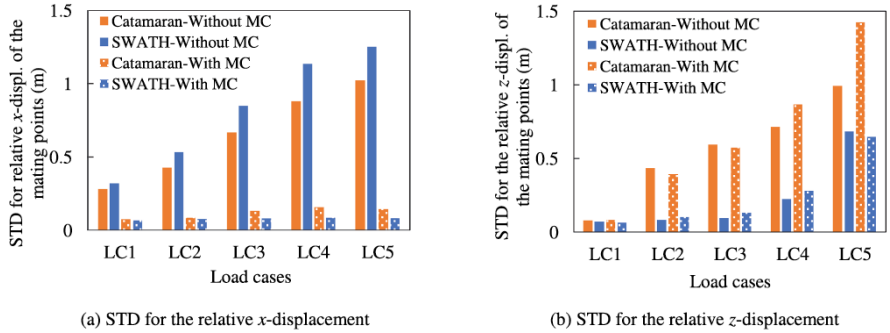

Figure 28. Standard deviation for relative response of the two mating points for both vessels (Liu et al 2023b).

CONCLUSIONS

A short summary of the most important findings from this study is given below.

- The proposed concept has shown to provide acceptable relative motions between the lifted OWT and the floating spar buoy, at least for wave headings mainly from bow and stern directions.
- The response pattern is dominated by the pitch motion of the installation vessel and the spar buoy.
- Because of the dominating pitch motion for the installation vessel, the position of the mating point will influence the relative vertical motion. Moving the mating point to the midship, reduces the relative vertical motion significantly.
- By introducing a mechanical coupling between the installation vessel and the spar buoy, the relative motion can be further reduced.
- By moving the mating point to the mid ship and introducing the mechanical coupling, the relative motion was reduced by 70-90% compared to the stern installation case.
- The flexibility of the lifting structure must be accounted for to provide precise dynamic response.
- The dynamics of the complex pay load can be controlled by a properly designed control algorithm.
- An alternative installation vessel less vulnerable to the wave excitation will improve the operability of the vessel.

The present base case for installation of floating wind turbines is to tow the fully assembled wind turbines from the assembly site in the Norwegian fjords to the final offshore site. The proposed concept has shown to be a promising alternative to the present base case.

DATA ACCESS STATEMENT

Data will be made available on request.

CONTRIBUTION STATEMENT

Karl H Halse: Project administration; supervision; conceptualization; writing – original draft.
Sunghun Hong: Conceptualization; formal analysis; writing – review and editing.
Befahr Ataei: Conceptualization; formal analysis; writing – review and editing.
Ting Liu: Conceptualization; formal analysis; writing – review and editing.
Shuai Yuan: Conceptualization; formal analysis; writing – review and editing.
Hans P Hildre: Supervision; conceptualization; writing- review and editing

ACKNOWLEDGEMENTS

This work was supported by the Research Council of Norway (RCN) through the Centre for Research-based Innovation on Marine Operations (SFI MOVE, RCN-project 237929). The paper summarizes the work of a project group of MSc students, PhDs, PostDocs, project associates and Professors in the SFI MOVE project (2015-2023). Key contributors to the publications used to prepare this summary included also: Zhiyu Jiang, Zhengru Ren, Jiafeng Xu, Lars Ivar Hatledal, David Vågnes, and Houxiang Zhang.

REFERENCES

Ataei, B., Yuan, S., Ren, Z., & Halse, K.H., (2023). Effects of structural flexibility on the dynamic responses of low-height lifting mechanism for offshore wind turbine installation, *Marine Structures, 89, 103399.* https://doi.org/10.1016/j.marstruc.2023.103399.

Ataei, B., Ren, Z., & Halse, K.H., (2024). Design of quick-connection device for installing pre-assembled Offshore Wind Turbines. In preparation.

Bereznitski, A., (2011). Wind turbine installation vessel of a new generation. In *Proceedings of the ASME 2011 30th International Conference on Ocean, Offshore and Arctic Engineering Volume 5: Ocean Space Utilization; Ocean Renewable Energy.* June 19-24, 2011. OMAE2011-49138. https://doi.org/10.1115/OMAE2011-49138.

DNV (2024a). Conceptual modelling of offshore and maritime structures – GeniE. https://www.dnv.com/services/conceptual-modelling-of-offshore-and-maritime-structures-genie-89128. (Accessed: 2024-02-08).

DNV (2024b). Hydrodynamic analysis and stability analysis software – HydroD. https://www.dnv.com/services/hydrodynamic-analysis-and-stability-analysissoftware-hydrod-14492. (Accessed:2024-02-08).

Gao, L., Liu, T., Halse, K.H., & Jiang, Z., (2023). Numerical analysis of the offshore wind turbine pre-mating process using a low-height lifting system for a nonconventional installation vessel. *Ocean Engineering, 286, 115555.* https://doi.org/10.1016/j.oceaneng.2023.115555.

Hatledal, L.I., Zhang, H., Halse, K.H. and Hildre, H.P., (2017). Numerical simulation of novel gripper mechanism between catamaran and turbine foundation for offshore win d turbine installation. In *Proceedings of the ASME 2017 36th International Conference on Ocean, Offshore and Arctic Engineering Volume 9: Offshore Geotechnics; Torgeir Moan Honoring Symposium.* June 25-30, 2017. OMAE2017-62342, V009T12A030, ASME. https://doi.org/10.1115/OMAE2017-62342.

Hong, S., Vågnes, D., Halse, K.H., & Nord, T.S., (2021). Mechanical coupling effect on the horizontal response of floating offshore wind turbine installation using a catamaran with a low height lifting system. In *Proceedings of the 31st International Ocean and Polar Engineering Conference*, June 20-25, 2021, ISOPE-I-21-1229.

Hong, S., Yuan, S., Zhang, H., & Halse, K.H., (2023a). Comparative study for numerical modelling and analysis of floating offshore wind onsite installation, In *Proceedings of the ASME 2023 42nd International Conference on Ocean, Offshore and Arctic Engineering*. *Volume 8: Ocean Renewable Energy*. June 11–16, 2023. OMAE2023-101206, V008T09A026, ASME. https://doi.org/10.1115/OMAE2023-101206.

Hong, S., Zhang, H., Nord, T.S., & Halse, K.H., (2022). Effect of fender system on the dynamic response of onsite installation of floating offshore wind turbines, *Ocean Engineering, 259, 111830.* https://doi.org/10.1016/j.oceaneng.2022.111830.

Hong, S., Zhang, H., & Halse, K.H., (2023b). Hydrodynamic and environmental modelling influence on numerical analysis of an innovative installation for floating wind, *Ocean Engineering, 280, 114681.* https://doi.org/10.1016/j.oceaneng.2023.114681.

Hong, S., Zhang, H., & Halse, K.H., (2024). Optimizing onsite installation methods for floating offshore wind: Effect of lifting arrangement strategies and mechanical damping on relative motion reduction, Submitted to *The 34th International Ocean and Polar Engineering Conference*. June 16–21, 2024. Rhodes, Greece.

Huisman, (2009). Press Release, https://www.huismanequipment.com/en/media_centre/press_releases/163-14_Huisman-launches-customised-range-of-Wind-Turbine-Installation-Cranes. (Accessed 2024-02-18).

Jiang, Z., Li, L., Gao, Z., Halse, K.H. and Sandvik, P.C., (2018). Dynamic response analysis of a catamaran installation vessel during the positioning of a wind turbine assembly onto a spar foundation. *Marine Structures, 61, pp.1-24*. https://doi.org/10.1016/j.marstruc.2018.04.010.

Krishnakanth, R., (2014). *Concept design of an installation vessel to install fully assembled next generation offshore wind energy turbines*. [Master's Thesis, Delft University of Technology]. http://resolver.tudelft.nl/uuid:2024b8f8-56a3-4bd5-a62f-8e1227d7eff4.

Larsen, T. J., & Hansen, A. M. (2007). *How 2 HAWC2, the user's manual*. Risø National Laboratory. Denmark. Forskningscenter Risoe. Risoe-R No. 1597

Lee, S.-K., Chen, Z., Pan, Q., Lu, H., & Xu, L. (2020). Hydrodynamic design of SWATH for offshore wind turbine transportation and installation. In *Proceedings of the 30th International Ocean and Polar Engineering Conference*, October 11-16, 2020, ISOPE-I-20-1191.

Liu, T., Halse, K.H., Leira, B.J., Jiang, Z., Chai, W., Brathaug, H.P. and Hildre, H.P., (2023a). Dynamic response of a SWATH vessel for installing pre-assembled floating wind turbines. *Marine Structures, 88, 103341.* https://doi.org/10.1016/j.marstruc.2022.103341.

Liu, T., Halse, K.H., Leira, B.J. and Jiang, Z., (2023b). Comparative study of the mating process for a spar-type floating wind turbine using two alternative installation vessels. *Applied Ocean Research, 132, 103452.* https://doi.org/10.1016/j.apor.2022.103452.

MARINTEK. (2016). SIMO - theory manual version 4.8.4.

NTNU, SFI MOVE – Marine Operations (2024). https://www.ntnu.edu/move (Accessed: 2024-02-13).

Offshoretronic, (2020). New Concept https://offshoretronic.tech/new-concept. (Accessed: 2024-01-21).

Orcina (2024). *OrcaFlex – World-leading software that goes beyond expectation*. https://www.orcina.com/orcaflex/. (Accessed: 20204-02-08).

Ren, Z., Skjetne, R., Verma, A.S., Jiang, Z., Gao, Z., & Halse, K.H., (2021a). Active heave compensation of floating wind turbine installation using a catamaran construction vessel. *Marine Structures, 75, 102868.* https://doi.org/10.1016/j.marstruc.2020.102868

Ren, Z., Verma, A.S., Ataei, B., Halse, K.H., & Hildre, H.P., (2021b). Model-free anti-swing control of complex-shaped payload with offshore floating cranes and a large number of lift wires. *Ocean engineering, 228, 108868.* https://doi.org/10.1016/j.oceaneng.2021.108868.

Skipsrevyen, (2011). Ulstein vokser i Nederland (in Norwegian), https://www.skipsrevyen.no/artikkelarkiv-idea-heavy-equipment-ulstein-idea-equipment-solutions-bv/ulstein-vokser-i-nederland/696009 (Accessed: 2024-01-21)

SINTEF Ocean, (2021). SIMO 4.20.3 Theory manual.

Ulstein, (2015). Winner of Statoil Challenge. https://ulstein.com/news/winner-of-statoil-challenge (Accessed: 2024-01-21)

Vågnes, D., Monteiro, T. G., Halse, K. H., & Hildre, H. P. (2020). Low-Height Lifting System for Offshore Wind Turbine Installation: Modelling and Hydrodynamic Response Analysis Using the Commercial Simulation Tool SIMA. In *Proceedings of the ASME 2020 39th International Conference on Ocean, Offshore and Arctic Engineering*. *Volume 9: Ocean Renewable Energy*. August 3–7, 2020. OMAE2020-19183, V001T01A030, ASME. https://doi.org/10.1115/OMAE2020-19183.

Xu, J., Ataei, B., Halse, K.H., Hildre, H.P. and Mikalsen, E.T., (2020). Virtual prototyping of a low-height lifting system for offshore wind turbine installation. In *Proceedings of the ASME 2020 39th International Conference on Ocean, Offshore and Arctic Engineering*. *Volume 9: Ocean Renewable Energy*. August 3–7, 2020. OMAE2020-19166, V009T09A074, ASME. https://doi.org/10.1115/OMAE2020-19166.

Yuan, S., Ataei, B., Halse, K.H., Zhang, H., & Hildre, H.P., (2022). FMI-based co-simulation of low-height lifting system for offshore wind turbine installation, In *Proceedings of the ASME 2022 41st International Conference on Ocean, Offshore and Arctic Engineering*. *Volume 8: Ocean Renewable Energy*. June 5–10, 2022. OMAE2022-79844, V008T09A045, ASME. https://doi.org/10.1115/OMAE2022-79844.

Proceedings of 15th International Marine Design Conference (IMDC-2024)
June 2-6, 2024
Amsterdam, the Netherlands

Concept Design of Typhoon Power Generation Ship Using System Simulation

Taiga Mitsuyuki[1,2,*], Haruki Ebihara[3] and Shunsuke Kado[1]

ABSTRACT

A concept of a typhoon power generation ship for utilizing enormous typhoon energy is proposed. This paper developed a system simulator for evaluating and designing the concept of a typhoon power generation ship using typhoon track history. A developed simulator was applied to the case study to design a typhoon power generation ship ship that operated near Japan. The case study showed that the annual power generation of the typhoon power generation ship tends to saturate and become constant earlier when the number of typhoons is small, in contrast to the improvement of power storage capacity. This result indicates that the appropriate size of the typhoon power generation ship exists at the current technology level.

KEY WORDS

Concept design; Typhoon power generation ship; System simulation.

INTRODUCTION

In recent years, demand for renewable energy has increased in Japan to realize a sustainable society. However, the inability to sustainably generate large amounts of renewable energy has become a problem. It is necessary to stabilize the renewable energy supply by increasing and diversifying options other than solar and wind power, which are currently used as the primary renewable energy sources. On the other hand, driven by global warming, disasters caused by typhoons are dramatically increasing in intensity. Japan's national and local governments have worked out a wide range of typhoon preparedness and damage-mitigation measures, yet typhoons remain as grave a threat as ever. However, if that enormous natural energy could be harnessed as an energy resource, it could provide a renewable energy source, contributing to a carbon-neutral society.

To realize this ultimate goal, our group has proposed a future marine movable power generation, storage, and transmission system utilizing typhoon mechanisms and high-accuracy prediction of typhoons. Specifically, we will develop a sailing ship with movable power generation and storage functions that utilize the strong winds of typhoons. Sails catch crosswinds within a typhoon's navigable semicircle and follow the typhoon track. Electric power is generated and stored in the sailing ship by turning a screw propeller underwater. The stored electricity is then transmitted to land by ship. High-precision typhoon forecasting provides high-precision estimates of power generation and risk in advance. Terao (2010) proposed Wind Hunter, one embodiment example of a typhoon power generation ship. Horinouchi and Mitsuyuki (2023) quantified the dynamic effects of large sailing vessels on typhoons. This paper showed that deploying numerous large sailing vessels for hydrogen production, proposed by Ouchi and Henzie (2017), near a typhoon and following it by operating their sails could

[1] Typhoon Science and Technology Research Center, Yokohama National University, Kanagawa, Japan; ORCID: 0000-0001-5181-5312

[2] Faculty of Engineering, Yokohama National University, Kanagawa, Japan

[3] Graduate School of Engineering Science, Yokohama National University, Kanagawa, Japan

[*] Corresponding Author: mitsuyuki-taiga-my@ynu.ac.jp

Submitted: 4 February 2024, Revised: 18 April 2024, Accepted: 1 May 2024, Published: 19 May 2024

Conference paper, DOI: https://doi.org/10.59490/imdc.2024.839 e-ISSN: 3050-4864

significantly affect the intensity of the target typhoon. Specifically, in one example, assuming a large sailing ship with a sail area of $25,600\,m^2$ per ship, the intensity of a typhoon could be reduced by 10 % by deploying 200 large-size sailing ships in a 100 km square around the center of the typhoon and having them follow the target typhoon.

The concept of a typhoon power generation ship has great potential for realizing a sustainable society. However, quantitative assessments with specific operational assumptions must be carried out to make this concept a reality. For example, we should examine whether a typhoon power generation ship can conduct physical operations as assumed in a typhoon. At the same time, we should accurately estimate in advance what kind of operations the typhoon power generation ship should perform, the amount of power generation that can be expected if operations are carried out as assumed, and the appropriate size of the typhoon power generation ship. These issues belong to the problem of designing the concept of a typhoon power generation ship. This paper develops a system simulator for quantitatively evaluating the operation concept of a typhoon power generation ship using typhoon track history data. By using the developed system simulator, this paper examines the appropriate size of the typhoon power generation ship.

PROPOSED METHOD

In this paper, a typhoon power generation ship is called a TPG ship. The operational concept, operation method, and necessary specifications of a typhoon power generation ship are collectively called the TPG ship concept model. The conceptual design and basic plan of the TPG ship are developed by defining its concept and quantitatively evaluating the defined TPG ship concept using a system simulator. Figure 1 shows the proposal to evaluate the TPG ship concept using a developed TPG ship operation simulator.

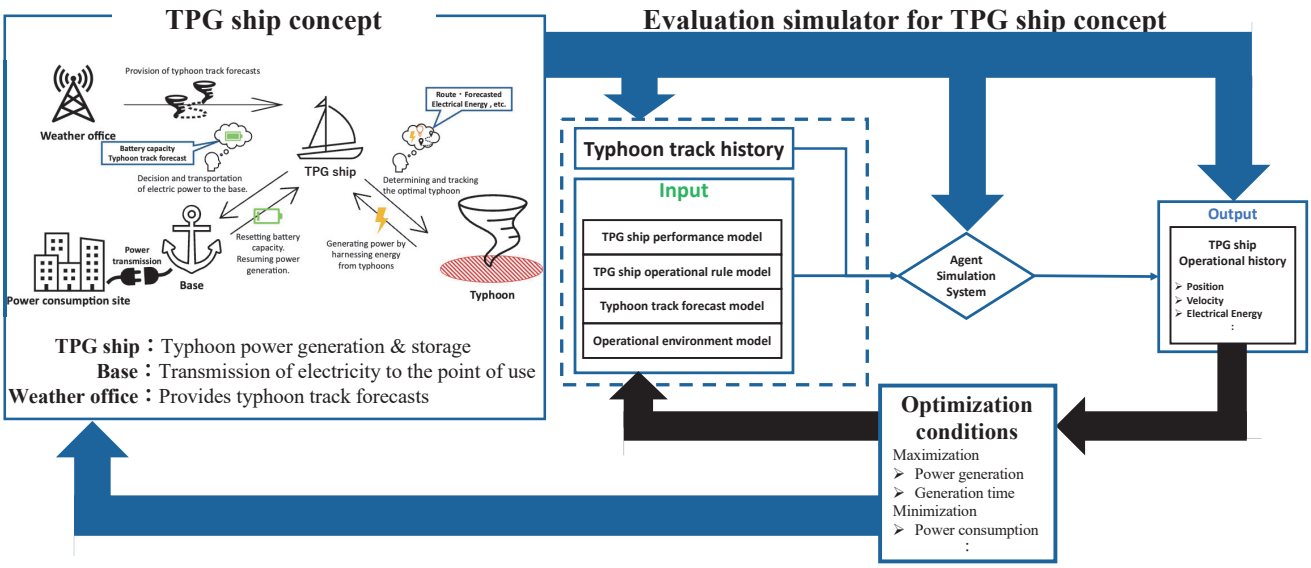

Figure 1: Overview of the proposed method

The TPG ship operation simulator must be able to reflect not only the ship body but also related technologies for power generation and storage and weather information as parameters. It also needs to be able to evaluate the impact of parameter changes on the TPG ship. An optimized TPG ship model is explored by continuously selecting and evaluating the TPG ship model based on the optimization conditions established, such as the maximization of power generation. We can quantitatively evaluate the TPG ship concept based on the required power generation targets and other issues.

TPG ship concept model

The TPG ship concept model consists of the operational concept, operation method, and necessary specifications of a target TPG ship. Figure 2 shows the operational concept of the TPG ship. In the proposed model, TPG ships can operate stably under typhoon conditions, generating and storing electricity. When sailing under typhoons, the TPG ship is propelled only by wind propulsion. When sailing in other conditions, the TPG ship is propelled using both wind and electricity propulsion stored on board. When sailing during power generation, even if the typhoon speed is slower than the TPG ship, this ship can keep the ship service speed by zigzag maneuvering under the typhoon. TPG ships can obtain accurate real-time typhoon track forecast information from the weather office. During periods when there are no typhoons in the surrounding area, the TPG ship waits in a predefined area. A base for accumulating the energy acquired by the TPG ship shall already be in place, and the base shall transport the energy to the use site by a different method from that of the TPG ship. The TPG ship must call at its base and manage its capacity before its storage capacity is full. The modeling of the TPG ship concept focuses only on the power generation from typhoons. Therefore, the entire supply chain, including transportation to the utilization sites, is not considered. The scope of the proposed model is limited to the transportation to the base, whose place is pre-determined.

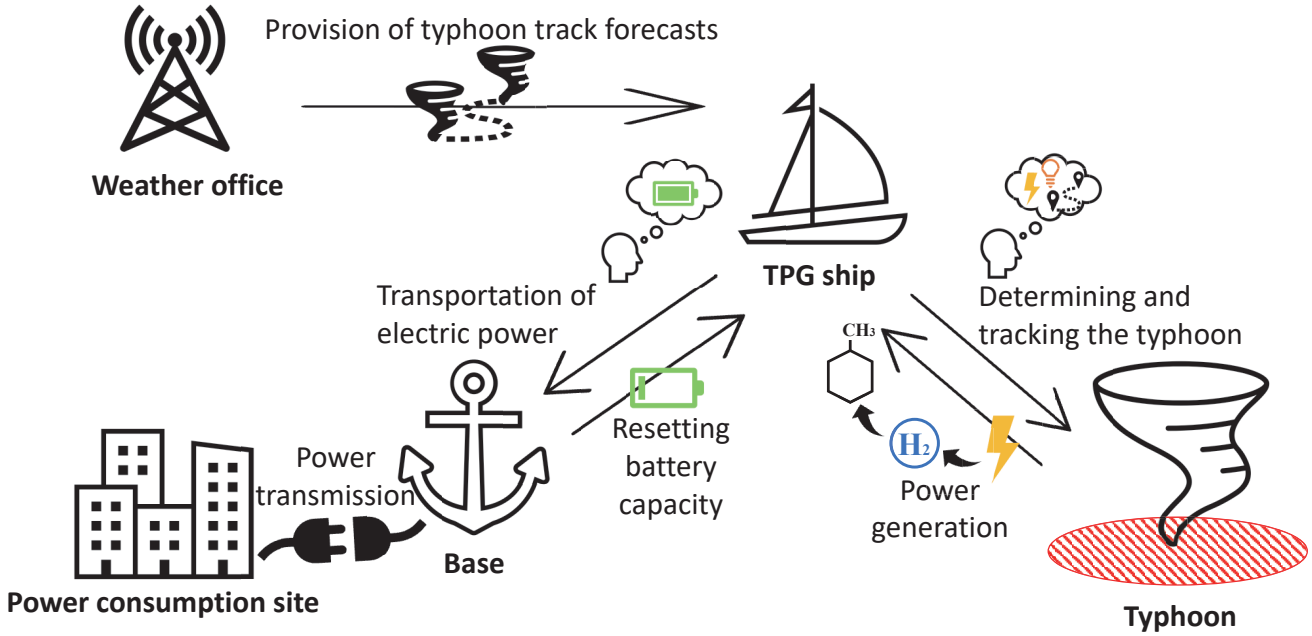

Figure 2: TPG ship operation concept

Developed TPG ship operation simulator

This paper has developed the TPG ship operation simulator as an agent-simulation system. The inputs consist of four models: the TPG ship performance model, the TPG ship operational rule model, the typhoon forecast model, and the operation environment model. This simulator conducts the agent simulation using these inputs and typhoon track history.

The TPG ship performance model defines the specification of functions, including power generation, power storage, wind propulsion, and electricity propulsion. The power generation function generates electricity when the TPG ship is propelled under typhoons. The power storage function stores the generated electricity or hydrogen converted from the generated electricity. The wind propulsion function uses winds to propel the TPG ship. The electricity propulsion function is a function in which the TPG ship is propelled by using the electric power stored on board. The TPG ship operational rule model reflects

how the TPG ship operates, corresponding to the environment. The TPG ship operational rule model is defined as an agent rule in the developed simulator. The typhoon forecast model defines the period and accuracy of typhoon track forecast. The operation environment model defines the position of the base and standby of the TPG ship.

The output of the TPG ship operation simulator includes the position, speed, power generation amount, and power generation time of the TPG ship at each time. Figure 3 shows one of the examples of the developed interface for visualizing the output of the TPG ship operation simulator. Figure 3 depicts a typhoon ship departing from a standby position to track, capture, and generate power from a typhoon. By specifying the period to be visualized, the behavior of the TPG ship in the simulator can be understood in detail and intuitively.

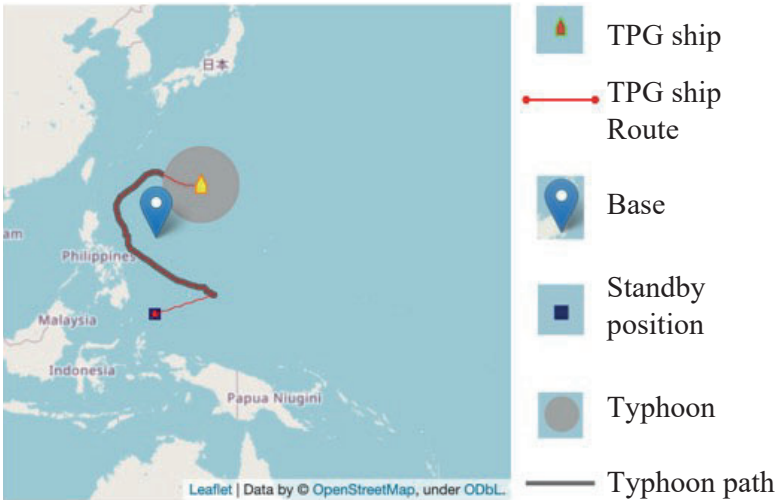

Figure 3: Interface for visualizing the result of TPG ship operation simulator

CASE STUDY

A primary design study of a TPG ship was conducted using the proposed method. Specifically, we performed sensitivity analysis on a simplified performance model of a TPG ship in which the specifications of the power generation function were set as fixed, and other performance functions of the TPG ship were automatically defined according to the storage capacity settings. This paper analyzed how the annual power generation of the typhoon power generation ship changes when the storage capacity setting is changed.

Problem setting

TPG Ship performance model

The TPG ship performance model defines the specification of functions, including power generation, power storage, wind propulsion, and electricity propulsion. In this case study, the specifications for the power generation function were fixed, and the specifications for the power storage function were adopted as the parameters for sensitivity analysis. The specifications of the wind propulsion and electric propulsion functions were calculated automatically from the power storage function's specifications by adopting a simple TPG specification model.

The specifications of the power generation function were set based on the studies conducted during the conceptual phase of

this research. Specifically, the rated output of a TPG ship under a typhoon P_{output} is set to 0.138 GW, and this specification is assumed to remain fixed as long as the ship is within 100km of the typhoon's center. It is assumed that the TPG ship cannot generate power outside the typhoon area. The specification of the power storage function can be entered into the developed simulator in units of 1 GWh. This case study will employ the organic hydride method to model the power storage function. The organic hydride method is a method in which electricity is converted to hydrogen and then added to toluene, an organic compound, for storage. The efficiency of converting the energy of the hydrogen produced by this method into electricity was set to 80 % by adopting the direct MCH method (Matsuoka et al. (2018), Kobayashi et al. (2021)) and in anticipation of future technological innovation. In other words, a 0.138GW TPG ship can store 0.110 GWh of electricity as MCH for one hour of power generation. The wind and electric propulsion function specifications are defined according to the deadweight ton (DWT). This case study uses a simple TPG specification model that transforms the deadweight ton to 379 tons per one GWh of power storage capacity, considering the physical properties of toluene, MCH and a ship hull similar to a tanker. Equation (1) shows the formula for calculating the energy output required for a deadweight ton of TPG ship hull to sail at speed V, which was adopted in this case study. This case study adopts $K = 2.2$, considering that the hull form of a TPG ship is similar to that of a tanker. Since the TPG ship is assumed to be a catamaran, Equation (1) divides the deadweight ton by two and multiplies by two at the end to calculate the energy output for two ship hulls that each ship hull has half deadweight ton.

$$P_{hull} = K \times \left(\frac{\mathrm{DWT}}{2}\right)^{\frac{2}{3}} \times V^3 \times 2 \tag{1}$$

The required energy output for the additional items other than the ship hull is calculated using Equation (2). For this simplified study, P_{add} is calculated as the energy output equivalent to 1 % of the rated output P_{output} at the service speed $V_{service}$ of the TPG ship. The required energy output for wind propulsion P_{wind} for speed V is always assumed to be 10 % of P_{hull} at service speed $V_{service}$. The energy output required for electric propulsion P_e is calculated from these three elements, as shown in Equation (3). Note that when the TPG ship generates electricity under a typhoon, it is assumed that $P_e = 0$, i.e., the TPG ship can sail at assumed service speed $V_{service}$ with wind power alone without power consumption.

$$P_{add} = 0.01 \times P_{output} \times \left(\frac{V}{V_{service}}\right)^3 \tag{2}$$

$$P_e = P_{hull} + P_{add} - P_{wind} \tag{3}$$

TPG ship operational rule model

The TPG ship operational rule model is a model that describes how a TPG ship makes decisions and acts according to the situation. The amount of power a TPG ship generates may vary depending on the operational rules for judging the situation. This case study implements the TPG ship operational rule model as an agent model. Figure 6 shows the overview of the adopted TPG ship operational rule model. We have implemented this TPG ship operational rule model to prevent the TPG ship's inefficient actions, such as tracking typhoons that the TPG ship cannot catch. In addition, we adopted a rule that the TPG ship's power generation output is frequently handed over to the base. This rule eliminates the need for massive power storage capacities and, thus, the need to adopt a huge TPG ship design proposal. As for the specific decision-making process in Figure 6, first, the system selects typhoons that can arrive and decides to call at the base when it is possible to do so via the base. Next, the destination is determined based on whether the TPG ship has stored at least 25 % of its storage capacity; if the TPG ship has arrived, it waits; otherwise, it takes action to move toward the destination. The developed simulator applies this operational rule at every time step in the simulation run.

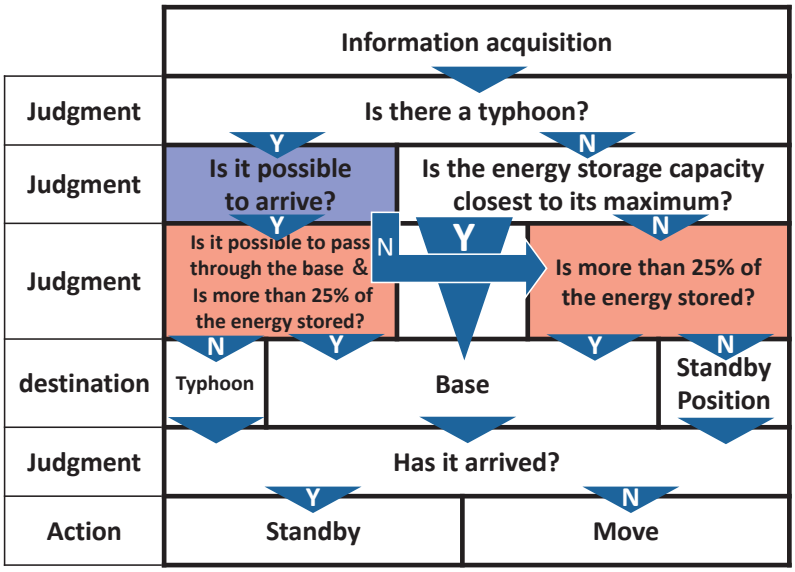

Figure 4: Overview of the TPG ship operational rule model

Typhoon forecast model

The developed typhoon forecast model focused only on the track and consisted of forecast period and accuracy. In this case study, the forecast period of the target typhoon track was set to five days from the time of the forecast, and the forecast accuracy of the track was set to 100 %. Although 100 % accuracy in typhoon track forecasting is unrealistic, the accuracy of typhoon track forecasting has been dramatically improved in recent years compared to typhoon intensity forecasting, and there is no significant difference in the judgment of TPG ship operations unless a typhoon makes landfall. Since the purpose of this case study is the primary design of a TPG ship, the above settings were adopted because they are expected to generate a considerable amount of power. In addition, the TPG ship can freely generate power outside the exclusive economic zone.

Operation environment model

The TPG ship is to be operated in Japan, and its base position is 24 degrees north latitude and 153 degrees east longitude, assuming MINAMITORISHIMA island. The standby position is where a TPG ship anchors at sea to capture typhoons efficiently. The TPG ship is assumed to be completely stationary in the standby position and does not generate power. Land and sea locations were roughly set up on the simulator from map data so that the TPG ship could only operate at sea locations. In addition, track information for each typhoon in the developed simulation was produced using the track history data of typhoons that passed near Japan from 2017 to 2022.

Results

By using the above settings, the annual power generation was calculated by varying the power storage capacity specification of the TPG ship performance model from 5 GWh to 150 GWh in 5 GWh increments. Figure 5 shows the annual power generation of the TPG ship for each power storage capacity specification. The horizontal axis represents the power storage capacity setting in the TPG ship performance model. The vertical axis represents the annual power generation resulting from the simulation. Each line shows the simulation results for each year. This figure shows that improving the power

storage capacity in any year becomes ineffective against annual power generation above a certain level. Table 1 shows the number of typhoons has occurred and past near Japan each year. From Table 1 and Figure 5, we can see that the amount of electricity generated tends to saturate and become constant earlier when the number of typhoons is small, in contrast to the improvement in storage capacity. It can also be read that the amount of electricity generated by the TPG ship is positively correlated with the number of typhoons and that the amount of electricity generated by the TPG ship is not simply proportional to the number of typhoons. A more detailed analysis of the simulation results shows that the amount of electricity generated is correlated with the number of typhoons. The time of occurrence or landfall also significantly affects the amount of electricity the TPG ship generates. Based on these results, it can be concluded that an power storage capacity of 50 GWh to 60 GWh is appropriate for the TPG ship in this problem setting.

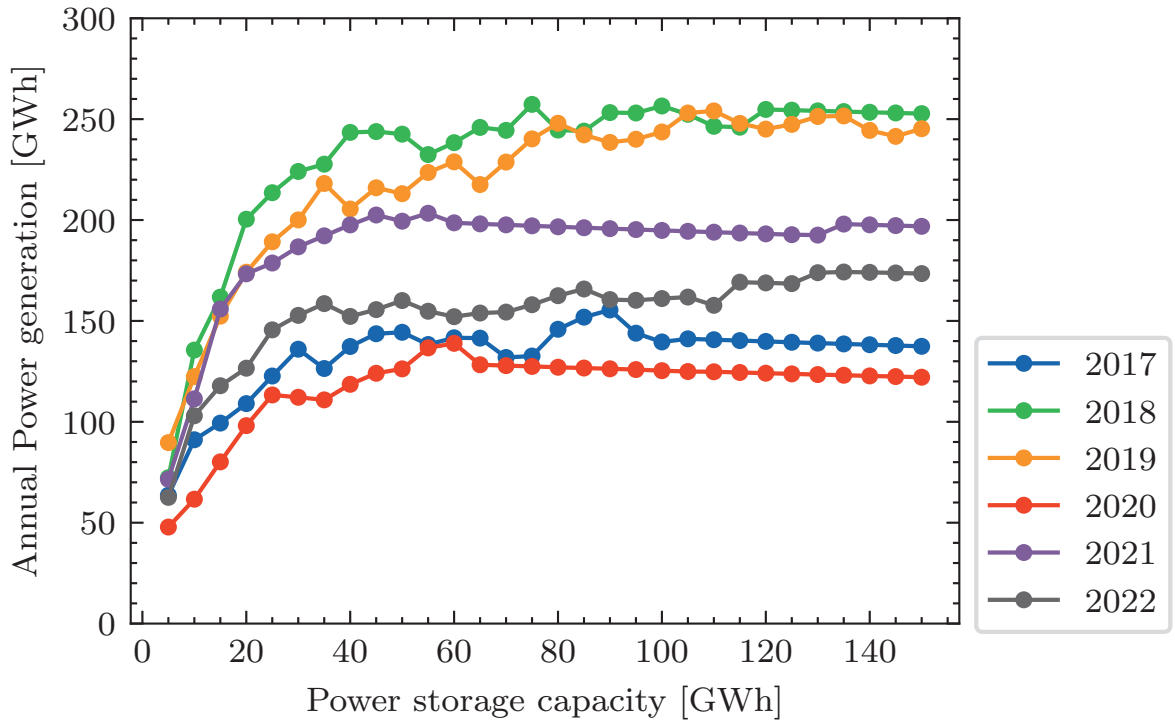

Figure 5: Annual power generation of TPG ship

Table 1: Number of typhoons has occurred and past near Japan each year

YEAR	NUMBER OF TYPHOONS
2017	27
2018	29
2019	29
2020	23
2021	22
2022	25

Sensitivity analysis

A sensitivity analysis was performed to see how the annual power generation would change if the standby position were moved slightly from this problem setting. Simulations were conducted by changing the standby location using the TPG

ship performance model setting of this case study when the power storage capacity specification was set to 60 GWh. In the case study, the standby position was set to MIMAMITORISHIMA island. However, this sensitivity analysis conducted four additional simulations with the center of MIMAMITORISHIMA island shifted ten degrees in latitude or longitude (about 1000 km) to the east, west, south, or north. Figure 6 shows the simulation results for each case from 2017 to 2022. From Figure 6, we can see that the annual power generation difference between each standby position setting is at most 5 % or less under the current conditions. The above results indicate that the effect of changing the standby location is small under this problem setting and simulation assumptions used in this study.

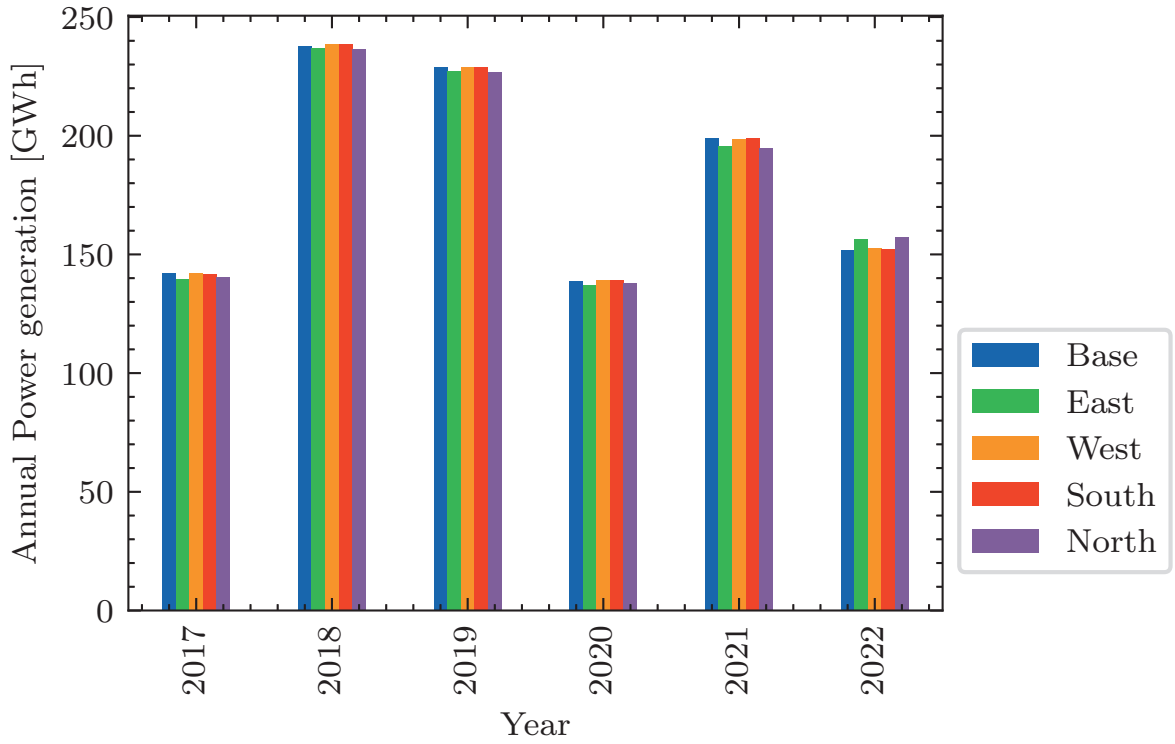

Figure 6: Annual power generation for standby position of TPG ship

DISCUSSION

This paper estimates the appropriate specifications of a TPG ship using a developed TPG ship operation simulator and simplified models. However, to provide a stable power supply, a TPG ship will be necessary to generate power not only from typhoons but also from ordinary ocean winds. This is because typhoons tend to occur more frequently in the summer, and typhoon power generation cannot occur during winter. On the other hand, the optimal decision on the extent to which typhoon power generation should be conducted and the extent to which power generation should be conducted using ordinary ocean winds is expected to vary depending on the specifications of a TPG ship. In this paper, simulations were conducted under the assumption that a TPG ship can operate as required, even in a typhoon environment. However, it is necessary to quantitatively estimate the extent to which operation is possible under a typhoon environment, reflect the results in the TPG ship operation simulator, and then develop the agent rule settings.

CONCLUSIONS

This paper proposes a typhoon power generation ship concept. The TPG ship concept model consists of the operational concept, operation method, and necessary specifications of a target TPG ship. For designing a preliminary concept of typhoon power generation ship, this paper developed a system simulator for evaluating the operation concept of a typhoon power generation ship using typhoon track history. Developed simulator was applied to the case study for designing a TPG ship which is operated near Japan. The case study showed that the annual power generation of the TPG ship tends to saturate and become constant earlier when the number of typhoons is small, in contrast to the improvement of power storage capacity. It can also be read that the amount of electricity generated by the TPG ship is positively correlated with the number of typhoons and that the amount of electricity generated by the TPG ship is not simply proportional to the number of typhoons. A more detailed analysis of the simulation results shows that the amount of electricity generated is correlated with the number of typhoons. The time of occurrence or landfall also significantly affects the amount of electricity the TPG ship generates. Based on these results, it can be concluded that an power storage capacity of 50 GWh to 60 GWh is appropriate for the TPG ship in this problem setting. This result indicates that appropriate size of TPG ship has existed in the current technology level. However, to provide a stable power supply, a TPG ship will be necessary to generate power not only from typhoons but also from ordinary ocean winds. In addition, it is necessary to quantitatively estimate the extent to which operation is possible under a typhoon environment, reflect the results in the TPG ship operation simulator, and then develop the agent rule settings.

CONTRIBUTION STATEMENT

Taiga Mitsuyuki: Conceptualization; methodology; writing – original draft. **Haruki Ebihara:** Data curation, methodology. **Shunsuke Kado:** conceptualization; writing – review and editing.

ACKNOWLEDGEMENTS

This work was supported by the Japan Science and Technology Agency Moonshot R&D Program Grant JPMJMS2282.

REFERENCES

Horinouchi, T. and Mitsuyuki, T. (2023). Gross Assessment of the Dynamical Impact of Numerous Power-Generating Sailing Ships on the Atmosphere and Evaluation of the Impact on Tropical Cyclones. *SOLA*, 19(0):57–62.

Kobayashi, A., Sato, Y., Miyoshi, K., Takami, H., Misu, Y., Nagatsuka, T., and Matsuoka, K. (2021). New Method for Producing Hydrogen Carrier: DIRECT MCH for Renewable Energy Use. In *23rd World Petroleum Congress*, page D041S018R001.

Matsuoka, K., Miyoshi, K., and Sato, Y. (2018). Development of Direct MCH Process using Renewable Energy and its Demonstration in Australia. *Journal of the Hydrogen Energy Systems Society of Japan*, 44(4):256–260.

Ouchi, K. and Henzie, J. (2017). Hydrogen generation sailing ship: Conceptual design and feasibility study. In *OCEANS 2017 - Aberdeen*, pages 1–5, Aberdeen, United Kingdom. IEEE.

Terao, Y. (2010). Typhoon Energy Utilization Using Mega-Yacht System. In *29th International Conference on Ocean, Offshore and Arctic Engineering: Volume 3*, pages 537–544, Shanghai, China. ASMEDC.

Proceedings of 15th International Marine Design Conference (IMDC-2024)
June 2-6, 2024
Amsterdam, the Netherlands

Conceptual design of shore station for an innovative waste collecting vessel

Niklas K.[1,*], Pruszko H.[2], Reichel M.[3], Jaworska J.[4], Marcinkiewicz E.[5]

ABSTRACT

Marine environment protection legislation in the EU requires ships to return waste they generate on voyages to waste-reception facilities in ports. In many harbors there is a need to expand the port infrastructure to enable the operation of Waste Collecting Vessels (WCVs). In addition, these vessels can perform new functions of cleaning port basins and adjacent waterways. A novelty in the presented research on the conceptual design of the shore station is the inclusion of new requirements for an autonomy and modularization of the vessel. The shore station was designed in the form of a floating pontoon, taking into account the various functional requirements addressed in the ship's conceptual design stage. The pontoon consists of modules corresponding to the ship segments moored in them. The conceptual design was intentionally defined in a generalized form to allow for further development and adaptation to local requirements at individual ports.

KEY WORDS

WCV autonomous; Station; Waste, Environment, Modular.

NOMENCLATURE

MARPOL - International Convention for the Prevention of Pollution from Ships
PRF - Port Reception Facilities
WCV – Waste Collecting Vessel

INTRODUCTION

At the international level, marine environment protection is addressed by the MARPOL Convention, which has been consistently extended to new areas including oil pollution (Annex I), sewage (Annex IV) and garbage (Annex V), air pollution (Annex VI). The most demanding environmental protection rules apply in so-called "special areas" which include the North Sea, the Baltic Sea, the Mediterranean, the Black Sea, the Red Sea and other basins that include a globally significant number of seaports. In European Union countries, the law is implemented on the basis of the relevant directives into national regulations. Recently, a directive was introduced on port reception facilities for the delivery of waste from ships (The European Parliament & Council of the European Union, 2019). The directive is a part of the circular economy policy (European

[1] Faculty of Mechanical Engineering and Ship Technology, Gdansk University of Technology, Gdansk, Poland; ORCID: 0000-0002-8652-765X

[2] Faculty of Mechanical Engineering and Ship Technology, Gdansk University of Technology, Gdansk, Poland; ORCID: 0000-0003-1902-2659

[3] Faculty of Mechanical Engineering and Ship Technology, Gdansk University of Technology, Gdansk, Poland; ORCID: 0000-0002-9876-9584

[4] Seatech Engineering Ltd, Gdansk, Poland; ORCID: 0009-0004-2239-7026

[5] Seatech Engineering Ltd, Gdansk, Poland; ORCID: 0009-0002-5152-9150

* Corresponding Author: karol.niklas@pg.edu.pl

Submitted: 23 February 2024, Revised: 15 April 2024, Accepted: 1 May 2024, Published: 19 May 2024

Conference paper, DOI: https://doi.org/10.59490/imdc.2024.840 e-ISSN: 3050-4864

Commission, 2018) and the plastics strategy (European Commission, 2020) of the European Commission. Under the requirements, ports are required to collect sewage and garbage from ships using land-based Port Reception Facilities (PRF). In practice, these are the most often adapted sections of existing port infrastructure. Garbage collection is particularly problematic, due to the fact that waste is segregated differently in various countries, and the way it is disposed of has not been standardized internationally. Thus, a ship returning garbage at each port can expect different formal rules and different collection methods, as well as different fees.

Port waters are at particular risk of pollution due to their high exposure to the negative effects of various human activities. It is port basins that often have the highest density of ship traffic in relation to water volume. It should be noted that these areas are often characterized by very limited exchange with the waters of the seas and further with the world ocean. Pollution is concentrated in port basins and is a growing challenge that should be addressed for environmental protection. It is worth noting that ships themselves and their traffic may account for only a fraction of a percentage of the various sources of pollution in many ports. In addition to ship traffic, port basins are exposed to impacts from various industrial companies, such as chemicals, heavy industry, ship repair yards, and cargo reloading companies. Particularly the latter in some locations pose a problem of heavy dusting of loose coal cargo, which, blown by the wind, partly ends up in the water and partly in nearby land areas. In many locations, harbor waters also experience pollution from various types of garbage, which, unlike that on land, is much more difficult and costly to remove, mainly because of the difficulties involved in finding, identifying, collecting, separating, transporting and disposing. Water pollution has been identified in many places as the most important environmental problem according to port authorities (Roberts et al., 2023). The survey was conducted among port authorities in 26 countries and city authorities in 13 countries. Air pollution and waste were identified as equally important aspects of environmental protection, where significant improvement measures are planned in the coming years. Currently, about half of the ports surveyed have facilities for re-use and recycling. This creates a lot of room for change with the growing awareness and ability to incorporate ports into circular economy (Roberts et al., 2021). For example, organic waste from ships can be used to produce feed for aquaculture (Strazza, Magrassi, Gallo, & Del Borghi, 2015). With the rapid development of many port cities and their revitalization, there is a need to address the challenge of cleaning port basins through special vessels, which are called Waste Collecting Vessels (WCS). It should be noted that they can have a variety of functionalities and range from picking up trash from commercial vessels, collecting trash from the water surface, to neutralizing small oil spills. The inadequate port infrastructure also poses a significant practical challenge to the operation of such vessels. In most port basins, the need for a systemic solution to the water treatment problem has not yet been addressed. Most port basins do not have a specially designed section dedicated to WCV and other environmental vessels. Garbage collection in ports is generally carried out in adapted portions of wharves, which have significant functional limitations. These are generally makeshift solutions that have been organized by local port authorities to comply with increasingly demanding environmental regulations. It should also be noted that a problem in vast port basins is also the presence of multiple stakeholders who use a common basin but are involved to varying degrees in its proper maintenance. Meanwhile, thinking ahead, in most port basins, since they are owned by a public entity, a systemic solution can be applied in the form of special municipal water services co-financed by all stakeholders. The next chapter presents the design assumptions for the selected conceptual design of a WCV-type vessel. This is followed by a description of the conceptual design of the shore station serving this new type of vessel. The conceptual design was made in the form of a universal modular concept adaptable to a variety of ports.

FUNTIONAL DESIGN ASSUMPTIONS OF THE WASTE COLLECTING VESSEL

The main functional design principles for the next-generation WCV vessel will be presented here. This is a conceptual design for a vessel with autonomous operation capability being developed through a consortium of an ongoing research and development project titled ‘Zero Emission Waste Collecting Vessel to Use in Ports and Close-to-Shore Areas’ carried out by a Polish-Taiwanese consortium. This description is intended to present a broader context on the various functionalities of the innovative vessel and the resulting requirements for the shore station. Various vessels of this type are currently being developed by design firms as conceptual designs in response to new demand from the niche sector of debris removal from port areas. It should also be added that the vessels currently operating in various ports are mainly the simplest solutions adapted from existing other vessels. A good example would be a towed transport barge with a container on board for collecting or picking up garbage by hand. Admittedly, this can be a quick and cheap temporary solution that works well in some places. At the same time, the large scale of needs and increasing environmental requirements are prompting the design of a dedicated special vessel that can safely and economically realize new functions. Functionally, a WCV vessel is envisioned for both collecting garbage from the water and areas near ports. In some cases, the functionality to pick up garbage directly from ships from the harbor roadstead is also required. An important task of this vessel is also to clean the harbor waters of trash, seaweed and minor oil spills. It is worth noting that statistically, as much as 80% of oil spills occur in ports and involve the normal operation of ships and port operations (Miola, Paccagnan, Massarutto, Perujo, & Turvani, 2009). These are unitary relatively small spills. However, their

negative effects accumulate over time in small volumes of port water. In summary, the following main functions were selected for the designed universal WCV vessel:

- collecting and removal of garbage floating on the surface of port waters,
- picking up of garbage containers from ships and yachts at anchorage,
- removal of minor oil spills from port waters,
- collecting seaweed from the water surface.

Since the required functionality may be different in different ports, the ship project was developed in the form of modules, which are connected according to the needs and tasks performed. The following modules of the WCV ship were defined:

- Module 1 (bow) occurs in different variants depending on the intended functions of collecting small oil spills. In Figure 1 the option of oil skimmer is shown.
- Module 2 (middle) which is the propulsion module of the vessel to which modules 1 and/or 3 are attached as required. The propulsion has been considered in two variants: the azimuth thrusters, or special water jets. This module also has consoles for optional manual control and suitable working conditions for a one-man crew. This module is equipped with tools for collecting trash from the water, a transport belt and containers for collecting waste.
- Module 3 (aft) provides additional transport volume for collected garbage. Optionally, this module can also have a transport belt.

Thanks to the hull's modularization, the ship can operate as a full three-module set or as a set consisting only of two modules, or as just the middle module as an independent unit. Modularization of the unit will ensure that it is multifunctional, allowing it to be used to its fullest potential, with the ability to select multiple modes of operation as needed. The vessel will be able to perform tasks in three operation modes: as a fully autonomous unit with pre-programmed operation mode, as a remotely controlled vessel and as a manned vessel controlled from aboard. In the last case, control will take place from a control panel located in the superstructure of the middle module. The use of Artificial Intelligence (AI) can also be considered in the autonomization of a ship of this type. In particular, to increase the operational energy efficiency and effectivities learned by the algorithms based on site-specific data. The conceptual design of a WCV-type vessel is analogous to that of other ship types and includes the design of the hull, propulsion and other equipment. At the same time, relatively more attention needs to be paid to maneuverability due to the functions performed and the often-tight area of operation. The initial design process shell include the selection of hull type between i.e. monohull and catamaran. The main dimensions are mainly driven by the desired functionalities. A key component of the project is the propulsion. Also in terms of its damage safety and operability in shallow waters. Overall, due to the multifunctionality and the required small hull size, the design process of a WCV-type vessel may be quite complex and demanding. A description of the innovative design approach for the new type of small special vessels like the WCV's is planned as the subject of a separate article. A visualization of the selected conceptual design of the WCV vessel in a catamaran version with an overall hull length of LOA=14 m is shown in Fig.1.

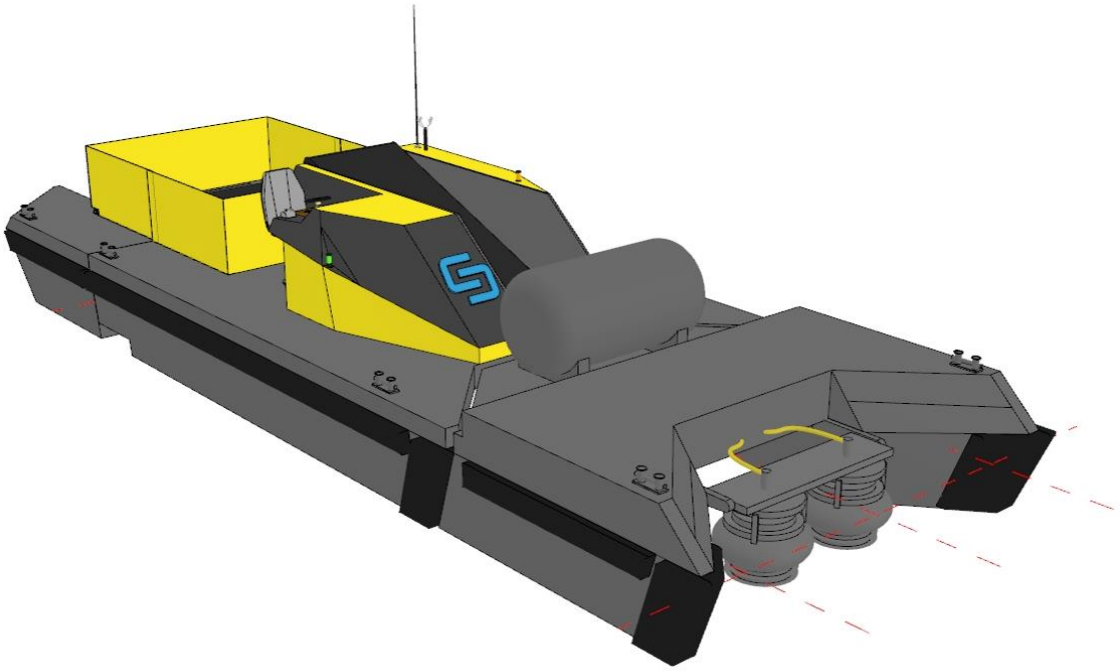

Figure 1: Conceptual design of the modular Waste Collecting Vessel

CONCEPT DESIGN OF THE SHORE STATION

The implementation of legislation on port reception facilities for the delivery of waste from ships assume fulfilling the following general requirements (The European Parliament & Council of the European Union, 2019). The main indication is that the port infrastructure shall be adequate to receive the types and quantities of waste from ships normally using that port. This needs to be done avoiding delays and without charging excessive fees. Also, ship waste needs to be managed in an environmentally appropriate way in accordance with the directive (European Parlament, 2008) and other EU legislation on waste. However, as the study shows, the current waste management at the vast majority of ports is insufficient (Özkaynak & İçemer, 2024). In large part, this may be due to the lack of proper port infrastructure, which was built when current environmental requirements did not apply. Effective logistics and management without a systemic solution of utilities is practically unfeasible. Thus, here the authors propose the modern idea of a shore station for Waste Collecting Vessels. The following functional assumptions are defined for the port quay:

a) The possibility of mooring a WCV-type vessel, which can operate in different modular configurations: as a single module designated as "2", as module "2" with attached modules "1" and "3". At the same time, module "1" comes in three variants depending on the function performed. In addition, the modularity of the ship and its multifunctionality is tailored to the individual needs of the specific area on which it is to operate and the selection of functionality with which it is to be equipped. No less, there is always at least module "2", which is also the propulsion module of the vessel. All modules should allow mooring in a position suitable for the connection and/or departure of the vessel. That is, bow modules marked "1" should be moored bow to quay, and stern modules marked "3" should be moored stern to quay. Module "2" should be moored with the stern to the quay, due to the easier transfer of containers with collected garbage to land. This positioning of module "2" influences the preferential location of the connection connectors for charging the electric drive batteries on the stern side of module "2". It is possible to use a different configuration of charging connections if there are other reasons for this. The functional diagram of the mooring of the modules of the WCV ship is shown in Fig.2. The arrows in the diagram indicate the direction in which the modules will sail when connected to each other.

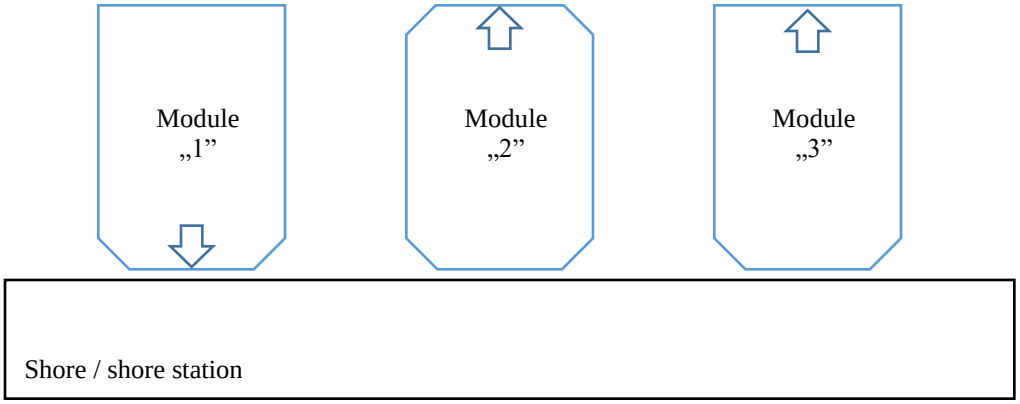

Figure 2: Functional diagram of the mooring of WCV ship modules to the shore

b) Mooring capability with different levels of autonomy of the WCV vessel. This functionality creates the need for an automatic mooring system. For a small vessel, it is possible to develop an automatic mooring system using suction pads and hydraulic actuator systems. Such solutions have already been developed commercially for larger vessels and their adaptation is relatively easy.

c) Capability of automated charging of electric propulsion batteries.

d) Ability to return collected waste to land. Each module is designed to collect waste of a different type. The quay at the docking point of module "1" should allow for the return of oil pollutants to land. This is usually done by pumping out the oily water to a vehicle (tanker) receiving the waste ashore. For this function, it is possible to automate the pump-out process (connecting, pumping, disconnecting). The second module is designed to drive the vessel and collect garbage and plants from the water surface has containers in the rear for collecting them on board the vessel. Again, it is possible to automate the replacement of containers. Replacement of the containers with empty ones, their cleaning is carried out by the city's municipal services. The third module is designed, like module "2", to store garbage and seaweed collected from the water. In addition, this module can receive garbage from ships, and this can be done similarly to module "2" using standardized site-specific containers. In all of the above cases, access to the quay and moored modules should be made available to vehicles dedicated to collecting each of the listed types of waste. Usually there will be special municipal vehicles – i.e. garbage trucks, cisterns, trucks with transport containers.

e) Ability to moor in defined weather conditions. Safety associated with mooring also in difficult weather conditions (e.g., strong wind, ice).
f) Ability to moor in tidal areas without restrictions (in practice, it is 15 m). For this purpose, the charging station was designed in the form of a floating modular pontoon. The movement of the station in relation to the quay can be carried out using guides attached to the quay, or by means of piles driven into the bottom of the basin. Depending on the expected loads from sea waves, the tidal guides and piles can have an additional function of stabilizing whole pontoon.
g) Safety capability. Selective access, the ability to access the modules for inspection.
h) Ability to disconnect modules and access each module for the purpose of performing maintenance work, and major repair work if needed.

Different variants of possible technical solutions have been analyzed in terms of the design assumptions set above. There are no dedicated design regulations for this type of facility. Therefore, design can take place based on i.e. the individual evaluation of the selected classification society. Design requirements for this type of object strongly depend on the choice of material to be used. For the design of a barge made of steel, the regulatory requirements for standard barges can be used directly. On the other hand, if one would like to use different material, the specific requirements must be agreed with the regulatory body. It should be noted that due to local regulations, in some countries it may be advantageous to classify the docking station as a hydro-engineering structure, and in others as a floating barge. This requires recognition in the country of intended use and is important because of differences in the costs of maintenance. The main design criteria concern structural strength and stability. When it comes to structural strength, the dominant load is dead weight and water hydrostatic pressure. In addition, there is a need to take into account the hydrodynamic pressure from wave action caused by passing ships. Particularly vulnerable elements at that time are the connections between modules and the junction area between the barge and the quay. Consideration needs to be given to both the loads from short waves hitting the side surfaces of the docking station and long waves that can induce additional bending moments on the entire hull of the barge. When designing a new type of docking station, stability requirements shall also be taken into account. This is not obvious, after all, the station is ultimately connected by movement to the guides or piles of the quay. At the same time, the transport of modules separately or combined to the site of use may include towing. The docking station does not have its own drive, which greatly simplifies the design process. On the other hand, the docking station is equipped with electric charging stations which introduces additional requirements specific to electric devices. However, from a practical point of view, the main determinant of the project concept presented below was economic criteria while allowing the design to be used in various ports around the world. Implementation in existing ports precisely for economic reasons is possible almost exclusively through the adaptation of existing port berths. A major challenge in most locations is ensuring the safety of the ship's mooring due to possible high wave loads, i.e. from passing vessels. Therefore, the individual modules of the WCV unit are docked in such a way that they do not protrude beyond the outline of the pontoon. A key aspect that improves the economics and flexibility of the proposed solution is the modularity of the shore station to match the modularity of the WCV. Each module reflects functional requirements of a particular vessel module. This means that the shore station will consist of such modules for which the need for mooring in a particular port is foreseen. Due to the optional different levels of autonomy of the WCV, all modules are suitable for both traditional human-operated mooring and different levels of autonomy. The design assumes applying universal connectors that allow different configurations of shore station modules. A visualization of the shore station conceptual design is shown in Figure 3. The stern and bow modules are to be moored in a way that enables their automatic connection with the middle propulsion module without the need to move or rotate and without human intervention. This means that the stern module will be moored aft, while the bow modules will have the bow facing the quay. Automatic mooring of all modules can be carried out using a dedicated pneumatic mooring system. After mooring, the module needs to be additionally secured by an automatically released mechanical holder. The reason for this is the need to reduce energy consumption during downtime. The charging of the middle module can be realized by dedicated automatic connector from the shore. At this stage of conceptual design technical details both for the pneumatic mooring system and the automatic charging connector were not analyzed. However, a review of the literature indicates that products with the required features could be available on the market very soon, if only they are desired. However, the implementation of the presented project to the technical design phase requires adequate research work for the components and the entire system. This may be the subject of further research work.

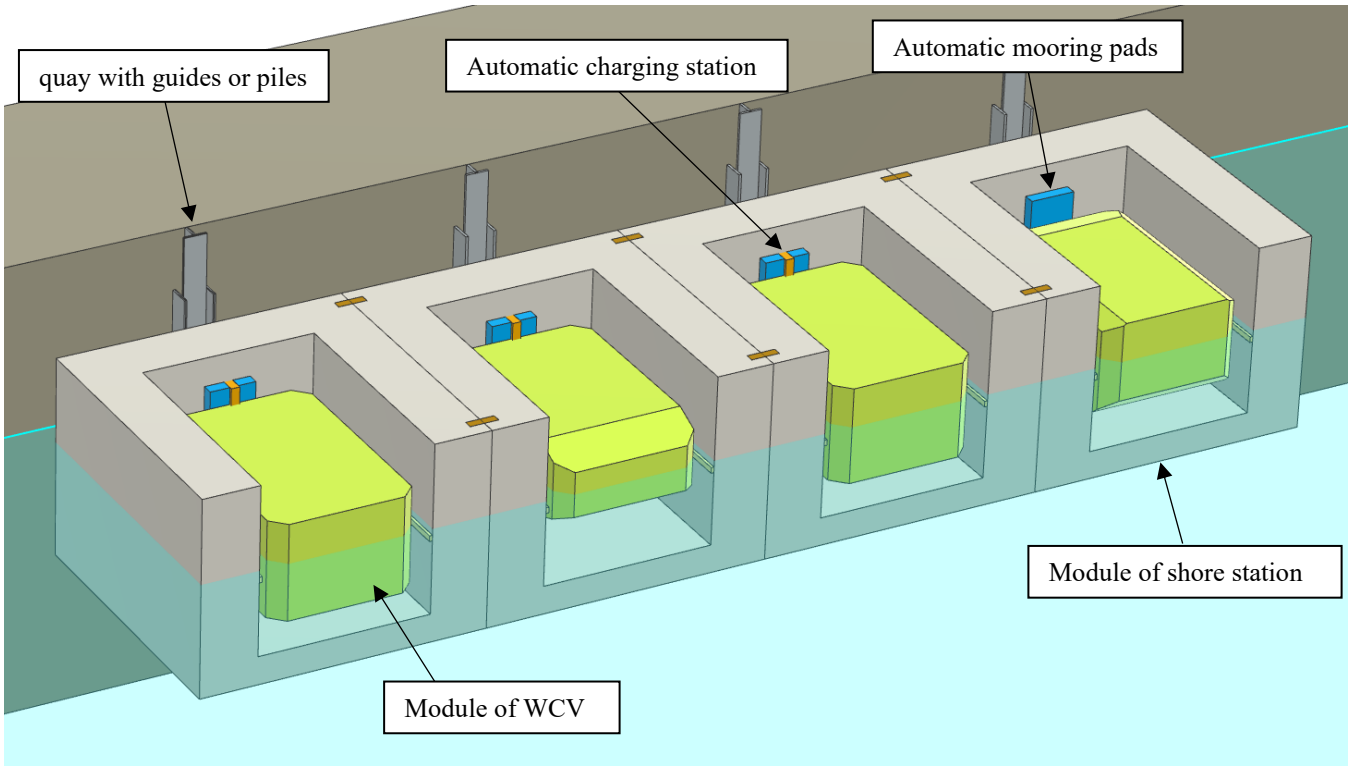

Figure 3: Conceptual design of the shore station for WCV vessel

SUMMARY

Progressive environmental regulations, especially in the port zones of SOLAS special areas, are forcing the development of port infrastructure and vessels related to the collection of waste from ships. On many basins, it is also important to clean port waters of various types of pollution - such as minor oil spills, garbage floating on the water surface and others. The problem, although it affects many ports and various locations, is particularly evident in developing countries where, for various reasons, waste management has not yet been properly addressed. It should be noted that the key challenges are the unification of solutions used in different ports, the application of affordable fees and the time of waste collection from ships.
The proposed conceptual design of shore station can be part of a key infrastructure for receiving waste from ships and pollution collected from the surface of port waters. The project uses a modern design approach based on modularity and versatility of various functionalities that can be tailored to the individual needs of a given port. They can also be changed or expanded relatively easily as the port grows. The presented shore station included new requirements for autonomy and modularization of a Waste Collecting Vessel. Finally, the form of modularized pontoon takes advantage of cost efficiency both for new and existing berths. Mooring the pontoon on piles or guides allows the station to be used in tidal areas. Also crucial for the mooring of small WCV-type vessels is their protection from waves, which has been achieved by the special shape of the station modules matching those of the ship. The presented conceptual design was made intentionally in a generalized form to allow for further development and adaptation to local requirements at individual ports. The project is under development being in line with the circular economy and industry 4.0 trends.

CONTRIBUTION STATEMENT

Author 1: Conceptualization; investigation; methodology; writing – original draft; writing – review and editing. **Author 2:** Conceptualization; investigation; methodology; writing – review and editing; funding acquisition. **Author 3:** Conceptualization; investigation; supervision; methodology; writing – review and editing; funding acquisition; project administration. **Author 4:** Conceptualization; investigation; visualization. **Author 5:** Conceptualization; investigation; visualization; writing – review and editing.

ACKNOWLEDGEMENTS

The research was supported by the National Center for Research and Development (NCRD) within the project ZeroWastePorts: Zero Emission Waste Collecting Vessel to Use in Ports and Close-to-Shore Areas. Agreement no PL-TW/IX/43/ZEROWASTEPORTS/2022. The project visualization was supported by the Academic Computer Centre in Gdansk (CI TASK). All support is highly appreciated by the authors. Authors thank the reviewers for their valuable comments.

REFERENCES

European Commission. (2018). *Strategy for Plastics in a Circular Economy*. *COM(2018) 28 final*. Brussels. https://doi.org/10.4325/seikeikakou.30.577

European Commission. (2020). *A new Circular Economy Action - Plan For a cleaner and more competitive Europe*. *COM(2020) 98 final COMMUNICATION*. Brussels. https://doi.org/10.7312/columbia/9780231167352.003.0015

European Parlament. (2008). DIRECTIVE 2008/98/EC OF THE EUROPEAN PARLIAMENT AND OF THE COUNCIL of 19 November 2008 on waste and repealing certain Directives. *Official Journal of the European Union*. https://doi.org/10.5040/9781782258674.0028

Miola, A., Paccagnan, V., Massarutto, A., Perujo, A., & Turvani, M. (2009). *External costs of Transportation, Case study : maritime transport*. *JCR Scientific and Technical Reports*. https://doi.org/10.2788/18349

Özkaynak, Ö. H., & İçemer, G. T. (2024). Based on stakeholder questionnaires of ship-derived waste, waste management re-planning in Ports and determining the need for inspection. *Marine Policy*, *159*(March 2023). https://doi.org/10.1016/j.marpol.2023.105912

Roberts, T., Williams, I., Preston, J., Clarke, N., Odum, M., & O'gorman, S. (2021). A virtuous circle? Increasing local benefits from ports by adopting circular economy principles. *Sustainability (Switzerland)*, *13*(13), 1–25. https://doi.org/10.3390/su13137079

Roberts, T., Williams, I., Preston, J., Clarke, N., Odum, M., & O'Gorman, S. (2023). Ports in a Storm: Port-City Environmental Challenges and Solutions. *Sustainability (Switzerland)*, *15*(12), 1–24. https://doi.org/10.3390/su15129722

Strazza, C., Magrassi, F., Gallo, M., & Del Borghi, A. (2015). Life Cycle Assessment from food to food: A case study of circular economy from cruise ships to aquaculture. *Sustainable Production and Consumption*, *2*(February), 40–51. https://doi.org/10.1016/j.spc.2015.06.004

The European Parliament, & Council of the European Union. (2019). Directive (EU) 2019/883 of the European Parliament and of the Council of 17 April 2019 on port reception facilities for the delivery of waste from ships, amending Directive 2010/65/EU and repealing Directive 2000/59/EC. *Official Journal of the European Union*, *2019*(November 2000), 116–142. Retrieved from https://eur-lex.europa.eu/legal-content/EN/LSU/?uri=CELEX%3A32019L0883

Proceedings of 15th International Marine Design Conference (IMDC-2024)
June 2-6, 2024
Amsterdam, the Netherlands

From Functional Arrangement to Vulnerability Assessment: Automating Naval Ship Design for Enhanced Survivability Analysis

H.J. den Ouden[1,*] and R. van der Wal[1]

ABSTRACT

A novel method has been developed to rapidly assess vulnerability of a new platform which has been generated through a packing approach. This method quickly transforms a volumetric packing model into a surface model that includes ship structure including doors and hatches, mission critical systems and the crew. A weapon model was developed taking into account the unpredictability of a threat by generating multiple scenarios with the Monte Carlo method. Based on this set of simulations vulnerability measures can be introduced in a weight efficient manner. This in turn will allow the naval architects to design safer naval ships in balance with other requirements. This paper describes the process of vulnerability analysis in early ship designs and the feedback loop of conclusions to the designers

KEY WORDS

Design; Vulnerability assessment; Naval ship; Internal Explosion; Fragmentation; Early ship design; Survivability.

INTRODUCTION

Command Materiel and IT (COMMIT) is responsible for the procurement and sustainment of the navy ships (van Oers et al. (2018)). The FIDES tool has been developed by COMMIT to facilitate the process of procurement, in which initial optimizations are performed with respect to layout and weight (Takken (2008)). Once a set of concept designs have been deemed acceptable, it becomes more important to test these designs on the aspect of ship vulnerability with the potential threats which this new navy ship can face. This analysis is directly performed after the initial early design process and should give insight on the ship design when it is still possible to alter the layout and component placement. The purpose of the paper is to demonstrate tooling and methodology in which TNO supports COMMIT with ship vulnerability assessment against damage from threat weapons. The tool entails the process of transforming the volumetric FIDES model that COMMIT produces into a model suitable for TNO's software RESIST (RESilience of Ship Targets), as well as the tooling used for developing the threat information and threat detonation locations. The tooling will be demonstrated in the following order: the model transformation of a volumetric model to surface model process by means of ShipMATe (Ship Modelling through Automated Technology) is demonstrated. Manual steps are performed to rapidly setup a RESIST model which includes both structural and systems information. Secondly the fragment distribution model of the threat weapon is explained. In-house developed tooling is used for determining the threat detonation locations. Lastly the RESIST tool is showcased in which the weapon effects are made visible for a specific case study. In this case study an initial ship layout is used with

[1] Department of Naval and Offshore Structures, TNO, Delft, The Netherlands

[*] Corresponding Author: hajo.denouden@tno.nl

Submitted: 23 February 2024, Revised: 1 May 2024, Accepted: 3 May 2024, Published: 21 May 2024

Conference paper, DOI: https://doi.org/10.59490/imdc.2024.858 e-ISSN: 3050-4864

specific conservative demands through which vulnerability improvements can be showcased. Various vulnerability reduction measures are applied to the ship and their effectiveness is determined based on the ship system state, after which a set of combined vulnerability measures are synthesized. These results are then communicated with the naval architects which concludes the vulnerability analysis process.

SHIP MODEL DEVELOPMENT PROCESS

As mentioned in van Oers et al. (2018) the Netherlands Defence Material Organisation (present day COMMIT) is responsible for the procurement of new navy ships. This includes the exploration of the naval ship design during the early stages of such a procurement process. During the exploration of the initial ship design, several different volumetric functional arrangement models are built with the tool FIDES (Functional Integrated Design Exploration of Ships), see Takken (2008). With the help of this tool various design routes are explored in which each route undergoes their own design loop in which stability, weight, costs and other requirements are assessed. Once such a design seems feasible, the model is shared so that more detailed analysis can be performed. Vulnerability requires more detail since it is influenced by a broad set of parameters: the ship structure, the placement and robustness of components, the routing of cables and pipes and the location of crew members. The threat definition based on the ship's mission is important for the assessment of vulnerability, which requires a different type of modelling effort. To quickly deliver a vulnerability assessment, the model building process from Figure 1 should be automated as much as possible.

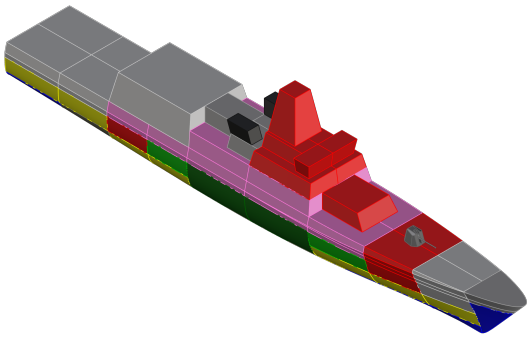

(a) The volumetric packing model in FIDES

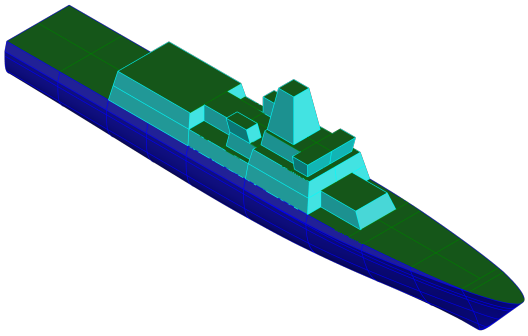

(b) The surface model that is automatically generated from FIDES model

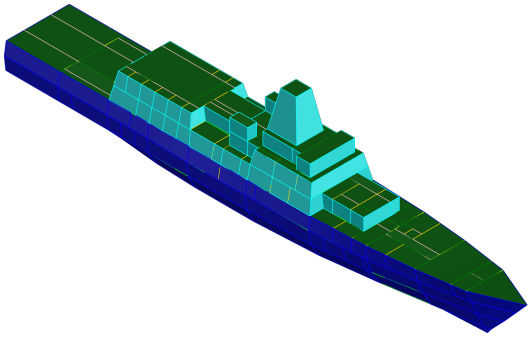

(c) The surface model transformed and simplified to a RESIST structural model

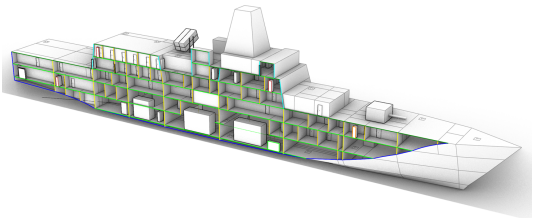

(d) RESIST model including passageways, components and systems

Figure 1: The process of model development through ShipMATe

During the early design stages, designers at COMMIT require an evaluation of design iterations within weeks. Next to the development of the initial arrangement, the designers also develop an initial plan of the routing and make an initial estimate of the primary component placement, see van Diessen et al. (2022). ShipMATe (Ship Modelling through Automated Tech-

nology) was developed to quickly prepare these initial ship arrangements into a model suitable for vulnerability assessment. The process is illustrated in Figure 1 and works in three distinct steps; The first step transforms the volume based FIDES model, portrayed in Figure 1a, into a surface model, shown in Figure 1b. The FIDES model that has been used for this paper is the same as the one developed for the automatic routing paper of COMMIT (Duchateau et al. (2018)). The reason for this surface model creation step is that most of the vulnerability analyses uses either a quadrangular surface with a specific thickness or shell elements in the case of FEM (Finite Element Method) model. This process is nearly completely automated while it allows the naval architect to make changes in the layout during the transformation process.

The second step in the process is to turn this surface model into a simplified surface model that only consists of quadrangular surfaces which is portrayed in Figure 1c. The reason for this simplification is that the current blast response model within RESIST requires a panel with two distinctive bending directions. This simplification affects the ship hull and panels that are in connection with the hull. These include: watertight bulkheads, transverse bulkheads and the hull panels. After this process is finished, the following steps will focus on including the structural data of the ship. Structural data is allocated to the various panels with the help of a 'scantling sheet'. This sheet appends the longitudinal and transverse stiffeners to various panels based on their type (deck, hull, longitudinal, watertight bulkheads and regular bulkheads) and their location (zonal position and deck level). The values for each of these properties are discussed with a naval architect specialised in the field of structural engineering. The inclusion of structural properties are essential for this type of vulnerability analysis since a more realistic approach for damage is used in this stage, which is where the analysis differs from other early design studies (Goodfriend and Brown (2018); Cramer et al. (2011)). The final structural properties of the panels can be modified if required. This allows the naval architect to add the necessary details to compartments which differ greatly in structural properties compared to the standard ship layout such as the ammunition storage rooms, the helicopter deck and the diesel generator room.

Once the structural model of the ship is completed, the systems on board of the ship can be created. Systems are included in a simplified manner because only limited information is available during the early design stages. Firstly the major components are approximated as filled bars, which include a skin material, skin thickness an internal material and a filling grade. This methodology is applicable to components ranging from small sensors to large components like diesel generators. The second step is to make an initial routing between the major components. Cable or pipe routing is often the more vulnerable part of the overall system. This process is currently performed manually, however tooling is in development to automate this process. The final step, see Figure 1d, in this process is to add the system logic to the model. The primary system logic is represented in a directed-graph, the requirements which check the ship state are represented in a tree structure. With all the necessary elements of the ship prepared an xml is generated by ShipMATe which allows for a direct transfer of the model into the RESIST software.

The ship has the following systems on board:

- The ship has a CODLAD (Combined diesel-electric and diesel) propulsion system
- The ship has a single anti surface weapon system and a single anti air system
- The ship has a single radar mast
- The ship includes for this study only the chilled water distribution and electrical distribution as auxiliary systems

THREAT MODEL

Where system studies commonly simplify the damage extend to compartment based rules , see (Duchateau et al. (2018); Jansen et al. (2020)), the damage extend for this systems study is based on physics-based model in which the threat consists of a blast and fragmenting warhead. A missile carries the warhead to the target and the fuse mechanism determines the detonation location, which could be either inside or outside the ship. The warhead is commonly a high explosive contained in a metal casing. The metal casing can be smooth resulting in natural breakup of the casing in fragments, or the casing can

contain pre-formed fragments of most any shape. In this paper we have assumed an anti-ship missile with a naturally fragmenting casing. There are several models available to describe the fragment distribution from such casings, one of which is given in ANEP43 (NATO Standardisation Office (NSO) (2014)). This describes a generic approach based on the warhead geometry and a mathematical mass distribution. For the current study, we have made use of the SPLIT-X tool from Numerics GmbH. SPLIT-X includes an elegant approach to natural fragmentation where the Hoop strain of the expanding metal is compared to the material tensile strength. SPLIT-X results in a spatial distribution and mass distribution of fragments. These stochastic distributions have a certain level of randomness, which is also witnessed in testing of shells or warheads. The break up process results in a unique distribution for each and every test. This requires a probabilistic approach when dealing with natural fragmentation, every run will yield in different fragment loading on the construction (although RESIST includes the option to fix the random seed, so that identical runs can be performed). Ejection velocities of the fragments are based on the Gurney velocity (Gurney (1943)).

The blast module in RESIST is deterministic in its approach. Every run of the same scenario will yield the same blast loading results on the structure. Reflected blast waves are determined using the mirror approach; the detonation charge is mirrored with identical charges in the plane where the reflection takes place. A target panel is divided in discrete loading areas and reflections up to first or second order from all other panels in the compartment are taken into account. Quasi-static pressure level is determined using a TNO-developed model for the rise time. Isentropic venting is based on leakage through failed decks, panels and doors. The response of the blast loaded panel is based on an advanced Single Degree of Freedom (SDOF) model (van Erkel (1992)) that is solved by time step integration. Failure is based on empirical strain values at the rim of the panels. RESIST combines the effects of fragments and blast: panels are weakened when fragments perforate before the blast wave arrives.

Threat physics definition

The threat considered in this case study is a sea skimming anti-ship missile. Sea-skimmers approach the ship a few meters above sea-level. Sea-skimmers have a circular error probability (CEP Webb (2012)) that is significantly smaller than the ships dimensions, and therefore can hit the ship at a specific spot. Weapon system ballistic performance is often expressed in CEP. In statistics the standard deviation is often used for expressing Gaussian distributions.

Here the assumption is made that the aim-point of the missile is selected near the bridge of the ship. This likely improves weapon effectiveness, because the centre of the ship contains more valuable compartments than the bow and the stern. The current model assumes no special manoeuvres. For optimal probability of hitting a target, a sea skimmer should hit the target from the side, with enough margin to miss the water, and low enough to not miss the freeboard. For users of the derived detonation point clouds it is recommended to check if the aim-point aligns well with the ship most important compartments. The model assumes an average impact altitude above sea-level, with a standard deviation. A dive angle is drawn from a uniform distribution, which corresponds to a slight dive in the terminal trajectory. Although not fully representative, the relative bearing of the missile with respect to the ship is chosen with a uniform distribution. For the fusing mechanism an impact delay fuse is chosen, with a delay that aims for a detonation near the centreline of the ship.

Uncertainty of the detonation location

The impact location of a threat on a naval vessel depends on a number of parameters in the flight trajectory of the missile, the seeker head, the fuse mechanism and the signature of the vessel. Therefore, a Monte Carlo Method is used to account for multiple scenarios. The Monte Carlo method that is used for the points distribution operates in the following manner: the impact location of the warhead on the ship is determined which can be achieved by either pulling a location from an uniform distribution (mostly applied for shells) or by using a Gaussian distribution. Limitations can be applied for the impact locations for threat, for instance the height range is limited for the sea-skimmer whereas the impact locations of the grenade threat is limited to impacts on the decks.

The other properties of the threat that are determined with a Monte-Carlo method are the elevation and azimuth angle. The

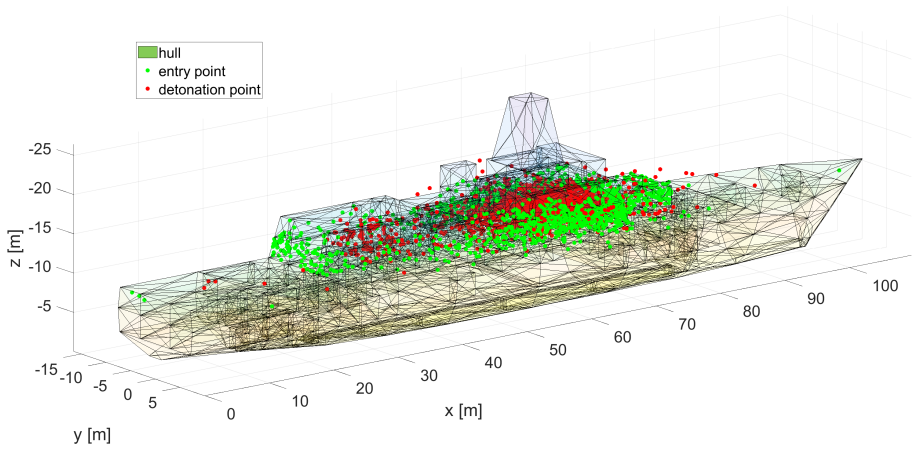

Figure 2: The impact and detonation points generated by the Monte Carlo detonation generator

velocity of the threat is fixed in this set of simulations since no distance based assumption is included for the determination of the threat properties. Finally the detonation mechanism of the threat needs to be defined, this can either be a deck counter or a proximity (delay) timer. With all these properties included a set of detonation locations are determined, similar to the example in Figure 2. The number of impact locations that is required for the analysis is dependent on both the type of analysis and the required confidence interval. As an example when we investigate the binary state of the ship with a confidence interval of 95% then about 1200 simulations are required to limit the error band to 5.7% (Clopper and Pearson (1934)).

CASE STUDY

With the ship model prepared and the threat impact points generated a set of Monte Carlo runs can be performed. The first results are the indicator to find improvements in the design. This ship model has been made so that it is not fully optimized with respect to vulnerability a priori. By performing an initial run of the Monte Carlo simulations on this baseline ship, the effectiveness of measures are demonstrated. The vulnerability is tested on the baseline ship by checking if the ”Mission Capability” state of the ship is still met. The ”Mission Capability” state is defined by the following conditions:

- Power must be available in each of the zones of the ship
- The SeWaCo (Sensor Weapons Communication) system must be active
  - The mast must available
  - Chilled Water must be available
  - 2 out of the 3 servers must be available and cooled
  - Either the anti-air or anti-surface weapon system must be available
- The ship must remain mobile
  - One of the propulsion lines must be operational
  - One of the propulsion machinery (diesel-electric or diesel) must be available
  - One of the steering gears must be available

The vulnerability of the ship can be minimized by intelligently combining the different measures. The second step of proposing effective vulnerability measures is to assess how effective various vulnerability measures are. To assess the effective-

ness of the vulnerability measures three variations of the ship have been made. Once a model is setup, it becomes easy to update the model with new additions to the design.

The first modified ship model has all its transverse bulkheads upgraded to blast and fragment resistant bulkheads (HARNESS bulkheads in this case , see van der Wal et al. (2018)). The outcomes of the simulations, visualized in Figure 3b demonstrate two areas in which the HARNESS bulkheads prove to be particularly effective when compared to the unprotected state. The first point is allocated at deck C underneath the bridge and close to a chilled water riser and a server room. The original 40 runs that take place in this compartment are rendered harmless due to the bulkhead taking more dynamic load of the blast wave and while also reducing the amount of fragments that would normally hit the servers. Similar effects are seen at deck D at the compartment second left to the furthest right bulkhead of the main superstructure. In this case a chilled water riser is protected significantly increasing the survivability of the local systems that require cooling like the server and the distribution board nearby.

The second vulnerability measure that is explored is increasing system redundancy. The ship design was improved with the redundancy of the electrical system of the ship, whereas the chilled water system remained unchanged. The chilled water system was not altered in this model since it required to add piping, whereas the electrical system does not require extra cable trays. The redundancy is increased by linking a load centre to two different distribution boards. The difference between the regular layout (Figure 4a) and redundant layout (Figure 4b) is the interconnection of the main switch board and that each load center is linked to two distribution boards.

Aside from the Monte-Carlo distribution, which is shown in Figure 3c, the actual performance of the systems can also deliver insight which parts of the systems benefit from the redundancy. For this case-study the system based comparison are made for the “Power to all zones” requirement of the ship and to investigate the performance of the mast which is a single point of failure within this ship design. Figure 5 shows how the overall “Power to all zones” criteria is met in more cases. It should be mentioned that the increased redundancy measure seems to be having the most effect in zone 3, whereas for example improving zone 2 does not increase the performance by much. The mast increases in survivability significantly as well, as shown in Figure 6. The load centre of the mast is in zone 3, meaning that increasing redundancy is a worthwhile effort.

The third vulnerability measure that has been investigated is that of hardening the components within ship. The ship model has been altered in such a manner that all the kill criteria of the components have been tripled. The kill criteria include the maximum pressure and maximum amount of kinetic energy that a component can withstand. Based on the results of this set of simulations, illustrated by Figure 3d it can be concluded that increasing the strength of the components is the most effective solutions. An analysis tool is used to see which hardened components improve the resilience the ship the most. This is done by correlating the increased “Mission Capable” states and see which components did not fail in these specific runs. The conclusion of this analysis is to harden the components that are close to the single points of failure like the chilled water piping close to the mast and the cables to the load centre of the mast.

By combining the lessons of the three sets simulations with different vulnerability measures, the following adaptations have been made to a final model:

- The HARNESS bulkheads will be placed in the areas where they caused reduction in vulnerability, this is highlighted in blue in the results
- Zone 3 and zone 4 will have redundant cables to significantly increase performance of the zonal power requirement
- The components with respect to the single point of failure (the mast and its subsystems) will be hardened

Each of these measures have been selectively chosen and the weight of the ship is only marginally increased by the adjustments:

- The cables and piping that have been strengthen has been limited to 100 meters. This is realised with an armoured

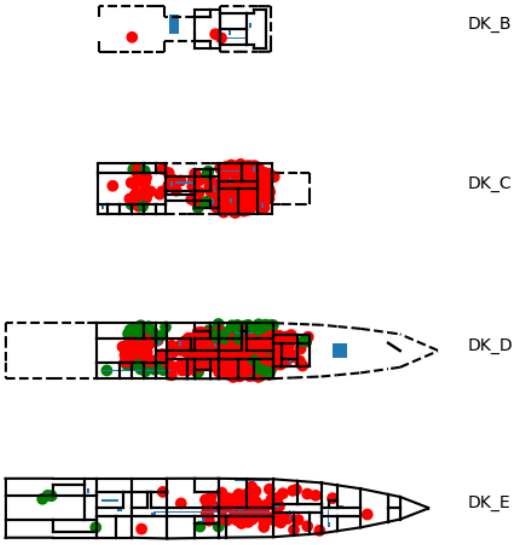

(a) The vulnerability of the unprotected ship

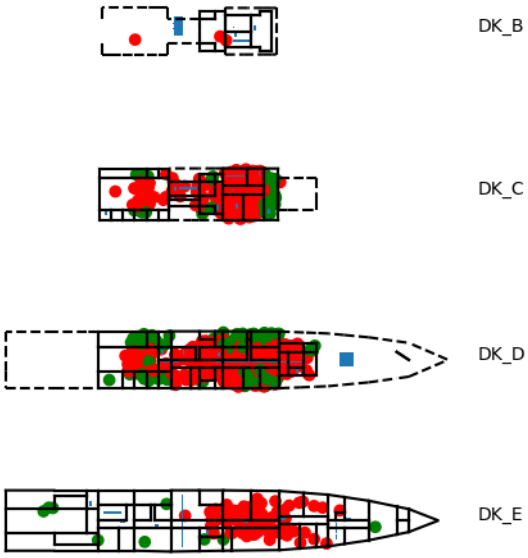

(b) The vulnerability of the ship with HARNESS bulkheads

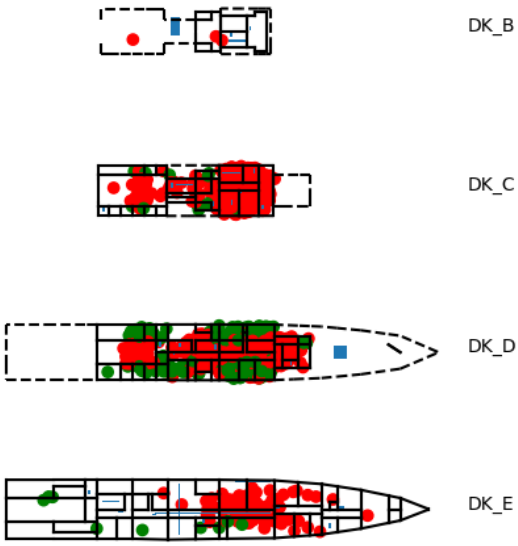

(c) The vulnerability of the ship with extra redundancy

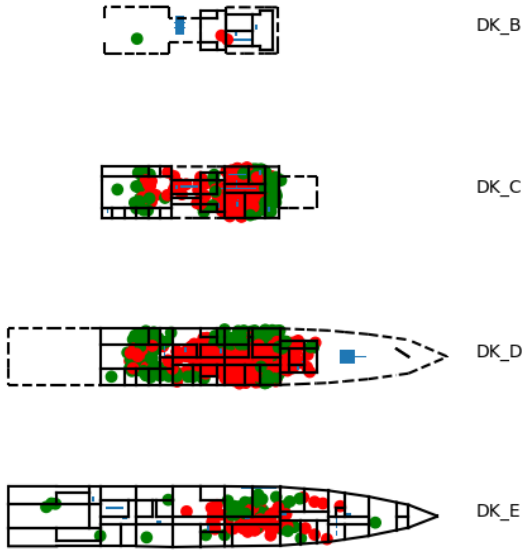

(d) The vulnerability of the ship with stronger components

Figure 3: Monte Carlo results with a sea-skimmer threat, showing when the ship is ”Mission Capable” in the colour green after impact

tray of about 0.1 m tall and 0.4 m wide, in which both cables and pipes can be protected. This would result in a weight increase of about 3 tonne

- The area of panels that have been turned into HARNESS bulkheads is about 100 square metre which results in a weight increase of about 9 tonne
- The increased weight increase of the redundancy is hard to estimate since the cable trays were already in the model. Extra cables would have to be introduced but this is more complicated to give insight in.

By performing a new set of Monte Carlo calculations there is a clear decrease in vulnerability as shown in Figure 7. The to-

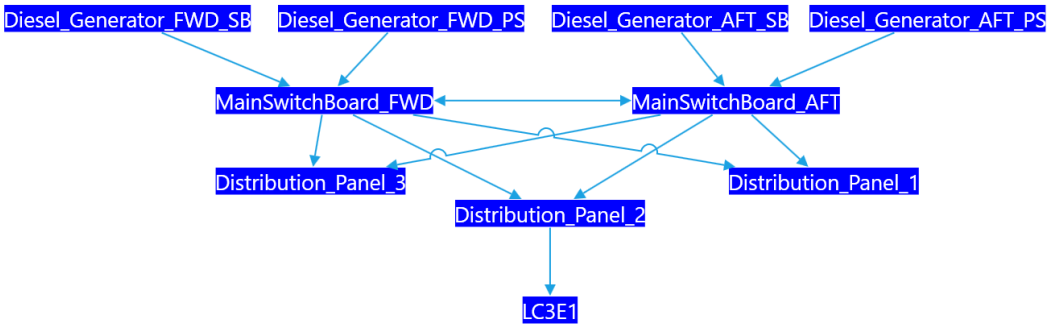

(a) Regular layout electrical system to a single load center

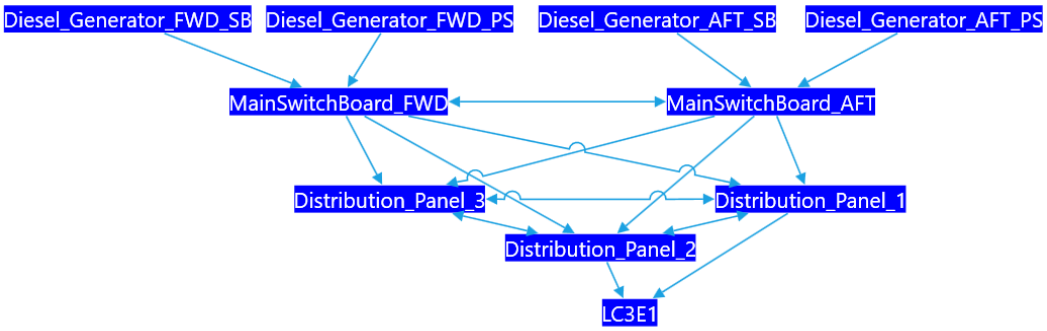

(b) Redundant layout electrical system to a single load center

Figure 4: Comparison of the system layout between the regular and redundant system

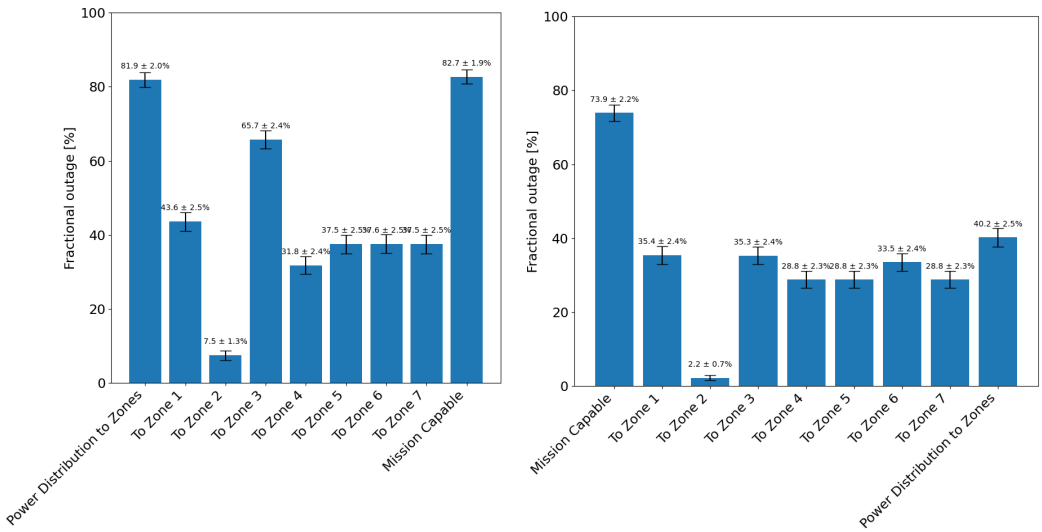

(a) System outage of the unprotected ship **(b)** System outage of the redundant ship

Figure 5: ”Power to each of zones” requirement in relation to the ”Mission Capable” state of the ship

tal availability, that is the 100% minus he percentage outage, of the mast increases from 34% to 43% , the availability of the power in zones from 18% to 60% and the overall ”Mission Capability” has been met from 18% to 33%. It does demonstrate that a ship with a lot of single points of failure it is impossible to retain the ”Mission Capability” state for all the impacts. However, using a smart selection of measures a great deal of vulnerability can be reduced. These upgrades to the ship de-

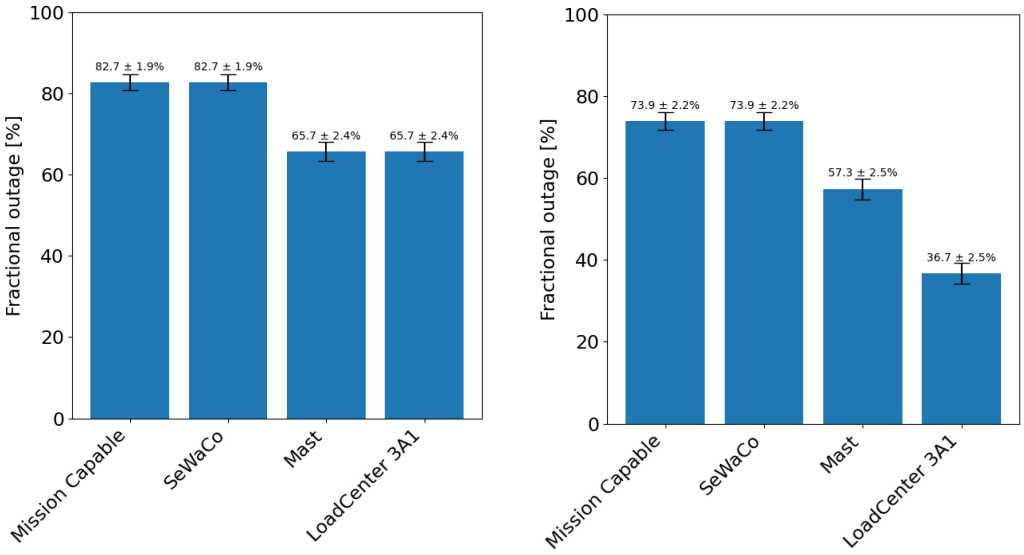

(a) System outage of the unprotected ship **(b)** System outage of the redundant ship

Figure 6: Mast availability requirement in relation to the ”Mission Capable” state of the ship

sign were verified and could be advised to the naval architects in the design department of COMMIT to include in the next iteration of the design. The naval architects review whether the vulnerability reducing measures can be accommodated taking into account volume, weight, estimated cost and other requirements. This review is based on a balance between the penalty on a specific requirement and the gain in survivability of the ship.

CONCLUSIONS

Through an automated process of model conversion it is now possible to evaluate an early stage ship design with respect to vulnerability. While the process requires the knowledge of a naval architect with respect to the structure and the component placement, quick simulation can aid the further improve the arrangement design. The threat modelling methodology demonstrates the need for the inclusion of both fragmentation and blast damage. Following from the probabilistic and non-uniform behaviour of the fragmentation model it is necessary to determine the detonation locations in a probabilistic manner. The detonation location tooling is based on specifics of a missile, such as the final flight trajectory, seeker head and fuse mechanism. When accounting for the variability of both the threat and threat detonation location a baseline for the assessment of the ship can be produced and weak points of the ship arrangement can be identified.

Based on the ship design variations the effectiveness of the vulnerability reduction measures could be determined and a smart selection of measures was made. This complete process shows how rapidly vulnerability of primary damage can be reduced, however for the inclusion of secondary damage and damage control, further model development and tooling should be developed. TNO and COMMIT continue to work closely together to further shorten the feedback loop of consequences by design choices on the vessel’s vulnerability. This allows for participation in concurrent design sessions, in which several disciplines work together on the design of a new vessel. Such sessions require on the spot answers to questions relating to vulnerability, or at least within weeks between subsequent sessions. Based on the work described in this paper COMMIT and TNO are able to iterate early ship designs to achieve a ”first time right” design that is compliant with the vulnerability requirements.

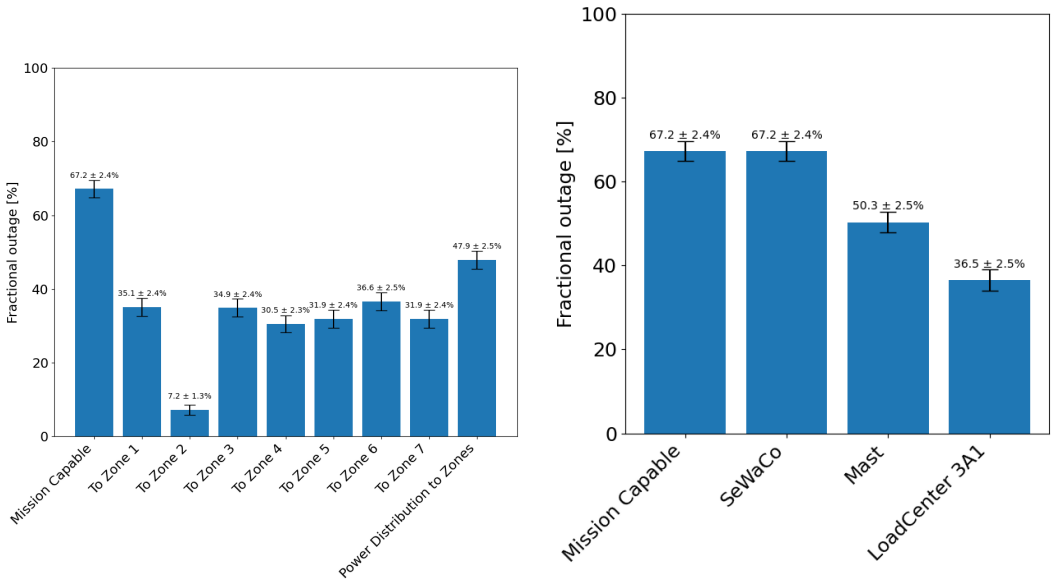

(a) Zonal system outage of the ship with survivability measures

(b) Mast outage of the ship with survivability measures

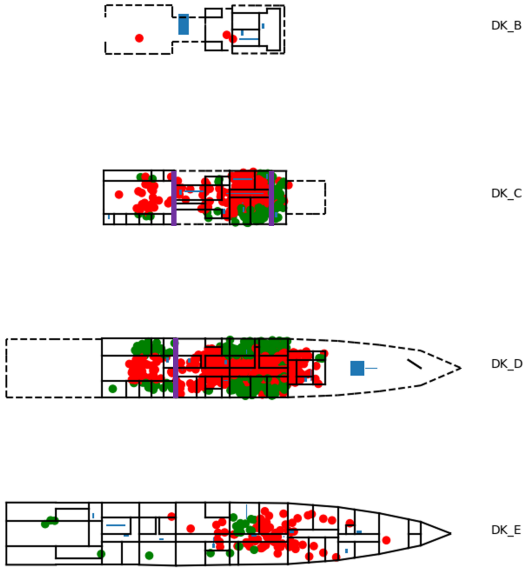

(c) The vulnerability of the ship survivability measures

Figure 7: Mast availability requirement in relation to the ”Mission Capable” state of the ship

FUTURE WORK

Further work focusses on combining the disciplines of susceptibility and recoverability, so that the entire chain of survivability of a naval vessel is covered. Vulnerability experts and experts on signatures (susceptibility) can for example work on technologies to predict and manipulate hit locations of particular missiles. When all countermeasures fail, the hit location may be steered to a spot with minimal crew attendance at that particular moment or to a spot with minimal consequences on operational availability of systems. A priori RESIST simulations can populate lists of such locations for a number of threats.

The future work could also aim to combine the routing optimisation that is performed by the designers with the a better definition of the damage extend that is defined by the analysts. This would bring the topic of vulnerability in a more realistic manner earlier into the design process.

CONTRIBUTION STATEMENT

H.J. den Ouden: Conceptualization, methodology investigation; writing – original draft. **R. van der Wal:** supervision; writing – review and editing.

ACKNOWLEDGEMENTS

We would like to acknowledge Rachiel de Boer for the development of the Graphic User Interface that helped us analysis the Monte-Carlo results. Furthermore we would like to acknowledge Mark Zijlstra for his input regarding the detonation location determination, Andre van Erkel for his input for the blast model and Noud Altinga for giving general input and creating the ship render.

REFERENCES

Clopper, C. J. and Pearson, E. S. (1934). The use of confidence or fiducial limits illustrated in the case of the binomial. *Biometrika*, 26(4):404–413.

Cramer, A. M., Sudhoff, S. D., and Zivi, E. L. (2011). Metric optimization-based design of systems subject to hostile disruptions. *IEEE Transactions on Systems, Man, and Cybernetics-Part A: Systems and Humans*, 41(5):989–1000.

Duchateau, E., de Vos, P., and van Leeuwen, S. (2018). Early stage routing of distributed ship service systems for vulnerability reduction. In *Marine Design XIII, Volume 2*, pages 1083–1096. CRC Press.

Goodfriend, D. and Brown, A. J. (2018). Exploration of system vulnerability in naval ship concept design. *Journal of Ship Production and Design*, 34(01):42–58.

Gurney, R. W. (1943). The initial velocities of fragments from bombs, shells, and grenades, brl-405. *Ballistic Research Laboratory, Aberdeen, Maryland. USA*.

Jansen, A. H., de Vos, P., Duchateau, E., Stapersma, D., Hopman, H., van Oers, B., and Kana, A. A. (2020). A framework for vulnerability reduction in early stage design of naval ship systems. *Naval Engineers Journal*, 132(2):119–132.

NATO Standardisation Office (NSO) (2014). Anep-43 ship combat survivability. Technical report, NATO.

Takken, E. (2008). Concept design by using functional volume blocks with variable resolution. Master's thesis, Delft University of Technology.

van der Wal, R., Carton, E., and Hilvers, F. (2018). The performance of armour steels with pre-layers against fragment simulating projectiles. In *EPJ Web of Conferences*, volume 183, page 04015. EDP Sciences.

van Diessen, M., Duchateau, E., Kana, A., and Hopman, J. (2022). Integrating vulnerability analysis into the early stage distributed naval ship system design process. *Journal of Marine Engineering & Technology*, 21(6):343–354.

van Erkel, A. (1992). The dynamic response of sdof systems loaded by a shock wave. Technical report, TNO.

van Oers, B., Takken, E., Duchateau, E., Zandstra, R., Cieraad, S., van den Broek-de Bruijn, W., and Janssen, M. (2018). Warship concept exploration and definition at the netherlands defence materiel organisation. *Naval Engineers Journal*, 130(2):63–84.

Webb, D. W. (2012). Circular probable error for circular and noncircular gaussian impacts. *US Army Research Laboratory Aberdeen Proving Ground United States: Adelphi, MD, USA*.

Proceedings of 15th International Marine Design Conference (IMDC-2024)
June 2-6, 2024
Amsterdam, the Netherlands

Special ship design and ocean space multi-use synergies

Sigurd S. Pettersen[1,*] and Arnstein Eknes[2]

ABSTRACT

This paper introduces the concept of synergistic multi-use between offshore wind and other sectors in the ocean space, to the ship design audience. We study the opportunities that arise when using special ships to service several ocean sectors, thereby realizing some of the synergies for multi-use. Multi-use of the ocean space becomes desirable due to the increasing demand for marine area by growth sectors like offshore wind and offshore aquaculture. We find that the primary opportunities to realizing multi-use synergies from vessels lie in the operational phase. Logistical support, crew transfer, emergency response, accommodation, and some inspection and repair tasks are sufficiently similar across offshore wind and fish farming that multi-use should be considered. The application of the synergistic multi-use concept also extends to other special ship types, such as offshore support vessels serving oil and gas production.

KEY WORDS

Special ships; Blue Economy; Ocean Space; Multi-use; Shared logistics

INTRODUCTION

The ocean is at the forefront of solutions to many of the world's most pressing problems, including the transition to green energy and more sustainable protein, for instance from seafood. Addressing the fight against climate change, the *High Level Panel for a Sustainable Ocean Economy* (Hoegh-Guldberg et al., 2023) recently suggested a number of mitigation opportunities across seven ocean-based sectors. Policy and market dynamics in key sectors that shape the blue economy suggest that buildout of renewable energy and food production in the ocean space will be highly geographically centralized. Locations with desirable ocean conditions will be highly sought after by several actors, meaning that there are opportunities for cross-sectoral collaboration and synergies, as well as a risk of competition for space (DNV, 2023d).

In Europe, the EU ambitions for offshore renewables have been reaffirmed by the countries surrounding the North Sea. The Ostend Declaration of April 2023 aims to grow offshore wind in the North Sea to 300 GW by 2050, signed by nine countries. Addressing the heightened concerns about use of marine space, the EU Maritime Spatial Planning Directive now requires all EU countries with a coastline to develop and implement a maritime spatial plan, to align energy production with other societal objectives depending on the ocean space. Following the introduction of MSP in the EU, a plethora of research projects have investigated multi-use as a solution where ocean industries make use of the same core or peripheral infrastructure (Schupp et al., 2019).

At DNV, multi-use challenges and opportunities are currently explored by the Ocean Space research programme. The *Ocean's Future to 2050* suite of reports provide forecasts of the Blue Economy on a global scale (DNV, 2021; DNV, 2023d), following the system dynamics methodology also applied in DNV's *Energy Transition Outlook* (DNV, 2023a). In 2023 we published our *Spatial Competition Forecast* (DNV, 2023d), showing that offshore wind area use will instigate competition for space among industries operating in the ocean. Later in 2023, we initialized a new project MARCO (*MARine CO-existence scenario building*), which investigates co-existence through a range of solutions turning the area conflict into a range of opportunities,

[1] DNV Group R&D, Høvik, Norway; ORCID: 0000-0003-1202-3413 [2] DNV Maritime, Høvik, Norway
* Corresponding Author: sigurd.pettersen@dnv.com

Submitted: 16 February 2024, Revised: 23 April 2024, Accepted: 1 May 2024, Published: 27 May 2024

Conference paper, DOI: https://doi.org/10.59490/imdc.2024.899 e-ISSN: 3050-4864

among them industry multi-use interlinkages (DNV, 2022c). Special ships are among several enabling infrastructures for multi-use, and already employed in service of many offshore industries, like offshore O&G, wind, and aquaculture.

The main purpose of this paper is to explore the challenges and opportunities for special ship design that targets multi-use synergies, which could exist when several ocean industries operate in close proximity of each other. How much of the vessel logistics involved in the operation of an offshore wind farm can be shared with an offshore fish farm? Which functionality is needed, and to what extent do the required vessel functions overlap? Can offshore charging systems near wind farms make battery-powered service vessels a reality? Can the chartering of service vessels with relevant functionality be shared between wind operators and fish farmers? How much would this reduce the OPEX of fish farmers and offshore wind operators?

Experiences from offshore support segments ten years back suggests that stakeholders in the wind and aquaculture sectors should take a cautious approach to designing in multi-functionality. Back then, ship design practice adapted to a "more is better" approach where more demanding operations, new rules and regulations, and a need for market differentiation allowed more costly vessels to be built, supported by high oil prices and chartering rates (Garcia et al., 2016). If multi-use opportunities for special ships are to materialize in an economically sustainable fashion in the emerging blue economy sectors, ship design needs to take a broad systems approach, and be conducted in smarter way, with respect to multi-functionality.

The paper is structured as follows: First, we review the relevant literature on marine multi-use and special ships. Second, we assess the primary drivers of multi-use between ocean industries. Third, we review the special ship types servicing offshore wind and aquaculture, through typical project lifecycles. Fourth, we assess the opportunities and challenges associated with multi-use that arises for special ships. Finally, we conclude.

LITERATURE REVIEW

We provide a brief literature review on key research across three distinct, but related domains. First, most advances related to the concept of multi-use recently has seen this in relation to the process of marine spatial planning, and hence has gained a lot of interest not only among engineers, but also from policymakers and marine science communities. Second, parts of the literature on design of special vessels that has ventured into concepts like multi-functionality, modularity, and future uncertainty, is highly relevant. Third, special ships are always part of a wider logistics system and it is difficult to understate the impact of the logistics system design on the capabilities needed in each ship.

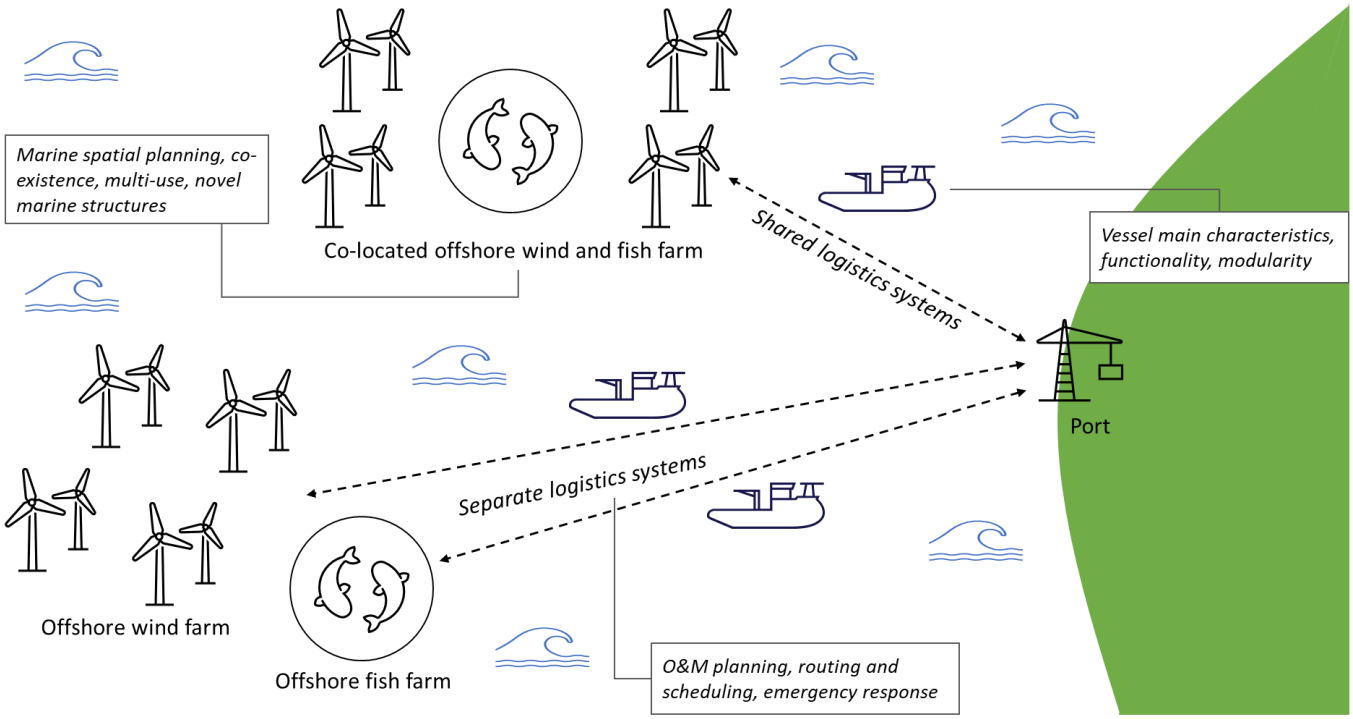

Figure 1: The main idea of the paper and topics addressed in the literature review.

Synergistic multi-use in marine spatial planning

Marine Spatial Planning is defined as "the public process of analysing and allocating the spatial and temporal distribution of human activities in marine areas to achieve ecological, economic and social objectives that have been specified through a political process" (Ehler & Douvere, 2007). In the EU, the Maritime Spatial Planning directive mandates every member state to introduce the concept into national legislation. On a global level, more than 75 states worldwide have some type of MSP process in place (Ehler, 2021).

Introducing MSP provides agency to stakeholders across ocean domains. However, in a world with rapidly evolving ambitions to build out offshore wind, the existence of trade-offs between societal objectives like energy production, seafood production and nature protection, could still lead to situations where some stakeholders remain unsatisfied. For instance, this has been seen between fishermen and the offshore wind sector over concerns that offshore wind will limit access to fishing grounds, when policymakers decide to prioritize renewable energy production. In some cases, considering synergies between sectors can reduce risk of conflict, and lead to identification of win-win opportunities.

Several large research projects have received funding from the EU to study the potential for multi-use of the ocean space, in order to reduce the potential for stakeholder conflicts, and to realize synergies. *MUSES (Multi-Use in European Seas)* developed seven multi-use case studies with a specific combination of production systems at a specific geographic location. Combinations with relevance to the food and energy sectors included offshore wind-wave energy, offshore wave energy-aquaculture, offshore wind-fisheries, offshore wind-aquaculture, and offshore O&G decommissioning with repurposing (Bocci et al., 2018). *MARIBE (Marine Investment for the Blue Economy)* investigated 24 sectoral combinations offshore, with more in depth demonstration of the most promising concepts (Dalton et al., 2019). Ongoing projects like OLAMUR (*Offshore Low-trophic Aquaculture in Multi-Use scenario Realization*) introduce pilot test sites for low-trophic aquaculture (e.g. mollusc and seaweed farming) inside existing wind farms (OLAMUR, 2024). Similar to the multi-use term, the concept of *Marine business parks* has been proposed by the *Center for the Ocean and Arctic* at the Arctic University of Norway, in a collaborative project involving stakeholders across the Norwegian offshore energy, seafood, shipping, non-governmental organization, and research sectors (Hersoug & Mikkelsen, 2022). Very little research has been done on the opportunities for designing special ships for this context.

In summarizing the results of the EU project *MUSES*, Schupp et al. (2019) provide a typology for multi-use, stretching from multi-purpose platforms to repurposing of offshore infrastructure, classified along four criteria; spatial, temporal, provisional, and functional. Table 1 introduces the typology proposed by Schupp, with examples prepared by Pettersen et al. (2023). In this paper, we build further on the concept with the second highest level of integration, called *symbiotic multi-use*. However, we will use the term *synergistic multi-use*, to emphasize more strongly the joint efforts by two actors to create an improved outcome for both, rather than to presume that a *symbiosis* emerges from the actor's mutual dependence. Under the concept of *synergistic multi-use*, offshore production systems may depend on the same logistics support and are located within proximity of each other. Hence, the two production systems make use of the *same space*, at the *same time*, and sharing *peripheral* infrastructure and services. Among several examples of multi-use, Pettersen et al. (2023) identify examples of potential for synergistic multi-use that includes special ships, highlighted in bold in Table 1.

As opposed to synergistic multi-use, multi-purpose platforms would reflect a fully integrated structure where a single infrastructure accommodates two or more distinct ocean uses. This means that multi-purpose platforms are also tightly functionally connected. Fully integrated multi-purpose structures face numerous barriers, both technically, economically, and regulatory (Van Den Burg et al., 2020). Naturally, they face difficulty meeting key design principles like functional independence (Braha and Maimon, 1998). Reporting on the results of the *MARIBE* project, Dalton et al. (2019) found that very few concepts for large-scale multi-use platforms were economically viable, according to a generalized "levelized cost of output" metric developed to compare unit costs for different production systems combined on a single marine platform. Other difficulties for scaling multi-use at sea are discussed by Van Den Burg et al. (2020) who, through a synthesis of the *MUSES* and *MARIBE* results, and other research on the topic, present an overview of the key barriers to multi-use, including economic, technical, social, administrative, legal, and environmental ones. Differing perspectives on risk among the stakeholders involved in multi-use will also influence the opportunity space, with distinct sector-specific frameworks dominating the sectors that will be involved in a multi-use concept (Van Hoof et al., 2020).

Table 1: Typology of multi-use concepts by level of system integration (Pettersen et al., 2023), based on Schupp et al. (2019). Examples in bold are particularly relevant for special ships.

Typology	Spatial	Temporal	Provisional	Functional	Description
Multi-purpose	X	X	X	X	Same area, same time, sharing core infrastructure and services
Examples	Combined floating offshore wind structure and finfish cage aquaculture Floating desalination plant powered by wave power Energy islands acting as hubs for grid connection and green hydrogen production plants				
Synergistic use	X	X	X		Same area, same time, sharing peripheral infrastructure and services
Examples	**Shared logistics systems and service vessels for offshore wind and aquaculture operations in the same area** Electricity from offshore wind to replace gas turbines on offshore oil and gas installations **Offshore wind farms to act as charging stations for electric ships** Floating solar photovoltaics replacing diesel generators at fish farms Integrated multi-trophic aquaculture: Fish farming combined with farming of low-trophic species like molluscs and seaweed				
Co-location	X	X			Same area, same time
Examples	Adoption of passive fishing gear to reduce risk of gear interference with offshore wind structures Requirements to reduce risk for trawling over pipelines and subsea structures				
Repurposing	X				Same area, subsequently
Examples	Ships and offshore structures decommissioned to become artificial reefs Area traditionally used as fishing grounds repurposed to fixed offshore wind farms				

Synergistic multi-use and research on design of special ships

Synergistic multi-use as described above will rely heavily on sharing of provisional functions, primarily provided by special ships that "go to sea to do something" (Andrews, 2018), besides transportation.

At the previous IMDC, Erikstad & Lagemann (2022) reviewed the state-of-art on ship design methodology, identifying four primary design strategies taking a hold, beyond the traditional design spiral approach; optimization-based, set-based, system-based, and configuration-based design. They argued that most design practice combines the four, but for practical purposes, the system-based approach (Erikstad & Levander, 2012) based on a "needs-function-form" mapping process, provides a useful starting point for understanding the role of special ships in synergistic multi-use. System-based ship design is a mission-centric approach where a good understanding of the market conditions and the main operational needs enables "right-sizing" of the vessel before concept exploration and design iterations take place. "Right-sizing" is becoming an essential aspect of teaching vessel owners in offshore wind service to specify requirements that correspond to the intended operational needs, rather than adding additional capabilities "just in case" (The Naval Architect, 2024).

Designing vessels for synergistic multi-use, considering the distinct needs of offshore wind and aquaculture markets, will require a deflection from previous run ins with concepts like multi-functionality in offshore support vessels. Up until nearly 10 years ago, offshore support vessels were increasingly designed for multi-functionality under the guise of high chartering rates due to high oil prices. Due to their high operating costs, some of these highly functional vessels turned "multi-useless" (Gaspar et al., 2015), as they could not find profitable work in a context with day rates dropping when the oil price collapsed (Garcia et al., 2016). The next generation of special ships, whether serving offshore wind, aquaculture, or the two sectors in combination, should adopt smarter design practices, aimed for instance at enabling future changes in configuration and mission-related equipment at a lower cost.

The EU-funded *NEXUS* project (*Next generation support vessels providing safe and more efficient offshore wind farm services)* investigated possible conditions for game-changing service operation vessels, with the objective of reducing maritime logistics

costs for offshore wind maintenance by 20%. Puisa et al. (2021) analyze the safety of SOV operations at a wind farm by introducing the concept of system variability as a proxy for the likelihood of incidents, finding that the most safety-critical interface during operations is between SOV gangway and the turbine. Also as part of the NEXUS project, the benefits of variable speed engines for fuel saving on vessels that spend a significant proportion of their operating profile in dynamic positioning (DP) were investigated (Holmefjord et al., 2020). Holmefjord et al. (2020) find a 20% fuel saving on an analysis of the Service Operation Vessel (SOV) *Edda Passat*. Similarly, in an earlier study by Lindstad et al. (2017), batteries were evaluated as a solution to hybridize offshore support vessels, thereby reducing the need for running redundant combustion engines at low loads when operating in DP mode.

Approaches to handle future uncertainty at the design stage will be needed to address new ocean sectors, exploit synergies in logistics support, new fuel types, and emerging mission-related requirements. To avoid overdesign, modularity and flexibility is desirable, and fits well with a "design for sustainability" perspective, where ship design considers long-term economic, environmental, and social objectives (Erikstad & Lagemann, 2022). Core design principles like modularity and flexibility are increasingly well-addressed in industry practice as a means to adapt to the energy transition (Willumsen et al., 2023). "Prepared for X" class notations exemplify the willingness of ship owners to pay a premium to prepare the vessel for future functionality, particularly in relation to upcoming fuel types (DNV, 2022b), exemplifying the designing of real options "into" ships. A number of recent vessel conversions of platform supply vessels to service operation vessels also illustrate that the industry sees retrofit as a more cost-efficient and sustainable option that newbuilding (Ulstein, 2022), particularly when the underlying marine platform is sufficiently versatile. Various methods have been developed to support offshore ship design viewed as decision-making under uncertainty with the goal of enabling flexibility through the lifecycle (Gaspar et al., 2015; Pettersen et al., 2020; Rehn et al., 2019; Zwaginga et al., 2021; van Lynden et al., 2022). In the offshore wind sector, Zwaginga et al. (2021) consider the uncertainty in future design requirements for installation vessels in offshore wind, for instance related handling turbines with increasing size and capacity. Similarly, van Lynden et al. (2022) apply epoch-era analysis (see for instance Gaspar et al. (2015)) to generation of future market scenarios for offshore wind installation vessels, combining this approach with parametric ship design modelling.

Pettersen et al. (2020) provide examples of latent capabilities existing in complex special vessels, enabling these vessels to perform a range of operations for which they were not originally designed, of particular importance for improving emergency preparedness. Latent capabilities refers to functional attributes vessels were not intentionally designed for. The idea of latent capabilities can be a powerful one in a context where possibly stranded assets from O&G service segments can be repurposed, possibly without large design changes, to new market segments. In the co-existence between offshore wind and other ocean users, one can consider concepts that use fishing vessels for ocean observation (Van Vranken et al., 2023), for instance providing new knowledge about the environmental impact of offshore wind. The use of fishing vessels for oil spill response or other emergency response tasks are also a prominent example of this (Pettersen et al., 2020).

Logistics of synergistic multi-use

A big operations research literature exists on use of optimization and simulation methods applied to complex special vessels and their logistics, serving both offshore oil and gas (Fagerholt & Lindstad, 2000), offshore wind (Irawan et al., 2023; Lazakis & Khan, 2021), and marine aquaculture (Slette et al., 2022, 2023). To the knowledge of the authors, very few studies have addressed the logistics of synergistic multi-use as described above, outside of emergency preparedness where e.g. oil spill response systems will address accidents regardless of in which industry they originate. We mention a few interesting examples from recent years, which has addressed logistical aspects relating to new ocean industries.

Lazakis & Khan (2021) propose an operational planning methodology for the optimal short-term route planning and scheduling of SOVs and crew transfer vessels (CTVs) taking into consideration characteristics for the wind farm, turbine failures, and the two vessel types, as well as environmental conditions. They find that the operational window increases when SOVs and CTVs are used together. Similarly, Irawan et al. (2023) construct a two-stage stochastic programming model accounting for weather uncertainty, and find that SOVs improve offshore wind maintenance efficiency, and that using SOVs in combination with a safe transfer boat (daughter craft) minimize the total maintenance costs. For the cases studies, SOV and the safe transfer boat combination are found to reduce maintenance costs by up to 70% over approaches that rely on CTVs.

Within aquaculture, Slette et al. (2023) provide an integrated simulation-optimization framework to evaluate the performance of alternative fleets composed of a combination of specialized vessels or multi-purpose vessels that service a set of fish farms. They find that the performance with respect to utilization of weather windows is generally higher for fleets composed of multi-purpose vessels, as appropriate functionality does not become a limiting factor when routing for the next service mission. Furthermore, they find that letting service vessels serve localities that are not correlated in terms of weather, also improves overall utilization of the fleet. The logistics of fish health emergency response has also been studied in another paper by Slette et al. (2022), focusing on the cost-benefit trade-off of dedicated emergency response vessels in fish farming.

The *North Sea Energy programme* report on *The Potential of Shared Offshore Logistics* analyses key scenarios for sharing of offshore logistics in the future offshore energy system of the southern North Sea (Omrani et al., 2022). The report focuses on logistical needs in the energy sector, considering wind farms and oil and gas platforms that increasingly turn to producing blue hydrogen and capturing carbon. In the scenario of the Dutch "Hub West 1", which includes the Hollandse Kust Noord wind farm and six O&G platforms close by, they find that 8% of the wind farm OPEX (1.9 MEUR) can be saved by using a shared logistics concept that uses CTVs for personnel transit to the oil and gas installations, without compromising the availability of the offshore wind farm. The effects of reducing PSV usage are not described in detail in the study but gives rise to the suspicion that the PSV functionality to be replaced is not sufficiently accounted for.

On top of sharing costs through multi-use synergies, European shipping will increasingly be forced to report on emissions (DNV, 2023b), meaning there is also an environmental dimension to the sharing of vessel capabilities among actors in the ocean industries.

KEY DRIVERS FOR MARINE MULTI-USE

DNVs efforts to forecasting the Blue Economy, the *Ocean's Future to 2050*, provide reference modes for developments across the ocean industries, a summary of which is shown in Figure 2. Offshore wind will by far be the fastest growing segment to mid-century and is forecast to see around a 20-fold growth between 2024 and 2050, as shown in blue. The floating offshore wind subsegment is forecast to rise even faster, but from a significant lower starting level than bottom fixed turbines, and is therefore not included in Figure 2. Marine finfish aquaculture, i.e. the farming of high-value fish like salmon in sea-based cages is forecast to triple, as shown in green (DNV, 2023c). Offshore fish farming grows much faster than other marine aquaculture, also growing around 20-fold, albeit from a much lower starting point than offshore wind. The prognoses of key developments within major ocean industries in Figure 2 is based on DNV (2023a), (2023c) and (2023d).

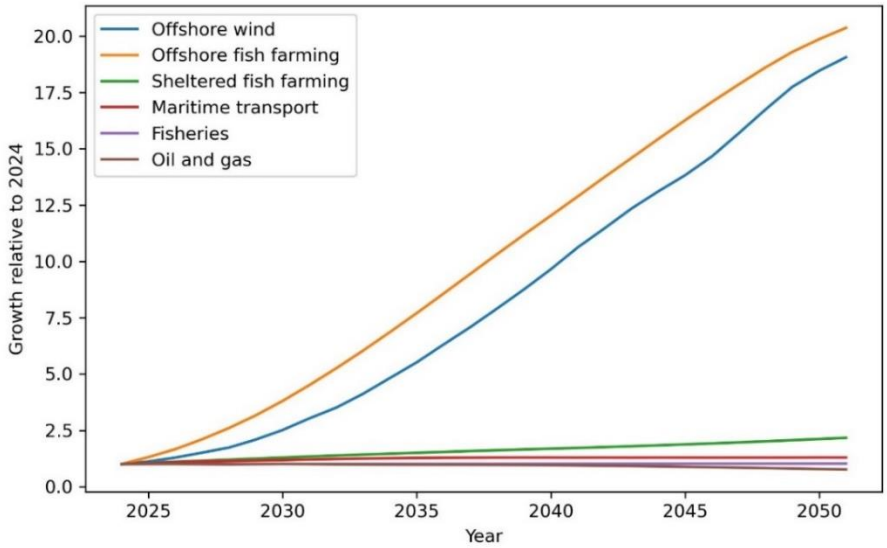

Figure 2: Prognosis for development in key ocean industries

Offshore wind

Offshore wind is the single, fastest growing sector in the ocean economy, spurred on by the need to decarbonize the energy system. By 2050, DNV (2023a) forecasts the installed capacity in the offshore wind sector to reach around 1,600 GW, which means 100,000 turbines globally if the average turbine rating by then reaches 16 MW. In Europe alone, the installed capacity reaches more than 400 GW, implying approximately 25,000 turbines. If all turbines globally require planned maintenance twice per year, more than 500 turbines need to be serviced every day, before considering unscheduled maintenance and repairs. With this, there will be a large demand for logistical support throughout the field lifecycle.

Geography largely determines the location of offshore wind, with wind speeds and proximity to existing electricity grids and other infrastructure, as some examples. Fixed offshore wind farms are build using monopiles or jackets, which may also be the

technically preferred solution down to around 80-100 m water depth, further limiting the availability of sites. Floating offshore wind is currently developed for deeper waters, with Hywind Tampen a first example of an industrial-scale floating wind farm built to electrify oil and gas production (Equinor, 2023). Future power-to-X solutions like green hydrogen production could alter the dependency of the sector on grid connectivity, but would introduce other logistical challenges, for instance related to hydrogen (DNV, 2023a).

In Europe, the geography of the North Sea basin makes it the most attractive sea basin for developments, with around two-thirds of installed capacity in 2050 (DNV, 2023d). Even if the North Sea will be the main market for European offshore wind, price cannibalization due to weather correlations between offshore wind fields, spatial conflicts at the most attractive sites, etc, will increasingly cause capacity to be developed far from shore and in deeper waters, where floating solutions will be needed.

Offshore wind, as a quickly emerging market segment, has seen rapid declines in cost (levelized cost of electricity (LCOE) over its first twenty years. In the last two years, high costs of raw materials and supply chain bottlenecks (ports, manufacturing, installation vessels) has contributed to large increases in the LCOE, resulting in delay of many investment decisions and poor turn-out in high profile offshore wind auctions (Equinor, 2024; Grønholt-Pedersen, 2023). Nevertheless, most forecasters believe this to mainly be a short-term problem, as many other industries face similar inflationary pressures. Over the longer run, LCOE is forecast to halve for fixed offshore wind between 2020 and 2050 and halve for floating offshore wind between 2030 and 2050 (DNV, 2023a).

Offshore wind is a capital-intensive industry as shown in Figure 3, based on data from the Crowne Estate and ORE Catapult (2019). Purchasing major components like turbines and balance of plant (non-generator supporting infrastructure like foundations, cables, etc.) constitutes around 40%, while installation costs add another 20%. In the operational phase, operations and maintenance costs contribute almost 30%.

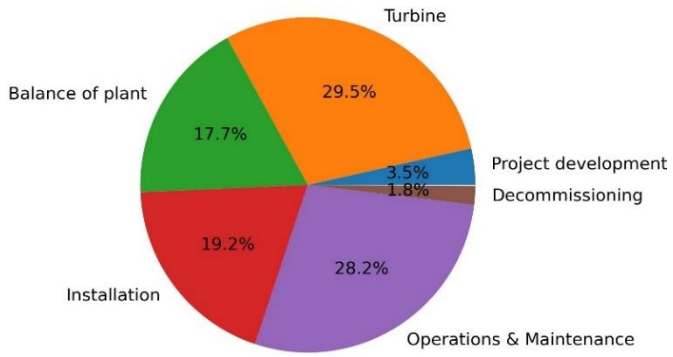

Figure 3: Generic levelized cost of electricity breakdown for offshore wind (based on The Crowne Estate and ORE Catapult, 2019)

As a relatively new market, Clarkson's Research (2024) historical time charter rates for key subsegments are available back to 2020 only (see Figure 4). In the three years following, there has been a significant increase in the chartering rates, with rates for e.g., large SOVs with walk-to-work (W2W) functionality and accommodation for more than 40 people have almost tripled from slightly more than 20,000 EUR/day to more than 55,000 EUR/day. In 2023, day rates for these vessels exceeded those of AHTS vessels operating in the North Sea. Smaller W2W vessels and non-W2W SOVs saw lower day rates over this period, owing to less functionality and hence likely lower operability (e.g. lack of gangway limiting time windows with sufficiently small waves). Compared to traditional offshore support segments, offshore wind will likely see lower rates, but likely also less volatility (The Naval Architect, 2024).

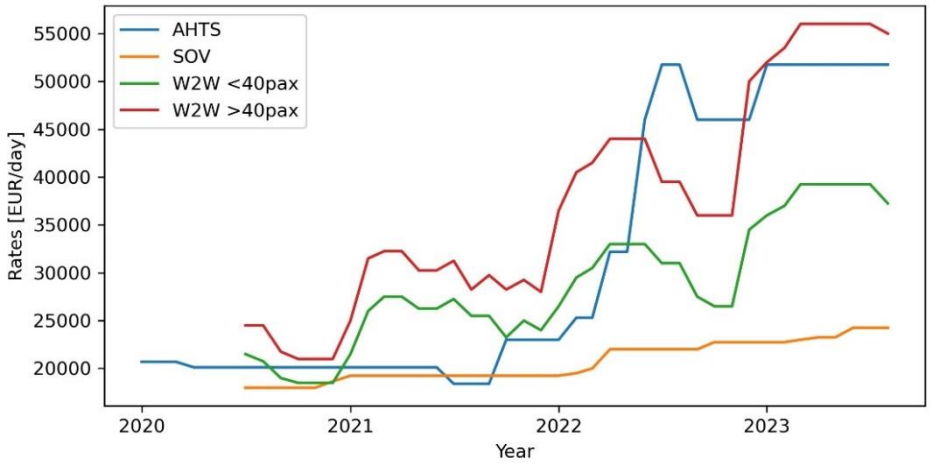

Figure 4: Charter rates for key vessel segments in offshore wind operations (Clarkson's Research, 2024)

A key driver for increasing vessel sizing and more advanced capabilities is the fact that offshore wind farms are being installed further from shore and in deeper waters. This is most critically pronounced in the construction phase, where novel solutions that can bring down the cost of installation will be desired. Also in the operating phase, new logistics support solutions may be favorable, due to the increased distance to shore. To great challenge will be for ship designers to advance offshore wind service vessel capabilities without adding excessive costs.

Offshore fish farming

Offshore fish farming is likely to become a fast-growing subsegment of marine aquaculture. Most current marine fish farming operations take place in benign waters (e.g. Mediterranean seabass and seabream production) or sheltered waters (fjords in Norway, Scotland, Iceland, Canada, or Chile). Over the last ten years, increasingly exposed localities have been tested out, particularly in Norway and the Faroe Islands. Some of the most promising concepts for offshore fish farms were awarded with development licences, with some key characteristics shown in Table 2 (Pettersen, 2022).

A key feature of the development licenses was that they allowed licenses free-of-charge for concepts with a sufficient degree of innovativeness. However, despite the introduction of development licenses several years, the regulatory framework for offshore fish farms is still lacking, causing many investments to be delayed in the short term as the developers see limited opportunity to scale to the increased number of units to trigger sufficient investment cost reductions. Another recent showstopper has been the decision that offshore fish farms will not be liable for a new resource rent tax, a scheme that would have opened for offsetting expenditures on offshore projects against high profits earned in coastal aquaculture.

Table 2: Some offshore fish farms awarded development licenses in Norway (based on Pettersen, 2022)

Name	Owner/operator	Concept description	Capacity [tonnes]	Operational year
Ocean Farm 1	SalMar Aker Ocean	Ocean fish cage based on offshore technology	6,000	2017
Havfarm Jostein Albert	Nordlaks	Ship-shaped ocean fish cage	10,000	2020
Arctic Offshore Farming	SalMar Aker Ocean	Semi-submersible fish cage	3,000 x 2	2021
Smart Fish Farm	SalMar Aker Ocean	Semi-submersible ocean fish cage	19,000	Planned 2022 (delayed)
Spidercage	Nova Sea	Heave-compensated, wave breaking, semi-closed ocean fish cage	3,120	Planned 2023 (delayed)

In the longer run, regulatory uncertainties will likely be sorted out, and one can expect other countries to explore offshore aquaculture including multi-use solutions, in Europe and beyond. Outside Europe, progress on offshore fish farming is also happening in China. A first structure called "Deep Blue" was launched in 2018 but saw operational problems and made its first

harvest of Atlantic salmon in 2021 (Pettersen, 2022). Following this, China has developed a variety of concepts for a number of species. The country also has high ambitions for offshore fish farming, e.g. as reported on by Feng (2023). DNV (2023c) finds that the offshore fish farming sector globally achieves a 7% market share by 2050.

A generic production cost breakdown for sheltered aquaculture is provided in Figure x, based on Iversen et al. (2020). Production costs in fish farming is mainly driven by the need for feed, which typically constitutes around 50%, or around 2.2 EUR/kg (Iversen et al., 2020). Investments, reflected through depreciations, constitute a relatively small cost share, but tripled over the period from 2006 to 2018 to 0.3 EUR/kg.

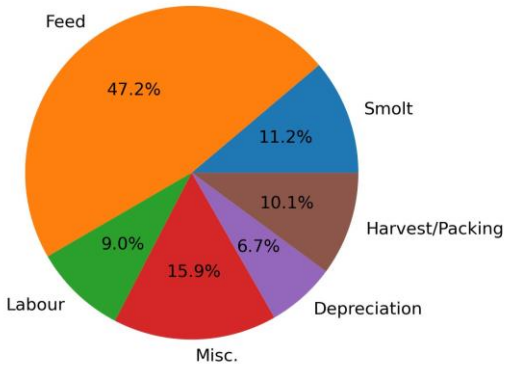

Figure 5: Generic production cost breakdown for sheltered aquaculture (based on Iversen et al., 2020)

For offshore fish farms, capital expenditures will make a much larger mark on production costs. Consider for instance a unit with a capacity of producing 3000 tonnes per year with a 25-year lifetime, and costing around 100 million EUR, then this would add around 1 EUR/kg to the production costs. To compete with existing aquaculture, offshore fish farming is therefore dependent on learning and scaling effects to reduce costs (Pettersen, 2022).

Additionally, with offshore locations comes more complex well boats and other specialized ships, which may further add to the costs. There is limited information about current chartering rates for well boats and other special vessels in aquaculture, with these costs often bundled with downstream processing activity in statistics (Iversen et al., 2020). For service vessels used for delousing operations, removal of sea lice, Iversen et al. (2017) cites day rates of up to 130 000 NOK, around 15 000 EUR. Some of the well boats retrofitted from laid off PSVs (AquaShip, 2021), will likely need to command rates similar to that market segment, which could be in the same range or higher.

Even though vessel-related costs constitute a relatively small fraction of costs associated with aquaculture today, more advanced vessels needed to support offshore operations, would require higher chartering rates. With a traditionally very cost-conscious industry (Iversen et al., 2020), and a low degree of willingness to be associated with the splurge associated with the golden-era of offshore support vessels (Garcia et al., 2016), offshore fish farmers might very well see the savings potential embedded in sharing of some logistical services with offshore wind.

Spatial impacts and benefits of sharing maritime resources

In area terms, 80% of the area reserved for permanent use by ocean industries will be taken up by offshore wind farms, not counting uses that are mobile, like shipping and fisheries, nor unproven offshore renewables (solar PV, tidal, wave power) (DNV, 2023d). Hence, by co-locating offshore wind with all other offshore installations (e.g. offshore oil and gas, marine aquaculture), the full potential of marine multi-use is estimated to reduce mankind's long-term use of marine area with 20%.

Apart from reducing the area footprint of marine use, this multi-use could come with potential synergies. Symbiotic use entails the use of marine space in a manner that exploits synergies, for instance by making use of shared peripheral infrastructures or services (Schupp et al., 2019). For example, there could exist a potential for cost saving when coupling the logistical support requirements of offshore wind with those of offshore aquaculture, if the production systems are in proximity of each other.

From the perspective of the overall production cost in aquaculture, or the levelized cost of electricity in offshore wind, chartering of vessels constitutes a relatively small share, indicating a need for further cost-benefit analyses for shared logistics concepts. Emerging regulatory and financial requirements can result in a stronger business case for the synergistic multi-use of

special ships, as carbon pricing is introduced (DNV, 2023b), and offshore wind tendering increasingly emphasizes co-existence with other ocean stakeholders (DNV, 2023d).

From 2027, offshore ships above 5000 GT will be included in the EU Emission Trading System (ETS), and smaller offshore vessels will also be considered for inclusion in this scheme. With the EU ETS, carbon prices will be brought into the maritime sector for the first time. The ETS implies a cap-and-trade philosophy, where a declining number of emission allowances will be auctioned and traded in the market (DNV, 2023b). The carbon price will rise over time due to declining allowances available, and the costs will eventually add to chartering rates, making ship operations that drive fuel consumption more expensive. Emissions will need to be reported on a voyage level, to settle transactions related to the emission allowance costs.

Synergistic multi-use of vessels for co-located offshore wind and aquaculture can reduce fuel consumption during transit by cutting the number of voyages needed, if one roundtrip voyage can support several production systems. The transparency that is needed for the cost of allowances to be allocated to specific charter parties, could also provide novel opportunities to define contractual terms for splitting the cost of carbon among several charterers, e.g., a collaboration between an offshore wind operator and an offshore fish farm operator.

Besides the impact of carbon pricing and reporting requirements related to fuel consumption for the vessels themselves, co-existence is increasingly taken into consideration in the tendering processes for new offshore wind farms (DNV, 2023d; Pettersen et al., 2023). Showcasing multi-use concepts like the dual use of vessels for offshore wind and aquaculture during an offshore wind tendering process could strengthen future applications, depending on the

SPECIAL SHIP CAPABILITIES IN THE PROJECT LIFECYCLE

In this section, we introduce key vessel segments that support marine operations in aquaculture and offshore wind, in order to assess whether the distinct operations allow for some sharing of vessel capabilities. Figure 3 provides an overview of the main lifecycle phases of any offshore wind or offshore fish farming project, emphasizing the marine operations where there is a need for support from vessels. Green shows operations with a lot of commonalities, light blue shows offshore wind operations, and dark blue shows offshore fish farming operations. Dashed green boundaries imply that there is some weaker commonality in the types of operations required.

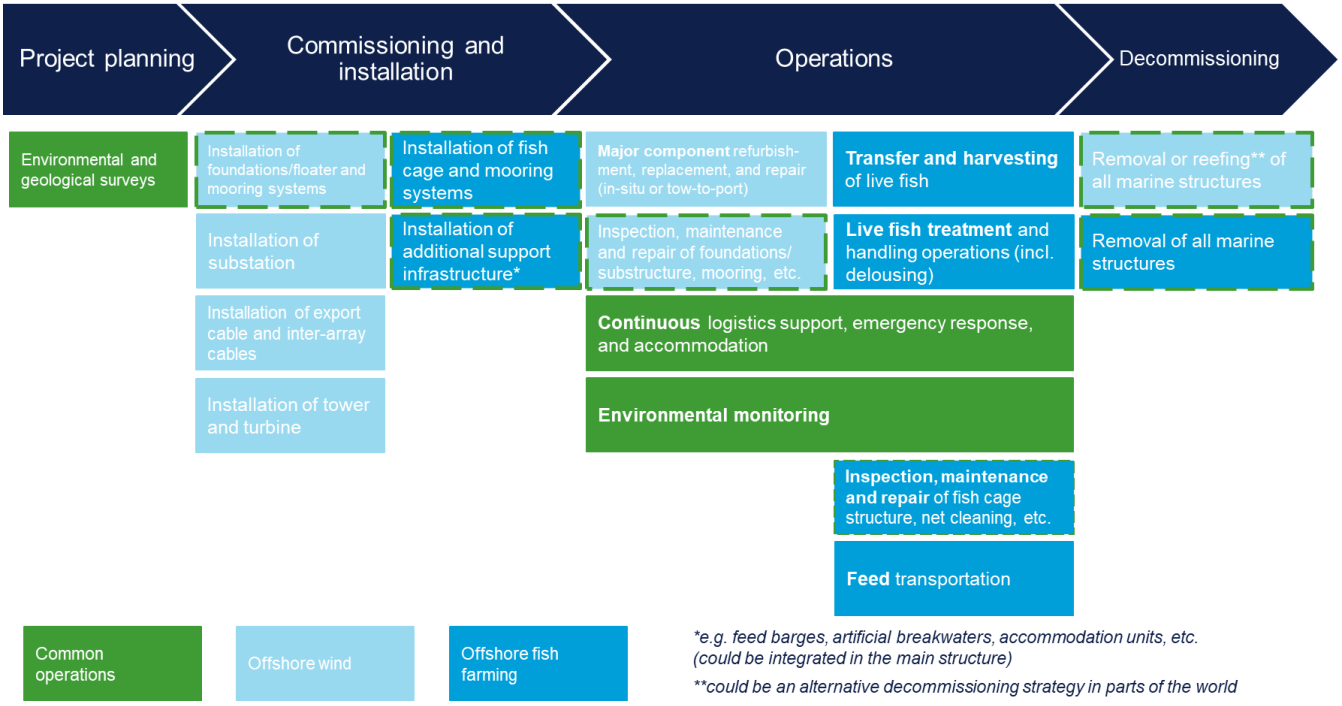

Figure 6: Lifecycle activities with main vessel operations reflected, for offshore wind and offshore fish farming.

From the lifecycle overview of key functions that need vessel support, it is clear to see that there are already some clear commonalities. We review the lifecycle phases, except decommissioning, and address common and distinct needs in offshore wind and offshore fish farming below. We then summarize the qualitative assessment of potential for multi-use synergies.

Project planning phase

During the project planning phase offshore wind makes use of both geophysical survey vessels and vessels for geotechnical surveys. Geophysical surveys make use of non-intrusive methods like multibeam echo soundings, sonars, and seismics to map the seafloor.

Geotechnical surveys are the more intrusive of the two and include sampling of rock and soil by methods like boreholes and cone penetration testing to understand specific seabed features and soil behavior under dynamic loading from wind, waves, and currents. Geotechnical survey vessels often have onboard laboratories for processing of the samples (The Crown Estate & ORE Catapult, 2019). To anchor larger offshore fish farm structures, many of the same methods will be required to verify the integrity of anchoring and mooring systems.

Environmental sampling of seabed (benthic) marine life is also becoming more important during project planning, as an understanding of ecological baselines becomes more important with ocean industries increasingly required to report on their biodiversity impacts (Pardo et al., 2023).

Commissioning and installation

During commissioning and installation, both offshore wind and aquaculture will require transportation of major equipment to the site, as well as anchoring. Bottom fixed offshore wind turbines need to be installed in multiple steps, with final assembly taking place on site. The installation of the tower and turbine itself (with nacelle and blades) is normally done by large wind farm turbine installation vessels (WTIVs) with large cranes having significant reach (+200 m above sea level) and capable of lifting 1500 tonnes or more. These vessels can also install the foundations unless these are lowered by use of heavy lift vessels.

Floating structures like large fish farms or floating wind foundations can be transported to site by towing or on the deck of semi-submersible heavy-lift vessels. Semi-submersible heavy-lift vessels have already been used for transportation of several high profile offshore fish farms, such as Nordlaks' Havfarm (Baird Maritime, 2020). New concepts for wind turbine installation are emerging, as floating offshore structures and larger turbines set new requirements to lifting capabilities (Zwaginga et al., 2021). When the wind farm is located close to shore, or the weather conditions are such that the technicians needed at the wind farm can be transported every day to/from a nearby port without getting seasick, crew transportation vessels (CTVs) are often used.

Commissioning support tasks in offshore wind are increasingly provided by commissioning service operation vessels (CSOVs). While SOVs typically provide support in the operations and maintenance phase of the lifecycle, CSOVs support the commissioning phase. CSOVs are often with larger capacity to accommodate people onboard, while many of the other capabilities are similar to the smaller SOVs. Helideck is one option you can find on both SOVs and CSOVs (but not a standard), while CSOVs are often outfitted with bigger cranes for offshore use. Since CSOVs can provide commissioning support, they are typically hired for shorter contract periods than SOVs., and may command much higher chartering rates. Both SOVs and CSOVs often work together with one or more daughter crafts or fast crew transport vessels (CTVs) to ensure faster mobilization of people to multiple turbines when this is required. With larger offshore wind farms, where rotor and turbine components increase in size, some developers are changing their O&M planning, so that CSOVs increasingly are engaged on long term contracts to meet the more complex maintenance needs. Notional design parameters for a typical SOV are contrasted with those of an CSOV in Table 3.

Table 3: Some key design parameters of SOVs

	SOV	**CSOV**
Length (incl **average**)	57-93 m **(80 m)**	80-108m (**90 m**)
Gross tonnage	2900-6800 GT	5500-7300 GT
Accommodation (People on Board - POB)	36-124 (**60** POB)	60-135 (**120 POB**)
Deck area	200-750 m^2	320-750 m^2 (one with 1000 m^2)
Gangway + Offshore crane	Motion compensated	Motion compensated
Fuel	Marine gas oil (MGO)+hybrid/battery + prepared for alternative fuel	MGO+hybrid/battery + prepared for alternative fuel

Anchor handling tug supply (AHTS) vessels commonly used during rig moves can contribute if there are towing operations, and during installation of mooring systems. AHTS vessels will likely be taking on role during the installation phase in both offshore wind and offshore fish farming. To some extent, offshore fish farms can be built to(be relatively easy to remove and for some concepts the primary maintenance strategy is to carry out repairs in port, potentially making AHTS day rates the driving factor in offshore aquaculture OPEX. Similarly, there may be opportunities for complex offshore support vessels to provide construction support, including lifting operations, as well as support to underwater inspection and repair services. These vessels will prioritize offshore O&G support work as long as the rates are higher in that market. One additional factor to consider for possible cross industry work is the limitations that may be imposed on the operators from investors or other important stakeholders, typically related to ESG (Environmental, Social, Governance)-aspects (e.g. some investors will not accept services to be delivered from the financed asset like an SOV to other industries than the renewable industry).

Other specialized offshore vessels at use in offshore wind operations includes cable-layers and subsea rock installation vessels. There could be some cable installation needs to connect offshore fish farms with nearby wind farms for powering. However, with a need for stable powering, such solutions will require storage to reduce intermittency challenges. Besides this, with a relatively low energy consumption in the first place, offshore fish farms will likely still be fueled by diesel.

Operations

During the operational phase, offshore wind and offshore fish farms share several needs. Both sectors will require inspection, maintenance, and repair operations, emergency preparedness, and accommodation for personnel. Additionally, continuous monitoring operations will likely be required for future operations to understand nature impacts.

Underwater inspection, maintenance, and repair tasks. Underwater inspection services will largely be performed by ROVs launched from service vessels through moonpool or over the side that inspect wind farm foundations, floating structures, fish farm nets, and mooring systems. Some diving support is also used both in established wind farm operations and in coastal aquaculture. In aquaculture, diving support operations are often carried out using smaller fast-moving vessels. With deeper waters, diving operations will potentially be reduced in favor of ROVs, as diving in deeper waters comes at higher risk and requires technically complex support systems found onboard offshore O&G diving support vessels.

O&M support, crew transfer, and accommodation. Operations and maintenance support to wind turbine components located above the foundations or floaters are normally done by technicians landed onto the turbines from either crew transfer vessels or from motion-compensated gangways onboard service operation vessels (Irawan et al., 2023; Lazakis & Khan, 2021). SOVs have quickly become the work horse of the offshore wind industry, as wind farms have grown and are located further from shore. Where crew transfer vessels, often catamarans, are used for transport of technicians to smaller wind farms close to shore, SOVs provide accommodation and a stable platform for safe crew transfer to turbines in rough weather, thereby increasing the size of weather windows for maintenance and repair (Irawan et al., 2023). With the space to carry spare parts and workshops to carry out smaller repair work, purpose-built SOVs have made it more challenging for PSVs repurposed from offshore oil and gas to compete in the offshore wind market (The Crown Estate & ORE Catapult, 2019), without first being retrofitted with additional accommodation space and W2W functionality.

SOV functionality will also be useful in the fish farming context. While the industry will want to move towards autonomy in offshore fish farms to reduce risk to crew, they will likely need to have personnel onboard often to manage the operation (e.g. managing feed distribution, inspecting structures, handling dead fish). A concept of operations where an SOV provides accommodation and safe transfer to wind farms and offshore fish farms that are located sufficiently close to each other, could result in shared, and thereby reduced, chartering costs. W2W functionality provided by actively motion-compensated gangways could be one example of a ship function from offshore wind that easily contributes to improved personnel safety in offshore fish farm operations.

On the other hand, there can only be a limited role for aquaculture service vessels in supporting wind farm operations. The types of services these vessels provide are often related to simple lifting operations, including net handling and cleaning.

Fish handling. Handling live fish requires a lot of specialized functionality that has no use in offshore wind. Figure 7 presents the key functions performed as part of the live fish logistics.

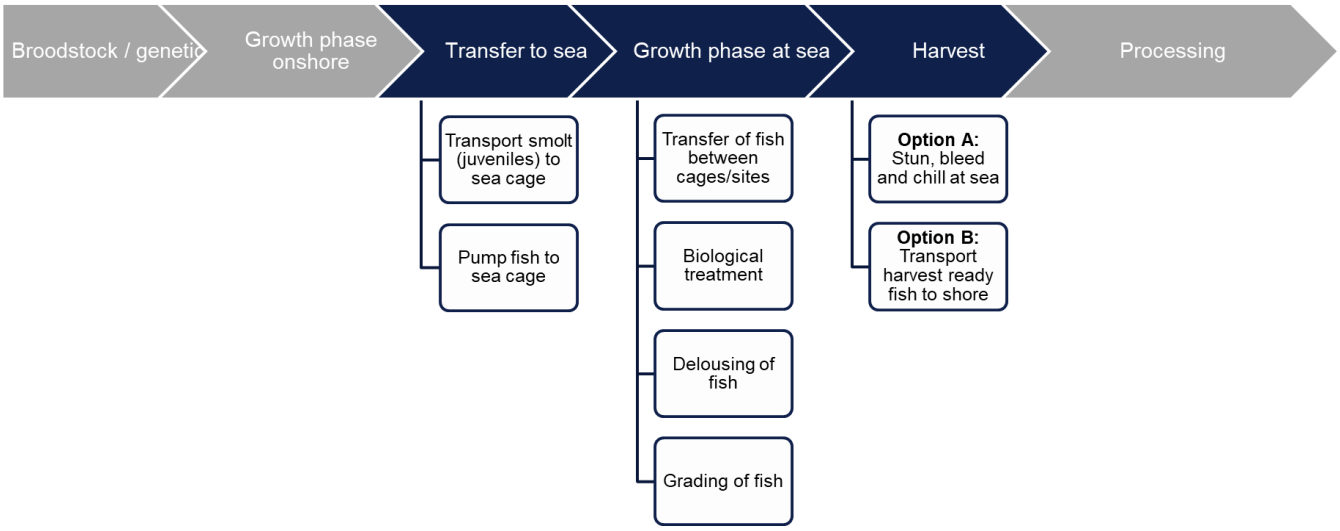

Figure 7: Salmon lifecycle with emphasis on key ship functions.

Well boats or live fish carriers play a key role in the transportation functions and are built around holding tanks designed to carry fish, with associated circulation systems to maintain good water quality. Importantly, well boat design considers biosecurity measures, to mitigate the risk of disease transfer between fish farm sites. Grading, delousing, and biological treatments are often also performed using well boats. In some cases, these functions are performed by specialized delousing vessels. Like in the offshore wind market, there have also been examples of PSVs retrofitted with delousing equipment for work in the aquaculture industry (AquaShip, 2021; Dixon, 2020).

Fish handling logistics could change because of larger distance to shore and more rough weather. With larger fish cages further from shore, newbuilt well boats have also become larger and more complex. More ships will likely be built with stun, bleed, and chill functionality to avoid detrimental fish health impacts from sloshing during transit from offshore cages to shore. Still, fish handling logistics will to little extent be affected by potential multi-use synergies.

Emergency response. Besides similarities in the need for accommodation for personnel, both offshore wind and offshore fish farming will need emergency preparedness. The emergency response needs of the sectors will only partially align, due to the presence of personnel working at sea. Beyond responding to incidents that could harm personnel, the emergency response system in aquaculture also needs to consider fish-related incidents. Compared to the use of emergency response and rescue vessels (ERRVs) in offshore oil and gas, the risk to personnel is smaller in both offshore wind and aquaculture.

Fish escape incidents, algal blooms, and disease outbreaks constitute key concerns in aquaculture that typically will be addressed using vessels with specialized fish handling capabilities (Slette et al., 2022). Disease outbreaks are often managed by removing dead fish and by slaughtering sick fish earlier than planned (Barrett et al., 2022).

Commonalities in mission requirements

We now turn to providing a summary, qualitative assessment of ship capabilities and commonalities in mission requirements. Table 4 summarizes vessel capabilities needed in offshore wind and offshore fish farming. Eight of the identified special ship types provide functionality that is interesting for both segments. The largest potential for exploiting synergies will be in the project planning and operational phases. In the commissioning and installation phases, highly specialized capabilities are needed on the offshore wind side, that do not lend themselves well to aquaculture.

Table 4: Ship types and use in marine operations in offshore wind and offshore fish farming. Ship types highlighted in italics score above 'Low' in technical feasibility for both offshore wind and fish farming.

Ship type	Lifecycle stage	Main functions	Offshore wind	Offshore fish farming
Geophysical survey vessels	*Project planning*	*Non-intrusive seafloor mapping, environmental monitoring*	*High*	*High*
Geotechnical survey vessels	*Project planning*	*Rock and sediment sampling, onboard processing, environmental sampling*	*High*	*High*
Wind turbine installation vessels	Commissioning and installation/ Decommissioning	Installation of wind turbines	High	Low
Heavy-lift vessels	*Commissioning and installation/ Decommissioning*	*Installation of substations, floating structures, turbine foundations*	*High*	*Medium*
Cable laying vessel	Commissioning and installation	Installation of inter-array cables inside wind farms, installation of export cables	High	Low
Subsea rock installation vessels	Commissioning and installation	Install scour protection for foundations and cables	High	None
Anchor handling, tug, supply vessels	*Commissioning and installation/ Operation/ Decommissioning*	*Towing operations, installation of mooring system*	*High*	*High*
Commissioning service operation vessel	*Commissioning and installation/Operation*	*Accommodation, walk-to-work (W2W) system, workshops, spare part storage, lifting operations, construction support, repair*	*High*	*Medium*
Offshore support vessels (O&G)	*Commissioning and installation/ Operation*	*Inspection, maintenance, and repair operations, lifting operations, diving support, ROV support*	*High*	*High*
Service operation vessel	*Operation*	*Accommodation, walk-to-work system, workshops, spare part storage, repair*	*High*	*Medium*
Delousing vessels	Operation	Biological treatments, removal of sea lice from fish	None	High
Well boat	Operation	Transport of live fish (smolts) to offshore fish farm; transport of live fish (mature) to harvest site on land; delousing operations	None	High
Slaughtering vessels	Operation	Onboard slaughtering facilities, cooling and freezing	None	High
Aquaculture service vessels	*Operation*	*Lifting operations, towing, (some) delousing operations, net cleaning*	*Medium*	*High*
Bulk carriers/multi-purpose vessels	Operation	Transport of fish feed, transport of frozen fish	None	High
Feed barges	Operation	Store and distribute fish feed (integrated in some offshore fish farm structures)	None	Medium

During project planning, the synergies mainly lie in about data and data sharing. By sharing data from previous surveys, impact assessments and seabed surveys could be fast-tracked for a second user of the same marine space.

In the operational phase of the lifecycle, multi-use synergies are present over a long period, making it potentially commercially interesting to take advantage of resource sharing schemes that is enabled by the fact that multiple users operate in the same area.

Estimate of potential savings

In the final part of this section, we provide a simple estimate of the power savings potential from multi-use synergies, considering the reduction in transit need if logistical demands can be coupled. We also comment briefly on potential fleet level impacts on capital expenditure.

A typical offshore support vessel spends close to 40% in transit, or around 3,000 hours per year (Lindstad et al., 2017). If we assume a similar pattern for special ships servicing the new offshore industries, and that half of the roundtrips are used to service both a wind farm and an offshore fish farm, then the transit time will be reduced by 25%. For simplicity, if we then assume that the same amount of time will be spent in transit at higher speeds, as these are likely missions with higher criticality, and therefore maintains some conservatism in the estimate of savings. If we then assume the average power requirement and specific fuel consumption for a variable speed engine with a specified operational mode, as suggested by Lindstad et al. (2017) and partially reproduced in Table 5, we observe fuel savings of around 5%, as the annual consumption reduces from almost 2,900 tonnes to just over 2,700 tonnes. This calculation assumes the use of diesel oil (for simplicity), and the actual savings potential will also depend on the dynamics of the future fuel mix (including new fuels) and the pricing of these alternative fuels. The effect of the reduced transit on costs might well be bigger, when taking into consideration the pricing of alternative fuels (DNV, 2023b).

Note that the share of time on dynamic positioning and for port loading operations increases when vessels are shared, meaning that there is an even greater potential for fuel saving, as batteries can play a key role during DP operations providing more flexible load. If offshore charging infrastructure is developed at wind farms, batteries may become an even more important part of the fuel mix of vessels serving offshore wind and could realize its potential to improving DP operations providing more flexible load (Lindstad et al., 2017; Holmefjord et al., 2020). Adding to this, we already discussed the role of the EU ETS in incentivizing shipping emission reductions (DNV, 2023b), and note that, all else kept constant, the carbon intensity of the fuel consumed will remain an important operational parameter in years to come.

Table 5: Example of change in operating profile and annual fuel consumption from shared offshore vessel capabilities.

Operational mode	**Original operational profile**		**Lower (75% of original) transit share of operational profile – due to co-location**		**Average power**	**Specific fuel consumption (variable engine speed)**	**Annual fuel consumption**	**Annual fuel consumption**
	Annual hours	**Share of time**	**Annual hours**	**Share of time**			**(original operating profile)**	**Lower transit share operating profile**
	Hours	**%**	**Hours**	**%**	**kW**	**g/kWh**	**Tonnes**	**Tonnes**
Dynamic positioning (DP)	*2400*	*27*	*2920*	*33*	*1600*	*210*	*806*	*981*
Standby	600	7	600	7	1500	205	185	185
Port	*2270*	*26*	*2500*	*29*	*336*	*265*	*135*	*149*
Transit ECO	*3000*	*34*	*2250*	*26*	*2300*	*200*	*1380*	*1035*
Transit 12 kn	400	5	400	5	3300	197	260	260
Transit 15 kn	90	1	90	1	6000	204	110	110
Total	8760	100	8760	100	-	-	2876	2720

Besides the effects on operational issues like emissions and operating costs, synergistic multi-use will also impact capital expenditure (CAPEX). For a single design case, the CAPEX will likely increase due to the need of catering to requirements for operations in several different market segments. Cost-related pitfalls of multi-functionality as pointed to by e.g. Gaspar et al. (2015) and Garcia et al. (2016) need to be avoided, and principles related to operational flexibility (Lindstad, et al., 2017; Rehn et al., 2019; Pettersen et al., 2020) adhered to, for this to remain a viable business case for ship owners. On the level of the support vessel sector as a whole, successful exploitation of synergistic multi-use logistics means that fewer vessels are needed to service a set of ocean assets. This means that less steel will be needed, further reducing the environmental footprint, and reducing CAPEX on the level of the whole industry. The same could hold true for the fleet design problem facing those ship owners that seek to take advantage of synergistic multi-use logistics.

OPPORTUNITIES AND BARRIERS

Sharing resources among several actors in the ocean space can be an opportunity to reduce costs, emissions, and to create a culture of collaboration across sectors that otherwise would compete for access to ocean area. We have established where the potential for sharing and synergistic multi-use lies, by identifying ship types that provide functions that can be useful in a multi-use setting. We now turn to discussing what key opportunities and barriers that exist to realizing this potential.

Opportunities

Reducing fuel consumption and operating costs by sharing logistics
From the perspective of an offshore wind farm or an offshore fish farm, the costs associated with chartering in special ships for the operational phase will constitute a relatively small share of the lifecycle cost. In offshore wind, operating costs overall constitute 25-30% of the lifecycle cost, of which a relatively small part will be vessel chartering during the operational phase. Still, sharing can constitute an interesting cost cutting measure, when seen along with developments like the introduction of carbon pricing. If shared logistics, as indicated in Table 5, in some cases can realize a 5% fuel saving, this is an opportunity that should be welcomed by ship owners and charterers.

The previously referred *NEXUS* project also provided some new insights into the feasibility of fully electrical operation of vessels at a wind farm (Holmefjord et al., 2020). Such operations are feasible provided sufficient infrastructure for charging is in place together with sufficient onboard energy storage (e.g. batteries). The opportunity to use renewable energy directly from a wind farm to charge offshore vessels is now being explored by several (Stillstrom, 2023; Memija, 2023), while ship designers are working on conceptual designs where space for sufficient energy storage and charging technology is integrated in close dialogue with owners and regulatory bodies (flag authorities and classification societies as DNV), see e.g. The Naval Architect (2024).

Reducing conflict potential through co-existence and multi-use
Besides the purely technical-economical argument above, the reduction of conflict potential that can be enabled by multi-use is substantial. From the discourse on the impact of offshore wind on other stakeholders, there is still a clear tendency to focus on the conflicts, which could hamper the "social license to operate" that any sector will be dependent on to some extent. This is most clearly seen in the relationship between offshore wind and the fisheries. Again, focusing on the potential synergies of this situation, rather than the trade-offs in what is quickly perceived as a zero-sum game, can create an atmosphere of collaboration between stakeholders.

The clearest marine design dimension to this question is the use of vessel capabilities for new types of operations. In the spatial relationship between offshore wind and the fisheries, compensation schemes to fisheries due to their exclusion from certain areas have been discussed. From other offshore sectors like oil and gas, there are examples of fishing vessels playing a key role in supporting emergency response operations, as exemplified by the Vessels of Opportunity-scheme deployed to participate in oil spill clean-up operations after the Deepwater Horizon accident (Pettersen et al., 2020). Identification of *latent capabilities* that were not intentionally designed for, can make fishing vessels useful in offshore wind operations or offshore aquaculture and could be a path to explore further.

Novel ways of meeting offshore wind tendering requirements
Co-existence is also finding its way into tendering requirements for offshore wind. In some cases, this could take the form of binary conditions, e.g. "it is required that the applicant has a co-existence plan". In other cases, non-price criteria are being shaped to award offshore wind tenders based on more quality parameters, including the design of specific measures that will ensure successful collaboration with other ocean stakeholders over the field lifecycle. This can be measures such as nature restoration by re-introduction of lost habitats (Pardo et al., 2024), or farming of blue mussels and kelp to extract excess nutrients from the sea, thereby improving water quality and/or providing human food.

Taking the arguments made in this paper further, these overarching government tender requirements could also percolate down to the specifications of chartering arrangements that ship owners will need to comply with to win contracts. For instance, could the future see chartering contracts being more explicit on the vessel's ability to also provide support to a co-located aquaculture operation?

Barriers

Technical barriers
Technical barriers to realizing synergistic multi-use related to the functionality of specific solutions. If there are significant amounts of mission-related systems onboard which are useful in the context of offshore wind, but without applications in the other sector to service, e.g. offshore aquaculture, then there is limited potential. The discussions in earlier parts of this paper largely screened for vessel types that can have applications in several sectors and sought to answer to what extent functionality from ship segments serving offshore wind, e.g. SOVs, could service offshore aquaculture. If similar solutions are sought out, for instance heavy-compensated gangways to improve operability and personnel safety, then the design features on the side of the offshore fish farm should be introduced to ease the compatibility with SOVs. For instance, the DNV class rules for floating fish farm installations lists "offshore gangways" as a relevant optional class notation (DNV, 2022a).

Operational barriers
Multi-use concepts have been observed to cause certain ambiguity in risk ownership, causing some authorities to impose operational restrictions for safety reasons (van den Burg et al, 2020). For instance, safety zones are one example where other activities are effectively banned from the vicinity of another. These might have good reasons, as in the case of oil and gas installations, but might be too strict for other types of offshore platforms.

Furthermore, if multi-use concepts are not restricted by e.g. safety zone issues, there still might be the need for development of appropriate operational procedures to allow for new types of vessel-structure interactions, for instance when an SOV services an offshore fish farm. In such cases, the successful operation of vessels in a multi-use logistics context also becomes a function of organizational factors like crew competence, training, and experience.

Finally, mission criticality considerations will also play a role as an operational barrier, seeing that an unplanned repair operation at the wind farm may need to take priority over a planned mission to service the offshore fish farm. If so, what should dictate when an unplanned mission at production system *A* should take priority over a planned mission at the co-located production system *B*? And who should pay?

Commercial barriers
The question posed above illustrates the core limitation to realizing synergistic multi-use logistics from the commercial point-of-view. Chartering arrangements need to reflect the co-use of vessels for both purposes and determine how the risks associated with the operations should be spread. The ease of creating a joint chartering arrangement could come down to factors such as organizational structure of the offshore wind/offshore fish farming operator. For instance, does common ownership over both production systems imply that establishing a joint chartering arrangement is easier? Would horizontally integrated companies that operate across several blue economy sectors like renewables and seafood more easily see the potential for multi-use synergies, and be more likely to realize them?

A second commercial barrier is related to the cost of managing the complexity of two disjoint operations. We observed earlier in the paper that the share of vessel-related costs during the operational phase of a wind farm (or a fish farm for that matter) is only a small share of the total operating costs. Hence, the increase in transaction costs related to managing a much more complex chartering arrangement may not be worth it, from the point of view of the charterer. Also on the supply side, a similar problem might exist, particularly in good times, when rates are high. Who would then bother taking on a more complex arrangement that may not pay a sufficient premium?

CONCLUSION

In this paper, we have introduced the concept of multi-use of marine space to the ship design audience. Where ideas of multi-use and co-existence have emerged in the marine spatial planning research community, there has so far been little work on understanding the roles special ships can take in a Blue Economy shaped by the need for sharing of maritime resources. We have provided an overview of some key drivers for marine multi-use and sharing of vessels in this setting and provided a qualitative assessment of key operations performed in offshore wind and aquaculture, aiming to identify areas for synergistic multi-use.

We have also provided insight on the key pros and cons of moving towards synergistic multi-use, pointing to drivers like reduced costs and emissions, as well as reducing conflict levels. The need for emission reductions and stakeholder collaboration appear to be the strongest drivers. On the side of barriers, chartering needs to take into consideration longer response times to missions of high criticality, and to consider how risks should be allocated.

While there are clear benefits, we ended the discussion with a set of more cautious remarks about the barriers. Further research could take a closer look at the shipping economics at play, the trade-offs, and the conditions under which synergistic multi-use would make sense. Assessments of multi-purpose platforms so far, at best, provide a mixed bag of results and with the previous experience from multi-functionality in offshore support vessels, there is reason to approach the concept with cost and emission reductions in mind first.

CONTRIBUTION STATEMENT

Sigurd S Pettersen: Conceptualization; writing – original draft; writing – review and editing. **Arnstein Eknes:** Conceptualization; writing – review and editing.

ACKNOWLEDGEMENTS

Sigurd S. Pettersen's contributions to this paper has been partially financed by the Norwegian Research Council through the *MARCO (MARine CO-existence scenario building)* project, grant no. 340998.

REFERENCES

Andrews, D. (2018). The sophistication of early stage design for complex vessels. *Transactions of the Royal Institution of Naval Architects: International Journal of Maritime Engineering.* https://doi.org/10.3940/rina.ijme.2018.SE.472

AquaShip. (2021, September 17). *AquaShip is expanding: Our new vessel Grip Explorer has arrived*. https://www.aquaship.no/eng/news/aquaship-is-expanding-welcome-to-our-new-vessel-grip-explorer

Baird Maritime. (2020, July 24). *VESSEL REVIEW | HAVFARM 1 – MAMMOTH, SEMI-SUBMERSIBLE, EXPOSED AQUACULTURE PEN ARRIVES IN NORWAY*. https://www.bairdmaritime.com/fishing-boat-world/aquaculture-world/vessel-review-havfarm-1-mammoth-semi-submersible-exposed-aquaculture-pen-arrives-in-norway/

Barrett, LukeT., Oldham, T., Kristiansen, T. S., Oppedal, F., & Stien, L. H. (2022). Declining size-at-harvest in Norwegian salmon aquaculture: Lice, disease, and the role of stunboats. *Aquaculture*, *559*, 738440. https://doi.org/10.1016/j.aquaculture.2022.738440

Bocci, M., Castellani, C., Ramieri, E. (2018). *Case study comparative analysis. MUSES project.* https://muses-project.com/wp-content/uploads/sites/70/2018/06/MUSES-WP3-D3.5-Case-study-comparative-analysis_20180510.pdf

Clarkson's Research. (2024). *Renewables Intelligence Network*. https://www.clarksons.net/rin/

Dalton, G., Bardócz, T., Blanch, M., Campbell, D., Johnson, K., Lawrence, G., Lilas, T., Friis-Madsen, E., Neumann, F., Nikitas, N., Ortega, S. T., Pletsas, D., Simal, P. D., Sørensen, H. C., Stefanakou, A., & Masters, I. (2019). Feasibility of investment in Blue Growth multiple-use of space and multi-use platform projects; results of a novel assessment approach and case studies. *Renewable and Sustainable Energy Reviews*, *107*, 338–359. https://doi.org/10.1016/j.rser.2019.01.060

Dixon, G. (2020, September 15). PSV to be converted into salmon delousing vessel as rates spike. *TradeWinds*. https://www.tradewindsnews.com/offshore/psv-to-be-converted-into-salmon-delousing-vessel-as-rates-spike/2-1-874607

DNV. (2021). *Ocean's Future to 2050.* https://www.dnv.com/oceansfuture/index.html

DNV. (2022a). *Floating fish farming units and installations* (DNV-RU-OU-0503). DNV.

DNV. (2022b, June 4). *DNV to class commissioning service operation vessels prepared for hydrogen operations*. https://www.dnv.com/news/dnv-to-class-commissioning-service-operation-vessels-prepared-for-hydrogen-operations-222725

DNV. (2022c, December 19). *DNV to lead research project to strengthen marine and offshore wind coexistence planning*. https://www.dnv.com/news/dnv-to-lead-research-project-to-strengthen-marine-and-offshore-wind-coexistence-planning-237122

DNV. (2023a). *Energy Transition Outlook 2023.* https://www.dnv.com/energy-transition-outlook/index.html

DNV. (2023b). *Maritime Forecast to 2050*. https://www.dnv.com/maritime/publications/maritime-forecast-2023/index.html

DNV. (2023c). *Seafood Forecast: Ocean's Future to 2050*. https://www.dnv.com/publications/seafood-forecast-250243

DNV. (2023d). *Spatial Competition Forecast: Ocean's Future to 2050*.

Ehler, C., & Douvere, F. (2007). *Visions for a sea change: Report of the First International Workshop on Marine Spatial Planning, Intergovernmental Oceanographic Commission and the Man and the Biosphere Programme UNESCO Headquarters*. IOC-UNESCO. https://doi.org/10.25607/OBP-1415

Equinor. (2023). *Hywind Tampen: The world's first renewable power for offshore oil and gas*. https://www.equinor.com/energy/hywind-tampen
Equinor. (2024, January 3). *Empire Wind 2 offshore wind project announces reset, seeks new offtake opportunities.* https://www.equinor.com/news/20240103-empire-wind-2-offshore-wind-project-announces-reset
Erikstad, S. O., & Lagemann, B. (2022). Design Methodology State-of-the-Art Report. *14th International Marine Design Conference*, D031S000R001. https://doi.org/10.5957/IMDC-2022-301
Erikstad, S. O., & Levander, K. (2012). System Based Design of Offshore Support Vessels. *11th International Marine Design Conference*.
Fagerholt, K., & Lindstad, H. (2000). Optimal policies for maintaining a supply service in the Norwegian Sea. *Omega*, *28*(3), 269–275. https://doi.org/10.1016/S0305-0483(99)00054-7
Feng, Y. (2023, October 15). China is Bringing Aquaculture to Deep Offshore Waters. *The Maritime Executive*. https://maritime-executive.com/editorials/china-is-bringing-aquaculture-to-deep-offshore-waters
Garcia, J. J., Brandt, U. B., & Brett, P. O. (2016). *Unintentional consequences of the golden era of the Offshore Oil & Gas industry*. International Conference on Ships and Offshore Structures, Hamburg, Germany.
Gaspar, H. M., Brett, P. O., Erikstad, S. O., & Ross, A. M. (2015). Quantifying value robustness of OSV designs taking into consideration medium to long term stakeholders' expectations. *12th International Marine Design Conference*.
Grønholt-Pedersen, J. (2023). Orsted hit by up to $5.6 billion impairment on halted US projects. *Reuters.* https://www.reuters.com/business/energy/orsted-cease-development-some-us-offshore-wind-projects-2023-10-31/
Hersoug, B., & Mikkelsen, E. (2022). *Marine næringsparker—Nye muligheter for samhandling til havs*. Senter for hav og Arktis. https://www.havarktis.no/files/Marine-n%C3%A6ringsparker-nye-muligheter-for-samhandling-til-havs.pdf
Hoegh-Guldberg, O., Northrop, E., Ashford, O. S., Chopin, T., Cross, J., Duarte, C., Geers, T., Gössling, S., Haugan, P., Hemer, M., Huang, C., Humpe, A., Kitch, G., Koweek, D., Krause-Jensen, D., Lovelock, C. E., Matthews, K., Nielsen, F. G., Parker, R., … Tyedmers, P. (2023). *The Ocean as a Solution to Climate Change: Updated Opportunities for Action* [Special Report]. World Resources Institute. https://oceanpanel.org/wp-content/uploads/2023/09/Ocean_Panel_Ocean_Climate_Solutions_Update_Full.pdf
Holmefjord, K. E., Husdal, L., de Jongh, M., & Torben, S. (2020). Variable-Speed Engines on Wind Farm Support Vessels. *Journal of Marine Science and Engineering, 8*(3), 229. https://doi.org/10.3390/jmse8030229
Irawan, C. A., Starita, S., Chan, H. K., Eskandarpour, M., & Reihaneh, M. (2023). Routing in offshore wind farms: A multi-period location and maintenance problem with joint use of a service operation vessel and a safe transfer boat. *European Journal of Operational Research*, *307*(1), 328–350. https://doi.org/10.1016/j.ejor.2022.07.051
Iversen, A., Asche, F., Hermansen, Ø., & Nystøyl, R. (2020). Production cost and competitiveness in major salmon farming countries 2003–2018. *Aquaculture*, *522*, 735089. https://doi.org/10.1016/j.aquaculture.2020.735089
Iversen, A., Hermansen, Ø., Nystøyl, R., & Hess, E. J. (2017). *Kostnadsutvikling i lakseoppdrett. Med fokus på for- og lusekostnader*. Nofima. https://nofima.brage.unit.no/nofima-xmlui/bitstream/handle/11250/2481501/Rapport%2b24-2017.pdf?sequence=1&isAllowed=y
Lazakis, I., & Khan, S. (2021). An optimization framework for daily route planning and scheduling of maintenance vessel activities in offshore wind farms. *Ocean Engineering*, *225*, 108752. https://doi.org/10.1016/j.oceaneng.2021.108752
Lindstad, H. E., Eskeland, G. S., & Rialland, A. (2017). Batteries in offshore support vessels – Pollution, climate impact and economics. *Transportation Research Part D: Transport and Environment*, *50*, 409–417. https://doi.org/10.1016/j.trd.2016.11.023
Memija, A. (2023). World's First Offshore Vessel Charging System Completes Harbour Trials. *offshoreWIND.biz.* https://www.offshorewind.biz/2023/03/15/worlds-first-offshore-vessel-charging-system-completes-harbour-trials/
OLAMUR. (2024). https://olamur.eu/
Omrani, P. S., Poort, J., Swamy, S. K., Uritsky, V., Dick, R., Peet, L., Egbertsen, J., & Winters, D. (2022). *The Potential of Shared Offshore Logistics*. North Sea Energy. https://north-sea-energy.eu/static/9890eefabe9a327a1cbad29d455a2f01/NSE-2020-2022-5.1-Logistics.pdf
Pardo, J. C. F., Aune, M., Harman, C., Walday, M., & Skjellum, S. F. (2023). A synthesis review of nature positive approaches and coexistence in the offshore wind industry. *ICES Journal of Marine Science*, fsad191. https://doi.org/10.1093/icesjms/fsad191
Pettersen, S. S. (2022). Design Novelty and Cost-Learning Dynamics in Offshore Fish Farming. *14th International Marine Design Conference*, D041S013R002. https://doi.org/10.5957/IMDC-2022-248
Pettersen, S. S., Aarnes, Ø., Arnesen, B., Pretlove, B., Ervik, A. K., & Rusten, M. (2023). Offshore wind in the race for ocean space: A forecast to 2050. *Journal of Physics: Conference Series*, *2507*(1), 012005. https://doi.org/10.1088/1742-6596/2507/1/012005
Pettersen, S. S., Garcia Agis, J. J., Rehn, C. F., Asbjørnslett, B. E., Brett, P. O., & Erikstad, S. O. (2020). Latent capabilities in support of maritime emergency response. *Maritime Policy & Management*, *47*(4), 479–499. https://doi.org/10.1080/03088839.2019.1710611
Puisa, R., Bolbot, V., Newman, A., & Vassalos, D. (2021). Revealing system variability in offshore service operations through systemic hazard analysis. *Wind Energy Science,* 6, 273-286. https://doi.org/10.5194/wes-6-273-2021

Rehn, C. F., Pettersen, S. S., Garcia, J. J., Brett, P. O., Erikstad, S. O., Asbjørnslett, B. E., Ross, A. M., & Rhodes, D. R. (2019). Quantification of changeability level for engineering systems. *Systems Engineering*, *22*(1), 80–94.

Schupp, M. F., Bocci, M., Depellegrin, D., Kafas, A., Kyriazi, Z., Lukic, I., Schultz-Zehden, A., Krause, G., Onyango, V., & Buck, B. H. (2019). Toward a Common Understanding of Ocean Multi-Use. *Frontiers in Marine Science*, *6*, 165. https://doi.org/10.3389/fmars.2019.00165

Slette, H. T., Asbjørnslett, B. E., Fagerholt, K., Lianes, I. M., & Noreng, M. T. (2023). Effective utilization of service vessels in fish farming: Fleet design considering the characteristics of the locations. *Aquaculture International*, *31*(1), 231–247. https://doi.org/10.1007/s10499-022-00974-9

Slette, H. T., Asbjørnslett, B. E., Pettersen, S. S., & Erikstad, S. O. (2022). Simulating emergency response for large-scale fish welfare emergencies in sea-based salmon farming. *Aquacultural Engineering*, *97*, 102243. https://doi.org/10.1016/j.aquaeng.2022.102243

Stillstrom. (2023). *Stillstrom A/S and North Star join forces to accelerate Vessel Electrification and Offshore Charging in the Offshore Wind Industry*. https://stillstrom.com/2023/08/stillstrom-north-star-mou-on-offshore-sov-charging-solution/

The Crown Estate & ORE Catapult. (2019). *Guide to an offshore wind farm*. https://guidetoanoffshorewindfarm.com/

The Naval Architect. (2024). *Offshore Wind Vessels. https://content.yudu.com/web/60wf/0A60wg/JetroOWV24/html/index.html?refUrl=https%253A%252F%252Frina.org.uk%252F&page=32*

Ulstein. (2022). *What makes vessel conversions a sustainable option?* https://ulstein.com/news/what-makes-vessel-conversions-a-sustainable-option

Van Den Burg, S. W. K., Schupp, M. F., Depellegrin, D., Barbanti, A., & Kerr, S. (2020). Development of multi-use platforms at sea: Barriers to realising Blue Growth. *Ocean Engineering*, *217*, 107983. https://doi.org/10.1016/j.oceaneng.2020.107983

Van Hoof, L., Van Den Burg, S. W. K., Banach, J. L., Röckmann, C., & Goossen, M. (2020). Can multi-use of the sea be safe? A framework for risk assessment of multi-use at sea. *Ocean & Coastal Management*, *184*, 105030. https://doi.org/10.1016/j.ocecoaman.2019.105030

Van Lynden, C., van Winsen, I., Westland, C. N., & Kana A. A. (2022). Offshore wind installation vessels: generating insight about the driving factors behind the future design. *International Journal of Maritime Engineering, 164,* No. A2. https://doi.org/10.5750/ijme.v164iA2.1175

Van Vranken, C., Jakoboski, J., Carroll, J. W., Cusack, C., Gorringe, P., Hirose, N., Manning, J., Martinelli, M., Penna, P., Pickering, M., Piecho-Santos, A. M., Roughan, M., De Souza, J., & Moustahfid, H. (2023). Towards a global Fishing Vessel Ocean Observing Network (FVON): State of the art and future directions. *Frontiers in Marine Science*, *10*, 1176814. https://doi.org/10.3389/fmars.2023.1176814

Willumsen, P., Oehmen, J., Vilsøe, M., Boserup, C. M., & Stilbo, R. (2023). *Making the green transition resilient: Adaptability by design*. Implement Consulting Group. https://cms.implementconsultinggroup.com/media/uploads/articles/2023/Making-the-green-transition-resilient/Making-the-green-transition-resilient-adaptability-by-design.pdf

Zwaginga, J., Stroo, K., & Kana, A. (2021). Exploring market uncertainty in early ship design. *International Journal of Naval Architecture and Ocean Engineering*, *13*, 352–366. https://doi.org/10.1016/j.ijnaoe.2021.04.003

Proceedings of 15th International Marine Design Conference (IMDC-2024)
June 2-6, 2024
Amsterdam, The Netherlands

Utilizing Amphibious AGVs to Optimize Container Transshipment for Deep Sea and Hinterland Operations

Abhishek Rajaram[1,*] and Lavanya Meherishi[2] and Jovana Jovanova[1] and Andrea Coraddu[1]

ABSTRACT

Transshipment is a key component of modern-day shipping logistics. Container supply chains rely on transhipment hubs to access remote locations. With globalisation driving growth in container trade, maritime congestion is rising at container terminals in ports worldwide. This is expected to worsen as demand continues to grow. This research explores novel maritime equipment designs that can contribute to solving problems in the trans-shipment chain. One such idea is that of the Amphibious Automated Guided Vehicle, an innovative concept that travels on both land and sea. Envisioned as a tool to minimise the rehandling of containers, the Amphibious AGV forms the heart of the new changes that this research proposes for the future of trans-shipment. Complementing swifter trans-shipment, the research also proposes complementary design concepts such as floating terminals to add more flexibility for container ships and Amphibious AGVs applied to exchange containers offshore. To validate these ideas, an agent-based modelling methodology was used and replicated in the environment of the Hong Kong- Pearl River Delta. This work, therefore, opens up an intriguing future scope for maritime transshipment that is both sustainable and adaptable while also discussing limitations and concerns that need to be carefully considered.

KEY WORDS

Marine Design, Transshipment network, Floating Terminals, Amphibious AGV, Agent-Based Modeling

INTRODUCTION

Globalisation has sprung up a huge surge in international trade. With the increase in international trade, container trade has also seen a substantial increase in the last few years. With container ships getting bigger, both inland and deep sea terminals are seeing massive volumes of container flow daily. Consequently, hinterland transportation networks have become extremely important for trade and accessibility worldwide. In this era of globalization, an increasing number of inland cities are playing pivotal roles in global trade by supplying electronics, essential goods, and even food items. However, with this growth, deep sea terminals that are often the gateways for inland container traffic become congested with the influx of multiple barges. In the ports of Rotterdam and Antwerp, terminals that often only see 1 ultra-large container ship a day would see 23 barges dock by the terminal (Shobayo and Van Hassel, 2019)

This number amplifies to 120 barges in busier ports like Hong Kong (Seatrade Maritime News, 2015). This contributes to arrival/departure problems, berth planning issues, and quay crane allocation problems in ports (Tang et al., 2022). Often, terminals are forced to use deep-sea berths to unload waiting container barges, preventing bigger ships from docking. Congestion in many other regions of the world, such as the United States, has taken a different turn, with the Port of Los Angeles

[1] Maritime and Transport Technology, Delft University of Technology,The Netherlands
[2] Faculty of Engineering, University of Exeter,United Kingdom
[1] Maritime and Transport Technology, Delft University of Technology, The Netherlands; ORCID: 0000-0001-8347-6386
[1] Maritime and Transport Technology, Delft University of Technology, The Netherlands; ORCID: 0000-0001-8891-4963
[*] Corresponding Author: rajaramabhishek@gmail.com

Submitted: 3 March 2024, Revised: 1 May 2024, Accepted: 3 May 2024, Published: 7 May 2024

Conference paper, DOI: https://doi.org/10.59490/imdc.2024.780 e-ISSN: 3050-4864

and Savannah seeing queues of up to 100 vessels, of which 70 of them were container vessels (Bu et al., 2023). Ports in the United States saw a massive increase in dwell times by 27.4% in 2021 compared to 2016. Similarly, in the Port of Rotterdam and Antwerp, only 41% of barges arrived/departed within a two-hour window that is usually reserved for barges From a policy side, congestion has caused tensions between barge operators and deep sea terminal operators since the former and latter do not share any contractual relationship (van der Horst et al., 2019), therefore not obligated to pay berth fees while spending 1/3rd of their operational time at deep sea terminals (Konings, 2007).

Compounding the issue, when the world's two busiest waterways, namely the Rhine and Yangtze rivers, were compared, their different upstream and downstream dynamics warrant solutions that are globally applicable to solve congestion (Notteboom et al., 2020). In the context of barges and inland waterways, congestion is also caused by multiple trips originating from the same inland port, which is a direct consequence of low container call sizes. Port of Rotterdam and Antwerp have seen this problem escalate at their deep sea terminals with call sizes as low as 6 TEU per barge trip with an average of just 33 TEU per deep sea terminal during a barge trip (Konings, 2007). This has meant that despite a priority for deep sea ships, some deep water berths are forced to block 3000 TEU+ ships to unload barges (Shobayo, 2023). This has also mounted to the congestion in container terminals with repetitive barge trips. Historically, this has called for better coordination and information exchange between deep-sea terminals and hinterland barge operators, but such alliances are not in place, and expect to take a long time before anything materialises (Wiegmans et al., 2018) When the issue is analyzed from a global perspective, the urgency to solve the problem of congestion is underlined by the fact that seaport/terminal inefficiency in handling container shipments will lead to higher maritime transport costs, which will eventually influence the prices paid by consumers for goods due to container holding costs (Sanchez et al., 2003). In its worst manifestation, COVID-19 showed how these prices could worsen when holding containers raised shipping costs 10-15 times in 2021 (Freightos, 2023). For instance, in 2021, freight rates for shipping a 40ft container from the USA to China skyrocketed to $20,600 (Regular cost- $1400). While congestion is never expected to impact trade as COVID-19 did, inefficiency in the supply chain can compound existing delays. Maritime congestion, therefore, sees terminal inefficiency as one of its leading causes. With the enormous growth in container trade and more markets and inland ports being breached, congestion at deep-sea terminals is imminent. This would essentially segue well into exploring terminal and port expansion through land reclamation, but this has many inherent issues. Singapore, one of the most prominent ports in the international shipping line, expanded in 2014 to increase the number of deepwater berths to 15, aiming to boost container throughput to 50 million in the coming years. However, this was not without its drawbacks, as the expansion severely impacted the ecological welfare of nature reserves despite preventive measures (Lian et al., 2015). This warrants a solution that is also sustainable. From a social sense, taking the example of the Port of Hong Kong, the terminals, which see 120 barges/day, are unable to expand due to the impending housing crisis in Hong Kong, which has threatened to close some terminals to create space for housing complexes and settlements (Chong and Li, 2020). Congestion in such circumstances will only worsen with fewer avenues of expansion. This has knock-on effects on daily schedules with worsening berth management issues. Shifting hub ports like Hong Kong to another place or creating new hubs is not viable in the maritime industry as various inland waterway ports are directly linked to these hubs. Some examples include Hong Kong- Pearl River Delta, Antwerp/Rotterdam- Rhine, and Shanghai- Yangtze. However it is not only the lack of expansion space affecting terminals, congestion is both a consequence and a cause of inefficient container handling operations that are seen today which is a constraint of technology and manpower. While ports have become more autonomous and have achieved the pinnacle of technology with the introduction of AGVs, automated quay, and yard vessels, it has still not solved vital issues such as rehandling of containers where a lot of time is lost even today (Caserta et al., 2011). Most containers lose time transiting between different types of vehicles, both in port and on water. A container transfer between two terminals would need the use of an AGV+Barge (Schroër et al., 2014), or the use of a truck which would have to travel 20+ km on land when the terminal is just 2km across water (Ghiridharan, 2023). Both transfer methods lead to delays in handling incoming and outgoing container consignments from partner terminals or inland entities, leading to higher dwell/waiting times for deep sea ships and especially barges, which generally look for quicker turnaround times (Chen and Schonfeld, 2010), given their low call sizes. This is also a domino effect, with rehandling often leading to container relocation problems in stacks/yards. Looking at the bigger picture to understand the cascading phenomenon, ship delays due to congestion have seen an increase in rehandlings by 44% in worse-case scenarios, and it gets worse with growing demand call sizes and container reshuffles aggravating maritime congestion (Gharehgozli et al., 2017).

Deep Sea- Hinterland transportation, therefore, has multiple challenges. It has to grow sustainably while addressing congestion, efficient inter-terminal and inland transport, and minimize or eliminate land reclamation while opening new avenues for expansion. With global trade set to grow by 70% in 2030 (Gibson, 2021), container handling at both deep-sea terminals

and hinterland must be efficient to enable seamless trade windows for international deep-sea vessels and domestic barges. The trade targets also bolster the need for new perspectives in container shipping for the future. Thus, this paper describes and analyzes the implementation of marine design concepts that can provide a novel outlook for deep sea to hinterland transportation.

According to the literature review, we identified four areas that would need new perspectives. These include: i) the minimization of container rehandling, ii) addressing low call sizes of barges, iii) identifying alternate avenues for expansion, and iv) an integrated network design and methodology to implement this novel trans-shipment idea. Most of the research carried out so far has emphasized on optimizing existing networks through various analytical and lean approaches to address bottlenecks(akin to point iv). However, as seen in the introduction and problem analysis, it is clear that certain design concepts are directly responsible for increasing container handling and barge congestion. This is where novel design approaches and methodologies are needed to enhance the performance of major container transshipment networks.

Therefore the goal of this work is to introduce such novel designs addressing each of the four points listed above and applying it to a real-world container transshipment network namely the Hong Kong- Pearl River Delta with the aim to reduce barge congestion, maintain stable container throughput and container transport time while also enabling future avenues for growth in such ports.This work aims to present preliminary design concepts that can enable a framework to address the four burning issues of this research.

The structure of this paper is organized as follows: Section **Related Work** introduces the state-of-the-art, providing a foundation for the research. This is followed by a detailed presentation of the methodology in Section **Methodology**, where we outline the authors' proposed approach for addressing the transshipment problem, encompassing both the theoretical design and practical implementation aspects. Subsequently, Section **Case Study** describes the validation of the proposed transshipment solution through a meticulously conducted case study. The findings from this case study are thoroughly examined in Section **Results**, where the effectiveness of the new transshipment method is evaluated. Finally, Section **Conclusions** concludes the paper, offering key insights derived from the research and suggesting directions for future work in this area.

RELATED WORK

This section is dedicated to providing a comprehensive overview of the existing literature and prior work that has significantly shaped the direction of our study. Much of the research in the maritime domain has traditionally been conducted with a focus either on design aspects or optimization techniques. However, instances where both design and optimization methods are integrated are notably rare. This gap highlights the unique contribution of our work, as we aim to synthesize these two approaches to address the challenges in the maritime field more effectively.

Barge Congestion Challenges- Addressing Call Size Variability: the congestion of barges at deep-sea terminals and along inland waterways presents a significant challenge, arising from a blend of operational and policy-related issues. This subsection explores the variability in call sizes across different ports, such as Hong Kong, and discusses the economic advantages of barge transport. It highlights the efficiency and cost benefits of barges compared to other modes of transport, emphasizing the global shift towards increased hinterland transport. The congestion of barges at deep-sea terminals and along the inland waterway has generally been caused due to a combination of operational and policy issues. One of the recent works aimed at solving barge congestion in part uses an agent-based modelling approach (Shobayo and Van Hassel, 2019) and makes important suggestions on how a mandate/contract needs to be agreed upon for a minimum number of containers that a barge calls at a terminal. The work suggests 30 TEU for the environment of Rotterdam and Antwerp as a minimum call size. The effects of this would be reduced port calls, and therefore reduced congestion. An earlier work which focused on opportunities to handle denser barges in the future (Konings, 2007) also corroborated the idea of having a minimum agreed-upon call size. This figure, however, is not universal with the port of Hong Kong recording call size anywhere between 50 TEU (Seatrade Maritime News, 2015) TO 120 TEU (Post, 1994) with 120 barges a day. The motivation to use a higher (and minimum agreed upon call size) is also complemented by research which has shown that barge transport costs as low as 12.6 Euros per 1000 Ton kilometers when compared to trucks and trains that cost 4 times as high (Gharehgozli and Zaerpour, 2018). Similarly, even regarding mileage, barge transport records 576 miles/ton/gallon compared to 413 in trains and 155 in trucks (Bu et al., 2023).

Ports worldwide are also increasing the proportion of hinterland transport given its cost and fuel benefits, with Rotterdam and Antwerp increasing the share to 45% by 2030 (Gumuskaya et al., 2020). Higher call sizes, in that sense, would benefit both barge companies and terminal operators in reducing trips. Congestion, when seen from a sustainable expansion point of view, brings numerous possibilities. A general deep sea terminal has provisions for deep sea ships, feeders, and barges.

Innovative Terminal Solutions to Combat Congestion: innovations such as dedicated handling spaces and the barge hub concept are explored here. These solutions aim to efficiently reconfigure terminal space, promoting larger call sizes and potentially reducing congestion, while also addressing their scalability and feasibility challenges. This section covers the development of integrated terminal ship transfer systems and other direct trans-shipment methods. Such advancements aim to streamline operations, reduce the use of unnecessary vehicles, and offer cost-effective alternatives for terminal expansion. Research has also explored dedicated handling spaces for barges and feeders, with the barge hub being a prominent example of reconfiguring existing terminal space without unnecessary land reclamation (Pielage et al., 2007) (Konings et al., 2013). A barge hub would be an intermediate terminal that extends hinterland services by shifting the centre of congestion from deep sea terminals to an area accessible by hinterland actors. This concept also encourages larger call sizes to flow in at once drastically reducing barge frequency. A major drawback of this shown in research (Nicolet et al., 2023) is that barge hubs work predominantly for small cargo volumes given that expansion would result in similar problems to deep-sea terminals and could cause similar levels of congestion. Location often would also become a contentious point if even feeders and deep sea ships had to be handled, reducing versatility (Konings, 2007). The Barge hub would still need investment in the yard, vehicles, and straddle carriers. A more flexible concept has been seen in floating terminals, which have been explored in various sustainable and modular forms. Initial concepts include repurposing post-panamax vessels with on-board harbour cranes for loading and unloading containers (Baird and Rother, 2013). The quay of 300 m would be long enough to support up to 3 standard rhine barges or two feeder ships and would cost 1/3rd of a regular terminal. Despite its cost benefits and stability certification, such a concept would not be able to accommodate as many quay cranes as needed and would lose time in loading, unloading, and transfer, thereby contributing to higher waiting times and congestion. When connecting this idea with container rehandling concepts are needed to reduce this rehandling, desirably through direct transfer trans-shipment between ships, minimising storage for repositioning (Shen and Zhang, 2015). These have been manifested in a 2020 work that discussed exploratory concepts for floating terminals (Jovanova et al., 2022). Simulated in the Port of Genoa, the floating extensions were modular and used carrier cranes that could simultaneously transfer containers overhead from one vessel to another. This would essentially reduce rehandling and the number of ground vehicles and space in the process. The drawback here was that the lack of yard space meant that even temporary storage was not possible. However, a work within the same timeline by Johannes March proposed an integrated terminal ship transfer system (March, 2020). While this is not a floating terminal out and out, the benefits of direct trans-shipment were shown using a similar over-the-head crane that spanned across an ultra-large container vessel, a feeder/barge, and also part of the quay/yard. This concept eliminates unnecessary vehicles and simplifies container access points from respective ships/yards. The research also claims a 50-80% reduction in overall investment and is an important consideration for alternate container expansion approaches. However, hub and spoke limitations and approaches concerning hinterland hubs also need to be considered regardless of floating terminal versatility as depicted in works done on Port of Antwerp and Rotterdam (Caris et al., 2011; Konings et al., 2013).

Rehandling of Containers during Inter-Terminal Transport to Reduce Congestion: technological innovations, including waterborne AGVs and the Amphibious AGV, are discussed for their potential to transform inter-terminal transfers and reduce container handling points, illustrating a shift towards autonomous and efficient maritime logistics operations. The port feeder barge concept is examined here, highlighting its potential to improve inter-terminal transport efficiency through faster loading and unloading processes. The potential resistance from traditional terminal operators to this innovation is also discussed. Addressing an identified problem of inter-terminal transport through trucks, another important idea in research that looks to solve container rehandling, call size issues, and congestion is the Port feeder barge idea (Malchow, 2020). This is essentially a crane-on-barge concept with a capacity of 168 TEU, aimed at serving small inland barges with swift loading, unloading and instant transfer. The port feeder barge has the potential to shorten multiple inter-terminal transfers on water (from 20km to 2km (Ghiridharan, 2023)) and reduce the overall time spent for barges within the port. While this idea is promising to solve congestion, as pointed out in another research (Nicolet et al., 2023), deep-sea terminal and hinterland operators could resist the involvement of a third party for stevedore operations. Eliminating the hassle of operators, the waterborne AGV was developed with a vision to enable swift inter-terminal transfer and transshipment. Envisioned to be operated by deep sea terminals, the waterborne AGV is essentially a 2 TEU AGV that traverses on water instead of land (Zheng et al., 2017). The waterborne AGV uses azipod thrusters for propulsion and is currently in the prototyping phase at TU Delft. The waterborne AGV is

promising, given its autonomous nature and the extensive research in inter-terminal transport. Complementing its significance, waterborne AGVs have also been simulated in cooperative control using a fleet of WAGVs either as a swarm or platoon in Port of Rotterdam conditions, displaying its versatility (Chen et al., 2019). Given the Maasvlakte's expansive layout, literature has also corroborated with Waterborne AGV's efficiency over trucks in reducing time, distance, and emissions for container transfers (Zheng et al., 2016). However, container rehandling remains an issue. Recalling previous literature accounts and sections, just as how an AGV or Truck + Barge is needed to move containers between terminals, similarly the waterborne AGV would still be involved in a switch with another truck or ground AGV. The handling points in the system would remain the same and in case of any ship delays, as seen earlier (Gharehgozli et al., 2017), handling times could compound by 44% or worse. Furthermore, this adds to the high number of trucks and AGVs that the terminal already has to operate, aggravating land and water-based congestion. The handling point can only be eliminated or reduced if a concept combines land and water handling capabilities. That is where the Amphibious AGV(AAGV) comes into the picture, a nascent yet significant concept in the broader terminal operations picture. The AAGV is again another 2 TEU vehicle that can travel on both land and water. Envisaged as an instrument to reduce container handling points in the supply chain, the AAGV was first designed as a general transport vehicle in 2019 (Kleefstra, 2019). It was subsequently redesigned by a TU Delft project team featuring the primary author of this research paper. The AAGV in preliminary findings (Abhishek Rajaram, 2023; Ghiridharan, 2023) produced a 21% saving in transfer times between container terminals. In both the aforementioned recent works, the AAGV reduced handling points, reducing barge/feeder waiting times and opening avenues for versatile implementation in tandem with concepts such as floating terminals.

Simulation Techniques for Congestion Analysis: this section delves into the use of simulation techniques, such as discrete event simulation and agent-based modeling, in analyzing maritime congestion and evaluating the effectiveness of proposed solutions. Recent advancements in addressing barge congestion have leveraged agent-based modelling techniques. Studies have effectively used agent-based modelling to address call size issues by implementing a minimum call size for barges at terminals, with recommendations for specific sizes in ports like Rotterdam and Antwerp, to alleviate congestion. When seen from an implementation point of view, maritime networks often follow either hub and spoke theories,point-to-point theories, or a combination of both (Tagawa et al., 2021). From a simulation standpoint, various approaches have been discussed to present the barge congestion situation accurately. One is by sequentially planning events, and this is discrete event simulation in research; this has been successful in modelling waterways (Bu et al., 2023), berth planning (Legato and Mazza, 2001) and also container yard management (Kotachi et al., 2016). However, this type of simulation is not capable of doing parallel processing, which would otherwise be possible in an agent-based modelling approach. Agent-based modelling (ABM) approach is an approach where every entity has autonomy while interacting with other entities. These entities are the agents in the simulation. For example, suppose a barge, Quay Crane, and Container terminal are considered agents. In that case, these agents have their functions, such as loading, unloading, and container inventory management, while they have separate interactive functions, such as loading and then leaving. ABM has found its relevance in various areas of container shipping, namely in frameworks for reducing congestion (Shobayo and Van Hassel, 2019), container terminal productivity (Mazloumi and van Hassel, 2021), and most importantly, in both inter-terminal transport (Iqbal, 2015) and interland (Feng et al., 2015).

A review of existing research and best practices has shed light on how to tackle the complexities of transshipment between deep sea and hinterland terminals. This exploration revealed four crucial areas demanding attention: i) minimizing the number of times containers are picked up, moved, and put down is essential. Streamlining container movement within terminals is key to achieving efficient operations; ii) traditional methods of expanding container terminals may not suffice. Exploring innovative solutions is crucial to accommodate the ever-growing volume of cargo; iii) currently, barges might not be filling to capacity, leading to inefficiencies. Optimizing barge loading schedules and sizes is essential for a smooth flow of goods.; iv) implementing a novel transshipment network requires a comprehensive strategy. This includes carefully planning and managing the system to ensure its effectiveness. This narrative approach uses figurative language and storytelling elements to make the content more engaging and easier to understand. It highlights the challenges in a way that is clear and memorable.

METHODOLOGY

The methodology of this work is divided into four distinct phases. The first phase targets the rehandling of containers. This is considered an important link, given that rehandling can only be addressed using a different transporter design. Subse-

quently, the next phase targets alternate avenues for expansion with the same design description. The third phase will focus on addressing existing barges' low call size situation. Since this is not a conceptual or cosmetic design change but merely an increase in call size, this will not be explained in detail. The final phase of the methodology describes a comprehensive design of the transport systems network implemented with a simulation approach. This methodology will then be validated through simulations in a real port environment that connects the deep sea and hinterland.

Phase 1 - Address Rehandling of Containers

Amphibious AGV Design

The review of the state of the art has helped identify key problem areas such as rehandling of containers between truck and barge, and longer and unnecessary routes for inter-terminal transfers. Several promising concepts were studied, namely waterborne AGVs, Port Feeder Barges, and Amphibious AGVs. Port feeder Barges suffer from operator compatibility issues (Nicolet et al., 2023). While waterborne AGVs were promising in their design and research availability, it became clear that rehandling issues still appear despite the reduction in inter-terminal transfer time and distance (Zheng et al., 2017). As the related work section states, Amphibious AGV is a container AGV that can traverse on land and water. This was specifically designed to address container re-handling problems and reduce inter-terminal distance. The Amphibious AGV went through various design cycles with three concepts being considered. This included a standard AGV chassis modification as the first idea, with hovercraft and catamaran designs also being considered. After being evaluated on a multi-criteria analysis of stability, complexity, manoeuvrability, efficiency, and cost, the standard AGV design was chosen owing to its design and dimensional compliance with current container AGVs on the market. As depicted, the design of the Amphibious AGV has been adapted specifically to handle geographical disparities. Changes in this include creating space for the water propulsion system. Since this is envisioned as a sustainable vehicle, the propulsion is all electric. Therefore, space is also made for the battery pack placed in the centre of the main chassis. This is shown in the form of boxes in Figure 2. The battery pack is estimated at 600 kWh. The battery pack itself is made up of 42 modules of 6.3 kWh each. These are stacked in three separate blocks of 12,12 and 18 modules, amounting to 710 kWh. The chassis itself measures 16.6 m (length) x 3 m (width) x 1.8 m (height). This allows enough space for mounting a fully loaded 40-foot container (or two 20-foot containers) and space in front and rear to accommodate the pump jet system, marked in red in Figure 2. The pumps are also flanked by 4 electric motors at the wheels for ground propulsion The Amphibious AGV also has more angled edges than regular ground AGVs. This makes it hydrodynamic, and the edges serve as a breakwater against waves should it encounter waves in port waters. The original design of the Amphibious AGV also had 4 holes to incorporate a SAE 316 stainless steel-based locking system to connect with other Amphibious AGV. However, this system has been disbanded for this work since such contraptions on water could create more instability. To enable floatation on water, the Amphibious AGV also has pontoons which will be delineated later. Given that the Amphibious AGV will also be in contact with water, choosing non-corrosive and water-resistant materials was important. While stainless steel would have been the best choice, due to cost concerns carbon steel was chosen for the body of the Amphibious AGV given that it offers similar performance levels as stainless steel. The pontoons have to be of high strength and flexibility. Taking inspiration from hovercraft designs, the pontoons are made of nylon base cloth, with the outer layer being made of natural rubber and neoprene. These are strong enough to resist the internal air pressure and buoyant force.

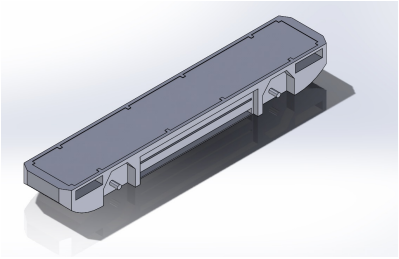

Figure 1: AAGV Body Exterior

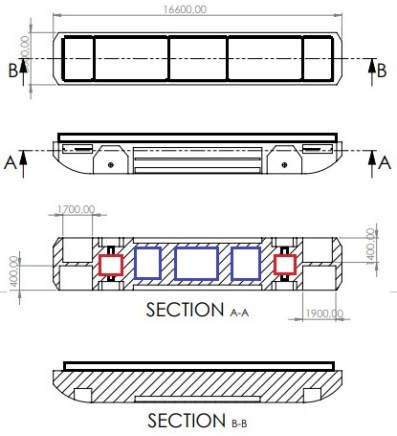

Figure 2: AAGV Body Interior

The land mode of the Amphibious AGV has been depicted in Figure 3. In this scenario, it is clear that the pontoons can be retracted because they would not be needed on land. Only the electric motors would be at work in land mode, drawing power from the battery pack. The Amphibious AGV was designed with the assumption that they would travel on ramps to enter or exit water. There will be a point between land and water where land and water-based propulsion and powertrains are used to enter water from land or vice-versa. The AAGV in water mode has been depicted in Figure 4. In this mode, the floatation pontoons are activated and marked in yellow in the figures. As mentioned earlier, the AAGV will engage both land and water-based propulsion systems while transitioning from the ramp to water. Subsequently, it will switch to completely water-based pump jet propulsion. The locking mechanism while still present can be used for locking with quays of container terminals but this is optional and does not affect the functionality of the Amphibious AGV.

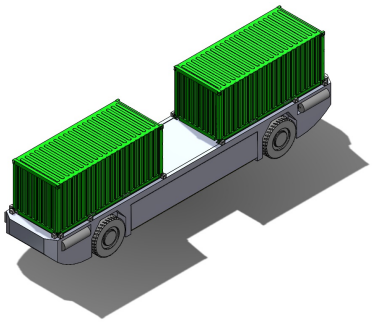

Figure 3: Land Mode- Isometric View

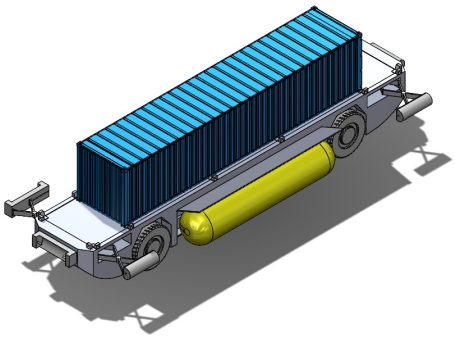

Figure 4: Water Mode of The AAGV

The amphibious AGV consists of salient mechanisms that stabilize it on water and lay frameworks for future dual powertrain concepts. The idea of pontoons on the AAGV was deemed necessary due to the low centre of gravity of the Amphibious AGV. This is caused due to the 5000Kg battery pack and 7000Kg propulsion. pump and powertrain systems installed.The Amphibious AGV was designed considering short-haul transfer between terminals on water and within, land. The above specifications on power were computed considering a slope of 3 degrees, wind speed of 20 m/s, a maximum operating speed of 12 Km/hr and acceleration of 1 m/s to support a maximum load of 75 Tonnes. Using these considerations, a maximum power rating of 457 kW is obtained for terrain with the slope. It is prudent to note that the ramps used for entry and exit of AAGV from land to water or vice versa are set to 3 degrees. In regular flat terrain conditions, the Amphibious AGV only requires 331 kW of power to transport 75 tonnes. In terms of energy consumption, a container AGV moves a few hundred metres to some km per day. Given the functionality of the Amphibious AGV, each cycle of operation is assumed at 25km over 8 hours after which the battery is swapped. The battery capacity is therefore calculated to be 710kWh. The same Amphibious AGV's

batteries will be swapped when empty and a standard swap takes between 6-7 minutes as mentioned in industry (Konecranes, 2023) and literature (Schmidt et al., 2015). Therefore 3 shifts of an Amphibious AGV is achievable with 75km of daily range. Summary of major power-train specifications are given in Table 1.

The water propulsion system will consist of 2 Schottel SPJ 30 C pump jets (Odetti et al., 2019) that can give a combined output of 200 kW. While a maximum of 250 kW was computed for a top speed of 8 knots, it must also be realised that if the admiralty formula (Giernalczyk et al., 2010) is considered, a lower velocity of 6 knots would deem 200 kW as sufficient power to propel 75000 Kg of load. These calculations have been done considering a pressure of 135 PSI at 85% volumetric efficiency. The speed considerations of the Amphibious AGV(initially developed for Port of Rotterdam) are based on their speed limits imposed by the Port of Rotterdam (Centre, 2014). With a near 70% of travel distance slated to be on water, the pumps would consume 495kWh of energy during an 8hr operational period. This is the full load capacity of the AAGV of which 54000 Kg is from the fully loaded containers which can be either a single 40 ft container (29000 Kg) or two 20 ft containers (54000 Kg). The remaining masses are comprised of the Amphibious AGV chassis (8000Kg), the electric drives and motors (8000 Kg), water-based propulsion system (4000 Kg) and the pontoon-based support structures (1000 Kg). On an operational level, the amphibious AGV is assumed to function 24 hours a (Liu et al., 2001) for 315 days a year since some days may also be used for servicing and maintaining the AAGV. This amounts to 7500 operational hours in a given year.

The stability aspect of the Amphibious AGV on water was not tested primarily but computed with logical assumptions. The Amphibious AGV when fully loaded with 2 TEU would weigh 75000 Kg and the design is akin to that of Inland barges which generally have fuller hulls(block coefficient of over 0.8). The Amphibious AGV features a fuller hull as well and places stability over maneuverability given the linear range of routes and guideways on land and water. The Amphibious AGV is also underlined by the fact that when fully loaded 75% of the body will be under water while 25% remain above. To enable this buoyancy, pontoons are inflated before the Amphibious AGV enters the water. With a requirement for 25% buoyancy, the pontoons should provide an upthrust of 185 kN(against a downward force of 735kN). The calculated volume of both pontoons are 24.505m^3 with a radius of 0.736m and a 7.2m pontoon length. The pontoons will be filled with air using Grundfos NB 150-315 pumps(Grundfos, 2024)capable of pumping at a flow rate of 447.8m^3/hr. This implies that the pontoons will be filled in 1.65 minutes. The pumps are rated at 37kW and at a maximum flow rate, each inflation/deflation would draw an energy of 2.035kWh for both pontoons which is 0.3% of the total battery capacity. It must also be noted that inflation holds more precedence over deflation as most port roads have space to accommodate Amphibious AGVs with fully inflated pontoons in the event of low battery. The pontoons also have 4 equally sized air-tight chambers, which implies that in the event of a puncture and water infilitration, only one out of the four pontoon segments would be impacted and the Amphibious AGV can return to safety. The Amphibious AGV also has space for ballast tanks placed over the battery with dimensions of 7.5m x 2.4 m x 1m translating to a capacity of 18000 Litres of Water which can be adjusted corresponding to on-board payloads or even a pontoon puncture as cited by the reviewers.

Table 1: Powertrain Specifications

Specifications	**Values**
Battery Voltage	720 V
Motor Power Rating(without slope)	331000 W
Motor Power Rating(with slope)	457000 W
Motor Maximum Loading Capacity	75000 Kg
Total Loading on Vehicles	54000 Kg
Distance Covered in a day (3 Shifts)	75 Km
Max Speed on Land	12 Km/hr
Operational Hours per day/AAGV (3 Shifts)	24 hours
Working days in a year	315 days
Operating Hours in a year	7500 hours
Travel in a year	23625 Km

While the author and previous works did not dive into the control system aspect of the Amphibious AGV, the Amphibious AGV is envisioned to function both by itself and in a coordinated control manner akin to the vessel train formation (Chen

et al., 2019) and cooperative control (Chen et al., 2020). The subsequent part of this research in phase 4 will discuss the agent-based modelling implementation that links terminals, containers, and transporters such as barges and feeders) with the Amphibious AGV's schedule. This is linked with routing systems that direct the Amphibious AGV to the concerned berth on water/yard position on land. This will fully utilize the Amphibious AGV's capabilities while also trying to ensure that it runs full-load trips on both journeys in the port conditions.From a stability point of view, ballast tank water levels can potentially be managed by a Model Predictive Control system (Negenborn et al., 2009) that uses a cost function that minimizes instability by maintaining appropriate tank levels.

The Amphibious AAGV will use ramps to enter and exit container terminals. These ramps resemble roll-on/roll-off ramps used in car carriers and ferries. The Amphibious AGV has been designed to handle slopes of 3 degrees at peak speeds The optimum speed assumed for roll-on roll-off slopes is 9km/hr based on literature (Di Ilio et al., 2021). These will be passive ramps installed at quays of container terminals to enable a smooth transition between entry and exit of the Amphibious AGV. Depending on the quay heights, the ramps can vary in length. For instance, in the author's earlier(Abhishek Rajaram, 2023) work, when the Port of Rotterdam was considered a testing ground, the ramp was 95 m length x 5 m width at barge terminals. In comparison, deep sea terminals with higher quays (12m and above because of draught) had ramp dimensions of 270 m length x 5 m width. Both were at an inclination of 3 degrees slope. Other accessibility details also include a travel delay of 40-100 seconds. The pontoon takes 1.65 minutes to deflate and inflate and this is initiated on the way to the ramp(S.A.S, 2018). This accounted only in the form of a setup/verification time used to check if pontoons are fully inflated and at required pressure(10 PSI) Depending on the length of the ramp, it is expected that the AAGV will spend 1.5 min to 2.5 min on the ramp when taken on a triangular distribution (Park et al., 2023). These assumptions and calculations will also be a part of the phase 4 implementation and validation section. When implemented, the Amphibious AGV will reduce the rehandling point since it can link the yardside and quayside of container terminals with other terminals by accessing both land and water modes and transit via the ramp. This means that any container to be transported to a nearby terminal can merely be loaded from the yard/ship, then take the water route and enter the other terminal. This prevents the need for the truck+barge mechanism or even the longer route of inter-terminal transfer generally taken by trucks. An added aim of the Amphibious AGV is to prevent additional barge and truck fleets in the process, which can also make the chain more sustainable while complementing existing barge networks.

Phase 2 - Alternative Means of Terminal Expansion

With saturation in terminal handling space, it has become clear that alternate but sustainable sources of expansion are needed to complement current deep-sea terminals. One such solution is the floating terminal, which provides a lot of flexibility regarding its modularity and location. The floating terminal will essentially provide the ability to split the feeder and deep-sea vessel traffic. With constraints in space, a floating modular terminal becomes the only choice that can alleviate congestion while providing more growth opportunities for existing container terminals worldwide. The Amphibious AGV becomes a crucial element in the chain since it is the only vehicle capable of transferring short packages of containers between an on-shore and offshore entity. This is the intersection point where, previously a combination of AGV and barge would have been needed but is now possible with just an Amphibious AGV. While this comes at the cost of some small-vehicle congestion, dedicated route corridors in the future will make it possible for large container ships and barges to not be affected. This is also where a modular floating terminal is needed to handle a versatile set of vehicles. The factors that warranted the need for a novel floating terminal design are lack of yard space in existing ideas (Jovanova et al., 2022) and lack of flexibility and efficiency in terms of loading and unloading (Baird and Rother, 2013). In concepts such as the port feeder barge, there is an issue of operator compatibility with current deep sea terminal and hinterland operators. It is prudent to mention that this research also considered several other concepts, such as barge hubs to handle traffic (Pielage et al., 2007). Still, it was deemed problematic because despite having dedicated space for barges, the barge hub would lack flexibility, especially in terms of location. As seen in the state-of-art section, distance plays a huge role in setting up a barge hub which is not a problem in the case of a floating terminal which can be modular and built anywhere. This also makes the research future-proof. A floating terminal would also require fewer ground resources in terms of vehicles.

From the study of major container hub ports such as the Port of Rotterdam, Port of Antwerp, and Port of Hong Kong, deep sea terminals are primarily congested with not only barge traffic but also feeder traffic. In all three ports where feeders

occupy deep sea berths by default, a feeder requires about 2-3 quay cranes (Meulenkamp, 2023) to load and unload containers. This means that freeing up two feeder berths would free up 4-6 quay cranes, typically needed for a deep sea vessel (Evers and De Feijter, 2004). To maximize the output of existing deep-sea terminals, the authors believe it will be prudent to assign deep-sea terminals to handle only deep-sea ships while the external floating terminal handles both feeder ships and super barges along with the Amphibious AGV. The design of the floating terminal is presented in Figure 5. The proposed design of the floating terminal has a 1km long quay with a yard that is 80 m wide. The terminal houses 10 rail-mounted gantry cranes with simultaneous transfer and exchange capabilities on both sides. of the bridge and over-reach. The crane used is akin to those used between rail barges and yard-side equipment. Therefore, the specifications and handling capabilities are based on the Liebherr Rail mounted gantry crane (Liebherr, 2024). The cranes are also equipped with twin spreaders, which enable two containers to be loaded, unloaded and transferred across in one go given the lifting capacity of 65 tonnes. The berths for the floating terminal design can be configured in different ways. A sample has been presented in Figure 5. Three rail-mounted gantry cranes have been enabled for feeder/feeder-max vessels with capacities between 800-3000 TEU depending on size and destination. The presence of twin spreaders will speed up feeder ships' loading and unloading process. Three such feeder ships can be accommodated at once in the floating terminal. Super barges which were introduced in the last phase will use two such rail-mounted gantry cranes to load and unload containers (Meulenkamp, 2023). Three berths have also been assigned for the super barge. The remaining 5 empty slots in the floating terminal will be occupied by Amphibious AGVs as marked in Figure 5. The Amphibious AGV will represent the impactful link between the floating and deep sea terminals for hinterland-bound containers and inter-terminal transfer. Regarding other terminal features, the floating terminal is designed to function without any vehicles and automated stacker cranes. The overhead rail-mounted gantry cranes will serve both yards and vessels, each crane can handle 30-50 moves/hour when modelled on a triangular distribution (Bartošek and Marek, 2013). When this is taken over 350 days across 10 cranes, the terminal can handle up to a maximum of 4.2 million TEU year-round. If the twin spreader is considered, the RMG crane will be operated at minimum speed for safety. However, it can still output 5.04 million TEU at maximum theoretical capacity. Regarding yard space, it has been designed to stack containers 90 length-wise, 25 width-wise, and 6 height-wise to give a total container storage capacity of 13500 TEU at once.

Figure 5: The Floating Terminal Design Configuration

The floating terminal will be located close to the deep sea terminal to handle feeder and barge traffic. Feeder ships generally carry containers destined for both inter-terminal transport and hinterland. The deep sea ships which arrive at the respective deep sea terminals also carry a mix of hinterland-bound and inter-terminal-bound containers. Considering the modal split of major ports such as Rotterdam, Antwerp and Hong Kong (Gumuskaya et al., 2020; Marine Department, Hong Kong, 2022), it is estimated that 30% of all containers coming into ports are transported by barges through inland waterways while the remaining 70% are comprised of inter- terminal/export transshipment containers. The research in general is only concerned

about the 30% containers transferred through the inland waterways. Once transporters such as super barges, feeders and Amphibious AGVs arrive at the floating terminal, the containers are sorted based on destination after which they are directly transferred overhead to the relevant transporter which could be either of the aforementioned. This is why the transporters dock only at berths which are parallel to the transporter to which the container needs to be transferred. For instance, in Figure 5, from the left, we see that the feeder is parallel to two Amphibious AGVs on the first berth. It can be assumed that the container from the feeder has to be transferred to the Amphibious AGV. After the direct container transfer, the transporters leave for the concerned destinations: Amphibious AGV to the deep-sea terminal, super barge to inland ports and feeder departs to the home port.

Phase 3 - Addressing Low Call Sizes

A predominant reason for the barge congestion today is the extremely low call sizes barges currently resort to. As seen in literature (van der Horst et al., 2019; Shobayo and Van Hassel, 2019), call sizes at deep sea terminals currently range from as low as 6 TEU to 48 TEU with an average of 33 TEU. The irregularities in call size result in less efficient use of berth space and time since many vessels with higher call sizes might be in the queue. This also includes deep-sea vessels despite priority for deep-sea vessels. This would put forth a case for higher call sizes and experience from Antwerp, urging barge operators to follow a standard minimum. Still, higher call sizes have yielded good results, with barge calls falling by 40%, decreasing congestion at DP World Antwerp Gateway (Buitendijk, 2019). Analysing the prevalence of common destinations in major waterways such as the Rhine Delta (Konings, 2007) and the Pearl River Delta, it makes more sense to have higher call sizes per barge trip to ensure lesser congestion along these waterways. These would be transported to the major inland ports. But the absence of such transporters thus far has made it hard to carry higher amounts of containers. However, a sustainable container ship concept has emerged in the form of COSCO's electric ship, which was introduced in 2023. This electric vessel has a total container capacity of 700 TEU currently plying across the waterways of the 1000km long Yangtze river (Lepic, 2023). This inland vessel is 119.8 m long and 23 m wide, falling in between the large Rhine Class Va and large Rhine Class Vb in terms of dimensions, implying that this vessel will fit within existing barge berth dimensions while having a notably higher capacity than current barges (Program, 2019). This vessel has a dead weight of 10,000 tonnes and is powered by two 900 kW propulsion engines. This electric ship has 36 portable container-sized batteries that hold a capacity of 50,000 kWh and are replaced accordingly at various ports of call along the inland waterways. This research will use this inland vessel concept and henceforth refer to it as "Super Barge" owing to its higher overall capacity. The call sizes for this super barge are set at 400-700 TEU, which is approximately 10 times higher than current call sizes. These again will be shipped to the main ports along the inland waterways, which can be distributed to destinations by truck or smaller barges. This would essentially reduce the congestion of barges at the main deep-sea terminal with the denser capacity configurations of 400-700 TEU. The COSCO electric container ship/Super Barge is also sustainable with projected CO_2 reductions of 32 metric Tonnes per 24 hours of operation (Lepic, 2023).

Phase 4 - Transport Network Systems Design

The methodology's final phase involves redesigning the transport systems network and a means to simulate and implement the networks as depicted in Figure 6. For this, an agent-based modelling is used. The predominant reason for this choice is that this simulation allows major entities in the system to have autonomy while interacting with other major entities. Discrete event simulation is a sequential simulation process which has also been often used for modelling container terminal operations. However, simulation process elements such as simultaneous berth planning and export/import container management warrant parallel processing, which can only be accomplished by agent-based modelling. This also allows for hierarchy in the system. But most importantly agent-based modelling opens up many research opportunities in integrated control for the future given its prevalence. The agent-based modelling system categorises all major elements into three agents: i) Ports and Terminals, ii) Containers, and iii) Transporters. These elements will possess their function besides the interaction with the other agents. To better understand these agents, they can either be a single agent (like a standalone container terminal) or a population of agents (like trucks, ships, or even multiple hinterland terminals). These will be mentioned below.

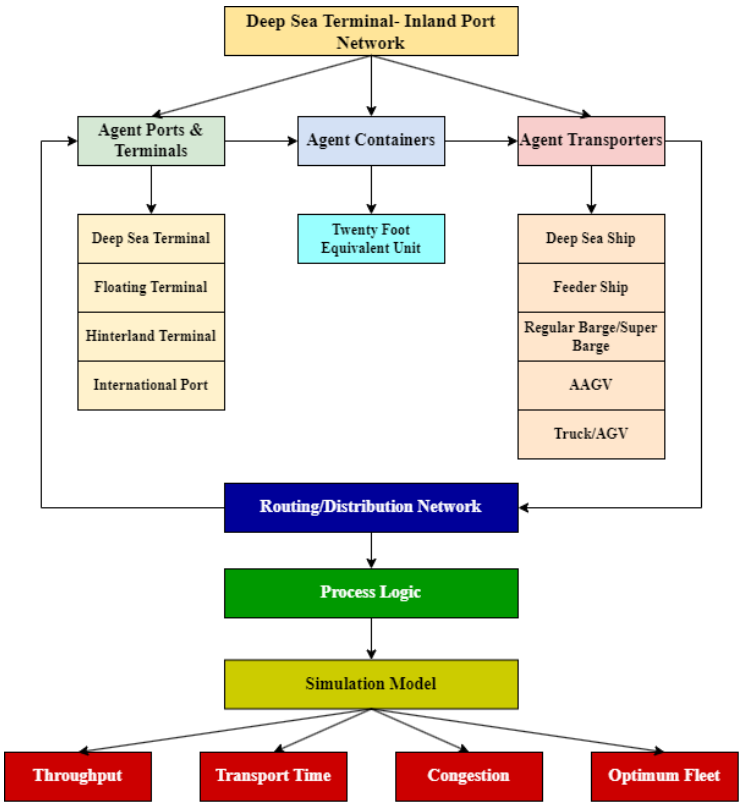

Figure 6: The agent-based modelling simulation of the deep sea terminal and inland network

1. **Agent Ports and Terminals**: this agent comprises international ports, deep sea terminals, floating terminals, and hinterland terminals. Depending on import, or export, this agent serves as the origin, destination or transit/transshipment hub for all containers in the system. Except for hinterland/inland ports, all the other terminals function as single agents. The international ports feature terminals themselves but will be classified as a single agent in this research. These are the origin points for containers in the system and they are picked by feeders and deep-sea ships. Deep sea terminals are intermediary points that function as transshipment hubs. They are a single agent and receive deep sea ships and feeders with containers. Hinterland terminals or ports are the final destination of these containers. In this research hinterland ports have been considered across various locations hence they function as a population of agents. The floating terminal is also a single agent and the new addition to the redesigned transshipment network. The floating terminal agent is also an intermediary transshipment hub complementing the deep sea terminal and handles transporters such as feeders, Amphibious AGVs, and super barges.

2. **Agent Containers**: these are a population of agents that originate from international ports and terminate at inland ports. This research considers standard twenty-foot equivalent units for classification and calculation purposes.

3. **Agent Transporters**: transporters refer to carriers of containers between various ports and terminals. Under this agent, existing concepts such as deep sea ships, feeders, barges, and trucks and the Amphibious AGV concept will form a crucial part of the proposed transshipment networks. All transporters are the population of agents. The Deep Sea Ships form the starting point of the entire process. These are considered vessels with a capacity of 3000 TEU and more, with the biggest capable of carrying 24000 TEU. Generally, they have a draught of 14m or more, hence the name deep sea. Deep sea Ships are also those ships that travel predominantly between major transhipment hub ports owing to the magnitude of containers they handle. They therefore require 6 quay cranes to unload containers (Bartošek and Marek, 2013). The second major actor responsible for bringing in containers are feeder/feedermax ships which have capacities in the range of 800-3000 TEU and travel to both hub ports and inland ports given their draught is less than 14m(Ogunsola, 2022).In most inland and deep sea terminals, barges arriving usually have call sizes ranging between 12 and 50 TEU with an average of 33 TEU(van der Horst et al., 2019). This research considers the upper bound of

50 TEU as the call size, and these are referred to as regular barges in this work henceforth. One of the gaps identified in the literature was the congestion consequences of using small container call sizes while transporting from deep sea terminals to the hinterland. The Super Barge is therefore an exploratory barge concept that addresses barge congestion by carrying larger call sizes of containers from deep-sea terminals to the hinterland. This concept is akin to the 700 TEU capacity electric container ship employed by COSCO in the waterways of Shanghai(Mandra, 2023). This research considers the call sizes from 400-700 TEU per barge trip. The Amphibious AGV envisaged to reduce the rehandling of containers forms the final piece of the puzzle, having the capability to travel on both land and water (Ghiridharan, 2023; Eijk et al., 2023). The Amphibious AGV will replace trucks/AGVs which are also modelled as the population of agents.

This multi-agent network of the aforementioned agents helps define the container transport environment from the international port to the deep sea terminals to the hinterland. This network is then paired with a routing and distribution network which distributes containers as a function of distance, which implies that the closer the destination is, the higher the number of trips to that destination and hence the higher container throughput. A process logic is then used to link all the agents and the routing networks. The process logic defines the container loading, unloading, and transfer sequence to subsequent destinations. This repeated throughout multiple change points. For instance, the benchmark involves entities like international ports, deep-sea terminals, and hinterland terminals therefore this process of loading, unloading, and transfer is seen in all the entities. This is then fed to a simulation model which processes the system's key performance indicators: congestion, container throughput, container transfer time and fleet trade-off. While the first three KPIs directly result from the agent-based modelling simulation, the fleet optimization is done with the help of a genetic algorithm (Yang et al., 2023) that works on the parameters, the objective and constraints shown in Table 2. This optimization aims to find the optimum transporter fleet size for the given utilization, which is set at 85%, considered a standard in literature for container equipment (Koo et al., 2004).

Table 2: Optimization Parameter, Variables, and Constraints

Objective	Maximize Utilization, U
Variables	
Total Transporters	N =[1,∞)
Transporters Used	T =[1,∞)
Utilization, U	T/N
Parameter	
Container Agent	Parameter as in ABM
Transporter Agent	Parameter as in ABM
Terminals Agent	Parameters as in ABM
Constraints	
Utilization	T/N <0.85
Total Transporters	N>0
Transporters Used	T>0
Output	
Transporters Used	Optimum T

This agent-based modelling implementation will now be applied to the current transshipment scenario, or the benchmark network design. Subsequently, the new transshipment scenario will also use this agent-based modelling methodology. The benchmark and new transshipment chain results will be compared to see if maritime congestion has been reduced.

Benchmark Network Design

The current transshipment network design is a hub and spoke design that has been followed for a substantial period of container shipping history (Langen and Van der Horst, 2008). An overview of the network with the concerned transporters, ports and terminals, and most importantly the interaction between the entities is shown in Figure 7. To summarise the agents, the

transporter agents involve the deep sea ship, feeders and container trucks. The ports and terminal agents involve international ports(example- Port Klang, Malaysia), deep sea terminals (example- Port of Hong Kong) and hinterland ports(example- the Pearl River Delta ports). Feeders/Feedermax (800-3000 TEU) and Deep Sea Ships(3000-24000 TEU) bring containers from international ports to deep-sea terminals in the home country. Deep sea ships and feeder ships bring in call sizes on an average of 2000 TEU and 1000 TEU per port, respectively (Shobayo and Van Hassel, 2019). These feeders and deep sea ships dock at the deep sea berths and unload their containers via quay cranes, after which they are sorted for inter-terminal transfer and hinterland-bound containers. The hinterland-bound containers are loaded onto container trucks, which transport the container to the barge berths at the deep sea terminal. This translates to ground congestion of trucks and waiting congestion of barges at berths in deep-sea terminals. The containers from trucks are subsequently loaded to regular barges via barge cranes. For the benchmark per current operation, the average call size of each barge is set at 50 TEU (Seatrade Maritime News, 2015; van der Horst et al, 2019). The barges then transport these containers to inland ports/terminals. A few details to be noted here are that in port waters and till the inland, barge speeds are set at 13 km/hr (Centre, 2014), the operational truck speed is set at 20 km/hr (Duisburg, 2018) with 30-50 moves/hour assumed for quay/barge cranes (Bartošek and Marek, 2013).

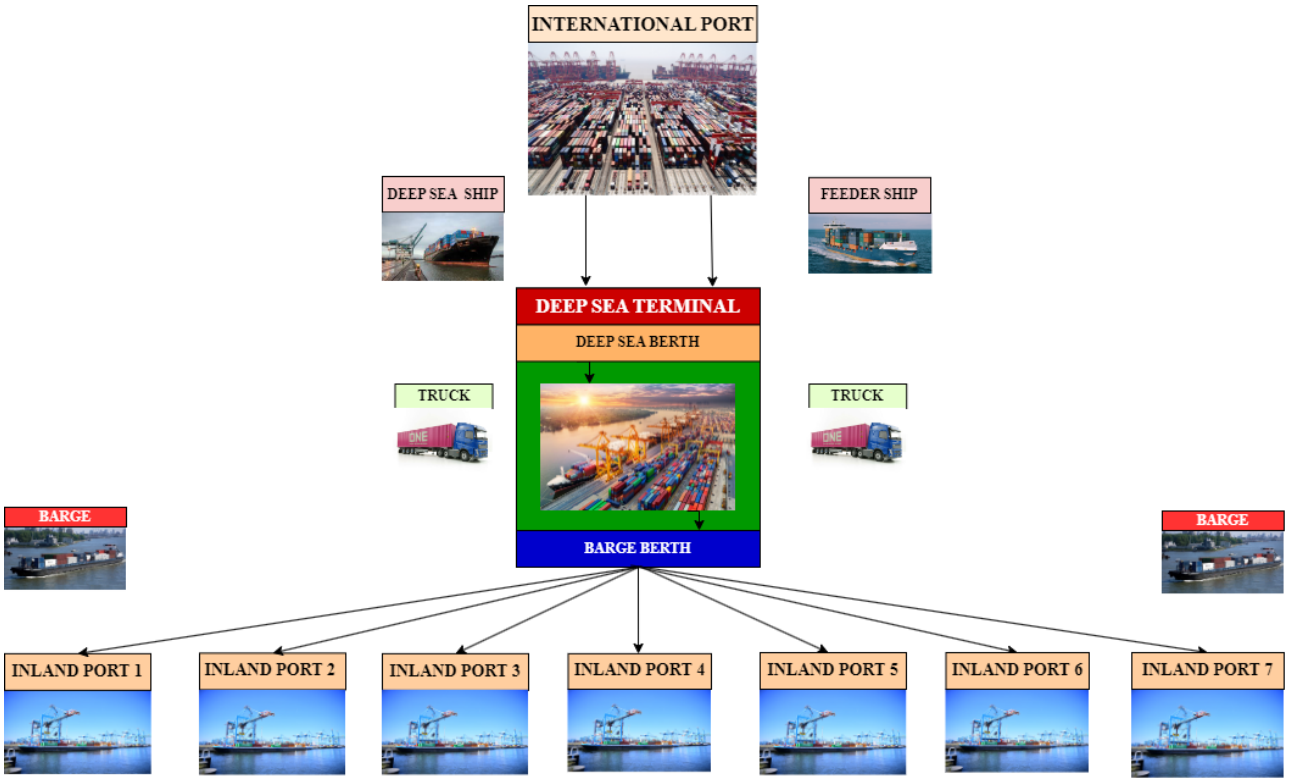

Figure 7: Current Transshipment Network- Benchmark

The New Transshipment Chain Solution

The new transshipment chain solution is also a hub and spoke approach implemented with the same agent-based modelling methodology as done for the benchmark. An overview of the network with respective transporters, ports, and terminals and their interaction is presented in Figure 8. For this network, the transporter agents involve deep sea ships, feeder ships, super barges, and amphibious AGVs. The ports and terminal agents involve international ports, deep sea terminals, floating terminals and hinterland ports. The process for the new transshipment scenario varies from the benchmark, especially concerning transporter and terminal interaction. As in the current scenario, both feeders and deep sea ships are loaded with containers from international ports (for example, Port Klang, Malaysia). However, after this, the process differs. To shift feeder traffic from deep sea terminals, the feeders from the international port dock at the floating terminal while the deep sea ships directly

dock at the deep sea terminal. The Amphibious AGVs now spring into action. The hinterland-bound containers present in the deep sea ship are transported from the deep sea terminal to the floating terminal via the Amphibious AGVs. The feeder docked currently at the floating terminal has a mix of hinterland-bound and inter-terminal transfer containers. The hinterland-bound containers stay at the floating terminal while the Amphibious AGVs take back the inter-terminal-bound containers on their return journey to the deep sea terminal. Upon their return, the Amphibious AGVs take inter-terminal containers to the relevant deep-sea berth or transfer them back to the yard. The hinterland-bound containers in the floating terminal are directly transferred to super barges that also dock at the floating terminal. These super barges take in call sizes of 400-700 TEU and transport them to hinterland ports (for example- Pearl River Delta ports). A subtle difference that is readily noticeable is the fact that in this new method, the Amphibious AGVs will have full load on most of the journeys to the floating terminal and the return back to the deep sea terminal. In the benchmark, this is a problem because trucks are guaranteed to be full only one way of the journey (during berth transfer). The Amphibious AGV's speed will be set at 12 km/hr, while the other parameters remain the same as the benchmark.

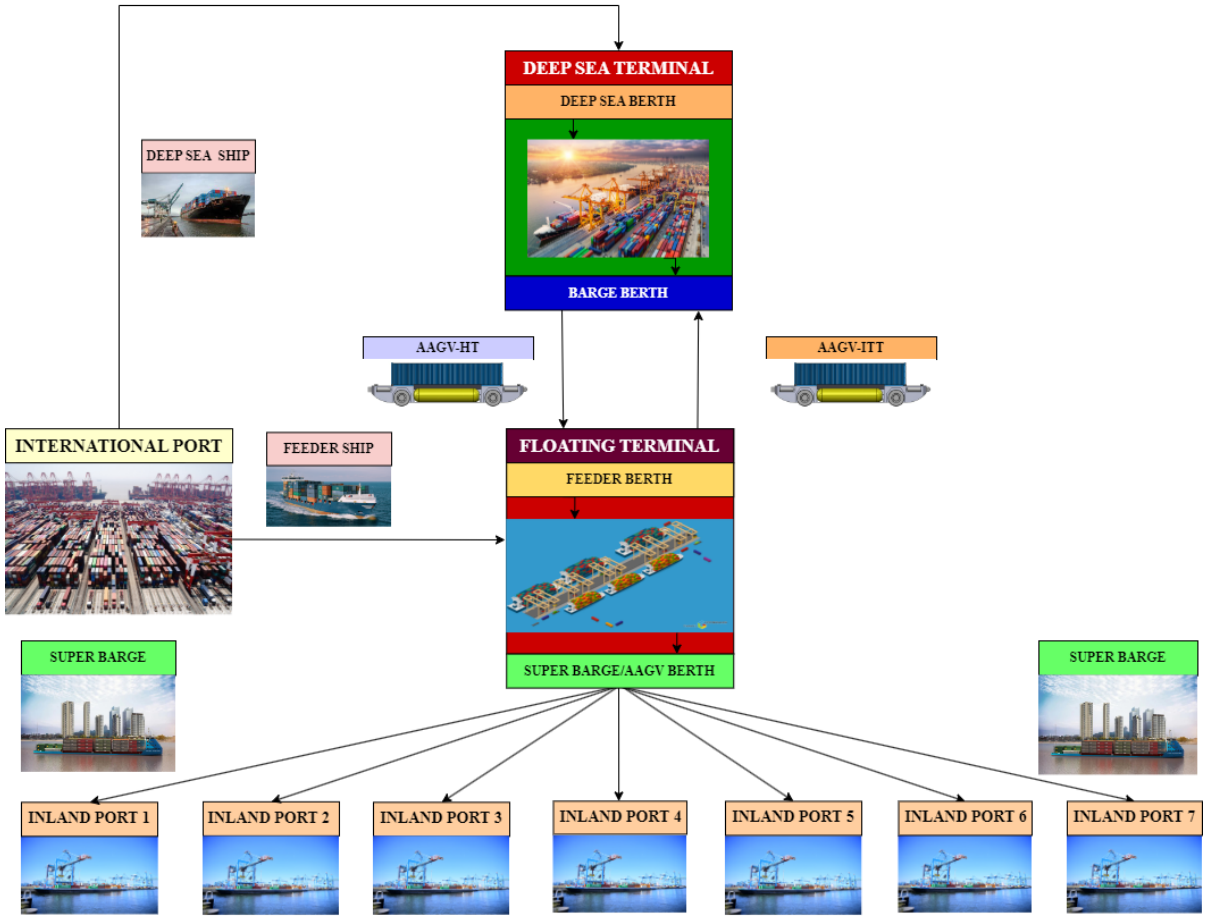

Figure 8: The New Transshipment Chain Solution

CASE STUDY

A case study is performed on the Port of Hong Kong and the hinterland of China's Pearl River Delta to validate the proposed transshipment network and simulate its performance. The Pearl River Delta is one of the largest inland waterway networks in the world, with an extensive range of industries from electronics and garments to plastics flanking the banks of the waterway. Due to this industrial productivity and the presence of multiple clusters of tech parks, the Pearl River Delta is also known as the world's factory or more recently the world's design studio of the world (Fuller, 2017). In terms of economic value,

the Pearl River Delta has a GDP of $1.2 Trillion forming 10% of China's GDP despite accounting for only 1% of China's territory. Of the 14000 Km stretch, 5000 km connects the southwest region through the extensive inland waterway network of barges (Wang and Li, 2012). The main trans-shipment ports here are Hong Kong, Guangzhou, and Shenzhen. Hong Kong stands out as a vital trans-shipment hub due to its robust connections with ports southward, including Port Klang in Malaysia and the Port of Singapore, and northward to the Port of Busan in South Korea and the Port of Taiwan. The Pearl River Delta, comprising nine major cities, contributes 18% to the nation's output and forms 73% of Hong Kong's inward trans-shipment. Despite a drop in Inland Waterway Transport (IWT) from 26% to 5% during 1980-2000, barge transport has rebounded, now holding 10% of the market. Calls for expansion in barge handling and trans-shipment services are increasing, driven by rising demand and sustainability needs, alongside local pressure to address the housing crisis. Recently, this crisis has threatened to close down a part of Kwai Tsing Terminals to build settlements (Chong and Li, 2020). This is where new transshipment solutions can help.

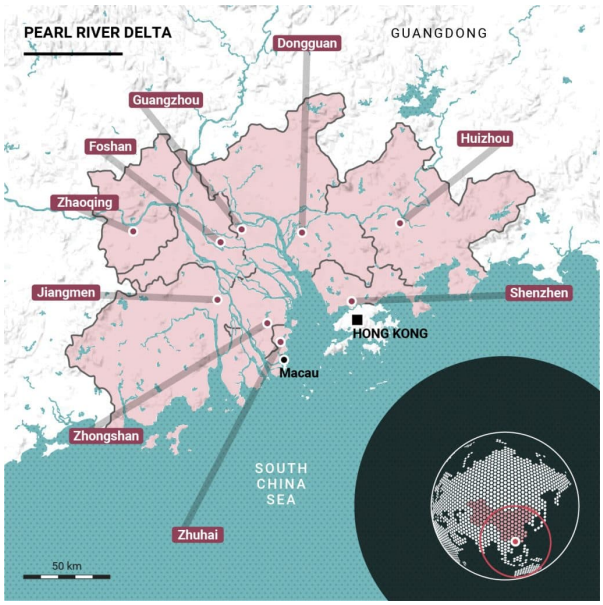

Figure 9: The Pearl River Delta (We Build Value, 2017)

Figure 10: Floating Terminal & Berths (Google, 2024)

Hong Kong Ports

The Hong Kong port is located in the South China Sea and comprises a river and deep water ports. The deep water port, commonly known as the Kwai Tsing Terminals, receives an average of 36000 TEU Per Day (Marine Department, Hong Kong, 2022). There are a total of 9 container terminals that are capable of handling 24 million TEU annually. Due to the COVID-19 pandemic, traffic at Hong Kong port declined to 12.869 million TEU in 2022 (Marine Department, Hong Kong, 2022). For this research, HIT and HIT-COSCO terminals with an annual throughput of 8.03 million TEU will be considered. They operate Container Terminal 9S(Left of image, berth in green), and Container Terminals 4, 6, 7 and 8 which are all marked in green in Figure 10. These also represent the 7 deep sea berths. The barge berths spread across terminals 4 and 6 are shown in red. Terminals 4 and 6 combined house 9 such barge berths (Hutchison Ports Trust, 2023). HIT and COSCO handled a peak of almost 6500 TEU per day in 2016, with 120 barges making footfall daily (Seatrade Maritime News, 2015). Looking at the current split between trans-shipment and PRD containers, the HIT-COSCO terminals receive 22000 TEU from international ports such as Singapore, Port Klang, Port of Busan and also from the west such as Colombo, Rotterdam and Port of Los Angeles (Bu et al., 2023; Marine Department, Hong Kong, 2022). This corroborates with the 70-30 split as derived in Phase 2. This translates to 6500 TEU headed to the Pearl River Delta and 15,500 TEU headed to other international ports. Apart from the 120 barges that make footfall, 15-18 (average -17) vessels dock at the deep sea berths daily. These mix feeder/feeder max vessels, panamax and ultra-large container ships (ULCS). The floating terminal is located in the region marked in yellow. This will use the large-scale floating terminal design (Figure 5), which has a 1 km quay with a theoretical

handling capacity of 2.52 million - 4.2 million TEU annually (5.04 million TEU with twin spreader). The berth configurations will be exactly used as shown in Figure 10. Among the 17 ships that dock at HIT-COSCO for benchmark case, 11 are feeder or feedermax vessels. The feeder/feeder max vessel traffic can be shifted to the floating terminal by the new transshipment chain methodology. Three RMG cranes per feeder max vessel will be used to unload and load containers. Owing to the length of these ships, realistically 3 feedermax ships (marked in pale pink in Figure 10), 3 Super Barges(marked in orange) and 5 Amphibious AGVs (marked in blue) can be accommodated at once in the floating terminal. It is also important to mention that despite the presence of the floating terminal, it will always be the deep sea terminal with the higher annual throughput. This is done to retain its competitiveness. Therefore the split of 22000 TEU between deep-sea terminals and floating terminals are tested in two configurations. The first is (14000 TEU at HIT-COSCO and 8000 TEU at the Floating Terminal) and second configuration is (12000 TEU at HIT-COSCO and 10000 TEU at the Floating Terminal).

Inland Ports in Pearl River Delta

The Pearl River Delta has 2000 inland ports within the region. Seven major import and export inland ports have been chosen for this research: Sanshui, Foshan, Jiangmeng, Shekou, Yantian, Zhongshan, and Humen. The ports are shown in Figure 9. These are ports quite prominent in the automotive, electronics and manufacturing industries given that Shenzhen and the Pearl River Delta region are hubs for mobile and communications OEMs. Currently, barges with call sizes of 50 TEU carry consignments from the Port of Hong Kong to the Pearl River Delta. This will be simulated in the benchmark network analysis. It is envisioned that when the new transshipment chain solution is employed, super barges will carry call sizes ranging from 400-700 TEU to the ports in the Pearl River Delta. The barges in the benchmark will depart from the barge berths marked in red from the HIT-COSCO deep sea terminals. Similarly, super barges will depart from the floating terminal to the Pearl River Delta for the new transshipment chain. The AAGVs will rotate between the deep sea and floating terminals, transporting containers for hinterland and other terminal transfers.

RESULTS

The Hong Kong-Pearl River Delta simulation presented a very intriguing set of results. The results are presented in Figure 11. The benchmark case from the simulation records 121 barges docking in at Hong Kong's HIT-COSCO terminal to transport 6500 TEU to the Pearl River Delta. This information corroborates with the terminal data of 120 barges a day (Seatrade Maritime News, 2015). As anticipated this causes an average congestion of 13 barges per berth per day which is disadvantageous given that the HIT-COSCO terminal is forced to use 2 barge quay cranes to unload barges when usually only one quay crane is used. When we shift the focus to the new transshipment scenario, it becomes clear that in both configurations of container split, there is a congestion of only 14 super barges per day. This is a direct result of the difference in call sizes of the respective barges. In the benchmark, the regular barges load or unload call sizes are 50 TEU, while the super barges in the new transshipment scenario take anywhere between 400-700 TEU (consider an average of 550 TEU) per barge trip. This makes it easier to have only two super barges visit each of the major ports in the Pearl River Delta daily instead of having up to 20 separate regular barges visit the hinterland ports in the benchmark case. This work also considered ground congestion as an important metric, and here it can be seen that in the benchmark, there are about 1788 daily truck visits to the berths to deliver containers to and from barge berths to/from deep sea berths/container yard compared to the 2104 and 2511 Amphibious AGV visits to the floating terminal. When the Amphibious AGV congestion is compared, it is clear that the Amphibious AGV has a higher frequency of visits given that it has to transport containers not only to the floating terminal but also on the return journey back to the deep sea terminal or the container yard. This also implies that the Amphibious AGV runs full load on at least 50% - 75% of the journeys (50% in the 12000 DST:10000 FT case, 75% in the 14000 DST:8000 FT case). This is not the case for trucks which run full on only one leg of the journey while transporting containers from the deep sea berths to barge berths. The trade-off is that the Amphibious AGV offers more productivity at the cost of slightly more added congestion. Furthermore, it must be realised that the Amphibious AGV is trying to replace the functions usually done in combination with a barge and a truck. When we analyse the fleet of both the benchmark and the new transshipment scenario in a graph 11, the fleet size of the new solution is 53% lower than the benchmark comprising 14 super barges and 70 AAGVs. This contrasts with the 126 regular barges and 54 trucks in the current solution. A large maritime fleet size and congestion scale have been reduced

by about 80%. The Amphibious AGVs have a larger fleet size than trucks but complete much longer round trip journeys (9km) than an average 2km back and forth berth transfer journey. This makes the Amphibious AGV more competitive per kilometre compared to trucks and justifies the increase in fleet. Also, to reiterate the Amphbious AGV is essentially covering for functions of both the truck and the regular barge. The new transhipment solution also has advantages when it comes to transporting containers to the hinterland. The benchmark posts a transfer rate of 2247 TEU/day to the Pearl River Delta while the new transshipment solution sees a marked 27%-30% improvement in throughput rate (2869 and 2953 TEU/Day) for both configurations. Complementing the throughput rate, the hinterland transport time also sees a 21%-23% improvement in the overall time recorded to move containers to the Pearl River Delta. While both the Amphibious AGV and super barge leg raised advantages over the conventional truck and regular barge, it was noticed that the biggest difference came in the AAGV transfer times which were 30% faster than that of trucks which transfer between deep sea and barge berths. This justifies the increase in the fleet of Amphibious AGVs over trucks. There were also marginal improvements in super barge transfer times compared to regular barges. One positive knock-on effect of implementing the new transshipment solution is that it frees substantial berth space. Since the floating terminal uses three cranes to unload a feeder/feeder max ship, at least 6 feeders can be accommodated over a day. This would essentially free space for two ultra-large container ship berths (18000+ TEU) requiring 6+ quay cranes. This translates to potentially handling 730 new ultra-large deep-sea ships year-round. The opportunities however do not end there. The barge berths at HIT-COSCO originally present in the benchmark also stand unused thanks to the new transshipment solution. These berths can also be repurposed to occupy feeder ships or a Panamax ship (5000TEU) (Ogunsola, 2022). This would mean that potentially 2 ultra-large container ship berths and 3 feeder berths have been identified as possibilities for expansion within HIT-COSCO's existing canvas. If all berths are used at full capacity as mentioned it would push up HIT-COSCO's handling capacity from the current 8.03 million TEU to 12.41 million TEU which represents a 54% increase in container handling capabilities. This makes the solution future-proof. The results also provided other crucial insights that have not been directly depicted in the graph. A pattern noticed here is that Amphibious AGVs become more effective when demand is higher. In the 14000-8000 case, maximum one-way demand is 5560 TEU (4270 TEU on way back) while in 12000-10000 case the max one-way demand is 6950 TEU (3660 TEU on way back). The AAGV performs the best in the latter. The super barges are used with call sizes from 400-700 TEU. Large call sizes can often be very uncertain owing to common delays that occur at points of origin. Therefore, this research deemed it important to experiment with call sizes for super barges ranging from 400-700 TEU. A short graphical analysis was done to find the optimum point for throughput, call size and congestion and here, a maximum throughput of 2927 TEU/Day was obtained at a congestion of 12 barges a day and a call size of around 600 TEU. For context, this result falls within the range seen in the average results for throughput (2869-2953 TEU/Day) and similar congestion for barges (12 v 14 a day). Similarly, when simulations with 400 TEU call sizes were done, a congestion of 17 barges a day was obtained.

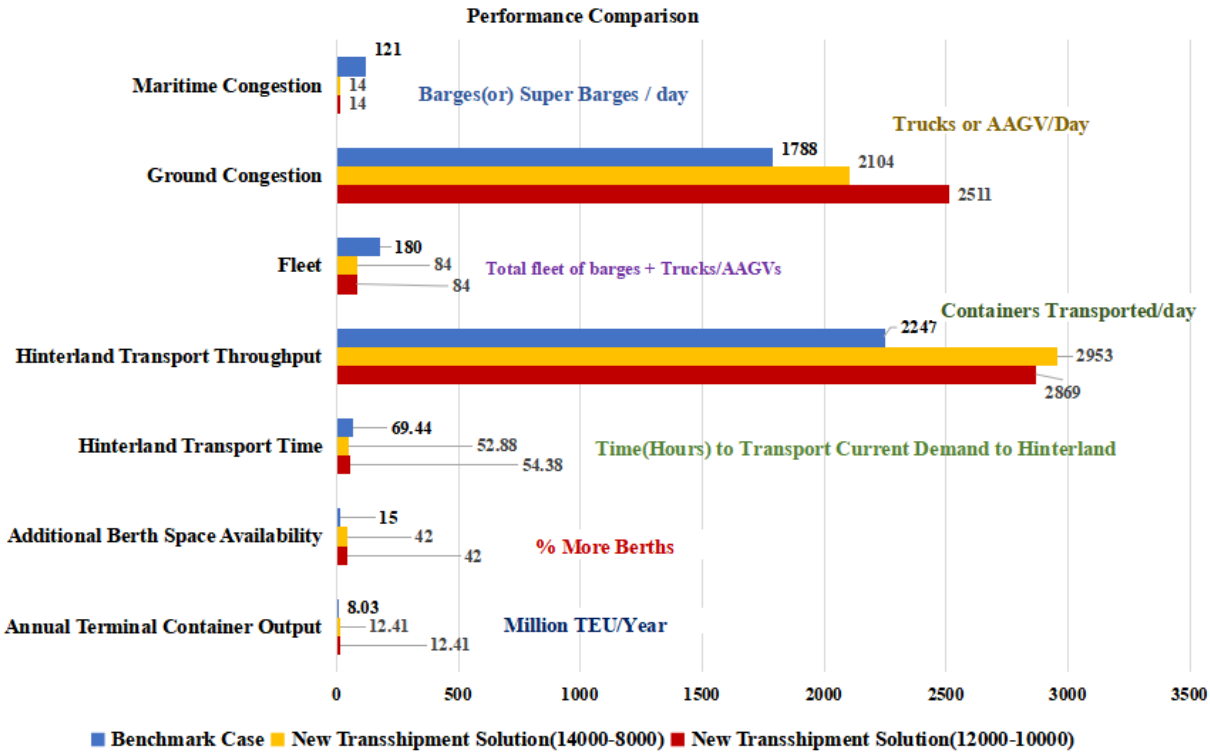

Figure 11: Performance Comparison

CONCLUSIONS

Trans-shipment forms a significant part of the services sector today and enables greater accessibility of industries and businesses located deep inside a country. This is also supported by the fact that the maritime industry takes care of 80% of the international trade volume. With increased trade, bigger ships, limited expansion space for ports, and growing congestion, there is an urgent need to develop future-proof solutions. Therefore this research was initiated to formulate new design and network solutions for the container shipping industry to facilitate efficient deep-sea to hinterland trans-shipment. A breakthrough in this research was introducing and using an Amphibious AGV for inter-terminal transportation. Being a 2 TEU vehicle, the Amphibious AGV provides the capacity of regular AGVs and trucks while providing the flexibility to travel on both land and water. This research also investigated the effectiveness of modular floating terminals as an alternate means of expansion, given the unsustainability of land reclamation. The author proposed a novel terminal design with a capacity of 4.2 million TEU annually. The design proposed a direct over-the-head instant transfer of containers from one transporter to the other, saving yard space and waiting time. To validate the problems faced today in trans-shipment, the Port of Hong Kong and the hinterland ports of the Pearl River Delta were chosen as the ground for the simulation. Using an agent-based modelling simulation on AnyLogic, it was clear that congestion was a serious issue with nearly 120 barges making footfall at HIT-COSCO terminals in Hong Kong, competing for just 9 berths. Essentially these barges were still using quay cranes generally used for deep-sea ships. This represented problems of congestion, saturation in handling capabilities, and other problems such as acute berth planning issues and quay crane allocation. With these constraints in mind, a new trans-shipment network solution involving the Amphibious AGV and the floating terminal was developed to boost handling capabilities by 50% as well as show how instrumental concepts like Amphibious AGV are in enhancing inter-terminal and hinterland transport. A salient feature of this new proposed network was also the use of a Super Barge, which took on higher container call sizes per trip to the tune of 400-700 TEU to reduce overall barge congestion by 80%. Under the new network, the feeder traffic was shifted from deep sea terminals to floating terminals enabling the berths to be occupied by extra deep sea ships. The simulations showed a container throughput increase from the current 8 million TEU to 12.41 million TEU when changes

were implemented. The takeaway from this research is that novel design solutions can indeed be found to address the current growth crisis. From a fleet transportation design perspective, novel network approaches have been implemented to address shortcomings of the status quo. Amphibious AGVs and floating terminals can potentially deliver more applications, such as liquid and dry bulk commodities. Amphibious AGVs were also envisioned to be sustainable and powertrain control is at the forefront with amphibious powertrains being relatively new. On a business level, Amphibious AGVs also have the potential to be effective for small and micro industries located on the hinterland and call for its investigation. The authors also believe that in the coming years, this work will be critically looked at to encourage impactful concepts like Amphibious AGVs and floating terminals to be introduced for the benefit of hinterland transportation that could eventually lower the prices of commodities that we use every day. From a design perspective, this work has proposed a preliminary concept that shows the potential of such an Amphibious AGV contraption is possible within a similar as canvas regular ground container AGVs. Future studies can move in the direction of certifying its stability and interaction with other equipment in the port.

ACKNOWLEDGEMENTS

This project has received funding from the European Union's Horizon 2020 (MFF 2014-2020) research and innovation programme under Grant Agreement 101036594.

REFERENCES

Abhishek Rajaram, A. (2023). Transshipment for the 21st century: A novel approach to deep sea-hinterland transportation.

Baird, A. J. and Rother, D. (2013). Technical and economic evaluation of the floating container storage and transhipment terminal (fcstt). *Transportation Research Part C: Emerging Technologies*, 30:178–192.

Bartošek, A. and Marek, O. (2013). Quay cranes in container terminals. *Transactions on Transport Sciences*, 6.

Bu, F., Liu, J., Liao, H., and Nachtmann, H. (2023). An alternative solution to congestion relief of u.s. seaports by container-on-barge: A simulation study. *Simulation Modelling Practice and Theory*, 129:102836.

Buitendijk, M. (2019). Antwerp sets minimum call size for container barges at twenty. *SWZ Maritime*.

Caris, A., Macharis, C., and Janssens, G. K. (2011). Network analysis of container barge transport in the port of antwerp by means of simulation. *Journal of Transport Geography*, 19(1):125–133.

Caserta, M., Schwarze, S., and Voß, S. (2011). Container rehandling at maritime container terminals. *Handbook of terminal planning*, pages 247–269.

Centre, H. C. (2014). Sailing speed.

Chen, C.-C. and Schonfeld, P. (2010). Modeling and performance assessment of intermodal transfers at cargo terminals. *Transportation research record*, 2162(1):53–62.

Chen, L., Haseltalab, A., Garofano, V., and Negenborn, R. R. (2019). Eco-vtf: Fuel-efficient vessel train formations for all-electric autonomous ships. pages 2543–2550.

Chen, L., Negenborn, R., Huang, Y., and Hopman, H. (2020). Survey on cooperative control for waterborne transport. *IEEE Intelligent Transportation Systems Magazine*, 13(2):71–90.

Chong, T. T. L. and Li, X. (2020). The development of hong kong housing market: Past, present and future. *Economic and Political Studies*, 8(1):21–40.

Di Ilio, G., Di Giorgio, P., Tribioli, L., Cigolotti, V., Bella, G., and Jannelli, E. (2021). Assessment of a hydrogen-fueled heavy-duty yard truck for roll-on and roll-off port operations.

Duisburg, H. P. (2018). Terminal rules.

Eijk, C., Hompes, J., Ghiridharan, V., Rajaram, A., V.S.Datta, Suryaa, V., Q.Colsen, and B.Groenhart (2023). Implementation of an amphibious agv in port of rotterdam.

Evers, J. and De Feijter, R. (2004). Centralized versus distributed feeder ship service: the case of the maasvlakte harbour area of rotterdam. *Transportation Planning and Technology*, 27(5):367–384.

Feng, F., Pang, Y., and Lodewijks, G. (2015). Integrate multi-agent planning in hinterland transport: Design, implementation and evaluation. *Advanced Engineering Informatics*, 29(4):1055–1071.

Freightos (2023). Global shipping costs are returning to pre-pandemic levels. *Aramex*.

Fuller, E. (2017). China's crown jewel: The pearl river delta. Accessed on February 23, 2024.

Gharehgozli, A., Mileski, J. P., and Duru, O. (2017). Heuristic estimation of container stacking and reshuffling operations under the containership delay factor and mega-ship challenge. *Maritime Policy & Management*, 44(3):373–391.

Gharehgozli, A. and Zaerpour, N. (2018). Stacking outbound barge containers in an automated deep-sea terminal. *European Journal of Operational Research*, 267(3):977–995.

Ghiridharan, V. S. (2023). Efficient inter terminal container transport using amphibious vehicles-a simulation approach.

Gibson, J. (2021). Global trade will grow by 70% to usd30 trillion by 2030.

Giernalczyk, A., Górski, Z., and Kowalczyk, B. (2010). Estimation method of ship main propulsion power, onboard power station electric power and boilers capacity by means of statistics. *Journal of Polish CIMAC*, 5(1):33–42.

Google (2024). Google Map: Port of Hong Kong. *Google*.

Grundfos (2024). Nb 150-315 specifications.

Gumuskaya, V., van Jaarsveld, W., Dijkman, R., Grefen, P., and Veenstra, A. (2020). Dynamic barge planning with stochastic container arrivals. *Transportation Research Part E: Logistics and Transportation Review*, 144:102161.

Hutchison Ports Trust (2023). COSCO-HIT Terminals (Hong Kong) Limited. *Hutchison Ports Trust Portfolio Overview*.

Iqbal, M. (2015). A multi-agent based model for inter terminal transportation.

Jovanova, J., van den Bos, W., and Schott, D. (2022). Design of floating terminals as integrated project for multi-machine systems. pages 475–490.

Kleefstra, T. (2019). Conceptual design of an autonomous amphibious container transportation vehicle.

Konecranes (2023). Automated guided vehicles.

Konings, R. (2007). Opportunities to improve container barge handling in the port of rotterdam from a transport network perspective. *Journal of Transport Geography*, 15(6):443–454.

Konings, R., Kreutzberger, E., and Maraš, V. (2013). Major considerations in developing a hub-and-spoke network to improve the cost performance of container barge transport in the hinterland: the case of the port of rotterdam. *Journal of Transport Geography*, 29:63–73.

Koo, P.-H., Jang, J., and Suh, J. (2004). Estimation of part waiting time and fleet sizing in agv systems. *International journal of flexible Manufacturing Systems*, 16(3):211–228.

Kotachi, M., Rabadi, G., Msakni, M. K., Al-Salem, M., and Diabat, A. (2016). A discrete event simulation for the logistics of hamad's container terminal of qatar. In *2016 Winter Simulation Conference (WSC)*, pages 2262–2271. IEEE.

Langen, P. and Van der Horst, M. (2008). Coordination in hinterland transport chains: A major challenge for the seaport community. *Maritime Economics and Logistics*, 10:108–129.

Legato, P. and Mazza, R. M. (2001). Berth planning and resources optimisation at a container terminal via discrete event simulation. *European Journal of Operational Research*, 133(3):537–547.

Lepic, B. (2023). Cosco electric vessel capable of 1,000 km yangze voyages launched. *Splash 247*.

Lian, T. L., Kang, L. C., Groen, S., Kit, L. C., and Kiong, O. A. (2015). Expansion of mega container port terminal close to nature reserve, singapore.

Liebherr (2024). Rail Mounted Gantry Cranes. Accessed: February 8, 2024.

Liu, C.-I., Jula, H., and Ioannou, P. A. (2001). Design and simulation of automated container terminal using agvs. In *2001 European Control Conference (ECC)*, pages 295–300. IEEE.

Malchow, U. (2020). Port feeder barges as a means to improve intra-port container logistics in multi-terminal ports. *Handbook of Terminal Planning*, pages 465–480.

Mandra, J. O. (2023). Cosco shipping's electric containership hits the water. *Offshore Energy*.

March, J. (2020). Itss: The integrated terminal ship system: Direct loading and unloading of transshipment containers between ultra large container vessels and feeder vessels. *Handbook of Terminal Planning*, pages 287–300.

Marine Department, Hong Kong (2022). Port and maritime statistics. *Marine Department, Hong Kong*.

Mazloumi, M. and van Hassel, E. (2021). Improvement of container terminal productivity with knowledge about future transport modes: a theoretical agent-based modelling approach. *Sustainability*, 13(17):9702.

Meulenkamp, A. (2023). A 3-stage approach to the berth allocation and quay crane specific problem in container terminals using cutting planes.

Negenborn, R. R., van Overloop, P.-J., Keviczky, T., and De Schutter, B. (2009). Distributed model predictive control of irrigation canals. *Networks and heterogeneous media*, 4(2):359–380.

Nicolet, A., Shobayo, P., van Hassel, E., and Atasoy, B. (2023). An assessment methodology for a modular terminal concept for container barging in seaports. *Case Studies on Transport Policy*, 14:101103.

Notteboom, T., Yang, D., and Xu, H. (2020). Container barge network development in inland rivers: A comparison between the yangtze river and the rhine river. *Transportation Research Part A: Policy and Practice*, 132:587–605.

Odetti, A., Altosole, M., Bruzzone, G., Caccia, M., and Viviani, M. (2019). Design and construction of a modular pump-jet thruster for autonomous surface vehicle operations in extremely shallow water. *Journal of Marine Science and Engineering*, 7(7):222.

Ogunsola, A. (2022). Container ships explained.

Park, S., Yun, S., and Kim, S. (2023). Autonomous vehicle-loading system simulation and cost model analysis of roll-on, roll-off port operations. *Journal of Marine Science and Engineering*, 11(8):1507.

Pielage, B.-J., Konings, R., and Schuylenburg, M. v. (2007). Barge hub terminals: a perspective for more efficient hinterland container transport for the port rotterdam.

Post, S. C. M. (1994). Tt club in plan to cover hk's barges.

Program, D. T. (2019). Overview vessel types on the danube. *Interreg European Union*.

Sanchez, R. J., Hoffmann, J., Micco, A., Pizzolitto, G. V., Sgut, M., and Wilmsmeier, G. (2003). Port efficiency and international trade: port efficiency as a determinant of maritime transport costs. *Maritime economics & logistics*, 5:199–218.

S.A.S, A. (2018). Preventing inadvertent slide deployments.

Schmidt, J., Meyer-Barlag, C., Eisel, M., Kolbe, L. M., and Appelrath, H.-J. (2015). Using battery-electric agvs in container terminals—assessing the potential and optimizing the economic viability. *Research in transportation business & management*, 17:99–111.

Schroër, H. J., Corman, F., Duinkerken, M. B., Negenborn, R. R., and Lodewijks, G. (2014). Evaluation of inter terminal transport configurations at rotterdam maasvlakte using discrete event simulation. In *Proceedings of the Winter Simulation Conference 2014*, pages 1771–1782.

Seatrade Maritime News (2015). HIT tops Pearl River Delta barge throughput in 2015. *Seatrade Maritime*.

Shen, Y. and Zhang, C. (2015). Loading sequencing with consideration of container rehandling. pages 1237–1241.

Shobayo, P. (2023). *Enhancing the competitiveness of inland waterway transport: a multi-methodological approach applied to port barge congestion and urban areas*. PhD thesis, University of Antwerp.

Shobayo, P. and Van Hassel, E. (2019). Container barge congestion and handling in large seaports: a theoretical agent-based modeling approach. *Journal of Shipping and Trade*, 4(1):1–26.

Tagawa, H., Kawasaki, T., and Hanaoka, S. (2021). Exploring the factors influencing the cost-effective design of hub-and-spoke and point-to-point networks in maritime transport using a bi-level optimization model. *The Asian Journal of Shipping and Logistics*, 37(2):192–203.

Tang, S., Xu, S., Gao, J., Ma, M., and Liao, P. (2022). Effect of service priority on the integrated continuous berth allocation and quay crane assignment problem after port congestion. *Journal of Marine Science and Engineering*, 10(9):1259.

van der Horst, M., Kort, M., Kuipers, B., and Geerlings, H. (2019). Coordination problems in container barging in the port of rotterdam: an institutional analysis. *Transportation Planning and Technology*, 42(2):187–199.

Wang, J. and Li, J. Y. (2012). Inland waterway transport in the pearl river basin, china. *Espace géographique*, 41(3):196–209.

We Build Value (2017). Pearl River Delta Area: China's Megacity. *We Build Value*.

Wiegmans, B., Menger, I., Behdani, B., and van Arem, B. (2018). Communication between deep sea container terminals and hinterland stakeholders: information needs and the relevance of information exchange. *Maritime Economics & Logistics*, 20:531–548.

Yang, X., Hu, H., Cheng, C., and Wang, Y. (2023). Automated guided vehicle (agv) scheduling in automated container terminals (acts) focusing on battery swapping and speed control. *Journal of Marine Science and Engineering*, 11(10):1852.

Zheng, H., Negenborn, R. R., and Lodewijks, G. (2016). Predictive path following with arrival time awareness for waterborne agvs. *Transportation Research Part C: Emerging Technologies*, 70:214–237.

Zheng, H., Negenborn, R. R., and Lodewijks, G. (2017). Closed-loop scheduling and control of waterborne agvs for energy-efficient inter terminal transport. *Transportation Research Part E: Logistics and Transportation Review*, 105:261–278.

Proceedings of 15th International Marine Design Conference (IMDC-2024)
June 2-6, 2024
Amsterdam, the Netherlands

Iron Powder as a Fuel on Service Vessels

Erik Scherpenhuijsen Rom[1], and Austin Kana[2,*]

ABSTRACT

This paper investigates the feasibility of iron powder energy generation systems on board a semi-submersible crane vessel. This is done using a design model that integrates design information and a simulated mission profile to determine a hybrid iron powder setup split. This setup is then placed within a set of vessel designs to calculate a base level feasibility looking at the draft, stability, and emissions decrease. For those concepts that were technically feasible, the new hybrid iron powder setup contributed to a reduction of CO_2 up to 25-50% and a reduction of NO_x emissions between 15-50%, depending on the mission profile.

KEY WORDS

Iron powder; alternative fuel; semi-submersible crane vessel design; feasibility study

INTRODUCTION

This paper explores the use of metal powder as a fuel on service vessels because they are a promising sustainable alternative to conventional energy sources since they are dense energy carriers. The main feature attributed to the iron powder power generation process that makes it such a high potential alternative fuel source is the fact that the combustion of this powder results in no CO_2 by-product (van Rooij et al., 2019). This paper is a follow on feasibility study to de Kwant et al (2023), who looked at the iron powder as a potential fuel on shipping vessels. De Kwant et al (2023) determined that short sea container vessels would be the most promising vessel class for shipping vessels, and that iron powder would could be technically feasible, however, it will likely not be as economically feasible as other alternative fuels.

This paper extends that research by looking into the feasibility within service vessels. This paper will start with a evaluation of the state-of-the-art of iron powder energy generation to determine the most optimal setup to be installed aboard a marine vessel. This will be followed by a study of the marine service vessels to determine which is best suited for an iron powder powertrain installation. The conclusions from these two studies will result in the creation of a design method to test iron powder feasibility on the chosen service vessel type. This method of testing feasibility will then be applied to a set of case study vessels.

Introduction to iron powder as fuel

Metal powder combustion is one of the promising sustainable power generating alternatives to conventional sources of power such as fossil fuels. Metal powders are dense energy carriers that can be turned into a power source using two processes (Bergthorson, 2018). The first is known as the wet cycle in which the metal is reacted with water at high temperatures for heat and hydrogen production (Dirven et al., 2018). The product can be used either in heat engines or in fuel cells. The second process is the dry cycle in which the metals are directly combusted in an external combustion chamber and converted into mechanical energy directly (Dirven et al., 2018). The dry cycle is a more direct form of energy generation as opposed to the two-step process of the wet cycle. This means that the dry cycle will be more compact in practical use than the wet cycle and require less volume. Therefore, the use of the dry cycle is far more practical onboard a ship with limited area and volume and will be the only one researched.

[1] Department of Maritime and Transport Technology, Delft University of Technology, Delft, the Netherlands;

[2] Department of Maritime and Transport Technology, Delft University of Technology, Delft, the Netherlands; ORCID: 0000-0002-9600-8669

* Corresponding Author: a.a.kana@tudelft.nl

Submitted: 22 january 2024, Revised: 26 April 2024, Accepted: 1 May 2024, Published: 21 May 2024

Conference paper, DOI: https://doi.org/10.59490/imdc.2024.870 e-ISSN: 3050-4864

Iron powder characteristics

The iron powder energy generation process has multiple characteristics that make it unique, such as its availability, recyclability, and zero-emission aspects of iron powder as an energy source. There are also other characteristics that serve as advantages such as low safety risks, ease of retrofit opportunities, and a significant energy density. Other characteristics such as abrasivity, moisture sensitivity, and a generally low efficiency serve as characteristics that will require further attention.

A key advantage of using iron as a power source is its overall abundance as a resource. Iron makes up around 5% of the earth's crust making it the 4th most common element in the crust (Bergthorson, 2018). This means that there will be enough resource availability for this particular use alongside the conventional uses of iron in construction and other sectors. Other metals that can be considered for electrofuels such as cobalt are far less abundant and more difficult to obtain, making them more expensive and less attractive as an alternative fuel.

As can be done with several other metal fuel sources, iron can be fully recycled after the process of energy generation. When iron powder is burned in a combustion chamber, the remaining products are iron oxides. These iron oxides cannot be used again for combustion in the state they are in as they have already been oxidized. Using either coke (a high-carbon distillate of coal) or hydrogen it is possible to reduce the iron oxides back into iron powder making the energy generation process fully circular process, as shown in Figure 1.

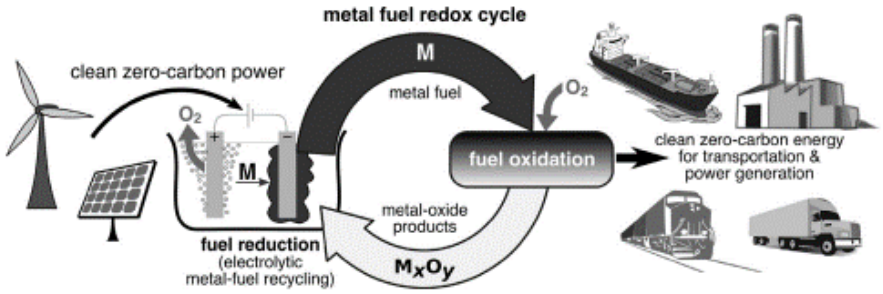

Figure 1: Metal reduction cycle applicable for iron (Bergthorson, 2018)

This has the main advantage that generally only one supply of iron powder is required for a specific application as this source can be infinitely reused through the reduction process. This is, of course, not possible with fossil fuels as their combustion products cannot be reduced back into the fuel.

The main advantage of using iron as a fuel source over fossil fuels is of course its extremely low emission in combustion. The combustion of iron releases no CO_2 as a by-product and very low levels of nitrous oxide with a maximum of 94 ppm of nitric oxide and 1 ppm of nitrogen oxide measured in a 100kW test setup by TU Eindhoven (van Rooij et al., 2019). The low level of nitrous oxide by-product is dependent on both the temperature of the combustion as well as the amount of hydrogen atoms present in combustion. For iron powder the temperature still reaches levels where some nitrous oxide may be released however the lack of hydrogen atoms in this combustion ensure this level is extremely low especially when compared to conventional diesel engine combustion (van Rooij et al., 2019).

Iron powder components

The iron powder powertrain consists of multiple systems to complete the entire cycle of power generation. A large array of infrastructure, systems and equipment are required both on land and onboard to complete the process (see Figure 2).

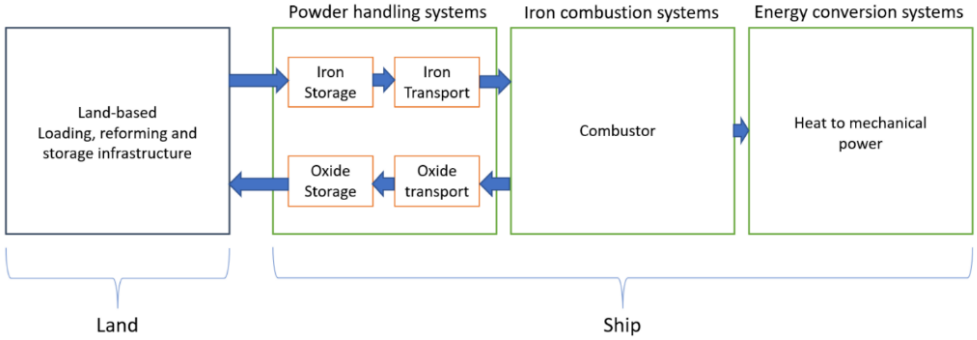

Figure 2: An overview of the components in the iron powder powertrain (de Kwant, 2021)

The land-based components are mainly the storage areas and regeneration plants. These are less important for the ship processes and will therefore not be further investigated in this paper. The components onboard the ship can be split into four different systems: storage, transport, combustion, and energy conversion systems. These systems will be further explored looking at the current state-of-the-art and will be analyzed in context of the challenges that arise with placement onboard a ship.

The storage of iron powder is fundamentally different to the storage of conventional liquid fuels such as marine diesel oil (MDO) and heavy fuel oil (HFO). Whereas liquid fuels are stored in tanks at around 40 degrees, iron powder cannot be stored in tanks and does not necessarily require a specific minimum temperature level (Seijger, 2020). As with all other bulk goods, iron powder is best stored in silos (van Rooij et al., 2019). The powdered form of the iron powder results in a higher volume requirement as well as high mass levels. There are two types of silos that can be used for iron powder storage, a horizontal or vertical silo. A horizontal silo is more comparable to the shape of a tank allowing for much lower placement to ensure a low center of gravity for the vessel. A key disadvantage of the horizontal silo, however, is its lower discharge level in comparison with the vertical silo. The vertical silo can discharge its bulk content through the hopper system mainly through gravitational forces and flow design. Due to its far more limited failure points, the vertical silo is currently preferred over the horizontal silo.

Transport of iron powder particles is best done using a two-phase pneumatic transport system. This transport system transports the bulk material through an air stream rather than direct contact. This air stream is created inside a tubular enclosed piping by a pump or high-power fan to push the bulk materials through the piping. This system can provide transport with sharp turns in any direction. Its high transport speed in the air stream makes it possible to minimize the size of the transport tubes while maintaining the minimum level of flow required. Flow level may need to be reduced to ensure minimal damage due to abrasiveness of the iron powder and oxide powder. The pneumatic two-phase transport system is also able to provide a homogeneous flow rate for transport from the dispersal system to the combustion chamber (van Rooij et al., 2019). This system has already been used for zinc transport whose properties are highly comparable to iron powder (Air-Tech System, 2024). The main concern with this system is the high amount of power required to operate in comparison to most other bulk transport systems.

The process of iron powder combustion is done in an external combustion chamber. This is because the combustion process for iron powder is much longer than is possible in an internal combustion chamber. This is coupled with the possibility of clogging of the iron powder particles in an internal combustion engine. To collect the iron oxide particles for storage and reduction back into iron powder, a combination of a cyclone filter and bag house filter setup are used. These are deemed sufficient to match the requirements for an iron powder system with an efficiency of around 38% to reach an oxide collection rate of 99.999% (van Rooij et al., 2019).

The energy generation from this combustion process is best done using a Mitsubishi (Ultra Steam Turbine) UST cycle (de Kwant, 2021). This is a reheated Rankine steam cycle. This setup is pictured in Figure 3. Is fitted with an economiser, evaporator, superheater and reheater. These are connected to a series of three turbines: a high-pressure turbine, intermediate pressure turbine, and a low-pressure turbine. This reheating of the working fluid and passing through this series of turbines increases the efficiency up to 15% compared to standard steam cycles. These systems are in commercial operation and are seen as suitable for iron powder application as well (van Rooij et al., 2019).

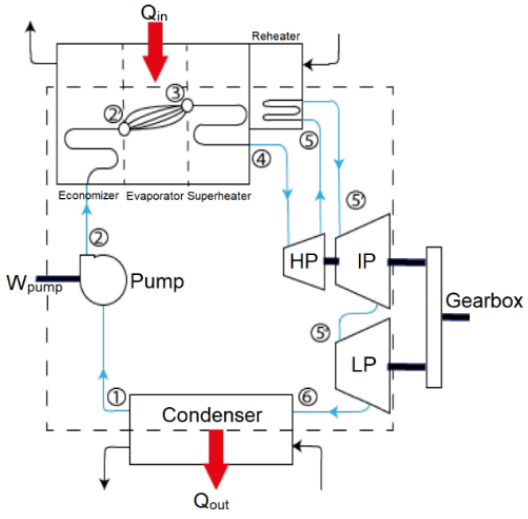

Figure 3: Schematic of Mitsubishi's UST plant, (de Kwant, 2021, Seijger, 2020)

Iron powder limitations

There are certain limitations that dictate the iron powder powertrain's output capability. These key limiters are the volume and mass concerns that come with iron powder storage systems, the part load and dynamic load issues that come with energy conversion, and potential filtration issues concerning the heat collection from oxides in the combustion system. Regardless of what combustion process, storage system, transport system or energy conversion system is used, there will be a high volume and mass requirement for the iron powder powertrain. From vertical storage silos to filtering systems to the boiler system and turbine the total volume taken up by the entire powertrain becomes significant with regards to ship stability. This requires a deep dive into the possibilities for different configurations of this system keeping in mind the high energy cost for pneumatic two-phase transport between these systems.

One of the main drawbacks of using a steam cycle for energy conversion is the low capability for part load conditions as well as dynamic loading. When the ship is in part load condition, the power requirement is lower than the design point of the power generation and conversion system. At this point the system is no longer working at optimum efficiency as this is only the case at the design point. This is the case with most power units however the drop in efficiency for a steam cycle can be quite stark. One of the most prominent solutions to the part load concern pertaining specifically to transit is the use of a controllable pitch propellers (van Rooij et al., 2019). This allows the ship to travel at different speeds without changing the steam cycle from its nominal power output. A hybrid configuration can be used to make up for the load variations (van Rooij et al., 2019). The main power source can be used for propulsive power and the secondary power source can be used for additional loads such as hotel, equipment, and crane loads.

Introduction to Service Vessels

The term service vessel encompasses a large variety of ship types with varying sizes and functions. These vessels were put through a two-phase down selection starting with the wide range of service vessels and ending with one, most optimal service vessel type. First, a list of different types of service vessels was made and their feasibility for an iron powder powertrain was determined based upon size and range. A select few vessel types were then further analyzed based on their operational modes and missions. These operational profiles were used to make an estimated load variation over the course of a mission and of the total output requirements along with their initial iron powder volume and mass requirements.

Phase one

Phase one of the down selection starts with a list of the service vessels to be considered, categorized into four areas: Transport, Support, Construction and Specialty, see Table 1.

Table 1: List of commonly used service vessels.

Transport Vessels	Support Vessels
- Walk-to-work Vessel - Platform Support Vessel - Heavy Lifting Cargo Vessel - Daughter Craft/Crew Transfer Vessel	- Tugboat - Anchor Handling Tug Supplier
Construction Vessels	**Specialty Vessels**
- Offshore Subsea Construction Vessel - Semi-submersible Crane Vessel (SSCV) - Jack-up Vessel	- Pipe-laying Vessel - Research Vessel - Dredger

These vessels were assessed for potential compatibility with an iron powder setup based upon their size, range, and functions. This very basic assessment allows certain vessels such as the daughter craft, tugboat, and pipe-laying vessels to be filtered out due to size and volume constraints. Long range research vessels can also be eliminated due to their likely high bunker requirement in comparison to their shape and size. Certain remaining vessels such as the walk-to-work and platform supply vessels are combined as they are highly similar in size and function.

Phase Two

From this first phase of the down selection, only four different vessel types remained: the platform supply vessel, the jack-up vessel, the semi-submersible crane vessel (SSCV) and the (limited range) research vessel. These vessel types were singled out in the 1st phase due to opportunities presented regarding either their size, their typical range of operation or the complexity of their functions. While all of these vessel types provided opportunities in one or two of these categories, none were ideal and would require a deeper dive to determine whether the opportunities presented were enough to make the idea potentially feasible. Through a further analysis of operational profile and load profile, an optimal vessel type of these four can be determined.

The main concern with platform supply vessels and research vessels is the relatively small capacity for extra volume and mass. These vessels are largely under 100m in length with largely varying loads over the course of a mission. Another issue is the densely packed state of the hulls of these smaller supply vessels, with minimal room on deck and below deck, placement of the silos will prove difficult. The main issue with the jack-up vessel is the high mass level in relation to its jacking-up process. The extra mass of an iron powder setup is considered too high for the jacking mechanism to still be able to lift the vessel.

The overall size and lightweight of the SSCV and its hull form make it far more ideal for iron powder powertrain implementation. From previous research testing the iron powder setup on short sea shipping vessels, one of the conclusions drawn from the results were that the volume and mass of the setup had a significant impact on the arrangement and performance of the vessel. These results were interpreted as, in order to minimize the impact of the mass and volume requirements of the iron powder powertrain a vessel with appropriate dimensions and tonnage is required. The large pillars connecting its pontoons to the deck box are ideal for silo placement. The general size of these SSCVs ranging from $130m$ up to $210m$ will likely decrease the total impact of the iron powder powertrain on the design of the vessel with regards to volume and mass constraints. While the level of power and energy required by a SSCV cannot be fully supplied by the iron powder powertrain, the load profiles have shown a potential for a hybrid installation which will ensure the power requirement of the vessel is satisfied while still decreasing the GHG emission. Therefore, the choice is made to test an iron powder setup on a SSCV.

METHOD

To test the feasibility of a hybrid iron powder setup on a SSCV, information is required on both the characteristics of the SSCVs as well as the systems to be placed aboard. The main inputs are the main dimensions and operating profiles of a selection of SSCVs. These are used to generate load profiles from which the hybrid split can be determined. With this hybrid split the weight estimations are made and used to test for stability and feasibility. Finally, an emissions comparison is made to assess the environmental impact of the hybrid setup. This process (Figure 4) is structured in a way that will maximize the limited inputs available for SSCVs where only main vessel dimensions, and high-level operating profile and load profile data is available.

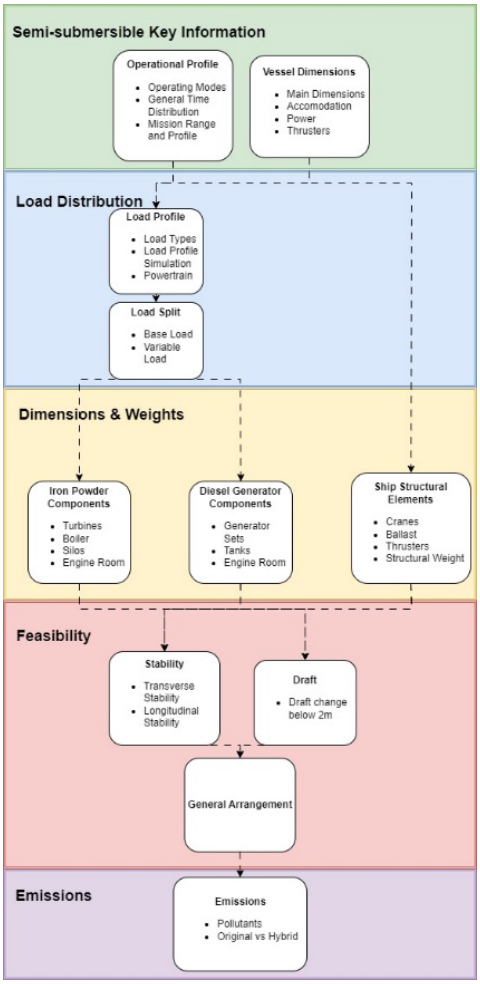

Figure 4: Method diagram showing steps to determine base feasibility.

Key Information

To ensure the reliability of results, existing vessel information is needed. In this case, a market study has been performed on the existing worldwide fleet of SSCVs. From this study, a set of four SSCV designs, each with differing main dimensions, power outputs and crane capacities were selected to form a case study. The information from these vessels is crucial in determining load distributions, weight estimations and stability calculations. Determining the operational profile of SSCVs means looking at the operating modes of the vessel, the distribution of time spent in a particular operating mode and using this information to create a realistic mission profile with an accurate range.

The operational profile of a semi-submersible crane vessel can be viewed over two timespans, over the space of a year and over the space of one mission. The standard SSCV has three operating modes; idle and repair, sailing, and working mode (Hagen, 2021). The idle and repair mode is assumed to be split between three sub modes: repair, idle at port and idle at sea. A SSCV mission can be described using a long and short cycle. In this case the 'long cycle' consists of the time spent loading, bunkering, and unloading at port coupled with the time taken to sail from port to the working area. The 'short cycle' then consists of all the time spent in the working area, this includes the time spent installing the offshore structures as well as potential idle times at sea and sailing time between offshore construction locations. This cycle is visualized in Figure 5.

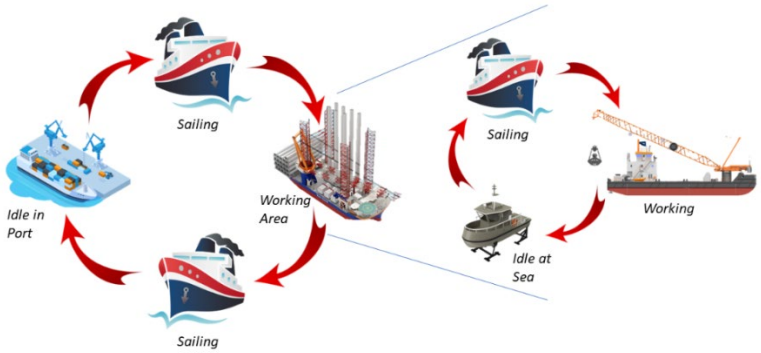

Figure 5: Diagram of the short and long cycles performed by a SSCV over the course of a mission.

The mission duration for SSCVs can vary greatly ranging from 7 weeks up to 15+, with bunkering occurring every 7-12 weeks. (personal communication, March 10, 2023). The missions for SSCVs vary significantly based upon what structures need to be installed, changed, or decommissioned. The sheer variety in operations makes it near impossible to simply take an average of all mission types and create a generic load profile. Therefore, the choice was made to focus on one specific mission type that is becoming increasingly common with installation vessels: wind turbine and mono-pile installation.

Load Distribution

Using the information provided about operating profiles, and general mission durations, the power and energy demands of the vessels can be estimated. The load profile determination starts with an understanding of the load types and how these power demands can be estimated from existing information to generate a time vs power graph. According to the results of the load profile simulations, the existing powertrain can be adapted to a hybrid powertrain. There are three main load types to be considered on a SSCV: the hotel load, thruster load, and crane load.

The load per operating profile is determined based upon the data available for one SSCV, to be used as a reference. The power level required for each operating mode is available for this vessel but not for the rest of the vessels. Due to most hotel systems being aimed at crew comfort or are systems used by the crew it is most likely that the hotel load can be scaled according to the crew capacity of the vessel. Using this reference vessel as a base, half of the factor difference in crew capacity is used as the difference in hotel load. This is because apart from the extra crew quarters, many areas such as the mess hall will not require as significant an increase in hotel load to accommodate for more crew. The thruster load of a vessel is mainly dependent on the installed thruster power. This is available for all vessels and can therefore be scaled to the same level as for the reference vessel. This can be assumed because of the tier III DP requirements applicable to all SSCV available reference vessels The thruster loads in dynamic positioning mode will be determined by a maximum thruster load and a base thruster load. Finally, the crane load is scaled based on the total powertrain of the vessel as the hotel load and thruster load have already been determined. This means that the remaining load for each operating mode is covered by the cranes. The variable crane loads are determined by a maximum crane load and a base crane load.

These loads per operating mode are the basis of the load profile estimation. Each operating mode is simulated for the previously determined mission type for the determined mission length. As the operating mode of the simulation varies over the mission, so does the power requirement of the vessel. This gives an indication of the total power requirement needed for each vessel as well as where the hybrid split should be made. Firstly, a load profile containing the three main consumers is created to show the variation of the power requirement over the course of a mission as well as where the peak loads occur. These are then summed up to create an estimation of the total power requirement of the vessel.

It is important to note that these load profiles are generated from assumptions made for the load requirement of each consumer. While the simulation of a relatively constant load such as the hotel load is quite simple, the simulation of a varying load is more complex and results in a wider range of results with each simulation. This is mainly the case for the thruster and crane load when the vessel is in working mode. With the base and peak load estimations made, the probability of the load requirement being any value between the base and peak load must be determined. This was done based on the existing crane energy demand data available from one of reference SSCVs, shown in Figure 6.

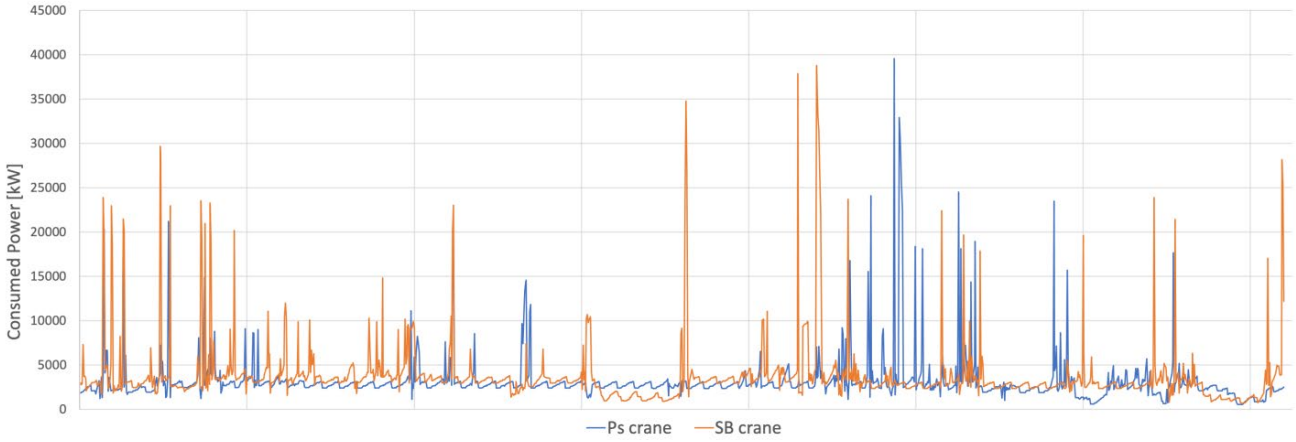

Figure 6: The energy demand of the reference SSCV's cranes during one day in working mode, (Hagen, 2021)

This frequency of peak power demand over one day for each crane was extrapolated for an entire operation in working mode. By calculating the number of times certain power demands were reached over the course of a day, a probability of a certain power demand could be generated and applied to each vessel. While this does not perfectly reflect the reality of the power demand for each vessel, it does give sufficient and reliable indication of the distribution of power demand for both the cranes and the thrusters. The thrusters in working mode are set to dynamic positioning mode and these often work in tandem with the crane operations. When the crane undergoes a large movement, it requires a large amount of power for lifting but also for the dynamic positioning to stabilise the vessel. This coupling of the thruster and crane in working mode allows this distribution of power demand to be used not only for the crane loads but also the thruster loads.

A full depiction of a typical powertrain from power generation to power consumption is given in Figure 7 depicting the full powertrain of one the reference SSCVs with 3 engine rooms. In this schematic the red, blue, and yellow components describe the generator sets in their respective engine rooms while the green components are the main power consumers such as the cranes and thrusters. This general layout of the powertrain systems will be used in the hybrid setup.

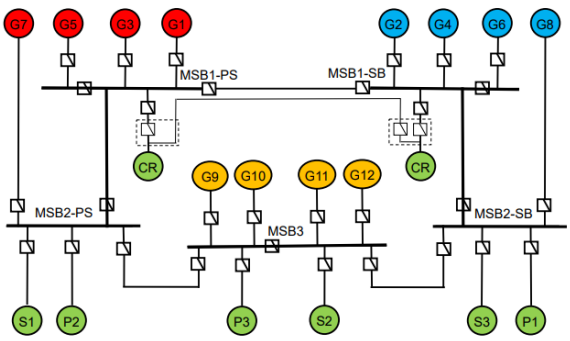

Figure 7: Powertrain schematic for one the SSCVs, (Lyu, 2016)

Keeping in mind that the power levels will differ significantly per vessel, an outline is made of the general layout of the hybrid powertrain. The main difference between the original powertrain and the hybrid powertrain is the addition of an extra engine room with an iron powder setup. Each vessel will consist of four engine rooms. Three of these engine rooms will be similar to the original engine rooms in that they will be equipped with diesel generator sets to provide the variable load required for the vessel. The iron powder engine room will be equipped with two boilers and turbine sets to provide redundancy. The rated power of each setup will be equal to the base load determined from the load profile. The rated power of the remaining diesel generator sets in the other three engine rooms will be determined based on the redundancy requirements used for the original powertrain design. Two of the remaining three engine rooms must be capable of providing the peak load requirement minus the output of the iron powder setup. The layout of this hybrid powertrain is modelled in Figure 8.

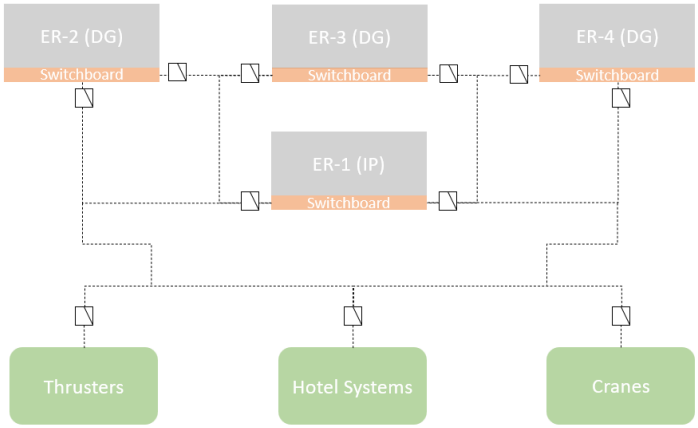

Figure 8: Simplified diagram of hybrid powertrain

Dimensions and weights

The load profiles show both the power and energy requirements of the vessels, the key information needed in order to properly size the powertrain components. The dimensioning and weight estimation is split into three main categories. First, the estimation of the iron powder components is done including everything in the engine room as well as the silos and filters. Next, the diesel generator sets are estimated as well as the bunker tanks. Finally, the main elements of the ship are estimated.

Iron powder components

The iron powder components to be estimated are the steam turbines, boiler, filters, and silos. These dimensions will vary per vessel as they are dependent on the base load required for each vessel as well as the overall kWh needed over the course of a mission. The method of dimensioning and weight estimation is based largely on the methods used by de Kwant er al (2023) for a similar iron powder setup.

Diesel generator components

The diesel generator components are far simpler to estimate as these are far more common and readily available for commercial use. This is also the case for the bunker tanks for the marine diesel fuel as the tanks have far more flexibility for placement compared to the silos for iron powder storage.

Ship main elements components

The ship structural elements consist of the remaining weights on the vessel required for an accurate stability calculation. These include the cranes, the ballast, thrusters, and the structural weight of the vessel. These elements are estimated separately despite the lightweight of all four reference vessels being given due to their varying placement aboard the vessel, these weights and their centres of gravity are required for a more accurate stability evaluation.

Feasibility

Using the information from the dimensioning and weight calculations, some base stability calculations can be made to determine both the feasibility of a hybrid setup on a SSCV as well as how this would look like. Due to a lack of information regarding the motions of these types of vessels as well as the exact internal layout of the vessels only the intact stability will be evaluated. Firstly, a look at the impact of the hybrid setup on the draft of the vessel is investigated. This is followed by the intact stability evaluation which is comprised of a transverse meta-centre height check and a longitudinal balancing leading to a general arrangement of the feasible vessels.

Draft
The draft of SSCV is used as a variable that can increase a vessels stability in working condition. The draft is lowest in sailing condition to minimize the underwater surface area and therefore resistance of the vessel. The draft is highest when performing heavy crane operations as the increased draft ensures a lower ship response to wave loading. The draft is essentially altered through creation of extra deadweight through pumping ballast water into the pontoons and occasionally pillars of the vessel. This increase in vessel weight increases the draft of the vessel. This change in draft is estimated for each vessel depending on their increased mass due to the iron powder setup.

This value is especially important for the transit draft condition as this cannot be compensated by simply pumping less ballast as is the case for the vessel's maximum draft. This increase in draft will certainly increase the underwater surface area which in turn will increase the resistance of the vessel changing its transit speed. This is an issue that may require a redesign of the vessel geometry to account for the added weight. If the draft at transit level increases to above the height of the pontoons, the issue is deemed serious and requiring significant redesign considerations. If the draft at transit level increases but not above the height of the pontoons, it is considered an issue requiring lass significant and far-reaching redesign considerations.

Transverse stability
The transverse stability of SSCVs is generally quite high to accommodate for large moments caused by crane operations. Although the vessel motions due to wave loading are significantly reduced at maximum draft, the metacentre height (GM) is significantly reduced. Therefore, the assumption is made that if the GM is acceptable at maximum draft in fully loaded condition, the GM will be acceptable for all other drafts and conditions as well. According to classification rules for heavy lift vessels in Part 5: Ship Types, Chapter 10: Vessels for special operations, 2021, the 'GM at equilibrium shall not be less than 0.3 m'. Further criteria include that the 'positive range of the GZ curve shall be minimum 15° in conjunction with a height of not less than 0.1 m within this range'. Finally, the 'maximum righting arm shall occur at an angle of heel not less than 7°'. To determine whether this vessel fulfils these criteria, the GM is determined as well as the GZ-curve for the first 15 degrees.

Longitudinal stability and general arrangement
The longitudinal stability is largely dictated by the distribution of ballast across the length of the vessel. This allows the trim of the vessel to be managed in different circumstances and drafts. The general arrangement of the vessel dictates to what degree the ship will trim and to what extent this trim must be controlled.

This placement of the various components to fulfil transverse and longitudinal stability creates a general arrangement of the vessel. The components are placed within the bounds of the geometry of the vessel at various heights along the length of the vessel. The placement will be symmetrical along the breadth of the vessel as is the case with almost all seagoing vessels. This general arrangement will be displayed in the 3D Rhinoceros model made for each vessel with side and top views of each level shown as well.

Emissions
The key advantage of iron powder as a power source is its significantly lower greenhouse gas emission in comparison the marine diesel fuels being used. It is assumed that the installation of an iron powder hybrid setup will likely incur technical concerns regarding the vessel design. The emissions decrease is weighed against these concerns to determine whether the degree of feasibility of installing an iron powder hybrid setup on a particular vessel is worth the effort and cost. This is done by having the emission reduction potential be a key factor alongside feasibility in making a final recommendation in the conclusion. Firstly, the pollutants to be considered are determined as well as their output for each power source and then the original powertrain is compared to the hybrid powertrain to determine the level of emissions reduction.

CASE STUDY
For this case study, a set of four semi-submersible vessel (SSCV) designs was chosen to be a representation of the SSCV fleet. Each vessel design has a slightly different geometry, size, and crane capacity. These four vessel designs are considered sufficient to represent the global SSCV fleet. The differing geometry and capacity allow for a clearer comparison between the vessels when evaluating the reasons for technical feasibility.

Key information
The four vessels have varying main dimensions, carrying/lifting capacities, and powertrain setups. The main information on each vessel is provided in Table 2, and will be used to help create suitable load profiles and general arrangements.

The only missing base information regarding these vessels was the powertrain configuration and total power output capability of Vessel C. The main features shared by all four vessels is the tier III dynamic positioning capability since this is a requirement

for the heavy lifting operations. This means that the thrusters for each vessel are azimuth thrusters. All vessels have a transit depth of 11-12m with maximum depths ranging from 25m to 32m. These maximum depths are only reached during heavy lifting operations in which the dynamic positioning is also active. The crew accommodation also vary from 400 persons up to 736 persons. These main points of information are used to determine the expected power requirements for each operating mode.

Table 2. SSCV main dimensions and key information

Dimension	Symbol	Vessel A	Vessel B	Vessel C	Vessel D	Unit
Length	L	220	201.6	154	137	m
Breadth	B	102	88.4	106	81	
Min Draft	T_{min}	12	11.9	11	11.28	m
Max Draft	T_{max}	32	31.6	25	26.4	m
Depth	D	49.5	49.5	42	39	m
Crane Capacity	C_{cap}	2x10,000	2x7,100	2,721 + 3,628	2x1,800	T
Transit Speed	V_{tr}	10	7	5	8	Kts
Thrusters	T	8x5.5	6x5.5	7x3.5	6x3.8	MW
Powertrain	P_E	12x8	6x4.9, 4x4.5, 2x5.5	N/A	8x3.86	MW
Total Power	P_T	96	58.4	N/A	30.88	MW
Accommodation	N_{per}	400	736	394	618	-

Load Distribution

Taking information from the power requirements of an existing SSCV (Hagen, 2021), the power ranges were extrapolated to each of the four vessels based on the information in Table 2 on each vessel. These estimated power requirements were split over the three main consumers: the thrusters, cranes, and hotel load, and are presented in Table 3.

Table 3: Estimated power ranges for each vessel

	Hotel Load [MW]				Thruster Load [MW]				Crane Load [MW]			
	Vessel											
Vessel	A	B	C	D	A	B	C	D	A	B	C	D
Idle	4-5	6-7	4-5	5-6	0.15-0.3	0.15-0.3	0.15-0.3	0.15-0.3	0-3	0-2	0-1	0-1
Sailing	6-7	9-10	6-7	8-9	29-31	22-23	16-17	15-16	0	0	0	0
Working	1-4	1-6	1-4	1-5	5-22	4-16	3-12	2-12	2-40	2-15	1-4	1-3

Using this information and the distribution of time spent in working, sailing and idle mode, the following load profiles were created shown in Figure 9. Each vessel was given the same mission time of 12 weeks and the loads were split between each main consumer; cranes, thrusters, and hotel load. From this split, a total power profile was created by summing the load requirements of each consumer. The total power consumption for each vessel was determined as the average over the 10,000 load profile simulations run.

Through further analysis of the range of load profile simulations of each vessel, the general split between iron powder and MDO power can be shown in the form of a percentage range of the total power requirement of the vessel. These values are shown in Table 4 for all four vessels.

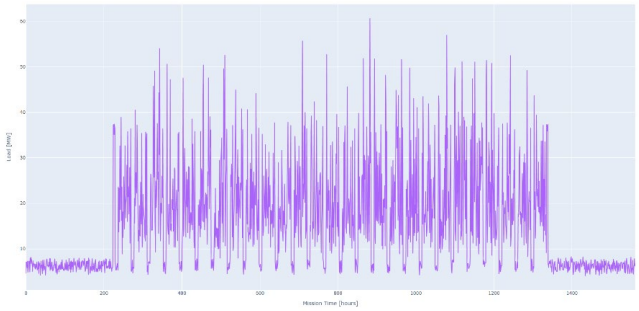

Figure 9a: Vessel A

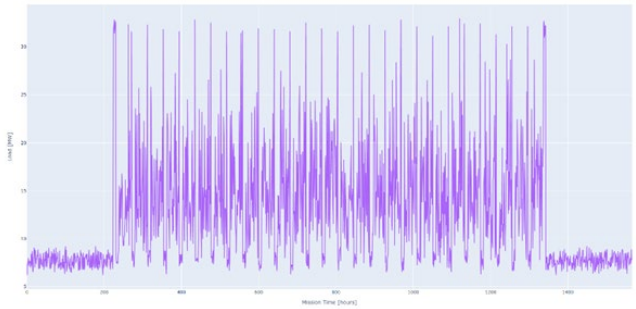

Figure 9b: Vessel B

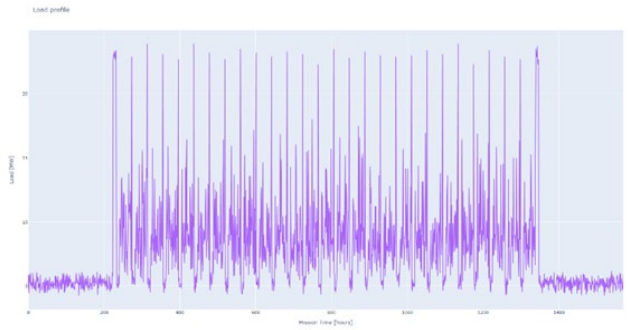

Figure 9c: Vessel C

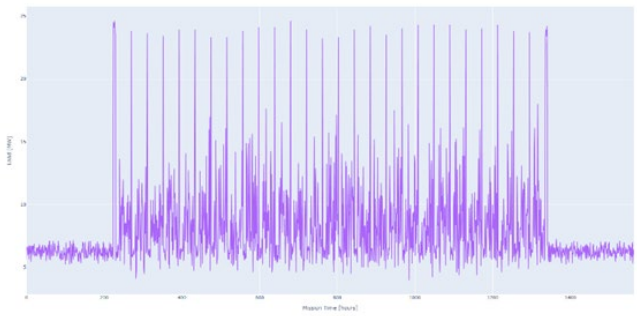

Figure 9d: Vessel D

Figure 9: The power profile of each vessel as the total load required

Table 4: Range of percentage total power demand covered by base and variable load.

	Base Load % of Total Demand	Variable Load % of Total Demand
Vessel A	18-45	55-82
Vessel B	31-63	37-69
Vessel C	41-67	33-59
Vessel D	45-73	27-55

Dimensions and Weights

The dimensions and weights were categorized into the engine room weights, bunker weights, and ship element weights.

Engine Rooms

One of the four engine rooms on each vessel will be fitted with the iron powder setup. This engine room will contain the turbines, boiler, and the electrical motor. The dimensions of the engine room are therefore determined by the dimensions of the turbines, boiler and electrical motor combined. A minimum additional margin 10% of length, breadth and height is added for other components as well as to give space for engineers. The length, breadth, height, and the total mass of each engine room is listed in Table 5.

Table 5: Main dimensions for each iron powder engine room

	Length [m]	Breadth [m]	Height [m]	Total Mass [t]
Vessel A	14	6	7	572
Vessel B	16	10	7	734
Vessel C	14	6	7	572
Vessel D	15	9	7	662

The breadth and total mass are double the amount needed for one UST setup as the engine room will need to fit two setups to ensure the strict redundancy criteria of semi-submersible crane vessels are fulfilled.

The diesel generator engine rooms are determined by the size and number of generator sets assigned to each vessel. Three of the four engine rooms to be placed on the vessels will be fitted with diesel generators. As with the iron powder engine room, a margin of at least 10% extra length, breadth and height are added for the remaining smaller components as well as room for engineers. The length, breadth, height and total mass of each engine room is listed in Table 6.

Table 6: Main dimensions for each diesel-powered engine room.

	Length [m]	Breadth [m]	Height [m]	Total Mass [t]
Vessel A	13.5	15	5	616
Vessel B	12	10	5	363
Vessel C	11	9	5	228
Vessel D	11	10.5	5	327

The mass and breadth of Vessel A are multiplied by four as this is the number of engines to be fitted in one engine room. The mass and breadth of the remaining vessels is multiplied by three as these engine rooms are fitted with one less generator set each.

Bunker

The design of the silos is dependent mainly on the dimensions of the vessels. These silos will be placed in the pillars of the main structures of each vessel and each vessel has different sized pillars. The height of the pillars is the main factor in determining the dimensions. The number of silos is taken as the number of silos needed to carry the required bunker including the bunker margin plus the additional 4 empty silos required for initial oxide deposit. The total number of silos must be an even number to allow for even distribution among the pillars on each side of the vessel. The main dimensions and volume of one silo as well as the number of silos required and total iron powder bunker mass for each vessel are listed in Table 7.

Table 7: Main dimensions for the silos on each vessel.

	Total Height [m]	Diameter [m]	Number of Silos	Total Mass [t]
Vessel A	21.6	3.93	34	16600
Vessel B	21.5	3.91	46	23200
Vessel C	20.7	3.76	38	16600
Vessel D	18	3.27	66	19900

The bunker level is determined based off of the specific fuel consumption of the chosen generator sets. The bunker will be placed in the remaining available area in the pillars. The total MDO bunker level required for each vessel as well as its mass are listed in Table 8.

Table 8: Required weight and volume of the MDO bunker on each vessel.

	Bunker Mass [t]	Bunker Volume [m^3]
Vessel A	5030	5650
Vessel B	2610	2930
Vessel C	2140	2400
Vessel D	1930	2170

Ship Elements

The ship structural elements contain the remaining significant elements of the vessel who have a significant mass and therefore significant impact on the ship stability calculations. These include the crane, ballast, thrusters, and structural weight of the vessel. The total mass of each of these elements are listed in Table 9.

Table 9: Mass estimations of key ship elements.

	Crane [t]	Ballast [t]	Thruster [t]	Structural [t]
Vessel A	6850	113000	512	83500
Vessel B	5980	120000	384	66100
Vessel C	5160	30000	329	44100
Vessel D	2240	21000	282	31100

These values alongside the other estimated masses for each engine room will be used to calculate an initial static stability to evaluate the feasibility of a hybrid iron powder configuration and to visualize how this would best fit.

Feasibility

The feasibility of an iron powder hybrid configuration on a SSCV can be measured in many ways. In this case, due to a limited amount of information about these vessels and their dynamic seakeeping behavior, the choice was made to keep to a base feasibility determination. This means that the main static stability criteria will be evaluated such as the draft, transverse stability, and longitudinal stability. Calculations will be made for each of these categories and the results will be compared to either the original powertrain setup of the vessel or the Det Norkse Veritas (DNV) classification bureau stability requirements for SSCVs [Part 5: Ship Types, Chapter 10: Vessels for special operations, 2021].

Draft

The draft is one of a SSCV's key feature in that it should be able to increase and decrease its draft according to its operating mode. A significant change in the total mass of the bunker will increase the draft of the vessel. By comparing the hybrid bunker mass level with a marine diesel fuel only mass level, the change in draft due to the increased bunker mass can be calculated. This is most important in the transit mode as ballast reduction is not possible in this mode meaning the draft increase cannot be simply compensated. The resulting draft increase is listed in Table 10.

Table 10: Draft increase due to increased bunker mass.

	Increase in Bunker Mass [t]	Increase in Draft [m]
Vessel A	15200	1.16
Vessel B	21200	2.22
Vessel C	15200	6.02
Vessel D	18300	8.06

The results are quite varied for each vessel as could be expected. This change in draft depends on both the mass increase as well as the ship's waterline area. The draft change was measured at minimum or transit draft as this is where the change in draft has the most impact. The maximum draft level can be much more easily maintained by adjusting the level of ballast. This is not the case for transit draft as there is no ballast to adjust. Of the four vessels, the only vessel indicating that the increased bunker will not necessarily require a redesign of the pillars and pontoons is Vessel A. The draft increase on Vessel C and Vessel D are mainly due to their small waterline area over all their pillars especially when compared to Vessel B and Vessel A. The substantial draft increase on these two vessels points to a need for a pontoon and pillar redesign if it is to accommodate the expected iron powder bunker level. While the increase in draft is not as severe as for Vessel C and Vessel D, Vessel B will likely also require a redesign of the vessel to a lesser extent. This is due to the draft now being above the pontoon height.

Transverse Stability

The metacentric height (GM) can be calculated for each vessel. Due to the limited information available for these vessels, only a base static transverse stability calculation can be made from which any reasonable conclusions can be drawn. Table 11 lists the KB, KG, BM, and GM values for each vessel in a fully loaded condition at the maximum draft.

Table 11: Transverse stability values for each vessel

	KB [m]	KG [m]	BM [m]	GM [m]
Vessel A	11.4	35.7	28	3.62
Vessel B	12.2	30.9	25.1	6.35
Vessel C	9.05	30.8	26.8	5.11
Vessel D	7.61	26.7	19.6	0.52

According to the classification rules by DNV [Part 5: Ship Types, Chapter 10: Vessels for special operations, 2021], the minimum allowed GM of 0.3m at maximum operating draft has been met by all four vessels. Vessels A, B and C even have a wide margin of safety above the minimum required GM value. This indicates that it may be possible for the iron powder hybrid configuration to be installed without negatively impacting the transverse static stability of the vessel. It must be considered that these GM values are determined based off rough estimations and may in fact not reflect reality. There are certain extra mass elements aboard the vessel that may not be as large as the ones considered but may add up alter the estimated KG value. This is why the margin of a few meters regarding the GM values of Vessels A, B and C are more promising than the 0.2m margin for Vessel D. If these estimations were to be altered and the GM were to lower, the chances of Vessels A, B and C still fulfilling the initial transverse stability criteria are far higher than that of Vessel D. On top of this, Vessel D has a righting arm that reaches only a maximum of 0.05m at 15 degrees of heel, which is only 50% of the minimum requirement stated by DNV. This means that Vessel D does not meet the stability requirements and cannot be deemed feasible with an iron powder setup.

Longitudinal Stability

The longitudinal stability of each vessel is largely determined by the trimming moment created by the vessel. The trimming moment is dependent on the longitudinal center of gravity of each component/element placed on the vessel. Each vessel has its own longitudinal center of buoyancy and its own structural longitudinal center of gravity. These elements cannot be altered same as the longitudinal center of gravity of the cranes, thrusters, and ballast. The trimming moment is minimized by keeping the total longitudinal center of gravity of each vessel within one meter of the longitudinal center of buoyancy of each vessel. The longitudinal center of gravity of the engine rooms and bunker tanks/silos have the largest impact on the longitudinal center of gravity of the vessel. Table 12 shows the needed longitudinal centers of gravity of the engine rooms, fuel bunker and iron powder bunker to ensure this minimal trimming moment.

Table 12: Longitudinal centers of gravity for each element that can be placed for each vessel.

	LCG Engine Rooms [m]	LCG MFO [m]	LCG Iron Powder [m]
Vessel A	75	156	90
Vessel B	70	163	80
Vessel C	50	100	60

These conditions alongside the vertical component placement conditions determined for the transverse stability can be used to create a general arrangement for Vessels A, B and C shown in figures 13, 14, and 15.

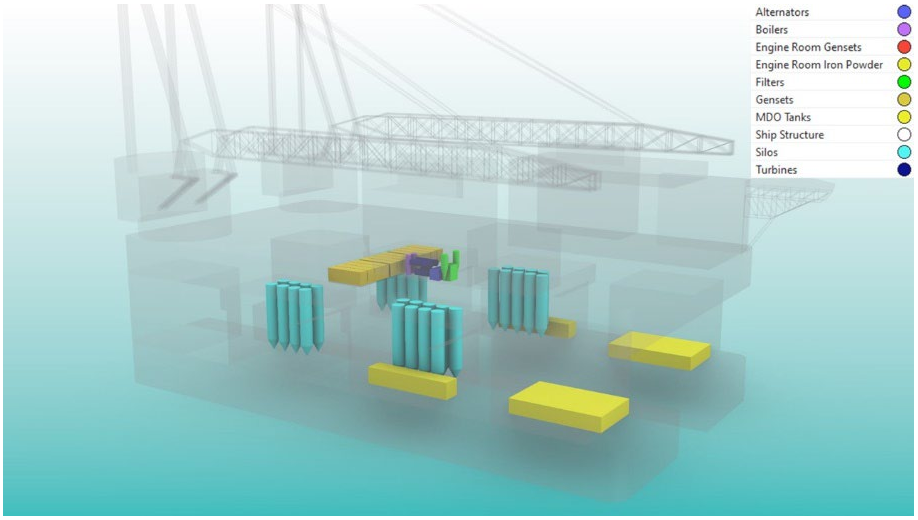

Figure 10a: Vessel A

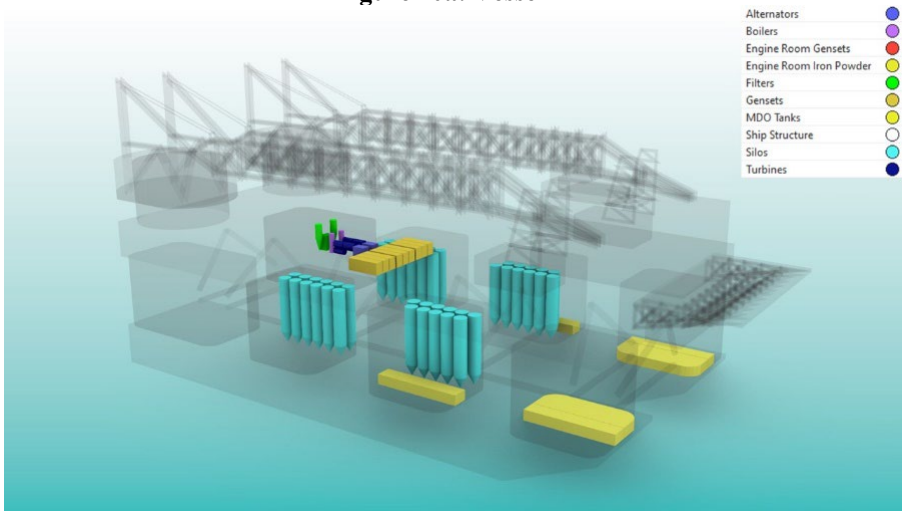

Figure 10b: Vessel B

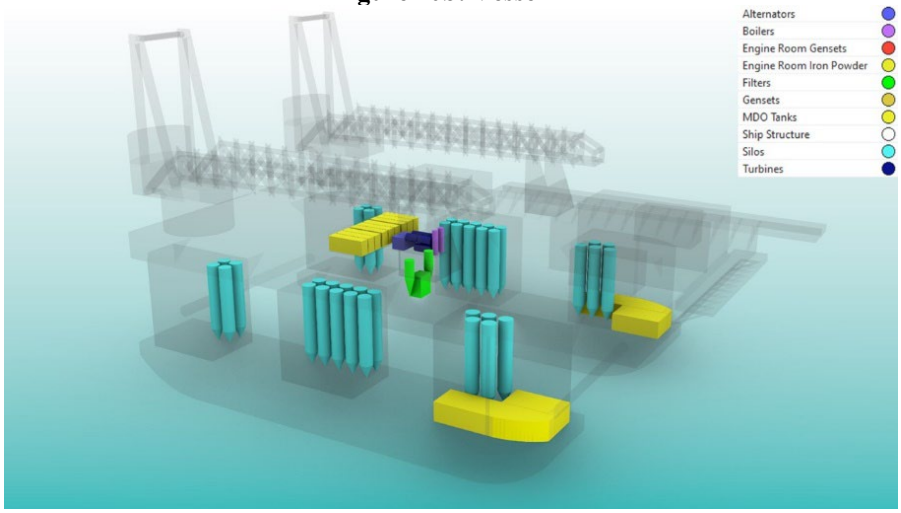

Figure 10c: Vessel C

Figure 10: Perspective view of each vessel's hybrid general arrangement

Emissions

The environmental impact of installing a hybrid iron powder powertrain on these SSCVs can be determined through an emissions comparison. The distribution of base versus variable power varies significantly for each vessel and is in this case taken as a range of output values as opposed to a singular value. This is due to the high variance in the variable load as it is simulated using probabilities of peak loads occurring. Table 13 shows the total calculated emissions output comparison for both carbon dioxide as well as nitrous oxide.

Table 13: Total CO2 and NOx output comparison for single year of 3 missions.

	CO_2 Total Output [kg/kWh]		NO_x Total Output [kg/kWh]	
Vessel	Hybrid	Original	Hybrid	Original
Vessel A	44100	66900	175	226
Vessel B	27900	46800	93	162
Vessel C	18300	31500	61	116

This comparison is based off of the assumption that three 12-week missions will be completed in a year to leave over 10 weeks for non-mission transit and potential maintenance and repair. The total CO_2 reduction is significant reaching around 20,000 tons of CO_2 a year for each vessel. The total NO_x reduction is not as large as the total output values are far lower than the CO_2 output. A reduction of around 50 tons of NO_x yearly can still be achieved which is in the case of Vessel C is around half of its total expected NO_x output.

CONCLUSION

Based on the results, certain feasibility evaluations can be made. First, it was determined that there is an optimal iron powder setup that can feasibly be placed aboard a marine service vessel. Furthermore, it was determined that a SSCV would be the most optimal vessel on which to place this iron powder setup. From this literature level research, the importance of implementing a hybrid setup was made clear. Through application of a model and simulation of said model on a case study of a set of SSCVs, the level of base feasibility can be determined for each vessel as shown in Table 14. In this table, the impact of the hybrid setup on the draft, stability and emissions of each vessel is compared. In the case of the draft, '1' indicates the lowest increase in vessel draft due to the increased mass while in the case of the stability '1' indicates the highest level of metacentric height and initial righting arm. In case of the emissions, '1' indicates the largest estimated decrease in CO_2 and NO_x emissions.

Table 14: Short comparison table ranking the feasibility of each case study vessel.

	Draft	Stability	Emissions
Vessel A	1	3	2
Vessel B	2	1	1
Vessel C	3	2	3
Vessel D	4	4	N/A

Vessel A claims the second highest feasibility level as it is least affected by the mass increase in terms of both draft and stability while still seeing significant emissions reductions. Vessel B has highest feasibility with only a minor concern regarding draft increase and satisfying the initial stability estimations whilst having an estimated highest emissions decrease. Vessel C is still considered base level feasible despite its issues with increased draft as its initial stability levels are more than sufficient. Vessel D is considered not feasible at a base level due to its lack of stability coupled with a high draft increase at a higher mass making an emissions comparison unnecessary. This leads to the main conclusion that the larger SSCVs are generally considered to be more feasible candidates for iron powder hybrid powertrain installation as they generally shaped to provide a larger water-plane area and equipped with a far larger deadweight carrying capacity. The key points of concern when trying to implement an iron powder powertrain on a SSCV include:

- Hybridization will be required due to the high variability in SSCV load profiles as well as increased mass of the iron powder bunker
- Balance needs to be found regarding the amount of power delivered by the iron powder powertrain (emissions saved) and the impact of its bunker on the vessel's stability and operability
- Larger SSCVs provide more sizing possibilities with comparatively lower vessel stability impact

FUTURE WORK

As the main concerns regarding iron powder implementation on marine vessels lies largely in the technical feasibility study, it was this area that was focused on most. There was not sufficient time to conduct a proper cost estimation for the vessels. This would provide interesting context to the technical feasibility as the initial costs of the setup can be compared to conventional

energy sources as well as the yearly bunker costs. This is especially interesting considering the iron powder cycle and the possibility of becoming a fully cyclical energy source meaning only one initial bunker cost is made for the lifetime of the powertrain. Redesign costs and port infrastructure costs can also be considered in this economic feasibility analysis to provide a full picture of the potential of iron powder as an energy source.

This research was done as an in-house project meaning that there was no continuous contact with companies within this field during the research. This meant that the information provided about certain iron powder powertrain components and the SSCVs was generally quite limited. The key information used as the main inputs of the method in were taken from official vessel brochures and reports that highlight the operating profile of select SSCVs. This information was then taken and extrapolated as carefully as possible to be applied to a wider range of SSCVs with the knowledge that the results would not be a complete reflection of reality. While these results were considered sufficient for evaluating a base level of feasibility for each vessel, more base information would allow for a more in-depth analysis of the impact of a hybrid iron powder setup. This includes a look at the impact of crane operations on the stability with a hybrid setup as well as a potential damage stability simulation to provide a more rigorous analysis of the stability of the vessel. More information regarding the performance and output of the existing SSCVs would contextualize the emissions results outside simply the estimated original setup for each vessel. With continuous contact with experts in these fields, it is likely that even more measures of feasibility can be considered to go beyond simply a base level feasibility.

CONTRIBUTION STATEMENT

Erik Scherpenhuijsen Rom: Conceptualization; Investigation, Methodology, Software, Writing – Original Draft, Review and Editing. **Austin Kana:** Conceptualization; Interpretation of data; Supervision; Writing – Review and Editing.

ACKNOWLEDGEMENTS

This work was performed as part of the academic thesis for the lead author, (Scherpenhuijsen Rom, 2023). The thesis was performed in Marine Technology at Delft University of Technology and the authors would like to acknowledge Delft University of Technology for their support of this research.

REFERENCES

Air-Tech System. (2024). Dilute phase pneumatic conveying. Retrieved October 16, 2023, https://www.air-tec.it/enau/pneumatic-conveying-techno

Bergthorson, J. (2018). Recyclable metal fuels for clean and compact zero-carbon power. *Progress in Energy and Combustion Science,* 68, 169-196. DOI: https://doi. org/10.1016/j.pecs.2018.05.001

Dirven, L., Deen, N., & Golombok, M. (2018). Dense energy carrier assessment of four combustible metal powders. *Sustainable Energy Technologies and Assessments*. 30, 52-58. DOI: https://doi.org/10.1016/j.seta.2018.09.003

Hagen, G. (2021). Hydrogen powered propulsion for an offshore crane vessel. *MSc thesis, TU Delft.*

de Kwant, J. (2021). Design implication and performance assessment of iron fuelled ships. *MSc thesis, TU Delft.*

de Kwant, J., Hekkenberg, R., Souflis-Rigas, A., Kana, A.A. (2023). Exploring the potential of iron powder as fuel on the design and performance of container ships. International Shipbuilding Progress. 70, 3-28. DOI: 10.3233/ISP-220012

Lyu, Z. (2016). Concept design of hybrid crane vessel. *MSc thesis, TU Delft.*

Part 5: Ship types, chapter 10: Vessels for special operations. (2021). DNV Rules for Classification. https://standards.dnv.com/explorer/document/DD751DE556864C6DA3C4F24616EF6CB2/26

van Rooij, N., Seijger, V., & Spee, T. (2019). Ijzer als brandstof voor schepen. Maritiem Kennis Centrum.

Scherpenhuijsen Rom, E. (2023) Iron Powder as a fuel on Service Vessels. *MSc thesis. TU Delft.*

Seijger, V.J.T. (2020). High-efficient heat engines for iron-fired power systems. *MSc thesis, TU Eindhoven.*

Proceedings of 15th International Marine Design Conference (IMDC-2024)
June 2-6, 2024
Amsterdam, the Netherlands

Grounded Ambitions: A Lean Approach for Assessing Beachability in Concept Design

Austin Shaeffer, PhD[1],* Sam Murply[1], Tim McIntyre[1], Alex Wiggins[1]

ABSTRACT

Littoral operations have become an increasing interest for defense stakeholders over the last several decades. Many navies currently operate ship-to-shore assets that are designed to travel shorter distances exclusively in the littorals between a ship and the beach. New concepts are being designed to transit much longer distances from shore-to-shore in both blue water and littoral regions. This Concept of Employment (CONEMP) drives these ships to displacements that are orders of magnitude larger. Compared to smaller vessels where seakeeping and maneuverability performance in the surf-zone are a significant area of interest, larger vessels have a comparatively greater risk with respect to the ability of the ship to get far enough up a beach to safely deliver assets and then get off the beach. This research presents the foundation for a new simulation tool to analyze how far up the beach a ship will be able to get given loading condition, initial speed, beach condition, and hull shape. The focus of this research is to provide a low computational-cost method for analyzing the beachability of a ship that still considers the dominating physical phenomena of grounding at early stages of design. The tool will need much faster turnaround times than high-fidelity Reynolds-Averaged Navier-Stokes (RANS) or Finite Element Analysis (FEA) simulations to support the rapid and evolving environment of concept design timelines.

KEY WORDS

Amphibious; Landing; Computational Methods; Ship Concept Design; Beaching

INTRODUCTION

Landing ships and craft play a critical role in delivering people and supplies to areas with limited infrastructure, during both war and peacetime. They have been the vanguard in many operations such as the Normandy landings during WWII, Incheon Bay during Korea, as well as being some of the first on the scene during disaster relief efforts such as during Operation Sea Angel following the 1991 Bangladesh cyclone and Operation Unified Assistance following the 2004 Indian ocean tsunami (Lewis, 2023; Smith, 1995; Tsunami aid: Who's giving what, 2009). Landing ships and craft enabled each of these operations by facilitating the movement of people and supplies in a way that was unachievable by air and ground means. Landing craft remain a major interest to the world's navies, with most major navies having a significant amphibious force in their fleet (Baker, 2023).

Amphibious landing operations conducted by the Allies during WWII often saw the use of Landing Ship Tanks (LST), which were ocean-going ships that would carry heavy equipment such as main battle tanks and smaller landing craft. LSTs could travel long distances in shore-to-shore scenarios, as shown in Figure 1, that smaller landing craft cannot. LSTs were not only important for large amphibious operations, but also for supplying troops in areas with no infrastructure such as the Pacific Islands as shown in Figure 2. The director of the Southwest Pacific forces during WWII, Daniel E. Barbey, said of the LST, "Without these ships there would have been no Southwest Pacific Force. Without these ships the major amphibious invasions of Europe and the Pacific could not have been undertaken" (Barbey, 1969). D-Day, in which over 4,000 landing craft of various types were deployed, was delayed in part due to the required 230 LSTs that were not yet ready, as they were necessary to deploy the five sea assault divisions and heavy armor companies (Koenig & Doerry, 2018).

[1] Naval Surface Warfare Center Carderock Division (NSWCCD) Department 80, Bethesda, Maryland, USA

Submitted: 23 February 2024, Revised: 25 April 2024, Accepted: 1 May 2024, Published: 21 May 2024

Conference paper, DOI: https://doi.org/10.59490/imdc.2024.859 e-ISSN: 3050-4864

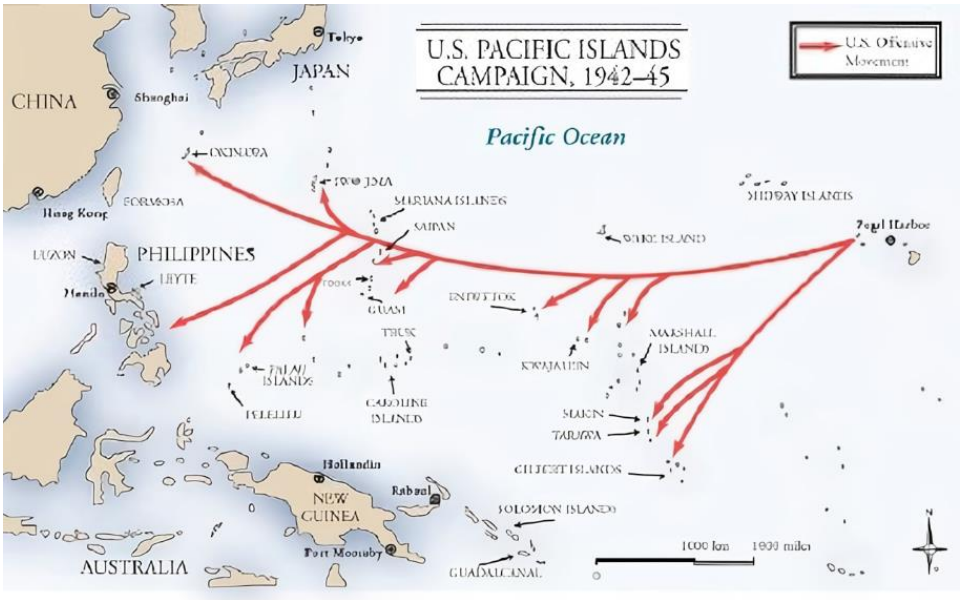

Figure 1: WWII Pacific Island Hopping Campaign (Kuehn, 2015)

Figure 2: LST Unloading Equipment at Iwo Jima (Navy History and Heritage Command, 2016)

Following WWII, changing operational needs drove the amphibious force away from the LST to the Landing Ship Dock (LSD), a type of ship that can carry several coastal, short range landing craft and does not beach itself, unlike the LSTs. The advantages of the LSDs are that they are generally faster than LSTs and can be outfitted for multiple roles when compared to the more restricted LST (Hope, 1991). Across the world, LSDs and LSD type ships like Landing Platform Docks (LPD) and Landing Helicopter Docks (LHD) are either being designed or acquired by many navies due to the flexibility that these types of ships offer (Keane et. al, 2009). The last major LSTs designed by the United States were built in the mid to late 1960s and have since all been decommissioned from the US fleet.

As a result, and demonstrated by the current United States amphibious fleet, most existing vessels that physically land on the beach are small craft like Landing Craft Air Cushion (LCAC), Landing Craft Utility (LCU) and Assault Amphibious Vehicles (AAV) that operate between the larger LSDs, LPDs, and LHDs and the beach. The LCAC, an unconventional landing craft, shown below in Figure 3 has an operation range of 200-300 nm (Naval Sea Systems Command, 2021). The average concept of employment (CONEMP), a use-case-oriented description of a system, for these crafts only necessitates shorter transit distances near the coast. This, in addition to host ship requirements has driven the size of these ship-to-shore

crafts much smaller than the LSTs of WWII. LCUs can be better categorized as boats, generally, due to their operational profile between the coast and host ship (Raunek, 2022). Because boats are generally smaller, a major focus during their design is on performance in a near-beach seaway as the waves can have a significant impact on their ability to safely arrive and land on the beach. This has prompted most of the research and development for landing craft to be focused on small craft with an emphasis on how they handle in the surf zone or very large ships that do not contact the beach directly. For purposes of this paper, large ships will be considered as those that must transit open ocean and usually have a displacement greater than 1000 tonnes.

Figure 3: LCAC Unloading (Naval Sea Systems Command, 2021)

The flexibility of the LSD type ships is not without its drawbacks. Reliance on multiple smaller craft to bring equipment and supplies to the shore functionally limits the missions and quantities the ship can deliver. To overcome this limitation, there has been a push in recent years to develop a larger beaching vessel, operationally similar to the LST that can land heavy equipment as well as transit the open ocean. The ability to perform both of these functions means that a large landing ship will be able to operate independently of ports and landing craft. This falls in line with the concept of the fast moving, self-supplied marine littoral regiment (MLR), which will provide mobility and flexibility for littoral combat operations (U.S. Marine Corps, n.d.). In addition to supporting an MLR, a large landing ship will be able to deliver supplies and troops across the area of operations with minimal infrastructure support and aid the Naval Construction Force (SEABEEs) in establishing infrastructure. An artist's rendering is shown in Figure 4 (Harper, 2022).

Figure 4: Artist's Rendering of Potential Large Landing Ship (Harper, 2022)

Due to the shift towards LSD type ships and small beaching craft, a knowledge gap exists for large, LST-like, landing ship design; which makes the acquisition of these ships particularly high-risk. Additionally, since WWII, ground vehicle weights have increased, with the heaviest vehicles, main battle tanks, increasing from 30.3 tons during WWII, to 61 tons when the

M1 Abrams was first developed, to the massive 75 tons the Abrams is currently (Larson, 2021). This increase in weight creates design challenges in landing these heavy vehicles, posing risk to new landing craft designs. Increased costs and complexities since WWII also means that ships are harder to build and replace, with Fletcher class destroyers costing $102 million in current USD per ship while the Arleigh Burke Flight III costs $1.45 billion per ship (Hill, 2023). Increased cost means that high risk factors, such as beaching ships' ability to get up the beach, need to be more heavily scrutinized in the early design stages.

To address knowledge gaps, larger ship acquisition costs, and increasingly short timeframes, modeling and simulation is being implemented across the ship design space to maximize ship performance regarding mission requirements (Cole, 2022). Modeling and simulation, a capability that didn't exist in a comparable state to the modern era when LSTs were designed, provides a low-cost solution to address potential risks in ship designs. To pare down risk and address the knowledge gaps specific to large landing ship beaching, this paper outlines the theory for developing a simulation tool for the large ship beaching problem.

If there was a tool that filled the knowledge gap identified, it would provide a critical new capability in the ship concept design space. Currently, the impacts of ship design characteristics on hydrodynamic performance, like resistance and seakeeping, are well known. Additionally, there exist an array of available ship design analysis tools to determine the seakeeping and resistance performance of a ship. This is not the case for beaching analysis; therefore, there is a need for development of an analysis method to accurately assess the beaching problem and determine the relationship between ship design characteristics and beaching performance. With a method available to assess beaching characteristics quantitatively, a trade off in performance for these three areas of hydrodynamic design can be determined, driving ship design forward and delivering well rounded ships to complete the specified mission.

Application of this tool in the design spiral paired with beaching Top Level Requirements (TLR) will be a driving factor for hull shaping and displacement. Using provided requirements for the beaching environment, ramp angle, ramp length, and fording depth, a designer would be able to assess bow shaping impacts and determine necessary ship conditions for beaching such as trim and displacement. These discoveries would inform the amount of payload the vessel would be able to carry, the arrangement and amount of ballast tanks to meet a required trim, and the opportune bow shape for a beaching operation. These impacts are critical components of the design of beaching ships and this tool provides a way for ship designers to identify risk and communicate capabilities of concept designs in a quantitative and comprehensive manner.

BACKGROUND

The United States Defense Acquisition Process can be summarized into multiple milestones as shown in Figure 5. Discussion in this paper is pre-Milestone B with a focus on Milestone A, Material Solution Analysis. According to Defense Acquisition University (DAU), "Phase activity will focus on identification and analysis of alternatives, measures of effectiveness, key trades between cost and capability, life-cycle cost, schedule, concepts of operations, and overall risk" (DOD Instruction 5000.84 "Analysis of Alternatives", 2020) During preliminary design, naval architects must deal with several technical challenges with tight timelines and budgets. Despite only 5% of costs being expended in preliminary design, 60%-80% of lifecycle costs are usually determined from decisions made in this stage. Visually, this is demonstrated in Figure 6. Being able to perform analysis early in the design process is a necessary way to buy down risk and lower program costs (Gaspar, 2011).

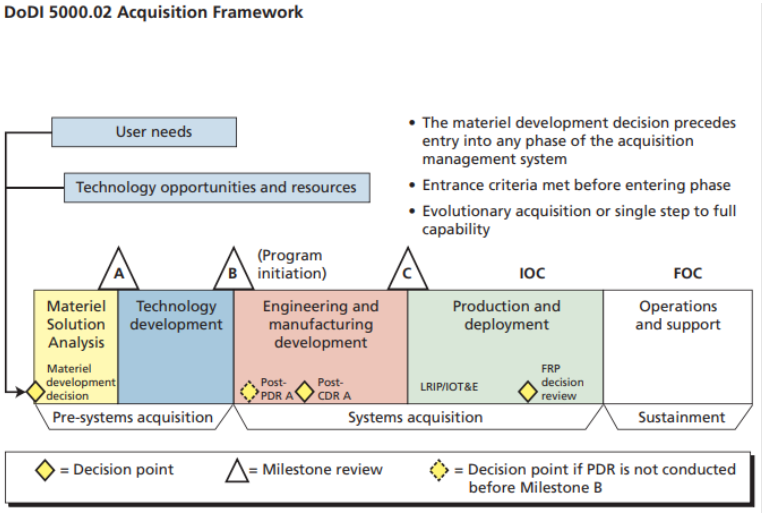

Figure 5: Defense Acquisition Lifecycle (Drezner, et al., 2011)

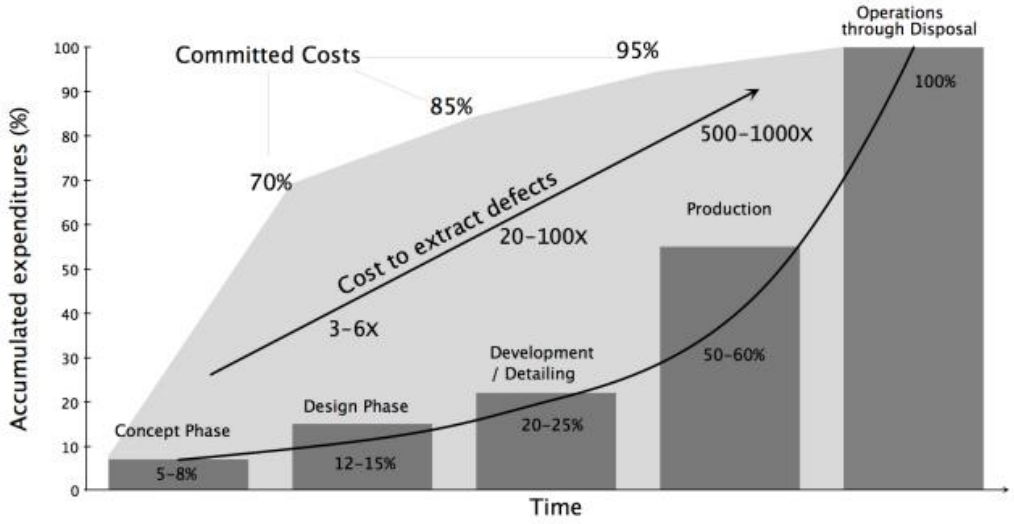

Figure 6: Overall Ship Cost by Milestone (Gaspar, 2011)

Due to the numerous, interrelated aspects of ship design, naval architects often refer to the design process as the design spiral shown in Figure 7 (Gaspar, 2011). Starting very broad and assessing one aspect of the design at a time, the design should eventually converge to meet requirements. It is expected that as the design changes, setbacks will occur, and specific aspects of the design will need to be assessed multiple times. For example, as displacement increases, draft increases and resistance on the hull form must be re-assessed. If resistance increases too much, larger engines must be selected to meet speed requirements, which will again increase displacement and have additional impacts on ship performance and cost. To add more complications, requirements at this stage of design are often fluid and design teams must adapt quickly and be flexible to these changes.

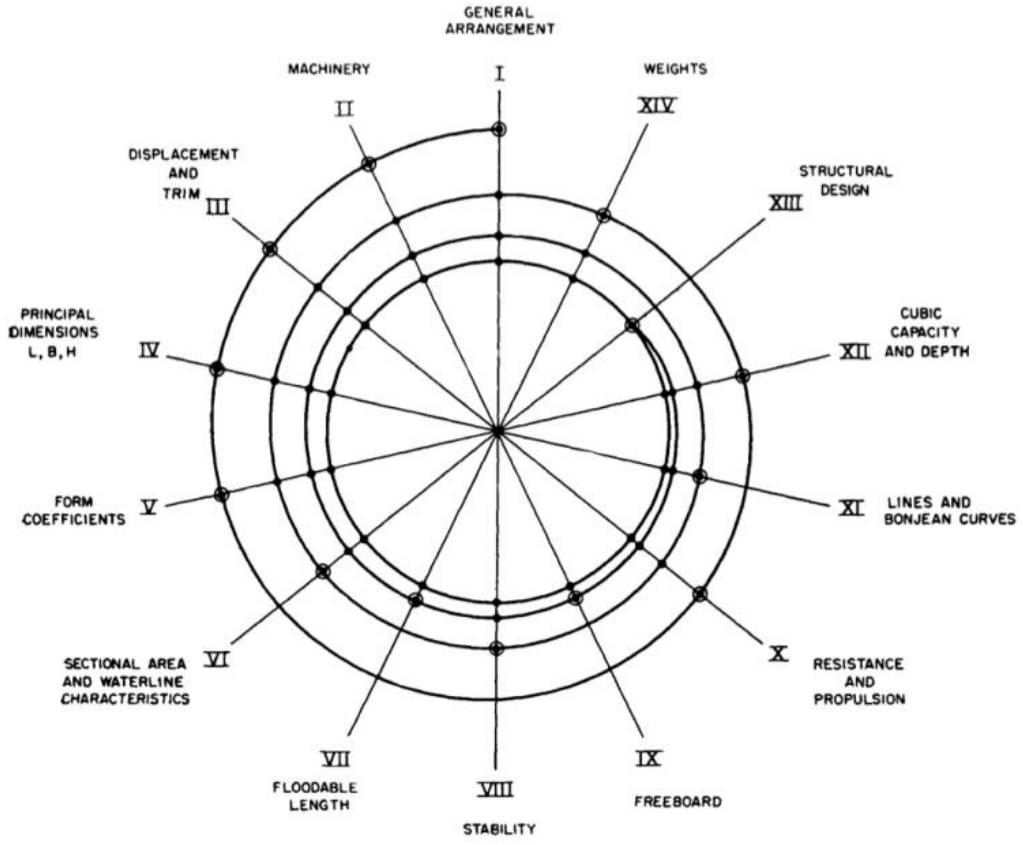

Figure 7: Ship Design Spiral (Gaspar, 2011)

Concept design makes up various aspects of the solutions analysis and concept refinement steps shown in Figure 8 (Schank, et al., 2014). Project durations often range from small 3-month excursions to large multiyear efforts. Each type of project having its own complexities and complications. In comparison to other design stages, this is a relatively short period of time for a ”typical” USN ship design cycles shown in Figure 9. Examples of the work naval architects do include integration studies, Analysis of Alternatives (AoAs), Requirements Evaluation Teams (RETs), and full ship concept designs sometimes referred to as indicative designs. During the CVX AoA, roughly 70 ship studies were developed and evaluated (Raber & Perin, 2000). The magnitude of these design programs creates a dire need for tools to deliver fast, accurate results. Fortunately, developments in recent years have made analysis in many areas of ship design quite agile. In the example of an AoA, it is necessary for technical experts to have the ability to assess several designs against Key Performance Parameters (KPPs). Design Space Exploration (DSE) is another growing area of interest in naval architecture in which a full range of parameters are varied in order to study a wider scope and gather quantifiable data to inform decisions (Robertson, et.al., 2022). DSE is increasingly valuable in situations when there may be design bias or a lack of clarity in requirements. An effort conducted at Naval Surface Warfare Center (NSWC) Carderock Division generated 2,916 individual hull forms to evaluate the impacts of varying hull characteristics on resistance, stability, and seakeeping (Strickland, Devine, & Holbert, 2018). Doing such analysis on hull shape provides valuable insight as to the preferred design for resistance, seakeeping, or other metrics such as beachability. This makes DSE yet another use case for a beaching tool that is capable of accurate results and short run times. The concept design environment can be fluid, fast paced, and often necessitates naval architects to be able to quickly run analysis, often with turnaround times less than 24 hours, or against hundreds to thousands of design points. Although concept design is a small portion of the overall ship design life cycle, it informs and drives the rest of the cycle, making it a critical step in ship acquisition.

Notional Durations of Acquisition Phases for Naval Ships

Phase	Duration (years)
Solutions analysis	1 to 3
Concept refinement	2 to 4
Design and build	4 to 7
Testing and trials	1 to 2

Figure 8: Notional Acquisition Durations for USN Vessels (Schank, et al., 2014)

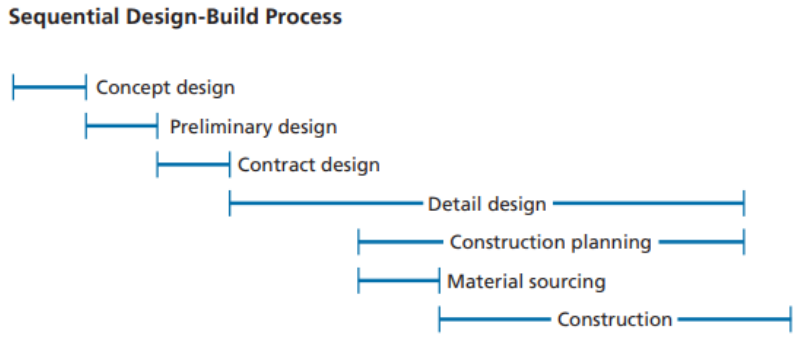

Figure 9: Ship Design Lifecycle (Schank, et al., 2014)

As mentioned previously, a majority of the beaching vessels currently in service are small craft (less than 1000 tons displacement) that can be carried by larger ocean-going ships. Extensive research has been done and is currently being executed to characterize the performance of these craft. The University of Iowa with the support of the Office of Naval Research (ONR) has recently executed research on surf zone dynamics and beachability of a small, single operator, craft called Quadski in which they experimentally and numerically defined the dynamics of the craft while beaching (Behra, 2020; Yamashita, et al. 2022). The Quadski work considers both the hydrodynamic and ground reactions when analyzing craft dynamics, with both interactions being major focuses of this paper. However, since the Quadski is small compared to the operational environment, there is a major concern with the seakeeping capabilities of the craft. It also has wheels that enable the craft to more easily get up a beach. This means that a majority of the research, has been allocated to the hydrodynamic reactions of the craft with respect to waves in the near-beach zone. In addition, the grounding work that has been completed uses a coupled CFD-MBD (computational fluid dynamics, model based definition) approach to define

ground reactions, which is computationally expensive and complex. As shown in Figure 10, this approach requires a well-defined mesh that is recalculated at every time step to account for soil deformation, driving up computation costs. The same group also worked on a lower fidelity solution which uses data from higher fidelity models to drive outputs, however this means large changes in the design will require additional simulations with the high-fidelity model (Yamashita, et al., 2023). Since concept design often requires significant design changes, this approach is not a viable method. In summary, due to high computational costs, long set up and run times of high-fidelity codes, as well as a heavy focus on seakeeping, small craft beaching research is not applicable to pre-Milestone B applications or for scaling to larger ship sizes.

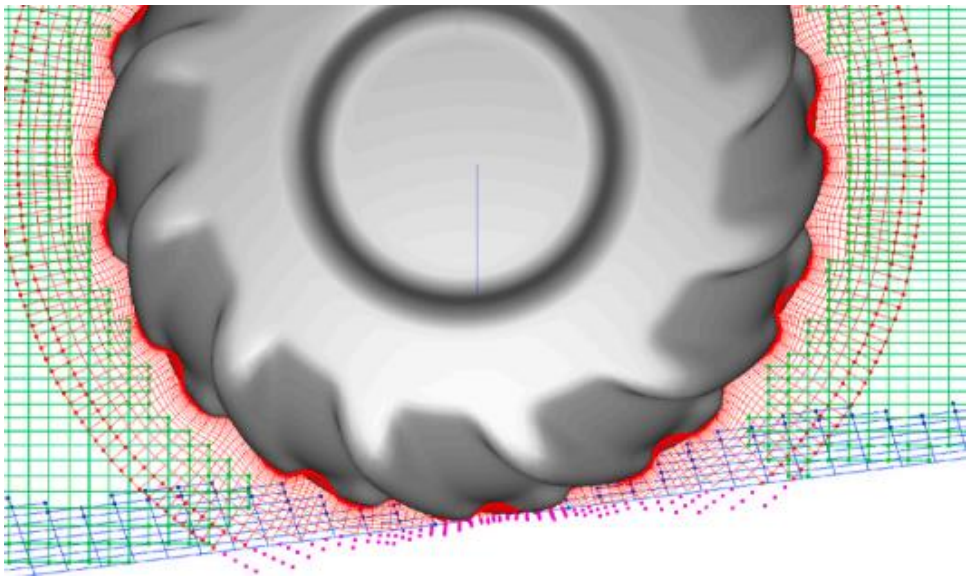

Figure 10: Boundary Mesh of the Wheel of the Quad Ski (Yamashita, et al., 2022)

Separate work has been done to characterize the deformation of saturated soil using LS-DYNA, a commercial structural deformation code that has large material libraries and experimental validation, making it ideal for quick simulation development (Flores-Johnson, et al., 2016). However, these studies and LS-DYNA solve material interactions on the grain scale, which leads to high computational costs and heavy reliance on user knowledge for setup (Flores-Johnson, et al., 2016; Sturt, et al., 2021). It has been used in applications of saturated sand deformation, making it applicable to the beaching problem, however, LS-DYNA does not calculate hydrodynamic interactions making it difficult to use in landing vessel applications (Flores-Johnson, et al., 2016). Additional research has been done on the effects of ship-structure interactions on larger commercial ships; generally, regarding the effect of grounding of the ship or the effect of a ship striking an offshore platform. Many of these studies used Finite Element Analysis (FEA) approaches within LS-DYNA to quantitatively define the effect of ship strikes on the sea floor as well as offshore platforms (Nguyen, et al., 2011; Yu, et al., 2016). Like other LS-DYNA codes, the main issue with these methods is that they require long setup times, large amounts of computational resources, and high user expertise, making them unsuitable for a concept design problem. Research done by Hansen, et al. (1995) attempted to define how far a ship will travel up a beach during grounding. They utilized a pressure method to calculate soil reaction, which was experimentally verified as shown in Figure 11. (Sterndorff & Pedersen, 1996). This method, while less computationally complex than LS-DYNA, still required a significant amount of computational resources and would require additional experimental data to support the analysis of vessels with other than simple, conventional bows.

Figure 11: Full Ship Grounding Experiments Conducted by Sterndorff & Pederson (1996)

In other technical disciplines related to naval architecture, there are concept design tools, such as Total Ship Drag (TSD) for resistance prediction and Ship Motion Program (SMP) for seakeeping evaluation, that allow naval architects to evaluate concepts rapidly (Wilson, et al., 2011). These concept design tools, while physics-based, generally have less fidelity than some of the more computationally intensive tools, however, they provide a reference point to compare multiple designs and inform the stakeholder on the best path forwards. These tools have quick setups and run times, which make them appealing for the fast-paced environment in pre-Milestone B work, but lack both accuracy and flexibility compared to more expensive solutions.

TSD is a low-fidelity tool that provides resistance predictions within seconds by reducing the physical problem using potential flow and Thin Ship Theory assumptions. A critical component of TSD that makes it well suited for early stage design work is that it is relatively easy to use. For example, the simulation is relatively insensitive to the input mesh, removing the need for sensitivity studies and allowing for reduced set up times. The low-cost of TSD make this tool ideal for evaluating a large trade space of concepts. The validation of TSD explains that TSD, "does a good job of providing quick and reasonably accurate evaluations for typical US Navy hull forms." (Wilson, et al. 2011).

The studies previously mentioned have demonstrated that there is work being done to evaluate beaching in a high-fidelity environment, however, there is a need for beaching analysis programs equivalent to TSD. Only one known method exists for evaluating beaching in a low fidelity realm: a quasi-static state solution, solving an energy balance equation. Based on a paper written by Pedersen (1995), this method considers a two phased approach in which; the first phase considers a ship with velocity V contacting a sloped beach and trims about a prescribed contact point until the ships trim is equal to the beach slope, and a second phase that considers the hull to then slide up the beach with the entire keel in contact with the beach. The second phase is only entered in this calculation if there is kinetic energy remaining after the ship reaches the trim of the beach. This model is limited in that the flat sloped beach is considered to not deform. This limits the effect of the beach on the ship to a simple frictional force in accordance with Amontons-Coulumb law, using a constant kinetic friction coefficient, μ (Pedersen, 1995).

The major limitations of this method are: the two phased quasi-static approach, and the severely limited consideration of hull shape on beach deformation. The quasi static approach limits the actions to large time-step phases where the physics is simplified using different methods in each phase. In both phases, this method ignores the interactions between the relevant physical features. For example, any translation of the hull up the beach as it rotates about its contact point in phase I is neglected. Additionally, ignoring hull shaping would reveal the same result for two hulls approaching the beach with the same velocity and mass, one having a broad blunt bow with a bulb and another with a skinny sharp bow, so long as they had the same contact point. Considering the large scale impacts of bow shaping on other hydrodynamics, like fluid resistance, this is a major problem that the current strategy overlooks and severely limits designers' ability to compare beaching results across a trade space of differing hulls, a common activity in pre-Milestone B. Therefore, ignoring the deformation of sand is an overly-broad simplification of the interaction and has resulted in low confidence in the results. Additionally, no validation of this method has ever been performed. Given this evaluation method, any engineer would be ill prepared to answer the questions they are currently being asked.

PROPOSED APPROACH

Language like beaching, beachability, or grounding are all terms that need definition before proceeding. For the purposes of this paper, beaching and grounding are synonymous in defining the act of a vessel impacting, riding up on, and embedding into a beach. This maneuver is intentional and a critical part of the prospective vessel's CONEMP. This does not include accidental grounding (i.e. a sandbar). Beaching and grounding start when the hull, likely to be near the intersection of the bow and keel, contacts the beach and ends when the vessel comes to a static equilibrium. Beachability is a qualitative measure of how reliably and safely a ship can deliver a payload from ship to shore.

Beachability is generally, quantitatively measured as an achievable fording depth or required ramp length or angle. Factors, such as the final position of a ship after beaching can be used to inform ramp design or evaluate against current ramp characteristics. Ramp angle defines the angle from the horizontal that the ramp contacts the beach. Ramp length defines how far, in any dimension, the ramp can extend from the hinge point. Fording depth represents the distance from the point where the ramp contacts the beach to the water free surface. This functionally represents the maximum depth of water the payloads will encounter during the beaching operation. Different payloads will have different requirements for each of these criteria. For example, vehicles with large separation between axels might have a minimum ramp length or maximum ramp angle to prevent chassis contact with the hinge point of the ramp. Other payloads might have fording depth requirements like vehicles, which cannot have their exhaust stacks submerged otherwise they risk down flooding into the engine. Additionally, ramp length, ramp angle, and fording depth can have significant impacts on the duration of the beaching mission, which can be a critical component of performance.

Assumptions

The proposed tool will consider a simplification of the physics of beaching to reduce runtime to fit within the discussed concept design framework. The considered physics include: kinetic energy transformed to potential energy from the vessel moving up the beach, energy losses from deformation of the beach, and other hydrostatic losses. These aspects of the physics have to take into account hull shape. The problem needs to be solved as a time series to capture the simplified physics to capture small changes in the state of the ship and the interaction of these changes over time. The theoretical assumptions that are taken to reduce the computational complexity of this problem are listed below. Should future Verification and Validation (V&V) efforts determine that any of these assumptions have significant detrimental impacts on the simulation, modifications will be made to remove or modify that assumption.

- The origin will be at the intersection of the stem and the waterline when the ship contacts the beach with the positive X axis traveling away from the bow of the ship. That means the stern will be at a negative length from the origin at t = 0. The Y axis will be 0 on the centerline, negative to port and positive to starboard. This assumes that the contact point is on the centerline. The Z axis travels from keel to weather deck with Z=0 at the waterline. The coordinate system can be seen in Figure 12.

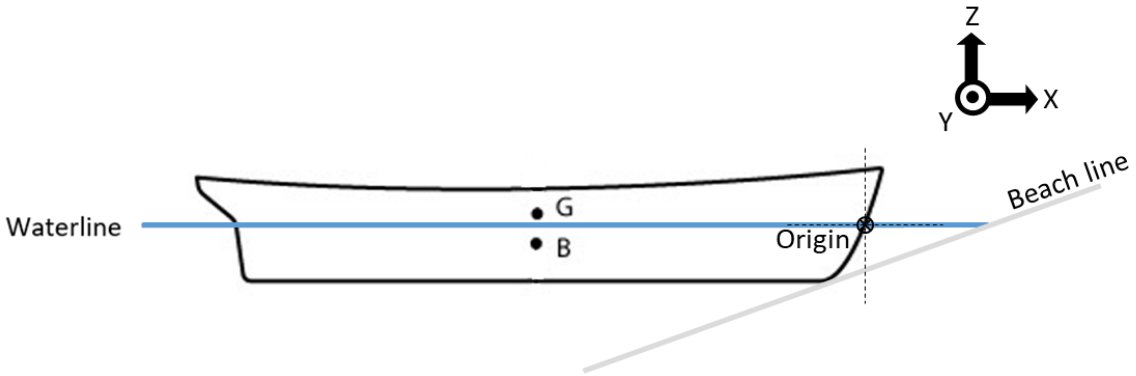

Figure 12: Coordinate System for beach modeling

- Sand is treated as a dense fluid with no viscous impacts on the simulation;
- Buoyant force from the beach acts normal to the beach surface;
- Sand friction will be calculated as a solid-on-solid interaction;
- Beach surface is a flat plane with a specified slope about the Y axis;
- Representative beach geometry will not undergo deformation as simulation progresses;
- Displaced sand moves vertically and once it is moved it is no longer considered in the simulation;
- C_F, coefficient of wetted frictional drag, is calculated via the ITTC ‘57 equation (Zubaly, 1996);
- C_r, coefficient of wetted residual drag, will be provided via external, supplementary analysis;
- Shallow water effect can be ignored at reasonably low speeds;
- Water is calm, environmental and ship generated waves can be ignored;
- Ship is not powered forward after contact with the beach;
- Ship motion is restricted to three degrees of freedom: surge, trim, and heave;
- Ship will rotate about a traditionally calculated center of flotation (CF);
- This simulation will occur ignoring the effects of a third fluid, being air.

The primary objective of this model is to consider the interaction of the hull form with the beach. Simplification of the beach definition, deformation, and interaction with the hull will be critical to the design purpose of this tool. Modeling the true physics of sand that can become saturated due to fluid interactions with the hull is an unreasonable problem to solve with current technology due to the sheer amount of interactions (Goodman, 2017). The proposed solution is to use first principles and basic definitions of fluids and solids interactions to reduce the complexity of the problem.

While a major component of the hull-beach interaction is the displacement of sand, capturing the true mechanics of this would likely require complex and computationally expensive meshes like the one shown in Figure 10. In order to account for the beach deformation in a computationally feasible manner, the beach will be assumed to be a dense fluid and be in a

constant shape and location. As a fluid, there is a simple computation to determine the normal force from the beach. This assumption is supported in a paper by Kang in Equation 1 which relates the buoyant forces (F_{ZB}) of granular media to, ρ, density of sand, g, gravity, and V, volume of displaced sand. This relation is reliant on an experimentally determined coefficient, K (Kang et al 2018). This assumption allows a computationally efficient method for accounting for the normal force caused by the beach.

$$F_{ZB} = K\rho gV \qquad \text{Equation [1]}$$

A difficult component of treating the sandy medium as a fluid is that it would complicate the computation of frictional force between the beach and the hull. The classic computation of force, shown in Equation 2, requires an empirically determined coefficient (Zubaly, 1996). A literature review reveals that no coefficients of frictional drag for a sandy beach handled as a fluid exists. Additionally, existing research has proven that the friction of a solid and a saturated granular medium adheres to the Amontons-Coulumb law which requires a direct relation of the quantity of frictional to the normal force on the medium. (Divoux & G'eminard, 2007). For these reasons, it is assumed the most reasonable approach to calculate the frictional force of the beach on the hull as if they act as solids. This assumption not only supports the Amontons-Coulumb law but also allows this simulation to utilize existing empirically derived frictional coefficients of sand which are only relevant for the solid-on-solid interaction.

$$Force = \frac{Coefficient * Density * Surface\ Area * Velocity^2}{2} \qquad \text{Equation [2]}$$

An additional complicated component of the beach problem is how to define the beach geometry, particularly complicated by handling the sandy beach as it acts as both a fluid and a solid. In order to simplify the problem, initial geometry of the beach is assumed to be a flat plane at an average slope representative of the desired operational area. This assumption seems reasonable considering beach topography changes relatively rapidly overtime when compared to acquisition timelines, and therefore modeling specific beach geometry is unnecessary, and computationally costly. It is known that as the hull displaces sand, some will rise above the presumed surface of the beach. This deformation would be influenced by the topography of the beach. If the beach is assumed to be flat then it must also be assumed that the sand is dissipated after it is deformed. With these assumptions, a geometrically varied and physically complex composite material is simplified to three inputs; a coefficient of friction, C_f, a beach slope, θ, and density, ρ_B.

While the physics of the interaction between the hull and the beach are considered primary in this simulation, the hydrodynamic and aerodynamic physics are considered secondary. Considering the relatively slow speeds associated with the beaching mission and the relatively large size of the ships of focus, fluid dynamic impacts are assumed to not be critical to consider to a high level of fidelity. Air resistance and wind heeling is assumed to be reasonably small, and can be ignored. Additionally, hydrodynamic effects and problems are generally complicated to implement and expensive to run. Assuming forward approach speeds, V_0, are less than roughly 5 knots, it should be reasonable to assume that hydrodynamics associated with forward speed and momentum can be neglected or simplified. For the purposes of calm water resistance, it is assumed that the coefficient of residual drag is constant throughout the simulation. With the availability of reliable resistance tools, residual resistance or C_r, will be provided externally for a single initial speed condition. Frictional fluid resistance or C_F will be approximated with the ITTC '57 equation. Sinkage due to sea floor interactions will be neglected at this level of detail due to a lack of inexpensive and reliable computational methods and for consistency with the already neglected seafloor topography.

As discussed at length in the background and introduction to this paper, the majority of recent research prior to this study has been invested in the interaction of small bodies in near-beach surf zone waves. Previous studies underline how difficult the seakeeping problem in the surf-zone is to simulate. In order to simplify the proposed simulation presented in this study, it is assumed that the ships used in this model are reasonably large (i.e. less than 1000 tonnes) to ignore significant wave-induced motions. Additionally, it is assumed that wave-induced motions do not have significant impacts on the final location of the ship with respect to the beach. Neglecting seaway-induced motions enables the simulation to be fixed in roll, sway, and yaw which offers additional computation cost savings and is relevant since the beach and hull geometry are assumed to be symmetric across centerline, y=0.

Proposed Solution

The backbone of this beachability tool is a time-domain solution, executed as a series of computations at discrete steps through time and space. The tool will be implemented in python in a modular format such that future levels of detail and fidelity could be easily added, based upon need and resources.

The hull form will be modelled as a coarse surface mesh and the fluid free surface will be modelled as a z-plane at location z=0 with the hull located such that the baseline is at the given load condition waterline. The code will begin at time = 0 and i=0 at the moment of impact with i being the time iterator and time being a scalar in seconds. The hull form will move forward in the x-direction through the stationary free surface (water) and into the static beach surface. At each time step the transformation of kinetic energy, KE_i, will be determined as follows in Equation 3, until the ship reaches zero kinetic energy. Based on Equation 4, the ship will have achieved a static condition, zero velocity, on the beach at this final iteration.

$$KE_i = KE_{i-1} - \Delta PE - W_w - W_B - W_D \quad \text{Equation [3]}$$

$$KE_i = (m_s * v_i^2)/2 \quad \text{Equation [4]}$$

KE_i will be determined as the remainder of kinetic energy at each iteration after considering the change in potential energy, ΔPE, as defined in Equation 5, work done on the wetted hull by water, W_w, as defined in Equation 6, work done by the friction with the beach, W_B, as defined in Equation 7, and work done by deforming the beach medium, W_D,as defined in in Equation 8. The change in potential energy will be variable with respect to the heave, z, of the ship at each time step with respect to the constants gravity, g, and ship mass, m_s.

$$\Delta PE = PE_i - PE_{i-1} = m_s * g * (z_i - z_{i-1}) \quad \text{Equation [5]}$$

$$W_w = \left(\frac{\rho_w * SA_w * v_i^2 * C_T}{2}\right) * \Delta x \quad \text{Equation [6]}$$

$$W_B = (m_B * g * C_f) * \Delta x \quad \text{Equation [7]}$$

$$W_D = W_{DZ} = \mathrm{m}_{Bk} * g * \Delta z_{Bk} \quad \text{Equation [8]}$$

Work done by the water, as defined in Equation 6 is the force caused by the fluid multiplied by the distance the ship travelled in the direction of the resisting force, Δx. The resistance on the hull caused by the fluid is proportional to the fluid density, ρ_w, wetted surface area, SA_w, velocity, v_i, and the coefficient of total drag, C_T. The wetted surface area, SA_w, will be computed at each iteration. The coefficient of total drag is a summation of residual, C_r, and frictional, C_F, coefficients of drag per Equation 9. As stated in the assumptions, the residual coefficient of drag will be provided by an external simulation. The frictional coefficient of drag will be computed via the ITTC '57 approximation in Equation 10 which related C_F to the Reynolds number, Re, defined with respect to length on waterline, LWL, ship velocity, v_i, and dynamic viscosity, μ, as defined in Equation 11 (Zubaly, 1996).

$$C_T = C_r + C_F \quad \text{Equation [9]}$$

$$C_F = \frac{0.075}{\log(Re - 2)^2} \quad \text{Equation [10]}$$

$$Re = \frac{(v_i * LWL)}{\mu} \quad \text{Equation [11]}$$

Work done by the friction with the beach, W_B, will be calculated as a coefficient, C_f times a normal force in Equation 7. The normal force is assumed to be equal to the weight of the vessel that the beach will support. Based on the assumption that the sandy beach acts as a dense fluid, this weight is being determined using the assumption that the deformed beach provides a buoyant force according to Archimedes principle (Kang et. al, 2018). This force will be determined at each times step via Equation 12, mass of the displaced beach, m_B, times gravity. The calculation of m_B can be seen in Equation 12 where ρ_B is the density of sand and ∇_B is the volume of displaced sand.

$$m_B = \rho_B * \nabla_B$$ Equation [12]

As stated in the assumptions, deformation of the beach will not be explicitly modelled geometrically, however the simulation will still consider the work done in the act of moving the displaced sand. To approximate this deformation work, W_D, the change in potential energy of the displaced sand will be determined at each iteration via Equation 8. The mass of sand that is displaced, m_{Bk}, will be determined at each time step as the difference in the total mass of the beach the ship displaces from the previous time step as explained by Equation 13. In order to determine the change in potential energy of the sand a segmented approach will be used, iterating over the mass, m_{B_k}, and calculating the vertical distance Δz_{Bk} required for that mass to be entirely above the beach plane as show in Figure 13.

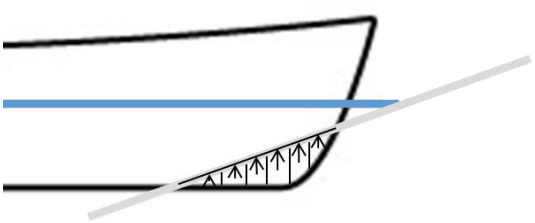

Figure 13: Sand Displacement

$$m_{B_k} = m_{B_i} - m_{B_{i-1}}$$ Equation [13]

Expanding and transforming Equation 13 by inserting Equations 4, 5, 6, 7, and 8 results in Equation 14. This allows Equation 3 to be rewritten in terms of v_i in Equation 14. This equation represents the proposed total energy conservation considered at each time step during the simulation. An additional system of equations will be required at each time step to determine the location in space of the hull form as it pitches and heaves. The pitch and heave of the hull will be calculated with a moment and force balance equations, Equation 15 and Equation 19 respectively. The moment balance equation, Equation 15, requires the sum of the moments caused by the buoyant force from the water, $m_w d_w$, buoyant force from the beach, $m_B d_B$, and the weight of the ship, $m_s d_g$ to equal zero. It is assumed that the sum of the mass of displaced water, m_W, and the mass of displaced sand, m_B, is equivalent to the mass of the ship, m_s as shown in Equation 19. It is assumed that the ship exclusively rotates around the center of floatation, CF_x, with the moment arms d_w, d_B, and d_g calculated as the difference between the center of action and the center of floatation in Equation 16, Equation 17, and Equation 18. The center of action for buoyancy due to water and beach are determined to be the center of volumes, x_{wCV} and x_{BCV} respectively. The center of action of the mass of the ship is the center of gravity, CG_x, and is a required input to the simulation.

$$v_i = \sqrt{\frac{2}{m_s} * \left(\frac{m_s * v_{i-1}^2}{2} - m_s * g * (z_i - z_{i-1}) - \left(\left(\frac{p_w * SA_w * v_{i-1}^2 * C_T}{2}\right) + \left(\mathrm{m}_B * g * C_f\right)\right) * \Delta x - \left(\mathrm{m}_B * g * (z_{Bk} - z_{Bk-1})\right)\right)}$$ Equation [14]

$$\sum M_{CF} = 0 = m_w d_w - m_s d_g + m_B d_B$$ Equation [15]

$$d_w = x_{wCV} - CF_x$$ Equation [16]

$$d_B = x_{BCV} - CF_x$$ Equation [17]

$$d_g = CG_x - CF_x$$ Equation [18]

$$\sum F_z = 0 = (m_s - \mathrm{m}_w - \mathrm{m}_B) * g$$ Equation [19]

Algorithms and Methods

The initial information required at the start of the simulation at which point the ship has just initiated contact with the beach and i=0, is listed below. The hull geometry is proposed to be a coarse surface mesh in the form of a PLY file. CAPSTONE, a HPCMP CREATE product can easily create simple surface meshes, from many of the classic geometry file types used in naval architecture. PLY is accepted in python mesh libraries Trimesh and VEDO (Haggerty, et al., 2019) (Musy, et al., 2021). These open source python libraries are proposed for handling mesh intersections. Working in python allows for plug-ins to the Leading Edge Architecture for Prototyping Systems (LEAPS) tool suite (Shaeffer, et al., 2020). Longevity of tools in the concept design space rely on integration with existing products or projects. Python is a well-known language commonly used in the naval architecture realm, therefore, generation of a python based tool will allow for integration in many existing projects.

Inputs:

- Coarse Hull Surface Mesh
- Ship Velocity (v_0)
- Ship Loading Condition
- Density of Water
- Beach Slope
- Density of Sand
- Coefficient of Friction of Sand

The proposed processes for the simulation are discussed below with the aid of flow charts in Figure 15 and Figure 16. These flow charts follow the color based key in Figure 14. Blue rectangles represent information that discuss inputs or conditional changes. Yellow squares use a calculation that is either represented by an equation in this paper or a query mesh intersections. Red triangle is a decision, evaluating against a criteria, typically in the form of an IF statement. Green ellipse represent output information.

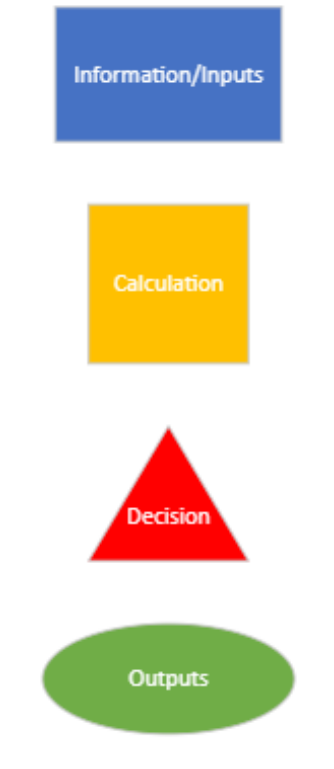

Figure 14: Flow Chart Key

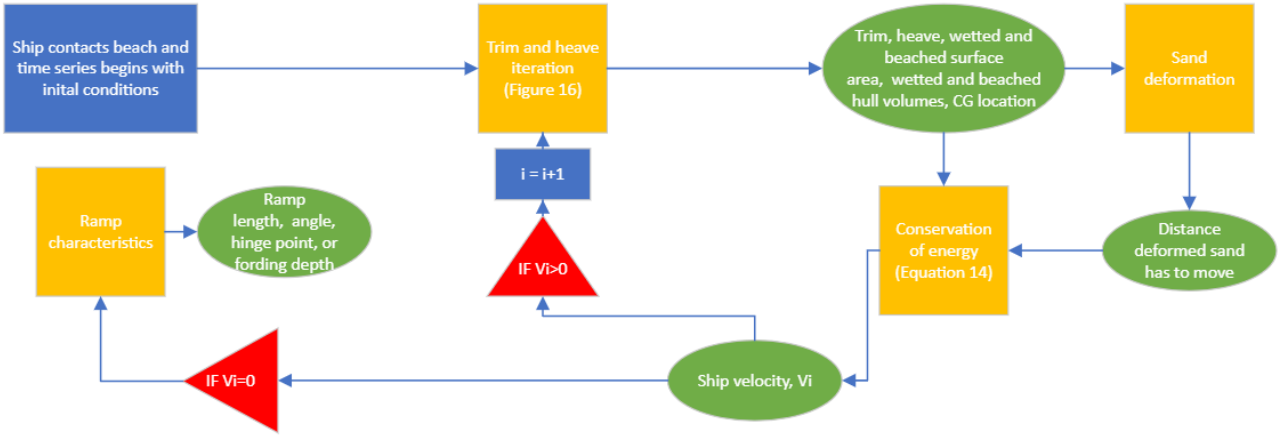

Figure 15: Beaching Tool Flow Chart

The objective of this simulation is to output ship position when ship reaches a static condition. The simulation will iterate over time and space to determine ship velocity, v_i, and hull position at each time step until the ship comes to a static equilibrium, $v_i = 0$, which is represented in the bottom left red triangle in Figure 15. Given this information, ramp characteristics and beachability can be determined easily. At the start of each time step, the new hydrostatic condition of the ship is calculated based on the workflow in Figure 16. Given the updated hydrostatic condition, change in velocity at each step is calculated via the conservation of energy given in Equation 3 and Equation 14. The simulation will continue to iterate until the ship velocity approaches very near to zero and is assumed to have met a static equilibrium.

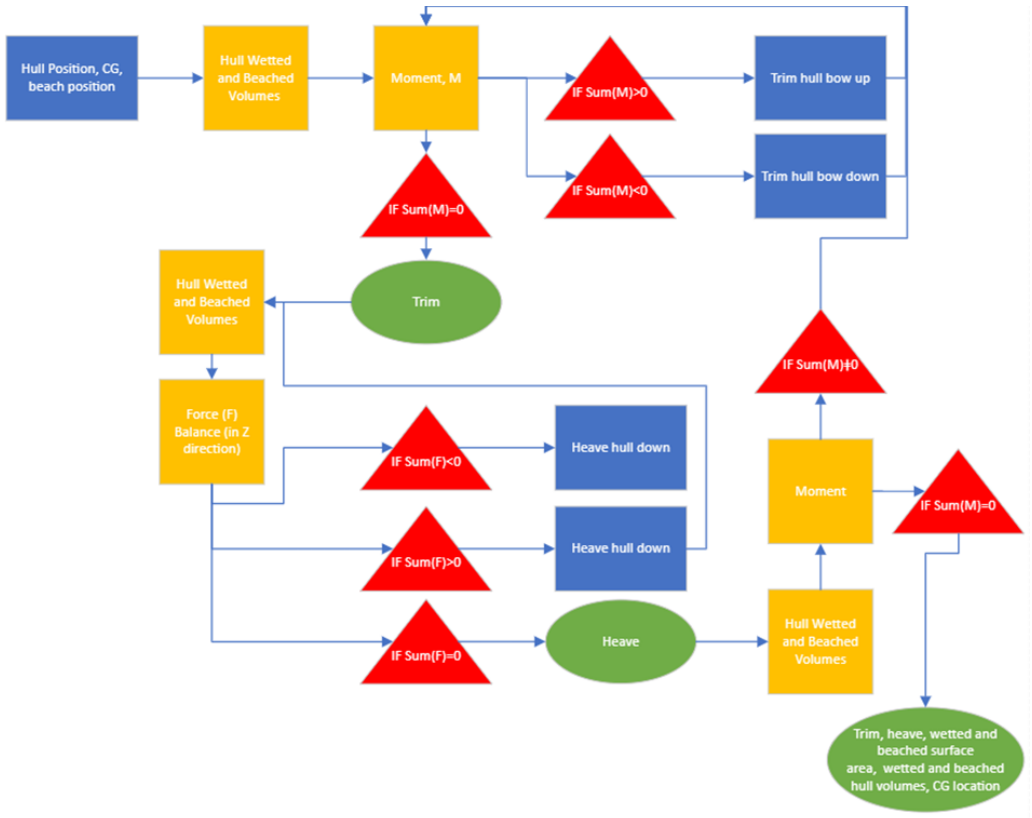

Figure 16: Trim and Heave Iteration Flow Chart

Separate trim and heave iterations occur at every time step. These loops are separate, but also dependent. This can be seen after the output of the force iteration returning to a moment calculation box on the right in Figure 16. The result is an iterative solution towards determining the ship's hydrostatic condition at each time step. In order to reduce computational time, the step size used in the iterative solution will be adaptive, dependent on how far the solution is from equilibrium. A critical component of this calculation is that the hull geometry directly drives the outcome which is a notable improvement over existing state-of-the-art beachability analysis in early-stage design discussed previously.

Following the flow chart in Figure 16, starting in the top left, these loops require information about the hull geometry, beach surface, wetted surface, and hull characteristics. The tool queries the mesh intersections to calculate wetted and beached volumes. The beached volume can be seen in yellow in Figure 17 and 18. Multiplying these volumes by their respective densities and distances to the center of rotation, CF, gives a moment balance equation seen in Equation 15. The assumed convention is a counterclockwise moment with the ship approaching the beach from the left being positive as seen in Figure 17. It is clear that a positive moment results in bow up trim and a negative moment results in bow down trim. The force and resulting moment are predicated on treating sand as a dense fluid that acts a buoyant force on the hull through the beached volumes centroid (Kang, et al. 2018).

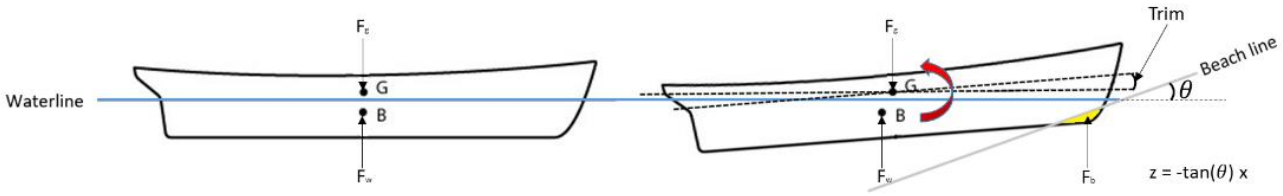

Figure 17: Trimming Moment

The trim angle will be adjusted as shown in the top right of the flow chart in Figure 16 until the moment is balanced, within a given tolerance, to zero using Equation 15. The updated trimmed position will provide new wetted and beached volumes to the force calculation in the middle of Figure 16. Equation 19 will then balance the forces in the z direction. With a positive force convention being up, if the force is positive the hull will experience positive heave and, if negative, negative heave. These heaving forces are shown in Figure 18. After $\sum F_z \approx 0$, the moment is calculated once more. If $\sum M \approx 0$ the hull mesh is queried.

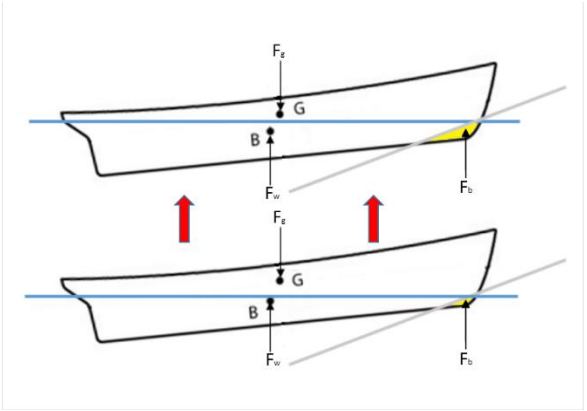

Figure 18: Heaving Force

CONCLUSIONS

As discussed in this paper, beaching has had a long and critical history in navies under taking amphibious operations around the globe. Delivering reinforcements and resources is vital to successfully providing disaster relief and maintaining a forward position in war. Both large and small beaching vessels are necessary to accomplish this during times when port infrastructure is contested or not available. Following WWII, the focus regarding beaching has shifted toward smaller craft. However, due to advances in technology and an uncertain warfighting environment, much is unknown as to the needs of the future. Looking objectively at the current amphibious fleet, a lack of knowledge in the areas of large beaching ships has been identified. This gap is aimed to be addressed through the development of a low fidelity beaching analysis tool.

With such a tool, naval architects will be able to quickly and accurately assess risk and costs associated with designing a large beaching ship. For the development of this tool, a first principals' approach has been taken to develop a time-series based simulation using conservation of energy. In order to evaluate a bounded and simplified trade space, the critical physical components of the beaching problem needed to be identified and fully considered. The interactions that will be evaluated or simplified in this tool are primarily focused on the beach-ship problem. Confirmation of these simplifications and assumptions is difficult due to a lack of Subject Matter Experts (SMEs) in the beaching domain problem and existing body of knowledge. Specifically, little research has been aimed at the hull form and beach interaction problem compared to the seaway induced motions problem. Due to the lack of available expertise, a verification and validation (V&V) effort

will be required to provide confident use of this tool within ship acquisition frameworks. As previously noted, decisions made early in the design, especially at the preliminary design stage, can ultimately determine the future success of a ship acquisition program.

Future work

The effort to develop the simulation discussed in this paper is intended to be completed by the end of FY24 (September 2024). A validation effort is planned to begin in late FY24 and completed in FY25. Due to a lack to higher fidelity simulation data, model testing is being pursued. Utilizing modeling expertise at NSWC Carderock Division and partnership with the model test basin at the Engineering Research and Development Center (ERDC) (ERDC Overview, n.d.), testing results can be obtained which a beaching tool should be able to emulate within some tolerance. Planning for this level of model testing began in early Calendar Year (CY) 24. Scaling as well as other unidentified topics are of concern and will be addressed as planning is refined and resources and time are available.

Additionally, future efforts aim at considering developmental improvements to the simulation based on time and resources. There are two notable features which have been identified. Firstly, the development of a method to objectively assess and compare the beachability of different concepts and enable automated design space exploration. The primary measure for beachability is the ability of the ship in its beached position to deliver its payload to the beach. This payload can vary depending on CONEMP. Different types of payloads have different requirements usually revolving around fording depth, ramp angle, and ramp length. These ramp characteristics that will enable objective assessment of beachability are included in the flow chart in Figure 15 with the path once v_i = 0 is satisfied. The approach is to find the intersection of a ramp line, starting at the hinge point with slope of ramp angle, and beach line, with the beach slope. Then, the vertical distance from the waterline to that intersection point has to be measured and reported as the fording depth. This final calculation has not been discussed as part of the current effort of the tool. This information is critical to the beaching design problem and can be calculated external to the tool, based on the solved final ship position. Integration in the tool is intended to reduce additional steps, total time, and errors.

Secondly, since these ships eventually need to extract themselves from the beach, it would be useful to integrate both beaching and extraction into the same tool. There are two possible methods for a vessel to get off the beach: under propeller load, utilizing the assistance of kedge anchors, or a combination of both. The force that the propeller and kedge anchor must overcome to get off the beach will be a result of wetted drag from water, skin drag from beach, etc... This will require additional investigation, however, it is likely to have an overlap with planned capabilities within the base version of the tool.

In later developments of the tool, adding options for specifying ship thrust throughout the simulation, seaway conditions, and beach approach angle are all areas of interest. In practice, many beaching vessels continue to generate thrust from the propellers after impact with the beach in order to increase the distance they can travel up the beach. In order to assess this, additional sources of power will need to be included in the energy balance. For seaway conditions and approach angles, a 6 degree of freedom (DOF) analysis will be required and assumptions of symmetry will have to be overcome. This adds more complexity to the simulation, however, is not unusual for tools to offer both 3-DOF and 6-DOF analysis options. This will be further considered and researched as development continues.

Rather than just adding additional features, future developments will also attempt to improve fidelity while retaining rapid assessment capability. This means exploring other potential simplifications and existing theory, such as resistive force theory (RFT) to achieve more defined ground reaction forces. RFT is a theory that uses linear superposition of experimental results to generate lift and drag forces on a body independent of the body's orientation (Zhang & Goldman, 2014). The advantage of using RFT for this project is that it can be computationally inexpensive while still being relatively high fidelity since it relies on experimental data to drive responses. Additionally, there are many well documented sources about its use in different environments since the theory was developed in the 1950's (Marcotte, 2016). There are a few potential disadvantages of RFT. It has only been used to predict interactions at very low Reynolds numbers (Re ~ 10^{-2}), beaching will mostly occur at higher Reynolds numbers (>Re ~ 10^{5}) so it will need to be explored if RFT can be reasonably scaled up (Rodenborn, et al., 2013, Zubaly, 1996). Most RFT tools also require experimental testing to quantitatively determine the reactions of the granular material and that is an expensive and lengthy process. Some work has been done to empirically define these reactions which may be useful for this project (Marcotte, 2016). RFT is just one of many potential methods for improving fidelity that could be explored. Hopefully, this paper will encourage conversation and gather attention from experts in the field with knowledge of other applicable theories. Truly and accurately solving the beaching problem could have wide impacts and will require collaboration from various disciplines beyond naval architecture.

REFERENCES

Altenburger, S., Bosworth, M., & Junge, M. (2013). A Landing Craft for the 21st Century. *U.S. Naval Institute, 139*(1,325).

Baker, S. (2023, August 6). *The World's Most Powerful Navies in 2023, Ranked*. Retrieved from Buisness Insider: https://www.businessinsider.com/most-powerful-navies-in-world-in-2023-ranked-ships-submarines-2023-8

Barbey, D. E. (1969). MacArthur's Amphibious Navy Seventh Amphibious Force Operations 1943-1945. Annapolis: United States Naval Institute.

Behara, S. A. (2020). Experimental and computational study of operation of an amphibious craft in calm water. *Ocean Engineering, 209*. doi:107460

Cole, C. (2022, May 5). *The Benefits of Integrating Simulation into the Ship Design Process*. Retrieved from Seimens: https://blogs.sw.siemens.com/marine/2022/05/05/the-benefits-of-integrating-simulation-into-the-ship-design-process/

Coussot, P. (2014). Yeild Stress Fluid Flows: A Review of Experimental Data. *Journal of Non-Newtonian Fluid Mechanics, 211*, 31-49. Retrieved from www.sciencedirect.com/science/article/abs/pii/S0377025714000895O

Divoux, T., & G'eminard, J. (2007). Friction and Diliatancy in Immersed Granular Matter. *Phys. Rev. Lett., 99*(25). Retrieved January 8, 2024

DOD Instruction 5000.84 "Analysis of Alternatives". (2020).

Drezner, J. A., Arena, M. V., McKernan, M., Murphy, R., & Riposo, J. (2011). *Are Ships Different? Policies and Procedures for the Acquisition of Ship Programs.* National Defense Research Institute. Retrieved from https://apps.dtic.mil/sti/pdfs/ADA552682.pdf

ERDC Overview. (n.d.). Retrieved from US Army Corps of Engineers, Engineering Research and Development Center Website: https://www.erdc.usace.army.mil/About.aspx

Flores-Johnson, E., Wang, S., Maggi, F., Abbas El-Zein, G. Y., Nguyen, G. D., & Shen, L. (2016). Discrete Element Simulation of Dynamic Behaviour of Partially Saturated Sand. *International Journal of Mechanics and Materials in Design, 12*, 495-507. doi:10.1007

Gaspar, H. M. (2011). *Handling Aspects of Complexity in Conceptual Ship Design.* NTNU Open.

Goodman, L. (2017, August 7). *The Physics of Sand*. Retrieved from Brandies Now: https://www.brandeis.edu/now/2017/august/sand-jamming-chakraborty.html

Haggerty, D., a, b, c, d, e, & f. (2019). Trimesh 4.0.5. Retrieved from https://trimsh.org/

Hansen, N.-E. O., Simonsen, B. C., & Sterndorff., M. (1995). Soil Mechanics of Ship Beaching. *Coastal engineering*. Retrieved from https://doi.org/10.1061/9780784400890.219

Harper, J. (2022, Febuary 9). *Navy Wants Agile Family of Logistic Ships.* Retrieved from National Defense Magazine: https://www.nationaldefensemagazine.org/articles/2022/2/9/just-in-navy-wants-agile-family-of-logistics-ships

Hill, J. (2023, September 7). *US Navy discloses cost of its order for ten new Arleigh Burke destroyers*. Retrieved from Naval Technology: https://www.naval-technology.com/news/us-navy-discloses-cost-of-construction-of-flight-iii-arleigh-burke-destroyers/

Hope, J. P. (1991, July 1). Naval Force Levels: Theory and Practice, with Naval Engineering Challenges for the 1990s. *Marine Technology and SNAME News, 28*(04), 224-235. doi:https://doi.org/10.5957/mt1.1991.28.4.224

Kang, W., Feng, Y., Liu, C. *et al.* Archimedes' law explains penetration of solids into granular media. *Nat Commun* 9, 1101 (2018). https://doi.org/10.1038/s41467-018-03344-3

Keane, R. G., Mcintyre, J., Fireman, H., & Maher, D. J. (2009, June 1). The LPD 17 Ship Design: Leading a Sea Change Toward Collaborative Product Development. *Naval Engineers Journal, 121*(2), 15-61. doi:https://doi.org/10.1111/j.1559-3584.2009.00189.x

Koenig, P., & Doerry, N. (2018, June 6). Naval Shipbuilding Expansion: The World War II Surface Combatant Experience. *SNAME Maritime Convention.* Providence: SNAME. Retrieved from Navy Times.

Kuehn, J. T. (2015). The war in the Pacific, 1941-1945. In *The Second World War* (pp. 420-454). Cambridge University Press. Retrieved from Island Hopping: https://wwtwointhepacific.weebly.com/

Landing Craft, Mechanized and Utility - LCM/LCU. (n.d.). Retrieved from Navy.mil: https://www.navy.mil/Resources/Fact-Files/Display-FactFiles/Article/2171588/landing-craft-mechanized-and-utility-lcmlcu/

Landing Ship, Dock (LSD)/ Amphibious Transport, Dock (LPD). (2023, December 2023). Retrieved from Global Security: https://www.globalsecurity.org/military/systems/ship/ld.htm

Larson, C. (2021, April 14). *Too Fat to Fight: M1 Abrams has a Weight Problem*. Retrieved from National Interest: https://nationalinterest.org/blog/reboot/too-fat-fight-m1-abrams-has-weight-problem-182670

Lewis, A. R. (2023, March 20). *Landing Ship Tank*. Retrieved from Encyclopedia Britannica: https://www.britannica.com/technology/landing-ship-tank

Ma, X., Wang, G., Lui, K., Chen, X., Wang, J., Pan, B., & Wang, L. (2022). Granular Resistive Force Theory Extension for Saturated Wet Sand Ground. *Machines, 10*(9), 721. doi:10.3390

Marcotte, B. (2016, September 29). *'No more magic' in predicting how objects move through sand, other terrain*. Retrieved from University of Rochester: https://www.rochester.edu/newscenter/model-makes-it-easier-to-predict-force-needed-to-push-objects-through-sand-and-other-materials-182152/

Musy, M., a, b, c, d, & f. (2021). Vedo, a Python Module for Scientific Analysis and Visualization of 3D Objects and Point Clouds. *Zenodo*. Retrieved from Zenodo: 10.5281/zenodo.2561401

Naval Sea Systems Command. (2021, October 14). *Landing Craft Air Cushion*. Retrieved from Navy.mil: https://www.navy.mil/Resources/Fact-Files/Display-FactFiles/Article/2170004/landing-craft-air-cushion-lcac/

Navy History and Heritage Command. (2016, January 19). *National Museum of the U.S. Navy*. Retrieved from Battle for Iwo Jima, February 19, 1945.: https://www.history.navy.mil/content/history/museums/nmusn/explore/photography/wwii/wwii-pacific/iwo-jima/us-marine-landing/80-g-304825.html

Nguyen, T.-H., Amdahl, J., Leira, B. J., & Garrè, L. (2011). Understanding ship-grounding events. *Marine Structures, 24*(4), 551-569. Retrieved from https://doi.org/10.1016/j.marstruc.2011.07.001

Pedersen, P. (1995). *Collision and Grounding Mechanics.* Denmark: Technical University of Denmark.

Raber, J. D., & Perin, D. A. (2000, May). Future USN Aircraft Carrier Analysis of Alternatives. *Naval Engineers Journal, 112*(3), 15-25. Retrieved from https://doi.org/10.1111/j.1559-3584.2000.tb03300.x

Raunek. (2022, Novemeber 20). *7 Differences Between a Ship and a Boat*. Retrieved from Marine Insight: https://www.marineinsight.com/types-of-ships/7-differences-between-a-ship-and-a-boat/

Robertson, N., McNabb, J., Balchanos, M., Sudol, A., & Mavris, D. (2022). A Design Decision-Support Environment for Evaluating the Impact of Ship Technologies. *14th International Marine Deisgn Conference*. Vancouver: SNAME. doi:https://doi.org/10.5957/IMDC-2022-353

Rodenborn, B., Chen, C.-H., Swinney, H. L., Liu, B., & Zhang, H. P. (2013, January 14). Swimming driven by a Helical Flagellum. *PNAS, 110*(5), 338-347. doi:https://doi.org/10.1073/pnas.1219831110

Schank, J. F., Arean, M. V., Kamarck, K. N., Lee, G. T., Birkler, J., Murphy, R. E., & Lough, R. (2014). *Keeping Major Naval Ship Acquisitions on Course.* National Defense Research Institute. Retrieved from https://www.rand.org/content/dam/rand/pubs/research_reports/RR700/RR767/RAND_RR767.pdf

Shaeffer, A., Wilson, W., & Yang, C. (2020). Application of Machine Learning to Early-Stage Hull Form Design. *SNAME Maritime Convention.* Virtual: SNAME.

Smith, C. R. (1995). *Angels from the Sea.* U.S. Government Printing Office.

Sterndorff, M. J., & Pedersen, P. T. (1996). Grounding experiments on soft bottoms. *Journal of Marine Science and Technology, 1*(3), 174-181. Retrieved from https://doi.org/10.1007/bf02391177

Strickland, J., Devine, T., & Holbert, J. (2018). A Design Space Generation Approach for Advance Design Science Techniques. *International Marine Design Conference.*

Sturt, R., Cengiz, C., Huang, Y., Go, J., Bandara, S., & Pillai, A. (2021). Modelling liquefaction of soils with LS-DYNA using a SANISAND-based material model. *13th European LS-DYNA Conference.* Ulm: DYNAmore GMBH. Retrieved from https://www.researchgate.net/publication/355155315_Modelling_liquefaction_of_soils_with_LS-DYNA_using_a_SANISAND-based_material_model

Tsunami aid: Who's giving what. (2009). Retrieved from BBC NEWS | Asia-Pacific |: http://news.bbc.co.uk/2/hi/asia-pacific/4145259.stm

U.S. Marine Corps. (n.d.). *Marine Littoral Regiment (MLR)*. Retrieved from United States Marine Corps Flagship: https://www.marines.mil/News/News-Display/Article/2708146/marine-littoral-regiment-mlr/

Wilson, W., Hendrix, D., Noblesse, F., & Gorski, J. (2011). Validation of Resistance Predicitons Using Total Ship Drag.

Yamashita, H., Arnold, A., Carrica, P. M., Noack, R. W., J. Ezequiel Martín, S. H., & Harwood, C. (2022). Coupled multibody dynamics and computational fluid dynamics approach for amphibious vehicles in the surf zone. *Ocean Engineering, 257*. doi:111607

Yamashita, H., Martin, J. E., Sugiyama, H., Tison, N., Grunin, A., & Jayakumar, P. (2023). Predicting Vehicle Motion in Shallow Water with Data-Driven Hydrodynamixs Model.

Yu, Z., Shen, Y., Amdahl, J., & Greco, M. (2016). Implementation of Linear Potential-Flow Theory in the 6DOF Coupled Simulation of Ship Collision and Grounding Accidents. *Journal of Ship Research, 60*(3), 119-114. doi:10.5957

Zhang, T., & Goldman, D. (2014). The effectiveness of resistive force theory in granular locomotion. *Physics of Fluids, 26*(10). Retrieved from https://doi.org/10.1063/1.4898629

Zubaly, R. (1996). Ship Resistance. In *Applied Naval Architecture* (pp. 238-271). Atglen, PA: Cornell Maritime Press.

Proceedings of 15th International Marine Design Conference (IMDC-2024)
June 2-6, 2024
Amsterdam, the Netherlands

Modernisation of Domestic Ro-Ro Passenger Ships Operating in the Philippines

D. Vassalos[1,*], D. Paterson[2], F. Mauro[2] and A. Salem[2]

ABSTRACT

This paper forms part of a wider study in the form of a Formal Safety Assessment of the domestic passenger ships operating in the Philippines, undertaken on behalf of the Philippines Government, and financed by the World Bank and the International Maritime Organisation. The paper focuses on design deficiencies of the domestic RoPax ships, primarily in damage stability. The process of ship selection for representation of the wider fleet risk assessment is explained, leading to one medium RoPax and one large RoPax, typical of some 500 of these ships, serving the open sea domestic trade in the Philippines. To this end, the selected designs have been subjected to a systematic process of damage stability and flooding risk analysis in order to identify design vulnerabilities, leading to risk estimation in the form of Potential Loss of Life. A number of risk control options have then been identified, enabling a thorough risk assessment and identification of cost-effective RCOs, as well as impact assessment, using IMO risk acceptance criteria as basis. Despite the poor state of the domestic Ro-Ro passenger vessels operating in the Philippines, many of these aged, badly retrofitted, poorly maintained, and operated, it has been possible to identify cost-effective design solutions to raise the damage stability (and safety) standard of these ships to international standards of newly designed ships; it seems an unprecedented achievement, but evidently true. This presents the Philippine Government and the owners of these vessels with a unique opportunity to upgrade their domestic fleet of RoPax vessels and showcase these against the best in the world. Because of the similarity in the approach, the selection of risk control options and the overall analysis adopted, only one of the typical RoPax vessels selected is presented in this paper.

KEY WORDS

Domestic Ro-Ro Passenger Ships; Damage Stability Failure; Flooding Risk; Cost-effective Risk Control Options

INTRODUCTION

One way of ensuring that action is taken before a disaster occurred is to use a process known as a Formal Safety Assessment (FSA, MSC-MEPC.2/Circ.12/Rev.2.). This has been described as "a rational and systematic process for assessing the risks associated with shipping activity and for evaluating the costs and benefits of IMO's options for reducing these risks.". Such options have invariably been extended to other stakeholders (Flags, Administrations, Class, Shipyards and Ship operators), aiming at identifying cost-effective solutions to improve the safety standards of existing ships and new buildings. As the nature of this undertaking is highly technical, it is vitally important that the proposed solutions in the form of recommendations are properly communicated to ensure that all stakeholders gain sufficient information at a level that is readily understood to support effective decision-making (Vassalos et al., 2022a). One way to achieve this is by comparing proposed changes with existing standards, targeting life-cycle implications (design, operation, emergencies) to enable a balance to be drawn between technical and operational issues, including the human element as well as between safety (Delta Risk) and cost (Delta cost) in the implementation of the proposed recommendations (Goerlandt, F. & Montewka, J., 2015, Puisa et al., 2021).
This paper focuses on describing the process of assessing the risk (Aven, 2012, 2022), as well as identifying and implementing cost-effective solutions for the design of new ships or for retrofitting existing ships (Vassalos et al., 2021,2022b) to achieve

[1] Maritime Safety Research Centre, Department of Naval Archiecture, Ocean and Marine Engineering, University of Strathclyde. Glasgow, Scotland, UK
[2] Sharjah Maritime Academy, Khorfakkan, UAE

Submitted: 23 February 2024, Revised: 29 April 2024, Accepted: 1 May 2024, Published: 23 May 2024

Conference paper, DOI: https://doi.org/10.59490/imdc.2024.877 e-ISSN: 3050-486

higher safety standards with focus on the highest risk contributor, as previously identified, namely inadequate damage stability and the ensuing risk to human life (Vassalos, 2012). To this end, following a ship selection process of representative ships from the whole fleet currently engaged in domestic voyages in the Philippines, three ships have been selected, namely (a) a small motor banca; (b) a medium-sized modern RoPax and (c) a large older design RoPax. In this paper, only the two latter categories are being addressed. The process of risk analysis and risk assessment is detailed, the latter providing a cost-benefit assessment to aid decision-making in the Risk Control Options (RCOs) selection, practical implementation, and impact.

ADOPTED METHODOLOGY FOR FLOODING RISK ESTIMATION

Survivability Assessment

The methodology adopted in the FSA Philippines project, has been tailored to cater for flooding risk estimation (using different risk metrics), pertinent to static assessment and statutory requirements, leading to risk-informed performance in relevant conditions and environments. This, in turn, facilitates the design and implementation of pertinent RCOs to prevent, mitigate and control flooding risk in domestic passenger ships and is comprised of eight distinct phases, as elaborated in the following and shown in Figure 1. The process begins by addressing damage stability assessment based upon conventional hydrostatic techniques (Bulian et al., 2016, Ruponen et al., 2019, Mauro & Vassalos, 2022). Such assessment is conducted in accordance with applicable IMO statutory instruments, which vary depending on vessel age, type, and size. When assessing new build vessels engaged in international voyage, this relates to the requirements of either SOLAS 2009 (IMO, 2009) or SOLAS 2020 (IMO, 2020), as applicable. This form of assessment enables a quantifiable baseline risk level to be established from which the impact of RCOs can then be measured and compared (Vassalos et al., 2022b). Unfortunately, a great deal of existing ships and domestic vessels are regulated based on older prescriptive regimes, with an implicit but not explicitly quantifiable safety level. This is by using the Index of Subdivision (A-Index) as the risk metric to facilitate comparisons in the attained "risk" level and for evaluation of various design options to enhance ship damage stability. This means that the choice of risk control options is somewhat shaped by the elements of assumption, generalisation and simplification that are commonplace within technical standards.

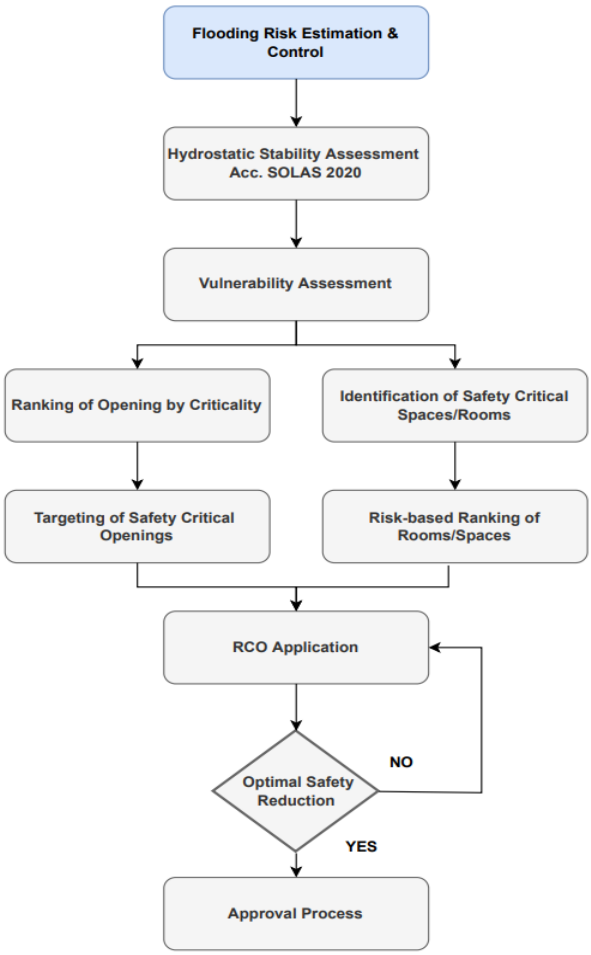

Figure 1: Methodology Adopted

Risk Assessment

Building upon the developments in risk models over the past 30 years, a generic risk quantification process and modelling is presented in this section, geared towards domestic passenger ships operating in the Philippines. In this respect, a generalised way of considering flooding risk in the form of Potential Loss of Life (pertinent to design evaluation; hence PLL Attamed, PLL_A) is given in equations [1] and [2], with a description in Figure 1.

$$PLL = Probabilty \times Consequence \quad [1]$$

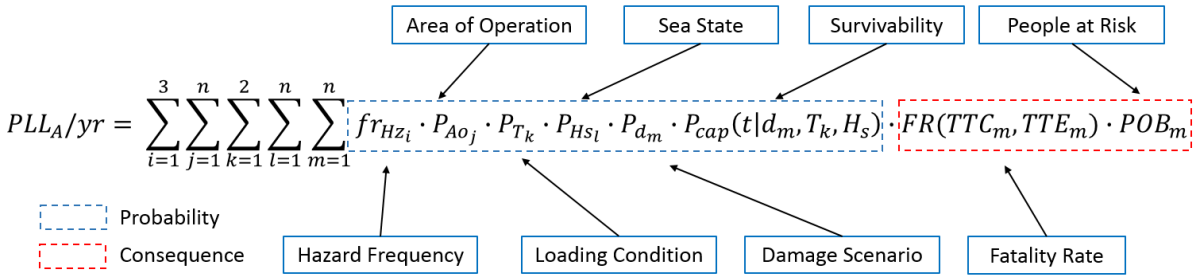

Figure 1: Description of Risk Estimation (PLL) Components

$$PLL_A/yr = \sum_{i=1}^{3}\sum_{j=1}^{n}\sum_{k=1}^{2}\sum_{l=1}^{n}\sum_{m=1}^{n} fr_{Hz_i} \cdot P_{Ao_j} \cdot P_{T_k} \cdot P_{Hs_l} \cdot P_{d_m} \cdot P_{cap}(t|d_m, T_k, H_s) \cdot FR(TTC_m, TTE_m) \cdot POB_n \quad [2]$$

Where,

i	denotes hazard (1=collision, 2=side grounding, 3=bottom grounding from the accident database devethe undertaking of this project
j	denotes area of operation (e.g., open sea, restricted, port)
k	denotes loading condition for the 3 SOLAS drafts (D_L D_S D_P)
l	denotes the 99th percentile of Hs pertinent to the area of operation
m	denotes a particular damage scenario up to the nth scenario of the sample
$FR(TTC_m, TTE_m)$	denotes Fatality Rate for each loss modality (transient, progressive, failure criteria, e.g., IMO/ITTC capsize criteria)
POB_m	denotes persons on board (people at risk) at each scenario
PPL_A/yr	denotes Potential Loss of Life per year of exposure at each scenario; hence PLL for life cycle needs to account for years, duration in service and POB in each.

For singular values of the variables i, j, k, l, m, (i.e., at scenario level) equation [2] becomes:

$$\frac{PLL_A}{yr} = hazardfequency\ x breach\ frequency\ x\ capzize\ probability\ x\ fatality\ rate\ x\ PoB \quad [3]$$

The process itself and the various terms depicted in Eq. [2] are expanded upon in the following.

Flooding Risk Quantification – Input Data and Parameters

Sample ships – Initial ship data and preliminary analysis

The first item considered in analysing domestic passenger fleet data pertaining to the Philippines, has been to observe the fleet demographics in terms of ship type and age, as shown in Figure 3.

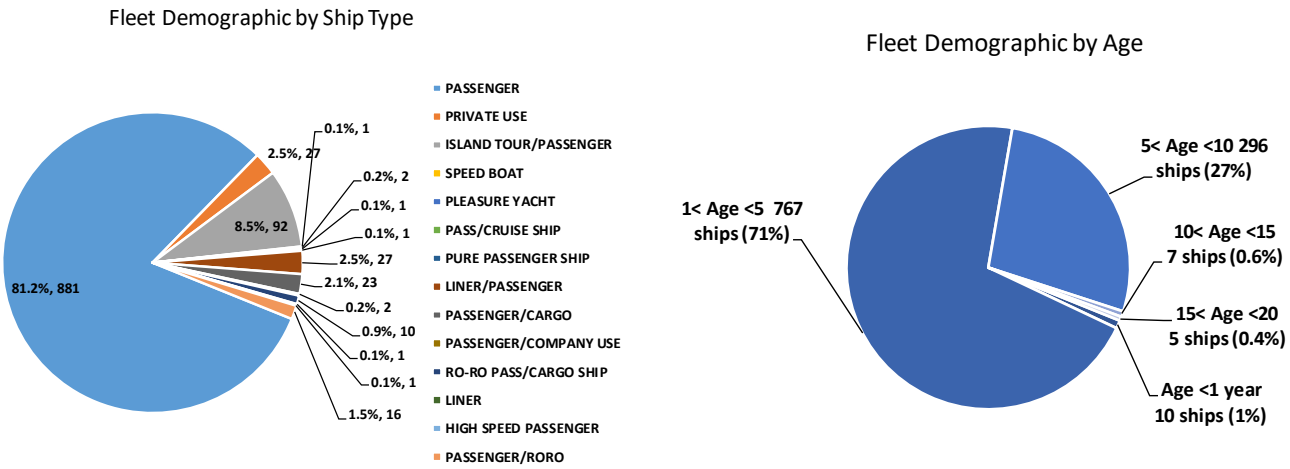

Figure 2: Ship Demographics by Ship Type and Ship Age

Here, the following key observations can be made:

- 93% of the fleet is less than 100 GT;
- 98% of the fleet is less than 1,000 GT;
- 37% of the fleet is less than 10 m length;
- 83% of the fleet is less than 20 m length.

In addition, the domestic passenger vessel fleet has also been analysed in terms of PAX capacity, Gross Tonnage and Length, as shown in Figure 3, Figure 4 and Figure 5.

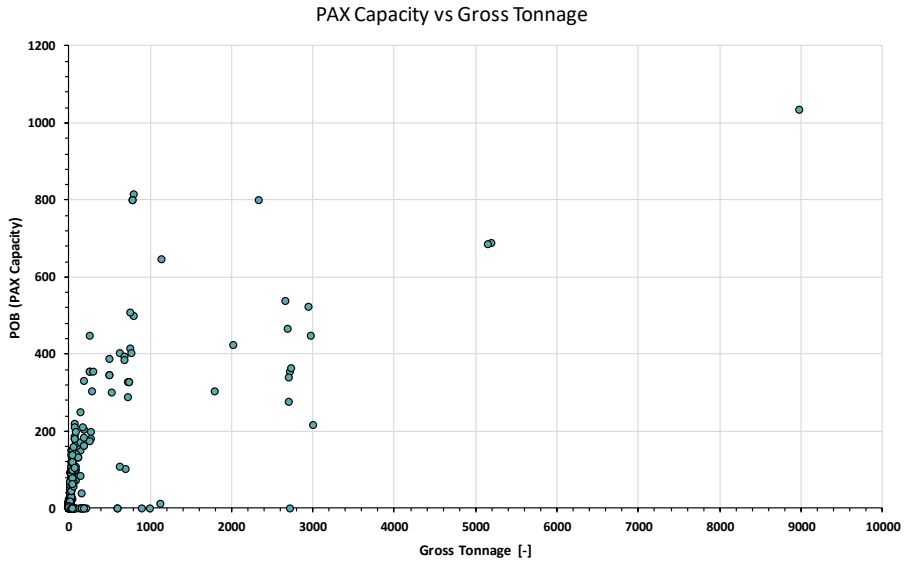

Figure 3: Fleet at Risk – PAX capacity Vs Gross Tonnage

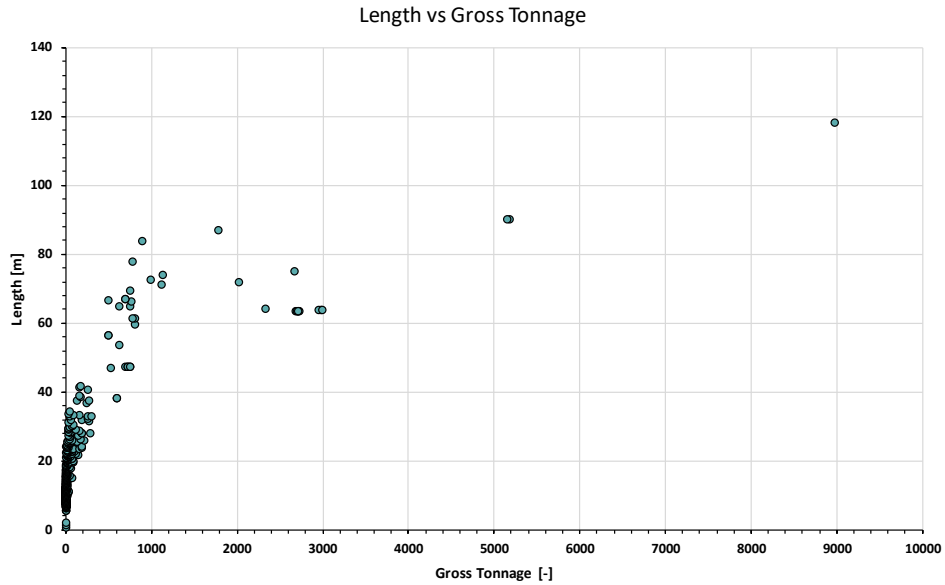

Figure 4: Fleet at Risk – Length Vs Gross Tonnage

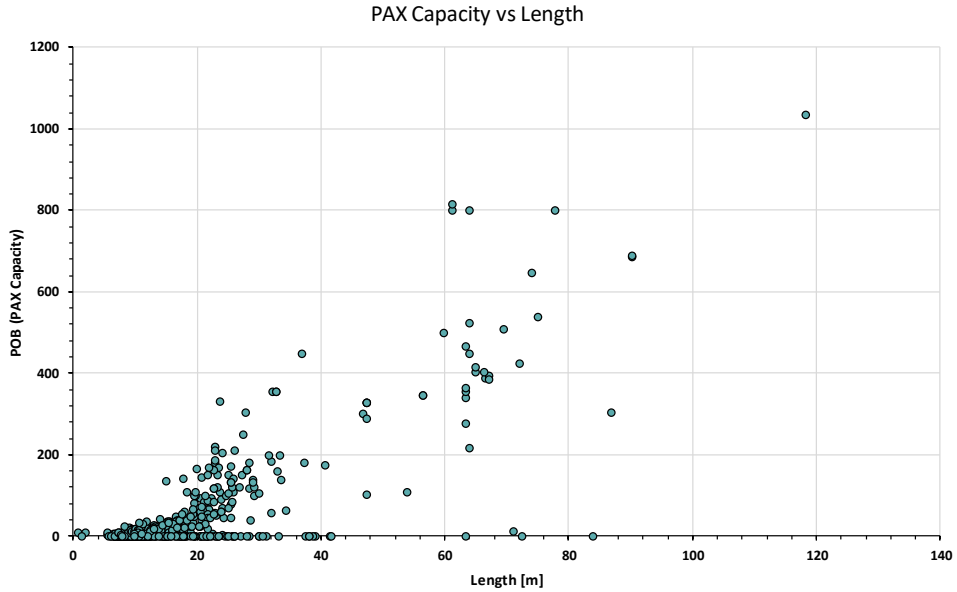

Figure 5: Fleet at Risk – Pax Capacity Vs Length

Sample ships selection

Figure 7 outlines the vessels selected for the FSA study, representing the full size-range, on the basis of which quantitative risk assessment will be undertaken, in particular damage stability calculations and risk analysis in the FSA study. The red markers in the figure are the ships selected in order to provide a representative picture of the whole range of vessels comprising the fleet at risk. This, in turn, supports the argument that a weighted (based on the number of ships in each of the four selected bands) risk evaluation will suitably represent the whole fleet at risk. However, it should be noted that the vessels selected have also been influenced by the availability of requisite information on the vessels to support calculations. Instead, the nearest representative vessels have been selected in such instances.

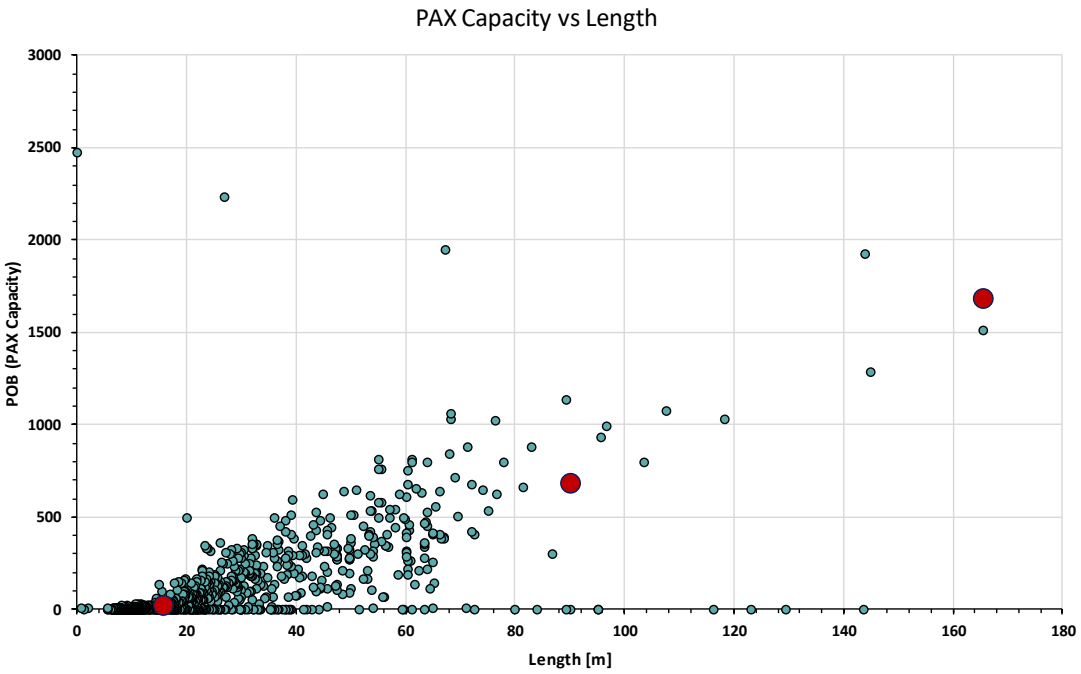

Figure 6: Vessel selection for the FSA study

Table 1: Representative ships and associated characteristics selected for the FSA study

Name	Service	Homeport	Registry	Build Yr.	Rig	Hull	Length	Breadth	GRT	PoB
Kate Alleson	Passenger	Surigao City	Surigao City	2019	MBCA	WOOD	15.75	1.24	3.86	24
Starlite Venus	Passenger	Batangas	Batangas	2020	MV	STEEL	90.11	16.3	1616	688
ST. Pope John Paul II	Passenger/Cargo	Manila	CEBU	1984	MV	STEEL	165.31	26.8	1931	1688

Frequency estimation of a loss scenario

1. Hazard frequency: This needs to be ship and area specific as well as hazard specific. In the absence of all the requisite information, we can take frequencies from the accident database, developed in the project purposely for the Philippines Domestic Passenger Ships, pertaining to each hazard in question (collision, bottom grounding, side grounding).

Table 2: Hazard frequencies for the domestic ferries in the Philippines (only collision has been considered)

Hazard type	Domestic Ferries in the Philippines	
	Frequency 1/ship year	
	Motor Banca	RoPax
Collision	4.55E-04	1.68E-03

2. Scenario frequency: This is the frequency of a given scenario occurring, conditional on the hazard being addressed, as defined by the p-factor. The product of 1 and 2 gives the frequency of the loss scenario being considered.
3. PLL calculation: Ship level PLL can be calculated by substituting scenario specific 1-s values, with the compliment of the Attained Index as an estimation of capsize probability.

PLL_A Quantification

Consequence estimation of a loss scenario

As the expected number of fatalities depends on the time to capsize and static analysis does not account for time, some approximation is called for to estimate the fatality rate. This is conditional on fast or slow capsize and assumptions relating to the percentage of People On Board (POB) lost. To simplify the methodology and to account for the dependencies between survivability and fatality rate, the following simplifying assumptions are made (based on work performed in Project FLARE), Eq. [4] and Eq. [5]:

If 0 < s-factor < 1 → Fatality rate = 5% [4]

If s-factor = 0 → Fatality rate= 80% [5]

This simple and conservative approach is in line with the method used in the EMSA III Project for capsizing and the development of SOLAS2020. Moreover, research in Project FLARE (Cardinale et al., 2022) indicated that collated information from time-domain simulations on cruise and RoPax vessels that the majority of damage scenarios in a survivability assessment are transient capsize cases, in which case no time for evacuation is available (on average 5 minutes for RoPax). In the absence of other evidence, it is assumed that for domestic ferries this value also applies.

Main assumptions and considerations

Drawing from Eq. [2], the following main assumptions are made for risk estimation:

i	Only collision is considered (1=collision)
j	Area of operation is considered with Hs=4 m, as per SOLAS
k	Three loading conditions are accounted for
$FR(s)$	Fatality Rate as a function of s-factor according to eq. [4] and eq. [5]
POB	Persons on board (people at risk) according for the operational profile of each selected vessel
$PLL_{A/yr}$	Attained Potential Loss of Life per year of exposure.

On the basis of the above, Eq. [2], with all the variables set to unit values, i.e., PLL for collision, per loading condition and scenario, becomes:

$$\frac{PLL_A}{yr} = hazard frequency \; x \; scenario \; frequency \; x \; capzize \; probability \; x \; fatality \; rate \; x \; PoB \quad [7]$$

Where,

- Hazard frequency for domestic ferries in the Philippines (
- Table 2).
- Scenario frequency is the p-factor corresponding to the breach being examined (damage scenario)
- Capsize probability is the complement of the scenario s-factor, i.e., (1-s)
- SOLAS breach distribution is used for collision.
- Calculations by software NAPA rel.2020.2

In the following sections, all three case studies are described in detail, including the initial damage stability evaluation, the process of implementing and measuring the impact of RCOs, and finally the approach adopted in judging the efficacy of each RCO.

CASE STUDY – MEDIUM SIZE ROPAX VESSEL

Vessel Principal Particulars

The following section details the vessel principal particulars, as outlined within
Table 3. Here, it is observed that the vessel is a moderately large Ro-Pax, with a length nearing 100 m and a capacity of 688 persons.

Table 3: Vessel Particulars

Property	Value
Length (O.A.)	97.78 m
Length (B.P.)	89.80 m
Breadth (MLD.)	16.30 m
Depth (MLD.)	9.90 m
Design Draft	4.90 m
GM	3.40 m
Deadweight	1094.89 ton
Passenger Capacity	688 persons
No. of Crew	50 persons

Coordinate System

A right-handed coordinate system has been used in defining the vessel stability model, as shown in Figure 7. The origin is located at frame #0, and locations in the ship are designated in accordance with a Cartesian coordinate system, where the axes are placed as follows:

- X-axis: longitudinal coordinate, positive in the direction of the bow, zero at frame #0,
- Y-axis: transverse coordinate, positive direction to port side, zero at the centre line,
- Z-axis: vertical coordinate, positive upwards, zero at the baseline.

In addition, trim is positive to stern and negative to bow.
The heeling angle is positive when the vessel heels to the port side.

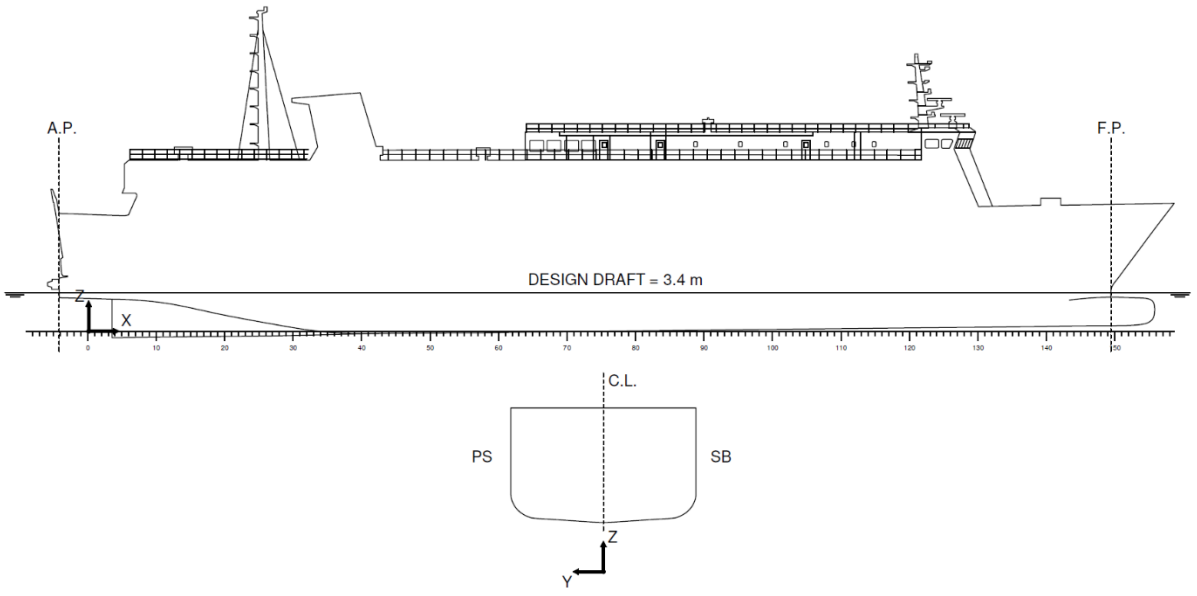

Figure 7: coordinate system

Stability Model

The ship model used in the damage stability calculations has been defined from the baseline up to, and including, the vessel ro-ro deck (9.9 m A.B.L.). In addition, one bow thruster has been reduced from the buoyant volume in the fore of the vessel. The resultant calculation sections of the model are shown in Figure 8 below, with the profile and body plan illustrated in Figure 9, and General Arrangement plan in Figure 10.

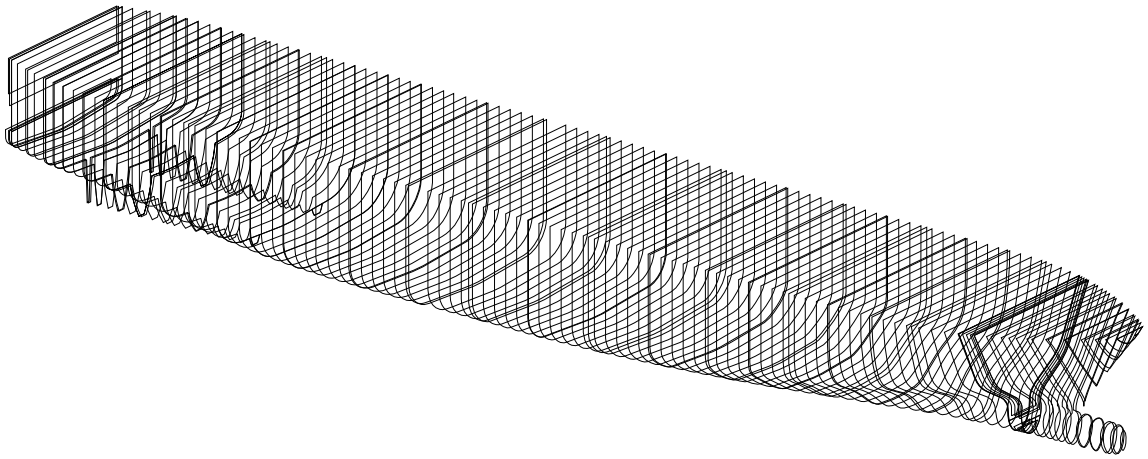

Figure 8: Stability Model Calculation Sections

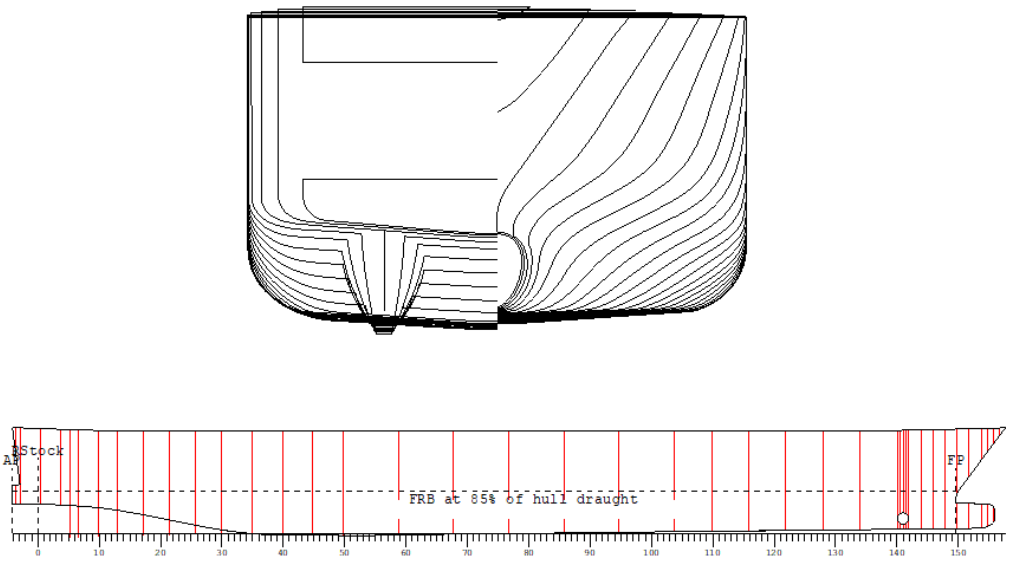

Figure 9: Stability Model Body Plan & Profile

Relevant Openings

When calculating the range of positive stability beyond the angle of equilibrium, the GZ curve has been truncated when an unprotected opening has been submerged. However, if an opening with a weathertight closing appliance has been temporarily submerged, it has had no effect on the range of positive stability. Instead, such openings are only accounted for if immersed in the final equilibrium floating position, resulting in s=0.

Subdivision Arrangement

In the calculation of the Attained Subdivision Index, the vessel subdivision has been discretised into 14 zones, Figure 11.

Permeabilities

The permeabilities used in the damage stability calculations are in accordance with the SOLAS 2020 prescribed values:

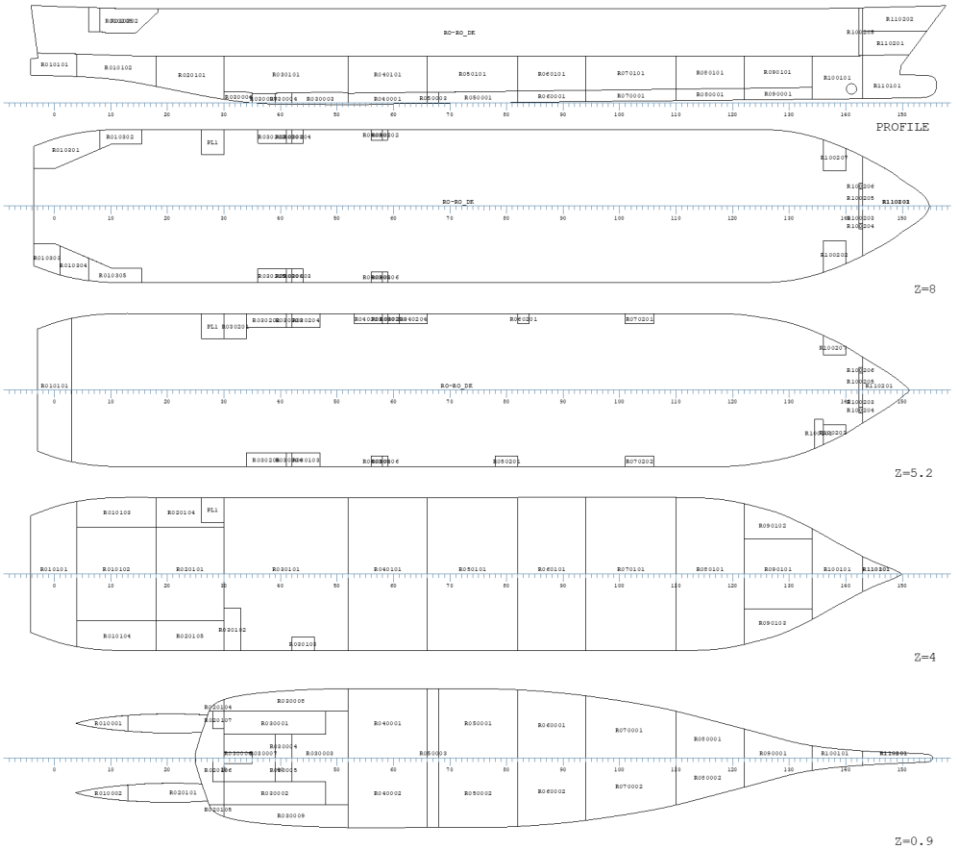

Figure 10: General Arrangement Plan

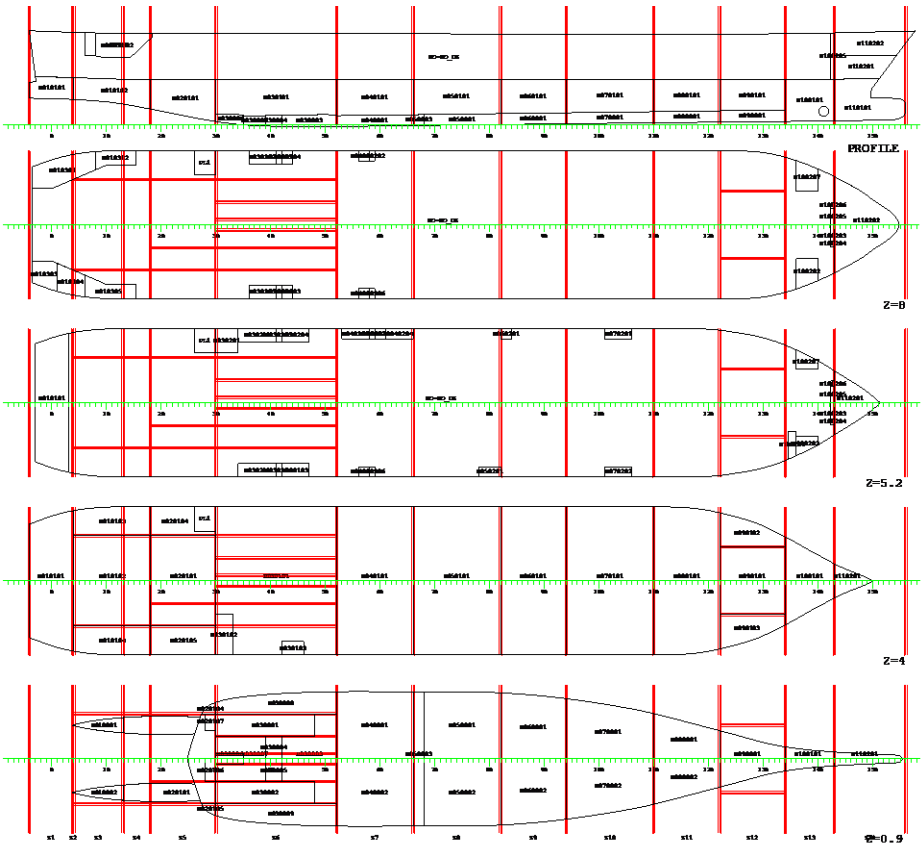

Figure 11: Subdivision Arrangement Plan

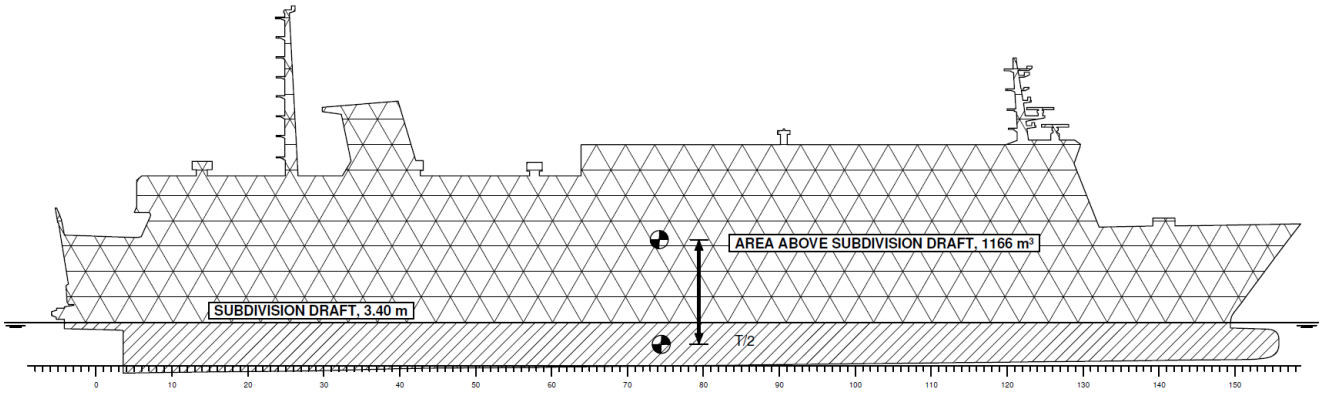

Figure 12: Wind Profile

Compartment Connections

As the vessel does not possess any A-class boundaries liable to inhibit floodwater equalisation, nor any cross-flooding arrangements, there are no damage cases flooded in stages.

Moments Due to Wind and Passenger Crowding

4.81 Wind-Induced Moment
The projected windage area of the vessel and corresponding moment lever are shown in Figure 12. The wind-induced heeling moment pertinent to damage stability calculations is estimated with the following formula:

$$\boldsymbol{M_{wind} = (P \cdot A \cdot Z)/9.806\ (tm)} \quad [8]$$

Where,
P = 120 (N/m^2)
A = Windage area (m^2), measured in accordance with the projected lateral area relating to each calculation draft.
Z = Distance from T/2 to the centroid of windage area (m)

Moment Resulting from Passenger Crowding

The moment resulting from passenger crowding has been calculated in accordance with the maximum number of persons onboard the vessel (738 persons). A conservative transverse lever of B/2 (8.15m) from the centreline has been assumed and the weight attributed to each passenger is 75 Kg.

Moment by crowding of passengers = 451.1 tm [9]

Initial Conditions

In accordance with Regulation 7, MSC.421(98), damage stability calculations shall be conducted with respect to three different drafts that define assumed upper and lower extremities of the vessel draft range, in addition to an intermediate condition. This includes the vessel deepest subdivision draft (3.41 m), the light service draft (2.89 m), and a partial subdivision draft determined by the following formula:

dp = dl+0.6(ds-dl) = 3.202* m [10]

The damage stability calculations are performed with a typical aft trim of -1.45 m for the light service draft and with zero trim (even keel) for the partial and deepest subdivision drafts. The draft, trim, intact GM and KG values applied in the calculations are summarised in Table 5. The assessment has been conducted under limiting GM conditions relating to Regulation 7 compliance, and hence the GM/KG values assigned to the calculation loading conditions, as detailed in Table 5, differ from those attributed to the statutory loading conditions of the vessel.

Table 4: Required Subdivision Index Acc. to MSC.421(98), Reg. 6

Persons on board	Required Index, R
N<400	R = 0.722
400 ≤ N ≤ 1,350	R = N/7,580 + 0.66923
1,350 < N ≤ 6,000	R = 0.0369 x Ln(N+89.048) + 0.579
N > 6,000	R = 1 – (852.5 + 0.03875 x N)/(N + 5,000)

Table 5: Attained Subdivision Index Calculation - Limiting GM

Initial Condition	T [m]	TR [m]	GM [m]	A/R	COEF	A*COEF
DL	2.890	-1.450	3.360	1.001	0.200	0.154
DP	3.202	0.000	3.195	1.021	0.400	0.313
DS	3.410	0.000	4.050	1.002	0.400	0.309
Attained Subdivision Index A						**0.775**
Required Subdivision Index R						**0.767**

Required Subdivision Index R

The vessel subdivision and damage stability performance are considered satisfactory when the Attained Subdivision Index A, as calculated in accordance with Regulation 7, is not less than the Required Subdivision Index, R. The details of this calculation are provided in Table 5, leading to a Required Index value of 0.767 for the vessel under assessment.

Attained Subdivision Index Calculation Under Limiting GM Conditions

Based on the assumptions outlined within the foregoing sections, the vessel Attained Subdivision Index has been calculated as summarised within
Table . Here, the Attained Index of the vessel has been optimised such that A=R for each of the calculation conditions, thus allowing limiting GM values to be derived.

Derivation of the Limiting GM Curve & GM Margins

Having optimised the Attained Subdivision Index in accordance with the requirements of SOLAS 2020, it has then been made possible to derive the limiting GM curve of the vessel. This represents the minimum required GM across the vessel draft range, such that statutory requirements are met. This is a significant design property as it dictates the boundary between safe and unsafe operation of the vessel. The results of this calculation are presented firstly within Figure 13. Here, plots of both the intact and damage stability limiting GM curves are shown relative to all statutory loading conditions, indicated as blue markers. Through examination of this diagram, a number of key observations can be made. Firstly, it is clear that the vessel limiting GM is dictated to a significant degree by the damage stability requirements according to SOLAS 2020. Secondly, by looking at the relative position of each loading condition to the limiting GM curve, it is clear that a number of conditions have notably low GM margins, with others failing to comply entirely (LD11 & LD9). This indicates that there is a requirement for improvements to be made in the vessel design in order to achieve compliance.

Vessel Risk Profile

A useful tool in identifying areas of heightened vulnerability within any vessel design, is to look upon the Risk Profile. This is a graph that maps collision risk across the vessel, allowing focus to be placed on those areas demonstrating the greatest vulnerability to flooding. Figure 14, shows the Risk Profile derived from the previously detailed calculations conducted under limiting GM conditions. Within the figure, collision risk is plotted along the vertical axis, and the damage centre is plotted along the horizontal axis. Differing damage lengths are distinguished by varying marker types, ranging up to four adjacent compartment damages.

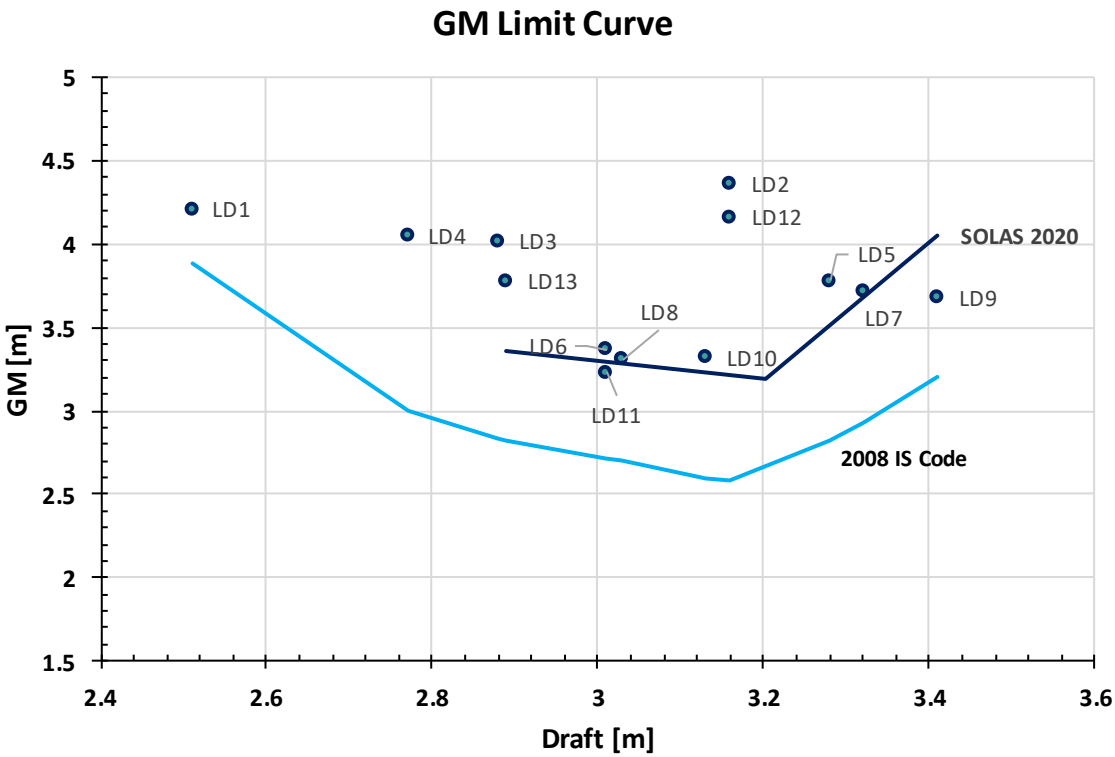

Figure 13: As-built Intact and Damage Limiting GM Curves

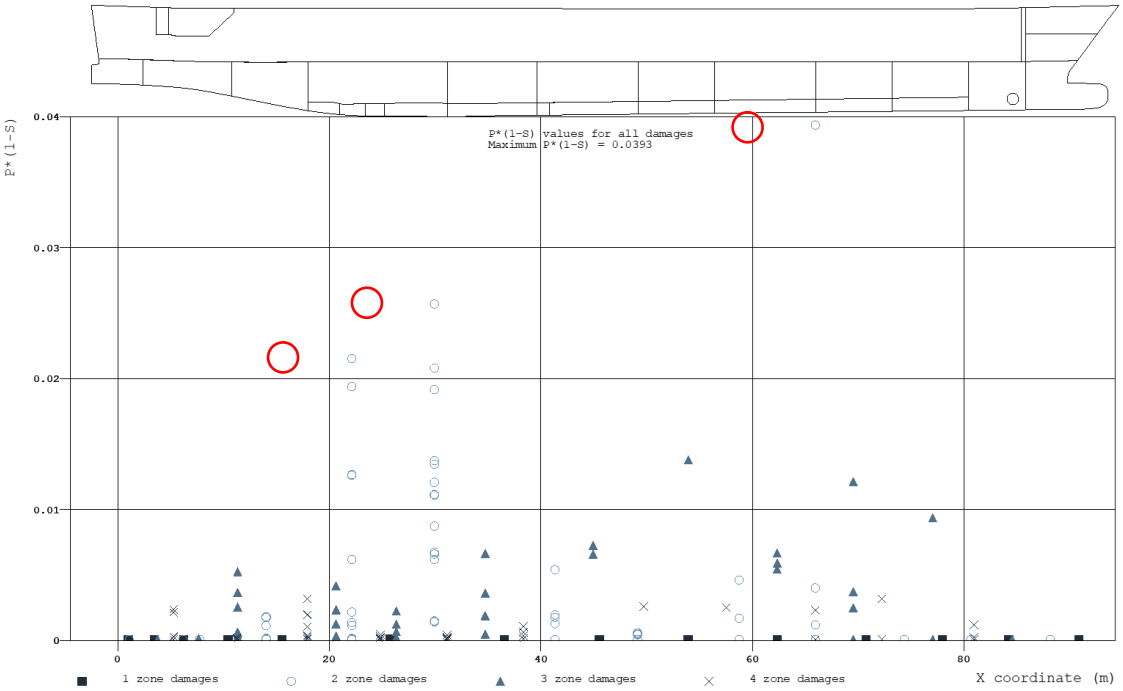

Figure 14: Vessel Risk Profile Under Limiting GM Conditions (High risk shown in red)

Observation of the Risk Profile indicates peak risk around the vessel fore shoulder, which is typical for RoPax vessels and, indeed, passenger ships in general. Heightened risk is also evident in damages affecting the two machinery spaces, located towards the aft shoulder of the vessel. In this location there is also a larger concentration of loss scenarios, meaning that the cumulative risk within this area will be significantly higher than that relating to any other part of the vessel. On the basis of these findings, the implementation of RCOs, as covered in the following sections, will target these areas. Through doing so, it

can be ensured that the design receives help where it is needed most, whilst at the same time allowing risk to be reduced in the most efficient and thereby cost-effective manner.

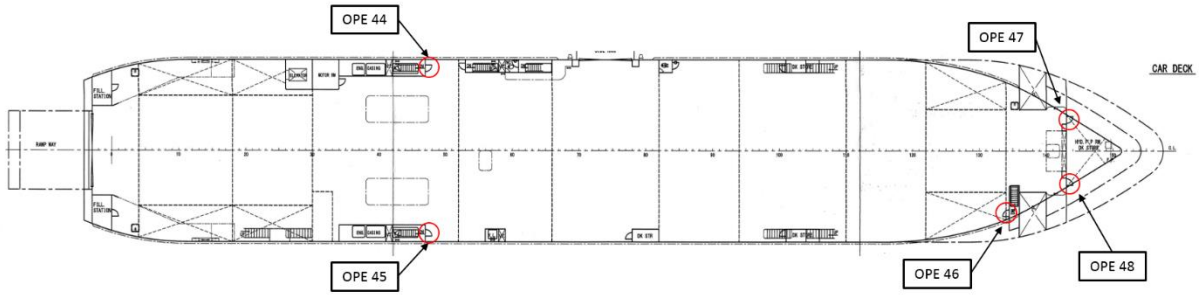

Figure 15: Critical Openings

Table 5: Attained Subdivision Index Calculation – As-Built Limiting GM Conditions + RCO 1

Initial Condition	T [m]	TR [m]	GM [m]	A/R	COEF	A*COEF
DL	2.890	-1.450	3.360	1.001	0.200	0.154
DP	3.202	0.000	3.195	1.033	0.400	0.317
DS	3.410	0.000	4.050	1.066	0.400	0.327
Attained Subdivision Index A						**0.797**
Required Subdivision Index R						**0.767**

RCO 1 – Critical Opening Protection

Description of RCO 1

On the basis of the results outlined within the foregoing, the first Risk Control Option explored has been to address critical openings identified within the vessel design. These are openings that have been found to adversely affect the magnitude of the Attained Subdivision Index, as a consequence of:

- Truncating the GZ curve, thus reducing GZ max,
- Truncating the GZ curve, thus reducing Range,
- Immersion in the final equilibrium condition, leading to a designation of $s_i = 0$

Details pertaining to each of those openings showing the highest risk can be seen in a plot of the openings in Figure 15 . Here, three of the openings (OPE 44, 45 & 46), represent non-watertight openings leading from the vessel ro-ro deck to spaces below the bulkhead deck. As such, this represents a particular downflooding risk in such cases where water accumulates on deck. Given that this is a significant hazard in the case of Ro-Pax vessels, this needs addressing. Furthermore, two openings leading to the fore hydraulic pump room have been identified as considerably impacting the vessel Attained Index.
The proposed solution to this problem is to uprate these doors to watertight status, using either hinged or sliding watertight doors. The impact of this design change has then been measured through re-calculating the vessel Attained Index, accounting for these modifications, the results of which are outlined in the following section.

Re-evaluation of Attained Subdivision Index

Table 5 outlines the results of the updated Attained Index calculations, conducted in light of uprating the watertight integrity of the openings described within the foregoing section. These calculations have been conducted with respect to the "as-built" limiting GM values of the vessel, as calculated previously, which provides a sound baseline from which to gauge improvement. The results demonstrate an impressive increase in the Attained Index from 0.775 to 0.797.

Re-evaluation of the Vessel Risk Profile

Once again, the vessel Risk Profile has been generated, this time accounting for the implementation of RCO 1. Here we can observe that the peak risk towards the vessel fore shoulder, having previously existed within the "as-built" condition, has now been eradicated. In addition, a number of high-risk cases towards the aft shoulder of the vessel have been mitigated. However, there still remain a number of high-risk scenarios situated around the vessel machinery spaces. This results from the fact that the majority of such cases are lost due to capsize and, as such, internal openings bear no significance on the outcome.

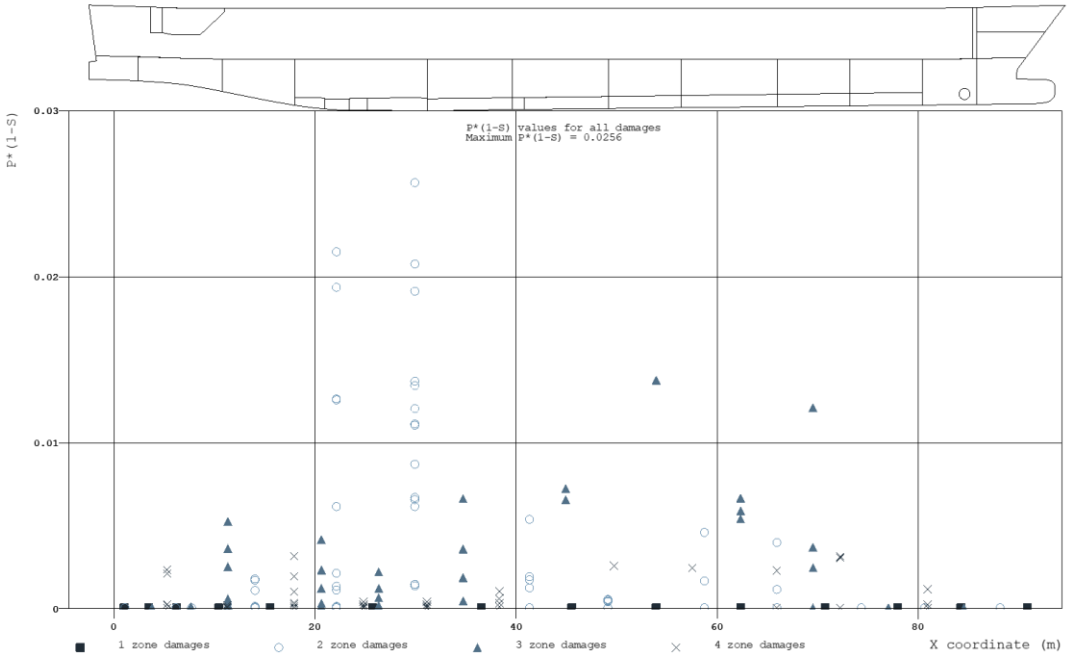

Figure 16: Vessel Risk Profile Under Limiting GM Conditions, with RCO 1 Applied

Table 6: Attained Subdivision Index Calculation - Limiting GM with RCO 1

Initial Condition	T [m]	TR [m]	GM [m]	A/R	COEF	A*COEF
DL	2.890	-1.450	3.355	1.000	0.200	0.153
DP	3.202	0.000	3.080	1.001	0.400	0.307
DS	3.410	0.000	3.440	1.002	0.400	0.307
Attained Subdivision Index A						**0.768**
Required Subdivision Index R						**0.767**

Derivation of the Limiting GM Curve & GM Margins

A further assessment has also been made in order to derive the updated limiting GM curve, thereby allowing the change in GM margins to be measured in light of the implemented RCO. The results of this process are provided in Table 6, including the limiting GM values.

Figure 17 contrasts the updated limiting GM curve to that of the existing vessel design. Here, it can be observed that a large improvement in limiting GM has been achieved, particularly towards the upper draft range. This is to be expected, as it is often deeper drafts having a tendency to suffer from lack of residual freeboard. As such, non-watertight openings pose a greater risk when the vessel is loaded to such conditions.

RCO 2 – Passive Foam Installations

Description of RCO 2

The second RCO considered has been the application of passive, high-expansion foam as a means of enhancing damage stability performance. This is achieved by strategically locating fixed-foam installations in vulnerable void spaces within the vessel design, resulting in a decrease in space permeability and leading to:

- A reduction in floodable volume, which preserves buoyancy, thus enhancing floatability, damaged freeboard, and reserve buoyancy.
- Enhanced stability in the form of increased damaged GM, as the foam installations increase waterplane area inertia and the metacentric radius.

The selected spaces for such applications are depicted in blue within Figure 18, and their location has been informed by the calculations pertaining to ship vulnerability.

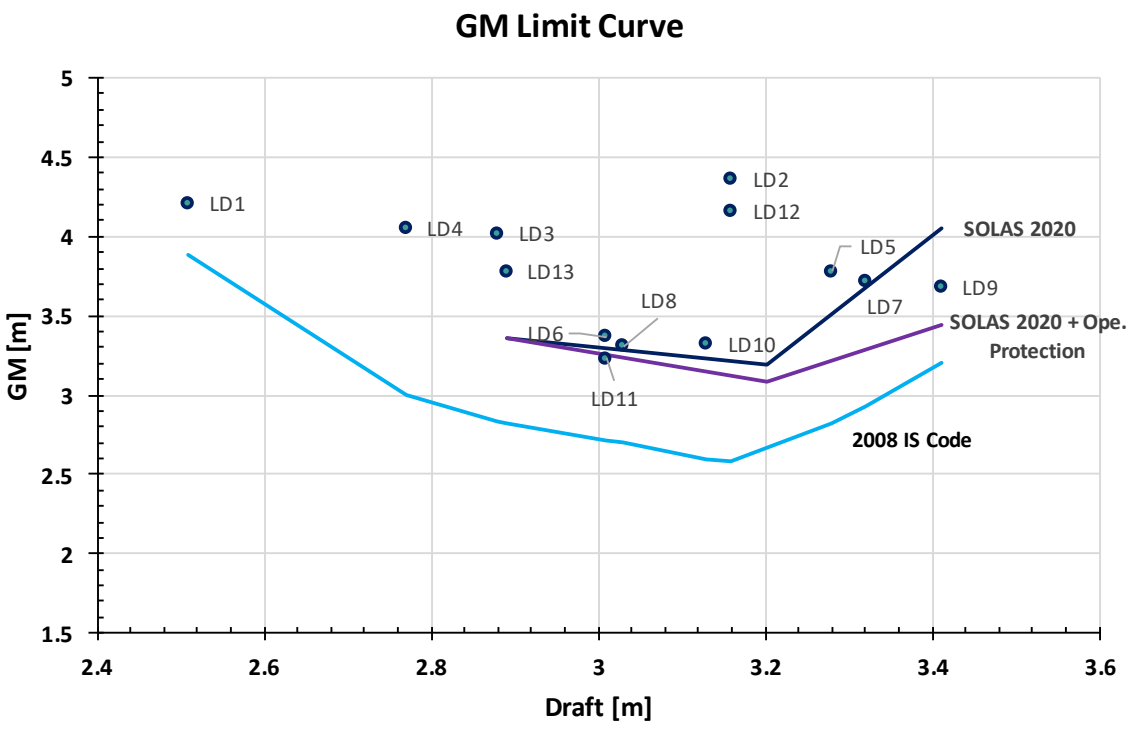

Figure 17: Intact and Damage Limiting GM curves comparison with RCO 1

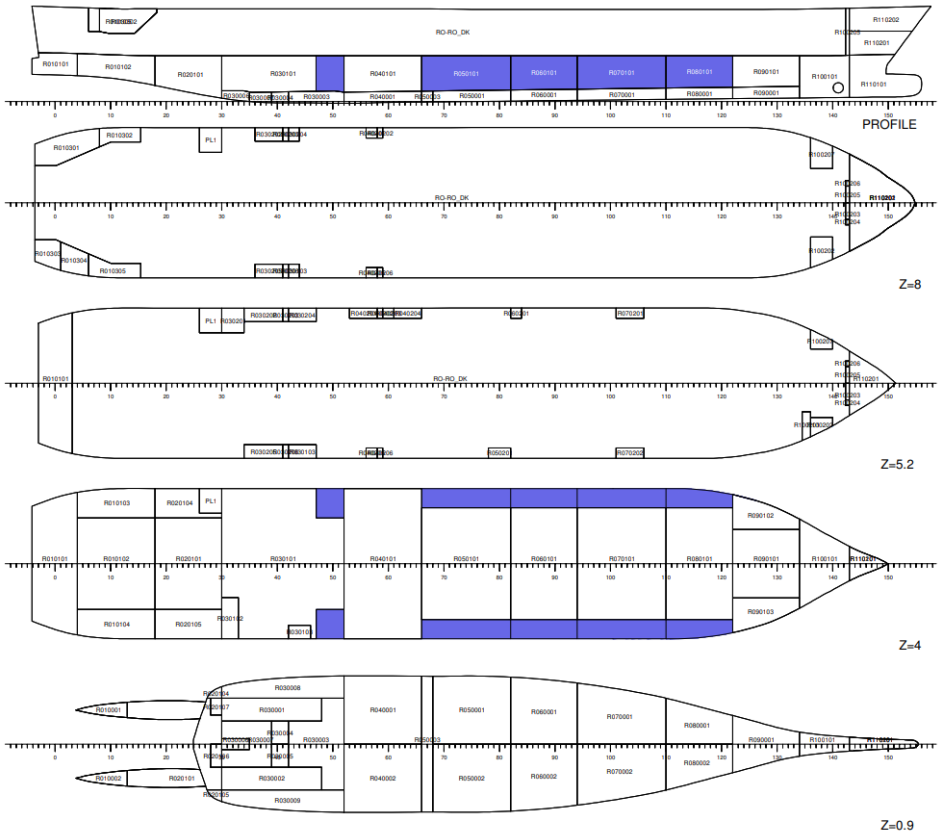

Figure 18: Spaces Subject to Foam Application (Shown in blue)

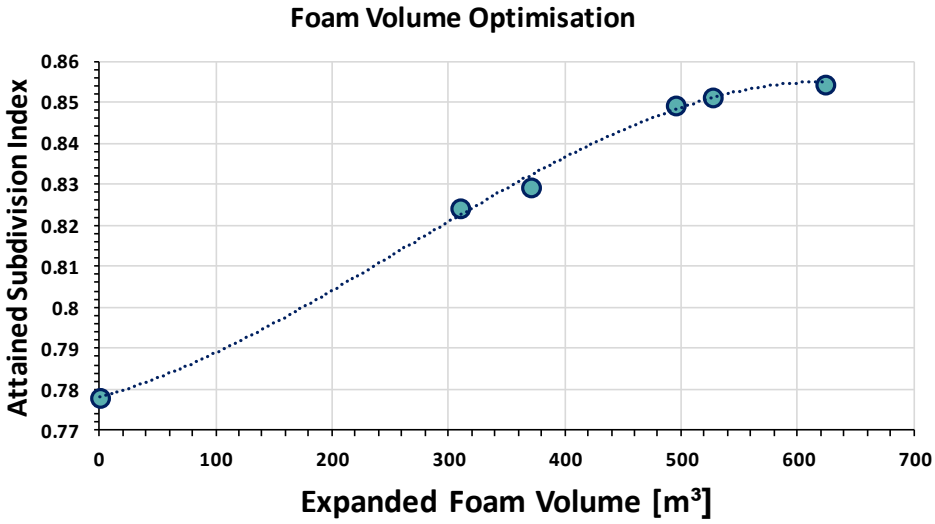

Figure 19: Foam Volume Sensitivity Analysis

Table 8: Foam Volume Vs. Attained Subdivision Index Value

A-Index	Foam Volume (m3)	Installation Weight (t)
0.8546	623.2	20.8
0.85142	**527.3**	**17.6**
0.84936	494.9	16.5
0.82934	370.8	12.4
0.82428	309.5	10.3
0.778 (As-built)	0.000	0.0

Table 9: Attained Subdivision Index Calculation with Passive Foam Installations (RCO 2)

Initial Condition	T [m]	TR [m]	GM [m]	A/R	COEF	A*COEF
DL	2.89	-1.45	3.36	1.064	0.2	0.1631
DP	3.202	0	3.195	1.087	0.4	0.3333
DS	3.41	0	4.05	1.083	0.4	0.8301
Attained Subdivision Index A						**0.829**
Required Subdivision Index R						**0.767**

Optimisation of Foam Volume

Having identified those spaces, which would be best served by passive foam protection, an optimisation process has been undertaken to determine the foam volume to be applied. This approach involves calculating the vessel Attained Subdivision Index for a series of incremental values of foam volume. This, in turn, allows the optimum foam volume to be determined as the point of diminishing returns in the relationship between the Attained Index and the volume of foam utilised.
The results of this process are outlined in Figure 19 in graphical form and within
Table in numerical form. Here, it can be observed that the optimal foam volume lies at approximately 500 m^3, leading to an installation weight of approximately 17 tonnes.

Re-evaluation of Attained Subdivision Index

Having identified the optimum foam volume solution, the damage stability performance of the vessel has been re-evaluated. Calculations have firstly been conducted with only the foam solution (RCO 2) in place, leading to the results presented within Table . Furthermore, an additional calculation has been conducted with consideration of opening protection (RCO 1) and foam protection (RCO 2) implemented simultaneously. Through doing so, it has been possible to measure the combined impact of both RCOs, as detailed within
Table . Quite remarkably, the results of this process show that with the foam solution in place the vessel has achieved an Attained Index of 0.829. Moreover, it has been possible to further raise the Attained Index to 0.850 when utilising both RCOs.

This indicates that the RCOs have been highly effective at reducing flooding risk, to the extent at which the damage stability performance of the vessel is now comparable with any modern RoPax operating today.

Table 10: Attained Subdivision Index Calculation with Opening Protection and Passive Foam Installations (RCOs 1 & 2)

Initial Condition	T [m]	TR [m]	GM [m]	A/R	COEF	A*COEF
DL	2.890	-1.450	3.360	1.102	0.200	0.169
DP	3.202	0.000	3.195	1.117	0.400	0.343
DS	3.410	0.000	4.050	1.100	0.400	0.337
Attained Subdivision Index A						**0.850**
Required Subdivision Index R						**0.767**

Table 11: Limiting GM Calculation - RCO 2

Initial Condition	T [m]	TR [m]	GM [m]	A/R	COEF	A*COEF
DL	2.89	-1.45	2.85	1.003	0.2	0.158
DP	3.202	0	2.56	1.001	0.4	0.307
DS	3.41	0	3.1	1.002	0.4	0.307
Attained Subdivision Index A						**0.768**
Required Subdivision Index R						**0.767**

Table 12: Limiting GM Calculation - RCOs 1 & 2

Initial Condition	T [m]	TR [m]	GM [m]	A/R	COEF	A*COEF
DL	2.89	-1.45	2.84	1.002	0.2	0.154
DP	3.202	0	2.56	1.001	0.4	0.307
DS	3.41	0	2.99	1.000	0.4	0.306
Attained Subdivision Index A						**0.767**

Derivation of the Limiting GM Curve & GM Margins

In this section, the impact of RCOs on the vessel GM limit curve and the scale of the GM margins has been explored. Firstly, the updated limiting GM values have been calculated for RCO 2 and then RCOs 1 & 2, as detailed within Table 11 and Table 12 .

Risk Analysis & Calculation of RCO Cost-Effectiveness

PLL Calculation

A good measure of Societal Risk is the Potential Loss of Life (PLL), which is defined as the expected value of the number of fatalities per year. PLL is a form of risk integral, being a summation of risk as expressed by the product of consequence and frequency. The integral is generally summed up over all potential undesired events that can occur, in this case limited to collision events. In the following, PLL values are calculated for the vessel in as-built condition, as well as having implemented each of the RCOs examined. Furthermore, the cost-effectiveness of each solution has been gauged by calculating the Net Present Value of each RCO and contrasting this value to a Gross Cost of Averting a Fatality (GCAF) limit, determined by the value of statistical life within the Philippines. The latter has been determined in accordance with estimates made by the Economy and Environment Program for Southeast Asia, where an estimation of $0.8 million per life within the Philippines is proposed.

In addressing cost, the following assumptions have been applied for each RCO:

- Watertight door - $20,000 per door installed.
- Passive Foam - $6/kg installed.

The results of the calculation are summarised in Table 13, where it can be observed that all RCOs are significantly cost-effective; each exceeding GCAF limits by at least a factor of two.

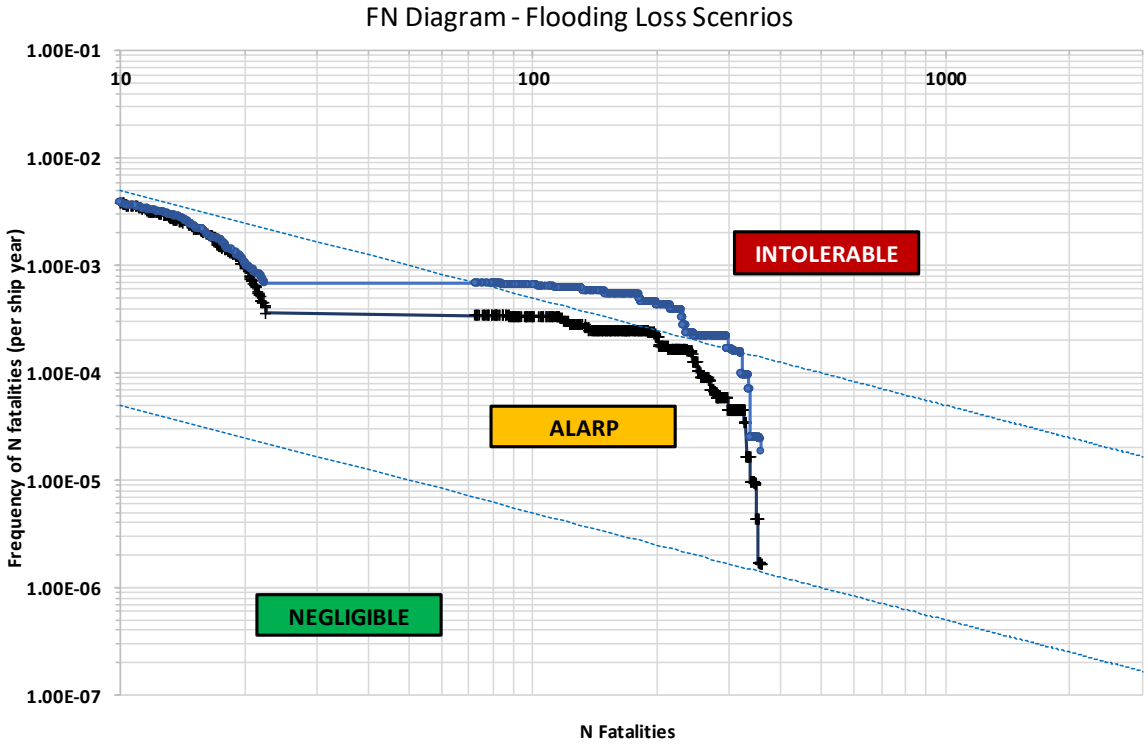

Figure 20: FN-Diagram Showing the Impact of RCOs

Table 13: Cost Effectiveness Calculation on the Basis of PLL, NPV & NCAF

Item	As-Built	RCO 1	RCO2	RCO1 & RCO 2
Attained Index	0.755	0.797	0.829	0.851
PLL	0.136	0.123	0.104	0.090
ΔPLL/ship-year	N/A	0.013	0.032	0.046
ΔPLL/ship-life	N/A	0.399	0.9624	1.387
Costs for financing, insurance etc ($)	N/A	8,000	7,127.6	15,128
CAPEX ($)	N/A	100,000	96,222.6	204,223
Net Present Value NPV ($)	N/A	118,800	105,844.86	224,645
GCAF Limit ($)	N/A	319,334.4	769,920	1,109,251
GCAF/NPV	N/A	2.69	7.27	4.94

Risk Acceptance Criteria – FN Diagram

Another useful approach to gauging the effectiveness of the RCOs, is by plotting what is known as an FN Diagram. This is a means of expressing societal risk, by illustrating the relationship between the frequency of an accident and the number of fatalities. Such diagrams are generally plotted against some form of risk-acceptance criteria, in this case taken as the IMO criteria expressed in MSC-MEPC.2/Circ.12/Rev.2. With consideration of the vessel in the as-built condition and also following the implementation of the combined RCO solution, an FN-diagram has been created as shown in Figure 20. Here, the blue curve represents the existing vessel design and the black curve the modified design with the RCOs implemented. The risk-acceptance criteria are plotted with light blue dashed lines, creating three regions within the chart, defined as follows:

- **Intolerable Region:** Risk cannot be justified and must be lowered.
- **ALARP Region:** Risk is tolerable if further risk reduction is impractical.
- **Negligible Region:** Risk is negligible.

If we observed the FN diagram, we could see that the existing vessel design falls within the intolerable region, indicating that action should be taken to bring the vessel into the ALARP region. In this respect, the application of the combined RCO solution

has achieved this aim, with all events considered now lying within the ALARP region. This again is another indicator that the RCOs considered hold significant potential to reduce flooding risk in a meaningful way.

CONCLUSIONS

General Conclusions

- One way of ensuring that action is taken before a disaster occurred is by using a process known as Formal Safety Assessment (FSA, MSC-MEPC.2/Circ.12/Rev.2.). This has been described as "a rational and systematic process for assessing the risks associated with shipping activity and for evaluating the costs and benefits of options for reducing these risks." Such options have been extended to other stakeholders (Flags, Administrations, Class, Shipyards and Ship operators), aiming at identifying cost effective solutions to improve safety standards of existing ships and new buildings.
- As the nature of this undertaking is highly technical, the proposed solutions in the form of recommendations are communicated with decision makers in mind, to ensure that all stakeholders gain sufficient information at a level that is readily understood to support effective decision making. To this end, proposed changes are compared with existing standards, targeting life cycle implications (design, operation, emergencies) to enable a balance to be drawn between technical and operational issues, including the human element, by contrasting safety (Delta Risk) and cost (Delta cost) in the implementation of the proposed measures, targeting identified hazard categories individually whilst considering cross-hazards implications.
- The focus on design solutions in the project and in this paper, is on the highest risk contributor, as previously identified, namely inadequate damage stability and the risk to human life. This comprises nearly 90% of the risk for all categories of passenger ships, as manifested by accident statistics. Contributing factors for such loss comprises not only deficiencies in design but also in environmental, human, organisational, regulatory, and other unknown factors, which are also addressed by the FSA_P team. Therefore, collectively the team covers the whole spectrum of hazards and their ensuing consequences, leading to balanced recommendations, accounting for feasibility, practical implementation, time scales, and cost.
- To this end, representative ships from the Philippines fleet currently engaged in domestic voyages are selected for risk analysis and risk assessment, the latter by using cost-benefit assessment to aid decision making in the RCOs selection, implementation, and impact. Based on this process of using representative ship designs in the risk assessment, any conclusions reached and recommendations ensuing on the basis of this sample of ships would, in principle, apply to the whole fleet of the domestic passenger ships operating in the Philippines. The selected ships include: (a) a medium size RoPax vessel; (b) a small motor banca vessel; (c) a large old design RoPax. This paper addresses ship (a).

Specific Conclusions

- Deriving from the analysis performed on the selected ship design, detailed in the report, it has been possible to identify and rectify design vulnerabilities to flooding hazards, typical of the fleet of domestic passenger ships operating internationally. Specific remarks pertaining to the selected RoPax ship, which apply to the whole fleet, include the following:
- Certain features, which make the Philippines fleet more susceptible to flooding risk, include: (a) low index of subdivision, (b) low freeboard, leading to water reaching the car deck (c) low GM margins; hence susceptible to overloading or heavy weather, (d) unprotected openings, (e) inappropriate verification, thus further exacerbating the potential for catastrophic loss of life.

General Recommendations

- Considering the current state of enforcement and verification of damage stability standards for domestic passenger ships operating in the Philippines (lack of fit for purpose regulations; gaps in enforcement and verification – frequency and rigor), ships must be made more robust to withstand flooding hazards by adopting risk control measures that are extremely cost-effective to incentivise the operator to meet higher standards, which in turn will fuel a virtuous cycle for continuous safety enhancement.
- Working with this incentive in mind, the most effective and practicable solutions, applicable to new and existing ships, in any time scale, have been selected and applied to the sample ships, enabling all categories of ship size to reach damage stability standards applicable to passenger ships engaged in any domestic or international voyages, including the proposed modified designs of the motor bancas.
- This is unprecedented and exciting, enabling Philippines in the short to medium term to showcase the safety of their domestic fleet against the best in the world.
- Based on this work, a clear pathway is outlined for consideration by the safety stakeholders in the Philippines, to facilitate a safety transformation for all domestic ships operating in the Philippines.

Specific Recommendations

- Based on the results detailed within the foregoing, the following specific recommendations can be made:

- In order to correctly inform the process of evaluating the damage stability performance of vessels and subsequently implement effective RCOs, it is essential that accurate and up-to-date information is available on all regulated vessels.
- As the RCOs assessed have proven highly effective in reducing flooding risk across a range of ship types, sizes and ages, due consideration should be given to providing alternative routes to compliance on the basis of implementing such measures, particularly where novel forms of RCO are to be employed.
- Guidelines should be produced detailing the approach that should be adopted in order to effectively implement and judge the efficacy of approved RCOs, in line with the approach adopted within this report.

ACKNOWLEDGEMENTS

We should like to express our appreciation to the International Maritime Organisation and the Word Bank for their support in this project, financial and otherwise, as well as our collaborators from the World Maritime University, Prof Jens-Uwe Schroeder-Hinrichs, Dr Anish Hebbar and Dr Serdar Yildiz for their unfailing support and comradeship during this project. We should also like to express our gratitude to all the Authorities and maritime industry in the Philippines for making us feel at home and for their help in every phase and aspect of this project

CONTRIBUTION STATEMENT

D. Vassalos: Conceptualisation, Methodology, Writing Original-Draft, Writing Review/editing, **D. Paterson**: Calculations, Data curation, Writing Review/editing, **F. Mauro**: Data curation, Writing Review-Editing, **A. Salem**: Writing Review/editing.

REFERENCES

Aven, T. (2012). The risk concept – historical and recent development trends. Reliability Engineering and System Safety, 99, 33-44.

Aven, T. (2022). A risk science perspective on the discussion concerning safety I, safety II and safety III. Reliability Engineering and System Safety, 217, 108077.

Bulian, G., Lindroth, D., Ruponen, P., Zaraphonitis, G. (2016). Probabilistic assessment of damaged ship survivability in case of groundings: development and testing of a direct non-zonal approach. Ocean Engineering, 120, 331-338.

Cardinale, M., Luhmann, H., Vassalos, D., Routi, A.L., Bertin, R., Murphy, A., Dalle Vedove, F., Sarkka, J., Ochs, T., Bolle, M., Tiscione, F., Auger, F., Mauro, F., Pine, E., Cantalupo, G., Mujeeb-Ahmed, M. (2022). D 7.1 Flooding risk calculations, Technical report, FLARE Project.

Goerland, F., Montewka, J. (2015). Maritime transportation risk analysis: review and analysis in light of some fundamental issues. Reliability Engineering and System Safety, 138, 115-134.

IMO (2009). SOLAS-International Convention for the Safety of Life at Sea, London, UK, International Maritime Organisation (IMO), 2009.

IMO (2020). SOLAS-International Convention for the Safety of Life at Sea, London, UK, International Maritime Organisation (IMO), 2020.

Mauro, F., Vassalos, D. (2022). The influence of damage breach sampling process on the direct assessment of ship survivability. Ocean Engineering, 250, 111008.

Puisa, R., McNay, J., Montewka, J. (2021). Maritime Safety: prevention vs mitigation. Safety Science, 136, 105151.

Ruponen, P., Linderoth, D., Routi, A.L., Aartowaara, M. (2019). Simulation-based analysis method for ship survivability of passenger ship. Ship Technology Research, 63, 182-194.

Vassalos, D. (2012). Design for Safety, Risk based design, Life cycle risk management. Keynote address. International Marine Design Conference, IMDC, Glasgow, June 2012.

Vassalos, D. Paterson, D., Mauro, F., Boulougouris, E. (2021). Life-cycle stability management for passenger ships. Proceedings of the International Offshore and Polar Engineering Conference, ISOPE 2021, Virtual event.

Vassalos, D., Paterson, D., Mauro, F., Mujeeb-Ahmed, M., Boulougouris, E. (2022a). Process, methods and tools for ship damage stability and flooding risk assessment. Ocean Engineering, 266, 113062.

Vassalos, D., Paterson, D., Mauro, F., Atzampos, G., Assinder, P., Janicek, A. (2022b). High expansion foam. A risk control option to increase passenger ship safety during flooding. Applied Science, 12(10), 4949.

Part 4:
OFFSHORE DESIGN METHODOLOGY

Proceedings of 15th International Marine Design Conference (IMDC-2024)
June 2-6, 2024
Amsterdam, the Netherlands

Effect of Platform Configurations and Environmental Conditions on the Performance of Floating Solar Photovoltaic Structures

M I Jifaturrohman[1], T Putranto[1], D Setyawan[1], L Huang[2], I K A P Utama[1*]

ABSTRACT

The growth and development of floating solar photovoltaic (FPV) power plants is a prominent topic within renewable energy technology. One reason contributing to this desired technology design concept is the possibility of land acquisition issues, whereas the usage of the ocean provides a greater technical alternative area. The objective of the research is to present an innovative design for a floating structure, focusing on investigating and comparing the seakeeping performance of several hull configurations: catamaran, trimaran, quadrimaran and pentamaran. The final computational simulation results indicate a linear negative trend in the motion response graphs, particularly in specific significant response values for heave (Global Z), roll (Global RX), and pitch (Global RY), as the hull configuration increases.

KEY WORDS

CFD; Floating photovoltaic; Multi-hull; Renewable energy; Seakeeping characteristics.

NOMENCLATURE

AP	=	Aft Perpendicular	H	=	Height of FPV
Aγ	=	Normalising Factor	ha	=	Hectare
B	=	Breadth	HDPE	=	High-Density Polyethylene
B1	=	Demihull Breadth	Hs	=	Significant Wave Height
Cb	=	Block Coefficient	IEA	=	International Energy Agency
CFD	=	Computational Fluid Dynamics	IESR	=	Institute for Essential Services Reform
CFPP	=	Coal-Fired Power Plants	Ixx	=	Inertia moment – X-Axis
CH_4	=	Methane	Iyy	=	Inertia moment – Y-Axis
CL	=	Center Line	Izz	=	Inertia moment – Z-Axis
CO_2	=	Carbon Dioxide	JONSWAP	=	Joint North Sea Wave Project
CoG	=	Center of Gravity	KB	=	Keel to Buoyancy
Cp	=	Prismatic Coefficient	kW	=	Kilowatt
FP	=	Forward Perpendicular	Kxx	=	Radii of gyration – X Axis
FPV	=	Floating Photovoltaic	Kyy	=	Radii of gyration – Y Axis
g	=	Acceleration due to Gravity	Kzz	=	Radii of gyration – Z Axis
GHG	=	Greenhouse gas	LCB	=	Longitudinal Center of Buoyancy
GHI	=	Global Horizontal Irradiation	LCG	=	Longitudinal Center of Gravity
GWp	=	Giga Watt peak	LoA	=	Length over All

[1] Department of Naval Architecture, Faculty of Marine Technology, Institut Teknologi Sepuluh Nopember, Surabaya, 60111, Indonesia.
[2] School of Water, Energy, and Environmental, Cranfield University, Bedford, MK 43 0AL, UK.
* Corresponding Author: *kutama@na.its.ac.id*

Submitted: 2 February 2024, Revised: 8 April 2024, Accepted: 1 May 2024, Published: 20 May 2024

Conference paper, DOI: https://doi.org/10.59490/imdc.2024.854 e-ISSN: 3050-4864

m	=	meter	ω	=	Angular Frequency (Wave Frequency)
MWp	=	Mega-Watt peak	S_J	=	JONSWAP's Wave Spectrum
N_2O	=	Nitrous Oxide	S_{PM}	=	Pierson-Moskowitz Wave Spectrum
NJR	=	New Jersey Resources Corporation	S_ζ	=	Wave Spectrum
R^2	=	Validity Error Values – R Squared	m_0	=	Area under the Response Spectrum Curve
RAOs	=	Response Amplitude Operators	∇	=	Laplace Operator
S	=	Spacing of FPV	ζ_{k0}	=	Amplitude of Motion in a Specific Mode
T	=	Draft of FPV	ζ_0	=	Wave Amplitude
Tp	=	Peak Wave Period	$S_{\zeta r}$	=	Response Spectra
UV	=	Ultra-Violet	ζ_s	=	Significant Amplitude
ϕ	=	Potential Velocity Function	γ	=	Non-dimensional peak shape parameter
Δ	=	Displacement	φ	=	Wave Heading
σ	=	Spectral Width Parameter			

INTRODUCTION

Indonesia strives to achieve a 23% renewable share of energy in the nation's overall energy composition within the next year based on the Minister of Energy and Mineral Resources of the Republic of Indonesia (2021), as depicted in Figure 1. a.
The high dependency on coal has the potential to result in a significant increase in greenhouse gas (GHG) emissions. As an example, by the end of 2021, the Institute for Essential Services Reform, IESR (2022) determined that the greenhouse gas emission profile in Indonesia was primarily comprised of CO_2, with a contribution of 93.10%. Following together was CH_4 at roughly 5.90%, whilst the remaining 1.00% is identified as N_2O following in Figure 1. b. Even though methane (CH_4) contributes less to emissions than CO_2, it can cause emissions which are as high as 29.80 times higher.
Furthermore, another extensive review of IEA (2022) data reveals that coal combustion, specifically in coal-fired power plants (CFPPs), is responsible for a considerable 72.10% of methane (CH_4) emissions. As shown in Figure 1c, the oil and gas industry contributes 23.40% of these emissions, with the remaining 4.50% going to the bioenergy sector.

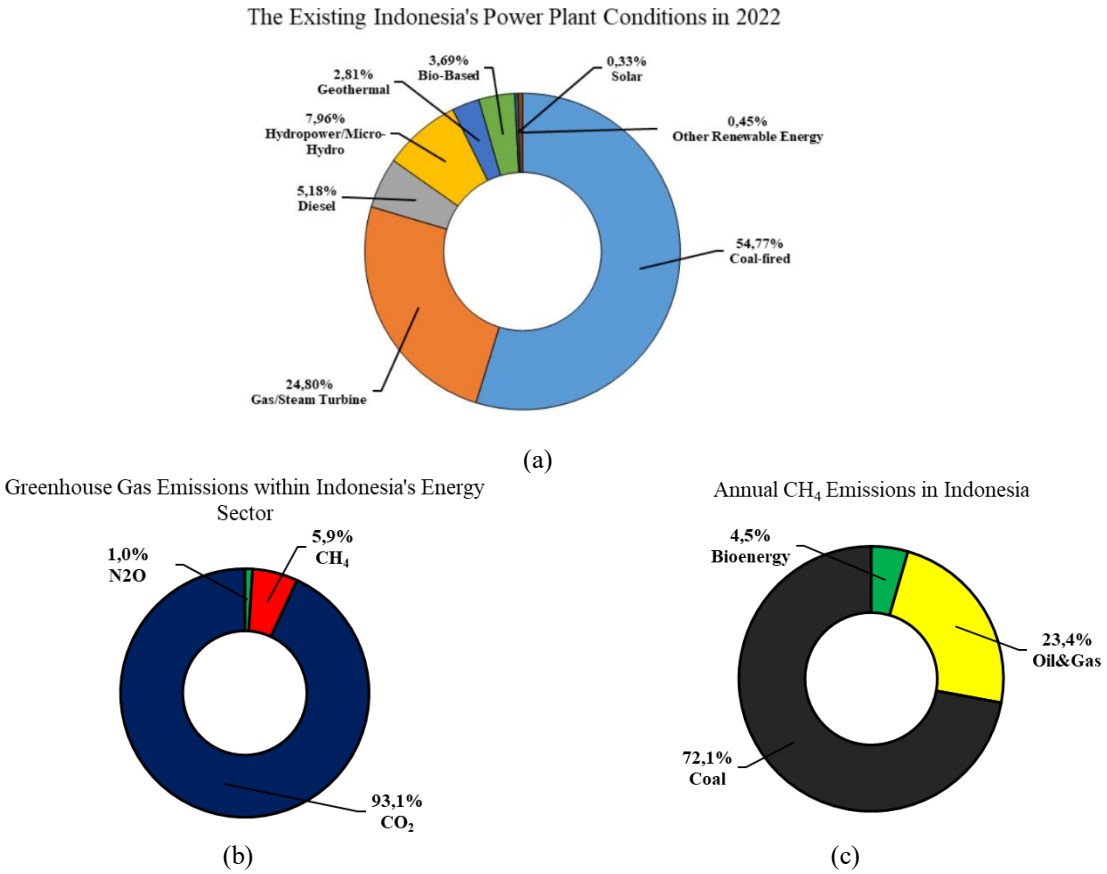

Figure 1. (a) The Ratio of Power Plant Conditions in Indonesia in 2022, (b) Greenhouse Gas Emissions within Indonesia's Energy Sector, (c) Annual CH_4 Emissions in Indonesia

Therefore, in a proactive action, the Indonesian government has issued a document Presidential Regulation 112 (2022), aiming to expedite the development of renewable energy for electricity supply. This regulation represents the gradual phase-out of coal-fired power plants (CFPPs). However, data from the Directorate General of Renewable Energy and Energy Conservation (2022), indicates that the share of Renewable Energy (RE) in the national energy mix was 12.16% in 2021, with a slight increase of 0.12% in 2022, which should be valued at 12.30%. Figure 2 illustrates the comparison of the percentage between the planned actions and the realization share mix of renewable energy implementation with a total target of 23% in the monitoring year 2022.

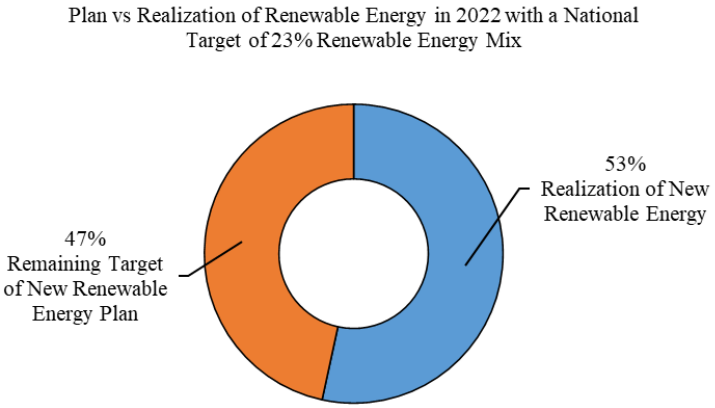

Figure 2. Realization vs Remaining Target of the Renewable Energy Plan in 2022

Approaching the year 2025, the State Electricity Company emphasizes the crucial role of expanding hydroelectric and geothermal power plants to achieve the 23% target in the national energy mix, as both sources can generate a significant energy by the Minister of Energy and Mineral Resources of the Republic of Indonesia (2021). However, these government projects have faced delays due to challenges related to land acquisition, environmental exploration, social concerns, and the high investment required. As a result, it is critical to take proactive actions toward discovering alternate renewable energy sources. An example is the deployment of solar energy converter systems.

Additionally, as highlighted by Shi et al., (2023), Solar energy is ecologically favourable, prominent, and widely distributed, warranting robust development. The solar photovoltaic (PV) system is a popular technology for directly converting solar energy into electricity using the photogenerated power effect of PV cells. Its wide range of uses includes both on-grid and off-grid power systems.

Implementing large-scale operations in photovoltaic (PV) power plants is a considerable difficulty due to the substantial land required for installation as explained by Sreenath et al., (2020). Then, as predicted by Rosa-Clot & Tina (2018), Land-based solar power facilities have an average demand of 0.50-0.70 MWp/ha. Furthermore, Pimentel & Branco (2018) explained that the forest destruction, extinction of birds due to habitat loss, erosion, runoff, and microclimate changes are some of the issues that arise throughout the installation and generation stages. Then a brief overview by Wang & Lund (2022), presents that in dealing with these challenges, researchers are actively investigating water-based PV systems, which include both fixed and floating PV (FPV) technologies from an offshore perspective. This novel technique is emerging as a promising alternative, searching to tackle the energy demand while limiting the environmental impact (Shi et al., 2023)

The fixed PV systems model, as described by Shi et al., (2023), illustrates that solar panels are secured to the seabed using pile foundations. However, the economic implications of this bottom-fixed technique reduce with increasing water depth, due to the substantially higher cost of piling. As a result, Rosa-Clot & Tina (2018) and World Bank Group (2019), give alternative solutions that are explored for deep water applications offshore, often using floating PV (FPV) systems. These FPV systems typically represent floaters or pontoons, PV modules, mooring systems, and cables as stated by Rosa-Clot et al., (2010) and Sen et al., (2015).

Over the past ten years, there has been an essential global study on floating photovoltaic (FPV) technology. The Aichi Project in Japan, with a capacity of 20 kW, represented the introduction of the first pilot FPV technology to the world in 2007, as may be noticed by Choi et al., (2016). Subsequently, the World Bank Group (2019) confirmed that in 2008, the first commercially operating FPV plant was presented in California, USA, with a capacity of 175 kW. Initially, these two initial projects are specifically designed for small-scale research projects. Trapani & Santafé (2015), confirmed that in 2015, Japan launched its first large-scale FPV plant, with a capacity of 7.55 MWp, followed by Boersma et al., (2019) revealed that a 40 – MWp plant was introduced in China in 2017. With the financial support of the African Development Bank and Clinton Foundation, Seychelles accomplished a historic milestone by establishing a 4 MW FPV plant in 2018 then becoming the first African nation to create history in FPV technology as explained by Beetz, (2018).

Proceeded into the year 2019, the Korea Energy Agency (2022) informed that the Korean rural community corporation was established to install 280 MW of FPV plants, whereas France built a 17 MW FPV system (Kenning, 2018). In the opening years of 2022, Shandong province in China delivered its largest FPV plant to the grid system, with a capacity of 320 MW (Lindholm et al., 2022). Furthermore, particularly in Indonesia, in collaboration with Masdar, is looking into a 60.00 MW FPV project to achieve 23% renewable energy by 2025 and 31% by 2030, with a significant milestone 145 MW project executed on a 250-hectare water area (Masdar, 2023). Singapore-based company "Sunseap" is developing a large 2.20 GW FPV in the Batam reservoir, expected completed by 2024 (Silalahi et al., 2021). Singapore has impressive goals to develop the world's biggest offshore FPV plant with a capacity of 2.00 GW by 2030 in its renewable energy sector (Liu et al., 2020). Additionally, the United States currently discovering the largest FPV project in progress, an 8.90 MW installation managed by New Jersey Resources Corporation (NJR) Clean Energy Ventures in Millburn, New Jersey. (Islam et al., 2023). Table 1 which follows provides further information and details on the ten largest FPV projects undertaken globally starting in 2020.

Table 1. The ten most extensive floating photovoltaic (FPV) projects worldwide

No	Country	Electric Capacity	Location	Provider / Investor	Years	Ref
1	Indonesia	2200 MW	Duriangkang reservoir, Batam Island	Sunseap, BP Batam	2024-2025	(Reuters, 2021)
2	South-Korea	2100 MW	Saemangeum floating solar energy project	SK E&S, Ocean Sun Hanwa Q Cells	2025-2030	(Frost&Sullivan, 2024)
3	India	600 MW	Omkareshwar reservoir, Madhya Pradesh	Tender process on going	2023-2024	(Frost&Sullivan, 2024)
4	China	550 MW	Wenzhou, Zhejiang Province	Chint Group	2021	(Emiliano Bellini, 2022)
5	Vietnam	500 MW	Laly hydropower reservoir, Dong Nai	Blueleaf Energy Asia	2021	(Japan International Cooperation Agency (JICA), 2020)
6	China	320 MW	Changhe and Zhouxiang reservoirs in Cixi	Hangzhou Fengling Electricity Science Technology	2020	(Frost&Sullivan, 2024)
7	Laos	240 MW	Nam Theun 2 hydropower plant, Khammouane	Electricté De France - EDF	2024	(Amir Garanovic, 2021)
8	Taiwan	181 MW	Chenghua County	Chenya Energy	2020	(Enerdata, 2020)
9	Indonesia	145 MW	Cirata, West Java	Masdar Solar Energy	2022	(Frost&Sullivan, 2024)
10	Thailand	45 MW	Sirindhorn Dam, Chanin Saleechan	B.Grimm Power, Energy China	2021	(Tom Kenning, 2019)

Table 1 shows Indonesia's ability to achieve a significant position among the top ten Floating Photovoltaic (FPV) projects globally supported by the highest potential Global Horizontal Irradiation (GHI), reaching up to 4.80 kWh/m2, as reported by (Silalahi et al., 2022), and represented in the subsequent Figure 3, when contrasted with other countries. This observation suggests that the adoption of FPV technology in Indonesia presents substantial and expansive opportunities, emphasizing the need for strategic planning to harness this potential for the future.

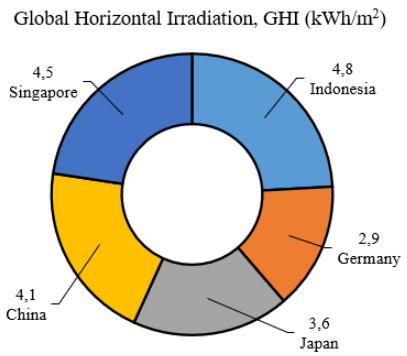

Figure 3. Global Horizontal Irradiation (GHI)

During the design process of a Floating Photovoltaic (FPV) system, a critical part is the floating structural component. It plays a crucial part in ensuring the system's buoyancy and stability. Following a research study by Sahu & Sudhakar (2019), the floating structure is often made of non-hazardous, UV light-resistant, and maintenance-free plastic materials recognised for their high tensile strength, for example, High-Density Polyethylene (HDPE). Several studies from Oliveira-Pinto & Stokkermans (2020); World Bank Group (2019) and Claus & López (2022) show that applying HDPE has numerous benefits, including a simple and easily implemented construction. Its lightweight characteristic contributes to reducing tension on the overall structure in response to offshore hydrodynamic pressures, and the use of minimum metal reduces susceptibility to corrosion. Furthermore, HDPE provides cost-effective beneficial effects when compared to other materials such as concrete (Mittal et al., 2017) and steel (Cazzaniga et al., 2017)

Taking these various factors into consideration, this study proposes a novel approach for floaters by utilizing the geometric shape of High-Density Polyethylene (HDPE) hulls. This material has several advantages, including resistance to the sea environment and protection against UV degradation effects. The research focuses on innovative floater design configurations in catamaran, trimaran, quadrimaran, and pentamaran. The impact of the hull configuration, administered as an initial design parameter, will be investigated by Computational Fluid Dynamics (CFD) simulations under the JONSWAP wave spectrum, including various sea-state situations.

The paper is organized as follows: **Section 2** describes the problem characterisation for the original concept of floating hull constructions. **Section 3** provides an extensive overview of the research methodology, as well as technical details about the Computational Fluid Dynamics (CFD) numerical setup. **Section 4** advances further into the CFD numerical simulation findings, investigating the effect of hull configuration on motion characteristics. Finally, **Section 5** provides a summary of the study, emphasizing its important findings.

PROBLEM CHARACTERIZATION

A multi-hull construction with several configurations starting from the catamaran (2 hulls), trimaran (3 hulls), quadrimaran (4 hulls), and pentamaran (5 hulls) is proposed. These hulls are identical geometric shapes and sizes, arranged in parallel to form an integrated structure (single-array) designed for energy farming. This numerical study considers several factors, including independent variables, dependent variables, and control variables. In a numerical/experimental study, the researcher manipulates or changes the independent variables to determine how they affect the dependent variables. Dependent variables are measured or observed in reaction to changes in independent variables, indicating the predicted outcomes of the numerical/experimental study. In numerical/experimental studies, control variables remain constant to ensure that changes in independent variables are the cause of observed effects on dependent variables. Table 2 describes the individual variables utilized in this numerical investigation.

Table 2. Utilized variables

Independent Variables	Dependent Variables	Control Variable

• Sea-State [Hs]
  o Sea-State 1 [0.1 m]
  o Sea-State 2 [0.5 m]
  o Sea-State 3 [1.25 m]
  o Sea-State 4 [2.50 m]
• Wave Heading
  o 0 Degree [Head Sea]
  o 45 Degree [Oblique Sea]
  o 90 Degree [Beam Sea]
• Hull Configuration
  o Catamaran
  o Trimaran
  o Quadrimaran
  o Pentamaran
	• Significant heave response ($\zeta_{s\ Global\ Z}$)
	• Significant roll response ($\zeta_{s\ Global\ RX}$)
	• Significant pitch response ($\zeta_{s\ Global\ RY}$)
		• LoA
		• Breadth Demihull
		• Spacing
		• Height
		• Draft

The dominant pure oscillatory response motions, particularly heave, rolling, and pitching characteristics in regular waves, will be determined by evaluating the free-floating conditions for all proposed design models. The results will be shown in a graph of Response Amplitude Operators (RAOs), where the frequency parameter is indicated on the horizontal axis (X-absis) and the ratio of motion amplitude in a specific mode to the wave amplitude is represented on the vertical axis(Y-ordinate), as explained by Djatmiko (2012).

As a result, the motion quality values for each proposed design will be presented as a representation of a curve, with the x-axis representing the type or number of hull configurations for the floaters and the y-axis representing the floating structure motion quality values (heave, roll, and pitch) for a specific sea-state. The trends of the scatter graph for each simulation result point

will be represented by the equation of a line that corresponds to the validity error values - R squared (R2) within the value that comes closest to 1.

METHODOLOGY

This numerical solution is based on a Computational Fluid Dynamics (CFD) simulation. The following subsection includes data for each proposed design with initial main principal dimensions, along with electrical capacity and weight distribution calculations then followed by a general layout. The seakeeping performance is evaluated by significant response spectra ($\zeta_{s\,[Z]}$, $\zeta_{s\,[RX]}$, $\zeta_{s\,[RY]}$,) , using further stochastic computations to calculate the area under the spectrum curve for specific sea situations.

Model Description & Initial Calculation

The stated numbers for floater hull dimensions are identical for each proposed design configuration, indicating that the addition of hull different forms is carried out by replicating the shape of the previous hull design laterally following Figure 4.

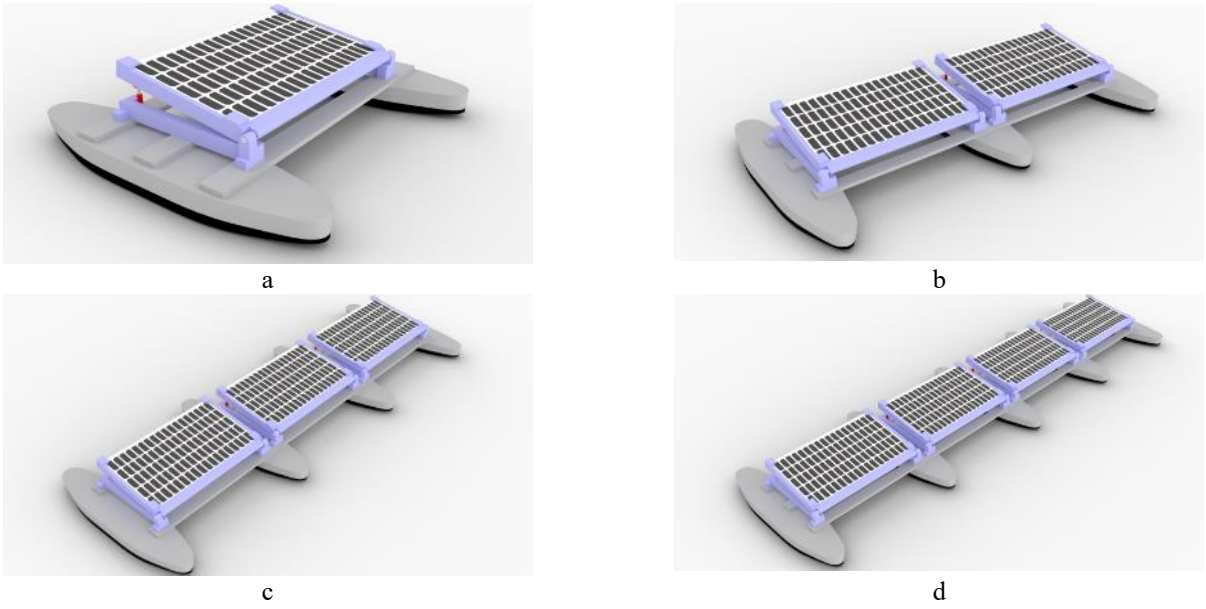

Figure 4. Novel design of hull geometry adaptation for FPV: (a) Catamaran, (b) Trimaran, (c) Quadrimaran, (d) Pentamaran

The main dimensions related to the hydrostatic properties of each design are tabulated in Table 3. It should be noted that, due to the identical values of the hull shape dimensions, this will result in hydrostatic properties of the identical FPV floating structure, except for the total width and displacement values of the FPV structure.

Table 3. Main principles dimension

Parameter	Catamaran	Trimaran	Quadrimaran	Pentamaran	Units
Length over All (LoA)	3.24	3.24	3.24	3.24	m
Breadth (B)	3.54	6.34	9.14	11.94	m
Height (H)	0.30	0.30	0.30	0.30	m
Draft (T)	0.12	0.12	0.12	0.12	m
Demihull Width (B1)	0.74	0.74	0.74	0.74	m
Spacing (S)	2.80	2.80	2.80	2.80	m
Hydrostatic properties					
Displacement (Δ)	437.31	655.31	874.74	1094.17	kg
Block coefficient (Cb)	0.75	0.75	0.75	0.75	-
Prismatic coefficient (Cp)	0.76	0.76	0.76	0.76	-
Keel to buoyancy (KB)	0.06	0.06	0.06	0.06	m
Longitudinal Center of Buoyancy (LCB) from AP	1.62	1.62	1.62	1.62	m

Table 4 shows the total installed power capacity for each proposed model, as well as the characteristics of the solar panel technology used.

Table 4. PV system specification and total power generation capacity

Parameter	Value	Unit	Remarks
PV capacity	665	Watt peak (Wp)	
Module efficiency	21.40	%	
Length of PV	2.38	m	(CSI Solar Co. Ltd, 2021)
Width of PV	1.30	m	
PV module weight	34.40	kg	
Total generating capacity			
Catamaran	665	Watt peak (Wp)	These calculations are
Trimaran	1330	Watt peak (Wp)	based on the maximum
Quadrimaran	1995	Watt peak (Wp)	capacity of the considered
Pentamaran	2660	Watt peak (Wp)	PV system technology

Governing Equations

The CFD simulation software's governing equation assumed a homogeneous, inviscid, irrotational, and incompressible fluid, as outlined by (Haug et al., 2018). This assumption aims to identify the potential velocity function, which serves as a criterion for determining fluid characteristics like velocity and pressure. The computation of Response Amplitude Operators (RAOs) within the Boundary Element Method (BEM) techniques were performed using (Ansys, 2019). The potential velocity can be expressed as equation (1), where i, j, and k represent unit vectors along the x-, y-, and z-axes, respectively.

$$V = \nabla_{\phi} = \frac{\partial \phi}{\partial x} i + \frac{\partial \phi}{\partial y} j + \frac{\partial \phi}{\partial z} k \tag{1}$$

Under the assumption that the fluid remains incompressible – implying a consistent mass within the flow entering and leaving a control surface – the Laplace equation is formulated by the following expression (2).

$$\nabla^2{}_{\phi} = \frac{\partial u}{\partial x} + \frac{\partial v}{\partial y} + \frac{\partial w}{\partial z} = 0 \tag{2}$$

Subsequently, to ensure compliance with the continuity equation, every potential velocity solution should be accompanied by the non-rotation condition outlined in equation (3). In simpler terms, an irrotational fluid is one in which the vorticity vector is uniformly zero across the entire fluid.

$$\omega_v = \nabla^2 \times V = 0 \tag{3}$$

In this scenario, fluid does not pass through the surface of a fixed body in motion. This condition indicates the impermeability of the object and is expressed in equation (4).

$$\frac{\partial \phi}{\partial n} = 0 \tag{4}$$

While equation (4) indicates the impermeability of a fixed body, such as the seabed, with n representing a normal vector pointing from the seabed and extending into the fluid, equation (5) expands this concept for a moving body with a velocity V

$$\frac{\partial \phi}{\partial n} = V \,.\, n \tag{5}$$

The kinematic free-surface condition states that in the presence of small waves, fluid particles at the surface are expected to remain on the free surface. Furthermore, the dynamic free-surface condition requires that the water pressure at the free surface becomes equal to a constant atmospheric pressure. The following equation (6) expresses the simplified and linearized formulations for the kinematic and dynamic free-surface conditions, which use linear theory and assume small waves, zero current, and zero forward speed of the body.

$$\frac{\partial^2 \zeta}{\partial t^2} + g\frac{\partial \phi}{\partial z} = 0 \qquad on\ z = 0 \tag{6}$$

In the end, as the vessel interacts with the waves, the potential velocity becomes an instrument for representing the wave flow field around the hull sections. Furthermore, the potential velocity is critical in computing the fluid force applied on the hull section, as well as determining hull motion and wave force. Consequently, the potential velocity generated by external waves can be combined using the method described in (7).

$$\phi = \phi_i + \phi_r + \phi_d \tag{7}$$

ϕ_i, ϕ_r, ϕ_d representing the potential functions for the incident wave, radiation wave, and diffraction wave, respectively. ϕ_i is computed using Airy linear theory, while the derivation of ϕ_r and ϕ_d relies on the application of diffraction theory. In diffraction theory, the potential function is determined by solving the Laplace equation, considering relevant boundary conditions, and subsequently calculating the pressure and resulting forces acting on the body. Additionally, pressure is extracted using the Bernoulli equation, and the potential function is determined. In conclusion, the integration of pressure over the entire wet surface area produces wave excitation forces, which are then utilized in the AQWA software.

Response Amplitude Operators (RAOs)

The Response Amplitude Operator (RAO) is a function of the dynamic motion of a structure induced by waves within a specific frequency range. RAO serves as a tool to convert wave forces into the dynamic motion response of the structure. Translation and rotational RAOs are described by equations (8) – (9).

$$RAO_{(k=x,y,z)} = \frac{\zeta_{k0}}{\zeta_0} \tag{8}$$

$$RAO_{(k=\theta,\phi,\psi)} = \frac{\zeta_{k0}}{\left(\frac{\omega^2}{g}\right)\zeta_0} \tag{9}$$

Calculation of Wave Spectral

JONSWAP's wave spectrum formulation is a modified version of the Pierson-Moskowitz spectrum with integrating parameters to accommodate the characteristics of waves in enclosed waters or island environment Djatmiko (2012) Therefore, it is suitable for application in Indonesia's archipelago with the following equation (10) – (14) based on DNV-GL recommendation Det Norske Veritas (2010)

$$S_J(\omega) = A_\gamma S_{PM}(\omega)\gamma^{exp\left[-0.5\left(\frac{\omega-\omega_p}{\sigma\omega_p}\right)^2\right]} \tag{10}$$

$$S_{PM}(\omega) = \frac{5}{16}.{H_s}^2{\omega_p}^4.\omega^{-5}exp\left[-\frac{5}{4}\left(\frac{\omega}{\omega_p}\right)^{-4}\right] \tag{11}$$

$$\omega_p = \frac{2\pi}{T_p} \tag{12}$$

$$A_\gamma = 1 - 0.287\ln(\gamma) \tag{13}$$

$$\sigma = 0.07 \text{ for } \omega \le \omega_p \textbf{ or } \sigma = 0.09 \text{ for } \omega > \omega_p \tag{14}$$

Where, $S_J(\omega)$ is the JONSWAP spectrum, $S_{PM}(\omega)$ is the Pierson-Moskowitz spectrum, ω_p is the angular spectral peak frequency, T_p is the spectral peak period, H_s is the significant wave height, A_γ is the normalizing factor, γ is the non-dimensional peak shape parameter, and σ is the spectral width parameter.

Calculation of Responses Spectral

The responses of a floating structure in irregular waves shall be obtained by correlating the RAO with the wave spectrum within transforming wave energy into response energy with the following equation (15). Subsequently, the amplitude significant response is calculated as equation (16).

$$S_{\zeta r}(\omega) = RAO^2 \times S_\zeta(\omega) \tag{15}$$

$$\zeta_s = 2\sqrt{m_0} \tag{16}$$

Where $S_{\zeta r}(\omega)$ is the response spectrum, $S_{\zeta}(\omega)$ is the waves spectrum and m_0 is the area under the response spectrum curve as shown in the following equation (17).

$$m_0 = \sum_{n=1}^{\infty} S_{\zeta}(\omega)\delta\omega = \int_0^{\infty} S_{\zeta}(\omega)d\omega \tag{17}$$

3-D Diffraction CFD Simulation Setup

The three-dimensional (3D) models of floating structures were developed using the Maxsurf modeler by Bentley System (2022). Subsequently, the 3D model was exported in .step format through Rhinoceros software to conduct seakeeping analysis using Ansys Aqwa. The statistical validation between Ansys Aqwa and the baseline for manual calculations was required to stay within a 2% threshold for all considerations, as detailed in the results presented in Table 4 (a) – (d) as recommended by Suastika et al., (2021)

Table 5. Statistical validation: (a) catamaran, (b) trimaran, (c) quadrimaran, (d) pentamaran

(a)

Parameter	AQWA	Manual Calculation	Difference (%)
Hydrostatic properties			
Displacement Δ (ton)	442.80	437.31	1.25
Water plane area (m^2)	3.86	3.86	0.21
Longitudinal center of gravity, LCG (m) from AP – CL	1.62	1.62	0.00
Inertia Properties			
Inertia moment – X Axis, Ixx ($kg.m^2$)	584.36	577.09	1.26
Inertia moment – Y Axis, Iyy ($kg.m^2$)	204.81	202.26	1.26
Inertia moment – Z Axis, Izz ($kg.m^2$)	779.81	770.12	1.26

(b)

Parameter	AQWA	Manual Calculation	Difference (%)
Hydrostatic properties			
Displacement Δ (ton)	663.40	655.31	1.23
Water plane area (m^2)	5.80	5.79	0.22
Longitudinal center of gravity, LCG (m) from AP – CL	1.62	1.62	0.00
Inertia Properties			
Inertia moment – X Axis, Ixx ($kg.m^2$)	2696.87	2663.35	1.26
Inertia moment – Y Axis, Iyy ($kg.m^2$)	299.65	295.81	1.30
Inertia moment – Z Axis, Izz ($kg.m^2$)	2982.29	2944.16	1.30

(c)

Parameter	AQWA	Manual Calculation	Difference (%)
Hydrostatic properties			
Displacement Δ (ton)	884.12	874.74	1.07
Water plane area (m^2)	7.74	7.72	0.21
Longitudinal center of gravity, LCG (m) from AP – CL	1.62	1.62	0.00
Inertia Properties			
Inertia moment – X Axis, Ixx ($kg.m^2$)	7241.88	7165.42	1.07
Inertia moment – Y Axis, Iyy ($kg.m^2$)	436.94	431.83	1.18
Inertia moment – Z Axis, Izz ($kg.m^2$)	7657.56	7575.05	1.09

(d)

Parameter	AQWA	Manual Calculation	Difference (%)
Hydrostatic properties			
Displacement Δ (ton)	1104.23	1094.16	0.92
Water plane area (m^2)	9.67	9.67	0.20
Longitudinal center of gravity, LCG (m) from AP – CL	1.62	1.62	0.00
Inertia Properties			
Inertia moment – X Axis, Ixx ($kg.m^2$)	15018.96	14883.71	0.91
Inertia moment – Y Axis, Iyy ($kg.m^2$)	542.62	537.30	0.99
Inertia moment – Z Axis, Izz ($kg.m^2$)	15536.47	15392.39	0.94

Furthermore, the motion characteristics are the combination of the mass properties and hull surface geometry of the floating structure. The mass properties such as inertia values and center of gravity (CoG) indicate how resistant a body is to changes in its rotational state. The mass properties are defined in Ansys Aqwa as a "point mass" with automatically calculated in mass and only input in radius gyration as can be seen Table 5.

Table 6. Radii of gyration of floating structures

Component	Catamaran (m)	Trimaran (m)	Quadrimaran (m)	Pentamaran (m)
K_{xx} (X-Axis)	1.15	2.02	2.86	3.69
K_{yy} (Y-Axis)	0.68	0.67	0.70	0.70
K_{zz} (Z-Axis)	1.33	2.12	2.94	3.75

The generating mesh provides to calculation of pressures and forces on each number element in hull surface geometry (Bosma et al., 2012). A finer mesh was used in interface between wet and dry surface region. Both of floating were meshed as shown in Figure 4.

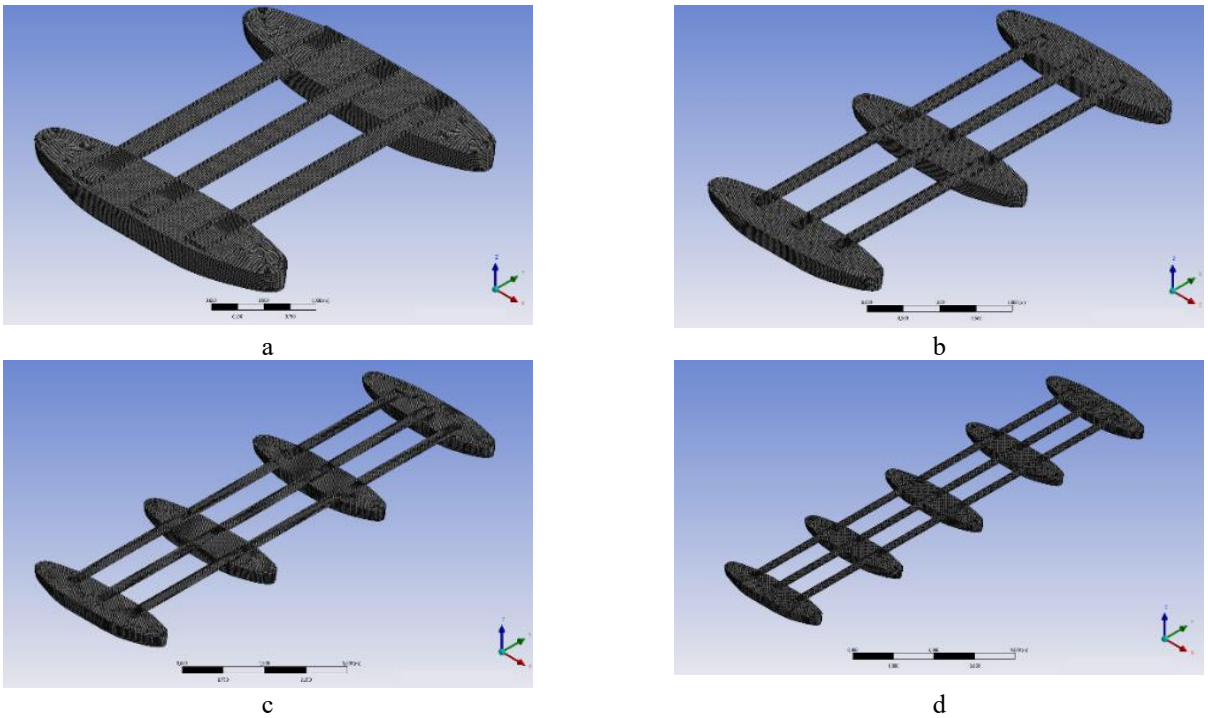

a b c d

Figure 5. Mesh visualization: (a) Catamaran, (b) Trimaran, (c) Quadrimaran, (d) Pentamaran

RESULT AND DISCUSSION

The results and discussions in this paper are divided into subsections: a key point of the fundamental proposed design, Response Amplitude Operators (RAOs) and JONSWAP's wave spectra under various sea states, including structural response spectra within stochastic values.

The main recommended design component emphasizes the importance of selecting hull-shaped floater concepts in PV technology, covering from catamaran to pentamaran shapes. This subsection examines several of the advantages of this multi-hull design in depth.
In the RAOs subsection, all graphs related to motion analysis in heave, roll, and pitch modes for each proposed design model are explained in the frequency range of 0.05 – 3.00 rad/sec. Explanations for the heave RAO graph will be presented for headings φ = 0, φ = 45, and φ = 90 degrees. The roll RAO graph is subsequently clarified for headings φ = 45 and φ = 90 degrees. The pitch RAO graph is described at headings of φ = 0 and φ = 45 degrees.
The significant response value of oscillatory pure motions subsection describes various aspects, including significant wave height values under each sea-state condition, and the visualization of JONSWAP wave spectra, followed by several graphical representations of motion quality calculations for each mode and sea-state condition for each proposed model.

A Key Point of the Fundamental Proposed Design

The floater structure, as a form of buoyant force, must be designed to withstand vertical and horizontal loads. The vertical load is less substantial than anticipated, as evidenced by the lightweight proportion of this FPV innovation design, which is just approximately 38% of the total displacement capacity, indicating that this technology was created with minimalism and lightness. Furthermore, horizontal cyclic loads such as wind, wave, and current loads must be considered because the technology will be utilized in nearshore locations (Liu et al., 2018). However, presently, HDPE blocks are commonly used in the implementation of FPV technology in lakes with generally calm water conditions – related to restricted limited wind fetch generating waves and mountains surrounded area (Allsop et al., 2018; Gudrun Sigtryggsdottir, 2022). Typically, certain designs involve only segments of the HDPE blocks, which are then arranged on the water surface to provide adequate buoyancy and serve as a platform for solar panel technology. Shifting the perspective toward nearshore areas is aimed at harnessing a significantly larger technical space compared to utilizing reservoirs – which are typically limited to only 5% of the total area as per Indonesia's Public Work and Housing regulation (IESR, 2021). Subsequently, to address the challenges of dynamic nearshore water conditions, the approach for developing a PV technology floater shape must be improved.
Many prior investigations have demonstrated the numerous advantages of multihull ship designs over monohulls. This ship with several hulls is a novel type of high-speed performance ship created in the late twentieth century (Molland et al., 2011). The multihull concept originated from their ability to handle more cargo than ordinary commercial containerships, resulting in improved capacity and lower emissions due to greatly decreased water resistance. This has a positive effect on environmental conservation (Zhao et al., 2023). Figure 6 might help demonstrate specific types of high-speed and low-resistance vessels.

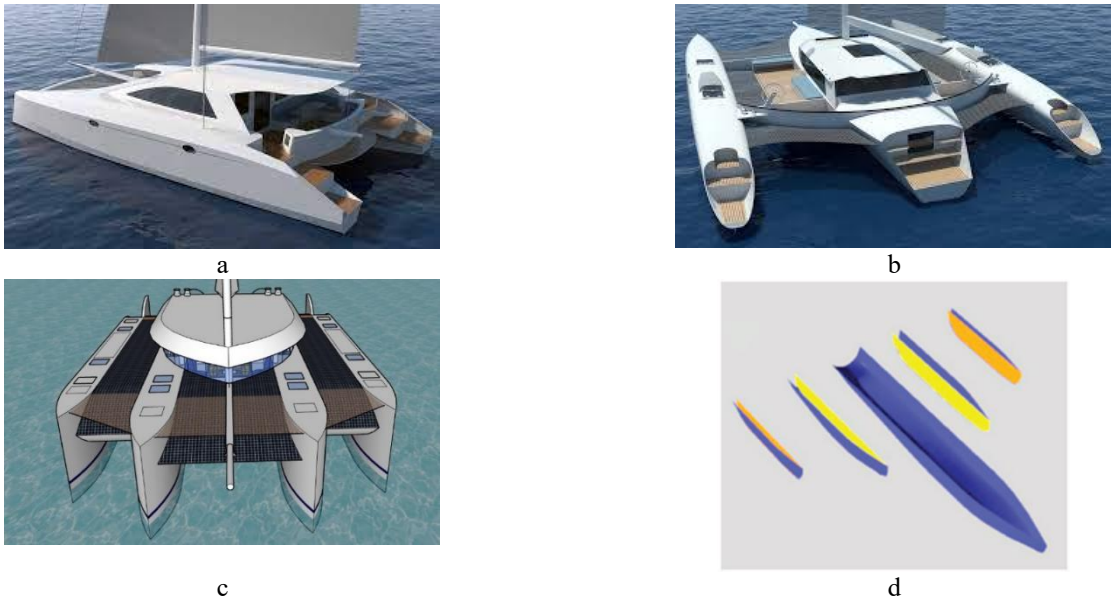

Figure 6. High-speed and low-resistance vessels: (a) Catamaran, (b) Trimaran, (c) Quadrimaran, (d) Pentamaran
Ref: (Dr. Hans, 2021; Schionning Designs International (Pty) Ltd, 2024; Yanuar & Waskito, 2017)

The innovative concept attempts to replicate the characteristics of high-speed boats in a stationary (non-propelled) PV floater system. However, the number of hulls utilized increases the cost component in manufacture, but this is rationalized by the size of the service deck along with the location of solar panels, where this renewable energy source is proportional to area. As explained by Bhattacharyya (1978) and (Zhao et al., 2023), the addition of lateral hulls enhances the metacenter height,

resulting in a significant reduction in excitation force due to the degree of roll motion, which is related to the natural period of the motion, lateral acceleration, and extra transverse stability.
Similar to other renewable energy technology concepts, the development of FPV technology is expected to evolve towards the concept of energy farming at sea. This involves a series of configurations, both laterally and transversally on the water surface where the incremental addition of floaters becomes inevitable. Hence, the complex and multi-analysis of CFD within fluid-structure interaction shall be conducted the key design of FPV energy farming (Wei et al., 2024).

Response Amplitude Operators (RAOs)

The results of seakeeping numerical simulations for all designs are presented in this section. Due to the symmetrical geometry in the stern and bow of all proposed floating structures, the wave heading is considered only at φ = 0° (following sea), φ = 45° (quartering sea), and φ = 90° (beam sea). From the three graphs provided, it becomes demonstrated that at a 0° heading, all heave response graphs, from catamaran to pentamaran, demonstrate zero differences. This is because when waves counter from the forward position (FP) or backside (AP), the FPV structural will be move (heave response mode) in a synchronized up-and-down action. This is due to the hull configuration in the design is arranged adjacent to one another.
The response degrees at φ = 45° and φ = 90° are significantly lower than at φ = 0°. The trend throughout all three graphs has been described as follows: The heave response motion decreases as the wave incidence angle approaches perpendicular to the longitudinal axis of the ship's centerline (φ = 90°). This behavior is also consistent with the increase of hull types. At headings of φ = 45° and φ = 90°, the pentamaran model demonstrates the lowest heave reaction.

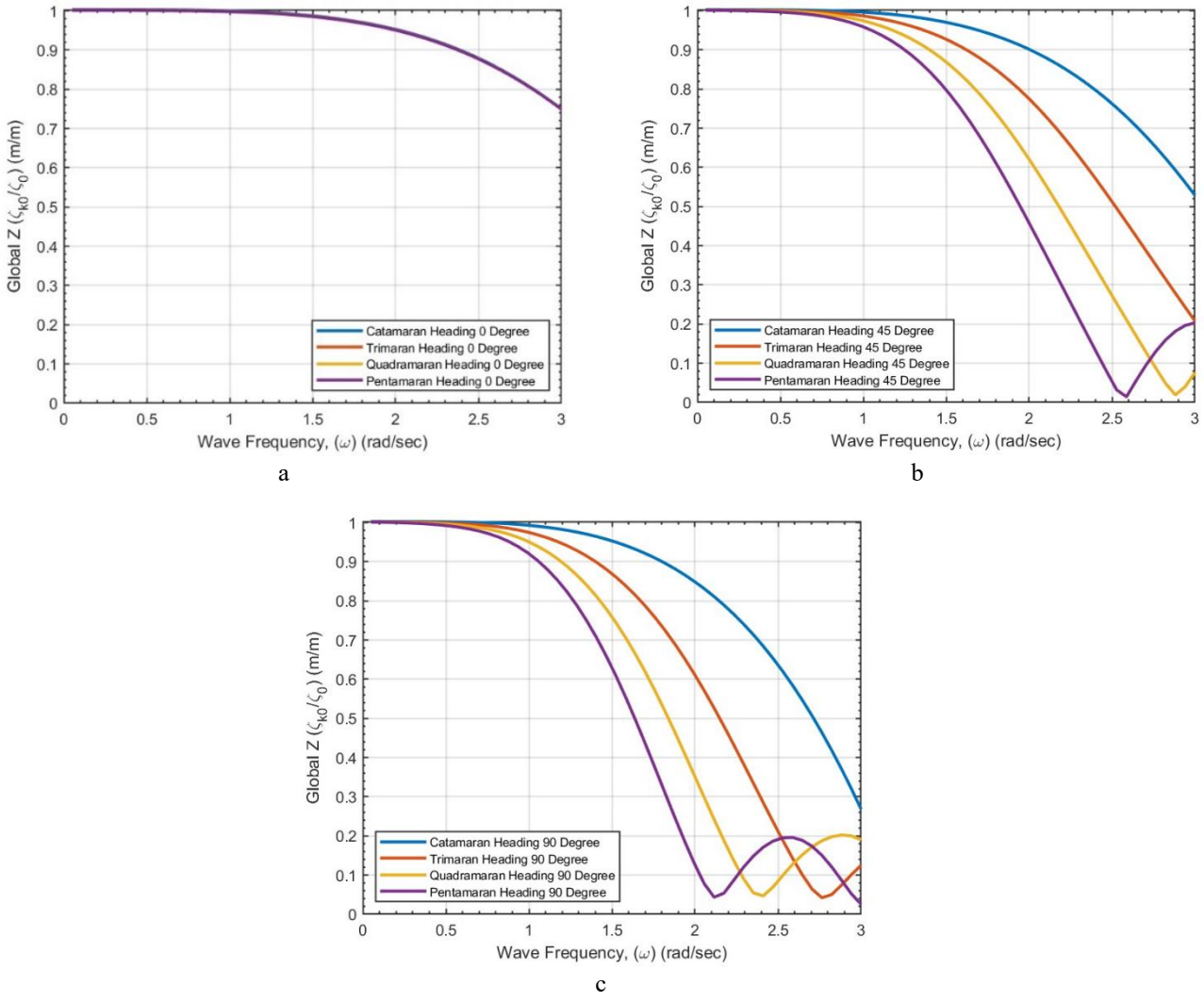

Figure 7. Heave RAO: (a) φ = 0°, (b) φ = 45°, (c) φ = 90°

Furthermore, the roll Response Amplitude Operator (RAO) curve of the FPV structure shows that the highest value of the peak roll response RAO occurs in the φ = 90° of wave incidence direction, indicating that this is the dominant direction leading to the roll response when compared to the 45° heading. Nevertheless, further investigation shows a significant discrepancy in peak values between the two headings (φ = 45 & 90°), particularly in the catamaran model (the difference can reach over 40% - nonetheles this percentage value will decrease significantly with the addition of configurations to the FPV structure). Then the addition of the hull configuration for the floater, the area under the roll motion response curve (RAO) will decrease, indicating that with an increasing number of float structure configurations, the roll motion can be dampened.

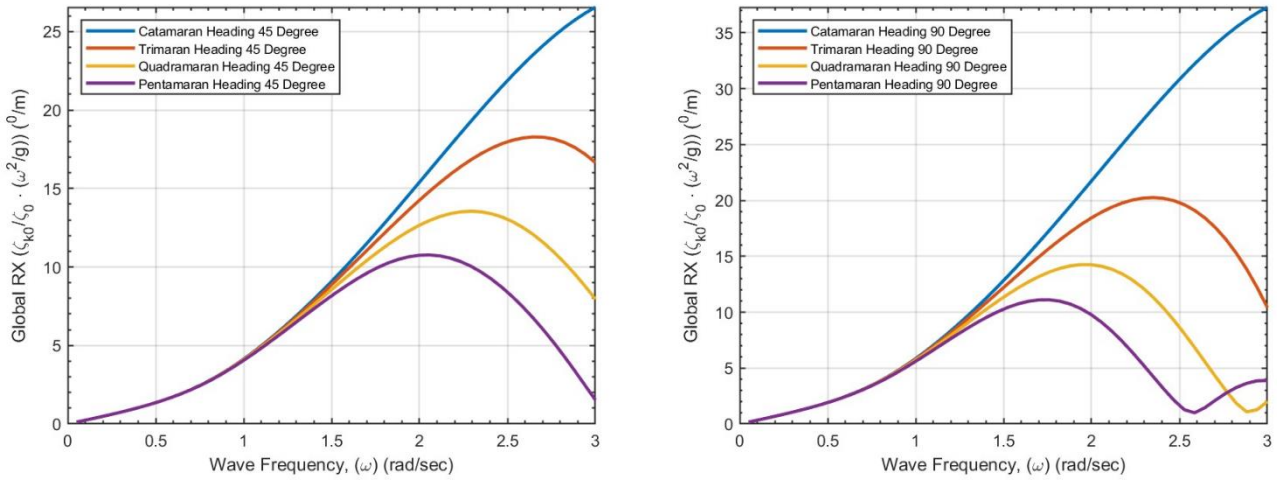

a b

Figure 8. Roll RAO: (a) φ = 45°, (b) φ = 90°

Then, the final response considered as pure oscillatory motion is the pitch motion. The findings of this investigation are unique, considering that the pitch response at the φ = 0° heading for all proposed designs is similar to the heave motion mode (no differences occur). When the structure is stimulated by waves from the dominant pitch motion direction (φ = 0°), all models will consistently provide identical response values throughout the specified wave frequency range. This also indicates that the addition of hull configuration to the FPV structure does not have a significant influence on the performance of this pitch motion mode.

However, there is a substantial difference at 45° heading, since the consequences of adding hull configurations to the FPV structure appear to have a significant effect. The pentamaran hull configuration has the lowest peak value of the pitch Response Amplitude Operator (RAO) response when compared to the other floater configuration.

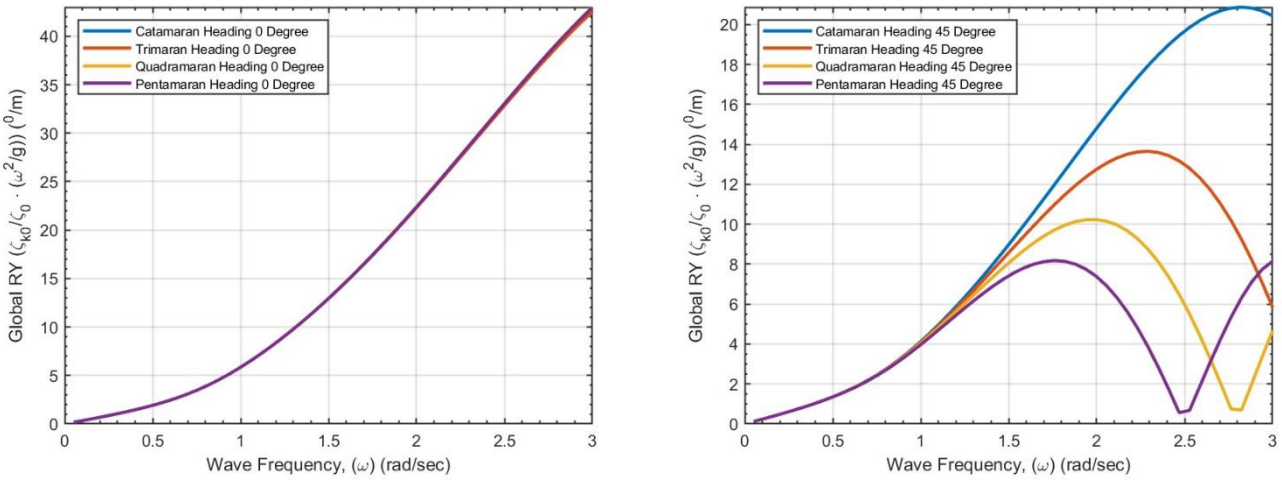

a b

Figure 9. Pitch RAO: (a) φ = 0°, (b) φ = 45°.

Significant Response Value of Oscillatory Pure Motions

Analyzing the wave spectrum is the subsequent process in evaluating the effect of the hull configuration. Figure 10 illustrates JONSWAP's wave spectra for sea states 1–4 based on Table 7, which indicate sea conditions.

Table 7. Sea-state codes

Sea-State	Description of sea	Significant Wave Height (m)
1	Calm (rippled)	0.10
2	Smooth (wavelets)	0.50
3	Slight	1.25
4	Moderate	2.50

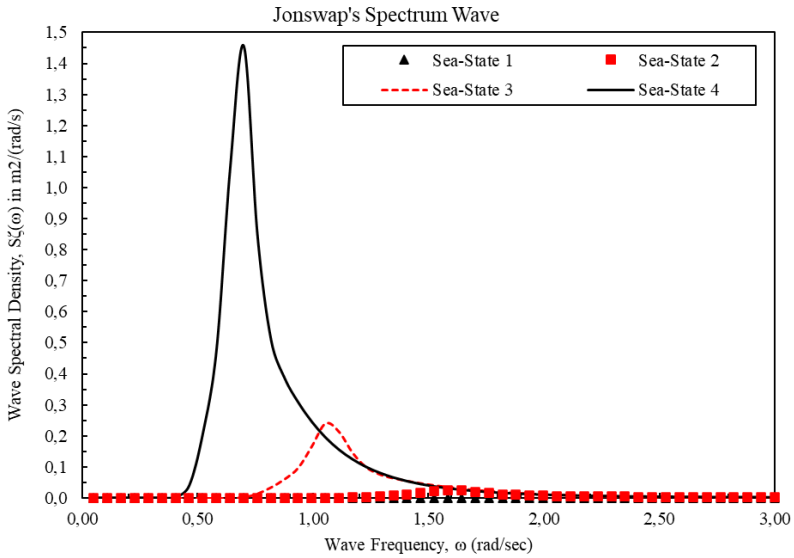

Figure 10. JONSWAP's wave spectra for various sea-state

Two key factors that influence the arrangement of response spectra are the wave spectrum and the RAO for specific modes. Moreover, stochastic parameters were computed based on the curves of response spectra for each mode. Nevertheless, the primary focus of this investigation will be restricted to determining significant response amplitudes, which represent an average measurement of the largest 33% of responses, within the sea-state range of 1-4.

Then, in Figures 11-14, it is shown that there is a negative linear trend in all three motion modes (pure oscillatory motion) when hull configurations have been added to the FPV floater structure under each sea-state scenario.

These graphs provide insightful data, particularly if there is an objective for developing an FPV floater structure using the single-array design concept with the addition of configurations laterally. The equation of each graph's negative linear regression line can be applied to predict the qualitative value of floating structure motion for an FPV structure with more than 5 hulls (pentamaran).

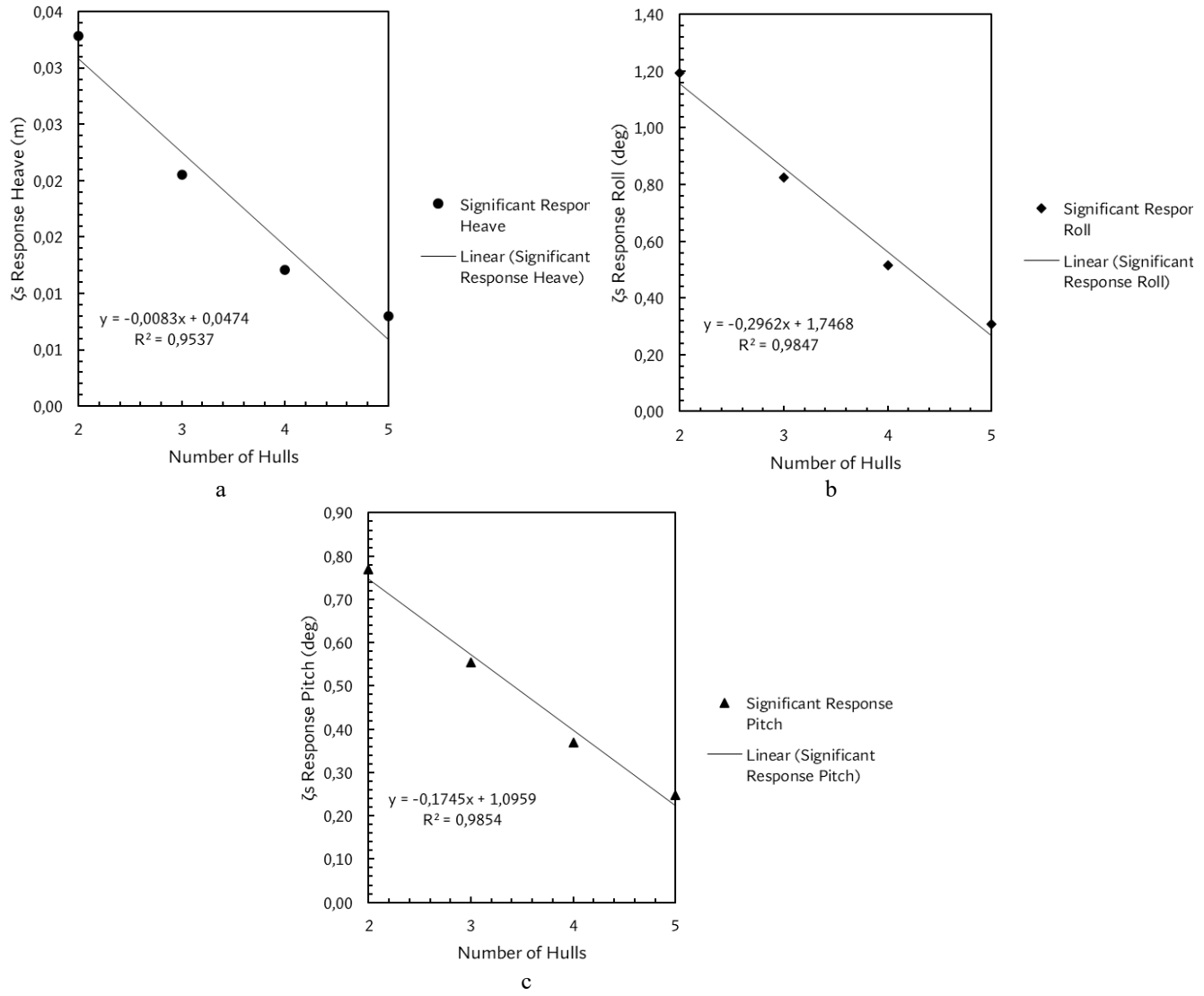

Figure 11. ζs Respons FPV – Sea-State 1: (a) Global Z, (b) Global RX, (c) Global RY

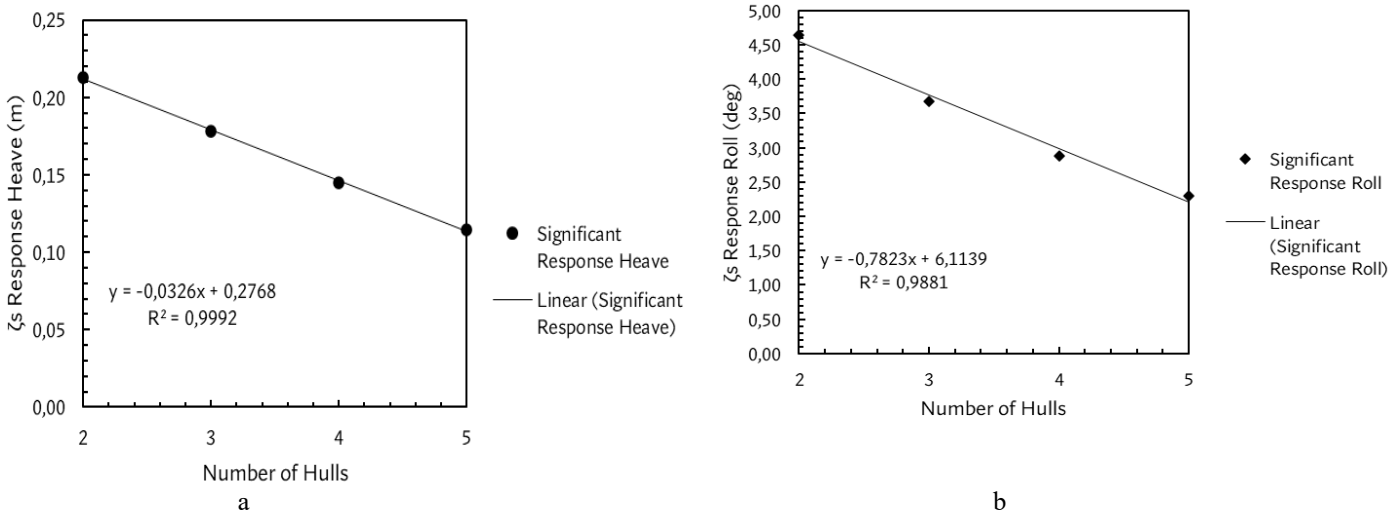

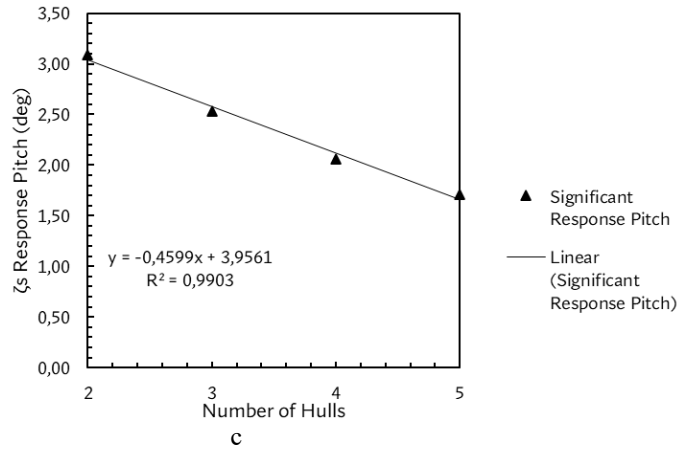

c

Figure 12. ζs Respons FPV – Sea-State 2: (a) Global Z, (b) Global RX, (c) Global RY

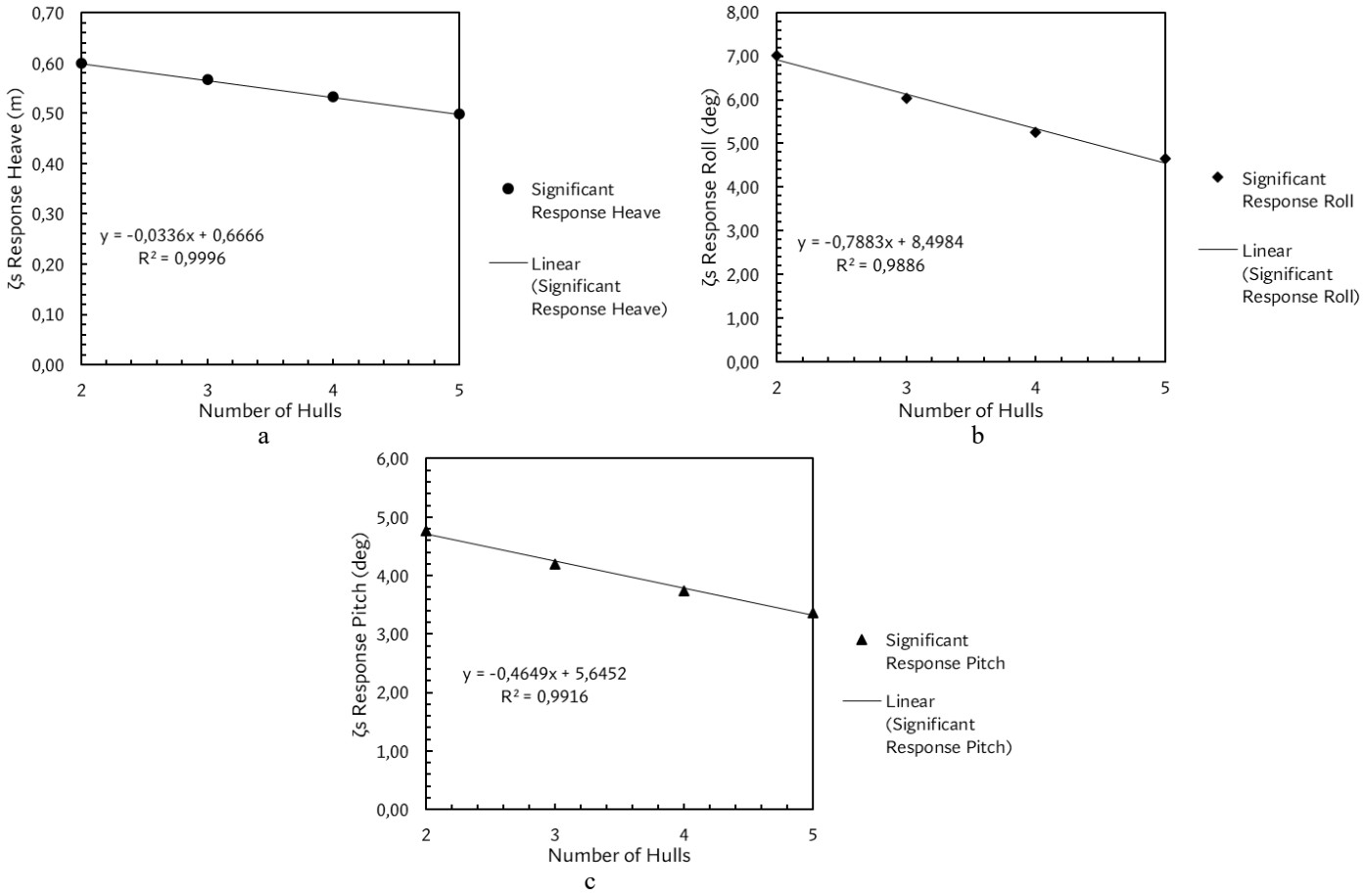

a b c

Figure 13. ζs Respons FPV – Sea-State 3: (a) Global Z, (b) Global RX, (c) Global RY

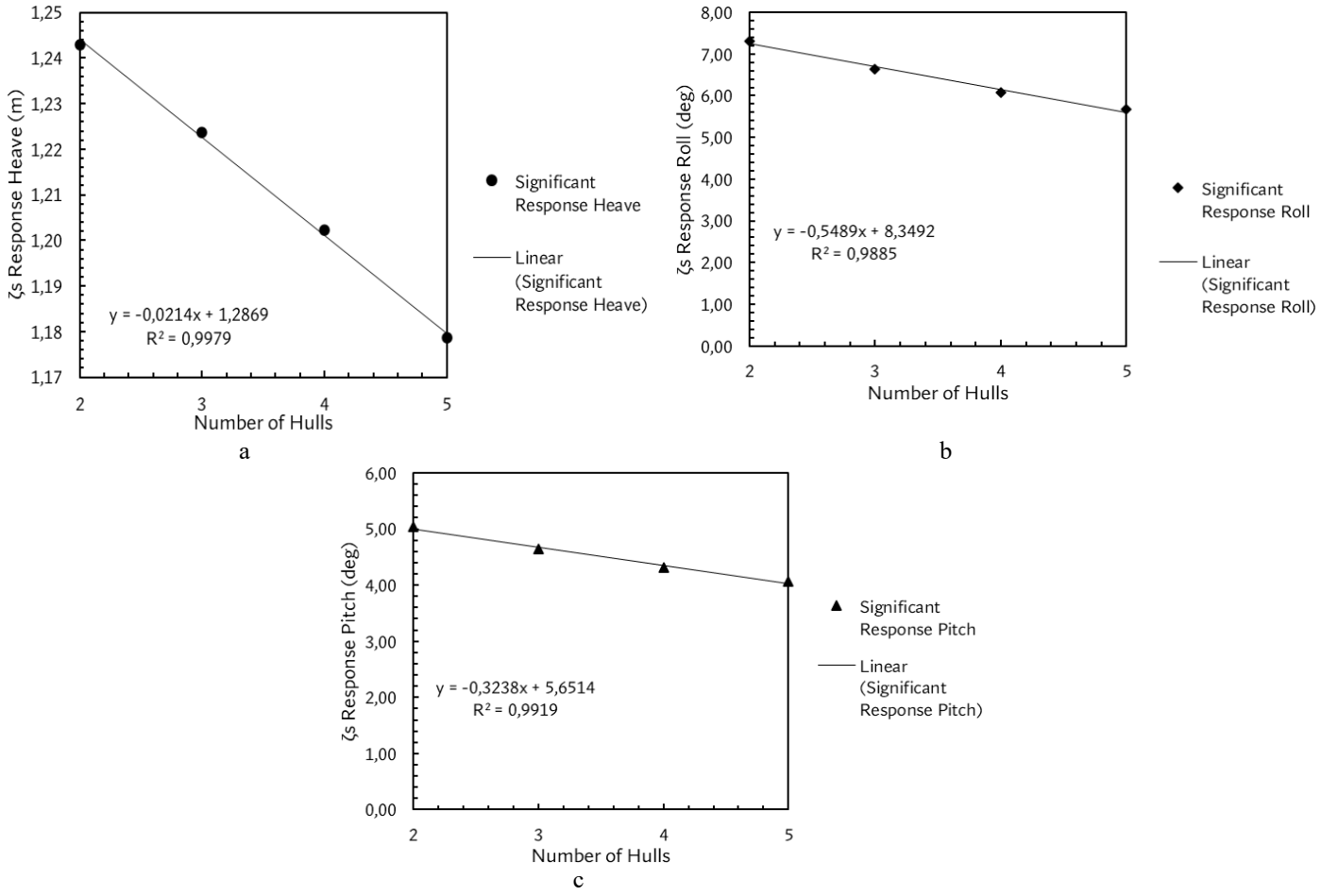

Figure 14. ζs Respons FPV – Sea-State 4: (a) Global Z, (b) Global RX, (c) Global RY

Table 8 illustrates the relationship between the variable reflecting the quantity of proposed floating structure configurations along the X-axis and its impact on the quality of each motion mode generated along the Y-axis under predefined sea-state conditions.

Table 8. Regression equation for each motion mode

Sea-State	Significant Responses	Equation	Curve Form	R^2
Sea-State 1	Heave	y= -0.0083x + 0.0474	Linear Negative	0.954
	Roll	y= -0.2962x + 1.7468		0.985
	Pitch	y= -0.1745x + 1.0959		0.985
Sea-State 2	Heave	y= -0.0326x + 0.2768		0.999
	Roll	y= -0.7823x + 6.1139		0.988
	Pitch	y= -0.4599x + 3.9561		0.990
Sea-State 3	Heave	y= -0.0336x + 0.6666		1.000
	Roll	y= -0.7883x + 8.4984		0.989
	Pitch	y= -0.4649x + 5.6452		0.992
Sea-State 4	Heave	y= -0.0214x + 1.2869		0.998
	Roll	y= -0.5489x + 8.3492		0.989
	Pitch	y= -0.3238x + 5.6514		0.992

CONCLUSIONS

A study was conducted to investigate the impact of platform configurations and environmental conditions on the performance of floating solar photovoltaic (FPV) structures. Numerical Computational Fluid Dynamics (CFD) simulations based on 3-D

diffraction were carried out to identify pure oscillatory motions in heave, pitch, and roll for all proposed designs. The numerical findings show that the FPV structure with 5 (five) floater hulls has the lowest motion response (pure oscillatory motion) compared to other configurations under each sea-state scenario. Furthermore, there is a negative linear trend in the motion response of the FPV structure from the catamaran configuration to the pentamaran. It is essential to note that if subsequent studies desire for a concept with several hull configurations exceeding 5 hulls, the negative linear regression equations for each motion under different sea-state conditions can be predicted, provided that the design concept, geometric shape, configuration arrangement, and several control variables remain similar to this study.
Furthermore, , The future works should consider the selection of mooring configurations and various types for the FPV structure's mooring system. The hydrodynamics responses of mooring lines and FPV structures could be investigated in the time domain analysis.

DECLARATION OF GENERATIVE AI AND AI-ASSISTED TECHNOLOGIES IN WRTITING

During the preparation of this work the author(s) did not use any generative AI and AI-assisted technologies in writing of this article.

CONTRIBUTION STATEMENT

Author 1:Methodology; software; validation; formal analysis; investigation; resources; writing – original draft; writing – review & editing; visualization. **Author 2:** Validation; investigation; writing – review & editing; supervision. **Author 3:** Investigation; writing – review & editing; funding acquisition. **Author 4:** Investigation; writing – review & editing; supervision. **Author 5:** Conceptual; investigation; writing – review & editing; supervision; project administration.

ACKNOWLEDGEMENTS

The authors express their gratitude to Institut Teknologi Sepuluh Nopember for providing research funding through the Outbound Researcher Mobility (ORM) program for the 2023/2024 period, batches 1, 2, and 3, under contract number 2432/IT2/T/HK.00.01/2023. The authors also appreciate the facilities, as well as scientific and technical support, provided by the Hydrodynamics Laboratory of Naval Architecture.

REFERENCES

Allsop, W., Goff, C., Wallingford, H. R., Pullen, T., Silva, E., & Williamson, T. (2018). *Wave and overtopping predictions on reservoirs and inland waterways*. https://www.researchgate.net/publication/327405119

Amir Garanovic. (2021, July 26). *EDF to develop 240MW floating solar project in Laos*. Offshore Energy. https://www.offshore-energy.biz/edf-to-develop-240mw-floating-solar-project-in-laos/

Ansys. (2019). *Ansys Aqwa Theory Manual*.

B. Beetz. (2018). Africa Announces Utility-Scale Floating Solar Tender. *PV Magazine*. https://www.pv-magazine.com/2018/04/09/africa-announces-utility-scale-floating-solar-tender/

Bentley System. (2022). *Maxsurf Modeler User Manual*.

Bhattacharyya, Rameswar. (1978). *Dynamics of marine vehicles*. John Wiley & Sons.

Boersma, T., Van der Laan, J., Noorduyn, O., & Mesbahi, M. (2019). *A Comprehensive Overview of 200+ Global Floating Solar Plants*. Solar Plaza. https://www.solarplaza.com/channels/future-grid/12067/200-global-floating-solar-plants/

Bosma Br, Zhang Zhe, Brekken Ted K.A, Ozkan H. Tuba, Mc Natt Cameron, & C Yim Solomon. (2012). Wave Energy Converter Modeling in the Frequency Domain: A Design Guide. *IEEE*, 2099–2106.

Cazzaniga, R., Cicu, M., Rosa-Clot, M., Rosa-Clot, P., Tina, G. M., & Ventura, C. (2017). Compressed air energy storage integrated with floating photovoltaic plant. *Journal of Energy Storage*, *13*, 48–57. https://doi.org/https://doi.org/10.1016/j.est.2017.06.006

Choi, Y. K., Choi, W. S., & Lee, J. H. (2016). Empirical Research on the Efficiency of Floating PV Systems. *Science of Advanced Materials*, *8*(3), 681–685. https://doi.org/10.1166/sam.2016.2529

Claus, R., & López, M. (2022). Key issues in the design of floating photovoltaic structures for the marine environment. *Renewable and Sustainable Energy Reviews*, *164*, 112502. https://doi.org/10.1016/j.rser.2022.112502

CSI Solar Co. Ltd. (2021, January). *Preliminary Technical Information Sheet of Canadian Solar*.

Det Norske Veritas. (2010). *Recommended Practice Environmental Conditions and Environmental Loads*. http://www.dnv.com

Directorate General of Renewable Energy and Energy Conservation. (2022). *Performance Report of the Directorate General of Renewable Energy and Energy Conservation for 2022* (Vol. 1, Issue). EBTKE Directorate General . https://globalsolaratlas.info/global-pv-potential-study

Djatmiko, E. B. (2012). *The Behavior and Operability of Offshore Structure in Random Waves*. ITS Press.
Dr. Hans. (2021, July 7). *Quadramaran: what do you think?* Cruisers & Sailing Forums. https://www.cruisersforum.com/forums/f48/quadrimaran-what-do-you-think-253004.html
Emiliano Bellini. (2022, January 7). *Chinese fish pond hosts 550 MW solar farm*. PV Magazine. https://www.pv-magazine.com/2022/01/07/chinese-fish-pond-hosts-550-mw-solar-farm/
Enerdata. (2020, April 23). *Chenya Energy reaches financial close for 181 MW floating PV park (Taiwan)*. Enerdata. https://www.enerdata.net/publications/daily-energy-news/chenya-energy-reaches-financial-close-181-mw-floating-pv-park-taiwan.html
Frost&Sullivan. (2024). *Global Solar Photovoltaic Growth Opportunities*. Frost&Sullivan Online Store. https://store.frost.com/global-solar-photovoltaic-growth-opportunities.html
Gudrun Sigtryggsdottir, F. (2022). *Environmental loads on embankment dams in mountainous regions*. www.nve.no
Haug, Ø., Trym, L., & Sjøberg, S. (2018). *Evaluation and Comparison of Operability and Operational Limits of Service Vessel Designs in Exposed Aquaculture*.
IEA. (2022). *International Energy Agency for Methane Tracker*. IEA. https://www.iea.org/data-and-statistics/data-tools/methane-tracker-data-explorer#comparison-sources
IESR. (2021). *Technical Potential of Floating Solar Photovoltaic in Central Java*. IESR. https://www.iea.org/reports/solar-pv
IESR. (2022). *Indonesia Energy Transition Outlook 2023: Tracking Progress of Energy Transition in Indonesia: Pursuing Energy Security in the Time*.
Islam, M. I., Maruf, M. H., Al Mansur, A., Ashique, R. H., Asif ul Haq, M., Shihavuddin, A. S. M., & Jadin, M. S. (2023). Feasibility analysis of floating photovoltaic power plant in Bangladesh: A case study in Hatirjheel Lake, Dhaka. *Sustainable Energy Technologies and Assessments*, *55*. https://doi.org/10.1016/j.seta.2022.102994
Japan International Cooperation Agency (JICA). (2020). *The Study on Power Network System Master Plan in Lao People's Democratic Republic*. https://openjicareport.jica.go.jp/pdf/12328027_01.pdf
Korea Energy Agency. (2022). *National Survey Report of PV Power Applications in Korea*. https://iea-pvps.org/wp-content/uploads/2024/01/IEA-PVPS-National-Survey-Report-KOREA-2022.pdf
Lindholm, D., Selj, J., Kjeldstad, T., Fjær, H., & Nysted, V. (2022). CFD modelling to derive U-values for floating PV technologies with large water footprint. *Solar Energy*, *238*, 238–247. https://doi.org/10.1016/j.solener.2022.04.028
Liu, H., Krishna, V., Lun Leung, J., Reindl, T., & Zhao, L. (2018). Field experience and performance analysis of floating PV technologies in the tropics. *Progress in Photovoltaics: Research and Applications*, *26*(12), 957–967. https://doi.org/10.1002/pip.3039
Liu, H., Kumar, A., & Reindl, T. (2020). *The Dawn of Floating Solar—Technology, Benefits, and Challenges* (pp. 373–383). Springer Link. https://doi.org/10.1007/978-981-13-8743-2_21
Masdar. (2023). *Cirata Floating Solar Photovoltaic*. Masdar. https://masdar.ae/en/news/newsroom/president-of-indonesia-inaugurates-floating-solar-plant
Minister of Energy and Mineral Resources of the Republic of Indonesia. (2021). *Electricity Supply Business Plan* (Vol. 1). State Electricity Company (PT. PLN).
Mittal, D., Saxena, B. K., & Rao, K. V. S. (2017). Floating solar photovoltaic systems: An overview and their feasibility at Kota in Rajasthan. *2017 International Conference on Circuit ,Power and Computing Technologies (ICCPCT)*, 1–7. https://doi.org/10.1109/ICCPCT.2017.8074182
Molland, A. F., Turnock, S. R., & Hudson, D. A. (2011). *Ship Resistance and Propulsion : Practical Estimation of Ship Propulsive Power.* Cambridge University Press.
Oliveira-Pinto, S., & Stokkermans, J. (2020). Assessment of the potential of different floating solar technologies – Overview and analysis of different case studies. *Energy Conversion and Management*, *211*, 112747. https://doi.org/10.1016/j.enconman.2020.112747
Pimentel Da Silva, G. D., & Branco, D. A. C. (2018). Is floating photovoltaic better than conventional photovoltaic? Assessing environmental impacts. *Impact Assessment and Project Appraisal*, *36*(5), 390–400. https://doi.org/10.1080/14615517.2018.1477498
Presidential Regulation 112/2022, Pub. L. No. 112, Presidential Regulation of the Republic of Indonesia 1 (2022).
Reuters. (2021, July 22). *Sunseap to build $2 billion floating solar farm in Indonesia, world's largest*. Reuters. https://www.reuters.com/business/energy/sunseap-build-2-bln-floating-solar-farm-indonesia-worlds-largest-2021-07-22/
Rosa-Clot, M., Rosa-Clot, P., Tina, G. M., & Scandura, P. F. (2010). Submerged photovoltaic solar panel: SP2. *Renewable Energy*, *35*(8), 1862–1865. https://doi.org/10.1016/j.renene.2009.10.023
Rosa-Clot, M., & Tina, G. M. (2018). Submerged PV Systems. *Submerged and Floating Photovoltaic Systems*, 65–87. https://doi.org/10.1016/B978-0-12-812149-8.00004-1
Sahu, A. K., & Sudhakar, K. (2019). Effect of UV exposure on bimodal HDPE floats for floating solar application. *Journal of Materials Research and Technology*, *8*(1), 147–156. https://doi.org/10.1016/J.JMRT.2017.10.002
Schionning Designs International (Pty) Ltd. (2024). *Tracer 1500TRi Preliminary Study Plans*. https://schionningdesign.com/sdi/

Sen, D., Sharma, P., & Muni, B. (2015). DESIGN PARAMETERS OF 10KW FLOATING SOLAR POWER PLANT. *International Advanced Research Journal in Science, Engineering and Technology*, *2*(1). https://doi.org/10.17148/IARJSETP10

Shi, W., Yan, C., Ren, Z., Yuan, Z., Liu, Y., Zheng, S., Li, X., & Han, X. (2023). Review on the development of marine floating photovoltaic systems. *Ocean Engineering*, *286*. https://doi.org/10.1016/j.oceaneng.2023.115560

Silalahi, D. F., Blakers, A., Stocks, M., Lu, B., Cheng, C., & Hayes, L. (2021). Indonesia's vast solar energy potential. *Energies*, *14*(17). https://doi.org/10.3390/en14175424

Silalahi, D. F., Gunawan, D., Wahyuni, E., Dipayana, G. F., Hardhi, M., Winofa, N. C., Ramadhan, R. A., & Hidayat, T. (2022). Indonesia Post-Pandemic Outlook: Strategy towards Net-Zero Emissions by 2060 from the Renewables and Carbon-Neutral Energy Perspectives. In *Indonesia Post-Pandemic Outlook: Strategy towards Net-Zero Emissions by 2060 from the Renewables and Carbon-Neutral Energy Perspectives*. Penerbit BRIN. https://doi.org/10.55981/brin.562

Sreenath, S., Sudhakar, K., Yusop, A. F., Solomin, E., & Kirpichnikova, I. M. (2020). Solar PV energy system in Malaysian airport: Glare analysis, general design and performance assessment. *Energy Reports*, *6*, 698–712. https://doi.org/10.1016/j.egyr.2020.03.015

Suastika, K., Silaen, A., Aliffrananda, M. H. N., & Hermawan, Y. A. (2021). Seakeeping analysis of a hydrofoil supported watercraft (Hysuwac): A case study. *CFD Letters*, *13*(5), 10–27. https://doi.org/10.37934/cfdl.13.5.1027

T. Kenning. (2018). *Independent power producer (IPP) Akuo Energy has started construction of a 17MW O'MEGA1 floating solar plant in France*. NS Energy. https://www.nsenergybusiness.com/news/akuo-energy-floating-solar-plant-france/

Tom Kenning. (2019, June 13). *Thai utility readies tender for 45MW floating solar on Sirindhorn Dam*. PV-Tech. https://www.pv-tech.org/egat-readies-tender-for-45mw-floating-solar-at-sirindhorn-dam/

Trapani, K., & Redõn Santafé, M. (2015). A review of floating photovoltaic installations: 2007-2013. In *Progress in Photovoltaics: Research and Applications* (Vol. 23, Issue 4, pp. 524–532). John Wiley and Sons Ltd. https://doi.org/10.1002/pip.2466

Wang, J., & Lund, P. D. (2022). Review of Recent Offshore Photovoltaics Development. In *Energies* (Vol. 15, Issue 20). MDPI. https://doi.org/10.3390/en15207462

Wei, Y., Zou, D., Zhang, D., Zhang, C., Ou, B., Riyadi, S., Utama, I. K. A. P., Hetharia, W., Wood, T., & Huang, L. (2024). Motion characteristics of a modularized floating solar farm in waves. *Physics of Fluids*, *36*(3). https://doi.org/10.1063/5.0199248

World Bank Group, E. and S. (2019). *Where Sun Meets Water: Floating Solar Handbook for Practitioners*. World Bank. www.worldbank.org

Yanuar, & Waskito, K. T. (2017). Experimental study of total hull resistance of pentamaran ship model with varying configuration of outer side hulls. *Procedia Engineering*, *194*, 104–111. https://doi.org/10.1016/j.proeng.2017.08.123

Zhao, B., Jiang, H., Sun, J., & Zhang, D. (2023). Research on the Hydrodynamic Performance of a Pentamaran in Calm Water and Regular Waves. *Applied Sciences (Switzerland)*, *13*(7). https://doi.org/10.3390/app13074461

Proceedings of 15th International Marine Design Conference (IMDC-2024)
June 2-6, 2024
Amsterdam, the Netherlands

A Fundamental Study on Inter-Array Cabling Methods Between Two Floating Offshore Wind Turbines in Shallow Waters

Kangho Kim[1], Chunsik Shim[1], Min Suk Kim[2], Daseul Jeong[1,*]

ABSTRACT

As the transition to renewable energy accelerates, interest in wind farms is heightening. There is a need to safely and economically transport energy produced from Floating Offshore Wind Turbines (FOWTs) to the shore. Consequently, this study conducted an analysis of inter-array cabling methods between two FOWTs in shallow waters, targeting the southwestern sea of South Korea. This research targeted four shapes of dynamic power cables: free hanging catenary, lazy wave shape, suspended and W-configuration type. To verify the economy of the dynamic power cable, the total lengths were compared, and to check safety, curvature and tension were examined. Insights obtained through this study indicate that among the four shapes of dynamic power cables, the lazy wave shape has substantial advantages in shallow waters.

KEY WORDS

Inter-array cable; Dynamic power cable; Motion analysis; Excursion.

INTRODUCTION

As interest in renewable energy grows, there is increasing attention to the production of eco-friendly electricity that can be mass-produced. Among these, the production efficiency of wind energy is relatively high compared to other green energy sources, making the construction of wind farms an essential role in decarbonization. The electricity from a wind farm, which comprises several wind turbines, is transmitted to a substation through power cables after each wind turbine generates it, as shows in Figure 1(Moon et al., 2014). In this study, we conducted a fundamental study on the methods of transmitting electricity from each wind turbine before it converges at the substation.

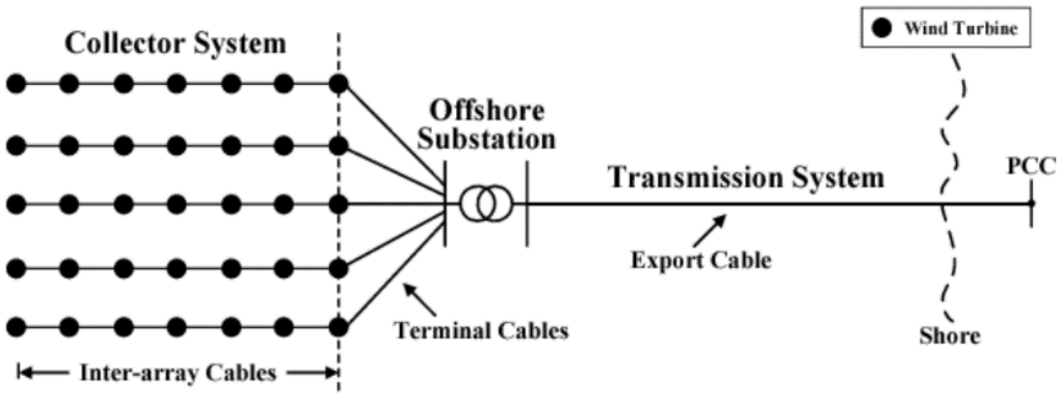

Figure 1: Power transmission system of floating wind farms

[1] Dept. of Naval Architecture and Ocean Engineering. Mokpo National Univ. Republic of Korea. [2] SURF R&D Center, Mokpo National Univ., Republic of Korea.
* Corresponding Author: dsjeoung@mokpo.ac.kr

Submitted: 13 February 2024, Revised: 2 April 2024, Accepted: 1 May 2024, Published: 21 May 2024

Conference paper, DOI: https://doi.org/10.59490/imdc.2024.823 e-ISSN: 3050-4864

Li et al. (2023) developed a dynamic response analysis model for ultra-deepwater cables with double-stepped configurations, focusing on the dynamic responses and robustness to moving boundaries during deep-sea mining operations. The study utilized finite element simulations combined with hydrodynamic models to analyze the cable's behavior under environmental excitations. It concluded that the double-stepped cable design offers improved compliance and effectiveness in buffering responses caused by moving boundaries, contributing to safer and more efficient deep-sea mining operations.

Chen et al. (2021) investigated the structural configurations and dynamic performances of flexible risers with distributed buoyancy modules, using Finite Element Method (FEM) simulations. Their study focused on assessing the influences of buoyancy module positioning and ratio on riser performance, especially under deep-sea mining conditions. The research concluded that the installation positions and buoyancy ratios significantly impact the riser's configuration, tension, and dynamic performance, contributing to the understanding of riser design for safe and effective deep-sea mining operations.

Okpokparoro and Sriramula (2023) conducted a reliability analysis of floating wind turbine dynamic cables under realistic environmental loads. Their research utilized an analytical model to evaluate the fatigue damage and reliability of these cables, considering environmental uncertainties and cable-soil interactions. The study offers significant insights into the structural reliability of dynamic power cables in offshore wind applications, highlighting the importance of considering realistic environmental loads in cable design and reliability assessment.

Poirette et al. (2017) presented a novel optimization methodology for the configuration of inter-array cables in floating offshore wind farms. This study utilizes FEM hydrodynamic simulations in conjunction with a derivative-free Sequential Quadratic Approximation (SQA) optimization algorithm. The research focuses on optimizing the cable layout for minimizing material costs while considering constraints to ensure cable integrity. This approach offers a new perspective on enhancing the efficiency and cost-effectiveness of cable configurations in floating offshore wind farm projects.

Zhao et al. (2021) conducted a study comparing two dynamic power cable configurations for floating offshore wind turbines in shallow water. Their research compared the hydrostatic and hydrodynamic performance of lazy wave and double wave configurations, utilizing a comprehensive numerical simulation approach. The study found that the double wave configuration exhibited superior performance, offering advantages in terms of reduced fatigue damage and better handling of high curvature tension.

Ahmad et al. (2023) explored an optimization methodology for suspended inter-array power cable configurations between two floating offshore wind turbines. Their research focused on the dynamic response of these configurations using a novel setup involving subsea buoys. The study demonstrated the feasibility of the suspended inter-array power cable concept, highlighting those smaller buoys yield more efficient designs and the copper cable configurations result in smaller horizontal excursions compared to aluminum cables.

Rentschler et al. (2019) focused on the design optimization of dynamic inter-array cable systems for floating offshore wind turbines. Utilizing a genetic algorithm, they analyzed cable configurations to improve fatigue life performance under extreme weather conditions. The research highlights the importance of considering dynamic behaviors and offers design recommendations for different water depths, contributing significantly to the development of efficient and reliable floating offshore wind technologies.

Schnepf et al. (2023) conducted a feasibility study on suspended inter-array power cables between two spar-type offshore wind turbines. This research involved exploring various cable configurations and their impact on structural behavior, focusing on buoyancy module placements. The study concluded that certain configurations, particularly those with strategically placed buoyancy modules, can lead to significant improvements in cable performance and cost-effectiveness in offshore wind turbine applications.

Jason Lavis (2021) argued that while shallow water was previously described as having depths of up to 91-121m, today, depths of less than 305m are now considered shallow. Tong (1998) identified the economic depth range for floating offshore wind turbines as typically between 100m and 300m. This study focuses on an area located in the Southwest Sea, with a water depth of 150m, falling well within Tong's suggested economic depth range. This placement offers optimal conditions for installing FOWTs, suggesting a strategic fit for this renewable energy technology in areas previously deemed challenging.

This study builds upon the 12MW FOWT model by SINTEF Norway and, to conduct a fully coupled dynamic analysis, using OrcaFlex to adapt to the ocean data measured from Uido island located in southwestern of Korea. The pivotal research endeavor involves the integration of a dynamic power cable into a 12 MW FOWT, thus considering the mooring system's intricate design. By adhering to the IEC 61400 regulations and realistic maritime conditions found in South Korea's southwestern sea, the study

carries out both Serviceability Limit State (SLS) and Ultimate Limit State (ULS) analyses, ensuring its findings' accuracy and practical relevance. The study focused on four types of power cables: free hanging catenary, lazy wave shape, suspended and W-configuration type.

METHOD

Three-column FOWT layout for optimal mooring and cable integration

Figure 2 shows the 12MW substructure model of SINTEF. The model consists of three columns and six pontoons. The main properties of the 12MW FOWT are summarized in Table 1 (SINTEF, 2022).

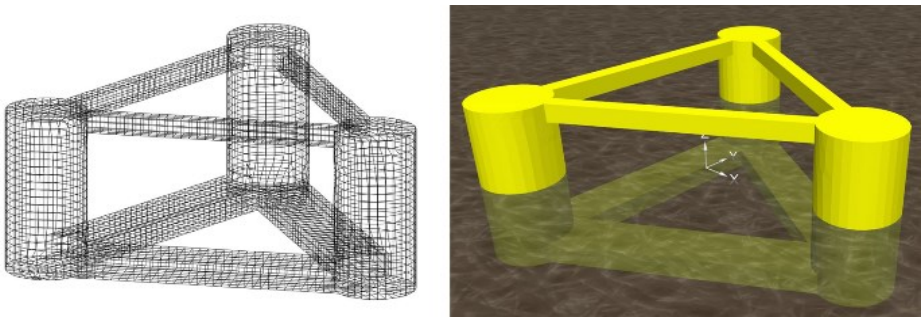

Figure 2: SINTEF 12MW substructure

The coordinate system of the analytical model is designed to align with the global coordinates of the substructure provided by SINTEF, as shown in Figure 3.

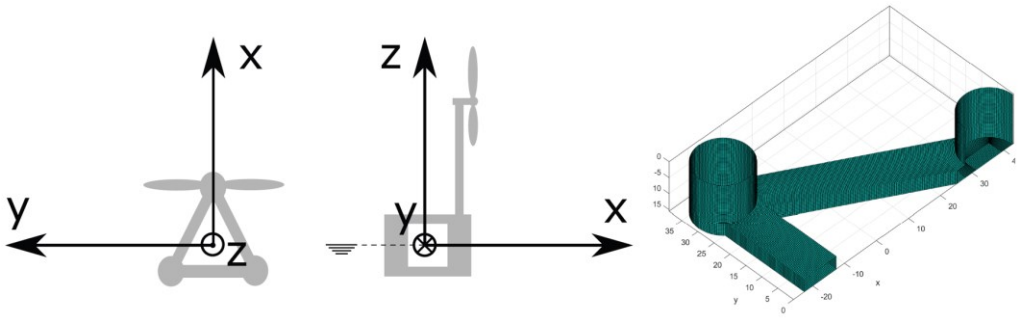

Figure 3: Coordinate system of SINTEF's 12MW offshore wind turbine substructure

To construct a wind farm using a substructure with three columns, the layout presented in Figure 4 by Aker Solutions (2019) is referenced. The model modeled using OrcaFlex is as shown in Figure 5. This configuration is an arrangement of a floater with three columns that shares anchors and ensures there is no interference between power cables and mooring lines. An advantage of using such an arrangement is that it facilitates the expansion for the construction of a wind farm, as illustrated in Figure 6.

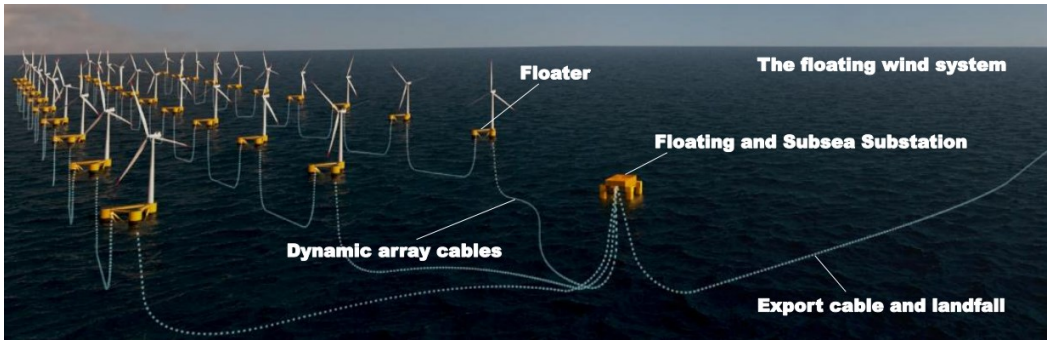

Figure 4: Inter array cable layout

Table 1: Main properties of the 12MW wind turbine

Parameter	Properties
Turbine rating	NREL 12MW
Blade length (m)	105.4
Hub diameter (m)	6
Hub Height (m)	131.7
Draft (m)	15.5
Nacelle mass (kg)	600,000
tower mass (kg)	1,161,600
Blade mass (kg)	3 * 63024
Hub mass (kg)	60,000
Total mass (kg)	14,176,000
Cut-in/rated/cut-out wind speed (m/s)	4.0 / 10.6 / 25.0
Cut-in/ rated rotor speed (rpm)	5.5 / 7.8
Generator efficiency (%)	94

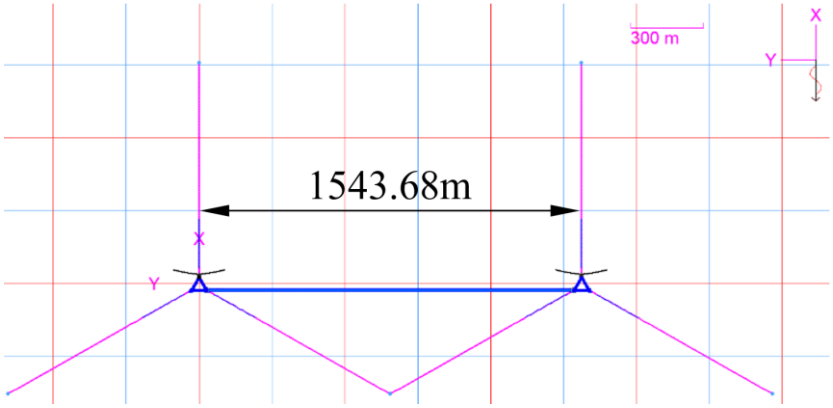

Figure 5: Layout of analysis model (top view)

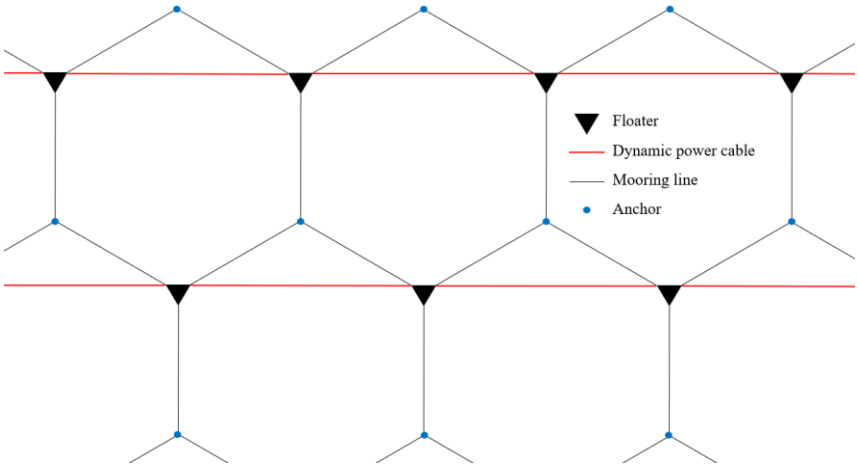

Figure 6: Expanding the floating substructure with three columns

The analysis model and the coordinate system used in this process are presented in Figure 7, and the specifications of the designed mooring line are detailed in Table 2. Additionally, Table 3 describes the positions of crucial points such as the fairleads and anchor points for each mooring line in their static state to understand the mooring system.

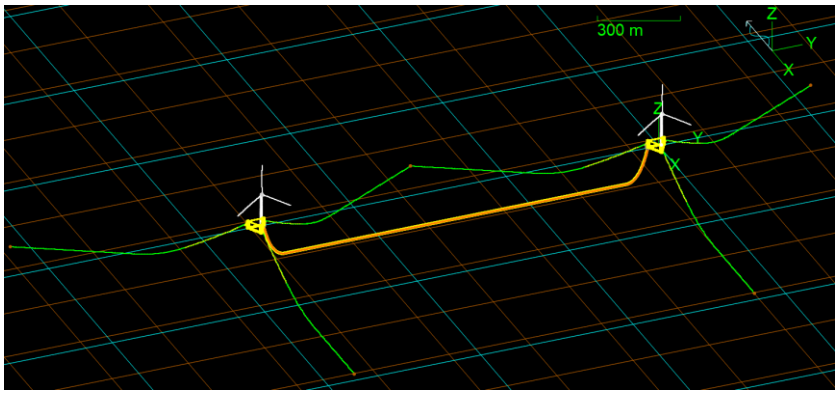

Figure 7: Overview of the analytical model for offshore wind farm cabling

Table 2: Mooring line material and length

Line type	ML 1	ML 2	ML 3
	Length (m)		
170mm R4 studless platform chain	32.4	32.4	32.4
210mm 6 strand rope	220.0	220.0	220.0
170mm R4 studless ground chain	665.0	660.0	660.0
Total length	917.4	912.4	912.4

Table 3: Main points of the mooring line position

		ML1	ML2	ML3	ML1-1	ML2-1	ML3-1
Fairlead point (m)	x	33.0	-31.1	-31.1	33.0	-31.1	-31.1
	y	0.0	-37.0	37.0	-1574.2	-1611.2	-787.1
	z	0.0	0.0	0.0	0.0	0.0	0.0
Anchor point (m)	x	906.1	-454.4	-454.4	906.1	-454.4	-454.4
	y	0.0	-787.1	787.1	-1574.2	-2361.3	-787.1
	z	-150.0	-150.0	-150.0	-150.0	-150.0	-150.0

Design of the dynamic power cable configurations

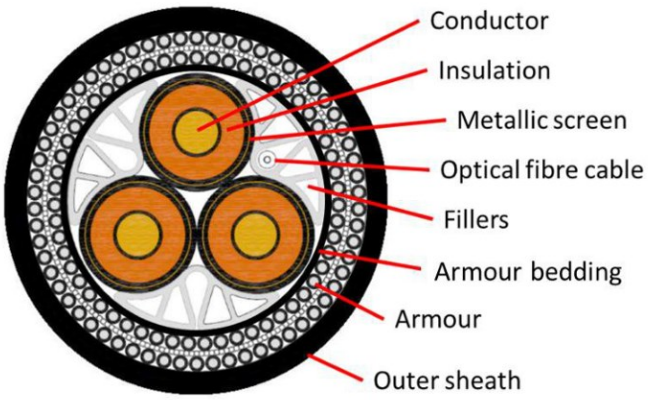

Figure 8: Typical dynamic cable cross section

The cross-section of the cable is composed of three conductor cores wrapped in insulation and two steel amours. In addition, it has four helical layers (circular helix type) including a copper shield and an outer sheath to protect the cores. The typical shape of a three-core power cable's cross-section is as shown in Figure 8 (CIGRE, 2022). The capacity of the power cable used in this study is 66kV.

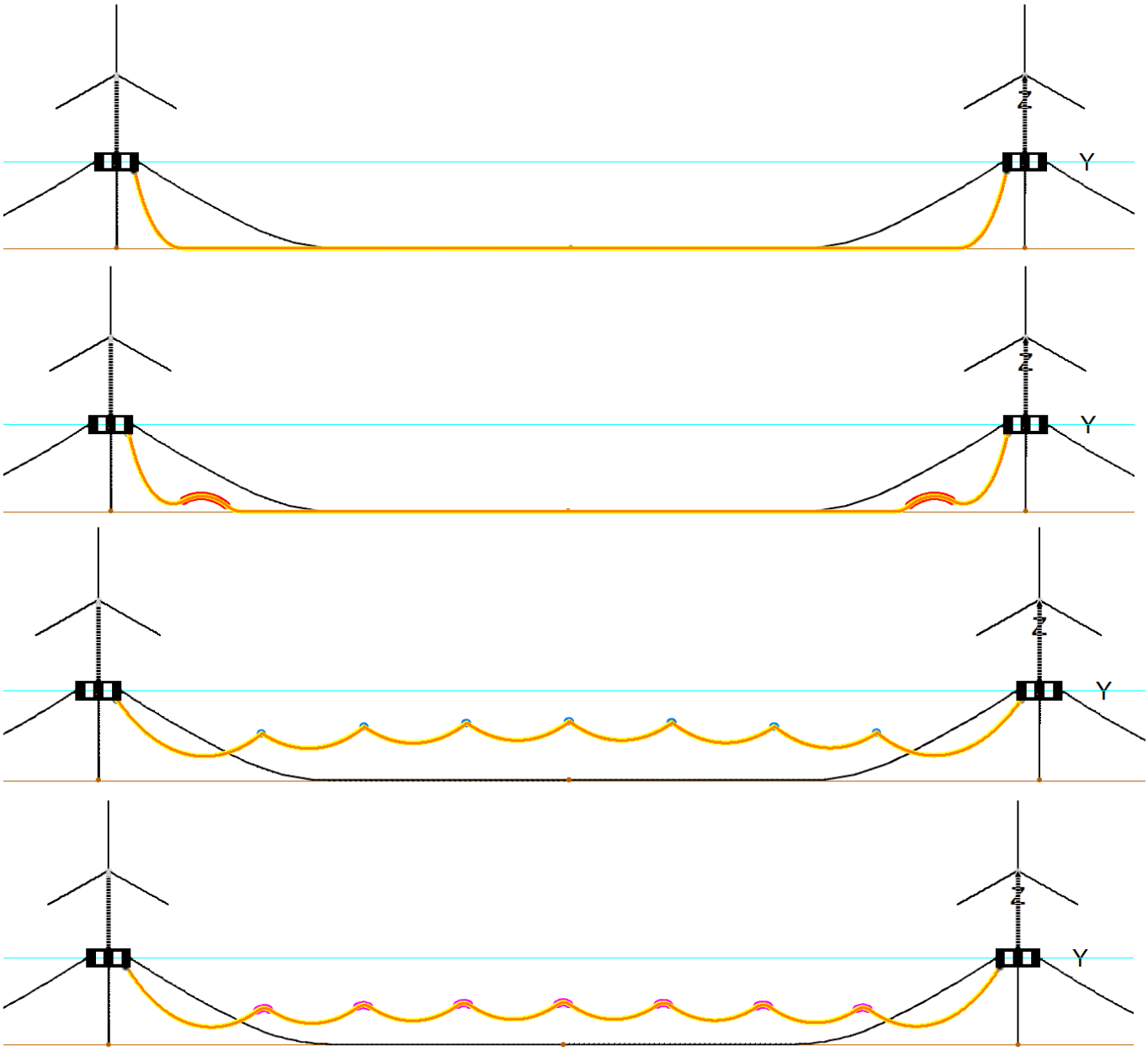

Figure 9: Cable configurations. From top, (a) free hanging catenary (b) lazy wave shape (c) suspended (d) W-configuration

Rentschler et al. (2020) conducted a parametric study on the inter-array cable systems of FOWTs. The optimal total cable lengths relative to water depth and buoy placements obtained through the parametric study are referenced for the design of the catenary and lazy wave shapes.

In this study, as shown in Figure 9, simulations are conducted for four types of power cables: (a) free hanging catenary, (b) lazy wave shape, (c) suspended and (d) W-configuration. The depth is set to 150 meters to determine which inter-array cable method is most suitable for shallow water depths.

The total length of the cable is 1681.9 meters, and different types of buoys are used to implement the lazy wave shape, suspended and W-configurations. For the lazy wave shape, relatively small buoys are attached, numbering 62 in total, while

for the suspended configuration, 7 large-capacity buoys are attached. In the W-configuration, 5 buoys are installed in each of the 7 sections, making a total of 35 buoys installed. Detailed specifications of the buoys are as presented in Table 4.

Table 4: Power cable attachment buoy specification

	Mass (te)	Volume (m^3)	Drag coefficient (x)	Drag coefficient (z)	Added mass coefficient (x)	Added mass coefficient (z)
Lazy wave shape buoy	0.069	0.197	1.100	1.100	1.000	1.000
Suspended buoy	2.700	8.615	0.209	1.000	0.459	0.600
W-configuration buoy	0.55	1.72	1.2	1.000	0.459	0.600

Figure 10 displays a detailed comparison between the suspended and W-configuration, zooming in on their structural differences. In the suspended configuration, a single buoy is installed in each section, resulting in a pointed appearance, whereas in the W-configuration, five buoys are installed in a single section, creating a smoother curve. The number and arrangement of buoys have been adjusted to prevent excessive curvature.

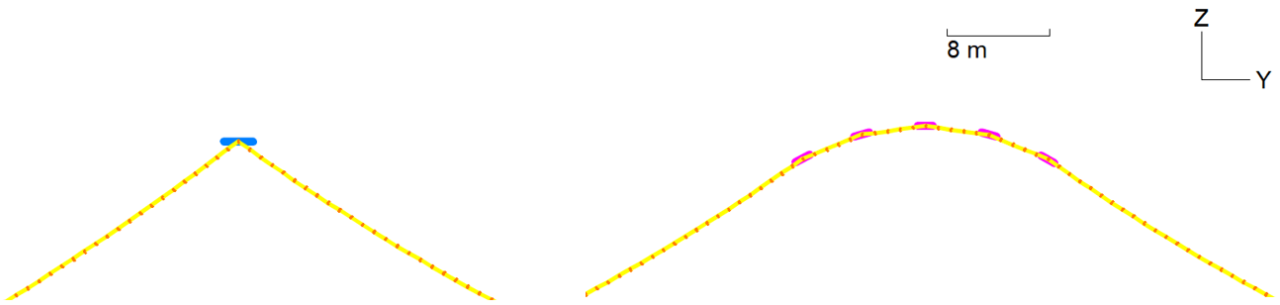

Figure 10: Detailed comparison between suspended and W-configuration

Environmental load case

Wave

To conduct simulations that closely resemble actual conditions at sea, numerous variables such as significant wave height (H_s), zero-crossing period (T_z), wave direction, tidal speed, and wind speed/direction are identified to establish comprehensive load cases. These variables are not arbitrarily chosen, but meticulously selected and optimized based on an extensive collection and processing of maritime environmental data. The data, harvested from Uido, Sinan, Jeollanam-do, South Korea, spans an entire year in 2021 and comprises 7,853data points observed at hourly intervals, as shows in Table 5. (KHOA, 2022) waves are implemented using the JONSWAP spectrum with the obtained values for T_z and H_s. (Hasselmann, K. et al.)

Table 5: Wave scatter diagram for Sinan Uido

	Hs (m)							
Tz (s)	0.5	1.5	2.5	3.5	4.5	5.5	6.5	sum
3.5	834	3	0	0	0	0	0	837
4.5	1,766	121	0	0	0	0	0	1,887
5.5	1,719	600	8	0	0	0	0	2,327
6.5	824	684	101	0	0	0	0	1,609
7.5	370	252	239	9	0	0	0	870
8.5	88	36	40	71	1	0	0	236
9.5	73	24	5	11	4	0	0	87
sum	5,644	1,720	393	91	5	0	0	7,853

Current

Current is calculated through wind-generated, tidal, and power law methods. (DNV, 2019) The current generated by the wind is determined by multiplying the average wind speed at an altitude of 10m by a coefficient k, as in Equation 1. The wind speed for the SLS is 18m/s, and for the ULS is 42.5m/s. Precise values of the coefficient k can be obtained from field measurements or detailed fluid dynamics models, but in this study, an intermediate value of 0.02 was used.

$$v_{c,wind}(0) = kU_{1\ hour,10m}\ where\ k = 0.015\ to\ 0.03 \quad [1]$$

For the current, the power law method, as detailed in Equation 2, was used to establish varying speeds at the 50m depth and the seabed. S_f and S_b denote the current speeds at the surface and seabed, respectively. Z_f and Z_b represent the Z coordinate of the 50m depth and seabed directly below the (X, Y) coordinates. This study set the power law exponent, denoted as p, to 7 (Orcina, 2023). The current profile used in this study is as depicted in Figure 11.

$$S = S_b + (S_f - S_b)\left[\frac{Z - Z_b}{Z_f - Z_b}\right]^{\frac{1}{p}} \quad [2]$$

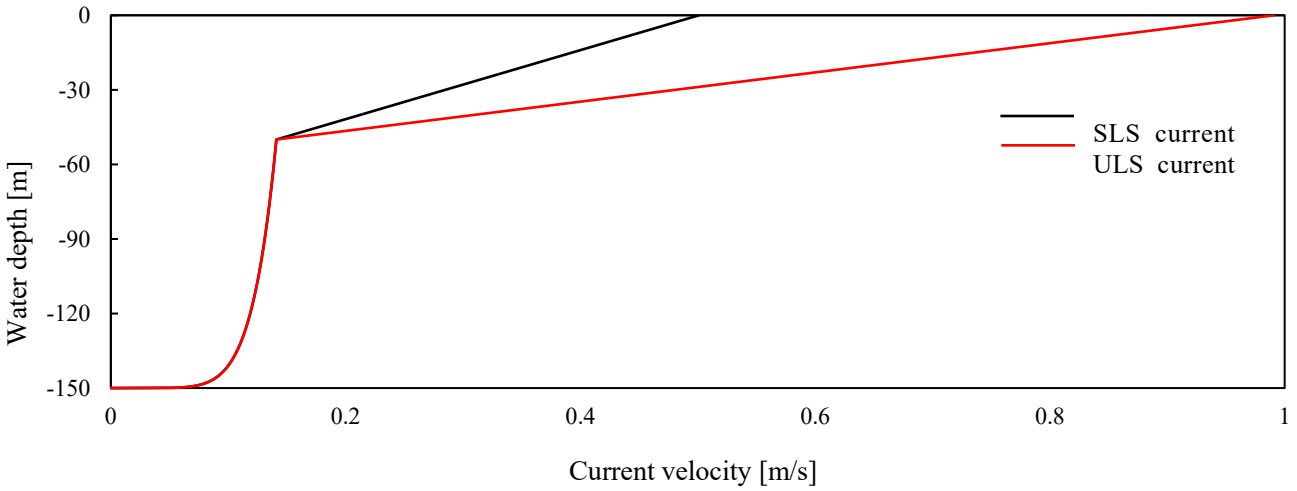

Figure 11: Current profiles in SLS and ULS

Environmental load in a 50-year cycle

The SLS analysis utilizes maximum values, such as significant wave height (H_s 4.5m), zero-crossing period (T_z 9.5s), and wind speed (18m/s). To recognize the potential impact of wave and wind directions on the mooring lines, these elements are set at 180 degrees, 300 degrees, and 60 degrees, resulting in a total of 9 SLS load cases. For the ULS analysis, assumptions are made based on Det Norske Veritas DLC 1.3 (DNV, 2016), with an understanding that the wind and wave directions are aligned.

Table 6 presents the wind speed, derived by examining the standard parameters that classify wind turbine stages in accordance with International Electrotechnical Commission 61400-1 (IEC, 2005). This research utilizes the wind speed recorded at the wind turbine class II stage. V_{ref} symbolizes the reference wind speed measured over 10 minutes, and A, B, C denote category designation values for high, medium, and low turbulence characteristics, respectively. Additionally, I_{ref} denotes the anticipated turbulence intensity value at a wind speed of 15m/s.

Table 6: Basic parameters for wind turbine classes

Wind turbine class		I	II	III	S
V_{ref}	(m/s)	50	42.5	37.5	Values specified by the designer
A	I_{ref}	0.16			
B	I_{ref}	0.14			
C	I_{ref}	0.12			

The extreme wind speeds corresponding to a 50-year return period are determined by referencing the IEC 61400-1 standard, which prescribes the standard wind speeds for three distinct turbine classes. The reference wind speed of 42.5m/s, associated with Class II, is employed in our analysis. For the evaluation of the significant wave height and the zero-crossing period under extreme wind scenarios, the American Petroleum Institute's (API, 2007) 2INT-MET guidelines are consulted. With a considered wind speed of 41.12m/s, the significant wave height is found to be 12.9m, and the zero-crossing period is recorded at 14 seconds. Hence, one ULS load case has been established in this research. The crucial details and visualizations for these load cases, vital for an all-encompassing understanding of the system's behavior, are shown in Table 7 and Figure 12.

Table 7: Environmental load case

	Load case	Waves			Wind	
		H_s	T_z	Dir.	Speed	Dir
		m	s	degree	m/s	degree
SLS	1	4.5	9.5	180	18.0	180
	2			180		300
	3			180		60
	4			300		180
	5			300		300
	6			300		60
	7			60		180
	8			60		300
	9			60		60
ULS	10	12.9	14.0	180	42.5	180

In this study, ten Environmental load cases are established, and the analysis is conducted targeting the shapes of four power cables. The names for the analysis cases are configured as C-LC1 (Catenary-Load Case1), L-LC1 (Lazy wave-Load Case1), S-LC1 (Suspended-Load Case1) and W-LC1(W-configuration-Load Case1).

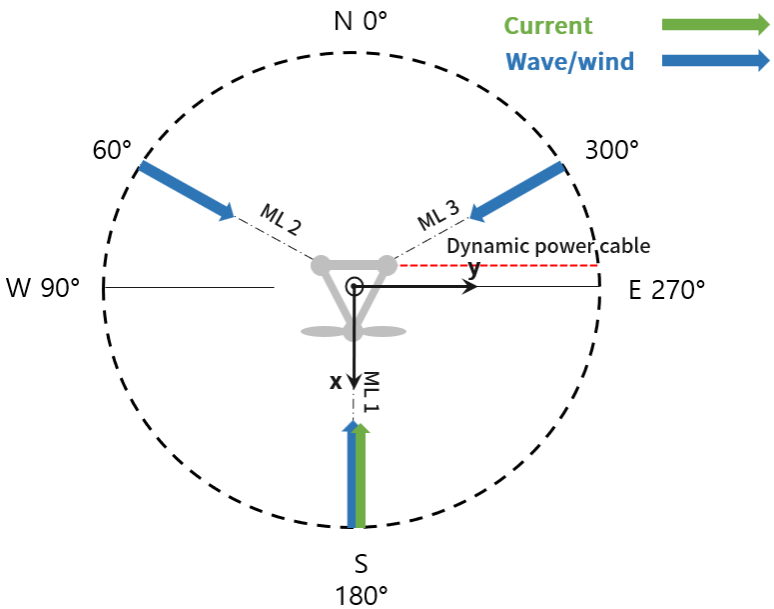

Figure 12: Load case diagram

RESULTS

Assessing cable configuration performance in LC10

In shallow water depth, a dynamic analysis is conducted using two FOWTs to determine the best method among four cable configurations. The simulation time is 10,800s (3 hours), with a start-up time of 300s, totaling 11,100s of dynamic analysis. Figure 13 shows the maximum elevation state at LC10 after completing the dynamic analysis for each shape. In the case of catenary and lazy wave, the cables lay on the seabed, while in suspended and W-configuration, they float in the middle. The suspended and W-configuration are designed to minimize the impact of wind-generated forces in the maximum elevation state, being set lower than 50 meters in depth.

Figures 14 and 15 illustrate the profiles of maximum effective tension and maximum curvature according to arc length, respectively. The maximum tensions and curvatures for each configuration are summarized in Table 8. The tension of the lazy wave is 19.00% lower than that of the catenary, 25.01% lower compared to the suspended and 26.28% lower compared to the W-configuration. Additionally, the lazy wave demonstrates superior performance in curvature as well, being 30.52% lower than the catenary, 77.42% lower than the suspended and 60.16% lower than the W-configuration. Overall, the performance of the lazy wave shape is confirmed to be superior, and it is advisable to use the lazy wave shape for ensuring long-term fatigue performance of dynamically behaving cables.

The W-configuration is a form designed to prevent the excessive curvature observed in the suspended configuration by installing five buoys in one section. While this significantly reduced the curvature, it was found to offer no substantial advantage in terms of tension. Considering installation and maintenance costs, it becomes evident that the lazy wave shape offers greater benefits.

Table 8: The rate of increase in tension and curvature for each configuration compared to the lazy wave

DLC	Maximum tension (kN)	Rate of increase compared to lazy wave (%)	Maximum curvature (m/m)	Rate of increase compared to lazy wave (%)
L-LC10	60.18	0.00	0.1218	0.00
C-LC10	74.29	19.00	0.1753	30.52
S-LC10	80.25	25.01	0.5393	77.42
W-LC10	81.57	26.28	0.3055	60.16

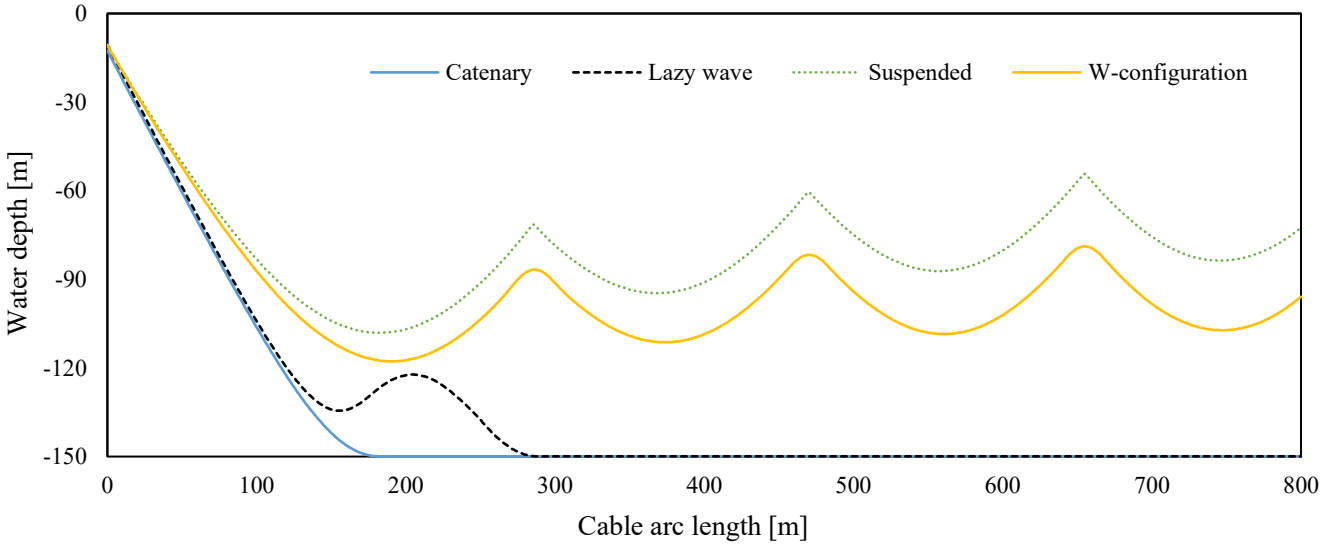

Figure 13: Cable configuration of maximum elevation state per arc length in LC10

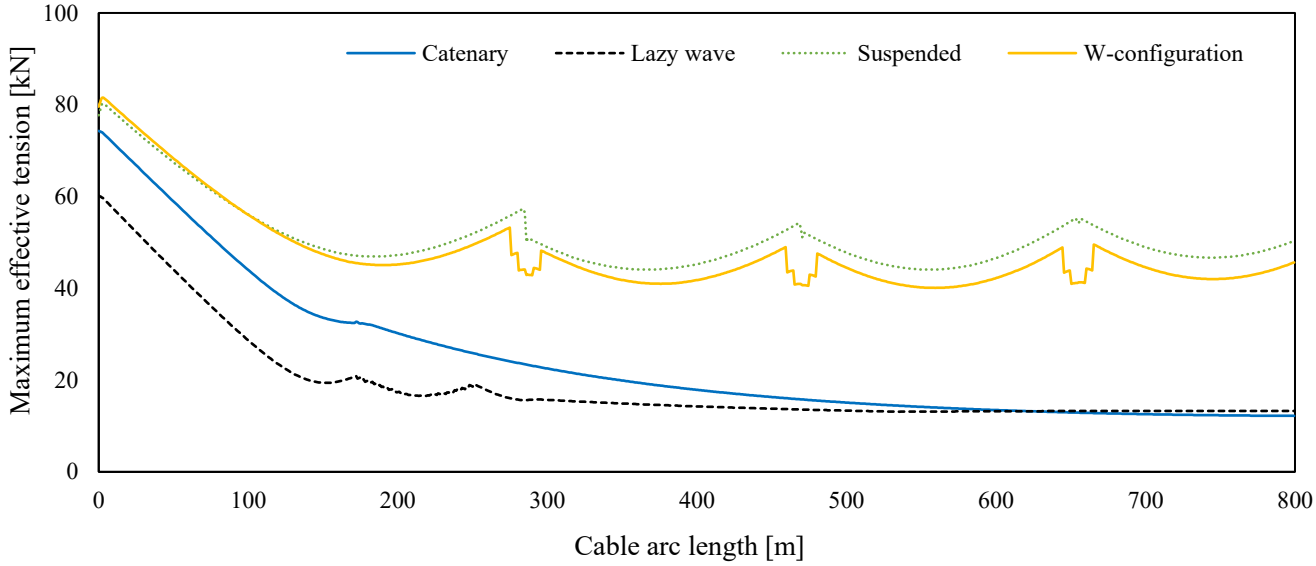

Figure 14: Maximum effective tension profile for each shape in LC10

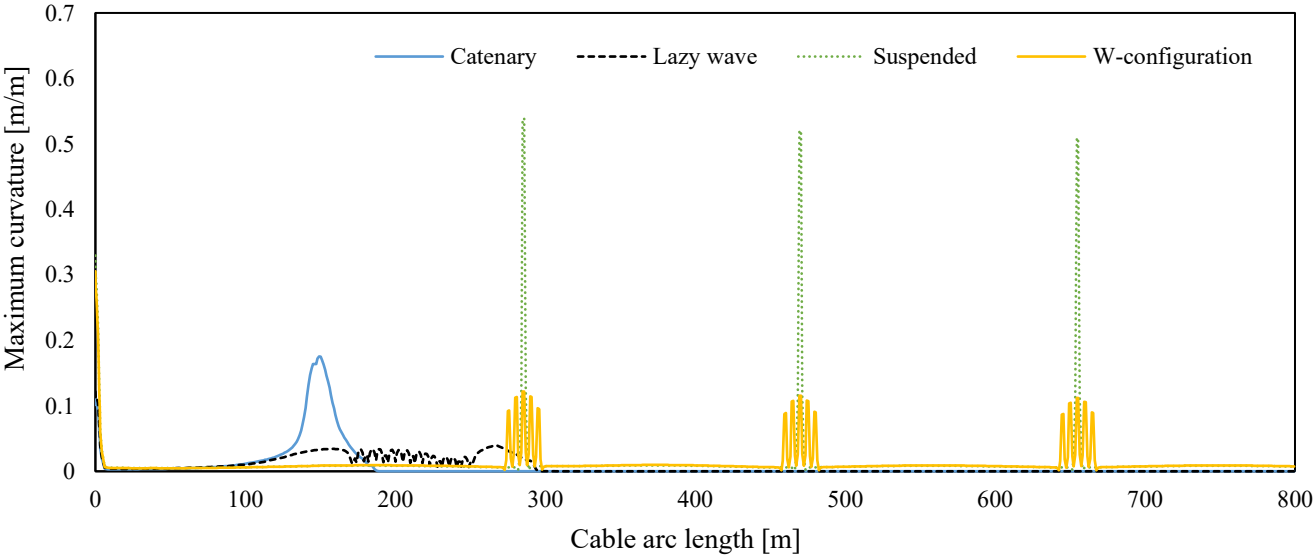

Figure 15: Maximum curvature profile for each shape in LC10

Evaluating all design load cases

Figures 16 and 17 respectively display the values of maximum effective tension and maximum curvature for all load cases. The points of highest tension and curvature in the cable occur at the hang-off connected to the substructure and the touch down point affected by the bottom drag. For the suspended case, since there is no touch down point, the tension and curvature at the buoy nearest to the hang-off are observed, denoted as the '1st buoy'.

In the case of C-LC10, the curvature and tension at the touch down point show significant differences between the SLS and ULS. This is deemed a characteristic of the free-hanging shape, where movements at the upper part of the power cable induce excessive motion at the lower part. For lazy wave and suspended, the difference between SLS and ULS is not substantial, indicating that the buoys placed in-between prevent excessive transfer of movements from the upper part of the power cable. However, considering the much higher curvature of the suspended compared to the catenary and lazy wave, the lazy wave method appears most suitable for inter-array cabling of power cables in shallow waters.

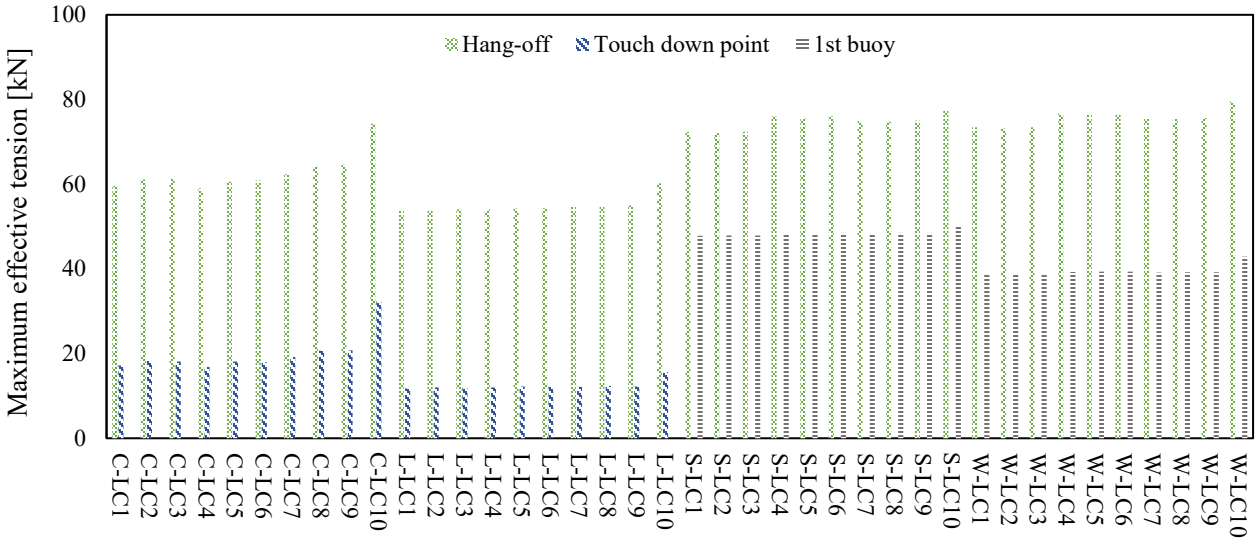

Figure 16: Maximum effective tension for all design load case

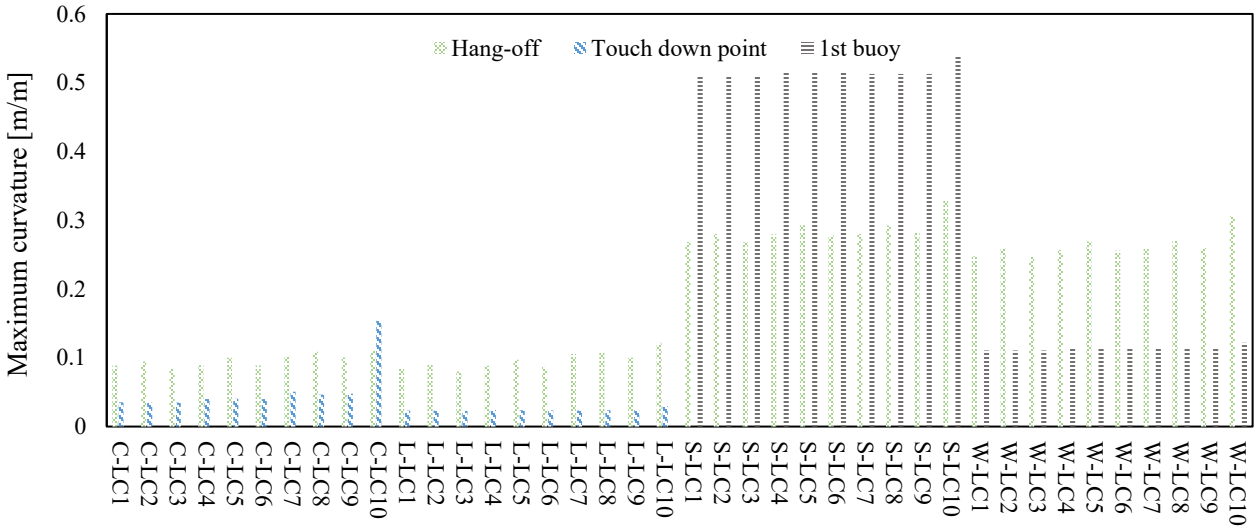

Figure 17: Maximum curvature for all design load case

Bird caging effect in helical cable

According to the study by Lu et al. (2017), the bird cage buckling phenomenon is likely to occur when the armor wires are subjected to high axial compression that exceeds their critical load, especially if there is damage to the cover sheath and strength tapes, as shows Figure 18.

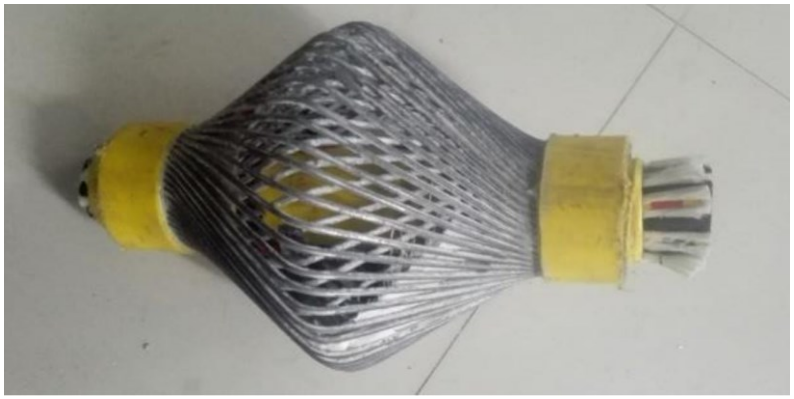

Figure 18: Bird caging failure mode of tension armor wires

The bird caging phenomenon can occur in steel armor cables that are twisted in one direction and can manifest when excessive compressive loads are applied. Among the four analytical models performed in this study, it was observed that a negative tension occurred at the touch down point of the catenary. As shown in Figure 19, the maximum compressive load was calculated to be 10.71 kN, which is not an absolute large value, but it suggests that caution is needed when designing FOWTs.

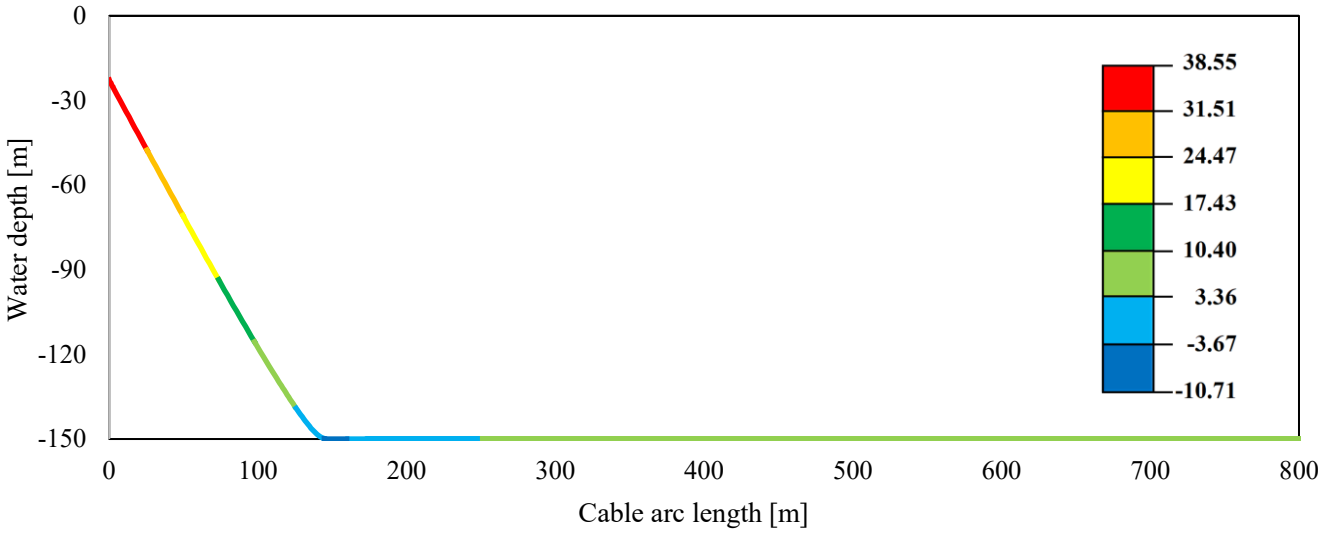

Figure 19: Minimum tension distribution on configuration profile in C-LC10

CONCLUSIONS

This study conducted research on inter-array cabling methods in shallow waters. A substructure with three columns was used to minimize interference between mooring lines and power cables. The power cables are analyzed in four types: catenary, lazy wave, suspended and W-configuration. To simulate a realistic environment, observational data and relevant standards are referenced. The obtained results are as follows.

1. Under ULS conditions, the lazy wave is found to have the best performance among the four shapes. It exhibited 19.00% lower tension compared to the catenary, 25.01% lower compared to the suspended and 26.28% lower compared to the W-configuration, along with 30.52% lower curvature than the catenary, 77.42% lower than the suspended and 60.16% lower than the W-configuration. The selection of the lazy wave is beneficial for ensuring long-term safety.

2. Additionally, the lazy wave shape showed low tension and curvature, with minimal difference in the impact on power cables between the SLS and ULS. Even in rapidly changing environmental conditions, it maintained low tension and curvature, proving superior in terms of shock load as well.

3. When a dynamic power cable has a catenary shape without any means to prevent direct contact with the seabed, it is observed that compressive loads can occur at the touch-down point. Although the values identified in this study are small compared to tensile loads, significant compressive loads may arise due to the cable's configuration deep water depth accompanied by heavy cable weight, and severe environmental conditions, potentially leading to bird caging. Careful consideration during design is necessary to prevent this phenomenon.

4. In this study, an analysis was conducted on four different cabling methods in terms of tension and curvature. However, the results of this study are to be considered preliminary, pending calibration with experimental data. Future research will involve comparative analyses with the free-decay test and regular wave test provided by SINTEF to enhance the reliability of the results.

5. Real ocean environment data obtained from the study will be utilized for fatigue analysis of mooring lines and dynamic power cables. Fatigue Limit State (FLS) will be generated using data observed in the targeted marine area to perform fatigue analysis. Moreover, an essential aspect to be addressed in further research is the cost-effectiveness. A comparative analysis between the installation costs and power production of the four different dynamic power cable configurations will be conducted to determine the payback period and profit based on fatigue life calculations.

CONTRIBUTION STATEMENT

Kangho Kim: Conceptualization; Data Curation; Formal analysis; Investigation; Methodology; Visualization; Writing – Original Draft. **Chunsik Shim**: Funding acquisition; Project administration; Supervision; Resources; Writing - Review & Editing. **Min Suk Kim**: Conceptualization; Supervision; Validation; Writing - Review & Editing. **Daseul Jeong**: Data Curation; Investigation; Writing - Review & Editing.

ACKNOWLEDGEMENTS

This results was supported by "Regional Innovation Strategy (RIS)" through the National Research Foundation of Korea(NRF) funded by the Ministry of Education(MOE) (Project Management Number of the Foundation: Gwangju Jeonnam Platform 2021RIS-002)
This work was supported korea institute for Advancement of Technology(KIAT) grant funded by the Korea Government(MOTIE) (P0017006 ,The competency Development Program for Industry Specialist)

REFERENCES

Aker Solutions, (2019). Predictable Offshore Execution – What Does It Take?, Fornebu, Norway.

Ahmad, I. B., Schnepf, A., & Ong, M. C. (2023). An optimisation methodology for suspended inter-array power cable configurations between two floating offshore wind turbines. Ocean Engineering, 278, 114406. Retrieved from https://doi.org/10.1016/j.oceaneng.2023.114406

American Petroleum Institute (API), 2005. Recommended Practice for Design and Analysis of Stationkeeping Systems for Floating Structures. API Recommend Practice 2SK, 3rd Edition. Washington, D.C.: API. Retrieved from https://www.api.org/news-policy-and-issues/hurricane-information/gulf-practices

Chen, W., Guo, S., Li, Y., Gai, Y., & Shen, Y. (2021). Structural configurations and dynamic performances of flexible riser with distributed buoyancy modules based on FEM simulations. International Journal of Naval Architecture and Ocean Engineering, 13, 650-658. Retrieved from https://doi.org/10.1016/j.ijnaoe.2021.07.003

Det Norske Veritas (DNV), (2016). STANDARD for Loads and site conditions for wind turbines, DNVGL-ST-0437, Oslo: DNV. Retrieved from https://www.dnv.com/energy/standards-guidelines/dnv-st-0437-loads-and-site-conditions-for-wind-turbines.html

Det Norske Veritas (DNV), (2019). DNV-RP-C205: Environmental Conditions and Environmental Loads. Oslo: DNV. Retrieved from https://www.dnv.com/oilgas/download/dnv-rp-c205-environmental-conditions-and-environmental-loads.html

Hasselmann, K., Barnett, T.P., Bouws, E., Carlson, H., Carwright, D.E., Enke, K., Ewing, J.A., Gienapp, H., Hasselmann, D.E. & Kruseman, P., (1973). Measurements of wind wave growth and swell decay during the Joint North Sea Wave Project (JONSWAP). Dtsch. Hydrogr. Z. 1973, 8, 1–95

International Council on Large Electric Systems (CIGRE), (2022). Recommendations for mechanical testing of submarine cables for dynamic applications, Paris: CIGRE. Retrieved from https://www.e-cigre.org/publications/detail/862-recommendations-for-mechanical-testing-of-submarine-cables-for-dynamic-applications.html

International Electrotechnical Commission (IEC) (2005). Wind turbines–Part 1: Design requirements, INTERNATIONAL STANDARD IEC 61400-1, London: IEC. Retrieved from https://webstore.iec.ch/publication/5426

Korea Hydrographic and Oceanographic Agency (KHOA) (2022). Ocean Data in Grid Framework, Retrieved from http://www.khoa.go.kr/oceangrid/khoa/koofs.do

Lavis, J. (2021). Shallow, Mid to Ultra-Deepwater Definitions. Drillers. Retrieved from https://drillers.com/shallow-mid-to-ultra-deepwater-definitions/#comments

Li, Y., Guo, S., Guo, Y., Yu, X., Chen, W., & Song, J. (2023). Dynamic responses and robustness performance to moving boundary of double-stepped cable during deep-sea mining. International Journal of Naval Architecture and Ocean Engineering, 15(2023), 100546. Retrieved from https://doi.org/10.1016/j.ijnaoe.2023.100546

Lu, Q., Yang, Z., Yang, Y., Yan, J., & Yue, Q. (2017). Study on the Mechanism of Bird-Cage Buckling of Armor Wires Based on Experiment. Proceedings of the ASME 2017 36th International Conference on Ocean Offshore and Arctic Engineering. OMAE2017, June 25-30, Trondheim, Norway. DOI: 10.1115/OMAE2017-61669. Retrieved from https://doi.org/10.1115/OMAE2017-61669

Okpokparoro, S., & Sriramula, S. (2023). Reliability analysis of floating wind turbine dynamic cables under realistic environmental loads. Ocean Engineering, 278, 114594. Retrieved from https://doi.org/10.1016/j.oceaneng.2023.114594

Orcina, (2023). Current theory Retrieved from https://www.orcina.com/webhelp/OrcaFlex/Content/html/Currenttheory.htm

Poirette, Y., Guiton, M., Huwart, G., Sinoquet, D., & Leroy, J. M. (2017). An optimization method for the configuration of inter array cables for floating offshore wind farm. Proceedings of the ASME 2017 36th International Conference on Ocean Offshore and Arctic Engineering, OMAE2017, Trondheim, Norway.

Rentschler, M. U. T., Adam, F., & Chainho, P. (2019). Design optimization of dynamic inter-array cable systems for floating offshore wind turbines. Renewable and Sustainable Energy Reviews, 111, 622–635. Retrieved from https://doi.org/10.1016/j.rser.2019.05.024

Rentschler, M. U. T., Adam, F., Chainho, P., Krügel, K., & Vicente, P. C. (2020). Parametric study of dynamic inter-array cable systems for floating offshore wind turbines. Marine Systems & Ocean Technology, 15(16-25). Retrieved from https://doi.org/10.1007/s40868-020-00071-7

Schnepf, A., Lopez-Pavon, C., Ong, M. C., Yin, G., & Johnsen, Ø. (2023). Feasibility study on suspended inter-array power cables between two spar-type offshore wind turbines. Ocean Engineering, 277, 114215. Retrieved from https://doi.org/10.1016/j.oceaneng.2023.114215

Stiftelsen for industriell og teknisk forskning (SINTEF), (2022). Definition of the INO WIND-MOOR 12MW base case floating wind turbine, Trondheim: SINTEF. Retrieved from https://hdl.handle.net/11250/2723188

Tong, K. C. (1998). Technical and economic aspects of a floating offshore wind farm. Journal of Wind Engineering and Industrial Aerodynamics, 74-76, 399-410. Retrieved from https://doi.org/10.1016/S0167-6105(98)00036-1

W.S. Moon, J.C. Kim, A. Jo & J.N. Won, (2014). Grid optimization for offshore wind farm layout and substation location, in ITEC Asia-Pacific 2014—Conference Proceedings, Beijing. Retrieved from https://ieeexplore.ieee.org/document/6941124

Zhao, S., Cheng, Y., Chen, P., Nie, Y., & Fan, K. (2021). A comparison of two dynamic power cable configurations for a floating offshore wind turbine in shallow water. AIP Advances, 11(3), 035302. Retrieved from https://doi.org/10.1063/5.0039221

Proceedings of 15th International Marine Design Conference (IMDC-2024)
June 2-6, 2024
Amsterdam, the Netherlands

Using a Design Exploration Model to Assess the Global Techno-Economic Feasibility of Far Offshore Green Hydrogen Production Towards 2050

T. Melles[1,2,*], J.F.J. Pruyn [1], J.L. Gelling [1] and J.J. de Wilde [2]

ABSTRACT

With space constraints onshore, strong renewable resources available far offshore and growing green hydrogen demand, far offshore green hydrogen production may be an attractive option. To assess this potential, a mixed integer quadratically constraint programming (MIQCP) optimization model was developed to find the cost per kilogram of far offshore green hydrogen in specific scenarios. The design of the far offshore green hydrogen supply chain was optimized with this model for six high potential scenarios in varying locations and the results were analyzed. It was found that far offshore green hydrogen costs are in the same order of magnitude as the costs of its alternatives. Far offshore green hydrogen may be considered marginally competitive with these alternatives from 2035 onwards in the analyzed scenarios when taking into account the considerable advantages of far offshore production, such as avoidance of scarce land usage in crowded areas and certain geopolitical considerations.

KEY WORDS

Far offshore; Green hydrogen; Green FPSO; LCoH; Optimization

INTRODUCTION

As the world attempts to slow down and eventually stop climate change, sustainability becomes increasingly important. According to Lapides et al. (2020), around 80% of the economy is relatively easy to decarbonize by electrification, with costs being reasonable and technologies already (widely) available. The other 20% consists of peak power generation, heavy duty transport (buses, trucks and ships) and industrial processes requiring combustion of a fuel to create high temperatures. For this last 20%, also referred to as the 'last mile' of decarbonization or hard-to-abate, hydrogen may play a key role in the path towards sustainability.

Hydrogen produced without any emissions using renewable energy is called green hydrogen. The production of green hydrogen occurs in a process called electrolysis, where electricity and water are used to produce hydrogen and oxygen. When renewable energy is used in this process, the hydrogen can be regarded as zero-emission and green. Since the production of green hydrogen will require large amounts of energy, a lot of additional renewable energy is needed. (Hague, 2021)

The demand for hydrogen is expected to rise strongly towards 2050 in many parts of the world (The Hydrogen Council & McKinsey & Company, 2021). Looking at the net-zero goals set by various countries (United Nations, n.d.), the demand

[1] Maritime and Transport Technology, Delft University of Technology, Delft, The Netherlands
[2] Maritime Research Institute Netherlands, Wageningen, The Netherlands
[*] Corresponding Author: tycho.melles@gmail.com

Submitted: 23 February 2024, Revised: 30 April 2024, Accepted: 1 May 2024, Published: 27 May 2024

Conference paper, DOI: https://doi.org/10.59490/imdc.2024.913 e-ISSN: 3050-4864

for green hydrogen and renewable energy in general will grow significantly, which means space restrictions onshore and near offshore may present problems. In addition, the development of floating energy generation, and the strong and steady wind resources available in many (far) offshore locations may make far offshore renewable energy generation attractive. To transport large amounts of energy over long distances, transport in the form of hydrogen is more economic than transport through electrical cables (d'Amore-Domenech et al., 2021). Therefore, far offshore green hydrogen production could be even more beneficial, as it will make long distance transport to shore more economic and therefore the distance to shore of the production location less important.

The actual techno-economic feasibility of far offshore green hydrogen production is however still largely unknown. Therefore, the main objective of this research is to create a first idea of the worldwide technological and economic feasibility of far offshore green hydrogen production over time, identifying the technologies to be used in its supply chains, looking at which factors influence its price, comparing it to its alternatives and showing the role it may play in a net-zero economy in and towards 2050. In this research, 'far offshore production' is defined as production in areas with water depths over 50 meters, where floating production is necessary (ESMAP, 2019).

Many factors can influence the far offshore green hydrogen supply chain and therefore the costs of far offshore green hydrogen. The right combination of energy generation devices, electrolyzers, conversion devices, storage size, FPSO size and hydrogen carrier must be determined in every scenario. In order to solve this design challenge and find the optimal combination of all these aspects leading to the lowest far offshore green hydrogen costs, an optimization model is needed when analyzing the scenarios to be considered. How to best set up the model for this research will be discussed in the literature review. In this literature review, the method of the literature retrieval and the technologies that were considered in this research will be discussed as well. Next, the methodology will show the model developed in this research and the scenarios that were analyzed. After this, the results will be analyzed, followed by a short discussion and the conclusions.

LITERATURE REVIEW

An extensive literature review was conducted to map the available knowledge regarding far offshore green hydrogen production and related topics. In this section, it will be discussed how the relevant literature was retrieved, how a suitable modelling method was found and which technologies were included in the model.

Literature Retrieval

For the literature retrieval, mainly SCOPUS was used. Eight combinations of search terms were used, which are shown in Figure 1. On the search results, a title scan and subsequently a quick abstract scan were performed which resulted in a list of possibly interesting references. Next, the selected references were analysed further by doing an extensive abstract scan and a quick scan of the rest of the paper. This lead to a further selection and structuring of the papers. In Figure 1, the literature retrieval process is shown visually and the amount of references is indicated for each part of the process. As can be seen, the initial scan resulted in a total of 247 references, which was brought down to 180 after the second scan. These references were then placed in four different categories (A, B, C and D), with categories A and B containing the literature with relevant general information on the various topics of interest (for example on the techno-economic feasibility of possibly interesting technologies) and categories C and D containing the literature describing possibly relevant methods. Furthermore, categories A and C contain the references that were expected to be relevant in their entirety, whereas categories B and D contain the references that are not relevant in their entirety, but contain relevant aspects, such as one or several specific input data values or a method for a specific (small) part of the model. Eventually, a total of 57 references were identified as most relevant (categories A and C). The literature review has been set up primarily based on these references. In all of the reviewed literature, only one reference was found describing a solution approach with a similar scope, which was used as a base for the modelling approach developed in this research, as will be explained below.

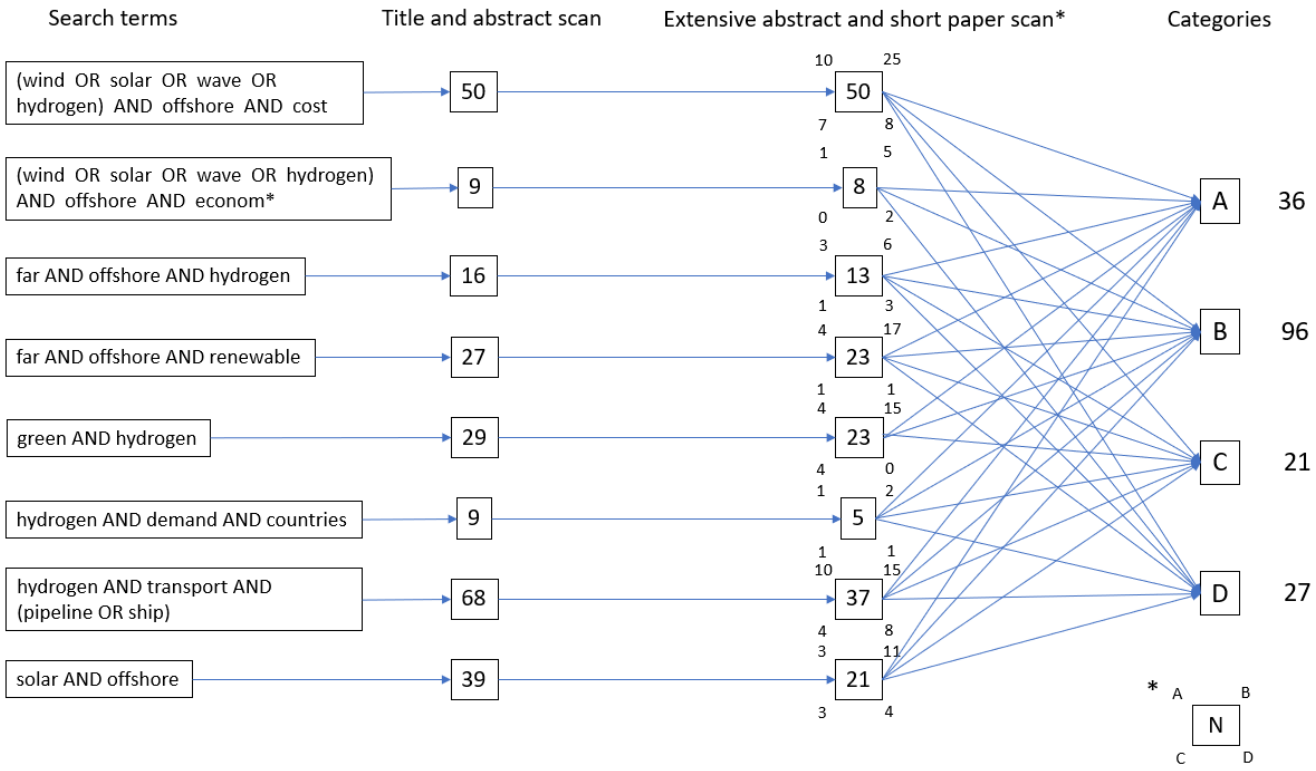

Figure 1: Flow chart literature retrieval (please note that the small numbers in the third column indicate how many references were placed into each category, as shown in the legend in the bottom right corner of the figure)

Suitable Modelling Method

During the reviewing, only one reference describing a solution approach with a similar scope to this research has been found. In this paper, Salmon and Bañares-Alcántara (2022) look at the worldwide feasibility of (far) offshore green ammonia production in 2030. Their main analysis is done on a global level, directly comparing the best onshore with the best offshore locations. This may however not show the full potential of far offshore production of green hydrogen and its derivatives. For example, if we directly compare an onshore production location in Morocco and an offshore production location off the coast of New Zealand to each other, the production costs of the onshore location in Morocco might be lower. However, if the demand is located in New Zealand, the delivered costs of the green hydrogen may still be lower from the offshore location when taking into account the conversion and transport costs. For this reason, comparing green ammonia production costs on a global level directly as done by Salmon and Bañares-Alcántara (2022) in their main analysis does not lead to a realistic comparison and approaches the potential of far offshore green ammonia from a very conservative side. This is a major limitation to their research and was therefore taken into account when setting up the modelling method for this research.

In order to assess the effect of infrastructure costs on the potential of far offshore green ammonia, Salmon and Bañares-Alcántara (2022) shortly look at its potential in two scenarios with usage in Germany and Japan (including transport). They conclude that far offshore green ammonia will be beneficial in Japan and not in Germany, with which they illustrate themselves that the specific scenario is highly important, which means an analysis based on specific scenarios is needed to make a realistic analysis. Therefore, the global potential of far offshore green hydrogen should be assessed ‘bottom-up’, where a representative set of specific scenarios is analyzed, from which conclusions are drawn about the global potential of far offshore green hydrogen. This means the main gap in literature to be filled by this research is an evaluation of the global potential of far offshore green hydrogen over time using local comparisons with specific scenarios. In addition to this, Salmon and Bañares-Alcántara (2022) only made predictions for 2030 and only considered ammonia. These shortcomings were ad-

dressed in this research as well. When defining the scenarios to be analyzed in this research, the highest potential scenarios were selected first, as it was still unknown whether far offshore green hydrogen production will become feasible at all. In the methodology, the scenarios considered in this research will be discussed in more detail.

In Figure 2, the modelling approach used by Salmon and Bañares-Alcántara (2022) is shown with the main adjustments as described in the previous paragraph (green blocks). This was used as a base for the model developed in this research. As can be seen, transport costs and technical data, several hydrogen carriers, and the period until 2050 are included. Also, the potential of far offshore green hydrogen is evaluated with local comparisons, shown by the fact that local demand and green hydrogen alternatives are used.

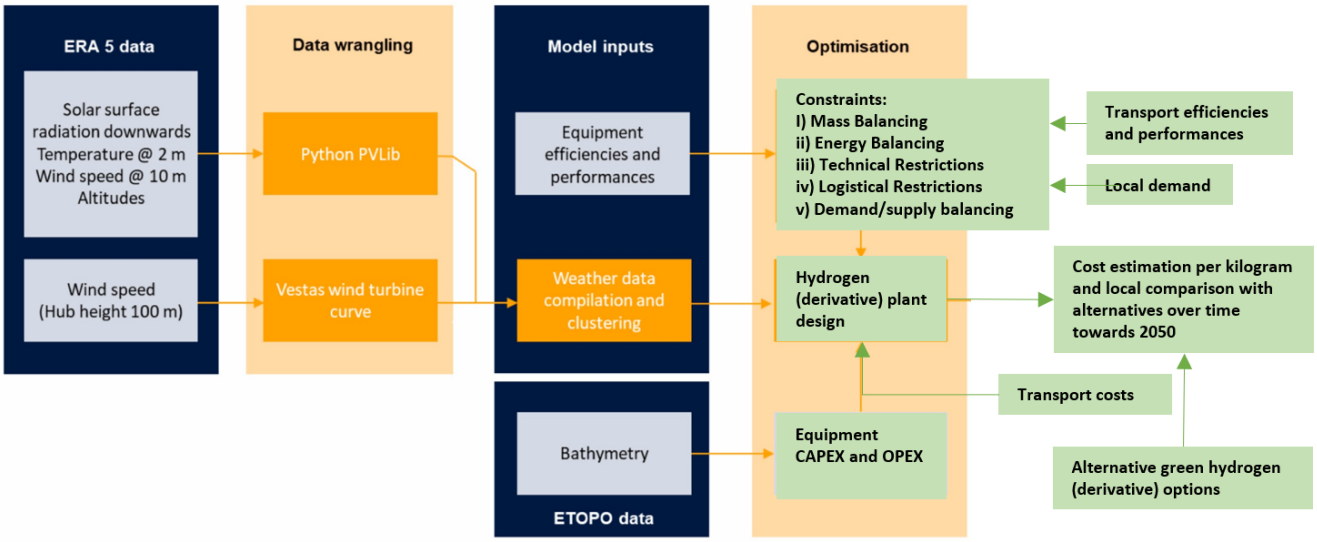

Figure 2: Basis for the modelling approach as adjusted from Salmon and Bañares-Alcántara (2022) (only main adjustments)

When following a modelling approach similar to the one shown in Figure 2, the focus is put on the optimization of the far offshore green hydrogen supply chain. The alternative would be to put the focus on a higher level supply/demand interaction in a global network of production and usage locations, and simplify the far offshore green hydrogen supply chain modelling. It is expected that putting the focus on the optimization of the far offshore green hydrogen supply chain will have a more direct practical relevance for the choices to be made in the development of far offshore green hydrogen production at this moment in time. In addition, it is expected that it will result in more complete and reliable insights into what technologies may become part of far offshore green hydrogen supply chains and how the potential will develop. Furthermore, when focusing on the optimization of the supply and demand interaction, too large uncertainties are expected to be introduced. More research must be performed to be used as a base for a research with such a focus. Therefore, the focus was put on the optimization of the far offshore green hydrogen supply chain in this research. Within this supply chain, the main optimization challenges included in the model developed in this research are (1) the optimization of the combination of various renewable energy generation devices with the electrolyzers, and (2) the choice between several hydrogen carriers as transport medium. Both of these optimizations integrate various parts of the far offshore green hydrogen supply chain. The outcome therefore depends on many different factors and the two optimizations are connected as well when solved simultaneously. How the model was set up to solve the two main optimization challenges and design the rest of the supply chain too will be discussed in more detail in the methodology.

Next to the focus of the model, the method to be used is of great importance. Salmon and Bañares-Alcántara (2022) applied an optimization model with mixed integer linear programming (MILP). MILP is preferred over genetic algorithms as it guarantees the optimality of the solution (EMD International, 2020). In addition, optimization is preferred over simulation, because the optimal supply chain must be designed by the model to assess the full potential of far offshore green

hydrogen and it is expected to be difficult to predefine a set of simulations due to the limited knowledge available on far offshore green hydrogen supply chains. So far, the approach of Salmon and Bañares-Alcántara (2022) is followed. However, because several hydrogen carriers were considered in this research, it was expected that not all constraints would be linear, since the value of certain variables would depend on which hydrogen carrier is used, which is defined in the model through a constraint. When those variables are then used in other constraints, quadratic constraints can arise. For the same reason, quadratic objective terms could also arise. Therefore, MILP cannot be applied in this research and mixed integer quadratically constraint programming (MIQCP) is used instead to deal with the quadratic constraints and objective terms. Lastly, the model is implemented in Python and the Gurobi optimization solver is used, which is freely available through an academic license.

Technologies to Be Included

The next step was to decide what exactly to include in the model, which was needed to be able to expand the general modelling approach presented in Figure 2 to a more detailed one. To do this, the retrieved literature was reviewed to assess what is already known about the techno-economic feasibility of the various aspects of a far offshore green hydrogen supply chain. An overview of the technologies included in the model is given in Table 1.

For the far offshore renewable energy generation, moored floating wind and solar energy production seem to be coming close to techno-economic feasibility (De Vries et al., 2021; Jan De Nul, 2023; SolarDuck, n.d.) and are therefore considered. The technological and especially cost development of wave energy converters is deemed too uncertain (Kasiulis et al., 2022; Rehman et al., 2022) and therefore, wave energy is left outside of the scope of the intended research.

With regards to the hydrogen production, it was found that PEM electrolyzers are expected to be most suitable for far offshore green hydrogen production due to their compact stacking possibilities and ability to handle the dynamic power input associated with renewable energy production (Jang et al., 2022). Furthermore, the focus of this research was put on centralized hydrogen production in an FPSO, leaving the option of decentralized hydrogen production out of the scope. Offshore hydrogen production with PEM electrolyzers will require a desalination plant as well (Jang et al., 2022).

Looking at the transport of hydrogen produced far offshore, the transport over sea seems most feasible from a techno-economic perspective if it is done by ship in the form of ammonia or liquid hydrogen. Whether ammonia or liquid hydrogen is more beneficial depends on the distance to be traveled and the quantity of hydrogen to be transported (International Renewable Energy Agency, 2022). Both options have therefore been included in the model. Methanol and compressed hydrogen are not considered in the model, since their costs are expected to be higher for most far offshore green hydrogen production scenarios (Cebolla et al., 2022). Other liquid organic hydrogen carriers (LOHCs) are also left out of the scope because there are multiple challenges that can limit their potential role in the global hydrogen trade, including limited availability, high costs, low hydrogen density, losses during recycling and high energy usage to recover the hydrogen from the carrier (International Renewable Energy Agency, 2022). Transport over land is assumed to be done with pipelines as gaseous hydrogen, since this seems to receive most attention at the moment. Long term storage onshore is not included in the model, but storage in the FPSO is. This storage may be done in the form of ammonia or liquid hydrogen, depending on which medium is used for transport.

Table 1: Technologies included in the model for each step of the far offshore green hydrogen supply chain

Step	Technologies included in the model
Power generation	Floating wind turbines Floating solar platforms
Electrolysis	PEM electrolyzers (with desalination) Centralized production on FPSO
Conversion and storage on FPSO	Ammonia Liquid hydrogen
Sea transport	Ammonia (by ship) Liquid hydrogen (by ship)
Land transport	Gaseous hydrogen (through pipelines)

METHODOLOGY

In this section, the model will be shown and its general outline will be discussed. In addition, the scenarios to be analyzed will be presented. In the report this paper was based on, a more detailed explanation of the model is given.

Model Overview
A schematic overview of the calculations belonging to an optimization of a far offshore green hydrogen supply chain, which forms the core of the developed model, is shown in Figure 3. It should be noted that only one optimization is visualized here, while a normal run of the model will include several optimizations for the chosen scenario in different years, meaning the visualized optimization will be run multiple times with changing input data. When looking at the input data for these optimizations belonging to different years, only the cost data will change, which is represented by the cell in the bottom right of Figure 3. This could lead to a different optimal far offshore green hydrogen supply chain for every considered year.

Next to the time domain included in the model by simulating several years, a second time domain is included within each optimization. From ERA5, hourly weather data is imported for a reference period of 10 months, which enters the model at the very left of Figure 3. From this hourly weather data, the hourly power production, the hourly power available for and used by the electrolyzers, and the hourly hydrogen production are determined over the reference period. Using these hourly production figures, the supply chain is optimized for production over a longer period of time, leading to more realistic results.

In Figure 3, the cells with yellow background color are ‘normal’, numeric input data or based on calculations with solely numeric data. The cells with red background color are variables, which are to be varied directly by the used optimization solver when finding the optimum. The cells with blue background color are based on calculations including other variables, meaning their value also changes while the optimization runs. Furthermore, the black arrows connecting cells represent ‘regular’ calculations, whereas the orange arrows represent constraints. Finally, the colors of the borders of the cells show to which part of the model they belong, as discussed further later in this section.

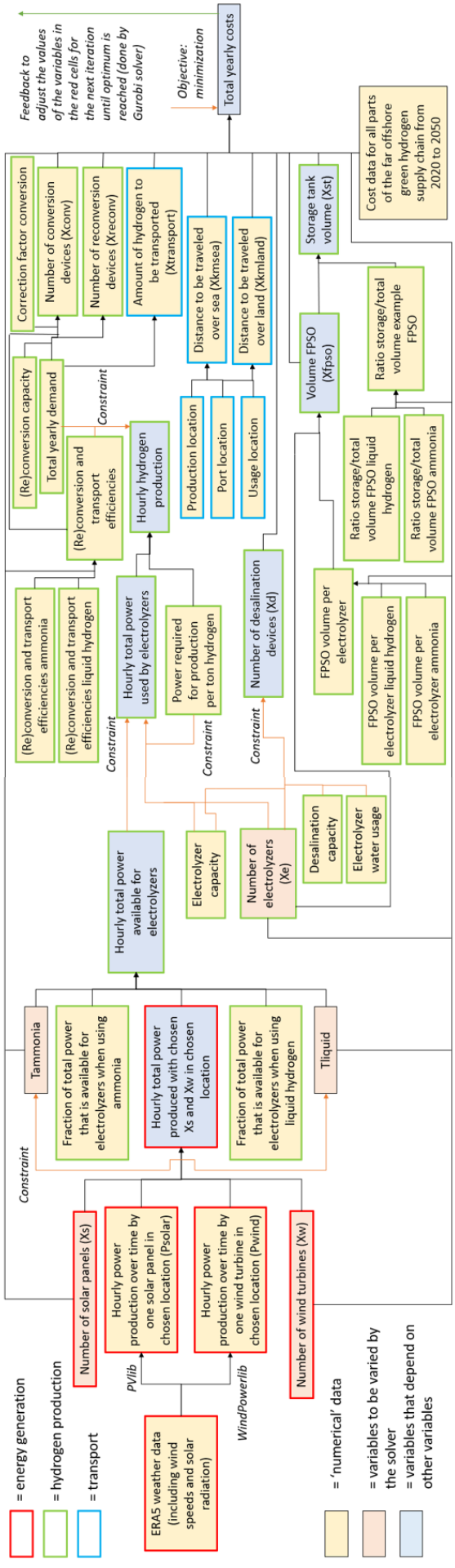

Figure 3: Model visualization

As can be seen in the figures, most calculations in the model eventually lead back to the calculation of the total yearly costs. As the yearly hydrogen production is given as a (constant) input to the optimization, these total yearly costs are directly related to the costs per kg of hydrogen. This means minimizing the total yearly costs is equal to minimizing the costs per kg of hydrogen for the analyzed supply chain. Therefore, the objective function to be minimized in the model is formulated as shown in Equation (1), where 'i' indicates the components of vectors x and C. Vectors x and C represent the number of units and the cost per unit respectively.

$$MIN(\sum_{i} x[i] * C[i]) \tag{1}$$

This means the sum that is minimized in the objective function is equal to the total costs for the far offshore green hydrogen supply chain in the defined scenario in the selected year. The elements of vectors x and C can be split up into three different groups: energy generation (X_{energy} and C_{energy}), hydrogen production ($X_{production}$ and $C_{production}$) and transport ($X_{transport}$ and $C_{transport}$). This gives the split shown in Equation (2). In Figure 3, it has been indicated which part of the model belongs to each group through the color of the borders of the cells. The meaning of these colors is given in the legend. The cells with $T_{ammonia}$, T_{liquid} and the cost data do not have a colored border, because the calculations in which they are used belong to multiple groups.

$$x * C = X_{\text{energy}} * C_{\text{energy}} + X_{\text{production}} * C_{\text{production}} + X_{\text{transport}} * C_{\text{transport}} \tag{2}$$

The three categories shown in Equation (2) can each be split up further, as shown in Equations (3) to (5). In Table 2, the variables and parameters used in these equations are explained. As indicated in the table, most of the equipment types are restricted to integer values.

$$X_{\text{energy}} * C_{\text{energy}} = X_{\text{w}} * C_{\text{w}} + X_{\text{s}} * C_{\text{s}} \tag{3}$$

$$\begin{aligned} X_{\text{production}} * C_{\text{production}} = {} & X_{\text{e}} * C_{\text{e}} + X_{\text{d}} * C_{\text{d}} + X_{\text{st}} * C_{\text{st}} + X_{\text{fpso}} * C_{\text{fpso}} \\ & + T_{\text{ammonia}} * X_{\text{convammonia}} * C_{\text{convammonia}} + T_{\text{liquid}} * X_{\text{convliquid}} * C_{\text{convliquid}} \\ & + T_{\text{ammonia}} * X_{\text{reconvammonia}} * C_{\text{reconvammonia}} + T_{\text{liquid}} * X_{\text{reconvliquid}} * C_{\text{reconvliquid}} \end{aligned} \tag{4}$$

$$X_{\text{transport}} * C_{\text{transport}} = X_{\text{basetransport}} * C_{\text{basetransport}} + X_{\text{kmsea}} * C_{\text{kmsea}} + X_{\text{kmland}} * C_{\text{kmland}} \tag{5}$$

Table 2: Meaning variables and parameters

Component	Meaning	Unit
X_w	Number of wind turbines (integer)	*dmnl*
X_s	Number of solar platforms (integer)	*dmnl*
X_e	Number of electrolyzers (integer)	*dmnl*
X_d	Number of desalination devices (integer)	*dmnl*
X_{st}	Volume of the storage tank on the FPSO	m^3
X_{fpso}	Volume of the FPSO	m^3
X_{kmsea}	Distance to be traveled over sea	*km*
$X_{basetransport}$	Amount of hydrogen to be transported	*tons*
X_{kmland}	Distance to be traveled over land	*km*
$X_{convammonia}$	Amount of conversion devices in case of transport as ammonia (integer)	*dmnl*
$X_{convliquid}$	Amount of conversion devices in case of transport as liquid hydrogen (integer)	*dmnl*
$X_{reconvammonia}$	Amount of reconversion devices in case of transport as ammonia (integer)	*dmnl*
$X_{reconvliquid}$	Amount of reconversion devices in case of transport as liquid hydrogen (integer)	*dmnl*
$T_{ammonia}$	Binary variable that indicates transport is done with ammonia when equal to 1	*dmnl*
T_{liquid}	Binary variable that indicates transport is done with liquid hydrogen when equal to 1	*dmnl*
C_w	Yearly costs of one wind turbine	*euros/year/unit*
C_s	Yearly costs of one solar platform	*euros/year/unit*
C_e	Yearly costs of one electrolyzer	*euros/year/unit*
C_d	Yearly costs of one desalination device	*euros/year/unit*
C_{st}	Yearly costs of one m^3 of storage tank	*euros/year/*$m3$
C_{fpso}	Yearly costs of one m^3 of FPSO	*euros/year/*$m3$
C_{kmsea}	Costs of ammonia or liquid hydrogen transport over sea for one tonkm hydrogen	*euros/ton of hydrogen/km*
$C_{basetransport}$	Base sea transport costs of ammonia or liquid hydrogen for one ton of hydrogen	*euros/ton of hydrogen*
C_{kmland}	Costs of gaseous hydrogen transport over land through pipelines per tonkm hydrogen	*euros/ton of hydrogen/km*
$C_{convammonia}$	Yearly costs of one ammonia conversion device	*euros/year/unit*
$C_{convliquid}$	Yearly costs of one liquid hydrogen conversion device	*euros/year/unit*
$C_{reconvammonia}$	Yearly costs of one ammonia reconversion device	*euros/year/unit*
$C_{reconvliquid}$	Yearly costs of one liquid hydrogen reconversion device	*euros/year/unit*

In Equations (3) to (5) and in some of the other calculations in the developed model, $T_{ammonia}$ and T_{liquid} are used, which are also mentioned in Table 2. $T_{ammonia}$ and T_{liquid} are binary variables used to include the choice between transporting with ammonia or liquid hydrogen in the optimization. To force the optimization solver to choose between the two, the constraint in Equation (6) has been implemented, which is also shown in Figure 3.

$$T_{ammonia} + T_{liquid} = 1 \tag{6}$$

In this section, the central cost calculation for the objective function as done by the developed model was shown. However, many related calculations and constraints are included in the model as well. As mentioned before, those are discussed in more detail in the report this paper was based on.

Scenario Definition

As explained before, the global potential of far offshore green hydrogen was assessed through the analysis of a representative set of high potential scenarios. To find these scenarios, usage locations were identified with high local production costs, as shown in Figure 4. In addition production locations were selected with strong wind resources and limited water depths, as shown in Figure 5.

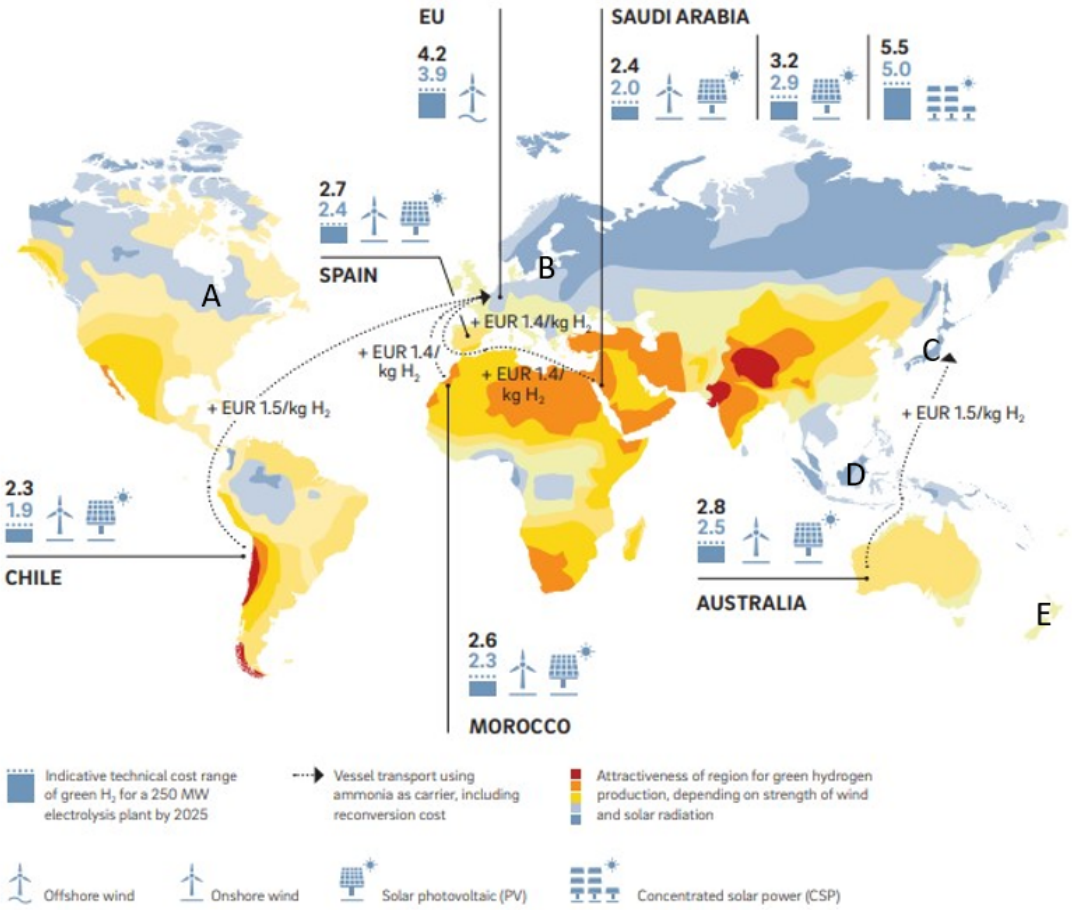

Figure 4: High potential far offshore green hydrogen usage locations A to E (modified from (De Vries et al., 2021))

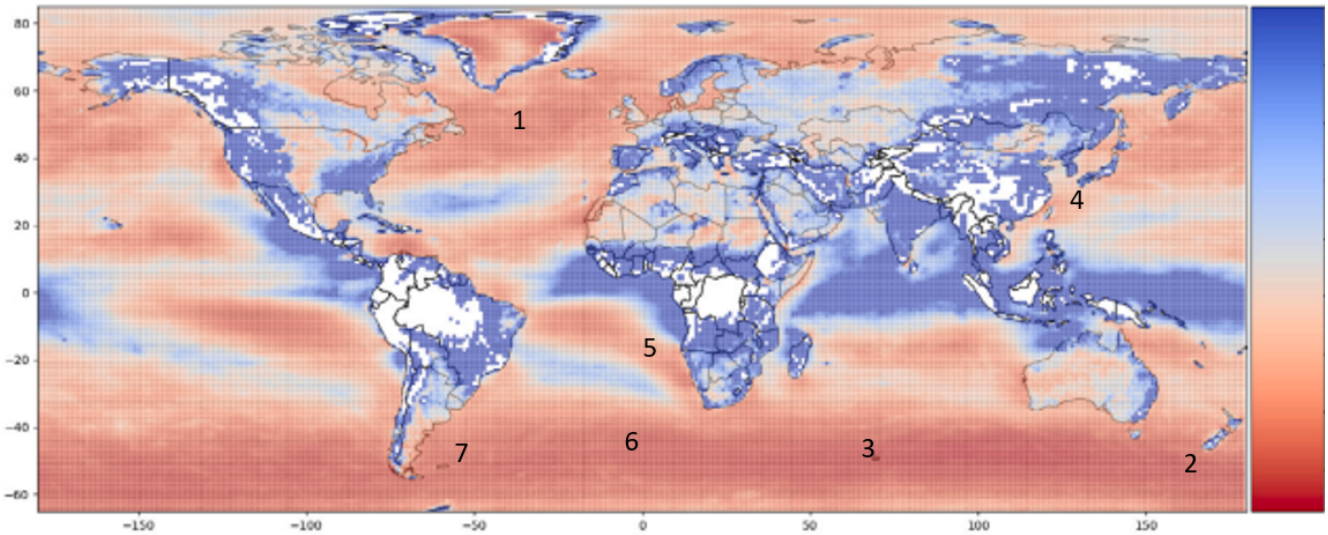

Figure 5: High potential far offshore production locations 1 to 7 (modified from (Salmon & Bañares-Alcántara, 2022))

The potential usage locations were combined with the closest production location to create the scenarios to be analyzed. For usage location D (Singapore), this could have been production location 2 (in the Southern Pacific Ocean), 3 (in the Indian Ocean) or 4 (in the East Chinese Sea). In this case, location 2 was chosen due to the strong renewable resource potential and relatively large area with limited water depth. The selection as described here lead to the selected scenarios shown in Table 3.

Table 3: High potential far offshore green hydrogen scenarios to be analyzed further in this research

	Production location	**Usage location**
Scenario 1	East Chinese Sea (4)	Tokyo, Japan (C)
Scenario 2	East Chinese Sea (4)	Seoul, South Korea (C)
Scenario 3	Northern Atlantic Ocean (1)	Cologne, Germany (B)
Scenario 4	Northern Atlantic Ocean (1)	New York, USA (A)
Scenario 5	Southern Pacific Ocean (2)	Singapore (D)
Scenario 6	Southern Pacific Ocean (2)	Christchurch, New Zealand (E)

RESULTS

After having formulated the model and defined a representative set of scenarios, the chosen scenarios could now be analyzed. The far offshore green hydrogen supply chain was optimized for all scenarios using the developed model and the accompanying costs per kilogram of hydrogen produced far offshore were compared to the costs of local green hydrogen production and green hydrogen import. The latter were determined primarily with the model made publicly available by Brändle et al. (2021). In the report this paper was based on, the general input data for the model (which stays the same across scenarios) and the scenario-specific input data can be found. In Figures 6 to 11, the results of the scenarios are presented, where the orange lines represent the far offshore green hydrogen costs.

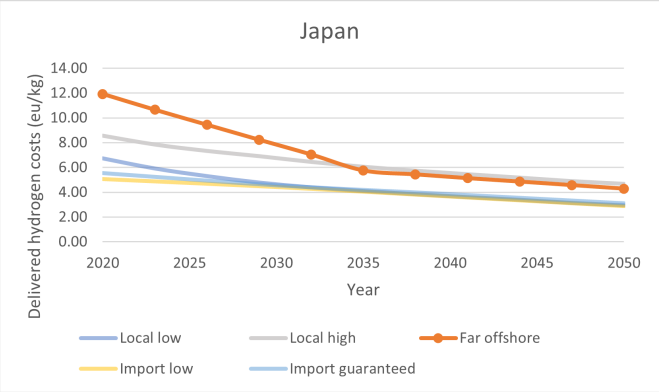

Figure 6: Results scenario 1

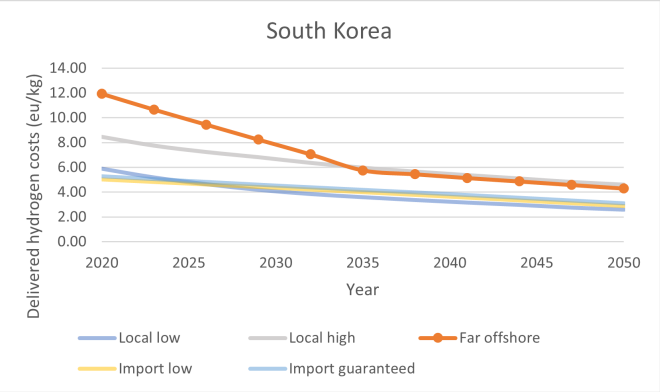

Figure 7: Results scenario 2

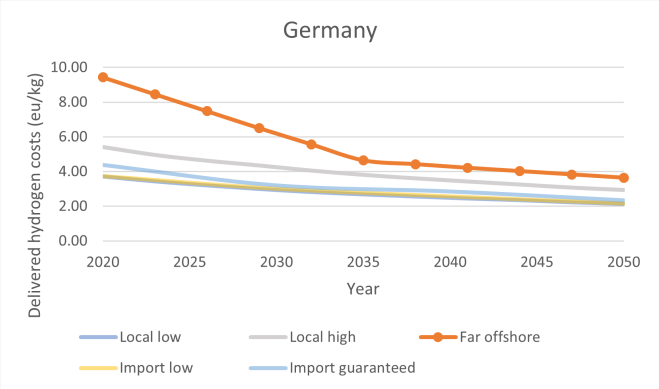

Figure 8: Results scenario 3

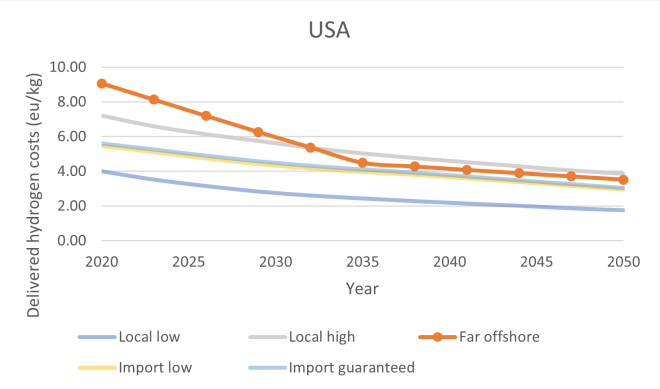

Figure 9: Results scenario 4

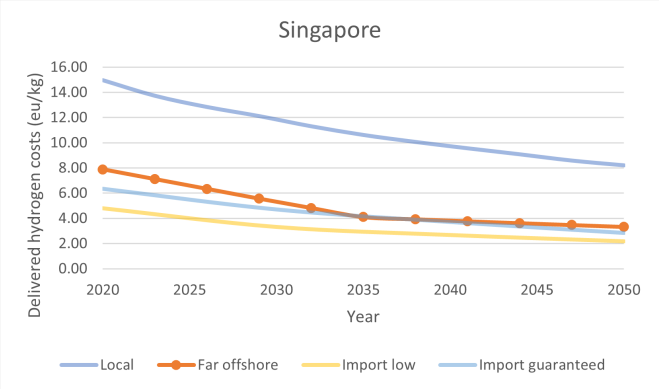

Figure 10: Results scenario 5

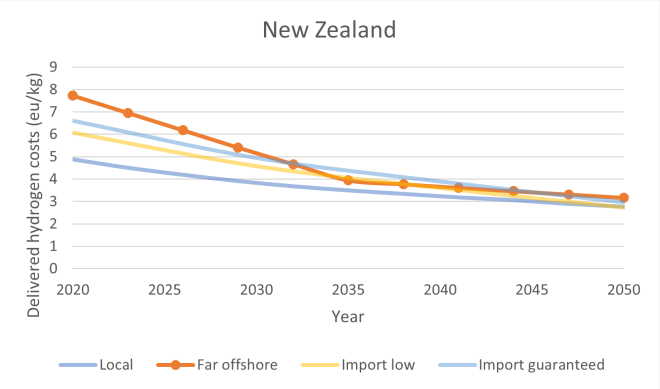

Figure 11: Results scenario 6

The results differ greatly between scenarios. In scenarios 1 and 2 (Figures 6 and 7), the far offshore green hydrogen costs are similar to the highest local production costs between 2035 and 2050. Green hydrogen import costs are clearly lower, which means far offshore green hydrogen does not have the preference from a purely techno-economic standpoint in these scenarios. However, since the cheap green hydrogen import options for Japan are mostly represented by China, Russia, Iran, Saudi Arabia and Oman, geopolitical factors may play in favour of far offshore green hydrogen. Based on the local production capacity of Japan (Brändle et al., 2021) and the expected demand in 2050 (The Hydrogen Council & McKinsey & Company, 2021), Japan is not expected to be able to be self-sufficient with onshore production, which means far offshore production will be necessary if Japan aims to be self-sufficient. The situation for South Korea is similar, although the onshore production capacity is higher there (Brändle et al., 2021).

When looking at scenario 3 (Figure8), it can be seen that far offshore green hydrogen is less economic than its alternatives over the entire period, but especially before 2035. The import options for Germany in this scenario include Spain, Italy, France, Norway and Morocco. It is therefore expected that the influence of geopolitical factors will be limited here. For scenario 4 (Figure 9), the far offshore green hydrogen costs are lower than the highest local production costs and similar to the import costs. However, the onshore green hydrogen production capacity in the USA is very large (Brändle et al., 2021), which means the local demand can be filled without any import. In scenarios 3 and 4, far offshore green hydrogen is not expected to be feasible from a purely techno-economic perspective based on these results. Societal factors such as the willingness to install renewable energy production onshore may however have an influence.

Finally, scenarios 5 and 6 (Figures 10 and 11) show relatively low far offshore green hydrogen costs, which can be attributed to the production location in the Southern Pacific Ocean, where very strong and steady winds can be found. From 2032 to

2050, the far offshore green hydrogen costs are similar to the import costs and also before 2032, the difference is relatively small. In Singapore (scenario 5), the local production costs are very high and the capacity is very small, so import is expected to be essential, either from a different country (in this case China) or from far offshore. Both options could share the market or the Singaporean government could choose between the two. In New Zealand, local onshore production is also relatively economic. It may depend on the capacity of this onshore production whether import from China or far offshore production is necessary. If one of these is necessary, again no strong preference can be given based on the costs.

Next to the scenario analysis based on the final costs, some additional analysis was done. It was found that combining wind turbines and solar platforms to create a more steady energy production is beneficial in most scenarios and that in every scenario, a different combination of wind turbines, solar platforms and electrolyzers is optimal. Figure 12 shows the installed wind and solar power generation capacity over the years for scenario 1 to illustrate this. In scenarios 1 and 2, a relatively large amount of solar power is used in the beginning, but this decreases over the years since the floating wind costs develop faster than the floating solar costs under the assumptions taken. After 2035, the model still uses some solar power in most years, but the capacity is small compared to the installed wind power capacity. The latter is the case for the entire period between 2020 and 2050 in scenarios 3 and 4. In scenarios 5 and 6, no solar power is used, indicating a relatively strong wind resource in the production location used in those scenarios.

Next, it was found that energy generation represents the biggest share of the total far offshore green hydrogen costs in 2020, but this decreases over the years. The percentage taken up by ammonia conversion, ammonia transport and the FPSO on the other hand grow because their costs stay constant while all other costs are decreasing over the years. This can be seen in Figure 13, which shows the development over the years of the far offshore green hydrogen costs and its distribution for scenario 1 as an example. In 2050, the ammonia (re)conversion costs are expected to be the biggest cost contributor, closely followed by the energy generation

Furthermore, ammonia is found to be the preferred transport medium for far offshore green hydrogen until at least 2050 in the analyzed scenarios. The choice between ammonia and liquid hydrogen based on the distance to be traveled over sea and the storage volume on the FPSO is illustrated in Figure 14 for scenario 1 in 2050. In this figure, it can be seen clearly that lower transport distances and lower storage volumes favor liquid hydrogen. The effect of reducing the liquid hydrogen transport, storage and (re)conversion costs by 10% is also shown.

Finally, in order to gain further insight in the influence of different input parameters on the costs per kilogram of far offshore green hydrogen, a sensitivity analysis was performed. In this analysis, it was found that the interest rate, floating wind costs, floating solar costs, ammonia (re)conversion costs, FPSO costs and large changes in water depth can have significant influence on the costs per kilogram of hydrogen. In addition, it was found that dampening and enhancing effects can be seen when changing the costs of floating wind, floating solar and the electrolyzers. Furthermore, it was found that the desalination costs, liquid hydrogen and ammonia transport costs, electrolyzer costs, distance to shore and size of the hydrogen demand have a relatively small influence within the variations performed. The small influence of the last one was however attributed to model simplifications.

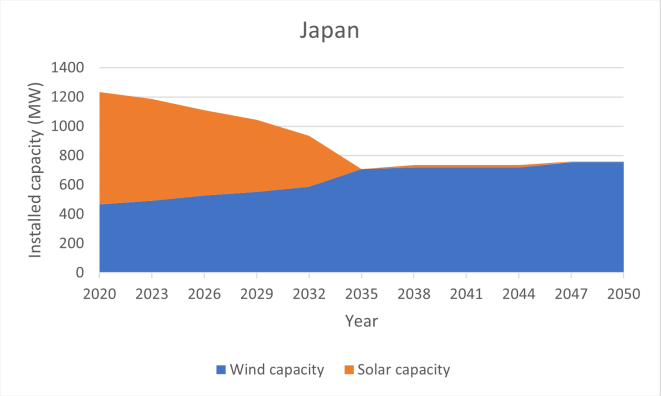

Figure 12: Total installed wind and solar power generation capacity from 2020 to 2050 in supply chains as optimized by the model for scenario 1

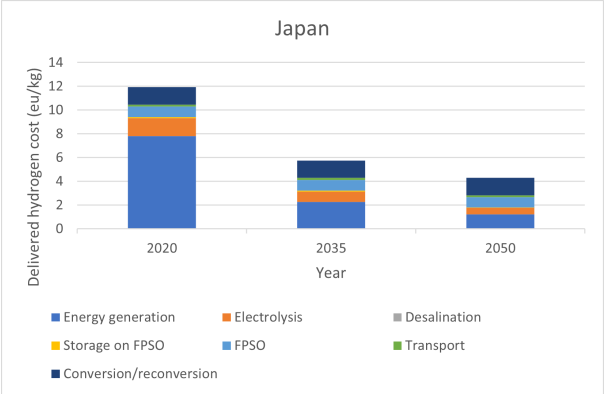

Figure 13: Cost distributions scenario 1 in 2020, 2035 and 2050

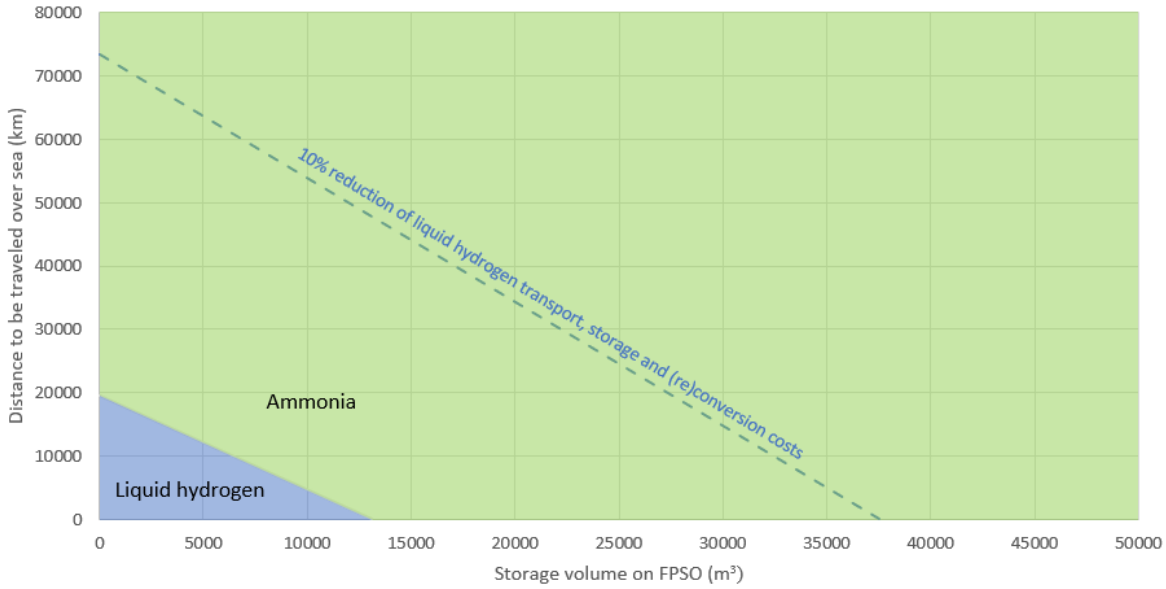

Figure 14: Visualization of preference for liquid hydrogen or ammonia based on distance to be traveled over sea and storage volume on the FPSO for scenario 1 in 2050

DISCUSSION

In the previous section, the results have been presented. Some side notes should however be placed with these results. First of all, as the field of far offshore green hydrogen is relatively new, data availability is limited. Therefore, the input data as used in this research should continuously be developed in follow-up research once more data becomes available.

Furthermore, follow-up research could look into further extending the model to make sure it becomes even more complete and accurate. The model could be extended by including size limitations of offshore locations, the effects of economy of scale, the costs of longer electricity cables for bigger wind parks (increasing the attractiveness of adding solar platforms),

differences in OPEX worldwide, and a more accurate estimation of the distance to be traveled over sea. These points are discussed in more detail in the report this paper was based on. Next to the model developed in this research, the model used to determine the green hydrogen local production and import costs also has several limitations, as discussed by Brändle et al. (2021).

Lastly, it should be mentioned that this research mostly looks at the techno-economic potential of far offshore green hydrogen, while geopolitical and social factors may also greatly influence its feasibility. Despite the comments mentioned in this section, valuable insights were created into what the global potential is of far offshore green hydrogen towards 2050 and what influences this potential. The conclusions drawn will be discussed further in the next section.

CONCLUSION

The techno-economic analysis of the selected scenarios in the present study shows a levelized cost of delivered green hydrogen from far offshore production locations of 3.5 to 5 euro/kg in 2050, coming from a cost of 7.5 to 12 euro/kg in 2020. A clear decreasing trend of the levelized cost of hydrogen (LCoH) can be observed for the coming decades up to 2050 across all scenarios. For two out of the six scenarios analyzed in our study (combination of far offshore production location and final delivery destination onshore), an LCoH below 5 euro/kg seems feasible from 2030 onwards, and from 2035 this is expected to be the case for another two scenarios. This cost may be considered as marginally competitive with alternatives such as local production of green hydrogen onshore or import of green hydrogen from other places in the world. Although the far offshore production costs are (slightly) higher in most scenarios, the considerable advantages of far offshore production, such as avoidance of scarce land usage in crowded areas and certain geopolitical considerations, should be taken into account when considering the competitiveness of the far offshore green hydrogen option and increase its feasibility. It should also be noted that techno-economic analysis of far offshore green hydrogen is still a relatively new research topic and that many aspects have not yet been thoroughly explored. Estimated cost may therefore still be lower or higher in certain specific scenarios, making or breaking the far offshore green hydrogen option. The most important uncertainty seems to be the development of the cost (CAPEX and OPEX) of critical components such as floating offshore wind, floating offshore solar and large size electrolysers for installation on a central floating production unit.

When going into a bit more detail, it was concluded that PEM electrolyzers would be most suitable for far offshore green hydrogen production. Furthermore, it was confirmed that combining wind and solar energy generation in far offshore hydrogen production can be beneficial, but it was also found that this not the case in every scenario. In addition, it was concluded that the optimal combination of wind turbines, solar platforms and electrolyzers strongly depends on the production location and the year considered. Furthermore, it was found that until at least 2050, ammonia appears to be the most suitable transport medium for green hydrogen produced far offshore under the current assumptions. In addition, it was found that the cost distribution of far offshore green hydrogen will develop strongly over the years. In 2050, the simulations predict the ammonia (re)conversion costs to account for the biggest part of the total costs, closely followed by the energy generation. Finally, it was found that the interest rate, floating wind costs, floating solar costs, ammonia (re)conversion costs, FPSO costs and large changes in water depth can have significant influence on the costs per kilogram of hydrogen.

Having come to these conclusions, a tangible outlook on the worldwide potential of far offshore green hydrogen towards 2050 has been created. This outlook, together with the developed model and gathered input data, will form a base from which future research will be able to explore this new and exciting research field in various directions. This research may be one of the first bricks in the wall for the development of a future where far offshore green hydrogen is a part of our energy mix. However, much research is still to be done, including further analysis with the existing model, expanding the model in different directions, and related research such as in depth technical studies of floating wind turbines and social studies to create insight into less tangible factors influencing the potential of far offshore green hydrogen production.

CONTRIBUTION STATEMENT

T. Melles: conceptualization; methodology; software; validation; formal analysis; investigation; data curation; writing - original draft; visualization; project administration. **J.F.J. Pruyn:** conceptualization; supervision; writing – review and editing. **J.L. Gelling:** conceptualization; supervision; writing – review and editing. **J.J. de Wilde:** conceptualization; supervision; writing – review and editing.

REFERENCES

Brändle, G., Schönfisch, M., & Schulte, S. (2021). Estimating long-term global supply costs for low-carbon hydrogen. *Applied Energy*, *302*, 117481. https://doi.org/10.1016/j.apenergy.2021.117481

Cebolla, O., Dolci, R., & Dolci, F. (2022). *Assessment of Hydrogen Delivery Options Feasibility of Transport of Green Hydrogen within Europe* (tech. rep.). Publications Office of the European Union. https://doi.org/10.2760/869085

d'Amore-Domenech, R., Leo, T. J., & Pollet, B. G. (2021). Bulk power transmission at sea: Life cycle cost comparison of electricity and hydrogen as energy vectors. *Applied Energy*, *288*, 116625. https://doi.org/10.1016/j.apenergy.2021.116625

De Vries, M., Albers. Bram, Goossens, S., & Van Dongen, B. (2021). *Innovate and industrialize: How Europe's offshore wind sector can maintain market leadership and meet the continent's energy goals* (tech. rep.). Roland Berger. https://www.rolandberger.com/publications/publication_pdf/roland_berger_offshore_wind_energy.pdf

EMD International. (2020). *The MILP Solver optimization method in energyPRO*. https://www.emd-international.com/files/energypro/HowToGuides/HowToGuide_MILP%20solver.pdf

ESMAP. (2019). *Going Global: Expanding Offshore Wind to Emerging Markets* (tech. rep.). World Bank. https://documents1.worldbank.org/curated/en/716891572457609829/pdf/Going-Global-Expanding-Offshore-Wind-To-Emerging-Markets.pdf

Hague, O. (2021). *What are the 3 Main Types of Hydrogen?* https://www.brunel.net/en/blog/renewable-energy/3-main-types-of-hydrogen

International Renewable Energy Agency. (2022). *Global Hydrogen Trade to Meet the 1.5°C Climate Goal Part II Technology Review of Hydrogen Carriers* (tech. rep.). https://www.irena.org/publications/2022/Apr/Global-hydrogen-trade-Part-II

Jan De Nul. (2023). *Jan De Nul, Tractebel en DEME Presenteren Drijvende Zonnepanelen Op Zee: SEAVOLT*. https://www.jandenul.com/nl/nieuws/jan-de-nul-tractebel-en-deme-presenteren-drijvende-zonnepanelen-op-zee-seavolt

Jang, D., Kim, K., Kim, K. H., & Kang, S. (2022). Techno-economic analysis and Monte Carlo simulation for green hydrogen production using offshore wind power plant. *Energy Conversion and Management*, *263*, 115695. https://doi.org/10.1016/j.enconman.2022.115695

Kasiulis, E., Jurasz, J., Sapiega, P., & Bochenek, B. (2022). Complementarity and application of renewable energy sources in the marine environment. In *Complementarity of variable renewable energy sources* (pp. 527–558). Elsevier. https://doi.org/10.1016/B978-0-323-85527-3.00007-8

Lapides, M., Kim, I., Fishman, D., & Ji, C. (2020). *Green Hydrogen: The Next Transformational Driver of the Utilities Industry* (tech. rep.). Goldman Sachs. https://www.goldmansachs.com/intelligence/pages/green-hydrogen.html#:~:text=This%20report%20focuses%20on%20Green,for%20the%20Utilities%20industry%20alone.

Rehman, S., Alhems, L. M., Alam, M. M., Wang, L., & Toor, Z. (2022). A review of energy extraction from wind and ocean: Technologies, merits, efficiencies, and cost. *Ocean Engineering*, *267*, 113192. https://doi.org/10.1016/j.oceaneng.2022.113192

Salmon, N., & Bañares-Alcántara, R. (2022). A global, spatially granular techno-economic analysis of offshore green ammonia production. *Journal of Cleaner Production*, *367*, 133045. https://doi.org/10.1016/j.jclepro.2022.133045

SolarDuck. (n.d.). *Unique Solution: Our technology differentiators*. https://solarduck.tech/unique-solution/

The Hydrogen Council & McKinsey & Company. (2021). *Hydrogen for Net-Zero: A critical cost-competitive energy vector* (tech. rep.). https://hydrogencouncil.com/wp-content/uploads/2021/11/Hydrogen-for-Net-Zero.pdf

United Nations. (n.d.). *Net Zero Coalition | United Nations*. https://www.un.org/en/climatechange/net-zero-coalition#:~:text=To%20keep%20global%20warming%20to,reach%20net%20zero%20by%202050

Part 5:
ENERGY TRANSITION

Proceedings of 15th International Marine Design Conference (IMDC-2024)
June 2-6, 2024
Amsterdam, the Netherlands

A review of the state-of-the-art Sustainable and Climate-resilient inland waterway vessels

Richmond Anku[1,*], Jeroen Pruyn[1,2] and Cornel Thill[1]

ABSTRACT

Inland water vessels are impacted by climate change in two respects. First of all, they will need to convert to low-impact power propulsion and energy (PPE) systems. Secondly, they will need to deal with the impact of climate change, especially longer periods of very low and high water. This paper reviews the multi facet impacts of climate change on inland waterway vessel performance and problems associated with the choice of alternative power energy and propulsion (PPE) system on the vessel's performance

KEY WORDS

climate-change, decarbonisation, inland waterway vessels, shallow-water

INTRODUCTION

Inland waterways play an important role in transportation, presenting a sustainable and energy-efficient means with better environmental performance than other transport modes in terms of CO_2 emissions by transport work (gCO_2e/tkm) (Doll et al., 2020). In the Netherlands, inland waterway transport accounts for approximately 41 % of the total freight transport among the main hinterland transport modalities according to ("Eurostat", 2023), contributing to the decongestion of road and rail networks (Vinke et al., 2022), and presents an economically competitive alternative in terms of cost and tonnage. Inland waterway vessels are affected by climate change in dual dimensions. First, there is an ambition to mitigate climate change by abating greenhouse gas (GHG) emissions, which, according to the European Environmental Agency (Doll et al., 2020), as of 2018, inland water transport emits 33 gCO_2/tkm, making up a share of about 17 % of CO_2 emissions from the transport sector. However, these vessels need to adapt to the predominant effects of climate change on waterways, ensuring sufficient cargo transport and navigation during prolonged periods of severe drought and flood, resulting in high and low water levels. To achieve a significant emission reduction, the use of low-impact energy carriers complemented by suitable energy converters is required (Zwaginga & Pruyn, 2022), and the adoption of alternative energy carriers poses inherent challenges owing to their lower energy densities. Meeting propulsion and power energy demands necessitate additional space and weight for storage, directly affecting vessel performance (Wang & Wright, 2021). In addition, the adverse effects of climate change influence vessel performance (Jonkeren et al., 2013).

Inland waterway vessels differ significantly from ocean-going vessels; given that they are much smaller in size and the environment in which they operate. Inland waterway vessels are designed to navigate and manoeuvre through confined and restricted waterways such as rivers with bridges and locks (Radojčić et al., 2021). Although ocean-going vessels sail under adverse weather conditions, they do not have the limitations of inland water vessels. The physical interaction between the hull and waterway, and thus the flow around the hull, influences the hull form design and maximum dimensions of inland

[1] Affiliation (Maritime and Transport Technology, Delft University of Technology, Delft, Netherlands); ORCID: 0009-0001-0942-792X
[2] Affiliation (CoE HRTech, Maritime Innovation, Rotterdam University of Applied Science, Rotterdam, Netherlands)
[*] Corresponding Author: R.s.a.anku@tudelft.nl

Submitted: 12 February 2024, Revised: 2 May 2024, Accepted: 3 May 2024, Published: 18 May 2024

Conference paper, DOI: https://doi.org/10.59490/imdc.2024.826 e-ISSN: 3050-4864

water vessels to suit the respective waterway classifications in which they operate (Zeng, 2019). The length is restricted by the lock length, the breadth is restricted by the lock width, the air draught (vessel height above the water line) is limited by the bridge vertical clearance, and the vessel draught is limited by the water depth (Guesnet et al., 2014). These distinguish inland waterway vessels from ocean-going vessels, which underpins the fact that their efficient operations are affected more by the effects of climate change. When this is not addressed, inland water transport would become a less reliable transport mode and could lead to a modal shift that is undesirable because the other transport modes do not have the capacity to compensate for the loss of capacity by inland water transport (IWT) (Vinke et al., 2022), whereas IWT has underexploited reserves. This would lead to a disruption of the supply chain, as well as an increase in environmental pollution from road transport. A fundamental element for ensuring the effective and safe transport of cargo along these routes involves a comprehensive understanding of ship hydrodynamics (Gebraad et al., 2021), actions required to adapt fleets, ensuring transportation reliability (Kempmann et al., 2023), and reducing the environmental footprint. The challenge however faced by ship designers and naval architects is finding the ”sweet spot”, an ideal balance between achieving zero-emission, adapting to climate change and vessel performance; thus, the trade-offs between adapting short-term measures and flexibility to meet uncertain future requirements are imperative, and hence careful consideration from the design point of view (Andrews & Erikstad, 2015).

This literature review focuses on current state-of-the-art research on the decarbonisation of inland water transportation and adaptation of inland water transport to climate change. The main research question for this literature review is:

“What is the current state of climate-resilient and sustainable inland water vessel design?”

The rest of this paper is structured as follows. In the next section, the Methodology is outlined, providing insight into the literature exploration approach. Following this, Results and Discussions presents and discusses the outcomes derived from the reviewed literature. Finally, in Conclusion and Future Study, a concise summary of the entire paper is provided, encapsulating the essential findings from the literature outcomes and the author’s reflection on future research directions from identified gaps.

METHODOLOGY

To comprehensively organise and evaluate findings from past research, we conducted a methodological exploration of the literature utilising specific search terms to answer the main research question highlighted in the previous section. The search strategy for this study stems from two concepts derived from the main research question: one concerns the climate change adaptation of inland waterway vessels and the decarbonisation of inland waterway vessels. For the first concept, the search terms included “climate change” OR “low water” OR “shallow water” AND “inland navigation” OR “IWT” OR “inland water*”. Whereas for the second concept, the search terms included “sustainability” OR “decarbonisation” OR “emission reduction” OR “GHG emissions” AND “inland navigation” OR “IWT” OR “inland water*”. The snowball technique was also used in the literature search, involving the examination and assessment of references cited in the selected primary literature for relevance and potential inclusion in this study. The initial search for resources was conducted using databases connected to the TU Delft library, as summarised in Table 1. The articles selected for this literature review provide a back-

Table 1: Search resources and types of documents

Information resources or database for preliminary search	**Types of documents**
Web of Science, Google Scholar, and TU Delft repository	Journal articles, conference papers, books
Secondary resources	**Types of documents**
Cited references of primary resources	Journal articles, conference papers

ground to answer the research questions. Selection and exclusion were performed first by scanning the titles and keywords, after which a detailed perusal of the abstracts, introductions, and conclusions of articles was performed to assess their relevance for this work.

RESULTS AND DISCUSSIONS

The search terms led to a selection of 392 papers, and after reviewing the titles, approximately 150 remained. Based on their abstracts, a further 65 were dismissed, as these primarily addressed logistics, policy management, or hydrology. The state-of-the-art review began by exploring the remaining 51 papers.

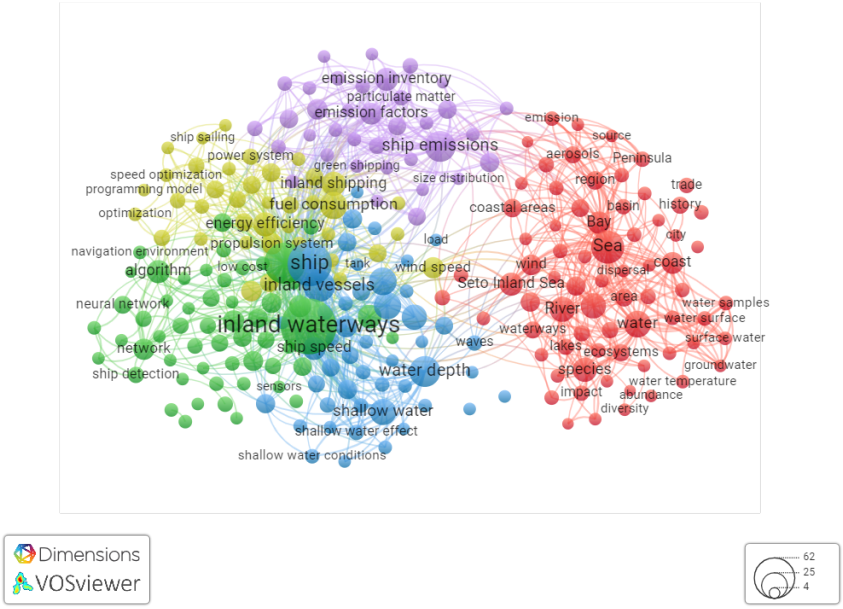

Figure 1: Literature clustering from database

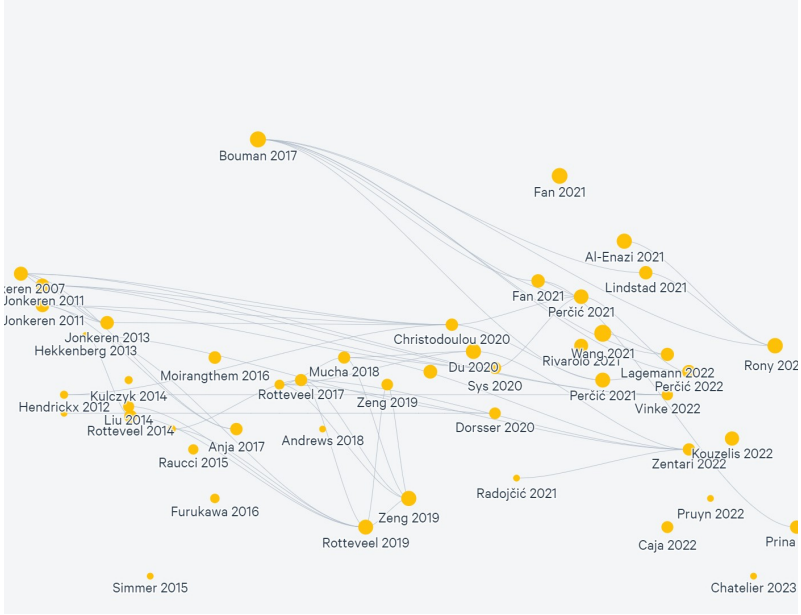

Figure 2: Map of reviewed literature

For the final review, 63 papers were studied in depth to arrive at the current state of the art, which will be presented next. The review is divided into two sections: the first section, which is covered in Climate Change and Inland Waterway Vessels, presents the impact of climate change on inland waterway vessels and the state-of-the-art options for adaptation, whereas Decarbonising Inland Waterway Vessels discusses the state-of-the-art decarbonisation of inland waterway vessels.

Climate Change and Inland Waterway Vessels

Climate change threatens the competitiveness and reliability of inland navigation, which also challenges the realisation of one of the objectives of the EU project NAIADES III action plan (Sys et al., 2020), which is to shift the significant share of freight transport from roads to more sustainable modes, such as inland waterways and rail transport. Several investigations have been conducted on the impact of climate change on inland water transport, and it is also interesting to note that many of these studies focused on the impact of low water depth on navigable fairways, because prolonged periods of droughts are expected to occur more often in the future and have even more severe consequences on efficiency, safety, and reliability than problems associated with high water levels or discharge on the fairways (Jonkeren, 2009). In many of these studies, various models were developed to predict the fairway conditions, estimate the hydrodynamic performance in shallow water, economic models to estimate revenue loss due to loss of payload capacity, and estimate the potential of modal shift from inland water transport to roads. In this section, we discuss the most prevailing impact of climate change on inland waterway vessels covered by current and past literature.

Resistance and Power Demand

Water depth severely impacts the resistance and power demands as this increases with decreasing water depth according to (Radojčić et al., 2021). ITTC, 2017 outlined that the shallow water effect on ship resistance must be taken into account when one or the combination of the following thresholds are met;

- Finite water depth to vessel draught ratio $h/T < 4$.
- Froude number of water depth $F_{\text{nh}} > 0.5$.

According to (Radojčić et al., 2021), total ship resistance of inland waterway vessels can be decomposed into two categories; the viscous resistance and the wave-making resistance (see equation 1). Zentari et al., 2022 did highlight that, when $F_{\text{nh}} < 0.6$, which characterises a subcritical flow regime, the wave-making resistance of a vessel in shallow water is comparable to deep water conditions. However, shallow water effect on wave-making resistance becomes more pronounced when the vessel approaches a critical flow regime of $F_{\text{nh}} = 1$. Nevertheless, this is not the case for inland waterway vessels given that most of these vessels operate within a speed range below the critical regime (Zentari et al., 2022). As such, viscous resistance emerges as the most dominant resistance component of inland waterway vessels, where the influencing factors are the friction coefficient and hull form factor.

In shallow water navigation, the keel clearance, which is the safety distance between the hull bottom and waterway bed is considerably reduced. This consequently causes ship squat, also known as dynamic sinkage, which as a result of increased water flow around the hull, leads to reduced pressure below the hull, a phenomenon based on Bernoulli principle (Radojčić et al., 2021; Zeng, 2019). The squat further amplifies the frictional resistance (Zeng et al., 2017), due to thinner boundary layer resulting from accelerated under-keel flow. The power required to propel the vessel depends on the total resistance and the ship's speed (see equation 2). As such given an increase in ship resistance as a result of shallow water, for the same sailing speed, the ship would require more propulsion power to perform its functions, and this translates into more energy consumption. Alternatively, for a given installed power, the speed may have to be reduced, and as a result, more time may be required to transport cargo over a distance (Schweighofer et al., 2022), which also translates into more energy consumption.

$$R_{\text{T}} = R_{\text{V}} + R_{\text{W}} \tag{1}$$

$$P_E = R_T \cdot V_s \tag{2}$$

In recent years, numerical methods using computational fluid dynamics (CFD) simulation tools have been used for both predictions and optimisation of ship resistance [9]. The traditional, model scale tests and use of empirical models such as the Holtrop & Mennen have been used for resistance estimations with some correction factors, applied to ship speed and form factor (Pompée, 2015), to account for shallow water effects. However, the Holtrop & Mennen empirical model was fundamentally obtained from datasets of ocean-going ships and hence applying this to inland water vessels may lead to inaccurate predictions. Moreover, the Schlichting (1934) empirical method was based on speed correction to account for the deviation of residual resistance in shallow water compared to the deep-water case (Pompée, 2015; Raven, 2012). The Schlichting speed correction method was further improved by Lackenby (1963) by extending its application to extreme shallow water conditions (Raven, 2012; Zeng et al., 2017). Jiang (2001) proposed another approach to estimate the shallow-water effect, based on effective Froude number influenced by dynamic sinkage (ship squat) to predict a new effective speed of the vessel. The weakness of these empirical methods is that they rely on correcting the resistance curve in deep water for shallow-water scenarios of ocean-going vessels.

Given that the presence of channel walls and the shallow nature of inland waterways significantly impact the hydrodynamic resistance of inland water vessels at a given speed. Rotteveel (Rotteveel & Hekkenberg, 2015) stated that the limited breadth of the waterway leads to backflow around the vessel, increasing the water speed around the hull and thereby amplifying frictional resistance, which is termed as the hydraulic effect. Additionally, the restricted water depth limits the wave speed, causing increased resistance from wave formation at the ship's specified speed, which is termed the undulatory effect (Pompée, 2015). For the reasons identified above, the empirical methods with shallow water corrections derived from seagoing vessels are characterised by higher speed and lower block coefficients, adding to the fact that the environment in which they operate differ considerably not only in terms of depth but also breadth and the presence of canals and locks. These methods may not be sufficient for application in inland waterway vessels. Hence, using CFD methods, recent studies (Zeng et al., 2019) and (Raven, 2012) focused on predicting the shallow-water effect on the frictional coefficient. While Furukawa et al., 2016 focused on predicting the hull form variation and shallow water on the viscous component of the total resistance of inland waterway vessels. Table 2 summarises recent studies performed to accurately estimate the resistance components of inland waterway vessels, accounting for shallow water effects.

Table 2: Summary of recent literature on shallow water effects on resistance of inland vessels

Reference	Method	Key findings
Zeng et al., 2019	Regression numerical friction line for shallow water correction obtained from CFD simulations.	Authors find that this method can be used to better estimate the frictional resistance of the ship's flat bottom (parallel middle body), however, should be combined with the ITTC57 correlation line for other wetted surfaces for accurate estimation of overall frictional resistance in shallow water conditions
Rotteveel and Hekkenberg (2015)	CFD approach to investigate the effect of hull form variation (block coefficient) and shallow water on resistance.	The authors' viscous pressure resistance component increases faster in shallow water than frictional resistance. Also, the water depth effect is larger than the hull form variation on the total ship's resistance as an effect of the hull for variation rather becomes smaller in shallow water.
Zeng et al., 2017	Numerical and experimental methods to investigate dynamic sinkage and ship resistance in extreme shallow water.	The authors found that flow under the keel accelerated as keel clearance reduced leading to a thinner boundary layer which increased the frictional resistance component. And this is further amplified by trim and squat effects. The trim correlation line was not linear or monotonic, and a piecewise function might best be used to represent the relation between trim and ship speed.

Table 2 continued

Furukawa et al., 2016	Captive model test to estimate the longitudinal hydrodynamic forces acting on bare hull in sufficient and shallow water conditions, to measure the shallow water effects on the longitudinal components of hydrodynamic derivatives.	Based on the results from the database of test cases performed on multiple types of vessels. The authors derived an empirical formula for estimating longitudinal hydrodynamic forces acting on a vessel.
Raven, 2012	CFD approach Using PARNASSOS, a RANS solver developed by MARIN to estimate the viscous resistance of 4 different ships accounting for shallow water effects.	The variations of viscous resistance against water depth were determined by the computational model. The authors also found a correction for model-to-full ship extrapolation of the viscous resistance in shallow water. It was mentioned the Froude extrapolation and form factor extrapolation can be applied for full-scale frictional resistance prediction, however, may lead to overestimation of residual resistance at full scale.
Raven, 2022	Numerical computation approach by MARIN to establish correction factors independently for viscous resistance, a wave-making resistance and an overall added resistance due to squat effect for extremely shallow water conditions. The results were then validated with full-scale ship trials and empirical estimates.	The author found a limiting Froude number Frh < 0.65 for which there is no influence of water depth on wave-making resistance. It was also observed that overall resistance increased as a result of sinkage, which is present due to low pressure underneath the hull in shallow water. Although this sinkage effect was somewhat uncertainty, stating that the estimated increase in sinkage was too large, and therefore may lead to inaccurate prediction of the overall resistance.
Mucha et al., 2018	An experimental study of the effects of water depth, separation distance and bank effects on resistance of inland waterway vessels.	Result of this study revealed that sinkage was more pronounced with increasing ship speed and decreasing water depth. Also, lateral restrictions (proximity of vessel to the sides of the fairway) further lead to increase in lateral forces and moment (hydrodynamic sway and yaw motions). The magnitude of these lateral force and moment as noted by the authors can even exceed that of the longitudinal force required to move the vessel forward.
Zentari et al., 2022	An experimental and numerical investigation of shallow water effects on resistance and propulsion of coupled convoys.	Although authors recorded some deviation 15 % when comparing the numerical results of resistance to the experimental result in shallow water. It was found that in deep water, the boundary layer is fully developed, and flow separation zones are smaller, and less vortex shedding occurs, however, that is not the case in shallow water. In shallow water it was observed that the under-keel clearance influenced the boundary layer, thereby altering the velocity pressure field, causing flow separation.

Table 2 continued

Du et al., 2020	Numerical simulation of confined waterway effect on resistance and ship-generated waves of two inland waterway vessels.	It was observed from the simulations results that stronger confinements characterised by smaller cross-section area ratio between channel and ship, increase the ship resistance. This effect becomes even more evident with higher values of ship speed and higher loaded draft. Also investigating the wave pattern, it was noted that the wave propagation is limited by the channel banks and bottom, causing reflection and refraction. This effect was also seen to amplify with larger loaded draught.

Propulsive Efficiency and Manoeuvring Capability

The heightened power demand is further exacerbated by the reduced propulsive efficiency, which is a result of increased thrust loading on the propellers when operating in extremely shallow water (Radojčić et al., 2021). With reduced keel clearance, the inflow to propellers considerably differs from deep-water conditions, and as a result, affects the open-water efficiency coefficients (Radojčić et al., 2021). In addition to the reduced propulsive efficiency caused by high thrust loading owing to increased resistance when operating under low water conditions, the risk of propeller emergence or ventilation is also higher when sailing on reduced draught owing to the limited water depth, resulting in the loss of thrust and low propulsive efficiency (Hagesteijn et al., 2015). The hydrodynamic propulsive efficiency applied to ocean-going ships is fundamentally the ratio of effective power (P_{E}) and the power delivered to the propeller through the shaft (P_{D}), as defined by (Radojčić et al., 2021) in equation 3:

$$\eta_{\mathrm{d}} = \frac{P_{\mathrm{E}}}{P_{\mathrm{D}}} = \eta_{\mathrm{H}} \cdot \eta_{\mathrm{o}} \cdot \eta_{\mathrm{R}} \tag{3}$$

$$\eta_{\mathrm{H}} = \frac{1-t}{1-w} \tag{4}$$

$$\eta_{\mathrm{o}} = \frac{J}{2\pi} \cdot \frac{K_{\mathrm{T}}}{K_{\mathrm{Q}}} \tag{5}$$

The hull efficiency η_{H} and the relative rotative efficiency η_{R}, both describe the overall hull and propeller interactions. The action of the propellers behind the hull induces additional resistance to the entire ship resistance. Consequently, an additional thrust force is required to overcome the ship towing resistance, and the added resistance is measured by the thrust deduction factor t. Also, for IW vessels navigating in restricted water, the changes in the inflow to the propeller tend to increase the wake fraction w. And if the wake fraction w becomes larger than the thrust deduction coefficient t, the hull efficiency increases according to (Rotteveel et al., 2017) and confirmed by research results of MARIN in (Mucha et al., 2018). However, this phenomenon is a complex one, given that, an increase in wake fraction means a reduction in advanced speed (V_{A}), translating into a reduction in open water efficiency η_{o} and relative rotative efficiency η_{R}, which could ultimately even lead to an overall reduction in propulsive efficiency η_{d} (Radojčić et al., 2021). An interesting observation by (Rotteveel et al., 2017) of the wakefield, is that the nominal wake fraction w which is usually estimated without the presence of propeller may lead to low power estimation, given that the presence of propeller suppresses the growth of wake and flow separation. Therefore, an effective wake fraction w_{e}, accounting for propeller action is rather accurate for estimating power.

Pompée, 2015 highlighted that, given the high block coefficient of inland vessels around 0.85 and 0.95, the wake fraction could easily be twice as high as that of ocean-going vessels. The high wake fraction value which is characterised by low inflow speed to the propeller is very difficult to measure as noted by (Rotteveel et al., 2014), that simply approximating with empirical formulas may give misleading results. Howbeit, according to (Pompée, 2015; Rotteveel et al., 2014), methods like the Holtrop & Mennen and Papmel commonly utilised in naval architecture for predicting propulsion efficiencies through thrust and wake fractions, primarily cater to ocean-faring ships, overlooking considerations for IW vessels. The

extended version of the Papmel formula was modified by A.M.Basin & Miniovich for inland vessels and pushers to accommodate inland vessels and pushers has been observed by (Pompée, 2015) and (Raven, 2022) to lack the incorporation of water depth effects. Most recently Rotteveel in (Rotteveel, 2019) analysed the influence of stern shape under varying waterway conditions on the propulsion performance of inland waterway vessels, this and other recent research have been summarised in Table 3 below.

Table 3: Summary of most recent literature on shallow water effect on inland waterway vessels propulsion

Reference	Method	Key findings
Rotteveel, 2019	In his thesis, Rotteveel used the CFD computation approach to analyse, the influence of stern shape variation of IWV on propulsion performance under different operating conditions. Further surrogate models were used to find trends and patterns for optimal design from the CFD results.	The author introduced novel design guidelines aimed at achieving an optimal stern design for efficient propulsion in low water conditions. This optimization process entailed balancing trade-offs between the ship's displacement and its propulsive performance across varying water depths. Through iterative adjustments of variables to attain the optimal design, the study identified the pivotal significance of stern length and the athwartship propeller position in enhancing propulsion efficiency.
Rotteveel et al. (2017)	Inland ship stern optimisation in shallow water. Optimising propulsion power based on aft-ship hull parameters which include; the lateral position of the propeller, stern bottom shape (V-shape and S-shape), stern bilge radius, and tunnel curvature.	It was observed the lateral propellers' position closer to the centerline, moves the propellers in a stronger wake field yielding increased hull efficiency. The V bottom shape showed stronger effect (increase) in thrust deduction compared to the S bottom shape in shallow water. The effect of the tunnel curvature was observed to be small and negligible with changing water depth. Also, the influence of the bilge radius was observed to decrease in shallow water, owing to the fact that in shallow water, the flow comes from the sides instead of the bottom.
Kulczyk and Tabaczek, 2014	Analysis of results of model tests, and numerical computation of the influence of ship loading, water depth, ship speed and stern height on thrust and wake coefficient for inland waterway motor cargo vessels and pushboats with stern tunnel	The authors found that both increase in ship speed and reduced h/T leads to decrease in wake fraction and corresponding increase in thrust deduction, owing to the reduction in under-keel clearance.
Hagesteijn et al., 2015	Model scale test in a Depressurized Wave Basin, to assess the performance reduction due to propeller ventilation.	Authors found from the experiment, speed reduction of 0.5knot due to ventilation. It was observed that, when propellers suck in air, the achievable thrust and torque required drop for a given advance coefficient. The resulting reduced thrust is sufficient to propel the vessel such that speed loss is inevitable.

The ideal design of propellers for IW vessels, especially to adapt to low-water conditions, as emphasised by (Hekkenberg, 2013), should be determined on a case-by-case basis. This involves finding a "sweet spot" such that, the propeller is small enough to remain fully immersed in water on the ballast draft, and also large enough to deliver sufficient thrust at the laden draft. This could also mean adopting the tunnel aft-ship to mitigate ventilation in ballast conditions or reduced draught im-

posed by low water depths; this was investigated by in (Rotteveel et al., 2017). However, (Hagesteijn et al., 2015) found that tunnel aft-ship does have added adverse effect on the hull resistance.

The manoeuvring and stopping capabilities of inland water vessels are also negatively impacted by shallow water effects. The change in hydrodynamic forces and moments acting on the hull and lifting surfaces influences the turning, stopping, and course-keeping performance, thereby compromising the safe operation of the vessel (Liu et al., 2014).

Cargo Capacity Utilisation

The loading capacity of inland water vessels is constrained by the available water depth. For a given ship size and dimension, the only variable that determines how much tonnes of cargo can be transported at a given time is the loaded draft, as the displacement in such instances depends on the depth of the vessel immersed in water. Total ship displacement can be decomposed into lightweight and deadweight; the deadweight tonnage is the component that determines the carrying capacity of the ship correlating directly to the loaded draft as investigated by (Hekkenberg, 2013) in a parametric inland ship design model. Given the draught restrictions imposed on vessels when navigating shallow water, the corresponding volume of cargo that can be transported is limited. The consequence of low water levels on the load factor differs for each ship type and size, depends on the vessel's empty and loaded draft (van Dorsser et al., 2020). The research findings from the EU joint research centre (JRC) in (Rothstein & Scholten, 2016), where they estimate the bearing capacity for different ship sizes and types, suggests that ships characterised by greater empty drafts are more prone to experiencing a reduction in their loading capacity at low level of water on the Danube river. In this work, for the lowest recorded water level of 177cm, the load factor of smaller vessels was about 50 %, whereas that of larger vessels ranged between 20 % and 30 %. Although not same quantified values of load factors were found by (van Dorsser et al., 2020) on the Rhine river, he also came to a similar finding that larger vessels experienced higher reduction and deadweight and payload capacity at low water levels.

Furthermore, a sensitivity analysis was conducted by (Al-Enazi et al., 2021), to deepen the understanding of the impact of capacity utilisation on the quantity of emissions produced. The findings revealed that an increase in capacity utilisation leads to a consistent decrease in CO2 emissions (Al-Enazi et al., 2021) per tonne-km. This is more related to the energy efficiency indices; an important operational performance metric, that quantifies carbon emission per transport work. Table 4 summarises recent literature on shallow water effects on cargo capacity utilisation

Table 4: Summary of the most recent literature on the effects of shallow water on cargo capacity utilisation

Reference	Method	Key findings
van Dorsser et al., 2020	Empirical model based on regression analysis of loading certificates of 157 ships, to analyse the relative effect of reduced or increased draft on loading capacity index	The model which was based on the operational loading of vessels during the extreme drought season of 2018, authors observed that vessels with higher empty draught are more vulnerable to low water conditions relative to vessels with low empty draft.
Rothstein and Scholten (2016)	Multi-regression analysis of the relation between water level and degree of capacity utilisation, transport volume per ship, total transport volumes and numberer of ships for transport on Danube river.	It was found from the analysis that, for every reduction in water depth by 10cm, the degree of capacity reduction was between (0.51 % and 0.66 %), for same water level reduction also, the transported cargo reduced by between (10t and 14t) for different ship types. Finally, also the total transported cargo on the corridor was observed to reduce in the range of (1188t and 3760t). For the lowest water condition recorded, they found from their model that smaller vessels could load about 50 % of their maximum capacity, whereas larger vessels only use up about 20 % to 30 %.

Vinke et al., 2022	Agent-Based and Discrete Event simulation using OpenCLSim; integrating hydrology data of corridor to estimate the cascading effects on navigation, transport performance, and economic impact	The authors observed a change in fleet composition with changing water levels, and also the number of trips required to make up for the volumes in normal conditions, although the simulation shows a loss of total transported volume

Transport Cost

The cost, among other factors, determines the competitiveness of inland water transportation. The restriction in the load factor, which results in reduced transport capacity caused by low water levels, leads to escalated transport expenses for the ship owner or operator. Moreover, (Jonkeren & Rietveld, 2007) says under certain demands, some negative relation between prices and water level is expected. These additional costs stem from the amplified voyage frequency, heightened handling expenses, prolonged waiting periods, and increased energy consumption. Consequently, these factors collectively account for a significant portion of operational expenditures (Jonkeren et al., 2013). Jonkeren, 2009 even found that the cost per ton could increase by as much as 75 % for vessels plying serious bottlenecks of the Rhine fairway at extreme water levels, noting that these additional costs are usually not borne by the operators or ship owners themselves, but the economic burden of low water periods is shifted to shippers and finally the consumers. As such shippers may consider alternative modes of transportation, potentially resulting in a decline in demand for inland water transport, and further worsening its competitive position (Krekt & van der Laan, 2011).

In a study conducted by (Jonkeren et al., 2011), the impact of prolonged drought on the cost of inland transport operations in Northwest Europe was evaluated. Their findings indicated that, in an extreme climate scenario, inland water transport could potentially experience a reduction in capacity of approximately 5.4 %. Furthermore, it was highlighted that road transport is likely to absorb a significant portion of this reduced capacity. Although (Krekt & van der Laan, 2011) also highlighted the potential loss of capacity to other transport modes due to climate change, they asserted that the majority of the shift would be towards rail transport, which contrasts the findings of (Jonkeren et al., 2011). Table 5 summarises recent literature on shallow water effect on the cost of cargo transport.

Table 5: Summary of most recent literature on shallow water effects on transport cost

Reference	Method	Key findings
Jonkeren and Rietveld, 2007	Multi-regression analysis to assess the impact of water level on the logarithms of load factor, freight rate per ton and freight rate per trip.	From the analysis of data on inland water transport activities on the Rhine River, authors found an empirical formula to estimate the welfare loss (economic implications) due to low water conditions between 2003 and 2005.
Jonkeren et al., 2011	Multimodal freight transport modelling with NODUS, a GIS-based software to assess the cost of transport operations for IWT over the Rhine River under varying climate scenarios	Authors discovered that the impact of extremely low water conditions extends beyond influencing the transportation prices of Inland Waterway Transport (IWT). These conditions may induce modal shifts, thereby compromising the competitive position of IWT in comparison to other modes of transportation.

Options for Technical Adaptation

To sustain competitiveness, cost-effectiveness, and reliability, it is imperative for inland water transport (IWT) to become less susceptible or more resilient to low-water periods, which are expected to become more frequent owing to climate change according to (Jonkeren, 2009). This necessitates a re-evaluation of vessel design trends, particularly for larger vessels that are inherently more vulnerable to low-water conditions (Radojčić et al., 2021; Rothstein & Scholten, 2016). From a design perspective, several research and development projects have been conducted to address the resilience of inland navigation to climate change. These projects consider technical adaptation measures aimed at efficient operation at a reduced draught, enabling flexible year-round navigation in both sufficient and shallow waters. Notable among them are concepts to achieve increased cargo capacity utilisation at reduced draught, by means of added buoyancy without altering the principal dimensions of the vessels. One of these concepts is the floatable side blisters investigated in the ECCONET project as referenced in (Zigic et al., 2012). The investigation of the concept of added buoyancy was further expounded and validated in the NOVIMOVE project (B. Ramne, 2021). In addition, measures to increase cargo transport on low draught by means of weight reduction, making use of lightweight materials for hull construction, were investigated in the INBAT project referenced by (Radojčić et al., 2021). Other options for maximising the capacity of a vessel by altering the principal dimensions of the ship have been investigated by (Bačkalov et al., 2016) and (Guesnet et al., 2014). To compensate for the loss of deadweight owing to shallow draught, it is possible to increase either the length or breadth of the ship. Bačkalov et al., 2016 noted that 'beamy' container vessels are more favourable than "lengthy" ones on restricted waterways, although the extent of beam increase is limited by canal and locks spaces on the fairway.

In a general context, it can be inferred from the previous subsection that operating under conditions of low water levels results in an increase in the thrust loading coefficient. Consequently, the open water efficiency is reduced, and when the draught is extremely low, the risk of propeller ventilation is high, impeding the generation of the thrust necessary to propel the vessel in water. The reduction in propulsive efficiency can be addressed by the concept of distributed thrust which was investigated by the notable STREAMLINE research project (Hagesteijn et al., 2015). Within this project, a novel design with six (6) thrusters was developed to attain higher efficiency at low propeller loading. The configuration of these propellers is such that forward propellers accelerate the flow to the trailing ones; at the same time, these propellers generate thrust instead of adding to the total ship resistance, as is the case with tunnels. The stern design is also such that the forward propellers again avoid flow separation and hence reduce the risk of propeller ventilation. In this research, for lower draughts, a new concept is proposed for streamlined cover plates to be fitted to prevent propeller ventilation which was originally investigated by DST. Given the relatively long lifespans of inland water vessels, climate change predictions must be factored into their design and planning. The careful design of the hull and propulsion, power, and energy (PPE) system configuration is imperative when accounting for low-water conditions in the early design phase (Kempmann et al., 2023). Table 6 summarises some notable adaptation measures and their application scenarios, as found in the state-of-the-art research projects and literature.

Table 6: Summary of Notable EU projects on Inland Waterway Vessels shallow-water adaptation

Reference	**Adaptability Measures**				**Application Scenarios**	**Key findings**
		Payload increase				
	Suitable Propulsion	*Additional buoyancy device*	*Lightweight construction*	*Beamy*		
ECCONET - Zigic et al., 2012	✓	✓	✓		Self-propelled cargo vessels	Retractable side blisters to increase buoyancy enabling improved cargo load factor at a reduced draught. Also, the use of high-tensile steel and aluminum was proposed to reduce the ship's weight

Table 6 continued

NOVIMOVE - B. Ramne, 2021			✓		Self proplled dry cargo vessel	Innovative Vessel concept, with added buoyancy to transport more cargo in shallow water conditions. Modular inflatable airpads which can be couple to the vessel's sides when needed to provide additional buoyancy during periods of low water levels.
VERBIS - Radojčić et al., 2021		✓	✓		Self-propelled cargo vessel and pushboats	Optimal hull form design for maximum payload at draughts. Also, a pump-jet propulsion was developed for push boats with draught (0.8-1.7m) to allow for shallow water operations
INBAT - Radojčić et al., 2021	✓			✓	Push boats and barge train	The application of lightweight construction materials and structural design was developed, realising weight saving of around 40 % if steel sandwich panels were used for small barge. Complimented with an innovative retractable middle propeller for additional thrust and manoeuvring during low draughts.
STREAMLINE - Hagesteijn et al., 2015	✓				Self-propelled Rhine class cargo vessel	A novel concept of distributed propulsion systems, offering efficient navigation advantage in extreme conditions. Although this comes with higher cost of investment, it offers the advantage of cheaper and smaller engines (usually road truck engines), which are also easier to maintain and replace. With the new stern design for 6 rudder propellers, it was also found that the cargo carrying capacity of the vessel could increase up to 3 %. In comparison with the reference vessel, an open water efficiency improvement of 21.5 % was recorded
IDV - Guesnet et al., 2014	✓			✓	Self-propelled container vessels for the Danube River	For the container vessel, the proposed concept is to increase the breadth of a standard 4-row container vessel from 11.4m to 11.65m to allow loading of 2.5 -2.55m wide domestic containers beside ISO containers, stowing up 2 tiers of container at 1.7 low draught. Also, for this concept, the author proposed an azimuth propeller for excellent manoeuvring optimised for low draught.
X-type - Bačkalov et al., 2016				✓	Self-propelled container vessels for the Danube River	The unconventional X-Type container vessel design. Increasing the breadth of a standard Class Va inland vessel carrying 4-row containers from 11.4 to 13.9 to stow an additional row. Increasing the beam was chosen over lengthening, for structural and cost considerations

Summary of Climate-Change Impact on Inland Waterway Vessels

The subsections Resistance and Power Demand to Transport Cost discussed the thematic literature on the state-of-art impacts of low water levels due to climate change on inland waterway vessels. The cascading effects could lead to a delay in the supply of goods, increased sailing time owing to reduced speed, and high transport costs for the given voyage, This culminating in an overall loss in transport efficiency and compounded by the undesirable modal shift to other transport modes with implications on the competitiveness of IWT. Identifying the main challenges, Options for Technical Adaptation, summarises some notable research projects and studies on adaptation measures to make inland waterway vessels more resilient to climate change. These projects primarily sought to address the issue of loss of cargo capacity utilisation with novel con-

cepts to transport sufficient cargo even at low draughts. Additionally, they explored the concepts of suitable propulsion systems to ensure navigation at both low draught and normal laden draught conditions. Moving on, the next section discusses the state-of-the-art decarbonisation of inland waterway transport and the current state-of-the-art report on greening pilot projects within the European region.

Decarbonising Inland Waterway Vessels

The EU stage V emission limits, which are sets of regulatory requirements established by the European Union, are considered the world's strictest emission standards for non-road mobile machinery (NRMM). These standards, outlined in Regulation (EU) 2016/1628 (Shao et al., 2016), set specific limits for the levels of local pollutants, including particulate matter (PM), nitrogen oxides (NOx), hydrocarbons (HC), and carbon monoxide (CO), emitted by new IWV engines higher than 300 kW. The current approach to curb the environmental footprint of inland water fleets is achieved through internal combustion engines fitted with exhaust filtering systems. Nevertheless, the most challenging aspect is reducing GHG emissions, which have global warming potential (GWP) and ozone depletion potential, by way of absorbing infrared radiation. The main anthropogenic GHG gases, according to, are;

- Carbon dioxide (CO_2) accounts for approximately 76 % of the total GHG emissions.
- Methane (CH_4) accounts for approximately 16 % of all GHG.
- Nitrous oxide (N_2O) accounts for approximately 6 % of all GHG.

Greenhouse gas (GHG) emissions emanating from ships primarily stem from conventional fossil-based fuels that are extensively employed as the primary energy source for ship propulsion, with carbon dioxide (CO_2) being the predominant gas. Nevertheless, the use of liquefied natural gas (LNG) as a fuel introduces emissions of methane (CH_4), whose environmental impact is significantly more potent than that of CO_2. It has been observed that there is a wide range of technical and operational measures with significant emission abatement potentials. Independent options and combinations of options may provide enormous benefits. The feasibility of the options, as highlighted by (Finney et al., 2022), is dependent on the vessel types and their operations. A typical example is an optimal hull design combined with the use of hull air lubrication, primarily focusing on reducing ship resistance during operation, which in essence reduces power demands and, hence, energy consumption. This can contribute to improving energy efficiency and CO_2 emission reduction, but (Bouman et al., 2017)[48] illustrates that its potential as a single measure may be limited. Although many abatement options are mutually exclusive, such that they are not practically and economically feasible to be adopted in combination with other options, others may need to be combined with other options to significantly contribute to emission reduction (Bouman et al., 2017). According to life-cycle (LCA) studies, the primary source of adverse environmental outcomes throughout a ship's life cycle is identified as the operating phase (Al-Enazi et al., 2021), with energy consumption emerging as its largest contributor. Consequently, the transition to greener alternative energy sources is regarded as a viable approach to attain environmental sustainability objectives, offering up to 100 % emission reduction.

State-of-the-art of IWV Greening Projects

The SYNERGETICS [1] project has been tracking and compiling a database of pilot projects and developments of inland water transport decarbonisation within Europe, and so far, a total of 115 diverse types and classes of inland waterway vessels are being retrofitted or newly built. Throughout these projects, the main sustainable alternatives considered of interest for the IWT are LNG, biofuels (FAME, HVO), methanol, hydrogen, and batteries (see Figures 3 and 4).

[1] https://www.synergetics-project.eu/downloads/

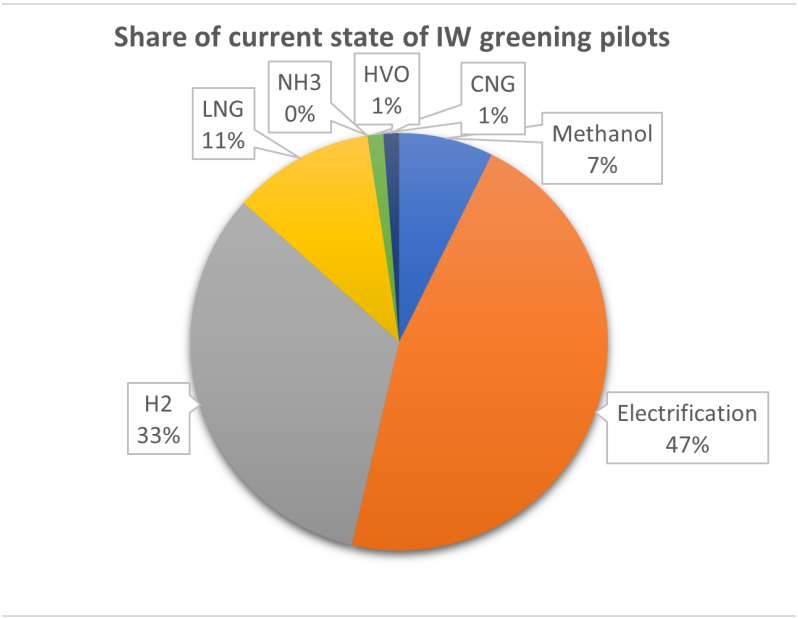

Figure 3: Shares Greening of IWV pilots in Europe

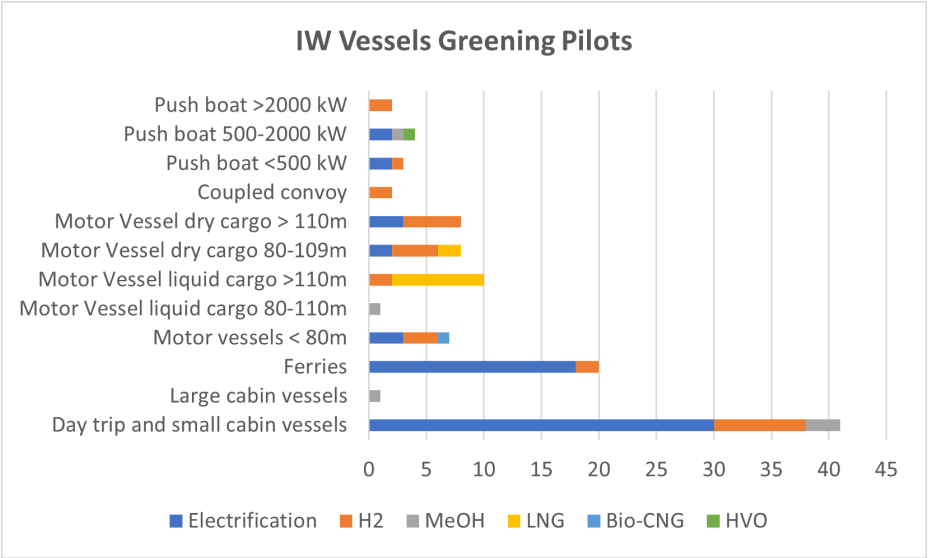

Figure 4: Classification of vessels and types of energy adopted for greening pilots.

Evidently, there are no ammonia-related projects, fundamentally because of toxicity and associated risks for IWT. A larger share of these projects is electrification, as shown in Figure 4, and the types of vessels that adopt batteries are those for short trips, such as day trip vessels and ferry boats.

Alternative Energy for Inland Waterway Vessels

The power train of a vessel is a system carefully designed to propel the vessel in water, primarily consisting of fuels as an energy source, internal combustion engines as convertors, and propellers as the device that produces thrust. Recognising the importance of tailoring newbuilds and retrofit solutions to specific vessels based on their operational profiles and power demands, it is necessary to explore viable options for alternative energy and power systems. Several studies have compared alternative propulsion, power, and energy (PPE) options based on their, environmental performance and economic viability, as well as the technology maturity. Table 7 summarises key literature on alternative fuels for inland navigation.

Table 7: Some key literature on Inland Water Vessels decarbonisation

Reference	Study	Alternative energy carrier	Key findings
Perčić, Vladimir, and Koričan, 2021	Electrification of Inland Waterway Ships Considering Power System Lifetime Emissions and Costs	Batteries	From the LCCA study on a cargo vessel, although electrification offered low environmental impact, it was found by the authors that reducing battery capacity onboard due to limited available space required reduction of sailing distance consequently extending the voyage duration by about 6 times hence the life cycle cost does not favour electrification for a cargo vessel. On the other hand, due to the lower required endurance of passenger ships, PV battery was found as most economical for passenger vessel, suggesting that electrification was more feasible for sustainable transition of passenger fleets.
Simmer et al., 2015	Multi criteria assessment of LNG as fuel for Inland Navigation	LNG	In considering the technical, logistic, financial, and environmental influence of adopting LNG as alternative fuel for inland navigation. Authors suggested that, the main factors influencing the adoption of LNG is the cost of investment, and regulatory barriers, although it was pointed out that the environmental gain are minimal and that because of methane slip.
Perčić, Vladimir, and Fan, 2021	Techno-economic assessment of alternative marine fuels for inland shipping in Croatia	LNG / Methanol / B20/ Hydrogen / Ammonia	The LCA revealed that the most environmentally friendly option is an electric powered vessel, however from the LCCA resulted in methanol as the most cost-effective option. A sensitivity analysis also showed that the not only does speed reduction influences the environmental performance of the alternatives, but also it influences the total cost of ownership. Indicating that although battery is the most expensive solution, reducing the speed by 30 % would result in 51 % reduction in net present value (NPV).
Rivarolo et al., 2021	Multi-criteria comparison of power generation and fuel storage solutions for maritime application	Hydrogen / Ammonia / Methanol / LNG	Comparative analysis based on weight, volume, cost, and emissions revealed, that the weight and volume limitations are more pronounce in the choice of alternative power and energy system than the emission reductions, given that this significantly reduced cargo loading and hence the revenue stream of the vessel.
Taccani et al., 2020	High energy density storage of gaseous marine fuels	Hydrogen	Efficient onboard storage containment for hydrogen fuel. The newly design storage “GASVESSEL” cylinders, requires volume of about 15.2m3 and total weight of 2.5 ton to store 140kg of hydrogen, compared to the type 1 cylinder which would have require 28m3 and 12.3 tons. This was a significant saving of about 2 time and 5 time in terms of space and weight respectively.

Table 7 continued

Prina et al., 2023	Optimal fleet transition modelling for sustainable inland waterways	Batteries	Analysing the fleet composition of small electric passenger boats required to replace diesel powered passenger boats on the Orta lake. Authors found that the number of charging stations and the capacity of these station play a critical role in determining the fleet composition required to replace existing fleet. It was concluded that with higher charging capacities of the stations, the entire diesel fleet can be replaced with equal number of new electric fleet without changes to the routes and travel scheduling, however with lesser charging capacity along the fairway, more vessels were required to replace the diesel fleet
Perčić et al., 2023	Holistic energy efficiency and environmental friendliness analysis of inland ships with alternative power systems	LNG / Batteries / Methanol / Hydrogen / Ammonia	Assessing the life cycle GHG and local pollutant (NOx and Sox) emission performance of cleaner fuels for inland navigation, it was established that batteries offer better GHG footprint, however batteries contribute significantly to SOx emission during its manufacturing phase. Although the NH3 and H2 do not produce tail pipe emissions, their current production from fossil fuel results in significant GHG pollutions.
Moirangthem and Baxter, 2016	Alternative Fuels for Marine and Inland Waterways	Biofuels / Hydrogen / Methanol / Batteries	This study suggests that LNG and Methanol could serve as transition fuels for mid-term, before making a major shift to cleaner fuels such as biofuels.

Challenges with Choice of Alternatives

Transitioning to cleaner energy and power systems for inland navigation is not devoid of challenges. The subsequent subsections shed light on the key hurdles associated with opting for alternative energy sources in inland navigation.

- **Space and weight requirements**
  A challenge related to the choice of alternative power and energy systems for inland vessels is related to onboard storage and integration. As mentioned earlier, compared with conventional diesel fuel as a baseline, the low energy densities of these alternatives necessitate an additional volume or deadweight to accommodate the equivalent capacity of diesel fuel. The storage of gaseous alternative fuels presents challenges because of their considerable space and weight requirements. This issue is exacerbated by specific storage containment methods, especially for naturally occurring gaseous fuels, such as hydrogen and ammonia, which necessitate the use of cylinders. Taccani (Taccani et al., 2020)[53] in the GASVESSEL project illustrated this challenge, revealing that a 1.8-ton storage system is required to contain 140 kg of hydrogen at 25°C and 250 bar in a type I pressure vessel. Additionally, adapting cylindrically shaped tanks to fit existing rectangular spaces leads to the suboptimal use of space. Furthermore, safety considerations for handling and storing Methanol and ammonia impose non-negotiable constraints on where these fuels can be stored, further limiting the use of available space. Indeed, in an investigation by (Rivarolo et al., 2021), a comparative analysis was undertaken to assess various alternative energy carriers and their respective converters for a small river passenger boat. The evaluation criteria encompassed volume, weight, cost, and emissions. The results of their scoring revealed that the limitations associated with weight, volume, and opportunity cost exerted a more substantial influence on the choice of greening technology than emissions.
  In a similar study conducted by (Lagemann et al., 2022) on retrofitting a deep-sea bulk carrier, accounting for the loss of payload, was expressed as opportunity cost within the total cost of ownership (TCO). In this situation the loss of revenue due to payload reduction when hydrogen is adopted was more pronounced. These observations arise from the impracticality of achieving zero emission when the utilization of zero-emission technology significantly takes up

cargo space and adds to the deadweight of the vessel. This limits the cargo carrying capacity of the vessel, which is the primary function of the vessel and thus the revenue stream of the owner.

- **Range and endurance (bunkering frequency)**
  Ship range and endurance are defined in terms of the maximum distance a ship can travel on its loaded fuel capacity and the maximum time of continuous operation without refilling respectively. When the cargo capacity in terms of volume and deadweight is maintained, the energy capacity is then constrained to the available space and deadweight. Consequently, given the low volumetric and gravimetric energy densities of the alternative energy carriers, the quantities that can be carried onboard may not suffice the required range and endurance. As such, the ideal distance that the vessel may cover is considerably reduced, requiring intermittent bunkering to complete a voyage. An important performance metric that measures the transport efficiency of a vessel is the voyage time, which would be inevitably influenced by bunkering time and the frequency of bunkering required to complete a voyage. An example of this inefficiency was analysed by (Perčić, Vladimir, & Koričan, 2021), where it was found that reducing battery capacity due to limited available space, required a reduction of sailing distance consequently extending the voyage duration by about 6 times for an inland cargo vessel. Lower range and endurance become more challenging, particularly in situations where bunkering infrastructures are limited on a specific operating corridor.

Summary of Inland Waterway Vessels Decarbonisation

The subsection State-of-the-art of IWV Greening Projects highlighted the state-of-art green pilot projects within Europe, whereas Alternative Energy for Inland Waterway Vessels summarises recent studies on alternative energy carriers for inland waterway vessels. The subsection Challenges with Choice of Alternatives also underscored some pivotal challenges impacting vessel performance as a result of opting for alternative energy and power systems.

CONCLUSION AND FUTURE STUDY

Conclusions

In this study, we conducted a scoping literature review, summarising the state-art-of-the-art "sustainable and climate-resilient inland waterway vessels". This study examines the multiple influences of climate change on vessels, as well as the problems associated with the choice of alternative energy on the performance of vessels. Altogether, this review first highlighted the most challenging impact of extreme shallow water conditions on the efficient operations of inland waterway vessels in terms of hydrodynamic performance and cargo transport performance, which threatens the ambitions to increase the modal share of inland water transport, that is already underutilised. Secondly, this work highlighted, the applicability of different alternative energy and power systems configurations on inland waterway vessels and how they also influence the performance of the vessel also in terms of cargo carrying capacity and voyage distance or endurance.

Fundamentally, there is yet to be found literature or study that takes into account, the dual facet problems of energy transition and climate-resilience of inland waterway vessel. These two have traditionally been tackled independently. While it is important to understand that the properties of the alternative energy carriers pose challenge to the overall transport efficiency of vessels, the impact of climate change on the conditions of the fairway also poses challenges to the transport efficiency of inland waterway vessels, and hence the need for both influences to be considered holistically. Having identified the gaps in the state-of-the-art, this presents an opportunity for further investigation, towards future-ready and climate-resilient inland waterway vessels.

Future work

To address the complexity of these challenges, a holistic approach in assessing the intricate interplay between these problems is crucial for consideration in early design stage. This comprehensive approach is important to find optimal design parameters for inland waterway vessels. The objectives of optimal design parameters are to ensure minimum energy consumption and maximise propulsive efficiency under different fairway conditions. Simultaneously, achieving maximum payload capacity, while maintaining a balance with the vessel's energy requirement and allowing cargo transport over longer range and endurance. Integral to this would be to concurrently ensure minimal environmental impact associated with the choice of alternative energy and power systems. This overall would ensure a harmonious balance between vessel performance and sustainability.

CONTRIBUTION STATEMENT

Author 1: Literature review and writing of manuscript. **Author 2:** Supervision, critical review and script - editing. **Author 3:** Supervision and critical review.

ACKNOWLEDGEMENTS

This research is conducted within the PATH2ZERO project, co-funded by NWA L2-Thema 2020 Zero emission shipping (ZES) program by Netherlands Organization for Scientific Research (NWO) with Grant NWA.1439.20.001, and by the Temporary research subsidy scheme Top Sector Logistics 2022-2026 of the Ministry of Infrastructure and Water Management.

REFERENCES

Al-Enazi, A., Okonkwo, E. C., Bicer, Y., & Al-Ansari, T. (2021). A review of cleaner alternative fuels for maritime transportation. *Energy Reports*, *7*, 1962–1985. https://doi.org/10.1016/j.egyr.2021.03.036

Andrews, D., & Erikstad, S. O. (2015). State of the art report on design methodology. *12th International Marine Design Conference 2015 - Tokyo, Japan*, 90–105.

B. Ramne, H. P., Sophie Martens. (2021). *Concepts and selection of innovative novimove concepts* (tech. rep.). NOVIMOVE Project.

Bačkalov, I., Kalajdžić, M., Momčilović, N., & Rudaković, S. (2016). A study of an unconventional container vessel concept for the danube. *13th International Symposium on Practical Design of Ships and Other Floating Structures (PRADS'2016)*.

Bouman, E., Lindstad, E., Rialland, A., & Strømman, A. (2017). State-of-the-art technologies, measures, and potential for reducing GHG emissions from shipping - a review. *Transportation Research Part D Transport and Environment*, *52*, 408. https://doi.org/10.1016/j.trd.2017.03.022

Doll, C., Brauer, C., & Köhler, J. (2020). *Methodology for ghg efficiency of transport modes* (tech. rep.). Fraunhofer-Institute for Systems and Innovation Research ISI, CE Delft.

Du, P., Ouahsine, A., Sergent, P., & Hu, H. (2020). Resistance and wave characterizations of inland vessels in the fully-confined waterway. *Ocean Engineering*, *210*, 107580. https://doi.org/10.1016/j.oceaneng.2020.107580

Eurostat. (2023). Retrieved November 24, 2023, from https://ec.europa.eu/eurostat/statistics-explained/index.php?title=Freight_transport_statistics_-_modal_split

Finney, H., Sikora, I., Baxter, B., Pons, A., Horton, G., Scarbrough, T., Ash, N., Powell, N., Parrett, M., Rogers, B., & Fischer, S. (2022). *Technological, operational and energy pathways for maritime transport to reduce emissions towards 2050* (tech. rep.). Ricardo Energy and Environment.

Furukawa, Y., Ibaragi, H., & Kijima, K. (2016). Shallow water effects on longitudinal components of hydrodynamic derivatives. https://doi.org/10.18451/978-3-939230-38-0_33
Gebraad, J., Quispel, M., Lisi, M. D., Wisselmann, R., Boyer, B., Roux, L., Rafael, R., de Schepper, K., & Schweighofer, J. (2021). *Report on the zero–emission strategy iwt* (tech. rep.).
Guesnet, T., Reinhold, D., Gerhard, S., Bačkalov, I., Milan, H., Aleksandar, S., & Dejan, R. (2014). *Innovative danube vessel* (tech. rep.). Development Centre for Ship Technology, Transport Systems, Austrian Institute for Regional Studies, and Spatial Planning, University of Belgrade, Faculty of Mechanical Engineering, Department of Naval Architecture, Ship Design Group srl.
Hagesteijn, G., van der Meij, K., & Thill, C. (2015). Distributed propuslion: A novel concept for inland vessels. *Proceedings of the ASME 2015 34th International Conference on Ocean, Offshore and Arctic Engineering OMAE2015 - Canada*.
Hekkenberg, R. G. (2013). *Inland ships for efficient transport chains*. s.n.
ITTC. (2017). Recommended procedures and guidelines-captive model test. *Proceedings of the 28th International Towing Tank Conference (ITTC)*.
Jonkeren, O. (2009). *Adaption to climate change in inland waterway transport*. PhD Thesis - Vrije Universiteit Amsterdam.
Jonkeren, O., Jourquin, B., & Rietveld, P. (2011). Modal-split effects of climate change: The effect of low water levels on the competitive position of inland waterway transport in the river rhine area. *Transportation Research Part A: Policy and Practice*, *45*(10), 1007–1019. https://doi.org/10.1016/j.tra.2009.01.004
Jonkeren, O., Rietveld, P., Van Ommeren, J., & Te Linde, A. (2013). Climate change and economic consequences for inland waterway transport in europe. *Regional Environmental Change*. https://doi.org/10.1007/s10113-013-0441-7
Jonkeren, O., & Rietveld, P. (2007). Climate change and inland waterway transport: Welfare effects of low water levels on the river rhine. *Journal of Transport Economics and Policy*, *41*.
Kempmann, K., Roux, L., & Wisselmann, R. (2023). *"act now!" on low water and effects on rhine navigation* (tech. rep.). Central Commission for the Navigation of the Rhine (CCNR).
Krekt, A., & van der Laan, T. (2011). *Climate change and inland waterway transport: Impacts on the sector, the port of rotterdam and potential solutions* (tech. rep.). ARCADIS, Port of Rotterdam,
Kulczyk, J., & Tabaczek, T. (2014). Coefficients of propeller-hull interaction in propulsion system of inland waterway vessels with stern tunnels. *TransNav, the International Journal on Marine Navigation and Safety of Sea Transportation*, *8*(3), 377–384. https://doi.org/10.12716/1001.08.03.08
Lagemann, B., Lindstad, E., Fagerholt, K., Rialland, A., & Ove Erikstad, S. (2022). Optimal ship lifetime fuel and power system selection. *Transportation Research Part D: Transport and Environment*, *102*, 103145. https://doi.org/10.1016/j.trd.2021.103145
Liu, J., Hekkenberg, R., & Rotteveel, E. (2014). A proposal for standard manoeuvres and parameters for the evaluation of inland ship manoeuvrability.
Moirangthem, K., & Baxter, D. (2016). *Alternative fuels for marine and inland waterways.* (tech. rep.). https://doi.org/10.2790/227559
Mucha, P., Moctar, O. E., Dettmann, T., & Tenzer, M. (2018). An experimental study on the effect of confined water on resistance and propulsion of an inland waterway ship. *Ocean Engineering*, *167*, 11–22. https://doi.org/10.1016/j.oceaneng.2018.08.009
Perčić, M., Vladimir, N., & Fan, A. (2021). Techno-economic assessment of alternative marine fuels for inland shipping in croatia. *Renewable and Sustainable Energy Reviews*, *148*, 111363. https://doi.org/10.1016/j.rser.2021.111363
Perčić, M., Vladimir, N., & Koričan, M. (2021). Electrification of inland waterway ships considering power system lifetime emissions and costs. *Energies*, *14*(21), 7046. https://doi.org/10.3390/en14217046
Perčić, M., Vladimir, N., Fan, A., & Jovanović, I. (2023). Holistic energy efficiency and environmental friendliness analysis of inland ships with alternative power systems. *PIANC America 2023 - Florida, USA*.
Pompée, P.-J. (2015). About modelling inland vessels resistance and propulsion and interaction vessel - waterway key parameters driving restricted/shallow water effects.
Prina, M. G., Zubaryeva, A., Rotondo, G., Grotto, A., & Sparber, W. (2023). Optimal fleet transition modeling for sustainable inland waterways transport. *Applied Sciences*, *13*(17), 9524. https://doi.org/10.3390/app13179524
Radojčić, D., Simić, A., Momčilović, N., Motok, M., & Friedhoff, B. (2021). *Design of contemporary inland waterway vessels: The case of the danube river*. Springer International Publishing. https://doi.org/10.1007/978-3-030-77325-0

Raven, H. (2022). *A correction method for shallow-water effects on ship speed trials* (tech. rep.). Maritime Research Institute Netherlands (MARIN).
Raven, H. (2012). A computational study of shallow-water effects on ship viscous resistance. *29th Symposium on Naval Hydrodynamics - Gothenburg, Sweden*.
Rivarolo, M., Rattazzi, D., Magistri, L., & Massardo, A. (2021). Multi-criteria comparison of power generation and fuel storage solutions for maritime application. *Energy Conversion and Management*, *244*, 114506. https://doi.org/10.1016/j.enconman.2021.114506
Rothstein, B., & Scholten, A. (2016). *Navigation on the danube - limitations by low water levels and their impacts* (tech. rep.). EU - Joint Research Centre (JCR). https://doi.org/10.2788/236234
Rotteveel, E., & Hekkenberg, R. G. (2015). The influence of shallow water and hull form variations on inland ship resistance. *12th International Marine Design Conference 2015 - Tokyo, Japan*.
Rotteveel, E. (2019). *Influence of inland vessel stern shape aspects on propulsive performance* [Doctoral dissertation, Delft University of Technology]. https://doi.org/https://doi.org/10.4233/uuid:8d8c14e3-cdfb-4e15-8314-35dc296fdbde
Rotteveel, E., Hekkenberg, R., & Liu, J. (2014). Design guidelines and empirical evaluation tools for inland ships. *European Inland Waterway Navigation Conference 2014 - Budapest, Hungary*.
Rotteveel, E., Hekkenberg, R., & Van Der Ploeg, A. (2017). Inland ship stern optimization in shallow water. *Ocean Engineering*, *141*, 555–569. https://doi.org/10.1016/j.oceaneng.2017.06.028
Schweighofer, J., Gebraad, J., & Seitz, M. (2022). *Options for shallow-water / climate resilient vessels* (tech. rep.).
Shao, Z., Dallmann, T., & Bandivadekar, A. (2016). *European stage v non-road emission standards* (tech. rep.). International Council on Clean Transportation (ICCT).
Simmer, L., Pfoser, S., & Schauer, O. (2015). Liquefied natural gas as a fuel in inland navigation: Barriers to be overcome on rhine-main-danube. *Journal of Clean Energy Technologies*, *4*(4), 295–300. https://doi.org/10.7763/JOCET.2016.V4.300
Sys, C., Van De Voorde, E., Vanelslander, T., & Van Hassel, E. (2020). Pathways for a sustainable future inland water transport: A case study for the european inland navigation sector. *Case Studies on Transport Policy*, *8*(3), 686–699. https://doi.org/10.1016/j.cstp.2020.07.013
Taccani, R., Malabotti, S., Dall'Armi, C., & Micheli, D. (2020). High energy density storage of gaseous marine fuels: An innovative concept and its application to a hydrogen powered ferry (K. Visser, F. Baldi, & L. Van Biert, Eds.). *International Shipbuilding Progress*, *67*(1), 33–56. https://doi.org/10.3233/ISP-190274
van Dorsser, C., Vinke, F., Hekkenberg, R., & van Koningsveld, M. (2020). The effect of low water on loading capacity of inland ships.
Vinke, F., Van Koningsveld, M., Van Dorsser, C., Baart, F., Van Gelder, P., & Vellinga, T. (2022). Cascading effects of sustained low water on inland shipping. *Climate Risk Management*, *35*, 100400. https://doi.org/10.1016/j.crm.2022.100400
Wang, Y., & Wright, L. A. (2021). A comparative review of alternative fuels for the maritime sector: Economic, technology, and policy challenges for clean energy implementation. *World*, *2*(4), 456–481. https://doi.org/10.3390/world2040029
Zeng, Q., Hekkenberg, R., Thill, C., & Rotteveel, E. (2017). A numerical an experimental study of resistance, trim and sinkage of an inland ship model in extremely shallow water. *International Conference on Computer Applications in Shipbuilding 2017 - Singapore*.
Zeng, Q. (2019). *A method to improve the prediction of ship resistance in shallow water* [Doctoral dissertation, Delft University of Technology]. https://doi.org/10.4233/UUID:D4D8524A-FEDC-4949-A953-F5848A1634BB
Zeng, Q., Thill, C., Hekkenberg, R., & Rotteveel, E. (2019). A modification of the ITTC57 correlation line for shallow water. *Journal of Marine Science and Technology*, *24*(2), 642–657. https://doi.org/10.1007/s00773-018-0578-7
Zentari, L., El Moctar, O., Lassen, J., Hallmann, R., & Schellin, T. E. (2022). Experimental and numerical investigation of shallow water effects on resistance and propulsion of coupled pusher-barge convoys. *Applied Ocean Research*, *121*, 103048. https://doi.org/10.1016/j.apor.2022.103048
Zigic, B., Holtmann, B., van Heumen. E, Ubbels, B., & Quispel, M. (2012). *Iwt fleet and operation* (tech. rep.). ECCONET.
Zwaginga, J. J., & Pruyn, J. F. J. (2022). An evaluation of suitable methods to deal with deep uncertainty caused by the energy transition in ship design. *Day 2 Mon, June 27, 2022*, D021S003R002. https://doi.org/10.5957/IMDC-2022-252

Proceedings of 15th International Marine Design Conference (IMDC-2024)
June 2-6, 2024
Amsterdam, the Netherlands

Simulation-based evaluation of concepts for short sea shipping of green hydrogen

M. Bergström[1,*], A. Niemi[2], B. Skobiej[3], Y. Dave[4], M. Begum[5], F. Schmid[6], F. Roland[7], M. Braun[8], and S. Ehlers[9]

ABSTRACT

In this study, a simulation-based approach is applied to develop concepts for short sea shipping of green hydrogen and to assess their overall energy efficiency. The study is conducted as a case study involving production of green hydrogen at an offshore site in the North Sea. Hydrogen produced at the site is first transported by pipeline to a port-based intermediate storage facility, from where it is transported onwards by ship. For the onward transport, four different hydrogen carriers are considered, namely compressed hydrogen, liquid hydrogen, ammonia, and a liquid organic hydrogen carrier.

KEY WORDS

Maritime transport; Short-sea shipping; Green hydrogen; North Sea; Discrete-event simulation

INTRODUCTION

In Europe, green hydrogen is expected to play an important role in the energy transition, in particular as a tool to decarbonize energy-intensive industries, such as heavy industry, shipping and aviation. To ensure a sufficient supply, the European Union (EU), as part of its plan REPowerEU, has set a target of reaching 10 million tons of domestic production of green hydrogen by 2030 (Notteboom & Haralambides, 2023). As many parts of the EU are densely populated, and thus have limited opportunities for increased local onshore production of green hydrogen, new offshore production facilities will be needed to reach the production target. Consequently, new transport infrastructure is also needed, and due to the general lack of hydrogen pipelines as well as challenges related to building new ones, especially through densely populated areas, we expect a growing demand for non-pipeline-based transport options. In this context, the aim of this study is to define and evaluate concepts for short sea shipping of green hydrogen.

[1] Institute of Maritime Energy Systems, German Aerospace Center, Geesthacht, Germany; ORCID: 0000-0001-7758-3038
[2] Institute for the Protection of Maritime Infrastructures, German Aerospace Center, Bremerhaven, Germany; ORCID: 0000-0001-6307-9826
[3] Institute for the Protection of Maritime Infrastructures, German Aerospace Center, Bremerhaven, Germany; ORCID: 0000-0003-0529-9454
[4] Institute of Maritime Energy Systems, German Aerospace Center, Geesthacht, Germany; ORCID: 0009-0002-7128-0065
[5] Institute of Maritime Energy Systems, German Aerospace Center, Geesthacht, Germany; ORCID: 0009-0004-9965-1723
[6] Institute of Maritime Energy Systems, German Aerospace Center, Geesthacht, Germany; ORCID: 0009-0007-7162-2092
[7] Institute of Maritime Energy Systems, German Aerospace Center, Geesthacht, Germany; ORCID: 0000-0000-0000-0000
[8] Institute of Maritime Energy Systems, German Aerospace Center, Geesthacht, Germany; ORCID: 0000-0001-9266-1698
[9] Institute of Maritime Energy Systems, German Aerospace Center, Geesthacht, Germany; ORCID: 0000-0001-5698-9354

* Corresponding Author: martin.bergstroem@dlr.de

Submitted: 23 February 2024, Revised: 30 April 2024, Accepted: 1 May 2024, Published: 24 May 2024

Conference paper, DOI: https://doi.org/10.59490/imdc.2024.898 e-ISSN: 3050-4864

The study is conducted as a case study involving the production of green hydrogen at an offshore site in the North Sea. Hydrogen produced at the site is first transported by pipeline to an intermediate port-based terminal, from where it is further transported by ship. For the onward transport, four different hydrogen carriers are considered, namely, compressed hydrogen (CH_2), liquid hydrogen (LH_2), ammonia (NH_3), and a liquid organic hydrogen carrier (LOHC) (Notteboom & Haralambides, 2023). Each considered concept is defined in terms of fleet characteristics (e.g. number of ships, ship type, ship size, and ship design speed), as well as the required intermediate port-based storage capacity. The study is limited to defining requirements for the fleet and port-based infrastructure considering energy efficiency and technical feasibility. Issues concerning safety, cost-efficiency, and regulations are not considered.

Related studies

Johnston et al. (2022) present a model developed to assist stakeholders in assessing the costs of maritime transport of hydrogen in various forms over different distances. In total five different options are considered, namely, transport of hydrogen in the form of LH_2, NH_3, liquified natural gas (LNG), methanol (CH_3OH), and LOHCs. Both fixed and variable costs, including port fees, canal usage charges, fuel costs, capital and operating costs, boil-off losses and expected future environmental taxes, are considered. For distances between 4 500 NM and 10 900 NM the study found that it is most cost-efficient to transport hydrogen in the form of NH_3 or CH_3OH. The study also analyzed the impact of using hydrogen, or the hydrogen carrier, as a low or zero carbon emission fuel for ships involved. However, it found that this would result in lower costs only in case hydrogen is transported in the form of LNG.

d'Amore-Domenech et al. (2023) compares the cost-efficiency of six different options for transport of hydrogen over sea including transport of LH_2 by ship with or without port-based storage facilities, transport of CH_2 by ship with or without port-based storage facilities, and transport of gaseous hydrogen by pipeline with or without intermediate compression stations. Each alternative was assessed for different transport distances and transport volumes. They found that for a transport distance of 100 km the most cost-efficient alternative is pipeline regardless of transport volume. For a distance of 2 500 km and an annual production volume of 1.0×10^5 ton, the most cost-efficient alternative was found to be shipping of CH_2 without port-based storage facilities. For a distance of 2 500 and an annual production volume of 1.0×10^6 ton, as well as for a distance of 5 000 km and an annual production volume of 1.0×10^5 ton, the most cost-efficient alternative was found to be shipping of either CH_2 or LH_2. For all other cases they found that the most cost-efficient alternative is shipping of LH_2.

EU Science Hub (2022) assessed the costs of different hydrogen transport options including CH_2, LH_2, NH_3, and LOHC. In brief, they found that for distances up to 3,000 km, the most cost-efficient option is the transport of compressed hydrogen by pipeline. For distances between 3,000-16,000 km, transport of LH_2 by ship was found to be the most cost-efficient options. For very long distances above 16,000 km, the most cost-efficient option was found to be transport of hydrogen in the form of LOHC or NH_3.

Based on the above studies it is evident that for distances up to 1,000 km, pipeline is generally the most cost-efficient option. However, none of the above-mentioned studies account for the fact that building a pipeline between two specific locations may not always be feasible for political, geographical, or other reasons. This study aims to assess what sea transport option is best for such cases.

CASE STUDY

Overview and design approach

In the case study, hydrogen is produced at an assumed offshore wind farm located in the North Sea within the exclusive economic zone of Germany at N54°26, E6°06. The location is indicated by a triangle in Figure 1. Hydrogen produced at the site is first transported along a 190 km long pipeline, whose approximate route is marked by a dotted line in Figure 1, to an intermediate port-based terminal storage located in Bremerhaven. From there all hydrogen is transported forward by ship to Kiel along an approximately 130 NM sea route marked by a dashed line in Figure 1. As per the figure, the sea route goes through Kiel Canal. If the intermediate port-based hydrogen storage in Bremerhaven becomes full, the H_2 production has to be limited or stopped. To avoid this, the capacity of the transport system must be sufficient. Moreover, the transport system must be energy- and resource-efficient.

The case study design process is carried out as follows. First, we define the hydrogen production rate based on a previous study. Second, we analyze the sea route, e.g., in terms of operational constraints, and make a preliminary assessment of the voyage time. Third, considering the hydrogen production rate and assessed voyage time, we define a preliminary conservative solution for each considered hydrogen carrier. Fourth, using the technique of discrete event simulation together with engineering

judgement, we derive a refined conceptual solution for each considered hydrogen carrier. Fifth, we assess the overall energy efficiency of each solution.

Hydrogen production

Following Eden et al. (2024), our considered assumed offshore wind farm consists of 42 Vestas V164 turbines with a total installed power capacity of 399 MW, which is reduced by 15 % due to wake effects. All electricity produced at the wind farm is used for producing hydrogen by electrolyzers requiring 3 kWh per produced kg of hydrogen. Following Eden et al. (2024), we simulate future hourly hydrogen production rates and volumes based on historical hourly wind speed data from the Copernicus ERA5 dataset specified for an altitude of 100 m covering the 11-year period 01.01.2012 – 31.12.2022 (Hersbach, et al., 2023). Accordingly, we assume that the wind conditions in the area will be similar as during the period represented by the data.

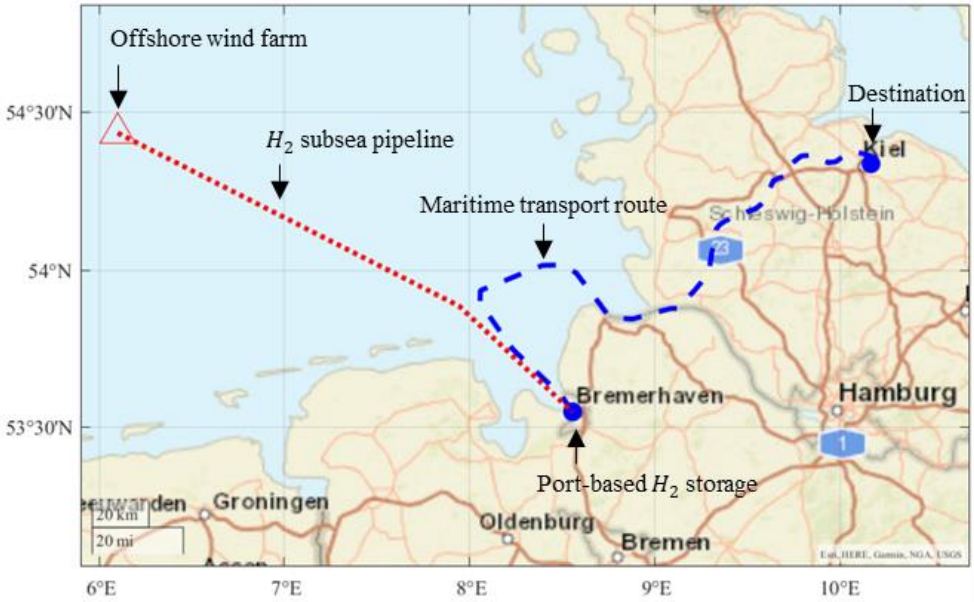

Figure 1: Production site and transport routes.

Over the considered 11-year period we simulated a total hydrogen production of around 244 000 ton. The corresponding annual, monthly, and daily averages are 22 182, 1 848, and 62 ton, respectively. However, due to variations in the prevailing wind conditions at the offshore site there are significant annual and interannual variations in the production rate. Specifically, as per Figure 2, the monthly production volume is estimated to vary between 780 and 3 050 ton.

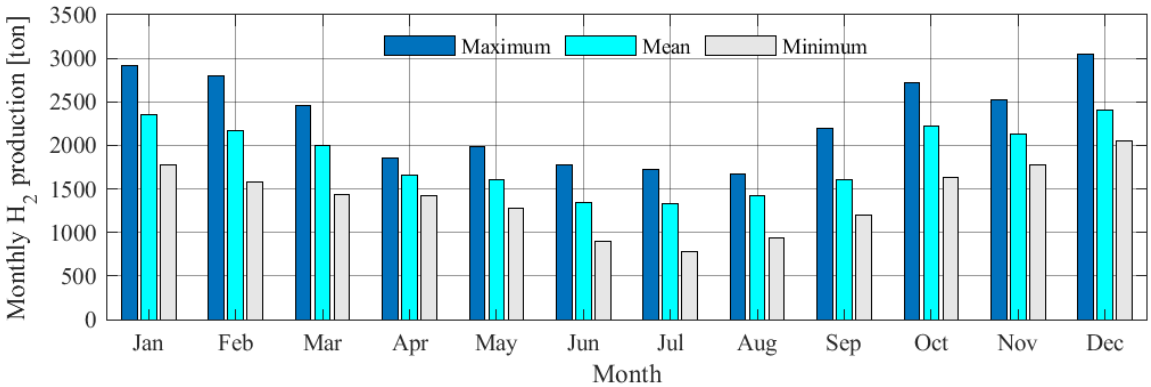

Figure 2: Annual and interannual variations in the production rate.

Sea route and operational constraints

The total distance of the sea route is 128.8 NM. Ship size and operational constraints are set primarily by the Kiel Canal as per Table 1. Following these constraints, ships are permitted to operate independently in all wind conditions without tug assistance

(UCA, 2023). The maximum allowed speed in and near Port of Bremerhaven and Port of Kiel is assumed to be 5 knots. In Elbe the maximum allowed speed is assumed to be 12 knots.

Table 1: Ship size and operational constraints set by the route (UCA, 2023).

Parameter	Maximum allowed value
Ship length	200 m
Ship beam	27 m
Ship draft	8 m
Ship speed, Kiel Canal	6.5 knots
Ship speed, port areas	5 knots
Ship speed, Elbe	12 knots

Considering the ship size and operational constraints determined as per Table 1, we choose to divide the route into 5 legs as per Table 2. Accordingly, some 40 % of the route is along Kiel Canal. As per the table, Kiel Canal has a lock at each end, i.e., in Brunsbüttel and Kiel-Holtenau, where the average locking times are assumed 45 and 25 minutes, respectively (WSV, 2022). As per WSV (2022), there are typically no additional waiting or queuing times. Assuming an open water speed of 14 knots, the total voyage time is estimated at 15.74 hour.

Table 2: Preliminary voyage time estimation.

Leg nr	Description	Distance [NM]	Speed [knots]	Time [hours]
1	Bremerhaven port area	3.8	5	0.77
2	Open sea (Bremerhaven - Elbe Estuary)	52.8	14	3.77
3	Elbe	16.5	12	1.37
	Lock 1 - Brunsbüttel	n/a	n/a	0.75
4	Kiel canal	53.4	6.5	8.22
	Lock 2 - Kiel-Holtenau	n/a	n/a	0.42
5	Kiel port area	2.2	5	0.43
	SUM	128.8		15.74

Elaboration of transport solutions

Assuming that the voyage time does not depend on the type of energy carrier, the voyage time for each option is preliminary estimated as per Table 2 to 15.74 hours. Assuming that the port-turn-around time in both Bremerhaven and Kiel is around 12 hours and independent of the type of energy carrier, the total duration of a round trip is estimated at 2 x 15.7 hours + 2 x 12 hours = 55.4 hours. Thus, assuming zero down time, the maximum number of round trips per month is 13. In order to meet the transport demand during a month of peak production (3 050 ton) using a single ship, the ship's required net transport capacity is estimated at $\frac{3\,050\ ton}{13} \approx 235$ ton of hydrogen.

To meet this transport demand, we derive a preliminary solution for each considered energy carrier (CH2, LH2, NH3, and LOHC) considering the operational constraints as follows:

1. Gas carrier ship carrying CH_2 at 350 bar. Assuming as per Table 3 a density of 23.2 kg/m^3, the required volumetric cargo capacity of the ship is estimate at $\frac{235}{0.0232}\frac{ton\ m^3}{ton} \approx 10\,129\ m^3$. Because we are not aware of any reference CH_2 carriers, we use an LNG tanker as reference instead. Based on Clarksons Research (2024), a typical LNG tanker with a capacity of around 10 000 m^3 do not exceed any of the route constraints defined as per Table 1.
2. Container feeder ship carrying LH_2 in 40 feet cryogenic tank containers, each with a LH_2 capacity of 3 ton (Decker, 2019). If a single ship is used, the required FEU capacity of the ship is estimated at $\frac{235}{3}\frac{ton*FEU}{ton} = 79\ FEU$ (158 TEU). Based on Clarksons Research (2024), a typical 160 TEU container ship do not exceed any of the route constraints defined as per Table 1.
3. Ammonia tanker ship. As per Table 3, a tone of NH_3 carries around 0.178 ton of hydrogen. Hence, in order to carry 235 ton of hydrogen, the ammonia tanker needs to carry 235 ton * (1/0.178) ≈ 1320 ton of NH_3. Based on Clarksons

Research (2024), a typical 1300 DWT LPG/Ammonia tanker does not exceed any of the route constraints defined as per Table 1.

4. Chemical tanker ship carrying LOHC. As per Table 3, one tone of a typical LOHC (benzyltoluene) is assumed to carry 0.063 ton of hydrogen. Hence, in order to carry 235 ton of hydrogen the tanker needs to carry 235 ton * (1/0.063) ≈ 3 730 ton of LOHC. Based on Clarksons Research (2024), a typical 3 730 DWT chemical tanker does not exceed any of the route constraints defined as per Table 1.

Table 3 Storage densities by volume and weight (Weichenhain, 2021).

Energy carrier	Storage volume density [kg H_2/m^3 of carrier]	Storage weight density [kg H_2/ ton of carrier]	Storage weight density [ton of carrier/ ton H_2]
CH_2	23	1 000	1 000
LH_2	71	1 000	1 000
NH_3	121	178	5.62
LOHC	55	63	15.87

The above defined preliminary solutions were derived without considering stochastic factors (e.g. variations in port-turnaround times), or more importantly, the role of the intermediate port-based storage in Bremerhaven acting as a buffer against short term variations in the production rate. Based on engineering judgement, we assume that it is preferable to store hydrogen in the intermediate storage in the same format in which it is to be transported forward. Hence, the type of storage tanks to be installed in Bremerhaven depends on the choice of hydrogen carrier for the maritime transport. Among the considered hydrogen carriers, we assume that the storage of LH_2 is the most challenging. The capacity of the largest commercial LH_2 storage tank that we are aware of is 2 500 m^3 (Kawasaki, 2021). As a preliminary solution we consider a hydrogen storage with a net capacity corresponding to four such tanks, providing a total capacity of 10 000 m^3, which assuming a LH_2 density of 70.9 kg/m^3, corresponds to around 709 ton.

In order to be able to consider both stochastic factors, and the role of the intermediate port-based storage, we simulate the operations of the system using the technique of Discrete Event Simulation (DES) using an approach originally presented by Bergström et al. (2016). An overview of the applied DES model is presented in Figure 3. As per the figure the model consists of five main blocks representing different components of the system. A more detailed presentation of the blocks representing the Port of Bremerhaven, the sea voyages, and the port of Kiel is provided in Figure 4. The time step of the simulation is one hour.

In the 'hydrogen production' - block, entities that each represent one ton of hydrogen, are produced at a rate corresponding to that simulated by Eden et al. (2024). All produced hydrogen entities proceed to the 'Port of Bremerhaven' block in which they are merged into a batch corresponding to that of the cargo capacity of the approaching or waiting ship. Once a cargo batch is completed, incoming cargo entities wait in a server with a capacity corresponding to the capacity of the port-based storage minus the capacity of the waiting cargo batch (ship load). If the port-based storage becomes full, entities are directed to a storage overflow block where they are terminated.

Figure 3: Overview of the applied DES model.

In the 'ship loading' block (in Port of Bremerhaven, see Figure 4), the completed cargo batch entity is merged with a waiting/incoming ship entity, resulting in a composite entity representing a fully loaded ship. Once a composite entity has been created, it will be held up for a time corresponding to the port-turnaround time, which is modelled as a normal distribution with a mean value of 12 hours and a standard deviation of 1 hour. Subsequently, the composite entity will proceed to the 'Voyage: Bremerhaven-Kiel' block, in which it will complete one leg at a time as shown in Figure 4. Once the composite entity has reached the 'Port of Kiel' block it will be split into its original components, i.e., an entity representing an empty ship plus a number of entities each of which represent one ton of hydrogen. Following a waiting time corresponding to the port turnaround time, which is modelled in the same way as the port-turnaround time in Kiel, the entity representing the empty ship will embark

on its return voyage towards Port of Bremerhaven and the entities representing hydrogen will enter the 'hydrogen market' block in which they are terminated.

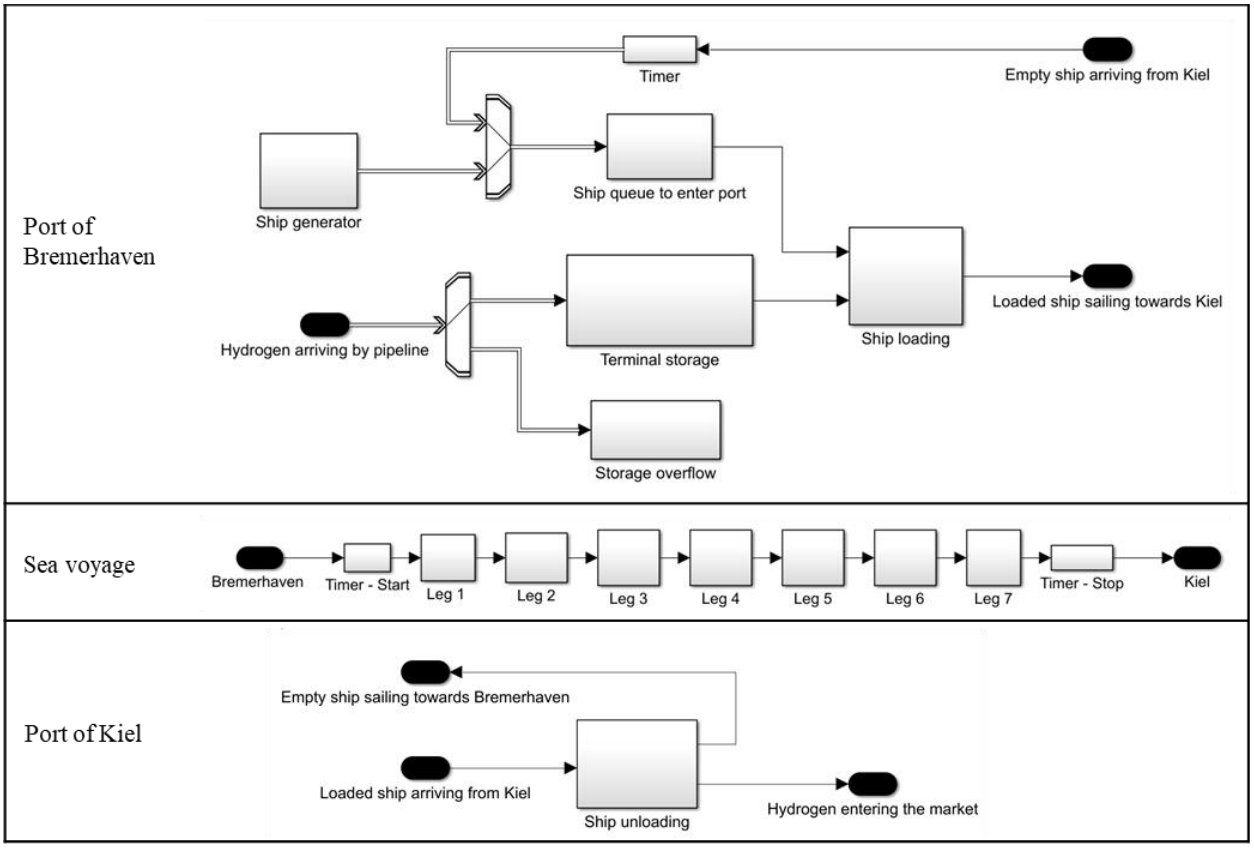

Figure 4: DES modelling of the Port of Bremerhaven, sea voyages, and Port of Kiel. The sea voyage Kiel-Bremerhaven is modelled in the same fashion as the distance Bremerhaven-Kiel.

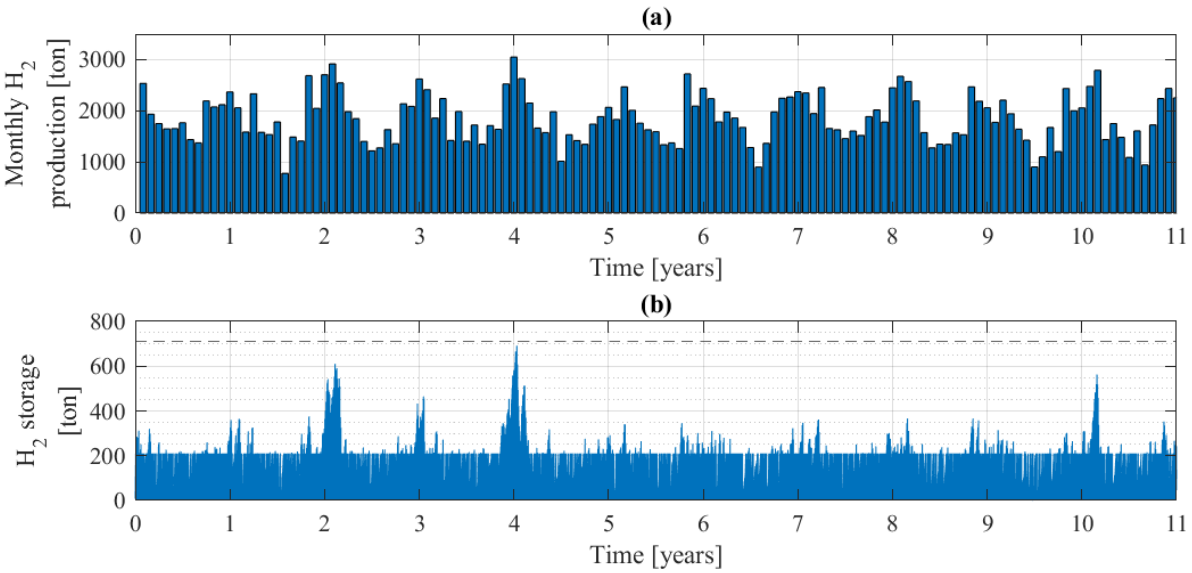

Figure 5: (a) Monthly hydrogen production and (b) the corresponding amount of hydrogen waiting for onward transport in Bremerhaven using a ship with net cargo carrying capacity of 209 ton operating as per Table 2. A storage capacity of 709 ton is sufficient to ensure that no production is lost.

With the help of the DES model, we iteratively find that a terminal storage capacity of 709 ton makes it possible to reduce the required net hydrogen cargo carrying capacity of the ship from the preliminary estimated 235 ton to 209 ton, assuming that the ship's speed is as per Table 2. For this solution, Figure 5 presents the amount of hydrogen waiting in the intermediate storage

in Bremerhaven as a function of time together with the corresponding monthly production rates. As per the figure, the peak storage value appears at the start of year 4 as a result of a slightly higher than normal hydrogen production, indicating that that the required storage capacity is sensitive to variations in the production rate. As shown in Figure 6, which shows in higher detail the development of the production rate together with corresponding development of the storage volume during the considered period, the increase in storage volume is a result of an increase in the frequency of days with high production.

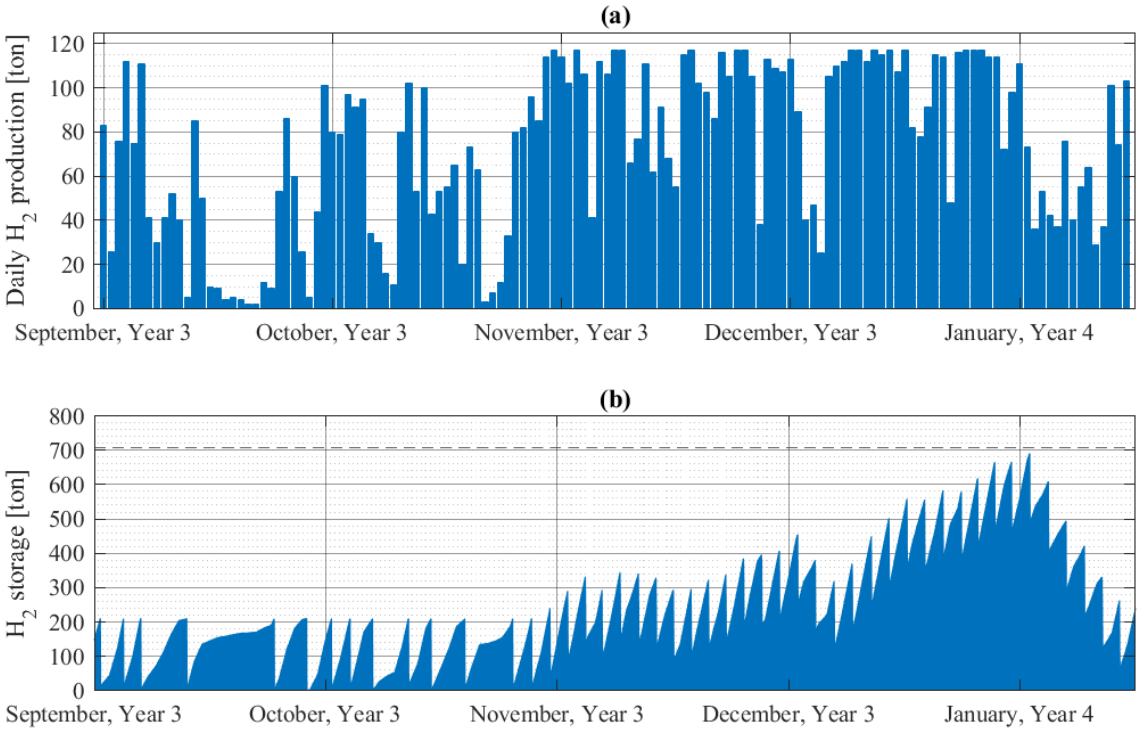

Figure 6: Detailed illustration of (a) the development of the daily production rate and (b) the resulting storage volume during the end of year 3 and start of year 4.

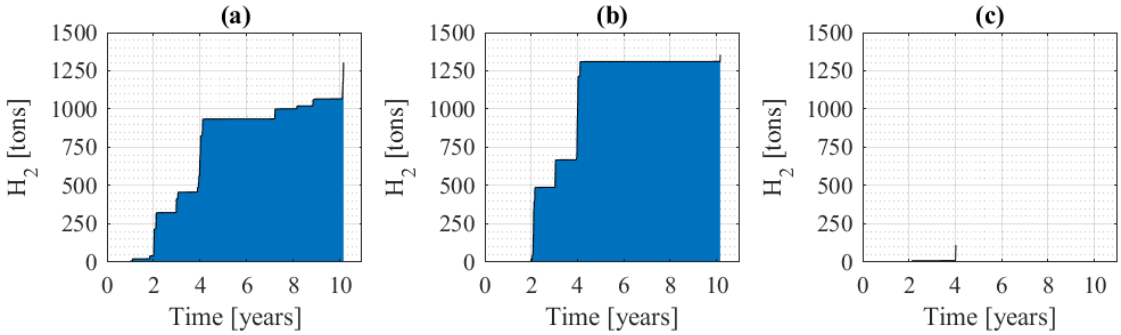

Figure 7: Amount of lost production for (a) 50 % reduced intermediate cargo storage (709 → 355 ton), (b) 10 % reduced ship cargo capacity (209 → 188 ton), and (c) reduced ship design speed (14 → 12 knots).

As also shown in Figure 5, except for a few short periods of high production, during most of the simulated operating years only a fraction of the storage capacity is utilized. This indicates that the solution is not particularly resource efficient. Measures that could be taken to reduce such waste during an average year include a reduction of the capacity of the intermediate storage and or of the transport system. To assess the cost of such measures in terms of the resulting production loss, we simulated the production losses resulting from the following system modifications: (a) reduction of the capacity of the intermediate storage by 50 % from 709 to 355 ton, (b) reduction of the ship's cargo carrying capacity by 10 % from 209 ton to 188 ton, and (c) reduction of the ship's design speed by 2 knots from 14 to 12 knots. Figure 7 presents the resulting production losses separately for each modification. As per the figure, both modification A and modification B results in a cumulated production loss of around 1 250 ton, corresponding to an annual average of 114 ton, which represents 0.5 % of the average annual production. Modification C results in an insignificant cumulated production loss of around 100 ton, corresponding to an annual average of

around 10 ton. Based on engineering judgement we assess that both modification A and C would result in significant savings that would exceed the costs associated with the resulting production loss. Hence, we decide to adopt both modifications.

For the selected system design modifications, involving an intermediate storage capacity of 355 ton and a ship with a net hydrogen carrying capacity of 209 ton and a design speed of 12 knots,
Figure **8** shows the simulated development of the storage volume, the cumulated production loss, and estimated monthly production losses.

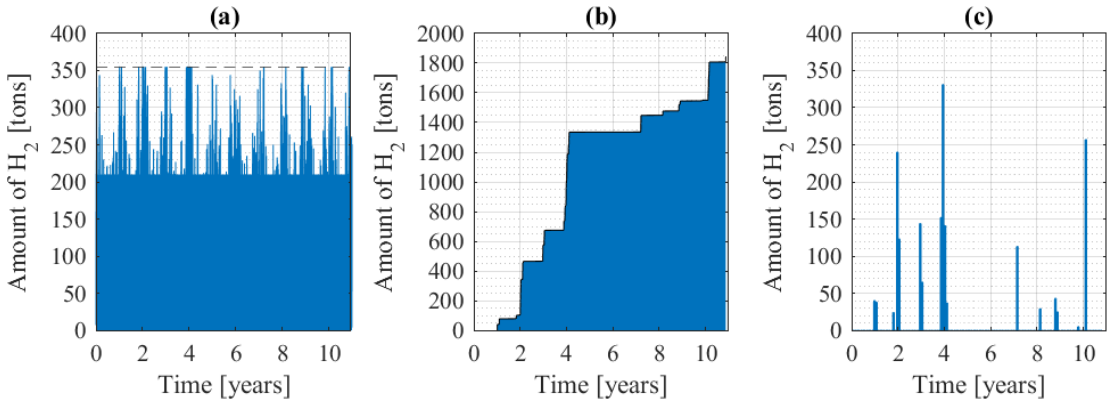

Figure 8: Development of the (a) storage volume, (b) cumulated production loss, and (c) monthly production losses for the selected system design involving an intermediate storage capacity of 355 ton and a ship with a net hydrogen carrying capacity of 209 ton and a design speed of 12 knots.

As per Table 4, for each considered hydrogen carrier we specify a simplified parametric ship design meeting the above defined requirements in terms of net hydrogen cargo carrying capacity and design speed. The dimensions and deadweight (DWT) of the ships are specified based on reference ships provided by Clarksons Research (2024), whereas the power demand at different speed are estimated as per Eq. 1.

$$V_{estimated} = \left(V_{ref\_avg} - m_v\right) \cdot \left(\frac{\sum P_{me}}{0.75 \cdot MCR_{avg}}\right)^{\frac{1}{3}} \quad (1)$$

, where V_{ref_avg} is a ship type- and size-specific statistical mean of distribution of ship speed defined as $V_{ref\_avg} = A\ x\ B^c$, where A, B, and C are given by IMO (2021). Parameter m_v is the considered ship's performance margin, defined as 5 % of V_{ref_avg}, or one knot, whichever is lower. MCR_{avg} is a ship type- and size-specific statistical mean of distribution of MCRs for main engines and is calculated as $MCR_{avg} = D\ x\ E^F$, where D, E, and F are given by (IMO, 2021). Because diesel engines should not be operated below around 30 % of their MCR, the ships' power demand at low speed is calculated per Eq. 2.

$$P_{min} = 0.3 * \frac{P_{me(14\ knots)}}{0.85} \quad (2)$$

Table 4: Specification of transport ships based on reference ships (Clarksons Research, 2024).

Hydrogen carrier	CH2	LH2	Ammonia	LOHC
Net H2 carrying capacity	209 ton	209 ton	209 ton	188 ton
Type of ship	Gas tanker	Container ship	LPG/Ammonia carrier	Chemical tanker
Required ship capacity (m^3, TEU, or DWT)	9010 m^3, 6800 DWT	140 TEU (70 FEU), 2010 DWT	209 ton x 5.62 ≈ 1175 ton	209 ton x 15.87 ≈ 3317 ton
Length	120 m	80 m	72 m	86 m
Beam	21 m	14 m	12 m	14 m
Draft	7 m	4 m	4 m	6 m
P_{me} (12 knots)	1660 kW	880 kW	1060 kW	1600 kW
P_{me} (6.5 knots)	590 kW	310 kW	375 kW	565 kW
P_{me} (5 knots)	590 kW	310 kW	375 kW	565 kW
Average specific fuel consumption	190 g / kWh	190 g / kWh	190 g / kWh	190 g / kWh

Each of the considered hydrogen carriers is associated with energy penalties related to the what is often referred to as 'packing' and 'unpacking, i.e., the processes of converting hydrogen to the desired transportation form, and subsequently to convert it back to hydrogen at the transport destination. For some of the energy carriers there is an additional loss in terms of boil-off. In the present study, such losses are assumed to be as per Table 5. As per the table, because many of the processes have not yet been applied on a large scale, there is a significant degree of uncertainty regarding their energy consumptions (IRENA, 2022). This appears to be especially true for LOHCs. There are many different types of LOHCs and there is a large variation between the energy consumption values reported in the literature for their "packing" and "unpacking". In part, this may be due to differences between theoretical values and the actual consumption of existing equipment. The values used in this study are intended to be indicative of 'typical' LOHCs.

Table 5: Energy penalties and boil-off estimates for the considered energy carriers (IRENA, 2022) (Parks, Boyd, Cornish, & Remick, 2014) (Melcher, George, & Paetz, 2021).

Energy carrier	Energy consumption, packing	Energy consumption, unpacking	Boil-off
CH_2	2 – 4 kWh/kg-H2	negligible	negligible
LH_2	10 – 12 kWh/kg-H_2	negligible	Boil-off 0.05-0.25 % / day
Ammonia	0.5 – 0.8 kWh/kg-NH_3	4 – 11 kWh/kg-H_2	Boil-off 0.004 % / day
LOHC	9 - 10 kWh/kg-H_2	6-12 kWh/kg-H_2	negligible

Based on the above defined data and assumptions we calculate the energy consumption for an average round trip as per Figure 9. As per the figure, for each energy carrier we calculate both an optimistic value, based on the lower values defined in Table 5, and a pessimistic value, based on the higher values of the same table. As can be seen from the figure, we find that for both the pessimistic and optimistic assumptions, CH_2 appears to be the overall most energy-efficient option. Whether LH_2 or NH_2 is the second most cost-effective solution depends on assumptions concerning energy penalties related to hydrogen packing and unpacking.

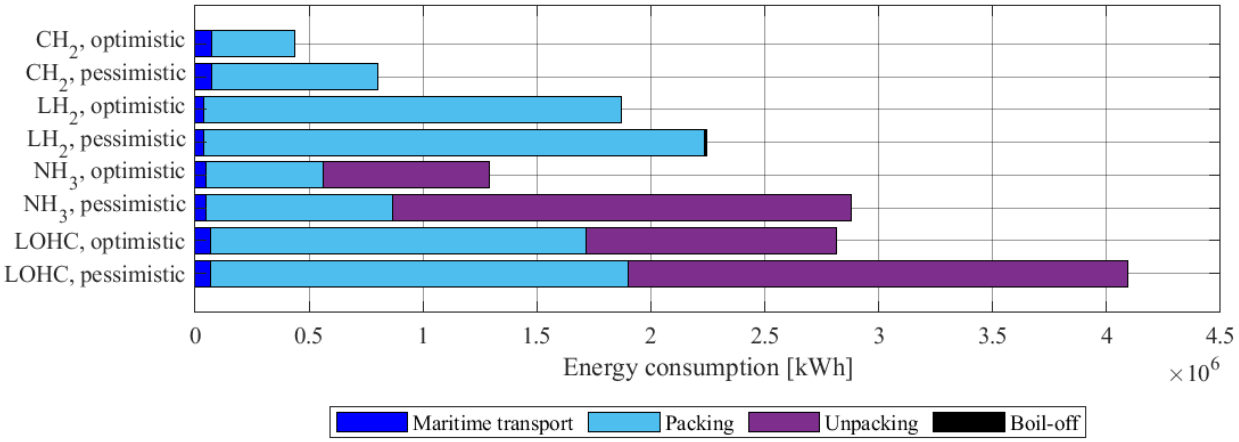

Figure 9: Comparison of the energy consumption of the different solutions for an average round trip.

CONCLUSIONS

In this study, a discrete-event simulation-based approach is applied to a case study to derive concepts for short sea shipping of green hydrogen produced at an offshore wind farm over a sea distance of around 130 NM. To meet the transport demand during a typical year, our simulation results indicate that a ship with a net hydrogen transport capacity of 209 ton and a design speed of 12 knots is needed. Among four considered hydrogen carriers, CH_2, LH_2, NH_3, and a LOHC, we find that CH_2 provides the overall best energy-efficiency. The simulation results further reveal that it does not appear resource-efficient to invest in the transport and storage capacities needed to be able to handle the expected 11-year maximum production peak without production limitations, as this would result in significant overcapacity most of the time. Future research is recommended to address safety, regulatory, and cost-efficiency aspects, as well as to investigate the required port infrastructure in detail, and to investigate potential hydrogen carrier specific differences in terms of loading/unloading times. Future research is also recommended to address uncertainties regarding how much energy is lost in the packing/unpacking of different hydrogen carriers, or through boil-off.

CONTRIBUTION STATEMENT

Author 1: Conceptualization; data curation, methodology; writing – original draft. **Author 2:** data curation, writing –review and editing. **Author 3:** data curation, writing –review and editing. **Author 4:** data curation. **Author 5:** data curation. **Author 6:** writing – review and editing. **Author 7:** conceptualization; supervision. **Author 8:** writing – review and editing. **Author 9:** conceptualization; supervision.

The authors declare that they have no conflict of interest. Neither the European Commission nor ECMWF is responsible for any use that may be made of the Copernicus information or data it contains.

REFERENCES

Bergström, M., Erikstad, S., & Ehlers, S. (2016). A simulation-based probabilistic design method for Arctic Sea transport systems. *Marine Science and Application, 15*(4), 349-369.

Clarksons Research. (2024). *World fleet register*. Retrieved 1 15, 2024, from https://www.clarksons.net

d'Amore-Domenech, R., Meca, V., Pollet, B., & Leo, T. (2023). On the bulk transport of green hydrogen at sea: Comparison between submarine pipeline and compressed and liquefied transport by ship. *Energy, 267*, 126621. doi:https://doi.org/10.1016/j.energy.2023.126621

Decker, L. (2019). Liquid hydrogen distribution technology. *HYPER closing seminar.* Brussels. Retrieved from https://www.sintef.no/globalassets/project/hyper/presentations-day-2/day2_1105_decker_liquid-hydrogen-distribution-technology_linde.pdf

Eden, S., Niemi, A., Skobiej, B., & Sill Torres, F. (2024). Brief review of options and risks in offshore green hydrogen production: A German case study. *Advances in Reliability, Safety and Security (ESREL 2024) (Accepted for publication).* Cracow, Poland.

Hersbach, H., Bell, B., Berrisford, P., Biavati, G., Horányi, A., Muñoz Sabater, J., . . . Thépaut, J.-N. (2023). ERA5 hourly data on single levels from 1940 to present. Copernicus Climate Change Service (C3S) Climate Data Store (CDS). doi:10.24381/cds.adbb2d47

IMO. (2021). *Resolution MEPC.333(76). Annex - 2021 Guidelines on the Method of Calculation of the Attained Energy Efficiency Existing Ship Index (EEXI).* London: International Maritime Organization. Retrieved from Website of the IMO: https://wwwcdn.imo.org/localresources/en/OurWork/Environment/Documents/Air%20pollution/MEPC.333(76).pdf

IRENA. (2022). *Global hydrogen trade to meet the 1.5°C climate goal: Part II – Technology review of hydrogen carriers.* Abu Dhabi: International Renewable Energy Agency.

Johnston, C., Khan, M., Amal , R., Daiyan, R., & MacGill, I. (2022). Shipping the sunshine: An open-source model for costing renewable hydrogen transport from Australia. *International Journal of Hydrogen Energy, 47*(47), 20362-20377. doi:https://doi.org/10.1016/j.ijhydene.2022.04.156

Kawasaki. (2021). *Kawasaki technical review no. 182 -Special Issue on Hydrogen Energy Supply Chain.* Akashi, Japan: Corporate Technology Division, Kawasaki Heavy Industries, Ltd. Retrieved from https://www.kawasaki-gasturbine.de/files/KAWASAKI_TECHNICAL_REVIEW_No_182.pdf

Melcher, B., George, M., & Paetz, C. (2021). Liquid Organic Hydrogen Carriers - A Technology to Overcome Common Risks of Hydrogen Storage. *International Conference on Hydrogen Safety.* Edinburgh (Online): Hydrogen Knowledge Centre. Retrieved from https://www.h2knowledgecentre.com/content/conference3532

Notteboom, T., & Haralambides, H. (2023). Seaports as green hydrogen hubs: advances, opportunities and challenges in Europe. *Maritime Economics & Logistics, 25*, pp. 1-27. doi:https://doi.org/10.1057/s41278-023-00253-1

Ortiz Cebolla, R., Dolci, F., & Weidner, E. (2022). *Assessment of Hydrogen Delivery Options: feasibility of transport of green hydrogen within Europe.* European Commission, Joint Research Centre. Brussels: Publications Office of the European Union. doi:https://doi.org/10.2760/869085

Parks, G., Boyd, R., Cornish, J., & Remick, R. (2014). *Hydrogen Station Compression,Storage, and Dispensing Technical Status and Costs.* Denver, USA: National Renewable Energy Laboratory (NREL).

UCA. (2023). *General Information about Kiel-Canal transits - part I.* Brunsbüttel: United Canal Agency.

Weichenhain, U. (2021). *Hydrogen transportation - The key to unlocking the clean hydrogen economy.* Munich, Germany: Roland Berger GMBH.

WSV. (2022). *The Kiel Canal - International lifeline for maritime traffic and maritime pearl of Schleswig-Holstein.* Bonn: Federal Waterways and Shipping Agency. Retrieved from https://www.gdws.wsv.bund.de/SharedDocs/Downloads/DE/Publikationen/_GDWS/Wasserstrassen/NOK_englisch.pdf?__blob=publicationFile&v=14#:~:text=Because%20of%20the%20larger%20tidal,and%20is%20thus%20significantly%20faster.

Proceedings of 15th International Marine Design Conference (IMDC-2024)
June 2-6, 2024
Amsterdam, the Netherlands

Technical and Economic Feasibility Study on Reducing CO_2 Emissions of Dutch Beam Trawlers

Arnoud de bruin[1,2], Walter van Harberden[2], Austin A. Kana[3,*]

ABSTRACT

This paper examines the technical and economic influence of CO_2 reduction measures on the design and operation of Dutch beam trawlers. This is done by means of a parametric model used to assess the influence on the overall design of the vessel. Technical feasibility is determined by meeting operational effectiveness requirements, maximum added draught, maximum added length, and a reduction of CO_2 emission by at least 40%. Secondly the model evaluates the new energy carrier and fish storage layout as a result of additional required volume. Additional volume is gained within the net store, fish hold, or by hull extension. Additionally, various propeller configurations, waste heat recovery, and regenerative braking systems are explored to reduce energy consumption. The economic performance is assessed using yearly operational requirements, capital expenses of configuration, and total cost of ownership.

KEY WORDS

Beam trawlers; feasibility study; parametric modeling; zero-emission

INTRODUCTION

The most recent estimates in the Fourth International Maritime Organization (IMO) Greenhouse Gas (GHG) Study 2020 show that GHG emissions of shipping have increased by 9.6% between 2012 and 2018 (IMO, 2020), while the IMO strives to reduce CO_2 emissions by at least 40% by 2030, pursuing efforts towards net zero by 2050, compared to 2008 (IMO, 2023). Although a Dutch beam trawler has a gross tonnage below or just above 400GT and the IMO regulations do not apply to it, there is nevertheless an aim to reduce GHGs of these vessels. The last decade the Dutch beam trawler fleet has been confronted with a lot of developments (MEPC, 2024) which has led to the reduction of profitability of the vessels. Two developments stand out in the last decade, namely: (1) BREXIT, which has resulted in a reduction of available fishing ground, and (2) the ban on pulse fishing, which is a method of fishing which reduced the operational expenses by around 30-40%. Due to the current state of the fishing fleet the Dutch government has introduced a plan called "Noordzee Visie (Northsea Vision)" (Rijsksdienst voor Ondernemend, 2019) which aims to reduce the environmental impact of the Dutch fishing fleet. This plan consists of buying out weak companies and investing money in the form of a subsidy to make the remaining fishing vessels more sustainable.

To continue fishing a Dutch beam trawler has to comply with these regulations, thus requiring implementing the use of sustainable fuels together with energy saving technologies. Vessel owners want to implement these technologies without sacrificing operational effectiveness. Therefore, this study aims to assess the technical and economic feasibility of reducing the CO_2 emissions of Dutch beam trawlers to meet the 2030 IMO CO_2 emission regulations, while maintaining vessel operational effectiveness.

[1] Department of Maritime and Transport Technology, Delft University of Technology, Delft, The Netherlands
[2] Padmos, Stellendam, the Netherlands
[3] Department of Maritime and Transport Technology, Delft University of Technology, Delft, the Netherlands; ORCID: 0000-0002-9600-8669
* Corresponding Author: a.a.kana@tudelft.nl

Submitted: 23 February 2024, Revised: 29 April 2024, Accepted: 1 May 2024, Published: 26 May 2024

Conference paper, DOI: https://doi.org/10.59490/imdc.2024.903 e-ISSN: 3050-4864

LITERATURE

With the buyout and high fuel costs on the horizon studies have been done on the reduction of CO_2 emissions by means of alternative energy carriers on new build (beam) trawlers. These research topics concern: feasibility study fishing on natural gas (‘t Hart, 2009), LNG potential energy source (Taal and Hoefnagel, 2012) and Design Green shrimp trawler (van Urk, 2012). This studies are limited to other fishing vessel types and only consider gas-like fuels. There are mainly three ways to reduce the emitted emission of a vessel: (1) reducing the energy consumption of the vessel, (2) after treatment of the rest product of energy converter or by (3) changing to an alternative fuel. All the mentioned and open source studies are done on new build beam trawlers, discuss one methods to reduce CO_2, and do not combine all three options and aspects together. Additionally, and the economic perspective has been missing from previous literature. Looking at emissions and fishing regulations there is large future uncertainty driven by future availability fishing grounds and alternative fuel characteristics. It is thus necessary to get insight in the performance of multiple propulsion configurations on economic and technical performance. The review below covers: (1) determining the current state and operation of a Dutch beam trawler, (2) exploring methods to reduce the CO_2 emissions, and (3) establishing requirements for an assessment model.

Vessel State

The latest study (Wageningen Marine & Research, 2023) showed the average age of the 284 active Dutch beam trawlers to be 32 years (build 1990), with 75% being older than 20 years. The vessels are powered by a conventional engine room set up. For these vessels this means the main engine is a MGO fueled 4-stroke medium speed internal combustion engine, and is indirectly coupled to the propeller by means of a gearbox. The installed Pb varies between 1000kW and 1450kW. The vessels average characteristics range from: Lpp: 35-42m, $B_{moulded}$: 6-9m, T_{mid}: 3-4.5m, D_{prop}: 2-3m and Prop-speed: 180−280rpm. The main energy consumers besides the engine propulsion the propeller onboard are the ice & cooling machines, safety & communication, and the winch. From which the cooling system is responsible for the preservation of caught fish and the winch for the setting and hauling of the nets.

The state of the art of beam trawlers limits itself to optimized propeller and diesel engine configurations but does not go any further. The operational profile of the vessel can be divided into the short and long cycle. The long cycle is the time from sailing out from port, the fishing and the return into port. The short cycle is the fishing cycle covering the repetition of setting, fishing and hauling the nets. Two types of long cycles exist in the Dutch fleet: a 100hr and a 160 hour per week, based on geographic and demographic preferences within the Netherlands. The short cycle has an average duration of 2.5 hours.

Emission Reduction Exploration

The energy converters, energy carriers and emission reduction methods identified in Table 1 have the highest potential in achieving the stated goals.

Table 1: Combination of systems, similar numbers indicate technical combinations

Converter	Energy Carrier	Energy Reduction
Diesel ICE (1)	MGO (1) HVO (1) FAME (1)	Propeller (1,2,3,4) - 3.4m 4 blade - 3.4m 5 blade - 4.0m 4 blade - 4.0m 5 blade
DF ICE (2)	Methanol (2)	Orcan, WHR (1,2,3)
LT PEMFC (3)	Hydrogen (3)	SRC, WHR (1,2,3)
NMC-Li battery (4)		Winch (1,2,3,4) - Regenerative braking - Operational optimization

The four energy converters identified demonstrate promising potential for implementation on a beam trawler. These converters were selected based on their capacity to reduce CO_2 emissions while ensuring technical reliability.

- ***MGO ICE*:** This engine was considered for its cost-effectiveness and its proven track record in efficiently converting chemical energy into mechanical or electrical energy (DNV, 2020; Streng et al, 2022).
- ***DF ICE**:* The DF (Dual Fuel) technology was chosen as it has already been validated by several engine manufacturers. Furthermore, its utilization of methanol fuel offers the potential to significantly decrease CO_2 emissions (Dierickx et al, 2021; Pendle Government, 2018).

- ***LT PEMFC*:** The Low-Temperature Proton Exchange Membrane Fuel Cell (LT PEMFC) was selected due to its reliability, high energy density, rapid response to load variations, and a simplified system compared to high-temperature fuel cells (Leon, 2008; Welaya et al, 2011).
- ***Nickel Manganese Cobalt-Lithium (NMC-Li) Batteries***: These batteries were preferred over other options because of their high energy density, extended cycle life, and relatively fast charging capability (Freudenberg E-power systems, 2022).

Additionally, five energy carriers are employed, carefully selected based on their ability to exhibit low Tank-To-Wake (TTW) emissions and ensure minimal safety risks for both the crew and the environment.

- ***MGO:*** MGO is being considered to assess its feasibility in meeting IMO targets without transitioning to alternative fuels.
- ***HVO and FAME***: Hydrotreated Vegetable Oil (HVO) and Fatty Acid Methyl Ester (FAME) are highly regarded by IMO for their exceptionally low TTW emissions due to their bio-based production (IMO, 2023). Their similarity to Marine Diesel Oil (MDO) makes their application relatively straightforward (DNV, 2019).
- ***Methanol***: Methanol is partially classified as a drop-in fuel, and its lower carbon content provides the potential to reduce TTW emissions.
- ***Hydrogen***: Hydrogen, chosen for its zero TTW emissions, is a favored fuel option. Hydrogen in liquid form is preferred due to its higher storage efficiency compared to compressed hydrogen, attributed to the significant reduction in volume resulting from its low temperature (DNV, 2022).

At last three types of energy reducing methods are explored. (1) Propeller: due to its high rotational speeds and high blade loading it is found that there is potential for efficiency improvement by increasing the diameter of the propeller, which would reduce blade loading and rotational speed, leading to an overall increase in efficiency (Laurens et al, 2013). (2) Winch: with the application of regenerative braking on the winch a small amount of electrical energy can be recovered during the setting of the nets. Secondly by optimizing the winch operation the required propulsion power during setting and hauling can be reduced. (3) Waste heat recovery (WHR): depending on the propulsion setup, energy can be recovered from exhaust gas or cooling water (Mat Nawi et al, 2019; Benvenuto, et al, 2016; Ouyang et al, 2020).

Combination of Systems

The proposed configurations consist of various combinations of energy converters, energy carriers, and energy consumption reduction strategies. However, certain combinations are not feasible due to system working principles. With the exception of the original propulsion configuration, all other combinations are designed to be either diesel-electric or fully electric, aligning with the Dutch subsidy regulations outlined in the Noordzee Visie. The calculations are designed to store the maximum amount of the main energy carrier on board, considering a 40% reduction in CO_2 emissions. The remaining required energy is stored as the secondary energy carrier. These hybrid combinations of energy carriers are chosen based on the assumption that they are the most economically feasible. The combination of Hydrogen and NMC-Li for example will result in significant capital investments, and complex combination of systems. HVO and FAME already achieve 40% CO_2 and are therefore not used in the hybrid configurations.

In addition to the mono-fueled configurations, four hybrid configurations are explored. The selection of these hybrid combinations is based on the goal of achieving the lowest initial investment while still achieving a 40% reduction in CO_2 emissions. Consequently, combinations involving HVO, FAME, Hydrogen, and batteries are not chosen, as they already comply with the TTW fraction requirements. The following four combinations remain:

1. MGO-Hydrogen (liquid) (MGO-H2(l))
2. MGO-Nickel Manganese Cobalt-Lithium (MGO-NMC-Li)
3. DF-Hydrogen (liquid) (DF-H2(l))
4. DF-Nickel Manganese Cobalt-Lithium (DF-NMC-Li)

The fraction of delivered energy in each combination is determined by using the maximum amount of MGO or DF, with the remaining energy supplied by the second energy carrier.

METHOD

To evaluate the potential of various combinations of systems, an assessment model was developed (Figure 1), consisting of three main components: literature, technical, and economical. The literature section gathered inputs from specific system characteristics found in a literature study. The technical segment involved calculations to determine the required energy and

new vessel dimensions for different storage options, ensuring compliance with all necessary requirements. In the economic part, proposed configurations that met the requirements were evaluated using three performance indicators: capital expenses, operational expenses, and total cost of ownership.

The primary focus of this research was to assess the technical and economic feasibility of reducing CO_2 emissions in a beam trawler. For this purpose, a parametric assessment model was employed. This method assigned points to various criteria and evaluated their fulfillment to assess the viability of the proposed solution. The model considered crucial factors such as emission reduction potential, cost-effectiveness, and alignment with existing infrastructure and regulations. By aggregating scores assigned to each criterion, a comprehensive and objective evaluation of CO_2 reduction measures was achieved. This parametric approach offered a systematic and transparent decision-making process, facilitating the selection of the most suitable emission reduction strategies for beam trawlers while considering both technical and economic aspects.

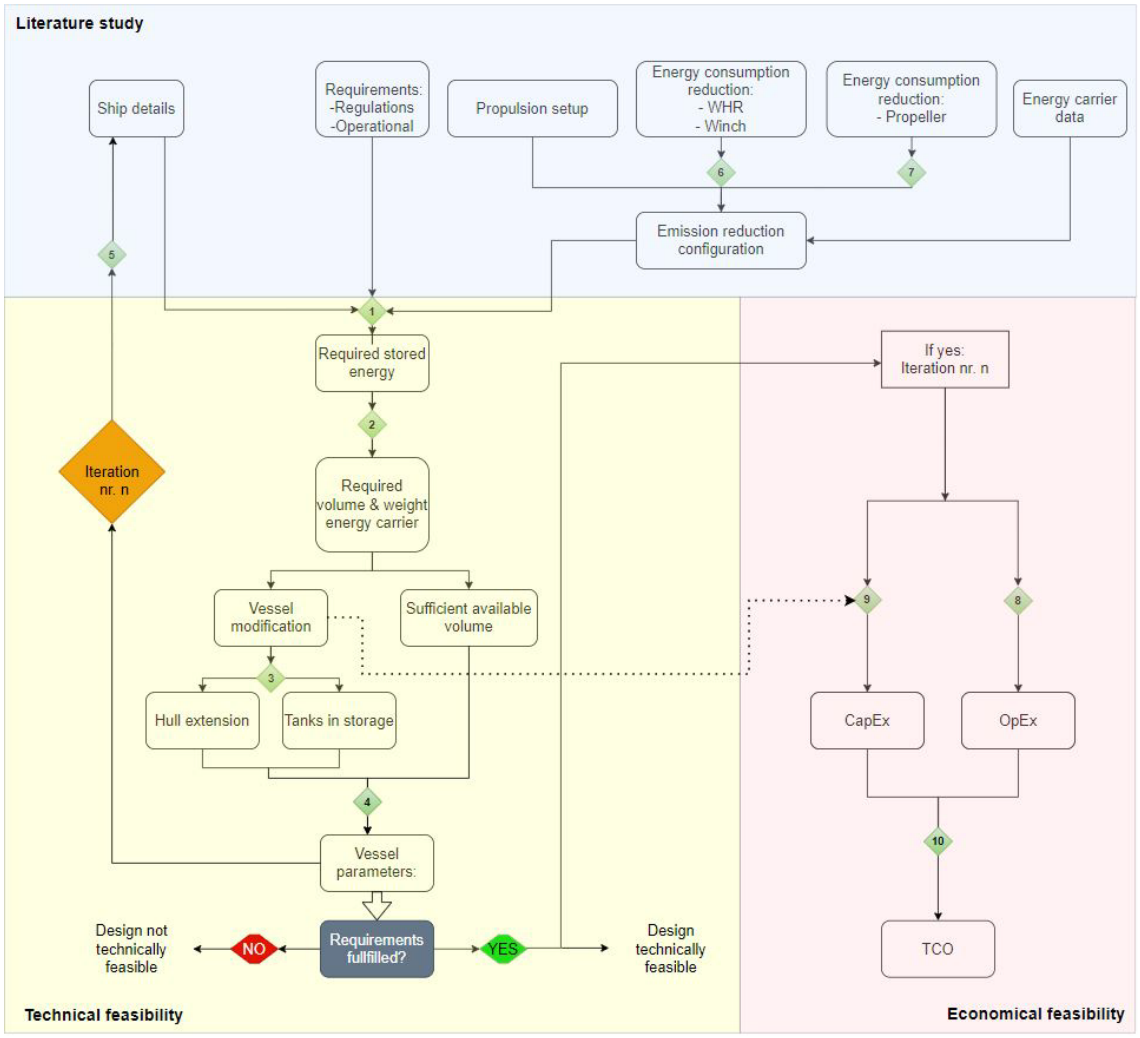

Figure 1. Flowchart of the assessment model.

Technical Feasibility Assessment

In this phase of the assessment, calculations are performed to transform the operational profile and propulsion configuration into new vessel parameters. By considering the system characteristics, vessel data, and operational requirements, the necessary energy per long cycle, volume of energy carrier, weight of energy carrier, and weight of propulsion configuration are determined. To accommodate the calculated volume of energy carrier, including the tank storage arrangement (See Figure 2), various storage methods are suggested. These methods involve combining the original storage tanks with additional volumes such as the net store, fish hold, or creating new storage space if the hull is extended.

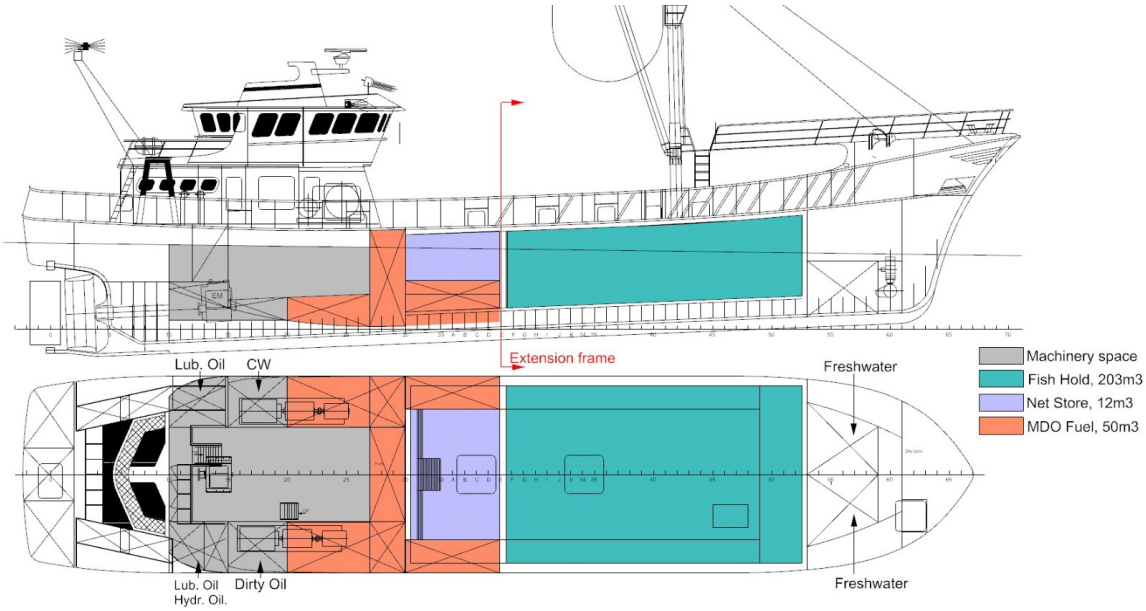

Figure 2: Original tank plan (Padmos, 1987)

Examining the energy density and storage arrangements of drop-in fuels such as MGO, HVO, and FAME requires relatively straightforward investigation. However, when dealing with energy carriers like methanol and liquid hydrogen, specific tank storage arrangements become necessary. In order to estimate the optimal position and quantity of tanks, this research took into account the average Dutch beam trawler, its energy carrier consumption, and hull dimensions. Additionally, the requirements for cofferdams and cryogenic tanks were considered, ultimately determining the average energy density, including the storage tank, used in this study.

Different organizations employ diverse formulas, often incorporating non-empirical values and correction factors, to calculate emission reduction. However, approaches like EEXI, EEDI, and CII, which work with emission ratios per ton of cargo per mile, are unsuitable for fishing vessels due to their limited transportation of goods, primarily consisting of a few tons of fish. Moreover, these ratios often use generalized correction factors that may not be applicable to specific sectors or may lack relevant data, leading to an insufficient understanding of the actual impact of various configurations.

To address these concerns, the assessment of CO_2 emission reduction for fishing vessels will be presented as a percentage relative to the original emission during the long cycle. The focus will be on considering TTW emissions, as Dutch, EU, and IMO regulations calculate, penalize, and evaluate emissions based on this criterion. It is important to note that fuel producers bear the responsibility for well-to-tank (WTT) emissions, and well-to-tank (WTT) emissions, being a separate study, are beyond the scope of this study.

Once the new estimated hull parameters are established, the configuration is examined for its technical feasibility. To be deemed feasible, the configurations must meet various types of requirements.

(1) Operational effectiveness requirements
- Towing capacity
- Endurance
- Fish hold capacity
- Cooling
- Winch
- Storage area

(2) Maximum 0.3m added average draught
(3) Maximum 3m hull extension
(4) Minimum 40% CO_2emission reduction

The maximum added draught and length of a vessel are unique to each vessel and determined by factors like minimum required freeboard, maximum GT, seaworthiness, and stability. If a configuration fails to meet these specific requirements, it is considered technically infeasible. Conversely, if it fulfills these criteria, it is deemed technically feasible, and the assessment model proceeds to evaluate its economic feasibility.

Economic feasibility assessment

This part assesses the economic performance of the configurations based on three indicators: (1) Operational expenses, (2) Capital expenses, and (3) Total cost of ownership.

Operational expenses

The operational expenses is the summation of the yearly costs of energy carrier consumption, the paid tax on CO_2 emission to the Dutch government, and the maintenance (Equation 1).

$$OpEx = Energy\ Carrier + CO_2\ emission\ taxes + maintenance \quad [1]$$

Using:

- Energy Carrier, required amount of energy carrier per year multiplied by price
- CO_2 emission taxes, CO_2 emission per year multiplied by tax price
- Maintenance, the yearly costs required to keep propulsion configuration and ship in good and reliable condition.

Maintenance costs

To obtain the most accurate estimate of the expected costs per propulsion configuration, the annual maintenance costs need to be determined. These costs will always be an approximation as they depend on various variables such as operational hours, whether the work is performed in-house or by a subcontractor, etc. Additionally, predicting breakdowns is challenging. However, through the expertise of Padmos and insights from case studies, an attempt has been made to determine an annual cost estimate for ship maintenance.

Capital expenses

With the propulsion configurations that meet the requirements, an estimation can be made on the system prices and vessel retrofitting prices. The propulsion configuration system prices can be estimated using average e/kW fractions. The retrofitting prices of the vessel are difficult to estimate, since they are vessel specific. Steel prices and labour prices are fixed but the required amount of hours and steel are difficult to estimate. The capital costs of retrofitting are significant and therefore must be included in the economic feasibility. The company's history in vessel retrofitting is used to estimate working hours for the different retrofitting options. With the cross section drawings and the weight of steel the added weight of the extension section is calculated. With an average price on steel welding, cutting and pre-forming costs this results in the overall costs to make the section. The CapEx is built up as the sum of propulsion configurations costs, propeller, winch modifications, WHR and vessel extension costs (see Equation 2).

$$CapEx = Propulstion\ configuration + Energy\ saving\ devices + Hull\ extnesion \quad [2]$$

Total cost of ownership (TCO)

TCO is one widely used approaches in the analysis of economic performance (see Equation 3). TCO takes into account not only the upfront investment costs but also the operational and maintenance expenses over the system's lifetime. A new propulsion configuration may require significant investment upfront, but its long-term cost implications are equally crucial. TCO analysis helps in identifying potential cost savings over the operational lifespan of the system. For instance, a propulsion configuration with higher fuel efficiency and lower maintenance requirements may result in substantial cost reductions over time, offsetting the initial investment. TCO analysis allows for a fair comparison of different propulsion configurations (Terun et al, 2022). By calculating and comparing the total costs associated with each option, decision-makers can identify the most economically viable solution.

$$TCO_{yearly} = CapEx + OpEx \quad [3]$$

- TCO_{yearly}, the yearly total cost of ownership[e/year]
- *Capex*, the capital expenditures[e]
- *Opex*, the operational expenditures[e/year]

In the context of the new propulsion configuration, the vessel's expected lifetime is considered to be 15 operational years. Consequently, the residual value of the investment, or the remaining value of the system after its useful life, is expected to be negligible or zero. This expectation arises from factors such as technological obsolescence, wear and tear, and the introduction of newer, more efficient propulsion technologies over time. Given the vessel's expected lifetime of 15 operational years, the TCO analysis typically focuses on this relatively short time horizon. Since the remaining value of the investment is negligible or zero by the end of this period, including it in the TCO analysis would not significantly impact the overall economic

assessment. Only at a later stage when a new build vessel is included into the configurations, a remaining value will be included since this vessels lifetime is more than 15 years. The remaining value is determined according to Equation 4.

$$TCO_{yearly,remaining} = CapEx + OpEx - remaining\ value \quad [4]$$

CASE STUDY

To obtain a realistic picture of the technically and economically feasibility of the configurations, a case study is conducted on an existing beam trawler. The vessel has the following characteristics (Table 2), and as can be seen from the literature it matches the average Dutch beam trawler parameters.

Table 2. Case vessel particulars

Lpp	33.75m
Beam	7.5m
Draught	3m
Displacement	500 tons
Block Coefficient	0.6
Main engine	1200kW Stork Werkspoor
Propeller diameter	2.5
Winch	100kW

Given the significant impact of operational expenses on the economic feasibility of the configuration, it is necessary to conduct scenarios with varying energy carrier prices and CO_2 emission tax prices. This analysis aims to determine whether the most promising configurations also perform well under different circumstances. By exploring different scenarios, insights can be gained into the robustness and versatility of the potential configurations beyond their primary conditions. Within this study three scenarios are explored: (1) high energy carrier price, and (2) high emission tax price, and (3) forecasted energy carrier and emission tax prices. The last scenario will be used to actually find the answer to the problem of this research.

Energy Carrier Prices

Although best estimates are used on forecasted carrier prices, the last decade showed large deviations from forecasted prices due to pandemics or wars (Olusanya et al. 2021; Pavlenko et al, 2020). By considering a case in which with high energy carrier prices, it allows for an analysis of the economic viability of different propulsion configurations under various cost conditions. The projection for 2050 is increased and decreased by 30% to find the influence of the price of the energy carrier on the economic feasibility of the beam trawler vessel. A 30% uncertainty is chosen after considering the enormous volatility that energy prices have shown.

Emission Tax Prices

The Dutch Government imposes taxes or levies on carbon emissions to incentivize emission reductions. This regulation has been set until 2030; however, this research aims to further explore the economic performance of the configuration. Therefore, there will be a need to make assumptions about the price trajectory post-2030 (Enerdata, 2023), introducing uncertainty into the model. To assess the model's sensitivity to these uncertainties, a scenario is applied assuming a high emission price. By evaluating this scenario with different emission tax prices, it helps in understanding the cost implications of environmental regulations and their influence on the economic viability of the proposed propulsion configurations. The scenario proposed will work with a upper limit of 50% above predicted prices. A 50% uncertainty is chosen after considering the enormous volatility that future regulations have shown. After finding the sensitivity of the model with Scenario 1 and scenario 2, the last scenario (3) uses the prices for both energy carrier prices and emission tax as forecasted in Table 3 and 4.

Table 3. Energy carrier price current and future, [e/GJ]

	Fuel Costs 2022	Fuels Costs 2050	Source
MGO	17	17	(LR, 2023)
HVO	31	31	(DNV, 2019)
FAME	28	28	(DNV GL, 2019)
Methanol	39	27	(Pothaar, 2022)
Hydrogen	70	33	(IEA, 2022, 2023)
Electricity	27	10	(GRO, 2020)

Table 4. Statutory price trajectory of carbon levy in 2021 (OECD, 2021)

	2021	2022	2023	2024	2025	2026	2027	2028	2029	2030
Levy rate (€ / tonne CO_2)	30	40.56	51.12	61.68	68.12	76.42	83.21	89.72	94.20	103.92

RESULTS

The results of the assessment model are presented for different configurations applied to the case beam trawler, sailing with both the 100hr and the continuous long cycle. In the economic evaluation, it is assumed that the retrofitted case vessel will have an operational lifespan of 15 years. The model generates various outputs, from which the required amount of energy per configuration per long cycle is the first value calculated. This is then converted into the necessary volume and weight. In this section, the required volume, including the storage tank, is presented to provide an overview of the quantities involved and to understand the impact of specific energy reduction methods. The outcome is presented in Table 5 and 6. The required volumes mentioned here are including storage tank.

Table 5. Required storage volume [m^3] for mono fuels configurations. Red indicates more volume than available.

			100 hr long cycle					Continuous long cycle				
			Propeller					Propeller				
Converter	Fuel	Config.	Original	T.1	T. 2	T. 3	T. 4	Original	T. 1	T. 2	T.3	T.4
ICE	MGO	D-D	22	18	15	18	15	36	29	25	29	25
ICE	MGO	D-E	23	19	16	19	16	38	30	26	30	26
ICE	HVO	D-E	25	21	18	21	18	42	33	28	33	28
ICE	FAME	D-E	25	20	17	20	17	41	33	28	33	28
ICE	DF	D-E	73	59	50	59	50	121	96	81	96	81
PEMFC	Hydrogen	E	117	93	79	93	79	191	151	128	151	128
Battery	NMC-lithium	E	232	188	161	188	161	380	305	259	305	259

Table 6. Required storage volume[m^3] hybrid configurations. Red indicates more volume than available.

			100 hr long cycle					Continuous long cycle				
			Propeller					Propeller				
Main energy carrier	Sec. energy carrier	Config.	Original	T.1	T. 2	T. 3	T. 4	Original	T. 1	T. 2	T.3	T.4
MGO	Hydrogen (1)	D-E	63	41	27	41	27	103	65	42	65	42
MGO	NMC-Li	D-E	99	61	37	61	37	163	97	58	97	58
Methanol	Hydrogen (1)	D-E	89	66	54	66	54	145	107	88	107	88
Methanol	NMC-Li	D-E	114	75	54	75	54	186	120	88	120	88

Both long cycles

None of the mono battery configurations are deemed feasible as they exceed the maximum added draught and extension length limitations. However, fuels like HVO and FAME show technical feasibility due to their similarity to MDO, provided the IMO continues to consider them as zero-emission fuels. Regarding the hybrid propulsion configurations, both MGO-H2(l) and DF-H2(l) are technically feasible for all propeller types, including the original propeller. This is mainly attributed to the relatively high energy density of methanol and MGO when compared to liquid H2.

It is worth noting that in all situations, the presence or absence of waste heat recovery (WHR) or regenerative braking, or a combination of these systems, does not directly determine whether the 40% CO_2 emission reduction target is met or not (see Table 7). However, this does not imply that installing these systems would not be beneficial. While they may contribute to additional complexity, volume, and weight in the overall machinery configuration, they may still provide other advantages and improvements.

Table 7: CO_2 emission reduction, green: configurations technical feasible

			Propeller				
Converter	Fuel	Conf.	Original	1	2	3	4
ICE	MGO	D-D	0%	19%	31%	19%	31%
ICE	MGO	D-E	-4%	16%	28%	16%	28%
ICE	HVO	D-E	90%	92%	93%	92%	93%
ICE	FAME	D-E	93%	94%	95%	94%	95%
ICE	DF	D-E	16%	32%	42%	32%	42%
PEMFC	Hydrogen	E	100%	100%	100%	100%	100%
Battery	NMC-Lithium	E	100%	100%	100%	100%	100%

100hr long cycle

The dual fuel configuration can achieve a 40% reduction in CO_2 emissions only when combined with the application of propeller type 2(4.0D). This is because carbon is still present in methanol and the pilot fuel, necessitating a larger diameter propeller to reduce energy consumption during the cycle. For a mono-fuel hydrogen configuration, upgrading the propeller to type 1 and type 2 is required to prevent exceeding the maximum extension limits. On the other hand, the hybrid configuration MGO-NMC-Li is feasible for all propellers, primarily due to MGO's high energy density, which requires only a small amount of energy from batteries. However, the hybrid configuration DF-NMC-Li is feasible only with propeller type 2, owing to the lower energy density of the batteries and methanol in comparison to MGO.

Continuous long cycle

The DF configuration can be feasible if combined with a type 2 propeller, even though it requires hull extension or storage in the fish hold. However, using H2(l) as a mono fuel is not technically feasible for any propeller type, as it exceeds the extension length or results in too much lost volume in the fish hold. The technically feasible hybrid configurations are generally similar to the 100hr long cycle, with the exception of DF-NMC-Li. This configuration requires additional volume of methanol compared to MGO, leading to the need for additional energy from batteries. Consequently, DF-NMC-Li is only feasible with the type 2 propeller.

Since the mono fuels use the same emission factor for both 100hr and continuous long cycles, their CO_2 emission reductions are equal. As previously mentioned, the hybrid fueled configurations are designed to achieve a 40% CO_2 reduction, and thus, their emission reductions are not visualized, as they all achieve the same reduction target of 40%. For the WHR systems, the battery is not taken into account since it does not have enough heat flow in the exhaust.

If it is found that the proposed configuration meets the requirements, it is considered technically feasible. Subsequently, further analysis will be conducted to assess the economic performance of the different configurations. The unfeasible configurations will be excluded from the scenarios which follow in the upcoming sections. Table 8 summarizes the technical feasibly propulsion configurations. Based on these developments it is assumed that using a larger diameter propeller is highly cost-effective regardless of the chosen energy carrier and thus it was decided to further analyze the configuration with the type 2 and type 4 propeller applied. Figure 3 demonstrates the economic performance of the 100-hour and continuous long cycle, combined with either a type 2 or type 4 propeller, for all technical feasible propulsion configurations. Figure 4 represents the total cost of owner ship, minus the remaining value of the ship including its propulsion configuration, (Equation 4).

Table 8. Technically feasible configurations

			100 hr long cycle	Continuous long cycle
	Fuel	Config.	Propeller type	Propeller type
Mono	HVO	D-E	Original, 1,2,3,4	Original, 1,2,3,4
	FAME	D-E	Original, 1,2,3,4	Original, 1,2,3,4
	DF	D-E	2,4	2,4
	Hydrogen	E	1,2,3,4	-
Hybrid	MGO-H2	D-E	All	All
	MGO-NMC-Li	D-E	2,4	2,4
	DF-H2	D-E	All	All
	DF-NMC-Li	D-E	1,2,3,4	2,4

A number of trends can clearly be spotted for the long term 15 year projection in Figure 3. First, the new build vessel surpasses all retrofit configurations in performance, primarily due to two factors. Firstly, the maintenance costs of the hull, including auxiliary systems, are significantly lower compared to retrofit configurations due to the age of the hull and systems. Secondly, fuel costs are low because MGO is relatively inexpensive, and the energy consumption is minimized due to the hull being optimized for a 4.0 meter diameter propeller. In contrast, the DF hybrid configurations yield poorer results compared to the MDO hybrid configurations. This is directly attributed to methanol being a more expensive fuel than MGO, and the carbon emission tax not compensating for the equal amount of emissions generated by both fuels. Although the HVO and FAME show promising numbers, they still exhibit a significant operational increase compared to the original configuration. However, over the long term, this difference diminishes as the emission tax rises. The TCO analysis for the 100-hour long cycle indicates that while the new build vessel has low operational costs, its performance is somewhat hindered by a high TCO resulting from substantial capital expenses in 2023. Despite higher operational expenses, the HVO and FAME demonstrate promising TCO lines due to being drop-in fuels, which require lower capital expenses. The MDO-Hydrogen, despite having higher capital expenses compared to fuels like MGO, HVO, FAME, or DF, shows good results owing to the low forecasted electricity prices.

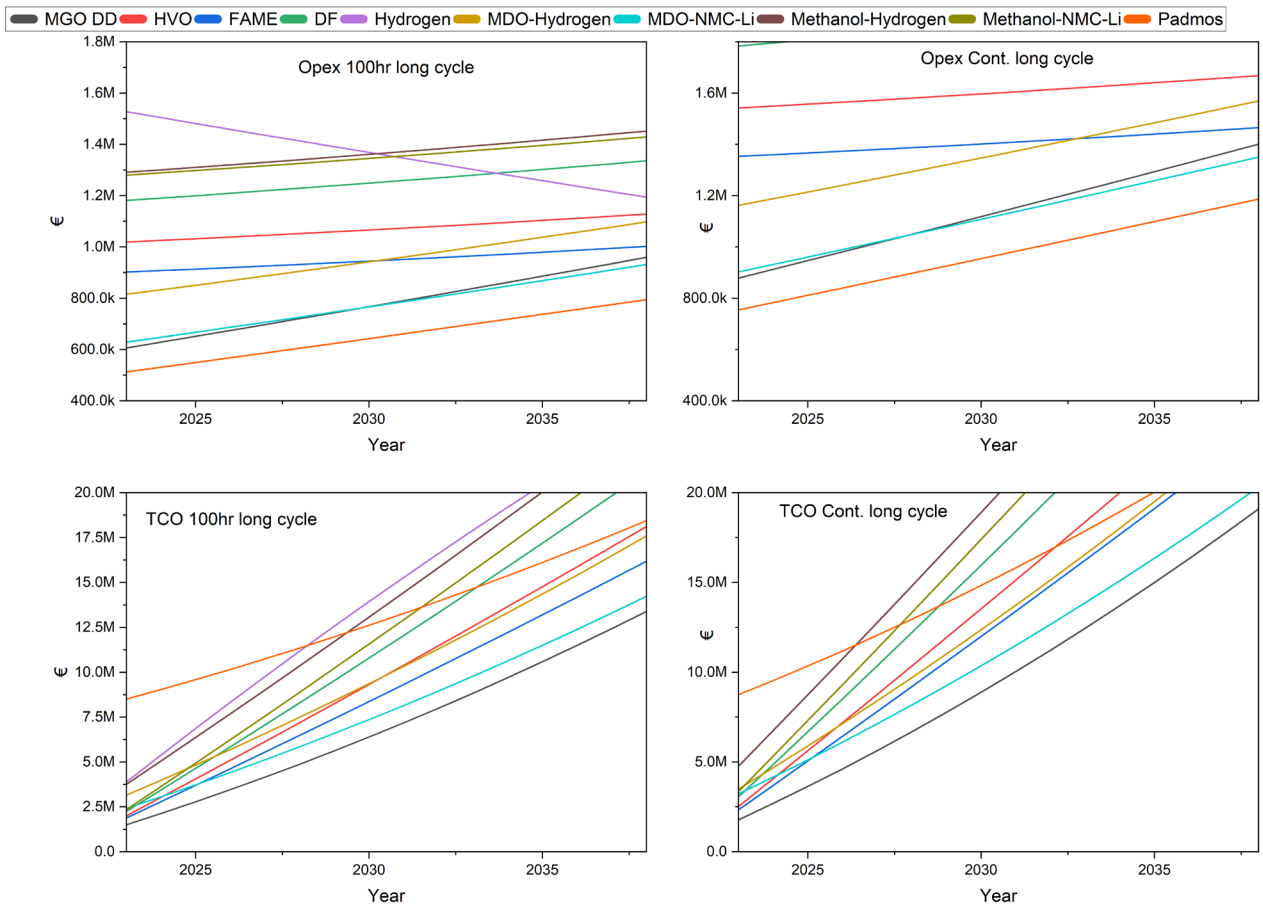

Figure 3: Opex and TCO, for type 2 propeller, 100hr and continuous long cycles, including new build vessel. The MGO DD is the reference to original costs

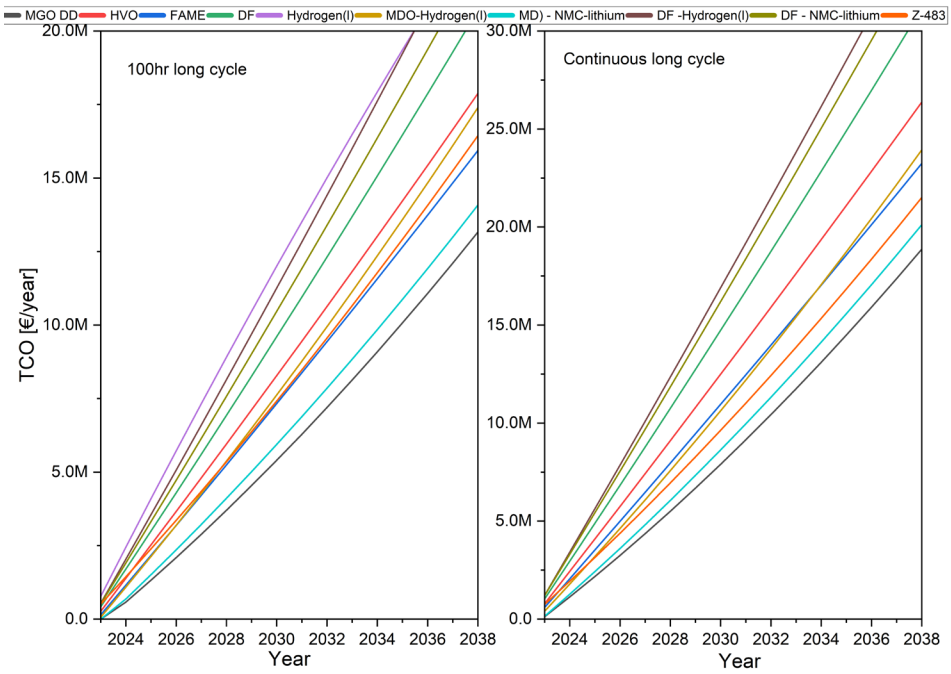

Figure 4: TCO – remaining value, for type 2 propeller including new build vessel. The MGO DD is the reference to original costs

Based on Figure 4 a short description is provided on what can be concluded when including the remaining value of ship and propulsion configuration into the TCO. In contraction to Figure 3 the high capital expenses in year 2023 are roughly included for in these figures. The hybrid MDO-NMC Li option shows promising performance despite its high capital expenses in 2023, this is again assumed to be caused by the low forecasted electricity. It is important to note that the average battery life is 15 years for the two long cycles, depending on the number and types of charges and charges. Therefore if, for any reason, there is a desire to proceed with the vessel, it would require a significant capital investment for the battery configurations. This is not the case for the other options. The options for mono hydrogen can be concluded to be technically or economically not feasible using the forecasted parameters from Table 3. The drop in fuels HVO and FAME actually show to be a very good option, but as mentioned their TTW factor is very sensitive to interpretation of IMO regulations, and thus could result in not being technically feasibly in 2030 when regulations change. To eliminate this uncertainty, an alternative option could be chosen, such as methanol. The main drawback of this option is the currently predicted higher energy carrier prices, which consequently increase the TCO.

CONCLUSIONS

This study employed an assessment model to evaluate various technical configurations of energy carriers, energy converters, and energy reduction methods on Dutch beam trawlers. The findings include analyses performed on different emission reduction techniques for a case vessel operating under either a continuous or 100-hour operational profile.

Technical Feasibility

Both long cycles:
None of the mono battery configurations are feasible due to exceeding the maximum added draught and extension length. However, fuels such as HVO and FAME are technically feasible as long as they are considered zero emission fuels by the IMO. The hybrid propulsion configurations MGO-H2(l) and DF-H2(l) are technically feasible for all propeller types, including the original propeller, due to the relatively higher energy density of Methanol and MGO compared to liquid H2. It can also be concluded that the implementation of WHR or regenerative braking systems, or a combination of both, does not determine whether the 40% CO_2 emission reduction target is met or not. However, installing these systems will contribute to additional complexity, volume, and weight of the overall machinery configuration.

100hr long cycle:
Dual fuel configuration only achieves the 40% CO_2 emission reduction target when combined with propeller type 2(4.0D) to reduce energy consumption. The mono-fuel hydrogen configuration requires propeller upgrades to prevent exceeding the maximum extension. The hybrid configuration MGO-NMC-Li is feasible for all propellers due to the high energy density of MGO, requiring only a small amount of energy from batteries. The hybrid configuration DF-NMC-Li is only feasible with propeller type 2 due to the low energy density of the batteries and methanol.

Continuous long cycle:
The DF configuration, when combined with a type 2 propeller, results in a feasible configuration, although hull extension or storage in the fish hold may be required. The mono fuel H2(l) is not technically feasible for any propeller type due to exceeding the extension length or losing volume in the fish hold. The technically feasible hybrid configurations are similar to the 100hr long cycle, except for DF-NMC-Li, which requires additional volume due to methanol requirements. The energy scale of batteries is such that this hybrid configuration is only feasible with a type 2 propeller.

Economic feasibility

Depending on the amount of available financial resources, available subsidy, and to what extent one is willing to take risks, the following conclusions can be made for different categories of initial capital expenses:

€0-€2.5M
The cheapest option to meet the 2030 regulations is the switch to bio-diesels HVO and FAME. Because these options are fully drop-in, there is no need for significant investments in system and vessel conversion, which applies to both types of long cycles. However, a major drawback of this strategy is the sensitivity to future regulations. This is partly due to the fact that the low CO_2 emissions for these fuels are entirely determined by regulations and the limited availability of raw materials. As a result, it is possible that within a short period, this option will no longer ensure IMO compliance.

A second option that can be recommended for any type of fuel and long cycles is to increase the propeller nozzle diameter. Although the Orcan WHR is estimated to have a payback period of 8-9 years (100-hour cycle) and 5 years (continuous cycle),

the investment of approximately €250k is still significant and does not determine compliance with the IMO regulations. Although in the long run the Orcan will result in a reduction of TCO compared to not applying it.

For both long cycles an option which requires more initial investments although less sensitive to regulations and can be cheaper in the long run is the conversion to methanol dual fuel configuration or to hybrid MDO-battery option, this applies to these configurations with 4.0m diameter propeller. The methanol option requires a lower investment, but the MDO-battery option outperforms it despite the high initial investment, thanks to the low predicted operational costs mainly caused by low forecasted electricity prices.

€2.5M+
In addition to the retrofit options, this option also includes the possibility of building a new ship. Once again, it is recommended to use a larger propeller for all configurations. Looking at Figure 3 and 4, it can be observed that in the long term, both types of long cycles show that the hybrid MDO-battery and the new build options deliver the best results in terms of TCO. For both options, it is again noted that they will be less sensitive to future prices of alternative fuels or the impact of (inter)national regulations on tax emissions.

In the assessment between the retrofit option to MDO-battery and the newbuild, it should be considered that after the assumed 15-year lifetime, the retrofit option will have virtually no remaining value, and the hull of the ship will be technically written off due to its age. This is not the case for the newbuild option, which still holds significant remaining value and is technically capable of many more years of service, provided it is well-maintained. As calculated with this model, no attempt has been made to calculate the labor hours required for installing the new propulsion configuration. However, the mentioned newbuild price does include the total cost of materials and labor. As a result, the lines for retrofit and new build may give a distorted picture. Therefore, despite the ease of saying it and the possibility of achieving it financially, committing the company to a large debt for many years, a newbuild ship is considered a better option when considering costs and lifespan.

Energy carrier storage
Due to practical considerations, it is not advised to use both the net store and fish hold to store the energy carrier. The costs to extend the vessel are very small compared to the costs for new propulsion configurations. This trend means that if one decides to extend the vessel, the extension length is not that important when looking at costs. This also reinforces why you wouldn't want to use a net store if you extend, since the costs to prevent giving up such a practical volume are very low.

The practical influence of using the fish hold is the reduction of storage volume for fish boxes. The practical influence of hull extension is a potential increase in operational costs due to increased hull resistance. The increase in operational costs, in reference to the original configuration, is very small. Only in the absence of financial resources would the choice be made to store the energy carrier in the fish hold. However, if an owner is convinced to have an excessively spacious fish hold and only a small additional volume is needed for energy carrier storage, then the fish hold can also be used.

CONTRIBUTION STATEMENT

Arnoud de bruin: Conceptualization; Investigation, Methodology, Software, Writing – Original Draft. **Walter van Harberden:** Conceptualization; resources; supervision; writing – review and editing. **Austin A. Kana:** Conceptualization; supervision; writing – review and editing.

ACKNOWLEDGEMENTS

This work was performed as part of the MSc thesis for the lead author, (de Bruin, 2023). The thesis was performed in Marine Technology at Delft University of Technology and the authors would like to acknowledge both Delft University of Technology and Padmos for their support of this research.

REFERENCES

Benvenuto, G., Trucco, A., Campora, U. (2016). Optimization of waste heat recovery from the exhaust gas of marine diesel engines". In: *Proceedings of the Institution of Mechanical Engineers, Part M: Journal of Engineering for the Maritime Environment* 230(1).

de Bruin, A. (2023). Technical and economical feasibility study on reducing CO_2 emissions of Dutch beam trawlers. *MSc thesis. TU Delft.*

Dierickx, J., Verbiest, J., Janvier, T., Peeters, J., Sileghem, L., Verhelst, S. (2021). Retrofitting a high-speed marine engine to dual-fuel methanol-diesel operation: A comparison of multiple and single point methanol port injection". *Fuel Communications* 7

DNV. (2019). Assessment of Selected Alternative Fuels and Technologies. Technical Report. June.

DNV GL. (2019). MARITIME FORECAST TO 2050, Energy transition outlook. Technical report.

DNV (2020). The role of combustion engines in decarbonization-seeking fuel solutions. *Maritime Insights*.

DNV (2022). Energy transition. Transition Outlook HYDROGEN FORECAST TO 2050. Tech. rep. DNV.

Enerdata. 2023. Carbon price forecast under the EU ETS. https://www.enerdata.net/publications/executive-briefing/carbon-price-projections-eu-ets.html

Freudenberg E-Power Systems (2022). *XMP 96P High power battery system*.

GRO. (2020). Global Renewables Outlook: Energy Transformation 2050. Report. International Renewable Energy Agency.

't Hart, P. (2009). Haalbaarheidsstudie Boomkorvissen op aardgas. Nederland Maritiem. Technical Report. September

IEA. (2022). World Energy Outlook. *International Energy Agency.*

IEA. (2023). End-use Prices Data Explorer. *International Energy Agency.*

IMO. (2020). Fourth Greenhouse Gas Study 2020. Technical Report. International Maritime Organization.

IMO. (2023). 2023 Resolution MEPC.377(80): IMO Strategy on Reduction of GHG Emissions from Ships. Report. July 7, 2023.

Laurens, J.M., Leroux, J.B., Coache, S. (2013). Design and retrofit of the propulsion of trawlers to improve their efficiency. DOI: 10.1201/b15813-136.

Leon, A (2008). *Hydrogen Technology: Mobile and Portable Applications (Green Energy and Technology)*. Springer.

LR. (2023). Lloyd's Register, Techno-Economic Assessment of Zero-Carbon Fuels report

Mat Nawi, Z., Kamarudin, S.K., Sheikh Abdullah, S.R., Lam, S.S. (2019) The potential of exhaust waste heat recovery (WHR) from marine diesel engines via organic rankine cycle. *Energy* 166.

MEPC 81. IMO. (2024). 2024: Marine Environment Protection Committee 81st session (MEPC 81)

Nooordzee Visie. 2022-2027. Noordzeebeleid, een halve eeuw in ontwikkeling URL: https://www.noordzeeloket.nl/beleid/

OECD. (2021). Policies for a Carbon-Neutral Industry in the Netherlands. Report.

Olusanya E., Akintande, O.J., Yaya, O.A., Ogbonna, A.E., Adenikinju, A.F. (2021). Energy pricing during the COVID-19 pandemic: Predictive information-based uncertainty indexes with machine learning algorithm. *Intelligent Systems with Applications.* 12.

Ouyang, T., Huang, G., Su, Z., Xu, J., Zhou, F., Chen, N (2020). Design and optimisation of an advanced waste heat cascade utilisation system for a large marine diesel engine. *Journal of Cleaner Production* 273.

Pavlenko, N., Searle, S. (2020). Assessing the potential advanced alternative fuel volumes in the Netherlands in 2030. *Working Paper 2020-12, International Council on Clean Transportation.*

Pendle Government, 2018. *Hydrotreated Vegetable Oil(HVO) fuel - briefing*.

Pothaar, M. (2022). Assessing the impact of sustainable fuels for Large Surface Combatants: A comparison between sustainable methanol and diesel for the Future Air Defender of the Royal Netherlands Navy. *MSc thesis. TU Delft.*

Rijksdienst voor Ondernemend Nederland. (2019). Duurzame kottervisserij op de Noordzee. Report.

Padmos. (1987) Dokmij Padmos designed and build beam trawler, drawing updated 2005.

Streng, J.E., Verbaan, J.H., Barendregt, I.P., Hopman, J.J., Kana, A.A. 2022. Alternative Energy Carriers in Naval Vessels. International Naval Engineering Conference and Exhibition (INEC2022). November 8 – 10. Delft, the Netherlands.

Taal, C., and Hoefnagel, A. (2012). Masterplan Duurzame Visserij: Haalbaarheidsonderzoek 2e fase. LEI Wageningen UR.

Terun, K., Kana, A.A., Dekker, R. (2022). Assessing Alternative Fuel Types for Ultra Large Container Vessels in Face of Uncertainty. *International Conference on Computer Applications and Information Technology in the Maritime Industries (COMPIT'22).* June 21-23. Pontignano, Italy.

van Urk. (2012). Ontwerp groene(energiezuinige) garnalenkotter. VCU. Project "Viskotter van de toekomst".

Welaya, Y., El Gohary, M., and Ammar, N. (2011). A comparison between fuel cells and other alternatives for marine electric power generation. *International Journal of Naval Architecture and Ocean Engineering* 3.

Proceedings of 15th International Marine Design Conference (IMDC-2024)
June 2-6, 2024
Amsterdam, the Netherlands

Ammonia Bunker Vessel: Ship Design for Energy Transition

Friederike Dahlke-Wallat[1], Katja Hoyer[1], Ljubisav Isidorović[1], Sophie Martens[1], Nathalie Reinach[1], Benjamin Friedhoff[1], and Igor Bačkalov[1,*]

ABSTRACT

This paper presents the basic design of a coastal ammonia carrier, intended to facilitate the energy transition by providing small-scale bunkering services to ferries in the South Baltic Sea. Due to the size and the purpose of the ship, a classic design process which builds on the experience and benefits from the prototype ships cannot be implemented in a straightforward manner. It follows that the energy transition may have a substantial impact on the design of otherwise conventional ship types, and that a hybrid approach to ship design comprising traditional design methodologies, advanced CAD tools, and experimentation is needed.

KEY WORDS

Ammonia; Energy transition; Bunker vessel; Coastal ship; CAMPFIRE.

INTRODUCTION

Alternative fuels play a major role in the energy transition of shipping, whereby one of the considered solutions is ammonia. While most of the ship design studies focus on the development of ships powered by novel fuels, this paper addresses the development of the infrastructure necessary for the reliable supply of such fuels, which also includes new bunker ships. Namely, the technologies for both the waterborne transport of liquid ammonia and the (ship-to-ship and truck-to-ship) refueling of ships with ammonia are being developed. This paper presents the design of a coastal ammonia bunker vessel, which is intended to provide small-scale bunkering services to future ammonia-powered ferries operating in the South Baltic Sea.

Liquefied gas carriers have been in use since the 1930s. The current fleet stands at approximately 1600 units (see SIGTTO, 2021), whereby some 200 ships can carry ammonia as cargo (see DNV, 2020). Thus, it may be concluded that substantial experience in design of ammonia carriers already exists. Such experience, however, may be of limited assistance in the present study, as the coastal ammonia bunker vessel has several unique features setting it apart from the conventional gas carriers. To compensate for the absence of an appropriate prototype ship, the design process described in the paper utilizes a "hybrid" approach, where the traditional ship design methodology (characteristic for the "design spiral") is blended with the advanced CAD tools, and the decision-making is supported by the statistical data on similar vessels, collected for the purpose of the study. Additional insights gained from the model tests are used primarily for the design appraisal but may also serve to assess the reliability of some of the classical methods for evaluation of powering requirements often used in early stages of design. Therefore, the purpose of the paper is two-fold. On the one hand, it explores the impact of energy transition on the design of bunker ships. On the other hand, it investigates the applicability of the classical methods in a design process which is handicapped by the lack of reliable data and by virtual nonexistence of the specific design guidelines.

[1] Development Centre for Ship Technology and Transport Systems (DST e. V.), Duisburg, Germany; ORCID: 0000-0002-1571-1361 (Friederike Dahlke-Wallat), 0000-0002-7366-1585 (Katja Hoyer), 0009-0001-1042-7134 (Nathalie Reinach), 0000-0002-5924-3563 (Benjamin Friedhoff), 0000-0002-6616-5516 (Igor Bačkalov)
* Corresponding Author: backalov@dst-org.de

Submitted: 12 February 2024, Revised: 12 April 2024, Accepted: 1 May 2024, Published: 18 May 2024

Conference paper, DOI: https://doi.org/10.59490/imdc.2024.829 e-ISSN: 3050-4864

OWNER'S REQUIREMENTS AND DESIGN OBJECTIVES

The "owner's requirements" follow from a scenario considered within the project. In future, the ammonia which can be supplied as fuel may be available from the tank storage in Peez situated in the vicinity of the port of Rostock. Alternatively, green ammonia may be collected from the offshore wind parks in the Baltic Sea. The ferries operating in the Baltic Sea have been identified as potential clients. Using Rostock as the homeport, the ship would supply with ammonia the long-range ferry sailing on the route Travemünde–Trelleborg and the short-range ferry sailing on the route Gedser–Rostock, see **Figure 1**. This determines the South Baltic Sea as the operational area of the ship. The principal "owner's requirement" – cargo capacity of the ship – is decided based on the estimated requirements for ammonia as fuel of the two ferries: 650 m^3 and 300 m^3 of ammonia would be necessary for the long- and the short-range ferries respectively to complete their round trips. It follows that the ship's cargo capacity should be around 1000 m^3.

Figure 1. Routes of (future) ammonia-powered ferries (base map: https://d-maps.com/).

The targeted ship speed is 11 kn. The ship is to be conventionally powered to overcome the initial "supply-demand" obstacle of the green transition, that is, the limited implementation of greening technologies due to the lack of infrastructure providing sustainable alternative fuels which is, in turn, justified by the limited number of potential customers. An ammonia bunker vessel powered by diesel and/or drop-in fuels would be, therefore, an initial step towards the acceleration of the shipping energy transition.

Design objectives follow from the owner's requirements. As with any cargo ship, the primary goal is to provide efficient transport and supply of the required cargo volume to the customers. The costs of the cargo tanks' production should be low and cargo space should be easy to maintain. Thus, the geometry and arrangement of cargo tanks – which have to comply with the safety regulations – have a decisive influence on the design as a whole. The design should facilitate the bunkering operations and safe handling of ammonia, which also affects the design of the cargo tanks as well as the deck arrangement and positioning of the related equipment. Considering that the cargo capacity is relatively small, the ship will be small as well, which is not favorable from the seakeeping point of view. The seakeeping performance of the vessel may be improved to an extent with a favorable hull form (or its operation may be limited with respect to the relevant seakeeping criteria).

SELECTION OF MAIN PARTICULARS

The ship design process usually benefits from a prototype vessel; if an adequate prototype is available, main dimensions may be selected with more confidence, weight estimation may be carried out with more precision, a range of technical solutions implemented on the prototype may be adopted, while the layout of the systems and the general arrangement of the prototype could be used as blueprints for the new design, and so on. It will be shown, however, that a suitable prototype is nonexistent in this case.

The initial selection of the main particulars (mass of displacement, length, beam, draught, depth, and hull form coefficients) was performed using the empiric regression formulae available from the literature (see Barras, 2006; Papanikolaou, 2014; Schneekluth and Bertram, 1998; Takahashi et al., 2006; Watson, 1998). However, it may be questioned how adequate such

formulae are considering that most of the authors used other ship types (such as e.g., general cargo ships and bulk carriers) in generating the underlying databases, with only occasional references to ship types which are only marginally relevant for this study, such as oil tankers. Additionally, it should be taken into account that some formulae were based on nowadays outdated hull forms and ship types, as pointed out by Papanikolaou (2014). Therefore, to verify the fitness of thus obtained values, a database containing the information on 41 relevant ships (liquefied gas carriers, chemical tankers, product carriers, bunker vessels, etc.) was created for the purpose of this study using a range of sources (hereinafter "DST database"). The features of the database are reported in the Appendix to this paper.

Assuming that the mass of deadweight is approximately:

$$m_{DWT} \approx 1.1 \cdot m_{cargo} \quad [1]$$

the first estimation of the mass of ship displacement may be done using the deadweight coefficient, expressed as the deadweight-over-displacement ratio:

$$\eta_{DWT} = \frac{m_{DWT}}{\Delta} \quad [2]$$

The deadweight coefficient may significantly vary depending on the ship type, so its value should be carefully selected. In the examined case, however, this is not a trivial task, because the references to adequate ship types (e.g., liquefied gas carriers) are seldom. In addition, a difference in density of liquefied ammonia (ρ_{NH3} = 0.68 t/m^3) when compared to LPG (ρ_{LPG} = 0.525–0.58 t/m^3) and LNG (ρ_{LNG} = 0.43–0.48 t/m^3) exemplifies the uncertainty related to a proper selection of the deadweight coefficient. Barras (2004) reports η_{DWT} = 0.62 for "LNG or LPG ships". Takahashi et al. (2006), on the other hand, report η_{DWT} = 0.72 for LNG ships. In addition to the difference in cargo density, this value is found not to be relevant for the present study, as it was obtained by analyzing mostly very large ships: gross tonnage of more than 90% of the analyzed LNG ships was greater than 30000 GT, while small ships made less than 2% of the database used by Takahashi et al. (2006). On the other hand, the LPG carriers analyzed by Takahashi et al. (2006) feature two distinct groups of vessels: ships up to 50000 GT and ships around 100000 GT. Considering that only the smaller ships are of interest for the present study, a displacement-gross tonnage relation applicable to ships up to 50000 GT was established. Based on this Δ–GT relation and the available m_{DWT}–GT relation, it follows that the deadweight coefficient of LPG carriers (of up to 50000 GT) would be η_{DWT} = 0.625. Finally, the DST database of relevant ships shows that there is a strong correlation between the displacement of the ships and their cargo capacity (coefficient of determination of the regression line is R^2 = 0.955), see **Figure 2**, which can be expressed as:

$$\Delta = 1.6374 \cdot V_{cargo} - 219.73 \,. \quad [3]$$

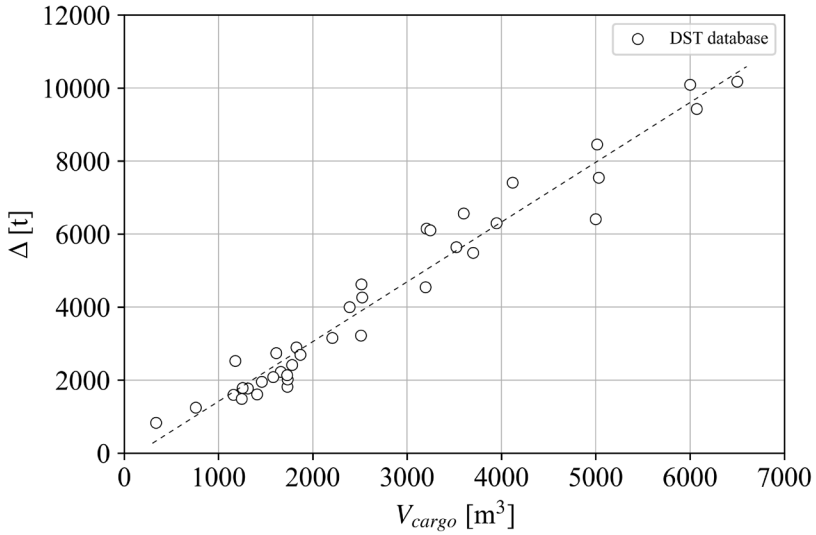

Figure 2. Correlation of ship displacement and volume of the cargo tanks of the relevant ships in the DST database.

The preliminary estimation of displacement is thus adopted as the average of the three values which are computed based on Barras (2004), Takahashi et al. (2006) for ships of up to 50000 GT, and equation [3]. This allows for assessment of the ship

length L which is computed as the average of five values ranging from 55.7 m to 60.8 m, obtained by regression formulae given in Papanikolaou (2014), Takahashi et al. (2006), and Watson (1998). The ship beam B is estimated based on considerations of Takahashi et al. (2006), and Watson (1998). The block coefficient C_B is decided based on the range of recommendations (mostly related to the Froude number of the ship) given in Schneekluth and Bertram (1998) and Watson (1998). The longitudinal center of buoyancy LCB is estimated based on the recommendations given in Schneekluth and Bertram (1998) and Papanikolaou (2014). Once the values of Δ, L, B, and C_B are known, calculating design draught d is straightforward. Nevertheless, each of the parameters could be subject to further refinement. In addition, even though the values of some of the parameters, such as the block coefficient, may be indicative of the existing designs if obtained by empiric formulae, they may as well be a matter of decision which deviates to an extent from the calculated values, depending on the targeted performance. A similar argument applies to the waterplane area coefficient C_{WL} which may be calculated using the empiric formulae as well (such as the ones provided by Papanikolaou, 2014) but may be also reconsidered in light of a specific design aspect. For instance, the C_{WL} value may be tuned aiming at improved seakeeping performance: to improve seaworthiness and diminish the resonance of heave and pitch in head seas, the non-dimensional natural heave and pitch periods should be as short as possible which may be achieved by the increase of the waterplane area coefficient (with unchanged values of the main dimensions, displacement, and speed). The midship area coefficient C_M is calculated as the average of three values obtained using formulae given in Schneekluth and Bertram (1998). The depth of ship D, as a minimum, should comply with the requirements of the International Convention on Load Lines (ICLL, 2003) for Type A ships. The first estimate of the main particulars is reported in **Table 1**.

Table 1: First estimate of the main ship particulars

Cargo capacity	V_{cargo}	1000 m^3
Mass of deadweight	m_{DWT}	750 t
Displacement	Δ	1275 t
Length	L	58 m
Beam	B	10.5 m
Draught	d	3.26 m
Depth	D	3.87 m
Freeboard	f	0.61 m
Block coefficient	C_B	0.626
Waterplane area coefficient	C_{WL}	0.790
Midship area coefficient	C_M	0.969
Longitudinal center of buoyancy	LCB*	-2 %L

* In reference to midships

The estimated main particulars were subsequently compared to the trends observed in the DST database of relevant ships (note that the trendlines shown in **Figure 3** are indicative only and were not used in the calculation of the main particulars). **Figure 3a** and **Figure 3b** show that the first estimates of length and beam fit well into the trends detected for the existing ships. This may not be stated for the estimated design draught, which appears to be lower than what could be expected for the ship of the given cargo capacity, see **Figure 3c**. As previously pointed out, the draught depends on the block coefficient, provided that L, B, and Δ are fixed. However, there is no clear trend in the C_B values of the existing ships, as may be seen in **Figure 3e**. The scatter of C_B values is particularly large for ships of smaller cargo capacity, up to 2500 m^3. An increase of the draught would imply a further decrease of the (already relatively low) block coefficient, which could result in a loss of volume available for the cargo space, and, consequently, complex geometry and high production costs of cargo tanks. On the other hand, increase of the block coefficient would lead to a further decrease of the draught, which is generally favorable from the cargo stowage point of view but may lead to a higher frequency of slamming. Block coefficient is equally poorly correlated to the Froude number, see **Figure 3f**. The absence of correlation of C_B to both V_{cargo} and Fr, confirms that the block coefficient is often a matter of a deliberate choice rather than an outcome of a statistical analysis. Ship depth is also well correlated to cargo volume of the existing ships, see **Figure 3d**. A weaker correlation is found between the freeboard f and ship length, see **Figure 4**. A higher freeboard implies improved safety (greater righting lever, larger reserve buoyancy, and lower frequency of shipping of green water) but comes at a cost (e.g., increase of operational costs related to higher gross tonnage). The deviation of the freeboard of the existing ships from the minimum freeboard as prescribed by the International Convention on Load Lines (ICLL, see IMO, 2003) may be substantial and may vary considerably for the ships of approximately the same length. It follows that the selection of f and D is not straightforward and that it is probably guided by the suitability of space for cargo stowage. As a first estimate, the selected freeboard is close to the minimum value required by IMO (2003) since the trends observed for the existing ships of similar lengths comply well with the ICLL provisions.

Finally, it should be noted there are only two ships with $V_{cargo} \leq 1000$ m^3 in the DST database (i.e., less than 5% of the total number of ships in the database): a chemical tanker and a product tanker. This highlights the difficulty of finding an adequate prototype ship.

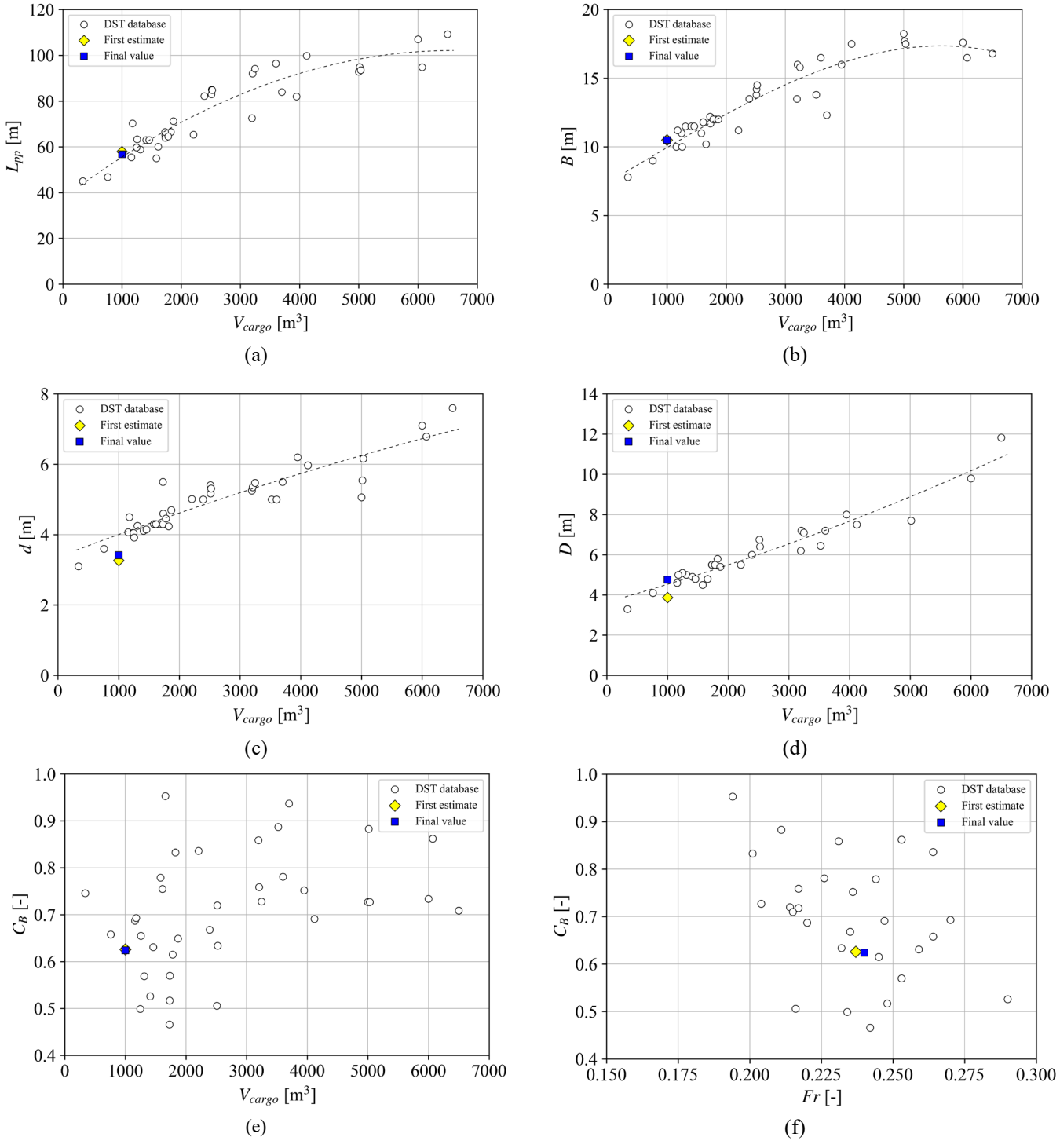

Figure 3. Comparison of estimated and adopted ship particulars to the trends observed in the DST database of relevant ships. Yellow diamonds correspond to the first estimate of the ship particulars (reported in Table 1). Blue squares correspond to the final values of the ship particulars (reported in Table 2).

Once the main particulars are selected, the preliminary stability assessment and resistance prediction may be performed, and the so-called "weight groups" may be estimated by means of approximate formulae, see e.g., Watson (1998) and Kalajdžić (2010). This allows for reassessment of the mass of displacement which can be calculated as the sum of the weight groups masses. At this stage, the weight groups are not detailed, primarily because the cargo tanks and the related systems and equipment are still undefined. For the sake of brevity these intermediate steps are not shown.

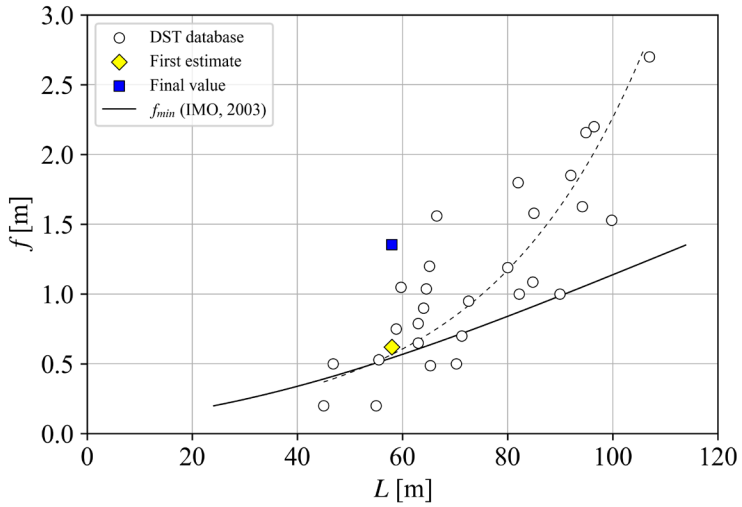

Figure 4. Comparison of estimated and adopted freeboard to the trend observed in the DST database of relevant ships (dashed line) and to the minimum values required by the International Convention on Load Lines (solid line). Yellow diamond corresponds to the first estimate of the ship freeboard (reported in Table 1). Blue square corresponds to the final value of the ship freeboard (reported in Table 2).

HULL FORM AND CARGO TANKS

In absence of the prototype vessel, the initial hull form (see **Figure 5**) was based on typical geometries of coastal cargo ships, as found in e.g., Journee and Versluis (1999). The hull form is subject to modifications which may be needed to accommodate sufficient space for cargo tanks and associated cargo-handling equipment and attain the targeted hull properties (hull form coefficients and the longitudinal center of buoyancy as given in **Table 1**). At this stage, the CAD tools (NAPA Designer and SolidWorks) are extensively used to check the effect of the hull modifications on the sizing and arrangement of the vessel's main "blocks": cargo space, machinery rooms, accommodation and working spaces, ballast and fuel tanks, etc.

The shape of cargo tanks intended for liquefied ammonia depends on whether the liquefaction is achieved by pressurizing the gaseous ammonia (resulting in fully pressurized ammonia), by pressurizing in combination with refrigeration (resulting in semi-refrigerated ammonia) or by refrigerating the ammonia to temperatures below -33°C at ambient pressure (resulting in fully refrigerated ammonia). All the above liquefaction methods are used on seagoing ships, whereby refrigeration is usually used for larger quantities while pressurizing is more often used for the transport of smaller ones. Thus, the decision on the cargo tank geometry and arrangement (which also affects the hull form) depends on the selection of the liquefaction approach. Pressurized and semi-refrigerated ammonia are carried in cylindrical pressure vessels (the so-called Type C tanks). Type C tanks may bring some benefits in view of the simpler (structural) design. On the other hand, the utilization of the hull volume available for cargo space is relatively low with the Type C tanks. Fully refrigerated ammonia is carried in prismatic Type A tanks where overpressure is managed by a boil-off management system, i.e. the re-liquefaction unit. The Type A tanks are self-supporting tanks, typically made of flat surfaces and shaped so as to maximize the space available for cargo. The prismatic tanks may allow up to 40% more cargo containment space (DNV GL, 2019). (For the main features of different types of cargo tanks used on liquefied gas carriers and typical design solutions see e.g. SIGTTO, 2021.) Characteristics of materials suitable for cargo systems of liquefied gas carriers (cargo tanks, process pressure vessels, and cargo piping) are detailed in the International Code for the Construction and Equipment of Ships Carrying Liquefied Gases in Bulk (IGC Code, see IMO, 2014). In view of the small cargo capacity, it was initially assumed that the ammonia would be pressurized and carried in Type C tanks. However, it will be shown that the final decision on the liquefaction method and, consequently, the design of the cargo tanks, depends on several design and operation aspects.

To attain sufficient volume of the cargo space and provide adequate room for the propeller, while maintaining the desired values of the block coefficient and the longitudinal center of buoyancy, it was necessary to increase the depth of the ship, from D = 3.87 m to D = 4.77 m. It was previously indicated that while the increase of freeboard is to the benefit of safety, it

also adds to the production costs (and some operational costs). Nevertheless, as it was pointed out by Schneekluth and Bertram (1998), the depth is the "cheapest" ship dimension since its increase results in a relatively small increase of steel weight. (Interestingly, the new depth value results in B/D = 2.2, which seems to be the most common ratio for the small gas carriers, see **Figure A1** in the Appendix to the paper.) Additionally, the raising of the deck caused the distortion of the hull lines which led to a decrease of the wetted surface at the stern, which is beneficial from the ship resistance point of view. The evolution of the hull lines of the vessel – from the initial hull form (shown in gray lines) to the final hull form with the raised main deck (shown in blue lines) – is reported in **Figure 5**. The cross sections from "0" to "54" are equally spaced at 1 m distance; the section "-1" is at -1.55 m. In both cases, the sections are shown up to the main deck (i.e., the geometry of the poop and the forecastle is not shown). In addition to attaining the targeted values of C_B and LCB, a positive "side effect" of the hull modification is the increase of the waterplane area coefficient in comparison to the first estimate given in **Table 1**, which is beneficial from the seakeeping point of view.

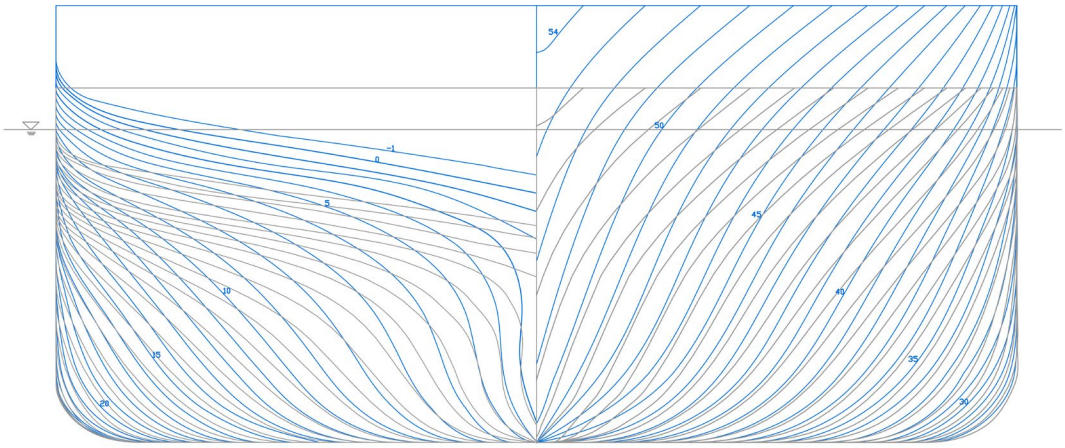

Figure 5. Body plan of the vessel. The initial hull form is shown in gray lines; final hull form is shown in blue lines.

The completion of the hull form was followed by the fitting of the cargo tanks. Despite the increase of the ship depth, the Type C tanks intended for pressurized ammonia could not be fitted without further considerable modification of the hull form. In order to comply with the ship survival capability and location of cargo tanks provisions of the 2014 IGC Code, that is, to attain the minimum distances between the cargo tanks and the hull, the diameters of the cylindrical tanks have to be limited. To attain the required cargo volume with the constrained tank diameters, the length of the cylinders has to be increased; this, however, results in the substantial loss of space available for forward and aft engine rooms. A compromise may be partly achieved by positioning the tanks higher relative to the baseline. In such a case, however, intact stability criteria cannot be satisfied. This led to reconsideration of the adopted liquefaction method.

Considering the toxicity of ammonia, a major factor to be accounted for when it comes to the selection of the liquefaction method is safety. As observed by the Society of International Gas Tanker & Terminal Operators, despite a good safety record of gas carriers, the risks related to accidents are greater in ports than at sea (see SIGTTO, 2021). The bunker vessel which is the subject of this study is supposed to serve passenger ferries; the vessel should, thus, operate in the vicinity of the passenger terminals in Travemünde and Rostock where an average of 10 and 20 passenger ships port calls respectively are recorded daily. Therefore, the consequences of potential accidents involving leakage of ammonia may be grave in view of the possibly large number of casualties. The spreading of ammonia in the event of leakage, however, differs depending on the liquefaction method. In the event of refrigerated ammonia leakage, the ammonia gas cloud forms due to evaporation of the cold pool of spilled ammonia (**Figure 6b**). The gas cloud formed as a consequence of pressurized ammonia leakage is significantly larger as it is fed by both a high flow velocity jet from the damaged tank and the evaporation of the pool of spilled ammonia (see **Figure 6a**). Once evaporated ammonia reaches ambient temperature, it will rise – this process will, however, take more time (i.e., the exposure to ammonia will be prolonged) if the ammonia was pressurized.

Some operational aspects may also affect the choice of the liquefaction method. Considering that the vessel should operate in ports and in a coastal area with dense traffic, less obstruction of the view from the wheelhouse could be advantageous. This becomes particularly important in view of complex systems and numerous equipment for handling ammonia and bunkering operations arranged on the main deck. Cylindrical tanks, required for carrying the pressurized ammonia, would have to be positioned higher with respect to the baseline, which could have a negative impact on the visibility from the bridge. Furthermore, in direct relation to the vessel's purpose – bunkering – it is to be noted that at high pressures required for compression liquefaction the dry disconnect couplings of bunkering hoses cannot be manually operated by the crew.

Therefore, based on the considerations given above (space utilization, safety, and operational aspects) it was decided to change the liquefaction method used on the bunker vessel. Instead of carrying pressurized ammonia in the cylindrical Type C tanks (**Figure 7a**), the vessel would carry refrigerated ammonia in the prismatic Type A tanks (**Figure 7b)** which would be a common solution on large liquefied gas carriers, rather than on small ones (see SIGTTO, 2021). The space utilization with Type A tanks would be indeed much better: the total length of the Type A tanks is 26.5 m, while the length of the Type C tanks would be (at least) 33.4 m. The visibility from the bridge would also improve: the highest point on the tank covers relative to the baseline would be 6.68 m for Type A tanks, as compared to (at least) 8.1 m for Type C tanks. The stability and survivability requirements can be satisfied in all relevant loading conditions if Type A tanks are utilized.

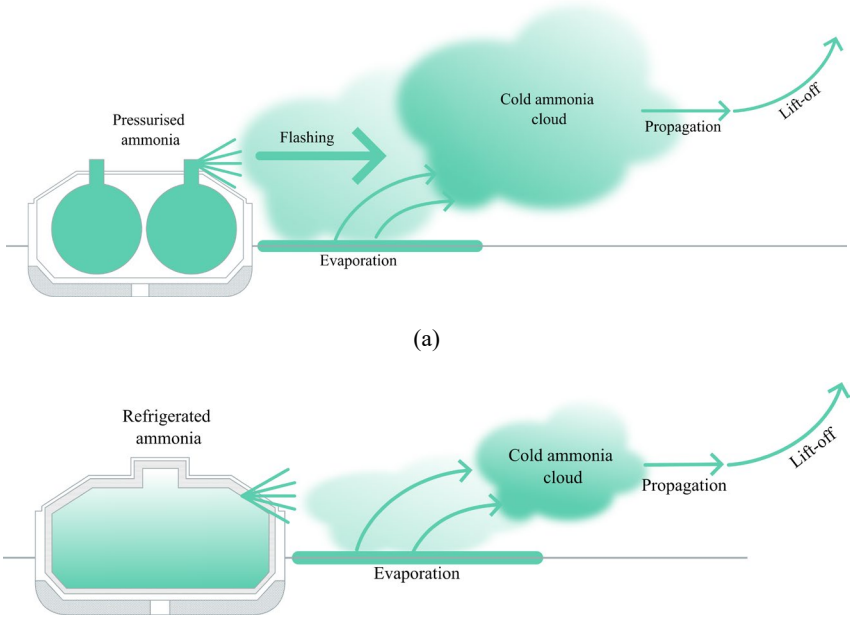

Figure 6. Spreading of ammonia in case of leakage of (a) pressurized ammonia and (b) refrigerated ammonia.

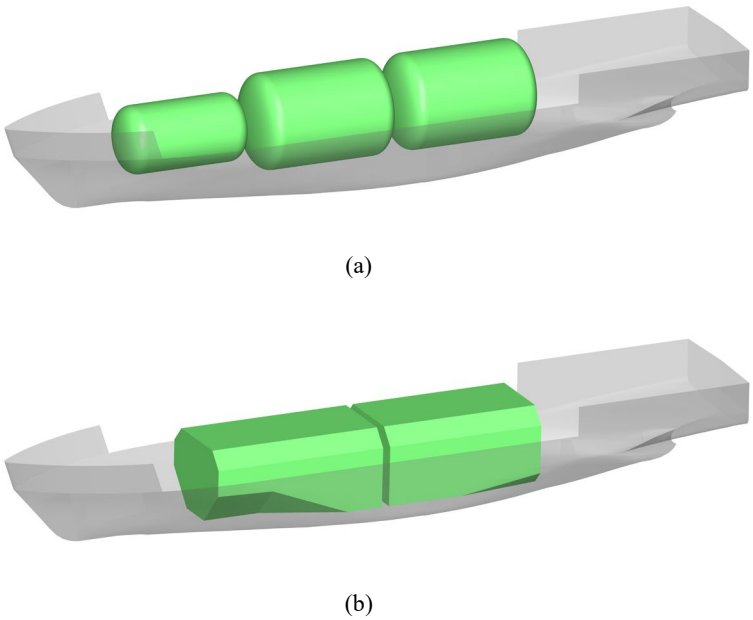

Figure 7. Comparison of the space requirements for (a) pressurized ammonia carried in the Type C tanks and (b) refrigerated ammonia carried in the Type A tanks.

This allows for a more precise estimation of weight groups' masses and centroids. The mass of the cargo tanks, which form a sizable part of the lightship mass and thus can significantly affect a range of design aspects, can be assessed based on the detailed CAD model of the tanks built in SolidWorks. The specific equipment and systems used for handling of ammonia could be itemized. Other weight groups may be determined with more reliability as well. The mass of machinery may be based on the actual main engine; the corresponding fuel consumption allows us to determine the required fuel supplies more precisely. The actual dimensions of the accommodations, poop and forecastle may be used in steel weight estimation, etc. The knowledge of the weight groups' masses and centroids makes it possible to determine the floating position of the ship in a range of relevant loading conditions and to calculate the ship stability parameters and compare them to the applicable regulatory requirements.

The main ship particulars, as adopted, are given in **Table 2**. The final value of the mass of displacement is less than 5% greater than the initially estimated value reported in **Table 1** (despite the increase of the depth), which is generally regarded to be within the acceptable boundaries. Greater differences would indicate that the main dimensions were not properly selected, which would require the process to be restarted, instead of advancing to the next stage of design. Considering the large initial uncertainty related to the type and size of cargo tanks and the related equipment, the questionable adequacy of formulae used in early stages, as well as the lack of an adequate prototype vessel which would be normally used in the estimation of the weight groups, the relatively low deviation of the mass of displacement from the preliminary assessment is most certainly a positive, yet (admittedly) somewhat unexpected outcome.

Table 2. Main ship particulars

Cargo capacity	V_{cargo}	1000	m^3
Mass of deadweight	m_{DWT}	746.4	t
Displacement	Δ	1337.8	t
Length over all	LOA	58	m
Length between perpendiculars	L_{pp}	56.869	m
Beam	B	10.5	m
Draught	d	3.415	m
Depth	D	4.77	m
Freeboard	f	1.355	m
Block coefficient	C_B	0.624	
Waterplane area coefficient	C_{WL}	0.833	
Midship area coefficient	C_M	0.992	
Longitudinal center of buoyancy	LCB*	-2.1	$\%L$

* In reference to midships

DECK ARRANGEMENT

One of the design objectives is safe and efficient handling of ammonia in the course of loading and bunkering operations. This requires the vessel to be outfitted with specific systems and equipment, which ought to be adequately arranged on the main deck. To facilitate a fitting positioning of the installations for handling of the ammonia, the 3D model of the ship built in SolidWorks was utilized, see **Figure 8**. The systems include manifolds (position 1 in **Figure 8**) to connect the bunker line (represented in green), the purge line (represented in light blue) and the vapor return line (represented in yellow) suitably positioned along the parallel midship. A vapor return line is necessary as during bunkering no gaseous ammonia in the customer's bunker tank may be vented to the open air; to avoid the pressure build-up, the gaseous ammonia shall be taken over by the bunker vessel. Via the purge line all lines can be purged with nitrogen. Via the condensate return line the reliquefied boil-off gas can be given back from the re-liquefaction unit in the forecastle to the cargo tanks. In case of an emergency such as tank over-pressure, both tanks are equipped with redundant pressure relief valves. The emerging ammonia is then led to the vent mast (position 2 in **Figure 8**). The IGC Code states that cargo tank venting openings "shall be arranged at distance at least equal to B or 25 m, whichever is less, from the nearest air intake, outlet or opening to accommodation spaces, service spaces and control stations, other non-hazardous areas, exhaust outlet from machinery or from furnace installations onboard" (IMO, 2014). Since the area around the manifold is regarded as a work area, the vent mast is placed furthest away.

In addition to the manifold, the vessel is equipped with a bunker arm (position 3 in **Figure 8**) to serve customers with a high freeboard. A set of all bunker lines is directly attached to the arm. Bunker hoses can be stored on deck. To keep a safe distance from customers, the bunker vessel has four Yokohama fenders (position 4 in **Figure 8**). The safe distance also ensures that the bunker hose is not pinched or kinked during the bunker process.

All the auxiliary equipment, such as the re-liquefaction unit and the nitrogen plant, is stored in the forecastle, away from the bunker area. Often, on board larger ships, there is a dedicated deck house in the midship area. For this design it is assumed that the vessel is mainly operated very close to the shore/the terminal and does not need the amount of inert gas that a large gas carrier would need. Also, the re-liquefaction unit is rather small, and the ammonia is only transported over a relatively short distance to the next customer.

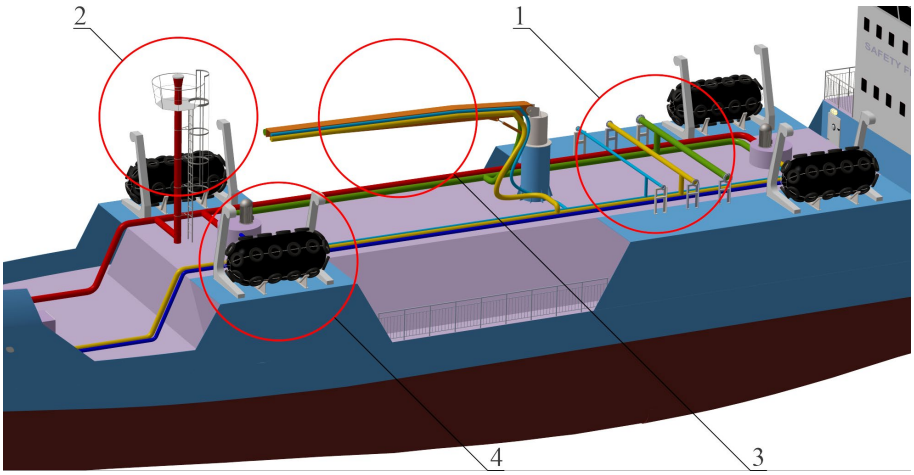

Figure 8. Simplified view of the main deck: arrangement of systems and equipment for handling of the ammonia

POWER PREDICTION AND MODEL TESTS

Ship resistance and power demand were estimated in each of the described design phases. The resistance estimations were carried out using the well-known empiric methods, such as the "Holtrop & Mennen" (see Holtrop, 1984) and the "Admiralty coefficient" approach (see Telfer, 1963) which is based on the data of comparable ships. Additionally, the resistance and propulsion model tests with a 1:14.5 scale model were performed in the large shallow water basin of DST, at two different water depths corresponding to h_w = 12.5 m and h_w = 5 m in full scale. Effective power calculated based on the resistance estimations made by the empiric methods and the model tests are reported in **Figure 9**.

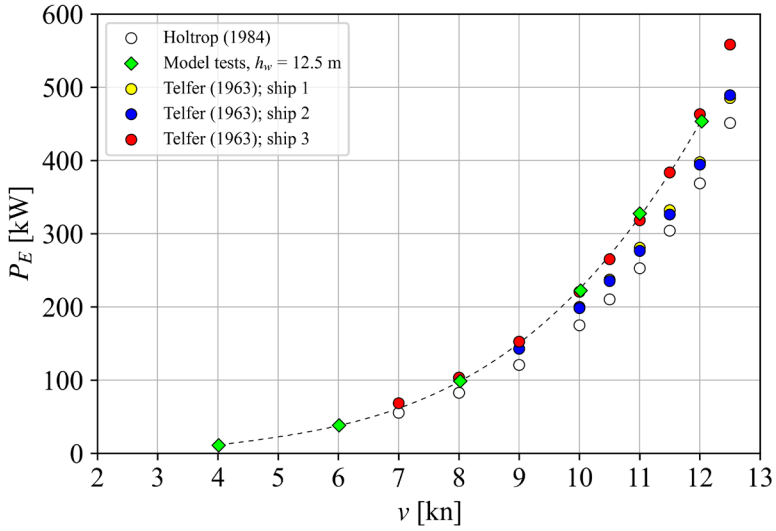

Figure 9. Comparison of effective power calculated using resistance estimations obtained with empiric methods and by means of model tests performed in the towing tank of DST.

The ship has a conventional drivetrain consisting of a diesel engine (691 kW@1406 rpm). The model was equipped with a four-bladed DST stock propeller (the propeller diameter being D_p = 1.84 m in full scale, and pitch ratio being P/D_p = 0.955). Since the main engine was selected based on the estimations done with empiric methods in the course of the basic design, the model tests were primarily used to verify if the predicted power would satisfy the owner's requirements. In addition, the model tests allow us to assess the reliability of the aforementioned empiric methods which are often used in the basic design. For instance, it may be observed that the Holtrop & Mennen method underestimates the resistance obtained in the model tests by some 20%. On the other hand, the best prediction was achieved using the Admiralty coefficient approach based on "ship 3" (red circles in **Figure 9**), which is indeed the most comparable one to the designed vessel (see **Table 3**).

Table 3. Features of the ships used in the ship resistance estimation based on the Admiralty coefficient approach.

		"ship 1"	"ship 2"	"ship 3"	design
L_{pp}	[m]	63.4	48	66	56.869
$L / \sqrt[3]{\nabla}$	[-]	5.62	4.71	4.95	5.21
B/d	[-]	3.58	3.53	3.41	3.07

Finally, the comparison of the total resistance recorded in model tests performed in two selected depths is reported in **Figure 10**. The chosen water depths are representative of the operational conditions in the designated area. As expected, a significant increase in resistance and, consequently, a reduction of speed in h_w = 5 m can be observed, which needs to be considered in the prediction of the operational profiles.

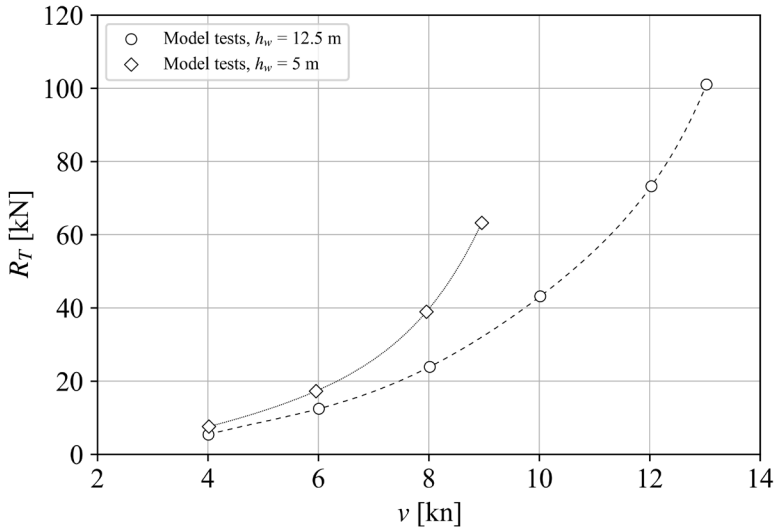

Figure 10. Comparison of total resistance obtained in model tests performed in the towing tank of DST in both tested water depths.

CONCLUSIONS

Energy transition of shipping goes beyond the modification of the ship propulsion and fuel systems and requires the development of the supporting infrastructure, including the vessels which could provide the bunkering service to ships utilizing novel fuels. The paper presented the basic design of a small ammonia bunker vessel, intended to provide ship-to-ship refueling services to future ammonia-powered ferries in the South Baltic Sea. Because of the size of the vessel (dictated by the cargo capacity at the lower boundary of capacities of the present ships) and its specific purpose (bunkering of passenger ships with toxic ammonia), the existing gas carriers could not be successfully used as prototypes. However, the formulae typically used in early stages of design (which may be found in the literature) proved to be robust enough to predict the vessel's mass of displacement and the main particulars with sufficient accuracy, despite not being developed with this specific ship type in mind. The inability to utilize the ship design spiral in a straightforward manner due to the absence of the prototype vessels was compensated for with an extensive use of CAD tools (NAPA Designer and SolidWorks) which facilitated architectural design of the vessel (i.e., arrangement of spaces and equipment) and minimized the uncertainties related to weight estimations.

The design is heavily influenced by the liquefaction method of ammonia, which in turn, depends on the ship operational profile and safety requirements. Even though liquefaction by pressurizing is typically used in maritime transport of smaller quantities of ammonia, in this case, the adopted liquefaction method was full refrigeration. Such a decision was driven by several design and operational aspects including much better cargo space utilization than it would be achieved by the pressurizing of ammonia, compliance with the survivability requirements of the IGC Code and intact stability requirements of the IS Code, more favorable dynamics of spreading of the toxic ammonia cloud in case of a spillage, and better visibility from the bridge (see Yang et al., 2022; SIGTTO, 2021; DNV, 2020; DNV GL, 2019). Again, the CAD tools enabled the sizing and positioning of the cargo tanks and arrangement of the associated systems and equipment, and fast verification of compliance with the design objectives and applicable regulations.

It is to be acknowledged that, considering the scarcity of adequate data which could be used in support of the decision-making, as well as the nonexistence of the design guidelines specifically intended for this kind of bunker ships, many decisions had to be made by the "designer" with the support of the CAD tools. This indicates that the design process could be further improved by implementing an automated multi-objective optimization (a "holistic ship design" as described in e.g., Papanikolaou, 2010; Marzi et al., 2018) provided that adequate software tools and computing resources are available. Such an approach allows for a fast analysis of dependencies between influential factors and exploration of a large number of (feasible) designs in search of an optimal solution. Nevertheless, regardless of accessibility of the tools and the implemented procedure, it is the designer who formulates the optimization criteria by considering the relevant regulatory, societal, and commercial aspects. In case of ammonia bunker vessel analyzed in this study, the formulation of criteria requires the knowledge of intricacies of energy transition, the understanding of operational risks associated with bunkering of ammonia, the specific environmental conditions in the operational area, etc.

The outcome of the study – presented in **Figure 11** – is a design which may be regarded as unconventional, primarily due to a fine hull form atypical for bunker ships and the adopted type of cargo tanks which is not common for small liquefied gas carriers. The success of the design was partly assessed with the model tests described in this paper, which addressed powering requirements in calm water. The design will be, however, the subject of the extended model tests which shall include the seakeeping performance and stability in waves of the vessel with partially filled cargo tanks. Only then, the success of the proposed design may be fully appreciated. Nevertheless, the outcome of the study indicates that the energy transition may require the development of new designs rather than reiteration of "off-the-shelf" ship design solutions.

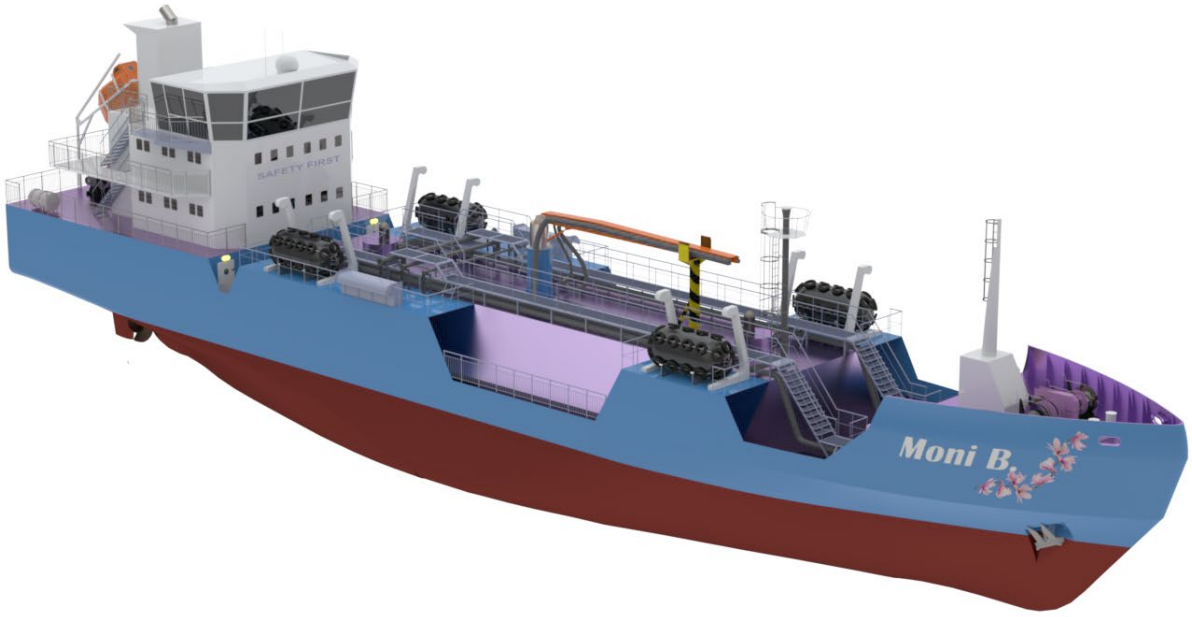

Figure 11. Final layout of the coastal ammonia bunker vessel

CONTRIBUTION STATEMENT

Friederike Dahlke-Wallat: Formal analysis, investigation, visualization, writing – original draft, writing – review & editing. Katja Hoyer: Formal analysis. Ljubisav Isidorović: Visualization. Sophie Martens: Formal analysis, investigation, writing – review & editing. Nathalie Reinach: Formal analysis, visualization. Benjamin Friedhoff: Funding acquisition, project administration, resources, supervision, writing – review & editing. Igor Bačkalov: Conceptualization, formal analysis, investigation, methodology, visualization, writing – original draft, writing – review & editing.

ACKNOWLEDGEMENTS

The research presented in this paper was funded by the German Federal Ministry of Education and Research (BMBF) within the framework of the hydrogen flagship project TransHyDE within the CAMPFIRE sub-project “Flexible NH3–refueling system” (No. 03HY209D).

REFERENCES

Barras, C.B. (2006). *Ship Design and Performance for Masters and Mates*. Second Edition. Oxford: Elsevier Butterworth-Heinemann.

DNV (2020). *Ammonia as a marine fuel safety handbook*. Retrieved from https://www.dnv.com/Publications/ammonia-as-a-marine-fuel-191385.

DNV GL (2019). *LNG containment systems: Finding the way for Type A*. Retrieved from https://www.dnv.com/expert-story/maritime-impact/LNG-containment-systems-finding-the-way-for-Type-A/.

Holtrop, J. (1984). *A statistical re-analysis of resistance and propulsion data*. International Shipbuilding Progress, 31(363), 272–276.

IMO (2003). *International Convention on Load Lines*. London: International Maritime Organization.

IMO (2014). *International Code for the Construction and Equipment of Ships Carrying Liquefied Gases in Bulk (2014 IGC Code)*. London: International Maritime Organization.

Journee, J.M.J. and Versluis, A. (1999). *Hull Form Series for SEAWAY*. Report No. 1206-M. Delft: Delft University of Technology, Faculty of Marine Technology, Ship Hydromechanics Laboratory.

Kalajdžić, I. (2010). *Cargo ships weight groups calculation*. Master thesis. Belgrade: University of Belgrade, Faculty of Mechanical Engineering.

Marzi, J., Papanikolaou, A., Brunswig, J., Corrignan, P., Lecointre, L., Aubert, A., Zaraphonitis, G., Harries, S. (2018). *HOLISTIC ship design optimisation*. Proceedings of the 13th International Marine Design Conference. Helsinki.

Papanikolaou, A. (2010). *Holistic ship design optimization*. Computer-Aided Design, 42(11), 1028–1044.

Papanikolaou, A. (2014). *Ship Design: Methodologies of Preliminary Design*. Dordrecht Heidelberg New York London: Springer.

Schneekluth, H. and Bertram, V. (1998). *Ship Design for Efficiency and Economy*. Second Edition. Oxford: Butterworth-Heinemann.

SIGTTO (2021). *Liquefied Gas Handling Principles on Ships and in Terminals*. Livingston: Witherby Publishing Group Ltd.

Takahashi, H., Goto, A., Abe, M. (2006). *Study on Standards for Main Dimensions of the Design Ship*. Technical note of National Institute for Land and Infrastructure Management. Tokyo: Ministry of Land, Infrastructure and Transport.

Watson, D.G.M. (1998). *Practical ship design*. Oxford: Elsevier Science Ltd.

Yang, M., Ng, C.K.L., Liu, M. (2022). *Ammonia as a marine fuel - bunkering, safety and release simulations*. Singapore: Singapore Maritime Institute.

APPENDIX

Features of the DST database of the relevant ships used in verification of the selected main particulars.

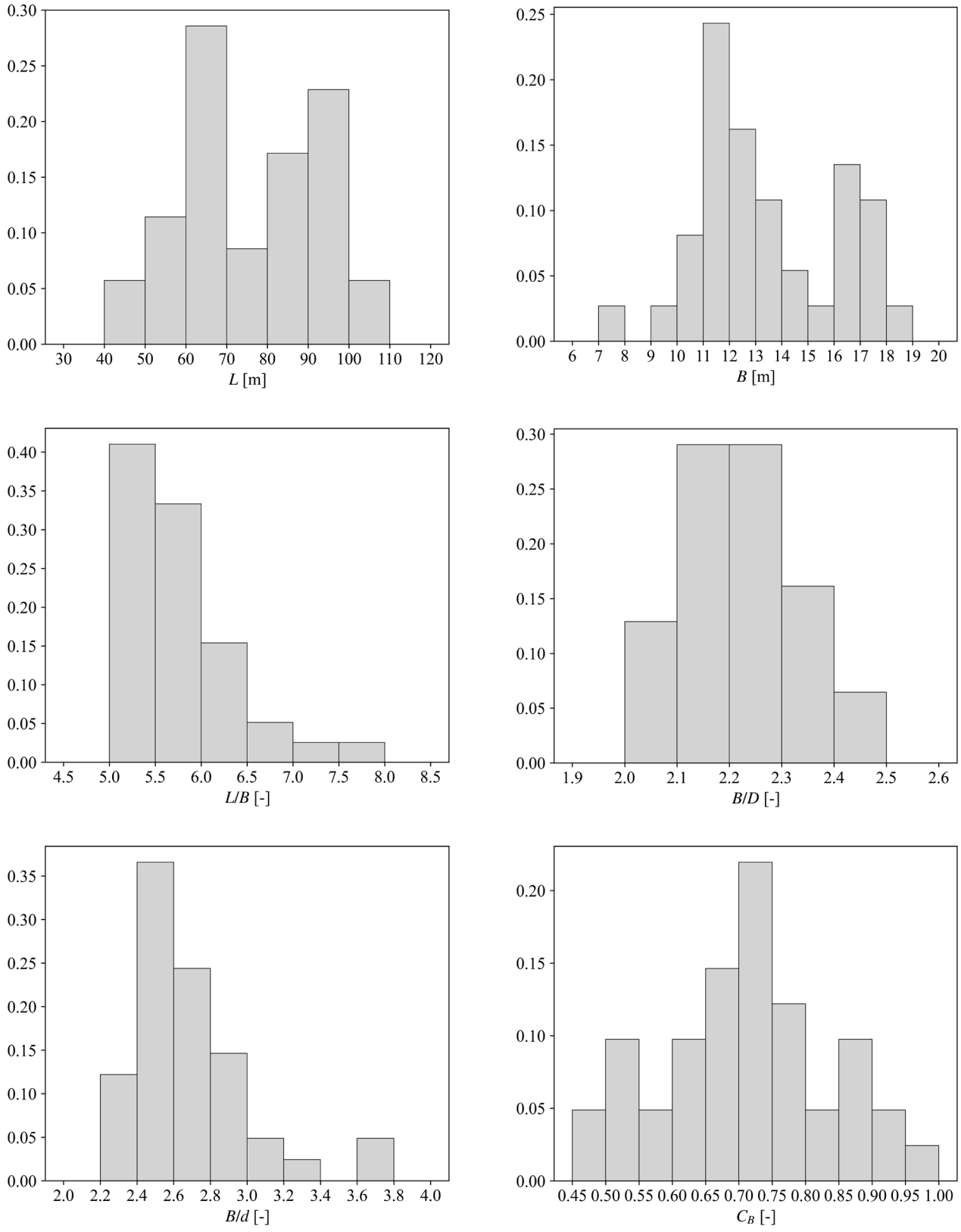

Figure A1. Distributions of the main dimensions, ratios, and hull form coefficients of the ships contained in the DST database of relevant ships.

Proceedings of 15th International Marine Design Conference (IMDC-2024)
June 2-6, 2024
Amsterdam, the Netherlands

Retrofit modeling for green ships

Julien J. M. Hermans[1] and Austin A. Kana[2,*]

ABSTRACT

This paper proposes a data-driven approach to reduce emissions in international shipping, aligning with the IMO's goal of achieving net-zero greenhouse gas emissions by around 2050. Digital twins (DTs) offer promise for maritime decarbonization due to their simulation and big data handling capabilities. However, fully realizing DTs for new-build is by definition challenging as it requires a real-time data connection. Thus, the research begins with retrofitting existing ships using operational data collected through Bunker Delivery Notes (BDNs), a mandatory method for larger ships since January 2019. The proposed framework constructs digital models to support the retrofit DT, that are tested on a 300m bulk carrier. A fuel consumption model is built using a gray box approach, while various wind-assisted ship propulsion systems are modeled using a white box approach. The study evaluates the design implications and emissions reduction potential of implementing these systems.

KEY WORDS

Retrofit; alternative power and energy; wind-assisted ship propulsion; bunker delivery notes; gray box modeling; Digital Twin for Green Shipping DT4GS.

NOMENCLATURE

ANN Artificial neural network

BBM Black box model

BDNs Bunker delivery notes

CII Carbon Intensity Indicator

DM Digital model

DS Digital shadow

DT Digital twin

DT4GS Digital Twin for Green Shipping

EEXI Energy Efficiency Existing Ship Index

FCM Fuel consumption model

GBM Gray box model

GDR Gap distance ratio

GHG Greenhouse gas

IMO International Maritime Organization

LLs Living labs

MAPE Mean absolute percentage error

WASP Wind-assisted ship propulsion

WBM White box model

[1] Delft University of Technology, Department of Maritime and Transport Technology, Delft, the Netherlands
[2] Delft University of Technology, Department of Maritime and Transport Technology, Delft, the Netherlands; ORCID: 0000-0002-9600-8669
[*] Corresponding Author: a.a.kana@tudelft.nl

Submitted: 23 February 2024, Revised: 19 April 2024, Accepted: 1 May 2024, Published: 23 May 2024

Conference paper, DOI: https://doi.org/10.59490/imdc.2024.890 e-ISSN: 3050-486

INTRODUCTION

During the United Nations Climate Change Conference near Paris in 2015, the Paris Agreement was adopted by the 196 parties present which stated that global warming must be limited to below 2°C (EC, 2015). Unfortunately, international shipping together with international aviation were not taken into account in this agreement. As a reaction, the International Maritime Organization (IMO) adopted in 2018 an initial strategy in order to reduce greenhouse gas (GHG) emissions by international shipping (IMO, 2018).

The goal of this initial strategy is set on a reduction of GHG emissions by 50% in 2050 compared to emission levels of 2008. During their annual meeting in July 2023, the strategy was revised to net-zero GHG goal close to 2050, addressing the IMO's environmental ambitions (IMO, 2023). The maritime industry generates vast amounts of data concerning vessel operations, route details, port activities, and more. Yet, much of this data remains underutilized due to factors such as manual processing and limited application beyond specific purposes like incident assessment or environmental impact measurement (Swider et al., 2018). This is due to the involvement of multiple stakeholders and the complexity of modern vessel design and operation. To address this challenge, researchers recommend focusing on research and innovation in digitalization and data usage within the shipping industry, exploring technologies such as artificial intelligence, augmented reality, virtual reality, high-performance computing, and big data analytics (Mouzakitis et al., 2023; Swider et al., 2018). These technologies hold potential for various maritime applications, including vessel traffic management, energy system design and operation, autonomous shipping, fleet intelligence, and route optimization. Despite ongoing digitalization efforts in other industries, such as aerospace and manufacturing, the maritime industry lags behind in embracing these advancements due to its complex and heavily regulated nature (Mouzakitis et al., 2023). However, leveraging shipping data has the potential to drive beneficial developments in marine engineering and propel the industry toward more digitally driven processes.

As a result of the Paris Agreement, the European Commission delivered in 2021 their European Green Deal in which they adopted a series of project proposals in order to achieve their own goal of reducing European GHG emissions by at least 55% by the year 2030, relative to 1990, and zero-net GHG emissions by 2050. By achieving this goal, the EC wants to become the first climate-neutral continent in the world, hence zero emission for international shipping (EC, 2021a,b). One of these projects is the Digital Twin for Green Shipping (DT4GS) project, funded by the European Union's Horizon research program. The goal of DT4GS is to eventually accomplish zero emissions by 2050 for the ship types of the collaborating companies within the DT4GS project; represented by an oil tanker, a container ship, a bulk carrier, and a ROPAX vessel. The collaborating vessels function as so-called 'Living Labs' (LLs), where operational data is collected to be used for improving green ship design based on digital twin (DT) methods. This research supported the DT4GS project by investigating the feasibility of a data-driven design method to reduce ship's CO_2 emissions.

WIND-ASSISTED SHIP PROPULSION

One obvious strategy regarding green shipping is the use of renewable energy, especially wind power. Due to its history with shipping and its availability at sea, the focus within renewable energy is shifting towards wind power (de Kat and Mouawad, 2019). Wind-assisted ship propulsion (WASP) systems have proven to achieve significant power reductions under favorable wind conditions: Thies and Ringsberg (2023) achieved a reduction between 10% and 14% by applying a Flettner rotor during the retrofitting of a ROPAX vessel, providing new-build design parameters for future ships with this WASP system. Bentin et al. (2018) investigated the energy-saving potential of using a towing kite, DynaRig sail, and Flettner rotor for a multi-purpose carrier, bulk carrier, and tanker. A saving potential of up to 35% was found when incorporating route optimization regarding favorable wind conditions. The investigated ship types were selected because they identified them to be suitable for WASP installation without changing the ship's capacity and the cargo loading and unloading function of the ship (Bentin et al., 2018). This is also addressed by Reche-Vilanova et al. (2021), where tankers and bulk carriers are identified to be especially suitable for WASP system installation due to their available deck space.

DEFINITION DIGITAL TWIN

In order to provide a clear explanation of the conducted research, a definition of a DT is chosen that is strictly followed during this study. Mauro and Kana (2023) identified that the term 'digital twin' is often falsely used throughout scientific research. In order to not contribute to this error in nomenclature, the model distinction adopted by Kritzinger et al. (2018) will be used throughout this research:

- A *digital model* (DM) which is a virtual representation of the physical product, but without any form of exchange of automated data between both. Data exchange could occur but only be performed manually. The DM is mostly used for simulation and planning-based operations which does not require automatic data integration.
- A *digital shadow* (DS) which is an extended version of a DM including only an automated data flow from the physical product towards the virtual product by which it is actively updated.
- And lastly a *digital twin* (DT) is, composed of a physical and virtual product including an automated data flow between both entities.

DT-SUPPORTED RETROFIT DESIGN

In order to investigate the state-of-the-art DT applications for maritime design, Mauro and Kana (2023) conducted a systematic literature review regarding maritime DT applications. Additionally, Hermans (2024) conducted a literature survey up to October 2023 for DT ship design. In these investigations, no publications are found on concrete DT applications for both new-build vessels and retrofits considering a whole vessel. Only theoretical frameworks and concepts are presented. In this research, a DT for retrofit design is investigated. First, the objective of the DT needs to be determined before starting with the actual modeling process for a DT-supported design. The objective covers the DT composition by indicating the required virtual models, and this composition consequently depends on the available data used by the final DT for performing simulations. The available operational data thus drives the modeling process of the DT (Giering and Dyck, 2021). The virtual models that are feasible to construct are identified by investigating this data. Finding the overlap between the required models (derived from the DT objective) and the feasible models (derived from the available data) provides the model selection for the final DT (see Figure 1).

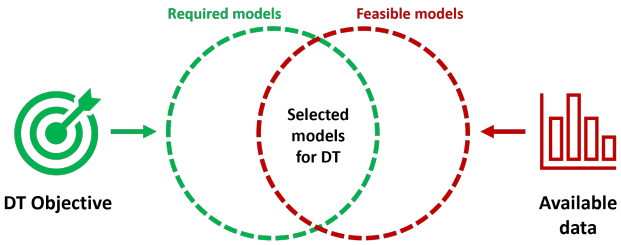

Figure 1: Selection process for DT models (Hermans, 2024)

After establishing the DT's objective and the model selection process, the modeling phase involves the following general steps, where the details can be found in Hermans (2024) and Papanikolaou et al. (2024):

1. Set-up the data acquisition
2. Choose modeling approaches for virtual models
3. Perform model training in case of statistical-based models
4. Integrate the virtual part with the physical part

Figure 2 shows a schematic representation of the transition towards a DT for retrofitting, where a detailed description can be found in Hermans (2024) and Papanikolaou et al. (2024).

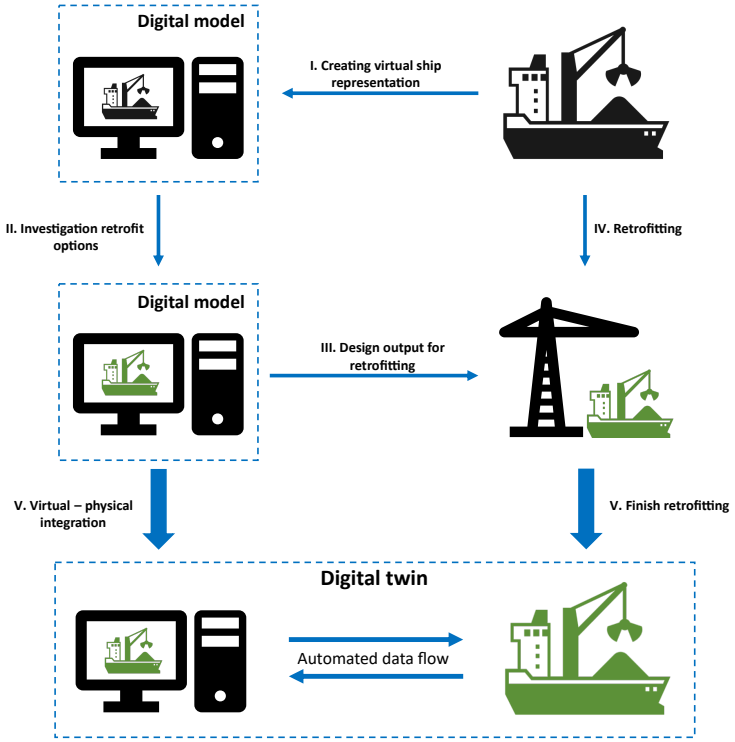

Figure 2: The development of the digital twin for retrofitting, based on the adopted DT definition (Hermans, 2024)

CONDUCTED RESEARCH

A DT with a retrofit design purpose starts as a digital model which becomes a DT after the retrofitting is completed. This research focuses on the modeling of the virtual part within the DT environment which will lay the basis for a green ship DT using this operational ship's data. Thus, using the definition by Kritzinger et al. (2018), this research will work on a green ship DM, supporting the process of constructing the DT (Figure 3).

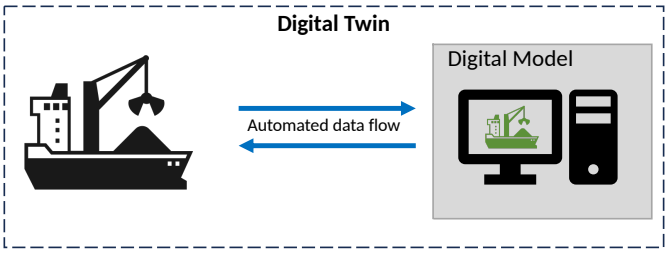

Figure 3: Focus of this research: representation of the green ship digital model (gray) within final digital twin

For the modeling construction, a model that represents the ship and a model that represents the green ship technologies are developed, which ultimately are integrated into one green ship DM. Within the DT4GS project, bunker delivery notes (BDNs) of a 300m bulk carrier are available as the data source. The main DT objective is set to reduce CO_2 emission through ship design, for which the Energy Efficiency Existing Ship Index (EEXI) and the Carbon Intensity Indicator (CII) are used

to evaluate this objective. The EEXI and CII are both IMO's environmental measurement tools which have been mandatory for most transport vessels since January 2018. Using these principles, the model selection (Figure 1) resulted in a fuel consumption model (FCM) which represents the ship, and three WASP models (towing kite, DynaRig sail, Flettner rotor), which represent the green ship technologies. The FCM will be composed of a resistance model and an artificial neural network (ANN). The resistance model will be modeled as a white box model (WBM), and the ANN as a black box model (BBM). Both are connected in a serial coupled fashion which results in an FCM constructed as a gray box model (GBM). The WASP models are all three modeled as WBMs. By combining these models into one green ship DM a potential retrofit design can be examined (Figure 4).

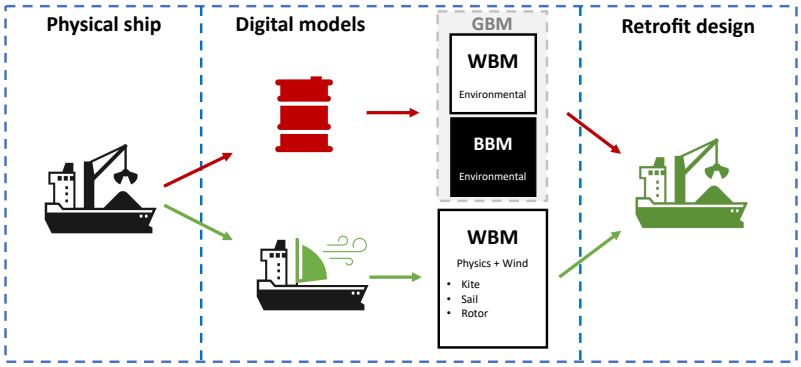

Figure 4: Overview of chosen method for constructing green ship DM. Combination of part representing the ship (red oil barrel) and part representing green ship technologies (green wind sail) resulting in one green ship DM for retrofit design (green bulk carrier)

A 300-meter bulk carrier is used as the case-study to investigate the proposed data-driven design approach. Besides evaluating the environmental impact of the EEXI and CII, a financial and feasibility assessment will be performed to investigate if the proposed retrofit of the respective vessel can be achieved. The payback period functions as the financial assessment. During the selection of WASP system configurations, the spatial feasibility per configuration is evaluated.

DATA PREPROCESSING

The available BDNs of the bulk carrier contain over 129,000 data points, with a time interval of 5 minutes during the following periods:

- Q2 2022: 02/06/'22 - 30/06/'22
- Q3 2022: 01/07/'22 - 30/09/'22
- Q4 2022: 01/10/'22 - 31/12/'22
- Q1 2023: 01/01/'23 - 24/02/'23
- Q2 2023: 01/04/'23 - 30/06/'23
- Q3 2023: 01/07/'23 - 30/09/'23

The abundance of operational data from the BDNs does not necessarily imply that all these data are of good quality and in the right format to be utilized. In order to be of use for the case-study, the data is first preprocessed. Figure 5 shows the steps performed within the adopted data preprocessing framework of this research. These preprocessing steps are based on the techniques described by García et al. (2016).

For the case study, only data points corresponding to sailing conditions of the ship are considered, with a minimum ship speed of 6 knots through water selected to filter out non-sailing data points during the data selection process (step 2). During the noise identification (step 3), outliers within the dataset are identified, as they can negatively impact the accuracy of the models if left untreated. To address this issue, outliers are either replaced through interpolation around the respective

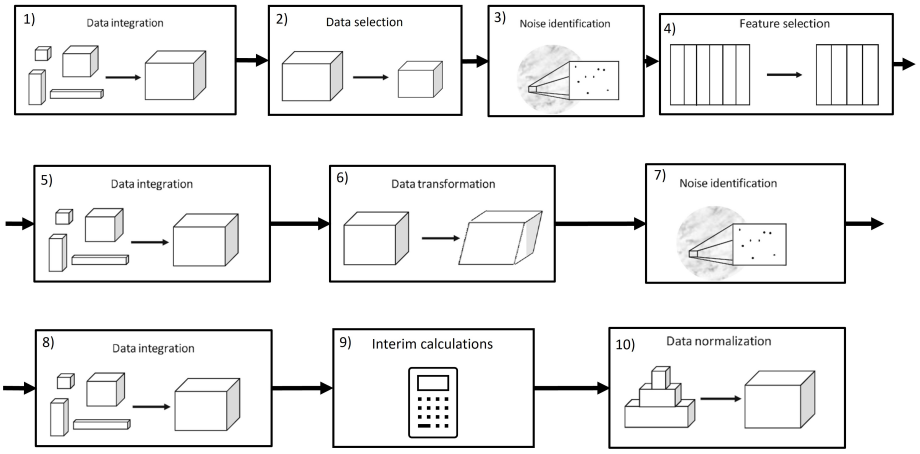

Figure 5: Adopted preprocessing data framework, based on techniques by García et al. (2016) (Hermans, 2024)

data points or entirely disregarded. In this research, identified outliers are simply disregarded. The following criteria are used during the noise identification process:

- Brake power is negative or zero
- The instant specific fuel consumption of the main engine is negative or zero (a result of a calculation)
- Sampling time is not 5 minutes
- Speed through water difference between 2 data points (= 5 min) is more than 3 knots, the second point is then disregarded

The other preprocessing steps within the adopted framework are discussed more thoroughly in Hermans (2024). The resulting amount of data points reduced per preprocessing step is provided in table 1. After performing the adopted data preprocessing steps, 5,687 data points remained. However, inspecting the resulting data points per period, significant anomalies were observed in Q2 2022, resulting in only 9 useful sailing hours. These 9 hours are just a tiny fraction of the resulting 5,687 hours (0.2%) and are therefore disregarded. This results in 5,678 data points, representing 'pure' sailing conditions, to be used for model construction.

Table 1: Data preprocessing results of BDNs data

	Data integration	Data selection	Noise identification				Data transformation
Period	Raw	$V_s \geq 6$ kts	$sfc_{ME} \leq 0$	$P_B \leq 0$	$T_s \neq 5$ min	$\Delta V_s \geq 3$ kts	Hour conversion
Q2 2022	8,267	3,165 (-5,102)	2,769 (-396)	148 (-2,621)	148 (0)	147 (-1)	9 (-39)
Q3 2022	26,488	15,582 (-10,906)	15,579 (-3)	15,572 (-7)	15,572 (0)	15,570 (-2)	1,284 (-162)
Q4 2022	26,493	18,281 (-8,212)	18,280 (-1)	18,280 (0)	18,279 (-1)	18,276 (-3)	1,514 (-108)
Q1 2023	15,697	9,756 (-5,941)	9,756 (0)	9,756 (0)	9,756 (0)	9,755 (-1)	802 (-131)
Q2 2023	26,207	12,586 (-13,621)	12,586 (0)	12,586 (0)	12,586 (0)	12,586 (0)	1,047 (-22)
Q3 2023	26,022	13,404 (-12,618)	13,353 (-51)	12,647 (-706)	12,645 (-2)	12,641 (-4)	1,031 (-269)
Σ	129,174	72,774 (-43.7%)				68,975 (-5.2%)	5,687 (-1.1%)

MODEL CONSTRUCTION

Fuel consumption model - GBM

Resistance model - WBM

The resistance model calculates the sum of the ship's calm water resistance (R_{cw}), according to the Holtrop and Mennen (1982), and the wind resistance (R_{AA}) using the method of Andersen (2013). The available sea trial report provides 6 runs with which the output of the resistance model can be verified. The R_{cw} and R_{AA} for each of these runs is calculated and compared with the measured value during the run. The mean errors from this comparison are listed in Table 2. The ship had a course direction of $60°$ during runs 1 to 3, and a course direction of $240°$ during runs 4 to 6.

Table 2: Mean percentage error resistance. Run 1 to 3 with course direction $\Psi = 60°$, run 4 to 5 with course direction $\Psi = 240°$

Resistance	Run 1	Run 2	Run 3	Run 4	Run 5	Run 6
$\Sigma(R_{cw} + R_{AA})$	+10.0%	+12.1%	+20.5%	-7.2%	-0.0%	+7.5%
R_{cw}	+12.9%	+14.4%	+24.2%	-7.1%	-0.0%	+7.6%
R_{AA}	-0.4%	-0.0%	-0.4%	-1.8%	-0.4%	+0.7%

As it can be noticed, the resistance prediction with a course direction of 240° is more accurate than the 60°. Moreover, the prediction of the additional wind resistance has a maximum error of 1.8%. The prediction of the calm water resistance fluctuates the most but within a 15% error when indicating run 3 as an outlier. There is no explanation found for the resistance difference between the two course directions and the relatively high error of run 3. The overall mean absolute percentage error is 9.6% which is deemed acceptable.

Artificial neural network - BBM

The ANN is constructed with Keras, which is an open-source neural network API written in Python (v3.11.5) that runs on top of the TensorFlow library (Keras, 2023). Before determining the architecture of the ANN, model inputs are chosen from the available data in the BDNs. The BDNs contain over 100 different data types. To ensure the accuracy and representativeness of fuel consumption predictions for future scenarios, an initial selection is made of potential model input parameters. This selection is based on the following assumptions:

- The goal is to predict fuel consumption with an operating WASP system, which will influence engine characteristics in a way that is currently unknown. Thus, parameters strongly related to the operating engine are left out of consideration
- Environmental parameters can be predicted for future situations by means of weather models, and are therefore taken into account
- Voyage characteristics such as ship speed and rudder position are route-dependent and can be chosen for future voyages

Following this filtering process, 12 potential model input parameters are identified. To refine the selection further, a Spearman correlation analysis is conducted for these parameters, specifically focusing on their correlation with the fuel consumption of the main engine. The analysis results, presented in Table 3, guide the final input selection process. Notably, in terms of engine output, engine torque is disregarded in favor of selecting brake power, as both parameters exhibit similar correlation factors, and power is deemed more suitable for WASP implementation.

Table 3: Spearman correlation for determination ANN inputs

Data types	Correlation with fuel consumption main engine	Selection
Brake power output	0.787	✓
Engine torque output	0.789	✗
Ship's heading	-0.082	✗
Rudder angle	-0.241	✓
Rudder rate of turn	0.002	✗
Relative wind direction	0.131	✓
Relative wind speed	0.226	✓
Speed over ground	-0.068	✗
Speed through water	0.142	✓
Speed difference	-0.170	✓
Total power diesel generators	0.041	✗
Sea water temperature	-0.174	✓
Fuel consumption main engine	1.000	—

From the Spearman correlation analysis, 7 parameters from the BDNs are chosen as model inputs. Additionally, the output of the resistance model, $\Sigma(R_{cw} + R_{AA})$, is incorporated as an additional input, which results in a total 8 model inputs for the ANN. This inclusion of the resistance as ANN input gives the model its gray box characteristic, and in this case, serially coupled. The 8 model inputs are:

- Brake power output
- Rudder angle
- Relative wind direction
- Relative wind speed
- Speed through water (ship speed)
- Speed difference
- Sea water temperature
- Sum of calm water and air resistance (result WBM)

The resulting 5,678 data points from the preprocessing are used for constructing the ANN. Initially, 500 data points are randomly selected for later cross-validation (referred to as the test set), leaving 5,178 points for training and intermediate validation to determine the optimal ANN architecture. These remaining data points are divided into a training set and a validation set at a ratio of 90% - 10%. The division is made using a specified random state (*rs*) parameter. During training, the weights of neurons are adjusted using the training set, while the validation set is used to monitor the ANN's loss.

The majority of research on ANNs for fuel consumption prediction suggests using a single hidden layer to balance complexity and accuracy (Hu et al., 2019; Bal Beşikçi et al., 2016). However, some studies propose the use of multiple hidden layers for improved prediction accuracy (Parkes et al., 2018; Fam et al., 2022). The accuracy of the ANN is closely tied to the number of hidden layers and neurons, with more units allowing for the modeling of complex relationships (Parkes et al., 2018). Nevertheless, networks with too few layers and neurons may struggle to capture all necessary relationships effectively. To address this, both one and two hidden layer configurations are explored, using the Fletcher-Gloss method described in da Silva et al. (2017) to determine the number of neurons. This resulted in 209 potential configurations of which the resulting configuration was chosen (Figure 6). The final ANN characteristics and training parameters are listed in Table 4. The choice and background of the training parameters are discussed more thoroughly in Hermans (2024).

The resultant ANN configuration with the highest accuracy is a network with 1 hidden layer containing 16 neurons. Three additional networks with the same configuration (1 hidden layer of 16 neurons) are constructed for cross-validation, each using a different *rs* value during training to yield networks with different weights per neuron. These networks are cross-validated using a test set of 500 data points that were set aside, ensuring that the achieved accuracy is independent of the specific data split used for training. The mean absolute percentage error (MAPE) for each network is listed in Table 5, along with the overall MAPE and corresponding standard deviation.

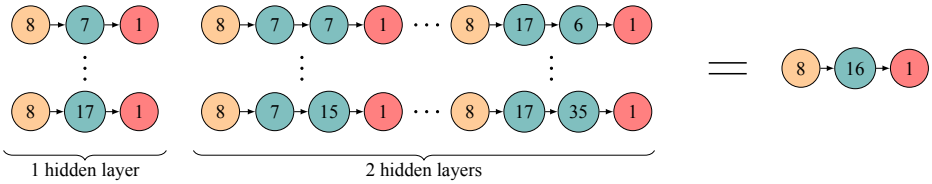

Figure 6: Investigated ANN configurations with 1 input layer (yellow), 1 or 2 hidden layers (green), and 1 output layer (red) (Hermans, 2024)

Table 4: ANN characteristics and training parameters

Characteristic - parameter	Value
Training algorithm	Adam
Activation function	ReLU
Number of inputs	8
Number of outputs	1
Number of hidden layers	1
Neurons in hidden layer	16
Dropout	0.2
Test set	500 data points
Training - validation set	90% - 10%
Batch size	16 data points
Max number of epochs	500
Learning rate	0.001
Patience	35 epochs
Monitor loss function	MSE

Table 5: Cross-validation using test data set between 4 models with equal configuration

Random state	MAPE
49	1.8%
59	2.1%
61	1.9%
80	1.9%
Overall	1.9%
Standard deviation	+/- 0.1%

The confidence interval is a common practice in statistics to indicate if the adopted method is within a desired accuracy (Carney et al., 1999). The minimum desired confidence interval for machine learning, and especially ANNs, is generally 90% (Carney et al., 1999). The constructed ANN is well within this interval, with an overall MAPE of 1.9% indicating the high accuracy of the network.

WASP models

In this research three distinctive WASP system models are constructed: a towing kite, a DynaRig sail, and a Flettner rotor. The selection for the towing kite and DynaRig sail is based on available literature (Bentin et al., 2018; Reche-Vilanova et al., 2021) on these models that use wind data that corresponds with the available data in the BDNs. Within the DT4GS project, a digital model of a Flettner rotor is constructed by Witzgall (2023) which is used in this research.

Wind conversion

The wind sensor which measures the wind speed and direction found in the BDNs is mounted on the mast on the bridge deck. As the wind profile is not constant over the height, the wind speed needs to be converted to the corresponding effective height of the respective WASP system. This conversion is calculated with Equation 1, which represents the power-law of the wind profile (Hsu et al., 1994).

$$V_{z_{WASP}} = V_{z_{measured}} \cdot \left(\frac{z_{WASP}}{z_{measured}} \right)^{P} \tag{1}$$

The power-law exponent (P) is a spatial parameter depending on the surroundings of the specific situation (e.g., at sea, open or undulating terrain). Hsu et al. (1994) concluded from their experiments that an exponent of $P = 0.11$ is an accurate approximation for the wind profile over the sea. This is also in line with the recommended procedures and guidelines provided by the ITTC (2021) concerning this wind speed conversion.

Towing kite - WBM

The constructed model is based on the research of Bentin et al. (2018). The resultant propulsion force by the towing kite is approximated with Equation 2.

$$F_{kite} = 0.5 \epsilon \rho_a V_a^2 S_{wi} F_{norm,kite} \tag{2}$$

The relative wind speed (V_a) acts on the effective wind surface of the kite (S_{wi}). Here $F_{norm,kite}$ is the normalized propulsion force of the towing kite as a function of only the relative wind direction and elevation angle (δ), and can be calculated with Equation 3.

$$F_{norm,kite} = \left(\cos\left(\frac{180^\circ - \varphi_{a,rel}}{2} \right) \right)^2 \cdot (\cos(\delta))^2 \tag{3}$$

Four kite configurations were investigated during the case-study, referred to as: *Kite300*, *Kite800*, *Kite1280* and *Kite2500*. These configurations vary in kite sail area, which are respectively: 300 m^2, 800 m^2, 1,280 m^2 and 2,500 m^2. The characteristics per kite configuration are listed in Table 6. It is assumed that the kite system is a fully autonomous system, including kite deployment and retrieving. An electric motor, included in the kite system, controls the flight and logistics. Such a fully autonomous system is also considered in the book chapter by Fritz (2013). The power usage of the electric motor is estimated at 2 kW with an electric efficiency of 0.95.

Table 6: Towing kite configurations

Kite characteristic	Kite300	Kite800	Kite1280	Kite2500
Kite sail area [m^2]	300	800	1,280	2,500
Height [m]	77.6	150	250	400
Elevation angle [°]	15	30	30	30

DynaRig sail - WBM

As with the kite model, the DynaRig sail model is also based on the modeling methods described by Bentin et al. (2018), together with the research conducted by Reche-Vilanova et al. (2021). The resultant propulsion force by the sail is calculated

with Equation 4. Here, the sail surface is represented by A_S. The normalized propulsion force $F_{norm,sail}$ is derived from the relative wind angle $\varphi_{a,rel}$ and the lift and drag coefficients (C_L and C_D). These coefficients characterize a specific sail. $F_{norm,sail}$ is calculated with Equation 5.

$$F_{sail} = 0.5 A_S \rho_a V_a^2 F_{norm,sail} \tag{4}$$

$$F_{norm,sail} = C_L \sin(\varphi_{a,rel}) - C_D \cos(\varphi_{a,rel}) \tag{5}$$

Bordogna (2020) conducted wind tunnel tests for 3 different DynaRig sail configurations and only investigated the lift and drag coefficients of the respective sail without interaction effects. For this reason, the derived force coefficients by Bordogna (2020) are used for this DynaRig model. The sails were virtually trimmed during Bordogna's experiments to optimize for the maximum thrust per apparent wind angle. During the experiments 3 different sail configurations are investigated: 1 sail, 2 sails with a gap distance ratio (GDR) of 2.5, and 2 sails with a GDR of 4. The GDR is defined as the ratio of the distance between two sails and the chord length of a sail. These configurations will be referred to as *DynaRig single*, *DynaRig double 2.5*, and *DynaRig double 4*. The resultant configurations are listed in Table 7, where the dimensions are determined based on the characteristics of the conducted experiments and the available spatial feasibility of the bulk carrier.

Table 7: DynaRig sail configurations

Sail characteristic	Single	Double 2.5	Double 4
Gap distance ratio [-]	-	2.5	4
Chord length [m]	20	20	12.5
Height sail [m]	37.1	37.1	23.2
Camber [%]	10	10	10

Flettner rotor - WBM

Unlike with the kite and DynaRig model, an already constructed model of a Flettner rotor adopted by Witzgall (2023) will be used. In collaboration with the DT4GS project, Witzgall (2023) used a non-linear regression method to develop a surrogate rotor model based on 7 distinctive studies conducted in the field of Flettner rotor lift and drag coefficients. Two rotor configurations are investigated: the installation of 1 rotor and 4 rotors. The configuration of 4 rotors consists of four times the same rotor as used for the configuration of 1 rotor. The goal of this research is to reduce the CO_2 emissions (i.e., fuel consumption), thus the largest feasible rotor available in the industry is selected to be investigated: a 35m high rotor with a diameter of 5m and an endplate with a diameter of 10m. Both configurations are referred to as *1x Rotor H35D5* and *4x Rotor H35D5*.

MODEL INTEGRATION

The goal of the green ship DM is to calculate the fuel consumption in case of an operating WASP. Comparing this with the fuel consumption without a WASP results in potential fuel reduction which provides an insight into the WASP's environmental and financial benefits. The output of the WASP's WBMs is propulsion force and possible power demand. One of the inputs of the ANN in the FCM is the ship's brake power. Thus, the ship's brake power including WASP force needs to be determined while maintaining the same ship speed and sailing time. The WASP's propulsion force is implemented with the propeller thrust demand in the ship's force balance to overcome the experienced resistance. This force balance is represented by Equation 6. Using this force balance a new working point of the propeller is derived, which is also known as the propeller-matching procedure. Vigna and Figari (2023) have performed this matching procedure including an operating Flettner rotor in order to derive the ship's brake power. The adopted integration framework is based on this procedure. The

ship speed and sailing time are kept the same as only the influence on the ship's brake power by the installed WASP system is being considered.

$$\underbrace{R_T = (1-t)\cdot T}_{\text{Without operating WASP}} \quad \Rightarrow \quad \underbrace{R_T = (1-t)\cdot T + F_{WASP}}_{\text{Including operating WASP}} \tag{6}$$

Equation 6 is rewritten to the forward equilibrium equation including the terms of the propeller characteristics and hull demand resulting from the required ship speed, to derive the new working point of the propeller (Vigna and Figari, 2023), resulting in Equation 7.

$$\underbrace{\frac{K_T}{J^2} - \frac{R_T}{\rho_{sw}\cdot(1-t)(1-w)^2\cdot V_s^2\cdot D_p^2} = 0}_{\text{Without operating WASP}} \quad \Rightarrow \quad \underbrace{\frac{K_T}{J^2} - \frac{R_T - F_{WASP}}{\rho_{sw}\cdot(1-t)(1-w)^2\cdot V_s^2\cdot D_p^2} = 0}_{\text{Including operating WASP}} \tag{7}$$

The established model integration framework for this research is depicted in Figure 7. The output of the WASP WBMs is firstly transformed into brake power, and next integrated into the FCM to predict the corresponding fuel consumption. The required steps for this integration are depicted in orange and are discussed in Hermans (2024). This presented framework is based on evaluating the known data from the BDNs. Necessary calculation adjustments in this framework for future data sets are also presented in Hermans (2024).

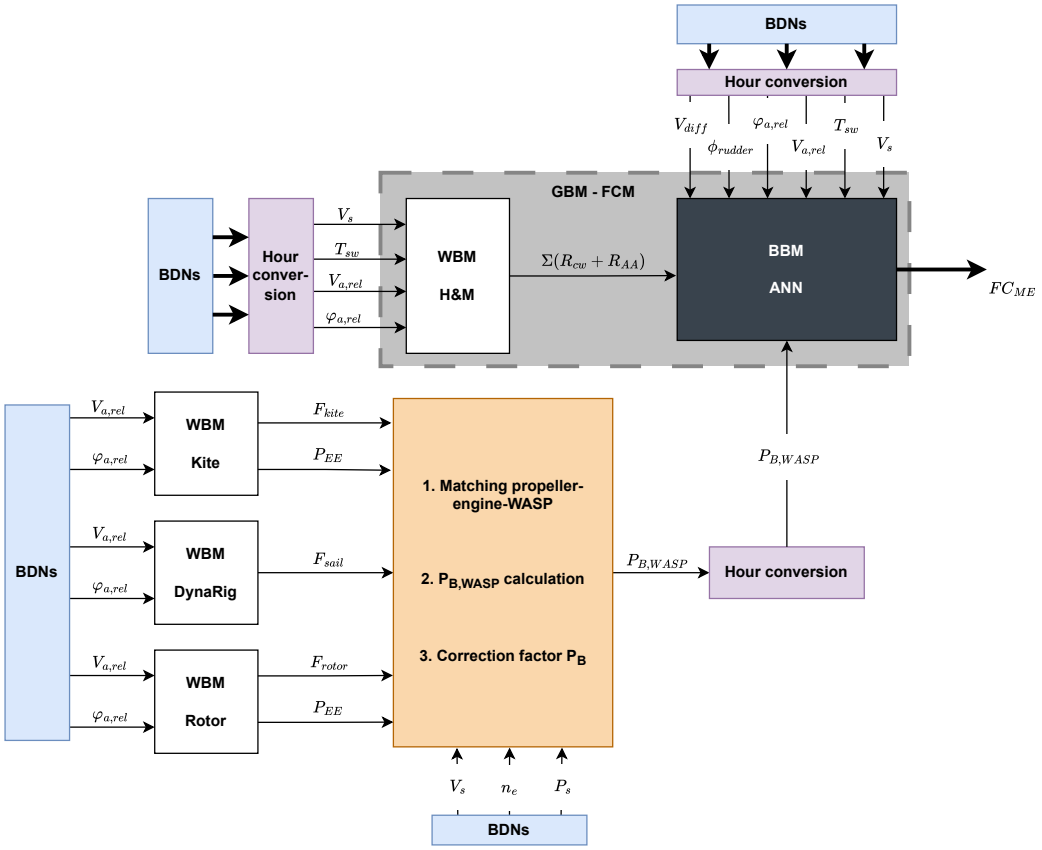

Figure 7: Schematic overview digital models including, the adopted model integration framework in orange (Hermans, 2024)

Step 3 in the integration framework (Figure 7) consists of a correction factor (*cf*) calculation of the ship's brake power. Because the current brake power is recorded in the BDNs, this *cf* can be calculated per data point to improve accuracy in the power computation. This *cf* can be seen as a variable value for all the efficiencies used in the brake power calculation (i.e., $\eta_S, \eta_{GB}, \eta_R$). The ship's forward equilibrium equation without operating WASP (in Equation 7), together with the derivation for the brake power (Equation 8) using the BDNs is used to calculate the ship's brake power. Because the bulk carrier does not have a gearbox, the propeller rotation (n_p) is assumed to be equal to the measured main engine rpm (n_e) available in the BDNs. This calculated value is compared with the measured brake power (BDNs) to derive the *cf* per data point (Equation 9). The correction factor is then multiplied by the ship's brake power with operating WASP.

$$P_B = \frac{2\pi\rho_{sw} D_p^5 n_p^3 K_Q}{\eta_S \eta_{GB} \eta_R} \tag{8}$$

$$cf = \frac{P_B \text{ (BDNs)}}{P_B \text{ (calculated)}} \tag{9}$$

RESULTS

Overall savings Q3 2022 - Q3 2023

For each configuration of the WASP systems, the money, fuel, and CO_2 savings are calculated over the 5,678 sailing hours ($\approx$ 237 sailing days) using a fuel price of \$618.50/mt-fuel. These results are presented in Table 8. Percentage reductions apply to all listed savings, as they are all directly linked to fuel consumption. The savings are computed as the difference between the predicted fuel consumption by the green ship DM with and without the WASP system. The MAPE between the actual fuel consumption (BDNs) and the predicted consumption (green ship DM), both without installed WASP, is 0.3%, indicating high model accuracy and reliability. This supports the validity of using the model. Calculating the difference between both predicted values by the green ship DM ensures consistency in accuracy.

Table 8: Total WASP savings during 5,678 sailing hours

WASP configuration	Fuel savings [mt]	\$-savings [K\$]	CO_2 savings [mt]	Percentage savings [%]
Kite300	1,031	637	3,240	-12.5
Kite800	1,048	648	3,293	-12.7
Kite1280	1,070	662	3,364	-13.0
Kite2500	1,129	698	3,549	-13.7
DynaRig single	1,145	708	3,599	-13.9
DynaRig double 2.5	1,148	710	3,610	-14.0
DynaRig double 4	1,068	660	3,357	-13.0
1x Rotor H35D5	1,197	740	3,762	-14.6
4x Rotor H35D5	1,598	989	5,025	-19.4

The overall results indicate a CO_2 reduction potential ranging from 12% to 19% across the investigated WASP configurations. This finding aligns with a literature study conducted by Bouman et al. (2017) on CO_2 reduction through green ship technologies, who found savings potentials between 7% and 22% of similar WASP technologies. When comparing individual configurations of each WASP system (1 kite, 1 sail, 1 rotor), it is observed that the rotor configuration offers the most significant savings potential. Additionally, kite configurations demonstrate progressively increasing savings potential with larger kite sail areas. Variations in the savings potential between the two double DynaRig configurations are attributed to differences in sail sizes as discussed in the WASP model construction.

Environmental assessment

EEXI

The power reduction due to an operating WASP is calculated according to the procedure presented in IMO (2021). Examining the sailing route of the bulk carrier during the period Q3 2022 - Q3 2023 showed that the vessel had sailed approximately 90% on the same shipping routes on which the IMO's wind probability matrix is based. This indicates that this wind prediction method, used in the EEXI calculation, has sufficient accuracy regarding this ship's operational area. The ship's current, required, and resulting EEXI values per investigated WASP configuration are provided in Table 9.

Table 9: New EEXI value per installed WASP configuration

WASP configuration	EEXI [g/(mt-nm)]	Reduction [%]
Required value (max)	2.370	-
No WASP (current)	2.120	-
Kite300	2.112	-0.4
Kite800	2.101	-0.9
Kite1280	2.085	-1.6
Kite2500	2.044	-3.6
DynaRig single	2.054	-3.1
DynaRig double 2.5	2.052	-3.2
DynaRig double 4	2.095	-1.2
1x Rotor H35D5	2.029	-4.3
4x Rotor H35D5	1.754	-17.2

All the investigated WASP configurations decrease the ship's EEXI value as suspected and consequently comply with the required EEXI value. Moreover, as noticed with the aforementioned overall savings, installing a rotor results in the highest CO_2 reduction. The *4x Rotor H35D5* configuration is simply a factor 4 environmental beneficial in terms of design potential, as the result of the calculation by the IMO.

CII

The evaluation of the ship's operational aspect involves calculating the CII. However, there are data gaps and errors in the data for March 2023 and in the period Q3 2023, rendering the CII calculation for those periods unreliable. As the CII calculation requires a complete calendar year, it cannot provide the official CII value. Nevertheless, the calculation is performed with the data of 11 consecutive months (Q3 2022 - Q2 2023) which still offers a useful indication of the vessel's operational impact. The required CII values for the years 2023, 2024, and 2025 for the specific bulk carrier used are illustrated in Figure 8.

For the calculations of the attained CII per installed WASP configuration, a fuel oil density of 0.8352 g/cm^3 is used. The fuel consumption is predicted with the constructed green ship DM. The results are provided in Table 10, including color labeling per CII corresponding to its rating for the year 2023.

The bulk carrier is currently above the required CII, in the C-rating. All the WASP configurations bring the bulk carrier in the B-rating regarding the year 2023, whereas both rotor configurations also comply with the B-rating regarding the year 2024 and *4x Rotor H35D5* extend B-compliance for the year 2025.

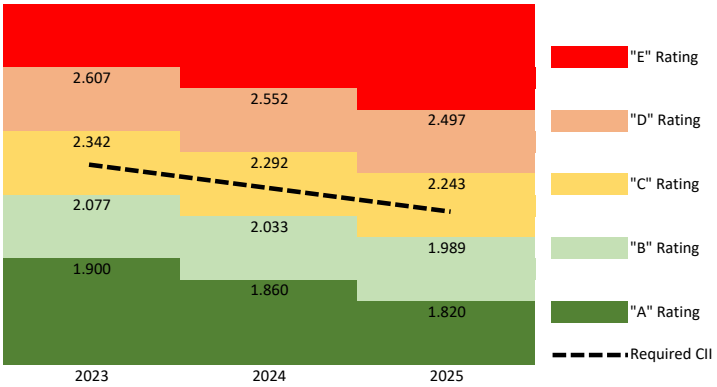

Figure 8: Attained CII values of the investigated bulk carrier; required CII values for 2023, 2024, and 2025 are respectively 2.212, 2.166, 2.119

Table 10: CII approximation of 11 months during Q3 2022 - Q2 2023

WASP configuration	Attained CII [g/(mt-nm)]
Required (2023)	2.212
No WASP	2.248
Kite300	2.059 (-8.4%)
Kite800	2.056 (-8.6%)
Kite1280	2.051 (-8.8%)
Kite2500	2.039 (-9.3%)
DynaRig single	2.035 (-9.5%)
DynaRig double 2.5	2.035 (-9.5%)
DynaRig double 4	2.052 (-8.8%)
1x Rotor H35D5	2.020 (-10.2%)
4x Rotor H35D5	1.931 (-14.1%)

Financial assessment - payback period

Even though the main objective is directly related to the environmental assessment, the financial assessment is done to give an idea of the feasibility in terms of time and money. The calculation of the payback period calculation per WASP configuration is performed with Equation 10, which is based on the financial assessments by Kiran (2022); van der Kolk et al. (2019).

$$P = \frac{B + C}{A - D} \tag{10}$$

Where the financial parameters represent:

A: $-savings per sailing hour using WASP

B: Purchase & installation system

C: Out of service costs & dry docking

D: Hourly operational & maintenance costs WASP

The $-savings per hour is the driving parameter (A) of the payback period. This parameter for each of the investigated WASP configurations (A) is derived by dividing its respective money savings in Table 8 by the total sailing hours (5,678 hrs). For the purchase and installation costs (B), the estimations provided by GloMEEP (2019) are used. GloMEEP is an international collaborating project established within the IMO aiming to support and provide insights into implementing energy-efficient measures for global shipping. Costs 'C' are not considered as there is no evident information available on these costs. This is mainly due to the fact shipping companies and maintenance docks only provide such information through a direct offer. The costs associated with the operations and maintenance of WASP systems are typically provided by the manufacturer. In this research, these costs are estimated to be annually equivalent to 2% of the WASP installation costs. This estimation aligns with a study conducted by van der Kolk et al. (2019), which performed a technological and economical assessment of WASP systems for transport vessels.

The payback period (P) for each WASP configuration can be calculated based on operational data, excluding costs 'C'. The results are presented in Table 11, considering the vessel in operational condition (minimum ship speed of 6 knots). To determine the total payback period accounting for all configurations, one must include the term $\frac{C}{A}$ to the provided payback period results, where 'C' represents the known value for costs and 'A' represents the annual savings.

Table 11: Payback period (P) of WASP configurations expressed in operating time, without costs 'C'

WASP configuration	P [hrs]	P [days]	P [years]
Kite300	4,091	170	0.5
Kite800	10,121	422	1.2
Kite1280	15,596	650	1.8
Kite2500	22,128	922	2.5
DynaRig single	1,368 $\sim$ 2,419	57 $\sim$ 101	0.2 $\sim$ 0.3
DynaRig double 2.5	2,735 $\sim$ 4,850	114 $\sim$ 202	0.3 $\sim$ 0.6
DynaRig double 4	2,943 $\sim$ 5,220	123 $\sim$ 218	0.3 $\sim$ 0.6
1x Rotor H35D5	5,437 $\sim$ 7,411	227 $\sim$ 309	0.6 $\sim$ 0.8
4x Rotor H35D5	16,696 $\sim$ 21,702	696 $\sim$ 904	1.9 $\sim$ 2.5

Analyzing the payback periods of the selected configurations indicates that the *Kite2500* and *4x Rotor H35D5* configurations require the longest time to become financially profitable. On the other hand, DynaRig configurations are generally the most favorable option in terms of payback period, averaging better results compared to other configurations.

CONCLUSION

Incorporating operational data into ship design through a DT-supported method allows for the evaluation of environmentally friendly ship designs, particularly focusing on reducing CO_2 emissions with WASP systems. The DT's capacity to handle vast amounts of data and conduct virtual simulations mitigates risks associated with such designs. Operational data from the IMO's mandatory BDNs serves as a valuable source for modeling construction, facilitating the development of a green ship DM. This DM incorporates ship characteristics, route-dependent factors, and environmental data to predict fuel consumption with and without a WASP system installed, thus estimating potential CO_2 emission reductions (environmental) and payback periods (financial). Environmental assessments conducted through IMO's EEXI and CII tools highlight the *4x Rotor H35D5* configuration as yielding the highest CO_2 reduction, while also with the longest payback time. Conversely, DynaRig configurations result as the most financially attractive on average, although dry-docking and out-of-service costs are not taken into account. Ultimately, ship owners' decisions will be guided by specific requirements and considerations, informed by the presented results.

DISCUSSION

The research focuses on integrating operational data into retrofit design, using high-level WASP models. However, these models are simplified, such as approximating aerodynamics in the towing kite model with a single value, the wind energy transfer efficiency (ϵ). To enhance the accuracy of propulsion force predictions, more refined WASP models are recommended. One key assumption is regarding fuel consumption prediction by the green ship DM with an operating WASP system. The FCM is validated with high accuracy for known sailing conditions, with one input being the ship's brake power. During the case-study, only the brake power value is altered to investigate the effect of an installed WASP system, assuming the resulting fuel consumption corresponds to that situation. To verify this assumption accurately, model or full-scale tests including WASP system installation are necessary. These tests would close the verification loop of the proposed method. The BDNs serve as a feasible data source for the modeling construction chosen in this research, providing ample data points related to route-dependent and environmental information for fuel prediction. However, there is a lack of information regarding the method and quality of the sensors used for data collection, raising uncertainty about potential errors within these values due to sensor sensitivity or recording methods. Additionally, despite the variety of recorded data types, important parameters such as waves, trim, and draft are absent. Incorporating these data types into the constructed resistance model could improve the estimation of the ship's resistance and total resistance. Although water depth data, which can influence speed loss due to shallow water effects, are present in the BDNs, they are incomplete and contain significant anomalies, leading to their exclusion from the research. Moreover, no interaction effects are considered regarding the WASP systems and the vessel during this research. While the IMO's calculations overlook these effects, deeming them significant only during unsafe operations that need to be prevented, they must be considered when investigating WASP retrofitting. The change in the center of gravity due to installing WASP systems can lead to differences in the power reduction prediction (Thies and Ringsberg, 2023). Moreover, induced trimming moments and heel angles as a result of operation WASP systems negatively influence the aero and hydrodynamic performance of the vessel's propulsion system (Smith et al., 2013; Stark et al., 2022).

DECLARATION OF GENERATIVE AI AND AI-ASSISTED TECHNOLOGIES IN WRTITING

During the preparation of this work, the authors used "OpenAI's ChatGPT 3.5" in order to guide the summarizing of several sections originating from the lead author's academic thesis. After using this tool, the authors reviewed and edited the content as needed and take full responsibility for the content of the publication.

CREDIT AUTHORSHIP CONTRIBUTION STATEMENT

Julien J. M. Hermans: Conceptualization; methodology; formal analysis; writing – original draft; writing – review and editing. **Austin A. Kana:** conceptualization; supervision; writing – review and editing.

ACKNOWLEDGEMENTS

This work was performed as part of the academic thesis for the lead author, (Hermans, 2024). The thesis was performed in Marine Technology at Delft University of Technology and the authors would like to acknowledge Delft University of Technology for their support of this research. The research also acknowledges the support by the European Union's Horizon research project DT4GS (Grant Agreement No 101056799).

REFERENCES

Andersen, I. (2013). Wind loads on post-panamax container ship. *Ocean Engineering*, 58:115–134.

Bal Beşikçi, E., Arslan, O., Turan, O., and Ölçer, A. (2016). An artificial neural network based decision support system for energy efficient ship operations. *Computers Operations Research*, 66:393–401.

Bentin, M., Kotzur, S., Schlaak, M., Zastrau, D., and Freye, D. (2018). Perspectives for a wind assisted ship propulsion. *International Journal of Maritime Engineering*, Vol 160.

Bordogna, G. (2020). Aerodynamics of wind-assisted ships : Interaction effects on the aerodynamic performance of multiple wind-propulsion systems.

Bouman, E. A., Lindstad, E., Rialland, A. I., and Strømman, A. H. (2017). State-of-the-art technologies, measures, and potential for reducing ghg emissions from shipping – a review. *Transportation Research Part D: Transport and Environment*, 52:408–421.

Carney, J., Cunningham, P., and Bhagwan, U. (1999). Confidence and prediction intervals for neural network ensembles. In *IJCNN'99. International Joint Conference on Neural Networks. Proceedings (Cat. No.99CH36339)*, volume 2, pages 1215–1218 vol.2.

da Silva, I. N., Spatti, D. H., Flauzino, R. A., Liboni, L. H. B., and dos Reis Alves, S. F. (2017). *Artificial Neural Networks - A Practical Course*. Springer International Publishing.

de Kat, J. and Mouawad, J. (2019). Green ship technologies. *Sustainable Shipping*.

EC (2015). Paris agreement. *Climate Action*. `https://climate.ec.europa.eu/eu-action/international-action-climate-change/climate-negotiations/paris-agreement_en`.

EC (2021a). A european green deal. *Green Deal*. `https://commission.europa.eu/strategy-and-policy/priorities-2019-2024/european-green-deal_en`.

EC (2021b). Reducing emissions from the shipping sector. *Climate Action*. `https://climate.ec.europa.eu/eu-action/transport-emissions/reducing-emissions-shipping-sector_en`.

Fam, M. L., Tay, Z. Y., and Konovessis, D. (2022). An artificial neural network for fuel efficiency analysis for cargo vessel operation. *Ocean Engineering*, 264:112437.

Fritz, F. (2013). *Application of an Automated Kite System for Ship Propulsion and Power Generation*, pages 359–372. Springer Berlin Heidelberg, Berlin, Heidelberg.

García, S., Ramírez-Gallego, S., Luengo, J., Benítez, J. M., and Herrera, F. (2016). Big data preprocessing: methods and prospects. *Big Data Analytics*, 1(1):1–22.

Giering, J.-E. and Dyck, A. (2021). Maritime digital twin architecture: A concept for holistic digital twin application for shipbuilding and shipping. *at-Automatisierungstechnik*, 69(12):1081–1095.

GloMEEP (2019). Kite. *GloMEEP - IMO*. `https://glomeep.imo.org/technology/kite/`.

Hermans, J. (2024). Retrofit modeling for green ships. Master's thesis, TU Delft. Report number: MT.23/24.021.M.

Holtrop, J. and Mennen, G. (1982). An approximate power prediction method. *International Shipbuilding Progress*, 29(335):166–170.

Hsu, S. A., Meindl, E. A., and Gilhousen, D. B. (1994). Determining the power-law wind-profile exponent under near-neutral stability conditions at sea. *Journal of Applied Meteorology and Climatology*, 33(6):757 – 765.

Hu, Z., Jin, Y., Hu, Q., Sen, S., Zhou, T., and Osman, M. T. (2019). Prediction of fuel consumption for enroute ship based on machine learning. *IEEE Access*, 7:119497–119505.

IMO (2018). Imo's work to cut ghg emissions from ships. *International Maritime Organization*. https://www.imo.org/en/MediaCentre/HotTopics/Pages/Cutting-GHG-emissions.aspx.

IMO (2021). 2021 guidance on treatment of innovative energy efficiency technologies for calculation and verification of the attained eedi and eex. *International Maritime Organization*.

IMO (2023). 2023 imo strategy on reduction of ghg emissions from ships. *International Maritime Organization*. https://www.imo.org/en/OurWork/Environment/Pages/2023-IMO-Strategy-on-Reduction-of-GHG-Emissions-from-Ships.aspx.

ITTC (2021). Preparation, conduct and analysis of speed/power trials. https://www.ittc.info/media/9874/75-04-01-011.pdf.

Keras (2023). Keras documentation: About keras 3. *Keras*. https://keras.io/about/.

Kiran, D. (2022). Chapter twenty-two - machinery replacement analysis. In Kiran, D., editor, *Principles of Economics and Management for Manufacturing Engineering*, pages 259–267. Butterworth-Heinemann.

Kritzinger, W., Karner, M., Traar, G., Henjes, J., and Sihn, W. (2018). Digital twin in manufacturing: A categorical literature review and classification. *IFAC-PapersOnLine*, 51(11):1016–1022. 16th IFAC Symposium on Information Control Problems in Manufacturing INCOM 2018.

Mauro, F. and Kana, A. (2023). Digital twin for ship life-cycle: A critical systematic review. *Ocean Engineering*, 269.

Mouzakitis, S., Kontzinos, C., Tsapelas, J., Kanellou, I., Kormpakis, G., Kapsalis, P., and Askounis, D. (2023). *Enabling Maritime Digitalization by Extreme-Scale Analytics, AI and Digital Twins: The Vesselai Architecture*, pages 246–256.

Papanikolaou, A., Boulougouris, E., Erikstad, S.-O., Harries, S., and Kana, A. (2024). Ship design in the era of digital transition - a state-of-the-art report. *15th International Marine Design Conference (IMDC 2024)*.

Parkes, A., Sobey, A., and Hudson, D. (2018). Physics-based shaft power prediction for large merchant ships using neural networks. *Ocean Engineering*, 166.

Reche-Vilanova, M., Hansen, H., and Bingham, H. B. (2021). Performance Prediction Program for Wind-Assisted Cargo Ships. *Journal of Sailing Technology*, 6(01):91–117.

Smith, T., Newton, P., Winn, G., and Grech La Rosa, A. (2013). Analysis techniques for evaluating the fuel savings associated with wind assistance.

Stark, C., Xu, Y., Zhang, M., Yuan, Z., Tao, L., and Shi, W. (2022). Study on applicability of energy-saving devices to hydrogen fuel cell-powered ships. *Journal of Marine Science and Engineering*, 10(3).

Swider, A., Wang, Y., and Pedersen, E. (2018). Data-driven vessel operational profile based on t-sne and hierarchical clustering. *OCEANS 2018 MTS/IEEE Charleston*, pages 1–7.

Thies, F. and Ringsberg, J. W. (2023). Retrofitting wasp to a ropax vessel—design, performance and uncertainties. *Energies*, 16(2):673.

van der Kolk, N., Bordogna, G., Mason, J., Bonello, J.-M., Vrijdag, A., Broderick, J., Larkin, A., Smith, T., Akkerman, I., Keuning, J., and Huijsmans, R. (2019). Wind-assist for commercial ships: A techno-economic assessment.

Vigna, V. and Figari, M. (2023). Wind-assisted ship propulsion: Matching flettner rotors with diesel engines and controllable pitch propellers. *Journal of Marine Science and Engineering*, 11(5).

Witzgall, F. (2023). Aerodynamic modelling of wind-assisted ship propulsion. Master's thesis, Institut Supérieur de l'Aéronautique et de l'Espace, Toulouse, France. Thesis completed at French Alternative Energies and Atomic Energy Commission (CEA).

Proceedings of 15th International Marine Design Conference (IMDC-2024)
June 2-6, 2024
Amsterdam, the Netherlands

Overall scheme design of green typical demonstration ship types under the background of Double Carbon Policy

ZhengChen Lian[1,*] and LiZheng Wang[2]

ABSTRACT

In order to explore the overall design and research issues of green typical demonstration ship types, this article takes Hunan Province's green typical demonstration ship types as an example. Using a combination of policy interpretation, research analysis, theoretical analysis, and overall design, with the Double Carbon Policy as the background, the overall positioning analysis of the ship type is conducted first. Then, the key technical features and application solutions of the ship type will be introduced to ultimately achieve the goal of matching the design ship type with the waterway conditions.

KEY WORDS

Green ship type scheme, ship type positioning, power mode selection, ship adaptability

INTRODUCTION

Inland waterway shipping has important strategic significance for the development of the national economy. With the completion of cascade development and a series of shipping construction projects, the conditions of China's inland waterways have greatly improved. However, it is also noted (Lian Zhengchen, Wang lizheng 2023) that the seasonal changes in the navigation conditions of China's inland waterways after channelization are significant, resulting in low load capacity, poor navigation performance, insufficient navigation safety, and potential safety hazards for ships navigating in such key sections. The comparative advantages of large transportation capacity, low cost, low energy consumption, and light pollution in inland waterway shipping have not been fully utilized. At the same time, in combination with the current implementation of the national strategy of "carbon peak and carbon neutrality" and the need for green and high-quality development of inland ships, there is an urgent need to promote the emission reduction and green upgrading of green standard ship types in the new era. This puts forward higher requirements for the overall plan research of ship types and is also an important prerequisite for the economic and efficient operation of ships. Therefore, it is crucial to explore the overall design and research issues of green typical demonstration ship types.

This article takes the green typical demonstration freight ship types in Hunan Province as the research object, with "carbon peak and carbon neutrality" as the policy background. At the same time, it strengthens the research on the "one river, one lake, and four water" ship types, especially the "four water" ship types, clean and environmentally friendly ship types, and new energy ship types in Hunan Province, and matches them with the Three Gorges ship type to achieve the urgent goal of connecting the river and the sea. Therefore, this article proposes an overall plan for Hunan Province's green typical standard demonstration ship type from the perspectives of market demand and navigation environment characteristics, overall positioning analysis, key technical characteristics analysis, and overall design scheme application. Through the above research, it points out the direction for the application and engineering demonstration of emission reduction technology for standard ship types in inland rivers in Hunan Province, and provides strong support for promoting the transformation and upgrading of the shipbuilding industry and green and high-quality development.

[1] Affiliation (Ship Engineering Department of Wuhan University of Technology, Wuhan University of Technology, Wuhan, China);

[2] Affiliation (Ship Engineering Department of Wuhan University of Technology, Wuhan University of Technology, Wuhan, China);

* Corresponding Author: email: zhengchen.lian@qq.com

Submitted: 15 February 2024, Revised: 1 May 2024, Accepted: 3 May 2024, Published: 23 May 2024

Conference paper, DOI: https://doi.org/10.59490/imdc.2024.885 e-ISSN: 3050-486

ANALYSIS OF THE OVERALL FRAMEWORK POSITIONING OF THE GREEN FREIGHT STANDARD DEMONSTRATION SHIP TYPE

Ship type positioning analysis

In terms of policy orientation, in order to achieve the strategic goals of "dual carbon", becoming a strong transportation country, and developing inland waterway shipping, and promoting high-quality development of inland waterway shipping, the selection of green standard demonstration ship types for waterway freight transportation in Hunan should meet the following three policy requirements (*Implementation Opinions of the Ministry of Industry and Information Technology and Five Other Ministries on Accelerating the Green and Intelligent Development of Inland River Ships*, 2022).

i. Guided by the goals of carbon peak and carbon neutrality, guided by promoting the green and standardized development of inland river ships in Hunan, and focusing on the development of new energy and clean energy powered ships, the typical scenarios of Hunan waterway freight transportation are selected to carry out demonstration applications according to local conditions, so as to accelerate the transformation and high-quality development of green energy applications of inland river ships in Hunan, implement the "14th Five-Year Plan" water operation and operation development plan in Hunan, and promote the green upgrading of inland river standard ship types in Hunan Province in the new era.

ii. Adhere to policy guidance, strengthen the coordination and linkage of departments, localities and enterprises, develop green and energy-efficient ships and green shipping, and improve the level of safe and green development. Promote scientific and technological innovation, adhere to demonstration and promotion, support representative enterprises in the inland river basin of Hunan to take the lead in the trial, summarize typical experience and practices, and steadily promote the basic principles.

iii. Comprehensively consider the perspectives of economy, energy efficiency and design optimization to create a standardized green energy ship type that meets the needs of typical scenarios of Hunan waterway freight, realize the demonstration application of Hunan inland river operation routes, form an experience that can be implemented, replicated and promoted, and form a green model of Hunan freight ships.

It was noted ("*Analysis Report on the Capacity Structure of Waterway Freight Ships in the Province"*, 2022) that, from the perspective of water transportation demand in Hunan Province in 2021, the province completed a freight volume of 212.72 million tons, an increase of 7.20% compared to the previous year, and a freight turnover of 45 billion ton-kilometer, an increase of 13.75% compared to the previous year. Among them, inland waterway transportation completed a freight volume of 211.31 million tons and a cargo turnover of 36.1 billion ton-kilometer; Ocean transportation has completed a freight volume of 1.41 million tons and a cargo turnover of 8.9 billion ton-kilometer. Although the water freight volume in the province has declined to a certain extent since 2014 due to the ban on sand and gravel mining in Dongting Lake and the significant decrease in water transportation volume, the development of container "water shuttle buses" has been actively guided to optimize and adjust the water freight structure, serving foreign trade transportation, and continuously optimizing the water freight transportation structure in recent years. The water transportation volume and proportion of bulk goods such as metal ores, coal, grains, and oil products in the province have significantly increased. In the long run, with the development of the economy and correct guidance, the structure of waterway freight transportation in Hunan will gradually transform and develop towards energy, steel, grain, equipment manufacturing, and more, serving the industrial development of Hunan Province. At the same time, considering further adjustment and optimization of the comprehensive transportation structure, with the adjustment of freight transportation from public transportation to water and from public transportation to rail, the medium and long-term water transportation volume will still show a gradual growth trend.

Subsequently, the Hunan Provincial Department of Transportation proposed key tasks for green transportation in the 2022 plan. Among them, in the key task of "optimizing transportation structure and innovating organizational methods," it was pointed out to deepen the promotion of the transportation of bulk goods and medium and long-distance goods from rail to rail and from water ("*Analysis Report on the Capacity Structure of Waterway Freight Ships in the Province"*, 2022). Focus on developing direct transportation between the Xiang River trunk line and the Dongting Lake area, consolidating the routes from Chenglingji Port to Yichang Port, Jingzhou Port in Hubei Province, and various ports in the upper reaches of the Yangtze River; In the key task of promoting resource conservation and intensive utilization, it is pointed out to promote the use of new and clean energy in highway service areas, ordinary national and provincial trunk highway service areas or overload control stations, CNG refueling stations and port shore power facilities, LNG refueling stations, and promote the use of new and clean energy in vehicles, ships, and other transportation equipment.

From an overall development perspective, from 2016 to 2020, the number of container arrivals and departures in Hunan Province has shown a continuous upward trend. In the first half of 2020, due to the impact of the epidemic, container transportation suffered a significant impact and demand declined. In the second half of 2020, with the gradual recovery of global trade, the demand for container waterway transportation increased, and the scale of transportation capacity quickly recovered. From 2016 to 2020, container waterway transportation ports in Hunan Province were mainly distributed in Changsha, Yueyang, Hengyang, and Changde cities. More than 60% of the export containers are shipped from Changsha New Port. Due to the limitations of the Xiangjiang River waterway, export containers from Hengyang Port, Changde Port, and Changsha Port need to transfer to Yueyang Chenglingji Port. In 2020, the total volume of container arrivals and departures in Hunan Province was 653693 TEUs, of which 327745 TEUs were inbound and 325948 TEUs were outbound ("*Analysis Report on the Capacity Structure of Waterway Freight Ships in the Province"*, 2022).Therefore, there is little possibility of a significant increase in the capacity of inland dry ship bulk cargo in Hunan Province in the future, and the development prospects of container transportation are promising. Therefore, this study chooses container waterway transportation as the demonstration object.

From the perspective of navigation environment, there are mainly two types of container transportation modes in Hunan Province: container "waterbus" transportation mode and river sea direct transportation mode. In the long run, with the development of the economy and correct guidance, the structure of waterway freight transportation in Hunan will gradually transform and develop towards multi-industry transportation such as energy, steel, grain, and equipment manufacturing, serving more industrial development, and the proportion of sand and gravel transportation will decrease. At the same time, considering further adjustment and optimization of the comprehensive transportation structure, with the adjustment of freight transportation from public transportation to water and from public transportation to rail, the water transportation volume in Hunan Province will continue to gradually increase in the medium and long term. Therefore, for the water container transportation mode in Hunan Province, this study chooses the inland river of Hunan as the research water area.

Determination of demonstration ship types

According to the current situation, development plan, and policy direction of water transportation in Hunan Province, the demand for typical demonstration ship types in Hunan Province has the following characteristics: firstly, the focus is on container cargo transportation; secondly, the development direction is based on the two transportation modes of inland river container "waterbus" (container liner shipping) and river sea direct transportation; thirdly, the development direction is driven by new energy and clean energy. Through market demand analysis, this article focuses on the transportation mode of container "waterbus" (container liner shipping) in Hunan's inland rivers, combined with transportation demand and typical scenarios of green energy application. From the perspective of adaptability, environmental protection, technological maturity, and economy of green technology application, short-term routes will be oriented towards electrification. At the same time, drawing on the development path of gasification and electrification of the Yangtze River, the demonstration ship selection is guided by building a green, low/zero carbon container benchmark ship for the Xiangjiang trunk line.

Based on the above analysis, in line with the national "dual carbon" strategy, meeting the urgent market demand, considering the navigable environment, the representativeness of transportation vessels, and scientifically positioning demonstration ship types. After market research, based on factors such as logistics environment, navigation environment, market environment, technology environment, and policy environment, a demonstration ship type suitable for the "waterbus" container transportation mode in inland rivers of Hunan has been determined as follows: considering adapting to the market's demand for multi cargo transportation, it is planned to use Lingji Port in Yueyang City as the hub port, and ports in Hunan Province such as Changsha Xianing Port, Changde Yanguan Port, Hengyang Songmu Port, etc Jinshi Port is a multi-purpose green container ship type fed to the port. The initial consideration of the deadweight of this ship type is 200 TEU container level, which is driven by electric motors.

For the determination of ship size, there has been a certain increase in the past two years for bulk carriers with a length exceeding 88m and a width exceeding 15.5m, as well as container ships with a length exceeding 85m and a width exceeding 15m. At the same time, a "shuttle bus" mode for containerized water transportation from various container ports in Hunan Province to Yueyang Chenglingji Port has been opened, and a 200TEU container level inland river container ship has been selected as the research object. This article is based on the limitation of ship size by the channel conditions of the Changsha Yueyang section, and calculated under the provided unified ship type demonstration platform to obtain the accuracy index results of each feasible ship type scheme. The trend chart of accuracy index changes with the main scale of the ship type is drawn, and the impact of variable changes in ship type schemes on the technical and economic performance of ship operation is analyzed. At the same time, the operation of the Changsha Yueyang route needs to pass through the Changsha hub, so the ship size needs to meet the requirements of the container ship series for the Yangtze River branch line lock transportation ships in the national mandatory standard GB38030.1. The preferred ship type size is CZ-J6 (with a length of 88m and a width of 15m), which is relatively close to the scale series. At the same time, considering that appropriately increasing the ship

width is beneficial for container stability, and combining the analysis of the changes in the above indicators with the ship size, it is advisable to choose the ship type with a length of 88m and a width of 15.00m. As mentioned above, the specific ship type parameters are obtained as shown in Table 1.

Table 1: Optimal ship type scheme for container ship

Project	Numerical Value
Length (m)	~88.00
Width (m)	~15.00
Draft (m)	~2.80
Container load capacity (TEU)	~200 container level

RESEARCH AND DEVELOPMENT OF DEMONSTRATION SHIP TYPES FOR ELECTRIC CONTAINERS IN HUNAN INLAND RIVERS

Based on factors such as logistics environment, navigation environment, market environment, technology environment, and policy environment, and considering adapting to the needs of multi cargo field transportation in the market, this demonstration ship type is planned to use Yueyang Chenglingji Port as the hub port, and Changsha Xianing Port, Changde Yanguan Port, Hengyang Songmu Port, and Jinshi Port as feeding ports to achieve a container "shuttle bus" water transportation mode, realizing Changsha Port, Hengyang Port, and Changde Port All containers entering and exiting Tianjin Port are transshipped at Yueyang Port. Develop a new generation of inland green container multi-purpose transport vessel that can sail on the ports and routes of Yueyang in Hunan Province, integrating safety, green, and economy. By optimizing the overall layout and line design, as well as applying advanced integrated power systems, we aim to reduce the carbon emissions of ships, improve the safety level of ship navigation, and create a "Hunan sample" of electric freight ships.

According to the previous analysis, the overall positioning of the demonstration ship type for inland electric containers in Hunan Province consists of the following parts. Firstly, from the perspective of transportation cargo types, the main focus is on loading containers and dry bulk cargo. Secondly, from the perspective of transportation routes, the transportation route of this demonstration ship type is from Changsha to Yueyang. Specifically, the container "shuttle bus" water transportation model is adopted, with Yueyang Chenglingji Port as the hub port and Changsha Xianing Port, Changde Yanguan Port, Hengyang Songmu Port, and Jinshi Port as the feeding ports. All containers entering and exiting Changsha Port, Hengyang Port, Changde Port, and Jinshi Port are transshipped at Yueyang Port. Finally, in terms of fuel power selection, in order to implement the national "dual carbon" strategy, starting from promoting green and low/zero carbonization of water transportation in Hunan, combined with the cargo demand and navigation environment conditions of Changsha Yueyang, considering various green energy energy density ratios, dynamic responsiveness of ships, container scheduling arrangements (*Green ship regulations*, 2020), distance and other factors, this ship adopts electric propulsion mode.

Next, this article introduces the overall overview of developing ship types. Firstly, for the main scale elements, the basic parameters of the ship are determined according to the applicable specifications based on its purpose and route (*Technical rules for statutory inspection of inland vessels*, 2019), as shown in Table 2.

Table 2: Basic parameters for developing ship types

Project	Numerical Value
Total length	88.00m
Length between perpendicular lines	85.36m
Molded breadth	15.00m
Molded depth	5.30m
Full load draft	3.52m
Load capacity	~3000t
Container capacity	208 TEU
Block coefficient	0.85
Maximum speed	18km/h
Rated power of propulsion motor	500kW×2

According to the Freund's number range and according to the speed requirements and characteristics of electric boats, this boat is a low-speed boat. It is also noted (Sheng Zhenbang et al, 2010) that educing shape resistance and improving propulsion efficiency are the main means to improve the speed of ships. In order to improve the flow of the tail propeller, improve the propeller propulsion efficiency, and adapt to the navigation environment of the inland river, the stern of the ship

adopts a double tail line type, which effectively reduces the deflow angle, and at the same time, the propeller of the ship is equipped with an energy-saving attachment with a vortex elimination fin, which is used to reduce the energy consumption loss of the propeller circulation and increase the auxiliary thrust. The schematic diagram and overall layout of the demonstration ship are shown in Figure 1 and Figure 2 respectively.

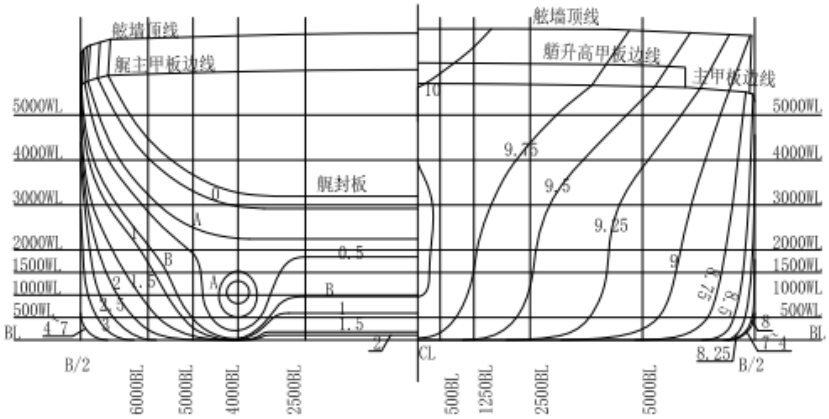

Figure 1: Schematic diagram of demonstration ship type line

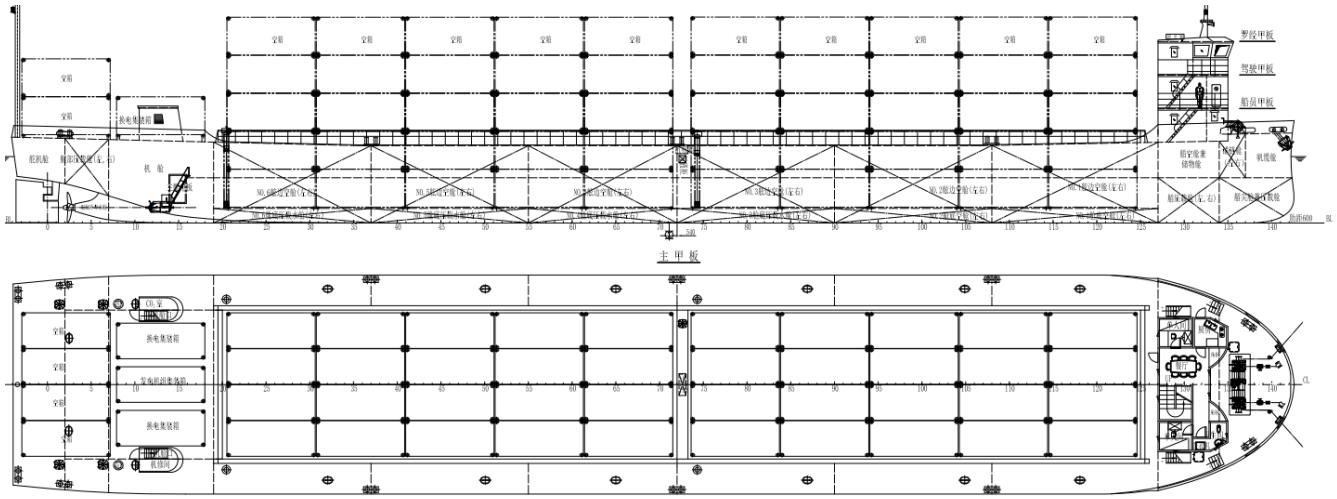

Figure 2: Schematic diagram of the overall layout of the demonstration ship

Regarding the adaptability of the overall demonstration scheme of inland electric container ship in Hunan Province, firstly, the modified Ayre method is used to evaluate the effective power of the ship to obtain the effective power curve of the ship, and the MAU spectrum propeller is used to design the propeller. In terms of ship accessibility, the adaptability of the main scale is judged from the perspectives of channel water depth, dock berthing and loading and unloading capacity, and clearance height. At the same time, with the goal of maximizing the length of the cargo hold, the principle of intensive layout is adopted to design the general layout of the ship to achieve the goal of maximizing the loading of the ship. In particular, the maximum height of the ship after lowering the mast does not exceed 12m, which is suitable for navigation in the Xiangjiang River and the Yangtze River waterway. If there are more special requirements, the ballast water can be adjusted to further reduce the height of the entire water surface of the ship and ensure the loading capacity of the container.

POWER MODE SELECTION

Technical analysis and battery capacity selection

There are various forms of electric propulsion. Such as pure electric ships, diesel powered electric propulsion, hybrid power, and extended range engines. Among them, hybrid vessels can be further divided into series hybrid, parallel hybrid, series parallel hybrid, and shaft generator modes(*Guidelines for Inspection of Hybrid Electric Ships*, 2019).

Series extended range hybrid mode refers to the configuration of a certain amount of chemical energy storage batteries and diesel or other internal combustion engine generator sets on board the ship. When the batteries are charged, pure electric propulsion is used, and when the batteries are depleted, the generator sets are used to generate electricity and charge the batteries to increase endurance. It is also noted (Tang Tianhao, Han Chaozhen 2015) that its biggest feature is that the batteries and generator sets can be placed in a fixed position inside the cabin, or can be placed in a container form and can be moved or suspended externally.

The container ships for inland water transportation in Hunan Province have a large tonnage and a long voyage. The biggest advantage of this method is that it solves the problem of navigation endurance and does not conflict with battery swapping and charging. In other words, in terminals with replaceable battery conditions, the battery can be directly swapped, and in terminals with charging piles, it can also be charged. If sailing in navigation areas where battery swapping and charging are not possible for a long time, the mode of generator range extension is adopted for continuous navigation. The use of series extended range in the transportation of bulk cargo can better solve the problem of endurance, improve the charging process and operational efficiency. In different situations, pure electric navigation, charging navigation, and charging or battery swapping can be flexibly selected. Its application can also meet the current policy implementation for new energy subsidies and development. Therefore, for the distance between Changsha and Yueyang, considering that the shore support is not yet sound and the route is not a short distance fixed point-to-point route, it can be seen from a technical perspective that the series extended range hybrid mode is more suitable for this demonstration ship.

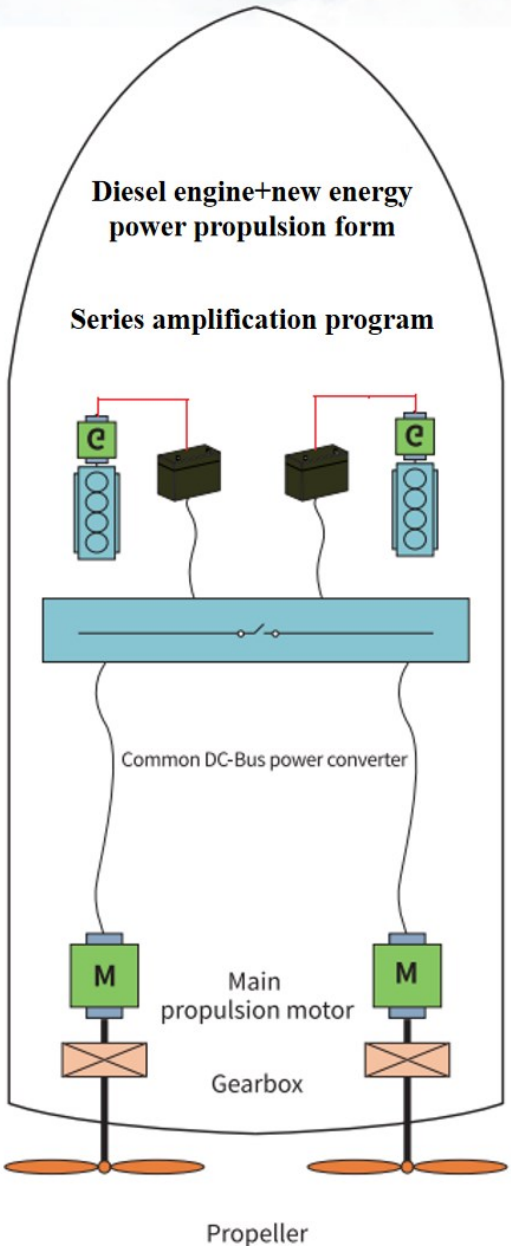

Figure 3: Series extended range hybrid mode

The selection of ship battery capacity should consider the following three factors: firstly, the main propulsion energy consumption of the ship mainly depends on the operating power and operating time of the ship; The second is the electricity consumption for crew members, which mainly depends on the power distribution and usage time of the ship's daily life; The third is the attenuation of the battery, taking 85% of the maximum capacity of the battery pack. Among them, the selection of energy consumption and the calculation of battery capacity adaptability are shown in Table 3.

Table 3: Battery Capacity Adaptability Analysis Table

Electricity consumption type	Project	Numerical Value
Main propulsion energy consumption	Route range	Approximately 150km
	Design Speed	18km/h
	Operational speed	12km/h
	Rated propulsion power	1000kW
	Operating propulsion power (12km/h)	Converted to approximately 297kW
	Single voyage time	12.5h
	Energy consumption for single voyage main propulsion	3713kWh
hotel load	Power of household distribution system	Approximately 30kW
	Waiting time for loading and unloading	1.5d
	hotel load and energy consumption	45kWh

According to Table 3, the ship is equipped with two box type power supplies. Due to the design specifications requiring that the capacity of each box type power supply should not exceed 2000kWh (*Battery Power Specification for Ship Applications*, 2023), two box type power supplies from 712 Institute were selected, each with a battery capacity of 1998kWh. The total battery capacity of this ship is 3996kWh. Calculated based on 85% effective capacity, it is 3397kWh, which cannot meet the energy demand of a single voyage of the ship, so diesel fuel range extension is still required.

Economic and Environmental Analysis

From the perspective of technological adaptability, container ships for trunk and branch transportation in Hunan Province have a smaller tonnage and shorter voyage. Diesel powered ships, extended range electric ships, pure battery powered ships, and LNG powered ships all have no endurance issues and are technically feasible. Among them, pure battery powered ships require more electricity per journey than the maximum carrying capacity of the ship itself, requiring one battery exchange midway.

By selecting the existing operating ship types in Hunan as the object, the comparison of cost, carbon emission and payback period under different power schemes was calculated according to the parameters given by the shipowner. The specific calculation results are shown in Figure 4. From the perspective of environmental benefit analysis, compared with pure diesel ships, the carbon emissions of extended-range electric ships are reduced by about 40% to 70%, while pure battery-powered ships can achieve zero emissions, and the carbon emissions of LNG-powered ships are reduced by about 10-15%.

Similarly, through the technical and economic calculation and analysis of different power schemes of sample ships, the relationship between ship cost subsidy and payback period in Hunan inland river transportation and trunk branch transportation container scenarios is obtained. Compared with pure diesel ships, the necessary freight rates for pure battery-powered ships have increased by about 15%, and the necessary freight rates for LNG-powered ships have decreased by about 10%. The economic analysis mainly focuses on the cost comparison of electric propulsion vessels with conventional diesel-powered vessels. When the ship cost subsidy is 10% to 20%, the payback period of extended-range electric ships can reach the level of pure diesel ships, while the payback period of pure battery-powered ships is difficult to reach the level of pure diesel ships through subsidies.

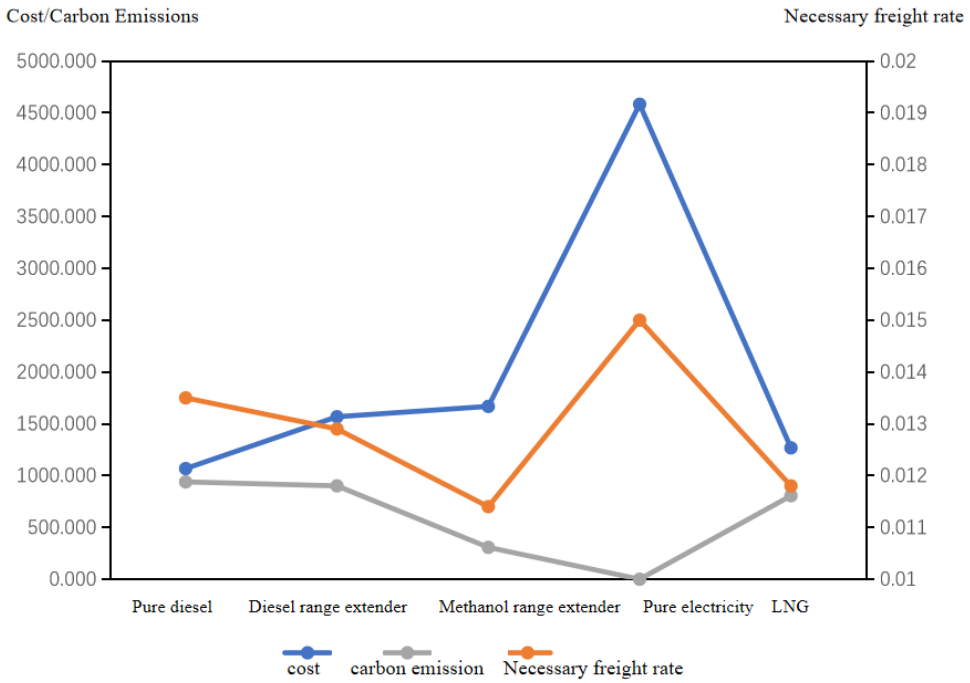

Figure 4: Calculation of cost, carbon emission and payback period of different power schemes in Hunan inland river transportation and trunk branch transportation container scenarios

Table 4: Comparison of prices between pure diesel and electric ship power systems

Serial Number	Cargo capacity (ton)	Pure diesel power (Ten thousand yuan)	Pure battery power (Ten thousand yuan)	Extended range electric boat (10000 yuan)		
				Pure electric range 120km	Pure electric range 100km	Pure electric range 80km
1	1000	~80	~530	~420	~382	~344
2	2000	~99	~730	~553	~494	~435
3	3000	~119	~984	~717	~642	~566
4	4000	~148	~1500	~910	~821	~732
5	5000	~179	~1976	~1068	~966	~865
6	6000	~203	~2452	~1232	~1120	~1008
7	7000	~238	~2938	~1394	~1272	~1151
8	8000	~260	~3014	~1535	~1405	~1275

According to Table 4, the main source of cost increase for electric powered ships is energy storage batteries. It can be seen that due to the increase in initial investment, the economic performance of electric powered ships is worse than that of traditional diesel powered ships without government subsidies. However, the environmental advantages of electric propulsion for ships are significant. Starting from achieving the "dual talk" goal of water transportation in Hunan, we should vigorously promote the electrification of medium and short distance freight ships. Before the design and construction of this vessel, the shipowner and relevant parties have conducted in-depth investigations and economic calculations, and even without any policy subsidies, the profitability of its operation is predictable.

In addition, the ultimate goal of the design, construction, and operation of this ship is to achieve complete pure electricity and zero emissions. Not only does it have zero emissions in terms of power, but it also includes zero emissions of dirty oil, sewage, and domestic sewage. The ship is equipped with oil and sewage collection tanks and domestic sewage collection tanks, which are used to collect and store all oil and sewage generated on board. Except for receiving at the shore or anchorage, the entire life cycle of the ship will not discharge any oily or domestic sewage outward.

Based on the analysis of the adaptability and economy of battery powered ship technology, and considering the adaptability, environmental friendliness, technological maturity, and economy of battery powered technology application, it is recommended to use diesel extended range hybrid power scheme at this stage. At present, the use of series extended range hybrid mode can better adapt to the current conditions of the Changsha Yueyang route where the shore based support for electricity supply is not yet sound and is not a short distance fixed point-to-point route. Therefore, it is feasible for this demonstration ship to adopt series extended range hybrid mode.

Overall Plan Description of 208TEU Inland River Electric Container Demonstration Ship Type

Based on the research and development concept mentioned earlier, and through the analysis of ship type positioning and ship power mode of the demonstration ship, modern design methods are adopted to meet the requirements of the latest applicable standards, conventions, and rules. Drawing on the research and development achievements of domestic and foreign inland river green ship types, the overall scheme design of the Changsha Yueyang 208TEU inland river pure electric distribution dual-use demonstration ship type is carried out. And introduce the plan from four aspects: cost estimation and construction progress of the hull, engine, electrical, and demonstration ship type.

Hull design

This ship is a dual engine, dual propeller, lithium battery + diesel generator hybrid electric propulsion, all steel structure, open hatch type container and distribution dual-purpose cargo ship. It mainly carries containers or containers containing some dangerous goods, and can also load dry and miscellaneous cargo such as sand, cement, stones, coal, grains, metal ores, etc. It mainly navigates within the A and B level navigation areas of inland rivers. A container capable of loading dangerous goods in packaging such as 1.3G, 1.4G, 1.4S, 2.2, 8, 9, 3, 4.1, 4.2, 5.1, 6.1, etc. (*Code for construction of steel inland vessels*, 2016)

For the selection of ship type, this ship is a multi-purpose cargo ship with a straight aft leaning slightly curved bow, square stern, twin engine, twin propeller, and stern electric drive. The entire ship is of steel fully welded structural type. The overall layout is as follows: below the main deck, from the front to the tail, there are bow peak tanks (ballast tanks), bow ballast tanks, cargo tanks, engine rooms, stern shaft tanks, stern ballast tanks, and rudder rooms. The head position on the main deck consists of three decks: crew deck, pilot deck, and compass deck. Set up battery swapping containers on both sides of the stern deck, with battery swapping generator containers placed in the center. Machine repair rooms, CO2 rooms, and lower engine stairwells are set up along the walkways on both sides of the stern deck. The front end of the upper structure at the bow is a raised deck, with wing bridges on both sides of the cab, and a full window in front. Since the ship is in the stage of actual ship construction and application, this paper models and displays an overview of the 208TEU inland river pure power distribution demonstration ship based on the software modeling and simulation platform based on the above overall layout, as shown in Figure 5.

For the performance analysis related to the demonstration ship type, this ship has two engines and two propellers, with a full load speed of 18km/h. Set up two streamlined balance helmets and equip them with a 160kN. m hydraulic servo. To effectively control vibration and noise, important compartments should be arranged away from noise sources; Optimize the shaft alignment and propeller design. Try to increase the gap between the propeller blade tip and the hull plate as much as possible, and design the propeller specifically to adapt to the uneven wake at the tail, delay the occurrence of cavitation or reduce the cavitation area, and reduce vibration; Properly strengthen the ship structure and ensure the reasonable strengthening and continuity of the entire ship structure. Strengthen the structure above the propeller and below the base. There is a good transition between bone materials and plates or between bone materials and bone materials.

Figure 5: Overview of 208TEU Inland River Pure Electric Distribution Demonstration Ship

Marine Engineering

This ship adopts a dual motor propulsion and dual fixed pitch propeller linear transmission method. The power device consists of a propulsion motor, high elasticity coupling, reduction gearbox, propeller and propeller shaft, control and monitoring system, etc. Two TYC500-6 propulsion motors from Xiangdian Corporation are selected as the main engine, with fixed pitch propellers. Each motor, shaft system, and its corresponding power system form an independent system, and the two propulsion motors can operate independently. The propulsion motor and gearbox are remotely controlled in the cab, monitored in the monitoring room, and controlled locally at the machine side. The main propulsion device consists of a propulsion motor, a high elastic coupling, a marine directional reduction gearbox (with clutch), a control and monitoring system, a shaft system and its accessories, and a fixed pitch propeller. The basic parameters of the selected propulsion motor and gearbox are shown in Table 5.

Table 5: Main propulsion device parameters

Propulsion device type	Project	Numerical Value
propulsion motor	Model	Xiangdian Corporation TYC500-6
	Rated power	500kW
	Speed	1450r/min
	Number of units	2
Gearbox	Model	HCD800
	Reduction ratio	5.889:1

Ship Electrical Design

It is recommended to use a range extender (diesel generator set) to meet the range extender requirements in the selection process of power mode for electric propulsion on this ship. This is mainly due to considerations of the operating scenario conditions being applied. At present, diesel power generation with extended range can be replaced with methanol power generation with extended range, hydrogen fuel cell with extended range, or other forms of power generation with extended range, which can increase the adaptability of new energy development to different new energy applications. In the design of this ship, sufficient design margin, interfaces, and equipment have been reserved to ensure charging, battery swapping, range extension, etc. Various modes can be freely switched, especially the range extension method. The system does not require any changes and can be directly connected for use.

In terms of power supply configuration, this ship is equipped with two containerized mobile power supplies and one generator set container on the main deck at the stern. Each containerized power supply is equipped with approximately 2000kWh of lithium iron phosphate battery packs and their supporting system equipment. Each generator set container is equipped with one 400kW marine diesel generator set and its supporting system equipment. The electrical protection level of the box type power supply shall not be lower than IP56, meeting the requirements for layout in outdoor deck spaces. There are emergency shutdown devices for each battery system on the driver's console and outside the box power supply, which can emit both visual and auditory signals during operation.

In addition, the box type power supply continuously provides power to the ship by replacing the fully charged box type power supply at the dock power station. The entire box type power supply includes a battery system, fire extinguishing system, plugging and unplugging system, fire protection design, air conditioning system, and seismic protection system. The battery system mainly consists of battery packs, high-voltage boxes, main control boxes, etc. The plug-in system mainly consists of plugs, sockets, and in place sensors. The fire protection system mainly consists of detectors, HFC-ea fire extinguishing, water sprinkler fire extinguishing, and monitoring. The fire protection design mainly consists of A60 compartments and A60 fire doors on both sides. The air conditioning system is mainly composed of air conditioning and air ducts, and the vibration isolation system uses steel wire isolators. The box type power supply is equipped with a BMS battery management system. The system has remote data monitoring function, which can be monitored and displayed in the cab.

This ship is a hybrid electric propulsion system consisting of lithium batteries, diesel generators, and dual engine propulsion. The propulsion motor is controlled by frequency conversion and commutation through a frequency converter to control the harmonic components of the ship's power grid. And there is an integrated transformer and distribution device in the engine room, which is the center of the ship's power system. The integrated transformer and distribution device distributes and converts the direct current output from lithium batteries and diesel generators into variable frequency and voltage alternating current required for propulsion motors and constant frequency and voltage alternating current required for daily electrical equipment, directly supplying power to the entire ship's propulsion motors and daily electrical equipment. The specific selection of the main propulsion motor is provided by Xiangdian Group with relevant technical information. The

specific parameters are shown in Table 5. The propulsion control system includes: 1 set of main propulsion driver control panel, 2 sets of machine side control boxes, 1 set of dual path propulsion motor tachometer, and 1 set of dual machine control handle. The main propulsion control box is located in the engine compartment. There is a remote control handle on the driver's console. In speed control mode, the speed signal can be sent to the distribution cabinet through the remote control handle, and the speed of the propulsion motor can be adjusted to achieve speed regulation.

This ship adopts a hybrid power scheme, and the propulsion control adopts an integrated design, collectively referred to as the integrated control system. It integrates the generation, use, and scheduling of energy in control functions and strategies, and is integrated into the integrated transformer and distribution device. This is mainly to reserve space for subsequent device upgrades. In addition, it is equipped with an intelligent ship system, which has functions such as remote transmission of information and data, real-time online detection of ship energy consumption parameters, and backend analysis and optimization. Many related interfaces are reserved for future upgrades and renovations of the intelligent system.

Cost estimation and construction application situation

The estimated cost of the Changsha Yueyang 208TEU inland pure electric distribution demonstration ship is about 13 million yuan, as shown in Table 6.

Table 6: Main propulsion device parameters

Serial Number	Project	Amount (Ten thousand yuan)
1	Hull materials	~350
2	Main equipment of the hull	~50
3	Marine equipment and materials	~120
4	Electrical equipment and materials	~540
5	labor cost	~200
6	Value added tax and surcharges	~110
7	Other Expenses	~30
8	Total cost of ship engineering	~1400

In terms of practical construction applications, the 208TEU inland pure electric distribution dual-purpose demonstration ship officially held a groundbreaking ceremony on June 12, 2023, and construction began in July at Xinyu Shipyard in Xiangtan County. The ship is expected to be completed and put into operation by the end of December. After the delivery of the vessel, it will become the largest 88m standard lock pure electric dual-purpose ship with container loading capacity in China, and also the first new energy pure electric dual-purpose ship in Hunan, serving the 160km container shuttle bus route from Lingji Port Area of Yueyang Port City to Xianing Port Area of Changsha Port in Hunan Ocean Shipping. The construction of a 208TEU inland pure electric distribution demonstration ship is shown in Figure 6.

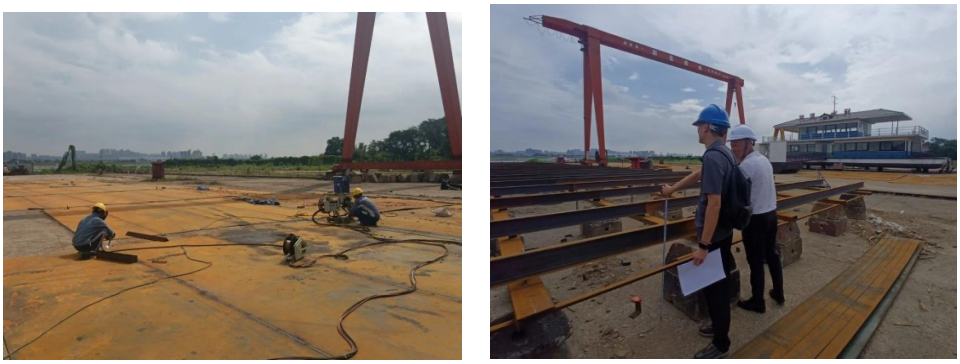

Figure 6: Construction status of a 208TEU inland pure electric distribution demonstration ship

With the construction and operation of the 208TEU inland pure electric dual-purpose demonstration ship, it is of milestone significance for promoting the green and low-carbon development of inland waterway navigation in Hunan Province's "one lake, four waters". In addition to the battery swapping function, in the future, ships will integrate digital and intelligent technology applications. After the formation of a large-scale network of ship charging and swapping stations, it is expected to achieve more than 10% of comprehensive energy-saving benefits.

CONCLUSIONS

This article aligns with national development strategies such as "dual carbon" to promote green, low-carbon, and high-quality development of shipping in Hunan. Adhering to the development concept of safe, applicable, green, efficient, economical, and low-carbon standard ship types, guided by the goal of "green, low-carbon/zero carbon", following relevant policies, regulations, standards, and technical requirements, adapting to the navigation environment of Hunan waterway freight ships, adapting to the "waterbus" transportation mode of Hunan inland river containers, and considering adapting to the market demand for multi cargo transportation. At the same time, combining green energy, power system technology and other applications, we will develop demonstration ship types for green, high-energy and direct river and sea transportation in Hunan Province, leading the development of green and standardized ships. Develop an overall plan for the demonstration ship type of pure electric distribution in the Changsha Yueyang inland river. This ship type has a load capacity of approximately 200TEU container level and is propelled by an electric motor. Its container capacity is 208TEU, with a total length of about 88.00m and a total width of about 15.00m. The designed draft is about 2.8m.

CONTRIBUTION STATEMENT

Zhengchen Lian[1]**:** Conceptualization; data curation, methodology; writing – original draft.
Lizheng Wang[2]**:** Conceptualization; supervision; writing – review and editing.

ACKNOWLEDGEMENTS

The authors are grateful for the Research on the Standard Ship Types for Green, High Energy Efficient Inland and River Sea Direct Transportation in Hunan Province.

REFERENCES

China Classification Society. (2016). Code for construction of steel inland vessels. Beijing: People's Transportation Publishing House.

China Classification Society. (2020). Green ship regulations. Beijing: People's Transportation Publishing House.

China Classification Society. (2023). Battery Power Specification for Ship Applications. Beijing: People's Transportation Publishing House.

China Classification Society. (2019). Guidelines for Inspection of Hybrid Electric Ships. Beijing: People's Transportation Publishing House.

China Maritime Safety Administration. (2019). Technical rules for statutory inspection of inland vessels. Beijing: People's Transportation Publishing House.

Department of Transportation of Hunan Province. (2022). Analysis Report on the Capacity Structure of Waterway Freight Ships in the Province. Retrieved from https://jtt.hunan.gov.cn/jtt/xxgk/jttj/202207/t20220715_27558285.html.

Hunan Provincial Department of Transportation. (2022). Hunan Province's 14th Five Year Plan for Transportation Development (Highway and Waterway). Retrieved from http://jtt.hunan.gov.cn/jtt/jjzdgz/jtghyj/ghyj/202203/t20220329_22724832.html.

Lian Zhengchen, Wang lizheng. (2023). SHIP PERFORMANCE EVALUATION AND GREEN SHIP TYPE SCHEME UNDER COMPLEX CHANNEL CONDITIONS. ASME Style Guide.

Ministry of Industry and Information Technology, Development and Reform Commission, Ministry of Finance, Ministry of Ecology and Environment, Ministry of Transport. (2022). Implementation Opinions of the Ministry of Industry and Information Technology and Five Other Ministries on Accelerating the Green and Intelligent Development of Inland River Ships. China's informatization, (10), 13-15.

Sheng Zhenbang et al. (2010). Ship Principles. Shanghai: Shanghai Jiaotong University Press.

Tang Tianhao, Han Chaozhen (2015). Ship Electric Propulsion Technology. Beijing: Machinery Industry Press.

Proceedings of 15th International Marine Design Conference (IMDC-2024)
June 2-6, 2024
Amsterdam, the Netherlands

Hybrid and Alternative Fuel Power Management Systems in Ships - Multi-Criteria Decision-Making Assessment

Amin Nazemian[1,*], Evangelos Boulougouris[2], and Sarath Krishnan Melemadom[3]

ABSTRACT

This paper addresses the maritime industry's imperative to cut greenhouse gas emissions by exploring hybrid propulsion systems for bulk carrier vessels, specifically focusing on battery systems and hybridized conventional four-stroke generator engines. Utilizing the Analytic Hierarchy Process (AHP) and MARCOS decision-making method, the study evaluates diverse factors, including capital and operational expenditures, risk, emissions, bunkering availability, and weight. The research delves into different power management system topologies, such as conventional diesel engines, ammonia, and methanol-fueled engines, along with battery hybrids. The study underscores the methodological significance of decision-making tools and anticipates that evolving regulations will drive the maritime industry towards carbon neutrality through hybrid power management systems.

KEY WORDS

Decarbonization; Multi-Criteria Decision-Making (MCDM); Hybrid Propulsion System; Alternative Fuel; Analytic Hierarchy Process (AHP).

INTRODUCTION

The shipping industry has been a significant contributor to global carbon dioxide (CO2) emissions, with recent estimates indicating a 4.6% increase to 833 million tonnes in 2022 compared to 794 million tonnes in 2020 (Richardson, 2022). This rise is attributed to the combustion of approximately 203 million tonnes of fuel, primarily sourced from environmentally unfriendly fossil fuels. In response to this environmental challenge, the International Maritime Organisation (IMO) has introduced regulations under the International Convention for the Prevention of Marine Pollution (MARPOL 73/78) Annex IV as part of its decarbonization strategy (IMO, 2018). The IMO's overarching goal is to reduce annual absolute greenhouse gas (GHG) emissions from international shipping by at least 50% by 2050, compared to 2008 levels (Seddiek & Ammar, 2023). Additionally, there is a concerted effort to completely eliminate GHG emissions from the shipping industry within this century. To achieve these objectives, the IMO aims to decrease the carbon intensity emissions of global maritime transport by a minimum of 40% by 2030 and a further reduction of 70% by 2050, relative to the baseline year of 2008 (Ammar & Seddiek, 2017; IMO. 2021).

Given the prolonged lifespan of vessels, achieving these targets necessitates significant modifications to the existing fleet. Current strategies employed by the maritime sector for emission mitigation include the adoption of emissions abatement technologies, the use of marine alternative fuels, and the potential implementation of hybrid power systems (HPS) (Inal et al., 2022). This study specifically explores the use of batteries and alternative fuels such as ammonia and methanol in the power supply system of large ocean-going vessels. Advancements in battery technology, extending beyond consumer electronics and

[1] Maritime Safety Research Centre (MSRC), Department of Naval Architecture Ocean and Marine Engineering, University of Strathclyde, Glasgow, UK; ORCID: 0000-0001-6861-4488

[2] Maritime Safety Research Centre (MSRC), Department of Naval Architecture Ocean and Marine Engineering, University of Strathclyde, Glasgow, UK; ORCID: 0000-0001-5730-007X

[3] Maritime Safety Research Centre (MSRC), Department of Naval Architecture Ocean and Marine Engineering, University of Strathclyde, Glasgow, UK; ORCID: 0009-0008-8300-6665

* Corresponding Author: amin.nazemian@strath.ac.uk

Submitted: 2 February 2024, Revised: 23 March 2024, Accepted: 1 May 2024, Published: 21 May 2024

Conference paper, DOI: https://doi.org/10.59490/imdc.2024.861 e-ISSN: 3050-4864

automobiles, have prompted consideration of their application in the maritime sector. The paper delves into the energy consumption and power demands of large ocean-going merchant vessels, exploring the feasibility of incorporating batteries into the electric grid system. This integration is identified as an area where batteries and hybridization can offer significant benefits, especially as forthcoming carbon-neutral fuels are expected to incur higher costs (MAN Energy Solutions, 2019).
Minimization of fuel consumption and reduction of emissions is one of the main objectives for designing the future generation of ship (Dedes et al., 2012). The development of hybrid vehicles, encompassing both terrestrial and marine applications, has emerged as a widely researched and implemented strategy to mitigate pollution within the transport sector (Chan et al., 2010). There are numerous advantages associated with the utilisation of electric hybrid systems in comparison to internal combustion engines, which pertain to both environmental and engineering considerations (Nazemian et al., 2024). The primary sources of air pollution from ships are NOx, CO2, SO2, and particulate matter. These emissions are generated either through direct combustion or as a result of chemical reactions occurring in the atmosphere. As a consequence of this, the implementation of hybrid electrical systems enables a significant decrease in pollutant emissions, as well as a substantial reduction in noise pollution (Padolecchia et al., 2023). In this context, it is imperative to thoroughly analyse power generation and power storage alternatives to identify more efficient solutions. In order to achieve an optimal and sustainable design that aligns with the ship's operation profile. Therefore, the existing scholarly literature predominantly emphasises the utilisation of batteries, supercapacitors, and flywheels as electric storage devices in conjunction with internal combustion engines and fuel cells as power generators when discussing hybridization technologies for ships (Geertsma et al., 2017; Nuchturee et al., 2020).
Batteries are the dominant energy storage technology due to their superior energy density, cost-effectiveness, and extensive knowledge in various transportation sectors. They consist of electrodes, electrolytes, and separators, with performance influenced by electrode material properties (Meng et al., 2017). The selection of battery type is crucial in the maritime industry, as there are various commercially available batteries suitable for transportation. Li-ion batteries are currently preferred due to their high energy densities and extended lifetimes, which are attributed to their industrial maturity and widespread availability. Despite the potential emergence of alternative technologies, lithium-ion batteries remain the preferred choice for shipping purposes (EMSA, 2022). Study by (Geertsma et al., 2017) examines the impact of a hybrid battery-diesel electric power management system on exhaust gas emissions within the global dry bulk carrier fleet. For more information, the comparison of different types of batteries is presented in the table below.

Table 1: Properties of different popular battery types. (Inal et al., 2022)

Battery type	Energy density (kWh/kg)	Power density (kW/kg)	Efficiency	Lifetime(cycle)	Capital Cost($/kWh)
Lead-Acid	30-50 * 10^{-3}	75-300* 10^{-3}	70-90%	500-1000	70
Nickel-cadmium	50-75* 10^{-3}	150-300* 10^{-3}	60-65%	2000-2500	300
Nickel Metal Hydride	60-100* 10^{-3}	200-1500*10^{-3}	65-90%	750	300-500
Lithium-ion	100-200*10^{-3}	80-2000* 10^{-3}	85-90%	600-2000	200-700

The duration for which the battery must provide power is contingent upon the anticipated duration of unforeseen operational interruptions of the auxiliary engine. Based on empirical evidence, a battery's 15-minute duration of operation is sufficient for preventing power outages, restarting a malfunctioning auxiliary engine, and achieving optimal power output. In this particular scenario, the battery system is not to be taken as substitute for auxiliary engines, but rather as an additional system. The optimal approach, in terms of both reliability and cost-effectiveness, would involve the implementation of a solution that enables a six-hour battery operation. This duration is assumed to be adequate for resolving any potential concerns related to the auxiliary engine. The implementation of an extended battery backup system guarantees the ability to restart and restore the auxiliary engine in the event of a significant failure, thereby ensuring uninterrupted operations. Additionally, it affords maintenance personnel a sufficient duration to identify and rectify the underlying cause of the problem, thereby reducing the likelihood of a reoccurrence. Moreover, an extended battery lifespan mitigates the necessity for prompt repairs or replacements, resulting in time and resource conservation. By implementing this solution, vessel management can attain a sense of assurance, as they can be confident that their supplementary engines are adequately supported and equipped to efficiently manage unforeseen periods of inactivity. Herein, different Power Management systems with different configurations of battery hybridization and alternative fuel (Ammonia and Methanol) will be analyzed and evaluated based on decision-making process.
Ammonia and methanol are regarded as viable alternative fuels and are duly acknowledged in various power management systems. Ammonia and methanol are widely recognized as the primary candidates for alternative fuel sources, both presently and in the foreseeable future. Accordingly, different power management systems (PMS) of ship propulsion will be evaluated in this paper by combination of Conventional, Ammonia, and Methanol fuels. When evaluating each alternative fuel, the following factors are taken into account, including capital expenditures (CAPEX), risk assessment, emissions, operating

expenditures (OPEX), availability, bunkering infrastructure, and weight considerations. Various combinations of conventional fuel, alternative fuel, and hybrid systems are being considered, which are explained as follows:

1. **PMS1**: Conventional Fuel ICE.
2. **PMS2**: Conventional fuel ICE + Battery
3. **PMS3**: Ammonia ICE
4. **PMS4**: Ammonia ICE + Battery
5. **PMS5**: Methanol ICE
6. **PMS6**: Methanol ICE + Battery

This paper discusses two various combinations of ship power supply systems Traditional diesel- Mechanic propulsion (Fig.1 (a)) and semi-hybrid diesel mechanic propulsion (Fig.1 (b)).

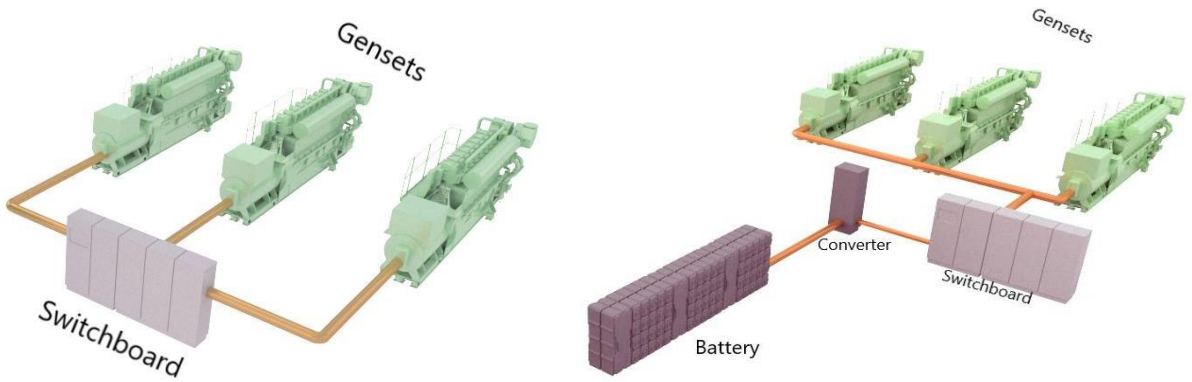

(a) (b)

Figure 1: (a) Conventional diesel-mechanic propulsion system, (b) Semi-hybrid diesel mechanic propulsion system (Latarche, 2021)

METHODOLOGY

The goal of this paper is to assess compare and contrast various power management systems (PMS) utilised in maritime vessels, considering multiple criteria including capital expenditure (CAPEX), risk, emissions, operational expenditure (OPEX), availability, and weight. The objective of this study is to offer a thorough examination that can inform decision-making within the maritime sector, specifically in the selection of the most suitable PMS for a particular application of vessel. Accordingly, the study has been conducted regarding the following **steps**:

S1. Evaluate Different PMS: This aims to evaluate the operational efficiency and effectiveness of different power management systems (PMS) including conventional diesel engines, diesel engine-battery hybrids, ammonia ICEs, ammonia ICE-battery hybrids, methanol ICEs, and methanol ICE-battery hybrids.

S2. Assess Criteria: This analysis will evaluate the primary factors to consider when choosing a PMS, encompassing the initial capital expenditure (CAPEX), risk assessment through the implementation of Failure Modes, Effects, and Criticality Analysis (FMECA), emissions quantified in terms of CO2 equivalents, ongoing operational expenses (OPEX), availability contingent upon fuel type and bunkering accessibility, and weight considerations.

S3. Dedicated Calculations: Conduct meticulous calculations for each criterion in order to determine a score for each PMS and subsequently establish a ranking based on these scores.

S4. Apply Analytic Hierarchy Process (AHP) and MARCOS method: Utilize the methodology known as AHP to rank the various PMS separately based on survey conduction, taking into consideration the relative relevance of each criterion. Furthermore, a dedicated calculation will be carried out using the MARCOS method on criteria and alternatives.

S5. Compare and Contrast: Compare the rankings derived from the dedicated calculations of MARCOS and the AHP to comprehend the effect of utilizing distinct evaluation techniques.

S6. Provide Recommendations: Based on the analysis, suggest to the maritime industry the most appropriate PMS for various scenarios, considering the vessel's specific requirements and constraints.

The composition of each system in EMS power plant varies with some systems employing conventional fuels, alternative fuels and hybrid configurations. Following is a summary of the six PMS systems currently under consideration:

PMS1: Conventional Fuel Internal Combustion Engine (ICE): This system uses conventional fuels such as LSMGO to generate power via an internal combustion engine. Currently, this is the most widely used PMS in the shipping industry.

PMS2: Conventional Fuel ICE + Battery: This system integrates a conventional fuel (LSMGO) internal combustion engine with a battery energy storage system. The hybrid nature of this system improves fuel economy, as the battery can store excess energy and provide additional power when required.

PMS3: This system uses ammonia as an internal combustion engine's fuel source and LSMGO as the pilot fuel.

PMS4: This system is a hybrid of an internal combustion engine powered by ammonia and LSMGO as pilot fuel with a battery storage system.
PMS5: This system employs methanol as an internal combustion engine's main fuel source and LSMGO as pilot fuel.
PMS6: This hybrid system combines an internal combustion engine fueled by methanol and LSMGO as pilot fuel with a battery storage system.
A typical configuration for an auxiliary system includes a minimum of 3 auxiliary engines. 2 engines are operating in modest loads, with another engine on standby while manoeuvring or cargo loading and unloading operations where blackouts must be avoided. This configuration permits an unexpected shutdown of one of the engines. During sailing in deep sea, 1 auxiliary engine is capable of supplying the load, the second is set to get started, and the third is undergoing maintenance. PMS1, PM3, and PMS5 do not have hybrid battery systems. These three systems are evaluated for use in important port operations with the configuration described. So, PMS1,3, and 5 will each have three engines, with two of them operating at 40% load simultaneously (Fig.2).

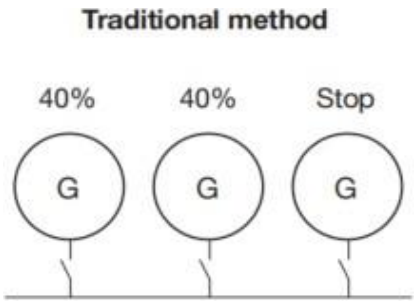

Figure 2: Traditional method

When two or more than two auxiliary engines operate at a low capacity for safety grounds, a battery has a substantial potential for savings. It can be used to mitigate sudden engine shutdowns and unforeseen events. Also, it has the capability to enhance the fuel efficiency of the auxiliary engines by selectively operating a single engine at elevated loads. The result leads to an enhancement in productivity while simultaneously decreasing operating expenses as well as repair costs. PMS 2, PMS 4, and PMS 6 have battery-hybrid systems, so in these three systems there will be two auxiliary engines, one operating at 80% capacity, second one in stop condition and battery (Fig.3).

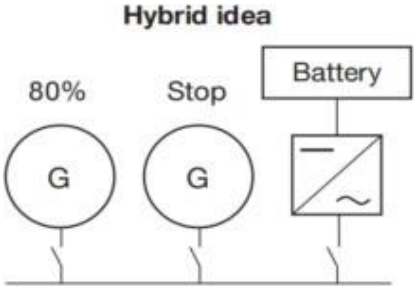

Figure 3: Hybrid Idea

Data collection of PMS scenarios for a Bulk Carrier

This study utilised data obtained from a variety of sources. This includes manufacturer data, data found in the literature, and data calculated based on established engineering principles. This section describes the methodologies used to collect data for each PMS system criterion. The ICE engines used for this study are shown in Table 2.

Table 2: Generator engine data (EMSA, 2022; Wärtsilä, 2023)

Power management system	Auxiliary engine	SFOC - g/kWh	Engine cost - USD/kW	Engine O&M cost USD/kW
PMS1, PMS2	Wartsila 6L25 auxiliary engine. 6-cylinder 2040kw ,900rprm	At 40% load - 198.2 At 80% load - 186.1	230	5

PMS2, PMS3, PMS4, PMS5	Wartsila 6L5DF Dual fuel Auxiliary engine, 6-cylinder 1890kW,900rpm	At 40% load - 202.1 At 80% load - 190.6	550	5.2

In both scenarios, total electric power is assumed to be 1480 kW, demanding 1560 kW from the auxiliary engine under the assumption that the generator is 95% efficient. The hotel load is assumed constant at the 560-kW required at port for operation. And the remaining power is required for port-critical activities, mainly the operation of cranes or bunker and ballast systems. In both scenarios, it is anticipated that the PMS will be operational for 1000 hours per year. For 6 hours of continuous operation in a hybrid system, the battery capacity required is 4230 kWh at a c-rate of 0.35. The Specific price of the battery in the system is taken at 500 USD/kWh, and the O&M cost is taken at 10 USD/kW (MAN Energy Solutions, 2019). Inverter installation is essential in Hybrid operation for the DC-AC conversion from the battery. The average inverter cost is 813 USD/kW (Brinsmead et al., 2015).
PMS3,4,5,6 is powered by a Wärtsilä 9L25DF engine. According to the manufacturer, this engine is already capable of running on multiple fuels and can therefore be readily upgraded to operate on future fuels like ammonia and methanol. In addition, the ratio considered for this study was influenced by Wartsila's announcement that their engine was effectively tested in full-scale operation with a blend of LSMGO (Wärtsilä, 2021).
For PMS3 and PMS 4 Fuel oil blend is: (Wärtsilä, 2021)

- GAS -> Ammonia - 70%
- Pilot fuel -> LSMGO - 30%

According to (Latarche, 2021) methanol exhibits a low ignitability when used as a fuel for internal combustion engines (ICE), as evidenced by its high ignition temperature of 470°C. Consequently, in order to ensure a consistent and stable combustion process as well as optimal engine performance, it is necessary to introduce 5% of pilot fuel, specifically LSMGO, into the combustion chamber. For PMS 5 and PMS 6 fuel oil blend is:

- GAS -> Methanol - 95%
- Pilot fuel -> LSMGO - 5%

Selective catalytic Reduction (SCR) is used as the after-treatment system for Ammonia powered PMS3 and PMS4.SCR Cost is taken 133USD/kW (EMSA, 2022).

Calculation and Assessment of evaluation criteria

This section will elucidate the process employed for calculating and assessing the evaluation criteria. Six power plant systems of bulk carrier ship will be evaluated based on the following criteria: capital expenditure (CAPEX), operational expenditure (OPEX), risk profile, availability/bunkering, weight, and emissions. Each criterion will be assigned a weighting based on its significance to the overall performance and feasibility of the system using AHP analysis.

CAPEX- Capital Expenditure

The capital expenditure (CAPEX) of a ship encompasses multiple components, which encompass the expenses related to the ship's asset acquisition and the financial costs associated with ship financing. In the context of ship-owners, CAPEX is typically regarded as a crucial cost component alongside OPEX within the financial statements. Numerous components, including the engine, aftertreatment system, storage tanks, and fuel supply system (FSS), are included in the fixed costs of a newly constructed vessel. The expenses incurred are not contingent upon the frequency and intensity of vessel utilization (EMSA, 2022). For the CAPEX, the cost of the engine, after-treatment system, battery, and inverter is taken into consideration as per the requirements of the PMS system.
PMS1:
CAPEX = Engine cost = 1,407,600USD

PMS2:
CAPEX= Engine cost + Battery cost + Inverter cost = 3,626,565 USD

PMS3:
CAPEX= Engine cost + SCR cost = 3,872,610 USD

PMS4:
CAPEX = Engine cost + SCR cost + Battery cost + Inverter cost = 5,269,905 USD

PMS5:
CAPEX = Engine cost = 3,118,500 USD

PMS6:
CAPEX= Engine cost + Battery cost + Inverter cost = 4,767,165 USD

OPEX- Operational Expenditure

Operational expenditures (OPEX) encompass variable costs that are based upon the utilisation of the vessel. These costs primarily include fuel expenses, bunkering charges, maintenance, and repair costs. The daily capital and operating cost per vessel are influenced by several factors, such as crew, ship size, insurance policy, and maintenance. Several factors have been identified as influential when making investments. These factors encompass fuel prices, the geographical area in which operations are conducted, relevant regulations, the duration of time at sea, and the lifespan of the vessel (Olaniyi et al., 2018). In addition, the weather and environmental conditions encountered by a maritime vessel can have a substantial influence on its operational costs. For instance, inclement weather conditions can potentially require the consumption of extra fuel or give rise to enhanced vessel deterioration, thereby resulting in added maintenance expenses (Olaniyi et al., 2018). For the OPEX Engine O&M, Battery O&M, SCR O&M, and fuel cost are taken into consideration. Fuel cost calculations are expressed below:
Global average cost of LSMGO Fuel is 840USD/Tonne (*Rotterdam Bunker Prices*, 2023);
Fuel Cost Ammonia = 650USD/Tonne (EMSA, 2022);
Fuel Cost Methanol = 350USD/Tonne (Korberg et al., 2021)

PMS1:

$$Fuel\ consumption\ at\ 40\%\ load\ =\ FC_{LSMGOonly}\ =\ SFOC\ *\ Load\ (40\%)*\ RunningHours,=\ 1560*\ 198.2*1000*10^{-6}\ =\ 309.19\ tonnes\ ,\text{Zincir, 2022.} \quad [1]$$

$$OPEX\ =\ (FC_{LSMGO}\ \times\ Fuel\ Cost)\ +\ Engine\ O\&M\ =\ 259{,}721.28\ USD \quad [2]$$

PMS2:

$$Fuel\ consumption\ at\ 80\%\ load\ =\ SFOC\ *\ Load\ (40\%)\ *\ RunningHours\ =\ 1560*186.1*1000*10^{-6}\ =\ 290.316\ tonnes \quad [3]$$

$$OPEX\ =\ (FC_{LSMGO}\times\ Fuel\ Cost_{LSMGO}\ )\ +\ Engine\ +\ Battery\ O\&M\ =\ 271{,}315\ USD \quad [4]$$

PMS3:

$$FC_{LSMGOonly}\ =\ SFOC\ *\ P_{design}\ *\ Load\ *\ RunningHours \quad [5]$$

$$FR_{ammonia}=\frac{M_{ammonia}*LHV_{ammonia}}{M_{ammonia}*LHV_{ammonia}+M_{LSMGO}*\ LHV_{LSMGO}} \quad [6]$$

$$M_{LSMGO}*\ LHV_{LSMGO}=\ FR_{ammonia}\ *\ M_{ammonia}\ *\ LHV_{ammonia}\ +\ FR_{LSMGO}\ *\ M_{LSMGO}\ *\ LHV_{LSMGO} \quad [7]$$

Equation (5) can be used to calculate the fuel consumption of a single engine that runs solely on LSMGO for 1000 hours:

$$FC_{LSMGOonly}\ =\ 202.1(g/kWh)\ *(780*2)\ (kW)\ *\ 1000\ hours\ *10^{-6}=\ 315\ tonnes \quad [8]$$

$FR_{ammonia}$	70%
$LHV_{ammonia}$(MJ/kg)	18.5
FR_{LSMGO}	30%
LHV_{LSMGO}(MJ/kg)	43.5

Fuel Ratios & LHV of Ammonia and LSMGO (Huang et al., 2022; Zincir, 2022).
Given that the FR_{LSMGO} = 0.3, Equation (6) can be used to determine the ratio between the mass in tonnes consumed by ammonia ($M_{ammonia}$) and the mass in tonnes consumed by LSMGO (M_{LSMGO}). In the instance of our engine, which burns 70% NH3 and 30% LSMGO as pilot fuel, the MLSMGO can be calculated as:

$$FC_{LSMGOonly}*FR_{LSMGO}\ =\ 315\ *\ 0.3\ =\ 95\ tonnes. \quad [9]$$

$$M_{ammonia}\ =\ 5.486\ *\ M_{LSMGO}=\ 5.486\ *\ 95\ =\ 521\ tonnes \quad [10]$$

As a result, the fuel consumption for 1000 hours of main engine operation was discovered to be:

- For 1000 hours of operation, 521 tonnes of NH3 are used.

- Which requires 95 tonnes of LSMGO (as pilot fuel).

$$OPEX = (FC_{LSMGO} \times Fuel\ Cost_{LSMGO}) + (FC_{Ammonia} \times Fuel\ Cost_{Ammonia}) + Engine\ O\&M\ Cost + SCR\ O\&M\ Cost = 453{,}577.4\ USD \quad [11]$$

PMS4:
Similar to Eqs (5-7) of the previous configuration for 1000 hrs operation:

$$FC_{LSMGOonly} = 190.6(g/kWh) * (1560)\ (kW) * 1000\ hours * 10^{-6} = 297\ tonnes \quad [12]$$

Given that the $FR_{LSMGO} = 0.3$, Equation (6) can be used to determine the ratio between the mass in tonnes consumed by ammonia ($M_{ammonia}$) and the mass in tonnes consumed by LSMGO (M_{LSMGO}).
In the instance of our engine, which burns 70% NH3 and 30% LSMGO as pilot fuel, the MLSMGO can be calculated according to Eq (13). The ammonia consumption mass in tonne can subsequently be calculated 89 tonnes, which takes into account the various fuel ratios.

$$FC_{LSMGOonly} * FR_{LSMGO} = 297 * 0.3 = 89\ tonnes. \quad [13]$$

$$M_{ammonia} = 5.486 * M_{LSMGO} = 5.486 * 89 = 489\ tonnes \quad [14]$$

As a result, the fuel consumption for 1000 hours of main engine operation was discovered to be 489 tonnes of NH3. Which requires 89 tonnes of LSMGO (as pilot fuel).

$$OPEX = (FC_{LSMGO} \times Fuel\ Cost_{LSMGO}) + (FC_{Ammonia} \times Fuel\ Cost_{Ammonia}) + Engine\ O\&M\ Cost + SCR\ O\&M\ Cost + Battery\ O\&M\ Cost = 424{,}629.8\ USD \quad [15]$$

PMS5:
Similar to Eqs (5-7) by changing the fuel from Ammonia to methanol:

$$FC_{LSMGOonly} = SFOC * P_{design} * Load * RunningHours \quad [16]$$

$$FR_{methanol} = \frac{M_{methanol} * LHV_{methanol}}{M_{methanol} * LHV_{methanol} + M_{LSMGO} * LHV_{LSMGO}} \quad [17]$$

$$M_{LSMGO} * LHV_{LSMGO} = FR_{methanol} * M_{methanol} * LHV_{methanol} + FR_{LSMGO} * M_{LSMGO} * LHV_{LSMGO} \quad [18]$$

Equation (18) can be used to calculate the fuel consumption of a single engine that runs solely on LSMGO for 1000 hours:

$$FC_{LSMGOonly} = 202.1(g/kWh) * (1560)\ (kW) * 1000\ hours * 10^{-6} = 315\ tonnes \quad [19]$$

FRmethanol	95%
LHVmethanol(MJ/kg)	19.9
FRLSMGO	5%
LHVLSMGO(MJ/kg)	43.5

Fuel Ratios & LHV of Methanol and LSMGO.
Given that the $FR_{LSMGO} = 0.3$, Equation (6) can be used to determine the ratio between the mass in tonnes consumed by Methanol ($M_{methanol}$) and the mass in tonnes consumed by LSMGO (M_{LSMGO}). In the instance of our engine, which burns 95% Methanol and 5% LSMGO as pilot fuel, the M_{LSMGO} can be calculated by Eq (20). The methanol consumption mass in tonne can subsequently be calculated using Equation (21), which takes into account the various fuel ratios.

$$FC_{LSMGOonly} * FR_{LSMGO} = 315 * 0.05 = 15.76\ tonnes. \quad [20]$$

$$M_{methanol} = 41.53 * M_{LSMGO} = 41.53 * 15.76 = 654.6\ tonnes \quad [21]$$

As a result, the fuel consumption for 1000 hours of main engine operation was discovered to be 654.6 tonnes of methanol usage. Which requires 15.76 tonnes of LSMGO (as pilot fuel).

$$OPEX = (FC_{LSMGO} \times Fuel\ Cost_{LSMGO}) + (FC_{Methanol} \times Fuel\ Cost_{Methanol}) + Engine\ O\&M\ Cost = 271860.3\ USD \quad [22]$$

PMS6:

Similar to Eqs (5-7) from the previous configuration, Eq (5) can be used to calculate the fuel consumption of a single engine that runs solely on LSMGO for 1000 hours:

$$FC_{LSMGOonly} = 190.6(g/kWh) * (1560)\,(kW) * 1000\,hours * 10^{-6} = 297\,tonnes \quad [23]$$

Given that the FRLSMGO = 0.3, Equation (2) can be used to determine the ratio between the mass in tonnes consumed by Methanol ($M_{methanol}$) and the mass in tonnes consumed by LSMGO (M_{LSMGO}). In the instance of our engine, which burns 95% Methanol and 5% LSMGO as pilot fuel, the MLSMGO can be calculated in Eq (24). The methanol consumption mass in tonne can subsequently be calculated using Equation (25), which takes into account the various fuel ratios.

$$FC_{LSMGOonly} * FR_{LSMGO} = 297 * 0.05 = 14.85\,tonnes. \quad [24]$$

$$M_{methanol} = 41.53 * M_{LSMGO} = 41.53 * 14.85 = 614.6\,tonnes \quad [25]$$

As a result, the fuel consumption for 1000 hours of main engine operation was discovered to be:

- For 1000 hours of operation, 614.6 tonnes of methanol are used.
- Which requires 14.85 tonnes of LSMGO (as pilot fuel).

$$OPEX = (FC_{LSMGO} \times Fuel\,Cost_{LSMGO}) + (FC_{Methanol} \times Fuel\,Cost_{Methanol}) + Engine\,O\&M\,Cost + Battery\,O\&M\,Cost = 255{,}290.48\,USD \quad [26]$$

Emissions

This study will evaluate the GHG emission of each PMS in a Tank to wake perspective, fueled by numerous fuels, including LSMGO, methanol, and ammonia. This investigation examined carbon dioxide (CO2), methane (CH4), and nitrous oxide (N2O), the three most important greenhouse gas emissions. After carbon dioxide, CH4 is the second largest contributor to greenhouse gas emissions. The vast majority of CO2 emissions result from the combustion of fuels, while a negligible amount is emitted during processing. The three primary sources of CH4 emissions were vented, furtive, and unburned emissions. Except for engines powered by ammonia, the contribution of N2O is minimal. Here, the greenhouse gas emissions are expressed in tonnes of CO2 equivalent (CO2eq), which is shown in Table 3. The following IPCC AR5 characterization parameters were used to calculate GHG emissions in order to evaluate the warming potential over the next hundred years: 1 for CO2, 28 for CH4, and 265 for N2O (IPCC, 2023).

$$Ef(GHG) = Ef(CO2) + 28 \times Ef(CH4) + 265 \times Ef(N2O) \quad [27]$$

For a medium-speed 4-stroke AE engine with:

LSMGO:

$$Ef(GHG) = 3.21 + (28 \times 5.35 \times 10^{-5}) + (265 \times 1.60 \times 10^{-4}) = 3.25\,\frac{ton\,CO2-eq}{ton\,fuel} \quad [28]$$

Ammonia:

$$Ef(GHG) = 0 + (28 \times 0) + (265 \times 5.02 \times 10^{-3}) = 1.33\,\frac{ton\,CO2-eq}{ton\,fuel} \quad [29]$$

Methanol:

$$Ef(GHG) = 1.38 + (28 \times 2.53 \times 10^{-5}) + (265 \times 7.59 \times 10^{-6}) = 1.38\,\frac{ton\,CO2-eq}{ton\,fuel} \quad [30]$$

Table 3: The engines' CO2 equivalent emission factors (tons/tons of fuel) (Huang et al., 2022)**.**

Fuel	CO2	CH4	N2O	Total (CO2-eq)
LSMGO	3.21	5.35×10^{-5}	1.60×10^{-4}	3.25
Ammonia	0	0	5.02×10^{-3}	1.33
Methanol	1.38	2.53×10^{-5}	7.59×10^{-6}	1.38

In our investigation of ammonia ICE and hybrid ammonia + diesel ICE, SCR is utilized to reduce N2O emissions. We assume that the SCR will contribute to a 70 percent reduction.

Table 4: NOx Emission factor

	Emission factor
N2O emission without SCR	1.33
N2O emission with SCR- 70% reduction	0.399

Consequently, the TTW Annual GHG Emissions have been estimated by multiplying the fuel consumptions for each scenario and shown in Table 5:

Table 5 Emissions of each PMS

Emissions (Ton CO2-eq)	Conventional Diesel engine	Diesel- Hybrid battery	Ammonia ICE engine	Ammonia + Diesel ICE-Hybrid	Methanol ICE	Methanol ICE+ Hybrid
	1005	944	514	485	955	900

Risk

A Failure Mode, Effects, and Criticality Analysis (FMECA) was performed in order to assess the risk of using different PMS onboard. For numerically evaluating each hazard and ranking the risk, the Risk Priority Number (RPN) indicator with the following formula has been utilised:

$$RPN = S \times P \times E \quad [31]$$

S = Severity, P = Probability, E = Ease of detection
After calculating the RPN values, a Threshold has been implemented to appropriately classify each hazard:

- Green colour, if <100 - Low risk hazard
- Yellow colour, if 100 ≤ medium risk hazard <180
- Red colour, if high risk hazard ≥ 180

For each system, potential failure modes in numerous components are identified. Here is an executive summary:

- All six systems share certain components, such as the engine (though the type of fuel varies), the alternator, the power management system, and the LSMGO bunkering procedure, and consequently share similar failure modes in these components.
- The fuel systems and safety systems differ based on whether the fuel is conventional, ammonia, or methanol, and each has its own failure mechanisms. For example, ammonia systems are susceptible to failures associated with nitrogen supply and leak detection, whereas methanol systems are susceptible to methanol pump failure or injector obstruction.
- The systems incorporating batteries, namely PMS2, PMS4, and PMS6, are equipped with supplementary components, namely the battery itself and the battery management system. These components possess essential dangers, including but not limited to battery overheating or thermal runaway, short circuit occurrences, cell degradation, and sensor malfunctions.
- It is important to note that the act of bunkering introduces various potential failure modes in all systems, and the specific nature of these failures is contingent upon the type of fuel being bunkered.

FMECA analysis for each PMS is done and the results obtained is as shown in the following risk plot.

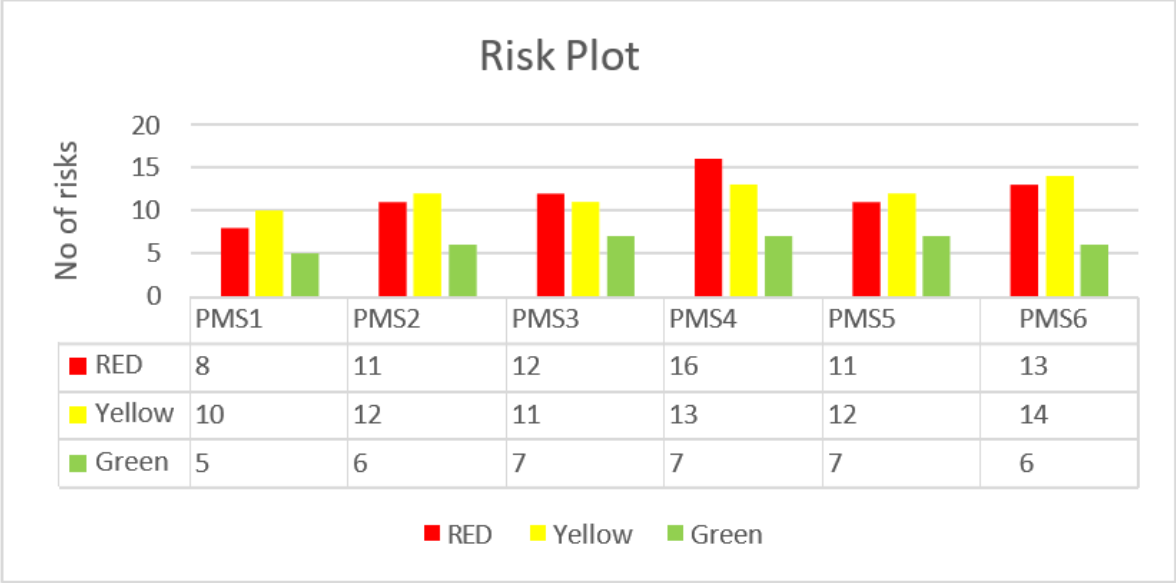

Figure 4: Risk plot from FMECA

Availability / Bunkering

The research conducted an examination of thirteen prominent international ports to determine the presence of various marine fuel options and shore-side battery charging (SBC) infrastructure. The ports were strategically chosen from three regions, namely Europe, Asia, and the Americas, with each region providing a total of five ports. The marine fuel options under consideration encompassed LSMGO, Ammonia, and Methanol. The findings revealed that LSMGO was widely accessible, as it was found to be offered in all thirteen ports. The widespread use of LSMGO as a primary marine fuel in various maritime operations is evident from its ubiquity. Ammonia and Methanol were found to be accessible in eight out of the thirteen ports, indicating a discernible transition towards environmentally friendly fuel alternatives in certain regions of the globe. The aforementioned fuels were readily accessible at all European ports (with the exception of London) and Asian ports (excluding Mumbai), as well as in the cities of New York and Los Angeles within the Americas. Shore-side Battery Charging (SBC) facilities, which constitute a significant component of the maritime sector's transition towards electrification, were found to be accessible in seven out of the total thirteen ports. These facilities were accessible in all European ports, with the exception of London, as well as in Shanghai and Singapore in Asia, and in Los Angeles in the Americas.
One noteworthy observation pertained to the presence of comprehensive marine fuel and SBC facilities at the ports of Rotterdam, Hamburg, Antwerp, Shanghai, Singapore, and Los Angeles. In contrast, it should be noted that ports such as London, Mumbai, and Panama exclusively offered LSMGO. The provided data offers a concise overview of the present state of marine fuel accessibility and the level of preparedness for the implementation of electrification within the shipping sector. The aforementioned statement underscores the regional disparities in the implementation of alternative fuels and electrification within the maritime industry. Specifically, European and Asian ports tend to exhibit a more extensive range of marine fuels and shore-based charging SBC facilities in comparison to their American counterparts.

Weight

This study entails the calculation of weights for different configurations of PMS. To determine the weight of a specific PMS, technical specifications provided by the engine manufacturer have been studied. These specifications typically include information on the engine's weight, dimensions, power output, and other relevant details.

Table 6: Engine weight data (Wärtsilä, 2023) (Latarche, 2021).

	Wartsila 6L25	Wartsila 6L25DF
Engine Weight- in tonnes	38.3	39.6
Battery weight-system (30 kg/kWh) in tonnes	126.9	

PMS1: The present configuration employs three 6L25 engines, each weighing 38.3 metric tonnes, resulting in a cumulative engine weight of 114.9 metric tonnes.
PMS2: system achieves improved efficiency by integrating two 6L25 engines, each weighing 38.3 tonnes, along with a battery weighing 126.9 tonnes, resulting in a combined weight of 203.5 tonnes.
PMS3: system incorporates three 6L25DF engines, with each engine weighting 39.6 metric tonnes. Consequently, the total weight of the engines employed in the project amounts to 118.8 metric tonnes.
PMS4: in this configuration, combines two 6L25 engines (76.6 t) with a battery (126.9 t) to attain a total weight of 203.5 t.
PMS5: in this configuration utilises a trio of 6L25DF engines, collectively weighing 118.8 tonnes.
PMS6: this configuration utilises a hybrid PMS system consisting of two 6L25 engines weighing 76.6 tonnes each, along with a battery weighing 126.9 tonnes, resulting in a total weight of 203.5 tonnes. This weight is comparable to that of PMS2 and PMS4. The significance of the engine and battery weights in determining the overall efficiency and performance of each PMS configuration cannot be overstated. The evaluation of these weights will greatly contribute to the findings of this study

AHP method

The Analytic Hierarchy Process (AHP) will be used to rank the PMS systems based on the importance of each criterion in terms of the overall performance and feasibility of the system. Fig.5 depicts hierarchical decision-making framework of the study regarding the goal of hybrid and alternative fuel power management systems in Ships.

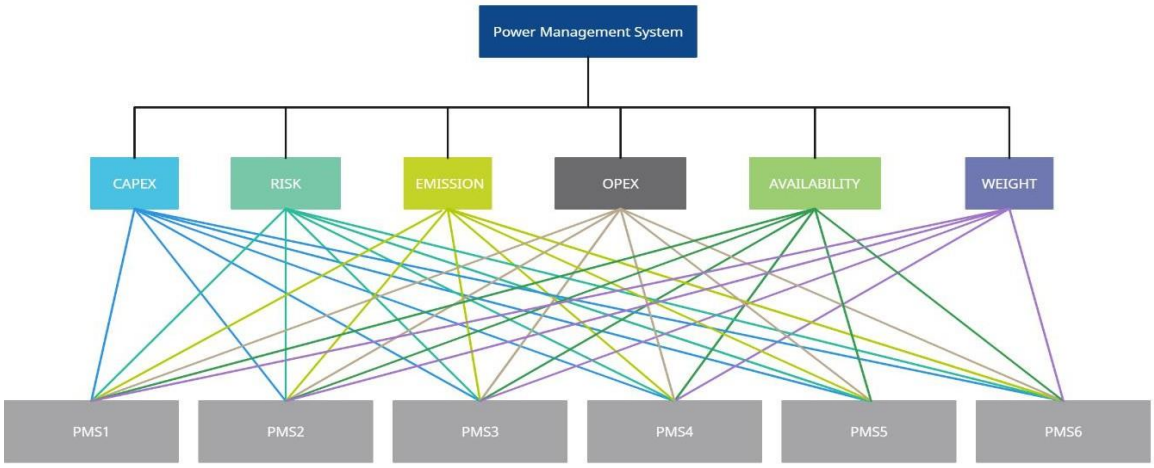

Figure 5: AHP flowchart for this study.

The research further demonstrates its practical application by employing a questionnaire to conduct surveys among identified Decision Makers (DMs). By using pairwise comparison and AHP techniques, managers can analyze many solutions based on various factors and prioritize them based on their preferences. The survey has been conducted among key stakeholders such as maritime industry, universities, technology companies, research and development (R&D) branches and etc.

Measurement of Alternatives and Ranking according to COmpromise Solution (MARCOS) method

The Measurement of Alternatives and Ranking according to MARCOS method is a decision-making technique used in multi-criteria decision analysis (MCDA). It is designed to help decision-makers evaluate and rank a set of alternatives based on multiple criteria or objectives. The MARCOS method uses a compromise solution that balances the conflicting objectives represented by the criteria. Pairwise comparison of criteria and defining the weight of each criteria have been obtained from AHP method section. The MARCOS method is performed through the following steps (Stević et al., 2020):
Step 1: Creating an initial fuzzy decision-making matrix.
Step 2: Formation of an extended initial matrix (X). In this step, the extension of the initial matrix is performed by defining the ideal (AI) and anti-ideal (AAI) solution.
Step 3: Normalization of the extended initial matrix (N).
Step 4: Determination of the weighted matrix (V). The weighted matrix V is obtained by multiplying the normalized matrix N with the weight coefficients of the criterion.
Step 5: Calculation of the utility degree of alternatives K_i.
Step 6: Determination of the utility function of alternatives $f(K_i)$.
Step 7: Ranking the alternatives based on the final values of utility functions.

The MARCOS method provides a structured approach that the best alternative is the one that is closest to the ideal and at the same time furthest from the anti-ideal reference. It aids decision-makers in identifying trade-offs and making informed choices aligned with their preferences and objectives.

RESULTS AND DISCUSSION

Survey and AHP results

The following report analyses six PMS options for ocean-going vessels: This pairwise comparison matrix in Table 7 illustrates, according to the evaluation, how each criterion (CAPEX, RISK, Emission, OPEX, Availability, and Weight) compares to each other in terms of importance. This matrix is used to determine the relative weights of the criteria, which are then used to rank the alternatives (in this case, the Power Management Systems). Priority weights are computed by normalising and then aggregating the values in each column and row.

Table 7: Pairwise comparison of criteria

	CAPEX	RISK	Emission	OPEX	Availability	Weight
CAPEX	1.00	5.00	0.20	1.00	5.00	7.00
RISK	0.20	1.00	0.20	0.33	3.00	5.00
Emission	5.00	5.00	1.00	5.00	7.00	9.00
OPEX	1.00	3.00	0.20	1.00	5.00	7.00
Availability	0.20	0.33	0.14	0.20	1.00	3.00
Weight	0.14	0.20	0.11	0.14	0.33	1.00

The resulting weights reflect the relative significance of each decision-making criterion. These weights are then used to perform a weighted evaluation of the alternatives, which ultimately results in the alternatives' final ranking. By calculating the priority vector using the pairwise comparison matrix, the priority of each alternative is determined, along with its rank. as shown in the table 8.

Table 8 Priority of each alternative

	Priority vector	Priority (%)	RANK
CAPEX	0.195	19.46	2
RISK	0.091	9.06	4
Emission	0.468	46.78	1
OPEX	0.172	17.17	3
Availability	0.049	4.89	5
Weight	0.026	2.64	6

About 47 percent of criteria preference devotes to emission reduction, which shows the most important parameter of propulsion system selection among ship operators and designers. CAPEX and OPEX are second and third rank in the survey in about equal priority. The following matrices show the alternatives for each criterion.

Table 9 Alternatives for criterion CAPEX

Alternatives	PMS1	PMS2	PMS3	PMS4	PMS5	PMS6
PMS1	1.00	5.00	5.00	9.00	3.00	7.00
PMS2	0.20	1.00	3.00	7.00	1.00	5.00

PMS3	0.20	0.33	1.00	7.00	0.33	5.00
PMS4	0.11	0.14	0.14	1.00	0.20	0.33
PMS5	0.33	1.00	3.00	5.00	1.00	5.00
PMS6	0.14	0.20	0.20	3.00	0.20	1.00

Table 10 Alternatives for criterion RISK

Alternatives	PMS1	PMS2	PMS3	PMS4	PMS5	PMS6
PMS1	1.00	3.00	3.00	9.00	5.00	7.00
PMS2	0.33	1.00	0.33	9.00	3.00	5.00
PMS3	0.33	3.00	1.00	5.00	1.00	3.00
PMS4	0.11	0.11	0.20	1.00	0.20	0.33
PMS5	0.20	0.33	1.00	5.00	1.00	3.00
PMS6	0.14	0.20	0.33	3.00	0.33	1.00

Table 11 Alternatives for criterion Emission

Alternatives	PMS1	PMS2	PMS3	PMS4	PMS5	PMS6
PMS1	1.00	0.33	0.14	0.11	0.33	0.20
PMS2	3.00	1.00	0.33	0.11	0.20	0.33
PMS3	7.00	3.00	1.00	1.00	5.00	3.00
PMS4	9.00	9.00	1.00	1.00	7.00	5.00
PMS5	3.00	5.00	0.20	0.14	1.00	0.33
PMS6	5.00	3.00	0.33	0.20	3.00	1.00

Table 12 Alternatives for criterion OPEX

Alternatives	PMS1	PMS2	PMS3	PMS4	PMS5	PMS6
PMS1	1.00	1.00	9.00	3.00	1.00	0.20
PMS2	1.00	1.00	9.00	7.00	1.00	1.00
PMS3	0.11	0.11	1.00	0.20	0.14	0.11
PMS4	0.33	0.14	5.00	1.00	0.20	0.14
PMS5	1.00	1.00	7.00	5.00	1.00	0.33
PMS6	5.00	1.00	9.00	7.00	3.00	1.00

Table 13 Alternatives for criterion Availability

Alternatives	PMS1	PMS2	PMS3	PMS4	PMS5	PMS6
PMS1	1.00	1.00	5.00	3.00	9.00	7.00
PMS2	1.00	1.00	5.00	3.00	7.00	9.00
PMS3	0.20	0.20	1.00	0.33	7.00	5.00
PMS4	0.33	0.33	3.00	1.00	5.00	7.00
PMS5	0.11	0.14	0.14	0.20	1.00	0.33
PMS6	0.14	0.11	0.20	0.14	3.00	1.00

Table 14 Alternatives for criterion Weight

Alternatives	PMS1	PMS2	PMS3	PMS4	PMS5	PMS6
PMS1	1.00	7.00	3.00	7.00	3.00	7.00
PMS2	0.14	1.00	0.20	1.00	0.20	1.00
PMS3	0.33	5.00	1.00	5.00	1.00	5.00
PMS4	0.14	1.00	0.20	1.00	0.20	1.00
PMS5	0.33	5.00	1.00	5.00	1.00	5.00
PMS6	0.14	1.00	0.20	1.00	0.20	1.00

Table 15 Mean Priorities by alternative AHP analysis

Crit./Alt.	Weight of criteria	PMS1	PMS2	PMS3	PMS4	PMS5	PMS6
CAPEX	19.46	8.64	3.51	2.32	0.54	3.52	0.93
RISK	9.06	3.76	1.77	1.70	0.25	1.08	0.49
Emission	46.78	1.42	2.76	13.41	18.68	4.35	6.17
OPEX	17.17	2.68	4.00	0.39	0.93	2.92	6.26
Availability	4.89	1.61	1.61	0.53	0.79	0.14	0.20
Weight	2.64	1.14	0.13	0.56	0.13	0.56	0.13

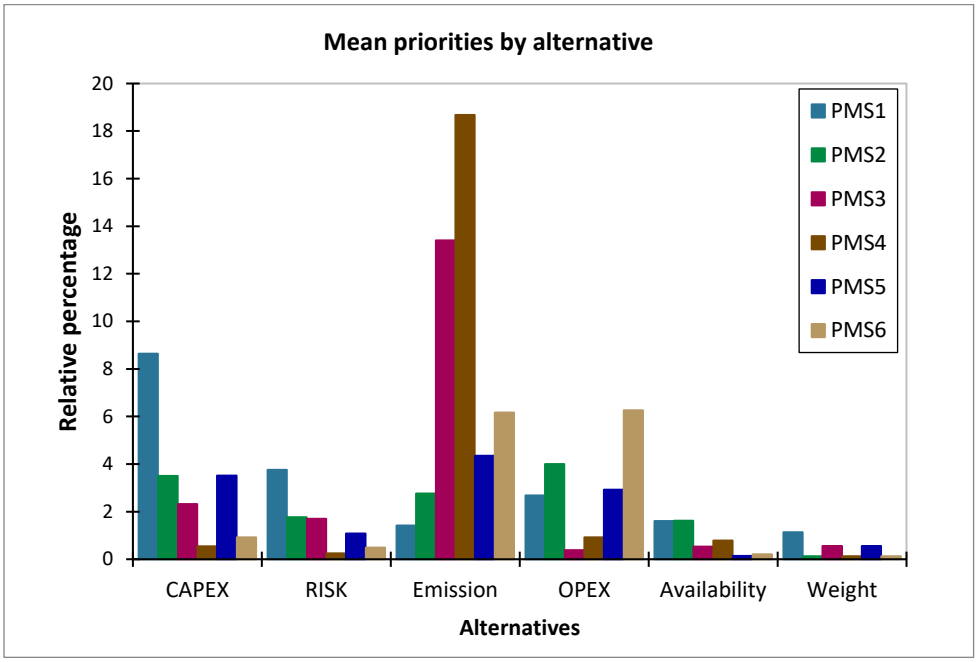

Figure 6: Mean prioritize of alternatives by percentage.

Table 16: PMS alternatives ranking.

Power system	Alt. num.	Rank
PMS1: Conventional Fuel ICE	3.259	**5**
PMS2: Conventional fuel ICE + Battery	2.903	**6**
PMS3: Ammonia ICE	6.985	**2**
PMS4: Ammonia ICE + Battery	9.068	**1**
PMS5: Methanol ICE	3.342	**4**
PMS6: Methanol ICE + Battery	4.197	**3**

According to AHP analysis results in Table 16, one may conclude hybridised system of ICE engines with battery (PMS 4) can be the best option among alternatives. The availability and cost of Ammonia as an alternative fuel make it appealing among stakeholders and can be a possible option for marine fuel in the future of the shipping industry. In the next section, another Multi-Criteria Decision-Making (MCDM) process will be carried out based on available data and dedicated calculations.

Criteria Evaluation for MARCOS Analysis

The specialised calculations provide a comprehensive evaluation of each power management system based on the values for each criterion. In the present section, these calculations are presented independently for each criterion, providing a clear overview of the performance of each PMS in each criterion. The sections that follow detail the calculations performed for each criterion. Measurement of Alternatives and Ranking according to COmpromise Solution (MARCOS) method will be applied to alternatives to rank them and compare them with AHP method.

CAPEX

Based on the cost of the systems and their installation, the CAPEX for each PMS was computed. The following are the results:

$$(If\ CAPEX = \$\,0\ \ then\ Score = 100\ @If\ CAPEX = \$\,8\,mil\ \ \ then\ Score = 0) \quad [32]$$

Table 17: CAPEX Results

Alternatives	USD	Score
PMS1 (Conventional Diesel Engine)	$1407600	82.41
PMS2 (Diesel Engine-Battery Hybrid)	$3626565	54.67
PMS3 (Ammonia ICE)	$3872610	51.59
PMS4 (Ammonia ICE-Battery Hybrid)	$5269905	34.13
PMS5 (Methanol ICE)	$3118500	61.02
PMS6 (Methanol ICE-Battery Hybrid)	$4767165	40.41

The conventional diesel engine system, PMS1, has the lowest CAPEX, whereas the most advanced and advanced system, the ammonia ICE-battery hybrid system, PMS4, has the highest CAPEX. The remaining systems range between these two extremes.

RISK

Calculated using Failure Modes, Effects, and Criticality Analysis (FMECA), The risk values for each PMS are as follows:
To determine these normalised values, all RPN for each FMECA analysis are added together. The PMS1 had the lowest risk score, with a value of 3,459. This was likely due to its long-standing use and continuous improvements. The PMS4, received the maximum risk score of 5816. The risk scores for the remaining systems, PMS2, PMS3, PMS5, and PMS6, were 4456, 4735, 4604, and 5195, respectively, due to the incorporation of alternative fuels and hybrid technologies. Comparing these risk scores assists in determining the tradeoffs involved in selecting an appropriate PMS for ocean-going vessels.

Table 18: Risk Results (Total of RPN values)

Alternatives	RISK	Score
PMS1 (Conventional Diesel Engine)	3459	50.59
PMS2 (Diesel Engine-Battery Hybrid)	4456	36.35
PMS3 (Ammonia ICE)	4735	32.36
PMS4 (Ammonia ICE-Battery Hybrid)	5816	16.92
PMS5 (Methanol ICE)	4604	34.23
PMS6 (Methanol ICE-Battery Hybrid)	5195	25.79

Conditions considered,

$$(If\ RISK = 1\ \ then\ Score = 100 @ If\ RISK = 7000\ \ \ then\ Score = 0) \quad [33]$$

Table 19: Risk analysis

	High	Medium	Low	
	RED	Yellow	Green	Total
PMS1	8	10	5	23
PMS2	11	12	6	29
PMS3	12	11	7	30
PMS4	16	13	7	36
PMS5	11	12	7	30
PMS6	13	14	6	33

Emission

These are the calculated emission values for every PMS in terms of carbon dioxide equivalents (CO2 eq):

Table 20 Emissions Results

Alternatives	Emission	Score
PMS1 (Conventional Diesel Engine)	1004	16.26
PMS2 (Diesel Engine-Battery Hybrid)	943	21.37
PMS3 (Ammonia ICE)	514	57.13
PMS4 (Ammonia ICE-Battery Hybrid)	485	59.57
PMS5 (Methanol ICE)	954	20.44
PMS6 (Methanol ICE-Battery Hybrid)	900	24.97

Conditions considered,

$$(If\ Emission = 0\ \ then\ Score = 100 @ If\ Emission = 1200\ \ \ then\ Score = 0) \quad [34]$$

The PMS1 had a high CO2 eq emission value of 1004,87 tonnes CO2 eq, indicating a substantial contribution to greenhouse gas emissions. At 485.16 tonnes CO2 equivalent, the PMS4 had the lowest emission value, highlighting the potential environmental benefits of using ammonia, a carbon-free propellant, and a battery hybrid system. Other systems, PMS2, PMS3, PMS5, and PMS6, demonstrated lower emissions, demonstrating the potential of alternative fuels and hybrid technologies to reduce the environmental impact of ocean-going vessels.

OPEX

OPEX represents the continual expenses associated with the PMS's operation and maintenance. The cost of fuel has the greatest impact on the OPEX. The following table shows the OPEX for each PMS:

Table 21: OPEX results

Alternatives	USD	Score
PMS1 (Conventional Diesel Engine)	$ 290321	51.61
PMS2 (Diesel Engine-Battery Hybrid)	$ 271315	54.78
PMS3 (Ammonia ICE)	$ 453577	24.40
PMS4 (Ammonia ICE-Battery Hybrid)	$ 424629	29.23
PMS5 (Methanol ICE)	$ 271860	54.69

PMS6 (Methanol ICE-Battery Hybrid)	$ 255290	57.45

Conditions considered,

$$(If\ OPEX = 0\ \ then\ Score = 100 @ If\ OPEX = 600000\ \ \ then\ Score = 0) \quad [35]$$

The cost of fuel has a significant impact on the OPEX values. Alternative fuels such as ammonia and methanol are not widely available and are more expensive than conventional fuels such as LSMGO. The highest OPEX for PMS3 is 453,577.36, indicating that ammonia-fueled systems incur greater operating expenses. PMS4 has 424,629.80, indicating that battery systems incur additional costs. At 255,290.48 USD, PMS6 has the lowest OPEX, demonstrating economic efficacy. Other systems have intermediate OPEX values, emphasising trade-offs between ongoing operational expenses and fuel expenses. The following figure shows the graphical representation of the OPEX.

Availability/Bunkering

The data on bunkering availability illustrates the availability of various fuel types at thirteen global ports. LSMGO is commonly used in the maritime industry, while alternative fuels such as ammonia and methanol are available in eight of thirteen ports. Seven out of thirteen ports offer shoreside battery charging (SBC) facilities, indicating the development of electric power infrastructure in the maritime industry but limited availability relative to traditional fuels. These bunkering availability statistics illustrate the current state of fuel infrastructure in the world's main ports, indicating that alternative fuels and electric power are becoming more prevalent but still lag behind traditional fuels such as LSMGO. This could have a negative effect on the viability and operational flexibility of ships powered by alternative fuels or hybrid systems.

Table 22: Availability/Bunkering evaluation based on operational ports.

	Ports	LSMGO	Ammonia	Methanol	SBC
1	Rotterdam	✓	✓	✓	✓
2	Hamburg	✓	✓	✓	✓
3	London	✓			
4	Antwerp	✓	✓	✓	✓
5	Barcelona	✓			✓
6	Shanghai	✓	✓	✓	✓
7	Singapore	✓	✓	✓	✓
8	Ulsan	✓	✓	✓	
9	Dubai	✓		✓	
10	Mumbai	✓			
11	New York	✓	✓	✓	
12	Los Angeles	✓	✓		✓
13	Panama	✓			
	Total	13	8	8	7

Table 23: Availability/Bunkering results.

Alternatives	Bunkering	Availability	Score
PMS1 (Conventional Diesel Engine)	LSMGO	13.00	90.91

PMS2 (Diesel Engine-Battery Hybrid)	LSMGO + SBC	13.70	95.80
PMS3 (Ammonia ICE)	Ammonia (70%)+LSMGO (30%)	9.50	66.43
PMS4 (Ammonia ICE-Battery Hybrid)	Ammonia (70%) +LSMGO (30%) + SBC	10.20	71.33
PMS5 (Methanol ICE)	Methanol (95%) +LSMGO (5%)	8.25	57.69
PMS6 (Methanol ICE-Battery Hybrid)	Methanol (95%) +LSMGO (5%) + SBC	8.95	62.59

Conditions considered,

SBC is given a 10% extra weightage in hybrid PMS.

$$(If\ Availability = 14.3\ \ then\ Score = 100 @ If\ Availability = 0\ \ \ then\ Score = 0) \quad [36]$$

Weight

The PMS1, PMS3, and PMS5 all utilise three engines with total weights of 114.9 tonnes, 118.8 tonnes, and 118.8 tonnes. The remaining three systems PMS2, PMS4, and PMS) are hybrid systems that include a battery weighing 126.9 tonnes. The total weight of these systems was determined by adding the weight of the two engines (79.2 tonnes) to the weight of the battery, resulting in a total weight of 206.1 tonnes for each system. The PMS's weight is a crucial factor in the decision-making process, as it impacts the performance of the vessel, its fuel efficiency, and the space required for the PMS.

Table 24: Weight assessment results.

Alternatives	Tonnes	Score
PMS1 (Conventional Diesel Engine)	115	77.35
PMS2 (Diesel Engine-Battery Hybrid)	206	23.42
PMS3 (Ammonia ICE)	119	75.04
PMS4 (Ammonia ICE-Battery Hybrid)	206	23.42
PMS5 (Methanol ICE)	119	75.04
PMS6 (Methanol ICE-Battery Hybrid)	206	23.42

Conditions considered,

$$(If\ Weight = 77\ \ then\ Score = 100 @ If\ Weight = 246\ \ \ then\ Score = 0) \quad [37]$$

Based on these calculations, each PMS can be evaluated and compared to determine the most suitable system considering the specific needs and constraints of the vessel.

MARCOS Analysis

After closely evaluating each PMS across the selected criteria using specialised calculations, the following ranking was determined by using MARCOS method. The MARCOS method is used for ranking alternatives based on multiple criteria while seeking a compromise solution. In order to determine the rank of each PMS, the values derived from the calculations are converted into unitless numbers and expressed as scores ranging from 1 to 100. All MARCOS process will be depicted in Tables 25 to 29.

Table 25: Criteria comparison and weight implementation.

	+	+	+	+	+	+
AHP Weight	0.19	0.09	0.47	0.17	0.05	0.03
Power system	**CAPEX**	**RISK**	**Emission**	**OPEX**	**Availability**	**Weight**
PMS1	82.41	50.59	16.26	51.61	90.91	77.35
PMS2	54.67	36.35	21.37	54.78	95.80	23.42

PMS3	51.59	32.36	57.13	24.40	66.43	75.04
PMS4	34.13	16.92	59.57	29.23	71.33	23.42
PMS5	61.02	34.23	20.44	54.69	57.69	75.04
PMS6	40.41	25.79	24.97	57.45	62.59	23.42
AI	82.41	50.59	59.57	57.45	95.80	77.35
AAI	34.13	16.92	16.26	24.40	57.69	23.42

Table 26: Normalization of criteria and alternatives

Normalized						
Power system	**CAPEX**	**RISK**	**Emission**	**OPEX**	**Availability**	**Weight**
PMS1	1.00	1.00	0.27	0.90	0.95	1.00
PMS2	0.66	0.72	0.36	0.95	1.00	0.30
PMS3	0.63	0.64	0.96	0.42	0.69	0.97
PMS4	0.41	0.33	1.00	0.51	0.74	0.30
PMS5	0.74	0.68	0.34	0.95	0.60	0.97
PMS6	0.49	0.51	0.42	1.00	0.65	0.30
AI	1.00	1.00	1.00	1.00	1.00	1.00
AAI	0.41	0.33	0.27	0.42	0.60	0.30

Table 27: Weighted values of criteria and alternatives

Weighted						
Power system	**CAPEX**	**RISK**	**Emission**	**OPEX**	**Availability**	**Weight**
PMS1	0.19	0.09	0.13	0.15	0.05	0.03
PMS2	0.13	0.07	0.17	0.16	0.05	0.01
PMS3	0.12	0.06	0.45	0.07	0.03	0.03
PMS4	0.08	0.03	0.47	0.09	0.04	0.01
PMS5	0.14	0.06	0.16	0.16	0.03	0.03
PMS6	0.10	0.05	0.20	0.17	0.03	0.01
AI	0.19	0.09	0.47	0.17	0.05	0.03
AAI	0.08	0.03	0.13	0.07	0.03	0.01

Table 28: MARCOS calculation

Power system	**Si**	**Ki+**	**Ki-**
PMS1	0.64	0.64	1.83
PMS2	0.58	0.58	1.67
PMS3	0.76	0.76	2.18
PMS4	0.71	0.71	2.04
PMS5	0.58	0.58	1.67
PMS6	0.55	0.55	1.57
AI	1.00		

AAI	0.35

Table 29: MARCOS ranking

Power system	F(Ki+)	F(Ki-)	F(Ki)	Rank
PMS1	0.74	0.26	0.59	**3**
PMS2	0.74	0.26	0.53	**5**
PMS3	0.74	0.26	0.70	**1**
PMS4	0.74	0.26	0.65	**2**
PMS5	0.74	0.26	0.54	**4**
PMS6	0.74	0.26	0.50	**6**

Table 30: MARCOS analysis result.

Power system	Rank
PMS1: Conventional Fuel ICE	**3**
PMS2: Conventional fuel ICE + Battery	**5**
PMS3: Ammonia ICE	**1**
PMS4: Ammonia ICE + Battery	**2**
PMS5: Methanol ICE	**4**
PMS6: Methanol ICE + Battery	**6**

As a result of the MARCOS method, PMS3 has been chosen as the first-rank PMS alternative for under-studied bulk carrier ship propulsion systems. The main difference between MARCOS results with AHP is the position of PMS3 and PMS4 in rank first and second, which are substituting each other. The reason for PMS3's advantage against PMS4 is two main parameters Risk and Weight.

CONCLUSIONS

This study delivered a thorough look at how well different power management systems (PMS) for vessels work, how much they cost, and what risks they pose. Using MARCOS method on dedicated calculations and the Analytic Hierarchy Process (AHP), important criteria of decision-making process have been evaluated. The dedicated calculations conducted involved comprehensive evaluations of various systems, considering the present circumstances, available data, and associated costs. The anticipated future developments, which were accomplished through the application of the Analytic Hierarchy Process (AHP), facilitated the comparison of each criterion and alternative from the perspective of a marine expert, aligning them with desired future outcomes. Based on the current circumstances that were taken into the calculations, the ammonia ICE (PMS3) emerged as the top option due to its lower pollution, acceptable operational costs, and reduced risk, closely followed by the ammonia ICE-battery hybrid (PMS4). However, when future scenarios are considered and criteria are prioritised using the AHP method, the rankings change, and the ammonia ICE-battery hybrid (PMS4) becomes the leading contender. This demonstrates the significant potential of ammonia as an alternative fuel and hybrid system to address the crucial challenge of reducing emissions when given priority. In the AHP classification, the standalone ammonia ICE system (PMS3) holds a firm second place, further demonstrating the potential of ammonia-fueled systems. In third place, the methanol ICE-battery hybrid (PMS6) is also a compelling future option, demonstrating the potential versatility of methanol fuel and hybrid systems.

The PMS5 and PMS6 systems that use methanol stand out as good choices to think about now and in the future. Their high carbon emissions, on the other hand, are a big problem. Innovations like onboard carbon capture units to reduce TTW emissions and the use of "green methanol" could reduce this pollution, making methanol-fueled systems more practical. In the same way, a machine that runs on ammonia could have a lot less pollution over its whole time if it used green ammonia in well to tank emissions. This study points out that infrastructure for alternative fuels and shoreside battery charging (SBC) at ports is one of the most important things to think about. As the company advances towards more environmentally friendly methods, there should be more of this kind of equipment. As technology improves, the costs of alternative fuels and the costs of buying the appropriate engine and safety systems are likely to go down in the future. This makes the case for using hybrid systems and alternative fuels even stronger, which could make them the best choice for future marine activities. Here are some conclusions about why dedicated calculations using the MARCOS method and AHP methods may have produced different rankings, as well as the strengths and weaknesses of each method.

DATA ACCESS STATEMENT

Research data must be shared via data repositories. The publisher, TU Delft OPEN Publishing, requires authors to cite any publicly accessible research data in their reference list and will verify this as a condition of publication. The publisher, TU Delft OPEN Publishing, encourages research data to be made accessible under open licenses that permit reuse freely. References to datasets (data citations) must include a persistent identifier (such as a DOI). The publisher, TU Delft OPEN Publishing, does not enforce particular licenses for research data, where research data are deposited in third party repositories.

CONTRIBUTION STATEMENT

Author 1: Conceptualization; data curation; methodology; validation; writing – original draft. **Author 2:** conceptualization; supervision; writing – review and editing. **Author 3**: conceptualization, data curation, formal analysis, investigation, writing – original draft.

REFERENCES

Ammar, N. R., & Seddiek, I. S. (2017). Eco-environmental analysis of ship emission control methods: Case study RO-RO cargo vessel. *Ocean Engineering*, *137*, 166–173. https://doi.org/10.1016/j.oceaneng.2017.03.052

Brinsmead, T., Graham, P., Hayward, J., Ratnam, E., & Reedman, L. (2015). *Future Energy Storage Trends: An Assessment of the Economic Viability, Potential Uptake and Impacts of Electrical Energy Storage on the NEM 2015–2035*.

Chan, C. C., Bouscayrol, A., & Chen, K. (2010). Electric, Hybrid, and Fuel-Cell Vehicles: Architectures and Modeling. *IEEE Transactions on Vehicular Technology*, *59*(2), 589–598. https://doi.org/10.1109/TVT.2009.2033605

Dedes, E. K., Hudson, D. A., & Turnock, S. R. (2012). Assessing the potential of hybrid energy technology to reduce exhaust emissions from global shipping. *Energy Policy*, *40*(1), 204–218. https://doi.org/10.1016/j.enpol.2011.09.046

EMSA. (2022). *Potential of Ammonia as Fuel in Shipping by ABS, CE-Delft & Arcsilea*. European Maritime Safety Agency (EMSA).

Geertsma, R. D., Negenborn, R. R., Visser, K., & Hopman, J. J. (2017). Design and control of hybrid power and propulsion systems for smart ships: A review of developments. *Applied Energy*, *194*, 30–54. https://doi.org/10.1016/j.apenergy.2017.02.060

Huang, J., Fan, H., Xu, X., & Liu, Z. (2022). Life Cycle Greenhouse Gas Emission Assessment for Using Alternative Marine Fuels: A Very Large Crude Carrier (VLCC) Case Study. *Journal of Marine Science and Engineering*, *10*(12), 1969. https://doi.org/10.3390/jmse10121969

IMO, 2018. (2018). *IMO. Adoption of the initial IMO strategy on reduction of GHG emissions from ships and existing IMO activity related to reducing GHG emissions in the shipping sector. UNFCCC Talanoa Dialogue.*

IMO. Resolution MEPC.336(76)—2021 Guidelines on Operational Carbon Intensity Indicators and the Calculation Methods (CII Guidelines, G1); IMO: London, UK. (2021).

Inal, O. B., Charpentier, J.-F., & Deniz, C. (2022). Hybrid power and propulsion systems for ships: Current status and future challenges. *Renewable and Sustainable Energy Reviews*, *156*, 111965. https://doi.org/10.1016/j.rser.2021.111965

IPCC. (2023). Climate Change Synthesis Report. In *Journal of Crystal Growth* (Vol. 218, Issue 2).

Korberg, A. D., Brynolf, S., Grahn, M., & Skov, I. R. (2021). Techno-economic assessment of advanced fuels and propulsion systems in future fossil-free ships. *Renewable and Sustainable Energy Reviews*, *142*, 110861. https://doi.org/10.1016/j.rser.2021.110861

Latarche, M. (2021). MAN Energy Solutions. In *Pounder's Marine Diesel Engines and Gas Turbines*. https://doi.org/10.1016/b978-0-08-102748-6.00022-0

MAN Energy Solutions. (2019). *Batteries on board in the*. Denmark: MAN Energy Solutions. https://www.man-es.com/docs/default-source/marine/tools/batteries-on-board-ocean- going-vessels.pdf

Meng, J., Guo, H., Niu, C., Zhao, Y., Xu, L., Li, Q., & Mai, L. (2017). Advances in Structure and Property Optimizations of Battery Electrode Materials. *Joule*, *1*(3), 522–547. https://doi.org/10.1016/j.joule.2017.08.001

Nazemian, A., Boulougouris, E., & Aung, M. Z. (2024). Utilizing Machine Learning Tools for Calm Water Resistance Prediction and Design Optimization of a Fast Catamaran Ferry. *Journal of Marine Science and Engineering*, *12*(2), 216. https://doi.org/10.3390/jmse12020216

Nuchturee, C., Li, T., & Xia, H. (2020). Energy efficiency of integrated electric propulsion for ships – A review. *Renewable and Sustainable Energy Reviews*, *134*, 110145. https://doi.org/10.1016/j.rser.2020.110145

Olaniyi, E. O., Atari, S., & Prause, G. (2018). Maritime Energy Contracting for Clean Shipping. *Transport and Telecommunication Journal*, *19*(1), 31–44. https://doi.org/10.2478/ttj-2018-0004

Padolecchia, D., Utzeri, S., Braidotti, L., & Marino, A. (2023). A Hybrid-Electric Passenger Vessel for Inland Waterway. *2023 IEEE International Conference on Electrical Systems for Aircraft, Railway, Ship Propulsion and Road Vehicles &*

International Transportation Electrification Conference (ESARS-ITEC), 1–6. https://doi.org/10.1109/ESARS-ITEC57127.2023.10114841

Richardson, M. (2022). *Simpson Spence Young Outlook 2022.* https://www.ssyonline.com/media/2016/ssy-2022-outlook-final.pdf

Rotterdam Bunker Prices. (2023). https://shipandbunker.com/prices/emea/nwe/nl-rtm- rotterdam

Seddiek, I. S., & Ammar, N. R. (2023). Carbon footprint and cost analysis of renewable hydrogen-fuelled ships. *Ships and Offshore Structures*, *18*(7), 960–969. https://doi.org/10.1080/17445302.2022.2093031

Stević, Ž., Pamučar, D., Puška, A., & Chatterjee, P. (2020). Sustainable supplier selection in healthcare industries using a new MCDM method: Measurement of alternatives and ranking according to COmpromise solution (MARCOS). *Computers & Industrial Engineering*, *140*, 106231. https://doi.org/10.1016/j.cie.2019.106231

Wärtsilä. (2021). *Wärtsilä and Shi agree to collaborate on ammonia fuelled engines for future newbuilds, Wartsila.com*.

Wärtsilä. (2023). *Wärtsilä 25 marine engine.*

Zincir, B. (2022). Environmental and economic evaluation of ammonia as a fuel for short-sea shipping: A case study. *International Journal of Hydrogen Energy*, *47*(41), 18148–18168. https://doi.org/10.1016/j.ijhydene.2022.03.281

Proceedings of 15th International Marine Design Conference (IMDC-2024)
June 2-6, 2024
Amsterdam, the Netherlands

The impact of hydro generation on board large sailing yachts

Marijn van der Plas [1,*], Wick Hillege[2] and Peter de Vos[3]

ABSTRACT

In response to the leading narrative of increasing sustainability in the yachting sector, a research collaboration is started between the Delft University of Technology and Dykstra Naval Architects (DNA) to examine the potential use of hydro generation on board large sailing yachts. By harvesting energy from the water flow when a yacht is sailing, diesel generator use can be limited, reducing overall emissions. However, it is a challenge to quickly identify the impact of a chosen hydro generation system on the overall design during the early stages of yacht design. A design method, with a primary focus on the propeller, is therefore developed to quantify this impact. This allows the designer to explore various hydro generation systems in an early design stage. This paper describes the developed method and presents results from a case study to provide insight into the applicability of the method.

KEY WORDS

Hydro generation; Sailing; Ship design; Sustainability

INTRODUCTION

The yachting industry is growing, as is the idea of sustainable yachting. Sailing yachts can limit emissions from the yachting sector with their ability to transit without using fossil fuels. However, a modern sailing yacht does require electricity to run its hotel, navigation, and sailing systems during sailing. The main engine or a dedicated engine-generator set usually provides this electricity. Alternative solutions for this exist. This paper focuses on one of these alternatives: hydro generation.

Hydro generation is the process of extracting momentum from a water flow to generate electricity. On board a sailing yacht this is achieved using the propulsion propeller or a separate dedicated turbine. This concept is realized in, among others, sailing yachts Black Pearl, Perseverance, and Project Zero, the latter currently under construction at Vitters Shipyards. The implementation of hydro generation serves two purposes: economic and ecological improvement, i.e. installing a hydro generation system limits the use of fossil fuel onboard, decreases related costs, and limits fuel-related emissions. However, it does give rise to several challenges that need to be overcome. These challenges find their origin in the required balance between the inevitable increase in system weight and size relative to, for example, emission reduction.

Today's approach towards analyzing a hydro generation system is characterized by detailed propeller calculations combined with refined flow analysis to converge to the optimum configuration. This approach requires detailed knowledge about the

[1] Department of Maritime and Transport Technology, Delft University of Technology, Delft, Netherlands
[2] Dykstra Naval Architects, Amsterdam, Netherlands
[3] Department of Maritime and Transport Technology, Delft University of Technology, Delft, Netherlands; ORCID: 0000-0002-5835-2450
[*] Corresponding Author: marijnvdplas@gmail.com

Submitted: 23 February 2024, Revised: 28 April 2024, Accepted: 1 May 2024, Published: 26 May 2024

Conference paper, DOI: https://doi.org/10.59490/imdc.2024.906 e-ISSN: 3050-4864

yacht's lines plan and chosen propulsion system making it unsuitable to use in the early stages of yacht design. The study presented here aims to overcome this difficulty by only utilizing first principles and main particulars. The method developed for this study allows the designer to efficiently investigate the impact of various configurations on the overall design, safeguarding the necessary flexibility.

The design method considers the impact of six major variables that influence hydro generation. The first three variables concern size and include the propeller diameter, battery capacity, and sail area. The remaining variables relate to operational and design choices and include decisions on energy consumption, fixed or controllable pitch propellers, and generation in the first or third quadrant of the propeller diagram. A case study for an ocean crossing with a sailing yacht aiming to limit fuel consumption demonstrates the influence of these design decisions. It shows that this method can support major design choices whilst having limited knowledge about the final design.

THEORY

Since this method is intended for an early-stage design assessment the calculations are very general. The energy balance is analyzed using only main dimensions and rough propeller data.

Turbine physics

A hydro turbine is designed to extract energy from a fluid flow and convert it to useful work. Since the turbine under consideration here is placed in an open flow, under a hull, the available power in the flow depends on the cross-sectional area, speed, and density of the fluid only:

$$P_{flow} = \frac{1}{2}\rho V_a^2 \cdot \dot{V} \tag{1}$$

$$P_{flow} = \frac{1}{2}\rho V_a^3 \cdot A_0 \tag{2}$$

Where in this case, ρ is the density of seawater, V_a is the advance velocity of the propeller, and A_0 is the propeller disc area. The efficiency of a turbine is often defined in literature by the fraction of the output of the turbine (in useful work) divided by the energy supplied to it; in case of a classical hydro turbine, this is the power present in the flow. For a turbine mounted on a moving object (the yacht), the energy supplied to it is not the power present in the flow, but rather the power required to move it through the water, so effectively, the drag of the unit multiplied by its speed through the water. The ratio between the power in the flow versus the output power is however significant property of the turbine, and is referred to as the power coefficient (C_p) in this paper, this in analogy to the power rating of wind turbines:

$$C_p = \frac{P_{extracted}}{P_{flow}} = \frac{P_{extracted}}{\frac{1}{2} \cdot \rho \cdot V_a^3 \cdot A_0} \tag{3}$$

$$P_{extracted} = C_p \cdot P_{flow} = C_p \cdot \frac{1}{2} \cdot \rho \cdot V_a^3 \cdot A_0 \tag{4}$$

The ratio between the useful power and the supplied power is, in analogy with common propeller theory, defined as the output power divided by the input power:

$$\eta_{regen} = \frac{P_{extracted}}{T \cdot V_a} = \frac{Q \cdot \omega}{T \cdot V_a} \tag{5}$$

Where T normally stands for thrust of the propeller, which in this case means the drag of the propeller in turbine mode as described above. Note that the extracted power here is defined at the propeller shaft, i.e. mechanical losses and conversion efficiencies are not incorporated in η_{regen} and C_p, as is depicted below.

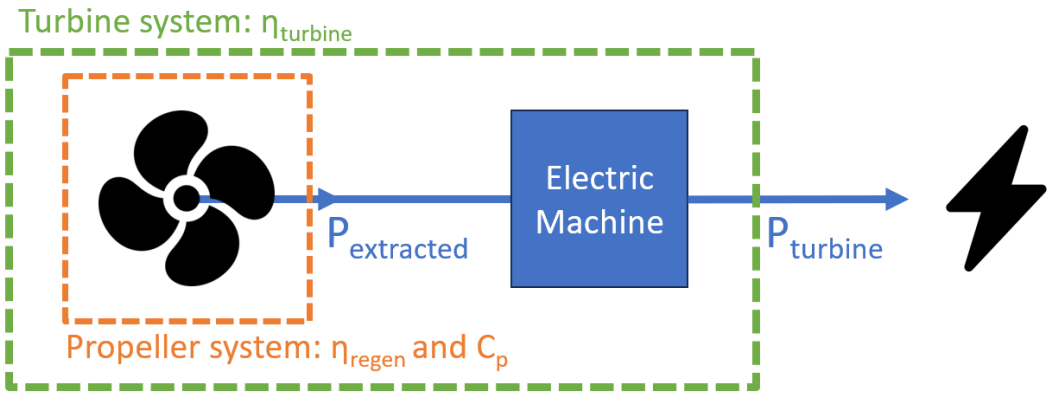

Figure 1: System definition for hydro generation systems

Turbines on sailing yachts

Every modern sailing yacht is fitted with a propeller for mechanical propulsion. With some adjustments and additions, this propeller can also function as a hydro generator. However, a propeller adds momentum to a flow, and a turbine is designed to extract the maximum energy from the available flow momentum. These are fundamentally different objectives combined with different physics. Propellers will generate a contracting flow and turbines an expanding flow. Furthermore, the flow around the blade is dissimilar for turbines and propellers. For propellers, lift is generated in the forward direction to deliver propulsion. For turbines, this lift is generated backwards resulting in drag. This is achieved by altering the angle of attack on the propeller blades. The main problem is the required shape. The shape differs for an optimal propeller from that of an optimal turbine. There are two adjustments that (partially) overcome this problem, either by adjusting the pitch of the blades, the flow direction, or both.

Fixed and controllable pitch propellers

Propellers can roughly be divided into two groups, fixed-pitch propellers (FPP) and controllable-pitch propellers (CPP). When considering an FPP, the pitch of the blades cannot be adjusted. The propeller is designed to work well in one operating point, likely a design point in propulsion. Outside this point, the propeller will not operate optimally and efficiency is compromised. Modern sailing yachts however operate at more than one operating point being propulsion, motor sailing, and free sailing. This requires a certain flexibility in different pitch settings. For this reason, the second propeller type, a CPP, is mostly applied on modern sailing yachts. Additional benefits of a CPP arise when considering hydro generation. During hydro generation, a sailing yacht is slowed down depending on the amount of energy extracted from the flow. Knowing this it can be reasoned that a CPP allows for more efficient hydro generation as the blade's pitch can be adjusted to meet the changing flow speed whilst tuning to the desired system energy output. This characteristic makes a CPP more suitable for hydro generation when compared to an FPP as it allows for better balancing the desired energy extracted with the desired sailing speed.

Generation quadrants

In this study the definition by Kuiper (1991) is adopted for the four propeller quadrants, it describes the transition between each quadrant as a function of the hydrodynamic pitch angle β. Several points of interest occur when increasing β for a fixed blade profile. In figure 2, points of interest on a fixed blade are shown:

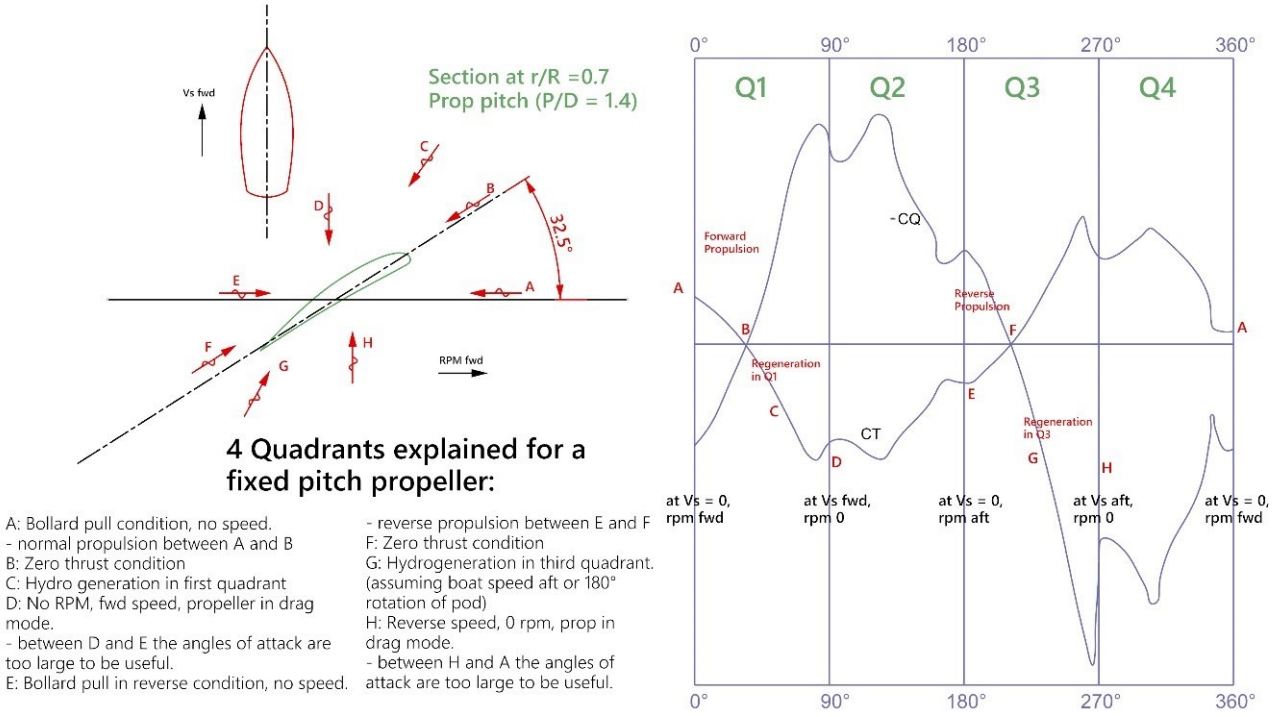

Figure 2: Four quadrants and the hydrodynamic pitch angles on a blade

FORCE BALANCE

During the simulations, the equations of motion are solved in 1 degree of freedom, x-direction only. For this, a force balance is defined for the conditions of motoring, free sailing, and for hydro generating. The latter is discussed in more detail below and shown mathematically in equation 6. The left-hand side of this equation represents the energy input in the system, driving force by the sails or propeller (not touched upon in this paper), whereas the right-hand side represents the energy output or loss.

When hydro generating, the total resistance comprises four parts: the hull resistance, the additional resistance due to side force, the resistance caused by the propeller blades ($R_{prop,generation}$), and the propeller related structure resistance ($R_{structure}$), equation 6.

$$F_{driving} = R_{hull} + R_{side} + R_{prop,generation} + R_{structure} \tag{6}$$

During the simulations the hull resistance and resistance due to side force are calculated adopting the relations developed

with the Delft Systematic Yacht Hull Series (DSYHS) as described by Keuning and Sonnenberg (1998). To determine the additional resistance due to hydro generation new formulations are derived. To better understand these formulations an understanding of feathered drag is necessary.

Feathered drag is the resistance of the propeller, in feathered condition, including surrounding structures. The presumption for this calculation is that the propeller blades are pitched into a setting where the least resistance occurs. Feathered drag is determined by multiplying a Prismatic Parameter (PiPa) with the pressure of water flow through the propeller area:

$$R_{feathered} = PiPa \cdot p_{flow} \qquad [\text{N}] \tag{7}$$

$$= \left(\left(\frac{A_e}{A_0} \cdot A_0 \right) \cdot C_d \cdot \frac{A_p}{A_d} \right) \cdot \left(\frac{1}{2} \cdot \rho \cdot V_a^2 \right) \qquad [\text{N}] \tag{8}$$

This formula encompasses all submerged propulsion system parts, such as hull bossing, shaft, struts, shaft brackets, and the propeller itself. The formula is based on the propeller area. It uses a coefficient C_d for the drag and a factor of $\frac{A_p}{A_d}$ to account for the difference between the developed area and the projected area of the propeller. Coefficient C_d for a feathered propeller is taken as 0.3 based on the findings of MacKenzie and Forrester (2008). The factor $\frac{A_p}{A_d}$ is based on formula 9 by Gerr (1989), adopting an average $\frac{P}{D}$ of 1.

$$\frac{A_p}{A_d} = 1.0125 - \left(0.1 \cdot \frac{P}{D} \right) - \left(0.0625 \cdot \frac{P}{D} \right)^2 \qquad [\text{-}] \tag{9}$$

To determine the total resistance during generation a distinction between drag caused by the structure and drag caused by the propeller is necessary as propeller drag varies with the propeller setting. It can be shown that roughly 50% of the total feathered resistance can be attributed to the structure, equation 10. Further research in this area is recommended to refine this ratio.

$$R_{structure} \approx \frac{1}{2} R_{feathered} \tag{10}$$

The remaining resistance contribution is the resistance caused by the propeller blades during generation. For this, propeller curves in the first and third quadrant are constructed based on the chosen propeller geometry. To construct the propeller curves the polynomials describing the B4-70 propeller family are used as published by MARIN, van Lammeren et al. (1969). The outcome presents itself in K_t and K_q values for different hydrodynamic pitch (β) angles and $\frac{P}{D}$ values. Matching the K_t value to the selected propeller setting allows for calculating the propeller blade drag.

The force balance described above is used to determine the possible output of a specific hydro generation setup for various environmental conditions. For this, a performance prediction program is developed of which results are shown in figure 3.

Figure 3 indicates in white the conditions when there is not enough or too much wind. It is for these wind angles and wind speeds that the yacht will not sail and her main engine(s) are used to provide the necessary driving force to allow travel at transit speed. Transit speed is the desired minimum speed at which a yacht can perform a transit, this speed is based on the yacht's length. The grey area in the graph represents a free sailing condition, i.e. when the desired transit speed can be reached under sail power alone and the engines are turned off. However, hydro generation does not occur yet, as this would result in the transit speed dropping below a preset limit. The colored part of the graph represents the hydro generation condition where the limit of the transit speed is surpassed under sail power alone. The excess energy can now be harvested through hydro generation.

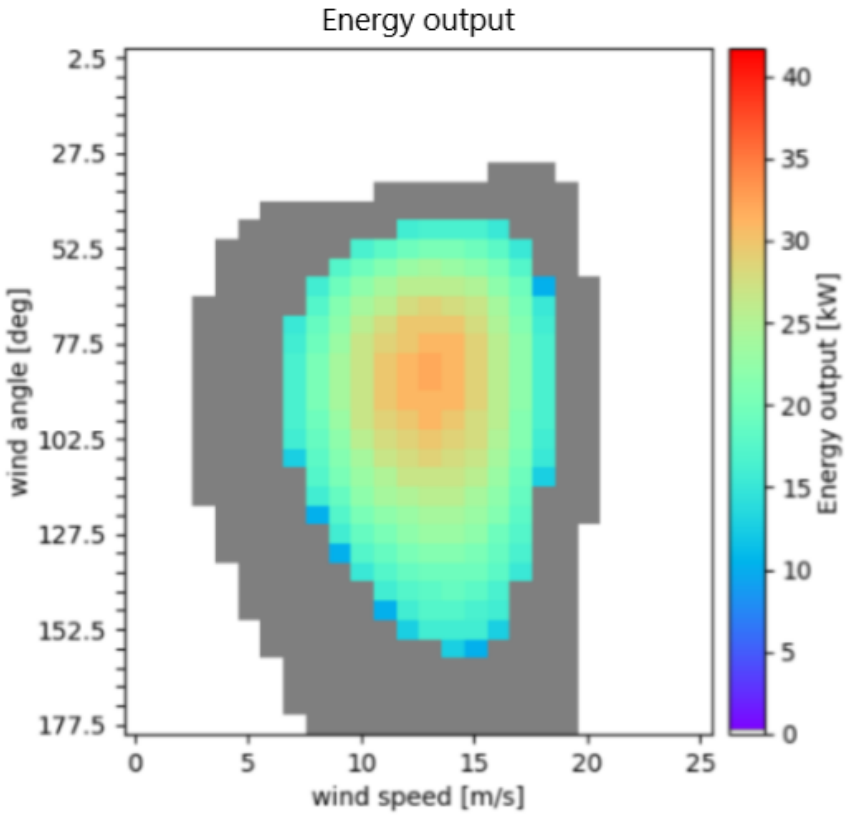

Figure 3: System energy output for the first quadrant

Hotel Load

The yacht's energy demand, or hotel load, is calculated adopting the method developed by Van Eesteren Barros and YETI van Eesteren Barros (2022). The yacht's operational profile is hereby taken into account. Following on board measurements and interviews with captains and crews, the values calculated via the YETI approach were deemed to be high, especially for sailing yachts. To better match the on board measured values a multiplication factor as a function of the yacht's waterline length is determined. For this a second-degree polynomial was drawn through the available data, resulting in a multiplication factor of roughly 0.42.

CASE STUDY

The goal is to perform a fuel-minimizing ocean passage. This means that the hotel load, modeled as a constant average, is compensated by utilizing hydro generation during the crossing where possible. A common ocean crossing for many big-class yachts is from the Mediterranean to the Caribbean once the European summer has ended. In this scenario, the sailing yacht leaves Gibraltar with a full battery and sets sail for the West Indies. The yacht's battery life is monitored for multiple crossings adopting a prediction for the chance of motoring, free sailing, and hydro generation. A crossing is considered a success if the crossing is completed without additional use of the diesel generator to supply the hotel load. A success rate is determined by dividing the number of successful crossings by the absolute number of crossings. For this case study five energy management rules are set to which the yacht adheres during each crossing.

- The engine covers the hotel load if turned on. The battery is not charged in this situation.
- The engine is used if the yacht cannot reach 80% transit speed using sails only.
- If 120% transit speed is reached under sail power alone, hydro generation is initiated. Transit speed is derived using the yacht's waterline length (l_{wl}) in meters, and relations shown in equation 11.
- Energy is supplied via the main engine, generators, and hydro generation only.
- A diesel generator supplies the hotel load if the battery state of charge reaches zero, and hydro generation is not possible.

$$F_n = \frac{V_{transit}}{\sqrt{g \cdot l_{wl}}}[-] \qquad \textit{in which:} \qquad F_n = 0.3 - 0.1 \cdot \left(\frac{l_{wl}}{150m}\right)[-] \tag{11}$$

Typically, a crossing would be planned based on the weather, resulting in the best route. In this case study the crossing starts at fixed time intervals, regardless of the weather. Also, the great circle route is sailed, even if a longer distance passage would be faster. Predicting the wind that a vessel might encounter on this route is done through a weather mapping calculation developed by DNA. This weather mapping calculation determines a probabilistic distribution of prevailing wind speed and direction along that particular route based on historical weather data. To create the distribution used for this study the crossing is completed 190 times in a straight line at transit speed. The crossing is executed between October and November, the usual time for a crossing like this. A crossing is completed every ten days using wind data from 1979 to 2009. All data is summarized in a wind probability matrix with wind speed and wind direction on its axis.

Event distribution

The information displayed in figure 3 shows the energy output for various wind direction and speed combinations. It also shows the conditions for which, motoring, free-sailing, and hydro generation occur. By multiplying this data with the wind probability matrix a probability distribution for motoring (A), free-sailing (B), and hydro generation (C) can be calculated. For this case the event distribution equals roughly, 30% motoring, 50% free sailing, and 20% hydro generating, 5. Each event is considered independent.

Adopting the chances for an event to occur, a route is simulated using a randomizing function. A route is characterized by a series of events where a new event occurs every three hours of the crossing. In other words, one time step lasts three hours. The battery state of charge is monitored over the entire crossing.

The success of one crossing does not guarantee future crossings to be successful as well, due to the underlying probability distribution. In other words, for the case of one crossing the sample does not represent the population. By simulating multiple crossings and monitoring their results, an overall success rate is determined that is representative of the population's success rate. For a population-representative sample, the distribution of the events is to be representative to the original distribution. Within such a sample, there might be crossings where almost the entire distance could be sailed, and there might be crossings with no sailing at all. An additional benefit of completing multiple crossings is the elimination of the dependency on how the events follow one another. To check whether the sample created is representative for the population a control mechanism is modeled that verifies if the acquired distribution of events, figure 5, adequately represents the input distribution. If not more crossings are calculated to extend the sample.

For each unsuccessful crossing, the number of hours a backup diesel generator was run is calculated and stored. A distribution of the sample is formed for the sum of backup generator hours per crossing. Figure 4 is an example of such a distribution. The distribution represents 100,000 crossings of the Atlantic with a notional sailing yacht using the calculated event distribution (30-50-20) in 300 hours. Note that the event distribution is design-specific. This sailing yacht has a hotel load

of 15 kW, an average hydro generation capacity of 30 kW, and a 700 kWh battery. The total success rate for a generator-less crossing is 1.51%. On average the diesel generator is running for 94 hours.

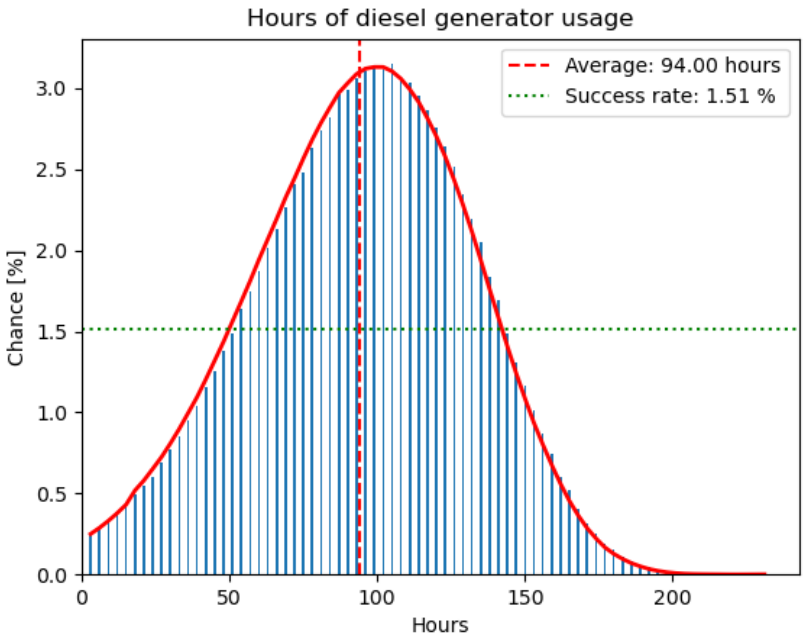

Figure 4: Sample distribution of generator hours, $n = 100.000$

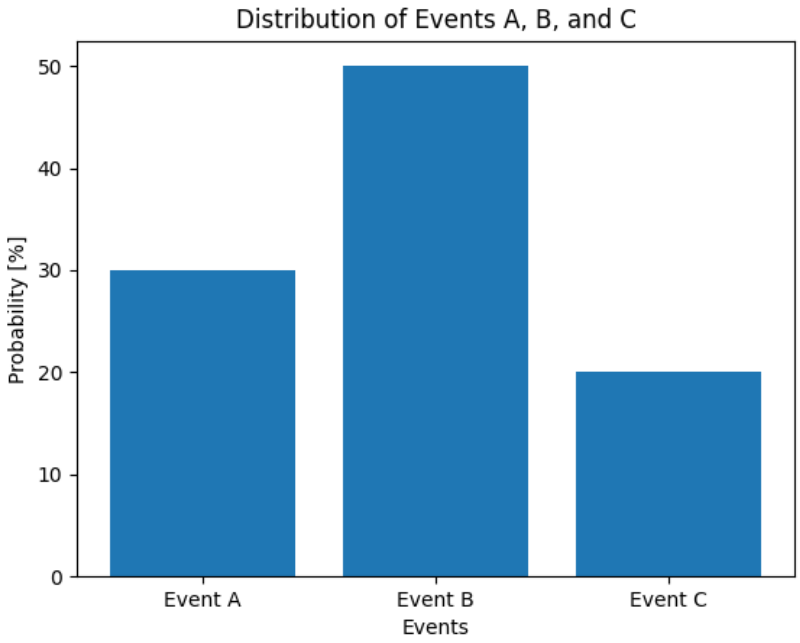

Figure 5: Sample event probability distribution, $n = 100.000$

Baseline

A 31-meter sailing yacht is set as a baseline for this case study. She is equipped with a shaft line mounted CPP that hydro generates in the first quadrant. The CPP allows four settings: feathering, maximizing η_{regen}, middle, and maximizing C_p. The design is characterized by a battery size of 200 kWh and a propeller with a diameter of 0.9 meters. The yacht runs an average hotel load of 26.2 kW. All simulations are done for $1 \cdot 10^6$ crossings.

The combined results of the crossings are shown for generator usage in figure 6. The success rate of this example is 0%, which indicates that the current design is under no conditions able to cross the ocean without running the diesel generator. On average, the diesel generator runs for about 232 hours during a crossing. From this baseline, design changes are introduced to the propeller, battery, and other factors such as the hotel load. In the following section, the impact of various changes on the expected average diesel generator running hours is shown.

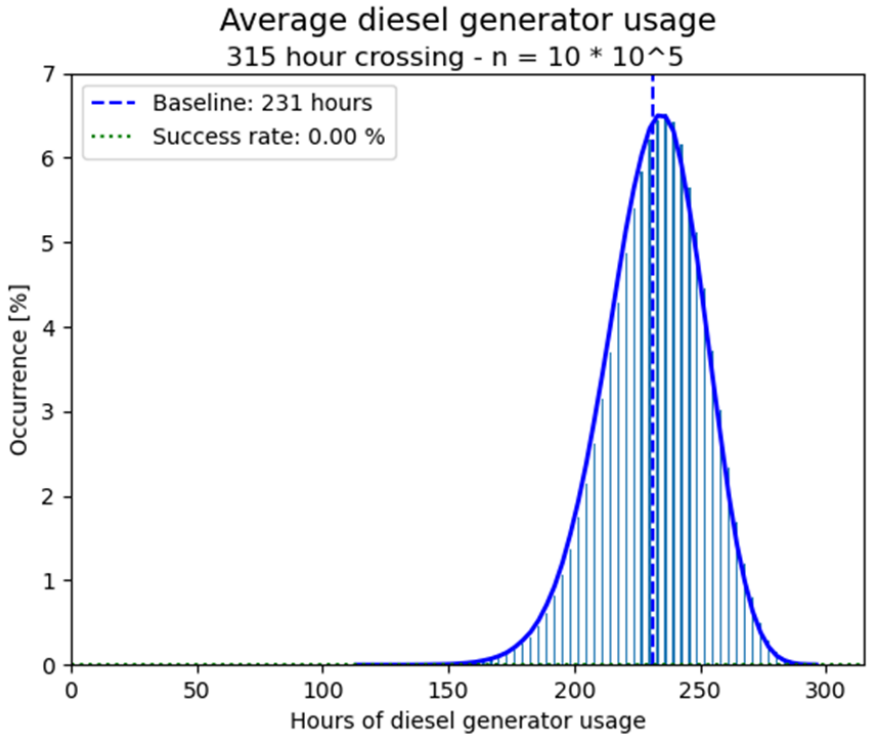

Figure 6: Baseline diesel generator usage

RESULTS

Several design changes are introduced to the baseline. These are a propeller diameter increase of 10%, a battery capacity increase of 100%, and a hotel load decrease of 30%. One variable is changed at a time in the baseline design after which its impact on average diesel generator usage is discussed. The reason for choosing above mentioned design alterations is that they do not require extensive changes to a yacht's design allowing for easy retrofitting if desired.

Propeller variation

The baseline's propeller measures at 0.9 meters which is increased to 0.99 meters. A larger change is deemed unrealistic without significant design changes. A larger propeller will result in more power output at the cost of additional resistance. This relationship is shown in figure 7. The impact on generator running hours is calculated and it is shown that increasing propeller size with 10% will lead to a decrease in diesel generator running hours of 5 hours. The chance for a successful crossing is not changed and remains 0%.

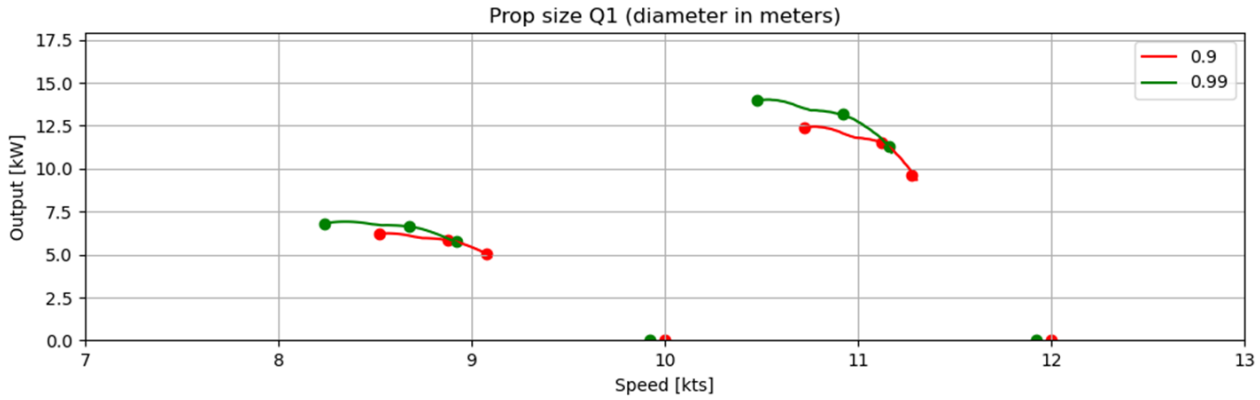

Figure 7: The effect of 10% increase in propeller diameter variation on the delivered power output.

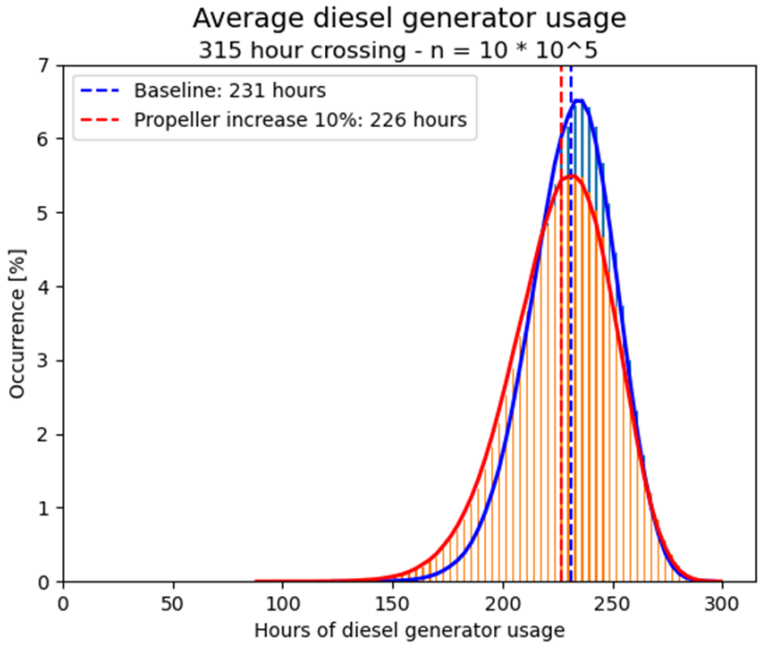

Figure 8: The effect of 10% increase in propeller diameter on average generator running hours.

Battery variation

Increasing the battery size by 100% leads to an increase in light ship weight of about 2%, based on phosphate batteries adopting a weight density of 0.133 $\frac{kWh}{kg}$, Verma and Kumar (2021). During the early design stage such a weight increase is considered within reason to implement. Calculations show that increasing the battery size will lead to a 21-hour decrease in average diesel generator usage, shown in figure 9. The chance for a successful crossing is not changed and remains 0%.

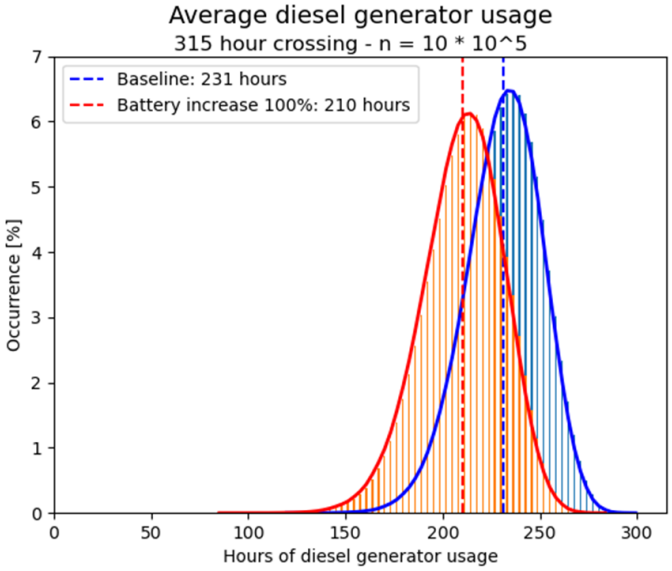

Figure 9: The effect of 100% increase in battery size on average diesel generator usage.

Hotel load variation

The final change deemed reasonable within the yacht's design without any significant design changes is a decrease in the hotel load. This can be achieved by incorporating more efficient systems together with better insulation. For the current design, a 30% decrease in average hotel load is considered feasible. A decrease of 30% of the hotel load reduces the generator hours from the baseline to 208 hours, indicating a 23-hour decrease, roughly equal to doubling the battery size. The chance for a successful crossing is not changed and remains 0%.

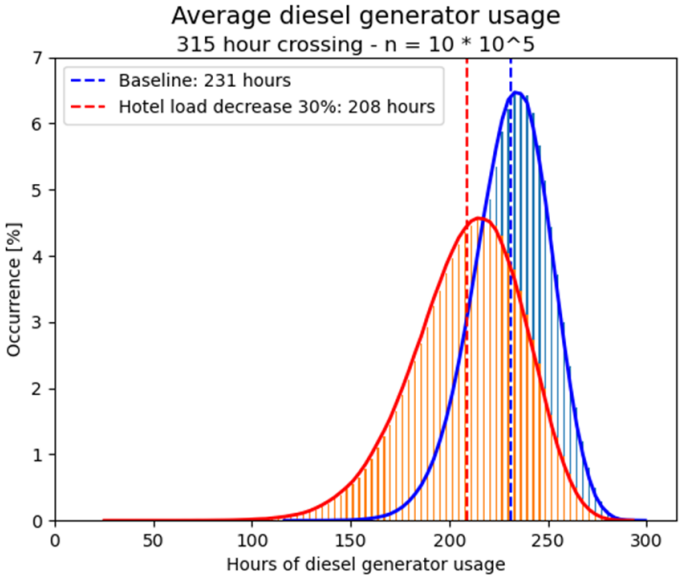

Figure 10: The effect of decreasing average hotel load with 30% on average diesel generator running hours.

Combined

The effect of combining above mentioned design alterations, i.e. implementing all at once, is also studied. It was found that changing the three variables at the same time shows a decrease in generator usage of 41%, as plotted in figure 11. A chance that the crossing succeeds is recorded at 0.02%, indicating that a crossing without any fuel consumption is possible, but not very probable. When compared to the other individual solutions it is found the combination of design alterations leads to a greater reduction in diesel generator hour usage than the sum of its parts, table 1.

Table 1: The effect of design alterations on average diesel generator usage.

	Baseline	**Propeller**	**Battery Capacity**	**Hotel Load**	**Combined**
Average generator running hours	231	226	210	208	139
Success Rate	0%	0%	0%	0%	0.02%
Diesel generator hours w.r.t Baseline	0	-5	-21	-23	-92

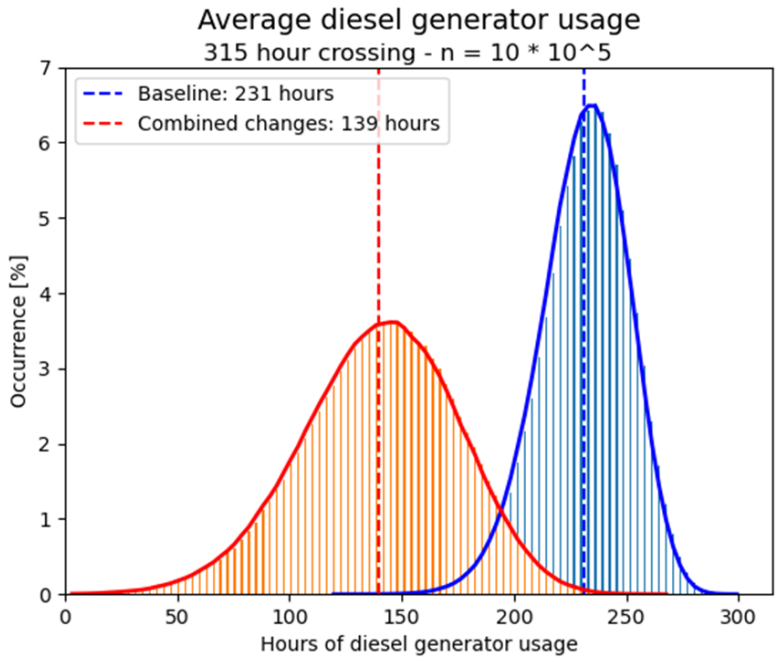

Figure 11: The effect of combined design changes on the average diesel generator running hours.

CONCLUSION

Hydro generation is expected to go from a niche to a common feature on sailing yachts in the coming years. A method is developed that allows for an exploration of various hydro generation components in the early design stage. This practical approach will assist yacht designers in designing more sustainable sailing yachts. Its applicability is shown by three examples for which a decrease in hotel load is found most effective in reducing the diesel generator running hours. For each design alteration, a total of 1 million routes were sailed to quantify its effect. The simulations were carried out using main particulars and first principles only. The design alterations proposed did not materialize in a significant increase of the success rate. Each design alteration did lead to a decrease in average diesel generator running hours; indicating less emissions.

The case study is concluded by combining the three design alterations and implementing them simultaneously. The calcu-

lations show this combination to be more effective than the sum of its parts. The 41% decrease in diesel generator running hours is 1.7 times larger than the sum of the separate solutions, which amounts to 22%. It suggests that the effect of one design alteration can benefit other alterations and act as a multiplier. The nature of this multiplier effect how it affects the outcome of the success rate, and whether it differs for different design change combinations, requires further research. This multiplier effect shows that it pays off to implement multiple small adjustments to a design rather than focusing on one major design change when considering hydro generation. A zero fuel crossing, as presented in the case study, is difficult to achieve by applying adjustments to an existing yacht. Using the design method during the initial design process helps to make this achievement more realistic on a new sailing yacht.

RECOMMENDATIONS

During this study, several assumptions and simplifications were made. It is recommended to further investigate these assumptions to improve the developed method.

- The current approach to determining the hotel load relies heavily on a database comprised mainly of motor yachts, hence it was chosen to correct for this with an average ratio based on on-board measurements. An improvement in the estimate for hotel loads of sailing yachts is therefore recommended. This can be achieved by using a database of sailing yachts within the design range of the method, and cross-reference with full-scale measurement data.
- At this moment the force and energy balance is considered for the yacht sailing in an upright condition. However, it is well known that sailing yachts tend to sail with heel and leeway. The effect of this on the performance of the hydro generation systems is to be further investigated.

CONTRIBUTION STATEMENT

Author 1: Conceptualization; data curation, methodology; writing – original draft.
Author 2: Supervision; writing – review and editing.
Author 3: Supervision; writing – review and editing.

REFERENCES

Gerr, D. (1989). The Propeller Handbook.

Keuning, J. and Sonnenberg, U. (1998). Approximation of the Hydrodynamic Forces on a Sailing Yacht based on the 'Delft Systematic Yacht Hull Series'. In *15th International Symposium on "Yacht Design and Yacht Construction "*, volume 15, pages 99–152.

Kuiper, G. (1991). *Resistance and Propulsion of Ships*. Delft University of Technology, Delft.

MacKenzie, P. M. and Forrester, M. A. (2008). Sailboat propeller drag. *Ocean Engineering*, 35(1):28–40.

van Eesteren Barros, J. P. (2022). *Modeling the Electric Power Consumption of a Yacht*. Master thesis, Delft University of Technology.

van Lammeren, W. P. A., van Manen, J. D., and Oosterveld, M. W. C. (1969). The Wageningen B-Screw Series. *SNAME Transactions*, page 43.

Verma, J. and Kumar, D. (2021). Recent developments in energy storage systems for marine environment. *Materials Advances*, 2(21):6800–6815.

Proceedings of 15th International Marine Design Conference (IMDC-2024)
June 2-6, 2024
Amsterdam, the Netherlands

Quantifying Flexibility for a Ship Power and Energy System Design

D. Platenberg[1], J. S. Chalfant[2*], W. Seering[3]

ABSTRACT

The pace of technology maturation and the uncertainty in magnitude and characteristics of future load types on Navy ships drive the need for robust power and energy system architectures that can adapt to future perturbations in requirements. The Naval design community needs a consistent method for evaluating ship system flexibility in the early design stages when informed decision making provides the greatest opportunity to influence the system's performance and lifecycle cost. The research presented herein develops quantitative, measurable metrics and applies them to applicable case studies for Naval power and energy system flexibility: the capability of the system to accommodate change in response to perturbations in requirements.

KEY WORDS

Ship Design; Flexibility; Metrics;

INTRODUCTION AND BACKGROUND

Naval ship design is a complex system-of-systems activity that balances the operational requirements, physical constraints, and logical connectivity of individual systems into an integrated platform. For a surface combatant, missions ranging from ballistic missile defense to antisubmarine warfare drive the required combat system, consisting of sensors, processing, communication, payload, and ordinance. To enable these mission systems, the ship must provide a stable, responsive power and energy system.

The U.S. Navy surface fleet is in a transition period and faces challenges related to the recapitalization of aging ships, the rate of technology change and uncertainty of the combat systems of the future, and the significant cost of investment to design and build new ship classes. The fleet as it exists today reflects a series of decisions based on the global geo-political environment dating back to the 1980s. Most of the Navy's destroyer and cruiser assets were designed and built following the end of the Cold War to host the top-of-the-line combat system technology of that era, the Aegis combat system, and the SPY-1D radar. Today, forty years later, they are approaching the end of their service lives, and the Navy needs new ships designed for the next fifty years of fleet operations.

At the same time, the rate of technology change has increased uncertainty in requirements for the major combat system elements of the future. System value is defined by its ability to affordably maintain mission relevance within an evolving operational context. The maturation of developmental mission system technologies, with new and increased electrical power demands, are driving requirements for emergent properties, or "ilities," for the naval power and energy system beyond the typical functional requirements. The need to understand and characterize these properties is further amplified by service life requirements of thirty to forty years per platform.

Affordability requirements dictate the need to conduct cost versus capability trade studies early in the design process. System metrics are necessary to quantify performance measures and provide the insight required to "right size" the system-of-system (SoS) architectures. The cost constraints of the recent Research and Development (R&D) and Acquisition environment, along with the timelines to develop and test new power and energy system designs, necessitates a robust evaluation of the design

[1] Sloan School of Management and Dept of Mechanical Engineering, Massachusetts Inst of Technology, Cambridge, MA, USA
[2] Dept of Mechanical Engineering, Massachusetts Inst of Technology, Cambridge, MA, USA; ORCID: 0000-0002-4932-2073
[3] Dept of Mechanical Engineering, Massachusetts Inst of Technology, Cambridge, MA, USA; ORCID: 0000-0001-8846-4851
[*] Corresponding Author: chalfant@mit.edu

Submitted: 23 February 2024, Revised: 17 April 2024, Accepted: 1 May 2024, Published: 23 May 2024

Conference paper, DOI: https://doi.org/10.59490/imdc.2024.889 e-ISSN: 3050-486

space to determine a dominant solution. Power and energy system metrics based on the required "ilities" provide the system designer a basis of differentiation between options within a large design space.

Platenberg (2024) presents the findings from a robust literature review of system of systems "ility" requirements and relationships, and methods for differentiating between preferred solutions within a design tradespace. The research was used to develop a hierarchy of "ility" relationships for the naval power and energy system and to generate a framework for decomposing top level requirements and ility-based requirements into metrics for identifying a dominant architecture within an early-stage design tradespace. The framework considers the physical, logical, and operational aspects of the architecture to generate a set of perturbations that are likely to impact the system's ability to maintain value over its lifecycle. A deep dive into Flexibility, a common "ility" of interest, is presented here with four case studies using proposed metrics for power and energy system flexibility. This work is intended to present metrics that can be integrated within early-stage design tools for generating and evaluating the naval power and energy system.

The Naval Power and Energy System

The power and energy system of a Navy ship is responsible for providing propulsion and shipboard electrical power required to conduct the platform mission requirements. Today's surface fleet primarily consists of ships with power and energy (P&E) system architectures that decouple propulsion and power generation functions through the implementation of dedicated propulsion turbines connected directly to the propeller shafts and separate ship service generators installed to provide distributed shipboard electrical power. This type of mechanical-electrical configuration has been a favorable and cost-effective design over the last century, as the demand for propulsion power has significantly outweighed the demand for combat system power. The DDG-51 class, for example, has approximately 78 MW of dedicated propulsion power on shaft, compared to 9 MW of separate ship service power.

The Navy's most recent class of destroyers, the Zumwalt class, introduced an alternative power and energy system architecture, the Integrated Power System (IPS), where all power generated onboard is shared between propulsion load demands and distributed electrical power demands, including mission system loads. The ability for this ship to share full power across all platform functions is enabled by the inclusion of electric propulsion motors, enhanced power distribution, and power controls.

Performance characteristics of the P&E system can be traced to the physical, logical, and operational characteristics of the sub-module configuration. It is important to decompose desired functional and non-functional requirements to the lowest level of measurable capability, as they can often be met by a variety of architectural configurations. For example, an IPS architecture provides increased flexible power capacity when compared to a traditional mechanical architecture based on the total installed power residing within the power generation module, vice split between the power generation and propulsion modules as in a mechanical architecture. However, alternative measures of flexibility, such as the ability to service high-magnitude-short-duration pulse load types, may be architecture agnostic and instead may depend more directly on the configuration of a particular sub-module, such as the energy storage module. When comparing alternatives, the designer needs to consider total integrated P&E system capability and the dependencies between applicable modules.

Design decisions are made at the system and subsystem levels throughout the Navy's ship design process to satisfy overarching performance and cost requirements. The permutation of architectural options within each subsystem domain creates a potential solution space of a high order of magnitude that is challenging to evaluate. Beyond the ability to meet predetermined requirements and specifications, additional performance metrics for non-functional requirements are necessary to evaluate and rank design options within the tradespace.

Development of Metrics for Ilities

Platenberg (2024) presents a hierarchy of ility relationships for the naval power and energy system and proposes a framework for decomposing top level requirements and ility-based requirements into metrics for identifying a dominant architecture within an early-stage design tradespace. The framework considers the physical, logical, and operational aspects of the architecture to generate a set of perturbations that are likely to impact the system's ability to maintain value over its lifecycle. Potential "preparations" that can mitigate perturbations are examined. Selection of preferred architectures requires a balance between uncertainty, performance, cost, and complexity to "right-size" the system.

The framework for development of metrics pertaining to ilities proceeds through six distinct steps:

1. Define the emergent system property of interest.
2. Characterize the system attributes in terms of their physical, logical, and operational architectures. Define the system boundary and required interfaces within the system logical model.
3. Establish a design tradespace of feasible solutions, defined by the lower-level system attributes of each option.
4. Identify a comprehensive set of potential perturbations impacting the emergent system property of interest.

5. Link potential preparations to the set of perturbations to verify the robustness of the potential design solution space. Decompose preparations into their base attributes within the physical, logical, and operational views of the system.
6. For perturbations of interest, generate design metrics for measuring system value under the influence of change caused by the given perturbation. Utilize the system physical, logical, and operational attributes to identify independent and dependent variables.

This framework was used to develop specific metrics for use in evaluating flexibility of a ship power and energy system; these metrics are described in the remainder of this paper.

LITERATURE REVIEW

A literature review was conducted to survey the existing body of knowledge related to "ilities", especially flexibility, in the design of complex systems-of-systems. The design community was found to use the term "ility" with a range of similar definitions, as summarized below.

Ilities. Beginning with a broad exploration of ilities for complex system of systems, several common themes and definitions were found throughout the published material reviewed. The primary objective of defining ilities centers on maintaining system value over time. This need arises from an identified difference between functional requirements used to define the current system's purpose and ilities used to measure the system's ability to respond to change. A temporal aspect of change is prevalent throughout the literature, including lifecycle performance and value discussions. However, there appears to be conflicting terminology used to articulate these purposes. One commonly discovered conflict is the overlap between the definition of ilities and metrics.

(Ricci, Fitzgerald, Ross, & Rhodes, 2014) define a system-of-systems' ilities by the lifecycle value properties that enable a system to "sustain value delivery over time by responding to exogenous changes in the operational environment." They suggest a temporal aspect of the ility, where the value provided isn't realized until after the system is in operation. This aspect differs from traditional functional requirements, which are set to determine the initial primary value of the system. The authors outline a System of System Architecting with Ilities (SAI) method that presents an example set of evaluation metrics for comparing design alternatives that include "optionability" alongside quantitative criteria such as cost and several uses. They go on to describe the need to evaluate SoS architecture alternatives against various metrics, including "value metrics," such as attributes and costs, and "ility metrics," which are determined by evaluating the impact of shifts in system context or requirements from one moment in time to another.

(Chin, Yau, Kok Wah, & Khiang, 2013) describe ilities as "attributes that characterize a system's ability to respond to changes, both foreseeable and unforeseeable." They are presented as non-functional requirements necessary to ensure value delivery over the lifecycle of a system of systems. The authors make a point to acknowledge the cost of implementing ilities and the potential conflict between certain ilities that would require tradeoff decision-making within the architecture. These considerations emphasize the need for a balanced design approach considering the broader system context and requirements.

(Doerry & Amy, 2019) discuss key requirements for surface combatant power and propulsion system design. The authors present a mixed discussion of three prioritized metrics (size, weight, cost) and ilities (flexibility and survivability) that greatly influence the metrics. They identify drivers of requirement implementation as a mix of metrics and ilities: projected future mission system loads, which is a metric, and system survivability criteria, including CONOPS, which is an ility.

(Guariniello & DeLaurentis, 2014) call out an essential role played by metrics in their definition of ilities as the impact of functional and developmental dependencies "on metrics that characterize global properties of a system of systems over its lifespan." They suggest that metrics represent capability at the individual system level but do not directly translate to the system of systems level. Higher level metrics at the SoS level are called ilities.

Design Metrics. To evaluate alternative power and energy system architectures, (Smart, et al., 2017) identified the need for metrics to distinguish between design alternatives. The study explored the impact of new technologies and alternative topologies. Several metrics were available within the designated design tool, S3D, including weight, volume, component count, and a fuel load-range calculation. The authors proposed several future areas for development within early-stage design tools, including various performance metrics.

(Toshon, et al., 2017) present a method for executing Set-Based Design within the shipboard power systems using metrics available in early-stage design tools. The authors discuss a 5 MW Modular Multilevel Converter (MMC) topology and identify pertinent metrics related to the choice of thermal facilities, power density, and cabinet sizing as selection criteria for preferred architectures.

(McNabb, et al., 2019) present a case study for quantifying the value of a particular electric-ship architecture within a broader tradespace using a methodical approach for implementing architectural variations in a baseline model within a robust design simulation environment. The example presented measured baseline performance metrics, displacement, speed, and range variation.

(Chalfant, Hanthorn, & Chryssostomidis, 2012) discuss several metrics typically used in early-stage P&E system design analysis of alternatives, such as weight, volume, fuel efficiency, and losses (based on location, size, and loading). They present an additional survivability metric, which relies on input data from loads, defined services, connectors, and their associated locations. These metrics and their underlying variables were identified within existing design tools, as they are required for defining the system's physical architectures and functional capabilities.

Options, Perturbations and Preparations. A reoccurring set of terminology was found throughout the literature review of system ilities. To establish a common vernacular, the various approaches for implementing ilities to maintain system value commonly refer to "options in design," "perturbations," and "preparations." To design for an ility and to preserve system value, the term perturbation is used to characterize an influence on the system that necessitates change. Design options are inherent capabilities in the design to accommodate future changes. They provide the system owner the option or right to implement the change later in the system's life once the need is identified (right to take action). Preparations refer to the specific architectural features or capabilities planned into the design to enable the system to positively respond to the perturbation (maintain value, value at cost, effectiveness).

(Ricci, Fitzgerald, Ross, & Rhodes, 2014) define perturbations as "unintended (i.e., imposed) state changes in a system's design, context, or stakeholder needs that could jeopardize value delivery;" and an option as "the ability to execute a design decision or feature at any point in the lifecycle that will change or prevent change to the SoS, to respond to variations in the operational context and in stakeholder preferences." The authors further decompose options into change options, which enable a change in the design in response to a perturbation, and resistance options, which enhance the system's ability to resist change.

(Mekdeci, Ross, Rhodes, & Hastings, 2012) decompose perturbations into disturbances and disruptions in their "Taxonomy of Perturbations." Disturbances and disruptions are defined as types of perturbances, with the distinction that disturbances occur over some period of time, but disruptions are nearly instantaneous.

System Views and Context. The naval power and energy system is a complex multidimensional system of systems, including architectures that perform various duties regarding the generation and supply of electrical power, cooling, and mechanical utilities, among others. (Brefort, et al., 2018) present a framework for analyzing distributed systems of naval ship design by decomposing the system characteristics into three primary architectures: physical, logical, and operational. Relationships between interconnected and interdependent systems are discussed in terms of their spatial, functional, and temporal characteristics. The authors present this framework with survivability specifically in mind but outline the applicability to other desired system characteristics. The primary architectures are defined as follows:

- Physical architecture represents the spatial and physical characteristics of the system and its environment.
- The logical architecture describes the functional characteristics of the system and the linkages between each component of the system, focusing on the multidisciplinary nature of the system.
- The operational architecture describes the temporal behavior of a system, including human-system interactions.

These overlapping areas combine information from each primary architecture to provide a deeper understanding of the design space: the physical and logical architectures produce a physical solution; the physical and operational architectures produce physical behaviors; and the logical and operational architectures produce the functional utilization. All three together produce the system response. This framework underpins our approach to defining flexibility metrics and the associated perturbations and preparations.

Flexibility. Flexibility was found to be a predominant ility considered throughout the literature review. Flexibility is frequently presented alongside the classic ilities of survivability and safety as a mechanism for easily enabling system change in response to various types of perturbations. Within the naval power and energy system community, the desire for system flexibility is clear; however, only a single accepted approach for implementation currently exists. Unlike survivability, where industry, government, and Navy-specific guidance has been issued to define system requirements, flexibility is still in the early stages of definition and implementation. This is partially due to the broad scope of requirements and system attributes commonly categorized as flexibility. Whereas the definition of survivability is widely accepted as being decomposed into susceptibility, vulnerability, and recoverability, the literature on flexibility ranges from intrinsic design properties to real options for stakeholder value.

(Chin, Yau, Kok Wah, & Khiang, 2013) define flexibility as "the degree of ease of effecting change(s) to the SoS, in response to external or internal changes, to maintain its mission effectiveness." They suggest that there are two different types of

flexibility – operational: the ability to transition between different modes of operation, and design: the design attribute that enables the system to incorporate changes more easily. Agility, adaptability, and scalability are considered subsets of flexibility.

(Doerry, 2014) identifies eight methods for global ship flexibility and how the electrical power distribution system should be considered within each approach. These flexibility approaches include physical shipboard arrangements of equipment to align with hull features and electrical zones, sizing of longitudinal electrical distribution busses, sizing of power cabling, use of interface standards for support equipment, use of modular equipment, use of commercial equipment, and incorporation of energy storage methods. Doerry specifically highlights the importance of flexibility in the electrical distribution system for servicing future electric weapon systems with significantly higher power ratings and load type demands and proposes several interfaces to be developed, including required power type, amount of power required, ramp rates, power quality, quality of service requirements, and monitoring and control conditions.

(Hein, 2022) defines flexibility as "the measure of a ship's ability to be upgraded quickly and cheaply to efficiently respond to a known or unknown perturbation." His thesis develops a framework for identifying and characterizing flexibility in design through cause-effect mapping.

(Doerry & Koenig, 2017) propose a framework for identifying what types and quantities of flexibility will "increase the ability of the ship to be quickly and economically reconfigured in the future." They acknowledge the temporal aspect of the required change as either a temporary mission capability or permanent reconfiguration. Their paper discusses modularity, adaptability, and flexibility as pertaining to specific types of technologies that can be incorporated, each with an independent impact on overall system affordability. The need for flexibility over the platform's service life is based on potential extensive unknown requirement changes, including high power and new variant combat and mission systems. The overarching framework is based on the principles of Real Options analysis, where design options are considered with respect to their cost per value delivered. In early-stage design and requirements formulation, this type of analysis is valuable for forecasting potential changes to the system requirements and evaluating cost-effective means for responding in the future, but it requires upfront investment in the design. The authors define a tradespace of type and quantity of modular and adaptable technologies, considering cost impacts in terms of weight/space/design effort. These technologies for a flexible ship are proposed considering future system locations, power capacity, sufficient power conversion and distribution, and cooling capacity to support future systems.

(Page J. , 2012) discusses the value of flexibility options in the early-stage design of naval warships instead of options on a project or design. The author argues that Real Options analysis and Net Present Value (NPV) need to be modified to evaluate capital projects (without revenue) and options in design based on needs, cost, and capability. The author identifies power generation and power distribution as top design considerations for historical ship platform upgrade enabling considerations, following general arrangements. Given the Navy's budgeting constraints that limit investment in new capabilities through the development of new ship classes, a framework is presented using an Overall Measure of Effectiveness based on a Choice Model for how capability can be added to a single ship class over time. The example compares an inflexible (current Navy) platform to a notional modular platform with several flexible preparations. The author suggests extending this framework to the subsystem-level or SoS-level analysis. The paper also suggests that the flexible platform has lower upfront acquisition costs, contrary to many discussions of the cost of flexibility.

(McCauley, Hannapel, Bassler, & Koleser, 2016) introduce the "SWAP Boxes" concept to decouple the ship payload (combat system) from the platform. This decoupling is intended to counter the observed tendency within Navy design programs to quickly lock in design requirements to reduce design time and constrain the ship's weight to control cost. The authors state that flexibility and modularity are two concepts: "flexibility is the ship design capability to accommodate combat system growth, and the ability to insert new technologies into the ship throughout the lifecycle of the individual ship and its class. Modularity is the platform's ability to accept a system as a self-contained unit with interface standards." They define flexibility as a function of four criteria: design flexibility, construction modularity, mission modularity, and mission flexibility. Some key benefits of implementing the SWAP Box approach are the ability to apply targeted system margins versus top-level margins and the ability to conduct sensitivity analysis against the maturity of the intended systems. For impact on the power and energy system, SWAP Box parameters would encompass the mission-related loads used to size distributed systems; however, the method is not obviously applicable to the design of the power and energy system architecture itself.

(Richards, Ross, Hastings, & Rhodes, 2009), in their discussion of various perspectives for defining survivability, introduces the ilities flexibility and robustness as "temporal system properties that specify the degree to which systems can maintain or even improve function in the presence of change." The authors emphasize that ilities are dynamic, based on changes to system needs, the system itself, or the system context.

(Doerry & Moniri, 2013) cite the need for improved survivability and reliability of naval power and energy systems as the systems evolve from traditional low-voltage systems to meet the demands of new high-power combat systems.

Ility Relationships. The collection of research presented in the literature review points to a common definition of ilities as emergent systems properties that impact the system's ability to maintain value over time. Ilities are not primary functional requirements, such as those defined in an Initial Capabilities Document or Capability Development Document that define the system's purpose, but rather, are attributes used to measure the system's ability to respond to change. Emergence refers to the resulting function or capability when multiple elements of a decomposed system architecture are integrated together. While the design community agrees on the perceived value in analyzing ilities, system architects and decision makers need a consistent method for prioritizing and quantifying ility requirements. U.S. Navy guidance identifies the need to assess such ilities as reliability, maintainability, sustainability, flexibility, and vulnerability. The Ship Specifications will typically detail the expected producibility, operability, and maintainability of the ship. However, these proprieties are typically measured within the late stages of design, once the ability to influence the system architecture has passed. Upfront understanding of the dependencies and relationships between ilities and functional requirements will enable the designer to identify more robust solutions when making architectural decision in the early stages of design.

While survivability is widely accepted as being decomposed into susceptibility, vulnerability, and recoverability, the literature on flexibility ranges from intrinsic design properties to real options for stakeholder value. Informally, in the field of Marine Engineering, the two ilities are interchangeably used to describe the ability to maintain system performance; however, a key distinguishing difference in application comes from the origin of the perturbation on the system, and the identification of enabling system attributes. A perturbation requiring system survivability is posed by a purposeful threat to degrade system performance, whereas flexibility perturbations are based on the own-system competitive performance or stakeholder desired capability. Survivability most closely relates to the short-duration sub-type of flexibility, due to the nature of real-time, finite duration disturbance.

FLEXIBILITY DEFINITION FOR SHIP DESIGN

Flexibility is an ility that frequently appears in the discussion of complex systems-of-systems' attributes and requirements but lacks a clear and consistent definition. From the literature review in Section 0, several authors have identified common characteristics of flexible systems within the context of Naval Architecture and ship design, but at varying levels of specificity. (Chin, Yau, Kok Wah, & Khiang, 2013) addressed a comprehensive maritime system of systems, relating flexibility to the degree of ease of effecting change to maintain mission effectiveness in response to external or internal perturbations. At the platform level, (Doerry & Koenig, 2017) have expanded the definition of "ease" to include a measure of speed, timeliness, and cost, and (Hein, 2022) identifies that the perturbations may be either anticipated or unknown at the time of making the required design decisions that determine the platform's capability. (McCauley, Hannapel, Bassler, & Koleser, 2016) identified the mission system as the driver of platform flexibility, which (Schank, et al., 2016) relates to the ability to change physical platform boundaries by providing excess space and flexible infrastructure.

From the commercial energy industry perspective, the International Energy Agency (IEA) defines power system flexibility as "the ability to respond in a timely manner to variations in electricity supply and demand" (Gutierrez Tavarez, 2019). This industry definition of flexibility can be tailored to the shipboard naval power and energy system application and used to develop metrics for early-stage design evaluation.

The definition of flexibility used in this work is as follows:

Flexibility is the capability of a system to accommodate change in response to perturbations in requirements.

The utility in application of flexibility depends on the defined system boundary and the distinction between near-term and long-term impacts. Requirements, such as Top-Level Requirements or system specifications, refer to the measurable needs of the stakeholders. The requirements can be organized into the system's physical, logical, and operational context to better understand the design drivers and determine the enabling design characteristics.

For the naval power and energy (P&E) system, flexibility is quantified within the system boundary, in response to perturbations from new and changing loads requiring power (**demand**) or changes at the source of an energy flow (**supply**). The following discussion defines the power and energy system within the physical-logical-operational capability construct introduced by (Brefort, et al., 2018). Together, these system views link the "right power, right location, right time, and right conditions" (Doerry, 2014).

Physical. The physical view relates to the spatial configuration of the system and the physical attributes of the individual subsystems and components. The P&E system is a distributed system that spans the full extent of the ship and comprises many components typically listed in a Machinery Equipment List (MEL). In this view, the system can be depicted as a series of nodes representing each component or enclosed subsystem. Each node is assigned a location using a coordinate system to establish

integration within the whole ship architecture and to define node locations in relation to each other. The metrics used to measure the system's physical requirements and characteristics include measures of distance and each component's physical attributes, including space, weight, power, and cooling (SWAP-C).

Flexibility within the physical view is system configuration driven. The selection of components that comprise the power and energy system and their integration within the ship platform determine the potential system flexibility. The component capacities are measured against the system requirements for supply and demand. Options for implementing flexibility within system attributes include provision of traditional Service Life Allowance margins on SWAP-C, the installation of excess capacity (e.g., installed power generation) beyond initial platform requirements, and defining system interface standards for future subsystem integration. Spatially, the P&E system architecture should be arranged to align with hull features and electrical zones. Options for implementing physical-spatial flexibility include designing reconfigurable spaces, providing access and outfitting paths, or reserving excess arrangeable area within the defined hull compartmentation. Modularity, the design feature that enables the swapping or plug-and-play capability of various system sub-modules within a defined location and interface standard, is defined within the physical view.

Logical. The logical view describes the functional characteristics of the system and the relationships between system components that enable emergent capability. The power and energy system is multidisciplinary, with components connected across the mechanical, electrical, thermal, and signals domains. Figure 1 depicts the flow of electrical power, thermal auxiliaries (water and air), and data across the electrical, thermal, and signals domains for a representative Integrated Power System architecture. In the IPS configuration, as described in Section 0, the propulsion module is considered within the power and energy system, vice as an external load. In the logical view, linkages are identified to connect the individual subsystem or component nodes established in the physical view. Each linkage requires a direction, type, and magnitude to represent a flow within a designated domain.

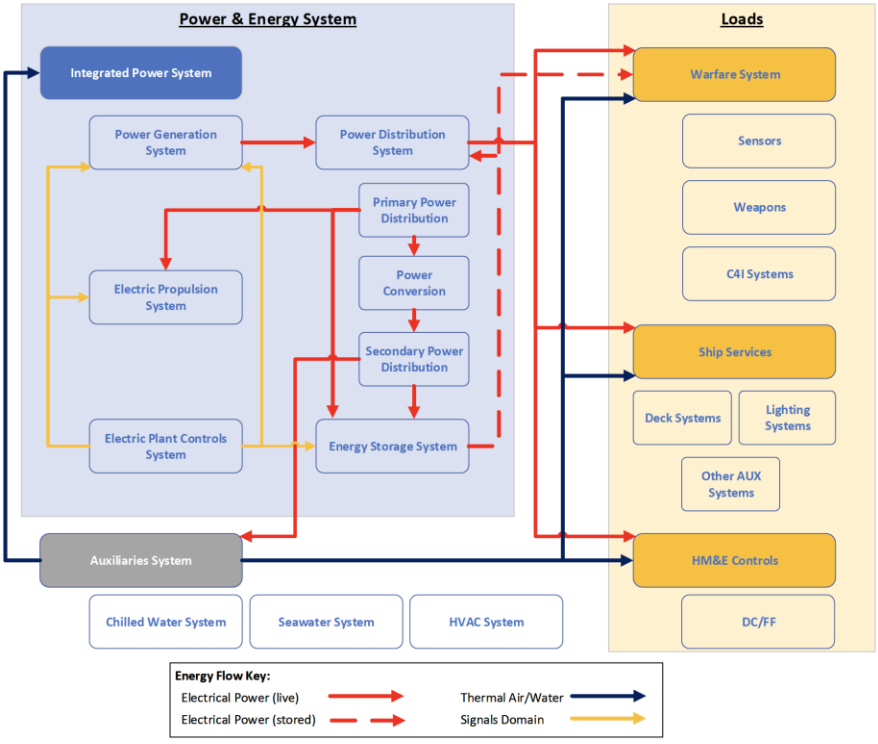

Figure 1: Power and Energy System Logical Model for an Integrated Power System (IPS) for a Combatant

Flexibility within the logical view focuses on the system's ability to provide the required linkages between supply and demand elements within each functional domain when the system realizes future perturbations in requirements. The power and energy system includes a network of distributed systems to enable flows within each domain. The functional flexibility of these systems often centers on the conversion and distribution of the flows and the type of compatible supply and demand elements. To facilitate system sizing and design decision-making, the SWAP Box method introduced by (McCauley, Hannapel, Bassler, & Koleser, 2016) can be used to represent unknown future elements requiring a range of potential P&E system services. The logical view also provides insight into the ability to reconfigure the system in response to realized perturbations.

Operational. The operational view defines the temporal behavior of the system required to accomplish a given mission, including the sequencing of system functions. This view relates a given architecture's physical and logical aspects to the system performance, often referred to as a Measure of Performance. Typical design requirements define the functional capability desired within a particular operating scenario. The time scale of a scenario can range from instantaneous system response to multiyear outlays, such as forecasting of technology maturation and integration. For the power and energy system, these requirements can target specific capabilities of components within each of the specified domains (supply side) or be derived from higher-level platform performance requirements (demand side), such as those related to platform energy consumption.

Operational flexibility is differentiated between requirements for instantaneous response to real-time changes in running conditions beyond the design requirements, and the reconfiguration of the system in response to an emerging requirement change over a large timescale (order of magnitude in years). The various combinations of the demand loads (combat system, ship service, and propulsion loads) requiring service and energy flows within each domain define operational scenarios for the power and energy system. Examples of operational flexibility include the ability to debit power from one category of load to service another, the use of energy storage in response to real-time operational changes or service interruptions, and the ability to incorporate future combat system elements with unique load profiles, such as pulse loads.

METRICS FOR FLEXIBILITY

Design metrics are quantitative or qualitative measures of a system's characterization and value. In the early stages of design, metrics are formulated to assess a system's ability to achieve design requirements and other desired capabilities, including ilities. When evaluating a large multi-attribute tradespace of potential system architectures, alternative designs are compared using metrics to understand the design trade-off and determine the preferred or non-dominated designs. A typical tradespace exploration will evaluate primary and secondary performance measures against cost requirements to uncover trends in system configurations within the open design tradespace.

Attributes of a system within the physical, logical, and operational views serve as the base elements for capability metrics. For ilities such as flexibility, any measure of performance can be traced to the physical attributes of the elements comprising the system; however, the logical and operational properties of these elements within the broader system configuration are required to achieve the desired emergent capability. Flexibility, as the capability to make changes within the system in response to perturbations, requires upfront consideration of how an architecture will respond within each design domain.

For U.S. Navy ship design, flexibility has been traditionally addressed using the Service Life Allowance (SLA) requirement, which equates each vessel's intended years in service to measures of future growth and fatigue capacities based on historical trends such as weight growth and increases in electrical load demands over time. The Navy's design authority, Naval Sea Systems Command (NAVSEA), decomposes SLA into the specific design domains of space, weight, power, and cooling (SWAP-C). These allowances are used to inform the design of the power and energy system and auxiliary systems, size the hullform, and design the hull structure. For the power and energy system, SLA represents flexibility by gross capacity, but doesn't address the necessary decomposition to the subsystem level such as preparations needed within the power distribution and energy storage modules to ensure the intended future capability is achievable.

The following sections identify metrics for evaluating flexibility of the power and energy system within early-stage design space exploration activities. The distinguishing factor of early-stage design is the relatively low amount of design-specific information available to specify a system architecture. Designers and decision makers will typically start with an initial machinery equipment list of components that drive acquisition cost and determine gross system capacity, such as prime movers, generators, power converters and transformers. Sizing and quantities of these components are balanced against first order estimates of load demands based on historical regression or ratiocination, known demands of required mission equipment, and initial system layouts within a conceptual ship stack-up arrangement. The following process traces perturbations to three categories of system flexibility requirements: power capacity, distributable power, and energy storage. Metrics for characterizing capability in each category are proposed using physical-logical-operational system attributes. These metrics should be considered within the overall design space exploration and weighed against functional requirement performance, other ility attributes, and system cost to identify the preferred, "right-sized," solutions.

Power Capacity

Flexible power capacity is dependent on the physical attributes of the power generation subsystem and the design ratings of its components. Within the operational view, flexible power capacity depends on the supply's specified running conditions from the power generation subsystem and demand from the mission system and ship service elements. While the overall power and energy system may be sized based on the prescribed Service Life Allowance requirement, the definition of operating conditions provides a realistic measure of the system's ability to accommodate future potential loads. For an IPS system, power flexibility is determined by the ship's power generation subsystem sizing criteria, including a requirements-driven loading condition. Sufficient power generation is required to energize electric propulsion motors, provide ship service power, and operate onboard

mission systems. The requirements-driven loading condition specifies the combination of ship speed and mission system electrical loads requiring simultaneous power supply. Typically, the power generation sizing requirement will specify the propulsion load required to ensure sustained speed, as this is the highest order of magnitude load onboard the ship. The corresponding mission system electrical load depends on the platform's intended use, which may require the ship to operate the most stressing mission load at sustained speed or a representative average of the daily loads experienced.

Flexible Power Capacity (FPC) Metric. Equation (1) defines flexibility power capacity (FPC) as the sum of the total distributable power available (P_{DST}), based on generation and distribution subsystem capacities; minus the sum of all required loads (L_{REQ}) within the system sizing criteria used for the calculation, such as the 24-hour average load or maximum-margined electrical load; divided by the total power installed (P_{tot}). Distributable power includes energy generated onboard that is available for mission systems and ship services, whereas, depending on the architecture topology, the total installed power includes all energy generated. For example, in an IPS architecture the distributable power may be equal to the total installed power, but a mechanical architecture will have separate ship service power generation and dedicated propulsion diesels or gas turbines directedly connected to the shaft line, so distributable power will be significantly lower than total installed power. The FPC metric provides a relative measure of flexibility for alternative architectures that meet similar mission requirements and should not be used to compare platforms of drastically different initial load requirements. For those types of high-level material solution considerations, a measure of total excess capacity in megawatts is more appropriate. Case Study 1 outlines the differences in applying this metric for different power and energy system architectures.

$$FPC = \frac{P_{DST} - L_{REQ}}{P_{tot}} \tag{1}$$

Debitable Power Flexibility (DPF) Metric. A second metric for the employment of flexible power capacity within an IPS architecture, where the total power generated is required to service the propulsion as well as the mission and ship service loads, is debitable power flexibility (DPF). Whereas the FPC Metric considers elements of the system's physical architecture in a defined loading condition, the Debitable Power Flexibility metric considers the operational architecture capability for applicable system topologies across a range of operational loading conditions, defined by combinations of load requirements. Debitable Power is the ability of the IPS system to prioritize the loads receiving power, effectively debiting power from one load category to service another. Because the largest magnitude load by category is the propulsion load at sustained speed (L_{ps}), the debitable power load available (L_{avail}) is the propulsion load used to size the propulsion subsystem (L_{pREQ}) less the propulsion load required to make a minimum acceptable mission speed (L_{pmin}); thus, $L_{avail} = L_{pREQ} - L_{pmin}$. The DPF is then the minimum of the new additional load demand above the initial design requirement (L_{add}) and the debitable power load available, divided by the new load demand; see equation (2). Case Study 2 will discuss the sensitivity of IPS power flexibility against the selected sizing criteria propulsion and mission loads.

$$DPF = \frac{\min(L_{add}, L_{avail})}{L_{add}} \tag{2}$$

An observed phenomenon when using this metric to compare power and energy systems in ship concepts of varying hullform efficiencies is that a less efficient hull requires larger installed power capacity to achieve the same top-end speed, thus providing a larger debitable power load available when propulsion requirements are reduced to the minimum acceptable speed. This perceived benefit, however, only sometimes leads to system selection within a tradespace when balanced against other attributes, such as cost. Right-sizing the power generation subsystem to align with the desired operating modes leads to a preferred architecture.

Case 1: Flexible Power Capacity Metric

The following examples demonstrate the application of the Flexible Power Capacity metric, equation (1), for three different power and energy system architectures: an Integrated Power System (IPS), a Hybrid power system, and a Mechanical propulsion system with separate ship service power generation. Within each architecture, the sensitivity to specified load conditions is demonstrated by varying the load criteria for ship service and mission elements between the max-margined and 24-hour average electrical load cases and the propulsion loads between the sustained speed and economical transit (cruise) conditions. Additionally, each demand load is evaluated at the initial delivery and end-of-service life conditions to demonstrate increases in demand over time.

For the basis of this analysis, a notional ship concept was leveraged from the NAVSEA Design Data Sheet (DDS 200-2) for 'Calculation of Surface Ship Annual Energy Usage and Cost' (2012). The concept has a design service life of 20 years, requiring a 15% power SLA. Table 1 shows the electrical loads for each design operating condition, including 50% of the SLA. Economical transit is conducted at 16 knots, surge to theater requires 30 knots, and the underway-mission propulsion load is based on a prescribed speed-time profile from DDS 200-2.

Table 1: Electric Load Conditions at various temperatures and operational scenarios (NAVSEA, 2012)

Temperature (°F)	In port - Shore Power (kW)	Underway - Economical Transit (kW)	Underway - Surge to Theater (kW)	Underway - Mission (kW)
10	1,000	3,000	3,000	4,800
59	500	1,800	1,800	3,200
100	900	2,400	2,400	4,000
Propulsion Load	-	7,100	46,800	7,208

Three representative ships were created using the same hullform, mission system loads, and propulsion requirements, but with three different P&E system topologies: IPS, Hybrid, and Mechanical. The DDS 200-2 representative ship concept was leveraged for the Integrated Power System, consisting of three Large Gas Turbine Generators (LTG), two Small Gas Turbine Generators (STG), and two electric Propulsion Motor Modules (PMM). For this basis of comparison, the hybrid and mechanical architecture alternatives were created to provide comparable power for propulsion and mission loads, as shown in Table 2. In the IPS concept, PMMs are sized to achieve the design sustained speed of 30 knots at eighty percent of the maximum continuous rating (MCR). The power generation subsystem, consisting of LTGs and STGs, is sized to provide sufficient power for the sustained speed condition plus the mission load at the end of service life (EOSL), accounting for motor efficiencies and power transmission losses. For the hybrid concept, the propulsion subsystem consists of PMMs, sized to achieve the economical transit speed of 16 knots, plus two propulsion gas turbines (PGT) directly coupled one to each shaft in an 'Or' configuration, such that the PMMs and PGTs do not combine to achieve sustained speed, and the required propulsion demand is supplied by one or the other. The hybrid power generation subsystem is sized to provide full power to the PMMs and mission loads at EOSL. Lastly, the mechanical concept propulsion subsystem consists of four PGTs, two per shaft, and the power generation subsystem is sized to provide mission loads at EOSL with one generator offline for redundancy, referred to as the (N-1) requirement. This (N-1) requirement is not required for IPS or hybrid architectures due to the order of magnitude greater amount of distributable power capacity installed which enables the system to debit propulsion load to compensate for a generator casualty.

Table 2: Major Machinery Equipment Lists

	IPS		**Hybrid (Or)**		**Mechanical**	
	Unit Count	Total kW	Unit Count	Total kW	Unit Count	Total kW
Large Turbine Generator (LTG)	3	72,000	0	-	0	-
Small Turbine Generator (STG)	2	6,000	5	15,000	3	9,000
Propulsion Motor Module (PMM)	2	60,000	2	8,000	0	-
Propulsion Gas Turbine (PGT)	0	-	2	60,000	4	76,000
Condition Driving Installed Power Generation	Sustained Speed Propulsion (30kt) + mission at EOSL		Max Electric Propulsion (16kt) + mission at EOSL		Mission at EOSL (N-1)	
Power Generation Required	-	67,370	-	12,938	-	5,136
Total Installed Power	5	78,000	7	75,000	7	85,000

IPS architecture case. In the IPS architecture, it is assumed that the full amount of power generated can be distributed throughout the ship for propulsion or ship mission loads; thus, the Power Distributable (P_{DST}) is equal to (P_{tot}) at 78 MW. In reality, there may be restrictions on the amount of power that can be distributed across a single bus, limiting the power available for non-propulsion loads based on the specific distribution architecture. The load required (L_{REQ}) is dependent on the specific combination of propulsion and mission load demands, and the amount of service life consumed. Table 3 determines the Flexible Power Capacity for the IPS architecture at sustained speed while operating in two different modes: the underway-mission at 10°F condition, requiring the maximum margined electrical load, and the underway-economical at 10°F condition, requiring the 24-hour average electrical load. Each load combination will evolve over the ship's service life as SLA is consumed and propulsion efficiency reductions are realized. The "at delivery" load required includes the propulsion shaft horsepower required with a 94% PMM efficiency at sustained speed and the stated mission load without SLA. The "at the end of service life (EOSL)" load applies an additional 25% growth factor to the propulsion SHP for hull fouling and plant degradation and a 15% growth factor to the mission loads for consumed SLA. Table 3 also provides the Flexible Power Capacity calculations for the same load conditions at cruise speed, where the PMM efficiency is 91%.

Hybrid architecture case. For the hybrid architecture, where the electric propulsion PMMs are required to cover a smaller portion of the propulsion speed-power curve than the IPS, the distributable power (P_{DST}) is significantly less, at 15 MW. In this configuration, propulsion power at the top end of the speed-power curve is provided by a dedicated PGT on each shaft, which are accounted for in the P_{tot} of 75 MW. In operating conditions with high-speed requirements, the PGTs are online to provide propulsion load, and the L_{REQ} only reflects the ship mission loads. In conditions with speeds up to 16 knots, the L_{REQ} includes the power for the electric propulsion PMMs in addition to the ship mission loads. Table 4 demonstrates the differences between

loading conditions requiring PGT and PMM propulsion service. In each example, L_{REQ} is calculated at the max-margined and twenty-four-hour average loads at delivery and at the end of service life, as evaluated in the IPS case. A 94% PMM efficiency factor is applied to the propulsion load in all cruise conditions (16 knots), and a 25% hull fouling and plant degradation factor is applied to the end of service life evaluations.

Table 3: IPS at Sustained Speed and Cruise Speed

	IPS: Sustained Speed				IPS: Cruise Speed			
	Max Margined Load at Delivery (w/o SLA)	Max Margined Load at EOSL (w/ SLA)	24 HR AVG at Delivery (w/o SLA)	24 HR AVG at EOSL (w/ SLA)	Max Margined Load at Delivery (w/o SLA)	Max Margined Load at EOSL (w/ SLA)	24 HR AVG at Delivery (w/o SLA)	24 HR AVG at EOSL (w/ SLA)
PDST (kW)	78,000	78,000	78,000	78,000	78,000	78,000	78,000	78,000
LREQ (kW)	54,253	67,370	52,578	65,444	12,268	14,889	10,593	12,963
Ptot (kW)	78,000	78,000	78,000	78,000	78,000	78,000	78,000	78,000
FPC	0.30	0.14	0.33	0.16	0.84	0.81	0.86	0.83

Table 4: Hybrid with Sustained Speed (PGT) Required

	Hybrid: Sustained Speed (PGT)				Hybrid: Cruise Speed (PMM)			
	Max Margined Load at Delivery (w/o SLA)	Max Margined Load at EOSL (w/ SLA)	24 HR AVG at Delivery (w/o SLA)	24 HR AVG at EOSL (w/ SLA)	Max Margined Load at Delivery (w/o SLA)	Max Margined Load at EOSL (w/ SLA)	24 HR AVG at Delivery (w/o SLA)	24 HR AVG at EOSL (w/ SLA)
PDST (kW)	15,000	15,000	15,000	15,000	15,000	15,000	15,000	15,000
LREQ (kW)	4,466	5,136	2,791	3,210	12,019	14,577	10,344	12,651
Ptot (kW)	75,000	75,000	75,000	75,000	75,000	75,000	75,000	75,000
FPC	0.14	0.13	0.16	0.16	0.04	0.01	0.06	0.03

Mechanical architecture case. In the mechanical architecture case, electrical power distribution capacity (P_{DST}) is not required for any portion of the propulsion load and, therefore, is sized solely based on the ship service and mission loads. The propulsion demand, an order of magnitude greater than the max margined electric load, is serviced by dedicated PGTs and included in the total installed power (P_{tot}). The load required (L_{REQ}) is calculated at the max margined and twenty-four-hour average loads at delivery and at the end of service life, as evaluated in the IPS and hybrid cases. The mechanical power flexibility, Table 5, is calculated based on the same loading requirements as the sustained speed hybrid case, using PGT propulsion power.

Table 5: Mechanical (not propulsion dependent)

	Mechanical: Not Propulsion Dependent			
	Max Margined Load at Delivery (w/o SLA)	Max Margined Load at EOSL (w/ SLA)	24 HR AVG at Delivery (w/o SLA)	24 HR AVG at EOSL (w/ SLA)
PDST (kW)	6,000	6,000	6,000	6,000
LREQ (kW)	4,466	5,136	2,791	3,210
Ptot (kW)	85,000	85,000	85,000	85,000
FPC	0.02	0.01	0.04	0.03

Discussion. When setting a flexible power capacity requirement, the selection of determinant loading conditions should be based on the platform's intended use and CONOPS. The comparison of cases above provides the requirement owner additional context into the differences between resulting architectures that a particular set of requirements will drive the designer to select. Evaluation of the FPC metric within a full-scale design space exploration will link the ility performance of the P&E system topologies to the physical attributes of their integrated platform, such as overall dimensions, displacement, and cost to better identify the preferred solution. Figure 2 depicts the flexible power capacity for each IPS, hybrid, and mechanical architecture considered across the range of potential loading requirements. Each of the eight loading conditions are plotted for the IPS and hybrid architectures, along with the four mechanical load cases. The flexibility metrics are plotted against a normalized balance of power required and power available to service the requirement due to the significant differences in capacities for integrated versus separated power systems. This normalization demonstrates the magnitude of power required for each individual load case versus the physical architecture capacity installed.

The IPS example architecture has installed capacity beyond the minimum requirement for end-of-service life based on the selected combination of LTGs and STGs. The plant lineup identified in DDS 200-2 (NAVSEA, 2012) targeted increased energy efficiency at each operating condition, requiring a mix of low- and high-power-rated turbines aligned to the required load combinations. This configuration provides flexible power capacity in each evaluation condition, including the most stressing case: sustained speed plus maximum-margined electrical load with full consumption of SLA. The IPS example has five times the amount of distributable power as the hybrid example and thirteen times the amount of the mechanical example. When evaluated for Flexible Power Capacity, including consideration of total installed power and propulsion plus ship service loads in each condition, the IPS example scored one and a half times greater than the FPC values of the hybrid PGT-propulsion on average across the four loading conditions, and eleven times greater on average than the FPC values of the mechanical architecture.

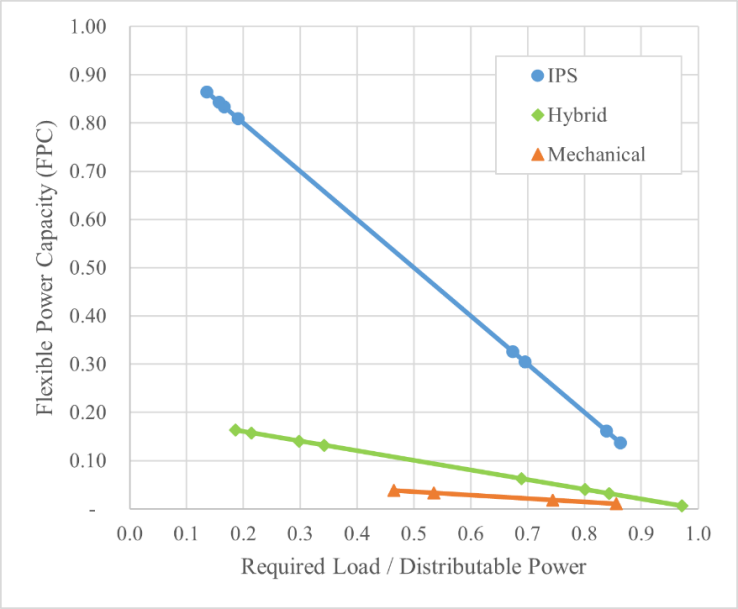

Figure 2: Flexible Power Capacity (FPC) Metrics for IPS, Hybrid, and Mechanical examples versus normalized power capacity, load case required over distributable power

Of interest, the case results determined that the hybrid architecture FPC flexibility is higher at high speeds, while the IPS architecture FPC flexibility is higher at low speeds. In the 'Or' condition with PMMs online (up to 8 MW), the hybrid architecture's measure of flexibility is significantly reduced from the flexible power capacity while using PGTs, as the electric propulsion consumes over half of the available power for distribution. It should be noted, however, that there may be limitations in minimum operating speeds for scenarios able to utilize the flexible power capacity of the PGT-only operating conditions based on the minimum RPM of the propulsion gas turbines and the shaft-propeller design.

The mechanical case requires the greatest amount of installed power of the three architectures, as the required loads for mission and propulsion are isolated to dedicated power supplies, resulting in the lowest amount of distributable power. Additionally, despite the mechanical concept requiring the installation of a redundant/backup ship service power generation to satisfy the (N-1) requirement, the third STG does not contribute to the distributable power.

Case 2: IPS Debitable Power Flexibility Metric

This case utilizes the notional IPS ship concept from DDS 200-2 (NAVSEA, 2012), as described in Case 1, to demonstrate the debitable power flexibility metric. Two variants of the IPS architecture, with a 30-knot and 27-knot sustained speed requirement (L_{pREQ}) respectively, are compared to isolate the impacts associated with a given architecture's sizing criteria for required propulsion load. The debitable power metric for each variant is evaluated for a 1-knot and 5-knot speed reduction in the minimum propulsion load required (L_{pmin}), at both initial delivery and end-of-service life conditions. Three sets of new load demands above the initial design requirement (L_{add}) are then used to represent a range of future mission system requirements.

Table 6 demonstrates the debitable power flexibility (DPF) for the 30-knot IPS architecture, given 1-knot and 5-knot speed reductions for minimum acceptable propulsion load at delivery and EOSL conditions. The additional 25% propulsion factor applied for the EOSL condition reduces the debitable power load available (L_{avail}) by 11 MW in the 1-knot reduction case and 7 MW in the 5-knot reduction case. This results in lower DPF values when assessed against the 15 MW load for the 1-knot

reduction case and the 30 MW load for both 1- and 5-knot reduction cases. In all minimum acceptable propulsion conditions, the 30-knot IPS architecture easily accommodates the 2 MW additional load case. The 5-knot speed reduction significantly increases debitable power load availability, a 94% increase in the delivery condition, and a 340% increase in the EOSL condition.

Table 6: Debitable Power 30 knot IPS

	1 Knot Reduction				5 Knot Reduction			
	Propulsion Condition	kW	Propulsion Condition	kW	Propulsion Condition	kW	Propulsion Condition	kW
LpREQ	30kt, 100% MCR	62,234	30kt, 100% MCR	62,234	30kt, 100% MCR	62,234	30kt, 100% MCR	62,234
Lpmin	29kt, Delivery	45,014	29kt, EOSL	56,268	25kt, Delivery	28,812	25kt, EOSL	36,015
Lavail		17,220		5,966		33,422		26,219
	Ladd (kW)	DPF	Ladd (kW)	DPF	Ladd (kW)	DPF	Ladd (kW)	DPF
Load 1	2,000	1.00	2,000	1.00	2,000	1.00	2,000	1.00
Load 2	15,000	1.00	15,000	0.40	15,000	1.00	15,000	1.00
Load 3	30,000	0.57	30,000	0.20	30,000	1.00	30,000	0.87

The 27-knot sustained speed variant of the notional IPS architecture assumes the same speed-power curve performance of the hull, but the reduced top-end speed requires less total installed power. Table 7 demonstrates the debitable power flexibility for the 27-knot IPS architecture, given 1-knot and 5-know speed reductions for minimum acceptable propulsion load at delivery and EOSL conditions. Based on the lower speed requirements, which correspond to significantly lower resistance and propulsion demand along the speed-power curve, this concept has less debitable power load available in both speed reduction conditions. Compared to the 30-knot concept, the available loads are 20-25% lower for the 27-knot concept cases. Despite the differences in the magnitude of the loads available in all conditions, the relationship between available load at delivery and EOSL conditions holds for the 27-knot concepts, with a 98% increase for the 1-knot reduction and a 330% increase in the 5-knot reduction cases. In summary, the 27-knot concept scored lower debitable power flexibility in all cases and failed to provide the available load threshold for the 15 MW load case 2 in the 1-knot reduction at delivery case, while the 30-knot IPS concept was able to provide sufficient flexible power in the all cases.

Table 7: Debitable Power 27 knot IPS

	1 Knot Reduction				5 Knot Reduction			
	Propulsion Condition	kW	Propulsion Condition	kW	Propulsion Condition	kW	Propulsion Condition	kW
LpREQ	27kt, 100% MCR	45,495	27kt, 100% MCR	45,495	27kt, 100% MCR	45,495	27kt, 100% MCR	45,495
Lpmin	26kt, Delivery	32,535	26kt, EOSL	40,669	22kt, Delivery	19,830	22kt, EOSL	24,787
Lavail		12,959		4,826		25,665		20,708
	Ladd (kW)	DPF	Ladd (kW)	DPF	Ladd (kW)	DPF	Ladd (kW)	DPF
Load 1	2,000	1.00	2,000	1.00	2,000	1.00	2,000	1.00
Load 2	15,000	0.86	15,000	0.32	15,000	1.00	15,000	1.00
Load 3	30,000	0.43	30,000	0.16	30,000	0.86	30,000	0.69

Whereas the flexible power capacity metric considers the architecture-specific installed power generation and electrical loading conditions, the debitable power flexibility metric focuses solely on the demand load conditions, given an established system sizing criterion. Figure 3 graphically displays the increase in available load as the propulsion load is debited for the 27 and 30 knot concepts in their EOSL state. Each curve represents the flexible power available at the given speed, as evaluated in the cases in Tables 13-16. Horizontal grey lines are placed at the three evaluation loads for 2, 15, and 30 MW. Where the dashed horizontal lines are above the L-avail curve, the debitable power flexibility is less than one, with scores decreasing as the distance between the two increases. Vertical arrows are drawn at the speed reductions of 1 and 5 knots, as evaluated above.

The debitable power flexibility metrics for each of the eight conditions are plotted in Figure 4 against the three added load requirements (2, 15, and 30 MW). The figure depicts the point at which each case is no longer able to satisfy the additional load when DPF drops below one. The 30kt IPS concept outscores the 27kt concept in each combination of delivery/EOSL and -1/-5 knot minimum propulsion load due to the exponential shape of the speed power curve. The higher the sustained speed required, the greater the available load when the minimum propulsion load is identified along the exponential curve. Additionally, as expected, we see that the 5 knot reductions for minimum propulsion load provide the largest available load and DPF values in each condition. Lastly, the impact of expected fact of life growth in propulsion load to achieve the minimum acceptable speed at EOSL reduces the available load and DPF for the 15 and 20 MW added loads in each case.

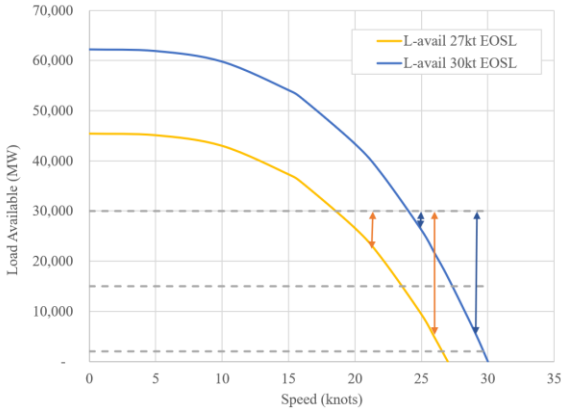

Figure 3: Flexible Power – Load Available at Speed

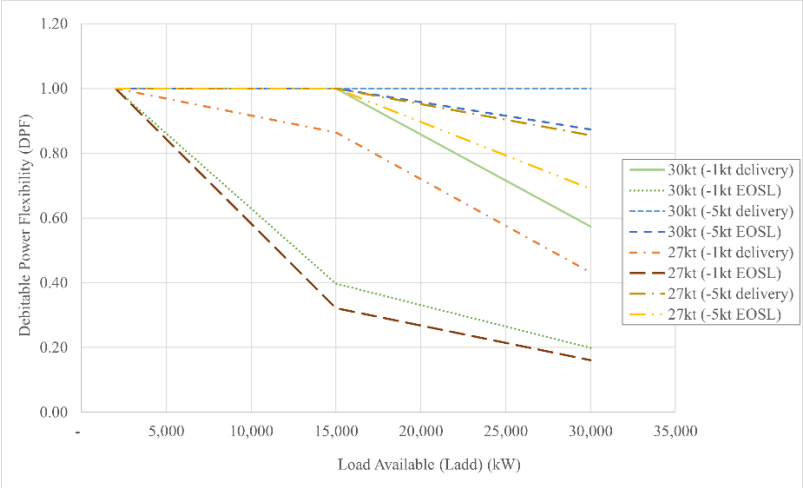

Figure 4: Debitable Power Flexibility versus Load Available for example speed delta cases

Distributable Power

Power distribution system flexibility is required to connect generation capacity to the component-specific load demands throughout the ship. Distribution includes the ship-wide transmission of energy flows and energy conversion into the voltage and quality required by the end users, as shown in the logical view, Figure 1. The physical configuration of the distribution system relies on the maximum distribution capacity, available voltage types and ratings, and the spatial considerations of where the loads are located on the ship, which are typically bound by the assignment of electrical zones. Load requirements will vary within each zone, depending on the interface needed for each individual end user. Therefore, power flexibility depends on each zone's local conversion and distribution capabilities.

Power Distribution System Flexibility (PDSF) Metric. The power distribution system flexibility metric utilizes an 'evaluation loading set' to represent the types of interfaces and the classification of potential future load demands within an individual zone. An evaluation loading set is a compilation of potential future load elements, beyond the initial system design requirements for demand services at delivery plus any required service life allowances. The set can be generated to include a variety of load characteristics required for service from the power and energy system to provide, such as voltage type, voltage rating, and power draw. Because propulsion load demands for an IPS ship significantly outweigh the mission and ship service loads in any zone, they are considered separately from the distribution evaluation loading set. Table 8 demonstrates five evaluation loading conditions based on four potential future mission elements and one representative set of their combination.

Each load element is differentiated by voltage type and power demand. The ~1000 VDC demands are typical of high-power mission systems like radar and laser weapons and may draw directly from the primary power distribution bus. Other low voltage demands, such as onboard computing and thermal auxiliary systems, require in-zone power conversion and distribution within the secondary power distribution system. In an early-stage design tradespace exploration, the full permutation of single

elements and their combinations can be used to determine a simple and indicative metric for distributable power flexibility. Further along in the design process, ship configuration details such as general arrangements and locations of mission stations are established, and the evaluation loading set should be tailored to reflect the revised open tradespace or uncertainty for a given zone.

Table 8: Example distribution system 'evaluation loading sets' for potential future load demands

Voltage Type:	1000 VDC	800-650 VAC	450 VAC
Load Condition (N)	Element* (Power - kW)	Element (Power - kW)	Element (Power - kW)
N1	Laser (1200)	Base Load (500)	Base Load (2000)
N2	Radar (1000)	Base Load (500)	Base Load (2000)
N3	EW (1500)	Base Load (500)	Base Load (2000)
N4	NA	Base Load (500) Energy Magazine (1000)	Base Load (2000)
N5	Laser (1200) Radar (1000) EW (1500)	Base Load (500) Energy Magazine (1000)	Base Load (2000)

*Electric loads for mission system elements of interest taken from (Smart et al., 2017)

The distribution capacity within a zone depends on the sizing of the primary power distribution system, which brings medium voltage power from the onboard generators, and the secondary power distribution system, which converts medium voltage power to lower voltages and currents directly compatible with end users' demand. The power distribution system can be configured in a variety of topologies, such as a radial bus, distributed, or zonal system, with each option having tradeoffs in space, weight, cost, and performance. The flexibility of a ship's power distribution system ($PDSF$), Equation (3), is the average distribution flexibility: the sum of the distribution flexibility in each zone (DST_{zone}), divided by the total number of zones (N_{zones}). Equation (4) determines each zone's flexibility score by assessing the in-zone distribution capability to satisfy the set of load conditions (N). If the zone has sufficient capacity in all defined assessment criteria categories, (N_j) will be scored as a 1, otherwise, if the distribution architecture cannot satisfy any one of the categories in the load condition, it will receive a 0. This approach provides a measure of the platform's distribution flexibility, regardless of the total number of electrical zones, as described below.

$$PDSF = \frac{\sum_{0}^{zone(i)} DST_{zone}}{N_{zones}} \tag{3}$$

$$DST_{zone} = \frac{N_1+N_2+N_3+\cdots+N_j}{N_{tot}} \tag{4}$$

Flexibility can be incorporated (and purchased) as capacity within the design at the initial delivery of the system, or through design preparations that enable future upgrades to the system when needed. The configuration of the primary and secondary power distribution (ring, distributed, zonal, or other) controls the inherent capabilities of the system that impact flexibility, as measured in equation (4). Table 9 provides three examples of power distribution system features that enable flexibility by increasing the total number of potential load cases either at initial system delivery or as a future reconfiguration. The case study provided below compares a split ring and a zonal distribution system architecture at different stages of the design specification process and at different points in the platform's service life.

Table 9. Examples of flexible distribution system features

Flexible Electrical Distribution	Impact
Dedicated electrical power distribution bus for expected high power loads.	Increases the number of potential load cases by enabling new mission system elements to be installed in any zone, with reduced dependence on in-zone power conversion capacity.
Use of high-temperature superconducting cable – variable current, temperature dependent.	Can increase the power distributed to the zone by decreasing the cable temperature without adding new cables. Requires additional cooling. (Note: not necessarily available instantaneously, design preparations needed)
Use of programmable and/or modular power conversion and power electronics: **- Power Electronic Building Blocks** **- Integrated Power Node Centers**	Reduces the total number of power conversion elements. Provides the ability to customize conversion within any given zone to the needs of future end-users using existing or common distribution equipment.

Case 3: Power Distribution System Flexibility Metric

This case demonstrates how to build an evaluation loading set and use it to assess power distribution system flexibility in P&E system architectures. The case study uses a common evaluation loading set to compare four variants:

- **Conventional split ring bus architecture (early-stage design)**: based on the ESRDC 10,000-ton IPS ship concept (Smart, et al., 2017)
- **Ring bus alternative (later design stage)**: a variant of the ESRDC concept case is presented to demonstrate the maturation of the evaluation criteria as the design space for potential future loads is reduced.
- **Zonal distribution architecture (base model)**: based on the Integrated Fight-Through Power (IFTP) concept described in the 'Next Generation Integrated Power System (NGIPS) Roadmap' (Doerry, 2007)
- **Zonal alternative (future block upgrade)**: a variant of the NGIPS concept is used to demonstrate the increase in flexibility associated with a future upgrade to the initial base architecture.

The evaluation loading set is built as a full permutation of the individual element loads in Table 10, which include the base loads required at delivery plus the potential future mission systems that the platform may be required to host in the future. The voltage types and power ratings for this evaluation set are notional, based on the payload list identified in (Smart, et al., 2017), and do not represent any actual Navy system values. Elements listed with multiple power ratings, separated by a comma, represent different configurations the future system may reflect in the future. Various options per element type may represent uncertainty of element rating or quantity. The two baseload LVAC options reflect potential differences across multiple zones of the ship at delivery. Inclusion of zero kW element loads enables the evaluation set to account for potential zone requirements that do not include the given mission element. A full permutation of these load elements generates 1,728 evaluation conditions; each of these evaluation conditions is assessed against each zone in the given distribution system architecture to determine the distribution score for that zone, then zonal scores are combined for an overall PDSF metric. To simplify the assessment of a given electrical distribution zone, the applicable loads for each set are summed by voltage type category, in this case as 1000V Medium Voltage Direct Current (MVDC), between 650-800V of either Alternating or Direct Current (MVAC/MVDC), or 450V Low Voltage Alternating Current (LVAC). For example, the 300th permutation consists of:

> [500 kW MVAC/DC Base Load, 1500 kW LVAC Base Load, 200 kW MVAC/DC Energy Magazine, 600 kW MVDC Laser, 0 kW MVAC/DC Processing, 0 kW MVAC/DC VLS, 1700 kW MVDC Radar, 4000 kW MVDC SEWIP, 450 kW MVAC/DC Sonar]

which sums to [6,300 kW MVDC, 1,150 kW MVAC/DC, 1500 kW LVAC]. The full set of permutations is available in Platenberg (2024).

Table 10: Evaluation Load Set Elements

Voltage Type:	MVDC (direct feed)	MVAC/MVDC	LVAC
Element	Power (kW)	Power (kW)	Power (kW)
Base Load	NA	500	1500, 2000
Energy Magazine	NA	0, 200, 1000, 2000	NA
Laser	0, 600, 1200	NA	NA
Processing Equipment	NA	0, 200	NA
Missile Launcher	NA	0, 400	NA
Radar	0, 1700, 3300	NA	NA
Electronic Warfare (EW)	0, 2000, 4000	NA	NA
Sonar	NA	0, 450	NA

Variant 1: Ring Bus (early-stage design evaluation). The conventional split-ring-bus architecture, shown in Figure 5, is based on the (Smart, et al., 2017) 10,000-ton IPS concept, with four electrical distribution zones, a primary power distribution system voltage of 10 kVDC, and dual paths of power on port and starboard sides of the ship through the fully connected ring bus. Power generation modules (PGMs) and propulsion motor modules (PMMs) are connected directly to the ring bus via appropriate converters or drives. The baseline architecture included dedicated converters for high power loads to connect two Radars and one Railgun to the primary distribution bus; however, for this case and the evaluation load set, the topology was modified to replace the Railgun converter with converters for the EW and Laser elements in Zone 1, add a second EW converter in Zone 2, and add a second Laser converter in Zone 4. The power conversion modules (PCMs) represent converters and inverters within each zone, connecting all other loads to the port and starboard bus. The sizing of these converters was taken directly from the ESRDC concept, and the total distribution capacity by zone is summarized in Table 11.

Each of the four electrical zones was assessed independently for its ability to satisfy the 1,728 potential future electrical loading conditions (N) in the evaluation set. If the zone had sufficient capacity in each of the three voltage categories, then a score of 1 was recorded for that Nth condition, otherwise, if there was insufficient capacity in any one of the three categories, a score

of 0 was recorded. The sum of the 1,728 N-scores divided by the total number of N load conditions determined the zone's flexibility metric (DST_{zone}), as shown in Table 11. The average of the four zones scores determined a total power distribution system flexibility score ($PDSF$) of 0.31.

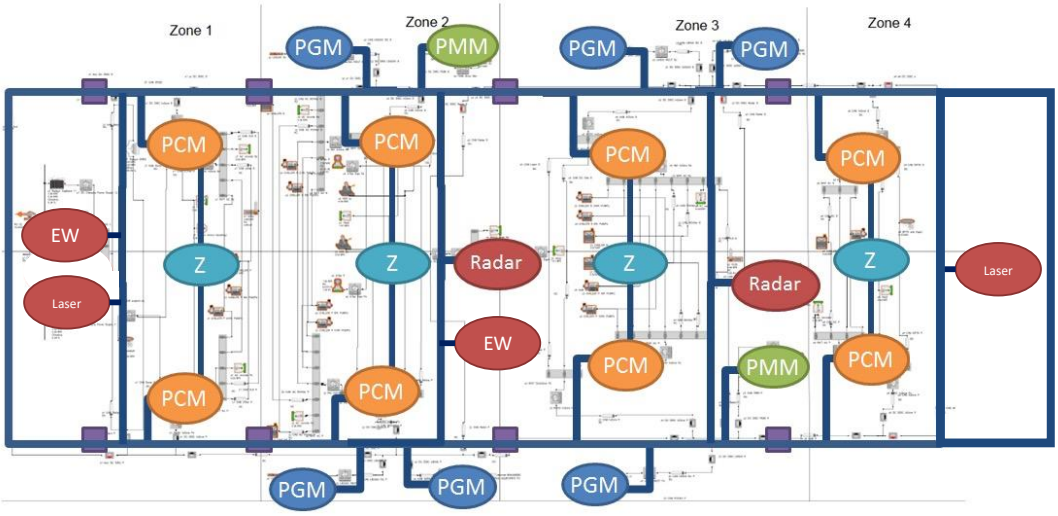

Figure 5: Conventional Split Ring Bus Distribution Architecture Topology. Based on (Smart, et al., 2017).

In each of the four zones, the limiting distribution category is the MVDC converter ratings for the dedicated mission elements. In a design space exploration activity, this finding might lead the designer to investigate the ability of the potential future elements to bring additional dedicated converters when needed for installation in the future, along with verification of the architecture's total flexible power capacity.

Table 11: Conventional Split Ring Bus Distribution Capacity by Zone and voltage category; with each zones distribution flexibility score considering the full evaluation loading set permutation.

	Zone 1 (kW)	Zone 2 (kW)	Zone 3 (kW)	Zone 4 (kW)
MVDC (direct feed)	3,200	3,700	3,300	1,200
MVAC/MVDC	8,000	17,800	12,400	5,800
LVAC	4,200	5,800	7,000	3,100
$\boldsymbol{DST_{zone}}$	0.33	0.41	0.37	0.11

*Distribution capacity based on (Smart et al., 2017)

Variant 2: Ring Bus (later stage design evaluation). To simulate the progression from a distribution flexibility analysis of an early-stage concept design to a more mature preliminary design baseline, the conventional ring bus architecture was used for a second flexibility evaluation. In this case, the design space for potential zone requirements is narrowed and the evaluation loading set is tailored to the requirements for each zone. Table 12 provides the refined requirements for evaluation loading set criteria applicable to Zones 1-4. Zone 1, the forward-most zone on the ship, is designated responsibility for the Sonar, due to shaping of the hullform and location of the sonar dome. Radar requirements are allocated to the zones 2 and 3, which are covered by the deckhouse for mounting the equipment topside. The Laser tradespace is unchanged; however, the energy magazine requirements are reduced to 1 MW and locations based in zones 2-4. The resulting flexibility score improvements are shown in Table 12, and the total power distribution system flexibility score ($PDSF$) improves to 0.64. Note that zone 1 scores a 1.0, as the evaluation loading set requirements were narrowed to match the MVDC converter for the mission elements as intended.

Variants 3 and 4: IFTP (Base Model and Block Future upgrade). The zonal distribution architecture is based on the Integrated Fight-Through Power concept described in the Next Generation Integrated Power System Roadmap (Doerry, 2007), with a notional in-zone topology depicted in Figure 6. For this case, the zonal electrical distribution system concept consists of 4 electrical zones, with a series of Power Conversion Modules (PCM) types to convert power within each zone. A PCM-4 serves as a transformer rectifier to convert MVAC power from the power generation module to 1000 VDC for distribution across the ship. Within each zone, PCM-1As convert 1000 VDC power to a variety of MVDC voltages based on user needs. PCM-2As then convert 750-800 VDC power from the PCM-1A into LVAC in-zone demands. Additionally, for this concept, a notional PCM-X is connected to the 1000 VDC bus in each zone to service high power MVDC loads throughout the ship. It is

assumed that the rating of each PCM is scalable based on the number of modular subcomponents included: Ship Service Inverter Modules (SSIM) or Converter Modules (SSCM).

Table 12: Refined Requirements Evaluation Loading Criteria

	Zone 1	Zone 2	Zone 3	Zone 4
MVDC (direct feed) Limiting Criteria	0x Radar 1x EW Unit 1x Max Laser	1x Radar Unit 1x EW Unit 1x Max Laser	1x Radar Unit 1x EW Unit 1x Max Laser	0x Radar 1x EW Unit 1x Max Laser
MVDC (kW)	3,200	4,900	4,900	3,200
MVAC/MVDC Limiting Criteria	1x Sonar 0x Energy Mag	0x Sonar <1MW Energy Mag	0x Sonar <1MW Energy Mag	0x Sonar <1MW Energy Mag
MVAC/MVDC (kW)	1,550	2,100	2,100	2,100
LVAC (kW)	2,000	2,000	2,000	2,000
DST_{zone}	1.0	0.65	0.59	0.33

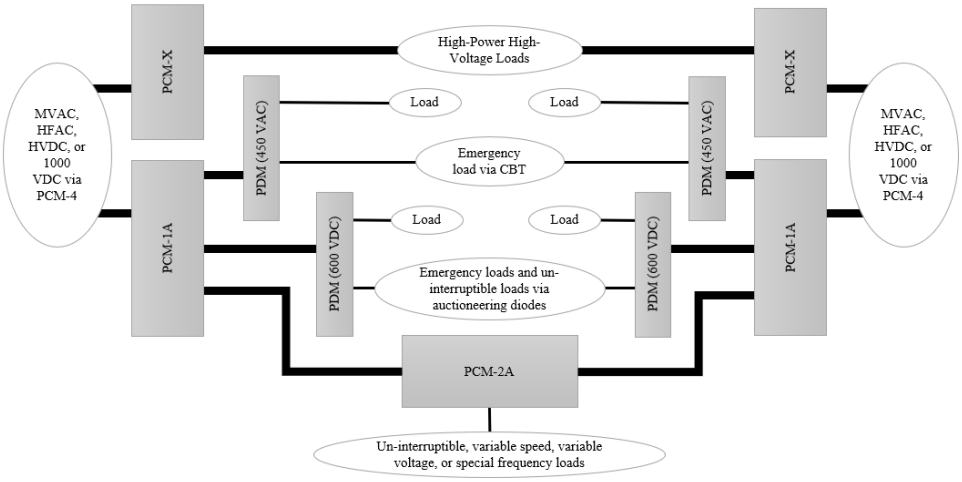

Figure 6: NGIPS Roadmap "Potential Future IFTP" In-Zone Topology, based on (Doerry, 2007)

Two variants of the zonal IFTP concept were evaluated to demonstrate the different flexibility scoring associated with a base model architecture as initially delivered, and a block future architecture, including some planned upgrades to the distribution system. These two zonal IFTP variants are consistent with this approach, as the base model architecture including design preparations in the form of planned PCM growth capacity to accommodate additional SSIM/SSCMs in the future, when needed. The base model is delivered with 5.5 MW of PCM-X, 12 MW of PCM-1A, and 10 MW of PCM-2A capacity, and design preparations for 22 MW of PCM-X and 4 MW of PCM-1A SSCM/SSIMs. Table 13 indicates the PCM capacity for the base model configuration by zone, with the associated zone's flexibility metric (DST_{zone}). The total power distribution system flexibility score ($PDSF$) for this configuration is 0.14. However, once the maximum PCM capacity is installed in the block future configuration, also shown in Table 13, the total PDSF score improves to 0.85.

Table 13: Zonal IFTP Distribution Capacity by Zone, Base Model and Future Distribution

	Base Model				Future Distribution				
	Zone 1 (kW)	Zone 2 (kW)	Zone 3 (kW)	Zone 4 (kW)	Zone 1 (kW)	Zone 2 (kW)	Zone 3 (kW)	Zone 4 (kW)	Total DST Capacity (kW)
PCM-X	0	2,000	3,500	0	6,875	6,875	6,875	6,875	27,500
PCM-1A	3,000	3,000	3,000	3,000	4,000	4,000	4,000	4,000	16,000
PCM-2A	2,500	2,500	2,500	2,500	2,500	2,500	2,500	2,500	10,000
DST_{zone}	0.03	0.16	0.32	0.03	0.85	0.85	0.85	0.85	0.85

The four architecture variants' power distribution system flexibility metrics and individual zone flexibility scores are plotted in Figure 7. Each architecture was modeled with four electrical zones, with varying distribution and conversion capacities in

each zone, across the MVDC, MVDC/MVAC, and LVAC assessment categories. The ring bus variants, each with the same distribution and conversion capacities, are shown in blue. The early-stage design assessment utilized the full permutation of the evaluation loads sets, whereas the later-stage design assessment tailored the evaluation loads based on other known design decisions to reduce the range of potential future load options desired in each zone. This maturation of design data resulted in a 100% increase in PDSF for the ring-bus architecture. The IFTP base model and block future variants are plotted in yellow, to demonstrate the increase in distribution flexibility provided by including preparations in the design to accommodate future (long-term) perturbations in required load demands. The ship concept for these IFTP variants remains constant other than the installation of additional distribution and conversion modules in the block future, to represent in-line upgrades at the same maintenance availability where the new load demand end-users are installed. In a design space exploration activity, a large number of representative architectures can be defined by their individual zone characteristics, and assessed against a common set of evaluation loads to identify the feasible options. In this limited example, the IFTP option is preferred based on the lower upfront cost of the architecture and the ability to achieve the higher power distribution system flexibility in the future, when the long-term perturbations are realized.

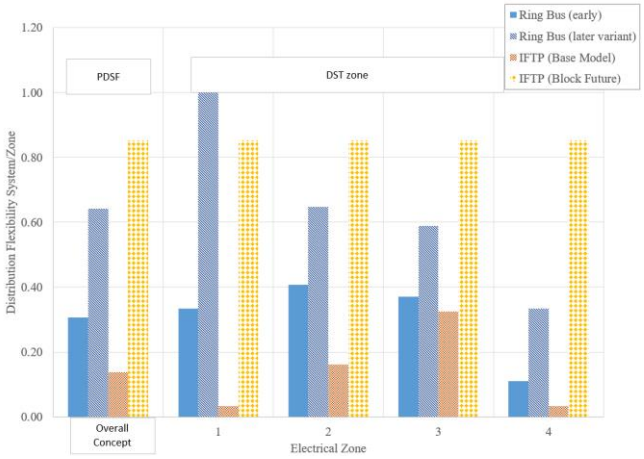

Figure 7: Power Distribution System Flexibility (PDSF) and individual zone (DSTzone) scores

CONCLUSIONS

This paper develops measures of power and energy system flexibility; this specific ility was chosen based on the frequency of its appearance in the literature review and interest within the broader naval design community. Flexibility is defined as the capability of the system to accommodate change in response to perturbations in requirements. For the naval power and energy system, flexibility is quantified within the system boundary, in response to perturbations from new and changing loads requiring power or changes at the source of an energy flow. Three case studies were conducted to develop metrics for Flexible Power Capacity, Debitable Power Flexibility, and Distributable Power Flexibility.

The maturation of developmental mission system technologies with new and increased electrical power demands are driving requirements for emergent properties, beyond the typical functional requirements. The U.S. Navy surface fleet is currently facing challenges related to the rate of technology change and uncertainty of the combat systems of the future, and the significant cost of investment to design and build new ship classes. Uncertainties impact the system's ability to affordably maintain mission relevance within an evolving operational context. Affordability constraints within the Navy acquisition environment, and the timelines for designing new and modified classes of ships, emphasize the need to make informed decisions in early-stage design.

Related and Future Work

Additional metrics were developed in conjunction with this work. Interested readers are referred to Platenberg (2024) for a description and case study of an energy storage system flexibility metric, and for a Real Options Analysis that balances system performance and cost to "right size" the P&E system at delivery with preparations in the design to react to future uncertainty.

The Navy and academic community should pursue validating and implementing the metrics presented here for power and energy system flexibility within the Smart Ship System Design (S3D) program and integrating with the standard early-stage design tools within the Leading Edge Architecture for Prototyping Systems (LEAPS) toolkit.

CONTRIBUTION STATEMENT

D. Platenberg: Conceptualization; data curation, methodology; writing – original draft. **J. Chalfant:** conceptualization; supervision; writing – review and editing. **W. Seering:** conceptualization; supervision.

ACKNOWLEDGEMENTS

This material is based upon research supported by the U.S. Office of Naval Research (ONR) under award number ONR N00014-21-1-2124 Electric Ship Research and Development Consortium; and by the National Oceanic and Atmospheric Administration (NOAA) under Grant Number NA22OAR4170126-MIT Sea Grant College Program, and was approved for public release under DCN #543-1521-24. The views expressed herein are the personal opinions of the authors and are not necessarily the official views of the Department of Defense or any military department thereof.

BIBLIOGRAPHY

Brefort, D., Shields, C., Jansen, A. H., Duchateau, E., Pawling, R., Droste, K., . . . Andrew. (2018). An architectural framework for distributed naval ship systems. *Ocean Engineering*, 147, 375-385.

Chalfant, J., Hanthorn, D., & Chryssostomidis, C. (2012). Development of a Vulnerability Metric for Electric-Drive Ship Simulations. *2012 Grand Challenges in Modeling and Simulation, GCMS '12* (pp. 8-11). Genova, Italy: SCS.

Chin, K. S., Yau, P. E., Kok Wah, S. K., & Khiang, P. C. (2013). FRAMEWORK FOR MANAGING SYSTEM-OF-SYSTEMS ILITIES. *DSTA Horizons*.

Cramer, A. M., Sudhoff, S. D., & Zivi, E. L. (2007). Performance Metrics for Electric Warship Integrated Engineering Plant Battle Damage Response. *2007 IEEE Electric Ship Technologies Symposium* (pp. 22-29). IEEE.

Doerry, N. (2007). Next Generation Integrated Power NGIPS Technology Development Roadmap. Washington, D.C.: Naval Sea Systems Command.

Doerry, N. (2014). Electrical Power System Considerations for Modular, Flexible, and Adaptable Ships. *ASNE Electric Machines Technology Symposium.* ASNE.

Doerry, N., & Amy, J. (2019). Key Requirements for Surface Combatant Electrical Power System and Propulsion System Design. *ASNE Advanced Machinery Technology Symposium.* ASNE.

Doerry, N., & Koenig, P. (2017). Framework for Analyzing Modular, Adaptable, and Flexible Surface Combatants. *SNAME Maritime Convention* (p. D033S011R003). SNAME.

Doerry, N., & Koenig, P. (2017). Modularity and Adaptability in Future U.S. Navy Ship Designs. *MECON 2017*, 21-23.

Doerry, N., & Moniri, K. (2013). Specifications and Standards for the Electric Warship. *2013 IEEE Electric Ship Technologies Symposium (ESTS)* (pp. 21-28). IEEE.

Guariniello, C., & DeLaurentis, D. (2014). Integrated Analysis of Functional and Developmental Interdependencies to Quantify and Trade-off Ilities for System-of- Systems Design, Architecture, and Evolution. *Procedia Computer Science*, 28, 728-735.

Gutierrez Tavarez, E. (2019). The who and how of power system flexibility. *International Energy Agency (IEA).* Paris: IEA.

Hein, C. (2022). *Quantifying Flexibility in Naval Ship Design.* Cambridge, MA: (Doctoral dissertation) Massachusetts Institute of Technology.

Jansen, A. H., de Vos, P., Duchateau, E., Stapersma, D., Hopman, H., van Oers, B., & Kana, A. A. (2020). A framework for vulnerability reduction in early stage design of naval ship systems. *Naval Engineers Journal*, 132(2), 119-132.

McCauley, P., Hannapel, S., Bassler, C., & Koleser, J. (2016). An Agile Method for Flexible Ship Architectures in Early Stage Naval Ship Design. *Naval Engineers Journal*, 128(3), 31-40.

McCoy, & Kuseian. (2013). *Naval Power System Technology Roadmap.* Washington, D.C.: Electric Ships Office, Naval Sea Systems Command (NAVSEA).

McNabb, J., Robertson, N. A., Steffens, M., Sudol, A., Mavris, D., & Chalfant, J. (2019). Exploring the Design Space of an Electric Ship using a Probabilistic Technology Evaluation Methodology. *2019 IEEE Electric Ship Technologies Symposium (ESTS)* (pp. 181-188). IEEE.

Mekdeci, B., Ross, A. M., Rhodes, D. H., & Hastings, D. E. (2012). A Taxonomy of Perturbations: Determining the Ways That Systems Lose Value. *2012 IEEE International Systems Conference SysCon* (pp. 1-6). IEEE.

NAVSEA. (2012). DDS 200-2; Calculation of Surface Ship Annual Energy Usage, Annual energy Cost, and Fully Burdened Cost of Energy. Washington, DC: Naval Sea Systems Command (NAVSEA).

Page, J. (2012). Flexibility in Early Stage Design of U.S. Navy Ships: An Analysis of Options. *Journal of Ship Production and Design*, 128-133.

Platenberg, D. (2024). *Characterizing Naval Ship Systems Power and Energy Metrics through Modeling and Analysis.* Cambridge, MA: (Master's Thesis) Massachusetts Institute of Technology.

Ricci, N., Fitzgerald, M., Ross, A. M., & Rhodes, D. H. (2014). Architecting Systems of Systems with Ilities: an Overview of the SAI Method. *Procedia Computer Science*, 28, 322-331.

Richards, M. G., Ross, A. M., Hastings, D. E., & Rhodes, D. H. (2009). *MULTI-ATTRIBUTE TRADESPACE EXPLORATION FOR SURVIVABILITY.* Cambridge, MA: (Doctoral dissertation) Massachusetts Institute of Technology, Engineering Systems Division.

Schank, J. F., Savitz, S., Munson, K., Perkinson, B., McGee, J., & Sollinger, J. M. (2016). *Designing Adaptable Ships.* RAND Corporation.

Smart, Chalfant, Herbst, Langland, Card, Leonard, & Gattozzi. (2017). Using S3D to Analyze Ship System Alternatives for a 100 MW 10,000 ton Surface Combatant. *IEEE Electric Ship Technologies Symposium (ESTS)* (pp. 96-103). IEEE.

Toshon, T., Soman, R. R., Wiegand, C. T., Israel, M., Faruque, M. O., & Steurer, M. (2017). Set-Based Design for Naval Shipboard Power Systems Using Pertinent Metrics from Product Development Tools. *2017 IEEE Electric Ship Technologies Symposium (ESTS)* (pp. 164-169). IEEE.

Proceedings of 15th International Marine Design Conference (IMDC-2024)
June 2-6, 2024
Amsterdam, the Netherlands

Optimization of Ship Design for the Effect of Wind Propulsion

Timoleon Plessas[1,*] and Apostolos Papanikolaou[2]

ABSTRACT

International regulations as well as strong market demand for zero-emission transport call for a radical change in the shipping industry. One very promising zero-emission propulsion system for shipping is wind propulsion. In this context, the EU-funded Orcelle Wind project (https://cordis.europa.eu/project/id/101096673) aims at using wind as the main source of ship propulsion and to demonstrate the effectiveness and viability of Wind Assisted Propulsion Systems (WAPS) by a retrofitting and new building demonstrator. In this paper, we explore the effect of wing sails on the concept design of a VLCC tanker in the frame of a newly parametric ship design optimization procedure.

KEY WORDS

Ship Design; Parametric Optimization; Wind Propulsion; Wing Sails; WAPS; Case Study

INTRODUCTION

The International Windship Association (IWSA) has declared 2021-2030 the 'Decade of Wind Propulsion' and the European Maritime Safety Agency (EMSA) recently issued a related report (EMSA, 2023) concluding that "wind-assisted propulsion is considered to have potential for the shipping industry". Thus, the maritime industry seems to be returning to its roots by experimenting with Wind Assisted Propulsion Systems (WAPS) in its effort to drastically cut its carbon footprint. The numerous regulatory requirements related to Green House Gas (GHG) emissions (IMO 2022)and the increased costs and problems with logistics of *green* fuels make wind propulsion a promising alternative for achieving the required environmental goals, to comply with related regulations and to reduce operational costs. Wind as an energy source offers numerous advantages for the shipping industry: it is freely available and future-proof, independent from the supply and price fluctuations of combustible and of alternative fuels. In addition, wind is a predictable energy source with zero emissions, which does not require new shore infrastructures and associated logistic systems. It is also one of the few technologies potentially offering double-digit fuel and emission savings.

Numerous recent studies have focused on the modeling and the simulation of wind assisted propulsion systems (e.g, Rosander & Bloch 2000; Bentin et al 2018; Talluri et al 2018), while potential fuel savings have been demonstrated by 3-DOF (Viola et al 2015; Ma et al 2023) and 4-DOF (Tillig & Ringsberg 2019) simulation methods. Although the main focus has been given to the performance prediction of vessels equipped with Wind Assisted Propulsion Systems (WAPS), *the effect of WAPS on ship design optimization* has not been yet systematically examined, namely *traditional ship design concepts* are being equipped with WAPS in the way of retrofitting and their performance is examined/optimized, even if they are newbuildings.

[1] Ship Design Laboratory, National Technical University of Athens, Athens, Greece
[2] Ship Design Laboratory, National Technical University of Athens, Athens, Greece; ORCID: 0000-0001-7464-9476
* Corresponding Author: Timoleon Plessas <timplessas@naval.ntua.gr>

Submitted: 25 February 2024, Revised: 16 April 2024, Accepted: 1 May 2024, Published: 23 May 2024

Conference paper, DOI: https://doi.org/10.59490/imdc.2024.884 e-ISSN: 3050-486

In this paper we present the development of a parametric ship design optimization framework to identify possible differences in the main dimensions and characteristics of ships, when considering the effect of WAPS, starting with the concept design of ships with fitted wing sails. It is noted that until now, the fitting of WAPS to ships has been as a retrofitting to an existing design, even in cases of newbuildings. For this, we developed and implemented a new methodology in MATLAB (Mathworks, 2023). It enables the fast simulation of the effect of alternative WAPS on the design of ships of various types and sizes, the identification of trends for the main ship design characteristics (main dimensions, hull form, main engine and propeller characteristics), while using only few input parameters and while all pertinent major design constraints are taken in to account. The developed method and s/w tool are herein applied to the design of a VLCC tanker with WAPS (here: generic wing sails) to demonstrate the applicability and limits of the presented approach.

WIND POWERED SHIP PROPULSION SIMULATION MODEL

Focusing on the concept design of ships with WAPS, a simplified one degree of freedom (1-DOF) hydrodynamic/maneuvering simulation model is utilized to conclude on the effect of WAPS on ship design. The main differences between a 1-DOF model (surge, movement in longitudinal direction) and a 4-DOF model (surge, sway, yaw and roll movement) are the consideration of the hydrodynamic forces that occur due to the added rudder resistance to maintain the required course and the drift resistance, which is the added resistance due to the fact that the vessel sails at a drift angle which results in a non-symmetrical flow around the hull. Regarding the effect of roll motion, a simplified way to compensate for the lack of consideration of the roll movement in the simulation is to examine the caused heel angle hydrostatically, meaning that the static heel is estimated based on the generated sail side force. Also, the effect of the heel angle on the projected sail area and the height of the center of effort is considered. Of course, this is a simplified approach that ignores the dynamic phenomena of a complete maneuvering model of ship's hydrodynamics (Papanikolaou et al, 2016); thus, it needs to be used with caution in cases where large heel angles are expected and when the hydrodynamic effect of hull appendages (bilge keel, sideboards, bottom daggerboards etc.) is significant. Tillig and Ringsberg (2019) showed in a case study on the utilization of WAPS for a tanker operating on a route in the Baltic Sea (from Gothenburg to St. Petersburg) that the difference in estimating the fuel consumption for wind assisted vessels with 1 DOF model compared to a 4 DOF model ranges from 2% (for smaller sail areas – e.g. 300 m2) to 7% (for larger sail areas – e.g. 900 m2), with the 4 DOF model giving more conservative predictions in terms of savings.

Following this reasoning and for the purpose of optimizing ship's concept deign, a one degree of freedom (1-DOF), quasi-steady model has been developed and coded for simulating and optimizing a ship operating in a pre-defined route with available weather data information. The developed model takes into account the interaction between hull, propeller, engine and sail, simulates and balances all forces in surge direction and estimates the power and fuel consumption needed for completing a scheduled voyage. In addition, the developed model allows the communication (exchange of data) between MATLAB and NAPA software packages (Figure 1). This enables the conduct of a more detailed analysis for each generated design alternative, which includes lightship & loading conditions determination, intact stability criteria assessment, environmental regulations assessment (e.g., oil outflow compliance for tankers) and overall performance analysis. The user can choose if NAPA should be utilized during the optimization. Alternatively, simplified calculations can be conducted within MATLAB without the need of NAPA, which may provide less details but it significantly speeds up the optimization procedure. Indicatively, when calling NAPA a single simulation takes approximately 40 seconds, whereas computations using semi-empirical formulas within MATLAB take approximately 1 second on a conventional computer. The results presented in this study were conducted using only MATLAB internal routines.

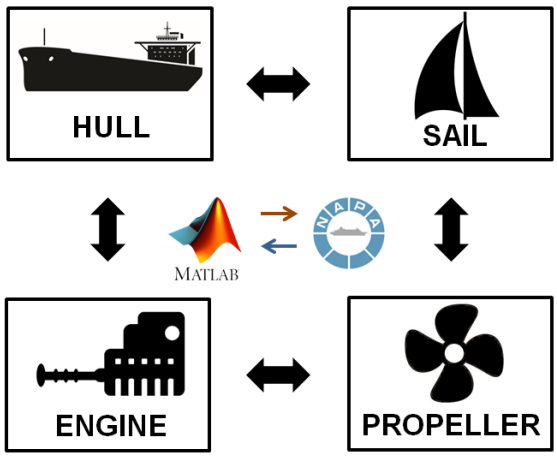

Figure 1. MATLAB code: Interaction between vessel modules

The developed simulation tool consists of three basic modules: “input creation”, “simulation” and “output”. The “Input creation” module is responsible for creating all the necessary input (power curves, engine curves, stability and weight relationships and calculations, etc.) while considering the input (selected) design variables (see subsection “Design Variables” for more information). Within this module it is possible to call NAPA for conducting more detailed weight, performance and stability calculations. Once all necessary input files are created, the “simulation” module estimates all acting hydrodynamic and aerodynamic forces and simulates the sailing of the vessel on the selected route considering the available weather information (wind and waves). Finally, the “output” module is responsible for printing the resulting figures and tables.

In the examined case study, the voyage is a typical tanker route between Corpus Christi (USA) to Rotterdam (Netherlands) (Figure 2). The voyage is subdivided into 12 legs and it is assumed that it is a round trip voyage, thus the vessel returns in ballast condition using the same route, therefore 24 voyage legs are considered in total (12 for laden condition and 12 for ballast condition). For each leg all ensuing parameters are estimated twice: once taking into account the effect of the wing sails and once as if the wing sails did not exist, for a fixed speed. This allows an instant comparison of the effect of wing sail on the required thrust to propel the ship and forms the foundation of the optimization process where the effect of the fitted wing sail on ship design is examined.

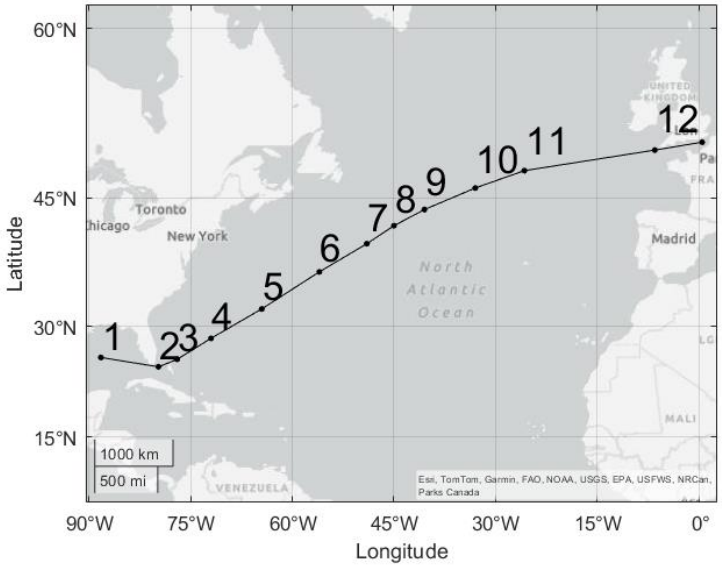

Figure 2. Selected Route

It is evident that the performance of fitted WAPS strongly depends on the route and the prevailing wind direction and strength, which are varying with location, time and season of the year. Thus, the shortest route between departure and arrival point is not necessarily the optimal one and traditional routing optimization procedures and software tools need to account for the best wind potential of the investigated route. An optimal routing methodology, which enables the operational energy savings to be assessed on various trading routes across the globe, has been developed by SSPA/RISE. The methodology considers the need for the vessel to fit into a logistics system regarding arrival time and lateness and considers European Centre for Medium-Range Weather Forecasts (ECMWF) weather data captured during the last decade (Werner 2021). This methodology is being utilized in the Orcelle project and supports the present study.

Wing Sail Characteristics

The main focus of the present methodology is development of tools in order to assess impact of WAPS on ship design in the frame of a design concept optimisation procedure. The herein examined wing sails system is based on a simplified, generic arrangement of symmetrical NACA airfoils (Abbott & Von Doenhoff 1959), which differs significantly from the *Orcelle Oceanbird* concept (Oceanbird 2024), whose sail consists of an optimized main wing and a controllable flap. This approach allows the development of the necessary WAPS simulation tools independently of the development and actual efficiency of

the Oceanbird concept, which will be integrated into the developed simulation tools in the future, while it is expected that its efficiency in terms of generated lift (and thrust) will be significantly higher.

Based on the above reasoning, the herein examined WAPS consists of eight rigid wing sails of an approximate height of 80 m and average chord length of 23 m. The assumed wing profile is a NACA0015 airfoil with a modified trailing edge. Each sail has sail area 1,844 m^2, mean chord length of 23 m and aspect ratio of 3.47 (Malmek et al 2020). The developed MATLAB simulation code has the flexibility to ultimately consider a variation of the number of fitted wing sails, their arrangement, size and wing profile. Also, alternative WAPS (different types of wing sails and rotors) may be considered, assuming the availability of aerodynamic data for the estimation of the induced lift and drag forces.

In the present case study, some assumptions regarding the position and the interaction of the wing sails are made in order to simplify the problem, reduce computational time and reduce the parameters of the optimization problem. Sail position (longitudinally and crosswise) is crucial for maximizing the effectiveness of the wings. However, for the 1-DOF model the exact position of the sails is not examined, thus it is implied that there is a feasible/optimized sail arrangement that maximizes the generated wind thrust and minimizes the effect of drift angle and rudder resistance for maintaining the required course and complies with all necessary requirements (e.g. bridge visibility, ship structural strength etc.) (Bordogna et al 2018).

In cases where the generated sail force is sufficient to move the vessel at the desired speed (100% wind generated thrust), there are various options regarding the operation of the propeller such as windmilling, feathering or harvesting (Gypa, 2023). For the optimization problem, harvesting the energy of the rotating propeller is herein not examined and the added resistance from the windmilling/feathering propeller is not taken into account.

Estimation of Forces

The developed model simulates the longitudinal/surge forces, so the voyage is divided into legs with constant speed and environmental conditions and for each leg, equation [1] is solved to estimate the thrust of the propeller.

$$X_{CW} + X_{AW} + X_W + X_S + T = 0 \quad [1]$$

where

X_{CW} is the calm water resistance (N) which is calculated using the Holtrop & Mennen method (Holtrop & Mennen 1982; Holtrop 1984), properly calibrated to predict the calm water resistance of the reference vessel.

X_{AW} is the added resistance due to waves (N) which is calculated using the semi-empirical SNNM method (Liu & Papanikolaou 2020)

X_W is the wind resistance (N) of ship's superstructure, which is estimated according to ISO 15016 (International Organization for Standardization 2015)

X_S is the generated sail force (N) for the assumed wing sails, which is calculated from tabulated aerodynamic forces provided by RISE Research Institutes of Sweden (personal communication)

T is the propeller thrust (N)

Vessel performance comparison with and without sails

The developed tool is capable of simulating the whole voyage with detailed calculations for each leg and a direct comparison between the same design with and without sails. Below some indicative figures are presented that compare the results of the various modules (hull, engine, propeller and sail). The figures refer to the 4th leg of the selected voyage for the reference vessel (Figure 3).

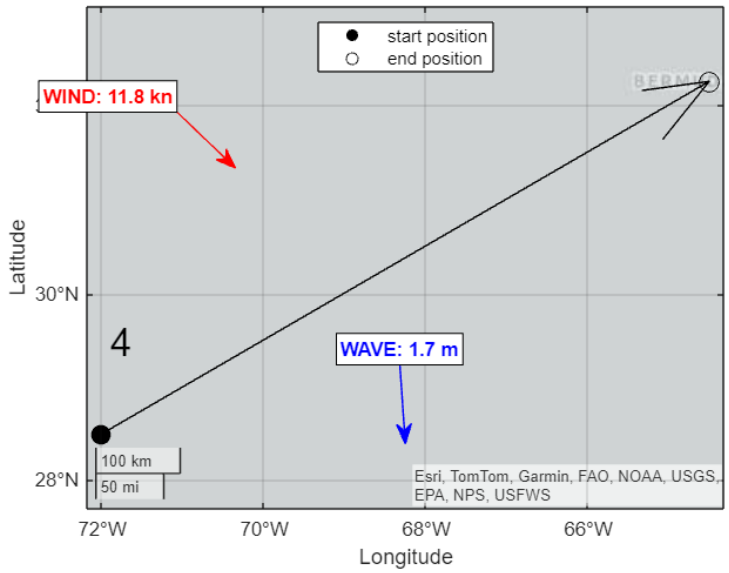

Figure 3. Leg 4

Forces

For each leg, all the forces are calculated (Figure 4) and the percentages of propulsion and resistance forces depicted in Figure 5.

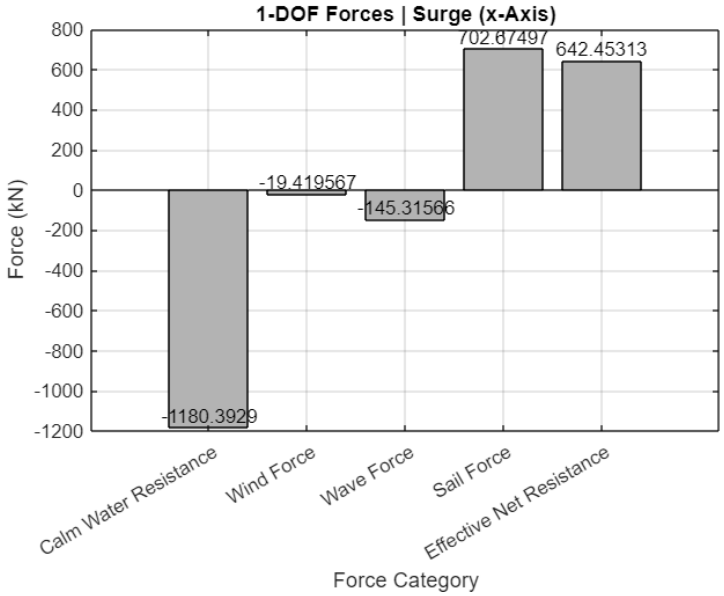

Figure 4. Estimated Forces for leg 4

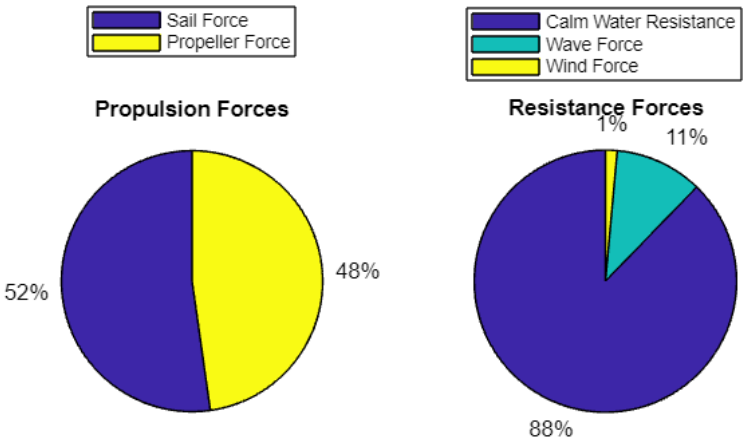

Figure 5. Force Percentages for leg 4

Hull

The calm water resistance of the vessel is plotted in Figure 6, along with the operational points. Speed is fixed to 12 knots.

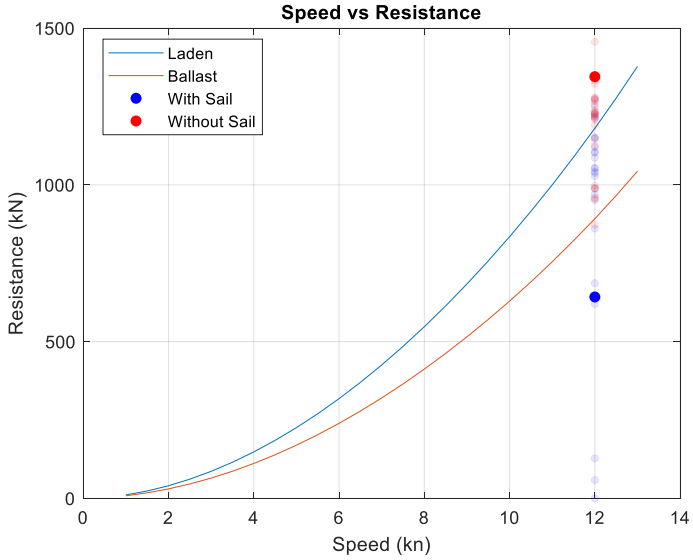

Figure 6. Speed vs Resistance
(Colored points refer to leg 4. Transparent points refer to the rest of the legs)

Main Engine

The engine layout diagram, along with the calculated operational points for all legs are shown in Figure 7 and the Specific Fuel Oil Consumption (SFOC) is shown in Figure 8. It should be noted that an assumption is made that the engine is always in operation (zero brake power is not allowed). In practice, operational points with very low engine loads (Reche-Vilanova et al 2023) need to be addressed with an operational strategy (e.g. increase vessel speed, trim sails etc.) in order to avoid operating at such low loads (and very high SFOC). During the herein conducted optimization, this is not taken into consideration because in the examined case study the majority of the operational points do not require very low engine loads, therefore the effect of an operational strategy for these cases does not have a significant impact on the optimization output.

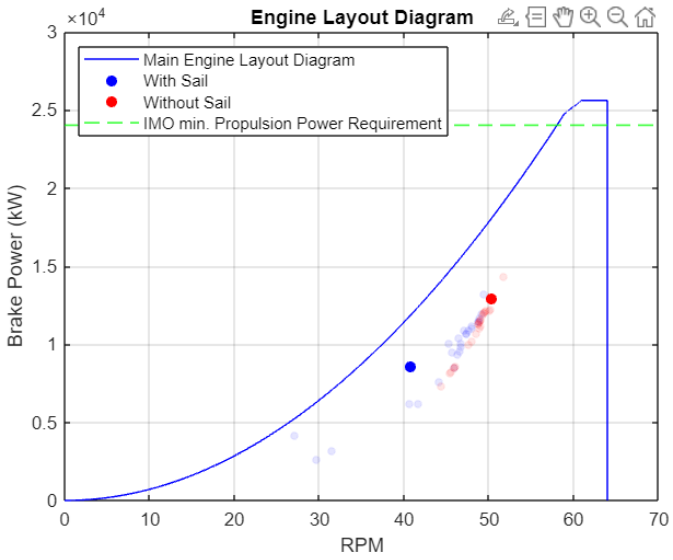

Figure 7. Engine layout diagram
(Colored points refer to leg 4. Transparent points refer to the rest of the legs)

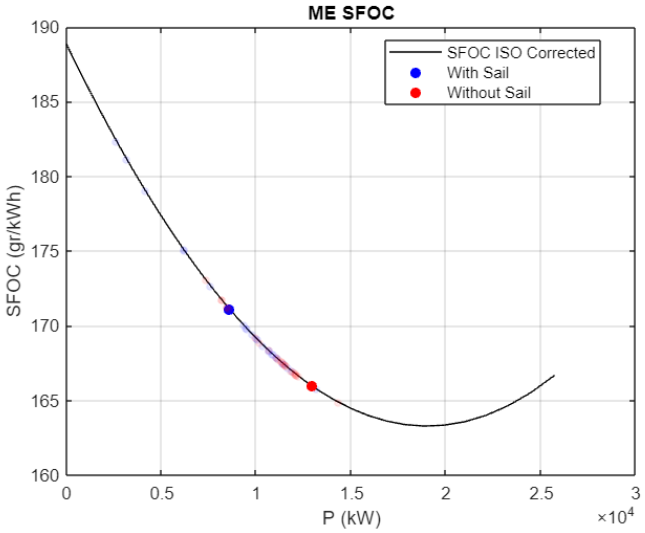

Figure 8. Power vs Specific Fuel Oil Consumption (SFOC)
(Colored points refer to leg 4. Transparent points refer to the rest of the legs)

Propeller

The examined Fixed Pitch Propeller (FPP) is modeled based on the polynomials of the Wageningen B-series (Lammeren et al 1969 and Oosterveld & Van Oossanen 1975). Propeller efficiency is estimated for the various operating points (Figure 9) and a check is conducted to ensure that we do not have extensive cavitation (Figure 10)

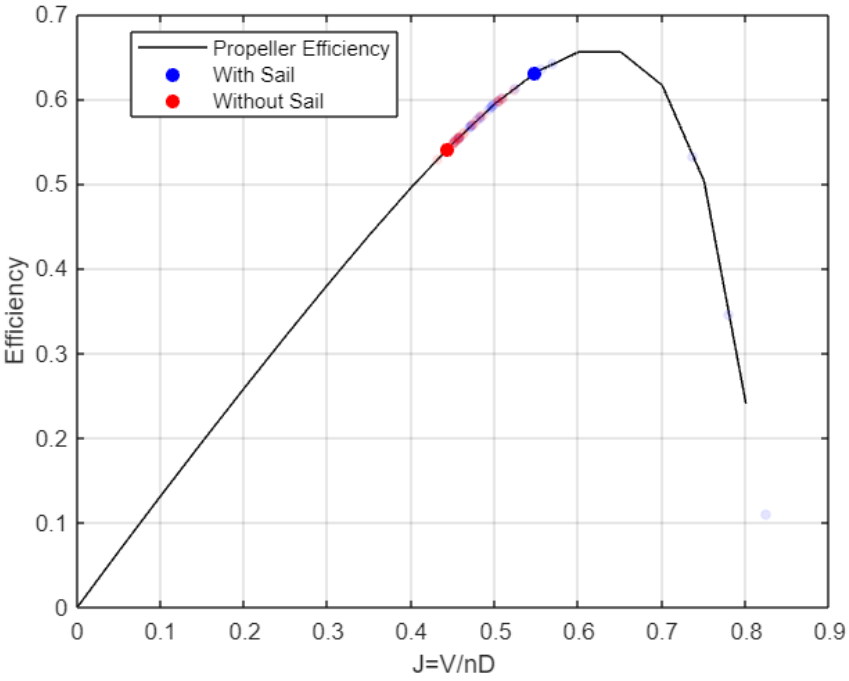

Figure 9. Propeller Efficiency
(Colored points refer to leg 4. Transparent points refer to the rest of the legs)

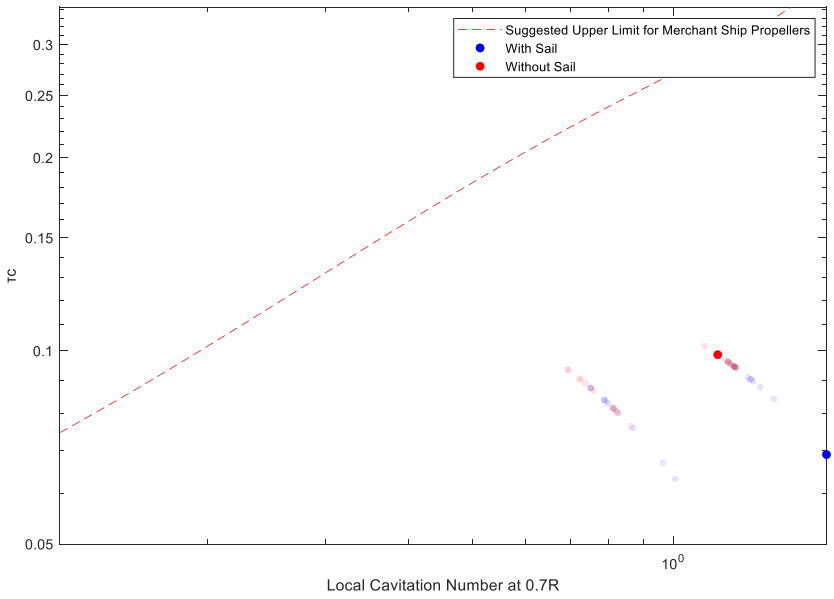

Figure 10. Checking for cavitation (Carlton 2007)
(Colored points refer to leg 4. Transparent points refer to the rest of the legs)

Wing Sail

Regarding the wing sail, the forces are calculated based on the apparent wind speed, apparent wind angle and lift/drag characteristics of the ensuing wing profile (Figure 11).

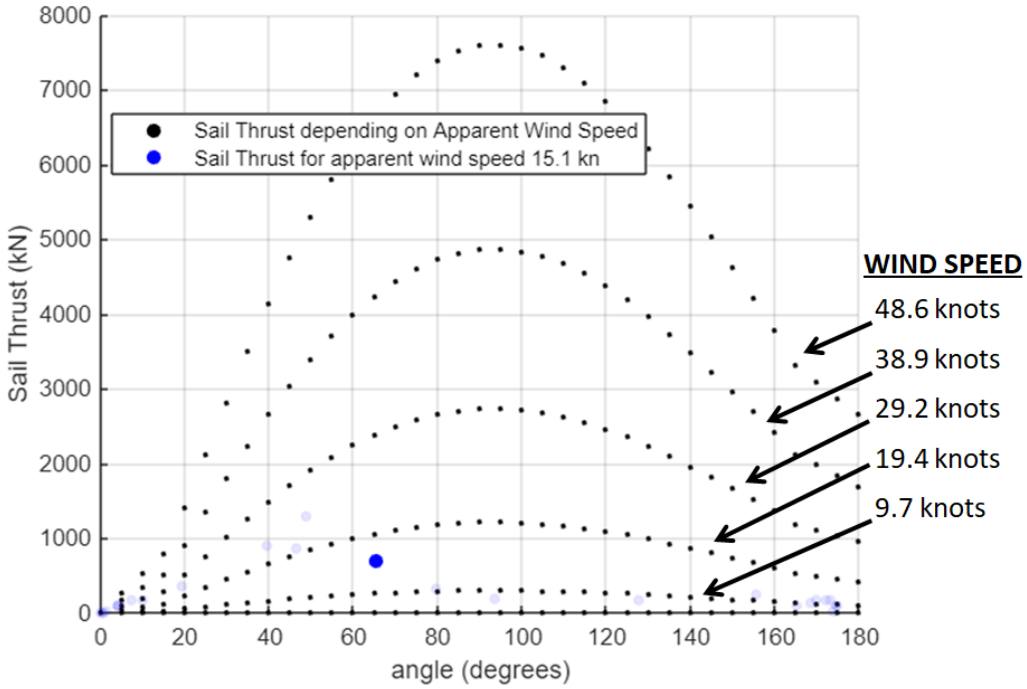

Figure 11. Wing Sails Thrust (8 Wing Sails) depending on wind angle and wind speed

DESIGN OPTIMIZATION METHODOLGY

A customized optimization problem for the design of ships with WAPS has been defined and appropriate methodology developed to handle the wind assisted propulsion problem. The output of the optimization process is the optimum combination of hull, engine and propeller that minimize the objective function, while including the effect of the examined WAPS. The MATLAB coded optimization module is capable of conducting both single- and multi-objective optimization studies and the main optimization process is sketched in Figure 12. The herein presented study focuses on a single-objective optimization problem. Below, some details regarding the optimization process are briefly mentioned.

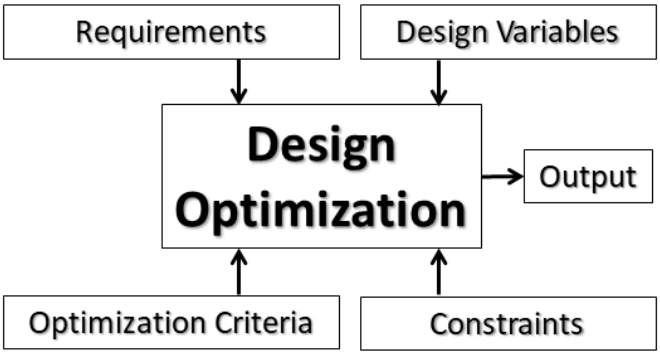

Figure 12. Generic design optimization process (Papanikolaou, 2014)

Optimization Algorithm Selection

Due to the nonlinear nature of the problem, a combination of optimization algorithms is utilized, both heuristic (genetic algorithm) and deterministic (sequential quadratic programming), in order to ensure that convergence to a global optimum solution and avoid possible local minimal solutions.

Design Space Exploration

In order to ensure that we have explored the design space sufficiently, a large number of initial designs is populated using the SOBOL sequence (Bratley & Fox 1988). A SOBOL sequence is a probabilistic sampling scheme that covers the design space more evenly compared with a pseudorandom number source. It increases the diversity of the population and leads to better

optimization results (Agushaka & Ezugwu 2022). In the examined case study 5,000 designs are generated and the best 50 feasible designs are used as initial population in the genetic algorithm.

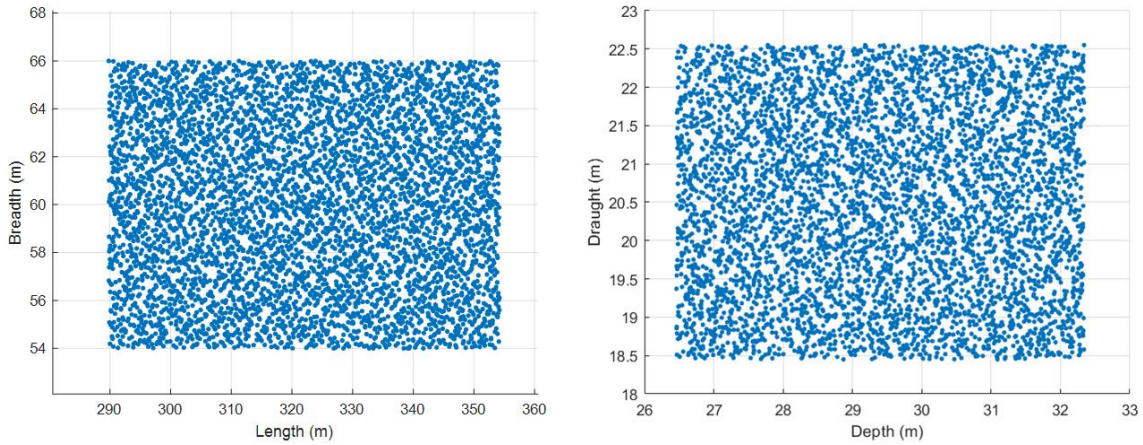

Figure 13. 5,000 Initial Designs Using Sobol Sequence

Heuristic Optimization Algorithm

The global optimization algorithm that is utilized is the genetic algorithm (Mathworks 2023). We optimize for 500 generations with each generation containing 50 individuals. The 50 "fittest" designs from the design space exploration process are used as initial population.

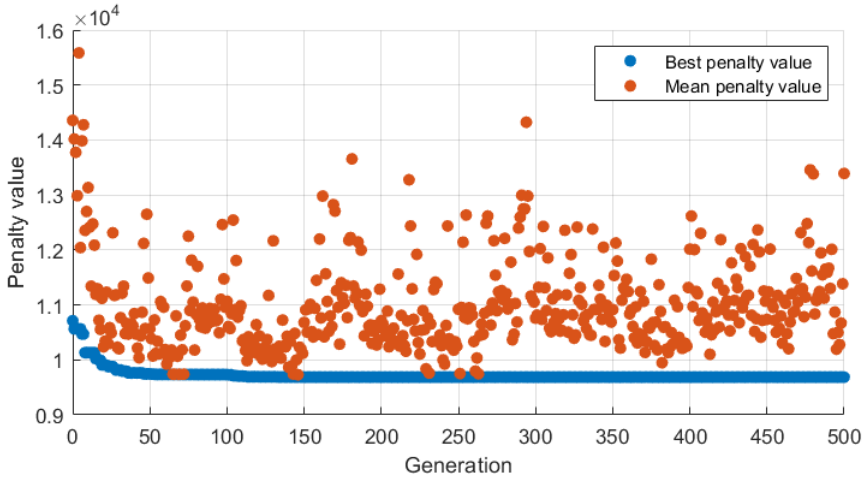

Figure 14. Genetic Algorithm Progress Example

Deterministic Optimization Algorithm

After the global optimization algorithm finishes, a deterministic optimization algorithm is utilized, namely Sequential Quadratic Programming (SQP). The initial value of the deterministic optimization algorithm is the output of the Heuristic Algorithm, thus optimizing further the design.

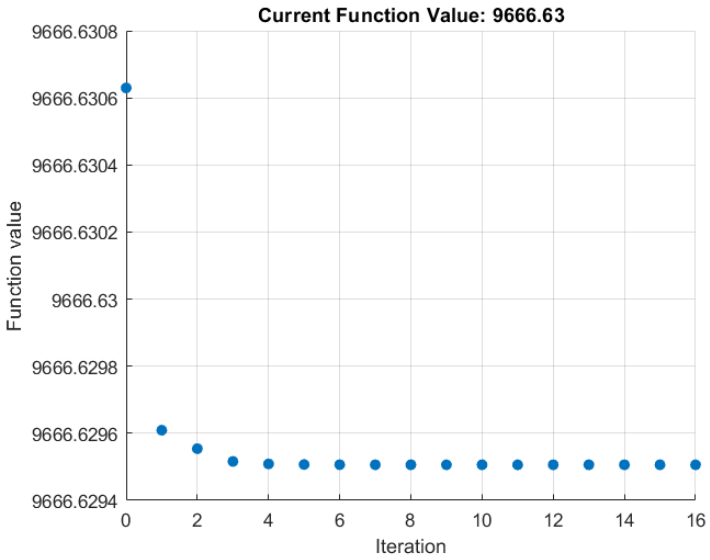

Figure 15. SQP Optimization Algorithm Iterations Example

IMPLEMENTATION

The developed WAPS simulation tool is implemented within the earlier defined design optimization methodology to approach the wind-assisted design optimization problem holistically (Figure 15). Some details regarding the implementation of the methodology are briefly outlined below.

Design Variables

In the herein presented application study, we consider 8 ship design variables: Length (L), Breadth (B), Depth (D), Draft (T), Block Coefficient (CB), Engine BHP/type (selected from a list), propeller pitch ratio (P/D) and propeller expanded area ratio (A_E/A_0). Due to the nature of the employed genetic algorithm that is used for optimization, it is more efficient to handle all design variables as integers (discrete optimization). For L, B, D and T we keep 2 decimals, thus $L_{integer} = L \cdot 100$, $B_{integer} = B \cdot 100$ etc. and for CB, P/D and A_E/A_0 we keep 3 decimals $CB_{integer} = CB \cdot 1000$ etc. The engine selection parameter is also an integer number that defines which engine has been selected from the provided engine list. This technique significantly speeds up the optimization process and allows a wider examination of the design space.

Once the genetic algorithm has completed the optimization process, the deterministic optimization algorithm uses the optimum result of the genetic algorithm to conduct a continuous optimization process, thus no longer treating the design variables as integers. This is due to the nature of the employed continuous optimization algorithm and allows the fine-tuning of the already optimized design by a genetic algorithm.

Objective Function

The objective function used in the present case study is the minimization of annual fuel oil consumption of the main engine (and indirectly of the associated GHG emissions). The fuel consumption per roundtrip is estimated for the provided weather conditions and then the annual consumption is estimated taking into consideration the activity of the reference vessel (yearly percentage of laden and ballast sailing time) and the number of roundtrip voyages that can be achieved yearly. It is noted that there is no restrictions in the implemented optimisation method and code to include more objective functions (multi-objective optimization possible)

Constraints

The set design optimization problem considers 15 constraints, which ensure that the derived results are feasible. More specifically, the constraints include limits for the DWT, limits for the form coefficients and main dimension ratios in order to ensure that the generated designs are meaningful and do not much deviate from relevant data of existing vessels (Papanikolaou 2014), they ensure that the propeller operates within engine limits with minimum cavitation (Burrill &

Emerson 1978), and the compliance with regulations regarding freeboard (IMO 1966) and minimum propulsion power (IMO 2021). A minimum metacentric height (GM) of 3 meters is also required as an initial check of the intact stability of the vessel. It should be noted that the EEDI constraint (IMO 2022) is herein excluded due to lack of information regarding the calculation of the possible reduction factor for the installed WAPS (presently under consideration at IMO).

The set constraints for the VLCC tanker considered in the following are summarized below:

1. Min. DWT ≥ 270000 tons
2. Max. DWT ≤ 330000 tons
3. Engine Limit Constraint
4. Less than approximately 5% cavitation at the propeller
5. 0.79 ≤ CB ≤ 0.88
6. 0.992 ≤ CM ≤ 0.996
7. 0.88 ≤ CWL ≤ 0.94
8. 0.835 ≤ CP ≤ 0.855
9. 5.1≤ L/B ≤ 6.8
10. 2.4 ≤ B/T ≤ 3.2
11. 10.5 ≤ L/D ≤ 14
12. IMO Minimum Power Requirement
13. Freeboard Constraint
14. GM ≥ 3 m
15. 0.2·T ≤ Propeller Diameter ≤ 0.55·T

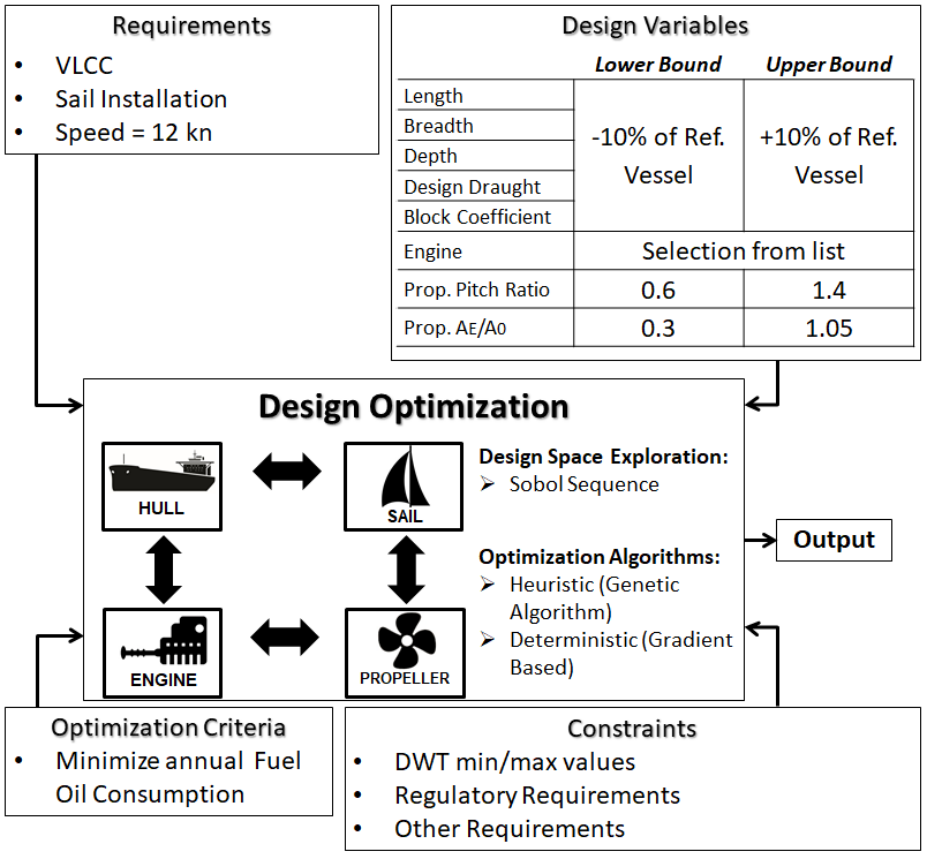

Figure 16. WAPS optimization process for VLCC case study

CASE STUDY

Reference Vessel

The reference vessel is an existing VLCC tanker. The main particulars of the reference vessel are presented in Table 1.

Table 1. Main particulars of reference vessel

Length B.P.	322.00 m
Breadth Mld.	60.00 m
Depth Mld.	29.40 m
Design Draught	20.50 m

Selected route and weather characteristics

The selected route for the case study is a common route from Corpus Christi (USA) to Rotterdam (Figure 2). The weather characteristics per leg were provided by the ORCELLE partner StormGEO and contain ERA5 data from 1980 to 2022. ERA5 (Hersbach et al. 2020) is the fifth generation atmospheric reanalysis of the global climate, produced by the Copernicus Climate Change Service (C3S) at ECMWF. In Table 2 the mean values of the provided data are presented. Seasonal changes in weather can also be taken into consideration but for the examined case study the weather information is herein considered constant.

Table 2. Weather information for the selected route

leg	Latitude	Longitude	TWS (kn)	TWA (deg)	Wave Height (m)	Wave Period (s)
1	26	-88.25	11.5	277.4	1.1	5.8
2	24.75	-79.75	11.0	276.6	0.9	5.4
3	25.75	-77	11.3	285.1	1.2	8.2
4	28.5	-72	11.8	310.7	1.7	8.7
5	32.25	-64.5	13.4	44.5	1.8	8.7
6	36.75	-56	16.3	64.4	2.5	9.2
7	40	-49	16.9	70.3	2.8	9.7
8	42	-45	17.8	75.3	3.0	9.8
9	43.75	-40.5	18.0	73.6	3.1	10.0
10	46	-33	18.1	70.0	3.3	10.3
11	47.75	-25.75	17.9	72.7	3.3	10.5
12	49.75	-6.5	15.7	86.2	2.5	10.4

It should be noted that the possible fitting of WAPS goes hand in hand with weather routing optimization, thus the examined conventional route (not optimized for prevailing winds) significantly underestimates the potential savings (Werner et al 2023).

Results

The results from the optimization algorithm are presented in Table 3 and a comparison of the main dimensions of the initial population (feasible and infeasible), the reference vessel (with and without sails) and the optimum vessel is presented in Figure 17

Table 3. Optimization Results

	Reference Vessel (without sail)	Optimized Vessel (with sail)	Difference (%)
L (m)	322	338.4	+5%
B (m)	60	54	-10%
D (m)	29.4	32.23	+10%
T (m)	20.5	22.12	+8%
CB	0.796	0.78	-2%
Main Engine MCR (kW)	25600	26437.61	+3%
Main Engine RPM at MCR (RPM)	60.9	63.5	+4%
Prop. P/D	0.803	0.787	-2%
Prop. AE/A0	1.05	0.459	-56%
Disp. (m3)	315264	315264	0%
DWT (t)	276902	276902	0%
Estimated Annual Main Engine Fuel Cons. (t)	13003	9666.6	-26%

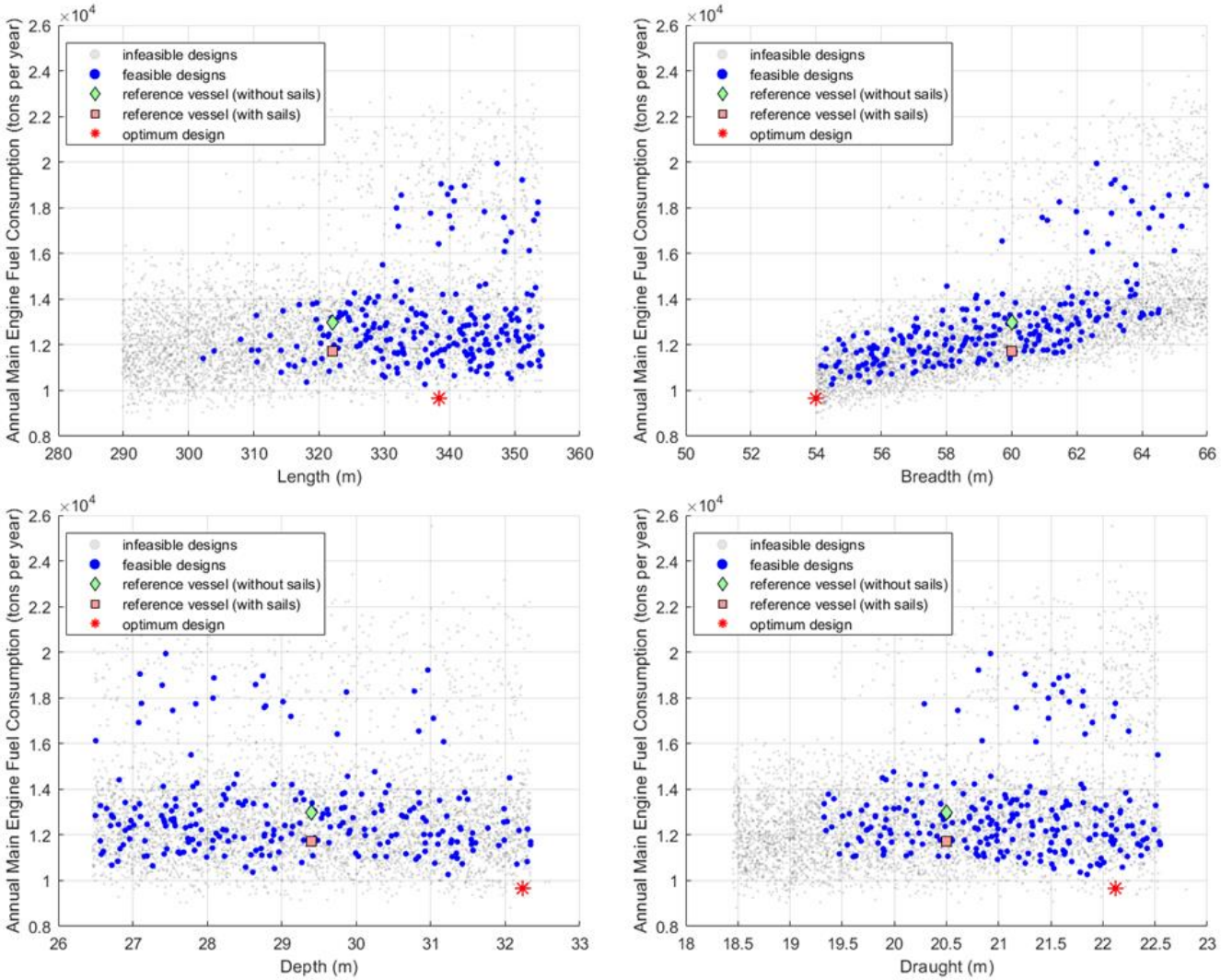

Figure 17. Comparing Main Dimensions of Explored Designs

In Figure 17 It can be observed that during the design exploration phase, a large number of infeasible designs is generated (grey points), which emphasizes the effect of the set constraints and the need of a sufficiently large and evenly-distributed

initial population in order to ensure that the optimization algorithm converges to the global optimum. In Table 3, it can be observed that the conducted optimization resulted in a vessel with the same DWT but longer, with smaller breadth and larger draught. The reduction of the annual fuel consumption compared to the reference vessel is about 26%. It is also interesting to note that if the present wing sail system were installed at the reference vessel (retrofitting), the estimated annual Main Engine consumption would be 11728 tons, thus we would have still a reduction of 17.5% that is attributed to the changed design characteristics. It should be finally noted that the effect of WAPS on ship's main dimensions can be expected to be more drastic for other ship types and sizes, considering that the wind potential may be assumed the same for all ships operating on the same route, but its effect on ship's propulsion and motions is directly dependent on ship's size (displacement) and on the magnitude of the generated wind thrust compared to ship's hydrodynamic (and air) resistance.

SUMMARY & CONCLUSIONS

In the present paper, we developed a new simulation tool for the assessment of the performance of ships equipped with WAPS, allowing the exploration of the effect of the wing sails on the concept design of ships with wing sails in the frame of a multi-parametric ship design optimisation procedure. The developed simulation tool has been applied to a VLCC tanker design case study. Several useful conclusions maybe drawn from the conducted research:

1. There are numerous ship design and operational parameters that have major effect on ship design, when the ship is fitted with WAPS, such as ship's main dimensions, engine and propeller characteristics, route, speed, size/number/arrangement of wing sails, logistics, WAPS alternatives etc. and all of them need to be included in a ship design optimization procedure.
2. The main characteristics of the resulting optimized VLCC tanker with WAPS significantly differ from those of traditional VLCC designs w/o WAPS. It may be expected that differences will be more pronounced for smaller vessels and other ship types (volume vs. deadweight carriers).
3. The predicted fuel saving and associated reduction of GHG emission of 26% for a VLCC tanker are remarkable. These savings may appear too optimistic, because of the limited accuracy of the employed 1DOF hydrodynamic modeling. However, using an optimized route with respect to wind potential, instead of the shorted root and advanced technology wing sails, like the Oceanbird concept, instead of the herein used NACA wing profiles, it may be expected that the encouraging outcome of this study is fully justified.
4. Way ahead: further investigation of the effect of WAPS by
    a. proceeding to ship's preliminary design (by use of, e.g., the NAPA® naval architectural software platform)
    b. applying the present concept design approach to other ship types and sizes
    c. using more advanced hydro- and aero dynamic models (3 and 4DOF maneuvering models, inclusion of Oceanbird wing sail characteristics, effect seakeeping on the sails and on the resistance/thrust estimations).

It seems evident only a holistic approach to the wind-assisted ship design process will reveal the true and full potential of wind assisted propulsion in shipping and facilitate its acceptance by the maritime industry.

CONTRIBUTION STATEMENT

TP: Conceptualization; data curation, methodology; writing – original draft. **AP:** conceptualization; supervision; writing – review and editing.

ACKNOWLEDGEMENTS

The support of this research by the European Com-mission research project ORCELLE WIND under the European Union's Horizon research and innovation program under grant agreement n° 101096673 is acknowledged. The European Commission and the authors shall not in any way be liable or responsible for the use of any knowledge, information or data presented, or of the consequences thereof. The authors also acknowledge the support the ORCELLE WIND project partners SSPA/RISE and StormGeo for the provision of aerodynamic data on wing sails performance and weather data pertaining to the presented case study, respectively. The provision of comparative ship data for the conducted case study by THENAMARIS is also acknowledged.

REFERENCES

Abbott, I.H., & Von Doenhoff, A.E. (1959) Theory of Wing Sections, Dover Publications, New York

Agushaka, J.O. & Ezugwu, A.E. (2022) Initialisation Approaches for Population-Based Metaheuristic Algorithms: A Comprehensive Review. Appl. Sci., 12, 896. https://doi.org/10.3390/app12020896

Bordogna, G., Keuning, , J. A., Huijsmans, R.H.M., & Belloli, M. (2018) Wind-tunnel experiments on the aerodynamic interaction between two rigid sails used for wind-assisted propulsion, International Shipbuilding Progress, 65(1): 93–125

Bratley, P., & Fox, B.L. (1988) "Algorithm 659 Implementing Sobol's Quasirandom Sequence Generator." ACM Transactions on Mathematical Software. Vol. 14, No. 1, 1988, pp. 88–100.

Burrill, L.C., & Emerson, A. (1978) Propeller cavitation: further tests on 16 in. propeller models in the King's College Cavitation Tunnel, Trans. NECIES, 195

Carlton, J.S. (2007) Marine Propellers and Propulsion, Butterworth-Heinemann (imprint of Elsevier)

European Maritime Safety Agency (2023), Potential of Wind-Assisted Propulsion for Shipping, EMSA, Lisbon

Gypa, I., Jansson, M., Gustafsson, R., Werner, S., & Bensow, R. (2023) Controllable-pitch propeller design process for a wind-powered car-carrier optimising for total energy consumption, Ocean Engineering, 269

Hersbach, H., Bell, B., Berrisford, P., Hirahara, S., Horányi, A., Muñoz-Sabater, J., Nicolas, J., Peubey, C., Radu, R., Schepers, D., Simmons, A., Soci, C., Abdalla, S., Abellan, X., Balsamo, G., Bechtold, P., Biavati, G., Bidlot, J., Bonavita, M., De Chiara, G., Dahlgren, P., Dee, D., Diamantakis, M., Dragani, R., Flemming, J., Forbes, R., Fuentes, M., Geer, A., Haimberger, L., Healy, S., Hogan, R.J., Hólm, E., Janisková, M., Keeley, S., Laloyaux, P., Lopez, P., Lupu, C., Radnoti, G., de Rosnay, P., Rozum, I., Vamborg, F., Villaume, S., & Thépaut, J.N. (2020) The ERA5 global reanalysis, Q.J.R. Meteorol. Soc., 146, 1999–2049

HOLISHIP (2016-2020), HORIZON 2020 – EU funded project, Grant Agreement n° 689074

Holtrop, J. (1984) A statistical Re-Analysis of Resistance and Propulsion Data, International Shipbuilding Progress, 31

Holtrop, J., & Mennen, G.G.J. (1982) An Approximate Power Prediction Method, International Shipbuilding Progress, 29

International Maritime Organization (1966) Convention on Load Lines

International Maritime Organization (2021) 'Guidelines for Determining Minimum Propulsion Power to Maintain the Manoeuvrability of Ships in Adverse Conditions', MEPC.1/Circ.850/Rev.3, 2021.

International Maritime Organization (2022) Resolution MEPC.351(78) - 2022 Guidelines on survey and certification of the Attained Energy Efficiency Existing Ship Index (EEXI)

International Maritime Organization (2022) Resolution MEPC.352(78) - 2022 Guidelines on operational carbon intensity indicators and the calculation methods (CII Guidelines, G1)

International Maritime Organization (2022) Resolution MEPC.364(79), 2022 Guidelines on the method of calculation of the attained Energy Efficiency Design Index (EEDI) for new ships

International Windship Association (2024), IWSA, www.wind-ship.org

ISO15016 (2015), Ships and marine technology - Guidelines for the assessment of speed and power performance by analysis of speed trial data, International Organization for Standardization

Lammeren, W.P.A., van Manen, J.D., & Oosterveld, M.W.C (1969) The Wagenigen B-screw series, Trans. SNAME.

Liu, S., & Papanikolaou, A. (2020) Regression analysis of experimental data for added resistance in waves of arbitrary heading and development of a semi-empirical formula, Ocean Engineering, 206

Ma, R., Wang, Z., Wang, K., Zhao, H., Jiang, B., Liu, Y., Xing, H., & Huang, L. (2023) Evaluation Method for Energy Saving of Sail-Assisted Ship Based on Wind Resource Analysis of Typical Route, J. Mar. Sci. Eng., 11, 789.

Malmek, K., Dhome, U., Larsson, L., Werner, S., Ringsberg, J.W., & Finnsgard, C. (2020) Comparison of Two Rapid Numerical Methods for Predicting the Performance of Multiple Rigid Wing-Sails, 5th INNOV'SAIL Conference, 15-17 June 2020

MATLAB (2024), Mathworks, www.mathworks.com

NAPA (2024), www.napa.fi

Oceanbird (2024), www.theoceanbird.com

Oosterveld, M. W. C., & Van Oossanen, P. (1975), 'Further computer-analyzed data of the Wageningen B-screw series', International shipbuilding progress, vol. 22, no 251, p. 251-262.

ORCELLE (2023-2027) HORIZON.2.5 Grant Agreement n° 101096673

Papanikolaou A. (2010), "Holistic Ship Design Optimization", Journal Computer-Aided Design (2010), Elsevier, Vol. 42, Issue 11, pp. 1028-1044

Papanikolaou, A., (2014) Ship Design Methodologies of Preliminary Design, Springer

Papanikolaou, A., (Ed.) (2019) A Holistic Approach to Ship Design | Volume 1: Optimisation of Ship Design and Operation for Life Cycle, Springer

Papanikolaou, A., Fournarakis, N., Chroni, D., Liu, S., Plessas, T. & Sprenger, F. (2016) Simulation of the Maneuvering Behavior of Ships in Adverse Weather Conditions, Proc. 31st Symposium on Naval Hydrodynamics, Monterey, California, 11-16 September 2016

Bentin, M., Kotzur, S., Schlaak, M., Zastrau, D. & Freye, D. (2018) Perspectives for a Wind Assisted Ship Propulsion, Trans RINA, Vol 160, Part A1, Intl J Maritime Eng, Jan-Mar 2018

Plessas, T., Papanikolaou, A., Liu, S., & Adamopoulos, N. (2018) Optimization of Ship Design for Life Cycle Operation with Uncertainties, Proceedings of the 13th International Marine Design Conference, Helsinki, Aalto University, 10-14 June 2018

Reche-Vilanova, M., Bingham, H. B., Psaraftis, H. N., Fluck, M., & Morris, D. (2023) Preliminary Study on the Propeller and Engine Performance Variation with Wind Propulsion Technologies, Paper presented at Wind Propulsion Conference 2023, London, United Kingdom.

Rosander, M. & Bloch, J.O.V. (2000) Modern Windships, Technical Report, Pelmatic Knud E. Hansen A/S

StormGeo (2024), www.stormgeo.com

Talluri, L., Nalianda, D.K. & Giuliani, E. (2018) Techno economic and environmental assessment of Flettner rotors for marine propulsion,

Tillig, F., & Ringsberg, J. (2019) A 4 DOF simulation model developed for fuel consumption prediction of ships at sea. Ships and Offshore Structures, 14(sup1), S112-S120.

Viola, I.M., Sacher, M., Xu, J., & Wang, F. (2015), A numerical method for the design of ships with wind-assisted propulsion, Ocean Engineering, 105, 32-42.

Werner, S., Kuttenkeuler, J., & Hörteborn, A. (2021) "Route Evaluation Methods For Long-Distance Sailing Vessel Performance Predictions" In the Proceedings of 7th High Performance Yacht Design Conference, Auckland, 11-12 March 2021

Werner, S., Papanikolaou, A., Razola, M., Fagergren, C., Dessen, L., Kuttenkeuler, J., Santen, V., & Steinbach, C. (2023) The Orcelle project - Towards Wind-Powered Ships for Deep Sea Cargo Transport, SNAME Maritime Convention 2023, 27-29 September 2023

Proceedings of 15th International Marine Design Conference (IMDC-2024)
June 2-6, 2024
Amsterdam, the Netherlands

Nuclear fusion as unlimited power source for ships

E.S. van Rheenen[1*], J.P.K.W. Frankemölle[2,3] and E.L. Scheffers[1]

ABSTRACT

Every now and then, every marine engineer dreams of a compact, lightweight and inexhaustible energy source to power large ships across the seven seas. Nuclear fusion of deuterium and tritium promises to be a safe, compact, carbon-free, and inexhaustible energy source. Even though it will take decades before conventional power plants may be replaced with nuclear fusion, the concept of nuclear fusion for marine propulsion has already been put on the table by commercial parties. This research investigates the potential of nuclear fusion onboard ships. The design investigates putting the smallest imaginable magnetic confinement reactor, ARC, on a ship. The only commercial ship requiring significant amounts of power is the Queen Mary 2. The large power output of ARC (200 MWe) is one of the major issues of putting a fusion reactor on a ship. Other issues may include intact stability, structural design and influences of vibrations on the fusion reactor. All in all, we found that a fusion reactor onboard a ship is unlikely to be feasible in the near future.

KEY WORDS

Nuclear Fusion; Nuclear ships; Powerful ships; Conceptual Design; Retrofit Design

INTRODUCTION

Like many other domains, the maritime industry needs to dramatically decrease its harmful emissions by 2050 (International Maritime Organization, 2023). Sustainable powering of ships is the key to reducing emissions during the ship's operational life cycle. Therefore, research into alternative fuels is essential to reach the emission goals. Those fuels range from hydrogen,hydrogen-based fuels such as methanol and ammonia, to nuclear-driven ships (Houtkoop et al., 2022). However, none of these fuels are a perfect match for maritime applications, as all have their drawbacks. Hydrogen has a low volumetric energy density and is extremely flammable (Van Rheenen et al., 2023). Both methanol and ammonia are toxic. Additionally, methanol still generates carbon emissions, and ammonia is hard to combust (Van Rheenen et al., 2023). Nuclear-powered ships currently refer to ships powered by fission reactors. While nuclear fission reactors are a proven technology, their use in commercial ships remains limited. Not only are nuclear-powered ships expensive, but the risks of meltdowns and long-lived radioactive waste have also slowed their adoption for marine power generation (Wang et al., 2023).

Nuclear fusion represents an alternative to nuclear fission, which can potentially mitigate many of the risks associated with conventional nuclear technology. While atoms are split in the nuclear fission process, the principle of nuclear fusion is to glue two atoms together. The most conventional form of nuclear fusion uses the deuterium–tritium (D–T) reaction:

$$ {}^{2}_{1}\mathrm{H} \; + \; {}^{3}_{1}\mathrm{H} \rightarrow \; {}^{4}_{2}\mathrm{He}\;(3.5\mathrm{MeV}) \; + \; \mathrm{n}\;(14.1\mathrm{MeV}). \tag{1} $$

[1] Department of Maritime and Transport Technology, Delft University of Technology, Delft, the Netherlands
[2] SCK CEN, Belgian Nuclear Research Centre, Boeretang 200, BE-2400, Mol, Belgium;
[3] KU Leuven, Dept. Mechanical Engineering, Celestijnenlaan 300, BE-3000, Leuven, Belgium;
[*] Corresponding Author: E.S.vanRheenen@tudelft.nl

Submitted: 23 February 2024, Revised: 22 April 2024, Accepted: 1 May 2024, Published: 23 May 2024

Conference paper, DOI: https://doi.org/10.59490/imdc.2024.880 e-ISSN: 3050-486

From left to right, the fusion of a deuterium atom (a hydrogen atom with an extra neutron, also noted as hydrogen-2) with a tritium (a hydrogen atom with two extra neutrons, also noted as hydrogen-3) yields an alpha particle (a helium atom, also noted as helium-4), a neutron and 17.6 MeV of energy split amongst the reaction products (Freidberg, 2007). Deuterium (hydrogen-2) is stable, and can be found naturally. Conversely, tritium (hydrogen-3) has a half-life of 12.3 years and decays to helium-3 under beta minus emission (Bé et al., 2006). Tritium needs to be generated on-site through a second nuclear reaction: neutron capture of lithium-6 and lithium-7, the neutron being supplied by the D–T reaction (equation 1).

So the only fuel a fusion-powered ship would have to carry would be deuterium and lithium, two light-weight isotopes. A ship would require only little fuel to travel far because D–T fusion has an energy density of approximately $340E6$ MJ/kg. Table 1 gives a comparison of the energy density of different fuels. Nuclear fusion fuels have the highest energy density. The difference in the energy densities of nuclear fusion and conventional marine diesel oil is extremely large. The amount of fuel that has to be bunkered for nuclear fusion is negligibly small compared to conventional fuels.

Table 1: Energy densities of different fuels (Freidberg, 2007; Aronietis et al., 2016)

Fuel	Energy density [MJ/kg]
Deuterium-tritium fusion	340 000 000
Fission (U-235)	88 000 000
Pure hydrogen	120
Heavy Fuel Oil	40

Nuclear fusion is an interesting ship fuel source, as it is safe, carbon-free and virtually inexhaustible. Ships powered by fusion would only need to be refuelled rarely and can thus have a higher up-time. Additionally, these ships would not only be carbon-free, but their only emissions would be helium, which is not considered a greenhouse gas or harmful. Moreover, fusion-driven ships would theoretically have a significantly larger range than fossil-fuel ships.

However, nuclear fusion is still under development. Currently, a reactor is being built in France, ITER, which aims to generate ten times more energy than is required to operate it. While ITER should hopefully be up and running by the late 2020s, it will be another fifteen years before it makes its first D–T fusion reactions (Lopes Cardozo, 2019). EUROfusion, the European fusion research consortium, aims to deploy the first European demonstration power plant (DEMO) by 2060 (Lopes Cardozo, 2019). An economy of scale will likely not be achieveable before 2100 (Lopes Cardozo, 2019). These plans all focus on land-based fusion power plants. Nonetheless, looking at fusion reactors on ships is still interesting, especially since companies are already advocating for fusion power on ships (Lockheed Martin, n.d.; DNV, 2021). Lockheed Martin (n.d.) not only promotes fusion on ships, but they also deem it to be one of the first applications of so-called compact fusion. DNV (2021), on the other hand, have made a preliminary calculation of placing a fusion reactor on a ship, based on a reactor designed by General Fusion. It is likely, that the main motivation for placing nuclear fusion reactors on ships is the resulting large range, combined with low fuel costs and no carbon emissions.

This paper aims to get insight into the implications of putting a nuclear fusion reactor onboard a ship from a design perspective. For this study, we decided to place a selected nuclear power plant onboard an existing ship, which provides a certain base in dimensions, mission and requirements. The selection of this ship is based on its suitability and adaptability for a nuclear fusion power plant. To structure our thinking, we loosely performed one iteration of the design spiral (Evans, 1959). We did not assume this would yield an exhaustive overview of all the pros and cons of nuclear fusion on a ship. However, we did feel it would give sufficient scoping to our research.

This work is structured as follows. First, we describe the basics of nuclear fusion (Section ”Basics of nuclear fusion”). This section describes the plant’s working process, basic design characteristics, and constraints. This theory is followed by an overview of design considerations and related challenges, loosely based on a first iteration of the design spiral (Section ”Stepping Through Design Spiral”). The part ”Mission and Owner Requirements” of this section contains the considerations regarding selecting a suitable vessel for our case study. The next section discusses scope boundary determination and overall design concept feasibility (Section ”Discussion”). In conclusion, we provide an overview of the drawn conclusions and future research recommendations (Section ”Conclusion and Outlook”).

BASICS OF NUCLEAR FUSION

Nuclear fusion of deuterium and tritium atoms does not readily take place. Under normal situations, the Coulomb force between the two nuclei – which are both positively charged – keeps them far apart. The nuclear force becomes dominant only when they get very close together. Then fusion can occur. Very high temperatures, on the order of several million Kelvins, are required for nuclei to brave the Coulomb barrier and for fusion to occur at all. At these temperatures, deuterium and tritium form a plasma: free electrons, deuterium ions, and tritium ions coexist in a gaseous state. Besides the temperature of the plasma, the number density is also important: if more deuterium and tritium are present, more reactions will occur. Finally, if we want to use fusion for net power generation, the plasma should be well enough insulated that the fusion power production offsets the thermal losses. A figure of merit that is often quoted in this context is the triple product $n\tau_{\mathrm{e}}T$, where n is the number density, τ_{e} is the energy confinement time – which is a measure of the insulation – and T is the temperature. Only when this triple product is larger than some value can a fusion reactor produce net power (Freidberg, 2007).

The main difficulty in achieving fusion on Earth is the energy confinement time τ_{e}. The materials of the wall limit the temperature at the wall of a fusion reactor, while the inside of the plasma has to be in the order of 150 million Kelvins. This large temperature difference results in extremely steep temperature gradients. Such gradients drive thermal transport, which turns the question of insulating the plasma into a huge problem. Several methods have been proposed to tackle this issue, but magnetic confinement fusion (MCF) is the most conventionally accepted method. MCF uses the Lorentz force to constrict charged particles within specially designed magnetic fields, limiting the heat transfer from the plasma to the reactor wall by several orders of magnitude. The large magnetic fields required for MCF can only be achieved using superconducting magnets, which operate at very low temperatures (Freidberg, 2007).

MCF-based designs are toroidally shaped. The best-known torus is a doughnut. The size of a doughnut is determined by its minor radius a, i.e. the radius of the uncurved cylinder, and its major radius R_0, i.e. the distance from the doughnut's central hole to the middle of the curved cylinder. They come in two flavours, tokamaks and stellarators, but the details of what sets them apart do not factor into the present study. Most reactors, including ITER, are tokamaks. Figure 1 visually represents a tokamak. This part houses the plasma, the layer around it, and its main auxiliary components. It is called the vacuum vessel. A near vacuum inside the vessel exists because of the low density. The magnets are placed outside the vacuum vessel. Nowadays, tokamaks are closer to curved elliptic cylinders, meaning that a can be larger in the vertical direction than in the horizontal, which is referred to as elongation and denoted by κ. For more information on the basics of nuclear fusion, we refer to Freidberg (2007).

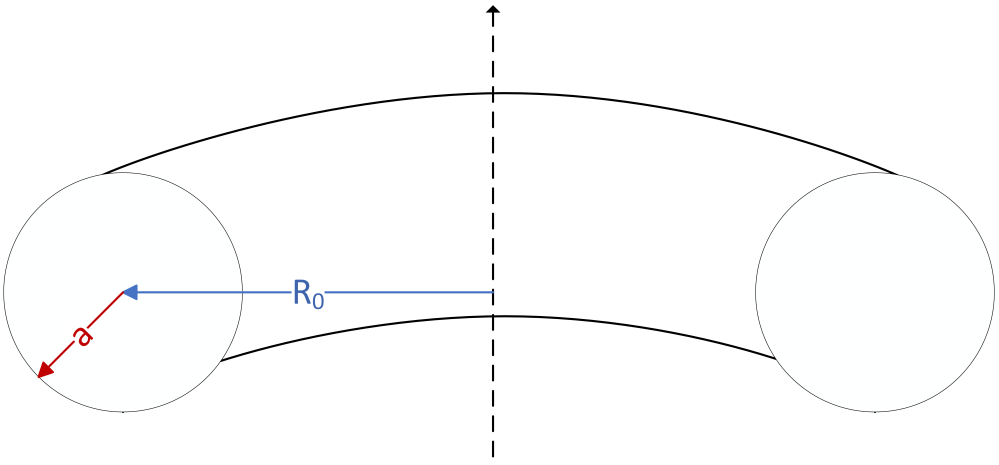

Figure 1: Representation of tokamak

Important for this study is that there exists a limit to how small toroidal reactors can become. This is caused by the choice of the D–T reaction on the one hand and the fact that MCF designs require superconducting magnets on the other. The D–T reaction produces a neutron with extremely high energy that, if it arrives at the superconducting magnet with sufficient en-

ergy, would quench the magnet, rendering the fusion reactor inoperable. These magnets are placed both on the inboard-side as well as on the outboard-side of the torus. To prevent quenching, the magnets are shielded by the blanket. The thickness of this shielding depends only on the shielding material and the energy of the neutron that it is meant to stop. The energy of the neutron is imposed by the D–T reaction (14.1 MeV, cf. equation 1) while other functions of the blanket impose constraints on the materials it can contain. As a result, the blanket will always have to be about a meter thick regardless of the reactor size (Freidberg, 2007), resulting in a minimal major radius and, thus, a minimal size of the torus.

More detailed 0D modelling based on plasma-physical considerations yields results that are largely in line with back-of-the-envelope reasoning. There is a strong coupling between the geometry of the reactor and the plasma performance, which means that not all parts of the design space are available. One cannot simply choose reactor size and power output. Using current-day superconducting magnet technologies (NbTi and Nb_3Sn) and available plasma physics regimes, economically viable reactors would need a major radius R_0 = 8–9 meters. Advanced superconducting magnet technologies like Rare-Earth Barium Copper Oxide (REBCO) might reduce R_0 to 5 meters. Such reactors generate power well over the level that can be utilised by a single ship. To make economically viable tokamaks that are smaller still, like the Affordable, Robust, Compact (ARC) reactor (Sorbom et al., 2015), one would need more optimistic assumptions on the physics performance (Zohm, 2019).

The concept of MCF could be disregarded completely, and alternative fusion concepts could be looked into. One that sometimes makes the news is inertial confinement fusion (ICF) using high-intensity lasers. While headway is being made (Betti & Hurricane, 2016) and ignition (a self-sustained fusion reaction) was even recently achieved (Osolin et al., 2023), it is unclear what an ICF-based power plant would look like. Then there is a host of more and less exotic designs that are championed by private industry. They often promise much shorter road maps to commercial reactors than presented in, e.g., the European road map (EUROfusion, 2018), but they usually rely on large technological breakthroughs. While such developments cannot be ruled out, they are far from certain. Although not much is known about the compact fusion concept for ship propulsion (Lockheed Martin, n.d.), we may assume that it will sit somewhere in this category. Alternatively, it might be a tokamak after all in which case all of considerations with regard to MCF apply to it.

In our opinion, ARC strikes a balance between being innovative enough to allow potential application on a ship – conventional fusion technology results in far too bulky machines – while being conservative enough – requiring limited technological development in some domains – to be deemed likely based on today's available technology. It also aids the present work that a rather detailed design study is already available (Sorbom et al., 2015). The ARC reactor produces 525 MW of fusion power and has a total thermal power of 708 MWth. After considering thermal efficiency and recirculating power in the auxiliary systems, 190 MW net electric power is left. The vacuum vessel has a major radius R_0 = 3.1 m, minor radius a = 1.1 m and elongation κ = 1.84. The on-axis magnetic field, i.e. the field at $r = 0$ where r runs from 0 to a, is 9.2 T while the peak on-coil magnetic field is 23 T. The entire reactor, excluding the balance of plant equipment, fits in as little as 1320 m^3, weighs 7190 tonnes and would cost 5.5 billion dollars. In this study, we will work with rounded numbers for convenience and install a reactor that has dimensions $10 \times 10 \times 10$ m^3, a weight of 7000 metric tonnes and that produces 200 MWe net power.

STEPPING THROUGH DESIGN SPIRAL

This study aims to provide a preliminary overview of the adjustments required and the feasibility of installing a fusion reactor as part of the ship power train. Therefore, all relevant aspects within the ship design process need to be addressed, as if the refit will take place in the near future. Several approaches to the ship design process exist, such as concurrent design (Sohlenius, 1992), set-based design (Doerry et al., 2014) or design-space exploration (de Vos, 2018). Since this study is not focused on design methodologies, one of the more basic design approaches is followed: an iterative design process following the design spiral as defined by Evans (1959). Since this study is, to our knowledge, the first paper on installing nuclear fission onboard a ship, developing a complete detailed design is considered unfeasible and premature at this moment. Therefore, following the six design stages as defined by Lamb (2003): (1) Concept Design, (2) Preliminary Design, (3) Contract Design, (4) Functional Design, (5) Transition Design, (6) Workstation/Zone Information Preparation, this study remains in the domain of concept or early-stage design.

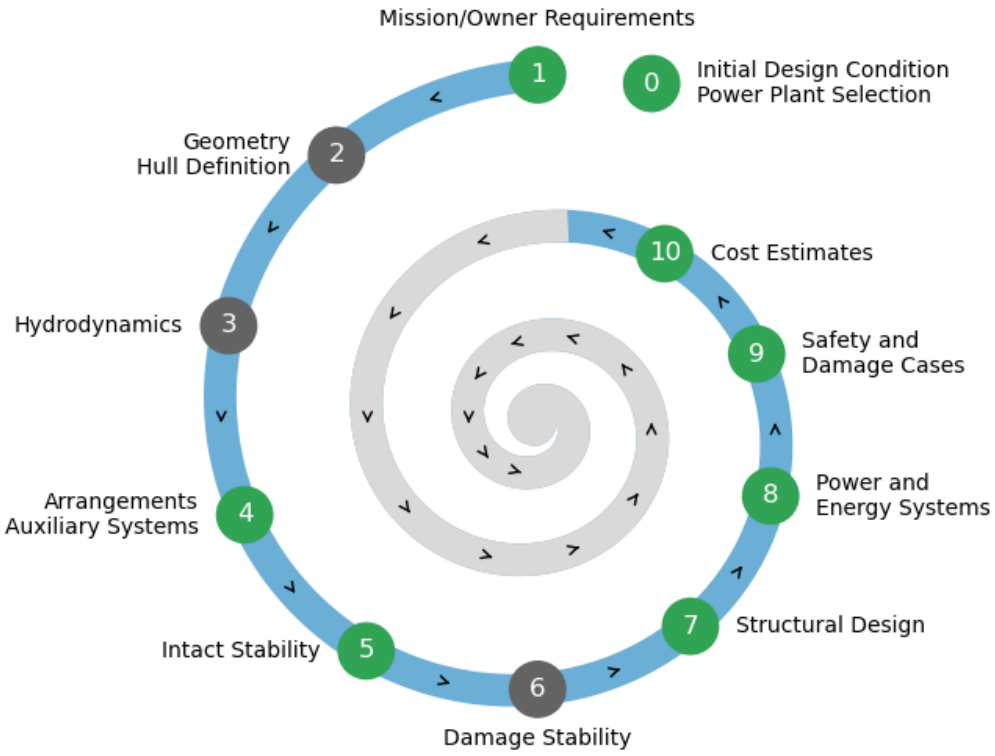

Figure 2: Ship Design Spiral (Evans, 1959) adjusted showing the first (blue) iteration of the ship design process: the concept design phase. The green design aspects are considered within the scope of this study, and the grey design aspects are either considered to be more fitting in later design stages or considered less relevant within a refit design process. All aspects are reconsidered in secondary and tertiary iterations.

Design spiral

In the design spiral representation of a design process (Figure 2), only a single iteration addressing the different design aspects is completed. Note that the power plant concept selection is considered ”design aspect 0” for it is an initial requirement in the design process within this study.

Disregarded Ship Design Aspects

Several of the design aspects are considered less relevant within this specific study. Some of these should be considered for later design phases, whereas others are generally less relevant for a retrofit. The hull form and by extension the hydrodynamics, for example, is assumed to remain rather constant. Therefore, this study does not consider the design aspects concerning hull lines, body plan, and Bonjean curves. The floodable length and freeboard calculations are considered unchanged as well. Thus, steps 2 and 3 from Figure 2 are left out in this study.

Damage stability refers to the case in which one or more watertight compartments have been damaged or breached, often caused by grounding (Costa Concordia) or collision (RMS Titanic). Stability considerations in these cases are a vital concept in guaranteeing the ship’s overall safety. However, current knowledge on the Queen Mary 2 with a nuclear fusion power plant refit does not permit a thorough damage stability analysis.

Mission and Owner Requirements

In this first step of the design spiral, the selection of a suitable case study is addressed. In the Theory Section, we described a lower limit to the power that can be generated by a fusion reactor of approximately 200 MWe. This is over the upper limit of the generators that drive the world's biggest commercial ships and is only surpassed by the newest naval fission power plants (Sea Forces, n.d.). As a result, only very few use ships are potentially compatible with a fusion reactor based on power requirements. We decided to reverse-engineer the mission/owner requirements from existing vessels. To this end, we looked at various extremely large or powerful ships.

Table 2 gives an overview of very powerful ships. The most powerful ships are aircraft carriers. However, aircraft carriers are naval vessels that play a vital role in national defence. Information on these ships is thus minimal, which is why they are disregarded as reference ships for this study. Icebreakers demand high power and significant autonomy, making nuclear propulsion an interesting option. The most powerful icebreakers are propelled by nuclear power (Brigham, 2022.; Manaranche, 2021.). However, information about these Russian nuclear icebreakers is extremely limited. Thus, they are disregarded as reference ships for this study.

Current cruise ships are all optimized for high energy efficiency and comfortable travel. Their speed is less important, and they have a low power demand compared to their size (Thakkar, 2023). Ocean liners, however, are generally sailing faster. The fastest ocean liner, the SS United States, required 185MWe to set the record for the fastest crossing of the Atlantic Ocean in 1952. Due to the ship's retirement, however, this ship is not considered. On the other hand, the second fastest ship was built more recently. The Queen Mary 2 is another ocean liner, with 117MWe installed power and top speeds of 30 knots. This ship was also featured in significant ships of 2003, the year she was delivered (Chanev, 2022.). Thus, the general arrangement and the power and propulsion layout of the Queen Mary 2 is known. Consequently, Queen Mary 2 was chosen as the reference ship for this study.

Table 2: Overview of powerful ships

Ship name	Ship type	Installed power	Power generation type	Source
Gerald R Ford	Aircraft carrier	600 MWe	Two nuclear reactors	(Sea Forces, n.d.)
Admiral Kuznetsov	Aircraft Carrier	150 MWe	Eight boilers, four steam turbines	(Naval Technology, 2021)
Charles de Gaulle	Aircraft Carrier	122 MWe	Two nuclear reactors	(Naval Technology, 2018)
Project 10510	Icebreaker	120 MWe	Nuclear reactor, planned	(Manaranche, 2021.)
Arktika	Icebreaker	60 MW shaft power	Nuclear reactor	(Brigham, 2022.)
Icon of the Seas (Largest cruise ship as of 2023)	Cruise ship	67.5MW	Six multi-fuel engines	(Thakkar, 2023)
SS United States	Ocean liner	185 MWe	Eight boilers, four steam turbines, ship retired	(Gibbs, 2021.)
Queen Mary 2	Ocean Liner	118 MWe	Diesel generators and gas turbines	(GE, 2017.; Chanev, 2022.)

The Queen Mary 2, visible in Figure 3, is the largest ocean liner ever built (Chanev, 2022.). It has a Combined Diesel Electric and Gas Turbine (CODEG) power plant layout, with four Wärtsilä diesel engines and two General Electric gas turbines (GE, 2017.; Chanev, 2022.). The diesel engines provide 16.8 MWe each, while the turbines provide 25 MWe each. The turbine sets, designed by GE, are about 35 tons lighter than similar turbines, resulting in more design freedom (GE, 2017.). The Queen Mary 2 has split engine rooms. The diesel engines are in one room, and the two gas turbines are in a different room (Cruise Industry News, 2004.). The power delivered by the power plant is used for propulsion, hotel, platform and auxiliary systems. The Queen Mary 2 has a small hospital with 11 beds. Its desalination plant can produce 2000 tons of fresh water daily. The garbage system requires heat of up to 1000 °C to burn trash (Chanev, 2022.). All these additional systems require energy, next to the energy needed for systems to keep the guests entertained. The ship currently takes up to 6 hours to fully bunker its fuel tanks (Chanev, 2022.). The Queen Mary 2 is 345m long, with a beam of 41m at the waterline (Chanev, 2022.). She is 72m high (including the funnel) and has a draft of 10m. The gross tonnage of the Queen Mary 2 is about 150000 GT. The block coefficient of the Queen Mary is 0.61 (Cruise Industry News, 2004.).

Figure 3: Queen Mary 2 in the port of Boston, from Oceanhistory46 (2013), Wikipedia, (https://commons.wikimedia.org/wiki/File:Qm2_portboston.jpg), CC BY-SA 4.0 Deed

Arrangements & Auxiliary Systems

The main consideration is adapting a standard diesel generator power plant with its related auxiliary systems into a fusion reactor power plant. Whereas the current systems of the selected vessel can be found in the ship's general arrangement (GA), such a list is less standardized for nuclear fusion plants. Therefore, land-based plants are assumed to provide sufficient information to estimate the required auxiliary systems' main dimensions on the concept design level.

The Queen Mary 2 has an integrated electric propulsion set-up featuring a CODEG plant layout, consisting of four diesel engines and two gas turbines (Chanev, 2022.). These engines, including their fuel, will not be required anymore when installing a fusion reactor. As a fusion reactor forms a single point of failure, an emergency generator set is advised that can generate sufficient power for emergency board systems such as fire fighting, communication and basic lighting. It is outside the scope of this paper to define the exact power required for these emergency systems. Next to removing three diesel engines and two gas turbines, the fuel tanks are not required anymore either. These fuel tanks can hold 3000 tonnes of fuel and are thus of significant size. As the ship is already operating on electric propulsion, this does not need to be changed; a fusion reactor produces electricity, too. The hotel systems are not expected nor required to change significantly. Therefore, the HVAC System, water desalination and distribution systems, and low-voltage electricity distribution systems remain intact.

Several additional auxiliary systems are required to keep a fusion reactor running. Some of these systems, such as the blanket and plasma diagnostics, are embedded inside the fusion reactor (Sorbom et al., 2015). Other fusion-specific auxiliary systems are not embedded into the system. Federici et al. (2017) estimates that the DEMO fusion power plant will need a tritium recovery plant, heating and current drive (H&CD) systems, control systems, a cryoplant and a vacuum system. Other auxiliary systems will be similar to those of fission power plants, such as the requirement of a secondary cooling system (Garcia et al., 2012; Lee et al., 2023). Table 3 gives an overview of the auxiliary systems and their estimated relative locations, while the estimated influence of removing the current engine room with ARC is visualised in figure 4 (Chanev, 2022.).

Auxiliary system	Location	Size
Cryoplant	Relatively close to power plant	Large
Tritium recovery plant	Relatively close to power plant	Small/medium
Heating and Current Drive	Next to reactor	Small
Control systems	Irrelevant	Medium
Vacuum system	Next to reactor	Small
Secondary cooling system	Close to reactor	Large
Turbines	Close to reactor	Medium

Table 3: Overview of auxiliary equipment and approximate locations of equipment

The cryoplant is significantly sized, as the cryoplant used in ITER will be approximately 6000m^2 with a maximum height of the buildings of 19m, excluding the storage required for storing the gaseous helium and liquid nitrogen (Fauve et al., 2017). In ITER, this cryoplant will require approximately 35 MW of electrical power to run. In contrast, the electrical power to run the cooling systems of ARC is estimated to be only 5.1 MW (Fauve et al., 2017; Sorbom et al., 2015). Despite this large difference, it is still assumed that the cryoplant will be the most significant auxiliary system. The cryopumps themselves will likely be small as the ITER exhaust pumping system will consist of 8 cryopumps (Day & Murdoch, 2008). A full-scale prototype torus cryopump has been developed by Day and Murdoch, which was 1.8m long and 1.6m in diameter.Next to the cryopumps, ITER also makes use of roughing pumps. These pumps themselves do not have to be located close to the reactor. In ITER, the vacuum systems are connected to a roughing pump in a vacuum pump room located 40m away from the torus (Day et al., 2004). Additionally, as there are only 8 pumps, the size they take up is considered to be relatively small. The tritium recovery plant is estimated to be small, especially if direct internal recycling is used (Day & Giegerich, 2013). The heating and current drive systems must be close to the main reactor. The size of these systems depends on their power and the choice of the system. For example, an ion cyclotron resonance heater capable of delivering 20 MW of power is approximately 14m^3 and weighs between 45 and 50 tonnes (Brans, 2020). As the external heating power for ARC is estimated to be approximately 25 MW, the size of this auxiliary system will be moderate. The control system is not fusion-specific, as fission reactors also need control systems. These systems do not have to be close to the reactor and can be distributed throughout the ship. They are also not expected to be extremely large. Comparison with the control system space in ITER is not likely useful, as this building in ITER will also be used as a visitor space next to ITER being a testing facility. The main control room of ITER will be able to house 60 to 80 people (ITER, 2023). The turbines are not specific to fusion-driven ships and are expected to be of medium size, similar to current turbines (No, Kim, & KIM, 2007; Houtkoop et al., 2022).

Intact stability

In this subsection, we consider the static stability effects of putting a nuclear fusion power plant onboard a ship. We study the effect of adding the reactor on the ship's draft and analyse the freedom in placing the reactor in terms of trim. We use the ship's length $L_{OA} = 345$m, width $B = 41$m, height $H = 62$m (including funnel $H_{total} = 72$m), draft $D = 10$m, displacement $\Delta = 79287$tonnes and block coefficient $C_B = 0.61[-]$, combined with the sea water density $\rho_{sw} = 1025$kg/m^3 and gravitational constant $g = 9.81$m/s^2. Figure 4 gives an overview of the main dimensions of the Queen Mary 2. The length at the waterline L_{WL} is calculated based on the given displacement and block coefficient:

$$L_{WL} = \frac{\Delta}{B \cdot D \cdot C_B \cdot \rho_{sw}} = 309[\text{m}] \tag{2}$$

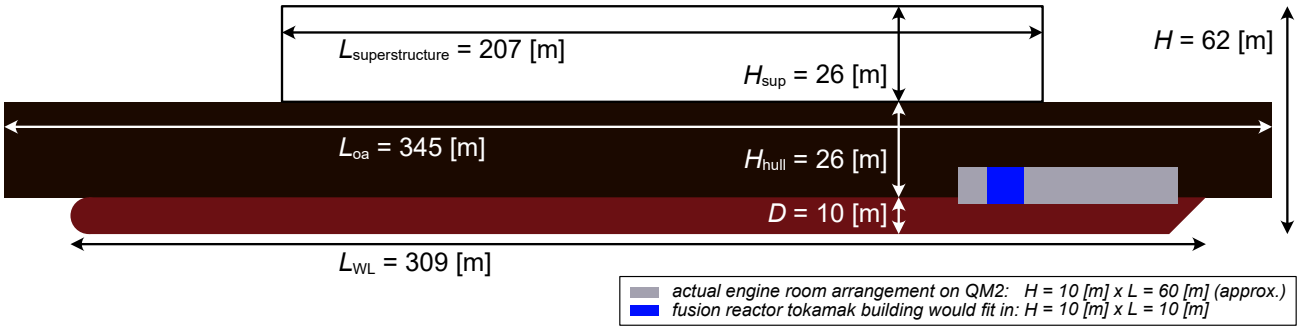

Figure 4: Schematic side view showing the main dimensions of Queen Mary 2 as well as the current location of the engine room approximately to scale. The tokamak building of the fusion reactor has been drawn, again to scale, inside this engine room to indicate that it would fit.

The fusion plant has a mass m of 7000 tonnes and is regarded as a point mass, due to its relatively small volume $V_m = 10 \times 10 \times 10 = 1000\text{m}^3$. In our calculations, we use dimensions as shown in Figure 4 and use the following notation:

$$\begin{array}{lll} K_z & 0 & [\text{m}] \\ K_{0,y} = B_{0,y} = G_{0,y} & 0 & [\text{m}] \\ G_{0,z}, G_{1,z} & \overline{KG_0}, \overline{KG_1} & [\text{m}] \\ y & G_{1,y} - G_{0,y} & [\text{m}] \\ z & \overline{KG_1} - \overline{KG_0} & [\text{m}] \\ M & \Delta_m & [\text{kg}] \end{array} \tag{3}$$

Draft

The change in draft is a relative simple calculation once the waterline area is known. We assume that the waterline area is

$$A_{WL} = L_{WL} \cdot B \cdot C_B^{2/3} [\text{m}^2]. \tag{4}$$

Where the block coefficient is adjusted to not take the draft into consideration. This gives us the difference in draft δD and the new draft D_m, which are

$$\begin{array}{lll} \nabla_m & = \frac{m}{\rho_{sw}} & [\text{m}^3], \\ \delta D & = \frac{\nabla_m}{A_{WL}} & [\text{m}], \\ D_m & = D + \delta D = 10.75 & [\text{m}]. \end{array} \tag{5}$$

This draft does not take the reduced mass by removing the fuels of the ship into consideration. If we address this reduced mass, m_{fuel} of 3000 tonnes, the new draft D_1 becomes 10.43m. Based on visual inspection of the ship's hull shape, this change in draft is not expected to change the waterline area markedly. It has, therefore, limited effects on the ship's stability.

Center of Gravity Height

The ship's current centre of gravity (CoG) has not been explicitly mentioned in the studied literature. Therefore, we calculate its location based on the three assumptions. First, we assume that the spaces below the waterline are mainly technical spaces. Second, that technical spaces have double the density of the hotel spaces. Third, that the block coefficient and main dimensions determine the volume below the waterline, while the volume above the waterline consists of two blocks that

represent the part of the hull above water and the superstructure (see Figure 4). Therefore, we find

$$\begin{aligned} M_{AWL} &= V_{AWL} \cdot \rho_{AWL} && \text{[tonnes]}, \\ M_{BWL} &= V_{BWL} \cdot \rho_{BWL} = V_{BWL} \cdot 2\rho_{BWL} && \text{[tonnes]}, \\ \overline{KG}_{tot} &= \tfrac{M_{AWL} \cdot \overline{KG}_{AWL} + M_{BWL} \cdot \overline{KG}_{BWL}}{M} = 21 && \text{[m]}. \end{aligned} \tag{6}$$

Here, subscript $_{AWL}$ refers to the volume V and mass M above waterline and $_{BWL}$ the submerged mass and volume. This gives the original CoG $\overline{KG}$ as 21m. It is known amongst ship designers that adding mass above the CoG leads to less stability, whilst adding mass below CoG increases the ship's stability. If, however, $\overline{KG}$ is too large, the ship's overall level of comfort reduces due to its movement. Therefore, placing the plant in the lower part of the hull but not in a fully submerged area is recommended.

Trim

The trim caused by placing the reactor at any other place than the CoG requires additional ballast (water) to be present at all times. Since this would lead to a certain increase in draft, it also causes an increased resistance. Therefore, this design aspect is chosen so that the maximum angle caused by the presence of the reactor is $5°$ degree. This degree can still be considered a "small angle" and is sometimes described as the angle of comfort: a larger angle would reduce comfort levels for the cruise passengers. All calculations regarding trim follow from (Moore, 2010), where GM is the difference between the center of gravity and the metacentric height. First, we calculate the maximum deviation in transverse direction (y-axis), which yields

$$\begin{aligned} \overline{GM} &= \overline{KB} + \overline{BM} - \overline{KG} && \simeq \frac{D}{2} + \frac{I_T}{\nabla} - \overline{KG} = 6.72 && \text{[m]}, \\ \frac{y_{max} \cdot m}{M+m} &= \overline{GM} sin(\phi_{max}) && && \text{[m]}, \\ |y_{max}| &= \overline{GM} sin(\phi_{max})(1 + \frac{M}{m}) && = 7.22 && \text{[m]}. \end{aligned} \tag{7}$$

Next, we calculate the maximum deviation in the longitudinal direction (x-axis), which yields

$$\begin{aligned} \overline{GM_L} &= \overline{KB} + \overline{BM_L} - \overline{KG} && \simeq \frac{D}{2} + \frac{I_L}{\nabla} - \overline{KG} = 1291 && \text{[m]}, \\ |x_{max}| &= \overline{GM_L} sin(\phi_{max})(1 + \tfrac{M}{m}) && = 1386 && \text{[m]}. \end{aligned} \tag{8}$$

Both values do not instantly constrain the placement of a reactor onboard the Queen Mary 2. It is self-explanatory that the location is more limited than the location of fuels onboard, but we consider the available positions to be within acceptable limits. In line with Payne et al. (2005), having a maximum longitudinal location of $|x_{max}|$ =1386m off-centre suggests that longitudinal stability, also in the case of head waves, is not a major issue for this ship.

Structural Design

Nuclear fusion reactors are known for their high density, with ARC weighing over 7000 tonnes with a volume of $V_{reactor} = 10 \times 10 \times 10\text{m}^3$. This gives the entire reactor a density $\rho_{reactor}$ of 7000 $\frac{\text{kg}}{\text{m}^3}$ and is equivalent to adding a solid block of lead of over 600m^3 near the heart of the ship. Structurally, we do not consider this mass to be a critical point within the design considerations.

A second consideration are the mechanical vibrations. Power spectra on a ship might differ considerably from those observed on land. In a first-order approximation, let us only consider the one-way couplings: ship-to-reactor vibrations and reactor-to-ship vibrations. Ship-to-reactor vibrations may come either from the ship itself or the interaction between the ship and its environment. Regarding the former, Van Dokkum (2005) identifies the two most common onboard sources of vibrations as the propellers and the engine. In the QM2 case, only the propellers survive the retrofit. Regarding the latter, wave-induced resonance-based vibrations like springing and whipping must be accounted for, as well as the potentially exacerbating effects of heavy weather. A perusal of the literature did not, in fact, yield a starting point for assessing the consequences of such ship-to-reactor vibrations outside of one. Land-based reactor designs consider the effect of seismic activity (also discussed in the ITER Preliminary Safety Report (Taylor et al., 2009)) on the structure of and components in the tokamak building (Ushigusa et al., 2000; Sorin, Barabaschi, & Sannazzaro, 2003), and ways of mitigating these via seismic pads (Syed et al., 2014). However, these studies do not seem principally interested in the reactor operation under vibrations but rather whether the structure would survive. This indicates that external vibrations do not seem top-of-mind in the operation of a fusion reactor. For the plasma itself, this makes sense in that it needs to be actively controlled for a large range of frequencies anyway.

Moving to reactor-to-ship vibrations, the story is quite different. While there are no large moving parts in a fusion reactor (hence no large vibrations during routine operation) and the thermal content of the plasma is negligible, there are large currents and magnetic forces at play. Failure modes that tap into these represent a serious risk. Plasma disruptions, Edge-Localised Modes (ELMs) and Vertical Displacement Events (VDEs) are to be avoided for various reasons(Hassanein, Sizyuk, & Ulrickson, 2008), but the mechanical stresses that they cause are certainly among them. In terms of mechanical stresses, the worst-case scenario is a VDE. For ITER, symmetric VDEs are expected to result in vertical forces on the reactor structure up to around 100 MN, while asymmetric VDEs result in horizontal forces up to 50 MN. While the vibrations that these cause in the ship will depend on the power spectra of these events – which are beyond the scope of this work – such vibrations are perhaps subordinate to the instantaneous mechanical stresses that VDEs cause in the ship's structure. Making a back-of-the-envelope estimation, a vertical force of 100 MN is equal to a weight of 10,000 tonnes. As a reactor weighs about 7000 tonnes, this amounts to a weight increase of +150%. While it is not clear how VDE forces in ITER translate to ARC (although they are similar in terms of fusion power) and the ship's structural material response to transient forces is not necessarily the same as to constant forces, this does indicate that the structural requirements need to take such failure modes into account.

Assuming that we design the ship to withstand these transient loads, it would seem that one-way coupled effects, both ship-to-reactor and from reactor-to-ship, are not showstoppers per se. It remains the case, however, that both fusion reactors and ships have eigenmodes that are best avoided. For example, the coil system of ITER has an eigenfrequency at around 1.5 Hz (Ushigusa et al., 2000). Designing ships such that they do not resonate at certain frequencies is already a complex issue (Kianejad et al., 2020) and adding a tokamak on board introduces a host of extra eigen frequencies that need to be taken into consideration. Two-way–coupled effects will start playing a role here: we want to prevent characteristic frequencies of the ship from exciting those of the tokamak and vice versa. Tackling such resonances would seem to be a challenge in the ship design. Further research in this area would be recommended.

Finally, damage stability is already considered outside the scope of this study. However, preventing the case where damage stability is required can be considered. Queen Mary 2 currently has a double hull for strength and collision protection, having a second function as storage space for fluids like ballast water and fuel. If the refit permits changing this structure, the "Y-Scheldehuid" could be considered as an alternative (Roller, 2012). This hull type, based on Y-shaped stiffeners, reduces the chance of crack formation in case of a collision. This hull type cannot prevent damage to the reactor resulting from the impact but might improve ecological preservation.

Powering and Energy Systems

The Queen Mary 2 has an installed power of 118 MWe, but it does not often use its full power. Payne et al. (2005) investigated several scenarios, ranging from constant power and accepting delays to using more power to recover delays. In all of these scenarios, the engines were mostly run at 60% or less. Engine usage of 60 to 80% was used in three of the four sce-

narios, and engine usages above 80% were very limited (Payne et al., 2005).

ARC, on the other hand, produces approximately 200 MW of electrical power available for the ship (Sorbom et al., 2015). Fusion and fission reactors are similar because they provide a large amount of high-quality heat. On fission-powered ships, a direct drive from the gas turbine to the shaft can be used to minimize conversion power losses (Houtkoop et al., 2022). Thus, a fusion reactor could also be coupled with a direct drive. It is estimated that this results in a system which is approximately 5% more efficient than using electrical power only. However, direct drive is disregarded here for several reasons. First of all, the Queen Mary 2 currently operates a full electric system and four azimuth thrusters for propulsion (Chanev, 2022.). Installing direct drive would result in significant changes in the propulsion system.

Secondly, a direct drive from the fusion reactor to the shaft results in more unnecessary power sources on board. When looking at the general arrangements, two turbines are required to transfer energy from the fusion reactor to electricity or the shaft. One or two backup engines are also required depending on the arrangement (Houtkoop et al., 2022). If an all-electric backup is chosen, only one backup engine is needed; otherwise, an additional one is necessary. Without direct drive, only one turbine is needed, and with an all-electric system, only one backup engine is required, resulting in two power sources instead of three or four. So the system becomes more complicated when using direct drive.

Finally, the Queen Mary 2 only requires 118 MWe at peak moments but usually requires around 75 MWe. It is not straightforward to reduce the power output of a fusion reactor, because of complex interplay of plasma parameters, which was also discussed in the context of reactor size (cf. Section ”Basics of nuclear fusion”) (“The resilience of an operating point for a fusion power plant”, 2015)[1]. A system optimized for energy efficiency is thus not necessary. However, in port lower power requirements are often in place. A useful approach to overcome this challenge would be ship-to-shore-power, which is feasible in case of an ocean liner only visiting a limited number of ports. On the other hand, a reliable electrical system is needed regardless for the hotel load. If the power surplus is to be used to charge batteries, create conventional fuels using the Fischer–Tropsch process or create hydrogen, an electrical system is needed. Thus, an electrical system results in more desirable flexibility of the system.

Safety and Damage Cases

Novel damage cases occurring on ships are hard to qualify or quantify exactly. Consequently, we will explore a non-exhaustive list of situations unique to ships that may influence fusion reactors and assess their potential impact on a fusion reactor. While crucial in the design of a ship, a traditional damaged stability analysis is far beyond the scope of this conference paper. However, a crude conceptual analysis is possible assuming the fusion reactor does not affect the rest of the ship in terms of safety and damage cases. Under that assumption, the only novel damage cases are those inherent to the fusion reactor design and those arising from putting that reactor on board a ship.

To understand the specific risks associated with a fusion reactor, we looked at a summary of the Preliminary Safety Analysis Report for ITER (Taylor et al., 2009). In this summary, it is described that the two main fusion-specific safety functions of ITER relate to the confinement of radioactive material and the limitation of exposure to ionising radiation. While ITER is an experiment and will not be used to generate electricity, at 500 MW of fusion power, it is in the same ballpark as ARC. Two risks that are not present in fusion reactors, as opposed to fission reactors, are runaway thermal reactions (meltdown) and proliferation. Other safety concerns exist, of course, but those are of the conventional types associated with large industrial facilities.

Worst-case: Confinement of Radioactive Waste in Case of Sinking

The current design phase does not consider the detailed effects of a ship sinking due to the complexity of predicting the outcome. Several factors significantly influence the consequences, including the specific design of watertight compartments

[1] This would clearly pose a challenge for vessel types with times of low or even no propulsion whilst at sea.

and bulkheads, the fusion reactor's location, and its compartment's size and contents. Additionally, the specific location of the sinking event itself can further impact the situation. It's important to note that while fission is considered a viable option for some ships, the potential consequences of a sinking event involving a fusion reactor are not necessarily deemed significantly worse. However, further research is necessary to fully understand the impact due to the numerous and unpredictable factors involved.

In this research, we only look at what could happen to the radioactive materials in case of a sinking. The confinement of radioactive material is probably the most pressing question in this case. Perfect safety cannot be guaranteed, and it stands to reason that incidents will happen. In 2001, IAEA released a tech doc listing the release rates due to wrecks that resulted from past marine accidents (*Inventory of Accidents and Losses at Sea Involving Radioactive Material*, 2001). Fusion reactors do not produce much long-lived radioactive waste compared to fission reactors, and much of that waste is locked into the structure – the vacuum vessel and components behind it are neutron-activated – so that the radioactivity cannot escape all at once. Besides activated structures, there is operational waste, the coolant may be activated and part of the fuel (tritium) is radioactive.

The operational waste for ITER is estimated at, at some 200 tonnes/year (Taylor et al., 2009). Only 5% of this is expected to be non-short-lived waste. It stands to reason that this waste can be stored such that it will not be released all at once in the case of an accident. For ARC, there is the additional consideration of FLiBe, which is used as coolant (as opposed to ITER, which uses water). However, FLiBe solidifies below 732 K (Sorbom et al., 2015), so we assume that it will be solid on the sea bed. Moreover, activity in FLiBe dies out rather quickly (Bocci et al., 2020). If it can be contained for a year, it does not pose a radiological risk afterwards (but it might still pose a chemical risk).

Finally, there is the question of the fuel. While deuterium is stable and naturally present in the sea, tritium is radioactive. The total amount of tritium in the plasma is negligible. For a fusion reactor of the size of ARC (with a plasma density of $n_e = 1.3 \times 10^{20}$ m^{-3} and a plasma volume of 141 m^3), the weight of the plasma is approximately 0.07 grams as can be seen from the simple calculation

$$m = n_{\mathrm{e}} V m_{\mathrm{a}} = 1.3E20[\mathrm{m}^{-3}] \cdot 141[\mathrm{m}^3] \cdot \frac{2+3}{2} \cdot 1.66E-24\mathrm{g} = 0.07[\mathrm{g}] \tag{9}$$

with m in kg, n_e in m^{-3}, V in m^3, m_{a} in u. However, there are orders of magnitude more tritium in the rest of the fusion system, mainly in the tritium recovery. The exact amount depends on, amongst others, the burn-up fraction and the throughput time. Our previous research showed for a burn-up fraction of 5%, a total tritium inventory of approximately 1 to 2kg per GW of fusion power, including an emergency inventory (Van Rheenen, 2021). The overall inventory can be as low as 500 grams per GW of fusion power without the emergency inventory. As ARC has a fusion power of 500 MW, the expected total tritium inventory is approximately 1 kg. At a specific activity of 358 TBq g^{-1}, this means that a total source term of 358 Pbq radioactivity is present. This is on the order of the total amount of tritium that has been released by the Le Hague reprocessing plant over the last thirty years (Bailly du Bois et al., 2020).

Whether this tritium source term is problematic depends strongly on how it is released, but that it is significant can be seen using a back-of-the-envelope approach. Regulatory recommendations for tritium in drinking water range from 30 kBq/L to 100 Bq/L (Dingwall et al., 2011). Taking these recommendations, we can calculate the equivalent bodies of water in which 358 PBq needs to be homogeneously dissolved to be compliant. For 30 kBq/L that would be 12 km^3, and for 100 Bq/L 3580 km^3. Of course, much depends on the mixing properties of the ocean. A surface release will disperse very differently than a release at depth. When the ship would sink in shallow water, and assuming a mixing depth of 100 m (D'Asaro, 2014), the tritium would have to spread over 2000 km by 2000 km to stay under 100 Bq/L or 10 km by 10 km to stay under 30 kBq/L. A very crude estimate of how far the effects range can be made using an analogy from atmospheric dispersion physics (Stockie, 2011). Assuming a Gaussian puff (a conservative approach, which assumes that the entire inventory is released as a single puff) and a horizontal eddy diffusivity on the order of 5–20 m^{2}s^{-1} (Döös & Engqvist, 2007), the distance that the puff needs to travel from the release point ranges between 500 km to 2000 km to go under the 30 kBq/L limit, and much further to go under 100 Bq/L. This tritium inventory thus poses a potential hazard to the environment, and suitable measures must be taken to ensure that it is not released to the environment in case the worst happens.

What the sinking of a fusion-driven ship would ultimately do to local and regional marine life and to human activities in

the area is too complex to answer in this conference paper. Taking a broader perspective, we feel that recommendations would need to be put into place, preferably at an international level by the IAEA, regarding the licensing of fusion reactors on ships. However, such policies at the moment appear insufficient even for conventional nuclear reactors on board ships (Wang et al., 2023).

Reactor Safety Risks caused by Motions of Vessels in Waves

A major difference between a fusion reactor based on a ship, contrary to on land, is the movements of a ship. As a ship moves in waves, the fusion reactor will also experience these movements. As the plasma has a very low density and is contained by magnets, we believe that the influence of the movement on the plasma itself may be negligible. These magnets, however, are suspended in concrete and may be influenced by ship motions. All auxiliary components, too, must be designed to withstand ship motions and movements. Placing the reactor at a height such that $\overline{GM}$ is positive but relatively small diminishes the ship's accelerations, possibly reducing the motions' influence on the reactor.

Cost Estimate

Capital expenditure (CAPEX) and operational expenditure (OPEX) costs of a fusion reactor are expected to change over time. The first fusion reactors will likely be significantly more expensive than later generations, the difference is estimated to be over a factor of 2 for small reactors (Lopes Cardozo, 2019; Lindley et al., 2023). Additionally, small, ARC-like reactors are estimated to be approximately 2.11 to 2.31 times relatively more expensive than larger, conventional fusion reactors (Lindley et al., 2023). Sorbom et al. have made an estimate for the CAPEX costs of ARC, which would lie at 428M USD for the materials, and a total fabrication cost of 5.56B USD. A nuclear fission reactor of a similar size would cost approximately 1.2B USD. The costs of building the Queen Mary 2 were approximately 780 million USD, in 2002 (Keck, 2003.). Thus, a fusion reactor of the size of ARC is approximately 7 times more expensive than the Queen Mary 2, while a fission reactor is only 1.5 times more expensive.

The operational costs are more difficult to estimate. Fuel costs are only a small part of the operational costs, estimated for a demonstration fusion reactor (DEMO2) to be 0.44 USD/MWh, only 1% of the total electricity cost (Entler et al., 2018). The total cost of electricity is estimated to be around 60 USD/MWh. The main part of the cost of electricity consists of the depreciation costs (57%), replaceable components (23%) and operation and maintenance (17%). The first of these costs, the depreciation costs, are likely to become much lower over time, as these are related to the CAPEX costs (Entler et al., 2018). To compare this with fission costs, the energy cost for a fission reactor is approximately 136 USD/MWh and is estimated to be around 99 USD/MWh in the future (Lindley et al., 2023). Thus, no overall cost estimate can be made due to the uncertainty of the operational costs. However, a nuclear fusion reactor's investment costs will be extremely high, both compared to fission reactors and to the overall cost of the ship in general.

DISCUSSION

Table 4 summarizes various aspects, data availability, and impacts of using fusion for ship propulsion from this research's design spiral. Drawing definitive conclusions based on the table is hindered by insufficient data for several aspects. Nevertheless, the available information highlights potential challenges with utilizing fusion as a ship's power source.

Two of the aspects were estimated to have a problematic influence on adding a fusion reactor as a power source on a ship. These aspects are matching the power supply and demand for the mission and owner requirements and the cost estimates. A fusion reactor will likely be too powerful and expensive for commercial ships. The influence on the arrangements and auxiliary systems, structural design and safety and damage cases all require additional data to estimate the influence of these aspects. Our first results show that the arrangements and auxiliary systems may not be problematic. Nothing can be said about the structural design and safety and damage cases with any certainty, as these aspects are too complex to estimate

Aspect	Availability Data	Estimated influence
Mission/Owner requirements	Sufficient	Problematic due to mismatch output power fusion reactor and required power ship
Arrangements/ Auxiliary systems	Insufficient	Not enough data, but does not seem to be problematic
Intact stability	Sufficient	Not a problem
Structural design	Insufficient	Adding a fusion reactor is likely to influence this Exact influence unclear
Powering	Sufficient	Additional power problematic, rest of system not a problem
Safety and damage cases	Insufficient	General safety too complex, more information required
Cost estimate	Sufficient	Likely too expensive for commercial application
Nuclear fusion power plant	Sufficient	Technology Readiness Level still too low for commercial application

Table 4: Summarizing table

their influence. The powering itself will, except for the large surplus of power, probably not form any large problems. Additionally, the fusion reactor can be placed in the ship without compromising the intact stability.

While this single iteration of the adjusted design spiral provided valuable insights, its scope is limited, and additional considerations are crucial. We highlight two such issues, acknowledging there are likely others to explore.

Constructing a vessel to meet specific power needs does not resolve the surplus power problem. An additional problem with fusion reactors is their constant power output, whereas conventional engines and fission reactors can adjust based on demand. Complex control systems with batteries or storage solutions are necessary to bridge this gap.

Additionally, current fusion reactor designs anticipate the need for regular significant maintenance activities. A component called the diverter, amongst others, has to be replaced every 2 years. As the diverter is in the centre of the reactor, this replacement process is believed to take 3 months. Maintenance will thus significantly influence the ship's operational time. This poses a major challenge for sectors that prioritize high availability, such as cruise ships and ocean liners.

CONCLUSION AND OUTLOOK

While nuclear fusion holds the potential to offer ships a virtually limitless energy source, its practical application remains distant. Despite this, this paper aims to identify specific challenges of implementing fusion technology on ships by exploring the influence of placing the fusion reactor ARC on the most powerful, commercial, available ship, the Queen Mary 2. Several factors have the potential to become critical roadblocks.

The minimum power output of an MCF fusion reactor, around 200 MWe, poses a challenge for its application in commercial shipping. While naval vessels may require such high power levels, current commercial ships operate at most with a maximum required power of about 120 MWe. This mismatch necessitates a significant increase in commercial shipping's power demands or the exploration of alternative applications for the surplus energy such as green fuel production. Additionally, a fusion reactor will likely require significant maintenance every two years, which poses a major challenge for

commercial ships focusing on high availabilities. Next to the power mismatch, deploying a fusion reactor on a ship introduces additional complexities. The influence of the ship's motions and vibrations on a fusion reactor is not trivial and could significantly influence the design and the working mechanisms of the fusion reactor. Researching these influences is crucial to determine potential mitigation strategies and the feasibility of a fusion reactor on a ship. Besides, placing a fusion reactor onboard a ship, a floating platform in the middle of the ocean, will result in safety and damage cases that have never been considered before. Because of the risks associated with nuclear materials, these safety and damage cases must be thoroughly addressed. The financial feasibility of a fusion reactor on a ship is a significant concern. A fusion reactor will be significantly more expensive than a fission reactor and additionally more expensive than the ship itself, as the estimated costs are 7 times more expensive than the Queen Mary 2.

Therefore, addressing these factors is crucial for fusion deployment onboard ships. Each of these factors may prove to be prohibitive to the use of fusion power on ships. While the idea of fusion on ships is captivating, its realization in the near (before 2100) future or with current technologies, appears unlikely. At least, these conclusions are true for 'conventional' fusion technology, i.e., those concepts based on magnetic confinement fusion (MCF). While more exotic, future fusion technologies might turn out to be the holy grail of ship propulsion, we believe it for the best that the nuclear fusion community should first vet such concepts.

With the current status of the technology behind nuclear fusion, using it as a power source on ships seems far-fetched. However, this research failed to present a single point of failure regarding the application of nuclear fusion onboard ships. Thus, only time will tell whether fusion will in the far future be used on ships.

CONTRIBUTION STATEMENT

E.S. van Rheenen: Conceptualization; methodology; investigation; writing – original draft; writing – review and editing; project administration. **J.P.K.W. Frankemölle:** Conceptualization; methodology; investigation; writing –original draft. **E.L. Scheffers:** Conceptualization; methodology; visualization; formal analysis; writing – original draft.

REFERENCES

Aronietis, R., Sys, C., van Hassel, E., & Vanelslander, T. (2016, 07). Forecasting port-level demand for lng as a ship fuel: the case of the port of antwerp. *Journal of Shipping and Trade*, *1*. doi: 10.1186/s41072-016-0007-1

Bailly du Bois, P., Dumas, F., Voiseux, C., Morillon, M., Oms, P.-E., & Solier, L. (2020). Dissolved radiotracers and numerical modeling in north european continental shelf dispersion studies (1982–2016): Databases, methods and applications. *Water*, *12*(6). doi: 10.3390/w12061667

Bé, M.-M., Chisté, V., Dulieu, C., Browne, E., Baglin, C., Chechev, V., … Lee, K. (2006). *Table of radionuclides* (Vol. 3). Pavillon de Breteuil, F-92310 Sèvres, France: Bureau International des Poids et Mesures. Retrieved from `http://www.bipm.org/utils/common/pdf/monographieRI/Monographie_BIPM-5_Tables_Vol3.pdf`

Betti, R., & Hurricane, O. (2016). Inertial-confinement fusion with lasers. *Nature Physics*, *12*(5), 435-448. doi: 10.1038/nphys3736

Bocci, B., Hartwig, Z., Segantin, S., Testoni, R., Whyte, D., & Zucchetti, M. (2020). Arc reactor materials: Activation analysis and optimization. *Fusion Engineering and Design*, *154*, 111539. doi: 10.1016/j.fusengdes.2020.111539

Brans, P. (2020). *How to pump 20 mw of power into 1 gram of plasma.* https://www.iter.org/newsline/-/3382. (Accessed on 19 february 2024)

Brigham, L. (2022.). *World's most capable icebreakers: Russia's new arktika class.* https://www.usni.org/magazines/proceedings/2022/may/worlds-most-capable-icebreakers-russias-new-arktika-class. (Accessed on 18 December 2023)

Chanev, C. (2022.). *Rms queen mary 2 ship.* http://www.queenmarycruises.net/rms-queen-mary-2-ship/. (Accessed on 18 December 2023)
Cruise Industry News. (2004.). *A ship for the sea.* https://cruiseindustrynews.com/cruise-news/2004/10/winter-03-04-a-ship-for-the-sea/. (Accessed on 18 December 2023)
D'Asaro, E. A. (2014). Turbulence in the upper-ocean mixed layer. *Annual Review of Marine Science*, *6*(1), 101-115. (PMID: 23909456) doi: 10.1146/annurev-marine-010213-135138
Day, C., Antipenkov, A., Dremel, M., Haas, H., Hauer, V., Mack, A., … Wykes, M. E. (2004). Validated design of the iter main vacuum pumping systems.. Retrieved from `https://api.semanticscholar.org/CorpusID:55649307`
Day, C., & Giegerich, T. (2013). The direct internal recycling concept to simplify the fuel cycle of a fusion power plant. *Fusion Engineering and Design*, *88*(6), 616-620. (Proceedings of the 27th Symposium On Fusion Technology (SOFT-27); Liège, Belgium, September 24-28, 2012) doi: 10.1016/j.fusengdes.2013.05.026
Day, C., & Murdoch, D. (2008). The ITER vacuum systems. *J. Phys. Conf. Ser.*, *114*, 012013.
de Vos, P. (2018). *On early-stage design of vital distribution systems on board ships* (Doctoral dissertation, Delft University of technology). doi: 10.4233/UUID:EB604971-30B7-4668-ACE0-4C4B60CD61BD
Dingwall, S., Mills, C., Phan, N., Taylor, K., & Boreham, D. (2011). Human health and the biological effects of tritium in drinking water: Prudent policy through science – addressing the odwac new recommendation. *Dose-Response*, *9*(1), dose-response.10-048.Boreham. (PMID: 21431084) doi: 10.2203/dose-response.10-048.Boreham
DNV. (2021). *Energy transition outlook 2021: Technology progress report.* Retrieved from `https://assets-global.website-files.com/643691764f0ee331841022ac/643691764f0ee323f810245c_DNV_Technology_Progress_Report_2021-compressed.pdf` (Accessed on 15 February 2024)
Doerry, N., Earnesty, M., Weaver, C., Banko, J., Myers, J., Hopkins, M., & Balestrini, S. (2014). Using Set-Based Design in Concept Exploration.
Döös, K., & Engqvist, A. (2007). Assessment of water exchange between a discharge region and the open sea – a comparison of different methodological concepts. *Estuarine, Coastal and Shelf Science*, *74*(4), 709-721. (Timescale- and tracer-based methods for understanding the results of complex marine models) doi: 10.1016/j.ecss.2007.05.022
Entler, S., Horacek, J., Dlouhy, T., & Dostal, V. (2018). Approximation of the economy of fusion energy. *Energy*, *152*, 489-497. doi: 10.1016/j.energy.2018.03.130
EUROfusion. (2018). *European research roadmap to the realisation of fusion energy*. Garching: EUROfusion. Retrieved from `https://euro-fusion.org/eurofusion/roadmap/`
Evans, J. H. (1959). Basic design concepts. *Journal of the American Society for Naval Engineers*, *71*(4), 671-678. doi: 10.1111/j.1559-3584.1959.tb01836.x
Fauve, E., Monneret, E., Voigt, T., Vincent, G., Forgeas, A., & Simon, M. (2017). Iter cryoplant infrastructures. *IOP Conference Series: Materials Science and Engineering*, *171*, 012008. doi: 10.1088/1757-899x/171/1/012008
Federici, G., Biel, W., Gilbert, M., Kemp, R., Taylor, N., & Wenninger, R. (2017). European demo design strategy and consequences for materials. *Nuclear Fusion*, *57*, 092002. doi: 10.1088/1741-4326/57/9/092002
Freidberg, J. (2007). *Plasma physics and fusion energy*. Cambridge University Press. doi: 10.1017/CBO9780511755705
Garcia, R. F., Carril, J. C., Catoira, A. D., & Gomez, J. R. (2012). Efficiency enhancement of gt-mhrs applied on ship propulsion plants. *Nuclear Engineering and Design*, *250*, 326-333. doi: 10.1016/j.nucengdes.2012.06.013
GE. (2017.). *Two 30 mw ge gas turbines propel queen mary 2, the world's largest transatlantic liner.* https://www.geaerospace.com/sites/default/files/30mw-queen-mary-case-history.pdf. (Accessed on 18 December 2023)
Gibbs, S. (2021.). *Op/ed: Ss united states, the maritime thoroughbred.* https://www.marinelink.com/news/oped-ss-united-states-maritime-484868. (Accessed on 18 December 2023)
Hassanein, A., Sizyuk, T., & Ulrickson, M. (2008). Vertical displacement events: A serious concern in future iter operation. *Fusion Engineering and Design*, *83*(7), 1020-1024. (Proceedings of the Eight International Symposium of Fusion Nuclear Technology) doi: 10.1016/j.fusengdes.2008.05.032
Houtkoop, K., Visser, K., Sietsma, J., & de Vries, N. (2022). New potential for integration of nuclear power in marine propulsion systems. *Conference Proceedings of INEC*. doi: 10.24868/10647
International Maritime Organization. (2023). *Revised ghg reduction strategy for global shipping adopted.* https://www.imo.org/en/MediaCentre/PressBriefings/pages/Revised-GHG-reduction-strategy-for-global-shipping-adopted-.aspx. (Accessed on 18 December 2023)
Inventory of accidents and losses at sea involving radioactive material (No. 1242). (2001). Vienna: INTERNATIONAL

ATOMIC ENERGY AGENCY. Retrieved from https://www.iaea.org/publications/6353/inventory-of-accidents-and-losses-at-sea-involving-radioactive-material
ITER. (2023). *Control building.* https://www.iter.org/construction/ControlBuilding. (Accessed on 19 february 2024)
Keck, G. (2003.). *Queen mary 2 101.* https://www.washingtonpost.com/archive/lifestyle/travel/2003/11/16/queen-mary-2-101/2f229ea0-ba30-43a1-b78b-e259c03ca83c/. (Accessed on 28 February 2024)
Kianejad, S. S., Enshaei, H., Duffy, J., & Ansarifard, N. (2020, October). Investigation of a ship resonance through numerical simulation. *Journal of Hydrodynamics*, *32*(5), 969–983. doi: 10.1007/s42241-019-0037-x
Lamb, T. (Ed.). (2003). *Ship design and construction* (New edition ed.). Jersey City, NJ: Society of Naval Architects and Marine Engineers.
Lee, W., Yoo, S., Park, D. K., & Lee, K.-Y. (2023). Design considerations of the supercritical carbon dioxide brayton cycle of small modular molten salt reactor for ship propulsion. *Progress in Nuclear Energy*, *163*, 104835. doi: 10.1016/j.pnucene.2023.104835
Lindley, B., Roulstone, T., Locatelli, G., & Rooney, M. (2023). Can fusion energy be cost-competitive and commercially viable? an analysis of magnetically confined reactors. *Energy Policy*, *177*, 113511. doi: 10.1016/j.enpol.2023.113511
Lockheed Martin. (n.d.). *Compact fusion.* https://www.lockheedmartin.com/en-us/products/compact-fusion.html. (Accessed on 28-2-2024)
Lopes Cardozo, N. J. (2019). Economic aspects of the deployment of fusion energy: the valley of death and the innovation cycle. *Philosophical Transactions of the Royal Society A: Mathematical, Physical and Engineering Sciences*, *377*(2141), 20170444. doi: 10.1098/rsta.2017.0444
Manaranche, M. (2021.). *Russian shipyard lays down leader nuclear-powered icebreaker.* https://www.navalnews.com/naval-news/2021/07/russian-shipyard-lays-down-leader-nuclear-powered-icebreaker/. (Accessed on 18 December 2023)
Moore, C. S. (2010). *Principles of naval architecture series - intact stability*. Society of Naval Architects and Marine Engineers (SNAME). Retrieved from https://app.knovel.com/hotlink/toc/id:kpPNASIS01/principles-naval-architecture-5/principles-naval-architecture-5 doi: 10.5516/net.2007.39.1.021
Naval Technology. (2018). *Charles de gaulle nuclear-powered aircraft carrier.* https://www.naval-technology.com/projects/gaulle/?cf-view. (Accessed on 18 December 2023)
Naval Technology. (2021). *Kuznetsov class (type 1143.5) aircraft carrier.* https://www.naval-technology.com/projects/kuznetsov/?cf-view&cf-closed. (Accessed on 18 December 2023)
No, H., Kim, J. H., & KIM, H. (2007, 02). A review of helium gas turbine technology for high-temperature gas-cooled reactors. *Nuclear Engineering and Technology*, *39*. doi: 10.5516/NET.2007.39.1.021
Oceanhistory46. (2013). *Queen mary 2 in port of boston.* Retrieved from https://commons.wikimedia.org/wiki/File:Qm2_portboston.jpg (Accessed on 28-2-2024)
Osolin, C., Kawamoto, J., Evangelista, B., Rhien, P., Koning, P., Thomas, J., … Fox, G. (2023). *The age of ignition: Inside lawrence livermore national laboratory's fusion breakthrough*. U.S. Department of Energy. Retrieved from https://lasers.llnl.gov/content/assets/docs/news/age_of_ignition_book.pdf
Payne, S., Dallinga, R., & Gaillarde, G. (2005). Queen mary 2 seakeeping assessment - the owner's requirements, the design verification and operational experience. In *Cruise & ferry.*
The resilience of an operating point for a fusion power plant. (2015). *Fusion Engineering and Design*, *98-99*, 2223-2226. (Proceedings of the 28th Symposium On Fusion Technology (SOFT-28)) doi: 10.1016/j.fusengdes.2014.11.021
Roller, E. t. (2012, 1). 'Scheldehuid' halveert kans op Schipbreuk.
Sea Forces. (n.d.). *Gerald r. ford class aircraft carrier - cvn.* https://www.seaforces.org/usnships/cvn/Gerald-R-Ford-class.htm. (Accessed on 18 December 2023)
Sohlenius, G. (1992). Concurrent Engineering. *CIRP Annals*, *41*(2), 645–655. doi: 10.1016/S0007-8506(07)63251-X
Sorbom, B., Ball, J., Palmer, T., Mangiarotti, F., Sierchio, J., Bonoli, P., … Whyte, D. (2015). Arc: A compact, high-field, fusion nuclear science facility and demonstration power plant with demountable magnets. *Fusion Engineering and Design*, *100*, 378-405. doi: 10.1016/j.fusengdes.2015.07.008
Sorin, V., Barabaschi, P., & Sannazzaro, G. (2003). Seismic analysis of iter tokamak including interaction with soil and building. *Fusion Engineering and Design*, *69*(1), 611-615. (22nd Symposium on Fusion Technology) doi: 10.1016/S0920-3796(03)00176-5
Stockie, J. M. (2011). The mathematics of atmospheric dispersion modeling. *SIAM Review*, *53*(2), 349-372. doi: 10.1137/10080991X

Syed, M., Patisson, L., Curtido, M., Slee, B., & Diaz, S. (2014). The challenging requirements of the iter anti seismic bearings. *Nuclear Engineering and Design*, *269*, 212-216. (Special Issue - The International Conference on Structural Mechanics in Reactor Technology (SMiRT21), New Delhi India, Nov 06-11, 2011) doi: 10.1016/j.nucengdes.2013.08.032

Taylor, N., Baker, D., Barabash, V., Ciattaglia, S., Elbez-Uzan, J., Girad, J.-P., … Topilski, L. (2009). Preliminary safety analysis of iter. *Fusion Science and Technology*, *56*(2), 573-580. doi: 10.13182/FST56-573

Thakkar, E. (2023). *First engine started on massive new royal caribbean cruise ship.* https://www.cruisehive.com/first-engine-started-on-massive-new-royal-caribbean-cruise-ship/96805. (Accessed on 18 December 2023)

Ushigusa, K., Isayama, A., Kurita, G., Ishida, S., Neyatani, Y., Ishiyama, S., … Ninomiya, H. (2000). Vibration analysis in jt-60su design. *Fusion Engineering and Design*, *51-52*, 371-376. doi: 10.1016/S0920-3796(00)00297-0

Van Rheenen, E. S. (2021). *Influence of the tritium system on fusion deployment and the thermal efficiency of a fusion reactor.*

Van Rheenen, E. S., Padding, J. T., Slootweg, J. C., & Visser, K. (2023). Hydrogen carriers for zero-emission ship propulsion using pem fuel cells: an evaluation. *Journal of Marine Engineering & Technology*, *0*(0), 1-18. doi: 10.1080/20464177.2023.2282691

Van Dokkum, K. (2005). *Ship knowledge: Covering ship design, construction and operation*. Enkhuizen, The Netherlands: DOKMAR.

Wang, Q., Zhang, H., & Zhu, P. (2023, February). Using nuclear energy for maritime decarbonization and related environmental challenges: Existing regulatory shortcomings and improvements. *International Journal of Environmental Research and Public Health*, *20*(4), 2993. doi: 10.3390/ijerph20042993

Zohm, H. (2019). On the size of tokamak fusion power plants. *Philosophical Transactions of the Royal Society A*, *377*. doi: 10.1098/rsta.2017.0437

Proceedings of 15th International Marine Design Conference (IMDC-2024)
June 2-6, 2024
Amsterdam, the Netherlands

Ship system design changes for the transition to hydrogen carriers

E.S. van Rheenen[1,*], J.T. Padding[2], A.A. Kana[1] and K. Visser[1]

ABSTRACT

Reducing the use of fossil fuels in shipping requires new, alternative maritime fuels. Hydrogen carriers offer a safe and energy-dense solution for storing hydrogen, a zero-emission alternative fuel. This research focuses on ammonia borane, $NaBH_4$, n-ethylcarbazole and dibenzyltoluene. Applying hydrogen carriers influences ship design significantly, as they require additional specialised equipment to remove hydrogen from the hydrogen carrier. This research estimates the size of the equipment. As this equipment will need to be stored and maintained on the ship, the exact sizing and sequence of the additional equipment will likely influence ship design. Results show that the reactor size is significant for all hydrogen carriers. The mixing tank is considerably sized for $NaBH_4$ and ammonia borane, while the heat exchangers are large for dibenzyltoluene and n-ethylcarbazole.

KEY WORDS

Hydrogen carriers; Heat exchangers; Dehydrogenation; Solid hydrogen carrier; LOHC

INTRODUCTION

Reducing fossil fuels in shipping requires new, alternative maritime fuels. However, applying alternative power sources can have significant implications for ship design and is thus extensively researched, mainly focusing on using ammonia or methanol as alternative fuel (Pawling et al., 2022; Souflis-Rigas et al., 2023; de Vos et al., 2022). Hydrogen is another of these alternative fuels, but it has a low volumetric energy density. Hydrogen carriers offer a safe and energy-dense solution for storing hydrogen, a zero-emission alternative fuel (van Rheenen, Padding, Slootweg, & Visser, 2023). Using hydrogen carriers will significantly influence the ship's power plant and, consequently, ship design, as additional components such as hydrogen release reactors are required. Additionally, these reactors cannot be placed everywhere on the ship, as they produce pure hydrogen and thus need to be in regulated and well-ventilated spaces. Besides the reactor, more components, such as heat exchangers, may be necessary. All these additional components that are required to release hydrogen from hydrogen carriers are components that are not necessary without hydrogen carriers. So, using hydrogen carriers may result in more components and, thus, more complexity.

As these additional components are of unknown size, it is unclear whether they are significantly sized to influence ship design. For other alternative fuels, such as methanol or LNG, it is clear that the additional components will influence ship design (Souflis-Rigas et al., 2023; de Vos et al., 2022). Research focuses on resulting required design changes because of the space other components take up (Souflis-Rigas et al., 2023; de Vos et al., 2022). However, the number of components

[1] Department of Maritime and Transport Technology, Delft University of Technology, Delft, the Netherlands
[2] Department of Process and Energy, Delft University of Technology, Delft, the Netherlands;
[*] Corresponding Author: E.S.vanRheenen@tudelft.nl

Submitted: 23 February 2024, Revised: 22 April 2024, Accepted: 1 May 2024, Published: 23 May 2024

Conference paper, DOI: https://doi.org/10.59490/imdc.2024.894 e-ISSN: 3050-4864

explicitly needed for hydrogen carriers as power sources, and the size of these specific components are unknown. The sequence, size, and number of this specialised hydrogen carrier equipment are required to see how they influence and perhaps limit ship design.

Our previous research identified a promising set of hydrogen carriers for use as alternative fuels on ships (van Rheenen, Padding, Slootweg, & Visser, 2023). The most promising ones were sodium borohydride ($NaBH_4$), potassium borohydride (KBH_4), ammonia borane (NH_3BH_3), n-ethylcarbazole (NEC), and dibenzyltoluene (DBT). Next, we developed a 0D thermodynamic model to evaluate the effective energy density of these hydrogen carriers in combination with various energy converters (van Rheenen, Padding, & Visser, 2023). The energy converters were a proton exchange fuel cell (PEMFC), solid oxide fuel cell (SOFC), hydrogen-powered internal combustion engine (ICE) and gas turbine (GT). Integration of the carrier with the energy converter is crucial to calculate the overall energy density. Heat integration can minimise losses, particularly for DBT and NEC, which require heat during the hydrogen release process. Findings from the model suggest that these hydrogen carriers hold significant promise as alternative fuels. However, the 0D model does not account for geometrical parameters or the ship's sizing restrictions.

Thus, this paper aims to identify and size the relevant components when using the hydrogen carriers mentioned earlier as power sources onboard ships. First, all the required components for each hydrogen carrier must be known. Only the specifically relevant components for hydrogen carriers are considered; general equipment for hydrogen-fueled ships is not regarded. Each of these components will then be sized. This will form a first step in designing hydrogen carrier-powered ships.

BACKGROUND

Sodiumborohydride, ammonia borane, N-ethylcarbazole and dibenzyltoluene are considered in this research. Table 1 gives an overview of the relevant parameters of these hydrogen carriers. As energy converters, same as in the previous model, the ICE, GT, PEMFC and SOFC are considered (van Rheenen, Padding, & Visser, 2023).

Hydrogen carriers

The hydrogen carriers will be divided into endothermic and exothermic release hydrogen carriers. Within these groups, the processes and, thus, the required equipment are very similar. The phase, energy density and energy requirements are also similar. All processes occur at relatively low pressures, around 1 to 10 bars; thus, specialised high-pressure equipment is unnecessary.

Endothermic release

The endothermic release hydrogen carriers are NEC and DBT. Both are liquid organic hydrogen carriers (LOHCs). The release mechanism for the LOHCs is very similar and is as follows:

$$\mathrm{LOHC}^{+} + \mathrm{Energy} \rightarrow \mathrm{LOHC}^{-} + n\mathrm{H}_2 \tag{1}$$

The significant difference is the temperatures at which they react and the heat required for dehydrogenation. DBT's dehydrogenation temperature lies between 553 and 593K; temperatures above 573K are required to reach full dehydrogenation, while DBT will start dissociating at temperatures above 563K. A temperature of 573K is chosen in the model, as this temperature is often used in experiments, and full dehydrogenation can be achieved without compromising the fluid too much (Asif et al., 2021). The dehydrogenation process requires 558 kJ/mol of full LOHC (Niermann et al., 2019). The dehydrogenation temperature for NEC lies between 453 and 523K. The dehydrogenation process is much slower at lower temperatures. The model uses a temperature of 503K. The dehydrogenation process is fast at this temperature, without having

Table 1: Parameters of hydrogen carriers

Parameter	DBT	NEC	$NaBH_4$	Ammonia borane
Theoretical energy density [MJ/kg]	7.44	6.98	25.56	23.52
Theoretical energy density [MJ/L]	7.0	6.63	27.34	14.4
Hydrogen yield per molecule of hydrogen carrier [mol/mol]	9	6	4	3
Molecular weight [g/mol]	290.54	207	37.8	30.8
Heat capacity fuel (incl. water if necessary [kJ/kgK]	1.96	2.04	4.54*	4.54*
Heat capacity spent fuel [kJ/kgK]	1.82	1.56	N.R.	N.R.
Dehydrogenation temperature [K]	573	503	353	353*
Dehydrogenation energy [kJ/mol Fuel]	558	318	-210	-156
Sources	(Lee et al., 2021) (Kwak et al., 2021)	(Stark et al., 2015) (Müller et al., 2015) (Teichmann et al., 2012)	(Zhang et al., 2006) (Kojima, 2019) (Ye et al., 2020)	(Sanyal et al., 2003) (Chandra & Xu, 2007)

Values denoted with * are estimated by the authors combined with data from Aspen as no precise information was available.
N.R. stands for 'Not required' as these values are not required in this calculation. When a solution is mixed, the heat capacity of the sol

high heating loads (Brückner et al., 2014). The hydrogenation process requires 318 kJ/mol of full LOHC (Niermann et al., 2019). van Rheenen, Padding, and Visser (2023) showed that, with an essential integration, a large part of the required heat could be supplied by the energy converter and heat available in the spent fuel, with similar results found by Preuster et al. (2018), who looked at a specific hydrogen carrier and energy converter. Figure 1 gives an overview of the specific components required for the hydrogen carrier to release hydrogen. After the carrier is transported from the tank, heat exchangers are used to preheat the carrier up to the dehydrogenation temperature. Part of this heat exchange already has to occur in the tank, as DBT is highly viscous; thus, preheating is required to get it out of the tank.

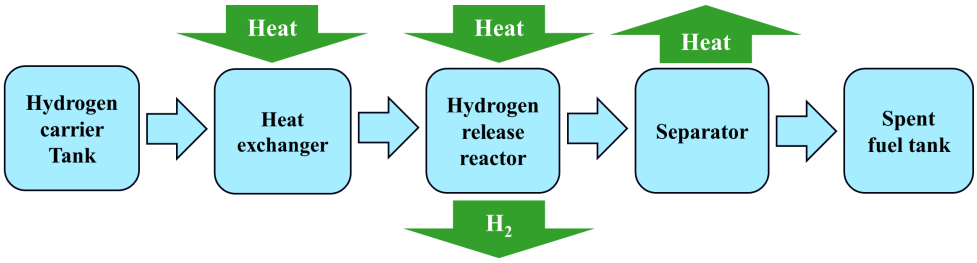

Figure 1: Simplified flow diagram with required components and main heat and mass flows for endothermic release hydrogen carriers

Exothermic release

Ammonia borane and $NaBH_4$ release hydrogen exothermically upon reacting with water, according to the following equations:

$$NaBH_4 + (2 + x)H_2O \rightarrow 4H_2 + NaBO_2.xH_2O \quad (2)$$

$$NH_3BH_3 + 3H_2O \rightarrow 3H_2 + B(OH)_3 + NH_3 \quad (3)$$

These reactions are similar, requiring water and releasing equally or more hydrogen than initially stored in the molecule, as the process also releases hydrogen within the water molecules. The boron-based spent fuel is also very similar. Regeneration of this spent fuel to the original molecule is possible but energy intensive due to the strong B-O bonds (Stephens et al., 2007). The exact composition of the spent fuel of $NaBH_4$ (equation 2) depends on the temperature of the reaction. At the optimal reaction temperatures of 333 to 353K, the composition is $NaBO_2.2H_2O$.

Equation 3 shows the release mechanism of ammonia borane, which produces hydrogen and ammonia. Ammonia gas can be burned in a heat engine, for example, in a dual-fuel ammonia-hydrogen internal combustion engine. Additionally, it can be decomposed into N_2 and H_2, after which the H_2 can be used in a fuel cell. Finally, ammonia gas can be stored on board. Storage is not considered feasible because of the required safety regulations and additional space. The decomposition process is also disregarded, as this process is highly energy-intensive. Thus, in this study, similar to in van Rheenen, Padding, and Visser (2023), only dual-fuel options of ammonia and hydrogen gas are considered. Only the PEMFC cannot run on the ammonia-hydrogen dual-fuel of the four investigated energy converters.

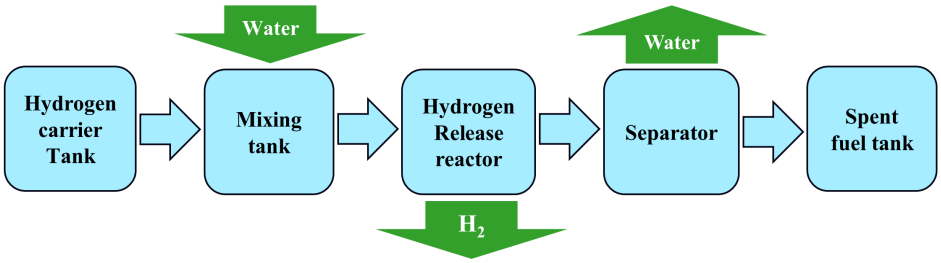

Figure 2: Simplified flow diagram with required components and main heat and mass flows for exothermic release hydrogen carriers

Energy converter

Energy converters convert the chemical energy inside hydrogen to electrical or mechanical energy. The model will simulate four different energy converters, namely a hydrogen spark ignition (SI) ICE, a PEMFC, SOFC and GT, as these are all considered possible alternatives within the shipping sector. At the moment, a compression ignition running on pure hydrogen is not feasible without a way to ignite the hydrogen and is thus not regarded (Dimitriou & Tsujimura, 2017). Additionally, SI ICEs are more researched, and more data is available for these heat engines (Wang et al., 2019). The output of both the SI ICE and GT is regarded as mechanical. Both are assumed to be able to run on pure hydrogen and a hydrogen-ammonia mixture (Gohary & Seddiek, 2013; Rosado et al., 2019; Wang et al., 2019).

Table 2: Parameters of energy converters, including sources.

Parameter	SI-ICE	PEMFC	SOFC	GT
T coolant [K]	363	348	-	-
P coolant [%]	30	44.8	0	0
P effective [%]	35	42.9	48	37.5
T flue gas [K]	623*	-	1023	790
P flue gas [%]	25	0	42.1	53
P losses [%]	10	12.3	9.9	9.5
Sources	(Wang et al., 2019)	(Zhao et al., 2017)	(van Veldhuizen et al., 2023)	(Gohary & Seddiek, 2013) (Rosado et al., 2019)

P is the percentage of overall power distribution, mainly based on Sankey diagrams. * Flue gas temperature of SI-ICE largely fluctuates depending on operating conditions and can range from 423 to 773K

METHOD

Using hydrogen carriers on ships results in additional components needed on board compared to using pure hydrogen or conventional fuels. Some of these components are specific to hydrogen carriers, whereas other components, such as the energy converter, may be different for hydrogen-based fuels in general. This research only covers the hydrogen carrier-specific components, not the hydrogen-specific components. These components are visible in figure 3, where the components that will be looked at in detail in this research are coloured green. The required input parameters, such as mass flows, compositions and temperatures, are calculated using the 0D model we previously created (van Rheenen, Padding, & Visser, 2023). Figure 4 shows a simplified model outline based on van Rheenen, Padding, and Visser (2023). The model is built so that each energy converter, regardless of the hydrogen carrier, will always have an output power of 2 MW, which is relevant for medium-sized vessels such as ferries and small cargo ships.

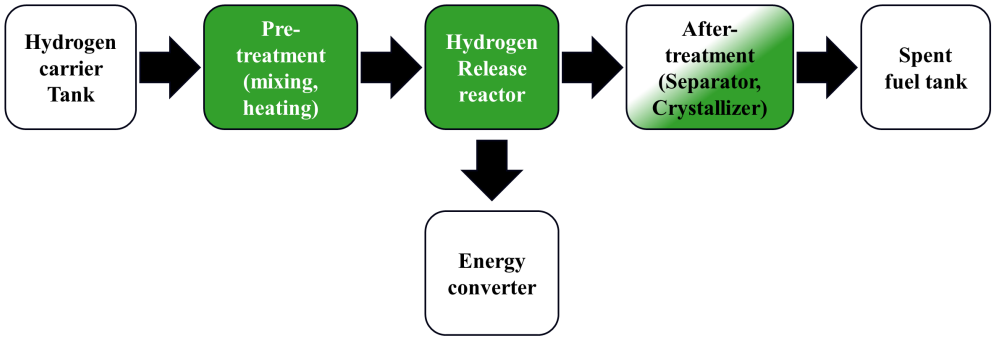

Figure 3: Overview of all components required on a ship when using hydrogen carriers as a power source. The components denoted in green are hydrogen carrier specific components and, thus, the main focus of this research

This section describes the necessary steps to upgrade them to get an overview of the sizing. A different approach is used for each component due to their significant difference in functionality. The parameters required for upgrading the components, such as mass flows and temperatures, are given by the 0D model. The following subsections will describe each critical component in detail and how they can be upgraded.

0D Model

Figure 4 gives an overview of the 0D thermodynamic model's layout, as implemented in Matlab Simulink. The power requirement, the hydrogen carrier and the energy converter can be chosen. These three parameters then define the mass flow of the hydrogen carrier. This mass flow, in its turn, defines the required energy for preheating and, if applicable, dehydrogenation. The model runs a complete iteration, including an energy balance check, and adjusts the mass flow accordingly if the required power and the output power do not match.

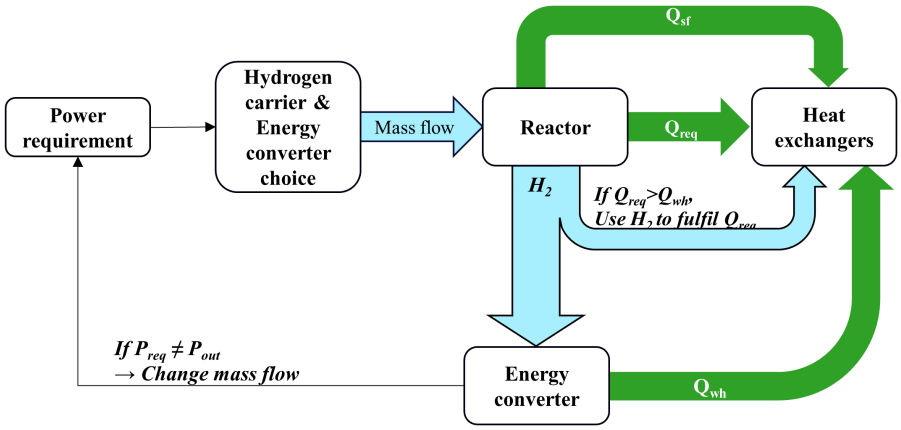

Figure 4: Simplified overview model. Flows that are used as a heat source can be turned on and turned off when necessary. Q_{wh} stands for waste heat, Q_{req} is the heat required for preheating and, if applicable, dehydrogenation and Q_{sf} stands for the heat inside the spent fuel

Tables 1 and 2 give an overview of the used parameters and the resources from which they were derived. The thermodynamic model provides estimates and a simplified representation of reality. For example, the model does not consider the preheating of air for a SOFC. In reality, this preheating, which is required, is a major, high-temperature heat sink (van Veldhuizen et al., 2023). When the heat needed for the dehydrogenation of the hydrogen carrier cannot be covered with waste heat from the energy converter, hydrogen will have to be burnt to cover the heat requirement. The heat required for preheating and dehydrogenation, Q_{req}, and the heat available inside the spent fuel, Q_{sf}, are calculated according to the following equation:

$$\dot{Q} = \dot{m} \cdot c_p \cdot \Delta T \tag{4}$$

With $\dot{Q}$ the heat in kW, $\dot{m}$ the mass flow in kg/s, c_p the heat capacity, in kJ/kgK and ΔT the temperature difference in Kelvin. In the Matlab model, c_p is considered constant, not temperature-dependent. Q_{wh} is defined by the percentage of heat going from the reactor to heat losses (denoted by P coolant and P flue gas in table 2). A fixed temperature difference is set for flue gasses and coolant, which is used to calculate the flue gas's or coolant's mass flow, using equation 4. The required mass flow of the flue gas or coolant to go into the heat exchanger is similarly calculated. However, if the heat (denoted by Q) is larger than required to heat the hydrogen carrier in that temperature window, the mass flow is adjusted, as equation 4 is always true (Cengel & Ghajar, 2014).

Pretreatment: mixing tank

The boron-based hydrogen carriers are mixed with water in the mixing tank. This mixture is then further heated in heat exchangers before entering the reactor. The mixing tank uses a stirrer. The size of the mixing chamber depends on the required power and the selection of spent fuel. The hydrolysis reaction of the boron-based carriers is visible in equation 2 and 3. The hydrolysis requires a surplus of water. The amount of water, defined by the (2+x) term, is the minimum amount

needed for the reaction to happen. Additionally, it defines the composition of the spent fuel. The (2+x) term depends on the temperature if enough water is available (Andrieux et al., 2012). More important, however, is the solubility of the fuel and spent fuel in water. The amount of water should be sufficient to avoid spontaneous crystallisation, which may result in clogging. For both ammonia borane and sodium borohydride, the spent fuel is less soluble in water than the fuel. As both the fuel and spent fuel are present in the reactor, the limiting substance defines the amount of water. For ammonia borane and its spent fuel product, boric acid, the limit at temperatures of 353K is about 19 wt% of ammonia borane in water (Crapse & Kyser, 2011). For sodium borohydride, this limit lies at around 44 wt% sodium borohydride in water (Andrieux et al., 2012). These limits thus define the minimum amount of water required in the mixing tank.

The size of the mixing tank is determined as follows. The amount of water required for the boron-based hydrogen carrier spent fuel to completely dissolve at 353K (the operating temperature of the reactor) is calculated. This amount of water is compared to the stoichiometric amount of water required for the reactions (as depicted in equations 2 and 3). The largest amount of water is taken. This amount should always be compared to the amount of boron-based hydrogen carrier that can be dissolved at room temperature (293K) without crystallisation (Demirci, 2020; Haynes, 2011). The spent fuel is the limiting factor for sodium borohydride and ammonia borane. The largest amount of water (stoichiometric or dissolvent value) must be held in the mixing tank. As the boron-based hydrogen carriers will completely dissolve, their volume is negligible.

Pretreatment: heat exchangers

All hydrogen carriers need to be heated before entering the reactor. The amount and type of heat exchangers depend on the energy converter chosen and the hydrogen carrier.

A heat exchanger with a large heat transfer surface per unit volume is a compact heat exchanger. The ratio of heat transfer surface area to the volume of the heat exchanger is called the area density, denoted with β(Cengel & Ghajar, 2014). Generally speaking, heat exchangers with a β in excess of 700 m^2/m^3 are classified as compact, with heat exchangers in microreactors reaching area densities of over 15000 m^2/m^3 (Cengel & Ghajar, 2014; Reay, Ramshaw, & Harvey, 2008). However, these high-area density heat exchangers, which also include printed circuit heat exchangers, have high pressure drops, making them less suitable for the specific applications addressed in this paper due to the high viscosity of some of the fluids, such as LOHCs (Cengel & Ghajar, 2014). To have an efficient heat exchanger, the thermal conductance of both fluids should be similar (Shah & Sekulić, 2003). This is more likely the case for liquids than for liquid-gas heat exchangers. Thus, liquid-liquid heat exchangers generally require different heat exchangers compared to liquid-gas heat exchangers (Shah & Sekulić, 2003).

The type of heat exchanger is defined by the fluids flowing through it. Generally, heat exchangers can differ depending on the fluid (gas or liquid), viscosity, fouling, pressure and temperature of the fluid (Cengel & Ghajar, 2014; Shah & Sekulić, 2003). As the pressures are similar for all four hydrogen carriers (1-10bars), different heat exchangers are unlikely to be required based on pressures. Fluid types differ, and both liquid-liquid and gas-liquid heat exchangers are required. Similarly, the temperature ranges of the hydrogen carriers vary significantly, as dehydrogenation temperatures range from 353K to 573K. Finally, the viscosity of the different hydrogen carriers differs. The boron-based hydrogen carriers are mixed with water, and these mixtures have viscosities that are relatively similar to water. Dibenzyltoluene is highly viscous at low temperatures, with viscosities of up to 4000 mPas (Müller et al., 2015).

Additionally, several other parameters must be known to evaluate the sizing of heat exchangers, namely, the mass flows, and in- and outlet temperatures of both the hot and cold sides. Thus, the 0D model should provide these mass flows. However, the 0D model uses a fixed heat capacity to calculate the mass flows of the hot side, which may result in small errors. The heat exchangers will all be designed in Aspen Exchanger Design & Rating (EDR), which will adjust the mass flow of the hot fluid when necessary. Aspen EDR can calculate the exact size and mass of heat exchangers and is widely used in industry and heat exchanger design research (K. Hooman, personal communication, November 27 2023). As a basis, the material properties from Aspen are incorporated. When a disagreement occurs between data obtained from any of the Aspen databases and experimental values from the literature, the data from the literature is taken. As the 0D model only incorporates a fixed, heat capacity value, the heat exchanged within a heat exchanger might differ between Aspen and the 0D

model. In these cases, the mass flow of the heat source is adjusted accordingly while checking if the mass flow does not exceed the maximum mass flow according to equation 4.

Expected amount and sequence of heat exchangers

Because we used the 0D model before, we can estimate the amount and sequence of the heat exchangers (van Rheenen, Padding, & Visser, 2023). The boron-based hydrogen carriers are mixed with water before entering the release reactor. This mixture has to be heated as well, and considering the difficulty of heating solid powders, the boron-based hydrogen carriers will be heated as a mixture. Heating the mixture will occur in a heat exchanger and requires only one heat exchanger, as they need to be heated to only 353K. No heat exchangers with spent fuel are used to avoid crystallisation inside heat exchangers. So, either flue gasses or coolant is used to preheat the exothermic-release hydrogen carriers, which are believed to contain enough heat to fulfil the requirements.

The endothermic-release hydrogen carriers, the LOHCs, will likely need more heat exchangers. When applicable, the LOHC will be heated in the first heat exchanger using the coolant from the energy converter. The second heat exchanger uses the spent fuel to heat the LOHC to almost the dehydrogenation temperature. A drawback for NEC here is that its spent fuel turns into a solid at temperatures lower than 343K. Thus, the fuel must be heated to at least 343K before entering the second heat exchanger. Finally, using flue gasses, a third heat exchanger will heat the LOHC until it reaches the dehydrogenation temperature.

After treatment: separator and crystallizer

If the conversion rate of the LOHC is below 100%, a separator may be advantageous. The threshold below which a separator becomes worthwhile depends on the energy density, desired ship range, and volumetric fuel tank requirements. However, if a separator is larger than the additional fuel required to compensate for the lower conversion efficiency, it would not be worth using.

Next to the separator, a crystalliser can crystallise the spent fuel from the water to avoid storing large amounts of spent fuel. This water prevents the spent fuel from crystallising and thus clogging the system. The water required depends on the spent fuel, as the solubility of the spent fuel is lower than that of the fuel itself (Andrieux et al., 2012; Sanyal et al., 2003; Crapse & Kyser, 2011). However, the water also adds a large amount of weight and volume to the spent fuel, reducing the energy density of the whole system. Thus, crystallising the spent fuel is essential, and a crystalliser has to be added to the system. For hydrogen carriers that exothermically release hydrogen, such as sodium borohydride and ammonia borane, the crystalliser's size must be at least as big as the reactor's. In an emergency, the content of the reactor can then be dumped in the cooled crystalliser to stop or at least significantly slow down the hydrogen release reaction. This is unnecessary for hydrogen carriers that release endothermically as withholding heat will stop the reaction.

The sizing of the crystalliser and the separator highly depends on the conversion rate inside the reactor. In turn, this depends on the choice of catalyst, the amount of catalyst, the temperature, the throughput time of the reactor and, for boron-based carriers, the amount of additional water. Especially the catalyst choice is of significant influence and is thus well-researched (Abdelhamid, 2021). Because of the depth of the studies on this subject, it was decided not to incorporate this.

Release reactor

The hydrogen release reactor is where the hydrogen is released from the hydrogen carrier. In this reactor, the hydrogen carrier passes by the catalysts, upon which it reacts and releases hydrogen. Many researchers are studying this process. We refer to Fogler (2016) for more detailed information on release reactors. In this work, however, the release reactor will be modelled as a plug flow reactor, with a jacket around it to provide the necessary heat or cold. The plug flow reactor is as-

sumed to have a membrane to remove the hydrogen. The hydrogen gas will expand vastly and thus significantly influence the reactor's working if not removed immediately.

The dehydrogenation of endothermic-release hydrogen carriers requires heat. A buffer fluid will be used when the heat has to be supplied to the reactor, and the heat source is not considered constant (such as flue gasses). This buffer fluid reduces the system's efficiency but controls the heating system. Using a buffer fluid can prevent overheating of the reactor, which can result in the decomposition of the hydrogen carrier and has to be avoided.

RESULTS AND DISCUSSION

This section discusses the main results. The model is first validated using pinch diagrams and a sensitivity analysis. The sizing of the mixing tank and reactor, as well as the type and sizing of the heat exchangers, is discussed next. It is important to realise that only the components from figure 3 are considered. The storage tanks, engines or fuel cells, and potential hydrogen burners are not considered, despite taking up significant amounts of space. The PEMFC is not considered in the case of ammonia borane. Ammonia borane releases both hydrogen and ammonia. Cracking or storage of ammonia is not deemed feasible and the ammonia will be used as fuel, together with hydrogen (van Rheenen, Padding, & Visser, 2023). This rules out a PEMFC, as ammonia is toxic to PEMFCs and strongly reduces the performance of the PEMFC (Halseid, Vie, & Tunold, 2006). Thus, the figures of ammonia borane will have only three results and the PEMFC is left out.

Validation

The model is validated in multiple ways. Pinch diagrams are used to check whether the heat flows from the 0D model are thermodynamically possible. A sensitivity analysis provides information on the influence of the viscosity on the size of a heat exchanger.

Pinch diagrams

Pinch diagrams are used to validate the results. Pinch diagrams show whether heat exchangers comply with the second law of thermodynamics and also where the design is most constrained. Heat exchangers will correctly transfer heat if the lines representing the hot fluid stay above the lines representing the cold fluid at all times; crossing lines means that the exchanger does not comply with the second law. The design is most constrained at the location where the hot and cold lines are closest, the 'pinch' (Kemp & Shiun Lim, 2020).

Figure 5 gives an overview of four of the pinch diagrams generated by the 0D model. As there are no crossing lines, the required heat exchangers all comply with the second law of thermodynamics. The figures, however, do show interesting differences. Figure 5a is an example of what all pinch diagrams look like for both $NaBH_4$ and ammonia borane: two straight lines, with a sufficiently significant temperature difference (at least 10 K or more). The lines are straight because the mass flow of the flue gas is calculated following the temperature and heat demand: it is less than the total mass flow of the flue gas. Mass flows are more straightforward to regulate than temperatures and lower mass flows require smaller heat exchangers.

Figure 5b gives an overview of an endothermic-release hydrogen carrier, DBT, combined with an ICE. The flue gas of the ICE does not contain sufficient heat to cover the heating demand of the dehydrogenation reactor. Hence, additional heat by burning hydrogen is required. Similarly, figure 5c shows that combining a PEMFC and DBT will result in hydrogen burning necessary for heating and dehydrogenation. The hydrogen used for burning is a loss, as it is first released from DBT but cannot be used for power. This combination is thus unfavourable. Finally, figure 5d shows the combination of NEC and a gas turbine. No additional heat is required as the flue gas (HT) line covers the whole dehydrogenation. Thus, no hydrogen has to be burned. As the spent fuel of NEC is solid at temperatures lower than approximately 343K, the preheating of the

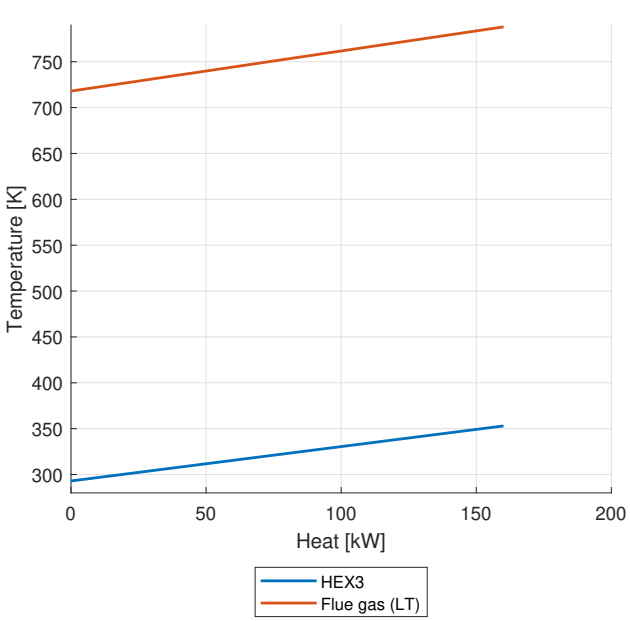

(a) Pinch diagram of $NaBH_4$ combined with an SOFC

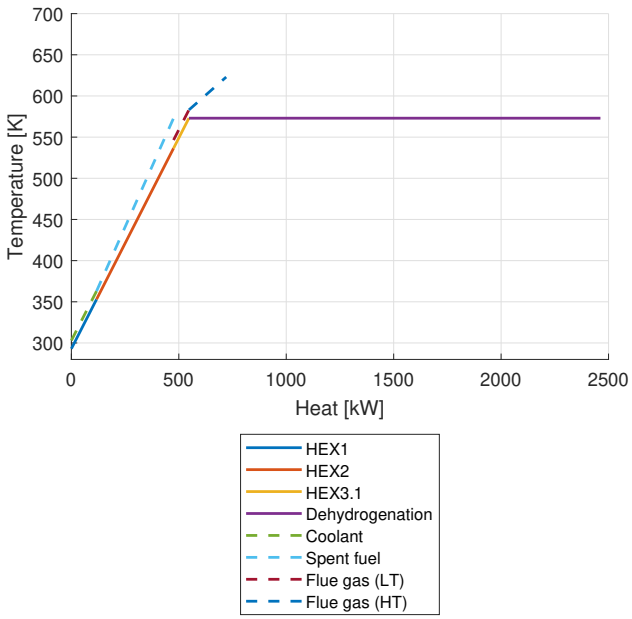

(b) Pinch diagram of DBT combined with an H2-ICE

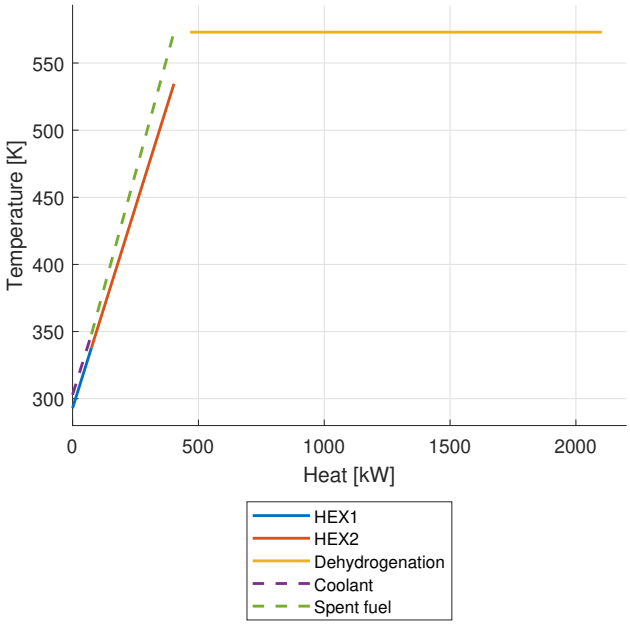

(c) Pinch diagram of DBT combined with a PEMFC

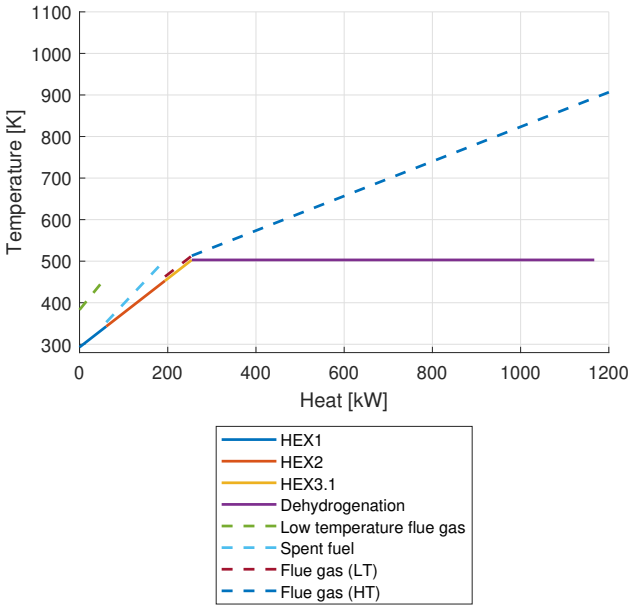

(d) Pinch diagram of NEC combined with a GT

Figure 5: Pinch diagrams for a selected group of hydrogen carriers and energy converters

fuel is done using low-temperature flue gas. This flue gas is not cooled below 373K to avoid condensation in the heat exchanger.

Validation: Influence of viscosity

The viscosity of ammonia borane mixed with water is unknown. Thus, we made an estimation. The level of ammonia borane in the water (3mol/L, (Crapse & Kyser, 2011)) is much lower than the solubility limit. Therefore, low viscosity (1-2 mPas) is assumed. A sensitivity analysis was used to control the influence of small changes in the viscosity on the output of Aspen EDR. The viscosity was changed with a factor of 1.5 and 2, without any changes in the heat exchanger. Thus, such small changes in viscosity are insignificant.

Mixing tank

To estimate the size of the mixing tank, the residence time and the mass flow of the mixture must be known. The residence time is defined by the dissolution time of the crystals, and is strongly influenced by the mixing equipment. The residence time should be sufficient to ensure sufficient mixing to avoid crystallisation. The residence time in mixing vessels for sodium borohydride and ammonia borane is estimated to be relatively short (about 3 minutes), resulting in small mixing tanks. The mixing time is based on data from Aspen for $NaBH_4$. The same mixing time for ammonia borane is taken, as no additional data is available for ammonia borane. Experiments should be performed on the mixing time to estimate the mixing tank size better. Figure 6 gives an overview of the mixing tank size without considering a safety factor.

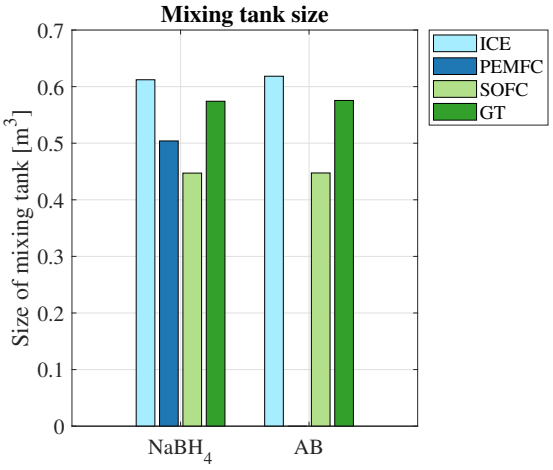

Figure 6: Size of mixing tanks, without safety factor

Heat Exchangers

This section will describe the choice and consequent size of heat exchangers.Table 3 gives an overview of the types of heat exchangers required for the different hydrogen carrier and energy converter combinations.

Choice of heat exchangers

Two main types of liquid-liquid heat exchangers exist: the shell-and-tube heat exchanger and the plate heat exchanger. The shell-and-tube heat exchanger is very common in industrial heat exchangers but is less suitable for the specific applications onboard ships, as they are relatively large and heavy (Cengel & Ghajar, 2014; Shah & Sekulić, 2003). This thus leaves plate

Cold medium	Hot medium	Mediums	Heat exchanger type	Sizing (Order of magnitude)
$NaBH_4$ and NH_3BH_3	Coolant	Liquid-Liquid	Plate	$8 \cdot 10^{-3}$ m^3
$NaBH_4$ and NH_3BH_3	Spent fuel	Liquid-Liquid	Avoided due to crystallisation resulting in possible clogging	N.A.
$NaBH_4$ and NH_3BH_3	Flue gas	Liquid-gas	Plate with fins	$5 \cdot 10^{-3}$ m^3
LOHCs	Coolant	Liquid-Liquid	Plate	$5 \cdot 10^{-3}$ m^3
LOHCs	Spent fuel	Liquid-Liquid	Plate	$8 \cdot 10^{-3}$ m^3
LOHCs	Flue gas (Preheat)	Liquid-gas	Plate with fins	$1 \cdot 10^{-3}$ m^3
Heat transfer fluid	Flue gas	Liquid-gas	Plate with fins	1 m^3
LOHC (dehydrogenation)	Heat transfer fluid	Liquid-Liquid	Jacketed reactor	4 m^3

Table 3: Summary heat exchangers and reactor types and sizes

heat exchangers, which are well suited for liquid-to-liquid heat exchange applications. The main limitation of plate heat exchangers is their unsuitability when large pressure or temperature differences between the hot and cold fluids occur (Cengel & Ghajar, 2014; Shah & Sekulić, 2003). Neither occurs in any of the heat exchangers. Plate heat exchangers are generally cheaper, have less fouling and have shorter residence times than shell and tube heat exchangers (Shah & Sekulić, 2003). As the dehydrogenation processes for all of the mentioned hydrogen carriers occur at only a few bars, and coolants are generally in a similar pressure range, this does not seem to be an issue. Thus, plate heat exchangers are the only type of heat exchangers considered in this research for liquid-to-liquid use.

The only exception to the plate heat exchangers is dehydrogenation reactors' heating (and cooling). The reactor design focuses on the reactor itself and less on the heating or cooling. For simplicity, a jacketed reactor is chosen. The jacket around the reactor can provide necessary heating or cooling. The reactors will be considered plug flow reactors, and the hydrogen is assumed to be immediately removed from the reactor. This latter is required as hydrogen is a gas and takes up a lot of volume. Removing hydrogen gas as soon as possible is essential for the reactor to keep working properly.

For liquid-gas use, plates with fins heat exchangers are used. A sensitivity analysis showed that plate heat exchangers would be significantly larger than plate-with-fins heat exchangers. Plate with fin heat exchangers are often used for liquid-gas heat exchangers, as they can have different surface areas for the gas and the liquid. Gasses usually require larger surface areas due to their lower heat capacities.

Table 3 gives an overview of the types of heat exchangers chosen for each combination of cold and hot fluids, including the type of fluid and the resulting order of magnitude.

Sizing of heat exchangers

Figure 7 gives a more in-depth overview of the sizes of the different heat exchangers. Clear differences between the boron-based hydrogen carriers and the LOHCs can be seen. The LOHCs require several heat exchangers, which are significantly sized, while the boron-based hydrogen carriers require a single, small heat exchanger with a size of several litres. Between the boron-based carriers, the heat exchangers required for heating sodium borohydride (represented in figure 7c) are smaller than those for ammonia borane (figure 7d). This difference is explained by the different amounts of water required for these carriers. Due to the higher solubility limits of the spent fuel of sodium borohydride, less water is required in the process. More water is required in the process for ammonia borane, resulting in a larger overall mass flow, greater heat demand and thus, a larger heat exchanger. These figures also show that heat exchangers that use hot gasses as heat sources can be smaller than liquid-liquid heat exchangers. The internal area of the plate with fins heat exchanger is larger than that of the plate heat exchangers.

The results of the heat exchanger geometry for liquid organic hydrogen carriers differ greatly. The heat exchangers are generally tenfold larger than those of the boron-based hydrogen carriers. From figures 7a and 7b, it appears that the heat ex-

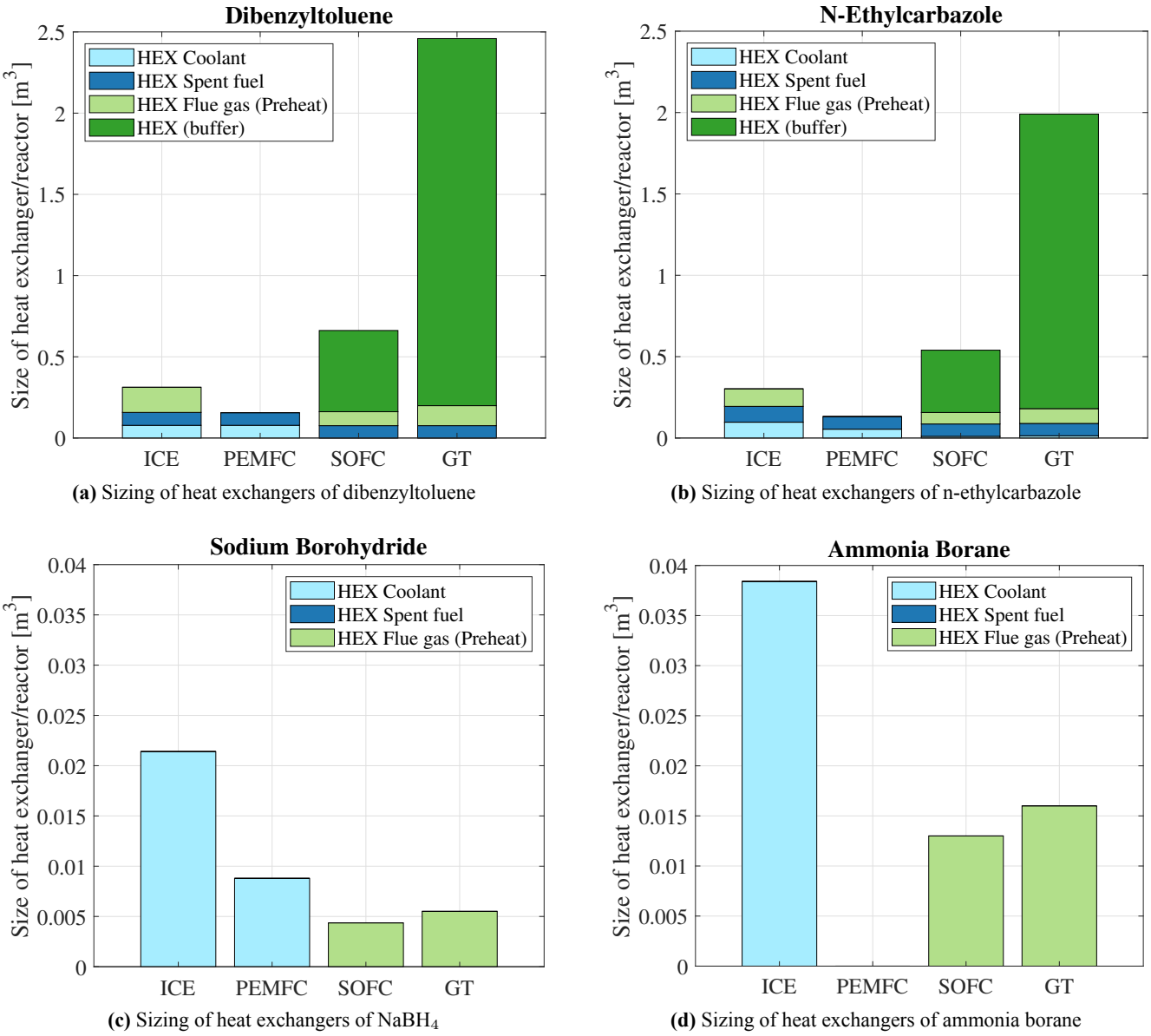

(a) Sizing of heat exchangers of dibenzyltoluene

(b) Sizing of heat exchangers of n-ethylcarbazole

(c) Sizing of heat exchangers of $NaBH_4$

(d) Sizing of heat exchangers of ammonia borane

Figure 7: Sizing of heat exchangers for different hydrogen carriers, additional possible hydrogen heaters are not taken into account

changers, when integrating with an ICE or PEMFC, are significantly smaller than those with a SOFC or GT. However, it should be noted here that the ICE and the PEMFC cannot cover the complete heat requirement of the preheating and dehydrogenation process of the LOHCs. An additional heat source, most likely hydrogen burning, is thus required. This reduces the energy density and efficiency of the system and requires an additional heater. This additional heater also needs to be sized. However, as this is a burner and not a heat exchanger, it is not considered here.

On the other hand, the complete system of heat exchangers required for the SOFC or GT integration can be simulated. Figure 7a shows that heating the buffer fluid results in an extremely large heat exchanger for this system. The large heat demand of the dehydrogenation process can explain this. The complete flue gas flow is required to heat the buffer fluid sufficiently. For both N-ethylcarbazole and dibenzyltoluene, the differences between the gas turbine and the SOFC buffer-fluid heat exchanger are significant. These differences occur due to the mass flow of the flue gas of a gas turbine and SOFC. The mass flows are calculated using equation 4. As the SOFC has a larger temperature difference, the mass flow is consequently less than for the GT, with a smaller temperature difference. Additionally, the SOFC has a higher efficiency and, as visible

in table 2, the overall component of the total available power going to heat is less for an SOFC than for a GT. Thus, combined, the mass flow of an SOFC is much lower than that of a GT, resulting in a smaller heat exchanger. However, figure 7a shows much larger heat exchangers in general, especially visible in the buffer, but also the other heat exchangers (for all energy converters) are larger. This difference occurs because dbt generally requires more heat, both for preheating and dehydrogenating. In figure 7b, a very small, additional heat exchanger is visible, which is required as the spent fuel of NEC should not be used to preheat the fuel at low temperatures. The spent fuel freezes at around 343K and should thus not be cooled down strongly. Thus, a heat exchanger must be added to do the first flue gas cooling step. These heat exchangers are generally very small, approximately 10L.

Knowing the size of the heat exchangers is not the only result of this study. The sequence and amount of heat exchangers is also an important input for ship design. As all the heat exchangers have to be connected to each other and different heat sources, they introduce limitations to the ship's design (Souflis-Rigas et al., 2023). These limitations occur less when using fewer and smaller heat exchangers; the design freedom when incorporating boron-based hydrogen carriers is thus much higher compared to LOHCs.

Reactor

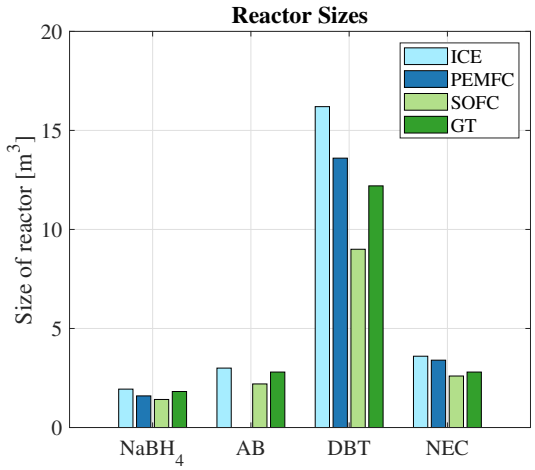

Figure 8: Estimated reactor sizes of different hydrogen carriers for different energy converters

Figure 8 gives an overview of the reactor sizes. The reactor size depends largely on the throughput time. In this case, a throughput time which results in a high conversion rate (>95%) is chosen. The throughput time can be shorter for lower conversion rates. The conversion rate depends on the temperature, catalyst, reaction rate, type of reactor, and more (Brückner et al., 2014; Abdelhamid, 2021). Additionally, catalyst packing influences the volume size. In all of the cases, a packing factor of 0.5 is considered. The throughput time and conversion rate do not depend on the energy converter. The differences for each energy converter, as visible in figure 8, occur due to different mass flows. Higher mass flows with the same throughput time result in a larger reactor size.

Experiments are generally required to calculate conversion rates and throughput times. These conversion rates and throughput times strongly influence the reactor size and the hydrogen release rate. Literature shows this as well. $NaBH_4$, for example, was reported to have throughput times of 1 to 2 hours (Li & Kim, 2012), whereas more recently, throughput times in the order of 20 minutes have been reported (Erat, Bozkurt, & Özer, 2022). Thus, they form an area of very active research, as the hydrogen release rate influences the suitability and usability of a hydrogen carrier. As this area of research is very specialised, we only considered known throughput times with a high conversion rate (Brückner et al., 2014; Qiu, Wu, Wu, Liu, & Huang, 2016; Erat et al., 2022). Figure 8 clearly demonstrates the requirement for low throughput times, as the difference in reactor size is large.

Overview of total required components

Figure 9 gives an overview of the total sum of the size of the required components. Each of the specific components is influenced by several factors, each with its own levels of reliability. Thus, the resulting sum of the sizes is an indication. The reactor size is the main influence of the components' total sizing. This figure clearly shows that the equipment's total size does not differ too much if the throughput time of the reactor is low enough. The relatively large heat exchangers required for NEC and DBT are only relevant if the reactor size is similar to that of $NaBH_4$ and ammonia borane. Even then, the overall sizing of the equipment is similar. The size of the mixing tank required for $NaBH_4$ and ammonia borane is similar to the heat exchangers required for DBT and NEC (except when combining these with a GT, in which case the heat exchangers are significantly larger).

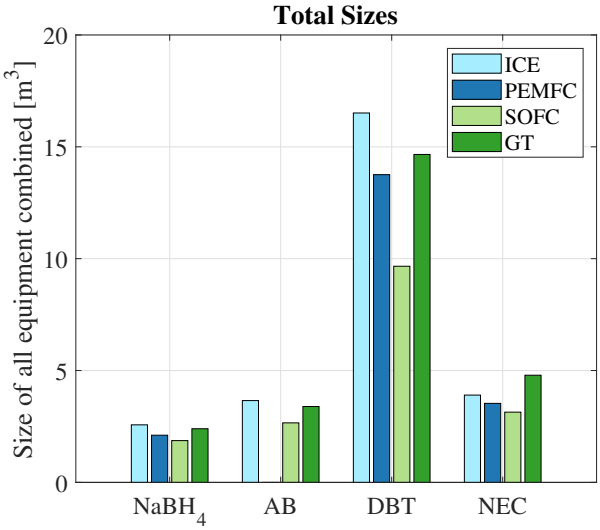

Figure 9: Overview of sizing of all components

CONCLUSION AND RECOMMENDATIONS

The sizing of all relevant components must be known to estimate the possible ship design changes required for incorporating hydrogen carriers as the power source. This research aims to give an overview of all the relevant components and their sizes.

The size of the release reactor is most significant for all hydrogen carriers. Further research on catalysts will hopefully result in shorter throughput times. This research clearly shows the benefit of shorter throughput times, as these strongly influence the reactor sizing. As this reactor has to be placed in a specialised room (due to the release of hydrogen), having an exact size is important. The reactors required for ammonia borane appear slightly larger than those for sodium borohydride reactors. This size largely depends on the throughput time and dehydrogenation rate. The other components, such as heat exchangers and a mixing tank, are significantly smaller than the reactor. The heat exchangers are of such small size that it is unlikely they will influence ship design.

The sizing of heat exchangers is of importance only for LOHCs. The heat exchangers required to heat the buffer fluid are especially large. When no buffer fluid is required, and the main part of heating has to be done using hydrogen, no estimates on equipment size have been made. In general, the heat exchangers required to preheat and, when possible, provide enough heat for the dehydrogenation process of LOHCs are large and numerous. As these heat exchangers need to be in a fixed sequence and use waste heat, they create limitations on the ship design. Additionally, all of the equipment for DBT is larger than that for NEC.

All in all, the boron-based carriers pose fewer limitations to ship design. The required equipment is smaller and less numerous, even though it is still in a fixed sequence. In all cases except for the PEMFC, only three components are necessary: a mixing tank, a single heat exchanger and a reactor vessel. When a PEMFC is used, a small hydrogen burner is also required. For LOHCs, more and larger components are needed. The only setups in which no hydrogen burner is required need at least 3 (for DBT) or 4 (for NEC) heat exchangers. Besides these, a reactor is also required.

To design ships using hydrogen carriers, knowing the amount of components and their sizing is imperative. This research has given an overview of all required components and estimated the sizing of each of these components. This is the first step in designing zero-emission ships powered by hydrogen carriers.

CONTRIBUTION STATEMENT

E.S. van Rheenen: Conceptualization; data curation; methodology; visualisation; writing – original draft. **J.T. Padding:** conceptualization; methodology; supervision; writing – review and editing. **A.A. Kana:** conceptualization; methodology; supervision; writing – review and editing. **K. Visser:** conceptualization; methodology; supervision; writing – review and editing.

ACKNOWLEDGEMENTS

This work was supported by the project SH2IPDRIVE, which has received funding from the Ministry of Economic Affairs and Climate Policy, RDM regulation, carried out by the Netherlands Enterprise Agency (RvO).

REFERENCES

Abdelhamid, H. N. (2021). A review on hydrogen generation from the hydrolysis of sodium borohydride. *International Journal of Hydrogen Energy*, *46*(1), 726-765. doi: 10.1016/j.ijhydene.2020.09.186

Andrieux, J., Laversenne, L., Krol, O., Chiriac, R., Bouajila, Z., Tenu, R., … Goutaudier, C. (2012). Revision of the nabo2–h2o phase diagram for optimized yield in the h2 generation through nabh4 hydrolysis. *International Journal of Hydrogen Energy*, *37*(7), 5798-5810. (XII International Symposium on Polymer Electrolytes: New Materials for Application in Proton Exchange Membrane Fuel Cells) doi: 10.1016/j.ijhydene.2011.12.106

Asif, F., Hamayun, M. H., Hussain, M., Hussain, A., Maafa, I. M., & Park, Y.-K. (2021). Performance analysis of the perhydro-dibenzyl-toluene dehydrogenation system—a simulation study. *Sustainability*, *13*(11). doi: 10.3390/su13116490

Brückner, N., Obesser, K., Bösmann, A., Teichmann, D., Arlt, W., Dungs, J., & Wasserscheid, P. (2014, 01). Evaluation of industrially applied heat-transfer fluids as liquid organic hydrogen carrier systems. *ChemSusChem*, *7*. doi: 10.1002/cssc.201300426

Cengel, Y. A., & Ghajar, A. J. (2014). *Heat and mass transfer: Fundamentals and applications* (5th ed.). New York, NY: McGraw-Hill Professional.

Chandra, M., & Xu, Q. (2007, 5). Room temperature hydrogen generation from aqueous ammonia-borane using noble metal nano-clusters as highly active catalysts. *Journal of Power Sources*, *168*, 135-142. doi: 10.1016/J.JPOWSOUR.2007.03.015

Crapse, K., & Kyser, E. (2011). *Literature review of boric acid solubility data* (Tech. Rep.). Savannah River National Laboratory (SRNL). doi: 10.2172/1025802

de Vos, P., de van der Schueren, T., Los, S., & Visser, K. (2022). Effective naval power plant design space exploration.. doi: 10.24868/10680

Demirci, U. B. (2020). Ammonia borane: An extensively studied, though not yet implemented, hydrogen carrier. *Energies*, *13*(12). doi: 10.3390/en13123071

Dimitriou, P., & Tsujimura, T. (2017). A review of hydrogen as a compression ignition engine fuel. *International Journal of Hydrogen Energy*, *42*(38), 24470-24486. doi: 10.1016/j.ijhydene.2017.07.232

Erat, N., Bozkurt, G., & Özer, A. (2022). Co/cuo–nio–al2o3 catalyst for hydrogen generation from hydrolysis of nabh4. *International Journal of Hydrogen Energy*, *47*(58), 24255-24267. (Hydrogen Sourced from Renewables and Clean Energy: Feasibility of Large-scale Demonstration Projects) doi: 10.1016/j.ijhydene.2022.05.178

Fogler, H. S. (2016). *Elements of chemical reaction engineering*. Prentice Hall.

Gohary, M. M. E., & Seddiek, I. S. (2013, 3). Utilization of alternative marine fuels for gas turbine power plant onboard ships. *International Journal of Naval Architecture and Ocean Engineering*, *5*, 21-32. doi: 10.2478/IJNAOE-2013-0115

Halseid, R., Vie, P. J., & Tunold, R. (2006). Effect of ammonia on the performance of polymer electrolyte membrane fuel cells. *Journal of Power Sources*, *154*(2), 343-350. (Selected papers from the Ninth Ulm Electrochemical Days) doi: 10.1016/j.jpowsour.2005.10.011

Haynes, W. M. (Ed.). (2011). *CRC handbook of chemistry and physics, 92nd edition* (92nd ed.). Boca Raton, FL: CRC Press.

Kemp, I. C., & Shiun Lim, J. (2020). Chapter 3 - key concepts of pinch analysis. In I. C. Kemp & J. Shiun Lim (Eds.), *Pinch analysis for energy and carbon footprint reduction (third edition)* (Third Edition ed., p. 35-61). Butterworth-Heinemann. doi: 10.1016/B978-0-08-102536-9.00003-5

Kojima, Y. (2019, 7). Hydrogen storage materials for hydrogen and energy carriers. *International Journal of Hydrogen Energy*, *44*, 18179-18192. doi: 10.1016/J.IJHYDENE.2019.05.119

Kwak, Y., Kirk, J., Moon, S., Ohm, T., Lee, Y. J., Jang, M., … Kim, Y. (2021, 7). Hydrogen production from homocyclic liquid organic hydrogen carriers (lohcs): Benchmarking studies and energy-economic analyses. *Energy Conversion and Management*, *239*, 114124. doi: 10.1016/J.ENCONMAN.2021.114124

Lee, S., Kim, T., Han, G., Kang, S., Yoo, Y. S., Jeon, S. Y., & Bae, J. (2021, 10). Comparative energetic studies on liquid organic hydrogen carrier: A net energy analysis. *Renewable and Sustainable Energy Reviews*, *150*. doi: 10.1016/j.rser.2021.111447

Li, Q., & Kim, H. (2012). Hydrogen production from nabh4 hydrolysis via co-zif-9 catalyst. *Fuel Processing Technology*, *100*, 43-48. doi: 10.1016/j.fuproc.2012.03.007

Müller, K., Stark, K., Emel'yanenko, V. N., Varfolomeev, M. A., Zaitsau, D. H., Shoifet, E., … Arlt, W. (2015). Liquid organic hydrogen carriers: Thermophysical and thermochemical studies of benzyl- and dibenzyl-toluene derivatives. *Industrial & Engineering Chemistry Research*, *54*(32), 7967-7976. doi: 10.1021/acs.iecr.5b01840

Niermann, M., Beckendorff, A., Kaltschmitt, M., & Bonhoff, K. (2019, 3). Liquid organic hydrogen carrier (lohc) – assessment based on chemical and economic properties. *International Journal of Hydrogen Energy*, *44*, 6631-6654. doi: 10.1016/j.ijhydene.2019.01.199

Pawling, R., Bucknall, R., & Greig, A. (2022). Considerations for future fuels in naval vessels. *Conference Proceedings of INEC*. doi: 10.24868/10676

Preuster, P., Fang, Q., Peters, R., Deja, R., Nguyen, V. N., Blum, L., … Wasserscheid, P. (2018, 1). Solid oxide fuel cell operating on liquid organic hydrogen carrier-based hydrogen – making full use of heat integration potentials. *International Journal of Hydrogen Energy*, *43*, 1758-1768. doi: 10.1016/J.IJHYDENE.2017.11.054

Qiu, X., Wu, X., Wu, Y., Liu, Q., & Huang, C. (2016). The release of hydrogen from ammonia borane over copper/hexagonal boron nitride composites. *RSC Adv.*, *6*, 106211-106217. doi: 10.1039/C6RA24000C

Reay, D., Ramshaw, C., & Harvey, A. (2008). Chapter 4 - compact and micro-heat exchangers. In *Process intensification* (p. 77-101). Oxford: Butterworth-Heinemann. doi: 10.1016/B978-0-7506-8941-0.00005-5

Rosado, D. M., Chavez, S. R., & de Carvalho Jr, J. (2019, 10). Determination of global efficiency without/with supplementary burning of a thermoelectric plant with combined cycle of natural gas.. doi: 10.26678/ABCM.COBEM2019.COB2019-0024

Sanyal, U., Demirci, U. B., Jagirdar, B. R., & Miele, P. (2003). Hydrolysis of ammonia borane as a hydrogen source: Fundamental issues and potential solutions towards implementation. *ChemSusChem*, *4*. doi: 10.1002/cssc.201100318

Shah, R. K., & Sekulić, D. P. (2003). *Fundamentals of heat exchanger design*. John Wiley & Sons.

Souflis-Rigas, A., Pruyn, J., & Kana, A. (2023). Establishing the influence of methanol fuelled power propulsion and energy systems on ship design. In *Proceedings of moses2023 conference.* doi: 10.59490/moses.2023.658

Stark, K., Emelyanenko, V. N., Zhabina, A. A., Varfolomeev, M. A., Verevkin, S. P., Müller, K., & Arlt, W. (2015, 8). Liquid organic hydrogen carriers: Thermophysical and thermochemical studies of carbazole partly and fully hydrogenated derivatives. *Industrial and Engineering Chemistry Research*, *54*, 7953-7966. doi: 10.1021/ACS.IECR.5B01841

Stephens, F. H., Pons, V., & Tom Baker, R. (2007). Ammonia–borane: the hydrogen source par excellence? *Dalton Trans.*, 2613-2626. doi: 10.1039/B703053C

Teichmann, D., Stark, K., Müller, K., Zoettl, G., Wasserscheid, P., & Arlt, W. (2012, 09). Energy storage in residential and commercial buildings via liquid organic hydrogen carriers (lohc). *Energy Environ. Sci.*, *5*, 9044-9054. doi: 10.1039/C2EE22070A

van Rheenen, E. S., Padding, J. T., Slootweg, J. C., & Visser, K. (2023). Hydrogen carriers for zero-emission ship propulsion using pem fuel cells: an evaluation. *Journal of Marine Engineering & Technology*, 1-18. doi: 10.1080/20464177.2023.2282691

van Rheenen, E. S., Padding, J. T., & Visser, K. (2023). A 0d model for the comparative analysis of hydrogen carriers in ship's integrated energy systems. In *Proceedings of moses2023 conference.*

van Veldhuizen, B., van Biert, L., Amladi, A., Woudstra, T., Visser, K., & Aravind, P. (2023). The effects of fuel type and cathode off-gas recirculation on combined heat and power generation of marine sofc systems. *Energy Conversion and Management*, *276*, 116498. doi: 10.1016/j.enconman.2022.116498

Wang, X., Sun, B.-G., & Luo, Q.-H. (2019, 2). Energy and exergy analysis of a turbocharged hydrogen internal combustion engine. *International Journal of Hydrogen Energy*, *44*, 5551-5563. doi: 10.1016/J.IJHYDENE.2018.10.047

Ye, L., Li, D., Dong, Y. P., Xu, B., & Zeng, D. (2020, 5). Measurement of specific heat capacity of nabo2(aq) solution and thermodynamic modeling of nabo2 + h2o, nabo2 + nacl + h2o, and nabo2 + na2so4 + h2o systems. *Journal of Chemical and Engineering Data*, *65*, 2548-2557. doi: 10.1021/ACS.JCED.9B01182

Zhang, J., Fisher, T. S., Gore, J. P., Hazra, D., & Ramachandran, P. V. (2006, 12). Heat of reaction measurements of sodium borohydride alcoholysis and hydrolysis. *International Journal of Hydrogen Energy*, *31*, 2292-2298. doi: 10.1016/J.IJHYDENE.2006.02.026

Zhao, L., Brouwer, J., James, S., Siegler, J., Peterson, E., Kansal, A., & Liu, J. (2017). Dynamic performance of an in-rack proton exchange membrane fuel cell battery system to power servers. *International Journal of Hydrogen Energy*, *42*(15), 10158-10174. doi: 10.1016/j.ijhydene.2017.03.004

Proceedings of 15th International Marine Design Conference (IMDC-2024)
June 2-6, 2024
Amsterdam, the Netherlands

Simulation of LNG-Battery Hybrid Tugboat Under the Influence of Environmental Loads and Manoeuvre

Sharul Baggio Roslan[1], Dimitrios Konovessis[2], Joo Hock Ang[3], Nirmal Vineeth[3] and Zhi Yung Tay[1,*]

ABSTRACT

This paper presents a system modelling approach aimed at designing and simulating real-time conditions, with a specific focus on extreme scenarios to assess the impact on the annual CO_2 emissions and the consumption of LNG and batteries in a hybrid tugboat. Environmental variables such as wave period, wave height, current speed, and wind speed are considered. The tugboat system model is validated using manually logged historical operational data from a similar tugboat profile using both AMESIM and MATLAB\Simulink to simulate diverse environmental conditions and estimate annual fuel operational costs and emissions. A comparative analysis of the different system configurations is then conducted between traditional diesel, LNG and several control configurations of LNG-battery hybrid. Results demonstrate a significant reduction of 96.5% in CO_2 emissions and a 95.3% decrease in annual fuel operational costs with the adoption of LNG-battery hybrid propulsion with the rule-based control system. The study notes a slight increase in vessel operational time by 10.8% due to higher wave heights and a 0.97% rise in added resistance from increased wind speed. Insignificant differences are observed in variations of wave period and current speed. Additionally, the CII ratings of the different system configurations were then compared and concluded with the LNG-battery hybrid with a rule-based control system being the most environmentally and economically sustainable.

KEYWORDS

Hybrid Marine Power System; LNG; Hybrid Tugboat; Energy Efficiency Operation Index; Carbon Intensity Indicator; System Modelling; System Optimisation; Control Strategies; Rule-Based Control; Energy Management System; Carbon Emissions; Fuel Cost

1. INTRODUCTION

Given Singapore's standing as home to one of the world's busiest ports, addressing greenhouse gas (GHG) emissions has become a top priority. The Marine Port Authority (MPA) targets ensuring that by 2030, all newly commissioned harbor vessels operating within Singapore's port waters will either be entirely electric, have the capacity to utilise B100 biofuel or be compatible with net-zero fuels like hydrogen. Vessel owners are mandated to collaborate with MPA on these designs by 2027 (Maritime & Port Authority Of Singapore, 2023). The MPA's initiative serves as a strategy to ready operational vessels for compliance with the MARPOL Annex VI, established by the International Maritime Organization (IMO) in 2016, aiming to halve annual GHG emissions by 2050 (International Maritime Organization, 2016), with an intermediate target of a 40% reduction by 2030 and an even more substantial 70% reduction by 2050. Additionally, stringent emissions limits, such as the 0.5% m/m marine sulfur content limit in emission-controlled areas (ECA) implemented in January 2020 (International Maritime Organisation, 2019), have necessitated vessel owners to explore diverse methods to curtail CO_2 emissions (Tadros *et al.*, 2023). This includes the adoption of scrubbers/exhaust gas clearing systems, carbon capture and storage, or net-zero fuel sources like

[1] Singapore Institute of Technology (Engineering, Singapore Institute of Technology, Singapore); ORCID: 0009-0007-4642-2216
[2] National Technical University of Athens (School of Naval Architecture and Marine Engineering, Athens, Greece); ORCID: 0000-0003-0085-4690
[3] Seatrium Limited (Seatrium Limited, Singapore)

[*] Corresponding Author: zhiyung.tay@singaporetech.edu.sg; ORCID: 0000-0003-3194-1965

Submitted: 23 February 2024, Revised: 30 April 2024, Accepted: 1 May 2024, Published: 24 May 2024

Conference paper, DOI: https://doi.org/10.59490/imdc.2024.897 e-ISSN: 3050-486

hydrogen, ammonia, or LNG (Mallouppas & Yfantis, 2021). With the various results from reducing emissions, the results are then assessed based on two new indexes introduced by the 76th Marine Environment Protection Committee (MEPC) (The Marine Environment Protection Committee, 2021). The Efficient Existing Ship Index (EEXI), the annual carbon intensity indicator (CII) operation report and the CII rating that was implemented in 2023. The EEXI applies to existing ships and requires these ships to fulfil the minimum energy efficiency standards, otherwise, the ship may need to implement technical and operational measures to improve its energy efficiency (ClassNK, 2021). CII ratings and annual CII operational reports are required for vessels of more than 5,000. CII ratings are based on the ship's CO_2 emissions during an operation, achieving a grade "A" CII rating signifies a highly efficient ship in reducing carbon emissions during operation. Ships with a rating of "D" or "E" for three consecutive years are required to develop a corrective action plan. A past study by Ejder and Arslanoğlu (2022) on CII explored using ammonia fuel engines, identifying potential savings of 12,660.07 tonnes of CO_2 and achieving an 'A' CII rating. However, the $5 million retrofitting cost makes building a new ship more economically viable. Another study by Gianni *et al.* (2022) assessed various power configurations for a cruise ship not meeting CII regulations. Only marine gas oil (MGO) failed to comply with the 2024 CII regulations, while LNG power was the sole option capable of securing an 'A' CII rating until 2026.

Given the urgent need to decrease GHG emissions, it is important to explore alternative solutions. Notably, there has been a surge in technological advancement and the widespread commercial adoption of electrical or hybrid propulsion in recent years. The earliest application of electrical propulsion in vessels existed since the 1990s, primarily used in military and cruise ships (Moreno, 2007) and the world's first electric-powered car ferry, the Ampere, was built later in 2015 (Ship Technology, 2015). The electrical propulsion system provides higher efficiency lower carbon emission or zero emission in low loading conditions (Tay & Konovessis, 2023), and overall reduces operational cost. Since LNG shrinks by a factor of 1/600 during liquification, it becomes easier to be transported around making it more accessible when compared to other alternative fuels, hybrid propulsion using natural gas-powered engines or batteries has also recently seen an increase in popularity (Roslan *et al.*, 2022). A few noteworthy research studies, including Vadset (2018) thesis which delved into LNG-powered systems. Vadset's research specifically explored LNG–battery hybrid systems, comparing those with variable speeds to full-LNG systems. The study revealed that a variable-speed LNG-battery system could achieve a 20% reduction in fuel costs compared to a fixed-speed fully LNG system. Another significant research from Lebedevas *et al.* (2021) conducted notable past research on the utilisation of LNG dual-fuel engines for tugboats. Their work achieved reductions of 10%, 91%, and 65% in CO2, SO2, and NOX emissions, respectively. Compared to utilising diesel, using a hybrid diesel-LNG propulsion system saves 33% on fuel costs. Moreover, LNG serves as a cost-efficient fuel with the potential to cut down CO_2 emissions by 26%, and it is sulphur-free, although the presence of methane slip may diminish its environmental advantages (Karaçay & Özsoysal, 2021). The authors are not aware of many studies focusing on the LNG–battery hybrid system, especially in the context of tugboats. This gap in research serves as the motivation for exploring this subject in the current paper.

In addition to enhancing emissions through the incorporation of renewable energy, it is important to explore ways to boost ship energy efficiency. This involves investigating the most optimised environmental conditions for optimal operation to achieve further reduction in emissions. Some noteworthy research on the impact of environmental factors on energy consumption has been conducted. A study done by Lindstad *et al.* (2013) revealed that a 4m head wave could increase energy consumption by up to 35%, while an 8m wave height might lead to a doubling of energy consumption for a bulk carrier. A study which explored different conditions of wind speed, wind direction and wave height conducted by Wang *et al.* (2023), managed to reduce fuel consumption by 3.38%. Currently, there is limited research employing system modelling on the impact of environmental loads on the performance and manoeuvrability of an LNG-battery hybrid system. This led to incorporating the topic into the current. While the selection of a route significantly influences a ship's efficiency, this paper specifically focuses on a fixed operational route. Future research is encouraged to explore route optimisation-based solutions based on the most efficient conditions discovered in this paper.

This study aims to evaluate the environmental and economic effects of adopting a LNG–battery hybrid propulsion system in a 65-ton tugboat in comparison to utilising diesel or LNG as the sole propulsion system. By utilizing data obtained from a comparable diesel-powered tugboat, the study profiles the loading operations of the modelled tugboat. The hybrid LNG–battery tugboat system is created in MATLAB/Simulink® and a diesel-powered tugboat is created in AMESIM, the full system breakdown is described in Section 2. The case study adopted for this study was obtained based on the design operational profile. Several different environmental conditions are tested to analyse the effects of varying environmental conditions on the engine load, annual fuel operation cost and annual CO_2 emissions emitted. Finally, an assessment was conducted to compare the CII rating of an LNG-battery hybrid system, employing rule-based control and various load distribution strategies, against conventional diesel and LNG systems. The goal was to identify the system with the best rating and economically and environmentally beneficial. Although CII ratings are not required for vessels below 5,000GT, this paper will neglect the weight requirements and categorise the tugboat as a cruise passenger ship for comparison purposes. The rule-based control and load distribution strategies adopted from this study are based on a past study conducted by the author (Roslan, Konovessis, *et al.*, 2023; Roslan, Tay, *et al.*, 2023). Further development of the system modelling could be conducted with the advancement of digital twins that incorporates machine learning (Abebe *et al.*, 2020; Cheliotis *et al.*, 2020; Fam *et al.*, 2022; Hadi *et al.*, 2022a; Tay, Z.Y.; Hadi, J; Konovessis, D.; Loh, D.J.; Tan, D.K.H; Chen, 2021; Tay *et al.*, 2021) and big data analytics (Hadi *et al.*, 2022b; Mirović *et al.*, 2018).

The paper is structured as follows: Section 2 provides an overview of the tugboat, details of the methodology for obtaining the vessel loading profile, and a brief description of both the diesel-powered tugboat system modelled on AMESIM and the hybrid LNG–-battery power system modelled on Simulink. In Section 3, a mathematical overview is presented for the comparison study. Section 4 compares the annual operation cost and annual CO_2 emissions across different cases and configurations. Finally, Section 5 concludes with a summary of the work and provides recommendations for future research.

2. SYSTEM OVERVIEW

The diagrams of both the diesel and LNG-battery hybrid tugboats are shown in Figure 1 and Figure 2, respectively. Figure 1 shows the system diagram of a diesel tugboat. Operational data from JMS Kappa was acquired due to its resemblance in operational requirements and vessel architecture. The diesel tugboat is equipped with two diesel engine generators as a primary source, with a rated output of 1,471kW, and rated speed of 750rpm and a low output nominal voltage of 400V generator with a capacity of 1,390kWe for the auxiliary load (IHI, 2022). The auxiliary load includes service and hotel loads, heating, ventilation and air-conditioning (HVAC), lighting and pumps. The two diesel engines are then directly connected to a gearbox, to reduce engine speed and reversing shaft rotation. Subsequently, connected to an azimuth thruster individually. The diesel power system is modelled in Simcenter AMESIM to replicate the dynamic response of the system.

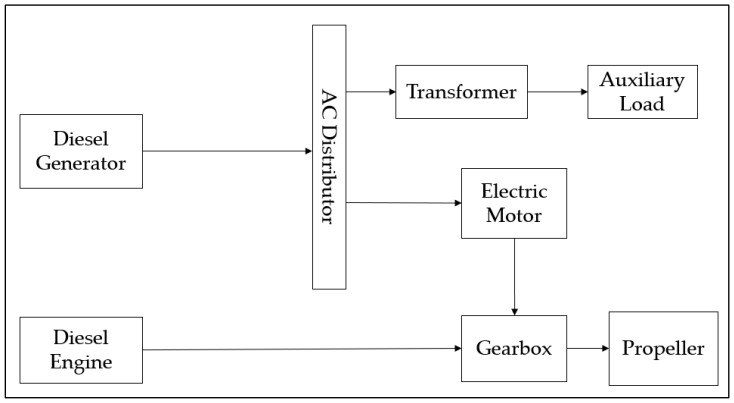

Figure 1. Simplified diagram of a diesel-electric vessel power system.

The tugboat's hybrid power system, shown in Figure 2, utilises two LNG generator sets (Gensets) with a maximum output of 1,492 kW, 1,600 rpm speed, and 545 V voltage for primary power generation. Additionally, two lithium-ion batteries, each with a 452 kWh capacity, provide energy storage. The vessel loads include the two azimuth thrusters with ducted propellers, service and hotel load, HVAC, lighting and pumps. A 1,000 V modern direct current (DC) distribution system is used in the present system due to its simplicity and fuel efficiency (Zahedi *et al.*, 2014). To streamline the system, AC power from the Gensets flows through a rectifier to become DC, while the battery directly feeds the DC distribution. This reduces equipment and boosts round-trip efficiency. The hybrid power system is modelled in MATLAB/Simulink® to simulate the dynamic response of the system.

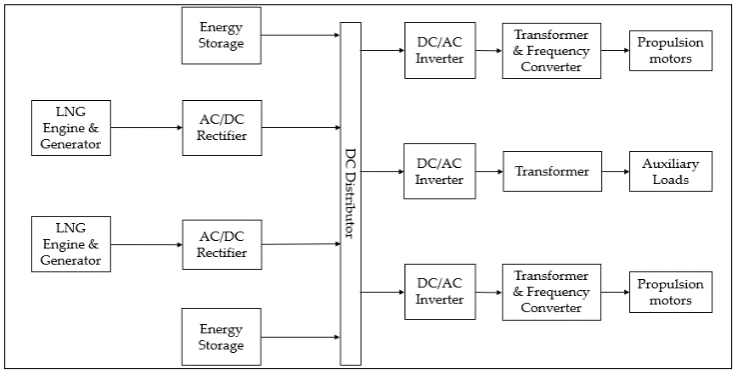

Figure 2. Diagram of LNG–battery hybrid vessel power system

2.1 Loading Profile

This study focuses on a 65-tonne tugboat equipped with two Gensets and batteries. The three primary operational modes categorised in this study are (i) idle or standby: in this mode, the vessel load ranges below 520kW and is either stationary or travelling along with the current. (ii) Transit: During transit, the speed and vessel load range between 6 - 12 knots 550kW and

1,100kW, respectively. (iii) Tugging: When performing tugging operations, the vessel load ranges up to a maximum load of 1,492kW, however, it averages 540kW with varying travelling speeds. The tugboat's operational time-domain load profile was created based on past studies done by the authors (Roslan, Konovessis, *et al.*, 2023; Roslan, Tay, *et al.*, 2023), utilising a combination of data manually recorded during an operational on the diesel tugboat, JMS Kappa, and the designed operational profile of the LNG-hybrid tugboat provided by the industrial collaborators.

2.2 Modelling of Diesel Propulsion System on Simcenter AMESIM

The Simcenter AMESIM model of the diesel propulsion tugboat consists of two major parts, i.e., the diesel generator set (genset) and vessel resistance shown in Figure 3. The system model shown is based on combinations of examples found in the Simcenter AMESIM library, with the values reconfigured to suit the parameters of JMS Kappa.

.

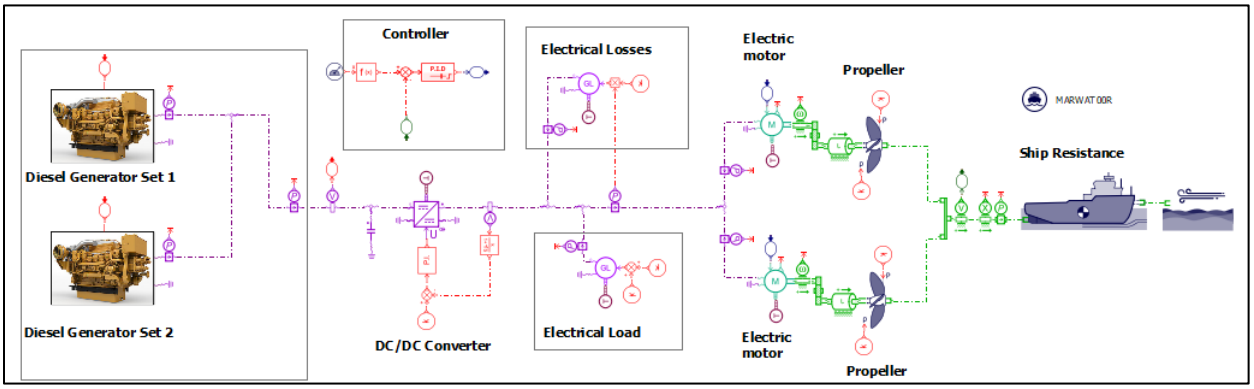

Figure 3. Model of the diesel power system in Simcenter AMESIM

2.2.1 Diesel Genset

The diesel engines are the main energy source for the diesel-powered tugboat. The generators are made up of diesel engines – DRVICE01H connected to electrical machines – DRVEMO3. The electrical generators then provide power through the DC/DC converter to two electrical motors that are connected to the propellers – MARPROP00, with a gear reduction system. The model also factors estimated auxiliary electrical load and electrical losses of 500kW and 0.5%, respectively. The parameters of the diesel genset – Niigata 6L26HLX, are based on the performance curves provided by the engine provider which are then replicated to the diesel engine model using the DRVICE table creator.

2.2.2 Vessel Resistance

The vessel resistance was based on CFD results shown in Figure 4, done on ANSYS Fluent and Finemarine with similar hull parameters to JMS Kappa. The results are then exploited and input into the vessel model, MARSHIP00, vessel resistance as a function of ship velocity. Speed ranging outside of the results provided are extrapolated linearly.

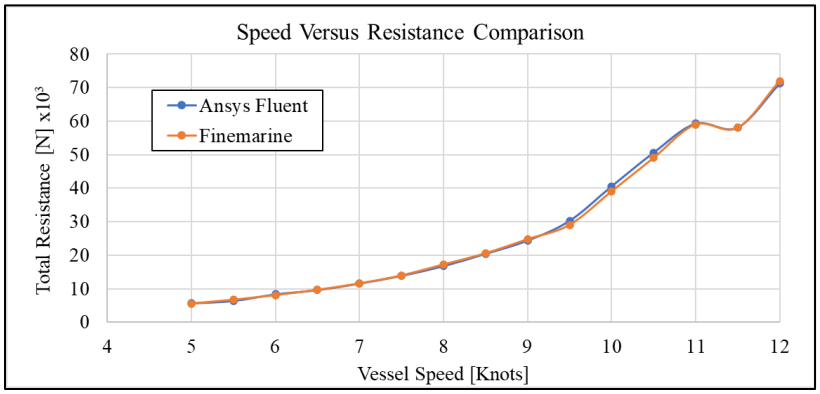

Figure 4. Vessel speed against resistance CFD results

The complete vessel route used in the study is shown in Figure 5, generated from the AMESIM Simcenter system simulation results and overlayed with Google Maps for easier visualisation. The operation observed in this study is based on data manually logged by the author during an operation. The route comprises segments of the tugboat cruising at high speed, tugging a vessel to an area near the shipyard and cruising back to the tugboat's original dock. The return trip of the tugboat in the example used

is assumed to be travelling along the same route taken to travel out, in reality the tugboat operator may prefer to use alternative routes depending on the traffic or other operation demands. The load distribution is discussed in Section 4.

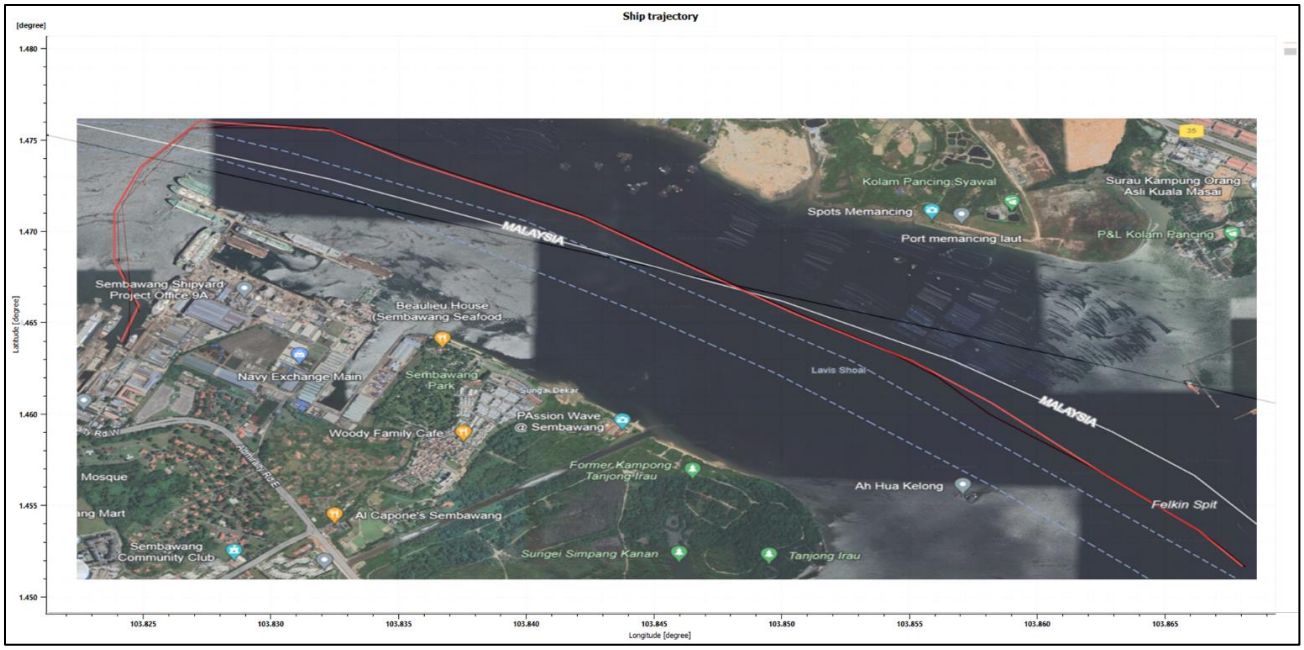

Figure 5. Vessel direction from Simcenter AMESIM results overlayed with Google maps

The environmental conditions during the specified route are based on several resources, i.e., the wave height is based on the MPA tide table (Maritime & Port Authority of Singapore, 2020) whereas the current speed and wind speed are based on data captured on a vessel with sensors capturing the current speed and wind speed along the similar route experience by the simulated vessel. The estimated average current speed and wind speed are also checked against online values from (Windfinder, 2020) for validation. These values along with the coordinates of the vessel operation route are then input into the marine environment model, MARWAT00R. The values used for this study are shown in Table 1. The added resistance due to the environmental conditions is computed through MARSEA00R using the Blendermann method and STAwave-2 for wind and wave resistance respectively. The Blendermann method is used to estimate the wind load based on wind tunnel test results and is one of the most accurate when compared to other methods such as the Isherwood and Gould method (Turk & Prpić-Oršić, 2009). STAwave-2 method is an empirical approach used to estimate the added resistance of a ship due to waves by STA-JIP (ITTC, 2021). The STAwave-2 is used due to its simplicity and one of the methods recommended by international standards (ISO, 2015). The controller in the system model - MARPOW00, determines the varying speed of the vessel during specific points of the operation.

Table 1. Parameters for MARWAT00R

Description	Value	Unit
Wind speed	2.21	m/s
Wave height	0.12	m
Current speed	0.387	m/s
Wave period	2.5	S
Water salinity	25	g/kg
Water temperature	30	°C

The control input table consists of the desired vessel speed at various coordinates during operation. It is noteworthy that the current system model is modelled with inputs from past operational data and not live data. Further development of the system modelling will be required to enable digital twinning of the system, where live data will be input instead. The system model's output incorporates diverse environmental factors and the vessel's added resistance to forecast the actual vessel speed, deviations in route, engine load requirements, added resistance, and estimated fuel consumption. The engine load results are subsequently compared with manually recorded data in Section 4 Case I. These findings are then used in the MATLAB/Simulink model detailed in the subsequent section to assess and compare the annual fuel operational costs and CO_2

emissions associated with LNG-hybrid propulsion. The AMESIM model is then employed to examine how different environmental conditions impact vessel loading in Section 4 Case II.

2.3 Modelling of Hybrid LNG-Battery Propulsion System on MATLAB Simulink

The Simulink model for the hybrid system discussed in this paper follows a similar approach to that presented in (Roslan, Tay, *et al*., 2023). However, this paper advances upon previous findings by incorporating operational condition results obtained from the AMESIM model. For a detailed explanation and parameters of the hybrid LNG-battery power system modelling using MATLAB/Simulink, readers are referred to (Roslan, Konovessis, *et al.*, 2023; Roslan, Tay, *et al.*, 2023). The LNG-hybrid model consists of three primary components: the Genset, the Gas Turbine (GAST), and the Battery, as illustrated in Figure 6. It is worth pointing out that the efficiency of the system components in both AMESIM and Simulink was assumed to be a constant of 90% and assumed that 10% is wasted due to heat. This assumption was made due to the lack of the component's efficiency curves. A system model that accounts for the efficiency curves of its components will be closer to real-world behaviour, important for digital twinning.

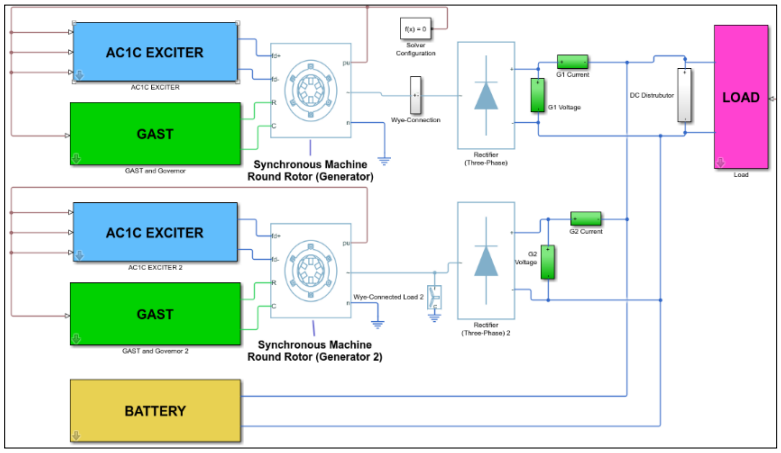

Figure 6. Model of Hybrid LNG–battery power system in Simulink.

2.4 Energy Management System

The energy management system (EMS) controls the different types of energy sources on board and fluctuating operational requirements. The optimal power distribution between the engine and energy storage system differs in the vessel fuel cost and emission emitted. To control and maintain the stability and distribution of the load required, a basic rule-based (RB) control strategy is added to the system model. The RB method is ideal with known loading conditions and past data of the system (Chua, 2019), where the past data are used as a benchmark for the RB control. This will then improve the power management of the hybrid system by allocating the different power sources efficiently to reduce operational costs and improve system longevity. The load-dependent RB control will be implemented in each case study similar to the one used in Roslan *et al.* (2023). The two types of RB strategy used in this paper are (1) LNG-RB: The Genset will be switched on/off to regulate the power switch to the fully battery-operated mode when the required load is consuming more than 200 g/kWh LNG or when each engine load of 300kW and below. (2) LNG/BAT: Based on the flexibility of the load sharing within the hybrid propulsions, different percentages of LNG and battery power in increments of 10% were investigated. A simple overview of the energy management framework is shown in Figure 7 below.

3. MATHEMATICAL OVERVIEW

3.1 Diesel Fuel Consumption

The calculation for diesel consumption is based on the method proposed by Hansen (2000) with some variations to accommodate the different systems. The mean specific fuel oil consumption ($\overline{SFOC}$) could be obtained from the specific fuel oil consumption ($SFOC$) for each Genset given in the diesel engine fuel consumption graph as follows,

$$\overline{SFOC} = \frac{1}{2t}\int_0^t [SFOC_{Gen\,1}(t) + SFOC_{Gen\,2}(t)]\,dt \tag{1}$$

where t is the total duration and the subscript in (1) denotes the $SFOC$ for the respective Genset.

The $\overline{SFOC}$ is then used to calculate the mean diesel consumption using the average generator power (P_{Avg}). The mean diesel consumption $\overline{C}_{diesel}$ calculation is shown in Equation (2).

$$\overline{C}_{diesel}\ [kg/h] = \overline{SFOC}\ [g/kWh]\ \times\ P_{Avg}[kW] \times 1000 \tag{2}$$

Note that the brackets in the equations represent the units for the variables and all the cost is in USD.
The annual operation cost $Cost_{annual}$ given in (3) is then calculated by taking the assumed diesel price P_{diesel}. As of writing, the average price of marine diesel oil is set to be USD 1.023/kg (Ship&Bunker, 2023).

$$Cost_{annual}\ [\text{USD}] = \overline{C}_{diesel}\ [kg/h] \times\ P_{diesel}\ [USD/kg] \times 24h\ \times 365 \tag{3}$$

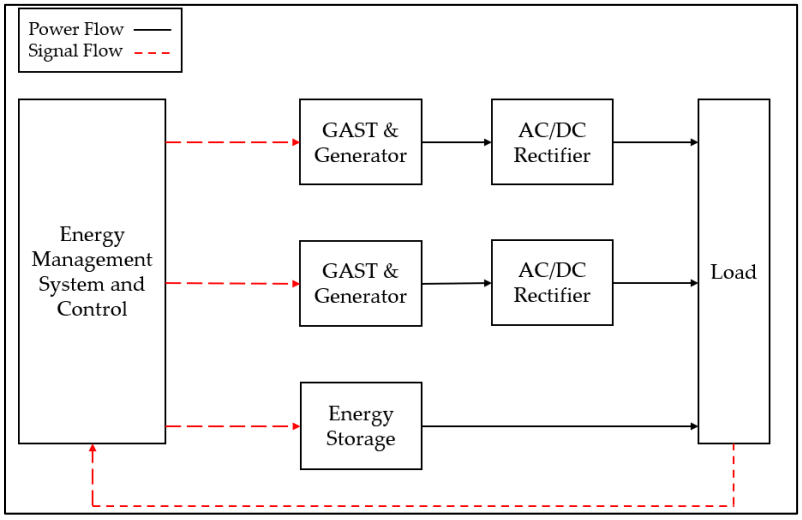

Figure 7. Simplified energy management framework (Roslan *et al.*, 2022)

3.2 LNG Consumption

For the LNG calculations, a similar concept to the diesel fuel counterpart is implemented. The mean LNG consumption $\overline{C}_{LNG}$ is directly calculated from the summation of the SGC at the active load obtained from the engine limit curve in Figure 4.

$$\overline{C}_{LNG}\ \left[\frac{Kg}{h}\right] = P_{Avg}[kW] \times \frac{1}{1000(2t)} \times \int_0^t \{SGC_{Gen\,1}(t) + SGC_{Gen\,2}(t)\}\,dt\left[\frac{g}{kWh}\right] \tag{4}$$

The annual operation cost of the LNG is given in (5). The price of LNG P_{LNG}, as of writing, is set to be USD 0.40/kg (IndexMundi, 2022).

$$Cost_{annual}[USD] = \overline{C}_{LNG}\ [kg/h] \times P_{LNG}\ [USD/kg] \times 24h\ \times 365 \tag{5}$$

3.3 Battery Consumption

The battery consumption for the example will be calculated based on the difference in the battery state of charge (SOC). Using the Coulomb counting method (Vadset, 2018) given in (6),

$$SOC(t) = SOC(t-1) + \int_0^t \frac{P\ [kW]}{E_{bat\ [kWh]}}\,dt \tag{6}$$

where $SOC(t)$ is the battery SOC at time t in %, $SOC\ (t-1)$ the battery's initial SOC in %, t the time in hour, P the charge/discharge power and E_{bat} is the battery capacity.

Charging the battery with 1800 kW for 130 s makes it possible to add USD 1.95 as claimed by Vadset (2018)with a rate of USD 0.03/kWh. A separate study from Kersey *et al.* (2022) used the price of electricity of USD 0.035/kWh. This paper, however, will utilise the average value of USD 0.033/kWh. The cost to charge the battery fully after every trip will be based on the formula in equation (7),

$$Battery\ Charging_{\text{Cost}}\ [\text{USD}] =\ (\text{SOC} - \text{SOC(t)}) \times E_{bat}\ [\text{kWh}] \times \text{Charging Cost}\ [\text{USD/kWh}] \tag{7}$$

where $SOC - SOC(t)$ is the percentage of battery to be fully charged, E_{bat} is the battery capacity and Charging Cost will be USD 0.033/kWh at 1800 kW. To obtain the annual operation cost with battery charging for configurations with a battery, the $Battery\ Charging_{\text{Cost}}$ is multiplied by the total number of trips completed in a year and added with $Cost_{annual}$ in (5), not factoring downtime and inactivity periods such as system breakdown or lunch. Charging duration will progressively improve as the technology matures, evidenced by successful cases in the automobile industry where the chargers are capable of charging one vehicle at 1 MW or three vehicles simultaneously at 360 kW (Heliox, 2022).

3.4 CO2 Emissions

The CO_2 emissions $Emission_{CO_2}$ calculation is based on MEPC.245 (66) (The Marine Environment Protection Committee, 2014). The total CO_2 emissions can be calculated using the following formula based on the total fuel oil consumption C_{fuel}.

$$Emission_{CO_2}\ (ton) = C_{fuel}\ (ton) \times C_F \tag{8}$$

where C_F represents the CO_2 emission coefficient based on the type of fuel oil consumed. The coefficients are based on MEPC.245 (66) Committee 2014. The diesel used in this paper is diesel oil and has a C_F value of 3.206, whereas the LNG has a C_F value of 2.75.

3.5 CII Ratings

Lastly, the $EEOI$ or CII attained will be calculated from (9), whereas the required annual operational *CII* is obtained from (10).

$$EEOI \text{ or } CII\ attained\ \left[\frac{g}{tonne - nm}\right] = \frac{Emission_{CO_2}}{DWT \text{ or } GT\ [tonne] \times Distance\ Sailed\ [nm]} \tag{9}$$

$$CII_R = aCapacity^{-C} \tag{10}$$

$$\text{Required Annual Operational } CII\ = \left(1 - \frac{Z}{100}\right) \times\ CII_R \tag{11}$$

where Z refers to the reduction factor, starting from 5% in 2023 and afterwards increasing by 2% each year. The CII reference value CII_R (10) is based on the respective ship type and capacity from the table found in MEPC.353 (78) (The Marine Environment Protection Commitee, 2022a). The values of *a* and *-c* are 930 and 0.383 respectively. The distance sailed in this study is the average distance travelled by the diesel operational tugboat of 10.4 nm. The calculated values will have a CII rating based on Table 3. The rating is based on the ratio of $EEOI$ or CII attained (9) to the required CII (11), where a higher ratio indicates a worse rating, and vice versa. Any values lower than column B in Table 3 are rated as A (Gianni *et al.*, 2022). As tugboats are not categorised under the list of vessel types in MEPC.354 (78) (The Marine Environment Protection Commitee, 2022a), this study adopts the cruise passenger ship values for $EEOI$ calculations and CII ratings.

Table 2 CII rating for the different types of ships (The Marine Environment Protection Committee, 2022b)

Ship Type	Ship Size	B	C	D	E
Bulk Carrier		0.86	0.94	1.06	1.18
Gas Carrier	DWT ≥ 65,000	0.81	0.91	1.12	1.44
	DWT < 65,000	0.85	0.95	1.06	1.25
Tanker		0.82	0.93	1.08	1.28
Container Ship		0.83	0.94	1.07	1.19
General Cargo Ship		0.83	0.94	1.06	1.19
Refrigerated Cargo Carrier		0.78	0.91	1.07	1.20
Combination Carrier		0.87	0.96	1.06	1.14
LNG Carrier	DWT ≥ 100,000	0.89	0.98	1.06	1.13
	DWT < 100,000	0.78	0.92	1.10	1.37
Ro-ro Cargo Ship (VC)		0.86	0.94	1.06	1.16
Ro-ro Cargo Ship		0.76	0.89	1.08	1.27
Ro-ro Passenger Ship		0.76	0.92	1.14	1.30
Cruise Passenger Ship		0.87	0.95	1.06	1.16

4. RESULTS AND DISCUSSION

The results and discussion in this section are of the following cases: (I) System validation and (II) Varying environmental conditions. The types of system of configuration considered in this paper include diesel, LNG with variable engine speed and two variations of LNG-battery hybrid with control strategies. The target of the study is to first provide validity of the system model based on past operational results in Case I. This is followed by studying the different effects on the vessel load, annual operational cost and CO_2 emissions when different environmental conditions are encountered in Case II. The study is then concluded with a comparison of the different system configurations and highlighting the most economically friendly based on the different results and design sustainability based on CII ratings. The load profile presented in this section represents a single tugboat operation based on the system models mentioned in the System Overview.

4.1 Case I: System Validation with Past Operational Data

The purpose of system validation of the system modelled is to showcase the reliability and accuracy of the profiles simulated when compared to real-time operations. The load profiles used in this study are based on a combination of manually logged engine load data from past operations conducted by JMS Kappa and the designed operation load profile distribution of the LNG-battery hybrid tugboat provided by the industry collaborator. The ideal distribution of the load profile used in this study is shown in Figure 8(a). Figure 8(a), however, does not factor in the distance of the operation including the environmental conditions, as shown in Figure 5, which will affect the duration during the specified operation.

On the other hand, Table 3 breaks down the load profile given in Figure 8(a) by the operational profile by using both the manual data obtained and the duration of the stated operation provided by the industrial collaborator. Figure 8(b) however shows the results of the same input from Figure 8(a), with the consideration of the distance, environmental conditions and added resistance in AMESIM. Results show that travelling at a higher speed of 10-12 knots in Figure 8(b) requires a shorter time when compared to Figure 8(a). The breakdown of the operational profile in Figure 8(b) by its distributed duration and simulated load, is given in Table 3 where a majority of the operation is spent on tugging. The average load for Figure 8(a) is 630kW. Compared to the average load of 606kW of Figure 8(b), that factors the added resistance throughout the trip. A lower average load since more than 50% of the operation was spent tugging and requiring a load less than 550kW, reducing the overall average load. As compared to Figure 8(a) which spent 35% of the operation tugging and spent a longer duration transiting at 10-12 knots, hence the higher average load. The following study in this paper references Case I results shown in Figure 8(b) as the controlled load profile.

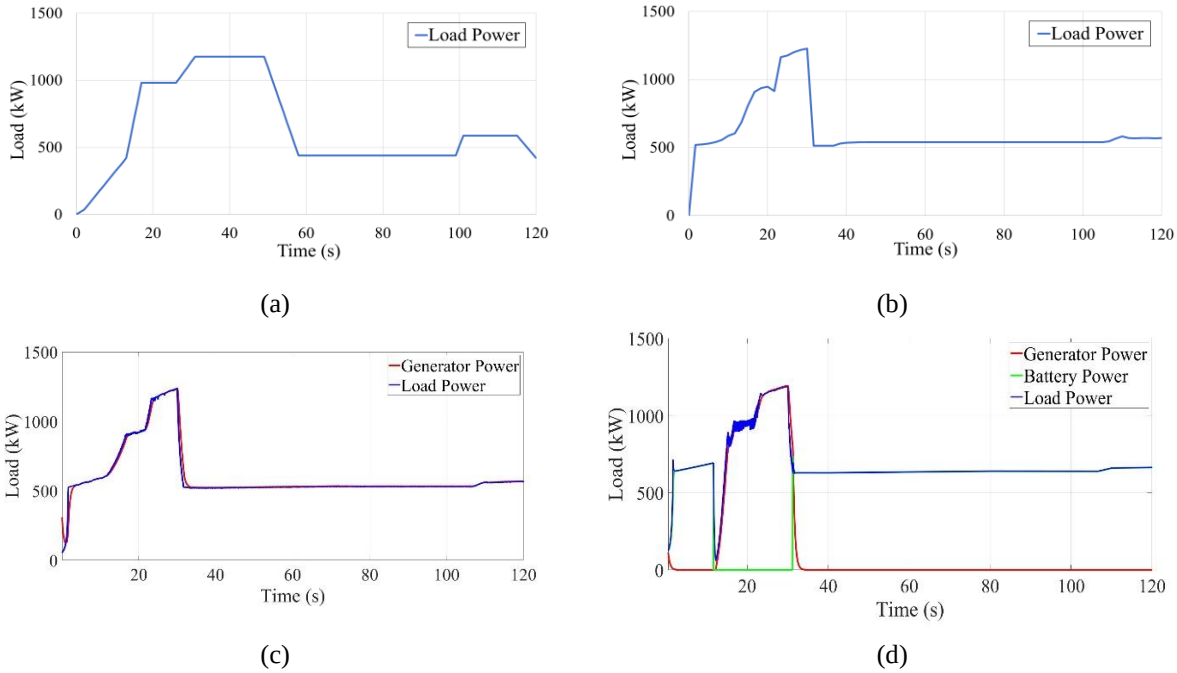

Figure 8: (a) Load profile based on past data (b) load profile based on operational conditions (c) Load profile simulated without battery (d) Load profile simulated with battery

Several types of system configurations such as diesel, LNG and LNG-battery hybrid with control strategies are then simulated to compare the annual cost and CO_2 emissions emitted based on the calculations in Section 3. Table 4 summarises the annual fuel cost and annual CO_2 emissions from the different system configurations. To simplify the annual calculations, no day off or downtime of the vessel throughout the year was assumed. Figure 8(c) and Figure 8(d) display the results of LNG

propulsion and LNG-battery hybrid systems on Simulink respectively. LNG-RB configuration displays the best results when compared to the other system configurations. The LNG-RB control strategy can reduce annual CO_2 emissions by up to 96.5% and save annual fuel operation costs of up to 95.3%. This is an improvement as compared to the results found in Roslan *et al.* (2023) because of the difference in the distribution of operation duration shown in Table 3 and the lower average load. It is worth mentioning that RB strategies will differ from study to study, it is not a one rule fits all solution. A separate RB study conducted by Diniz *et al.* (2023) controls the operational performance of the generators of an escort tug to perform at optimal efficiency and to have bi-directional battery control, which reduced CO_2 emissions by 10.7% for a single load profile.

Although LNG-RB results in having the best results concerning cost and emission, the number of daily trips is lesser than the conventional diesel system. This is due to the high battery usage per trip of 73.2% when compared to the other hybrid control configurations as shown in Table 4. The total number of trips completed daily is calculated based on the total duration of a day divided by the total time to complete an operation and the time to charge the battery fully. Therefore, with a higher SOC used, it will require the ship to return to port to charge after every trip. Without a bi-directional converter the battery will not be able to charge offshore, hence limiting the number of trips daily. With the current battery system configuration, the only means of charging is by connecting to shore power or swapping batteries. Therefore, with the current battery system configuration the LNG/BAT at 80% LNG and 20% battery load distribution configuration is ideal, since it consumes 16.2% SOC. A more operational-orientated configuration where a fully charged battery is capable of a single operation of up to 10 hours or five 120-minute operations, with varying loading conditions between idle, transiting and tugging up to an average of 3150kWh power consumption. While still having a reduction of annual fuel cost and CO_2 emissions by 65.9% and 27.7% respectively.

Table 3 Operation Profiles

Operation	Logged Load (kW)	Designed Duration (%)	Simulated Load (kW)	Simulated Duration (%)
Idle	420	10	521	6.9
6-knot Transit	588	25	549	26.4
10-knot Transit	980	10	927	5.6
12-knot Transit	1176	20	1083	8.3
Tugging	440	35	538	52.8

Table 4: Case I results in comparison using different system configurations.

Fuel Type	Annual Fuel Cost ($USD)	Annual CO_2 Emission (tonne)	Battery SOC used per trip (%)	Number of trips Daily	% Reduction*	
					in Cost	in CO_2 Emissions
Diesel	2,571,224	8,050.1	-	12	-	-
LNG	917,906	6,245.5	-	12	64.3	22.4
LNG-RB	121,678	278.2	73.2	10	95.3	96.5
LNG/BAT (10/90)	210,632	900.8	80.1	10	91.8	88.8
LNG/BAT (20/80)	334,662	1,788.9	76.5	10	87.0	77.8
LNG/BAT (30/70)	427,341	2,480.1	66.6	11	83.4	69.2
LNG/BAT (40/60)	489,659	2,937.3	49.9	11	81.0	63.5
LNG/BAT (50/50)	551,321	3,343.0	52.6	11	78.6	58.5
LNG/BAT (60/40)	653,281	4,139.9	37.6	11	74.6	48.6
LNG/BAT (70/30)	710,903	4,594.4	29.3	11	72.4	42.9
LNG/BAT (80/20)	876,038	5,822.4	16.2	12	65.9	27.7
LNG/BAT (90/10)	1,016,854	6,851.4	7.7	12	60.5	14.9

* concerning diesel system configuration results

4.2 Case II: Varying Environmental Conditions (Extreme and Operational Cases)

4.2.1 Loading and Energy Consumption of Battery

The four environmental conditions that investigated in this paper are based on the capabilities of the Simcenter/AMESIM module MARWAT00R, i.e., wind speed, wave height, current speed and wave period. The data are based on the data mentioned in Section 2.2 The required vessel loads of the varying extreme environmental conditions are then simulated between the minimum and maximum values based on past data experienced along the vessel route shown in Figure 5. Figure 10(a) compares the vessel load with varying wind speeds ranging between 0 m/s and 9.5m/s. An increase in the load is observed when a

variation of vessel speed is required. Significant observation can be seen at 30 – 40 minutes where a change of speed is required to accelerate back up. A surge of load is observed to increase incrementally with the wind speed. However, the average vessel load only increased by 0.93% when the wind speed increased to 9.5m/s from 0 m/s as observed from the AMESIM simulation. Table 5 summarises the comparison of the extreme results between the minimum and maximum environmental conditions. Aside from the vessel load, the vessel's added resistance and specific fuel consumption (SFOC) are also compared using the Simcenter/AMESIM software. A decrease of 0.24% and an increase of 0.97% were observed for the average SFOC and vessel's added resistance respectively.

A major difference could be observed when comparing the results of varying wind speeds against varying wave heights. In Figure 10(b), the vessel load of varying wave heights is shown, ranging from 0m to 5m. Notably, two key variances emerge in terms of the total time required to complete the operation and the maximum load. The total duration for completing the same operation extended from 120 minutes to 133.3 minutes, while the maximum load surged from 1228kW to 3121kW. Comparing between 0m and 5m wave heights, the average load doubled. This increase in the average vessel load led to a rise in the average vessel's added resistance by 50.3kN, nearly seven times higher than the results obtained without considering any wave height. From past studies found in Roslan *et al.* (2023), the higher the vessel load required the lower the SFOC. A decrease of 9.6% in the average SFOC was observed due to the higher average load in general.

However, simulating extreme conditions of current speeds and wave periods produced minimal to negligible effects on the vessel load, SFOC, and added resistance. Figure 10(c) illustrates the absence of effects on the vessel when varying current speeds within the range of 0 m/s to 1.2 m/s. Additionally, Figure 10(d) depicts the variation in wave periods between 0 seconds and 9 seconds, resulting in a mere 0.06% increase in average load and a 0.80% increase in the average vessel's added resistance observed in the AMESIM simulation (see Table 5). A summary of the findings from the varying environmental conditions is shown in Table 5, concerning the difference in percentages between the minimum and maximum results. Based on the summary Table 5, the environmental conditions that govern the loading and energy consumption of the vessel are the varying wind speeds and wave heights.

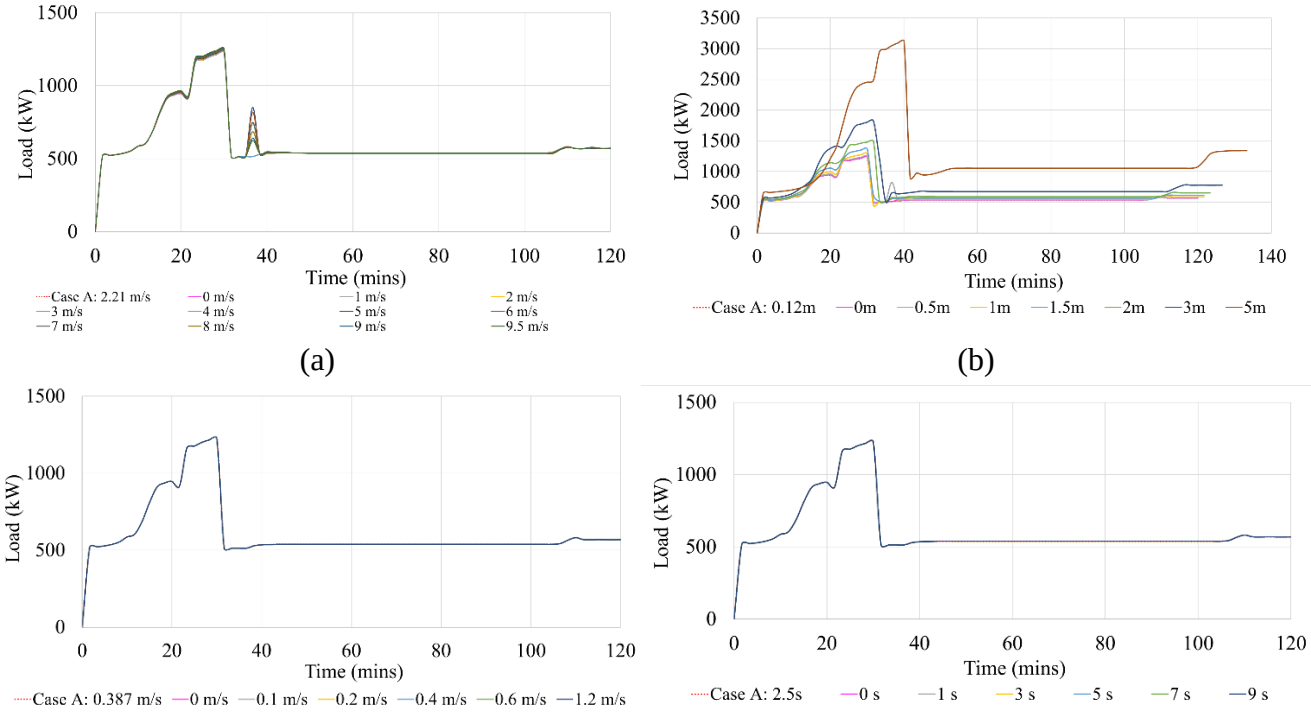

Figure 9: Load profiles of (a) varying wind speeds (b) varying wave heights (c) varying current speeds (d) varying wave periods

Table 5: Results comparisons between the minimum and maximum results from varying environmental conditions

	Wave Period	Current Speed	Wind Speed	Wave Height
Load	0.06%	0.00%	0.93%	104.03%
SFOC	-0.02%	0.00%	-0.24%	-9.62%
Added Resistance	0.80%	0.00%	0.97%	681.96%

4.2.2 Annual Costs and CO2 Emissions

Next, the study focuses on studying the average load, annual fuel operational cost and CO_2 emissions for the different system configurations under varying environmental conditions of the specified route. The range of values of wave heights is based on the average values obtained from past data (Windfinder, 2020) where the typical wave height along the route and around Singapore typically averages between 0.5 m and 1.0 m (Bricheno *et al.*, 2015).

The annual fuel operation cost and annual CO_2 emissions for the varying operational conditions under different wave heights are shown in Table 6 and Table 7, respectively. A small difference in the average load is observed between 1.0m and 0.5m wave height at 608.14kW and 608.20kW respectively. The change in speed from high speed to low speed causes the vessel's average load to be higher at 0.5m wave height. The 1.0m wave height, however, takes more time (1.67 minutes more in the simulation) to complete the operation. The results for the annual cost and annual CO_2 emissions are found to correlate with the increase in average load where the cost and emission increase with the increase in average load. The highest increase in the annual fuel operation cost and CO_2 emissions along the route due to wave heights is by 4.8% and 16.3% respectively, at 0.5m wave height using LNG-RB system configuration. This is likely due to the increase in the average load from 604.45kW to 608.20kW, although a higher load typically leads to having lower SGC. The period where the increase in load for this configuration occurred was less than 800kW, therefore 200g/kWh SGC was consumed instead of 195g/kWh resulting in a higher cost and emission.

Table 6: Annual Cost results from varying operational wave heights

Fuel Type	Annual Fuel Cost ($USD) – Case I*	Annual Fuel Cost ($USD) – 0.5m	Annual Fuel Cost ($USD) – 1m	% Increase*	
				in Cost – 0.5m	in Cost – 1m
Diesel	2,571,224	2,462,561	2,491,973	-4.2%	-3.1%
LNG	917,906	898,764	898,194	-2.1%	-2.1%
LNG-RB	121,678	127,459	122,973	4.8%	1.1%
LNG/BAT (10/90)	210,632	211,569	211,503	0.4%	0.4%
LNG/BAT (20/80)	334,662	336,250	336,021	0.5%	0.4%
LNG/BAT (30/70)	427,341	428,964	429,108	0.4%	0.4%
LNG/BAT (40/60)	489,659	492,029	491,428	0.5%	0.4%
LNG/BAT (50/50)	551,321	553,460	553,658	0.4%	0.4%
LNG/BAT (60/40)	653,281	656,594	656,437	0.5%	0.5%
LNG/BAT (70/30)	710,903	714,122	713,646	0.5%	0.4%
LNG/BAT (80/20)	876,038	880,555	878,759	0.5%	0.3%
LNG/BAT (90/10)	1,016,854	1,021,319	1,019,921	0.4%	0.3%

* concerning respective Case I results

Table 7: Annual CO_2 Emissions results from varying operational wave heights

Fuel Type	Annual Emissions (ton) – Case I*	Annual Emissions (ton) – 0.5m	Annual Emissions (ton) – 1m	% Increase*	
				in CO_2 Emissions – 0.5m	in CO_2 Emissions – 1m
Diesel	8,050.1	7,709.9	7,802.0	-4.2%	-3.1%
LNG	6,245.0	6,115.0	6,111.1	-2.1%	-2.2%
LNG-RB	278.2	323.5	284.3	16.3%	2.2%
LNG/BAT (10/90)	900.8	904.1	903.5	0.4%	0.3%
LNG/BAT (20/80)	1788.9	1,796.7	1,794.9	0.4%	0.3%
LNG/BAT (30/70)	2480.1	2,488.2	2,489.1	0.3%	0.4%

LNG/BAT (40/60)	2,937.3	2,950.8	2,946.3	0.5%	0.3%
LNG/BAT (50/50)	3,343.0	3,354.6	3,355.9	0.3%	0.4%
LNG/BAT (60/40)	4,139.8	4,160.3	4,159.0	0.5%	0.5%
LNG/BAT (70/30)	4,594.3	4,614.4	4,610.9	0.4%	0.4%
LNG/BAT (80/20)	5,822.4	5,852.1	5,839.5	0.5%	0.3%
LNG/BAT (90/10)	6,851.4	6,881.2	6,871.6	0.4%	0.3%

* concerning respective Case I results

The operational wind speed experienced by the vessel along the route changes from 0 m/s to 9.5 m/s, as indicated by data collected from sensors on a vessel navigating the same route. Table 8 and Table 9 present the differences in annual cost and annual CO_2 emissions, respectively. The average load is 602.16kW at 0m/s and 606.55kW at 9.5m/s wind speed. This load is lower when compared to the impact of wave height. The increase in average wind speed along the route results in a 2.8% rise in annual fuel operation cost and a 9.4% increase in annual CO_2 emissions at a wind speed of 9.5m/s using the LNG-RB system configuration. The results with 0m/s wind speed are expected to be lesser in cost and emissions because Case I was simulated with an average wind speed of 2.25m/s.

Table 8: Annual cost results comparison of varying wind speeds

Fuel Type	Annual Fuel Cost ($USD) – Case I*	Annual Fuel Cost ($USD) – 0 m/s	Annual Fuel Cost ($USD) – 9.5m/s	% Increase*	
				in Cost – 0m/s	in Cost – 9.5m/s
Diesel	2,571,224	2,437,919	2,453,265	-5.2%	-4.6%
LNG	917,906	890,217	896,355	-3.0%	-2.3%
LNG-RB	121,678	122,612	125,123	0.8%	2.8%
LNG/BAT (10/90)	210,632	210,113	211,168	-0.2%	0.3%
LNG/BAT (20/80)	334,662	335,652	335,647	0.3%	0.3%
LNG/BAT (30/70)	427,341	426,601	427,906	-0.2%	0.1%
LNG/BAT (40/60)	489,659	488,455	490,761	-0.2%	0.2%
LNG/BAT (50/50)	551,321	549,639	552,079	-0.3%	0.1%
LNG/BAT (60/40)	653,281	651,943	654,960	-0.2%	0.3%
LNG/BAT (70/30)	710,903	709,271	712,495	-0.2%	0.2%
LNG/BAT (80/20)	876,038	874,027	878,402	-0.2%	0.3%
LNG/BAT (90/10)	1,016,854	1,014,480	1,018,958	-0.2%	0.2%

* concerning respective Case I results

Table 9: Annual CO_2 emissions results comparison of varying wind speeds

Fuel Type	Annual Emissions (ton) – Case I*	Annual Emissions (ton) – 0m/s	Annual Emissions (ton) – 9.5m/s	% Increase*	
				in CO_2 Emissions – 0m/s	in CO_2 Emissions – 9.5m/s
Diesel	8,050.1	7,632.8	7,680.8	-5.2%	-4.6%
LNG	6,245.5	6,057.1	6,098.9	-3.0%	-2.3%
LNG-RB	278.2	285.7	304.3	2.7%	9.4%
LNG/BAT (10/90)	900.8	899.1	902.6	-0.2%	0.2%
LNG/BAT (20/80)	1788.9	1,798.2	1,793.8	0.5%	0.3%
LNG/BAT (30/70)	2480.1	2,476.9	2,482.0	-0.1%	0.1%
LNG/BAT (40/60)	2,937.3	2,930.7	2,943.1	-0.2%	0.2%
LNG/BAT (50/50)	3,343.0	3,333.0	3,346.2	-0.3%	0.1%
LNG/BAT (60/40)	4,139.9	4132.2	4,149.9	-0.2%	0.2%
LNG/BAT (70/30)	4,594.4	4584.4	4,603.9	-0.2%	0.2%
LNG/BAT (80/20)	5,822.4	5809.4	5,837.8	-0.2%	0.3%
LNG/BAT (90/10)	6,851.4	6835.6	6,865.4	-0.2%	0.2%

* concerning respective Case I results

In summary, the results summarised in Table 5 show the extreme results for load, SFOC and added resistance between the minimum and maximum environmental conditions. Varying wave heights are found to have the highest effect on the results followed by varying wind speed. The results from varying operational wave heights show an increase of up to 4.8% and 16.4% in the annual fuel operation cost and annual CO_2 emissions, respectively. As for the varying operational wind speeds, an increase of up to 2.8% and 9.4% in the annual fuel operation cost and annual CO_2 emissions, respectively. Additionally, different system configurations were tested. Similar to Case I, the LNG-RB configuration demonstrated the most significant reduction in cost and emissions when compared to the diesel configuration. The capabilities of the system model used in this study to simulate the effects of environmental loads to the system performance will be beneficial for vessel operator or machine learning algorithms. Algorithms such as route optimisation-based solutions based on the most efficient conditions discovered in this paper. Having knowledge of which environmental conditions to avoid will save valuable operational cost and emissions.

4.3 Economical and Sustainability System Comparison

With the results of the different system configurations in Case I and Case II, the CII ratings of the respective system are then calculated using the equations (9) – (11) expressed in Section 3. Table 10 summarises the results of the CII ratings for the following years based on the results simulated. Achieving a grade "A" CII rating signifies a highly efficient ship in reducing carbon emissions during operation. With future readiness for a more environmentally friendly maritime industry. Vessel designs with a score of "D" or "E" for three consecutive years are required to develop a corrective action plan. Based on the CII ratings of the configuration tested, it is highly recommended that the vessels operate with at least 30% of the load with battery and 70% on LNG. Operating on diesel and LNG is not recommended since it is the least efficient with a grade "E" CII rating.

Table 10: CII Ratings of the respective configurations through the years

Configuration \ Year	2024	2025	2026	2027
Diesel	E	E	E	E
LNG	E	E	E	E
LNG-RB	A	A	A	A
LNG/BAT (10/90)	A	A	A	A
LNG/BAT (20/80)	A	A	A	A
LNG/BAT (30/70)	A	A	A	A
LNG/BAT (40/60)	A	A	A	A
LNG/BAT (50/50)	A	A	A	B
LNG/BAT (60/40)	A	B	C	D
LNG/BAT (70/30)	B	C	D	E
LNG/BAT (80/20)	D	E	E	E
LNG/BAT (90/10)	E	E	E	E

Although the CII ratings play a big part in selecting a system configuration with efficient carbon emission and sustainability, the reality in operation is to have a system design capable of providing both efficiency in completing more operations and in reducing emissions. LNG-RB demonstrated the best in performance with the biggest reduction in annual fuel operation cost and annual CO_2 emission and obtained a grade "A" CII rating. However, the total number of trips capable of completing within a day is limited to 10 trips as compared to the 11 trips using a 30% LNG and 70% battery load distributed system. The single increase in operation leads to an increase in the annual fuel operation cost and CO_2 emissions by $USD 305,663 and 2,202 tons, respectively. It is imperative, therefore, to refrain from increasing the trip count to 11, and instead allocate the extra time for battery charging due to the significant surge in costs and emissions. With the cost saved, an enhancement to the configuration could involve incorporating a bi-directional converter due to their electrical isolation capabilities and high reliability in renewable energy sources (Dung *et al*., 2017), and also enabling the battery to be charged by the LNG generators onboard.

The annual fuel operation cost and CO_2 emissions results from this paper could be used for a further study on the life cycle assessment (LCA) and life cycle cost assessment (LCCA) of the LNG-battery hybrid system model. A similar study done by Fan *et al.* (2021) where the economic and environmental impact of the lifetime of a LNG-battery hybrid river ship was assessed and compared to a diesel propulsion. The annual emissions reduced by 33.44% and fuel cost reduced by 39.15%, including carbon emission tax, when compared between the LNG-battery hybrid to diesel system. For future LCA assessment on CO_2 emissions, factors to consider include but not limited to the following: emission during equipment manufacturing stage, energy production stage and energy transportation. For LCCA on the other hand considers the total cost including investment cost,

operation cost (maintenance cost, fuel cost and carbon credit cost) and decommission cost. The results from Fan's LCCA concluded with LNG-battery hybrid system costing less than the diesel-powered system. Future works alternative tugboats propulsion systems should consider comparing different renewable energies such as methanol and hydrogen. A similar work had been done by Perčić *et al.* (2021), where he investigated on the LCA and LCCA of various ships using alternative fuels. The study concluded with fully electric ships being the most environmentally and cost-effective solution, followed closely by methane and LNG. A similar study could be conducted in the near future for tugboats with the results obtained from the current study which will benefit potential vessel owners before converting current diesel systems to an alternative renewable energy propulsion system.

5. CONCLUSIONS

The paper presented the influence of environmental loads and manoeuvre on the vessel load in several different system configurations. The configurations include a full diesel system, LNG system, LNG-battery hybrid system with rule-based control and LNG-battery hybrid system with flexible load sharing. The annual fuel operation cost, annual CO_2 emissions and CII ratings for each system configuration at the varying environmental load were calculated and discussed in the paper. The cases covered in this paper are as follows: Case I: System Validation and Case II: Varying environmental conditions. Case I validates the system modelled with past results manually captured from similar tugboats. The model was created on Siemen/AMESIM for the diesel system configuration and MATLAB/Simulink for the LNG and LNG-battery hybrid systems. The LNG-RB system showcased its capabilities with the lowest annual fuel operation cost and annual CO_2 emissions when compared to the conventional diesel system with a reduction of 95.3% and 96.5% respectively.

The results in Case I were set as a benchmark when compared to results from Case II with the varying environmental conditions. The conditions included in the study are wind speed, wave height, current speed and wave periods. Each environmental condition was tested between zero and the extreme condition experienced through the route. The results concluded that wave height had the biggest impact on the vessel load performance, with an average increase of 104.03% and 681.96% in load and added resistance respectively. The varying wind speed displayed a slight increase in the load and added resistance, unlike the varying current speed and wave periods that had no impact on the vessel's performance. The wave height and wind speed are then simulated using operational conditions to calculate the respective annual fuel operational cost and annual CO_2 emissions. The operational wave height along the route ranges between 0.5m and 1m. An increase of up to 4.8% and 16.3% to the annual fuel operational cost and CO_2 emissions when compared to Case I results. The operational wind speed experience along the route simulated ranges between 0 m/s to 9.5m/s . An increase of up to 2.8% and 9.4% in annual fuel operational cost and CO_2 emissions can be obtained between extreme wind speed and average wind speed at 2.25 m/s.

The paper concludes with the CII ratings of each system configuration to find the most efficient system for reducing emissions. LNG-RB and LNG/RB load sharing with more than 40% battery load had the best CII rating of grade "A". However, based on the number of daily trips capable of completing with a fully charged battery, LNG-RB was limited to 10 trips whereas LNG/RB with 30% LNG and 70% battery load sharing was able to complete 11 trips. The annual increase in cost and emission for the additional trip increased by $USD 305,663 and 2,202 tons, respectively. Therefore, it is more economical and efficient to maintain 10 trips using LNG-RB system configuration. Using the allowance of time to travel back to shore for charging or battery swap. Moreover, the funds designated for this purpose could be redirected to enhance the vessel system by integrating a bi-directional converter. This converter facilitates better control over the battery's voltage and current, crucially enabling offshore charging by the LNG generators. To enhance the credibility of the modelled system, future investigations should encompass a broader range of case studies, including diverse routes and varying operational vessel loads. Subsequent studies could involve integrating live sensor data into the model to create a digital twin capable of producing route optimisation and load predictions.

CONTRIBUTION STATEMENT

Sharul Baggio Roslan: Conceptualization, methodology, data collection, validation, writing – original draft preparation, data collection, visualization. **Dimitrios Konovessis:** supervision, funding acquisition. **Joo Hock Ang:** validation, data collection. **Nirmal Vineeth:** validation, data collection. **Zhi Yung Tay:** methodology, writing – review and editing, supervision, project administration, funding acquisition.

ACKNOWLEDGEMENTS

This research was funded by MOE, Grant Number R-MOE-A403-E002.

REFERENCES

Abebe, M., Shin, Y., Noh, Y., Lee, S., & Lee, I. (2020). Machine learning approaches for ship speed prediction towards energy efficient shipping. *Applied Science*, *10*(7), 2325.

Bricheno, L., Cannaby, H., Howard, T., Mcinnes, K., & Palmer, M. (2015). Extreme Sea Level Projections. *Centre for Climate*

Research Singapore.
Cheliotis, M., Lazakis, I., & Theotokatos, G. (2020). Machine learning and data-driven fault detection for ship systems operations. *Ocean Engineering*, *216*(May), 107968. https://doi.org/10.1016/j.oceaneng.2020.107968
Chua, L. W. Y. (2019). *A Strategy for Power Management of Electric Hybrid Marine Power Systems* [Nanyang Technological University]. https://doi.org/10.32657/10220/48078
ClassNK. (2021). *Outlines of EEXI regulation EEDI Section of Marine GHG Certification Department*. https://www.classnk.or.jp/hp/pdf/activities/statutory/eexi/eexi_rev3e.pdf
Diniz, G. H. S., Miranda, V. dos S., & Carmo, B. S. (2023). Dynamic modelling, simulation, and control of hybrid power systems for escort tugs and shuttle tankers. *Journal of Energy Storage*, *72*, 108091. https://doi.org/10.1016/J.EST.2023.108091
Dung, N. A., Hieu, P. P., Hsieh, Y., Lin, J., Liu, Y., & Chiu, H. (2017). A novel low-loss control strategy for bidirectional DC–DC converter [Article]. *International Journal of Circuit Theory and Applications*, *45*(11), 1801–1813. https://doi.org/10.1002/cta.2373
Ejder, E., & Arslanoğlu, Y. (2022). Evaluation of ammonia fueled engine for a bulk carrier in marine decarbonization pathways [Article]. *Journal of Cleaner Production*, *379*. https://doi.org/10.1016/j.jclepro.2022.134688
Fam, M. L., Tay, Z. Y., & Konovessis, D. (2022). An artificial neural network for fuel efficiency analysis for cargo vessel operation. *Ocean Engineering*, *264*, 112437. https://doi.org/10.1016/J.OCEANENG.2022.112437
Fan, A., Wang, J., He, Y., Perčić, M., Vladimir, N., & Yang, L. (2021). Decarbonising inland ship power system: Alternative solution and assessment method. *Energy*, *226*, 120266. https://doi.org/10.1016/J.ENERGY.2021.120266
Gianni, M., Pietra, A., Coraddu, A., & Taccani, R. (2022). Impact of SOFC Power Generation Plant on Carbon Intensity Index (CII) Calculation for Cruise Ships [Article]. *Journal of Marine Science and Engineering*, *10*(10), 1478. https://doi.org/10.3390/jmse10101478
Hadi, J., Konovessis, D., & Tay, Z. Y. (2022a). Achieving fuel efficiency of harbour craft vessel via combined time-series and classification machine learning model with operational data. *Maritime Transport Research*, *3*, 100073. https://doi.org/10.1016/J.MARTRA.2022.100073
Hadi, J., Konovessis, D., & Tay, Z. Y. (2022b). Filtering harbor craft vessels' fuel data using statistical, decomposition, and predictive methodologies. *Maritime Transport Research*, *3*, 100063. https://doi.org/https://doi.org/10.1016/j.martra.2022.100063
Hansen, J. F. (2000). *Modelling and Control of Marine Power Systems*. Norwegian University of Science and Technology.
Heliox. (2022). *The Future is Megawatt Charging*. Heliox. https://www.heliox-energy.com/blog/the-future-is-megawatt-charging
IHI. (2022). *Niigata Marine Selection Guide*. https://www.ihi.co.jp/ips
IndexMundi. (2022). *Natural Gas vs Diesel - Price Rate of Change Comparison*. https://www.indexmundi.com/commodities/?commodity=natural-gas&currency=sgd&commodity=diesel
International Maritime Organisation. (2019). *The 2020 global sulphur limit: FAQ*. International Maritime Organization. http://www.imo.org/en/MediaCentre/HotTopics/GHG/Documents/FAQ_2020_English.pdf
International Maritime Organization. (2016). *Prevention of Air Pollution from Ships*. International Maritime Organization. https://www.imo.org/en/OurWork/Environment/Pages/Air-Pollution.aspx
ISO. (2015). ISO 15016:2015 - Ships and marine technology — Guidelines for the assessment of speed and power performance by analysis of speed trial data. In *ISO*. https://www.iso.org/standard/61902.html
ITTC. (2021). ITTC-Recommended Procedures and Guidelines. *International Towing Tank Conference* .
Karaçay, Ö. E., & Özsoysal, O. A. (2021). Techno-economic investigation of alternative propulsion systems for tugboats [Article]. *Energy Conversion and Management. X*, *12*, 100140. https://doi.org/10.1016/j.ecmx.2021.100140
Kersey, J., Popovich, N. D., & Phadke, A. A. (2022). Rapid battery cost declines accelerate the prospects of all-electric interregional container shipping. *Nature Energy 2022 7:7*, *7*(7), 664–674. https://doi.org/10.1038/s41560-022-01065-y
Lebedevas, S., Norkevičius, L., & Zhou, P. (2021). Investigation of Effect on Environmental Performance of Using LNG as Fuel for Engines in Seaport Tugboats. *Journal of Marine Science and Engineering 2021, Vol. 9, Page 123*, *9*(2), 123. https://doi.org/10.3390/JMSE9020123
Lindstad, H., Asbjørnslett, B. E., & Jullumstrø, E. (2013). Assessment of profit, cost and emissions by varying speed as a function of sea conditions and freight market. *Transportation Research Part D: Transport and Environment*, *19*, 5–12. https://doi.org/10.1016/J.TRD.2012.11.001
Mallouppas, G., & Yfantis, E. A. (2021). Decarbonization in Shipping Industry: A Review of Research, Technology Development, and Innovation Proposals. *Journal of Marine Science and Engineering 2021, Vol. 9, Page 415*, *9*(4), 415. https://doi.org/10.3390/JMSE9040415
Maritime & Port Authority of Singapore. (2020). *Singapore Tide Tables*. https://www.mpa.gov.sg/who-we-are/newsroom-resources/publications/singapore-tide-tables
Maritime & Port Authority Of Singapore. (2023). *Strengthening Singapore's Competitiveness as a Hub Port and International*

Maritime Centre. https://www.mpa.gov.sg/media-centre/details/strenghtening-singapore-s-competitveness-as-a-hub-port-and-international-maritime-centre

Mirović, M., Miličević, M., & Obradović, I. (2018). Big data in the maritime industry. *NAŠE MORE: Znanstveni Časopis Za More i Pomorstvo*, *65*(1), 56–62.

Moreno, V. M. (2007). Future trends in electric propulsion systems for commercial vessels. *Journal of Maritime Research*, *4*(2), 81–100.

Perčić, M., Vladimir, N., & Fan, A. (2021). Techno-economic assessment of alternative marine fuels for inland shipping in Croatia. *Renewable and Sustainable Energy Reviews*, *148*, 111363. https://doi.org/10.1016/j.rser.2021.111363

Roslan, S. B., Konovessis, D., Ang, J. H., Menon, N. V., & Tay, Z. Y. (2023). Modelling and Operation of a Hybrid LNG Propulsion Tugboat. *Volume 5: Ocean Engineering*. https://doi.org/10.1115/OMAE2023-100911

Roslan, S. B., Konovessis, D., & Tay, Z. Y. (2022). Sustainable Hybrid Marine Power Systems for Power Management Optimisation: A Review. *Energies 2022, Vol. 15, Page 9622*, *15*(24), 9622. https://doi.org/10.3390/EN15249622

Roslan, S. B., Tay, Z. Y., Konovessis, D., Ang, J. H., & Menon, N. V. (2023). Rule-Based Control Studies of LNG–Battery Hybrid Tugboat. *Journal of Marine Science and Engineering 2023, Vol. 11, Page 1307*, *11*(7), 1307. https://doi.org/10.3390/JMSE11071307

Ship&Bunker. (2023). *Singapore Bunker Prices - Ship & Bunker*. https://shipandbunker.com/prices/apac/sea/sg-sin-singapore#MGO

Ship Technology. (2015, June 1). *Ampere Electric-Powered Ferry*. Ship Technology. https://www.ship-technology.com/projects/norled-zerocat-electric-powered-ferry/

Tadros, M., Ventura, M., & Soares, C. G. (2023). Review of current regulations, available technologies, and future trends in the green shipping industry. *Ocean Engineering*, *280*, 114670. https://doi.org/10.1016/J.OCEANENG.2023.114670

Tay, Z.Y.; Hadi, J; Konovessis, D.; Loh, D.J.; Tan, D.K.H; Chen, X. (2021). Efficient harbour craft monitoring system: Time-series data analytics and machine learning tools to achieve fuel efficiency by operational scoring system. *Proceedings of the ASME 2021 40th International Conference on Ocean, Offhsore and Arctic Engineering OMAE 2021*, OMAE2021-62658.

Tay, Z. Y., Hadi, J., Chow, F., Loh, D. J., & Konovessis, D. (2021). Big Data Analytics and Machine Learning of Harbour Craft Vessels to Achieve Fuel Efficiency: A Review. *Journal of Marine Science and Engineering 2021, Vol. 9, Page 1351*, *9*(12), 1351. https://doi.org/10.3390/JMSE9121351

Tay, Z. Y., & Konovessis, D. (2023). Sustainable energy propulsion system for sea transport to achieve United Nations sustainable development goals: a review. *Discover Sustainability*, *4*(1). https://doi.org/10.1007/S43621-023-00132-Y

The Marine Environment Protection Commitee. (2014). *Resolution MEPC.245(66)-2014 Guidelines on the Method of Calculation of the Attained Energy Efficiency Design Index (EEDI) for New Ships*. https://wwwcdn.imo.org/localresources/en/OurWork/Environment/Documents/245(66).pdf

The Marine Environment Protection Commitee. (2021). *Resolution MEPC.328(76) - Amendments to the Annex of the Protocol of 1997 to Amend the International Convention for the Prevention of Pollution from Ships 1973, As Modified by the Protocol of 1978 Relating Thereto 2021 Revised MARPOL Annex VI*. https://wwwcdn.imo.org/localresources/en/OurWork/Environment/Documents/Air pollution/MEPC.328(76).pdf

The Marine Environment Protection Commitee. (2022a). *Resolution MEPC.353 (78) - 2022 Guidelines on the Reference Lines for Use with Operational Carbon Intensity Indicators (CII Reference Lines Guidelines, G2)*. https://wwwcdn.imo.org/localresources/en/OurWork/Environment/Documents/Air pollution/MEPC.353(78).pdf

The Marine Environment Protection Commitee. (2022b). *Resolution MEPC.354(78) - 2022 Guidelines on the Operational Carbon Intensity Rating of Ships (CII Rating Guidelines, G4)*. https://wwwcdn.imo.org/localresources/en/OurWork/Environment/Documents/Air pollution/MEPC.354(78).pdf

Turk, A., & Prpić-Oršić, J. (2009). *ESTIMATION OF EXTREME WIND LOADS ON MARINE OBJECTS Anton TURK 1 Jasna PRPIĆ-ORŠIĆ 2 Estimation of Extreme Wind Loads on Marine Objects*. *2*, 147–156.

Vadset, M. S. (2018). *Modeling and operation of hybrid ferry with gas engine, synchronous machine and battery*. Norwegian University of Science and Technology.

Wang, Z., Chen, L., Wang, B., Huang, L., Wang, K., & Ma, R. (2023). Integrated optimization of speed schedule and energy management for a hybrid electric cruise ship considering environmental factors. *Energy*, *282*, 128795. https://doi.org/10.1016/J.ENERGY.2023.128795

Windfinder. (2020, May). *Wind, waves, weather & tide forecast Sembawang*. https://www.windfinder.com/forecast/sembawang

Zahedi, B., Norum, L. E., & Ludvigsen, K. B. (2014). Optimized efficiency of all-electric ships by dc hybrid power systems. *Journal of Power Sources*, *255*, 341–354. https://doi.org/10.1016/J.JPOWSOUR.2014.01.031

Proceedings of 15th International Marine Design Conference (IMDC-2024)
June 2-6, 2024
Amsterdam, the Netherlands

An optimisation-based approach to reduce fuel consumption and emissions from shipping navigation

Ribeiro e Silva, S.[1,*] and Bento Moreira, M.[2]

ABSTRACT

This study presents an optimisation-based approach to reduce fuel consumption and emissions from shipping navigation. The main objective is to improve energy efficiency and simultaneously turn a case-study vessel compliant with Carbon Intensity Indicator (CII) proposed by IMO. This optimisation module has been devised as part of a new robust integrated real-time digital solution that will involve a significant number of both technical and operational measures in practice aiming to optimise operational efficiency (during navigation and port calls). Namely, the tool will be capable of situational awareness and decision support to reduce fuel consumption and Green House Gas (GHG) emissions from shipping and must be combined with intrinsic vessel systems to improve vessel hydrodynamic performance, resulting also in improved vessel safety and widening of the operational weather window.

KEY WORDS

Ship energy efficiency; Real-time fuel consumption estimation; Hydrodynamic optimisation; Weather routing; Vectorized simulated annealing.

INTRODUCTION

As the most energy efficient mode of transportation, the maritime transport sector is one of the major sectors of cargo shipping of goods around the world, but is also responsible for 681 [t] of $C0_2$ every year (see Hieminga and Luman (2023)). Hence, IMO is targeting a drastic reduction of Green House Gas (GHG) and $C0_2$ for shipping (see IMO (2023)). These ambitious targets involve major changes in the way ship owners, in general, and the maritime industry sector operates, bringing the need to adopt new technologies, investing in greener alternative fuels and adopting practical measures to improve current energy efficiency of the means of transportation.
In addition to this most challenging context of the maritime industry sector, many weather routing service providers claim the ability to save fuel and increase safety and schedule reliability. However, many seaman lives are frequently put at risk since more than 3,000 containers are lost overboard every year. According to the most recent report issued by the World Shipping Council ((see Larsson (2023)), the average annual loss for the two-year period 2020-2021 saw an increase to 3,113 from the 779 of the previous period, driven by major incidents. In 2020 the ONE Opus lost more than 1,800 containers in severe weather. The Maersk Essen also experienced severe weather in 2021 that resulted in the loss of some 750 containers. Also a study conducted by Gershanik (2011) revealed that weather routing helped to reduce ship rough weather damages by 73% and costs of maintenance and cargo damage law suits by 29% and 87%, respectively. At the same time the length of ship delays due to unfavourable weather reduced by 80% and fuel savings amounted to about 6%. With exaggerated capabilities and unsubstantiated benefits being advertised by weather routing companies, port authorities, ship owners,

[1] MARETEC (Department of Mechanical Engineering, Instituto Superior Tecnico, University of Lisbon, Portugal); ORCID: 0000-0003-0977-0629

[2] CENTEC (Centre for Marine Technology and Ocean Engineering, Instituto Superior Tecnico, University of Lisbon, Portugal); ORCID: 0000-0002-4948-6668

[*] Corresponding Author: ribeiro.e.silva@tecnico.ulisboa.pt

Submitted: 12 March 2024, Revised: 16 April 2024, Accepted: 1 May 2024, Published: 18 May 2024

Conference paper, DOI: https://doi.org/10.59490/imdc.2024.832 e-ISSN: 3050-4864

operators or charterers often face the difficult task of selecting the right service provider and level of technology suitable for their operations.
Anticipating that fuel prices in years to come will remain high due to war in Ukraine (see International Energy Association (2023)) and the conflict in the Middle-East plus the recent emphasis on reducing GHG emission in Europe, have resulted in renewed interest in further optimising ship performance. A recent DnV study (see DNV (2022)) indicated that while hydrodynamic performance (hull coating, hull form and trim optimisation and regular propeller cleaning) can achieve 5 to 15% reduction in fuel consumption and associated GHG emissions, more than 20% improvement can be achieved through technical and operational measures such as speed management, fleet planning and weather routing (the so-called logistics and digitalisation). Moreover, an experimental campaign conducted by HSVA with scaled models of a containership have demonstrated that hydrodynamic performance can be further improved in case an anti-rolling tank is installed to reduce ship motion waves (see HSVA (2020)).
To tackle the problem above, firstly, a numerical program has been developed at University of Lisbon, IST to evaluate added resistance in waves using output data of a standard strip theory seakeeping program developed by Ribeiro e Silva (2008). In this case, the strip theory code is based on Frank's Close-Fit method and the added resistance in waves is evaluated using the formulation originally proposed by Salvesen (1978). The program has provided good results against experimental data available in literature, especially for slender ship forms (see Ribeiro e Silva et al. (2011)). The numerical predictions presented in here have been compared against experimental data relative to ship's models with the same L/B ratio. Additionally, another Computational Fluid Dynamics (CFD) solver of the Navier-Stokes (N-S) type has been utilised to provide additional numerical predictions of the ship's total resistance in calm water and more detailed information on the flow characteristics around the ship's hull for distinct trim angles (see further details in Ribeiro e Silva and Eça (2024)).
More recently progressive increase in memory and speed of computers favours the utilisation of CFD N-S solvers, for current voyage planning purposes (i.e., simulations close to real-time for variable meteocen conditions) in conjunction with Salvasen method to predict added resistance in waves seems to be the most suitable decision support tool. Where a multi-dimensional (velocity and heading), multi-disciplinary constrained (rms ship motions and eventually with prevention of dynamic instabilities in waves), single objective (fuel consumption) optimisation algorithm has been proposed in order to take into account not only the pertinent fuel savings, but also the safety aspects of the voyage. Efforts have been focused so far on key technical-economic challenges that can demonstrate cost effectiveness and applicability of the concept. In particular, use of CFD simulations have been conducted with the aim of obtaining reliable predictions of calm water resistance, which combined with corrections for current, wind and wave effects lead to the development of this optimisation-based approach to reduce fuel consumption and emissions from shipping navigation.
Furthermore, development of a voyage planning module based on weather routing to save fuel and increase safety and schedule reliability (in terms of Just in Time arrival to port) has been envisaged. Hence, prior to integration of voyage planning module with the other Ship Operation Optimisation System (SOOS) modules and their full-scale demonstration during sea trials, all these modules must be extensively tested in a virtual environment to proper de-risk this new technology.
Firstly, the methodology used in this paper is presented in the Theoretical Background section, where an optimisation-based approach for enhanced fuel efficiency and safety aboard is described.
Secondly, in the Numerical Results section, some preliminary figures on the performance of the newly developed voyage planner are shown for a synthetic environment to demonstrate the capabilities of the tool. Namely, the range of surface currents, wind loading conditions and sea states which a typical containership usually operates in the Atlantic West coast of Portugal were simulated in order to set a numerical model that could be utilised to calculate the optimised fuel consumption for a desired average speed between two ports.
As mentioned in Conclusions, it is believed that calculation of specific hydrodynamic responses such as added resistance in waves for a real-time loading condition of the vessel, represents a major advantage in comparison with other commercial available tools, allowing as well the designer to define the most suitable hullform and superstructure area for the most energy efficient mode of operation of the vessel.

THEORETICAL BACKGROUND

In general, the hydrodynamic performance of a ship is influenced by the surrounding environmental conditions. In this context the existing space and time realizations of wind, waves and ocean current conditions can be defined as the environmental factors in any voyage. These factors will affect the fuel consumption by changing the power requirements for the propul-

sion of the vessel. Hence, this section attempts to presents a summary of the basic concepts in the realm of power estimates for the ship propulsion.

Power Curve Estimation

Ship's resistance is particularly influenced by the ship's hullform, speed, displacement and trim. In addition to these calm water parameters, added-resistance in waves or even wave-induced roll motion can also have a significant impact in the power delivered by the propeller. The total resistance R_T consists of several resistance components acting on the ship, which will be briefly describe in this section, while also referring to some relevant works that provide a more thorough and analytical presentation of methodologies to estimate those components of ship's resistance.
Hydrodynamic analysis for a specific hullform and ship loading condition can be used to calculate the components resistances acting on the ship by means of dimensionless resistance coefficients (see for example Harvald (1983)). This analysis may consist of using towing tank tests with scaled models, developing CFD models to simulate the flow around the ship, quasi-experimental methods using results of experiments and calculations. In case, calm water resistance is obtained, then seakeeping models can be utilised to estimate ship motions in irregular waves. In terms of CFD applications there are open source or commercial software that can be used in modelling ship resistance. In this study, CFD Simerics MP software considering a marine template to calculate ship resistance is used to determine calm water effective hull resistance at a given loading condition and range of ship speeds, i.e., the so-called power curve in calm water.
Calm water resistance is what a vessel would face in the event of total calm weather conditions, with an absolute lack of waves excluding the waves created by the ship moving in otherwise calm deep water condition. Calm water is very seldom encountered in real world conditions, particularly in ocean going voyages. For example, in the North Atlantic the probability of encountering calm water conditions is only 26 days in a year, i.e., 0.7%.
According to Scheekluth and Bertram (1998), calm water total resistance of a ship is made up of a number of different components, which are caused by a variety of hydrodynamic factors, and interact one with each other in a extremely complex way. Adopting a reductionist approach, calm water resistance consists of a viscous resistance plus the resistance due to the Kelvin waves generated by the hull. Viscous resistance is due to the viscosity of the water, which creates friction with the hull of the ship and depends, among other things such as the hull surface curvature, on the hull roughness and cleanness of the hull. With regard to the second component of calm water resistance component, wavemaking resistance, R_W, is closely associated with Kelvin wave system (i.e., waves generated from a moving pressure field with divergent and transverse systems). As it can be seen in Fig. 1, the wave system of a ship is composed of different Kelvin wave systems. Note that waves are generated by every point of the containership, where larger waves (more visible) are generated at the bow and stern.

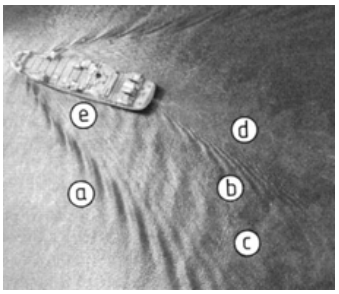

Figure 1: Different Kelvin wave systems of a typical containership, where: a) divergent bow wave; b) divergent stern wave; c) transverse wave; d) turbulent wake; e) quarter wave.

Ship calm water resistance, R_T, can be calculated as a function of the total resistance coefficient, $C_T = C_V(Rn)+C_R(Fn)$, the density of seawater, ρ_{sw}, the ship's speed over water, V_s, and the total wetted area of the hull, S_w, given by Eqn. (1).

$$R_T = \frac{1}{2}\rho_{sw} S_w V_s^2 C_T = \frac{1}{2}\rho_{sw} S_w V_s^2 (C_V + C_R) \tag{1}$$

Note that equation above is a simplified formulation of the complex nature of ship resistance in calm water, where viscous resistance coefficient, C_V, is assumed to be only dependent of Reynolds number (Rn), whereas the coefficient of residuary resistance, C_R, mainly composed by wavemaking resistance, C_W, is assumed to be dependent on Froude number (Fn). Once the main resistances have been estimated, it is possible to calculate the required effective power with appendages, P_{EA}, to move the ship through the water at the required sailing speed. Note that the effective power is simply the product of the total resistance times the speed over water, V_S. Based on that, the required nominal power at the main engine shaft (P_S) can be calculated using the shaft-line efficiencies, given by Eqn. (2).

$$P_S = \frac{P_{EA}}{PC} = \frac{R_{EA} V_S}{QPC \eta_S} = \frac{(R_T + R_{APP})\, V_S}{\eta_H \eta_O \eta_R \eta_S} \tag{2}$$

Hull efficiency, $\eta_H = \frac{P_{EA}}{P_T}$, is the ratio between the effective power with appendages and the power thrust, which depending on hydrodynamic pressure distribution around the hull, may attain values larger than 1.0. Open water propeller efficiency, $\eta_O = \frac{P_T}{P_{Do}}$, ranges approx. 0.60-0.75, whereas relative rotative efficiency, $\eta_D = \frac{P_{Do}}{P_D}$, of a conventional propeller ranges approx. 0.95-1.02. Note that power thrust (P_T) of the propeller is the power output that can be measured at thrust block bearing, whereas the open water delivered power or propeller power in open water (P_{Do}) is the power input measured during scaled model test of the propeller in open water, i.e., either towing tests or cavitation tunnel tests to measure thrust and torque developed by the rotating propeller without the presence of the ship's hull. Hence, propulsive coefficient (PC) can be calculated from quasi-propulsive coefficient (QPC) once shaft transmission efficiency is known, which is given by the ratio between delivered power with the propeller installed behind the hull (power measured at propeller flange) by power at the main engine shaft, i.e., $\eta_S = \frac{P_D}{P_S}$. Shaft transmission efficiency in conventional propulsion systems ranges 0.97-0.99 depending whether a simple or reversible reduction gearbox is intercalated in the shaft line or not (cases where 2-stroke low-speed diesel engine is installed).

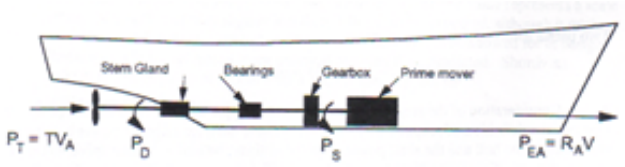

Figure 2: Different power and efficiencies along the shaft-line of a propulsion system, and locations where: a) effective power with appendages; b) shaft power; c) delivered power; d) thrust power can be measured.

As illustrated in Figs. 1 and 2, the behaviour of the flow around the hull determines the ship resistance and the wake at the propeller, which are interrelated. While the magnitude of the resistance directly determines the power requirements, the magnitude of the wake and its distribution at the propeller plane also affects the power requirements as well as the performance characteristics. When the wake distribution is highly non-uniform at the propeller plane, this is a major source of poor propulsive efficiency (η_R), cavitation, vibration and noise. Assuming some simplifications, the main engine that satisfies the propeller's demands, and allows the ship to sail at its nominal speed during voyage, can be selected. Note that this main engine rated power should cover the propulsion demands considering as well an appropriate power margin that will depend on certain cost elements (acquiring, operating and maintenance), reliability and adaptability to different operating patterns of the vessel.

Wind Resistance

In first place, it is recalled that wind is the cause to the creation of waves so that their incoming direction is sometimes practically the same, and simultaneously wind acts as a force on the vessel known as wind resistance. Wind resistance will affect all surfaces of the ship above the sea-surface as well as cargo when the latter is above the hull, as it is the case of most containerships. According to Bernoulli's equation, wind resistance either in the x or y direction is directly proportional to the projected transverse cross-sectional (A_T) or lateral (A_L) areas of the ship above the waterline, the density of the air,

ρ_{air}, and the square of the wind speed. These two projected areas are defined by the above-water part of the main hull and any superstructures (e.g., cargo, bridge, funnel, and equipment). Normally wind represents around 2% of the total resistance, with the notable exception of containerships where due to both large projected transverse cross-sectional and lateral areas of the vessel (due to 60% of containers on-board are pilled-up above main deck) the contribution can reach up to 10%.

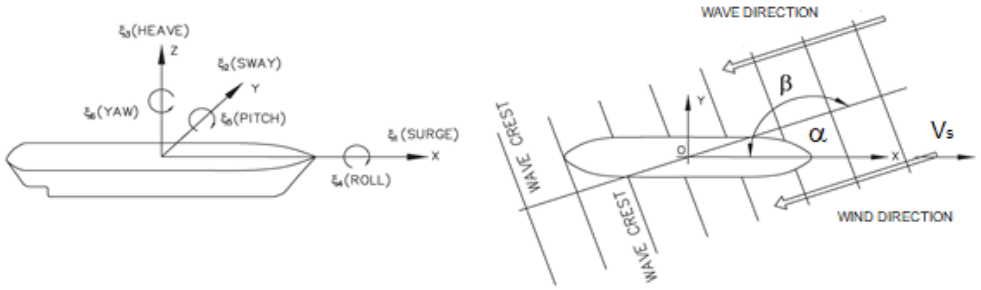

Figure 3: The non-inertial body-fixed tri-axial coordinate system of the ship, illustrating the six modes of motion and the definition of the true wind vector (α) and wave (β) incoming direction angles.

The wind force is typically divided into two components: the fair wind, which is what the ship is facing during sailing (same speed but opposite direction of the vessel), and the true wind, which is the actual wind speed and direction at the current position at sea. The former can be computed using either a semi-empirical formulation proposed by Gould (1982) or a standard CFD tool Ribeiro e Silva and Eça (2024) and is essentially the wind that the vessel would face due to the fact it is sailing, while the latter would be the wind the vessel would face at the same location if she was anchored. Adding these two vector components, the resulting apparent wind vector can then be used to calculate the total wind resistance. As illustrated in Fig. 3, the true wind induced longitudinal and transverse force components and the yawing moment can be calculated using the following equations originally derived by Isherwood (1972),Gould (1982) and Blendermann (1994):

$$\begin{bmatrix} F_{wx} \\ F_{wy} \\ M_w \end{bmatrix} = \frac{1}{2}\rho_{air} V_w^2 \begin{bmatrix} C_{wx}\left(\alpha_w\right) A_T \\ C_{wy}\left(\alpha_w\right) A_L \\ C_w\left(\alpha_w\right) x_{wc} \end{bmatrix}, \tag{3}$$

where x_{wc} represents the distance between the center of the lateral area of the ship above waterline and midships and the force components are given by Eqns. (4) and (5):

$$F_{wx}\left(\alpha_w\right) = F_w\left(\alpha_w\right)\cos\left(\alpha_w\right) \tag{4}$$

$$F_{wy}\left(\alpha_w\right) = F_w\left(\alpha_w\right)\sin\left(\alpha_w\right) \tag{5}$$

Assuming that wind force Cartesian components in surge and sway are expressed by $F_{wx}(0°)$ and $F_{wy}(0°)$, respectively, then the resulting true wind induced force at any given incoming angle, α_w, may be expressed as:

$$F_w\left(\alpha_w\right) = F_{wy}\left(90°\right)\left\{\frac{2\sin^2\left(\alpha_w\right)}{1+\sin^2\left(\alpha_w\right)}\right\} + F_{wy}\left(0°\right)\left\{\frac{2\cos^2\left(\alpha_w\right)}{1+\cos^2\left(\alpha_w\right)}\right\} \tag{6}$$

Note that more precise wind load calculations could have been performed to take into account as well a given vertical wind profile. In this case, an effective wind speed and the lateral center of pressure for a gradient wind could be also estimated by

subdividing the frontal and lateral projections into small elements so that after surface integrals have been conducted new non-dimensional wind load coefficients $C_{wx}(\alpha_w)$, $C_{wy}(\alpha_w)$ and $C_w(\alpha_w)$ could be obtained.

Added-Resistance in Waves

Both involuntary and voluntary speed reductions are taken into account to avoid over-predicted ship speed and wrong diversion decisions when facing rough weather, not to mention inaccurate estimates of fuel consumption and time of arrival. To prevent this problem, added-resistance in waves for a specific loading condition and a given hullform will be computed as well using a state-of-the art numerical tool. Note that this additional component of resistance called added-resistance in waves, R_{aw}, is heavily non-linear. In fact, estimating added resistance is a complex process, as this generally depends on hullform, hydrodynamic characteristics of the ship and the encountered sea spectrum. For the calculation of the added resistance in waves, Salvesen 1978 method using strip theory approximation has been adopted. In this case, the strip theory code is based on Frank's Close-Fit method and the added resistance in waves is evaluated using the formulation originally proposed by Salvesen plus a correction for short waves. Hence, using this strip theory, Salvesen introduce the added-resistance in waves, given by Eqn. (7):

$$R_{aw} = -\frac{1}{2} k \cos\beta \sum_{j=3,5} \zeta_k \left\{ \left(F_j^I\right)^* + \hat{F}_j^D \right\} + R_7, \tag{7}$$

where $(F_j^I)^*$ is the Froude-Krylov force and moment, $(F_j^D)^*$ is the diffraction force and moment, R_7 is the added-resistance due to diffraction potential, ζ_k is the ship's displacement induced by waves in k direction.
In case head waves scenario is considered, in this study, the equation can be more conveniently expressed as Eqn. (8):

$$R_{aw} = \frac{i}{2} k \left\{ \zeta_3 \hat{F}_3 + \zeta_5 \hat{F}_5 \right\} + R_7, \tag{8}$$

where the incident and diffracted components are given by Eqn. (9):

$$\hat{F}_j = \left(F_j^I\right)^* + \hat{F}_j^D \tag{9}$$

The complex amplitude for the incident wave potential for head waves having wave amplitude ζ_w^a and angular frequency ω can be expressed by Eqn. (10).

$$\phi_0 = \frac{ig\zeta_w^a}{\omega} e^{ikx+kz} \tag{10}$$

Hence, heave components of added-resistance in waves are given by Eqn. (11):

$$\hat{F}_3 = \zeta_w^a \int_L e^{-ikx} e^{-kds} \left\{ \rho g b - \omega_e \left(\omega a_{33} - i b_{33} \right) \right\} dx, \tag{11}$$

and pitch components of added-resistance in waves are given by Eqn. (12):

$$\hat{F}_5 = -\zeta_w^a \int_L e^{-ikx} e^{-kds} \left\{ \rho g b - \omega_e \left(x + \frac{iV_S}{\omega} \right) \left(\omega a_{33} - i b_{33} \right) \right\} dx, \tag{12}$$

where $d =$ sectional draft, $s =$ sectional area coefficient, $b =$ sectional breadth, $\omega_e = \omega - \frac{\omega^2}{g} V_S cos\beta =$ encountering wave frequency, $a_{33} =$ sectional heave added mass coefficient and $b_{33} =$ sectional heave damping coefficient.
Added-resistance due to diffraction potential can be expressed as Eqn. (13) for calculating head sea result:

$$R_7 = \frac{i}{2} \left(\zeta_w^a\right)^2 k \frac{\omega_e^2}{\omega} \int_L e^{-2kds} b_{33} dx \tag{13}$$

Note that a non-dimensional added-resistance in waves can then be simply defined by the summation of the three dimensional components $R_{aw} = \hat{F}_3 + \hat{F}_5 + R_7$ as:

$$R'_{aw} = \frac{\hat{F}_3 + \hat{F}_5 + R_7}{\rho_{sw} g \left(\frac{B^2}{L_{pp}}\right) \left(\zeta_w^a\right)^2} \tag{14}$$

Next, a practical simplification can be introduced to estimate added-resistance in waves directly from head sea result, where added-resistance in waves at any angle β relatively to head waves is given by Eqn. (15):

$$R_{aw}\left(H_S, T_P, \beta\right) = R_{aw_{180^\circ}}\left(T_P\right) \left(\frac{H_S}{2}\right) \cos^2 \beta \tag{15}$$

Trim Effect on Ship Resistance

CFD with RANS turbulence models can address a wide variety of flows including external flows around bodies of a certain shape, i.e., statistically steady flows that require streamlined shapes aligned with the incoming flow where boundary-layers do not exhibit significant flow separation. However, for trim optimisation these simulations must be supported by relevant background experience in the realm of CFD tools utilisation and must be subjected to a dedicated Verifcation and Validtion (V&V) procedure.

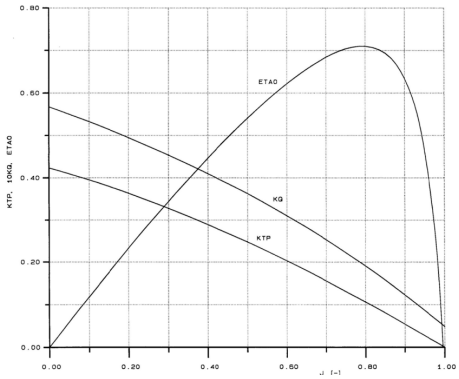

Figure 4: Schiffbau Versuchsanstalt Potsdam GmbH: Open-water propeller test diagram of a variable pitch propeller (VP 1124)

.

CFD simulations of ship performance in waves will be mainly built around an advanced actuator disk model implemented either in or Simerics MP, which reads the open water performance of a real propeller (see Fig. 4). Notice should be given to the fact that being able to remove the actual propeller geometry from the numerical computations considerably simplifies the physics and speeds up the process. Moreover, experimental results from scaled model testing or sea trials having sys-

tematic draught and trim variations are expected to be compared and contrasted against CFD simulation results in the near future.
Firstly, considering the geometry of the hull, accurate ideal trim predictions of the total CFD resistance in calm water must be determined for enhanced stability and fuel consumption optimisation purposes. Secondly, the vessel floatation, and the corresponding flow characteristics at the propeller plane during operation must be optimised to attain the least required power solution for a specific design loading condition by means of altering the vessel's position of centre of gravity of the ship, $CG(x, y, z)$. Note that instantaneous location of the center of gravity of the ship, $CG(x, y, z, t)$ depends on magnitude and location of a large number N of i discrete weights aboard, including fuel and ballast water in the aft and peak tanks, is given by:

$$CG\left(x, y, z, t\right) = \frac{\sum_{i=1}^{N}\left[m_i\left(t\right) \times \left(x_i, y_i, z_i\right)\right]}{\sum_{i=1}^{N} m_1\left(t\right)} = \frac{M_i\left(x, y, z, t\right)}{\Delta\left(t\right)} \tag{16}$$

Next, using one particular hydrostatic parameter called unit moment to change trim (M_U), the required instantaneous trim angle variation, $\delta\theta(t)$, for enhanced stability and fuel consumption optimisation purposes can be easily calculated by SOOS from the instantaneous variation in the longitudinal inclining moment, $\delta M_I(x, t)$, using the Eqn. (17):

$$\delta\theta(t) = \frac{\delta M_I(x, t)}{M_U} \tag{17}$$

Finally, added-resistance in waves component for this particular new loading condition as well as wave induced roll motion component of total ship's resistance will be computed in the near future using SOOS.

Vectorized Simulated Annealing (VSA)

Fuel consumption C while sailing from points A to B, depends on the route L chosen and can be computed using the following line integral with respect to the arc length:

$$C = \int_L \frac{\frac{\partial M}{\partial t}}{V} ds, \tag{18}$$

where $\frac{\partial M}{\partial t}$ and V stands respectively for fuel consumption time rate and the speed along L. Note that $\frac{\partial M}{\partial t}$ and V depends particularly on environmental conditions such as wind, currents and waves. Therefore, the route that minimizes global fuel consumption, in such conditions, is not the straight (or geodesic) path from A to B.
The approach that has been adopted to find the route L that minimizes the global fuel consumption is the Vectorized Simulated Annealing (VSA) technique which is based on the Simulated Annealing (SA) method, see Press (2007). This method can be roughly described using the analogy with the metallurgical process of annealing to bring a metal from an high energy/temperature state to a crystal lattice state of minimum/temperature energy. At a high temperature, the different elements that characterize the system register significant variations in their respective positions, resulting from their high kinetic energy. As the temperature decreases, the system assumes lower energy and more stable configurations and the changes in position of the system's constituents occur with a smaller amplitude. In case the temperature decrease is not too rapid and if during it the system has the possibility of assuming less probable configurations (of higher energy), the retention of the system in meta-stable configurations will be less likely. A slow and gradual decrease in temperature will allow the system to properly explore the search space and assume the configuration of minimum energy by the end of the annealing process. SA method was developed by Metropolis and co-workers, see Metropolis et al. (1953). A comprehensive description of this method, also known as the Metropolis-Hastings algorithm, can be found in Hitchcock (2003). The VSA method applies components of the SA algorithm in parallel to a population of systems that constitute the components of a vector. This methodology has been successfully applied in previous works such as Maurício and Moreira (2022).

In the application of the VSA method, paths will be modelled by a process of proper concatenating oriented segments. Note that any path between A and B can be arbitrarily approximated in the aforementioned manner. So, define N concatenated oriented segments L_i(legs) that establish a route L between points A and B. This path is thus defined by $N-1$ yaw points P_i. The global fuel consumption C in L is given by:

$$C\left(L\right)=\sum_{i=1}^{N}C\left(L_i\right), \tag{19}$$

where $C\left(L_i\right)$ is the fuel consumption in leg L_i.

Note that Eqn. (19) can be numerically integrated (with respect the arc length) using a standard numerical integration method (e.g., trapezoidal rule) and adopting an appropriate spatial discretization of the leg over the corresponding leg L_i.

$$C\left(L_i\right)=\int_{L_i}\frac{\frac{\partial M}{\partial t}}{V}ds \tag{20}$$

The aim is to determine the positions of the yaw points P_i thus determining the path L that minimize the global fuel consumption C. As previously mentioned, fuel consumption rate $\frac{\partial M}{\partial t}=\frac{\partial M}{\partial t}\left(x,y\right)$ and speed $V=V\left(x,y\right)$ along the routes depend on environmental conditions.
Note that (x,y) stand for the spatial coordinates. The estimation of the fuel consumption time rate will consider the effect of wind (intensity and direction), the resistance associated with waves (significant height, period, and direction), and the effect of drift produced by currents. Later on consideration of the effects of roll motion in formulating this fuel consumption optimisation problem will be considered.

VSA NUMERICAL MODELLING

Main details in the implementation of the heuristic to minimize Eqn. (18) comprises five main steps as follows:

(i) Generate a set U, of $2M$ different routes L^j from A to B, each one defined by sequences of $N-1$ yaw points in randomly distributed spatial positions;

(ii) Compute de fuel consumption $C\left(L^j\right)$ on each one of the routes in U and retain an ordered subset $V\subset U$ of the routes with the lower global fuel consumption. Typically $\#V=\frac{\#U}{2}$. Note that routes L^j, in

$$V=\left\{L^1,L^2,\ldots,L^j,\ldots,L^k,\ldots,L^M\right\},$$

must be ordered such that $C\left(L^j\right)<C\left(L^k\right)\Rightarrow j<k$;

(iii) Construct a new set U concatenating a new set of V with previous set of best performers V and apply a randomly uniformly distributed $2-D$ spatial perturbation of maximum semi-amplitude ε to the positions of each one of the yaw points that define each of the $2M-1$ last routes in U. The first and better route in the current epoch remain undisturbed and survive to integrate the set U in the next epoch without any perturbation imposed in order to prevent that a top performer candidate prematurely detected could be discarded;

(iv) Repeat steps $(ii)-(iii)$ using in each repetition a smaller semi-amplitude ε of the maximum spatial perturbation;

(v) Stop when the best route in V route fails to show significant improvements or, after P repetitions.

Note that the successive repetition of steps $(ii)-(iv)$ allows us to define a sequence $U\left(i\right)$, $i=1,\ldots,P$ of route sets and a related sequence $\varepsilon=\varepsilon(i)$, $i=1,\ldots,n,\ldots,P$ of maximum semi-amplitude spatial perturbation of the yaw points, where

each i define an "*epoch*". Moreover, $\varepsilon = \varepsilon(i)$, $i = 1, \ldots, n, \ldots$, must be a slowly decreasing function in order to ensure an adequate survey of the search space. In particular, the slow decreasing negative exponential function given by the Eqn. (21) can be used:

$$\varepsilon\left(i\right) = d \times e^{-\sigma \times i}, \tag{21}$$

where d stands for a characteristic length, related with the distance from A to B, for instance. The decreasing coefficient σ is given by Eqn. (22):

$$\sigma = \frac{\ln\left(\frac{d}{\delta}\right)}{P}, \tag{22}$$

where δ is small residual distance and P is the global number of epochs. Note that when $i = P$, the following detection is obtained:

$$\varepsilon\left(P\right) = \delta, \tag{23}$$

which means that δ and P must be selected assuring the decrease of ε is slow enough and the spatial perturbations of the position of the yaw points of semi-amplitude of δ will be irrelevant.
Before real-data is utilised, a synthetic environment has been proposed to obtain preliminary checks on performance of this decision-support tool. After these V&V studies, the newly developed voyage planner must be compared and contrasted with available sea-trials results.

NUMERICAL RESULTS

In this section the numerical results of a fully integrated voyage planner for enhanced fuel efficiency and safety aboard a 712 TEU geared containership (see Appendix) are presented. Firstly, a synthetic environment is utilised to check consistency of the fuel consumption results under three scenarios: (i) ocean currents, (ii) wind loads and (iii) wave conditions. Moreover, navigation interdiction zones such as traffic corridors or islands have been introduced to check consistency of the optimisation-based approach to reduce fuel consumption and emissions from shipping navigation.
Finally, using a scenario of real-case meteocean conditions for a given geographical area (obtained from the numerical model MOHID) still in a synthetic environment, some preliminary figures on the performance of the newly developed voyage planner in terms of fuel consumption reduction can be obtained. Note that MOHID is a large circulation hydrodynamic model able to provide either hindcast or forecast predictions of wind, waves, and currents for distinct design-points, i.e., either small domestic routes or long hauls (transoceanic crossings).

Calm Water Power Estimation

As shown in Figs. 5 and 6, the power curve [knots versus kW], can be modelled by means of a 3rd order polynomial fit of the type $f(x) = a_3x^3 + a_2x^2 + a_1x + a_0$, where the coefficients of this polynomial obtained by means of linear regression reads $a_2 = -0.275$, $a_3 = 6.510$, and $a_1 = a_0 = 0.0$. Note that the polynomial function obtained must be equal to zero at the origin so that effective power will be extinct at ship's zero speed ($a_0 = 0.0$). Moreover, a second condition has been imposed to this polynomial fit of the effective power in terms of having also zero resistance at zero speed, so that at the slope of the effective power at the origin must be also zero, i.e., $dP_E/dV_s = 0.0$ at $V_s = 0$ implying additionally that $a_1 = 0.0$.

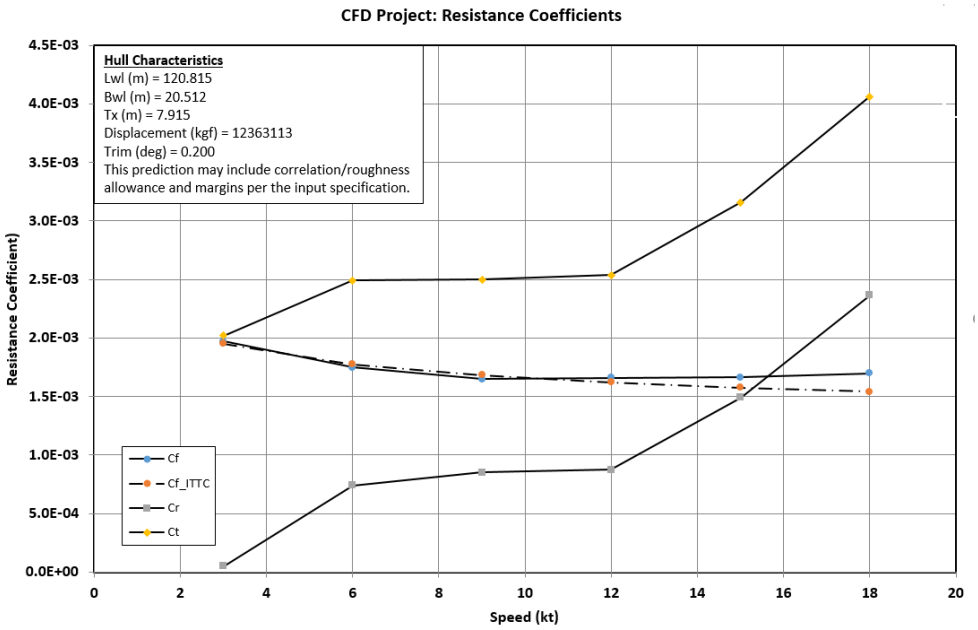

Figure 5: CFD resistance coefficients in calm water from Simerics MP of the containership

.

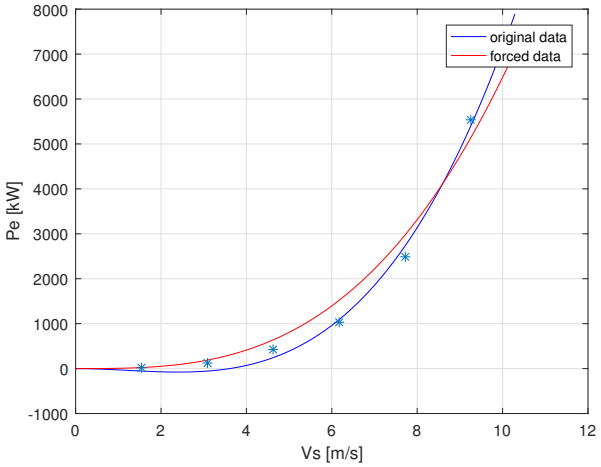

Figure 6: Power curve in calm water of the containership [m/s versus kW]

.

Finally, to prevent the power curve to take negative values at low speeds (see Fig. 5) a third local condition has been imposed to force the polynomial to move upwards by means of introduction of an extra point located upwards. This extra point that can be interpreted as an outlier point, whose magnitude is large enough to obtain a forced power curve always positive (see forced data curve of Fig. (6) coloured in red).
From the rated power of the CFD effective power curve at an ideal trim of $\theta = 0.2^o$ by the stern, a propulsive coefficient of the containership at top speed of $PC = 0.656$ has been determined.

Wind Loads Estimation

Firstly, estimation of forces (and moments) caused by wind resistance have been conducted for the containership facing head and beam winds. Next, as shown in Fig. (7), trigonometric relations given by Eqn. (3) can be used to determine the wind loads coefficients at different incoming angles of direction of the wind relatively to the ship's heading.

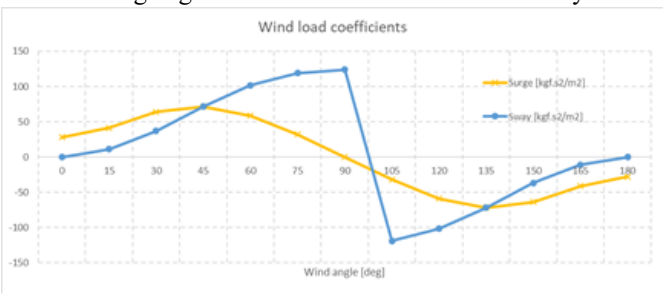

Figure 7: Wind load coefficients in surge and sway of the containership

.

Note that instead of using Gould's semi-empirical formulation, a more accurate assessment of the impact of wind on this containership could have been conducted by means of CFD. In that case, CFD presents many advantages, of which the most obvious is adequacy for flow visualization and for design optimisation of all surfaces of the ship above the sea-surface as well as cargo. However, proper selection of the choice of the CFD method as well as a grid convergence study should be adopted in first place to prevent results become affected by the mesh and input data selection. Hence, in this preliminary study a faster methodology has been adopted for demonstration purposes.

Added Resistance in Waves and Speed Loss Estimation

As shown in Figs. (8) and (9), there is a fair agreement between Salvesen (1978) and Gerritsma and Beukelman (1979) numerical predictions of added resistance in head waves. In close or open quartering waves the added resistance curves obtained by Gerritsma&Beukelman (1979) present larger deviations and in the opposite direction practical experience of the authors as seafarers, therefore Salvesen (1978) is considered to provide more accurate predictions when compared with experiments, so that this will be the adopted methodology in this study.

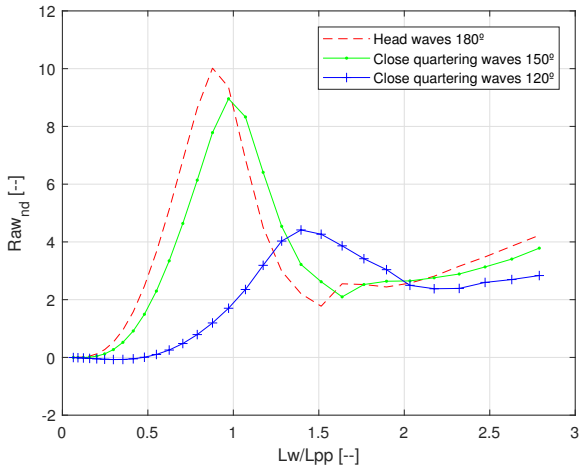

Figure 8: Transfer functions of non-dimensional added resistance in wave ($R_{aw} = R_{aw}/(\rho_{sw} g B^2/L_{pp}\zeta_w^{a\,2})$ versus ratio of wave to ship's length between perpendiculars (λ_w/L_{pp}) in head waves (180^o in red dashed line), close quartering waves (150^o in green line) and open quartering waves (120^o in blue line with cross) of the containership at top speed, calculated by the Salvesen, 1978 method

.

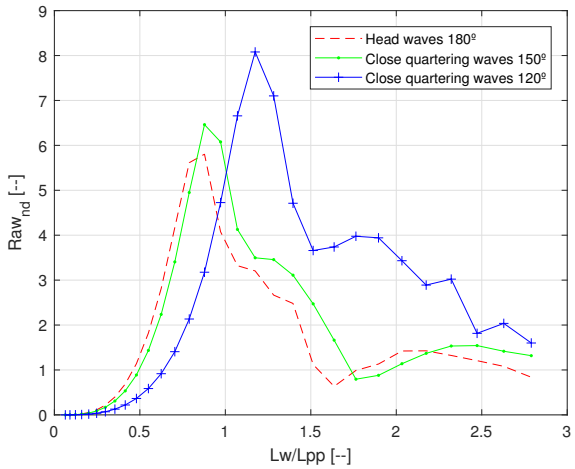

Figure 9: Transfer functions of non-dimensional added resistance in wave ($R'_{aw} = R_{aw}/(\rho_{sw} g B^2/L_{pp})\zeta_w^{a\,2}$) versus ratio of wave to ship's length between perpendiculars (λ_w/L_{pp}) in head waves (180^o in red dashed line), close quartering waves (150^o in green line) and open quartering waves (120^o in blue line with cross) of the containership at top speed, calculated by by Gerritsma&Beukelman, 1979 method

.

Non-dimensional added resistance in waves estimates versus wave frequency for top speed ($Fn = 0.26$) are shown in Figs. (8) and (9). Next, considering the design-point peak wave period and wave height along with Eqn. (15) the added resistance in waves for any wave condition encountered at sea with a certain relative incoming wave direction can be easily calculated. For example, considering the containership is facing the most statistically frequent wave train with a peak period around $T_P = 9$ [s] and a significant wave height of $H_S = 1.25$ [m], the resulting added resistance in head waves is 13.42 [kN], which represents 1.7% of the total resistance or 2.9% of the residuary resistance at top speed.

Weather Routing Assumptions

Considering the effect of environmental conditions in the ship's resistance in otherwise calm water. Namely: wind, waves and ocean currents. The present implementation of VSA allows to find the route that minimizes global fuel consumption under the influence of these most relevant environmental conditions. Notice should be given to the fact that, at this initial stage, either synthetically generated or MOHID predicted environmental conditions are assumed to be steady, so that preliminarily testing of the developed algorithms and the proposed heuristic can be conducted via numerical simulations.
The encoding of land presence and prohibited passage zones (e.g., marine traffic corridors) has been also added to the heuristic with the aim of equipping SOOS to handle such unavoidable and common restrictions in determining a realistic route. Programming this functionality involves assuming a practically zero speed of the ship in land or prohibited zones.
The trajectory from point A to B is planned to be carried out at a ship's advance base speed V_0 to reach the destination within the estimated or desired time. At this stage of the development of SOOS, the estimation of the effects of wind, waves, and ocean currents on speed and fuel consumption involved the formulation of some simplifications, namely:

(i) In considering the effects of environmental conditions, the principle of superposition will be applied, i.e., implicitly linearity in the dynamic behaviour of the system in the neighbourhood of V_0 and C_0 is assumed . Hence, the variation (either increase or decrease) in speed or fuel consumption stemming from environmental conditions will simply be added to the base velocity V_0 and the base fuel consumption C_0.

(ii) In the calculation of wind, drift, and current effects it has been assumed that vessel's heading is equal to her course;

(iii) Vessel drifting associated with wind loads has been neglected, and the wind loads will only impact the increased or decreased resistance to ship's advance. Consequently, leeway corresponds only to either increments or decrements to the base consumption C_0. The increased or decreased resistance to ship's advance is computed using the formalism condensed in Eqn. (4);

(iv) The increases or decreases in speed along the course caused by ocean currents at the free-surface will simply be added to the ship's advance base velocity V_0. The leeway produced by ocean currents will be considered only as an increase in the base consumption C_0, i.e., the corresponding increase in the velocity to maintain the ship's advance base velocity V_0 along the defined course over ground;

(v) Waves will be characterised by significant wave height, H_S, spectral peak period, T_P, and a relative incoming incidence angle, β, which will induce an additional ship's resistance component. This ship's resistance component will be varying from a maximum to zero depending on a spreading function, which is defined by an incidence angle in the range $-\frac{\pi}{2} \leq \beta \leq \frac{\pi}{2}$ radians, using the formalism exposed in Eqn. (15).

In the absence of wind, waves, and currents, let P be the power required to maintain speed V, let R be the resistance offered by the water and air to the displacement of the ship at speed V, and let C be the corresponding fuel consumption time rate, it has been assumed that:

$$P = a_1 V^2 + a_2 V^3, \tag{24}$$

$$R = a_1 V + a_2 V^2, \tag{25}$$

and

$$C = k\left(a_1 V^2 + a_2 V^3\right), \tag{26}$$

where k, a_1 and a_2 are fitting coefficients to be computed from previously obtained using CFD or empirical data.

Combining Eqns. (25) and (26) it is obtained:

$$\triangle C \approx \frac{k\left(2a_1 + 3a_2V_0\right)V_0}{\left(a_1 + 2a_2V_0\right)}\triangle R, \tag{27}$$

and

$$\triangle C \approx k\left(2a_1V_0 + 3a_2V_0^2\right)\triangle V. \tag{28}$$

These expressions will be used to estimate the consumption increments, $\triangle C$, associated with the computed increases in resistance, $\triangle R$, and velocity, $\triangle V$, resulting from the effects of the above mentioned considered environmental conditions. It should be stressed that linearity in the dynamic behaviour of the system in the neighbourhood of V_0, has been assumed, so that the present formulation will only be valid in a context where the effects of wave wind and currents are sufficiently moderate.
At a later stage of this work, the results will be experimentally validated by means of sea-trials, so that simplifications made in the formalism used in here might be appropriately adjusted.
In the implementation of the VSA technique, synthetic environmental conditions have been defined in an appropriate spatial grid. Namely, a non-uniform wind velocity field having a maximum wind speed of approximately 23 [kts], an uniform ocean current of 2.14 [kts] with direction 270^o and an uniform field of regular waves with direction 270^o characterized by a significant wave height H_S of 1.25 [m] and period T_P of 10 [s] has been adopted. The starting point A, with Cartesian coordinates: $(x_A, y_A) = (-100, 70)$ and the destination point B with coordinates: $(x_B, y_B) = (100, -10)$ were also defined. Note these points were only approximately 215 [m] apart from each other to speed up the process.

The power curve (P in [kW] and V in [m/s]), given by: $P = a_1V^2 + a_2V^3$, and the fuel consumption time rate curve (C in [kg/s]), given by: $C = k\left(a_1V^2 + a_2V^3\right)$, used in the simulations where characterized by the following parameters:

Table 1: Parameters defining the power and the fuel consumption time rate curves.

a_1	-0.275
a_2	6.510
k	$5.069\,4 \times 10^{-5}$

The minimal global fuel consumption route was defined by 5 yaw points and the heuristic was executed in a set U with 200 routes evolving over 750 epochs.
In Fig. 10 the evolution of minimum global fuel consumption from epoch to epoch is shown. Also, the corresponding determination of the optimal path is represented in Figure 11. Notice should be given to the fact that in this particular simulation less than 100 epochs were necessary to obtain the minimal route.

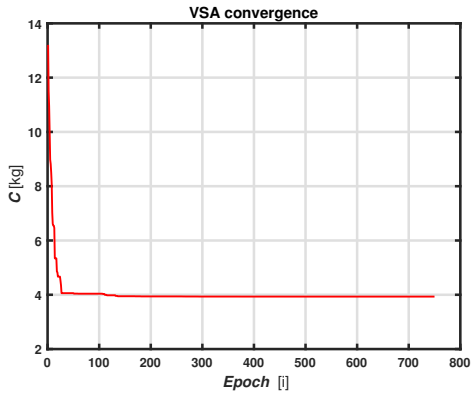

Figure 10: Evolution of minimum global fuel consumption from epoch to epoch.

In Fig. 11 results provided by the heuristic under the aforementioned conditions are shown. It can be observed that minimal route exhibits a lower global fuel consumption than the global fuel consumption associated with the direct route. Actually, the fuel savings observed in the minimal route determined are, approximately, 9% with respect to the fuel consumed in the direct route, which is considered quite promising at the fuel prices nowadays.

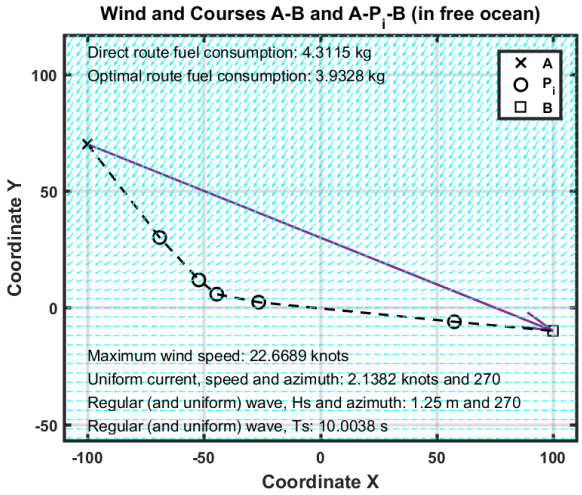

Figure 11: Minimal route from A to B in free ocean.

As illustrated in Fig. 12, all the simulation conditions remained unchanged, an exception being made for the addition of an ”island” to the original grid in an exact location corresponding to the passage zone of the minimal route represented in Fig. 11. In this new situation, as expected, the minimal route determined circumvents the island. Despite this change, the new determined route still allows for a fuel saving of approximately 8%, compared to the global fuel consumption over the direct route.

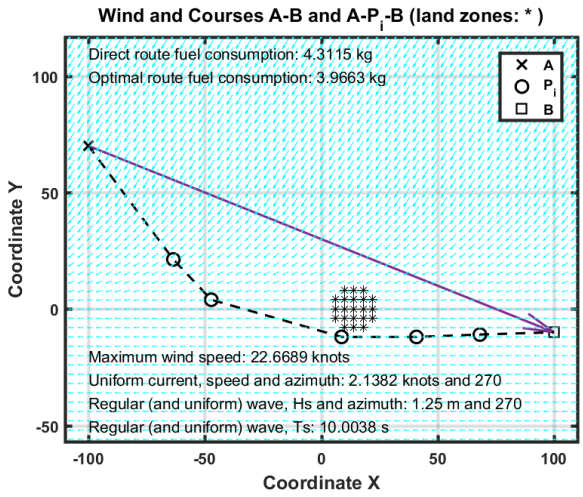

Figure 12: Minimal route from points A to B with land zones.

The simulation results are considered very satisfactory and highlight the potential of the developing application. The results obtained so far demonstrate that a rational weather routing is conducive to an increase in ship safety and energy efficiency. In fact, from these numerical simulations, the fuel consumption of a given voyage can be significantly reduced to 9% or 8% (see ratios of fuel consumed between optimal and direct route shown in Figs. 11 and 12). At the same time, fuel consumption reduction will create the double benefits of reducing the cost of ship operations while also reducing engine gas emissions that come from burning extra fuel, i.e., making the vessel compliant with new CII regulations proposed by IMO. In the near future, more simulations will be conducted with realistic environmental forecasts provided by a large circulation hydrodynamic model, such as MOHID (see (Neves, 1985)).

CONCLUSIONS AND FUTURE WORK

In this study the development of an optimisation-based approach to reduce fuel consumption and emissions from shipping navigation has been presented. The current study demonstrates that hydrodynamic performance can be substantially improved by means of trim optimisation that allows ships to reduce fuel consumption and simultaneously operate in adverse weather conditions with minimum degradation of their mission effectiveness.
Firstly, from a set of synthetic environments some preliminary figures on the performance of this newly developed voyage planner based on Vectorized Simulated Annealing (VSA) method was assessed in terms of fuel consumption as a function of speed over ground due to ocean currents and wind loads. Next, the assessment of added-resistance in waves induced by local wave conditions was introduced still as a synthetic environment to check consistency of the fuel consumption results. The simulation results are considered very satisfactory and highlight the potential of the developing a practical application where land zones or traffic corridors are taken into consideration. Actually, the fuel savings observed in the minimal route determined are, approximately, 9% with respect to the fuel consumed in the direct route, which is considered quite promising at the fuel prices nowadays.
In the near future, using a real-case environment scenario the performance of the Ship Operation Optimisation System (SOOS) in terms of fuel consumption reduction along with its comparison with other commercial available tools will be obtained. Moreover, next results are expected to allow the containership operator to have confidence that this containership after mid-life refit to convert an existing anti-heeling tank into an anti-rolling U-type tank will be capable of meeting and in some cases exceeding their operational requirements in terms of energy efficiency due to its superior hydrodynamic performance in a real scenario sea conditions. Contrarily to other decision-support tools systems, SOOS will provide enhanced energy efficiency and roll stabilisation at zero as well as at any advance speed. Therefore, SOOS will be a very attractive option for vessels performing operations that require a large range of speeds. Moreover, the objective of describing the selection process of the most appropriate decision-support tool and roll stabilisation system at the ship's life cycle will be also

achieved.
Looking ahead, there is a significant potential for innovation in this field of providing the maritime transport sector with customised decision-support systems, and further applied R&D is necessary to develop this potential. This is reinforced by current trends toward increased automation and reduced manning of maritime operations and the regulation requirements in the European context.

DECLARATION OF GENERATIVE AI AND AI-ASSISTED TECHNOLOGIES IN WRTITING

Statement: During the preparation of this work the author(s) have not used generative AI neither AI-Assisted Technologies in writing.

CONTRIBUTION STATEMENT

Author 1: SOOS conceptualization; supervision; MOHID hydrodynamic model data curation; methodology; CFD simulations of ship's resistance in calm water; Strip theory method calculations of hydrodynamic coefficients in FORTRAN; Salvesen (1978) and Gerritsma&Beukelman (1979)'s added resistance and roll motion responses in waves modules programming in MatLab; writing – original draft, review and editing. **Author 2:** VSA conceptualization; Synthetic model data curation; VSA module programming in MatLab; writing – original draft, review and editing.

ACKNOWLEDGEMENTS

This work was partially funded trough MARETEC project ASTRIIS (Atlantic Sustainability Through remote and In-situ Integrated Solutions), where a large group of partners (Tekever Space, CoLAB +ATLANTIC, CEiiA - Centro de Engenharia e Desenvolvimento, IST, Abyssal S.A., Hidromod, Spinworks, ISQ, WavEC, Universidade do Algarve, Universidade do Minho, Faculdade de Engenharia do Universidade do Porto, Oceanscan) aims to develop an Autonomous Surface Vehicle for Search and Rescue (SaR) along with a scalable tool for simulation and training of SaR operations (with a sustainable business model) using an high-fidelity immersive virtual marine environment.

REFERENCES

Blendermann, W. (1994). Parameter identification of wind loads on ships. *J. Wind Eng. Ind. Aerodyn.*, 51:339–351.

DNV (2022). Maritime forecast to 2050 – energy transition outlook 2022. Technical report, Download at https://www.dnv.com/publications/.

Gerritsma, J. and Beukelman, W. (1979). Analysis of the resistance increase in waves of a fast cargo ship. Technical Report 169S, Netherlands Ship Research Centre.

Gershanik, V. I. (2011). Weather routing optimisation–challenges and rewards. *Journal of Marine Engineering and Technology*, 10(3):29–40.

Gould, R. W. F. (1982). The estimation of wind loads on ship superstructures. *The Royal Institution of Naval Architects*, 8:1–34.

Harvald, S. A. (1983). *Resistance and Propulsion of Ships*. John Wiley & Sons.

Hieminga, G. and Luman, R. (2023). Synthetic fuels could be the answer to shipping net-zero goals, but don't count on them yet. Technical report, Download at https://think.ing.com/.

Hitchcock, D. B. (2003). A history of the metropolis–hastings algorithm. *The American Statistician*, 57(4):254–257.

HSVA (2020). Development of an automated test procedure for efficient determination of roll damping of ships equipped with bilge keels (autoroll). Technical Report 1695, HSVA.

IMO (2023). Resolution mepc.377(80): The 2023 imo strategy for the reduction of greenhouse gas emissions from ships. Download at https://wwwcdn.imo.org/localresources/en/MediaCentre/PressBriefings/Documents/Resolution20MEPC.377(80).pdf.

International Energy Association (2023). World energy outlook 2023. Technical report, Download at https://iea.blob.core.windows.net/assets/ed1e4c42-5726-4269-b801-97b3d32e117c/.

Isherwood, R. M. (1972). Wind resistance of merchant ships. *Trans. of the Royal Institution of Naval Architects*, 38:114–327.

Larsson, A. (2023). Containers lost at sea 2023 update. Technical report, Download at https://www.worldshipping.org/statements/containers-lost-at-sea-2023-update.

Maurício, F. and Moreira, M. (2022). Optimization of sailboat routes under non-uniform wind velocity fields. *Trends in Maritime Technology and Engineering*, pages 391–396.

Metropolis, N., Rosenbluth, A. W., Rosenbluth, M. N., Teller, A. H., and Teller, E. (1953). Equation of state calculations by fast computing machines. *The journal of chemical physics*, 21(6):1087–1092.

Neves, R. J. J. (1985). *Étude experimentale et modélisation des circulations transitoire et résiduelle dans l'estuaire du Sado*. PhD thesis, Univ. Liége.

Press, W. H. (2007). *Numerical recipes 3rd edition: The art of scientific computing*. Cambridge university press.

Ribeiro e Silva, S. and Eça, L. (To be published in 2024). Solution verification of cfd simulations of a drowning body at sea. In *Proceedings of the ASME Symposium on Verification, Validation, and Uncertainty Quantification Symposium (VVUQ 2024)*, Texas, USA.

Ribeiro e Silva, S., Uzunoglu, E., Guedes Soares, C., Marón, A., and Gutierrez, C. (2011). Investigation of the hydrodynamic characteristics of asymmetric cross-sections advancing in regular waves. In *Proceedings of the 30th International Conference on Ocean, Offshore and Arctic Engineering (OMAE 2011)*, Rotterdam (The Netherlands).

Ribeiro e Silva, S. B. N. (2008). *Instabilidades no Comportamento Dinamico Nao-Linear de Navios no Mar*. PhD thesis, Instituto Superior Técnico, Universidade Técnica de Lisboa. In Portuguese.

Salvesen, N. (1978). Added resistance of ships in waves. In *Journal of Hydronautics*, volume 12(1), pages 24–34.

Scheekluth, H. and Bertram, V. (1998). *Ship Design for Efficiency and Economy*. Butterworth & Heinmann.

APPENDIX

The vessel studied in here corresponds to a 712 TEU geared containership, whose $Fn = 0.26$. As regards the case-study selection, containerships are the highest emissions producers in the world fleet due to their higher sailing speed that requires larger propulsion engines.
Considering the design load condition of 712 TEU, the main characteristics of the vessel are shown in Table 2.

Table 2: Main characteristics of the 712 TEU geared containership.

Length between perpendiculars	L_{pp}, in [m]	119.50
Breadth, maximum	B, in [m]	20.4
Draught, mean	T_m, in [m]	7.75
Displacement, light condition	Δ_l, in [t]	3936
Crew	N_{crew}, in [pax]	16
Gross tonnage	GT, in [t]	7580
Cargo capacity	N_{TEU}, in [TEU]	712
Crane elevation capacity (x2)	C_{crane}, in [t]	40
Power (effective)	P_E, in [kW]	4665
Power at MCR (shaft)	P_S, in [kW]	7200
Propeller diameter (CPP)	D_P, in [m]	4.2
Cruise speed	U_{cruise}, in [kts]	16
Lateral projected area (above MWL)	A_L, in [m^2]	1883
Transverse projected area (above MWL)	A_T, in [m^2]	444

Fig. 13 shows a 3D geometric model which has been utilised to perform the CFD resistance and propulsion simulations and the semi-empirical wind loads calculations of the vessel. Considering the origin of the right handed system of coordinates located along the ship keel, in the symmetrical plan, at mean distance between the two perpendiculars, with z-axis pointing upwards and x-axis pointing through the ship bow.

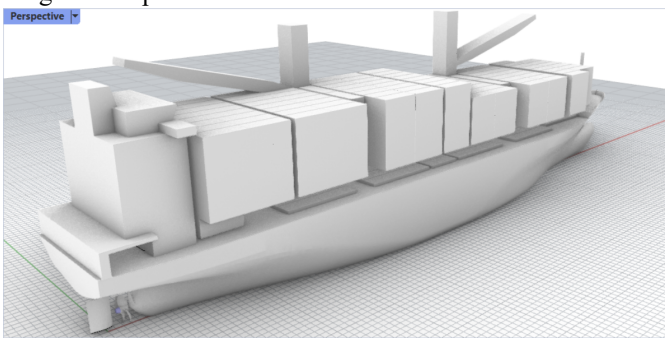

Figure 13: 3D geometric model of the containership.

Proceedings of the 15th International Marine Design Conference (IMDC-2024)
June 2-6, 2024
Amsterdam, the Netherlands

Functional analysis of speed, battery pack capacities and chargers of small electric ships - Adriatic Sea case study

Vedran Slapničar[1]*, Jerolim Andrić[2] and Smiljko Rudan[3]

ABSTRACT

Electric propulsion refers to propulsion using a combination of an electric motor and batteries. Electric motors powered by batteries represent a significant solution within the broader context of sustainability, energy efficiency, and technological advancement. As energy containers, batteries are characterized by low energy and power density and are currently not considered suitable for use on large displacement ships. Consumption of electric ships depends on numerous factors and the performance of the vessel's energy system requires great attention. The basic limitations are the ship's size and speed, the built-in capacity of the batteries, charging infrastructure, and sailing distance. These limitations are discussed and justified in two case studies in which the existing diesel-powered ships are replaced with electric ones.

KEY WORDS

functional analysis; electric ships; batteries; chargers; speed

INTRODUCTION

Today's challenging replacement of internal motor combustion with electric motors powered by batteries or other alternative energy sources includes many variables and we can say that it is very difficult to recommend the best solution. In principle, each case should be considered independently. In this paper, 9 shipping lines were analysed, namely 7 existing ones on which existing ships with diesel propulsion are already sailing, and 2 potentially new ones. For existing lines and potentially new lines, an analysis was made of which electric-powered ships could replace the existing ships. In this paper, batteries are treated as a potential energy source on board as an option that has already been applied. Considering the topicality of this issue, a relatively large number of papers have been published that consider the problem from various points of view but do not give a unique solution which is understandable. So, the literature review would take a quite lot of references without a serious sense of it. Here, we are referencing characteristic papers dealing with certain important topics. We can say that the sort of endless loop of solutions spins between the following topics, but not exclusively:

- Photovoltaic modules, solar energy
- Batteries
- Chargers
- Economics, cost
- Repowering, energy transition
- Operational profile, speed optimisation
- Coastal region, rivers, inland waters
- Lifecycle analysis

[1] Faculty of Mechanical Engineering and Naval Architecture, University of Zagreb, Zagreb, Croatia); ORCID: 0000-0002-3175-2542

[2] Faculty of Mechanical Engineering and Naval Architecture, University of Zagreb, Zagreb, Croatia); ORCID: 0000-0001-5968-5807

[3] Faculty of Mechanical Engineering and Naval Architecture, University of Zagreb, Zagreb, Croatia); ORCID: 0000-0002-5904-5938

* Corresponding Author: vedran.slapnicar@fsb.unizg.hr

Submitted: 23 February 2024, Revised: 27 April 2024, Accepted: 1 May 2024, Published: 7 May 2024

Conference paper, DOI: https://doi.org/10.59490/imdc.2024.782 e-ISSN: 3050-4864

The possibilities of isolated energy systems of islands by the usage of photovoltaic power systems for charging battery-powered electric ferries are discussed in (Frković et al, 2022). The paper (Kortsari et all, 2022) aims to present and explore the economic performance of a pure electric ferry, E-ferry. The E-ferry prototype is a viable commercial solution from a purely economic standpoint, according to the results of the economic examination. The E-ferry prototype, for example, has greater building expenses, but it has far lower operating costs overall, especially when it comes to fuel and energy resulting in a 5-8-year payback period. Comparably, even while battery systems have contributed significantly to the cost of the E-ferry, the ongoing decline in battery prices positions completely electric ships as a sustainable option. The auxiliary charging system is another significant factor in the E-ferry prototype's overall cost. To conclude, this is valid for the specific routes and belonging infrastructure. Evaluation of the possibility of using alternative fuels for small ferries based on several parameters, including technical readiness, regulations, GHG emission reduction, capital expenditure, and operational expense is elaborated in the paper (Laasma et all, 2022). When concentrating on the ferry business, it is crucial to take regional peculiarities and chances for lines into account. To attain carbon neutrality in the area, the paper's conclusion calls for more research to be conducted, including case studies of more specialized ecosystems with more obvious answers and possible courses of action. Considering the repowering option with battery-electric technology authors of the paper, (Mao et all, 2021), found out that passenger ferries up to 55 m that sail on legs up to 50 NM would replace 50% of fossil fuel use with electricity. But it must be considered that they had considered 10 MW chargers, which is still very doubtful in most countries.

We can agree, with the general conclusion given in (Pense & Akinoglu, 2020), that in the era of intelligent transportation systems, fully electric drive systems in the maritime industry may represent a significant step toward safer, more environmentally friendly, and more sustainable shipping globally, particularly when paired with solar energy or other renewable energy sources. In recent years, the most flexible approach to ship decarbonization may have been to build an entirely electric, battery-powered vessel. Battery-powered ships have a lower energy redundancy and a higher initial investment cost than conventional ships. Thus, it is essential to have an energy management plan that may reduce operating costs while ensuring the safety of energy use. The non-linear ship energy and speed optimization model describes energy usage under various sailing circumstances and speeds (Sun et al, 2022). Batteries and the safety of usage are another important issue (Trombetta et al, 2024). To guarantee ship efficiency and ensure high survivability and reliability, battery systems and their auxiliaries must be arranged. This could be done by complexly designed integrated power and energy systems that can link, track, and manage numerous onboard systems, including those for cooling, heating, detecting, alerting, and firefighting. The Filipino study (Vakili & Ölçer, 2023) also examines the environmental effects of battery-powered versus traditional diesel ferries, revealing that eco-friendliness pivots upon the nation's electricity mix. Battery-powered ships show promise for decarbonizing local waterways, provided there is a shift toward cleaner energy sources. The authors present a novel location problem called the electric riverboat charging station location problem, which is inspired by river operations with an electric vessel (Villa et al, 2020). This problem considers the necessary infrastructure for an electric vessel to be able to perform a round trip. The size of the electric vessel battery system and the placement of the solar-assisted charging stations are designed to keep expenses to a minimum. It incorporates both the charging function and the variation of solar radiation as a nonlinear behaviour function.

A case study (Wang et al, 2021) of a battery-powered fast catamaran ferry is employed, The various ship life phases and activities are taken into consideration by LCA and LCCA to create a life cycle emission inventory and calculate the associated costs. The findings show that when grid mix electricity from 2019 is used, the battery-powered system has life cycle greenhouse gas emissions decreased by approximately 30% and life cycle expenses lowered by 15% when compared to a conventional power system. Finally, it is necessary to properly plan the service network to offer high-quality transportation services. Thus, under service time constraints, the study (Wang et al, 2022) concurrently examines the positioning of charge stations, charging plans, route planning, ship schedule, and ship deployment. A literature review shows us the importance of carefully planning the sailing route of a ship powered by electric energy, speed, and consumption, as well as the necessary infrastructure for a certain ship to sail smoothly on a certain line. An insight into the conditions and limitations of the application of electrically powered ships was intended to be given in this work.

In the following sections, the elaboration of the work follows. Section 2 elaborates basic features of the ships' electrical eco-system and gives a comparison of features of the electric ships. For the selected lines, existing and new ones, the analysis of passenger ships is done in Section 3. The estimation of power and energy for the passenger ships of 45 m and 17 m together with the case studies is given in Section 4. A preliminary proposal of technical specifications for the new battery-powered solar-electric passenger ships to be deployed on selected lines is presented in Section 5. Finally, at the end, the Conclusion is given.

BASIC FEATURES OF THE SHIPS' ELECTRICAL ECO-SYSTEM

Electric drive refers to a system using a combination of an electric motor and a battery pack. Batteries, as energy storage, are characterized by low energy and power density and are currently not considered suitable for use on larger ships. In recent years, significant progress has been made in the development of batteries, especially when it comes to charging speed and reducing the memory effect of charging. Lithium batteries' current energy storage capacity is about 300 Wh/kg (Thunder Said Energy, 2024). In most batteries the critical metal is lithium and the world's lithium reserves are estimated at 23 million tons, most of which are stored in Chile (Statista, 2024). An alternative is to use magnesium, which is much more abundant, but it is still in the research phase. Table 1 depicts the advantages and disadvantages of using electric energy.

Table 1: The advantages and disadvantages of using electric energy

Advantages	Disadvantages
• Complete absence of greenhouse gas emissions during vessel operation. • Batteries seem suitable for powering smaller ships in the short to medium term. • In combination with other types of drives, it is possible to realize a hybrid drive, applicable for propelling smaller and medium-sized ships.	• The size and mass of the batteries currently limit the application of the batteries mostly to smaller-sized ships and very short distances. • Battery-powered ship's propulsion needs to be further developed, and even with significant progress, it is likely to expect the installation of such propulsion only on smaller-sized ships. • The battery pack must be replaced and disposed of at the end of its working life, which is determined by the total number of charging and discharging cycles.

Consumption of electric battery-powered ships depends on numerous factors and the performance of the vessel's energy system requires great attention. The basic limitations are the built-in capacity of the batteries, the permissible percentage of battery discharge (DOD-Depth of discharge), the value of the upper limit of the battery charge, the speed and frequency of charging, the sailing route, weather conditions, and the way the vessel is operated. If we consider only navigation, energy consumption depends on a series of manoeuvres of acceleration, deceleration, docking, manoeuvring in the port, and an adaptation of the driving style to sea conditions, environmental temperature, and other conditions. Energy consumption needs to be compensated by charging battery systems, whereby chargers differ in terms of installed power and charging speed, ease of use, charging losses, etc. The construction of chargers is regularly associated with significant infrastructure costs and sometimes administrative and technical difficulties. It can be concluded that the electric battery-powered ship is part of an energy ecosystem in which each component of the system needs to be adjusted optimally for the system.

Designing an energy ecosystem for electric battery-powered ferries requires knowing the answers to the following related questions:

1. What are the prices of energy from the local utility?
2. Are there special prices for off-peak energy consumption or permitted service interruption?
3. What will be the infrastructure needed for shore charging?
4. Is there a large-capacity power supply on-site at the terminal?
5. Is there a possibility of a power supply at both ends or all parts of the route?
6. Who pays/finances the charging infrastructure?
7. What emergencies are allowed?
8. What happens if the energy grid is temporarily unavailable?
9. How "green" is the energy that is purchased/used?
10. What is the durability of batteries and what about their disposal?
11. What new technologies are in the pipeline that can improve performance and reduce costs?
12. How far is the location for the ship overhaul?
13. Does the vessel have to react to emergencies such as rescue actions?

The main part of the energy ecosystem, questions 1-9, should be addressed by governmental administrative activities and by building the infrastructure. Questions 10-11 depend on market development and certainly, the designer will choose the best batteries on the market when designing the battery system that satisfies safety issues and has valid certificates. Question 12 is the question for the ship operator, it depends on the specific area but also it is a part of the infrastructure because if we don't

have repair places nearby, then it will be almost impossible to deploy any ships on certain lines. Question 13 depends on some specific needs that could be prescribed by the classification rules and/or national statutory rules.

Energy supply and battery systems for maritime applications

The supply of energy to ships that use batteries as the main or auxiliary energy source is only possible with the existence of a dedicated infrastructure. To be able to electrify ships on certain lines, it is necessary to provide infrastructure for fast/adequate battery charging at least at one of the endpoints of these lines. Therefore, energy supply must be ensured for each case within the framework of long-term transportation network planning.

One of the problems that should be stated is that the energy supply infrastructure, specifically intended for the supply of new solar-electric battery-powered ships on the selected existing and potentially new lines, currently doesn't exist, so the problem of deploying the new ships is even greater. Generally, the battery systems for maritime applications can be considered by very high reliability, large system capacity, modularity, and high safety in use. System certification is performed by classification societies and one of the most important tests includes a detailed heat transfer simulation. The risk of excessive heat transfer is reduced by the battery management system (BMS), integrated heat dissipation, and fire protection system. Although classification societies allow the use of new types of batteries with great caution, unlike lead batteries, due to the risk of ignition.

Comparison of features of electric ships

Table 2 shows the part of the basic features of 10 electric ships that are publicly available. Some data were slightly different due to the different data sources, and some data were not even publicly available. Also, some inconsistencies in the data can be seen, although they are given on the manufacturer's website. Given the fact that only the data of installed engine power is available, and not the data of the required engine power for the corresponding service speed, it can be concluded that the power of the installed engines on some lines is quite higher than necessary, i.e. the larger power reserve was taken. Data in the table are presented in the wide range of ship length, 24.5 m -144 m, and number of passengers, 132 – 1250. It is also visible from the table that the sailing time is mostly less than 30 min., except in two cases.

Table 2: Presentation of basic features of electric ships

Name of the ship	**Ampere 2015** (Ship Technology, 2015)	**Aurora and Tycho Brahe 1991-2017** (Wikipedia, 2023)	**Ellen 2019** (Wikipedia, 2024)	**Ika Rera 2022** (Danfos, 2022)	**Amherst Islander II 2019** (Damen, 2024)	**Wolfe Islander IV 2019** (Damen, 2024)	**Basto Electric 2020** (Ferry Shipping News, 2020)	**M/S Sjövägen 2014** (Wikipedia, 2024)	**Legacy of The Fjords 2020** (Baird Maritime, 2020)	**BB Green 24 2020** (Jackson, 2021)
Hull type*	CAT	MONO	MONO	CAT	MONO	MONO	MONO	MONO	CAT	MONO
Length, m	80	111	59.4	19	71.7	99.3	144	24.50	42	24.8
Number of passengers /cars	360/120	1250/240	198/31	132	300/42	399/75	600/200	150	400	147
Sailing time-one direction, approx.. min.	20	20	100	30	20	20	30	50	60	30
Speed, kn	10.00	14.50	12.10	20	12	12	12.80	10	20	35
Engines. kW	900	6000	1500	650	2080	2080	2250	320	900	660
Batteries, kWh	1000	4160	4300	540	1940	4500	4000	500	1800	500
Mass of batteries, t	10.0	57.0	56.0	5.5	25.0	58.5	52.0	5.0	23.4	5.0

*CAT - Catamaran; MONO - Monohull

ANALYSIS OF PASSENGER SHIPS ON SELECTED LINES – EXISTING/NEW ONES

As stated in the introduction 9 lines listed in Table 3 were analysed, 7 existing ones and 2 potentially new ones. The first 4 are served by high-speed catamarans (Lines Nos. 1-4), with service speeds between 14.8 - 21.03 kn, while Lines Nos. 5-7 are served by slow-speed monohull ships, with service speeds between 10-11 kn. Based on the previous work it was decided to investigate the possibility of placing slow-speed catamarans on potentially new lines, Line Nos. 8-9, with a speed of 10 kn. Catamaran was chosen for potentially 2 new lines due to the size of the ferry ports at the destination points and because it has a relatively large available area for passenger accommodation about the ship's length. The paper aimed to analyse the feasibility of replacing the existing diesel-powered ships with fully electric ships using batteries as an energy source, but also, to deploy the same kind of ships on the new lines. In Table 3 the 2 values per shipping line are presented, namely, distance per trip and consumption per trip. Distance per trip represents the total distance that a ship navigates in one direction. Consumption per trip depends on the required engine power for the service speed, hotel consumption, maximum voyage time, and efficiency coefficient (from the battery to the propeller), taken here as 0.92. Required engine power is obtained by in-house software based on the Holtrop-Mennen method (Holtrop & Mennen, 1978),

Table 3: List of analysed shipping lines

	Line No.	Line name	Distance per trip NM	Consumption per trip kWh
Exisitng lines	1	9601-Split-Rogač-Stomorska-Sutivan-Milna	33.00	1706
	2	9602-Split-Milna-Hvar-Vis	29.80	2036
	3	9406-Zadar-Zaglav-Zadar	22.20	675
	4	9604-Split-Hvar-Vela Luka-Ubli	61.13	4870
	5	310-Mali Lošinj-Srakane Vele-Unije-Susak	36.83	1201
	6	505-Šibenik-Zlarin-Prvić Luka-Prvić Šepurine-Vodice	20.18	658
	7	807-Dubrovnik-Koločep-Lopud-Šipan	22.79	1068
New lines	8	Split-Postira-Omiš	16.80	229
	9	Gaženica-Zadar-Borik	8.40	115

All these lines with their schedules and existing ship data (Row Nos. 1-9) were preliminarily analysed as follows (Table 4):

- Considering the navigation route and the schedule, the real service speed was calculated since these values were not available (Row No. 10). The available data were the maximum speed and total engine power.
- Using the in-house computer program the required power for the service speed was estimated (Row No. 11).
- Considering the navigation route and schedule the navigation distance without charging is determined (Row No. 12)
- Considering the battery depth of discharge (80% DOD + 10% reserve), the losses in the system, the ship's speed, the required power for service speed, available charging time and assumed charger power, the capacity of the batteries was calculated (Row No. 13).
- The fuel oil mass was obtained from the available ship's documentation (Row No. 19).
- The mass of the required batteries was calculated conservatively by multiplying the capacity of the batteries with the coefficient 13 kg/kWh (Row No. 24).
- The ratio of the mass of the required batteries and the fuel oil mass obtained from the existing ship documentation was calculated. The criterion of the feasibility indicators for replacing energy sources from fossil fuels with batteries is set (Row Nos. 26 and 28).
- A Feasibility Indicator 1 shown in Figure 1 was introduced as the ratio of the required mass of batteries and the fuel oil mass of existing ships, mBATT/mFUEL (Row No. 26) . According to this indicator, the existing ship on the existing line is feasible if it is less than or equal to 1. The feasible lines are Line Nos 5,6,7, and 9, while Line No. 8 could be probably feasible with some additional adjustments.
- Another indicator, Feasibility Indicator 2 shown in Figure 2, is the relation between the energy source and deadweight. Namely, fuel oil mass and deadweight, mFUEL/mDWT (Row No. 27), and required mass of batteries and deadweight, mBATT/mDWT (Row No. 28). This indicator should be less than 35%.

Considering the Feasibility Indicator 1, the high-speed ships lines 9602, 9601, 9604, and 9406 are not feasible since the values of this indicator range from 3.0 to 7.1. To conclude, the lines on which it would be possible to replace energy sources from

fossil fuels with batteries must generally have lower speeds, larger charging time frames and shorter sailing distances. The sailing schedule must be harmonized to enable the daily charging of the batteries also, otherwise, the battery pack capacity needs to be too large. In any case, each line should be analysed individually with the existing parameters and limitations, and if the lines are not feasible, it is necessary to design a new ship considering the realistic requirements for passenger capacity, required speed, and sailing schedule to enable consumption of electric energy as low as possible. Last, but not the least, any changes to the existing sailing schedule and passenger capacities should be coordinated with the needs of the users and the local community. This is because they are already accustomed to a certain sailing schedule with existing passenger ships powered by diesel engines, so it is necessary to explain why changes would be necessary for the ships powered by batteries.

Table 4: Preliminary calculation of capacity of the battery pack for the passenger ships on selected lines

			Line No.	1	2	3	4	5	6	7	8	9
			Line name	9601	9602	9406	9604	310	505	807	Split-Postira-Omiš	Gaženica-Zadar-Borik
			Hull type	CAT	CAT	CAT	CAT	MONO	MONO	MONO	CAT	CAT
Row No.		Unit	Data/calculation									
1		m	L - length	37.37	36.85	24.5	36.00	45.00	45.00	45.00	17.00	17.00
2		m	B - breadth	11.00	11.00	9.00	10.10	10.00	10.00	10.00	7.00	7.00
3		m	T - draft	1.19	1.20	1.28	1.79	2.50	2.50	2.50	0.97	0.97
4		m	b - demihull width	2.83	2.83	2.32	2.60	-	-	-	2.10	2.10
5		-	CB - block coefficient	0.480	0.480	0.480	0.480	0.607	0.607	0.607	0.486	0.486
6		t/m3	ro - sea density	1.025	1.025	1.025	1.025	1.025	1.025	1.025	1.025	1.025
7		t	LS - Lightship mass	85.6	84.8	49.2	113.89	612.9	612.9	612.9	22.05	22.05
8		t	DWT - Deadweight	38.7	38.3	22.2	51.3	80.1	80.1	80.1	12.5	12.5
9		t	Displacement	124.3	123.1	71.5	165.0	702.0	702.0	702.0	34.5	34.5
10		čv	v - service speed	18.4	21.0	14.8	21.0	10.0	10.0	11.0	10.0	10.0
11		kW	Pb - Required power for service speed	850.3	1297.0	389.2	1514.0	275.1	275.1	449.2	110.5	110.5
12		NM	d - navigation distance without charging	33.00	59.60	44.40	61.13	36.83	20.18	22.79	16.80	8.40
13		kWh	ENG - Battery capacity	2900	6800	2300	8150	2100	2100	2150	430	250
14		kWh	maxENG - maximum consumption between charging	1706	4072	1350	4870	1201	658	1068	229	115
15		h	t - maximum voyage time	1.79	2.83	3.00	2.92	3.68	2.02	2.07	1.68	0.84
16		kW	Maximum charger power on the route	1250	500	400	975	335	665	1000	350	450
17		g/kWh	SFOC - specific fuel oil consumption	170	150	185	170	170	170	170	170	170
18	**=8/9**	-	etaDWT = DWT/Displacement	31.1%	31.1%	31.1%	31.1%	11.4%	11.4%	11.4%	36.1%	36.1%
19		t	mFUELdoc (fuel mass obtained from ship documentation)				16.68	32.1	32.1	32.1		
20	**=19/8**		etaFUEL = mFUELdoc/DWT				0.325	0.401	0.401	0.401		
21	**=14*17/10^6**	t	equiFUEL=maxENG*SFOC/1000000 (Equivalent fuel consumption per voyage)	0.29	0.61	0.25	0.83	0.20	0.11	0.18	0.04	0.02
22	**=20*8**	t	mFUEL = etaFUEL*DWT (Assumed fuel mass based on the mFUELdoc)	12.57	12.45	7.22	16.68	32.10	32.10	32.10	4.05	4.05
23	**=22/21**	-	nVOYAGE = mFUEL/equiFUEL (The number of voyages a ship can make using diesel fuel without refuelling)	43.3	20.4	28.9	20.1	157.2	287.0	176.8	104.0	207.2
24	**=13*(13 kg)**	t	mBATT = ENG*13 kg (Battery mass)	37.70	88.40	29.90	105.95	27.30	27.30	27.95	5.59	3.25
25	**=22-24**	t	deltaDWT=mFUEL-mBATT ("-" means that the ship lacks deadweight)	-25.13	-75.95	-22.68	-89.27	4.80	4.80	4.15	-1.54	0.80
26	**=24/22**	-	mBATT /mFUEL (Relation of battery mass and fuel mass)	**3.0**	**7.1**	**4.1**	**6.4**	**0.9**	**0.9**	**0.9**	**1.4**	**0.8**
27	**=22/8**	-	mFUEL/DWT (Relation of fuel mass and deadweight)	32.5%	32.5%	32.5%	32.5%	40.1%	40.1%	40.1%	32.5%	32.5%
28	**=24/8**	-	mBATT/DWT (Relation of battery mass and deadweight)	97.5%	230.8%	134.5%	206.5%	34.1%	34.1%	34.9%	44.9%	26.1%

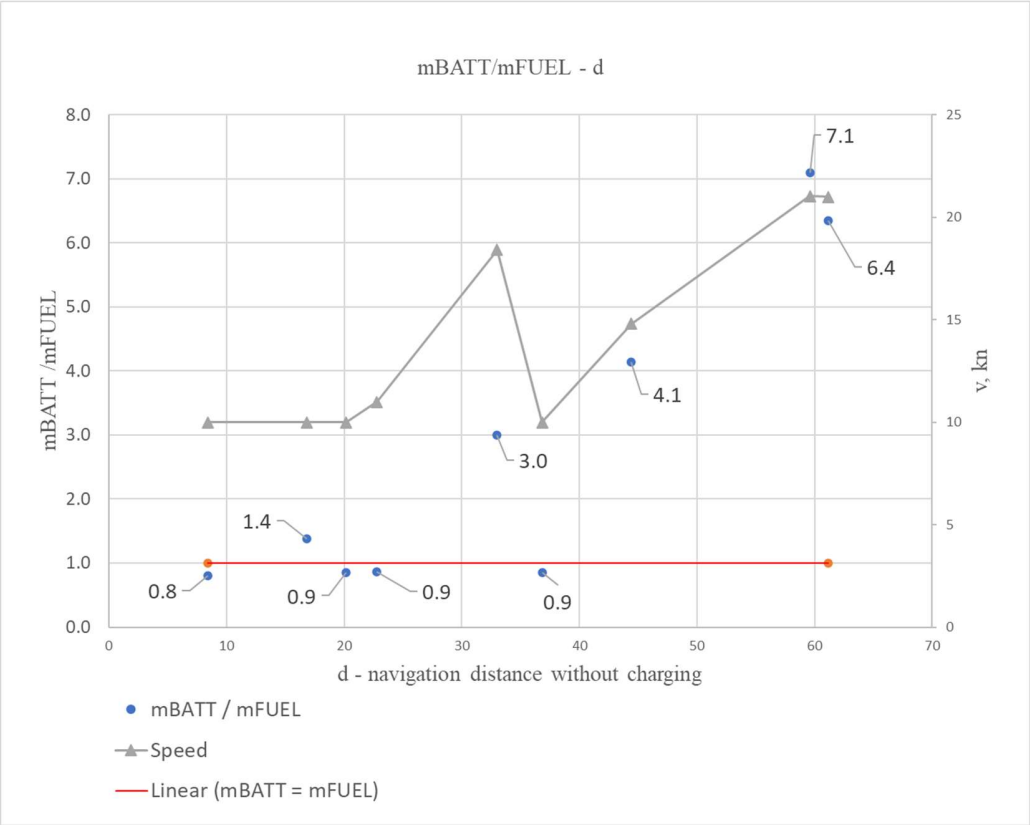

Figure 1: Feasibility Indicator 1 - relation of required mass of batteries and fuel oil mass

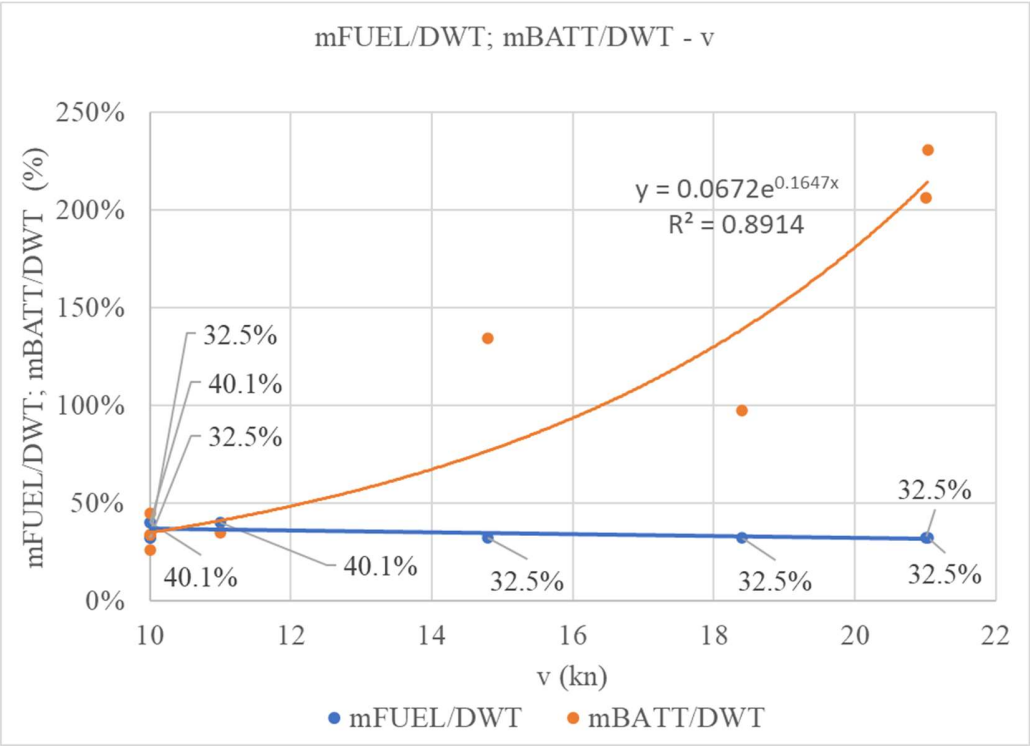

Figure 2: Feasibility Indicator 2 – the relationship between the mass of the energy source and deadweight

ESTIMATION OF POWER AND ENERGY - CASE STUDIES

Estimation of power and energy for a 45 m passenger ship

For a passenger ship with a length of 45 m for lines 310, 505, and 807, Table 4, Line nos. 5-7, the required engine power was estimated (Holtrop & Mennen, 1978) as shown in Figure 3. For the speed of 10 kn, the required engine power is 275,08 kW, while for the speed of 11 kn, the value is 449.19 kW. Considering that these values represent 90% of MCR (Maximum continuous rating), the built-in engines should have a total power of 300 kW, or 2 x 150 kW for the speed of 10 kn, and 500 kW, or 2 x 250 kW for the speed of 11 kn. The bow thruster power is assumed to the 20% of the main engine power, or 2 x 15 kW for the speed of 10 kn and 2 x 50 kW for the speed of 11 kn. Together with the required engine power, the required battery pack capacity as well as the required charger power were calculated for the original sailing schedules. To avoid unnecessarily high battery pack capacity as well as high charger power, an analysis of the schedule was performed. This analysis showed that the small changes in the schedule would enable daily charging of the batteries, and consequently lower battery pack capacities and charger powers. Regarding the gain of solar energy, the average daily value in kWh per 1 kW of installed photovoltaic module, for the location of Mali Losinj, is 3.21 kWh (PVGIS, 2024). The number of 350 W photovoltaic modules, considering the assumed allowable free superstructure roof area of 360.00 m^2 amounts to 180, and they provide 201.95 kWh, which is 9.4% of the battery pack capacity. Considering the electric motor voltage of 705.6 V, the battery pack has 2150.67 kWh with a total weight of 27.95 t. The battery pack consists of 42 modules and 10 strings, where each module has 32 battery cells of capacity 38.1 Ah and voltage 4.2 V.

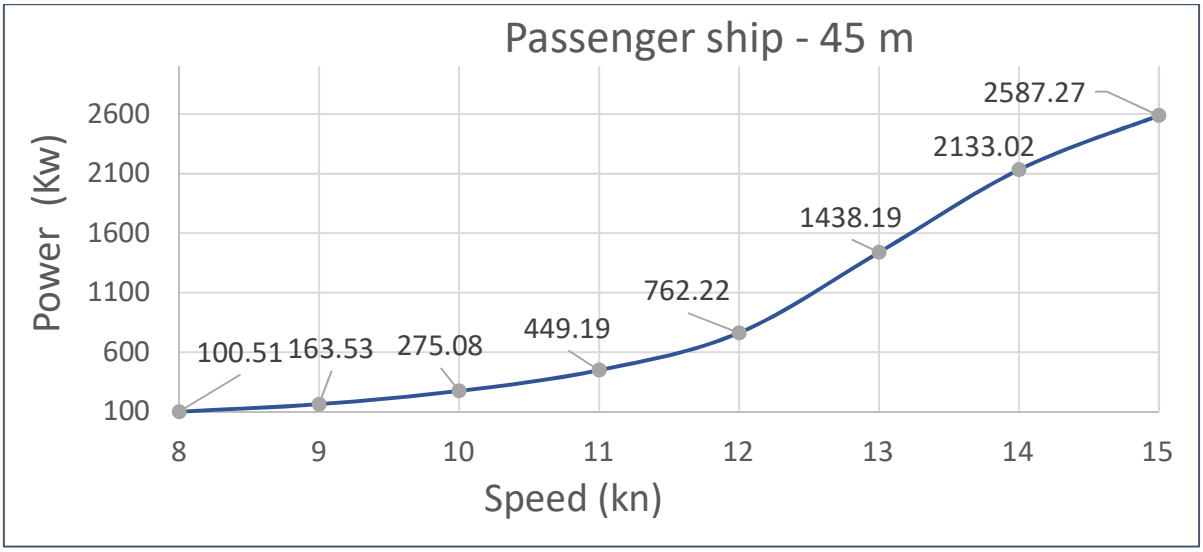

Figure 3: Power-speed diagram for a 45 m passenger ship

Hotel consumption of a 45 m passenger ship (air conditioning, vessel devices, lighting) is assumed during navigation 25 kW, and by the night charging 10 kW.

Analysis: Case study 1 - State line no. 807

"Case study 1" gives a detailed analysis of the state line no. 807 as an example of a 45 m passenger ship. The original sailing schedule for the high season is shown in Figure 4, and the navigation distance is 22.79 NM. Although the service speed for line 807 is 11 kn, the required battery pack capacities and chargers were calculated for 3 speeds (Table 5), so the battery pack capacity ranges from 3450 kWh to 6800 kWh and daily charger in Dubrovnik from 1000 kW to 3000 kW.

HIGH SEASON

01.07. - 28.08.

MONDAY - SATURDAY				SUNDAY AND HOLIDAY				PORTS	MONDAY - SATURDAY				SUNDAY AND HOLIDAY			
I	II	III	IV	I	II	III	IV		I	II	III	IV	I	II	III	IV
06:00	11:55	15:20	18:30	07:30	10:20	17:00	19:35	SUĐURAĐ	11:15	15:15	17:45	21:15	10:15	13:00	19:30	22:15
06:15	12:10	*	18:45	07:45	10:35	–	19:50	LOPUD	11:00	15:00	17:30	21:00	10:00	12:45	19:15	22:00
06:20	12:15		18:50	07:50	10:40		19:55		10:55	14:55	17:25	20:55	09:55	12:40	19:10	21:55
06:40	12:35	15:45	19:10	08:10	11:00	17:25	20:15	KOLOČEP	10:35	14:35	17:05	20:35	09:35	12:20	18:50	21:35
06:45	12:40	15:50	19:15	08:15	11:05	17:30	20:20		10:30	14:30	17:00	20:30	09:30	12:15	18:45	21:30
07:15	13:10	16:20	19:45	08:45	11:35	18:00	20:50	DUBROVNIK	10:00	14:00	16:30	20:00	09:00	11:45	18:15	21:00

Figure 4: Original schedule for the state line no. 807

Table 5: Required capacity of battery packs and chargers for speeds of 10, 11 and 12 knots for the state line no. 807 - original schedule

V=12 kn	No schedule change
Sudurad: min charging power (kW)	**650 kW**
Dubrovnik: min charging power (kW)	**3000 kW**
Input: nominal battery capacity (kWh)	**6800 kWh**

V=11 kn	No schedule change
Sudurad: min charging power (kW)	**430 kW**
Dubrovnik: min charging power (kW)	**1850 kW**
Input: nominal battery capacity (kWh)	**4500 kWh**

V=10 kn	No schedule change
Sudurađ: min charging power (kW)	**330 kW**
Dubrovnik: min charging power (kW)	**1000 kW**
Input: nominal battery capacity (kWh)	**3450 kWh**

It is necessary to provide two power chargers, a higher capacity charger in Dubrovnik for daytime charging and a lower capacity charger in Sudurad for overnight charging. Considering the very high required battery pack capacities and the chargers' power (Table 5), a slight modification of the original schedule is necessary. With a slightly changed schedule, the required battery pack capacities and chargers' power have been significantly reduced compared to the obtained for the original schedule (Table 6). This gives us an overview of the possible combinations for the speed options 10, 11, and 12 kn.

Table 6: Possible options for the battery pack capacities and chargers for speeds of 10, 11, and 12 knots for the state line 807 - slightly changed schedule

V=12 kn

Sudurad: min charging power (kW)	260	280	315	345	375	400	430
Dubrovnik: min charging power (kW)	1630	1570	1480	1410	1330	1275	1200
Input: nominal battery capacity (kWh)	2800	3000	3300	3600	3900	4200	4500

V=11 kn

Sudurad: min charging power (kW)	180	210	245	270	290	320	345
Dubrovnik: min charging power (kW)	1075	975	900	825	775	715	640
Input: nominal battery capacity (kWh)	1900	2200	2500	2800	3000	3300	3600

V=10 kn

Sudurad: min charging power (kW)	125	160	185	215	240	270
Dubrovnik: min charging power (kW)	750	660	590	525	450	375
Input: nominal battery capacity (kWh)	1300	1600	1900	2200	2500	2800

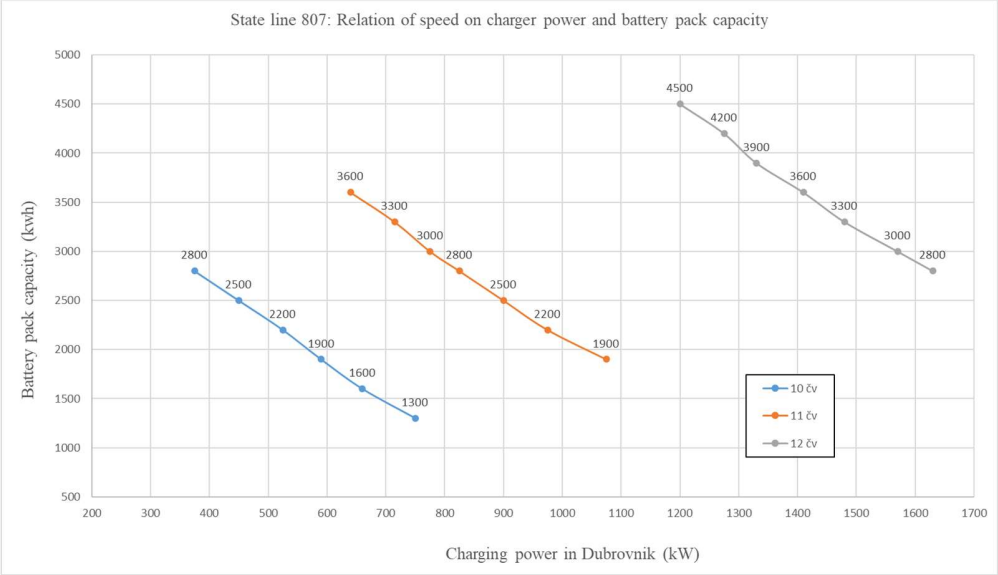

Figure 5: State line 807: Effect of speed on charger power and battery capacity

Table 7: State line 807: slightly changed schedule to enable more time for charging

Trip	Original harbour time, min	New proposed harbour time, min	Charging=harbour time-10, min	Harbour time, hours	Battery trip start, kWh	Consumption per voyage, kWh	Battery trip ends, kwh	Available battery charger capacity, kWh
1	165	105	95	1.58	1935	534	1401	1326
2	50	80	70	1.17	1935	1068	867	977
3	10	80	70	1.17	1844	1068	776	977
4	15	50	40	0.67	1753	1068	685	558
					1243	534	709	

Daily charging in the Dubrovnik, 1000 kW charger

Overnight charging in Suđurađ, 7 hours including 10 kW for hotel consumption, 200 kW charger

Estimation of power and energy for a 17 m passenger ship

For a passenger ship with a length of 17 m for lines Split-Postira-Omis and Gazenica-Zadar-Borik, Table 4, Lines Nos. 8 and 9, the required engine power was estimated (Holtrop & Mennen, 1978). For the speed of 10 kn, the required engine power is 110.49 kW as shown in Figure 6. Taking into account that this value represents 90% of MCR, the built-in engines should have a total power of 130 kW, or 2 x 65 kW. The bow thruster power is assumed to the 20% of the main engine power, or 2 x 12 kW. The required engine power, battery pack capacity, and charger power are calculated considering the following parameters:

- the assumed sailing schedule on the line Gazenica-Zadar-Borik is 11 departures per day, but the charging is done only in Gazenica port in 20 min. after each round voyage. Assumed nominal charger capacity is 450 kW and battery pack capacity 250 kWh.
- assumed sailing schedule on the line Split-Postira-Omis, 2 departures per day, charging is done in both ports after each voyage with the assumed nominal charger capacity of 350 kW and battery pack capacity of 430 kWh.

Since these two lines are supposed to be completely new, considering the estimated engine power and hotel consumption, the required battery pack capacity as well as the required charger power the schedule proposal was given by the authors to avoid unnecessarily higher capacities. Regarding the gain of solar energy, the average daily value in kWh per 1 kW of installed photovoltaic module, for the location of Mali Losinj, is 3.21 kWh (PVGIS, 2024). The number of 350 W photovoltaic modules, considering the assumed allowable free superstructure roof area of 95.20 m^2 amounts to 48, and they provide 53.85 kWh, which is 12.5% to 21.54% of the battery capacity, depending on the line.

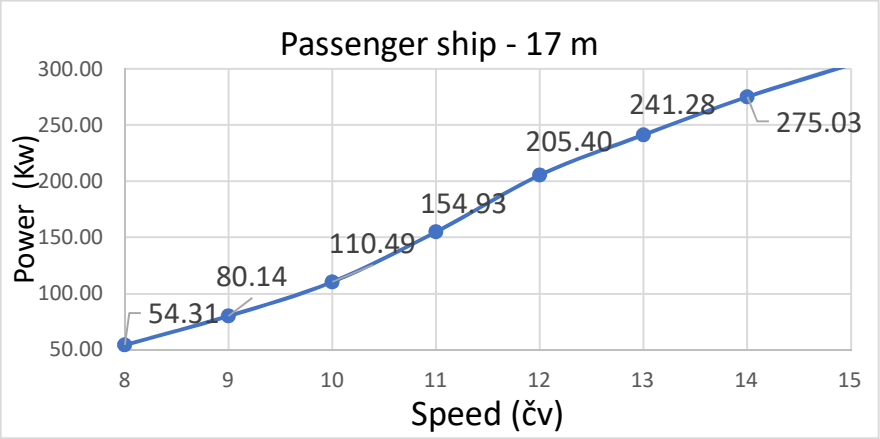

Figure 6: Power-speed diagram for a 17 m passenger ship

Hotel consumption of a 17 m passenger ship (air conditioning, vessel devices, lighting) is assumed during navigation 15 kW, and the night charging 5 kW.

Analysis: Case Study 2 - Line Gaženica – Zadar – Borik

"Case study 2" gives a detailed analysis of the state line Gazenica-Zadar-Borik as an example of a 17 m passenger ship. The assumed schedule for the line Gazenica-Zadar-Borik and back takes 70 min. for a round trip including the necessary time for boarding and disembarking the passengers, with 30 min. for a break in Gazenica port, of which 20 min. is for charging (Table 8). For the speed of 10 kn the possible options of the combinations for the battery pack capacities and chargers are given in Table 9.

Table 8 Voyage and charging description for line Gaženica – Zadar – Borik

Harbour time, min	Trip	Charging= Harbour time-10, min	Harbour time, hours	Battery trip start, kWh	Consumption per voyage, kWh	Battery trip ends, kWh	Available battery charger capacity, kWh
30	1	20	0.33	225	115	110	125
30	2	20	0.33	225	115	110	125
30	3	20	0.33	225	115	110	125
30	4	20	0.33	225	115	110	125
30	5	20	0.33	225	115	110	125
30	6	20	0.33	225	115	110	125
30	7	20	0.33	225	115	110	125
30	8	20	0.33	225	115	110	125
30	9	20	0.33	225	115	110	125
30	10	20	0.33	225	115	110	125
30	11	20	0.33	225	115	110	

Daily and overnight charging in Gazenica, 450 kW charger

Table 9: Possible options for the battery pack capacities and chargers for the speed of 10 kn for the line Gaženica – Zadar – Borik

V=10 kn

Gazenica: min charging power (kW)	425	405	390	365	450
Nominal battery capacity (kWh)	200	250	300	400	250

The consequence of the proposed schedule and charger option is that the batteries will be charged 12 times per day, so they will be replaced approximately within 3 years.

PRELIMINARY PROPOSAL OF TECHNICAL SPECIFICATIONS FOR NEW SOLAR-ELECTRIC BATTERY-POWERED PASSENGER SHIPS ON SELECTED LINES

After the detailed analysis of all lines, in terms of rationalizing design and construction costs, it is proposed that the two types of fully electric battery-powered passenger ships could replace existing passenger ships on selected lines (Table 3)

- **Ship I** – monohull, length up to 45 m, for the service on existing lines 310, 505 and 807.
- **Ship II** – catamaran, length up to 17 m, for the service on new lines Split-Postira-Omis -Omiš and Gazenica-Zadar-Borik.

When proposing the preliminary dimensions of the new ships, the following aspects were considered:

- The technical specifications were chosen as an envelope of requirements for lines for which the same type of vessel is proposed.
- The proposed passenger capacity results from an analysis of the existing ships and shipping lines, which showed that the maximum capacity of the existing ships is sufficient to cover long-term needs on the selected lines.
- The speed of the ships, 10 to 11 kn, is specified in such a way that fits the schedule and as low as possible lower battery pack capacities and chargers.
- For lines 310, 505, and 807, the option for loaded cargo is 25 t, which can be breakbulk /pallet/container loaded by crane, together with the 3 medium-sized supply vehicles and 5 passenger cars loaded by a stern ramp.
- The proposed approximate dimensions of the larger ship, length up to 45 m, will be in line with the existing ships that currently operate on lines 310, 505, and 807. The passenger capacity for all lines is not the same and consequently, the length should not be the same, but since line 310 (Line No. 5, Table 3 and Table 4) is an open-sea line exposed to severe weather conditions that has by far the largest number of cancelled voyages, it is assumed that the same size ship should serve this line to ensure a reduction in the number of cancelled voyages.
- The proposed dimensions of smaller-sized ships consider the limitations of the potential berths at the ports of destination.

Table 10 provides a preliminary proposal for the technical specifications of new passenger ships on the selected lines.

Table 10: Preliminary proposal of technical specifications of new passenger ships on selected lines

	Ship I		**Ship II**	
	310, 505	**807**	**Gazenica-Zadar-Borik**	**Split-Postira-Omis**
Type of vessel	Pasenger ship		Pasenger ship	
Classification	HRB★50A1 IWS SD★M1 AUT3		HRB★50A1 IWS SD★M1 AUT3	
Class-passenger vessel	Class C-Rules for statutory certification		Class C-Rules for statutory certification	
Navigation area	national navigation 5/6		national navigation 6	national navigation 6
Length L [m]	up to 45 m		up to 17 m	
Width B [m]	Monohull, about 10 m		Catamaran, up to 7 m	
Draft T [m]	up to 2.5 m*		up to 1 m*	

Height H [m]	up to 4.2 m		up to 2.0 m	
Minimum speed, kn	10	11	10	10
Drive	Twin-screw, separate control systems		Twin-screw, separate control systems	
Type of propulsion –	electric		electric	
Passenger capacity	max 390 passengers		max 100 passengers	
Passengers open deck	140		-	
Passengers closed space	250		max. 100	
Cargo capacity	25 t		deck area 3 m2	
Crane capacity	-		-	
Number of crew	9		3	
Construction material	hull/superstructure: steel/aluminium		hull and superstructure: steel/aluminium alloy/	
Special requirements	Bow thruster, energy shore connection		Bow thruster, energy shore connection	
Flag	Croatia		Croatia	
Type of lines	Open sea	Open sea	Coastal	Open sea

*Note: regarding the maximum permissible draft, when finalizing the project, it is necessary to consider in detail the max. the depth of the pier according to the latest data.

CONCLUSION

Nine shipping lines were examined in this paper, 2 possibly new lines and 7 existing lines that are currently served by ships using diesel propulsion. An analysis was conducted to determine which electric-powered ships could replace the current ships on both existing and possibly new lines. Batteries are discussed in this paper as a potential onboard energy source that has already been used on certain lines and is a reasonably simple alternative to implement. In terms of the rationalization of design and construction costs, as previously stated, it is proposed to build two types of passenger ships, a 45 m Ship I and a 17 m Ship II, which could be deployed on selected lines with solar-electric-battery propulsion. The final dimensions and all technical characteristics of the ships will be defined by the initial design and technical descriptions, considering additional technical requirements and the actual depth condition at the intended piers. Some remarks must be stressed:

- The introduction of solar-electric battery-powered ships requires a deep analysis of the minimum necessary speed, for each line independently, to keep the energy consumption as low as possible.
- It is also necessary to harmonize the schedule to enable the daily charging of the batteries.
- For some existing lines, such as line 807 (shown as Case Study 1), the analysis showed that with a slightly changed schedule, the required battery pack capacity and charger power can be significantly reduced compared to the original schedule.
- Proposed changes to the sailing schedule should be harmonized with the needs of the users.
- The contribution of energy that can be obtained from photovoltaic modules installed on the superstructure roof area, ranges from 9.4% to 21.5%, depending on the particular line.
- The feasibility indicators are defined, as Feasibility Indicator 1 and Feasibility Indicator 2, and they must be within certain limits, i.e. under 1 and 35% respectively.

We see that electric energy for the propulsion of ships that use batteries as a potential energy source on board is not largely used and has not taken off as much as we might expect, in fact, its application, for now, is just on mostly very specific lines. The reason for this is the lack of infrastructure, the relatively small capacity of batteries and their large mass compared to diesel propulsion systems, engine rooms and supplies. Also, the cost of the batteries, as well as the problem of recycling batteries after a certain number of charging cycles is a real problem. In summary, the lines that may potentially replace energy sources from fossil fuel with batteries need to have slower speeds, longer charging times, shorter sailing distances, and with the sailing schedule carefully adjusted. In future work, it is planned to analyse the application of electric energy to larger ships that would have a hybrid drive, diesel-electric-battery, where the energy obtained from the batteries would be for ship departure and arrival, as well as during the ship's stay at the berth. The benefit of such a system would be the reduction of exhaust gases in the port as well as less noise.

CONTRIBUTION STATEMENT

Vedran Slapnicar: Conceptualization; data curation, methodology; writing – original draft.
Jerolim Andric: review and editing.
Smiljko Rudan : review and editing.

REFERENCES

Baird Maritime. (2020, August). *Vessel Review | Legacy of the Fjords*. Retrieved from Baird Maritime: https://www.bairdmaritime.com/work-boat-world/passenger-vessel-world/maritime-tourism/vessel-review-legacy-of-the-fjords-second-all-electric-newbuild-joins-the-fjords-sightseeing-fleet/

Damen. (2024). *Damen*. Retrieved from Road Ferries: https://www.damen.com/vessels/ferries/roro-ferries?view=models

Danfos. (2022, January). *Engineering Tomorrow*. Retrieved from Danfos: https://www.danfoss.com/en/about-danfoss/news/dps/southern-hemisphere-s-first-fully-electric-passenger-ferry-launches-in-new-zealand/

Ferry Shipping News. (2020, December). *The World's Largest Electric Ferry Delivered*. Retrieved from Ferry Shipping News: https://ferryshippingnews.com/the-worlds-largest-electric-ferry-delivered/

Frković, L., Ćosić, B., Pukšec, T., & Vladimir, N. (2022). The synergy between the photovoltaic power systems and battery-powered electric ferries in the isolated energy system of an island. *Energy*, 28. doi:10.1016/j.energy.2022.124862

Holtrop, J., & Mennen, G. (October 1978). A statistical power prediction method. *InternationalShipbuilding Progress, 25*(290), 253-256.

Jackson, R. (2021, May). *BB Green ferry*. Retrieved from E-Mobility Engineering: https://www.emobility-engineering.com/bb-green-ferry/

Kortsari, A., Mitropoulos, L., Heinemann, T., Mikkelsen, H., & Aifadoupoulou, G. (2022). Evaluating the Economic Performance of a Pure Electric and Diesel Vessel: The Case of E-ferry in Denmark. *Trans. marit. sci.*, 15. doi:10.7225/toms.v11.n01.008

Laasma, A., Otsason, R., Tapaninen, U., & Hilmola, O.-P. (2022). Evaluation of Alternative Fuels for Coastal Ferries. *Sustainability*, 13. doi:10.3390/su142416841

Mao, X., Georgeff, E., Rutherford, D., & Osipova, L. (2021). Repowering Chinese coastal ferries with. *2021 International Council on Clean Transportation-working paper*, 17.

Pense, C., & Akinoglu, B. G. (2020). Using Renewable Energy on Electric Vessels in. In IEEE (Ed.), *2nd International Conference on Photovoltaic Science and Technologies (PVCon)* (p. 4). Ankara, Turkey: IEEE. doi:DOI: 10.1109/PVCon51547.2020.9757767

PVGIS. (2024). *Photovoltaic Geographical Information System*. Dohvaćeno iz re.jrc.ec.europa.eu: https://re.jrc.ec.europa.eu/pvg_tools/en/tools.html

Ship Technology. (2015, June). *Ampere Electric-Powered Ferry*. Retrieved from Ship Technology: https://www.ship-technology.com/projects/norled-zerocat-electric-powered-ferry/

Statista. (2024, March). *Reserves of lithium worldwide from 2010 to 2023*. Retrieved from Statista: https://www.statista.com/statistics/1253739/lithium-reserves-worldwide/

Sun, L., Zhang, Y., Ma, F., Ji, F., & Xiong, Y. (2022). Energy and speed optimization of inland battery-powered ship with considering the dynamic electricity price and complex navigational environment. In E. Institute (Ed.), *3rd International Conference on Power Engineering (ICPE 2022)* (p. 12). Sanya, Hainan Province, China: Elsevier. doi:10.1016/j.egyr.2023.04.267

Thunder Said Energy. (2024, January). *Lithium ion batteries: energy density?* Retrieved from Thunder Said energy-the research consultancy for energy technologies: https://thundersaidenergy.com/downloads/lithium-ion-batteries-energy-density/

Trombetta, G. L., Leonardi, S. G., Aloisio, D., Andaloro, L., & Sergi, F. (2024). Lithium-Ion Batteries on Board: A Review on Their Integration for Enabling the Energy Transition in Shipping Industry. (MDPI, Ed.) *Energies*. doi:10.3390/en17051019

Vakili, S., & Ölçer, A. I. (2023). Are battery-powered vessels the best solution for the domestic ferry segment? Case study for the domestic ferry segment in the Philippines. *Energy*, 11. doi:10.1016/j.energy.2023.128323

Villa, D., Montoya, A., & Herrera, A. M. (2020). The Electric Riverboat Charging Station Location Problem. *Journal of Advanced Transportation*, 16. doi:10.1155/2020/6527924

Wang, H., Boulougouris, E., Theotokatos, G., Zhou, P., & Priftis, A. (2021). Life cycle analysis and cost assessment of a battery powered ferry. *Ocean Engineering*, 11. doi:10.1016/j.oceaneng.2021.110029

Wang, W., Liu, Y., Zhen, L., & Wang, H. (2022). How to Deploy Electric Ships for Green Shipping. *J. Mar. Sci.* doi:10.3390/jmse10111611

Wikipedia. (2023, November). *MF Tycho Brahe*. Retrieved from Wikipedia: https://en.wikipedia.org/wiki/MF_Tycho_Brahe
Wikipedia. (2024, February). *E/S Sjövägen*. Retrieved from Wikipedia: https://sv.wikipedia.org/wiki/E/S_Sj%C3%B6v%C3%A4gen
Wikipedia. (2024, April). *E-ferry Ellen*. Retrieved from Wikipedia: https://en.wikipedia.org/wiki/E-ferry_Ellen

Proceedings of 15th International Marine Design Conference (IMDC-2024)
June 2-6, 2024
Amsterdam, the Netherlands

The Potential of Next Generation Nuclear Power for Marine Propulsion of Commercial Vessels

Niels de Vries[1*], Koen Houtkoop[2] and Zeno Leurs[3]

ABSTRACT

Nuclear energy has the potential to become one of the main alternatives to achieve sustainable marine shipping and reduce its greenhouse gas emissions. This study defines a power generation arrangement and evaluates design speed for nuclear powered vessels. Higher design speeds show promising economic results. This includes higher revenue and trade while maintaining a relatively low operational expenditures when compared with conventional powered ships. This study is carried out for a large container vessel and a large bulk carrier to support the implementation of nuclear energy technology. This study reviews reactors designed to a 25- to 75-year service life, using a fully electric power generation and propulsion layout.

KEY WORDS

Nuclear energy, commercial shipping, marine design, molten salt reactor, comparative study.

NOMENCLATURE

B	Breadth	O&M	Operation and maintenance
CapEx	Capital expenditures	OpEx	Operational expenses
Cb	Block coefficient	Pb	Brake power
DWT	Deadweight	Pd	Propulsion power
EIRP	Energy Innovation Reform Project	Pne	Nuclear electrical power
FEU	Forty-foot equivalent unit	PWR	Pressurized water reactor
Fn	Froude Number (Fn = v / √(g·L))	sfc	Specific fuel consumption
GT	Gross tonnage	SMR	Small modular reactor
IAEA	International Atomic Energy Agency	T	Draft
Lbp	Length between perpendiculars	TEU	Twenty-foot equivalent unit
LSW	Lightship Weight	v	Ship speed
VLSFO	Very low sulphur fuel oil (0.5% Sulphur)	VHTR	Very high temperature reactor
MSR	Molten salt reactor	WNA	World Nuclear Association
NEA	Nuclear Energy Agency		

INTRODUCTION

With the need for shipping to become more sustainable and reduce its harmful emissions, nuclear marine propulsion has potential to be one of the solutions. Earlier research (Houtkoop, 2022) has shown the initial potential of next generation nuclear technology for shipping with replacement of conventional power generation. However, the full potential of nuclear on marine applications, especially for new builds, is not fully known yet. Therefore, the goal of this study is to develop new build cases and explore their potential focusing on design speed, propulsion and power generation, and ship design.

This paper is built up as follows. The first section studies parts of nuclear power generation and propulsion and establishes a technically feasible basis for the propulsion configuration and arrangement. This is followed by a section introducing the case studies with their own background for further economic analysis in the second section. The third and fourth section elaborate on the speed-dependent total cost of ownership and shipping income respectively that serve as input for the analysis of the cases. The fifth section clarifies the overall calculation method to determine the most economic speed for the complete range investigated in this research. The sixth section presents the results with initial review followed by the seventh section discussing the results further. This final sections of this paper cover the conclusion and recommendations.

[1] C-Job Naval Architects (Hoofddorp, The Netherlands);
[2] Delft University of Technology (Marine Technology, Delft, The Netherlands);
[3] Delft University of Technology (Marine Technology, Delft, The Netherlands).

*Corresponding Author: n.devries@c-job.com

Submitted: 29 January 2024, Revised: 26 April 2024, Accepted: 1 May 2024, Published: 27 May 2024

Conference paper, DOI: https://doi.org/10.59490/imdc.2024.912 e-ISSN: 3050-4864

POWER GENERATION AND PROPULSION

This section describes the considered and selected options to convert and distribute nuclear power to propulsion and other electrical consumers. It does so by reviewing the main topics covering reactor, shielding, heat exchangers, turbines, propulsion configuration, and arrangement.

System Design

The system design of a nuclear power plant can be made in various ways. This study is not exclusive for one reactor type or one system design. Instead this study aims to be representative for a range of designs. For a better understanding of the principles of a nuclear power plant a basic system design is shown in Figure 1. It is based on primary loop going through the reactor, an intermediate loop and an open air loop. Two hypothetical options for the reactor and mediums for the respective loops are shown in Table 1. The reasoning for the respective design options are provided in subsections *Heat Exchangers* and *Turbines*. Alternative nuclear power plant designs with a different number of loops are also possible. Furthermore, different types of mediums with respective open or closed cycles are also possible. However, both are not further reviewed in this study.

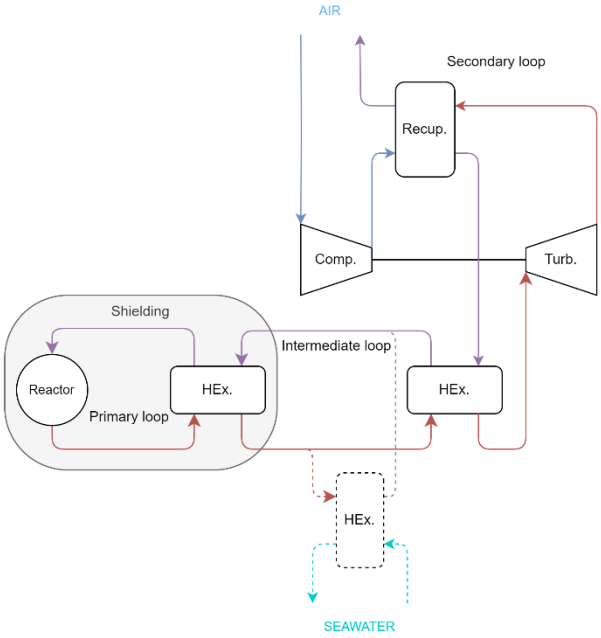

Figure 1: Basic system design of a nuclear power plant

Table 1: Hypothetical options for (V)HTR and MSR and heat transfer loop mediums

Hypothetical option	Reactor	Primary loop	Intermediate loop	Secondary loop
1	(V)HTR	Helium	Salt	Open Air
2	MSR	Salt	Helium	Open Air

Reactor

This study is not exclusive to one reactor type, and researches a bandwidth of reactor capital expenditures (CapEx). As examples of reactor types, earlier research (Houtkoop, 2022) has indicated that for a number of reasons, (Very) High Temperature Reactors ((V)HTRs) and Molten Salt Reactors (MSRs) have a lot of potential for the maritime industry. An important reason is the passive safety properties which prevent issues with stability and thus ensures reactor safety without outside intervention. Another reason is the high burn-up of these reactor types. Burn-up is an effectivity measure indicating how much thermal energy the reactor can extract from a given quantity of nuclear fuel. A higher burn-up is favorable as it reduces the amount of required nuclear fuel and produced waste per power produced (Houtkoop, 2022). Furthermore, both these reactor types have the potential to (partially) use the thorium fuel cycle. In addition to thorium being three times more abundant than uranium, the thorium fuel cycle has a higher proliferation resistance, meaning it is a very unattractive route to create nuclear weapons with it. This eliminates (or greatly reduces) the potential of weaponization. With thorium, the high-level nuclear waste longevity can be reduced from more than 10,000 years to approximately 300 years (Hargraves, 2010).

Shielding

The shielding around the reactor, to contain the respective forms of radiation, has a substantial mass and volume primarily consisting of water or concrete and additionally lead (Houtkoop, 2022). This partially clarifies why nuclear power generation onboard vessels is primarily interesting for large ocean-going vessels, as the shielding could become disproportionally large in terms of mass and volume for smaller vessels. This is further reflected upon in sub-section Background of section Case Studies. Future developments of making (reactors and) shielding more compact could change this. An example of this development for both reactors and shielding is Westinghouse and other parties developing SMR of the range of 5000kWe. This is believed to be ideal for the smaller size of ocean-going vessels (Petrakakos, 2024).

Heat Exchangers

Heat exchangers are essential to transfer the heat from the nuclear reactor to the turbines as shown in Figure 1. In the earlier research (Houtkoop, 2022) three heat exchanger types were compared as shown in Table 2.

Table 2: Summary of heat exchanger evaluation *(Houtkoop, 2022)*

Heat exchanger → Property ↓	**Shell and tube**	**Helical coil**	**Printed circuit**
Heat transfer coefficient [$W/m^2 \cdot K$]	500	1000	2000
Surface density [m^2/m^3]	75	80	1100

Printed circuit heat exchangers have the best volumetric power density. However, it has a low technical readiness level at the size under consideration. Therefore, helical coil heat exchangers are selected as the most suitable as these are more developed and proven.

The hypothetical option 1, as shown in Table 1, with (V)HTR, uses an intermediate salt loop. Hypothetical option 2, as shown in Table 1, with MSR, uses an intermediate helium loop. The main reason for this is the containment of radiation. In alternative designs supercritical CO2 could also be considered.

Turbines

In earlier research (Houtkoop, 2022) multiple turbine concepts have been investigated for marine nuclear power generation, namely:

- Rankine cycle (Steam)
  - Superheat
  - Superheat and reheat
  - Superheat and feedwater heating
- Closed Brayton cycle
  - Simple cycle
  - Recuperation
  - Intercooling and/or recuperation
- Open Brayton cycle
  - Simple cycle
  - Recuperation
  - Intercooling and/or recuperation

To evaluate these options, multiple performance indicators, being weight, volume, system complexity, and load response were used. The open Brayton cycle was found to be the most suitable as shown in Table 3.

Table 3: Summary of turbine evaluation *(Houtkoop, 2022)*

Turbine → Property ↓	**Rankine (steam)**	**Closed Brayton**	**Open Brayton**
Efficiency	++	+	+
Volume (system)	-	+	0
Weight (system)	-	+	0
Complexity (system)	--	-	+
Load response	+	+	++

The open Brayton cycle turbine is, in terms of its development close to the current marine gas turbine, operating with air as the medium. The main difference with the conventional marine gas turbine is the use of a heat exchanger to supply heat instead of using a combustion process. One of the benefits of open cycle is that it does not require a condenser or heat exchanger for cooling, as the used air is simply rejected (Houtkoop, 2022). This however comes at the expense of having inlet and outlet ducting that are associated with performance and pressure losses and a space requirement (Stapersma, 2019).

For load response the open Brayton cycle turbine is again limited by the reactor and its heat exchanger. The aeroderivative open Brayton turbine can operate on far greater load responses than gas turbines operating on the combustion process. A greater load response similar to this can be achieved when considering load rejection strategies (Houtkoop, 2022). The resulting concept applying heat rejection to improve load response is shown in Figure 2. This configuration also shows the separation of compressor turbine and the load turbine. The benefit of this is that the compressor operation upon load change is not disturbed resulting in a larger load envelope (Stapersma, 2019). In alternative designs supercritical CO2 could also be considered.

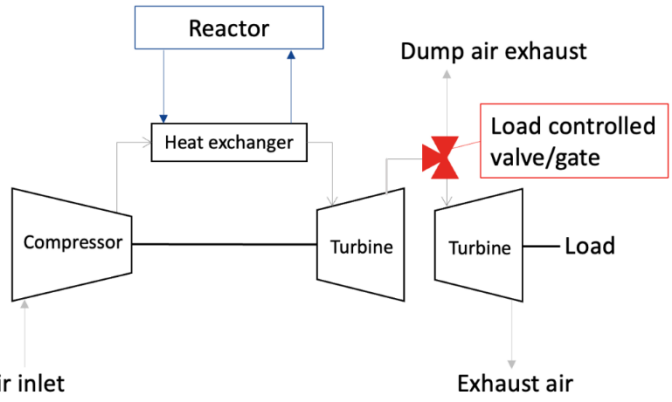

Figure 2: Open Brayton, heat rejection and load turbine (Houtkoop, 2022)

Propulsion Configuration

To convert the power generated by turbine to propulsion multiple propulsion configurations can be considered. In principle this comes down to three options namely, turbine-direct, turbine-electric, or a hybrid form of both. For this study a complete electric propulsion is selected. By doing so, a conservative approach in terms of efficiency for the nuclear option is established, assuring that the results are not overly optimistic. Additionally, full electric propulsion offers flexibility in arrangement and options for easy integration of peak shaving with batteries for improved load response. Furthermore, it also offers options for reverse cold ironing while in port and easy integration of back-up power by means of diesel generators. Nevertheless, future studies are encouraged to review options to further optimize the nuclear option with, for example, turbine-direct propulsion or hybrid propulsion.

Arrangement

Combining the found options discussed in each subsection, an initial overall arrangement is formed and shown in Figure 3. It has the reactor, shielding, and intermediate heat exchangers in the middle. There are two power generation rooms each with a primary heat exchanger, turbine, and generator. Furthermore, it has a redundant electrical propulsion system. This is supplemented with batteries and emergency diesel generators.

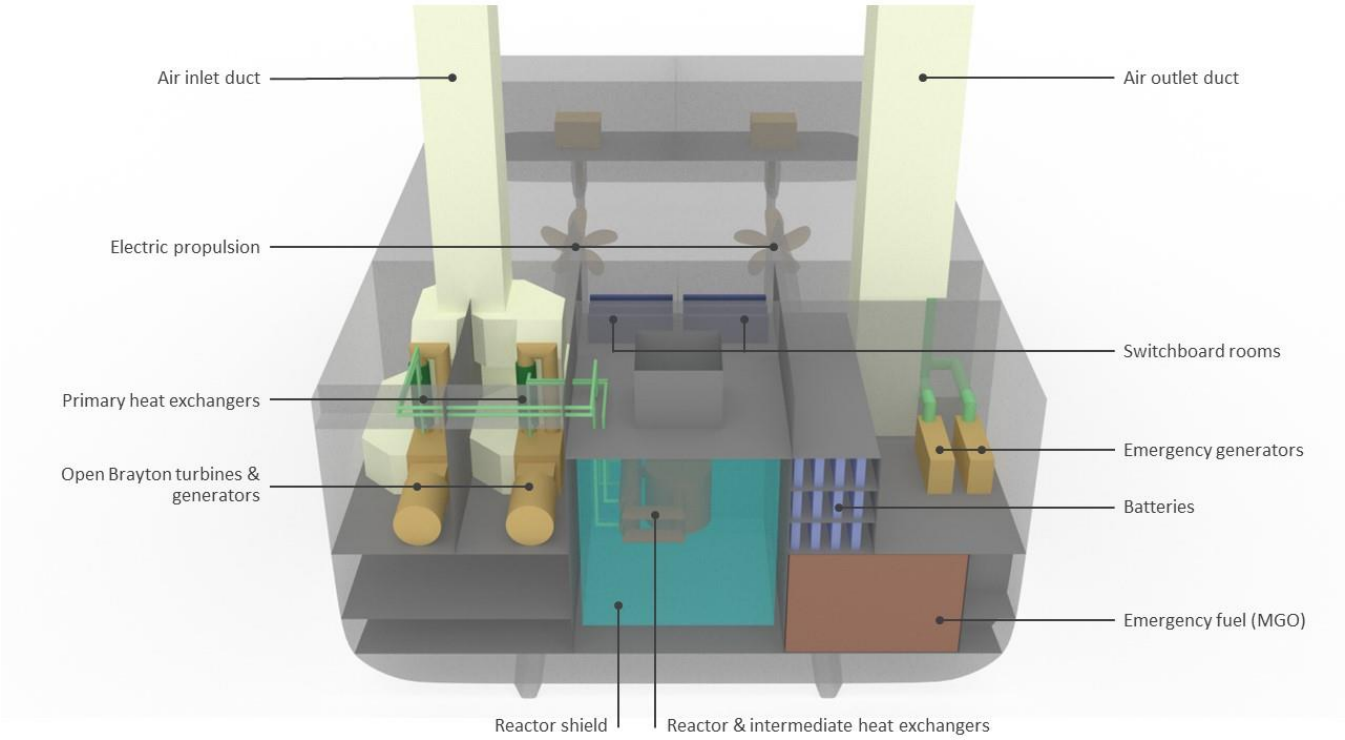

Figure 3: Nuclear power generation and propulsion arrangement

CASE STUDIES

In this section the case studies to evaluate design speed are defined. In order to explain the selection of these case studies more background on nuclear energy and marine propulsion is reflected upon first.

Background

Earlier research has shown that Generation IV (Gen-IV) nuclear reactors have a lot of potential to decarbonize the power sector effectively (Buongiorno, 2018). Furthermore, specifically Gen-IV Molten Salt Reactors (MSR) designs, which enable use of the thorium fuel cycle, are expected to be cost-competitive with other energy sources (Mignacca, 2020). In addition to onshore nuclear power plants other concepts are also being developed for floating nuclear power plants (Lobner, 2021). Additionally, studies have reviewed MSR application on vessels and have shown it to be economically competitive with other alternatives (Emblemsvåg, 2021) (Gennaro, 2020).

Furthermore, research work of (Houtkoop, 2022) *Nuclear reactors for marine propulsion and power generation systems* has shown that nuclear marine propulsion has a lot of potential for large ocean-going vessels to reduce harmful emissions. The completion of the study (Houtkoop, 2022) inspired to explore the potential of higher design speeds with nuclear marine propulsion. It could potentially make the ship more profitable. This is because fuel cost, as part of operational expenditures (OpEx), only grows marginally with higher speeds for nuclear powered vessels. Ultimately the main limiting factor would be the CapEx of the installation with more power. Additionally, the reactor can be used for a longer period of time by either reusing it in a new ship or by extending the service life of the initial ship. This would allow to depreciate the CapEx of the reactor over more years thus improving the economic model of the investment and enabling considerations for higher speeds further. Of the high potential ship types covered in (Houtkoop, 2022), two are selected for this study as new build cases, a container vessel and a bulk carrier. As shown in Figure 4, the weight of reactor and shielding is smaller than the conventional fuel weight, plotted as dots, for a ship set containting built vessels from the last decades, it would replace in like-for-like replacement. The blue and red lines represent the lower and upper weight estimates of the nuclear reactor and shielding. The dashed black line is a trend line of the respective data point. Therefore, the integration is considered to be managable with limited design impact for large ocean going container and bulk vessels.

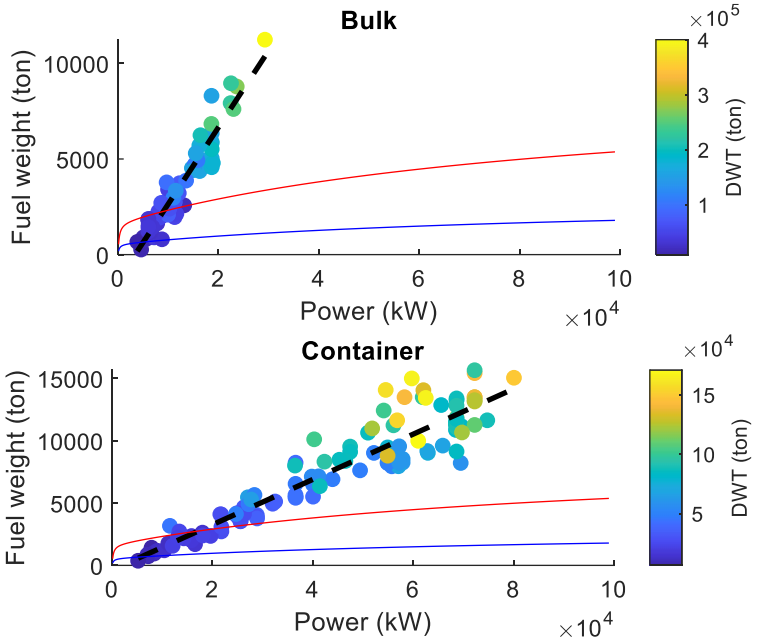

Figure 4: Plots of vessels fuel weights vs reactor and shielding weight estimates *(Houtkoop, 2022)*
Blue and red lines: Lower and upper bound of weight estimates of the nuclear reactor and shielding
Black dashed line: trend line of data points

Container

To study container cases a market representative selection of ship size and route is made. For this study this results in the selection of a ship size of 20,000 TEU with two routes as described below in Table 4.

Table 4: Container cases

Case	Route (Baltic Exchange, 2023)	Distance [nm] (Ports.com, 2010-2023)	Port duration* [day]	Suez canal duration* [day]
I	North Europe – China/East Asia (FBX11 & 12)	11,999 (Rotterdam – Shanghai)	3	1
II	Europe – North America East Coast (FBX21 & 22)	3,918 (Rotterdam – New York)	3	Not applicable

*No additional considerations are made with respect to port congestion that could result in waiting times. (C-Job Naval Architects, 2024)

Bulker

To study bulk carriers cases a market representative selection of ship size and route is made. For this study this results in the selection of a ship size of 300,000-ton DWT with the vessel transporting iron ore along two routes, as described below in Table 5.

Table 5: Bulker cases

Case	Route (Baltic Exchange, 2023)	Distance [nm] (Ports.com, 2010-2023)	Port duration* [day]	Suez canal duration [day]
III	Tubarao, Brazil to Qingdao, China (C3)	13,555 (Tubarao to Qingdao)	5	Not applicable
IV	West Australia to Qingdao China (C5)	4,059 (Hedland to Qingdao)	5	Not applicable

*No additional considerations are made with respect to port congestion that could result in waiting times. (C-Job Naval Architects, 2024)

SPEED-DEPENDENT TOTAL COST OF OWNERSHIP

To determine the most economical speed, the speed-dependent costs need to be identified which then can be deducted from the shipping income. As a result, it will show where the optimal speed lies. The speed-dependent total cost of ownership is divided into capital expenditures and operational expenditures. In this calculation, only main contributors are considered. Cost components that are not (substantially) influenced by speed are not included in this analysis, as this is an initial evaluation for optimum design speed and its design implementation.

Capital Expenditures

Speed-dependent capital expenditures (CapEx) are identified in two main components. The first is the nuclear reactor, which not only includes the reactor, but also its shielding, the heat exchangers, turbines, generators, and other respective auxiliaries. The second component includes electrical system elements, the electric motor, gearbox, propeller shaft and the propeller. Other components are not included in this study.

Nuclear Reactor

Small Modular Reactors (SMR), which are defined as nuclear reactors with 300,000 kWe or less, are the most suitable to establish a cost reference. Based on literature research, the estimated costs of SMRs are as presented in Table 6. Most references include estimated costs of Pressurized Water Reactors (PWRs) and only a few cover multiple reactor types. This study is not exclusive to one reactor type, as stated earlier, and instead it researches a bandwidth of reactor CapEx.

To estimate the nuclear reactor cost, the reactor size, in terms of power, needs to be defined. Referring to the range of installed brake power of large ocean-going vessels fitted with diesel engines, generally directly connected to the propeller shaft, as presented in Figure 4, the installed brake power ranges from 5,000 to 80,000 kW.

Table 6: Nuclear reactor CapEx *(Leurs, 2023)*

Source	Cost [$/kWe]	Power [MWe]	Type
(Abdulla A., 2013)	*2,000-9,200	45	PWR
(Abdulla A., 2013)	**9,200-25,500	45	PWR
(Stewart W.R., 2022)	5,230	160	PWR
(Vegel Benjamin, 2017)	4,790	225	PWR
(EIRP, 2016)	2,053-5,855	<300	Various
(Lloyd, 2018)	5,720	300	PWR
(Lloyd, 2018)	5,000	400	PWR
(Lloyd, 2018)	4,500	500	PWR
(Lloyd, 2018)	4,225	600	PWR
(Stewart W.R., 2022)	4,059	685	PWR
(Black Geoffrey A., 2019)	3,611	720	PWR

*11 experts
**5 experts

As can be seen in Table 6 there is a relative cost decrease with higher power generated. Furthermore, there are still quite some deviations between the calculated cost estimates. Based on these results a bandwidth of 3,000-9,000 $/kWe is selected for the analysis in this study. Respective decommissioning cost estimates show similar deviations as shown Table 7. For this analysis, since a large bandwidth of CapEx is investigated, the decommissioning cost is assumed to be included in the CapEx.

Table 7: Nuclear reactor decommissioning cost *(Leurs, 2023)*

Source	Cost [$/kWe]
(NEA, 2016)	1,070-1,220
(The World Bank, 1990)	144-254
(Sayres and Associates Corporation, 2008)	3,153
(United States General Accounting Office, 1992)	242-432

Other
For the other CapEx items, design guidelines and estimations of C-Job are used. The resulting costs are shown in Table 8.

Table 8: Other CapEx *(C-Job Naval Architects, 2024)*

Item	Cost
Electrical System	500 $/kW
Electric Motor	250 $/kW
Gearbox	75 $/kW
Propeller and Shaft	75 $/kW

Operational expenditures
Yearly speed-dependent operational expenditures (OpEx) are identified in three parts. The first is fuel cost. The second is the operations and maintenance cost. The third cost aspect is the voyage cost including port, canal, pilot, and tug fees. Whereas the fuel and operation and maintenance cost are evidently speed dependent, the voyage cost is also directly proportional to the vessels speed, because with higher speeds, ports and canals are visited more frequently, resulting in a higher yearly costs.

Fuel Cost
To determine the fuel cost per kWh ($/kWh), the respective specific fuel consumption (sfc) in g/kWh and cost of fuel $/kg of the respective fuel needs to be established. The efficiency g/kWh can be defined by assuming a burnup (IAEA, 2020) of 45 GWd/tHM (Gigawatt per day per ton of heavy metal) and a reactor efficiency of 33% (Shultis, 2002), resulting in 0.0028 g/kWh. To put this in perspective, marine diesel engines are generally in the order of 170 g/kWh (MAN Energy Solutions, 2024) using Very Low Sulphur Fuel Oil (VLSFO).

The World Nuclear Association (WNA) divides the front-end fuel cycle costs into four categories. The natural uranium mining cost, the conversion cost, the enrichment cost, and the fuel fabrication cost. These account for 51%, 7%, 24% and 18% of the cost respectively (Leurs, 2023). In summary, an average of 2,500 $/kg Uranium 5% enrichment was found (Leurs, 2023). Alternatively, in future work Uranium 20% enrichment or Thorium could also be investigated.

Combining 0.0028 g/kWh and 2500 $/kg one can find 0.0070 $/kWh as fuel cost for nuclear. To put this in perspective, for marine diesel engines this would be 0.102 $/kWh, based on 600 $/ton VLSFO (Ship and Bunker, 2024) and the earlier defined 170 g/kWh. With these prices, in terms of fuel cost, based on energy output, nuclear is roughly a factor of 15 cheaper than VLSFO.

Operations & Maintenance Cost
The operation and maintenance (O&M) cost of a nuclear power plant are the costs to maintain and operate a nuclear power plant. They consist of all non-fuel costs which are, for example, plant staffing, purchased services, replaceable materials, and equipment. Further, these can be divided into fixed and variable costs where fixed (plant staffing) are considered the biggest, which for a marine application will be assumed as nuclear power plant crew cost (Mignacca, 2020). The fixed costs are based on the installed electrical power and expressed in $/kW per year. Furthermore, the variable costs are based on MWh output expressed in $/MWh. An overview of O&M cost estimates is shown in Table 9. For this study, a round average is taken resulting in 130 $/kW per year and 4.0 $/MWh are used.

Table 9: Nuclear O&M cost *(Leurs, 2023)*

Source	O&M Fixed [$/kW per year]	O&M Variable [$/MWh]
(EIRP 2016)	96	3.0
(EIRP 2016)	158	5.0
(EIRP 2016)	206	6.5
(US Energy Information Administration 2022)	99	3.1
(US Energy Information Administration 2022)	114	2.8
(Vegel Benjamin 2017)	123	3.9
Round average	**130**	**4.0**

Voyage Cost

In this analysis the voyage cost consist of fees for ports, canals, pilots, and tugs. Based on reviews of the ports an average estimate has been established to be used in this analysis. An overview of the defined cost is shown in Table 10.

Table 10: Voyage cost *(Leurs, 2023)***

Item	Cost
Port Case I & II (Rotterdam, Shanghai, New York)	0.50 $/GT + *6.00 $/TEU
Port Case III & IV (Tubarao, Qingdao, Hedland)	0.80 $/GT
Pilotage Case I & II (Rotterdam, Shanghai, New York)	7,500 $/per visit
Pilotage Case III & IV (Tubarao, Qingdao, Hedland)	20,000 $/per visit
Tugs Case I & II (Rotterdam, Shanghai, New York)	6,000 $/tug 3 tugs per visit
Tugs Case III & IV (Tubarao, Qingdao, Hedland)	15,000 $/tug 3 tugs per visit
Suez Canal Case I	4.50 $/GT

*Based on 0.50 $/ton per TEU and 12 ton per TEU
**Rounded estimates from respective sources

SHIPPING INCOME

In this study, a range of freight rates is investigated to determine their influence on design speed. To obtain a realistic and market representative range of freight rates, historical data of the past 5 years from the Baltic Exchange (Baltic Exchange, 2023) has been studied.

Container Case I & II

Case I, with FBX11 and FBX12, and Case II, with FBX21 and FBX22, generally has an average freight rate between $1,000-$3,000 per FEU (Baltic Exchange, 2023). There are certain periods above and below this average range, but these are excluded from this study as they do not occur very often. Because container vessels do not always sail fully loaded, a utilization factor of 0.85 (Leurs, 2023) is used in this study.

Bulker Case III & IV

Case III, with C3 and Case IV, with C5, generally have an average freight rate between $5-$30 per ton of ore (Baltic Exchange, 2023). Similar to container freight rates, ore freight rates have certain periods above and below this average range. However, these are not included in this study. For utilization of the DWT for cargo 0.98 has been defined. 1.3% (0.013) of the DWT, being 4000 ton, is deducted to compensate for additional lightship weight (LSW) of the nuclear power plant as derived from earlier work (Houtkoop, 2022). The remaining 0.7% (0.007) of the DWT, being 2000 ton, is available for the consumables. The reference conventional base case Brasil Maru (Royal Institution of Naval Architects, 2008) has approximately 7500 ton of its DWT allocated for VLSFO. VLSFO is no longer present on the nuclear option and other consumables are only a fraction of fuel DWT. Therefore, the 2000 ton is deemed more than sufficient for other consumables. It is recommended to study the consequences of the integration of reactor and shield on LSW. The reason for this is that the longitudinal strength for bending and shear is different than with VLSFO storage.

DESIGN SPEED CALCULATION METHOD

In this section the design speed calculation method is clarified by defining the specifications of the ships. Furthermore, the economic speed determination is elaborated upon and illustrated showing how the cost are deducted from the shipping income resulting in a profit line.

Nuclear Options

With the income and speed-dependent costs identified, various scenarios can be calculated for different freight rates, reactor CapEx, and speeds. To do this, the vessel's total resistance is calculated for various speeds. Because relative high speeds are the area of interest, with large ocean going vessels, wave making resistance is a substantial part of the total resistance. To calculate it in a preliminary design stage a smaller vessel (Maersk-B Class (Leurs, 2023)) of the same type with a high Froude number is scaled up to the size and capacity of interest. Keeping the Froude number constant the total resistance is calculated. By doing so, for speeds up to the respective Froude number, it can be stated that the wave making resistance is not underestimated, which is considered a conservative approach for the initial designs. These estimates are then compared to Holtrop & Mennen (Leurs, 2023) to validate the order size of the respective resistance for the actual calculations. The initial estimates for the container cases are shown in Table 11.

Table 11: Initial design estimates container *(Leurs, 2023)**

Container	**Model**	**Ship**
Name	Maersk-B Class	Nuclear Container
Lbp x B x T [m]	278.20 x 32.18 x 12.20	475.72 x 55.03 x 20.86
Cb [-]	0.59	
Displacement [ton]	66,051	330,255
Froude number [-]	0.29	
Speed [kts]	29.2	38.2
Capacity [TEU]	4,000	20,000
Scale factor [-]	1.71	
Pd [MW]	68.0	444.3
Pb [MW]	68.6	457.9
Pne [MWe]	-	512.6

*Further clarified with power figures.

The power listed is brake power (Pb) for the existing vessels, listed under Model. Pb is the power provided by the engine on the shaft. The listed power for the nuclear option, listed under Ship, is the installed nuclear electrical power (Pne). This is calculated by correcting the translated Pb with 0.89 which is clarified in Figure 5.

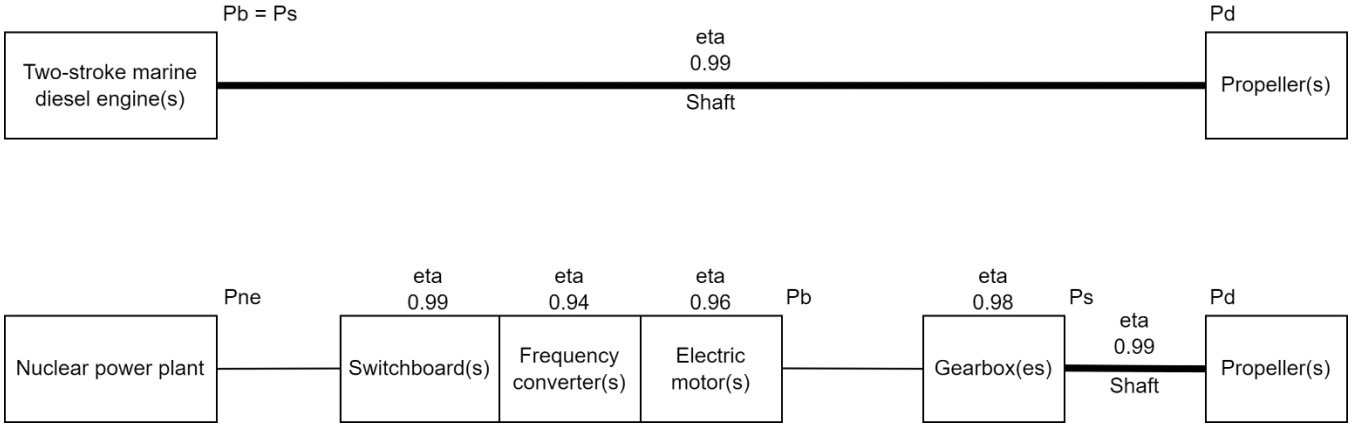

Figure 5: Conventional and nuclear power train (applied in this study) *(C-Job Naval Architects, 2024)*

The gearbox is included as a conservative approach but it might not be needed. This study aims to represent a broad range of designs. To make this tangible with a hypothetical speed of 30 knots it would result in roughly 249 MWe Pne. For a hypothetical vessel that uses two electric motors, this would translate into a power output of roughly 111 MWe per electric motor. The impact of the size of such electric motors without gearbox is not fully known. Additionally, similar to the selection of full electrical propulsion, adding the gearbox, with efficiency loss, contributes to a conservative approach in terms of efficiency. By doing so there is additional margin that assures that the results are not overly optimistic for the nuclear option. Therefore,

the gearboxes are included in this study, in addition to making sure that the size of the electric motors are manageable. Nevertheless, future studies are also encouraged to review options to further optimize the nuclear option with (full) electrical propulsion without gearbox in addition to other propulsion configurations.

The same method used for scaling the container vessel has been used for the bulk carrier using Golden Wealth bulk carrier as reference vessel which has Fn 0.25 with 18,842 ton DWT (Ship Spotting, 2011). However, it was found that the resulting economic speeds were not in the high speed region (Fn>0.2) but clearly in the lower speed region (Fn<0.2). Therefore, using this reference vessel and method was not found suitable as the results were reasonably accurate on the high speeds but too conservative for the lower speeds. Therefore, a different reference vessel was selected, Brasil Maru, with a lower Froude number and larger deadweight resulting in a smaller scale factor. Here it should be noted that any potential results above this Froude number could be considered too optimistic. The initial estimates for the bulker cases are shown in Table 12.

Table 12: Initial design estimates bulker

Bulker	**Model**	**Ship**
Name	Brasil Maru*	Nuclear Bulker
Lbp x B x T [m]	325.00 x 60.00 x 18.10	336.31 x 62.09 x 18.73
Cb [-]	0.85**	
Displacement [ton]	307,508	330,255
Froude number [-]	0.15	
Speed [kts]	16.0	16.3
DWT [ton]	270,728	300,000
Scale factor [-]	1.03	
Pd [MW]	23.4	26.4
Pb [MW]	23.6	27.2
Pne [MWe]	-	30.4

*Data Brasil Maru: (Royal Institution of Naval Architects, 2008) & (Class NK, 2023)
**Estimate based on trend line derived from (C-Job Naval Architects, 2024)

As discussed in the background section of this study, the service life of nuclear reactors, approximately 75 years, are substantially longer than the service life of a conventional vessels, approximately 25 years. A first consideration would be to extend the service life of the vessel to make the use of nuclear reactor more attractive economically. However, an alternative form of economic use of the nuclear reactor is to decommission the ship, at its service of life of 25 years, and preserve the nuclear reactor which can then be used for a new vessel. Reviewing the options, this study views that the selection of either option on how to extend the use of the nuclear reactor, is independent on the design speed analysis. Therefore, in this study only the potential of extended use of the nuclear reactor is investigated with 50 and 75 years in addition to the conventional 25 years of service life of a vessel as illustrated in Figure 6. This study does not include evaluation of either option on how to extend the service life of the ship with nuclear reactor as illustrated in Figure 7. Future studies are encouraged to review these options, including all aspects of the ship and nuclear reactor, in order to determine the most attractive strategy.

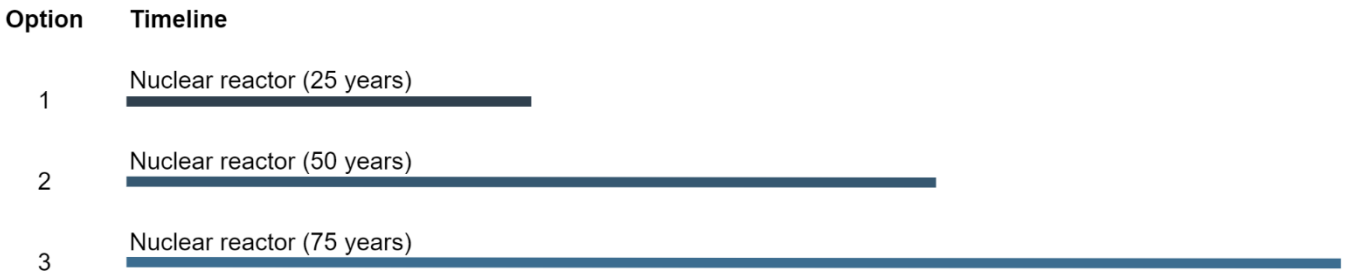

Figure 6: Service life options nuclear reactor (investigated in this study)

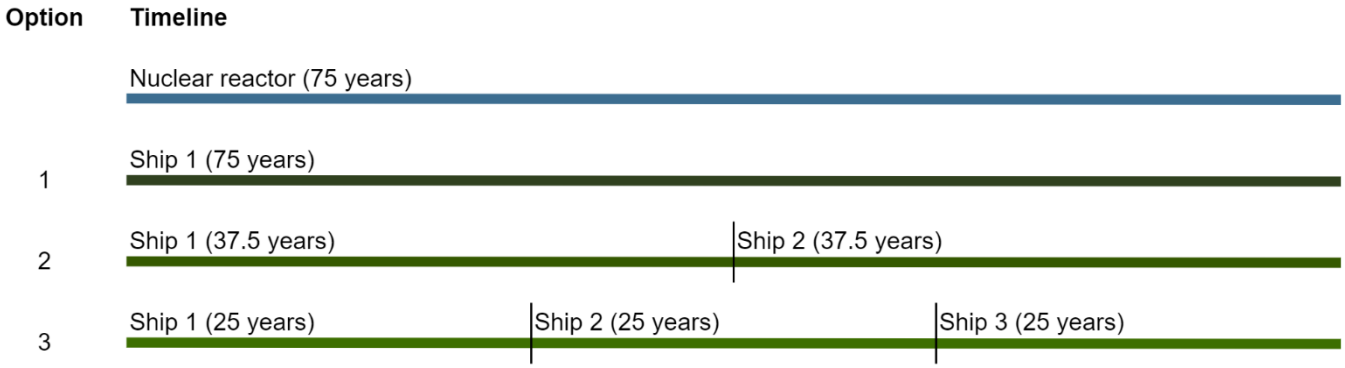

Figure 7: Service life options ship with nuclear reactor 75 years (not investigated in this study)

Conventional Option

To determine whether the resulting speeds of the nuclear options are actually higher compared to conventional configurations, as anticipated, a conventional option as reference is established. This conventional option will use the parameters as per Table 13 based on established design guidelines.

Table 13: Conventional option parameters

Item	Parameters	Source
Income	Same as Nuclear	-
CapEx: Marine diesel engine (2-stroke)	350 $/kW	(C-Job Naval Architects, 2024)
OpEx: Fuel cost (VLSFO) Specific fuel consumption	300-800 $/ton 170 g/kWh	(Ship and Bunker, 2024) (MAN Energy Solutions, 2024)
OpEx: O&M Fixed per year	35 $/kW	(Leurs, 2023)
OpEx: O&M Variable	10 $/MWh	(Leurs, 2023)
OpEx: Voyage	Same as Nuclear	-

Case Calculations

With the shipping income, and all cost components defined each case can be evaluated accordingly to determine the maximum profit and thus the optimum speed. An example of an individual scenario calculation is shown in Figure 8 which regards Case I, Nuclear, service life 75 years, freight rate $2000 per FEU, reactor CapEx $6,000 per kW. By combining all maximum profit scenario results an overview can be made with most economic speeds. These results are presented in the next section for all 4 cases with 3D graphs.

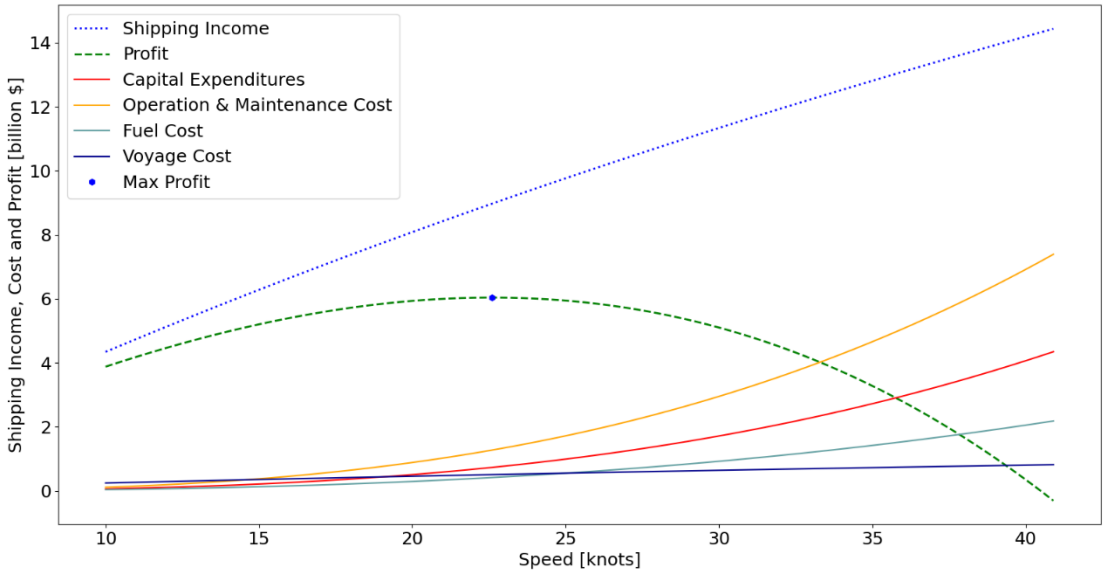

Figure 8: Example of individual scenario calculation
(Case I, Option Nuclear service life 75 years, scenario freight rate $2000 per FEU, reactor CapEx $6,000 per kW)

DESIGN SPEED RESULTS

Results covering the entire range of scenarios are presented in 3D graphs per case. Additionally, three specific scenarios are listed in tables for further considerations as shown in Table 14. For the conventional option, three specific scenarios are defined as per Table 15, similarly as with the nuclear options.

Table 14: Specific nuclear scenarios

Scenario	Freight rate	Nuclear reactor CapEx
A	High	Low
B	Average	Average
C	Low	High

Table 15: Specific conventional scenarios

Scenario	Freight rate	Fuel cost
A	High	Low
B	Average	Average
C	Low	High

Container

In this subsection the results of the container cases are presented and initially reflected upon. More extensive evaluation is covered in the section *Discussion*.

Case I

Using the figures of shipping income and speed-dependent cost with the described calculation method, Case I can be calculated with the results shown in Figure 9 (where the color gradient covers the resulting speed levels). The principal coding to generate these figures is sourced from (Leurs, 2023) and is adjusted with refined assumptions for this study. Furthermore, the results of the specific scenarios of nuclear with both 25, 50, and 75 years of service life, and the conventional VLSFO reference with 25 years are shown in Table 15.

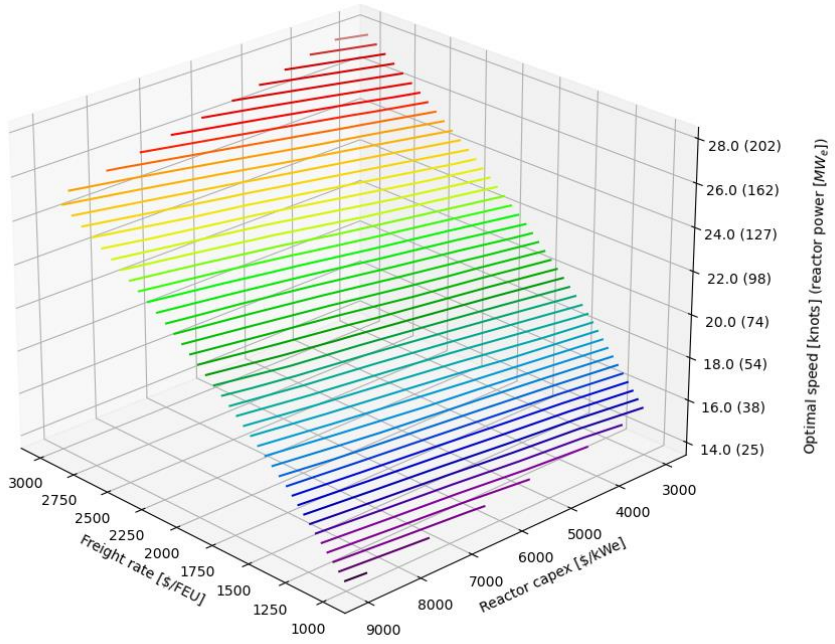

Figure 9: Case I, Nuclear, service life 75 years (color gradient covering speed levels)

Table 16: Case I design speed results of specific scenarios [kts]

Scenario	VLSFO 25y	Nuclear 25y	Nuclear 50y	Nuclear 75y
A	22.9	24.3	27.0	28.2
B	14.6	17.2	19.9	21.2
C	8.0	10.5	12.6	13.7

As can been seen in the nuclear options, 25, 50, and 75 years of service life, have higher economic speeds than the conventional VLSFO case of 25 years. Results of scenario A and B seem realistic as the conventional VLSFO case with speeds from 15 to 23 knots is considered very representative to current container vessel operation. For example, the Triple-E class of Maersk has a service speed of 16 knots and a maximum speed of 23 knots. Reviewing scenario C, which is the low-speed scenario, it should be noted that the current resistance estimate is done with a basic initial approach aiming for a good accuracy for the higher speed range, as explained earlier in the section Design Speed Calculation Method. As a result, it is too conservative for lower speeds (meaning speeds below 14 knots Fn<0.2). Hence the lower resulting speeds for scenario C. Furthermore, nuclear with 75 years of service life has an increase in economic speed compared to nuclear with 25 years of service life. This confirms the earlier statement about its potential and quantifies the additional gain. Additionally, freight rate seems to have the biggest influence whereas reactor CapEx has a less substantial role in the range investigated in this study.

Case II

For Case II, the results are shown in Figure 10 and the results of the specific scenarios are shown in Table 17.

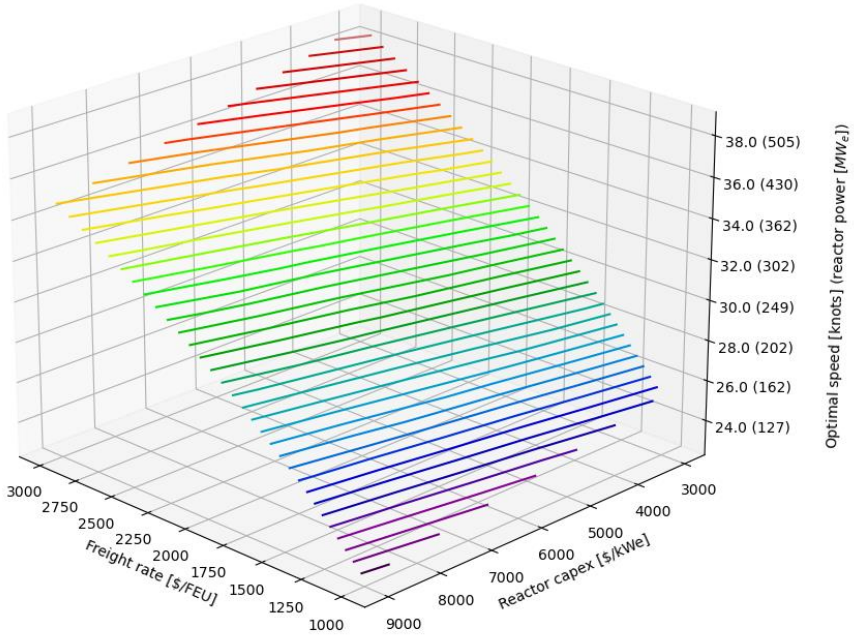

Figure 10: Case II, Nuclear, service life 75 years

Table 17: Case II design speed results of specific scenarios [kts]

Scenario	VLSFO 25y	Nuclear 25y	Nuclear 50y	Nuclear 75y
A	35.9	33.9	37.3	38.8
B	24.6	25.6	29.2	30.9
C	15.3	17.8	21.0	22.6

With Case II covering a substantially shorter distance than Case I, the resulting speeds are clearly higher. This can be explained by the investigated ranges of cost and freight rates. The freight rates are kept the same resulting in the same amount of income. On the other hand, lower cost associated with a shorter distance, lead to higher economic speeds. So, in general similar trends can be observed compared to Case I, where the actual speeds are higher. However, scenario A does not seem representative for Case II for current container vessel operations with speeds up to 36 knots for the VLFSO case. One might consider those respective conditions to be too optimistic with a very low likelihood of occurring. Here the results of scenario B and C are deemed more representative.

Bulker

In this subsection the results of the bulker cases are presented and initially reflected upon. More extensive evaluation is covered in the section Discussion.

Case III

For Case III, the results are shown in Figure 11 and the results of the specific scenarios are shown in Table 18.

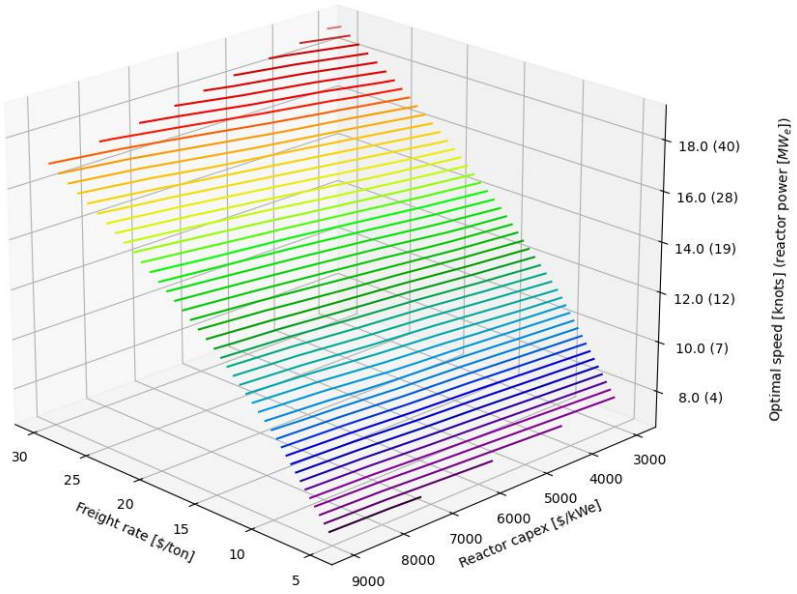

Figure 11: Case III, Nuclear, service life 75 years

Table 18: Case III design speed results of specific scenarios [kts]

Scenario	VLSFO 25y	Nuclear 25y	Nuclear 50y	Nuclear 75y
A	15.2	16.5	18.3	19.1
B	8.9	10.8	12.5	13.3
C	3.7	5.2	6.2	6.8

As can been seen in the nuclear options, 25, 50, and 75 years of service life, have higher economic speeds than the conventional VLSFO case of 25 years. The result of scenario A of the conventional VLSFO case, with 15 knots, are deemed representative as current bulk carrier operations are considered to generally range between 11 and 16 knots. Additionally, freight rate seems to have the biggest influence whereas reactor CapEx has a less substantial role in the range investigated in this study.

Case IV

For Case IV, the results are shown in Figure 12 and the results of the specific scenarios are shown in Table 19.

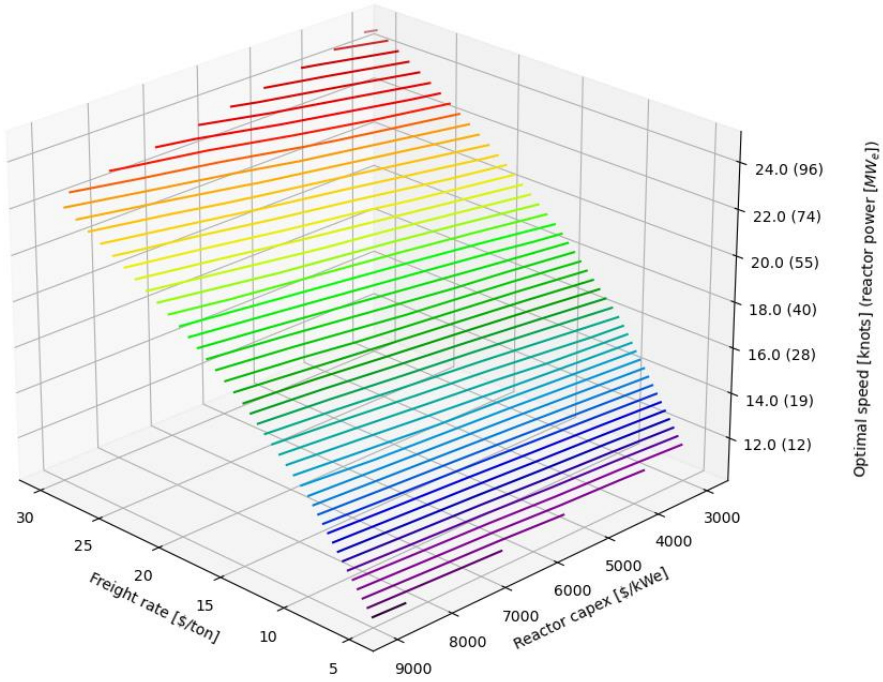

Figure 12: Case IV, Nuclear, service life 75 years

Table 19: Case IV design speed results of specific scenarios [kts]

Scenario	VLSFO 25y	Nuclear 25y	Nuclear 50y	Nuclear 75y
A	23.2	21.8	24.1	25.0
B	14.5	15.2	17.3	18.4
C	6.5	8.1	9.6	10.4

As can been seen in the nuclear options, 25, 50, and 75 years of service life, have higher economic speeds than the conventional VLSFO case of 25 years for scenario B and C. Scenario A does not seem representative for current bulk carrier operations with speeds up to 23 knots for the VLFSO case. Besides that, the shorter distance in Case IV logically has also higher speeds than Case III since the freight rates are kept the same and the effective cost is lower for the shorter distance. The result of scenario B of the conventional VLSFO case, with 15 knots, is deemed representative with respect to current bulk carrier operations.

DISCUSSION

In this section the results are further reflected upon. Additionally, an outlook is given on the design development including considerations for propulsion configurations.

Design Speed

This sub-section evaluates the design speeds of both cases for both ship types and envisions a guideline for future research.

Container

Reviewing the container cases with the specific scenarios, the range between scenario A and B for Case I and the range between scenario B and C for Case II seem most representative for the current container vessel operations. Considering the respective results of these cases and scenarios, it is found that 28-31 knots with a service life of 75 years would be a good range to explore nuclear powered container vessels further. This is a considerably higher speed than conventional container vessels. This is based on the assumption that the service life of the reactor is 75 years which is derived from existing nuclear power plants (Petrakakos, 2024). If the service life of the reactor changes, this design guideline would need to be revisited. As this is an initial design review, further analysis is recommended to cover more details, reduce uncertainty, and confirm or adjust these findings accordingly.

Bulker

Reviewing both bulker cases, similar principle results as with the container cases can be observed. Namely, both nuclear options, 25, 50, and 75 years of service life, have higher economic speed than the conventional VLSFO case, expect in scenario A of the shorter distance case. Furthermore, nuclear vessels with 75 years of service life have an increase in economic speed compared to nuclear vessels with 25 or 50 years of service life. Additionally, freight rate seems to have the biggest influence whereas reactor CapEx has a less substantial role. Considering the respective results of these cases and scenarios, it is found that 18-19 knots with a service life of 75 years would be a good range to explore nuclear powered bulk carriers further. This is a somewhat higher speed than conventional bulk carriers. This is based on the assumption that the service life of the reactor is 75 years which is derived from existing nuclear power plants (Petrakakos, 2024). If the service life of the reactor changes this design guideline would need to be revisited. As this is an initial design review further analysis is recommended to cover more details, reduce uncertainty, and confirm or adjust these findings accordingly.

Sensitivity

This study analyzed a bandwidth of reactor CapEx and freight rate and studied its impact on design speed. Besides these factors, also other cost aspects were quantified based on various references and design guidelines. Primarily the OpEx is considered of interest to be studied further to identify its sensitivity with respect to the design speed. This includes, but is not limited to, operations and maintenance cost of the nuclear power plant, and nuclear fuel cost, which is derived from the level of enrichment, the burnup and the price per kilogram. Further sensitivity analysis will help improve the robustness of the overall assessment. This will support the decision making process for the design speed of nuclear powered vessels.

Design Development

In this section the design development considerations for both the container vessel and bulk carrier are given. This covers main dimensions, resistance, and hybrid propulsion configurations.

Container

For this analysis the main dimensions of the container vessel exceed current port restrictions. Furthermore, a volume and displacement check needs to be done to confirm the cargo capacity (TEU), and adjust main dimensions where needed, to assure it is not too large. Therefore, for further design development it is envisioned to change the dimensions as shown in Table 20.

Table 20: Container vessel development of main dimensions

Parameter	**Nuclear Initial**	**Nuclear Iteration 1**	**Nuclear Iteration 2***	**Port restriction** (Leurs, 2023)
Lbp [m]	475.72	475.72	399.90	Rotterdam
B [m][	55.03	55.03	61.50	Rotterdam
T [m]	20.86	20.86	15.00	Shanghai
Cb [-]	0.59	0.59	TBD	-
Froude number [-]	0.29	0.23	0.25	-
Speed [kts]	38.8	30.0	30.0	-

*Envisioned dimensions based on port restrictions

Reviewing this design development it is noted that the length over breath ratio is reduced from 8.6 to 6.5 which is less favorable with respect to wave making resistance. However, at the same time, the actual Froude number is also reduced as the initial

speed of 38.8 knots is reduced to 30.0 knots (derived as rounded average from the earlier identified range of 28-31 knots) based on the economic analysis. Thus, this also implies that the relative part of wave making resistance is reduced in the total resistance. So, these changes are not expected to change the overall total resistance significantly. Regardless, it is recommended to further develop the design, starting with the second iteration to reduce uncertainty, and confirm or adjust these findings accordingly.

Besides the envisioned development in main dimension, the propulsion can also be studied further. It might be possible that the initial defined arrangement of two propellers, as shown earlier in Figure 3, is not optimal for the considered speeds. The speed of 30 knots will require a substantial amount of thrust which thus might opt for a three propeller arrangement to reduce thrust loading coefficients and improve overall efficiency. An initial design of a 3 propeller arrangement is shown in Figure 13.

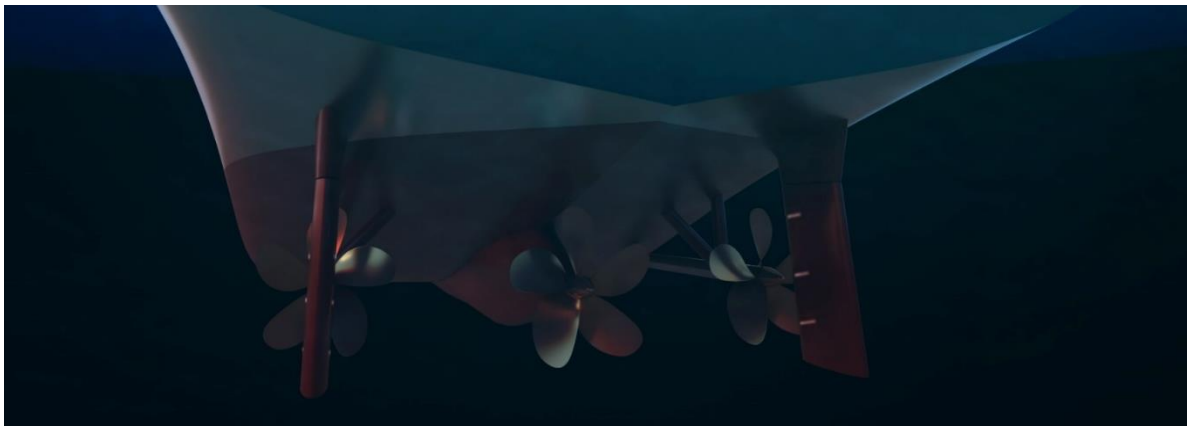

Figure 13: Initial design 3 propeller arrangement *(C-Job Naval Architects Visualization Discipline, 2024)*

The proposed arrangement with more propellers would offer further potential for hybrid propulsion configurations such as, but not limited to:

- 2 electric driven shafts + 1 direct turbine driven shaft
- 2 electric pods + 1 direct turbine driven shaft
- 1 electric driven shaft + 2 direct turbine driven shafts
- 3 hybrid driven shafts (turbine + power take in/off)

To further visualize this vision an initial integrated design of 3 hybrid driven shafts (turbine + power take in/off) is shown in Figure 14, Figure 15 (and Figure 16 under the acknowledgement).

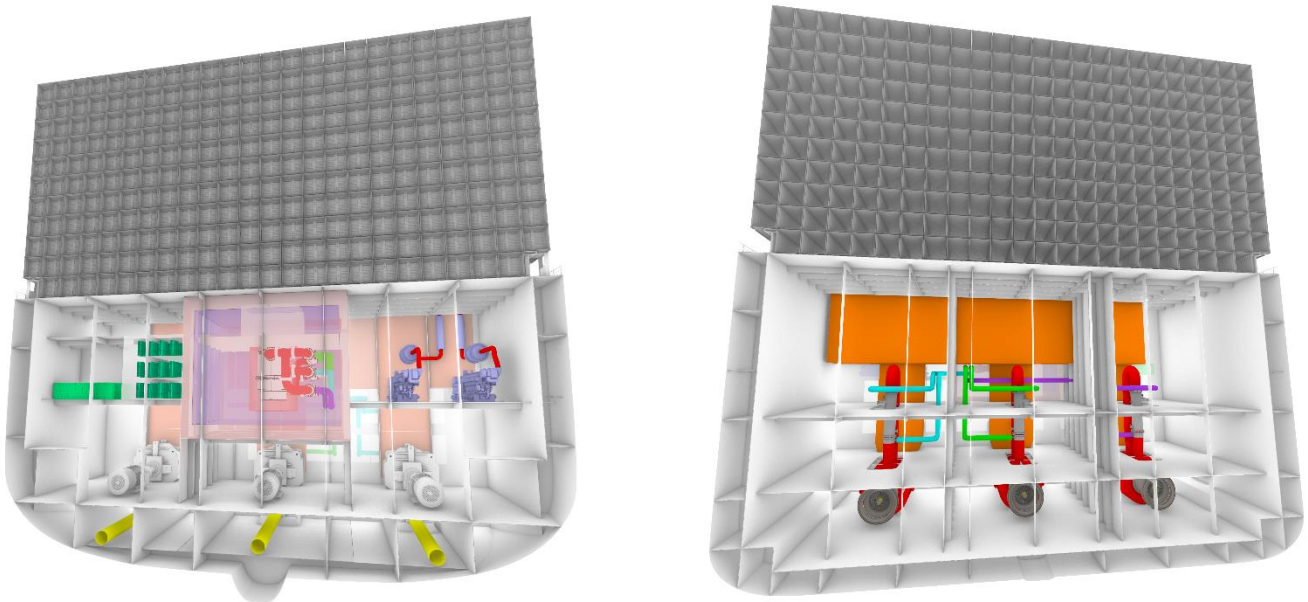

Figure 14: Initial ship design with integrated nuclear power and 3 hybrid driven shafts (turbine + power take in/off) part 1 *(C-Job Naval Architects Visualization Discipline, 2024)*

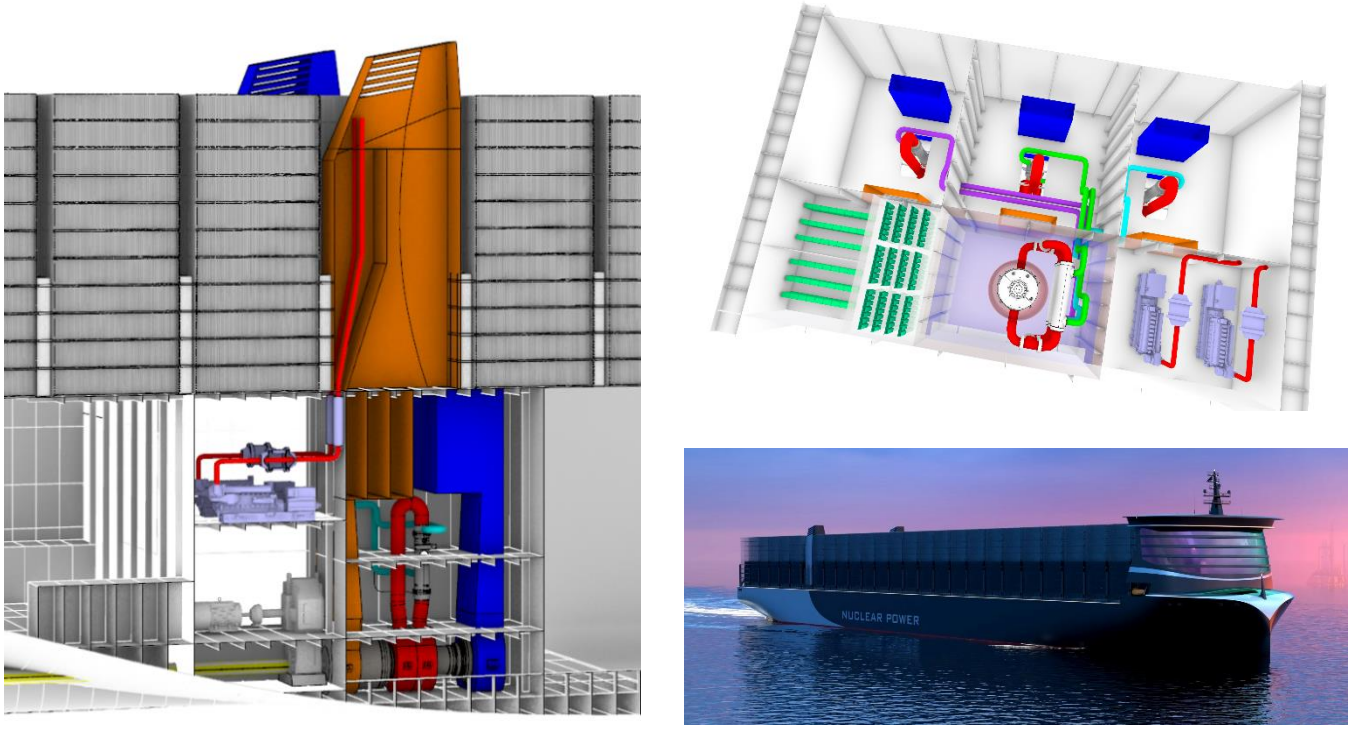

Figure 15: Initial ship design with integrated nuclear power and 3 hybrid driven shafts (turbine + power take in/off) part 2 *(C-Job Naval Architects Visualization Discipline, 2024)*

Bulker

Reviewing the bulk carrier dimensions, no adjustments seem absolutely necessary based on port restrictions. Furthermore, the considered speed range of 18-19 knots, defined in the earlier discussion, would suggest two propellers are adequate. Based on that a number of hybrid propulsion configurations can be considered, such as, but not limited to:

- 2 hybrid driven shafts (turbine + power take in/off)
- 1 electric pod + 1 direct driven shaft line

Contribution and Future Work

The work of (Houtkoop, 2022) identified the initial potential of next generation nuclear technology for shipping with replacement of conventional power generation. The work of (Leurs, 2023) expanded on this for container vessels by developing new build cases and explore their potential focusing on design speed, propulsion and power generation, and ship design. As additional expansion, this study also added the bulk carriers focusing on the same aspects. With this combined material, this study aims to inspire other naval architects and marine engineers to look beyond conventional design and operations, and punch technical boundaries to ultimately make shipping more sustainable.

CONCLUSION

Both nuclear options, 25, 50, and 75 years of service life, have higher economic speeds than the representative conventional VLSFO case. Furthermore, nuclear with 75 years of service life has an increase in economic speed compared to nuclear with 25 and 50 years of service life. Additionally, freight rate seems to have the biggest influence whereas reactor CapEx has a less substantial role. Besides that, the shorter distance cases logically also have higher speeds than longer distance cases since the freight rates are kept the same and the effective cost are lower for the shorter distance.

Considering the respective results of the container cases it is found that 28-31 knots with a service life of 75 years would be a good range to explore nuclear powered container vessels further. For the bulker cases it is found that 18-19 knots with a service life of 75 years would be a good range to explore nuclear powered bulk carriers further. This is based on the assumption that the service life of the reactor is 75 years which is derived from existing nuclear power plants. If the service life of the reactor changes this design guideline would need to be revisited.

In the initial review of options on how to convert nuclear power to propulsion and electrical power each part was evaluated. A primary and intermediate loop was used for heat transfer to the secondary loop to assure containment of radiation. For the turbines, an open Brayton cycle concept with load turbine and heat rejection capability was found to be most suitable, as it has improved load response capabilities and is relatively compact.

RECOMMENDATIONS

In this section the recommendations are given which serve as inspiration for future research and are part of the authors vision and understanding of the topic acknowledging various aspects that require more attention for the next steps.

Cost

The studied bandwidth of reactor CapEx, which included decommissioning cost in this study, is still quite broad and should be narrowed down further to reduce the uncertainty on the total cost of ownership. To do so, more detailed input from nuclear power plant developers is required to evaluate initial investment cost and the connected decommissioning cost at the end of the service life. Additionally, the effects of inflation on these costs over longer periods, considering the 75 years that is investigated in study, should also be incorporated in future work to reduce the uncertainty.

Besides CapEx, also OpEx of nuclear power plants should be studied further to reduce the uncertainty on the total cost of ownership. Especially, operations and maintenance cost of the nuclear power plant, and nuclear fuel cost are considered to be very relevant in future studies.

The effect of higher speeds and potential longer service life of other ship cost components such as the steel hull and other components besides the nuclear power plant should also be included in future studies. Despite the fact that these cost components are anticipated to be smaller than the nuclear power plant, incorporating them will improve the accuracy of the total cost of ownership which is the foundation for investment decisions.

Another cost component that requires more attention is the insurance. At this time, the difference in ship insurance cost between conventional and nuclear-powered ships is unknown and is not included in this study. Nevertheless, considering the sensitive nature of nuclear power, it deserves more attention from an insurance perspective as well. Therefore the respective insurance cost should also be studied.

Regulatory Framework

The current regulatory framework for nuclear powered vessels are outdated and considered a hurdle for nuclear power to be applied in (commercial) marine applications. Therefore, further development of nuclear power on marine applications is needed to clarify various parts on national and international level. This development should include all involved stakeholder such as, but not limited to, equipment manufacturers, ship designers, shipyards, classification societies, shipowners, local governments and nuclear regulators.

Main Particulars

The studied container vessel design has main dimensions that exceed current port restrictions. Furthermore, a volume and displacement check needs to be done to confirm the cargo capacity (TEU). Therefore, it is recommended to further develop the design, starting with the second iteration to reduce uncertainty, and confirm or adjust these findings accordingly. Furthermore, it is recommended to do a more detailed resistance analysis to reduce the uncertainty.

Propulsion Configuration

In this study a fully electric the propulsion configuration was selected as it offers flexibility in arrangement and options for easy integration of peak shaving with batteries for improved load response. Furthermore, it also offers options for reverse cold ironing while in port and easy integration of back-up power by means of diesel generators. Nevertheless, future studies are encouraged to review options to further optimize the nuclear option with for example turbine-direct propulsion, hybrid propulsion or full electrical propulsion without gearbox.

Operational Challenges

Where conventional VLSFO fueled vessels have low CapEx for their marine engines, it is observed that big(ger) engines can be installed with relatively little additional cost. With that, one gains the operational flexibility to adjust speed economically based on freight rate and fuel cost, as part of OpEx. For nuclear powered vessels this operational flexibility is limited as the CapEx of the nuclear reactor is relatively large. Therefore, it is recommended to further study all costs of nuclear marine propulsion where the share of CapEx, fuel, O&M, and others are better understood. Based on that the economic risks can be better assessed in order to determine the actual design speed for a nuclear-powered cargo vessel. An additional challenge, for the container vessel cases, considering their high speeds, is heavy weather conditions were it could be the case that ship speed needs to be temporary lowered to avoid damages caused by such conditions at higher speeds. The potential effect of this should be further studied.

Service Life

The service life of nuclear reactors is understood to be approximately 75 years and thus substantially longer than the service life of a conventional vessels, with approximately 25 years. So in general it seems logical to use the full service life of 75 years of the nuclear reactor on one or more vessels. This is further supported by findings of higher operational speeds, and thus more profitability, for service life of 75 years. However, it is not known what option, on how to facilitate utilization of the nuclear for 75 years, on one, two or three vessels is most economical. Therefore, future studies are encouraged to review these options in order to determine the most attractive strategy.

Ship Types

Besides container vessels and bulk carriers, it is recommended to consider other ship types, such as, but not limited to, tankers and offshore vessels, to further explore the potential of nuclear marine propulsion.

DECLARATION OF GENERATIVE AI AND AI-ASSISTED TECHNOLOGIES IN WRTITING

No AI or AI-assisted technologies have been used by the authors in the receptive research or in writing this paper.

CONTRIBUTION STATEMENT

Author 1, Niels de Vries: Research of the bulk carrier cases, supervision of nuclear marine propulsion and power generation research, supervision of the container vessel cases research, writing and editing of this paper.

Author 2, Koen Houtkoop: Research of nuclear marine propulsion and power generation, writing the referenced thesis report (Houtkoop, 2022) and reviewing this paper.

Author 3, Zeno Leurs: Research of the container vessel cases, writing the referenced thesis report (Leurs, 2023) and reviewing this paper.

ACKNOWLEDGEMENTS

Multiple versions of this paper have also been reviewed by Harilaos Petrakakos, Rick Ashcroft and Roy de Winter and provided constructive feedback. Therefore, the authors would like to thank all of them and acknowledge their contribution to this paper. Furthermore, we would like to thank the support of the C-Job Visualization Discipline to develop the various renders presented in this study.

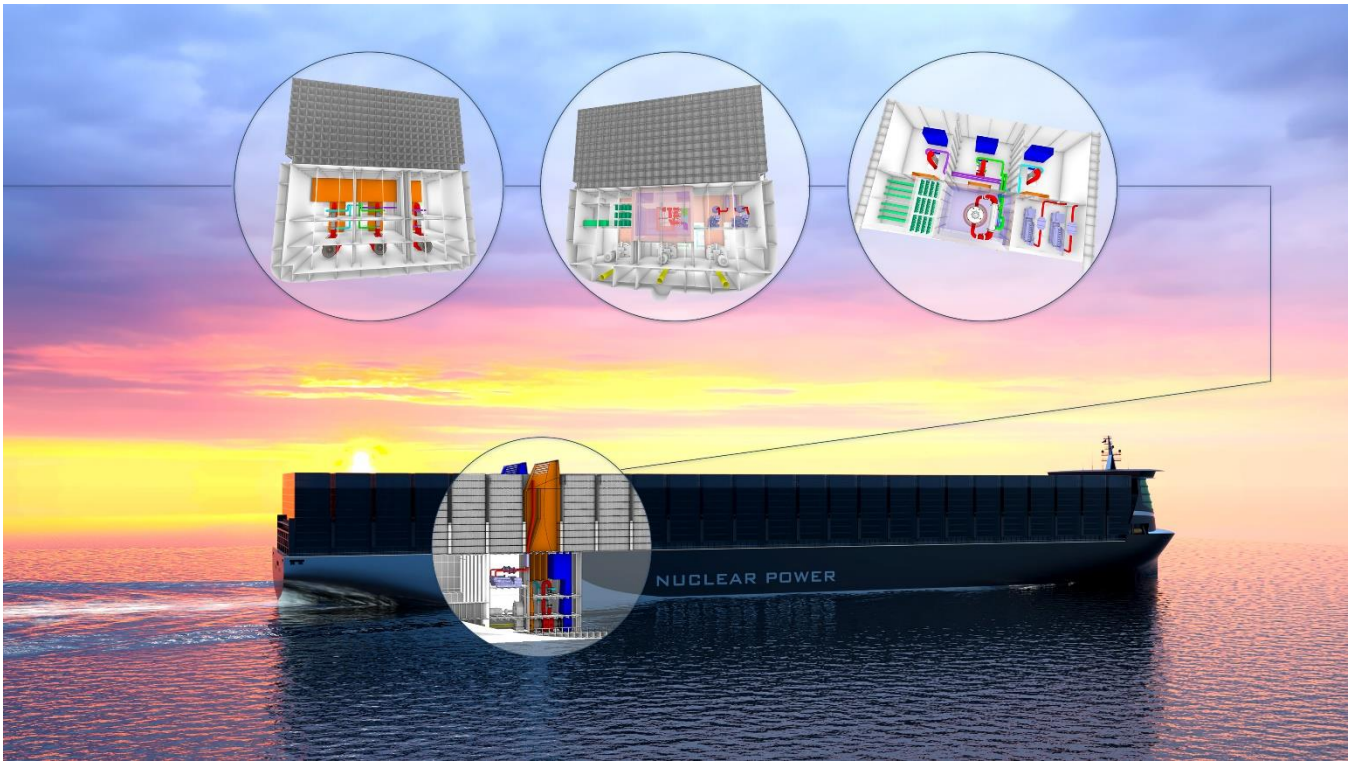

Figure 16: Initial ship design with integrated nuclear power and 3 hybrid driven shafts (turbine + power take in/off) part 3 *(C-Job Naval Architects Visualization Discipline, 2024)*

REFERENCES

Abdulla A., A. I. (2013). Expert assessments of the cost of light water small modular reactors. *Proceedings of the National Academy of Sciences*, (pp. 9686-9691).

Baltic Exchange. (2023). *Baltic Exchange*. Retrieved March 2023, from https://www.balticexchange.com/en/index.html

Black Geoffrey A., A. F. (2019). Economic viability of light water small modular nuclear reactors: General methodology and vendor data. In *Renewable and Sustainable Energy Reviews* (pp. Volume 103, Pages 248-258).

Buongiorno, J. C. (2018). *The Future of Nuclear Energy in a Carbon-Constrained World.* Massachusetts Institute of Technology.

C-Job Naval Architects. (2024). Anonymised data from multiple projects converted to an average as design guideline for initial concepts + Internal ship database (RefWeb).

C-Job Naval Architects Visualization Discipline. (2024). C-Job Nuclear Propulsion IMDC Paper Renders.

Class NK. (2023). *ClassNK Register of Ships - M/S BRASIL MARU.* Retrieved from ClassNK: https://www.classnk.or.jp/register/regships/one_dsp.aspx?imo=9321275

EIRP. (2016). *What will advanced nuclear power plants cost?* EIRP.

Emblemsvåg, J. (2021). How Thorium-Based Molten Salt Reactors Can Provide Clean, Safe, and Cost-Effective Technology for Deep-Sea Shipping. *Marine Technology Society*, Volume 55 Number 1.

Gennaro, G. a. (2020). Sustainable decarbonization of ocean transportation from marine Molten Salt Reactors (m-MSR) for zero-emission electric propulsion . *SNAME Maritime Convention.* Society of Naval Architects and Marine Engineers (SNAME).

Hargraves, R. a. (2010). Liquid Fluoride Thorium Reactors: An old idea in nuclear power gets reexamined. *American Scientist*, pp. 304-313.

Houtkoop, K. (2022). *Nuclear reactors for marine propulsion and power generation systems.* Delft: TU Delft Mechanical, Maritime and Materials Engineering.

IAEA. (2020). *Advances in small modular reactor technology developments: A SUPPLEMENT TO THEIAEA Advanced Reactors Information System (ARIS).* IAEA.

Leurs, Z. (2023). *Design of a high-speed 20,000 TEU nuclear container vessel.* Delft: TU Delft Mechanical, Maritime and Materials Engineering.

Lloyd, C. M. (2018). The impact of modularisation strategies on Small Modular Reactor Costs. *ICAPP*, (pp. 1-8). Atlanta.

Lobner, P. (2021). *China's CNNC ACP100S and ACP25S Floating Nuclear Power Plant (FNPP) Concepts* .

MAN Energy Solutions. (2024). *Project guide G90ME-C10.5-GI.* Copenhagen: MAN ES.

Mignacca, B. a. (2020). Economics and finance of Molten Salt Reactors. *Progress in Nuclear Energy*, Volume 129.

NEA. (2016). *Costs of decommissioning nuclear power plants.* OECD Publishing.

Petrakakos, H. (2024). PNP Marine, SNAME.

Ports.com. (2010-2023). *Sea route & distance*. Retrieved March 29, 2023, from http://ports.com/sea-route/

Royal Institution of Naval Architects. (2008). *Significant Ships of 2008.* London: RINA.

Sayres and Associates Corporation. (2008). N.S. Savannah. In *U.S. Department of transportation* (pp. pp. 1–47).

Ship and Bunker. (2024, April 22). *Rotterdam Bunker Prices*. Retrieved from Ship and Bunker: https://shipandbunker.com/prices/emea/nwe/nl-rtm-rotterdam

Ship Spotting. (2011). *GOLDEN WEALTH - IMO 7712640*. Retrieved from https://www.shipspotting.com/photos/1270779?navList=moreOfThisShip&imo=7712640&lid=1291287

Shultis, J. a. (2002). *Fundamentals of nuclear science and engineering.* New York: 3th ed. US: Marcel Dekker.

Stapersma, H. a. (2019). *Design of propulsion and electric power generation systems.* Witherby publishing group ltd.

Stewart W.R., a. S. (2022). Capital cost estimation for advanced nuclear power plants. In *Renewable and Sustainable Energy Reviews* (p. Volume 155).

The World Bank. (1990). Decommissioning of Nuclear Power facilities. In *Industry and energy department* (pp. pp. 1–45).

United States General Accounting Office. (1992). *Nuclear submarines, Navy efforts to reduce inactivation.*

Vegel Benjamin, Q. J. (2017). Economic evaluation of small modular nuclear reactors and the complications of regulatory fee structures. In *Energy Policy* (pp. Volume 104, Pages 395-403).

Proceedings of 15th International Marine Design Conference (IMDC-2024)
June 2-6, 2024
Amsterdam, the Netherlands

Simulation Method of Decarbonization of International Shipping for Evaluating the Impact of Possible Regulation Limiting GHG Intensity of Marine Fuels

Shinnosuke Wanaka[1,*] Kazuo Hiekata[2], Tomohito Takeuchi[3] and Masanobu Taniguchi[3]

ABSTRACT

This study explored how the GHG fuel standard (GFS) regulation affects international shipping quantitatively by simulating future fleet transformation, fuel consumption, and well-to-wake GHG emissions based on an inputted GHG fuel intensity pathway and scenario of transportation demand, fuel availability and costs, and technology availability. The method comprises three steps: calculating the amount of scrapped and built ships, allocating fuel type and mix, and calculating fuel consumption. We simulated how the regulation changes fleet composition and the mix of fuel consumption. From the perspective of feasibility and alternative fuels' availability, some meaningful insights to implement the GFS regulation were delivered.

KEYWORDS

Simulation of fleet transformation; GHG fuel standard; Decarbonization of shipping.

INTRODUCTION

In 2023, the International Maritime Organization (IMO) revised its GHG reduction strategy to include net-zero emissions by 2050 (IMO MEPC, 2023). The strategy includes targets for introducing green fuels and total emission reduction, that is, the indicative checkpoints. These checkpoints were set for 20-30% and 70-80% reduction by 2030 and 2040 respectively. However, the technology to achieve decarbonization is in the R&D stage and has not yet been established. Although various fuels have been studied as marine fuels such as ammonia (Kim et al, 2020; Inal et al., 2022), biofuels (Tan et al. 2022), eMethane, eMethanol, and hydrogen (Shi et al., 2023), it remains undetermined which fuels and energy sources will be used in international shipping (Balcombe et al., 2019) and the fuels' availability is highly limited (Grzelakowski et al., 2022).

To encourage technological and infrastructure development to achieve this goal, various regulations, including technical and economic elements, are being discussed by the IMO. As for the economic elements, market-based measures (MBM), such as feebate and carbon levy, are being considered (Psaraftis, 2021), and the impact and implementation of these measures have been studied. For example, Wang et al. (2015) developed an economic model and evaluated the emission-trading scheme (ETS). They compared open-ETS and maritime-only ETS and discussed the economic impacts on container and bulkcarrier shipping. Metzger (2022) evaluated the impact of carbon pricing on the valuation of investments in

[1] Knowledge and Data System Department, National Maritime Research Institute, Mitaka, Japan; ORCID: 0000-0002-1958-4013

[2] Graduate School of Frontier Sciences, The University of Tokyo, Tokyo, Japan; ORCID: 0000-0002-8646-8506

[3] Japan Transport and Tourism Research Institute, Tokyo, Japan
* Corresponding Author: wanaka-s@m.mpat.go.jp

Submitted: 21 February 2024, Revised: 26 April 2024, Accepted: 1 May 2024, Published: 24 May 2024

Conference paper, DOI: https://doi.org/10.59490/imdc.2024.896 e-ISSN: 3050-486

greening technologies using the fuzzy pay-off method. Masodzadeh et al. (2022) discussed MBM complications and proposed a new hybrid MBM to fill the gap between short-term measures and the MBM.
However, mid-term technical measures, such as the GHG fuel standard (GFS) have not yet been studied. The GFS is a regulation that requires ships to use fuels with well-to-wake (WtW) GHG intensity (gCO_2eq/MJ) below the defined limit called the GHG fuel intensity (GFI) (IMO, 2021). A similar regulation will be introduced in FuelEU Maritime (ClassNK, 2023), which is a local regulation to be introduced in EU/EEA Member States in 2025. The framework is considered to be a certain promise, and the impact should be evaluated before implementation. When discussing the GFS, one of the important issues is whether to introduce a flexibility mechanism that allows the ships to share their GHG emission reductions in the fleet. Without this mechanism, all ships must individually comply with the GFS. However, with the flexibility mechanism, ships using better fuel than the required GFI can provide a surplus to ships that cannot comply with the required GFI. This means that the overall fleet complies with the regulations. As the path to shipping decarbonization varies depending on whether the mechanism is introduced, the impact of the flexibility mechanism must be evaluated. Moreover, the IMO's indicative checkpoints are based on total emissions from the fleet, and a macro analysis of the fleet is necessary to determine whether the GFS adequately contributes to the IMO's target.
Modeling and simulation are powerful tools for quantitatively evaluating the impact of future regulations. Eide et al. (2011) built a model to assess the cost and GHG reduction of various measures by combining a fleet projection model with activity-based CO_2 calculations and evaluated the amount of GHG reduction and the required cost by using the marginal abatement cost curve (MACC). Halim et al. (2018) developed a future CO_2 estimation model combining the International Freight Model and Activity, Structure, Intensity, and Emission factor methods and conducted impact assessments of various GHG reduction measures until 2035. Wada et al. (2021) used system dynamics to model the shipping and shipbuilding market and forecast future shipbuilding demand affected by the EEDI, slow steaming, and penetration of LNG to reduce GHG emissions. Zwaginga et al. (2022) pointed out that future uncertainties including regulation make designing ships difficult and utilized three methods to deal with the deep uncertainty in designing alternative fueled ships: dynamic adaptive policy pathways (DAPP), responsive system comparison (RSC), and robust decision making (RDM). By comparing the three methods, it demonstrates what insight could be obtained and how the ship design is affected by the uncertainties. However, a simulation method that can model GFS regulation and analyze its behavior, to the best of our knowledge, has not yet been developed.
The objective of this paper is to study how the GFS regulation affects international shipping in the future, and a simulation method is proposed for this purpose. The simulation projects future fleet transformation, fuel consumption, and well-to-wake (WtW) GHG emissions based on an inputted GFI pathway and enables us to study the regulation quantitatively from the perspective of feasibility, fuel, technology availability, and so on. In the case study, we assumed a GFI pathway considering the revised IMO GHG reduction strategy and simulated several cases with and without the flexibility mechanism. By comparing these results, we have analyzed how international shipping is affected by the presence or absence of the flexibility mechanism. Moreover, another case shows how the simulation can be used to search for GFI pathways that are feasible and contribute to GHG reduction as much as possible and demonstrates that the proposed method can support the design of the GFS regulation.

SIMULATION METHOD

Overview of the Method

Figure 1 shows an outline of the proposed simulation method, which consists of three parts: a model of shipbuilding and scrapping, a model for selecting the introduced ships and calculating the fuel mix, and a calculation of fuel consumption. The proposed method requires fleet composition data that defines the initial fleet status and five scenarios as follows: transportation demand, ships' survivor rate to age, GFI pathway that defines how WtW emission regulation in the simulation will be tightened, ship data including ships using alternative fuels, and fuel data including costs, emission factors, and availability. In this simulation, the GFS is defined by the GFI pathway, and ships and fuels are operated on the assumption that the GFI is not exceeded. The figure describes what data and scenarios are required for each part, and what kind of output is produced by the part. The simulation flow is run iteratively from 2021 to 2050 with a timestep of one year and outputs WtW emissions, WtW GHG intensity (gCO_2eq/MJ), and costs including those of fuel and ship. In addition, the amount of shipbuilding and scrapping, the ships' fuel type introduced at each time step, and the fuel mix

utilized for the operation were considered. The remainder of this section explains the data and calculation procedures for each part.

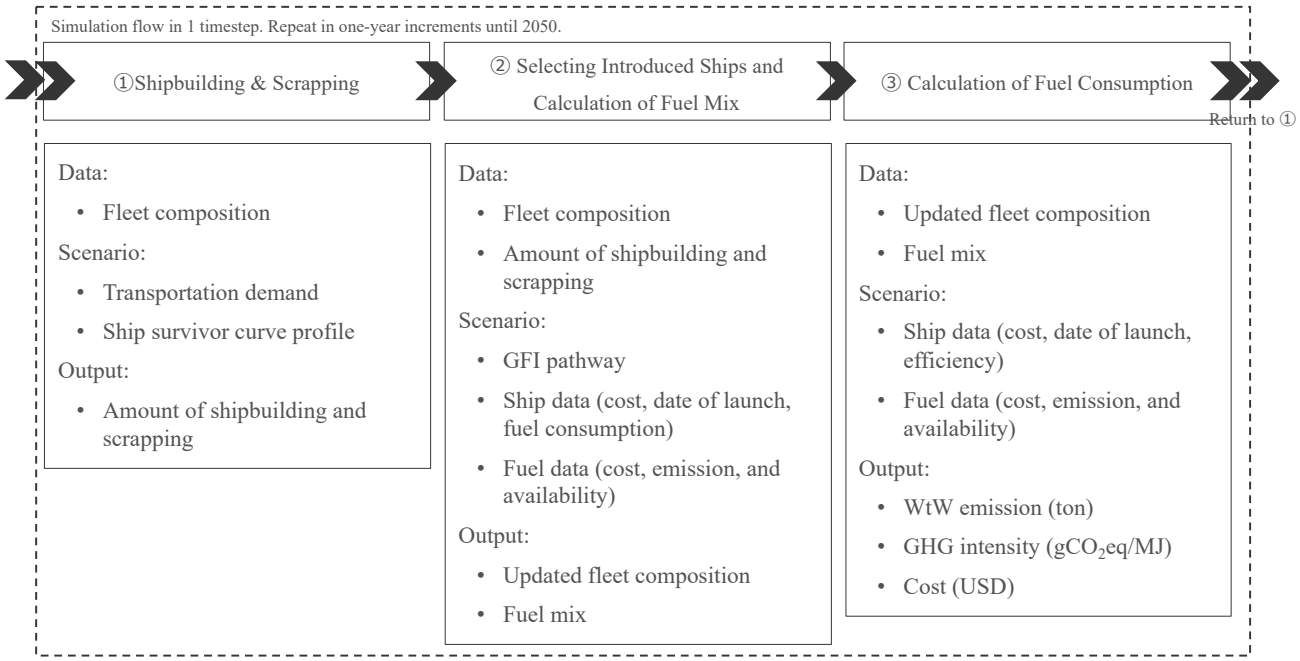

Figure 1: Outline of the proposed simulation flow

Models of Shipbuilding and Scrapping

As for the model of shipbuilding and scrapping, the method assumes that shipbuilding is related to transportation demand, and the amount of scrapping is related to ship age distribution. First, the amount of scrapping was calculated based on fleet composition data defined by age, ship type, and the number of ships. The number of ships scrapped $Scrap_{t,a}^{type}$ is shown in equation 1. The fleet data are represented by $Ship_{t,a}^{type}$, which indicates the number of ships whose age is a and ship type is $type$ at time t. $Sr(a)$ is the survivor rate at the ship age. The ship type is a label indicating the fuel that the vessel can use, such as LNG, NH_3, and Methanol. Note that the fuel type in the method mentioned afterward is a more detailed fuel label such as eAmmonia(Blue), eAmmonia(Green), and so on, and is different from the ship type. Ship type defines a set of fuels that can be utilized. This is described in more detail in the "Case Study" section.

$$Scrap_{t,a}^{type} = Ship_{t,a}^{type} \cdot (1 - Sr(a+1)/Sr(a)) \quad [1]$$

The number of newly built ships was calculated by adding the number of new buildings to meet the growth in transportation demand to the amount of scrapping calculated by Equation 1. The number of newly built ships B_t is calculated by Equation 2.

$$Built_t = \sum_{type}\sum_{a} Scrap_{t,a}^{type} + \sum_{type}\sum_{a} Ship_{t,a}^{type} \cdot (1 - Transportwork_{t+1}/Transportwork_t) \quad [2]$$

$Transporwork_t$ is the amount of transport work (billion-ton mile) that is supposed to be transported by the fleet at time t. Through this process, the amount of scrapping for each ship type and age and the amount of shipbuilding for the fleet are calculated. Because the objective of this method is to analyze the regulation's behavior from a macro perspective, the fleet is represented as a set of averaged vessels with no distinction between cargo and size, and the average size of the vessels is constant in the future.

Model of Selecting Introduced Ships and Calculation of Fuel Mix

In this subsection, a model is used to select the ship types that will be built for the shipbuilding volume calculated in the previous step and to calculate the fuel mix consumed by the fleet in the next time step. The process differs in the GFS with and without the flexibility mechanism. First, the model in the case without the flexibility mechanism is explained, followed by the differences in the case with the mechanism.

Without the flexibility mechanism, each ship in the fleet complies with the regulations and does not share the emission reductions. The model for selecting the introduced ship types and calculating the fuel mix consists of four steps: take n types of ships from the set of ship types that can be introduced and create a list of combinations of these types a pre-defined share rate, optimize the fuel mix in the fleet as each combination is introduced, and extract the combination with the lowest cost among all combinations. The ships to be introduced are selected according to their costs, including ship and fuel cost. The details of the equation in the optimization are as Equations 3 – 8, where FU_{fuel}^{type} is the percentage of fuel mix used by a specific ship type, is DFC is fuel consumption (MJ) by a ship in 1 year, $Ship_t^{type}$ is the number of ships whose type is $type$, FP_{fuel} is fuel cost(USD/MJ), SP_{type} is ship cost (USD), CI_{fuel} is carbon intensity (gCO_2eq/MJ) of each fuel, GFI is a defined GFI value for the regulation, $Limit_{fuel}$ is the fuel's availability (MJ), $FUEL$ is the set of fuel being calculated, and $SHIP$ is the set of ship types defined in the simulation.

$$\min \sum_{type} \left(\sum_{fuel} FU_{fuel}^{type} \cdot DFC \cdot FP_{fuel} + \frac{1}{20} SP_{type} \right) \cdot Ship_{t+1}^{type} \quad [3]$$

s.t.

$$\sum_{fuel} FU_{fuel}^{type} \cdot CI_{fuel} \leq \frac{GFI}{100} \cdot CI_{LSFO} \quad [4]$$

$$\sum_{type} FU_{fuel}^{type} \cdot DFC \cdot Ship_{t+1}^{type} \leq Limit_{fuel}, \forall fuel \in FUEL \quad [5]$$

$$\sum_{fuel \in MAIN,PILOT} FU_{fuel}^{type} = 1, \forall type \in SHIP \quad [6]$$

$$\sum_{fuel \in MAIN} FU_{fuel}^{type} \leq 1 - pfr, \forall type \in SHIP \quad [7]$$

$$\sum_{fuel \in PILOT} FU_{fuel}^{type} \geq pfr, \forall type \in SHIP \quad [8]$$

Equation 3 represents the objective function to be minimized, which is the total cost including the fuel cost and the ship cost. As for the ship cost, the value is depreciated over 20 years. Equations 4 and 5 represent constraints, respectively, to comply with the regulation, and of fuel availability. Equations 6-8 are constraints around fuel usage. $MAIN$ is the set of fuels primarily used on the ship, and $PILOT$ is the set of pilot fuels. For example, in a dual-fuel ship of LNG, LNG, eMethane, and BioMethane are primarily used, and LSFO and bio-heavy fuel oil (BioHFO) are used as pilot fuels. pfr is the pilot fuel rate required to operate; in the simulation, it is defined as 0.05 until 2040 and 0.03 thereafter.

In the case with the flexibility mechanism, ships in the fleet can share their emissions to comply with the regulation so that Equation 4 in the optimization differs as shown in Equation 9.

$$\sum_{type} \sum_{fuel} FU_{fuel}^{type} \cdot CI_{fuel} \cdot Ship_{t+1}^{type} \leq \frac{GFS}{100} \cdot CI_{LSFO} \cdot \sum_{type} Ship_{t+1}^{type} \quad [9]$$

All possible combinations are optimized, and ships with the lowest minimized cost are selected for construction. For the calculation, it is necessary to determine the number of types of ships that will be introduced in the future and the market share of these types. To simplify the calculation, we assume that three types of ships have constant market shares of 50%, 30%, and 20%, respectively. Although it is difficult to establish the market situation in the future, the authors interviewed multiple shipping companies in Japan and developed the above-mentioned assumptions. This step outputs

the types of newly built ships and the percentage of fuel utilized by each type of ship in the fleet. Once the type of newly built ships is determined, the updated fleet composition for the next year's operation can be calculated. When using the model, depending on the input GFI pathway and fuel availability scenario, no optimization solution may exist, which means that the input GFI pathway cannot be complied with by the scenario. In this case, to continue the calculation, the constraint on the GFI is removed (Equation 4) and a penalty for emissions is added to the objective function. This minimizes costs and emissions. As for the penalty, this simulation applied the penalty of FuelEU Maritime, which is calculated by multiplying the energy consumption that exceeds the regulation value by 0.06 EUR/MJ.

Calculation of Fuel Consumption

The fuel consumption is calculated based on the updated fleet composition and fuel mix obtained in the previous step. After calculating the fuel consumption, the WtW emissions, WtW GHG intensity, and costs were calculated. Equations 10–13 represent the calculation, where FOC_{fuel} is the fuel consumption (MJ) of each fuel, FU_{type}^{fuel} is the fuel mix used by a specific ship type, $Emission_{WtW}$ is WtW emissions (ton), $Emission_{intensity}$ is a the GHG intensity of the fleet normalized by the LSFO's intensity, and $FuelCost$ is the fuel cost of the fleet. The consumption of each fuel is calculated by multiplying the fuel mix, average fuel consumption per ship, and the number of ships. Because there are fuels that can be used in multiple ship types, such as LSFO, aggregation by ship type is performed. In the output cost data, CAPEX is added to the fuel cost as the total cost. For the CAPEX, only the ship cost is considered and 1/20 of the total ship cost is accounted for, assuming that the depreciated period is 20 years.

$$FOC_{fuel} = \sum_{type} FU_{type}^{fuel} \cdot Ship_{t+1}^{type} \cdot DFC \quad [10]$$

$$Emission_{WtW} = \sum_{fuel} FOC_{fuel} \cdot CI_{fuel} \quad [11]$$

$$Emission_{intensity} = \sum_{fuel} (FOC_{fuel} \cdot CI_{fuel}) / (CI_{LSFO} \cdot \sum_{fel} FOC_{fuel}) \quad [12]$$

$$FuelCost = \sum_{fuel} FOC_{fuel} \cdot FP_{price} \quad [13]$$

CASE STUDY

Overview and Scenarios

This case study aims to demonstrate how the proposed method of this paper evaluates the GFS, and what kind of insight can be delivered. In this paper, two cases are conducted. In Case 1, a comparison of the GFS with and without the flexibility mechanism was conducted. When the GFS is applied without the flexibility mechanism, all vessels should align with the GFI pathway. However, when the GFS with the flexibility mechanism is applied, not all vessels need to align with the GFI pathway, rather, the GFI pathway should be achieved at the fleet level. The comparison demonstrates that the proposed method enables a quantitative evaluation of the advantages of the flexibility mechanism. In Case 2, a GFI pathway that achieves as much decarbonization as possible and does not have much impact on the shipbuilding market is explored in a more severe scenario. The GFI pathway to achieve IMO's indicative checkpoint depends on the transportation demand scenario, and the higher the transportation demand, the more stringent the GFI pathway should be set. However, setting too stringent a GFI pathway would make it difficult to adapt to existing HFO vessels and would greatly reduce the regulation's feasibility. If existing vessels cannot be adapted, conversion or replacement can be considered; however, too much conversion or replacement will have a significant impact on the shipbuilding market. In Case 2, we input several GFI pathways, and explore which pathway can best lower GHG emissions and does not require conversion or replacement. The remainder of this subsection summarizes the scenarios of transportation demand, fuels, and ships used in the case study.

Ship scenarios

In this case study, 32275 vessels with a gross tonnage of 5000GT or more that operate worldwide were set as the initial fleet. The dataset is based on the IHS Sea-web (S&P Global, 2023), which is the largest web-based ship database service and is generated by excluding offshore-related ships, tugs, barges, and patrol ships from all vessels listed in the database. In this case study, ships of various cargoes and sizes are averaged, and the fleet is represented only by the number of ships, ship age, and ship type. Figure 2 shows the initial fleets' age distribution. To calculate the fuel consumption and emissions, it is necessary to define the average fuel consumption per ship, which is defined as 2.85×10^8(MJ) in this case study. This setting is based on the IEA reporting that energy consumption in international shipping in 2022 is 9.2 (EJ) in total (IEA, 2023). Fuel consumption will be improved in the future because energy efficiency regulations such as EEDI and EEXI are applied, and to align the regulations, propulsion technology is refined. In this case study, based on fuel efficiency in 2008, the. efficiency would improve by 22%, 40%, and 50% in 2018, 2030, and 2050, respectively. This assumption is based on the 4th IMO GHG Study (Faber et al, 2020) and the IMO GHG reduction strategy adopted in 2018(IMO, 2018). The 4th IMO GHG Study reported a 22% improvement in the annual efficiency ratio in 2018 compared with that in 2008, and the reduction strategy adopted in 2018 targeted a 40% improvement in energy efficiency by 2030.

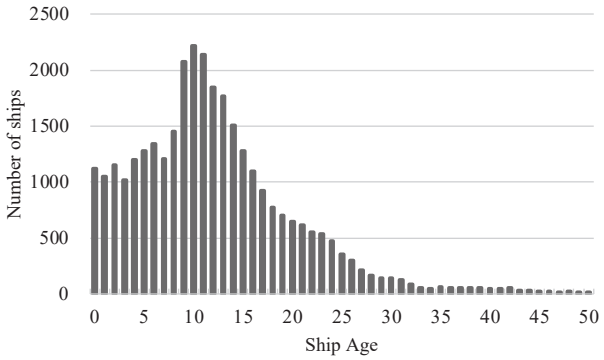

Figure 2: Ship age distribution of the initial fleet

This case study considered the following five types of ships, heavy fuel oil ship (HFO), dual fuel ship of HFO and LNG (DF(HFO, LNG)), dual fuel ship of HFO and Ammonia (DF(HFO, NH_3)), dual fuel ships of HFO and Methanol(DF(HFO, Methanol), and H_2 fueled ship. DF(HFO, LNG) has already been widely used and the DF(HFO, Methanol)'s technology is considered sufficiently mature. However, DF(HFO, NH3) and H_2-fueled ships are at the R&D stage and are unlikely to be implemented soon. In this case study, it is assumed that DF(HFO, NH3) and H_2-fueled ships can be introduced in 2028. This assumption is based on Japan the Ministry of Land, Infrastructure, Transport and Tourism of Japan's development roadmap (MLIT, 2021), which shows that the implementation of the alternative fuel technology will begin to be introduced in 2028 at the earliest. In the proposed simulation method, the introduction rate of each ship type can be inputted as a scenario. For the near future, it is possible to estimate the percentage of ships introduced from the information in the order book. Based on the Clarkson Shipping Intelligence Network (SIN) data (Clarkson, 2023), a scenario was developed for the percentage of ships that will be deployed from 2022 to 2026. The SIN provides data on deliveries and orderbooks. By aggregating data on containers, bulkcarrier, tankers, PCC, and general cargo, the percentage of each ship type was calculated. The results are shown in Figure 3. The proportion of both LNG- and methanol-fueled ships has increased.

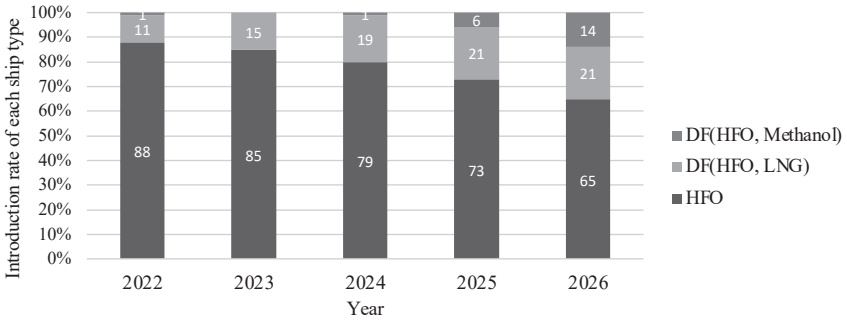

Figure 3: Percentage of ships introduced from 2022 to 2026

Figure 4 shows the setting of the ships, which was assumed based on the IHS Seaweb's ship cost data and references from the IMO 4th GHG Study's MACC calculation. The values at the top of the bars in the figure indicate the ratio of the costs when based on HFO-fueled ships. DF(HFO, Methanol) ship was set as the cheapest ship and the H_2-fueled ship was set as approximately 40% more expensive than the HFO ship.

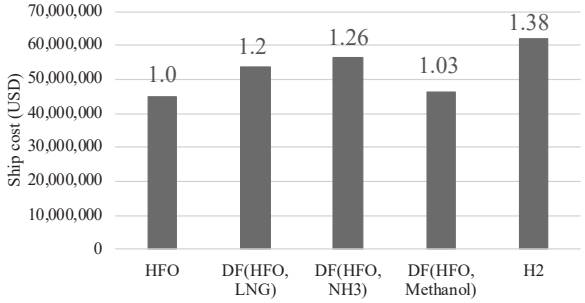

Figure 4: Setting of ship costs in case study

Figure 5 presents the survivor curve profile for this case study. Historical data on scrapped ships from the IHS Sea-web database were compiled to create a relationship between age and scrapping, with the maximum age set at 50 years old.

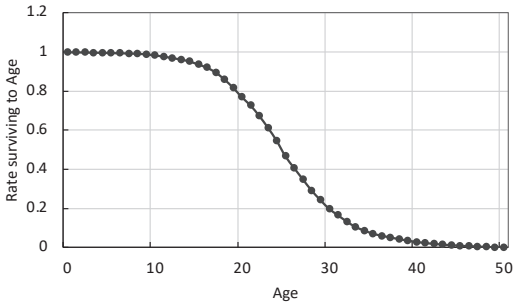

Figure 5: Survivor curve profiles for the case study

Fuel scenarios

To conduct a simulation based on the proposed method, it was necessary to define the fuel WtW emission factors, future costs, and availability. Although it is difficult to predict future trends in fuels owing to significant future uncertainties, the simulation in this study was based on the results of the JTTRI internal study in which scenarios were developed based on the literature and available data.

Table 1 presents the assumed WtW GHG emission intensity (gCO2eq/MJ). The fuels' tank-to-wake (TtW) GHG emission intensity does not vary with time because of its chemical properties, but the WtT GHG emissions can change based on trends in the decarbonization of the energy production industry, such as renewable energy penetration.

Therefore, the case study assumes that the WtW emission intensity changes with time. The IMO's newest GHG reduction strategy describes decarbonization around 2050, which is based on the IEA NZE scenario and the WtW GHG intensity of biofuels and e-fuels (green) decreases to 0. Table 2 presents the assumed fuel costs (USD/GJ).

Table 1: WtW GHG intensity (gCO_2eq/MJ) setting of 2030, 2040, and 2050.

Fuel label	2030	2040	2050
LSFO	90.0	90.0	90.0
LNG	71.7	65.1	58.3
BioHFO	4.9	2.4	0
BioMethane	7.5	3.1	0
BioMethanol	6.9	2.9	0
eMethanol(Brown)	91.7	90.8	90.7
eAmmonia(Brown)	114.2	112.3	111.2
H_2(Brown)	93.1	91.1	90.2
eMethane(Blue)	28.4	13.5	5.4
eMethanol(Blue)	31.4	14.7	5.9
eAmmonia(Blue)	15.6	7.3	2.9
H_2(Blue)	13.3	6.1	2.4
eMethane(Green)	4.6	0	0
eMethanol(Green)	5.8	0	0
H_2(Green)	5.3	0	0

Table 2: Fuel cost (USD/GJ) setting for 2030, 2040, and 2050.

Fuel label	2030	2040	2050
LSFO	6.8	5.9	4.9
LNG	14	13.8	13.7
BioHFO	63.2	60.2	57.6
BioMethane	32.3	29.2	26.2
BioMethanol	24.6	21.6	18.7
eMethanol(Brown)	13.8	13.2	12.6
eAmmonia(Brown)	19.2	18.7	18.2
H_2(Brown)	40.2	37.7	35.2
eMethane(Blue)	39.3	38.4	37.5
eMethanol(Blue)	35.3	34.1	32.9
eAmmonia(Blue)	23.8	23.3	22.7
H_2(Blue)	44.2	41.7	39.1
eMethane(Green)	40.7	38.2	35.6
eMethanol(Green)	40.8	37.6	34.4
H_2(Green)	35.9	33.3	30.8

As for the fuels' availability, we assumed two kinds of scenarios, "High Bio" and "Low Bio". Biofuels are essential alternative fuels for the shipping decarbonization. Fuels are also promising for the aviation and land transportation industries. In the high-biofuel scenario, assuming that other industries would implement more decarbonization through electrification, the availability of biofuels was set. However, it was assumed that biofuels would be used more in other industries and that their availability in the maritime industry would be significantly reduced. Figure 6 shows the fuel availability for each scenario.

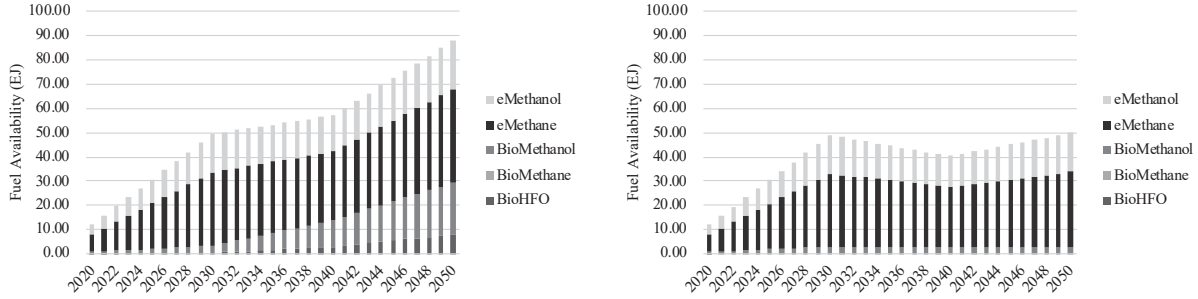

Figure 6: Fuel availability scenarios (Left: High Bio, right: Low Bio)

Other Scenarios

For transportation demand, two scenarios were chosen from the 4th IMO GHG Study's assumptions; RCP2.6 OECD and RCP2.6 SSP2. They are called "Low" and "High" in this paper. Various scenarios were considered in the IMO study. From these scenarios, we selected the maximum and minimum scenarios to comply with the 2°C target of the Paris Agreement. The indicative checkpoints in the 2023 IMO target are defined for the total GHG emissions from international shipping; thus, the GFI pathways for implementing them have different individual values for each transportation demand. In this case study, the indicative checkpoints were defined as a 20%, 70%, and 100% reduction in 2030, 2040, and 2050, respectively, in WtW emissions compared to that in 2008. Table 3 summarizes the transportation demands and GFI pathways used in the case study. Notably, the GFS regulation is under discussion at the IMO, and the GFI pathways described in the table are based on the assumption that the IMO indicative checkpoints are achieved by GFS regulation alone.

Table 3: Transportation demand and GFI pathways of 2030, 2040, and 2050

Transportation demand label		2030	2040	2050
Low	Demand (billion ton mile)	6.7×10^4	7.6×10^4	8.2×10^4
	GFI (LSFO = 100)	95.2	34.7	0
High	Demand (ton mile)	8.2×10^4	1.0×10^5	1.2×10^5
	GFI (LSFO = 100)	78	26	0

Results

Case 1: Comparison of cases with/without the flexibility mechanism

In Case 1, simulations of cases with and without a flexibility mechanism were conducted, and the impact of the flexibility mechanism was evaluated by comparing the results. The fuel availability scenario was set as High Bio, and the RCP2.6 OECD (scenario: low) was selected for transportation demand. For the notation, the case without the flexibility mechanism is Case 1-1, and the case with the flexibility mechanism is Case 1-2. Figure 7 presents the result of Case 1-1, which shows fuel consumption and WtW emissions from the overall fleet until 2050. The WtW emissions are normalized by the 2008's emission. The bar chart shows each fuel consumption (EJ=10^{12}MJ). In this case study, 15 fuels were assumed to be potential candidates for alternative fuels; however, by selection based on the cost, fuel decomposition can be expressed by the seven fuels in the figure. HFO-fueled ships are adapted to the GFS regulations by using BioHFO as a drop-in fuel. The DF(HFO, LNG) utilizes a combination of LNG and eMethane(Green) as the most cost-effective option. The DF(HFO, Methanol) primarily consumes BioMethanol. The DF(HFO, NH_3) was operated mostly with a mixture of LSFO and eAmmonia(Blue) and eAmmonia(Green) was used only in the last two years of the simulation. Especially for HFO-fueled ships, biofuels must be utilized to adapt the regulation in the case without the flexibility mechanism. Based on the simulation result, 0.30 EJ of BioHFO will be required as of 2030. Moreover, owing to the insufficient availability of BioHFO, the GFI pathway cannot be implemented from 2033 to 2036, as indicated by the shaded areas in the Figure 7.

This implies that more BioHFO is required for HFO ships to comply with the GFI pathway. Although the indicative checkpoints for 2030, 2040, and 2050 are achieved, it is a possible risk factor that parts of the pathway cannot be achieved.

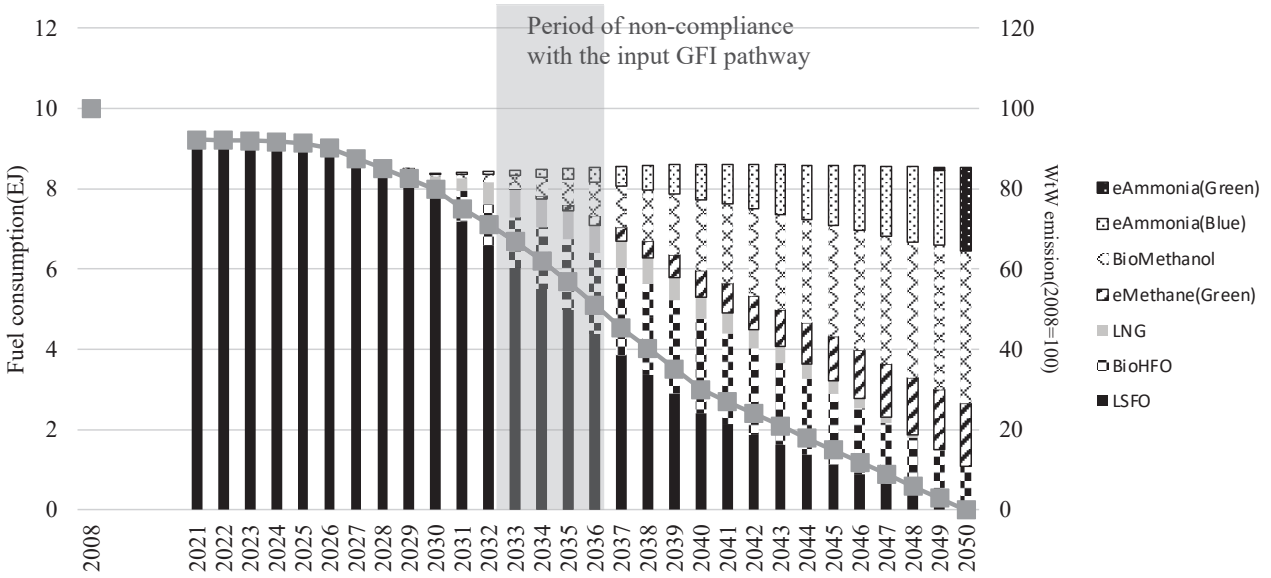

Figure 7: Fuel consumption and WtW emissions (Case 1-1, case without flexibility mechanism)

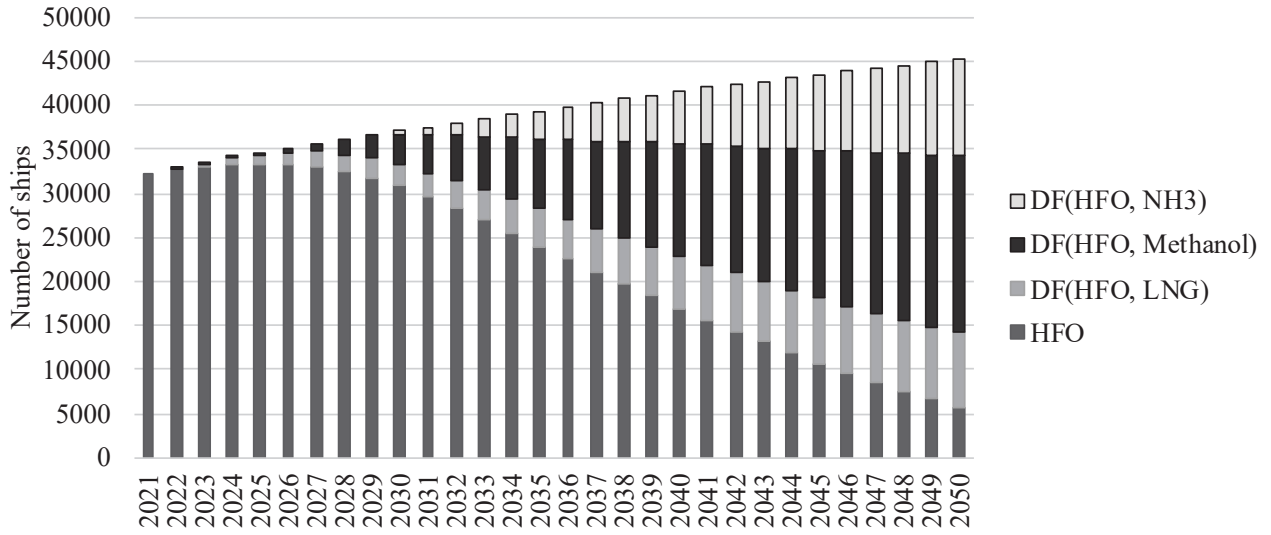

Figure 8: Fuel decomposition (Case 1-1, case without flexibility mechanism)

Figure 8 shows the results of the fleet decomposition from 2021 to 2050. The vertical axis represents the number of ships operating annually. From 2026 to 2028, the introduction of DF(HFO, NH_3), DF(HFO, LNG), and DF(HFO, Methanol) penetrated the fleet to adapt to the GFS regulation. Finally, DF(HFO, NH3), DF(HFO, Methanol), and DF(HFO, LNG) were introduced in that order. This is due to the total cost of CAPEX and fuel cost, and the high availability of inexpensive BioMethanol.

The results of Case 1-2 are shown in Figures 9 and 10, respectively. They are the results of the flexibility mechanism. As shown in Figure 10, there is not much difference in the fleet decomposition to comply with the GFS regulation, except that the introduction period of HFO ships is extended by two years. However, Figure 9 indicates that the fuel consumption composition is significantly different from that in Case 1-1. While in Case 1-1, HFO-fueled ships utilized BioHFO to comply with the regulation, in Case 1-2 with the flexibility mechanism, HFO-fueled ships did not utilize biofuels, and ships fueled by others compensated to achieve the GFI pathway. In this scenario, although BioHFO is more

expensive and not as abundant in supply as other green fuels, the results indicate that it is possible to promote emission reduction by ships fueled by other fuels and implement the GFI pathway for the entire period.

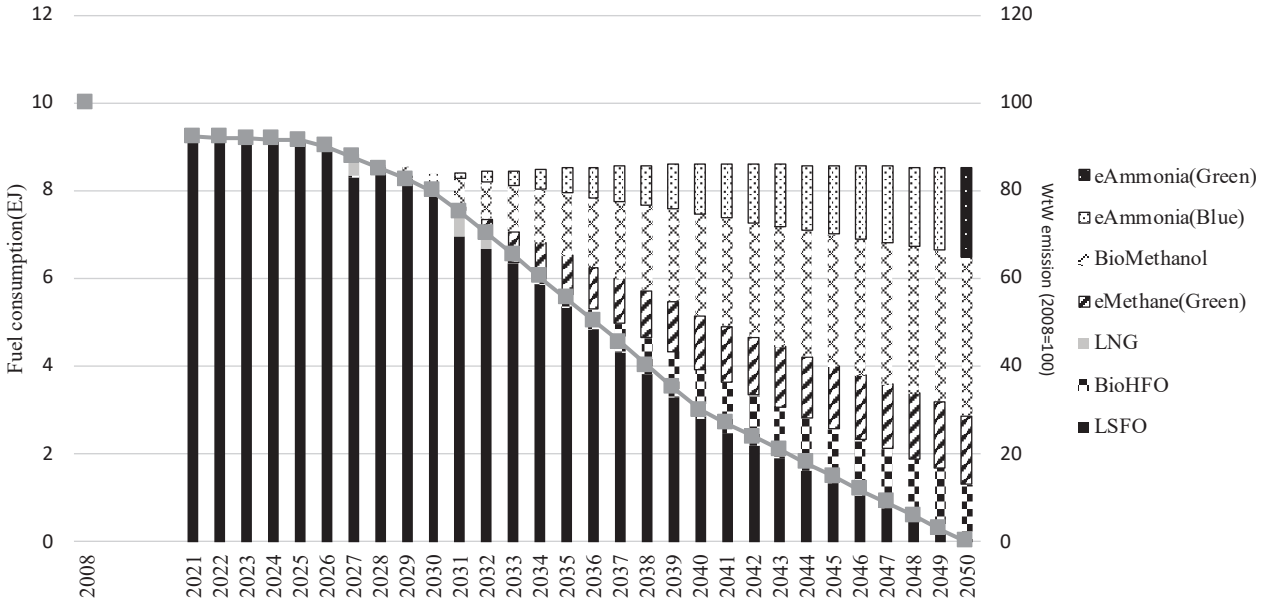

Figure 9: Fuel consumption and WtW emissions (Case 1-2, case with flexibility mechanism)

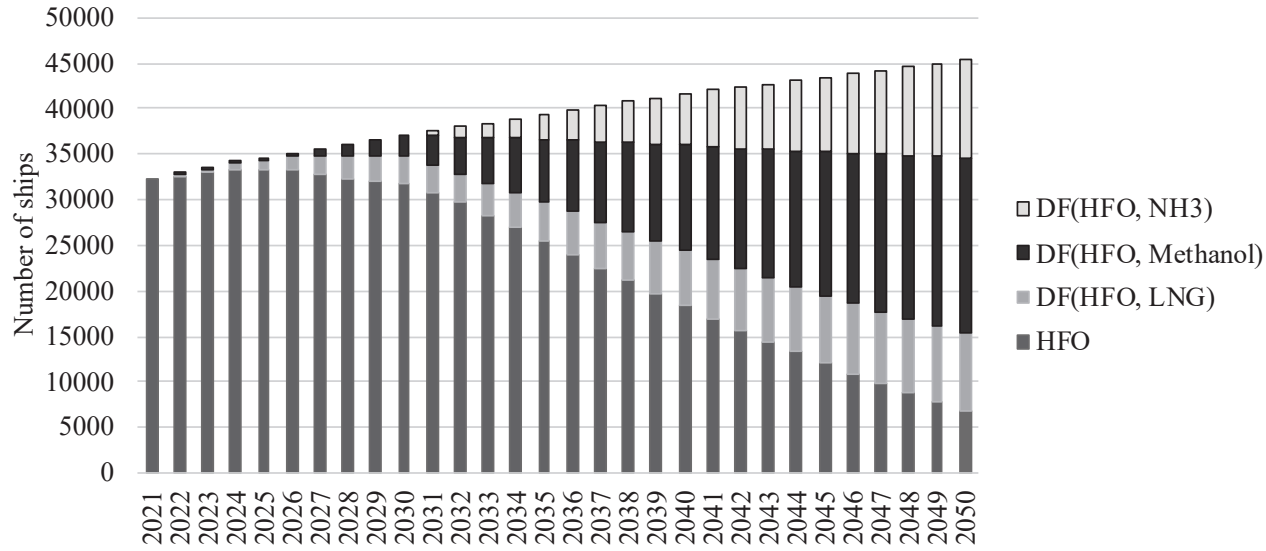

Figure 10: Fleet decomposition (Case 1-2, case with flexibility mechanism)

A cost comparison between Cases 1-1 and 1-2 is shown in Figure 11 to illustrate the effect of the flexibility mechanism in more detail. Figure 11 indicates that the fuel cost is affected by the flexibility mechanism, especially for 2040. When the flexibility mechanism is applied, the fleet can select a more cost-effective fuel mix according to fuel costs and availability beyond the constraints of the fuel type of individual ships, thereby, reducing transportation costs in the overall shipping market when complying with the regulations.

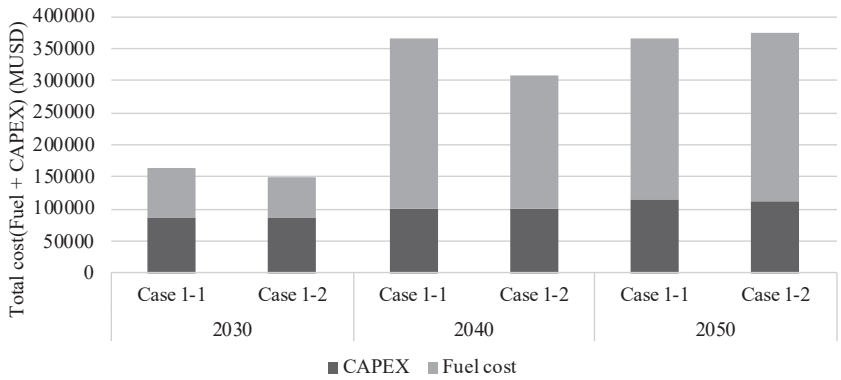

Figure 11: Comparison of costs between Cases 1-1 and 1-2 in 2030, 2040 and 2050

Case 2: Exploration of feasible GFI pathway

Shipbuilding can take years; thus, the replacement cannot proceed rapidly, and deployment of the fuel supply chain is an unaddressed issue. Therefore, setting the GFI pathway incorrectly would render the GFS regulation unfeasible. In this case study, assuming that a severe scenario is applied (transportation demand is "High" and "Low Bio"), a GFI pathway that is feasible and contributes most to GHG emission reduction should be explored.

The exploration process is as follows: First, in addition to the GFI pathway presented in Table 3, four pathways with less restrictive GFI values were prepared. The FuelEU Maritime reduction target was adopted as the most feasible pathway. Each of these pathways was input into the simulation to examine their feasibility for 2030 and 2040. A feasible line that contributes as much as possible to GHG emission reductions up to 2040 is defined as a solution. The final GFI target for 2050 is the input in increments of 5 from 0 to 20 to find a feasible point that contributes to GHG emission reduction as much as possible. The input GFI pathway candidates are listed in Table 4.

Table 4: Input GFI pathways of 2030, 2040, and 2050 for Case 2.

Year	2030	2040	2050
GFI candidates (LSFO=100)	94	69	20
	90	58.25	15
	86	47.5	10
	82	36.25	5
	78	26	0

The discovered solution pathway is presented in Figure 12. For reference, the GFI pathways that comply with the IMO GHG reduction strategy and FuelEU Maritime are also illustrated. As a result of the exploration, the pathway that complies with the IMO's reduction indicative checkpoint until 2030, passes between FuelEU Maritime and the IMO target, and finally reduces the GFI by 80% compared to LSFO was found. This result means that if the transportation demand becomes high, and biofuel availability is low, it is difficult to achieve the IMO's indicative checkpoint using only the GFS regulation. When the proposed pathway is applied, 26% more reduction in 2040 and 25% more reduction in 2050 by other measures such as the MBM, is required to achieve the IMO's indicative checkpoints.

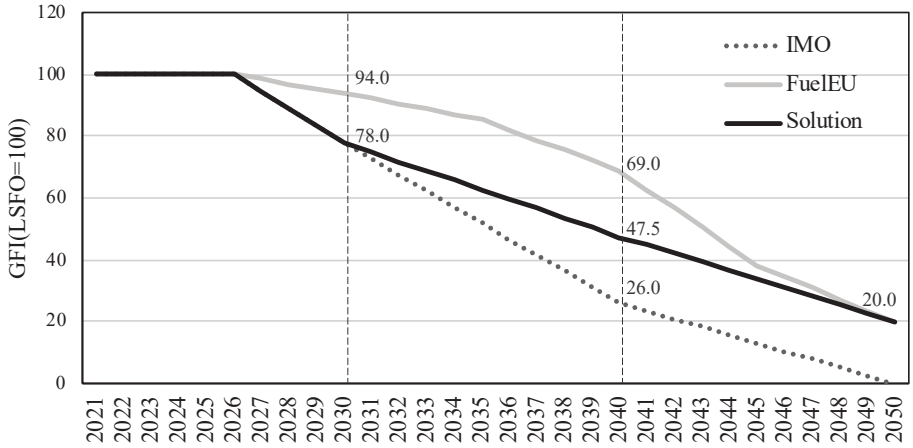

Figure 12: Exploration result of the feasible GFI pathway under a severe scenario

DISCUSSION

Case 1 compares the GFS regulation with and without the flexibility mechanism via the simulation. In addition to introducing alternative fuel ships, it is important to consider how existing ships comply with the regulations. The results of the comparison show that the presence of the flexibility mechanism can eliminate the period of non-compliance with the regulations owing to the availability of BioHFO. Moreover, the cost comparison shows that the flexibility mechanism can reduce the costs, especially fuel costs, required to adapt to the regulation. This results from the flexibility mechanism, allowing the fleet to utilize not only BioHFO but also more diverse and cost-effective fuels to adapt existing ships to the regulations. While these results are limited to the specific scenario assumed in the case study, the general insight from the results is that the flexibility mechanism can diversify options to comply with the regulation, especially for the existing ships, and thus promote more efficient decarbonization across the fleet.

However, the introduction of the flexibility mechanism has disadvantages, as it requires a more complex implementation, such as an emission trading mechanism. Decisions on whether to introduce the mechanism should be based on a consideration of these advantages and disadvantages. The proposed method allows for a quantitative evaluation of its advantages and is useful for supporting the decision-making processes.

In Case 2, a feasible GFI pathway that contributes to decarbonization as much as possible was explored with a higher transportation demand and lower biofuel supply than in Case 1. The results show that the proposed method can support the design of the GFS, as it can output a feasible GFI pathway and the amount of the GHG reduction required to achieve the IMO's indicative checkpoints by other measures such as MBM.

The case study in this paper is based on a specific scenario out of many future scenarios, and a more detailed consideration of future uncertainties is required in the actual regulation design. Specifically, the transport demand, fuel costs, and availability scenarios are highly uncertain, and the results of the case studies can change if the scenario is different.

Lagouvardou, et al. (2020) pointed out the uncertainty of the market conditions, and it is estimated that there are deep uncertainties in the fuel scenario, the cost of alternative fuel ships, and transportation demand. The results of the case study should be read with this limitation, and it is one of the future works to consider the impact of such deep future uncertainty. Hiekata et al. (2015) generated large scenarios based on a binomial lattice model and utilized the Monte Carlo simulation method to evaluate the scenarios. Irena et al. (2021) considered the uncertainties by sensitivity analysis when calculating the MACC of CO_2 mitigation measures for the decarbonization of shipping. The approach used in these studies will be useful for future research.

In addition, improving the model for the share of fuel ship types in the simulation is a topic for future research. It is difficult to model this behavior because there has never been a situation in international shipping where multiple fuels have been candidates for use, and they constitute market share. However, at present, various fuels are being handled in development projects for alternative fuel ships, and because best practices have not yet been established, they are considered to form a market share. In automotive studies, discrete choice models such as logit models are utilized to model users' behavior in choosing vehicle and fuel types based on preference data and interviews with users (Hess et al., 2012;

Khan et al., 2020; Yoo et al., 2021). Incorporating the current shipping company's preferences into the model through surveys and the modeling is a possible direction for the model improvement.

CONCLUSIONS

This study quantitatively examined how the GFS regulation affects international shipping through simulations that project future fleet transformation, fuel consumption, and WtW GHG emissions based on an inputted GFI pathway and scenario of transportation demand, fuel availability and costs, and technology availability. The method consists of three models, shipbuilding and scrapping, fuel and ship selection, and calculation of emissions and cost, and enabling us to study the regulation quantitatively from the perspective of feasibility and cost. The fuel and ship section model can express the difference between the cases with and without the flexibility mechanism, and in the simulator, it is possible to quantify the differences. Two case studies were conducted using simulation. First, we compared the simulation results with and without the flexibility mechanism. It was shown that the introduction of the flexibility mechanism allows more options for achieving the regulation as of 2030, especially for existing vessels, and that there are benefits for the cost of overall international shipping. In the second case, GFI pathways that are feasible and contribute to GHG reduction as much as possible were explored by using the simulation. As shown in the results of Case 2, the simulator can search the pathways by inputting transportation demand, fuel availability scenario, and candidates of GFI pathways, demonstrating that the proposed method is useful in designing the feasible GFS regulation according to the transportation demand, and fuel availability.

CONTRIBUTION STATEMENT

Shinnosuke Wanaka: conceptualization; data curation; methodology; software; visualization; writing – original draft. **Kazuo Hiekata:** conceptualization; supervision; writing – review and editing. **Tomohito Takeuchi**: conceptualization; project administration; writing – review and editing. **Masanobu Taniguchi**: conceptualization; investigation; writing – review and editing.

ACKNOWLEDGEMENTS

This research was supported by the JSPS KAKENHI (Grant Numbers: JP20K14967 and JP21K04501).

REFERENCES

Balcombe, P., Brierley, J., Lewis, C., Skatvedt, L., Speirs, J., Hawkes, A., & Staffell, I. (2019). How to decarbonise international shipping: Options for fuels, technologies and policies. *Energy Conversion and Management*, *182*, 72–88.
ClassNK (2023). Adoption of the FuelEU Maritime Regulation, Technical Information, TEC-1308.
Eide, M. S., Longva, T., Hoffmann, P., Endresen, Ø., & Dalsøren, S. B. (2011). Future cost scenarios for reduction of ship CO2 emissions. *Maritime Policy & Management*, *38*(1), 11–37.
Clarkson (2023, August 1) *Shipping Intelligence Network,* Retrived from https://sin.clarksons.net/
Faber, J., Hanayama, S., Zhang, S., Pereda, P., Comer, B., Hauerhof, E., & Yuan, H. (2020). Fourth IMO greenhouse gas study. London, UK: IMO.
Grzelakowski, A. S., Herdzik, J., & Skiba, S. (2022). Maritime shipping decarbonization: Roadmap to meet zero-emission target in shipping as a link in the global supply chains. *Energies*, *15*(17), 6150.
Halim, R. A., Kirstein, L., Merk, O., & Martinez, L. M. (2018). Decarbonization pathways for international maritime transport: A model-based policy impact assessment. *Sustainability*, *10*(7), 2243.
Hess, S., Fowler, M., Adler, T., & Bahreinian, A. (2012). A joint model for vehicle type and fuel type choice: evidence from a cross-nested logit study. *Transportation*, *39*, 593–625.
Hiekata, K., Mitsuyuki, M., Yamato, H., Koyama, M., Wanaka, S., Saito, T., & Moser, B. (2015). A Ship Design Evaluation Method to Maximize Operational Value under Uncertainty. In Proc. of the 12th International Marine Design Conference (Vol. 2, pp. 287–295).
IEA (2023, August 1) *International Shipping*, Retrieved from https://www.iea.org/energy-system/transport/international-

shipping
IMO (2018). Initial IMO Strategy on Reduction of GHG emissions from ships, Resolution MEPC, *304*(72).
IMO (2022). Proposal for a GHG Fuel Standard, ISWG-GHG 12/3/3.
IMO MEPC (2023). 2023 IMO strategy on reduction of GHG emissions from ships Retrieved from https://wwwcdn.imo.org/localresources/en/MediaCentre/PressBriefings/Documents/Clean%20version%20of%20Annex%201.pdf
Inal, O. B., Zincir, B., & Deniz, C. (2022). Investigation on the decarbonization of shipping: An approach to hydrogen and ammonia. *International Journal of Hydrogen Energy*, *47*(45), 19888–19900.
Irena, K., Ernst, W., & Alexandros, C. G. (2021). The cost-effectiveness of CO2 mitigation measures for the decarbonisation of shipping. The case study of a globally operating ship-management company. *Journal of Cleaner Production*, *316*, 128094.
Khan, U., Yamamoto, T., & Sato, H. (2020). Consumer preferences for hydrogen fuel cell vehicles in Japan. *Transportation Research Part D: Transport and Environment*, *87*, 102542.
Kim, K., Roh, G., Kim, W., & Chun, K. (2020). A preliminary study on an alternative ship propulsion system fueled by ammonia: Environmental and economic assessments. *Journal of Marine Science and Engineering*, *8*(3), 183.
Lagouvardou, S., Psaraftis, H. N., & Zis, T. (2020). A literature survey on market-based measures for the decarbonization of shipping. *Sustainability*, *12*(10), 3953.
Masodzadeh, P. G., Ölçer, A. I., Ballini, F., & Christodoulou, A. (2022). How to bridge the short-term measures to the Market-Based Measure? Proposal of a new hybrid MBM based on a new standard in ship operation. *Transport Policy*, *118*, 123–142.
Metzger, D. (2022). Market-based measures and their impact on green shipping technologies. *WMU Journal of Maritime Affairs*, *21*(1), 3–23.
Psaraftis, H. N., Zis, T., & Lagouvardou, S. (2021). A comparative evaluation of market-based measures for shipping decarbonization. *Maritime Transport Research*, 2, 100019.
MLIT (The Ministry of Land, Infrastructure, Transport and Tourism of Japan) (Sep. 22, 2021). Roadmap to Zero Emission from International Shipping. Retrieved from https://www.mlit.go.jp/common/001354314.pdf
Shi, J., Zhu, Y., Feng, Y., Yang, J., & Xia, C. (2023). A prompt decarbonization pathway for shipping: green hydrogen, ammonia, and methanol production and utilization in marine engines. *Atmosphere*, *14*(3), 584.
S&P Global (2023, August 1). *Sea-web Vessel Search.* Retrieved from https://www.spglobal.com/marketintelligence/en/mi/products/sea-web-vessel-search.html
Tan, E. C., Harris, K., Tifft, S. M., Steward, D., Kinchin, C., & Thompson, T. N. (2022). Adoption of biofuels for marine shipping decarbonization: A long‐term price and scalability assessment. Biofuels, Bioproducts and Biorefining, *16*(4), 942–961.
Wada, Y., Yamamura, T., Hamada, K., & Wanaka, S. (2021). Evaluation of GHG emission measures based on shipping and shipbuilding market forecasting. *Sustainability*, *13*(5), 2760.
Wang, K., Fu, X., & Luo, M. (2015). Modeling the impacts of alternative emission trading schemes on international shipping. *Transportation Research Part A: Policy and Practice*, 77, 35–49.
Yoo, S., Wakamori, N., & Yoshida, Y. (2021). Preference or technology? Evidence from the automobile industry. *Transportation Research Part D: Transport and Environment*, 96, 102846.
Zwaginga, J. J., & Pruyn, J. F. (2022). An evaluation of suitable methods to deal with deep uncertainty caused by the energy transition in ship design. In SNAME International Marine Design Conference, p. D021S003R002.

Proceedings of 15th International Marine Design Conference (IMDC-2024)
June 2-6, 2024
Amsterdam, the Netherlands

Design Lab: a simulation-based approach for the design of sustainable maritime energy systems

Kevin Kusup Yum[1,2,*], Sadi Tavakoli[1], Torstein Aarseth Bø[1], Jørgen Bremnes Nielsen[1] and Dag Stenersen[1]

ABSTRACT

The process of achieving decarbonization in the maritime industry relies on tackling complex issues related to ship design. Designers require tools that can integrate the processes of providing relevant operational profile, configuring a target design, evaluating the design and exploring possibilities. Design Lab framework innovatively addresses this need by creating realistic operational profiles, simulating vessel performance and machinery systems, and providing comprehensive system evaluations.

The framework promotes a comprehensive design process that starts by creating an operational profile. This profile is used to simulate the vessel's propulsion power considering statistical weather conditions. Then, machinery systems are configured and simulations are performed. The performance of these systems is evaluated against key performance indicators such as total cost of ownership, carbon intensity indicator, etc., and the process is iterated with new design candidates.

A case study of a hydrogen-fueled RoPax vessel is presented to validate the framework and demonstrate its capabilities. By focusing on simulation-based predictions and performance indicators, it provides a quantitative assessment, thereby supporting the decision-making process for stakeholders.

KEY WORDS

Maritime energy system; Simulation-based design; Decarbonization; Design framework

INTRODUCTION

The shipping industry plays a crucial role in our endeavors to address climate change. It is imperative to achieve significant reductions in carbon emissions within this sector. To meet the goals set by the International Maritime Organization (IMO) IMO (2023), we must focus on two key areas: improving energy efficiency and adopting alternative technologies that produce little or no greenhouse gases. This includes a variety of strategies, such as reducing ship speed, better route planning based on weather conditions, maintaining and upgrading propellers and engines, using carbon capture and storage onboard the ships Tavakoli et al. (2023), taking care of the ship's hull Yuan et al. (2016), and using alternative low-carbon fuel.

In addition, as the regulations evolve and a broad spectrum of technological options emerge, designers need tools capable

[1] SINTEF Ocean, Trondheim, Norway;
[2] HD Hyundai Europe R&D Center, Düsseldorf, Germany; * Corresponding Author: kevin.koosup.yum@gmail.com

Submitted: 23 February 2024, Revised: 1 May 2024, Accepted: 3 May 2024, Published: 19 May 2024

Conference paper, DOI: https://doi.org/10.59490/imdc.2024.843 e-ISSN: 3050-4864

of incorporating future scenarios, including fuel price fluctuations and potential carbon taxes, into total cost of ownership calculations.

To explore the impact of various technologies and the effectiveness of alternative fuels on marine power systems, a framework can be established. This framework will facilitate the optimal design and operation of ship propulsion systems, providing a comprehensive assessment of their technical and economic performance. A study by Thaler et al. (2022) explored the optimal design and operation of maritime energy systems that use renewable methanol and closed carbon cycles. They focused on the integration of onboard carbon capture technologies in shipping, evaluating both pre- and post-combustion carbon capture methods. The study employs a mixed integer optimization framework to analyze the techno-economic performance of these systems on a case study of a ferry operating in the Baltic Sea. The findings reveal cost advantages and robustness against various technological and economic conditions for systems that employ closed carbon cycle strategies. Furthermore, Buonomano et al. (2023) studied a new approach to energy design for ships with the aim of reducing fuel consumption and environmental impact. They integrated two methods, Building Information Modeling (BIM) with Building Energy Modeling (BEM), to create a dynamic, 3D physics-based simulation of a ship's energy performance under real operating conditions. The case study named "Allure of the Seas", a 6000-passenger cruise ship, was used to analyze energy performance and potential waste heat recovery. Significant primary energy savings and reduced emissions are highlighted, demonstrating the effectiveness of the methods in sustainable ship design and operation.

The study by Hansson et al. (2020) investigates the viability of ammonia as a marine fuel compared to other fuel options. It combines energy systems modeling to assess cost-effectiveness in achieving climate targets and multi-criteria decision analysis (MCDA) to rank marine fuels based on various criteria including fuel performance and stakeholder preferences.

The study by Bordin and Mo (2019) optimized the battery lifetime in vessels using a developed model. The model helps to make battery investment decisions, considering factors such as battery degradation and desired lifetime. It was designed to evaluate how the different operating modes of a vessel influence investment choices in energy storage.

Moreover, Tang et al. (2018) presented an exploration of energy management in green shipping by examining the challenges posed by emission regulations that sometimes limit or even prohibit the use of diesel in ports, necessitating alternative power sources such as shore power. The study focuses on ships equipped with onboard photovoltaic (PV) systems and how the management of a hybrid energy system (HES) combining PV, battery, diesel, and cold-ironing can lead to significant electricity cost reductions.

Therefore, the design of the entire marine propulsion system plays a central role in predicting and optimizing the power requirements of maritime vessels. An integrated system design considers not only the engine's performance but also the interaction of various components such as propellers, hull shape, and energy recovery systems. This holistic approach enables accurate power predictions, essential for fuel efficiency and reducing emissions. In addition, it allows for the adaptation of innovative technologies such as hybrid power systems and alternative fuels, ultimately leading to more sustainable and cost-effective maritime operations.

The primary objective of this paper is to present the development of a comprehensive framework designed to analyze the power system of a ship power plant, focusing on its operational profile and general arrangement using a case study as a reference. Thus, in the following section, we will introduce and discuss this framework in more detail. Subsequently, the chosen case study will be described, highlighting its specific operational profile. The core aspects of the framework, which are central to our analysis, will be elaborated upon in the following. Finally, the results derived from applying this framework to the case study will be thoroughly presented and examined in the last section, providing information on the practical implications and effectiveness of the proposed system analysis.

DESIGN LAB AND PROCESSES

Design Lab is a framework developed to evaluate the performance of the vessel with realistic operational scenario and ship models that account for all relevant technical aspects of the vessel. The evaluation process is shown in Figure 1 in an iter-

ative process for the analysis and design of a power system of a ship based on various operational parameters. The process is made of four subprocesses: defining operational profile, ship operation simulation, machinery simulation, and analysis of the design and redesign if necessary. The cycle begins with the ”Operational Profile”, which includes the route, speed profile, timetable, and weather conditions. The next phase is to run the ”Ship Operational Simulation,” using the specific ship and propulsor model from the vessel design to predict the propulsion and hotel power with the input from the operational profile. The output of the simulation is fed into the ”Machinery Simulation,” where the actual energy conversion, incorporating the machinery system model and the control strategy for the machinery system, is simulated to obtain fuel consumption and emissions. The output of the fuel consumption and emissions and the cost information from the system configuration leads to ”Analysis and Redesign,” a phase in which the total cost of ownership is considered to evaluate the economic feasibility of potential changes. This stage can influence the operational profile, signifying a feedback loop for iterative improvement and optimization of the ship’s energy system design.

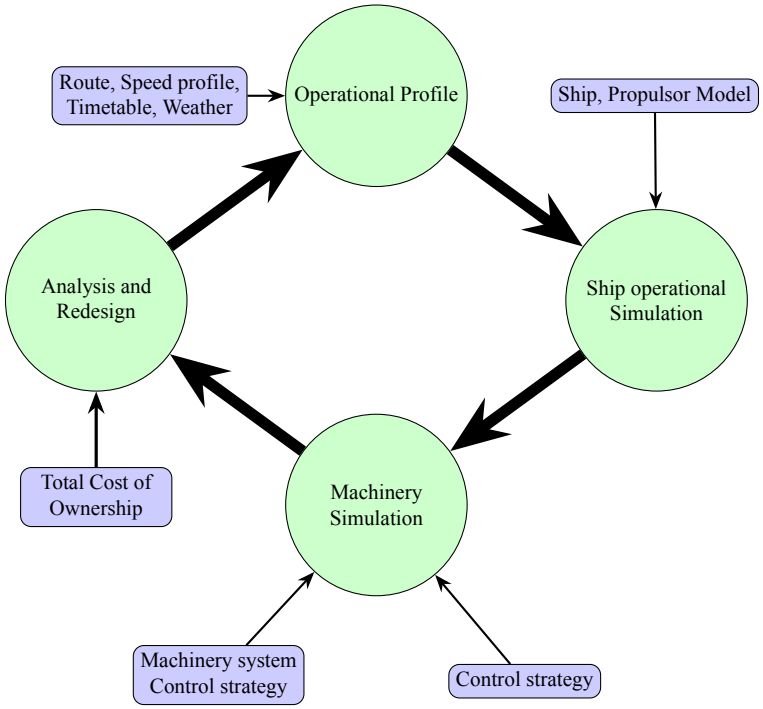

Figure 1: Design Lab process for marine propulsion systems modeling.

The framework suggests the process of the design evaluation and iteration rather than a specific implementation of the software. The framework allows designers to customize the specific models and implementation of the process fit for the purpose, providing the guidance for the implementation for defining operational profile, making ship models, performing ship and machinery performance simulation and converting the output of the simulation to KPIs. It also provides the guidance for flow of data along the design process, suggesting data interfaces between the processes. The processes should be as holistic as possible to entail all the aspects of the operation of the ship, environmental load, response of the ships, and the systems onboard as well as control strategy for the systems. At the end of the evaluation chain, the designer should define his or her own KPIs based on the output of the simulation. The most common KPI would be carbon intensity indicator and total cost of ownership or levelized cost.

For the operational profile, there are basically two ways to define it for a vessel. The first method is to define the power consumption of the vessel using the measurement data. This data can be a time series of required power or a statistical input of power vs frequencies. If such data are given, the ship performance can be skipped as the required power for the machinery system is already given. On the other hand, one can define the behavior of the vessel using its speed, route and the operation mode of the vessel. The most simple input would be to provide the design speed, length of the route and time spent in the port. Or one can define the speed profile with frequency data that provides information how much the vessel spends time with various speeds. If more information is available, one can define the route using specific way points along the path

that provides spatial information for the vessel. In addition, the metocean data within the area of vessel operation can be added to the operational profile to estimate the environmental load on the ship. These information will be provided to the next step of the process, ship performance simulation.

In the ship performance simulation, the main purpose is to estimate the required power demand on the vessel, including the propulsion and hotel load. The information from the operational profile defined in the previous stage will be used as main input for the process. The hull resistance and propulsion model is created using the specific information of the design candidate such as main dimensions of the hull form and particulars of the propellers. The hull resistance and propulsor model can be as simple as a speed power curve from a model test or can be a parametric model extracted from computational fluid dynamics (CFD) models. For the propulsor model, it can be a static efficiency value, Wageningen ”B” series propeller model or a open water characteristic curve extracted from the CFD analysis. If the environmental load should be considered, added resistance due to wave and wind should be considered. One can either just add a sea margin, use an empirical model or use potential-theory-based methods to calculate the vessel response which converts to the resistance. At the end, the hull resistance and propulsor model will convert the location, heading, speed and the time of the vessel into the propulsion power. The output may be a time series, a histogram or a single value depending on the type of the input values.

In the machinery simulation, the main purpose is to calculate total fuel consumption, emissions and the degree of usage of power sources. The required power for propulsion and hotel load is the input for the simulation. A machinery system is a system that converts the energy source to usable form of energy such as shaft work or electricity and deliver them to the consumers. The machinery system can be described as a single conversion efficiency or a full blown system in which each energy converter and consumer is modeled. If various energy converters are used such as gensets, fuel cells or multiple fuels are used, there must be a control strategy for the system how the energy is shared among them. Together with the system configuration, this control strategy will affect the performance of the machinery system in terms of fuel consumption and emissions. For the purpose of calculation of fuel consumption and emissions, it is usually sufficient to use only efficiency of each component or brake specific fuel consumption to model the component. For a sophisticated system model with multiple energy convereters, the component should be described with the mode of energy sharing and whether the power source is available.

When the total fuel consumption and emissions are simulated with the machinery model, one can now calculate relevant KPIs. A common KPI is total cost of ownership (TCO). TCO must entail all the cost incurred in the lifetime of the vessel. It is usually divided into capital expenditure (CAPEX) and operational expenditure (OPEX). CAPEX comprises mainly of the cost related to build a ship, and, retrofitting cost if necessary. OPEX comprises mainly of the fuel cost traditionally, and other cost for crewing, maintenance, insurance and adminication is added. In recent development of carbon tax, pricing and penalty, additional cost for emissions may be considered. Regulaion related KPIs such as the carbon intensity indicator set by IMO can be considred for the design evaluation. Other qualitative KPIs such as safety, complexity and maturity can be considered if the design envolves nobel technolgy. At the end of the analysis, the designer makes decision if the design candiate is satisfactory to the requirements. Otherwise, the designer should create a new candiate and start a new process of evaluation. A new evaluation process can be evoked by an update of the design or when more detail information is available for more sophiscated modeling and evaluation.

CASE STUDY AND OPERATIONAL PROFILE

The case study focuses on the Stena Hydra, a conceptual ship designed to push the boundaries of marine engineering by incorporating hydrogen fuel cells.

As shown in Figure 2, the Stena Hydra design blueprint shows the integration of hydrogen fuel cell technology into its structure (light green boxes).

The main specifications of Stena Hydra, listed in Table 1, include an overall length of 212 meters and a beam of 26.7 meters, ensuring ample space for both cargo and passenger facilities.

The requirement for the design is defined as follows:

1. The ship shall travel back and forth between Göthenburg and Fredrikshaven for the given time table as of today.

2. The speed of the vessel shall be determined to meet the time table given.

3. The vessel shall be able to perform three crossings without bunkering fuel.

4. The vessel shall be able to provide at least 22 MW power for the ship to operate in the harsh weather.

5. The vessel shall be powered by hydrogen fuel cells of mature technology and achieve zero emission operation.

The use of hydrogen as the primary fuel in large ships presents a series of technological challenges.

While the core technology for such storage is readily provided by various suppliers, the maritime adaptation of this technology requires specialized systems, particularly for efficient bunkering operations within the strict time constraints specific to the type of ship in question. The low volumetric density of hydrogen makes storage a significant challenge; It requires containment in a liquid state at -252 ^{o}C or as a pressurized gas at 350∼700 bar to enhance density, both of which entail substantial installation costs. Consequently, identifying the optimal storage capacity is essential to ensure the economic feasibility of the system.

Currently, Proton Exchange Membrane Fuel Cells (PEMFCs) are commercially available for maritime applications. These fuel cells (FCs) are provided as modules with a typical rated power of 200kW. Furthermore, FCs have different efficiency characteristics from diesel engines. The efficiency is typically highest in the low load range and lower as the load increases. This is almost opposite to the case for diesel engines. Therefore, fuel cell operating should be different from diesel engines, especially for determining the optimal number of modules to engage for a given load. The configuration of fuel cell modules according to the power level will affect the size of the fuel cells and the fuel consumption.

The last challenge is the cost of fuel and fuel cells. They are expected to be much higher than conventional fuel and diesel engines. The size of the power capacity of the power plant should be determined to minimize the total cost of ownership. To do this, a system model that simulates the power demand for the vessel and power distribution depending on the power load and fuel consumption at each fuel cell is needed. The power demand should be realistic and stochastic to reflect the real operation requirement and the environment conditions.

The main purpose of the design study is to size the fuel cell based power plant that provides the lowest total cost of ownership. Fuel cells will ensure that the vessel will emit no emissions for the energy conversion as long as the hydrogen is coming from green sources. One of the challenges with utilizing hydrogen fuel cell is sizing. The typical efficiency curve of a fuel cell has highest efficiency at 30% and the lowest at the rated power. The study will address the challenges mentioned to arrive at the reasonable design. The following steps will demonstrate how the design lab framework is implemented to perform such a complex design evaluation process.

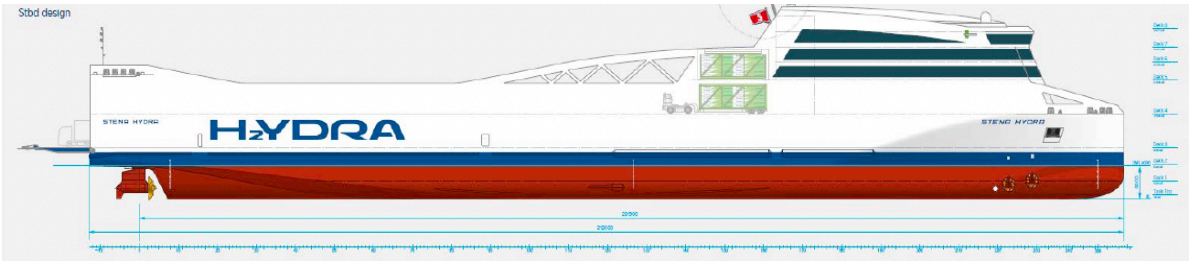

Figure 2: Ship design drawing of the hydrogen fuel cell concept named Stena H2YDRA.

Table 1: Main specification of the case study.

Item	Value
Length O.A. (meters)	212.0
Length P.P (meters)	201.9
Beam (meters)	26.7
Design Draft (meters)	6
Scantling draught (meters)	6.3
Propulsion power	15 MW
Operational range	150 NM
Speed	22 kn
Deadweight (metric tons)	6000
Payload (metric tons)	4500
Lane meters	2500
Passenger facilities	Day ferry

Definition of the operation profile

The frequency of travel and the transit time from one place to another are determined from the weekly time table of the current operation of the vessel, Stena Jutlantica. However, it doesn't provide exact way points and actual speed profile along the path including maneuvering in the confined water and transit. In order to find such detailed information, AIS data were used to create a representative operational profile. The AIS data were collected from Kystdatahuset Kystverket (2024) for Stena Jutlantica for the entire year of 2022. 339002 points were collected with many missing points in between. Figure 3 shows the spread of the points in the space with the speed of the vessel presented in a color map. The spread is rather wide, and to get the representative route of the ship, a machine learning method to find a piece-wise spline regression curve was used. The route is represented with 100 points between two ports. For the speed profile, the speeds of AIS points that are nearest to a point on the representative route are averaged and assigned to the the point. Figure 4 show the route on the map and the speed profile along distance and time.

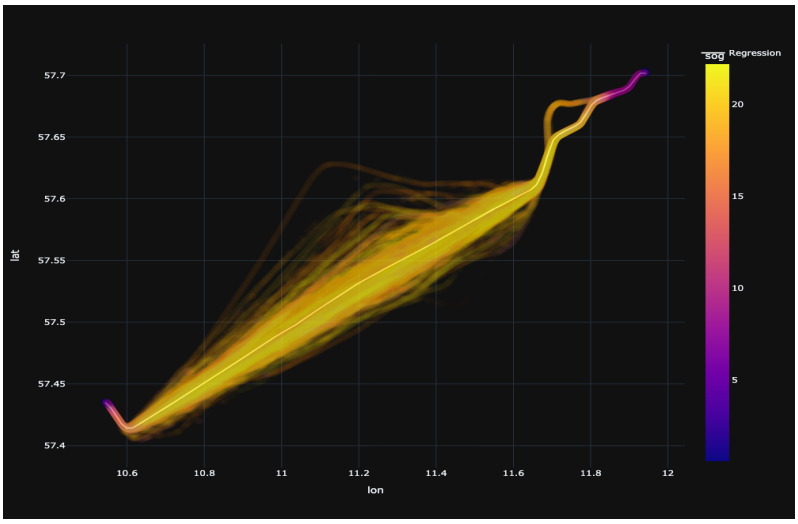

Figure 3: Actual positions and speeds of the ship on multiple voyages between Frederikshavn and Gothenburg.

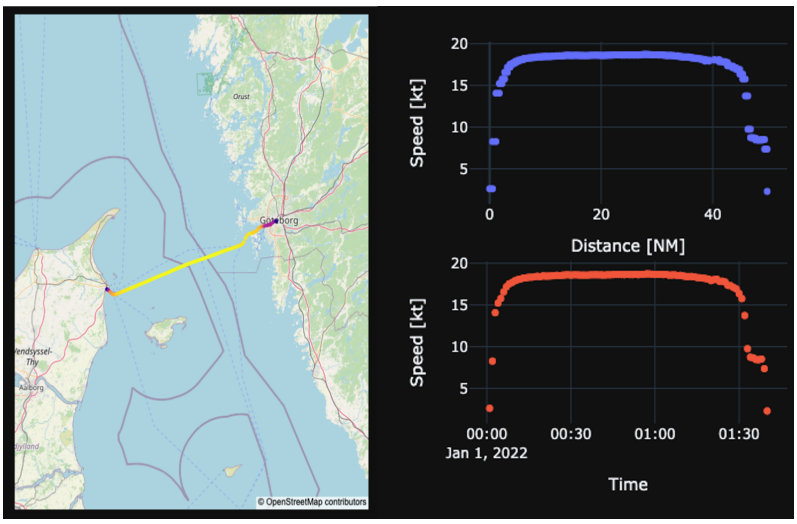

Figure 4: The representative route presented on the map and the speed profile along the length and time of the voyage

Ship Operational Simulation

With the input of the operational profile, a vessel performance simulation is performed to reproduce the propulsion power time series for entire year of 2021 and 2022. Trips are scheduled according to the weekly time table of the real operation. Each trip from one port to the other is simulated along the way points where a specific time for a way point is determined with the given the speed profile. Metocean data from the Norwegian Meteorological Institute (Institute (2023)) is used to find the wave and wind information at the way point at that specific time. The speed and the heading of the vessel together with the metocean information are provided as an input to the hull resistance model. The total resistance calculated will be converted to the shaft power using the propulsor model. In this case study, Hollenbach method is used for estimation of the calm water resistance, SNNM method by Wang et al. (2021) for added resistance due to waves, ITTC method for wind resistance and open water propeller curve for converting the required thrust to shaft power. The ship propulsion performance model is presented in Figure 5

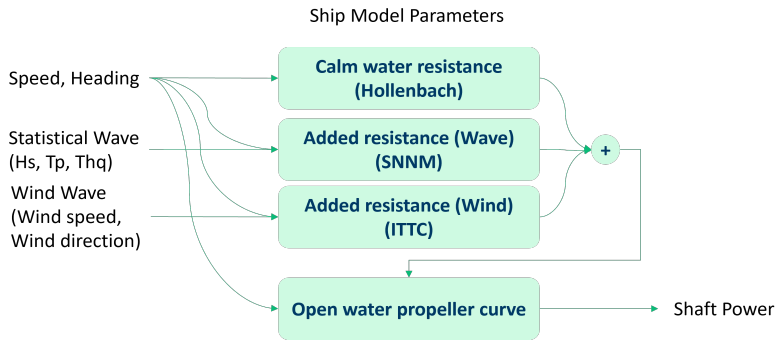

Figure 5: Components of the hull resistance models and the propulsion model used in the case study and their interfaces

The result of the ship propulsion performance simulation is shown in Figure 6. The simulation includes 2400 one-way trips from Frederikshavn to Gothenburg and vice versa throughout the year. The variation among each trip accounts for various weather conditions that the ship encounters in different time and location. There are a couple of trips where the maximum power is over 15 MW that is the maximum propulsion power of the vessel. The limitation of the simulation is that there is no involuntary speed loss due to weather condition where the speed cannot be achieved due to limitation of the installed power. However, such cases accounts less than 0.1% of the trips and, therefore, statistically.

To validate the result, the result is compared to the measured total power on the STENA Jutlandica in year 2021 and 2022 that was provided by STENA as shown in Figure 7 and 8. The results are generally in good agreement while there are some difference for high loading region. The differences are results of both model uncertainties and discrepancy in operational profile. The resistance models are based on the statistical dataset for various vessels that may lead to a certain degree of errors, and having a static speed profile may have led to inaccurate boundary conditions for the model.

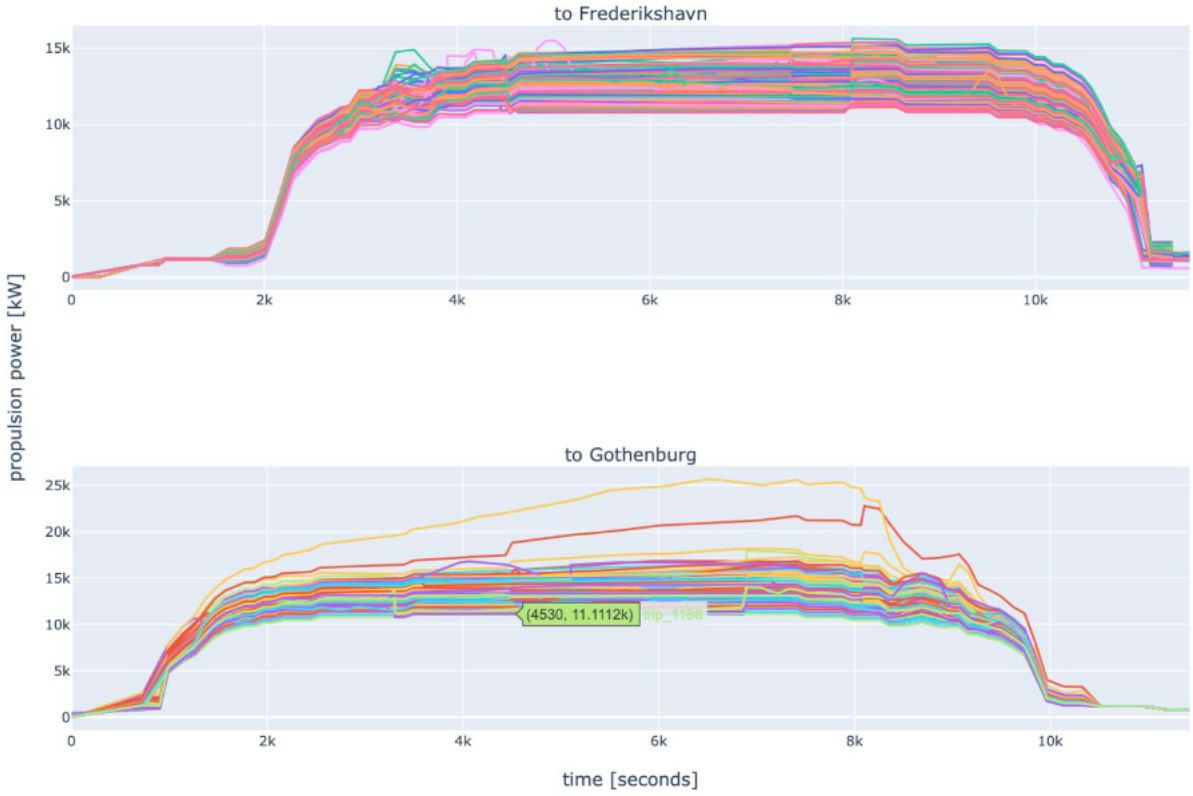

Figure 6: Prediction of the propulsion power from the simulation given as a time series for all trips in 2021 and 2022

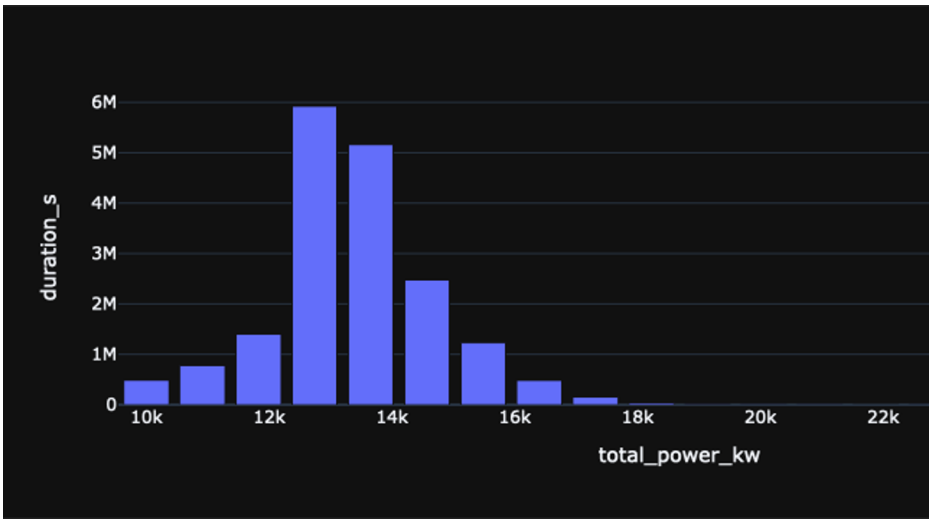

Figure 7: Histogram of the predicted propulsion power from the simulation for all trips in 2021 and 2022

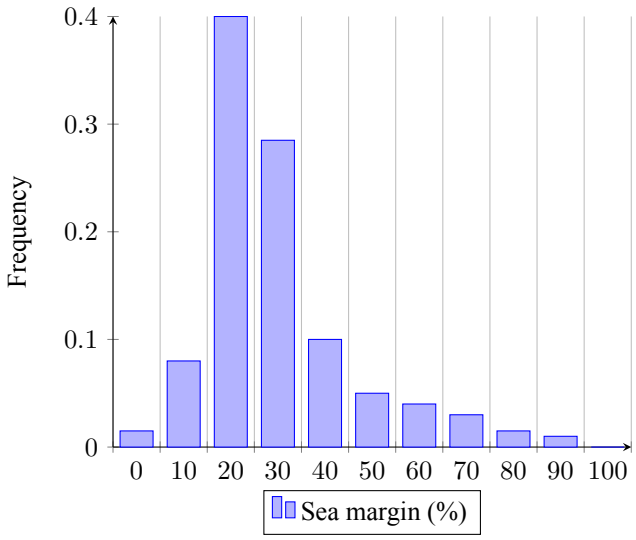

Figure 8: The histogram of the power load on gensets of STENA Jutlandica measured in 2021 and 2022.

Machinery Simulation using FEEMS

FEEMS (Fuel Energy Emissions Calculation for Machinery System) is a modeling framework designed for marine power and propulsion systems, created by the Author. It is available as a open source Python library (https://github.com/SINTEF/FEEMS/tree/main). It calculates fuel consumption, emissions, and energy balance by considering various operating modes and external power loads. The framework allows modelers to configure power systems using a component library and a single line diagram. It supports different types of power and propulsion systems, including hybrid/conventional diesel electric propulsion, hybrid propulsion with power take-in/power take-off (PTI/PTO) and mechanical propulsion with a Separate Electric Power System. The unique advantage of using FEEMS is that it will be possible to apply energy management strategy to the power sources such as load dependent start/stop of power sources, load smoothing/peak shaving operation with batteries, PTI/PTO operation, and choosing optimal power sources depending on the power demand, availability, and criticality of the operation. At the same time, FEEMS is designed to handle a large set of inputs, such as a year-long operational profile, with a short calculation time. Typically, it will give the result of calculation with over 100,000 points input within a couple of seconds. In FEEMS, a system model is created in a bottom-up approach starting with a component model to create a subsystem of components and then a system of subsystems. The system model holds both the architecture of the system and the components as objects. Typical information required to create a component model is the rated output power, the type of component in terms of functionality and power, and a load-dependent efficiency curve. For an engine component, a load-dependent brake specific fuel consumption (BSFC) curve should be given instead of the efficiency curve. For the component that converts fuel to energy, fuel information and/or emissions information should be specified as well.

When the system model is all specified, one needs to go through the following steps to arrive at the result. The first step is to define the load input for power consumers, such as propellers and auxiliary loads. Following this, it is essential to specify the operational status (either ’on’ or ’off’) and the load sharing mode for each power sources and energy storage units. If there are PTI/PTO machines, it is also necessary to specify the same for them as well as their PTI/PTO mode. Additionally, if the electric system includes a bus tie breaker, its status (closed or open) must be set.

Once all these settings are in place, the system model can perform a power balance calculation. This calculation is carried out for a bus and a shaft line. It involves determining the total power consumption at the switchboard or shaft line level. This process takes into account power losses in each component. The total power consumption is then distributed among power sources, energy storage units, and PTI/PTO machines. This distribution is based on their respective statuses, load-sharing modes, and PTI/PTO modes.

After completing the power balance calculation, the output power values for each power source are obtained. From these values, it is possible to calculate the fuel consumption, emissions, and running hours for the system. The final result is given as structured data that contains:

1. Duration of the operational profile input,
2. Total fuel consumption for each kind of fuel,
3. Total GHG emissions as CO2 equivalent value,
4. Running hours of power sources, PTI/PTO machines, and batteries,
5. Net energy saved in the energy storage units,
6. Total energy consumption of propulsion and auxiliary loads,
7. Above information for each power source, PTI/PTO machines and batteries.

These steps are shown in the visualization way in Figure 9.

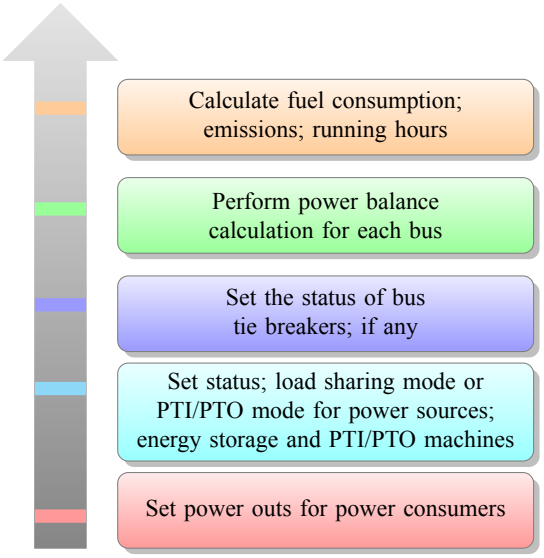

Figure 9: Procedure of calculation of the vessel's fuel consumption and corresponding emissions.

The base configuration of the machinery system has the total installation power of 20MW from fuel cells. Each fuel cell model has rated power of 200 kW. Five fuel cells are connected to a common DC link that is connected to a switchboard by a DC/DC converter. This means that there are 20 groups of fuel cell modules in total. There are two propulsion drives that are connected to each switchboard. Other load at each switchboard represents hotel and auxiliary load. The configuration is shown in Figure 10

The fuel cell group will be turned on and off depending the load level of the power sources to achieve the optimal number of fuel cells. Because the fuel cells have the best efficiency between 20% and 30% of their rated power, the number of fuel cells providing power will be determined so that the number is minimum where the power load on each fuel cell does not exceed 30%. Using this simple energy management makes sure that the plant can run at the best efficiency point depending on the load.

The fuel consumption for each trip and accumulated consumption for three consecutive trips are shown in Figure 11

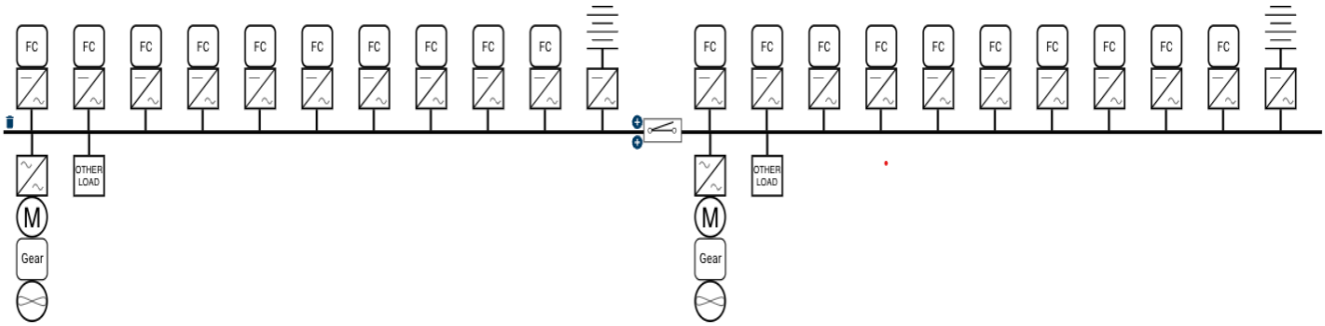

Figure 10: A machinery system with 20MW installed power from fuel cells as a base case for the design study

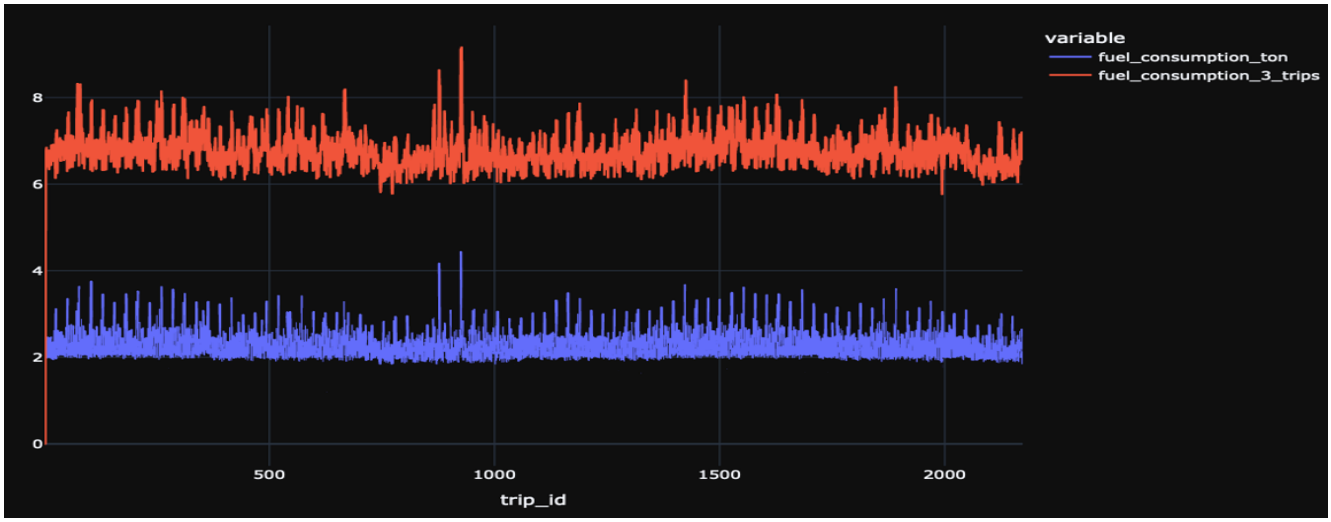

Figure 11: Fuel consumption for each trip and three consecutive trips from the machinery simulation using FEEMS

Analysis and redesigns

Among other KPIs, total cost of ownership (TCO) is a single value that expresses the system efficiency, capital cost and emissions as a single value. The calculation of TCO can be done with the input of the system configuration, fuel consumption results and running hours of fuel cells from the machinery simulation. The overall analysis is shown in Figure 12.

For hydrogen powered vessel, the cost of hydrogen storage constitutes a significant part. Deciding capacity based on the simulation results, therefore, prevent the system from over- and under-sizing of the storage. From the design requirements, the vessel must be able to make three trips without bunkering. In Figure 11, accumulated fuel consumption for three consecutive trips are presented. The maximum value is 9.2 tons. Therefore, storage capacity of 10 tons will be capable of fulfilling the design requirement while it is kept in a reasonable range.

The TCO is calculated as a levelized cost, cost per trip. The cost is calculated only for the machinery system using the following equation.

$$LC = \frac{CAPEX + \sum OPEX_i \cdot (1+r)^{-i}}{\sum n_{trip} \cdot (1+r)^{-i}}$$

$$CAPEX = 1.2 \cdot (P_{rated} \cdot C_{PS} + M_{storage} \cdot C_{storage})$$

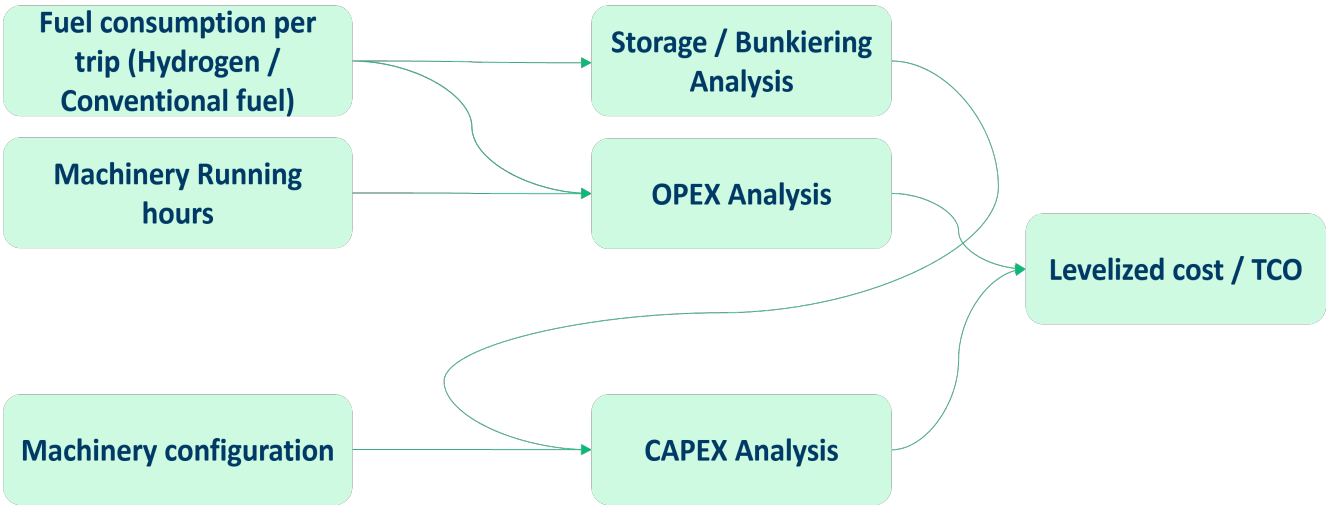

Figure 12: Analysis of the simulation results to arrive at the total cost of ownership for the design case

Table 2: Calculated TCOs for three design cases with different intalled power

	20MW	25MW	30MW
CAPEX [mEUR]	46.3	54.1	62.1
OPEX [mEUR/year]	18.308	17.497	17.008
Number of trips per year	1,353	1,353	1,353
Energy production [kWh/trip]	38,458	38,458	38,458
Fuel consumption [ton/trip]	2.36	2.241	2.168
Levelized cost [EUR/trip]	16,392	16,271	16,403

$$OPEX_i = m_{fuel} \cdot (C_{fuel} + c_{CO_2} \cdot C_{CO_2}) \cdot n_{trips} + E_{PS} \cdot C_{mt}$$

where,

r :	Discount rate
n_{trip} :	Number of trips per year
P_{rated} :	Total installed power of power sources [kW]
C_{PS} :	Unit cost for the power plant [EUR/kW]
$M_{storage}$:	Storage capacity [ton]
$C_{storage}$:	Unit cost for storage [EUR/ton]
m_{fuel} :	Fuel consumption per trip [ton]
C_{fuel} :	Fuel unit cost [EUR/ton]
c_{CO_2} :	CO2 conversion factor for fuel [kg/kg]
C_{CO_2} :	Cost of CO_2 emission [EUR/ton]
E_{PS} :	Energy production per year [kWh]
C_{mt} :	Maintenance cost [EUR/kWh]

The overall procedures are performed in three design cases: 20MW, 25MW and 30MW for total installed power. With the assumption of fuel cost of 5 EUR/kg, fuel cell cost of 1400 EUR/kW, maintenance cost of 0.045 EUR/kWh and storage cost of 1,000,000EUR/ton, the TCOs are calculated as shown in Table 2.

RESULTS AND DISCUSSION

Within the maritime industry, the transition to hydrogen fuel is based on a wide range of economic factors. Figures 13 through 16, complemented by detailed specifications based on our case study, form a comprehensive analytic structure. The Design Lab framework enables the assessment of the operational costs associated with this innovative vessel. Sensitivity analysis underscores the crucial role of hydrogen pricing, which emerges as a primary determinant of overall costs, more than the purchase of fuel cells. This paper has conducted a sensitivity analysis focusing on the three key factors:

- Fuel cell unit cost: 800 – 1400 EUR/kW
- Fuel cell maintenance cost: 0.02 – 0.045 EUR/kWh
- Hydrogen cost: 3-9 EUR/kg

The cost analysis further suggests that hydrogen pricing provides valuable insights into determining the most suitable size of the vessel's power plant. Reduced hydrogen prices support the selection of a power plant with smaller installed capacity to reduce initial investment, whereas higher hydrogen prices may favor a larger power plant to capitalize on economies of scale. The main goal is to create maritime energy solutions that maintain environmental and economic sustainability. The Stena Hydra serves as a model or example, highlighting the necessity for strategic power configuration and smart energy management for the promotion of environmentally friendly maritime operations.

The graphical representation in Figure 13 correlates the levelized cost of maritime transport with the fluctuating prices of marine gas oil (MGO), in the context of diverse CO2 pricing under the European Union Emissions Trading System (ETS). This relationship highlights the financial consequences of carbon emissions within the maritime sphere and the requirement for shipping companies to develop strategies that can effectively address the potential effects of carbon pricing on their operational expenses. Figure 14 also shows a visualization of the effects of the MGO price on maritime transport costs per kWh, further analyzed under different ETS CO2 price scenarios. Moreover, Figure 15 represents the impact of the price of liquid hydrogen on the levelized transport costs in different vessel power capacities. The increasing prices of liquid hydrogen have a direct impact on the levelized cost, particularly for vessels that require more energy. This emphasizes the significance of taking into account fuel costs in the early stages of ship design. The diagram illustrates a comprehensive evaluation of liquid hydrogen prices and fuel cell prices, represented by the colored shapes, within the 800 to 1400 EUR/kW range. As demonstrated, the rate at which the levelized price increases is reduced as the size of the power plant increases. The reason behind this is the influence of reduced fuel usage in the larger machinery setup of the case study, despite the additional investment in the power plant, by the increased capacity of the fuel cell from 20 to 30 MW. Lastly, Figure 16 shows the assessment of levelized transport costs per kWh in the context of liquid hydrogen prices and fuel cell prices.

CONCLUSION

In summary, the Design Lab has emerged as a key tool, providing a robust and iterative framework to evaluate the designs of maritime vessels that use hydrogen fuel cells. The ability to analyze AIS data has resulted in the creation of operational profiles, which offer a comprehensive understanding of vessel behavior in real-world scenarios. These profiles serve as the basis for the design process. Furthermore, the semi-empirical approach enables the prediction of power requirements that are statistically validated, ensuring that the design of the ship is robust to the variation of maritime environments. Meanwhile, simulations conducted via FEEMS offer detailed insights into the machinery's performance, revealing system efficiency and fuel consumption patterns across a spectrum of operational loads.

Economic analysis has made it clear that while hydrogen-fueled propulsion systems currently cost more than conventional fossil-based solutions, it is possible to achieve a balance. As technological advancements continue and carbon taxation becomes a global norm, the cost of operating hydrogen-powered vessels is expected to decrease, potentially aligning with those of traditional maritime fuels. This shift would mark a significant milestone in the maritime industry's journey towards

sustainability, positioning hydrogen as a viable and environmentally responsible fuel choice for the future of global shipping.

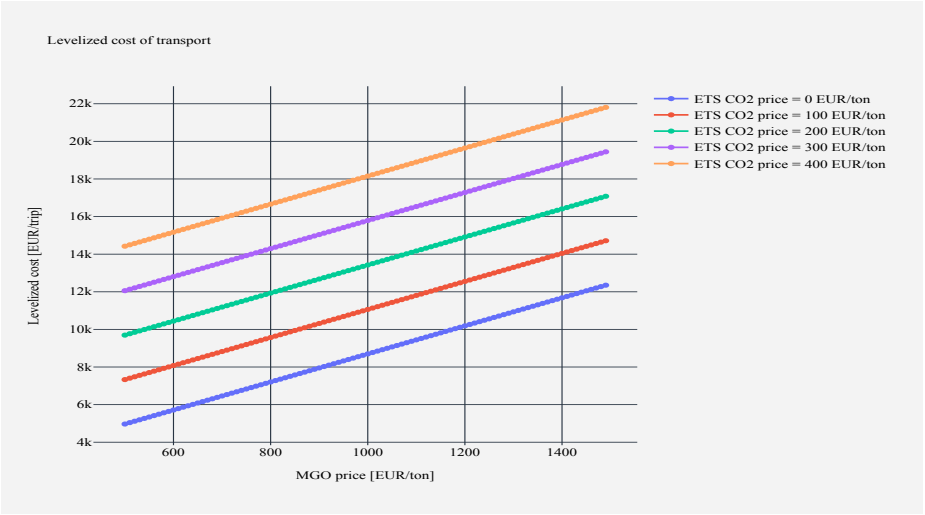

Figure 13: Levelized cost of transport regarding the marine gas oil price and the ETS.

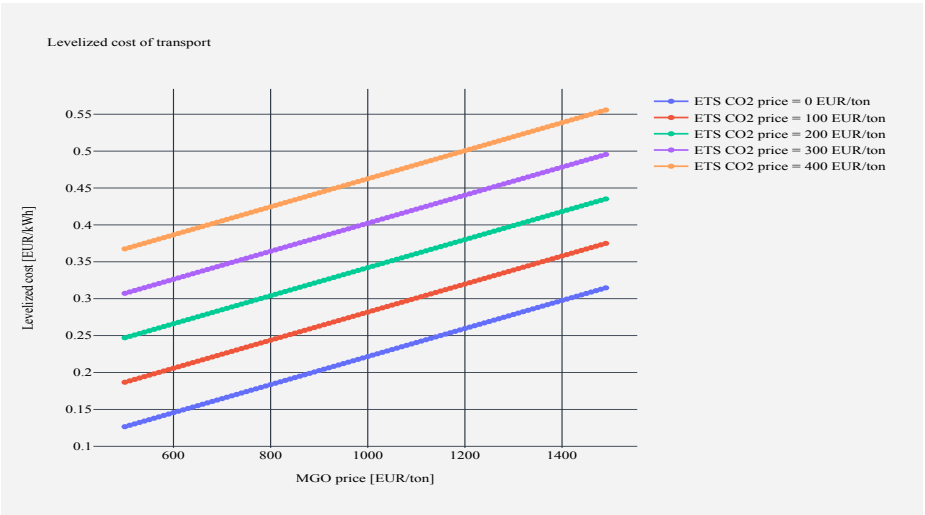

Figure 14: Levelized cost of transport per kWh regarding the marine gas oil price and the ETS.

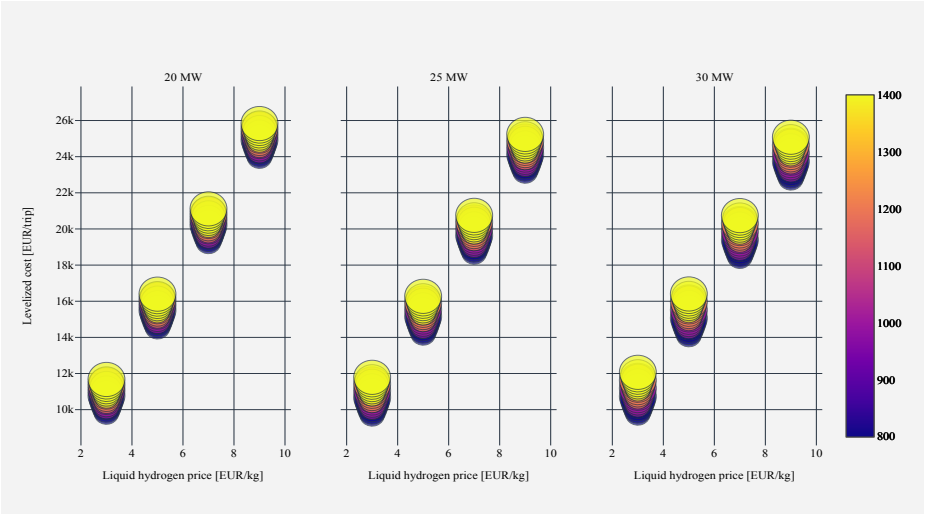

Figure 15: Levelized cost of transport based on hydrogen price.

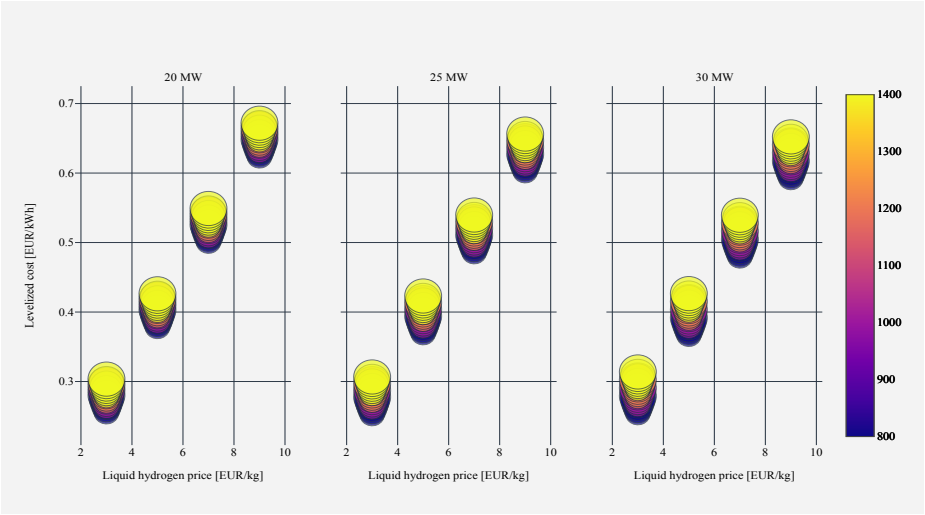

Figure 16: fig: Levelized cost of transport per kWh based on hydrogen price.

CONTRIBUTION STATEMENT

Kevin Kusup Yum Conceptualization; data Creation, methodology; writing – original draft. **Sadi Tavakoli** Conceptualization; data Creation, methodology; writing – original draft. **Torstein Aarseth Bø** writing – review and editing. **Jørgen Bremnes Nielsen** writing – review and editing. **Dag Sternesen** conceptualization; supervision; review and editing.

ACKNOWLEDGEMENTS

We acknowledge the financial support received from the HOPE Project (https://www.nordicenergy.org/project/hope/), focusing on hydrogen fuel cells in maritime shipping from a Nordic perspective. This support has been crucial in the advancement of our research on low-carbon maritime solutions. The authors thank all the project partners and stakeholders for their valuable contributions.

REFERENCES

Bordin, C. and Mo, O. (2019). Including power management strategies and load profiles in the mathematical optimization of energy storage sizing for fuel consumption reduction in maritime vessels. *Journal of Energy Storage*, 23:425–441.

Buonomano, A., Del Papa, G., Francesco Giuzio, G., Maka, R., and Palombo, A. (2023). Advancing sustainability in the maritime sector: energy design and optimization of large ships through information modelling and dynamic simulation. *Applied Thermal Engineering*, 235:121359.

Hansson, J., Brynolf, S., Fridell, E., and Lehtveer, M. (2020). The potential role of ammonia as marine fuel—based on energy systems modeling and multi-criteria decision analysis. *Sustainability*, 12(8).

IMO (2023). IMO strategy on reduction of GHG emissions from ships. *International Maritime Organization London, UK*.

Institute, N. M. (2023). Met norway thredds service - mywavewam. Accessed on 6 May, 2023.

Kystverket (2024). Kystdatahuset. Accessed on 5 May, 2023.

Tang, R., Wu, Z., and Li, X. (2018). Optimal operation of photovoltaic/battery/diesel/cold-ironing hybrid energy system for maritime application. *Energy*, 162:697–714.

Tavakoli, S., Gamlem, G. M., Kim, D., Roussanaly, S., Anantharaman, R., Yum, K. K., and Valland, A. (2023). Exploring the feasibility of carbon capture onboard ships. *LAPSE*, 2023(36831v1). Record ID: LAPSE:2023.36831v1.

Thaler, B., Kanchiralla, F. M., Posch, S., Pirker, G., Wimmer, A., Brynolf, S., and Wermuth, N. (2022). Optimal design and operation of maritime energy systems based on renewable methanol and closed carbon cycles. *Energy Conversion and Management*, 269:116064.

Wang, J., Bielicki, S., Kluwe, F., Orihara, H., Xin, G., Kume, K., Oh, S., Liu, S., and Feng, P. (2021). Validation study on a new semi-empirical method for the prediction of added resistance in waves of arbitrary heading in analyzing ship speed trial results. *Ocean Engineering*, 240:109959.

Yuan, J., Ng, S. H., and Sou, W. S. (2016). Uncertainty quantification of co2 emission reduction for maritime shipping. *Energy Policy*, 88:113–130.

Part 6:
UNMANNED AND AUTONOMOUS TRANSITION

Proceedings of 15th International Marine Design Conference (IMDC-2024)
June 2-6, 2024
Amsterdam, the Netherlands

Large Uncrewed Surface Vessel: An opportunity for Energy Transition?

T Beard[1,*] and J Rigby[2]

ABSTRACT

Driven by the IMO target to make the maritime industry net-zero in its carbon emissions by 2050, the maritime industry now has the question of how to create both technically feasible and economically viable solutions. While many are looking at how this can be achieved for currently crewed vessels, even those service vessels such as naval combatants, there is also a real benefit that could be had by combining autonomy with the challenge of meeting the energy transition. Without people onboard there are options to completely change assumptions on layout, deck height and operations that could provide greater available space and counter energy density challenges. Additionally the removal of human life could open the line for other fuels such as ammonia with significant toxicity concerns. This paper investigates the benefits and difficulties that a Large Unmanned Surface Vessel (LUSV) utilising alternative fuel can bring, building on the recent BMT LUSV vision.

KEY WORDS

Autonomous Vessels; Energy Transition; Alternative Fuels; Modularity.

INTRODUCTION

The maritime industry accounts for ~3% of global emissions (EU Horizon, 2022), if it were a country it would rank 6th, although accounting for ~90% of global trade. Clearly reducing maritime emissions will have a significant impact on global warming. The updated IMO GHG emissions strategy is for a ~50% reduction by 2030 and net zero by 2050 (IMO, 2023). There is also a clear ambition globally to maximise the opportunity of autonomy, thus reducing people in hazardous scenarios and increasing the ability to conduct tasks in a world with a skills shortage across many industries (World Economic Forum, 2023).

BMT have created a vision known as the Large Uncrewed Surface Vessel (LUSV). This is exploring not only an autonomous vessel, but how it can contribute to the maritime net zero targets. By combining autonomy with the energy transition there are many advantages to be gained. However, there are some technical challenges that must be overcome to ensure not only compliance with regulations, but also ensuring safe operation.

This paper introduces the BMT LUSV concept, which while it has been designed for a specific purpose the lessons learnt are applicable across the autonomous vessel range of operations and sizes. The advantages an LUSV has for supporting the energy transition are explored, alongside the general technical challenges.

One of the major advantages of autonomy is the removal of people. This not only provides more space it also has the added benefit of significantly reducing the energy demands of a vessel. This is due to the reduction in hotel load, which could around 15% of the required power compared to a crewed vessel and is explored in more detail in subsequent sections.

This provides two options for an owner/operator. The vessel could be reduced in size or endurance while cargo capacity could also be increased. Although it is likely that a combination of both of these will be sensible. However, one of the likely key drivers when starting out is acknowledging that the key ship impact of fuel would no longer be internal space but the impact of the mass of the fuel at the start of deployment.

[1] Affiliation (BMT Ltd, Glasgow, UK)
[2] Affiliation (BMT Ltd, Bath, UK)
* Corresponding Author: Thomas.beard@uk.bmt.org

Submitted: 24 February 2024, Revised: 2 April 2024, Accepted: 1 May 2024, Published: 21 May 2024

Conference paper, DOI: https://doi.org/10.59490/imdc.2024.872 e-ISSN: 3050-4864

LARGE UNCREWED SURFACE VESSEL (LUSV)

The LUSV vision is a simplified supporting vessel that can utilise the full benefits of autonomy to help reduce costs. The concept of a LUSV is not new; LUSVs have been seen as the key component of the United States (US) Navy's ASW Continuous Trail Unmanned Surface Vessel programme since 2010. More recently, the US Navy has also looked at LUSVs to address the projected reduction in vertical launch strike missile capacity as their Ticonderoga Class cruisers are retired. The key element which makes these systems "large" is their requirement to operate on open ocean and higher sea states as well as the scale/size required to host the modular capability and support it for long durations of time. While the Royal Navy is keen to integrate and exploit uncrewed systems and is making significant progress in areas such as mine warfare and maritime air power, it has yet to formally consider the use of LUSVs to enhance its surface fleet. This means there is an opportunity to take a holistic design approach to the challenge; to outline the design drivers and help fuel discussion on the topic.

This LUSV vision has been created predominantly with an Anti-Submarine Warfare (ASW) application in mind but it could be utilised for a range of other surface warfare functions. ASW is especially appealing as it is a resource intensive endeavour. In order to counter a threat from entering a sensitive area, such as the Greenland Iceland UK (GIUK) Gap, a mixed fleet approach will often be used deploying a combination of submarines, Maritime Patrol Aircraft and expensive, high-performance front-line warships (UK Defence Journal, 2023). In the future LUSVs could be deployed to cover the GIUK Gap or similar maritime area on a permanent / near-permanent basis as required by intelligence-led indicators and warnings. Equipped with towed array and sonar buoys, these vessels would be capable of proceeding to a patrol station and maintaining a pre-planned patrol pattern (or respond to remote orders) to conduct either barrier operations or search functions. They would be capable of exchanging real-time data with both shore-based control centres and other assets (crewed and uncrewed) including those from other NATO countries. In this scenario, the crewed assets need only be activated once a positive detection is made. This means other more complex assets spend less time away from other, planned, commitments and the impact on personnel is also reduced.

Key Requirements

Following the creation of a potential Concept of Operations (CONOPS) for the LUSV, Table 1 below outlines the key driving requirements for the vessel that became the input to the vision.

Title	Requirement	Measure of Performance
Endurance / Duration	Remain on mission for the duration of a mission with no physical maintenance or support required	Threshold 1 month
Seaworthiness	Maintain all systems operation in deep ocean conditions and survive extreme conditions,	Upper SS6 full performance
Speed loiter	Maintain a loiter speed on mission for extended duration	10kts – 12kts
Speed cruise	Deploy to AoA or maintain deployment with TG ships	20kts
Speed sprint	Sprint speed for short period to avoid obstacle or threat	Objective 25kts
Payload	Provide ability to deploy towed array over the stern and flexible mission modules	Space for 6+ TEU
Above Water Signature	Low observable, IR, and radar signature	tbd
Below Water Signature	Low in water acoustic noise and magnetic signature	Commercial ICES standard with margin
Command and Control	A constant connection to a human in/on the loop is required, this drives the need for a layered approach to communication and connection.	tbd
Offboard Systems	Although the primary function does not require an organic airborne capability it may be advantageous to facilitate modular drone capabilities.	tbd
Cost	Provide added mass to the fleet at less than half the cost of a traditional vessel. Through Life Cost should also be minimised, although onboard crew may be removed from the scenario, there is still a significant shore based maintenance crew.	£50m - £100m per vessel UPC TLC tbd

Table 1: Key Requirements

The LUSV concept is not constrained by the requirement to have humans onboard; there will be humans in the loop but not onboard. This unlocks huge potential to design a flexible and adaptable ship optimised for its operational roles, free of the compromises usually made to accommodate humans. Additionally it breaks the link between fleet mass and number of trained personnel; not all LUSVs need to be exercised all the time and they can be kept ready for a future surge in requirement (with suitable minor re-activation/work up). Autonomy opens the door to synergies that combine to bring significant operational, financial, sustainability and safety benefits.

Whilst there are benefits, there are also a number of challenges to overcome in order to provide a credible autonomous solution. These include, the increased cost of autonomy, ongoing ethical, security risk of capture and a requirement for a person in the loop for command and control. As part of our wider work we looked at all of these issues, categorising them into six key themes of development as outlined in Figure 1.

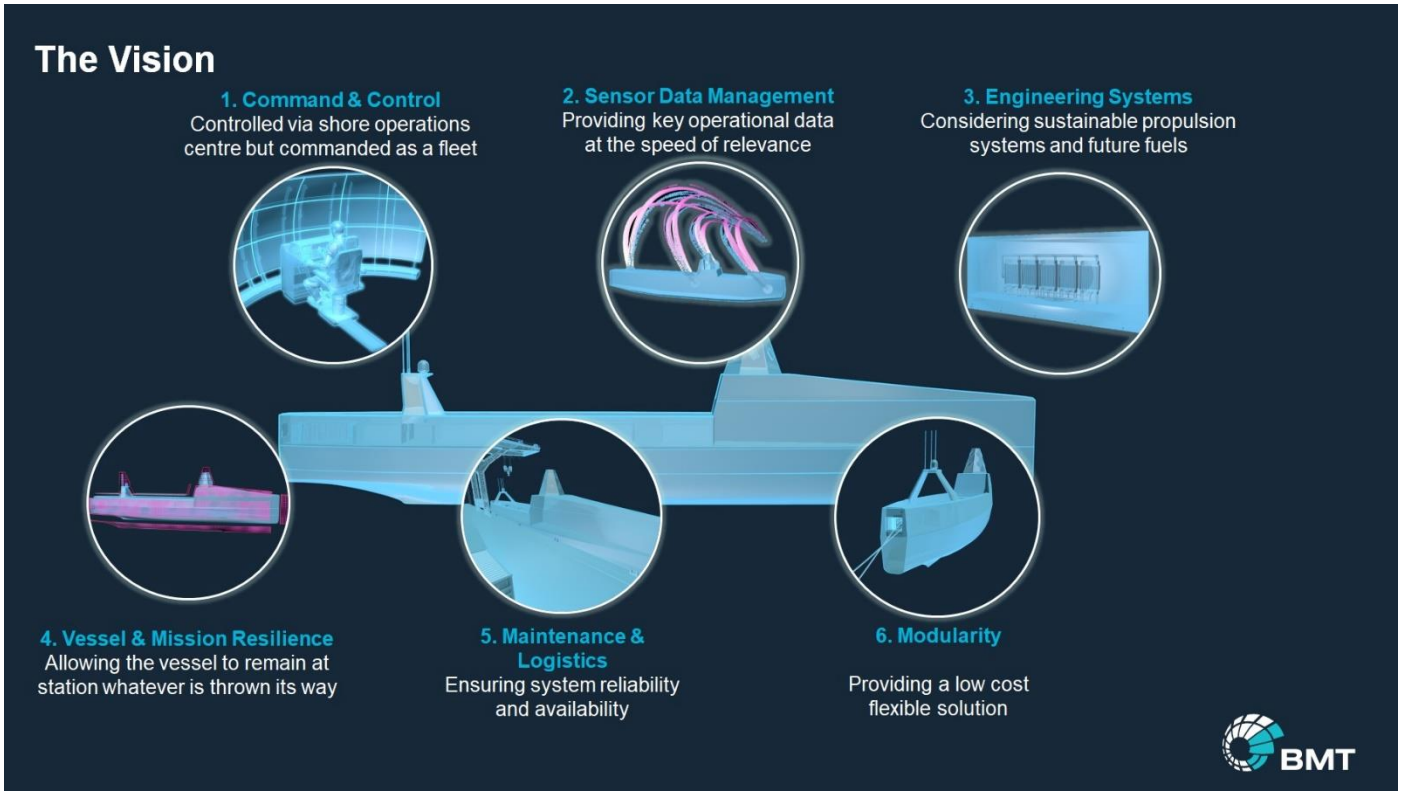

Figure 1: The Six Core Challenges of a Large Uncrewed Surface Vessel

Although six different and complex challenge areas have been investigated as part of the project, this paper only explores one, the engineering systems and the opportunity for future fuel insertion.

Engineering Systems

By creating a vision for the future, it is important to consider that the regulatory and operational environment of the future will likely require alternative power and energy solutions. The LUSV provides an opportunity to incorporate alternative fuel solutions, without the same safety concerns of a crewed vessel. Although removing people from the vessel allows a re-evaluation of space for machinery and/or fuel, the energy density of alternative fuels still causes a significant headache for Naval Architects, with the alternative being more frequent replenishment. The minimum requirement is for 30 days operation, but greater endurance could provide even greater capability and perhaps reduce the number of hulls required.

To future proof the vessel and allow for through life alterations, an all-electric propulsion solution is proposed; this has the primary benefit of reducing mechanical maintenance, but it will also allow for changes in the power generation plant as technology develops. In addition, by utilising modular prime movers it can simplify the maintenance process in port allowing the key equipment to be removed and replaced with working items, this has an added bonus of enabling greater flexibility in the choice of future fuel. This modular design allows for the use of Fuel Cells, which would decrease vessel signatures whilst

allowing for improved maintainability and reliability. However, it should be noted current fuel cells (e.g. Proton-exchange membrane) require dehydrogenation for any alternative fuel except pure (99.999%) hydrogen. Solid Oxide Fuel Cells (SOFCs) can utilize various alternative fuels such as methanol, LNG or ammonia. Although the technology readiness level is lower, with a score of 7 given by IEA Fuel Cells (2024).

As previously discussed, removing people frees up space for more fuel, but the hull size will still limit the weight. Different fuels change the volume, weight and energy density balance, but alternatives to fossil fuels will have a lower volumetric energy density and this will create a challenge when the objective is to increase range beyond the baseline 30days at 10kts. It is also hard to select a specific fuel option as the apparent best systems are also the most immature.

The energy demand for the vessel will be different to a crewed variant, whilst the propulsive power required is anticipated to be equivalent or similar, the hotel load profile will vary. A comparison between crewed and uncrewed vessels for key sub-categories of the hotel load is provided in Table 2. This is an average over three operating climates and as such there is some variability for some of the sub-systems.

Hotel Load Sub Category	**Crewed Energy Demand (%)**	**Uncrewed Energy Demand (%)**
Hull	5	5
Propulsion & Generation	8	8
General Distribution & Lighting	5	0
Command & Control (including Communication)	15	20
Auxiliary Systems	30 ± 10	30 ± 10
HVAC	30 ± 10	15
Outfit & Furnishings	2	0
Armament	5	5
TOTAL	**100**	**83**

Table 2 Hotel Load analysis and comparison for Crewed and Uncrewed vessels

The following steps are a breakdown of the energy demand changes for the hotel load due to the removal of people, this is the view of the authors.

1. Hull load is likely to remain constant with potential for a minor decrease;
2. Propulsion & generation is likely to remain constant, although this could decrease as less power is required overall;
3. General distribution and lighting will be negligible;
4. Command and Control will increase due to a requirement to relay more information as well as computing power to execute decisions;
5. Auxiliary systems will remain constant, there is variability depending on the operating climate.
6. HVAC will decrease but there will still be a requirement for some HVAC to be onboard. This is because there will be a need to maintain suitable conditions for machinery and equipment;
7. Outfit & furnishings will be negligible as no people are onboard;
8. Armament is kept constant for this analysis but could change increase to account for the decrease in other demand.

This change in the energy demand is likely to result in a reduction required to maintain the vessel, which could be leveraged for the energy density reduction of the novel fuels. Conversely, this could lead to an increase in the mission systems onboard the vessel.

FUEL OPTIONS

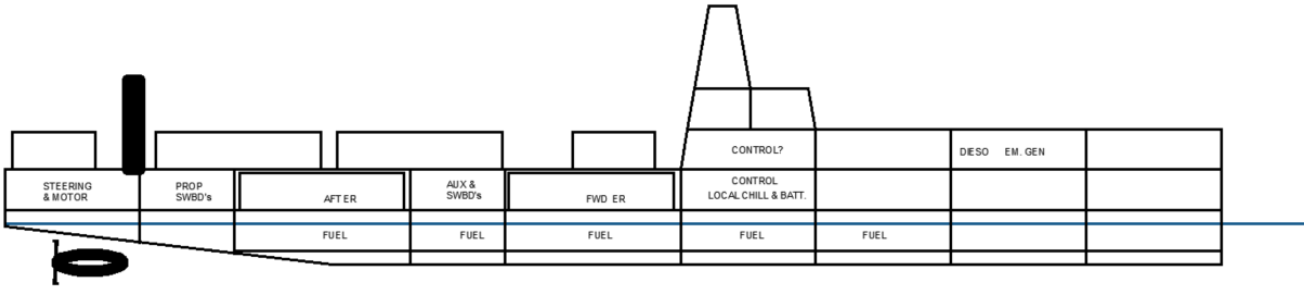

Figure 2: Cross section of potential LUSV

The LUSV has the space to potentially consider almost an entire deck for alternative fuel. Basing the fuel quantity on volume would provide circa 1000 m^3 of space for liquid (stored at or near ambient conditions), based on a LOA of 80m and a beam of 10m. However, when accounting for standalone storage tanks (pressurised or cryogenic/refrigerated) then the space significantly decreases to ~300 m^3. However, the volume available is no longer the driving case for the quantity of fuel, instead the mass is now the driver. When accounting for mass of fuel required, one should be cognisant not to base any calculations on diesel alone and should at least account for the gravimetric energy density ratios.

There are a number of potential future fuel options offering different levels of future viability:

- Methanol is a viable alternative but is not completely emission free, emitting carbon locally and only being low carbon when the production is taken into consideration, but it remains a near term solution.
- Compressed or liquid forms of hydrogen are not considered viable due to the spatial constraints of stand-alone tanks.
- Ammonia may have potential if it can be stored in such a way that it can avoid the stand-alone tanks, this is only possible on a LUSV due to the lack of people onboard. Utilising associated Solid Oxide Fuel Cells (SOFC) would also overcome the challenges of dehydrogenation as it is not required.
- Liquid Organic Hydrogen Carriers (LOHC) could be the best long term solution. It supports the vessel efficiency by having a minimal impact on trim due to storing the dehydrogenated carrier liquid onboard. However, it will always require dehydrogenation but this could be supported with associated technology developments.

The fuels chosen for investigation on the LUSV to be operating at end of life are ammonia and Liquid Organic Hydrogen Carriers (LOHCs). This is because methanol can only be net zero, whilst these have the potential to be truly zero. Hydrogen was ruled out due to the spatial constraints previously mentioned since it requires standalone tanks.

Whilst normally ammonia requires standalone tanks, there is potential to utilise pressurised ammonia rather than refrigerated. Pressurised ammonia at ~10 bar has similar storage to refrigerated ammonia (Engineering Toolbox, 2024). This would require the plate structure to be 23 mm thick, for a plate with spans 2100mm long and 600mm wide. This could be optimized by altering the stiffener spacing such that it can withstand this pressure and any operating constraints as well.

The use of a LOHC provides an opportune method to utilise hydrogen whilst having minimal impact on the vessel design. This is also truly zero since only hydrogen is utililsed. LOHCs are generally aromatic carbon compounds that are cyclic in nature. They hydrogenate (replace carbon double bonds with hydrogen) and dehydrogenate (replace hydrogen with carbon double bonds)

However, it is acknowledged that these fuels may not be available in the near future, or at least not globally. Therefore the use of modularity for power generation should be incorporated into the design. This allows the vessel to be designed to utilise any ambient liquid fuel through the life of the vessel. The use of modularity for power generation does require an electrical architecture for the propulsion system. However, this is now encouraged to minimise risk of obsolescence and ability to change prime mover moving forwards.

Placing power generation equipment just below the weather deck is advisable, since it is then possible to locate soft patches to support the removal of the equipment when required. This also minimises the spatial impact on the cargo/equipment onboard the LUSV.

BENEFITS & RISKS

There are several benefits to utilizing a uncrewed vessel but there are also risks that need to be accounted for, both of which will be expanded on further within this section.

BENEFITS

Electric propulsion allows the use of modular power generation. This provides flexibility of the fuel, which mitigates the risk of availability. Whilst this requires changes to the prime movers, this can be achieved via suitable removal routes and soft patches. This also gives a planned route to net zero if the chosen fuel is not available at time of build or during in operation.

The fuels chosen for the long term solution are LOHC or ammonia, whilst there can be transitions from MGO via methanol to the end solution. Currently the difference between the fuel is determined by the energy density and storage conditions. The ability to alter fuel through life, allows greater flexibility to accommodate emerging technologies and provides the flexibility to be included in a fleet-wide solution.

The use of the modular power generation provides an increase to the maintenance of the vessel and systems. The removal of equipment also means that there is less risk to operators conducting maintenance.

The removal of crew provides additional power due to the reduction in the hotel load. This could be used to offset the energy density or increase the capability of the vessel.

RISKS

Currently firefighting and damage control are significantly human intensive actions. A USV will require far more information to be created, assessed and actioned to ensure a vessel is operationally still effective. However, the removal of people allows the potential to utilise different firefighting techniques due to a lack of requirement to sustain human life (Savage & Glockling , 2023). The potential to loss of situational awareness and by extension control is a key risk and issue for any autonomous vessel, but more so during the event of damage and fire. The use of hypoxic environments could be a beneficial way to mitigate the fire risks, reducing the oxygen content below 12% v/v for conventional fuels (Savage & Glockling , 2023).

Recoverability is split into seven areas, as shown in Figure 3, some of which are far more difficult to mitigate on a USV. Whilst technology can support some elements, for example situational awareness, it is more difficult to recover the vessel with no humans onboard. The use of external assistance to support recoverability could be more difficult when using novel fuels.

Figure 3: Pillars of recoverability (Savage & Bartlett, 2023)

The recoverability could be supported by the use of robots which could be stored onboard and activated as required. Although this seems like science fiction, humanoid or other robots could support the recoverability and remove potential risks to human life during an emergency.

Similar to crewed vessels inspections would still be required. However, it is possible to utilize drones to support this and as such remove the risk to people. The other option would be to ensure the system is fully safe, by the removal of fuel and ensuring there is no hypoxic environment.

The vessel is designed for no humans onboard and if this were required then it would likely need to be on the mission deck. Otherwise, it removes the benefits of operating a LUSV and the potential benefits that are offered.

CONCLUSIONS

This paper presents a vision for a LUSV that has the potential to significantly contribute to the maritime industry's net-zero targets. The LUSV concept, which combines autonomy with alternative fuels, is adaptable and affordable, and is capable of performing a variety of surface warfare functions, with a particular emphasis on anti-submarine warfare. The engineering systems and fuel options for the LUSV, such as ammonia and liquid organic hydrogen carriers, have been thoroughly examined, and the benefits and risks of operating an uncrewed vessel have been discussed. In conclusion, the LUSV appears to be a promising and feasible solution that could enhance the mass and capability of future blue water fleets, while addressing the challenges associated with the energy transition.

A review of the concept is required to ensure optimal energy transition fuels are more realistic, due to many vessels originally being designed based on mass rather than volume of fuel. The main challenge is the mass of the new fuel which will have a lower energy density. The removal of people supports this due to the decrease in hotel load and increase in available space. Although this doesn't meet the full decrease in energy density when moving from diesel.

A secondary challenge is the recoverability of such an asset if damage were to occur. Smarter systems are required that can reduce the risk of the asset being lost. For example flood alarm switches that are linked to pressure to allow more information about the state of flooding, that is lost with the removal of people. Graceful degradation of systems would enhance the time for recoverability and allow for human intervention as required.

The use of autonomy has significant potential to support the energy transition of vessels by allowing the use of less energy dense and potentially more hazardous fuels to be used.

CONTRIBUTION STATEMENT

T Beard: Conceptualization; investigation, methodology; writing – original draft. **J Rigby:** conceptualization; supervision; writing – review and editing.

REFERENCES

Brækken, A., Gabrielii, C., & Nord, N. (2023). Energy use and energy efficiency in cruise ship hotel systems in a Nordic climate. *Energy Conversion and Management*, *288*, 117121. https://doi.org/10.1016/j.enconman.2023.117121

Engineering Toolbox. (2023). *Ammonia—Properties at Gas-Liquid Equilibrium Conditions*. https://www.engineeringtoolbox.com/ammonia-gas-liquid-equilibrium-condition-properties-temperature-pressure-boiling-curve-d_2013.html

EU Horizon. (2022, September 6). *Emissions-free sailing is full steam ahead for ocean-going shipping | Research and Innovation*. https://projects.research-and-innovation.ec.europa.eu/en/horizon-magazine/emissions-free-sailing-full-steam-ahead-ocean-going-shipping

Glockling, J., & Savage, I. (n.d.). *Fire Fighting Systems for Autonomous Vessels*.

IEA Fuel Cell. (n.d.). *TRL*. Retrieved 23 February 2024, from https://www.ieafuelcell.com/index.php?id=44

IMO. (2023). *2023 IMO Strategy on Reduction of GHG Emissions from Ships*. https://www.imo.org/en/OurWork/Environment/Pages/2023-IMO-Strategy-on-Reduction-of-GHG-Emissions-from-Ships.aspx?refresh=1

Savage, I & Bartlett, S. (2023). *Naval Autonomous Surface Vehicle Recoverability* [Preprint]. https://doi.org/10.24868/11073

World Economic Forum. (2023). *The Future of Jobs Report 2023 | World Economic Forum*. https://www.weforum.org/publications/the-future-of-jobs-report-2023/digest/

Proceedings of 15th International Marine Design Conference (IMDC-2024)
June 2-6, 2024
Amsterdam, the Netherlands

Simulation for Designing the Transition to Autonomous Shipping – Japanese Coastal Shipping -

Kazuo Hiekata[1], Yuki Maeda[1,*], Takuya Nakashima[1]

ABSTRACT

In Japanese coastal shipping, there is a need to introduce automation technology to alleviate the shortage of seafarers, but its introduction has an indirect impact on coastal shipping due to the interaction between transportation demand and freight rates in a market with a variety of stakeholders. Therefore, it is difficult to make decisions about its introduction. This study uses a simulator that mimics the Japanese cargo market to evaluate the impact of the deployment. The results show that the introduction of autonomous vessels, even in the middle of development, may bring benefits, and that remote maneuvering technology with a crew on board may not produce positive impacts.

KEY WORDS
Simulation, Autonomous ship, Technology adoption, Mobility transition, Coastal Shipping

1. INTRODUCTION

Background

On a kilometer basis, more than 90% of Japan's domestic freight transportation is by automobile. However, on a ton-kilometer basis, coastal shipping accounts for about 40%, and coastal shipping plays a large role, especially in long-distance transportation (MLIT, 2022). However, coastal shipping is facing a serious shortage of labor, which is reflected in the fact that in recent years the ratio of effective job offers to applicants has consistently exceeded 2 and is even above 2.5 (MLIT, 2019). The aging of the seafarer population is also a problem, with about half of the seafarers over the age of 50 (MLIT, 2021). The number of seafarers is expected to decrease further soon. Therefore, the introduction of automation technology is expected to reduce the demand for seafarers and secure a stable supply of new seafarers. In addition to reducing the demand for seafarers, the introduction of automation technology is also expected to reduce accidents caused by human error, which is estimated to account for 80% of maritime accidents and reduce carbon dioxide emissions by reducing fuel consumption through optimization of routes and vessel shapes.

For these reasons, various projects are underway in Japan and abroad to develop automation technology. In Japan, a project called MEGURI2040 was launched in 2020 with the goal of commercializing unmanned vessels by 2025 and of having half of all domestic vessels operated by unmanned vessels by 2040 (The Nippon Foundation, 2022). At the same time, the Maritime Unmanned Navigation through Intelligence in Networks (MUNIN) project is one of the big projects held in 2015-2020 outside of Japan. Project Report (MUNIN, 2015) concluded that autonomous vessels are feasible, although some barriers still remain. The MUNIN project is not only developing the technology but is also investigating the economic evaluation of autonomous vessels and discussing their feasibility. According to Bellingomo et al. (2023), the technology to develop autonomous vessels has been well developed by these projects, and it is technically feasible to introduce autonomous vessels in the near future.

The economics of autonomous vessels were analyzed by MUNIN (2015) and Kretschmann (2017). They compare the operating costs of autonomous vessels with conventional vessels for the bulk vessels envisaged in the MUNIN project. Akbar (2019) analyzes the total costs of introducing autonomous vessels on Norwegian coastal routes, based on actual routes and cargo volumes. These studies show that autonomous vessels are economically profitable, and when operated on actual routes,

[1] Graduate School of Frontier Science, The University of Tokyo, Japan,
* Corresponding Author: maeda-yuki086@g.ecc.u-tokyo.ac.jp

Submitted: 22 February 2024, Revised: 1 May 2024, Accepted: 3 May 2024, Published: 24 May 2024

Conference paper, DOI: https://doi.org/10.59490/imdc.2024.895 e-ISSN: 3050-486

costs can be further reduced through route optimization. Dantas et al. (2023) compare the operating costs of a typical Norwegian short-haul vessel with those of a conventional autonomous vessel (TAS), and a new configuration of autonomous vessels (NGAS) with reduced crew living space and other functions made unnecessary by unmanned autonomous vessels and concluded that the reduction of crew facilities on autonomous vessels helps to reduce costs. As for the impact of automation technology on crewing demand, Kretschmann (2017) proposed a system in which instead of crewing autonomous vessels, autonomous vessels are monitored from a remote operations center (ROC). They estimate that 112 people would be needed for one ROC, including standby operators, watchkeepers, and managers. It also estimates that one ROC can operate 90 vessels. Kooij (2021) also conducted a study on the impact of the introduction of automation technology, analyzing the tasks required to operate a 750 TEU container ship with a crew of 12 and the tasks that could be replaced by the introduction of automation technology. The analysis showed that the number of seafarers required was reduced by only one second officer, but the workload of the seafarers was significantly reduced. Therefore, the study concluded that for shipowners, the economic benefit of reducing automation technology is small because it does not significantly reduce the demand for seafarers, but the reduction in workload improves the working environment and contributes to a reduction in maritime accidents, which account for 80% of all maritime accidents due to seafarer fatigue. Further research on policies that promote automation technology includes Nakashima et al. (2023). This study estimated that a combination of deregulation and appropriate assistance could hasten the introduction of fully autonomous vessels by more than 10 years.

Although the introduction of automation technology in coastal shipping is ongoing due to the background described in the previous part, the introduction of autonomous vessels with no crew on board will not be possible anytime soon. Therefore, until the introduction of autonomous vessels becomes feasible, one measure to maintain the market share of coastal shipping and ensure stable transportation is to eliminate the shortage of seafarers by utilizing the automation technology to be introduced in autonomous vessels and reduce the number of seafarers required. On the contrary, if automated technologies are rapidly introduced, a rapid drop in the demand for seafarers could lead to an oversupply of seafarers, which could worsen the employment environment for seafarers, and an oversupply of seafarers could lead to extra labor costs. Under these circumstances, it is desirable to introduce automated technology to match the shortage of seafarers. However, while there have been studies on the economics of autonomous vessels and the number of seafarers that would change with the introduction of automation technology, few studies have analyzed the impact of the introduction of such technology on seafarer employment and how the early introduction of automation technology used on autonomous vessels would improve shipping capacity by reducing the seafarer shortage in the transitional period.

Purpose of this study

The introduction of automation technology also has a direct impact on seafarer demand and operating costs and an indirect impact on coastal shipping due to the interaction between transportation demand and freight rates in a market with a variety of stakeholders. In the presence of such complex factors, it is difficult for coastal shipping to make decisions to introduce automation technology more quickly while maintaining its transportation capacity as an industry in terms of employment and economics. Therefore, this study aims to support this decision-making process through a simulator that models the costs of coastal shipping and car transport in Japan and designs the transition to autonomous shipping driven by the introduction of automation technology.

2. PROPOSED METHOD

Overview of the proposed method

We propose a method to evaluate the impact of the introduction of automation technology by shipping companies. As shown in Figure 1, the method begins by developing a simulator that models the domestic freight market in Japan, including the estimated parameters. The simulator models how to calculate costs and set freight rates for coastal shipping and automobile transport, and at each step, decisions are made on factors related to the calculation of costs, such as investment in facilities and hiring of employees for each transportation demand. In addition, changes in the determined freight rates change the transportation demand for each means of transport in the next step. These complex interactive demands represent the Japanese freight market. Next, the case study is conducted as shown below using the simulator developed. The inputs to the case study are a combination of a shipping company's decision-making strategy regarding the introduction of automation technology and future trends in total transportation demand. The strategy regarding the introduction of automation technology relates to whether to introduce each of the four stages of technology envisaged as stages in the development of automation technology. The future trend of total primary demand is a set of future trends in total transportation demand from 2010, the starting year of the simulation. Based on these inputs, the simulation is run for a one-time step of 1 week between 2010 and 2070, and output results include the transition of shipping costs. Finally, the result is transformed into three indexes between 2025, when we assume that automation technology can be implemented, and 2070, when the simulation ends, as the NPV considered for the time discount rate, the total lost transportation opportunity ratio, and the cumulative early retirement crew ratio, by total transportation demand. After that, they are plotted on a scatter plot. The scatter plots are plotted on the

horizontal axis with the cumulative percentage of early retired seafarers on the right decreasing, and on the vertical axis with the percentage of lost transportation opportunities on the bottom decreasing. The color of the plotted points expresses the NPV of the shipping company's ton-kilometer-based costs and the larger the costs are, and the closer to yellow, the smaller the costs are red. The above methodology is proposed in this study as a method for evaluating the impact of shipping companies on the adoption of automation technology.

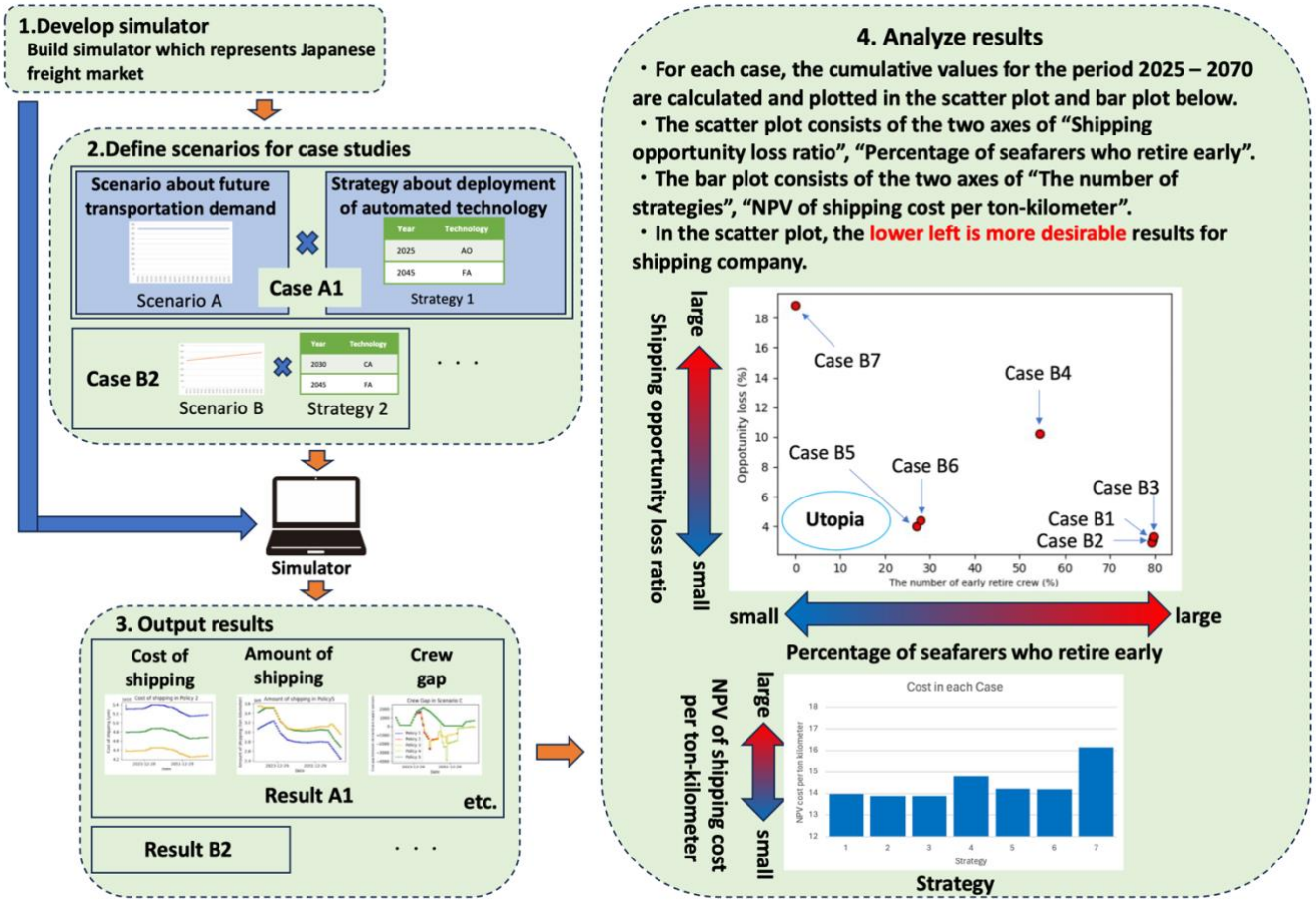

Figure 1: The abstract of proposed method

Simulation calculation flow

In the previous part, we proposed a method to provide decision support to shipping companies regarding the introduction of automation technology. In this section, we describe the specific computational flow of the simulator. Firstly, variables that are considered necessary for the simulator to be developed are selected based on previous studies and will be described later in subsequent parts. At each time step, the variables for the next time step are also calculated. As shown in Figure 2, the simulator was conducted with a time unit of 1 week from 2010 to 2070, the year when autonomous ships and self-driving cars are expected to be widely used. The simulator is divided into two parts: a transportation demand estimation model and a transportation cost estimation model. The transportation demand estimation model calculates transportation demand by transportation agency according to the freight market conditions. Then, based on the transportation demand, the transportation cost estimation model calculates transportation costs for each transportation. The relationships between the variables represented by the arrows in Figure 3 were developed based on previous studies. The sequence of calculations in the transportation cost estimation model is likewise shown in Figure 3.

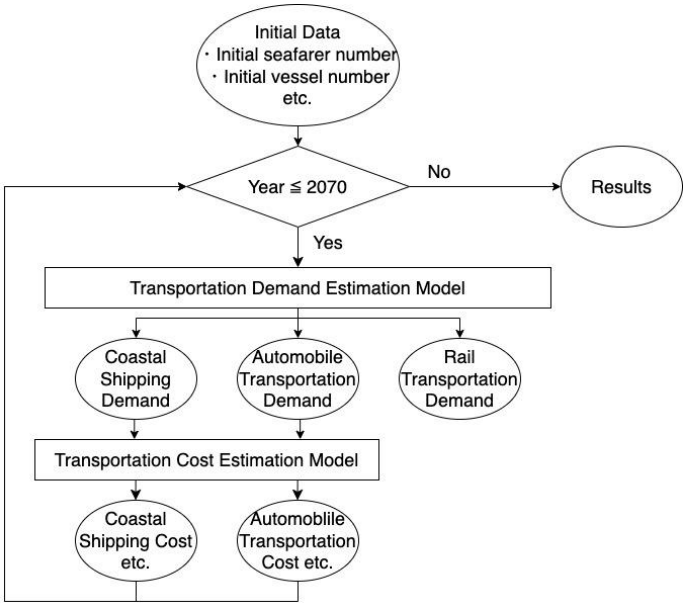

Figure 2: The abstract of simulator

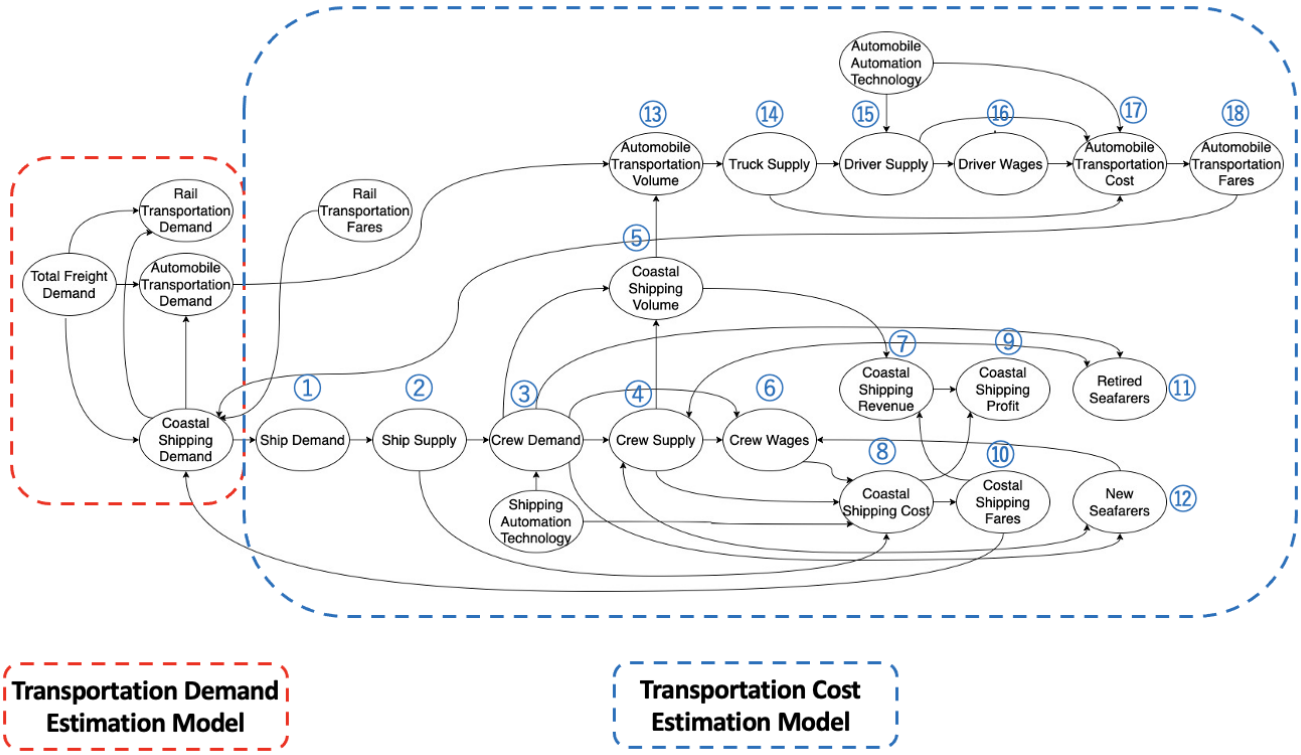

Figure 3: The relationships among variables in one loop. Source: Prepared by the authors from (Shinke, 2007), (Kretschmann, 2017) and (Lee, 2023)

Simulation model variables

Air transportation was not treated in this study because its share of transportation is small (less than 1%). In addition, rail transportation was treated with fixed freight rates because the percentage of transportation has been fixed in recent years, although there is a certain amount of transportation (The Japanese Shipowners' Association, 2021). For the variables used, the variables necessary for transportation demand allocation (Shinke, 2007) and for calculating the costs of coastal shipping (Kretschmann, 2017) (Lee, 2023) and automobile transportation were selected (Table 1) with reference to previous studies.

Table 1: The variables in the simulator

modes of transportation	variable
Coastal shipping	Transportation demand, number of vessels demanded/supplied, crew demand/supply, crew labor costs, transportation expenditures, fare, and transportation revenues
automobile	Transportation demand, truck demand/supply, truck driver demand/supply, truck driver labor costs, transportation expenditures, freight rates, and transportation revenues
railroad	Transportation demand, freight rates

Estimation of transportation demand

In this study, 47 prefectures are treated as nodes, and the links connecting these nodes are treated as a domestic freight transportation network. Transportation demand by each mode of transportation is distributed by a multinomial logit model. The calculation of the probability $P_{m,o,d,t}$ of transportation m from node o to node d at time t is defined in Equation [1], and the transportation demand $X_{m,o,d,t}$ is obtained by the expected value using the total transportation demand $G_{o,d}$ and $P_{m,o,d,t}$ as shown in Equation [5]. The utility calculated by the logit model $V_{m,o,d,t}$ is the freight rate per ton-kilometer $F_{m,t}$ (discussed after) and transport distance $L_{m,o,d}$ (discussed in Appendix) and time $T_{m,o,d}$ (discussed in Appendix) based on previous studies and defined in Equations [2] through [4]. The parameters α used in these equations are described below in Appendix.

$$\boldsymbol{P_{m,o,d,t} = \frac{\exp\left(V_{m,o,d,t}\right)}{\sum \exp\left(V_{m,o,d,t}\right)}} \quad [\mathbf{1}]$$

$$V_{ship,o,d,t} = \alpha_{time} T_{ship,o,d} + \alpha_{cost} F_{ship,t} L_{ship,o,d} \quad [2]$$

$$V_{rail,o,d,t} = \alpha_{time} T_{rail,o,d} + \alpha_{cost} F_{rail,t} L_{rail,o,d} + \alpha_{rail} \quad [3]$$

$$V_{truck,o,d,t} = \alpha_{time} T_{truck,o,d} + \alpha_{cost} F_{truck,t} L_{truck,o,d} + \alpha_{truck} \quad [4]$$

$$X_{m,o,d,t} = G_{o,d} P_{m,o,d,t} \quad [5]$$

Shipping

Automation progress

Referring to IMO's definition (IMO, 2016) for automation technology and AUTOSHIP's roadmap (Nordahl, 2023), the following stages of automation technology development were established as Table 2.

Table 2: Automation technology development stage (Nordahl, 2023)

Automation phase	Description.
AO (Automatic Operation)	Automated technologies such as automatic ship holding and automatic ship release are beginning to be implemented, but decisions are made by the ship's crew.
RC (Remote Control)	Predictive breakdowns of machinery will be possible, and maintenance of machinery will be performed when the vessel makes port calls. The ship will be constantly monitored from shore, and the conventional control system will remain, but decisions will be made remotely from the RCC.
CA (Constrained Autonomy)	The vessel operates autonomously under general conditions, although its autonomy is limited. The vessel no longer requires a crew to be on board and is only operated remotely from a remote-control center (RCC) under complex conditions, such as bad weather.
FA (Full Autonomy)	Full autonomy is achieved, with no crew on board or in the RCC. However, the operator of the RCC must deal with fallback recovery.

Fleet configuration

The demand for the number of vessels of each size $D_{ship,size,t}$ is calculated based on transport demand and defined in Equation [6]. The weekly transport volume β_{ship} per pair of vessels calculated from the past data to calculate the total tonnage required by the vessel. The ship types described in this study are four typical ship types (MLIT, 2021) is

assumed that the ratio of the number of vessels by ship size $A_{ship,size}$ does not change, we calculate the demand for the number of vessels for each ship size.

$$D_{ship,size,t} = \left\lceil \frac{A_{ship,size}}{\beta_{ship}} \sum_{o,d} X_{ship,o,d,t} \, L_{ship,o,d} \right\rceil \quad [6]$$

Number of vessels supply

The shipping company determines the supply of vessels of ship age age, $S_{ship,size,phase,age,t}$ based on the demand $D_{ship,size,t}$. In this study, it is assumed that ships are used for 14 years, which is the statutory service life of a ship in Japan, and that they are not scrapped in the middle of their service life. The number of new vessels is determined by the difference between the demand for vessels and the number of existing vessels in the current time step for each vessel type to meet the demand. The number of vessels in each automation phase is defined by Equations [7] and [8] to be allocated to the number of vessels in each automation phase according to the C_{phase}.

$$S_{ship,size,phase,age+1,t} = S_{ship,size,phase,age,t-1} \; if (0 \le age \le 13) \quad [7]$$

$$S_{ship,size,phase,0,t} = \left(D_{ship,size,t} - \sum_{phase} \sum_{age}^{13} S_{ship,size,phase,age,t-1} \right) C_{phase} \quad [8]$$

Seafarer demand

The demand for seafarers $D_{crew,t}$ is the supply of number of vessels $S_{ship,size,phase,t}$ and the demand for seafarers per vessel $B_{ship,size,phase}$ is calculated using Equation [9]. One of the purposes of introducing automated technology is to solve the shortage of seafarers, and the demand for seafarers is greatly affected by the introduction of automated technology. The factors affecting the demand for seafarers at each stage of automation technology are summarized in Table 3 with reference to AUTOSHIP (Nordahl, 2023). The demand for seafarers for conventional vessels is based on the Ministry of Land, Infrastructure, Transport and Tourism (2021).

Table 3: Factors influencing the demand for seafarers at each stage (Nordahl, 2023).

Automation phase	Seafarer services to be reduced
AO	The demand for seafarers on deck will decrease with the introduction of automated technologies such as sensors on the hull, automatic ship holding and automatic ship release.
RC	Machinery maintenance will be performed by the port's machinery mechanics when they call at the port as machine failures can now be predicted MUNIN Project Report. (2015) According to the MUNIN project report (2015) the maintenance that used to be performed during the 216-day voyage is now performed during the 120-day voyage when the vessel is in port. It was assumed that the number of seafarers in the machinery department would effectively increase by a factor of 120/216 as they would be serviced. At the same time, the demand for seafarers in the deck section would be substantially reduced as remote monitoring facilities would provide around-the-clock monitoring and decision making.
CA	Ships will navigate autonomously under all but the most complex conditions, such as bad weather, reducing the number of seafarers required at remote monitoring facilities MUNIN Project Report. (2015) According to the MUNIN project report (2015), the MUNIN project envisions a single remote monitoring facility to monitor 90 autonomous vessels with a crew of 112.
FA	If no abnormalities occur on the vessel, it will operate autonomously, further reducing the number of crew members required at the remote monitoring facility.

$$D_{crew,t} = \sum_{i,j} S_{ship,size,phase,t} B_{ship,size,phase} \quad [9]$$

Seafarer supply

Seafarers are divided into two categories: staff and departmental staff. Staff members are required to obtain national certification by graduating from a seafarer training school, but they are indispensable to the operation of a ship. Therefore, in this study, it is assumed that new seafarers are hired at the age of 20, when licenses can be issued, and retire at the age of 70 defined by Equation [10]. New Seafarers $S_{crew,20,t}$ is the new potential seafarer $N_{crew,t}$ and is calculated as the minimum of the gap between seafarer supply and demand, defined by Equation [11]. New potential seafarers $N_{crew,t}$ is calculated using Equation [12], assuming that the number of potential new seafarers will decrease by 1% each year from the current number of 900, which is the number of new seafarers in Japan, taking into account the decline in Japan's population. $E(=0.01)$ is the seafarer retirement rate for each year. In this study, based on the number of seafarers in 2010, the initial values for seafarers are used, separated by age groups by one year of age. Equation [13] and [14] defines the actions of shipping companies with respect to the dismissal of seafarers. In this model, shipping companies are assumed that they lay off seafarers when the number of seafarers exceeds a certain ratio $\kappa(=1.1)$ of the current demand for seafarers. The model is set up so that when dismissing a seafarer, the older seafarers would be dismissed first.

$$S_{crew,age,t} = (1-E)S_{crew,age-1,t-1} - I_{crew,age,t}\ if\ (21 \le age \le 70) \quad [10]$$

$$S_{crew,20,t} = \min\{N_{crew,t}, (D_{crew,t} - S_{crew,t})\} \quad [11]$$

$$N_{crew,t} = 900 * \{1 - 0.01 * (t - 2010)\} \quad [12]$$

$$I_{crew,t} = \sum_{age}(S_{crew,age,t}) - \kappa D_{crew,t} \quad [13]$$

$$I_{crew,age,t} = max\left(0, I_{crew,t} - \sum_{i=0}^{70-age} S_{crew,70-i,t}\right) \quad [14]$$

Worker labor costs

The wage of workers is calculated as defined in Equations [15] and [16] from the effective job openings ratio (the gap between supply and demand for seafarers divided by the number of potential new seafarers) with reference to the Bank of Japan's past analysis (2017).

$$Q_t = 1 + 0.5\left(\frac{D_{crew,t} - S_{crew,t}}{N_{crew,t}} - 1\right) \quad [15]$$

$$W_{crew,t} = W_{crew,t-1}\left(1 + \frac{Q_t}{100}\right) \quad [16]$$

Vessel transportation expenditures

The multiple subcontracting structure of the Japanese transportation industry has become a problem because it leads to lower profit margins. In this study, we assume a "time-charter contract" as one of these employment types. In this type of employment, the shipowner pays operating costs such as crew costs and ship repair costs, as well as capital costs such as depreciation, and earns charter fees by leasing the ship to an operator who actually carries the cargo. The operator, on the other hand, rents the people and equipment necessary to operate the ship from the shipowner, and in addition pays voyage expenses such as fuel to actually transport the cargo. The operator's source of income is the freight charges from the shipper.

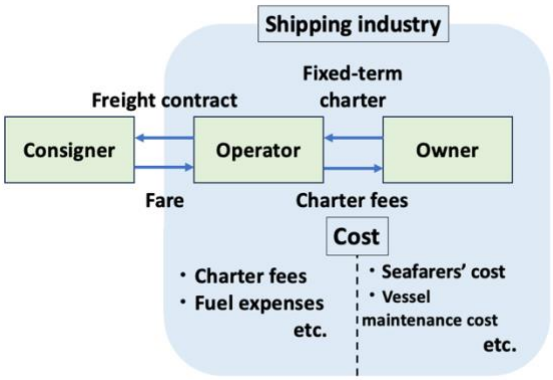

Figure 4: The market structure of Japanese coastal shipping (MLIT, 2020)

In this study, the cost to the owner was calculated with reference to the Maritime Industry Research Institute (2004). The operator's costs were calculated based on a survey by the Ministry of Land, Infrastructure, Transport and Tourism (2010). The following are the costs for each of the conventional sizes. Since only data for 199 GT, 499 GT, and 699 GT were available for the owner's costs, data for 799 GT and 5000 GT were prepared assuming that all costs except crew costs are proportional to the size of the vessel.

Table 5: The change of cost in each phase (MUNIN, 2015), (Dantas, 2023)

	existing ship	admission office	reinforced concrete reactor	CA	FA
capital cost	0	+7.5%	+15%	+10%	
freight costs	0				
fuel expenses	0		-5%		
harbor charges	0		+20%		
remote facility	0		Construction costs are $2,100 thousand. Maintenance costs are $874 thousand.		

There are also several possible costs that will increase or decrease with the autonomous vessels. Below is a summary of equipment costs that will vary with the introduction of autonomous vessels. The MUNIN report (2015) analyzes the costs associated with remote monitoring facilities to monitor autonomous vessels. It also points out the increased costs associated with port employees performing berthing tasks that would traditionally be performed by the crew. The cost of vessel construction is also expected to change. Various methods have been proposed in the past to estimate the cost of building a conventional ship (Caprace, 2009). Based on these methods, MUNIN (2015) and Dantas et al (2023) have estimated costs. Based on the above, this study has determined that the cost of transportation by ship is shown in the following Table 5.

Marine transportation revenues

Revenues from shipping $R_{ship,t}$ are calculate by freight rates $F_{ship,o,d,t}$. In this study, freight rates are calculated as in Equation [17] in a way that is consistent with the actual situation.

$$R_{ship,t} = F_{ship,t} \sum_{o,d} F_{ship,o,d,t} X_{ship,o,d,t} L_{ship,o,d} \quad [17]$$

Maritime transportation profit

Profit from shipping $H_{ship,t}$ is calculated as in Equation [18] from the difference between income $R_{ship,t}$ and expenditure $C_{ship,t}$.

$$H_{ship,t} = R_{ship,t} - C_{ship,t} \quad [18]$$

Shipping freight rates

In this study, shipping companies try to keep profit margins. In other words, freight rates fluctuate according to the shipping companies' costs. Using historical data (Maritime Industry Research Institute, 2004), the shipping company was set to maintain a 2% profit margin. Overall freight rates and standard overall freight rates calculated from J_{ship} and standard freight rates for each link $E_{m,o,d}$ (discussed below in Appendix), as shown in Equation [19].

$$F_{ship,o,d,t+1} = \frac{C_{ship,t} E_{m,o,d}}{J_{ship} \sum_{o,d} X_{ship,o,d,t} L_{ship,o,d}} \quad [19]$$

Automobile transport

Automation progress

Automation is being promoted not only in coastal shipping, but also in the automobile industry. Already in 2023, there have been demonstrations of Level 4 automated trucks on highways (unmanned operation under certain conditions) (LNEWS, 2023). In addition, the Japanese government's roadmap sets the goal of social implementation of Level 4 automated trucks at 2026 (MLIT, 2023a). Automated driving outside of expressways will be available after 2026, but in terms of modal shift to and from marine transportation, the modal shift in automobile transportation is mainly for long-distance transportation, and

many of them use expressways. Therefore, we assumed that the demand for transportation will change with shipping due to automation on highways, and that the introduction rate of automated trucks will increase linearly between 2026 and 2060.

Number of trucks

Truck demand at time t $D_{truck,t}$ is calculated from the ton-kilometer-based transportation demand calculated and weekly transport volume per vehicle β_{truck} (All Japan Trucking Association, 2010) as defined in Equation [20].

$$D_{truck,t} = \left\lceil \frac{\sum_{o,d} X_{truck,o,d,t}\, d_{truck,o,d}}{\beta_{truck}} \right\rceil \quad [20]$$

In addition, the supply of trucks $S_{truck,t}$ The supply of trucks is assumed to be equal to the demand as shown in Equation [21] because the number of trucks produced is large and the lead time of production is small, so the supply can be changed flexibly in response to fluctuations in demand.

$$S_{truck,t} = D_{truck,t} \quad [21]$$

Number of truck drivers

In this study, we assumed that the proportion of trucks $S_{truck,t}$ and the number of drivers is not likely to change. In addition, the results of a comparison of the number of trucks and drivers using historical data (All Japan Trucking Association, 2022) are shown that the number of drivers per vehicle has not changed significantly over the last eight years. Therefore, as shown in Equation [22], B_{driver} drivers are needed per vehicle $(B_{driver} = 0.60)$.

$$D_{driver,t} = S_{truck,t} B_{driver} \quad [22]$$

In addition, there are fewer barriers for people to obtain a license to drive trucks. Although a license is certainly required to transport medium-sized or larger trucks, the demand for small truck drivers is also high, so we assumed that supply and demand would almost balance, as in the case of the number of trucks, as in Equation [23], and that demand and supply $S_{driver,t}$, as in the case of the number of trucks.

$$S_{driver,t} = D_{driver,t} \quad [23]$$

Trucking expenditures

Trucking expenditures are calculated from the number of trucks and the number of drivers. In this study, per-vehicle costs were calculated based on data from the All Japan Trucking Association (2022), and costs were divided into four major categories: labor, fuel, insurance, and other vehicle-related costs. In addition, the variation in transportation costs when automated technology is implemented. Lee et al. (2023) conducted a cost analysis of the implementation of automation technology in 1-ton trucks. With reference to those analyses, this study established the costs of automobile transportation as shown in Table 6.

Table 6: The change of cost of trucking

	Conventional (thousand yen)	Autonomous (thousand yen)
personnel expenses	1.25 Wages	0.125 Wages
fuel expenses	246	196.8
insurance premium	41	36.9
Other expenses related to the vehicle	775	775

Trucking fare

Trucking freight rates $F_{truck,o,d,t}$ is the cost to maintain a profit margin similar to that of shipping companies. In this study, the formula was set up as shown in Equation [24], assuming that the profit margin is kept at 2% with reference to past data (All Japan Trucking Association, 2022).

$$F_{truck,o,d,t+1} = \frac{C_{truck,t} E_{truck,o,d}}{J_{truck} \sum_{o,d} X_{truck,o,d,t} L_{truck,o,d}} \quad [24]$$

3. CASE STUDY

Case study subject

The purpose of this study is to analyze how coastal shipping can introduce automation technology that is desirable from the perspective of employment and economics while maintaining shipping capacity in a market that includes complex interactions between freight rates, transportation demand, and other factors. Therefore, the case study will focus on which stage of automation to choose when building a ship.

Case study settings

With regard to the strategy for introducing automation technology, the roadmap created by AUTOSHIP, as mentioned earlier in Section 2, aims to develop automation technology in four phases. In this study, assuming that the development of automation technology will proceed according to the roadmap, whether or not shipping companies will start introducing automation technology when vessels in each phase are ready for introduction is defined in Figure 5 divided into Strategy 1 to 16. as follows. Furthermore, these strategies are divided into Group 1 through Group 4 based on the introduction of CA and FA.

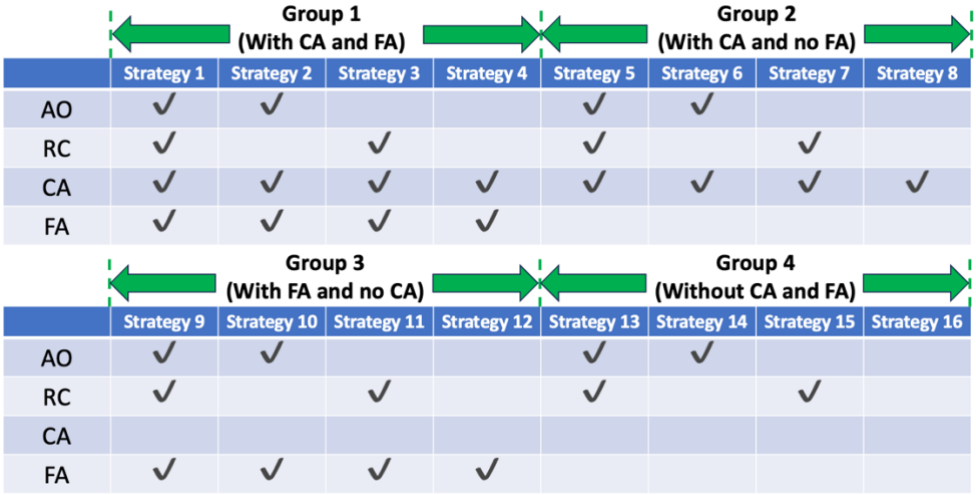

Figure 5: The strategy of deploying automated technology

In addition, three scenarios of future demand for freight transportation were considered: "demand will increase," "demand will remain unchanged," and "demand will decrease". The three scenarios were developed as shown in Table 7.

Table 7: Total transportation demand assumptions for each scenario

scenario	Description.
Scenario A	Total transport demand increases by 0.5% per year
Scenario B	Aggregate demand for transportation does not change
Scenario C	Total transport demand decreases by 0.5% per year

Results and Discussions

The results of the case study described in the previous part are presented below. The scatter plot shows the cumulative percentage of seafarers who retired early due to the oversupply of seafarers [%] on the horizontal axis, the percentage of lost transportation opportunities [%] due to the shortage of seafarers on the vertical axis. The lower right of the graph is the preferred result because the cumulative percentage of seafarers who retire early is smaller, and the cumulative transportation opportunity loss percentage is also smaller. Also, the bar plot shows the cumulative cost [yen/ton-kilometer] on a ton-kilometer basis for shipping companies calculated using a discount rate of 3% in the marker color for simulation results for 2025 to 2070 when automated technologies can be introduced.

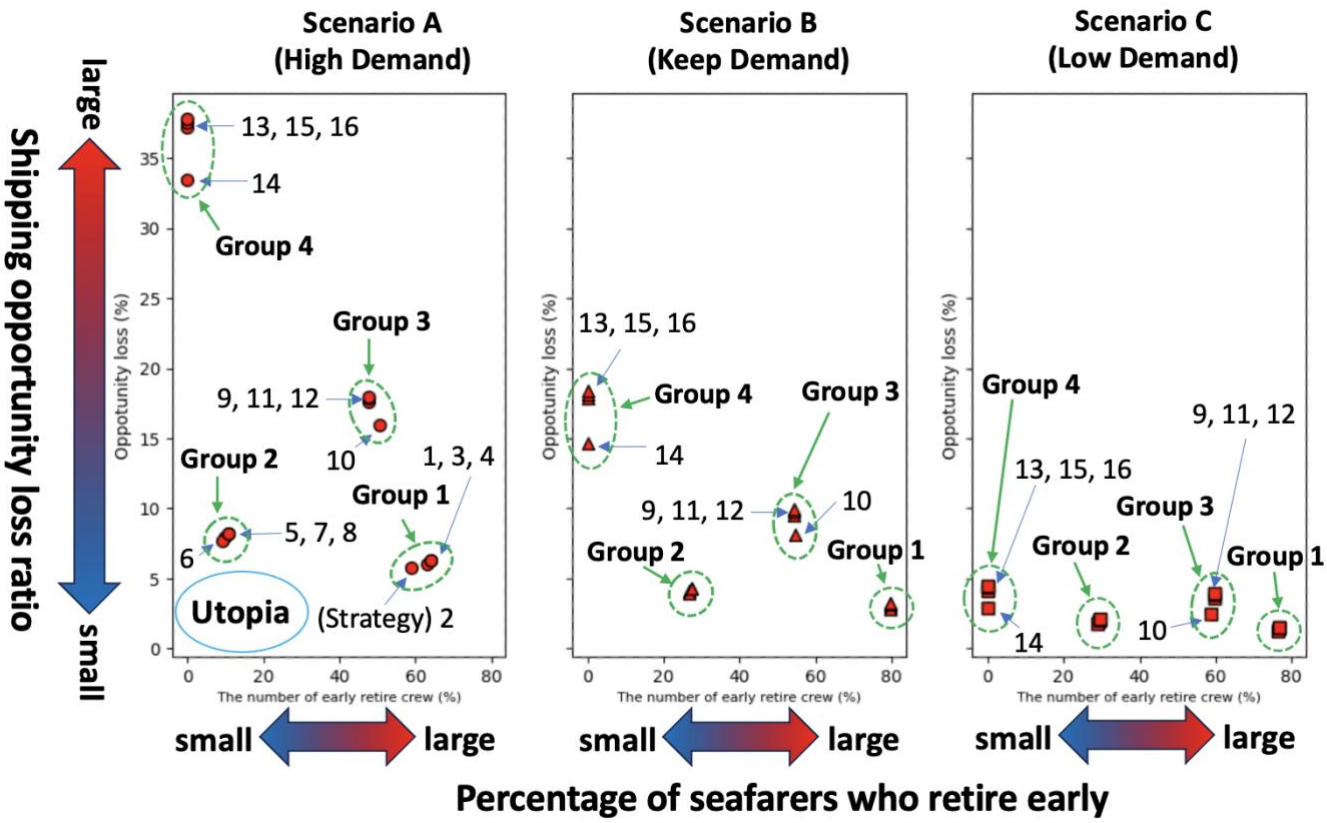

Figure 6: The results by case in Model A

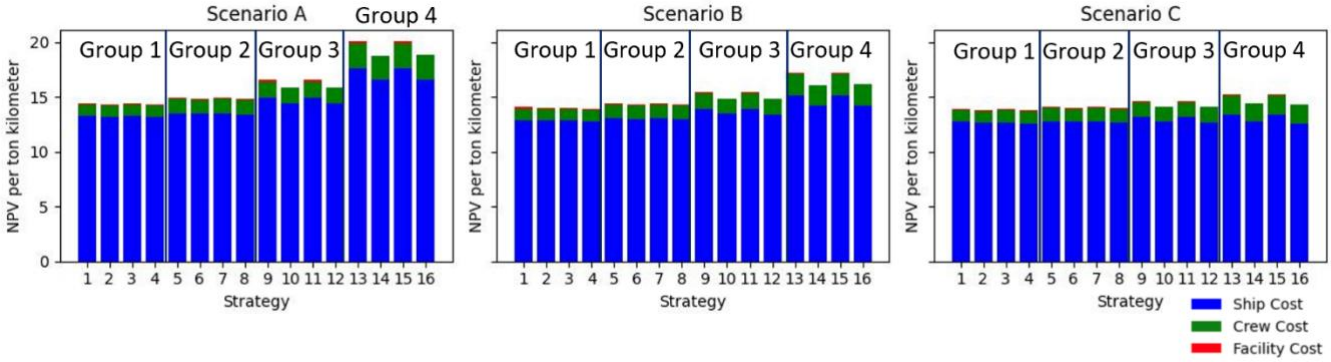

Figure 7: The results by case in Model A

Table 8: The influence of each technology

	Retirement of seafarers	Opportunity loss	Shipping cost
AO	+ (in most cases)	+	+
RC	almost zero	almost zero	—
CA	——	++	++
FA	—— (when used with CA, —)	++ (when used with CA, +)	++ (when used with CA, +)

・"+" means positive influence and "—" means negative influence.
・The number of icons represents the size of influence.

From the assumptions of this research, these results can be divided into four Groups, and it can be read that the impact of the introduction of CA and FA is significant. A comparison of each of these groups shows that Group 3 is completely inferior to

Group 2, while Group 1, 2, and 4, are in a trade-off relationship, with no strategy superior to the other strategies in all indicators, indicating that the decision to introduce automation technology is difficult. The overall result of the three indicators shows that as the total demand for transportation increases, the strategy that does not introduce autonomous ships significantly increases “Shipping opportunity loss ratio” and “NPV cost per ton kilometer”, indicating the superiority of Group 2 that only introduces CA in these scenarios, while in the scenario where the total demand for transportation decreases, the strategy that only introduces autonomous ships is superior to Group 2. In the scenario where the total demand for transportation decreases, Group 4, which does not introduce autonomous vessels, shows a smaller difference in the two indicators, indicating that the demand for introducing autonomous vessels in this scenario is small.

In the following parts, we will discuss in detail the impact of the introduction of automation on each of these indicators.

Retirement of seafarers

1) The impact of deploying CA and FA is larger than that of deploying AO and RC, and these results are divided into four groups.
2) The ratio of early retired seafarers increases with the introduction of CA and FA regardless of the scenario of the transport demand, while the introduction of AO has reduced the percentage of early retired seafarers in most cases.
3) The number of early retired seafarers fluctuates with changes in total transportation demand, but not monotonically.

In discussing these results, we use Figure 8, a graph on the supply-demand gap for seafarers, with positive values on the y-axis indicating a shortage of seafarers and negative values indicating a surplus of seafarers. At the same time, the x-axis represents the year. In Figure 8, Strategy 1 is used to represent Group 1, Strategies 6, 7 and 8 to represent Group 2, Strategy 12 to represent Group 3, and Strategy 16 to represent Group 4. And to evaluate the impact of the introduction of AO, and Strategy 7 to evaluate the impact of the introduction of RC by comparing Strategy 7 and Strategy 8. It is clear from these comparisons that the introduction of CA and FA has significantly changed the supply and demand for seafarers, indicating the magnitude of the impact of the introduction of CA and FA as described in 1).

Regarding 2), the introduction of CA and FA has caused an excess of seafarers. Figure 8 shows that the introduction of FA without CA has caused a temporary large overcrowding of seafarers due to the rapid alleviation of the seafarer shortage. Comparing Strategy 6 and Strategy 8 for the introduction of AO, the number of seafarer shortages during the period when a seafarer shortage is occurring is mitigated by a decrease in the demand for seafarers per vessel. At the same time, the reduction in the number of seafarers employed in the cases where AO was introduced due to the reduction in the seafarer shortage also alleviated the seafarer surplus during the period after the seafarer shortage was resolved.

With regard to 3), the percentage of early retired seafarers is expected to decrease as the demand for transport increases because the demand for seafarers also increases, but no significant change was observed between Scenario B, where the demand for transport is maintained, and Scenario C, where the demand for transport decreases (Figure 6). The simulation results indicate that when transport demand declines, shipping companies hire fewer new seafarers, which reduces the supply of seafarers, and as a result, the number of seafarers who retire early also declines. However, there is a slight difference in the trend between policies, suggesting that changes in transport demand affect the environment of seafarers’ employment.

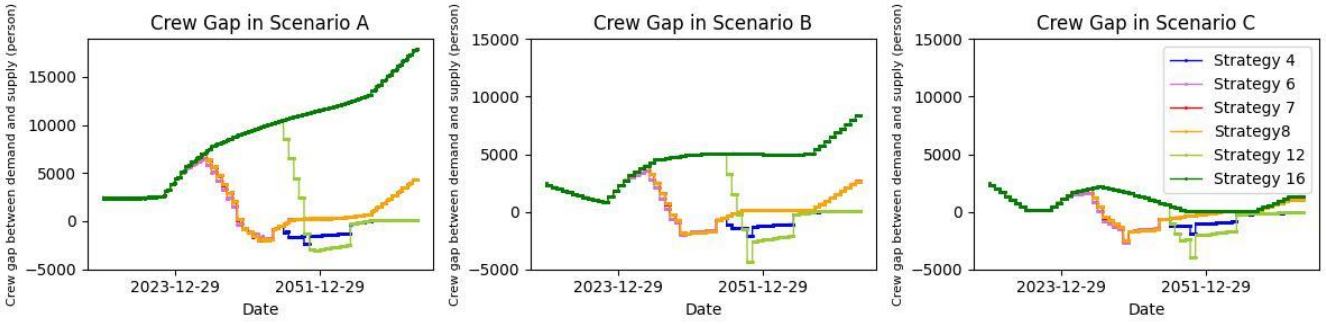

Figure 8: The difference between the supply and demand of seafarers in each case

Opportunity loss

1) Under different total transportation demand scenarios, the opportunity loss rate increases with an increase in total transportation demand.
2) Groups 1, 2, and 3 with autonomous technology successfully reduce the impact of the increasing total transportation demand compared to Group 4 without autonomous technology.

3) With respect to the introduction of AO and RC, both reduced “Opportunity loss”, but the impact was less than that of CA and FA. The reduction in Opportunity loss due to AO implementation can be read from the Figure 6 in most cases, while the reduction due to RC implementation was very small.

Figures 9 and 10 are used to discuss these results. In both graphs, the horizontal axis represents years and shows the results for each scenario in Strategy 1. The left graph in Figure 9 shows the volume transported by coastal shipping, while the middle graph shows the difference between supply and demand for seafarers, as discussed in Figure 8. Finally, Figure 10 shows the number of seafarers in each age group.

As can be read from the middle graph in Figure 8, before the introduction of autonomous vessels such as CA and FA, the shortage of seafarers accelerated as total transport demand increased. This is due to the aging of seafarers in Japan's coastal shipping industry, which is resulting in the retirement of currently elderly seafarers on a large scale (Figure 9). This shortage of seafarers is causing the drop in coastal shipping volumes seen through the second half of 2020, as seen in the left graph in Figure 8, and leads to the result in 1), "As total transportation demand increases, the proportion of lost transportation opportunities due to the shortage of seafarers increases.

In addition, as described in 1), the shortage of seafarers accelerates in line with the increase in total transportation demand before the introduction of CA and FA autonomous vessels, while the supply-demand balance for seafarers after the introduction of CA and FA does not differ significantly between scenarios (Figure 8), indicating the benefits of introducing autonomous vessels, especially in a scenario where total transportation demand increases, as described in 2).

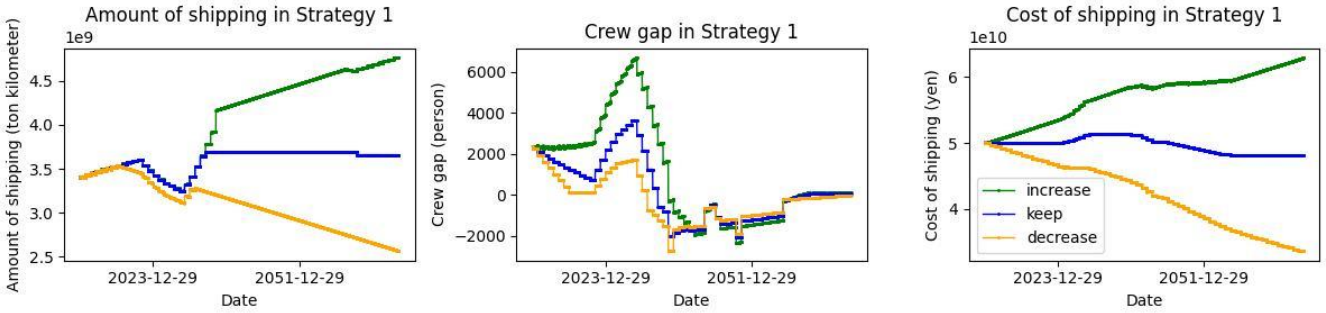

Figure 9: Shipping volume, crew gap, and shipping costs of Strategy 1 under each scenario.

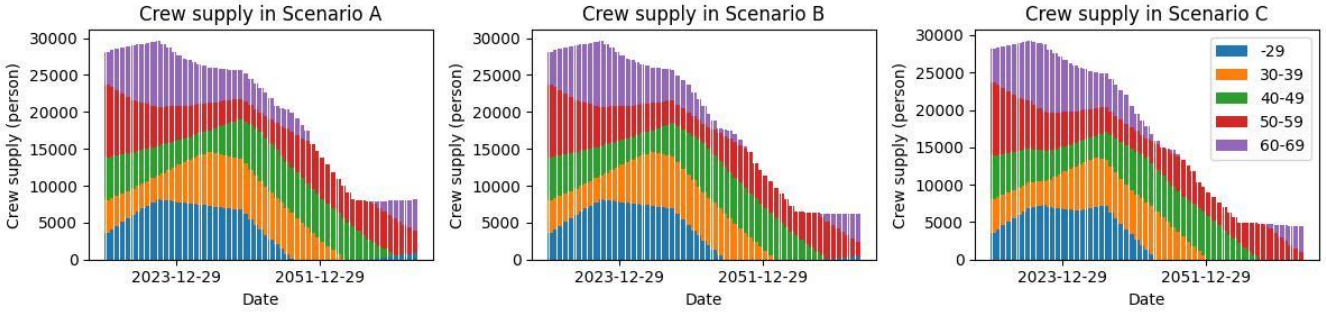

Figure 10: Change in the number of seafarers in Strategy 1 under each scenario.

Shipping cost

1) Except AO and RC, the deployment of autonomous technology helps shipping companies to reduce their shipping cost.
2) Under different total transportation demand scenarios, the transportation cost increase with an increase in total transportation demand.
3) As opportunity loss, Groups 1, 2, and 3 with autonomous technology successfully mitigate the impact of the increase compared to Group 4 without autonomous technology.

Firstly, 1): the impact of each strategy on costs is discussed. Figure 11 shows the costs for each of all transportation demand scenarios. The results show that for all transport demand scenarios, the impact of automation technologies other than FA on pure costs was not significant. However, the introduction of AO and RC increases costs, while the introduction of CA slightly decreases costs, and the introduction of FA significantly decreases costs. However, the difference between Strategies when comparing costs based on the volume of transportation activity is due to the increase in the volume of transportation due to

the introduction of automation technology, which will alleviate the labor shortage. This effect for AO results in the cost increase due to the introduction of AO almost offsetting the increase in transport volume, while for CA and FA, the increase in transport volume results in a significant decrease in cost per transport volume on a ton-kilometer basis.

As for 2), as can be read from Figure 8, the greater the scenario of aggregate demand for transport, the more the shortage of seafarers accelerates, resulting in higher wages for seafarers. Figure 6 shows that this effect raises the labor cost of seafarer wages, resulting in higher costs. However, even in scenarios where demand increases, the introduction of autonomously operated vessels has succeeded in mitigating the adverse effects, as mentioned in 3) and like “Opportunity loss” 2).

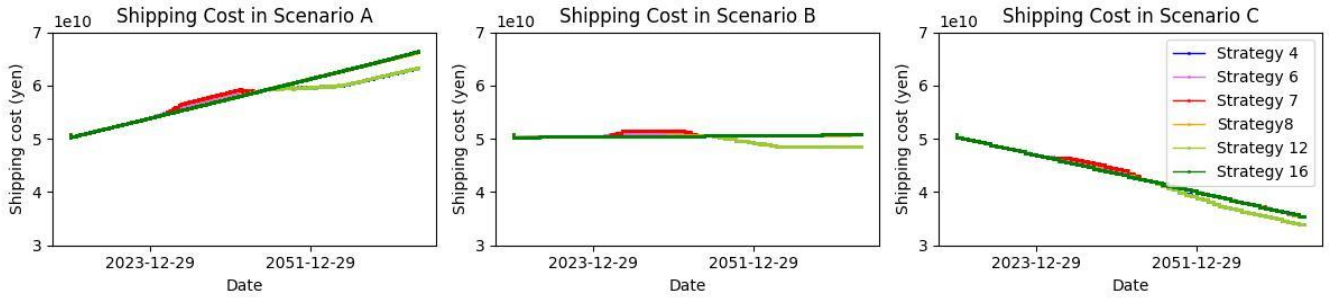

Figure 11: Transportation costs in each case.

4. SUMMARY

The following findings were obtained from Section 3 in the assumption of this research.

・While the introduction of autonomous vessels reduced transportation costs and lost transportation opportunities, the number of early retired seafarers increased significantly with their introduction. At the same time, the introduction of automation technology to support navigation has had a positive impact in many cases, and there are advantages to early deployment even in this model, which does not consider the experimental introduction of new technology to promote technology maturity.

・In the case where automation technology was introduced, a case with RC (Remote Control) was inferior to strategy without RC in all three indicators and in the transportation demand scenario. However, the other policies had a trade-off relationship with each other on one of the indicators, so it was not possible to conclude which strategy was better.

・The current Japanese domestic logistics transportation mode choice has low sensitivity to freight rates, and the decrease in transportation demand due to higher freight rates is smaller than the increase in freight rates, making higher freight rates one effective means for shipping companies to pursue profits.

5. CONCLUSION

In this study, we developed a simulator based on a Japanese cargo transport model and proposed a method to evaluate the impact of introducing automation technology. The results of the simulation showed changes in the impact of several policies on the economics and employment of seafarers and provided decision-making support for shipping companies on the introduction of desirable automation technology.

ACKNOWLEDGEMENT

This research was made possible by the support of many people, and I would like to take this section to thank them. First, I would like to thank the Ph.D., M.S., and undergraduate students of this laboratory for their various advice in my research activities. Thank you very much. Second, I would like to thank the technical specialists and secretaries of this laboratory for their generous support in the procurement of research equipment, administrative procedures, schedule coordination, and so on. I would like to express my sincere gratitude to them.

AUTHOR CONTRIBUTION

Author 1: Conceptualization; methodology; writing – review & editing.
Author 2: Conceptualization; data curation; investigation; methodology; software; writing – original draft.
Author 3: Writing – review & editing.

References

Akbar, A., Aasenn, A. K. A., Msakni, M. K. et al. 2019. An Economic Analysis of Introduction Autonomous Ships in a Short- Sea Liner Shipping Network. International Transactions in Operational Research. 28(4). 1740-1764.

All Japan Trucking Association. 2010. Survey Report on Freight Rates and Costs at the Truck Transportation Board (in Japanese). URL: https://www.mlit.go.jp/common/000167957.pdf. (Access on 28 December 2023).
All Japan Trucking Association. 2022. Japan's Truck Transportation Industry Current Situation and challenge (in Japanese). URL: https://jta.or.jp/wp-content/themes/jta_theme/pdf/yusosangyo2022.pdf. (Access on 28 December 2023).
Bank of Japan. 2017. Outlook for Economic and Price Trends (in Japanese). URL: https://www.boj.or.jp/mopo/outlook/box/data/1707BOX1a.pdf. (Access on 28 December 2023).
Bellingmo, P. R., Wille, E., Nordahl, H., et al. 2023. Analyzing the Feasibility of an Unmanned Cargo Ship for Different Operational Phases, TransNav the International Journal on Marine Navigation and Safety of Sea Transportation, 17(2).
Caprace, J. D., Rigo, P. 2009. Multi-Criteria Decision Support for Cost Assessment Techniques in Shipbuilding Industry. URL: https://orbi.uliege.be/bitstream/2268/9967/1/03_Caprace.pdf.
Dantas, J. L. D., Theotokatos, G. 2023. A framework for the Economic – Environmental Feasibility Assessment of Short – Sea Shipping Autonomous Vessels. Ocean Engineering. 279(114420).
Kooji, C., Hekkenberg, R. 2021. The Effect of Autonomous
Kretschmann, L., Burmeister, H. C. 2017. Analyzing the Economic Benefit of Unmanned Autonomous Ships: An Exploratory Cost – Comparison between an Autonomous and a Conventional Bulk Carrier. Research in Transportation Business & Management. 25. 76-86.
IMO. 2018. IMO Takes First Steps to Address Autonomous Ships. https://www.imo.org/en/MediaCentre/PressBriefings/Pages/08-MSC-99-MASS-scoping.aspx#:~:text=For%20the%20purpose%20of%20the,operate%20independently%20of%20human%20interaction.&text=Fully%20autonomous%20ship%3A%20The%20operating,and%20determine%20actions%20by%20itself. (Access on 28 December 2023).
Japan Shipping Association. 2013. Domestic Distance Table.
Lee, S. Cho, K., Park, H. et al. 2023. Cost-Effectiveness of Introducing Autonomous Trucks: From the Perspective of the Total Cost of Operation in Logistics.
LNEWS. 2023. Aiming to Autonmate Truck Transportation with Self-Driving Trucks in 2026 (in Japanese). URL: https://www.lnews.jp/2023/08/p0829406.html. (Access on 28 December 2023).
Maritime Industry Research Institute. 2004. Coastal Shipping Cost Analysis Study Group Report (in Japanese). URL: http://www.e-naiko.com/kaiun_data/scale.pdf. (Access on 28 December 2023).
MLIT (Ministry of Land, Infrastructure, Transport and Tourism). 2000. Current Status of Inward Cargo Transportation (in Japanese). URL: https://www.mlit.go.jp/hakusyo/kaijireport/kaihaku00/kaihaku00-12.pdf. (Access on 28 December 2023).
MLIT (Ministry of Land, Infrastructure, Transport and Tourism). 2010. Operator-Owner Cost Structure (in Japanese). URL: https://www.mlit.go.jp/common/001012639.pdf. (Access on 28 December 2023).
MLIT (Ministry of Land, Infrastructure, Transport and Tourism). 2016. Current Situation in Coastal Shipping (in Japanese). URL: https://www.mlit.go.jp/sogoseisaku/transport/sosei_transport_fr_000074.html. (Access on 28 December 2023).
MLIT (Ministry of Land, Infrastructure, Transport and Tourism). 2019. Workplace Reforms for Coastal Seafarers (in Japanese). URL: https://www.mlit.go.jp/common/001226206.pdf. (Access on 28 December 2023).
MLIT (Ministry of Land, Infrastructure, Transport and Tourism). 2020. Types of Employment in Coastal Shipping (in Japanese). URL: https://www.mlit.go.jp/common/001328224.pdf. (Access on 28 December 2023).
MLIT (Ministry of Land, Infrastructure, Transport and Tourism). 2021. Current Situation of Seafarers (in Japanese). URL: https://www.soumu.go.jp/main_content/000727908.pdf. (Access on 28 December 2023).
MLIT (Ministry of Land, Infrastructure, Transport and Tourism). 2022. National Freight Forward Flow Survey (in Japanese). URL: https://www.mlit.go.jp/sogoseisaku/transport/sosei_transport_fr_000074.html. (Access on 28 December 2023).
MLIT (Ministry of Land, Infrastructure, Transport and Tourism). 2023a. Initiatives for Utilizing Self-Driving Cars, ets. That Contribute to Solving Social Issues (in Japanese). URL: https://www.mlit.go.jp/policy/shingikai/content/001623770.pdf. (Access on 4 January 2024).
MLIT (Ministry of Land, Infrastructure, Transport and Tourism). 2023b. Freight / Passenger Regional Flow Survey (in Japanese). URL: https://www.mlit.go.jp/k-toukei/kamoturyokakutiikiryuudoutyousa.html. (Access on 4 January 2024).
MUNIN. 2015. D9.3: Quantitative Assessment. URL : https://www.unmanned-ship.org/munin/wp-content/uploads/2015/10/MUNIN-D9-3-Quantitative-assessment-CML-final.pdf. (Access on 28 December 2023).
Nakashima, T., Moser, B., Hiekata, K. 2023. Accelerated Adoption of Maritime Autonomous Vessels by Simulating the Interplay of Stakeholder Decisions and Learing. Technological Forecasting & Social Change. 194. 122710.
Nordahl, H., Rødseth, J. Ø., Nesheim, D. A. et al. 2023. AUTOSHIP [D8.2] Roadmap for Autonomous Ship Adoption and Development. URL: https://www.researchgate.net/publication/369657905_AUTOSHIP_D82_Roadmap_for_Autonomous_ship_adoption_and_development. (Access on 28 December 2023).
Shinke, T., Ishida, T., Abe, H. 2007. Effects of Modal-Shift Policies on the Reduction of Carbon Dioxide Emissions from Freight Transportation in Japanese Prefectures (in Japanese), Studies in Regional Science. 37(4). 1079-1096.
The Japanese Shipowners' Association. 2021. SHIPPING NOW2020-2021. URL: https://www.jpmac.or.jp/img/relation/pdf/2020pdf-p46-49.pdf. (Access on 28 December 2023)

The Nippon Foundation. 2022. Unmanned Ships are Expected to be Put to Practical Use in 2025 by Bringing Together the Latest Technology: How will the Future of the Sea Change? (in Japanese). URL: https://www.nippon-foundation.or.jp/journal/2022/71652. (Access on 28 December 2023).

A. Appendix

Transportation choice model

Various models of transportation mode choice have been studied. Typical examples include the logit model and the sacrifice quantity model. In this study, the logit model was employed to express the interaction between each transportation mode and the equilibrium that results from the interaction. In addition, many studies on modal shifts take a wide area as the target region or limit the routes to be covered, however, we wanted to create a model that covered the entire country. Therefore, this study calculates utility based on time and cost with reference to the study by Shinke et al (2007). In this study, 47 prefectures are considered as nodes, and the links connecting these nodes are treated as a transportation network.

Transportation distance for each transportation agency

Regarding transport distances, the transport distances for coastal shipping are listed in the domestic shipping distance table published by the Nippon Kaiun Syukaijyo (2013). The distance between representative ports in each prefecture was used as a shipping distance. For automobiles and railroads, Google Map was used, and distances between prefectural offices were used. Transportation distances within the same prefecture were calculated from transportation time and average speed using the average speed described below. For links for which transport time data was not available, the average transport distance within the same prefecture was used. Also, National Freight Forwarding Survey (MLIT, 2022) and the distances collected in the above method were used to calculate transport volume on a ton-kilometer basis, and the transport volume calculated by the Ministry of Land, Infrastructure, Transport and Tourism (MLIT, 2023b). A discrepancy was observed when two statistics were compared. Therefore, we adjusted the transport distances for each transportation mode by multiplying them by a constant in order to match the latter transport volume. The following are the transport distances for each transport mode. Inland shipping links with no ports are indicated by 0.

Transportation time for each transportation agency

Comparing transport times in 2005, 2010, and 2015 collected from the Logistics Census (MLIT, 2022) with the transport distances, there is a proportional relationship between transport distance and transport time for coastal shipping and rail transport, while transport time for automobile transport increases slowly as the distance increases. Therefore, in this study, the transport m from node o to node d, $T_{m,o,d}$ is calculated using the following Equations [A1] ~ [A3]. They are calculated using $L_{m,o,d}$ and average transport speed v_m for ocean and rail transport, and the square root of transport distance and parameters γ_{truck} and δ_{truck} for automobile transport. For auto transport, we used the minimum transport time in the 2005, 2010, and 2015 data because in some cases the transport distances were small, and the time was negative.

$$T_{ship,o,d} = \frac{L_{ship,o,d}}{v_{ship}} \quad [A1]$$

$$T_{rail,o,d} = \frac{L_{rail,o,d}}{v_{rail}} \quad [A2]$$

$$T_{truck,o,d} = \gamma_{truck}\sqrt{L_{truck,o,d}} + \delta_{truck} \quad [A3]$$

Fares for each mode of transportation

Comparing freight rates per ton-kilometer for 2005, 2010, and 2015 obtained from the Logistics Census (MLIT, 2022) and the transport distance, it can be said that freight rates per unit ton-kilometer decrease with increasing transport distance for all transport modes. Therefore, as well as the transport time, the fare of transport m from node o to node d, $E_{sm,o,d}$ is calculated by the following Equations [A4] ~ [A6], respectively $L_{m,o,d}$ and the parameters ε_m, θ_m. Note that when calculating freight rates, negative values may be obtained due to long transport distances, in which case the lowest freight rates from the 2005, 2010, and 2015 data were used.

$$E_{ship,o,d} = \varepsilon_{ship}\sqrt{L_{ship,o,d}} + \theta_{ship} \quad [A4]$$

$$E_{rail,o,d} = \varepsilon_{rail}\sqrt{L_{rail,o,d}} + \theta_{rail} \quad [A5]$$

$$E_{truck,o,d} = \varepsilon_{truck}\sqrt{L_{truck,o,d}} + \theta_{truck} \quad [A6]$$

Parameter optimization of logit model

When optimizing the parameters, in the National Net Freight Flow Survey (MLIT, 2023b), there were some routes that did not have any transportation performance. Since this study focuses on the variation in transportation demand among transportation agencies, the parameters are divided among the cases of "routes with a track record of transportation by coastal shipping and a track record of transportation by rail or trucks", "coastal shipping & automobiles & rail". In this case, the amount of transportation may be biased toward one mode of transportation on a particular route, and modal shift is unlikely to occur on that route due to the large dominance of that particular transportation agency. Therefore, the case classification of routes is defined as follows.

・Coastal & Automobile & Rail": Ratio of coastal shipping, automobile, and rail transportation to all transportation is 0.1 or more.
・Coastal & Automobile": Ratio of coastal shipping and automobile transportation is more than 0.1 and that of rail transportation is less than 0.1.
・Coastal & Automobile": Ratio of coastal shipping and automobile transportation is more than 0.1 and that of rail transportation is less than 0.1.
・"Coastal & Rail": characteristics of each link based on the definition of a transport ratio of more than 0.1 between coastal and rail transport and less than 0.1 between car transport.

Freight and Passenger Regional Flow Surveys (MLIT, 2023b) in 2005, 2010 and 2015 were used to determine the characteristics of each link. For parameter optimization, the 2005, 2010, and 2015 national freight net flow surveys (MLIT, 2022). freight hours, fare per ton-kilometer were used. The results are shown in Table A-1 below.

Table A-1 Parameters of the logit model in each case

＼parameter case	α_{time}	α_{cost}	α_{rail}	α_{truck}
Coastal & Automobile & Railroad	$-1.02 * 10^{-2}$	$-1.24 * 10^{-5}$	$-6.87 * 10^{-1}$	$-7.34 * 10^{-1}$
Coastal & automobile	$3.27 * 10^{-3}$	$-2.00 * 10^{-6}$	$-5.12 * 10^{-1}$	0
Coastal Shipping & Railroad	$4.95 * 10^{-3}$	$-2.20 * 10^{-6}$	0	$1.27 * 10^{-2}$

Using the parameters obtained, the 2010 Freight and Passenger Regional Flow Survey (MLIT, 2023b) to predict the data. The obtained ton-kilometer-based transport volumes are shown in Table A-2 shows that 15~30% of the total transport volume is subject to modal shift.

Table A-2 Comparison of predicted and measured values on a ton-kilometer basis

		coastal shipping	automobile	railroad
Measured value		179,898	20,398	246,175
Predicted value	whole	162,122	22,750	271,231
	fixed content	114,504	15,617	231,417

Model with greater impact by transportation cost (Model B)

The previous part discussed the impact of automation technology on shipping companies. However, in the freight transportation demand estimation model within the simulator, the impact of the cost term was small, and transportation demand did not change much in response to changes in freight transportation costs and associated changes in freight rates. This may be due to a lack of explanatory variables, the limited impact of freight rates on the Japanese freight market, or other factors. The model reflects the impact of freight rate changes on transportation demand by setting the parameters in the cost term to the same order as the parameters in the constant term. This new model is called Model B and the previous one is called Model A thereafter.

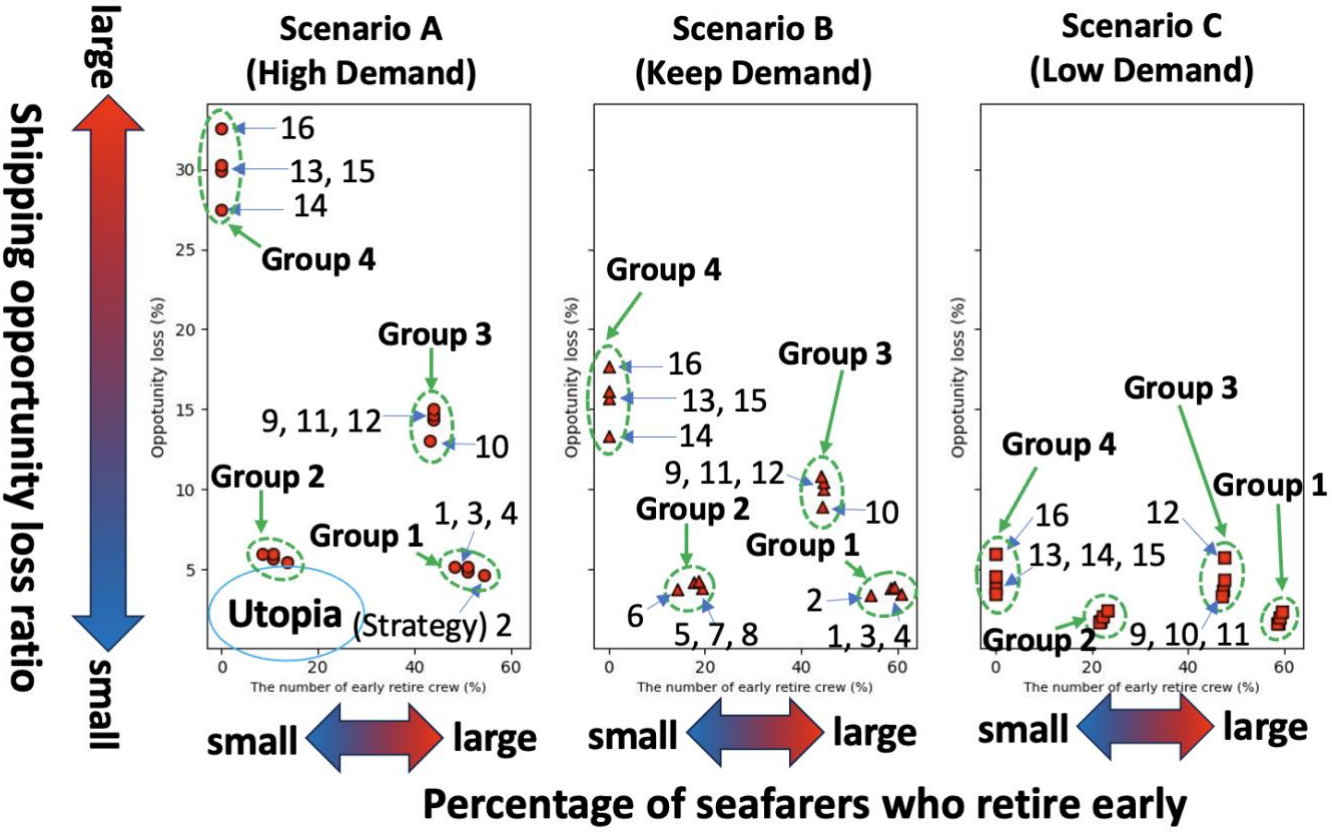

Figure 12: The results by case in Model B

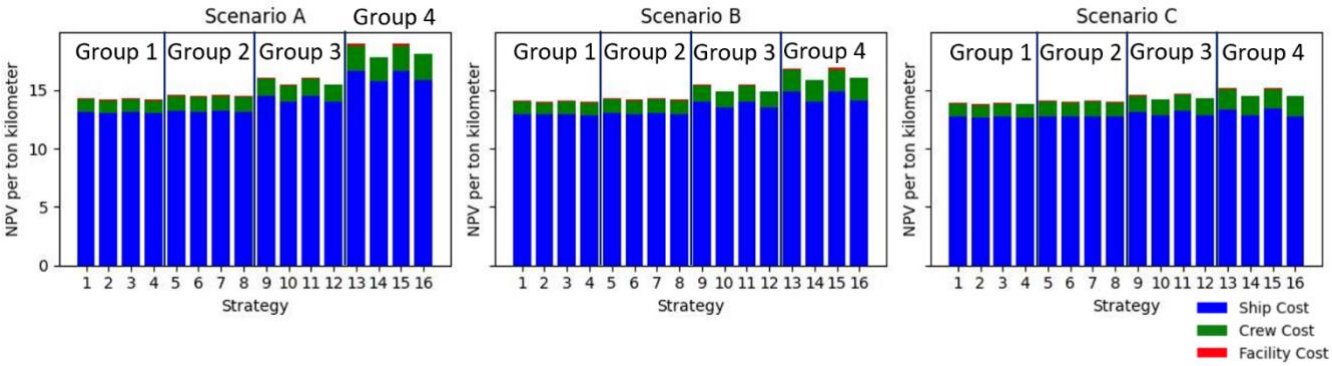

Figure 13: The results by case in Model B

The general shape of the results for Model B (Figure12, 13) was similar to Model A (Figure 6, 7). However, some differences were observed. In Groups 1, 2, and 3 with CA or FA, Scenario B, where transport demand is maintained, and Scenario C, where it decreases, the case with AO only has smaller values for all three indicators than the cases with both AO and RC. In comparison with the case with neither AO nor RC, the case with only AO showed smaller values for the loss of transport opportunities and the ratio of early retired seafarers, but only for the NPV of transport costs in the case with neither AO nor RC. On the other hand, in Scenario A, where total transportation demand increased, the case with AO only, the case with both AO and RC, and the case with RC only were compared, and the case with AO only showed smaller transportation cost and opportunity loss ratio, but the case with AO only showed smaller NPV in the ratio of early retired crews. However, the percentage of seafarers who retired early was higher in the AO-only case.

These results show that when total transport demand is maintained or decreases, AO implementation benefits shipping companies in all three indicators, but when total transport demand increases, AO implementation adversely affects shipping companies only in terms of seafarer employment.

Initially, as a consideration of the improvement in transportation costs due to the introduction of AO that was seen in the results of Model B but not seen in the results of Model A. This phenomenon is caused by a decrease in demand for marine transportation and seafarers is triggered by the increase in costs due to the introduction of AO (Figure 14). This is a decrease not seen much in the Model A due to the smaller impact of the cost term (Figure 15). The timing of this decline coincides with the retirement of seafarers currently aged 60 and over, as discussed before, causing a shortage of seafarers, which combined with the effect of the reduction in seafarer demand per vessel due to the introduction of AO, alleviates the seafarer shortage. This, in turn, is thought to have reduced the cost of shipping per ton-kilometer by reducing the rising labor costs of seafarers.

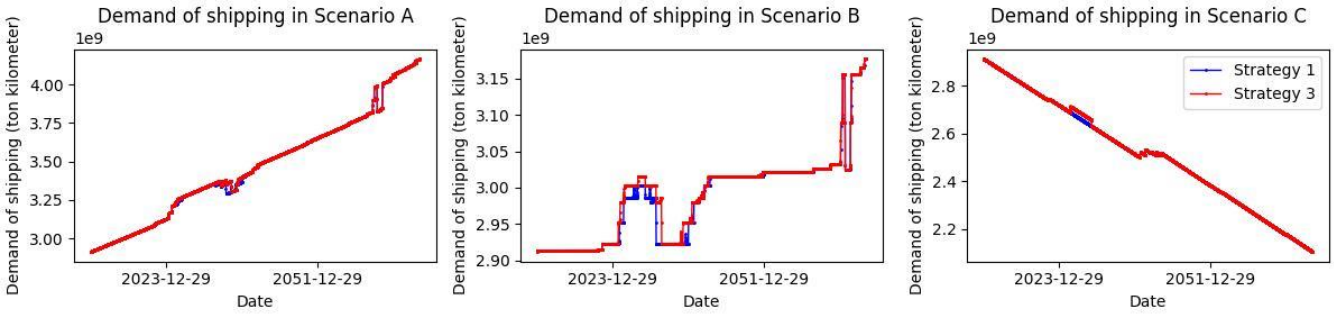

Figure 14: Result of shipping demand in Model B.

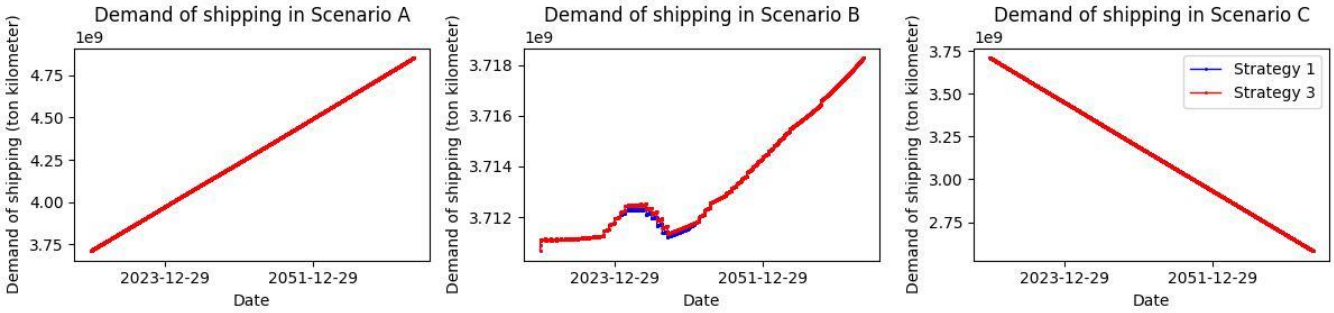

Figure 15: Result of shipping demand in Model A.

The next part discusses the cases in Model B where the introduction of AO has a positive impact on seafarer employment in scenarios where aggregate transport demand is maintained (Scenario B) or reduced (Scenario C), and where the introduction of AO has a negative impact in scenarios where aggregate transport demand is increased (Scenario A). In Model A, the introduction of AO had a positive impact on seafarer employment in all scenarios. This is one of the advantages of phasing in automation technology. Furthermore, as discussed in the previous part, the percentage of early retired seafarers decreased when aggregate transport demand increased, but there was no significant difference in the percentage of Scenario B and C. In Model B, the latter phenomenon is confirmed, but the former phenomenon, in which the ratio of early retired seafarers improves as aggregate demand increases, is not observed in the case where AO is introduced.

One factor contributing to this is that the recruitment of seafarers is done on an annual basis rather than in one time step. As a result, in Model A, the seafarer shortage is eliminated one year earlier in the case where AO were introduced (left graph in Figure 16). On the other hand, in Model B, the seafarer shortage was eliminated in the same year regardless of introduction of AO (right graph in Figure 16). This means that in Model A, where the seafarer shortage was solved a year earlier by the introduction of AO, the working environment for seafarers improved, while in Model B, where the seafarer shortage was solved in the same year regardless of the introduction of AO, the working environment for seafarers worsened in Strategy 1, which employed the same number of seafarers in both cases but introduced more automation through the introduction of AO. This suggests that even a one-year delay in eliminating the seafarer shortage by introducing automated technology can have a significant impact on the employment environment for seafarers, and that it is necessary to introduce automated technology with caution.

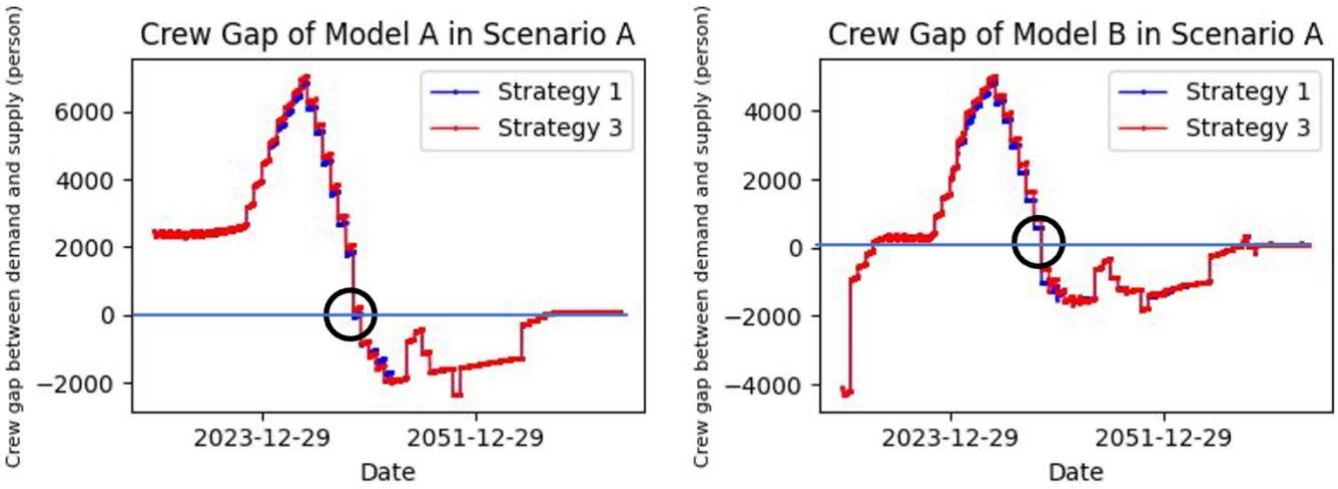

Figure 16: Result of crew gap (Left is Model A. Right is Model B).

Part 7:
DIGITAL TRANSITION

Proceedings of 15th International Marine Design Conference (IMDC-2024)
June 2-6, 2024
Amsterdam, the Netherlands

Exploring the Opportunities of Generative Artificial Intelligence in Concept Ship Design

Grech La Rosa Andrea[1,*], Simpson Peter[1] and Zammit Ryan[2]

ABSTRACT

Designing vessels is a complex process requiring the consideration of numerous aspects to develop a successful design. Ship and submarine design often requires the designer to approximate, make assumptions, consider scenarios and imagine how the vessel may be used in operation. Having the ability to consult for feedback or request additional information may be a welcome aid.

The onset of Generative AI (GENAI) presents a new opportunity to integrate this resource into the workflows of the concept ship design process. Augmenting the design process could have a positive impact on the outcome of the design, further improving various qualities such as performance, sustainability, equality, diversity and inclusion. Aspects associated with weight groups, payload catalogues, technical analysis and layout set out will be explored to investigate whether GENAI could add value to the design process. A case study will be used to facilitate this investigation, taking note of GENAI's content throughout the process.

KEY WORDS

Generative Artificial Intelligence, concept ship design. text to text, text to image, Chat GPT, Gemini, Dal E

BACKGROUND

Generative Artificial Intelligence (GENAI)

Generative AI (GENAI) refers to a class of artificial intelligence systems that can generate new content, such as images, text, video, voice, or even music, often indistinguishable from content generated by humans. These systems are based on generative models, which are trained on large datasets to learn patterns and relationships within the data. GENAI has made significant strides in recent years, leading to advancements in creative content generation, data augmentation, and problem-solving across various domains (Fui-Hoon Nah et al., 2023).

In contrast to internet search engines, GENAI is designed to create novel content by learning patterns from datasets. It generates completely new and possibly realistic images, text, or other forms of media as opposed to finding existing media like in traditional search. Jason Allen famously won an art competition in 2022 by submitting a digital art piece to the Colorado State Fair's annual art competition, won an award, and only then did the submitters announce that it was created using GENAI (Kevin Roose, 2022).

Search engines such as Google, are focused on retrieving and presenting existing content from the web in response to user queries. They index and rank pre-existing information rather than generating new content, making their functionality distinct from that of GENAI. From a practical perspective, AI query data sources and generate answers based on the prompt, whilst with search engines, the user is expected to manually go through the results, assess applicability and apply the results.

The models produce these outputs based on a prompt or a series of prompts. This is a specific input or instruction given to the model to generate output. The prompt serves as a guide for the model to produce content based on the provided input, and if it's a follow-up prompt, previous prompts, and answers will be taken into consideration as context. The format and content of the prompt depend on the type of generative AI model and the desired output. Different types of models exist, mostly

[1] University College London (Mechanical Engineering, UCL, London, UK); ORCID: 0009-0008-5829-8635

[2] Affiliation (department, institution, city, country); ORCID: 0000-0000-0000-0000 (if available)

* Corresponding Author: a.grechlarosa@ucl.ac.uk

Submitted: 2 March 2024, **Revised**: 30 April 2024, **Accepted**: 1 May 2024, **Published**: 6 May 2024

Conference paper, DOI: https://doi.org/10.59490/imdc.2024.752 e-ISSN: 3050-4864

specialising in one format such as text to text or text to image. The specificity and clarity of the prompt play a crucial role in influencing the quality and relevance of the generated content however it is important to note that the same prompt will not necessarily generate the same exact results.

A new field of specialisation is emerging that is not limited to computer engineering called "prompt engineering". The term prompt engineering can refer to the process of crafting effective prompts or inputs for generative AI models, to receive optimal outputs (MsKinsey&Company, 2023). Prompt engineering involves understanding the capabilities and limitations of the model and designing prompts that elicit the desired responses or outputs. Individuals may specialize in prompt engineering as part of their broader roles in machine learning engineering, data science, or AI research, however we speculate that in the near future most jobs aided by AI will require a basic understanding of prompt engineering.

Generative AI has applications in various fields, including:

1. **Image Generation:** Creating images that may resemble photographs, sketches, drawings, etc.
2. **Text Generation:** Writing coherent and contextually relevant text, which has applications in natural language processing, content creation and technical writing.
3. **Code Generation:** Writing computer code in a specified language to fulfill a design brief.
4. **Video Generation**: Creating video, including accompanying audio, based on user input prompts (OpenAI, 2024).

There is a large selection of commercially available GENAI tools available. Chat Generative Pre-Trained Transformer (ChatGPT) by OpenAI has arguably brought GENAI to the public limelight. The current GENAI tools are built on fields of research that pre-exist the current technology. Fields such as Machine Learning, genetic algorithms, sentiment analysis, data mining, etc. have been around for years. However, it was only fairly recently that the interest in GENAI has boomed. Competition is heating up with Google quickly attempting to catch-up by hastily launching Bard, only to rebrand to Gemini within a few months (Ortiz, 2024). It is well-accepted that OpenAI is the leading model with Chat-GPT, a text-text algorithm and Dall-E, a text-image algorithm, and now having demoed Sora, a text-to-video generating algorithm.

Challenges with AI

When new technologies and processes are introduced to an established industry, new challenges, risks and uncertainties become apparent. GENAI is no different, with several industries becoming increasingly concerned about how this technology can be improperly utilised in applications that may not be suitable for it yet. For example, the education industry is concerned of generative AI's negative influence on learning (Michel-Villarreal et al., 2023) and the creative industry is aware of the impact it will have as algorithms are improved (Amankwah-Amoah et al., 2024).

While the potential of GENAI is undisputable, there are inherent risks associated with using such a platform. Some of the more noteworthy points for technical industries include:

1. Hallucinations (Alkaissi et al., 2023):
    - AI models, including generative ones, can sometimes produce erroneous or factually incorrect responses, but are presented by the model in a convincing manner. These "hallucinations" occur due to their reliance, and possible limitations, on training data and algorithms used to build the model.
    - Users may encounter misleading or blatantly wrong answers, especially when relying on AI chatbots for information. It is always recommended to check the response, which means the human using GENAI ultimately requires some field-knowledge to be able to check the response.
    - Detecting these biases or inaccuracies can be challenging as AI solutions become increasingly believable, especially to novice or inexperienced users.
2. Cybersecurity Risks (Gupta et al., 2023):
    - GENAI can inadvertently expose sensitive and proprietary enterprise data.
    - Interactions with AI chatbots may inadvertently leak confidential information, posing cybersecurity threats.
    - GENAI could be used by malicious actors (e.g. cyber criminals) to try and circumvent current security protocols or practices (Stanham, 2023)
3. Copyright Issues (Ren et al., 2024):
    - As GENAI is built on existing content to learn and train the model, there are ethical and legal copyright considerations on permission of using this data to generate new content (Appel et al., 2023)
    - As GENAI produces content, questions arise about intellectual property rights and copyright infringement.
    - Ensuring that AI-generated works respect existing copyrights is crucial to avoiding legal disputes.
4. Computational Power (Crawford, 2024):

- GENAI uses large amounts of computational power to train the model, keep it running, and to produce results to prompts. In a world where we are seeking to reduce our power consumption, there is an argument that the increased use of GenAI will increase the need of using more power.

Industry Specific GENAI platforms

As stated earlier, the performance of an AI model is heavily influenced by the data used to train and develop it. Platforms like Chat-GPT have been trained on a myriad of data, and is able to provide answers about most generic questions. However, if there is a lack of specific information in its training model, it wouldn't be able to provide a specific answer to the prompt. One way of mitigating such risks is to develop and implement customized models for specific industries. These models are tailored to address the unique challenges and requirements of specific industries, domains, or applications, offering specialized capabilities and domain-specific knowledge. Some examples of how different industries can benefit from GENAI are:

1. **Engineering** (Kar et al., 2023)
   - GENAI models can aid in product design, optimization, and simulation across various manufacturing processes, such as additive manufacturing, CNC machining, and supply chain management.
   - Natural language processing models can generate technical documentation, automate parts cataloging, assist in troubleshooting and maintenance tasks as well as support project management tasks.
2. **Architecture**(Liao et al., 2024; van Hooijdonk, 2023)
   - GENAI can be used to streamline design processes, explore innovative solutions, and optimize complex systems and support technical designs.
   - Conduct parametric design, urban planning, spatial analysis and facilitate brainstorming sessions.
   - Natural language processing models can generate technical documentation, automating construction sequences and assist in project management.
3. **Healthcare** (Lan et al., 2023)
   - Generative models trained on medical imaging data can assist in tasks such as image reconstruction, disease detection, and medical image synthesis.
   - Natural language processing models can generate clinical notes, summarize medical records, or assist in medical literature review.
4. **Finance** (Cao, 2022)
   - GENAI can generate synthetic financial data that mimics real-world patterns without compromising privacy or security to help train models. It could also process large volumes of financial data, generate reports, and perform analyses and learn from historical fraud cases and identify suspicious patterns.
   - Natural language processing models can generate financial reports, summarize market trends, and analyze financial news articles

Ship Design Procedure

Ship design is a complex iterative process used to design vessels needing to fulfill a role. Figure 1 illustrates a summary of the design method, showing the multitude of relationships between the different aspects needed to design a vessel. The aspects illustrated are technical and administrative that vary based on the scenarios being considered (UCL, 2024).

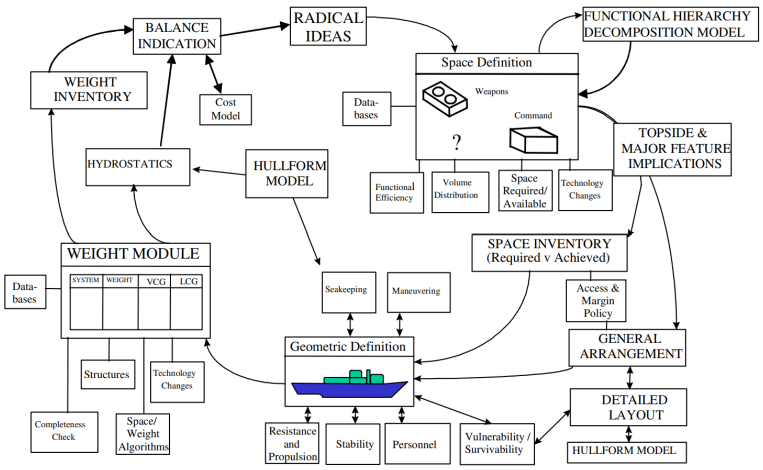

Figure 1 – Illustration of the Design Building Block Methodology applied to Surface Ships (Andrews et al., 2008)

The major milestones in the ship design process are setting the requirements, the initial sizing, conducting a cost capability trade off, payload selection, parametric survey and finally the design refinement (UCL, 2024). Each of these milestones require different skills and resources to complete however they all entail diligent project management to ensure the project is successful. The naval architect must also carry out supplementary analysis to determine what capabilities are essential and where compromises can be incorporated to create a vessel that is able to fulfill its role.

New maritime regulations, conflicting requirements and tight budgets are some of the reasons why ship designers must constantly keep up-to-date with the latest technologies and procedures to identify the best compromise for the design to be successful. As Figure 1 shows, radical ideas may also be required to satisfy some requirements however the consideration and/or implementation of such ideas typically requires the knowledge of a team of naval architects and marine engineers having experiences. While there isn't a standard procedure to follow when considering and implementing radical ideas, typical approaches include brainstorming, research and consultations with third parties who may have had to consider such options for other projects.

GENAI and Ship Design

The ship design process presents a number of opportunities to explore the use of GENAI. While limited literature is available to show examples of how this has been done so far, models such as Chat GPT suggest that they would be able to conduct:

- Conceptual design exploration
- Feasibility analysis
- Performance Optimisation
- Material selection and Sustainability
- Risk assessment and Safety Analysis
- Integration of advanced technologies
- Documentation and Reporting.

No publicly available resource was found saying that GENAI was used in full or in part to design a vessel, but there is no doubt that it is being explored. Although such algorithms have been in existence for some time, their integration in company processes is limited. This new technology is pushing boundaries in a similar way to how the introduction of the internet in 1993 led to radical change to facilitate communication, knowledge transfer, collaboration and much more. In this instance, ship designers were not immediately drawn to this service. However, as technology evolved, the marine industry recognized the potential benefits of integrating the internet into ship design and operations. They now recognize its potential to create smarter, more connected vessels that benefit shipowners, crew, and passengers alike.

Direct evidence to demonstrate how each of these points were determined was not found however Khan S et al (Khan et al., 2023) conducted an analysis showing a Hullform parametric study using a customised genetic algorithm called ShipHullGAN, that was trained using 52,591 validated designs differing in features. The algorithm successfully generated valid designs that were deemed feasible however future work will involve integrating CFD solvers to continue building on the tool's capabilities (Khan et al., 2023).

SCOPE OF WORK

The literature review highlights the need to explore how GENAI, particularly commercially available software, can help facilitate the ship design procedure. Different aspects of the concept design were investigated using commercially available text to text and text to image GENAI tools. The research aims to identify whether some examples of commercially available tools can add value to the ship design process by supporting, conducting or improving it.

METHOD

A range of commercially available text-to-text and text-to image GENAI platforms were queried with questions relating to ship design. In addition to general questions that aim to establish the GENAI's confidence in conducting such analysis, the prompts were used to explore the early concept design aspects of potential designs. The latter was focused on two vessel types, a regular fishing boat for text-to-text and a cruise liner that pushes boundaries of the status quo for text-to-image. A summary of the requirements of each vessel can be found in Table 1.

Table 1 – Requirements for the 2 vessels being considered in this study

	Fishing Boat	Cruise Liner
Role	Utilitarian fishing vessel to operate in Indonesian waters to catch tuna	Extravagant Cruise Liner for young families to operate in the Mediterranean Sea having a floating zoo and entertainment.
Primary Tasks	Making new technology accessible to Indonesian communities	Embrace green technology
		Full of activities
Area of Operation	Indonesian Coast	Mediterranean Sea
Duration of Mission	4 days	10 days
Passengers	20	600
Accommodation	basic	luxury
Environmental	Net Zero	Net Zero
In Service Date	2030	2040

Each text-to-text GENAI model was provided with the same initial data associated with the requirement of each respective vessel. The current study was linear in its approach where only one GENAI model was considered at a time. Further studies exploring how responses one model could be linked to another GENAI model for increased utility and analysis.

The GENAI model was then asked a range of questions becoming more specific based on the responses received. The text-to-image models on the other hand were utilized to generate visualisations of the vessel or particular features. The outcomes of each respective query were recorded, and additional refinement was requested when needed.

RESULTS

A selection of the results recorded in the study will be presented below showing the prompt and response. In those cases where the responses consisted of a series of bullet point outputs, up to 3 list levels are published..

Text-to-Text

Chat GPT 3.5

How does an AI machine such as Chat GPT think it can support the Ship design process?
As an AI language model, I can indeed provide assistance in the ship design process by offering guidance, generating ideas, and answering questions related to various aspects of ship design. Here's how I can support the ship design, knowledge base, idea generation, problem solving, simulation and modelling, regulatory compliance, collaboration and communication and continuous learning and adaptation

While I cannot replace the expertise and experience of human naval architects, engineers, and designers, I can complement their skills and knowledge by offering valuable insights, information, and support throughout the ship design process. Ultimately, the combination of human creativity, expertise, and AI assistance can lead to innovative and successful ship designs that meet the needs of the maritime industry

You are a naval architect tasked to design the fishing vessel in Table 1, what are your thoughts?
Designing a fishing boat for Indonesian waters with a focus on catching tuna and incorporating new technology while ensuring environmental sustainability presents both challenges and opportunities. Here are some initial thoughts:
Size and Stability, Efficient Tuna Fishing Equipment, Accessibility of Technology, Environmental sustainability, accommodation and amenities, Safety features, local regulations, durability and maintenance. By integrating these considerations into the design process, the fishing boat can effectively fulfill its role while contributing to sustainable fishing practices and technology accessibility in Indonesian communities.

How should this vessel be sized?
The size of the fishing boat for tuna fishing in Indonesian waters should be determined by several factors including the number of passengers, the duration of the mission, the type of fishing equipment onboard, and the intended area of operation. Here are some considerations for determining the size of the vessel passenger capacity, cargo capacity, deck space, stability and seaworthiness, maneuverability and fuel efficiency. Considering these factors, the fishing boat should be sized to strike a balance between accommodating passengers and crew, providing adequate storage and deck space for fishing operations, ensuring stability and seaworthiness, and optimizing fuel efficiency. The specific size and dimensions will depend on the

detailed requirements of the mission and the preferences of the operators. Working closely with naval architects and marine engineers can help determine the optimal size of the vessel based on these considerations.

How should the calculations be carried out
Calculating the dimensions and specifications of a fishing boat involves several technical considerations and calculations. Here's an overview of the key aspects to be taken into account hydrostatics and stability analysis, weight estimation, hull design, propulsion system sizing, structural design, systems engineering, regulatory compliance and cost estimation. These calculations and analyses are typically carried out by naval architects, marine engineers, and other specialized professionals using advanced software tools, mathematical models, and engineering principles. Collaboration between various disciplines is essential to ensure that the vessel meets its performance, safety, environmental, and operational objectives.

What are the big ticket payload items that should be considered?
In the context of designing a fishing boat, "big ticket payload items" refer to significant components or equipment that directly contribute to the vessel's functionality, operational capabilities, and mission objectives. These items are crucial for the vessel's primary task of catching tuna and ensuring operational efficiency. Here are some of the big ticket payload items that should be considered fishing gear and equipment, fish storage and holding facilities, navigation and communication systems, safety and survival equipment, fuel and propulsion systems and deck machinery and handling equipment. These big ticket payload items constitute essential components of a fishing boat designed for tuna fishing in Indonesian waters. Each item plays a crucial role in the vessel's operational effectiveness, safety, and ability to fulfill its mission objectives. Integrating these payload items into the vessel's design requires careful consideration of space, weight distribution, operational requirements, and regulatory compliance.

Can you give me a weight estimate in kg for Longline fishing equipment for a vessel like this?
Estimating the weight of longline fishing equipment for a vessel depends on several factors, including the vessel's size, the fishing method employed, the target species (in this case, tuna), and the operational requirements. While it's challenging to provide an exact weight without specific details, I can offer a rough estimate based on common components and considerations. Here's a breakdown of the typical longline fishing equipment and their approximate weights:

- Mainline The mainline is the primary line that extends from the vessel and supports the branch lines and hooks. Depending on the length and diameter, a mainline can weigh anywhere from 1 kg to 5 kg per 100 meters
- Branch Lines: Branch lines are attached to the mainline and hold the baited hooks. The weight of branch lines varies depending on their length, diameter, and the number of hooks per line. On average, branch lines can weigh between 0.5 kg to 2 kg per 100 meters.
- Hooks: Hooks are essential components of the longline setup. The weight of hooks depends on their size, material, and design. On average, a hook can weigh between 20 grams to 100 grams, depending on the type and size of the target species
- Buoys and Floats: Buoys and floats are used to mark the position of the mainline and provide buoyancy. The weight of buoys and floats varies depending on their size and material. A typical buoy or float can weigh between 0.5 kg to 5 kg each
- Weights and sinkers: Weights or sinkers are used to keep the mainline and branch lines submerged at the desired depth. The weight of weights and sinkers depends on their size and material. They can range from 50 grams to 500 grams each

What propulsion system should be considered for this design?
Selecting the appropriate propulsion system for a fishing boat designed to operate in Indonesian waters and catch tuna involves considering factors such as efficiency, reliability, maneuverability, environmental impact, and operational requirements. Here are several propulsion options to consider: Diesel propulsions, Hybrid propulsion, outboard motors, pod propulsions, sterndrives and waterjet propulsion. The choice of propulsion system should be based on a comprehensive evaluation of the vessel's size, intended use, operating conditions, budget constraints, and environmental considerations. Collaborating with marine engineers, naval architects, and propulsion system manufacturers can help identify the most suitable propulsion solution for the fishing boat design, ensuring optimal performance, efficiency, and sustainability throughout its service life.

Are these options appropriate for Net Zero?
Achieving a "Net Zero" designation for a fishing boat involves minimizing or offsetting the vessel's greenhouse gas emissions and environmental impact over its operational lifecycle. While some propulsion options inherently produce fewer emissions or can be optimized for reduced environmental impact, others may require additional measures to achieve Net Zero status. Here's how each propulsion option mentioned previously aligns with Net Zero goals and considerations. Diesel propulsion, hybrid propulsion, outboard motor, pod propulsions, stern drives and waterjets
Should alternative options like wind propulsion or electric drive be considered

Yes, alternative propulsion options such as wind propulsion and electric drive should definitely be considered, especially in the context of designing a fishing boat with a Net Zero objective. Here's a closer look at these alternative options and their potential benefits:

- Wind propulsion,
  - Wind propulsion systems, such as sails or wind-assist technologies like Flettner rotors or kite sails, harness the power of the wind to supplement or replace traditional propulsion methods
  - Benefits include reduced fuel consumption, lower emissions, and increased energy efficiency, particularly during favorable wind conditions
  - Wind propulsion can be especially effective for vessels engaged in long-range voyages or coastal navigation where wind patterns are favorable
  - Integrating wind propulsion systems requires careful consideration of vessel design, stability, and operational requirements, but they can significantly contribute to reducing the vessel's carbon footprint and achieving Net Zero goals
- Electric drive
  - Electric propulsion systems, powered by batteries or fuel cells, offer a clean and efficient alternative to traditional diesel engines
  - Benefits include zero emissions at the point of use, reduced noise and vibration, and potential cost savings over the vessel's lifecycle
  - Electric drive systems are well-suited for short-range operations, harbor maneuvering, and low-speed cruising, making them ideal for fishing boats operating in coastal waters or protected areas
  - Charging infrastructure, battery capacity, and range limitations are important considerations when integrating electric drive systems, but advancements in battery technology and charging infrastructure are making electric propulsion increasingly viable for marine applications

How achievable would it be to integrate wind propulsion on this fishing vessel being designed?

Integrating wind propulsion on a fishing vessel designed for tuna fishing in Indonesian waters can be achievable, but it requires careful consideration of various factors including vessel design, operational requirements, cost-effectiveness, and regulatory compliance. Here are some key points to consider when evaluating the feasibility of wind propulsion integration:

1. Vessel Design and Compatibility
   - The fishing vessel's hull design, size, and stability characteristics must be compatible with the installation of wind propulsion systems such as sails, Flettner rotors, or kite sails.
   - Modifications to the vessel's superstructure and deck layout may be necessary to accommodate the additional equipment and rigging associated with wind propulsion.
2. Operational Profile
   - The vessel's operational profile, including typical routes, wind patterns, and sailing conditions, will influence the effectiveness of wind propulsion systems.
   - Wind propulsion may be more suitable for vessels engaged in coastal navigation or longer voyages where favorable wind conditions are more prevalent.
3. Performance and Efficiency
   - Wind propulsion systems can enhance the vessel's overall performance and fuel efficiency by harnessing wind power to supplement or replace traditional propulsion methods.
   - Computational fluid dynamics (CFD) simulations and performance modeling can help assess the potential impact of wind propulsion on the vessel's speed, maneuverability, and fuel consumption.
4. Costs and Return on Investment (ROI)
   a. The initial investment and ongoing maintenance costs associated with integrating wind propulsion systems must be carefully evaluated against potential fuel savings and operational benefits.
   b. Factors such as equipment costs, installation expenses, and crew training should be considered when assessing the economic viability of wind propulsion.
5. Regulatory Considerations
   - Compliance with maritime regulations and classification society standards is essential when integrating wind propulsion systems into the vessel's design.
   - Safety, stability, and seaworthiness requirements must be met to ensure the safe operation of the vessel and its crew.
6. Technology Readiness and Support
   - Availability of reliable and proven wind propulsion technologies, as well as access to technical expertise and support, are critical considerations during the integration process.
   - Collaborating with experienced wind propulsion providers and naval architects can help mitigate risks and ensure successful implementation.

What design features do Indonesian fishers desire on their vessels?
Indonesian fishers typically desire fishing vessels that are well-suited to the local maritime environment, meet their operational needs, and enhance their productivity and safety at sea. Here are some design features that are commonly sought after by Indonesian fishers for their vessels: seaworthiness, maneuverability, deck space and layout and storage and seaworthiness, maneuverability, deck space and layout and storage and fish handing facilities, safety equipment and features, comfort and accommodation, fuel

What budget would an Indonesian fisher have to purchase a vessel like this?
The budget required for an Indonesian fisher to purchase a fishing vessel can vary widely depending on several factors, including the vessel's size, age, condition, equipment, and specifications. Additionally, market conditions, availability of financing, and regional differences in pricing can also influence the cost of acquiring a fishing vessel in Indonesia. Generally, fishing vessels range in price from tens of thousands to several million dollars, with smaller vessels typically being more affordable than larger ones.

Gemini

How does an AI machine such as Gemini think it can support the Ship design process?
My approach to supporting the ship design process differs slightly from other large language models like ChatGPT due to my specific capabilities and the ongoing advancements in the field of GENAI. Here's how I envision contributing:

1. Enhanced Information Access and Deeper Analysis:
    - Similar to other language models, I can access and process vast amounts of ship design data, including regulations, technical specifications, and case studies.
    - However, leveraging my advanced natural language processing (NLP) capabilities, I can go beyond simple information retrieval. I can analyze this data to identify trends, correlations, and potential design implications not readily apparent through basic summaries.
2. Collaborative Design Exploration and Iteration:
    - I can assist with design exploration by generating variations based on your initial specifications, similar to other models.
    - However, my ability to understand and respond to natural language prompts and feedback allows for collaborative design iteration. You can provide feedback on my generated concepts, and I can then refine them based on your input, iteratively leading towards the optimal design solution.
3. Advanced Optimization and Generative Design:
    - Beyond basic calculations, I am capable of utilizing machine learning algorithms to perform more complex optimization tasks. This could involve optimizing hull shapes for fuel efficiency or analyzing various configurations to maximize stability and payload capacity.
    - Additionally, I can leverage generative design techniques to explore entirely new design solutions by learning from existing successful models and identifying innovative layouts and structures.
4. Integration with Design Tools and Automation:
    - My ability to understand and generate code allows for potential integration with existing ship design software. This could involve automating repetitive tasks, extracting data from various sources into the design software, or even generating code to perform specific design calculations.
5. Evolving Capabilities and Adaptation:
    - As the field of generative AI continues to evolve, my capabilities will continue to improve and expand. This includes ongoing advancements in NLP, knowledge representation, and reasoning, allowing me to better understand the intricacies of ship design and provide even more comprehensive support.

Limitations:
Similar to other AI models, I cannot replace the expertise of human ship designers or engineers. My role is to augment their capabilities by providing efficient information access, facilitating design exploration, performing advanced optimization, and potentially supporting automation. Ultimately, the responsibility for creating a safe, functional, and compliant vessel lies with qualified professionals.

In conclusion, while other language models can offer valuable support in the ship design process, I believe my unique capabilities in information analysis, collaborative design exploration, advanced optimization, and potential integration with design tools offer a more comprehensive and evolving approach for the future of AI-assisted ship design.

You are a naval architect tasked to design the fishing vessel in Table 1, what are your thoughts?
I think this initial design concept for a tuna fishing vessel in Indonesia has great potential! As a large language model, I can't fully design the vessel myself, but I can offer some key considerations and suggestions based on the information you provided:

Strengths and Objectives:
- Utilitarian: Focusing on functionality for tuna fishing is a good starting point.
- Technology Accessibility: Integrating new technologies to benefit Indonesian communities aligns with a noble goal.
- Net Zero: Aiming for zero emissions is commendable and aligns with future sustainability goals.

Considerations and Suggestions:
- Vessel Size and Type: Based on the 4-day mission duration, 20 passengers, and basic accommodation, a medium-sized vessel (around 20 meters) could be suitable. Depending on the chosen technology, explore options like purse seiners, longliners, or even innovative designs like electric or hybrid fishing vessels.
- New Technologies: Identify specific technologies that address local needs. This could include:
    - Fuel-efficient engines or alternative fuel sources (e.g., biofuels) for net-zero emissions.
    - Advanced fish detection and tracking systems for sustainable fishing practices.
    - On-board pre-processing facilities to improve catch quality and value.
- Local Context:
    - Regulations: Ensure the vessel design complies with Indonesian maritime regulations.
    - Infrastructure: Consider local infrastructure like available ports and fuel supplies for the chosen technology.
    - Community Needs: Engage with local fishing communities to understand their specific needs and challenges to incorporate them into the design.
- Cost and Feasibility:
    - Net-zero technology is still under development and might be expensive.
    - Analyze the cost-effectiveness and long-term sustainability of implementing such technology.

Next Steps:
1. Conduct further research on specific technologies and their feasibility in this context.
2. Consult with naval architects, marine engineers, and local stakeholders to refine the design based on technical expertise and community needs.
3. Create detailed plans and cost estimates for building and operating the vessel.

With proper research, design, and collaboration, this project has the potential to be an innovative and impactful contribution to the Indonesian fishing industry.

How should this vessel be sized?
Determining the optimal size for your fishing vessel involves several factors, but based on the information provided, here are some considerations to guide you:

Key factors influencing size:
1. Mission duration (4 days): This suggests the need for sufficient fuel storage and provisions for the crew, but doesn't necessarily require a massive vessel exclamation
2. Number of passengers (20): This translates to basic accommodation needs explanation. Bunk beds and shared spaces can be employed efficiently on smaller vessels.
3. Catch target (tuna): Tuna fishing techniques like longlining or purse seining require varying degrees of space for equipment and catch handling.
4. Net-zero goal: Depending on the chosen technology (e.g., batteries for electric propulsion), you might need space for additional equipment, potentially impacting size.

Considering these factors:
- A medium-sized vessel (around 20 meters) could be a good starting point. This size offers a balance between accommodating basic needs, maneuverability, and potentially adhering to net-zero goals with advancements in technology.
- However, it's important not to solely rely on estimations.

Next steps for determining size:
1. Refine your understanding of the chosen technology: Different net-zero technologies like electric or biofuel engines might have varying space requirements.
2. Consult with a naval architect: They can provide expertise in calculating the necessary space for crew, equipment, fuel, and catch based on specific chosen technologies and fishing practices.
3. Consider regulations and local context: Indonesian maritime regulations might define minimum or maximum size limitations for specific fishing vessel types.

Additional points:

- Smaller vessels generally offer increased maneuverability and might be more fuel-efficient (excluding the potential impact of net-zero technology).
- Larger vessels can offer more space for catch processing, which might be relevant depending on your goals and chosen technology.

Ultimately, the optimal size will be a result of careful consideration of all these factors and collaboration with professionals like naval architects and local stakeholders.

How should the calculations be carried out?

While I cannot perform the specific calculations myself, I can guide you through the general process of determining the optimal size for your fishing vessel. Here's how it might unfold:

1. Gather detailed information:
   - Specific net-zero technology: Finalize the type of technology you plan to implement (e.g., battery capacity for electric propulsion, biofuel storage tanks). Each technology has specific space requirements.
   - Fishing practices: Determine the exact fishing technique you'll utilize (e.g., longlining, purse seining) as it dictates the space needed for equipment and catch handling.
   - Regulations: Research any size limitations or regulations set by Indonesian maritime authorities for your chosen fishing vessel type and technology.
2. Consult a naval architect:

   With the gathered information, collaborate with a professional naval architect. They can perform the following:
   - Space estimation: Based on your chosen technology, fishing practices, crew size, and basic accommodation needs, the architect can estimate the required space for various onboard elements.
   - Weight and stability calculations: They can perform crucial calculations to ensure the vessel maintains proper stability and buoyancy while accommodating the planned weight of passengers, equipment, fuel, and catch.
   - Regulations compliance: The architect can verify if the proposed size adheres to Indonesian maritime regulations for the chosen vessel type and technology.
3. Software tools for visualization and optimization:

Naval architects often utilize specialized software to:

- Create 3D models: These models help visualize the vessel layout, ensuring efficient use of space and optimal placement of equipment.
- Perform simulations: Software can simulate the vessel's performance with different sizes and equipment configurations, providing valuable insights into fuel efficiency, stability, and maneuverability.

4. Iteration and refinement:

The initial size estimate from the architect might not be the final solution. Based on the calculations, simulations, and potential regulatory limitations, you might need to:

- Adjust the chosen technology: If space constraints arise due to the initial net-zero technology choice, explore alternative options that might offer a smaller footprint.
- Optimize the layout: The architect can work with you to refine the internal layout to maximize space utilization and ensure efficient workflow.
- Remember, this is a collaborative process. By providing detailed information, working closely with a naval architect, and utilizing specialized software, you can arrive at the optimal size for your fishing vessel, ensuring it meets your operational needs, adheres to regulations, and adheres to your net-zero goal.

What are the big ticket payload items that should be considered?

For your utilitarian tuna fishing vessel aiming for net-zero operation, several "big ticket" payload items need careful consideration:

1. Net-Zero Propulsion System:
   - This is likely the most significant investment and will depend on the chosen technology:
     - Electric: High-capacity batteries will be needed for extended operation. Their size and weight significantly impact available space and overall vessel size.
     - Biofuels: Requires storage tanks for the chosen biofuel, with capacity considerations based on mission duration and fuel efficiency of the engine.
     - Hybrid: Combines elements of both, requiring space for both traditional fuel tanks and the chosen net-zero technology (e.g., batteries).
2. Fishing Gear:
   - The specific equipment varies based on the chosen fishing technique:
     - Longlining: Requires longlines, reels, hooks, and bait storage.
     - Purse seining: Needs purse seines, winches, and potentially fish sorting and processing equipment.
3. Catch Handling and Processing (Optional):

- Depending on your goals, you might consider:
    - Refrigeration units: To preserve catch quality, especially for longer missions.
    - Processing equipment: If you plan to pre-process the catch onboard for increased value.

4. Navigation and Communication Equipment:

- Essential for safety and efficient operation:
    - GPS and navigation systems: For accurate positioning and course plotting.
    - Communication equipment: Radios and satellite communication devices for emergency situations and staying connected.

5. Safety Equipment:

Mandatory and crucial for crew safety:

- Life rafts and life jackets: For emergency situations.
- Firefighting equipment: To address potential onboard fires.
- First-aid kits: To provide basic medical care for crew members.

Additional Considerations:

- Spare parts: Carrying essential spare parts for critical equipment minimizes downtime and ensures operational continuity.
- Freshwater and provisions: Enough freshwater and food supplies are essential for the crew's well-being during the 4-day mission.

Remember, the final selection and cost of these big-ticket items will depend on the chosen net-zero technology, fishing technique, and specific functionalities you prioritize. Carefully analyzing your needs and conducting thorough research on each item is crucial for making informed decisions within budgetary constraints.

Can you give me a weight estimate in kg for Longline fishing equipment for a vessel like this?

Providing a precise weight estimate for longline fishing equipment for a vessel intended for your project is challenging due to several factors:

- Specificity of equipment: The weight can vary significantly depending on the specific longline configuration chosen. Factors like:
    - Mainline length: Longer mainlines require more weight.
    - Number of hooks: More hooks contribute to increased weight.
    - Hook size and material: Larger and heavier-duty hooks weigh more.
    - Buoy type and number: The type and quantity of buoys used to mark the mainline can impact weight.
- Fishing vessel size: While your project outlines a medium-sized vessel (around 20 meters), slight size variations can still influence the amount of equipment typically carried.
- However, to provide a rough estimate, a vessel of this size engaged in longline fishing in Indonesia might typically carry longline equipment weighing between 1,000 and 3,000 kg. This includes:
- Mainline: 5,000 to 10,000 meters, typically made of synthetic materials like nylon or Dyneema, weighing around 0.2-0.3 kg per 100 meters.
- Hooks: 1,000 to 3,000 depending on the target species and spacing, with individual hook weights varying based on size and material (typically 50-200 grams each).
- Swivels and clips: Used to connect the mainline to leaders and hooks, contributing a relatively small overall weight.
- Buoys: Several dozen buoys might be used, with varying weights depending on size and material (typically 1-5 kg each).

Important Note:

This is just a general estimate, and the actual weight of your longline equipment will depend on the specific choices you make regarding the factors mentioned above. It's crucial to consult with experienced longline fishermen and fishing gear suppliers in Indonesia to get a more accurate estimate based on your specific needs and local practices.

What propulsion system should be considered for this design?

Choosing the most suitable propulsion system for your net-zero fishing vessel in Indonesia involves careful consideration of several factors:

1. Net-Zero Goal:

- Electric:
    - Pros: Zero emissions, quiet operation, potential for efficiency improvements.
    - Cons: High initial cost of batteries, limited range based on current battery technology, requires access to charging infrastructure.

- Biofuels:
    - Pros: Reduced emissions compared to traditional fuels, potentially aligns with local sustainability initiatives if using regionally produced biofuels.
    - Cons: Emissions still present, engine modifications might be needed, availability and cost of suitable biofuels in Indonesia need evaluation.
- Hybrid:
    - Pros: Combines the benefits of electric and traditional fuel sources, offering extended range and flexibility.
    - Cons: Increased complexity, potentially higher maintenance costs.

2. Operational Needs:

- Mission duration (4 days): This suggests needing sufficient range or the ability to recharge/refuel efficiently.
- Area of operation (Indonesian Coast): Accessibility of charging infrastructure (for electric) or biofuel availability needs evaluation.

3. Local Context:

- Regulations: Indonesian regulations on net-zero technologies and emissions might influence your choice.
- Infrastructure: Availability of charging stations (electric) or biofuel suppliers is crucial for operational feasibility.

Considering these factors:

- Hybrid systems might be a good initial option. They offer the flexibility of using a combination of electric and traditional fuels, providing extended range while reducing emissions compared to solely relying on traditional fuels. This might be suitable until battery technology and charging infrastructure in Indonesia advance significantly.
- Biofuels could be a future alternative. If sustainable and cost-effective biofuel production and distribution become established in Indonesia, biofuels could become a viable option for achieving net-zero goals.

Additional Considerations:

- Emerging technologies: Explore advancements in hydrogen fuel cells or other promising net-zero options, keeping in mind their current feasibility and long-term potential.
- Consult with experts: Collaborate with naval architects, marine engineers, and local stakeholders to understand the best fit for your project based on technical expertise and the evolving landscape of net-zero technologies in Indonesia.

Remember, there is no single "perfect" solution at this stage. Carefully evaluating the factors mentioned above and staying updated on technological advancements will guide you towards choosing the most suitable and sustainable propulsion system for your innovative fishing vessel.

Are these options appropriate for Net Zero?

The appropriateness of the proposed propulsion systems (electric, biofuels, and hybrid) for achieving net-zero emissions for your fishing vessel project depends on a nuanced understanding of the concept of "net-zero" and the specific context of your project:

Understanding Net-Zero:

- Net-zero emissions: This doesn't necessarily mean zero emissions during operation. It signifies that any emitted greenhouse gasses are balanced by removing equivalent amounts from the atmosphere elsewhere in the lifecycle of the vessel and its operation.

Evaluating the Options:

- Electric:
    - Pros: During operation, electric propulsion produces zero emissions directly.
    - Cons: Emissions are potentially generated during electricity generation if the source isn't renewable. Additionally, battery production and disposal might have environmental impacts.
- Biofuels:
    - Pros: Some biofuels, like sustainably produced biodiesels or advanced biofuels, can offer significant emissions reduction compared to traditional fossil fuels.
    - Cons: Even "cleaner" biofuels still generate emissions during operation. Additionally, sustainability concerns exist regarding potential land-use change and potential indirect emissions associated with biofuel production.
- Hybrid:
    - Net-zero potential: Hybrid systems can be considered partially net-zero if they combine electric propulsion with renewable energy sources (e.g., solar panels for battery charging) and biofuels with extremely low lifecycle emissions.

Contextual Considerations:

- Indonesian energy mix: If Indonesia's electricity grid relies heavily on fossil fuels, electric propulsion might not be truly net-zero due to indirect emissions during electricity generation.

- Biofuel sustainability: If the chosen biofuel isn't demonstrably sustainable, it might not contribute meaningfully to net-zero goals.

Therefore:

- None of the options might be fully "net-zero" in the strictest sense, considering the current limitations and potential upstream emissions. However, they represent steps towards achieving net-zero by reducing direct emissions compared to traditional fossil fuels.

Recommendations:

Focus on maximizing the use of renewable energy sources whenever possible, regardless of the chosen propulsion system. This could involve:

- Onboard solar panels for partially charging batteries in an electric or hybrid system.
- Investing in renewable energy sources for charging infrastructure if opting for electric propulsion.
- Prioritize biofuels with demonstrably low lifecycle emissions if biofuels are considered.
- Continuously monitor and refine your approach as technology advances and the understanding of "net-zero" becomes more comprehensive.

Ultimately, achieving true net-zero requires a holistic approach that extends beyond the vessel itself, encompassing the entire lifecycle, energy sources, and potential environmental impacts of all involved elements.

Should alternative options like wind propulsion or electric drive be considered?

- While your initial options (electric, biofuels, and hybrid) offer promising paths towards reduced emissions, including alternative options like wind propulsion and electric drives in your evaluation is definitely worthwhile. Here's a breakdown of their potential:

Wind Propulsion:

- Pros:
    - Harnessing natural wind power can significantly reduce reliance on fossil fuels and associated emissions.
    - Simple and low-maintenance technology compared to some other options.
    - Environmentally friendly and aligns with net-zero goals.
- Cons:
    - Highly dependent on wind conditions, making them unreliable for consistent operation and requiring a backup propulsion system like a diesel engine.
    - Limited effectiveness in calm winds and might not be suitable for all fishing activities.
    - Potentially lower maneuverability compared to traditional engines.
- Electric Drive (assuming you meant electric motors powered by on-board batteries or other renewable sources):
- Pros:
    - Zero emissions during operation if the electricity source is renewable (e.g., solar panels on board).
    - Quiet operation compared to traditional engines, potentially reducing underwater noise pollution.
    - High potential for efficiency improvements as battery technology advances.
- Cons:
    - Limited range due to current battery limitations, potentially requiring frequent recharging.
    - High initial cost of batteries and charging infrastructure.
    - Weight and space constraints associated with batteries might require careful design considerations.

Considering your project's specific context:

- Indonesian Coast: While wind patterns might be favorable in some regions, relying solely on wind propulsion might not be feasible due to potential calm periods.
- Mission duration (4 days): Current battery technology might limit the range of an electric drive system for a 4-day mission without recharging options.

Therefore:

- Wind propulsion can be considered as a supplementary option. In conjunction with another propulsion system (e.g., hybrid with a diesel engine), it could be used in favorable wind conditions to reduce fuel consumption and emissions.
- Electric drive has potential but requires further investigation. Evaluating advancements in battery technology, potential for onboard solar charging, and exploring hybrid configurations with a smaller battery pack for limited electric operation are recommended.

Additionally:

- Emerging technologies like hydrogen fuel cells might offer future possibilities for net-zero operation, but their current stage of development needs to be factored in.
- Seek expert advice from naval architects, marine engineers, and wind propulsion specialists to understand the feasibility and practical applications of these alternative options in your specific context.

- By exploring various options and conducting thorough research, you can choose the most suitable and sustainable propulsion system for your innovative fishing vessel, contributing to advancements in net-zero fishing practices in Indonesia.

How achievable would it be to integrate wind propulsion on this fishing vessel being designed?
Integrating wind propulsion into your fishing vessel design has potential but comes with challenges and considerations for achieving practical and operational success. Here's an assessment of its feasibility:

Feasibility factors:
- Technical feasibility: Integrating wind propulsion systems onto vessels is technically possible. Different configurations exist, such as rigid sails, soft kites, or Flettner rotors.
- Partial emissions reduction: Wind power can significantly reduce reliance on fossil fuels and associated emissions when conditions are favorable.

Challenges and limitations:
- Dependence on wind: Wind is unreliable and unpredictable. Calm periods or unfavorable wind directions would require a backup propulsion system like a diesel engine, negating some environmental benefits during those times.
- Limited effectiveness: Wind propulsion is less effective in calm conditions and might not be suitable for all fishing activities requiring precise maneuvering or maintaining specific speeds.
- Maneuverability concerns: Depending on the chosen wind propulsion system, vessel maneuverability might be impacted, potentially affecting fishing operations and safety.
- Design considerations: Integrating wind propulsion requires careful design integration with the existing vessel structure and other equipment, potentially impacting layout and functionality.
- Safety and operational training: Crew members need training on operating and maintaining the wind propulsion system and adapting fishing practices to variable wind conditions.

Considering your project's specific context:
- Indonesian Coast: While wind patterns are generally favorable in some regions, relying solely on wind propulsion might not be feasible due to potential calm periods.
- Mission duration (4 days): A backup propulsion system is highly recommended for completing the mission in case of unfavorable wind conditions.

Therefore, integrating wind propulsion on this vessel is achievable but with limitations. Here are some recommendations:
- Treat wind propulsion as a supplementary system. Combine it with another, more reliable propulsion system (e.g., hybrid) to provide flexibility and ensure operational continuity when wind is insufficient.
- Carefully evaluate the chosen wind propulsion system's impact on maneuverability and ensure it aligns with the intended fishing practices.
- Consult with naval architects and wind propulsion specialists to design the system effectively and integrate it seamlessly into the vessel's design.
- Remember, achieving true net-zero requires a multifaceted approach. While wind propulsion offers potential, it's crucial to consider its limitations and combine it with other sustainable solutions for a comprehensive and practical net-zero fishing vessel design.

What design features do Indonesian fishers desire on their vessels?
Understanding the specific needs and desires of Indonesian fishers is crucial for designing a truly useful and sustainable fishing vessel. While specific preferences might vary based on factors like location, fishing techniques, and target species, here are some general design features often desired by Indonesian fishers:

Efficiency and Functionality:
- Fuel efficiency: Reducing fuel costs is a significant concern, so features like efficient hull design, optimized engine selection, and potential for alternative fuels (e.g., biofuels) are often desired.
- Ease of operation: Simple and intuitive controls, user-friendly layouts, and minimal maintenance requirements are valued, especially for smaller-scale or less experienced operators.
- Durability and reliability: Vessels operating in potentially harsh marine environments need robust construction materials and reliable equipment to minimize downtime and ensure safety.

Safety and Comfort:
- Safety features: Adequate life-saving equipment, proper navigation and communication systems, and adherence to safety regulations are essential for ensuring crew well-being at sea.
- Basic comfort: While space might be limited on smaller vessels, providing comfortable sleeping quarters, designated cooking areas, and basic sanitation facilities is crucial for longer missions.

Storage and Processing:

- Adequate storage space: Sufficient space for fishing gear, catch, provisions, and other equipment is essential for efficient operation.
- Basic processing capabilities: Depending on the target catch and market demands, on-board processing facilities like sorting, icing, or refrigeration might be desired to improve catch quality and value.

Additional Considerations:

- Cultural and religious considerations: Incorporating design elements that respect the cultural and religious beliefs of Indonesian fishers can foster a sense of ownership and comfort onboard.
- Environmental sustainability: While the project aims for net-zero emissions, features that minimize waste generation, promote fuel efficiency, and encourage responsible fishing practices are generally appreciated by environmentally conscious fishers.

It's crucial to emphasize that these are general considerations. To gain a deeper understanding of the specific needs and preferences of Indonesian fishers in your target region and fishing practices, it's highly recommended to:

- Conduct interviews and focus groups swith local fishers and fishing communities.
- Engage with local boat builders and maritime experts familiar with the regional context.
- Research existing literature and studies on the needs and challenges faced by Indonesian fishers.

By involving the intended users in the design process and understanding their specific needs, you can create a fishing vessel that is not only technologically innovative and environmentally friendly but also practically useful and well-received by the Indonesian fishing community.

What budget would an Indonesian fisher have to purchase a vessel like this?

Unfortunately, it's impossible to provide a definitive budget for a vessel like the one you're conceptualizing without more specific details. Several factors significantly influence the cost:

- Net-zero technology: The chosen net-zero propulsion system (electric, biofuels, hybrid) has a substantial impact on the overall cost. Currently, electric propulsion systems with sufficiently powerful batteries are still expensive, while the cost of biofuels and their infrastructure can vary significantly.
- Final design and size: The finalized size and complexity of the vessel design directly impact the cost of construction materials, equipment, and labor.
- Local market and regulations: Costs of materials, labor, and permits can vary depending on the specific location in Indonesia where the vessel is built.

However, considering the features and target functionalities mentioned, here's a general range to provide context:

- A medium-sized (around 20 meters) fishing vessel with basic accommodation, designed for longlining in Indonesian waters, and utilizing traditional fuel sources might cost between US$200,000 and US$500,000.
- Integrating net-zero technologies like electric propulsion or biofuels can significantly increase the cost, potentially doubling or tripling the base price depending on the chosen technology and its current market state.

It's important to remember:

- This is just a rough estimate based on general market trends and might not accurately reflect the actual cost.
- Obtaining accurate pricing requires consulting professional naval architects and shipbuilding companies in Indonesia. They can provide cost estimates based on your specific design, chosen technologies, and local market factors.

Additionally:

- Consider exploring available government subsidies or financing options for sustainable fishing vessels in Indonesia. Some initiatives might offer financial support to encourage the adoption of net-zero technologies in the fishing industry.
- Collaborate with local communities: Partnering with fishing communities and organizations might offer opportunities for collective investment or innovative financing models to make these types of vessels more accessible to Indonesian fishers.

Remember, the primary goal is to design a sustainable and affordable solution for Indonesian fishers. By carefully considering their needs, exploring cost-effective options, and seeking potential financial support mechanisms, your project can contribute to a positive transformation in the Indonesian fishing industry.

Text to Image

A sample of the images created using the requirements for the cruise liner will be presented below.

Microsoft Copilot with Dal-E (OpenAI tech)

Microsoft Copilot generates 4 images for each prompt submitted. The GENAI's initial response to the requirements set can be seen in Figure *2* to Figure *5*.

Figure 2 – AI Generated cruiser liner 1

Figure 3 - AI Generated cruiser liner 2

Figure 4 - AI Generated cruiser liner 3

Figure 5 - AI Generated cruiser liner 4

Additional prompts were then implemented to coerce the GENAI model to add different features. Similarly, four images per updated prompt were generated however only the best outcome each of the updates is being reproduced here in Figure 6 to Figure 9.

Figure 6 – Add wind propulsion

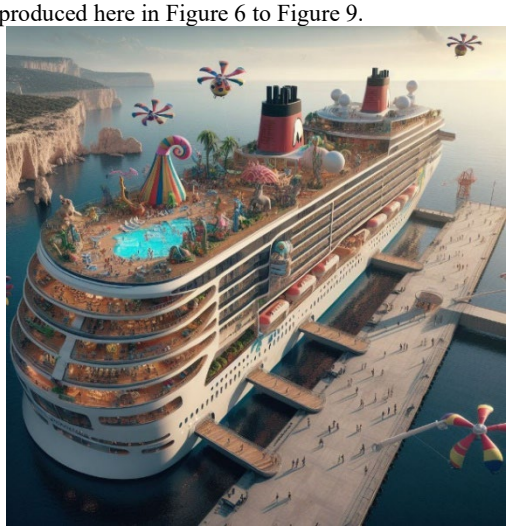

Figure 7 – Add Flettner Rotors

Figure 8- Add solar panels

Figure 9 – Interior shot of dinning lounge

Additional results recorded from this explorative study can be found in Figure 10 and Figure 11.

Figure 10 - AI Generated energy efficient Cruise liner 1

Figure 11 – AI Generated energy efficient Cruise liner 2

Deep AI

The fantasy Deep AI model was prompted to create images of cruise liners meeting the design requirements. A sample of the results can be seen in Figure 12 and Figure 13.

Figure 12 – AI generated fantasy cruiseliner

Figure 13 - Interior of fantasy cruise liner

DISCUSSION

The results presented showcase the outcomes of the investigative study into using text to text and text to image GENAI models for concept ship design. A total of four models were used independently from each other utilizing similar prompts depending on the type of GENAI model throughout the process. The study yielded some interesting results that will be expanded upon to ultimately determine whether ship designers should consider using such tools and who stands to benefit the most from them.

When using either of the text to text GENAI models, plausible results were recorded that would be suitable to consider at an early stage of the design. When reflecting on whether the responses were elevating the ship design process or returning elementary aspects that should already be known by the designer, it was concluded that this is highly dependent on the experience of the designer and on the past portfolio of the studio. This means that design studios that have designed a particular vessel type for many years stand to gain far less than those exploring new business and design opportunities in the particular sector.

Naturally, when one lacks experience, there is a greater chance of acting on incorrect, incomplete or false knowledge. While the same argument could be put forward when utilizing open source non peer reviewed material, the GENAI algorithms are able to frame responses in a convincing and well framed manner. To counter this risk, studios should consider carrying out a risk assessment on the utilization of such algorithms for each respective project and confining the scope of the GENAI exploration. Such an approach would enable safer use of while acknowledging the embedded risk is the design process.

Both text to text GENAI algorithms recognized their limitations and suggested contacting naval architects and marine engineers despite having told the algorithm that they are that capacity. This outcome is reassuring as it sobers the user to acknowledge the uncertainty in response and provides them with good direction with what to do next.

This study also showed the importance of generating prompts well to try and tap in to useful information that be included in the design process. Users must be aware of the language used to generate responses and make use of action words to empower the algorithm to divulge data that would be otherwise time consuming to determine. As with any numerical or analytical model, verification and validation should be conducted to try and quantify the error and uncertainty in the predicted results. Since ship design is a heavily iterative process, it is commonly known that the initial parameters considered for a design don't need to have high accuracy or confidence as they are sure to change as the design evolves. The GENAI models can add value by accelerating this process and empowering the designer to continue advancing. A GENAI register should be created to complement the assumptions register to help trace and troubleshoot any parameters formally established by a GENAI machine.

The responses from the current study didn't suggest or recommend novel technologies despite having set the algorithm design requirements to do that. When emphasizing this and even suggesting some possible options such as wind or electrical propulsion, the algorithm didn't dispute them but it is clear that they weren't the first option of choice for it to recommend. A potential reason for this is that the data used to form these models is heavily biased by technologies that claim to be reach net zero but isn't able to verify that using technical knowhow. In light of this, it is unlikely for the algorithm to produce something new in way of technology.

The legal aspects of acting on the advice of such models that could later be traced to misinformation generated by GENAI are interesting and valid to be aware of. The maritime industry is heavily regulated and already has rigorous regulations, procedures and protocols to safeguard all parties, irrespective of how the vessel was designed. Prescriptive regulations may limit the use of such models but goal based regulations are already heavily scrutinized, irrespective of whether the proposals were generated by AI. It would be interesting to investigate whether GENAI models could be used to assist in scrutinizing designs or narratives before they are submitted for assessment. Similarly, regulating bodies could consider developing dedicated models to aid them in processing requests. Such an approach would leave more resources to instances or cases in the regulating body that require more attention.

An interesting outcome of this study was becoming aware of the potential information overload produced by the GENAI models. The study presented in this paper took longer than expected due to the volume of information and data returned by the models. Although this was not initially expected, design studios should be conscious of this and introduce measures to limit the breadth of direction and time sunk into a project through AI. The barrier to access knowledge and data is so minimal that it encourages further prompting in areas that may not necessarily add value to the project.

The results from the study conducted with text to image GENAI models produced a range of images that were refined with further prompts through the same GENAI algorithms. The ship design process rarely uses images to facilitate design but they can be helpful to start conversations and get ideas of layout and payload integration on similar vessels.

The images created by the GENAI models have minimal value from a technical perspective but do present the opportunity of visualizing radical ideas. Although none of the images are suitable for construction, they could be useful to demonstrate to clients requiring bespoke aesthetic statement features on a particular vessel. Figure 12 is a good example of this where despite the vessel not being practical to construct in that format does have a visual appeal that may be appropriate for the target end user it was trying to attract. The fantasy elements of the vessels produced did offer the opportunity to have some interesting discussions with no effort needed to create them in the first place. In particular, the visualization of a zoo on a cruise ship could be seen as a useful output to the client requesting it to understand the extent the zoo would dominate the vessel. This could have been used to help facilitate a conversation with the client to reel back the design requirement to something more manageable or determine a constructive way of how the radical idea may be implemented.

Similar to text-text models, text to image models also generated incorrect responses that are not even physically possible to create. Interestingly, Gemini took more of an initiative with the design process. In some instances, the output was unquestionable, even to a non-technical person such as in Figure 10. Other AI generated images with irregular proposals may not necessarily be as clear to no technical people such as Figure 11 where water jets were fitted to the proposed cruise liner.

Nonetheless, there is no doubt that these GENAI models are powerful and increasingly becoming more capable. Should a dedicated GENAI tool be developed specifically for ship design that is coupled with physics models to introduce technical rigor, it is fair to assume that more sensible outputs would be created. Although not available yet, new GENAI models that would do text to CAD or IMAGE to CAD would enable quicker transitions between formats. Software such as Autodesk Fusion already makes use of generative design as part of its offering where products being designed are modified according to different constraints and criteria. Similar approaches can be found in literature for different hull form analysis models but they require substantial training and expertise to use.

CONCLUSIONS

The study undertaken successfully explored the utiliasation of text to text and text to image GENAI models for concept ship design. Two differing case studies were considered to explore the type of content that the GENAI models could generate to determine whether they would be an added asset to the ship design process.

GenAI is very easy to engage with, breaking the barrier between thoughts and actions. The experience is similar to talking with a colleague when asking questions. This differs to search engines what require selecting key words for the speech. The models are also able to remember the previous responses an use this to understand the context of the questions and influence the next prompts.

The results and analysis recorded suggest that overall, GENAI would be help the ship design process but should only be used in an assistive role. Until the design studio is confident with how to use if and gain confidence in the results, greater care should be implemented to minimise risk of acting on invalid recommendations. It is evident that not having the relevant technical background and understanding in both ship design and AI could result in poor decision making.

The GENAI models used for this study were trained and modelled against an existing catalogue of items that are not topic specific. A ship design studio could build their own version of an AI tool by inputting appropriate research papers, past designs and relevant content that could be a useful source of information to influence future designs. Such models could be tailered for initial sizing, parametric modelling or other ship design milestones.

Based on the study conducted, GENAI models can be a useful addition to the ship design process but their use should be limited to an assistive role. The text-text GENAI models were able to produce more useful results than the text-image models however the benefits of being able to cycle through new images to facilitate brainstorming did not go unnoticed. The models utilized were unable to propose new ideas, methods or technologies for the ship design process. Coupling such models with a physics model or numerical analysis may yield more complex but plausible results. Other possibilities to explore include the linking of different GENAI models to determine whether there exists a benefit of having them work together.

A genuine opportunity exists to develop tailored GENAI models for the ship design process. Future work should explore this option further and work closer with ship designers to record their feedback when using this technology.

DECLARATION OF GENERATIVE AI AND AI-ASSISTED TECHNOLOGIES IN WRTITING

Statement: During the preparation of this work the author(s) used [CHAT GPT 3.5, Microsoft CoPilot, Dal E and Deep AI] in order to conduct the research and support the report writing process. After using this tool/service, the author(s) reviewed and edited the content as needed and take(s) full responsibility for the content of the publication.

CONTRIBUTION STATEMENT

Author 1: Conceptualization; data curation, methodology; writing – original draft.
Author 2: Conceptualization; supervision; writing – review and editing.
Author 3: Conceptualization; – review and editing.

BIBLIOGRAPHY

Alkaissi, H., & McFarlane, S. I. (2023). Artificial Hallucinations in ChatGPT: Implications in Scientific Writing. *Cureus*. doi: 10.7759/cureus.35179

Amankwah-Amoah, J., Abdalla, S., Mogaji, E., Elbanna, A., & Dwivedi, Y. K. (2024). The impending disruption of creative industries by generative AI: Opportunities, challenges, and research agenda. *International Journal of Information Management*. doi: 10.1016/j.ijinfomgt.2024.102759

Andrews, D., & Pawling, R. (2008). *Concept Studies for a Joint Support Ship*.

Appel, G., Neelbauer, J., & Schweidel, D. (2023, April 7). *Generative AI Has an Intellectual Property Problem*. Retrieved from https://hbr.org/2023/04/generative-ai-has-an-intellectual-property-problem

Cao, L. (2022). AI in Finance: Challenges, Techniques, and Opportunities. *ACM Computing Surveys*, *55*(3). doi: 10.1145/3502289

Crawford, K. (2024). Generative AI is guzzling water and energy. *Nature*. Retrieved from https://arxiv.org/

Fui-Hoon Nah, F., Zheng, R., Cai, J., Siau, K., & Chen, L. (2023). Generative AI and ChatGPT: Applications, challenges, and AI-human collaboration. In Journal of Information Technology Case and Application Research (Vol. 25, Issue 3, pp. 277–304). Routledge. doi: 10.1080/15228053.2023.2233814

Gupta, M., Akiri, C., Aryal, K., Parker, E., & Praharaj, L. (2023). From ChatGPT to ThreatGPT: Impact of Generative AI in Cybersecurity and Privacy. In IEEE Access (Vol. 11, pp. 80218–80245). Institute of Electrical and Electronics Engineers Inc. doi: 10.1109/ACCESS.2023.3300381

Kar, A. K., Varsha, P. S., & Rajan, S. (2023). Unravelling the Impact of Generative Artificial Intelligence (GAI) in Industrial Applications: A Review of Scientific and Grey Literature. *Global Journal of Flexible Systems Management*, *24*(4), 659–689. doi: 10.1007/s40171-023-00356-x

Kevin Roose. (2022, September 2). *An A.I.-Generated Picture Won an Art Prize. Artists Aren't Happy.* NY Times. Retrieved from https://www.nytimes.com/2022/09/02/technology/ai-artificial-intelligence-artists.html

Khan, S., Goucher-Lambert, K., Kostas, K., & Kaklis, P. (2023). ShipHullGAN: A generic parametric modeller for ship hull design using deep convolutional generative model. *Computer Methods in Applied Mechanics and Engineering*, *411*. doi: 10.1016/j.cma.2023.116051

Lan, G., Xiao, S., Yang, J., Wen, J., & Xi, M. (2023). Generative AI-based Data Completeness Augmentation Algorithm for Data-driven Smart Healthcare. *IEEE Journal of Biomedical and Health Informatics*. doi: 10.1109/JBHI.2023.3327485

Liao, W., Lu, X., Fei, Y., Gu, Y., & Huang, Y. (2024). Generative AI design for building structures. In Automation in Construction (Vol. 157). Elsevier B.V. doi: 10.1016/j.autcon.2023.105187

Michel-Villarreal, R., Vilalta-Perdomo, E., Salinas-Navarro, D. E., Thierry-Aguilera, R., & Gerardou, F. S. (2023). Challenges and Opportunities of Generative AI for Higher Education as Explained by ChatGPT. *Education Sciences*, *13*(9). doi: 10.3390/educsci13090856

MsKinsey&Company. (2023, September 22). *What is prompt engineering?* Retrieved from https://www.mckinsey.com/featured-insights/mckinsey-explainers/what-is-prompt-engineering#/

OpenAI. (2024, February 17). *Introducing Sora — OpenAI's text-to-video model*. Youtube. Retrieved from https://www.youtube.com/watch?v=HK6y8DAPN_0

Ortiz, S. (2024, February 8). *Google rebrands Bard to Gemini, now available for the first time in mobile*. ZDNET. Retrieved from https://www.zdnet.com/article/google-rebrands-bard-to-gemini-now-available-for-the-first-time-in-mobile/

Ren, J., Xu, H., He, P., Cui, Y., Zeng, S., Zhang, J., Wen, H., Ding, J., Liu, H., Chang, Y., & Tang, J. (2024). *Copyright Protection in Generative AI: A Technical Perspective*. Retrieved from http://arxiv.org/abs/2402.02333

Stanham, L. (2023, November 27). *Generative AI (GENAI) in Cybersecurity*. Retrieved from https://www.crowdstrike.com/cybersecurity-101/secops/generative-ai/

UCL. (2024). UCL SDX. In Zenith Database.

van Hooijdonk, R. (2023, August 4). *Building the future: how generative AI is redefining architectural design*. Richardvanhooijdonk. Retrieved from https://blog.richardvanhooijdonk.com/en/how-generative-ai-is-redefining-architectural-design/

Proceedings of 15th International Marine Design Conference (IMDC-2024)
June 2-6, 2024
Amsterdam, the Netherlands

A Novel Application of Tensor Networks for the Investigation of Design Optimization Tools in the Marine Domain

Connor W. Arrigan[1,*], Alexander D. Manohar[1], Matthew D. Collette[1], and David J. Singer[1]

ABSTRACT

Traditional optimization methods often struggle to map the unique interactions between design variables, operational constraints, and performance objectives. Tensor networks, a mathematical framework rooted in quantum physics, address this challenge by providing a tool to model state relationships within multidimensional data structures. In the context of bulk carrier synthesis and optimization, tensor networks enable the simultaneous analysis of multiple constraints and their interactions via a state space representation. A state space representation offers a holistic understanding of the optimization landscapes by providing insights that add to traditional optimization analysis techniques. This paper presents a methodology for converting the optimization problem into multiple tensor network representations, details the implementation of tensor network algorithms, and showcases implementation results. The findings underscore the capacity of tensor networks to provide a deep, data-driven understanding of complex optimization landscapes, thus enabling novel decision-making opportunities.

KEY WORDS

Tensor Networks, Early-Stage Design, Optimization, Concept Design Tools, Informed Decision Making

INTRODUCTION

In recent years, optimization techniques have emerged as indispensable tools in the pursuit of efficient, autonomous, eco-friendly, and high-performance marine solutions. This conference paper delves into the multifaceted challenges faced when applying optimization methodologies in the nascent stages of marine design. From the intricate dance between hydrodynamics and structural integrity to the intricacies of incorporating sustainability criteria, this paper illuminates the complexities that must be navigated by designers and engineers in this dynamic and evolving field.

The maritime industry stands at the precipice of transformation, driven by the demands for greater efficiency, sustainability, autonomy, and performance in marine vessels. As designers and engineers embark on the challenge of designing the next generation of vessels, they are increasingly turning to optimization techniques to guide their decisions from the very inception of a project. However, this endeavor is not without its challenges, as optimizing marine designs at the early stages presents a unique set of challenges. Engineers and designers, driven by the promise of improved efficiency, cost-effectiveness, and innovation, often embrace optimization results with unwavering trust. However, this "blind faith" in optimization outcomes may have unintended consequences that warrant careful consideration.

[1] Department of Naval Architecture and Marine Engineering, University of Michigan, Ann Arbor, MI, USA; ORCID: 0009-0002-8243-9086 (CWA), ORCID: 0009-0000-5924-5887 (ADM), ORCID: 0000-0002-8380-675X (MDC), ORCID: 0000-0002-5293-6236 (DJS)
[*] Corresponding Author: arriganc@umich.edu

Submitted: 23 February 2024, Revised: 2 April 2024, Accepted: 1 May 2024, Published: 18 May 2024

Conference paper, DOI: https://doi.org/10.59490/imdc.2024.824 e-ISSN: 3050-4864

Traditional optimization methods and optimization analysis methods often struggle to comprehensively map the complex interactions between design variables, operational constraints, and performance objectives Papalambros and Wilde (2000) Marler and Arora (2004). No current methods exist for mapping populations of solutions in relation to design variables, objectives, or constraint activation across a solution space. The case study presented in this manuscript aims to help provide a framework for understanding how to better formulate and understand the results of optimization in early-stage design. The methodology and framework presented in this manuscript employ tensor networks and concepts from ontological commitment.

There has been limited research utilizing the philosophy-based side of ontologies within engineering, but there can be crucial implications for marine design. One concept that is of great interest in this domain is ontological commitment. Ontological commitment is a concept from philosophy that pertains to assertions of existence and entities of kinds of entities Jubien (1998).In the context of engineering and design, ontological commitment refers to the assumptions and pre-conditions about the fundamental nature of the design variables, objects, functions, and relationships that comprise the design. Ontological commitment in this context yields the possibility to enable the understanding of potential design implications associated with the integration of the multiple contextual views of design artifacts within a singular framework. To enable the use of ontologies and ontological commitment in the marine domain, tensor networks show promising capability as a framework. Tensor networks, a mathematical framework rooted in quantum physics, have found promising utility in diverse domains due to their ability to capture intricate patterns and correlations within large, highly entangled datasets, such as those seen in the marine domain Klishin (2020). The main question addressed by this research is how one understands a-priori the encoded and non-encoded relations and inter-dependencies that exist within design tools from an ontological lens. In the case of this research, an encoded relation is one captured by a direct relation of input variables or objectives in relation to constraints or intermediate functions. A non-encoded relation is a relation that may exist between variables, constraints, intermediate functions, or objectives that is not directly codified in the formulation of a problem. A tensor network framework is able to capture the impact of non-encoded and encoded relations by having the ability to investigate all possible couplings in n-dimensions.

While networks and network science have proven to be invaluable tools, in most cases researchers are simply analyzing networks that already exist with some innovative modifications and representations. However, within the naval design domain, standard networks (e.g., social networks) do not exist. For this reason, naval design researchers have been forced to create unique novel network frameworks and associated novel network metrics, tailored to specific naval design problems. As with other naval design research, a critical step is the proper abstraction and creation of not only a ship-centric ontological framework but also the methods needed to populate the network. How one structures the nodes, edges, layers, and population will determine the framework's ability to uncover the desired insights. Based on the challenges presented by the problem, tensor networks show promise in their ability to provide insights. Tensor networks address the challenge of investigating optimization tools by providing a powerful framework to unravel intricate relationships within multidimensional data structures.

This manuscript presents a novel tensor network framework for investigating optimization codes, which is used in the presented case study. The case study presented in this manuscript is based on the Sen and Yang Bulk Carrier multi-objective optimization problem Sen and Yang (1998). The problem is well studied and provides a simple example to investigate the capabilities of tensor networks while providing novel insights. The Sen and Yang Bulk Carrier Optimization is governed by three objectives, six design variables, 13 constraints, and 34 intermediate functions. In the performed case study, both optimization-based data and Monte Carlo-based data from the model were analyzed using the novel tensor network framework. The novel framework developed provided several insights detailed later in this paper. These insights included the ability to investigate constraint activation, the nature of constraints and regions of binding, and the ability to identify regions of viability within the solution space.

The investigation completed in this case study provides a few important insights for the marine domain. First, as engineers and designers, one must recognize that one's design tool predicts the resulting trade space. The way one defines inputs and objectives directly impacts and commits the resulting solution space of the problem. Second, one must investigate what assumptions or constraints bind a design space. This will help ensure that the solutions from an early-stage design optimization tool have a meaningful impact on the designs made and prevent later design re-work. Third, the case study shows that it is critical to investigate whether one's inputs and their ranges and constraints are reasonable. Fourth, it is essential to

know if the preferred solution is valid and robust. Finally, the case study presented provides a framework to evaluate the crucial question of can a design tool give the designer what they want relative to a specified objective.

BACKGROUND

The following sections detail the necessary background for the case study presented in this manuscript.

Ontological Commitment

The notion of ontological commitment stemming from the realm of metaphysics has not found widespread application within the field of engineering design, especially not directly or overtly. In metaphysics, ontological commitment refers to the necessity of positing certain entities for a theory or system to be deemed valid or true Rayo (2007). In the context of engineering design, ontological commitment holds relevance concerning the presumptions and prerequisites that underlie a design. This concept is formally defined as "a relation that holds between persons or existence assertions, on the one hand, and specific entities or kinds of entities, on the other" Jubien (1998). This implies that "assertions of the existence of specific entities or kinds of entities are the intuitive source of the notion of an ontological commitment" Jubien (1998).

In simpler terms, ontological commitment signifies the recognition that one assigns significance to something by inferring belief within an established domain or context, and its validity hinges on its connection to some notion of prior existence. There are numerous instances illustrating ontological commitments. For instance, within the realm of physics, the field is ontologically committed to the existence of entities such as atoms, quarks, and space-time. To expand on this, physics theory is ontologically committed to the concept of electrons, meaning that the authenticity of physics demands the existence of electrons, adhering to specific behavioral patterns.

Another perspective on ontological commitment is that it discloses the "demands imposed on the world" Rayo (2007). Nevertheless, despite extensive discussions in philosophy, the term "ontological commitment" is not commonly utilized in engineering design as a technical term or framework. Engineering primarily concerns itself with practicality and concrete outcomes, prioritizing tangible requirements over abstract metaphysical considerations.

However, the notion of ontological commitment does hold relevance in engineering design in the sense that the design process often entails decisions regarding which types of entities should be included or excluded from a design. In certain instances, engineers or designers may need to make assumptions or commitments about the nature of reality or the existence of specific entities to develop a functional design. For instance, in the field of software engineering, choices about the inclusion of particular data structures or classes in a program may carry ontological implications. Similarly, in the design of complex systems, decisions about the incorporation of various components or subsystems may involve ontological commitments. Nonetheless, in both scenarios, the language and concepts employed to address these matters typically belong to the engineering domain, rather than being derived from metaphysics.

Two critical concepts within ontological commitment are explicit and implicit ontological commitment. The concepts are directly a bi-product of the modern efforts to try to quantify all entities involved in a commitment and were originally presented by Peacock and Krämer and expanded upon by Österblom Peacock (2011) Krämer (2014) Österblom (2017). Explicit ontological commitments are defined by the entities that are claimed to exist that are directly stated in the statement of a theory or statement Peacock (2011) Österblom (2017). Put simply, "a theory is explicitly ontologically committed [to an entity] if it contains some sentence that means there are X" Krämer (2014) Österblom (2017). Explicit ontological commitment is a pretty clear notion and covers any direct statement of existence. To cover the commitments that are not directly stated or directly related to a theory or statement, there is implicit ontological commitment. Implicit ontological commitment is defined by two criteria. The first of the criteria for determining implicit ontological commitments is "the theory could not be true unless X existed," and the second is "the theory is committed to X and not explicitly committed to X" Peacock (2011)Österblom (2017). One important aspect to note about ontological commitments is that they are an

“unavoidably modal notion” Österblom (2017). Specifically, this means with implicit ontological commitment, it is not necessarily always clear whether an entity is involved in the commitment of a statement or theory or not. A more in-depth discussion of the use of ontological commitment in the marine domain can be found in a previous conference paper written by the author Arrigan et al. (2022).

Within the domain of naval architecture, there is a multitude of ontological commitments that go into a ship’s design. For example, one can explore the ontological commitment to ship stability, which is inherently acknowledged as a paramount design principle. This is exemplified by the explicit prioritization of a positive, non-zero metacentric height (GM), which serves as a fundamental criterion for a vessel’s ability to right itself after being heeled by external forces. The acceptance of this constraint reveals a naturally embedded ontological commitment to ensuring the stability of a ship, a necessity for operational safety and seaworthiness. Consequently, the solution space for ship design is inherently limited to configurations that yield a positive, non-zero GM. In this case, there is an explicit commitment to ships with positive, non-zero GMs and an implicit commitment to their stability. Digging deeper into the components that contribute to the calculation of GM, which includes the distance from the keel to the center of buoyancy (KB), the distance between the metacenter and center of buoyancy (BM), and the distance from the keel to the center of gravity (KG), one stumbles upon a series of implicit commitments. These pertain to the various elements and design choices that influence KG, such as weight distribution, onboard systems, and cargo loading protocols, which themselves are circumscribed by a myriad of other constraints and linguistic stipulations. Simultaneously, KB and BM are predominantly dictated by the engineered geometry of the hull. Thus, there are clearly ontological commitments in ship design regarding stability. In this context, they can be classified as high-order commitments due to the layering of explicit and implicit first-order commitments that make up the ontological commitment of stability.

STATISTICAL PHYSICS

Statistical physics is a branch of quantum physics concerned with understanding the behavior of large-scale systems based on the interactions between their individual components largely via tensor networks Huang (2009). Tensor networks are networks of n-dimensional arrays, referred to as tensors. Tensor networks can be utilized as a powerful tool for investigating highly correlated and entangled, complex systems. Tensor networks efficiently represent all possible combinations of components’ states and their connections to other components and their respective states. This ability directly allows one to rapidly query the state space and obtain probability distributions across different components and their respective states through performing contractions and studying the statistical properties of their collective behavior. In the marine domain, tensor networks have just started to be used and are in the nascent stages of being introduced to their many use cases. Currently, within the marine domain, tensor networks have been used to shed new light on the problem of ship arrangements and routing Klishin (2020) Klishin et al. (2019). Additionally, tensor networks are being used for decoupling diagnostic decision-making from the scale of the state space to enable self-adaptive health monitoring Manohar and Singer (2022).

In the view of the authors, tensor networks enable a strong framework for investigating optimization codes as one can easily investigate the impact of individual or multiple components across certain or changing states. Traditional optimization analysis methods, design of experiments, and sensitivity analysis struggle to comprehensively map the complex interactions between design variables, operational constraints, and performance objectives. Tensor networks provide a powerful tool to unravel intricate relationships within multidimensional data structures since it is native for data to be represented as high-dimensional tensors in the tensor network. Tensor networks enable the simultaneous analysis of multiple constraints, design variables, and their interactions simultaneously and offer a holistic understanding of the optimization landscape. Furthermore, tensor networks allow for the identification of constraint activation regions, shedding light on the conditions under which specific constraints come into play. This ability directly provides the design process with insights that would otherwise remain hidden. To fully understand the results presented from the case study detailed in this manuscript, it is critical to lay out the technical details of a few important statistical physics and tensor network-based concepts.

Statistical physics largely utilizes the Variation Principle of Maximum Entropy Cimini et al. (2019). This principle states that the probability distribution best representing the current state of (knowledge on) a system maximizes Shannon entropy subject to the context of any prior information on the system itself. In more common terms this means that the lowest en-

ergy is the most probable. In quantum mechanics, the ground state of a system is the state in which the quantum mechanical Hamiltonian operator has its lowest eigenvalue Klishin (2020). The wave function corresponding to the ground state contains information about the probability distribution of finding a particle in various positions and momentum states. This same idea applies to tensor networks where one can obtain position and state probability information from a given network. Within statistical physics there are two primary information structures: partition functions and tensor networks Klishin (2020). The partition functions describe the statistical properties of a system and can be manipulated to obtain statistical properties, such as probability distributions, about the system Klishin et al. (2019). The partition function directly provides a connection between the microscopic properties of individual particles and the macroscopic properties of the entire system. It is defined as the sum of the Boltzmann factors (meant to obtain the Boltzmann Distribution), which are exponential functions of the system's energy at each state. In work done by Klishin et al., they developed a method for integrating a partition function into a tensor network such that the tensor network can be modified and contracted to evaluate the partition function and learn statistical information about the system Klishin et al. (2019) Klishin (2020). The partition function $\mathcal{Z}$ sums over all possible system state configurations α. The energy of the system in configuration α is given by the objective function $\mathcal{O}_i(\alpha)$. The partition function is defined below.

$$\mathcal{Z} = \sum_{\alpha} e^{-\sum_i \lambda_i \mathcal{O}_i(\alpha)} \tag{1}$$

From this partition function, the probability of specific configurations can be derived. By taking the specific configuration α, it can be extracted from the equation and normalized as in Eq. 2. This gives the probability of the system being in configuration α.

$$p_\alpha = \frac{1}{\mathcal{Z}} e^{-\lambda \mathcal{O}(\alpha)} \tag{2}$$

In the above formulation λ is $\frac{1}{T_{Critical}}$. In statistical physics, the critical temperature of the system represents when phase transition occurs. The value selected for the critical temperature, or in this case λ, is essential. A lower value of λ suggests that the behavior of a system is more random. A higher value of λ suggests that the behavior of a system is more known. A value around the transition point suggests the behavior of the system is largely unknown. In terms of a probability distribution, a lower λ suggests a more uniform distribution, and a higher λ suggests a centered or skewed distribution. A second important component of the partition function is the objective function $\mathcal{O}_i(\alpha)$. The objective function $\mathcal{O}_i(\alpha)$ returns the system's energy while at state configuration α. $\mathcal{O}(\alpha)$ is equivalent to the system's Hamiltonian at configuration α. The objective function can be configured for varying goals. For the case study presented in this manuscript, the objective function was configured to favor extreme high or low displacements. λ could also be thought of as a configuration pressure, favoring more random or known behavior of the system. Fundamentally, the objective function defines state-to-state relationships via the energy between states. This is the point where the Principle of Maximum Entropy comes into play since the lowest objective state will have the highest probability.

The second information structure of statistical physics is tensor networks. Tensor networks are networks of tensors where the edges between tensors represent contractions, which are summations over a shared index Ran et al. (2022). The first important concept to understand in relation to tensor networks is the concept of rank. Rank refers to the order of the tensor. A rank zero tensor is a scalar, a rank one tensor is a vector, a rank two tensor is a matrix, and so on. Since contractions represent a summation over a shared index between two tensors, a tensor network represents a series of mathematical operations. Therefore, by encoding a partition function into a tensor network, contracting the tensor network evaluates the partition function Klishin (2020). As an example, consider the contraction between two two-rank tensors A_{ij} and B_{jk} over a shared index i. The result of the contraction is a new two-rank tensor, C_{ik}.

$$A_{ij}B_{jk} = A_{i1}B_{1k} + A_{i2}B_{2k} + ... + A_{in}B_{nk} = C_{ik} \tag{3}$$

Within this partition-encoded tensor network, there are two types of tensors. The first type of tensors are those which represent particles in the system and their states. The second type of tensor is a coupling tensor which represents all state-to-state energy combinations between two particles in the system. In the tensor network, particle tensors are connected to other particle tensors via an intermediary coupling tensor if those two particles directly impact one another. The states represented within the particle tensors and the energy represented within the coupling tensors are determined by their use case. The values utilized in these tensors will be detailed in the later sections of this manuscript.

When the tensor network is contracted, the result is a probability distribution over that system's state space. There are two other critical concepts related to contractions that should also be mentioned. To obtain statistical information about a system via a tensor network, there are two critical concepts related to contractions that need to be presented. These are the concepts of external legs and anchors. In addition to being able to perform constrictions of the tensor network, to aid querying one can add external legs and or anchors. An external leg artificially adds a rank to a tensor to prevent it from being fully summed in the partition function. If there are no external legs on a tensor network, a contraction of the tensor network yields a single number. Multiple external legs can be added to a network. A single external leg will yield a marginal probability relative to the node it was placed and multiple external legs will result in a joint probability relative to the respective nodes. Similar to external legs, none, one, or multiple anchors can be added to a tensor network. Anchors condition the system on being in a specific state. Thus, the specified configuration is held constant over partition function summation. This in turn yields a conditional probability for the system conditioned on a specific state or multiple states.

To wrap up this brief introduction to statistical physics and tensor networks, it should be noted that tensor networks require three pieces of information to be constructed. The first is a logical network of nodes of a system. The second is the state space of these nodes. Finally, there needs to be an objective function that describes the cost or energy of the system being in specific configurations.

Sen and Yang Bulk Carrier Problem Formulation

The following section details the formulation of the Sen and Yang Bulk Carrier optimization.Sen and Yang (1998). Additional information may also be found in Yang et al. (1990) and Yang and Sen (1996).

Inputs and Intermediate Functions

The model defines six inputs: length (L), beam (B), draft (T), depth (D), speed (V), and block coefficient (C_B).

Using these inputs, the model defines a host of intermediate functions:

$$\begin{aligned}
\text{annual cost} &= \text{capital charges} + \text{running cost} \\
&\quad + \text{voyage cost} + \text{RTPA} && (4)\\
\text{capital charges} &= 0.2 \times \text{ship cost} && (5)\\
\text{ship cost} &= 1.3 \times (\text{steel mass})^{0.85} \\
&\quad + 3500 \times \text{outfit mass} + 2400 \times P^{0.8} && (6)\\
\text{steel mass} &= 0.034 \times L^{1.7} \times B^{0.7} \times D^{0.4} \times C_B^{0.5} && (7)\\
\text{outfit mass} &= L^{0.8} \times B^{0.6} \times D^{0.3} \times C_B^{0.1} && (8)\\
\text{machinery mass} &= 0.17 \times P^{0.9} && (9)\\
\text{P} &= \Delta^{2/3} \times V^3 \times \frac{1}{b(C_B) \times \frac{V}{(g \times L)^{0.5}} + a\,(C_B)} && (10)\\
\Delta &= 1.025 \times L \times B \times T \times C_B && (11)\\
\text{running cost} &= 40000 \times DW^{0.3} && (12)\\
DW &= \Delta - \text{light ship mass} && (13)\\
& && (14)
\end{aligned}$$

$$\text{voyage cost} = \text{fuel cost} + \text{port cost} \tag{15}$$
$$\text{fuel cost} = 1.05 \times \text{daily consumption} \times \text{sea days} \times \text{fuel price} \tag{16}$$
$$\text{daily consumption} = P \times 0.19 \times 0.024 + 0.2 \tag{17}$$
$$\text{sea days} = \frac{\text{round trip miles}}{24 \times V} \tag{18}$$
$$\text{round trip miles} = 5000\,(\text{nautical miles}) \tag{19}$$
$$\text{fuel price} = 100\,(\text{pounds/ton}) \tag{20}$$
$$\text{port cost} = 6.3 \times DW^{0.8} \tag{21}$$
$$\text{RTPA} = \frac{350}{\text{sea days} + \text{port days}} \tag{22}$$
$$\text{port days} = 2 \times \left(\frac{\text{cargo deadweight}}{\text{cargo handling rate}} + 0.5 \right) \tag{23}$$
$$\text{cargo deadweight} = DW - \text{fuel carried} - \text{crew, stores, and water} \tag{24}$$
$$\text{fuel carried} = \text{daily consumption} \times (\text{sea days} + 5) \tag{25}$$
$$\text{crew, stores, and water} = 2.0 \times DW^{0.5} \tag{26}$$
$$\text{cargo handling rate} = 8000\,(\text{tons/day}) \tag{27}$$

where $RTPA$ is round trips per annum, DW is deadweight, and g is the gravitational constant ($g = 9.8065\ \ m/s^2$). The functions $a(C_B)$ and $b(C_B)$ are regression equations based on Froude Number and a coefficient referred to as the *Admiralty Coefficient*, detailed in the original paper. Functions $a(C_B)$ and $b(C_B)$ are defined as follows:

$$a(C_b) = \eta_1 \times C_B^2 + \eta_2 \times C_B + \eta_3 \tag{28}$$
$$b(C_b) = \zeta_1 \times C_B^2 + \zeta_2 \times C_B + \zeta_3 \tag{29}$$
$$\eta = [4977.06, -8105.61, 4456.51] \tag{30}$$
$$\zeta = [-10847.2, 12817, -6960.32] \tag{31}$$

Objectives

The model defines three objectives:

$$\text{transportation cost} = \frac{\text{annual cost}}{\text{annual cargo}} \tag{32}$$
$$\text{light ship mass} = \text{steel mass} + \text{outfit mass} + \text{machinery mass} \tag{33}$$
$$\text{annual cargo} = \text{cargo deadweight} \times \text{RTPA} \tag{34}$$

$$\Omega_1 = \min(\text{transportation cost}) \tag{35}$$
$$\Omega_2 = \min(\text{light ship mass}) \tag{36}$$
$$\Omega_3 = \max(\text{annual cargo}) \tag{37}$$

Constraints

The model defines dimensional and displacement constraints:

$$L/B \geq 6 \tag{38}$$
$$L/D \leq 15 \tag{39}$$
$$L/T \leq 19 \tag{40}$$
$$T \leq 0.45 \times DW^{0.31} \tag{41}$$
$$T \leq 0.7 \times D + 0.7 \tag{42}$$
$$DW \geq 3000 \tag{43}$$
$$DW \leq 500000 \tag{44}$$

Powering constraints:

$$C_B \geq 0.63 \tag{45}$$
$$C_B \leq 0.75 \tag{46}$$
$$V \geq 14 \tag{47}$$
$$V \leq 18 \tag{48}$$
$$\frac{V}{(g \times L)^{0.5}} \leq 0.32 \tag{49}$$

Stability constraint:

$$GM \geq 0.07 \times B \tag{50}$$

where

$$GM = KB + BM - KG \tag{51}$$
$$KB = 0.53 \times T \tag{52}$$
$$BM = \frac{(0.085 \times C_B - 0.002) \times B^2}{T \times C_B} \tag{53}$$
$$KG = 1.0 + 0.52 \times D \tag{54}$$

CASE STUDY DATA

The following sections detail the data collected and used for the case study presented in this manuscript. Included in the table below are the selected limits that were used with the Sen and Yang Bulk Carrier problem for this study.

Table 1: Lower and Upper Bounds Defined for Case Study

Design Variable	Lower Bound	Upper Bound
Length (m)	195	500
Draft (m)	10	27
Depth (m)	13	46
Block Coefficient	0.63	0.75
Beam (m)	24	80
Speed (kts)	14	18

In the case study presented in this manuscript, the states of the tensor network were determined to be a change in the dimension of a meter, a change in speed of a meter per second, and a change in the block coefficient of one hundredth. Some cases were run for the case study where each of the design variables was given 100 different possible states over the range of the lower and upper bound.

In this work, point-wise mutual information was utilized in the creation of the tensor networks for the case study presented. The point-wise mutual information takes the form as shown below.

$$PMI(a,b) = log(\frac{P(a,b)}{P(a) * P(b)}) \tag{55}$$

The point-wise mutual information represents comparing the joint probability of $P(a,b)$ occurring to the marginals of $P(a)$ and $P(b)$. In this case study, the point-wise mutual information was used as a surrogate for the energy needed in tensor building and contracting the tensor networks. For the investigated case, the objective function was defined following the formulation below.

$$\mathcal{O}(\alpha) = e^{PMI(\alpha) \times Cost(\alpha)} \tag{56}$$

$$Cost(\alpha) = e^{-\frac{Displacement(\alpha)}{1{,}000{,}000}} \tag{57}$$

$$Displacement(\alpha) = L(\alpha) \times B(\alpha) \times T(\alpha) \times C_b(\alpha) \tag{58}$$

In the above equations, α represents a given state configuration. The displacement is averaged based on the data points in each respective state configuration. The state configurations are determined by the number of states for each node. In this case, the states are as defined earlier in this section.

Two methods for developing data for this case study were used. The first approach used was to output the iterations of a multi-objective optimization of the Sen and Yang bulk carrier. The optimization was formulated using the equations detailed in this manuscript and using MATLAB's built-in fminimax optimizer. The algorithm for the optimizer is gradient-based. The data from the optimizer is compromised of multiple runs from multiple initial starting conditions, some including those mentioned in the original formulation. The other data set developed for this case study was a Monte Carlo simulation of the Sen and Yang Bulk Carrier Optimization. The Monte Carlo simulation was run with the upper and lower bounds detailed in this manuscript. These were also used as the upper and lower bounds for the optimization. The Monte Carlo simulation was run for 1,000,000 iterations. The data sets are comprised of the values of the inputs, output, constraints, and every intermediate function value for each iteration of the optimization or the Monte Carlo. In both data sets only the feasible solutions were considered for this initial case study. It was noted from looking at the results including the in-feasible solutions that the trends seen did not largely vary from those seen in the feasible solutions.

DEVELOPED CASE STUDY NETWORKS FOR INVESTIGATING RELATIONS

To investigate a priori the encoded and non-encoded relations and inter-dependencies that exist within the Sen and Yang Bulk carrier design tool multiple tensor networks were formulated. The formulation used for the case study presented in this manuscript is similar to some of the work done by Klishin et al Klishin et al. (2019). In this case study, each variable or node in the tensor networks presented later in this manuscript represents a rank one tensor acting as a possible state vector. The tensor networks formulated were developed to be able to easily place external legs and anchors on important variables within the tool. Based on the input tensor network to the framework, the data was populated for the network to enable necessary calculations and queries. The following sections delve into the four networks developed and their states.

Input to Output Network

The first of the four networks developed sought to investigate one of the most fundamental relations that exist, the relation of the input variable to the output final objective values. In the developed bipartite network, the input variables are on the left and each is connected to each of the relevant output objectives that they impact. In this case, each input is connected to each of the outputs. This can be seen in the developed network below.

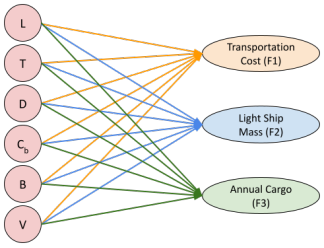

Figure 1: Developed Tensor Network for Investigating Input Output Relations

In the developed network above, the states for each of the nodes were defined as a change in the value of the input variable or the output objective.

Input to Constraint Status Network

The second network developed sought to begin to capture some of the more hidden relations in the tool. The bipartite network consists of the input variables on the left and three nodes on the right indicating a constraint status of non-binding, near binding, or binding. In this case, the values of each constraint in the data were pre-processed to determine the associated node to which each belonged. In this case study near binding was defined to be a value of ϵ away from the binding value. Each constraint was re-arranged so that when the constraint was bound or violated the value would become zero or greater than zero. For the presented data, ϵ was determined using best judgment as an engineer. In this case, ϵ was defined to be 0.5 for when a constraint was near binding.

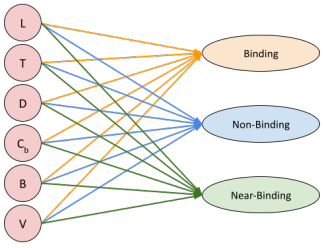

Figure 2: Developed Tensor Network for Investigating Constraint Status (Non-Binding, Near Binding, Binding

In the developed network above, the states for each of the input nodes were defined as a change in the value of the input variable. For the status nodes of non-binding, near binding, or binding, the states were determined to be the number of constraints falling under non-binding, near binding, or binding for each data point.

Input to Solution Status Network

The third network developed again sought to capture some of the relations that are not typically apparent in a tool. The bi-partite network consists of the input variables and the output objectives on the left and one node on the right for the solution status.

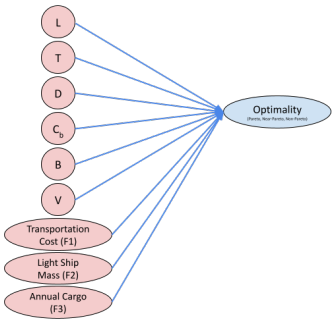

Figure 3: Developed Tensor Network for Investigating Solution Status (Non-Pareto, Near Pareto, Pareto)

In the developed network above, the states for each of the input and output objective nodes were defined as a change in the value of the variable. For the solution status node, only three possible states were defined, non-Pareto, near Pareto, or Pareto referring to the optimally of the solution. In this case, the values of output objectives in the data were pre-processed to determine if a solution was non-Pareto, near Pareto, or Pareto. In this case study, near Pareto was defined to be a value of ϵ away from the Pareto front. For the presented data, ϵ was determined using best judgment as an engineer.

Input to Constraint Network

The final network developed sought to capture some of the relations in terms of constraint activation that are not typically apparent in a tool. The bipartite network consists of the input variable nodes on the left and constraint nodes on the right. Each of the input nodes is connected to each of the relevant constraints that they impact.

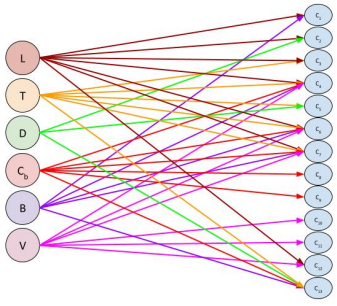

Figure 4: Developed Tensor Network for Investigating Constraint Activation over the Solution Space

In the developed network above, the states for each of the input nodes were defined as a change in the value of the variable. For the constraint nodes, each of the nodes had the possible states of non-binding, near binding, or binding. In this case, the values of each constraint in the data were pre-processed to determine the associated state for each of the constraint nodes. As stated above, near binding was defined to be a value of ϵ away from the binding value. For the presented data, ϵ was determined using best judgment as an engineer.

RESULTS

The following section details the results from performing quires in the developed networks with different external legs. Numerous more contractions were performed, not detailed in this manuscript, to further validate the findings. The contraction results presented in this manuscript are intended to provide insight into the tool and to demonstrate the capabilities of tensor networks in relation to optimization.

One of the first sets of contractions performed was done to help begin to understand the results of a tensor network contraction and to be able to easily check the result against one's instincts as a naval architect. The contraction was done on the input to output relation network and an external leg was placed on length. In evaluating the contraction, the tensor network objective was defined to maximize or minimize displacement. As a naval architect, with a simple ship like a bulk carrier, one would expect if one minimizes displacement, they would get a very short ship close to the minimum, and if one maximizes displacement, they would get a long ship close to the maximum. Included below are the contraction results for the queries. In this case, a higher probability indicates a higher likelihood of a ship with that given length.

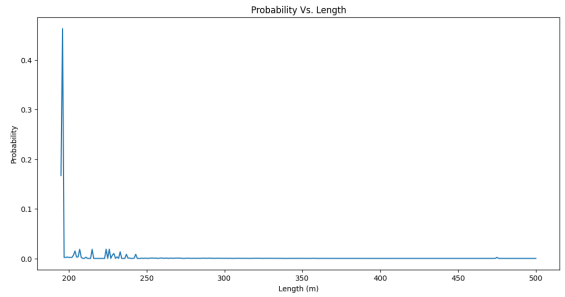

Figure 5: Input Output Tensor Network Contraction Result from Gradient-Based Optimization Data with Objective of Minimizing Displacement with External Leg on Length

As expected, the results from performing the contraction indicate that the smallest ship is the most probable. The contraction from the Monte Carlo data set shows some interesting dynamics. The reason for the lack of a single line as in the above figure is due to the Monte Carlo data set having a more limited number of feasible solutions in the shorter length range. However, it can be noted that the trends and behavior between the data are the same and that the Monte Carlo data has a higher level of fidelity due to the increased number and range of coverage of the points. This behavior can be seen in the figure below.

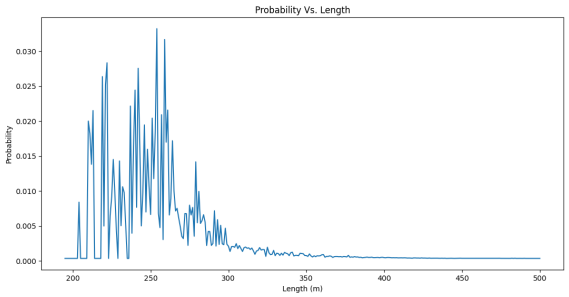

Figure 6: Input Output Tensor Network Contraction Result from Monte Carlo Data with Objective of Minimizing Displacement with External Leg on Length

Further, one can investigate the results of maximizing the displacement instead of minimizing it. Included below again are

figures of the same contraction from the optimization data set and the Monte Carlo data set.

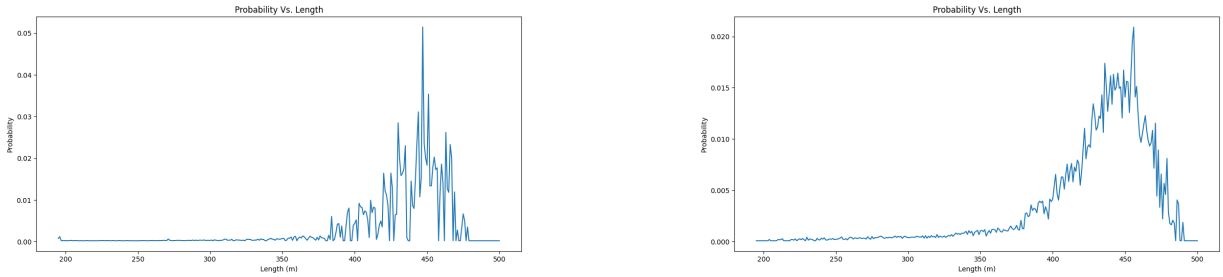

Figure 7: Input Output Tensor Network Contraction Result from Gradient-Based Optimization Data with Objective of Maximizing Displacement with External Leg on Length (Left) and Input Output Tensor Network Contraction Result from Monte Carlo Data with Objective of Maximizing Displacement with External Leg on Length (Right)

One can see from these contractions that the trends and behavior between the data are the same and that the Monte Carlo data has a higher level of fidelity. Additionally, one interesting behavior can be noted. As a naval architect, one would expect if one maximizes displacement they would get a long ship close to the maximum length. However, this is not the case in either of the contractions. In both, the most probable lies approximately 50 meters shorter than the maximum length. This result does not logically make sense. To investigate the reasoning for this, several other contractions using the other developed tensor networks were performed.

The next set of contractions performed to investigate the findings from maximizing the displacement was looking at the constraint activation across the solution space. One would naturally think that based on the behavior seen above one of the constraints is probably binding. Included below is a sample contraction of the constraint activation network with multiple external legs. The contraction shows the relation of the constraint state of non-binding, near binding, or binding to the entire state space. In the following contractions, the color bar on the right of the plot indicates the probability value for the contraction. In this case, the displacement was maximized and again similar behavior to the previous set of contractions can be seen. The constraint referred to in the contraction is the length-to-beam constraint detailed in Eq. 38.

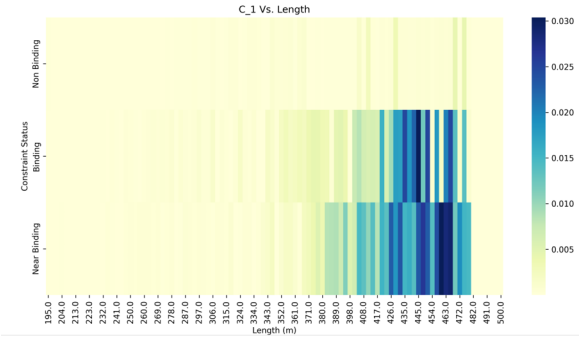

Figure 8: Constraint Activation Tensor Network Contraction Result from Monte Carlo Data with Objective of Maximizing Displacement with External Legs on Constraint 1 and Length

From the figure above, it can be noted that over the majority of the state space, the constraint is non or near binding but not binding. While the above figure supports the conclusions, it does not provide insight into the behavior of solutions when maximizing displacement. To provide insight, more contractions were performed. Some interesting results were found from the draft constraints over the solution space. The following contractions are of the same contraction of the constraint activation network just with different external legs. The constraint referred to in the contraction is the draft constraint detailed in Eq. 41.

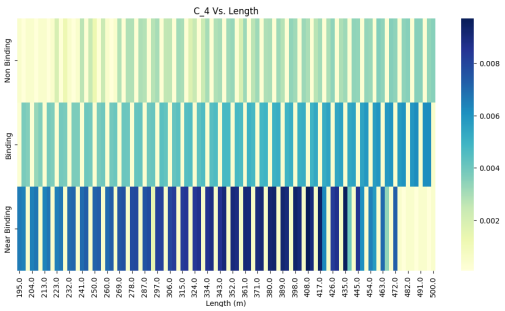

Figure 9: Constraint Activation Tensor Network Contraction Result from Monte Carlo Data with Objective of Maximizing Displacement with External Legs on Constraint 4 and Length with $\lambda = 1$

In the above contraction, one can notice the behavior of interest. In the contraction's result, it looks like a barcode for each of the states of the constraints. To investigate the meaning of the result, the value of λ was increased to see if the critical temperature had an impact. The figure below demonstrates the results.

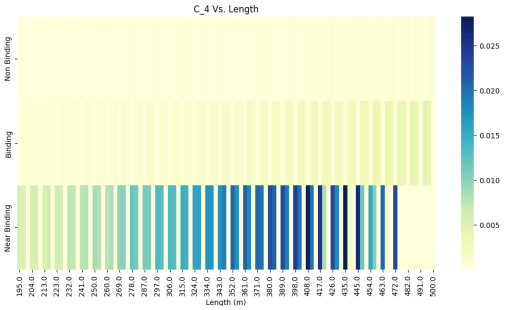

Figure 10: Constraint Activation Tensor Network Contraction Result from Monte Carlo Data with Objective of Maximizing Displacement with External Legs on Constraint 4 and Length with $\lambda = 3$

From the figure above it can be seen that the lower probability values become more muted and the same behavior of the near binding and binding states can be observed. Largely, a higher value of λ suggests that the behavior of a system is more known. In terms of the probability distribution seen, the higher λ highlights the underlying or grounding behavior of the contraction. In addition to performing the contraction with an external leg on length, the same contraction was performed with an external leg on draft.

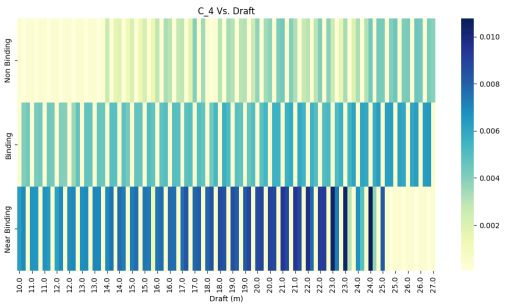

Figure 11: Constraint Activation Tensor Network Contraction Result from Monte Carlo Data with Objective of Maximizing Displacement with External Legs on Constraint 4 and Draft with $\lambda = 1$

The results from the contraction in the figure above can largely be seen showing the same behavior as that from the contraction of the same constraint but in relation to the length. Upon further investigation, one can notice that at each small range of states for the length and the draft, the constraint is going from non-binding to near binding and then to binding. This is the reason for not being able to achieve large vessels with the tool. What is happening is that as the design tool tries to increase the size of the vessel, the deadweight increases and causes the draft constraint to bind. This in turn forces smaller vessels and is exaggerated at that upper limit. It can also be noted that a second draft constraint also exists in the code seen in Eq. 42. However, this constraint is not dominant and does not impact the solutions in the same way as in Eq. 41. The origins of this constraint are largely unknown and it is assumed that it is most likely from older regression data of bulk carriers when the code was developed. In the Sen and Yang bulk carrier tool, deadweight is known to be the main driving variable, and as a result, directly impacts the allowable size of the vessel through the draft constraint. To check this, the deadweight limit was increased to see if the solution space changed. To see the change, a Monte Carlo data set was created for the increased deadweight limit. A contraction was then performed on the input to output relation network and an external leg was placed on length. The following figure can directly be compared to Fig. 7.

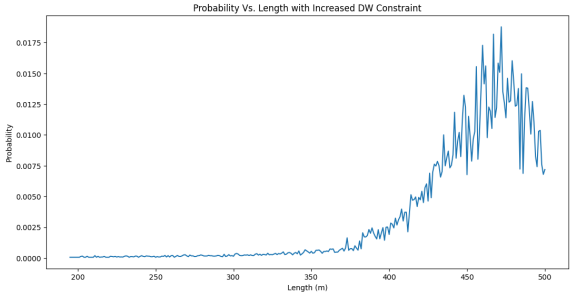

Figure 12: Input Output Tensor Network Contraction Result from Monte Carlo Data with Objective of Maximizing Displacement with External Leg on Length with Deadweight Constraint Upper Limit Increased to 800,000

From performing the contraction above and increasing the deadweight constraint upper limit to 800,000 tons, it can be seen that the peak shifted to the right. The peak value sits around 473 m in length which is a large increase from that of the contraction with the deadweight constraint upper limit set to 500,000 tons. This shows that it is a combination of the deadweight and the draft constraint that is limiting the size of the vessel. In other words, the model is ontologically committed to deadweight and the draft constraint in Eq. 41. Without tensor networks, discovering this behavior and the reasoning would be extremely difficult and time-consuming, whereas with tensor networks, performing the contractions only takes seconds.

DISCUSSION

The following section provides a discussion of the results presented above. To verify the results in Fig. 7 the Sen and Yang bulk carrier model was run as a single objective optimization with each of the three objectives in the formulation presented in this manuscript having equal weighting. The optimization was run five times using multiple different optimization algorithms in MATLAB. The results are included in the figure below. The red lines indicate the solution from the optimizer plotted in Fig. 7 or in the case of the genetic algorithm the range of optimal solutions found.

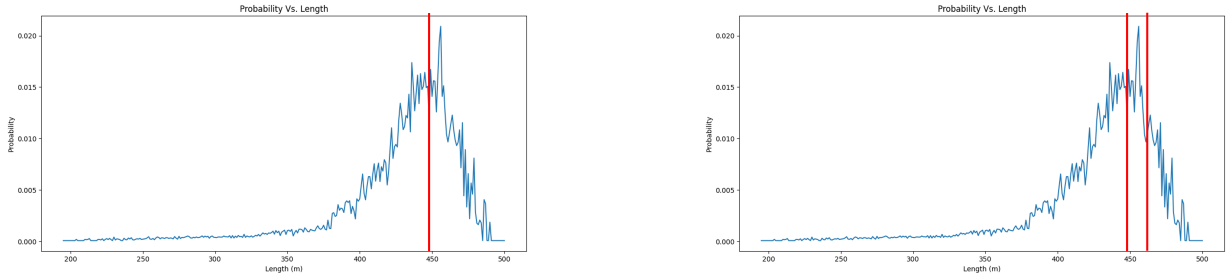

Figure 13: Feasible Length from Running fmincon Equal Weighting Single Objective Sen and Yang Bulk Carrier Optimization (Left) and Feasible Length Range from Running GA Equal Weighting Single Objective Sen and Yang Bulk Carrier Optimization (Right)

In both of the cases presented above, the single objective optimization with the objective of maximizing displacement provided solutions close to that found from the tensor network contractions. These results from running the tool as a single objective optimization support the findings in the result section and validate the peak value found. In the results presented in the section above most of the contractions were performed on the data set from the Monte Carlo simulation instead of the optimization data. It was found that both data sets had the same behavior and that the Monte Carlo just provided higher fidelity. The figure below shows this between the two data sets.

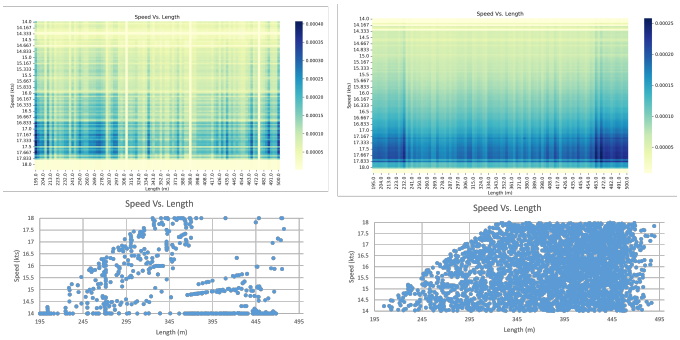

Figure 14: Comparison of Tensor Network Contraction Result and Data from Monte Carlo and Gradient-Based Optimization Data with Objective of Maximizing Displacement with External Legs on Length and Speed

From the figure above it is clear that the Monte Carlo data set provides a better picture of the solution space. Many of the gaps seen in the optimization data are filled from the Monte Carlo data. Another interesting point to note is that when looking at the data plotted on its own, the trends seen in the data support the conclusions derived from the tensor network contractions.

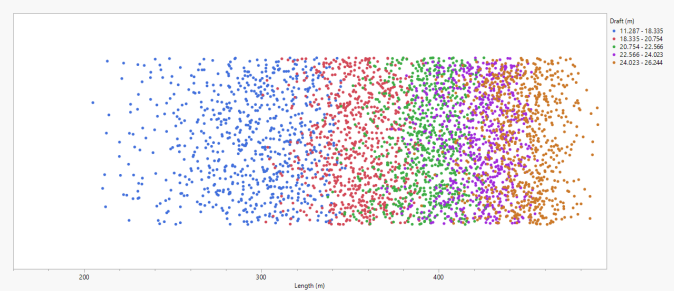

Figure 15: Population of Feasible Solutions Plotted Over Length Solutions Overlaid by Draft

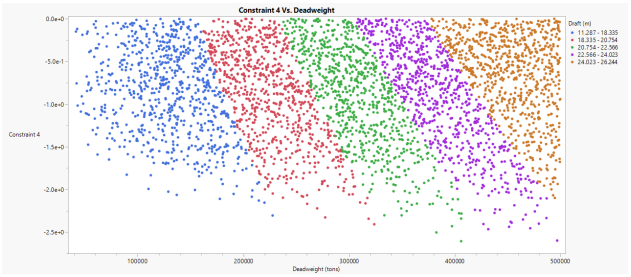

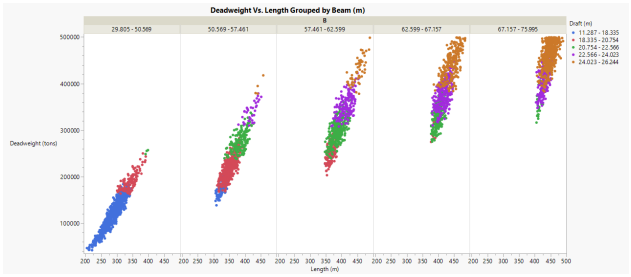

Figure 16: Draft Constraint Eq. 41 Versus Deadweight Overlaid by Draft (Left) and Deadweight Versus Length Grouped by Beam Overlaid by Draft (Right)

From the three figures included above, very distinct populations of solutions can be seen in relation to the length, draft, and deadweight. This suggests constraint or function is heavily impacting feasible solutions. This result can especially be seen in Fig. 16 where there is almost no mixing of different draft populations. One would largely expect there to be mixing in the solutions. These plots support the conclusions found from the contractions presented in the results section of this manuscript.

Through the results found and detailed from the presented case study some interesting insights can be made when looking at the case study from an ontological lens. From the presented results, one can directly see that the optimization model for the bulk carriers is highly committed to deadweight and the identified draft constraint. What this means is that the solutions of the model are predicated on these commitments. This was directly shown by how the set of solutions changed when the deadweight was increased. In the case of the draft constraint discussed earlier in this manuscript, there is an explicit commitment to the constraint from its inclusion in the model, but there is also an implicit commitment to the unknown origin or meaning of the constraint. These simple commitments to the deadweight and the discussed draft constraint significantly impact the optimization and the results that are possible to be obtained from the optimization. The insights from this analysis are more than what one could get from a Design of Experiments analysis and it is much more efficient in terms of finding the information necessary to be able to make similar conclusions.

CONCLUSIONS

In conclusion, the application of tensor networks to the Sen and Yang bulk carrier model has shed light on the intricate relationships between design variables, operational constraints, and performance objectives that are often challenging for traditional optimization methods to capture. The results from the case study highlight the unique capabilities of tensor networks, rooted in quantum physics, to effectively model state relationships within multidimensional data structures.

The analysis of the bulk carrier synthesis and optimization through tensor networks has allowed for the simultaneous examination of multiple constraints and their interactions using the state space representation. This holistic approach has proven invaluable in unraveling hidden relations within the Sen and Yang model, particularly when attempting to maximize displacement while navigating the complex behavior of the draft constraint.

The presented methodology, which involves converting the optimization problem into multiple tensor network representations and implementing tensor network algorithms, demonstrates the practical efficacy of this approach. The implementation results not only showcase the capacity of tensor networks to provide a deep, data-driven understanding of complex optimization landscapes but also emphasize their potential to uncover novel decision-making opportunities.

As one reflects on the outcomes of this study, it becomes evident that tensor networks offer a promising avenue for addressing the challenges posed by intricate and interconnected optimization parameters in the maritime industry. By providing insights that complement traditional optimization analysis techniques, tensor networks contribute to a richer understanding of optimization landscapes. The findings presented in this paper serve as a catalyst for further exploration of tensor network methodologies in tackling complex optimization challenges across diverse domains. Ultimately, this research opens new horizons for innovative decision-making support processes and underscores the transformative potential of tensor networks in the realm of optimization. There are many opportunities for future work in creating general, easily applicable frameworks for diverse optimizations and engineering design tools.

DECLARATION OF GENERATIVE AI AND AI-ASSISTED TECHNOLOGIES IN WRITING

Statement: During the preparation of this work the author(s) used ChatGPT 3.5 to help improve language and readability. After using this tool/service, the author(s) reviewed and edited the content as needed and take(s) full responsibility for the content of the publication.

CONTRIBUTION STATEMENT

CWA: Conceptualization; data curation, methodology; software; writing – original draft. **ADM:** conceptualization; software; writing – review and editing **MDC:** conceptualization; supervision; writing – review and editing **DJS:** supervision; writing – review and editing.

ACKNOWLEDGEMENTS

We would like to thank Dr. Jessica Dibelka from the Office of Naval Research for providing support for this project. This work was funded under grant number N00014-21-1-2795, Data Model Fusion: Design, Experiments, and Frameworks for Surface Platforms. Additionally, this work received Government support awarded by the Department of Defense, Office of Naval Research, National Defense Science and Engineering Graduate (NDSEG) Fellowship, 32 CFR 168a.

REFERENCES

Arrigan, C. W., Emmitt, R., and Singer, D. J. (2022). Ontologies in the marine domain and use cases for autonomous vessel design and other novel designs. In *Proceedings of the 14th International Marine Design Conference*.

Cimini, G., Squartini, T., Saracco, F., Garlaschelli, D., Gabrielli, A., and Caldarelli, G. (2019). The statistical physics of real-world networks. *Nature Reviews Physics*, 1(1):58–71.

Huang, K. (2009). *Introduction to Statistical Physics*. CRC Press.

Jubien, M. (1998). Ontological commitment. In Taylor and Francis, editors, *The Routledge Encyclopedia of Philosophy*. Accessed 22 June 2022.

Klishin, A. A. (2020). *Statistical Physics of Design*. PhD thesis, University of Michigan.

Klishin, A. A., Shields, C. P., Singer, D. J., and Anders, G. V. (2019). Corrigendum: Statistical physics of design (new j. phys. (2018) 20 (103038) doi: 10.1088/1367-2630/aae72a). *New Journal of Physics*, 21.

Krämer, S. (2014). *On What There is For Things To Be: Ontological Commitment and Second-Order Quantification*. Vittorio Klostermann, Frankfurt Am Main.

Manohar, A. and Singer, D. J. (2022). State space scalability to enable smart ships with statistical physics and multi-agent based reinforcement learning. In *Proceedings of the Interdisciplinary Conference on Mechanics, Computers, and Electronics*.

Marler, R. and Arora, J. (2004). Survey of multi-objective optimization methods for engineering. *Structural and Multidisciplinary Optimization*, 26:369–395.

Papalambros, P. Y. and Wilde, D. J. (2000). *Principles of Optimal Design: Modeling and Computation*. Cambridge University Press, 2 edition.

Peacock, H. (2011). Two kinds of ontological commitment. *The Philosophical Quarterly (1950*, 61(242):79–104.

Ran, S.-J., Tirrito, E., Peng, C., Xi, Luca, C., Gang, T., and Lewenstein, S. M. (2022). Lecture notes in physics 964 tensor network contractions methods and applications to quantum many-body systems.

Rayo, A. (2007). Ontological commitment.

Sen, P. and Yang, J.-B. (1998). Multiple Objective Decision Making. In *Multiple Criteria Decision Support in Engineering Design*, chapter 4.4.1, pages 150–157. Springer.

Yang, J.-B., Chen, C., and Zhang, Z. J. (1990). The Interactive Step Trade-Off Method (ISTM) for Multiobjective Optimization. *IEEE Transactions on Systems, Man and Cybernetics*, 20(3):688–695.

Yang, J.-B. and Sen, P. (1996). Interactive trade-off analysis and preference modeling for preliminary multiobjective ship design. *Systems Analysis, Modelling and Simulation*, 26:25–55.

Österblom, F. (2017). What is a neutral criterion of ontological commitment?

Proceedings of 15th International Marine Design Conference (IMDC-2024)
June 2-6, 2024
Amsterdam, the Netherlands

C-ShipGen: A Conditional Guided Diffusion Model for Parametric Ship Hull Design

Noah J. Bagazinski[1*] and Faez Ahmed[2]

ABSTRACT

Ship design is a complex design process that may take a team of naval architects many years to complete. Improving the ship design process can lead to significant cost savings, while still delivering high-quality designs to customers. A new technology for ship hull design is diffusion models, a type of generative artificial intelligence. Prior work with diffusion models for ship hull design created high-quality ship hulls with reduced drag and larger displaced volumes. However, the work could not generate hulls that meet specific design constraints. This paper proposes a conditional diffusion model that generates hull designs given specific constraints, such as the desired principal dimensions of the hull. In addition, this diffusion model leverages the gradients from a total resistance regression model to create low-resistance designs. Five design test cases compared the diffusion model to a design optimization algorithm to create hull designs with low resistance. In all five test cases, the diffusion model was shown to create diverse designs with a total resistance less than the optimized hull, having resistance reductions over 25%. The diffusion model also generated these designs without retraining. This work can significantly reduce the design cycle time of ships by creating high-quality hulls that meet user requirements with a data-driven approach.

KEY WORDS

Hull Design Generative Artificial Intelligence Diffusion Model Design Constraint Satisfaction Drag Reduction

INTRODUCTION

Generative artificial intelligence has shown to be a promising tool for engineering design. By training models on engineering datasets, generative models have created designs with high performance. These tools are particularly useful in ship design, as the complexity of balancing competing trade-offs in a ship requires long design cycles for human design teams. A hull's shape affects several key aspects of a ship's performance, including buoyancy, upright stability, hydrodynamics, and general arrangements. A generative model specifically trained to generate ship hulls can improve this workflow by creating high-quality designs quickly and inexpensively. The availability of open-source datasets on ship hull designs enables the use of generative artificial intelligence for design. This work builds on prior work, a guided diffusion model called *ShipGen* (Bagazinski and Ahmed, 2023a).

Hull design was chosen as the application for this work as hulls have a direct impact on over 70% of the cost of a ship (Lin and Shaw, 2017) and they are the first step in the traditional workflow for ship design (Evans, 1959). Ship hulls can exist

[1] Department of Mechanical Engineering, Massachusetts Institute of Technology, Cambridge, USA; ORCID: 0000-0001-9893-8619

[2] Department of Mechanical Engineering, Massachusetts Institute of Technology, Cambridge, USA; ORCID: 0000-0002-5227-2628

[*] Corresponding Author: noahbagz@mit.edu

Submitted: 15 February 2024, Revised: 2 May 2024, Accepted: 3 May 2024, Published: 19 May 2024

Conference paper, DOI: https://doi.org/10.59490/imdc.2024.841 e-ISSN: 3050-4864

across many length scales, ranging from a few meters to over three hundred fifty meters in length. In addition, hulls can exhibit large ranges in relative dimensions such as the beam, draft, depth, and volume displacement. A well-designed generative model for hull design should consider the scale and diversity of ship hulls in its training. This would allow the generative model to create ship hulls based on a designer's needs.

This work proposes a model called C-ShipGen, which generates early-stage hull designs considering a designer's inputs: length, beam, draft, depth, volume displacement, and intended velocity. C-ShipGen is a conditional diffusion model that implements guidance algorithms to create ship hull designs with low resistance while constraining to a user's desired principal characteristics. Figure 1 shows an overview of C-ShipGen, highlighting how the model utilizes a combination of input conditioning and guidance algorithms during the design sampling process. The following sections detail prior research on generative artificial intelligence for engineering design and computational ship design; the methods for training and sampling hull designs with C-ShipGen; the evaluation of hulls generated by C-ShipGen; and a discussion on the work. C-ShipGen generates ship hulls with low resistance for future design analysis. These generated hulls do not necessarily resemble real-world ship hulls as many other factors influence the design of hulls in addition to total resistance. Through the development of C-ShipGen, the contributions of this paper are:

1. The use of a conditional diffusion model to generate diverse ship hulls within a 5% volume error tolerance given desired principal characteristics across the full spectrum of hull sizes and relative dimensions found in real-world hull designs.
2. The use of guidance in a conditional diffusion model to generate hulls with lower total resistance than optimized hulls, having resistance reductions greater than 25% while maintaining the displaced volume within 5% of a target.

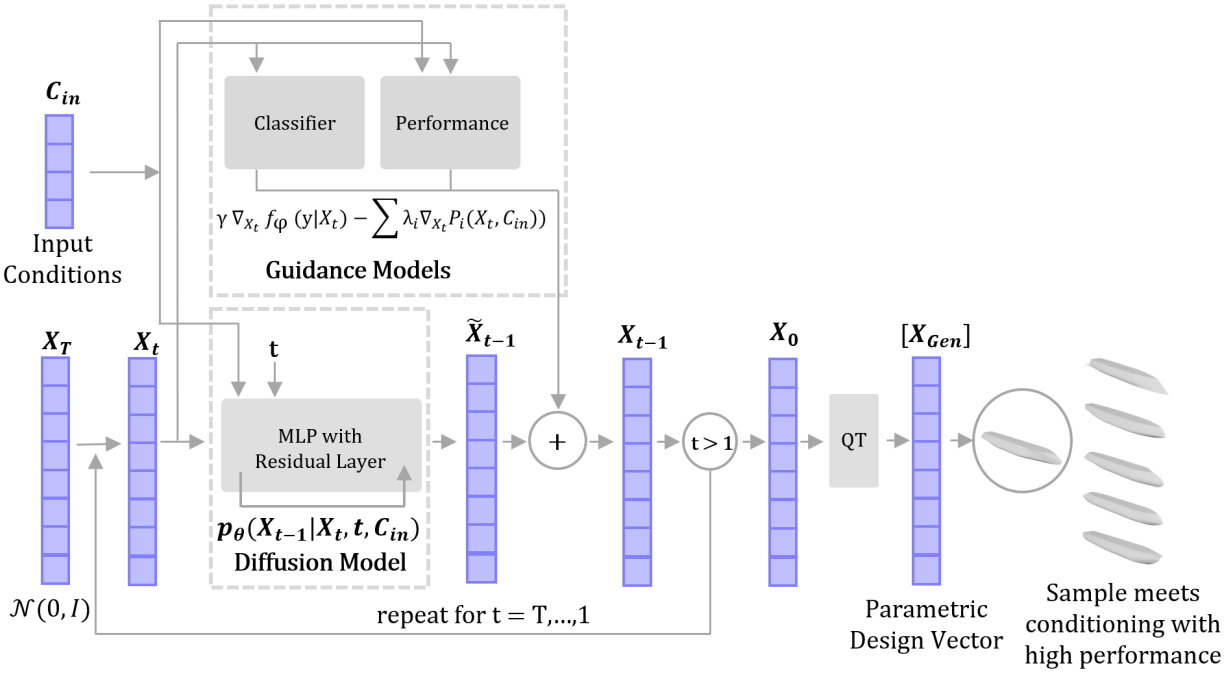

Figure 1: C-ShipGen is a guided conditional diffusion model that generates hull designs with low resistance while maintaining the principal dimensions provided by the user during sampling. The model leverages guidance gradients from pre-trained regression models to improve the performance of the hulls.

PRIOR WORK

Computational ship design refers to the application of computer-based modeling, simulation, and optimization techniques in the design and analysis of marine vessels. This facilitates more efficient, innovative, and integrated design solutions. Historically, computational ship design can be divided into three categories: design representation, forward modeling which includes surrogate regression models, and inverse design or synthesis, which includes optimization methods. Recently, generative artificial intelligence methods have emerged as a powerful technique, which has been used to represent and synthesize ship hull designs.

In order to computationally design a product, a design representation is needed that allows a computer to manipulate the design. For ship design, the two most popular modes to represent the design of a ship hull are parameterized vectors (Brown and Salcedo, 2003; Feng et al., 2022; Read, 2009; Zhang et al., 2018; Chrismianto and Kim, 2014; Lu et al., 2016; Knight et al., 2014, 2015; Hodges et al., 2022; Bagazinski and Ahmed, 2023a) and free form deformation techniques (Wang et al., 2022; Ao et al., 2021, 2022; Peri et al., 2001; Demo et al., 2021; Abbas et al., 2023). With a design representation, a dataset of designs can can be created by calculating or simulating performance metrics for each design. With the dataset, data-driven models can be trained to make inferences on new designs. For ship design specifically, the works of Khan et al. (Khan et al., 2022b,a, 2023), Shaeffer et al. (Shaeffer, 2023; Shaeffer et al., 2020), and Bagazinski et al. (Bagazinski and Ahmed, 2023a) have looked at various methods to create diverse design spaces and datasets for ship hull design.

With a dataset of designs and performance metrics of a hull as inputs, data-driven surrogate models, using methods such as neural networks, provide a computationally inexpensive way to predict performance. Significant research has been done on predicting the hydrodynamics of hulls with neural network-based surrogates due to the high cost of performing computational fluid dynamics simulations (Ao et al., 2021, 2022; Khan et al., 2022a,b; Peri et al., 2001; Read, 2009; Lu et al., 2016; Feng et al., 2022; Wang et al., 2022; Marlantes and Maki, 2021; Silva and Maki, 2023).

Generative artificial intelligence models are designed to create new content or data that resemble the input they were trained on. These models can produce a wide range of outputs, from text to images, and even complex design structures. In the context of ship design, datasets facilitate quick performance predictions and serve as a foundation for training generative artificial intelligence models to innovate in hull design. Prior work has explored various generative approaches, including variational autoencoders (Hodges et al., 2022), generative adversarial networks (Yonekura et al., 2023; Khan et al., 2023), and diffusion models (Bagazinski and Ahmed, 2023b), each contributing uniquely to the field.

Diffusion models, in particular, iteratively modify a noisy data vector over many specified steps. This transforms random data to mirror the statistics of training data (Ho et al., 2020). The development of diffusion models has shown that they can generate complex data and already have applications for engineering design. For example, diffusion models were shown to create higher quality images compared to generative adversarial networks (Ho et al., 2020). Subsequent advancements in diffusion models introduced guidance, where gradients from a classifier neural network guide image synthesis to match a specific image classification label (Dhariwal and Nichol, 2021). This evolution enabled text-to-image diffusion models that employ text-based guidance to craft custom, lifelike images (Ramesh et al., 2022; Rombach et al., 2022). Guided diffusion models have found applications in generating 3D shapes from image data (Liu et al., 2023). In addition, guided diffusion can be applied to engineering design generation. For example, guided diffusion has been used to create two-dimensional structures (Mazé and Ahmed, 2023; Giannone et al., 2023b,a), room layouts (Ploennigs and Berger, 2023), thermometers (Yang et al., 2023), architected materials (Lew and Buehler, 2023), and vehicles (Arechiga et al., 2023). A notable advantage of diffusion models is their adaptability, allowing the incorporation of new design constraints or objectives without necessitating retraining the entire model. This attribute is particularly beneficial for iterative design processes, where continuous adjustments are essential for optimizing performance.

The work presented in this paper builds on the prior work in training diffusion models for hull design. A prior model called *ShipGen* can generate parametric ship hull designs that have 91.4% lower wave drag and 47.9x higher internal volume on average compared to the original training data (Bagazinski and Ahmed, 2023b). *ShipGen* implements seven different guidance models to create these designs. A major shortcoming of this model is that there is no control to generate desired principal characteristics in a hull design, such as length, beam, draft, depth, and displacement. All hull designs generated by *Ship-*

Gen are purely influenced by the guidance models and not by a human designer. This makes *ShipGen* impractical for some real-world design applications, where designers may seek more freedom in imposing constraints. To address this gap, we propose a model that utilizes an additional feature called conditioning, where the diffusion model is given a hull design's principal characteristics during training. This way, the diffusion model will generate designs that satisfy the principal characteristics provided by a designer during sampling. The following subsections detail this improvement and showcase a few design applications with this diffusion model.

METHODS

This section outlines the methodology for developing C-ShipGen (Conditional *ShipGen*). The first subsection explores the training dataset of ship hulls, including formulae for geometric and performance measurements of the dataset hulls. The second subsection details the model training for the regression models used in this study. The third subsection details training and sampling with a conditional diffusion model. The fourth subsection details the methodology for analyzing designs generated with the diffusion model.

Dataset

To train the regression and generative models, a dataset of ship hulls and their respective performance metrics was created. The training dataset consists of 82,168 parametric ship hull designs. These dataset hulls were derived from the following sources:

- 30,000 hulls from the *Ship-D* dataset (Bagazinski and Ahmed, 2023a)
- 41,752 hulls generated using *ShipGen* (Bagazinski and Ahmed, 2023b)
- 10,416 hulls subset from the former *ShipGen* hulls with the addition of randomly parameterized bulbous bows and sterns

These parametric hull designs are represented with a forty-five-parameter scheme that algebraically defines the hull's surface. The *Ship-D* hulls cover the full design space possible with the parametric design scheme. The *Ship-D* hulls do not represent realistic-looking or performing hullforms. The hullforms, however, provide a large diversity of feature combinations that encompass realistic hull designs for machine learning applications (Bagazinski and Ahmed, 2023a). A few examples of the *Ship-D* dataset hulls are shown in Figure 2. Using the initial 30,000 *Ship-D* hulls, a guided tabular diffusion model called *ShipGen* was trained to generate high-performing hull designs. The mean performance of the 41,752 *ShipGen* hulls and the mean performance of the 30,000 *Ship-D* hulls was calculated and non-dimensionalized. Comparatively, the generated *ShipGen* hull designs have a mean wave drag that is 91.4% lower and a mean internal volume that is 47.9x higher than the mean performances found among the *Ship-D* dataset hull designs (Bagazinski and Ahmed, 2023b). A selection of *ShipGen* hulls is shown in Figure 3. The *ShipGen* hulls are much more representative of realistic hull designs compared to the *Ship-D* hulls. Among the *ShipGen* hulls, it was observed that few were generated with bulbous bows and bulbous sterns, a feature that can reduce the drag on hulls when designed well. To increase the presence of bulbs in the training dataset, bulbs were added to 10,416 hulls by randomly sampling the design parameters for bulbs. These bulbs were not tuned for hydrodynamic performance. Only a smaller subset of the *ShipGen* hulls were selected for bulbs as these were the hull designs that allowed for the generation of feasible bulb designs.

The feasibility of hulls is calculated using a set of forty-nine algebraic constraints. These constraints ensure that a parametric hull surface is watertight and non-self-intersecting. These algebraic constraints are solved with the parameter values for a given hull design without generating the hull's surface, reducing the total computation time. Full documentation of the hull design parameters and constraints is provided at `https://decode.mit.edu/projects/ShipGen/`.

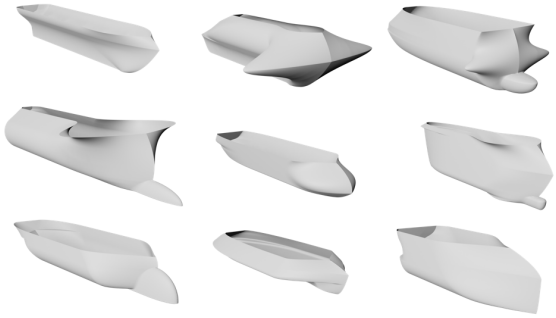

Figure 2: A selection of hulls from the *Ship-D* dataset, showing the variability possible with the hull parameterization. A random sampling from the dataset may lead to unrealistic hulls, containing combinations of features that do not resemble real-world ships and features that lead to poor performance.

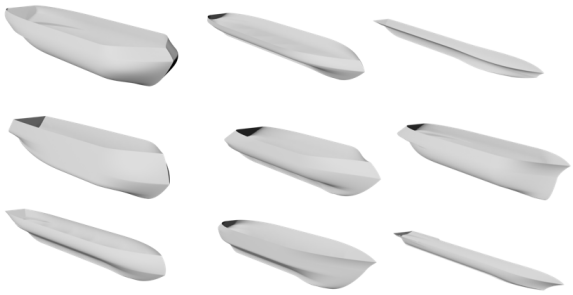

Figure 3: A selection of hulls generated with multi-objective guided performance generation. Notice the relative slenderness of the hulls leading to drastically reduced drag coefficients relative to the *Ship-D* dataset hulls.

Measures of Hull Geometry

In addition to the parametric hull designs, the dataset includes geometric measures for each hull. The displaced volume, wetted surface area, and waterline length were calculated at 100 evenly spaced draft marks across the depth of each hull. To generate designs regardless of scale, these geometric measures are scaled using the first parameter in the hull representation: length overall, or LOA. The equations for the normalized volume, surface area, and waterline length are provided in Equations 1, 2, and 3.

$$V_{t*} = \left(\frac{\int_0^{T/D=t*} \delta V(z)\, \delta z}{\text{LOA}^3} \right) \tag{1}$$

$$SA_{t*} = \left(\frac{\int_0^{T/D=t*} \delta SA(z)\, \delta z}{LOA^2} \right) \tag{2}$$

$$WL_{t*} = \left(\frac{X_{fwd}(t*) - X_{aft}(t*)}{LOA} \right) \tag{3}$$

In each equation, LOA scales the value based on its dimensionality: LOA^n. The other terms, $t*$ is ratio of draft, T, to depth, D. During model training, $t*$ will be used as an additional embedding to hull shape to predict the geometric measures of a hull at a specific draft mark.

Calculation of Total Hull Resistance

In addition to the geometric measures of each hull, the total resistance of each hull is calculated for many speed and draft conditions. Total resistance, R_T is estimated to be the sum of wave-making resistance, R_w, and skin friction resistance, R_f, as seen in Equation 4. Wave drag calculations were computed using Michell's integral. Michell's integral was chosen as the simulation for this study as it considers the full 3D geometry of a hull in the total resistance prediction while being computationally inexpensive to calculate. In practice, any fluid simulation would work for this study as the methodology of training generative models is the same. For this study, 2.6 million fluid simulations were performed using the Michell integral. The Michell integral balances the need for accurate simulation data with reduced computational cost of performing the simulation. For this study, thirty-two wave drag coefficients for each hull across four different drafts and eight velocity conditions. The four drafts are $t*$ = 0.25, 0.33, 0.50, and 0.67. The eight velocity conditions are normalized using Froude

scaling as seen in Equation 5, where g is gravitational acceleration, U is the ship's speed, and WL_{t*} is the non-dimensional waterline length for a given draft. In the denominator, WL_{t*} is multiplied by LOA to balance the dimensions of U and the denominator.

$$R_T = R_w + R_f \tag{4}$$

$$F_n = \frac{U}{\sqrt{gWL_{t*}LOA}} \tag{5}$$

The eight ship speeds are scaled between $F_n = 0.10$ and $F_n = 0.45$ in increments of 0.05, corresponding to typical operating conditions of traditional displacement hulls (Zubaly, 1996; Newman, 2018). Given the 3D surface of a hull submerged to $t*$ and a velocity, U, the wave-making resistance is calculated with Equation 6.

$$R_w = \frac{A\rho g^2}{\pi U^2} \int_1^\infty (I^2 + J^2) \frac{\lambda^2}{\sqrt{\lambda^2 - 1}}\, d\lambda \tag{6}$$

where ρ is the density of water, and A, I, and J are integrated terms relating to the surface normal across the hull and the direction of wave propagation. Further insight into these terms is in Michell's paper from 1898 (Michell, 1898). With these thirty-two wave drag measurements, a given hull's wave-making resistance for a given $t*$ and F_n is interpolated between these calculations.

Skin friction resistance is calculated using the ITTC-1957 formula in Equations 7 and 8.

$$C_f = \frac{0.075}{(\log(Re) - 2)^2} \tag{7}$$

$$R_f = \frac{1}{2} C_f \rho U^2 SA_{t*} LOA^2 \tag{8}$$

The Reynolds number of the hull, Re, scales with forward velocity, U, and waterline length, WL_{t*}. SA_{t*} is the non-dimensionalized wetted surface area of the hull for a given draft. Together, R_w and R_f can be used to calculate the coefficient of total resistance, C_T. To learn with the dataset, C_T is scaled by LOA^2 as opposed to the more traditional use of wetted surface area. This was done so that a regression model can embed LOA and $t*$ to predict C_T without explicitly providing SA_{t*}. Additionally, C_T is on a logarithmic scale so that the distribution of C_T is approximately Gaussian for model training. The calculation of C_T is provided in Equation 9.

$$C_T = \log_{10}\left(\frac{R_w + R_f}{\frac{1}{2}\rho U^2 LOA^2}\right) \tag{9}$$

With this representation, C_T will be predicted using the 45 design parameters, $t*$ for a draft embedding, and F_n for a speed embedding. The predicted coefficient of total resistance, $\hat{C_T}$, can then be scaled to a prediction of total resistance. $\hat{R_T}$ with Equation 10.

$$\hat{R_T} = 10^{\hat{C_T}} \frac{1}{2} \rho U^2 LOA^2 \tag{10}$$

The following subsection will detail training the regression models and the diffusion model with a dataset made from these equations.

Regression Modeling with Neural Networks

Using neural networks, four regression models were trained with the dataset: displaced volume, coefficient of total resistance, waterline length, and design feasibility. A trained neural network for regression provides two key benefits for computational design. The first benefit is a fast prediction of performance directly from design parameters. The second benefit is the ability to calculate the gradient of a performance metric with respect to the design parameters. This subsection will detail the process of training the regression models.

Following prior work, the forty-four (not including LOA), design parameters are quantile normalized and then scaled between -1 and 1 (Bagazinski and Ahmed, 2023b). Quantile normalization bins values of the design parameters so that the distributions of the design parameters are approximately Gaussian. This parameter scaling improves the diffusion model training. Scaling the parameters for the regression models allows them to work in conjunction with the diffusion model during sampling. This process, called guidance, will be described in the following subsection.

The process for training the coefficient of the total resistance regression model is described in Table 1. In the algorithm, the neural network is represented as P_{C_T}. The inputs to the regression model are a quantile normalized design vector, X_i, a draft embedding, $t*$, a speed embedding, F_n, and a length embedding, $\log(LOA)$. The loss function is the mean-squared error loss between the ground truth and the prediction of C_T. The draft and speed embeddings are restricted to the limits of the range of draft and Froude numbers used in the dataset calculation of wave-making resistance. The length embedding is on a logarithmic scale for hulls with a length between 3 meters and 450 meters. This range of values allows the model to learn the relative influence of skin friction across velocity and length scales. Given the diversity of hull forms in the dataset and the range of length scales, this regression model is trained to predict the coefficient of total resistance on a large diversity of shapes, speeds, and sizes. This model was trained with a batch size of 1024 for 50,000 batches. The resistance prediction model predicts the total resistance coefficient across the full spectrum of the dataset hulls, draft ratios, and Froude numbers. This regression model predicts the total resistance coefficient derived from the simulation with an R^2 of 0.997. Results of the training accuracy relative to the simulation data are shown in Figure 6 and Figure 8.

1:	**repeat**
2:	**select** X_i from Dataset
3:	$t* \sim Uniform([0.25, 0.67])$
4:	$F_n \sim Uniform([0.05, 0.45])$
5:	$\log(LOA) \sim Uniform([0.47, 2.65])$
6:	**interpolate** $R_{w_{t*,F_n}}$, SA_{t*}, and WL_{t*} from Dataset
7:	**calculate** C_f, R_f, and C_T
8:	$\hat{C_T} = P_{C_T}(X_i, t*, F_n, \log(LOA))$
9:	Take gradient descent step on: $\nabla_{P_{C_T}}(C_T - \hat{C_T})^2$
10:	**until** converged

Table 1: The training algorithm for the total resistance coefficient regression model. The algorithm randomly samples a Froude number and draft ratio for a hull in each batch so the model is trained on a full spectrum of speeds and drafts for the hulls in the dataset.

The training for the volume regression model, P_V, and the waterline regression model, P_{WL}, is similar. The volume regression model was trained to predict $\log(V_{t*})$ given X_i and $t*$. The model was trained to predict the logarithm of volume as this term has an approximate Gaussian distribution across the dataset. Similar to the C_T regression model, the volume regression is trained to predict the displaced volume for any draft on a large diversity of hullforms. The waterline regression model predicts the waterline length of a given hull at a given draft. This model is used with the coefficient of total resistance regression model when WL_t* is unknown.

The final regression model is a feasibility classifier, f_ϕ. The feasibility classifier provides guidance gradients to influence the diffusion model to generate parametric designs that satisfy the forty-nine algebraic feasibility constraints (Bagazinski

and Ahmed, 2023b). The only input to the feasibility classifier is a design vector, X_i. To learn the distinction between feasible and infeasible designs, a set of 82,793 design vectors that violate at least one constraint was generated. The loss function in training was binary cross-entropy loss, which is better for classifier training than mean-squared-error loss.

Conditional Diffusion Model

A diffusion model is a generative artificial intelligence model that generates new instances of data by denoising random information over many steps. The generated sample will fall within the statistical distribution of the training dataset samples. Conditional diffusion models are similar to the standard diffusion model described by (Ho et al., 2020), however, their structure includes extra layers that embed information in the training and sampling process. This conditional diffusion model is a modified version of the *ShipGen* model, a tabular diffusion model for ship hull design (Bagazinski and Ahmed, 2023b). The conditioning for the model is the principal characteristics of the hull: draft, beam, depth, and displaced volume. The diffusion model and the conditioning use parameters that are scaled by the length overall, which is the first term in the forty-five parameter representation used to generate the hull designs. After sample generation, the parameter terms are re-scaled by LOA to measure the scaled design. By training with parameters scaled with respect to LOA, the model does not have to learn "length" in addition to the statistical relationships between the parameters to generate a hull design. This reduces the complexity of the learning task. The training algorithm for the conditional diffusion model is stated in Table 2 and illustrated with Figure 4.

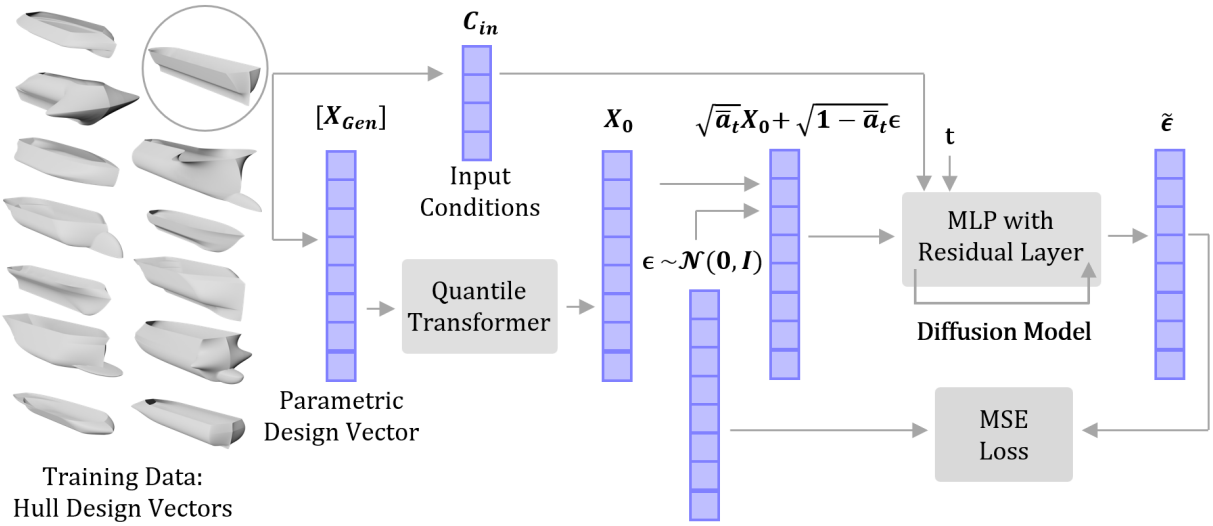

Figure 4: During training, the diffusion model predicts a denoising step, given a timestep embedding and a partially noised sample design vector. The model is informed by the input conditioning at each denoising step.

The diffusion model is conditioned with the draft, $t*$; volume, V_{t*}; Beam, B, and depth, D of each hull. During training, the original design vector is partially noised to a timestep, t, and the conditional diffusion model predicts the noise of the sample at that timestep. Conditioning is applied to the diffusion model to influence the denoising process to satisfy input conditioning. To clarify in the algorithm, t is the timestep embedding of the denoising process, while $t*$ is the draft embedding of the hull design in the conditioning vector.

After training, the diffusion model can be sampled to create design vectors that satisfy the input conditioning. While the diffusion model can generate hull designs that satisfy the input conditioning, the sampling process does not consider the total resistance of the hull. To generate hulls with reduced total resistance, the total resistance coefficient regression model is implemented in the sampling process as a guidance algorithm. Guidance leverages the gradients of the regression model

1:	**repeat**
2:	$X_0 \sim q(X_0)$
3:	$t* \sim Uniform([0.01, 1.0])$
4:	**interpolate** V_{t*}, B, and D from Dataset
5:	$C = [t*, \log(V_{t*}), B, D]$
6:	$t \sim Uniform(\{1, ..., T\})$
7:	$\epsilon \sim N(0, I)$
8:	Take gradient descent step on: $\nabla_\theta \|\|\epsilon - \epsilon_\theta(\sqrt{\bar{a}_t}X_0 + \sqrt{1-\bar{a}_t}\epsilon, t, C)\|\|^2$
9:	**until** converged

Table 2: This is the training algorithm for a conditional diffusion model. The diffusion model is represented by the function $\epsilon_\theta(X_0, \epsilon, t, C)$ in step 8. The conditioning for hull design is the draft,$t*$; displaced volume, $\log(V_{t*})$; beam, B; and depth, D, of the hull, X_0

at each timestep to influence the denoising process toward producing designs with reduced total resistance. In addition to resistance guidance, the feasibility classifier and the volume prediction regression models are also used as guidance. The feasibility classifier aims to improve the likelihood that a generated design vector leads to a feasible hull design. The volume guidance assists the diffusion model in generating a design that satisfies the input conditioning for displaced volume. This was implemented to prevent the resistance guidance from over-influencing the sampling process and producing hulls that do not satisfy the input conditioning. Each guidance algorithm is tuned with a hyperparameter: γ tunes the classifier guidance, while λ_0 and λ_1 tune the performance guidance. The sampling process is illustrated in Figure 1. The sampling algorithm is stated in Table 3.

1:	**input** $C = [t*, V, B, D,]$ and U, LOA
3:	$X_T \sim N(0, I)$
4:	**for** $t = T, ..., 1$ **do**
5:	$Z \sim N(0, I)$ if $t > 1$, else $z = 0$
6:	$F_n = \frac{U}{gP_{WL}(X_t, t*)LOA}$
7:	$X_{t-1} = \frac{1}{\sqrt{\alpha_t}}\left(X_t - \frac{1-\alpha_t}{\sqrt{1-\bar{\alpha}_t}}\epsilon_\theta(X_t, t, C)\right) + \sigma_t(Z(1-\gamma)) + \gamma\nabla_{X_t} f_\phi(y\|X_t)$ $-\lambda_0 \nabla_{X_t} P_{C_T}(X_i, t*, F_n, \log(LOA)) - \lambda_1 \nabla_{X_t}\left(V - P_V(X_t, t*)\right)^2$
8:	**end for**
9:	**return** X_0

Table 3: This is the sampling algorithm for a guided conditional diffusion model. The diffusion model is represented by the function $\epsilon_\theta(X_t, t, C)$ in step 7.

In the sampling algorithm, γ is equal to 0.2, while λ_0 and λ_1 are equal to 0.3. The performance guidance hyperparameters are set equal so that no model overpowers the others. The λ values are set low so the guidance models do not overpower the denoising process from the diffusion model. One advantage to leveraging performance guidance is that the diffusion model does not need to be retrained to produce designs when considering different objectives. The guidance model can simply be replaced with a new one. Using an *NVIDIA GeForce RTX 4090*, 512 samples are generated in approximately 2.5 seconds. The feasibility check, total resistance calculation, and geometric measurements are computed on a single *Intel Core i9-13900K* core in approximately 2.5 seconds per sample. After sampling, the parallel CPU process across 32 cores for the 512 samples is less than 30 seconds.

Diffusion models rely on a degree of randomness in the denoising process. Sampling from the guided conditional model will not guarantee that every generated design will be high-quality. Therefore, studies on designs generated from the model evaluate the statistics from a set of generated designs. In addition, high-quality designs will be filtered from a set of generated designs to select potential candidates for further design evaluation. This is distinctly different from other data-driven design approaches, such as optimization, which provides some guarantee of design performance and constraint satisfac-

tion among generated designs. Assuming that intended designs fall within the statistical distribution of the training dataset, conditional diffusion models can produce a large diversity of designs without needing to retrain the model, significantly decreasing the computational effort to create high-quality designs compared to optimization methods.

Evaluation of Diffusion Model for Low-Drag Design

A baseline comparison is needed to evaluate the ability of the guided conditional model to generate high-quality hull designs. Design optimization for drag reduction was selected as the baseline comparison. To conduct the study, five design test cases compare optimized hull forms to diffusion-generated hull forms. The purpose of this test is twofold:

1. Evaluate the diffusion model's ability to design low-resistance hulls while meeting specific dimensional properties.
2. Evaluate the accuracy of the total resistance regression model for a wide array of designs, scales, and relative speeds.

The five test cases were selected to create a unique set of dimensional requirements for both the design optimization and the diffusion model to satisfy. The designs of real-world ship classes inspired the dimensions of the five test cases. The design inspirations are a supercarrier [1] , a kayak [2] , a NeoPanamax container ship [3] , a frigate [4] , and a ROPAX ferry [5] . These test cases encompass two military-style ships, two large ship designs, one small hull design, two small block coefficient designs, and one high beam-to-draft ratioed hull. The principal dimensions and design speed of the test cases are provided in Table 4.

Test Case	**LOA** (m)	**BOA** (m)	**T** (m)	**D** (m)	$\boldsymbol{\forall}$ (m^3)	$\boldsymbol{C_B}$ $(-)$	$\boldsymbol{U_s}$ (m/s)	$(knots)$
Supercarrier [1]	333.0	42.1	11.3	29.6	97,561	0.617	16.0	31.1
Kayak [2]	3.8	0.787	0.15	0.438	0.166	0.372	1.50	2.92
NeoPanamax [3]	366.0	50.0	15.2	40.0	182,114	0.654	10.3	20.0
Frigate [4]	127.0	16.0	6.90	11.0	4,488	0.320	14.4	28.0
ROPAX Ferry [5]	72.0	20.0	3.2	4.8	3,917	0.850	6.17	12.0

Table 4: This table provides the dimensions of hull design test cases inspired by real-world ship designs. These test cases cover a diversity of principal characteristics, hull speeds, and length scales.

It is not expected for the diffusion model nor the optimization algorithm to produce designs that look like real-world ship designs with the same principal characteristics. Real-world hull designs satisfy many additional performance objectives in addition to total resistance; such as seakeeping, upright stability, cargo packing, general arrangements, etc. Since these hulls are generated only considering total resistance and principal dimensions, they are not expected to resemble real-world hull designs. For each design test case, 512 hull designs were generated with the full diffusion model, 512 were generated with the diffusion model and classifier guidance only, and 100 designs were generated using design optimization. In each test case, the diffusion-generated designs will be evaluated on drag, dimensional target satisfaction, and design diversity compared to optimized designs.

The optimization algorithm used for these studies is *NSGA-II* (Deb et al., 2002). *NSGA-II* is a state-of-the-art genetic algorithm for optimizing two or more objectives. Genetic algorithms are a set of optimization algorithms that act similarly to biological evolution to drive the optimization over several "generations". These tests were performed with a population

[1] supercarrier Inspiration: `https://www.nvr.navy.mil/SHIPDETAILS/SHIPSDETAIL_CVN_68.HTML`

[2] Kayak Inspiration: `https://oldtownwatercraft.johnsonoutdoors.com/us/shop/kayaks/recreation/loon-126`

[3] NeoPanamax Inspiration: `https://www.cmacgm-group.com/en/group/at-a-glance/fleet/ships/9780873/cma-cgm-t-roosevelt`

[4] Frigate Inspiration: `https://www.dcms.uscg.mil/Our-Organization/Assistant-Commandant-for-Acquisitions-CG-9/Programs/Surface-Programs/National-Security-Cutter/`

[5] ROPAX Inspiration: `https://www.steamshipauthority.com/about/vessels`

of 100 samples for 200 generations. The initial population consisted of randomly selected designs from the dataset. For each test case, the optimization algorithm constrains the design parameters to be within 2% of the beam target, 1% of the depth target, and $\geq$ 99% of the volume target, while also constraining the design with the forty-nine feasibility constraints to maintain design feasibility. The target draft is held constant, so $t*$ is scaled appropriately for each design at each generation during optimization. This provides a buffer for the optimization algorithm to find low-drag designs around the test case targets. In this study, the two objective functions were the total resistance of a hull and the total resistance coefficient of a hull, which were evaluated using the total resistance coefficient regression model, P_{C_T} at the test case's target speed. By leveraging the same regression model in both optimization and diffusion generation, we can directly compare the ability of each design method to produce low-drag designs. The optimization is expected to exploit the regression model, likely finding local minima and not a true minimum. This will be seen as a significant loss in accuracy when comparing predictions from the regression model to the original total resistance simulation. With the combined use of parallelized CPU computation (*Intel Core i9-13900K*) and GPU (*NVIDIA GeForce RTX 4090*), this optimization is performed in approximately 80 minutes per test case.

RESULTS

This section contains the results of the studies described in the Methods Section. The first subsection provides error measurements of diffusion-generated samples meeting the principal dimensions from the five test cases. The second subsection provides the results by generating low-resistance designs using the conditional diffusion model and the design optimization algorithm.

Targeted Design Sampling with Conditional Diffusion Model

For each design test case, 512 samples were generated with the full model, and 512 samples were generated with only feasibility guidance, $\nabla_{X_t} f_\phi(y|X_t)$. The feasibility rate and adherence to principal dimensions in each test case are provided in Table 5.

Test Case	Model	Feasibility Rate	Volume Error		Beam Error		Depth Error	
			Mean	*Std.*	*Mean*	*Std.*	*Mean*	*Std.*
Supercarrier	Full Model	67.77%	-3.17%	8.83%	2.03%	2.98%	-2.14%	1.82%
	$\nabla_{X_t} f_\phi$ Only	88.28%	2.53%	5.97%	1.46%	4.94%	-1.65%	1.82%
Kayak	Full Model	86.91%	0.05%	4.52%	-0.50%	2.75%	-0.45%	1.77%
	$\nabla_{X_t} f_\phi$ Only	95.70%	0.62%	3.50%	0.40%	3.55%	0.06%	1.63%
NeoPanamax	Full Model	71.09%	-2.89%	5.63%	1.41%	3.60%	-0.44%	1.69%
	$\nabla_{X_t} f_\phi$ Only	92.19%	2.26%	4.66%	0.18%	3.74%	-0.01%	1.70%
Frigate	Full Model	91.99%	-0.87%	6.60%	0.22%	8.06%	-0.31%	2.44%
	$\nabla_{X_t} f_\phi$ Only	94.53%	0.83%	6.93%	1.65%	10.27%	0.19%	1.93%
ROPAX ferry	Full Model	58.98%	-16.73%	7.57%	-4.74%	6.78%	-1.02%	1.86%
	$\nabla_{X_t} f_\phi$ Only	88.48%	-2.80%	5.52%	0.38%	7.37%	-0.34%	2.15%

Table 5: This table provides the design feasibility rate and principal dimension errors relative to each test case for diffusion-generated samples using the full model and with feasibility guidance only.

The general trend among these test cases is that designs sampled with feasibility guidance only have higher feasibility rates and have tighter adherence to the test case's principal dimensions compared to hulls generated with the full model. This trend is seen in all five test cases. Generated hull designs within a 5% error tolerance will be selected for further design analysis. This tolerance is a reasonable margin for large ship hull designs. A ship's displacement can easily vary by this much through changes in cargo, fuel, water, etc. Sampling with only feasibility guidance yields, on average, 58.3% of hulls

generated within a 5% volume error across the five test cases. Sampling with the full model gives 37.0% of total samples within a 5% volume error tolerance. This measure was calculated with Equation 11 for each design test case.

$$\eta_{E_{V_{t*}}} = \eta_{fease}\Phi\left(\frac{+5\% - \mu_{E_{V_{t*}}}}{\sigma_{E_{V_{t*}}}}\right) - \Phi\left(\frac{-5\% - \mu_{E_{V_{t*}}}}{\sigma_{E_{V_{t*}}}}\right) \tag{11}$$

In the equation, $\eta_{E_{V_{t*}}}$ is the percentage of samples within a 5% volume error tolerance. This metric relies on the feasibility rate, η_{fease}, and the Gaussian cumulative distribution between +5% and -5% error given the mean ($\mu_{E_{V_{t*}}}$) and standard deviation($\sigma_{E_{V_{t*}}}$) of volume error.

Drag Reduction with Guidance During Sampling

For each design test case, hull designs were optimized using *NSGA-II* to minimize the total resistance while satisfying the principal dimensions of the test case. After optimization, the total resistance of the 100 optimized hulls was calculated with the Michell Integral. The minimum total resistance calculated with the Michell Integral is listed in Table 6 for each test case. Similarly, the total resistance was calculated for the feasible hull designs among the 512 designs generated for each test case. The feasible hull designs were sorted into groups with volume errors less than 1%, 5%, and 10% relative to the target volume for each design test case. Then, the number of hulls with a total resistance less than the optimized minimum total resistance was collected. The number of these low resistance samples within each volume error tolerance is listed in Table 6. The final column in Table 6 lists the minimum total resistance among the diffusion-generated designs within a 5% volume error tolerance for each design test case. These results will be further analyzed in the Discussion Section.

Test Case	***NSGA-II* Min. R_T** *[N]*	**Model**	**Number of Low R_T Hulls with $E_{V_{t*}}$** $\leq 1\%$	$\leq 5\%$	$\leq 10\%$	**Sample Min. R_T** *[N]*	**ΔR_T**
Supercarrier	7,332,137.7	Full Model	0	5	11	4,883,089.3	-33.4%
		$\nabla_{X_t} f_\phi$ Only	0	1	1		
Kayak	11.18	Full Model	8	50	56	6.98	-37.6%
		$\nabla_{X_t} f_\phi$ Only	1	2	2		
NeoPanamax	3,931,834.1	Full Model	37	157	239	1,220,057.3	-69.0%
		$\nabla_{X_t} f_\phi$ Only	5	23	28		
Frigate	1,177,601.3	Full Model	30	130	178	874,617.0	-25.7%
		$\nabla_{X_t} f_\phi$ Only	26	87	114		
ROPAX ferry	2,512,677.3	Full Model	1	9	41	206,537.0	-91.8%
		$\nabla_{X_t} f_\phi$ Only	42	208	307		

Table 6: This table lists the number of feasible, diffusion generated hull designs having a total resistance less than the minimum total resistance found through optimization. The number of hulls with low resistance increases as the volume error tolerance is increased. The final column lists the reduction in total resistance seen by a hull within a 5% volume error generated by C-ShipGen.

In general, as the volume error tolerance is loosened, more diffusion-sampled hull designs will have lower total resistance than the optimized hull design. This trend is seen in samples generated using the full model and among samples generated using only classifier guidance. Additionally, for four test cases, the full diffusion model produces low resistance designs within a 5% volume error tolerance at a rate of 1.5x to 25x more frequently than without using performance guidance. In addition, the full diffusion model generated hulls with at least 25% less total resistance than the *NSGA-II* generated hulls while still aligning to the principal dimensions of each design test case. For the *ROPAX* test case, the diffusion model with only classifier guidance created low-resistance designs with much higher success than the full diffusion model. Further analysis of the test cases can be found in the Discussion Section.

To illustrate the diversity of designs generated by the diffusion model, a two-dimensional principal component analysis

(PCA) was performed with the design parameters from the training dataset, the diffusion-generated designs, and the *NSGA-II* sampled designs. The PCA was fitted with the training dataset. Figure 5 shows this PCA. The diffusion-generated samples maintain a high degree of diversity. This is expected as the diffusion model is trained to randomly generate designs that match the statistics of the training data. The optimized designs, however, are clustered around a single location on the PCA plot, suggesting these samples have low diversity.

After sampling, all feasible diffusion-generated designs and *NSGA-II* generated designs were simulated with the total resistance simulation. This was done to compare the regression model accuracy to the simulation data. Figure 6 shows the total resistance of each hull using both regression and simulation plotted against each other for the supercarrier design test case. The red dashed line shows perfect regression, meaning that the regression predicts the exact simulation. The generated samples show high accuracy with the regression, except for a few outliers. This is expected as the diffusion-generated samples statistically resemble the training dataset. This dataset was used to train both the regression model and the diffusion model. Because diffusion-generated designs will statistically resemble the training data, they should have higher accuracy with the regression model. The hull designs created through optimization are significantly under-predicted compared to the total resistance calculated with the simulation. As mentioned in the methods section, this result was expected as the optimization algorithm exploited the regression model to find a minimum in the model that does exist in the simulation. This trend is seen across optimized hulls from the other four test cases, shown in Figure 8.

To further visualize the resistance across the diffusion-generated samples, a kernel density estimate (KDE) of the distribution of the simulated total resistance is shown in Figure 7. Also included in the plot is the minimum simulated total resistance among hulls sampled with *NSGA-II*. The KDE shows that approximately fifteen percent of diffusion-generated samples for this design test case will have lower total resistance than samples generated with *NSGA-II* using the same surrogate model for drag prediction. This relative trend also appears with the other four test cases shown in Figure 9.

The optimized designs from the ROPAX ferry design test case exhibit the worst regression-simulation similarity among the test cases. The regression prediction for the optimized ROPAX ferry was off by nearly a factor of 10 compared to its simulation-calculated resistance. Further analysis of the error in simulation prediction is in the Results Section.

To exhibit some of the diffusion-generated hull designs, Figure 10 showcases the station lines of hulls from each test case. The Figure showcases the hull design sampled among the 512 with the minimum resistance within the 5% volume error tolerance for each design test case. The total resistance of these hulls is listed in Table 6.

DISCUSSION

This section provides a discussion of the results of the study. The first subsection analyzes the diffusion model's ability to satisfy the principal characteristics from the design test cases. The second subsection discusses the study on generating low-resistance designs. A third subsection discusses the ROPAX design case study compared to the other design test cases. The final subsection discusses the limitations of the C-ShipGen model in designing real-world hulls.

Targeted Sample Generation

The study's findings underscore the effectiveness of the conditional diffusion model in generating feasible designs that closely adhere to design requirements. The tolerance to the user-defined principal characteristics decreases when performance guidance is implemented with the model during sampling. Performance guidance reduces the diffusion model's ability to generate hulls within a 5% volume error tolerance by 36%. The next subsection will discuss how performance guidance produces low-resistance hull designs more frequently while maintaining the 5% volume error tolerance.

While not every individual design meets the entirety of the specifications provided by a user during sampling, the diffusion model proves to be a computationally inexpensive tool for producing samples closely aligned with intended principal di-

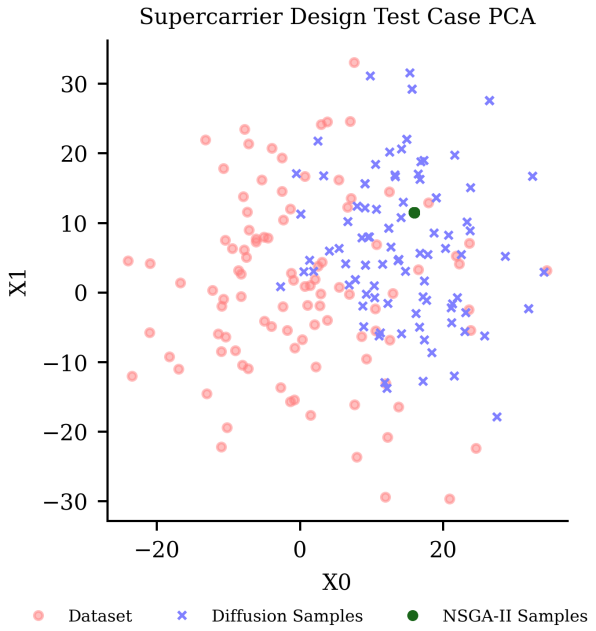

Figure 5: Two-dimensional principal component analysis of the hull parameterization shows the relative distribution between dataset hull designs, diffusion-generated hull designs, and optimized hull designs for the supercarrier test case. The optimized hulls have much less design diversity than the diffusion-generated designs.

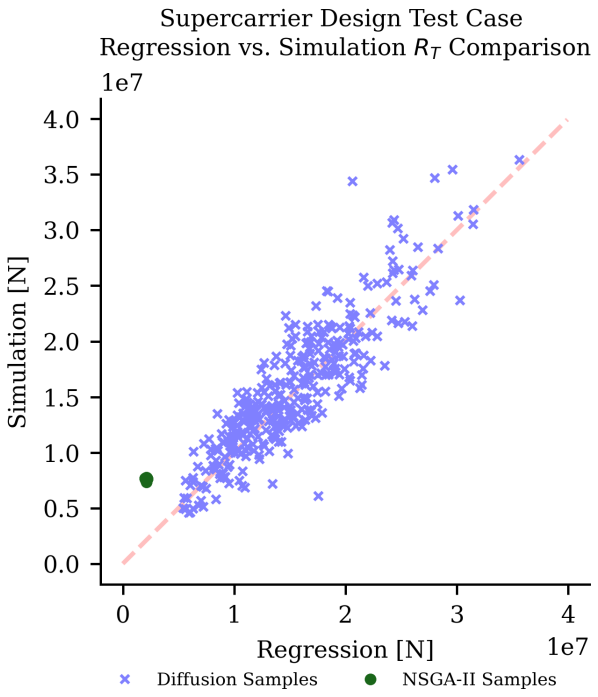

Figure 6: Comparison of total resistance between simulation and regression for hull designs produced for the supercarrier design test case. The optimized designs have lower regression accuracy than the diffusion-generated designs.

mensions. This characteristic makes it particularly advantageous for early-stage design processes, where loosely following requirements allows for design exploration. The diffusion model produces many diverse designs for further in-depth design analysis. With an efficient down-selection process, many useful hull designs are quickly identified within a user-desired tolerance with C-ShipGen.

Optimization versus Diffusion Models for Design Generation

Optimization represents a powerful approach to design exploration but has strong advantages and disadvantages. One key strength is the optimization's ability to generate samples within tighter tolerances to user-defined targets. Additionally, the optimization process excels at producing feasible designs with low resistance. On the other hand, design optimization for each test case can be slow and computationally expensive. For *NSGA-II*, increasing the population size increases the time complexity of the algorithm by $O(N^2)$. Increasing the number of objectives increases its time complexity by $O(N)$ Deb et al. (2002). Optimization is limited by the diversity of samples and the computational complexity arising from increasing the number of samples. This inhibits design space exploration in early-stage design. Finally, as seen in the results, optimization exploits regression models, which leads to a loss in accuracy of the optimized design's prediction versus ground truth performance calculated with simulation. In this instance, the loss in accuracy of the total resistance regression surrogate model compared to the simulation leads to sub-optimal hull designs compared to those generated with the C-ShipGen model.

The diffusion model presents a contrasting set of advantages and challenges. The computation to generate designs is signif-

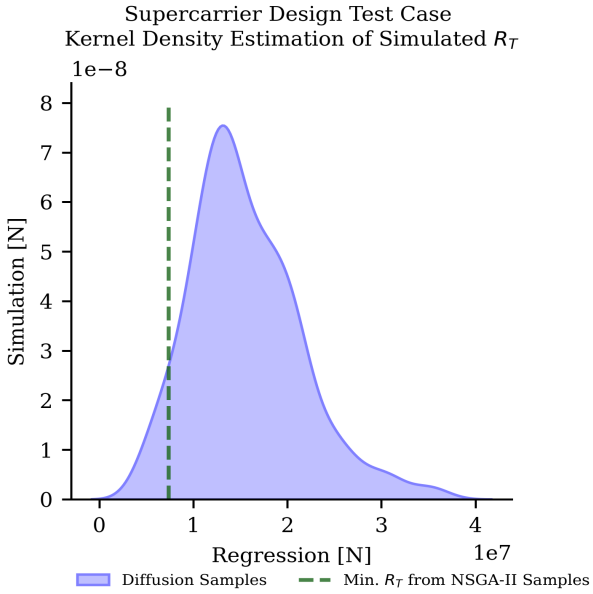

Figure 7: Kernel Density Estimate (KDE) of the distribution of the simulated total resistance across the diffusion-generated samples for the supercarrier test case. The distribution shows that some of the generated samples have a total resistance less than the minimum total resistance found using the total resistance prediction as a surrogate model with *NSGA-II*.

icantly faster, allowing more design space exploration and discovery over-optimization methods. Increasing the number of generated samples increases the time complexity of C-ShipGen by $O(N)$. Increasing the number of objectives increases the time complexity of C-ShipGen by $O(N)$. Secondly, this diffusion model produces new designs without model retraining, which allows significant flexibility in its use. This flexibility permits hull design across all scales of real-world displacement hulls within a large range of typical operating speeds. This flexibility is thanks to the diversity of the samples in the training data. Thirdly, leveraging the total resistance regression model during the diffusion sampling process is particularly advantageous. The regression model and the diffusion model were trained with the same dataset. Since the diffusion model is trained to generate designs with statistical similarity to the training dataset, the regression model has high prediction accuracy for diffusion-generated designs. This similarity between the training data and sampled designs is why C-ShipGen saw a significant improvement in total resistance among generated samples compared to *NSGA-II* using the same total resistance regression model. This trend was seen across the five design test cases in Figure 6 and Figure 8. This accuracy did not hold in optimization-generated designs. In addition, the diffusion model better leveraged the regression model in sampling. This is shown through the proportion of designs in each test case with lower total resistance than the samples generated with *NSGA-II* using the same regression model. Figure 7 and Figure 9 show that depending on the test case, roughly fifteen percent or more of the diffusion-generated samples will have a lower total resistance than samples generated using *NSGA-II*. However, the diffusion model has its own set of limitations. One major flaw is that the generated design needs to be sorted and filtered to identify low-resistance hull forms that meet the input conditioning within a desired tolerance. Additionally, while the diffusion model facilitates rapid design exploration, it does not provide a guarantee of finding an optimal solution, introducing an element of uncertainty into the design process.

Additionally, the diffusion model with performance guidance produces designs within a specified tolerance less frequently than the diffusion model without performance guidance, and even less frequently than optimization. Despite this compromise in tolerable design generation, these designs demonstrate a notable reduction in drag compared to their counterparts without performance guidance. Implementing performance guidance produces low resistance designs at a rate of 1.5x to 25x than the model without the implementation. The simultaneous benefits of lower drag and decreased feasibility highlight the nuanced impact of performance guidance on design outcomes.

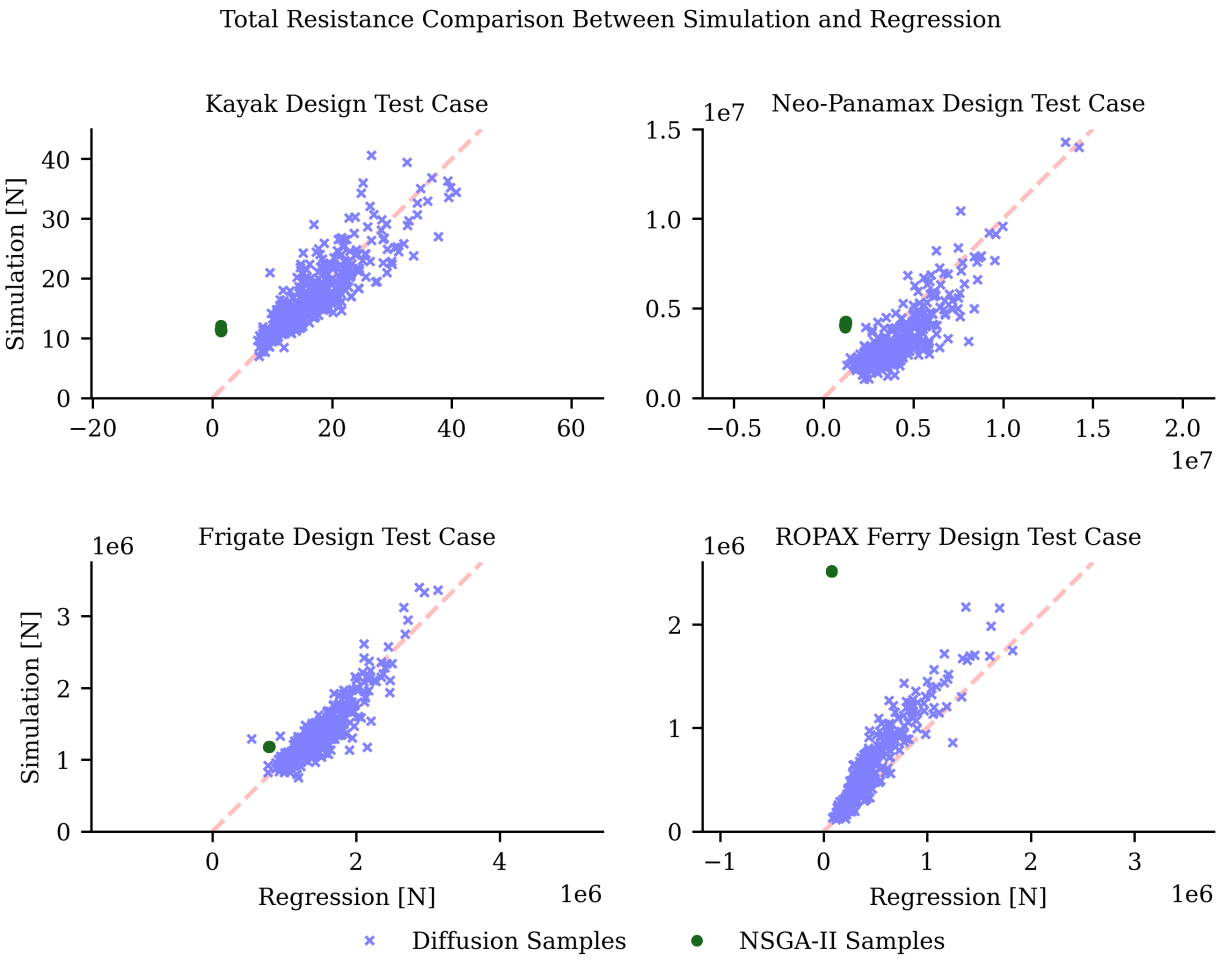

Figure 8: Comparison of total resistance between simulation and regression for hull designs produced for the other design test cases. The total resistance of optimized designs is less accurately predicted by the regression model than the diffusion-generated designs.

Analysis on ROPAX Ferry Design

Despite the general success of the other design test cases, the ROPAX ferry design proved difficult for the diffusion model, the regression model, and the optimization algorithm. This design test case was inspired by a real-world ferry operating in the State of Massachusetts in the United States. This particular hull has a significantly higher length-to-draft ratio, beam-to-draft ratio, and block coefficient compared to other design test cases. These comparisons are also true compared to hulls in the training data. As this design is different than most of the training data, the outcomes of the test case were expected to be poorer. This is particularly true with the total resistance prediction model. The regression model had completely inaccurate predictions of total resistance for the *NSGA-II* generated samples. The diffusion-generated designs also had poor regression accuracy as well. A third consideration with this particular design that is outside the project's scope is that the resistance simulation itself is also highly inaccurate for this design. Michell's integral relies on the assumption that the hull is a slender body (Michell, 1898). The ROPAX design is not necessarily slender compared to the other hulls. A new simulation method is needed to reasonably calculate the drag on a hull design like this one.

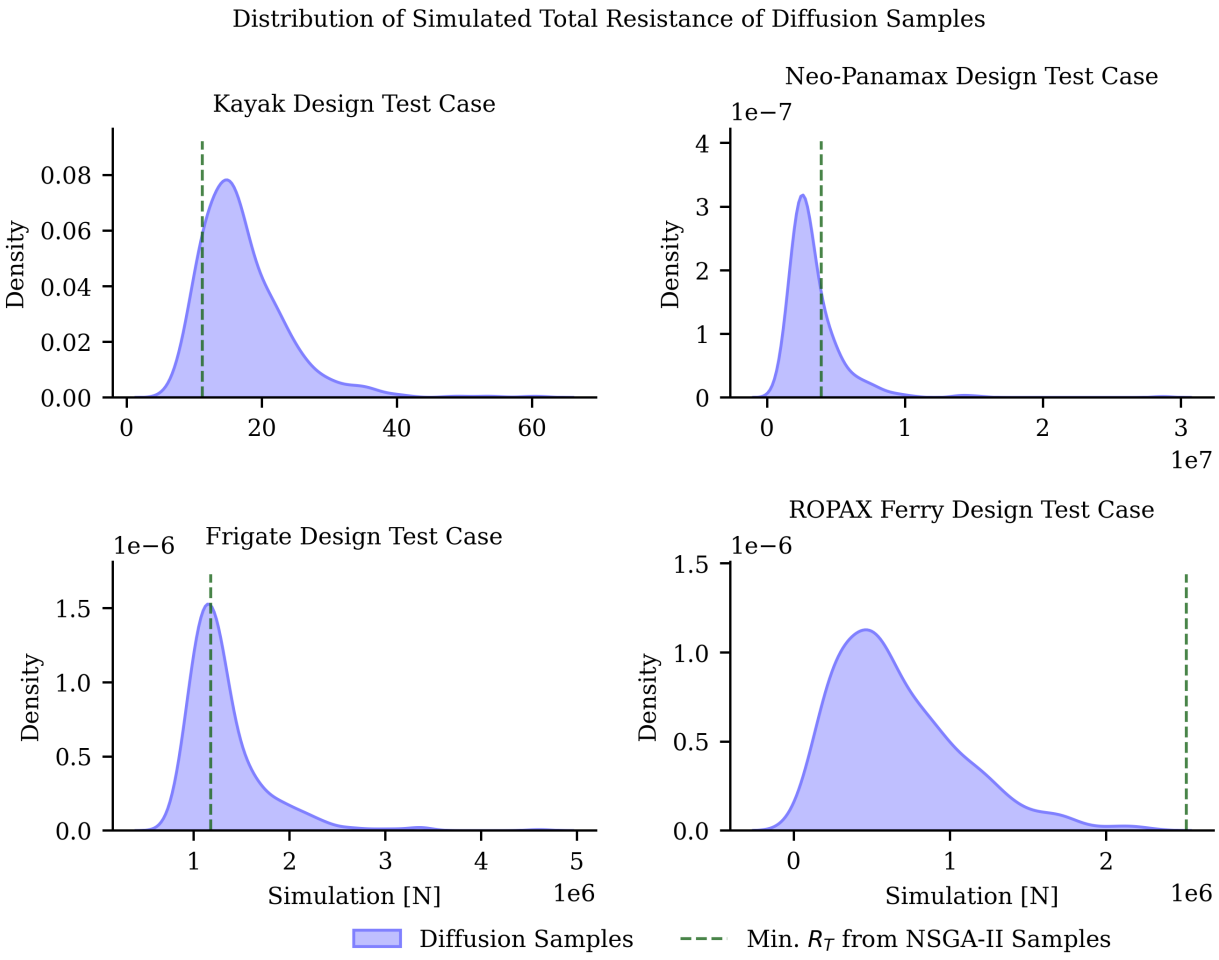

Figure 9: KDE plots of the remaining four design test cases. The plots showcase the statistical distribution of total resistance among the diffusion-generated samples compared to the *NSGA-II* generated samples. Depending on the test case, 15% or more of the generated samples will have less total resistance than samples produced using *NSGA-II* with the same surrogate model for total resistance prediction.

Limitations of Hull Design with C-ShipGen

When designing any product with generative artificial intelligence, understanding the model's limitations will avoid negative consequences on real products designed with the model. C-ShipGen has several limitations. The first limitation of this model is the training data. C-ShipGen and other diffusion models generate designs statistically similar to the training data. Since C-ShipGen was trained on hulls that are not necessarily representative of real-world hull designs, C-ShipGen generates hulls that are not necessarily representative of real-world designs. The second limitation of C-ShipGen is the simulation used to generate the total resistance training data. While the Michell integral is not the most accurate simulation for real-world hull design, it was chosen to balance accuracy and computational cost. Creating training data with higher fidelity and more accurate simulations will give these models data with a better representation of real-world hull designs in water. In addition, leveraging more accurate simulations for creating training data will enhance claims of increased performance with generative design. The third limitation of C-ShipGen in its current implementation is that it only considers total resistance and volume displacement for design generation. Real ship hulls are designed considering other performance metrics such as seakeeping, stability, general arrangements, draft limitations, and countless other considerations for hull design.

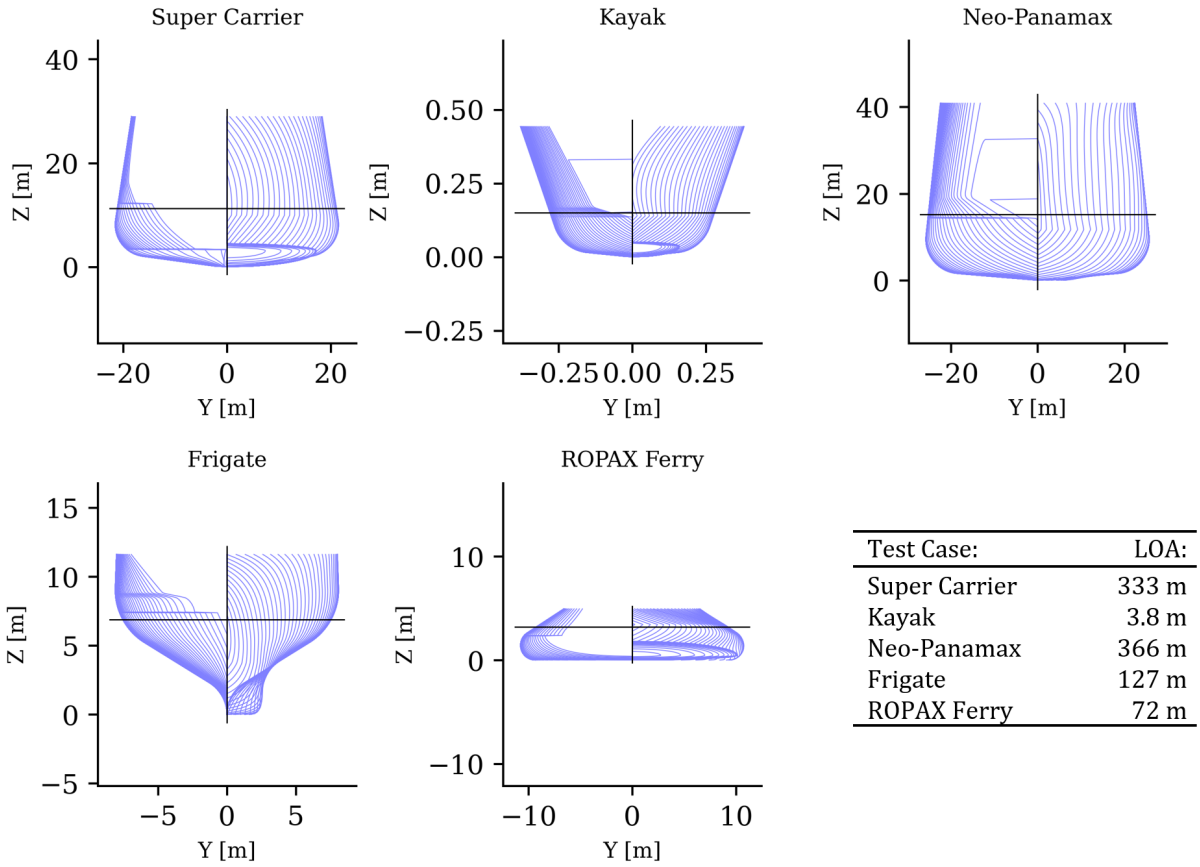

Test Case:	LOA:
Super Carrier	333 m
Kayak	3.8 m
Neo-Panamax	366 m
Frigate	127 m
ROPAX Ferry	72 m

Figure 10: The five hulls depicted are diffusion-generated hulls with the minimum total resistance within the 5% volume error tolerance for each design test case. The cross-section drawings showcase station lines for the bow on the right side and the stern on the left side. Also included is the LOA for each design.

Therefore, hulls designed with C-ShipGen are not necessarily capable of performing safely in the real world without further analysis. These are some of the limitations of the current implementation of C-ShipGen to create hull designs with low total resistance.

CONCLUSION

This work generated ship hulls with low resistance using a conditional diffusion model that considers the desired principal dimensions of the hull during design generation. This diffusion model is trained on a large set of nearly 83,000 diverse hull designs that allow for a comprehensive design space exploration with the model. In addition, a regression model was trained to predict the total resistance of a hull with variable speed and draft. The gradients of this regression model allowed the diffusion model to generate designs with low resistance. This regression model was also used as a surrogate model to optimize hulls while constraining the designs to user-defined principal dimensions and design speeds. The optimization study was performed using *NSGA-II*. Five design test cases demonstrated the ability of C-ShipGen to generate hull designs across all scales of displacement hulls and many different dimensional properties found in different ship classes. Additionally, C-ShipGen was able to generate designs with greater diversity than *NSGA-II*, while creating designs with better predictive alignment between the regression model and the simulation used in the training data. A proportion of the diffusion-generated designs in each test also had a total resistance less than the samples generated with *NSGA-II*. In all five test cases,

C-ShipGen produced hull designs with at least 25% less total resistance than *NSGA-II* generated samples. An additional advantage of the diffusion model is that the diversity of these designs allows for efficient design space exploration in early-stage design.

Creating hull designs with reduced resistance will reduce the need to fuel ships, reducing the cost to operate the ship and reducing its emissions. Future work with generative artificial intelligence for ship design will continue to explore the systems-level design of ships. Training models to explore the nuanced complexity of designing a ship system can yield better efficiencies and reduce costs for the marine industry. Through this work, the economic prospect of leveraging generative artificial intelligence to design ship hulls is demonstrated by C-ShipGen.

ACKNOWLEDGEMENTS

This research is funded by the United States Department of Defense, Office of Naval Research, via the National Defense Science and Engineering Graduate (NDSEG) Fellowship program. The authors thank MIT Supercloud for providing some of the computational resources needed to perform this work (Reuther et al., 2018).

DATA ACCESS STATEMENT

Data, Code, and Trained models for C-ShipGen will be available upon publication at `https://decode.mit.edu/projects/C_ShipGen/`.

DECLARATION OF GENERATIVE AI AND AI-ASSISTED TECHNOLOGIES IN WRITING

Statement: During the preparation of this work the author(s) used OpenAI's *ChatGPT* (version 3.5) and *Grammarly* to reduce word count. After using this tool/service, the author(s) reviewed and edited the content as needed and take(s) full responsibility for the content of the publication.

CONTRIBUTION STATEMENT

Noah J. Bagazinski: Conceptualization; data curation, methodology; writing – original draft. **Faez Ahmed:** supervision; writing – review and editing.

REFERENCES

Abbas, A., Rafiee, A., and Haase, M. (2023). Deepmorpher: deep learning-based design space dimensionality reduction for shape optimisation. *Journal of Engineering Design*, 34(3):254–270.

Ao, Y., Li, Y., Gong, J., and Li, S. (2021). An artificial intelligence-aided design (aiad) of ship hull structures. *Journal of Ocean Engineering and Science*.

Ao, Y., Li, Y., Gong, J., and Li, S. (2022). Artificial intelligence design for ship structures: A variant multiple-input neural network-based ship resistance prediction. *Journal of Mechanical Design*, 144(9):091707.

Arechiga, N., Permenter, F., Song, B., and Yuan, C. (2023). Drag-guided diffusion models for vehicle image generation. *arXiv preprint arXiv:2306.09935*.

Bagazinski, N. J. and Ahmed, F. (2023a). Ship-d: Ship hull dataset for design optimization using machine learning. In *International Design Engineering Technical Conferences and Computers and Information in Engineering Conference*. American Society of Mechanical Engineers.

Bagazinski, N. J. and Ahmed, F. (2023b). Shipgen: A diffusion model for parametric ship hull generation with multiple objectives and constraints. *Journal of Marine Science and Engineering*, 11(12):2215.

Brown, A. and Salcedo, J. (2003). Multiple-objective optimization in naval ship design. *Naval Engineers Journal*, 115(4):49–62.

Chrismianto, D. and Kim, D.-J. (2014). Parametric bulbous bow design using the cubic bezier curve and curve-plane intersection method for the minimization of ship resistance in cfd. *Journal of Marine Science and Technology*, 19:479–492.

Deb, K., Pratap, A., Agarwal, S., and Meyarivan, T. (2002). A fast and elitist multiobjective genetic algorithm: Nsga-ii. *IEEE Transactions on Evolutionary Computation*, 6(2):182–197.

Demo, N., Tezzele, M., Mola, A., and Rozza, G. (2021). Hull shape design optimization with parameter space and model reductions, and self-learning mesh morphing. *Journal of Marine Science and Engineering*, 9(2):185.

Dhariwal, P. and Nichol, A. (2021). Diffusion models beat gans on image synthesis. *Advances in neural information processing systems*, 34:8780–8794.

Evans, J. H. (1959). Basic design concepts. *Journal of the American Society for Naval Engineers*, 71(4):671–678.

Feng, Y., el Moctar, O., and Schellin, T. (2022). Parametric hull form optimization of containerships for minimum resistance in calm water and in waves. *Journal of Marine Science and Applications*.

Giannone, G., Regenwetter, L., Srivastava, A., Gutfreund, D., and Ahmed, F. (2023a). Learning from invalid data: On constraint satisfaction in generative models. *arXiv preprint arXiv:2306.15166*.

Giannone, G., Srivastava, A., Winther, O., and Ahmed, F. (2023b). Aligning optimization trajectories with diffusion models for constrained design generation. *arXiv preprint arXiv:2305.18470*.

Ho, J., Jain, A., and Abbeel, P. (2020). Denoising diffusion probabilistic models. *Advances in neural information processing systems*, 33:6840–6851.

Hodges, J., Wheeler, M., Belhocine, M., and Henry, J. (2022). Ai/ml applications for ship design. *ICCAS 2022*.

Khan, S., Goucher-Lambert, K., Kostas, K., and Kaklis, P. (2023). Shiphullgan: A generic parametric modeller for ship hull design using deep convolutional generative model. *Computer Methods in Applied Mechanics and Engineering*, 411:116051.

Khan, S., Kaklis, P., Serani, A., and Diez, M. (2022a). Geometric moment-dependent global sensitivity analysis without simulation data: application to ship hull form optimisation. *Computer-Aided Design*, 151:103339.

Khan, S., Kaklis, P., Serani, A., Diez, M., and Kostas, K. (2022b). Shape-supervised dimension reduction: Extracting geometry and physics associated features with geometric moments. *Computer-Aided Design*, 150:103327.

Knight, J. T., Singer, D. J., and Collette, M. D. (2015). Testing of a spreading mechanism to promote diversity in multiobjective particle swarm optimization. *Optimization and Engineering*, 16:279–302.

Knight, J. T., Zahradka, F. T., Singer, D. J., and Collette, M. D. (2014). Multiobjective Particle Swarm Optimization of a Planing Craft with Uncertainty. *Journal of Ship Production and Design*, 30(04):194–200.

Lew, A. J. and Buehler, M. J. (2023). Single-shot forward and inverse hierarchical architected materials design for nonlinear mechanical properties using an attention-diffusion model. *Materials Today*, 64:10–20.

Lin, C.-K. and Shaw, H.-J. (2017). Feature-based estimation of preliminary costs in shipbuilding. *Ocean Engineering*, 144:305–319.

Liu, R., Wu, R., Van Hoorick, B., Tokmakov, P., Zakharov, S., and Vondrick, C. (2023). Zero-1-to-3: Zero-shot one image to 3d object.

Lu, Y., Chang, X., and Hu, A.-k. (2016). A hydrodynamic optimization design methodology for a ship bulbous bow under multiple operating conditions. *Engineering Applications of Computational Fluid Mechanics*, 10(1):330–345.

Marlantes, K. and Maki, K. (2021). Modeling vertical planing boat motions using a neural-corrector method. In *SNAME International Conference on Fast Sea Transportation*, volume Day 1 Tue, October 26, 2021.

Mazé, F. and Ahmed, F. (2023). Diffusion models beat gans on topology optimization. *Proceedings of the AAAI Conference on Artificial Intelligence*, 37(8):9108–9116.

Michell, J. H. (1898). Xi. the wave-resistance of a ship. *The London, Edinburgh, and Dublin Philosophical Magazine and Journal of Science*, 45(272):106–123.

Newman, J. N. (2018). *Marine hydrodynamics*. The MIT press.

Peri, D., Rossetti, M., and Campana, E. F. (2001). Design optimization of ship hulls via cfd techniques. *Journal of ship research*, 45(02):140–149.

Ploennigs, J. and Berger, M. (2023). Diffusion models for computational design at the example of floor plans. *arXiv preprint arXiv:2307.02511*.

Ramesh, A., Dhariwal, P., Nichol, A., Chu, C., and Chen, M. (2022). Hierarchical text-conditional image generation with clip latents. *arXiv preprint arXiv:2204.06125*.

Read, D. (2009). *A drag estimate for concept-stage ship design optimization*. The University of Maine.

Reuther, A., Kepner, J., Byun, C., Samsi, S., Arcand, W., Bestor, D., Bergeron, B., Gadepally, V., Houle, M., Hubbell, M., Jones, M., Klein, A., Milechin, L., Mullen, J., Prout, A., Rosa, A., Yee, C., and Michaleas, P. (2018). Interactive supercomputing on 40,000 cores for machine learning and data analysis. In *2018 IEEE High Performance extreme Computing Conference (HPEC)*, pages 1–6.

Rombach, R., Blattmann, A., Lorenz, D., Esser, P., and Ommer, B. (2022). High-resolution image synthesis with latent diffusion models. In *2022 IEEE/CVF Conference on Computer Vision and Pattern Recognition (CVPR)*, pages 10674–10685. IEEE.

Shaeffer, A. (2023). *Application of Artificial Neural Networks to Early-Stage Hull Form Design*. PhD thesis, George Mason University.

Shaeffer, A. K., Wilson, W., and Yang, C. (2020). Application of machine learning to early-stage hull form design. In *SNAME Maritime Convention*, page D043S019R002. SNAME.

Silva, K. M. and Maki, K. J. (2023). Implementation of the critical wave groups method with computational fluid dynamics and neural networks. *arXiv preprint arXiv:2301.09834*.

Wang, Y., Joseph, J., Aniruddhan Unni, T., Yamakawa, S., Barati Farimani, A., and Shimada, K. (2022). Three-dimensional ship hull encoding and optimization via deep neural networks. *Journal of Mechanical Design*, 144(10):101701.

Yang, C., Liu, F., and Ye, J. (2023). A product form design method integrating kansei engineering and diffusion model. *Advanced Engineering Informatics*, 57:102058.

Yonekura, K., Omori, K., Qi, X., and Suzuki, K. (2023). Designing ship hull forms using generative adversarial networks. *arXiv preprint arXiv:2311.05470*.

Zhang, Y., Kim, D.-J., and Bahatmaka, A. (2018). Parametric method using grasshopper for bulbous bow generation. In *2018 International Conference on Computing, Electronics & Communications Engineering (iCCECE)*, pages 307–310. IEEE.

Zubaly, R. (1996). *Applied Naval Architecture*. Cornell Maritime Press.

Proceedings of 15th International Marine Design Conference (IMDC-2024)
June 2-6, 2024
Amsterdam, the Netherlands

Digital Twin-Enabled Response Function Analysis: A Synthetic Approach to Ship's Propulsion System Assessment

Oleksiy Bondarenko[1,*] and Yasushi Kitagawa[2]

ABSTRACT

Analyzing the behavior of vessels in actual sea conditions is crucial for conceptual system design, safety and energy efficiency considerations. However, the essential seakeeping problem is reduced to the analysis of wave-hull interactions often neglecting consideration of the propulsion. But in the meantime, the synthetic consideration of wave–propulsion interactions is a key for safety and energy efficiency. Furthermore, safety evaluation of a ship's design with reduced propulsion power in adverse seas is vital for risk management. Response functions are commonly used to estimate propulsion system responses in incoming seaways. This paper proposes a synthetic approach using digital twin technology for rapid response function estimation. It introduces a companion linearized state-space model linked with the digital twin, enabling immediate retrieval of coefficients for response function analysis at the desired operating point. This integrated methodology provides a comprehensive representation of ship propulsion behavior in wave environments, offering a comprehensive framework for system performance assessment.

KEY WORDS

Propulsion system; state-space model; propulsion system dynamics; describing function analysis.

INTRODUCTION

Over the last decade, concerns about environmental issues have spurred the maritime industry to undergo a major shift towards zero-emission shipping. Digital transformation is considered one of the drivers in transforming the maritime industry into a more sustainable and efficient transportation sector. With the advent of the Internet of Things (IoT) and the development of sensors and monitoring systems, a wide variety of data has become available for processing onboard or at on-shore data centres, delivering a number of new possibilities. However, raw data is of little value until it is turned into information to enable knowledge. In this context, the advancement in the digitalization of ship operations and the imperative to turn the raw data into knowledge for informed decision-making, have given rise to the development of another emerging technology – a digital twin. The digital-twin is an accurate virtual replica of its physical counterpart, that delivers valuable information by mapping the dynamic behavior in real time. For example, simulation-based analysis of operational data, where the error between predicted and actual responses may uncover system abnormalities. However, the utilization of such a complex tool cannot be justified as a universal tool for all kinds of applications. In particular, when it comes to predicting the expected significant value of a response ahead of time for a known spectrum of input disturbance, the response functions (derived from linear models) are preferable. Furthermore, the ship's hull seakeeping performance is commonly evaluated by using the response functions which translate waves into hull motion responses for a given wave frequency. In turn, wave and hull motions are the main cause of propeller torque fluctuation that disturbs the operation of the propulsion engine. Thus, the synthetic representation of the hull-propeller-engine mutual responses is highly relevant for the safety assessment of the ship propulsion system operation, especially in operation under extreme propeller load torque fluctuations (Sui 2022).

[1] Marine Environment and Engine System, National Maritime Research Institute, Tokyo, Japan;
[2] Fluid Engineering and Ship Performance Evaluation, National Maritime Research Institute, Tokyo, Japan;

* Corresponding Author: bond@m.mpat.go.jp

Submitted: 14 February 2024, Revised: 11 April 2024, Accepted: 1 May 2024, Published: 20 May 2024

Conference paper, DOI: https://doi.org/10.59490/imdc.2024.850 e-ISSN: 3050-4864

An early attempt at a synthetic consideration of ship propulsive performance in waves dates back to the late 70s (Naito 1979), where the linearized representation of the mutual relations among the functions of a ship propulsion system was derived and used for the prediction of speed loss of the ship in waves. Later Kim (1985) expanded the consideration of the ship propulsion system for the evaluation of propulsive dynamics in rough sea conditions. Recently, a notable effort on propulsion system dynamics and behavior in the time and frequency domains was made by Xiros (2002), where a linearized model is used for engine speed control synthesis, also taking into account turbocharger-engine interaction. An analysis of complex and extreme propeller-engine interaction in the case of ventilation and racing is reported by Bondarenko (2011, 2012). A more recent development of a linear representation of the core propulsion system is reported by Stapersma (2017) and in a companion paper by Vrijdag (2017). In that research, the linearized model of both uncontrolled and controlled systems was derived and used for time and frequency domain analysis of propulsion plant behavior in waves. It was concluded that the linearized model is a suitable tool for system analysis and controller development as long as the limitations of linearization are kept in mind.

Although a variety of linearization procedures and response function models can be found in the literature, an accurate estimation of the propulsion system response function requires detailed information about characteristics intrinsic to propulsion components such as hull, propeller, and engine; in the early stages of ship design, might not be available. Furthermore, ship in-service is characterized by a significant degree of uncertainty, and for this reason, the response function estimated from the "ideal" theoretical characteristics may not fit the actual system. At the same time, the digital twin binds information/data sources of the physical space, a set of dynamic models describing the physical counterpart, and a set of parametrized characteristics, parameters of which are instantiated explicitly for the specific ship in service. Thus, owing to the explicit functional relationships and parametrized characteristics at the core of the digital twin, the linearized representation of the propulsion system can be derived analytically.

This paper intends to provide a synthetic approach binding the identified parametrized models of the digital twin and the companion linearized state-space model, where the data feedback from the ship in service can be used to assess the propulsive performance in waves and review future ship designs. Moreover, to account for the engine torque limit function, the linearized model of the propulsion system was extended with a describing function - a quasi-linear representation of the hard nonlinearity.

THE BASE SHIP PROPULSION SYSTEM

In the context of the defined objective, which is the assessment of the propulsive performance of a ship in waves, a generic ship propulsion system may be considered to be made of three main components: an engine producing the torque, a shaft transmitting the torque from the engine to the propeller, and a propeller delivering thrust to a hull. Additionally, the engine speed governor, which is a part of the engine, forms the shaft speed control loop. Figure 1 details the composition and mutual relations among the functions of the components.

The ship's hull translation (surge) motion is based on a force balance between propeller thrust and hull resistance:

$$\left(m + m_x\right)\frac{dV_s}{dt} = T_p - R_t, \quad R_t = R_c + X_w \qquad [1]$$

where m and m_x are the constant hull mass and added mass, correspondingly; T_p is the effective propeller thrust, R_t is the total water resistance composed of calm water component, R_c, and the added resistance due to waves, X_w,. Here, it is worth noting that only time-averaged steady waves-induced forces acting on the ship hull are considered. In contrast, the time-varying oscillatory forces are neglected since the time scale is much shorter than that of the hull longitudinal velocity, Vs. Thus, equation [1] determines the steady-state position of the engine operating point.

The propulsion engine is directly interfaced with the propeller by means of shaft rotational dynamics, expressed as:

$$2\pi I_{sh}\frac{dn_{sh}}{dt} = Q_e - Q_p \qquad [2]$$

where Q_e, Q_p are the engine and propeller torques, respectively, I_{sh} is the moment of inertia of the rotating shaft system, including the engine, propeller and added mass of water, n_{sh} is the propeller shaft rotational speed which is also equivalent to the engine rotational speed, in case of direct coupling of propeller and engine. Note that the shaft speed control loop is also a part of the propulsion system, and the details will be covered later.

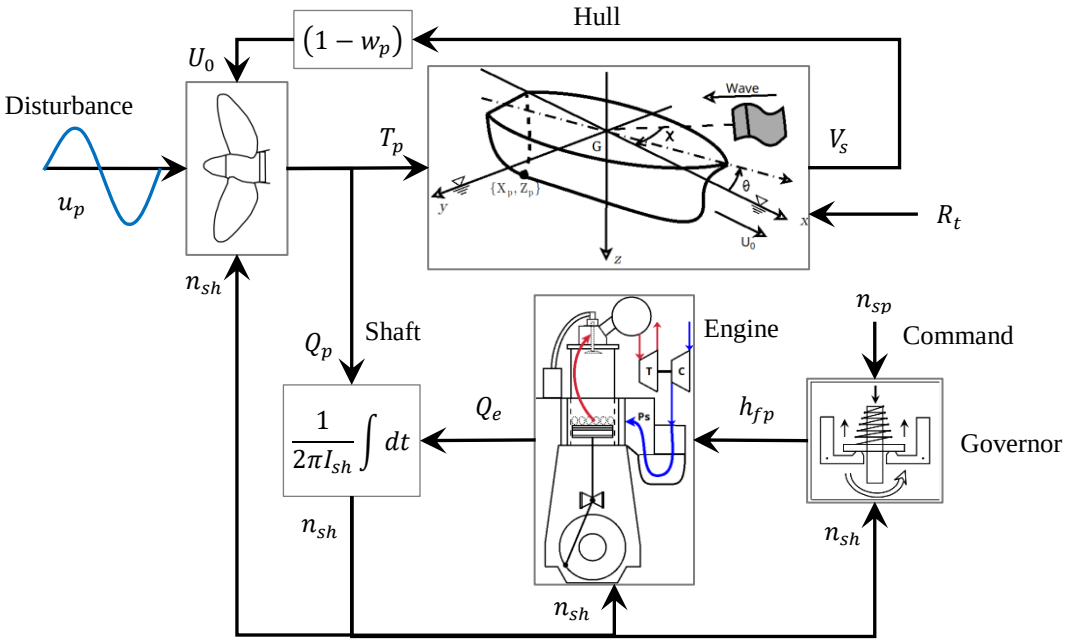

Figure 1: The base ship propulsion system

The static models of the effective propeller thrust and torque are based on the propeller open-water characteristics obtained in calm water conditions. These are given as follows:

$$
\begin{aligned}
T_p &= \left(1-t_p\right)\rho n_{sh}^2 D_p^4 K_t\left(J\right) \\
Q_p &= \rho n_{sh}^2 D_p^5 K_q\left(J\right)\tfrac{1}{\eta_r} \\
J &= \frac{U_p}{n_{sh}D_p}, \quad \because U_p = U_0 + u_p\left(t\right), \quad U_0 = V_s\left(1-w_p\right)
\end{aligned}
\qquad [3]
$$

where t_p is the thrust deduction ratio, w_p is the wake fraction, ρ is the water density, D_p is the propeller diameter, J is the propeller advance ratio, K_q, K_t are the torque and thrust coefficients expressed as polynomial functions of the J, defined by an open propeller characteristic, η_r is the propeller relative rotation efficiency, and U_p is the effective inflow velocity composed of the steady-part, U_0, and fluctuating part, $u_p(t)$. The time-varying forces induced by waves on the ship's hull excite oscillatory hull motions, which, in turn, along with the wave orbital motion, induce a time-varying velocity field around the propeller. The in-line or axial component, $u_p(t)$, of the velocity field, gives rise to a change in the advance velocity U_p and consequently the advance ratio J. With time-varying J, the propeller operating point is moving on the K_q curve, inducing fluctuation in the propeller torque and, consequently, engine torque and revolution. Thus, effective inflow velocity acts as a link between wave-hull interaction and propeller-engine response, provided that the base ship propulsion system can be split into separate parts, and each can be investigated independently. Figure 2 illustrates the boundaries of each part.

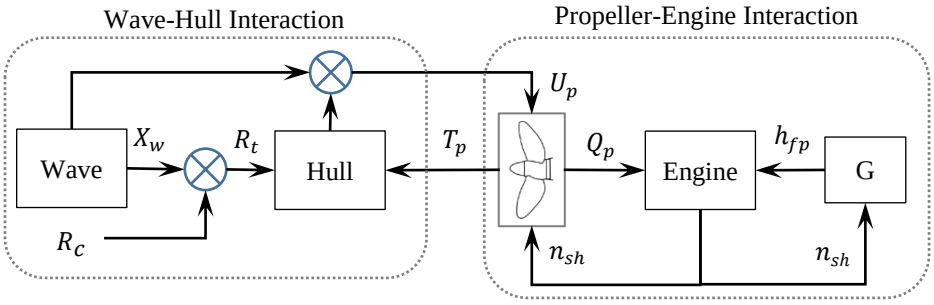

Figure 2: Decomposition of base ship propulsion system

Engine Model

Internal combustion engines remain an unavoidable part of the ship propulsion system, owing to the efficient conversion of fuel chemical energy into mechanical energy. The vast majority of merchant ships use low-speed, two-stroke marine Diesel engines as a prime mover. The objective of the engine model is to represent an external characteristic of the engine concerning the developed torque, which in the general case is a function of engine states such as rotational speed and air and fuel mass flows (Xiros 2002). In the field of propulsion system simulation, a cycle-mean value (CMV) engine modelling approach is commonly used for steady-state and transient performance evaluation (Hendrics 1989, Theotokatos 2010). The central assumption in the CMV modeling approach is that air and exhaust gases flow continuously irrespective of the intermittent nature of a cylinder scavenging process. Thus, the engine is considered a series of control volumes connected through flow restrictions, ensuring continuity of air and exhaust gas flows. The engine is decomposed into a finite number of elements, including the cylinder, air and exhaust gas receivers, turbocharger (TC) with a compressor and turbine, and an air cooler, as shown in figure 3 below.

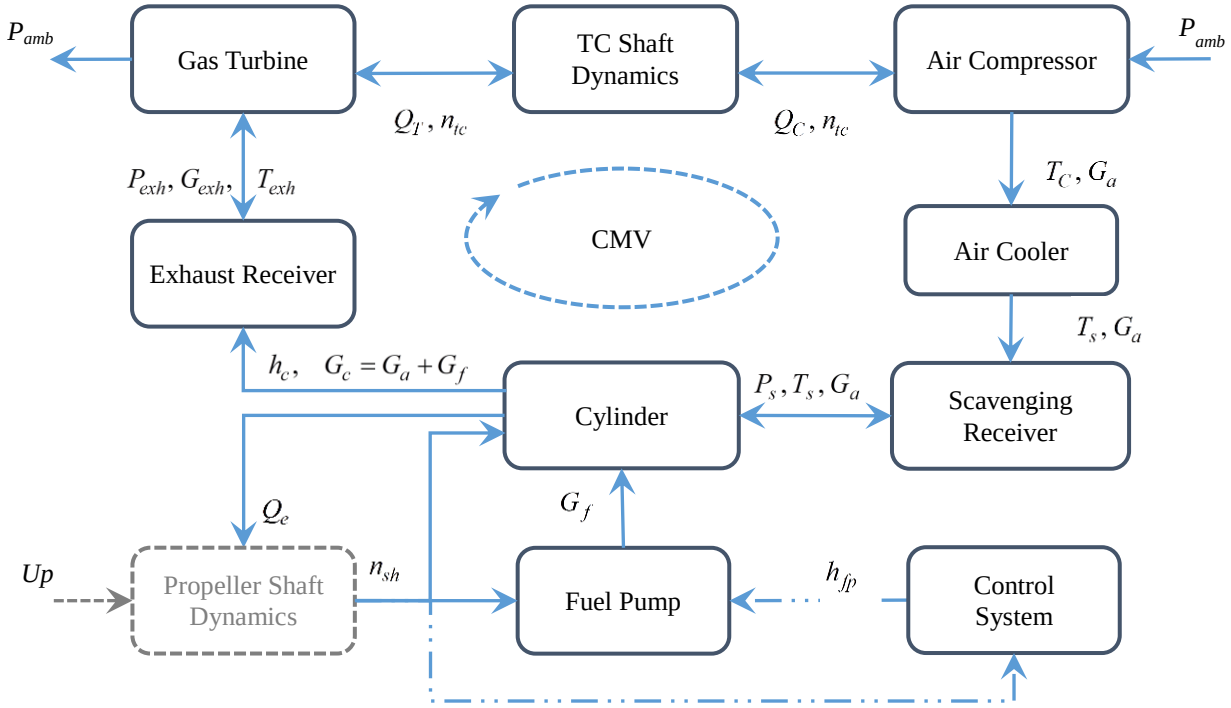

Figure 3: Composition of the propulsion engine

The compressor and turbine are mechanically linked via the TC shaft. An air cooler is connected between the compressor and the air receiver. The fuel pump, i.e. fuel injector, is directly connected to the cylinder. The engine's cylinders are linked with the propeller through shaft rotational dynamics, expressed by the equation [2]. In turn, the engine torque is the result of an indicated mean effective pressure (IMEP), P_i, developed in the cylinder volume V_s during one cycle, minus a friction mean effective pressure (FMEP), P_f:

$$Q_e = \frac{\left(P_i - P_f\right)V_s}{2\pi} \qquad [4]$$

The developed IMEP is a function of the engine states such as pressures, p, temperatures, T, and mass flows, G. The fundamental equations necessary to describe the temporal evolution of the engine state variables can be obtained from the following mass and energy conservation laws along with the ideal gas equation:

$$\frac{dm}{dt} = \sum_i G_i, \quad i \in \{a, exh, f\} \qquad [5]$$

$$p = \frac{m}{V}\tilde{R}T \quad \Rightarrow \quad \frac{dp}{dt} = \frac{dm}{dt}\frac{\tilde{R}T}{V} = \frac{\tilde{R}T}{V}\left(\sum_i G_i\right), \quad \because T = \text{const} \tag{6}$$

$$c_v m\frac{dT}{dt} + u\frac{dm}{dt} = \sum_i h_i G_i \tag{7}$$

here u is the internal energy, $\check{R}$, c_v are the thermodynamic constants, and m is the mass of the gas.
The air and exhaust gas mass flow rates, through the engine and turbine, respectively, are calculated under the assumption that an orifice with the equivalent mean effective flow area $\mu\check{A}$ can characterize the engine cylinder as well as turbine. Thus, the flow of compressible gas is evaluated according to:

$$G_{(a,exh)} = \mu\tilde{A}\frac{p_{in}}{\sqrt{RT_{in}}}\Psi\left(p_{in}, p_{out}\right) \tag{8}$$

here, the subscripts, in/out, represent the inlet and outlet parameters of the considered element, correspondingly. $\Psi = f(p_{in}, p_{out})$ is the throttling characteristic of the orifice.

The turbocharger, which is an integral part of the engine, contributes to the assurance of sustainable airflow necessary for optimal and efficient fuel combustion. The dynamic of the turbocharger, in terms of the rotational speed, is derived by applying the angular momentum conservation in the following form:

$$2\pi I_{tc}\frac{dn_{tc}}{dt} = Q_T - Q_C \tag{9}$$

$$Q_T = \frac{\eta_{iT}}{2\pi n_{tc}} G_{exh} C_{p.e} T_{exh}\left[1 - \left(\frac{P_{amb}}{P_{exh}}\right)^{\frac{k_e-1}{k_e}}\right] \tag{10}$$

$$Q_C = \frac{G_a C_{p.a} T_{amb}}{2\pi\, n_{tc}\, \eta_{iC}}\left[\left(\frac{P_s}{P_{amb}}\right)^{\frac{k_a-1}{k_a}} - 1\right] \tag{11}$$

where Q_T is the torque developed by the turbine due to the expansion of exhaust gas from pressure P_{exh}, Q_C is the torque required by the compressor to compress the air to pressure P_s in the scavenging receiver, n_{tc} is the turbocharger rotational speed, I_{tc} is the inertia of the turbocharger shaft, η_{iC}, η_{iT} are the isentropic efficiencies of the compressor and turbine, correspondingly.

The energy flow rate, $h_c G_c$, exiting the engine cylinder and taking part in the energy balance of the exhaust gas receiver in equation [7], is calculated by taking into consideration the energy conservation in the cylinder, averaged over one engine cycle, thus:

$$h_c G_c = G_a C_{p.a} T_s + G_f H_U - W_i, \quad \because W_i = \oint p_c dV \tag{12}$$

where W_i is the engine cylinder indicated work, which is the result of one complete engine cycle calculation. In the CMV approach, however, the complete combustion cycle simulation, as commonly accepted (Xiros 2002, Theotokatos 2010), has been seamlessly embedded by the coefficient ζ_a, which denotes the proportion of the fuel chemical energy retained in the exhaust gas:

$$\zeta_a = 1 - \frac{W_i}{G_f H_U} \tag{13}$$

Thus, the energy rate of exhaust gas is considered an increase in the energy rate of scavenging air due to combustion in the following form:

$$h_c G_c = G_a C_{p.a} T_s + \zeta_a G_f H_U \tag{14}$$

This, admittedly, fosters the successful transition to the transfer function representation.
The engine fuel mass flow rate, G_f, is calculated as a linear function of the fuel pump index, F_p, as follows:

$$G_f = Z_c m_{fc_{mcr}} h_{fp} n_{sh} \quad [15]$$

where m_{fc_mcr} is the mass of fuel injected per cycle at MCR, Z_c is the number of engine cylinders, and h_{fp} is the fuel pump index determined by the engine control system. The subscript 'mcr' denotes values at the MCR point of the engine.
Finally, in the quasi-steady context of CMV, the IMEP is considered proportional to the fuel pump index, as follows:

$$P_i = \eta_{C_{eff}} P_{i_{mcr}} h_{fp} \quad [16]$$

Indeed, increasing the fuel index leads to an increase in the fuel amount per cycle per cylinder and thus a higher IMEP, provided that a perfect combustion regime is maintained. The latter holds true for the most practical operating points along propeller lines. However, in actual sea conditions, when the engine operating point most likely shifts towards a region of low speed and high torque the ability of the compressor to supply air for combustion tends to decrease. Consequently, the combustion process becomes more susceptible to variations in air-to-fuel ratio (AFR). Moreover, in transient conditions, the fuel amount, determined by the fuel index, h_{fp}, adjusts sufficiently fast following the demand in engine torque to keep the engine speed constant, as shown by equation [2]. At the same time, the air mass flow may be delayed compared to that of fuel due to the large inertia of the TC and the lack of a mechanical connection between the TC and the engine shaft. Indeed, the energy of the exhaust gas delivered to the turbine must first accelerate the TC shaft for the compressor to develop air pressure before the cylinder, imposing additional delay due to the presence of the exhaust gas and air receivers in between. Thus, in transient conditions, due to the engine response to propeller load fluctuation, the optimal AFR ceases to hold due to the delay in air supply, leading to engine performance degradation. Such a phenomenon clearly must be accounted for in the dynamic engine model. Therefore, the IMEP in equation [16] is modified with the coefficient η_{Ceff}, introduced (Medica 1988, Xiros 2002) to take into account the losses due to incomplete fuel combustion. Furthermore, a series of theoretical and experimental studies (Bondarenko, 2018; Bondarenko, 2023) have revealed the characteristics of combustion process degradation due to the depletion of air charge in the cylinder. Thus, the following combustion efficiency coefficient is introduced into the model:

$$\eta_{C_{eff}} = f\left(AFR\right) = C_0 AFR^{\frac{b_0}{AFR}}, \quad \therefore AFR = \frac{G_a}{G_f} \quad [17]$$

where C_0 and b_0 are the coefficients that represent the sensitivity of combustion efficiency to the AFR. Figure 4 illustrates a family of characteristics for different coefficient selections. As can be observed, the adopted model demonstrates a consistent decline in combustion efficiency when AFR falls below the nominal value (AFR < 1.0), grounded on the experimental results.

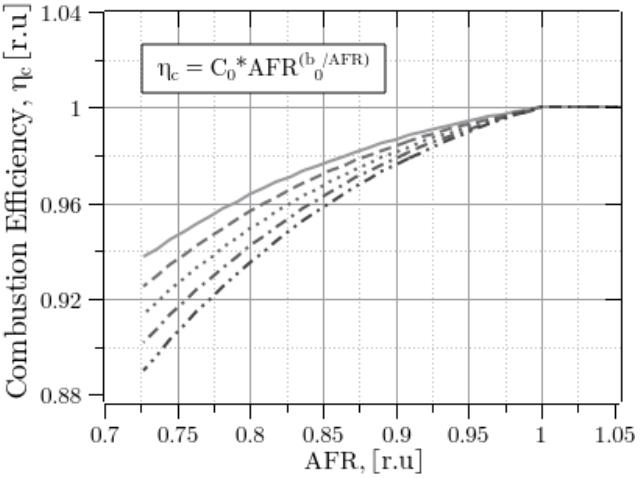

Figure 4: Combustion efficiency characteristics

Apart from the presented fundamental algebraic and differential equations describing the engine components' behavior, there are certain empirical characteristics required to complete the model. These include effective turbine area, $\mu\tilde{A}$, compressor isentropic efficiency, η_{iT}, remained fuel energy proportion in exhaust gas, ζ_a, FMEP, P_f, defined as follows:

$$\mu\tilde{A} = c_{\mu_0} + c_{\mu_1}\left(\frac{P_{amb}}{P_{exh}}\right) + c_{\mu_2}\left(\frac{P_{amb}}{P_{exh}}\right)^2 \quad [18]$$

$$\eta_{iT} = \eta_{iT_0}\left[\frac{n_{tc}}{C_s}\left(c_{T_0} - \frac{n_{tc}}{C_s}\right) + c_{T_1}\right] \quad [19]$$

$$\zeta_a = c_{\zeta_0} + c_{\zeta_1}\frac{Q_e}{Q_{e_{mcr}}} \quad [20]$$

$$P_f = P_{i_{mcr}}\left(c_{f_0} + c_{\zeta_1}\frac{n_{sh}}{n_{sh_{mcr}}} + c_{\zeta_2}h_{fp}\right) \quad [21]$$

The outlined CMV modelling approach results in continuous, nonlinear, and fully parameterized first-order ordinary differential equations, describing the time evolution of the key engine states, as shown below. Such model formulation allows for the analytical transition to the linear state-space model, ensuring the effective binding of the linear counterpart to the original nonlinear model.

$$\frac{d}{dt}\boldsymbol{Y}(t) = \boldsymbol{F}\left(\boldsymbol{Y}, \boldsymbol{\theta}, h_{fp}, u_p\right), \quad \boldsymbol{Y} = \left[n_{sh}, n_{tc}, P_s, M_{exh}, T_{exh}\right]^T \quad [22]$$

here $\boldsymbol{Y}$ is the vector of state variables, $\boldsymbol{\theta}$ is a set of constants that parametrize the static characteristics of the engine components, h_{fp} is the input from a control system, and u_p is the disturbance resulting from the wave-hull interaction.

In past research (Bondarenko 2020, Bondarenko 2023) the adaptive parameters identification framework was developed. The framework integrates the core of the digital twin - a set of parametrized dynamic models - with information/data sources of the physical space. It is possible to identify the constants that parametrize the static characteristics of the engine components, tailored to the specific ship in service, in this way.

Engine Control System

The control system of marine diesel engines aims at controlling their speed and load operating regimes. Inadequate control system dynamics may lead to incomplete fuel combustion, thermal and mechanical overload of the engine components, and excessive oscillation of the shaft rotational speed. As a rule, the control system of propulsion engines consists of a speed governor and several functional modules for protection against torque and thermal overloading. For the purpose of the present study, a Proportional-Integral (PI) + Proportional (P) governor structure is used as shown in figure 5 in the form of the Laplace domain block diagram (Gorb 1989). The PI+P structure mimics a popular and classic hydro-mechanical governor of Woodward. The linear part of the governor's dynamic can be represented in state-space form, as demonstrated below:

$$\begin{aligned} &\frac{d}{dt}\boldsymbol{x} = \boldsymbol{A}\,\boldsymbol{x} + \boldsymbol{B}\,u, \quad \boldsymbol{x} = \left[\bar{X}_{efb}, \bar{X}_{pp}\right]^T, \quad u = \left[\left(n_{sp} - n_{sh}\right)\right] \\ &y = \boldsymbol{C}\,\boldsymbol{x}, \qquad y = h_{fp} \end{aligned} \quad [23]$$

$$\boldsymbol{A} = \begin{bmatrix} -\left(\frac{K_i K_m K_{su}}{T_{ss}} + \frac{1}{T_i}\right) & -\frac{K_i K_m K_{fb} K_{su}^2}{T_{ss}} \\ -\frac{K_m}{T_{ss}} & -\frac{K_{fb} K_m K_{su}}{T_{ss}} \end{bmatrix}, \boldsymbol{B} = \begin{bmatrix} -\frac{K_i K_m K_{su}}{T_{ss}} \\ -\frac{K_m}{T_{ss}} \end{bmatrix}, \boldsymbol{C} = \begin{bmatrix} 0 & 1 \end{bmatrix}$$

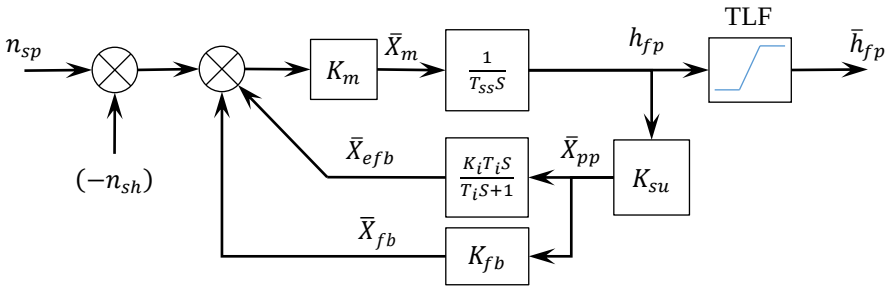

Figure 5: Governor functional block diagram

In order to prevent the engine from thermal and mechanical overloads, the engine control system includes a torque limiter function (TLF). The TLF provides saturation of the governor output at the upper boundary, limiting the fuel injection amount, and thus engine torque. Figure 6 illustrates characteristics of TLF implemented in the governor.

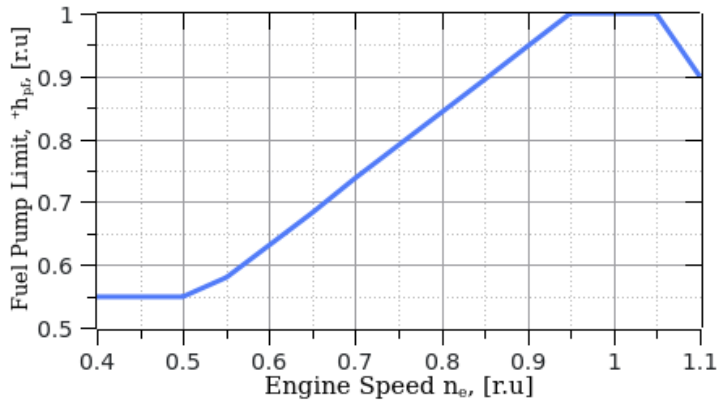

$$h_{fp} = \begin{cases} h_{fp}, \text{if } h_{fp} \le {}^{+}h_{fp} \\ {}^{+}h_{fp}, \text{if } h_{fp} > {}^{+}h_{fp} \end{cases}$$

$$ {}^{+}h_{fp} = \begin{cases} 0.55, \text{if } n_e \le 0.5 \\ \dfrac{n_e}{0.95}, \text{if } 0.5 < n_e \le 0.95 \\ 1.0, \text{if } n_e > 0.95 \end{cases} \quad [24]$$

Figure 6: The TLF characteristic

THE STATE-SPACE MODEL OF THE PROPELLER-ENGINE SYSTEM

As noted earlier, wave and hull motions are the main causes of propeller torque fluctuation, disturbing the operation of the propulsion engine. The response functions conveniently relate the system's response to a forcing function with the aid of appropriate Laplace transforms. Thus, the response functions, which translate waves into hull motions and, in turn, into propeller torque fluctuation, characterize the wave-hull-propeller interaction in the frequency domain (Bondarenko 2011). It is desirable to interface these characteristics into the analysis of propeller-engine interaction, resulting in a comprehensive assessment of hull-propeller-engine interaction. Since the equations representing propeller-engine interaction are non-linear differential equations, the linearization about an operating point is required. The response functions are obtained from the linear state-space representation for input disturbance.

Different types of nonlinearities intrinsic to the system require different linearization techniques. Thus, for weak types, such as nonlinearity due to the product of variables or nonlinearity due to polynomial characteristics, the standard approach, often called small signal increments, is the most suited. Whereas hard nonlinearity, such as saturation, requires a special technique often called harmonic linearization. At first, the linearization of the base propulsion system without TLF will be presented, followed by the introduction of describing function for a (quasi) linear description of the TLF.

Linearization

The basic method of small increments is commonly used for the linearization of propulsion engine models (Mezherickiy 1971, Naito 1979, Stapersma 2017). The method allows for interpreting a nonlinear function as an explicit linear combination of the small increments of the constituent variables, simultaneously getting rid of constant parameters. For the sake of simplicity and illustration of the application of the method, the nonlinear equation of propeller shaft dynamics, equation [2],

will be processed from now on. Let's rewrite the equation [2] in the form of finite increments of the constituent variables about a steady-state operating point, simultaneously introducing normalization at that point:

$$\begin{gathered}\frac{2\pi I_{sh}}{Q_{p_0}}\frac{d\Delta n_{sh}}{dt}\frac{n_{sh_0}}{n_{sh_0}}=\frac{\Delta Q_e}{Q_{p_0}}-\frac{\Delta Q_p}{Q_{p_0}},\quad Q_{e_0}\equiv Q_{p_0},\quad \frac{\Delta n_{sh}}{n_{sh_0}}\equiv\delta n_{sh},\quad \frac{\Delta Q_e}{Q_{p_0}}\equiv\delta Q_e,\quad \frac{\Delta Q_p}{Q_{p_0}}\equiv\delta Q_p \\ \Downarrow \\ \frac{d}{dt}\delta n_{sh}=\frac{1}{\tau}\left[\delta Q_e-\delta Q_p\right],\quad \tau=\frac{2\pi I_{sh}}{Q_{p_0}}n_{sh_0}\end{gathered} \tag{25}$$

Equation [25] requires further detailing of the torque functions, and following the method of small increments, the composite functions are decomposed by applying a logarithm, and then the partial differentiation is performed. Finally, by introducing coefficients of influence and substituting finite increments for differentials, the composite function is replaced by a linear combination of constituent variables. Thus, the transformation of the propeller torque function defined in equation [3] yields:

$$\begin{gathered}Q_p=\rho n_{sh}^2 D_p^5 K_q\left(J\right)\frac{1}{\eta_r} \\ \Downarrow \\ \ln\left(Q_p\right)=\ln\left(\rho\right)+2\ln\left(n_{sh}\right)+5\ln\left(D_p\right)+\ln\left(K_q\right)-\ln\left(\eta_r\right) \\ \Downarrow \\ \frac{dQ_p}{Q_{p_0}}=2\frac{dn_{sh}}{n_{sh_0}}+\frac{dK_q}{K_{q_0}},\quad \frac{dQ_p}{Q_{p_0}}\approx\frac{\Delta Q_p}{Q_{p_0}}\equiv\delta Q_p,\ldots \\ \Downarrow \\ \delta Q_p=2\delta n_{sh}+\delta K_q\end{gathered} \tag{26}$$

The torque coefficient, K_q, holds the nonlinear functional relation in the polynomial form with the engine speed and inflow velocity and thus requires further linearization. Applying the Taylor series expansion, neglecting higher order term, the transformation yields:

$$\begin{gathered}K_q\left(J\right)=q_o+q_1 J+q_2 J^2,\quad J=\frac{U_p}{n_{sh}D_p} \\ \Downarrow \\ \Delta K_q=\frac{\partial K_q}{\partial n_{sh}}\Delta n_{sh}+\frac{\partial K_q}{\partial U_p}\Delta U_p \\ \Downarrow \\ \frac{\Delta K_q}{K_{q_0}}=\underbrace{\frac{\partial K_q}{\partial n_{sh}}\frac{n_{sh_0}}{K_{q_0}}}_{k_{q_1}}\frac{\Delta n_{sh}}{n_{sh_0}}+\underbrace{\frac{\partial K_q}{\partial U_p}\frac{U_{p_0}}{K_{q_0}}}_{k_{q_2}}\frac{\Delta U_p}{U_{p_0}},\quad \frac{\Delta K_q}{K_{q_0}}\equiv\delta K_q,\ldots \\ \Downarrow \\ \delta K_q=k_{q_1}\delta n_{sh}+k_{q_2}\delta u_p\end{gathered} \tag{27}$$

Substituting the result of equation [27] into the result of equation [26] and collecting coefficients for the same variables, the transformation yields the following result:

$$\delta Q_p=\left(2+k_{q_1}\right)\delta n_{sh}+k_{q_2}\delta u_p \tag{28}$$

Under similar considerations, the finite increment of engine torque, δQ_e, can be derived in the following form:

$$\begin{aligned}\delta Q_e &= k_{imep} k_{C_{eff}} \left(\delta G_a - \delta G_f \right) + k_{imep} \delta h_{fp} - k_{fmep} \delta n_{sh} \\ \delta G_a &= \left(1 - k_{\Psi_a}\right) \delta P_s + k_{\Psi_a} \left(\delta M_{exh} + \delta T_{exh} \right) \\ \delta G_f &= \delta h_{fp} + \delta n_{sh}\end{aligned} \qquad [29]$$

The unwieldy expression for the engine torque results from the presence of the combustion efficiency coefficient in equation [16]. At the same time, it shows the interrelation of the engine torque increment with the increments of other engine state variables. Finally, by substituting equations [28] and [29] into equation [25], collecting and grouping coefficients for the same variables, the linearized and normalized equation of the engine shaft speed dynamics gains the following form:

$$\frac{d}{dt} \delta n_{sh} = a_{11} \delta n_{sh} + a_{13} \delta P_s + a_{14} \delta M_{exh} + a_{15} \delta T_{exh} + b_{11} \delta h_{fp} + k_{q_2} \delta u_p \qquad [30]$$

Likewise, the linearized and normalized version of the rest of the state variables in equation [22] can be obtained, resulting in the linearized state-space description of the engine propulsion system (uncontrolled part) in terms of variables finite increments in the following form:

$$\begin{aligned}&\frac{d}{dt} \delta \boldsymbol{x} = \boldsymbol{A}\, \delta \boldsymbol{x} + \boldsymbol{B}\, \delta \boldsymbol{u}, \quad \delta \boldsymbol{x} = \left[\delta n_e, \delta n_{tc}, \delta P_s, \delta M_{exh}, \delta T_{exh} \right]^T, \quad \delta \boldsymbol{u} = \left[\delta h_{fp}, \delta u_p \right]^T \\ &\delta \boldsymbol{y} = C\, \delta \boldsymbol{x}\end{aligned}$$

$$\boldsymbol{A} = \begin{bmatrix} a_{11} & 0 & a_{13} & a_{14} & a_{15} \\ 0 & a_{22} & a_{23} & a_{24} & a_{25} \\ a_{31} & a_{32} & a_{33} & a_{34} & a_{35} \\ a_{41} & 0 & a_{43} & a_{44} & a_{45} \\ a_{51} & 0 & a_{53} & a_{54} & a_{55} \end{bmatrix}, \quad \boldsymbol{B} = \begin{bmatrix} b_{11} & k_{q_2} \\ 0 & 0 \\ 0 & 0 \\ b_{41} & 0 \\ b_{51} & 0 \end{bmatrix}, \quad \boldsymbol{C} = \begin{bmatrix} 1 & \cdots & 0 \\ \vdots & \ddots & \vdots \\ 0 & \cdots & 1 \end{bmatrix} \qquad [31]$$

The coefficients of the system matrix $\boldsymbol{A}$ and input matrix $\boldsymbol{B}$ are analytically bound up with the original nonlinear equation [22], and thus can easily be evaluated at arbitrary operating points of the propulsion system. Furthermore, the uncontrolled state-space representation of the propulsion system can be turned into a controlled version simply by expanding and combining the state matrix $\boldsymbol{A}$ and input matrix $\boldsymbol{B}$ with the linear part of the governor's state-space description [23]. The transformation results in the updated matrices and vectors:

$$\delta \boldsymbol{x} = \left[\delta n_e, \delta n_{tc}, \delta P_s, \delta M_{exh}, \delta T_{exh}, \delta X_{efb}, \delta X_p \right]^T, \quad \delta \boldsymbol{u} = \left[\delta u_p \right]^T$$

$$\begin{matrix} \\ \text{Engine} \\ \\ \\ \\ \text{Governor} \\ \end{matrix} \boldsymbol{A} = \begin{bmatrix} a_{11} & 0 & a_{13} & a_{14} & a_{15} & 0 & \frac{b_{11}}{K_{su}} \\ 0 & a_{22} & a_{23} & a_{24} & a_{25} & 0 & 0 \\ a_{31} & a_{32} & a_{33} & a_{34} & a_{35} & 0 & 0 \\ a_{41} & 0 & a_{43} & a_{44} & a_{45} & 0 & \frac{b_{41}}{K_{su}} \\ a_{51} & 0 & a_{53} & a_{54} & a_{55} & 0 & \frac{b_{51}}{K_{su}} \\ b_{61} & 0 & 0 & 0 & 0 & a_{66} & a_{67} \\ b_{71} & 0 & 0 & 0 & 0 & a_{76} & a_{77} \end{bmatrix}, \quad \boldsymbol{B} = \begin{bmatrix} k_{q_2} \\ 0 \\ 0 \\ 0 \\ 0 \\ 0 \\ 0 \end{bmatrix}, \quad \boldsymbol{C} = \begin{bmatrix} 1 & \cdots & 0 \\ \vdots & \ddots & \vdots \\ 0 & \cdots & \frac{1}{K_{su}} \end{bmatrix} \qquad [32]$$

The obtained state-space description, either uncontrolled or controlled, defines the system's dynamic behavior in the time domain. However, in the context of propeller-engine interaction, the frequency domain behavior is of primary interest. Thus, the transition from the time domain to the frequency domain representation, in the form of the transfer function of the linear system from input, δu, to output, δy, can be easily obtained by applying the Laplace transformation to the state-space system in the following form:

$$\boldsymbol{W}(s)=\frac{\delta \boldsymbol{y}}{\delta u}=\boldsymbol{C}\left(s\boldsymbol{I}-\boldsymbol{A}\right)^{-1}\boldsymbol{B},\quad s\equiv\frac{d}{dt}-\text{the Laplace operator}$$

$$\boldsymbol{H}(\omega)=20\log_{10}\left|\boldsymbol{W}(i\omega)\right|,[dB] \qquad [33]$$

Equation [33] provides the plotting of Bode charts, which quantify the ratio of the system response magnitudes to the magnitude of the input disturbance in the range of frequencies. There are seven responses to the input disturbance of the inflow velocity in the context of the presented propulsion system.

Time and Frequency Domain Validation

The linearization comes with a cost: the model is only valid for small variations around the steady-state point. So, the important question is how the state-space linearized model compares to the numerical non-linear model in both the time and frequency domains. To get insights into how both models behave, a numerical simulation was implemented in MATLAB/Simulink. The Panamax-size bulk carrier is used as a prototype ship for the numerical model. The hull form was designed at the National Maritime Research Institute (NMRI) with a target speed of 14.5 kt at 90% MCR. The principal dimensions of the hull and propeller are listed in Table 1. The required engine power was assessed as a result of propeller-hull matching for the desired target speed. The engine particulars are listed in Table 2. It is assumed that a ship advances with a constant speed, U_0, in head waves and experiences longitudinal (surge) motion. As mentioned before, the axial component of the velocity field around the propeller influences the behavior of the propulsion engine directly, thus is the most important for the investigation of wave-propeller-engine interaction (Bondarenko 2012, Taskar 2016).
The model of inflow velocity is composed of two terms (Nakamura 1975): due to the hull surge motion, u_{pm}, and due to the wave orbital motion, u_{pw}, as follows:

$$\begin{cases} u_p = u_{p_m} + u_{p_w} \\ u_{p_m} = \left(1-w_p\right)\left\{U_0 - \omega_e\,\xi_a \sin\left(\omega_e t-\varepsilon_\xi\right)\right\} \\ u_{p_w} = \alpha_w \omega \zeta_w e^{-k z_p}\cos\chi\cos\left(\omega_e t - k\,x_p\cos\chi\right) \end{cases} \qquad [34]$$

where ω_e is the encounter wave frequency, ξ_a and ε_ξ are the surge motion amplitude and phase, correspondingly; ω is the incident wave frequency, χ is the heading angle to waves, ζ_w is the wave amplitude, k is the wavenumber (=$2\pi/\lambda$) and λ is the wavelength, x_p and z_p are the coordinates of propeller position with respect to the hull centre of gravity, G. The dynamics of the subject hull dynamics as well as an effective wave amplitude coefficient α_w are discussed in details by Kitagawa (2019). The time histories of inflow velocity fluctuation in irregular waves are generated based on linear wave theory and detailed discussion is not in the scope of this paper.

Table 1: Principal particulars of a ship and propeller

Item	Design Value
L_{pp} (m)	217.0
B (m)	32.3
D (m)	12.2
Displacement (ton)	7.17e4
Service Speed U_0 (kt)	14.5
C_B	0.84
Propeller Series	Wageningen B
D_p (m)	6.6
Blades	4
Pitch Ratio	0.65

Table 2: Propulsion engine specification @ MCR

Engine Type	Mitsui-MAN S50ME-T9
No of Cylinders	6
Bore/Stroke, [mm/mm]	500/2214
Power, [kW]	9640
Speed, [rpm]	119
IMEP, [bar]	22
Scav. Air Pressure, [barA]	4.4

Figure 7, the engine envelope, visualizes the combined engine speed and power responses to the generated inflow velocity fluctuation in irregular waves, followed by figure 8, where the time histories of the corresponding engine state variables'

responses, relative to the MCR point, are shown. These graphs clearly show that the behavior of the state-space linear and non-linear models is indistinguishable, except for a slight difference in the exhaust gas temperature responses. This variation can be attributed to the nonlinearity of the characteristic. The presented results do not directly include the effect of resistance increase in waves, as mentioned from the beginning; equation [1] is neglected due to the negligible effect of varying added resistance in waves on the propulsion engine. Instead, the focus is put on understanding the responses in waves due to fluctuating inflow velocity, which indirectly includes the effect of the resistance fluctuation. Finally, figure 9 shows the responses in the frequency domain. A general observation is that both systems show similar response magnitudes for the range of frequencies typical for ocean waves. Additionally, as expected from the time-domain results, the magnitude of the exhaust temperature response is lower in the linear case.

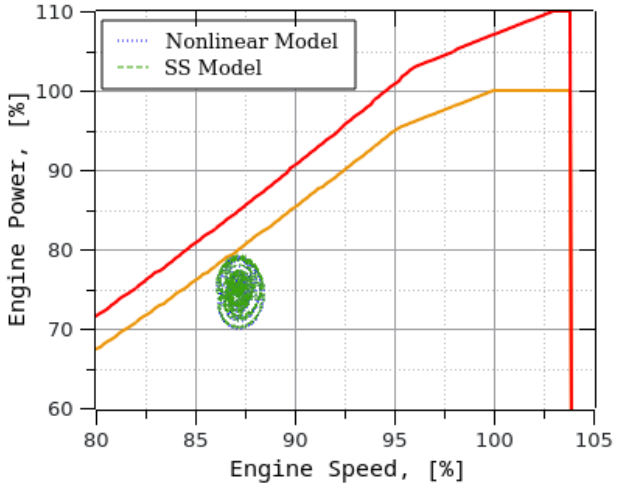

Figure 7: Engine operating point response on the engine envelope

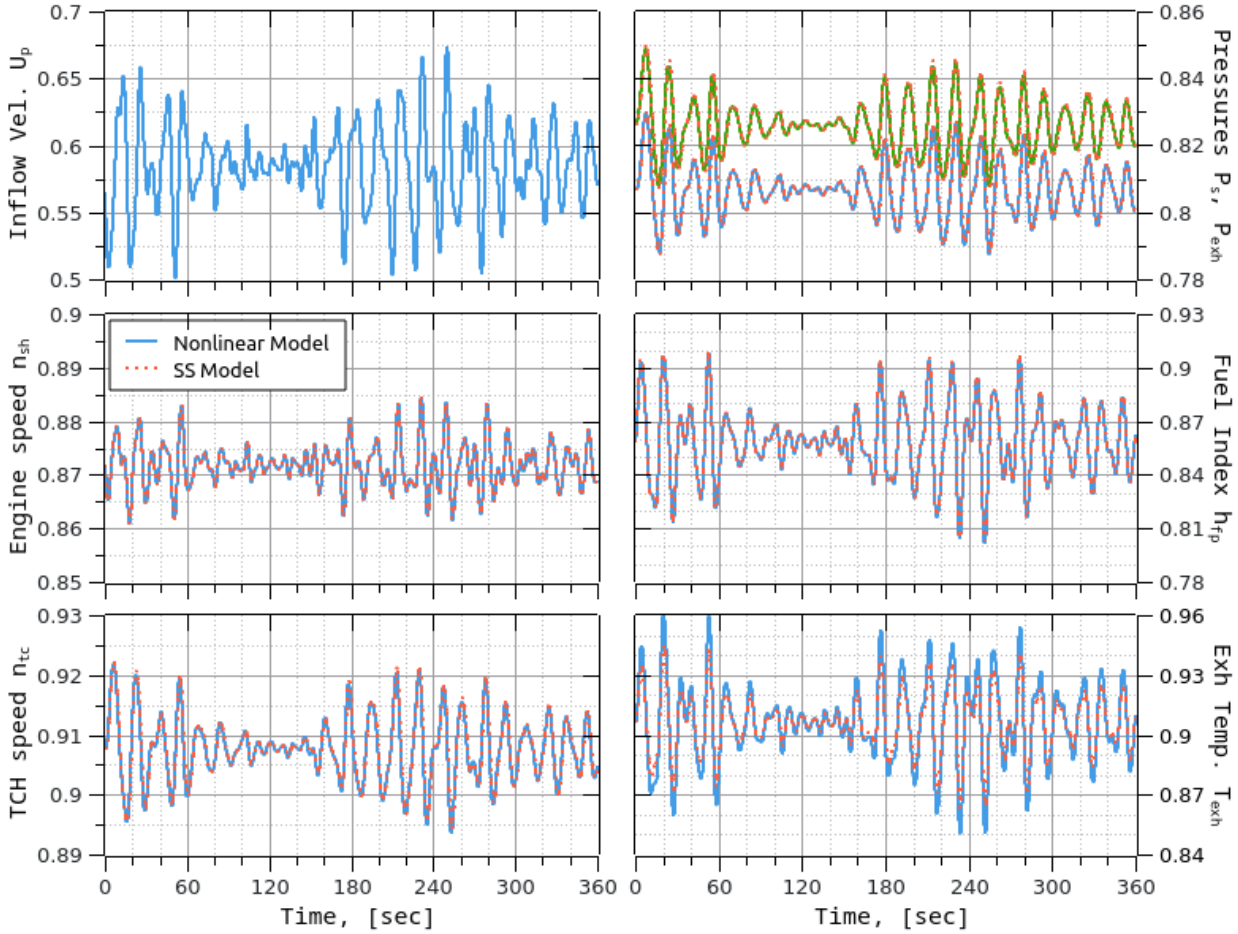

Figure 8: Propulsion engine responses in time domain

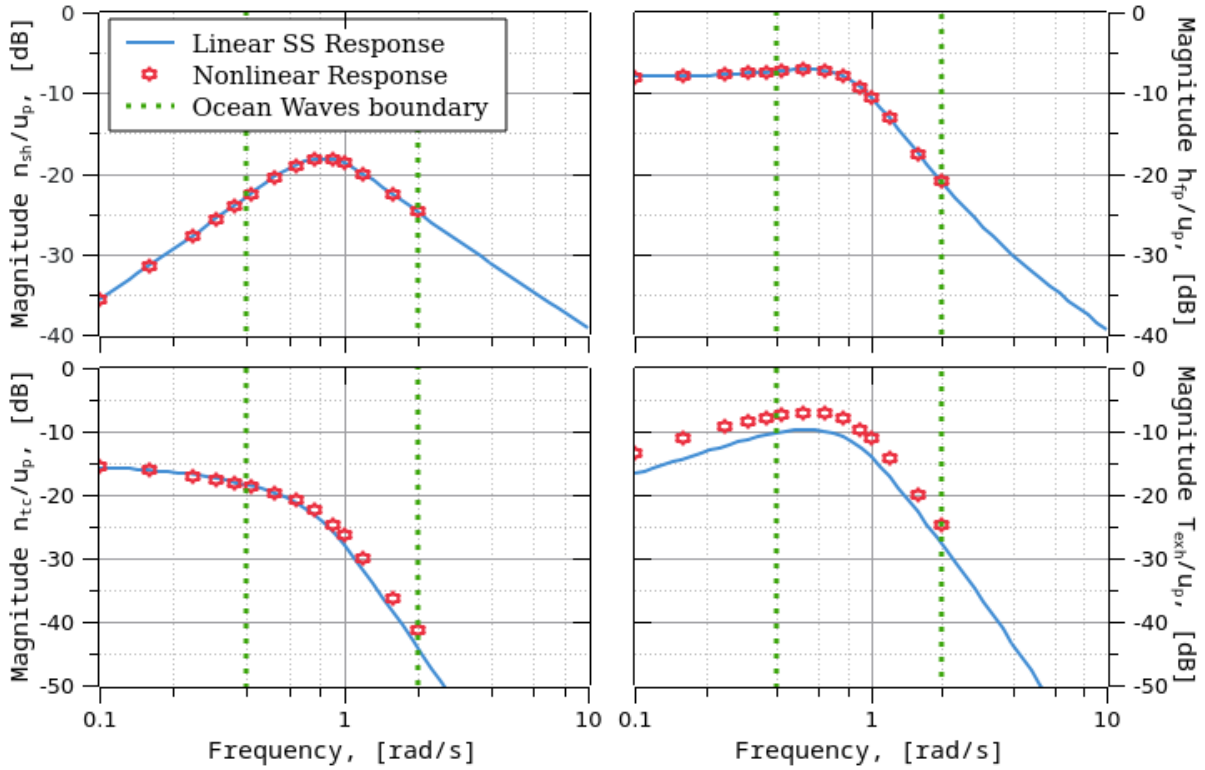

Figure 9: Propulsion engine responses in frequency domain

Although the behavior of the linearized model compares fairly well with the full non-linear model, it has a major limitation: the non-linearity of the TLF that cannot be captured by a linear model in a straightforward manner. However, there is an approximate method of analysis in the frequency domain, also known as harmonic analysis, providing the replacement of each nonlinear element with a quasi-linear describing function. A brief description is provided in the subsequent subchapter.

Describing Function Representation of the TLF Function

One way to deal with a nonlinear system is to linearize it with the help of a finite increment method. Linearization in the time domain requires the system under consideration to be composed of continuous and differentiable characteristics. However, this approach is ill-suited for studying the limiting or detrimental effects of nonlinearity. On the other hand, harmonic linearization is a way of describing hard nonlinear functions in the frequency domain (Csaki 1972).

Let's assume the nonlinear transformation function $f(x,t)$ of the harmonic signal of the form $x(t) = a \sin(\omega t)$. The transformation results in the output $y(t) = f(a \sin(\omega t), t)$. The describing function gain, $N(a, \omega)$ is the fundamental harmonic of the Fourier series representation of this periodic output $y(t)$, divided by the input amplitude a, as follows:

$$y(t) \cong A_0(a,\omega) + N(a,\omega) \cdot a\, e^{j\omega t}, \qquad [35]$$

$$N(a,\omega) = q(a,\omega) + jq'(a,\omega)$$

The coefficients A_0, q, q' can be found through the Fourier series expansion of the non-linear transformation function $f(\bullet)$ as follows:

$$A_0 = \frac{1}{2\pi}\int_0^{2\pi} f\left(a\sin(\Psi)\right)d\Psi, \quad \because \Psi \equiv \omega t$$
$$q = \frac{1}{a\pi}\int_0^{2\pi} f\left(a\sin(\Psi)\right)\sin(\Psi)d\Psi \qquad [36]$$
$$q' = \frac{1}{a\pi}\int_0^{2\pi} f\left(a\sin(\Psi)\right)\cos(\Psi)d\Psi$$

In the context of the nonlinear characteristic of TLF described by equation [24], and schematically shown in figure 10, the describing function gain can be derived as follows:

$$A_0(a) = \frac{1}{2\pi}\left[\int_0^{\beta} a\sin(\Psi)d\Psi + \int_{\beta}^{\pi-\beta} {}^{+}h_{fp}\,d\Psi + \int_{\pi-\beta}^{2\pi} a\sin(\Psi)d\Psi\right]$$
$$= \frac{{}^{+}h_{fp}}{2} - \frac{{}^{+}h_{fp}}{\pi}\sin^{-1}\left(\frac{{}^{+}h_{fp}}{a}\right) - \frac{a}{\pi}\sqrt{1-\left(\frac{{}^{+}h_{fp}}{a}\right)^2}$$
$$q = \frac{1}{a\pi}\left[\int_0^{\beta} a\sin^2(\Psi)d\Psi + \int_{\beta}^{\pi-\beta} {}^{+}h_{fp}\sin(\Psi)d\Psi + \int_{\pi-\beta}^{2\pi} a\sin^2(\Psi)d\Psi\right] \qquad [37]$$
$$= \frac{1}{2} + \frac{1}{\pi}\sin^{-1}\left(\frac{{}^{+}h_{fp}}{a}\right) + \frac{1}{\pi}\frac{{}^{+}h_{fp}}{a}\sqrt{1-\left(\frac{{}^{+}h_{fp}}{a}\right)^2}$$
$$q' = \frac{1}{a\pi}\left[\int_0^{\beta} a\sin(\Psi)\cos(\Psi)d\Psi + \int_{\beta}^{\pi-\beta} {}^{+}h_{fp}\cos(\Psi)d\Psi + \int_{\pi-\beta}^{2\pi} a\sin(\Psi)\cos(\Psi)d\Psi\right]$$
$$= 0$$

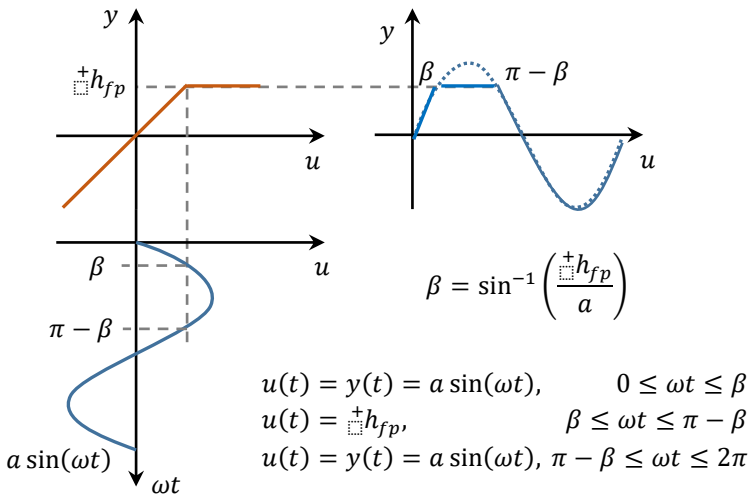

Figure 10: Schematic of nonlinear transformation of TLF

The components obtained in equation [37] define the describing function as frequency-invariant and input amplitude-dependent, though. In order to confirm the obtained characteristics, a simple numerical experiment was set up: a harmonic signal of varying amplitude at a single frequency passes through the saturation non-linearity, and the estimated amplitudes ratio is plotted in figure 11 along with the corresponding describing function. The presented results of the numerical simulation suggest the non-linearity analysis capability by the describing function method.

Finally, it should be observed that the saturation type non-linearity, such as TLF, also introduces the DC component (A_0), and to some extent, the AC component ($N(a)$) is dominant; however, the larger the amplitude, the larger the bias. Definitely, in

harsh sea conditions when the engine operation in close vicinity of the limit is inevitable, the effect of the DC component becomes prominent, exacerbating the safety concerns of propulsion system operation. For the purpose of this research, investigating the wave-propeller-engine interaction, only the AC component is considered at the moment, while the simultaneous consideration of both components will be left for future analysis.

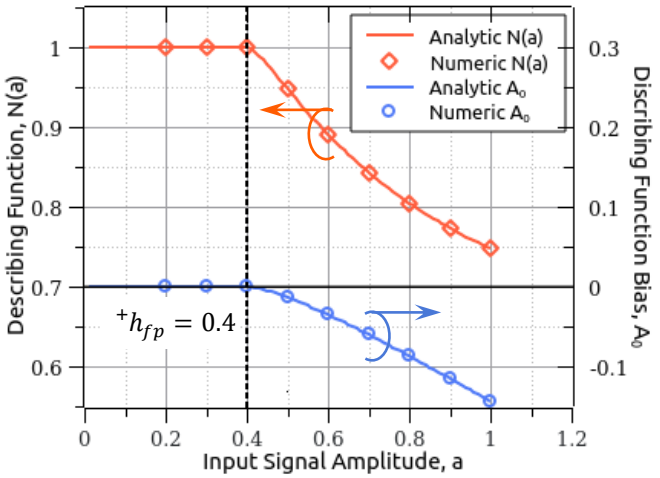

Figure 11: Describing function for saturation non-linearity

State-Space Model of the Propulsion System with TLF in Frequency Domain

The describing function method has traditionally been used for two primary purposes: limit-cycle stability analysis and characterizing the input-output behavior of a non-linear system in the frequency domain. In this paper, the focus is put on the latter purpose, particularly to determine the amplitude-dependent frequency response of a nonlinear system.

The TLF is placed between the governor and the engine to saturate the fuel pump index input to the engine and prevent thermal overload. Thus, the describing function coefficient, *N(a)*, is introduced to the system matrix *A*, to the part related to the governor-engine interface, as shown by equation [38], and delivers the quasi-linear response function as in equation [39]

$$\delta \boldsymbol{x} = \left[\delta n_e, \delta n_{tc}, \delta P_s, \delta M_{exh}, \delta T_{exh}, \delta X_{efb}, \delta X_p\right]^T, \quad \delta \boldsymbol{u} = \left[\delta u_p\right]^T$$

$$\text{Engine}\left\{\boldsymbol{A} = \begin{bmatrix} a_{11} & 0 & a_{13} & a_{14} & a_{15} & 0 & \frac{b_{11}}{K_{su}} N(a) \\ 0 & a_{22} & a_{23} & a_{24} & a_{25} & 0 & 0 \\ a_{31} & a_{32} & a_{33} & a_{34} & a_{35} & 0 & 0 \\ a_{41} & 0 & a_{43} & a_{44} & a_{45} & 0 & \frac{b_{41}}{K_{su}} N(a) \\ a_{51} & 0 & a_{53} & a_{54} & a_{55} & 0 & \frac{b_{51}}{K_{su}} N(a) \\ \hline b_{61} & 0 & 0 & 0 & 0 & a_{66} & a_{67} \\ b_{71} & 0 & 0 & 0 & 0 & a_{76} & a_{77} \end{bmatrix}\right. \text{Governor}, \quad \boldsymbol{B} = \begin{bmatrix} k_{q_2} \\ 0 \\ 0 \\ 0 \\ 0 \\ 0 \\ 0 \end{bmatrix}, \quad \boldsymbol{C} = \begin{bmatrix} 1 & \cdots & 0 \\ \vdots & \ddots & \vdots \\ 0 & \cdots & \frac{1}{K_{su}} \end{bmatrix} \qquad [38]$$

$$\boldsymbol{W}(i\omega, a) = \frac{\delta \boldsymbol{y}}{\delta u} = \boldsymbol{C}\left[i\omega \boldsymbol{I} - \boldsymbol{A}(a)\right]^{-1} \boldsymbol{B} \qquad [39]$$

Here, *a* stands for the amplitude of the governor's response before the TLF, that is:

$$a \equiv \delta h_{fp} = \left|\boldsymbol{W}(i\omega, a)\right| \delta u_p, \quad \boldsymbol{C} = \begin{bmatrix} 0 & \cdots & 0 \\ \vdots & \ddots & \vdots \\ 0 & \cdots & \frac{1}{K_{su}} \end{bmatrix} \qquad [40]$$

Thus, to produce the frequency response of such a quasi-linear amplitude-dependent response function, an iterative solution is required until the convergence of the describing function value. The elaborated procedure is as follows: set a specific value for δu_p from a range of input amplitudes covering the expected operating range of the system and set a range of frequencies [ω_{min}, ω_{max}] to span a frequency range of interest. Then, set $N(a) = 1$ and evaluate the amplitude of response, a, for every frequency in the range, update $N(a)$ and repeat the calculation until the convergence. It was found that a converged solution appears within a few iteration steps.

To illustrate the frequency response of the state-space system given the TLF activation, the simulation condition is set similar to that of figure 7, where the operating point is close enough to the limit line. To generate the amplitude-dependent DF, the six inflow velocity amplitudes in the range [0.08…0.20] were selected, and a set of frequencies covering the typical range of the ocean waves. Figure 12 illustrates the evolution of the describing function magnitude in the frequency domain. It is evident that the larger the input disturbance, the larger the response of the governor and, thus, the activation of the TLF function. Furthermore, figure 13 shows the frequency response of the propeller-engine system, and, as evident, the engine speed response increases as the input disturbance increases. This is because the increasing response, X_{pp}, of the governor linear part, also shown in figure 13, cannot reach the engine because of the TLF, whereas the response of the fuel pump index, h_{fp}, is suppressed. As for the air supply subsystem, including the compressor, receivers, and turbine, whose response is indicated by the TC rotating speed, n_{tc}, the effect of TLF is negligible owing to the large inertia.

Although the demonstrated effect of TLF is relatively small, it can be prominent for other operating points and dynamic properties of the speed control system, and the developed approach allows for the evaluation of various conditions in a straightforward and integrated manner.

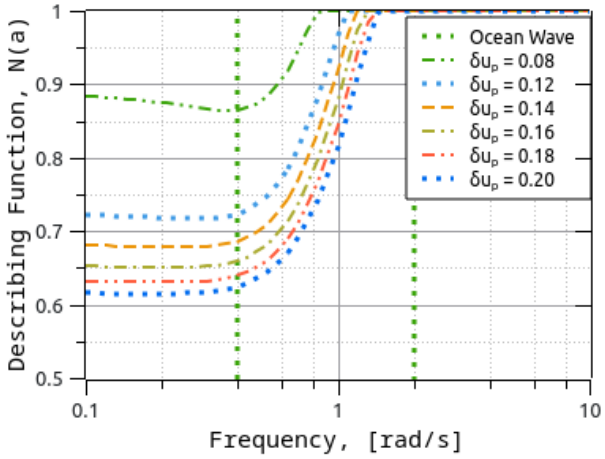

Figure 12: Describing function coefficient in frequency domain for a range of amplitudes

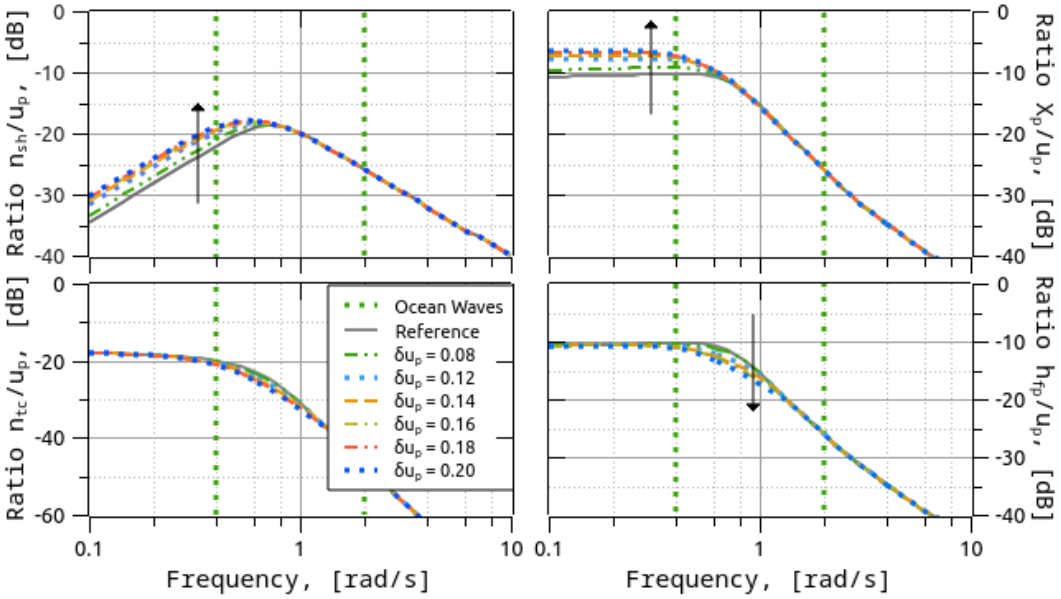

Figure 13: Frequency response of propeller-engine system in view of the TLF activation

CONCLUSIONS

Frequency-response techniques and the use of response functions are valuable tools in the analysis of the ship propulsion system behavior in waves. However, accurate calculation of the propulsion system response function requires detailed information about characteristics intrinsic to constituent components. This paper proposes the digital-twin-enabled response function analysis technique for the problem of wave-propeller-engine interaction assessment. The core part of the digital twin is the nonlinear, fully parametrized model of propeller-engine dynamics. The parameters identification framework from past research ensures that models are tailored to the specific ship in-service. The companion linearized state-space model was derived analytically based on the structure of the digital twin. A remarkable aspect of the developed linearized state-space model is the introduction of the air supply subsystem (compressor, receivers, and turbine), which has a notable effect on engine performance. The coefficients of the derived state-space system are bound up with the nonlinear models underlying the digital twin. Thus, at any point in the ship operation, reflected by the digital twin, the state-space system matrices can be readily obtained, and then a variety of analyses can be performed. This is valid only under moderate sea conditions, though. On the other hand, in adverse sea conditions, the increased propeller load forces the engine operating point to move closer to the upper bound of the engine operation limit. At the same time, significant propeller torque fluctuations occur. As a rule, the governors of modern engines are equipped with torque-limiting functions, preventing the engine from overloading, and simultaneously restricting the maneuverability of the ship. The latter circumstance has raised serious safety concern about ships with reduced propulsion power, used for better energy efficiency (Shigunov 2018). The presence and activation of torque saturation make the problem of propeller-engine interaction highly nonlinear. Therefore, it is desirable to extend the analysis of linearized state-space systems to the consideration of systems with nonlinear components such as TLF. In this work, the effect of the nonlinear function was approximated by using the theory of harmonic linearization. Specifically, the output of the nonlinear function is represented by its Fourier series by assuming a pure sinusoidal signal of constant amplitude with no bias at the input and no subharmonics at the output. Thus, the describing function is then defined as the complex ratio of the fundamental term of the output to the input sinusoid. A simple example considered in the paper showed that the system responses to a variety of disturbance amplitudes can be studied in the frequency domain utilizing the linear system theory.

To wrap up, this paper proposes a synthetic approach to evaluating and assessing a ship's propulsion system. A digital twin precisely reflects the characteristics intrinsic to the ship in-service, and the companion state-space system, bound up with the digital twin, provides a foundation for wave-propeller-engine interaction analysis in the frequency domain. The harmonic linearization extends the technique to consider the nonlinearity of TLF. All components are mutually supportive, ensuring that the data feedback from the ship in service can be used to assess propulsive performance in waves and review future ship designs.

Besides all the aforementioned aspects, there is also a desire to extend the technique by combining the wave-hull interaction problem, providing a holistic assessment of ship operation in actual sea conditions, as shown by Bondarenko (2012). The required component is the response function of hull motions in waves, and Nielsen (2021, 2022) proposed a simple and practical method that can be used to tune the transfer function from in-service data of hull response measurement. This is the subject of ongoing research.

CONTRIBUTION STATEMENT

Author 1: Conceptualization; propeller-engine interaction methodology; describing function analysis; writing – original draft. **Author 2:** Wave-hull interaction methodology; review and editing.

REFERENCES

Bondarenko, O., Kashiwagi, M. (2011), Statistical Consideration of Propeller Load Fluctuation at Racing Condition in Irregular Waves. *J. of Mar. Sci. and Techn.*, 16(4), 402-410

Bondarenko, O, Kashiwagi, M. (2012). Ensuring safe operation of ship propulsion plant in extreme sea condition. *In Proc.: 11th International Marine Design Conference*, 3, 83-96

Bondarenko, O., Fukuda, T. (2018). Intelligent Air Management for Ultimate Flexibility of Ship Propulsion Plant Operation. Part 1: Experiment and Simulation. *J. Japan Institute of Marine Engineers*, 53

Bondarenko, O., Fukuda, T., Kitagawa Y., Omiya T. (2020). Problem of Identification and Adaptation of Main Engine Digital Twin Based on Operational Data. *J. Japan Institute of Marine Engineers*, 57(2), 30-34

Bondarenko, O., Kitagawa, Y., et.al. (2023). Development of a free-Running model test methodology for evaluation of a full-scale ship propulsion system performance. CIMAC Congress, Paper No.328
Bondarenko, O., Fukuda, T., Miura, S. (2023). Empowering Propulsion Engine Digitalization Utilizing Digital Twin, Kalman Filter and Data Assimilation. *Jpn Soc. Nav. Arch. Ocean Eng*., 36, 95-101
Csaki, F. (1972). *Modern Control Theories: Nonlinear, Optimal and Adaptive Systems*, Budapest: Akademiai Kiado
Sui, C., et.al. (2022). Effects of Adverse Sea Conditions on Propulsion and Maneuvering Performance of Low-Powered Ocean-Going Cargo Ship. Ocean Engineering, 254
Gorb, S.I. (1989). *Analysis of automatic speed control systems of ship's diesel engine plants*. Moscow: Mortechinformreklama (In Russian)
Hendrics, E. (1989). Mean value modelling of large turbocharged two-stroke diesel engines. *SAE*, technical paper No 890564
Kim, SK, Naito, S., Nakamura, S. (1985). Propulsive performance of lower speed ship in a seaway. *J Kansai Soc Naval Arch Japan*, 196
Kitagawa, Y., Bondarenko, O., et al. (2019). An experimental method to identify a component of wave orbital motion in propeller effective inflow velocity and its effects on load fluctuations of a ship main engines in waves. *App Ocean Res*., 92
Mezherickiy, A.D., (1971). *Turbochargers of the Diesel engines*. Leningrad: Shipbuilding (in Russian)
Medica V., (1988). Simulation of turbocharged diesel engine driving electrical generator under dynamic working conditions. Manuscript of dissertation: University of Rijeka. Croatia
Nakamura, S., Hosoda, R., Naito S. (1975). Propulsive performance of a container ship in waves (3rd report). *J.Kansai Soc Nav Archit Japan*., 158, 37–46 (in Japanese).
Naito, S, Nakamura, S, and Hara, S. (1979). On the prediction of speed loss of a ship in waves. *J Kansai Soc Naval Arch Japan*, 146
Nielsen, U.D., Mounet, R.E.G., Brodtkorb, A.H. (2021). Tuning of transfer functions for analysis of wave-ship interactions. *Mar. Struct*., 79, 103029
Nielsen, U.D., Mounet, R.E.G., Brodtkorb, A.H. (2022). Parametrized transfer functions with associated confidence bands. *App Ocean Res*., 125, 103250
Shigunov, V. (2018) Manoeuvrability in adverse conditions: rational criteria and standards. *J. Mar. Sci and Tech*., 23(4), 958-976
Stapersma, D., Vrijdag, A. (2017). Linearization of a ship propulsion system model. *J. Ocean Eng*., 142, 441-457
Taskar, B., Yum, K., K., et.al. (2016). The effects of waves on engine-propeller dynamics and propulsion performance of ships. *Ocean Eng*., 122, 262–277
Theotokatos, G. (2010). On the cycle mean value modelling of a large two-stroke marine diesel engine. *Proc. IMechE Part M: J. Engineering for the Maritime Environment*, 224, 193-205.
Vrijdag, A., Stapersma, D. (2017). Extension and application of a linearized ship propulsion system model. *J. Ocean Eng*. 143, 50-65
Xiros, N. (2002). *Robust control of diesel ship propulsion*. Springer

Proceedings of 15th International Marine Design Conference (IMDC-2024)
June 2-6, 2024
Amsterdam, the Netherlands

Leveraging the concept of information-theoretic entropy to improve a multi-fidelity design framework for early-stage design exploration of complex vessels

Nikoleta Dimitra Charisi[1,*], Hans Hopman[1] and Austin Kana[1]

ABSTRACT

Early-stage design exploration is crucial since most of the major design decision are locked-in and only small design modifications are possible at later stages. To assess the performance of the various design candidates while performing design exploration, there are available methods and tools of various fidelities. These methods can be combined to form a multi-fidelity (MF) framework that guarantees accuracy through the high-fidelity model and achieves faster computational speeds through low-fidelity models. The present study proposes the adoption of information-theoretic entropy to improve a MF design framework based on Gaussian Processes (GPs). Entropy quantifies the uncertainty associated with the prediction of the design space. We propose using this uncertainty metric both as a criterion to determine whether further designs should be sampled to construct a reliable approximation of the design space and as a criterion to establish in which optimization step the optimization of the covariance matrix for the MF-GPs should be performed. The approach was tested to benchmark analytical functions and to a ship design problem of an AXEfrigate. The approach holds potential in practical applications, as it aids in the determination of whether additional resources should be allocated for high-fidelity analysis to support early-stage exploration.

KEY WORDS

Early-stage design; Design exploration; Complex vessels; Multi-fidelity models; Information theory; Entropy; Gaussian Processes; Compositional kernels.

INTRODUCTION

Early-stage design of complex engineering systems is critical since it involves making the majority of key design decisions Mavris et al. (1998); Andrews (2018). These design decisions determine the overall configuration of the vessel, including main dimension selection, hull shape, and propulsion plant, among others. Committing to these decisions early in the design process results in a swift reduction of design freedom and entails a substantial overall cost allocation Mavris et al. (1998). Hence, it is crucial to perform a thorough exploration of the design space to identify trends and trade-offs, ultimately guiding well-informed design decisions.

In the initial stages of design, the primary focus is on recognizing design trends and crucial trade-offs within the broad design space Duchateau (2016). Typically, during this design stage, low-fidelity (LF) methods are employed. LF methods are

[1] Maritime and Transport Technology Department, Technical University of Delft, Delft, the Netherlands
[*] Corresponding Author: N.D.Charisi-1@tudelft.nl

Submitted: 23 February 2024, Revised: 22 April 2024, Accepted: 1 May 2024, Published: 21 May 2024

Conference paper, DOI: https://doi.org/10.59490/imdc.2024.874 e-ISSN: 3050-4864

computationally cheap but fall short in terms of accuracy. Thus, with such tools, it becomes feasible to evaluate a vast number of designs. For instance, when assessing motions and loads, linear methods like potential flow can be employed as LF models. Yet, in certain scenarios, LF methods prove inadequate for the following reasons: (1) LF models may fail to capture the complex physical behavior of complex engineering systems, and (2) LF methods, by their very nature, are simplifications derived from more advanced methods, simplified based on assumptions that may not apply to novel designs. When LF models fail to accurately capture the physical behavior of the system, it becomes necessary to incorporate HF analysis earlier in the design process. For example, Sapsis (2021) demonstrated the influence of nonlinearities on the seakeeping and vertical bending moment of the tumblehome hull.

A promising approach to integrating HF analysis earlier into the design process involves the creation of multi-fidelity (MF) models. In essence, MF models combine LF models with a HF model, aiming to harness the accuracy offered by the HF model while benefiting from the computational efficiency provided by the LF models. Beran et al. (2020) assert that 'analysis or design of a system is considered MF when there is synergistic use of different mathematical descriptions ... in the analysis or design procedure'. MF models have shown promise in diverse engineering fields, particularly in applications demanding computationally expensive iterations, such as design applications (e.g., Ng and Willcox (2015)), prediction of extreme loads (e.g., Drummen et al. (2022)), and solving partial differential equations (e.g., Perdikaris et al. (2017)).

In the context of information theory, entropy serves as a metric for quantifying the amount of information inherent in a message Shannon (1948). This concept can be extended to compute the information associated with an event, random variable, or probability distributions Murphy (2012). In the context of design applications, entropy can function as a metric for assessing the uncertainty associated with predicting the design space. Consequently, entropy can be utilized to enhance design exploration by quantifying such uncertainty.

Different entropy metrics have been employed to support engineering applications. Nevertheless, to the authors' best knowledge, a research gap exists in utilizing entropy to enhance a MF design framework for the early-stage design of complex vessels. Therefore, this research establishes a MF design framework and explores the role of entropy in facilitating the design exploration of complex vessels. More specifically, the utilization of entropy is proposed to determine the necessary number of HF simulations for MF design optimization. As noted by Mainini et al. (2022), a mathematical formulation to determine the required number of HF simulations for MF analysis is currently lacking. The authors suggest that entropy can be considered as a suitable mathematical formulation for this purpose. Furthermore, as an expansion of Charisi et al. (2022b), we suggest that entropy can act as an indicator to perform kernel optimization throughout the optimization process.

RELEVANT WORK

Early-stage design exploration of novel vessels with multi-fidelity models

As previously stated, the importance of early-stage design lies in the crucial decisions that shape a vessel's performance. To achieve a good design, ship designers must make well-informed decisions. This involves conducting a broad exploration of the design space, considering various concepts Van Oers et al. (2018). The goal of such exploration is to discern design trends and crucial trade-offs Andrews (2018), rather than offering highly precise values for specific key performance indicators (KPIs). The difficulty lies in striking a balance between attaining the necessary accuracy and managing computational costs, given our constraints in terms of both computation and time. When designing novel vessels, it becomes essential to incorporate HF analysis early in the process to effectively capture design trends Charisi et al. (2022a). However, achieving the required accuracy through HF tools results in escalated costs. These costs can be offset by integrating HF analysis via MF analysis.

State-of-the-art research incorporates MF analysis in ship design. In this section, characteristic examples of studies are presented, without aiming for an exhaustive literature review. The design optimization of SWATH hull forms was explored by Bonfiglio et al. (2018, 2020), who evaluated the vessel's seakeeping using two methods: a strip theory and a boundary element method based on the potential flow assumption Bonfiglio et al. (2018). Additionally, the hull forms were assessed

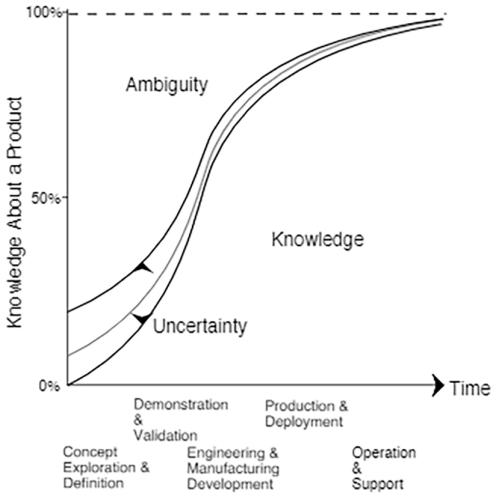

Figure 1: Variability in uncertainty across the design process Mavris et al. (1998)

for calm water resistance using a Boundary Element Method (BEM) formulated approach, assuming a potential flow-like behavior as the LF model, and a solver based on the unsteady Reynolds-averaged Navier-Stokes (RANS) equation, serving as the HF model Bonfiglio et al. (2020). The MF model was built based on GPs. Serani et al. (2022) addressed the design problem of optimizing the DTMB 5415 hull form for seakeeping and resistance. The researchers employed various analysis models, ranging from potential flow to Reynolds-Averaged Navier-Stokes equations, to solve the physical problem. Different methods were employed to construct the MF surrogates, namely stochastic radial basis functions, Kriging partial least squares, augmented expected improvement-based Kriging, and mixed-fidelity neural networks. Gaggero et al. (2022) tackled the problem optimizing a marine propeller through two methods—utilizing an inviscid potential flow-based BEM approach as the LF method and employing an inviscid finite volume RANS solver as the HF method. All the studies report promising results.

As mentioned earlier, the primary objective in early-stage design is to identify the concept that best addresses the design problem through key decisions. However, a substantial portion of relevant research, including the research studies presented, has concentrated on hull optimization, primarily emphasizing quantities of interest like resistance or seakeeping. The authors have envisioned the possibility of advancing such frameworks to earlier stages in the design process to enhance decision-making effectiveness. The uncertainty of the design space prediction is a significant factor that can be utilized to facilitate the introduction of such methods earlier on in the design process.

Uncertainty is associated with the lack of knowledge North (2017). While uncertainty is closely connected to risk, the primary distinction lies in the ability to assign a quantifiable value to risk, a task that proves challenging in the realm of uncertainty Silver (2012). Mavris et al. (1998) highlighted that there is heightened uncertainty in the early phases of the design, as shown in Figure 1. This uncertainty is introduced by the assumptions, the analysis codes of various fidelities, economic uncertainty, or technological risks. Using information-theoretic entropy as a metric enables the quantification of uncertainty in predicting the design space. In this study, the objective is to leverage this uncertainty, measured through entropy, to facilitate the early-stage design of innovative vessels.

Information theory: the entropy

According to Martignon (2001), information theory ‘is the mathematical treatment of the concepts, parameters and rules governing the transmission of messages through communication systems’. In 1948, Claude Shannon laid the foundation for information theory. The concepts and principles of information theory have expanded far beyond their original appli-

cation. Nowadays, they find application in various domains, including cryptography, machine learning, economics, and neuroscience. In the context of early-stage design, there is a direct link between design exploration and information theory via uncertainty. Krus (2013) states that 'design theory should really be a theory of design information'.

Entropy, a foundational concept in information theory, can be understood as either the measure of information content or the degree of randomness associated with a discrete random variable Duplantier and Rivasseau (2018). Various mathematical formulations exist for entropy, with some of the most commonly used ones encompassing relative entropy, or commonly known as KL divergence, and mutual information. The relevant equations to be employed in this study are presented in a subsequent section.

Entropy has found application in research problems related to design optimization. Saad and Xue (2023) proposed using entropy as a means to identify design configurations with a high likelihood of attaining optimal solutions. In such content, entropy was applied to assess the partial configuration candidates represented as branches in the AND-OR tree, aiding in the elimination of improbable branches to lead to the optimal outcome. In addition, Krus (2013) suggested that the entropy rate, which is based on Shannon's information entropy, can be a performance criterion to characterize the difficulty of different optimization problems. Farhang-Mehr and Azarm (2008) proposed an entropy-based metric to assess the quality of solution sets obtained during design optimization. The assessment is based on the distribution of the solution set over the pareto optimal frontier. Finally, Chaudhuri et al. (2020) proposed a MF design framework for risk-averse design optimization. The method is based on importance sampling and cross-entropy.

In this study, entropy serves as a metric to quantify the uncertainty within the early-stage design space. The proposal is to employ this metric as a termination criterion for concluding the design exploration process. The rationale behind this recommendation lies in the observation that, to the best of our knowledge, these problems typically operate under a predetermined budget. Thus, entropy can form a criterion to make an informed decision regarding the termination of the optimization process. Furthermore, the authors advocate for using entropy as an indicator for optimizing the covariance matrix via the optimization of the kernel function, as an extension of the method proposed in Charisi et al. (2022b). The technical details of the framework are elucidated in the following section.

PROPOSED METHOD

This section outlines the technical aspects of the methods employed in constructing the proposed framework. Specifically, it offers a comprehensive overview of the framework itself and presents the mathematical formulation of MF-GPs, compositional kernels, Bayesian optimization, and information entropy.

Proposed Framework

The flowchart illustrating the design architectural framework (DAF) is depicted in Figure 2. Organized around three primary blocks—generation, analysis, and optimization engines—the design framework shares commonalities with other design frameworks. However, the distinctive feature of this particular framework lies in the way the analysis and optimization engines are constructed to encompass the information entropy metrics. The analysis engine is dedicated to constructing the MF surrogate model for the design space. To enhance the precision of design space predictions, compositional kernels, as kernel functions, are employed to discern trends within the design space Charisi et al. (2022b). Entropy serves as a criterion for determining the optimization step where kernel optimization is most beneficial. Additionally, the optimization engine is designed to efficiently identify the optimal design point using Bayesian optimization. Entropy is incorporated into this phase of the framework as a criterion for terminating the optimization process.

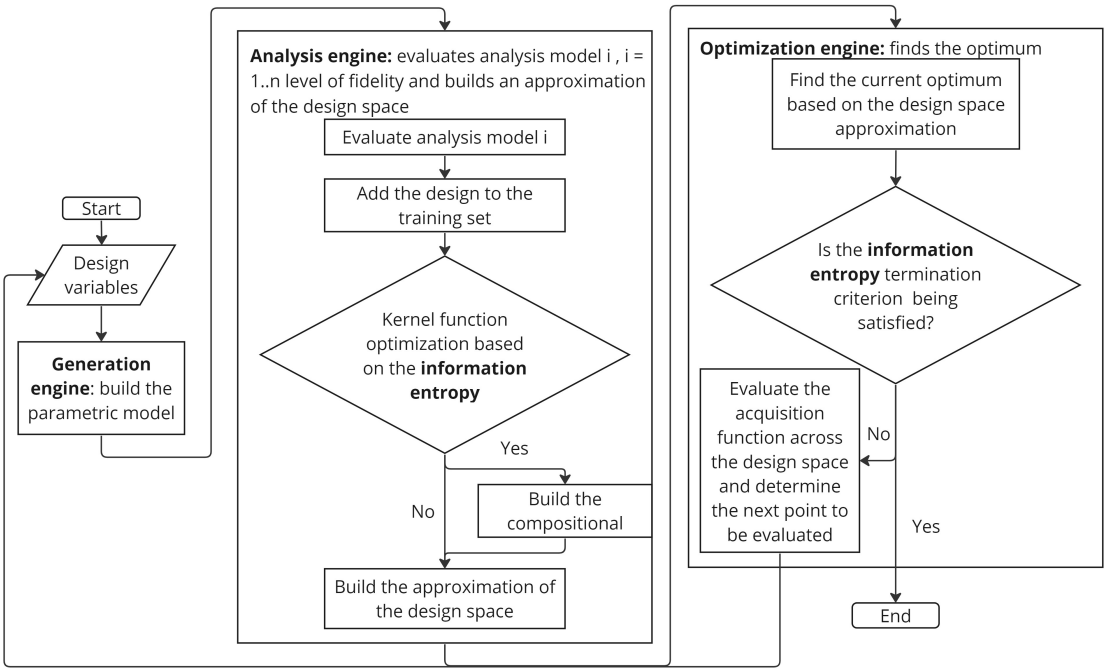

Figure 2: Flowchart of the design framework

Gaussian Processes, MF-Gaussian Processes and Compositional Kernels

Gaussian Processes

GPs are used to build approximations of real-world processes $f(x)$. Mathematically, a GP is defined as "a collection of random variables, any finite number of which have a joint Gaussian distribution, and it is fully characterized by its mean and covariance function Rasmussen (2003)". The mathematical formulation for the GPs is taken from Rasmussen (2003). The GP is fully defined by a mean $\mu(x)$ and a covariance function $k(x, x')$ according to Equations 1, 2, and 3. A common practice is to assign the prior a zero mean and a kernel function $K_{ij} = k(x_i, x_j; \theta)$.

$$f(x) \sim \mathcal{GP}(m(x), k(x, x')) \tag{1}$$

$$m(x) = \mathbb{E}[f(x)] \tag{2}$$

$$k(x, x') = \mathbb{E}[f(x) - m(x)][f(x') - m(x')] \tag{3}$$

The available analysis or experimental data can be described according to Equation **??**:

$$y = f(x) + \epsilon, \epsilon \sim \mathcal{N}(0, \sigma_{\mathrm{n}}^2 \mathcal{I}) \tag{4}$$

where f represents the function to be approximated and ϵ represents the error term which is assumed to be normally distributed with variance σ_{n}^2.

GPs are part of the Bayesian methods, where a pivotal aspect of the analysis involves the prior distribution. The prior distribution encapsulates our pre-existing knowledge or assumptions about the unknown function f. The prior distribution of the observed data X and the test data X' is determined according to Equation 5.

$$\begin{bmatrix} y \\ f_* \end{bmatrix} \sim \mathcal{N}\left(\begin{bmatrix} 0 \\ 0 \end{bmatrix}, \begin{bmatrix} K(X,X) + \sigma_n^2 I & K(X,X_*) \\ K(X_*,X) & K(X_*,X_*) \end{bmatrix} \right) \tag{5}$$

where f_* are the function values evaluated at the test locations X_*. In Bayesian learning, the prior distribution is revised by incorporating the observed data, resulting in the formation of the predictive distribution. Mathematically, the prior distribution is conditioned on the observed data to form the predictive distribution according to Equations 6, 7, and 8:

$$f_*|X, X_*, y \sim \mathcal{N}(\mu_*, \sigma_*^2) \tag{6}$$

$$\mu_* = k_*^T (K + \sigma_n^2 I)^{-1} y \tag{7}$$

$$\sigma_*^2 = k_{**} - k_*^T (K + \sigma_n^2 I)^{-1} k_* \tag{8}$$

where $K = K(X,X)$, $k_{**} = k(x_*, x_*)$ and $k_* = k(x_*)$. In order to optimize the model's hyperparameters, , the marginal log-likelihood was applied. The marginal log-likelihood is defined according to Equation 9.

$$\log p(y|x,\theta) = -\frac{1}{2}\log|K + \sigma_n^2 I| - \frac{1}{2} y^T [K + \sigma_n^2 I]^{-1} y - \frac{n}{2}\log 2\pi \tag{9}$$

MF Gaussian Processes

The present study adopts the autoregressive scheme AR1 introduced by Kennedy and O'Hagan (2000). The scheme is based on the assumption that there is a linear dependency among different fidelity models. The mathematical formulation follows the description in Le Gratiet and Garnier (2014). The mathematical description of the bifidelity model is given since the case studies deal with bifidelity problems. The sub-models are linked according to Equation 10 and 11. The HF function connects to the LF function via a scaling function ρ and an additive function δ. It is assumed that F_2 refers to the HF function and F_1 refers to the LF function. The function δ is a GP which is independent of F_1.

$$F_2(x) = \rho(x) F_1(x) + \delta(x) \tag{10}$$

$$F_1(x) \perp \delta(x) \tag{11}$$

The predictive model is a multivariate normal distribution described by Equation 12, with a mean function according to Equation 13 and a variance according to Equation 14.

$$[F_2(x)|\boldsymbol{F} = \boldsymbol{f}, (\boldsymbol{\beta_1}, \boldsymbol{\beta_2}, \rho), (\sigma_1^2, \sigma_2^2), (\boldsymbol{\theta_1}, \boldsymbol{\theta_2})] \sim \mathcal{N}(m_{F_2}(x), s_{F_2}^2(x)) \tag{12}$$

$$m_{F_2}(x) = \mathbf{h}(x)^T \boldsymbol{\beta} + k(x)^T \boldsymbol{V}^{-1}(\boldsymbol{f} - \boldsymbol{H}\boldsymbol{\beta}) \tag{13}$$

$$s_{F_2}(x) = \rho^2 \sigma_1^2 + \sigma_2^2 - \boldsymbol{k}^T \boldsymbol{V}^{-1} \boldsymbol{k}(x) \tag{14}$$

where the trend parameters $\boldsymbol{\beta} = \begin{pmatrix} \beta_1 \\ \beta_2 \end{pmatrix}$, and $\boldsymbol{f} = \begin{pmatrix} f_1 \\ f_2 \end{pmatrix}$. The variance parameters σ_1^2, σ_2^2 and the parameters θ_1, θ_2 are the model's hyperparameters.

$$\boldsymbol{H} = \begin{pmatrix} \boldsymbol{f}_1'(x_1^{(1)}) & 0 \\ \vdots & \vdots \\ \boldsymbol{f}_1'(x_{n_1}^{(1)}) & 0 \\ \rho \boldsymbol{f}_1'(x_1^{(2)}) & \boldsymbol{f}_2'(x_1^{(2)}) \\ \vdots & \vdots \\ \rho \boldsymbol{f}_1'(x_{n_2}^{(2)}) & \boldsymbol{f}_2'(x_{n_2}^{(2)}) \end{pmatrix} \tag{15}$$

$$\boldsymbol{h}(x)^T = (\rho \boldsymbol{f}_1'(x), \boldsymbol{f}_2'(x)) \tag{16}$$

The covariance matrix is calculated as described in Equation 17.

$$\boldsymbol{V} = \begin{pmatrix} \sigma_1^2 R_1(\boldsymbol{D_1}) & \rho\sigma_1^2 R_1(\boldsymbol{D_1}, \boldsymbol{D_2}) \\ \rho\sigma_1^2 R_1(\boldsymbol{D_2}, \boldsymbol{D_1}) & \rho^2\sigma_1^2 R_1(\boldsymbol{D_2}) + \sigma_2^2 R_2(\boldsymbol{D_2}) \end{pmatrix} \tag{17}$$

Compositional Kernels

The covariance matrix conveys the degree of resemblance among data points Rasmussen (2003) and integrates prior beliefs and knowledge regarding the function f. The validity of the covariance matrix requires both symmetry and positive semi-definiteness. Prior research has examined basis functions used as kernel functions, which are defined as functions generating valid covariance matrices. For instance, the periodic kernel is employed for modeling repetitive functions. In this study, the framework introduced in Charisi et al. (2022b) was employed. The core idea was the development of compositional kernels, aiming to facilitate early-stage design analysis and optimization.

Compositional kernels, introduced by Duvenaud et al. (2013), are defined as a combination of a limited number of basis kernels through addition or multiplication. Choosing the basis kernels is intended to mathematically encapsulate the key features of the function f or, in the context of this specific research problem, the design space. The compositional kernels are built via discrete optimization. As the objective function, the Bayesian Information Criterion (BIC) was used as proposed in the original paper Duvenaud et al. (2013). BIC is defined according to Equation 18.

$$\mathcal{BIC} = k_{hyp} \ln n - 2 \ln L \tag{18}$$

where n is the number of training data, k_{hyp} is the number of hyperparameters, and L is the maximized likelihood value. BIC comprises two elements: a penalty term determined by the count of model parameters and a term derived from the likelihood function. The advantage of opting for BIC over maximizing the marginal log-likelihood is its attention to the complexity of the kernel function. By favoring functions with fewer hyperparameters, BIC aids in preventing overfitting.

Bayesian Optimization

Bayesian optimization (BO) has found extensive application in addressing optimization problems characterized by objective functions that are costly to evaluate. It comprises three fundamental components: establishing the prior distribution, refining the prior distribution to derive the posterior distribution, and determining the subsequent sampling point Brochu et al. (2009). The initial two components are associated with shaping the surrogate model, while the last one is linked to the acquisition function. The MF surrogate model in the proposed framework was built via MF-GPs as described in the previous sections. The acquisition function establishes a strategy for assessing the utility of evaluating the objective function at specific points within the search space Di Fiore and Mainini (2024). The objective of the acquisition function is to strike a

balance between exploring new areas and exploiting known areas within the search space. For this research, Expected Improvement (EI) was employed as the acquisition function, as described in Equation 19.

$$\alpha_{\text{EI}}(y_{\text{best}}, \mu.\sigma) = -\left(\phi\left(\frac{y_{\text{best}} - \mu}{\sigma}\right) + \frac{y_{\text{best}} - \mu}{\sigma} \cdot \Phi\left(\frac{y_{\text{best}} - \mu}{\sigma}\right)\right) \cdot \sigma \tag{19}$$

y_{best} represents the current optimum, μ and σ denote the mean and covariance matrix, respectively, while ϕ and Φ refer to the probability density function and the cumulative distribution function, respectively.

Information Entropy

Entropy measures the uncertainty that observers have about the state of a random variable X Varley et al. (2023). The entropy $H[p(x)]$ of a distribution $p(x)$ is a measure measuring the uncertainty in the distribution Rasmussen (2003). The integral can be replaced by a sum of discrete variables. The differential entropy for continuous variables is calculated according to Equation

$$H(X) = -\int_s f(x) \log f(x)\, dx \tag{20}$$

where S is the support of the probability density function. Regarding the multivariate Gaussian distribution, the entropy is defined according to Equation 21.

$$H[\mathcal{N}(\mu, \Sigma)] = \frac{1}{2} \log |\Sigma| + \frac{D}{2} \log 2\pi e \tag{21}$$

where D is the number of dimensions. Unlike entropy for discrete random variables, differential entropy can take negative values. The covariance matrix is guaranteed to be symmetric positive semi-definite. However, in instances where the covariance matrix becomes singular, the entropy value tends toward negative infinity. To mitigate this issue for singular matrices, the eigenvalues are computed. Any zero eigenvalues are replaced with a value of 10^{-6}, and the covariance matrix is then reconstructed based on the adjusted eigenvalues using Equation 22.

$$A = U \Lambda U^{-1} \tag{22}$$

where A represents an $n \times n$ matrix, U is an $n \times n$ matrix containing the eigenvectors of A, with each column of U representing an eigenvector of A, and Λ is an $n \times n$ diagonal matrix containing the eigenvalues of A along its diagonal elements.

The termination of the optimization loop occurs when the quantified uncertainty of the design space prediction, assessed through entropy, reaches a predetermined threshold. To ensure robustness, the criterion includes the condition that the value of entropy should not increase by more than a predetermined margin for n iterations. In summary, the formulation of the termination criterion can be found in Algorithm 1. A comparable concept was applied to the optimization criterion for compositional kernels. Entropy serves as an indicator to decide whether compositional kernel optimization should be conducted. The rationale behind this approach is that a notable decrease in entropy signifies a significant change in the predictive distribution. The formulation of the kernel optimization criterion is detailed in Algorithm 2.

input : $\Delta H_{\text{critical}}, \Delta H_{\text{margin}}, nr_{\text{iter}}^{\text{critical}}, nr_{\text{iter}}^{\text{max}}$; /* critical value of entropy change, acceptable margin of entropy change, critical number of optimization iterations, maximum number of optimization iterations */

output: $\epsilon_x, \epsilon_f, \epsilon_t, \text{RMSE}, nr_{\text{iter}}^{\text{terminate}}$; /* performance, metrics, step to terminate the optimization loop */

$nr_{\text{iter}}^{i} \leftarrow 1$;
$comp\_cost \leftarrow 0$;
$counter \leftarrow 0$;
while $nr_{\text{iter}}^{i} \leq nr_{\text{iter}}^{\text{max}}$ **do**
  Compute μ, σ from Equations 7, 8 ; /* MF surrogate model */
  Compute entropy H_{iter_i} from Equation 21;
  if $nr_{\text{iter}}^{i} = 1$ **then**
    $H_0 \leftarrow H_{iter_i}$; /* Reference entropy value */
  end
  else
    if $H_{iter_i} > H_0$ **then**
      $H_0 \leftarrow H_{iter_i}$
    end
  end
  Compute $comp\_cost_i$;
  $comp\_cost \leftarrow comp\_cost + comp\_cost_i$; /* Computational cost */
  Compute $\epsilon_x, \epsilon_f, \epsilon_t$, RMSE from Equations 24,25,26,23; /* Performance metrics */
  if $H_0 - H_{iter_i} \geq \Delta H_{\text{critical}}$ **then**
    $counter \leftarrow counter + 1$; /* Counting optimization steps */
    if $counter = nr_{\text{iter}}^{\text{critical}}$ **then**
      $nr_{\text{iter}}^{\text{terminate}} = nr_{\text{iter}}^{i}$;
      break;
    end
  end
  if $H_{iter_i} - H_{iter_i - 1} \geq \Delta H_{\text{margin}}$ **then**
    $counter \leftarrow 0$
  end
  $nr_{\text{iter}}^{i} \leftarrow nr_{\text{iter}}^{i} + 1$;
end

Algorithm 1: Termination criterion

input : $\Delta H_{\text{critical}}, \Delta H_{\text{margin}}, nr_{\text{iter}}^{\text{max}}, nr_{\text{iter}}^{\text{critical}}$; /* critical value of entropy change, acceptable margin of entropy change, maximum number of optimization iterations, critical number of optimization iterations */

output: $\epsilon_x, \epsilon_f, \epsilon_t$, RMSE; /* performance, metrics */

$nr_{\text{iter}}^{i} \leftarrow 1$;
$bool_{ker\_opt} \leftarrow$ False ;
$counter \leftarrow 0$;
while $nr_{\text{iter}}^{i} \leq nr_{\text{iter}}^{\text{max}}$ **do**
  Compute μ, σ from Equations 7, 8 ; /* MF surrogate model */
  Compute entropy H_{iter_i} from Equation 21;
  if $nr_{\text{iter}}^{i} = 1$ **then**
    $H_0 \leftarrow H_{iter_i}$; /* Reference entropy value */
  end
  Compute $\epsilon_x, \epsilon_f, \epsilon_t$, RMSE from Equations 24,25,26,23; /* Performance metrics */
  if $|H_0 - H_{iter_i}| \geq \Delta H_{\text{critical}}$ **and** $(H_0 - H_{iter_i})(H_0 - H_{iter_i - 1}) > 0$ **then**
    $counter \leftarrow counter + 1$; /* Counting optimization steps */
    if $counter = nr_{\text{iter}}^{\text{critical}}$ **then**
      Perform compositional kernels optimization;
      $H_0 \leftarrow H_{iter_i}$;
    end
  end
  if $|H_{iter_i} - H_{iter_i - 1}| \geq \Delta H_{\text{margin}}$ **and** $(H_{iter_i} - H_0)(H_{iter_i} - H_{iter_i - 1}) < 0$ **then**
    $counter \leftarrow 0$
  end
  $nr_{\text{iter}}^{i} \leftarrow nr_{\text{iter}}^{i} + 1$;
end

Algorithm 2: Kernel optimization criterion

Error metrics

Various error metrics were employed to evaluate the accuracy of the proposed framework. The Root Mean Squared Error (RMSE), as defined in Equation 23, was used to quantify the accuracy of the models in predicting the design space. Furthermore, the error metrics ϵ_x, ϵ_f, ϵ_t characterize the normalized error in the design space, the objective function, and the Euclidean distance in the normalized x-f hyperspace. Detailed descriptions of these metrics are provided in Equations 24, 25, and 26.

$$\varepsilon_{RMSE} = \frac{1}{y_{max} - y_{min}} \sqrt{\frac{1}{N} \sum_{i=1}^{N} (y_i - \hat{y}_i)^2} \tag{23}$$

$$\epsilon_x = \frac{\|\hat{x}^* - x^*\|}{\sqrt{N}} \tag{24}$$

$$\epsilon_f = \frac{f(\hat{x}^*) - f_{\text{min}}}{f_{\text{max}} - f_{\text{min}}} \tag{25}$$

$$\epsilon_t = \sqrt{\frac{\epsilon_x^2 + \epsilon_f^2}{2}} \tag{26}$$

CASE STUDIES

The case studies encompass a simplified example, using the Jump Forrester function, to illustrate the rationale behind integrating information entropy into an early-stage design framework. Subsequently, two analytical problems will the addressed: the 1D Heterogeneous function and the 2D shifted rotated Rastrigin function. Finally, a realistic ship design is showcased, addressing the 2D design of the AXE frigates focused on optimizing the wave-induced vertical bending moment (VBM).

A toy example: the Jump Forrester function

This simplified design problem aims to give a better understanding on how and why entropy is integrated in the design framework. The toy case study assumes a one-dimensional design space characterized by the Jump Forrester function as described in Equations 27 and 28. The initial dataset comprises 5 HF and 35 LF observations.

$$f_1(x) = \begin{cases} (6x-2)^2 \sin(12x-4), & 0 \leq x < 0.5 \\ (6x-2)^2 \sin(12x-4) + 10, & 0.5 \leq x \leq 1 \end{cases} \tag{27}$$

$$f_2(x) = \begin{cases} 0.5 f_1(x) + 10(x-0.5) - 5, & 0 \leq x < 0.5 \\ 0.5 f_1(x) + 10(x-0.5) - 2, & 0.5 \leq x \leq 1 \end{cases} \tag{28}$$

Figure 3 illustrates the evolution of error metrics and entropy throughout the optimization process. Evidently, an augmented

dataset correlates with heightened accuracy in the obtained results. This is a general trend which can be observed in both the evolution of H and ϵ throughout the optimization. Figure 3a illustrates a notable decrease in entropy between iteration 10 and 11. The decrease in entropy is correlated with a reduction in the error metrics, as depicted in Figure 3b. It is evident that the variations in entropy do not perfectly align with changes in the error metrics. This underscores the importance of treating entropy as an indicator rather than an absolute measure.

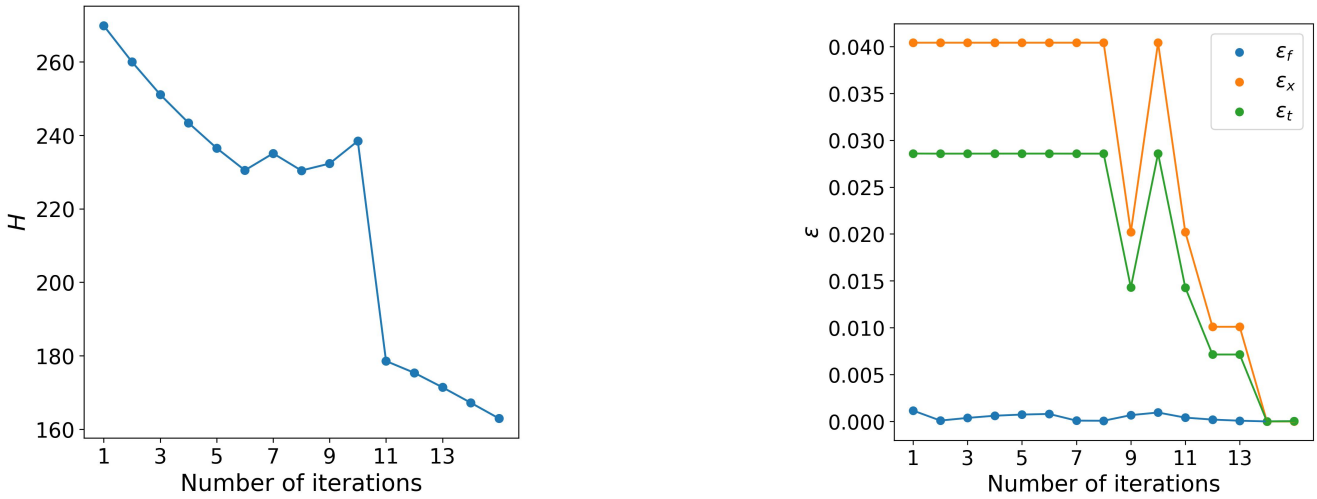

(a) Tracking H throughout the optimization iterations

(b) Tracking ϵ throughout the optimization iterations

Figure 3: Comparing H with ϵ error metrics

To further analyze the results, the design spaces for iterations 9, 10, and 11 are plotted in Figure4. Specifically, Figure 4a displaying the prediction of the design space at step 9, reveals that the prediction is inaccurate across the domain and the variance is high. However, the area where the optimum lies is further explored, resulting in a lower calculated error. This localized behavior cannot be captured via entropy which is calculated over the entire design domain. Similarly, the design space in iteration 10, depicted in Figure 4b, is characterized by an inaccurate prediction of the design space and high uncertainty bounds. Entropy is slightly increased between iteration 9 and 10. In addition, the measured error is higher since the prediction fails to capture the area containing the optimum. Moving on to iteration 11, illustrated in Figure 4c, the prediction aligns more closely with the true design space, resulting in a significant reduction in both calculated error and entropy.

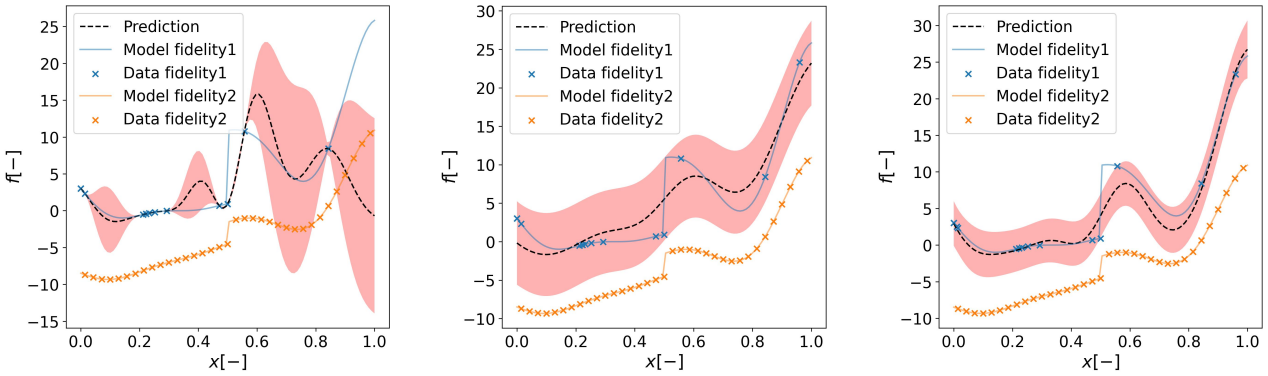

(a) Optimization Step 9

(b) Optimization Step 10

(c) Optimization Step 11

Figure 4: Design space for various optimization steps

Analytical function 1D: the Heterogeneous function

A commonly employed analytical function is the Heterogeneous function, known for its localized and multi-modal behavior Mainini et al. (2022). The 1D Heterogeneous function is described by the Equations 29 and 30. The Heterogeneous function can be visualized in Figure 5.

$$f_1(x) = \sin 30(x - 0.9)^4 \cos 2(x - 0.9) + (x - 0.9)/2 \tag{29}$$

$$f_2(x) = (f_1(x) - 1.0 + x)/(1.0 + 0.25x) \tag{30}$$

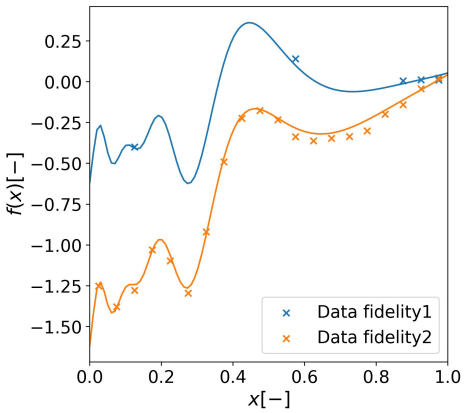

Figure 5: Heterogeneous function

where $0 \leq x \leq 1$. In this case study, the initial training set comprised included 10 HF data fused with 35 LF data. The base case underwent 15 optimization steps. The parameters of this case study remained consistent when evaluating both the entropy-driven termination criterion and entropy-driven kernel optimization. Furthermore, recognizing the substantial impact of the training set on model performance, statistical insights were derived by employing 20 distinct training sets in both scenarios.

Regarding the entropy-driven optimization criterion, relevant statistics can be found in Tables 1 and 2 for the proposed and the base model, respectively. Six scenarios were examined, involving the increase of noise in the training data from 0.00 to 0.05. The comparison of mean error metric values is presented and visualized in Figure 6. The main observation is that, as anticipated, the error generally rises with an increase in noise level. In most instances, the proposed model demonstrates comparable or slightly elevated errors compared to the base model, while concurrently achieving significant computational savings. For instance, when $\sigma_n = 0.04$, the average number of iterations is 10.5, resulting in a 30% improvement compared to the 15 iterations in the base scenario.

Regarding the entropy-driven kernel optimization, the results can be found in Tables Tables 3 and 4 for the proposed and base models, respectively. The visualization of mean error metrics is presented in Figure 7. As illustrated in Figure 7, the proposed model demonstrates a comparable performance to the base model, and their results are closely aligned, thus the performance of the two models is similar.

Analytical function 2D: the Shifted Rotated Rastrigin function

In this case study, the 2D shifted-rotated Rastrigin function was employed. This function is characterized by multi-modal behavior. To investigate this, a noise term e_{data} was added to the 2D shifted-rotated Rastrigin function, taken from Mainini et al. (2022). Thus, for this analysis, Equations 31 and 34 were used. The function can be visualized in Figure 8.

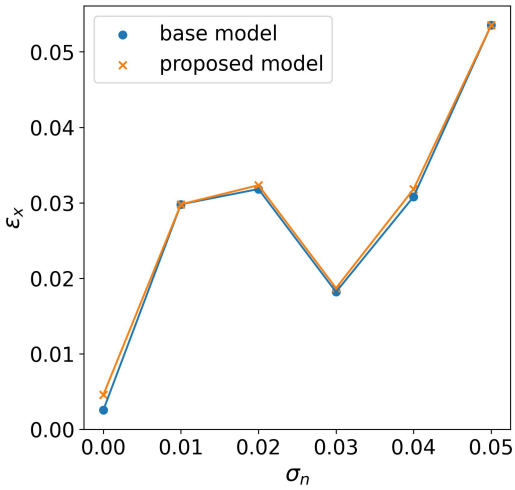

(a) Graph depicting the relationship between ϵ_x and σ_n

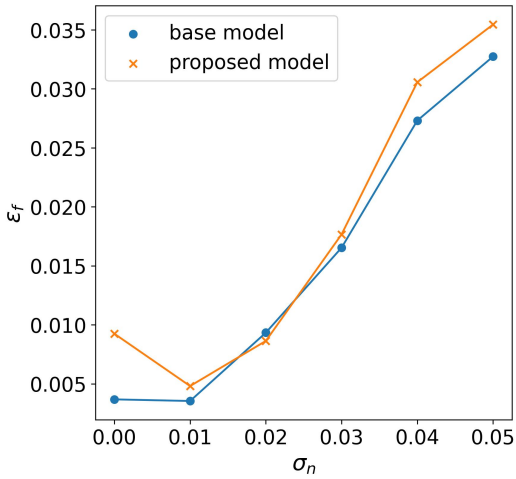

(b) Graph depicting the relationship between ϵ_f and σ_n

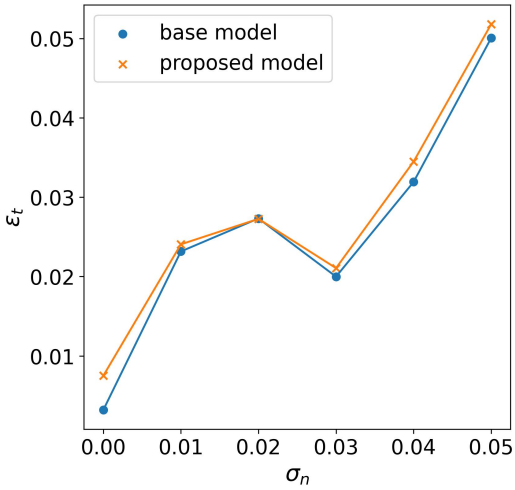

(c) Graph depicting the relationship between ϵ_t and σ_n

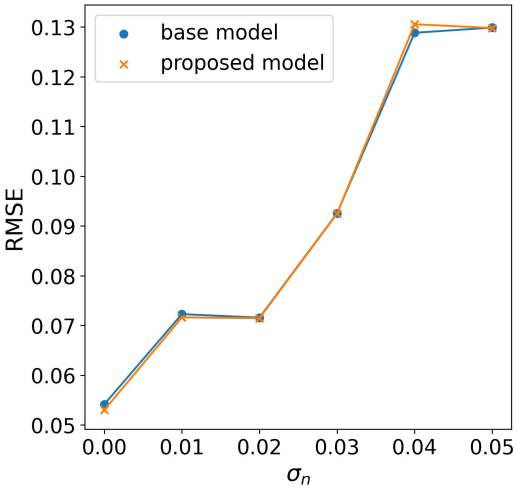

(d) Graph depicting the relationship between $RMSE$ and σ_n

Figure 6: Heterogeneous function: Entropy-driven termination criterion, while varying the noise σ_n

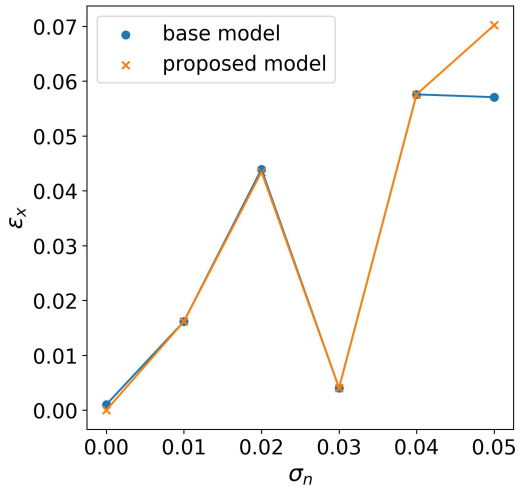

(a) Graph depicting the relationship between ϵ_x and σ_n

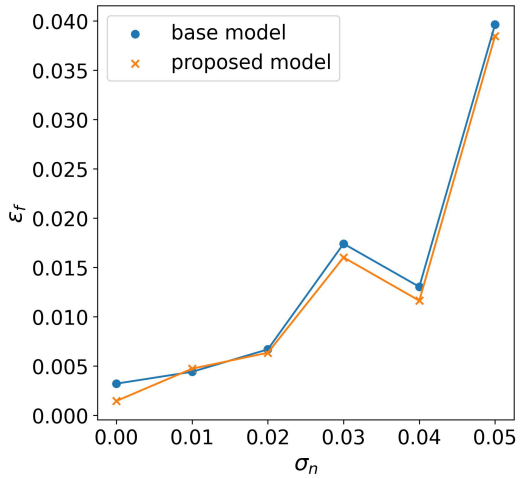

(b) Graph depicting the relationship between ϵ_f and σ_n

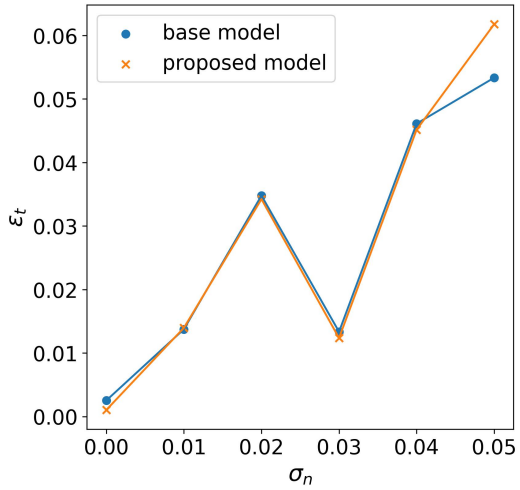

(c) Graph depicting the relationship between ϵ_t and σ_n

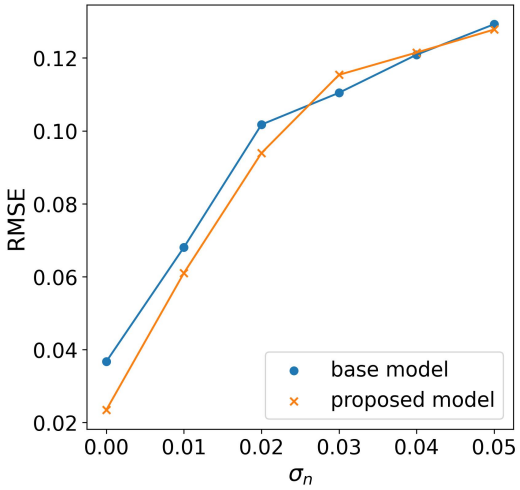

(d) Graph depicting the relationship between $RMSE$ and σ_n

Figure 7: Heterogeneous function: Entropy-driven kernel optimization, while varying the noise σ_n

Table 1: Proposed model performance (entropy-driven termination criterion, Heterogeneous function)

σ_n	ϵ_x **(std)**	ϵ_f **(std)**	ϵ_t **(std)**	$RMSE$ **(std)**	**computational cost (std)**	**optimization steps (std)**
0	0.0045 (0.0050)	0.0092 (0.0104)	0.0075 (0.0079)	0.0530 (0.0387)	2.21 (0.71)	10.45 (4.00)
0.01	0.0298 (0.0811)	0.0048 (0.0062)	0.0241 (0.0564)	0.0716 (0.0231)	2.91 (0.39)	14.5 (2.18)
0.02	0.0323 (0.0803)	0.0086 (0.0131)	0.0273 (0.0559)	0.0715 (0.0126)	2.6 (0.74)	12.75 (4.11)
0.03	0.0187 (0.0585)	0.0177 (0.0223)	0.0211 (0.0430)	0.0925 (0.0222)	2.38 (0.97)	11.6 (5.31)
0.04	0.0318 (0.0772)	0.0306 (0.0408)	0.0345 (0.06)	0.1306 (0.0528)	2.18 (1.03)	10.5 (5.62)
0.05	0.0535 (0.0991)	0.0354 (0.0362)	0.0518 (0.0703)	0.1298 (0.0485)	2.67 (0.79)	13.2 (4.29)

Table 2: Base model performance (entropy-driven termination criterion, Heterogeneous function)

σ_n	ϵ_x **(std)**	ϵ_f **(std)**	ϵ_t **(std)**	$RMSE$ **(std)**	**computational cost**	**optimization steps**
0	0.0025 (0.0044)	0.0037 (0.0062)	0.0032 (0.0053)	0.0542 (0.0516)	3	15
0.01	0.0298 (0.0811)	0.0035 (0.0024)	0.0232 (0.0566)	0.0723 (0.0230)	3	15
0.02	0.0318 (0.0804)	0.0093 (0.0130)	0.0273 (0.0559)	0.0716 (0.0126)	3	15
0.03	0.0182 (0.0586)	0.0165 (0.0217)	0.02 (0.0431)	0.0925 (0.0223)	3	15
0.04	0.0308 (0.0776)	0.0273 (0.0410)	0.0319 (0.0606)	0.1288 (0.0512)	3	15
0.05	0.0535 (0.0991)	0.03273 (0.0376)	0.05 (0.0713)	0.1299 (0.0486)	3	15

$$f_1(z) = \sum_{i=1}^{D=2} (Z_i^2 + 1 - \cos(10\pi z_i)) \tag{31}$$

where

$$z = R(\theta)(x - x*) \tag{32}$$

$$R(\theta) = \begin{bmatrix} \cos\theta & -\sin\theta \\ \sin\theta & \cos\theta \end{bmatrix} \tag{33}$$

where $x_i \epsilon [-0.1, 0.2]$ for $i = 1, .., D$, R is the rotation matrix, and $\theta = 0.2$.

$$f_2(z, \phi_i) = f_1(z) + e_r(z, \phi_i) + e_{data} \tag{34}$$

where the resolution error e_r is defined according to Equation 35.

$$e_r(z, \phi_i) = \sum_{i=1}^{D=2} \alpha(\phi) \cos^2(w(\phi) z_i + \beta\phi + \pi) \tag{35}$$

Table 3: Proposed model performance (entropy-driven kernel optimization, Heterogeneous function)

σ_n	ϵ_x **(std)**	ϵ_f **(std)**	ϵ_t **(std)**	$RMSE$ **(std)**
0	0.0	0.0015	0.0010	0.0235
	(0.0)	(0.0030)	(0.0021)	(0.0279)
0.01	0.0162	0.0047	0.01396	0.0610
	(0.0590)	(0.0047)	(0.0412)	(0.0218)
0.02	0.0434	0.0063	0.0342	0.0939
	(0.0964)	(0.0059)	(0.0668)	(0.0618)
0.03	0.0040	0.0160	0.0124	0.1154
	(0.0049)	(0.0131)	(0.0091)	(0.0633)
0.04	0.0576	0.0116	0.0452	0.1215
	(0.1077)	(0.0081)	(0.0743)	(0.0468)
0.05	0.0702	0.0385	0.0618	0.1278
	(0.1114)	(0.0562)	(0.0847)	(0.0529)

Table 4: Base model performance (entropy-driven kernel optimization, Heterogeneous function)

σ_n	ϵ_x **(std)**	ϵ_f **(std)**	ϵ_t **(std)**	$RMSE$ **(std)**
0	0.0010	0.0032	0.0025	0.0367
	(0.0030)	(0.0052)	(0.0042)	(0.0359)
0.01	0.01616	0.0044	0.0137	0.0681
	(0.0590)	(0.0050)	(0.0413)	(0.0172)
0.02	0.0439	0.0067	0.0348	0.1017
	(0.0962)	(0.0059)	(0.0665)	(0.0665)
0.03	0.0040	0.0174	0.01334	0.1105
	(0.0049	(0.0141)	(0.0097)	(0.0557)
0.04	0.0576	0.0130	0.0461	0.1209
	(0.1077)	(0.0086)	(0.0738)	(0.0451)
0.05	0.0571	0.0396	0.0534	0.1293
	(0.1018)	(0.0558)	(0.0794)	(0.0522)

with $\alpha(\phi) = \Theta(\phi)$, $w(\phi) = 10\pi\Theta$, $\beta(\phi) = 0.5\pi\Theta(\phi)$, $\Theta(\phi) = 1 - 0.0001\phi$. For the present case study, we chose $\phi = 2500$.

In this case study, the initial training set consisted of 10 HF data combined with 50 LF data. The base case underwent 15 optimization steps. Consistent with other studies, parameters were maintained constant during the assessment of both the entropy-driven termination criterion and entropy-driven kernel optimization. Statistical insights were obtained by using 20 different training sets in both scenarios.

Regarding the entropy-driven optimization criterion, relevant statistics can be found in Tables 5 and 6. The visualization of mean error metrics is presented in Figure 9. A notable observation is that, similar trends to the previous case study are observed, where the suggested model displays errors that are comparable or slightly higher than those of the base model, yet it concurrently realizes computational savings. The discrepancy between the models is more apparent, possibly due to the increased complexity of this problem. Notably, in this instance, the error does not escalate with the noise level.

Regarding the entropy-driven kernel optimization, the results can be found in Tables Tables 7 and 8 for the proposed and base models, respectively. The visualization of mean error metrics is presented in Figure 10. The findings indicate a substantial enhancement in error metrics of the proposed model compared to the base case across various scenarios. These results are noteworthy, with a more pronounced improvement compared to the previous case study. This heightened improvement could be attributed to the increased complexity of the problem or the ability of compositional kernels to better capture the structure of the function.

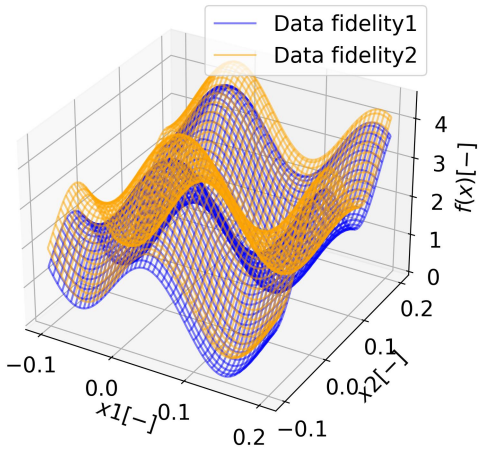

Figure 8: Rastrigin function

Table 5: Proposed model performance (entropy-driven termination criterion, Rastrigin function)

σ_n	ϵ_x **(std)**	ϵ_f **(std)**	ϵ_t **(std)**	$RMSE$ **(std)**	**computational cost (std)**	**optimization steps (std)**
0	0.1192 (0.2064)	0.0068 (0.0103)	0.0875 (0.1443)	0.1110 (0.0386)	0.9 (0.0696)	14.15 (1.53)
0.01	0.2007 (0.2475)	0.0151 (0.0207)	0.1464 (0.1722)	0.1212 (0.0570)	0.8969 (0.0845)	14.15 (1.74)
0.02	0.0239 (0.1042)	0.0035 (0.0082)	0.0192 (0.0733)	0.1094 (0.0348)	0.8875 (0.1129)	14 (2.17)
0.03	0.1044 (0.2121)	0.0097 (0.0196)	0.0775 (0.1489)	0.1538 (0.0718)	0.8844 (0.1330)	13.9 (2.45)
0.04	0.0717 (0.1706)	0.0049 (0.0093)	0.0528 (0.1199)	0.0997 (0.0351)	0.9031 (0.0850)	14.15 (1.68)
0.05	0.1924 (0.2658)	0.0121 (0.0298)	0.1367 (0.1889)	0.1312 (0.0658)	0.8875 (0.0980)	13.8 (1.91)

Ship design problem 2D: the AXE frigates

The AXE frigates are characterized by the inclusion of an AXE bow, a design initially conceived by Keuning et al. (2015). The AXE bow offers the potential to enhance a vessel's seakeeping capabilities, making it a compelling choice for frigates that must effectively carry out missions even in challenging weather conditions. The key performance indicator (KPI) for this design problem focuses on predicting the wave-induced VBM.

The VBM emerges as a significant load with substantial implications for ship structural design. It results from the uneven distribution of water pressure and gravity, resulting in the bending of the elastic hull structure Molland (2008). Wave loading conditions are assessed independently for each design variation. More specifically, we have chosen to examine the vessel in a sea state that maximizes wave-induced VBM, specifically when the wavelength equals the ship's length. Consequently, a regular sea state is selected and characterized by Equations 36 and 37 Tupper (2004). The vessel's speed was set to 0 knots. The problem is simplified into a 2D case, where only the vessel's length (L_{pp}) and breadth (B) are varied.

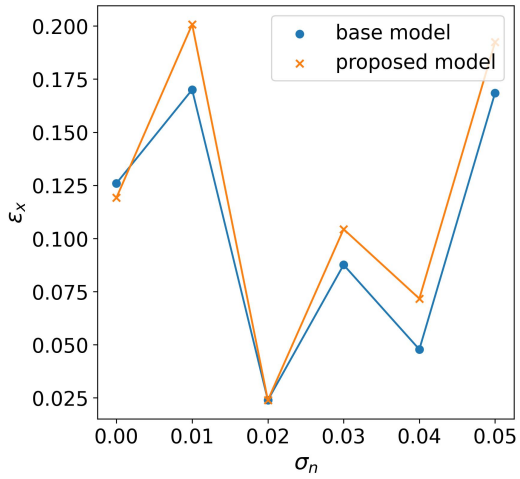

(a) Graph depicting the relationship between ϵ_x and σ_n

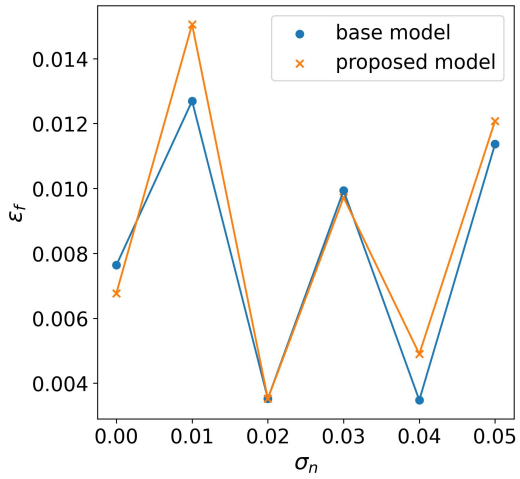

(b) Graph depicting the relationship between ϵ_f and σ_n

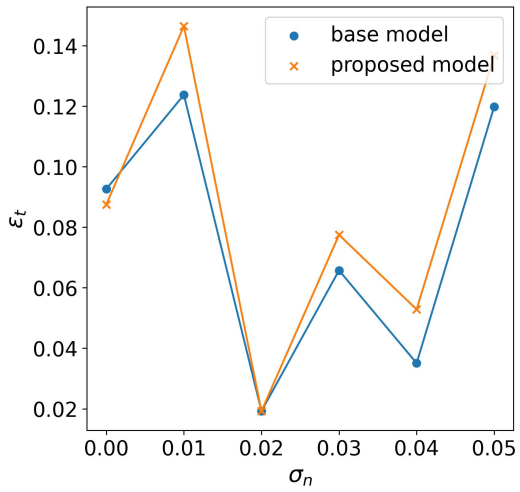

(c) Graph depicting the relationship between ϵ_t and σ_n

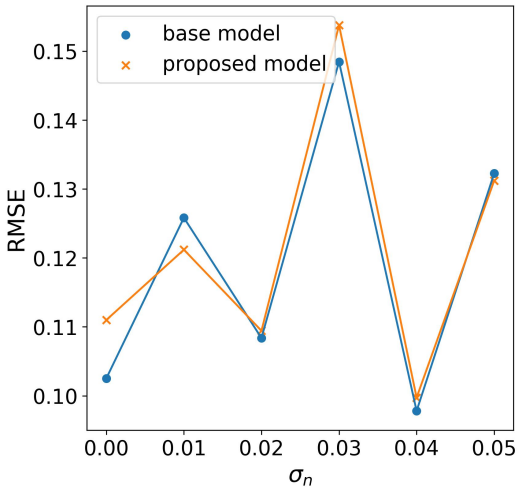

(d) Graph depicting the relationship between $RMSE$ and σ_n

Figure 9: Rastrigin function: Entropy-driven termination criterion, while varying the noise σ_n

$$\lambda = L_{pp} \tag{36}$$

$$H = 0.607 \cdot \sqrt{Lpp} \tag{37}$$

In the frequency domain (FD) calculation of the wave-induced VBM, PRECAL software, developed by Marin, was employed. PRECAL is a dedicated tool designed to predict linear responses through potential flow calculations. The tool operates by: (1) dividing the wetted hull into multiple quadrilateral panels and defining flexural modes, (2) calculating hydrodynamic coefficients through solving the linearized boundary value problem, and (3) determining ship motions and loads using linearized potential flow. Additionally, it incorporates adjustments for viscous damping based on empirical corrections.

Furthermore, the time domain (TD) results were obtained using PRETTI_R, a 3D time-domain nonlinear seakeeping and hydroelasticity tool. In contrast to PRECAL, PRETTI_R is specifically crafted for predicting motions in high sea states, en-

Table 6: Base model performance (entropy-driven termination criterion, Rastrigin function)

σ_n	ϵ_x **(std)**	ϵ_f **(std)**	ϵ_t **(std)**	$RMSE$ **(std)**	**computational cost (std)**	**optimization steps (std)**
0	0.1259 (0.2200)	0.0076 (0.0104)	0.0926 (0.1536)	0.1025 (0.0324)	0.9375 (0.0)	15 (0.0)
0.01	0.1700 (0.2320)	0.0127 (0.0209)	0.1237 (0.1623)	0.1258 (0.0557)	0.9375 (0.0)	15 (0.0)
0.02	0.0239 (0.1042)	0.0035 (0.0082)	0.0192 (0.0733)	0.1084 (0.0344)	0.9375 (0.0)	15 (0.0)
0.03	0.0876 (0.2109)	0.0099 (0.0196)	0.0657 (0.1483)	0.1485 (0.0718)	0.9375 (0.0)	15 (0.0)
0.04	0.0478 (0.1434)	0.0035 (0.0082)	0.0351 (0.1011)	0.0978 (0.0326)	0.9375 (0.0)	15 (0.0)
0.05	0.1685 (0.2606)	0.0114 (0.0299)	0.1198 (0.1852)	0.1323 (0.0643)	0.9375 (0.0)	15 (0.0)

Table 7: Proposed model performance (entropy-driven kernel optimization, Rastrigin function)

σ_n	ϵ_x **(std)**	ϵ_f **(std)**	ϵ_t **(std)**	$RMSE$ **(std)**
0	0.0902 (0.2177)	0.0076 (0.0183)	0.0663 (0.1536)	0.1070 (0.0597)
0.01	0.7382 (0.2700)	0.0150 (0.0288)	0.1245 (0.1912)	0.1349 (0.0691)
0.02	0.1115 (0.2262)	0.0096 (0.0254)	0.0796 (0.1607)	0.1175 (0.0437)
0.03	0.0543 (0.1643)	0.0015 (0.0039)	0.0389 (0.1160)	0.0961 (0.0189)
0.04	0.0756 (0.1699)	0.0035 (0.0069)	0.0540 (0.1200)	0.1043 (0.0529)
0.05	0.1050 (0.2132)	0.0069 (0.0138)	0.0759 (0.1503)	0.1012 (0.0494)

compassing rigid-body motion, elastic deformation, and hydrodynamic loads. It is also capable of considering slamming and whipping loads. Developed as part of the Cooperative Research Ships (CRS) initiative, this software calculates the Froude Krylov force by integrating incident wave hydrodynamics and hydrostatic pressure across the vessel's hull surface. The diffraction force is estimated by scaling the FD diffraction force Response Amplitude Operator (RAO) with the incident wave amplitude. The radiation force is computed through a convolution integral involving an impulse function, and slamming force can be assessed using either the Generalized Wagner Model or the Modified Logvinovich Model. PRETTI_R utilizes FD results to derive the required impulse functions.

The initial training set consists of 2 HF PRETTI_R simulations (TD data) and 20 PRECAL simulations (LF data). The LF and the HF design space can be visualized in Figure 11. The optimization steps were configured to be 10. The outcomes are presented in Tables 9 and 10 for the entropy-driven termination criterion and kernel optimization, respectively. The data was gathered through 20 simulations utilizing various initial Design of Experiments (DoEs). In general, the results exhibit similar trends to previous case studies. The performance metrics of the proposed model slightly surpass those of the base model, with an associated reduction in computational steps to an average of 8.55 from the set 10 steps. Concerning the kernel optimization scenario, the performance metrics of the proposed model are improved compared to the base model.

Table 8: Base model performance (entropy-driven kernel optimization, Rastrigin function)

σ_n	ϵ_x **(std)**	ϵ_f **(std)**	ϵ_t **(std)**	$RMSE$ **(std)**
0	0.1377 (0.2432)	0.0087 (0.0181)	0.1001 (0.1709)	0.1178 (0.0571)
0.01	0.1966 (0.2743)	0.0217 (0.0364)	0.1424 (0.1938)	0.1615 (0.0710)
0.02	0.1932 (0.2682)	0.0135 (0.0273)	0.1382 (0.1897)	0.1396 (0.0570)
0.03	0.1260 (0.2223)	0.0096 (0.0212)	0.0912 (0.1570)	0.1086 (0.0494)
0.04	0.1036 (0.2117)	0.0140 (0.0765)	0.0765 (0.1468)	0.1468 (0.0703)
0.05	0.1528 (0.2366)	0.0081 (0.0141)	0,1098 (0.1666)	0.1131 (0.0524)

Table 9: Models' performance (entropy-driven termination criterion, AXE frigates)

model	ϵ_x **(std)**	ϵ_f **(std)**	ϵ_t **(std)**	$RMSE$ **(std)**	**optimization steps (std)**
base	0.0 (0.0)	0.0436 (0.0285)	0.0308 (0.0202)	0.1300 (0.0405)	10 (0)
proposed	0.0068 (0.0172)	0.0513 (0.0304)	0.0376 (0.0232)	0.1388 (0.0416)	8.55 (2.5)

CONCLUSIONS

In summary, the paper proposes the integration of entropy, a mathematical concept from information theory, to improve a MF design framework for early-stage design exploration. Two concepts, namely the entropy-driven termination criterion and entropy-driven kernel optimization, were formulated and illustrated. The case studies encompassed analytical benchmark problems, including the 1D Jump Forrester and the 2D Shifted Rotated Rastrigin function, along with a 2D physical problem involving AXE frigate design where variations in L and B were considered.

Similar patterns were observed across the different case studies. Concerning the termination criterion, the performance metrics slightly exceeded those of the base model while concurrently achieving computational savings. This suggests the potential for a potent tool in design exploration, particularly when the goal is to discern design trends. Furthermore, the outcomes related to kernel optimization exhibited enhancements in most cases and comparable results in others. This underscores the concept's potential in integrating compositional kernels within a design optimization loop.

The inclusion of entropy in design exploration is rooted in the concept that entropy can serve as an indicator of how comprehensively the design space has been investigated. It is crucial to emphasize that entropy is not presumed to be an absolute performance measure akin to error metrics. Instead, its significance lies in the fact that in practical design exploration problems, calculating error metrics is not feasible. To advance this concept, exploring its scalability to higher-dimensional problems is an area that needs further research. Additionally, determining the critical parameters for the method is a case-dependent and challenging aspect in real-world applications.

CONTRIBUTION STATEMENT

Nikoleta Dimitra Charisi: Conceptualization; methodology; writing – original draft. **Hans Hopman:** supervision; writing – review and editing. **Austin Kana:** supervision; writing – review and editing.

Table 10: Models' performance (entropy-driven kernel optimization, AXE frigates)

model	ϵ_x (std)	ϵ_f (std)	ϵ_t (std)	$RMSE$ (std)
base	0.0 (0.0)	0.0349 (0.0298)	0.0247 (0.0210)	0.1295 (0.0523)
proposed	0.0 (0.0)	0.0180 (0.0301)	0.0127 (0.0213)	0.1133 (0.0303)

ACKNOWLEDGEMENTS

This publication is part of the project "Multi-fidelity Probabilistic Design Framework for Complex Marine Structures" (project number TWM.BL.019.007) of the research program "Topsector Water & Maritime: the Blue route" which is (partly) financed by the Dutch Research Council (NWO). The authors thank DAMEN, the Netherlands Defence Materiel Organisation (DMO), and MARIN for their contribution to the research.

REFERENCES

Andrews, D. (2018). The Sophistication of Early Stage Design for Complex Vessels. *International Journal of Maritime Engineering*, Vol 160(SE 18).

Beran, P. S., Bryson, D. E., Thelen, A. S., Diez, M., and Serani, A. (2020). Comparison of multi-fidelity approaches for military vehicle design. *AIAA AVIATION 2020 FORUM*, 1 PartF:1–34.

Bonfiglio, L., Perdikaris, P., and Brizzolara, S. (2020). Multi-fidelity Bayesian optimization of SWATH hull forms. *Journal of Ship Research*, 64(2):154–170.

Bonfiglio, L., Perdikaris, P., Vernengo, G., De Medeiros, J., and Karniadakis, G. (2018). Improving SWATH seakeeping performance using multi-fidelity Gaussian process and Bayesian optimization. *Journal of Ship Research*, 62(4):223–240.

Brochu, E., Cora, M., and De Freitas, N. (2009). A Tutorial on Bayesian Optimization of Expensive Cost Functions, with Application to Active User Modeling and Hierarchical Reinforcement Learning. Technical report, Department of Computer Science, University of British Columbia.

Charisi, N. D., Hopman, H., and Kana, A. (2022a). Early-Stage Design of Novel Vessels: How can we Take a Step Forward? In *SNAME 14th International Marine Design Conference*, Vancouver, Canada. SNAME.

Charisi, N. D., Kana, A., and Hopman, H. (2022b). Compositional kernels to facilitate multi-fidelity design analysis: Applications for early-stage design. In *AVT-354 Multi-Fidelity Methods for Military Vehicle Design*.

Chaudhuri, A., Peherstorfer, B., and Willcox, K. (2020). Multifidelity cross-entropy estimation of conditional value-at-risk for risk-averse design optimization. *AIAA Scitech 2020 Forum*, 1 PartF.

Di Fiore, F. and Mainini, L. (2024). Physics-aware multifidelity Bayesian optimization: A generalized formulation. *Computers and Structures*, 296:107302.

Drummen, I., Hageman, R. B., and Stambaugh, K. (2022). Multifidelity Approach for Predicting Extreme Global Bending Load Effects. In *9th International Conference on HYDROELASTICITY IN MARINE TECHNOLOGY*, Rome.

Duchateau, E. (2016). *Interactive evolutionary concept exploration in preliminary ship design*. PhD thesis, Technische Universiteit Delft, Delft, the Netherlands.

Duplantier, B. and Rivasseau, V., editors (2018). *Information Theory: Poincaré Seminar 2018*. Birkhäuser.

Duvenaud, D., Lloyd, J. R., Grosse, R., Tenenbaum, J. B., and Ghahramani, Z. (2013). Structure Discovery in Nonparametric Regression through Compositional Kernel Search. *30th International Conference on Machine Learning, ICML 2013*, (PART 3):2203–2211.

Farhang-Mehr, A. and Azarm, S. (2008). On the Entropy of Multi-Objective Design Optimization Solution Sets. *Proceedings of the ASME Design Engineering Technical Conference*, 2:829–838.

Gaggero, S., Vernengo, G., and Villa, D. (2022). A marine propeller design method based on two-fidelity data levels. *Applied Ocean Research*, 123:103156.

Kennedy, M. C. and O'Hagan, A. (2000). Predicting the Output from a Complex Computer Code When Fast Approximations Are Available. *Biometrika*, 87(1):1–13.

Keuning, J. A., van Terwisga, P. F., and Nienhuis, B. (2015). The Possible Application of an AXE Bow on a 5000 Ton Frigate. *SNAME 13th International Conference on Fast Sea Transportation, FAST 2015*.

Krus, P. (2013). Information Entropy in the Design Process. pages 101–112.

Le Gratiet, L. and Garnier, J. (2014). Recursive co-Kriging model for design of computer experiments with multiple levels of fidelity. *International Journal for Uncertainty Quantification*, 4(5):365–386.

Mainini, L., Serani, A., Rumpfkeil, M. P., Minisci, E., Quagliarella, D., Pehlivan, H., Yildiz, S., Ficini, S., Pellegrini, R., Di Fiore, F., Bryson, D., Nikbay, M., Diez, M., and Beran, P. (2022). Analytical Benchmark Problems for Multifidelity Optimization Methods.

Martignon, L. (2001). Information Theory. *International Encyclopedia of the Social & Behavioral Sciences*, pages 7476–7480.

Mavris, D., DeLaurentis, D., Bandte, O., and Hale, M. (1998). A stochastic approach to multi-disciplinary aircraft analysis and design. In *36th AIAA Aerospace Sciences Meeting and Exhibit*, Reston, Virigina. American Institute of Aeronautics and Astronautics.

Molland, A. F. (2008). Chapter 4 - ship structures. In *The Maritime Engineering Reference Book*, pages 116–180. Butterworth-Heinemann, Oxford.

Murphy, K. P. (2012). *Machine learning: a probabilistic perspective*. Cambridge, MA.

Ng, L. W. T. and Willcox, K. E. (2015). Multi-fidelity Monte Carlo Information-Reuse Approach to Aircraft Conceptual Design Optimization Under Uncertainty.

North, D. W. (2017). *Decision Analytic and Bayesian Uncertainty Quantification for Decision Support*, pages 1361–1399. Springer International Publishing, Cham.

Perdikaris, P., Raissi, M., Damianou, A., Lawrence, N. D., and Karniadakis, G. E. (2017). Nonlinear information fusion algorithms for data-efficient multi-fidelity modelling. *Proceedings of the Royal Society A: Mathematical, Physical and Engineering Sciences*, 473(2198).

Rasmussen, C. E. (2003). Gaussian Processes in Machine Learning. *Lecture Notes in Computer Science (including subseries Lecture Notes in Artificial Intelligence and Lecture Notes in Bioinformatics)*, 3176:63–71.

Saad, M. H. and Xue, D. (2023). Initial selection of configurations based on information entropy for multi-level design optimization. *Procedia CIRP*, 119:533–538.

Sapsis, T. P. (2021). Annual Review of Fluid Mechanics Statistics of Extreme Events in Fluid Flows and Waves.

Serani, A., Ficini, S., Grigoropoulos, G., Bakirtzogou, C., Broglia, R., Diez, M., Papadakis, G., Goren, O., Danisman, D. B., Scholcz, T., Hayriye, J. K., Solak, P., and Yıldız, S. (2022). Resistance and Seakeeping Optimization of a Naval Destroyer by Multi-Fidelity Methods. In *AVT-354 Research Workshop on "Multi-Fidelity Methods for Military Vehicle Design"*, Varna.

Shannon, C. E. (1948). A Mathematical Theory of Communication. *Bell System Technical Journal*, 27(3):379–423.

Silver, N. (2012). *The Signal and the Noise: Why So Many Predictions Fail–but Some Don't*. Penguin, New York.

Tupper, E. (2004). 14 - main hull strength. In Tupper, E., editor, *Introduction to Naval Architecture (Fourth Edition)*, pages 276–303. Butterworth-Heinemann, Oxford, fourth edition edition.

Van Oers, B., Takken, E., Duchateau, E., Zandstra, R., Cieraad, S., Van Den Broek De Bruijn, W., and Janssen, M. (2018). Warship Concept Exploration and Definition at The Netherlands Defence Materiel Organisation Introduction: The Netherlands Defence Materiel Organisation. Technical report.

Varley, T. F., Pope, M., Faskowitz, J., and Sporns, O. (2023). Multivariate information theory uncovers synergistic subsystems of the human cerebral cortex. *Communications Biology 2023 6:1*, 6(1):1–12.

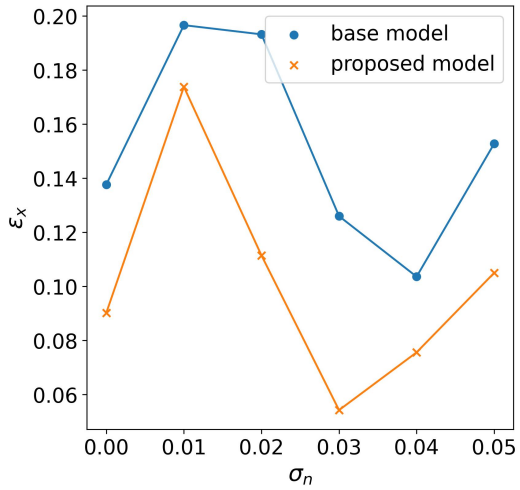

(a) Graph depicting the relationship between ϵ_x and σ_n

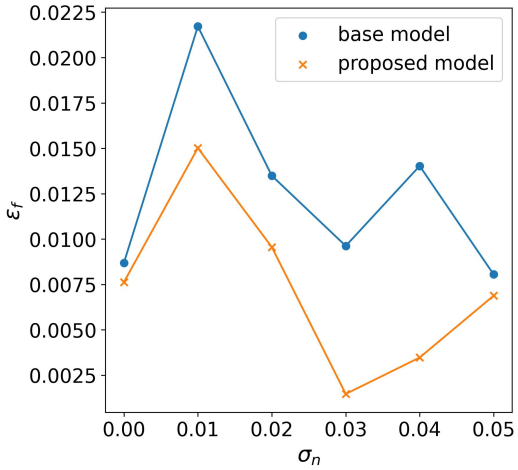

(b) Graph depicting the relationship between ϵ_f and σ_n

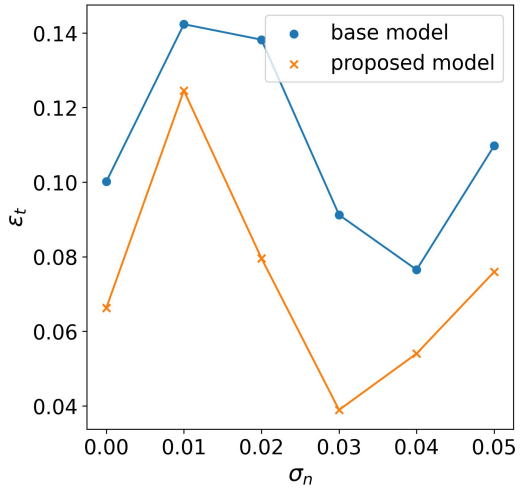

(c) Graph depicting the relationship between ϵ_t and σ_n

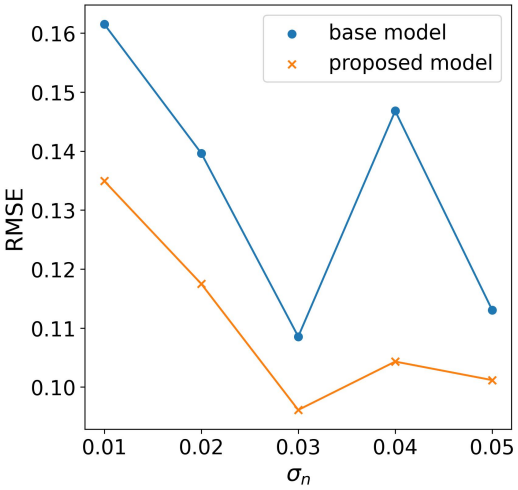

(d) Graph depicting the relationship between $RMSE$ and σ_n

Figure 10: Rastrigin function: Entropy-driven termination criterion, while varying the noise σ_n

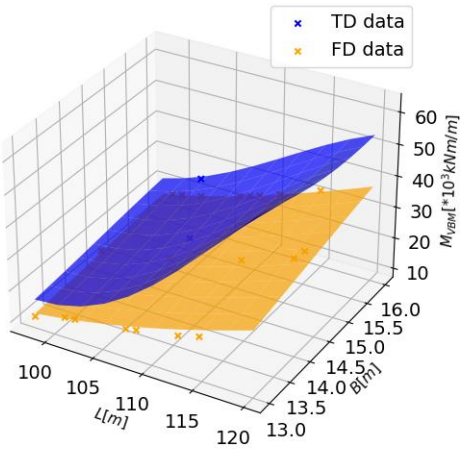

Figure 11: MF design space for the AXE frigates

Proceedings of 15th International Marine Design Conference (IMDC-2024)
June 2-6, 2024
Amsterdam, the Netherlands

Operational Data for Sea Margin Calculations in Early Ship Design

Sietske de Geus-Moussault [1a,2,*] Henk Seubers[3], Harry Linskens[3], Andrea Coraddu [1b] and Jeroen Pruyn[1c,4]

ABSTRACT

The current sea margin estimate applied in early ship design, commonly assumed 15-20% extra installed engine power, is not based on calculations, but has nonetheless become an industry standard. These sea margin estimations, applied in early ship design, are insufficiently accurate. This paper evaluates if a data driven approach is suitable to more accurately predict the sea margin in early ship design. Using operational data this method considers the whole operational profile of the vessel not limited to design or calm water conditions. A case study is performed where a data driven model is trained to make power predictions, subsequently this trained model is used to make calm water predictions. This proof of concept illustrates the potential of proposed method to be utilised for sea margin estimations in early ship design.

KEY WORDS

Sea Margin; Early Ship Design; Operational Data; Data Driven Model; Calm Water Predictions.

INTRODUCTION

In the early design stage of a vessel, many characteristics of the vessel are determined and fixed. When considering the propulsion system and power train, these choices have a large impact on the future emissions of the vessel, and care is required so as not to install too much power. A key parameter in this estimation is the sea margin, an addition of 15-20% to compensate for any unknowns and issues related to sailing on the oceans instead of in calm water (Esmailian et al. (2022), Islam and Soares (2022)). To the best of the authors' knowledge, there is no clear explanation for this value, and it has been maintained at this value despite improvements in estimation techniques and other scientific advances. As this directly impacts the installed power, reconsidering this value is warranted.

As explained, the sea margin is additionally installed engine power to attain added resistance due to external conditions, such as resistance from wind, waves, and/or fouling. To more accurately estimate the sea margin, the required extra power is needed to accurately estimate the added resistance. Based on the added resistance, a more accurate assumption for the required sea margin can be made, or at least a start can be made with understanding how this sea margin ensures safety and comfort during operations. To enhance the accuracy of models that predict the sea margin, it is essential to first assess the existing methods used to calculate added resistance. The following paragraphs will detail this evaluation.

[1] Department of Maritime and Transport Technology, Delft University of Technology, Delft, the Netherlands; [a] ORCID: 0000-0002-5116-1491; [b] ORCID: 0000-0001-8891-4963; [c] ORCID: 0000-0002-4496-4544; [2] Maritime Institute Willem Barentsz, NHL Stenden University of Applied Sciences, Leeuwarden, the Netherlands; [3] DEKC Maritime, Groningen, the Netherlands [4] CoE HRTech, Maritime Innovation, Rotterdam University of Applied Sciences, Rotterdam, the Netherlands [*] Corresponding Author: s.r.a.degeus-moussault@tudelft.nl
Submitted: 29 March 2024, Revised: 1 May 2024, Accepted: 3 May 2024, Published: 23 May 2024

Conference paper, DOI: https://doi.org/10.59490/imdc.2024.882 e-ISSN: 3050-486

Literature Review

This section evaluates the current methods for calculating the added resistance: traditional methods, towing tank testing, and computational fluid dynamics.

Traditional Methods

A significant component of added resistance is wave resistance, which is defined as the resistance encountered by a ship as it moves through water. More precisely, *"the steady motion of a ship in initially smooth water assuming an ideal fluid"* (Bertram (2012)). Often considered to be the first breakthrough in wave resistance calculations is the 1898 paper of J.H. Michell, using a triple integral to calculate the wave resistance of a ship (Michell (1898)).

Another well-known method is Holtrop-Mennen, which can predict the resistance and propulsion data for different hull designs using regression analysis. First, in 1982, their method was used to develop a formula based on full-scale data and model experiments (Holtrop et al. (1982)). Subsequently, in 1984, the method was refined with more data and model tests to improve overall power predictions. The earlier method proved insufficient for more high-speed vessels at Froude numbers above 0.5 (Holtrop (1984)). In 1984, Holtrop and Mennen developed a formula to calculate the resistance, Equation 1, (Holtrop (1984)).

$$R_{Total} = R_F(1+k) + R_{APP} + R_W + R_B + R_{TR} + R_A \tag{1}$$

In which R_F is the frictional resistance; $(1 + K)$ is the form factor of hull; R_{APP} is the appendage resistance; R_W is the wave resistance; R_B is the additional pressure resistance of bulbous bow near the water pressure; R_{TR} is the additional pressure resistance due to transom immersion and R_A is the model ship correlation resistance. This is a parameter-set that describes the hull and is used to calculate the total resistance, the formula is made up out of the; frictional resistance, dependant on the form factor of the hull, the appendage resistance, wave resistance, bulbous bow pressure resistance, transom immersion pressure resistance and model-ship correlation resistance.

As this method relies on analysis of a finite combination of full-scale data and model tests, estimations and assumptions within the used parameters allow for less detail and robust results. When unorthodox combinations of parameters are used, it leads to inaccurate results (Holtrop et al. (1982)). This causes the regression method not to be the best fitting method analysing the vessel after construction (Petersen et al. (2012)).

As ship resistance calculations tend to focus on the resistance of ships through water, an under-exposed factor in overall resistance is wind loading. Not surprising as water is approximately 800 times more dense than air, however the surface area of ships above water can impact overall resistance (Blendermann (1994)). Particularly in the case of cargo ships, for instance, the surface area of the loaded vessel above water can be quite substantial. Blendermann (1994) identified parameters to calculate aerodynamic forces and moments to numerically simulate ship behaviour. This experiment was executed with different wind tunnel tests on scale models.

Resistance factors of hull coating are generally neglected, or general assumptions are made in traditional resistance calculations. Almost all ships have anti-fouling paint applied to their underwater hulls. The general state of this coating, combined with slime, shell, and weed growth, adds resistance as the ship moves through the water. Townsin (2003) describes a general roughness parameter to calculate the penalty of fouling, the ship's speed loss at constant power.

Direct Model Testing in Towing Tanks

Experimental Fluid Dynamics, based on scaled ship models tested in towing tanks, provide an alternative to the traditional methods. The first internationally recognised towing tank experiments, are the results of the experiments executed by David Watson Taylor, published in his 1910 book ”The speed and power of ships”. In his book, Taylor describes the estimation of the flow resistance of 80 vessels that were model-tested in a towing tank. The sequential testing of variations in design characteristics of the models led to estimations of ship resistance (Taylor (2013)). The experiments by Taylor attributed a great deal to the knowledge of the impact of certain design choices that can be made in ship design. As experimental research relies on the repeatability of experiments in a fixed set of conditions, the smallest variation in conditions will lead to different results. Neglecting to conduct the experiments in identical temperature conditions by Taylor led the US Navy to carry out a re-analysis of the Taylor Standard Series in 1954 to correct for this variation in experimental conditions (Gertler (1954)).

The downsides to model tests are accuracy due to scaling and the overall costs of the experiments. Furthermore, the accuracy of towing tank can fluctuate as scaling problems tend to lead to a difference in wave behaviour between scale models and full size ships (Bertram (2022)). Testing in a towing tank is an expensive and time-consuming experiment that can cost tens of thousands of euros per test (Barczak (2020)).

Computational Fluid Dynamics

Computational fluid dynamics (CFD) is a form of fluid mechanics that uses numerical analysis and data structures to analyse fluid flows, and it can be used to simulate and calculate the flow around and, therewith, the added resistance of a hull-form. CFD was first developed in the 1950s with the emergence of the computer, as this opened up an more efficient method of the computation of complex partial differential equations like finite element methods (FEM) and finite difference methods (FDM) (Chung (2002)). Dynamic flows over intricate shapes can be calculated and analysed for both aerodynamics and hydrodynamics (Anderson and Wendt (1995)). In the 1960s simplified boundary layer equations were solved for ship hulls, those more basic elementary flow models led to less accurate results (Bertram (2022)). A Reynolds Averaged Navier-Stokes Solver (RANS) method was developed in the 1980s and was improved greatly with stern flow prediction in the 1990s and a numerical method for three dimensional flows was described (Chen et al. (1990)). However, because of insufficient knowledge about modeling of turbulence, propeller simulations were largely inaccurate (Zhang et al. (2006)).

To verify CFD model calculations a ship model was made open source available. The KVLCC (KRISO Very Large Crude Carrier model) was designed, analysed in both towing tank and CFD (Van et al. (2000)). Later, in 2005, a second model with a slight difference in hull shape was developed (Hino et al. (2021)). The hull lines, rudder, and propeller data are open source and available for validation and verification (Kvale (2014)). This model is used on a large scale in academics to increase the accuracy of CFD calculations. Sadat-Hosseini et al. (2013) verified a technique to calculate the added resistance of short and long waves using the KVLCC2 vessel.

Using numerical models for predicting ship performance in the design phase is becoming more common since the computational power of computers is far greater than it used to be, and RANS equations can now be more easily solved using CFD. The KVLCC2 vessel was used to predict and verify added resistance at constant forward velocity (Ozdemir and Barlas (2017)). In recent years, an effort has been made to make CFD more efficient. The CFD modelling process, which can last several weeks to months, is aided by the experience of ship designers. Because of this experience, the engineer can set design parameters to control the overall design process. The effectiveness of this process relies on the engineer’s skill.

Cui et al. (2012) adopted a machine learning approach to the early design phase in an effort to increase the robustness of the design. Weatheritt et al. (2017) used a machine learning approach on data in a CFD experiment to study linear and non-linear relationships using the least-squares regression technique. Zhao et al. (2020) build on this research using machine learning to develop a CFD training framework of RANS models.

CFD is often perceived to be time-consuming, complex, and expensive. With the computational power increase of computers and the user interface changes, this image problem might be fading, as the alternative, model testing in towing tanks, is time-consuming and expensive as well (Gatin (2019)).

Problem Definition

From the literature, it can be concluded that currently used methods to estimate the added resistance have their upsides and downsides. The traditional methods are more than 80 years old, based on ships from then and on only a selection of hull forms, making them not widely applicable to currently designed vessels. Towing tank tests lack accuracy due to scaling, are time-consuming, and expensive. Finally, CFD simulations are also expensive and considered time-consuming and complex. This illustrates that the current methods to calculate added resistance are not the most suitable to incorporate in a model to predict the sea margin in early ship design. Therefore, this research investigates whether we can utilise operational data to estimate the added resistance more accurately.

METHOD

A novel model has been developed and proposed to explore the possibility of using operational data to estimate added resistance. This model, which is currently based on operational data from a single cargo vessel, serves as a proof of concept. Successful validation of this model would allow for its expansion to include data from additional vessels, thereby enhancing its applicability and robustness In this section, the method is presented. First, the scope of the research is described. Then, in the second section, a description of the data is given. Finally, in the third section, the model description is presented.

Scope

This research covers the development of a model based on the data of one cargo vessel. The dataset consists of approximately 90,000 data points. The developed model is, in principle, suitable to make predictions based on data from this same vessel or sister vessels with similar dimensions. Nonetheless, when desired it is also possible to train the developed model with data from other vessels and therewith also make it able to make predictions about different vessels. However, this will not be investigated in this paper.

Data Description

In this research, real-world operational data from a single cargo vessel over a time span of two years is used. This data is combined with meteorological data from the Copernicus C3S Knowledge Base (Hersbach et al. (2023)). The data can be grouped into two categories: i) endogenous data, which describe the behaviour of the vessel, such as consumption of the main engine, the speed over ground, and the course over ground, and ii) exogenous data, which describe the metocean conditions, such as wind speed and direction, and wave height and direction. A summary of the operational data categorised by source is presented in Table 1.

Table 1: Summary of the Selected Operational Data categorised by Source

Source	Feature	Unit
Royal Wagenborg	Fuel Oil Consumption of ME	[t/day]
	Speed over Ground	[knots]
	Speed through Water	[knots]
	Draft Forward	[m]
	Draft Aft	[m]
	Shaft Generator Power	[kW]
	Deadweight	[t]
	Mean Engine Fuel Type	[MGO/HFO]
Copernicus Knowledge Base	Wind speed at 10 m (north-south)	[m/s]
	Wind speed at 10 m (west-east)	[m/s]
	Temperature at 2m	[K]
	Pressure at Mean Sea Level	[Pa]
	Mean Wave Direction	[deg]
	Significant Wave Height	[m]
	Wave Peak Period	[s]

Royal Wagenborg has provided data logs from a single cargo vessel over the period between April 13th, 2020, and April 13th, 2022. With a sampling interval of 5 minutes, various measurements, control settings, and manually entered voyage parameters were logged. Based on the GPS position and time, this data has been combined with hindcast weather data from the ERA5 dataset (Hersbach et al. (2023)). This weather data is available at one-hour intervals and a spatial scale of 0.5 degrees latitude and longitude (about 55 km). Relevant variables were selected, for the selection see Table 1, and interpolated in space along the ships track.

Model Description

In this paragraph, the setup and development of the model are explained. The explanation is divided into a few separate sections due to the nature of the work. First, the data preparation and combining of the two datasets is explained. Following, the model development and training are explained, and finally, the model implementation to predict the vessel's performance in calm water is elaborated upon.

Data Preparation

The first step in preparing the data is combining the two datasets to determine the weather conditions the ship is encountering. This is done based on location and time. For nondimensionalisation and scaling of derived variables some fixed reference values are applied, these are presented in Table 2.

Table 2: Fixed Reference Values

Variable	Symbol	Value	Unit
Length between Perpendiculars	LPP	130	[m]
Beam	B	15	[m]
Lightship Weight	LSW	3300	[t]
Height to top of Wheelhouse	H	25	[m]
Water Density	ρ_{water}	1025	[kg/m^3]
Acceleration of gravity	g	9.81	[m/s^2]

Following this first step, to evaluate the performance of the vessel, all measured conditions are expressed relative to the vessel, this means for example an apparent wind angle and apparent wind speed (Figure 1). In addition, derived variables are calculated that aid in interpreting the data, such as the wave encounter angle (WEA)

and rate of turn (ROT). All the derived variables calculated based on the measured variables are presented in Table 3.

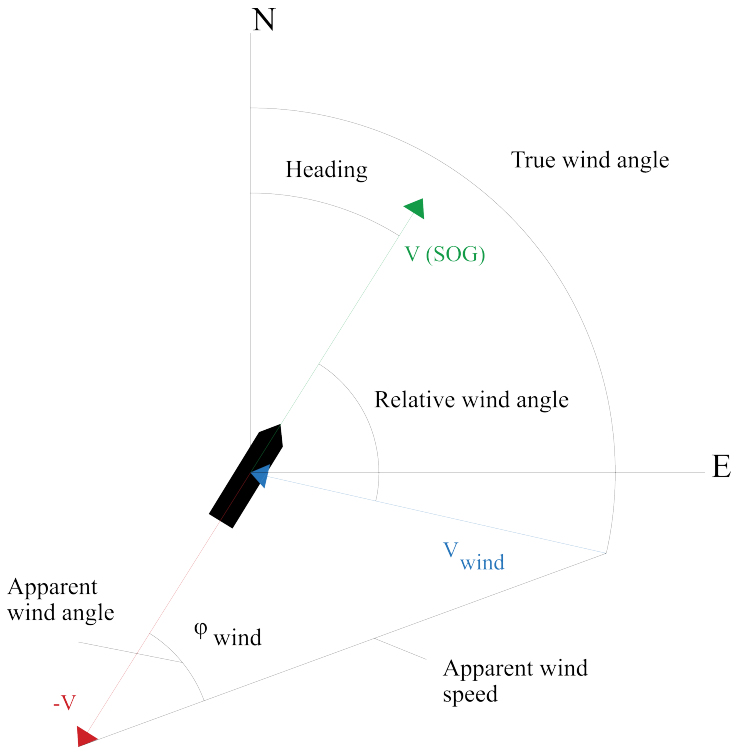

Figure 1: Graphical Representation of Relative Wind and Speed Calculation

Based on the length, the deadweight, the light ship weight, the forward and aft trim and textbook knowledge the *trim* (T), the *displacement* (D), and the *mean draft* (MD) are calculated. With the course over ground, ship speed, wind speed, ρ_{air}, and Equation 2 the *relative wind* (v), the *apparent wind angle* (AWA), and the *dynamic wind pressure* (Q_{wind}) are calculated, a graphical representation of this calculation is presented in Figure 1.

$$Q_{wind} = \frac{1}{2}\rho_{air}|v|^2 \tag{2}$$

With the course over ground, the mean wave direction, and Equation 3, the *WEA* is determined.

$$WEA = mean\ wave\ direction + 180 - course\ over\ ground \tag{3}$$

As a final step, also based on the graphical representation in Figure 1 and with the course over ground, the ships speed, and Equations 4 and 5, the *rate of turn* (ROT), *longitudinal acceleration* (A_x), and the *transverse acceleration* (A_y) are calculated. With that, all necessary derived parameters (Table 3) required as input for the model have been determined, and thus, the model can be developed.

$$ROT = \frac{dCOG}{dt} \tag{4}$$

$$A = \frac{dV}{dt} \tag{5}$$

Table 3: Derived Variables

Derived Variable	Symbol	Unit
Trim	T	[rad]
Displacement	D	[t]
Mean Draft	MD	[m]
Relative Wind Intensity	v	[m/s]
Apparent Wind Angle	AWA	[rad]
Dynamic Wind Pressure	Q_{wind}	[Pa]
Mean Wave Drift Force	MWDF	[N]
Wave Encounter Angle	WEA	[rad]
Rate of Turn	ROT	[deg/min]
Longitudinal Acceleration	A_x	[m/s^2]
Transverse Acceleration	A_y	[m/s^2]

Model Development

For the power prediction model a two step approach is required. First, the model needs to be developed and trained based on the parameters mentioned above. In the second step, the developed model is used to predict the required power in calm water conditions. The goal is to develop a model that can predict the required power given (average) speed, loading, and environmental conditions. Subsequently, the model will be implemented to predict the corrected required power, given speed, the design draft, and calm environmental conditions. Before constructing the model, some dependencies between the input variables have to be established.

In ship design, the power at the propeller shaft is of interest because this is measured during sea trials and separates the hydrodynamic performance from mechanical and thermal efficiencies. However, from the operational data, only fuel consumption is usually available to measure propulsive power when the shaft power is not measured. Therefore the model will aim to predict fuel consumption in ton per day.

The resistance is split into individual contributions, which are modelled independently. Some modelling assumptions have already been made here to avoid infinite values in the model. Towing power is defined by speed through water, not speed over ground. The reason is that the towing speed-power curve (corrected to calm-water) is a property of the ship, while the speed-over-ground-power curve is a property of the ship and the local current. In other words, the corrected power data will not coincide with a single curve when plotted against speed-over-ground. The resistance contributions are modeled linearly using coefficients such as, calm water, wind, and wave influence.

$$P_{tow} = V_w(R_{calm} + R_{wind} + R_{wave} + R_{inertia}) \tag{6}$$

The friction, pressure, and wave-making resistances are all modeled to scale with the dynamic pressures.

$$Q_w = \frac{1}{2}\rho_w V_w^2\,, \quad Q_a = \frac{1}{2}\rho_a V_a^2 \tag{7}$$

No Froude-number effect is modelled, so the model should only be applied to displacement vessels well below the critical Froude number. The reference area for calm water resistance is an indication of the wetted area based on the main dimensions and the draft. The reference area for wind resistance is an approximate frontal area above the waterline, including the accommodation.

$$R_{calm} = LPP * (C_{calm}B + C_{draft}T) * Q_w \tag{8}$$

$$R_{wind} = C_{wind}(\alpha_{wind}) * (H - T)B * Q_a \tag{9}$$

The wave-induced resistance is based on the significant wave height H_s, the wave encounter angle α, and the wave length λ_p at the peak period, resulting in Equation 10. This is, in essence, the mean wave drift force (Journée et al. (2015)) with a coefficient consisting of a spline (in the frequency/wavelength) (Press et al. (2011)) and a Fourier series (in the wave encounter angle).

$$R_{wave} = C_{wave}\left(\alpha, \frac{\lambda_p}{LPP}\right)\frac{1}{16}\rho_w g B H_s^2 \tag{10}$$

We aim to develop a model that defines the speed-power curve under specific conditions: calm water, no wind, and constant speed and direction. This model will consider a vessel at its design draft, maintaining an even keel and consistent power output. To extract this knowledge from the model, we first need to develop and train it. Earlier sections have already established the model's input parameters and their interdependencies. The model's input features and target feature are summarised in Table 4.

Table 4: Input Parameters of the Model

Input and Target Features	**Symbol**
LPP	LPP
Beam	B
Speed	V
Trim	T
Displacement	D
Relative Wind Intensity	v
Apparent Wind Angle	AWA
Dynamic Wind Pressure	Q_w
Wave Encounter Angle	WEA
Rate of Turn	ROT
Longitudinal Acceleration	A_x
Transverse Acceleration	A_y
Measured Fuel Consumption	FOC

One of the objectives of this study is to develop a model for predicting the FOC based on the input parameters outlined in Table 4. This learning problem can be formulated as a supervised Machine Learning (ML) problem, specifically a regression problem (Shalev-Shwartz and Ben-David (2014)). In regression analysis, an input space $\mathcal{X} \subseteq \mathbb{R}^d$ is comprised of d features (in this case, the parameters in Table 4) and the output space, $\mathcal{Y} \subseteq \mathbb{R}$, corresponds to FOC. A dataset of n examples, denoted as $\mathcal{D}_n = (\boldsymbol{x}_1, y_1), \cdots, (\boldsymbol{x}_n, y_n)$, represents input/output relationships where $\boldsymbol{x}_i \in \mathcal{X}$ and $y_i \in \mathcal{Y}\ \forall i \in 1, \cdots, n$. The aim is to learn the unknown input/output function $\mu : \mathcal{X} \to \mathcal{Y}$ based solely on $\mathcal{D}n$. An ML regression algorithm A, characterized by its hyperparameters $\mathcal{H}$, selects a model f from a set of potential models $\mathcal{F}$ based on available data $A_{\mathcal{H}} : \mathcal{D}_n \times \mathcal{F} \to f$. The set $\mathcal{F}$ is typically unknown and depends on the choices of A and $\mathcal{H}$.

Many different ML algorithms exist in the literature (Shalev-Shwartz and Ben-David (2014); Chandrashekar and Sahin (2014)) but, as the no-free-lunch theorem states (Wolpert (2002)), there is no way to determine a-priori the best ML algorithms to use for a specific application. Since our goal is to establish a proof-of-concept, we have opted to use a Regularized Least Squares (RLS) model as our benchmark. This decision is supported by the fact that linear regression models are frequently employed in similar engineering contexts. Additionally, preliminary exploratory data analysis revealed a linear correlation between several input parameters and the target feature FOC. Thus, initiating our investigation with a linear model as a benchmark provides a logical and strategic starting point. RLS is a regression method that introduces a regularization term to the traditional least squares problem to control the complexity of the model and prevent overfitting. The objective of RLS is to minimize the sum of squared residuals, similar to ordinary least squares, but with an additional penalty term that discourages

large values of the model parameters. The regularization term is typically a function of the model parameters, such as the L2 norm (also known as Ridge regression) or the L1 norm (also known as Lasso regression). The L2 norm encourages small parameter values, leading to a more stable model with lower variance, while the L1 norm can lead to sparse solutions, where some parameters are exactly zero, effectively performing feature selection. The balance between the fit to the data and the regularization is controlled by the only hyperparameter of this algorithm λ. A larger λ increases the impact of the regularization term, leading to a simpler model, while a smaller λ allows the model to fit more closely to the data, potentially at the risk of overfitting. The accuracy of model f in approximating μ is evaluated using a prescribed metric $M : f \rightarrow \mathbb{R}$. Multiple metrics are available for regression analysis in ML (Aggarwal (2015)). However, due to the physical significance of FOC, this study will focus on three primary metrics: Mean Absolute Error (MAE), Mean Absolute Percentage Error (MAPE), and the Coefficient of Determination (R^2). A statistically consistent model selection and error estimation process was conducted to identify the optimal hyperparameters and evaluate the performance of the final model based on the desired metrics.

We divide all available data into two subsets: training and test sets. Specifically, 80% of the data is allocated for training the model, which uses measured power as its input (as shown in Model in Figure 2). Following the training phase, we utilize the remaining 20% of the data as a test set to validate the model's performance. This approach ensures that we can assess the model's accuracy and generalizability to unseen data.

The results from this validation of the model are described in the model implementation paragraph.

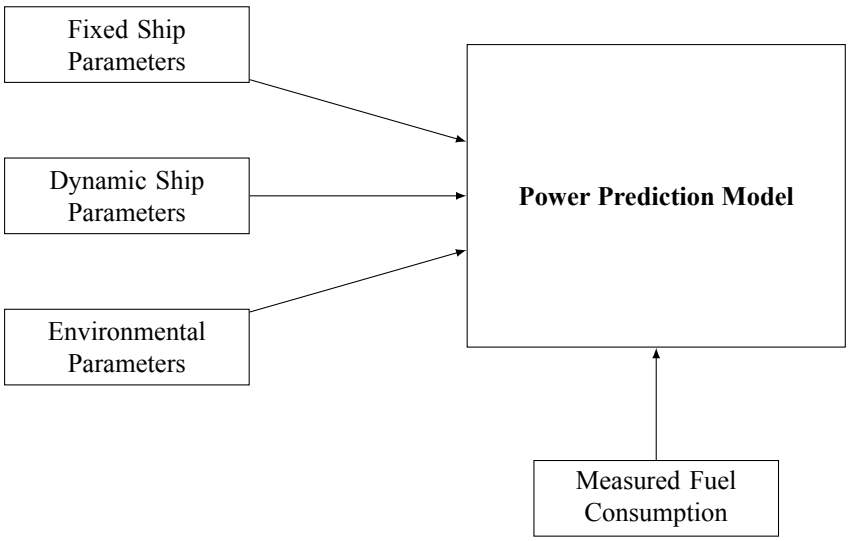

Figure 2: Training and Development of Power Prediction Model

Model Implementation

The first step is to employ the model developed in the previous section to predict the calm water speed-power curve, which assumes no wind, constant speed and direction, design draft with even keel, and constant power take-off. The performance of the model is assessed through error estimation and model validation, as depicted in Figure 3 and summarized in Table 5. These visual and tabular representations indicate that the model achieves a satisfactory level of accuracy. However, there remains potential for enhancement. Consequently, pursuing further research with alternative (non-linear) modeling approaches represents a viable direction for future studies.

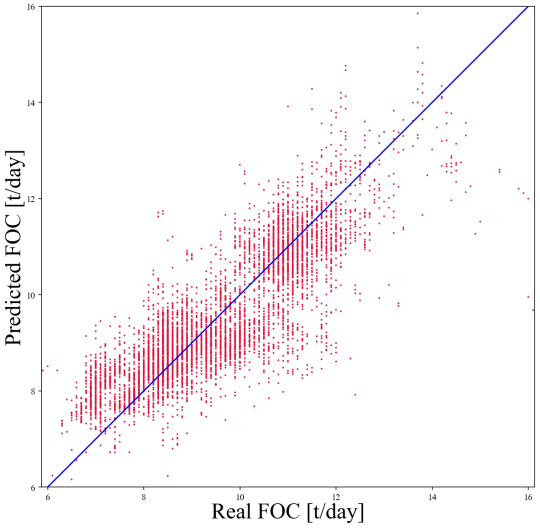

Figure 3: Scatterplot Predicted versus Measured

Table 5: Error Estimates of the Model

Metric	**Accuracy**
MAE	0.64 ± 0.0070
MAPE	17.79 ± 0.1281
R^2	0.706 ± 0.0163

The second step involves using the model to generate power predictions under calm water conditions. This step requires modifications to some of the input parameters previously utilized for model development, as detailed in Table 4 and Figure 2. These parameters are adjusted to reflect calm water conditions and are displayed in blue in Table 6 and Figure 4. Additionally, it is important to note that the power measurements, which were initially used as inputs in the model, are no longer included.

Table 6: Input Features of the Model

Input Feature	**Alteration**
LPP	as before
Beam	as before
Speed	as before
Trim	Design Draft
Displacement	Design Draft
Relative Wind	No wind
Apparent Wind Angle	No wind
Q_{wind}	No wind
Wave Encounter Angle	No waves
Rate of Turn	No Rate of Turn
Longitudinal Acceleration	No Acceleration
Transverse Acceleration	No Acceleration
Measured Fuel Consumption	No input

With these altered input features we will test our hypothesis, *that it is possible to make calm water predictions based on real-world operational data*. In the next section, the results are presented and discussed.

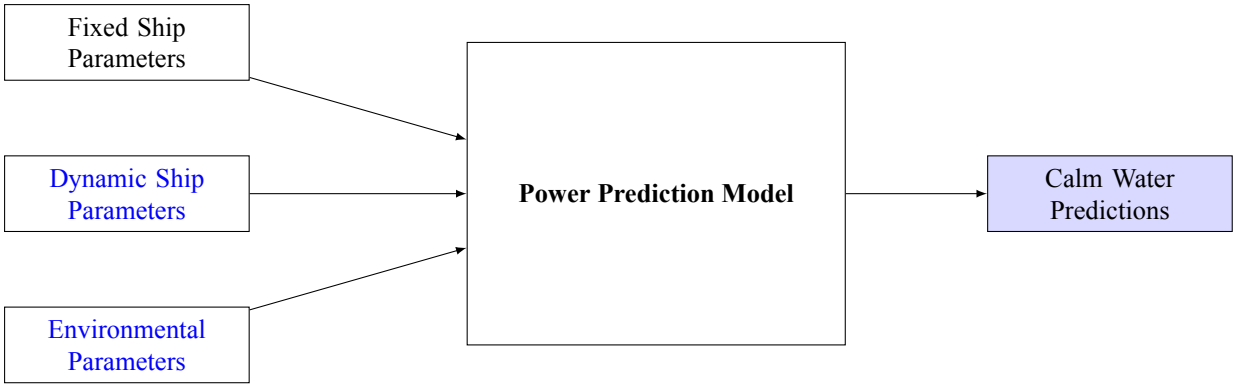

Figure 4: Implementation Power Prediction Model

RESULTS & DISCUSSION

In this section, the results of the calm water predictions are presented and discussed. In the scatter plots, the fuel consumption (t/day) is on the y-axis, and the speed over ground (knots) is on the x-axis. The original measured fuel consumption of the main engine, denoted by y, is depicted in blue, while the predictions of fuel consumption, corrected for factors such as draft, maneuvering, and weather conditions, are illustrated in orange.

Figure 5 shows a scatter of the measured fuel consumption, and in Figure 6, the measured and the corrected are reported.

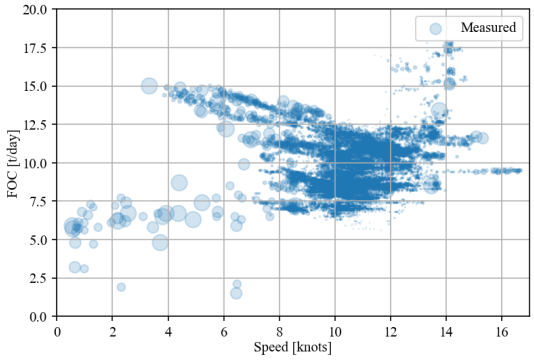

Figure 5: Speed-Power Plot based on the Measured Operational Data

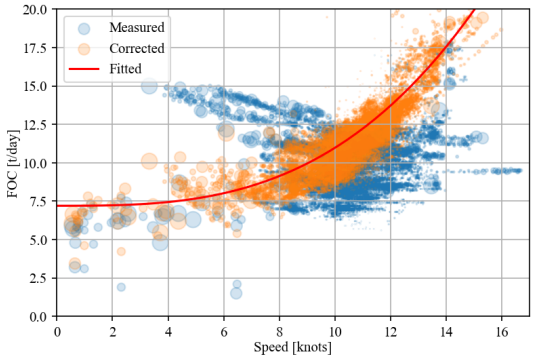

Figure 6: Speed-Power Plot with Measured and Corrected

In Figure 6, it is clear that the corrected data points (orange) are less scattered than the original measured operational data (blue). Furthermore, it is observed that the orange scatters approach the fitted red line. This fitted line is an ideal representation of the developed model, meaning the calm water situation. The orange scatters approaching the fitted line illustrate that the proposed methodology is capable of correcting for weather conditions, but also that there is still room for improvement. Moreover, it can be observed that the two cloudy protrusions in the blue scatter (coming from the center of the plot pointing towards the top left of the plot, between 4 and 8 knots, and 12.5 and 15 t/day) are no longer visible in the calm water predictions. This is a positive confirmation of correcting for weather conditions, as these two protrusions represent two storms (on 27 December 2020 and 11 March 2021). Also, these two protrusions make it clear that the weather conditions (in this case, the two storms) result in a significant involuntary speed reduction, leading to a speed between 4 and 8 knots with a fuel consumption between 12.5 and 15 t/day.

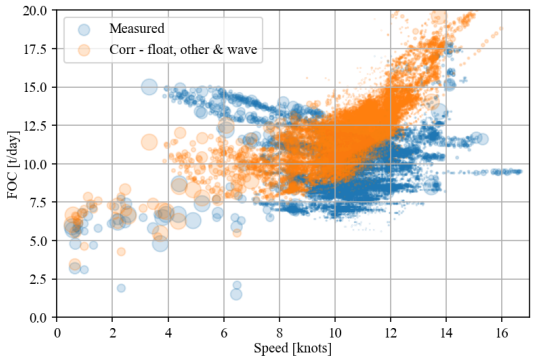

Figure 7: Speed-Power Plot with Corrections for All Parameters Except Wind

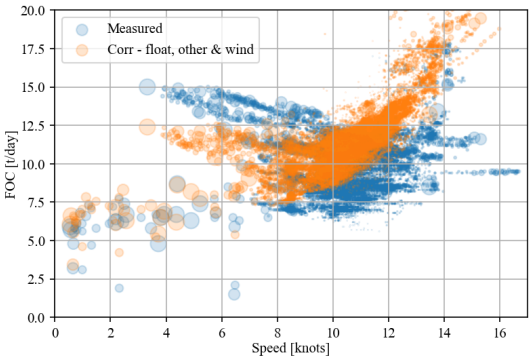

Figure 8: Speed-Power Plot with Corrections for All Parameters Except Waves

When making the calm water predictions, several intermediate steps are taken between Figure 5 and Figure 6. The intermediate steps most interesting to discuss are the situations without the correction for wind (Figure 7) and without the correction for waves (Figure 8). When making the corrections for all parameters except for wind, we get the results plotted in Figure 7. Alternatively, when making the corrections for all parameters except for waves we get the results plotted in Figure 8. When evaluating the difference between the two situations, Figure 7 and Figure 8, it can be seen that for the conditions the vessel encountered between April 2020 and April 2022, the waves appear to have a larger impact on the fuel consumption. This can be best seen when looking at the orange scatter clouds between 4 and 8 knots and comparing the change in these clouds between the measured data (Figure 5), the corrections except wind (Figure 7), and the corrections except waves (Figure 8). When comparing these two predictions with the measured data and each other, it is evident that the effect of the waves is larger than the effect of the wind. Furthermore, when looking at Figure 6, it can be observed that the model still has some difficulty completely filtering out the effect of these two storms, as the orange cloud between 4 and 8 knots remains more scattered than at higher speeds.

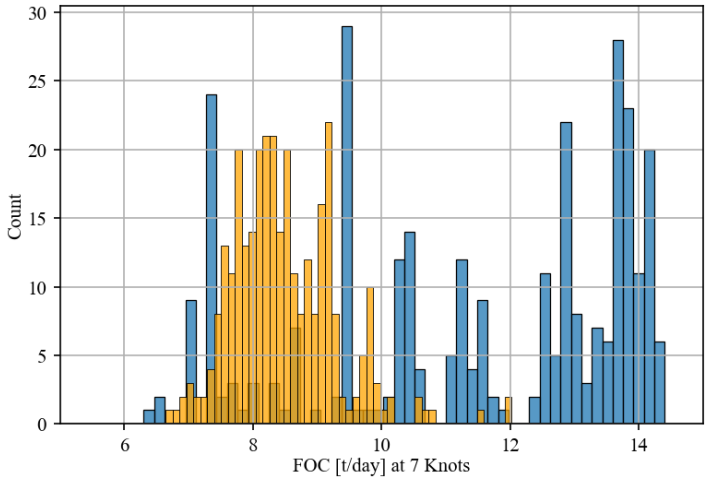

Figure 9: Histogram of the Distribution of the Fuel Consumption at 7 knots

To properly evaluate and compare the distribution, three histograms are plotted in Figures 9, 10, and 11. These histograms are cross-sections of the distribution of the fuel consumption at low, design, and high speed. Furthermore, a summative table presenting the mean and variance at all speeds between 7 and 14 knots is given in Table 7. When evaluating the distribution of the fuel consumption at low speed, 7 knots (Figure 9) it is clear that the spread has decreased between the measured (blue) and the predicted calm water (orange) fuel consumption. The measured fuel consumption is spread between 6.5 and 14.5 tonne per day, and the calm water predictions are spread between 6.75 and 12. This reduced the range from 8 for the measured data to 5.25 for the predicted

calm water. Also, when comparing the distribution of the measured and predicted, it can be observed that the orange graph is far more like a bell curve than the blue distribution.

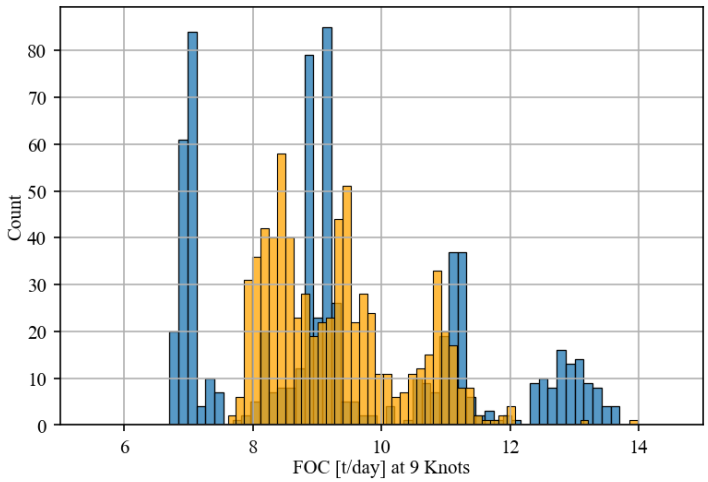

Figure 10: Histogram of the Distribution of the Fuel Consumption at 9 knots

When evaluating the distribution of the fuel consumption at the design speed, 9 knots (Figure 10), it is clear that also at this speed, the spread has decreased between the measured (blue) and the calm water (orange) fuel consumption. The measured fuel consumption is spread between 7 and 14 tonne per day, and the calm water predictions are spread between 8 and 12. This results in a reduction from 7 for the measured data to 4 for the predicted calm water. Furthermore, when comparing the distributions, it can be observed that, in this case, the orange distribution is more in the shape of a bell curve than the original blue distribution.

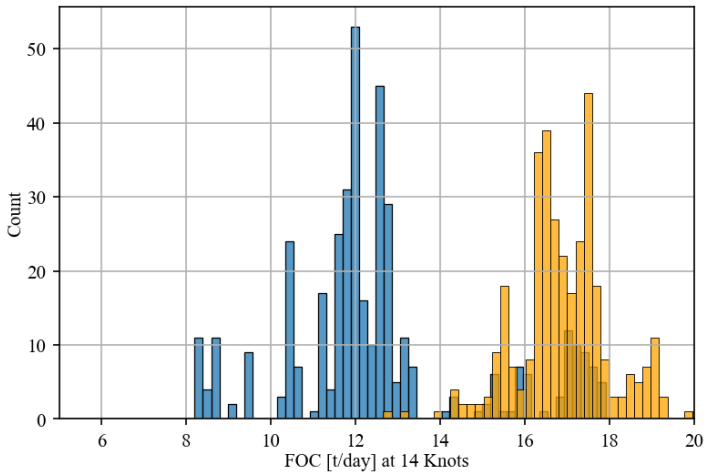

Figure 11: Histogram of the Distribution of the Fuel Consumption at 14 knots

When finally also evaluating the distribution of the fuel consumption at high speed, in this case, 14 knots (Figure 11), it is clear that also at this speed, the spread has decreased between the measured (blue) and the calm water (orange) fuel consumption. The measured fuel consumption is spread between 8 and 18 tonne per day, and the calm water predictions are spread between 14 and 20. Meaning that also, for this situation, there is a significant decrease in the range, from 10 for the measured to 6 for the calm water predictions. Furthermore, when comparing the distributions in Figure 11, it can be observed that the orange graph is more in the shape of a bell curve than the blue distribution. However, for this speed it is also noted that the bell curve has shifted from the original center around 12 tonne per day to a new center around 17.

Table 7: FOC Mean and Variance at Different Speeds

Speed	FOC Mean [t/day]		FOC Variance [t/day]	
[knots]	Measured	Calm Water	Measured	Calm Water
7	11.41	8.48	5.62	0.65
8	9.96	9.29	4.86	0.99
9	9.37	9.29	3.90	1.08
10	8.89	10.19	2.05	0.92
11	9.38	11.42	2.03	0.99
12	9.85	12.51	1.77	1.19
13	10.73	14.80	2.64	2.16
14	12.54	17.65	5.32	4.10

When comparing the mean and variance of the measured and the calm water prediction in Table 7, it can be seen that the variance has decreased at all speeds. Furthermore, it becomes clear that at the lower speeds, the mean in the calm water predictions is lower than the corresponding mean of the measured data, while at the higher speeds, the calm water mean is higher than the corresponding mean of the measured data. These reductions in range and shifts of the mean to lower fuel consumption at reduced speeds not only validate the concept of the proposed method but are also highly explicable. In Figure 9, it can be seen that the corrected predicted fuel consumption (orange) has shifted to the left, a lower fuel consumption. When evaluating Figure 10, it can be seen that for this speed, the predicted fuel consumption is more centered compared to the measured fuel consumption. Finally, when looking at Figure 11, the fuel consumption at 14 knots, it can be seen that the predictions have moved more to the right. This seems very logical because the lower and higher speeds are outside the normal operating envelope of the vessel. The lower speeds with high fuel consumption are involuntary, in this case mostly due to storms. The higher speeds with low fuel consumption are only possible with positive help from a tailwind and/or current. This means that when we remove the meteorological effects, low speeds with high fuel consumption and high speeds with low fuel consumption no longer occur.

Overall, it is observed that the predicted calm water fuel consumption has a decreased variance relative to the variance of the original measured fuel consumption. Furthermore, the histograms in Figures 9, 10, and 11 confirm what is also observed in Figure 6 that the developed method for making calm water predictions works as it results in less scattered data points, all more centered around the fitted line. Implying the developed method works.

CONCLUSIONS

This paper presents a method to make calm water power predictions. This is achieved through a data driven model based on operational data. A case study proved the concept and showed the potential of this method. It illustrated that operational data can be used to make calm water predictions, correcting for meteorological effects. When comparing the calm water power predictions with the actual delivered power the sea margin can be calculated. The proposed methodology will enable a more accurate sea margin calculation in early ship design and will thus allow for a better understanding of the required power. This will lead to a better-informed decision-making process regarding the propulsion system and/or the possibilities of alternative fuels, thus having a positive effect on the footprint of a vessel.

This novel approach for sea margin estimation offers a quick and substantiated estimation in the early-design stage of a ship, making it a promising starting point for further research. Recommendations for further research comprise further developing the model by testing different algorithms, including more data from different vessels to train and test the model, and finally evaluating whether a pattern in sea margin for certain passages can be recognised.

CONTRIBUTION STATEMENT

Sietske de Geus-Moussault: Conceptualization; data curation, methodology; writing – original draft. **Henk Seubers:** conceptualization; data curation, methodology; writing – review and editing. **Harry Linskens:** conceptualization; data curation, methodology; writing – review and editing. **Andrea Coraddu:** conceptualization; supervision; writing – review and editing. **Jeroen Pruyn:** conceptualization; supervision; writing – review and editing.

ACKNOWLEDGEMENTS

This research was performed based on data from a cargo vessel of Royal Wagenborg the authors would like to acknowledge and thank Royal Wagenborg for their support of this research.

This research has been performed within the TODDIS project, partially funded by the Dutch Research Council (NWO) under grant agreement Raak-Pro program 2018, n° 03.023.

This research contains Copernicus Climate Change Service Information (2024), neither the European Commission nor ECMWF is responsible for any use that may be made of the Copernicus information or data it contains.

REFERENCES

Aggarwal, C. C. (2015). *Data mining: the textbook*. Springer.

Anderson, J. D. and Wendt, J. (1995). *Computational fluid dynamics*, volume 206. Springer.

Barczak, N. (2020). *The ship towing tank*. DMS.

Bertram, V. (2012). *Practical ship hydrodynamics*. Elsevier.

Bertram, V. (2022). Realistic assessment of saving potential for energy saving options. In *Sustainable Energy Systems on Ships*, pages 451–467. Elsevier.

Blendermann, W. (1994). Parameter identification of wind loads on ships. *Journal of Wind Engineering and Industrial Aerodynamics*, 51(3):339–351.

Chandrashekar, G. and Sahin, F. (2014). A survey on feature selection methods. *Computers & Electrical Engineering*, 40(1):16–28.

Chen, H. C., Patel, V. C., and Ju, S. (1990). Solutions of reynolds-averaged navier-stokes equations for three-dimensional incompressible flows. *Journal of Computational Physics*, 88(2):305–336.

Chung, T. J. (2002). *Computational fluid dynamics*. Cambridge university press.

Cui, H., Turan, O., and Sayer, P. (2012). Learning-based ship design optimization approach. *Computer-Aided Design*, 44(3):186–195.

Esmailian, E., Steen, S., and Koushan, K. (2022). Ship design for real sea states under uncertainty. *Ocean Engineering*, 266(5). doi.org/10.1016/j.oceaneng.2022.113127.

Gatin, I. (2019). Cfd in the marine industry: Today and tomorrow.

Gertler, M. (1954). *A reanalysis of the original test data for the Taylor Standard series*. Department of the Navy, Washington.

Hersbach, H., Bell, B., Berrisford, P., Biavati, G., Horányi, A., Muñoz Sabater, J., Nicolas, J., Peubey, C., Radu, R., Rozum, I., Schepers, D., Simmons, A., Soci, C., Dee, D., and Thépaut, J.-N. (2023). Era5 hourly data on single levels from 1940 to present. copernicus climate change service (c3s) climate data store (cds), doi: 10.24381/cds.adbb2d47 (accessed on 01/02/2023).

Hino, T., Hirata, N., Stern, F., Larsson, L., Visonneau, M., and Kim, J. (2021). Introduction, conclusions and recommendations. In *Numerical Ship Hydrodynamics: An Assessment of the Tokyo 2015 Workshop*, pages 1–21. Springer.

Holtrop, J. (1984). A statistical re-analysis of resistance and propulsion data. *Published in International Shipbuilding Progress, ISP, Volume 31, Number 363*.

Holtrop, J., Mennen, G. G. J., et al. (1982). An approximate power prediction method. *International Shipbuilding Progress*, 29(335):166–170.

Islam, H. and Soares, C. (2022). Head wave simulation of a kriso container ship model using openfoam for the assessment of sea margin. *ASME. J. Offshore Mech. Arct. Eng.*, 144(3). doi.org/10.1115/1.4053538.

Journée, J. M. J., Massie, W. W., and Huijsmans, R. H. M. (2015). Offshore hydromechanics. *3rd edition*. Delft.

Kvale, J. M. (2014). Revised simulation model for a very large crude carrier (vlcc). Master's thesis, Institutt for marin teknikk.

Michell, J. H. (1898). The wave-resistance of a ship. *Philosophical Magazine*, 45(5):106–123.

Ozdemir, Y. H. and Barlas, B. (2017). Numerical study of ship motions and added resistance in regular incident waves of kvlcc2 model. *International Journal of Naval Architecture and Ocean Engineering*, 9(2):149–159.

Petersen, J. P., Jacobsen, D. J., and Winther, O. (2012). Statistical modelling for ship propulsion efficiency. *Journal of marine science and technology*, 17:30–39.

Press, W. H., Teukolsky, S. A., Vetterling, W. T., and Flannery, B. P. (2011). *Numerical Recipes: The Art of Scientific Computing*. Third Edition. ISBN 978-0-521-88068-8.

Sadat-Hosseini, H., Wu, P.-C., Carrica, P. M., Kim, H., Toda, Y., and Stern, F. (2013). Cfd verification and validation of added resistance and motions of kvlcc2 with fixed and free surge in short and long head waves. *Ocean Engineering*, 59:240–273.

Shalev-Shwartz, S. and Ben-David, S. (2014). *Understanding machine learning: From theory to algorithms*. Cambridge university press.

Taylor, D. W. (2013). *The speed and power of ships*. BoD–Books on Demand.

Townsin, R. L. (2003). The ship hull fouling penalty. *Biofouling*, 19(S1):9–15.

Van, S.-H., Kim, W.-J., and Kim, D.-H. (2000). Experimental investigation of local flow around kriso 3600teu container ship model in towing tank. *Journal of the Society of Naval Architects of Korea*, 37(3):1–10.

Weatheritt, J., Pichler, R., Sandberg, R. D., Laskowski, G., and Michelassi, V. (2017). Machine learning for turbulence model development using a high-fidelity hpt cascade simulation. In *Turbo Expo: Power for Land, Sea, and Air*, volume 50794, page V02BT41A015. American Society of Mechanical Engineers.

Wolpert, D. H. (2002). The supervised learning no-free-lunch theorems. In *Soft computing and industry*.

Zhang, Z.-r., Hui, L., Zhu, S.-p., and Feng, Z. (2006). Application of cfd in ship engineering design practice and ship hydrodynamics. *Journal of Hydrodynamics, Ser. B*, 18(3):315–322.

Zhao, Y., Akolekar, H. D., Weatheritt, J., Michelassi, V., and Sandberg, R. D. (2020). Rans turbulence model development using cfd-driven machine learning. *Journal of Computational Physics*, 411:109413.

Proceedings of 15th International Marine Design Conference (IMDC-2024)
June 2-6, 2024
Amsterdam, the Netherlands

Knowledge Graphs underpinning ship digital twins for decarbonisation options assessment

Bill Karakostas[1,*] and Antonis Antonopoulos[2]

ABSTRACT

We propose the concept of a Knowledge Graph as a data management and inference machinery that underpins digital twins of ships. The Knowledge Graph is a directed graph connecting dependent and independent model variables of interest in the digital twin, where the correlations between variables are continuously updated based on data received from the physical ship. The paper outlines a methodology for constructing the Knowledge Graph and proposes metrics that help to calculate the effectiveness of decarbonization solutions based on changes to the strength of data correlations. The proposed methodology allows for the extrapolation of decarbonization technology potential across specific vessels, fleets, operational patterns, and lifecycle phases.

KEY WORDS

Digital Twin, Knowledge Graph, Correlation Graph, Ship Decarbonisation, Wind Assisted Propulsion

INTRODUCTION

The digitalisation of shipping to accelerate decarbonisation, supported by data gathered from sensors and ship systems (Agarwala et al, 2022), is a promising approach (Ksetri, 2021). Particularly relevant is *Digital Twin* (DT) technology, initially used by NASA, but applied in recent years to smart manufacturing, transport, smart cities and other areas. DTs enable the creation of a digital representation of a ship, which is fed with data acquired by the physical ship via sensors. These digital representations can then be used to analyse ship-related functions and processes, and actuate systems on the physical ship responsible for engine management, navigation and others.

A ship digital twin therefore, can be viewed as a virtual replica of its physical counterpart that is not static but dynamic, with a bidirectional relationship to the physical system. Use of DT in shipping can result in reducing costs and improving time effectiveness and quality.

A broad definition of a knowledge Graph is as a graph of data intended to accumulate and convey knowledge of the real world, whose nodes represent entities of interest and whose edges represent relations between these entities (Hogan et al, 2022). Knowledge graphs are knowledge-based models that utilize graph links to connect entities in a particular domain and to augment the existing knowledge by using queries and other types of inferences. A knowledge graph therefore is ideally suited for modelling knowledge in the domain represented by the physical counterpart of the DT. Moreover, the knowledge graph links data about the physical system as these are collected by the digital twin. Such data types may include:

- geometrical data, e.g. CAD models of the ship
- event based data for events generated by the physical ship throughout its operation, and
- time series data such as speed, fuel consumption, etc, collected from the ship, as well as data such as sea state, direction, collected from the ship's environment.

A knowledge graph can be used as the data engine management, and also as the inference engine of the DT, that acts on the datasets received from the physical ship to make inferences such as predictions of future states of the ship, and also to evaluate

[1] Inlecom Systems, Brussels, Belgium
[2] Konnecta, Dublin, Ireland
* Corresponding Author: bill.karakostas@inlecomsystems.com

Submitted: 29 January 2024, Revised: 25 April 2024, Accepted: 1 May 2024, Published: 23 May 2024

Conference paper, DOI: https://doi.org/10.59490/imdc.2024.871 e-ISSN: 3050-4864

the actual current state of the ship and compare with the expected one, thus supporting anomaly detection (the existence of an abnormal state), and error and fault diagnosis.
This paper builds upon foundational work on digital twin technology and knowledge graphs as tools for supporting the decarbonization of the shipping industry (Antonopoulos et al, 2023). In the research presented in (Antonopoulos et al, 2023), a digital twin of maritime vessels was developed to provide a platform for simulating and evaluating the impacts of various decarbonization technologies. Key to that approach is the use of knowledge graphs for maintaining ontologies, storing simulation models, and correlating these models with a combination of measured and estimated variables.
The novel contribution of this paper is on enriching knowledge graphs with dynamic features by introducing a computational framework that establishes quantifiable links between system parameters. By utilizing measures such as correlation, we enable precise comparisons between data-driven ship models and their theoretical counterparts.
The paper is structured as follows: Initially, the paper outlines the methodological framework within which the proposed technique is applied. The next section provides a formal definition of the Knowledge Graph and illustrates it with an example. Then, a procedure for constructing a Knowledge Graph is proposed. Next, we introduce metrics that are based on statistical analyses of the datasets collected by the digital twin. Again, an example is used to illustrate the various proposed metrics. Following that, a case study is shown where a sample data set and Knowledge Graph is used to analyse and quantify the effectiveness of a hypothetical wind-based decarbonisation technology introduced on a ship. We conclude the paper with an overview and critique of the proposed approach and with suggestions for further research.

ENCODING DOMAIN-SPECIFIC KNOWLEDGE OF DIGITAL TWINS USING KNOWLEDGE GRAPHS

Within the maritime sector, a DT is conceptualized as a real-time digital counterpart of a physical entity, such as a ship, port, or maritime operation [Madusanka et al, 2023]. Specifically, a ship's DT represents an exact digital reflection of the physical vessel, encapsulating its structural design (like hull type and layout, hull parameters), onboard equipment (engines, propellers, rudders), and operational functionalities (propulsion, navigation, cargo handling). This comprehensive digital model integrates technical specifications, component designs, and operational data within a fleet management framework, facilitating the computerized simulation and optimization of ship operations across various performance metrics with a focus on environmental sustainability.
Digital Twins engage in a two-way communication with the ship's Information and Communication Technology (ICT) infrastructure [Tao et al, 2018], utilizing data collection techniques and devices to continuously update the digital model with real-time information from the physical vessel. This dynamic learning process allows the DT to accurately reflect the physical ship's lifecycle, offering insights into its present condition and forecasting future states through simulations and predictive analytics.
A ship DT is built around measurable parameters and can be structured into a network of interconnected modules, such as propulsion systems, voyage and fleet management systems. These modules may also be integrated with broader digital twins that encompass ship operations management or the entire spectrum of ship design, construction, and lifecycle management. The primary goal of employing a ship DT is to facilitate both reactive and predictive decision-making processes, aiming to achieve objectives that include reducing environmental impact. The insights gained from one ship's DT can often be applied to others, enabling data and knowledge sharing in advancing green shipping practices. This prerequisite a degree of interoperability between digital twin instances, which can be achieved by using a common ontology, as suggested by (Hiekata et al, 2010).
Digital Twin technology has found application across various maritime domains, including shipbuilding, offshore oil and gas exploration, marine fisheries, and renewable marine energy production (Zhihan et al, 2023). For instance, (Coraddu et al, 2019), have developed a data-driven digital twin for ships, capitalizing on vast datasets from onboard sensors to estimate speed loss due to marine fouling, showcasing the practical utility of digital twins in enhancing maritime operations.

KNOWLEDGE GRAPH FORMAL DEFINITION

Rationale

Knowledge graphs are sophisticated semantic networks acting as knowledge bases, structured like directed graphs (Qiu et al, 2017). They function by organizing data into triples of (subject, predicate, object) from semi-structured or unstructured sources, thereby enabling advanced knowledge retrieval and reasoning capabilities (Wei et al, 2018). Knowledge graphs are adept at modelling complex relationships within domains, linking disparate pieces of information, and supporting a wide range of applications including knowledge retrieval, question and answer (Q&A) systems, recommendations, and visualization.
Initially developed for extracting knowledge from extensive datasets, knowledge graphs are now a cornerstone in the semantic web, setting a benchmark for efficient information retrieval and usage. Their utility spans various sectors, notably in industry

for tasks such as maintenance planning of sophisticated equipment (Xia et al, 2023), and predictive maintenance for hydraulic systems (Yan et al, 2023).

Within the maritime and shipping sector, knowledge graphs have found applications in analyzing ship collision accident reports to enhance maritime traffic safety. (Zhang et al., 2020), have developed a knowledge graph for maritime dangerous goods, streamlining the knowledge retrieval of hazardous materials, automating the assessment of cargo stowage and segregation, and advancing the intelligent transport of dangerous goods. Similarly, (Langxiong et al, 2023) crafted a Ship Collision Accident Knowledge Graph, aiding in uncovering accident correlations and streamlining the judicial and investigative processes for marine accidents.

Crucially, knowledge graphs have become integral to augmenting the functionality of Digital Twins. By mapping entities, their relationships, and attributes in an organized fashion, they offer a systematic approach to collating and interlinking data within the DT framework. In maritime contexts, they enable comprehensive representations of vessel ecosystems, covering equipment, maintenance histories, and compliance with regulations. These interconnected networks support predictive analytics, risk evaluations, and the simulation of various scenarios, enhancing operational decision-making. By bridging real-time and historical data, knowledge graphs also underpin predictive maintenance strategies, facilitating early detection of potential failures, thus ensuring operational reliability and safety.

A related modelling formalism, *dependency graphs*, have been studied as part of engineering design (Rötzer et al, 2022). There is a variety of such graphs based on their formal underpinning and role in the design/manufacturing cycle. Effect Graphs, for instance are qualitative models built to produce early qualitative statements about the system behaviour. Directed Acyclic Graphs (DAG) or causal diagrams as described by (Pearl, 1995).

The Knowledge Graph we propose is a dependency network of dependent and independent model variables of interest, where the links show the strength of correlation associations between the variables. The Knowledge Graph utilizes the ship data collected by the DT to learn the strength of the correlations between system variables and to represent them as rule nodes. Association rule learning is a rule-based machine leaning method for discovering interesting relations between variables in large databases. (Agrawal et al, 1993). Association rule mining has been studied since the 1990s in domains such as supermarket transactions. However, in such domains there are not many theoretical models to cross validate against the empirically mined association rules. In contrast, the association rule we propose utilizes both theoretical and data driven ship models.

The Knowledge Graph can therefore, be considered as a qualitative statistical summarizer of the ship's models parameters of interest, reflected in the strength of associations between the key variables that represent the system and its environment.

As shown in Figure 1, the knowledge graph models dependency rules such as statistical correlations of the data collected from the physical ship and its environment. The rules describe statistical dependencies (correlations) between independent variables (factors) and dependent variables (factors) of interest. For instance, independent factors include ship speed and direction as well as environment factors such as ship state. Dependent factors include ship fuel consumption and emissions.

The exact relationships between independent and dependent variables are complex and mostly nonlinear. Complexity means that the independent variables may be correlated with each other as well as with the dependent variables

To calculate the strength of the influence of each independent variable on a dependent variable, standard correlation analysis techniques such as Person for linear, and Spearman, for nonlinear correlations, can be employed. For instance, although ship sped is positive related to fuel consumption for very low speeds the polarity of the relation is reversed as in such speed, the friction is increased and requires more power to overcome.

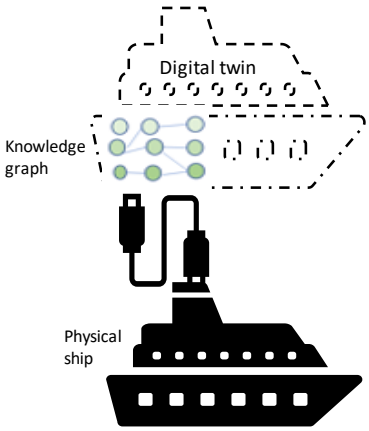

Figure 1: Knowledge Graph in the context if the digital twin

Formal Definitions

Let X be a finite set of independent variables ('factors') $x_1, \ldots x_2, \ldots$ and Y a finite set of dependent variables $y_1. y_2, \ldots$

Each factor x in X draws values from a finite countable set of ordered values called the domain of X and denoted as $Dom(x)$
We use $val(x_i)$ to refer to a value drawn from $Dom(x_i)$
Similarly, each dependent variable y in Y draws values from a finite countable set of ordered values demoted as $Dom(y)$
We define a *record type r* of variables $x_1,..,x_k$ $k>1$, as a tuple $(val(x_1)\ldots,val(x_k))$ with $k >= 1$ where $xi \neq xj$ for all i, j.
We define a set of correlation rules C where $c \in C$ *is a tuple* $(x_1,..,x_n, y)$, and the strength of the rule *c corr(c)* as a function *corr* returning a value between 0 and 1.
We define a Knowledge Graph as a directed graph $<V,E>$ where $v \in V$ is a variable from $X \cup C \cup Y$ and $e \in E$ is a tuple (x, c) where $x \in X$ and $c \in C$ or $\{c, Y)$ where $c \in C$ and $y \in Y$.
Informally, factors are connected to rules and rules are connected to dependent variables. A rule $(x_1,..,x_n, y)$, shows the correlation of factors $x_1,..,x_n$ with the dependent variable y, while the weight on the edge between rule and dependent variable corresponds to the strength of the correlation . The correlation strength can be the result of a theoretical formula or an empirical (e.g. regression) formula.

Example

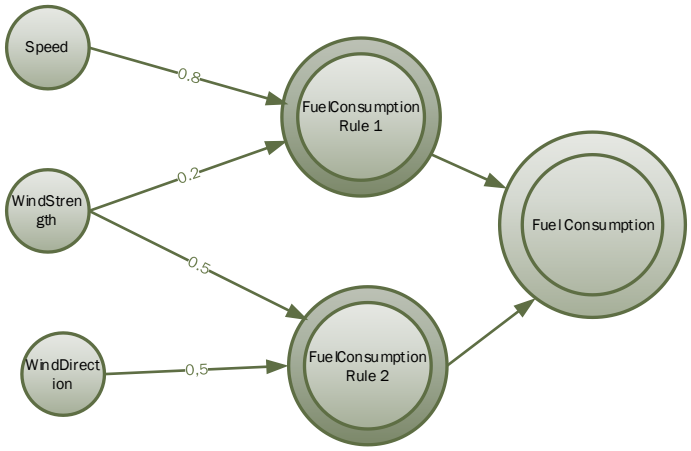

Figure 2: Knowledge Graph for Fuel Consumption

Figure 2 shows a small sample Knowledge Graph. The modelled factors are *Speed*, Wind *Strength* and *Wind Direction*. All these factors are quantized as discussed in the next section, and draw values from their respective domains. For instance, *Wind Strength* draws values from the domain of integers between 0 and 9 following the Douglas Sea Scale units of measurement. The three factors are connected to rule nodes. Consequently, the rule nodes connect to dependent variables of interest, in this case to *Fuel Consumption*. The labels on edges between rules and dependent variables show the strength of the correlation.

PROCEDURE FOR CONSTRUCTING KNOWLEDGE GRAPH

The main steps in constructing a Knowledge Graph are as follows

1. Identify subsystems and components of the ship system.
2. Identify additional systems that the current system interacts with/is part of.
3. Identify model variables (endogenous as well as exogenous) that describe the behaviour/performance of the system/subsystem/component.
4. Define the Knowledge Graph vertices (nodes) in terms of the variables in Step 3.
5. Discretise continuous or numerical variables into categorical variables.
6. Determine dependencies between independent variables and dependent ones using theoretical models, experimental data and expert knowledge/Create one rule vertice per rule in the Knowledge Graph.

Discussion on the proposed Knowledge Graph construction procedure.

In general, quantizing/binning of continuous variable introduces non-linearity and tends to improve the performance of the model. It can be also used to identify missing values or outliers. We quantise the values of the independent factors using natural (e.g. physics dictated, as well as business related criteria, using ordered categorical variables.

Example

Although vessel speed can be modelled as a continuous variable, we discretise it according to speed categorisation that is dictated by physics/ operational and legislation constraints So, speed is discretised according to the categories of normal, slow steaming and extra slow steaming. Table 1 shows examples of quantizing ship and environment variables.

Table 1: quantizing variables

Record id	Avg. Speed (knots)	Speed quantized	Avg wave height (m)	Waves in Douglas Sea Scale	Fuel consumption rate (lt/min)	Fuel consumption rate quantized
T1	22	*n* (normal)	6.5	7	14	*h*(high)
T2	19	*ss* (slow steaming)	3	5	10	*m* (medium)
T3	21	*n* (normal)	2	4	8	*l*(low)
T4	15	*ess* (extra slow steaming)	1	3	6	*vl* (very l(ow)

Metrics

In this section we define metrics related to the numbers, frequency of occurence and correlations in the dataset vailable to the DT and consisting of measurements taken from the physical ship, discretised and grouped into records. We define a record instance of a record *r* an appearance of a record of type *r* in the dataset.

Expected Frequency

Expected frequency *Ef(r) is* a measure of how frequently instances of record of type *r* are expected to appear in the dataset. It is based on the strength of correlation between variables appearing in the record according to the existing knowledge (theoretical and/or empirical) of the domain.

Example

Assuming high (0.9) correlation between ship speed and fuel consumption and the following quantization of speed and fuel consumption:

Dom(*Speed*):{ *ss*,*n*} with *ss* < *n*

Dom(FuelConsumption) : {*l*, *h*} with *l* < *h*.

If speed and fuel consumption were totally uncorrelated we would expect to find all combinations (*ss, l*),(*ss*,*h*),(*n*,*l*),(*n*,*h*) with equal probability of 0.25.

However because of the assumed correlation we expect to find record types (*ss*,*l*),(*n*,*h*) with probability 0.9 and record types (*n*,*l*) , (*ss, h*) with probability 0.1

However, not all combinations are equally represented in the dataset due to measurement limitations. For instance, it may be possible to measure some particular combinations of factors due to technical and physical limitations such as very strong winds co-occurring with high vessel speeds. Therefore, we introduce the concept of *support* below.

Coverage

Coverage for a record of type *r* is the number of record instances in the dataset divided by the number we could theoretically find in a dataset of that size. For example, because of the strength of the correlation between speed and fuel, we could expect on average 10 instances of record (*low speed, high fuel*) in a sample of 100 instances, If we find instead 5 instances of the record the coverage is 5/10 or 0.5

When *coverage* < 1 for a record type it means that the record type is *underrepresented* in the dataset while > 1 means the record type is *overrepresented*

Counterrecord

A counterrecord of record type $r:(x_1, x_2, .., x_k, y)$ with respect to some correlation rule *c is a record type* ř:$(x_1, x_2,..,x_k,y')$ where y ≠ y' has expected frequency $\mathbb{E}f(\check{r}) < \mathbb{E}f(r)$
For instance, if the association between speed:(l,h) and fuel consumption:$(l,$h$)$ is strong positive (with for example, 0.9 strength) we expect to find record instances of type (l, l) and speed: (h, h) with high frequency and records of type (l,h) and (h,l) with lower frequency in the dataset. Thus record types (l,h) and (h,l) are counterrecords of (h, h).
We use $\hat{R}_c$ for the set of all counterecord types of *r* under correlation rule *c*.

Association rule strength

The strength of an association rule *c* for a record of type *r* is defined as

$$\Sigma_{\check{r}\in\hat{R}_c}\left(\mathrm{E}f(\check{r})\right) * \frac{|r|}{|\check{r}|* \mathrm{E}f(r)} \quad [1]$$

Where |ř| is the cardinality of the set of all counterexamples found in the data set.

The summation of expected frequencies of counterrecords in formula [1] can be explained with this example: If we have 3 types of counter records and we find one instance per counter record and the expected frequency of each counter record is 1/30 and 5 record instances with frequency 0.9 ,we obtain the association rule strength as 3 x 1/30 x (5/3*0.8= 0.13

CASE STUDY

Background

We illustrate our approach with a hypothetical example about the introduction on a ship of a fuel consumption reduction technology that is based on wind assist propulsion (WASP). It is well known today that the use of wind is one of the solutions to substitute existing fossil-based propulsion technologies. The sizing of wind assists devices such as sails and kites needs to take into account the propulsion system. Therefore, vessels equipped with variable pitch provide a greater range of applicability. Moreover, analytical models for kite have been developed (Leloup et al, 2016). Models of the operation of wing sails have calculated the Energy Efficiency Design Index (EEDI) change for specific commercial routes, identifying a potential reduction of 18% (Yong et al, 2919).

Estimating the correlation strengths

The correlation graph of Figure 3 is small as it is only used to illustrate the principles of our approach. A real life scale knowledge graph would also include variables such as fuel consumption/mile, wind direction, wind speed, vessel speed and propeller pitch. The new WASP technology is expected to negatively correlate fuel consumption with wind power, i.e. as the wind power increases, the new technology will utilize it to reduce required engine power, and hence, fuel consumption. The size of our synthetic data is small compared to a real life scenario where the data set could contain thousands or millions of records collected over large time periods, and is used to illustrate the proposed approach. It is envisaged that the Knowledge Graph would periodically carry out the calculations described below as the ship conditions change, on very large datasets that are updated over the ship's lifecycle. The impact of both speed and wind strength on fuel consumption has been investigated both empirically and theoretically. More specifically, the weather a ship encounters during voyage has significant influence on her fuel consumption, in particular relating to prevailing wind and waves (Bialystocki and Konovessis, 2016). Accordingly, prior to introducing the new technology the correlation between wind strength, speed and fuel consumption rate for the particular vessel was calculated experimentally and theoretically as shown in the Knowledge Graph of Figure 3. As

per Figure 3, there is a very strong positive correlation between speed and fuel consumption rate (0.9) and a strong (0.7) positive correlation between wind strength and fuel rate consumption.

The factors' corresponding domains after discretization are:
Speed: {(*n*)ormal, (*s*)low steaming. *m*(anouvring)}
Wind Strength:{*0..9*}
Fuel Consumption Rate: {*n*(ormal), *l*(ow), *h*(igh)}

The sample dataset received by the digital twin is shown in Table A1 in appendix A.

To assess the effectiveness of the decarbonisation technology based on the collected data we need to pose several questions and analyse the dataset using the metrics that we defined previously. The different analyses are further discussed below.

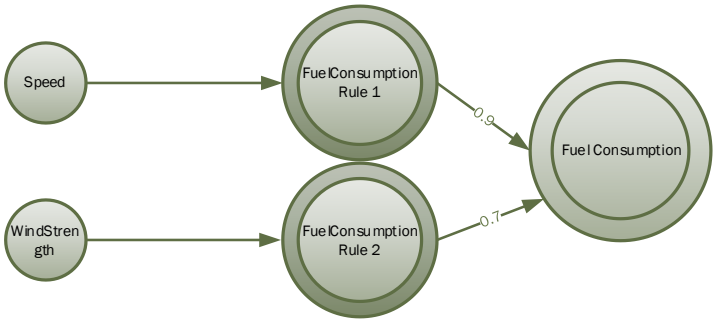

Figure 3: Correlation graph for Speed, Wind Strength and Fuel Consumption

The coverage of the dataset for every speed-wind strength combination

The total number of record types is ||*Dom(Speed*)|| x ||*Dom(WindStrength*)|| i.e. 30. The coverage of the different record types *Speed* x *WindStrength* is shown in Table 2.

Table 2: Coverage of record types

Record type	(n,0),(n,2),(n.3),(n,4),(n,5),(n,6),(n,7),(n,8),(n,9) (ss,0),(ss,1),(ss,2),(ss,5),(ss,6),(ss,7),(ss,8),(ss,9) (m,0),(m,1),(m,2),(m.3),(m,4),(m,5),(m,6),(m,7),(m,8),(m,9)	(n,1), (ss,3), (ss,4)
Expected Coverage	2/3	2/3
Actual Coverage	0	2

The reasons that most record types are underrepresented on this occasion is the small size of our dataset. In real life underrepresentation could be interpreted as caused by:

- Data corresponding to underrepresented record types were difficult to collect due to limitations of the measuring apparatus, Measuring or recording errors
- Due to the rarity of the physical events corresponding to the record type. For instance, sea scales of strength between 3-5 are more commonly experienced in open seas than those of strength 0, 1, 8, 9.

Examine the sensitivity of the new technology to wind strength i.e. whether it works better with higher or lower wind strengths

To analyse that, we compare the frequency of occurrence of record types (S*:*any*, WindSrength:0-4, FuelConsumption:h*), with those of record types (S*:*any*, WindStrength:5-9, FuelConsumption:h*)

According to the dataset of Table 1, the new technology tends to be more strongly associated with low fuel consumption at low wind strengths. Of course, that can be explained that other confounding factors such as ship wind resistance have a stronger effect on fuel consumption than the new technology at high wind speeds.

Identify potential situations where the technology causes increased fuel consumption results

For this type of analysis we need to enumerate all counterrecord types of records where fuel consumption is medium or low and compare the frequency of the record with that of the counterrecords.
Counterecord types of (*m,l*) are (*m,m*),(*m,h*). From the association rule strength we expect to find 2 counterecord instances, however 5 instances where found in the dataset. This means that the new technology can have unintended increase in fuel consumption at maneuvering speeds.
Counterecord types of (*s,m*) are (*s,h*),(*s,l*). From the association rule strength we expect to find 2 counterchord instances, however 4 instances where found in the dataset. This means that the new technology can have unitentended increase in fuel consumption at slow steaming speeds.

However, all above analysis results should be interpreted in the context of the dataset size and coverage of each record type.

Calculate the overall fuel improvement potential of the new technology

We need to test whether the new tech reduces the strength of the association between speed and fuel consumption and increases the strength of the association between wind strength and fuel consumption
By applying equation [1] to the dataset we obtain the revised correlation strengths as shown in Table 4.

Table 3 revised correlation strengths after new decarbonization technology

$\lvert R_{Speed} \rvert$	$\lvert \hat{R}_{speed} \rvert$	*c*(Speed→Fuel Consumption)	$\lvert R_{\text{Wind Strength}} \rvert$	$\lvert \hat{R}_{\text{Wind Strength}} \rvert$	*c*(Wind→Fuel Consumption)
4	5	~0.11	4	11	~0.65

From the results shown in table 3 we observe that the strength of the correlation between speed and fuel consumption has been reduced from 0.9 to 0.11. This means that speed is no longer the main determinant of fuel consumption. Similarly, the strength of the wind and fuel consumption has increased from 0.1 to ~0.65, meaning that wind strength is now the significant determinant of fuel consumption. This of course assume that all other factors have remained unchanged after the introduction of the new technology.

CONCLUSIONS

In this paper we presented the theoretical foundation of an approach to encode quantified domain-specific knowledge, followed by practical examples, and demonstrate its application in a use case focused on wind-assist technology. While this work primarily explores the methodology's principles and provides a preliminary report, it lays the groundwork for future development and implementation of a holistic decision-support framework aimed at decarbonizing the shipping industry with the use of DTs and knowledge graphs. The proposed Knowledge Graph correlates independent and dependent variables that model the physical system in a digital twin. Knowledge Graphs in general, are an important technology for data representation and knowledge inference in many industrial domains. (Abu-Salih, 2021). The Knowledge Graph connects theoretical and empirical ship knowledge with the data received from the ship throughout its operation.
The purpose of the proposed Knowledge Graph is to compare the theoretical with empirical model of the ship in order to identify discrepancies. Such discrepancies can then be interpreted as anomalies, or as changes to physical ship parameters, and used to compare 'before' and 'after' scenarios. This is also the approach employed in this paper where the Knowledge Graph is used to analyse the impact of decarbonization technologies on the ship's operational parameters. This dynamic characteristic of the knowledge graphs enables the optimization of predictive capabilities for computational efficiency, and facilitates the encoding of knowledge patterns that can be transferred across different instances of digital twins. By leveraging quantifiable associations, we can effectively analyze and quantify the effectiveness of newly introduced decarbonization technologies within an existing ship's system. Such analyses allow for the drawing of insightful conclusions regarding system changes brought about by the integration of new subsystems and their impact on system parameters. Through this novel integration of dynamic knowledge graphs and digital twin technology, our work lays a foundation for a more informed and

effective application of decarbonization technologies across the maritime industry, ensuring a strategic approach to mitigating environmental impact while maintaining operational efficiency.

The research presented in this paper aims to support the development of a knowledge graph for encoding domain-specific knowledge generated by the digital twin. The knowledge graph is not just a static repository of data but a dynamic system that integrates, processes, and standardizes knowledge for easy access and application. The proposed knowledge graphs catalogs simulation outcomes, operational insights, and environmental data, transforming raw data into actionable intelligence.

The encoding process involves several key steps: Firstly, simulation models within the digital twin generate data reflecting the performance and environmental impact of various decarbonization technologies under different operational scenarios. This data, along with measured data, is then contextualized within the knowledge graph, which correlates it with existing operational parameters, environmental conditions, and technology performance metrics. Through semantic tagging and linkage, the knowledge is not only stored but also interconnected in meaningful ways, facilitating complex queries and analysis (Fonseca et al, 2022).

Using ontologies to maintain a shared vocabulary and structure, allows for the consistent interpretation of data across different digital twin instances. This standardization is crucial for enabling the transfer of knowledge between instances, ensuring that insights gained from one vessel or fleet can inform decisions on others, even if they operate under differing conditions.

The ultimate goal of this methodology is to enable the extrapolation of decarbonization technology potential across various maritime contexts. By analyzing data from specific vessels or fleets, our approach can predict the effectiveness of decarbonization technologies in different operational patterns (e.g., speed, route, and cargo type) and throughout different phases of a vessel's lifecycle (e.g., design, mid-life retrofitting, and decommissioning). This predictive capability allows ship owners, operators, and industry stakeholders to make informed decisions on adopting decarbonization technologies, tailored to their specific needs and circumstances.

To conclude, our work seeks to bridge the gap between theoretical decarbonization potential and its practical application, offering a scalable and adaptable tool for accelerating the shipping industry's transition towards a more sustainable future.

It must be emphasized that a knowledge graph is never complete or entirely encompassing the modelling perspectives for a ship. It is instead modelled from the perspective of the stakeholders who use the Knowledge Graph/ digital twin in order to study and understand the physical ship. Also, some types of data that may be of interest may not be represented in the digital twin due to technology limitations or even due to non technical reasons (e.g. confidentiality issues).

Additionally, the increasing utilization of Knowledge Graphs as parts of digital twins raises questions about their quality and robustness. (Abu-Salib, 2021). Both model quality and the quality of the underlying data needs to be present for the inferences and predictions made with the use of the Knowledge Graph to be trustworthy. The size and dynamicity of the data sets handled by the DT requires data quality assurance techniques to be automated and integrated in the overall Knowledge Graph infrastructure. As part of future research, we propose techniques of self-reflection and self-correction to be utilized by the Knowledge Graph in order to always remain a reliable and up to date representation of the physical ship.

DATA ACCESS STATEMENT

No research datasets or repositories were used in this paper.

DECLARATION OF GENERATIVE AI AND AI-ASSISTED TECHNOLOGIES IN WRITING

Statement: During the preparation of this work the author(s) did not use any generative AI and AI-assisted technologies

CONTRIBUTION STATEMENT

Author 1: Conceptualization; data curation,; writing – original draft. **Author 2:** methodology**,** review and editing.

ACKNOWLEDGEMENTS

Research described in this report has received funding from the European Union's Horizon Europe research and innovation program under grant agreement no. 101056799 (Project 'DT4GS')

REFERENCES

1. Abu-Salib , B. (2021). Domain-specific knowledge graphs: A survey. Journal of Network and Computer Applications. 185(1).

2. Agarwala P., et al. (2021). Using digitalisation to achieve decarbonisation in the shipping industry, Journal of International Maritime Safety, Environmental Affairs, and Shipping 5(4).

3. Agrawal, R., Imieliński, T.; Swami, A. (1993). Mining association rules between sets of items in large databases. Proceedings of the 1993 ACM SIGMOD international conference on Management of data - SIGMOD '93. p. 207.

4. Aggarwal, CC and Philip S. Yu. (1998). A New Framework For Itemset Generation. PODS 98, Symposium on Principles of Database Systems

5. Antonopoulos, A., Karakostas, B., Katsoulakos, T., Mavrakos, A., Tsaousis, T., Zavvos, S. (2023). A Digital Twin Enabled Decision Support Framework for Ship Operational Optimisation Towards Decarbonisation. In: Yang, XS., Sherratt, R.S., Dey, N., Joshi, A. (eds) Proceedings of Eighth International Congress on Information and Communication Technology. ICICT 2023. Lecture Notes in Networks and Systems, vol 694. Springer, Singapore. https://doi.org/10.1007/978-981-99-3091-3_38.

6. Bialystocki, N. and Konovessis, D. (2016). On the Estimation of Ship's Fuel Consumption and Speed Curve: A Statistical Approach March 2016Journal of Ocean Engineering and Science 1(2).

7. Coraddu Andrea, Luca Oneto, Francesco Baldi, Francesca Cipollini, Mehmet Atlar, Stefano Savio. Data-driven ship digital twin for estimating the speed loss caused by the marine fouling. Ocean Engineering. 2019 ; Vol. 186.

8. Fonseca Ícaro Aragão & Henrique Murilo Gaspar (2021) Challenges when creating a cohesive digital twin ship: a data modelling perspective, Ship Technology Research, 68:2, 70-83, DOI: 10.1080/09377255.2020.1815140.

9. Hiekata Kazuo , Hiroyuki Yamato b , Sho Tsujimoto. Ontology based knowledge extraction for shipyard fabrication workshop reports. Expert Systems with Applications 37 (2010) 7380–7386
.
10. Hogan, Aidan, Eva Blomqvist, Michael Cochez, Clau dia D'amato, Gerard De Melo, Claudio Gutierrez, Sabrina Kirrane, José Emilio Labra Gayo, Roberto Navigli, Sebastian Neumaier, Axel-Cyrille Ngonga Ngomo, Axel Polleres, Sabbir M. Rashid, Anisa Rula, Lukas Schmelzeisen, Juan Sequeda, Steffen Staab, and Antoine Zimmermann. 2022. Knowledge graphs. ACM Computing Surveys, 54(4):1–37.

11. Kshetri, N. (2021). "The Economics of Digital Twins" IEEE Computer, 54(4): 86-90.

12. Langxiong Gan, Beiyan Ye, Zhiqiu Huang, Yi Xu , Qiaohong Chen, Yaqing Shu. Knowledge graph construction based on ship collision accident reports to improve maritime traffic safety. Ocean & Coastal Management Volume 240, 1 June 2023, 106660

13. Leloup R, K. Roncin, M. Behrel, G. Bles, J.-B. Leroux, C. Jochum, Y. Parlier, A continuous and analytical modeling for kites as auxiliary propulsion devoted to merchant ships, including fuel saving estimation,Renewable Energy, Volume 86, 2016, https://doi.org/10.1016/j.renene.2015.08.036

14. Madusanka, Nuwan Sri, Yijie Fan, Shaolong Yang, and Xianbo Xiang. 2023. "Digital Twin in the Maritime Domain: A Review and Emerging Trends" Journal of Marine Science and Engineering 11, no. 5: 1021. https://doi.org/10.3390/jmse11051021

15. Mauro, F. and Kana, AA. (2022). Digital twin for ship life-cycle: A critical systematic review. Ocean Engineering.

16. Pearl J. (1995). Causal diagrams for empirical research. Biometrika, 82:669–710..

17. Qiu Lirong and Zhang Huili. 2017. Review of development and construction of uyghur knowledge graph. In Proceedings of the 2017 IEEE International Conference on Computational Science and Engineering and IEEE/IFIP International Conference on Embedded and Ubiquitous Computing. Institute of Electrical and Electronics Engineers Inc., 894–897.

18. Rötzer S., Schweigert-Recksiek , S., Thoma, D. and Markus Zimmermann. (2022). Attribute dependency graphs: modelling cause and effect in systems design. Published online by Cambridge University Press.

19. Tao, Fei & Sui, Fangyuan & Liu, Ang & Qi, Qinglin & Zhang, Meng & Song, Boyang & Guo, Zirong & Lu, Stephen & Nee, Andrew. (2018). Digital twin-driven product design framework. International Journal of Production Research. 57. 1-19. 10.1080/00207543.2018.1443229.

20. Wei Yan, Yu Shi, Zengyan Ji, Yuan Sui, Zhenzhen Tian, Wanjing Wang, Qiushi Cao, Intelligent predictive maintenance of hydraulic systems based on virtual knowledge graph, Engineering Applications of Artificial Intelligence, Volume 126, Part A, 2023,106798, ISSN 0952-1976, https://doi.org/10.1016/j.engappai.2023.106798

21. Yan, J, Lv, T, Yu, Y. Construction and recommendation of a water affair knowledge graph. Sustainability 2018, 10, 3429.

22. Yong Ma, Huaxiong Bi, Mengqi Hu, Yuanzhou Zheng, Langxiong Gan, Hard sail optimization and energy efficiency enhancement for sail-assisted vessel, Ocean Engineering, Volume 173, 2019, https://doi.org/10.1016/j.oceaneng.2019.01.026.

23. Zhang Yimeng, Yuanqiao Wen, Fan Zhang, Chunhui Zhou, Lei Du, Liang Huang,Changshi Xiao. Semantic model of ship behaviour based on ontology engineering. The 2nd 2018 Asian Conference on Artificial Intelligence Technology(ACAIT 2018).

24. Zhang Qi, Yuan Q Wen, Dong Han, Fan Zhang, Chang S Xiao. Construction of knowledge graph of maritime dangerous goods based on IMDG code. The 3rd Asian Conference on Artificial Intelligence Technology (ACAIT 2019) 22 May 2020 https://doi.org/10.1049/joe.2019.1147

25. Zhihan Lv, Elena Fersman, 2022, Digital Twins: Basics and Applications, Springer Cham, https://doi.org/10.1007/978-3-031-11401-4

APPENDIX A

Table A.1: Sample dataset

Record id	Speed	Wind Strength	Fuel consumption rate
T1	n	1	n
T2	n	2	n
T3	n	5	l
T4	s	2	l
T5	s	3	n
T6	s	4	n
T7	s	3	l
T8	m	8	h

T9	m	6	h
T10	m	4	h
T11	n	1	n
T12	s	4	l
T13	s	7	n
T14	s	6	h
T15	n	8	h
T16	n	3	h
T17	m	7	l
T18	m	3	h
T19	n	4	l
T20	n	7	h

Proceedings of 15th International Marine Design Conference (IMDC-2024)
June 2-6, 2024
Amsterdam, the Netherlands

Prediction of main engine power of oil tankers using artificial intelligence algorithms

Darin Majnarić[1,*], Nikola Anđelić[2], Sandi Baressi Šegota[2], and Jerolim Andrić[1]

ABSTRACT

In the preliminary ship design, the accurate determination of a vessel's main engine power is one of the most critical aspects next to service speed, main particulars, and cargo capacity. However, this task can be quite intricate due to its reliance on an extremely great number of influencing factors. In the research that is presented in this paper dataset of 357 oil tankers was gathered and developed to research the idea in which genetic programming is applied to the mentioned dataset to obtain mathematical equations (MEs) that can estimate the ship's main engine power with high accuracy. The highest estimation accuracy of MEs is achieved by tuning the GP hyperparameter values through the random hyperparameter search (RHS) method. The initial dataset was divided into train and test datasets in a 70:30 ratio. The train dataset was used to train GP in a 5-fold cross-validation process and after the process was done the obtained MEs were evaluated on the test dataset. To evaluate the GP training testing process several evaluation metrics were used i.e., coefficients of determination (R2), mean absolute error (MAE), root mean square error (RMSE), and length of obtained MEs. The conducted investigation showed that GP generated MEs that can estimate ship main engine power with high accuracy.

KEY WORDS

Preliminary ship design; Genetic programming; Main engine power; Random hyperparameter search; 5-fold cross-validation

INTRODUCTION

In the initial design phase of ship design, it is necessary to select key values that define the general characteristics of the ship. These initial values can be specified as requirements by the client or determined by the naval architect. Main particulars, cargo capacity, service speed, and main engine power are among the values that form the foundation of the ship design process.

Upon defining the primary project inputs, the naval architect can roughly estimate the main engine power required to propel the ship and consequently determine the type of main engine needed. When establishing these initial values, which serve as the starting point for the entire design process, the designer must consider limiting factors such as port and channel specifications. The sizes of channels significantly constrain ship dimensions, as evident from the names of standard oil tanker categories such as Panamax and Suezmax, which are designed to navigate through specific channels. Therefore, initial ship design phase takes into consideration the mentioned requirements but also the limits of the environment in which the ship will be operating. It's evident that the entire design process relies heavily on accurately establishing initial values. Improved estimation of these values will likely result in fewer iterations later in the process, thereby shortening the design time. This correlation is evident in the widely adopted ship design spiral, where naval architects encounter fewer cycles. Ship design spiral was introduced by Evans (7) and is set up in a way in which as mentioned designer starts with rough design values and is through iterations arriving at final ship values and final design. There were many modifications made to the entire process

[1] Affiliation (Department of Naval Architecture and Offshore Engineering, Faculty of Mechanical Engineering and Naval Architecture, University of Zagreb, Zagreb, Croatia)

[2] Affiliation (Department of Automation and Electronics, Faculty of Engineering, University of Rijeka, Rijeka, Croatia);
* Corresponding Author: darin.majnaric@gmail.com

Submitted: 23 February 2024, Revised: 1 May 2024, Accepted: 3 May 2024, Published: 23 May 2024

Conference paper, DOI: https://doi.org/10.59490/imdc.2024.887 e-ISSN: 3050-486

with the goals of shortening it, reducing required effort, automating certain aspects, and enhancing the overall quality of the process. For example, the design spiral itself was modified by Andrews (1), later on, Watson developed two design spirals of which one was for warships and the other for merchant ships (18). Further Rawson and Tupper have introduced more steps in their design spiral with which main design parameters were separated into the components (15). To reduce the number of iterations in the design spiral and to ”prepare” the process, so that it can accommodate different types of vessels Papanikolaou (12) has presented a ship design procedure in the form of a straightened spiral. As presented there was constant effort to improve the process itself and through time new methods are being developed and proposed. Besides improvements on the process itself as already mentioned it was recognized that initial values have a significant impact on the rest of the design process and also the final results. Therefore efforts were also placed into the improvement of the initial values with which the design process is starting. Multiple approaches were developed and utilized to predict initial values. Most efforts were directed toward predicting the main particulars. Among the first to develop and apply statistical regression equations was Piko who used the nonlinear approximation method (14). Later on, Papanikolaou used the power regression model for initial values prediction as deadweight as an input (13). Linear 2nd-degree polynomial together with a power regression model was used by Kristensen to predict initial values which were in his research focused on container ships (8).

In recent years, new approaches for predicting initial ship values have been developed and used. Among them most significant is the utilization of artificial intelligence algorithms. Specifically, a lot of research has been conducted on the possible usability of artificial neural networks (ANN). For example, in his research, Clausen has (4) used Bayesian network and regression analysis at the same time as ANN for the estimation of ship main particulars. Ekinci (6) was predicting the main parameters of oil tankers as well by using ANN and the method that has shown as most successful was the Model Trees (M5P) method. When considering ship types most of the research was been conducted on container ships, Majnaric et al. (10) developed a database of 250 container ships which was analyzed with ANN to get high accurate estimation of initial ship values. Additionally, research was also conducted on the utilization of synthetic data to get to the amount of data that can be usable for ANN (9). The research focused on the estimation of ship length between perpendiculars was conducted by Cepowski et al. (2) and by using ANN they have produced two equations for preliminary design purposes. Part of the overall research focused on the implementation of artificial intelligence algorithms was also focused on the prediction of main engine power. In the research (3) authors have used a set of ANNs to update the design equations for the estimation of main engine power and fuel consumption on top of which it was proposed how to estimate CO2 emissions. Similar research was carried out by Ozsari (11) at which ANN was used to predict main engine power and pollutant emission. Develop model was presented and proposed for future studies on fuel consumption and energy efficiency.

From the previous literature overview, it can be noticed that the majority of used AI algorithms were ANNs. The main problem with ANNs is that they can’t be easily transformed into simple mathematical equations due to a large number of interconnected neurons. The other problem is that they require considerable computational resources for storing trained models (memory) and for processing new data samples (CPU power). So, in this paper, the idea is to apply genetic programming symbolic regressor (GPSR) to obtain symbolic expressions (SEs) that could estimate the ship’s main engine power with high estimation accuracy. The benefit of using GPSR is that the trained AI model does not require string after it was trained since it after each execution generates SEs i.e. mathematical equation that connects input variables with the target (output) variable). In order to determine the optimal combination of GPSR hyperparameter values for generating SE with high estimation accuracy, the random hyperparameter value search (RHVS) method was developed and applied. To create a robust system of SEs the GPSR will be trained using a 5-fold cross-validation method. A database of Oil tankers was developed so that genetic programming could be applied to obtain mathematical equations that can be used for accurate estimation of main engine power. However, the dataset created for this research had to be preprocessed (outliers removed, synthetically oversampled). Based on the detailed literature overview and the idea in this paper the following questions arise:

- Is it possible to obtain SEs using GPSR that could estimate main engine power with high estimation accuracy?
- Do data preprocessing techniques (outliers removal) and synthetic oversampling have any effect on the estimation accuracy of the trained GPSR model i.e. obtained SEs?
- Can the RHVS method be utilized to find the optimal combination of GPSR hyperparameters, leading to SEs with the highest estimation accuracy achieved by GPSR?
- Is it possible to obtain a robust system of SEs using a 5-fold Cross-Validation process for the estimation of electrical power output?

The outline of this paper consists of the following sections: materials and methods, results and discussion, and conclusion. In materials and methods, the dataset is described as well as the statistical analysis performed. Besides that, in the materials

and methods section, the GPSR is described as well as, the evaluation metrics used and the training-testing procedure. The results section contains the description of the best set of SEs obtained with the optimal combination of GPSR hyperparameter values, and evaluation metric values. The conclusion section contains the conclusions drawn from this research ed based on the results and discussion given in the previous section.

MATERIALS AND METHODS

This section of the paper will begin by detailing the initial creation of the database, emphasizing its quality assurance measures. Subsequently, an analysis of the database will be presented. Finally, dataset statistics will be provided and analyzed at the conclusion of this section.

Database

For this study, a dataset of 357 oil tankers was developed. Information for each ship was collected, including net tonnage (NT), service speed (v), and main engine power.

Additionally, to the mentioned data deadweight tonnage (DWT) and length overall (LOA) were collected as well but were not used in this study other than for the representation purposes of main data.

The decision was made to collect data directly from classification society databases, as the quality of results and analysis depends on the input data. Three maritime classification societies had open and maintained databases available to the public (Register; Veritas; DNV) and were used to collect the data. The databases of these classification societies exhibited some inconsistencies in data presentation, and at times, information was missing. Inconsistencies were observed in the form of misplaced commas in values, leading to physically impossible scenarios, as well as incorrect numbers resulting in significantly inflated or deflated values. For example, incorrect values, when located at the first digit of the ship's service speed, introduced significant oscillation from the usual speed expected for a ship of a certain length and main machine power. Therefore, all of these questionable values were identified, checked, and either corrected or obsoleted. For Genetic programming, it is preferable to have larger databases, so that training and validation sets can be of sufficient size, ensuring that the database size does not limit the analysis. Because of this, the intention was to gather as much data as possible. In cases where data was missing or incorrect, best efforts were made to fill in the gaps. Missing or incorrect values were addressed only if the information was available from shipowners' websites or by directly contacting shipping companies. The important quality check performed on the developed database aimed to identify sister ships and recurring vessels, which were subsequently removed to prevent any distortion of the final results. In order to keep the database relevant it was filled in only by the ships built from the year 2000 and onwards. Distribution of the ships through the years is visible at the figure 1.

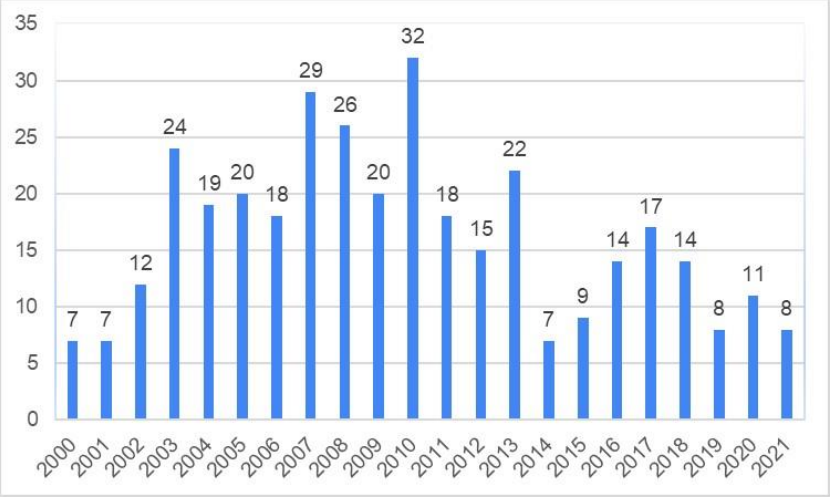

Figure 1. Distribution of ships in the database through the built years

The mentioned deadweight tonnage that was as already specified collected additionally, was used in this research only to

present the ship categorization. In 1 ship categorization is presented based on typically used ship categorization in the industry.

As expected, most of the collected ships belong to the smallest Panamax category, while there are only two records of ultralarge crude carriers (ULCCs). Although more ULCC records were initially present in the database, some were obsoleted. For example, in one instance, there were four sister ships, but only one record was retained. Including records of sister ships in the database would introduce clusters that could distort the dataset and compromise the reliability and realism of the analysis.

Table 1: Distribution of ships through classes

Sub-types	DWT range		Number of ships
Panamax	-	79,999	197
Aframax	80,000	119,999	68
Suezmax	120,000	199,999	47
Very large crude carrier (VLCC)	200,000	319,999	43
Ultra large crude carrier (ULCC)	320,000	-	2

Dataset statistics

The dataset consists of 357 samples and three variables i.e. net tonnage, service speed, and main engine power. The initial statistical analysis of the dataset i.e. the number of samples (count), mean, standard deviation (std), minimum (min), maximum (max), and GPSR variable representation is listed for each dataset variable in Table 2.

Table 2: Initial statistical analysis of the dataset

	Net Tonnage (NT)	Service	Engine Power (KW)
count	357		
mean	30213.52	14.03221	11890.5
std	32342.13	1.360539	8332.385
min	5.49	8	1118
max	112192	16.8	51913
GPSR Variable Represntation	X_0	X_1	y

From Table 2 it can be seen that all three dataset variables have the same number of samples (357) which means that there are no missing values in the dataset. The mean, std, min, and max values show that net tonnage and engine power have a larger value range than the service variable. This variation in the value range of the dataset variable would indicate that the scaling/normalization technique is required. However, the idea in this paper was to perform the investigation with the original range of dataset variable values. The GPSR variable representation shows how the dataset variables will be represented in the symbolic expressions obtained with this method. The input variables Net Tonnage (NT) and Service (input variables) will be represented in symbolic expressions as $X0$ and $X1$, respectively. The plots Engine Power versus Net Tonnage (NT) and Engine Power versus Service are shown in Figure 2.

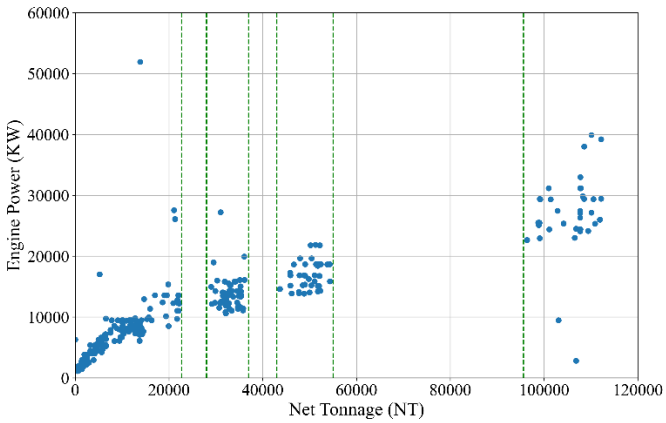

(a) Engine versus Net Tonnage (NT) plot (The green lines represent the gaps)

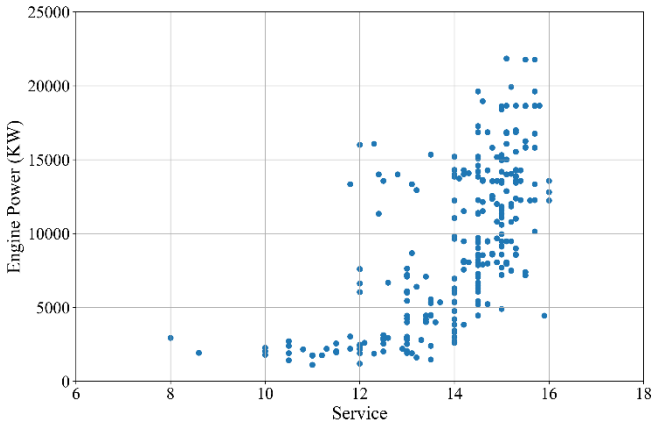

(b) Engine versus Service plot

Figure 2: Initial plots of dataset input variables versus the Engine power

From Figure 2 it can be noticed that data is scattered. However, some general trends can be noticed for lower values of net tonnage (NT) (0-60000). There are also gaps where no samples consist for example net tonnage (NT) first gap (22700 - 28000), second gap (37000 - 43000), and third gap (55000 - 95600). Besides the gaps in the general data trend, there are also a number of outliers i.e. samples that greatly deviate from the general data trend and should be somehow handled. Regarding the Engine power versus service plot, the general trend could be noticed for lower values of the engine power however the majority of data is scattered in 12 to 16 range Service values. The next step in dataset analysis is to perform Pearson's correlation analysis to determine the correlation between input and output variables. Pearson's correlation between two variables can be in the -1 to 1 range. The -1 value indicates perfect negative correlation between two variables and indicates that if the value of one variable increases the value of the other variable will decrease and vice versa. The value of 1 indicates a perfect positive correlation where an increase of one variable will increase the value of the other variable and vice versa. The worst possible correlation value is 0 between two variables which indicates that the increase/decrease in one variable value will not affect the other variable. The results of the Pearson's correlation analysis in the form of the heatmap are shown in Figure 3.

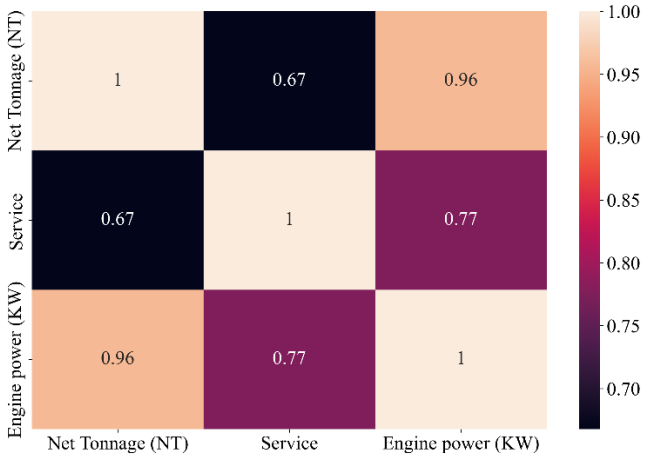

Figure 3: Results of Pearson's correlation analysis in the form of the heatmap

From Figure 3 it can be noticed that the Net Tonnage (NT) has a high positive correlation value (0.86) with the main engine power while the Service has a low positive correlation (0.29) value with the main engine power. Regarding the correlation between the net tonnage (NT) and the service speed variable, the correlation value is 0.18 which is the lowest correlation between the two variables in this dataset. This value indicates that the change in Net Tonnage (NT) will have a very small

effect on the Service variable, and vice versa. The value of 1 on the diagonal line in the heatmap indicates that the variable is correlated with itself. Outliers and boxplots play crucial roles in data analysis. Outliers, which are data points significantly different from others, can distort interpretations and analyses, making their identification important. Boxplots offer a concise visual representation of data distribution, displaying key summary statistics such as median, quartiles, and outliers. They facilitate a quick understanding of data spread, central tendency, and variability, aiding in comparison across different groups or categories within a dataset. Moreover, boxplots are robust to skewness and outliers, providing reliable insights even with non-normally distributed data. Their effectiveness in communicating findings makes them valuable tools for analysts to convey insights to stakeholders succinctly. Overall, outliers and boxplots are essential in detecting anomalies, summarizing distributions, comparing groups, and communicating data characteristics effectively. The results of outlier detection are presented in the form of the boxplot and shown in Figure 4.

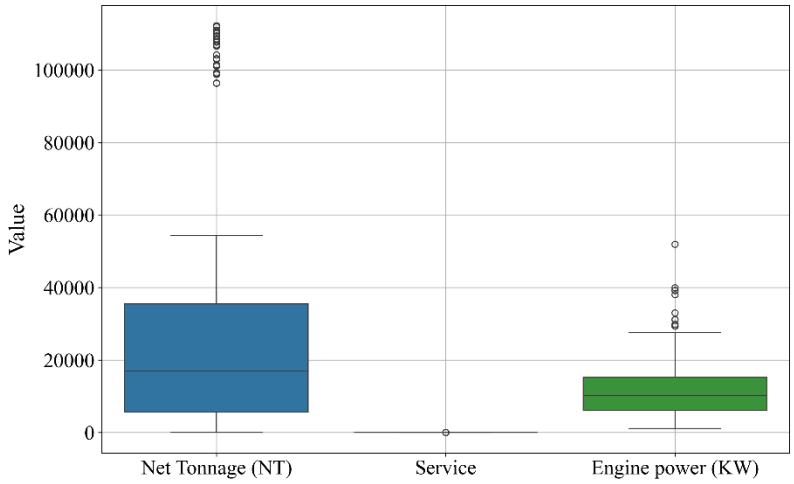

Figure 4: Distribution of dataset variables.

As observed in Figure 4, all dataset variables exhibit outliers to some extent. To enhance estimation accuracy with the GPSR, these outliers need to be addressed. The capping method known as median absolute deviation (MAD) was employed for outlier removal. MAD is a robust statistical measure of dispersion, offering reduced sensitivity to outliers compared to measures such as standard deviation. To apply the MAD method for capping outliers, the following steps were followed: Firstly, the median of the dataset was calculated to establish the central tendency. Next, the absolute deviations of each data point from the median were computed to capture the variability. Subsequently, the median of these absolute deviations (MAD) was determined. Finally, MAD was multiplied by a constant factor, typically 2 or 3 (in this case, 3), to establish the threshold for identifying outliers.

$$LT = \text{median} - (3 \cdot \text{MAD}), \quad (1)$$

$$UT = \text{median} + (3 \cdot \text{MAD}), \quad (2)$$

Here, LT and UT denote the lower and upper thresholds, respectively, beyond which any data points are regarded as outliers and may be either capped or removed. Any data points outside these thresholds can be considered outliers and in this paper, these outliers were removed. Generally, this is a very useful method when dealing with skewed or non-normally distributed data where traditional methods like standard deviation may not be appropriate due to sensitivity to outliers. With the application of this outlier removal method, the outliers were successfully removed from the dataset as seen from Figure 5.

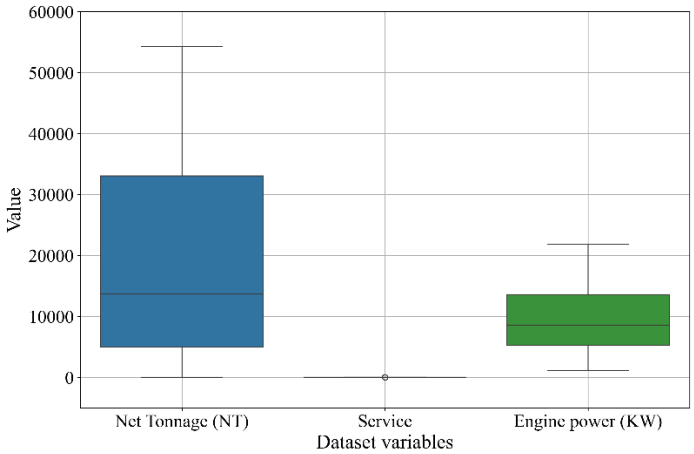

Figure 5: The distribution of dataset variables after application of MAD outlier capping method.

When Figure 4 and 5 are compared it can be noticed that the outliers (black dots) were removed from dataset variables (Net Tonnage (NT) and Engine Power (KW)), however, some small number of outliers remains in the Service dataset variable. With the application of the MAD capping the majority of outliers were successfully removed however the number of dataset samples was reduced from the original 357 to 307 samples. After the outliers were removed from the dataset using the MAD method the plots Engine versus Net Tonnage (NT) and Engine versus Service are shown in Figure 6.

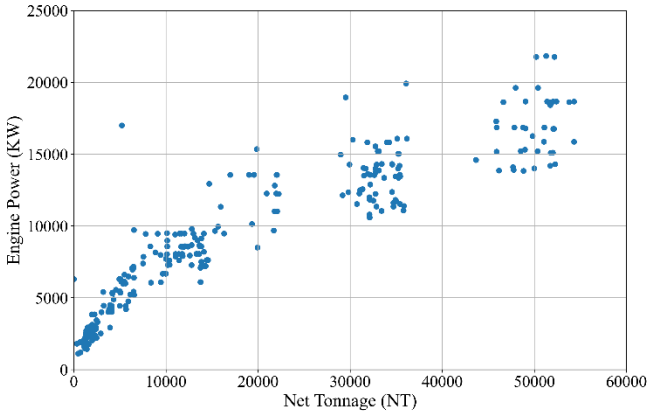

(a) Engine versus Net Tonnage (NT) plot after outliers were removed using MAD technique

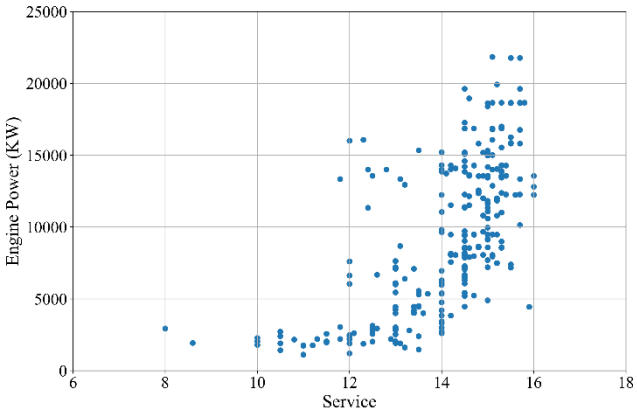

(b) Engine versus Service plot after outliers were removed using MAD technique

Figure 6: The Engine power versus net tonnage and service after outliers were removed using MAD technique

As seen form Figure 6 it can be noticed that the MAD technique has removed outliers from the dataset. This is especially valid when Figure 6a is compared to Figure 2a. Besides outliers that greatly deviate from the general data trend a large number of samples where removed in which Net Tonnage (NT) exceeded 90000. This is due to the large gap in data since the majority of samples in terms of Net Tonnage (NT) are concentrated in the 0 to 60000 range.
The other problem with the obtained dataset is the small number of samples and the idea is to see if somehow the number

of samples could be synthetically generated. In this paper the averaging method is considered that consists of the following steps:

1. sort the dataset samples from minimum to maximum value of the target variable (main engine power),
2. for dataset samples in range from 1 to the maximum number of dataset samples:
    - create an average dataset sample between the current sample and the sample + 1, sample +2, sample +3, sample +4, sample +5, sample + 6, and sample +7 for all dataset variables,

3. concatenate the original dataset with newly created samples,
4. repeated the process an arbitrary number of times.

In this paper, the process of creating the average values was repeated 3 times. By doing so the number of samples was enlarged from 307 up to 76460.

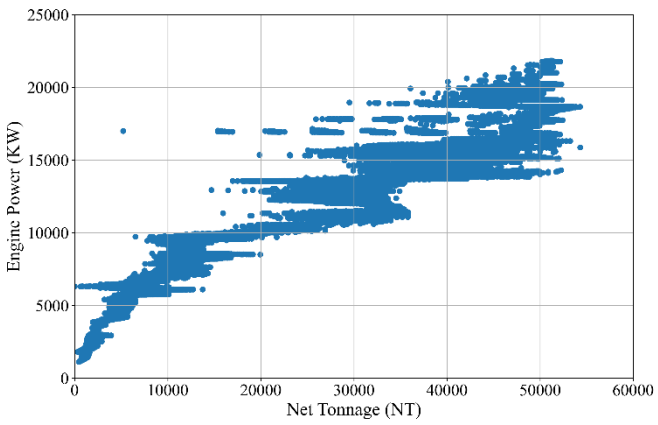

(a) Engine versus Net Tonnage (NT) plot after average oversampling was performed 3 times

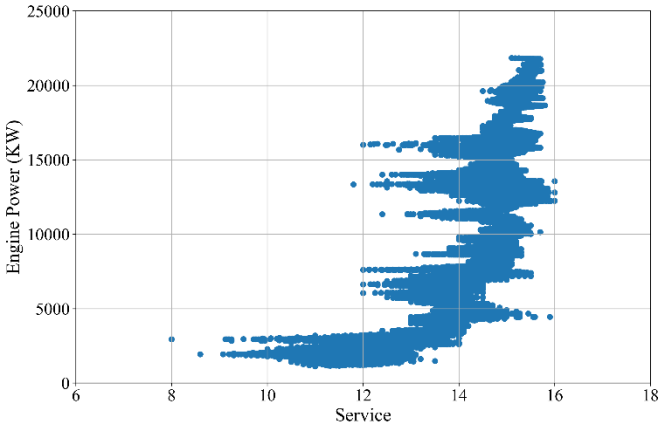

(b) Engine versus Service plot after average oversampling was performed 3 times

Figure 7: The Engine power versus net tonnage and service after average oversampling was performed

As seen from Figure 7 visually the number of samples was greatly increased. The advantage of the average oversampling is that the gaps (in the case of Net Tonnage) are filled but the problem is the small number of outliers generated (samples that deviate from the general data trend). The correlation plot of the final synthetically oversampled dataset is shown in Figure 8.

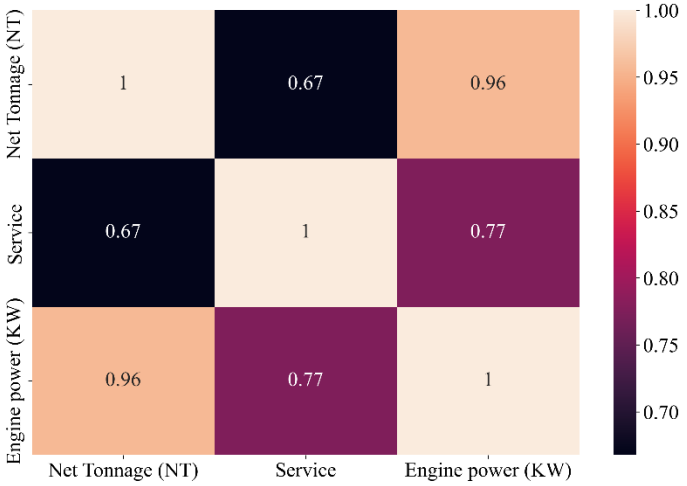

Figure 8: The correlation heatmap of the synthetically enlarged dataset.

When Figures 3 and 8 are compared it can be noticed that with the application of outlier removal and the synthetic oversampling, the correlation between Net Tonnage (NT) and the main engine Power was increased from 0.86 to 0.96, between Service and main engine power (KW) the correlation was increased from 0.29 to 0.77. It can be also noticed that the correlation between Net Tonnage and Service speed was increased from 0.18 to 0.67. This final version of the dataset obtained using outlier removal and synthetic oversampling will be used in genetic programming symbolic regressor to obtain symbolic expressions for estimation of main engine power.

Genetic programming symbolic regressor

The genetic programming symbolic regressor begins its execution by randomly creating the population of naïve symbolic expression by random selection of input variables, constant values, and mathematical functions to estimate the target value. The estimation accuracy of the initial population is generally very low. However, with the application of genetic operations such as crossover and mutation through a consecutive number of generations in the end the symbolic expression is obtained that estimates the target variable with certain accuracy. Since the GPSR has a large number of hyperparameters the random hyperparameter values search method was developed and applied to find the optimal combination of hyperparameter values using GPSR will produce the SE with high estimation accuracy. The process of developing the RHVS includes the following steps:

1. Definition of the initial value range for each GPSR hyperparameter value,
2. Testing the lower and upper boundaries of each GPSR hyperparameter to see if the GPSR can successfully be executed i.e. produce the SE,
3. If the GPSR fails in its execution due to a specific hyperparameter boundary value adjust the hyperparameter value
range.

In the RHVS method, the optimal values of the following hyperparameters were searched:

- Population size – the size of the population (SEs) that will be evolved during its execution
- Number of generations – The maximum number of generations for which GPSR will executed. This is also one of the termination criteria which means that GPSR will terminate the execution after the predefined number of generations is reached.
- Tournament size – the tournament size is the size of a randomly selected population in each generation that will compete to become the parents of the next generation. In every tournament selection, there is only one winner and on this winner, genetic operations such as crossover or mutation are performed.
- Initial depth size – inside the GPSR the population members are represented as tree structures which means that the size of the population member is presented in terms of depth measured from the root node up to the deepest leaf in the tree structure. It should be noted that the initial depth size is defined as a value hyperparameter indicating the range of the population member's depth size. For example (3,12) indicates that the initially created population the depth of population members will be in 3 to 12 depth.
- Crossover probability value – probability value of crossover operation performed in each generation. The crossover is performed using two tournament selection winners. On both tournament selection winners, the random sub-tree is selected and the sub-tree from the second tournament winner replaces the sub-tree of the first winner to create offspring for the next generation.
- Subtree mutation probability value – the probability value of the subtree mutation. This operation and other mutations used in this research require only one tournament selection winner on which the random sub-tree is selected and replaced with a randomly created sub-tree by randomly picking constant values (from a predefined range), input variables, and mathematical functions.
- Point mutation probability value – is the probability value of the point mutation genetic operation. In point mutation, the nodes are randomly selected on the tournament winner and replaced. In other words, the randomly selected constant value node is replaced with a constant value, the input variable with other input variables, and mathematical functions with randomly picked mathematical functions. However, when mathematical functions are replaced with other randomly selected mathematical functions the number of arguments in the original mathematical function must be the same in the mathematical function that will replace the original one.
- Hoist mutation probability value – In hoist mutation, the random subtree is selected on the tournament winner, and on that tree a random node is selected. Then the randomly selected node is "hoisted" i.e. it replaces the entire randomly selected subtree.
- Range of constant values – the range of constant values that will be used in GPSR to develop the initial population, to perform the different mutation operations.
- Stopping criteria – is the predefined minimum value of the fitness function. In the case of GPSR, the fitness function is the Mean Absolute error defined with the equation:

$$MAE = \frac{\sum_i^n (y_{ti} - y_{pi})}{n}, \tag{3}$$

Where y_{ti}, $y_{pi,}$ and n are the true target value, predicted target value and the number of dataset samples. So, in the case of stopping criteria if the fitness function value of only one population member falls below the predefined stopping criteria value the GPSR execution will terminate and the GPSR will give as the output the best SE. In other words, the stopping criteria are the second GPSR termination criteria, alongside the number of generations.

- Max Samples – the fraction of the samples that will be drawn from the training dataset and used to evaluate each SE. The max samples are a useful tool to see how the SE performs on the unseen data during the execution. The output value in this case will be out of bag or raw fitness value. For example, if you use a training dataset you can specify a very small portion of that dataset that will not be used during training i.e. it will be unseen by SEs during training, and in each generation, the majority of the training dataset will be used to calculate the fitness value while this small portion will be used to calculate the raw fitness value. Generally, the raw fitness value should be close to the real fitness value in order to at the end obtain SE with high estimation accuracy.
- Parsimony coefficient – is the coefficient used in the parsimony pressure method to stop the bloat phenomenon. This phenomenon occurs when the size of the population members rapidly grows from generation to generation without any indication of lowering the fitness value. In extreme cases, this bloat phenomenon can cause the GPSR to quickly terminate due to memory overflow or it can execute after a long time with an extremely large size (1000 or more elements in SE). The coefficient is the most sensitive one which means that small values can lead to extremely large population members (SEs) while large values can lead to small SEs with low estimation performance.

It should be noted that the sum of all genetic operations (probabilities) must be equal to 1 or slightly lower than 1 for example 0.99. If the value is smaller than 1 then some tournament selection winners enter the next generation unchanged i.e. the genetic operations were not applied to some tournament selection winners. In all GPSR investigations, the following mathematical functions were used addition, subtraction, multiplication, division, square root, absolute value, sine, cosine, tangent, natural logarithm, and logarithm with bases 2 and 10. However, division, square root, natural logarithm, and logarithm with bases 2 and 10 had to be modified to avoid imaginary or not number values which could lead to failed GPSR executions.

The division function was modified in the following way:

$$y_{\text{DIV}}(x_1, x_2) = \begin{cases} \frac{x_1}{x_2} & \text{if } |x_2| > 0.001 \\ 1 & \text{if } |x_2| \leq 0.001 \end{cases} \tag{4}$$

The square root function was modified in the following way:

$$y_{SQRT} = \sqrt{|x|} \tag{5}$$

The natural logarithm and logarithm with bases 2 and 10 are modified in the following way:

$$y_{LOG}(x) = \begin{cases} \log_i(|x|) & |x| > 0.001 \\ 0 & |x| < 0.001 \end{cases} \tag{6}$$

Where *i* represents the base of the logarithm (e, 2, and 10). It should be noted that x_1, x_2, and x in previous equations do not have any connection with the input variables used in this research. They are only used here to describe the modifications made to the aforementioned mathematical functions.

Table 1: The RHVS ranges for previously described hyperparameters are listed

Hyperparameter	Range
Population size	1000-2000
Number of generations	25 - 50
Tournament size	100-500
Initial depth size	3-18
Crossover	0.001-1
Subtree mutation	0.001-1
Point mutation	0.001-1
Hoist mutation	0.001-1
Range of constant values	-10000 - 10000
Stopping criteria	$1 \times 10^{-9} - 1 \times 10^{-3}$
Max samples	0.99-1
Parsimony coefficient	1×10^{-6} - 1×10^{-1}

Evaluation metrics

The evaluation metrics used in this research were coefficient of determination (R^2), mean absolute error (MAE), and Root mean square error (RMSE). The R^2 can be defined as:

$$R^2 = 1 - \frac{\sum_i (y_i - f_i)^2}{\sum_i (y_i - \overline{y}_i)^2}, \tag{7}$$

Where y_i is the real value (target variable), f_i is the predicted value and the y_i is the mean value of the real data. The MAE was previously defined in the description of GPSR as it was used as a fitness function for the evaluation of population members. RMSE stands for Root Mean Square Error. It is a commonly used metric to evaluate the performance of a regression model. RMSE measures the average magnitude of the errors between predicted values and actual values. Mathematically, RMSE is calculated as follows:

$$RMSE = \sqrt{\frac{1}{n}\sum_{i}^{n}(y_i - f_i)^2} \tag{8}$$

Where n is a total number of samples.

Training-Testing Procedure

The training-testing procedure is graphically shown in Figure 9.

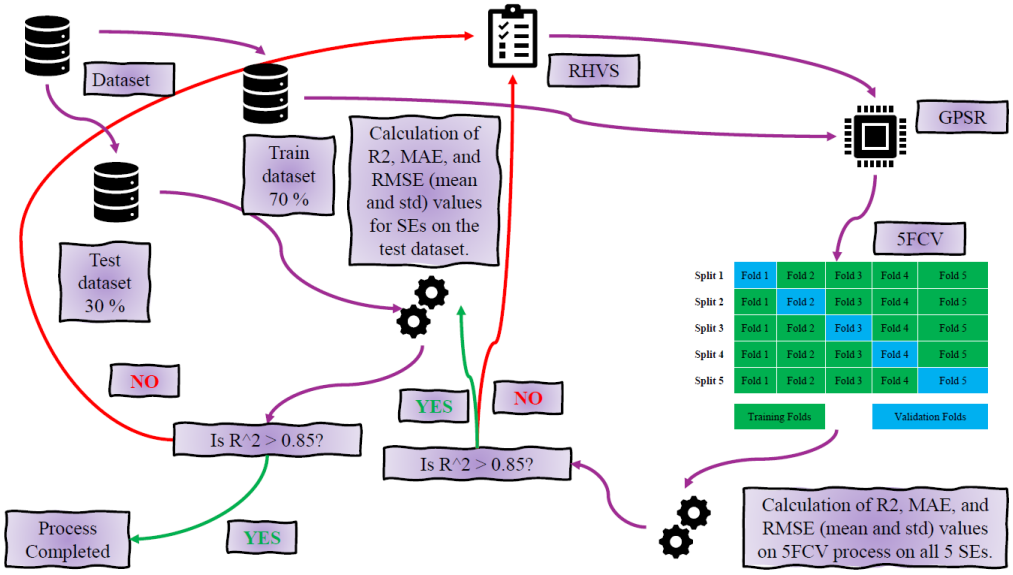

Figure 9: The scheme of training GPSR using the 5FCV process and RHVS method for GPSR random hyperparameter selection.

The training-testing procedure shown in Figure 9 consists of the following steps:

1. The dataset obtained after preprocessing (elimination of outliers and oversampling) is divided on training and testing
   datasets in 70:30 ratio. The training dataset will be used in GPSC and will be trained using 5FCV while the test dataset will be used from the evaluation of SEs obtained with GPSC.
2. The random selection of GPSC hyperparameter values using the RHVS method and training of GPSC using 5FCV. It
   should be noted that after each split in 5FCV (5 splits in total) the SE is obtained so this means that after 5FCV a total of 5 SEs will be obtained using GPSC.
3. After training was done evaluate the obtained SEs using R2, MAE, and RMSE evaluation metric methods. Since after 5FCV, the GPSC generated 5 SEs the evaluation metric values have to be obtained for each SEs on train and validation sets. The mean and std values of the aforementioned metric methods are obtained and if the mean value of R2 is higher than 0.85 the process continues to the testing phase. However, if the R2 is lower than 0.85 the process continues from the beginning i.e. by selecting the random GPSC hyperparameter values using the RHVS method.
4. In the testing phase the test dataset (30% of the initial) dataset is provided to the 5 SEs and the output is generated. This output is compared to the original output and the R2, MAE, and RMSE mean and std values are obtained. Finally, if the mean R2 value is higher than 0.85 the process is completed. Otherwise, the process starts from the beginning i.e. from the RHVS method.

RESULTS AND DISCUSSION

The best set of SEs obtained in this research was achieved using the following combination of hyperparameters listed in Table 4.

Table 4: Optimal combination of GPSR hyperparameter values

	Population size	Number of generations	Tournament size,	Initial depth size	Crossover	Subtree mutation
Case 1	1126	25	350	(6, 11)	0.0035	0.9667
	Point mutation	Hoist mutation	Range of Constant Values	Stopping Criteria	Max Samples	Parsimony Coefficient
Case 1	0.019	0.0102	(-8861.28, 1162.32)	6.91×10^{-7}	0.995	0.0098

As seen from Table 4 the best set of SEs was obtained with GPSR in which the population consisted of 1126 population members that were evolved for 25 generations. These two hyperparameters are near the lower boundary used in the RHVS method (Table 3). The dominating genetic operation was subtree mutation (0.9667) while other genetic operations had values in the 0.0035 to 0.019 range. The stopping criteria value was defined so low any population member never reached it during the execution of GPSR which means that the dominating termination criteria in all these investigations was the number of generations. The parsimony coefficient was near the upper boundary (Table 3) which prevented the occurrence of bloat phenomenon and generated smaller SEs. The example of SE is shown in Eq.(9).

$$
\begin{aligned}
y \;=\; & 67.06\sqrt{|X_0|}\Big(\tan(\log(\max(\min(-3953.5, 1.443\log(0.43|\log(X_0)|)),\\
& \min(0.93\log(X_1), 1.2\sqrt{\log(\frac{X_0}{X_1}+\sqrt{X_0})} - \sin(\log(\min(|X_1|,\\
& 1.4\log(\min(-7556.63, X_0)))))))))\Big)^{\frac{1}{2}} - \sqrt{|\log(0.00031\log(X_0))(X_0+\sqrt[9]{X_0}-7073.28)|} + 10.31
\end{aligned}
\tag{9}
$$

As seen the Eq.(9) is not so large however it requires both input variables. It should be noted that using the 5FCV training process the GPSR generated five different SEs to estimate the target variable. The evaluation metric values (R2, MAE, and RMSE) were obtained on both training and testing datasets. The mean and standard deviation values are shown in Figure 10.

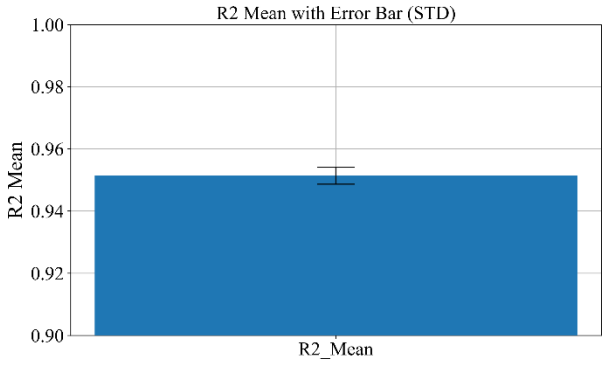

(a) Mean R^2 value with standard deviation obtained with GPSR generated SEs on the synthetically oversampled dataset.

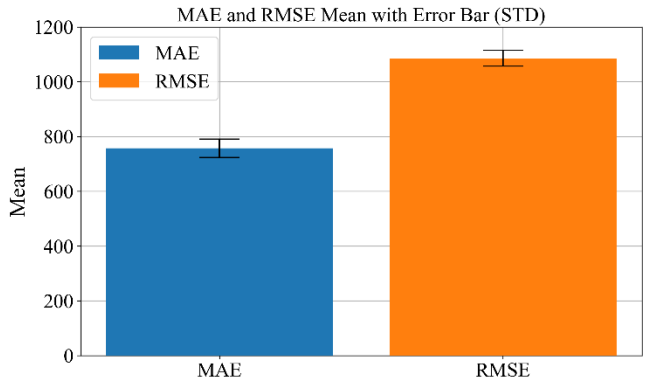

(b) Mean *MAE* and *RMSE* values with standard deviation obtained with GPSR generated SEs on the synthetically oversampled dataset.

Figure 10: Evaluation metric values of SEs obtained with GPSR trained on the synthetically oversampled dataset.

As seen from Figure 10 the mean value of R^2 is pretty high with a small standard deviation value. The *MAE* and *RMSE* values are low when these values are compared with the range of the target variable (Table 5). After the 5 SEs obtained on the synthetically oversampled dataset are evaluated on the initial dataset (307 samples) i.e. the dataset obtained after outlier removal using MAD capping the following evaluation metric values are obtained and listed in Table 5.

Table 5: Summary of Data

Metric	Value
R^2 Mean	0.883
R^2 STD	0.0113
MAE	1205.92
$\sigma(MAE)$	105.094
RMSE	1736.75
$\sigma(RMSE)$	83.67

The results from Table 5 have shown that the obtained SEs using GPSR on the synthetically oversampled dataset have slightly lower estimation accuracy when applied on the initial dataset (outliers removed). This is because the obtained SEs follow the general trend of the data however there are some samples that deviate from the general trend. The graphical representation of the Engine versus Net Tonnage (NT) and Engine versus Service is shown in Figure 11.

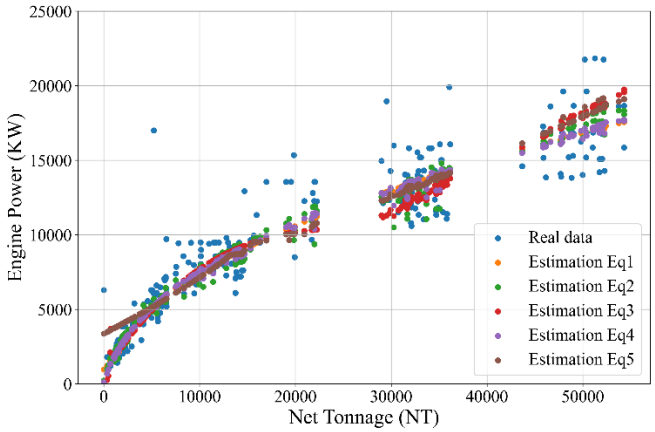

(a) Engine versus Net Tonnage (NT) comparison of real data and estimation made by all five best equations obtained with GPSR.

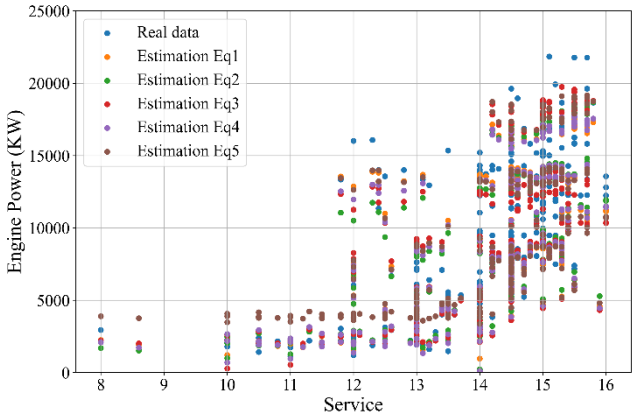

(b) Engine versus Service comparison of real data and estimation made by all five best equations obtained with GPSR.

Figure 11: Comparison of estimation made by five best equations obtained with GPSR and the real data (dataset with removed outliers).

As seen from Figure 11 the best SEs captured the trend in the data. This can be seen from Figure 11a where Engine Power (KW) versus Net Tonnage (NT) is shown.

CONCLUSIONS

As presented in this paper, a dataset was developed that consisted of 357 oil tankers for which data was collected as net tonnage (NT), service speed (v), and main engine power. The original dataset variables contained several outliers which had to be removed since they greatly influenced the estimation accuracy of the trained AI model. After the removal of the majority of outlier dataset samples the dataset was synthetically oversampled by the introduction of averaging samples. This modified dataset was used in GPSR with the RHVS method that was trained using 5FCV. After the application of this procedure, the 5SEs were obtained. The best set of SEs achieved great estimation accuracy of main engine power on synthetically oversampled datasets and the initial dataset without outliers. Based on the conducted investigation the following conclusions can be drawn:

- The SEs with high estimation accuracy of main engine power can be obtained using GPSR however the accuracy is dependent on two factors i.e. dataset quality, a combination of hyperparameters.
- Dataset preprocessing methods (outliers removal) and synthetic oversampling greatly contributed to the GPSR-generated SEs since the GPSR produced the SEs with high estimation performance.
- The RHVS method proved to be useful in finding the optimal combination of GPSR hyperparameters using which the SEs obtained with GPSR have achieved high estimation performance
- The 5FCV proved to be a useful method for training the GPSR since using this approach a robust set of 5 SEs was obtained.
- Approach can be used in the preliminary phase of ship design to generate a value of main engine power.
- Based on the results initial main engine power value will be an accurate estimation and therefore close to the value that will be reached at the end of the design. With that fewer iterations will be needed during the design development process.

  The equations developed through this approach have the potential to be utilized during the initial design phase of ship development. The practicality of this approach lies in its speed and accuracy, making it a valuable complement to existing methods for estimating initial engine main power. Furthermore, based on this research equations produced by this method can eventually even be used as a sole source of initial values.

The proposed approach in this paper has its pros and cons. The pros are:

- The outlier removal and synthetic oversampling are great approaches in dataset preparation which will be used for train of AI algorithm,
- The GPSR in combination with RHVS and 5FCV is a great method to obtain a robust set of SEs with high classification Performance.

The cons of the proposed research are:

- Removing outliers removes the number of original dataset samples, and in general, the trained AI model on the dataset without outliers cannot predict the outliers. The other problem with outliers removal using this approach is that the majority of outliers i.e. values of Net Tonnage (NT) higher than 50000 were removed from the original dataset. So this approach could be used for Net Tonnage in the 0 to 55000 range.
- The GPSR with RHVS and 5FCV can take some time to obtain a robust set of 5SEs with high estimation performance because the optimal combination of GPSR hyperparameters cannot be found instantly and each combination of GPSR hyperparameter values had to be tested in GPSR which is trained using 5FCV. This means that GPSR will be trained 5 times on different splits of the training sets i.e. generating 5 SEs in the process.
- This approach may not be suitable for designing oil tankers that deviate from typical designs.

Based on the pros and cons of the proposed research methodology future work will be focused on exploring alternative artificial intelligence algorithms (Neural networks) to see if better estimation accuracy of engine power could be obtained.
Besides the alternative artificial intelligence algorithms in the future work different input variables will be considered since the correlation between Net Tonnage (NT) and the Service with the Engine Power (KW) is initially too low.

DATA ACCESS STATEMENT

The dataset used in this study is available on request.

DECLARATION OF GENERATIVE AI AND AI-ASSISTED TECHNOLOGIES IN WRTITING

Not applicable.

CONTRIBUTION STATEMENT

Author 1: Conceptualization; Investigation; Data curation; Writing original.
Author 2: Conceptualization; methodology; Software; Validation; Formal analysis; Writing original draft; visualization.
Author 3: Conceptualization; methodology; writing – original draft.
Author 4: Supervision; writing - review and editing; project administration; funding acquisition.

ACKNOWLEDGEMENTS

This research has been (partly) supported by the CEEPUS network CIII-HR-0108, the Erasmus+ project WICT, under the grant 2021-1-HR01-KA220-HED-000031177; the University of Rijeka, under scientific grants uniri-tehnic-18-275-1447 and uniri-mladi-technic-22-61.

REFERENCES

[1] Andrews, D. (1986). An integrated approach to ship synthesis. *Trans. RINA*, 128:73–102.

[2] Cepowski, T. and Chorab, P. (2021a). Determination of design formulas for container ships at the preliminary design stage using artificial neural network and multiple nonlinear regression. *Ocean Engineering*, 238:109727.

[3] Cepowski, T. and Chorab, P. (2021b). The use of artificial neural networks to determine the engine power and fuel consumption of modern bulk carriers, tankers and container ships. *Energies*, 14(16):4827.

[4] Clausen, H. B., Lutzen, M., Friis-Hansen, A., and Bjørneboe, N. (2001). Bayesian and neural networks for preliminary ship design. *Marine technology and SNAME news*, 38(04):268–277.

[DNV] DNV. Dnv gl vessel register. https://vesselregister.dnvgl.com/vesselregister/vesselregister. html. Accessed: 14.2.2023.

[6] Ekinci, S., Çelebi, U. B., Bal, M., Amasyali, M. F., and Boyaci, U. K. (2011). Predictions of oil/chemical tanker main design parameters using computational intelligence techniques. *Applied Soft Computing*, 11(2):2356–2366.

[7] Evans, J. H. (1959). Basic design concepts. *Journal of the American Society for Naval Engineers*, 71(4):671–678.

[8] Kristensen, H. O. (2013). Statistical analysis and determination of regression formulas for main dimensions of container ships based on ihs fairplay data. *University of Southern Denmark: Odense, Denmark*.

[9] Majnarić, D., Baressi Šegota, S., Anđelić, N., and Andrić, J. (2024). Improvement of machine learning-based modelling of container ship's main particulars with synthetic data. *Journal ofMarine Science and Engineering*, 12(2):273.

[10] Majnarić, D., Šegota, S. B., Lorencin, I., and Car, Z. (2022). Prediction of main particulars of container ships using artificial intelligence algorithms. *Ocean Engineering*, 265:112571.

[11] Ozsari, I. (2023). Predicting main engine power and emissions for container, cargo, and tanker ships with artificial neural network analysis. *Brodogradnja: Teorija i praksa brodogradnje i pomorske tehnike*, 74(2):77–94.

[12] Papanikolaou, A. (2009). Andersen p, kristensen ho, levander k, riska k, singer d, vassalos d. state of the art design for x. In *Proc. 10th Int. Marine Design Conference-IMDC09, Trondheim*.

[13] Papanikolaou, A. (2014). *Ship design: methodologies ofpreliminary design*. Springer.

[14] Piko, G. (1980). *Regression analysis ofship characteristics*. Australian Government Publishing Service.

[15] Rawson, K. J. and Tupper, E. C. (2001). *Basic Ship Theory: Hydrostatics and Strength*, volume 1. Butterworth-Heinemann.

[Register] Register, L. Lloyd's ships in class. https://www.lr.org/en/about-us/who-we-are/ lr-ships-in-class/. Accessed: 14.2.2023.

[Veritas] Veritas, B. Bv fleet. https://marine-offshore.bureauveritas.com/bv-fleet/#/bv-fleet/. Accessed: 14.2.2023.

[18] Watson, D. G. (1998). *Practical ship design*, volume 1. Elsevier.

Proceedings of 15th International Marine Design Conference (IMDC-2024)
June 2-6, 2024
Amsterdam, the Netherlands

MariData – Digital Twin for Optimal Vessel Operations Impacting Ship Design

Jochen Marzi[1,*], Stefan Harries[2], Benjamin Schwarz[3], Martin Scharf[4], Katharina Demmich[5], Martin Pontius[5]

ABSTRACT

Energy efficiency is a key element for reduced shipping emission to meet future environmental regulations. Both design and operation play an important role to meet this goal and the perfection of the interplay between these aspects promises quick improvements to meet the requirements of short term emission standards. The MariData project [https://maridata.org] developed a forward-looking energy management and decision support system (DSS) for ship operation based on rational methods and data created during ship design and sets out to bridge the gap between design and optimized operation. The "digital performance twin" of a vessel, which is based on design data, is enhanced with lifecycle data covering the entire operational envelope and provides valuable feedback into design processes.

KEY WORDS

Simulation; Operational profile; Digital twin; Weather routing; Navigational support; Design Feedback.

INTRODUCTION

Shipping emissions are increasingly in the focus of public interest and political as well as regulatory attempts are being made to reduce such GHG emissions. While the majority of the maritime industry appears to concentrate on new generations of e-fuels to meet future emission standards, the question of sufficient availability and price is still uncertain. On the other hand, perfections of design and operational performance promise significant improvements of the energy efficiency of individual vessels and thus the whole of maritime operations, likely to meet emerging requirements for the 2030 emission goals. Departing from a vast experience of design improvements, the MariData project and its team members set out to develop a forward-looking energy management and decision support system (DSS) for ship operation based on rational methods and data created during ship design. In a first step, a digital twin of the vessel and its performance related properties is created, which can be derived from design data. Here, technologies from the EU HOLISHIP project (Papanikolaou, et al., 2022), (Papanikolaou, 2018) are applied to generate extensive surrogate models which cover the entire operational envelope including also degradation of the hull surface condition due to fouling which leads to increased resistance over time. This "digital design twin" is a fundamental prerequisite to determine optimal energy consumption during all phases of operation. In a second step a model of the engine / machinery system on board is created which provides another facet of the digital twin. In combination, these models allow to determine the total energy consumption on board for a large variety of operational conditions experienced during the lifetime of a vessel and form the basis for a continuous comparison of the target performance of the ship with actual data provided by comprehensive on-board data collection. Combining this energy model with advanced route planning is done on the basis

[1] The Hamburg Ship Model Basin (HSVA), Hamburg, Germany
[2] FRIENDSHIP SYSTEMS AG (Strategy and R&D), Potsdam, Germany
[3] Institute of Multimedia and Interactive Systems, University of Lübeck, Lübeck, Germany; ORCID: 0000-0003-3998-5161
[4] Institute for Fluid Dynamics and Ship Theory, TU Hamburg, Hamburg, Germany; ORCID:0000-0003-1755-2349
[5] 52°North Spatial Information Research GmbH, Münster, Germany; ORCIDs: 0009-0006-1626-9647, 0000-0002-2279-2593
* Corresponding Author: marzi@hsva.de

Submitted: 22 February 2024, Revised: 17 April 2024, Accepted: 1 May 2024, Published: 21 May 2024

Conference paper, DOI: https://doi.org/10.59490/imdc.2024.875 e-ISSN: 3050-4864

of a combination of different geographic information and satellite weather data as well as weather forecasts. While ship safety is a key prerequisite, the information how the vessel will behave under projected environmental forecast data allows optimizing voyage planning using a variety of different target functions including minimal voyage time and / or fuel consumption or emissions. On the operational end, MariData presents planning and actual information to the ship crew through a dedicated advanced user interface, which allows for a permanent target performance comparison and decision support for corrective measures. By using advanced design data, MariData bridges the gap between modern design systems and operation. In one direction, the wealth of information created during design will be applied for optimized operation whilst in the other direction, statistical information obtained during – practical – operation will influence future designs.

DIGITAL TWIN FOR OPTIMAL VESSEL OPERATIONS

R&D Project MariData

The German national R&D project MariData (Comprehensive technologies for ship energy management) started in 2019 to explore the efficient use of energy during shipping operations. Energy efficiency has always been a key concern for both, shipbuilding and shipping. Whereas in the past it was mainly economic reasons that motivated the search for a low power requirement for a ship, nowadays ecological reasons and compliance with statutory regulations to reduce emissions are coming strongly to the forefront with at least equal weight. These concerns call for a consistent strategy of energy efficiency as well as a significant reduction of exhaust emissions not only in the construction but also substantially in the operation of ships.

The energy consumption of merchant ships is largely determined by their hydrodynamic characteristics and the systems onboard. In some cases, up to 90% of primary energy consumption is used for propulsion and must, therefore, be optimally managed. MariData's goal is to develop, improve and classify simulation-based modules for ship energy management based on information created during the design phase of a vessel.

Together with geospatial information and a DSS that brings together technical, environmental and economic data, energy consumption information is integrated into a platform that can be used both onboard the ship and shore-based by a shipping company. The platform provides on-line simulations for decision support to the ship's management, as well as assistance with short-, medium- and long-term forecasts and decisions related to ship operations.

A key element of the project's development is the energy model in form of a Digital Twin. Today, Digital Twins play an increasingly important role in the maritime industry: during design, production and operation of ships and other assets, they offer a large potential to improve the "product" in terms of (i) better understand the performance of the asset, (ii) study possible ways of improving it and (iii) predict and optimize operational behavior (e.g. with regard to scheduling maintenance, avoiding failure and improving energy efficiency). The concept applied in MariData is founded on a sophisticated and accurate simulation based energy which is in turn largely based on design data. This is accomplished with on-board measurements and allows to provide instant feed back for the operational optimisation. Although we consider the crew as part of the system, i.e. there will be no automatic manipulation of operational parameters, this concept can be regarded as a Digital Twin, though possibly not in the strict definition of the term. Rather than acquiring only measured operational data, often affected by sensor errors, the model is made up from large sets of simulations, e.g. for the energy requirements due to resistance and propulsion under various conditions of operation. This allows, together with reliable forecasts of environmental conditions, to plan and optimize voyages with increased reliability. The knowledge of all relevant parameters, wind, waves, currents etc. and the respective behavior of the vessel increases the accuracy of predictions and forecasts for the energy consumption during passages which in turn will yield a much higher accuracy in predicted and achieved fuel consumption for a planned voyage. This is a fundamental prerequisite for actual voyage optimization and makes fuel / energy savings accessible. The design contribution in this respect is that actual operational conditions are gathered and allow to produce more precise design briefs for similar or likewise ships in the future. The present system allows to feed experience gained from operation into detailed specifications for a new design brief which will be much improved by more precise weighting of different (operational) conditions and hence allow for a more specified design optimization, e.g. focusing more on the role of efficient behavior in waves, wind or other conditions which are typically considered to be "off design" at present.

Carl Büttner Tanker

Within the MariData project the main application is a tanker of 183 m length overall, 32 m maximum beam, 16 m depth, a design draft of 9.50 m (scantling draft of 10.5 m) and a cargo capacity of about 45 000 m3 (see Figure 1) is studied with regard to its energy consumption. The ship is an oil-chemical tanker, the CB Adriatic (called CBT for brevity), was built in 2019 after having been jointly optimized for an anticipated operational profile, i.e., for multiple speeds and drafts. The hull features an asymmetric stern, the propulsion system a tip rake propeller and the rudder a Costa bulb. Results from model tests showed a performance in the top of its class.

Figure 1: CB Adriatic (oil-chemical tanker, IMO 9851696), operated by Carl Büttner Shipmanagement

The project sets up a digital twin in order to compare consumptions as computed by means of simulations and as measured onboard and to suggest how to further improve energy efficiency. To this end, the ship's hydrodynamic performance needed to be simulated for many different operational scenarios, e.g. in calm water, in sea states representative of its operational profile, in both deep and shallow water, when maneuvering and when under the influence of heavy winds and current. As can be readily appreciated, this calls for suitable geometric representations of the ship hull, the propulsion system, appendages and the superstructure. Besides the tanker, also two heavy lift carriers have been equipped and investigated.

Data Acquisition

One cornerstone of our investigation was the acquisition of sensor-driven ship data alongside navigational data. To do this, custom-tailored hardware has been deployed on 6 ships of two fleets, representing a range of carrier vessel usages (tankers and heavy lift / project cargo vessels). The minimum specifications included access to navigational and performance-related data, such as Speed Over Ground (SOG) and Fuel Oil Consumption (FOC). To streamline data management and accessibility, a common interface has been established using the Navis Bluetracker Suite (Kaleris, 2024). This well-established platform, combining sensor and reporting data, serves as the backbone for data integration and pre-processing. In addition to this, a proprietary high-frequency data interface has been implemented to address the additional demands of model validation and onboard route monitoring. This interface supports archiving for historical analysis and facilitates local use, providing a robust foundation for real-time decision-making and continuous improvement of the digital twin. After initial sensor deployment, the acquired data on actual trips has been verified through plausibility checks and crew feedback, ensuring the reliability and practical relevance of the information obtained from sensor and onboard systems data.

Figure 2 illustrates the data flow within our system. The Navis Bluetracker Suite (B6, Figure 2) acts as the primary conduit for information, seamlessly integrating with the proprietary high-frequency data interfaces. On the shore side, this setup is enhanced by a proprietary server for geodata (e.g., environmental and navigational data; B3, Figure 2) and routing services. This architecture ensures a smooth and efficient flow of data from onboard sensors to centralized systems and back to the onboard decision support system (B1, Figure 2), enabling comprehensive monitoring and analysis. The visualization of this data provides valuable insights into vessel navigation and performance, empowering stakeholders to make informed decisions for enhanced maritime operations. Additionally, on shore side, extensive evaluation of recorded ship parameters for both system improvements and crew training is facilitated.

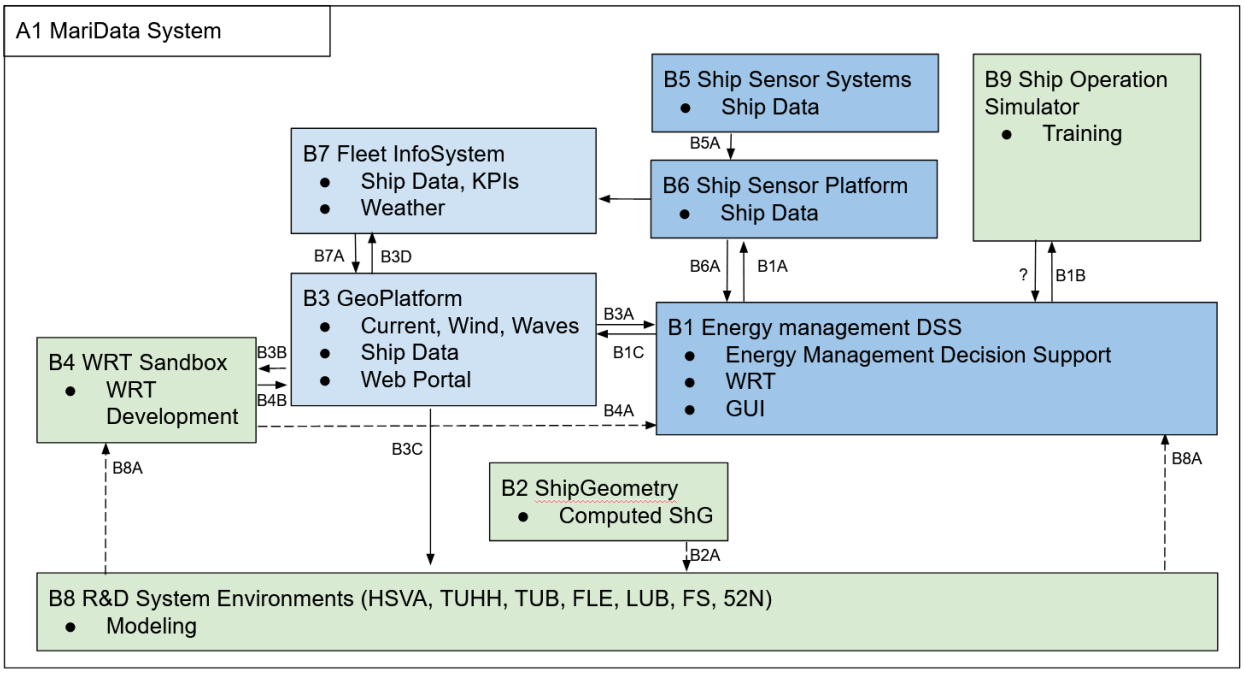

Figure 2: Data Flow and System Map (excerpt; initial planning stage)

SIMULATIONS AND SURROGATES

Components

A ship traveling through water is influenced by many factors, all of which contribute to some extent to its total energy consumption. Assuming that interactions are sufficiently small in comparison to any component's direct contribution, a superposition ought to give reasonably good estimates. For the sake of simplifying the analysis often calm-water at infinite water-depth is considered, see Figure 3a, while the actual situation at sea comprises wind, waves, current, fouling along with possible effects from shallow water and/or canals, see Figure 3b. All components need to be suitably considered. Here, only the key contributors shall be discussed in some detail, namely calm-water resistance, added resistance in waves and propeller performance.

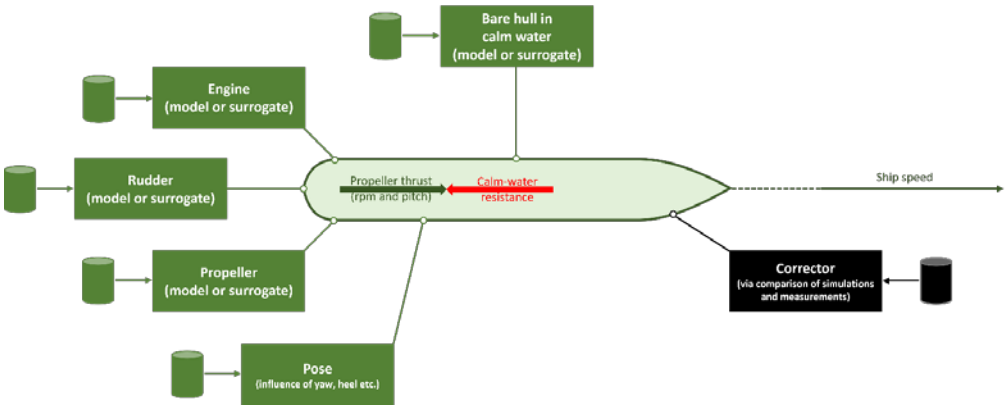

(a) Calm-water conditions (idealized)

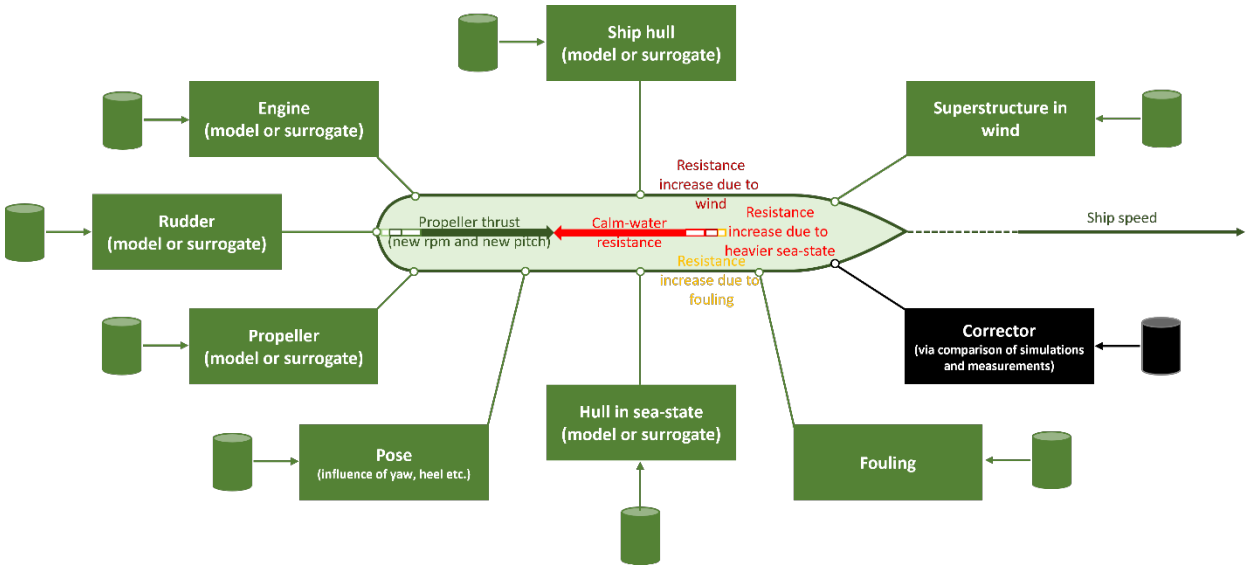

(b) Conditions under the influence of wind, sea-state, restricted water conditions (e.g., shallow water), fouling etc. (realistic)

Figure 3: Components for which data are produced by simulations

Calm Water Resistance

Calm water resistance is typically the first and often foremost element of all hydrodynamic considerations. It is made up of two different components: (i) the pressure or form-related wave resistance and (ii) the viscous drag. The added resistance due to wind and waves is treated in the following section. The calm water contributions to the overall power requirements of a vessel typically amount to 70% of the overall power required on board. The pressure related component depends – besides speed and draft of the ship – on the hull form and hence is invariant over the lifetime. Viscous resistance however changes a lot over time due to increased hull roughness due to fouling. As the overall share of the viscous or frictional resistance can be large, especially for typical merchant vessel cases, this has to be taken into account not only during operational optimization but already during design as to make sure that the selected engine meets the requirements of increased water resistance over time.

For the surrogate model used in the digital twin of the CBT, a set of design predictions formed the basis. This concept follows an approach developed in the HOLISHIP project, see e.g. (Marzi, et al., 2018; Papanikolaou, 2018).

A first evaluation of the operational conditions of the tanker revealed that more draught and trim conditions than considered during design were required to cover the entire envelope. This meant that an extra set of predictions had to be performed. As the design predictions all were performed using a standard roughness according to ITTC guidelines, further analysis of additional hull roughness conditions was included in the data set which finally resulted in a model comprising more than 190 different conditions for the calm water resistance. This was considered sufficient for use during operational optimization. Predictions were performed using HSVA's in-house RANS code FreSCo^{+} (Hafermann, 2007)

using different roughness models. An example of the calm water predictions is shown in the following figure which illustrates also the complex wave formation at the bow of the ship.

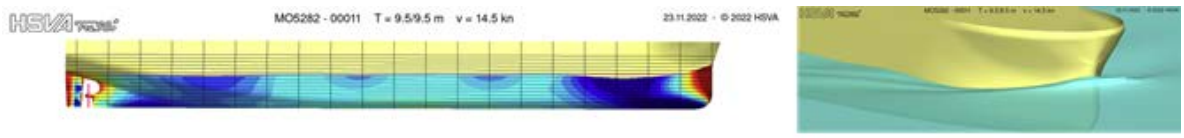

Figure 4: Example CFD prediction for the CBT – fully laden at design speed

The entire set of predictions resulted in a response surface shown in Figure 5 indicating total resistance as a function of speed and draft (even keel situation). Due to confidentiality, these and all following resistances are normalized with the calm water resistance $R_{calm,ref}$ at a ship speed of 13 kn and a draught of 9.5 m.

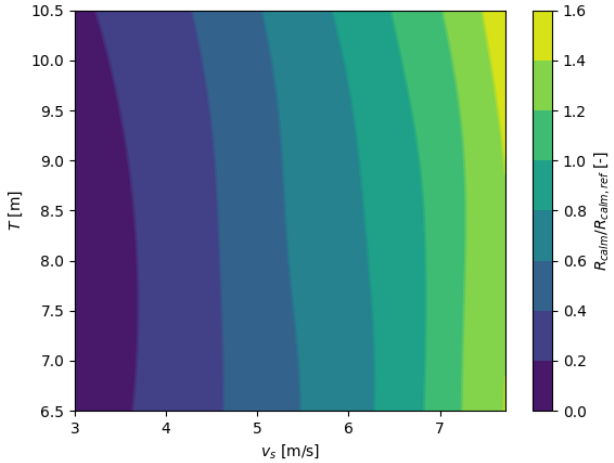

Figure 5: CBT calm water resistance as a function of speed and draft, even keel

The effect of hull roughness has been accounted for using a dedicated new wall function model in FreSCo+ developed in the MariData project. This allows to choose between different wall functions and even to specify local distributions of roughness based on a sand grain equivalent. The following Figure 6 indicates the effects of different distributions of roughness on the hull of the CBT: On the left, variable sand roughness distributions on tanker hull are indicated: from bottom to top: constant fouling, positive fouling gradient, negative fouling gradient and variable fouling fraction. On the right, friction coefficients on the hull and along hull center line are shown based on the different mean (spatially constant) sand roughness.

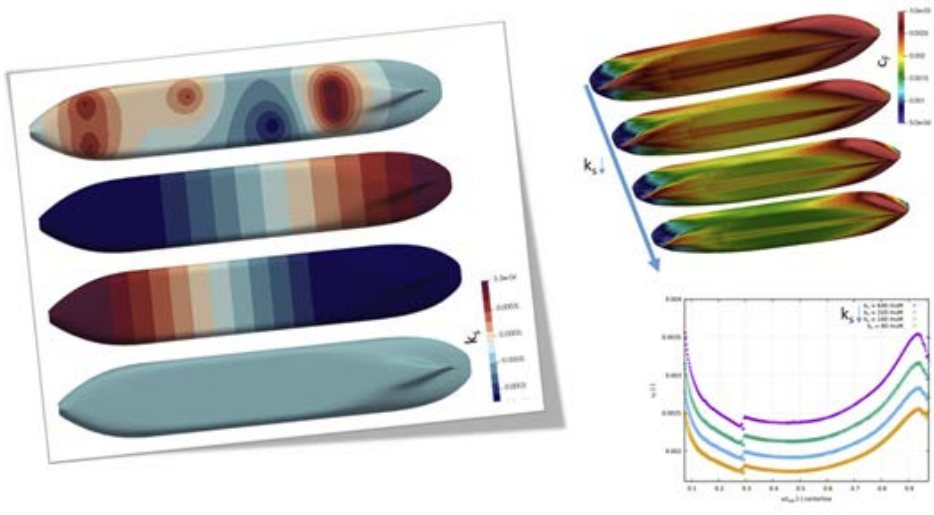

Figure 6: Effect of local roughness distribution on shear forces

Alternatively, roughness effects can of course also be modelled using the well-known ITTC roughness model. Figure 7 indicates the respective response surface for additional resistance according to roughness as a function of speed.

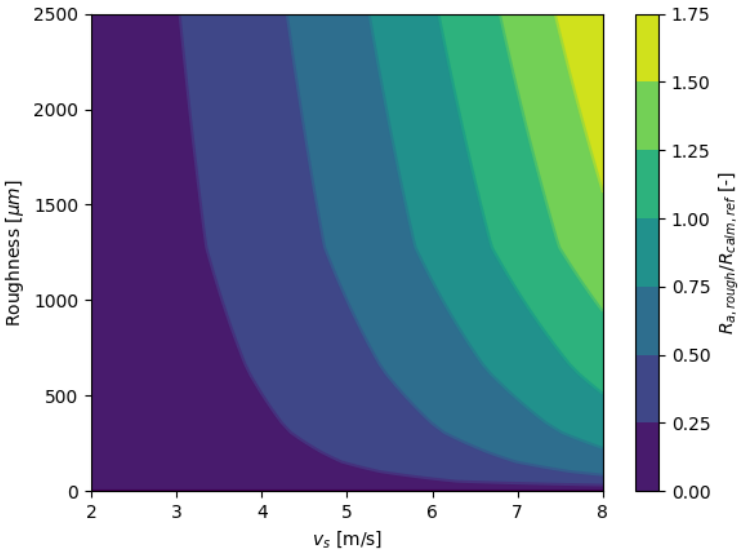

Figure 7: Added resistance due to hull roughness on CBT

Added Resistance in Waves

The contribution of added resistance in a seaway to the total resistance can be quite significant, depending on the ship type and weather conditions. To obtain a good estimate of the resistance, the following parameters must be considered:

- draught at aft perpendicular
- draught at forward perpendicular
- vertical position of center of gravity
- ship speed
- main direction of incoming waves
- peak period of wave spectrum
- significant wave height of incoming waves

Because of the number of relevant parameters, methods like RANSE-based simulations are not feasible to build the surrogate model. Instead, simulation methods based on potential flow theory are used. The 3D panel code NewDrift, developed at National Technical University of Athens (NTUA), was used in the scope of the MariData project to create large sets of training data. To generate penalizations for many different floating conditions, a process using the CAD environment CAESES was set up. About half of the generated dataset of approx. 6000 points is used to train the surrogate model using a Kriging approach. The remaining points serve as control set to check the model quality.

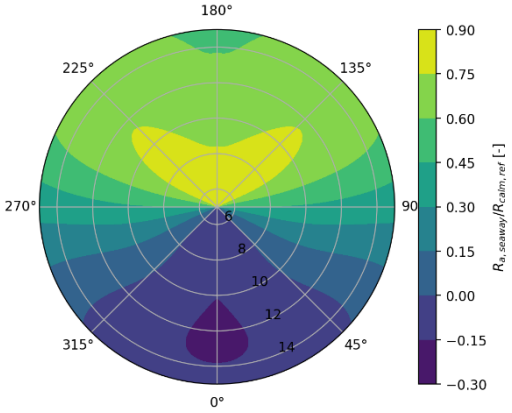

Figure 8: Added resistance due to seaway in $T_p = 9.5\ s, H_s = 2\ m$

Propeller Performance

Simulations were performed in the panel code panMARE (Hundemer, 2005) developed at the Institute of Fluid Dynamics and Ship Theory. A grid study resulted in a blade discretization with 20 panels in chord wise direction and 25 panels in radial direction, shown in Figure 9.

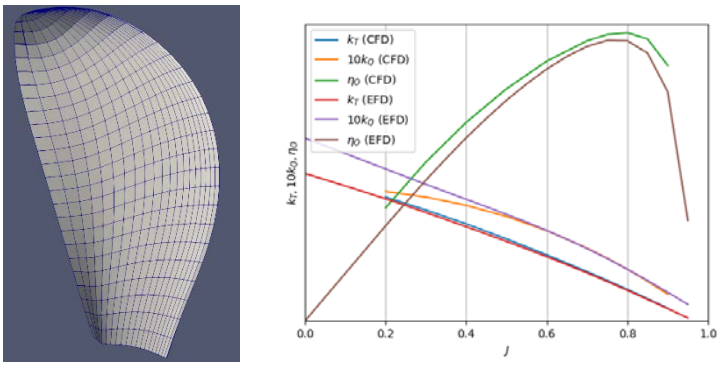

Figure 9: CBT propeller blade panel grid and open water comparison of simulated and measured results

A Sobol sequence was used for the sampling in parameter space of rotation rate and blade pitch θ. Only operating conditions from the first quadrant were simulated until the absolute of the second statistical moment of thrust coefficient, torque coefficient and open water efficiency fell below 1E-4. 736 operating conditions remained for the generation and testing of the two surrogate models under the condition $c_{Th} < 10$. The models are designed to determine the advance coefficient J and torque coefficient k_Q from the ship loading curve coefficient $k_T/J\text{^}2$ and θ, see Figure 10 for the resulting response surfaces.

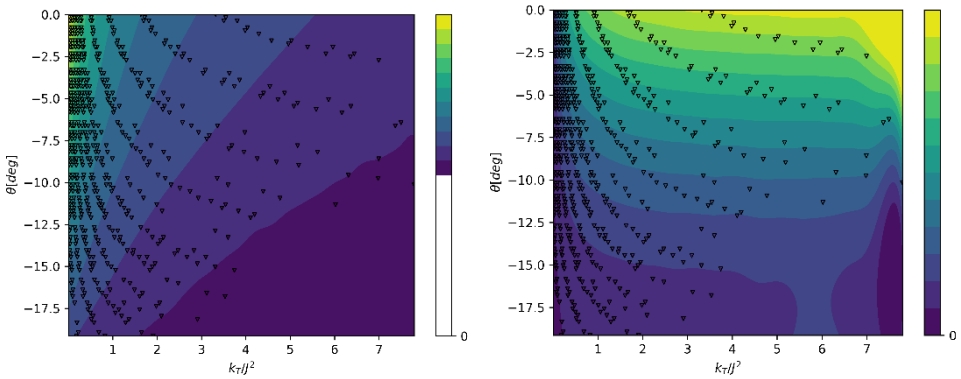

a) Advance coefficient **b) Torque coefficient**

Figure 10: CBT propeller surrogate model response surfaces

Various Additional Components

Environmental factors not only introduce parts to the added resistance but can also introduce transversal forces as well as yaw moments. The reaction of the ship to these components in form of drift motion and necessary rudder angle to neutralize yaw moments is modeled with a set of maneuvering coefficients. These also contain parts for the longitudinal force due to sway motion and rudder angle.

Aerodynamic Resistance

For the wind influence, forces were determined through hybrid RANS/LES simulations for two geometries, a detailed geometry and a simplified one regarding deck and deckhouse superstructure. The difference in longitudinal and transversal force for the two versions in apparent wind angles of 0°, 45° and 90° were between –5% and 8% of the force on the detailed version. The surrogate model was built with a coefficient-based interpolation approach with ship speed, wind speed, wind angle, draught and material properties of the air as input parameters,

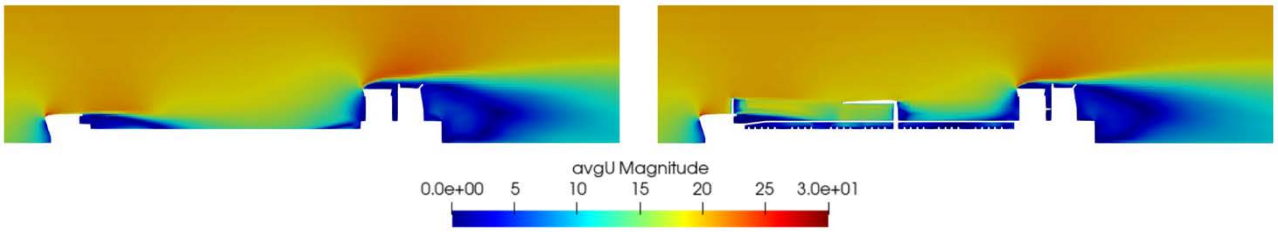

Figure 11: Air velocity distribution on midship plane for two geometry detail levels

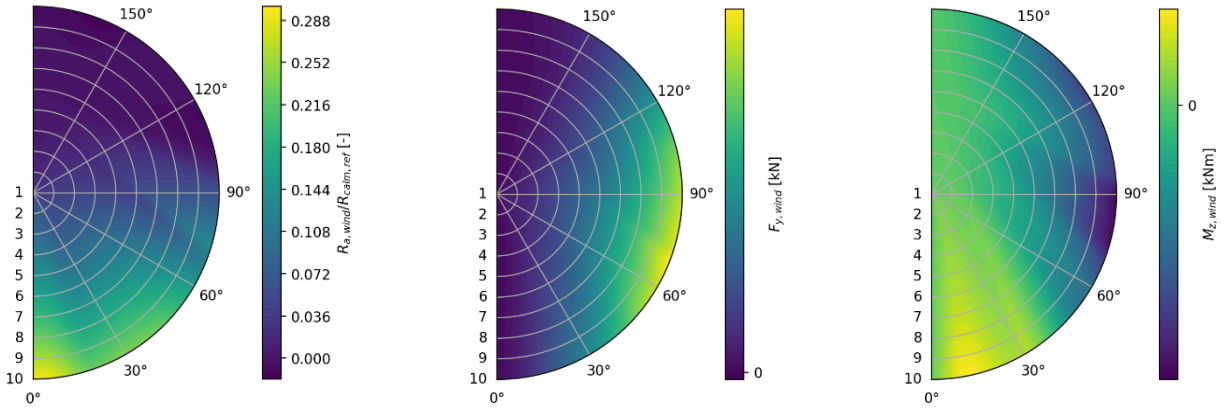

a) Added resistance **b) Side force** **c) Yaw moment**

Figure 12: CBT wind force surrogate model results for 5 m/s ship speed as a function of apparent wind angle and wind speed

Added Resistance in Shallow Water

Simulations with the CBT hull in restricted water depths were carried out using a Finite-Volume method. The results were used as training data for a Kriging-based surrogate model, as previously published e.g. in (Harries, et al., 2019) and (Harries, et al., 2017) for the added resistance due to shallow water with the parameters water depth, ship speed and draught. Exemplary results of this model are shown in Figure 13.

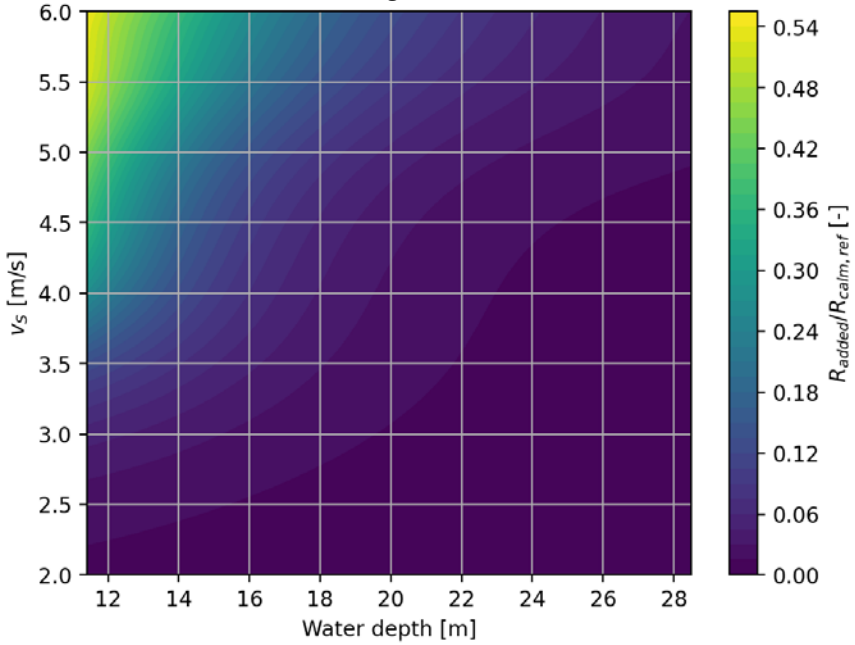

Figure 13: Added resistance due to shallow water effects for CBT at T=9.5m

Uncertainty considerations and analysis

Given the complex structure and interdependencies between different elements of the overall MariData development, it is evident that here are several sources of errors, causing uncertainty. Prominent sources of uncertainty are:

- Simulations: System behavior is only approximated by simulations which themselves are sufficiently converged numerical solution to chosen mathematical model that describe the physics of interest. In some cases certain phenomena are deliberately neglected to be able to undertake simulations with reasonable effort, e.g., potential theory for sea-keeping analyses in which viscous effects are not taken into account.
- Interactions: Assuming that various resistance components can be superimposed linearly omits any interaction between them. For instance, hull fouling not only changes calm-water resistance but might change the wake field into the propeller.
- Surrogates: The various components are captured by means of surrogates, i.e., meta-models that are fed with simulation data and which interpolate (or approximate) these data, yielding quantitative results for system behavior where no simulation actually took place. Previous work has shown good accuracy for surrogates representing calm-water resistance (±1% difference between the approximation and the simulations) and added resistance in waves (uncertainty of ±2.5%), see Harries et al. (2019) and Harries et al. (2017), respectively.
- Biofouling: This component has a huge impact on ship resistance while its assessment is often rather difficult. Without regular inspections, the amount and location of biofouling can only guessed by the crew while in port. In the present case timely and well documented hull inspections were available which allowed to determine a fairly accurate level of hull roughness increase during the periods for which historic voyages were analyzed.
- Representation: The geometry of various components is not taken into account as built but as designed, causing additional uncertainty in the simulation set-ups.

There are further uncertainties which are related to the weather fore- and/or hindcast as well as in the sensors installed on board. These will be briefly addressed in the sections below.
Ideally, a through analyses of the error propagation would be undertaken. This, however, was beyond the scope of the project and is certainly beyond the scope of this paper. Still, an attempt was made to develop an appreciation of the influence of uncertainty by assuming ±5% of change in calm-water resistance, independent of its origin, and ±20% of change in added resistance in waves. Further investigations would be needed.

Engine Model

The main engine model was supplied by project partner AVL and predicts the fuel oil consumption based on engine operational data as shown in Figure 14.

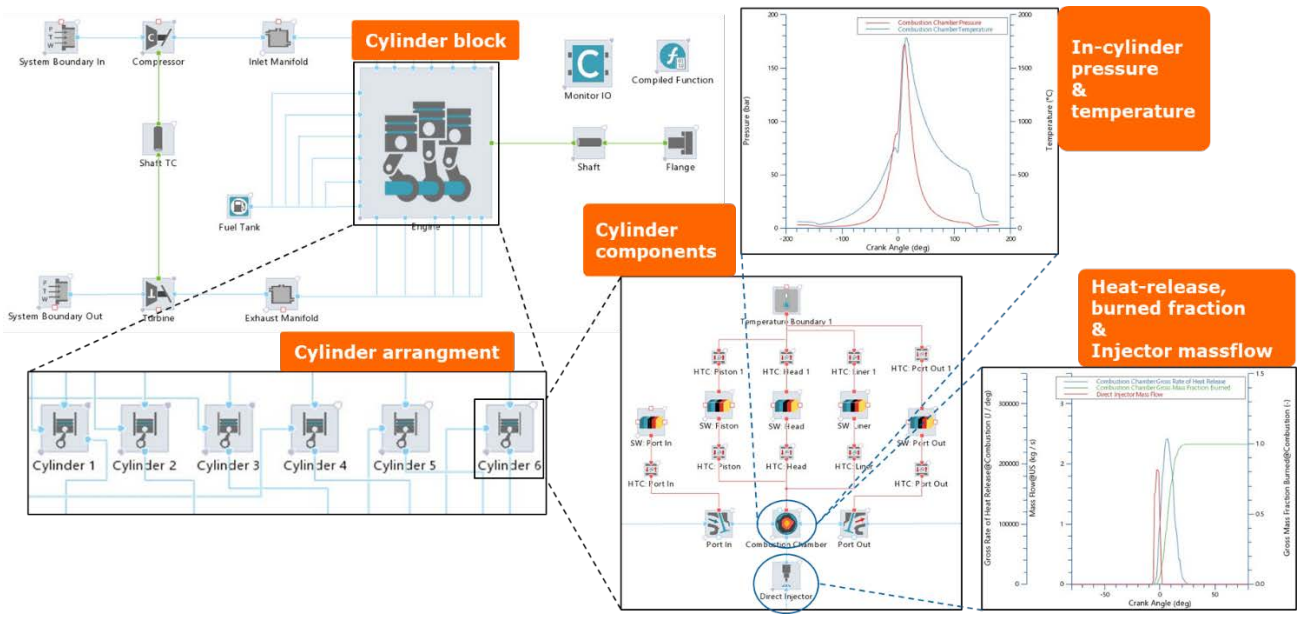

Figure 14: Detailed main engine model derived from design data

The core of the model consists of six cylinders, which in turn are divided into a combustion chamber and an integrated injector model. All geometric design parameters have already been considered in the model parameterization. The model can calculate and output both transient, i.e. time-resolved, engine variables (e.g. total engine power, fuel consumption, engine speed, etc.) and traces resolved via crank angle position (e.g. cylinder pressure curve, heat release rate, etc.). Combustion and heat release in the combustion chamber are approximated using the empirical vibe model. The calorific

value of the fuel was stored using the fuel tool integrated in the AVL CRUISE M tool and is used as the basis for calculation in combustion modeling.

The injector model receives a variable injection mass flow as a transient target value as an actuator signal and distributes the corresponding fuel quantity during the conversion between the time/crank angle domain in accordance with the stored injection profile via a working cycle. The engine shaft, which is mechanically coupled to the cylinder bank, can be operated both speed-controlled and torque-controlled. Depending on the set mode, either the applied speed or the applied torque can be applied directly as a control variable. The transient response of the motor model after the manipulated variables have been changed can be checked for plausibility using the calculated engine power, consumption, and speed.
A turbocharger has been added to the main engine model, which means that charge air conditioning and energy recovery from the engine exhaust are considered in the model. A simplified representation without operating maps for the compressor and turbine was selected: the turbine component is equipped with an internal wastegate sub model, which adjusts the wastegate opening depending on the power requirement.

In addition, two auxiliary blowers were added to the main engine model. The pressure increase that the intake air experiences as it flows through the blowers is taken into account using adapted maps. These are used to maintain charge air control even at low engine loads, where the turbocharger alone cannot achieve the desired compression on the intake side. With the implementation of the turbocharger and the auxiliary fans, the gas path representation of the main engine is complete.

Due to the limited measurement data available, which does not allow a detailed comparison of the internal cylinder condition with detailed combustion curves over a working cycle, no changeover was made to a predictive combustion model with detailed, phenomenologically based parameterization. Instead, an empirical Vibe combustion model was used and its parameters were adjusted as part of the parameter variation plan so that the simulation results approximate the consumption/power and torque figures in the data sheets with sufficient accuracy. The purpose of the Vibe function is to reproduce the typical S-shaped profile of the integrated heat release of combustion engines (Stiesch, 2003). The start of combustion and the combustion duration in the cylinder were defined as load point-dependent parameters of the Vibe model. The shape factor used was also represented as a function of the load point. It was possible to achieve a high level of agreement between the simulation results and the characteristic values from the data sheets by taking the above-mentioned measures when parameterizing the Vibe model. The accuracy was examined over five stationary operating points: 25%, 50%, 75%, 100% load and then at 10% overload. Table 1 shows the resulting model reference deviation for absolute fuel consumption (FOC) and power-specific fuel consumption (BSFC). Depending on the selected operating point, the deviation ranges between 0.3% and 0.98%.

Table 1: Deviation of the simulated fuel consumption over five reference load points

Load Points	25	50	75	100	110
Deviation percentage FOC	0.594	0.332	0.886	0.269	0.745
Deviation percentage BSFC	0.522	0.299	0.983	0.167	0.622

WEATHER ROUTING

Weather Data

To evaluate the simulations – i.e. by comparison with measured data – and to perform route optimization for historical and planned routes, we need to know the physical state of the atmosphere and the ocean at the time of travel. The in-situ data from the sensors deployed on the ships are not sufficient as they do not cover all necessary variables and provide only information about the current state. Today, multiple operational forecast and reanalysis systems exist which can fill this gap. For oceanographic data we use two products, “Global Ocean Waves Analysis and Forecast” (EU Copernicus Marine Service Information (CMEMS). Marine Data Store) and “Global Ocean Physics Analysis and Forecast” (EU Copernicus Marine Service Information (CMEMS). Marine Data Store) and for atmospheric data we use the Global Forecast System (National Centers for Environmental Prediction/National Weather Service/NOAA/U.S. Department of

Commerce, 2015). The data come in different spatial and temporal resolutions. Table 2 shows an overview of those variables expected as input for our fuel consumption model.

Table 2: Overview of the environmental variables downloaded from CMEMS and GFS

Variable	Platform	Space	Time
Wind speed u-component[1]	GFS	1/4°, global	3 h, 10 days-forecast
Wind speed v-component[1]	GFS	1/4°, global	3 h, 10 days-forecast
Air pressure reduced to mean sea level	GFS	1/4°, global	3 h, 10 days-forecast
Air temperature at water surface	GFS	1/4°, global	3 h, 10 days-forecast
Spectral significant wave height	CMEMS	1/12°, global	3 h, -1 Y to 10 days-forecast
Wave period at spectral peak	CMEMS	1/12°, global	3 h, -1 Y to 10 days-forecast
Mean wave direction from	CMEMS	1/12°, global	3 h, -1 Y to 10 days-forecast
Total[2] surface sea water zonal velocity (u)	CMEMS	1/12°, global	1 h, -2 Y to 10 days-forecast
Total[2] surface sea water meridional velocity (v)	CMEMS	1/12°, global	1 h, -2 Y to 10 days-forecast
Sea surface salinity	CMEMS	1/12°, global	1 h, -2 Y to 10 days-forecast
Sea water potential temperature	CMEMS	1/12°, global	1 h, -2 Y to 10 days-forecast

[1] available at 10 m, 20 m, 30 m, 40 m, 50 m, 70 m, 100 m height above ground
[2] Eulerian + Waves + Tide

As the system being developed in the MariData project aims at providing decision support in real time, the focus is on actual forecast data. However, for the evaluation of the models we also need historical data. The CMEMS products include analysis data for the last 1-3 years and thus also cover the period for which we collected data on the ships. For GFS, analysis data is not available. Instead, we use the archived forecasts from the temporarily closest forecast cycle.
In addition to the temporarily varying environmental data, we also use static data on water depth from the ETOPO 2022 15 Arc-Second Global Relief Model with a 30 arc second resolution (NOAA National Centers for Environmental Information).

Routing

A variety of algorithms has been explored in the past to optimize time and/or fuel consumption during sea journeys for a given weather scenario (Walther, Rizvanolli, Wendebourg, & Jahn, 2016). Due to the large interdisciplinarity of the MariData consortium, it is not only possible to investigate the performance of individual algorithms in the project context but also to elaborate on the interplay between the respective hydrodynamic simulations for power and fuel consumption on the one hand and the weather routing tool (WRT) on the other hand. In this paper, the measured power consumptions for historical routes traveled by a CBT are compared to routes provided by the routing tool as a general proof of concept. In addition, the effect that different weights on added resistances have on the simulation of power consumption for a specific historical route as well as on the routing procedure will be investigated.

The routing algorithm which has been utilized in this paper is an ‘isofuel’ algorithm – i.e. it provides routes that are optimized for fuel consumption – based on the concept of the modified isochrone method by Hagiwara (1989). Similar to the latter, the routing is performed in individual routing steps. For every step, it is calculated how far the ship can travel in different directions with a fixed amount of fuel considering the respective weather conditions and properties of the environment. All environmental variables listed in Table 2 are considered in this process. Tides are only considered as part of the overall ocean currents. Water depth is assumed to be static based on bathymetry data. At present the ship is assumed to sail at constant speed and fore and aft draught for the full route. Adaptations will be considered in the next step. Weather conditions are considered to be constant for every individual routing step.

The optimization is achieved by grouping routes according to their courses and selecting only the route segment per group for the next routing step that maximizes the travel distance. Using this concept, a wide angular range is scanned systematically for optimal routes as it can be seen in Fig. 15. The algorithm considers constraints by landmasses and shallow water by eliminating routes that cross the latter from the optimization process. Thereby, shallow waters are defined as areas with a water depth below the sum of the ship’s draught and an under keel clearance of 20 m.
Due to the nature of the algorithm choices in an early routing step might lead to an overall worse fuel consumption later. This is partially mitigated by scanning a large number and wide range of angles and by using many groups in the

selection process thus keeping a sufficient number of segments for the subsequent routing step. In the future, it is planned to evaluate algorithms which consider always the complete route like genetic algorithms.

Uncertainty of environmental data

Further uncertainties in the model evaluation and the route optimization are related to the environmental data. The reanalysis and forecast data used to feed the power and fuel consumption models represent average values for a coarse grid where one grid cell covers an area in the order of tens to hundreds of square kilometers and time periods from 1 to 3 hours. In contrast, a ship experiences conditions at a specific position in space and time which might vary significantly from the average values. Moreover, the reanalysis and forecast models come with their own uncertainties.

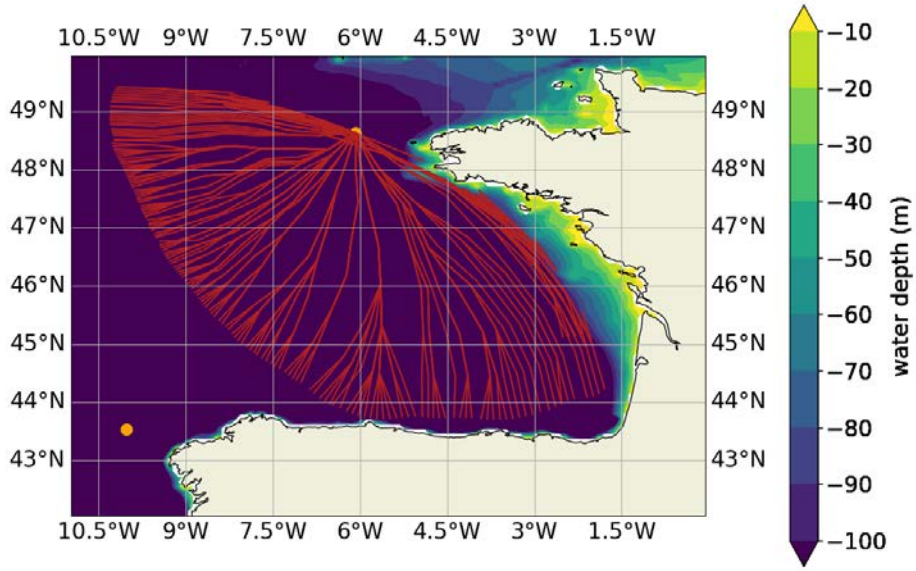

Figure 15: Visualization of route segments at an intermediate routing step of the Isofuel algorithm for a CBT traveling in the Bay of Biscay

SYNTHESIS AND SHIP OPERATIONS

Synthesis

It would be rather resource-intensive – if not prohibitively expensive – to compute the performance of a ship by means of direct simulation, i.e., by computing the behavior of all components at full-scale and bringing them into the correct balance of total resistance encountered and thrust delivered, providing the engine power and fuel oil consumption for any given speed in any environmental condition. As shown in Fig. 2 the approach taken here is to subdivide the overall system into manageable components. This follows the approach developed in HOLISHIP (Papanikolaou, 2018), and used for design synthesis. Based on (many) upfront simulations, realized via Design-of-Experiments, the various contributions are captured in surrogates that provide quantitative results within split-seconds for any condition of interest.

A python module called mariPower was implemented that connects all described surrogates for (added) resistance components and propulsion to consider every factor during the power and fuel consumption prediction. It takes loading conditions along a route specified by a discrete trajectory and ship speeds and determines the encountered weather from a forecast or hindcast for all points along the route. Then, it iterates the unknown ship motion parameters (propeller rotation rate, drift angle and rudder angle), continuously updating the surrogate model results as their inputs change. After convergence or the maximum number of iterations is reached the fuel oil consumption is estimated from the resulting engine power and rotation rate.

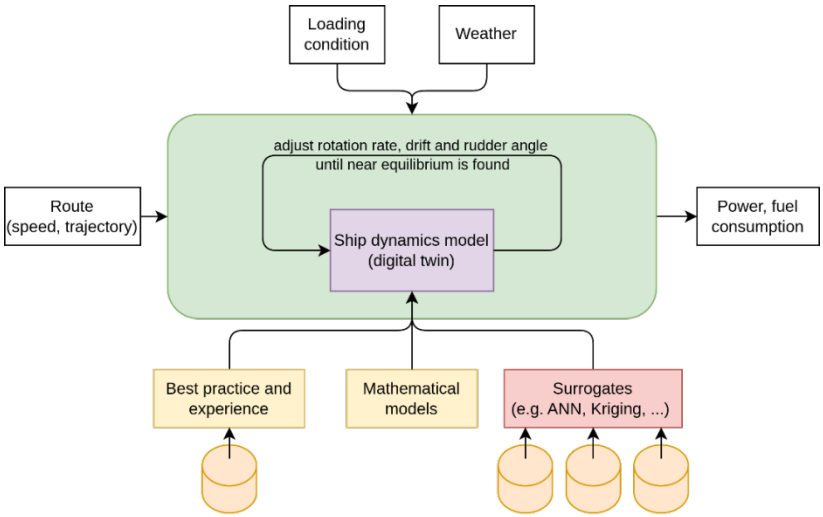

Figure 16: Process flow within mariPower

Ship Operations via mariPower

The described module mariPower was implemented as a general framework to take into account various environmental factors in the prediction of necessary engine power. In the current state, it is able to consider additional forces due to wind, seaway, fouling and shallow water. In the latter three cases also wake fraction changes can be included. The base class in the module implements the functionality to iterate the ship and engine motion state. It updates the added forces in longitudinal and transversal direction as well as the yaw moment of all available sources iteratively and estimates a drift and rudder angle to keep its course based on maneuvering coefficients. The total required thrust and forward velocity through water are used as inputs to the propeller model which predicts the resulting rotation rate and torque. This continues until an equilibrium of longitudinal forces is found or the maximum number of iterations is reached. Its child classes allow the connection to individual user-defined surrogate models for the added forces and wake fraction changes due to each of the described environmental factors. Those only need to comply with the defined input and output parameters and units. The code uses vectorized functions where possible to increase efficiency.

STATISTICAL ANALYSES

Data Lake

Within the research project MariData extensive measurements of onboard data with high sampling rate were performed. Those data were used to find predominantly encountered weather conditions as well as periods where the operating conditions were steady with a certain tolerance.

For the latter, the sensor data was synchronized first and resampled to a frequency of 1Hz to ensure a shared time stamp before filtering with a minimum ship speed and several other conditions regarding draught and engine load to remove sections before and after berthing. This combined data was then separated into voyages whenever a pause of more than two hours was found. Since this could also happen due to technical issues with the sensors, the endpoints of resulting routes are not necessarily near ports of call. Each voyage data is then evaluated regarding the standard deviation on rolling windows of 30 minutes compared to an individual tolerance for each sensor. If all tolerances are met, the window is marked as steady. In a second step, the slope of this evaluation result is calculated to determine starts and ends of steady intervals. Finally, all values in between stops and starts are marked as unsteady as well as those values between starts and stops where the time difference is less than the window length. The results are then resampled to a period of one hour and enriched with hindcast weather data.

To determine the representative operating conditions used in the following chapter, histograms were calculated from the operational data and manually analyzed.

Representative Operating Points

Two representative weather situations were picked from available operational data of seven months. For a ship speed of 6 m/s (11.7 kn) at a draft of 9.5 m on even keel the calm water case was selected having a low wind speed of 2 m/s with the rough weather case set at 12 m/s wind speed. Since no onboard wave measurements were available the seaway was approximated using a Pierson-Moskowitz spectrum for the two wind speeds (see Table 3). Water and air temperature were chosen as 293 K and the air pressure at 101350 Pa. The roughness of the hull was assumed to be hydraulically smooth in this case.

Table 3: Wind and seaway conditions for representative operating points

Weather	calm	rough
Wind speed	2 m/s	12 m/s
Significant wave height	0.09 m	3.25 m
Peak period	1.5 s	9 s

INFLUENCES IN REPRESENTATIVE OPERATING POINTS

Resistance Components

The digital twin was simulated in both weather conditions from all directions. In calm weather, the added resistance due to seaway is almost zero. The wind forces cause some yaw especially for crosswinds while the added resistance is highest for the frontal wind directions. Still, the maximum total added resistance is only around 3% of the calm water resistance. For rough weather, the added resistance due to seaway causes a drastic rise of the total added resistance, contributing 50% and more of the calm water resistance. The wind forces cause maximum drift angles of around 4° while increasing the total added resistance in head wind by another 30% to a total of 80% of the calm water resistance.

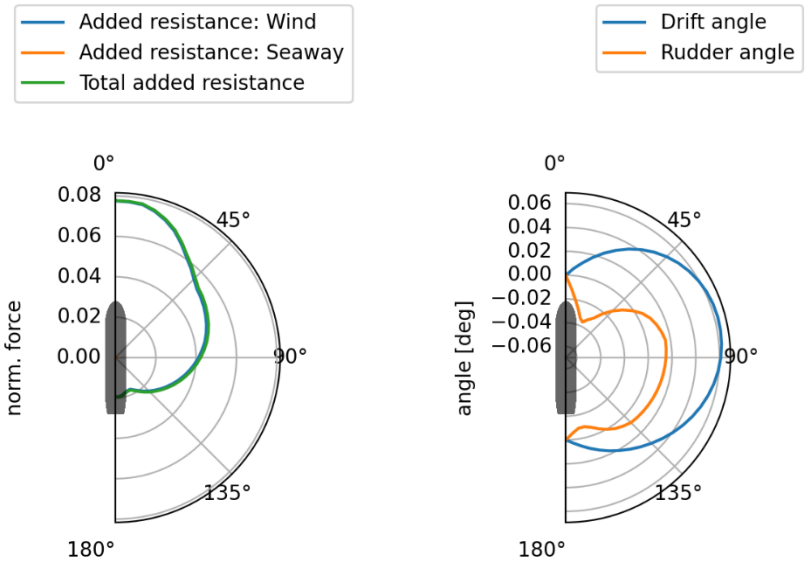

Figure 17: Added resistance components and drift and rudder angle in calm condition (forces normalized by calm water resistance)

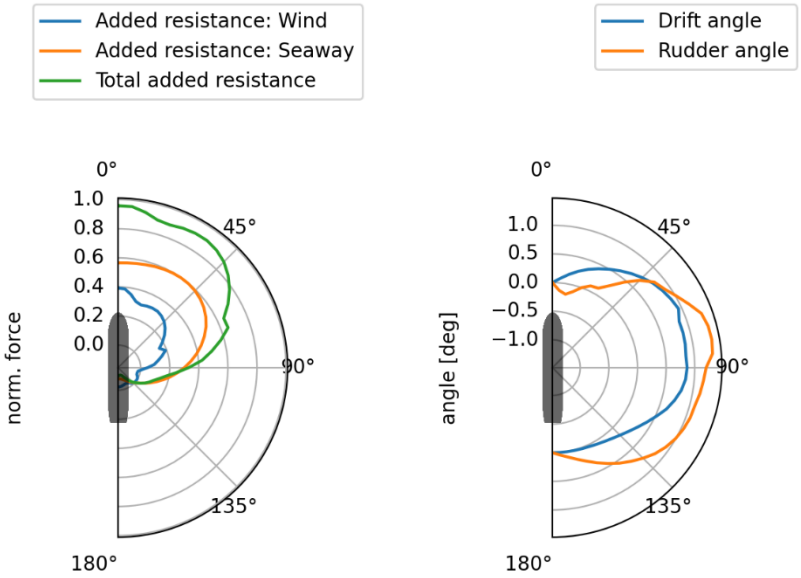

Figure 18: Added resistance components and drift and rudder angle in rough condition (forces normalized by calm water resistance)

Hypothetical Variation of Resistance Components

In the following, the effect of adding weights to the calm water resistance as well as the added resistances for waves and sea state on the power consumption is investigated. By these manipulations, it is possible to mimic imperfect hydrodynamic simulations and study the respective differences of the power prediction. As in the previous paragraph, angles between wind and waves on the one hand and the ship's course on the other hand are scanned in steps of ten degrees for two weather scenarios. The ratio of the power consumption calculated for the modified resistances over the results for the original settings is visualized. The results for changing the calm water resistance by +-5%, the added resistance for wind by +-20% and the added resistance for waves by +-20% can be seen in Figure 19.

For the calm-weather scenario, the effect of the modifications for the added resistances for wind and sea state are negligible while a +-5% modification of the calm-water resistance directly translates into a +-5% deviation for the power consumption. For the rough-weather scenario, the effect of the modifications for the added resistances for wind and sea state are most significant if wind and waves are coming from the front. In these cases, a 10% deviation for wind and 5% deviation for waves is reached. Due to the significant contribution from the added resistances for wind and sea state in this scenario, the modifications of the calm water resistance have a smaller effect (~3%) on the overall power consumption if wind and waves are coming from the front.

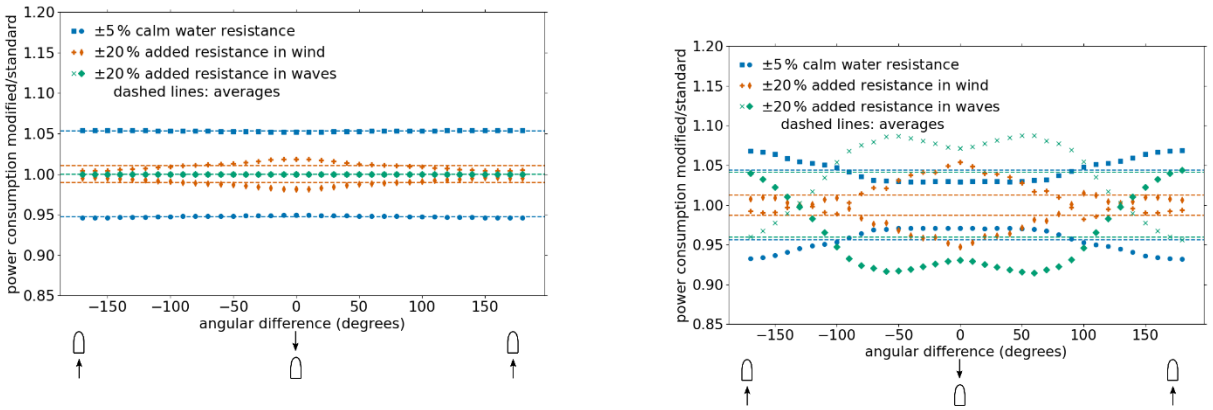

a) Calm weather **b) Rough weather**

Figure 19: The ratios for simulations of the power consumptions for manipulated resistances over those for standard settings in dependence of the angular difference between the CBT's course and the directions of winds and waves in ideal weather

INFLUENCES IN REAL CONDITIONS

Two routes have been selected from the analyzed operational data of one of the tankers in 2023. They were chosen based on long periods of quasi-steady ship motion and operation as well as being different regarding the severity of the weather conditions encountered during those periods. Their trajectories are shown in Figure 20.

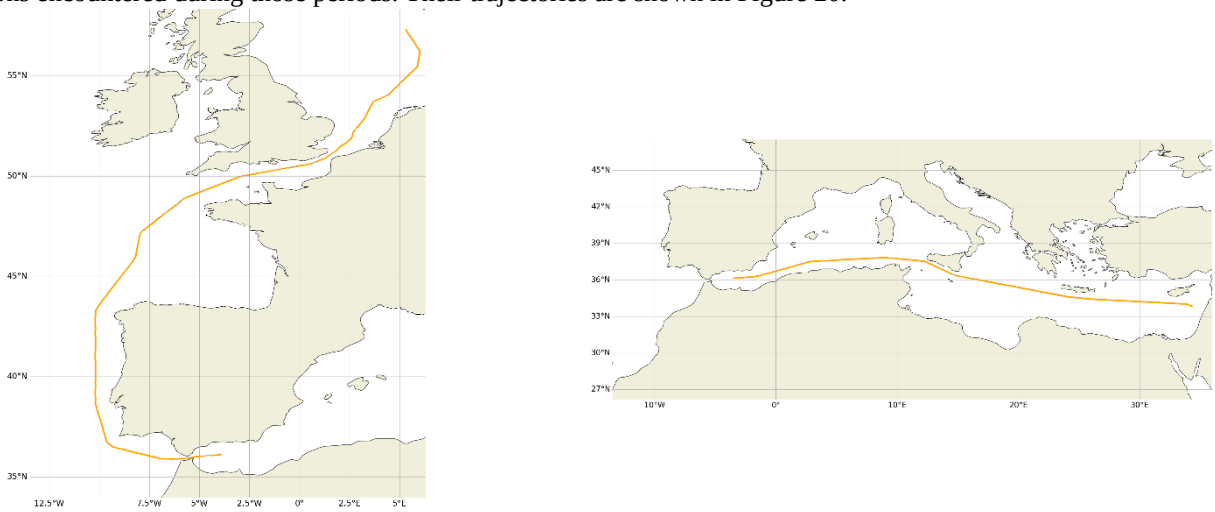

a) British channel **b) Mediterranean sea**

Figure 20: The historical routes traveled by a CBT which have been selected for investigations on the simulated power consumption in real weather conditions

Comparison of Operations and Simulations

When comparing predicted and measured engine power in Figure 21 the surrogate models clearly are able to predict the power with a certain error (RMS error across all routes in 2023 was 6.5%). Correlation coefficients showed that the main cause for the apparent fluctuations in the predicted power between all input parameters was the speed through water with a correlation coefficient of -0.657. The measured propeller pitch was usually above 98%, so the error due to predicting the propeller operating point for the maximum pitch only is assumed to introduce little error. Since the response surfaces of all surrogate models shown in previous chapters are continuous, we suspect the measured speed through water or the engine power to have some kind of measurement error.

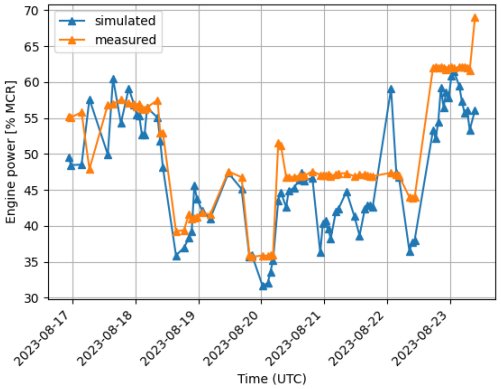

Figure 21: Predicted and measured engine power along "Mediterranean sea" route

Hypothetical Variation of Resistance Components

To investigate the effect of manipulated resistances on realistic routes, the power consumption has been simulated for historical routes traveled by a CBT under real weather conditions. In addition to the simulations for the standard settings, the calm water resistance as well as the added resistances in wind and waves have been varied by the same values as for the previous investigations for the representative operating points. The routes that have been selected pass the Mediterranean Sea as shown in Figure 20a and the British Channel as shown in Figure 20b. While the weather conditions

are mild in the Mediterranean Sea, the route through the British Channel traverses a low-pressure region roughly at the middle of the full travel distance.

The results for both routes are provided in Figure 22. It can be found that for the rough weather conditions in the British-Channel scenario, the modifications of the added resistances for wind and waves have a more significant effect than for the calmer conditions in the Mediterranean-Sea scenario. In contrast, the effects of the manipulations of the calm water resistance are more significant in the Mediterranean-Sea scenario than in the British-Channel scenario.

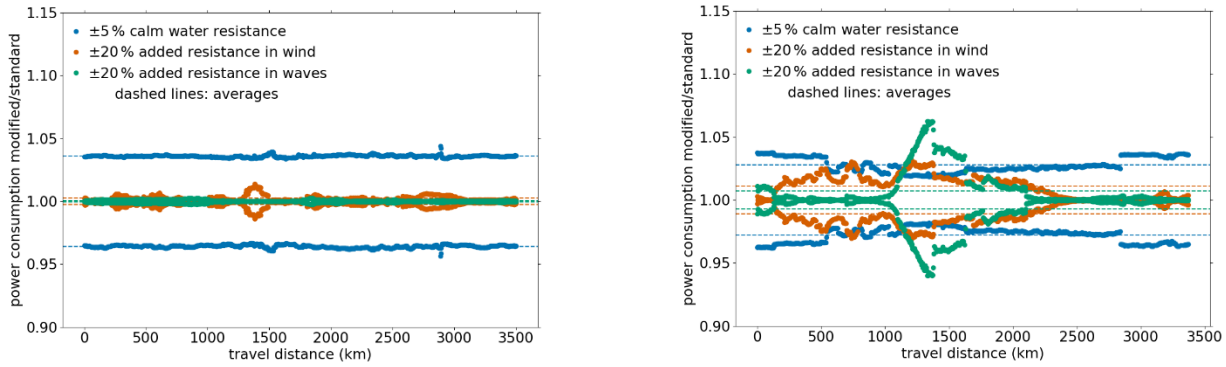

a) Mediterranean-Sea scenario **b) British Channel scenario**

Figure 22: The ratios for simulations of the power consumption for manipulated resistances over those for standard settings in dependence of the travel distance for historical routes traveled by the CBT

Routing in Actual Weather

In this section, it shall be demonstrated that the WRT of the MariData DSS provides alternatives to historical routes that reduce the overall fuel consumption. In addition, the effect of manipulations of the resistances on the routing procedure will be elaborated.

Naturally, the effect of the routing will be most significant in regions where restrictions like water separation zones or danger areas are rare. This is why two segments from the Mediterranean and the British-Channel scenario that meet these conditions have been selected for the investigations. The corresponding areas are displayed in Figure 23 and Figure 24 and shall be referred to as the Biscay and the Crete scenario.

For the routing procedure, the constant speed of the tanker is set to the average speed of the historical route. The inputs for fore and aft draught are averaged over the full historical route. In addition, the settings for the hull roughness are adapted to those which were found to describe the measured power consumption best (see Sec. 21).

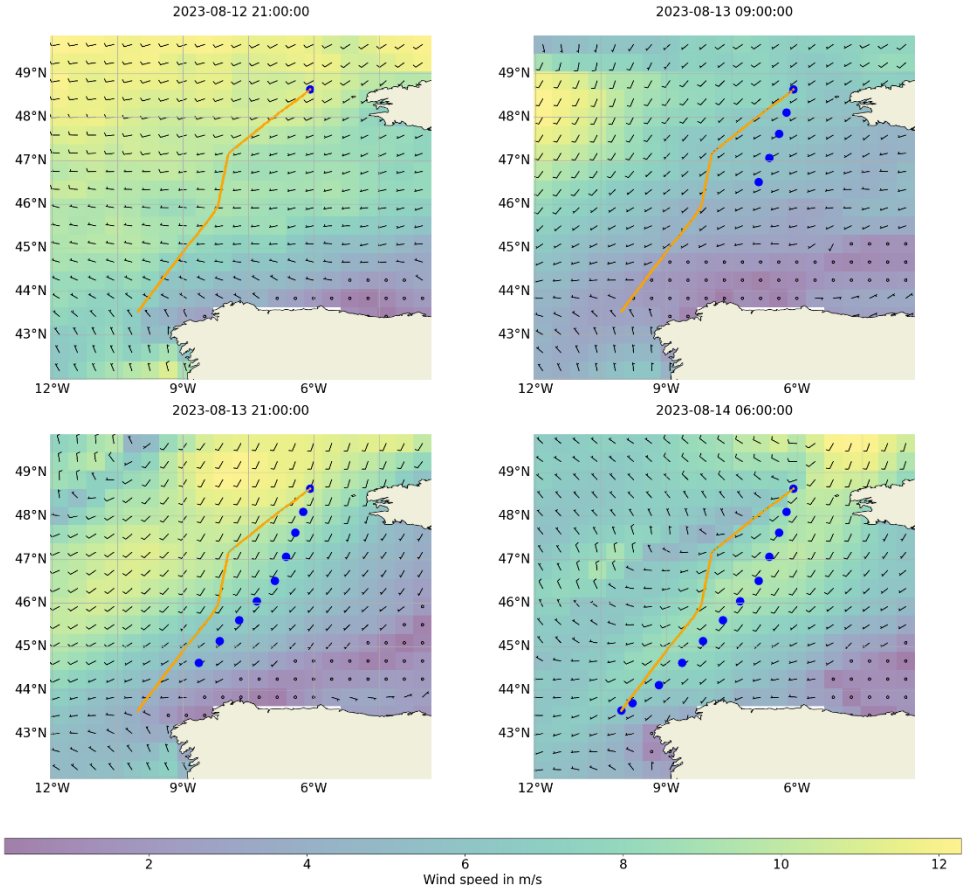

Figure 23: Trajectories of reference (orange) and optimized (blue) routes in the Biscay scenario for four snapshots. The background map shows wind speed and wind direction as heat map and wind barbs.

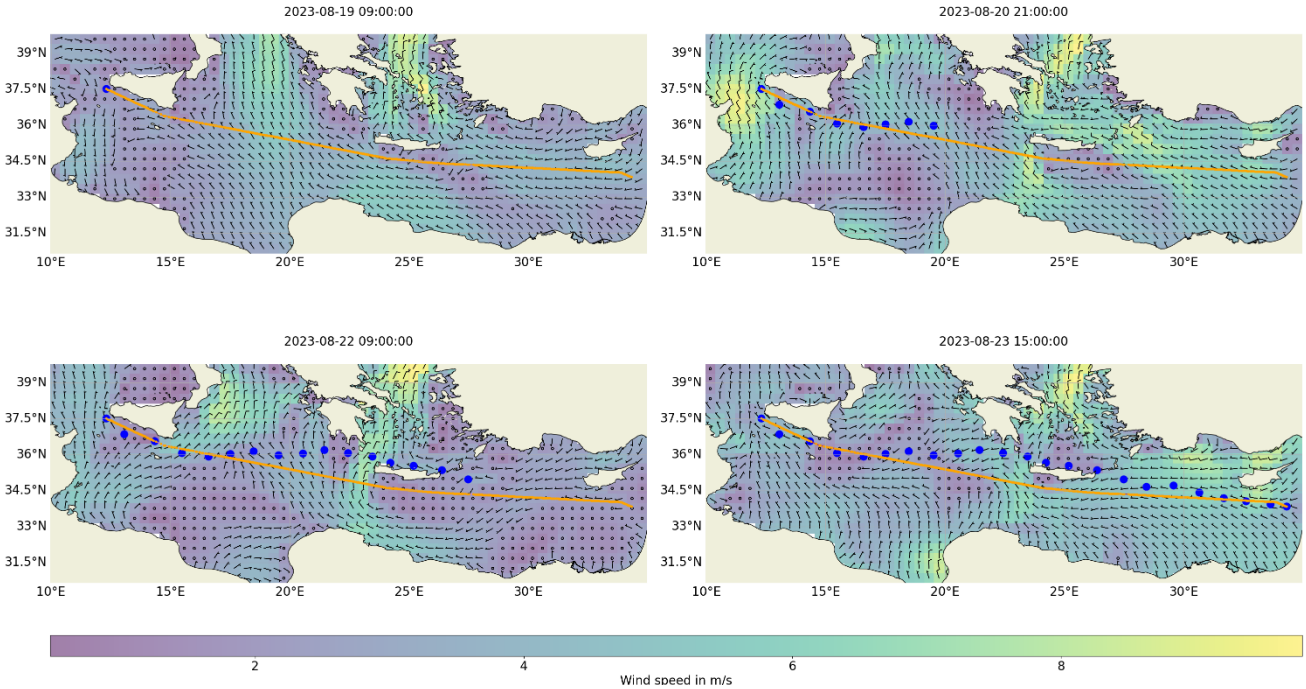

Figure 24: Trajectories of reference (orange) and optimized (blue) routes in the Crete scenario for four snapshots. The background map shows wind speed and wind direction as heat map and wind barbs.

The alternative routes for both scenarios are compared to the historical routes in Figure 23 and Figure 24. The differences between the historical routes and the routes from the WRT are significant. In the Biscay scenario, the WRT tanker travels

farther east than the historical route and in the Crete scenario, the WRT tanker passes by Crete on the northern side, while the historical CBT is traveling on the southern side. Looking at the corresponding weather conditions, these differences are plausible as in both scenarios, the wind speed and wave heights are more suitable for the routes selected by the WRT. In particular, both wind speed and wave heights are decreasing from west to east in the Biscay scenario making routes that reach farther to the east more fuel-efficient. In the case of the Crete scenario, the WRT tanker traveling on the northern side of Crete experiences stronger tail wind than the original CBT tanker traveling on the southern side.

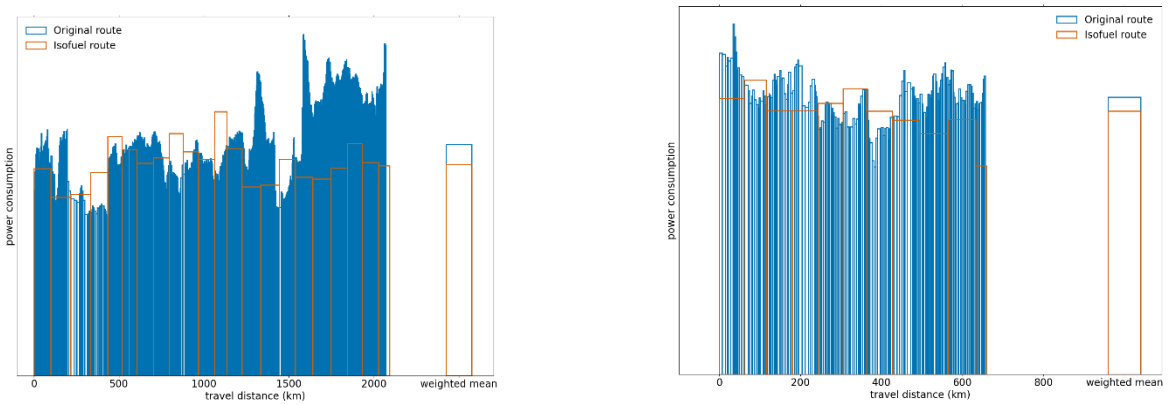

a) "Crete" **b)"Biscay"**

Figure 25: Power consumption of reference and optimized routes in two scenarios

Figure 25a and Figure 25b compare the resulting power consumptions for the historical and the WRT routes. For both scenarios, a smaller mean power consumption can be observed for the WRT routes which, in particular, results from a significantly smaller power consumption towards the end of both routes. Considering the absolute values and differences with respect to the historical route for travel time, travel distance and fuel consumption provided in Table 4 and Table 5, the WRT routes tend to be slightly longer, they reach the destination in roughly the same travel time (differences are smaller than an hour) and they spare about 8.7 % (Crete scenario) and 6.4 % (Biscay scenario) of the total amount of fuel that has been consumed for the historical routes.

Similar to the previous sections we investigate how a variation of individual resistances influences the routing process. We selected only the Biscay scenario as the effects are more significant here due to rougher weather. Figure 26 shows how the proposed routes differ geographically for variations of added resistance in wind. Table 4 and Table 5 summarize the key characteristics of travel distance and time and accumulated fuel consumption for both routes. Here, also values for variations of added resistance in waves and calm water resistance are included.

Generally, it can be observed that with a higher resistance ships can travel less far in each routing step and vice versa for lower resistances. Higher and lower resistances also naturally result in a different accumulated fuel consumption along a given track. However, the optimized routes also tend to travel in different areas to the originally proposed route without variation. If the added resistance in wind is 20 % higher, the ship can save fuel by traveling farther in the east where wind speeds decrease. For the last few waypoints, the opposite effect can also be observed when resistance is 20 % smaller. The specific behavior of the routing algorithm depends on a multitude of factors, so one has to be cautious with drawing specific conclusions from the given examples. In particular, the temporal evolution of the weather conditions can smear definite effects by the resistance variations. As a general conclusion, varying resistance components can not only change the overall consumption but also the track proposed by a routing optimization tool itself.

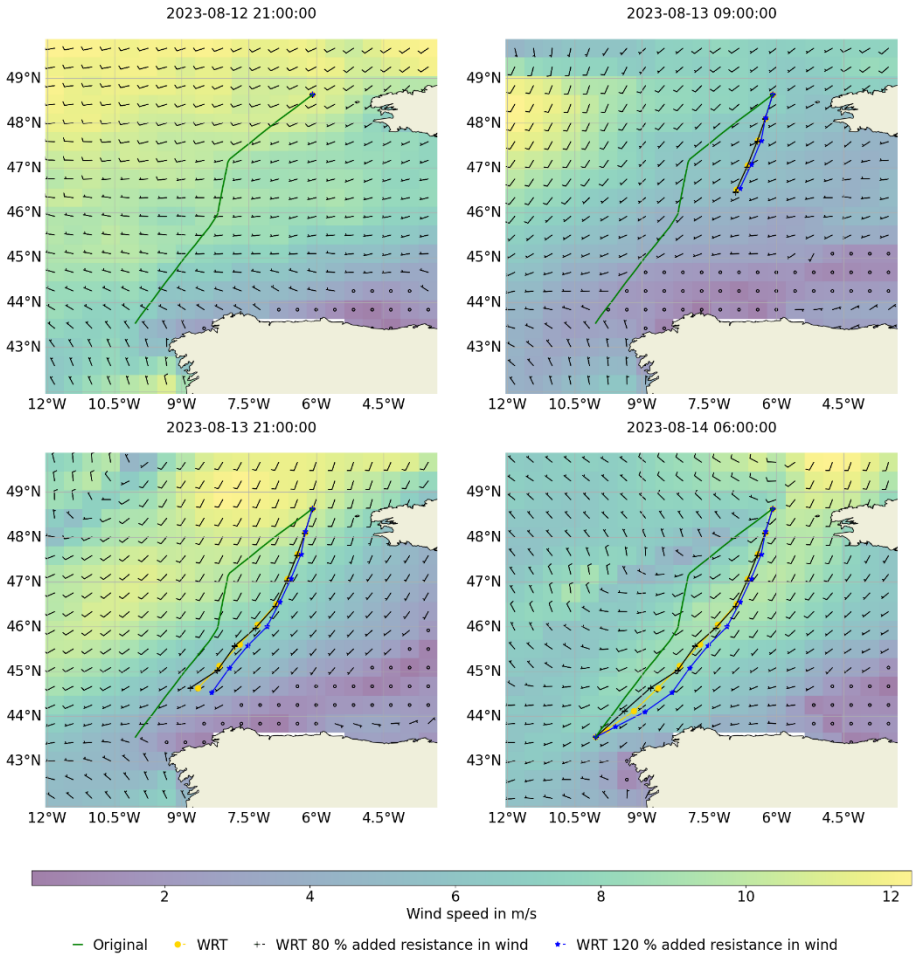

Figure 26: Trajectories of optimal routes found by varying the added resistance in wind by +-20 %

Table 4: Key characteristics of the routes in the Crete scenario

Route	Fuel consumption difference	Travel distance	Travel distance difference	Travel time	Travel time difference
Original	-	2071 km	-	4 days, 03:14:36	-
WRT	8.7 % less	2092 km	21 km (1.0 %) more	4 days, 04:10:15	00:55:39 (0.9 %) more

Table 5: Key characteristics of the routes in the Biscay scenario

Route	Fuel consumption difference	Travel distance	Travel distance difference	Travel time	Travel time difference
Original	-	657 km	-	1 day, 7:35:23	-
WRT	6.4 % less	660 km	3 km (0.5 %) more	1 day, 7:35:07	00:00:16 (0.0 %) less
WRT (120% Wind)	4.6 % less	670 km	13 km (2.0 %) more	1 day, 8:06:09	00:30:46 (1.6 %) more
WRT (80% Wind)	10.1 % less	660 km	3 km (0.5 %) more	1 day, 7:37:31	00:02:08 (0.1 %) more
WRT (120% Wave)	4.1 % less	661 km	4 km (0.6 %) more	1 day, 7:38:53	00:03:30 (0.2 %) more
WRT (80% Wave)	10.5 % less	659 km	2 km (0.3 %) more	1 day, 7:33:57	00:01:26 (0.1 %) less
WRT (105% Calm)	3.4 % less	661 km	4 km (0.6 %) more	1 day, 7:38:16	00:02:53 (0.2 %) more
WRT (95% Calm)	11.3 %	665 km	8 km (1.2 %) more	1 day, 7:49:58	00:14:35 (0.8 %) more

NAVIGATIONAL SUPPORT

Defining the relevant operational points is critical for custom-tailored ship design as currently practiced. According to our research, there is a high variance in how these operational points are defined. Making a digital twin of the prototype available at design time, we want to engage in a discourse on the differentiation of an optimization project or making compromises transparent and discussable at the design stage. The role of virtual prototyping (VP) and related concepts in ship design has been identified as crucial in the highly individualized field of ship design, with even sister ships having significant design variations (Hassani, et al., 2016). Effective VP requires an interdisciplinary effort, covering hydrodynamics, machinery and power systems, structural engineering, navigation, and control. Current contributions in the field focus on methodological innovation in the design processes (Dodero, Bertagna, Braidotti, Marinò, & Bucci, 2022), the discourse on Human-Centered Digital Twins (Preuss, et al., 2023), and review the “clean” integration of Digital Twins (DT) in Marine Engineering (Mauro & Kana, 2023) or industry in general (Sharma, Kosasih, Zhang, Brintrup, & Calinescu, 2022). This paper aims to contribute to and expand upon the framework relating virtual Prototyping/Digital Twins and Ship Design.

Our goal is to provide early-stage information to operators on how a ship might behave in future scenarios and inform ship design by how operators will actually conduct the vessel—and in which typical range of environmental conditions. On one hand, we used this constant comparison of virtual ship operation and actual journeys to inform and validate model construction. On the other hand, having the DTs and actual environmental data available during design-time enables designers and operators to compare the performance of design variants, including current ships, all performing under the same conditions. In this project, we derived actual typical operational points from previous journeys, combined them with actual trips and environmental conditions encountered, and enabled operators to drive the digital representations of existing ships and prototypes in a highly realistic ship simulator in identical conditions, e.g., actual weather data. Repeated with design variants, this enables a much more detailed look into, e.g., added resistance (e.g., wind, wave and even hull fouling effects), resulting in requirements analysis of unprecedented depth, matching the custom-tailored approach to carrier vessel design aimed for today to ensure peak energy efficiency.

Ship design is always a compromise. Designers today already account for added resistance, but can seldom base calculations on detailed data of, e.g., how often a ship will actually face specific conditions. In this project, a broad parameter space is explored, including the analysis of a crew’s decision-making between avoiding and confronting weather situations in simulator runs where, on historical routes with actual weather data, and equipped with a next generation energy efficient operational decision support system developed in this project, future operators determine the sweet spots informing design decisions. Gathering these data during design time enables addressing operational aspects

during simulations (e.g., prioritizing cargo space upfront in the ship, even if it negatively impacts seakeeping resistance). Additionally, our system allows for the detailed exploration of future propulsion systems, such as diesel-electric drives, with the ability to connect multiple engines to an electrical power supply, and its design implications, when existing ships on established routes are to be replaced.

Supporting this virtual prototyping and test-driving, a novel Onboard-Decision Support System (DSS) for navigational and operational support was designed and implemented (Schwarz, et al., 2023), enabling differentiated control over route optimization processes. A novel module allows for the inspection of simulation data quality (i.e., uncertainties), pertaining to chart accuracy, up-to-date weather, and model fitness for the current operational point, among others. This digital-twin powered tool also enables logging and evaluating user actions (Zoubir, et al., 2023), again driving the optimization process in the ship design phase. Factors considered in the DSS include Requested Time of Arrival as multiple distinct windows (i.e., encouraging slow steaming to match external conditions in tide waters, ship lock operational times or port arrival time frames), CO_2e emissions, and energy efficiency, enabling the analysis of crew decisions in specific contexts. The DSS hereby interacts with the DT for route optimization, realistic simulation, and simultaneously feeds and optimizes the DT. Insofar, the DSS functions as both a research vessel and an outcome.

Figure 27: Photograph of Crew Member System Use During Navigational Task "Enroute Re-Planning"

FEEDBACK FOR DESIGN

Ship operational patterns have changed drastically over the past decades. On the one hand enhanced digital systems on board support the crew in operating the vessels leading to a large amount of data which are often only used for optimizing part of the operation. Often based on purely data driven and machine learning algorithms these are also prone to errors resulting from erroneous data collection and sensors if not properly validated. On the other hand, vessels are – still – often designed for a limited range of operational conditions while in practice they encounter all conceivable conditions during their life-cycle often not considered during the early stages of vessel design. This is often due to the fact that a number of operational constraints are not known a priori and may change over time. This may have economic, environmental or even political reasons which are barely predictable at the beginning of a 25 + years lifecycle of a new ship. Present striking examples being the situations around the two major canals, Suez and Panama which call for significant changes of operational patterns, due to different causes but having similar effects. A digital twin in turn which uses all available information from design stages onwards helps to optimize operations and provides valuable feedback to ship design in that collected data will both improve the quality of design data and will form the basis for more holistic considerations of future designs.

During design, predictions of operational and environmental performance are traditionally based on a forecasted, limited range of environmental conditions. Due to limited resources, a design team always needs to decide where to put a focus and hence resources for further improvements and where an existing solution would be sufficient. Similarly, it is important to understand if an improvement at design stage will actually show during operations and to which extent. In

the present example for a medium-size tanker all components which contribute to resistance at representative trim and draft conditions and in specific weather conditions so as to maintain certain speeds were studied. The composition of total resistance followed the classic approach in naval architecture of superposing calm-water resistance, added resistance in waves, wind resistance, resistance due to fouling, resistance when sailing with (small) yaw angles at non-zero rudder angles while keeping the course and, finally, resistance increases in shallow and/or restricted waters. It was generally assumed that secondary influences are negligible, for instance, that mean wind resistance does not change with ship motions in heavy seas. Furthermore, added drag due to openings such as bow thrusters, sea chests, sacrificial anodes, potential asymmetries from production etc. were not accounted for.
There are several findings that this study suggests, some of which are not surprising while others may indicate that further attention should be given in the future:

- Calm-water resistance, unsurprisingly, is the governing component. A decrease or increase of resistance yields similar improvements or drawbacks, respectively, provided the propulsive efficiency is not determinately affected. At least for the tanker design at hand and for the routes considered any improvement – independent of where it comes from – leads to reductions in fuel oil consumption to almost the same extent.
- The increase of resistance due to hull and propeller fouling has very tangible effects. While maintaining good conditions is controlled by the operator the design team may be able to contribute to the ease of cleaning the wetted surface.
- Wind resistance turns out to be a component that deserves more attention. Even though air is considerably less dense than water (factor around 800) the air resistance is non-negligible and should be considered when designing superstructures for higher energy-efficiency.
- Added resistance in waves naturally also contributes to overall resistance. However, tangible increases lead to less severe drawbacks in fuel oil consumption and, vice versa, tangible decreases – while being hard to realize when keeping the main dimensions constant – also do not show considerable effects.

While these findings are based on the current example it is evident that the concept of a design based Digital Twin for energy efficient operation can yield equivalent conclusions also for other ships and ship types. Using the complete design information collected in the surrogate models introduced in the Resistance chapter, the Digital Twin allows analyzing the effect of any special focus in form of a “What if?” analysis once weighted changes to either factor influencing the performance are introduced. This feedback will allow designers to more efficiently decide on the focus for further improvements. In the future this will particularly apply to so-called green ships, for which the use of alternative fuels or energy sources (e.g. wind propulsion) introduces additional constraints not addressed in traditional design processes.

CONCLUSIONS

The MariData project developed a simulation based digital twin for improved energy management of ships, based on available design information which was further enhanced using the same concepts as during design to cover the broader range of operational conditions encountered during the life-cycle so far. As an example, a medium sized tanker was investigated in a white-box approach for its major resistance components and its propulsion system, comprising the propeller, the rudder and the main engine. All components were simulated with appropriate and validated numerical methods for large sets of representative conditions. The data were captured in dedicated surrogates equivalent to those already applied during design optimization for a fast and repetitive look-up. Subsequently, a simulation tool was established that takes environmental conditions – wind, waves, currents and bathymetry – along with the ship’s loading – draft and trim – into account and computes the fuel-oil consumption for any given speed. Uncertainties in each of the modelling and simulation steps have been considered, This allows running routing optimizations in which all important contributors are considered. For each leg along a certain route the simulation tool thus determines the expected FOC.

Comparing onboard measurements for several routes, primarily along Europe’s Atlantic coast and in the Mediterranean, with the white-box simulations fed with the weather and bathymetry encountered and the speed (through water and over ground) measured on the ship has shown realistic accuracy. Nevertheless, some erratic differences which are visible when comparing simulated and measured engine power could not be resolved yet. The question whether these relate to the reliability of acquired sensor data from onboard measurements needs to be solved in the final phase of the project. An uncertainty is also introduced in the comparison of simulations as local weather phenomena could still have been slightly different to the hindcasts interpolated from the European weather grid. The surrogates which represent the digital twin of the ship are smooth and, therefore, cannot be held responsible for higher frequency variations of the solution. While the simulations may not always yield results that are accurate in absolute terms, they indicate clear tendencies. Looking at the relative FOC for various routes gives confidence that the major elements which determine overall energy consumption were well captured. The system combining weather routing and FOC was further utilized to check sensitivities regarding hypothetical changes of various resistance components. Those changes are representative of two scenarios: (i) What should a design team focus on when spending resources on improving a ship and (ii) which components need to be captured accurately to yield reliable suggestions for safe, economic and environmentally friendly routes. To this end,

hypothetical changes to three resistance components were undertaken: (i) What if calm-water resistance, i.e., the lion's share of resistance, could be improved by 5% and vice versa. This is typical of many hull form optimization campaigns that often yield three to seven percent of improvements over good baselines. (ii) What if added resistance in waves is under- or overestimated by 20%. Of course, added resistance in waves cannot be influenced so easily at the design stage, save for modifying main dimensions which, however, are often more or less fixed. Yet, for routing, unless a rather high-fidelity seakeeping code is employed, the accuracy of the predictions, at least in many routing routines, might only be within that range, see Harries et al. (2023). (iii) What if the estimate for wind resistance is +-20%, wind resistance not being considered often at the design stage with more than reasonable estimates.

As expected, though not often shown, changes in calm-water resistance are fully apparent, i.e., any improvement leads to a reduction in energy consumption of almost the same amount. Added resistance in waves and wind resistance often being substantially smaller than calm-water resistance do not influence the FOC to the same extent. Yet, they affect the optimal route by avoiding detrimental and by taking advantage of favorable conditions. Therefore, it appears questionable if a routing algorithm can produce reliable predictions for energy savings if the underlying models are too simple, e.g., if calm-water resistance is merely taken from series data via the input of a handful of main dimensions, see Harries et al. (2022) for additional discussion.

Consequently, for design work it seems fair to still focus on calm-water performance as has been done in the past. However, aerodynamics should no longer be simply estimated. While this might be obvious for ships that should be retrofitted with wind-assisted propulsion systems (WASPs) or new buildings that shall benefit from WASPs from the start this may well be worthwhile to consider for ships in service and for new buildings, especially in view of retro-fit options which can offer reductions in aerodynamic resistance for a range of vessels (Voß & Marzi, 2020).
While here a white-box model for the simulation of FOC was used it should not be forgotten that there are black-box models, too. They are trained on data measured onboard a ship over considerable periods of time without building on any physics-based simulations or using low fidelity models. Black-box models may potentially be more accurate regarding actual FOC, in particular when applying machine learning on large data sets. However, from black box models it is likely more difficult to understand which components contribute how much to the overall performance, making them less valuable for designers. In the future, a hybrid approach may show benefits, i.e., as suggested in the synthesis model presented here, see Fig. 2, the major contributors are determined from a white-box while deviations could be captured from a black-box. This, however, is subject to additional research. Based on the experience made here, one should be cautious with data from onboard measurements. They should not be used without supervision and intelligent filtering.

Naturally, it needs to be kept in mind that the study presented here only covers a single ship. It stands to reason, however, that similar influences could be seen for other ships. For smaller ships, for instance, the effect of added resistance in waves might be more important since they experience larger motions. For ships with sizeable loads on and above deck, meanwhile, the impact of wind resistance might have greater importance. Additional work is needed to quantify which components show an especially strong influence on both energy consumption as considered at the design stage and routing recommendations as made for efficient ship operation.

CONTRIBUTION STATEMENT

Conceptualization: All authors
Data Curation: Katharina Demmich, Martin Pontius, Martin Scharf
Formal Analysis: Katharina Demmich, Martin Pontius, Martin Scharf
Funding acquisition: All authors
Investigation: Katharina Demmich, Martin Pontius, Martin Scharf, Mourad Zoubir
Methodology: Katharina Demmich, Martin Pontius, Martin Scharf
Project administration: All authors
Software: Jörg Brunswig, Katharina Demmich, Jan Heidinger, Jan Kaufmann, Malte Loft, Rupert Pache, Martin Pontius, Martin Scharf
Supervision: Jochen Marzi, Stefan Harries
Resources: Mirco Schomburg, Xin Gao, Scott Gatchell, Christian Schyr
Validation: Katharina Demmich, Martin Pontius, Martin Scharf
Visualization: Katharina Demmich, Martin Pontius, Martin Scharf, Rupert Pache
Writing – Original Draft: All authors
Writing – Review & Editing: All authors

ACKNOWLEDGEMENTS

The presented work is part of the German national research project MariData, http://maridata.org/, which is partly funded by the German Ministry of Economic Affairs and Climate Action (BMWK) on the orders of the German Bundestag and PTJ as the conducting agency (FKZ 03SX528). The authors wish to acknowledge the support given by the MariData partners, specifically Carl Büttner Shipmanagement.

This study has been conducted using E.U. Copernicus Marine Service Information; https://doi.org/10.48670/moi-00016; https://doi.org/10.48670/moi-00017

We acknowledge the National Center for Atmospheric Research (NCAR), for providing public access to the GFS forecast data products (https://doi.org/10.5065/D65D8PWK; NCEP, 2015).
We also acknowledge the NOAA National Centers for Environmental Information for providing public access to the ETOPO 2022 global relief model (https://doi.org/10.25921/fd45-gt74).

REFERENCES

Dodero, M., Bertagna, S., Braidotti, L., Marinò, A., & Bucci, V. (2022). *Ship design assessment through virtual prototypes* (Vol. 200). Retrieved from https://linkinghub.elsevier.com/retrieve/pii/S1877050922003325

EU Copernicus Marine Service Information (CMEMS). Marine Data Store. (n.d.). *Global Ocean Physics Analysis and Forecast.*

EU Copernicus Marine Service Information (CMEMS). Marine Data Store. (n.d.). *Global Ocean Waves Analysis and Forecast.*

Hafermann, D. (2007). The new RANSE Code FreSCO for ship applications. *Jahrbuch der Schiffbautechnischen Gesellschaft*, p. 103.

Hagiwara, H. (1989, 11). *Weather routing of (sail-assisted) motor vessels.* Retrieved from http://resolver.tudelft.nl/uuid:a6112879-4298-40a6-91c7-d9a431a674c7

Harries, S., Cau, C., Marzi, J., Papanikolaou, A., Kraus, A., & Zaraphonitis, G. (2017). Software Platform for the Holistic Design and Optimisation of Ships. *Jahrbuch der Schiffbautechnischen Gesellschaft 2017.*

Harries, S., Dafermos, G., Kanellopoulou, A., Florean, M., Gatchell, S., Kahva, E., & Macedo, P. (2019). Approach to Holistic Ship Design – Methods and Examples. *Computer Applications and Information Technology in the Maritime Industries (COMPIT 2019).*

Hassani, V., Rindarøy, M., Kyllingstad, L., Nielsen, J., Sadjina, S., Skjong, S., . . . Pedersen, E. (2016, 6). *Virtual Prototyping of Maritime Systems and Operations.* Busan, South Korea: ASME. Retrieved from https://asmedigitalcollection.asme.org/OMAE/proceedings/OMAE2016/49989/Busan,%20South%20Korea/281064

Hundemer, J. (2005). *Erstellung eines Verfahrens zur Berechnung der Auftriebskräfte von dreidimensionalen Tragflügeln mit Hilfe der Potentialtheorie.*

Kaleris. (2024). *CVS Fleet Performance Bluetracker.* Retrieved from https://kaleris.com/solutions/cvs-fleet-performance-bluetracker/

Marzi, J., Papanikolaou, A., Brunswig, J., Corrignan, P., Lecointre, L., Aubert, A., . . . Harries, S. (2018). *HOLISTIC ship design optimisation.* CRC Press.

Mauro, F., & Kana, A. (2023, 2). *Digital twin for ship life-cycle: A critical systematic review* (Vol. 269). Retrieved from https://linkinghub.elsevier.com/retrieve/pii/S0029801822027627

National Centers for Environmental Prediction/National Weather Service/NOAA/U.S. Department of Commerce. (2015). NCEP GFS 0.25 Degree Global Forecast Grids Historical Archive.

NOAA National Centers for Environmental Information. (n.d.). *ETOPO 2022 15 Arc-Second Global Relief Model.*

Papanikolaou, A. (2018, 12). *A holistic approach to ship design: Optimisation of ship design and operation for life cycle* (Vol. 1). Springer International Publishing.

Papanikolaou, A., Harries, S., Hooijmans, P., Marzi, J., Le Néna, R., Torben, S., . . . Boden, B. (2022, 3). *A Holistic Approach to Ship Design: Tools and Applications* (Vol. 66). Retrieved from https://onepetro.org/JSR/article/66/01/25/453209/A-Holistic-Approach-to-Ship-Design-Tools-and

Preuss, K., Schulte, S., Rzazonka, L., Befort, L., Fresemann, C., Stark, R., & Russwinkel, N. (2023). *Towards a Human-Centered Digital Twin* (Vol. 118). Retrieved from https://linkinghub.elsevier.com/retrieve/pii/S2212827123002809

Schwarz, B., Zoubir, M., Heidinger, J., Gruner, M., Franke, T., & Jetter, H. (2023). Investigating Challenges in Decision Support Systems for Energy-Efficient Ship Operation: A Transdisciplinary Design Research Approach. In T. Ahram, & C. Falcão (Ed.), *AHFE Open Access, 114.* USA. doi:10.54941/ahfe1004281

Sharma, A., Kosasih, E., Zhang, J., Brintrup, A., & Calinescu, A. (2022, 11). *Digital Twins: State of the art theory and practice, challenges, and open research questions* (Vol. 30). Retrieved from https://linkinghub.elsevier.com/retrieve/pii/S2452414X22000516

Stiesch, G. (2003). *Modeling Engine Spray and Combustion Processes.* Springer. doi:10.1007/978-3-662-08790-9

Voß, J.-P., & Marzi, J. (2020, September). Cheating the Wind – at sea. *The Naval Architect* (September 2020), pp. 46-48.

Walther, L., Rizvanolli, A., Wendebourg, M., & Jahn, C. (2016). *Modeling and Optimization Algorithms in Ship Weather Routing* (Vol. 4).

Zoubir, M., Gruner, M., Schwarz, B., Heidinger, J., Jetter, H., & Franke, T. (2023). Charting the Course: Human Factors Research for Shipping Energy-Efficient Operations. *AHFE 2023 Hawaii Edition.* USA. doi:10.54941/ahfe1004338

Proceedings of 15th International Marine Design Conference (IMDC-2024)
June 2-6, 2024
Amsterdam, the Netherlands

Industry 5.0: Transforming ship design through human-centered approach

Ludmila Seppälä[1,*]

ABSTRACT

Industry 5.0 heralds a paradigm shift by reinstating the significance of human centricity alongside technology. Incorporating human collaboration into the design methodology aligns with general project management methodology and addresses the imperative of facilitating sustainable goals in the industry. Focusing on human skills and aspirations offers a viable path to expedite the adoption of new technology into the mainstream, aligning with the evolving needs of the shipbuilding industry and green targets of society development. The article delves into the implications of the Shipbuilding 5.0 paradigm to design process and methodology, the potential changes it brings, and the potential benefits it can offer to the evolution of the shipbuilding industry.

KEYWORDS

Shipbuilding 5.0; Human aspects of technology; Digital transformation; Design methodology

INTRODUCTION

The ship design process is often perceived as a primary engineering discipline focused on functionality. There are numerous methodologies and approaches to managing and organizing this process and many forums where such topics are discussed. A recently introduced concept to the shipbuilding world is Industry 5.0. Initially developed by the EU (European Union Publications, 2021), it takes the previous idea of Industry 4.0 to the next level. The levels of the Industrial Revolution are conceptual simplifications capturing the core changes in the social-technology landscapes and related processes understanding. These levels should not be interpreted as an assessment of the technology use, readiness, or advancement in digitalization, as these only indicate the industry's transformation stage and a conceptual framework.

Changes described in Industry 5.0 can be reflected in the evolution of the shipbuilding industry and ship design process. This article explores what changes in ship design can be expected in the context of Industry 5.0. It starts by providing an overview of the Industrial Revolution concepts focusing on ship design and shipbuilding, identifying impact areas, examining each area in detail, and offering a framework approach for considering the human-centricity perspective.

SHIP DESIGN METHODOLOGIES AND HUMAN CENTRICITY

The slow evolution of the ship design activities and methodology development reflects the society and technology development process. Figure 1 presents a very simplified version of the main changes in shipbuilding, primarily triggered by industrial evolution. From sailing ships to steam engines and steel hulls, these changes directly impacted the designs and purposes of vessels. It enabled longer sailing routes and larger cargo holds, and it is impossible to say what the cause and the reasons were

[1] CADMATIC, Turku, Finland
* Ludmila.seppala@cadmatic.com

Submitted: 18 March 2024, Revised: 24 April 2024, Accepted: 1 May 2024, Published: 21 May 2024

Conference paper, DOI: https://doi.org/10.59490/imdc.2024.865 e-ISSN: 3050-4864

- the desire for stronger vessels or the enablement of longer sailing due to more reliable ships. Later, CAE/CAD/CAM technology enabled more complexity and opened the doors to robotized production processes. This process is still ongoing; however, hardly any ship design is performed without the involvement of IT technology. Now, we witness the next leap forward with data management systems, advanced simulation, and a human-centricity finding its space in the IT technology serving shipbuilding. The latest stage of evolution, Shipbuilding 5.0, is expected to focus on placing human needs and capabilities at the heart of intelligent IT to take cyber-physical systems to the next level.

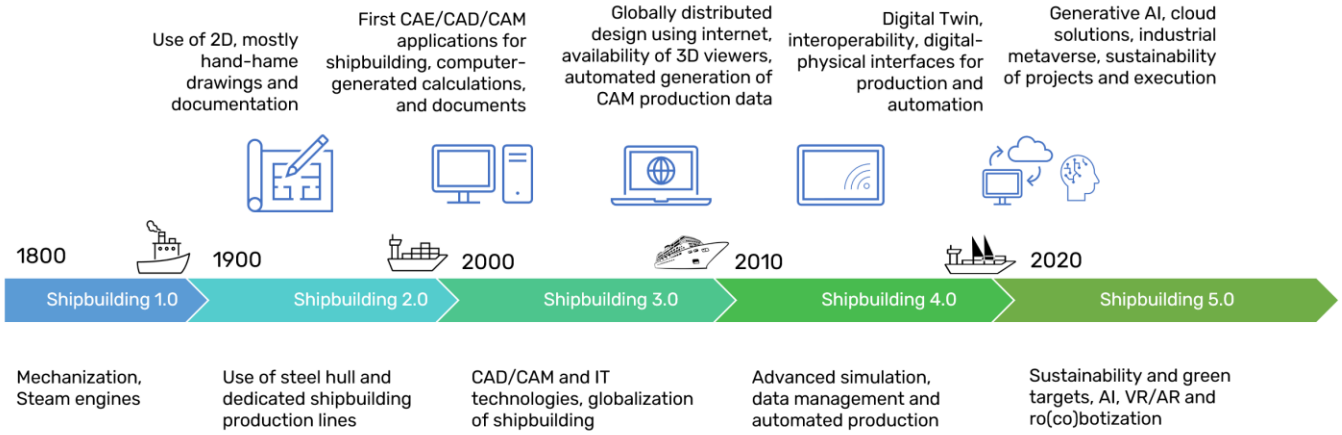

Figure 1: Evolution of concepts towards Industry/Shipbuilding 5.0 and main driving forces behind the concept levels and ship design technology.

For the ship design process, these steps can be described as a change from manually made design to technology-creating design based on human input. Only 30 years ago, it was a mainstream practice to do calculations and prepare all documentation using pen and paper or a calculating machine at best. Some 20 years ago, the first applications for engineering calculations were employed for ship design. At about the same time, the first CAD application provided the possibility to create a digital model and 3D model to evaluate engineering decisions and generate semi-automated output. There are technical possibilities to present the design model in Virtual Reality (VR), use simulation to assess hull forms and propulsion alternatives, and involve any expert anywhere in the world in the design process. These are undeniable advancements of the change that affected the ship design process due to technology and societal evolution. Industry 4.0 emphasizes a connection between digital models and physical products, while Industry 5.0 adds a human-digital-physical layer of complexity. Considering the latest stage, Shipbuilding 5.0, expectations are high with generative AI applications popping up in all areas, the industrial metaverse making its first steps into the industry, and co-bots and robots being employed in many shipyards for various tasks. What makes it unique is its overall focus on sustainability and resilience. It can be expected that the ship design process will be affected by these changes, and the following sections outline some of them.

AREAS OF SHIP DESIGN WHERE HUMAN-CENTRIC APPROACH CAN INFLICT CHANGES

The primary goals of shipbuilding lay in large-scale transportation, with various goals in rivers, sea, and ocean exploration. There are numerous purposes for waterborne transportation and human activities on and underwater. These goals are often substituted in ship design with derived imperatives, such as "delivering value for owners and operators" and ensuring the safety of operations. We must return to the origin and address the initial question - why does society need waterborne transportation and exploration of the rivers, seas, and oceans? While the response to these questions might be obvious, the presentation of the question in this form opens the core of the Industry 5.0 concept, placing human intentions and interests at the core of all processes. Focusing on the core of the initial reason provides a key to evaluating how to fulfill the request. This way, the discussion is taken from the context of shareholders, such as the owner or operator perspective, into a more comprehensive background of stakeholders, such as society goals, regional differences in communities, and people who will operate and use the vessels. This is a primary shift towards human-centricity, which should be performed before functional requirements.

The shipbuilding industry is different from other transportation industries. There are many explanations for this, ranging from the narrow specific expertise required for naval architecture to the complexity of projects closer in scale to onshore production facilities, such as power plants. Additional differences can be found in the methodology approach - product versus project. While most similar industries refer to the end product as a product and hence apply product design and management

methodology, shipbuilding often refers to vessels as projects. It is even sometimes said that shipbuilding projects are similar to the R&D process. However, there is no mainstream discussion about applying methodologies from the R&D approach, such as software development, to ship design processes. As a separate industry focusing mainly on shipbuilding-specific needs, there is little cross-dissemination with other industries and practices. On one side, this helps to facilitate a significant amount of complexity and stay in one direction, but on the other hand, this deprives shipbuilding of experiences in similar industries and technologies, as well as general management practices.

To summarise, ship design has the following differentiators: rapid advancement to the functional approach, lack of connotation with other industries, and approaches to design. The next part presents a more detailed discussion about the areas with the most potential to evolve under the concept of Shipbuilding 5.0.

Change of focus from shareholders to stakeholders

The purpose of building vessels should primarily focus on the intention of its use and, consequentially, on human intention. Therefore, decisions made during the design stage should be verified against the design's intended purpose. One might say that ship technical specifications outline all these intentions and purposes, and indeed, this is the expected flow of information—the ship owner would describe in a relatively detailed manner the main expectations and limitations for the future vessel. Ideally, it should incorporate the expectations of people who need to "keep vessel at seas" and those who "need to make it functional" onboard. However, the technical specifications are often copied from previous vessels and projects, and requirements are significantly affected by personal preferences or beliefs. It is a very human way, but unfortunately, such misconceptions placed in the first steps of the design process significantly affect the later stages.

Two examples of the early identification of the end user need tackled early in the process are twin x-stern by Ulstein and double-acting technology (DAT) by Wärtsilä. In both cases, identification of the primary intentions of the vessels and expected operations in the early stages led to an entirely new design. In the case of Twin X-stern, a step away from traditional thinking with one stern, they proved maximum maneuverability and fuel savings, especially for offshore operations requiring a ship to remain in position in rough weather (Ulstein, 2021). In the case of DAT, the new design was identified during tests, leading to a whole new class of designs optimized for bow performance in open water and stern designed to break the ice (Warsila, 2024). Another similar example is a barge and pusher or puller combination, initially created to address the challenges of inland shipping and insurance requirements for unmanned vessels. Instead of having a manned vessel, having an unmanned barge and a pusher tug operating alongside is a more economically feasible solution.

The examples illustrate how addressing human centricity at the very early stages of the design can change the course of the design process and challenge standard practices or intentions to reuse previous project practices. Changing the focus from the shareholders' perspective of the ship owner to stakeholders of the future vessel, such as the primary purpose of the new-build project, its goals, and expectations, might significantly affect the design outcome and the later design stages.

Future use of ships and how to address unknowns

A typical lifespan of commercial vessels is about 20 years, and the navy fleet might be extended to 30 or more years. This means that many unknown and unpredictable factors exist when defining the main characteristics of future designs. Such concerns are repeatedly addressed in the methodology research, and a comprehensive overview is presented in IMDC 2022 (Erikstad, 2022). The questions brought to the discussion are uncertainty when designing for the future and the needed flexibility to meet this uncertainty. Some industry design companies experience the same concerns and look for a methodology to tackle these design aspects (Yrjänäinen, 2023). The approach proposed revolves around a typical engineering approach – to account for the changing factors, such as technologies, regulations, and environmental changes, and integrate these into the operational scenarios accounted for in the design. This approach is propagated to the simulation of operations, and while being a viable alternative, it exercises a linear approach to a complex design problem. One may argue that similar problems are addressed in variant management for a typical PLM approach and scenario-building technique in general and strategic management.

A possible approach to tackling this area would be to employ one or several approaches from other fields of study or industries. The shipbuilding industry often dismisses experience from other fields as distinctively different from its own. However, there might be a suitable methodology for approaching complex projects with high uncertainty levels and multi-stakeholders. This approach can be taken from general project management, where many similar or even more complex organizational, process, and methodology issues are actively researched and tested in industrial settings. A more specific methodology, such as agile development principles (Rigby, 2016), can be adopted, similar to the design spiral approach in an iterative nature of incremental development to handle complexity and uncertainty. Considering the ship design project from a typical research and

development perspective, the process outcome changes along the project's progress, and external factors may significantly change the scope and outcome.

Systems thinking (Forrester, 1961) (Ford, 2009) offers yet another way to look at ship design methodology. Currently, it is often applied in a way that limits the scope of functional systems of the ship and system architecture. A broader perspective can be taken to look at a future vessel as a part of the system of stakeholders, such as owner, operator, transportation, or research systems - as a part of the system of shipyards, suppliers network, technology providers, etc. It can offer a more holistic view of design and address human centricity in a large context, leading to innovations, sustainable factors accounted for early, and greater flexibility compared to a standard approach, which gets into the specifics of functional design very early.

An additional way of tackling uncertainty would be to employ futures studies methodology. Futures studies is a field of science that researches the uncertainty and complexity of futures. A classic example of this methodology is scenario building, which offers a way to structure unknowns and include unexpected factors. One of the main principles of future studies is to involve stakeholders in the discussion and, through this discussion, to identify possible, probable, and plausible paths. This approach was presented in the research (Jokinen, 2022), where the influence of creativity shaping long-term futures for decisions made about ship design was examined using foresight methods. Looking at the ship design problem as a task to create a design that serves in the future is a novel perspective to ship design methodology.

Change of design process elements: workforce, expectations, tools, and expertise

The third area of the transformation is the process elements affected by a change of perspective. These elements are workforce, expectations, tools, and expertise. The first one is the change in the workforce, which the industry and academia have witnessed already, and these changes are expected to accelerate in the future – changes in the workforce involved in the design process. Generations XYZ engineers gradually replace the stereotypical image of the past with experienced engineers solving challenges and striving for the best outcome. New generations of engineers expect technology to serve their needs and facilitate a significant part of the design process, including encapsulated best industry practices and tacit knowledge to be embedded in the tools. One aspect of this change is accessibility and user experience of the technological tools interactions – instead of the laborious process of creating 2D drawings to use interactive AI-assisted Mixed Reality (MR) headsets and generate engineering output automatically. Software providers continuously fostered this shift of the paradigm process, and expectations often exceeded reality in this area and sometimes even created unrealistic expectations of technology solving all imaginable problems, which remain unsolved for now.

Expectations are another area that can be affected by incorporating human perspective. Based on the human perspective, marketing promises and sometimes science fiction publications often elevate expectations, creating an image from limitless possibilities. Managing the expectations early enough can help allow a realistic approach and leave space for innovation. It requires a conscious and systematic effort to manage this process instead of considering it taken care of by itself.

Tools are arguably the fastest-evolving element of the design. The tools refer to various ship design packages for modeling, simulations, etc. Within the last decade, only the advancements in hardware and software alone have gone that far to take designers from 2D reality with paper drawings into Mixed Reality, where design can be created and designed full scale with immersing experience in 3D. Digital Twin concepts are enabled by the possibility of handling large and increasingly complex amounts of data and connectivity. The original vision of a unified Digital Twin was gradually substituted with a more practical Digital twin for a particular purpose and now slowly moves into the direction of a digital thread or backbone, enabling the storage and use of Digital Models and Twins for specific purposes. Software developers increasingly place User Experience (UX) at the center of the software development process and recognize the importance of technology adaptation instead of focusing on functionality exclusively.

In the previous wave of evolution, Industry 4.0, the main focus was on the connectivity of digital models and the physical world to enable manufacturing and automation. Blurring the borders between the digital and physical worlds provided numerous applications to send ship design data directly to production or machinery. It became mainstream to use general cutting and welding programs automatically based on 3D data and created many automated interfaces and applications for robotic assembly in the industry. Now, attention from the software development teams is dedicated to the usability of the data, tools, interfaces, and user experience. Therefore, the focus is no longer on the tool's functionality; a human-centric perspective is gradually incorporated, addressing the previously described challenges: workforce and expectations. Fully robotized production lines remain a vision for shipbuilding while using co-bots, and AI-generated planning and scheduling are a reality enabled by advanced ship design technology.

Expertise or skills is the last element of the change process. It refers to specialized expertise required for ship design and knowledge management systems facilitation of organizational knowledge management. Modern shipbuilding's complexity

exceeds a single person's capacity to handle all aspects or disciplines, elevating the need for expertise management, different teams' involvement, and tacit knowledge facilitation. Newer generations of shipbuilders expect technology to store and offer embedded knowledge, skills, and expertise that previous generations needed years to acquire. Here, technology plays an even more critical role as a storage and facilitator of knowledge.

IMPACT ON SHIP DESIGN PROCESS METHODOLOGY

Based on the discussion from the previous part, the following additions can be suggested to the system-based ship design process methodology. Conceptually, these additional additions are presented in Figure 2 as a development for Levander's illustration (Levander, 2006).

Adding the human-centricity aspects calls for additional points in the "design spiral". These points allocate the space in the design process for analyzing stakeholders, building scenarios for functional design as a representation of alternatives, and similarly for the project's economic feasibility. These might be already accounted for in the other stages of the design process; however, making these steps explicitly visible provides a more comprehensive view of the methodology. It highlights three points where the human-centric approach has the most significant impact and can change the course of the whole design process. Figure 2 shows these additions: stakeholder analysis, scenario analysis for functional design, and scenario analysis for economics design.

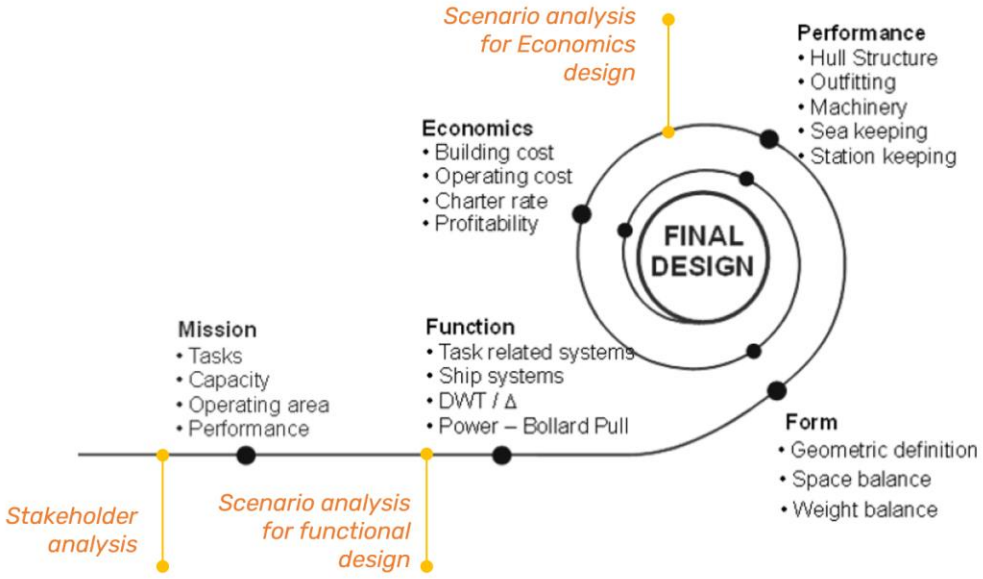

Figure 2: Adapted system-based ship design, a leading figure from (Levander, 2006)**, additional points for stakeholder analysis, scenario analysis for functional and economical design points added based on the proposal from the proposal in the article.**

Stakeholder analysis is suggested as a first step of design activities. Before defining the mission parameters, the initial question should be how and who will benefit from the future vessel. This way, the focus will shift from stakeholders to stakeholders. Analyzing stakeholders can provide insights into the differences between involved groups and potential conflicts of interest among these groups. It would help to map potentially conflicting expectations and also identify sustainability characteristics. As in the examples used above, it can lead to innovative designs and more tailor-made solutions where challenging stereotypes or previous designs have significant potential to offer radically new approaches to design. Such analysis can be arranged as one or several workshops, including as wide a range of shareholders as possible. Ideally, it should include ship owners, naval architects, building yard representatives, and any other potential stakeholders, such as local authorities or local communities that will exploit the potential of a new build.

Scenario analysis (Ramírez, 2016) for functional design is another step after the main characteristics are defined in the two previous steps – stakeholder analysis and mission identification. It should precede the functional design stage and can serve as a foundation for developing several alternative design variants. There are many possible techniques to perform scenario building and analysis. It can be an elaborated process with several workshops, steps, and a thorough study of alternatives, or it can be a simple identification of the central axis for differences and main different scenarios. For example, one axe can be GHG emissions (extremes can be a traditional heavy fuel engine and methanol engine), and another axe can be the shape of a bow

affecting cargo capacity and stability. The natural objection here would be that typically, in the design, there is a multitude of parameters and variations significantly exceeding 2 or 3 extremes, which would lead to the exponential growth of a number of scenarios – 4 in the case of 2 axes, 16 in the case of 3 axes, and so on. To avoid this unnecessary complexity, previous steps from stakeholder analysis and mission clarification can help identify the most valuable criteria for design and focus on these. The outcome of this activity would be a set of distinctively different scenarios for discussion and selection of 1-2 for further development. It can provide a structured way to manage innovation and avoid opinion-influenced decisions.
Scenario analysis for economics design, similar to the functional analysis scenarios, economic scenarios can be built to evaluate the financial feasibility of the project. It can be performed for one functional design or for a set of designs and can include known economic characteristics and future.

Both of the previous steps offer not only a framework to consider different variants and specs of the designs but, most importantly, a tool to address uncertainty in the future. Scenario building is a method in strategic management and futures studies that facilitates the exploration of alternative futures by constructing plausible and consistent narratives of potential developments (Schwartz, 1991). It helps to think systematically about uncertainties, test assumptions, and consider the implications of different future contexts. All of these can enhance design decisions and help avoid design mistakes by providing a structured way of evaluation in complex projects. Along with the scenario methodology, many other tools, such as systems thinking and foresight techniques, can be employed. These can offer a more holistic setting to address the growing complexity of ship design projects, uncertainty of future requirements and regulation changes, and provide a sustainability focus to the maritime industry.

The overall change of the perspective based on human centricity impacts the whole design process. The steps discussed above are explicit actions that can impact the methodology. Besides the methodology, the overall process and its parts are gradually changing. Societal and technological changes impose a significant impact on these. Slow changes from a hierarchical management style in organizations give way to a more flexible way of working, which impacts how decisions are made and how innovations are fostered, allowing the creation of new designs and unleashing human imagination and creativity. Society's goals change from continuous economic growth to sustainability and green targets, giving a prevailing imperative to all activities. Generations of designers change and bring differences in how work is done and what parts are perceived as the most critical. Technology develops fast, allows us to benefit from the digital twin, and opens possibilities for the use of virtual possibilities in simulation, harvesting operational data, and creating an immersive experience in visualization. The whole separate area of potential development is related to Machine Learning (ML) and Artificial Intelligence (AI) applications for ship design and digital twin data management. In addition to the above steps, the design process itself evolves. The management process for ship design as a project, the effect on tools UX or expertise management, including HR aspects or knowledge management systems in organizations—all of these changes will take place gradually in the future and result in updated methodology and, hopefully, the enablement of better designs.

As discussed above, the influence of human-centricity on design process management provides an exciting area for research and application. Ship design methodology can benefit from adopting selected practices from project management – agile methodology, stakeholder and impact analysis, systems thinking, and foresight techniques. This cross-use of methodology from other fields can enrich the narrowly focused ship design process with human-centricity and a broader interpretation of stakeholders' intentions and tackle the uncertainty of future changes. An alternative possibility for such an approach is a service design methodology, with the first research of its application presented (Kim, 2024).

CONCLUSIONS

This article reviewed some aspects of the evolution of the ship design process and methodology based on the framework of the Shipbuilding or Industry 5.0 concept discussion. Without being exhaustive, the main paradigm shift for human centricity was presented as an influential factor in ship design, and possible results of such a shift were discussed. The main areas where the changes can be expected are a change of focus from shareholders to stakeholders, the inclusion of the future uncertainty element in the design decisions, and a change of several aspects of the process: workforce, expectations, tools, and expertise management. Possible impacts on the ship design methodology are identified as three additional steps in the commonly used methodology based on design spiral – stakeholder analysis, scenario analysis for functional design, and scenario analysis for economic evaluation. The expected implications are identified as a structural approach for uncertainty, innovations, and expectations management. The potential benefits include a higher degree of alignment between stakeholders and with the society goals, expectations of new designs and applications of waterborne transport in maritime industry.

The future is not carved in stone, and while some of the implications of human centricity appear most likely, some might take a completely different turn or unexpected directions. While predictions were never the intended outcome of this article, the discussion about Shipbuilding 5.0 and its effects on the ship design process should positively impact the industry overall.

REFERENCES

Erikstad, S. L. (2022). Design Methodology State-of-the-Art Report. *14th International Marine Design.* Vancouver.

European Union Publications. (2021). *Industry 5.0, Towards a sustainable, human-centric and resilient European industry.* Luxemburg: Publications Office of the European Union.

Ford, A. (2009). *Modeling the Environment: An Introduction to System Dynamics Modeling of Environmental Systems.* Washington, D.C.: Island Press.

Forrester, J. W. (1961). *Industrial Dynamics.* Cambridge, MA: MIT Press.

Jokinen, L. (2022). *Ideation for future cruise ships. Collaborative interorganizational foresight in cruise ship concept ideation.* Turku: University of Turku.

Kim, Y. S. (2024). A Service Blueprint Approach in SHipbuilding Activity Mapping. *IMDC 2024.* Amsterdam.

Levander, K. (2006). System Based SHip Design. *TMR 4110 Marine Design and Engineering*. Trondheim.

Ramírez, R. &. (2016). *Strategic Reframing: The Oxford Scenario Planning Approach.* Oxford, UK: Oxford University Press.

Rigby, D. S. (2016). *Embracing Agile.* Retrieved from Harvard Business Review: https://hbr.org/2016/05/embracing-agile

Schwartz, P. (1991). *The Art of the Long View: Planning for the Future in an Uncertain World.* New York: Doubleday.

Ulstein. (2021, 06 10). *The TWIN X-STERN® design provides fuel savings and maximum manoeuvrability*. Retrieved from Ulstein: https://ulstein.com/news/two-sterns-provide-fuel-savings-and-maximum-manoeuvrability

Warsila. (2024, 02). *Wartsila Encyclopedia*. Retrieved from Wartsila: https://www.wartsila.com/encyclopedia/term/double-acting-technology-(dat)

Yrjänäinen, A. (2023, 05 25). *Designing a future-proof solution – being prepared for the carbon-free marine fuel*. Retrieved from Elomatic Top Engineer: https://www.elomatic.com/top-engineer/designing-a-future-proof-solution-being-prepared-for-the-carbon-free-marine-fuel/

Proceedings of 15th International Marine Design Conference (IMDC-2024)
June 2-6, 2024
Amsterdam, the Netherlands

A novel usage of rough sets in design of data fusion systems

Brendan Sulkowski[1,*] and Matthew Collette[2]

ABSTRACT

Design changes for crewless vessels are unexplored compared to the maritime design processes that have been utilized and updated for hundreds of years. This paper presents an exploration into how autonomous and unmanned systems can impact maritime design, specifically focusing on how well they can fuse multiple types of information. Currently, formal and informal communication onboard crewed vessels between various departments is critical in constructing a view of the vessel's current health and future capability. A major focus area is determining whether utilizing data classification techniques can replace these human-centered decision processes, and what the design implications of losing the human synthesis will be. This paper proposes a mechanical spring-mass-damper system with base excitation using real-world ocean data to be used to perform analyses. Rough Set Theory (RST) is a data classification technique that can be used for the characterization of a set of objects, finding dependency between attributes, and creating rules for making decisions. RST is compared with other data classification techniques to determine where each classifier succeeds and how they can generate information useful in design. By integrating the results of these analyses, this paper identifies ways to begin fusing multiple information types and how this will impact marine design in the future of crewless systems.

KEY WORDS

Digital Twin; Machine Learning; Design Uncertainty; Wave Forecast; Safety Prediction

INTRODUCTION

As human safety becomes increasingly more important in every aspect of life, the desire for crewless platforms grows in the ground, air, and marine domains. However, the necessity for operating crewless platforms for weeks to months is a challenging endeavor that separates the naval world from many other domains using autonomous or human-less systems. Designers currently lack guidance on which types of systems may be successful for these long-term applications. While a range of machine learning approaches have been proposed in the computer science literature, it is not clear how these methods could help the overall design process. This work compares a Rough Sets based approach to two conventional classifiers, looking at both accuracy and how the classifiers generate design-relevant information.

Collette et al. (2022) interviewed human crew members who had served or were serving on several types of ships and were involved in different roles both on and off the vessel. Crew members discussed that they were still deeply involved with making sure ship systems were healthy and functional even though there are preventative maintenance systems and sensors

[1] Naval Architecture and Marine Engineering, University of Michigan, Ann Arbor, USA; ORCID: 0009-0000-9970-3918
[2] Naval Architecture and Marine Engineering, University of Michigan, Ann Arbor, USA; ORCID: 0000-0002-8380-675X
[*] Corresponding Author: bsulkow@umich.edu

Submitted: 21 February 2024, Revised: 15 April 2024, Accepted: 1 May 2024, Published: 18 May 2024

Conference paper, DOI: https://doi.org/10.59490/imdc.2024.825 e-ISSN: 3050-4864

onboard that work without humans constantly in the loop. Through years of experience, humans can sense when or where there may be an issue even if it is not noted by a fault sensor or other component. Therefore, a major issue with crewless platforms is exposed – how will we be able to predict failure? This is imperative both in the design phase of a vessel and across the vessel's lifespan.

Remaining Useful Life (RUL) is an estimate of how long an item, component, or system can operate and fulfill its intended purpose before repair or replacement becomes necessary. Gebraeel et al. (2004) developed neural network models around bearing parameters and a parameter-updating algorithm that computed bearing failure time predictions. Liao et al. (2006) present a proportional hazards model and a logistic regression model in predicting the RUL of an individual unit. They also use a bearing test to demonstrate their proposed approach. Li et al. (2018) proposed a data-driven approach for prognostics using deep convolution neural networks. They then used their approach to perform and cross-compare an experimental study with NASA's C-MAPSS Dataset with other approaches. Cai et al. (2020) contributes a hybrid physics-model-based and data-driven remaining useful life (RUL) estimation methodology of structure systems considering the influence of multiple causes by using dynamic Bayesian networks. Finally, Aivaliotis et al. (2017) present an approach to try and provide a satisfactory solution for calculating RUL of machines in a production plant through PHM technique, leading to the idea of using a Digital Twin (DT).

A digital twin is a dynamic virtual representation of a physical object, person, system, or process that absorbs data and replicates processes to predict possible performance outcomes and issues. It will last the entire life of its physical twin, can be updated from real-time data, and can aid in the decision-making process of its twin. Kritzinger et al. (2018) provided a thorough review of DT in manufacturing at that time and showed that development was still relatively new but increasing in effort. Zhao et al. (2020) described a modeling method using DT for a manufacturing process, proposing a hierarchical model and mapping strategy for generating DT data, and Liu et al. (2023) proposed an updating method for DT knowledge based on a memorizing-forgetting model. On the maritime side, Raza et al. (2022) conducted research for applying DTs for autonomous vessels, and stated that DTs can be used to optimize path planning models using real world data such as sea charts and wave disturbance estimates. Mauro and Kana (2023) review the present-day status of DT research, and they state that the shipping industry is a few years delayed compared to other industry sectors, especially manufacturing. Finally, Kinaci (2023) discusses the need for DT for full autonomy in the seas, using a maneuvering math model to represent a physical ship. They developed a digital twin environment for a model ship and tested a control algorithm for sailing automation. Collectively, the prior research on digital twins contains several component examples, but digital twins are not discussed thoroughly from a design perspective, especially regarding autonomous vessels.

Failure prediction will be one of the most important aspects of autonomous vessels, especially in the design phase. These are platforms that do not have the experience of human crews and do not have enough underway data to learn from themselves yet. This work outlines a proposed system model which can be used to model component degradation. Several different classifiers are used on data generated from the model to predict failures and are compared with each other. Finally, rough sets was used to classify and analyze the data to be looked at from a design perspective. Background information on rough sets is included in the machine learning classifiers subsection of the next section.

SYSTEM SETUP AND CLASSIFIERS

Studying vessels designed for long-term autonomy is challenging, as full-scale prototypes are only in the early stages of development. Based on the literature review above, a model system was created to stand in for the autonomous vessel. The model system should have multiple interacting components whose health could be assessed in differing ways and a single output parameter to stand in for the capability of the overall vessel. The model system should also allow realistic weather forecasts and uncertainty to be included in the system. After some discussion, a spring-mass-damper system, excited by stochastic wave systems, was selected. The spring, mass, and damper can be modeled as degrading components; as the value for each change, the overall response of the system also changes. By setting a maximum allowed displacement on the system, an equivalent of a safety threshold, dependent on the health of all three components and the weather prediction, can be modeled. This section introduces the spring-mass-damper system, ocean wave parameters, and the overall setup of the simulation. The parameters used for each trial are described, and the machine learning classifiers are also introduced

and detailed in this section.

Spring-Mass-Damper System

A spring-mass-damper system was developed to model component degradation and is composed of a mass block, a stiffness component, and a damping component, as well as using an ocean wave input as base displacement. The system can use different input parameters such as significant wave height and peak frequency to excite the dynamic system and track its response. Figure 1 is a physical drawing of the system. In the figure, y represents the base displacement, x represents the mass displacement, m is the mass component, k is the stiffness component, and c is the damping component.

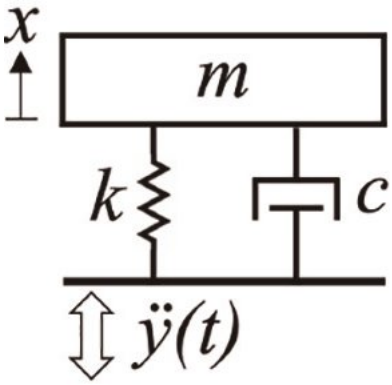

Figure 1: Spring-Mass-Damper system diagram

Simulations using Ocean Weather Data

Using the correct system model and setup is critical for accurate, reusable, and scalable results. The weather data, i.e. the significant wave heights and peak periods used to model the base excitation, were taken from the European Centre for Medium-Range Weather Forecasts (©2023 European Centre for Medium-Range Weather Forecasts (ECMWF) ECMWF (2023)). This data is published under a Creative Commons Attribution 4.0 International (CC BY 4.0).

The ECMWF has open weather data containing wave data from across the Earth, and the ECMWF provides "global forecasts, climate reanalyses, and specific datasets". The data used for this project is five predictions for one specific time on one specific date, which was the 00:00 hour on May 22, 2023. Data was collected at 1000 points distributed across the world's oceans in order to collect a range of different significant wave heights and peak periods. The five different datasets are the real-time data from May 22, and weather predictions from 24, 72, 144, and 240 hours out. Figure 2 displays the significant wave heights at the 00:00 hour on May 22. The regions on the map filled with black markers are the coordinates where weather data was collected for this project.

The mass and stiffness values were chosen to generate a certain range of natural frequencies, which can be converted to natural periods. The periods were selected to correlate with the peak periods seen in the ocean data. The mass, stiffness, and damping values were generated using Latin Hypercube Sampling (LHS) with three dimensions and 1000 data points for each component. LHS distributed m, k, and c values between the selected minimum and maximum for each component, which are shown below in Table 1. The Bretschneider ocean wave spectrum was used to create the wave spectra used for the base excitation. Equation 1 displays the equation used for the Bretschneider wave spectra. This equation comes from the textbook *Offshore Hydrodynamics* (Journée (2001)).

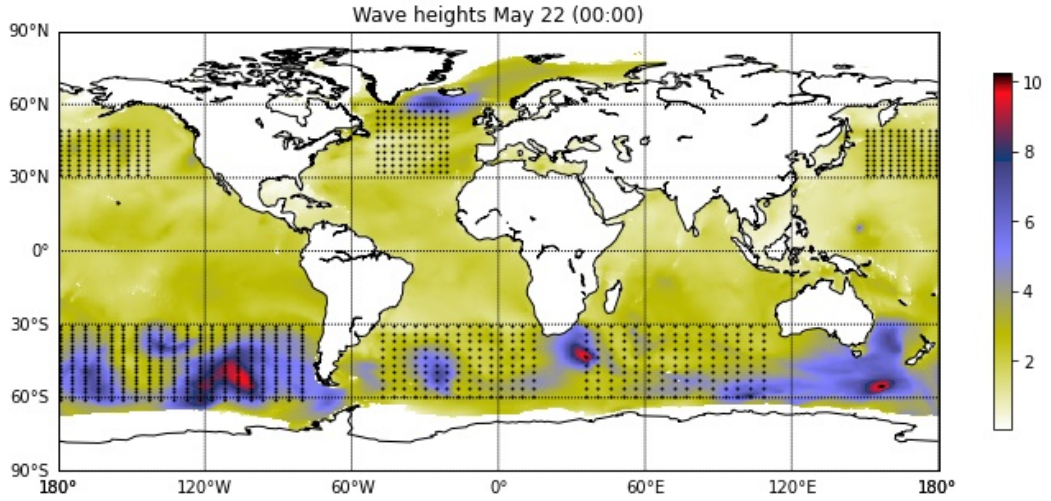

Figure 2: Significant wave heights for 00:00 hour on May 22, 2023 with data collection regions overlaid

Table 1: Minimum and Maximum values for mass, stiffness, and damping components

	Mass (kg)	Stiffness (N/m)	Damping (Ns/m)
Minimum	1	1	0.1
Maximum	10	9	9.5

$$S_\zeta(\omega) = \frac{173 \cdot {H_{\frac{1}{3}}}^2}{{T_1}^4} \cdot \omega^{-5} \cdot exp(\frac{-692}{{T_1}^4} \cdot \omega^{-4}) \tag{1}$$

$$T_1 = 0.772 \cdot T_p \tag{2}$$

Using the mass, stiffness, damping, and wave data values, the average maximum displacement of the mass was calculated for each of the 1000 data points. Equation 3 shows the amplitude for the vibration of a base-excited spring-mass system, and then, using the square root of the moment, multiplied by 3.85, the greatest response amplitude expected on 1000 independent observations is generated. An arbitrary threshold value was selected such that a mix of maximum displacements both exceeded the threshold and remained below the threshold. If the maximum displacement exceeded the threshold, the trial result was considered a 'failure', and if it remained below the threshold, the result was a 'pass'.

$$x = \frac{Ky(1 + (2\zeta\omega/\omega_n)^2)^{1/2}}{((1 - \omega^2/{\omega_n}^2)^2 + (2\zeta\omega/{\omega_n}^2))^{1/2}} \tag{3}$$

The first set of trials looked at how failure prediction accuracy changed with decreasing weather forecast accuracy. For these five trials, the exact m, k, and c values from the LHS results were used. For the base excitation, all 5 weather forecasts were used to determine how prediction accuracy is affected between the real-time zero-hour data and the 240-hour predicted weather data.

Simulations using Alternate Parameters

A major part of the Collette et al. (2022) report revolved around the human interviews with crew members. They reported that human crew members onboard marine vessels are deeply involved in the preventative maintenance process to the point that they are sometimes able to notice a fault or failure before a sensor or machine can report it. However, especially in the design space of autonomous vessels, human inspection will not exist and sensors will be necessary for sensing component health. This puts on the designers the need to choose sensors, sensor accuracy, and decision methods that will use the sensor data. However, very little guidance exists in this space right now.

Therefore, an additional column was added to the data table utilizing a 'visually inspected' spring. The stiffness values were taken from the LHS generations, and using three levels of accuracy, given a label. Results were labeled 'healthy', where the spring is in a healthy and optimal state, 'worn', where the spring is well-used but still functional, and might not work as optimal as in the 'healthy' state, and 'failed', where the spring is no longer operational. For a crewless vessel, this could correlate with an onboard imaging system or periodic human inspection between voyages. A trial was conducted using the visually inspected stiffness results, the same LHS results for mass and damping, and the zero-hour weather data to see how decreasing stiffness component knowledge accuracy affected the prediction accuracy.

Machine Learning Classifiers

Ultimately, a crewless vessel will need to be able to make its own assessment of safety, given its current understanding of its health and the forecasted weather. Collette et al. (2022) noted that this process was highly human-dependent at the moment, with extensive discussion among senior crew members used to arrive at integrated, vessel-level assessments. In designing a crewless vessel, this process will need to be automated. As a first approach, a machine learning classifier could be used to integrate component health information and weather forecasts to assess if the system is safe. In this work, three machine learning data classification techniques were applied to these test cases. Support vector machines (SVM) are supervised learning methods used for classification and regression, and this work features SVM from scikit-learn in Python with the default SVC method (Pedregosa et al. (2011)). An advantage of using SVM is that it uses a subset of training points in the decision function (called support vectors), so it is also memory efficient. SVMs are adaptable and can manage high-dimensional data and nonlinear relationships, however, they are black-box models and the method of finding the final product may not always be understood. In Adadi and Berrada (2018), the authors discuss how black-box models do not disclose anything about internal design or structure, meaning users are finding results without thorough knowledge of how the model is working. On the other hand, glass-box models are completely exposed to the user from start to finish, so users have full knowledge of how the model works.

The second technique is a Decision Tree, which is a glass-box supervised learning method that makes predictions by learning simple decision rules from data features and previous data. A decision tree is a flowchart-like tree structure where internal nodes denote features, branches denote rules, and leaf nodes denote the results of the algorithm. This work uses the tree.DecisionTreeClassifier from sklearn to predict outcomes. It is used for both classification and regression problems, and because decision trees are glass-box models, they present options that allow for informed decisions to be made. For the design phase of the vessel, such rules are useful as they indicate to the designer which parameters and values are most important to understand. However, decision trees can be less accurate than SVM and other black-box models, depending on the problem.

Finally, Rough Set Theory (RST) was also compared. RST can be used for both classification and to give a deeper understanding of the problem and decision space, which is attractive for use in a design setting. RST was orginally proposed by Polish scientist Zdzislaw Pawlak and is a technique for identifying and learning on common patterns in data, especially in the case of uncertain and incomplete data (Pawlak (1982)). The mathematical foundations of this method are based on the set approximation of the classification space. The theory allows for a description of objects to be used which can contain information about various features. The precision, or amount of detail in the description can vary based on the knowledge of the feature and other limitations. RST uses indiscernibility relations to recognize and discover attribute relations. Therefore, it needs data to be in a discretized form to properly function, so the input data for rough sets was sorted into bins for

the data analysis and performance accuracy test.

Also in RST, two approximations are developed: The upper approximation is the set of objects which possibly but do not definitely belong to the target set, and the lower approximation is the set of objects which positively belong to the target set. Objects that fall between the lower and upper approximation are said to be in the boundary region. If the boundary region is non-empty, the set is said to be rough, otherwise it is a crisp set and all cases can be classified without fail.

Large volumes of data can be difficult to classify into specific categories through visual inspection, and RST can discern and classify objects in large data sets. RST uses the indiscernibility relations and lower and upper approximations to characterize and express an information system, and therefore does not require additional parameters to extract information. Rough Sets results were generated in this paper using the RoughSets package in R (Janusz et al. (2020)). The process for performing the data analysis in R begins with taking in the dataframe with the simulation results and converting it into a decision table. Then, the indiscernibility relation is computed and utilized with the decision table to compute the lower and upper approximations. Like with the SVM and decision tree classifiers, the data was split into training and testing sets, and the classifier was then able to compute the predictions for the test set, determine the overall accuracy of the predictions, and generate a list of rules.

Assessment Approach

From the 1000 data points, 700 were used for training the classifiers and 300 were used for the testing phase. The overall accuracy of the predictions was the main focus point for each classifier in comparing them to each other and is defined as the percentage of test trials where the predicted outcome matches the true outcome. The results and comparisons between classifiers are given in the following sections.

RESULTS AND DISCUSSION

The results from the simulations were used with the previously described data classification approaches to predict possible failures. Two different approaches were simulated, the first being the case where the mass, stiffness, and damping values all come from the Latin Hypercube Sampling. These are run with each weather data-set out to 240 hours to see how each classifier handles the changing weather uncertainties. The results are shown in Table 2, with the classifiers bolded in each row, the trial bolded in each column, and the table filled out with the accuracy percentages.

Table 2: Table of prediction accuracies (in percentage) for each classifier in each trial case

	0-hour	**24-hour**	**72-hour**	**144-hour**	**240-hour**
SVM	95.28	95.28	94.85	93.06	90.66
Decision Tree	91.50	91.50	90.72	88.55	85.74
Rough Sets	91.95	91.95	89.70	86.30	84.20

The results show that overall, SVM outperforms the other two classifiers in prediction accuracy. Rough sets performs similar to but better than the decision tree for the 0 and 24 hour trials, but worse than the decision tree for the other three weather prediction cases. In the case of SVM and decision tree, the prediction accuracies remain similar from the 0 hour trial to the 72 hour trial, and then the accuracies drop significantly as the weather prediction becomes increasingly inaccurate. Rough sets performs similarly, except it loses its accuracy at 72 hours instead.

When thinking about how these results can be thought of in the design space, the drop off in accuracy as the weather knowledge weakens should be the main focus point. It emphasizes how designs need to focus on not only overall vessel safety, but also the unpredictability of the oceans. On crewed vessels, humans have the ability to make decisions based on their past experiences and knowledge of how well their ship can handle a certain weather obstacle. On uncrewed vessels however, the vessel itself may need to make the decision on whether to change its mission or remain on course. Being able to

do this from 72 to 144 hours out is much more optimal than only having 24 hours to make a well-informed and accurate decision.

The second approach involves using the same mass and damping component values, but using a 'visually inspected' stiffness component to emulate the findings from the human crew interviews mentioned in Collette's paper. The prediction accuracy results for this approach are shown in Table 3 along with the initial result from the first trial.

Table 3: Table of prediction accuracies (in percentage) for each classifier in the trial case with a visually inspected stiffness component compared to the original test case. The new trial case also uses the 0-hour weather data.

	0-hour	Visually Inspected
SVM	95.28	93.67
Decision Tree	91.50	90.17
Rough Sets	91.95	91.90

The 0-hour result from the first trial is included and compared to the visually inspected trial results because that case contains the most knowledge about the system. The results show that the SVM and decision tree results drop in accuracy by about 1.6 percent and 1.33 percent respectively from the 0-hour, full data case to the 0-hour, visually inspected stiffness component case. However, the rough sets prediction accuracy remains about level with only a drop of 0.05 percent.

The decrease in accuracy is expected with less knowledge about the system as a whole, but rough sets holding its accuracy was unexpected. Again, rough sets prove to be better than the decision tree at this stage and slightly worse than SVM, but closer than before. Rough sets also provides other options for data analysis as opposed to SVM and decision tree, which is detailed in the following section.

IMPACT ON DESIGN

While Rough Sets may not have outperformed the SVM and decision tree classifiers in terms of failure prediction accuracy, it also provides other information that can be more useful in design. The boundary region was defined as being the area between the lower and upper approximation, where the lower approximation was the set of objects that positively belonged to the target set.

The accuracy results show that from the real-time data to the 72 hour prediction data, there is not much of a drop in accuracy. However, there is a significant drop in prediction accuracy when moving to the 144 hour weather prediction data. Therefore, we looked at how the boundary region changes while using Rough Sets from the 0 hour case to the 144 hour case. Six different bin sizes were used for each case, with the bin sizes meaning how knowledgeable the system is on component accuracy. The number of bins ranges from 3 to 20, where the number of bins means that the exact numeric values of mass, stiffness, and significant wave height data have been placed into the corresponding number of bins between their minimums and maximums to discretize them. Such binning is also related to the accuracy of potential sensors for each component.

The trial used for this test case is the visually inspected spring component, along with the bin values in place of the previous mass, damping, and significant wave height components. Table 4 shows the number of cases (out of 1000) that were placed in the boundary region for the different number of bins in each trial.

Table 4: Number of test cases in the boundary region for differing numbers of bins

# of Bins	3	5	7	10	15	20
0h Trial	542	261	143	29	4	8
144h Trial	609	303	150	45	8	10

Looking at the table, the number of bins and the number of cases in the boundary region are clearly related. With a lower

number of bins, such as 3 or 5, there are more cases in the boundary region than at 10 or 15 bins. This shows that the number of bins affects our knowledge accuracy. As we begin knowing more about the system and can better differentiate between data, we can place them more accurately where they belong.

This can be related to design in looking at things such as sensor fidelity. If a sensor can only offer 3 or 5 different knowledge states about a part or product, it might not be worth selecting over one that offers 10 knowledge states. This is especially relevant in autonomous vessels, where knowing the difference between a component being healthy, worn, or failed may make the difference between a successful mission and a lost or compromised asset. However, at the extreme right hand side of the table, a different story is shown. Here, there is little advantage in selecting a sensor accuracy corresponding to 20 bins over one with 15, at least in terms of how well the data can be classified into sets.

Also being compared was the 0 hour trial to the 144 hour trial. The immense fall-off in prediction accuracy for the 144 hour case allowed for analysis in this situation as well to see if a similar pattern developed. While there was not an exact pattern, the superior knowledge of the 0 hour trial outperformed the 144 hour trial at every number of bins. Some cases, such as 7 bins and 20 bins did not have much difference, but with 10 and 15 bins, the 144 hour trial had 66 percent more cases and twice as many cases in the boundary region, respectively. This difference shows how more accurate knowledge about one aspect of a system, in this case the weather component, can allow for better design choices to be made.

Being able to visualize the impact on classification via the size of the boundary region is an important advantage in using a system like rough sets. Compared to black-box classifiers, whose performance may change with hyperparameter settings and the pipeline used to build the model, the boundary region is a fixed property of the engineering data set used to describe the problem. It provides a second way of looking at the potential for classifiers to work on the base problem that is quickly humanly understandable. Differing sensor accuracy and real-world uncertainty can also be examined.

CONCLUSION

This paper presented a system that was used to model component degradation and knowledge degradation. The spring-mass-damper system was combined with real-world ocean data to excite the system and 1000 test cases were simulated. Different machine learning classifiers were used to predict operational successes and failures and were compared to each other based on their accuracies. Support vector machines (SVM) was the best classifier in the sense of prediction accuracy, as compared to decision tree and rough sets. However, Rough Sets provided opportunities to look at the system in different ways, specifically how we can use it to think about design.

Rough sets have the ability to not only predict results from learning on training data, they also can perform other operations. Here, rough sets was used to look into how changing knowledge accuracy about a system or component can affect design knowledge. We saw that as we increased our sensor fidelity, the number of cases that could be positively classified increased immensely. This has design implications where rough sets can be used to determine which configurations or components can be considered in an optimal design region, or if they might need to be worked on further to narrow down the feasible design space.

CONTRIBUTION STATEMENT

Brendan Sulkowski: Conceptualization; Investigation; Data curation; Software; Methodology; Writing – original draft.
Matthew Collette: Conceptualization; Writing – review and editing; Supervision; Funding.

ACKNOWLEDGEMENTS

The authors would like to thank Dr. Jessica Dibelka, ONR code 331 for supporting work to date under grant Number N00014-21-1-2795.

REFERENCES

Adadi, A. and Berrada, M. (2018). Peeking inside the black-box: A survey on explainable artificial intelligence (xai). *IEEE Access*, 6:52138–52160.

Aivaliotis, P., Georgoulias, K., and Chryssolouris, G. (2017). A RUL calculation approach based on physical-based simulation models for predictive maintenance. In *2017 International Conference on Engineering, Technology and Innovation (ICE/ITMC)*, pages 1243–1246.

Cai, B., Shao, X., Liu, Y., Kong, X., Wang, H., Xu, H., and Ge, W. (2020). Remaining Useful Life Estimation of Structure Systems Under the Influence of Multiple Causes: Subsea Pipelines as a Case Study. *IEEE Transactions on Industrial Electronics*, 67(7):5737–5747. Conference Name: IEEE Transactions on Industrial Electronics.

Collette, M., Bielski, R., Rohrer, P., Magistro, A., Sulkowski, B., and Houten, J. V. (2022). Needs Exploration for Long-Term Autonomous Marine Systems: Working Report.

ECMWF (2023). ECMWF | Use of data accessed via this service.

Gebraeel, N., Lawley, M., Liu, R., and Parmeshwaran, V. (2004). Residual Life Predictions From Vibration-Based Degradation Signals: A Neural Network Approach. *Industrial Electronics, IEEE Transactions on*, 51:694–700.

Janusz, A., Jankowski, D., Fiedukowicz, A., and cbergmeir (2020). Roughsets. `https://github.com/janusza/RoughSets`.

Journée, M. (2001). *Offshore Hydromechanics by J.M.J. Journée, W.W. Massie - Download link*.

Kinaci, O. K. (2023). Ship digital twin architecture for optimizing sailing automation. *Ocean Engineering*, 275:114128.

Kritzinger, W., Karner, M., Traar, G., Henjes, J., and Sihn, W. (2018). Digital Twin in manufacturing: A categorical literature review and classification. *IFAC-PapersOnLine*, 51(11):1016–1022.

Li, X., Ding, Q., and Sun, J.-Q. (2018). Remaining useful life estimation in prognostics using deep convolution neural networks. *Reliability Engineering & System Safety*, 172:1–11.

Liao, H., Zhao, W., and Guo, H. (2006). Predicting remaining useful life of an individual unit using proportional hazards model and logistic regression model. In *RAMS '06. Annual Reliability and Maintainability Symposium, 2006.*, pages 127–132. ISSN: 0149-144X.

Liu, S., Zheng, P., Xia, L., and Bao, J. (2023). A dynamic updating method of digital twin knowledge model based on fused memorizing-forgetting model. *Advanced Engineering Informatics*, 57:102115.

Mauro, F. and Kana, A. A. (2023). Digital twin for ship life-cycle: A critical systematic review. *Ocean Engineering*, 269:113479.

Pawlak, Z. (1982). Rough sets. *International Journal of Computer & Information Sciences*, 11(5):341–356.

Pedregosa, F., Varoquaux, G., Gramfort, A., Michel, V., Thirion, B., Grisel, O., Blondel, M., Prettenhofer, P., Weiss, R., Dubourg, V., Vanderplas, J., Passos, A., Cournapeau, D., Brucher, M., Perrot, M., and Duchesnay, E. (2011). Scikit-learn: Machine learning in Python. *Journal of Machine Learning Research*, 12:2825–2830.

Raza, M., Prokopova, H., Huseynzade, S., Azimi, S., and Lafond, S. (2022). Towards Integrated Digital-Twins: An Application Framework for Autonomous Maritime Surface Vessel Development. *Journal of Marine Science and Engineering*, 10(10):1469. Number: 10 Publisher: Multidisciplinary Digital Publishing Institute.

Zhao, P., Liu, J., Jing, X., Tang, M., Sheng, S., Zhou, H., and Liu, X. (2020). The Modeling and Using Strategy for the Digital Twin in Process Planning. *IEEE Access*, 8:41229–41245.

Proceedings of 15th International Marine Design Conference (IMDC-2024)
June 2-6, 2024
Amsterdam, the Netherlands

Human digital twins to inform ship design

Nicole Catherine Taylor[1,*], Anriëtte Bekker[2,*] and Karel Kruger[3]

ABSTRACT

A key building block of digital twin solutions is a virtual counterpart for an asset that can be coupled to the asset throughout its lifecycle – predicting an asset's potential performance at design and providing insight into operation during service. This paper presents the development of human digital twins that integrate human factors into conventional ship design procedures, particularly focussing on seakeeping performance assessments. A novel method for incorporating human-centric performance criteria in seakeeping analyses is proposed and initial validation thereof is detailed. Human digital twins are seen to provide a platform for informing the ship design process using data captured during vessel operation.

KEY WORDS

Digital Twins; Ship Design; Human-Centred Design; Seakeeping; Motion Sickness

INTRODUCTION

A visible rise in research interest is evident in reviews of digital twins in the maritime domain. Digital twin solutions comprise of virtual counterparts linked to assets and communication between the coupled digital and physical entities. This is not to be confused with geometric models that mimic the structural components of assets, particularly in the case of ships. Ship digital twins are recommended to be created at the inception of the physical ship lifecycle, at the beginning of design, to be coupled with the physical asset through production and operation to retirement. (Mauro and Kana, 2023; Madusanka *et al.*, 2023)

The most recent International Marine Design Conference state-of-the-art report on ship design methodology identified exploiting operation data from digital twins as an emerging development that will become an intrinsic part of future design processes (Erikstad and Lagemann, 2022). It is likely that a digital twin of an asset will contribute design data to the design stage of its coupled asset, shown by arrow (a) in Figure 1 for Ship 1. However, it is unlikely that a digital twin of an asset will contribute operation data to the design stage of the asset, as the design precedes the operation of the asset. It is more likely that digital twin of an asset already in operation may inform the design of next-generation or new, similar assets, as shown in Figure 1 for two ships, particularly by arrow (b).

[1] Department of Mechanical and Mechatronic Engineering, Stellenbosch University, Stellenbosch, South Africa; ORCID: 0000-0002-1176-9021

[2] Department of Mechanical and Mechatronic Engineering, Stellenbosch University, Stellenbosch, South Africa; ORCID: 0000-0001-8697-6503

[3] Department of Mechanical and Mechatronic Engineering, Stellenbosch University, Stellenbosch, South Africa; ORCID: 0000-0003-0932-2850

* Corresponding Authors: nctaylor@sun.ac.za, annieb@sun.ac.za

Submitted: 8 February 2024, Revised: 15 April 2024, Accepted: 1 May 2024, Published: 21 May 2024

Conference paper, DOI: https://doi.org/10.59490/imdc.2024.860 e-ISSN: 3050-4864

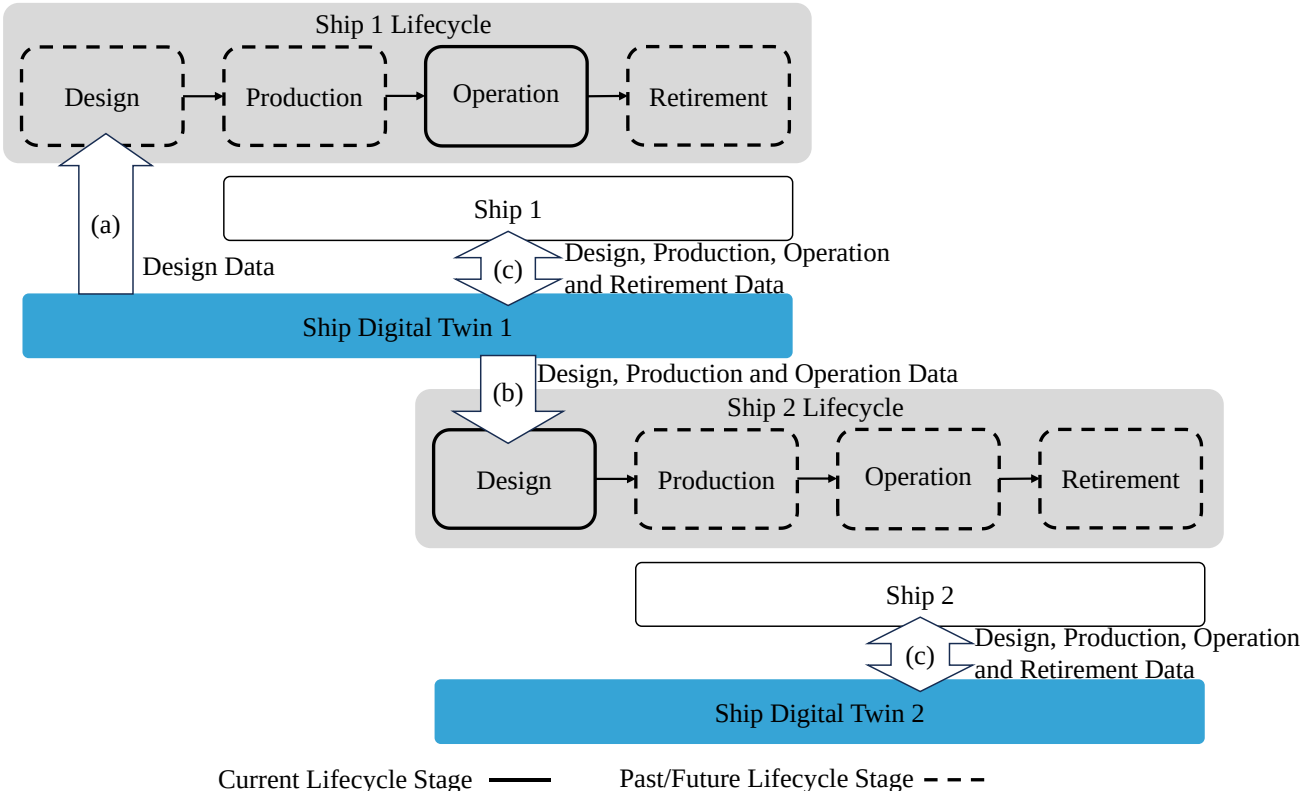

Figure 1: A Digital Twin in Operation Informing the Design Stage of Another Asset.

It is evident that data should be exchanged between the digital and physical entities within a digital twin solution throughout the physical ship lifecycle, represented by arrows labelled (c) in Figure 1 (Madusanka *et al.*, 2023). However, a gap in information flow from digital twin solutions that capture data during ship operation and send data to a new ship's design stage is highlighted in literature, represented by arrow (b) in Figure 1 (Fonseca *et al.*, 2023). The objective of the work presented is to propose information feedback from digital twins used during vessel operation to aid the ship design stage.

In maritime literature, as presented until now, digital twin developments are typically referred to for ships. However, human digital twins are the focus of attention in the work presented. Where a ship digital twin is coupled to a vessel, a human digital twin virtually mimics the identity, condition and behaviour of a person.

A human digital twin for a seafarer, called Mariner 4.0, was developed and trialled on board the SA Agulhas II (Taylor *et al.*, 2023a). Mariner 4.0 facilitated the study of motion sickness in real time during ship operation on a research expedition. Subjective feedback was captured from vessel occupants through a mobile application and sensor readings from a full-scale motion measurement system. The human digital twin developed personalised motion sickness criteria that can aid the diagnoses of motion sickness incidence (MSI), an estimate of the percentage of individuals in a group that may vomit on board (O'Hanlon and McCauley, 1974), using the motion sickness dose value (MSDV), a human-weighted metric of a level of ship motion that is known to induce motion sickness (ISO 2631-1, 1997). An MSDV can be calculated with Equation 1,

$$\text{MSDV} = \int_0^T a_w(t)\,\mathrm{d}t, \qquad [1]$$

where a_w is the frequency-weighted acceleration measured by z-oriented accelerometers and T is the duration of exposure in seconds (ISO 2631-1, 1997). The z orientation is vertically aligned with the heave motion of a ship, but comprises additionally of roll and pitch components.

The work presented starts with a description of a baseline method to assess seakeeping performance that contextualises the proposed means for constructing an information loop from ship operation to design through human digital twins. A Mariner 4.0 deployment and results are detailed as an illustrative use case of the method for informing ship design using human digital twins. Thereafter, potential benefits and drawbacks of integrating human digital twins in ship design procedures are discussed.

It is envisioned that human digital twins will venture out to sea with their seafarer counterparts, returning to land with human-centric insight gained from ship operation that is of value for seakeeping assessments typically conducted in ship design.

SEAKEEPING PERFORMANCE ASSESSMENT METHODS

It is common practice to define the specifications that a ship should achieve or criteria that a ship should not exceed during missions it is designed for, irrespective of the methodology selected for ship design (Erikstad and Lagemann, 2022). Performance criteria are selected to assess ship seakeeping, typically through forming operability envelopes (Tezdogan *et al.*, 2014). Figure 2 presents a foundational procedure for applying conventional seakeeping performance methods. The work presented does not intend to amend the extensively used procedure shown in Figure 2. Instead, the focus is on Step 9, which incorporates the development and selection of human-centric performance criteria.

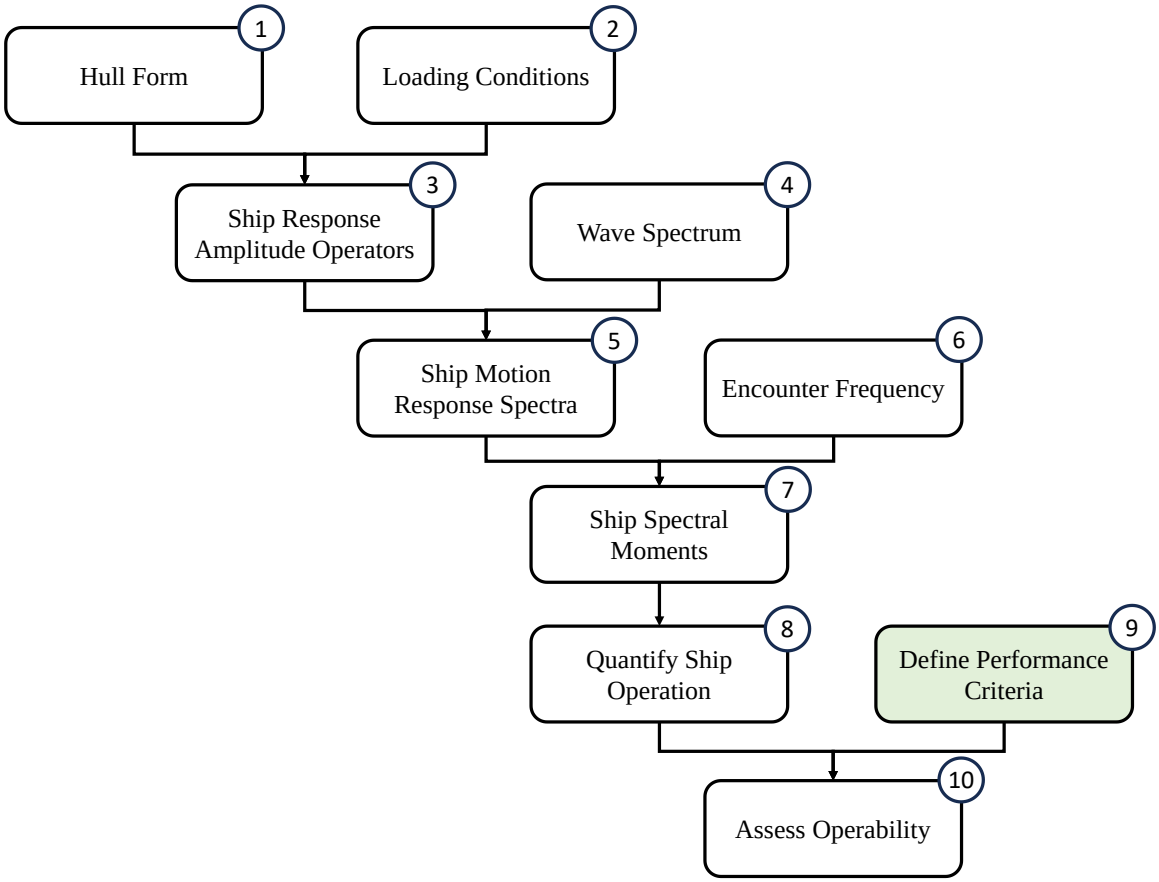

Figure 2: Basis of Conventional Seakeeping Performance Methods (adapted from Tezdogan *et al.*, 2014; Scamardella and Piscopo, 2014; 2015).

DEVELOPMENT OF HUMAN-CENTRIC PERFORMANCE CRITERIA USING HUMAN DIGITAL TWINS

Taylor *et al.* (2023b) proposed that seafarers each be coupled with a unique virtual representation of their state and behaviour, which describes their condition of well-being while performing tasks on board. The virtual representations are human digital twins devoted to acquiring and managing data related to the seafarers they are coupled with during ship operation. The core functions of human digital twins are to acquire data, process data and provide information to support decision making. Data acquired could be related to a seafarer in particular, such as their heart rate measured by a wearable sensor, or their environment, such as rigid body motion of a ship that a seafarer is exposed to, measured by sensors installed on the ship structure. Information that human digital twins should inform seafarers of should be related to seafarers' virtual representations. For example, a seafarer could be notified if their vibration exposure associated with a task that they have scheduled will go above a safety threshold for whole-body vibration when completing a dangerous task. Thresholds in the work presented are values for metrics

that quantify ship performance above which ship operation would be deemed unacceptable (NATO, 2000). If the task does exceed the safety threshold, then rescheduling to when the vibration of the ship is more acceptable would be advised.

Individualised data analyses can be conducted by each human digital twin in such a way that thresholds are determined to aid prediction of human response incidences, such as motion sickness (Taylor *et al.*, 2023a). It is common practice that a threshold is qualitatively selected or, more rarely, estimated from experiments (NATO, 2000). The work presented proposes the development of human-centric performance criteria during ship operation to capture invaluable real-world experiences that are not present during structured experiments traditionally performed at sea trials (NATO, 2000). This incorporates phenomena encountered during the full duration of a voyage into criteria development, such as adaptation to motion. Furthermore, criteria can be tailored to specific voyage scenarios and missions, including various durations of assessment.

Human-centric performance criteria are best developed for seafarers at an individual level that is associated with attributes unique to each seafarer, such as their age or previous seafaring experience. Thresholds are not strictly to be linked to the ship(s) a seafarer lives and works on, but rather metrics of ship operation. Hereby, seafarer-specific collections of human-centric performance criteria developed through human digital twins can be generated so that stakeholders can extract thresholds relevant to their ship or voyage missions. For example, a cruise ship designer may prefer to select characteristics of individuals that best describes an unadapted cohort. Comparatively, naval ship designers would be more inclined to work with thresholds of seafarers that are more tolerant to vessel motion.

OBTAINING AND IMPLEMENTING SEAKEEPING PERFORMANCE ASSESSMENT METHODS THROUGH DIGITAL TWINS

Service-oriented architectures based on digital twins have been developed for maritime solutions (Erikstad and Bekker, 2021). The development and servitisation of the diagnostic motion sickness criteria through human digital twins is recommended, additionally motivated by service-oriented approaches being widely accepted (IEC, 2017). The architecture that displays the interactions between digital and physical counterparts to generate and use diagnostic motion sickness criteria is presented in Figure 3.

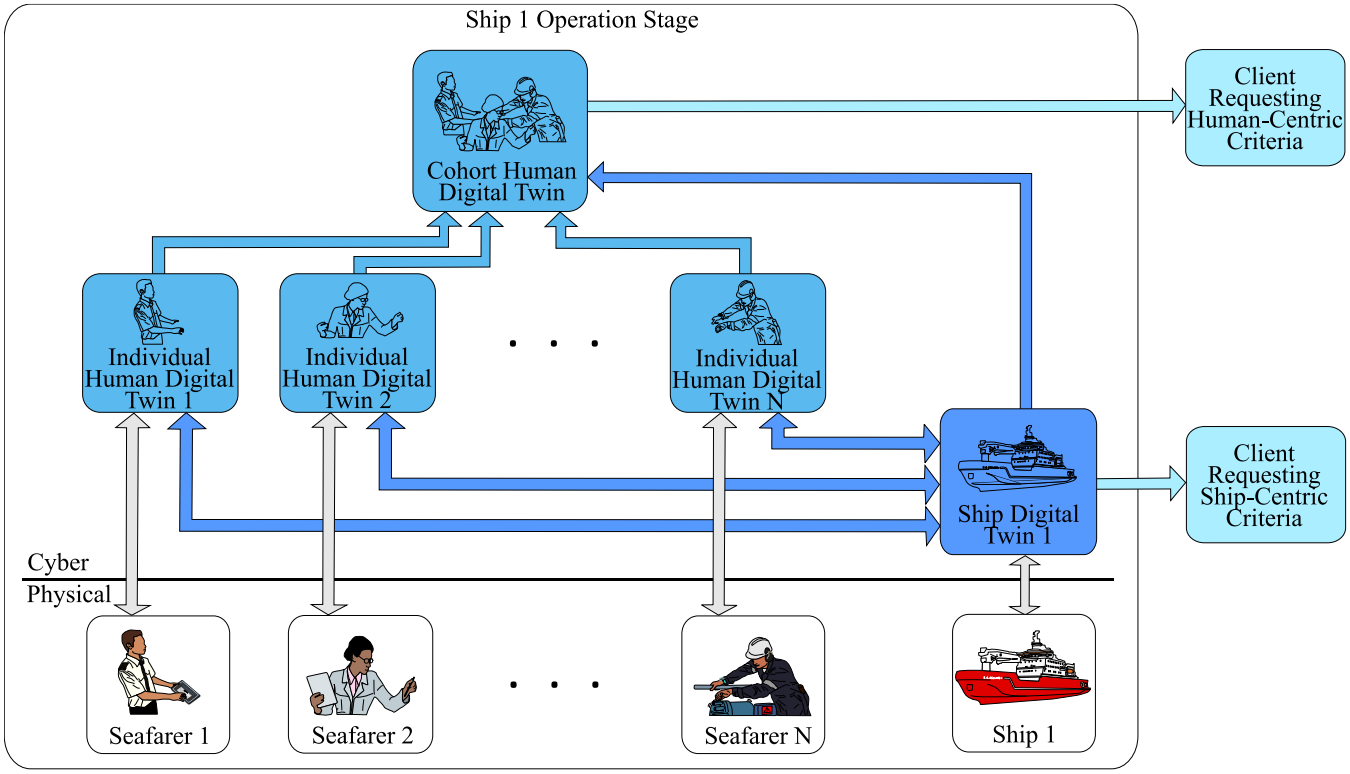

Figure 3: Architecture Displaying the Interactions Required for the Development and Use of Diagnostic Human-Centric Performance Criteria Through Human Digital Twins.

In Figure 3, the individual human digital twins are each coupled to unique seafarers, which generate personalised thresholds. Hierarchically, the thresholds from individual human digital twins are aggregated at a cohort level. The Cohort Human Digital Twin acts as a service provider that offers clients relevant human-centric thresholds.

Clients in the work presented could be any entity that is interested in retrieving a human-centric threshold based on seakeeping methods conducted for the purposes of performance assessments, which is recommended to be included in the functionality of Ship Digital Twin 2 shown in Figure 1. Moreover, full-scale ship measurements are managed by Ship Digital Twin 1, which provides information regarding the state and behaviour of the vessel, such as rigid body motion while travelling through open water during a voyage, or ship-centric criteria.

The work presented does not focus on automated control of the seafarer, but rather on informing stakeholders of relevant information at the appropriate time for making decisions. For example, the Cohort Human Digital Twin could provide the average motion sickness level of passengers to the navigating officers in a ship's Bridge via a user interface, which may be used to inform their next actions, such as adjust the ship speed and course.

ILLUSTRATIVE USE CASE

Motion sickness is focussed on in this illustrative use case as it is a prevalent natural human response to ship motion. Symptoms can include nausea, vomiting, tiredness and bouts of depression in severe cases, none of which are conducive to comfort or productivity aboard (Stevens and Parsons, 2002; Mansfield, 2005). The effects of motion sickness on passengers and crew are sought to be minimised through seakeeping in ship design, which is detailed as a conventional means of motion sickness assessment. A proposed method of enhancing human-centric performance criteria development is then described, followed by a real-world deployment to showcase human digital twins in operation, working towards exploiting operation data to inform ship design.

Conventional Motion Sickness Assessment

The MSI is widely adopted in seakeeping performance assessments (Tezdogan *et al.*, 2014; Scamardella and Piscopo, 2014; 2015). Criteria for the MSI that are reported in literature include:

- 5 % at 0.5 hours of exposure for naval crew (Baitis *et al*., 1994);
- 10 % of general passengers (ABS, 2021);
- 20 % of naval crew at 4 hours of exposure (NATO, 2000);
- 35 % over 2 hours (Tezdogan *et al.*, 2014).

The MSI can be computed from the second and fourth ship spectral moments. The MSI is related to absolute acceleration shipboard as described by Equation 2,

$$\mathrm{MSI} = 100 \cdot \frac{1}{\sqrt{2\pi}} \int_{-\infty}^{z} \mathrm{e}^{\left[-\frac{1}{2}x^2\right]}, \qquad [2]$$

which expresses a cumulative distribution function using the standard normal distribution, where z is given by Equation 3,

$$z = \frac{\log_{10}\bar{a} - \mu}{\sigma}, \qquad [3]$$

and σ and μ can be determined empirically, and $\bar{a}$ is the absolute acceleration (O'Hanlon and McCauley, 1974; McCauley *et al.*, 1976). McCauley *et al.* (1976) found that μ is suitably estimated by Equation 4,

$$\mu = k_1 + k_2 \cdot \log_{10}\left(\frac{1}{2\pi}\sqrt{\frac{m_4}{m_2}}\right) + k_3 \cdot \left[\log_{10}\left(\frac{1}{2\pi}\sqrt{\frac{m_4}{m_2}}\right)\right]^2, \qquad [4]$$

where k_x are constants to be resolved empirically, m_2 and m_4 are the second and fourth ship spectral moments described by Equations 5 and 6, respectively,

$$m_2 = \int_0^\infty \omega_e^2 \, S_z(\omega_e) \mathrm{d}\omega_e, \quad [5]$$

$$m_4 = \int_0^\infty \omega_e^4 \, S_z(\omega_e) \mathrm{d}\omega_e, \quad [6]$$

and are functions of the encounter frequency, ω_e (Lloyd, 1998; Scamardella and Piscopo, 2014; 2015). The absolute acceleration, $\bar{a}$, in Equation 3 can further be defined in terms of the fourth ship spectral moment (Lloyd, 1998). Only vertical ship motion is considered in recommended motion sickness assessments, hence the z subscript in the ship motion response spectra symbol, S_z (ISO 2631-1, 1997).

Contrastingly to seakeeping performance assessments conducted in ship design, the MSI computed with the MSDV is adopted in international standards for the evaluation of motion sickness performed during vessel operation, such as full-scale sea trials, using Equation 7 (ISO 2631-1, 1997; Lawther and Griffin, 1987),

$$\mathrm{MSI} = K_m \cdot \mathrm{MSDV}. \quad [7]$$

K_m is a constant that can empirically be determined for a specific seafaring group or be used as 1/3 for a mixed population of male and female adults that are unadapted to motion (ISO 2631-1, 1997). The MSDV can be computed with sensor measurements, using Equation 1, or seakeeping methods, using Equation 8,

$$\mathrm{MSDV} = \sqrt{m_{4w} T}, \quad [8]$$

where T is again the duration of motion exposure and m_{4w} is the weighted fourth ship spectral moment. m_{4w} is denoted by Equation 9,

$$m_{4w} = \int_0^\infty \omega_e^4 \, S_z(\omega_e) G^2(\omega_e) \mathrm{d}\omega_e, \quad [9]$$

where G is the frequency weighting function (Scamardella and Piscopo, 2014).

Proposed Motion Sickness Assessment

The presented method suggests developing diagnostic motion sickness criteria using real-world sensor measurements and feedback from seafarers through human digital twins. Then, the results are to be integrated into seakeeping methods conventionally performed in ship design. The operational and design methods of computing the MSDV are associated with the knowledge that the MSDV in Equation 1 can equivalently be computed using Equation 10,

$$\mathrm{MSDV} = \sqrt{T} \cdot a_{\mathrm{wRMS}} \quad [10]$$

and that the square root of the weighted fourth ship spectral moment equates to the root mean square value of the weighted time signal of vertical ship acceleration, a_{wRMS}, measured over duration T in seconds (ISO 2631-1, 1997; Lloyd, 1998).

It is observed that the relationship between the MSI and MSDV is not strictly linear or necessarily proportional with a 3:1 ratio for all cases. Factors, such as age and sex, influence susceptibility to motion sickness (ISO 2631-1, 1997). A criterion of 30 $\mathrm{m/s^{1.5}}$ for the MSDV is reported (ABS, 2021), considering Equation 6, however Taylor *et al.* (2023a) suggest that a cumulative distribution function, using a normal distribution of MSDV thresholds, provides a more relevant fit for relating the MSI and MSDV. This suggestion aligns with findings of the relationship between MSI and vertical ship acceleration in literature (O'Hanlon and McCauley, 1974; McCauley *et al.*, 1976). Linking the MSI and MSDV through a cumulative distribution function enables the development of diagnostic motion sickness criteria, as shown in Figure 4 with 95 % confidence intervals for an exposure duration of 6 hours.

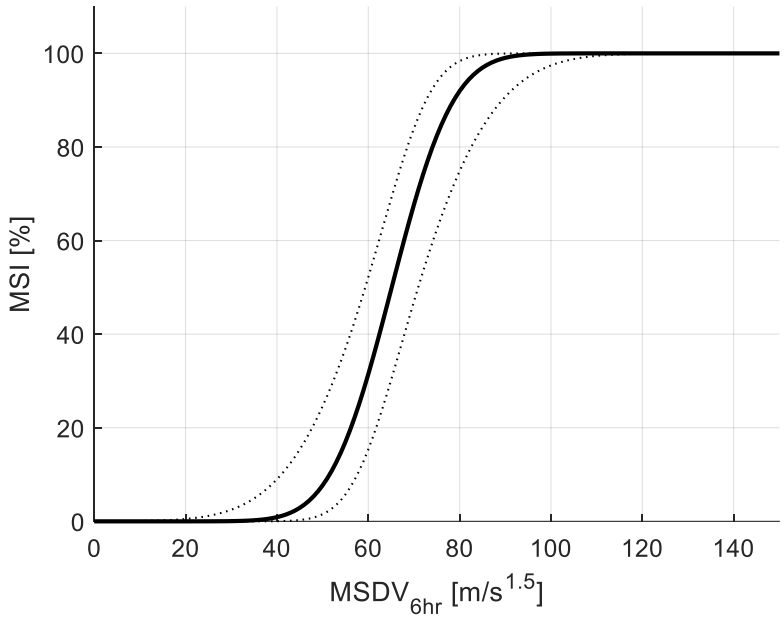

Figure 4: Cumulative Distribution Function with 95 % Confidence Intervals Serving as Diagnostic Motion Sickness Criteria.

Novel motion sickness criteria such as this can be used to estimate the MSI for a cohort of seafarers from ship motion predicted using seakeeping methods. The proposed method recommends computing the MSDV using Equation 8 and estimating the MSI from the generated diagnostic motion sickness criteria. The estimated MSI can then be assessed against the desired criterion for seakeeping performance. Alternatively, an MSI criterion could guide the selection of the associated MSDV threshold if there is a preference for working with the MSDV.

Human Digital Twin Deployment During Ship Operation

Human digital twins were deployed on board the SA Agulhas II to monitor the motion sickness of participating passengers (Taylor *et al.*, 2023a). A mobile application deployed on participant cell phones collected subjective feedback from seafarers that indicated whether they experienced any motion sickness symptoms or not (MSI) and tracked their location as they moved throughout the ship using near field communication (NFC) technology. In parallel, ship motion was measured by a full-scale measurement system, which computed an MSDV at all NFC tag locations over consecutive 5-minute durations.

Each seafarer human digital twin integrated the seafarer's present location with MSDV's in real time, computing an equivalent MSDV over 6 hours every 5 minutes that represented their extended motion exposure on a 3-week long research voyage. The human digital twins additionally fused the subjective feedback with the equivalent MSDV's to analyse the measurements of motion exposure against subjective observations. Individual MSDV thresholds, which were unique to each participating passenger, were computed using receiver operating characteristic curve analysis.

The individualised thresholds were used by a human digital twin that represented the motion sickness state of the cohort to generate a cumulative distribution curve with a normal distribution, which linked the MSI and MSDV metrics. In this way, the Cohort Human Digital Twin enabled the determination of a cumulative distribution curve within a real-world contextual environment, managing the evolution of the curve throughout the voyage. The equivalent MSDV computation duration was extended to accommodate durations from 0.5 to 6 hours in 0.5 intervals. A unique final cumulative distribution curve was generated for each duration, as shown in Figure 5.

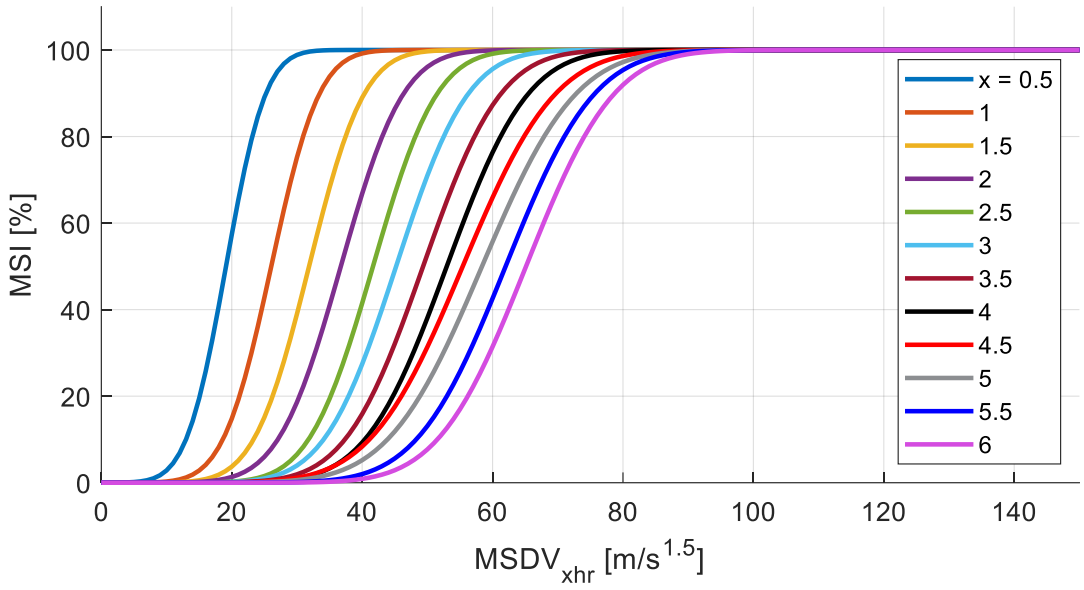

Figure 5: Diagnostic Motion Sickness Criteria Over Various Durations of Motion Exposure (adapted from Taylor *et al.*, 2023a).

The use of diagnostic motion sickness criteria managed through the Cohort Human Digital Twin was validated. The validation procedure included requesting the MSI from the Cohort Human Digital Twin each time a new mean equivalent $MSDV_{6hr}$ was computed based on the individually tracked locations of participating passengers. The procedure was run over the course of the 3-week research voyage to show that the latest cumulative distribution curve was accessible throughout the expedition.

Results of the estimated and observed MSI values are presented in Figure 6, of which the Spearman correlation was found to be 0.78 (Taylor, 2023). In Figure 6, MIZ is the marginal ice zone in the Southern Ocean. Ship motion in the MIZ was marginal compared to open water transits, hence the smaller values of observed MSI for participating passengers. Moreover, the MIZ separates the first and second open water voyage legs, such that adaptation to motion was observed by personnel having smaller MSI values (both estimated and observed) after the MIZ than at the start of the voyage.

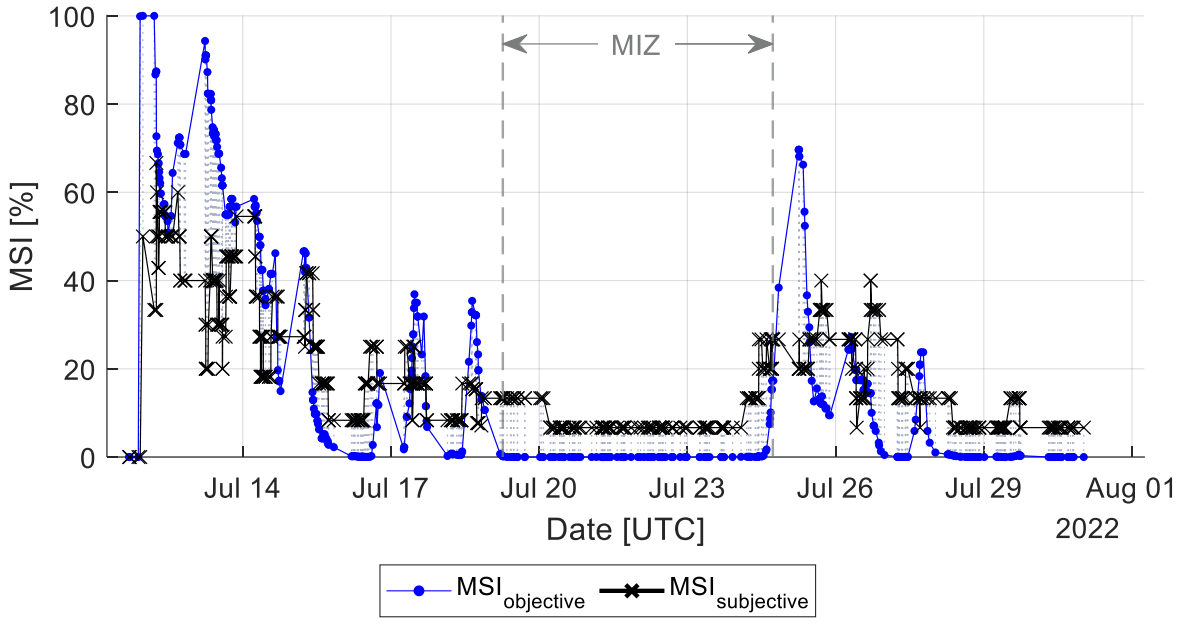

Figure 6: MSI Estimated (Objective) versus Observed (Subjective).

DISCUSSION OF BENEFITS AND DRAWBACKS FROM THE INTEGRATION OF HUMAN DIGITAL TWINS TO INFORM SHIP DESIGN

Human digital twins for seafarers trialled in situ during a research voyage were seen to be effective systems for human-centred data acquisition and analysis on board a ship. The human digital twins enabled the development of diagnostic motion sickness criteria throughout the voyage, evolving with newly acquired data from both a full-scale ship measurement system and participating passengers.

The motion sickness criteria development was driven by data acquired from seafarers based on their actual experiences on board through a mobile application installed on participant cell phones. Therefore, the human digital twins tailored motion sickness criteria to a unique cohort based on individual responses. In this way, more detailed information is gathered about the MSI in relation to a human-centric ship motion dose metric (MSDV) than typical human response studies, which report using daily metrics acquired through paperbound questionnaires (Taylor, 2023). Moreover, the duration of motion sickness assessment can be tailored to specific voyage or vessel scenarios with periods ranging from 0.5 to 6 hours (see Figure 5). Motion sickness criteria identified in literature are applicable to a single duration only or do not provide related exposure times, which the MSDV computation is dependent on.

The diagnostic motion sickness criteria provided MSI estimates that were positively associated with the observed MSI, excluding the time in the MIZ. Here, a single participant stopped participating with their MSI showing a false positive while in the MIZ. The estimate of MSI is, therefore, more strongly associated with the observed MSI. The customised functionality of the human digital twins is considered beneficial for better understanding the real-world experiences of seafarers on board specific vessels, which could transpire motion sickness diagnoses. For example, the cruise industry could characterise customer satisfaction levels for their fleet.

It is envisaged that the best benefit of operational digital twins for informing design would be for fleets that operate with similar vessels, such as in the cruise and naval sectors. Human digital twins enabled production of data and results from analyses, which can provide access to results beyond a single operational voyage or the operational service of a vessel. Information flow could be facilitated from one voyage to the preparation phase of the next expedition, or from the service of one ship to the design of its or similar successors, as presented in Figure 7. The Cohort Human Digital Twin could make the cumulative distribution function accessible to Ship Digital Twin 2, which would need to define performance criteria for completing a seakeeping performance assessment. The motion sickness criteria provide an artefact of operation data acquisition and analysis that quantify the real-world experience of seafarers for informing ship design when defining performance criteria.

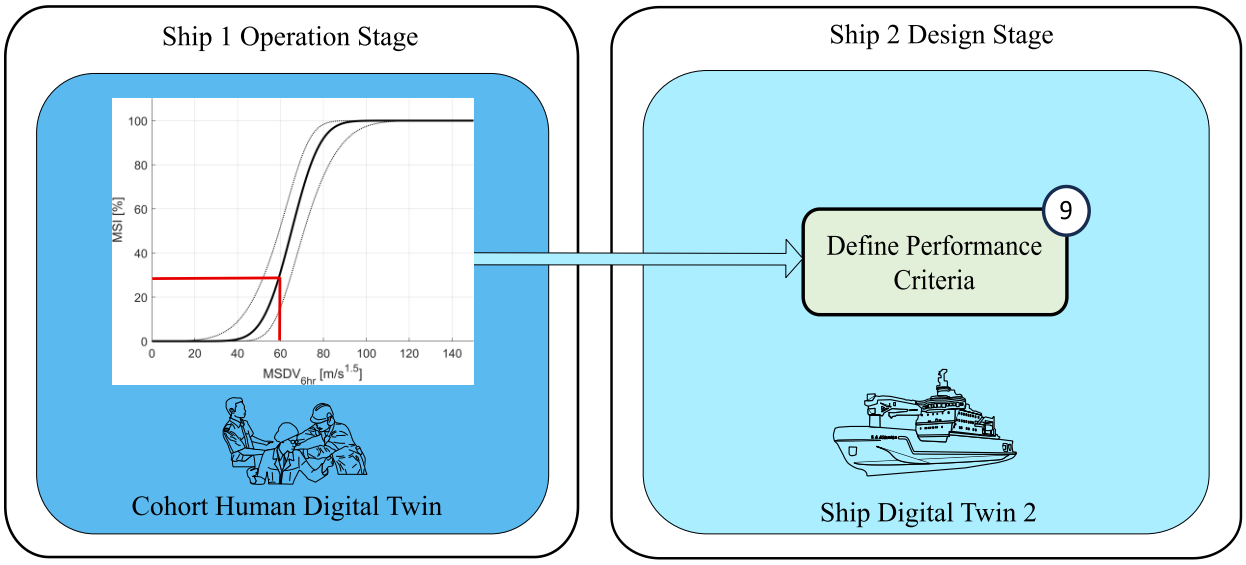

Figure 7: Cohort Human Digital Twin in Ship 1 Operation Stage Informing Ship Digital Twin 2 in Ship 2 Design Stage.

It is noted that the human digital twins require at least one deployment to incorporate real-world data. Results could be generated from simulations prior to a debut voyage, but would have to omit the inclusion of the actual experience of seafarers. The latter would provide the same results as seakeeping analyses performed previously. The human digital twins facilitated a quantitative,

empirical means of generating human-centric diagnostic criteria, compared to qualitative results readily employed during conventional seakeeping performance assessments. Such a system can be regarded a form of real-world seakeeping trials, which capture invaluable data for rare operational occurrences in situations beyond that of controlled, systematic seakeeping trials (NATO, 2000). The implication for ship design is an increase in information about ship operability that is captured during operation, which can be made available and used to guide strategic decisions. Nonetheless, it is noted that ship design is inherently complex, and the work presented provides evidence of a proof of concept that requires further development to comprehensively construct an information pipeline from ship operation to design.

CONCLUSIONS

Constructing information feedback from data acquired and analysed during ship operations to the design stage has been proposed through digital twins for people and a ship. Human digital twins captured feedback from participating passengers, which allowed the automated generation and use of diagnostic motion sickness criteria that link the MSI and MSDV. A ship digital twin that implements seakeeping performance assessment procedures acted as a client of a cohort human digital twin to integrate the diagnostic motion sickness criteria. A real-world validation of the use of diagnostic motion sickness criteria was offered, highlighting that data managed through human digital twins can be made accessible beyond the scope of an operational voyage. Human digital twins are regarded as beneficial for integration with ship digital twins during vessel operation aiming to inform decision making throughout the lifecycles of seafarers and ships, but particularly back into ship design. In this way, human digital twins refine the practical understanding of operational situations at the time of ship design through data-driven artefacts produced during ship operation.

Future work includes using the proposed seakeeping performance methods with weather forecasts to predict ship motion and human motion sickness responses for a voyage. Results could be compared with in-situ, full-scale ship motion measurements and observed human responses over the duration of the same voyage. Moreover, MSDV thresholds extracted from the diagnostic motion sickness criteria are to be used to generate novel MSDV operability envelopes for comparison with results of real-world ship operation measured through ship and human digital twins.

DATA ACCESS STATEMENT

Research data used to generate the plotted results is publicly accessible in an institutional repository (Taylor *et al.*, 2023c).

CONTRIBUTION STATEMENT

NC Taylor: Conceptualisation; data curation; methodology; writing – original draft. **A Bekker and K Kruger:** Conceptualization; supervision; writing – review and editing.

ACKNOWLEDGEMENTS

The financial assistance of the National Research Foundation (NRF), through the South African National Antarctic Programme (SANAP Grant No. 110737), towards this research is hereby acknowledged. Opinions expressed and conclusions arrived at are those of the author and are not necessarily to be attributed to the NRF.

The crew and managers of the SA Agulhas II, AMSOL, and vessel owners, the Department of Forestry, Fisheries and the Environment of South Africa are thanked for providing access to the ship and their significant research support during voyages. The passengers that participated in the human response research activities are greatly appreciated and thanked for their contribution.

Prof Martin Kidd is thanked for his guidance and assistance with statistical data analyses.

REFERENCES

American Bureau of Shipping (ABS) (2021). Guide for Passenger Comfort on Ships. Spring: ABS

Baitis, A.E., Bennet, C.J., Meyers, W.G., Lee, W.T. (1994). Seakeeping Criteria for 47-ft, 82-ft and the 110-ft United States Coast Guard Cutters. Technical Report ADA291162. Bathesda: United States Coastguard

Erikstad, S.O., Bekker, A. (2021). Design Patterns for Intelligent Services Based on Digital Twins. Proceedings of the Conference on Computer and Information Technology Applications in the Maritime Industries, pp. 235-245. Mülheim,

Germany

Erikstad, S.O., Lagemann, B. (2022). Design Methodology State-of-the-Art Report. Proceedings of the 14th International Marine Design Conference. Vancouver, Canada

Fonseca, Í.A., de Oliveira, F.F., Gaspar, H.M. (2023). Open Framework for Digital Twin Ship Data: Case Studies on Handling of Multiple Taxonomies and Navigation Simulation. International Journal of Maritime Engineering, 165, Part A1, pp. A-23-A-42

International Electrotechnical Commission (IEC) (2017). Smart Manufacturing – Reference Architecture Model Industry 4.0 (RAMI4.0). Publicly Available Specification (PAS). IEC PAS 63088. Geneva: IEC

International Organisation for Standardisation (ISO) (1997). Mechanical Vibration and Shock – Evaluation of Human Exposure to Whole-Body Vibration – Part 1: General Requirements. ISO 2631-1. Geneva: ISO

Lawther, A., Griffin, M.J. (1987). Prediction of the Incidence of Motion Sickness from the Magnitude, Frequency and Duration of Vertical Oscillation. Journal of the Acoustical Society of America, 82(3), pp. 957-966

Lloyd, A.R.J.M. (1998). Seakeeping: Ship Behaviour in Rough Weather. Doctoral Dissertation. Chichester: Ellis Horwood Ltd

Madusanka, N.S., Fan, Y., Yang, S., Xiang, X. (2023). Digital Twin in the Maritime Domain: A Review and Emerging Trends. Journal of Marine Science and Engineering, 11, 1021

Mansfield, N.J. (2005). Human response to vibration. Boca Raton: CRC Press

Mauro, F., Kana, A.A. (2023). Digital Twin for Ship Life-Cycle: A Critical Systematic Review. Ocean Engineering, 269, 113479

North Atlantic Treaty Organisation (NATO) (2000). Standardisation Agreement (STANAG): Common Procedures for Seakeeping in the Ship Design Process. STANAG 4154 (Edition 3). Brussels: Military Agency for Standardisation

O'Hanlon, J.F., McCauley, M.E. (1974). Motion Sickness Incidence as a Function of the Vertical Frequency and Acceleration of Vertical Sinusoidal Motion. Aerospace Medicine, 45(4), pp. 366-369

McCauley, M.E., Royal, J.W., Wylie, C.D., O'Hanlon, J.F., Mackie, R.R. (1976). Motion Sickness Incidence: Exploratory Studies of Habituation, Pitch and Roll, and the Refinement of a Mathematical Model. Technical Report 1733-2. Goleta: Human Factors Research, Incorporated

Rumawas, V. (2016). Human Factors in Ship Design and Operation: Experiential Learning. Doctoral Dissertation. Trondheim: Norwegian University of Science and Technology

Scamardella, A., Piscopo, V. (2014). Passenger Ship Seakeeping Optimisation by the Overall Motion Sickness Incidence. Ocean Engineering, 76, pp. 86-97

Scamardella, A., Piscopo, V. (2015). The Overall Motion Sickness Incidence Applied to Catamarans. International Journal of Naval Architecture and Ocean Engineering, 7, pp. 655-699

Stevens, S.C., Parsons, M.G. (2002). Effects of Motion at Sea on Crew Performance: A Survey. Marine Technology, 39(1):29-47

Taylor, N.C. (2023). A Human Cyber-Physical System to Study the Motion Sickness of Seafarers. Doctoral Dissertation. Stellenbosch: Stellenbosch University

Taylor, N.C., Bekker, A., Kruger, K. (2023a). Operational Development of Diagnostic Motion Sickness Criteria Through a Human Cyber-Physical System. Under Review at Applied Ergonomics

Taylor, N.C., Bekker, A., Kruger, K. (2023b). Mariner 4.0: Integrating Seafarers into a Maritime 4.0 Environment. Transactions of the Royal Institution of Naval Architects Part A: International Journal of Maritime Engineering, 164, pp. 373-384

Taylor, N.C., Bekker, A., Kruger. (2023c). Ship Motion Measurements and Human Responses Captured on the SA Agulhas II - Winter Cruise 2022 [Online]. Available: https://doi.org/10.25413/sun.24331114

Tezdogan, T., Incecik, A., Turan, O. (2014). Operability Assessment of High Speed Passenger Ships Based on Human Comfort Criteria. Ocean Engineering, 89, pp. 35-52

Proceedings of 15th International Marine Design Conference (IMDC-2024)
June 2-6, 2024
Amsterdam, the Netherlands

Integration of the Power Corridor Concept in the Early-Phase Design of Electric Naval Ships using Mathematical Design Models

Giorgio Trincas[1], Luca Braidotti[1,*] Andrea Vicenzutti[1], Andrea Alessia Tavagnutti[1], Chathan M. Cooke[2], Julie Chalfant[2], Vittorio Bucci[1], Chryssostomos Chryssostomidis[2] and Giorgio Sulligoi[1]

ABSTRACT

The aim of this paper is to illustrate the process of identifying the 'best compromise' solution for an all-electric destroyer at the concept design level. The design strategy reflects a paradigm shift from a sequential approach towards a holistic multicriterial approach. The destroyer is required for an extensive range and endurance, fully operable in rough sea states. A mathematical design model (MDM) that includes a set of metamodels, is implemented to evaluate the overall performance of feasible, then non-dominated designs. The power corridor concept is integrated into the MDM to optimize the location and functionality of the individual units of the power train. The fuzzy sets theory is used for normalizing and weighing incommensurable properties of candidate designs, so resolving many of the ill-defined requirements and criteria. The final result of this study is a top-level specification for the destroyer with enhanced performance and reduced power demand.

KEY WORDS

Concept ship design; destroyer; all-electric ship; power corridor; fuzzy-sets

NOMENCLATURE

Symbols

A_X	area of maximum section area
B_{MAX}	beam, maximum
B_{WL}	beam at design draft
BM	transverse metacentric radius
BM_L	longitudinal metacentric radius
C_B	block coefficient at design draft
C_{BD}	block coefficient at ship deck
$C_{GM/B}$	stability coefficient
C_{WP}	waterline area coefficient
C_P	longitudinal prismatic coefficient
C_{VP}	vertical prismatic coefficient
C_{WP}	waterline area coefficient
C_X	wind resistance coefficient
D_P	propeller diameter
D_{tac}	tactical diameter

Acronyms

AAC	annual average cost
AC	alternating current
AS	attribute space
DC	direct current
$DESMAD$	destroyer multiattribute design
DOE	design of experiments
$DTMB$	David Taylor Model Basin
DWT	deadweight
DS	design space
$HVAC$	heating, ventilation, air conditioning
IMO	International Maritime Organization
$ITTC$	International Towing Tank Conference
LSW	lightship weight
$MADM$	multiattribute decision-making
$MCDM$	multicriterial decision-making

[1] Department of Engineering and Architecture, University of Trieste, Italy
[2] Massachusetts Institute of Technology, 77 Massachusetts Ave, Cambridge, MA 02139, USA
* Corresponding Author: lbraidotti@units.it

Submitted: 23 February 2024, Revised: 30 April 2024, Accepted: 1 May 2024, Published: 6 May 2024

Conference paper, DOI: https://doi.org/10.59490/imdc.2024.753 e-ISSN: 3050-4864

GM	metacentric height	MCR	maximum continuous rating
$H_{1/3}$	significant wave height	MDM	mathematical design model
i_E	entrance half-angle	MDO	marine diesel oil
KB	vertical center of buoyancy	MIT	Massachusetts Institute of Technology
KG	vertical center of mass	$MODM$	mathematical design model
KM	metacentric height from baseline	MOP	measure of seakeeping performance
KQ	propeller torque coefficient	MSI	motion sickness incidence
KT	propeller thrust coefficient	MVZ	main vertical zones
LCB	longitudinal center of buoyancy	NA	number of attributes
L_{PC}	length for future power corridor	ND	number of non-dominated designs
T_ϕ	natural roll period	$NORDFORSK$	Nordic Co-operative Organization for Applied Research
V_{MAX}	maximum ship speed		
S_ζ	spectral value of the sea	NV	number of variables
W_{FL}	full load weight	$PEBB$	power electronics building blocks
W_{HS}	hull steel weight	RMS	root-mean-square
W_{PL}	payload weight	RSM	response surface methodology
α_{cut}	threshold for fuzzy attributes	$STANAG$	standardization agreement
μ	membership grade function	$SWBS$	ship work breakdown system
ρ_a	air density	$UNITS$	University of Trieste
ζ_a	wave amplitude	VLS	vertical launch system
ω_e	encounter frequency	$ZEDS$	zonal electric power distribution system
Δ	full load displacement		
∇	volume of displacement		

INTRODUCTION

The modern destroyer, born in response to the threat posed by torpedo boats to larger fleet vessels at the end of the 19th century, has evolved into a highly versatile and heavily armed surface unit. It is capable of escorting naval groups and merchant convoys, conducting anti-submarine operations, and engaging in air and surface combat with missiles, electronic warfare, and counter missions. Despite the vague classification between frigates and cruisers, destroyers often represent the most dominant surface units in the fleets of major navies.

In recent decades, there has been a steady increase in the size of naval vessels, and destroyers are no exception. Displacement and length have surpassed 10,000 tons and 160 meters, respectively, with vessels like the Zumwalt of the US Navy reaching 14,564 tons and 182.8 meters. This growth is driven by the escalating power demands of new sensors and onboard systems, as well as by the anticipated introduction of disruptive technologies such as direct energy weapons and railguns, currently under development or testing by several navies. These advancements underscore the heightened focus on the onboard electric power system, its architecture, and its arrangement. Specifically, there are increased requirements for safety, redundancy, and modularity to enhance ship survivability and facilitate retrofits and upgrades throughout the ship's operational lifespan, especially on full-electric ships.

To face these challenges, the main scope of this paper is to develop an innovative design approach for an all-electric destroyer where the integration of a power corridor plays a fundamental role in concept design and decision-making processes. This poses increasing challenges to naval ship design, which has to find new solutions and arrangements to cope with the increasing space and power demand (and thus, installed power, amount of fuel, etc.).

Destroyers are fast warships intended to escort larger vessels and equipped for antisubmarine warfare, with missiles for surface and air combat, as well as for electronic warfare. The new destroyer will have to guarantee high-level operability from the conceptual design phase, taking into account the following basic factors:

- the hydrodynamic quality of the ship hull, and the interaction of equipment, subsystems, and military installations between them and the ship body;
- the hull-environment interaction in rough sea states
- a set of crisp and soft criteria to be satisfied which respect all requirements of physical and normative nature.

To include simultaneously all these factors, it is necessary to change the paradigm in the ship design process. A multicriterial approach in ship design is the best answer for overcoming heuristic approaches such as the classic design spiral. In particular, more than the multiobjective design method, the multiattribute decision-making approach was found to be the most suitable for the concept design (Triantaphyllou, 2000; Trincas, 2001; Trincas et al., 2018). The theory of fuzzy sets was incorporated into the decision-making procedure to provide a simple mathematical tool to handle uncertainty and imprecision in the concept design phase.

Decades of experience on naval ships have shown that the order of importance to attach to the various hydrodynamic disciplines is seakeeping first, then stability and control both in the vertical plane and in maneuvering, then propulsion, and finally resistance. To respond to this scale of priorities right from the concept design, it is necessary to develop seakeeping metamodels to rapidly evaluate responses in a seaway while ensuring ship safety.
To define the new compartmental configuration with a deck dedicated to the power corridor with systems and equipment it contains, reference is made to the seminal papers of Nehrling (1985) and Cort & Williams (1987).
The paper has seven main sections. Section 2 illustrates the concept design strategy based on the principles of the multiattribute decision-making process. Section 3 describes the main feature of the power corridor designed to satisfy the destroyer's overall energy requirement. Section 4 describes the main modules that make up the mathematical design model. Section 5 deals with the decision support system where the attributes' outcomes are fuzzified. Section 6 develops the design of the baseline destroyer as an anchor point for competing designs. Section 7 contains the two phases of the multiattribute decision making process: generations of feasible designs and selection of the preferred design. Finally, section 8 draws some conclusions.

METHODOLOGY

Ship Design Methods

Successful engineering design, including ship design, is mainly a matter of fast and efficient decision-making in a conflicting environment. This is especially worthwhile for concept design, which is the most important phase of the global design process since it gives the highest opportunity to influence the overall efficiency and effectiveness of the ship a long way ahead. Even though evaluation of design alternatives requires rational decision-making, so far the usual way is still to reduce target complexity by using a heuristic approach in order to arrive at final technical decisions. Major weak points and ineffectiveness of still popular design methods mainly relate to the poor integration of different subsystems and the lack of mutual influence of design responses to different requirements.
Design theory has evolved to evaluate design alternatives in an integrated shell rationally, where multiple conflicting requirements, external environments, and mandatory rules are to be tackled simultaneously. This limit was overcome by the development of the multiple criteria decision-making (MCDM), which was also the name of the first conference on the subject held at the University of South Carolina in 1972. The basic concepts (optimization, satisficing solution, compromising set, ideal solution) of the MCDM can be found in the fundamental work of Zeleny (1982).
A profound debate conducted in the 1990s between naval experts and researchers, especially during IMDC and PRADS conferences, led to the distinction between multiple attribute decision-making (MADM) and multiple objective decision-making (MODM), different in application scope and underlying mathematical approach. The generally accepted conclusions were that the MADM approach is more suitable for the concept design phase (where analytical mathematics is generally used), while the MODM approach is recommended in the preliminary/contractual design phase when it comes to optimizing ship systems and subsystems. Trincas et al. (2018) summarized the impossibility of applying MODM methodologies in the concept design stage, also supported by the conclusions of recognized naval field MODM experts: Campana et al. (2007) among others. Therefore, the aim of this work is not to confirm the validity of the MADM methodology in developing a concept ship design, but to use it to propose a feasible project of an innovative all-electric naval vessel based on the power corridor concept.

Concept Design Modeling

Many design teams forego a concept design altogether and proceed directly to the preliminary design phase. They usually follow the iterative design spiral procedure although mostly not in a formal way. Firstly, main dimensions are determined on a statistical basis; then a lines plan is developed and the general arrangement plan is fitted in. Hydrostatics and stability assessment, overall power estimate, engine selection, strength evaluation, seakeeping and manoeuvring qualities then follow from the analytical/numerical procedures applied to the single lines plan. A tedious trial and error process brings the relevant features of the design in balance. Such a design process is time-consuming, as no complete definition of the ship exists before a balance is reached at each turn of the design spiral.
The concept design is not a substitute for the traditional preliminary design; rather, it should precede it, yielding a top-level specification based on the primary characteristics and performance requirements of the preferred design. This early design stage has the aim of avoiding a redesign in a later stage, as often is necessary with descriptive methods (Trincas et al., 1994; Hubka and Eder, 1996) in ship design. The concept design is conceived as a new paradigm where the key words are selection, concurrency and multidimensional design space. The early phase of the ship design process requires reliable and fast time decisions, allowing the design team to explore a wide range of feasible solutions and offering increased assurance for benefits throughout the ship's lifetime. Such a demand requires that several fundamental features, normally associated with later phases of the design process, should be anticipated at the level of concept design. In the present study, one of these features is the

integration of the power corridor into the general arrangement plan and evaluation of its effect on the optimal choice of the main characteristics of the destroyer (ship dimensions, general plans, hydrodynamic properties).
The concept design process follows a prescriptive model (Andreasen, 1992) that is broken down into three basic interrelated activities:

- *design analysis*: random generation and performance assessment of a large number of design alternatives that have to meet the required targets subject to crisp and soft constraints; this activity is performed by executing the mathematical design model so many times as to fill the design space enough;
- *design synthesis*: filtering the feasible designs (i.e., designs not eliminated automatically by crisp constraints); creating the set of non-dominated designs that constitute the Pareto frontier;
- *design selection*: based on different metrics and multiple attribute decision-making techniques, aimed at selecting the preferred design from the ones in the Pareto frontier.

The quality and accuracy of the *design analysis* is crucial, since it dramatically affects the target of obtaining a successful ship. Unfortunately, at concept design stage the design team is often faced with imprecise information on the functional requirements and uncertainties in the ship performance, as well as with the significant interaction and interconnectivity of the main ship design disciplines. All these aspects make ships complex systems that requires highly evolved decision tools to handle this high degree of complexity. Since it becomes impractical to rely on simulation and numerical codes for the purpose of concept design, a preferable strategy is to use approximation models, which are referred as metamodels as they provide a 'model of the model' (Kleijen, 1987), to replace the expensive detailed simulation models. A metamodel-based approach (i.e., artificial intelligence applied to ship design) is the solution also to limit uncertainties across the predicted performance, functional requirements, building costs, and so forth (Derelöv, 2009), while reducing the computational expense and the design cycle time, and providing quick tradeoff for evaluation. Evaluation (*design synthesis*) and decision making (*design selection*) are key parts of the design process. In conventional ship design they are generally poorly structured and depend significantly on designers' own perceptions, which often imply a subjective (and thus suboptimal) assessment as a result. To improve on the latter, the Authors propose an evaluation strategy that combines a MADM approach (Trincas et al., 1994; Pahl et al., 1996) with different techniques (feasibility judgement, ELECTRE method and Pareto frontier), to reduce the number of candidate solutions (Ulrich and Eppinger, 2007).

POWER CORRIDOR

Cooke et al. (2017) introduced the concept of Power Corridor: a single entity incorporating distribution, conversion, isolation and storage of main bus power throughout the ship. The aim was to introduce significant advantages in terms of higher level of survivability, a simplified general arrangement plan of the ship as well as reduction of building and life-cycle costs.
Thanks to the on-land construction of the power corridor modules, and the subsequent easy onboard assembly, the cost of initial construction and repair (and future modernization) of the power corridor will be reduced compared to standard onboard power plants. Advantages in terms of standardization in modules' production (e.g., power electronics converters based on the Power Electronics Building Blocks – PEBB – concept) and the possibility to de-risk new modules in the factory are also present. Thus, a reduction in production, installation, supply chain, and training costs is expected. The use of identical pieces of hardware and control interfaces rather than many bespoke units also provides improved maintainability.
The installation of two redundant power corridors, installed onboard in separated locations, together with the centralization of the distribution, isolation, and energy storage functions, provides improved survivability. The interchangeability of the power corridor modules enables fast and easy replacement of faulted elements during service (without requiring ship docking).
The definition of a single entity dedicated to most of the functions related to electric power generation, distribution, and utilization, provides advantages in terms of quality of the ship design. In fact, the onboard arrangement can benefit from the Reserved Space approach, where the length and volume dedicated to the power corridor can be defined in the early phases of the ship design (Chalfant, 2015). This simplifies the process of allocating onboard the power system components, leading to the possibility of considering the power system design of an all-electric ship much earlier in the ship design process, enhancing the design results. This is because it encourages the ship's design team to consider the power system as an integral part of the ship design, optimizing it dually in relation to the overall ship. The use of uniform modules also aids in this regard.
A representation of the Power Corridor is depicted in Figure 1. It is composed of the following main components:

- bus cable and conduit (magenta)
- power converter stack (dark blue and brown)
- interface junction box (orange)
- energy storage (salmon)
- circuit breaker or disconnect (teal)
- bulkhead penetration (gray)

The details about the Power Corridor concept can be found in Cooke et al. (2017).

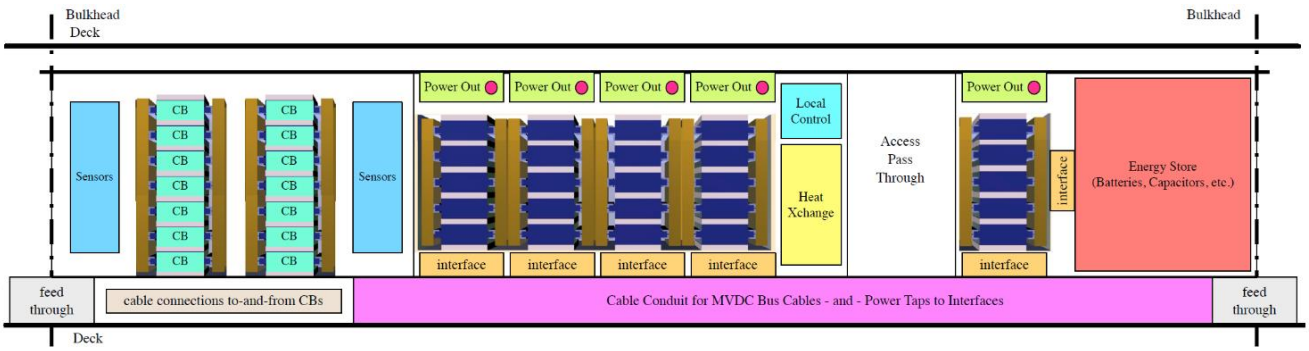

Figure 1: Modular integrated power corridor (Cooke et al., 2017)

The Power Corridor concept briefly presented above is here used as a key point in the design process. Thanks to its modular nature, it enables the integration of critical components of the power system directly into the concept mathematical design model, thus expanding its capabilities. The expected result is the definition of a set of feasible ship designs, evaluated considering not only the usual ship design parameters and constraints, but also the electrical related ones (power, space, weight, cooling, etc.).

MATHEMATICAL DESIGN MODEL

Ship properties that are likely to influence the identification of viable alternatives and their selection must be determined and analyzed as early as possible, that is, at the concept design phase. In fact, the success of the decision-making process in the concept design depends on how effectively the mathematical design model (MDM) simulates the real performance of the ship taking into account a sufficient number of primary properties (attributes). The MDM yields a large set of alternative solutions that have to be feasible in terms of the selected attributes. The candidate designs are randomly generated employing an adaptive Monte Carlo method. The structure of MDM is modular to allow the design team to vary or include different sets of analytical formulations and data to model the problem at hand with the greatest possible accuracy. It contains various design relationships for calculating areas, volumes, sizes, weights, electric power, stability, and so forth.
The MDM employs relationships based on practical design skills, scientific-based methods and metamodels based on statistical analysis of databases of similar ships, e.g. destroyers. It is written in Fortran 90 language.

Structure of the Model

The general structure of the MDM for destroyers, denoted as DESMAD and described in Figure 2, evaluates the attributes by a number of analytical modules, some of which consist of metamodels.
Unlike other mathematical models developed by various naval design centres, DESMAD does not include any iterative process except in the hull steel weight module. The approach adopted is non-compensatory: if a candidate design does not overcome any crisp constraint of geometric, physical and/or regulatory nature, it is immediately discarded. Only the designs in which both primary and secondary attributes overcome the constraints are feasible and are stored in the decision matrix.

Hullform Definition

This module selects the hull dimensions and relationships, which determine the technical requirements and capabilities of the candidate designs. The choice of appropriate form parameters has to comply with many constraints, mainly related to main dimensions and longitudinal prismatic coefficient. One crisp constraint is to have a natural roll period higher than 10 seconds to avoid the installation of large anti-rolling devices. As capability to sustain medium-high speed in rough weather and good ride quality are desired targets, a slender hullform is mandatory. The design waterline must have an entrance half-angle below 10 degrees. V-shaped sections are recommended even if at the expense of a slight extra building cost. In order to reach high efficiency at high speeds with minimum pressure pulses against the hull from the propellers, a hull/tip clearance not lower than 25 percent of the propeller diameter is imposed.
In each generation, some geometrical characteristics, such as C_B and $C_{WP} = C_B/C_{VP}$ are immediately derivable from the independent variables. For this purpose, starting from four basic hulls and using the Box-Behnken four-level design DoE technique (Myers et al., 2016) a database of one hundred hulls was constructed whose geometric characteristics of interest (BM, BML, KB, WS, LCB, LCF) were determined by statistical analysis with the Response Surface Methodology (RSM).

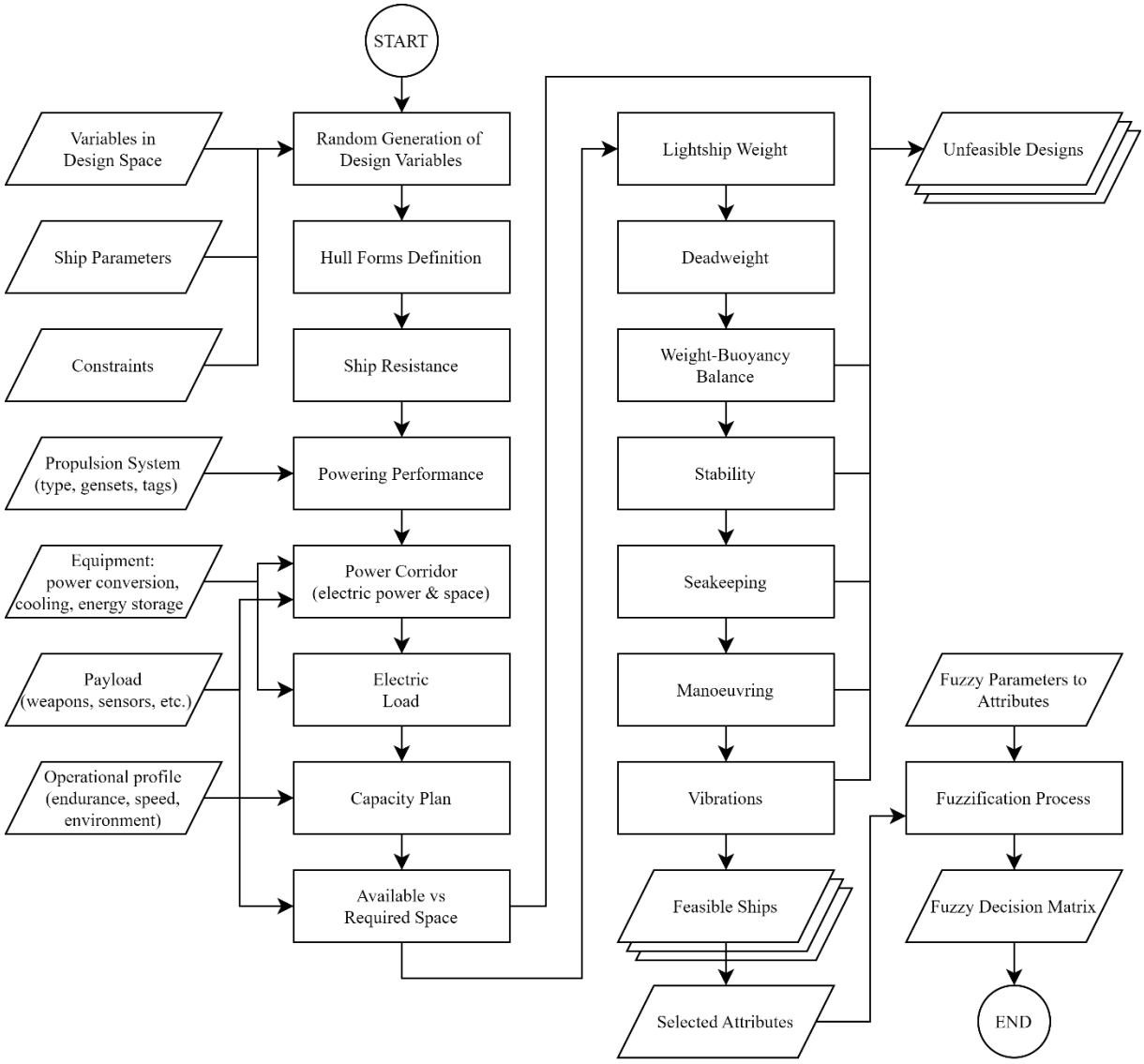

Figure 2: Flowchart of the mathematical design model

Ship Resistance

The still water resistance is evaluated by summing the bare hull resistance and the added resistance due to appendage as:

$$R_{CW} = R_{BH} + R_{APP} \quad [1]$$

Bare Hull Resistance. The resistance module estimates the resistance of the ship in calm water as well as in sea states 4, 5 and 6, at speeds ranging from 10 to 33 knots. Values of added resistance due to wind and hull roughness of 18 months are evaluated too.

The resistance in calm water is calculated following the DTMB methodology, where the residual resistance component is evaluated according to the algorithm of Fung (1991) that is statistically based on experimental measurements made on destroyer models with large transom sterns. The added resistance due to hull roughness and fouling is taken into account adding the allowance correlation according to formulas proposed by Townsin et al. (1981).

Appendage Resistance. A set of empirical formulas (Kirkman et al., 1979) are used to calculate separately the added resistance of each appendage, such as bilge keels, propellers, rudders, and shaft lines. The area of the bilge keels is taken as 2.5% of the waterplane area at the design draft to make more effective their contribution to roll damping. The sonar dome is considered as a part of the hull so contributing to the frictional resistance component of the bare hull. Added resistance due to steering is estimated using approximate formulas given by Norrbin (1972).

Added Resistance due to Wind and Waves. The added resistance in an irregular sea is based on the superposition principle for the components of the wave, motion and resistance spectra as well as on the assumption of linearity for the ship response. In a wave spectrum, the mean added resistance in regular waves is then calculated from

$$\bar{R}_{AW} = 2 \int_0^\infty \frac{R_{AW}}{\zeta_a^2}(\omega_e) \cdot S_\zeta(\omega_e)\, d\omega_e \qquad [2]$$

where ζ_a is the wave amplitude, ω_e is the encounter frequency, S_ζ is the spectral value. R_{aw} is determined using the formulation of Lang and Mao (2020) in unidirectional head regular waves:

$$R_{AW} = \frac{1}{2}\rho g\, \zeta_a^2\, B\, B_f\, \alpha_T (1 + \alpha_V) \left(\frac{0.19}{C_B}\right) \left(\frac{\lambda}{L_{PP}}\right)^{Fn-1.11} \qquad [3]$$

where λ is the wave length, B_f is the bluntness coefficient of the design waterline, α_V is the speed correction factor depending on Froude number (Liu and Papanikolaou, 2016), and α_T is the draft correction factor (Kwon, 2008).
Calculations are performed at SS4, SS5 and SS6, which correspond to significant wave heights of 1.875, 3.250, and 5.000 meters according to the WMO. They account for a frequency of 43% in the North Atlantic.
The resistance due to wind is calculated for head wind as:

$$R_W = 0.5\, C_X\, \rho_a\, V_R^2\, A_T \qquad [4]$$

where $V_R = V_S + V_W$, ρ_a is the air density, and A_T is the transverse ship area esposed to wind. The wind resistance coefficient in the longitudinal direction, C_X, given by the Isherwood formula (1973). The wind speed is correlated to the significant wave height as follows:

$$V_W = 6.851\sqrt{H_{1/3}} \qquad [5]$$

Powering Performance

This module calculates the power developed at the speeds of interest in the required operating conditions, and determines the fuel consumption for each speed. The 'design point' of the fixed-pitch propeller is selected at the combat speed in a given sea state in order to take into account the increased loads the propeller will encounter over the years.
When a ship sails in a rough sea, the quasi-propulsive performance, η_D, decreases compared to calm water, since the open-water propeller efficiency decreases much more than the increase in hull efficiency. Minsaas et al. (1983) provided the following approximations for the reduction of thrust and torque coefficient because of lower propeller submergence due to waves and ship motions:

$$K_{T_\beta} = \beta \cdot K_T \qquad K_{Q_\beta} = \beta^{0.8} \cdot K_Q \qquad [6]$$

where $= 1 - 0.675[1 - 0.769\, h/R]^{1.258}$ for $h/R < 1.3$, while the hull efficiency increases slightly due to the increase in the wake fraction and the irrelevant variation of the thrust deduction factor.
Change in the effective wake fraction due to hull roughness is estimated by applying a modified version of ITTC-1978 formula for full-scale wake prediction. Losses in propeller efficiency due to roughness and fouling are evaluated as proposed by Townsin (1983).

Power Corridor

In DESMAD, the power corridor keeps its width and height constant for each generated ship, whereas its length varies depending on the ship length and its subdivision. These values dictate the allocation of dedicated volumes and areas for each design alternative within the required space module. By determining the total power requirements for payload, propulsion, and other non-vital loads through the Electric Load and Powering Performance modules, the volume required by all modules positioned in the power corridor can be assessed. Assuming a standard-sized cabinet within the power corridor (1.60 m wide, 2 m high) and employing a volume-to-power conversion for all main components, the occupied length in the power corridor can be calculated and compared to the available length. In this way, non-feasible solutions can be excluded and free length in

the power corridor reserved for future upgrades can be assessed. If a zonal distribution system is implemented, the available, required and free lengths are defined zone by zone to ensure proper accommodation of all components.

Electric Load

The electrical load module assesses the maximum electric load in the winter cruise condition, including margins, since it is associated with the highest fuel consumption. The electric power value is obtained from the gensets, where a factor 0.91 is introduced to transform mechanical power into electrical power. The latter is the sum of payload electric power and non-payload functional electric load, including auxiliaries, outfitting, crew accommodations, heating, ventilation, and air conditioning (HVAC). In particular, the HVAC electric load power value is a function of the net volume of the ship, which is calculated by subtracting from the total volume of hull and superstructures the volumes of the engine and auxiliary rooms, the fuel tanks, the fore and aft peaks, the lavender water and grey water tanks, the trunks for aspiration and exhausted gas, as well as the volumes occupied by the military system. The payload electric load is considered an input, whose power value is determined by summing all the electric loads that are required to be installed onboard for performing the ship-specific missions (e.g., weapon systems, sensors, etc.). The non-payload electric load is automatically evaluated based on the ship's propulsion and manoeuvring performance, the number of crew members, and so on. All formulas introduced in this module are empirical. A margin is added to compensate for voltage fluctuations.

Capacity Plan

To assess the required volume of tanks, first the fuel consumption required for the generators shall be assessed. Since it is the sum of the propulsion and electric consumptions, it turns out to vary significantly with different speeds, with the electric load associated with each operating condition, and with the demand of the military equipment (weapons, sensors, cooling).
In this respect, we deem that at the concept design level it is useless to try to make the gensets operate at the optimal load, i.e. the one with the lowest consumption. This strategy has the advantage of ensuring that the range constraint at cruising speed is respected with a safe margin. The fuel amount for the gas turbines is the same for all designs, whilst for the gensets the fuel rate is a function of the delivered power for the low, cruise and endurance speed, and of the power demand not satisfied by the gas turbines at combat and top speeds.
Fuel tanks must have sufficient volume to guarantee the range required at endurance speed. Other tanks are needed for lubrication oil, fresh water, ballast water, sewage, waste oil, and helicopter fuel. The volume of these tanks is calculated by means of simple empirical formulas.

Available vs Required Space

The space balance of a ship has an overriding importance on the overall ship's effectiveness. Arrangement of spaces in the general arrangement plan is evaluated concurrently with hullform selection. Design whose available spaces (areas and volumes) are lower than required, are discarded immediately.
The subdivision scheme considers constraints on the location of machinery spaces, the need to have a discrete number of subdivisions of at least minimum length, as well as safety considerations. Subdivision arrangement and compartment arrangement follow the requirements of RINAMIL (2017a). The Available vs Required Space module evaluates available space within the hull against power corridor volume, machinery arrangement and tankage requirements based on length, height, and volume of machinery spaces for the required propulsion plant and auxiliary machinery. Tankage volume is validated against the required endurance fuel. Available ship areas and volumes are calculated for payload items and a variety of ship functional purposes. The superstructure and deckhouse above the main deck are specifically sized to meet design requirements for the remainder of the required payload, crew, and ship functions.

Lightship Weight

The destroyer employs an all-steel construction. The components of the lightship weight (LSW) are classified by the US Navy Ship Work Breakdown System (SWBS). LSW is divided into six main groups, consisting of groups 100 through 600. Assessment of the hull steel weight (group 100) requires an iterative process since the weight of foundations can be determined only after having calculated the weight of the groups from 200 to 600, with due accuracy for 200-machinery group, 300-electric plant and 500-auxiliaries. A weight margin factor of 7.5 percent is added to the computed LSW; it includes 2.5% for future growth.
The longitudinal centre of gravity is assumed to coincide with LCB, whilst KG is increased with a margin of 3 percent.
The hull structure is divided into three primary components: longitudinal structures, transverse structures and super-structures. The weight of each component is calculated using the metamodels obtained from the statistical analysis of the results obtained from the structural calculations on the hundred ships in the database. All other weights in LSW are evaluated using empirical formulas as a function of the ship's main dimensions and coefficients.

Deadweight

The deadweight (DWT) is the sum of the consumables (fuel weight, lubrication oil weight) and payload. It also includes the ballast water for trim adjustment through a compensation system.
The payload is mostly determined by the military payload in Group 400 and the entire Group 700, which consists of a fixed payload and a variable payload. The latter includes weights of the crew, provisions and required stores, which depends on the crew size and the required stores period, as well as on the helicopters, JP-5 fuel, missiles and ammunition. The fixed payload is basically the combat system weight (vertical launch system, railgun, weapons handling, etc.).

Weight-Buoyancy Balance

The balance between the ship buoyancy and ship weight is assured through applying a crisp constraint. In detail, the relative difference between full load displacement Δ_{FL} and the total ship weight W_{FL} shall be within 2.5 percent. This condition is stated as:

$$\frac{|\Delta_{FL} - W_{FL}|}{\Delta_{FL}} \leq 0.025 \quad [7]$$

Stability

The general intact stability criteria of naval ships (RINA, 2017b) to be fulfilled for the righting lever curve are more stringent than the IMO criteria for merchant ships. Intact stability criteria are verified using empirical formulas for calculating cross curves of stability, as outlined by Degan et al. (2021). Subsequently, the righting lever curve is evaluated at the design draft to ensure compliance with stability criteria. A further criterion for intact stability is the feasibility range of the ratio $C_{GM/B}$ between the metacentric height GM and ship beam at the design waterline B_{WL}. According to values assumed for the DDGx ship model, it can be expressed as:

$$0.090 \leq C_{GM/B} \leq 0.135 \quad [8]$$

Damage stability compliance is evaluated by determining the geometric floodable length using regression equations, following the approach of Mauro et al. (2019). These floodable lengths are then utilized to guide bulkhead allocation, as described by Braidotti & Prpić-Oršić (2023).

Seakeeping

First of all, the module calculates the natural periods of heave, pitch and roll, subject to two crisp constraints: i) the natural roll period must be higher than 10 seconds; ii) the double heave and pitch periods must be quite different from the roll period.
For seakeeping assessment, various tools are available such as linear numerical codes based on "strip theory", completely reliable for single-hull ships up to Froude numbers equal to 0.35, nonlinear numerical codes, experimental tests on physical models and nonlinear numerical simulations. As stated above, the strategy underlying the concept design does not involve any direct calculation. Therefore, several metamodels were built at the University of Trieste (UT) where many ship responses were evaluated for the hundred ships generated with the DoE. Calculations were performed for the annual average significant wave height in the North Atlantic ($H_{1/3} \approx 2.450$ m) at endurance speed. The sea was described by the two-parameter Bretschneider spectrum. The metamodels refer only to the root-mean-square (RMS) of motions and effects induced in the vertical plane in head sea. This hypothesis is entirely consistent with what was stated by Bales (1980): “It was further assumed that both the index and the relationship could be adequately quantified using analytically-based results for long-crested, head seas. The implications of this assumption are that rolling motion can be adequately controlled by subsequent appendage design, and that coupling effects from the lateral modes at oblique relative headings and/or in short-crested seas will not significantly alter trend identified under the relatively simple conditions evaluated”.
The valued responses are heave, pitch, vertical acceleration at the bridge, relative motion and relative velocity at the propeller tip at 12 o’clock, relative motion at helideck, relative motion at sonar dome, vertical acceleration at railgun foundation, slamming and deck wetness. Corresponding metamodels may be expressed in functional terms as:

$$MS = f\left(\frac{BM_L}{L}, \frac{L}{B}, \frac{L}{T}, \frac{B_{tr}}{T}, \frac{LCB - LCF}{T}, C_{WP}, C_{VP}\right) \quad [9]$$

The operability limits for naval ships are given in Table 1. The more stringent ones are selected as crisp criteria in the mathematical design model. The RMS responses of the metamodels are unified in the seakeeping measure of performance (MOP) after weighing each seakeeping characteristic using the AHP method (Saaty, 1980).

Table 1. Seakeeping criteria

Recommended and Default Criteria	NATO STANAG (2020)	NORDFORSK (1987)	RINA (2017c)
Pitch (RMS)	1.5 deg		
Vertical acceleration at bridge (RMS)	2.0 m/s2	2.75 m/s2	
Motion sickness incidence (MSI)	20% in 4 hrs		35% in 2 hrs
Slamming		3% probability	20/hr
Deck wetness		5% probability	30/hr
Propeller emergence			90/hr

Manoeuvring

As with the other properties of the destroyer, in the ship concept design a quick computation is required to assess the ship's maneuverability. This module predicts the attributes of course keeping, advance and turning ability, quantified by the tactical diameter, using the metamodels built on the basis of results obtained by calculations on ships of the destroyers' database, carried out with a code (Nabergoj, 2000) made available to UNITS. The code integrates the manoeuvring nonlinear equations by means of a fourth-order, variable step Runge-Kutta method. It uses hydrodynamic derivatives calculated using the formulas of Yoshimura and Masumoto (2011). The manoeuvring model is applied only in calm water.
To evaluate the path keeping, the evolution index of Norrbin (1971) – the so-called P-number -is used.
Maneuverability criteria for merchant ships are generally not applicable to the special requirements of naval ships. The attributes are subject to rules established by RINA (2017c). A bounding value of 3.5 ship lengths is applied for a minimum tactical diameter, whereas the P-number is required to have a minimum value of 5.0.

Vibrations

The module calculates the first four natural frequencies of vertical hull vibration mode based on regression analysis of a large number of full-scale measurements, made available to UNITS. Then, the risk of unwanted resonance is estimated by comparing these hull natural frequencies with three excitation frequencies, i.e. engine second-order frequency, propeller imbalance and propeller blade frequency. An averting membership grade function is used to assign aspiration level to avoid the worst case of resonance between the excitation and hull natural frequency.

DESIGN OF THE BASELINE DESTROYER

Technical Specification

The technical specification is a more stringent variant than that formulated by the Italian Navy regarding the operating conditions. The military payload is that assumed for the USA Notional Ship (Chalfantet al., 2015; Chalfant 2017). The destroyer is required to operate in the wider Mediterranean Sea, the Arabian Gulf, and the Red Sea, as well as in the Atlantic, Indian and Pacific Oceans.
The ship must be capable of carrying out its functions for at least thirty years, in which operation must be guaranteed for at least 70% of the time, assuming as a reference employment away from national basins periods of up to 8 months (6 in the area and 2 for transfer). It must ensure compliance with MARPOL TIER III regulations, ensure transit of 1000 miles at a minimum speed of 12 kt and stay in port for 7 days in ECA zones.
The ship propulsion system shall be based on a conventional twin propeller/rudder solution, powered by electric motors, realizing an all-electric ship. The onboard gensets have to supply both propulsion and onboard loads, exploiting an integrated power system.
The crew is assumed to have 26 officers, 25 non-commissioned officers, 78 sergeants, 80 troops, plus 21 additional accommodations. The standard reference for living spaces on board, food storage and waste treatment is the SMM-100 regulations of the Italian Navy (Marina Militare Italiana).
The ship shall be characterized by logistical autonomy of at least 45 days and must be energy efficient neutral, e.g. green plus notation. It must be able to retain black and grey water on board for at least 7 days. Regarding military payload, the ship is required to include (Chalfant, 2017):

- 1 x railgun (impulse of 10 MW)
- 1 x laser gun
- 2 x 76/62 naval gun
- 2 x machine guns close-in weapon system

- 2 x multipurpose rocket launcher
- 3 x fixed face radar in both S and X bands
- 2 x integrated topside array
- 2 x 48-cell Vertical Launching Systems (VLS)
- 1 x sonar in the bulbous bow

Power System Design

As the ship is all-electric, it is required to supply full power by means of electric generators, through a suitably sized integrated power system. The Power Corridor concept described above has been selected for this ship, and the Zonal Electric Power Distribution System (ZEDS) of Figure 3 has been defined. This solution offers significant advantages in terms of survivability and flexibility a ZEDS provides (Sulligoi et al., 2020) and is capable of managing large power level variations due to direct energy systems (Bosich et al., 2023), which are even more important for naval ships. The electrical zones follow the subdivision of the ship into Main Vertical Zones, and each can operate separately from the rest of the power system (provided that sufficient electrical power is available in the zone for the installed loads). Each load group is interfaced to one or both the power corridors by means of suitably sized power electronics converters, which have multiple functions. First, they step-down the voltage to the level required by the loads; second, they convert the DC voltage of the main buses in AC, if required by the loads; third, they manage the power flows in and out of the power corridors. Some of the loads (i.e., the chillers and the railgun) have no dedicated converter installed on the power corridor, because they either require specifically designed power supply systems (it is the case of the railgun), or they are supposed to already integrate conversion phases to perform their expected functions (it is the case of the chillers).
In relation to the onboard electric loads listed above, the definition of the interface converters' power has been made as follows:

- the 10 MW railgun requires a 17 MW power supply (Chalfant, 2017), which can be fully powered by either power corridor; the power supply is integrated into the railgun subsystems, thus interface converters are not required.
- the 300 kW laser requires a 0.5 MW interface converter, and can be fully powered by either power corridor.
- the 3 fixed-face radars in both S and X bands (3 MW total) and the integrated topside arrays (3 MW total) are powered by the same interface converters. The latter has a 4 MW size, thus being capable of supplying two-thirds of the total power from each power corridor. This is because contemporary and usage factors of these two loads are supposed to be not equal to one; despite this, full power operation is possible with both power corridors working and partial operation with half the power system down.
- the VLSs (0.5 MW for each set) are supposed to be fully operable also with one power corridor down, as well as the sonar in the bow (0.5 MW total), thus requiring equally sized interface converters on each side.
- the chillers, sized at 3.8 MW each to correctly manage all heat sources onboard and providing a 2 to 1 redundancy level, are fed alternatively by the two power corridors.
- other loads are also present onboard (e.g., the steering systems depicted in Figure 3, the cabin loads, and so on), which are alternatively supplied by the two power corridors through 2 MW interface converters. The latter are oversized by nearly 50%, to enable the supply of only the vital loads in the nearby zone in case of a fault (requiring a load shedding system to be put in place). This is highlighted by the dotted lines connecting such loads across zones in Figure 3.

The 80 MW all-electric propulsion system, which requires one 40 MW electric motor on each shaft, is designed to be capable of powering both the propellers (albeit at reduced power) with one power corridor down. To this aim, the electric motors are dual stator winding induction machines, where each winding can provide half of the power. The two windings are thus supplied by 20 MW converters, integrated into the power corridors (thus not located inside the engine rooms).
The electric power generation system (composed by two 22.7 MW gas turbines, two 16.3 MW diesel generators, and two 9.16 MW diesel generators) follows the same approach as the propulsion system, with dual stator winding machines providing half the power to each power corridor. This enables to deliver up to 48 MW of power to the ship loads also with one power corridor faulted. As can be seen in Figure 3, the power corridor is distributed in five zones. whose lengths are shown in Table 2.
Payload weight and volumes have been taken from (Chalfant, 2017), while the non-payload and the HVAC loads weights and volumes are calculated by the above-described mathematical model.
The Power Corridor main distribution, located in its bottom part (refer to Figure 1), operates in medium voltage, at 12 kV. It has been sized to transport up to 60 MW from one extremity to the other in each power corridor, providing a 25% margin with respect to the generators' power for future refitting. Different solutions can be used to deliver such power, here a busbar system has been selected, leading to a minimum required space of 44 cm in height and 15 in width, to which cooling, and power tap systems, must be added. Similarly, a weight of 50 kg/m must be considered for the busbars only, to which additional weight for power tap and enclosures must be added. To reduce the overall weight and volume of this element, a possible solution is to reduce its power sizing in the more external zones (i.e., zones 1 and 5), where only the power needed by the local loads is to be delivered. However, a full distribution sizing has been here used, to both enable the installation of more loads in these external zones and promote standardization of the power corridor components.
For what it concerns the power electronics converters installed in the power corridor, their weight and volume follow the values defined in Chalfant (2017), depicted in Table 5 for reference.

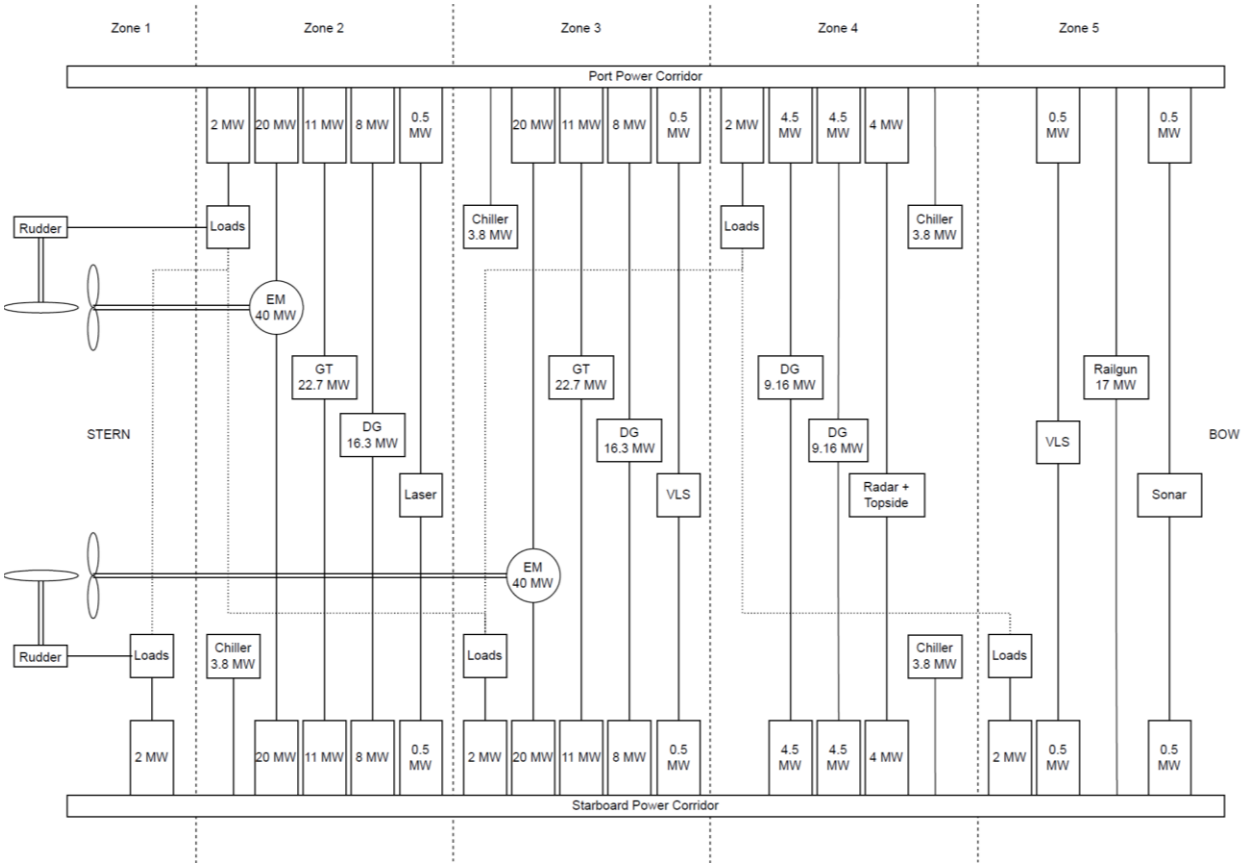

Figure 3: Zonal Electric Distribution System based on Power Corridor concept

Table 2: Available lengths of the zones

Zone	1	2	3	4	5
Length (m)	14.0	24.8	32.4	29.8	10.0

The overall Power Corridor sizing has a width of 1.6 m, which requires a total reserved space of 3.8 m on each ship side for ensuring correct accessibility for maintenance, and a converter rack height of 1.9 meters maximum, to be installed on top of a 0.6 m height distribution conduit (refer to Figure 1). The total length of the power corridor can be inferred from the ship GAP, while the single converters length has been evaluated as the one required to obtain the Table 3 volume, when the above-mentioned width and height are fixed.

Table 3: Nominal Power Converter Sizing Chart

Power Rating (MW)	1	2	3	4	6	8	10	12	14	18	22	24
Weight (t)	2.55	2.73	2.91	3.09	3.72	3.78	3.90	3.96	5.61	5.73	6.44	6.62
Volume (m^3)	12.9	12.9	12.9	12.9	15.1	15.1	15.1	15.1	20.8	20.8	24.2	24.2

Preliminary Design

The concept of the prototype design is that of a multi-mission ship whose combat system is fundamentally based on that of the Notional Ship (Chalfant, 2017). It is an all-electric twin-screw and two-rudder destroyer with a “tumblehome” hull form to reduce radar signature. It has a wide flaring bow, which significantly allows high speed in heavy sea conditions. A representative rendering of the ship model is shown in Figure 4 with its main characteristics listed in Table 4.
The main data of the individual fixed-pitch propeller and rudder is listed in Table 5. The propellers are designed based on the hydrodynamic load present in the battle scenario.
The operating profile is assumed on an annual basis and is given in Table 6 in terms of the percentage of time during which the destroyer sails at speeds and related operative conditions given in Table 4.

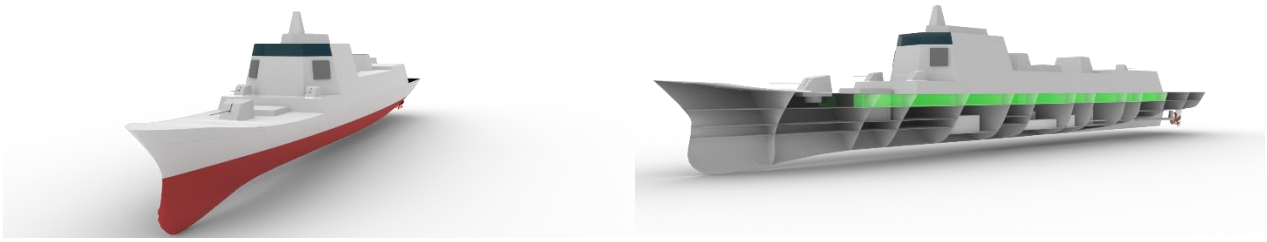

Figure 4: Rendering of the reference destroyer (in green: the port power corridor)

The total electrical power is obtained by adding the vital and non-vital electrical loads to the electrical demand requested by the sensors, weapons and chillers. It is worth noticing that the total power installed on board (95,780 kW) is more than 15,000 kW in excess of the maximum power required at a speed of 31 knots in sea state 4, in anticipation of an increase in power to be installed in the power runner in the future. For powering the full electric propulsion system at low and medium speed, it is sufficient to operate only the Diesel gensets (the size of the running ones depends on the speed, as shown in Table 6), while at peak and combat speed the ship operates with all the Diesel and the Gas Turbine gensets running. Finally, the MCR percentages of the gensets are reported for each speed. The values of baseline ship's attributes are given below in section "Ranking for the Best Compromise Design".

Table 4: General characteristics of the baseline ship

Length overall	L_{OA} = 179.000 m	Range at endurance speed	8000 nm
Length between perpendiculars	L_{PP} = 170.500 m	Low speed	12 kn @ SS6 + wind
Length at waterline	L_{WL} = 170.500 m	Cruise speed	18 kn @ SS5 + wind
Beam, maximum	B_{max} = 24.180 m	Endurance speed	20 kn @ SS5 +wind
Beam at design draft	B_{WL} = 22.250 m	Battle speed	28 kn @ SS4 + wind
Draft	T = 6.520 m	Top speed	31 kn @ SS4 + wind
Displacement	Δ = 12592 t	Complement	209
Longitudinal center of buoyancy	LCB = 84.24 m	Engines	2 x 9160 kW gensets
Longitudinal prismatic coefficient	C_P = 0.614		2 x 16030 kW gensets
Waterplane area coefficient	C_{WP} = 0.732		2 x 22700 kW tags
Vertical prismatic coefficient	C_{VP} = 0.675	Sensors, weapons, cooling	see Chalfant (2017)
Metacentric height	KM = 11.024 m	system, power conversion	
Vertical center of gravity	KG = 8.684 m	& distribution equipment	

Table 5: Propeller and rudder characteristics

Propeller		*Rudder*	
Diameter	= 4.620 m	Area	= 17.620 m^2
Pitch ratio	= 1.257	Span	= 4.895 m
Expanded rea ratio	= 0.986	Tip chord	= 3.600 m
Number of blades	= 5		

Table 6: Powering Performance

Ship Speed	V_S = 12 kn	V_S = 18 kn	V_S = 20 kn	V_S = 28 kn	V_S = 31 kn
Operating Time	10.0%	52.5%	30.0%	2.5%	5.0%
Delivered Power	P_D = 9592 kW	P_D = 12968 kW	P_D = 17852 kW	P_B = 39055 kW	P_B = 70855 kW
Total Electric Power	P_{EL} = 14726 kW	P_{EL} = 19796 kW	P_{EL} = 25164 kW	P_{EL} = 75415 kW	P_{EL} = 79740 kW
Fuel Consumption	2.701 t/h	3.636 t/h	4.622 t/h	5.752 t/h	6.518 t/h
Main Engines	Wärtsilä 8L46	Wärtsilä 14V46	Wärtsilä 14V46	LM 2500 + Wärtsilä 8V46 + Wärtsilä 14V46	LM 2500 + Wärtsilä 8V46 + Wärtsilä 14V46
Cont. Service Rating	80.6% MCR	61.9% MCR	78.6% MCR	35.6% MCR	58.7% MCR

FUZZIFIED DECISION SUPPORT SYSTEM

In the multiattribute design process, a large number of feasible designs is created by execution of the mathematical design model with a set of design variables generated by an adaptive Monte Carlo method. Constraints of min-max, crisp or fuzzy type may be applied to any attribute value generated within the MDM. A design is feasible if all attributes are within the given limits. Among all feasible designs, only non-dominated ones in the Pareto sense are retained. The product is a hypersurface of non-dominated designs subject to a final selection strategy.

Membership Grade Function

Ship design is a decision-making process whose nature generally involves uncertainty, vagueness or imprecision in the design attributes and constraints. Some of them are hard, i.e. based on physical laws or statutory norms, whereas some may be soft, i.e. based on the design team's aspiration level with uncertainty included. Moreover, in modeling the concept design process, deterministic algorithms are implemented to predict the attributes' values, which often cannot be determined exactly due to vagueness of many parameters and limited reliability of prediction methods. That is why the decision making necessitates a fuzzified decision support system. In fact, the concept design is intrinsically a fuzzy-logic problem where attributes may be weighed by the degree of membership reflecting the design team's knowledge and experience with the specific ship type.
To present the notion that an attribute is a member of a set A (for example, the RINA weather criterion rules) either fully or not at all, the function μ is introduced in Boolean terms as:

$$\mu_A(x) = \begin{cases} 1 & \text{if and only if} \quad x \in A \\ 0 & \text{if and only if} \quad x \notin A \end{cases} \qquad [10]$$

stating that the design x has either a 0 or a 1 membership grade in the given set. When $\mu_A(x)$ contains only the two points 0 and 1, the set A is non-fuzzy (crisp); in the above example, the weather criterion determines whether design x is feasible or unfeasible.
The i^{th} attribute's scores of a feasible design are viewed as a fuzzy set A, defined as the ordered set of pairs:

$$\{x_i, \mu_A(x_i)\} \qquad i = 1, 2, \dots, n \qquad [11]$$

where x_i denotes a design in the fuzzy set, whereas $\mu_A(x_i)$ represents the degree of truth, i.e. the membership grade function $0 \leq \mu_A(x_i) \leq 1$ for any $x \in A$
The mathematical theory of fuzzy sets (Zadeh, 1965), also referred to as fuzzy logic, is concerned with the aspiration level $\mu_A(x)$ reached by the outcome of an attribute, hence of a design.
Fuzzy sets may be treated as a collection of crisp sets by using the concept of an α-cut. An α-cut determines the crisp set A_α having all elements of A with a membership grade greater than α:

$$A_\alpha = \{x \in A \mid \mu_A(x) > 0\} \qquad [12]$$

Thus, α-cut sets correspond to discarding those elements of a fuzzy set that are 'extreme' in the sense of having 'low' membership grade in the set.
Among the three most important operations on any fuzzy sets, e.g. complement, union and intersection, the latter is the one useful in the MADM decision-making process. According to the intersection operation, the membership grade value of design x_i belonging to set A_1 and to set A_2 cannot be greater than the minimum of the two membership grade values:

$$\mu_{A_1 \cap A_2}(x_i) = \min\left[\mu_{A_1}(x), \mu_{A_2}(x_i)\right] \qquad [13]$$

Generalizing for n attributes, we can write for the degree of total membership grade $\mu_{\tilde{A}_j}$ of design x_i:

$$\mu_{\tilde{A}_j}(x_i) = \min\left[\mu_{A_1}(x_i), \dots, \mu_{A_k}(x_i), \dots, \mu_{A_n}(x_i)\right] \qquad j = 1, \dots, k, \dots, n \qquad [14]$$

Fuzzy MADM Selection

After generating a number of projects that adequately fill the design space, a fuzzy multiattribute decision-making method was implemented to identify the non-dominated designs and select the optimal vector of design attributes, e.g. the ideal design. It consists of six steps:

1. structuring the decision matrix;

2. determining the membership grade $\mu(x_i)$ for each attribute;
3. establishing the relative importance of the attributes by pairwise comparison;
4. weighing the degrees of attribute attainment $\mu(x_i)$ by the respective w_j so creating the intra-attribute fuzzy sets $\tilde{A}_j$;
5. finding the fuzzy set $\widetilde{D}$ of the non-dominated designs and the ideal design x_i^*;
6. selecting the preferred design x_i that has the minimum distance from $\widetilde{D}$ as the preferred design.

Decision Matrix. The decision matrix organizes the data available to the decision maker at the beginning of the selection process. A design problem with a total of m feasible designs described by n attributes is structured in a $m\ x\ n$ matrix $\tilde{A}$. Each element a_{ij} of the matrix is the performance rating of the design A_i with respect to attribute x_j.
The decision matrix should include only those attributes which vary significantly among the alternative designs and for which the design team considers this variation significant.

Intra-Attribute Preference and Attribute Normalization. Intra-attribute preference reflects the objective importance of the different values of the same attribute according to the maximum target the design team aspires to. Although different approaches look alike (e.g. value function concept), the membership grade approach from the fuzzy set theory is considered the most suitable tool for the purpose (Kosko, 1994). Among different formulations of membership grade functions developed so far, the generalization of Nehrling's function (Nehrling, 1985) is introduced in this study. Four types are defined, i.e. attracting, ascending, descending, and averting, whose formulation is provided in Table 7.

Table 7: Formulation of membership grade functions

Attracting	$\mu(x_i) = \dfrac{1}{1 + \left\lvert\dfrac{x_1 - x_i}{d}\right\rvert^N}$	*Averting*	$\mu(x_i) = 1 - \dfrac{1}{1 + \left\lvert\dfrac{x_1 - x_i}{d}\right\rvert^N}$
Ascending	for $x_i < x_1$ $\quad \mu(x_i) = \dfrac{1}{1 + \left\lvert\dfrac{x_1 - x_i}{d}\right\rvert^N}$ for $x_i \geq x_1$ $\quad \mu(x_i) = 1$	*Descending*	for $x_i \leq x_1$ $\quad \mu(x_i) = 1$ for $x_i > x_1$ $\quad \mu(x_i) = \dfrac{1}{1 + \left\lvert\dfrac{x_1 - x_i}{d}\right\rvert^N}$

Two points on the membership grade curve are important and may be defined as
$x = x_1$ the level of an attribute that is 100% satisfactory - $\mu(x) = 1$ -, i.e. the level that may be expected to be reached by the best design with respect to the specific attribute;
$x = x_1 \pm d$ the level that is only 50% percent satisfactory - $\mu(x) = 0.5$ -, where d is the variation imposed subjectively by the decision maker compared to the aspiration level.
Selecting the proper type and assigning appropriate values to d and N (2, 4, 6, 8), the design team may shape the membership function for each attribute.

Inter-Attribute preference. Design attribute values serve as a basis for selection of the final design among all non-dominated designs. As the attributes are not equally influential, in order to reflect their relative importance it is necessary to weigh them. One solution is to obtain a weighted membership grade by multiplication with a weighting factor reflecting the subjective preferences of the design team. In this respect, the Analytical Hierarchy Process (AHP) method, which was pioneered and developed by Saaty (1980), converts subjective assessments of relative importance to a set of weights. It provides a useful mechanism for checking the consistency of the evaluation measures for attributes generated by the mathematical design model.

Weighing the Intra-Attribute Fuzzy Sets. According to Nehrling (1985), weights were originally applied to membership grade as:

$$\left[\mu_j(x_i)\right]^{w_j} = \frac{\mu_j(x_i)}{1 + w_i} \qquad [15]$$

which did not take into account the number of attributes n.
To obtain better resolution of small weights when $n > 5$, a better solution was derived by Grubišić et al. (1997, 1998) as:

$$\left[\mu_j(x_i)\right]^{w_j} = \frac{\mu_j(x_i)}{1 + n\ (w_i - w_{min})} \qquad [16]$$

Hence, membership grades are multiplied by 1 for $w_i = w_{min}$ and by values progressively smaller than 1 for other weights.

Choice of the Preferred Design. Among a large set of feasible designs, no dominant design will exist that is better than all other designs in terms of all attributes. At the same time, it is impossible to minimize/maximize all attributes simultaneously. Since good values of some attributes inevitably go with poor values of others, the goal of the MADM method is to find the 'best compromise' solution following the concept introduced by Zeleny (1982). It can be obtained from a set of design alternatives referred to as the Pareto frontier, which consists of designs having a simple and desirable property, i.e. dominance (Pareto, 1906). According to this strong normative statement, a design is non-dominated, denoted as ND, when no attribute can be further improved without causing at least one of the other attributes to decline. Non-dominance can be expressed in terms of a simple vector comparison. If $x^j = \left(x_1^j, x_2^j, \dots, x_n^j\right)$ and $x^k = (x_1^k, x_2^k, \dots, x_n^k)$ are two designs of n attributes x^j dominates x^k if $x_i^j \geq x_i^k$ and $x_i^j > x_i^k$ for at least one attribute i and thus design x^k is discarded. Further pairwise comparison between feasible alternatives creates a set of non-dominated designs. At the same time, the collection of the highest achievable membership grades (attribute maxima) with all considered attributes form a composite, an ideal design x^* or 'utopia point' (Yu, 1973), denoted as $x^* = (x_1^*, x_2^*, \dots, x_n^*)$.
The hypersurface of the non-dominated designs defines the boundary of the production possibility, e.g. the limits attainable with each primary attribute depending on constraints of technological (and economic) nature. Then for each non-dominated design a fuzzy set $\tilde{A}$ in X is the set of ordered pairs:

$$\tilde{A}_j = \left\{x_i, \left[\mu_j(x_i)\right]^{w_j}, \quad x_i \in X\right\} \qquad [17]$$

The intersection of all $\tilde{A}_j$ forms the fuzzy decision set $\tilde{D}$ represented by the membership function $\mu_D(x_i)$ which describes the 'utopia point'.
The final step is to identify the 'best compromise' design from those contained in the fuzzy decision set $\tilde{D}$ represented by the membership function $\mu_D(x_i)$. As the rationale of the designers' choice is to prefer the solutions that are closer to the 'ideal design', the 'best compromise' design is that one with the minimum distance to the ideal design. In a fuzzy environment, the degree of closeness to the anchor value is measured via the Čebyšev metric as follows:

$$L_\infty = \min_j \left\{1 - \min_i \left[\mu_j(x_i)\right]_{i=1,n}^{w_j}\right\}_{j=1,ND} \qquad [18]$$

where the distance parameter ∞ means that the maximum possible weight is given to the largest deviation according to Equation [16].

MADM SELECTION PROCESS

The goal of the decision model is to simulate the decision-making of the design team in selecting the 'best compromise' destroyer from the Pareto frontier. The selection process is modelled as a MADM problem. The overall process for generating feasible designs, filtering non-dominated designs and selecting the preferred solution flows through the following steps: (i) identification of design variables, parameters, attributes and definition of individual min-max design space; (ii) generation of feasible design via an adaptive Monte Carlo method; (iii) definition of intra-attribute fuzzy functions and interactive inter-attribute preference; (iv) structuring the non-dominated design hypersurface; (v) selection of the 'best compromise' design.

Generation of Feasible Designs. The implemented mathematical design model is applied to the concept design of a class of destroyers whose main novelty is the presence of the power corridor. The propulsion system, the power from the electrical generators, the crew size, the vital and non-vital loads, the weapons and ammunition, the sensors, and the conversion and equipment distribution system are the same for all candidate designs. Viable and feasible solutions were generated subject to crisp constraints and soft constraints treated as attributes.

Variables, Parameters, Attributes and Constraints. The generated designs are uniquely defined by six independent variables given in Table 8, which define the design space through min-max values.

Table 8: Initial design space

Variable	L_{PP}/B_{WL}	B_{WL}/T	L_{PP}/T	C_P	C_{VP}	$L_{WL}/\nabla^{1/3}$
Minimal Value	7.250	3.000	23.750	0.615	0.600	7.000
Maximal Value	8.000	3.750	27.250	0.675	0.700	7.750

All candidate ships have data that is held fixed in a generation run, such as deck heights, number of zones, gas turbines, gensets, weapons, sensors, radars, cooling equipment, power conversion and equipment data, power corridor size, etc. The geometric topology and equipment are determined in advance as a result of the initial design of a destroyer prototype, which can be considered as the guess value to activate the mathematical design model.
Note that only the hull is defined by the random generation and not the superstructure. The size of the superstructure and deckhouse is a function of the length and beam of the hull. Not all generated ships yield feasible solutions since many other geometrical constraints are introduced which implicitly further restrict the multidimensional design space. The primary min-max constraints, which further restrict the design space, are illustrated in Table 9.
The mathematical design model calculates the primary and secondary attributes of feasible designs given in Table 10 together with their codes to simplify the writing of subsequent tables.
Attributes Y5 and Y10 are given as grades to reduce the number of attributes. Due importance is assigned to seakeeping and manoeuvring attributes because they heavily influence the operability of the ship.

Table 9: Geometrical constraints

Parameter	C_B	B_{ML}/L_{PP}	KB/B	Δ [t]	B_{MAX} [m]	$L_{WL}/\nabla^{1/3}$	i_E [deg]
Minimal Value	0.450	2.015	0.150	12250	23.750	7.000	5
Maximal Value	0.525	2.925	0.205	13000	25.250	7.750	10

Table 10: Attributes in the design process

Primary Attribute	Code	Secondary Attributes	Code
Fuel consumption at endurance speed (t/h)	Y1	Tankage volume (m3)	Y11
Power coefficient (-)	Y2	Metacenter height-to-beam ratio (-)	Y12
Weight-buoyancy balance (-)	Y3	Delivered power at endurance speed (kW)	Y13
Maximum speed (kn)	Y4	Delivered power at top speed (kW)	Y14
MOP membership grade function (-)	Y5	Electric load (kW)	Y15
Tactical diameter-to-length ratio (-)	Y6	Non-vital payload electric load (kW)	Y16
P-number (-)	Y7	HVAC electric load (kW)	Y17
Payload fraction (-)	Y8	Pitch (deg)	Y18
Available length for extra power corridor (m)	Y9	Volume of engine rooms (m3)	Y19
Vibration membership grade function (-)	Y10	Volume of power corridor (m3)	Y20

Outcomes of the Generation Process. The concept design starts with the generation of feasible designs. Fifty thousand destroyers were randomly generated. Only a little more than two thousand designs were found to be acceptable, overcoming all constraints. The cause of the unfeasibility of most of the ships was due to the fact that they had one or more geometric characteristics external to the design space. Other causes of elimination were, in decreasing order, an excessive detachment from the weight-thrust balance and non-compliance with the criteria of stability, seakeeping and manoeuvrability.
The process of design selection is interactive since designers might change and refine their preferences (sensitivity study). It is, therefore, of great importance to provide the design team with fast insight into multidimensional design and attribute spaces. To help in guiding the decision-making process a graphic support should be added.
For this purpose, three types of diagrams are proposed with the following combinations:

variable – variable	X-design space projection
variable – attribute	cross projection
attribute – attribute	Y-attribute space projection

The first group that relates the main dimensions and geometric coefficients to each other, serves to immediately identify the design space of feasible designs, so allowing to carry out an initial reduction of the feasible design space.
The second group is used to analyze the influence of any variable upon any attribute. It is useful for quantitatively predicting the effect of changing any variable on any attribute and for reducing the spans within which the variables are going to be generated in a next try. In this way, density of the non-dominated designs close to the ideal design may be increased.
The third group may be used as a guide to identify advantageous regions and to gain an impression of what may be the penalty for departing from the ideal solution.
Two examples in the X-design space are given in Figure 5. As can be seen, the feasible range of B/T ratio is dramatically reduced and reduces as the L/B ratio increases, making it unthinkable to have destroyers with L/B ratios tending towards 8. Relationship between C_B and C_{VP} allows to determine the feasible range for the waterline design coefficient, e.g. $0.685 \leq C_{WP} \leq 0.748$.

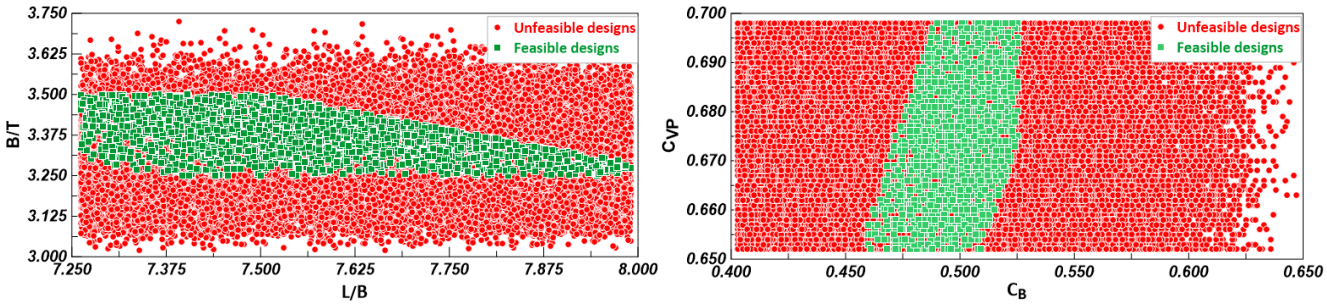

Figure 5: Variable-variable diagrams

Selecting the Preferred Designs

The purpose of the following analysis is to rate the overall performance of the feasible alternatives via the proper assignment of numerical grades to attributes and to rank the best designs.

Defining the Fuzzy Functions. The subjective decision on the aspiration level and relevance of each attribute is summarized in Table 11. A more stringent aspiration level (n = 2) is assigned to the hourly fuel consumption and free space in the power corridor for future storage of batteries.

Table 11: Selection of the membership grade functions

Attribute	Y1	Y2	Y3	Y4	Y5	Y6	Y7	Y8	Y9	Y10
Target	4.075	0.455	0	32.500	1.000	2.350	0.600	0.080	12.00	1.000
d	0.275	0.020	250	1.000	0.300	0.500	0.030	0.005	8.000	0.400
n	2	6	4	6	4	4	6	8	2	2
Fuzzy	Z-type	Z-type	Ω-type	S-type	Z-type	Z-type	S-type	S-type	S-type	U-type
α-cut	0.60	0.50	0.75	0.50	0.70	0.40	0.35	0.25	0.50	0.60

Non-dominated and Ideal Designs. The ideal solution (zenith) is characterized by the values of the attributes shown in Table 12, which represent the highest membership grades reached by different non-dominated designs in the multidimensional attribute space.

Table 12: Attributes of the Ideal Design

Fuel consumption	MDO = 4.025 t/h	Vertical acceleration at bridge	ACC_V = 1.466 m/s2
Power coefficient	C_{Power} = 8.08x10-2	Relative motion at helideck	RM_{hel} = 0.836 m
Maximum speed	V_{Max} = 32.44 kn	Nondimensional tactical diameter	D_{tac}/L = 2.526
Natural roll period	$T_{\emptyset}$ = 10.82 s	Available length for future power corridor	L_{PC} = 11.650 m

It is worth noting that the cross projections in Figure 6 show that both the baseline ship and ideal ship are very close to the Pareto frontier. Since both diagrams represent the power-speed relationship, this attests to the excellent quality of the resistance prediction in calm and confused seas and the design of the propulsion system.

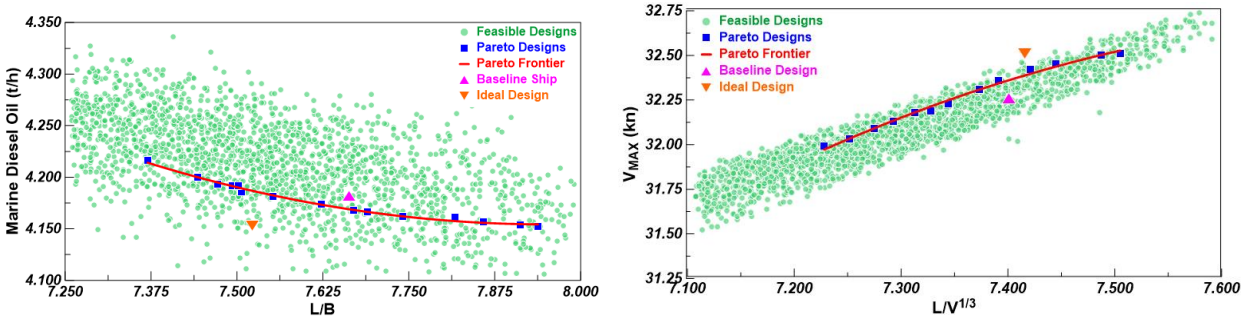

Figure 6: Variable–attribute graphs

Projection in the Y-space of the attribute-attribute relationship between available length for future enlargement of the power corridor and fuel consumption at endurance speed (left graph in Figure 7) shows that there are many possible designs with a longer power corridor than the baseline ship, but at the expense of a higher hourly rate.

Ranking for the Best Compromise Design. Measuring the distance of the non-dominated designs from the ideal point allowed us to build the ranking of the 'best possible' designs. Table 13 shows the comparison between the baseline ship and the 'best compromise' designs, where Design_1 and Design_3 are first and third in the ranking, respectively.

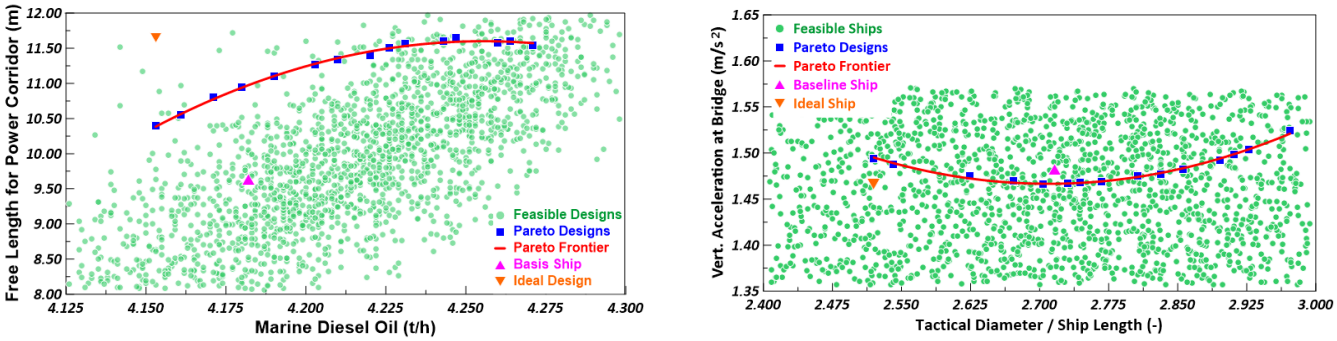

Figure 7: Attribute–attribute graphs

Table 13. Comparison between basic ship and the best possible designs

Item	*Baseline Ship*	*Design_1*	*Design_2*	*Design_3*
Main characteristics				
L_{OA}	179.00 m	180.18 m	181.75 m	180.52 m
L_{PP}	170.50 m	171.60 m	173.10 m	172.92 m
B_{MAX}	24.18 m	24.50 m	24.35 m	24.16 m
B_{WL}	22.25 m	22.52 m	22.40 m	22.18 m
T	6.52 m	6.37 m	6.48 m	6.56 m
Δ	12592 t	12500 t	12577 t	12413 t
C_P	0.612	0.613	0.606	0.604
C_{WP}	0.752	0.768	0.759	0.746
C_{VP}	0.656	0.629	0.649	0.642
KM	11.024 m	11.029 m	11.008 m	11.459 m
Primary attributes				
Y1	4.082 t/h	4.179 t/h	4.167 t/h	4.168 t/h
Y2	4.57 x 10-2	8.32 x 10-2	8.28 x 10-2	8.11 x 10-2
Y3	32.11 kn	32.03 kn	32.07 kn	32.04 kn
Y4	10.83 s	10.91 s	10.19 s	10.81 s
Y5	0.972	0.986	0.974	0.979
Y6	2.515	2.414	2.538	2.532
Y7	0.512	0.533	0.535	0.525
Y8	8.24 x 10-2	8.35 x 10-2	8.40 x 10-2	8.37 x 10-2
Y9	9.00 m	9.35 m	9.31 m	9.50 m
Y10	0.984	0.987	0.974	0.980
Secondary attributes				
Y11	3908 m3	3924 m3	3951 m3	3961 m3
Y12	0.109	0.110	0.106	0.122
Y13	19913 kW	20031 kW	20201 kW	20318 kW
Y14	74703 kW	74269 kW	76185 kW	75830 kW
Y15	3737 kW	3740 kW	3771 kW	3739 kW
Y16	1695 kW	1698 kW	1714 kW	1697 kW
Y17	1436 kW	1436 kW	1458 kW	1428 kW
Y18	1.145 deg	1.137 deg	1.125 deg	1.079 deg
Y19	3371 m3	3407 m3	3487 m3	3458 m3
Y20	2246 m3	2252 m3	2309 m3	2223 m3

Final Design Space. To conclude, one of the most important results of this study is that of having reduced the multidimensional design space, as shown in Table 14, where the initial design space is put in comparison with the final one as limited by the non-dominated designs.

Table 14. Design space before and after the concept design

Variable	L_{PP}/B_{WL}	B_{WL}/T	L_{PP}/T	C_P	C_{VP}	$L_{WL}/\nabla^{1/3}$
Initial Design Space						
Minimal Value	7.250	3.000	23.750	0.615	0.600	7.000
Maximal Value	8.000	3.750	27.250	0.675	0.700	7.750
Final Design Space						
Minimal Value	7.370	3.250	23.950	0.615	0.620	7.225
Maximal Value	7.920	3.500	23.720	0.675	0.675	7.5050

CONCLUSIONS

The contents of this paper are the result of a multidisciplinary cooperation project between MIT and UNITS, where the primary interest is to transfer know-how and technologies between still separated areas of naval architecture and electric-electronic engineering. We started from the belief that the introduction of advanced electrical and electronic technologies with integration of a power corridor requires a breakthrough in the design methodology (Sulligoi et al., 2016). To this purpose, a multiattribute decision-making process was applied to effectively select the 'best compromise' design which incorporates the power corridor. The results of the present work confirm the tendency towards increasing size of main surface combatants. It is about proposing ships that guarantee in the medium and long term the integration of additional systems and equipment that will absorb further electric and electronic power and require adequate space. It is for this reason that due importance has been given to the space available for future lengthening of the power corridor which is treated as a primary attribute in the decision-making process. Nevertheless, it has been here proved that in a main surface combatant, 2 power corridors, instead of original 4, might be sufficient to allocate all the required equipment with some margin.

The current MDM, although capable to provide reliable and interesting insights, can be further improved. Future enhancement of the mathematical model should include: (i) peak shaving to maximize the overall ship propulsive efficiency; (ii) competitive analysis of alternative power trains; (iii) optimization of power corridor layout; (iv) performance evaluation for energy storage systems to mitigate electric load fluctuations; (v) estimate of exhaust emissions by improvement of power distribution; and (vi) preliminary economic feasibility.

A limitation of this work is that all the primary and secondary attributes determined in the mathematical model are technical only. An economic module that calculates the annual average cost (AAC) index is completely missing. For a full picture of life-cycle costs, the economic module should include operating costs during the destroyer lifetime in addition to building costs including shipyard installation cost (excluding procurement cost) for command and armament. The AAC will be a dominant design criterion in a final analysis and selection of the 'best possible design'. This future activity requires knowledge of cost constraints.

CONTRIBUTION STATEMENT

Giorgio Trincas: Conceptualization, Methodology, Software, Investigation, Writing – Original Draft, Visualization, Project administration. **Luca Braidotti**: Conceptualization, Methodology, Software, Validation, Formal analysis, Resources, Data Curation, Writing – Original Draft, Visualization. **Andrea Vicenzutti**: Conceptualization, Validation, Formal analysis, Investigation, Data Curation, Writing – Original Draft, Visualization. **Andrea Alessia Tavagnutti**: Formal Analysis, Investigation. **Chathan M. Cooke**: Conceptualization, Investigation. **Julie Chalfant**: Conceptualization, Investigation, Writing – Review & Editing, Project Administration. **Vittorio Bucci**: Conceptualization, Investigation. **Chryssostomos Chryssostomidis**: Conceptualization, Investigation, Supervision. **Giorgio Sulligoi**: Conceptualization, Investigation, Resources, Writing – Review & Editing, Supervision, Funding acquisition.

ACKNOWLEDGEMENTS

Co-funded by the European Union, Horizon Europe Program - V-ACCESS Project; Grant agreement ID: 101096831. "Views and opinions expressed are however those of the authors only and do not necessarily reflect those of the European Union. Neither the European Union nor the granting authority can be held responsible for them".

This material is based upon research supported by, or in part by, the Office of Naval Research under award number ONR N00014-21-1-2124 Electric Ship Research and Development Consortium, by the National Oceanic and Atmospheric Administration (NOAA) under Grant Number NA22OAR4170126- MIT Sea Grant College Program, and by the Italian PNRM research projects “Naval Smart Grid (NaSG)” and "ETEF - Electric Test Facility".

REFERENCES

Andreasen, M.M. (1992). *The Theory od Domains*, Working Paper, Institute for Engineering Design, Technical University of Denmark, Lundby.

Bales, N.K. (1980). Optimizing the Seakeeping Performance of Destroyer-Type Hulls, 13th *Symposium on Naval Hydrodynamics*. Tokyo.

Bosich, D., Chiandone, M., Sulligoi, G., Tavagnutti, A. A., Vicenzutti, A. (2023). High-Performance Megawatt-Scale MVDC Zonal Electrical Distribution System Based on Power Electronics Open System Interfaces, *IEEE Transactions on Transportation Electrification*, 9(3), 4541-4551. DOI: 10.1109/TTE.2023.3244360

Braidotti, L., Prpić-Oršić, J. (2023). Bulkheads’ Position Optimisation in the Concept Design of Ships under Deterministic Rules, *Journal of Marine Science and Engineering*, 11(3), 546. DOI: https://doi.org/10.3390/jmse11030546.

Campana, E.F., Peri, D., Pinto, A, (2007), Multiobjective Optimization of a Containership Using Deterministic Particle Swarm Optimization, Journal of Ship Research, 51 (3), 217-228.

Chalfant, J. (2015). Early Stage Design for Electric Ship, *Proceedings of the IEEE on Electric Ship Technologies*, 103 (12), 2252-2266.

Chalfant, J., Ferrante, M. and Chryssostomidis, C. (2015). ‘Design of a Notional Ship for Use in the Development of Early-Stage Design Tools, *IEEE Electric Ship Technology Symposium* (ESTS), Alexandria, VA, 239-244.

Chalfant, J. (2017). ESRDC Notional Ship Data, *Electric Ship Research and Development Consortium*, Massachusetts Institute of Technology, Cambridge, available in https://esrdc.com/library/?q=node/762..

Cooke, M., Chryssostomidis, C. and Chalfant, J. (2017). Modular Integrated Power Corridor, *Proceedings of the 2017 IEEE Electric Ship Technologies Symposium* (ESTS), Arlington, VA, USA, 91-95

Cort, A. and Hills, W. (1987). Space Layout Design Using Computer Assisted Methods, *Naval Engineers Journal*, 249-260.

Degan, G., Braidotti, L., Marinò, A., Bucci, V. (2021). LCTC Ships Concept Design in the North Europe-Mediterranean Transport Scenario Focusing on Intact Stability Issues, *Journal of Marine Science and Engineering*, 9(3), 278. DOI: https://doi.org/10.3390/jmse9030278.

Derelöv, M. (2009). Identification of Potential Failure: On Evaluation of Conceptual Design, *Journal of Engineering Design*, 201-225.

Fung, S.C. (1991). Resistance and Powering Prediction for Transom Stern Hull Forms During Early Phase Ship Design, *Transactions SNAME*, 99, 29-84.

Grubišić, I., Zanić, V. and Trincas, G. (1997). Sensitivity of Multiattribute Design to Economic Environment: Shortsea Ro-Ro Vessels, *6th International Marine Design Conference, IMDC'97,* Newcastle upon Tyne, 201-216.

Grubišić, I., Zanić, V. and Bender, M. (1998). Fuzzy Attributes in Multi-Criterial Ship Concept Design Procedure, *International Design Conference - Design* ’98, Dubrovnik.

Hubka, V. and Eder, W.E. (19962). Design Science, Springer-Verlag, Berlin, ISBN 3-540-19997-7.,

Isherwood, R.M. (1973). Wind Resistance of Merchant Ships, *Transactions RINA*, 115, 327-338.

Kirkman, K.L., Sanders, D.G. and Slager, J.J. (1979). Methodology for Computation of Appendage Resistance, *NAVSEA*, Report 3213-79-40.

Kleijnen, J.P.C. (1987). *Statistical Tools for Simulation Practitioners*, Marcel Dekker, New York.

Kosko, B. (1994), *Fuzzy Thinking*, Flamingo, London.

Kwon, Y.J. (2008). Speed Loss due to Added Resistance in Wind and Waves, *The Naval Architect*, 14-16.

Lang, X. and Mao, W. (2020). A Semi-Empirical Model for Ship Speed Loss Prediction at Head Sea and Its Validation by Full-Scale Measurement”, *Ocean Engineering*, 209, 1-17.

Liu, S. and Papanikolaou, A. (2020). Regression Analysis of Experimental Data for Added Resistance in Waves of Arbitrary Heading and Development of a Semi-Empirical Formula, *Ocean Engineering*, 206, 1-17. doi.org/10.1016/ j.oceaneng.2020.107357.

Mauro, F., Braidotti, L., Trincas, G. (2019). A Model for Intact and Damage Stability Evaluation of CNG Ships during the Concept Design Stage, *Journal of Marine Science and Engineering*, 7(12), 750. DOI: https://doi.org/10.3390/jmse7120450.

Minsaas, L., Faltinsen, O.M. and Persson, B. (1983). On the Importance of Added Resistance, Propeller Immersion and and Propeller Ventilation for Large Ships in a Seaway, 2nd *International Symposium on Practical Design in Ship Building*, Tokyo & Seoul.

Myers, R.H. Montgomery, D.C. and Anderson-Cook C.M. (2016): *Response Surface Methodology*: *Process and Product Optimization Using Designed Experiments*, 3rd edition, Wiley, ISBN: 978-1-118-91601-8.

Nabergoj, R. (2020). Program MEDUSA, User's Guide, NASDIS PDS, Izola, Slovenia.
NATO (2000). Standardization Agreement (STANAG 4154). Common Procedures for Seakeeping in the Ship Design Process, NATO, *Military Agency for Standardization*.
Nehrling, B.C. (1985). Fuzzy Set Theory and General Arrangement Design, *Computer Applications in the Automation of Shipyard Operation and Ship Design, ICCAS 85*, Trieste, 319-328.
Norrbin, N.H. (1971). Theory and Observation on the Use of a Mathematical Model for Ship Manoeuvring in Deep and Confined Waters, 8th *Symposium in Naval Hydrodynamics*, Pasadena, California, 1971.
Norrbin, N.H. (1972). On the Added Resistance due to Steering on a Straight Course, *Proc. 13th ITTC*, Berlin & Hamburg.
NORDFORSK (1987). Assessment of Ship Performance in a Seaway, *The Nordic Co-operative Organization Project*: *Seakeeping Performance of Ships*, Copenhagen. ISBN 8798263714, 9788798263715, 1987.
Pahl, B., Beitz, W., Feldhusen, J. and Grote, K-H. (2007). *Engineering Design – A Systematic Approach*, Springer-Verlag, London, ISBN 978-1-84628-318-5.
Pareto, V. (1906). Handbook of Political Economics with an Introduction to the Social Science (in Italian), Società Editrice Libraria, Milan.
RINA (2017a). *RINAMIL, Rules for the Classification of Naval Ships*, Pt. B, Ch. 2, General Arrangement Design, 31-39.
RINA (2017b). *RINAMIL, Rules for the Classification of Naval Ships*, Pt. B, Ch. 3, General Arrangement Design, 47-55.
RINA (2017b). *RINAMIL, Rules for the Classification of Naval Ships*, Pt. B, Ch. 3, General Arrangement Design, 66-67.
Saaty, T.L. (1980). *The Analytical Hierarchy Process*: *Planning, Priority Setting, Resource Allocation*, McGraw Hill International, New York.
Sulligoi, G., Vicenzutti, A. and Menis, R. (2016). All-Electric Ship Design from Electrical Propulsion to Integrated Electrical and Electronic Power Systems, IEEE Transactions on Transportation and Electrification, 2(4), 507-521.
Sulligoi G., Bosich, D., Vicenzutti, A. and Khersonsky, Y. (2020). Design of Zonal Electrical Distribution Systems for Ships and Oil Platforms: Control Systems and Protections, *IEEE Transactions on Industry Applications*, 56 (5), 5656-5669, doi: 10.1109/TIA.2020.2999035.
Townsin, R.L. (1983). Bottom Condition and Fuel Conservation, VIII *WEGEMT Graduate School*, Gothenburg.
Townsin, R.L., Byrne, D., Svensen, T.E and Milne, A. (1981). Estimating the Technical and Economic Penalties of Hull and Propeller Roughness, *Transactions SNAME*, 89, 295-318.
Triantaphyllou, E. (2000). *Multi-Criteria Decision Making Methods*: *A Comparative Studies*, Kluwer Academic Publishers.
Trincas, G. (2001). Survey of Design Methods and Illustration of Multiattribute Decision Making System for Concept Ship Design (keynote paper). *Proceedings of MARIND 2001*, Varna, III, 21-50.
Trincas, G., Grubišić, I. and Žanić, V. (1994). Comprehensive concept design of fast ro-ro ships by multiattribute decision making. *Proceedings of 5th International Marine Design Conference, IMDC'94*, Delft, 403-418.
Trincas, G., Mauro, F., Braidotti, L. and Bucci, V. (2018). Handling the Path from Concept to Preliminary Ship Design, *Proceedings of IMDC 2018*, Espoo, Helsinki.
Ulrich, K.T. and Eppinger, S.D. (2007). *Product Design and Development*, 4th edition, Mc-Graw Hill, New York, ISBN 007123273-7.
Yoshimura, Y. and Masumoto, Y. (2011). Hydrodynamic Force Database with Medium High Speed Ships and Investigation into a Maneuvering Prediction Method, *JASNAOE*, 14, 63-73.
Yu, P.L. (1973). A Class of Solutions for Group Decision Problems, *Management Science*, 19(8), 936-946.
Zadeh, L.A. (1975). Fuzzy Sets and Their Application to Cognitive and Decision Processes, *Academic Press*.
Zeleny, M. (1982). Multiple Criteria Decision Making, *McGraw-Hill Book Company*, New York.

Proceedings of 15th International Marine Design Conference (IMDC-2024)
June 2-6, 2024
Amsterdam, the Netherlands

Comparison and Evaluation of Learning Capabilities of Deep Learning Methods for Predicting Ship Motions

Mingyang Zhang [1,*] , Cong Liu [1], Pentti Kujala [1,2], and Spyros Hirdaris [3]

ABSTRACT

The development of intelligent ship control systems in real-world conditions relies heavily on the accurate identification and prediction of ship seakeeping and maneuvering trajectories. In this study, we comprehensively evaluate a selection of deep learning methods to assess their learning capabilities in terms of idealizing ship motion behavior in realistic operational environments. To recover real conditions, we utilize historical Automatic Identification System (AIS) data and a time domain 6 Degree of Freedom (6-DoF) grounding dynamics model to generate ship motion sequences for a Ro-Ro passenger ship operating in the Gulf of Finland. Via a rigorous evaluation process, we validate the performance of these methods using extensive data streams. The analysis includes the identification and estimation of uncertainties between two ports. The paper demonstrates the proficiency of the selected deep learning methods in capturing ship maneuvering features, their potential use in the design of ship control and intelligent decision support systems.

KEY WORDS

Seakeeping, Maneuvering, Deep learning methods, Design for safety, Ship systems.

INTRODUCTION

Seakeeping prediction methods can enhance our understanding of the dynamic behaviour of ships in stochastic seaways. The models are valuable for improving ship design operational efficiency and safety of ship operations. The development and use of intelligent decision support systems should account for motions and manoeuvres in real operational conditions. Predicting ship motions under real conditions provides a unique opportunity to help crew members understand ship dynamics in advance of a collision or grounding event (Zhang et al., 2023). The integration of empirical data with neural networks in deep learning models shows great promise. However, among the multitude of neural network models, the method that best captures ship manoeuvring features requires comparison and evaluation. Therefore, this paper aims to evaluate the learning capabilities of selected deep learning methods.

With the ongoing advancement in sensor and identification technologies, ship maneuvering system identification methods have emerged as a distinct set of techniques for predicting ship motions. Ship maneuvering parameter identification models are categorized into parametric and non-parametric. Parametric estimation models quantify ship dynamics using established ship theory (e.g., Maneuvering Modelling Group - MMG or Abkowitz models), to train large data sets. Recently the nu- Support Vector Machine (SVM) and a 3-DOF Abkowitz model have been utilized (Wang et al., 2019), while the extended Kalman Filter (EKF) has been coupled with the MMG model (Zeng et al., 2021) to predict hydrodynamic derivatives (Liu et al., 2021). Taimuri et al., (2022) introduced a predictive analytics approach for grounding avoidance using a rapid 6-DoF ship manoeuvring model. However, incorporating hydrometeorological conditions (wave, wind, current, etc.) into these methods poses challenges.

1. Aalto University, Department of Mechanical Engineering, Marine and Arctic Technology Group, Espoo, Finland
2. Tallinn University of Technology, Estonian Maritime Academy, Tallinn, Estonia
3. American Bureau of Shipping - ABS, Athens, Greece
* Corresponding Author: mingyang.0.zhang@aalto.fi

Submitted: 15 February 2024, Revised: 18 April 2024, Accepted: 1 May 2024, Published: 19 May 2024

Conference paper, DOI: https://doi.org/10.59490/imdc.2024.838 e-ISSN: 3050-4864

Non-parametric estimation methods quantify ship dynamics without relying on predefined models. Prominent models include Artificial Neural Networks (ANN) (Silva et al., 2022), machine learning methods, such as Gaussian Process Regression (GPR) (Ouyang et al., 2021; Ramirez et al., 2022), Recurrent Neural Networks (RNN) (D'Agostino et al., 2023), Long Short-Term Memory models (LSTM) (Sun et al., 2022; Zhang et al., 2021), Gated Recurrent Units (GRU) (Zhou et al., 2023), and Transformers (Zhang et al., 2023). These models can be trained using data from simulated free-running tests or sea trials. Recently, Luo et al. developed an ANN model to predict the 3-DOF motion of unmanned surface vehicles (Luo et al., 2022). Non-parametric models have shown potential in identifying ship motion features and rapidly predict ship motions.

To analyze the differences in predicting ship motions using deep learning methods this paper evaluates and compares the learning efficacy and capabilities of the above-mentioned methods.

SHIP MOTIONS AND DATA

The analysis of ship motions often treats the ship as a rigid body moving in six degrees of freedom (6-DOF), using an earth- and ship body-fixed systems. In this paper, to capture the 6-DOF ship motions in real operational conditions, AIS (Automatic Identification System) ship trajectories are reconstructed for a ship operating between two ports. Time-domain hydro-meteorological data are sourced from now-cast data providers, and GEBCO (General Bathymetric Chart of the Oceans). Bathymetry data are employed to map the waterway (see Zhang et al., 2023 and Figure 1).

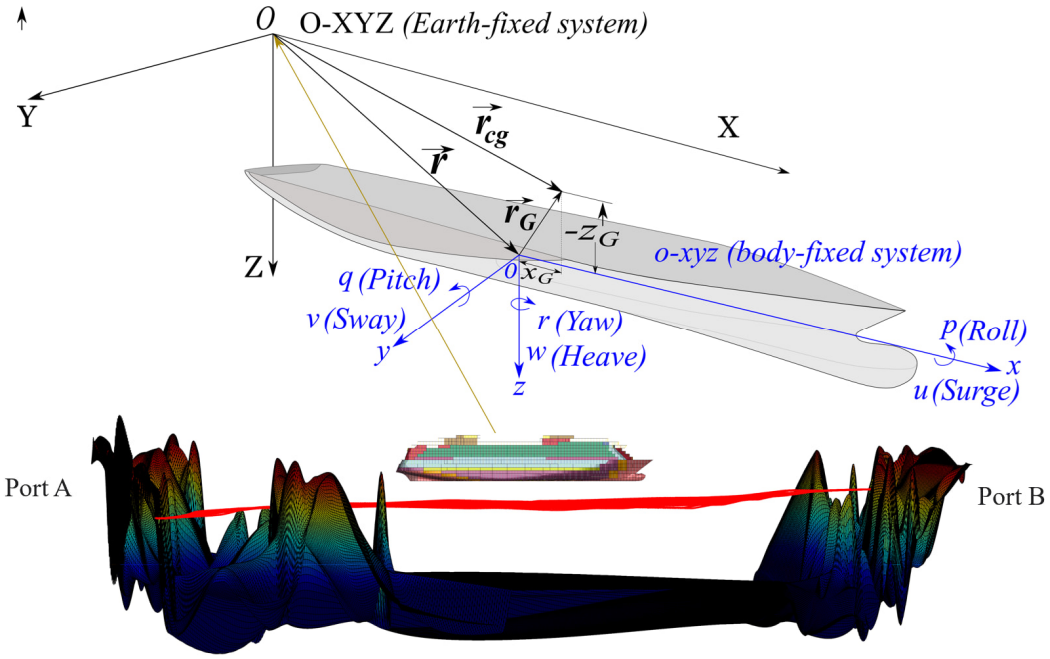

Figure 1: 6-DoF ship motions along ship trajectories between two ports.

The data collected serve as inputs to the FSI model of Taimuri et al., (2022) which idealizes the impact of operational conditions and control devices on ship motions. A Proportional Derivative (PD) controller is utilized to adjust the rudder according to the ship predefined heading, thus autonomously maintaining the desired AIS track for each voyage in real-time, see Zhang et al. (2023). The 6-DOF motions of the ship are depicted in Figure 2. The data utilized to compare and evaluate the learning capabilities of the selected deep learning methods are outlined in Section 3.

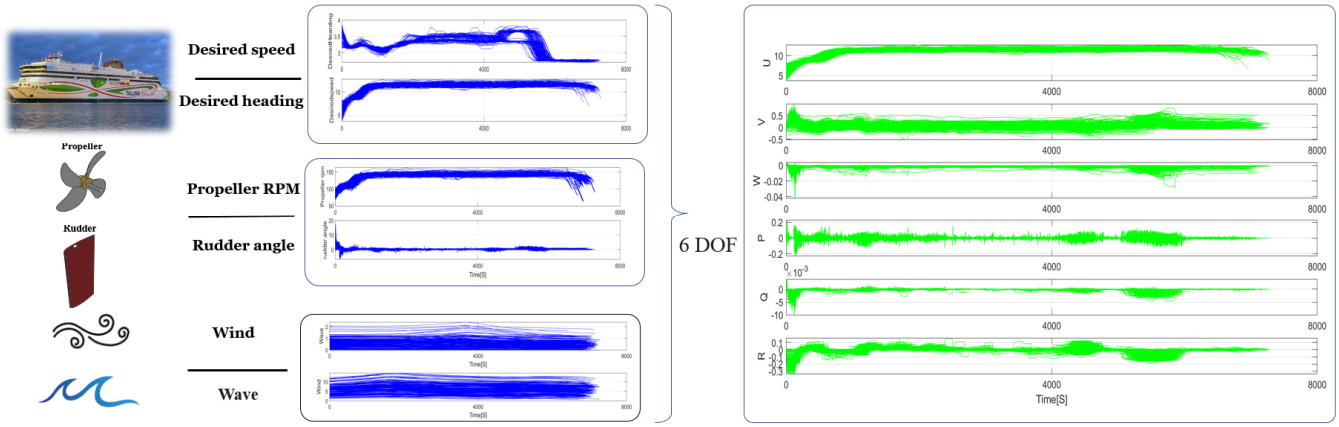

Figure 2: The ship maneuvering commands and the corresponding 6 DOF ship motions

METHODS

This section offers an overview of 6 deep learning methods used for ship motion predictions, illustrating the operating principles of them and briefly describes the underlying mathematical logic of each method. In addition, these models are used to train ship motion prediction models using varying length of training dataset for the evaluation of model learning capabilities, as shown in Figure 3.

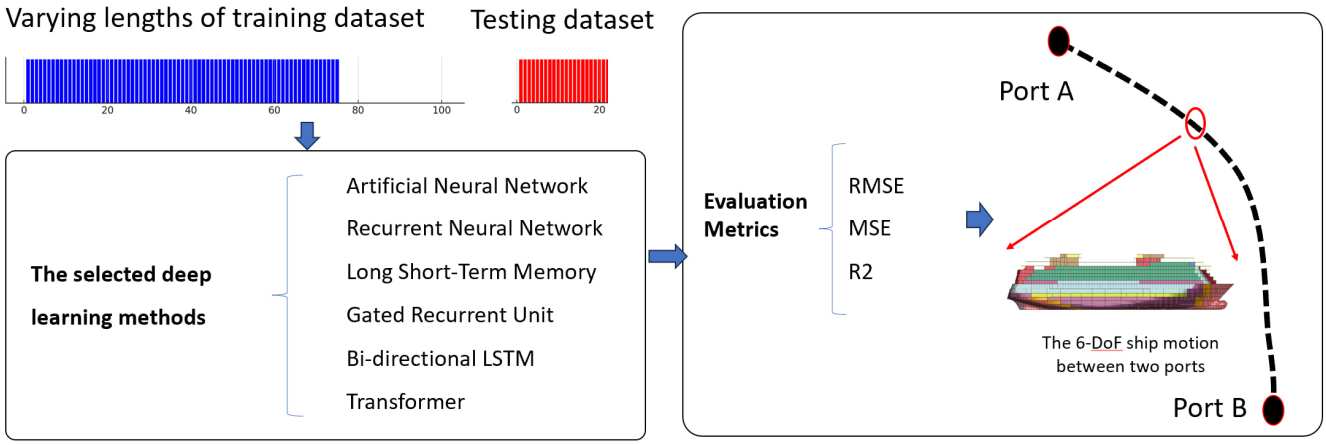

Figure 3: The flowchart of comparison and evaluation of learning capabilities of selected deep learning methods

Selected Deep Learning Models

In this section, the theories behind the 6 deep learning methods (ANN, RNN, LSTM, Bi-LSTM, GRU, and Transformer) used in existing studies are presented to help understand the mathematical logics and the advancements in deep learning technologies for predicting ship motions.

(1) Artificial Neural Networks (ANN)

ANN are a foundational neural network type and a critical component of deep learning technology that may be utilized to predict ship motions (Luo et al., 2022). It comprises of three main layer blocks, namely, an input layer, one or more hidden layers, and an output layer. Each neuron in a layer is connected to every neuron in the preceding and following layers, see Figure 4, where the connections (represented by arrows) contain learnable parameters. The principle of back propagation is employed to adjust the network parameters, by effectively mapping inputs to outputs to approximate various nonlinear functions as follows:

$$h = XW^h + b^h \quad (1)$$
$$y = hW^y + b^y \quad (2)$$

where W^h, W^y are weights and b^h, b^y are biases.

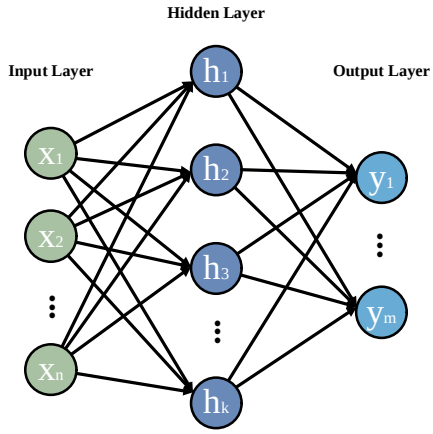

Figure 4: Diagram of ANN architecture

(2) Recurrent Neural Networks (RNN)

RNN represent a type of neural network known for their robust processing of time-series data. Recently, they have been used to predict ship motions (D'Agostino et al., 2023). Unlike ANN, RNN models excel at considering temporal correlations by integrating historical and current information. RNN also serve as a comprehensive framework of neural networks, encompassing various variants, see Figure 5. In a standard RNN, the process begins with an initial hidden state, denoted as H_0. At each time step t, the input X_t is fed into the hidden layer of RNN, where it is combined with the hidden state from the previous time step, see Eq. (3). This combination introduces nonlinearity to the model through an activation function. The activation function, see Figure 5, is typically the hyperbolic tangent - $tanh$. Ultimately, this process results in the generation of the current output and the updated hidden state.

$$H_t = tanh(X_t W_x + H_{t-1} W_h + b_h) \quad (3)$$

where W_x, W_h are the weight matrices and b_h is the bias.

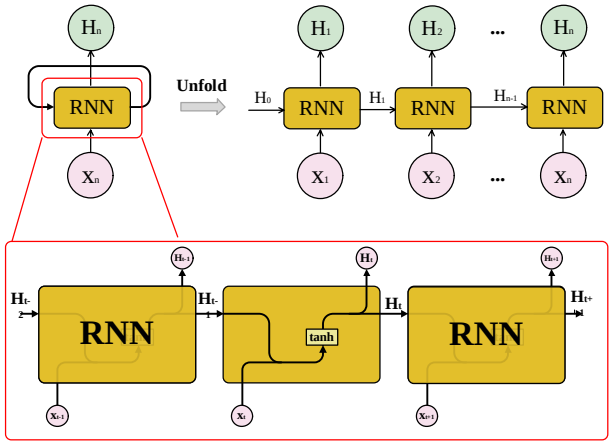

Figure 5: The framework and architecture of RNN

(3) Long Short-Term Memory (LSTM)

In conventional RNN, the issues of gradient explosion and gradient vanishing often arise, hindering a network's ability to predict long sequences effectively (Bianchi et al., 2017). To address this limitation, the LSTM model introduced by Graves, et

al. (2012) was used to train ship motion prediction models (Sun et al., 2022). The LSTM enhances the standard RNN architecture by incorporating three distinct gates namely input, output, and forget gates. These gates allow to selectively retain or discard information, thereby enabling it to effectively utilize long-distance temporal information and significantly improve the model's learning capability.

As illustrated in Figure 6, at a time step t, the current input information is fed into the LSTM, along with the hidden state from the previous time step. This information is then nonlinearly processed by the Sigmoid (σ) activation function to compute the values of the three gates. The computations for these gates are defined as follows:

$$F_t = \sigma(W_F \cdot [H_{t-1}, X_t] + b_F) \quad (4)$$
$$I_t = \sigma(W_I \cdot [H_{t-1}, X_t] + b_I) \quad (5)$$
$$O_t = \sigma(W_O \cdot [H_{t-1}, X_t] + b_O) \quad (6)$$

where W_F, W_I, W_O are the weight matrices of the forget, input and output gates respectively, and b_F, b_I, b_O are the biases of the three gates respectively.

The candidate memory element $\tilde{C}_t$ is calculated as shown in Eq. (7), utilizing the hyperbolic tangent activation function $tanh$. This process determines the information to forget or retain by multiplying the forget gate output F_t with hidden state H_{t-1} at the previous moment. The new cell state C_t is then obtained by adding the memory cell to the information selected by the forget gate. Finally, the latest hidden state H_t is derived by combining the output gate O_t and the new cell state C_t as indicated in Eqs. (8) - (9).

$$\tilde{C}_t = tanh(W_O \cdot [H_{t-1}, X_t] + b_O) \quad (7)$$
$$C_t = F_t * H_{t-1} + I_t * \tilde{C}_t \quad (8)$$
$$H_t = O_t * tanh(C_t) \quad (9)$$

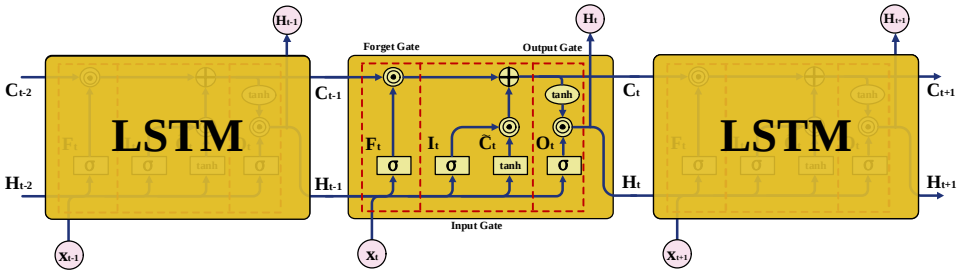

Figure 6: Diagram of LSTM architecture

(4) Gated Recurrent Units (GRU)

GRU are RNN models improved via LSTM and designed to address issues of gradient explosion and vanishing gradients (Chung et al., 2014). Their application for ship motion predictions are presented in Zhou et al. (2023). As compared to LSTM, the GRU simplifies the model architecture by featuring only two gates namely the update gate Z_t and the reset gate R_t, see Figure 7. This streamlined structure allows the GRU to achieve performance comparable to that of LSTM while enhancing training efficiency and computational speed. The computational process of the GRU is outlined as follows:

$$Z_t = \sigma(W_Z \cdot [H_{t-1}, X_t] + b_Z) \quad (10)$$
$$R_t = \sigma(W_R \cdot [H_{t-1}, X_t] + b_R) \quad (11)$$
$$\tilde{H}_t = tanh\,(W_H \cdot [R_t * H_{t-1}, X_t] + b_H) \quad (12)$$
$$H_t = (1 - Z_t) * H_{t-1} + Z_t * \tilde{H}_t \quad (13)$$

where W_Z, W_R, W_H, are weight matrices, b_Z, b_R, b_H are biases, σ is the Sigmoid function, and tanh is the hyperbolic tangent function.

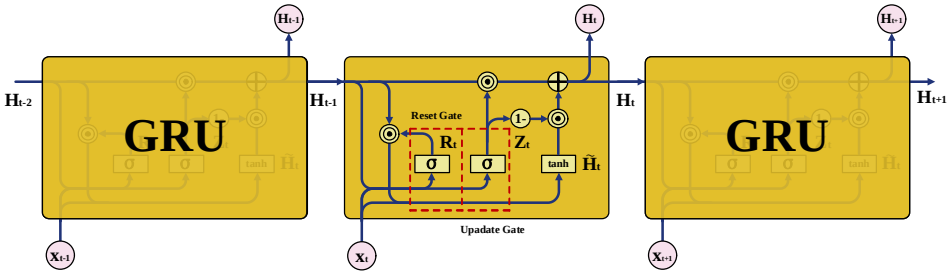

Figure 7: Diagram of GRU architecture

(5) Bi-directional LSTM

In the traditional LSTM model, information can only be recorded from the past, propagating from front to back. However, Bi-directional LSTM (Bi-LSTM) networks are also capable of combining information from both the past and the future (Zhang et al., 2024). This is achieved by constructing associations between the current time step information and the information from both preceding and succeeding time steps, see Figure 8. By leveraging this approach, Bi-LSTM models can learn more complex temporal features, leading to improved prediction accuracy and robustness, see Eqs. (14)-(16).

$$H_t^{fwd} = LSTM_{fwd}(X_t, H_{t-1}^{fwd}) \tag{14}$$

$$H_t^{bwd} = LSTM_{bwd}(X_t, H_{t+1}^{bwd}) \tag{15}$$

$$H_t = [H_t^{fwd}, H_t^{bwd}] \tag{16}$$

where X_t is the input at moment t, H_t^{fwd} is the state of the forward LSTM, H_t^{bwd} is the state of the reverse LSTM, and H_t is the output of the Bi-LSTM after combining the positive and negative states.

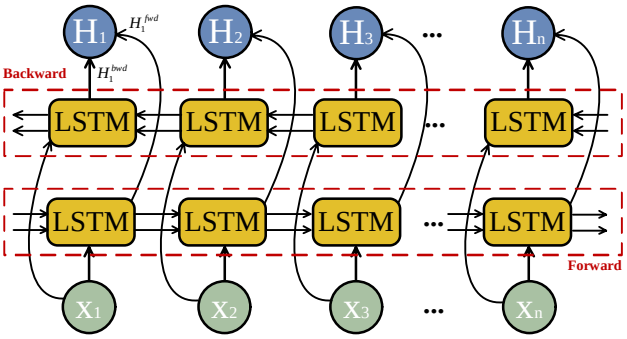

Figure 8: Diagram of Bi-directional LSTM structure

(6) Transformers

The introduction of attention mechanisms has significantly enhanced deep learning methods with widespread application in time series prediction (Zhang et al., 2023). Transformer models employ a multi head self-attention mechanism and an encoder-decoder architecture to extract deep features from training data. Supervised learning trains on historical data, with model parameters updated via back-propagation to progressively approximate true values. The Transformer encoder comprises a series of N identical layers, each containing two sub-layers: a multi-head self-attention mechanism and a fully connected feed-forward network. Both sub-layers undergo normalization operations and incorporate residual connectivity to facilitate information flow. The decoder, similarly, comprises of N identical layers. However, it includes an additional third sub-layer in each sub-layer. This additional sub-layer tasks with masking the self-attention mechanism to ensure predictions for a given position can only depend on previously known outputs, see Figure 9. To incorporate position information within the model, positional encoding is applied at the base of both encoder and decoder layers as follows:

$$PE_{(pos,2i)} = sin(pos/10000^{2i/d_{\text{model}}}) \tag{17}$$

$$PE_{(pos,2i+1)} = cos(pos/10000^{2i/d_{\text{model}}}) \tag{18}$$

where pos is the position and i is the dimension of the d_{model}.

The attention mechanism utilized in the Transformer model is the scaled dot-product attention. This mechanism involves stitching together multiple attention heads to form distinct subspaces, enabling the model to learn features from various perspectives. Additionally, each layer includes a fully connected feed-forward neural network. This network is independent and applied to each position identically across the sublayers. The computation within this network proceeds through the ReLU (Rectified Linear Unit) activation function, as follows:

$$Attention(Q,K,V) = softmax(\frac{QK^T}{\sqrt{d_k}})V \tag{19}$$

$$MultiHead(Q,K,V) = Concat(head_1,\ldots,head_h)W^O \tag{20}$$

$$\text{where head}_i = Attention(QW_i^Q, KW_i^K, VW_i^V) \tag{21}$$

$$FFN(x) = max(0, xW_1 + b_1)W_2 + b_2 \tag{22}$$

$$ReLU(x) = (x)^+ = max(0,x) = \begin{cases} x & if x > 0 \\ 0 & if x \leqslant 0 \end{cases} \tag{23}$$

Where Q, K, V are query, key, and value respectively, $\sqrt{d_k}$ is the vector dimension, h is the number of parallel attention heads, W_i^Q, W_i^K, W_i^V are the weight matrices, W_1, W_2 are the weights, and b_1, b_2 are the biases.

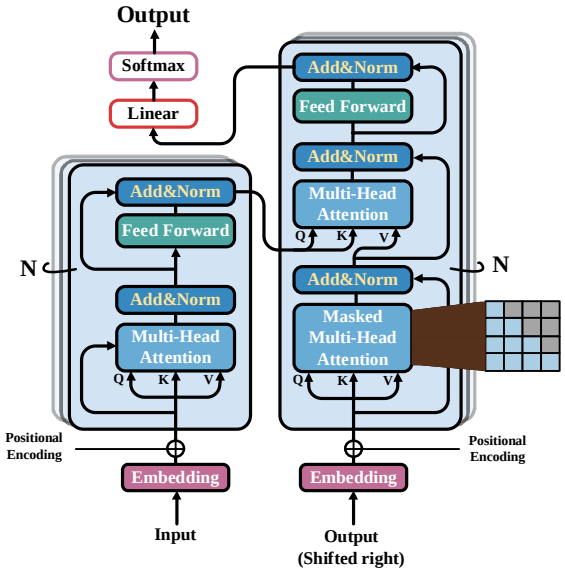

Figure 9: Diagram of Transformer architecture

Model Evaluation Metrics

To evaluate the performance of these selected deep learning models and quantify the errors between the real and the predicted ship motions, Root Mean Square Error (RMSE), Mean Square Error (MSE), and R^2 value (coefficient of determination) were evaluated, as:

$$RMSE = \sqrt{\frac{1}{N}\sum_{n=1}^{N}(y_n - \hat{y}_n)^2} \tag{24}$$

$$MSE = \frac{1}{N}\sum_{n=1}^{N}(y_n - \hat{y}_n)^2 \tag{25}$$

$$R^2 = 1 - \sum_{n=1}^{N}(y_n - \hat{y}_n)^2 / \sum_{n=1}^{N}(y_n - \bar{y}_n)^2 \tag{26}$$

In the above expressions, y_n is the actual value, $\hat{y}_n$ denotes the predicted value, $\bar{y}_n$ is the mean value.

RESULTS AND DISCUSSION

The results presented utilise 400 (80%) of the 500 ship trajectories from Section 2. A 6 DOF ship motions model of each ship trajectory is used to train the selected 6 deep learning models presented in Section 3.1. The remaining 100 (20%) ship trajectories serve for validation purposes. (See Section 4.1). To keep the hyperparameters of these deep learning models unchanged, training sessions encompassing different data volumes are used to examine how the amount of data influences model efficacy, see Section 4.2. Through this comprehensive analysis, attempts to pinpoint the predictive accuracy of models and identify the data volume necessary to achieve training saturation. In this sense the results presented may be useful to develop ship motion prediction models that possess the ability to learn and adapt.

Results of Ship Motions Prediction Using Various Deep Learning Models

Based on the data presented in Section 2, different machine learning models have been utilized to train predictors for ship motions. The inputs to these models are propeller RPM and rudder angle. The outputs are the 6 DOF of ship motions along ship trajectories. Their configurations are outlined in Table 1. Hyperparameters are optimized using a grid search method, with the best parameters determined by the lowest MSE obtained during validation (Zhang et al., 2024).

Table 1: The characteristics of the selected models and the optimal hyperparameters

Model	ANN	RNN	LSTM	Bi-LSTM	GRU	Transformer
Data	2 input variables and 6 output variables					
Architecture	3 layers; 64 hidden units per layer; Early stopping: Patience=10; Optimizer: Adam; Dropout rate: 0.2; Regularization param: 0.1					Encoder: 6 Decoder: 6
Leaning rate	0.001	0.001	0.001	0.001	0.001	Batch Size: 8
Epochs	18	32	17	21	28	Epochs: 48
Batch size	10	15	5	10	10	Inner layers: 1,024

The training and validation losses were calculated based on the basis of training 80% and 20% of 500 ship trajectories, respectively. Table 2 showcases the validation losses for various models, illustrating that the Transformer model exhibits a stronger capability for handling the degrees of freedom in ship motions as compared to models like ANN, RNN, LSTM, GRU, and Bi-LSTM. Theoretically, a Transformer model's advantage stems from its extensive parameter scale, which enhances its predictive performance and learning capabilities. It is also possible that the observed superiority of the Transformer model is partly due to the relatively simplistic complexity settings of the ANN, RNN, LSTM, GRU, and Bi-LSTM models.

Table 2: The performance evaluation on the teasing dataset of the selected ship models

	ANN	RNN	LSTM	Bi-LSTM	GRU	Transformer
RMSE	0.096	0.098	0.067	0.055	0.042	0.022
R^2	0.365	0.375	0.487	0.511	0.574	0.837

To further assess these models, propeller RPM and rudder angle, were chosen to evaluate the generalization capabilities of the trained models. The results indicate that the trained deep learning models are proficient in capturing the characteristics of ship maneuvering under real conditions. However, their accuracy varies. This difference is observed not only in the overall accuracy of the models but also in the prediction accuracy for various motions (Surge, Sway, Heave, Roll, Pitch, Yaw), see Figure 10. Overall, the results indicate that the Transformer model is more effective in capturing nonlinear ship motions that mirror actual operational conditions. This also suggests that its learning capabilities are superior for predicting ship motions in real conditions, as compared to selected deep learning methods.

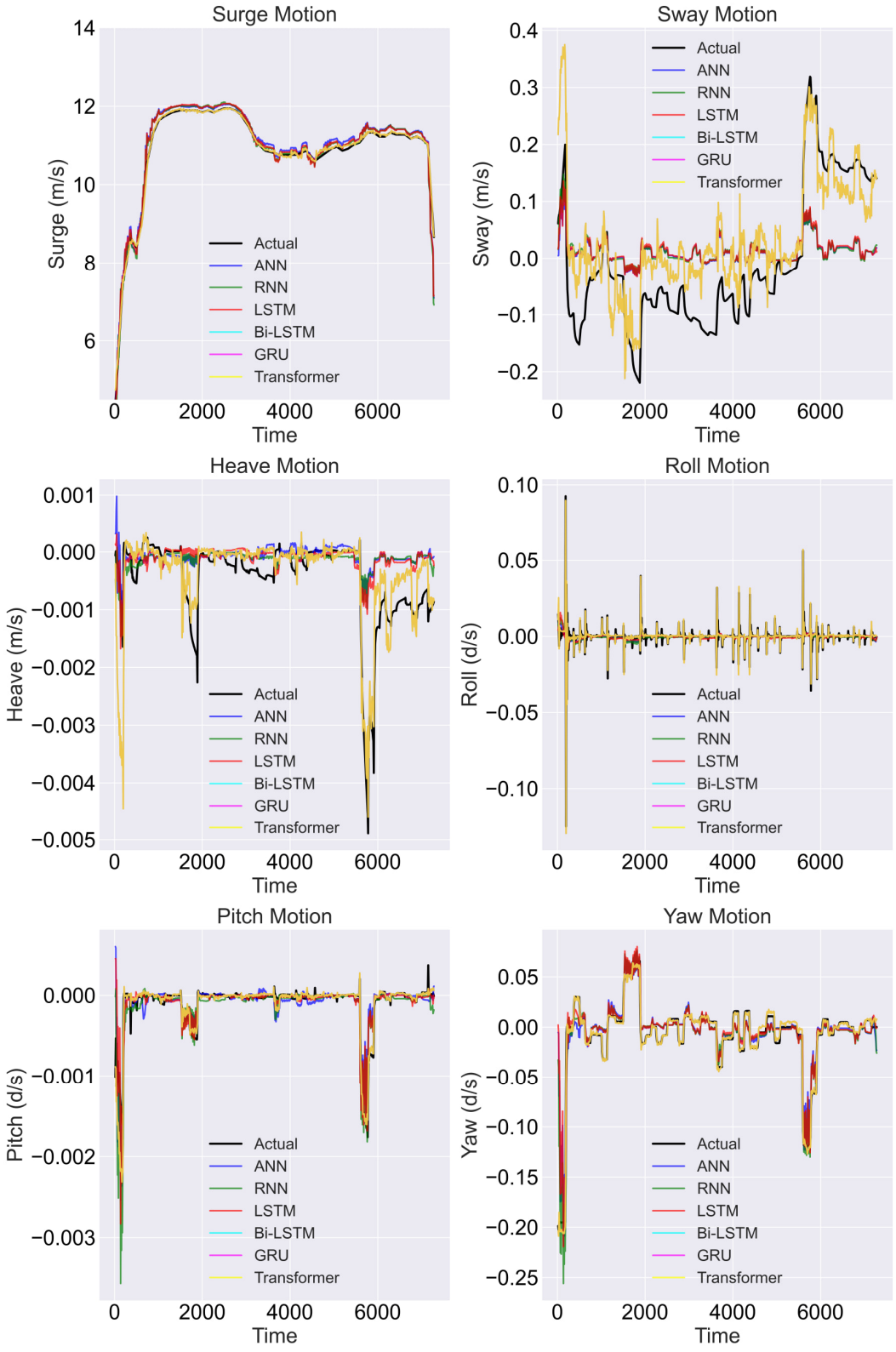

Figure 10: The results of the prediction of ship motion dynamics using different models

Evaluation of Learning Capacities

In Section 4.1, this paper trains and predicts the 6 DOF ship motions using the selected deep learning models. Subsequently, the paper explores how much data is required to saturate results, i.e., to the point where increasing the amount of data no longer

reduces the accuracy. Initially, 400 ship trajectories have been divided into 20 datasets, with the first dataset containing the first 20 trajectories, the second set containing the first 40 trajectories, and so on, until the 20th dataset, which includes all 400 trajectories. An additional 100 trajectories have been reserved as a fixed testing dataset, see Figure 3. The selected deep learning models have been trained, keeping the hyperparameters from Section 4.1 unchanged. This allowed for the incremental increase in the amount of training data against the same testing set and the calculation of test loss, thereby identifying the data volume at which model training reaches saturation.

The test error curves for the various models have been plotted based on the given data with different lengths, see Figure 11. Each line represents the change in error as the lengths of training dataset increases, which could represent iterations in training ship motion predictors using the selected models. It displays the general trend that as the number of ship trajectories increases, the testing loss for each model decreases. This indicates an improvement in the prediction accuracy of these models with the increase of the training database. Figure 11 illustrates that upon reaching saturation, the loss error of these models ranges from 0.4e-3 to 12.5e-3. Among them, the transformer model exhibits the highest accuracy, while the RNN model performs the poorest, with its error being threefold higher than that of the transformer. The losses of LSTM, Bi-LSTM, and GRU are between them.

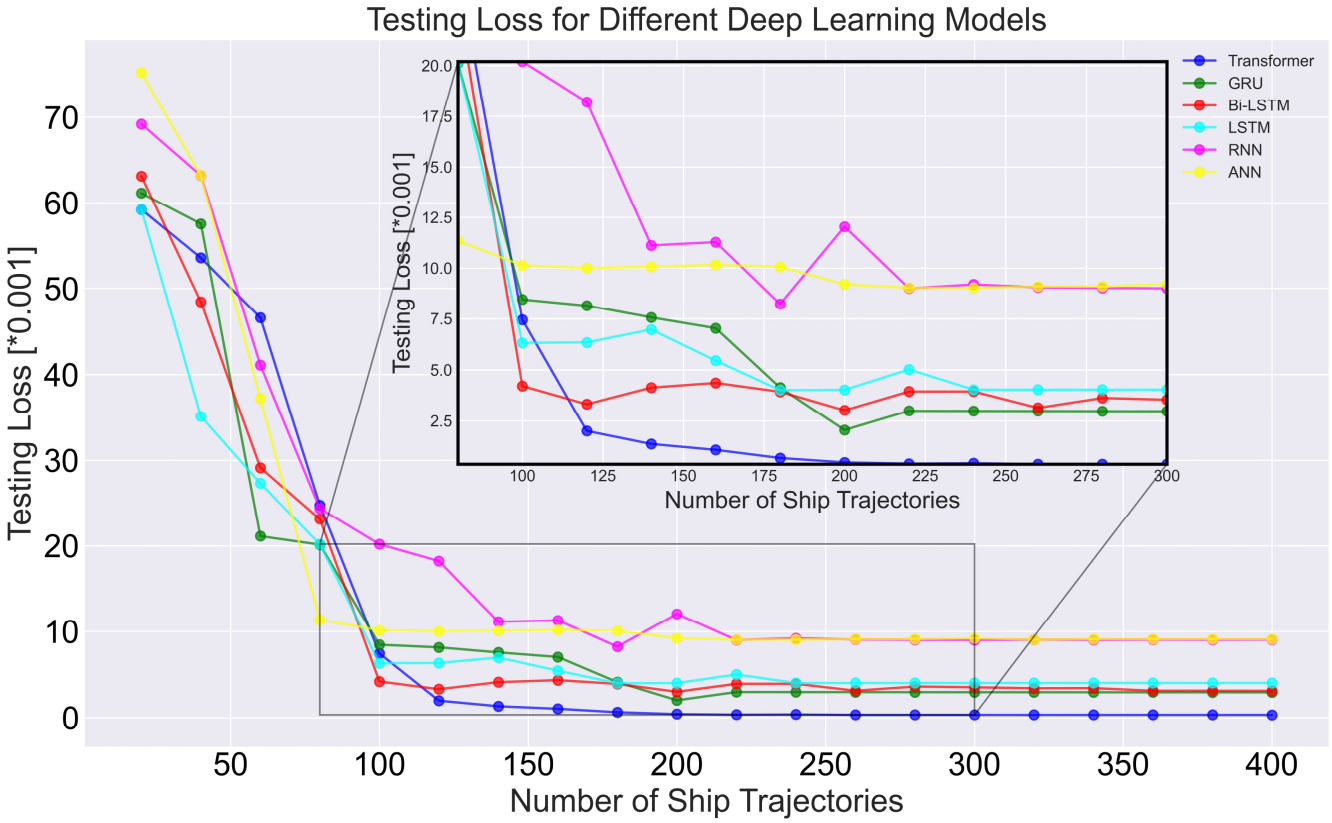

Figure 11: The influences of different lengths of training data on testing loss evaluation

Figure 12 illustrates the data volume thresholds at which various deep learning models reach saturation, demonstrating that each model requires a different dataset size to achieve optimal performance. For instance, the Transformer model reaches peak efficiency at a data volume of 280, while the RNN model achieves its best performance with a data volume of 140, and the ANN requires only 80. Overall, as the training dataset expands, the increase in predictive accuracy halts, indicating that the models have reached their maximum learning capabilities. The ANN and LSTM models appear to plateau earlier than others. This suggests that they require less data to reach their performance limits. It is noted that reaching performance limits does not imply that these models have attained the highest prediction accuracy for ship motions. It merely indicates that the deep learning model may not process additional data to further enhance the model's prediction ability to capture ship motion characteristics.

Other models continue to show improvements with additional data before reaching a plateau. Notably, when data is scarce, the Transformer exhibits the highest accuracy, implying that it has superior learning ability compared to the others and is more adept at capturing the nonlinear movements of ships influenced by hydrological and meteorological conditions. An RNN model requires a substantial amount of data to train effectively, and even then, their accuracy may not be sufficient.

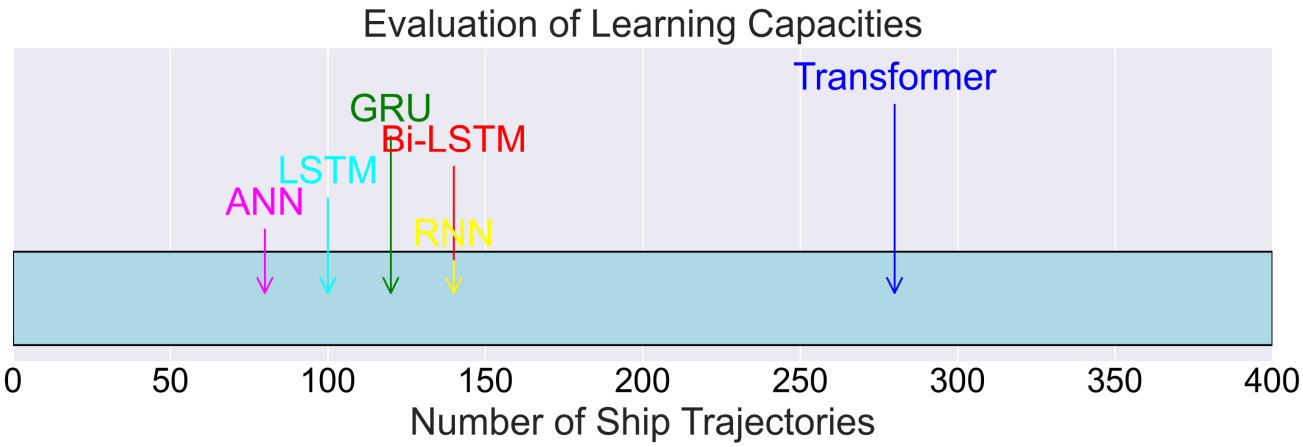

Figure 12: The learning capacities of the selected deep learning model

In predicting nonlinear ship motions, the Transformer model excels due to its remarkable accuracy, especially when dealing with complex dependencies over long sequence in the time domain. However, this model requires substantial computational power and a large volume of training data. Bi-LSTM and GRU models provide a compromise, handling sequences with moderate complexity more efficiently and using fewer resources while maintaining dependable accuracy. On the other hand, traditional ANNs and RNNs are quicker but faultier. The intricacies involved in predicting nonlinear ship motions, render them less effective for sophisticated tasks.

Figure 10 highlights the diverse proficiencies of various models in capturing the six degrees of freedom (6 DOF) of ship motions in the time domain. The Transformer model significantly outperforms others in predicting sway motion. However, for roll and surge predictions, other models also exhibit high accuracy and require less data. There is potential for future research to explore combining two or more models to predict each motion separately. Such hybrid approaches could enhance the precision of predictions by leveraging the strengths of diverse modelling techniques.

CONCLUSIONS

The paper presents a framework for the comparison and evaluation of learning capabilities of the selected deep learning methods that could be used for the prediction of ship motions. To validate the framework, six existing deep learning methods for ship motion predictions are selected, namely ANN, RNN, LSTM, Bi-LSTM, GRU, and Transformer. The models are used to train 6 DOF ship motions predictors displaying the influence of nonlinear effects by using the same data streams along ship trajectories between two ports. It is concluded that their level of accuracy varies (see Table 2 and Figure 11). The paper also evaluates the learning capacities of these selected models in analyzing the impact of data volumes on their effectiveness by utilizing datasets of varying lengths. Generally speaking, the transformer model stands out in terms of accuracy.

In the future, results of this comparison and evaluation of the selected deep learning models may assist in selecting appropriate models for the development of online ship motion prediction tools with adaptive learning capabilities. Such tools are a crucial component of intelligent navigational decision-making systems.

CONTRIBUTION STATEMENT

Mingyang Zhang: Conceptualization; data curation, methodology; writing – original draft. **Cong Liu:** methodology; writing – original draft; writing – review and editing. **Pentti Kujala**: conceptualization; writing – review and editing. **Spyros Hirdaris**: conceptualization; supervision; writing – review and editing.

ACKNOWLEDGEMENTS

The authors express gratitude for the financial support provided by the "RETROFIT solutions to achieve 55% GHG reduction by 2030 (RETROFIT55) – Project No.: 101096068," funded under the Horizons Europe project, as well as by Merenkulun Säätiö. They also extend special thanks to CSC Finland for offering access to their parallel computing facilities. It is important to note that the opinions and findings presented in this paper represent those of the authors alone and may not coincide with the positions of their funding bodies.

REFERENCES

Bianchi, F. M., Maiorino, E., Kampffmeyer, M. C., Rizzi, A., Jenssen, R., Bianchi, F. M., ... & Jenssen, R. (2017). Properties and training in recurrent neural networks. Recurrent Neural Networks for Short-Term Load Forecasting: An Overview and Comparative Analysis, 9-21.

D'Agostino, D., Serani, A., Stern, F., & Diez, M. (2021). Recurrent-type neural networks for real-time short-term prediction of ship motions in high sea state. arXiv preprint arXiv:2105.13102.

Graves, A., & Graves, A. (2012). Long short-term memory. Supervised sequence labelling with recurrent neural networks, 37-45.

Liu, Z., Wu, Z., Zheng, Z., Wang, X., & Soares, C. G. (2021). Modelling dynamic maritime traffic complexity with radial distribution functions. Ocean Engineering, 241, 109990.

Lou, J., Wang, H., Wang, J., Cai, Q., & Yi, H. (2022). Deep learning method for 3-DOF motion prediction of unmanned surface vehicles based on real sea maneuverability test. Ocean Engineering, 250, 111015.

Ouyang, Z. L., & Zou, Z. J. (2021). Nonparametric modeling of ship maneuvering motion based on Gaussian process regression optimized by genetic algorithm. Ocean Engineering, 238, 109699.

Ramirez, W. A., Leong, Z. Q., Nguyen, H., & Jayasinghe, S. G. (2018). Non-parametric dynamic system identification of ships using multi-output Gaussian Processes. Ocean Engineering, 166, 26-36.

Silva, K. M., & Maki, K. J. (2022). Data-Driven system identification of 6-DoF ship motion in waves with neural networks. Applied Ocean Research, 125, 103222.

Sivaraj, S., Rajendran, S., & Prasad, L. P. (2022). Data driven control based on Deep Q-Network algorithm for heading control and path following of a ship in calm water and waves. Ocean Engineering, 259, 111802.

Sun, Q., Tang, Z., Gao, J., & Zhang, G. (2022). Short-term ship motion attitude prediction based on LSTM and GPR. Applied Ocean Research, 118, 102927.

Taimuri, G., Zhang, M., & Hirdaris S. (2022). A Predictive Analytics Method for the Avoidance of Ship Grounding in Real Operational Conditions. SNAME Maritime Convention 2022 26-29 September, Houston, TX, 2022, p. 18.

Wang, Z., Zou, Z., & Soares, C. G. (2019). Identification of ship manoeuvring motion based on nu-support vector machine. Ocean Engineering, 183, 270-281.

Woo, J., Yu, C., & Kim, N. (2019). Deep reinforcement learning-based controller for path following of an unmanned surface vehicle. Ocean Engineering, 183, 155-166.

Zeng, D., Xia, G., & Cai, C. (2021, October). Parameter Identification of Hydrodynamic Model of Ship Using EKF. In 2021 China Automation Congress (CAC) (pp. 1427-1432). IEEE.

Zhang, M., Kujala, P., Musharraf, M., Zhang, J., & Hirdaris, S. (2023). A machine learning method for the prediction of ship motion trajectories in real operational conditions. Ocean Engineering, 283, 114905.

Zhang, M., Taimuri, G., Zhang, J., Hirdaris S. (2022 d). A deep learning method for the prediction of 6-DOF ship motion in real conditions. Proceedings of the Institution of Mechanical Engineers, Part M: Journal of Engineering for the Maritime Environment, Doi 14750902231157852.

Zhang, M., Tsoulakos, N., Kujala, P., & Hirdaris, S. (2024). A deep learning method for the prediction of ship fuel consumption in real operational conditions. Engineering Applications of Artificial Intelligence, 130, 107425.

Zhang, T., Zheng, X. Q., & Liu, M. X. (2021). Multiscale attention-based LSTM for ship motion prediction. Ocean Engineering, 230, 109066.

Zhou, T., Yang, X., Ren, H., Li, C., & Han, J. (2023). The prediction of ship motion attitude in seaway based on BSO-VMD-GRU combination model. Ocean Engineering, 288, 115977.

Part 8:
INFLUENCE OF REGULATIONS

Proceedings of 15th International Marine Design Conference (IMDC-2024)
June 2-6, 2024
Amsterdam, the Netherlands

A time-dependent ice accretion model for trap-setting fishing vessels with filigree structures

Thomas DeNucci[1,*], Daniel Brahan[2], Peter McGonagle[1], Colman Schofield[1] and Delaney Taplin-Patterson[1]

ABSTRACT

This paper describes a time-dependent methodology for calculating the rate of ice accretion on vessels with filigree structures. It combines Newton's Second Law for spray droplet trajectories with time varying flow velocities determined using computational fluid dynamics (CFD). The mass flux of ice is determined by solving a set of partial differential equations describing the conservation of mass, heat, and salt in the boundary layer of brine near the ice surface. Icing predictions numerically generated by this approach are evaluated against current stability regulations for fishing vessels.

KEY WORDS

Ice Accretion; Safety; Stability; Fishing Vessels; Porous Surface

INTRODUCTION

The fishing vessel *Scandies Rose* capsized off the coast of Alaska, USA, in heavy spray-icing conditions on December 31, 2019, with five of the seven onboard perishing. A Marine Board of Investigation conducted by the U.S. Coast Guard and the National Transportation Safety Board (NTSB) identified inaccurate accounting of ice on deck gear, specifically fishing pots, as a causal factor, National Transportation Safety Board (2021).

This tragedy follows in the wake of another capsize event. In 2017, the fishing vessel *Destination* sank off St. George Island, Alaska, under heavy spray icing conditions with the loss of all six crew members onboard. Figure 1 shows icing on *Sandra Five*, a vessel operating in the same vicinity as *Destination* during the fatal storm.

Since *Scandies Rose* and *Destination* were operating on domestic voyages, they were subject to the stability standards identified in US 46 CFR Part 28 Subpart E instead of those prescribed by international regulation and survey requirements of Safety of Life at Sea (SOLAS) set forth by the International Maritime Organization (IMO). However, the maximum assumed icing quantities on fishing vessels are identical between these two codes – 30 $\frac{kg}{m^2}$ of ice on horizontal surfaces and 15 $\frac{kg}{m^2}$ on vertical surfaces.

[1] U.S. Coast Guard Academy, Department of Naval Architecture & Marine Engineering, New London, CT, USA)
[2] U.S. Coast Guard Academy, Department of Naval Architecture & Marine Engineering, New London, CT, USA) ORCID: 0009-0000-9997-5366
[*] Corresponding Author: thomas.w.denucci@uscga.edu

Submitted: 8 February 2024, Revised: 26 April 2024, Accepted: 1 May 2024, Published: 18 May 2024

Conference paper, DOI: https://doi.org/10.59490/imdc.2024.828 e-ISSN: 3050-4864

Figure 1: Ice accumulation on *Sandra Five*, National Transportation Safety Board (2017).

There are limitations to these rule-sets. First, both regulatory schemes assume uniform ice loading and do not consider the effects of list due to off-center weight additions. Uniform ice loading in storm conditions is a rare occurrence because fishing vessels rarely have wind and seas directly off their bows. Second, these rule-sets assume that icing is applied over the top and sides of the fishing pots, commonly referred to as the "shoebox method." However, crab pots are porous, being constructed of steel tubing with netting, which enables ice to accumulate in the interior of the crab pot stack.

The goal of this paper is to develop an icing model that specifically considers both the time-varying effects of icing on fishing pots and the nature of ice formation on filigree structures themselves. Knowing how, where and the rate of ice accretion will provide opportunities to develop fishing vessel designs less prone to icing. This work forms the foundational knowledge required before changes to regulations may be proposed. The results have the potential to change the modeled icing quantity and location for naval architects performing stability analysis on fishing vessels subsequently improving safety conditions for mariners onboard while protecting the marine environment.

BACKGROUND

The effects of marine icing on vessels at sea can be catastrophic. Ryerson (2009) cites hazards including a reduction in stability, damage to vessel structure, damage to equipment including winches, cranes, and antennas and slipping hazards on decks, ladders, and handrails. In the worst case, rapidly accumulating ice can cause a rise in the vessel centre of gravity which can result in a reduction of the righting arm and possible vessel capsize.

Scandies Rose and other trap-set fishing vessels are distinctive because their deck load ices differently than solid plates and cylinders because they are porous. Ice can accumulate not only on exterior surfaces, but also inside the fish pot itself, filling up space normally assumed to be empty voids on deck, National Transportation Safety Board (2021).

Table 1: *Scandies Rose* on-scene weather conditions reported by rescue team and survivors, National Transportation Safety Board (2021).

Weather Element	Value
Wind Velocity	18 – 25 m/s (35 – 50 kts)
Wind Direction (Relative to the Vessel)	045^o
Significant Wave Height	6 – 10 m
Wave Period	9 – 10 sec
Water Temperature	3^oC
Air Temperature	-12^oC

All too often, all hands are lost on vessels that capsize in the Bering Sea. However, weather conditions on the night of *Scandies Rose* capsize, shown in Table 1, have been corroborated by the may-day call, survivor testimony and on-scene reports from the rescue helicopter and offer unique insight into the on-scene conditions. This paper applies these weather data and the knowledge gained from survivor testimony to the ice accretion approach outlined next.

APPROACH

Figure 2 highlights the key elements of the presented approach. The model assumes that a thin layer of ice already exists on all surfaces. The velocity flow across the vessel and crab pots are solved using CFD. The flow field is important because it influences both droplet trajectory and heat convection coefficients. However, as ice accumulates on the crab pot netting, the crab pot geometry and flow field change DeNucci et al. (2023). To account for this, the flow field is recalculated after every 30 minutes of simulation.

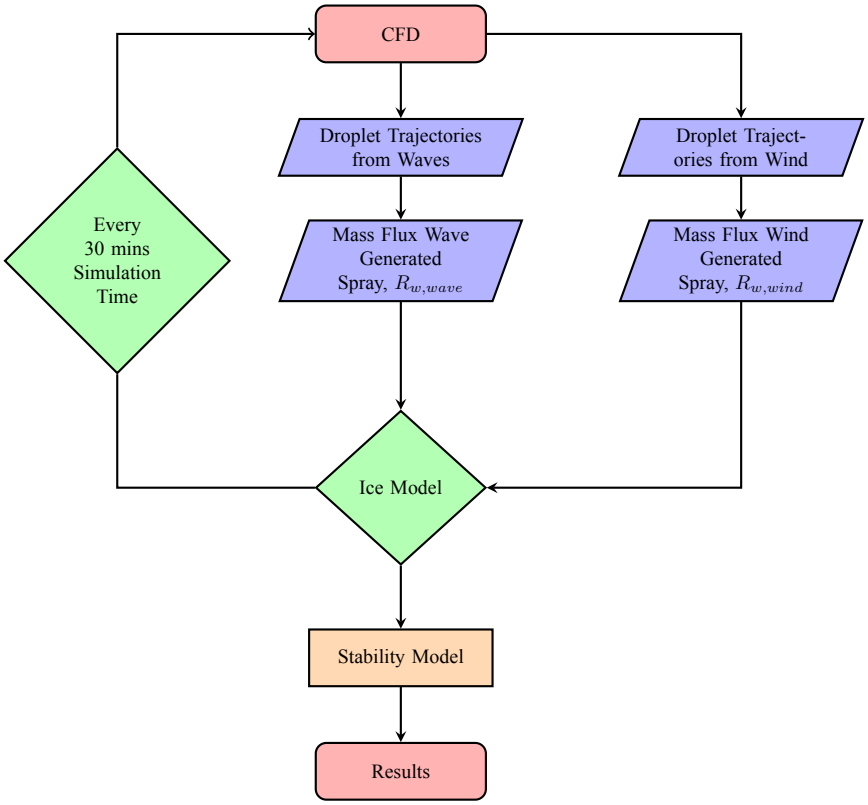

Figure 2: Flow chart of ice accretion analysis on porous surfaces.

Using the environmental conditions described in Table 1, the mass flux of spray striking the vessel is calculated. A thermodynamic heat balance between the mass and salinity of brine is solved to determine the rate of ice accretion. After 30 minutes, the crab pot porosities, flow field, mass flux and heat convection coefficient are recalculated and the rate of ice accretion is again solved using the updated data.

After the simulation finishes, the impact of ice on overall vessel stability is analysed using General Hydrostatics Software (GHS). Stability is evaluated using the wind magnitude and direction reported on the night of the capsize. Details of this approach follow.

TIME VARYING VELOCITY FLOW FIELDS

One challenge with filigree structures, crab pots on fishing vessels, are their nature of icing. As ice accumulates on the netting structure, the pot porosity changes, which results in new geometry, and subsequently, different velocity flow across the pot structure. These changes have an important effect on ice accretion and have not been accounted for in previous icing models.

Darcy-Forchheimer Law

Computational fluid dynamics is used to determine velocity flow across the crab pots. To achieve this, the pots are modelled as porous surfaces using the Darcy-Forchheimer law so that the permeability and drag coefficient of the pot structure can be determined. The Darcy-Forchheimer law serves as an augmented version of Darcy's law, which characterizes the flow of fluids through porous media. Unlike Darcy's law, the Darcy-Forchheimer equation accommodates non-linear effects observed at elevated flow velocities within porous media, offering a more comprehensive understanding of fluid dynamics at higher flow speeds.

The law, shown in equation 1, is comprised of a linear and quadratic term. At low Reynolds numbers, the pressure loss is directly proportional (linear) to the flow velocity. At higher Reynolds numbers, the pressure losses across the medium increase rapidly and become a quadratic function of velocity.

$$\Delta P = -(\frac{\beta}{\alpha}\mu\overrightarrow{V} + \frac{\beta^2}{\sqrt{\alpha}}\rho C_d|\overrightarrow{V}|\overrightarrow{V})\delta \tag{1}$$

where

$C_d =$ quadratic drag coefficient ($\frac{1}{m}$)

$\Delta P =$ change in pressure (Pa)

$\overrightarrow{V} =$ velocity magnitude ($\frac{m}{s}$)

$\alpha =$ permeability (m^2)

$\beta =$ porosity

$\delta =$ the thickness of medium (m)

$\mu =$ dynamic viscosity (Pa s)

$\rho =$ density ($\frac{kg}{m^3}$)

To solve for permeability and drag coefficient, the pressure drop across a singular crab pot of specific porosity is measured for various wind velocities (0 to 40 knots). The net orientation and webbing thickness of the crab pot match those loaded on *Scandies Rose*. After varying the wind speed across the pot, the pot porosity is changed and the pressure drop is measured again at the new porosity. Changes in porosity, illustrated in Figure 3, are achieved by changing the web thickness to achieve the desired porosity value (80% - 10%). Results are shown in Table 2.

Using the Darcy-Forchheimer Law, a second-order polynomial is fit to the data describing the pressure drop and wind velocity at each crab pot porosity. The coefficients of this polynomial curve describe the crab pot permeability (m^2), a linear term, and quadratic drag-coefficient (m^{-1}), a quadratic term. Results are shown in Table 3.

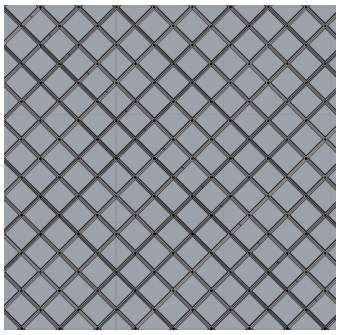

80% porosity

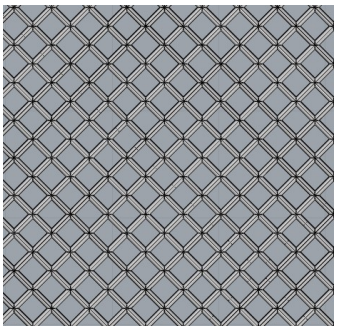

50% porosity

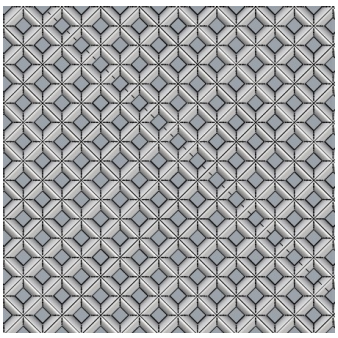

20% porosity

Figure 3: Crab pot netting at various porosities.

Table 2: Change in pressure across crab Pot netting at different wind velocities [Pa]

Wind Velocity		Crab Pot Porosity (γ, %)							
$(knots)$	(m/s)	80	70	60	50	40	30	20	10
0	0	0	0	0	0	0	0	0	0
2.5	1.29	0.22	0.27	0.35	0.48	0.50	0.63	0.69	0.82
5	2.57	0.86	1.05	1.33	1.64	1.98	2.49	2.88	3.26
10	5.14	3.37	4.15	5.30	6.54	7.99	10.01	11.59	13.05
15	7.72	7.52	9.335	11.89	14.69	17.97	22.56	26.14	29.38
20	10.29	13.39	16.25	21.09	25.91	31.93	40.14	46.45	52.26
25	12.86	20.96	25.78	32.90	40.75	49.95	62.3	74.5	81.54
30	15.43	30.13	37.08	47.33	58.66	71.8	90.57	104.5	117.5
40	20.58	53.6	65.89	84.17	100.15	127.55	158.20	184.7	208.8

Using values in Table 3, the crab pot stack can then be modelled as a porous surface and the velocity field is again determined using CFD. Local icing quantities (kg/m^2) are directly related to porosity by assuming the ice accumulates on the crab pot webbing in a half-cylindrical fashion. This is discussed later in the paper.

SEA SPRAY FLUX, R_w

Sea spray flux is the precursor to ice formulation and is required to accurately predict the rate of ice accretion on the vessel. Spray originates from both wind-wave and vessel-wave interactions, although the majority of the sea spray striking the vessel comes from vessel-wave interactions. Wind-generated sea spray is caused by lifting droplets from wave crests on the ocean surface. Wind-spray is a small, but constant water flux present in the air when the wind speed is greater than nine metres per second. Deterministic methods to calculate wind-generated spray flux are found in Jones and Andreas (2012). Wave-generated sea spray is caused by the collision of waves with the vessel. Wave-generated sea spray is generally the source of large but brief periodic water flux that originates near the bow of the vessel Hansen (2012). Zakrzewski (1986) and Lozowski et al. (2000) provide methods to calculate this flux. Sea spray flux calculations specific to *Scandies Rose* can be referenced in Brahan et al. (2023).

Using Newton's Second Law for droplet motion, individual water droplets were injected into the velocity flow field and tracked throughout their flight to determine if they intersect the vessel. Since it is impractical to simulate every droplet of water generated by sea spray, droplets are re-characterized as "parcels" of the mass flux Brahan et al. (2023). Jones and Andreas (2012) determined the size and quantity of droplets at a given height above a free surface for given wind speeds. Since the total water mass present in a cubic meter of air can be calculated, a relationship between percent contribution of

Table 3: Permeability and drag coefficient values for crab pots as a function of porosity.

Porosity	Permeability (α)	Drag Coefficient (C_d)
80	1.02E-02	1.59E-02
70	4.82E-03	1.77E-02
60	1.32E-03	1.61E-02
50	1.07E-04	9.96E-03
40	6.82E-04	3.64E-02
30	4.96E-05	2.14E-02
20	1.95E-05	3.78E-02
10	2.43E-04	6.16E-01

mass for a given droplet size was established Brahan et al. (2023). An analogous correlation was developed by Ryerson (1995), who measured the droplet number concentration and droplet size distribution of a wave-spray cloud using a stroboscopic camera on the U.S. Coast Guard Cutter *Midgett* in the Bering Sea.

Since wave-generated spray only occurs when encountering a wave and for the duration of the wave encounter, the wave-generated flux behaves like a step function. When the vessel encounters a wave, wave flux comes into the system; it is zero at all other times Brahan et al. (2023).

ICING MODEL

A system of partial differential equations governs the ice and brine flux. The ice flux depends on several factors including the incoming latent heat of mass from the ocean, heat flux, brine flux, and brine salinity. The set of differential equations which follow are analyzed as a series of nodes on the side of the crab pot stack. These are numerically solved for each time step at each node using the method of lines DeNucci et al. (2023).

Wet Icing

Normally, marine icing occurs in a wet state. This occurs when atmospheric conditions are conducive to freezing, but only part of the incoming spray flux freezes. The remaining spray flows off the surface as brine. Modelling the crab pot net as series of nodes, each node receives water from the free surface and brine flux. Conservation of mass, heat and salt give the approximate differential equations of the brine film, Horjen (1990); DeNucci et al. (2023):

$$\frac{\delta X}{\delta t} + \nabla_t(v_b X) = R_w - I \tag{2}$$

$$c_b X(\frac{\delta}{\delta t} + v_b \nabla_t) T_b = Q + (1-\sigma) l_f I \tag{3}$$

$$\frac{X}{S_b}(\frac{\delta}{\delta t} + v_b \nabla_t) S_b = I(1-\sigma) - R_w(1 - \frac{S_w}{S_b}) \tag{4}$$

where X is the local brine amount per unit area ($\frac{kg}{m^2}$), T_b is the brine temperature and S_b the brine salinity (in parts per thousand). R_w is the impinging sea spray flux ($\frac{kg}{m^2 s}$) and I ($\frac{kg}{m^2 s}$) is the rate of accretion of both the ice and the brine trapped in the ice. The variable v_b is the brine velocity and ∇_t is the differential operator in the tangential direction, i.e., along the direction in which the brine will move. c_b is the specific heat capacity of the brine, σ is the fraction of entrapped brine in

the accretion, l_f is the latent heat of freezing and S_w is the salinity of seawater. Mass flux due to evaporation is neglected.

Dry Icing

If the sea spray flux is relatively low, and the weather is sufficiently cold, it is possible for all the incoming spray to freeze on impact, Hansen (2012). This condition, referred to as dry icing, occurs when the heat transport away from the brine is greater than or equal to the latent heat produced if all the impinging spray freezes. The initial assumption was that only wet icing occurred on the vessel. However, initial simulations revealed that certain portions of the crab pot stack do not receive heavy quantities of mass flux into the system. Furthermore, the cyclical nature of heavy then light mass flux due to vessel-wave interaction causes different locations on the crab pot stack to freeze differently.

These factors combine to create a cycle of wet and dry icing, where dry icing often occurs between the wave-generated sea spray events. Initial simulations showed that wet and dry icing occurred concurrently on different nodes and at the same node for different instances of time, DeNucci et al. (2023). This phenomenon impacts the rate of ice accretion because residual brine flux may still be present at a given node location as the process of icing repeats itself. One important result of this phenomenon, shown in equation 5, is the modification of established icing equations to include the impact of brine on the different icing modes DeNucci et al. (2023).

$$R_w + X \leq \frac{Q}{l_f(1-\sigma)} \tag{5}$$

where R_w is the spray flux during a spray event and σ is the interfacial coefficient, assumed to be 0.34. X is the local brine amount per unit area ($\frac{kg}{m^2}$) and l_f is the latent heat of freezing.

Heat Balance

The icing model requires a thermodynamic heat balance governed by a set of differential equations Horjen (1990). When water droplets strike a vessel, they freeze due to various heat fluxes. The heat fluxes are convective heat flux (Q_c), evaporative heat flux (Q_e), radiant heat flux (Q_r),and the heat capacity of impinging water droplets (Q_d). The heat flux due to viscous aerodynamic heating (Q_v), conduction (Q_a), and kinetic energy of in-coming droplets (Q_a) are usually neglected because they are small. The icing model uses a parameterized form in which heat flux equations are presented as functions of T_s, where T_s is the equilibrium freezing temperature of the surface brine.

The convective heat flux is the sensible heat flux between the freezing surface and the surrounding air and is given by equation 6.

$$Q_c = h_c(T_s - T_a) \tag{6}$$

where h_c is the heat transfer coefficient, where T_s the temperature of the water at the air-water interface, and T_a the air temperature.

The heat transfer coefficient is given by equation 7:

$$h_c = \frac{Nuk_a}{L} \tag{7}$$

where k_a is the thermal conductivity of air and L is the characteristic length of the component, which for cylindrical com-

ponents is the diameter. Nu is the is the Nusselt number defined for cylindrical components.

Q_e, the evaporative heat loss to the surrounding air flow is given as equation 8.

$$Q_e = h_c(\frac{Pr}{Sc})^{0.63}\frac{\epsilon l_f}{P_{c_a}}(e_s(T_S) - RHe_a(T_a)) \tag{8}$$

where h_c is the heat transfer coefficient, Pr is the Prandtl number, Sc is the Schmidt number, ϵ is the ratio of molecular weights of water vapor and dry air, P is the atmospheric pressure, l_v is the latent heat of vaporization for water at the surface temperature, c_a is the specific heat capacity of dry air at constant pressure, RH is the relative humidity of the air, and $e_s(T)$ is the saturated water pressure.

Q_r, the radiative heat flux is given by equation 9.

$$Q_r = \sigma(\epsilon_s T_s^4 - \epsilon_a T_a^4) \tag{9}$$

where ϵ is the Stefan Boltzmann constant, and ϵ_s and ϵ_a are the emissivity of the air flow and icing surface, both considered to be 1.

Q_d, the heat capacity of impinging water droplets, is presented as equation 10, Zarling (1980).

$$Q_d = R_w c_w (T_s - T_d) \tag{10}$$

where c_w is the specific heat capacity of water, T_d the droplet temperature of the wave spray prior to impingement, and R_w the total mass flux of water. Although the droplet temperature, T_d, can be calculated on the individual droplet scale using a method proposed by Kato (2012), a simplified assumption proposed by Stallabrass (1980) is used. The total heat out of the system, Q, is the summation of the individual heat fluxes.

Using relationships between brine salinity and brine temperature by Assur (1958) and Horjen and Vefensmo (1987), equations 3 and 4 are combined to determine the ice accretion rate:

$$I = \frac{(1 - \frac{S_w}{Sb})R_w\frac{F(S_b)}{l_f}Q}{(1-\sigma)(1+F(S_b))} \tag{11}$$

CALCULATING RELATIONSHIP BETWEEN ICE ACCRETION AND POROSITY

Across the fishing industry, there is a high degree of variation in the size of pots vessels carry due to the many species, regions, and state or federal regulations they may operate under. Accordingly, the approach should not be bound by any set dimensions. Therefore, a general geometric relation between ice accretion and porosity was created to accommodate the majority of pot types and configurations with little to no change between each simulation.

Assuming the crab pot netting is flat, continuous, and at a 45^o bias across the entire face presented towards the oncoming spray, it is possible to subdivide the large net into individual squares show in Figure 4. This approach allows full simulation of icing event given only two dimensions, R, the thickness of webbing material in the net, and L, the distance between intersections in the net.

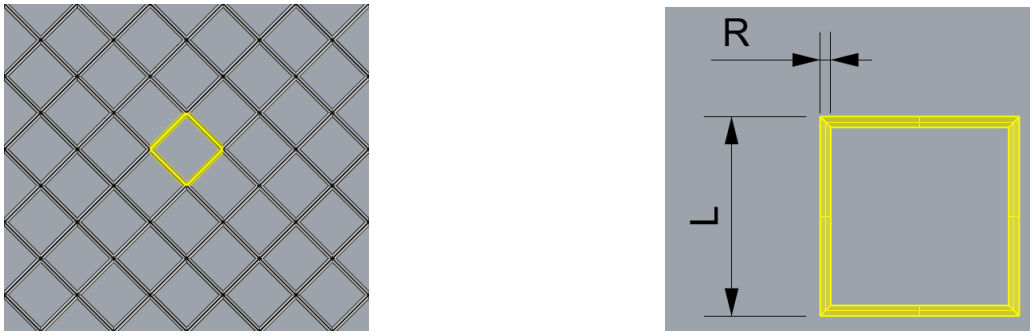

Sub square within net

Geometry of sub square

Figure 4: Location and geometry of a sub-square in the net structure.

Initially, we assumed that ice would form in a cylindrical manner around each line in the netting. However, this reflects the behavior of *snow* accretion on power lines, which, given their ubiquity around the world, are well documented and researched.

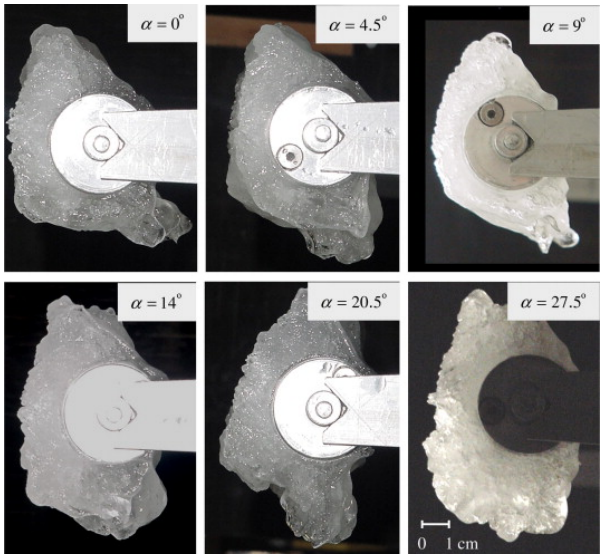

Figure 5: Profiles of ice accretions for various values of angle from horizontal, α, around stream wise axis under freezing rain conditions, Kollár and Farzaneh (2010).

Admirat (2008) notes that the *cylindrical accretion mechanism* seen on power lines is dependent on their ability to rotate due to the low torsional resistance seen by the long wires. While this rotational ability seen in the netting of crab pots, it is the accumulation of ice rather than snow drastically affects the resulting shape, making the initial cylindrical model inadequate.

Kollár and Farzaneh (2010) demonstrate that icing events on shorter, fixed, cylindrical objects, while certainly not uniform, appear much closer to a semi circle as seen in Figure 5. To better reflect this new *semi-cylindrical icing accretion mechanic*, equation 12 shows that the amount of mass due to icing is such that only half of the line would be covered in ice, thereby doubling the amount of radius (R) "consumed" per kg of ice accumulated (m_{Ice}).

$$m_{Ice} = \frac{\rho\pi}{2}\left[L(R^2 - r^2) - \frac{4}{3}R^3 + \frac{4}{3}r^3\right] \tag{12}$$

where

m_{Ice} = mass of ice accumulated per sub square (kg)

L = side length of net sub square (m)

ρ = density of ice ($\frac{kg}{m^3}$)

R = overall radius of line and accumulated ice (m)

r = initial radius of line (m)

γ = porosity of netting (%)

Equation 13 shows the relationship between icing volume and porosity. Given R, L and r, crab pot porosity is determined from the weight of ice onboard the vessel. This information is then fed back into the CFD solver, droplet trajectory and icing models to change droplet trajectory, mass flux of water into the side of the crab pot, and convection coefficients in the icing model.

$$\gamma = \frac{4r(L-R)}{L^2} \tag{13}$$

MODEL IMPROVEMENTS

One significant improvement in this approach is the incorporation of a feedback loop. Previous simulations only considered constant crab pot porosity. To implement the time varying nature of porosities in crab pots as they ice, the CFD model was updated to allow varying porosity values.

The previous model had five tiers of crab pot stacks with uniform porosity within each layer of the crab pot stack. Early simulations showed that porosity varied only in the forward third of the stack, DeNucci et al. (2023). Additionally, icing was non-uniform, meaning certain areas saw ice form at a rapid pace and indicated that the original model was not representative of the location or rate of ice accumulation. An updated model, shown in Figure 6, subdivides the crab pots into 14 clusters to more accurately capture the localized areas where porosity varies the most. Since ice rapidly accumulates on the forward starboard side of the vessel, eight smaller clusters are modelled in that location.

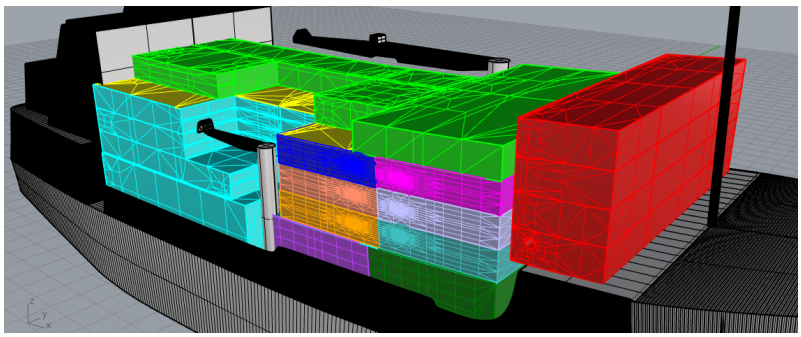

Figure 6: *Scandies Rose* CFD model. The different colored regions represent areas where porosity can be individually defined.

The CFD solver and the icing model were run at 30 minute intervals. The 30 minute interval balanced computational time with obtaining an accurate model of the phenomenon. After each interval, the porosities of the crab pots would be updated

based on the amount and extent of icing that occurred. The total simulation time was four hours, mirroring the total time icing occurred on *Scandies Rose*. Initial porosity was set to 90% throughout the crab pot stack and then reassessed for the 14 subdivided regions after every 30 minutes of simulation time.

RESULTS

Figure 7 shows the simulation results from the model presented in this paper. Ice accretes in a non-linear fashion, both in total mass accumulated and vcg of the ice on the crab pot stack. Previous simulations with 90.5% porosity (constant), shown in Figure 8, did not show any appreciable change in icing distribution.

The results showed the that vertical center of gravity (vcg) of the ice in the crab pot stack rises, as does the rate of ice accretion on the crab pot stack. This is an important point. If constant porosity is assumed throughout the simulation, the vcg remains constant and therefore underestimates the stability impact of added weight.

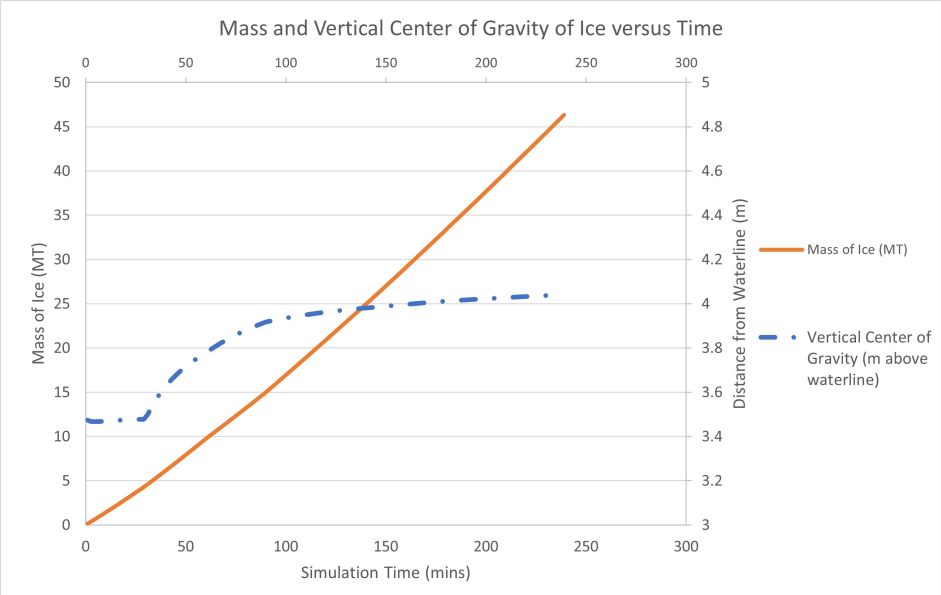

Figure 7: Mass versus vcg of ice versus time for the simulation length.

Figure 9 shows ice progression as it begins to accumulate in the upper forward region of the crab pot stack. Note, the icing scales are different between the two images. Simulation results highlight the need for a time-dependent model in order to more accurately simulate the phenomenon of icing on porous surfaces.

Stability Analysis

After obtaining ice data (mass and vcg) from the icing simulation, vessel stability was analyzed using GHS software. Figure 10 shows the hydrostatic righting curves from the icing simulation compared to the regulatory icing requirements in US 46 CFR 28.550 and International Code on Intact Stability (IS Code) 6.3 using the "shoebox" method DeNucci and Brahan (2022). The regulations required the addition of 19.89 MT of ice on the centerline of the vessel. The righting arm curve for this condition is shown as the dashed line in Figure 10.

The simulated results most nearly match the regulatory icing after a half hour of simulation time with *only* 4.26 MT (vs. 19.89 MT) of ice added to the vessel. It is important to note that the resultant ice from the simulation only accounts for ice

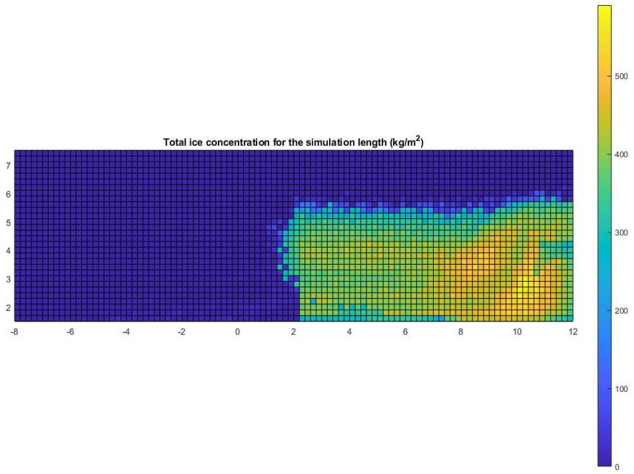

Figure 8: Ice mass per unit area (kg/m^2) for a one hour simulation with constant porosity (no feedback loop implemented). Figure displays ice accumulation for outboard starboard side of pot stack on main working deck. Origin - point (0,0) - is located at amidship and based at waterline.

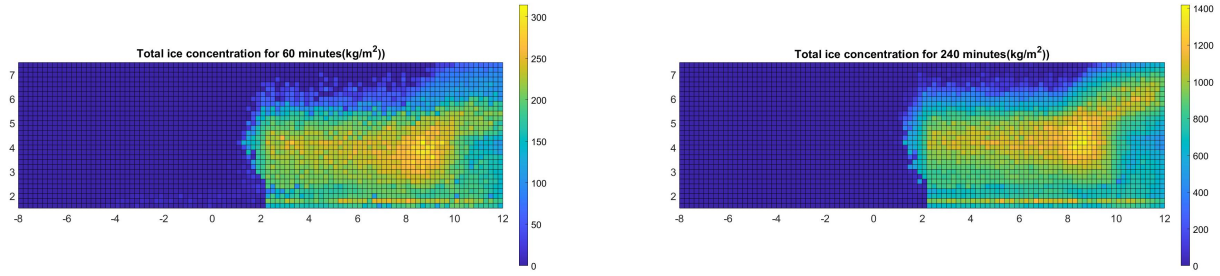

1 hour simulation 4 hour simulation

Figure 9: Ice mass per unit area (kg/m^2) at discrete times in the simulation. Crab pot porosity values are updated every 30 minutes.

on the *outer edge* of the crab pots, whereas the regulatory icing applies ice across the entire surface area of the vessel. Simulated icing also occurs farther forward on the vessel than assumed by regulation, as the centroid of ice is forward of amidships. This creates an increased righting arm at higher angles due to the large buoyant volume in the forward location of the vessel. This assumes the forward volume in the hull is watertight throughout all angles analyzed and did not take into account downflooding points.

The icing model also induces a list from off-center ice loading. Regulations require ice to be loaded uniformly centerline, whereas this icing model puts the ice loading on the outer edge of the crab pot stack. The righting arms show an induced list of almost 3^o after one hour and 5^o after an hour and a half. Additionally, the hour and a half case shows a lolling condition possible - an indicator the vessel is in dire circumstances. This lolling condition is a result of less ice onboard than what is applied by regulation (approximately 15 MT versus 20 MT) DeNucci and Brahan (2022). Given the extreme environment which induces these icing conditions, the righting area may not be enough to absorb the dynamic effect of wind and waves on the vessel.

Initially, *Scandies Rose* experienced wind off the starboard bow. Applying this wind as a restoring moment created an almost-imperceptible change to the righting arm and angle of list.

This analysis highlights the importance of modeling ice accretion in an off-center fashion. A comparison of righting arms

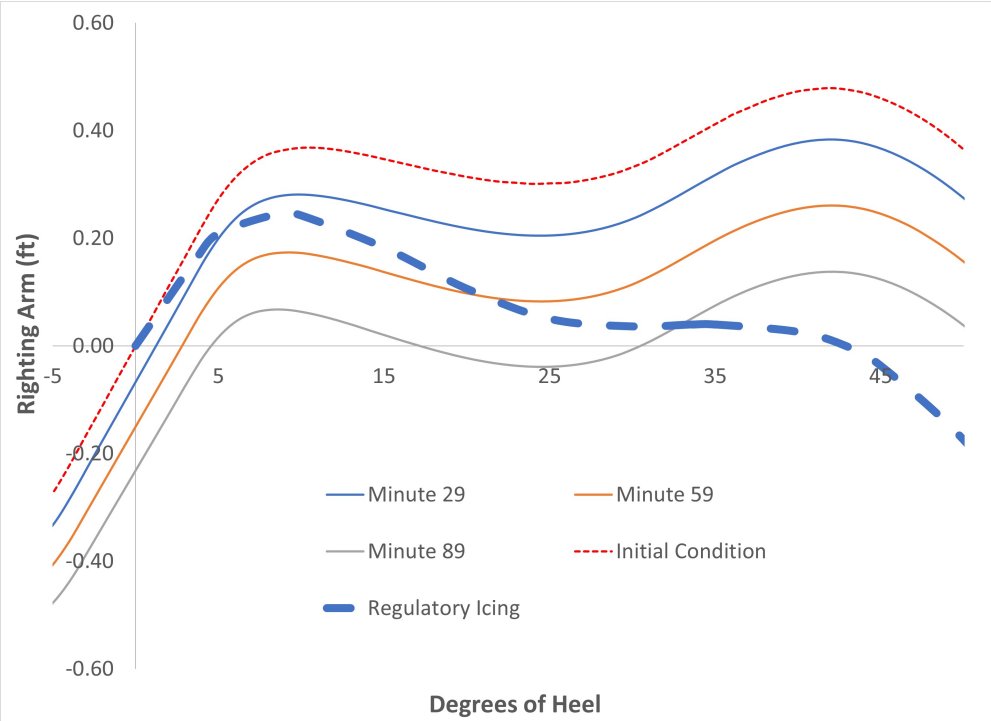

Figure 10: Static Righting Arm of *Scandies Rose* for the icing simulation. Regulatory icing, 46 CFR 28.550, is shown in the bold dashed line. Of note, downflooding points were not taken into account. Ice loads from the longer simulations capsized the vessel.

using regulatory icing requirements and the results after 89 minutes show the stark difference in a vessel's ability to withstand external forces.

CONCLUSIONS

With this model, a more accurate depiction of crab pot icing is captured. Implementing a feedback loop in the vessel icing model, while concurrently updating the pot porosities as they ice, showed both an increased rate of icing and a rise in the center of gravity of the ice over time. The accumulating ice:

1. changes the flow field, causing subsequent droplets to land in higher regions than previous simulations showed, and
2. decreases crab pot porosity, thereby increasing the sea spray flux into the system.

If permitted to continue, the center of gravity of ice will continue to rise, thereby increasing the vessel's overall center of gravity.

Off-center weight, which negatively impacts the vessel's stability, can ultimately cause vessel capsize. The effect of off-center ice is clear: less ice than required by regulation modeled in an off-center fashion puts the vessel in a worse situation than witnessed in with regulations. This paper presents an accurate, time-dependent study of how quickly ice can accumulate on the outer surface of the crab pot stack. The goal of future regulation should be to provide reasonable amount of time for the crew to intervene to prevent catastrophic capsizing.

FUTURE WORK

This study presents an ice accretion model that improves the quantitative understanding of icing phenomena on filigree structures. It only considered the outer edge of the crab pot stack and does not take into account all the intermediate surfaces where ice can accumulate. Future work should aim to quantify the ice accumulation on the interior surfaces and equipment (coiled line and buoys) of each crab pot.

While modeling the events leading up to *Scandies Rose's* capsize was one aim of this research, another is to prevent these occurrences in the future. This might be accomplished by updated stability regulations, but it is also of interest to reduce the amount of icing on the structure in the first place.

To match the net orientation on *Scandies Rose*, crab pot netting was arranged at a 45^o bias to the structure of the crab pot. As a result, the brine flows in both the x- and z- directions along the webbing. Modeling the nets in the vertical direction might reduce ice accumulation because the amount of time the brine is exposed to the high convection coefficients may decrease. Other areas of interest are the effects of spray rails and the addition of flare to the hull design. All three design changes have the potential to impact the quantity of ice accumulation on a vessel in extreme weather conditions such as those *Scandies Rose* and *Destination* were subject.

CONTRIBUTION STATEMENT

Thomas DeNucci: Conceptualization; porous surface methodology; computational fluid dynamics modelling; writing – original draft. **Dan Brahan:** Methodology; droplet and ice accretion modelling; stability calculations; writing – original draft. **Peter McGonagle** Methodology; ice accretion modelling; writing - review and editing. **Colman Schofield:** Computational fluid dynamics vessel model; porosity calculations; writing - review and editing. **Delany Taplin-Patterson:** Computational fluid dynamics vessel model; porosity calculations; writing - review and editing.

REFERENCES

Admirat, P. (2008). *Wet Snow Accretion on Overhead Lines*, pages 119–169. Springer Netherlands, Dordrecht.

Assur, A. (1958). Composition of sea ice and tensile strength, arctic sea ice. *US National Academy of Science, National Research Council Publication 508*.

Brahan, D., DeNucci, T., and Glivar, G. (2023). Numerical simulation of sea spray events in extreme weather conditions. 22^{nd} *International Conference on Computer Applications and Information Technology in the Maritime Industries*.

DeNucci, T. and Brahan, D. (2022). A digital twin for the formulation of ice accretion on vessels. 21^{st} *International Conference on Computer Applications and Information Technology in the Maritime Industries*.

DeNucci, T., Brahan, D., Kerst, A., and Oyola, O. (2023). Improving ship safety with a digital twin for ice accretion. 22^{nd} *International Conference on Computer Applications and Information Technology in the Maritime Industries*.

Hansen, E. (2012). *Numerical modelling of marine icing on offshore structures and vessels*. PhD thesis, Norwegian University of Science and Technology.

Horjen, I. (1990). *Numerical modelling of time-dependent marine icing, anti-icing and de-icing*. PhD thesis, Norwegian University of Science and Technology.

Horjen, I. and Vefensmo, S. (1987). Time dependent sea spray icing on ships and drill rigs - a thoeretical analysis. *Offshore Icing - Phase IV, NHL Report STF60 F87130*.

Jones, K. and Andreas, E. (2012). Sea spray concentrations and the icing of fixed offshore sea structures. *Quarterly J. Royal Meteorological Society*, 138:131–144.

Kato, R. (2012). *Modelling of ship superstructure icing: Application to ice bridge simulators*. PhD thesis, Norwegian University of Science and Technology.

Kollár, L. E. and Farzaneh, M. (2010). Wind-tunnel investigation of icing of an inclined cylinder. *International Journal of Heat and Mass Transfer*, 53(5):849–861.

Lozowski, E., Szilder, K., and Makkonen, L. (2000). Computer simulation of marine ice accretion. *Philosophical Transactions: Mathematical, Physical and Engineering Sciences,*, 358:2811–2845.

National Transportation Safety Board (2017). Marine accident report: Capsizing and sinking of fishing vessel destination. *U.S. Coast Guard*.

National Transportation Safety Board (2021). Marine accident report: Capsizing and sinking of commercial fishing vessel scandies rose. *U.S. Coast Guard*.

Ryerson, C. (1995). Superstructure spray and ice accretion on a large US Coast Guard Cutter. *J. Atmospheric Research*, 36:321–337.

Ryerson, C. (2009). Assessment of superstructure ice protection as applied to offshore oil operations safety. *US Army Cold Regions Research and Engineering Laboratory, Report 09-4*.

Stallabrass, J. (1980). Trawler icing. a compilation of work done at the national research center. *Mechanical Engineering Report MD-56, N.R.C. No. 19372*.

Zakrzewski, W. (1986). Icing of fishing vessels, part i: Splashing a ship with spray. 8^{th} *International Association for Hydro-environment Engineering and Research on Ice*.

Zarling, J. (1980). Heat and mass transfer from freely falling drops at low temperatures. *US Army Cold Regions Research and Engineering Laboratory, Report B0-1B*.

Proceedings of 15th International Marine Design Conference (IMDC-2024)
June 2-6, 2024
Amsterdam, the Netherlands

Integrated infection and crowd behavior model for COVID-19 infection risk assessment onboard large passenger vessels

N.A. de Haan[1], A.A. Kana[1,2,*] and B. Atasoy[1,3]

ABSTRACT

The development of the global COVID-19 pandemic from 2020 onward has had significant impact on the world and specifically the maritime industry. Striking examples were COVID-19 outbreaks onboard the Diamond Princess cruise vessel and the U.S.S. Theodore Roosevelt aircraft carrier at the start of the pandemic. Contagious disease management onboard large passenger ships remains a complex issue, amplified by the international character of the industry, confined environment and shared facilities. This paper therefore presents an integrated infection and crowd behavior model used to calculate agent-specific infection risk, incorporating guest and crew circulation through a passenger ship layout. The integrated model is used to investigate the effect of ship layout design, capacity reduction and mask wearing on COVID-19 airborne infection risk onboard large passenger vessels.

KEY WORDS

Contagious disease; passenger vessel; layout design; COVID-19; infection risk

INTRODUCTION

The development of the global COVID-19 pandemic from 2020 onward has had a significant impact on the world and specifically the maritime industry. The shipping industry had to deal with restricted travel, changing trade volumes, increased waiting times and stricter security measures in ports (Yazir et al., 2020). As seafarers kept working through the COVID-19 pandemic, quarantines, travel restrictions and country entering measures became standard practice (Keçeci, 2022). Striking examples of the pandemic's impact were COVID-19 outbreaks onboard the Diamond Princess cruise vessel and the U.S.S. Theodore Roosevelt aircraft carrier at the start of the pandemic. During these outbreaks, over 20% of the total population tested positive for SARS-CoV-2 with major implications (Kasper et al., 2020; Turvold and Mcmullin, 2020). Contagious disease management onboard large passenger ships remains a complex issue, amplified by the international character of the industry, confined environment and shared facilities. This paper therefore aims to:

Investigate the effect of ship layout design, capacity reduction and mask wearing on COVID-19 airborne infection risk onboard large passenger vessels

Since the COVID-19 pandemic, significant research has been done into the characteristics of this contagious coronavirus, covering incubation periods, (asymptotic) infection rates and transmission mechanisms (Zhao et al., 2022; Rocklöv et al.,

[1] Department of Maritime and Transport Technology, Delft University of Technology, Delft, the Netherlands
[2] ORCID: 0000-0002-9600-8669
[3] ORCID: 0000-0002-1606-9841
[*] A.A.Kana@tudelft.nl

Submitted: 23 February 2024, Revised: 30 April 2024, Accepted: 1 May 2024, Published: 21 May 2024

Conference paper, DOI: https://doi.org/10.59490/imdc.2024.867 e-ISSN: 3050-4864

2021; Lipsitch et al., 2020). Other literature focuses on ways to prevent or control disease spread, like the research by Gupta et al. (2021) discussing the choice between ship quarantine or disembarkation of suspected cases and the article by Li et al. (2021) proposing "A timeline and system framework for cruise ship disease risk management". Additionally, there is a wide availability in research relating COVID-19 disease spread to behavioral measures like mask wearing, social distancing and personal hygiene. Besides operational and behavioral measures, layout adjustment might be an option for disease prevention and control. This can be connected to the concept of prevention through design (PtD) Brewster et al. (2020). The layout design should thus aim to prevent a disease outbreak and facilitate disease control in case prevention fails. Research connecting ship layout design with contagious disease was done by Ruggiero et al. (2008) as they present a retrofit design for an Italian fast medical support vessel. Furthermore, the Healthy Sailing HORIZON EUROPE research project specifically supports "substantially reducing the spread of communicable disease on board passenger ships" (Healthy Sailing, 2024).

The novelty of this paper lies with the integrated infection and crowd behavior model used to calculate agent-specific airborne infection risk, incorporating guest and crew circulation through a passenger ship layout. These location- and agent-based infection risks can be considered complementary to COVID-19 studies onboard large passenger vessels presenting retrospectively calculated attack rates and reproduction numbers (Rocklöv et al., 2021; Mizumoto and Chowell, 2020; Liu et al., 2020; Rosca et al., 2022).

The scope of this paper is described by the details in the research objective. The ship type is defined and the scope of the measures and interventions tested is limited to capacity reduction, mask wearing and ship layout adaptions. The effect of these measures will be investigated by means of model simulations. The study of ventilation and ventilation system design onboard large passenger vessels in relation to contagious disease spread falls outside the scope of this research.

This paper starts by describing the required background information related to contagious disease transmission, disease prevention and control. This background leads into the development of the integrated model. The first part of the method covers the model requirements where after a specific movement model and infection model were selected for integration. The second part of the method handles the model architecture implemented in order to integrate the movement and infection model. Three interventions are investigated using the integrated model and the results are compared against two sample cases. The interventions feature layout adjustments, capacity reductions and mask wearing. The paper closes with a discussion and concluding summary.

BACKGROUND

Diseases have been a part of daily human life throughout history and the recent COVID-19 pandemic showed the impact of a contagious disease on a global level. Next to coronaviruses; Tuberculosis, Noroviruses and influenza have been linked to life at sea (Mangili and Gendreau, 2005; Kak, 2007). These diseases can spread via four modes of disease transmission as described by Mangili and Gendreau (2005):

- *Contact transmission*
  Contact transmission includes person-to-person contact, contact with a contaminated intermediate host and large droplet transmission; if someone for example inhales large droplets generated when an infector sneezes or coughs. The contaminated intermediate host might be something like a surface or door handle. The densely populated environment, confined and shared spaces onboard large passenger vessels may amplify contact transmission.
- *Airborne transmission*
  Airborne transmission covers very small droplet residua (nuclei) that travel over long distances. These aerolized infectious agents move around because of circulation inside a space, mechanical ventilation or they end up in filtration systems (Tan et al., 2022).
- *Common vehicle transmission*
  Common vehicle transmission route is associated with food and water sources.

- *Vector-borne transmission*
  Vector-borne transmission relies on insects or rodents to spread a disease.

Measures to prevent or control disease transmission onboard large passenger vessels cover three categories: ship layout adjustments, operational measures and behavioral measures. An improved ship layout could feature additional medical facilities, optional isolation and quarantine zones and a lower passenger-space ratio (Rosca et al., 2022; Li et al., 2021). Also, high-risk spaces might benefit from an area or location change. Possibilities for operational measures are: embarkation requirements, extensive onboard disease management and monitoring, and restricted movement onboard or on-shore (Mouchtouri et al., 2010; Kordsmeyer et al., 2021; Moon and Ryu, 2021). Another measure with large potential can be found in the research by Guagliardo et al. (2022). They investigate the effect on COVID-19 infection cases when the general capacity onboard a cruise ship is reduced. The last group of measures is related to the behavior of crew and guests who can improve their personal hygiene, get vaccinated, keep a social distance and wear personal protective equipment like a mask (Noakes et al., 2006; Nicolaides et al., 2020; Kak, 2007; Sun and Zhai, 2020).

METHOD

The development of the integrated movement and infection model followed a two-step approach. The first step is the integrated model analysis. In this step, the model requirements are presented after which a model combination is selected from the various investigated movement and infection models. The second step describes the developed model architecture in order to achieve integration between the movement and infection model.

Integrated Model Requirements

The integrated model requirements are given in Table 1. These requirements can be connected to the scope and specific boundaries of this research. R1 and R9 are related to the considered design stage as converging results are required within a time frame that is acceptable for *initial stage retrofit design*. R2 specifies the population size which is related to the ship type: *large passenger vessels*. The preferred result of this investigation is the *limitation of contagious disease spread* which can be linked to R3 and R12. R10 and R11 specify requirements to monitor the time spent in specific spaces and the space occupation. These requirements can be used to inform *layout adjustments* and the exposure time and space occupation might be relevant when implementing *operational and behavioral measures*. Finally, R4 up to R8 are formulated to achieve two key model specifications: *incorporating crew and guest circulation* and *incorporating movement through a ship layout*.

Keeping the requirements in mind, different types of agent movement and infection models were investigated. Both the investigated movement and infection models describe varying levels of detail, from macroscopic pipe flow models to microscopic agent-based movement models. Widely used compartment models, infection risk models and complex agent-based models were investigated as options to cover the medical aspect of the integrated model. The movement and infection models were brought together in twelve combinations and their integration compatibility was evaluated. After careful consideration, the combination of a mesoscopic route-choice model developed by Narayan et al. (2021) as used in van Gisbergen (2022) and the modified Wells-Riley infection model presented by Sun and Zhai (2020) was selected. Comparing all model combinations against the requirements, this option showed the most potential. The combination is less complex and time-intensive than an agent-based model but it does provide a strong disease performance indication. The performance indication is layout dependent and agent specific.

Table 1: Integrated model requirements

Requirement		Details
1	Convergence	The simulation results converge within an acceptable time frame
2	Population size	3000-4000 Individual agents can be modelled (guests and crew)
3	Disease performance indication	Model results indicate scenario performance for contagious disease spread
		Model results indicate *where* in the layout agents are most at risk for infection
		Model results enable performance comparison between different scenarios
4	Layout incorporation	Model is layout dependent
		Model support layout dimensions from 5 up to 50 meters per space.
5	Space capacity and flow	Model takes limited capacity of spaces into account
		Model takes limited flow between spaces into account
6	Individual movement	Movement can be modelled for each individual agent
		Individual agent movement can be tracked and movement data is stored
7	Random movement	There is controlled randomness in the activities that agents undertake
		There is controlled randomness in *when* agents start different activities
		There is controlled randomness in the routes agents take to their destinations
8	Multi-leg movement	Agents can move between multiple destinations in one simulation
		The time an agent stays at a single destination can be adjusted
9	Medical complexity	Medical model is as simple as possible while producing relevant results
10	Time spent	Time spent at each location is known for every agent
		Time spent at each location is incorporated when calculating infection risk
11	Space occupation	Space occupation is known for each time step
		Space occupation changes with the agents entering and exiting spaces
		Space occupation is incorporated when calculating infection risk
12	Disease specific	Model should (to a degree) take differences between diseases into account

Integrated Model Architecture

The chosen route choice model simulates the normal-day movement of guests and crew onboard a cruise ship based on an activity schedule. The activity schedule provides the destinations and duration of activities while the agents choose their individual routes between destinations based on a mixed logit route choice model. The agents can hold four different states in the route choice model: activity, wayfinding, stay and walk. The ship layout is converted into nodes representing one or multiple spaces and these nodes are connected via bi-directional links.

The implemented infection model presented by Sun and Zhai (2020) calculates Wells-Riley infection probability for airborne disease transmission in confined spaces, taking the social distance into account. The social distance index is shown in Equation 1 where d equals the social distance in meters. The modified Wells-Riley infection risk is given in Equation 2 with the following parameters: P_I: probability of infection, C: new cases, S: susceptible individuals, I: number of infectors, p: pulmonary ventilation rate of susceptible individuals $[m^3/s]$, q: quanta production rate per infected individual [q/s], t: time [s], Q: room ventilation rate $[m^3/s]$ and E_z: ventilation index.

$$P_d = \frac{-18.19\ ln(d) + 43.276}{100} \tag{1}$$

$$P_I = \frac{C}{S} = 1 - exp(-P_d \frac{Iqpt}{QE_z}) \tag{2}$$

An overview of the integrated model architecture can be found in Figure 1. The route choice model (RCM) is coded in C++ and run in Microsoft Visual Studio 2022 with an academic license. The output for every RCM simulation consists of five .CVS files. The integrated infection and crowd behavior and model itself is coded in Python and run in Spyder. Every investigated case was repeated five times and the infection results in this paper correspond to an average over these five repetitions.

The parameters from Equation 2 are recognized in Figure 1 as start parameters, except the ventilation rate Q. This parameter is no longer a constant start parameter as the ventilation rate Q has become location specific based on the Air Change per Hour ACH, the location floor area and the space height H_c. The node occupancy and local ventilation rate is calculated using the start parameters and RCM output. The last step consists of the modified Wells-Riley infection risk calculation. The infection risk is given in a matrix format with the infection risk for every agent per timestep. The size of this matrix covers approximately 60000 time steps (rows) and 2848 agents (columns) for the total population. The exposure time is tracked for the time an agent stays in the same location and the exposure time is reset when an agent changes node location.

In the infection risk calculation, two assumptions have been made. The first assumption is related to the situation where the social distance is more than $10.8m$. At social distances greater than this, the social distance index becomes negative which results in a negative infection risk. This situation lies outside the scope of the modified Wells-Riley equation and one could question if there is infection risk at all when the infector and the susceptible agent are so far apart. Therefore, the infection risk is set to zero for negative social distance index results. The second assumption concerns the time when agents are not yet moving to their first destination or when agents have finished their activity schedule. The infection risks for these situations are also assumed to be zero. The assumption does not affect the risk calculations for the rest of the day as the exposure time is reset. The reasoning behind this assumption can be found in the fact that the implemented ship layout does not realistically model the guest and crew cabin spaces. For example, the guest cabins are modelled in large groups, as if agents are staying together in one large space. This situation leads to unexpected high risks before starting and after finishing the activity schedule. Also, the focus of this research is not the infection risk calculation for long-term risk inside a cabin, but infection risk during normal-day movement. Normal-day movement is still captured in the model results when the described assumptions are implemented.

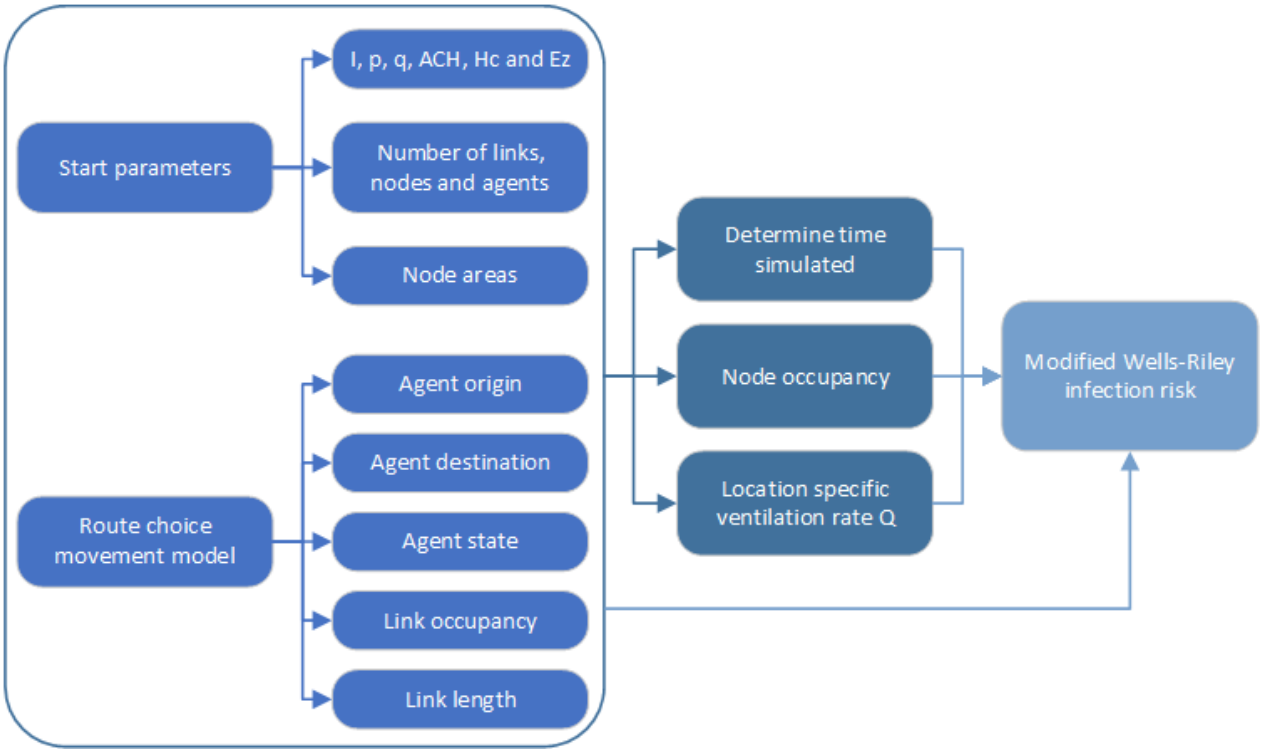

Figure 1: Integrated model architecture

SAMPLE CASES AND VALIDATION

This section presents two sample cases for the integrated infection and crowd behavior model. These sample cases are continuously presented as a reference when investigating ship layout adjustments, capacity reductions and mask wearing. The sample cases can be described covering three main topics: the ship layout, the activity schedule and the chosen start parameters. The ship layout is based on the second data-set from the SAFEGUARD project which features the layout from a cruise ship operated by Royal Caribbean International (Galea et al., 2012; Brown et al., 2021). The layout corresponds to the Radiance of the Seas cruise ship as seen in Figure 2. The ship characteristics are provided in Table 2. It is relevant to note that the Radiance of the Seas has undergone retrofitting after the SAFEGUARD project and the deck plans are no longer a complete match (Royal Caribbean Press Center, 2024). The current dataset is sufficient for this research as it does provide a realistic representation of 'a large passenger vessel'.

Figure 2: Radiance of the Seas (CruiseMapper, 2024)

Table 2: General characteristics Radiance of the Seas (Royal Caribbean Press Center, 2024)

Ship	Radiance of the Seas
Owner	Royal Caribbean Group
Maiden Voyage	7 April 2001
Tonnage	90,090 GT
Length (LOA)	293.2 m
Beam	32.2 m
Draft	8.63 m
Decks	13 (12 guest accessible)
Speed	25 kts

The activity schedule prescribes the node destinations per individual agent over the course of a day. The structure of the schedules can be found in Table 3 and Table 4. The guests complete seven legs per day: cabin → breakfast → activity → lunch → activity → dinner → activity → cabin. All agents follow the same trend (seven legs) but the activity and meal locations are chosen arbitrarily. The crew schedule specifies eight legs: cabin → shift → break → shift → break → shift → break → shift → cabin. The cruise ship can host over 850 crew of which 700 crew are modelled. These crew members have frequent contact with the guests.

Table 3: Sample case guest activity schedule characteristics

Number of agents	2148
Groups	Every 4 agents follow the same schedule
Activity/Meal duration	140 minutes $\pm$ 10 minutes
Moving to breakfast	Uniform distribution 08:00 till 09:00
Final move to cabin	Between 21:00 and 24:00

Table 4: Sample case crew activity schedule characteristics

Number of agents	700
Shift duration	180 minutes (4x)
Break duration	30 minutes (3x)
Early shift	07:30 $\pm$ 3 minutes till 21:00 $\pm$ 3 minutes
Late shift	10:30 $\pm$ 3 minutes till 00:00 $\pm$ 3 minutes

Next to the layout and schedule, the start parameters were investigated and defined. The start parameters can be found in Table 5. The I parameter is set to 1 infected person per space, introducing a fundamental assumption for the integrated model: the agent risk is determined 'as if there were a single infected agent in every space the agent enters'. In reality, there might be multiple infectors or no infectors at all in a particular space. However, tracking the actual amount of infectors would require the model to assign disease states like 'infected', 'susceptible' or 'recovered'. The model would then become a microscopic agent-based model while the choice has been made to work with a less complex risk-based model instead.

The pulmonary ventilation rate p is set to 8 L/min associated with resting, sitting and light indoor activities. The quanta production rate and air change per hour have a significant impact on the infection risk results. The quanta production rate q is set to 100qph as a compromise dealing with the variation for this medical parameter in literature (Gaddis and Manoranjan, 2021; Dai and Zhao, 2023; Buonanno et al., 2020). Increasing the ACH value to 25 or even 30 air changes per hour leads to lower infection risks in the integrated model. However, there is also research that suggests that higher ventilation rates might increase virus spread because droplets spread further (Ritos et al., 2023). This phenomenon is not captured in the integrated model as droplet spread itself is not modelled. This consideration, together with ventilation values mentioned in literature, led to the choice of 15 air changes per hour for the ACH parameter (Sodiq et al., 2021; Azimi et al., 2021; Zheng et al., 2016). The space height H_c is set to 2.35m and the ventilation index lies outside the scope of this research and is therefore determined to be 1.

Table 5: Start parameters for integrated model

I	1
p	8 L/min
q	100 qph
ACH	15
H_c	2.35 m
E_z	1
Number of links	968
Number of nodes	389
Number of agents	2848

The two sample cases were validated against similar cases presented in literature. Most COVID-19 studies onboard large passenger vessels present attack rates and reproduction numbers based on real-life cases (Rocklöv et al., 2021; Mizumoto and Chowell, 2020; Liu et al., 2020). These attack rates and reproduction numbers are retrospectively calculated. The National Institute for Infectious Diseases in Japan determined that over a 20-day COVID-19 outbreak, 22% of the population

onboard the Diamond Princess cruise vessel was “detected to have been infected with SARS-CoV-2” (Rosca et al., 2022). Using the average daily infection risk for sample case 1 (0.807%) and sample case 2 (1.05%), the attack rates were calculated to be 15% and 18% for a 20-day outbreak. This calculation directly removes infected cases from the susceptible population, assuming that infected cases isolate directly. Additionally, the average infection risk does not change over the 20-day period. In reality, infected individuals might not isolate because they are pre-symptomatic or asymptomatic and it is possible that symptomatic agents do no isolate at all. The result will be an increase of infected individuals in the agent population, increasing the average infection risk over time. The actual number of cases and therefore attack rate will thus be higher which explains the slight difference between the calculated attack rates for the sample cases and the value reported for the Diamond Princess outbreak.

The sample cases were also compared to the infection risk inside a single office space described by Dai and Zhao (2022) and a multi-room office space from the research by Srivastava et al. (2021). The single office space scenario in Dai and Zhao (2022) features the Wells-Riley infection risk equation adjusted to include a regression equation based on a CFD analysis. For a 40 m^2 office hosting six people, the infection risk over an eight hour period is described to be 13.2%. Using the developed integrated model, an infection risk of 19.6% was calculated. Differences might be attributed to the presence of portable air cleaners and the incorporation of complex air/particle circulation (CFD) in the research by Dai and Zhao (2022).

For the multi-office space, Srivastava et al. (2021) used a CFD tool to simulate the air-flow within a 59-person office geometry which resulted in an average infection risk of 3.10%. The average infection risk was calculated to be 1.97% implementing the integrated model while assuming the office space to be a single open space. Taking the geometry and calculation approach differences into account, equal results were not expected but the integrated model does present a result in the same range as the CFD-based average infection risk.

Specifically focusing on location based infection risks, the top 20 high-risk locations from sample case 1 were compared to 20 waiting rooms in an out-patient hospital building in Shenzhen, China (Li and Tang, 2021). The day average infection risk for the SC1 locations ranges between 0.75% and 3.58% with an average of 1.49%. The day average infection risks for the 20 hospital rooms ranges between 0.19% and 2.63% with an average of 0.79% (Li and Tang, 2021). Lastly, infection risk at one of the restaurants onboard was validated against a reception scenario with similar space characteristics, occupation and exposure time (Lelieveld et al., 2020). The average infection risk for the restaurant over a three hour exposure period was calculated to be 3.2% compared to 1.6% reported by Lelieveld et al. (2020).

SHIP LAYOUT DESIGN

The integrated model was used to investigate the effect of ship layout adjustments on COVID-19 infection risk. For sample case 1, the average infection risks per node and links are presented in Figure 3 and Figure 4. The average infection risk is calculated as the average risk over all agents at that location for a specific timestep. These values are then averaged over time. The figures show that the node locations reach average infection risks 10000 times higher than the infection risks at links. There is one outlier at node 107 with an average infection risk of 16.8% which is not completely visible in Figure 3 because of the limited y-axis. This outlier concerns a local schedule inconsistency which does not affect the full-scale infection risk results. The inconsistency was resolved for the combined tested measures. The modified Wells-Riley infection equation only covers airborne transmission and the occupancy and extended exposure times at nodes cause higher infection risks compared to the links.

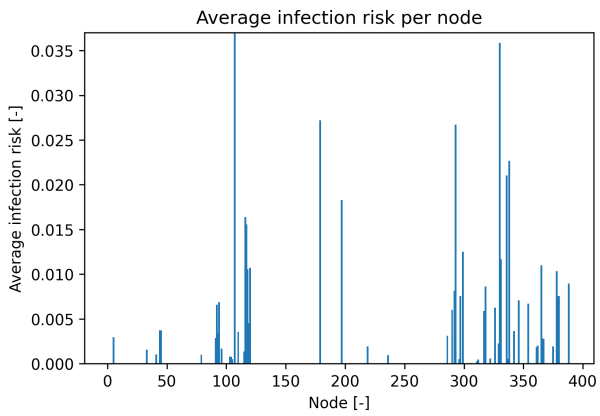

Figure 3: Average node infection risk (limited y-axis)

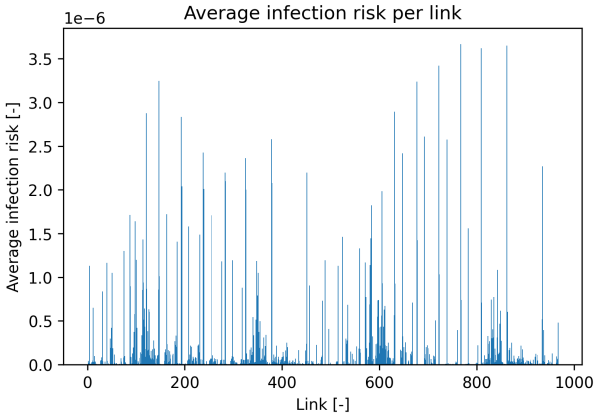

Figure 4: Average link infection risk

Based on the average infection risks and number of agents who reach their maximum infection risk at a certain node, two high-risk node locations were selected for further investigation. These nodes feature a restaurant on deck 11 (N293) and a restaurant on deck 12 (N330). The partial deck plans corresponding to these locations can be found in Figure 5 and Figure 6. The floor area of N293 was increased with $12m^2$, decreasing the area associated with neighboring corridor N295. The N330 restaurant is located next to a sundeck (N331) which was converted to become part of the N330 restaurant. The agents originally visiting the sundeck were relocated to adjacent sundeck nodes on the same deck.

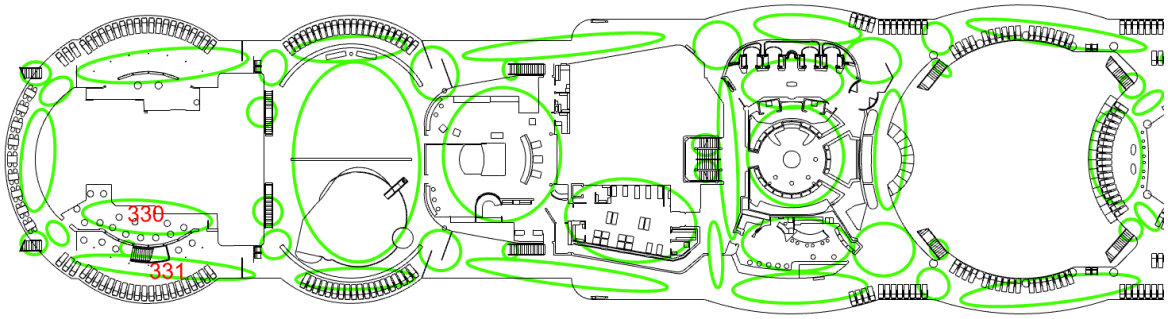

Figure 5: Deck 12 SAFEGUARD layout at N330 (Galea et al., 2012)

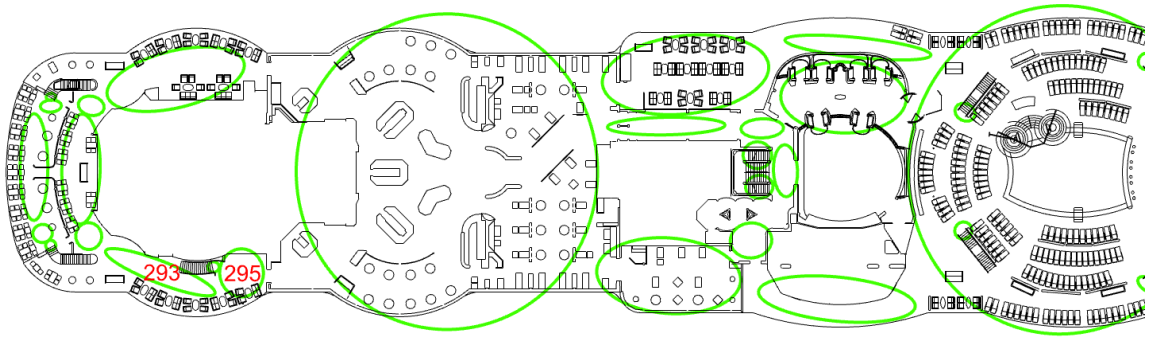

Figure 6: Deck 11 SAFEGUARD layout at N293 (Galea et al., 2012)

The location-specific infection risk for N293 and N330 can be found in Figure 7 and Figure 8. In Figure 7, there is a significant local risk improvement for the N293 restaurant. The average infection risk at N293 decreases to 1.57%, compared to 2.67% for sample case 1 (SC1) and 2.61% for sample case 2 (SC2). The N293 layout adjustment does not lead to higher infection risks for the surrounding nodes. Figure 8 presents a different picture as the N330 layout adjustment does not improve the local risk to a similar degree as the N293 adjustment. The average risk for N330 only decreases from 3.59% (SC1) or 3.51% (SC2) to 3.30% for the adjusted layout. The infection risk of adjacent node 331, which was converted from sundeck to restaurant, shows a risk increase to 1.57% compared to 1.17% for SC1 and 1.07% for SC2. The rerouted guests who are now using other sundecks do not significantly increase the infection risks for these sundeck nodes. If a local risk improvement for node 330 is to be achieved, a larger layout adjustment might be required. The N330 adjustment also shows that in trying to decrease the infection risk for a specific location, surrounding nodes might present with increased risk. This compromise should be considered whenever discussing layout adjustments in an effort to improve local infection risk.

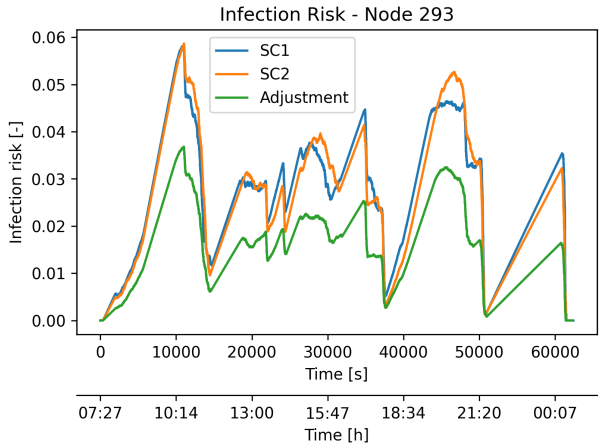

Figure 7: Infection risk at N293

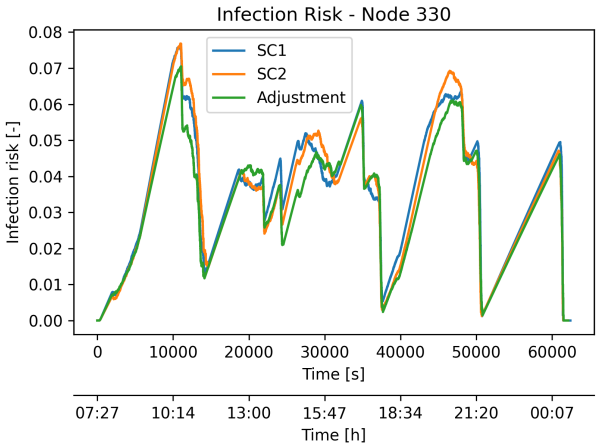

Figure 8: Infection risk at N330

Moving from local risk results to overall ship infection results, local improvements are not distinguishable from the risk variation related to the randomness in the route choice model output. This was expected as the layout adjustments were small compared to the size of the complete ship. Also, the agents affected by the layout change only cover part of the population. Thus, the improvements are simply too small to be visible in full-ship infection results even if local risk improvements are achieved.

CAPACITY REDUCTION

The integrated model was also used to test an operation measure, namely the capacity reduction for both the crew and guests. This measure was implemented for the following reductions CR = [2562, 2280, 1994, 1708, 1422, 1140, 711] agents corresponding to reduction percentages $CR = [10, 20, 30, 40, 50, 60, 75]\%$. The guest-to-crew ratio was kept constant and the reduced number of guests and crew was randomly removed from the activity schedule.

Figure 9 gives the total infection risk for the investigated capacity reductions. Sample case 1 and 2 are presented in the figure for 0.807% (SC1) and 1.05% (SC2). The average infection risk reveals a decreasing trend for increasing capacity reductions. The main mechanism behind this risk improvement can be related to increasing social distances through lower space occupancies. The average risk increase between 20% and 30% is unexpected but can be connected to the randomness in the integrated model input. This randomness is found in the population draws for the capacity reductions and in the route choice model outcomes used as integrated model input. This variation can also be recognized in the two sample cases for which the first sample case provides more favourable infection risk results. During the simulations, SC1 was used as a conservative reference in the sense that this sample already has low infection risks without any layout intervention or

implemented operational measures. Sample case 2 presents a more average situation related to infection risk. All capacity reductions lead to smaller infection risks than the second sample case with risk reductions from 4.8% (CR=10%) up to 40% (CR=75%). Compared to SC1, capacity reductions above 50% result 2.6% (CR=50%), 6.5% (CR=60%) and 22% (CR=75%) risk reductions.

In Figure 10, the percentage of the population with an infection risk above 50% over time is visualized. The capacity reduction below 50% are not presented in the figure as they only showed small improvements for the number of high-risk agents around 13:00. However, the capacity reductions above 50% show an infection risk improvement compared to sample case 2, especially for the risk peaks around 13:00 and 15:30. These times correspond to the end of the morning activity and the end of lunch.

Combining the results from Figure 9 and Figure 10, some general conclusions can be drawn. Improvements are achieved in the average infection risks, especially for higher capacity reductions. Additionally, for higher capacity reductions, the percentage of agents at high risk decreases compared to sample case 2. The improvements for smaller capacity reductions remain limited. A possible reason for this could be linked to the initial crowdedness onboard cruise vessels. When the number of guests and crew is slightly reduced, the ship remains crowded and social distance might not significantly improve. In this situation, large capacity reductions are required in order to achieve larger infection risk improvements. These increased capacity reductions might introduce issues around economic and operational feasibility. A possibility could be to implement a small capacity reduction as part of an intervention plan; also covering other operational or behavioral measures which together achieve infection risk improvements.

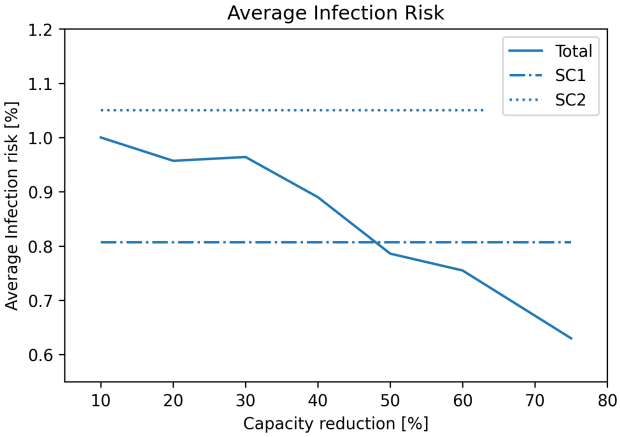

Figure 9: Average infection risk over CR

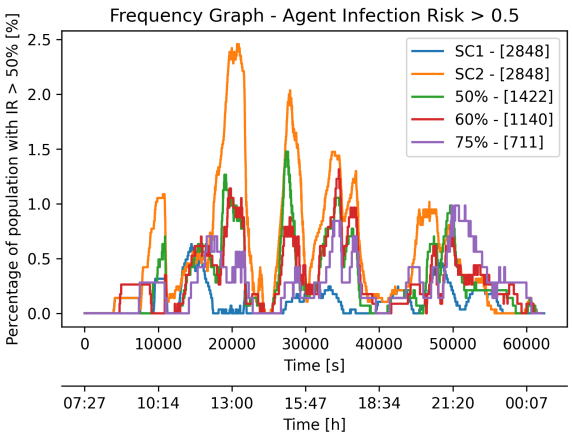

Figure 10: Infection risk above 50% for CR

MASK WEARING

A third investigated scenario is the behavioral intervention covering mask wearing by guests and crew. Mask wearing can be conveniently implemented in the modified Wells-Riley from Equation 2 through the definition of an adjusted pulmonary ventilation - and quanta production rate. The adjusted pulmonary ventilation rate is given in Equation 3 with respiratory filtration efficiency η_R. Equation 4 defines the adjusted quanta production rate q for an exhalation filtration efficiency η_E. The respiratory and exhalation filtration efficiencies are assumed to be 50% for surgical masks (Zheng et al., 2016; Dai and Zhao, 2020).

$$p_{adjusted} = p(1 - \eta_R) \tag{3}$$

$$q_{adjusted} = q(1 - \eta_E) \tag{4}$$

Three measure variations were formulated, specifying in which conditions guests and crew wear a mask. In the first case (MASK1), guests are wearing masks whenever they are moving between locations and crew members wear their masks continuously over the course of the day. The second case (MASK2) features a situation where guests are continuously wearing a mask except when they are at breakfast, lunch or dinner. The crew is, again, wearing their masks for the entire day. The final case (MASK3) relates mask wearing to the actual local social distance. In this situation, the crew and guests are obliged to wear a mask when the social distance becomes smaller than a specified safe distance. This safe distance is set to be $1.5m$ (CDC, 2020; European Centre for Disease Prevention and Control, 2023).

For all scenarios involving face masks, the average total risk results are lower than both sample cases as seen in Table 6. For MASK1, the average infection risk reduction is 2.4% compared to SC1 and 25% compared to SC2. This improvement can be solely attributed to a decreased risk for the crew who are wearing masks. The average guest risk shows no significant improvement compared to both SC1 and SC2. Notable average risk improvements are found for MASK2 and MASK3 with a risk reduction over 40% compared to SC1 and more than 50% compared to SC2. The guest infection risk for continuous and social distance-based mask wearing lie close together. A possible reason could be that the guests in MASK3 are almost continuously wearing a mask because the social distance is smaller than the set safe distance for the majority of the time.

Table 6: Average infection risks for mask wearing

Result [%]	SC1	SC2	MASK1	MASK2	MASK3
Average infection risk	0.807	1.05	0.787	0.451	0.487
Average guest infection risk	0.730	0.935	0.925	0.478	0.481
Average crew infection risk	1.04	1.39	0.362	0.369	0.506

Figure 11 presents the average infection risk over time for the three mask wearing scenarios. In scenarios MASK2 and MASK3, a pronounced risk decrease is recognized for the activities in between the meals around 13:00, 17:00 and after 21:30 for the evening activity. The 10:15 risk peak presents different behavior which can be explained by the fact that passengers do not wear a mask during breakfast. Continuing on this reasoning, the end of lunch peak around 15:30 and end of dinner peak around 20:00 are also expected to show less risk improvement. The figure indeed shows that for these timings there is little risk improvement for the tested cases compared to sample case 2.

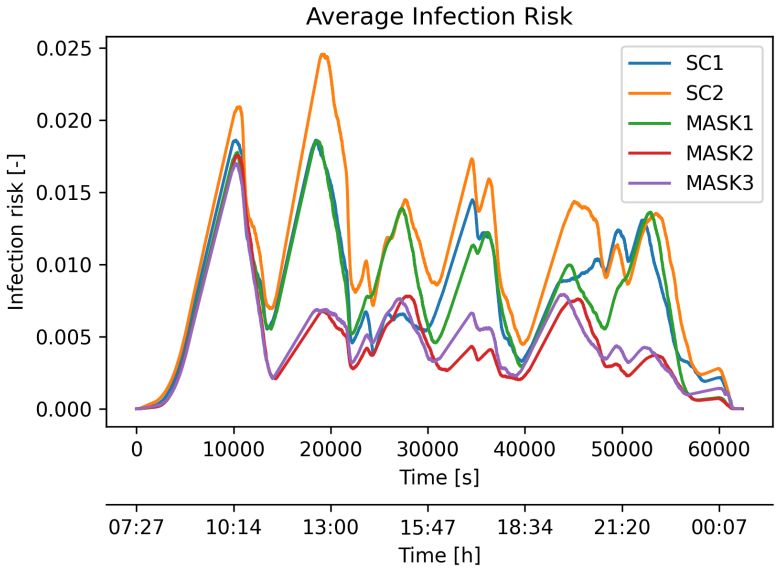

Figure 11: Average infection risk for mask wearing

In Figure 12, the guests at high risk are presented. MASK1 follows a similar trend as sample case 2, with a peak increase around 15:30. This increase might be the result of route choice model output variations. In general, wearing a mask solely during movement does not significantly improve the infection risks experienced by the guests. This matches with the findings for the ship layout design, where the nodes presented with higher infection risks than the links. The figure also shows that for MASK2 and MASK3, there are no guests with a risk above 50% except around 13:00. This is a major improvement compared to sample case 2. Looking at Figure 13, the crew at high risk is reduced for all scenarios involving masks, especially compared to SC2. The maximum number of crew members at high risk is 6 (MASK1-3) compared to 9 (SC1) and 38 (SC2) crew members.

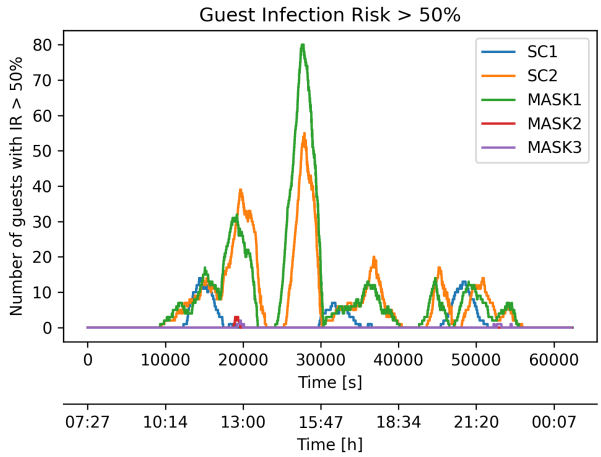

Figure 12: Guest infection risk above 50%

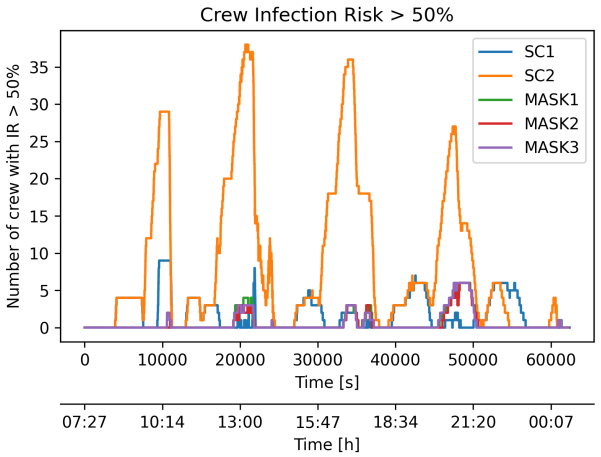

Figure 13: Crew infection risk above 50%

Continuous (MASK2) and social distance based mask wearing (MASK3) show most potential. Choosing between these two behavioral measures, with similar infection risk results, might instead be a question of preferred policy. Continuous mask wearing provides more clarity because guests and crew know when to wear a mask. Additionally, this measure avoids the situation where agents are frequently switching between mask on and mask off. Social distance based mask wearing could increase awareness around social distancing and crowded spaces. Guests might actually choose a different activity or route based on crowdedness and whether or not they have to wear a mask. Leaving these considerations aside, both measures do present significant average risk improvements and a reduction in the number of guests and crew at high risk.

COMBINED MEASURES

The previous sections described the implementation of capacity reduction, mask wearing and possible layout adjustments. The interventions can also be combined to further reduce COVID-19 infection risk. The combinations can be found in Table 7. The N293 layout adjustment was applied as it proved to decrease local infection risk without compromising surrounding nodes. The 50% capacity reduction is tested as this was the first scenario which presented with lower average risk results than sample case 1. Also, a 30% capacity reduction is investigated. This capacity reduction functions as a compromise between infection risk, profitability and operability. These two capacity reductions and N293 layout adjustment are combined with continuous mask wearing (MASK2) and social distance based mask wearing (MASK3).

Table 7: Specifications combined measures

	Layout adjustment	Capacity reduction	Mask wearing
C1	N293	CR = 30%	MASK2
C2	N293	CR = 50%	MASK2
C3	N293	CR = 30%	MASK3
C4	N293	CR = 50%	MASK3

The average infection risks are given in Table 8. The highest risk improvements are achieved for C1 and C2 when capacity reductions are combined with continuous mask wearing. The average risk from SC1 is reduced by 57% for C1 and by 64% for C2; compared to a 44% risk reduction when continuous mask wearing is applied as a stand-alone measure. The difference between a 30% and 50% capacity reduction is visible between C1 and C2 (-0.05%) and between C3 and C4 (-0.03%). Although, these differences seem rather small compared to the economic and operational impact that a 50% capacity reduction might have compared to a 30% capacity reduction. Figure 14 shows that for the combined cases, the average infection risk over time significantly decreases. The infection risk peak for breakfast does remain for the combined cases even as the other peak moments significantly decrease. A possible explanation for this is the fact that in a relatively short time, all guests move to breakfast and both crew shifts start in the same period. The movement of the guests still needs to spread out as they experience variations in activity duration over the day. For C1 and C3 there are no agents with an infection risk above 50%. C2 and C4 respectively have a maximum number of 2 guests and 2 crew with a risk above 50% at a single moment during the day. This is a significant improvement for the crew compared to Figure 13 for mask wearing without capacity reduction.

Table 8: Average infection risks for combined measures

Result [%]	SC1	SC2	C1	C2	C3	C4
Average infection risk	0.807	1.05	0.343	0.295	0.427	0.396

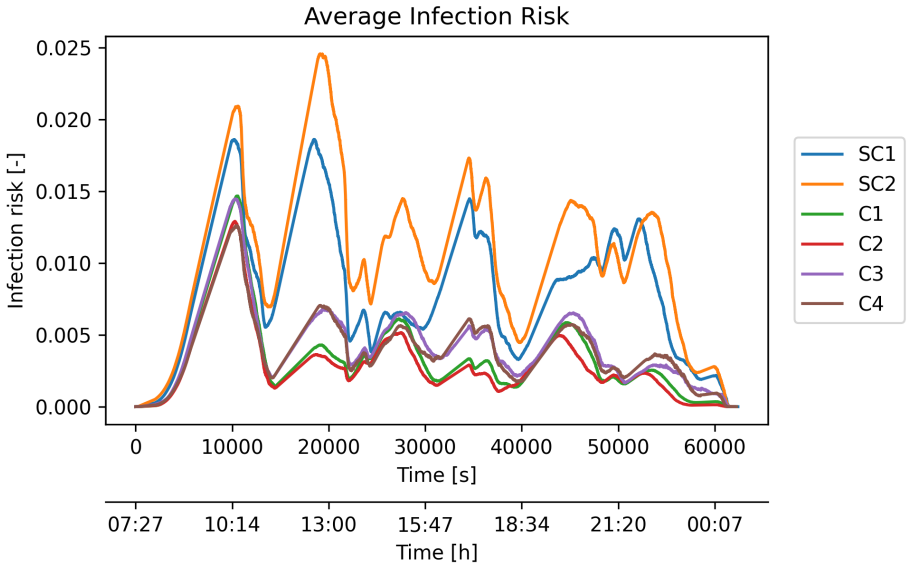

Figure 14: Average infection risk for C1-C4

DISCUSSION

The developed model presents a proof of concept for integrating a route choice movement model and a modified Wells-Riley infection model with the goal of investigating COVID-19 airborne infection risk onboard large passenger vessels. During the development and scenario evaluation, certain assumptions were required in order to move forward. These assumptions concerned the ship layout, agent activity schedule, compliance with implemented measures and chosen parameters. The infection results of the two sample cases revealed the variation related to the route choice model output. This in itself is also a strength of the integrated model because the movement of people is difficult to predict and should therefore feature a degree of randomness. However, to further improve the consistency of results it would be beneficial to increase the number of repetitions for further research. This also includes the repetition of population draws for the capacity reduction cases.

With respect to the integrated model, there are several areas available for further improvement and research. Firstly, the social distance calculation in the model is purely based on the location floor area and occupation. It was assumed that the agents distribute themselves over the available space and do not group together. In reality, the agents will probably group together and use the available space less efficiently, leading to smaller social distances and higher infection risks.

Secondly, the ship layout presents an opportunity for further improvement. The current layout does not model crew accommodation and the guest cabins are modeled in large groups. It could be interesting to implement a risk indication for the time agents spent in their cabins. This might require a different infection model than the one currently implemented. Also, the SAFEGUARD dataset was specifically created for the evaluation of large passenger evacuation models. During evacuations, elevators are not in use and they are thus not included in the current ship layout. These elevators are small spaces where agents stand close together, potentially resulting in high infection risks.

Thirdly, the integrated model only accounts for the airborne transmission of COVID-19. There are other modes of transmission, like contact transmission, which are relevant for infection risk onboard large passenger vessels because of the crowded spaces and shared (sanitary) facilities. These other transmission modes can increase the infection risks and specific control or preventive measures might show inferior or superior results when additional transmission modes are taken into account. Next to the transmission modes, there are medical parameters with a constant value that require further attention. For example, the pulmonary ventilation rate is constant for the integrated model. When someone is exercising in the gym, this ventilation rate will increase significantly and a crew member at work might have a higher pulmonary ventilation rate compared to the guests.

Suggestions for future research can move in either a microscopic or macroscopic direction. For the macroscopic direction, it is relevant to notice the boundaries of the current infection risk calculation, as the integrated model assumes the passenger vessel to be a confined environment without any outside influences. Additionally, the model is focused on infection risk and does not specify disease progression in terms of cases. If the ship were considered in its environmental setting, ports and travel routes become relevant because infected individuals might embark or disembark the vessel. In summary, the integrated model could be further developed describing cases over an extended period of time while incorporating the environmental setting of the passenger vessel.

Future research could also move in the microscopic direction, related to the ship layout, the investigated disease and the tested measures and adaptions. This research might describe an extended sensitivity study for the base cases where the activity schedule and the ship layout are radically changed. Additionally, the current research covered a COVID-19 application of the integrated model for a cruise vessel layout. The integrated model could also be applied to a large naval vessel or a ferry to investigate the risk of another contagious disease in different circumstances. A final suggestion beyond retrofit design is the option to determine infection risk performance for a set of initial stage design plans. This could provide infection risk insight before a ship design is finalized and the ship is built.

CONCLUSIONS

This paper aimed to: *Investigate the effect of ship layout design, capacity reduction and mask wearing on COVID-19 airborne infection risk onboard large passenger vessels*. This investigation is based upon the development of an integrated model that calculates agent-based infection risk, incorporating guest and crew circulation through a passenger ship layout. Various movement and infection models were studied in an effort to find the model combination that best fits the proposed model requirements. After careful consideration, a mesoscopic route choice model and a modified Wells-Riley infection model were selected for model integration. The integrated model was validated for two sample cases without any applied measures or layout adjustments.

Ship layout design, capacity reductions and mask wearing measures were evaluated using the integrated model. The node locations presented with higher infection risks than the links, caused by high occupancy and extended exposure time at nodes. The proposed layout adjustments resulted in local risk improvements. Investigating these layout changes is important as risk reduction for one location might lead to a risk increase somewhere else in the layout. For increasing capacity reductions, the average infection risk decreases. This is specifically visible for higher capacity reductions above 50%. A possible reason could be the initial busy and crowded environment onboard a large cruise ship, which requires large capacity reductions in order to achieve larger infection risk improvements. These large capacity reductions do raise questions regarding operational and economic feasibility. It might be interesting to combine a 'smaller' capacity reduction with other control or prevention measures like mask wearing. For the mask wearing scenarios, the highest average risk improvements from the three tested interventions were achieved. Continuous and social distance based mask wearing reduced the average risk over 40% compared to the sample cases.

When continuous mask wearing is combined with a 30% or 50% capacity reduction, average infection risk reductions over 55% are achieved compared to the sample cases. The average risk improvement between a 30% and 50% capacity reduction, combined with mask wearing, is relatively small compared to the economic and operational impact of a 50% capacity reduction. For all tested combined measures, there is a significant reduction in the number of agents that present infection risks above 50% over the course of a day.

Considering the evaluated infection risk for the different layout adjustments, measures and combined scenarios; the aim of this paper was reached using the developed integrated infection and crowd behavior model. Additionally, the model presents opportunities for further research and evaluation of different interventions, alternative ship layouts and application during the initial design stage.

CONTRIBUTION STATEMENT

N.A. de Haan Conceptualization; investigation; methodology; validation; visualization; writing – original draft. **A. A. Kana** Conceptualization; supervision; writing – review and editing **B. Atasoy** Conceptualization; supervision; writing – review and editing.

ACKNOWLEDGEMENTS

This work was performed as part of the academic thesis for the lead author, (de Haan, 2024). The thesis was performed in Marine Technology at Delft University of Technology and the authors would like to acknowledge Delft University of Technology for their support of this research.

REFERENCES

Azimi, P., Keshavarz, Z., Laurent, J. G. C., Stephens, B., and Allen, J. G. (2021). Mechanistic transmission modeling of COVID-19 on the Diamond Princess cruise ship demonstrates the importance of aerosol transmission. *PNAS*, 118.

Brewster, R. K., Sundermann, A., and Boles, C. (2020). Lessons learned for COVID-19 in the cruise ship industry. *Toxicology and Industrial Health*, 36(9):728–735.

Brown, R., Galea, E. R., Deere, S., and Filippidis, L. (2021). Passenger Response Time Data-sets for Large Passenger Ferries and Cruise Ships derived from sea trails. *International Journal of Maritime Engineering*, 155(A1).

Buonanno, G., Stabile, L., and Morawska, L. (2020). Estimation of airborne viral emission: Quanta emission rate of SARS-CoV-2 for infection risk assessment. *Environment international*, 141.

CDC (2020). Social distancing : keep a safe distance to slow the spread.

CruiseMapper (2024). Radiance Of The Seas deck plan.

Dai, H. and Zhao, B. (2020). Association of the infection probability of COVID-19 with ventilation rates in confined spaces. *Building Simulation*, 13(6):1321–1327.

Dai, H. and Zhao, B. (2022). Reducing airborne infection risk of COVID-19 by locating air cleaners at proper positions indoor: Analysis with a simple model. *Building and Environment*, 213:108864.

Dai, H. and Zhao, B. (2023). Association between the infection probability of COVID-19 and ventilation rates: An update for SARS-CoV-2 variants. *Building Simulation*, 16(1):3–12.

European Centre for Disease Prevention and Control (2023). Questions and answers on COVID-19: Travelling.

Gaddis, M. D. and Manoranjan, V. S. (2021). Modeling the Spread of COVID-19 in Enclosed Spaces. *Mathematical and Computational Applications*, 26(79).

Galea, E., Deere, S., and Filippidis, L. (2012). THE SAFEGUARD VALIDATION DATA SET – SGVDS2 A GUIDE TO THE DATA AND VALDIATION PROCEDURES. Technical report, University of Greenwich.

Guagliardo, S. A. J., Prasad, P. V., Rodriguez, A., Fukunaga, R., Novak, R. T., Ahart, L., Reynolds, J., Griffin, I., Wiegand, R., Quilter, L. A., Morrison, S., Jenkins, K., Wall, H. K., Treffiletti, A., White, S. B., Regan, J., Tardivel, K., Freeland, A., Brown, C., Wolford, H., Johansson, M. A., Cetron, M. S., Slayton, R. B., and Friedman, C. R. (2022). Cruise Ship Travel in the Era of Coronavirus Disease 2019 (COVID-19): A Summary of Outbreaks and a Model of Public Health Interventions. *Clinical Infectious Diseases*, 74(3):490–497.

Gupta, A., Kunte, R., Goyal, N., Ray, S., and Singh, K. (2021). A comparative analysis of control measures on-board ship against COVID-19 and similar novel viral respiratory disease outbreak: Quarantine ship or disembark suspects? *Medical Journal Armed Forces India*, 77:S430–S436.

Healthy Sailing (2024). Prevention, mitigation, management of infectious diseases on cruise ships and passenger ferries.

Kak, V. (2007). Infections in Confined Spaces: Cruise Ships, Military Barracks, and College Dormitories.

Kasper, M. R., Geibe, J. R., Sears, C. L., Riegodedios, A. J., Luse, T., Von Thun, A. M., McGinnis, M. B., Olson, N., Houskamp, D., Fenequito, R., Burgess, T. H., Armstrong, A. W., DeLong, G., Hawkins, R. J., and Gillingham, B. L. (2020). An Outbreak of Covid-19 on an Aircraft Carrier. *New England Journal of Medicine*, 383(25):2417–2426.

Keçeci, T. (2022). Importance and applicability analysis of the health and safety measures taken against the coronavirus disease on merchant vessels Tuba KEÇECİ. *Aquatic Research*, 5(3):171–185.

Kordsmeyer, A. C., Mojtahedzadeh, N., Heidrich, J., Militzer, K., Münster, T. v., Belz, L., Jensen, H. J., Bakir, S., Henning, E., Heuser, J., Klein, A., Sproessel, N., Ekkernkamp, A., Ehlers, L., de Boer, J., Kleine-Kampmann, S., Dirksen-Fischer, M., Plenge-Bönig, A., Harth, V., and Oldenburg, M. (2021). Systematic review on outbreaks of sars-cov-2 on cruise, navy and cargo ships. *International Journal of Environmental Research and Public Health*, 18(10):5195.

Lelieveld, J., Helleis, F., Borrmann, S., Cheng, Y., Drewnick, F., Haug, G., Klimach, T., Sciare, J., Su, H., and Pöschl, U. (2020). Model Calculations of Aerosol Transmission and Infection Risk of COVID-19 in Indoor Environments. *International Journal of Environmental Research and Public Health*, 17(8114).

Li, C. and Tang, H. (2021). Study on ventilation rates and assessment of infection risks of COVID-19 in an outpatient building. *Journal of Building Engineering*, 42:103090.

Li, H., Meng, S., and Tong, H. (2021). How to control cruise ship disease risk? Inspiration from the research literature. *Marine Policy*, 132:104652.

Lipsitch, M., Chan, H. T., Emery, J. C., Russell, T. W., Liu, Y., Hellewell, J., Pearson, C. A., Covid, C., Group, W., Knight, G. M., Eggo, R. M., Kucharski, A. J., Funk, S., Flasche, S., and MGJ Houben, R. (2020). The contribution of asymptomatic SARS-CoV-2 infections to transmission on the Diamond Princess cruise ship. *eLife*.

Liu, F., Li, X., and Zhu, G. (2020). Using the contact network model and Metropolis-Hastings sampling to reconstruct the COVID-19 spread on the "Diamond Princess". *Science Bulletin*, 65(15):1297–1305.

Mangili, A. and Gendreau, M. A. (2005). Transmission of infectious deceases during commercial air travel. *Lancet*, 365:989–996.

Mizumoto, K. and Chowell, G. (2020). Transmission potential of the novel coronavirus (COVID-19) onboard the diamond Princess Cruises Ship, 2020. *Infectious Disease Modelling*, 5:264–270.

Moon, J. and Ryu, B. H. (2021). Transmission risks of respiratory infectious diseases in various confined spaces: A meta-analysis for future pandemics. *Environmental Research*, 202.

Mouchtouri, V. A., Nichols, G., Rachiotis, G., Kremastinou, J., Arvanitoyannis, I. S., Riemer, T., Jaremin, B., and Hadjichristodoulou, C. (2010). State of the art: public health and passenger ships. *International maritime health*, 61(2):53–98.

Narayan, J., Kana, A., Atasoy, B., and Alonso-Mora, J. (2021). Activity and Agent Based Simulation Model with Path-Size Logit Mixture for Passenger Flow to Evaluate Ship Layout. Unpublished.

Nicolaides, C., Avraam, D., Cueto-Felgueroso, L., González, M. C., and Juanes, R. (2020). Hand-Hygiene Mitigation Strategies Against Global Disease Spreading through the Air Transportation Network. *Risk Analysis*, 40(4):723–740.

Noakes, C. J., Beggs, C. B., Sleigh, P. A., and Kerr, K. G. (2006). Modelling the transmission of airborne infections in enclosed spaces. *Epidemiology and Infection*, 134(5):1082–1091.

Ritos, K., Drikakis, D., and Kokkinakis, I. W. (2023). Virus spreading in cruiser cabin. *Physics of Fluids*, 35(10).

Rocklöv, J., Sjödin, H., and Wilder-Smith, A. (2021). COVID-19 outbreak on the diamond princess cruise ship: Estimating the epidemic potential and effectiveness of public health countermeasures. *Journal of Travel Medicine*, 27(3):1–7.

Rosca, E. C., Heneghan, C., Spencer, E. A., Brassey, J., Plüddemann, A., Onakpoya, I. J., Evans, D., Conly, J. M., and Jefferson, T. (2022). Transmission of SARS-CoV-2 Associated with Cruise Ship Travel: A Systematic Review. *Tropical Medicine and Infectious Disease*, 7(10).

Royal Caribbean Press Center (2024). Radiance of the Seas Fact Sheet.

Ruggiero, V., Guglielmino, E., and Filippo, C. (2008). An interactive approach for the design of an Italian fast medical support ship as consequence of world emergency due to Sars2-Covid 19. *International Journal on Interactive Design and Manufacturing*, 16:409–417.

Sodiq, A., Khan, M. A., Naas, M., and Amhamed, A. (2021). Addressing COVID-19 contagion through the HVAC systems by reviewing indoor airborne nature of infectious microbes: Will an innovative air recirculation concept provide a practical solution?

Srivastava, S., Zhao, X., Manay, A., and Chen, Q. (2021). Effective ventilation and air disinfection system for reducing coronavirus disease 2019 (COVID-19) infection risk in office buildings. *Sustainable Cities and Society*, 75.

Sun, C. and Zhai, Z. (2020). The efficacy of social distance and ventilation effectiveness in preventing COVID-19 transmission. *Sustainable Cities and Society*, 62:102390.

Tan, S., Zhang, Z., Maki, K., Fidkowski, K. J., and Capecelatro, J. (2022). Beyond well-mixed: A simple probabilistic model of airborne disease transmission in indoor spaces. *Indoor Air*, 32(3).

Turvold, W. and Mcmullin, J. (2020). Ships Become Dangerous Places During a Pandemic. *Asia-Pacific Center for Security Studies*.

van Gisbergen, D. (2022). Development of a crowd behavioral model for large-scale simulation on large vessels. Technical report, Delft University of Technology, Delft.

Yazir, D., Şahin, B., Yip, T. L., and Tseng, P. H. (2020). Effects of COVID-19 on maritime industry: a review. *International Maritime Health*, 71(4):253–264.

Zhao, X., Liu, S., Yin, Y., Zhang, T., and Chen, Q. (2022). Airborne transmission of COVID-19 virus in enclosed spaces: An overview of research methods. *Indoor Air*, 32(6):e13056.

Zheng, L., Chen, Q., Xu, J., and Wu, F. (2016). Evaluation of intervention measures for respiratory disease transmission on cruise ships. *Indoor and Built Environment*, 25(8):1267–1278.

Proceedings of 15th International Marine Design Conference (IMDC-2024)
June 2-6, 2024
Amsterdam, the Netherlands

Introduction to the Concept of the German Navy Stability Standard DMS 1030-1

P. Russell[1,*]

ABSTRACT

Following World War II and the founding of the German Armed Forces, lessons learned from ship accidents as well as scientific advancements called for a new stability regulation specific to the Federal German Navy, the BV 103. While certain minor modifications have been made through the years since then, the basic concept behind this standard still remains effective up to the succeeding regulation DMS 1030-1 of this day. With the most recent additions it has been proven to keep up with and even outclass the safety levels of current civilian stability regulations. The key to this success is early adaptation of available scientific techniques outside the usual constraints of large regulatory bodies.

KEY WORDS

Stability; Standard; German Navy; Regulation; Code

INTRODUCTION

Just by their designed purpose, naval vessels are subject to use cases and loads different from regular civilian merchant craft. At the same time, they still have to work on a day-to-day basis during peacetime operations. As sufficient stability and floatability form the necessary baseline of any functioning ship, having an appropriate regulation for these parameters has a major impact on the viability of a ship design and needs to accommodate both scenarios.

Therefore, the German Armed Forces (Bundeswehr) decided early after its (re)founding past World War II, that a specific stability standard was needed for the new Federal German Navy (Bundesmarine), especially since existing regulations at that time considered stability issues very simplified, if at all. This code was originally called BV (Bauvorschrift, meaning construction regulation) 103. It was later renumbered to BV 1033-1, according to the numerical identifier for “intact stability” as per the structured breakdown in the official German list of naval components and assemblies, “-1” denoting the applicability for surface vessels.

In 2001, it was again renumbered to BV 1030-1, referring to the numerical identifier for “stability” as a whole, as it also integrated inclining test requirements now. Following a recent new approach in requirement engineering of the 2020s within the German procurement organization BAAINBw (Federal Office of Bundeswehr Equipment, Information Technology and In-Service Support), the code was renamed DMS (Deutscher Marinestandard, meaning German Navy Standard) 1030-1.

This paper explains the rationale behind the creation of the original standard in the 1960s, its philosophy of stability criteria and the principal steps in its further development into the most recent edition DMS 1030-1 of 2023. A short comparison of safety levels with respect to current civilian standards is also outlined within the paper. It thereby provides the necessary basic understanding, given by the actual regulatory body responsible for said regulation, to further evaluate its impact on current as well as future navy ship designs. These design impacts themselves and the improvements to the standard derived from them are then presented by Krüger (2024).

[1] German Navy Stability Authority (Department 112, Marinearsenal, Wilhelmshaven, Germany) *
PhilippRussell@bundeswehr.org

Submitted: 23 February 2024, Revised: 6 April 2024, Accepted: 1 May 2024, Published: 21 May 2024

Conference paper, DOI: https://doi.org/10.59490/imdc.2024.869 e-ISSN: 3050-4864

HISTORICAL CONTEXT

Early Regulation Efforts

Historically, the very first regulations for seagoing ships established in the 19th century considered reserve buoyancy, i.e. sufficient freeboard, to be of most importance for ship safety. In principle, these early considerations still remain in effect up to today in form of the International Convention on Load Lines (ICLL), with every ship above a certain size being subject to corresponding calculations and markings.

Stability issues were of course also considered, at least academically, over the course of several past centuries. However, most of the time this work focused on the initial stability in form of the metacentric height GM. While it was found around the same time as the first local freeboard regulations entered into force, that ships with the same GM might have different stability issues at higher heeling angles (Reed, 1868), no mandatory rules for stability were established for quite some time after that.

Regulation efforts at those times were of course also impeded by choosing international competition rather than cooperation. Following the TITANIC disaster for example, a very early version of SOLAS was discussed for the first time internationally, but was thwarted by the outbreak of World War I. Both the impact of TITANIC as well as the World Wars also meant, that the safety of damaged ships got a lot more focus than intact stability. And even then, the safety of damaged ships was mostly considered a problem to be solved rather with freeboard and subdivision than with stability requirements – that might have developed differently if TITANIC had capsized before it sunk due to progressive flooding.

Therefore, safe ship design from a stability point of view relied mostly on experience and best practice by naval architects and generally not on mandatory requirements. Even after Rahola (1939) came up with his famous basic intact stability criteria, it was not until late into the 1960s that the Inter-Governmental Maritime Consultative Organization (IMCO, todays International Maritime Organization IMO) finally adopted these officially, albeit first as a recommendation (!) for fishing vessels only, becoming mandatory for all ships as late as with the 2008 International Code on Intact Stability (IS Code). Mandatory damage stability criteria also were not available until 1960 at the earliest, and even then, they were very basic and not applicable for all ship types.

Rationale for a New German Navy Stability Standard

The Federal German Navy was founded on January 2, 1956 after the reestablishment of the German Armed Forces in late 1955. In its very early days, it consisted mostly of ship designs from World War II as well as ships bought from allies. However, the new role of Germany within NATO as well as technological advancements soon required a new quality and quantity of naval ships and corresponding designs.

On the other hand, rebuilding efforts after World War II lead to an increase in commercial shipbuilding activity around the world, now trying to keep to the non-mandatory Rahola criteria as the newest best practice as far as reasonably possible. Having lost the war, Germany was limited to a certain size of ships under its flag, which then were designed and operated with very little regard even to these still very basic criteria to maximize payload. As a result of this, a lot of stability accidents including capsizings of undamaged German-flagged merchant ships happened in the 1940s and 1950s, which were noticed especially in the German scientific community of the time (Wendel, 1958).

The German government as the responsible flag authority of course had to investigate these accidents and therefore cooperated closely with these scientific institutions, in this case the Technical University of Hanover and the University of Hamburg. Implementing the German lessons learned from these investigations on an international level for the merchant navy had to wait due to the number of nations involved, as described above. Germany however took initiative trying to avoid the failure modes leading to said accidents at least for its new military, as regulations for warships were in the own interest of each nation and therefore excluded from IMO regulations up to this day. Furthermore, the special stability needs due to the varying military usage of navy ships are not accounted for by civilian standards, e.g. maneuvering a tight turning circle at full speed for example.

Therefore, it was decided to create a new stability standard for the Federal German Navy together with the mentioned German scientific institutions. Ironically, the first ship these rules were applied to was the sail training vessel GORCH FOCK of 1958, a modified design of the 1930s and in service up to this day. A preliminary version of the standard then became official in 1961, incorporating full-scale stability measurements and experiences from designing and operating the GORCH FOCK, and applied to other vessels as well.

As a baseline, the German researchers looked at the Rahola criteria (Arndt, 1965), as they were best practice at the time. While they appreciated that these took the whole righting lever curve beyond the initial stability GM into account, they reasoned that general safe criteria for the righting lever curve cannot be formulated without considering the individual inclining levers for each ship and load case as well. In principle, they also looked back into the work of Reed (1868), who had already found out about decisive effects of the same inclining lever acting on ships with different righting levers, and argued to combine his approach (with modified and additional inclining levers) with modified criteria of Rahola.

In addition, and as their investigations into the post-war accidents had shown, it was also deemed necessary to formulate requirements for stability in a seaway. Due to the failure modes encountered in these accidents, stability in longitudinal waves had been found especially important to consider.

These two main factors, comparison of individual righting versus inclining levers and consideration of stability in a seaway, form the successful backbone of the German Navy stability standard up to this day and are at least in combination still somewhat unique to other regulations.

REGULATORY FRAMEWORK OF THE DMS 1030-1

Every basic concept explained in this section applies to the original edition of BV 103 of the 1960s as well as its later variants BV 1033-1/1030-1 in several following editions and the newest DMS 1030-1. For ease of readability however, within the text the regulation referred to will always be DMS 1030-1, with differences to earlier editions being outlined as they apply.

Universal Design Assumptions

The starting point for applying DMS 1030-1 is given by the so-called operating area group, see Table 1, which has to be chosen depending on the use cases of the ships by the navy and by the procurement organization. Historically, larger ships like frigates, destroyers and tankers were assigned to the highest operating area group A, medium-sized ships like corvettes and squadron tenders were designed for operating area B, while operating area C was intended for small combatants like minehunters and offshore patrol vessels. These three operating areas were already present in the first version of the standard and have remained unchanged to this day. The operating areas D to F were added later and are used for small craft, which will not be subject of this paper.

Table 1: Operating area groups in DMS 1030-1 (BAAINBw, 2023)

Operating area group	Operating area	Design wind speed in knots	Additional limitations
A	Worldwide, unlimited	90	n/a
B	Worldwide, outside tropical storms	70	n/a
C	Coastal	50	n/a
D, E, F	Shore-based, harbors, inland	20 - 40	restricted wave height and distance to the shore, decreasing from D to F

Nowadays, the military focus of the German Navy has generally shifted from operating mainly in the Baltic and North Sea to being able to perform missions worldwide, while relying more on single ships per mission rather than small squadrons. Thereby range and endurance considerations have made former small ship types bigger and so operating area group A is demanded more and more as a de-facto default for most of the ongoing newbuilds of the German Navy.

Then there are several standard load cases defined in DMS 1030-1, the most important ones are given in Table 2. These have been heavily modified in their total extent, numbering structure and detailed definition since the original BV 103, but the principles shown in Table 2 have always been implemented in the standard. These standard load cases consider the special purpose of navy ships with many details, e.g. with respect to endurance requirements and ammunition depletion during the mission they are designed for. There are some additional standard load cases defined for special mission requirements, but they are seldom design-driving and therefore omitted in this paper.

Each of the seagoing load cases 1, 1A, 2 and 2A however also has a variant with heavy ice accretion of up to 15 cm thickness, depending on the operating area group. As Figure 1 shows, this is not an academic problem, because being able to operate all-year around also in colder regions is mission-critical for a navy faced with potential adversaries in said cold regions. These ice

load cases do not have to fulfil damage stability requirements, but are regularly design-driving for intact stability, as several hundred tons of ice mass at a very high center of gravity have to be considered in the calculations.

Table 2: Standard load cases in DMS 1030-1 (BAAINBw, 2023)

Load case ID	Designation	Explanation
0	Light displacement	Non-seagoing, empty vessel with crew and specified equipment and system fillings
0V	Short move displacement	Same as load case 0, but with additional ballast due to trim restrictions for docking and warping
1	Limit displacement	End of mission, ammunition only partly depleted, other consumables fully depleted
1A	End-of-life limit displacement	Same as load case 1, but with commissioning reserves
2	Full-load displacement	Begin of mission
2A	End-of-life full-load displacement	Design load case, same as load case 2, but with commissioning reserves

Another factor not to be overlooked is the commissioning reserve, which started at 2 to 6 percent of the light ship weight at delivery (depending on the ship type) in older versions of the standard. It has now been increased to 10 percent of this value and at a higher center of gravity, as the lifetime of German Navy ships tends to be extended more and more and lots of weight-intensive retrofits accumulate over this period, so that several older ship classes now operate at their stability limits and can only be modified further with expensive countermeasures, if at all. As a side note, the German Navy also uses a realistic person weight derived from several actual measuring campaigns resulting in 91 kg per soldier, which of course is also used in other areas such as the design of life saving equipment.

Figure 1: Ice accretion (Source: NATO)

Especially for naval auxiliaries carrying large amount of supplies, additional variants and/or intermediate stages of the mentioned load cases need to be added. As per DMS 1030-1 all tank fillings are assumed at a maximum of 95% filling of the net tank volume and the tanks are actually built to physically achieve only this limit. This is done to achieve at least a basic protection against hull ruptures from underwater explosion shock pressures by allowing the incompressible fluids to move. As a side effect, this also leads to a clearly defined maximum free surface moment of the tanks.

In this context, it is important to note that in DMS 1030-1 the effect of free surfaces is always considered as an inclining lever l_f with the actual tank moments, not some simplification using the surface moment of inertia, see Equation 1 with p denoting the individual tank masses and b(φ) denoting the tank cross-curves of stability.

$$l_f = \frac{\sum_i p_i \cdot b_i(\varphi)}{\Delta} \quad [1]$$

This inclining lever is always present in all load and damage cases and used in every stability criterion. In addition, all hydrostatic calculations are to be done with free instead of fixed trim.

As a consequence, this also means that the actual righting lever curve has to be treated and presented separately without free surface correction in the German Navy stability documentation. This documentation follows a unified approach for every ship class designed according to DMS 1030-1 and presents a lot of data at a quick glance on a single page per load or damage case, which is useful for training purposes as well as quick decision making under pressure in combat. For this purpose and some ship classes, a stability computing software with decision making support is developed by the Bundeswehr itself and supplied to the contractors responsible for the automation software, whose hardware (operating station and sensors) it then uses.

The complications mentioned in the paragraphs before had to be argued for quite a lot back in the 1960s – and even today for some projects –, as they meant a calculation effort at the yards hitherto unknown, and later also made a solid business case for the increasing use of computers and corresponding software programs in naval architecture developed in cooperation with the German scientific community.

General Criteria Approach

As a first step for every load or damage case to be investigated according to DMS 1030-1, a lever balance with the applicable righting and inclining levers has to be established. Then, all of the stability criteria follow the same basic concept, as two conditions have to be satisfied. Firstly, the inclining angle has to stay below a certain value, depending on the condition (still water, seaway, damaged, special) and operating area group. Secondly, a reference angle is determined, at which a minimum residual righting lever "GZ_S-Rest" has to be reached, see Figure 2. The reference angle Φ_{ref} for the intact condition is then determined by

$$\phi_{ref} = max\left(2 \cdot \phi_{equi} + 5°; 35°\right) \quad [2]$$

from the inclining angle at the equilibrium Φ_{equi}, while the reference angle for damaged conditions is derived from

$$\phi_{equi} + 15° \leq \phi_{ref} \leq min\left(40°; \phi_{df}\right) \quad [3]$$

with Φ_{df} denoting the angle of downflooding. The limit for the residual righting lever depends on the inclining angle in the equilibrium, but is never lower than 0.1 m in the intact and 0.05 m in the damaged condition.

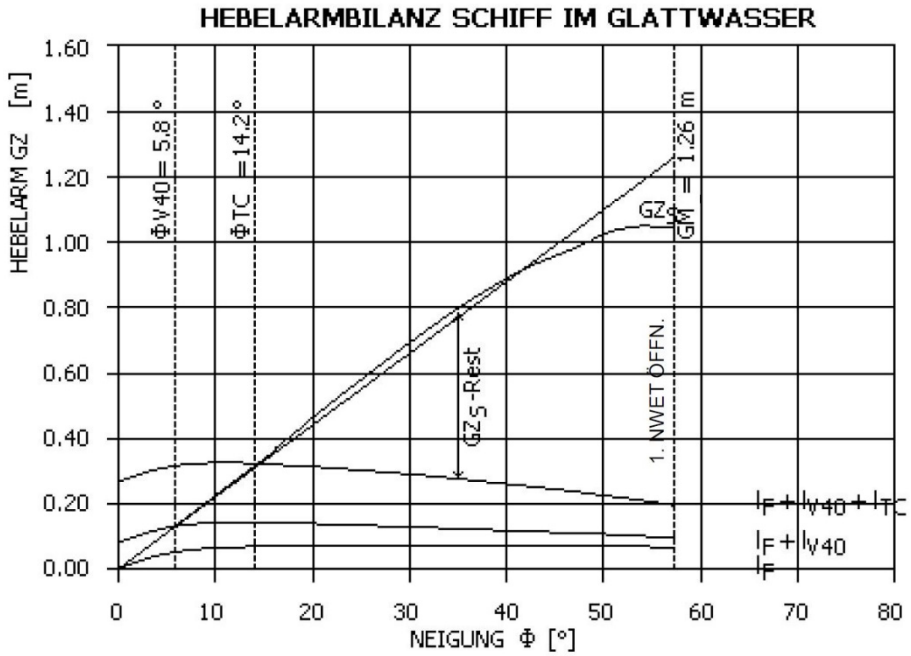

Figure 2: Typical DMS 1030-1 lever balance with inclining levers, reference angle and residual righting lever (BAAINBw, 2023)

This two-part approach allows to account for several requirements. First off, the inclining angle part of the criteria is able to consider limits set by the crew and operations on board and is in itself not primarily driven by safety concerns. The necessary safety is then given by the residual righting lever part of the criteria, which is intelligently coupled with the inclining angle at the equilibrium resulting from the applied inclining levers. Due to the third factor, the use of minimum values for the reference angle, at which the residual righting lever is to be achieved, a minimum safety level is always guaranteed, even for very little inclining levers. Lastly and maybe most importantly, the reference angle concept implicitly also leads to restoring energy reserves in addition to the pure static requirements, as should be immediately clear from Figure 2, if the areas between the righting and inclining lever curves left and right of the equilibrium angle (in this case Φ_{TC}) up to the reference angle (in this case 35°) are compared.

As a boundary condition of course, sufficient freeboard with regard to watertight and weathertight integrity has to be achieved for the stability assessment. Historically, the revisions of BV 103/1033-1/1030-1 up to 2015 required the bulkhead deck to be not submerged in any condition. Since per the standard and in difference to civilian regulations the bulkhead deck had to be completely watertight anyway and as a result of investigations explained further down below, it was decided for the 2015 revision of BV 1030-1 to review this approach and now allow consideration of individual watertight and weathertight openings in the same way as in civilian standards.

Intact Stability in Still Water

The intact stability requirements of DMS 1030-1 for still water conditions focus on the main use cases of navy ships in general as well as the individual ship type. This means, that as a baseline every ship subjected to the regulation has to be able to perform a turning circle at maximum speed and maximum rudder angle in every seagoing standard load case, while at the same time being subjected to a steady cross wind of 40 knots and the actual fluid shifting moments, with sufficient stability. This means that a maximum heeling angle of 15° and a minimum residual righting lever at the reference angle of in this case 35° have to be complied with. These criteria have to be met even with up to 15 cm of ice accretion, depending on the operating area group. Until BV 1030-1 was revised in 2015, this criterion with ice accretion often was design-driving in the intact condition.

Figure 3: High speed turning circle (Source: Bundeswehr / Carsten Vennemann)

As Figure 3 shows, the actual turning circle at full rudder can be quite tight, while the speed loss might be quite significant. Because the actual turning circle parameters can be quite difficult to compute properly (and were nigh impossible to do back in the 1960s), DMS 1030-1 uses an equation with an empirical factor C_D derived from a range of real ship types (Arndt, 1965):

$$l_{TC} = \frac{C_D \cdot v_{max}^2 \cdot (\overline{KG} - 0.5 \cdot T)}{g \cdot L_{DWL}} \cdot cos\,\Phi \qquad [4]$$

As a matter of fact, and despite all shifts in naval design since the 1960s, this factor (default value 0.3) holds up quite well until this day if no other data is available. The wind inclining lever is then derived from Equation 5, the factor 0.25 ensuring proper developing of values at higher angles (Arndt, 1965).

$$l_V = \frac{A_V \cdot (A_{VZ} - 0.5 \cdot T)}{\Delta \cdot g} \cdot p_V \cdot (0.25 + 0.75 \cdot cos^3\Phi) \qquad [5]$$

Explicit values for the wind pressure are prescribed in the standard for every 10 knots increase of wind speed. To determine the windage area A_V, individual drag coefficients for different shapes are required in the standard, e.g. for lattice structures often found on radars in older navy ship designs.

Factors other than turning circle, wind and free surfaces in still water conditions are then considered depending on the ship type. Replenishing ships for example need to be able to withstand an inclining lever of its replenishment-at-sea (RAS) gear,

basically a pulling force (equivalent to the breaking strength of the gear already including safety margins) acting very high up in the supply mast. This is because for technical reasons the RAS gear is fastened much higher on the supplying ship than on the supplied ship, see Figure 4. The criterion for the RAS residual righting lever at the reference angle of 35° remains the same as for other criteria, the permissible inclining angle however is project-specific to the type of supply ship, but generally lower than 15°.

Figure 4: RAS maneuver (Source: Bundeswehr)

Tugs are designed using a similar approach to the RAS inclining lever, albeit with slightly modified parameters. In addition, smaller ships (operating area group E especially) are generally subject to unsymmetrical loading criteria in DMS 1030-1 as they are vulnerable to persons shifting positions, but are as mentioned omitted in this paper. Lastly, if the ship type calls for it, project-specific inclining levers can very easily be integrated using the described criteria philosophy.

Intact Stability in a Seaway

In addition to the intact stability requirements in still water, DMS 1030-1 requires every ship in intact condition to be resistant to lateral wind pressure as per Table 1, while at the same time being underway in longitudinal waves. This combination of longitudinal and lateral influences might seem contradictory and too conservative at first, but in conditions with such high wind speeds, wind direction might change much quicker than wave direction (Arndt, 1965).

The design wave length λ in DMS 1030-1 is set to the length between perpendiculars L_{PP} of the ship, while the wave height H is derived from this length as per Equation 6 and both are then combined to a sinusoidal wave. It should be noted that the aft perpendicular (AP) of German Navy ships usually is defined by the intersection of the design waterline with the transom instead of the civilian definition with AP at the rudder post.

$$H = \frac{\lambda}{10 + 0.05 \cdot \lambda} \qquad [6]$$

Using Equation 6, for a typical navy ship of 120 m in length a wave height of 7.5 m is the result, resulting in a wave steepness of 1/16. On the one hand, this is quite a large design wave for this ship size, especially compared to some other standards. On the other hand, this steepness is close to the breaking limit of natural waves, so the approach is also very conservative.

With this wave length, righting and inclining levers for three conditions have to be calculated and evaluated for different criteria: ship on wave crest, ship in wave trough and the average of these two, called “ship in a seaway”. Historically, the investigation of different wave phases between these extrema as well as trochoidal waves had also been used in the standard, but were omitted at some time in favor of the current conservative approach of just these three conditions.

In the condition “ship in a seaway”, the inclining levers due to free surfaces and wind pressure as per Equation 1 and 5 are combined and then subjected to the general criteria approach explained above. The permissible inclining angle is depending on the operating area group and can be up to 25° for operating area group A, leading to a reference angle of up to 55°, which then can be of consequence design-wise for the placement of non-weathertight openings such as large gas turbine air intakes.

In a second requirement, the worst of these three righting lever curves, usually ship on wave crest, has to be subjected to the inclining lever curve from free surfaces. It then still has to achieve positive residual righting lever values all the way from the equilibrium with this inclining lever up to 45° inclining angle, reaching 0.05 m at least once during this range. Both requirements have to be reached including ice accretion also, although the wind speeds for the first requirement may be reduced in this case to as low as 40 knots, depending on the operating area group.

With these two steps, the German Navy stability standard had already considered two out of the five failure modes as per the IMO Second-Generation Intact Stability Criteria, namely "dead ship" and "pure loss of stability", back in the 1960s, i.e. several decades beforehand. This was only possible due to the circumstances mentioned in the historical summary above, which presented Germany with the opportunity to come up with something better than what was (insufficient) best practice at that time. One decisive factor to achieve this was of course also the relatively small and at the same time scientifically open-minded regulatory body responsible for the German Navy stability, being able to make quick decisions, which has continued to be like that until this day. In that sense, in the early 2010s it was decided to enhance the German Navy stability standard, finally resulting in BV 1030-1 of 2015 with an additional criterion for the intact stability in waves (Krüger, 2012).

This was deemed necessary because the design of German Navy ships had changed quite a bit over the 50 years since its founding. These design changes can be attributed to a number of factors. One major step was the increased use of helicopters now requiring large flight decks, a trend which also afflicted supply vessels. Another one was the introduction of more complex gun systems requiring more space on deck as well as below deck at the bow. Both trends are illustrated by Figure 5 with two ship pairs, each of a comparable base type but several decades apart.

Then there was a general trend to increase the endurance of ships, leading to larger tank volumes. With growing endurance – and also increasing demands for more comfort on board, i.e. bigger and less crowded rooms, by crews of younger generations – the ship hulls got bulkier and have much more enclosed decks now. At the same time service speed requirements were lowered from 35+ knots down to 20 to 30 knots due to changes in mission profiles, allowing for this increase in block and midship section coefficient in the first place.

Figure 5: Development of German Navy ship types (Sources: Bundeswehr / Christian Klöcking, Marcel Kröncke and Carsten Vennemann)

As a consequence of more flared frames and increased bulkiness, German Navy ships got generally more susceptible to righting lever alterations in waves and therefore parametric excitation of roll motions, which called for an additional criterion to limit these. The scientific background applied for this is described in more detail by Kluwe (2009), Krüger (2012) and Krüger (2024). Using the conditions ship on wave crest GZ_C and ship in wave trough GZ_T in DMS 1030-1, the criterion is then formulated using Equation 7 with the areas defined in Figure 6.

$$A_2 \overset{!}{\geq} 2 \cdot A_1 \qquad [7]$$

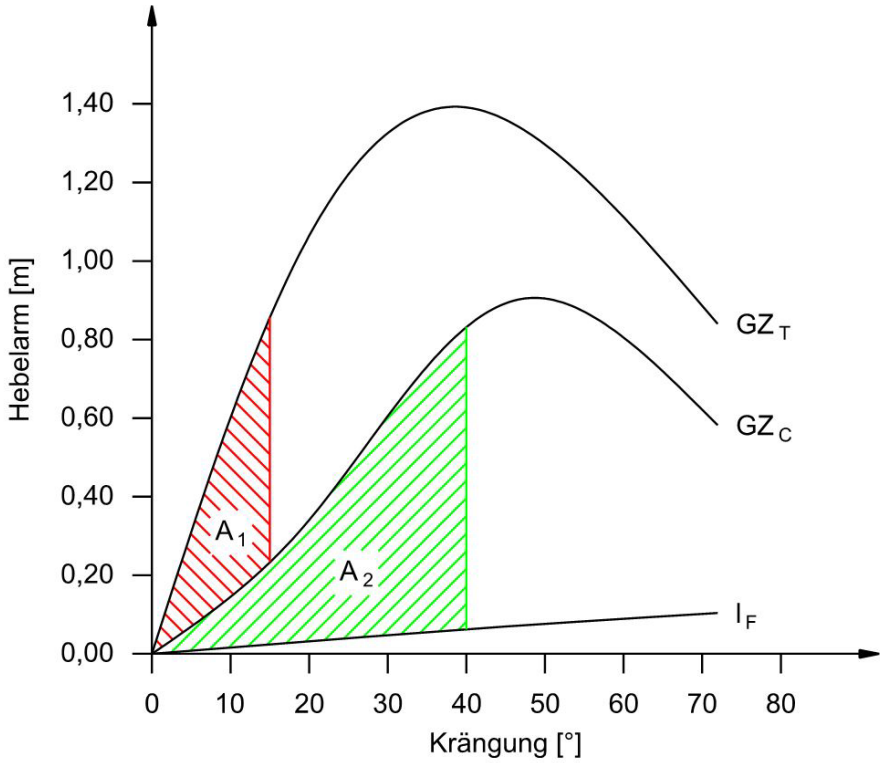

Figure 6: DMS 1030-1 area criterion (BAAINBw, 2023)

With this new area criterion, DMS 1030-1 now also directly addresses a third failure mode of the IMO Second-Generation Intact Stability Criteria, namely "parametric rolling". Ever since its introduction in 2015, it has now become the design-driving intact stability criterion of DMS 1030-1 in several projects, especially if ice accretion is involved. This then leads designers to rethink their approaches and reintroduce some features from older proven hull forms, such as V-hulls, larger bilge radii and lines with less flare of frames and buttocks (especially in the bow area), because the righting lever alterations in waves are primarily governed by the change of waterplane area in vertical direction.

Damage Stability

The damage stability in DMS 1030-1 follows a deterministic approach with a given damage length as per Equation 8. Keeping an absolute upper limit for the damage length is considered to be a sufficient compromise as a result of investigations into the safety levels described further down below, even for larger ship types.

$$L_l = min(0.18 \cdot L_{DWL} - 3.6\,m; 18\,m) \qquad [8]$$

This damage length is then to be applied with half the ships breadth penetration depth (up to centerline and excluding centerline bulkheads, if applicable) and unlimited penetration height at any given point (!) in longitudinal direction. That means there is not a specific number of compartments to be damaged like in some civilian standards, which could be directly derived from the damage length, but instead the actual damage resulting from the described cuboid is to be assumed, so compartment-internal additional subdivisions are also of importance. If a lesser extent of this baseline damage at one position leads to a more severe condition, this condition is to be evaluated with regard to the damage stability criteria and shown in the stability documentation. The same principle holds true for several cases of intermediate flooding stages differentiated in DMS 1030-1.

With respect to watertight integrity, there has to be one defined bulkhead deck as a horizontal watertight barrier to prevent up- and downflooding, which means any staircase or elevator casing penetrating the bulkhead deck also has to be watertight at minimum at that deck, but not necessarily below the bulkhead deck. Doors and hatches below the bulkhead deck are not permitted since the 2022 revision of DMS 1030-1 and are assumed open if above the bulkhead deck (no V-lines). This has two main reasons derived from experience: firstly, in general operation of the ship and especially in combat any existing opening will generate traffic of persons and often remain open, when it should not be. This has been proven time and again to be a contributing factor to many total losses including ships of foreign navies. Secondly, it presents an immense challenge to design a door or hatch, which can uphold its integrity even after a shock incident from weapon damage. For these reasons, if a door or

hatch is to be fitted below the bulkhead deck as an exemption, it will be considered open in the damage stability evaluations. From experience, ammunition and cold storage rooms provide a sufficient pressure resistance to be assumed watertight in DMS 1030-1.

The DMS 1030-1 damage stability criteria follow the same general concept as the intact stability criteria, i.e. a lever balance has to be established first, in this case with the inclining levers from free surfaces and 40 knots of wind pressure. It should be noted in this context, that ice accretion as well as waves are not considered in the damaged condition in DMS 1030-1. Damage stability however is required for every seagoing load case of the intact condition, with an exchange of fluids in damaged tanks to sea water, if applicable.

The maximum permissible inclining angle at the equilibrium from this lever balance has to be less or equal than 25°. Cross-flooding devices to achieve this angle are generally not permitted in the standard. The latter also implicitly drives designers to choose a more symmetrical layout, which has additional value beyond stability in combat situations, where situational awareness and short routes are beneficial. The reference angle then has to be reached as per Equation 2, with at least 0.05 m of residual righting lever in the range between the equilibrium and 40° inclining angle and at the same time a minimum righting lever range of at least 15° before reaching 40° heeling angle or the downflooding angle. Again, the applied reference angle concept also means that there is an inherent level of safety against residual energy from rolling motion even in the damaged condition.

With regard to freeboard requirements, until 2015 any submergence of the bulkhead deck described above was the permissible limit within the standard. Starting with the 2015 revision of BV 1030-1, it was then decided to switch freeboard requirements from considering a whole deck, which had to be completely watertight anyway, to considering individual openings. This had been deemed acceptable from a safety point of view (see also below), allowed designers more freedom of arrangement for new ships, while at the same time making no discernible difference in evaluating already existing designs. Since then, the minimum freeboard in the damaged condition required in DMS 1030-1 is 0.5 m for weathertight openings. With the latest revision of DMS 1030-1, it was decided to enhance this approach with a requirement of half the height of the design wave as per Equation 6 for non-weathertight openings to consider the effect of a seaway also in the damaged condition.

SAFETY LEVELS

Comparison with 2008 IS Code

The safety level of intact ships in a seaway can be quantified using the so-called Insufficient Stability Event Index (ISEI), developed by the Institute of Ship Design and Ship Safety at Hamburg University of Technology (Kluwe, 2009). A summarized introduction into the concept is given by Krüger (2022). In very short terms, an ISEI value indicates the probability of a specific failure criterion of a ship – generally a special criterion for capsizing is used, but the concept allows for other criteria also – to be reached during a calculation of a significant timeframe in a seaway with a significant statistical parameter distribution.

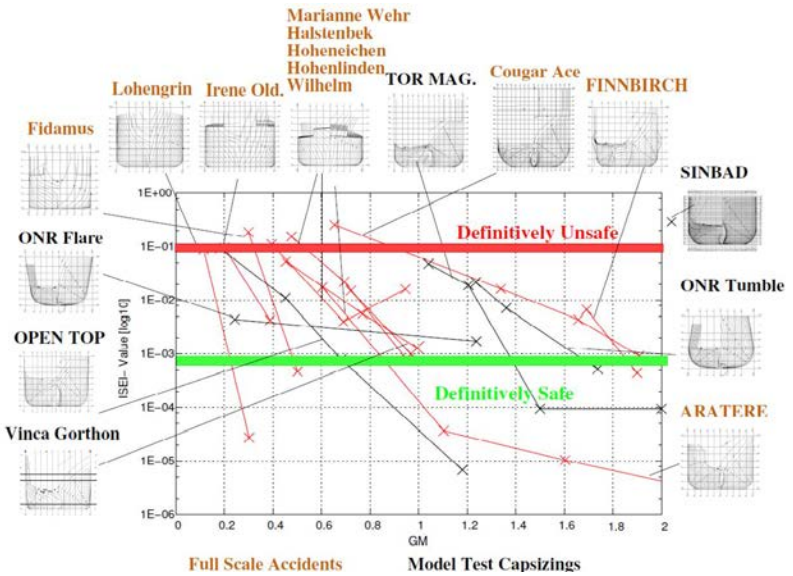

Figure 7: Safety levels of different civilian ships in a seaway (Krüger, 2022)

Figure 7 shows the ISEI values derived from several full-scale accidents and later model tests for ships designed according to the six Rahola criteria and the later added weather criterion, i.e. the minimum set of criteria as per the 2008 IS Code applied to any civilian ship nowadays. In a first step, the ISEI values for the actual stability – represented by the value of GM – in each accident condition are computed, resulting in the upper threshold of definitely unsafe values at 0.1 and above. In a second step, the same calculations are done after raising the stability in several steps until all of the mentioned IS Code criteria are only just fulfilled. Using the assumption that the ship loss rate resulting from applying these criteria is deemed socially acceptable, the lower threshold of definitely safe values of 0.001 and below is then determined.

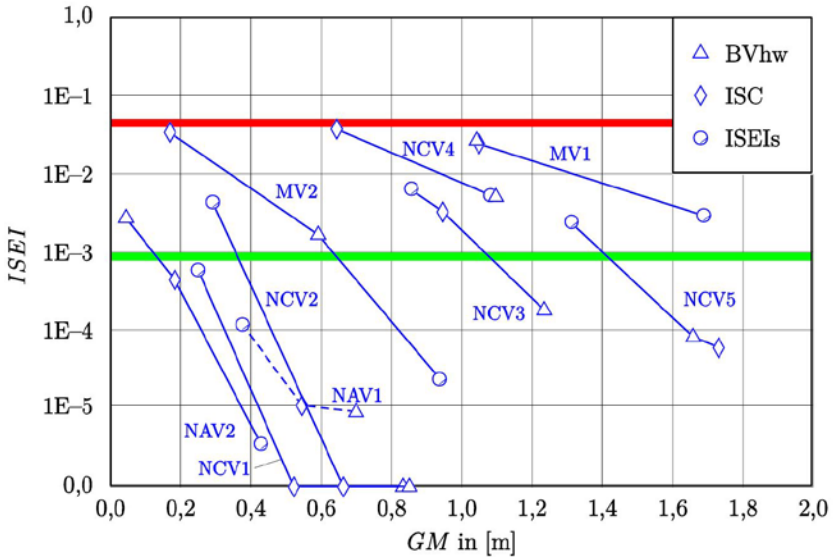

Figure 8: Safety levels of ships designed to different standards in a seaway (Krüger, Hatecke, Rinke & Tammen, 2014)

The same concept is applied by Krüger et al (2014) to determine the safety level of BV 1030-1 for a select number of ship types of combat vessels (NCV) and auxiliary vessels (NAV) designed to said standard and compared to two merchant vessels (MV), see Figure 8. These ship types are then given stability values to only just fulfil the minimum stability criteria for the IS Code (diamonds in Figure 8) and BV 1030-1 (triangles in Figure 8) respectively.

As a result, ISEI values for ships designed and operated according to BV 1030-1 are found to be two to three order of magnitudes smaller than those designed and operated according to the 2008 IS Code. This implicitly means that the probability of capsizing in heavy weather is lower by said magnitude, which is underlined by the fact that there has never been a single loss of any German Navy ship over 60 years since the introduction of the first BV 103 and with a sizeable fleet especially during the Cold War. Even if these naval ships were to be operated with the lower stability values according to IS Code, they still would be a lot safer than any merchant vessel thanks to their design according to BV 1030-1.

However, two particular naval ship types are identified, which get a lot closer to the investigated merchant vessels with regard to safety levels than the rest of the group, even if given BV 1030-1 stability values. Looking into the source of this, the reasons described above (see around Figure 5) are found and counteracted by the introduction of the new area criterion. This means that the picture painted by Figure 8 will look even with the most recent edition of DMS 1030-1 applied for future ships. In return of course this also means, that the 2008 IS Code without the application of Second-Generation Intact Stability Criteria presents a severe safety deficit for civilian vessels, which is only somewhat healed by stability values required for damage stability – which, mind you, generally only apply for ships over 80 m in length.

Comparison with SOLAS 2009

As described above, DMS/BV 1030-1 follows a deterministic approach to damage stability, opposed to SOLAS, which since 2009 uses a probabilistic damage stability approach for all types of ships. The damage safety index in SOLAS is determined by using the probability of a specific damage condition derived from accident statistics, then evaluating the survivability of this damage condition by fulfilment of SOLAS stability criteria to a value between 0 and 1, multiplying probability and survivability of this damage condition and then repeating the process for additional damages by adding up damage safety index until a minimum index at several draughts is reached. As the potential damage suffered by navy ships is not just inflicted by collision

or grounding, which are statistical events, but by weapon impact, which is impossible to predict and can be aimed at any part of the ship, the mentioned deterministic approach is the only viable solution for evaluating the damage stability of navy ships.

However, to compare the two standards, a theoretical design of a civilian RoPax vessel only just fulfilling the minimum damage stability requirements of SOLAS 2009 B1 is used by Krüger (2012). The damage safety index resulting from this then forms the baseline for the comparison, see the uppermost line in Figure 9. Using a comparable set of damages and damage probability, but now evaluating the survivability of each damage case with the damage stability criteria from DMS/BV 1030-1 described above, results in less than half the damage index than as per SOLAS 2009 B1 for the same ship, see the lowermost line in Figure 9. In other words, even the minimum damage stability criteria of DMS/BV 1030-1 result in more than double the safety compared to SOLAS 2009 B1.

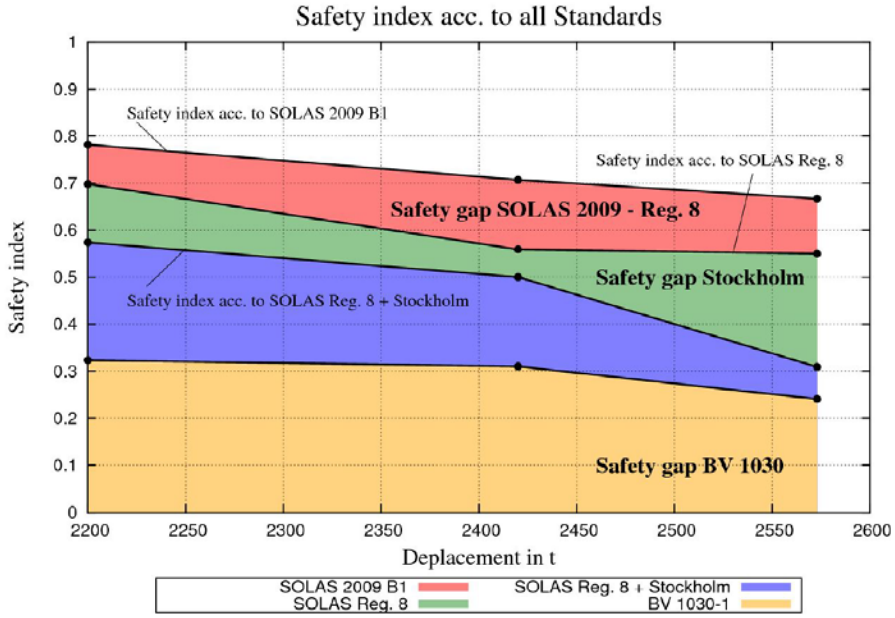

Figure 9: Damage safety index of the same ship design assessed by different standards (Krüger, 2012)

In the same investigation, the survivability of a recent German Navy ship beyond its design damage cases is investigated. As a result, it is found that the default scope of deterministic damage cases to be investigated as per DMS/BV 1030-1 covers about 82% of all theoretically possible probabilistic damage cases. The same ship however was able to survive about 95% of all theoretical damage cases beyond its design, even with DMS/BV 1030-1 stability criteria applied, which implies a lot of implicit additional safety generated by the deterministic approach used in DMS/BV 1030-1.

CONCLUSIONS

This paper has presented the basic principles of the German Navy Standard DMS 1030-1 as well as the rationale behind individual criteria decisions and their development over the years. Furthermore, the main reasons for its technical success were discussed upon in detail and related to the historical background during the creation of the standard. The safety levels achieved by the standard have been quantitively shown and compared to civilian regulations. As a result, it should be clear that proper stability regulations will drive a ship design to work well in everyday civilian usage first before it then will be a good warship in combat usage as well. This is achieved by naval administrations being able and willing to react quickly to scientific developments in working closely with competent academic communities. Finally, it is found that the standard remains valid and up to date until this day and with relatively minor improvements – compared to civilian standards over the same timeframe – will continue to provide successful designs for the foreseeable future.

REFERENCES

Arndt, B. (1965). Ausarbeitung einer Stabilitätsvorschrift für die Bundesmarine. Jahrbuch der STG, Band 59. Berlin / Göttingen / Heidelberg, Germany.

BAAINBw (2023). Deutscher Marinestandard (DMS) für Wasserfahrzeuge der Bundeswehr, Teil 1030-1: Stabilität von Überwasserschiffen. Regulation, issued November 6th, 2023 (not published), Federal Office of Bundeswehr Equipment, Information Technology and In-Service Support. Koblenz, Germany.

Kluwe, F. (2009). Development of a Minimum Stability Criterion to Prevent Large Amplitude Roll Motions in following Seas. PhD thesis, Institute of Ship Design and Ship Safety at Hamburg University of Technology. Hamburg, Germany.

Krüger S. (2012). Bewertung des Sicherheitsniveaus der BV 1030. Final study report (not published), Federal Office of Bundeswehr Equipment, Information Technology and In-Service Support. Koblenz, Germany.

Krüger, S., Hatecke, H., Rinke, A. & Tammen, K. (2014). Analysis of the German Navy Stability Standard BV 1030 with Respect to Operability in Heavy Weather. Proceedings, OMAE 2014. San Francisco, California, USA.

Krüger, S. (2022). The insufficient stability event index (ISEI) - an easy overview. Schriftenreihe Schiffbau, Institute of Ship Design and Ship Safety at Hamburg University of Technology. Hamburg, Germany.

Krüger., S. (2024). The Impact of the new DMS-1030 Stability Standard on the Future Design of Navy Ships. Proceedings, IMDC 2024. Amsterdam, The Netherlands.

Rahola, J. (1939): The Judging of the Stability of Ships and the Determination of the Minimum Amount of Stability. PhD thesis. Helsinki, Finland.

Reed, E.J. (1868): On the Stability of Monitors under Canvas. Transactions of the Royal Institution of Naval Architects, Volume 9. London, UK.

Wendel, K. (1958): Sicherheit gegen Kentern. VDI-Zeitschrift 100. Düsseldorf, Germany.

Proceedings of 15th International Marine Design Conference (IMDC-2024)
June 2-6, 2024
Amsterdam, the Netherlands

The Impact of the new DMS-1030 Stability Standard on the Future Design of Navy Ships

Stefan Krüger[1,*]

ABSTRACT

In 2022, the German BAAINBw launched a revised issue of their 1030-1 stability regulations for Navy surface vessels. The improvements of the revised code concerned (inter alia) a new stability criterion for minimizing the effect of parametric rolling combined with pure loss of stability on the wave crest and revised damage stability calculation assumptions, which mainly focus on the submergence of openings and a special treatment of watertight doors. The improvements of the code were found to be necessary to keep track of recent developments in IMO for commercial ships and to update the safety level represented by the code. At the same time, the revised code gives more freedom to the ship designer, a fact which may allow novel and more cost effective concepts of Navy Ships in the near future, provided, the evaluation of the stability according to the code takes place immediately during the very early design phase of the ship. The present paper gives insight into the important updates of the code and it demonstrates at the same time how the design of Navy Ships may benefit from the revised code, if it is applied throughout the very first design phase of the ship. The paper will further present an improved design regime for the early design stage.

KEY WORDS

Navy Ship Design, Navy Ship Stability

INTRODUCTION

Due to their mission profile, Navy Ships encounter more and different threats compared to commercial vessels. As a consequence, Navy Ships require higher safety levels with respect to the survivability in intact and damaged conditions. Consequently, commercial safety standards such as the International Code on Intact Stability or the SOLAS, which define minimum requirements only, cannot be applied to Navy Vessels, as one of their core abilities is to survive extreme situations. This holds for the intact stability in adverse weather conditions as well as for the survivability after a damage. For this reason, Navy Ships have to comply with other, more demanding stability standards compared to commercial ships. Navy Ships may be in principle subdivided into surface ships and submarines. The present paper addresses solely Surface Vessels, which may be further subdivided into Navy Combatants and Auxiliary Ships. In 2022, the German Federal Office of Bundeswehr Equipment, Information Technology and in Service Support (Bundesamt für Ausrüstung, Informationstechnik und Nutzung der Bundeswehr), abbreviated BAAINBw) published a revised version of their stability standard for surface ships of the German Navy. The revision of this well proven and established stability standard, which was developed by Wendel in the mid-sixties of the last century (Wendel 1964) seemed to be necessary for the following reasons:

- New hull forms of Navy Ships lead to a higher risk of experiencing large roll angles due to parametric rolling. This was not explicitly addressed by the standard.
- Recent developments in damage stability assessment of the SOLAS 2009 and the SOLAS 2020 showed that the consideration of intermediate flooding stages and the treatment of openings should be reconsidered.

[1] Institute of Ship Design and Ship Safety, Hamburg University of Technology, Hamburg, Germany * Corresponding Author: krueger@tuhh.de

Submitted: 29 January 2024, Revised: 8 April 2024, Accepted: 1 May 2024, Published: 26 May 2024

Conference paper, DOI: https://doi.org/10.59490/imdc.2024.908 e-ISSN: 3050-4864

- In some aspects, the existing stability standard was found to be unnecessarily prescriptive, and it was suspected that this might prevent novel designs of Navy Surface Ships.

When reviewing recent developments in the stability assessment of commercial ships, the following problems were identified which should be definitively avoided when assessing the stability of Navy Vessels:

- Due to the more demanding damage stability requirements in the SOLAS, the limiting GM is strongly dominated by damage stability, but the ships shall operate most of the time in intact conditions, and they should be designed for intact conditions.

- Some types of ship (e.g. large Container vessels) operate with GM- Values which are far away from those the ship was designed for.

- The commercial standard allows to make use of additional operational guidance if problems in the fulfilment of the stability are identified (2nd Generation Intact Stability Criteria). This is certainly not an adequate option for Navy Ships.

Overall, there were several reasons identified which made a revision of the Navy Stability Code necessary. The following sections explain why certain amendments of the code became necessary and how the identified problems were solved. These amendments are compared with existing stability standards and it is shown where elements of these standards (e.g. SOLAS, IS-Code) could be used and where alternatives needed to be developed. The impact of these amendments on the future design of Navy Surface Ships is demonstrated afterwards.

INTACT STABILITY

A brief Introduction into the Intact Stability Part of the BV 1030-1

A detailed description of the BV 1030-1 (now DMS 1030-1) is given by Russel (2024). Explanations about the development of the original stability code are given by Wendel (1964). The governing principle of the BV1030-1 is the determination of ship specific individual heeling levers, which are then checked against the righting levers of the ship as lever balances. The code does not make explicit differences between Auxiliaries and Combatants, but it specifies service categories where a ship is intended to operate. Depending on the defined service area, loading conditions, external forces and groups of stability criteria are then defined. If any German Navy Ship shall operate in a region which is characterized by a higher service category than the one the ship was originally designed for, a decision of the German Parliament (Deutscher Bundestag) is required to permit the operation of the ship. For ships in unrestricted service, which are solely treated in this paper, these lever balances have to be determined for the still water condition as well as for the ship in waves, where the two situations “ship on wave crest” and “ship in wave trough” are to be analysed. Several loading conditions including reserve deadweight for future service have to be analysed during the stability assessment, and, before each voyage, the individual loading condition has to be individually checked against the criteria by the crew by making use of the stability booklet and, if available, the loading computer. It should be noted in this context that typically, the stability booklet and the loading computer are not provided by the industry, but by the German Navy Arsenal. As the BV 1030-1 deals with explicit loading conditions, no $GM_{required}$ (or KG_{max}) curves are in use. For the still water condition (see Fig. 1, top right), the following heeling levers have to be determined:

- Shifting of fluids by heeling levers for each tank (the maximum permissible filling level for any tank is 95%)

- Beam Wind of 40 knots

- Turning circle at full speed (eventually, the permissible speed is limited during the operation of the ship)

- Icing

- Unsymmetrical loading

- RAS supply, if applicable

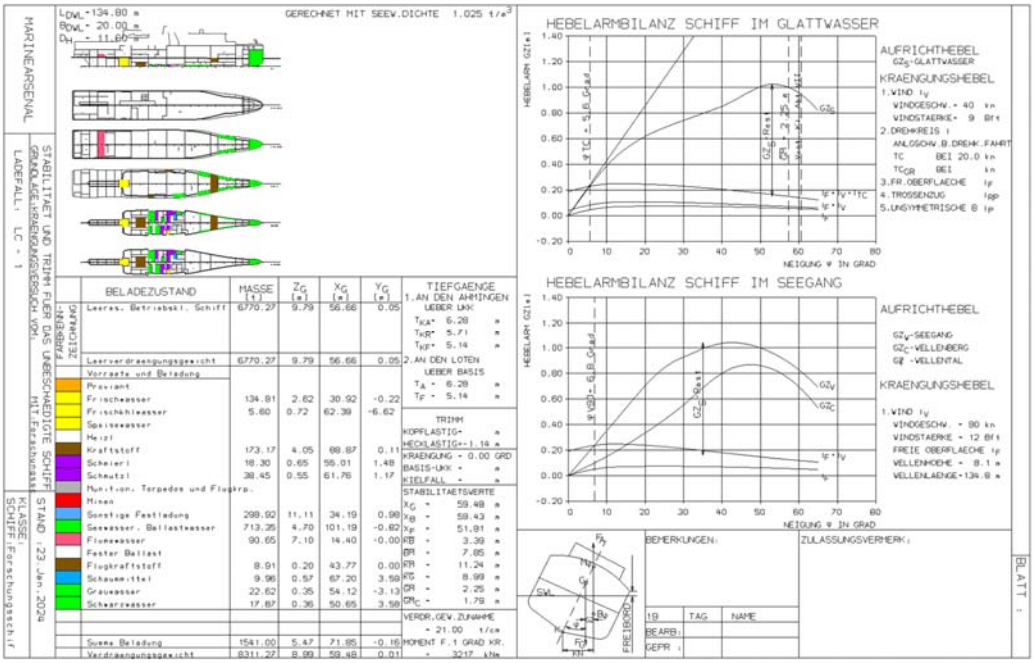

Figure 1: Lever arm balance still water (top right) and in waves with the crest curve (GZ_C) and the crest-trough average (GZ_V)

For Navy Auxiliary Ships, additional loading conditions may be defined and must be investigated. The sum of these heeling levers is compared with the righting lever of the ship, see Russel 2024. Additionally, a lever balance of the ship in waves has to be determined, where the wave length λ equals ship length, and the related wave height H has to be taken from the formula $H=\lambda/(10+0.05\lambda)$ (Wendel 1964, Russell 2024). For this design wave, the two situations "ship on crest" and "ship in trough" have to be computed, see Fig. 1, bottom right. For the "ship on the crest" condition (which is typically the weaker of the two curves), the maximum stability must equal at least 0.05m in minimum to prevent a pure loss of stability failure. The reference curve in waves for the lever balance is computed as the average of the crest and the trough curve, and the following heeling levers have to be computed (for ships in unrestricted service):

- Beam wind of 90 knots
- The shifting of fluids in tanks

For this lever balance, the same limiting criteria as for the still water condition apply, see Fig. 1 bottom right. The BV 1030-1 stability standard includes a stability criterion against the "pure loss of stability" failure mode, but righting lever alterations in waves which are responsible for parametric rolling (or a combination of parametric rolling and pure loss of stability on the wave crest) are only indirectly addressed when taking into account the crest-trough average for the lever balance.

Improvements the BV 1030-1 Intact Stability Part

Parametric roll and pure loss of stability. It is a general understanding in the commercial ship stability community that the existing stability regulations -represented by the International Code on Intact Stability- have not solved all relevant problems concerning ship safety (IMO 2008, Preamble Para 4, P. 9). As a consequence of this insight, the IMO has initiated the development of the so called 2nd Generation Intact Stability Criteria (SGIT), which are presently part of the recommended Intact Stability criteria of the IMO. In parallel, investigations by Krüger et al (Krüger 2014) have shown that the safety level against large roll angles represented by the BV 1030-1 is indeed substantially larger compared to the safety level of the IS code (due to the fact that the BV 1030-1 already includes pure loss of stability on the wave crest), but there remains a nonnegligible probability of encountering large rolling angles for hull forms which have substantial righting lever alterations in waves, even for ships designed according to the BV 1030-1. Therefore, it was concluded to integrate a criterion into the code which takes into account the identified problem. When analysing the SGIT, namely the criteria suggested for parametric rolling, it was

found that too many physical problems existed which prohibited to make further use of any of these criteria in the context of the BV 1030-1. The problems identified were the following (e.g. Krüger 2013, Gualeni 2015):

- The SGIT- Criteria do not sufficiently take into account that the real GZ-curve may deviate substantially from its linearization by GMφ. As a consequence, it is neglected that the natural roll period of the ship varies with the amplitude of the roll motion.

- The natural roll period of the ship is calculated from the still water stability, but it should be calculated from the stability in waves. And it does additionally vary in waves, as the stability permanently changes.

- The criteria do not take into account any combination of parametric rolling and pure loss of stability on the wave crest, and they additionally fail if the initial stability on the wave crest becomes negative. But that is exactly the failure mode which is to be addressed by the BV 1030-1 (in following seas).

- The computation of the righting lever curve in waves in the SGIT-regulations is incorrect, as it shall be computed for several longitudinal positions of the wave crest with free trimming at the same time. This is certainly not correct, as the real trim of a ship in longitudinal wave comes from the pitching motion. And this has a strong effect on the phase shift between heeling and pitching motion and therefore on the stability alterations.

Besides the above mentioned deficiencies of the SGIT, the BV 1030-1 already includes a stability regime in waves, and the newly developed criterion should be developed as an addendum to the existing code.

The newly implemented addendum is explained in the following, and it is now a mandatory part of the new DMS 1030-1 which has replaced the BV 1030-1.

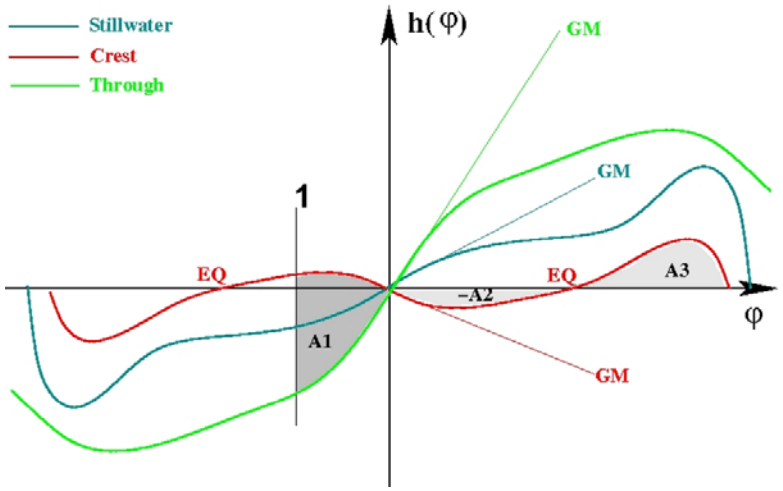

Figure 2: Stability in waves (following seas)

As the BV 1030-1 aims on minimum stability requirements, the critical situation for surface ships is certainly their operation following seas. This is due to the following reasons:

- The most critical resonances (two or one pitch cycle(s) per roll cycle) occur only in following seas if the stability is low or moderate.

- In following seas, the ship stays sufficiently long on the wave crest which makes a large roll angle more probable.

- Due to the low relative velocity between ship and waves, roll damping (e.g. from bilge keels) is less effective.

For these reasons, the addendum shall focus on the stability behavior in following seas. Fig. 2 shows a typical stability situation in following seas, and it shows the righting lever curves for crest (red), trough (green) condition as well as the still water

condition (blue). The latter is not relevant for the problem addressed, nor is the linear representation of this curve. In Fig. 2, the initial stability on the wave crest has become negative, which means that the upright equilibrium is not stable anymore. If we assume for a moment that the wave crest situation would remain forever, then the ship will start to heel towards the stable equilibrium on the wave crest (EQ). If the ship reaches this equilibrium, she has taken up an energy level which is equivalent to the area under crest curve A2 (if dissipation by roll damping is neglected). As the remaining energy under the crest curve (A3) is larger than |A2|, the ship will not heel over the angle of vanishing stability and she will (after some time, damping included) return to the stable equilibrium EQ and she will then remain there. A long as A3 is larger than |A2|, the ship will not capsize due to pure loss of stability alone. The relation of A2 and A3 is mainly dominated by the wave height (for a given stability).

If one takes into account now that the ship is permanently oscillating between the wave crest and the wave trough situation, it is well known that this oscillation can build up a large and sudden roll motion (parametric roll). If the ship experiences such a roll motion, she sees the maximum roll angle when she is in the wave trough situation (green) and she is always close to the upright position when she is on the wave crest. In Fig. 2 we assume that when the ship is in the wave trough condition, she may have rolled to a certain roll angle, denoted by "1" in Fig. 2. If the ship is accelerated from the heeled position (1) to the upright position again, the wave passes by until the ship stays on the wave crest again in the upright position. During this heeling motion toward the upright position, the sea state feeds energy into the ship which can be expressed as the difference of the areas under the crest and the trough curve. In Fig. 2, this area difference is denoted by "A1". When the ship reaches the upright position on the wave crest, she has taken up an energy equivalent to A1. When the ship now heels on the wave crest towards the crest equilibrium EQ, her energy level equals A1 + |A2| when she reaches this equilibrium. As the sum A1 + |A2| is certainly larger than A3, the ship will be forced over the angle of vanishing stability and she will capsize due to a combination of parametric rolling and pure loss of stability on the wave crest.

This concept was for the first time put forward by Kluwe (Kluwe 2009). He suggested 15 Degrees for the roll angle denoted by "1" in Fig. 2 and 40 Degrees as the maximum permissible roll angle. It is of further interest to underline that the Area A1 solely depends on the individual hull form of the ship and not on the stability (as this area is basically a difference between two righting lever curves, the ZCGsinφ and YCGcosφ- terms cancel out themselves), whereas the areas A2 and A3 depend on both the hull form and the stability. This criterion is therefore a strong motivation for the ship designer to minimize the righting lever alterations in following seas during hull form design. If he is not able to do so, the designer has to accept that the ship requires larger values of stability (on the crest) as a consequence.

In the context of the BV 1030-1 this criterion can easily be implemented if it is applied for the design wave which is already included in the BV. Rinke (Krüger 2014) has applied this criterion to several existing Navy Ships of the German Navy and he concluded that the Area A3 should have twice the value of the sum of the areas A1 and |A2|. Further, it was found that the GM on the wave crest must never become negative, which does then result in a crest righting lever which must be positive from zero to 40 degrees. (A3 then disappears, and A3 should amount 2A1). Concluded, the revised requirements of the DMS 1030-1 are the following (Russell, 2024):

- For the given design wave of λ equalling ship length, and the related wave height $H=\lambda/(10+0.05\lambda)$, the area under the wave crest curve up to 40 Degrees must amount to two times the area difference between trough and crest up to 15 Degrees (where the wave crest righting lever curve must be corrected for free surface effects).

- The stability on the wave crest (including free surface corrections) must meet a minimum value of 0.05m, which must occur before 40 Degrees. From the equilibrium up to 40 degrees, the righting lever on the wave crest must be positive.

It is further recommended to present the stability results in form of $GM_{Required}$ -Curves. This is to prevent the situation that only one single criterion dominates the whole ship design or that damage stability deviates significantly from intact stability.

Openings. Originally, the treatment of openings was not foreseen in the BV 1030-1 as the hull (and the superstructure) needed to be watertight up to 60 degrees. During all stability calculations the only criterion was that the side of the bulkhead deck must never be submerged in any equilibrium (intact or damaged). This requirement was found to be too stringent, impeding to many interesting design alternatives. Consequently, the side of deck criterion was deleted and replaced by exactly the same opening concept as it is part of the SOLAS. Openings are subdivided into weathertight and not weathertight openings. During any equilibrium (the balance between heeling and righting levers), no openings are allowed to be submerged. Not weathertight openings may limit the range of stability if they become submerged. For the stability evaluation in waves, the freeboard of weathertight openings in the equilibrium is calculated as the average value between the crest and the trough condition. The means that a weathertight opening may be submerged either in crest or trough condition, provided, that the sum of both freeboards is clearly positive.

Ballast water. The DMS 1030-1 requires that no additional ballast water shall be taken in any loading condition for stability reasons. This means that the designer of a Navy Ship must be aware of the operational profile of the ship.

$GM_{Required}$-Curves. The DMS 1030-1 requires that curves of $GM_{Required}$ are to be computed for the intact and the damaged ship during the planning phase of any Navy Ship. These curves shall be computed without taking into account fluid shifting moments. It must be demonstrated that the limiting GM- values for the damaged condition do not differ significantly from those obtained for the intact condition. If there is a significant difference found, the design should be revised, otherwise it must be demonstrated by appropriate calculations that in none of desired operational conditions, excessive accelerations do occur.

DAMAGE STABILITY

A brief Introduction into the Damage Stability Part of the BV 1030-1

Other than the SOLAS, the damage stability part of the BV 1030-1 examines the same predefined loading conditions as the intact part (or part of them). This includes not only the exchange of fluids in case a filled tank is damaged, but also the correction for the free surface effects of all partly filled tanks which are not damaged. One should note that the BV does not permit filling levels of more than 95% of a tank, which results in the fact that especially Auxiliary Navy Vessels may have large initial free surface corrections. The BV 1030-1 damage stability standard is a deterministic standard with a maximum damage length L_l of

$$L_l = 0.18\ L_{DWL} - 3.6\text{m, but not more than 18m.} \qquad [3]$$

The maximum penetration depth is assumed not to breech the center line of the ship, the damage height is infinite. Like the SOLAS, any combination of lesser extent is to be examined. The BV generally requires to minimize the amount of longitudinal bulkheads, as the flooding should be kept as symmetrical as reasonably possible. During the damage stability evaluation, the following heeling levers have to be computed:

- Beam wind of 40 knots
- The shifting of fluids in tanks

The resulting equilibrium (including the heeling levers) must be less than 25 Degrees, and the residual righting lever must be larger than 0.05m up to 40 degrees or the submergence of a not weathertight opening. The range of positive stability from the equilibrium must be larger or equal to 15 degrees, for details see Russell 2024. Fig. 3 shows an example of the damage stability assessment according to BV 1030-1. It should be noted that the output of the stability assessment (both intact and damage) is quite extensive as this information is not only part of the stability booklet of the ship, but it is also used for crew training purposes in stability matters.

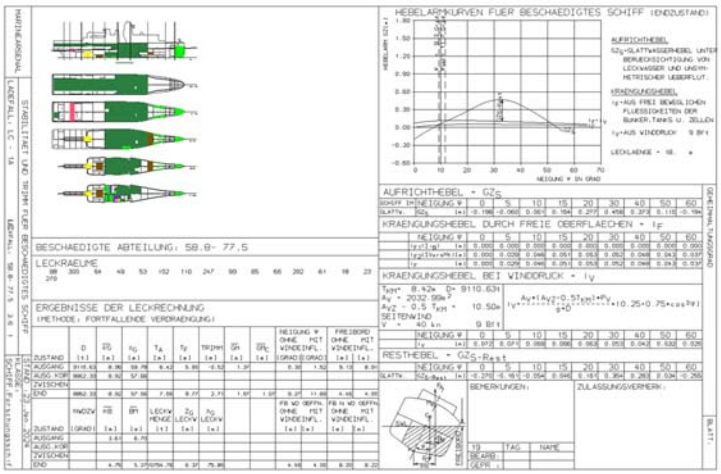

Figure 3: Damage stability assessment according to BV 1030-1

Improvements the BV 1030-1 Damage Stability Part

Intermediate stages of flooding. In the BV 1030-1, the assessment of intermediate stages of flooding was not explicitly mentioned. Nevertheless, the BAAINBw could request that intermediate stages should be analysed, but this was typically not done. The reason is that the BV requires that flooding shall be kept as symmetrical as ever possible, and the use of longitudinal bulkheads was restricted to the absolute minimum. For the same reason, cross flooding devices were not fitted. Another assumption was that the investigation of lesser extent damages was typically restricted to investigate only the effect of double bottom compartments. The effect of A- class bulkheads on the possible flooding sequence was never requested to analyse, although Navy Ships have quite complex internal subdivisions in this respect, see Fig. 4.

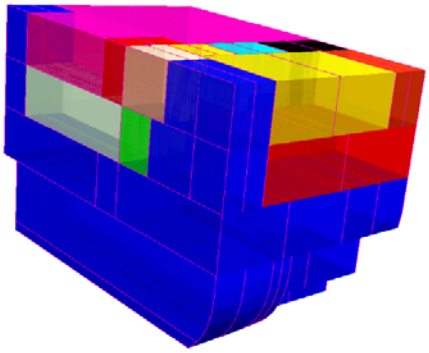

Figure 4: A-class sub-compartments of a single watertight compartment

The revision of the SOLAS with the 2009 and 2020 edition has put more emphasis on intermediate stages of flooding (see Russell 2024), and now, also cross flooding arrangements of cargo ships have to be checked against intermediate stages of flooding. Consequently, it was found that there was a certain gap between the commercial standard, represented by the SOLAS 2020, and the damage stability part of the BV 1030-1. In contrast to the IS-Code developments, it was found to be useful to integrate the most important updates of the SOLAS 2020 more or less directly into the damage stability part of the BV 1030-1 as follows:

- If cross- flooding devices are fitted, intermediate stages shall be considered and cross flooding times shall be computed. The procedure is equivalent to the former A266.

- If A-class bulkheads are fitted, the most critical lesser extent combination of not flooded sub compartments has to be determined and investigated, eventually together with cross flooding examinations.

- In cases of large compartments with unrestricted floodwater flow, these may be additionally investigated as being partly filled.

The maximum permissible heeling angle of any intermediate stage must not exceed 25 degrees (including wind and shifting of fluids in partly filled tanks), the maximum residual righting lever must be 50mm. This is roughly equivalent to the SOLAS 2020 requirement for passenger ships.

Openings. The consideration of openings was originally not foreseen in the BV as it was required to design the complete hull and superstructure watertight until 60 degree. During the stability assessment (both intact and damage) it had to be checked that the deck edge must never be submerged. This concept was replaced by the opening concept which is used in the SOLAS 2020 standard, distinguishing between weathertight and not weathertight openings. None of these openings might be submerged during any equilibrium floating, but weathertight openings are allowed to submerge during the calculation of the righting levers.

Watertight doors. The new stability standard DMS 1030-1 does generally not permit the installation of watertight doors below the bulkhead deck.

APPLICATION TO NAVY SHIP DESIGN

Intact stability

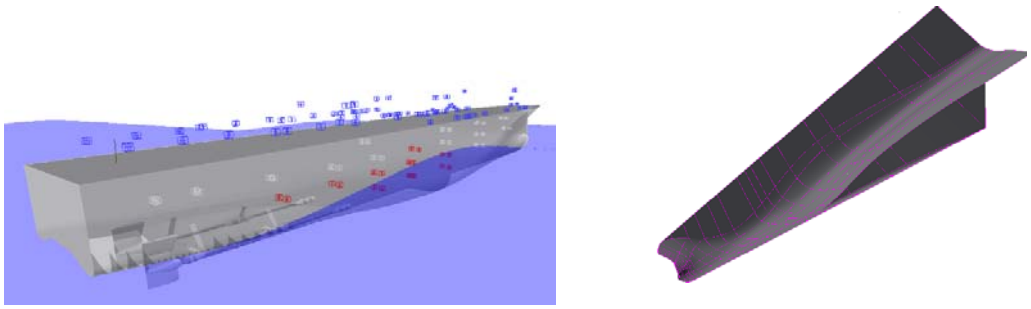

Figure 5: Navy Ship in wave crest condition of the design wave and a hull form optimized for righting lever alterations

The newly implemented stability criterion puts an additional challenge on the hull form design of all Navy Ships built according to this new standard. Besides optimizing the hydrodynamics with respect to minimum speed power requirement and optimal underwater pressure signature, the designer must now additionally try to minimize the righting lever alterations in waves (see Fig. 5, left, and Fig. 2). This is certainly an additional design constraint for the development of the hull form and the subdivision. To keep the good hydrodynamics (also with respect to the underwater noise signature) of existing designs, it was found beneficial to conduct the following strategy during hull form design, which increases the stability on the wave crest and reduces the stability in the trough at the same time, while keeping the basic hydrodynamic efficiency of the hull:

- The LCB should be as far aft as reasonably possible. This leads to an increased trim down by stern in the wave crest condition and this increases the phase shift between rolling and pitching motion. At the same time it is also beneficial to design the ship in such a way that the ship will always operate with slight trim down by stern. This should be taken into account when optimizing the hydrodynamics of the aft body.

- The bilge radius should be as large as reasonably possible. This increases the immersion of the ship on the wave crest and increases the effective water plane moment of inertia.

- Where ever possible, buoyancy should be moved to the outer parts of the hull which are immersed in the crest condition.

Hulls which have been designed according to this strategy easily comply with the area ratio requirement. An additional problem now arises for all Navy Supply Vessels: As these ships have large tank capacities for aircraft fuel and marine diesel, this results in substantial free surfaces at small heeling angles, resulting in a righting lever curve which immediately deviates from its initial GM (see Fig. 6).

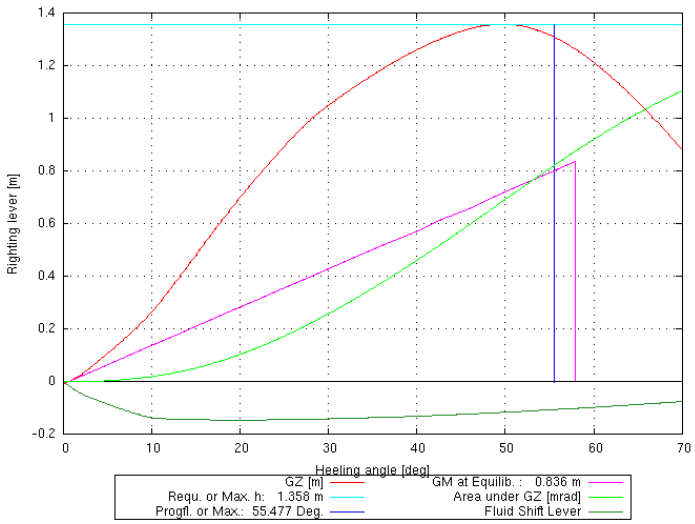

Figure 6: Righting lever curve (red) of a Navy Auxiliary for a loading condition with large free surfaces

In this context it must be noted that all fluid shifting moments have to be directly calculated, taking into account heel and free trimming. As the maximum permissible filling level of all tanks is 95%, this leads to large initial free surfaces which decrease with larger heeling angles. The wave crest curve in the area ratio criterion must be corrected for free surface effects. This may result in a situation where it is reasonable to subdivide large tanks to reduce the initial free surface.

It is further well possible that the ship may be sensitive with respect to trim. This mostly holds for Navy Auxiliaries which have a larger variety of possible loading conditions compared to Navy Combatants. For these ships, the tank arrangement must be well designed for all possible operating conditions as only limited possibilities exist to use extra ballast water.

Damage stability

The revised damage stability regulations of the DMS-1030 result in two major challenges and opportunities for the design of the hull and the internal subdivision: First of all, the position of the bulkhead deck can be selected freely now, as it is explicitly allowed that the bulkhead deck becomes submerged during a damage case, provided, no openings become submerged. Secondly, it puts a hard challenge on the ship design if no water tight doors are allowed below the bulkhead deck. This is hardly a problem for Navy Combatants, but some Navy Auxiliaries are strongly restricted in their operability when heavy goods need to be transferred longitudinally below the bulkhead deck.

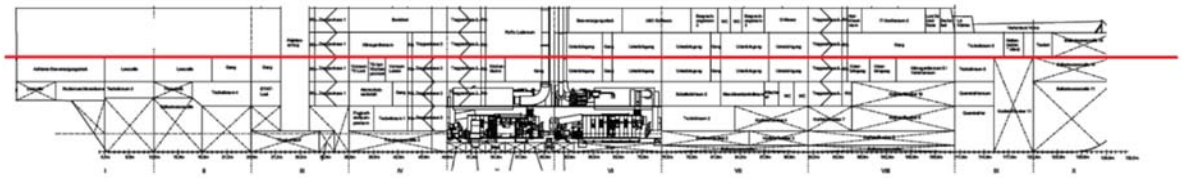

Figure 7: Possible location of the bulkhead deck (red)

This leads to one possible solution that the bulkhead deck must not necessarily be the uppermost water tight deck. It is now well possible to lower the bulkhead deck and to extent the watertight transversal bulkheads into the superstructure, see Fig. 7. This leads to an increased reserve buoyancy on one hand and allows the installation of water tight doors on the bulkhead deck and the superstructure decks. Due to the increased reserve buoyancy, the compartments can become longer which is cost effective. Below the bulkhead deck of Navy Auxiliaries, there may exist the possibility to install water tight doors in the main traffic routes, provided, the ship fulfils all damage stability requirements when the doors of interest are assumed to be open, see Fig. 8.

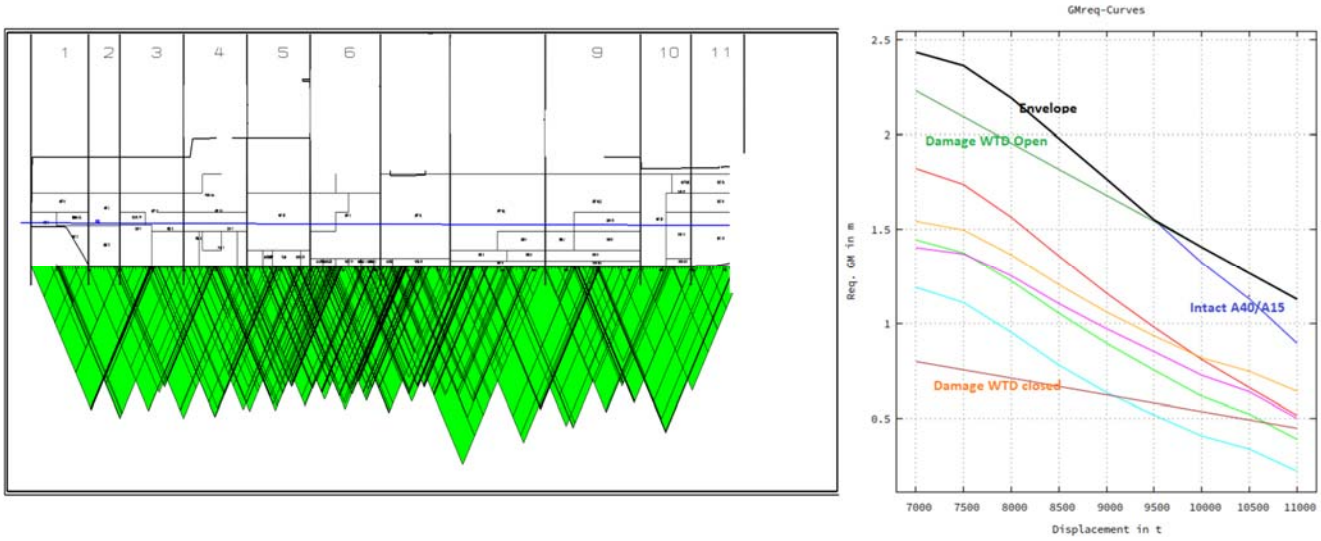

Figure 8: Damage stability assessment and $GM_{Required}$- Curves

Fig, 8, left, shows the results of the damage stability assessment where it is assumed that the most critical water tight door is open. Due to the large reserve buoyancy, this does not pose large problems for the damage stability assessment. The curves of $GM_{Required}$ (Fig. 8, right) show that the required values of GM are not substantially larger compared to the intact stability values, even if the most critical water tight door is assumed do be open. The damage stability curve denoted by "Damage WTD closed" shows the effect of the most critical open watertight door on the damage stability.

CONCLUSIONS

The present paper has given an insight into recent developments of the German Navy Stability Code DMS 1030-1 (former BV 1030-1) and to the resulting effects on Navy Ship design. The necessity to update the code was shown, and it was also discussed when it seemed to be reasonable to integrate well proven elements of stability standards for commercial ships into the BV code. It was also shown that for the problem of intact stability in waves, it seemed to be useful to deviate from available commercial standards. The idea that the limiting values of GM shall not differ substantially between intact and damaged condition, which is not reflected in commercial standards, assures that the design of a Navy Ship is well balanced with respect to stability. For typical ship design problems, recommendations have been presented how to deal with this new standard. Most important is that the stability assessment of a Navy Ship is thoroughly performed during the very first stages of the planning phase.

REFERENCES

BAAINBw (2022). Deutscher Marinestandard (DMS) für Wasserfahrzeuge der Bundeswehr. Stabilität von Überwasserschiffen (German Navy Standard, Stability of Surface Vessels), Koblenz, Germany, 2022

Gualeni, P., di Donato, L., Krüger., S., Hatecke, H. (2015). On the application of the 2nd Generation of Intact Stability Criteria to RoRo-Passenger Vessels. Proc. Stab 2015, Glasgow, UK

International Maritime Organization (IMO) (2008). International Code on Intact Stability, 2008. 2009 Edition. IMO, London, UK

Kluwe, F. (2009). Development of a Minimum Stability Criterion to Prevent Large Amplitude Roll Motions in following Seas. Dissertation, Inst. Of Ship Design and Ship Stafety, TU Hamburg, 2009.

Krüger, S., Hatecke, H., Rinke, A., Tammen K. (2014). Analysis of the German Navy Stability Standard BV 1030 with Respect to Operability in Heavy Weather. Proc. OMAE 2014, San Francisco, California, USA

Krüger, S., Hatecke, H. (2013). The impact of the 2nd Generation of Intact Stability Criteria on RoRo-Ship Design. Proc. Stab 2013, Changwon City, Korea.

Russell, P. (2024). Introduction to the Concept of the German Navy Stability Standard DMS 1030-1. Proc. IMDC 2024, Amsterdam, The Netherlands.

Wendel, K. (1964). Erläuterungen zur Bauvorschrift für die Sicherheit der Überwasserschiffe der Deutschen Bundesmarine gegen Sinken und Kentern (Explanations to the Stability Standard for the Safety of Surface Ships of the German Navy against Sinking and Capsizing. Archive Inst. for Ship Design and Ship Safety, TU Hamburg, Hamburg, Germany

Proceedings of 15th International Marine Design Conference (IMDC-2024)
June 2-6, 2024
Amsterdam, the Netherlands

The importance of first-principles tools for safety enhancement in the design of passenger ships in the case of flooding events.

Dracos Vassalos[1,2], Francesco Mauro[1,*], Donald Paterson[1] and Ahmed Salem[1]

ABSTRACT

The design of a passenger ship is a complex process covering multiple aspects of naval architecture and marine engineering to address performance, functionality safety, and cost as primary objectives. Between them, safety is a key element focusing on the people on board. In this sense, ship safety in the case of flooding events needs proper estimation from the first stages of the design process employing an appropriate metric. To this end, safety can be evaluated as a risk by calculating the Potential Loss of Life. Thanks to a multi-level framework developed during project FLARE, it is possible to calculate the risk associated with an accident, increasing the level of reliability as the design process advances. The framework aims at employing first-principles tools from the early stages of the design process, abandoning static calculations and empirical formulae as soon as data is available to set up advanced calculation techniques. Then, the framework adopts rigid-body time-domain calculations for the flooding simulations, advanced evacuation analysis tools, and direct crash simulation to evaluate collision damages. The process allows for testing alternative design solutions for the ship to enhance safety. Investigating risk control options is also possible, considering active or passive systems such as fixed foam installations, deployable barriers, or crashworthiness. Such an approach allows for evaluating safer solutions, respecting other design constraints and cost-related aspects. The present work describes the risk assessment framework for the case of flooding events, together with the different levels of accuracy that can be achieved, showing the improvements that could be reached by employing alternative risk control options.

KEYWORDS

Risk-based design; flooding risk assessment; passenger ships; risk control options.

INTRODUCTION

The design of passenger ships is a complex process involving the concurrent evaluation of multiple aspects of Naval Architecture and Marine Engineering. Between them, damage stability is a key part of the design process, providing a lifecycle flooding risk management for the vessel (Vassalos, 2020). Consequently, the estimation of flooding risk is a relevant attribute for the design of new passenger vessels (Atzampos, 2019, Papanikolaou et al., 2013, Vanem et al., 2007). However, the approach to risk has never been deeply applied by designers, who prefer to adopt a compliant-based approach to damage stability. In recent years the trend has changed, giving more importance to the application of first principles tools in the design process of passenger ships (Vassalos, 2016), and providing designers with suitable guidelines for their application (Mauro et al., 2023a).
The application of this different kind of approach led to the formulation of a multi-level flooding risk assessment framework during the EU-founded project FLARE (Vassalos et al., 2022a), suitable for the flooding risk estimation through the whole

[1] Sharjah Maritime Academy, Khorfakkan, Sharjah, UAE; ORCID: 0000-0003-3471-9411 (F. Mauro), [2] University of Strathclyde, Glasgow, Scotland, UK.
* Corresponding Author: Francesco.Mauro@sma.ac.ae

Submitted: 23 Febraruy 2024, Revised: 2 April 2024, Accepted: 1 May 2024, Published: 26 May 2024

Conference paper, DOI: https://doi.org/10.59490/imdc.2024.909 e-ISSN: 3050-4864

ship lifecycle. The advantages of this framework are given by the implementation of a multi-level approach to risk, allowing a designer to choose the most appropriate tools to use during the design process, starting from simple assumptions and simulations up to perceiving fully first-principles-based predictions. The application of first-principles tools concerns principally three aspects of the flooding risk assessment, namely the damage generation, the survivability analysis and the evacuation analysis. For each topic, suitable options are available to achieve different levels in the reliability of predictions as indicated by the multi-level framework for risk assessment. Furthermore, the flexibility of the provided framework allows for the use of the first-principles tools as a design instrument for the identification and evaluation of the benefits of suitable risk control options (RCOs).

This paper presents the main concept of the multi-level framework for risk assessment for the specific case of the design phase of a passenger ship. A description of the main first-principles tools is provided for the generation of breaches, flooding simulations and evacuation analysis. To demonstrate the applicability and flexibility of the multi-level framework, a worked example is presented on two reference ships, a cruise and a Ro-pax, highlighting how first-principles-based tools can be used also for the design of RCOs, like the implementation of fixed foam installations, deployable barriers, and crashworthy structures. Simulations are performed with different levels of reliability, highlighting how the application of first principles tools influences not only the general estimation of the risk level but also the impact of each selected RCO on the reduction of risk. Finally, the obtained results raise questions on the actual praxis in passenger ships'design, highlighting how the application of active or passive RCOs may change the attained flooding risk level of a vessel without the need for searching for more capillary compartmentation of the internal layouts.

FLOODING RISK ASSESSMENT FRAMEWORK

The assessment of flooding risk during the design phase of a passenger ship (or ship in general) passes through the recursive execution of the following main points:

1. Definition of calculation scenarios and ship main particulars.
2. Flooding risk evaluation.
3. Identification of suitable vulnerability mitigation measures.
4. Reassessment of the flooding risk.

These steps relate to the design of a new unit as well as to the retrofitting of an existing vessel or a change in the operational profile of the ship.

The risk can be measured through the Potential Loss of life (*PLL*), which follows the general formulation of risk as given by the following equation:

$$PLL = p_f \cdot c_f \quad [1]$$

p_f represents the probability of flooding and c_f is the consequence of the flooding event. For the evaluation of risk during the project of a passenger ship it is necessary to identify an attained index PLL_A to be compared with a tolerable level of risk. In case all the vessel life-cycle has to be taken into account, a more general model for PLL_A can be considered, evaluating the attained PLL_A per year of service (PLL_A^*), which provides more flexibility to assess multiple operational scenarios. Then, the definition of PLL_A^* for every single scenario has the same form of equation [1] but with a more in-depth definition of p_f and c_f.

$$PLL_A^* = \sum_{i=1}^{N_{hz}} \sum_{j=1}^{N_{op}} \sum_{k=1}^{N_{ld}} \sum_{h=1}^{N_c} p_{f_{i,j,k,h}} \cdot c_{f_{i,j,k,h}} \quad [2]$$

In equation [2], N_{hz} is the number of possible hazards (which corresponds to collision, bottom and side groundings, i.e. N_{hz}=3), N_{op} is the number of operational areas (open seas, restricted or port areas), N_{ld} is the number of loading conditions and N_c is the number of flooding cases (depending on the ship subdivision). Consequently, the associated probabilities and consequences of an event have the following formulations:

$$p_{f_{i,j,k,h}} = p_{hz_i} \cdot p_{op_j} \cdot p_{ld_k} \cdot p_{c_h} = p_{hz_i} \cdot p_{op_j} \cdot p_{ld_k} \cdot p_{c_h}^* \left(1 - s_{c_h}\right) \quad [3]$$

$$c_{f_{i,j,k,h}} = FR_{i,j,k,h} \cdot POB_{i,j,k,h} \quad [4]$$

The probabilities described by equation [3] result from the statistical analysis of damage databases, specifically for passenger ships. The probabilities of the damage case can be described by employing the common definition of the p and s-factors (Pawlowski, 2004, IMO,2009, Vassalos et al., 2022b). On the other hand, equation [4] describes the consequences of a hazard, which are given by the fatality rate *FR* and the number of people onboard *POB*. All the quantities change scenario by scenario, thus, the final risk assessment requires the execution of $N=N_{hz}N_{op}N_{ld}N_c$ scenarios to be assessed with flooding survivability and passenger evacuation tools.

The resulting number of scenarios is considerably high as is the computational load, but they can be reduced by applying the concept of a multi-level framework, employing different types of tools according to the level of accuracy required by different stages in the vessel life cycle. This is of utmost importance, especially for the design phase.

Multi level-framework

The studies performed during Project FLARE led to the definition of calculation frameworks, initially oriented to survivability only and subsequently extended to risk. Such frameworks provide a connection between the research-oriented vision of the flooding problem and the designer and operators' practical point of view (Mauro et al. 2023a). A global first-principle characterization of flooding risk is difficult to achieve because of the calculation time and availability of suitable codes. Therefore, a multi-level approach, with consequent multi-fidelity results, significantly improves in-force damage stability frameworks for passenger ships.

The main assumptions of the multimodal framework refer to three characteristics of the flooding process determination: the occurrence, the survivability and the fatality in a given scenario. Therefore, the definition of *PLLA** of equation [2] assumes the following form for the case of a single scenario:

$$PLL^*_{A_{i,j,k,h}} = p^*_{i,j,k,h}\left(1-s_{i,j,k,h}\right)c_{f_{i,j,k,h}} \quad [5]$$

According to equation [5], the probabilities and weights associated with the scenario occurrence are identified by p^*, while s describes the scenario's survivability and c_f the consequences as per equation [4]. Concerning the probabilities, the occurrence is identified during the input preparation phase of a Level 1 survivability assessment. Level 1 or Level 2 damage stability calculations determine survivability, while evacuation analyses determine fatality.

Therefore, the definition of the levels in the multi-level framework is as follows:

- *PLL Level 1*: the approach is fully based on static damage stability calculations. The expected number of fatalities depends on the time it takes the vessel to capsize, and the static analysis does not account for time. Then, the estimation of fatality rate in this stage needs some approximation. To keep the methodology as simple as possible and to account for the dependencies between survivability and fatality rate, the following extremely simplifying assumption is made:

$$FR = \begin{cases} 0.8 & \text{if } s < 1 \\ 0.0 & \text{if } s = 1 \end{cases} \quad [6]$$

  This simple and conservative approach follows the method used in the EMSA III Project, the results of which were used to support political decisions at IMO, leading eventually to SOLAS 2020 regulations for damage stability.
- *PLL Level 2*: The main additional parameters distinguishing Level 2 from Level 1 flooding risk estimation are the Time to Capsize *TTC* and the Time to Evacuate *TTE*. The *TTC* describes the time it takes the vessel to capsize/sink after a flooding event occurs. Therefore, the use of *TTC* requires the execution of time-domain flooding simulations, thus neglecting the static approach. The *TTE* defines the time necessary for an orderly evacuation of passengers and crew onboard a passenger ship after a flooding hazard occurred. Hence, the *TTE* determination implies the execution of time-domain evacuation analyses. However, according to the multi-level framework, also simplified methods oriented to a fast TTE evaluation are available, providing two sub-levels for the Level 2 analysis. Such options are:
  - *PLL Level 2.1*: for this level of approximation, only time domain flooding simulations are required to determine TTC. Evacuation analyses for TTE evaluation are omitted; therefore, an empirical formulation is needed to derive *FR* as follows:

$$FR = \begin{cases} 0.0 & \text{if } TTC > n \\ 0.8\left(1-\dfrac{TTC-n}{30-n}\right) & \text{if } 30 \le TTC \le n \\ 0.8 & \text{if } TTC < 30 \end{cases} \quad [7]$$

    where n is the maximum allowable evacuation time in minutes according to MSC.1/Circ. 1533. The assumption on *FR* intrinsically considers the nature of the capsize event as a function of the *TTC*, assuming the impossibility of evacuating the ship during fast transient capsizes cases.
  - *PLL Level 2.2*: In this level the direct evaluation of *TTE* is considered. Starting from significant cases described by time-domain flooding simulations, where it is realistic to proceed with an evacuation analysis, ship motions and floodwater can be imported in the evacuation software. Such a coupling allows comparing the evacuation process and the associated *TTC*.

The full details, justifications and also applied examples for the FLARE multi-level risk framework are provided by Vassalos et al. (2022b) and are not rediscussed here for the sake of brevity. The individual definition of probabilities and values associated with occurrences, survivability and fatality changes not only with the selected level between the above-presented options but is also depend upon the phase of interest during the vessel life-cycle. Here the focus is on the design phase.

Design Phase framework

The application of a risk framework for the design phase of a passenger ship implies the definition of the main inputs and all parameters in equation [2] to allow the evaluation of PLL_A*, with input and information available in this specific stage of the vessel life cycle. Moreover, the application of the framework during the design phase requires to refer to regulations, assumptions, and outputs relevant to the statutory damage stability framework. This reflects in the selection of the frequencies and probabilities associated with the occurrence, survivability and fatality of a scenario and, consequently, in the generation of the cases to be analysed. The focal points can be summarised as follows:

- *Possible hazards*: the framework handles three kinds of casualties (N_{hz}=3); collisions, side, and bottom groundings. These hazards imply the adoption of specific frequencies of occurrence $p_{hz,}$ corresponding to the relative weights *w* used to define the *A*-index in the damage stability frameworks. Suitable values for p_{hz} derive from database analyses and are reported in Vassalos et al. (2022b) with the associated *w*.
- *Operational areas*: Only the open sea (N_{op}=1) is taken into account for design purposes, restricting the wave conditions to a representative sea state that corresponds to a significant wave height H_s of 4 metres. When assessing risks at Level 1 or Level 2, such an assumption is taken into account.
- *Loading conditions*: the framework adopts two drafts T_1 and T_2 with the same weight on the final assessment and corresponding to 0.45 and 0.75 times the design draught of the ship, respectively. Such an assumption is maintained across the levels and does not follow the SOLAS standards, which are based on three draughts. The assumption has been promoted by designers during the activities of Project FLARE (Vassalos et al, 2022c).
- *Calculation scenarios*: Depending on the level chosen for the risk assessment, there are a different number of scenarios. 10,000 breaches are created for every type of danger in order to produce a Level 1 prediction, sampling the location and dimensions from relevant cumulative distributions. The number of scenarios is lowered to 1,000 breaches for each danger since time-domain simulations take longer to complete than a static approach. The damage distributions mentioned in Levels 1 and 2 are the same as those in SOLAS for collisions and EMSA III for bottom and side groundings.

According to the given assumptions, equation [2] can be modified by rewriting the occurrence terms provided by equation [3], resulting in the following final formulations valid for Level 1 and Level 2 predictions, respectively:

$$PLL^*_{ALevel1} = \sum_{i=1}^{3}\sum_{k=1}^{2}\sum_{h=1}^{N_c^*} p_{hz_i}\, p_{ld_k}\, p^*_{c_h} \left(1-s_{c_h}\right) FR_{i,k,h} POB_{i,k,h} \quad [8]$$

$$PLL^*_{ALevel2} = \sum_{i=1}^{3}\sum_{k=1}^{2}\sum_{h=1}^{1{,}000} p_{hz_i}\, p_{ld_k}\, p^*_{c_h} \left(1-s_{c_h}\right) FR_{i,,k,h} POB_{i,k,h} \quad [9]$$

the two equations differentiate themselves mainly in the determination of the scenario's occurrence p_c* and the final number of scenarios N_c. Such differences are strictly connected with the level of damage stability calculations. The generation of breaches is equivalent between Level 1 and Level 2, following a non-zonal approach requiring the sampling damage characteristics with an enhanced Randomised Quasi-Monte Carlo technique. But by using a static assumption (Level 1), it makes no sense to make a distinction between instances that harm the same set of internal compartments. Therefore, the final amount of scenarios to evaluate is N_c*<10,000 and strictly depends on the ship's internal layout. All cases referring to the same damaged compartments are grouped to determine the scenario occurrence p_c*. Conversely, when using dynamic simulations (Level 2), the grouping becomes impossible because the breach's diameter affects how much water enters and exits the system. Then, for Level 2 calculations, all cases are equiprobable and all the 1,000 scenarios are considered with the same p_c*. The Level 2 framework permits a hybrid approach, taking into account only the case with the higher breach longitudinal area resulting from static calculations (Mauro et al. 2023a). Regardless, FLARE's recommendations and advancements are meant to standardise the use of dynamic analyses in the damage stability evaluation of passenger ships, leading to the selection of Level 2 flooding risk assessment.

Concerning evaluating the consequences and *FR* in particular, preliminary calculations performed during the FLARE project highlight small differences between Level 2.1 and Level 2.2 assessments (Vassalos et al., 2022c). The application of Level 2.2 design phase evaluation on one cruise ship and one Ro-pax highlights the significant equivalency of the final risk level that is reached, whether or not sophisticated evacuation analyses are used.

However, it is of utmost importance to encourage the application of first principle tools for increasing the reliability of the results since the first stages of a design, promoting their application for the generation of breaches, the flooding simulations and the evacuation analyses. This will be discussed in the following sections, together with the applications of measures to mitigate the risk and how to use first-principles tools to reduce the global risk onboard a passenger ship.

FIRST PRINCIPLES TOOLS FOR FLOODING RISK

The determination of flooding risk during the design process of a passenger ship implies the evaluation of different components of risk, both for the frequencies and consequences estimation. In dealing with the flooding of ships, the first step is determining the source of the flooding, which means establishing how the flooding breach has been generated. Secondly, the flooding process needs to be analysed for the associated environmental conditions, determining the flooded compartments and the time to a possible sinkage/capsize event. Finally, in case there is sufficient time before a capsize event, it is necessary to simulate the evacuation process for the ship.
For all the issues mentioned above, there are different available solutions for identifying the associated relevant quantities, with different levels of approximation. Here, the focus is on employing first principle tools for the prediction of risk; therefore, the principal direct method for modelling breach dimension, flooding dynamics and evacuation will be shortly described.

Breach generation

The generation of breaches derived from collisions with other ships or grounding has a serious implication on the evaluation of flooding risk in the design process of a passenger ship. The common practice is to use simplified breach models, referring to box-shaped damages or unrealistic prismatic damages which follow the shape of the waterline of the ship (Mauro et al. 2023a). The breach dimensions and location are derived from statistical distributions based on database analyses of real accidents (Bulian et al. 2019).
However, to generate the breaches necessary to perform risk analysis, a first-principles approach can be pursued by performing a set of crash analyses. Such kind of approach implies the execution of a large number of Finite Elements Methods (FEM) analyses, considering a proper population of potential striking ships (Conti et al., 2022). Using conventional FEM simulations to assess the internal mechanics of the collision problem would be prohibitive in terms of total computation time. Therefore, the simulations can be carried out based on the Super Element Method. This method, which was introduced by Lützen (2001), consists of splitting the ship into very large-sized independent structural units (the so-called Super-Elements), for which closed-form analytical formulations are available. These formulas, which describe the resistance and energy dissipation of the Super-Element based on its type and deformation mechanism, are derived from experimental and numerical data.
Regarding the ship's external dynamics (rigid body movements of the ship due to the action of the hydrodynamic loads and the collision forces) during the collision event, they are addressed using a semi-coupled approach via the use of the MCOL solver (Le Sourne et al., 2001), the ships hydrodynamic properties being obtained using Bureau Veritas seakeeping analysis code Hydrostar (BV, 2019).

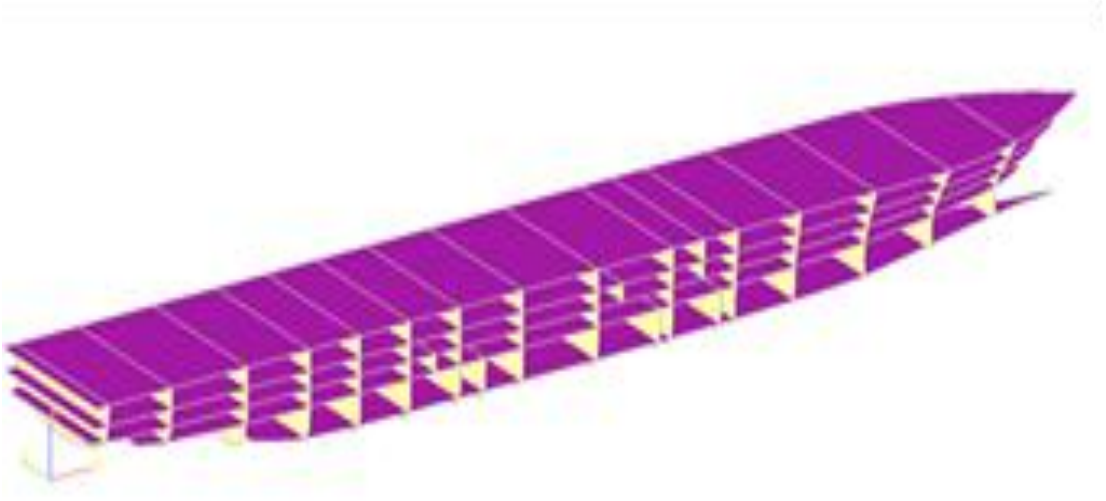

Figure 1: Example of super-element model for crash analyses.

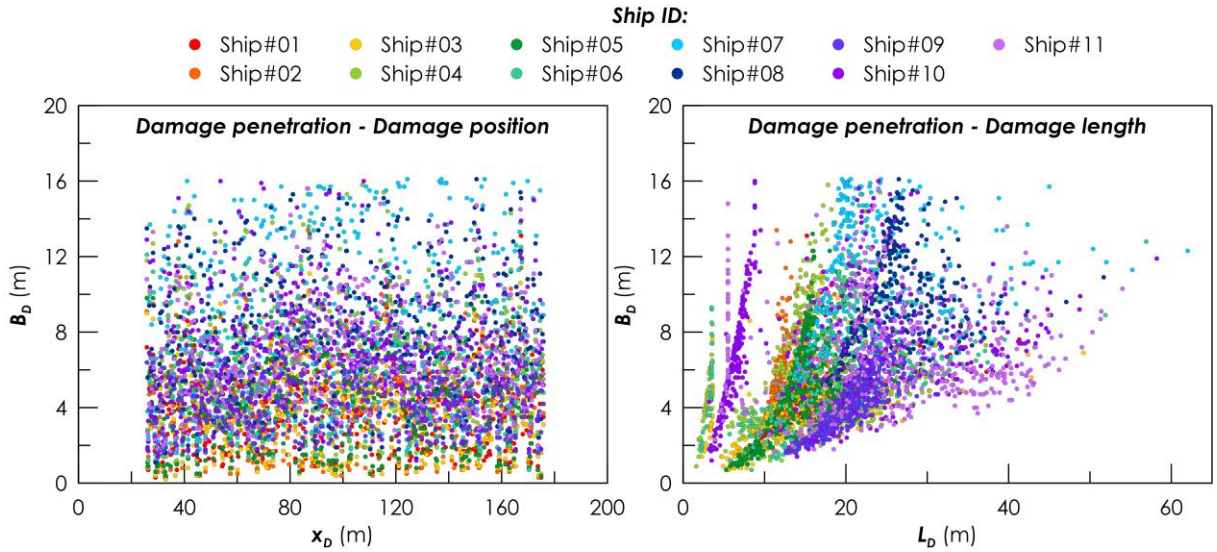

Figure 2: Example of damage dimensions derived from super-element calculations.

These two principal features are considered in the software SHARP, which allows for performing fast collision simulations. The accuracy of this method was recently reconfirmed during Project FLARE, by benchmarking against Finite Element codes (Kim et al., 2022). Furthermore, the methodology allows for building damage databases suitable not only for the generation of damages in the design stage (Conti et al., 2022) but also for the estimation of risk in real-time applications (Mauro et al., 2023b). Figure 1 gives an example of the super-element modelling of a passenger ship, while Figure 2 shows an example of the damage penetration derived from crash analyses as a function of the damage position and length.
The adoption of this direct technique to estimate the damage dimensions permits the generation of a reliable input for the damage simulations, but still following the approximation of box-shaped damages.

Flooding simulations

The assessment of the flooding process after a casualty with direct calculations implies the modelling of a complex phenomenon, coupling the motion of the ship with the behaviour of the flooding process and their relative interaction with the ship and the wave environment (Vassalos, 2020). Different levels of simplification apply to the problem modelling with associated different levels of confidence for the obtained results.
Among the possible solutions, the adoption of time-domain simulations on rigid bodies offers a good compromise between calculation time and the accuracy of the provided results. The damaged ship motions derive from fundamental motion equations as the law of conservation of linear and angular momentum. These laws normally apply to rigid bodies, thus systems where the mass is constant during the simulations; here, the floodwater changes at each time interval. The problem is approximated by extending the rigid body motion equation to the internal fluid mass, resolved in a body-fixed reference system. Then, six scalar equations are defined for linear and angular motions having the following vector form in the case of angular motions:

$$\begin{aligned}&\left(I_s^{'}+I_w^{'}\right)\cdot\frac{\mathrm{d}}{\mathrm{d}t}\vec{\omega}^{'}+M_w\cdot\left[\vec{r}_w^{'}\times\frac{\mathrm{d}}{\mathrm{d}t}\vec{v}_{Gs}^{'}\right]+M_w\cdot\left[\left(\vec{\omega}^{'}\times\vec{r}_w^{'}\right)\times\vec{v}_w^{'}\right]+\\&+M_w\cdot\left[\vec{r}_w^{'}\times\left[\frac{\mathrm{d}}{\mathrm{d}t}\vec{v}_w^{'}+\vec{\omega}^{'}\times\left(\vec{v}_{Gs}^{'}+\vec{v}_w^{'}\right)\right]\right]+\\&+\frac{\mathrm{d}}{\mathrm{d}t}M_w\cdot\left[\vec{r}_w^{'}\times\left(\vec{v}_{Gs}^{'}+\vec{v}_w^{'}\right)\right]+\left(\frac{\mathrm{d}}{\mathrm{d}t}I_w^{'}\right)\cdot\vec{\omega}^{'}+\vec{\omega}^{'}\times\left[\left(I_s^{'}+I_w^{'}\right)\cdot\vec{\omega}^{'}\right]=\vec{M}_{Gs}^{'}\end{aligned}\qquad[10]$$

where I_s and I_w are the ship and internal fluid mass moment of inertia, ω is the rotational velocity vector, M_w is the internal fluid mass and r_w and v_w are the position and velocity vectors of the internal fluid mass centre. v_{Gs} is the ship velocity vector and M_{Gs} is the external moment acting on the ship. A more detailed explanation of all relevant terms together with the complete model in six degrees of freedom is available in Jasionowsky (2001). The right-hand side of equation [10] represents the external forces and moments acting on the ship with respect to its centre of mass. The sloshing motions of the floodwater can be modelled as a lumped mass (Papanikolaou et al, 2000), while water ingress/egress, the water accumulation and progression follow a simplified model based on the Bernoulli equation. These methods are implemented in the software PROTEUS3, used in this study, which has been recently tested and compared with other software during project FLARE (Ruponen et al., 2022a, 2022b), highlighting its suitability for the modelling of critical scenarios in waves for passenger ships

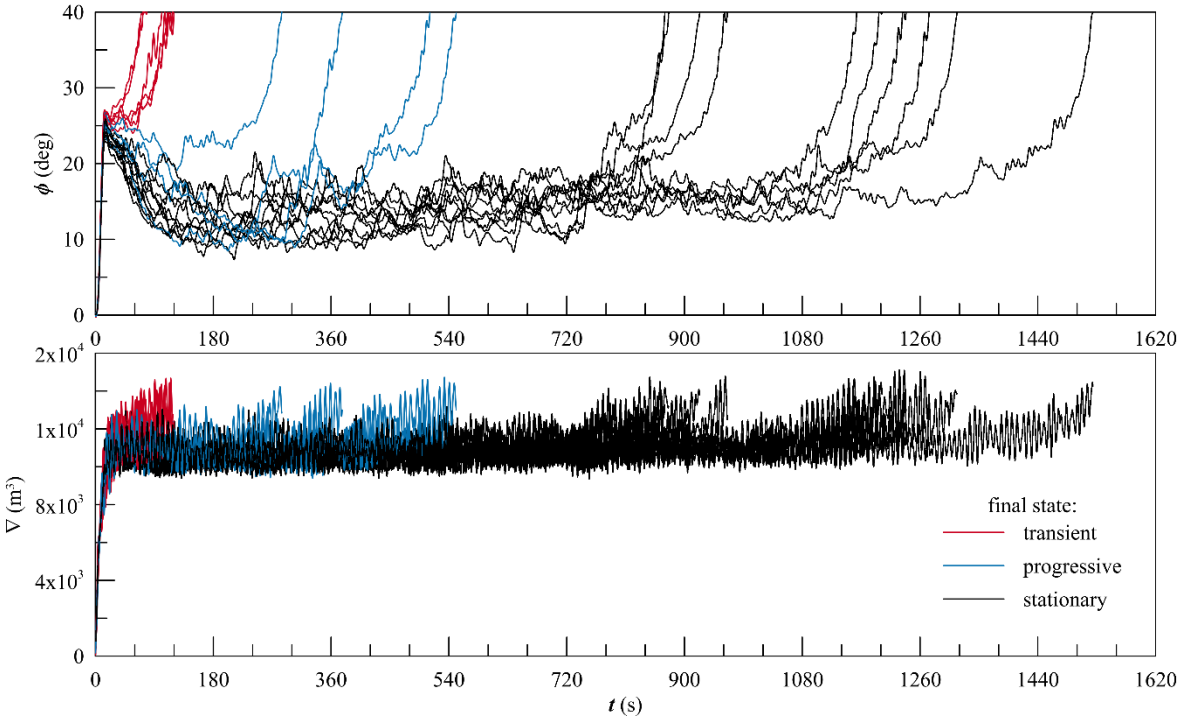

Figure 3: Example of roll (up) and floodwater (down) time histories derived from flooding simulations.

(Mauro et al., 2023a). Figure 3 shows the outputs of a set of dynamic simulations, representing the roll time history from the occurrence of the hazard until the ship capsizes and the amount of mass water entering/leaving the ship.
The time-domain simulations imply the modelling of water ingress/egress from/to the ship; therefore, the breach dimensions strongly influence the dynamics of the flooding process and the evaluation of the time to a possible capsize/sinkage event (The time to capsize).

Evacuation analysis

Another aspect of a risk assessment is related to the evacuation of the ship. Once there is sufficient time before an upcoming sinkage/capsize event, it is worth assessing the time needed to evacuate the ship. This, in turn, allows for evaluating how many fatalities may occur by comparing the Time to capsize obtained by flooding analyses and the time to evacuate derived from the evacuation analysis.
There are different approaches to the evacuation analysis, employing different kinds of simplifications and modelling of the evacuation path. In fact, it is possible to perform the evacuation with simplified methods by employing the hydraulic analogy (Nasso et al., 2019), assuming that corridors are like pipes and the passengers are the mass flow flowing through them. This method is admitted by the MSC.1/Circ. 1533 for evacuation analyses of passenger ships; however, the methodology is too simplified to capture well the evacuation process and the possible occurrence of some congestion points during the evacuation path. For such a reason, it is convenient to employ more advanced methodologies based on the direct evaluation of the pedestrian path of each evacuee, considering the interaction with the rest of the environment (Vassalos et al., 2003, Azzi et al, 2011, Kwee-Meier et al, 2016).
Among the different software that provides the possibility to perform the advanced evacuation analysis of a passenger ship, there is software EVI. EVI, developed by the University of Strathclyde and distributed by Safety at Sea, is based on the concept of “evacuability”, meaning the ability of an individual to evacuate the ship. The resulting evacuation index takes into account a wide range of parameters, which can be collected in two separate groups, namely the Initial Conditions and the Evacuation Dynamics. The first group considers the layout of the ship, the demography of the population its initial distribution and the response time to danger, while the second group takes into account the walking speed of each agent, the interaction between passengers and crew and between agent and layout of the ship. Figure 4 shows the modelling layout of a Main Vertical Zone in EVI for a passenger ship.

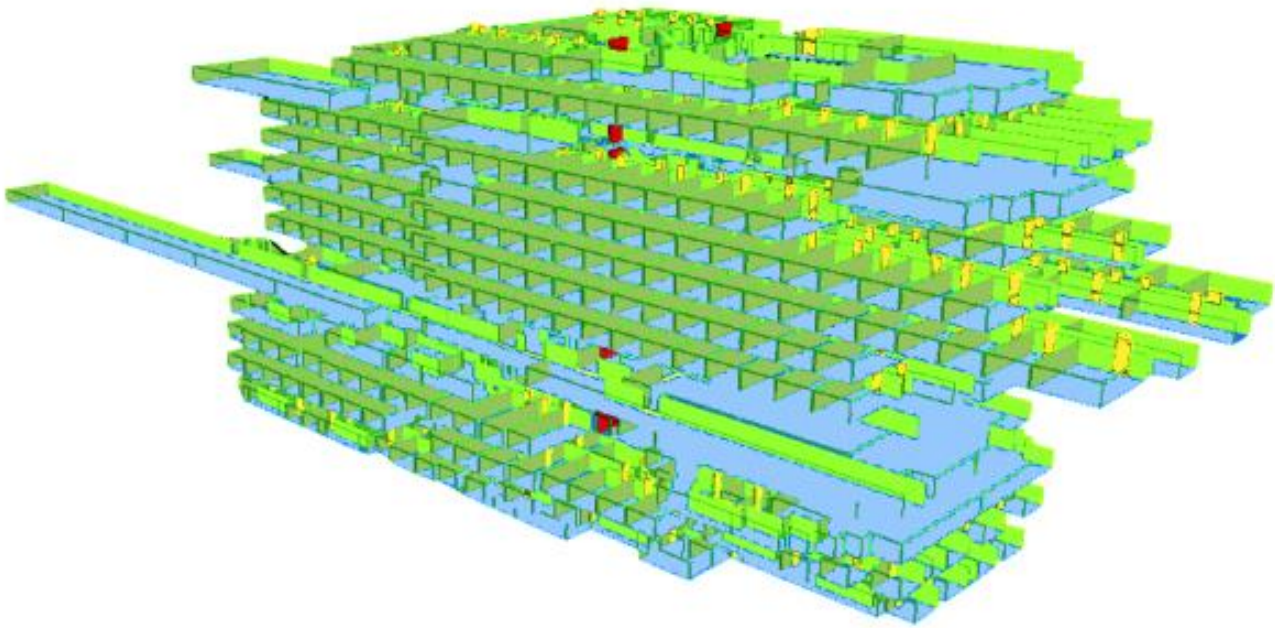

Figure 4: Example of modelling a Main Vertical Zone with software EVI.

Furthermore, the evacuation analysis could be performed by imposing the dynamic motions and the flooding progression determined by dynamic flooding analysis. Such a coupling allows for extending the reliability of evacuation results as the dynamics of the ship and its interaction with the evacuees are implicitly considered.

RISK CONTROL OPTIONS

The safety of a passenger ship is strictly related to its internal layout, as highlighted by dynamic flooding analyses and evacuation simulations. Nonetheless, a passenger ship's interior design must take into account unique considerations for passenger comfort as well as safety regulations pertaining to additional potential death threats, such as fire. Increasing internal layout restrictions in an attempt to reduce flooding may compromise the ship's ability to make money. Therefore, it is necessary to look at possible solutions aimed at increasing safety in a possible accident during the ship operation, thus increasing ship resilience to a failure event. Such solutions are usually referred to as Risk Control options (RCOs), as they aim to the reduction of the risk, i.e., in our case, of the Potential Loss of Life.
The risk control options can be passive, thus fitted permanently on the ship like fixed foam installation in ship voids or the adoption of a crashworthy structure, or active like watertight deployable barriers used only during emergencies. The following section describes a set of possible solutions to be installed onboard or to be considered during the design phase of a modern passenger ship.

Permanent foam installation

In order to increase the ship's initial stability and restoration forces in the event that these areas are directly or indirectly flooded after an incident, permanent foam is installed in the void spaces of the ship as part of a passive flooding protection system.
These installations function similarly to buoyancy tanks and have the extra advantage of being impermeable, which allows them to provide buoyancy in the damaged region instantaneously. Reducing the likelihood of transient capsize cases, which are also closely linked to insufficient reserve of stability during the early stages of flooding, is the goal of this type of improvement in initial stability and additional reserve of stability. Figure 5 shows a possible site for foam installation in available void spaces on the lower decks of a passenger ship.

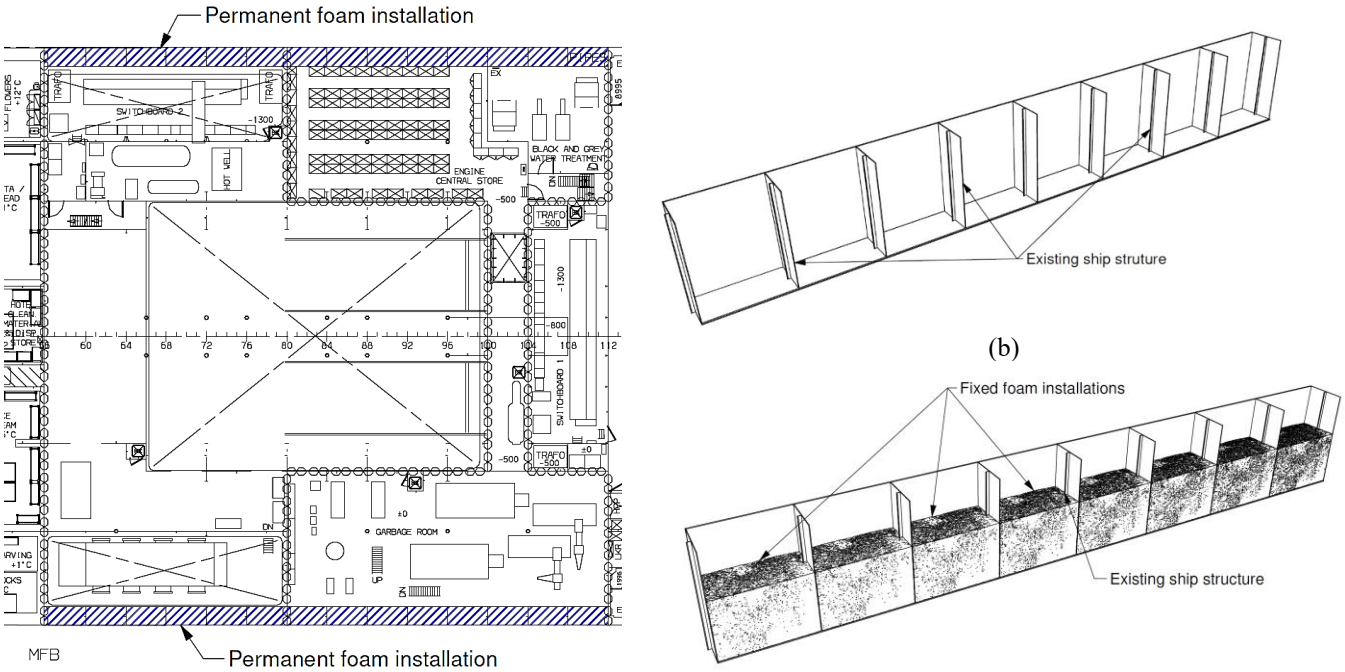

Figure 5: (a) permanent foam installation sites (blue) in a double hull. (b) Existing ship structures in the installation site. (c) Void spaces filled with foam.

Figure 6: (a) main (red) and minor (blue) flooding path on a cruise ship deck zone. (b) Vertically deployable shutters. (c) Horizontally deployable shutters.

Deployable watertight barriers

During the flooding process of a complex environment, like the internal geometry of a ship, the progressive flooding paths can be divided into major progressive floodwater paths. Minor paths are narrow passageways and areas that are connected to one another inside a certain area; they are thus routes that permit the ship to collect water locally. The main paths are essentially wide passageways that link two adjacent areas of the ship, acting as arteries that might quickly disperse floodwater throughout the vessel (refer to Figure 6a). The best course of action for managing progressive flooding in ships is

to restrict the main arteries. Deployable barriers are a good way to prevent flooding in this situation without changing the interior design of the ship. Deployable barriers consist of two lightweight shutters spaced 30 cm apart, usually composed of steel laths or GRP with an A-class fire rating. Shutters can be deployed also in case of fire casualties or drills. In case of flooding, the cavity between shutters is filled with expanding foam delivered from a compressed foam canister. In order to comply with specific local structural characteristics and arrangements, the shutters can be mechanically adjusted to be deployed either vertically (see Figure 6b) or horizontally (see Figure 6c). In addition, the barrier may be extended up to 30 metres over intermediate supports in a matter of minutes, limiting and managing floodwater channels that were previously determined to be crucial.

In this way, an appropriate damage control plan may be established and adequately carried out based on the outcomes of time domain flooding simulations, perhaps with the help of an appropriate decision support system. This makes it possible to isolate the affected area after any critical flooding event that is predicted and for which progressive flooding is the cause of the loss. The implementation of evacuation evaluations for certain important instances is implied by this technique, which aims to determine whether deployable impediments impede the evacuation process. This provides a clear benefit over current damage control strategies, which are mostly based on fixed design measures and are therefore less flexible and effective in likely critical loss circumstances.

Crashworthy structure

Another kind of RCO is crashworthiness, studied as a mitigation measure for damage stability since early 1990s. However, the lack of suitable tools to undertake this analysis as a routine has discouraged its application by designers since the early stages of the design process of passenger ships. In fact, crashworthiness is the ability of a structure to protect its occupant during an impact; therefore, the determination of a crashworthy structure for a passenger ship implies the dedicated study of a new layout for the main longitudinal and transversal elements of the ship.

In project FLARE, a dedicated study has been performed in an attempt to implement crashworthiness as a suitable risk control option to mitigate flooding risk. The scope was to derive a general scaling method from the conventional distributions used for damage dimension determination (Mauro & Vassalos, 2022) to new distributions considering the implementation of specific reinforcement to the hull (Cardinale et al. 2022). Thanks to the application of super-elements codes, as mentioned earlier, it was possible to derive corrections for specific damage dimensions according to the damage type:

1. Collisions: damage length, damage penetration, damage height.
2. Bottom groundings: damage length.
3. Side groundings: damage length

The correction has the form of a scaling function as reported in the following equation:

$$d^* = \lambda \cdot d \qquad [11]$$

Where λ is the scaling function, d is the original breach dimension derived from pertinent distributions and d^* is the new breach dimension.

The following possibilities have been analysed in the study, pertinent to different damage types:

1. Doubling of hull thickness: for collision only.
2. Increase of side shell plating thickness by 10 mm: side grounding only.
3. Installation of the double hull at B/20 with transversal web frames and an inner plate of 12 mm: collision and side groundings.
4. Installation of the double hull at B/10 with transversal web frames and an inner plate of 12 mm: collision and side groundings.
5. Installation of the double hull at B/30 with transversal web frames and an inner plate of 12 mm: collision and side groundings.
6. Installation of the double hull at B/20 with transversal web frames and an inner plate of 7 mm: collision and side groundings.
7. Installation of the double hull at B/20 with transversal web frames and an inner plate of 17 mm: collision and side groundings.
8. Doubling of inner bottom plating thickness: for bottom groundings
9. Doubling the number of girders within the inner bottom: for bottom groundings.
10. Increase of bottom structures material grade to AH36: for bottom groundings.

The above 10 possibilities have been implemented on a reference ship, considering possible collisions with a database of 11 striking ships (Conti et al., 2022, Mauro et al., 2023b).

Thanks to this modelling it is possible to take into account the crashworthiness of the new structure in all the levels of approximation of the risk assessment framework, as the correction for crashworthiness is directly applied to the inputs, thus allowing assessments from Level 1 up to Level 2.2.

RISK MITIGATION EXAMPLES

The present section presents two test cases for the implementation of RCOs on passenger ships. The cases refer to a Cruise Ship (Ship A in the following) and a Ro-Pax (Ship B). The general particulars of the ships are reported in Table 1, while the general overview is given in Figures 7 and 8. The two cases present the evaluation of different RCOs according to the following scheme:

1. Ship A:
   1.1. Change of internal layout with the installation of passive permanent foam
   1.2. Insertion of a double hull at B/20 with a plate shell thickness of 12 mm.
2. Ship B:
   2.1. Change of internal layout with application of permanent foam.
   2.2. Insertion of deployable barriers with foam.

The resulting combination of the two examples covers all the mentioned RCOs possibilities, having fixed foam applications (Cases 1.2 and 2.1), deployable barriers (Case 2.2) and crashworthiness (Case 1.2). For all the conditions, the PLL has been calculated at Level 1 and Level 2.1. No calculations have been performed at Level 2.2 because studies in project FLARE highlight that the differences between Level 2.1 and Level 2.2 are negligible for the tested vessels (Cardinale et al. 2022).

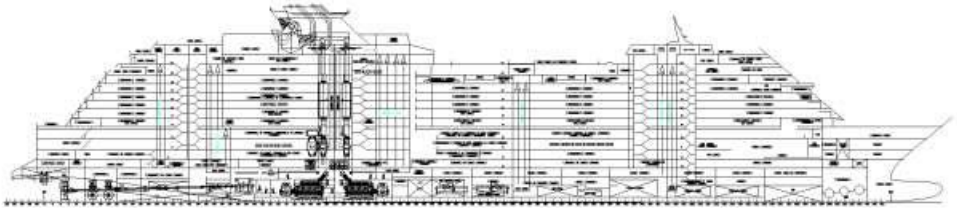

Figure 7: General Overview of Ship A

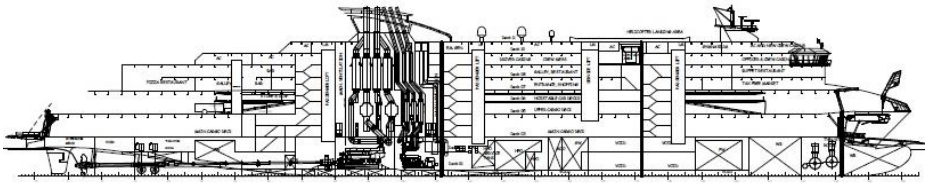

Figure 8: General Overview of Ship B

Table 1: Main particulars for Ship A and Ship B

Parameter	Symbol	Ship A	Ship B
Length overall	L_{OA}	300.00 m	211.30 m
Length between perpendiculars	L_{PP}	270.00 m	195.30 m
Subdivision length	L_S	296.74 m	212.25 m
Beam	B	35.20 m	25.80 m
Draught	T	8.20 m	6.70 m
Construction height	D	11.00 m	9.40 m
Number of passengers		2750	2315
Number of crew		1000	185
Gross tonnage	GT	95,900	36,822
Deadweight	DWT	8,500 t	5,581 t

Ship A

Ship A is an example of a large cruise ship. The ship was first assessed in its original configuration employing static and dynamic analyses for flooding risk assessment. The first round of calculations allows for identifying the attained PLL at both Level 1 and Level 2.1 according to the process described in the previous sections. However, the execution of detailed analyses offers also the possibility of identifying the most critical and vulnerable areas for flooding, thus giving the possibility to select the most suitable zones for the implementation of risk control options.

Figure 9 gives an overview of the critical damage location with the associated penetration resulting from the first analysis. The graph reports in a non-dimensional form the penetration L_y and the location x of the damage highlighting the presence of two main vulnerable areas located in the presence of the ship aft and fore shoulder. Those locations correspond to the presence of the heeling tanks in the fore shoulder and of the engine room in the aft. Due to the internal configuration of the ship, it is easier to fit risk control options in the aft shoulder instead of in the fore shoulder. For such a reason, two solutions have been applied to the re-design of the aft-shoulder space: the implementation of a crashworthy structure and the installation of permanent foam.

Figure 10 presents the first option, which means the creation of a crashworthy structure consisting of a watertight double-hull located at B/20 with local reinforcements with a thickness of 12 mm. The configuration gives a significant improvement in terms of achieved PLL, indicating a decrease of 14.6% compared to the original value for Level 1 and a decrease of 15.5% compared to the original for Level 2.1 prediction.

Figure 11 reports the second option, consisting of the installation of permanent foam inside void spaces in a double hull positioned at B/20. Such a technique allows for reducing the permeability of the void space in the double hull, thus increasing the "floatability" of the vessel. The configuration gives a lower reduction compared to the previous solution, providing a decrease of PLL of 11.9% compared to the original configuration for Level 1 and a decrease of 12.3% compared to the original configuration for Level 2.1 prediction.

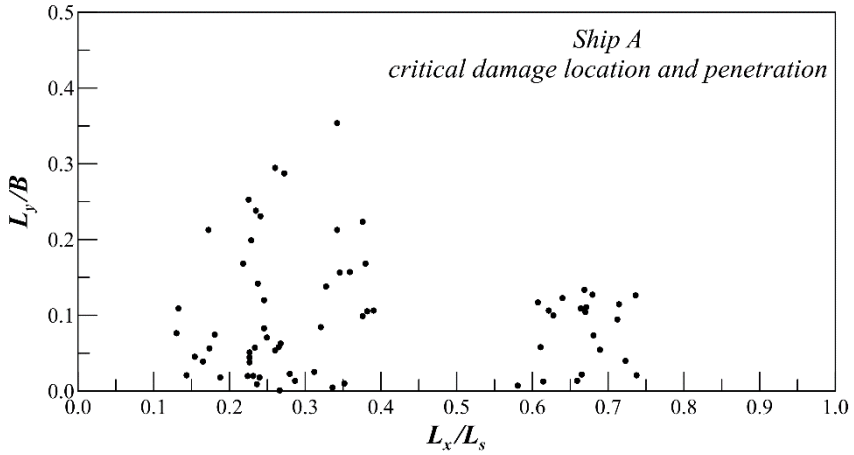

Figure 9: Critical damages location and penetration for Ship A.

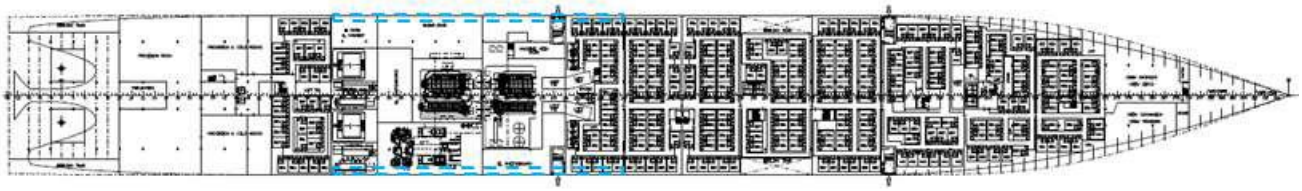

Figure 10: Crashworthy structure for Ship A.

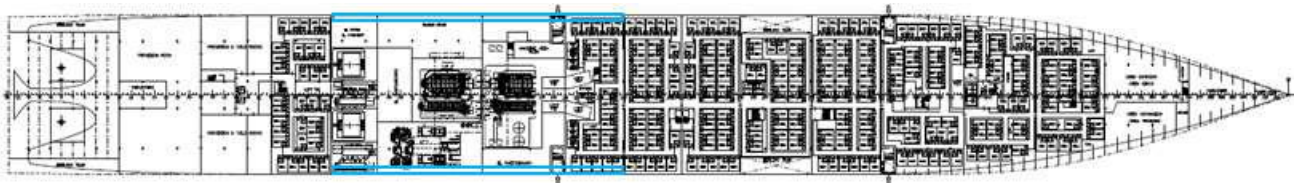

Figure 11: Double hull with foam installation for Ship A.

Ship B

Ship B is an example of a Ro-Pax vessel. As for the previous ship, the vessel was initially assessed for its original configuration through static and dynamic analyses, providing Level 1 and Level 2.1 predictions for the attained PLL. Also, in this case, the execution of detailed analyses allows for identifying the most vulnerable areas of the ship, allowing for providing the correct location of possible RCOs.

Figure 12 shows the most vulnerable areas of the ships, highlighting two main areas of risk, one in the fore shoulder and one in the aft shoulder. Compared to Ship A, most of the critical damages lie in the fore-shoulder, thus, this is the most critical area to be re-engineered by employing suitable risk control options. In this case, having the configuration of the Ro-pax 2 full car decks, it is not possible to change the volumetry in that space or change the structures of the decks, therefore it is possible to use deployable barriers as a risk control option in combination with fixed foam installation under the car decks.
Figure 13 shows the first risk control option implementation, consisting of the installation of permanent foam in void spaces under the car deck. The location of foam is concentrated in the fore shoulder, where most of the criticalities have been detected by initial analysis. It is these cases in particular that can benefit the greatest from the introduction of passive foam, as such installations work to significantly increase damage GM (restoration). Furthermore, as a passive system, the permanent foam is immediately available following the opening of the damage breach and is therefore effective during the transient phase. As void spaces have been targeted, the resultant solution is non-intrusive by nature and converts what is essentially "dead space" into an asset. The configuration gives a considerable improvement in terms of achieved PLL, registering a decrease of 47.04% compared to the original value for Level 1 and a decrease of 42.57% compared to the original for Level 2.1 prediction.

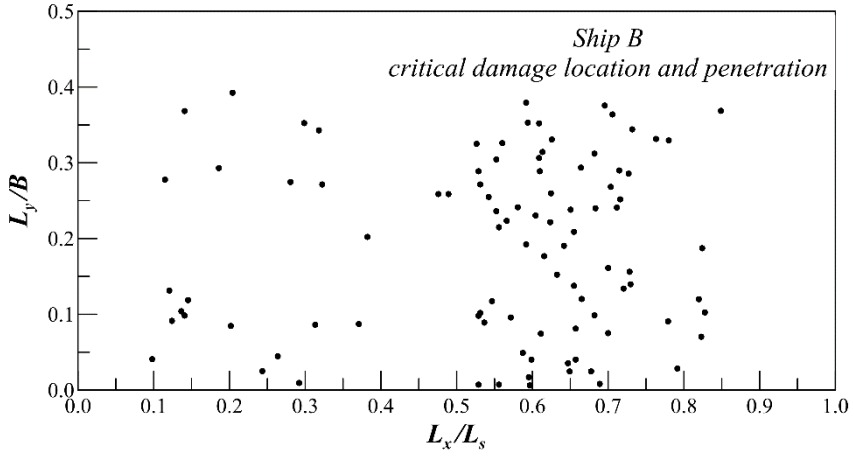

Figure 12: Critical damages location and penetration for Ship B.

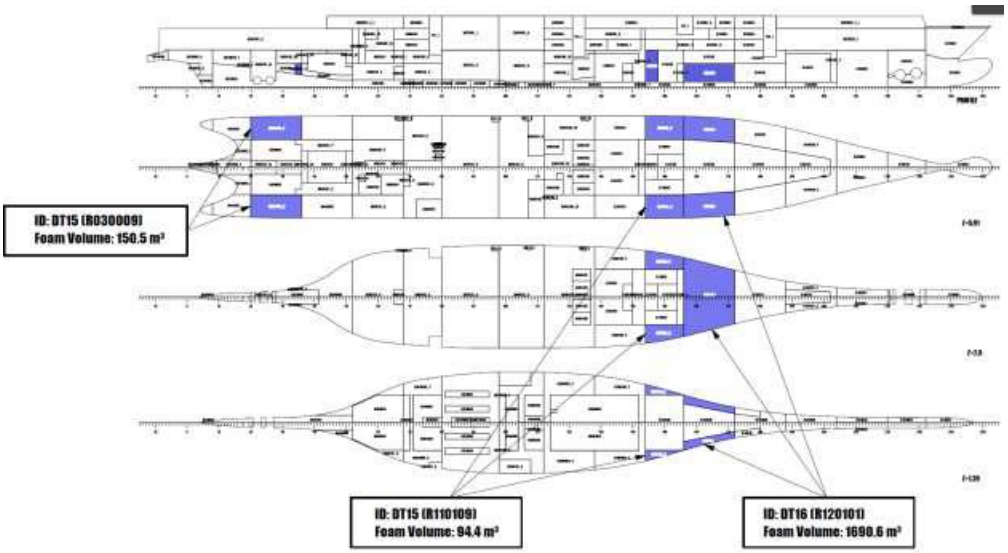

Figure 13: passive foam installations on Ship B.

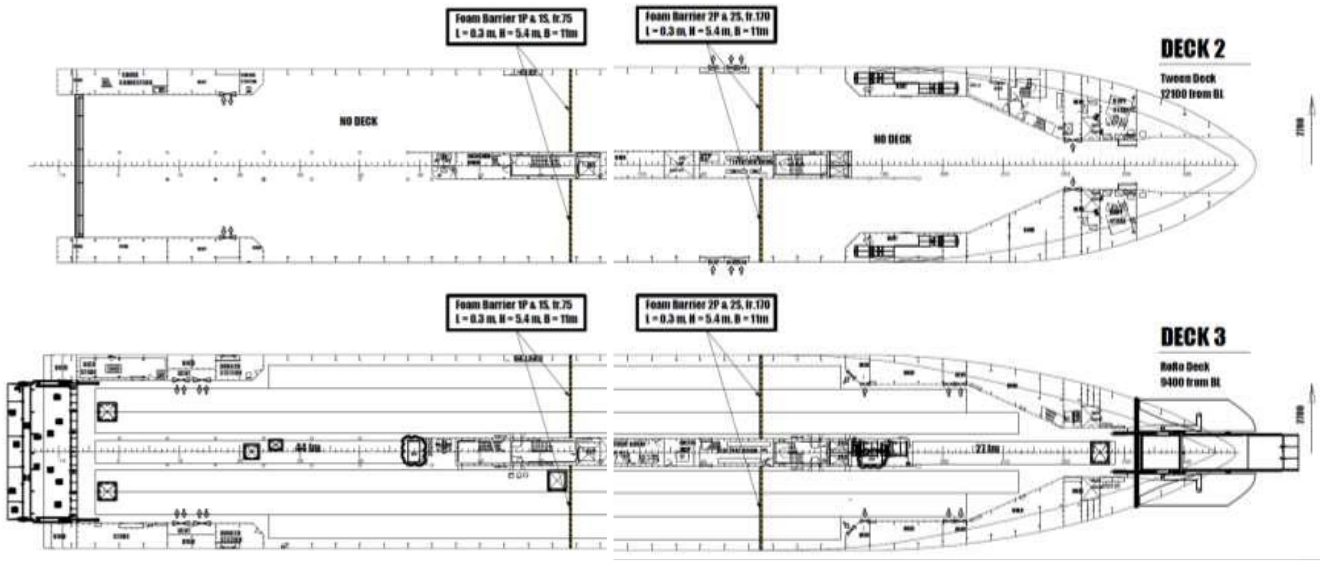

Figure 14: Deployable barriers in the car deck for ship B.

Figure 14 shows the second risk control option implementation, consisting of the installation of deployable barriers. In determining where best to locate the foam barriers, the first consideration has been to target areas of heightened vulnerability within the vessel design. These can be identified where there are concentrations of loss scenarios. Secondly, the barriers have been located to limit, as far as possible, the number of breaches overlapping the barriers. This works to maximise the number of cases that will be positively influenced by the presence of the barriers, whereas if they were to lie within the breach extent, they would offer little to no protection. The resultant configuration has seen the implementation of 4 barriers, protecting both the fore and aft shoulders in pairs across the car deck. The configuration gives an improvement in terms of achieved PLL, registering a decrease of 15.74% compared to the original value for Level 1 and a decrease of 22.94% compared to the original for Level 2.1 prediction.

Concluding Remarks

The previous sections presented the implementation of three different kinds of RCOs to the two reference ships. The implementation results in evaluating the PLL with both simplified and advanced methodologies. More precisely, Level 1 considers only static calculations while Level 2.1 employs dynamic simulations, thus a first principle tool. Table 2 reports a resume of all the PLLs evaluated for the reported cases for Level 1 prediction, while Table 3 reports the results for Level 2.1.
The implementation of RCOs led to different results comparing Ship A and Ship B, especially for the installation of the passive fixed foam system. This is essentially due to the differences in the amount of foam installed in the two designs. For Ship A, the quantity of foam is limited to the small space of the double hull in the engine room area (see Figure 11) thus ensuring few reserves of buoyancy compared to Ship B, where the total amount of foam is about 1935.5 m^3, equivalent to almost 30 % of the volume in deadweight conditions. Such a massive installation of foam was possible on Ship B because of the large number of void spaces available under the car decks, something not possible to achieve for Ship A or a cruise vessel in general. Other studies on foam application highlight that there is some margin to put more foam volume on cruise vessels, just by slightly changing the internal layout of the ship (Vassalos et al., 2021, 2022a).

Table 2: PLL Level 1 values for Ship A and Ship B.

	Damage type	No RCO	Passive foam	Crashworthy structure	Deployable barriers
Ship A	Collision	0.3549	0.3182	0.2716	-
	Side grounding	0.5349	0.4555	0.4721	-
	Bottom grounding	0.1990	0.1859	0.1859	-
	Total	**1.088**	**0.9596 (-11.90%)**	**0.9296 (-14.60%)**	**-**
Ship B	Collision	0.3412	0.1862	-	0.2622
	Side grounding	0.1603	0.0820	-	0.1546
	Bottom grounding	0.0357	0.0163	-	0.0358
	Total	**0.5372**	**0.2845 (-47.04%)**	**-**	**0.4526 (-15.74%)**

Table 3: PLL Level 2.1 values for Ship A and Ship B.

	Damage type	No RCO	Passive foam	Crashworthy structure	Deployable barriers
Ship A	Collision	0.3173	0.2674	0.2268	-
	Side grounding	0.3353	0.2956	0.3086	-
	Bottom grounding	0.1809	0.1683	0.1686	-
	Total	**0.8334**	**0.7312 (-12.30%)**	**0.7040 (-15.50%)**	**-**
Ship B	Collision	0.3284	0.1894		0.2281
	Side grounding	0.1041	0.0632		0.0988
	Bottom grounding	0.0352	0.0161		0.0334
	Total	**0.4677**	**0.2686 (-42.57%)**		**0.3604 (-22.94%)**

In any case, with the application of foam being really effective in reducing flooding risk, it could be reasonable to start thinking about different layouts for the passenger ship interior design and abandon the actual trend of extensively capillary compartmentation aimed to increase asymptotically the static A-index, which of course is not possible as saturation is reached after a small increase of the empirically determined number of bulkhead spacing of $0.03Ls+10$ m.

On the other hand, the crashworthy structure for Ship A and the deployable barriers for Ship B highlight comparable levels of flooding risk reduction while considering a Level 1 assessment. The difference between the effectiveness increases while considering the Level 2.1 characteristics where the effect of the deployable barriers in the car deck became more effective due to the reduction of water progression in the car deck, something that can be reliably evaluated with dynamic simulation only as highlighted by recent benchmarking activity on several flooding simulation codes (Ruponen et al. 2022a).

It is important to underline the differences between the PLLs evaluated with Level 1 and Level 2.1 for both ships as it underlines the relevance and impact of using first principle tools for the flooding risk assessment. All the PLLs evaluated with dynamic simulations have lower values than those obtained by Level 1. The differences arise both for Ship A and Ship B, regardless of the RCO adopted for the calculations. For the Ship A original configuration, the Level 2.1 risk is 23.40% less than the Level 1.1. For Ship B the difference in the original configuration is in the order of 12.94%. Considering the fixed foam installations, the difference for Ship A is about 23.80% and for Ship B 5.5%. For the crashworthy structure, the difference attests to 24.27% while for the deployable barriers in Ship B is 20.37%.

The difference between the values obtained with the two prediction levels is not negligible as it is always above 5%, reaching peaks around 25%. Such a matter stresses the importance of using first principle tools for flooding risk assessment in the design process of passenger ships. Furthermore, the obtained results suggest how different strategies should be pursued to design safer passenger ships, thanks to the adoption of proper cost-effective risk control options instead of relying only on the excessive compartmentation of internal spaces.

CONCLUSIONS

The present work details the application of a multi-level flooding risk assessment framework for the design phase of passenger ships, highlighting the possibility of implementing different kinds of risk control options to reduce the final risk. The paper describes the primary first-principle tools that can be used to increase the reliability of the risk analysis during the design phase of a passenger vessel, focusing on the adoption of super-element methods for breach generation and design of crashworthy structures and the application of dynamic flooding simulations to estimate the vessel survivability to a given hazard. The execution of advanced evacuation analyses has also to be taken into account to pursue a fully first-principle-based risk analysis, however, the study within project FLARE demonstrates that the gain in terms of PLL by using evacuation analyses or analytical approximation is negligible. Therefore, the implementation of a risk assessment framework for flooding is achievable by using first principle tools up to Level 2.1, thus employing dynamic simulations for vessel survivability.

The paper offers also the possibility to appreciate the flexibility of the given framework to implement different design solutions for risk mitigation. The example provided on a cruise ship (Ship A) and a Ro-pax (Ship B) allows for the testing of three different risk control options: fixed foam installation, deployable barriers and crashworthy structure. Calculations have been performed for all the configurations highlighting the efficacy of the proposed measures to the reduction of risk, always above 10% compared to the original configuration. At the same time, the calculation provided at both Level 1 and Level 2.1 for the PLL highlights differences from 5 to 25% in the final value of attained risk. Such a matter underlines the importance of using more reliable tools (thus at least a Level 2.1 prediction) in the flooding risk assessment of passenger ships.

Finally, the paper underlines how the adoption of a risk control option may increase the safety of a passenger ship and how the use of first principles tools allows for the quantification of the risk reduction provided by the RCOs themselves. The results show how active or passive solutions may significantly reduce the flooding risk on a ship, without the need for

increasing the capillarity of the internal compartmentation of the vessel. Therefore, the adoption of such tools in the design process of passenger ships may result in a new design strategy for the achievement of a generation of safer passenger vessels. It is important to stress that the first-principle tools employed for the reference study have all been validated against experiments in the last 20 years, with continuous activity of benchmarking. Such a matter gives confidence in the reliability of the final results.

CONTRIBUTION STATEMENT

D. Vassalos: Supervision; writing – review and editing. **F. Mauro:** Conceptualization; data curation, methodology; writing – original draft; writing – review and editing. **D. Paterson**: data curation, writing – review and editing. **A. Salem**: writing – review and editing

ACKNOWLEDGEMENTS

The authors want to acknowledge the partners of the EU founded Project FLARE for the constructive work leading to the findings of the present paper.

REFERENCES

Atzampos, G. (2019). A holistic approach to damage survivability assessment for large passenger ships. PhD Thesis, University of Strathclyde, Glasgow, Scotland, UK.
Azzi, C., Pennycott, A., Mermiris, G., Vassalos, D. (2011). Evacuation Simulation of Shipboard Scenarios. Proceedings of Fire and Evacuation Modelling Technical Conference, Baltimore.
Bulian, G., Cardinale, M., Francescutto, A., Zaraphonitis, G. (2019). Complementing SOLAS damage ship stability framework with a probabilistic description for the extent of collision damage below the waterline. Ocean Engineering, 186, 106073.
BV (2019). Hydrostar for experts user manual. *Technical Report*, Paris, Bureau Veritas.
Cardinale, M., Särkka, J., Bertin, R., Wurst, S., Murphy, A., Hamann, R., Paterson, D., Conti, F. (2022). D7.2 Analysis of Risk Control Options, FLARE Project.
Conti, F., Le Sourne, H., Vassalos, D., Kujala, P., Lindroth, D., Kim. S., Hirdaris, S. (2022). A comparative method for scaling solas collision damage distributions based on a ship crashworthiness application to probabilistic damage analysis of a passenger ship. Ship and Offshore Structures 17(7), 1498-1514.
IMO, (2009). SOLAS-International Convention for the Safety of Life at Sea, London, UK: International Maritime Organisation (IMO).
Jasionowski, A. (2001). An integrated approach to damage ship survivability assessment. PhD Thesis, University of Strathclyde, Glasgow, Scotland, UK.
Kim, S.; Taimuri, G.; Kujala, P., Conti, F.; Le Sourne, H. Pineau, J.; Looten, T.; Bae, H.; Mujeeb-Ahmed, M., Vassalos, D.; Kaydihan, L., Hirdaris, S. (2022). Comparison of numerical approaches for structural response analysis of passenger ships in collisions and groundings. Marine Structures 81, 103125.
Kwee-Meier, S.T., Mertens, A., Schlick, C.M. (2016). Evacuations of passenger ships in inclined positions - Influence of uphill walking and external stressors on decision-making for digital escape route signage. International Conference on Human Factors in Transportation, AHFE 2016.
Le Sourne, H. Donner, R., Besnier, F., Ferri, M. (2001). External Dynamics of Ship-Submarine Collision. Proceedings of the 2nd International Conference on Collision and Grounding of Ships (ICGS): 137-144.
Lützen, M. (2001). Ship Collision Damage. PhD thesis, Technical University of Denmark.
Mauro, F., Vassalos, D. (2022). The influence of damage breach sampling process on the direct assessment of ship survivability, Ocean Engineering, 250, 1-17
Mauro, F., Vassalos, D., Paterson, D., Boulougouris, E. (2023a). Evolution of ship damage stability assessment – transitioning designers to direct numerical simulations. Ocean Engineering, 268, 113387.
Mauro, F., Conti, F., Vassalos, D. (2023b). Damage surrogate models for real-time flooding risk assessment of passenger ships. Ocean Engineering, 285, 115716.
Nasso, C., Bertagna, S., Mauro, F., Marino, A., Bucci, V. (2019). Simplified and advanced approaches for evacuation analysis of passenger ships in the early stage of design. Brodogradnja, 70(3), 43-59.
Papanikolaou, A., Hamman, R., Lee, B.S., Lemoine, L., Mains, C., Olufsen, O., Tvedt, E., Vassalos, D., Zaraphonitis, G. (2013), GOALDS: goal-based damage stability of passenger ships", Transactions SNAME.

Pawlowski, M. (2004). Subdivision and Damaged Stability of Ships, F. P. Przemyslu, Ed., Gdansk, Poland: Euro-MTEC Book Series.
Ruponen, P., Valanto, P., Acanfora, M., Dankowski, H., Lee, G., Mauro, F., Rosano, G, van't Veer, R. (2022a), Results of an international benchmark study on numerical simulation of flooding and motions of a damaged ropax ship, Applied Ocean Research, 123, 103153.
Ruponen, P., van Basten-Batemburg, R., van't Veer, R., Bu, S., Dankowski, H., Lee, G., Mauro, F., Ruth, E., Tompuri, M. (2022b) International benchmark study on numerical simulation of flooding and motions of a damaged cruise ship, Applied Ocean Research, 129, 103403.
Vanem, E., Rusas, S., Skjong, R., Olufsen, O. (2007). Collision damage stability of passenger ships: Holistic and risk-based approach. International Shipbuilding Progress, 54(4), 323-337.
Vassalos, D., Guarin, L., Vassalos, G.C., Bole, M., Kim, H.S., Majumder, J. (2003). Advanced evacuation analysis – Testing the ground on ship. Second International Conference in pedestrian and evacuation dynamics, London.
Vassalos, D. (2016). Damage survivability of cruise ships – Evidence and Conjecture. Ocean Engineering, 121, 89-97.
Vassalos, D. (2020), The role of damaged ship dynamics in addressing the risk of flooding, Ship and Offshore Structures, 1-25.
Vassalos, D., Paterson, D., Mauro, F., Boulougouris, E. (2021). Life-cycle stability management for passenger ship. ISOPE International Ocean and Polar Engineering Conference, ISOPE-I-21-4187.
Vassalos, D., Paterson, D., Mauro, F., Mujeeb-Ahmed, M., Murphy, A., Michalec, R. Boulougouris, E. (2022a). A multi-level approach to flooding risk estimation of passenger ships. SNAME 14th International Marine Design Conference, IMDC 2022, Vancouver, BC, Canada.
Vassalos, D., Mujeeb-Ahmed, M., Paterson, D., Mauro, F., Conti, F. (2022b). Probabilistic Damage Stability for Passenger Ships—The p-Factor Illusion and Reality. Journal of Marine Science and Engineering, 10(3), 348.
Vassalos, D., Paterson, D., Mauro, F., Mujeeb-Ahmed, M.P., Murphy, A., Michalec, R., Boulougouris, E. (2022c). A lightning intact and damage stability in a multi-level assessment framework. 18th International Ship Stability Workshop, Gdansk, Poland.
Vassalos, D., Paterson, D., Mauro, F., Atzampos, G., Assinder, P., Janicek, A. (2022d). High-Expansion Foam: a risk control option to increase passenger ship safety during flooding. Applied Science, 12(10), 4949.

Part 9:
DESIGN EDUCATION

Proceedings of 15th International Marine Design Conference (IMDC-2024)
June 2-6, 2024
Amsterdam, the Netherlands

Designing a marine systems design specialization track at NTNU

Stein Ove Erikstad[1,*] , Per Olaf Brett[1,2] , Benjamin Lagemann[1,3]

ABSTRACT

In this paper we describe and discuss the current and future MSc specialization programme in marine systems design at the Norwegian University for Science and Technology (NTNU). We follow the structure of a design process. First, we identify relevant stakeholders. That includes industry, society and the students themselves, and we discuss what are their key needs and requirements for a master level education. Further, we outline what can be considered a conceptual solution for the marine systems design specialization programme´s structure and content. We apply two basic types of learning elements. First, a set of focused topic blocks covering central systems design models and methods to develop the required theoretical competence platform. Second, the students perform a series of creative, 'use case'-oriented collaborative development projects based on CDIO (Conceive, Design, Implement, Operate) principles. We discuss the "educational design solution" in terms of learning objectives vs. achieved results and evaluate the impact both from an academic and an industrial perspective.

KEY WORDS

Marine systems design; Education; Study programme

INTRODUCTION

"Everyone designs who devises courses of action aimed at changing existing situations into preferred ones" (Simon 1996). In this paper the "situation" refers to our marine technology study programme, unlike in most IMDC papers, where the design object is typically a ship.

Globally, there are only a few universities offering an integrated five-year MSc track in marine technology. Our marine technology programme at NTNU graduates around 120 MSc students each year. This reflects the importance and size of the maritime industries in Norway, traditionally being shipping and fisheries, shipbuilding, ship equipment systems, later including offshore oil & gas and aquaculture in the 70s, and more lately offshore energy, autonomous ocean space surveillance and now also deep-sea mining.

NTNU is also among the even fewer universities having a dedicated specialization in marine systems design (MSD). In our MSc programme, about 20-30 students each year have chosen this specialization, alongside those specializing in marine structures, hydrodynamics, cybernetics, or energy systems. The historical roots of the MSD programme date back to the late 60s, with the establishment of a separate department of *ship design*, and with Professor Stian Erichsen pioneering the development of *design* as a research and education field at NTNU beyond what was then considered a typical naval architecture and shipbuilding programme. Later, with the advent of the new ocean industries both in Norway and beyond, the specialization changed its name to *marine systems design*. This was reflecting both the shift of importance to "industry Norway" expanding from shipping to offshore oil and gas related design objects', but also the importance of a *systems* focus in developing everything from integrated multi-modal logistics to the installation and operation of subsea oil & gas fields, aquaculture, offshore wind farms, to name a few.

[1] Department of Marine Technology, Norwegian University of Science and Technology (NTNU), Trondheim, Norway
[*] Corresponding author, email: stein.ove.erikstad@ntnu.no
[2] Ulstein International AS, Ulsteinvik, Norway
[3] SINTEF Ocean, Trondheim, Norway

Submitted: 23 February 2024, Revised: 23 April 2024, Accepted: 1 May 2024, Published: 20 May 2024

Conference paper, DOI: https://doi.org/10.59490/imdc.2024.846 e-ISSN: 3050-4864

As will be discussed in more detail later in this paper, we have a current string of both more general systems analysis courses as well as marine design methodology courses that is the backbone of the MSD specialization. However, we steadily see the need to review and re-design this track. There are several reasons for this. One is simply to critically evaluate the status quo at regular intervals as part of a continuous education quality process. Further, internal factors such as student exchange periods (80% of our student go abroad for at least one semester), changes in human resources and internal organization, and changing expectations from industry, all drive change and require adaption. Finally, external developments such as the focus on sustainability and net zero emissions towards 2050, and developments in digitization and artificial intelligence, are additional instigators for change.

Asbjørnslett et. al. (2022) presented much of the concept ideas and some more details about the NTNU perspective on educating the next generation marine system design engineer. The NTNU future technology studies project was reviewed and discussed as to its consequences and implications for the organization and upgrades of the marine technology study and outline of the study plan. It was also explained how the trajectory of human expansion into the ocean represented by new and expanded ocean activities like marine aquaculture, deep-sea minerals, offshore wind energy generation, etc. in addition to the more conventional and well-established ocean activities like shipping, offshore oil & gas, fisheries, and others, may be seen as an accelerated demand for marine systems design architects and engineers. The CDIO (Conceive, Design, Implement, Operate) approach introduction in the study syllabus, the use of field studies to improve the understanding of operational matters, the introduction of sustainability and digitalization into the study plan, and finally, a short review and argumentation for the introduction of the marine system design (MSD) "diamond" as a realization and implementation tool of the needs-function-form mapping in engineering design, on different levels, meeting the diverse stakeholders' demand, were all addressed.

Thus, the overall objective of this paper is to *outline the goals, structure and content of a marine systems design MSc specialization track that meets anticipated needs and requirements for the next decade(s)*. Based on this, the important questions we want to address here and discuss at IMDC are as follows:

- Who are key stakeholders for such a programme, and what are their needs and requirements?
- How can we map these needs and requirements into specific learning objectives for the specialization programme in marine systems design?
- What should be the corresponding learning content, in terms of theory, models, processes, tools and skills?
- What should be the structure of the study programmes?
- How do we handle and include the interdisciplinary challenges of future study programmes?
- What should be the role of industry and industrially relevant design business cases in this education track?
- What is a good balance between a classical naval architecture approach and the exploration and implementation of new topic areas and technologies, such as artificial intelligence, digital twins, model-based systems engineering?

Needs and requirements

Before we start to define needs and requirements for a revised MSc education track, we must define *who* are actually our "customers". What immediately comes to mind for most technical universities is the industry and their needs since they are the main receivers of graduates which they subsequently turn into value-creating employees. This "what-the-industry-want" is also easily accepted by the students, since an education targeted towards their needs, make them attractive in the labour market after graduation. It is here important to keep in mind the tendency of industry to be short-sighted and very topical in their demands and expectations' setting. From experience, we know that study programmes are not that quickly to change and sometimes topics and expectations of industry can only be met by inter-departmental (institutes) set-ups, because they are multi-disciplined by nature and the universities and departments are not necessarily arranged such that cross-discipline challenges experienced by industry, can easily be handled by existing course programmes and syllabuses. Industry demands and expectations must, therefore, be carefully scrutinized and evaluated, and study programmes gradually adapted to these needs if at all possible. So, not all industry expectations can necessarily be met by universities.

Beyond the value-creating employee perspective, the students themselves are important stakeholders. A master level education is essential for the formation of an intellectual and competency platform for the individual that gives meaning, mastery and self-realisation throughout their life. The report "Worth knowing" (NOU 2000) points out that "higher education should not only provide society with competent professionals, but also aim for developing independent and insightful people." The first sets of Generation Z have arrived and already finished their MSc study at the universities. More student groups have or are about to finish their studies. As the first social generation to have grown up with access to the internet and portable digital technology from a young age, members of Generation Z, even if not necessarily digitally literate, have been dubbed "digital natives" (McKinsey 2023). Moreover, the negative effects of screen time are most pronounced in adolescents, as compared to younger children. Members of Generation Z tend to live more slowly than their predecessors when they were their age. This is

reflected in being more concerned than older generations with academic performance and job prospects and spend more time on electronic devices and less time reading books than before, with implications for their attention spans, vocabulary, academic performance, and future economic contributions.

For the society as such, it is desirable that we train master level engineers who can contribute constructively to the public debate with understanding, perspectives and opinions that stretch out over narrow commercial interests. This will be both a counterweight and a complementary voice in a public debate which is characterized to a greater extent by social scientists and economists than by engineers. Such a public debate will demand engineers who dare to challenge and question existing structures and to use their knowledge to point out errors and shortcomings in a world characterized by technology - including topics that may not always be in the industry's interest to raise. Most of the students we educate will, to a greater or lesser extent, work with research and development. Here, in addition to solving technology challenges in a short-term perspective, they must be trained to address more long-term, fundamental issues that often fall outside the industry's interest, but where a holistic understanding is important. The importance of this has increased by the need to curb greenhouse gas emissions. The solution is multifaceted, but technology does play a vital role - both in creating the problem in the first place, but also for developing solutions. And it should be said that industry representatives have told NTNU that we should listen to what they say – but we should not listen too carefully.

We are part of a knowledge society, where knowledge is perceived to have an intrinsic value beyond its usefulness from an industrial perspective. Knowledge is a crucial pillar in an enlightened, rational, and democratic society. The interaction between technology and society, and technology and humanity, is as such an important perspective which, both directly and indirectly, must be communicated as an important end goal for an education.

What is then the future role of the naval architect?

Previous IMDC contributions have addressed and seriously challenged the future role of the naval architect – to be strengthened and expanded upon as an integrator or manager of the ship design project – sometimes even administering the new building project development on behalf of the customer from idea to ship in operation. Thus, the naval architect becomes an integral part of the customer's business development process – as in current project-making activity (Ulstein & Brett et al. 2012, 2015). In addition, it has been argued that it is paramount that the naval architect retains his or her expertise and skills, and even continually improves them, in designing the better ship or marine object to meet all stakeholders' expectations.
Andrews (2018b) approaches the challenge by asking the question "is a naval architect an atypical designer – or just a hull engineer?" He continues: "It seems appropriate…to question whether the engineering discipline – that of naval architecture – which has to date dominated ship design practice, still remains best placed to continue in that role." In the conclusion, it is said that: " …despite the increasingly demanding safety (and decarbonization) regime in ship design, that emphasizes the naval architect's role as "the hull engineer", the naval architect's role remains that being the overall ship (solution) designer." In short, Andrews (2018a) put forward three main reasons for that assertion: a) "Everyone's problem is the naval architect's problem, " b) "There is a need to have a whole ship perspective to ensure design balance is achieved from the initial synthesis and maintained through-out design development and through life", c) "Architecture is seen to be the key to both initial ship design synthesis and to achieving and maintaining design balance".

In addition to the appropriate academic qualifications a naval architect needs to also expand from wider engineering practice with a set of additional applied and social science expertise and skills such as finance, human resources, organization, marketing and communication and finally, project leadership and management skills, (Ulstein & Brett, 2015, 2018). Thus, more naval architects need to expand their multi-disciplinary expertise and skills to better support and be able to respond better to increasing industry demands. Again, it is suggested that "the ship designer of the future" must master equivalent expertise and knowledge within the fields of commercial, operational, and technical challenges related to a new building project realization. Thus, a new type of competent naval architect must be developed by academic education and training and put into practice situations different from the past.

Marine systems design - a managerial process

Over the years, it has become clearer to us that handling the whole process of a ship design project, with its apparent complexity, uncertainty, and ambiguity are more of a managerial mastery task rather than a classic naval architecture and marine engineering-based ship design and ship-hull engineering task. Another challenge is the conflict-oriented situation, which often arises in the ship design approach and how to turn it into something positive for the process and the parties involved. Conflict situations are generated within or among stakeholders in the ship design process as a manifestation of contesting differences in viewpoints, competence, and experiences. They occur when the views that are involved in the ship design discussions collide to produce cognitive turbulence, which can result in instable patterns of conflicting behaviour. Typically, three classes of conflict situation can arise in a ship design approach: i) tensions that may have no discernible cause, ii) disputes caused by

misreading and interpretations *and* minor provocations, and iii) conflicts represented as a manifestation of differences in opinions, experience, and expertise. Consistent with the systems viewpoint, it has been suggested that a conflict modelling cycle can contribute to the exploration of the undesirable behaviour patterns and inherent attitudes among the participants in the ship design process.
Under such a regime, we believe that traditional ship design approaches will gradually become an extended project management process to be offered owners rather than a given design package. Classic naval architecture and marine engineering skills and expertise will rather become an integral part of it. Hence, state-of-the-art naval architect education must gradually reflect these challenges.

New challenges – time for change

In line with RINA, it seems as if the traditional naval architecture and marine engineering basic bachelor and or master's degree educational disciplines and existing study programmes do not suffice as the basis for further enlightenment and proper handling of appearing multi-faceted, "wicked" problems. The wicked problem(s) being described by typically 10 propositions put forward by Rittel and Weber, (1973): "1. There is no definite formulation of a wicked problem. 2. Wicked problems have no stopping rule. 3. Solutions to wicked problems are not true or false, but good or bad. 4. There is no immediate and no ultimate test of a solution to a wicked problem. 5. Every solution to a wicked problem is a 'one-shot operation'; because there is no opportunity to learn by trial-and-error, every attempt counts significantly. 6. Wicked problems do not have enumerable set of potential solutions, nor is there a well-described set of permissible operations that may be incorporated in the plan (business concept). 7. Every wicked problem is essentially unique. 8. Every wicked problem can be a symptom of another problem. 9. The existence of a discrepancy representing a wicked problem can be explained in numerous ways. The choice of explanation determines the nature of the problem's solution. 10". The planner (naval architect) has no right to be wrong. Head and Alford (2015) propose some strategies for dealing with wicked problems – such as going beyond technical/rational thinking, collaborative working, new modes of leadership, and reforming the managerial infrastructure. These strategies can enable partial and provisional responses to problems, amounting to shared understanding about the nature and about ways of dealing with them, they conclude.

RINA (Andrews, 2018) suggests that such additional problem-solving expertise and skills training should take place after the formal degree-based education is finished. The authors of this article argue that such training is not only a question of future on-the-job training for a certain period but requires proper education in relevant non-technical subjects too.
It is, therefore, time to reconsider how we educate and train future naval architects. Future technology study programmes (Asbjørnslett et al., 2023) should expand their knowledge territories and or let other complementary trained expertise, team up with them each time and in such a way to create the necessary inter-disciplinary expertise and skills to advance the relationship between academic staff and students. Project-related work where students can achieve valuable collaborative experience, go beyond technical/rational thinking, take real leadership of their innovation projects, ensure that the different subjects of the marine technology study-programme is fully explored and utilized, seem to be in line with contemporary plans for the future of technology studies. Complementarity, openness and improved interpretive schemes for interfacing different subjects and study programme approaches and their corresponding project tasks and course work are most likely what we need. NTNU IMT is moving quickly in this direction. It will be interesting to see whether other academic marine design schools move into the direction of broadened and multi-disciplinary study programmes too.

THE CURRENT STUDY TRACK TO MEET NEW CHALLENGES

Programme structure

The integrated Master of Science programme extends over five academic years (10 semesters) and constitutes a course load of 300 ECTS credits. All 5-year master's programmes offer a combination of compulsory and elective courses. To graduate from a Master of Science programme a student must have completed all compulsory courses, as well as enough elective courses to achieve the total 300 ECTS credits required to complete the programme.

For a student that will graduate with a master's in marine technology, with a specialization in marine systems design, the study will comprise the following, see Table 1:

- There is a string of marine technology courses starting from the first semester, that is meant to cover all basic naval architecture topic areas, such as hydrostatics and stability, hydrodynamics, structures, cybernetics & power systems. This string is compulsory for all students. It converges towards the 6th semester with a capstone design project that will synthesize and integrate the different marine technology disciplines, providing hands-on training for the students to apply their knowledge in a realistic design setting.

- In parallel, the first three years will develop a sound foundation in mathematics (4x 7.5 ECTS), physics and chemistry, as well as covering basic engineering topics such as mechanics, fluid dynamics and thermodynamics.
- In the last part of the study, the students are obliged to dive deeper into selected marine technology topics, such as sea loads, advanced structural analysis, propulsion, etc.
- Additionally, a number of non-technical topics are compulsory, such as technology management and electives from economics, finance, or social sciences.

Table 1: The five year MSc programme in marine technology at NTNU. Yellow cells are common cross-specializations naval architecture courses, while the blue are courses specifically for the marine systems design specialization

Year	Sem	7.5 ECTS	7.5 ECTS	7.5 ECTS	7.5 ECTS
5	10	Master's Thesis			
	9	Complementary	MT elective	Simulation/Fleet design	Specialization Project
4	8	Experts in Team	MT elective	MT elective	Design methods II
	7	Complementary	MT elective	Other elective	Design methods I
3	6	MT elective	OR & Optimization	Machinery systems	MT6 Capstone design
	5	Mathematics 4N	Techn management	MT5 Marine dynamics	MT4 Propulsion&control
2	4	Statistics	Thermodynamics	Material Technology	MT3 Hydrodynamics
	3	Mathematics 3	Physics	Fluid Mechanics	MT2 Structures
1	2	Mathematics 2	Programming	Mechanics 2	Philosophy of science
	1	Mathematics 1	IT Introduction	Mechanics 1	MT1 Intro

The specialisation in Marine Systems Design starts off after the capstone design course. According to the learning goals, the specialization shall provide the students with knowledge and competence for the design and realization of complex, innovative marine systems, such as ships, marine transportation systems, offshore platforms, offshore logistics and systems for offshore energy production. After completing this specialisation, the candidates shall be able to:

- perform a technical analysis of relevant marine systems, such as stability and hydrostatics, resistance and propulsion, strength, reliability, and availability.
- analyse the economic, environmental, risk and safety-related performance of a vessel or fleet in a life cycle perspective.
- design and verify systems for operation in harsh marine environments, with a particular focus on Arctic conditions.
- use methods from operations research and risk analysis for optimization, simulation and decision support.
- apply a holistic perspective to the development and realization of marine systems, based on methods from design theory and systems engineering.

They should also develop skills that make them able to:

- develop holistic, complex innovative systems solutions both individually and as part of teams.
- make relevant ICT tools for computer aided design, technical analyses, optimization, simulation and risk and safety analysis.
- verify design solutions with respect to regulations and requirements from trade, customers, and society as such.
- efficiently present and communicate the final design solutions and corresponding documentation, both written and orally.

The overall programme

The new study programmes in marine systems design must be structured in such a way that not only "filtered" industry needs are catered for but also some of the needs of the incoming Generation Z students. Compared to previous generations, the alternative characteristics of Generation Z: live more slowly, more concerned with academic performance and job prospects,

more time spent on electronic devices and less time reading books, with implications for their attention spans, it is argued by the authors of this paper that in many ways, a perfect situation is now to make a new marine design course programme work based on the following synthesized assertions:

1. Traditional course time thieves, like making computer programmes work, and traditional library-oriented data-source searches can be replaced by more creative project 'use case'-oriented collaborative development work – idea creation, comparing different solution alternatives by performance indexed benchmarking and massive, big data web-based information solicitation – a real collaborative project expectation elucidation process.
2. Take a broader stand to a full project realization, get in charge with the project team and argue your project team's case and pursued project business proposition – a full practical project work and findings communication process – read less and do more innovation work – take leadership.
3. Use all subject disciplines related to commercial, operational, and technical matters, by engaging all the subject disciplines of a marine technology institute and thereby – make use of the knowledge infrastructure and network - apply the full CDIO (Conceive, Design, Implement, Operate) principles.
4. Prepare and document a real time series of decision-making related to the project development and ship design solution drawings, specification, and analyses – practical application of lessons learned to date and beyond.

CORE METHODOLOGY MODULES OF THE SPECIALIZATION

Still, “the proof lies in the pudding”. Given the needs and requirements developed so far, and the statements on the high-level learning objectives, what should be the specific content of the core specialization track? We have chosen to take a modular approach to this. At NTNU, the standard course is 7.5 ECTS[4]. We have chosen to break this up into 2.5 ECTS “virtual” modules, thus giving us 9 topical building blocks as a replacement for the three courses considered. The question then becomes: What should be those 9 modules?

We are still in the process of developing these modules. Our first draft contained the modules outlined in Figure 1. Each of these is supposed to provide one or a few tangible tools to the designer's toolbox, both from a theoretical and an application-oriented perspective. These modules will of course need to build on the other basic courses that the students have already covered, both generic topics (mathematics, mechanics, etc.), NAME topics and basic systems analysis (e.g. operations research, data analysis, statistics, etc.). In the following, we will briefly describe each of these and discuss the rationale for including them:

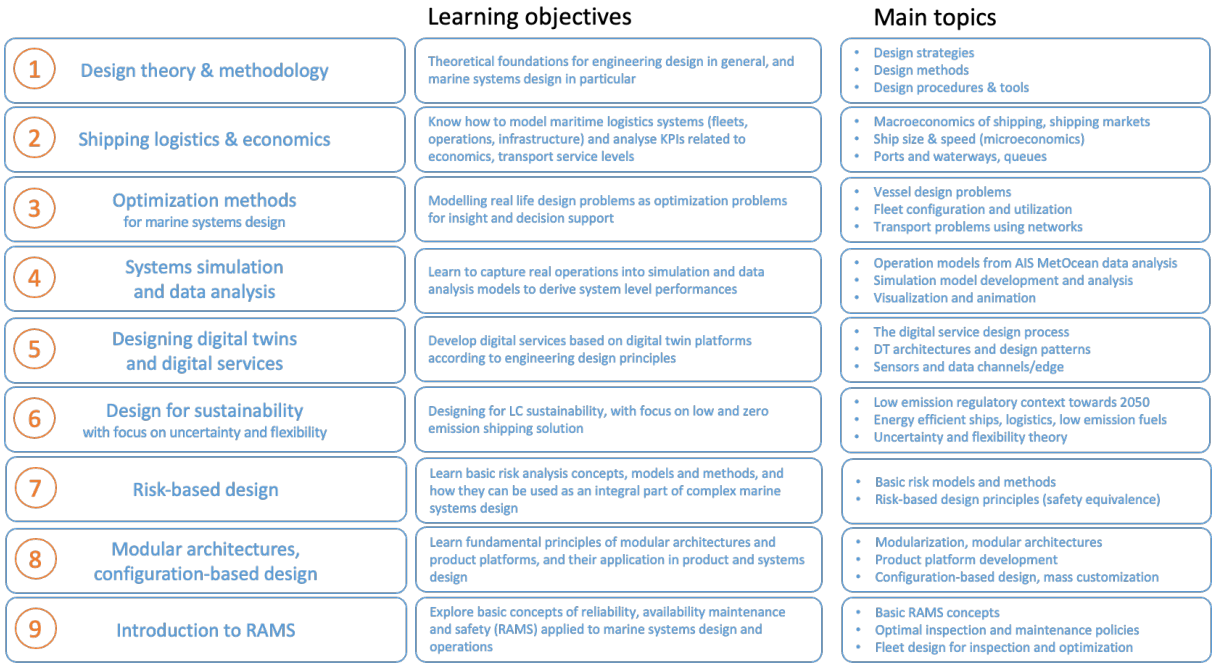

Figure 1: A preliminary outline of core theory and method modules as part of the systems design specialization

[4] European Credits Transfer System

Design theory and methodology

This module will cover the theoretical foundations for engineering design in general, and marine systems design in particular. This includes different design models, the design processes at shipyards and ship designers, and provide a basis for understanding of design as a mapping from needs via functions to form. From before, the students have covered most topics related to marine systems analysis pertaining to hydrodynamics, structures, power systems, etc., and they have already a "hands-on" experience of a guided and relatively complete design process from their capstone project in the 6th semester.

The "function-to-form" principles in engineering design requires a fundamental logical shift for the students. Their previous engineering subjects typically has a form-to-function approach ("given this description, analyse the performance using this method algorithm"). They have already been exposed to the practical reality in the 6th semester capstone subject, which provides a good starting point for reflection and a more theoretical understanding of fundamental design principles. This includes the realization that there is not one "deductive" correct solution for real world design problems, motivating for the introduction of system architectures and corresponding conceptual choice theory. This is akin to "style" being a fundamental element of design according to Andrews (2018a), both as a mental and practical construct of design classes as archetypes that can be further developed and optimized by prototype refinement, (Coyne et al. 1990).

Shipping logistics & economics

A systems perspective on marine design requires a fundamental understanding of the operating context in which the ship will operate. The ship is typically part of a fleet, and the fleet a part of a logistics system. Further, we see the need for a deeper understanding of both the ship and fleet operations, as well as the operational context in terms of e.g. regulatory framework, economics & financing, fuel infrastructure, and technology development – and this from a lifecycle perspective.

This module should link relevant topics from the technical disciplines with topics from operations research and economics, with an emphasis on the strategic design decisions towards fleet renewal and retrofit under a high degree of uncertainty.

Optimization methods for marine systems design

Intrinsically, *design is about finding the best possible solutions* within a set of constraints. Thus, optimization is naturally a core topic for the marine systems design specialization. This includes reflections towards the challenges of capturing large, complex, multi-faceted problems, as real-world design problems typically are, into the relatively strict and formalized framework of mathematical optimization (Simon 1973, Ackoff 1979). Still, our experience is that the students gain considerable insight into a design problem by the modelling process itself, independently of the final optimal solution. This module is planned on the assumptions that all students have a basic course in operation research and optimization from before, so that the focus can be on application-oriented modelling of industry-relevant design problems.

Systems simulation and data analysis

We always design for operation. To understand, visualize and be able to analyse operations that are complex, dynamic, and typically stochastic, simulation and data analysis models become an important part of a designer's toolbox as a means to derive system level performances.

Designing digital twins and digital services

Recent advancements in digitalization and the Internet of Things (IoT) have enabled various digital twin (DT) solutions, facilitating closer collaborations among ship designers, equipment manufacturers, and shipbuilders throughout the vessel's lifecycle. An important aim of DT solutions is to offer value-added services by based on real-time data streams from onboard sensors. For instance, one such service could involve monitoring the vessel's inventory from its inception to decommissioning, actively providing docking services for maintenance, upgrades, and retrofits as needed. Another example includes the establishment of online shore-based operation centres, capable of delivering specialized expertise and economies of scale through the simultaneous management of multiple vessels. These examples illustrate how digital twins become an import outcome from a systems design process, alongside the delivery of the physical vessel. Furthermore, these DT-based value-added services should be *designed* based on the same underlying principles and using a similar methodology as for the ship design itself (Erikstad 2019b).

Design for sustainability with focus on uncertainty and flexibility

We always design for the future, and the future is intrinsically uncertain. Still, we do not have the luxury of waiting for these uncertainties to be uncovered. Design decisions must be made today, increasingly for the long horizon to meet sustainability goals following the 2050 zero emission target defined by IMO. At NTNU, we have an ongoing process towards defining and developing what should be the curriculum related to sustainability, both for the engineering education as such, as well as for the marine technology programme. We believe this topic should be combined with teaching theory, models and methods for designing for uncertainty, flexibility and changeability, such as real options, stochastic programming, epoch-era analysis, scenario development, combined with lifecycle analysis methods.

Risk-based design

Understanding fundamental concepts of risk is a necessary element in all systems-oriented programmes. Many students will take elective courses covering this topic in depth, predominantly from other perspectives than design. A basic module here should cover fundamental risk analysis concepts, models, and methods, and how they can be used as an integral part of complex marine systems design process. It is already central to core topics in naval architecture, e.g. probabilistic damage stability, (Papanikolaou 2012), and it will be increasingly important for developing new and innovative solutions for which there is a limited existing regulatory framework, say, new zero emission fuels, new energy-saving technologies, etc. Here, principles of "equivalent-risk" and "equivalent-safety" are needed for validating design solutions.

Introduction to RAMS

Covers basic concepts of reliability, availability, maintenance, and safety (RAMS) applied to marine systems design and operations. RAMS concepts are important for the operation of the system as such, but also for understanding and modelling important service operations (say, service vessels/fleet for wind farm inspection and maintenance).

Modular architectures, configuration-based design

This module covers fundamental principles of modular architectures and product platforms, and their application in product and systems design, (Erikstad 2019a).

Alternative modules

The nine modules proposed here were the first attempt to define a specialization track for marine systems design. With each module covering 2.5 ECTS, this corresponds to three normal courses, which is our current planning constraint. There will be good arguments for including other topics in this track, though this will have the consequence that one of these nine will have to be removed. Some of the alternatives considered are:

- Project-making and business development, focusing on how shipping and maritime projects are initiated and matured from both technical, commercial/financial and operational perspectives. This includes stakeholder's perspectives, requirements elucidation, and analysis of markets and competitors using tools like Accelerated Business Development (ABD), (Ulstein & Brett, 2015).
- Strategic business models for the design firm. In the DREAMS[5] project, NTNU and Ulstein have investigated the relation between strategic business models, the organisation of the design firm, the structure and content of alternative design processes, and the technical and commercial outcome of the process. It remains an open question to us whether this should be a part of a systems design specialization curriculum.
- Model-Based Systems Engineering (MBSE). This is an approach to systems development that has strong historical roots, as well as having received renewed attention lately. It puts emphasis on the explicit modelling of all central aspects of the system using formal, standardized models, and thus have a relevance to the students beyond systems design. MBSE could be a separate module in our 9-module collection, or it could be integrated as a common modelling framework in most of the other modules.
- Artificial Intelligence in design. At present, with AI application beyond "classical machine learning" is still relatively immature, this would basically be raising relevant discussions and exploring opportunities towards using

[5] Design Re-Engineering and Automation for Marine Systems

AI in design. Though with the present pace of development in this area, it is likely that more substantial models, methods, skills, and applications will have reached a level of readiness to be an unavoidable part of the curriculum.

This list could have been longer. A key point is that we live in an uncertain dynamic world, thus we should design our study programme so that we can continuously adapt – and to the extent possible open up for a certain degree of choice for each student. Over time, it is expected that this list of complementary study modules will be expanded upon to for example meet special contemporary topical needs of the industry and political trends. Other existing modules might be frozen for some years if demand and student interests do not prevail and later on to be revised and revitalized if need be.

From subject theory to project making - Capstone design course

NTNU IMT decided in fall 2023 to adjust and enhance their 3rd level 6th semester TMR4256 Design of Marine Systems Course (previously PMS) into a capstone project that became compulsory for all specializations. The capstone project being a unique opportunity to carry out independent group work to devise an innovative solution for a real-world problem. Figure 2 depicts the international development and search for a modernization approach to existing and traditional training of engineers, particularly at MSc level. Table 1 showed how the Capstone initiative is positioned in the middle of the 10-semester long MSc-course structure of NTNU. In this way, it is thought that students after 5 semesters of basic theoretical training of engineering subjects like maths and physics and others, will need and experience a challenging course in the 6th semester where they will have to develop their innovative skills, handle commercial, operational and technical aspects related to a real problem-solving project.

An important change was that this course was made compulsory for all specializations – so that, e.g., a student who wants to study hydrodynamics should understand the setting for supporting the hull form and propeller design as part of an integrated process.

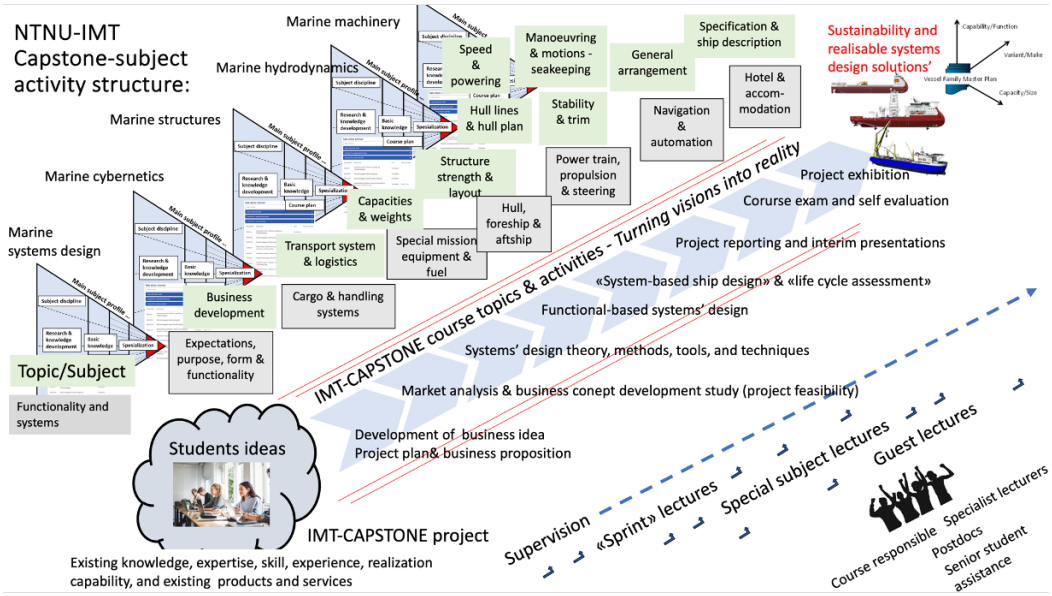

Figure 2: The outline of the new capstone design course

The idea is that students with their 6th semester start background and with additional core lectures, external guest contributions and many "sprint" training sessions can make the students develop an idea almost into a "sellable" and "producible" marine system design solution.

All the traditional naval architecture and marine engineering disciplines are there and applied by the students. In addition, they must also expand their horizon in the early part of the course project work in being introduced, for the first time, with market, business, commercial, and operational matters that influence their project problem solving process. A new important feature of the Capstone initiative is that academic staff (subject specialists) from other main subject disciplines are directly involved in the course execution by particularly running the ad hoc "sprint" training sessions on subject matters arising as the progress of student work takes place and project problems arise – "problem solving at your fingertips". A comprehensive course project

plan is needed and a tight control of course time-plan is executed. Continual facilitation of project work and supervision of student students are practiced.

Interaction with industry is important and is encouraged. Industry representatives are, therefore, involved by web, telephone or physical presence. A lot of emphasis is placed on presentation of ongoing and final work and the course finish off with a two-day oral exam and a two-week exhibition of project work done at the end of the semester.

Almost midway through the Capstone effort, it is still too early to summarize the experiences so far. We, therefore, promise to return to IMDC at a later stage and report on more thought through and well documented experiences.

CONCLUSIONS

In this paper we have outlined a revised plan for a specialization track in marine systems design at NTNU. This is indeed a complex design process, starting with defining the needs of multiple stakeholders, such as students, industry, and society at large, and ending up with, though somewhat fragmented, propositions for what should be part of a marine systems design master-level specialization. We have further described our revised Capstone design course that serves as the introduction to a holistic systems design thinking.

We live in a time where new areas are being opened for exploration, energy production and extraction, where typically deep water, long supply lines, and challenging climatic conditions require new expertise and technology. Energy shortages and a focus on the environment pave the way for profitable exploitation of wind power far offshore. Global warming demands significant reductions in emissions to the air from maritime transport, where a vision of zero emissions from the industry itself sets high expectations for technology that has not yet been developed. Our northern areas are becoming more accessible for marine activities, with associated challenges for vessel technology, logistics, risk, and environment, and where commercial exploitation of a trans-Arctic route is increasingly seen as a real possibility. Aquaculture is moved out into exposed waters.
All this paints a picture of an industry where the most important constant factor is change. And the pace of change seems to be accelerating. The future for which we are educating our engineers appears, however, unpredictable, unclear, and complex. We, therefore, see the need to understand multidisciplinary and complex issues, while important areas of knowledge continue to be developed, accompanied by a need for bringing fragmented expertise within narrow areas closer together. This creates significant challenges in terms of what knowledge and skills we should convey so that our students are as well-prepared as possible for a 40-year plus career after completing their education.

CONTRIBUTION STATEMENT

Stein Ove Erikstad: Conceptualization; writing – original draft, review and editing. **Per Olaf Brett:** Conceptualization; writing – original draft. **Benjamin Lagemann**: Writing - review and editing.

REFERENCES

Ackoff, R. L. (1979). "The Future of Operational Research is Past." *Journal of the Operational Research Society* 30

Adi, A., & Stoeckle, T. (2022). “Public relations as responsible persuasion: Activism and social change.” In *The Routledge Companion to Public Relations* (1st edition, pp. 302–314). Routledge.

Andrews, D. J. (2003). “Marine Design - Requirement Elucidation rather than Requirement Engineering.” *International Marine Design Conference (IMDC)*.

Andrews, D. J. (2018a). “Choosing the Style of a New Design - The Key Ship Design Decision.” *International Journal Maritime Engineering*, *160*(Part A1). https://doi.org/10.3940/rina.ijme.2018.a1.457

Andrews, D. (2018b). “Is a naval architect an atypical designer – or just a hull engineer?”, *International Marine Design Conference*, Helsinki.

Asbjørnslett, B. E., Brett, P. O., Lagemann, B., & Erikstad, S. O. (2022). “Educating the Next Generation Marine Systems Design Engineer – The NTNU Perspective”. *14th International Marine Design Conference*, Vancouver, CA

Brett, P. O., Carneiro, G., Horgen, R., Konovessis, D., Oestvik, I., & Tellkamp, J. (2006). "LOGBASED: Logistics-Based Ship Design". *International Marine Design Conference (IMDC)*.

Coyne, R. D., Rosenman, M. A., Radford, A. D., Balachandran, M., & Gero, J. S. (1990). "Knowledge-Based Design Systems*"*. Addison-Wesley.

Erikstad, Stein Ove (2019a), "Design for Modularity: Volume 1: Optimisation of Ship Design and Operation for Life Cycle", Chapter in book: "A Holistic Approach to Ship Design", ed. Apostolos Papanikolaeu, pp 329-356, Springer Verlag, ISBN 978-3-030-02809-1

Erikstad, S. O. (2019b). "Designing Ship Digital Services". In V. Bertram (Ed.), *COMPIT'19 - 18th Conference on Computer and IT Applications in the Maritime Industries*. Tullamore, Ireland

McKinsey (2023). "What is Gen Z?" Web-based article, https://www.mckinsey.com/featured-insights/mckinsey-explainers/what-is-gen-z, dated March 20, 2023, accessed April 22, 2024

NOU (2000), "Freedom and responsibility – on higher education and research in Norway", *NOU* 2000:14

Papanikolaou, A. (2012), "Risk-based Design", *Springer Verlag*

Head, B. W., & Alford, J. (2015). "Wicked Problems: Implications for Public Policy and Management". *Administration & Society*, 47(6), 711-739. https://doi.org/10.1177/0095399713481601

Horst, W. J. R., & Webber, M. M. (1973). "Dilemmas in a General Theory of Planning". *Policy Sciences*, *4*(2), 155-169. http://www.jstor.org/stable/4531523

Simon, H. A. (1973). "The Structure of Ill-structured Problems." *Artifical Intelligence* 4: pp. 181-200.

Simon, Herbert A. (1988). "The Science of Design: Creating the Artificial". In: *Design Issues* 4.1/2, pp. 67–82. issn: 07479360, 15314790. doi: 10.2307/1511391. url: http://www.jstor.org/stable/1511391.

Simon, H. A (1996). "The Sciences of the Artificial". 3 ed. Cambridge, Massachusetts: MIT Press. https://doi.org/10.7551/mitpress/12107.001.0001.

Ulstein, T., Brett, P. O. (2012). "Critical Systems Thinking in Ship Design Approaches." In *IMDC 2012: 11th International Marine Design Conference*, 1:365–83. Glasgow, Scotland.

Ulstein, T., Brett, P. O. (2015). "What Is a Better Ship? - It All Depends." *In IMDC 2015: Proceedings of the 12th International Marine Design Conference*, 1:49–69. Tokyo, Japan: International Marine Design Conference.

Proceedings of 15th International Marine Design Conference (IMDC-2024)
June 2-6, 2024
Amsterdam, the Netherlands

Educating for an unknown future: How to prepare students of ship design for the propulsion of tomorrow

Carmen Kooij[1,*]

ABSTRACT

It is very likely that the students that we educate today will work with what we currently refer to as modern propulsion or alternative fuels in their career. As educators, the goal is to best prepare our students for their working life. This article looks into what a naval architecture student would need to know about these modern propulsion systems and fuels when they graduate. In this article, two types of knowledge are defined; adaptive knowledge, knowledge that spans multiple areas, and routine knowledge, that addresses a specific case. By identifying what competencies fall under the adaptive knowledge and which fall under routine knowledge, it is possible to advice on changes that should be made to the curriculum in order to best prepare students for the future.

KEY WORDS

Design education; green propulsion; green shipping; marine engineering

INTRODUCTION

Last year, in 2023, the IMO published the common ambition of its member states to bring the greenhouse gas (GHG) emissions close to zero. Additionally, they made a commitment to use more alternative, zero and near zero GHG fuels by 2030 (IMO, 2023). These goals, together with the general trend towards cleaner and greener fuels and propulsion methods means that the students we educate today will need to work with these alternative fuels and propulsion systems in their career. However, as we are still at the beginning of the green revolution in shipping there are many different types of fuel and corresponding propulsion systems to choose from. Unfortunately, we cannot simply address them all in detail.

Education has always had to deal with adapting to innovations made in the industry. Especially in the last decades, technology and tools used in industries are changing rapidly, making educational institutions play catch-up. There is a field of tension between teaching students traditional skills and adding new skills. This is influenced by the wishes of the industry, but also by the skillset of the lecturers and the available time to set up a curriculum surrounding these new technologies.

In this article, we look at how we can best prepare students for the unknown future, allowing them to excel regardless of how a ship's propulsion system will look in the future. We start of with an analysis of the current curriculum for the marine engineering. From there, we define the competencies that a student who graduates with a bachelor degree has. Next, we make the transition to identifying what competencies students should have in the future. This is based on three parts; the first is an analysis of a project performed by our third year students who were tasked with designing a Crew Transfer Vessel (CTV) powered by fuel cells, without them receiving specific training in this area. Additionally, a literature review is performed to find if a trend can be found there. Finally, the industry is asked for their input to see what competencies recent graduates lack. Together, this leads to an overview of what changes should be made to better prepare our students for the future. The article ends with an advice on where the focus should lie.

[1] Maritiem Instituut Willem Barentz, NHL Stenden, Leeuwarden, The Netherlands

* Corresponding Author: carmen.kooij@nhlstenden.com

Submitted: 7 March 2024, Revised: 26 April 2024, Accepted: 1 May 2024, Published: 20 May 2024

Conference paper, DOI: https://doi.org/10.59490/imdc.2024.853 e-ISSN: 3050-4864

In this article the focus lies on modern propulsion systems such as batteries and fuel cells and different (low flash point) fuels. Other methods to reduce GHG emissions on ships such as scrubbers and wind assisted sailing also exist. However, the use of these types of systems is assumed to not be as disruptive for the industry and therefore the curriculum. This means that they are out of scope.

CURRICULUM MAPPING

Currently, the curriculum at NHL Stenden mostly focusses on ships powered by conventional propulsion. In the first year, students are introduced to the main drivers and auxiliary systems. They learn about the most important values of the propulsion systems and make some basic calculations to determine the type and size of engine a ship requires. In the second year, as part of a project, students are asked to make a more detailed design of the engine room. They determine the required power to propel the ship, calculate the amount of additional power that is required and make technical drawings of the engine room such as a detailed design of the engine room and a one line diagram. In the third year students are tasked to design a more complex ship design which requires a better understanding of the required power on board.

To identify the skill that students now have when they leave their study program a method known as curriculum mapping is used. Generally, it is used to identify how generic skills, such as literacy, numeracy and interpersonal skills of students are evaluated, however, it also works for technical skills. Curriculum mapping is used to identify in which subject specific competencies are taught. For example, it can be used to identify where students learn to present their work orally, or where they learn to write a comprehensive report (Sumsion & Goodfellow, 2004). For this article, the method was inverted. Using the study guide of the NHL Stenden University of Applied Sciences as well as input from the lecturers for the different subjects and projects the current competencies within the bachelor curriculum related to the propulsion of ships is investigated.

Defining main educational themes

The mapping of the competencies leads to a long list of different skills related to the propulsion of the ship. In many cases the competencies could be directly derived from the learning outcomes of the different subjects, leading to well defined competencies. The competencies are then grouped together under overarching themes. By identifying the different themes, it is easier to define where changes to the curriculum are required and what elements can remain the same.

The themes are identified conceptually, as is a common approach in this type of research (Male et al., 2011). For this research six themes have been defined; technical theory, design; knowledge of systems and components; operations and economics; safety and fit for 2050. Within these themes, the competencies are identified. Below, each of the six themes are explained further, explaining which current competencies would fall under the relevant theme. The full list of the competencies belonging to the six themes can be found in Table 1. These competencies are used in the end of this article to identify what changes need to be made to the curriculum and what can remain the same.

Technical theory

Technical theory is a very broad theme than encompasses the general knowledge students should have to understand the working principles of the propulsion systems. This includes a general understanding of basic thermodynamic principles but also electrical engineering. The competencies in this theme form the basis on which students build with the other themes.

Design

The theme design covers the competencies related to the design of the engine room. This means that students are able to select the required machinery based on a set of requirements, place it in the allocated space and identify how their choices might influence the rest of the design. As this study only looks at the design of the engine room. Design strategies, although a key part of education of a naval architect, are left out of the scope of this research.

Knowledge of systems and components

This theme covers the understanding of different components that make up the propulsion system. In a traditional system, this would include the diesel engine, (shaft) generators, gearbox etc. Additionally, it includes, but might not be limited to, auxiliary systems and fuel systems. In addition to understanding the different propulsion types, this theme also covers the ability to connect ship types with common or favourable propulsion types.

Operations and economics

It is not enough for a naval architect to be able to design an engine room, they should also understand the effects the chosen propulsion has on the operational profile or building cost of the ship. This theme covers the effect that the choice of propulsion type will have on the operation of the ship, as well as the influence on building cost and operational cost.

Safety

Safety is always a key aspect in any operation, but is also a very broad term. For this article, safety is everything that has to do with safe operation of the ship, with regards to the propulsion system. A main competency in this area is the understanding of the dangers of different propulsion and fuel types. This also includes a basic understanding of the rules governing the design of the engine room and knowing how to apply them.

Fit for 2050
The final theme already looks towards the future. The current curriculum already has an aspect that looks into elements of modern propulsion. Covered in this theme are calculations regarding the emissions of a ship, knowledge of the EEDI, EEOI and EEXI and benefits of electrification on board of ship. However, the competencies within this theme are still fractured and not very well defined.

Table 1 Summary of the themes and corresponding competencies

Theme	Included competencies
Technical theory	- The student can apply the basis laws of thermodynamics (e.g., first and second law, ideal gas law etc.) - The student can apply basic electric principles (e.g., Kirchhoff, AC, DC, Lorentz force etc.)
Design	- The student can translate functional requirements to system solutions which are subsequently integrated into a ship design that meets the requirements of the client. - The student can select required machinery based on system requirements. - The student can perform a matching procedure to determine the required propellor and main driver characteristics. - The student is capable of placing the selected propulsion system and auxiliary systems into the general plan of the ship. - The student understands the logic behind the general plan of different types of cargo ships. - The student can compare different types of conventional propulsion systems with regards to performance, efficiency, manoeuvrability, comfort, design and cost.
Knowledge of systems and components	- The student can explain the components and processes that are part of the following propulsion systems: o A conventional internal combustion engine o A gas turbine o A blue fuel system - The student knows the capabilities of the following propulsion systems o A conventional internal combustion engine o A gas turbine o A blue fuel system - The student knows the auxiliary systems of a conventional propulsion system.
Operations and economics	- The student is aware of the different operational profile of conventional propulsion systems - The student can determine the operational cost of conventional propulsion systems
Safety	- The student knows and is conscious of the technical, human and organisational dangers and risk of different propulsion systems
Fit for 2050	- The student knows the different types of ship emissions and the influence of the environment. - The student can determine the environmental impact of a specific design. - The student knows the advantages and disadvantages of different modern propulsion types.

Comparison with other study programs
While a detailed analysis of other study programs has not been done at this time, a cursory comparison is made to see if there are large differences. Within the Netherlands, two other universities offer a bachelor's degree in naval architecture; the Delft

University of Technology and the Rotterdam University of Applied Sciences. The study programs are not the same, Delft has a more theoretical focus, and in Rotterdam they specifically mention marine engineering as separate subjects instead of being integrated into projects as is the case at NHL Stenden (Delft University of Technology, 2023; Hogeschool Rotterdam, 2023). However, based on the short study guide descriptions and discussions with lecturers from the other schools it can be concluded that many of these competencies overlap.

Adaptive expertise

Adaptive expertise is a term first introduced by Hatano and Inagaki (Hatano & Inagaki, 1984). They stipulate that in learning one can have two types of expertise; routine expertise and adaptive expertise. Routine expertise means a person is highly skilled at a specific task, but lack the flexibility to use the skills and knowledge related to this tasks to new problems. Adaptive expertise on the other hand means that creativity and flexibility are used to solve a problem. This also means that the "standard" procedures for solving a problem are not always followed. To allow for students to thrive not only in the current state of technology but also in the future, they should gain adaptive expertise. However, educational institutes struggle with how to help students develop the creativity and flexibility to become an adaptive expert when needed, without forgoing the need for standardised routine expertise (McKenna et al., 2006). An efficient study program prepares students to have both areas of expertise (Pierrakos et al., 2016).

COMPETENCIES IN PRACTICE: DESIGN OF A FUEL CELL POWERED CTV

In the second semester of their third year, the marine technology students at NHL Stenden are tasked with the full design of a vessel for a specific client. They will run through the entire design process, from identifying the clients wishes to the drawing of the general plan. Last year (2022/2023) the students were tasked with designing a crew tender vessel that was powered by fuel cells. They did not receive any specific training or lectures on the detailed workings of the fuel cells, they had to find the relevant information for themselves. This project therefore provides a good insight into what further information the students would require to fully understand how to design a ship with this type of propulsion.

The final report of the project shows that the students are capable of performing the calculations that determine the required power that needs to be installed on the ship. This is, of course, no different when designing a ship with conventional propulsion. They also calculate the amount of energy they can get out of a m^3 of hydrogen, giving them a reasonable assumption in the amount of hydrogen they would need to take. This, once again, is no different from designing for HFO or MDO. In the next step the students select a fuel cell, as they have been taught.

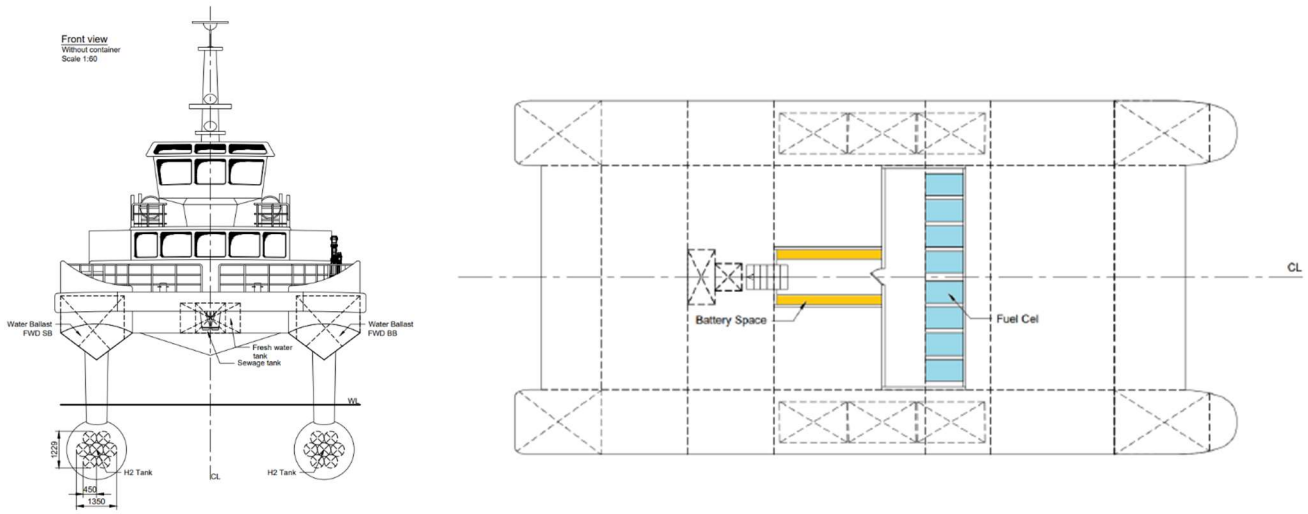

Figure 1 - general plan of the CTV designed by the third year students

The steps the students take up to here show that they have the competencies that one would expect them to have given the list presented in Table 1. However, after this, we see what happens when students try to apply routine expertise as adaptive expertise. It becomes clear that the students have not understood the different equipment that is required for a fuel cell system to operate. The choice they made in the design and the general arrangement show that they do not know enough about the set-up of a system that uses fuel cells. Additionally, the report shows that they have a limited understanding how a fuel cell system generates energy and how this energy is used to power the ship. One example of this is the battery pack. Although the report mentions the fact that a battery pack of 45 batteries is required and it is also drawn into the general arrangement of the ship (see

Figure 1), it is never explained how much power can be stored in these batteries. The confusion seems to stem from how a system with a fuel cell works. Basically, they have designed a system that gets its power from the fuel cell, and provides this to an electrical engine and the propellor directly, as can be seen in Figure 2. This shows that they have a very good understanding of how a propulsion system with a diesel engine works, but that they failed to make the translation towards a fuel cell system. Figure 3 gives a very basic representation of the main components of a fuel cell system.

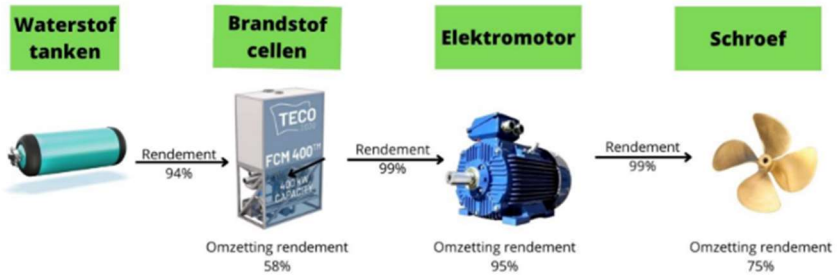

Figure 2 - Basic setup of a fuel cell system according to the students, showing that they designed it as they would a diesel direct system and misunderstood the fundamental differences between these systems.

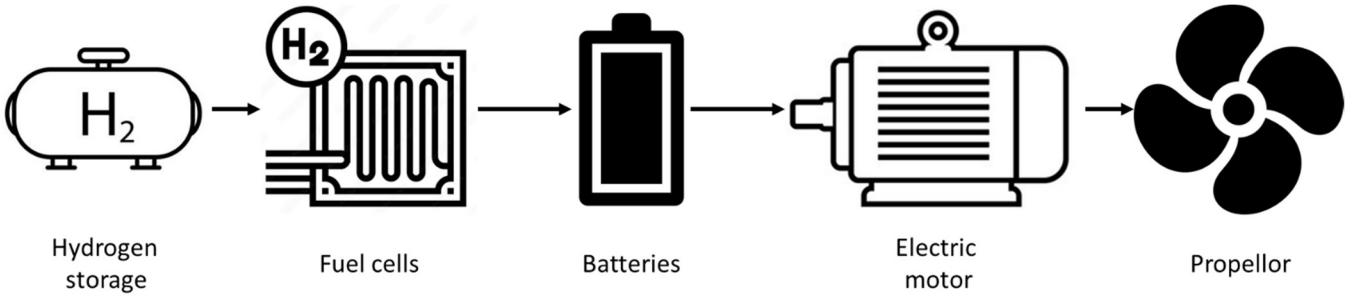

Figure 3 Very basic overview of the main components of a propulsion system with fuel cells

The analysis of this project shows that the competency regarding the matching procedure; t*he student can perform a matching procedure to determine the required propellor and main driver characteristics;* can be classified as adaptive expertise. Regardless of the requirements of the propulsion system, the students can perform the required calculations. The students also show that they can change from conventional fuel types to different types of fuel to calculate the consumption and thus the size of the tanks. The students also made a reasonable estimation of the production cost of the system, based on basic figures they had found. However, for a functioning design, the theme of Knowledge of systems and components should be expended with knowledge of the fuel cell and its corresponding systems. Likely, the same argument can be made for a system that runs on batteries.

It would be beneficial for the students to not only learn about the different systems that a modern propulsion system consists of, but also work with them in a project. By applying the knowledge they have gained in practice it cements. Additionally, they might run into situations not covered by the theory, leading them to use what they have learned creatively, making the step towards adaptive knowledge.

REQUIREMENTS ACCORDING TO LITERATURE

In literature, the terms green propulsion, automation and digitalisation are often used together when it comes to the future of the shipping industry (Skillsea, 2022). As we are still at the beginning of the transition to other types of propulsion, much of the literature focusses on the possibilities and capabilities of different types of batteries and fuel cells and the systems that manage them. To the authors knowledge, no research has been published on what naval architecture students should know.

There are however, articles that look into very specific calculations or estimations that can be done to determine specific details about, for example, determining the power demand or determining the degradation of batteries in a system. In these articles machine learning and AI is used to perform the calculations or the analysis. A bachelor student of naval architecture is not required to understand the machine learning and AI that is used, but might, at some point be working with the resulting programs, tools, or calculation methods. This means that some understanding of the working principles of machine learning and AI might be required or beneficial.

Existing training and documentation in modern propulsion systems

Although there is seemingly no standard or advice in what naval architects should know about modern propulsion, there is a wide variety of introductory courses, books and other documentation available that cover different types of modern propulsion. In general, everything seems to follow the same set-up. It starts with an introduction on the main engineering principles of the technology that is discussed. From there the operating characteristics are introduced and finally the link is made to the system operating in a maritime context (Baldi et al., 2022; MAN Energy Solutions, 2019; Maritime Hydrogen Safety (MarHySafe) Joint Development Project, 2021; Netherlands Maritime Technology, 2024; Stoiber & Valøen, 2016)

This makes sense. Before being able to grasp the benefits and abilities of a propulsion type, one should have a basic understanding of how this works. The main difference in this case will be the electro-chemical propulsion, as it is substantially different from the current propulsion systems. Both the chemistry required to grasp the working principles of these types of propulsion systems and the electrical engineering required to understand how the power is distributed throughout the ship are not currently part of the standard curriculum.

Adjusting requirements for seafarers

The training and education of the seafarers that work on the ships is much more regulated than that of the designers. The IMO is looking to make large changes to the International Convention of Standards of Training, Certification and Watchkeeping for Seafarers (STWC). In a large review of the current STCW code it was decided that a committee should look into how the changes in propulsion should be anticipated (IMO Subcommittee on Human Element Training and Watchkeeping, 2024).

A large European project, Skillsea, looked into the skills that seafarers should have now and should have in the future (Oksavik et al., 2020; Zec et al., 2020). They mainly identify a skill gap in digital skills, such as understanding the complex digital architecture of modern systems, and green skills, which focusses on energy efficient and environmentally friendly ship operations.
In the results of this project, it is suggested that additional specialisation can be offered, without (currently) making changes to the STCW. They suggest, among others, the following technical skills (Oksavik et al., 2020):

- Knowledge of logistic and optimisation methods in terms of the operation of ship and machinery
- Operation of complex hybrid and zero-emission machineries
- Measurement, calculation and documentation of emissions
- In-depth knowledge of the complex systems on board
- Advanced skills in analytics and use of data in optimisation of the fleet

There is an overlap between the observation made regarding the student project and the skills that are suggested here. The Skillsea project finds that the knowledge and understanding of the modern systems on board is lacking for seafarers, as we also found during the student project. The measurement and calculation of emissions is already covered in the curriculum and mentioned under the theme Fit for 2050 in Table 1.

The optimisation methods have not come up yet. For the seafarers, this mostly focusses on the operation, for example by sailing at ideal speeds, or having the propulsion system function at peak efficiency. At the moment, there is not a lot of focus on the operational profile of the ship, as a diesel engine does not offer a lot of flexibility in operational modes. However, an electrical system has much more adaptability and flexibility, making use case calculations more important (Klein Woud & Stapersma, 2008).

THE WISH OF THE INDUSTRY

Finally, we look at the wishes of the industry. As ships powered by modern propulsion systems are already operating and with more in the order books, companies that work with these systems are looking for personnel that has knowledge of these systems. To determine what companies require, informal interviews have been held. During these interviews the competencies of the students were discussed, to see if the list of competencies is complete, and more importantly, if they feel that knowledge should be added.

One of the main findings is that companies that design and install modern electro-chemical propulsion systems in house find it difficult to find recent graduates that have the required knowledge and interest to work at their company. In general, these companies state that the lack of knowledge with regards to electrical engineering is lacking. They do not generally expect student to be completely familiar with different types of modern propulsion systems but having a stronger basis in theory would help them be better prepared to work with these systems. Many of the companies provide in house training, either on the job or as a course for their new employees to make them more familiar with modern propulsion systems. Interestingly one company stated that they were also hiring engineers from ships who have a specialisation as an Electro Technical Officer, because they

are currently the best qualified to understand how the systems work. Companies have also branched out, hiring mechanical or electrical engineers who have no direct knowledge of ships, training them in that area, as they cannot find employees who have both knowledge of electrical engineering and ships.

HOW TO BEST PREPARE OUR STUDENTS

With the analysis completed, it is time to look at the competencies defined at the start of this article. This is the current starting point for bachelor students, but from the analysis, several changes can be proposed. The summary of the findings can be found in Table 2.

Table 2 Summary of the findings per defined theme and suggested changes to the competencies within the theme

Theme	Type of expertise	Summary and suggested changes
Technical theory	Adaptive expertise	Talking with industry shows that the interest and knowledge with regards to electrical engineering is lacking. While it is listed as a competency, the students' knowledge in this department is generally not sufficient to work with more electrified systems. Suggested change: A broader focus on the theory of electrical engineering and chemistry to help students better understand how electrochemical propulsion works.
Design	Adaptive expertise	The analysis of the design of the CTV shows that most of the competencies in this theme are adaptive knowledge that translates very well to other types of propulsion. Suggested change: Adapt the final competency: *The student can compare different types of conventional propulsion systems with regards to performance, efficiency, manoeuvrability, comfort, design and cost* to also include modern propulsion systems.
Knowledge of systems and components	Routine expertise	From the analysis it has become clear that this theme requires some changes. While other types of fuel do not seem to be a problem for the students, as the design process remains the same, the systems that are not based around an internal combustion engine are more difficult. Therefore, these should be added to the list for both of the competencies listed under this theme. At this point, this seems to be fuel cells and batteries, however, this could be completely different in the future. Suggested change: knowledge of a system working with fuel cells and or batteries should be added to both competencies.
Operations and economics	Adaptive knowledge	The operational profile of a system with a modern propulsion system can be very different from that of a system with a conventional propulsion system. However, with the additional knowledge provided in the previous two theme, the skills and methods taught in this theme should translate well enough for students to work with modern systems as well. Suggested change: The competencies should be adapted to include modern propulsion systems, however, this does not necessarily change the content of this theme.
Safety	Adaptive and routine knowledge	Safety has not been a significant area within this article. Every different power generation configuration has different safety risks. However, the process of identifying and handling these risks remains the same. Some additional attention could be paid to specific risks of other types of propulsion and fuel, but a change to the competency is not required. Suggested change: When focussing on the working principles of modern propulsion systems, additional attention should be paid to additional risks that are present when a ship is equipped with different fuel and/or propulsion systems.

Fit for 2050	Adaptive knowledge	There are not many changes required to this theme. The effects of the emissions and the influence of shipping on the environment will remain a factor. The fact that we are teaching students about low and no carbon fuels doesn't mean that learning about emissions is suddenly obsolete.

CONCLUSIONS

Table 2 shows that the competencies in most of the themes can be classified as adaptive knowledge. The competencies that require the most attention are the once under the theme knowledge of systems and components. This knowledge very much counts as routine knowledge, meaning that each type of new propulsion needs to be addressed separately. In addition to the specific knowledge regarding the working principles of the new propulsion types and the required auxiliary systems, the connection between the themes *operations and economics* and *safety* might need additional attention. However, the competencies here does not necessarily change, it is mainly using the competencies from the theme *knowledge of systems and components* in a different way.

REFERENCES

Baldi, F., Coraddu, A., & Mondejar, M. E. (Eds.). (2022). *Sustainable Energy Systems on Ships Part 2 Novel technologies for energy conversion and integration* (1st ed.). Elsevier.

Delft University of Technology. (2023). *Course browser searcher*. https://studiegids.tudelft.nl/menuAction.do?toolbarSelection=tree

Hatano, G., & Inagaki, K. (1984). Two Courses of Expertise. *Hokkaido University Collection of Scholarly and Academic Papers*.

Hogeschool Rotterdam. (2023). *Maritieme Techniek Voltijd*. https://www.hogeschoolrotterdam.nl/opleidingen/bachelor/maritieme-techniek/voltijd/

IMO. (2023). Resolution Annex 15. In *Resolution* (Vol. 377, Issue July, pp. 1–17). https://wwwcdn.imo.org/localresources/en/OurWork/Environment/Documents/annex/MEPC 80/Annex 15.pdf

IMO Subcommittee on Human Element Training and Watchkeeping. (2024). *Sub-Committee on Human Element, Training and Watchkeeping (HTW 10), 5-9 February 2024*. Meeting Summary. https://www.imo.org/en/MediaCentre/MeetingSummaries/Pages/HTW-10th-session.aspx

Klein Woud, H., & Stapersma, D. (2008). *Design of Propulsion and Electric Power Generating Systems* (2nd ed.). IMarEST.

Male, S. A., Bush, M. B., & Chapman, E. S. (2011). Understanding Generic Engineering Competencies. *Australasian Journal of Engineering Education*, *17*(3), 147–156. https://doi.org/10.1080/22054952.2011.11464064

MAN Energy Solutions. (2019). Batteries on board ocean-going vessels. In *Investigation of the potential for battery propulsion and hybridisation by the application of batteries on board*. https://www.man-es.com/docs/default-source/marine/tools/batteries-on-board-ocean- going-vessels.pdf

Maritime Hydrogen Safety (MarHySafe) Joint Development Project. (2021). *Handbook for hydrogen-fueld vessels*. https://www.dnv.com/maritime/publications/handbook-for-hydrogen-fuelled-vessels-download.html

McKenna, A. F., Colgate, J. E., Olson, G. B., & Carr, S. H. (2006). Exploring adaptive expertise as a target for engineering design education. *Proceedings of the ASME Design Engineering Technical Conference*, *2006*(January). https://doi.org/10.1115/detc2006-99711

Netherlands Maritime Technology. (2024). *Netherlands Maritime Technology - Agenda*. Webpage. https://maritimetechnology.nl/nl/agenda/?type=Training

Oksavik, A., Hildre, H. P., Pan, Y., Jenkinson, I., Kelly, B., Paraskevadakis, D., & Pyne, R. (2020). Future Skill and Competence Needs. In *Skill Sea, Co-funded by the Erasns+programme of the European Union, Norwegian University of Science and Technology, Liverpool John Moores University*. https://ntnuopen.ntnu.no/ntnu-xmlui/handle/11250/2648963

Pierrakos, O., Welch, C. A., & Anderson, R. D. (2016). Measuring adaptive expertise in engineering education. *ASEE Annual Conference and Exposition, Conference Proceedings*, *2016-June*. https://doi.org/10.18260/p.25690

Skillsea. (2022). *Summary of SkillSea strategy, key findings and recommendations*.

Stoiber, R., & Valøen, L. O. (2016). *DNV GL Handbook for Maritime Offshore Battery Systems*. www.dnvgl.com

Sumsion, J., & Goodfellow, J. (2004). Identifying generic skills through curriculum mapping: A critical evaluation. *Higher Education Research and Development*, *23*(3), 329–346. https://doi.org/10.1080/0729436042000235436

Zec, D., Maglic, L., Šimić, H. M., & Gundić, A. (2020). *Current Skills Needs: Reality and Mapping*. https://www.skillsea.eu/index.php/news-events/spotlight/106-read-the-full-report-on-currents-skills-needs

Proceedings of 15th International Marine Design Conference (IMDC-2024)
June 2-6, 2024
Amsterdam, the Netherlands

"Are You Sure About That?": Handling Uncertainty in an Early-Stage Ship Design Process

Rachel Pawling[1,*]

ABSTRACT

UCL teaches ship design at postgraduate and undergraduate level, using a combination of spreadsheets and commercial computer aided ship design tools. These tools produce single values for a given input and so uncertainty is only incorporated via margins. Experience has shown that students do not develop an effective understanding of engineering uncertainty using the current tools and approaches. This paper describes ongoing work to develop an "add on" to the existing UCL toolset to allow the representation of various ship parameters as uncertainty distributions. This is with the aim of better understanding of uncertainty in ship design, primarily for ship design education but with broader applications for concept design tasks.

KEY WORDS

Design methodology; design education; uncertainty; margins

INTRODUCTION

UCL has taught ship design since 1967 when the RCNC course moved to the Department of Mechanical Engineering from the Royal School of Naval Architecture in Greenwich. The Naval Architecture and Marine Engineering (NAME) group, part of the Department of Mechanical Engineering (UCL, 2024a) teaches ship design at two levels; MScs in Naval Architecture or Marine Engineering; and a Maritime Design module as part the "Integrated Engineering Programme" (UCL, 2024b). The author has run the undergraduate module since its inception in 2018 and, after providing support for several years, took over the running of the postgraduate module in 2019. With a background in early-stage design methodology research, frequently presented to IMDC (Andrews & Pawling 2003, 2006, 2009, Pawling et al 2015) the author has sought ways to combine research and teaching interests. This paper briefly describes the UCL postgraduate course, focusing on observations regarding the way in which uncertainty manifests in the teaching of twentieth century students. The concepts of uncertainty, margins and design robustness are explored, and a possible approach illustrated via a modification to existing UCL design tools.

SHIP DESIGN TEACHING AT UCL

This paper mainly focusses on the postgraduate course, as it is a longer module (450 hours commitment) with time to explore design in detail. The course and some of the details of the various design tasks are described in more detail in Pawling et al (2018). The Ship Design Exercise (SDX) module follows six months of taught modules covering aspects such as ship stability, structures, resistance and powering (for naval architects); thermodynamics, power electronics and control (for marine engineers). Students on the course are generally industry sponsored but may be early in their employer's graduate schemes so have little practical experience. The module sees the cohort split into small groups of 2-4 naval architects and marine engineers. Design requirements for each group are generally warships and service vessels and they are characterized by being challenging and relatively open. Table 1 provides some examples of recent design requirements. The SDX requires the students to integrate the subject specific technical knowledge gained during the MSc into a coherent design. Emphasis is placed on decision making and justification, and the understanding of influences and interactions in the design.

[1] Department of Mechanical Engineering, UCL, London; ORCID: 0000-0002-5214-9566
* Corresponding Author: r.pawling@ucl.ac.uk

Submitted: 7 March 2024, Revised: 8 May 2024, Accepted: 9 May 2024, Published: 16 May 2024

Conference paper, DOI: https://doi.org/10.59490/imdc.2024.821 e-ISSN: 3050-4864

Table 1: Examples of UCL MSc SDX design requirements

Year	Title	Summary
2020	Optionally Crewed Territorial Defence Vessel	A small, high speed vessel for patrol and defence of home waters against a numerically superior adversary.
2021	Family of Zero Emissions Island Ferries	An adaptable design for a Ro-Pax ferry serving island routes around the British Isles
2022	Seaplane Logistics Mothership	A ship to act as a hub for logistics seaplanes including large ground-effect machines.
2023	Adaptable Export Patrol Combatant	A trimaran vessel designed for export and to be completed in several roles via design and construction modularity.

A Typical UCL Design Model

Both undergraduate and graduate design exercises involve the construction of a parametric model composed of a number of line items for weight and space, with the general iterative structure shown in Figure 1.

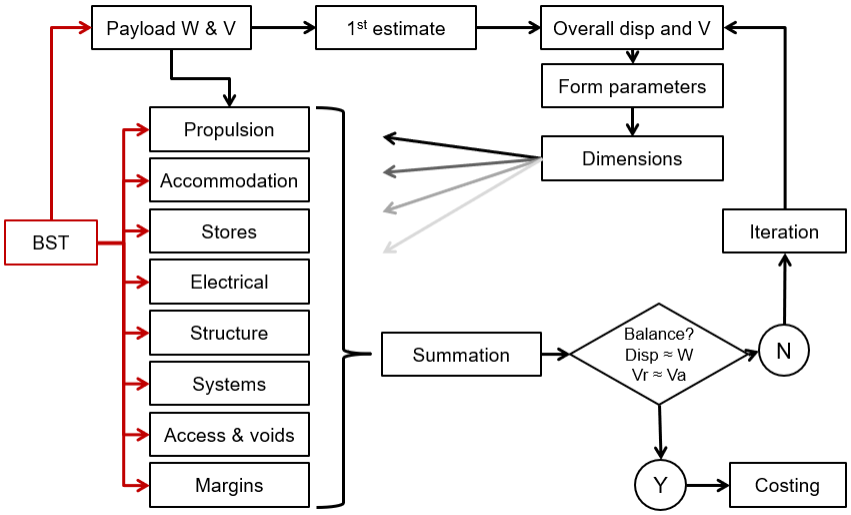

Figure 1: The general structure of a UCL student sizing model

This model is then used to examine different capability variants (cargo, speed, weapons etc.), and also the impact of different technology options, e.g. directed energy weapons or all-electric machinery. The students are provided with a template Excel file with the UCL Weight Breakdown System and various housekeeping functions such as the generation of summary tables already implemented. This spreadsheet becomes not only a design tool but also a method of managing work allocation between design team-members, integration with simplified analysis tools such as initial resistance estimates, prior to later development of Paramarine or Maxsurf design models. Screenshots of the spreadsheet are shown in Figure 2 overleaf.

MARGINS, UNCERTAINTY AND ROBUSTNESS IN SHIP DESIGN

Within the UCL SDX, general uncertainty in design is handled in a relatively simplistic manner. Margins are added to weight, space and other characteristics. Stability is generally assessed in the extremes of deep and light load, and many systems such as propulsion or electrical generation will be designed to meet the worst-case scenario. Students are expected to consider more general operational scenarios, but there is not a formalised process to specify what these should be, other than some very specific cases (e.g. harbour load is a specified condition for electrical generation).

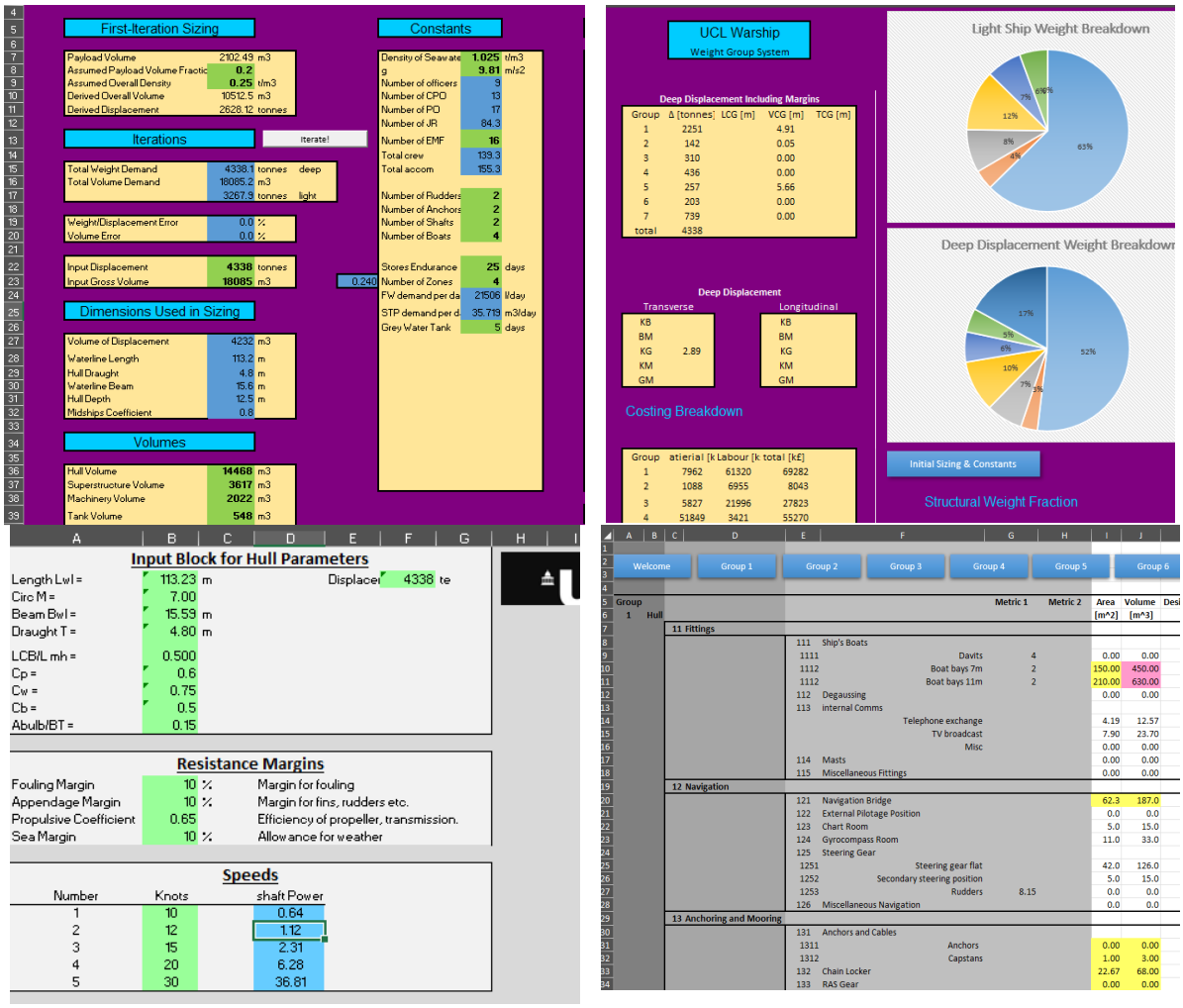

Figure 2: Screenshots of the template sizing tool, clockwise from top left; iteration to numerical balance; summary tables and charts, typical weight entry table; resistance estimation

Fixed Design Margins

The use of various types of margins is an important part in any engineering design activity, however these margins have different conceptual meanings. Design and build margins are used to account both for possible changes that *may* occur with the design but also for weight growth that *will* occur during detail design but is not captured in the early-stage design estimates. In the theoretical case of perfect and complete detailed data collection and perfect and completely detailed design models, this latter type of design and build margin would not be needed, or at least could be limited to that required due to mechanical variation (e.g. plate rolling). Growth margins are also applied to prevent design limits being exceeded through life.

UCL ship design education employs several types of design and operational margins, and these are summarised in Table 2. These are ultimately derived from UK naval practice and experience in the post war period. For example, the “Board Margin” refers to the RN Admiralty Board who would authorise additional equipment to be added during the ship’s life (Brown, 1991), whilst the electrical load margin originates in the rapid growth of shipboard electronics in the post-war period (Gates & Rusling, 1982). Growth margins for UK warships were derived from historical experience of 0.5% per year between major refits (Brown, 1991). It can be seen that these are all linear, additive margins that simply make the initial design larger, heavier and more expensive, firstly to account for changes in detail design and build and then to account for changes through life.

Table 2: Typical UCL MSc SDX margins

Group	Name	Weight %	Space %
		Design and Build Margin	
1	Hull	5-10	0
2	Personnel	0-5	5-10
3	Ships services	5-15	2-10
4	Propulsion	4-10	0-2
5	Electrical services	5-10	0-10
6	Payload	5-25	5-25
7	Variables	4-7	4-7
Board margin, for additions through life		2-10% light weight @ no 1 deck	5% volume
Growth margin, for unattributed growth through life		5% light weight	
Sea margin, to prevent overloading engine		25% on shaft power	
Fuel margin		5% on fuel tankage	
Electrical load margin, for design and build		25% on design load	
Electrical growth margin, for additions through life		20% on design load + design margin	

Simply adding linear margins to design characteristics is not the only solution, and can cause problems with compounding margins (Hockberger, 1976). A ship with excessive stability margins may in fact be too stable early in life or in some light load conditions. A generator with the total margins applied in the traditional UCL approach will be lightly loaded much of the time, with consequences for efficiency and reliability. This was illustrated in Lyster and Pawling (2019) where a Monte-Carlo analysis applied to a statistical model of ship through-life operations showed that the conventional approach of designing for the worst-case, or a set of specific loadings, was poorly matched to the wide range of possible displacements and load cases that would occur once the total range of variability was incorporated into the model. This is illustrated in Figures 3 and 4 which show the probability distributions of displacement and fuel consumption for a light frigate / OPV type vessel.

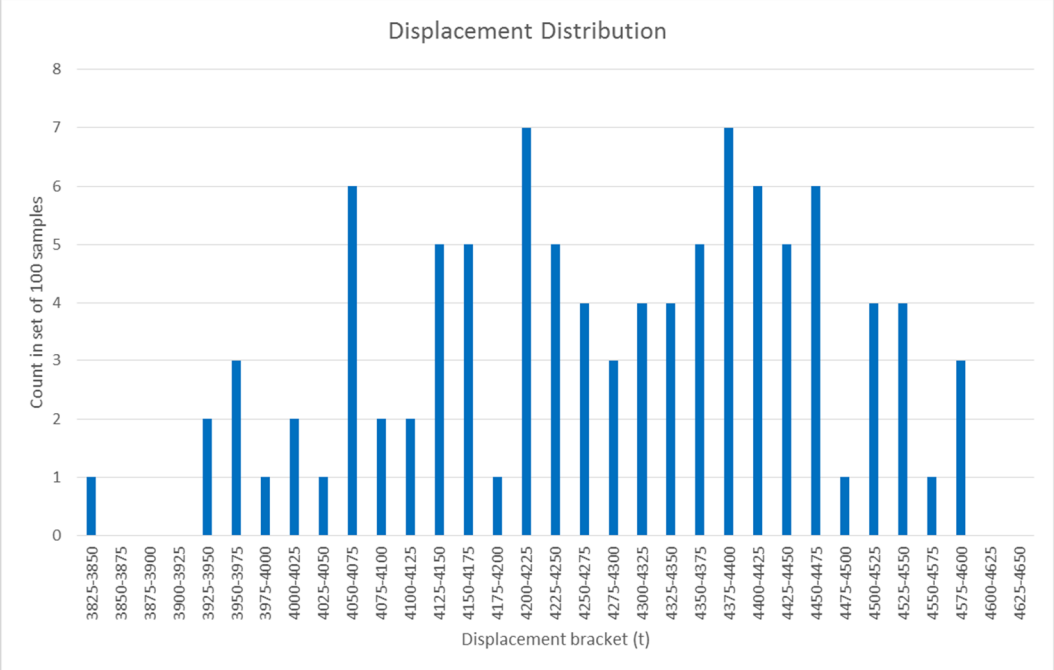

Figure 3: Probability distribution of displacement over ship life (Lyster & Pawling, 2019)

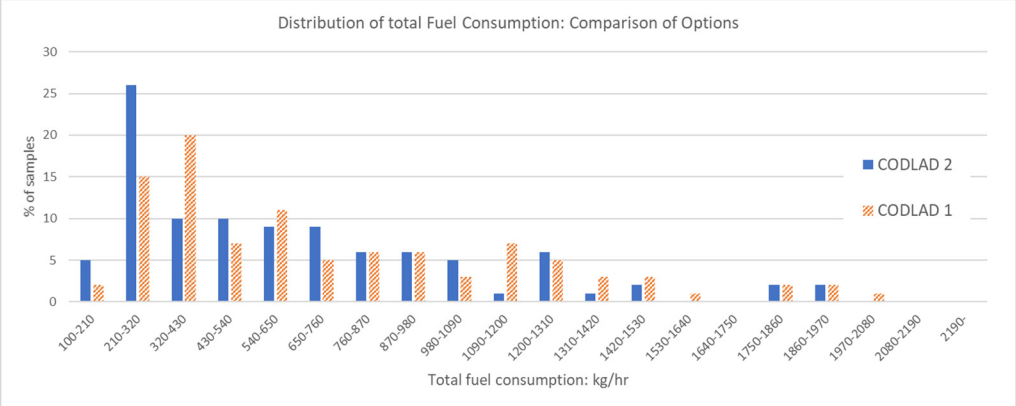

Figure 4: Probability distribution of fuel consumption for different machinery types applied to a statistical through-life model (Lyster & Pawling, 2019)

Design and build margins can however be consumed by uncertainty due to new technologies not developing as first estimated. As exceeding design margins can have undesirable consequences, the appropriate margin to be applied can be related to not just the novelty and confidence in a design estimate, but also the acceptable risk (ISAWE, 2001). Both design and through life margins can be regarded as similar in some respects to the safety margins applied when calculating loads, as they ensure a system remains within a safe (or low risk) region. However, risk here is a broad case including financial and programmatic risk rather than only structural failure or stability problems. As risk is probability multiplied by consequence, this suggests margins should be selected using an approach that examines a range of consequences for different margin choices, as different outcomes may be permitted; as noted by Brown (1991) RN practice was that the vessel had to meet its performance requirements with all design and build margins consumed, but growth margins were permitted to degrade performance but not safety. The importance of considering a range of possible outcomes increases if margin policy is derived from historical designs, technologies and operational practices which may not be appropriate for modern systems. An example is a fuel-cell based generator system. Given the higher UPC for fuel cells compared to diesel engines, oversizing the generator is undesirable. But if a large fuel cell generator is composed of multiple smaller modules, it becomes possible to remove the growth margin by allowing for easy addition of more modules later in life.

Uncertainty

Uncertainty and variation in design can take many forms and have many implications, and it is not truly captured by simple linear margins added to properties such as weight and space. Hockberger (1976) used a probabilistic approach to describe design margins in general, with the demand and supply both being probability distributions as illustrated in Figure 5.

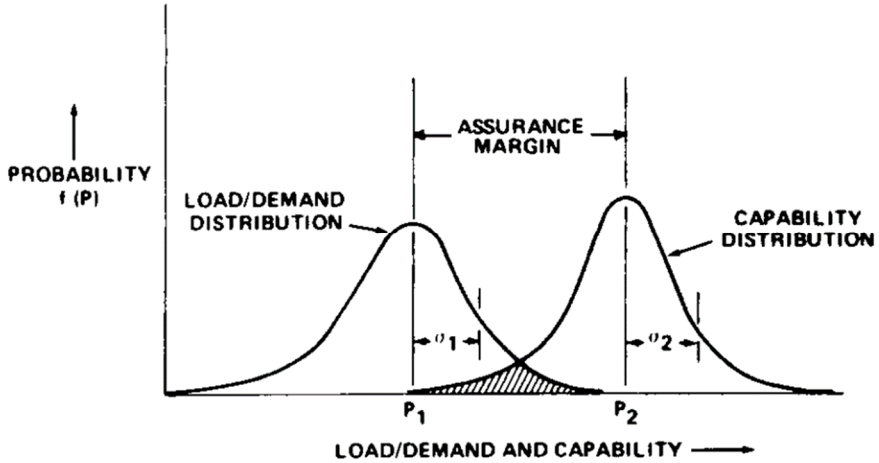

Figure 5: Representation of design demand and capability as probabilisty distributions with associated range of uncertainty (Hockberger, 1976)

Uncertainty can be inherent in the mathematical models used in ship design, as the final product produced via detailed design may vary from estimates due the vast range of possible detail solutions that can be produced to meet the same high-level requirements. Some items such as recreation spaces may also be regarded as “rubber” in that they can expand to fill available space or be compressed if the design is cramped. Table 3 illustrates this with a sample of cabin areas for five ships (all service

vessels), for the same rate of cabin on that ship, normalised to the smallest example for that ship, with variations as high as 90% on the smallest size. The distribution of the ratios-to-smallest is summarised as a histogram in Figure 6.

Table 3: Example of variation in cabin sizes for the same rate

Ship	Cabin Sizes, Normalised to Smallest				
A	1	1.5	1.9		
B	1	1.2	1.1		
C	1	1.2	1.1	1.3	
D	1	1.2	1.1	1.2	
E	1	1.2	1.2	1.2	1.1

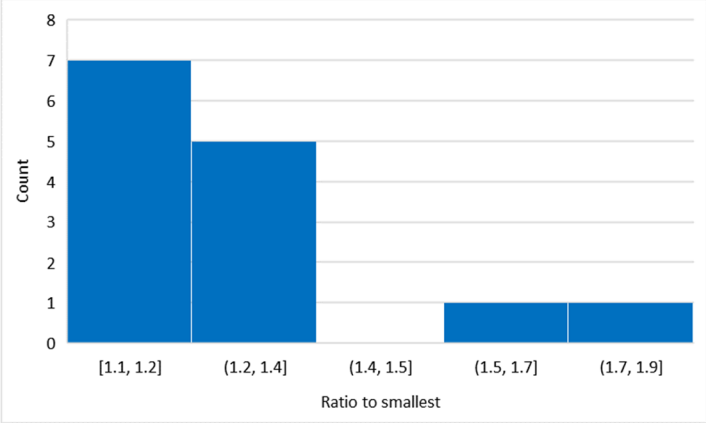

Figure 6: Histogram of ratios-to-smallest cabin

Much of the design data in the UCL database is derived from multiple datapoints with subsequent curve fitting and this type of model leads to an uncertainty of plus or minus some percent, as illustrated in Figure 7 for a generic linear diesel generator. Based on specific machinery data, the Excel trendline (using the default least-squares method built into Excel) is only around +/-20% accurate to any specific item. Figure 7 also shows the error between the linear estimator and individual data points as a histogram, with a maximum error of +/-32%.

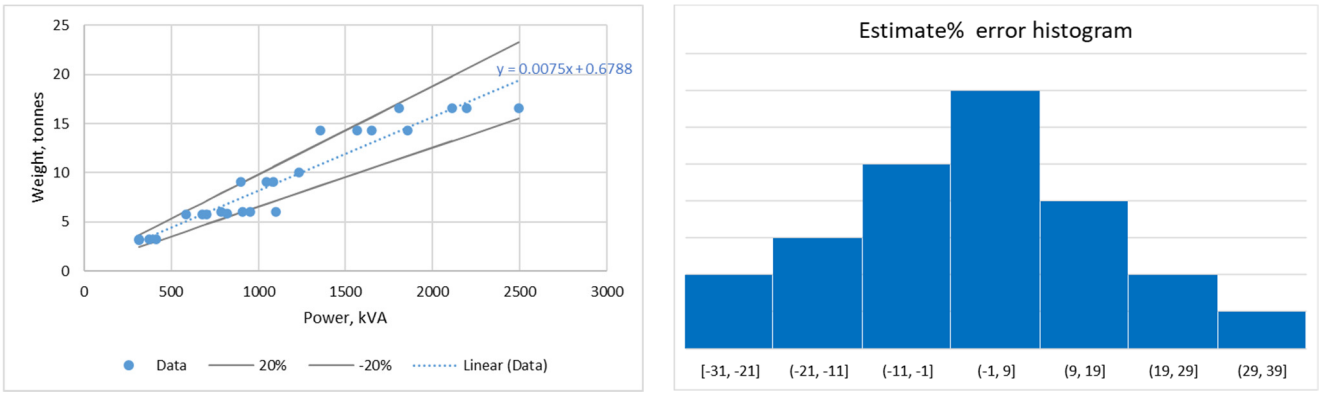

Figure 7: Example of a UCL single line sizing algorithm and error distribution

Uncertainty can also manifest as a type of prediction, i.e. a new technology might be expected to become cheaper or lighter as it is refined, thus having a wider "-%" than "+%". Porche et al (2004) described the use of BetaPERT distributions, more typically used to describe uncertainty in task durations for project management, to evaluate the effect of uncertainty in propulsion machinery technology. Figure 8 below shows such a distribution applied to the case where a trendline has been fitted to a set of data points.

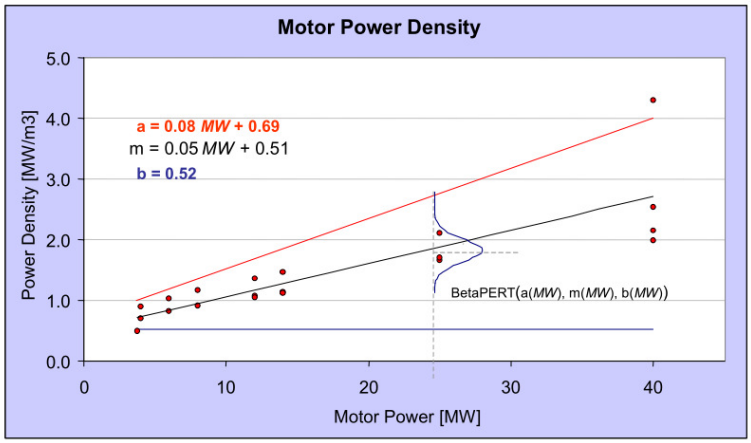

Figure 8: An example of a trendline fitted to data being the "most likely" value in a Beta distribution (Porche et al, 2004)

The Beta distribution was adopted by Porche et al as it can be used to represent a three-point estimate, itself being a simple way of describing the error or uncertainty in a numerical evaluation. In particular a Beta distribution, for the same three inputs (minimum, maximum, most likely value), weights the most-likely value more heavily. This approach can be particularly useful in comparing various options, such as electric motor technologies as shown in Figure 9, where both general trends and the potential for different technologies to have very similar outcomes can be shown.

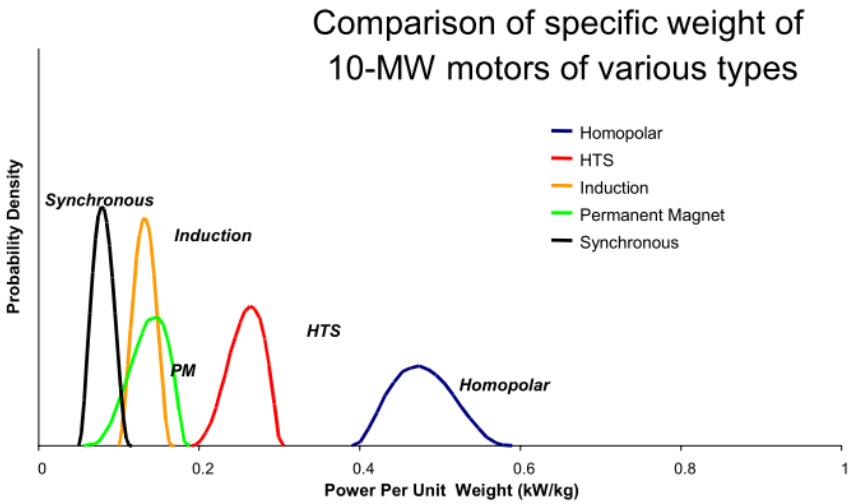

Figure 9: Representation of different motor technologies having different power density and different uncertainty ranges (Porche et al, 2004)

Whilst most mathematical and procedural methods for incorporating uncertainty have focused on the detail design and component level, e.g. structural design (Claus & Collette, 2018) or planing craft resistance (Brefort & Singer, 2018), other approaches have looked at higher level aspects, such as market and regulatory uncertainty has also been considered (Zwaginga et al 2021), (Puisa, 2015) extending to through life operation (Plessas et al, 2018). Olivier et al (2012) used a structured approach to capture subject matter expert input and develop a probabilistic model of ship cost at the weight group and total ship level. They illustrate the major difference between uncertainty inherent to the ship design ("epistemic factors") and uncertainty due to external factors ("aleatory factors"), with quite broad ranges as illustrated in Figure 10, where were then used to define the sample ranges in a Monte-Carlo analysis using a ship costing model. The importance of working with SMEs and stakeholders was also described by Brett et al (2022), in their comprehensive survey of the subjects of uncertainty and complexity in ship design.

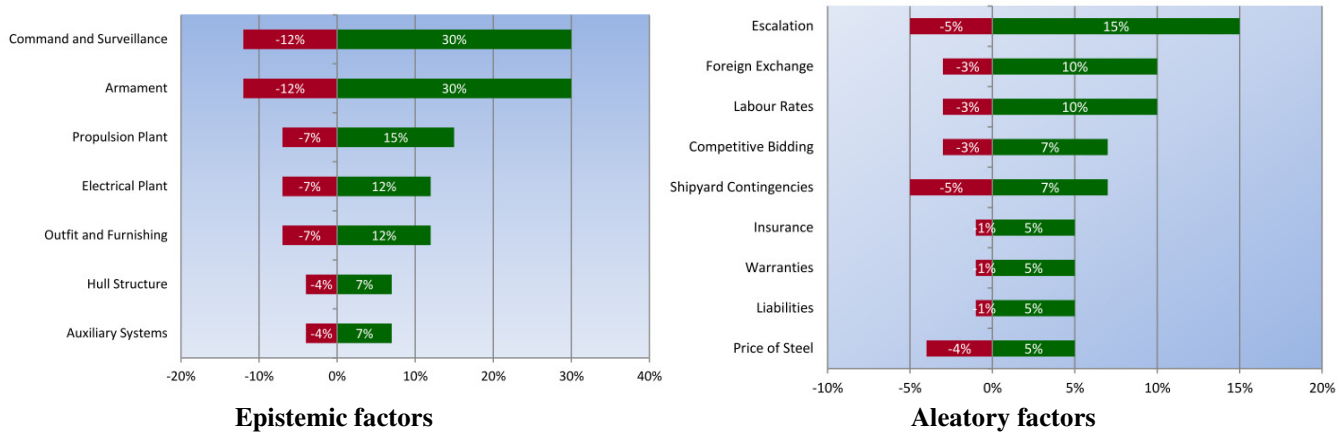

Figure 10: Broad ranges of uncertainty resulting from design and environmental factors (Olivier et al, 2012)

Whilst this paper focusses on the UCL postgraduate course, which mainly covers warship design, uncertainty and robustness were introduced to the undergraduate course, specifically concerning the assumed values of container or vehicle weight. Provided with data such as that illustrated in Figure 11, taken from Kristensen (2013), the students were expected to justify their assumptions for tonnes per unit cargo and discuss the likelihood and consequences of variations in service. Similarly, the students are provided with representative data on vessel utilisation and operational speed profiles and expected to consider scenarios where these differed from the theoretical optimum.

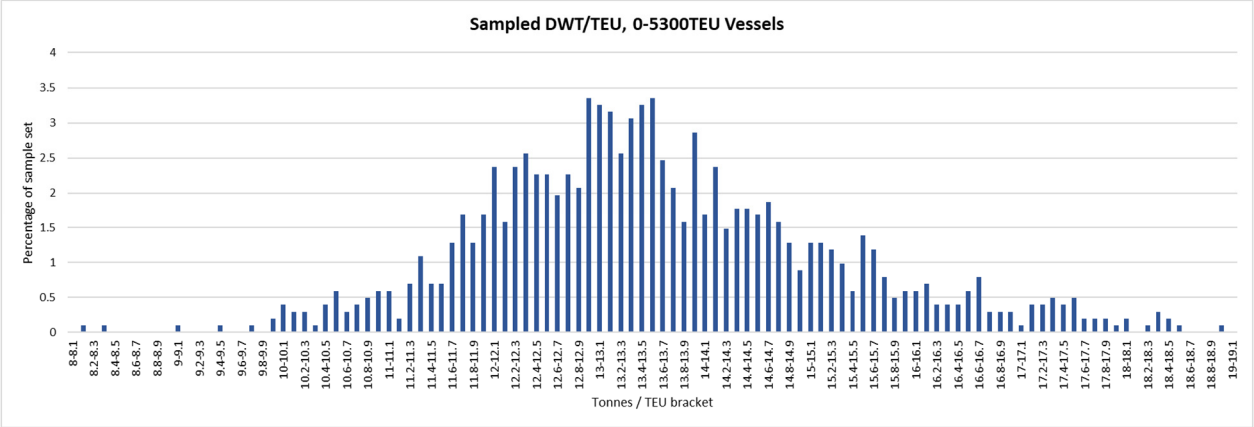

Figure 11: Example of variation in probability of occurrence with laden container mass in tonnes (n = 1013, digitised from Kristensen (2013), 0-5300 TEU range)

Robustness

Design margins and uncertainty also relate to the concept of robustness in design. The concept of robust design originated with Taguchi's robust design method, developed in Japanese manufacturing, which sought to create "a design that has minimum sensitivity to variations in uncontrollable factors" (Simpson, 2000). A graphical representation of design robustness is provided by Karl et al, (2011) and shown as Figure 12. This shows a notional design space with a surface representing possible solutions. On the left, a solution is shown that has been selected for peak performance. Whilst it easily meets the customer requirement, the steep shape to the local solution space means that any change in design or operational characteristics leads to its performance rapidly falling to below the requirement. To the right of the figure is an example of a more robust solution, which may not have such high performance, but will remain above the customer requirement for a range of design or operational characteristics.

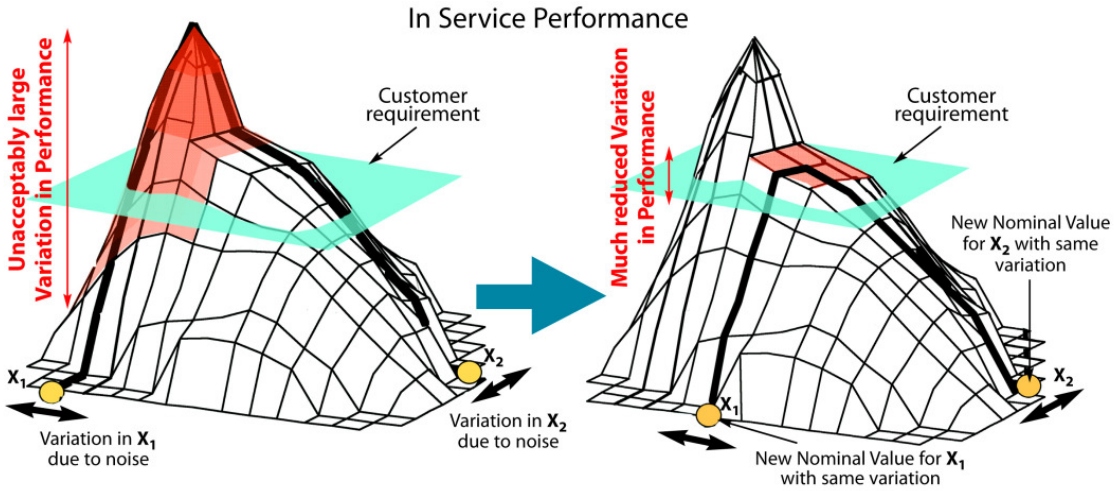

Figure 12: Example of highly optimised (left) and robust design (right) (Karl et al, 2011)

Summarising literature on robust design methods that would of interest in ship design, Puisa et al (2014) outlined four ways of dealing with uncertainty:

- Resistance: plan for the worst possible case of future situation – this is similar to the conventional approach used in the current UCL MSc SDX.
- Resilience: whatever happens in the future, make sure that the system can recover quickly – this is a key part of warship survivability, being the crew-centric concept of recoverability.
- Static robustness: aim at reducing vulnerability in the widest possible range of conditions.
- Dynamic robustness (or flexibility): plan to change over time in case conditions change.

Various mathematical approaches have been applied to the problem of robust design, including real options valuation (Puisa, 2015), the use of response surfaces providing meta-models of more complex engineering models (Karl et al, 2011), Epoch-era analysis (Gaspar et al, 2015) whilst the US Department of Defense's Engineered Resilient Systems (ERS) effort sought to improve the resilience and robustness of US defence procurement through the application of high-performance computing tools (Neches, 2012).

Adaptability and Changing Design Styles

The design of both warships and commercial vessels has changed in recent years, with cargo vessels, previously having been seen as the perfect example of a ship "optimised" for a single operational point, now having a much broader range of operational speeds (Banks et al, 2013) and in general a greater understanding of operational variation in the design, leading to changes in hull design for example or considerations of designing for adaptability through later refits (Puisa, 2015). The long operational life and rapidly changing strategic and technological environments mean adaptability has long been of concern for warship designers (Andrews, 2001) and recently warships have seen ever greater use of modularisation e.g. Doerry (2014), an approach introducing substantial uncertainty as to system weight and service demands, even if volume is constrained (Abbott, 1977).

Whilst some items in the UCL ship design database are derived from a technologically similar set of datapoints, such as a range of high speed marine diesel engines from one or two manufacturers, the majority of the scaling algorithms were generated using weight and space data from RN warships of the 1970s and early 1980s and so inherit the design style of those vessels. Pawling et al (2013) proposed a definition of "Style" in the engineering context of warship design as "a cross-cutting concept, where one decision explicitly influences a wide range of solution areas", with one example being how the approach to survivability will impact the number of bulkheads and detail design to resist shock. Some stylistic aspects of warship design have changed since this database was defined, such as the adoption of "Naval Ship Rules" and semi-commercial approaches, that do not explicitly call for heavier structure, but frequently lead to it. That warships are subject to change in their general style and proportions is well documented, e.g. Gates & Rusling (1982), implying a need to capture possible (but not certain) changes in general design style from current concept design algorithms.

THE PERCEIVED NEED FOR A NEW APPROACH IN THE SDX

Whilst the UCL design process features several stages of option exploration and selection, ultimately it results in a single point design assessed over a limited set of operational conditions. Although students are expected to consider aspects such as uncertainty and robustness in their designs, and justify their choice of margins, it is generally difficult to ensure they do so purely through lecture material and discussion – if default margins are provided, students will usually adopt them. There is thus a need for a method and toolset for students to examine possibilities and determine margins as a structured part of the exercise. Another reason for introducing improved handling of uncertainty within an educational concept is an observed trend for many engineering students to view engineering as simply "applied mathematics", with any value calculable with high precision. It can be a challenge to assist students in internalising the changes in engineering systems with increasing detail, and the difference between a sizing algorithm applicable to a wide range and data representing single points, i.e. the importance of being "approximately right" rather than "precisely wrong".

Against this educational and engineering background, as the co-ordinator for the two UCL ship design modules, the author has been examining how concepts such as uncertainty, robustness and margin selection can be better examined in the course, through the use of software tools. The author has previously presented some aspects of software tools for ship design education (Pawling et al, 2015), with specific attention to teaching general arrangements design. Nine properties were identified as being important for tools to be usable by students. Based on these, the approach has been to take the existing Excel spreadsheet templates and add additional functionality;

1. Wide availability:
2. Low learning and familiarisation overheads:
3. Fast operation:
4. Not type ship based:
5. Task focused:
6. Not automated:
7. Integration of models, datasets and evaluation:
8. Flexible levels of detail:
9. Appropriate levels of precision:

THE MODIFIED MODEL

The existing UCL MSc ship sizing template Excel sheet was modified with additional characteristics for each line item and VBA macros to carry out various studies. The most visible change is that the weight, space, cost etc. defined for each item becomes the “most likely” value in a beta distribution, with a percentage +/- defined for each item. This is illustrated in figure 13 below.

		Area	Volume	Weight	Uncertainty				Multiplier Used	
					Volume		Weight		Volume	Weight
		[m^2]	[m^3]	[tonne]	Minus %	Plus %	Minus %	Plus %	m3	te
s										
611	Weapon Control Systems									
6111	Operations Room	70.30	210.90	2.85	25	10	25	10	1.00	1.00
6112	CMS Computer Room	19.00	57.00	1.58	25	10	25	10	1.00	1.00
6113	Briefing Room	13.50	40.50	0.45	12	30	9	23	1.00	1.00
612	Weapon Datalinks									

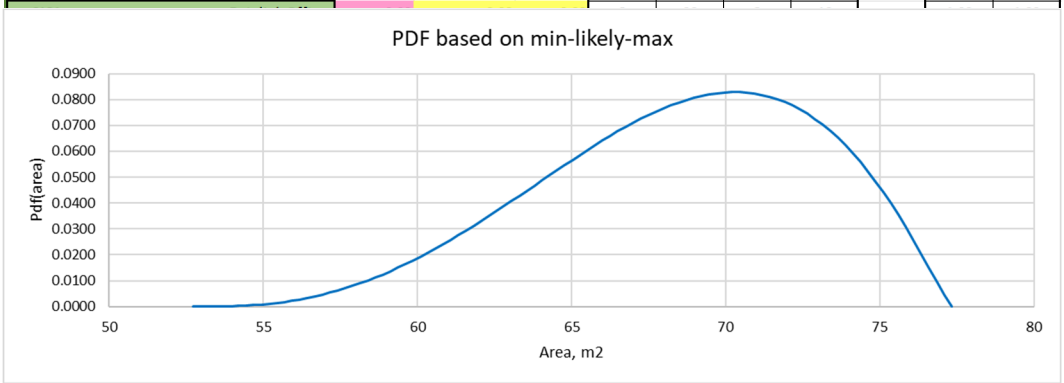

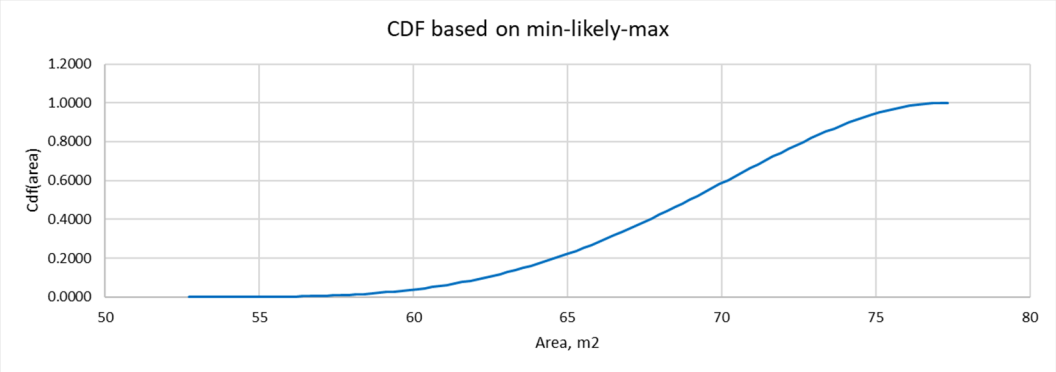

Figure 13: Top: modified table with +/- percentages for weight and volume. Middle: Resulting Beta Probability Density Function (PDF). Bottom: Cumulative Density Function (CDF).

Sampling was carried out using the Cumulative probability Density Function (CDF). For a required number of samples, the CDF was sampled at a random point within each sample window. Figure 14 below illustrates a sample taken at 0.275 within the sample window 0.2-0.4 (i.e. the window resulting from a sample number of 5).

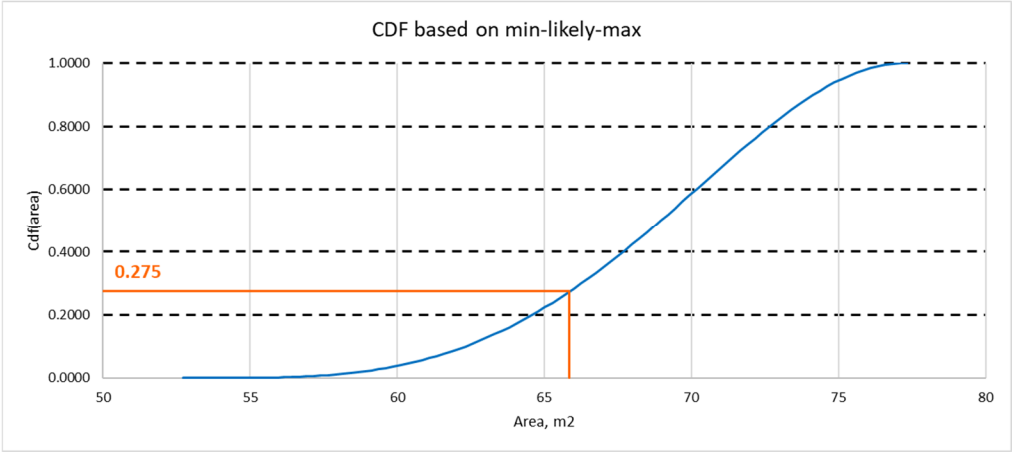

Figure 14: Example of a sample taken from a CDF

At the time of writing, the following studies have been implemented using VBA macros:

MOST LIKELY Run: This macro sets the values to their most likely value and balances the design.

MAX Run: This macro sets all values to their maximum value and balances the design.

MIN Run: This macro sets all values to their minimum value and balances the design.

X% Run: This macro sets all values to their Xth percentile value and balances the design. Currently this is set to the 50th percentile. The aim of this function is to allow students to quickly identify a "most likely" outcome.

Weight Group X Sensitivity Study: This macro conducts a simple sensitivity study for a selected weight group "X", varying each item from its minimum to maximum value and recording the impact on the design. The aim of this function is to assist students in determining which items have the most impact on the overall design.

Special Item Study: This macro conducts a sensitivity study on specified variables. This is intended for variables such as hullform coefficients, specific fuel consumption etc. It requires more input from the user as they must specify the sheet and cell in which the variable is located.

System Sensitivity Study A: Deterministic: This macro conducts a complex sensitivity study on multiple items, using the mid-point of each range within the CDF.

System Sensitivity Study B: Random: This macro conducts a complex sensitivity study on multiple items, using a random point within each range of the CDF. System sensitivity studies are defined in a tabular structure illustrated in Figure 15. Up to six line items can be defined. There is no restriction on the number of samples, other than user preference for run time.

Selected Items for System Sensitivity

Item #	Item Name	Item Group	Samples
1	DG size 1	5	5
2	Electric Motors	4	5
3	GT GB	4	5
4	EM GBs	4	5
5	DG size 2	5	5
6			

Figure 15: Definition of the system sensitivity study

The tool currently uses a simple full factorial approach, examining every combination of every item. The tool generates 2 to 3 options per second, with typical run times for a study summarised in the table below. Keeping run times short is important to ensure student use, as unless they are directly assessed on the use of the tool, any activity that takes too much time will generally be deprioritised. The UCL design exercise emphasises interactivity and the explorative "sketching" model of concept design described by Pawling and Andrews (2011) where the design model is used to explore alternatives and aid in discussion. In this model of design, time spent developing and running models should be reduced as much as possible, as it can be an impediment to understanding.

Table 4: Typical run times for the tool

Items	Samples per Item	Run Time (minutes)
1	4	<1
	5	<1
2	4	<1
	5	<1
3	4	<1
	5	1
4	4	2
	5	5
5	4	7
	5	21
6	4	28
	5	105

EXAMPLE DESIGN STUDY

To demonstrate the functions currently implemented, the sizing model was populated with data representing a generic frigate, with the broad characteristics outlined in Table 5.

Table 5: Principal particulars of the example design

Combat Systems	Baseline (most likely option)	
1 x 127mm and 2 x 30mm guns	Deep displacement	4338 tonnes
20 short range and 16 medium range SAM	Light displacement	3268 tonnes
Single face AESA radar	Internal volume	18088 m3
12 long range SSM	Waterline length	113.2m
10 tonne helicopter with hangar	Waterline beam	15.6m
3 x 1.5 tonne UAV	Depth amidships	12.5m

2m 7m and 2 x 11m boats	Draught amidships	4.8m
Hull sonar	UPC	398 M£
Triple torpedo tubes	Max speed	29.5 kn
Decoys	Cruise speed	15 kn
16 x Embarked personnel	Complement	139
Machinery	CODLOG – twin shaft, single boost GT with splitter gearbox	

Example Single Weight Group Sensitivity Study

In this study the tool sets all weights to their "most likely" value, then for each item in the selected weight group performs two runs – one with that item set to its maximum value, and one with it set to the minimum. Comparison charts are produced showing several metrics; the ratio of item change (in tonnes and m^3) to overall ship change; the total range of variation (in tonnes and m^3 and as a percentage of the group totals); the percentage of the group total that that particular item makes up. These are presented in bar charts as shown in Figures 16-19 for weight group 2 (personnel).

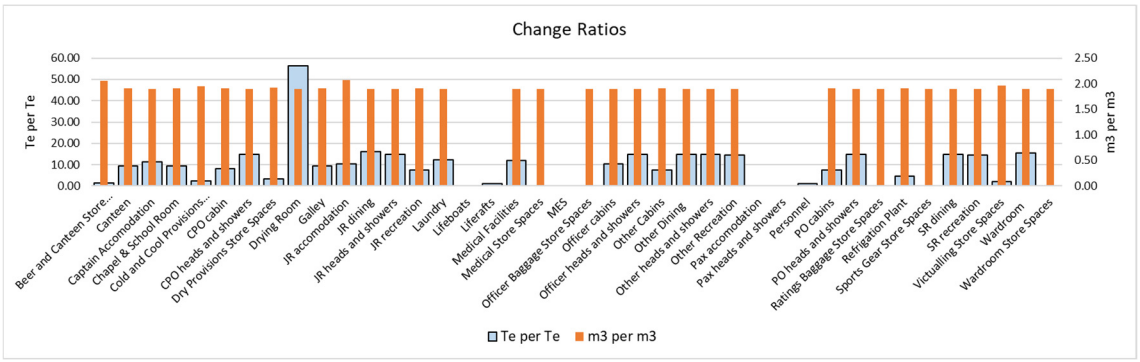

Figure 16: Ratios of item to overall ship change for group 2

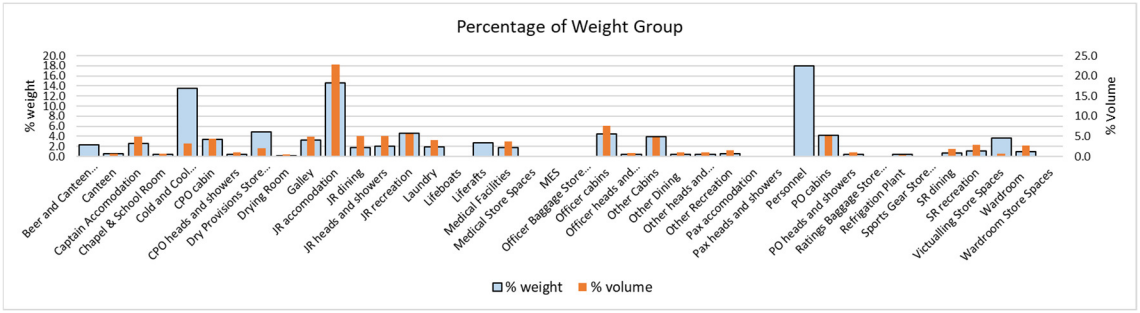

Figure 17: Composition of weight group 2 by percentage

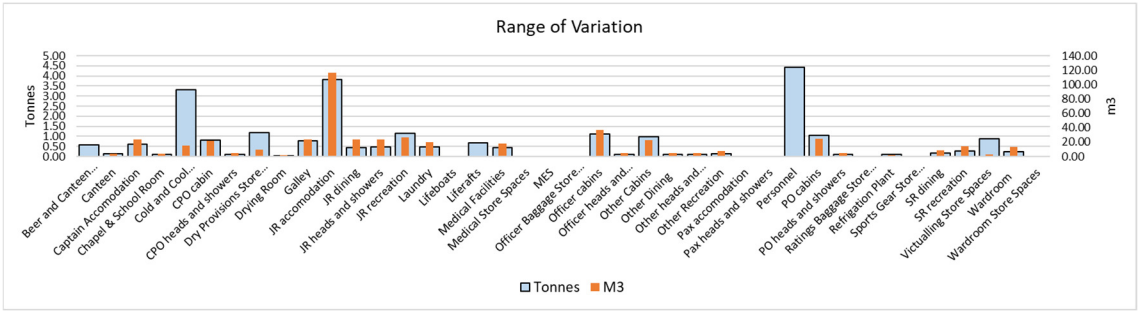

Figure 18: Total range of variation for each item

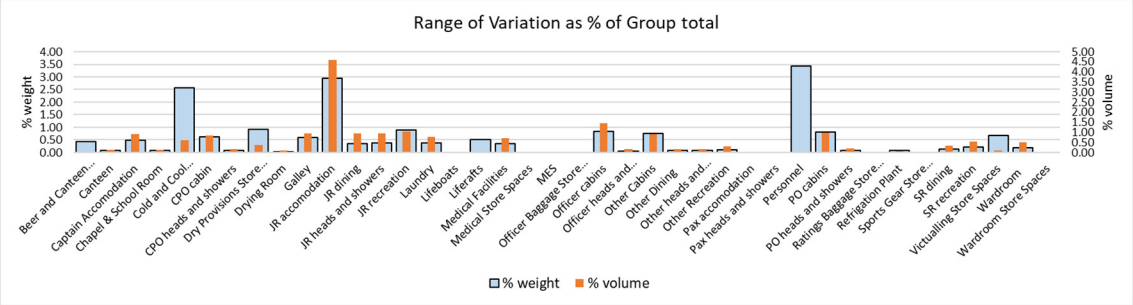

Figure 19: Total range of variation for each item as a percentage of the group totals

Example System Sensitivity Study

A trail was run on the main components of the propulsion system; gas turbines; diesel generators; electric motors and their power electronics. Figure 20 shows; a histogram of the deep displacements with the corresponding approximation of the CDF produced by compiling the runs. A generic beta PDF is also shown, generated by varying the specific components to their minimum and maximum values. Figure 21 shows the same plots for the overall ship volume. The current concept for use of the tool is that the CDF plots would be used to derive the design point to be used for analysis, based on a required level of certainty.

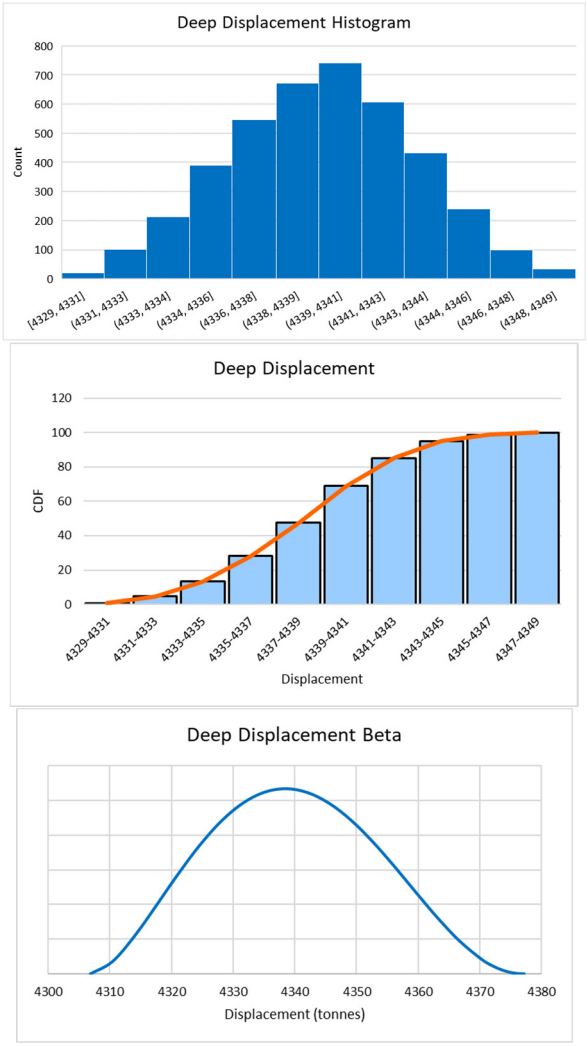

Figure 20: Displacement results

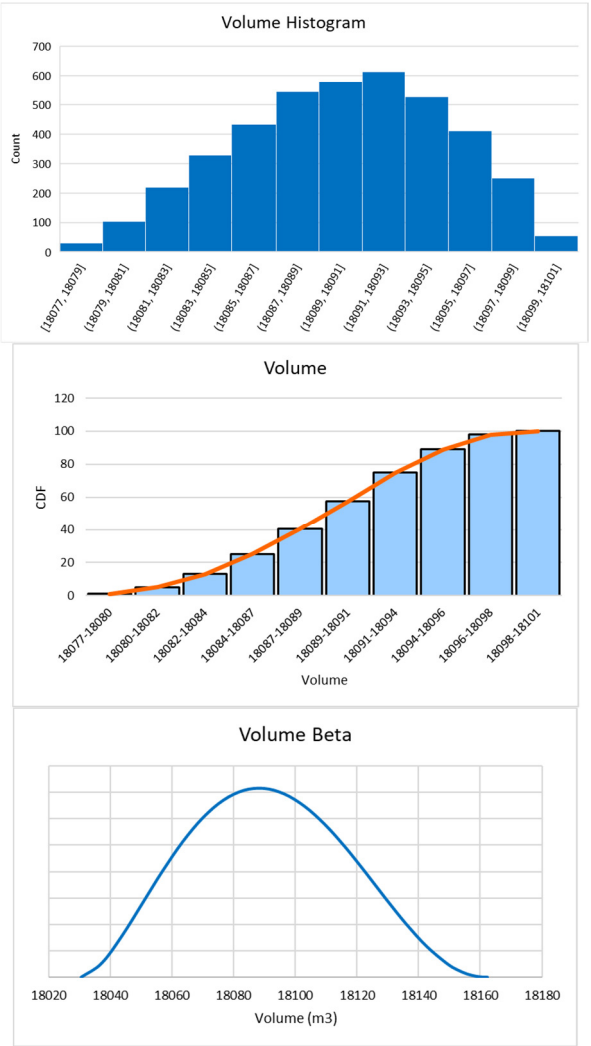

Figure 21: Volume results

Figures 20 and 21 show that the overall distribution is not necessarily well represented by a simple beta, or by a normal distribution (as would be expected as per the central Limit theorem). However, it should be remembered that this study only examined a small set of the many line items in the sizing model.

SPECIFYING UNCERTAINTY RANGES

For this approach to be used in the design exercise, guidance will be required regarding the choice of uncertainty ranges. This should be linked to some characteristic to allow a reasoned selection. Some references may describe uncertainty using +/- values. These can range from specific components to entire weight groups.

From Data

As noted previously, UCL sizing algorithms derived from multiple date points have an inherent uncertainty, and this can be provided in the existing design database. Histograms of the error between the actual values and fitted curve can be used to determine the most appropriate +/- values to generate the min and max inputs to the beta distribution. This is illustrated for the case of diesel generator weight in Figure 22.

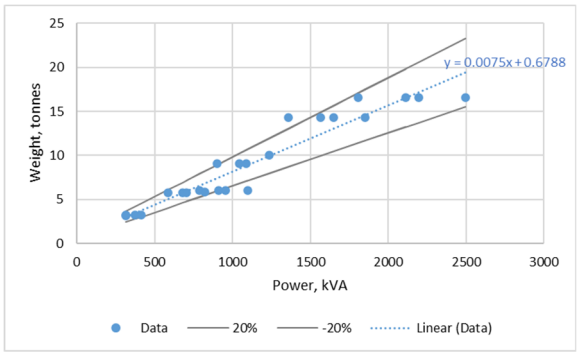

Basis data, fitted curve and example limits

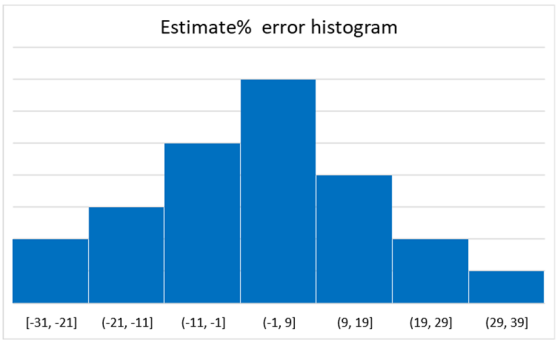

Histogram of errors between fitted curve and input data

Figure 22: Example uncertainty range for a fitted curve

To support the development of the new design tool, similar histograms have been developed based on reference papers containing historical values such as Kehoe et al (1983). A range of general arrangement drawings for commercial and naval ships have also been analysed to determine possible distributions for the area of certain spaces, some of which are shown in Figure 23. The figure also compares the area per rating for accommodation sizes in commercial and naval vessels in the database and whilst there is some overlap in the values, the distributions are quite different. This is due to the dominance of offshore support vessels and research vessels from the 1990s onwards in the commercial ship database, all being designed to broadly similar standards of crew comfort, whilst the warships database contains ships as old as the 1970s designed RN Type 22 frigate (with mess decks for accommodation) and as modern as the RNZN Otago class OPV (with cabins).

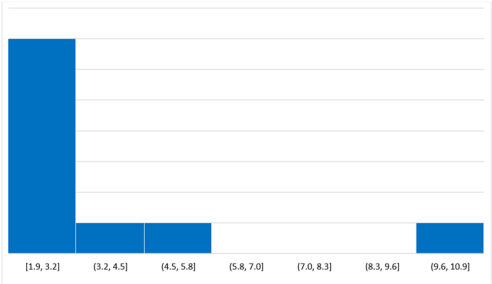

Operations rooms, area per operator

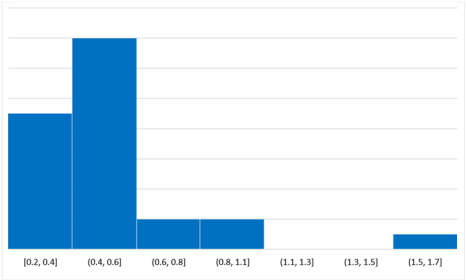

Galleys, area per crewmember

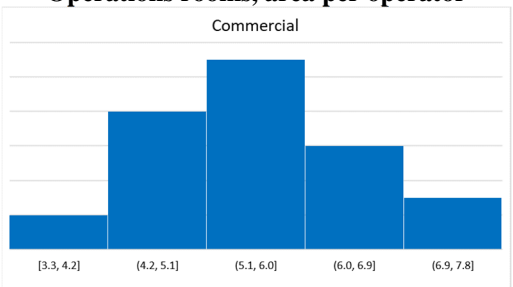

Ratings accommodation, area per rating, commercial

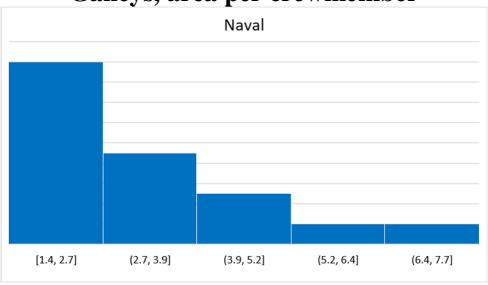

Ratings accommodation, area per rating, naval

Figure 23: Example histograms for spaces extracted from general arrangement drawings

From Design Margins

The recommended weight and space margins summarised in Table 2 may also be used to generate a beta distribution, under some assumptions. If a weight margin is assumed to be the value that captures 90% of all possible outcomes (for example) then it is possible to define a Beta distribution that reflects this. Figure 24 shows how this might be represented for the assumption that the baseline value is the most likely value (left) or that the margin value is most likely (right). The margin value has a CDF of 90% in both cases. This approach has the advantage of aligning with the existing approach to design margins.

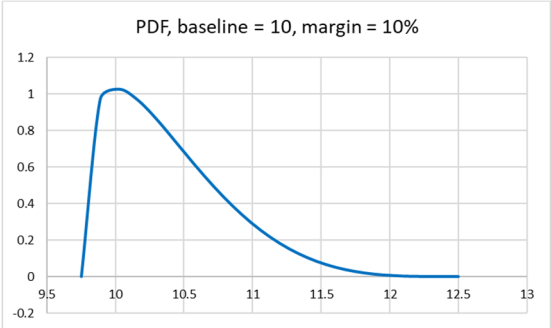

PDF assuming baseline value is most likely

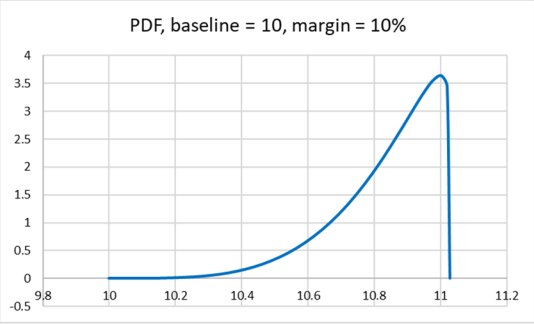

PDF assuming margin value is most likely

Figure 24: PDFs derived from existing margins and assumption that margin = 90% cumulative probability

From Confidence Levels

Linking uncertainty values with standardised definitions of confidence, is attractive for a teaching environment as the definitions can be clearly stated and understood. The NASA Technology Readiness Levels (Manning, 2023) are already used within both the SDX and its sister Submarine Design and Acquisition Course at UCL, but do not have any formal margins or uncertainty values associated with them. Past NASA programmes have shown that novel concepts can experience huge weight growth as the design develops (NASA, 1971) however, a ship would usually not be entirely composed of new technologies so TRL-linked weight margins or uncertainty levels should be selected for the specifics of shipbuilding rather than aerospace. Pedatzur (2016) proposed specific ship weight margins associated with the Bonen scale – a similar concept to TRL – and stage of the design. These are shown in Table 6 below and could be used to generate a PDF as per other weight margins. The Bonen scale having four levels listed below.

Level 1—Duplicating an Existing System
Level 2—Upgrading an Existing System
Level 3—Development of a New System
Level 4—Technological Breakthrough

Table 6: weight margins based on design stage and Bonen scale (after Pedatzur (2016))

Complexity and risk level according to the "Bonen Scale"	Stage of the project			
	Feasibility study	Contract design	Detailed design	Construction
Level 1	5%	4%	2%	1%
Level 2	10%	8%	5%	2%
Level 3	15%	12%	8%	4%
Level 4	25%	15%	10%	5%

DISCUSSION AND CONCLUSIONS

Within the UCL SDX, general uncertainty in design is handled in a relatively simplistic manner via margins added to various characteristics, and a limited set of operating conditions to be analysed. It has proven difficult to ensure students consider the concept of uncertainty in their design, either at the whole ship or system level, and this has, ironically, been made more difficult

by the greater numerical precision easily available with modern tools. This paper has described a work-in-progress on developing new tools and approaches to address this issue. Whilst a need for a different approach to educating future engineers about uncertainty in design has been identified, the tool demonstrated is only viewed as a step along the way. As the ship design exercise represents one quarter of the total credits for the MSc some caution is warranted when making changes to the tools or material. This paper is intended as part of the discussions on the way to improving ship design teaching at UCL. Implementation of an Excel based uncertainty model using the beta distribution at individual line-item and component level has proven relatively straightforward. More complicated is the development of the supporting material, such as recommended numerical uncertainty values associated with concepts such as TRL and the phase of the design process.

FURTHER WORK

Currently the tool performs a simple analysis, generating all possible combinations of the selected items. This full factorial approach does not scale to larger numbers of samples or components of a system without an unacceptable run time. A further development would be to incorporate a method such as Latin Hypercube Sampling to generate a statistically representative set of results over a large range of design components. As a typical UCL sizing sheet would contain around 250 individual line items this would be a challenge to cover the entire design within a run-time acceptable to maintain the desired level of interactivity. However, it would permit the extension of single-system analyses to cover more components.

Additional visualisations and aggregations of results will be required for deployment, as experience with other UCL-developed tools has shown that students frequently output the results from multiple runs with the tool, to compare and discuss with teammates. A further area of development is to automate the process of generating the complete definition of a beta distribution from only a baseline and additive margin. The beta distribution is defined by three input parameters; minimum, maximum and most likely, so a method is required to derive the values such that the CDF reaches the required value (e.g. 90%) at the margin, as shown in Figure 24. Currently this is done by a pre-calculated set of ratios arrived at by numerical approximation.

REFERENCES

Abbott, J., W., (1977), “Modular Payload Ships in the U.S. Navy”, Trans. SNAME

Andrews, D J, (2001), "Adaptability - The Key to Modern Warship Design", Proc. Warship 2001: Int. Symp. On Future Surface Warships, London: RINA

Andrews, D.J., Pawling, R.J., “SURFCON – A 21st Century Ship Design Tool”, IMDC 2003, Athens, May 2003.

Andrews, D.J., Pawling, R.J., “The Application of Computer Aided Graphics to Preliminary Ship Design”, IMDC 2006, Ann Arbor MN, May 2006.

Andrews, D.J., Pawling, R.J., “The Impact of Simulation on Preliminary Ship Design”, IMDC 2009, Trondheim, Norway, May 2009.

Banks et al., (2013), “Understanding ship operating profiles with an aim to improve energy efficient ship operations”, Low Carbon Shipping Conference, UCL, London

Brefort, D., Singer, D., (2018), “Managing epistemic uncertainty in multi-disciplinary optimization of a planing craft”, International Marine Design Conference (IMDC) 2018, Helsinki, Finland, June 2018.

Brett, P.O., Garcia Agis, J.J., Ebrahimi, A., Erikstad S.O., Asbjørnslett B.E., (2022), “A Rational Approach to Handle Uncertainty and Complexity in Marine Systems Design”, International Marine Design Conference (IMDC) 2022, Vancouver

Brown, D. K., (1991), “The Future British Surface Fleet”, London: Conway Maritime Press

Claus, L.R., Collette, M.D., (2018), “An optimization framework for design space reduction in early-stage design under uncertainty”, International Marine Design Conference (IMDC) 2018, Helsinki, Finland, June 2018.

Doerry, N.H., (2014), “Institutionalizing Modular Adaptable Ship Technologies”, Journal of Ship Production, Vol. 30, No. 3, August 2014

Gaspar, H. M, Brett, P O, Erikstad, S O & Ross, A M "Quantifying value robustness of OSV designs taking into consideration medium to long term stakeholders' expectations", International Marine Design Conference (IMDC) 2015, Tokyo, May 2015.

Gates, P. J. & Rusling, S. C, (1982), "The Impact of Weapons Electronics on Surface Warship Design", Trans. RINA 1982

Hockberger, W.A., (1976), "Ship Design Margins- Issues And Impacts", ASNE Naval Engineers Journal, April 1976

International Society of Allied Weight Engineers, Inc, (2001) "Weight Estimating and Margin Manual For Marine Vehicles", Recommended Practice Number 14, May 22, 2001

Karl, A., Farris, B., Brown, L., Metzger, N., (2011), "Robust design and optimization: key methods and applications", Rolls-Royce PLC

Kehoe, J.W., Brower, K.S., Meier, H.A., Runnerstrom, E., (1983), "US and Foreign Hull Form, Machinery and Structural Design Practices" ASNE Naval Engineers Journal, November 1983

Kristensen, H.O. (2013), Statistical Analysis and Determination of Regression Formulas for Main Dimensions of Container Ships Based on IHS Fairplay Data, Project no. 2010-56, Emissionsbeslutningsstøttesystem, WP 2, Report no. 03, University of Southern Denmark

Lyster, C., Pawling, R., "A proposed framework for developing an Energy Efficiency Design Index (EEDI) for Warships", Mari-Tech 2019, Canada

Manning, C.G., (2023), "Technology Readiness Levels", https://www.nasa.gov/directorates/somd/space-communications-navigation-program/technology-readiness-levels/

NASA (1971), "Fundamental Techniques of Weight Estimating and Forecasting for Advanced Manned Spacecraft and Space Stations", Technical Note 0-6349

Neches, R., (2012), "Engineered Resilient Systems (ERS)", 15th Annual NDIA Systems Engineering Conference San Diego, CA, USA, October 25, 2012

Olivier, J.P., Balestrini-Robinson, S., Briceño, S., (2012), "Ship cost-capability analysis using probabilistic cost modeling and hierarchical functional decomposition methodologies", International Naval Engineering Conference (INEC) 2012, IMarEST

Pawling, R.J., & Andrews, D.J., (2011), "Design Sketching for Computer Aided Preliminary Ship Design", Ship Technology Research / Schiffstechnik, Vol.58, No. 3, September 2011, Institute of Ship Technology and Ocean Engineering, ISSN 0937-7255.

Pawling, R.J., Andrews, D.J., Piks, R., Singer, D., Duchateau, E., Hopman, H., (2013) "An Integrated Approach to Style Definition in Early Stage Design", 12th COMPIT, Cortona, Italy, 15-17 April 2013.

Pawling, R.J., Piperakis, A.S., Andrews, D.J., (2015), "Developing Architecturally Oriented Concept Ship Design Tools for Research and Education", International Marine Design Conference (IMDC) 2015, Tokyo

Pawling, R.J., Bilde, R., Hunt, J., "HYDRA – multipurpose ship designs in engineering and education", International Marine Design Conference (IMDC) 2018, Helsinki, Finland, June 2018.

Pedatzur, O., (2016), "Weight Design Margins in Naval Ship Design—A Rational Approach", ASNE Naval Engineers Journal, June 2016, No. 128-2

Plessas, T., Papanikolaou, A., Liu, S., Adamopoulos, N., (2018), "Optimization of ship design for life cycle operation with uncertainties", International Marine Design Conference (IMDC) 2018, Helsinki, Finland, June 2018.

Porche, I., Willis, H., Ruszkowski, M., "Framework for Quantifying Uncertainty in Electric Ship Design", RAND National Defence Institute, DB-407-ONR, March 2004

Puisa, R., Pawling, R., Bliault, C., Pratikakis, G., Tsichlis, P., (2014), "Description of uncertainty in design and operational parameters", Deliverable n. 6.3, FAROS, EC Project no 314817

Puisa, R., (2015), “Integration of Market Uncertainty in Ship’s Design Specification”, International Conference on Computer Applications in Shipbuilding (ICCAS) 2015, Bremen, Germany

Simpson, T., (2000), “Taguchi’s Robust Design Method”, in IE 466: Concurrent Engineering, course notes, Penn State University, https://www.mne.psu.edu/simpson/courses/ie466/ie466.robust.handout.PDF

UCL, 2024b: UCL IEP page: https://www.ucl.ac.uk/centre-for-engineering-education/integrated-engineering-programme

UCL, 2024a: UCL Mechanical Engineering homepage: https://www.ucl.ac.uk/mechanical-engineering/ucl-mechanical-engineering

Zwaginga, J., Stroo, K., Kana, A., (2021), “Exploring Market Uncertainty in Early Ship Design”, International Journal of Naval Architecture and Ocean Engineering 13 (2021)

Proceedings of 15th International Marine Design Conference (IMDC-2024)
June 2-6, 2024
Amsterdam, the Netherlands

Empowering Adolescents through Hands-on Wooden boatbuilding Training: Adapting Javanese Wooden Boat Design and Construction for a Teenage-Friendly Training Experience

Daniel M. Rosyid[1] and Samodra[2,*]

ABSTRACT

In the realm of educational and cultural enrichment, empowering adolescents through hands-on wooden boatbuilding training connects them with Javanese maritime heritage. This scholarly exposition outlines a modern path for youth to engage in traditional wooden shipbuilding, emphasizing tangible skill acquisition and intangible heritage appreciation. The curriculum navigates the confluence of woodworking, mentorship, and cultural identity, fostering youth empowerment. This innovative pedagogical approach views wood sculpting as a vehicle for empowerment, creating a framework for youth-friendly learning inspired by Javanese shipwrights. The proposed model not only crafts seaworthy vessels but also shapes resilient, confident, and empowered young minds, navigating the waves of growth and identity.

KEY WORDS

Empowerment; Adolescents; Training; Adaptation; Boatbuilding.

.

INTRODUCTION

At the heart of adolescent development lies the need for an education that equips youth with more than just academic knowledge; it calls for the development of holistic skills that prepare young minds for the challenges and opportunities that await them in the future. Integral to this comprehensive educational experience is the incorporation of innovative, engaging, and practical teaching methodologies that groom adolescents into competent, creative, and culturally aware adults.

A paradigm that fulfills these criteria is the art of traditional Javanese wooden boatbuilding, an Indonesian cultural hallmark that is as much about craftsmanship as it is about heritage and communal identity (Clark et al., 1993).

Tucked away within the vast maritime expanse of the Indonesian archipelago, the island of Java quietly harbors a tradition that encapsulates both the essence of cultural ingenuity and the spirit of nautical exploration that has come to define the region for centuries. Javanese wooden boatbuilding is not merely a craft; it is a limbic narrative, interwoven with the lives of the people who build these vessels and the seas they navigate. It speaks of a symbiosis between nature and human endeavor, between the trees that furnish the material and the hands that mold it into form. This intrinsic relationship, filled with lessons of sustainability, resilience, and engineering, holds untapped educational potential, particularly for the youthful learner (Barker, 1993).

[1] Department of Ocean Engineering, Institut Teknologi Sepuluh Nopember, Surabaya, Indonesia
[2] Department of Naval Architecture and Shipbuilding, Muhammadiyah University, Gresik, Indonesia
* Corresponding Author: nfsamodra@gmail.com

Submitted: 2 February 2024, Revised: 8 April 2024, Accepted: 1 May 2024, Published: 20 May 2024

Conference paper, DOI: https://doi.org/10.59490/imdc.2024.854 e-ISSN: 3050-4864

The present paper endeavors to explore the transformative prospect of adapting the Javanese boatbuilding tradition for adolescent training programs with a particular emphasis on empowerment as a fundamental outcome. The need for such an interventional approach in educational systems cannot be overstated, especially in an era that is rapidly shifting towards abstract, disconnected modes of learning. By bringing this centuries-old maritime artisanry into training modules, the contemporary youth can be imbued with a rich concoction of hard skills such as woodworking, design, and physics, coupled with soft skills like teamwork, problem-solving, and cultural intelligence (Belasus & Daly, 2023; Ellis, 2009).

This fusion of practical know-how and socio-emotional development embedded within a cultural context promises to deliver a multi-faceted learning experience. Adolescents engaged in this hands-on woodworking journey will not only inherit the rich legacy of their forebearers but also arm themselves with a suite of applicable skills and competencies. Moreover, by crafting something tangible and enduring, such as a wooden boat, they participate in a rite of passage that instills a robust sense of self-efficacy, accomplishment, and pride (Bogucki, 2008).

However, the question remains: how does one translate an involved and intricate tradition such as Javanese wooden boatbuilding into an accessible, engaging, and rewarding experience tailored for the young modern learner? It is a task that involves a careful balance of respect for tradition with the pragmatism of educational application (Mitsuyuki et al., 2020).

Modifications and adaptations are necessary to cater to the learning requirements and safety of adolescents, all while ensuring the essence of the craft is not lost but rather emphasized and cherished (Roberts et al., 1994).

Moreover, the process must be cognizant of the current societal trends and the adoption of technological advancements. Youths today are digital natives, and the use of technology must be adeptly integrated into the learning process to heighten their engagement and to bridge the gap between traditional craftsmanship and contemporary learning environments (H. De Rosa et al., 2012).

Such an endeavor also brings forth considerations of pedagogical theory, instructional design, and curriculum development. It is about curating an experience that respects the cognitive and psychological developmental stages of adolescents (Hunt, 2012). It is about embracing a multidimensional teaching approach that fosters not just skills but also an awareness of environmental stewardship, an appreciation for cultural diversity, and a sense of connectedness with the global historical narrative (Allen, 2022).

Through a pedagogical lens, the paper examines the theoretical frameworks and educational underpinnings that support such an integration of tradition into teaching. It delves into constructivist theories, experiential learning models, and the latest in educational psychology to discern methodologies that both resonate with the targeted age group and deliver on instructional goals. The manuscript also explores the socio-cultural importance of maintaining such crafts, the potential impact on local communities, and how engaging the youth in this tradition can foster a new generation of custodians for intangible cultural heritage (Zhao et al., 2023).

In dissecting the role that this adaptation of Javanese boatbuilding can play in the broader scope of adolescent empowerment, the discussion extends to include the expected outcomes and deliverables of such a program. These include the development of technical acumen, enhancement of socio-emotional intelligence, promotion of cultural pride, and ultimately, the cultivation of a self-empowered individual ready to navigate the complex seas of the contemporary world (Allen, 2022; H. M. De Rosa et al., 2015).

As such, the paper sets the stage for a comprehensive exploration of how the ancient lore of Javanese wooden boatbuilding can be reframed and restructured as a potent instrument for modern education, a tool that does not merely impart knowledge but actively empowers the learner. It provides the foundation upon which a rich tapestry of cultural education can be woven, never losing sight of the ultimate goal: to mold adolescents who are not just learned but empowered, not just skilled but also enlightened; individuals who are the very embodiment of the fusion of tradition with modernity, of the past with the future.

THE RELEVANCE OF BOATBUILDING TRAINING IN ADOLESCENTS FORMATTING

In the multidimensional world of education, specific approaches and disciplines serve as pivotal gateways to a spectrum of learning outcomes and skill development. Notably, among such methods, boatbuilding training has emerged as a remarkable platform that dissipates its echoes across diverse dimensions such as the mechanical, structural, aesthetics, and historical.

This craft, particularly as it unfolds in the context of traditional Javanese boat design and construction, possesses inherent potential to not only stimulate intellectual growth but also cultivate personal attributes and codify cultural connections for adolescents, a transformative experience that amalgamates the richness of heritage, the wisdom of age-old techniques, and the value inculcation of priceless transferable skills (Hunt, 2012).

When analyzed closely, the intricate process of boatbuilding offers numerous touchpoints of mechanical understanding for the learner. It introduces students to the basic principles of woodworking, from selecting and preparing the right materials to understanding the various types of tools, their uses, and safe handling methods.

Beyond learning the pragmatic value of creating something tangible and useful, young learners gain exposure to concepts such as buoyancy, load bearing, balance, and propulsion, which inadvertently steep them in the fundamentals of physics and engineering (Stammers, 2001).

The hands-on application of these principles not only serves as a practical demonstration of theoretical knowledge but also promotes an in- depth comprehension of how different mechanical aspects merge to give life to a complete sea-going vessel.

On a more sophisticated level, the design and construction of a boat demand an understanding of structural concepts. Students learn about the importance of creating a durable, robust framework that can withstand the elements, the steps to ensure symmetry and balance, and the elements that contribute to a boat's overall stability and functionality.

This exposure cultivates an appreciation for how integral the combination of various constituents, wood pieces, hull design, deck arrangement, is to the working of the complete, structural entity. Understanding these concepts prepares adolescents for potential interests and careers in architecture, structural engineering, and product design (Kahanov et al., 2012).

Inescapably, boatbuilding is not a process devoid of artistry. The craftsmanship requires an eye for detail and an aesthetic sense that ensures the finished product is pleasing to the eye. Javanese boat design is well-regarded for its distinct, intricate detailing that can be seen as an expression of cultural art inherited through generations.

The opportunity to learn, appreciate, and contribute to this retained aesthetic appreciation in adolescents can help foster a belief in the value of traditional art and the potential for its modern reinterpretation (Martín Seijo et al., 2021).

Equally significant is the historical facet woven into the very fabric of Javanese boatbuilding. As the adolescents attune to innovative building techniques, they inadvertently uncover layers of historical information lurking beneath. They explore a rich tapestry of maritime history, socio-cultural norms, and philosophical underpinnings that have shaped the very tradition they are engaging with. This understanding bridges generations and fosters respect for the wisdom and skills of ancestors, thereby building a profound connection with their cultural lineage (Domínguez-Delmás et al., 2023).

Delving deeper beyond academic growth, engaging adolescents in the process of boatbuilding offers a fertile landscape for the germination of essential character traits. The art of crafting a boat is a testament to patience since the process requires careful precision and does not permit haste. Dedication and persistence are instilled as the project demands time, effort, and a consistent commitment to see the craft move from an idea to reality (Grieco et al., 2020).

Moreover, since boatbuilding is rarely a solitary endeavor, students learn the essence of teamwork and cooperation. They experience the division of labor, the necessity of communication, and the shared responsibility that fosters a communal spirit. It births an understanding of collective responsibility and helps students grow into more collaborative, thoughtful individuals, attributes that are invaluable for personal growth and career success (Teo et al., 2021).
Simultaneously, the boatbuilding journey amplifies the spirit of determination and resilience. The path to completion might be strewn with failed attempts, challenging stages, and moments of self-doubt. However, overcoming these obstacles instills a sense of accomplishment, self-efficacy and nurtures the courage to persist amid adversity, an experience resembling the arduous but rewarding voyage of a boat on the sea (Imron & Abdullah, 2023).

By engaging youth in the Javanese tradition of boatbuilding, the educational prospect goes a step further, infusing cultural appreciation alongside practical wisdom. These adolescents gain first-hand insight into the philosophy and principles echoed in every curve, joint, and finishing touch of the boats they build. They unwittingly become custodians of a rich cultural legacy, appreciating, preserving, and potentially passing on their knowledge to future generations (Barker, 1993).

The acquisition of practical, transferable skills through boatbuilding initiatives imparts a unique edge to adolescents, preparing them for versatility in various fields in the future. They become equipped not only with technical knowledge but also insights into project management, problem-solving, and critical thinking, proficiencies that persist beyond the boatbuilding classroom and into their adult life (Allen, 2022; Szubska et al., 2023).

In its essence, the pedagogy of traditional boatbuilding embodies a worldview on education: a journey of self-exploration, discovery of heritage, initiation into adulthood, and protocols of community living. Simultaneously, it is an experiential journey that opens young minds to the infinity of their potential (Rodzala & Saat, 2018). A pathway to empowerment, the relevance of teaching Javanese boatbuilding to adolescents can be seen as a catalyst in their evolution: an evolution from learners to creators, from students to skilled practitioners, and ultimately, from adolescents to empowered adults ready to navigate the vast ocean of life's opportunities.

ADAPTING THE JAVANESE WOODEN BOAT DESIGN FOR ADOLESCENT TRAINING

The encapsulation of traditional Javanese wooden boat designs within an adolescent training program brings about an intriguing challenge. It necessitates adapting an age-old craft, complex, nuanced, and routed in layers of cultural knowledge and skill, into an accessible, appealing, yet formative educational experience for youth. The process of adaptation needs to strike a thoughtful balance between preserving the essence of the craft and making the experience stimulating, relevant, and youth-friendly. This section explores addressing this challenge by simplifying complex techniques, incorporating technological integration, and enhancing engagement strategies for a holistic learning environment fostering adolescent development (Liu et al., 2019).

The Boat Design

Javanese traditional wooden boats, known for their cultural significance and historical roots, provide a unique foundation for innovative adaptations in modern boat design. The general arrangement of Javanese traditional wooden boats can be creatively integrated with contemporary elements, fostering a harmonious blend of heritage and functionality. Adapting their design for contemporary use involves respecting and drawing inspiration from the cultural heritage embedded in these vessels. The general arrangement reflects a balance between preserving the authenticity of the original design and incorporating practical modern features.

Ergonomics in the general arrangement should be approached with a focus on preserving the traditional aspects of Javanese boat design. The arrangement should be strategically positioned to reflect the cultural context, ensuring a comfortable and authentic experience This integration of ergonomic principles with traditional aesthetics contributes to a seamless fusion of old and new.

Building the wooden boat for this training purpose should also involve a commitment to sustainable construction methods. Emphasizing the use of locally sourced, renewable materials and traditional building techniques contributes not only to the authenticity of the design but also to the environmental sustainability of the vessel. This approach aligns with the ethos of Javanese craftsmanship, which historically prioritizes harmony with nature. The construction of this training wooden intentionally avoids the use of wood from natural forests and exclusively utilizes wood sourced from cultivation which are Teak wood (Tectona grandis) and Mahogany (Swietenia mahogani) harvested from managed cultivated forest.

Adapting the general arrangement of Javanese traditional wooden boats for contemporary use involves a delicate dance between heritage and innovation. Preserving cultural authenticity, optimizing spatial arrangements, infusing ergonomics with tradition, embracing sustainable construction methods, and integrating technology with sensitivity are crucial aspects of this transformative process. In doing so, designers can create vessels that not only pay homage to Javanese maritime traditions but also serve as a bridge between the past and the future of wooden boat design.

The frames are made using wood lamination techniques in which wooden materials are placed together to form a strong and water-resistant structure. Lamination techniques are employed to reduce the use of natural bent timber for the frames constructions and to improve structural performance. By utilizing lamination techniques, boats can be designed with better durability without sacrificing the sustainability of resources This technique enables manufacturers to achieve an optimal combination of strength, lightweight construction, and resistance to environmental conditions in water.

The boat name is Putri Mayangmadu, translated into English as 'The Daughter of Mayangmadu.' The name originates from a local folklore featuring Prince Mayangmadu, whose name literal translation means Sugar Palm (Arenga pinnata). Prince Mayangmadu served as a prominent local chief during the Javanese classical era, possibly acting as the Harbor Master of the Paciran coastal area, where the boatyard for the training project is located.

Principal Dimension of the Boat:

LOA	: 12.85 meter
LBP	: 11.10 meter
B	: 4.00 meter
H	: 1.65 meter
T(max)	: 1.10 meter

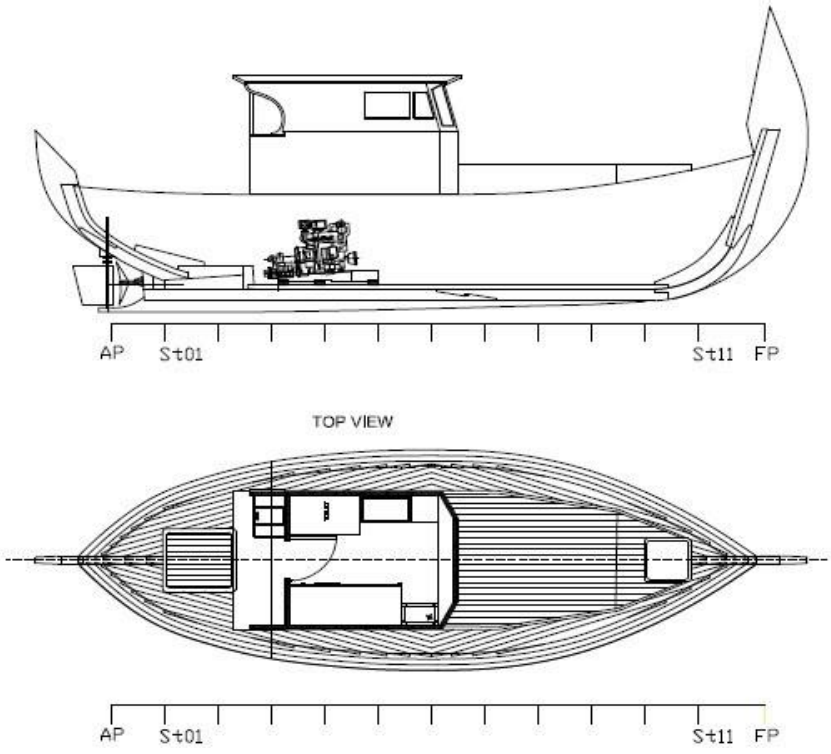

Figure 1: General Arrangement

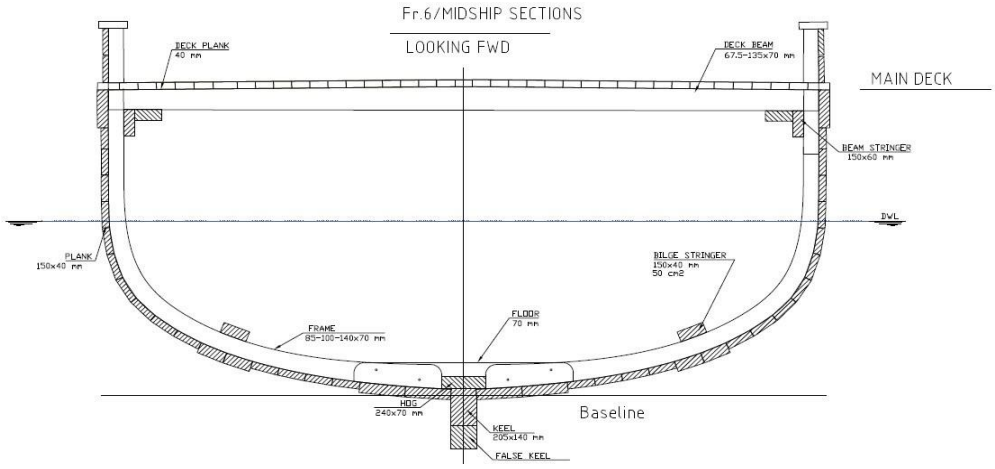

Figure 2: Midship Section

Figure 3: The Daughter of Mayangmadu is seen side by side with a traditionally built Javanese wooden fishing boat

The Builders Team

The boat was constructed in a traditional wooden boatyard in Kandangsemangkon Village, Paciran East, Java (Coordinates 6052'17.02"S - 112018'50.02"E) as a training project for a team of students from SMK Negeri 3 Buduran Sidoarjo – a state-owned Vocational High School – and students from SMK Sunan Drajat, Paciran – a local Islamic Vocational Boarding High School. The teamwork involved 45 male and female students, guided by 4 Master Boatbuilders as trainers. The training lasted for 8 months, with 6 months dedicated to fieldwork. Throughout the training period, the students stayed in provided housing next to the boatyard.

Figure 4: The students are constructing the boat's laminated frames in the school workshop

Figure 5: The students are working on setting the frames in the boatyard.

Figure 6: Completing the hull construction

Figure 7: Pre-launching

Figure 8: Sea Trial

Simplification of Technical Aspects

An accurate replication of traditional Javanese boatbuilding techniques may involve intricate processes, high-end tools, and a level of skill mastery typically earned over years, if not decades, of practice. For an adolescent demographic, some of these aspects could appear daunting, unnecessarily arduous, or even unsafe, potentially hampering youth's buy-in into the learning process. Therefore, it becomes crucial to devise a simplified model of boatbuilding that retains the core elements of the tradition yet is streamlined, achievable, and safe for younger learners (Belasus & Daly, 2023).

The first step would be to distill the techniques into their most basic elements, ensuring that the fundamental concept, approach, or principle that drives the technique remains intact. This simplified design needs to be easily comprehensible to the adolescent mind, scaffolding upon students' existing abilities and understanding. By strategically reducing the complexity, it ensures the learners are not overwhelmed, thus promoting a sustainable and fulfilling learning journey that gradually grows in depth and sophistication (Indruszewski, 2008).

One example of simplifying boat construction involves utilizing lamination techniques for futtock constructions and designing jigs to facilitate students in forming the futtock and assembling other frame parts without excessive complexity.

While preserving cultural authenticity, the use of age-appropriate, modern tools becomes instrumental in maintaining safety, efficiency and reduced physical effort. Protective gear, accompanied by strict safety protocols, can ensure that the students can engage in the process without posing unnecessary risks. Moreover, the incorporation of simpler, ergonomically designed tools mitigates the risk of injury and drastically increases the students' sense of mastery and confidence in handling the tools, empowering them to explore deeper into the craft (Kahanov et al., 2012; Khalilieh, 2005).

Use of Technology

In an era where adolescents are essentially digital natives, a crucial aspect of the adaptation process lies in integrating technology within the traditional boatbuilding training. This adoption not only makes the training more relatable to modern youth but also expands the horizons of their understanding, application, and interest in the craft (Ma et al., 2023).

One compelling tool for this purpose could be Learning Management System. This tool will enable online distance learning, anywhere anytime as long as the internet connection is available.

The learning management system employed is Moodle, an open-source platform software, complemented by instructional videos developed specifically for boat construction tasks. These videos guide students through various stages of the construction process, offering detailed demonstrations and explanations. By integrating video instruction into Moodle, students benefit from visual aids that enhance their understanding and retention of complex concepts and techniques involved in boat building. This multimedia approach not only facilitates learning but also allows students to review and reinforce their skills at their own pace, ensuring comprehensive mastery of the construction process.

In the intricate planning and design stages of boatbuilding, Learning Management System can provide an immersive way for students to understand and visualize the project before they even lift a single tool. They can study the technical and the 3D drawings of the proposed boat, inspect it from every angle, and comprehend the structural nuances, a previsioning process that could significantly intensify their conceptual understanding. The 3D Drawing could also provide a safe, virtual sandbox where students can practice certain construction methods or procedures before replicating them in the real world. This risk-free, immersive experience allows for learning through practice minus the risk, fostering a heightened sense of preparation and confidence when transitioning to real-world application.

Moreover, using modern software to design, simulate, and test the boats on a computer allows adolescents to align their insights about traditional craftsmanship with contemporary design principles. This computer-aided design (CAD) integration opens an engaging dialogue between tradition and technology, an exciting arena of exploration that could be massively appealing to technological affinities of modern youth. Introducing technology in the teaching of traditional boatbuilding is, therefore, about creating relevant bridges between the traditional and modern worlds of learning. It's about using tools that adolescents are familiar with, to teach them skills that have their roots in the distant past but are still as relevant today.

Enhanced Engagement

The art of teaching, more so when it involves encapsulating culturally rich traditional skills within an adolescent learning net, lies in thoughtfully enhancing student engagement. The efficacy of the boatbuilding training program will pivot upon the ability to capture students' curiosity, sustain their interest, and motivate them towards continual growth in mastering the craft.

Consequently, designing the program thoughtfully with ample opportunities for hands-on activities, group collaboration and gamification could be the catalysts in transforming the experience into an engaging, empowering journey rather than a mere technical skill-learning endeavor (Grieco et al., 2020).

Firstly, hands-on activities present an experiential learning environment where students can tangibly interact with the processes and see the fruits of their efforts materialize in real-time. The amalgamation of 'thinking' and 'doing' fosters deeper comprehension, retention, and satisfaction stemming from active learning. It positions the students as active creators rather than passive receivers, thereby continually cultivating their intrinsic motivation (Eggenberger & Backes-Gellner, 2023).

Secondly, the incorporation of group tasks within the boatbuilding process fosters students' interpersonal and collaborative skills. Building a boat in teams not only lightens the workload but also births an atmosphere of mutual reliance, shared accomplishment, and communal kinship, values that resonate with the societal orchestration of traditional Javanese boatbuilders (Erstad & Siddiq, 2023).

Lastly, incorporating gamification elements in the boatbuilding process can convert learning tasks into challenges, making the process more enjoyable and motivating for adolescents. Leaderboards, progress bars, badges, or other rewarding elements can boost student motivation. Also, integrating positive reinforcements such as certifications, rewards, or school credits can serve as powerful incentives to spur interest and induce motivation, ensuring progress is recognized and valued, fostering a sense of accomplishment and ownership among the learners (Hassan et al., 2017; Omar et al., 2020).

Gamification can take the form of students circling the boat and playing while inspecting various parts of a ship's construction that are perceived to be incorrect. They are discussing and arguing about the result of the inspections with an instructor supervising and acting as the judge. Rewards can be given to those who identify the most errors. Rewards can also be given to students who provide arguments explaining why a particular error occurred.

In adapting the Javanese wooden boat design for adolescent training, an essential consideration remains harnessing the profoundness of formative skills nestled in cultural wisdom. It's about simplifying while preserving, modernizing without losing authenticity, and engaging without overwhelming. Continual careful calibration of these components can ensure that the resulting training program rhetorically communicates its relevance to adolescents, both as a tribute to their shared cultural heritage and as a skillset geared towards their future prospects (Ciarli et al., 2021).

OUTCOMES AND EMPOWERMENT

The fruition of a well-adapted Javanese wooden boat design training program for adolescents must be seen not just in completed boats or acquired skills, but in the broad-sweeping developmental accomplishments, and ultimately, empowerment, of its participants. This experience is expected to yield multifaceted outcomes, propelling students into a realm where they are not only cognizant of the value of traditional craftsmanship but also possess enhanced capabilities that span the technical, social, and cognitive domains (Belasus & Daly, 2023; Roberts et al., 1994). They are likely to emerge with a fortified sense of accomplishment, cultivated teamwork dynamics, a deepened cultural understanding, and a profoundly entrenched sense of personal empowerment. This section delves into the expected outcomes from such a transformative educational journey.

Appreciation of Traditional Craftsmanship

Upon successfully completing training that interlaces the historic threads of Javanese boatbuilding with innovative teaching methods aimed at modern adolescents, students are likely to develop a robust appreciation for traditional craftsmanship. This appreciation stems from understanding the effort, skill, and artistry involved in creating something magnificent from raw materials, all while honoring the time-tested practices of their ancestors. However, their admiration would extend beyond mere recognition; they will internalize the craftsmanship as part of their cultural identity and legacy, a precious heritage to be preserved and cherished (Indruszewski, 2008).

Enhancement of Technical Skills

Naturally, through the detailed and immersive process of boatbuilding, technical skills are honed to a significant degree. Students learn to work with various tools, materials, and methodologies that are both traditional (in respect to Javanese designs) and modern (in relation to contemporary tools and safety practices). The practical knowledge encompassing woodworking, material selection, design principles, and structural integrity interwoven with the efficiency of modern technology provides these adolescents with a unique edge. They add to their toolbox of competencies an array of valuable skills that serve them in various fields, from engineering to design to environmental science (Kahanov et al., 2012).

Social Skills Acquisition

A crucial part of the learning process during the boatbuilding training is the enhancement of social skills. Given that boatbuilding is often a communal effort, students learn valuable lessons in teamwork, communication, leadership, and cooperation. The necessity to collaborate with peers, respect different roles, and contribute effectively to a shared goal is a powerful life lesson that transcends the context and becomes a guiding principle for community life and work environments they will enter later on (Imron & Abdullah, 2023; Jaaffar et al., 2016).

Cultivation of Problem-Solving Abilities

Problem-solving is an inherent part of any constructive or creative task, and boatbuilding is no exception. Adolescents engaged in building a boat face various challenges that demand innovative solutions, whether it's adapting a design to better suit materials at hand or rectifying a structural issue uncovered during a trial. Learning to troubleshoot in the workshop, students apply logical reasoning, critical thinking, and creativity, which becomes a habit of mind beneficial in all aspects of life (Hudnall & Kopecky, 2020).

A Sense of Accomplishment

There is a monumental sense of accomplishment that comes from completing a boat. It's a tangible testament to the students' efforts and skills, a visible, floatable product of their dedication. This sense of accomplishment is profound and resonates deeply, often contributing to heightened self-esteem, a reinforced belief in one's abilities, and a validation of personal effort. The process from start to finish is a journey through which students confirm to themselves that they are creators, builders, and finishers (Messinis & Ahmed, 2013).

Teamwork Dynamics

The collaborative nature of the boatbuilding process fosters not just an ability to work in a team but an intrinsic understanding of group dynamics. Students experience first-hand how a team functions efficiently with the distribution of tasks, reliance on fellow team members, and productive synergy required to achieve a common goal. These teamwork dynamics are invaluable not just in their immediate educational environment but as preparation for their professional life and as active citizens (Eggenberger & Backes-Gellner, 2023; Erstad & Siddiq, 2023).

Deepened Cultural Understanding

By its very nature, the program is steeped in cultural education. By learning the traditional methods of Javanese boat construction, students gain more than just a superficial textbook understanding of their heritage. They gain hands-on, pragmatic comprehension of their cultural history, imbuing within them a respect for their cultural identity and a passion for its conservation and celebration (Hensel et al., 2021).

Personal Empowerment

Finally, and perhaps most importantly, the experience of learning to build Javanese wooden boats culminates in a heightened sense of personal empowerment. Adolescents learn that they can wield tools, create complex designs, work collaboratively, overcome challenges, and complete significant projects. This empowerment transcends the immediate skills learned, it's the realization that these young individuals can engage with their tradition in meaningful ways and are equipped to contribute their inherited knowledge and novel insights to their communities and the wider world (Hassan et al., 2017).

In essence, the outcomes of Javanese wooden boat design training for adolescents are both immediate and enduring. Participants benefit from a unique confluence of skill acquisition and personal development. They are apprentices not only in the artistry of boatbuilding but also in the more subtle art of weaving their newfound skills, cultural understanding, and collaborative experiences into the broader tapestry of their lives (Omar et al., 2020). These outcomes do not just empower students as individual artisans or technicians; they empower them as custodians of a rich cultural heritage, responsible community members, and proactive contributors to society.

CONCLUSIONS

Integrating traditional Javanese wooden boat design into an adolescent training program represents a compelling, holistically beneficial endeavor. It's an innovative crossroads where tradition meets modernity, enriched cultural heritage greets empowering skill learning, and youthful vigor finds a constructive, purposeful outlet. With strategic adaptation that appropriately aligns with adolescents' cognitive capacities and interests, this fusion of boatbuilding craft with modern

pedagogical techniques emerges as a promising avenue for engaging, empowering, and educating the next generation.
By creating a learning space that respects and highlights the intricacies of Javanese boatbuilding craftsmanship while ensuring the experience remains appealing and relatable to modern youth, the training bring about a vibrant educational panorama. It encompasses skill-building, character shaping, and cultural education in an integrated, immersive, and hand-on manner. The process is just as striking as the product, a unique educational journey where adolescents explore, indulge their curiosity, challenge their creativity, and apply their problem-solving acuity.

This harmonious amalgamation of traditional knowledge and contemporary teaching approaches equips youth with an array of tangible and intangible skills. It fosters in them a sense of pride in their cultural identity, a conviction in their capacity to work constructively and collaboratively, and a confidence in their hands-on abilities. The training embodies a symbiotic blend of imparting proven craftsmanship, transmitting cultural essence, and cultivating personal capabilities.
At its core, the adapted training program aims to retain the essence of traditional Javanese boat design while making it a lively, appealing, and empowering learning environment for youth. With both physical and digital tools, fostered team dynamics, and an engaging curriculum that seamlessly interweaves learning with application, the program sets sail to craft an experience as unique as the boats themselves.

It unfolds as a pathway that not only introduces the intricacies of Javanese tradition to a younger demographic but also tangibly empowers them with a tactile, innovative craft. But importantly, the empowerment transcends the confines of the workshop, it is the empowerment of self-confidence, creative expression, cognitive flexibility, and cultural appreciation. So, with every wooden plank carved and every boat finished, students don't just learn to build boats, they learn to navigate new avenues of personal growth, societal contribution, and cultural preservation.

In conclusion, the promising prospect of adapting Javanese wooden boat design for an adolescent training program speaks of an engaged, meaningful, and empowering educational experience. It represents a steppingstone towards connecting young minds with their cultural roots on a personal, relatable, and impactful level. By bridging the gap between the old and the new, the practical and the conceptual, the individual and the collective, the training project create an educational space that resonates with the dynamism, curiosity, and potential of adolescence. This adaptation, therefore, guiding the younger generation to create a future that respects the past and readily shapes the present in the pursuit of “mastery for the seas.”

CONTRIBUTION STATEMENT

Author 1: Conceptualization; methodology; writing **Author 2:** conceptualization; writing and editing, figures and pictures.

REFERENCES

Allen, S. J. (2022). House and Boat: Reuse of Ship Planking in a 10th Century Building at Hungate, York. International Journal of Wood Culture, 3(1–3), 152–160. https://doi.org/10.1163/27723194-BJA10015

Barker, R. (1993). John Patrick Sarsfield’s Santa Clara: an addendum. The International Journal of Nautical Archaeology, 22(2), 161–165. https://doi.org/10.1111/j.1095-9270.1993.tb00404.x

Belasus, M., & Daly, A. (2023). Just Bad Quality or Just Good Quality? The Meaning of Macroscopic Growth Features of Timber in Ship-Archaeological Analyses. International Journal of Wood Culture, 3(1–3), 161–191. https://doi.org/10.1163/27723194-BJA10026

Bogucki, P. (2008). The Bronze Age of Temperate Europe. Encyclopedia of Archaeology (Second Edition), 1–10. https://doi.org/10.1016/B978-0-323-90799-6.50061-5

Ciarli, T., Kenney, M., Massini, S., & Piscitello, L. (2021). Digital technologies, innovation, and skills: Emerging trajectories and challenges. Research Policy, 50(7). https://doi.org/10.1016/j.respol.2021.104289

Clark, P., Green, J., Vosmer, T., & Santiago, R. (1993). The Butuan two boat known as a balangay in the National Museum,Manila, Philippines. The International Journal of Nautical Archaeology, 22(2), 143–159. https://doi.org/10.1111/j.1095-9270.1993.tb00403.x

De Rosa, H., Lucchetta, M. C., & Svoboda, H. G. (2012). Characterization of Sternpost Gudgeon of a Ship Found in the City of Buenos Aires. Procedia Materials Science, 1, 666–673. https://doi.org/10.1016/j.mspro.2012.06.090

De Rosa, H. M., Ciarlo, N. C., Pichipil, M., & Castelli, A. (2015). 19th Century Wooden Ship Sheathing. A Case of Study: The Materials of Puerto Pirámides 1, Península Valdés. Procedia Materials Science, 9, 177–186. https://doi.org/10.1016/j.mspro.2015.04.023

Domínguez-Delmás, M., Schroeder, H., Kuitems, M., Haneca, K., Archangel, S., van Duin, P., & Piena, H. (2023). A stepwise multidisciplinary approach to determine the date and provenance of historical wooden objects. Journal of Cultural Heritage, 62, 430–440. https://doi.org/10.1016/j.culher.2023.06.023

Eggenberger, C., & Backes-Gellner, U. (2023). IT skills, occupation specificity and job separations. Economics of Education Review, 92. https://doi.org/10.1016/j.econedurev.2022.102333

Ellis, R. (2009). Whaling, Aboriginal. Encyclopedia of Marine Mammals, 1227–1235. https://doi.org/10.1016/B978-0-12-373553-9.00281-9

Erstad, O., & Siddiq, F. (2023). Educational assessment of 21st century skills—novel initiatives, yet a lack of systemic transformation. International Encyclopedia of Education(Fourth Edition), 245–255. https://doi.org/10.1016/B978-0-12-818630-5.09038-2

Grieco, G., Fix, P., Kennedy, C., Herbst, J., Shultz, L., Borrero, R., & Dostal, C. (2020). Integrating digital and conventional recording techniques for the documentation and reconstruction of an 18th-Century wooden ship from Alexandria, VA. Digital Applications in Archaeology and Cultural Heritage, 16. https://doi.org/10.1016/j.daach.2020.e00136

Hassan, C. N., Md. Shahid, S. A., & Yunus, N. H. (2017). Soft skills: An evaluation. Pertanika Journal of Social Sciences and Humanities, 25(S), 383–390.

Hensel, R., Visser, R., Overdiek, A., & Sjoer, E. (2021). A small independent retailer's performance: Influenced by innovative strategic decision-making skills? Journal of Innovation and Knowledge, 6(4), 280–289. https://doi.org/10.1016/J.JIK.2021.10.002

Hudnall, J. A., & Kopecky, K. E. (2020). The Empathy Project: A Skills-Development Game: Innovations in Empathy Development. Journal of Pain and Symptom Management, 60(1), 164-169Muhhamd.e3. https://doi.org/10.1016/j.jpainsymman.2020.02.008

Hunt, D. (2012). Properties of wood in the conservation of historical wooden artifacts. Journal of Cultural Heritage, 13(3 SUPPL.). https://doi.org/10.1016/j.culher.2012.03.014

Imron, M. A., & Abdullah, M. R. T. L. (2023). Environment and Benchmarking: Industry 4.0 Sustainable Work Readiness Framework. KnE Social Sciences, 2023, 374–392–374–392. https://doi.org/10.18502/KSS.V8I20.14616

Indruszewski, G. (2008). Ships and seafaring. Encyclopedia of Archaeology, 1985–1994. https://doi.org/10.1016/B978-012373962-9.00282-X

Jaaffar, A. H., Ibrahim, H. I., Annuar, K., Shah, M., & Zulkafli, A. H. (2016). Work-integrated learning and graduate employability skills: The employers' perspective. Social Sciences (Pakistan), 11(21), 5270–5274. https://doi.org/10.3923/sscience.2016.5270.5274

Kahanov, Y., Tresman, J. B., Me-Bar, Y., Cvikel, D., & Hillman, A. (2012). Akko 1 shipwreck: The effect of cannon fire on the wooden hull. Journal of Archaeological Science, 39(7), 1993–2002. https://doi.org/10.1016/j.jas.2012.02.013

Khalilieh, H. S. (2005). Capacity and regulations against overloading of commercial ships in Byzantine and Islamic maritime practices. Journal of Medieval History, 31(3), 243–263. https://doi.org/10.1016/j.jmedhist.2005.06.004

Liu, W., Demirel, Y. K., Djatmiko, E. B., Nugroho, S., Tezdogan, T., Kurt, R. E., Supomo, H., Baihaqi, I., Yuan, Z., &
Incecik, A. (2019). Bilge keel design for the traditional fishing boats of Indonesia's East Java. International Journal of Naval Architecture and Ocean Engineering, 11(1), 380–395. https://doi.org/10.1016/j.ijnaoe.2018.07.004

Ma, X., Zhao, J., Weng, Y., Fei, L., Zhang, H., Liu, J., & Zhao, D. (2023). 3D structural deformation monitoring of the archaeological wooden shipwreck stern investigated by optical measuring techniques. Journal of Cultural Heritage, 59, 102–112. https://doi.org/10.1016/j.culher.2022.11.007

Martín Seijo, M., Cruz Berrocal, M., Serrano Herrero, E., & Tsang, C. (2021). Wooden material culture and long-term historical processes in Heping Dao (Keelung, Taiwan). Journal of Archaeological Science, 133. https://doi.org/10.1016/j.jas.2021.105443

Messinis, G., & Ahmed, A. D. (2013). Cognitive skills, innovation and technology diffusion. Economic Modelling, 30(1), 565–578. https://doi.org/10.1016/j.econmod.2012.10.002

Omar, M. K., Zahar, F. N., & Rashid, A. M. (2020). Knowledge, skills, and attitudes as predictors in determining teachers' competency in Malaysian TVET institutions. Universal Journal of Educational Research, 8(3 3C), 95–104. https://doi.org/10.13189/ujer.2020.081612

Roberts, O. T. P., Barker, R., Parker, A. J., Gőttlicher, A., & McGrail, S. (1994). Review of Wooden Ship Building and the Interpretation of Shipwrecks, by J. R. Steffy; 500 Years of Change-Underwater... The International Journal of Nautical Archaeology, 23(3), 255–259. https://doi.org/10.1006/ijna.1994.1032

Rodzala, S. A., & Saat, M. M. (2018). Factors influencing the improvement of students' communication skill: An industrial training intervention. Journal of Social Sciences Research, 2018(Special Is), 899–906. https://doi.org/10.32861/jssr.spi6.899.906

Stammers, M. K. (2001). Iron knees in wooden vessels - An attempt at a typology. International Journal of Nautical Archaeology, 30(1), 115–121. https://doi.org/10.1016/s1057-2414(01)80012-1

Szubska, M. I., Szubski, M. J., Klisz, M., Pilch, K., Wojnar, J., & Zin, E. (2023). Advantages and limitations of an interdisciplinary approach in woodland archaeology: An example of 18th-19th century tar production in European temperate forest. Quaternary International, 659, 63–73. https://doi.org/10.1016/j.quaint.2022.09.010

Teo, T., Unwin, S., Scherer, R., & Gardiner, V. (2021). Initial teacher training for twenty-first century skills in the Fourth Industrial Revolution (IR 4.0): A scoping review. Computers & Education, 170, 104223. https://doi.org/https://doi.org/10.1016/j.compedu.2021.104223itchell, J.A. (2017). Citation: Why is it so important. Mendeley Journal, 67(2), 81-95

PROCEEDINGS OF THE 15TH

INTERNATIONAL MARINE DESIGN CONFERENCE

The aim of the **15th International Marine Design Conference (IMDC 2024)** is to promote all aspects of marine design as an engineering discipline. The focus of IMDC-2024 is on the key design challenges and opportunities in the maritime field with special emphasis on the following themes:

- **Ship design methodology**
- **Novel marine design concepts**
- **Offshore design methodology**
- Influence of the **energy transition** on maritime design
- Influence of the **unmanned and autonomous transition** on maritime design
- Influence of the **digital transition** on maritime design
- **Influence of regulations on maritime design**
- **Maritime design education.**

IMDC 2024
INTERNATIONAL MARINE DESIGN CONFERENCE

TU Delft OPEN

TU Delft

9 789463 668965

https://doi.org/10.59490/mg.113